HANDBOOK OF FOOD ENZYMOLOGY

edited by

John R. Whitaker
University of California–Davis
Davis, California, U.S.A.

Alphons G. J. Voragen
Wageningen University
Wageningen, The Netherlands

Dominic W. S. Wong
U.S. Department of Agriculture
Albany, California, U.S.A.

MARCEL DEKKER, INC. NEW YORK • BASEL

Cover figure reprinted with permission from Figure 3, page 643 of Architecture of RNA Polymerase II and Implications for the Transcription Mechanism, P. Cramer, D. A. Bushnell, J. Fu, A. L. Gnatt, B. Maier-Davis, N. E. Thompson, R. R. Burgess, A. M. Edwards, P. R. David, and R. D. Kornberg. Science 288(5466): 640–649, 2000. Copyright 2000 American Association for the Advancement of Science.

Library of Congress Cataloging-in-Publication Data
A catalog record for this book is available from the Library of Congress.

ISBN: 0-8247-0686-2

This book is printed on acid-free paper.

Headquarters
Marcel Dekker, Inc.
270 Madison Avenue, New York, NY 10016
tel: 212-696-9000; fax: 212-685-4540

Eastern Hemisphere Distribution
Marcel Dekker AG
Hutgasse 4, Postfach 812, CH-4001 Basel, Switzerland
tel: 41-61-260-6300; fax: 41-61-260-6333

World Wide Web
http://www.dekker.com

The publisher offers discounts on this book when ordered in bulk quantities. For more information, write to Special Sales/ Professional Marketing at the headquarters address above.

Current printing (last digit):
10 9 8 7 6 5 4 3 2 1

PRINTED IN THE UNITED STATES OF AMERICA

Preface

Enzymes are the catalysts of life. They perform the majority of reactions in all living systems—all animals, plants, and microorganisms. Our lives are absolutely dependent on them. Even inhaling in oxygen and exhaling carbon dioxide are dependent on enzymes. Our plants take up minerals, water, and air, and combine them with carbon dioxide and ammonia to provide our fruits and vegetables, via enzymes.

The *Handbook of Food Enzymology* is a single source that can answer questions about what enzymes are, how they function catalytically, and how we depend on them and use them every minute of our life. This is not a book that can be read in a single day. Rather, it is a handbook to be used to find the answers to various questions: Who are we biologically and chemically? How do we function biologically? How do our foods, most of our clothing, and much of our shelter depend on enzymes? What are enzymes? What do they do? How can we manage them in the most effective way to live a long and healthy life with an abundance of food?

The *Handbook* is divided into two major parts. The first 26 chapters deal with general aspects of enzymology. There are two chapters (1 and 2) on the history of enzymology, which discuss protein structure and the kinetics of enzyme reactions and emphasize food production, and the trail of knowledge that led to this handbook. The next two chapters (3 and 4) deal with how enzymes are highly specific and highly efficient catalysts and the environmental factors that affect their activities. Chapter 5 describes how to inactivate enzymes when their action is no longer desirable. Chapters 6 and 7 deal with regulatory issues pertaining to using enzymes in our foods to change the taste, flavor, aroma, color, texture, and nutritional quality. Chapter 8 deals with the evolution of enzymes under extreme conditions of pH, temperature, salinity, toxicity, and pressure, and how these enzymes with special extremophilic characteristics can be used effectively in foods. Chapters 9 through 16 deal with how enzymes produce the components of our foods—the proteins, lipids, carbohydrates, and nucleic acids—as well as the enzymes that make it possible to synthesize our food components rapidly, efficiently, nutritiously, and in the quantity needed to feed 6 billion persons each day. The last 10 chapters (17–26) in Part I deal with management of enzymes postharvest and as tools for increasing the quality and consumability of our foods.

Part II describes specific prototypic enzymes of the six chemical types of reactions catalyzed by enzymes: oxidoreductases, transferases, hydrolases, lyases, isomerases, and ligases. The contributors of these 57 chapters have followed a common format in which they discuss what the enzyme(s), does, its importance to feed and food production, its chemical and biological properties, how to measure activity of the enzyme(s) and how to purify it from raw animal, plant, or microbial sources. Being catalysts, the enzymes are produced in rather small amounts (0.01 to 1% by weight of the total protein).

The contributors were carefully selected on the basis of their specific knowledge of the importance of enzymology to food production, food preservation, and food quality. We are very proud and fortunate to have attracted first-

rate, active scientists worldwide (20 countries are represented) as contributors to the *Handbook*. We hope the *Handbook* will be prominently displayed in all college and university libraries, especially those in which food production, nutrition, and food quality are important subjects, on the bookshelves of all food manufacturing companies, and in many faculty offices at major universities worldwide. When questions arise as to what enzymes are, what they do, and their importance in food supply and quality, we hope students, educators, and researchers will find the answers rapidly and satisfactorily in the *Handbook*.

We thank all the authors for joining us in this endeavor. Their contributions are excellent, up-to-date, and well written. Bringing together over 100 first-rate, active contributors to provide chapters in their selected area of food enzymology was our first objective. We wish to thank all the editors and authors who permitted use of copyrighted material, as well as those who typed the manuscripts. Marcel Dekker, Inc., and its staff were especially helpful as editors and contributors alike struggled to meet deadlines that extended over four years.

To the reader, may you find answers to all your questions on food enzymology in this handbook. If you don't, please ask any of us to help you find additional material and/or clarification.

John R. Whitaker
Alphons G. J. Voragen
Dominic W. S. Wong

Contents

Preface

PART I. GENERAL ASPECTS

INTRODUCTION

Protein Structure and Kinetics of Enzyme Reactions: A Historical Perspective
John R. Whitaker

History of Enzymology with Emphasis on Food Production
Poul Børge Poulsen and Klaus Buchholz

What Enzymes Do and Why They Are Highly Specific and Efficient Catalysts
John R. Whitaker

Enzyme-Catalyzed Reactions: Experimental Factors that Affect Rates
John R. Whitaker

Inactivation of Enzymes: From Experimental Design to Kinetic Modeling
Ann Van Loey, Indrawati, Chantal Smout, and Marc Hendrickx

REGULATORY ISSUES

Regulatory Issues of Enzymes Used in Foods from the Perspective of the E.U. Market
Danielle P. Praaning

Regulatory Issues of Food Enzymes Used in the United States
John R. Whitaker

EXTREMOPHILIC ENZYMES

Properties of Extremophilic Enzymes and Their Importance in Food Science and Technology
Magnús M. Kristjánsson and Bjarni Ásgeirsson

THE FOOD CHAIN AND ENZYMES

Nitrogen Fixation and the Enzyme Nitrogenase
William E. Newton

Enzymes in Amylose and Amylopectin Biosynthesis
Bruce P. Wasserman and Ying Yu

Fatty Acid Biosynthesis and Triacylglycerol Assembly
Allan Keith Stobart and Gareth Griffiths

Phospholipid Biosynthetic Enzymes in Plants
Ralph E. Dewey and Anthony J. Kinney

Applications of Oxidoreductases in Foods
Colja Laane, Yvonne Bruggeman, and Chris Winkel

Transgenic Plants for Production of Enzymes
Anne S. Ponstein, Rob F. Beudeker, and Jan Pen

Enzymes in Protein Biosynthesis
John R. Whitaker

Nucleic Acid Biosynthesis
Dominic W. S. Wong

ENZYMES AS TOOLS TO MODIFY FOOD COMPONENTS

Protein Modification to Optimize Functionality: Protein Hydrolysates
Ton Kunst

Production and Modification of Acylglycerides
Rob M. M. Diks

ENZYMES IN FOODS POSTHARVEST

Significance of Indigenous Enzymes in Milk and Dairy Products
Patrick F. Fox

Exogenous Enzymes in Dairy Technology
Patrick F. Fox

Flavor Enhancement in Fruit Juices and Derived Beverages by Exogenous Glycosidases and Consequences of the Use of Enzyme Preparations
Ziya Günata

IMMOBILIZED ENZYMES AND THEIR APPLICATIONS

Entrapment of Biocatalysts by Prepolymer Methods
Takuo Kawamoto and Atsuo Tanaka

Genetic Immobilization of Enzymes on Yeast Cell Surface
Mitsuyoshi Ueda, Toshiyuki Murai, and Atsuo Tanaka

Use of Immobilized Enzymes in the Food Industry
Harold E. Swaisgood

ENZYME UTILIZATION AND DEVELOPMENT

Enzymes and Food Analysis
Philip O'Connell and George G. Guilbault

Recent Advances in Enzyme Development
Dominic W. S. Wong

PART II. SPECIFIC ENZYMES

OXIDOREDUCTASES

Catalase
Dominic W. S. Wong and John R. Whitaker

Horseradish Peroxidase
Zhong Yi Yuan and Tai Jiao Jiang

Glutathione Peroxidase
Jun-qiu Liu and Gui-min Luo

Glucose Oxidase
A. J. Vroemen

Lactate Dehydrogenase
Hayao Taguchi

Alcohol Dehydrogenase
Sabato D'Auria

Alcohol Dehydrogenase
Sandrine Dallet, Marie Trovaslet, and Marie Dominique Legoy

Amine Oxidase
Akio Ito and Jichun Ma

Prolyl 4-Hydroxylase
Robert B. Rucker, Ana Samimi, and Jerold A. Last

Lysyl Hydroxylase
Ana Samimi, Jerold A. Last, Lucas C. Armstrong, and Robert B. Rucker

Lysyl Oxidase
Robert B. Rucker, Alyson E. Mitchell, Eskouhie Tchaparian, and Jerold A. Last

Superoxide Dismutase
Hirokazu Hara, Tetsuo Adachi, and Kazuyuki Hirano

Polyphenol Oxidase
Edna C. Ramírez, John R. Whitaker, and Victoria M. Virador

Laccase
William H. Flurkey

Mammalian Sulfhydryl Oxidase
Harold E. Swaisgood and Violeta G. Janolino

Xanthine Oxidase
John R. Whitaker

Lipoxygenase and Associated Enzymes
Harold W. Gardner

Sorbitol Oxidase
Kohei Oda and Kazumi Hiraga

TRANSFERASES

Starch Phosphorylases
Ying Yu

Amylosucrase
Volker Büttcher

Dextransucrase
Klaus Buchholz and Pierre F. Monsan

Levansucrase
Ki-Bang Song and Sang-Ki Rhee

Cyclodextrin Glycosyltransferase
Lubbert Dijkhuizen and Bart A. van der Veen

Limonoid Glucosyltransferase
Shin Hasegawa, Masayuki Kita, and Mitsuo Omura

Transglutaminase
Chang-Rak Ha and Ichiro Iuchi

HYDROLASES

Feruloyl Esterases
Craig B. Faulds and Gary Williamson

Lipase
Dominic W. S. Wong

Chlorophyllase
Roger F. McFeeters

Phytase
Onno Misset

α-Amylases
Dominic W. S. Wong and George H. Robertson

β-Amylases
Dominic W. S. Wong and George H. Robertson

Glucoamylase
Peter J. Reilly

Limit Dextrinase/Pullulanase
E. Ann MacGregor

Limit Dextrinase
James Hutchison Bryce

Methodologies for Assaying the Hydrolysis of Cellulose by Cellulases
David Johnston

Cellulases in Food Processing
Maija Tenkanen, Marja-Leena Niku-Paavola, Markus Linder, and Liisa Viikari

β-Glucosidase
Asim Esen

β-D-Fructofuranoside Fructohydrolase
Laura Cantarella, Francesco Alfani, and Maria Cantarella

β-Galactosidase
Raymond R. Mahoney

Pectic Polysaccharides
H. A. Schols and Alphons G. J. Voragen

Pectic Enzymes
Jacques A. E. Benen, Alphons G. J. Voragen, and Jaap Visser

Pectic Esterases
Jacques A. E. Benen, Gert-Jan W. M. van Alebeek, Alphons G. J. Voragen, and Jaap Visser

Polygalacturonases
Jacques A. E. Benen and Jaap Visser

Enzymes Releasing L-Arabinose and D-Galactose from the Side Chains of Pectin
Ronald P. de Vries and Jaap Visser

Xylanolytic Enzymes
Peter Biely

Enzymes with Activity Toward Xyloglucan
Jean-Paul Vincken

Enzymes Degrading Rhamnogalacturonan and Xylogalacturonan
Jean-Paul Vincken, Alphons G. J. Voragen, and Gerrit Beldman

Enzymic Hydrolysis of Cereal (1→3, 1→4)-β-Glucans
Maria Hrmova and Geoffrey Fincher

Enzymology of Endo-1,4-β-Mannanases
Henrik Stålbrand

Lysozyme
Akio Kato

Ribonucleases
Jaap J. Beintema and Wei Zhao

Proteolytic Enzymes
John R. Whitaker

Thermolysin
Kuniyo Inouye

LYASES

Pectate and Pectin Lyases
Jacques A. E. Benen and Jaap Visser

Alliinases
Edna C. Ramírez

Cystine Lyases in Plants
Edna C. Ramírez

ISOMERASES

Xylose (Glucose) Isomerase
Onno Misset

Contributors

Tetsuo Adachi Laboratory of Clinical Pharmaceutics, Gifu Pharmaceutical University, Gifu, Japan

Francesco Alfani† Department of Chemistry, Chemical Engineering and Materials, University of L'Aquila, L'Aquila, Italy

Lucas C. Armstrong Division of Pulmonary and Critical Care Medicine, Toxic Substances Research and Training Program, Department of Internal Medicine, University of California, Davis, Davis, California, U.S.A.

Bjarni Ásgeirsson Department of Biochemistry, Science Institute, University of Iceland, Reykjavik, Iceland

Jaap J. Beintema Department of Biochemistry, University of Groningen, Groningen, The Netherlands

Gerrit Beldman Laboratory of Food Chemistry, Department of Agrotechnology and Food Sciences, Wageningen University, Wageningen, The Netherlands

Jacques A. E. Benen Laboratory of Microbiology, Department of Agrotechnology and Food Sciences, Wageningen University, Wageningen, The Netherlands

Rob F. Beudeker DSM Food Specialties, Delft, The Netherlands

Peter Biely Institute of Chemistry, Slovak Academy of Sciences, Bratislava, Slovakia

Yvonne Bruggeman Functional Biomolecules, Unilever Research, Vlaardingen, The Netherlands

James Hutchison Bryce International Center for Brewing and Distilling, Department of Biological Sciences, Heriot-Watt University, Edinburgh, Scotland

Klaus Buchholz Carbohydrate Technology, Braunschweig Technical University, Braunschweig, Germany

Volker Büttcher Aventis CropScience GmbH, Frankfurt, Germany

†Deceased.

Laura Cantarella Department of Industrial Engineering, University of Cassino, Cassino, Italy

Maria Cantarella Department of Chemistry, Chemical Engineering and Materials, University of L'Aquila, L'Aquila, Italy

Sabato D'Auria Institute of Protein Biochemistry and Enzymology, Naples, Italy, and Center for Fluorescence Spectroscopy, University of Maryland, Baltimore, Maryland, U.S.A.

Sandrine Dallet Laboratory of Protein and Cellular Engineering, University of La Rochelle, La Rochelle, France

Ronald P. de Vries Microbiology, Utrecht University, Utrecht, The Netherlands

Ralph E. Dewey Department of Crop Science, North Carolina State University, Raleigh, North Carolina, U.S.A.

Lubbert Dijkhuizen Department of Microbiology, University of Groningen, Haren, The Netherlands

Rob M. M. Diks Unilever Research and Development, Vlaardingen, The Netherlands

Asim Esen Department of Biology, Virginia Polytechnic Institute and State University, Blacksburg, Virginia, U.S.A.

Craig B. Faulds Food Materials Science Division, Institute of Food Research, Colney, Norwich, England

Geoffrey Fincher Department of Plant Science, University of Adelaide, Glen Osmond, South Australia, Australia

William H. Flurkey Department of Chemistry, Indiana State University, Terre Haute, Indiana, U.S.A.

Patrick F. Fox Department of Food Chemistry, University College, Cork, Ireland

Harold W. Gardner* National Center for Agriculture Utilization Research, Agricultural Research Service, U.S. Department of Agriculture, Peoria, Illinois, U.S.A.

Gareth Griffiths Horticulture Research International, Wellesbourne, Warwick, England

George G. Guilbault Department of Chemistry, University College, Cork, Ireland

Ziya Günata Department of Bioengineering and Food Science, University of Montpellier II, Montpellier, France

Chang-Rak Ha Life Science Institute, Sophia University, Tokyo, Japan

Hirokazu Hara Laboratory of Clinical Pharmaceutics, Gifu Pharmaceutical University, Gifu, Japan

Shin Hasegawa Western Regional Research Center, Agricultural Research Service, U.S. Department of Agriculture, Albany, California, U.S.A.

Marc Hendrickx Laboratory of Food Technology, Katholieke Universiteit Leuven, Leuven, Belgium

Kazumi Hiraga Department of Applied Biology, Faculty of Textile Science, Kyoto Institute of Technology, Kyoto, Japan

Kazuyuki Hirano Department of Pharmaceutics, Gifu Pharmaceutical University, Gifu, Japan

Maria Hrmova Department of Plant Science, University of Adelaide, Glen Osmond, South Australia, Australia

*Retired.

Indrawati Laboratory of Food Technology, Katholieke Universiteit Leuven, Leuven, Belgium

Kuniyo Inouye Laboratory of Enzyme Chemistry, Division of Food Science and Biotechnology, Graduate School of Agriculture, Kyoto University, Kyoto, Japan

Akio Ito Department of Chemistry, Faculty of Science, Kyushu University, Fukuoka, Japan

Ichiro Iuchi Life Science Institute, Sophia University, Tokyo, Japan

Violeta G. Janolino Department of Food Science, North Carolina State University, Raleigh, North Carolina, U.S.A.

Tai Jiao Jiang Institute of Biochemistry and Cell Biology, Chinese Academy of Sciences, Shanghai, China

David Johnston Eastern Regional Research Center, Agricultural Research Service, U.S. Department of Agriculture, Wyndmoor, Pennsylvania, U.S.A.

Akio Kato Department of Biological Chemistry, Yamaguchi University, Yamaguchi, Japan

Takuo Kawamoto Department of Synthetic Chemistry and Biological Chemistry, Graduate School of Engineering, Kyoto University, Kyoto, Japan

Anthony J. Kinney DuPont Experimental Station, Wilmington, Delaware, U.S.A.

Masayuki Kita Department of Plant, Cell, and Environment, National Institute of Fruit Tree Science, Tsukuba, Ibaraki, Japan

Magnús M. Kristjánsson Department of Food Science, Science Institute, University of Iceland, Reykjavik, Iceland

Ton Kunst Quest International, Naarden, The Netherlands

Colja Laane DSM Food Specialties, Delft, The Netherlands

Jerold A. Last Division of Pulmonary and Critical Care Medicine, Department of Internal Medicine, University of California, Davis, Davis, California, U.S.A.

Marie Dominique Legoy Laboratory of Protein and Cellular Engineering, University of La Rochelle, La Rochelle, France

Markus Linder VTT Biotechnology, Espoo, Finland

Jun-qiu Liu Key Lab of Molecular Enzymology and Engineering of Ministry of Education, Jilin University, Changchun, China

Gui-min Luo Key Lab of Molecular Enzymology and Engineering of Ministry of Education, Jilin University, Changchun, China

Jichun Ma Department of Chemistry, Faculty of Science, Kyushu University, Fukuoka, Japan

E. Ann MacGregor Department of Chemistry, University of Manitoba, Winnipeg, Manitoba, Canada

Raymond R. Mahoney Food Science Department, University of Massachusetts, Amherst, Massachusetts, U.S.A.

Roger F. McFeeters Agricultural Research Service, U.S. Department of Agriculture, and Department of Food Science, North Carolina State University, Raleigh, North Carolina, U.S.A.

Onno Misset DSM Patents & Trademarks, Delft, The Netherlands

Alyson E. Mitchell Department of Food Science and Technology, University of California, Davis, Davis, California, U.S.A.

Pierre F. Monsan Department of Biochemistry and Food Engineering, National Institute for Applied Sciences, Toulouse, France

Toshiyuki Murai Department of Synthetic Chemistry and Biological Chemistry, Graduate School of Engineering, Kyoto University, Kyoto, Japan

William E. Newton Department of Biochemistry, The Virginia Polytechnic Institute and State University, Blacksburg, Virginia, U.S.A.

Marja-Leena Niku-Paavola VTT Biotechnology, Espoo, Finland

Philip O'Connell Laboratory of Sensor Development, Department of Chemistry, National University of Ireland, Cork, Ireland

Kohei Oda Department of Applied Biology, Faculty of Textile Science, Kyoto Institute of Technology, Kyoto, Japan

Mitsuo Omura Department of Citrus Research, National Institute of Fruit Tree Science, Shimizu, Shizuoka, Japan

Jan Pen PlantZyme, Leiden, The Netherlands

Anne S. Ponstein Syngenta Mogen, Leiden, The Netherlands

Poul Børge Poulsen Novozymes A/S, Bagsvaerd, Denmark

Danielle P. Praaning DSM Food Specialties, Delft, The Netherlands

Edna C. Ramírez University of California, Davis, Davis, California, U.S.A.

Peter J. Reilly Department of Chemical Engineering, Iowa State University, Ames, Iowa, U.S.A.

Sang-Ki Rhee Biomolecular Engineering Laboratory, Korea Research Institute of Bioscience and Biotechnology (KRIBB), and Real Biotech Co., Ltd., KRIBB, Daejeon, Korea

George H. Robertson Western Regional Research Center, Agricultural Research Service, U.S. Department of Agriculture, Albany, California, U.S.A.

Robert B. Rucker Department of Nutrition, University of California, Davis, Davis, California, U.S.A.

Ana Samimi Pharmacology and Toxicology Graduate Program, University of California, Davis, Davis, California, U.S.A.

H. A. Schols Laboratory of Food Chemistry, Department of Agrotechnology and Food Sciences, Wageningen University, Wageningen, The Netherlands

Chantal Smout Laboratory of Food Technology, Katholieke Universiteit Leuven, Leuven, Belgium

Ki-Bang Song Biomolecular Engineering Laboratory, Korea Research Institute of Bioscience and Biotechnology (KRIBB), and Real Biotech Co., Ltd., KRIBB, Daejeon, Korea

Henrik Stålbrand Department of Biochemistry, Lund University, Lund, Sweden

Allan Keith Stobart School of Biological Sciences, University of Bristol, Bristol, England

Harold E. Swaisgood Department of Food Science, North Carolina State University, Raleigh, North Carolina, U.S.A.

Hayao Taguchi Department of Applied Biological Science, Faculty of Science and Technology, Tokyo University of Science, Noda, Chiba, Japan

Atsuo Tanaka Department of Synthetic Chemistry and Biological Chemistry, Graduate School of Engineering, Kyoto University, Kyoto, Japan

Eskouhie Tchaparian Agricultural and Environmental Sciences, Department of Nutrition, University of California, Davis, Davis, California, U.S.A.

Maija Tenkanen VTT Biotechnology, Espoo, Finland

Marie Trovaslet Laboratory of Protein and Cellular Engineering, University of La Rochelle, La Rochelle, France

Mitsuyoshi Ueda Department of Synthetic Chemistry and Biological Chemistry, Graduate School of Engineering, Kyoto University, Kyoto, Japan

Gert-Jan W. M. van Alebeek Laboratory of Food Chemistry, Department of Agrotechnology and Food Sciences, Wageningen University, Wageningen, The Netherlands

Bart A. van der Veen Department of Microbiology, University of Groningen, Haren, The Netherlands

Ann Van Loey Laboratory of Food Technology, Katholieke Universiteit Leuven, Leuven, Belgium

Liisa Viikari VTT Biotechnology, Espoo, Finland

Jean-Paul Vincken Laboratory of Food Chemistry, Department of Agrotechnology and Food Sciences, Wageningen University, Wageningen, The Netherlands

Victoria M. Virador National Institutes of Health, Bethesda, Maryland, U.S.A.

Jaap Visser Fungal Genetics and Technology Consultancy, Wageningen, The Netherlands

Alphons G. J. Voragen Laboratory of Food Chemistry, Department of Agrotechnology and Food Sciences, Wageningen University, Wageningen, The Netherlands

A. J. Vroemen DSM Food Specialties, Delft, The Netherlands

Bruce P. Wasserman† Department of Food Science, Rutgers University, New Brunswick, New Jersey, U.S.A.

John R. Whitaker Department of Food Science and Technology, University of California, Davis, Davis, California, U.S.A.

Gary Williamson Nestlé Research Centre, Lausanne, Switzerland

Chris Winkel Department of Enzyme Research, Quest International, Naarden, The Netherlands

Dominic W. S. Wong Western Regional Research Center, Agricultural Research Service, U.S. Department of Agriculture, Albany, California, U.S.A.

Ying Yu Department of Food Science, Rutgers University, New Brunswick, New Jersey, U.S.A.

Zhong Yi Yuan Institute of Biochemistry and Cell Biology, Chinese Academy of Sciences, Shanghai, China

Wei Zhao Department of Biochemistry, University of Groningen, Groningen, The Netherlands

† Deceased

1

Protein Structure and Kinetics of Enzyme Reactions

A Historical Perspective

John R. Whitaker
University of California, Davis, Davis, California, U.S.A.

I. INTRODUCTION

This opening chapter focuses primarily on the history of applications of enzymes in food science and technology. The evolution of knowledge on proteins and food enzymology must also be understood from the fundamental aspects. Enzymes are proteins. Therefore, the history of food enzymology is a composite of advances in both understanding the chemistry of protein structure and environmental behavior, as well as the physicochemical properties (kinetics and thermodynamics) of enzyme behavior.

This chapter will first treat the history of food enzymology from the evolution of protein chemistry and then the physicochemical behavior of enzymes in relation to environmental conditions, including the effects of enzyme, substrate, cofactor and inhibitor concentrations, and the effects of pH and temperature.

II. PROTEIN CHEMISTRY DEVELOPMENT

During the period 1820–1840 crude purifications of proteins began to be made by heat coagulation and precipitation with organic solvents and high concentrations of salts, such as ammonium sulfate.

A. Amino Acid Composition

Glycine and leucine were the first amino acids to be isolated (from hydrolyzed gelatin and wool, respectively) (1). This was during the time when the word "protein" was coined to describe these compounds that have the compositional formula of carbon, hydrogen, oxygen, and nitrogen ($\sim 16\%$), with small amounts of sulfur and phosphorus. Methionine was discovered in 1922 by Mueller (1) and in 1935 threonine, the last amino acid, was discovered by Rose. It was very difficult to determine the amino acid composition in the earlier days. With the discovery in 1952 by Moore and Stein (2) that the amino acids of protein hydrolyzates could be separated and identified readily within 24 h by ion exchange chromatography, the amino acid composition of many proteins became readily available. Today, the complete amino acid composition of a protein is done by automated analysis in 2–24 h using nano- or picogram amounts of hydrolyzed protein, at a cost of $25–35 per total analysis.

B. Primary Structures of Proteins

Real proof of the importance of the peptide bond in proteins was when this bond joining individual amino acids into a longer polymer was discovered in 1903 by Emil Fischer, who synthesized the first peptides (3). Fischer synthesized many peptides during his scientific career. Höfmeister also reported the peptide bond in 1903 (4). Sanger developed the methodology for determining the amino acid sequences of proteins in 1955 (5) using insulin (a polypeptide of 5737 daltons). Edman developed a chemical method of sequencing

proteins in 1949 (6); the automated Edman degradation method, invented in 1967 by Edman and Begg (7), is used routinely now for sequencing picogram quantities of protein within 24 h. The methods are so sensitive these days that one must wear plastic gloves in all operations. A typical cost per amino acid residue is about $20–25. The time required for sequencing depends on the size of the protein, since most proteins must be hydrolyzed to 25–50 amino acid residue fragments by two or more highly selective proteases in order to produce overlapping protein fragments. Each of the peptides must then be purified before sequencing.

The fastest, most economical, and most precise method of determining the sequences of proteins, since the 1980s, is by determining the nucleotide sequence of the gene for a protein. Extremely low amounts of DNA or sRNA are needed since PCR (protein chain reaction) catalyzed by S-polymerase can be used to make many copies of the gene. However, it is important to remember that the amino acid sequence determination via gene sequence does not include posttranslational modifications, including proteolysis, that are required to produce the active mature protein. The relationship between the primary sequence of proteins and gene nucleotide sequence was first postulated in the 1950s—the ''one gene–one protein'' hypothesis.

C. Secondary Structures of Proteins

The α-helix secondary element of proteins was first postulated in 1950 by Linus Pauling (8) and was found in myoglobin by Kendrew et al. (9) by x-ray crystallography in 1960. The determination of β strands in the primary structures of proteins, subsequently resulting in β sheet formation by folding of the polypeptide chain back on itself, was reported in 1951 by Pauling and Corey (10). The β and γ turns, loops, and bulges were clearly established in proteins by 1987, based on Milner-White and Poet's reported observation of reproducible x-ray crystallographic conformation in previously described loops (random folding) of a number of proteins (11). The key roles of glycine and proline in forming γ and β turns are now well established, with subclasses of each of these turns. Therefore, the key secondary components of proteins are α-helices (a few other types of helices also occur in some proteins), β strands, and β and γ turns and loops. Supersecondary folding patterns (motifs), involving a minimum of three secondary structures, are well known (12, 13).

D. Tertiary Structures of Proteins

Tertiary structures of proteins, along with secondary structures, were determined by x-ray crystallography of myoglobin by Kendrew et al. in 1960 (9). Even though hemoglobin was crystallized in 1848, and the law of x-ray diffraction was established by Bragg in the 1920s, computer capabilities for quantitatively analyzing the complex x-ray patterns of proteins were not available until the late 1950s.

The primary sequence of amino acids, while determining the folding pattern of proteins, is not responsible for the folding. The aqueous system is. To be more precise, the H-bonded clusters (6–8 water molecules) forces the proteins to fold with predominately hydrophobic amino acid residues inside and predominately hydrophilic amino acid residues on the outside, along with 20–40% (on average) bound water of hydration around the protein. Folding of proteins is an entropy-driven process. The entropic energy from the hydrogen-bonded clusters of water molecules is used to force the protein to fold so as to occupy its smallest possible surface area, generally a sphere. Proteins, and life, have evolved in an aqueous environment. No other solvent could have caused the evolution of biological functions as we know them.

Aqueous protein solutions contain three types of water—structural (constitutional) water (~ 0.003 g water/g protein), interfacial water (~ 0.3–0.5 g water/g protein on the surface of the protein, and free water (14). The structural water molecules are bound tightly and are not removed by lyophilization or drying of the protein or by displacement of water by acetonitrile (15). In the serine superfamily of enzymes, 20 structural water molecules are found in identical locations in all (16). The surface of native proteins contains, on the average, 20–40% by weight of bound water molecules. The first monolayer (vicinal) of water molecules binds primarily to the charged and neutral side chains of the surface amino acid residues by hydrogen bonds. Water molecules surround surface hydrophobic side chains as a cage but do not interact with them. The second and subsequent layers (multilayers) of water molecules bind less tightly by dipole interaction with the monolayer water. Bound water and free water can be distinguished readily by nuclear magnetic resonance (NMR).

E. Quaternary Structure

The importance of subunits in some proteins was recognized in 1970 by Klotz et al. (17), when it was

discovered that a 0.4 M sodium chloride solution caused hemoglobin to change from 68,000 daltons to 34,000 daltons. Later, it was shown that the tetrameric protein was cleaved to give two identical subunits containing two polypeptide chains, α and β, and that higher concentrations of salts caused further dissociation to subunits (α and β) of 17,000 daltons. Perutz et al. (18) determined the x-ray crystallography pattern of hemoglobin in 1960. A number of other proteins and enzymes have subunits (17). Subunits of proteins were found to be devoid of biological activity; in time, a molecule of a protein was defined as the smallest unit that has biological activity.

F. Macromolecular Structure

By the late 1960s, it was recognized that the skeletal muscles of animals are composed of several different proteins, myosin, actin, tropomyosin, and troponin (three types) that, when associated correctly, had contractile properties in the presence of the cofactor ATP. Later, it was shown that pyruvate dehydrogenase, the electron transport system, and other systems performing complex functions require association of several different proteins to perform the overall biological function (19, 20).

G. Folding of Proteins from the Primary Structure

By the 1960s, physical chemists such as Harold Scheraga at Cornell University, Phillip Handler at North Carolina State University, Ronald Baldwin at Stanford University, and others began to ask how protein folding occurs and how fast it occurs. Dr. Scheraga, using the hypothesis that every atom of the protein had to find its proper location by a random process, and using high-speed computers, predicted that it would take $\sim 10^{50}$ years for a 100–amino acid residue polypeptide to fold properly. About the same time, Hantgan et al. (21) and others (22, 23) began to unfold proteins by heat, urea, pH changes, etc., to remove the unfolding agent and measure the rate of regain of activity. Lu and Whitaker (24) and others found that denatured proteins could regain most of their activities in $\sim$ 6–10 min at 35°C. Not too long after, sufficient data accumulated to show clearly that the primary sequence of amino acids contained the information needed to permit the protein to fold into the native structures, including quaternary and macromolecular structures. But it is appropriate to mention that many proteins are posttranslationally modified in $\sim$135 ways (collectively among proteins) and that posttranslational modification plays a very important, sometimes essential role in the folding and stabilizing of a protein in its biologically functional form.

Detailed analyses of the data from x-ray diffraction of protein crystal structures became available in the 1960s owing to advances in computers. NMR was developed sufficiently by the 1980s to be used for determining the tertiary structures of proteins. Modern x-ray diffraction and new methods of intense beam magnification, using a synchrotron, permit the tertiary structures to be determined at 1.2 Å, sufficient to identify primary amino acid sequence, the secondary structure, the tertiary structure, and in some cases the quaternary structure. In some cases crystallographic structures of proteins are now being determined at a faster pace than the biological function of the proteins.

The most complex protein in which the tertiary structure has been determined recently is that of yeast RNA polymerase II (25).

H. Protein Crystallization

Hemoglobin was the first protein to be crystallized, by accident, in 1848. Almost anyone can crystallize hemoglobin from blood, but recognizing that it is a protein is more difficult. Ovalbumin from chicken egg white was crystallized in the 1880s. But it was the crystallization of urease in 1926 by J.B. Sumner that finally proved that enzymes are proteins (26). Again, serendipity (being at the right place at the right time and recognizing it) played an essential role in this discovery. As the story goes, Professor Sumner of Cornell University made a water/alcohol extract of jack beans on a Friday, removed the solids, and placed the extract on the window sill of the laboratory and went home. On Monday, a solid had formed that, when the liquid/solid was swirled, refracted light—a biofringence. Recognizing this as unusual, he determined under the microscope that crystals were present. He showed that the crystals were protein with urease activity, so he suggested that enzymes are proteins. Despite the earlier "finding" by Willstätter in 1926 that highly purified peroxidase was not a protein (27), Sumner has been proven correct that all enzymes known to date are proteins. Willstätter made the mistake that many scientists make at one time or another; the ability to measure the peroxidase activity was much

more sensitive than the ability to measure the protein concentration.

Protein crystallization is a science these days permitting most proteins, including even glycoproteins and lipoproteins, to be readily crystallized as demonstrated, for example, by the crystallization of yeast S-RNA polymerase II (25).

I. Active Sites of Proteins

Active sites of proteins are the locations where the biological function of a protein resides in the native protein. Study of active sites of proteins became a major field of study for enzymologists and protein chemists beginning in the 1960s. But as early as 1902, Brown (28) and Henri (29) independently proposed that enzymes must bind the substrate prior to conversion to product. Fischer in 1894 (30) proposed that the active site must fit the substrate as stereospecifically as a key fits a lock (lock-and-key analogy) in order to be bound properly and be converted to product. Koshland in 1965 (31) introduced the "induced fit" hypothesis to explain how apparently dissimilar molecules could sometimes serve as substrates for the same enzyme.

Initially, study of active sites of enzymes was approached by use of chemical modification of the side chain groups of amino acid residues of the native protein, using loss of biological activity as the measure. Also, the unfolding and refolding of proteins such as myoglobin and ribonuclease, especially around cofactors, hematin, etc., gave much information on active sites. Much was learned about essential amino acids in the active site. For example, in lysozyme chemical modification established that Glu35, Asn37, Asn44, Asp52, Asp59, Try62, Try63, Asp101, and Arg114 are a part of the active site (32). Asp52 and Glu35 are the key catalytic general acid/general base residues (–COOH and $–COO^-$ are the catalytic groups). X-ray crystallography was key to determining that His69, Glu72, and His196 (chelates the essential cofactor Zn(II)), Arg71, Arg145, Tyr198, Tyr248, and Phe279 are in the active site of carboxypeptidase A (33). Zn(II) is responsible for catalysis. The other amino acid residues are key to binding the substrate properly in the active site.

The best current method of determining the essentiality of amino acid residues in the active site is the use of recombinant biotechnology to replace one amino acid at a time, thereby determining its effect on activity, is much more certain than the two methods above. Absence of binding and/or activity based on a single amino acid replacement is about as close to the truth as one might get of the role of that amino acid.

III. DISCOVERY OF ENZYMES AND DEVELOPMENT OF ENZYME KINETICS

A. Discovery of Enzymes

There is some overlap between this section and that of Chapter 2. This is justified based on the need to present a complete picture in the book.

1. Catalase appears to be the first enzyme discovered. This occurred in 1812. In reality, the discovery was that something in blood caused the evolution of bubbles, shown to be O_2, when hydrogen peroxide was added. The reaction observed was

$$2\ H_2O_2 \rightarrow 2\ H_2O + O_2$$

2. Diastase was discovered in wheat flour by Payen and Persoz in 1833 (34), when they reported that the enzyme caused the solubilization of starch. In addition, they found the enzyme to be thermolabile and precipitated by alcohol. They named the substance "diastase" because it separated, by solubilization, the starch from the bran. They further used "ase" in the name to designate it as an enzyme. The reaction observed was

$$\text{Starch} + H_2O \rightarrow \text{dextrins}$$

3. Peroxidase in plants was reported by Schöenbein in 1855 (35, 36). Schöenbein used gum guaiac which changes in color from light tan to blue when H_2O_2 was added to an extract containing peroxidase. Several other compounds can be used to assay easily for peroxidase as shown by the equation:

$$\underset{\text{(colorless)}}{4\ \text{Guaiacol} + 8\ H_2O_2} \rightarrow \underset{\text{(brown)}}{\text{tetraguaiacol} + 8\ H_2O}$$

4. Polyphenol oxidase was discovered by Schöenbein in plant extracts in 1856 (36). It was named polyphenol oxidase because of its ability to oxidize phenols, cause browning of plant extracts and bruised plant tissues. The enzyme can use a number of mono- and polyphenols plus O_2 as substrates as shown by:

$$\text{Phenol} + 0.5\ O_2 \rightarrow o\text{-dihydroxyphenol}$$

$$o\text{-Dihydroxyphenol} + 0.5\ O_2 \rightarrow o\text{-benzoquinone} + H_2O$$

5. Invertase was discovered in 1860 by Berthelot in yeast (37). The enzyme catalyzes the hydrolysis of sucrose to glucose and fructose:

$$\underset{(56.5^\circ)}{\text{Sucrose}} + \text{H}_2\text{O} \rightarrow \underset{(65.5^\circ)}{\text{glucose}} + \underset{(-79.2^\circ)}{\text{fructose}}$$

where the numbers in parentheses are optical rotation.

During this period of enzymology, polarimeters were developed that could manually or continuously follow the changes in optical rotation during the conversion of sucrose to glucose and fructose by the change in optical rotation from 56.5° to –23.7° based on the difference in optical rotation of the sucrose (the substrate) to the products (glucose and fructose). This ability eventually led to discovery and quantitation of the effect of pH, temperature, and substrate concentration on the kinetics of enzyme reactions.

The discovery of enzymes continues even today. In the last listing in 1992 of well-studied enzymes there were 3196 enzymes listed (38). The types of enzymes so far discovered based on the chemical reactions catalyzed are oxidoreductases, transferases, hydrolases, lyases, isomerases, and ligases. Many of the individual enzymes have isozymes (same reaction catalyzed but they differ in primary structure of the protein). The nucleotide sequence of the genes that code for the biosynthesis of the enzyme can be modified by researchers to give multiple forms of enzymes via one or more amino acid changes of the primary sequence. Posttranslational modification of the protein can also lead to multiple forms.

B. Enzyme Specificity

In the period 1894 to the 1930s Emil Fischer, a German chemist, and his associates developed and refined the concept of enzyme specificity and of the close stereospecificity between an enzyme and its substrate(s) (30). Based on their careful studies of enzyme action on numerous compounds his group synthesized, Fischer enunciated the now famous "lock-and-key" analogy of enzyme–substrate interaction. Other compounds, called competitive inhibitors, bind into the active site in competition with the substrate but they are not converted to products because they lack the overall keylike fit to the active site.

In 1959, Koshland emphasized the importance of the "induced fit" concept of enzyme specificity (31). His detailed research showed that compounds that do not have identical shapes can be substrates for the same enzyme and that this is possible because of accommodation (flexibility) of the active site of the enzyme in binding the substrate. Further research has shown that the induced fit concept is an important factor in the specificity of numerous enzymes and perhaps less important in more rigid active sites of some enzymes, such as urease, which converts only urea to products.

C. Quantition of Rates

The importance of quantitation of rates was introduced briefly in Section III.A above. This section will expand on the topic.

1. Effect of Temperature on Velocity

In 1889, after a large amount of research on invertase using a polarimeter to study the effect of temperature on velocity of reaction, Arrhenius developed the empirical equation:

$$dlnk/dT = Ae^{-E_a/RT}$$

which is still in use by most biologists today (39). Physical chemists derived de novo an equation (Gibbs equation; 40) that gives a slightly different numerical value from that of Arrhenius. The difference is given by

$$E_a = \Delta H^{\neq} + RT$$

At 25°C E_a is 0.6 kcal/mol larger than $\Delta H^{\neq}$ given by Gibbs' equation because a slight temperature effect on E_a is removed by using $\Delta H^{\neq}$. For most purposes the two methods of calculation agree within experimental error.

2. Effect of Substrate Concentration on Velocity

Studies of effect of substrate concentration on velocity of enzyme-catalyzed reactions advanced primarily owing to the availability of the polarimeter, permitting the effect of substrate (sucrose) concentration on the velocity of the invertase-catalyzed reaction to be studied in great detail. The results showed a "saturation-type" curve (Fig. 1). At very low substrate concentrations, the velocity increased in direct proportion to the increase in substrate concentration. At higher concentrations, the relationship was curvilinear and at high concentrations, the rate reached a maximum (and even decreased in some cases) owing to substrate inhibition.

In 1903 Brown (28) and Henri (29) independently proposed that the "saturation curve" for the relation-

ship between velocity and substrate concentration $[A]_o$ could be explained by the equation

$$E + A \rightarrow E \cdot A \rightleftharpoons E + P$$

where $E \cdot A$ is an obligatory intermediate; i.e., E and A must form a noncovalent complex before conversion of substrate to products can occur. This concept is now universally accepted.

In 1913, Michaelis and Menten (41) showed that the enzyme–substrate saturation curve can be expressed mathematically by the equation of a right hyperbola

$$v_o = V_{max}[A]_o/(K_m + [A]_o)$$

where v_o is the observed initial velocity, V_{max} is the maximum velocity when the enzyme is fully saturated with substrate, and K_m is $[A]$ at which $v_o = 0.5\ V_{max}$.

In 1918, Langmuir (42) showed independently that the same-shape curve is found for adsorption of gases onto metal surfaces, soluble solutes onto charcoal, etc. The Langmuir equation is:

$$\text{Fraction of surface covered} = n_s x/(n_e + n_s x)$$

where n_s is number of molecules striking 1 cm^2 of surface per second, x is the quantity of molecules that binds on the surface, and n_e is the number of molecules leaving the surface per second.

In 1934, Lineweaver and Burk (43) showed that a reciprocal plot of v_o versus $[A]_o$ (i.e. $1/v_o$ vs. $1/[A]_o$) converts the Michaelis-Menten equation to a form in which V_{max} and K_m can be determined in an unambiguous manner (Fig. 2). There are two other methods that give linear plots—the Augustinsson method (44), and the Eadie-Hofstee method (45); however, the Lineweaver-Burk method continues to be the most widely used method.

3. Effect of pH on Enzyme-Catalyzed Reactions

In 1909, Sörensen published a classic paper on the effect of pH on invertase activity (46). Not only did he show that the activity of enzymes is affected by the pH of the reaction, he was able to differentiate the effect on reaction rates and on stability of the enzyme.

Detailed studies of pH effects on rates of enzyme-catalyzed reactions were largely ignored until the 1960s when Bender, Whitaker, and others gave much attention to the interpretation of the results from a mechanistic standpoint. See Whitaker (47) for more details of the studies.

4. Further Refinements of Kinetics

During 1957–1963, there were substantial advancements in better understanding of the effect of concentrations of one, two, or multiple substrates on enzyme-catalyzed reactions. These advancements were made by

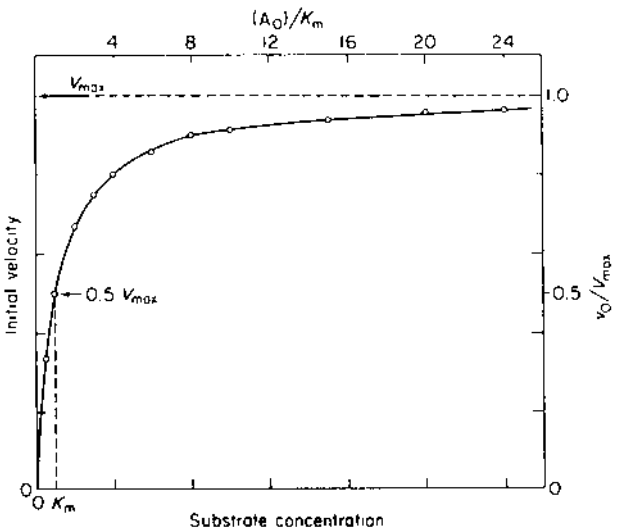

Figure 1 Variation of initial velocity with substrate concentration for an enzyme-catalyzed reaction according to the Michaelis-Menten equation. (From Ref. 41.)

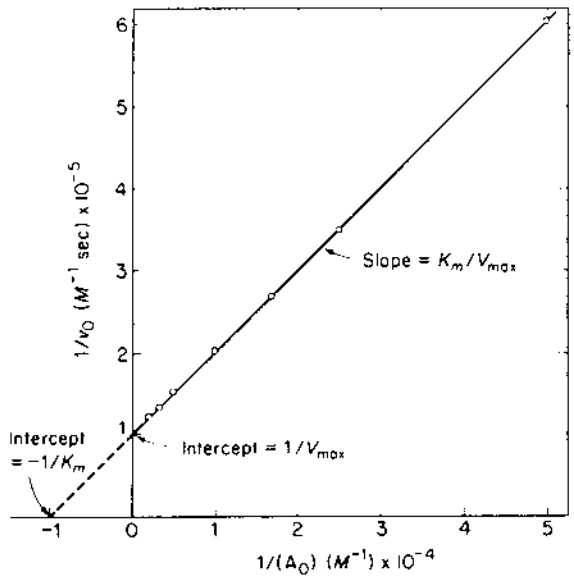

Figure 2 Plot of reciprocal of initial velocity versus reciprocal of initial substrate concentration by the Lineweaver-Burk method. (From Ref. 43.)

Alberty (48), Wong and Haines (49), Cleland (50), and Segel (51). Cleland's descriptive nomenclature (50), ordered BiBi sequential mechanism, random BiBi sequential mechanism, and Ping Pong BiBi mechanism terms and methodology are used most frequently. See Whitaker (47) for a detailed discussion and use of these methodologies.

5. Concept of Initial Velocity

The concept of initial velocity, v_o, arose in the 1960s and is universally used by those interested in detailed studies of enzymes. v_o is determined as near time zero of the reaction as possible. No more than 5% of the original $[A]_o$ should be converted to product in determining v_o. The method requires that the velocity be determined on a continuous time basis, generally by continuous recording of the data.

There are several reasons for using v_o. It largely eliminates problems caused by change in degree of saturation of the enzyme with substrate during the reaction time. It eliminates influence of the back reaction ($P + E \rightleftharpoons E + A$). It eliminates effect of product inhibition of the enzyme. It eliminates effect due to instability of the enzyme, since the reaction is normally done within ~ 5 min. Since it is based on a continuous recording, not on a one-point assay, the substrate concentration ($[A]_o$) at time zero can be used.

6. Sigmoidal Kinetics

Experimentally, not all enzyme-catalyzed reactions follow Michaelis-Menten kinetics. In 1965, Monod et al. (52) published the first paper conclusively showing that some enzyme-catalyzed reactions do not follow the Michaelis-Menten equation. The kinetics are said to be *sigmoidal* or *allosteric* in nature. The form of the equation developed to express the results is:

$$v_o = V_{max}[S]_o^n/(K_m + [S]_o^n)$$

Sigmoidal kinetics are sometimes found when more than one substrate molecule binds to the enzyme molecule. Generally, sigmoidal kinetics may be shown in enzymes that have quaternary structure. If binding of substrate into the active site of the first subunit affects, positively or negatively, the binding of substrate into the active site of the second subunit, sigmoidal behavior will be seen. Enzymes in metabolic pathways often show sigmoidal behavior (53).

IV. ANALYTICAL TOOLS IN ADVANCEMENT OF ENZYMOLOGY

Advancement of enzymology, as with all chemical and biological sciences, has been influenced very much by the development of tools and methodology. Perhaps one of the first tools was the microscope, which permitted Pasteur to discover the asymmetry of molecules leading to discovery of isomeric differences among L-, D-, and DL-tartaric acid crystals in wine. A specific enzyme can use only one of the forms as a substrate. Another was the development of polarimetry which permitted detailed studies on the effect of pH, temperature, and substrate concentration effects on invertase particularly and other enzymes in general. These studies led to Sörensen's contribution to understanding the effect of pH on enzyme activity (46), to Arrhenius' study of temperature effect on rates of invertase-catalyzed reactions (the Arrhenius equation [39], and data on the velocity–substrate concentration relationships leading to the Henri (29) and Brown (28) hypothesis on essentiality of the EA complex, the Michaelis-Menten equation (41), and the Lineweaver-Burk reciprocal plot (43).

Kinetic analyses are used to determine how much enzyme is present in tissues. But their primary use is to determine the mechanism of action of enzymes via a detailed study of the kinetic effect of substrate concentration, enzyme concentration, pH, temperature, and inhibitors on the v_o of the reaction. Early investigations in this area were by Koshland and Neet (54) and by Vallee and Riordan (55). Many articles, books, and treatises of this subject have appeared over the past 30 years.

A. Tools for Purification of Enzymes

Not much was done on the purification of proteins until the 1920s when Willstätter purified horseradish peroxidase to the point that no protein could be detected by the method used, but the peroxidase activity could be determined, leading to the conclusion that horseradish peroxidase could not be a protein (27). But Sumner (26) crystallized jackbean urease and showed it to be a protein. In 1930 Haldane (56) and others expressed the view that except for urease, next to nothing was known about the chemical nature of proteins.

In the 1930s, several enzymes, including pepsin, trypsin, chymotrypsin, and carboxypeptidase A, were crystallized by Northrop, Kunitz, Herriott, and Anson (57, 58) at the Rockefeller Institute. All were found to be proteins. The ultracentrifuge (59) and free boundary

electrophoresis (60) were developed and used to determine the molecular weight and purity of enzymes.

From 1930 to 1955, use of differential solubility of proteins at different pH's, as well as differential temperature stability, were used to purify proteins. Large amounts of protein were needed. In the late 1940s and early 1950s Moore and Stein (2) developed ion exchange chromatographic methods for separating the amino acids from hydrolysates of proteins, including enzymes.

But it was the period beginning in 1956 and extending to the 1980s that chromatographic methods based on cellulose ion exchangers for separation by charge (61), size (62, 63), surface hydrophobicity (64), affinity chromatography (65), and chromatofocusing chromatography (66) really made it possible to purify proteins routinely. Along with the advances in chromatography were advances in determining the purity of proteins, including molecular weight and subunit structure by polyacrylamide gel electrophoresis (67) and SDS-polyacrylamide gel electrophoresis (68). Further advances in procedures permit microgram amounts of enzymes to be purified and sequenced by the Edman degradation method within 24–72 h.

Fred Sanger and colleagues (5) worked out methodology for determining the amino acid sequence of insulin in 1955 (5737 daltons; 53 amino acid hormone). By 1958, ribonuclease (13,683 daltons; 121 amino acids) was sequenced by Moore and Stein (69) and Hirs et al. (70, 71). As noted above, small proteins up to $\sim$ 50,000 daltons can be automatically sequenced within 24 to 48 h by the Edman degradation method.

The three-dimensional structure of an enzyme, ribonuclease, was determined by Kartha et al. in 1967 by use of x-ray crystallography (72). Major advances in x-ray crystallography have been made so that it used routinely to determine the tertiary and quaternary structures of proteins, even though the biological function of the protein is not known. In 2000, the complete tertiary structure of yeast S-polymerase II was determined (25); it consists of 10 different subunits.

In 1969, the first and only complete chemical laboratory synthesis of an enzyme, ribonuclease, was done (73, 74).

In the 1980s and 1990s three-dimensional structural analyses of enzymes in solution were elevated to high levels by NMR spectroscopy. This is the only technique that can determine the three-dimensional structure of proteins in solution. Fortunately, the three-dimensional structures of enzymes determined by x-ray crystallography and NMR spectroscopy are essentially identical.

The latest tools to be used in enzymology involve identification of presumed primary amino acid structure of enzymes by sequencing the genes that encode enzymes, by the replication of enzymes by the polymerase chain reaction, and the mutagenesis of enzymes by replacement of one or more nucleotide bases or by combinational methods. As noted earlier, significant posttranslational modification of the enzyme can occur after translation of the amino acid sequence.

REFERENCES

1. HB Vickery, CLA Schmidt. History of the discovery of the amino acids. Chem Rev 9:169–318, 1931.
2. S Moore, WH Stein. Chromatography of amino acids on sulfonated polystyrene resins. J Biol Chem 192:663–681, 1951.
3. E Fischer. Synthese von polypeptiden. Chem Ges 36:2982–2992, 1903.
4. F Höfmeister. Uber den Bau des Eiweissmoleculs. Verh Ges D Natf 74:33–50, 1903.
5. F Sanger, EOP Thompson, R Kitai. The amide groups of insulin. Biochem J 59:509–518, 1955.
6. P Edman. Determination of the amino acid sequence in peptides. Arch Biochem 22:475–576, 1949.
7. P Edman, G Begg. A protein sequenator. Eur J Biochem 1:80–91, 1967.
8. L Pauling. Atomic coordinates and structure factors for two helical configurations of polypeptide chain. Proc Natl Acad Sci USA 37:235–240, 1950.
9. JC Kendrew, RE Dickerson, BE Strandberg, RG Hart, DR Davies. Structures of myoglobin. A three dimensional Fourier synthesis at 2 Å resolution. Nature (Lond) 185:422–423, 1960.
10. L Pauling, RB Corey. Configurations of polypeptide chains with favored orientations around single bonds: two new pleated sheets. Proc Natl Acad Sci USA 37:729–740, 1951.
11. EJ Milner-White, R Poet. Loops, bulges, turns and hairpins in proteins. Trends Biochem Sci 12:189–192, 1987.
12. ST Rao, MG Rossmann. Comparison of super-secondary structures in proteins. J Mol Biol 76:241–256, 1973.
13. C Branden, J Tooze. Introduction to Protein Structure. New York: Garland Publishing, 1991.
14. O Fennema. Water and protein hydration. In: JR Whitaker, SR Tannenbaum, eds. Food Proteins. Westport, CT: Avi Publishing Company, pp 50–90.
15. PA Fitzpatrick, ACU Steinmetz, D Ringe, AM Klibanov. Enzyme crystal structure in a neat organic solvent. Proc Natl Acad Sci USA 90:8653–8657, 1993.
16. U Sreenivasan, PH Axelsen. Buried water in homologous serine proteases. Biochemistry 31:12785–12791, 1992.

17. IM Klotz, DW Darnell, NR Langerman. Quaternary structure of proteins. In: H Neurath, RL Hill, CL Boeder, eds. The Proteins. 3rd ed. Vol 1. New York: Academic Press, 1975, pp 293–411.
18. MF Perutz, MG Rossmann, AF Cullis, H Muirhead, G Will. Structure of haemoglobin. A three-dimensional Fourier synthesis at 5.5 Å resolution, obtained by x-ray analysis. Nature 185:416–422, 1960.
19. LJ Reed, RM Oliver. Multienzyme α-keto acid dehydrogenase complexes. Brookhaven Symp Biol 21:397–412, 1968.
20. PK Stumpf. Metabolism of fatty acids. Annu Rev Biochem 38:159–212, 1969.
21. RR Hantgan, GG Hammes, HA Scheraga. Pathways of folding of reduced bovine pancreatic ribonuclease. Biochemistry 13:3421–3432, 1974.
22. AW Burgess, HA Scheraga. A hypothesis for the pathway of thermally-induced unfolding of bovine pancreatic ribonuclease. J Theor Biol 53:403–420, 1975.
23. FN Joffe, CO Ball. Kinetics and energetics of thermal inactivation and the regeneration rates of a peroxidase system. J Food Sci 27:587–592, 1962.
24. AT Lu, JR Whitaker. Some factors affecting rates of heat inactivation and reactivation of horseradish peroxidase. J Food Sci 36:1173–1178, 1974.
25. P Cramer, DA Bushnell, J Fu, AL Gnatt, B Maier-Davis, NE Thompson, RR Burgess, AM Edwards, PR David, RD Kornberg. Architecture of RNA polymerase II and implications for the transcription mechanism. Science 288:640–648, 2000.
26. JB Sumner. Note. The recrystallization of urease. J Biol Chem 70:97–98, 1926.
27. R Willstätter. Advances in the isolation of enzymes. Ber 59B:1–12, 1926.
28. AJ Brown. Enzyme action. J Chem Soc 81:373–379, 1902.
29. V Henri. General Laws of the Action of Diastases. Paris: Hermann, 1903.
30. E Fischer. Influence of configuration on the action of enzymes. Ber 27:2985–2993, 1894.
31. DE Koshland Jr. Mechanisms of transfer enzymes. In: PD Boyer, H Lardy, K Myrbäck, eds. The Enzymes, Vol 1. 1st Ed. New York: Academic Press, 1959, pp 305–346.
32. LN Johnson, DC Phillips, JA Rupley. Activity of lysozyme: an interim review of crystallographic and chemical evidence. Brookhaven Symp Biol 1:120–138, 1969.
33. WN Lipscomb, JA Hartsuck, GN Reeke Jr, FA Quiocho, PH Bethage, ML Ludwig, TA Steitz, H Muirhead, JC Coppola. Structure of carboxypeptidase A. The 2.0-angstrom resolution studies of the enzyme and its complex with glycyltyrosine, and mechanistic deductions. Brookhaven Symp Biol 1:24–90, 1969.
34. FW Payen, JF Persoz. Treatise on diastase, the principal products of its reactions and their application to industrial arts. Ann Chim Phys 53:73–92, 1833.
35. CF Shöenbein. Ueber ozonisirten sauerstoff. J Prak Chem 66:286–289, 1855.
36. CF Schöenbein. On ozone and ozonic actions in mushrooms. Phil Mag 11:137–141, 1856.
37. M Berthelot. Sur la fermentation glucosique du sucre de canne. CR Acad Sci 50:980–984, 1860.
38. Enzyme Nomenclature. Recommendations of the Nomenclature Committee of the International Union of Biochemistry, published for the International Union of Biochemistry. San Diego: Academic Press, 1992.
39. S Arrhenius. Ueber die Reaktions geschwindigkeit bei Inversion von Rohrzucker durch Sauren. Z Physik Chem 4:226–248, 1889.
40. RA Alberty, RJ Silbey. Physical Chemistry. New York: Wiley, 1992.
41. L Michaelis, ML Menten. The kinetics of invertase action. Biochem Z 49:333–369, 1913.
42. I Langmuir. The adsorption of gases on plane surfaces of glass, mica and platinum. J Am Chem Soc 40:1361–1402, 1918.
43. H Lineweaver, D Burk. Determination of enzyme dissociation constants. J Am Chem Soc 56:658–666, 1934.
44. KB Augustinsson. Substrate concentration and the specificity of choline ester-splitting enzymes. Arch Biochem 23:111–126, 1949.
45. BHS Hofstee. The evaluation of the constants V_{max} and K_m in enzyme reactions. Science 116:329–331, 1952.
46. SPL Sörensen. Enzyme studies. II. The measurement and importance of the hydrogen ion concentration in enzyme reactions. Biochem Z 21:131–304, 1909.
47. JR Whitaker. Principles of Enzymology for the Food Sciences. 2nd ed. New York: Marcel Dekker, 1994.
48. RA Alberty. The rate equation for an enzymic reaction. In: PD Boyer, H Lardy, K Myrbäck, eds. The Enzymes, Vol 1. New York: Academic Press, 1959, pp 143–155.
49. JT Wong, CS Hanes. Kinetic formulations for enzymic reactions involving two substrates. Can J Biochem Physiol 40:763–804, 1962.
50. WW Cleland. The statistical analysis of enzyme kinetic data. Adv Enzymol 29:1–32, 1967.
51. IH Segel. Biochemical Calculations. New York: Wiley, 1976.
52. J Monod, J Wyman, JP Changeux. On the nature of allosteric transitions: a plausible model. J Mol Biol 12:88–118, 1965.
53. DE Koshland Jr, G Nemethy, D Filmer. Comparison of experimental data and theoretical models in proteins containing subunits. Biochemistry 5:365–385, 1966.

54. DE Koshland Jr, KE Neet. The catalytic and regulatory properties of enzymes. Annu Rev Biochem 73:359–410, 1968.
55. BL Vallee, JF Riordan. Chemical approaches to the properties of active sites of enzymes. Annu Rev Biochem 38:733–794, 1969.
56. JBS Haldane. Enzymes. London: Longmans, Green, 1930.
57. M Kunitz, JH Northrop. Isolation of a crystalline protein from pancreas and its conversion into a new crystalline proteolytic enzyme by trypsin. Science 78:558–559, 1933.
58. M Kunitz, JH Northrup. Isolation from beef pancreas of crystalline trypsinogen, trypsin, a trypsin inhibitor and an inhibitor-trypsin compound. J Gen Physiol 19:991–1007, 1936.
59. A Tiselius, KO Pedersen, T Svedberg. Analytical measurements of ultracentrifugal sedimentation. Nature 140:848–849, 1937.
60. A Tiselius. Electrophoresis of serum globin. Biochem J 31:313–317, 1937.
61. EA Peterson, HA Sober. Chromatography of proteins. I. Cellulose ion-exchange adsorbants. J Am Chem Soc 78:751–755, 1956.
62. P Flodin. Dextran Gels and Application in Gel Filtration. Uppsala, Sweden: Pharmacia, 1962.
63. JR Whitaker. Determination of molecular weights of proteins by gel filtration on Sephadex. Anal Chem 35:1950–1953, 1963.
64. S Shaltiel. Hydrophobic chromatography. Methods Enzymol 34:126–140, 1974.
65. P Cuatrecasas. Protein purification by affinity chromatography. Derivatives of agarose and polyacrylamide beads. J Biol Chem 245:3059–3065, 1970.
66. EH Cooper, R Turner, JR Webb, H Lindblom, L Fagerstam. Fast protein liquid chromatography scale-up procedures for the preparation of low-molecular-weight proteins from urine. J Chromatogr 327:269–277, 1985.
67. O Vesterberg. Isoelectric focusing of proteins. Methods Enzymol 22:389-412, 1971.
68. K Weber, M Osborn. Proteins and sodium dodecyl sulfate: molecular weight determination on polyacrylamide gels and related procedures. In: H Neurath, RL Hill, CL Boeder, eds. The Proteins, Vol 1. 3rd ed. New York: Academic Press, 1975, pp 179–233.
69. S Moore, WH Stein. Determination of the structures of proteins. Studies on ribonuclease. Harvey Lect 52:119–143, 1958.
70. CHW Hirs, S Moore, WH Stein. Sequence of the amino acid residues in performic acid oxidized ribonuclease. J Biol Chem 235:633–647, 1960.
71. DH Spackman, WH Stein, S Moore, AM Zamoyska. Disulfide bonds of ribonuclease. J Biol Chem 235:648–659, 1960.
72. G Kartha, J Bello, D Harker. Tertiary structure of ribonuclease. Nature 213:862–865, 1967.
73. B Gutte, RB Merrifield. Total synthesis of an enzyme with ribonuclease A activity. J Am Chem Soc 91:501–502, 1969.
74. R Hirschmann, RF Nutt, DF Veber, RA Vitali, SL Varga, TA Jacob, FW Holly, RG Denkewalter. Total synthesis of an enzyme V. Preparation of enzymatically active material. J Am Chem Soc 91:507–508, 1969.

2

History of Enzymology with Emphasis on Food Production

Poul Børge Poulsen
Novozymes A/S, Bagsvaerd, Denmark
Klaus Buchholz
Braunschweig Technical University, Braunschweig, Germany

I. INTRODUCTION

The scientific development in biocatalysis goes back to the beginning of the 19th century. The first enzymatic actions, notably starch hydrolysis by Diastase, was acknowledged as a catalytic effect by Berzelius in 1835 and utilized industrially following the findings and developments of Payen and Persoz on diastase and its application in the brewing industries about 10 years later. Continuous scientific investigations, with emphasis on alcoholic fermentation, can be traced to the 1850s with investigations of Berthelot and Béchamp, the school of Pasteur, and the controversy with the chemical school of Liebig and his influence.

The first company based on applied biocatalysis also dates back to the 19th century, when in 1874, Christian Hansen started a company in Copenhagen named Christian Hansen's Laboratory which exists to this day, producing an enzyme preparation, rennet (chymosin), for cheese making.

After this early period, research in the subsequent decades brought about significant progress with the important findings of E. Fischer in 1894 on enzyme specificity, and E. Buchner in 1897 on the pure chemical nature of alcohol formation, and the key steps by Sumner and Northrup in crystallizing enzymes in 1926 and 1930, respectively. These represented turning points in identifying the nature of the catalytic agent. A continuous technical development can be traced to the beginning of the 20th century, where Röhm and the foundation of the Röhm and Haas company in 1907 may be seen as a major technical and economic breakthrough.

II. THE EARLY PERIOD TO 1880

Applied biocatalysis has its roots in ancient China and Japan in the manufacture of food and alcoholic drinks. Without knowing, mankind utilized microbial amylases and proteases, in particular for the production of soy-derived foods. In Europe also, applied biocatalysis has a long history. Cheese making has always involved the use of enzymes. As far back as about 400 B.C., Homer's *Iliad* mentions the use of kid stomach for making cheese. It was discovered that milk, which was stored in a bag made of a stomach of a recently slaughtered calf, lamb, or kid was converted into a semisolid substance. Upon pressing of this substance a drier material was obtained (namely cheese) which showed preferred properties over milk, could be easily transported, and gained a flavor after some time. These ancient applications may best be described as an art and not as a technology, a scientifically based technique. The context of biotechnology has been described in a profound analysis by Bud (1).

A. Findings and Empirical Results

Stahl explored in his book *Zymotechnika Fundamentalis* (1697) the nature of fermentation as an important industrial process, where zymotechnique should be the scientific basis (2). About a hundred years later the liquefaction of meat by gastric juice, as an enzymatic activity, yet not recognized as such, was noted by Spallanzani in 1783 (3). The enzymatic hydrolysis of tannin was described by Scheele in 1786 (4: p. 30). In 1814 Kirchhoff observed that a glutinous component of wheat was capable of converting starch to sugar and dextrin, and Vogel showed in 1817 that an infusion of oats would produce a fermentable sugar from milk (5: p. 5).

Some vital factor, *le principe vital*, was considered an important principle in the chemical processes associated with the synthesis of materials isolated from living matter.

> All simple bodies in nature are subject to the action of two powers, of which one, that of attraction, tends to unite the molecules of bodies one with another, while the other, produced by caloric, forces them apart.... A certain number of these simple bodies in nature are subject to a third force, to that caused by the vital factor, which changes, modifies and surpasses the two others, and whose limits are not yet understood (6).

In one of the books on technology in the period preceding Berzelius and Payen, Poppe (7) discussed mysterious ideas concerning fermentation:

> Fermentation is seen as a—at a time and under circumstances spontaneous—occurring mighty movement in a liquid of different compounds..., which is due to the fact that several compounds act in harmony with each other, others in opposition to each other, so that the first attract, the latter reject each other.... The sugar and a...gum extract material act by antagonist forces on each other so heavily, that they decompose and thus cause the formation of alcohol (*Weingeist*) (7: p. 229).

Gay-Lussac had postulated a *generatio spontanea*, the hypothesis that a continuing, rather mysterious chain should be the cause of spontaneous generation (of organisms) (summary in Ref. 8). Pasteur showed that this assumption was without any empirical basis.

Remarkably, a most significant change in the theoretical background, a change in paradigm, took place in textbooks on chemical technology within a few years. Poppe's *Technology* (7) was prescientific insofar as it did not show any chemical formula, working on a strictly descriptive level. In contrast, Knappe's *Chemical Technology* (9) gave chemical formulae, thus for sugar (not yet fully correct) based on the atomic composition of the molecules. Most clearly Payen's textbook (10, Vol. 1: p. 1) reflected the theoretical background of chemistry based on atomic and molecular composition and constitution, differentiating theoretical, applied, and technical chemistry.

The book by Knapp (9: pp. 300–303), about a decade after Poppe's (7) view of fermentation, develops a rather distinct picture of the action of ferments (mainly referring to diastase and the work by Payen and Persoz), and these views are expressed more precisely by Payen (10: pp. 399–403). Fermentation is seen as a contact (catalytic) process of a degradation (*Spaltungs-*) or addition process (with water). It can be performed by two substances or bodies: a nitrogen-containing organic (nonorganized) substance, such as protein material undergoing degradation; or an organized body, a lower-class plant or an "infusorium," such as with alcoholic fermentation. Probably the type of effect is the same insofar as the ferment of the second class produces a body of the first class, possibly a big number of singular ferments. In 1878 Kühne named the latter class of substances "enzymes".

A breakthrough occurred with the observations of Dubrunfaut and subsequently Payen and Persoz. Dubrunfaut discovered the transformation of starch into sugar and some kind of gum by means of water and germinated barley, as well as the application of this finding for technical and economic purposes (11). Payen and Persoz in 1833 (12) prepared the acting principle in isolated form, which they named diastase, with the following characteristics: it is a white, amorphous solid insoluble in alcohol and soluble in water. For the production of diastase they macerated germinating barley in cold water, then pressed and filtered it. The filtrate was heated to 70°C, filtered again, then precipitated with alcohol. The precipitate was collected on a filter and subsequently, by repeated redissolving and precipitating with alcohol, separated from the accompanying residual nitrogenous substances (12). The dextrin production was performed in a reaction vessel as shown in Figure 1 (10). The vessel inserted in a water bath could be heated to 75°C, the optimal temperature for the formation of dextrin by diastase. The reaction progress was controlled by the iodine test and stopped by heating to 100°C. The product solution was subsequently filtered, collected in a reservoir, and

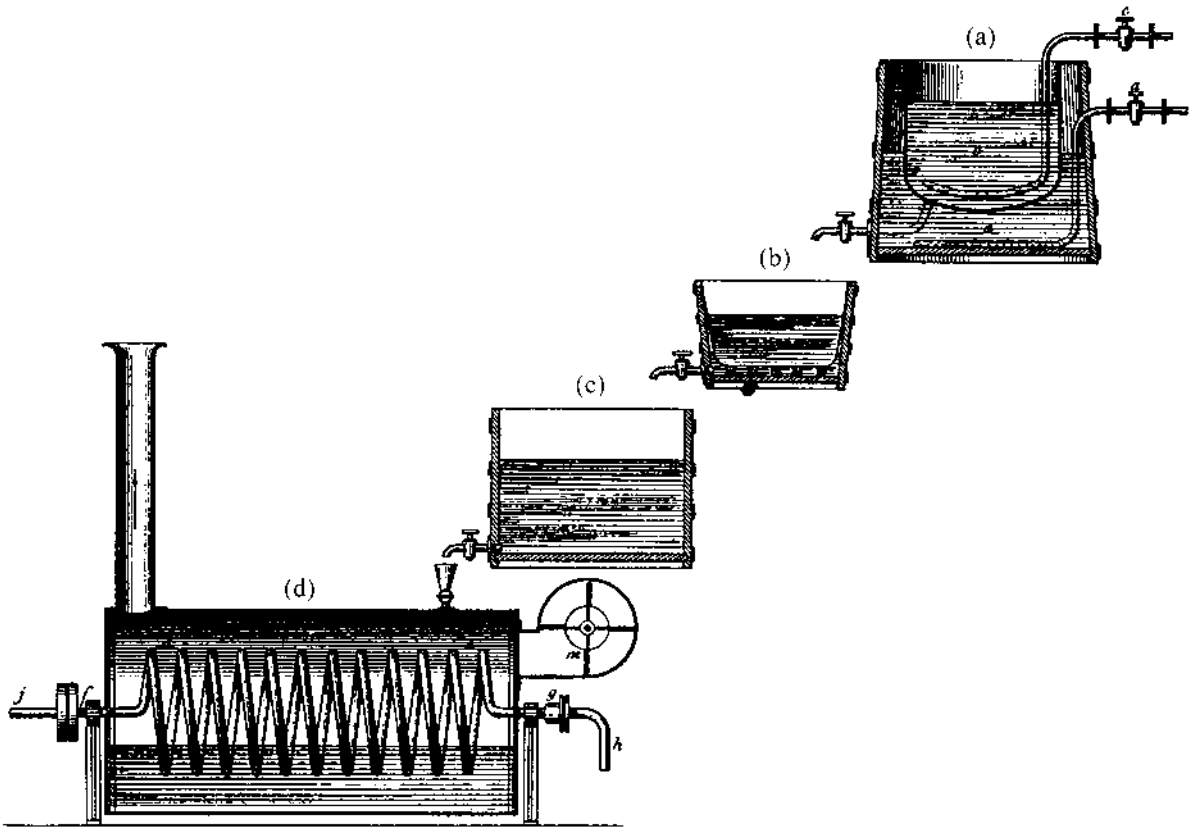

Figure 1 Process for dextrin production with reaction vessel (a), filter (b), reservoir (c), concentration unit (d). (From Ref. 10.)

concentrated by heating with steam. The product rapidly found industrial application.

Payen and Persoz (12) identified numerous topics for further research, such as the existence of diastase in plants, its molecular weight and elementary composition, and the reaction products from different substrates. Diastase was the dominating object of research on enzymes throughout the century with ~ 10–20% of publications dealing with this topic owing to its economic importance. Nevertheless the overall research activities remained very weak in this field, as compared to chemistry (see below).

A few further activities were discovered in subsequent years. Pectase was found in plants, both in soluble and nonsoluble form. It was able to break down pectose into pectinic acid, and was attributed to have some similarity to diastase. Neither material could be crystallized (10: p. 30). Claude Bernard was the first to show lipolytic activity in pancreas in 1856 (4: p. 25). Dobell (13) found that an extract from pancreas hydrolyzed both fat and starch; he gave a procedure for extraction and stabilization and named this preparation *pancréatine*.

Further enzymatic conversions (ferment actions) observed in that early period summarized in Frankland's list of soluble ferments (14) and by Sumner and Somers (3) are summarized in Table 1.

Alcoholic fermentation was a dominating topic of the time in the field called physiological chemistry which attracted a good deal of interest and activity of leading scientists (5). Trying to identify the active principle, Bethelot (15) showed, according to his own interpretation, that a peculiar nitrogen-containing substance, formed by yeast and precipitable by alcohol (he used casein) and comparable to diastase, could transform sugar into alcohol. He stated that this substance was different from yeast and that there was no production of yeast cells (8, 15). Thus, he claimed to have observed the transformation of sugar into alcohol without the participation of any activity of living organisms. He was convinced that the formation of alcohol from sugar was a genuine chemical process. However, his experiments were not performed under sterile conditions, and obviously unknown in part, anaerobic bacteria (in tests where oxygen was excluded) must have produced scarce amounts of alco-

Table 1 Ferments (Enzyme Activities) Known Up to 1880

Enzyme	Ferment source	Catalyzed reaction	Author
Protease	gastric juice	meat liquefaction	Spallanzani, 1783[a]
Cyanogen	plant roots	substrate: guaiacum	Planche, 1810[a]
Glutin compound	wheat	starch hydrolysis	Kirchhoff, 1814[a]
Emulsin	bitter almonds	amygdalin hydrolysis	Robiquet and Boutron, 1830[a]; Chalard, Liebig and Wöhler, 1837[a]
Diastatic activity	ptyalin	starch hydrolysis	Leuchs, 1831[a]
Amylase	malt	starch hydrolysis	Payen and Persoz (1833) (12)
Sinigrinase			Faure, 1835[a]
Pepsin		protein hydrolysis	Schwann, 1836[a]
Trypsin		protein hydrolysis	Corvisart, 1856[a]
Saccharase	yeast	sucrose hydrolysis	Berthelot, 1860[a]
Pectase	plants	pectin hydrolysis	Payen (1874) (10)
Pancreas		lipolytic activity	Bernard, 1856[b]
Pancreas extract		fat and starch hydrolysis	Dobell (1869) (13)
Pancreatic ferment	pancreas	fat hydrolysis	Frankland (1885) (14)

[a] In (3).
[b] In (4).

hol, carbon dioxide, but also hydrogen and acetic and butyric acid (16). It was 40 years later when Buchner succeeded in demonstrating cell-free alcohol formation unequivocally (see below).

Pasteur presented a series of experimental results showing unequivocally that alcoholic fermentation proceeded only in the presence of living organisms. And he showed that in all cases where fermentation could be observed under precisely controlled conditions, it was microorganisms (of different kinds, also present in the air) that must be present to initiate fermentation. So he presented strong evidence against the assumption of a *generatio spontanea* postulated by Gay-Lussac. He definitely changed, about two decades later, the disciplinary context of fermentation away from chemistry, redefining the subject to a new autonomous discipline—microbiology (1).

The overall research activity on soluble ferments, meaning enzymatic reactions, was scarce in this period. Thus, in the German *Annalen der Pharmacie* in the period from 1833 to 1850, four articles were published on ferments and fermentation, three of them on diastase. The key paper was essentially a translation from Payen and Persoz (12, 17). In the German *Journal für Praktische Chemie* in the period from 1850 to 1860 no paper dealt with soluble ferments (enzymatic activities; eight papers were published on fermentation [*Gährung*], meaning microbial activity). In the *Bulletin de la Société Chimique de Paris*, one of the most important of the time for fermentation research, there was about one article per year in the 1860s dealing with soluble ferments, meaning enzyme activity, and three or four dealing with fermentation. It was only in the 1880s that research and publication activities increased significantly.

B. Technology

Work on technological issues was more important and even dominating over that on basic aspects from the beginning of the 19th century, especially for brewing, wine, bread, and acetic acid production. These topics made up important parts of the chemical technology of the time (7, 9, 10, 18). Knapp (9) considered scientific and practical industrial interests as equally important.

Diastase application was a major issue from the 1830s onward. "The diastase presents the best means for production of dextrin and dextrin syrup. These products not only become cheaper, but also more pure and tasty." This latter argument was used in favor of the application in food and beverage production. Thus, it was recommended for the manufacture of bread, pastries, chocolate, and soups; furthermore, it was recommended for cider and fruit wine, but especially beer production, where a specific advantage was that the formation of haze at low temperature could be prevented (12, 17). Also, a sugar could be isolated after extended action of diastase on starch. A mass balance gave, in two experiments where the sugar was subsequently fermented by yeast and the amount of carbon

dioxide measured, sugar equivalents of 86.91 and 77.64 parts, with respect to 100 parts of starch. By means of crystallization the authors obtained a "completely pure sugar (which) is white, without smell...." It was less sweet than cane sugar. As a chemical formula they presented $C_{12}H_{28}O_{14}$ (12).

The manufacture of dextrin was established: "Fouchard's dextrin syrup is produced by the factory of Mr. Fouchard at Neuilly as a commercial product" (12). It remained so for decades, and was mentioned in most of the major books and series on technology and chemical technology (9:144–150, 10:125–131, 19, 20a). The treatment of starch by acids or diastase yielded a gummy syrup. Notably, French products seemed to have been produced enzymatically, as was obvious by their smell of malt (recognized by Knapp [9]). Payen (10) gave a short calculation showing that the application of malt is more economical than the use of sulfuric acid.

A further application of enzymes was the use of lab products to produce cheese (9:39, 40). Berzelius was cited with details stating that one part of lab ferment preparation coagulated 1800 parts of milk, and that only 0.06 parts of the lab ferment is lost.

The first company based on applied biocatalysis dates to the 19th century. In 1874, Christian Hansen started a company in Copenhagen. His company, named Christian Hansen's Laboratory to this day, was the first in the industrial market with a standardized enzyme preparation, rennet, for cheese making. Rennet, a mixture of chymosin (earlier called rennin) and pepsin, was and still is obtained by salt extraction of the fourth stomach of suckling calves.

III. THE PERIOD FROM 1890 TO 1940

A. Growing Interest

A pronounced increase in published papers on soluble ferments indicated the growing interest, and several key findings initiated the enzymology of the 20th century. Thus, the numbers of articles on soluble ferments summarized in the abstract service *Chemisches Zentralblatt* rose from ~ 15 per year in the mid-1880s to 35 in 1895 and to 94 in 1910.

From about 1894, Emil Fischer investigated in a series of experiments the action of different enzymes using several glycosides and oligosaccharides of known structure; the results revealed specificity as one the key characteristics of enzymes. Fischer derived therefrom his theory on specificity with the famous picture of a lock and key (21:836–844). A second aspect referred to the protein nature of enzymes. In 1894 Fischer (21:829–835) stated that among the compounds that serve the living cell the proteins are the most important. He was convinced that enzymes were proteins. However, Willstätter, in 1927, denied that enzymes were proteins (22).

A few years after Fischer's investigations, Eduard Buchner published a series of papers (23, 24) which signaled a breakthrough in fermentation and enzymology. The experiments began in 1893 (24c). In his first paper on alcoholic fermentation without yeast cells (23) he stated, in a remarkably short and precise manner, that "a separation of the (alcoholic) fermentation from the living yeast cells was not successful up to now"; in the following year (24) he described a process that solved that task. He gave the experimental details for the preparation of a cell-free press juice from yeast cells with disruption, filtration under high pressure, and further filtration. He then described the formation of carbon dioxide from carbohydrates (sucrose, glucose, fructose, and maltose). No fermentation was observed with lactose or mannitol. No microscopic organisms were present. Chloroform, an antiseptic inhibiting microbial growth, did not inhibit the "fermentation" (the enzymatic reaction). At elevated temperature protein was precipitated and the activity decreased and was finally destroyed. From these results, Buchner derived essential new insights into the nature of alcoholic fermentation. So the concept of enzyme action as a general principle in biochemical reactions was initiated by Berthelot (16) in the 1850s as to priority. The experimental verification, however, was Buchner's work, and he earned the credit for it.

Many more details make up the demarcation of a breakthrough against an established paradigm which taught that processes in living organisms, where alcoholic fermentation was the most important example, were not of pure chemical nature but required a *vis vitalis*. The chemical paradigm, which reduced all reactions in physiological (or bio-) chemistry to chemistry without further hidden forces, began to play the dominant role.

Further findings relevant for establishment of the chemical nature of enzymatic catalysis and technical application followed within a rather short time. Croft-Hill performed the first enzymatic synthesis, that of isomaltose, in 1898, by allowing a yeast extract (α-glycosidase) to act on 40% glucose solutions (3). In 1900, Kastle and Loevenhart found that the hydrolysis of fat and other esters by lipases was a reversible reaction and that enzymatic synthesis could occur in a dilute mixture of alcohol and acid (25). This principle

was utilized for the synthesis of numerous glycosides by Fischer and coworkers in 1902 and by Bourquelot and coworkers in 1913 (26).

After a long period of ~ 100 years, with mysterious hypotheses and several technical applications, where one (diastase) was even economically important, research on enzymes obtained a chemically scientific status. The activity in research increased significantly owing to the new direction, and technical development also got a new scientific basis on which to proceed in a rational way. The definitive establishment of the chemical paradigm was the crystallization of urease by Sumner in 1926, and further enzymes (trypsin etc.) by Northrup and Kunitz in 1930/31. In every known case the pure enzyme turned out to be a protein (25).

B. Technical Development

With the exception of Christian Hansen's rennet, the industrial development of enzymes was very slow initially. Takamine began isolating bacterial amylases in the 1890s in what later became known as Miles Laboratories (today a part of Genencor). In 1894 he obtained a patent for the production of a diastatic enzyme preparation from molds, which he called Takadiastase. The production was performed in a surface culture with wheat bran as a substrate and inoculation by spores of *Aspergillus oryzae* (Fig. 2) (4:401). Additional early applications and patents on enzyme application in the food industry have been collected by Neidleman (27) (Table 2).

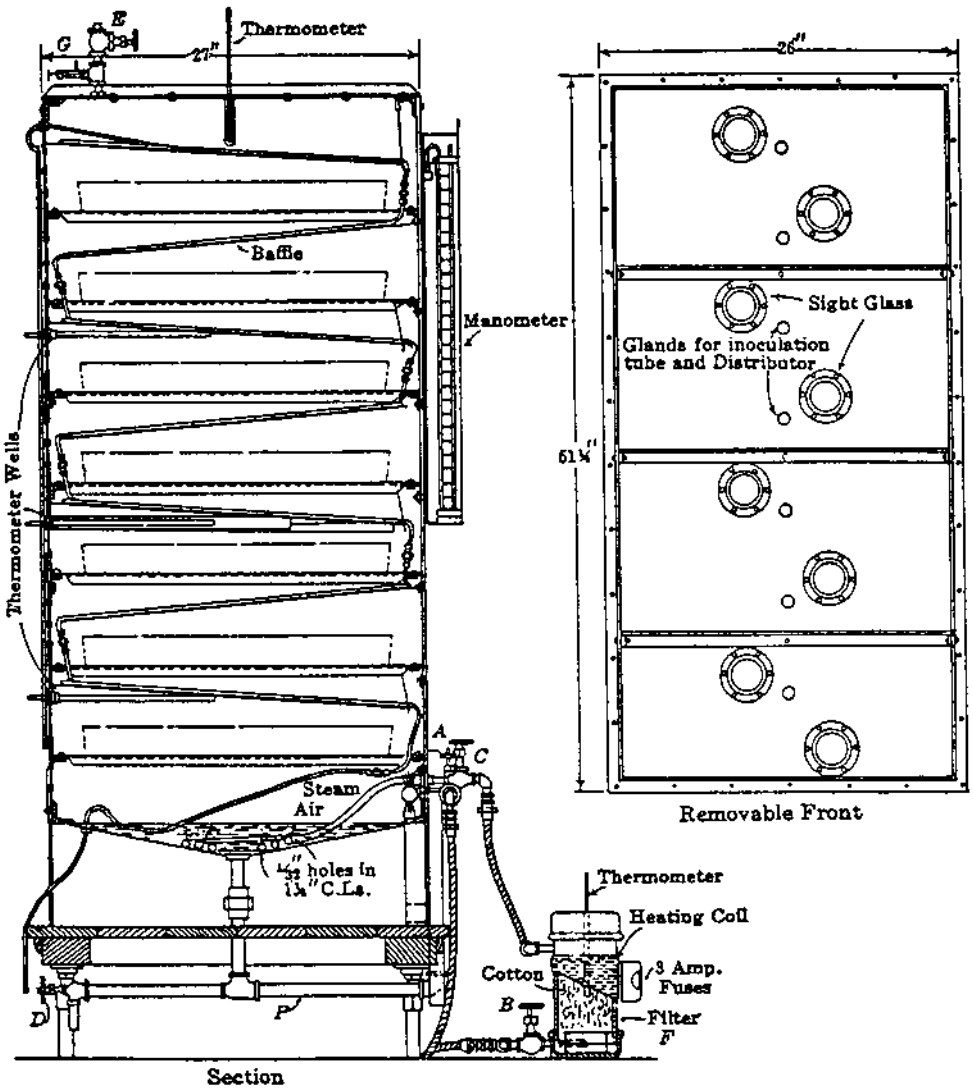

Figure 2 Surface culture with *Aspergillus* in a cabinet incubator. (From Ref. 4.)

Table 2 Selected Early Enzyme Patents

Inventor	Year	Enzyme	Title
J. Takamine	1894	Amylases	Process for making diastatic enzyme
J. Takamine	1906	Amylases	Diastatic substance and production procedure
O. Röhm	1908	Trypsin, steapsin	Preparation of hides for the manufacture of leather
J. Takamine	1911	Amylases	Enzyme
J. Takamine	1911	Amylases	Amylolytic enzyme
L. Wallerstein	1911	Malt protease	Beer and production procedure
L. Wallerstein	1911	Proteases	Preparation of use in brewing
L. Wallerstein	1911	Pepsin	Method of treating beer or ale
L. Wallerstein	1911	Papain	Method of treating beer or ale
L. Wallerstein	1911	Bromelain	Method of treating beer or ale
L. Wallsterstein	1911	Yeast	Method of treating beer or ale
O. Röhm	1915	Pancreatin	Process for cleaning laundry of all types
S. Frankel	1915	Amylase	Manufacture of diastase
I. Pollak	1915	Amylase	Diastase preparations and production procedure
I. Pollak	1915	Amylases	Malt extract and production procedure
A. Boidin/J. Effront	1917	Amylases	Process for treating amylaceous substances
A. Boidin/J. Effront	1917	Amylases	Process of manufacturing diastases and toxins by oxidizing ferments
V.G. Bloede	1918	Amylase	Process of manufacturing vegetable glue
H.S. Paine/J. Hamilton	1922	Invertase	Process for preparing fondant or chocolate soft cream centers
J. Takamine	1923	Amylases, protease, lipase	Enzymatic substance and production procedure
A. Boidin/J. Effront	1924	Amylase, protease, lipase	Treatment of textile fabrics or fibers
Wallerstein Co.	1931	Amylases, protease, lipase	Improvements in process of depilating hides
M. Wallerstein	1932	Amylases or papain	Method of making chocolate syrups
R. Douglas	1932	Amylases	Process of preparing pectin
L. Wallerstein	1933	Invertase	Invertase preparation and production procedure
L. Wallerstein	1937	Proteases	Process of chill-proofing and stabilizing beers and ales
L. Wallerstein	1937	Proteases	Rubber
L. Wallerstein	1938	Proteases	Deproteinization of rubber latex

Source: Ref. 27.

At the beginning of the 20th century the production of plant lipase was performed by mechanical disruption of the seed of ricinus by procedures of Nicloux and Hoyer. These seeds had to be stored for several days with some acid added, which then developed a much higher activity owing to the activation of lipase. These were then utilized for the production of fatty acids from oils and fats. A production vessel is shown in Figure 3. The vessel A can be heated by steam and mixed by compressed air from the compressor L and the storage vessel W. The procedure was as follows: oil or fat was mixed with 35% water, the temperature held at 20–25°C, the ferment (enzyme 4–8%) added to the liquid mass, along with manganese sulfate for activation of the enzyme. Mixing was performed for 15 min, then intermittantly. Eighty percent conversion was obtained after 24 h, 90% after 2 days. The

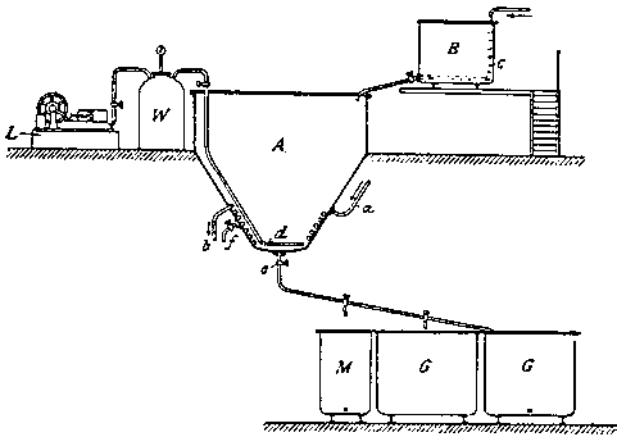

Figure 3 Reactor for fatty acid production. Details of reaction vessel *A*; water reservoir *B*; tube for steam *c*, entrance of steam *a*, exit of steam *b*, compressor *L*, storage vessel for steam *W*, tube for air *d*, valves at positions *e* and *f*, *M* storage vessel for medium layer, *G* storage vessels for glycerol. (From Ref. 20b.)

enzyme was inactivated by heating to 80–85°C. Glycerol was taken from the lower valve e, fatty acid from that in the higher position f. Details for manufacture of 10 tons/week were given. It was pointed out that the reaction is reversible and that an enzymatic synthesis of fat from glycerol and fatty acid was described by Welter in 1911 (20b).

In 1895, Boidin discovered a new process for the manufacture of alcohol called the *amyloprocess*. It comprised cooking of the cereals, inoculation with a mold which formed saccharifying enzymes, and subsequent fermentation with yeast. Together with Effront, working on enzymes for alcohol production since 1900, Boidin founded the Société Rapidase (today a part of DSM-Gist-brocades) in 1920 (28:6). For chill-proofing of beer, proteolytic enzymes (produced by Wallerstein, later Bayter Travenol) have been used successfully since 1911 in the United States (4:337). So urgent was the demand throughout the brewing industry in the United States for a practical solution to this problem of sedimentation that in 1909 and again in 1910 the then U.S. Brewmaster's Association offered two cash awards (27). Lintner, as early as 1890, observed that wheat diastase was important in dough making. This effect was extensively studied, the addition of malt extract came into practice, and American bakers in 1922 used 30 million pounds of malt extract valued at $2.5 million (4:422). The production of pectinases began around 1930 for use in the fruit industry (Schweizerische Ferment, now part of Novozymes).

The use of enzymes for the manufacture of leather played a major role for the industrial-scale production of enzymes. Wood was the first in 1898, to show that the bating action of the unpleasant dungs used at that time was caused by the enzymes (pepsin, trypsin, lipase) they contained. In the context of Wood's investigations the first commercial bate, called Erodin, was prepared from cultures of *Bacillus erodiens*, based on a German patent granted to Popp and Becker in 1896. The bacterial cultures were adsorbed on wood meal and mixed with ammonium chloride (4: 491). In 1907, Röhm patented the application of a mixture of pancreatic extract and ammonium salts as a bating agent (4:488). With this perspective he founded his company in 1907, which successfully entered the market. In 1913 the company had 22 chemists, 30 other employees, and 48 workers (29:101). A systematic approach toward the interrelation of scientific development and engineering aspects, which played a major role in this development, has been published by Buchholz (30).

IV. DEVELOPMENTS SINCE 1940

Even the development of citric acid by fermentation, (Pfizer) and penicillin (Beecham, Glaxo, Merck, Pfizer, Squibb, Bristol-Myers) in the 1940s did not really trigger a scale-up of industrial applications of enzymes. We must go forward to around 1955 before the development of enzyme production was gaining speed by growing sales of bacterial amylase and protease. It began in a very modest fashion. As an illustration, the turnover of the enzyme division of Novo Industri (now Novozymes), the leading enzyme manufacturer, did not exceed $1 million (U.S.) annually until 1965. However, with the appearance of the detergent proteases, the use of enzymes increased. Everybody wanted Biotex, the protease-containing detergent. At the same time, an acid/enzyme process to produce dextrose using glucoamylase was used increasingly in starch processing. By 1969, within only 4 years, Novo's enzyme turnover exceeded $50 million (U.S.) annually; in 1997 Novozyme's enzyme division had a turnover of ~ $650 million (U.S.). The present global market is estimated to be around $1.6 billion (U.S.) (31).

One question, which is as old as industrial enzyme, is: Can enzymes be reused? Some of the first attempts to reuse enzymes were described by Nelson at the beginning of the 20th century. But the enzymes adsorbed to charcoal were very unstable. In the 1950s, Manecke was the first really to succeed in making relatively stable systems; however, he could not convince industry of the importance of further development of his systems (30). It became the group of chemists working with Katchalski-Katzir in Israel who really opened the eyes of industry to the world of immobilized enzymes. Among Katchalski-Katzir's coworkers were Klaus Mosbach, Daniel Thomas, and Malcolm Lilly. The first immobilized enzyme products to be scaled up to pilot plant and industrial application (in 1969) were immobilized amino acid acylases (i.e., I. Chibata and colleagues at Tanabe Seiyaku Co. in Japan [32]) and penicillin G acylase (M. D. Lilly/University College, London, Beecham Pharmaceuticals, England, and G. Schmidt-Kastner, Bayer, Germany) (33, 34:7).

The largest immobilized enzyme product still today in volume is immobilized glucose isomerase. The first commercial enzymatic production of high-fructose corn syrups (HFCS) was in Japan in 1969 (Takasaki and coworkers), utilizing heat treated *Streptomyces* cells containing glucose isomerase in a batch reactor. In the United States, Clinton Division of Standard

Brands (now ADM) was the first company using "Takasaki immobilized glucose isomerase" to make industrial quantities of HFCS around 1971 (33). The skyrocking sucrose prices, during 1973–75, where the price of sucrose increased from 5–7¢/lb to ~ 30¢/lb speeded the interest for HFCS. Thereby, immobilized glucose isomerase increased dramatically in price. Companies like Novozymes, and later Gist-brocades developed more stable enzyme products, which were easier and cheaper to use. Resources were spent on optimizing fermentation for glucose isomerase production, immobilization processes, and the application processes for the immobilized glucose isomerases. As a result, productivities of the commercial immobilized glucose isomerase products increased from ~ 500 kg HFCS/kg immobilized enzyme product (1975) to ~ 15,000–20,000 kg/kg (1997).

Other immobilized enzyme product successes (where annual production of immobilized enzymes has surpassed 1 ton/year) comprise: aminoacylase (Amano), hydantoinase (Smith Beecham), lactase (Valio), lipase (Novozymes), penicillin G acylase (Gist-brocades, Smith Beecham, Röhm), and penicillin V acylase (Novozymes/Gist-brocades) (33).

Numerous efforts and papers, as well as standardized procedures for the characterization of immobilized biocatalysts, have been published in recent decades. The scientific and technical progress may be questioned in the majority of the papers (35). A remarkable issue, however, might be the application of biocatalysts for synthesis of a broad range of products, most importantly in the sectors of food, food ingredients, and pharmaceuticals, and recently in glycobiology for making oligosaccharides and glycosides, and in organic chemistry, including nonaqueous systems and the hydrolysis and modification of fats and products derived therefrom, for surfactants (34:141–190).

Recombinant techniques have been established during the last two decades for much improved yields of enzymes by fermentation, modification of stability, and even selectivity and specificity (36). These techniques have pushed the application, and tend to considerably extend the scope of potential applications, of enzymes in diverse fields including food technology.

REFERENCES

1. R Bud. The Uses of Life, A History of Biotechnology. Cambridge: Cambridge University Press, 1993.
2. R Bud. The zymotechnic roots of biotechnology. Br J His Sci 25:127–144, 1992.
3. JB Sumner, GF Somers. Chemistry and Methods of Enzymes. New York: Academic Press, 1953, pp 13–16.
4. H Tauber. The Chemistry and Technology of Enzymes. New York: Wiley, 1949.
5. SM Roberts, NJ Turner, AJ Willets, MK Turner. Introduction to Biocatalysis. Cambridge: Cambridge University Press, 1995, pp 1–33.
6. MPJ Beral. Notes sur la fermentation. J Pharm Sci Access 1:358–361, 1815.
7. JHM von Poppe. Volks-Gewerbslehre oder allgemeine und besondere Technologie. Stuttgart: Carl Hoffmann, 1842.
8. Anon. Ueber die Gährung und die sogenannte generatio aequivoca. (summary article). J Prakt Chem 85:465–472, 1862.
9. F Knapp. Lehrbuch der chemischen Technologie, Vol 2. Braunschweig: F. Vieweg und Sohn, 1847.
10. A Payen. Handbuch der technischen Chemie. Nach A. Payens Chimie industrielle, frei bearbeitet von F. Stohmann and C. Engler, Vol II. Stuttgart: E. Schweizerbart'sche Verlagsbuchhandlung, 1874, p 127.
11. Guerin-Vary. Wirkung der Diastase auf Kartoffelstärkemehl. Ann Pharm 17:261–267, 1836.
12. A Payen, JF Persoz. Mémoire sur la diastase, les principaux produits de ses réactions, et leurs applications aux arts industriels. Ann Chim Physique 2me Sér 53:73–92, 1833.
13. H Dobell. Action du pancréas sur les graisses et sur l'amidon. Bull Soc Chim 506, 1er semestre, 1869.
14. E Frankland. On chemical changes in their relation to microorganisms. J Chem Soc 47:159–183, 1885.
15. M Berthelot. Remarques sur la note de M. Béchamp relative à la fermentation alcoolique. Bull Soc Chim 392–393, 1864.
16. M Berthelot. Ueber die geistige Gährung. J Praktische Chem 71:321–325, 1857.
17. Anon. Diastase und Dextrin. Ann Pharm 12:295–299, 1834.
18. R Wagner. Die chemische Technologie. Leipzig: O. Wiegand, 1857.
19. Brockhaus. Diastase, Vol 5, p 255, 1894; Fermente, Vol 6, p 679, 1894.
20. F Ullmann. Enzyklopädie der technischen Chemie, (a) Vol 3, pp 749–773, 1916; (b) Vol 5, p 445, 1914. Berlin: Urban und Schwarzenberg.
21. E Fischer. Untersuchungen über Kohlenhydrate und Fermente. Berlin: J Springer, 1909; Ber D Chem Ges 27:2985, 1894; 27:2031, 1894.
22. JS Fruton. Early theories of protein structure. In: PR Srinivasan, JS Fruton, JT Edsall, eds. The Origins of Modern Biochemistry. New York: New York Academy of Sciences, 1979, pp 1–18.
23. E Buchner. Alkoholische Gährung ohne Hefezellen. Ber D Chem Ges 30:117–124, 1897.
24. (a) E Buchner. Ueber zellfreie Gährung. Ber D Chem

Ges 31:568–574, 1898. (b) E Buchner, R Rapp. Alkoholische Gährung ohne Hefezellen. Ber D Chem Ges 31:209–217, 1898. (c) E Buchner, R Rapp. Alkoholische Gährung ohne Hefezellen (5). Ber D Chem Ges 31:1084–1090, 1898. (d) E Buchner, R Rapp. Alkoholische Gährung ohne Hefezellen (6). Ber D Chem Ges 31:1090–1094, 1898. (e) E Buchner, R Rapp. Alkoholische Gährung ohne Hefezellen (7). Ber D Chem Ges 31:1531–1533, 1898.
25. JB Sumner, K Myrbäck. The Enzymes, Vol 1, Part 1, 1950, pp 1–27.
26. K Wallenfels, H Diekmann, Glykosidasen. Hoppe-Seyler/Thierfelder, Handbuch der physiologisch- und pathologisch-chemischen Analyse, Vol 6B. Berlin: Springer, pp 1156–1210.
27. SL Neidleman. Enzymes in the food industry: a backward glance. Food Technol 45(1):88–91, 1991.
28. H Uhlig. Enzyme arbeiten für uns. Munich: Hanser Verlag, 1991.
29. E Trommsdorf. Dr. Otto Röhm—Chemiker und Unternehmer. Düsseldorf: Econ, 1976.
30. K Buchholz. Reflections on the history and scientific character of biochemical engineering. Adv Mol Cell Biol 15A:117–134, 1996.
31. WH Stroh. Industrial enzymes market: growth experiences from new products and movement into global market. Genet Eng News March 1:11, 38, 1998.
32. T Tosa, T Mori, N Fuse, I Chibata. Studies on continuous enzyme reactions. 6. Enzymatic properties of DEAE-Sepharose aminoacylase complex. Agr Biol Chem 33:1047–1056, 1969.
33. PB Poulsen. Biotechnology and Genetic Engineering Review, Vol 1. Newcastle-upon-Tyne: Intercept Inc., 1984.
34. K Buchholz, V Kasche. Biokatalysatoren und Enzymtechnologie. Weinheim: VCH, 1997, p 7–11.
35. K Buchholz. Criteria for the analysis of scientific quality. Scientometrics 32:195–218, 1995.
36. SB Petersen. Protein engineering. In: AJJ Straathof, P Adlercreutz, eds. Applied Biocatalysis. Amsterdam: Harwood Academic Publishers, 2000, p 229–270.

3

What Enzymes Do and Why They Are Highly Specific and Efficient Catalysts

John R. Whitaker
University of California, Davis, Davis, California, U.S.A.

I. INTRODUCTION

Enzymes are the key to all life. Therefore, it is not surprising that all organisms contain hundreds of different enzymes. It is common to find isoenzymes, which are multiple protein forms of an enzyme within the same organ, with qualitatively the same enzymatic activity. Therefore, each isoenzyme is encoded by a different gene. With so many different organisms in the world, all with hundreds of different enzymes, how is it possible to systematize enzymes and enzyme nomenclature? This was a problem that the biochemical and chemical community faced in 1955.

As indicated in Chapter 1, the first enzyme recognized, based only on its activity, was catalase, in 1812. It converts hydrogen peroxide to water and oxygen; the oxygen bubbles out of the solution. As described in Chapter 1, several other enzymes were discovered over the years. By 1955, more than 600 enzymes were known and partially characterized. The naming of enzymes was largely left to the discoverer. Some enzymes, such as catalase, diastase (now amylase), polyphenol oxidase, peroxidase, etc., used "-ase" to indicate that the compound was an enzyme. However, naming of other enzymes, such as trypsin, chymotrypsin, ficin, and papain, did not use "-ase". Warburg and Christian in 1935 discovered an enzyme that, when partially purified, was yellow because of the cofactor riboflavin. They named it the "yellow enzyme." Soon after, Warburg discovered a different yellow enzyme so he named it the "new yellow enzyme." When a crude preparation of enzymes that synthesized proteins was first discovered it was named "the pH 5 extract" because maximum enzyme activity occurred at that pH.

An International Commission on Enzymes was established in 1955 by the International Union of Biochemistry with the charge "to consider the classification and nomenclature of enzymes and coenzymes, their units of activity and standard methods of assays, together with the symbols used in the description of enzyme kinetics." The Commission on Enzymes contained one or more members from each of the countries that were publishing significant research on enzymes. The first Report of the Commission on Enzymes in 1961 contained 712 enzymes. Subsequent updates have been issued. The most recent report in 1992 contained 3196 enzymes (1). In order for the enzyme to appear in the list, the researcher must isolate the enzyme and characterize it with respect to substrate(s) specificity, product(s) formed, nature of the overall reaction, and protein properties, and clearly demonstrate that it is unique.

II. THE THREE-TIER CLASSIFICATION OF ENZYMES

The 1955 Commission on Enzymes recommended that each enzyme have three designations. These are: a

systematic name, a trivial name, and an Enzyme Commission (EC) number.

The systematic name consists of the name(s) of the substrate(s). In the case of two or more substrates (or reactants), the names of the substrates are separated by a colon. The second part of the systematic name, ending in -ase, is based on one of the six types of chemical reactions catalyzed (see below). When the overall reaction involves two different chemical reactions, such as oxidative demethylation, the second type of reaction is listed in parenthesis following the name of the first type of reaction—for example, "sarcosine:oxygen oxidoreductase (demethylating)."

The trivial name is one that is generally recognized and is in common usage such as trypsin, chymotrypsin, α-amylase, cellulase, peroxidase, or catalase.

The number system derives directly from the classification scheme. Each enzyme number contains four digits, separated by periods, and preceded by EC. The numbers are permanent. Newly discovered enzymes are placed at the end of a list under appropriate headings. When the classification of an enzyme is changed, the original number remains in the listing, but the user is directed to the new listing, including the new number of the enzyme. For example, the listing of the proteases has been changed recently. A new arrangement of the carbohydrases will be published soon.

A. Rules for Naming of Enzymes

1. Classification into Six Groups Based on Type of Chemical Reaction Catalyzed

As noted above, the Enzyme Commission classified the enzymes into groups based on the type of chemical reaction catalyzed. Together with the name(s) of the substrate(s), this provides the basis for systematically naming individual enzymes.

There are six chemical types of reactions catalyzed by enzymes. These are (with the general group name of the enzymes in parentheses): (a) oxidoreduction (oxidoreductase), (b) group transfer (transferase), (c) hydrolysis (hydrolase), (d) formation of double bonds without hydrolysis (lyase), (e) isomerization (isomerase), (f) ligation (ligases).

The first digit in the EC number system is based on the type of chemical reaction catalyzed, with (a)–(f) above being listed as EC 1–6.

2. The Overall Reaction as Basis of Nomenclature

The overall reaction catalyzed, based on the formal chemical equation [for example, Eq. (1)] is the basis for the nomenclature. The mechanism of the reaction is not indicated. Therefore, an enzyme cannot be named systematically until the substrate(s), product(s), and the chemical nature of the reaction catalyzed are known.

The overall reaction catalyzed by a specific enzyme is shown in Eq. (1):

$$\underset{\text{Ethanol}}{CH_3CH_2OH} + NAD^+ = \underset{\text{Acetaldehyde}}{CH_3CHO} + NADH + H^+ \quad (1)$$

According to the Enzyme Commission, the systematic name of the enzyme is ethanol:NAD^+ oxidoreductase (more commonly called acohol:NAD^+ oxidoreductase. The substrate (ethanol) that donates the hydrogens (becomes oxidized) is listed first, followed by the substrate (NAD^+) that accepts the hydrogens (becomes reduced). According to the number system, alcohol:NAD^+ oxidoreductase is EC 1.1.1.1). The first digit designates it as an oxidoreductase. The second digit indicates that the donor of the hydrogens is an alcohol ($R_2CH–OH$). The third digit indicates that NAD^+ (or $NADP^+$) is the specific acceptor of the hydrogen(s), and the fourth digit indicates that the alcohol is ethanol. The trivial name of alcohol:NAD^+ oxidoreductase is alcohol dehydrogenase. In a publication the systematic name would be given at the first mention of the enzyme, along with the trivial name and EC number; i.e., alcohol:NAD^+ oxidoreductase (alcohol dehydrogenase; EC 1.1.1.1). Thereafter in the publication, the trivial name, alcohol dehydrogenase, would be used. Table 1 contains the general listing of enzymes through the second digit as recommended by the Enzyme Commission.

B. Six Groups of Enzymes

The six groups of enzymes, based on the chemical reaction catalyzed, are described in more detail in this section.

1. Oxidoreductases

Oxidoreductases are enzymes that oxidize or reduce substrates by transfer of hydrogen or electrons or by addition of oxygen. The systematic name is formed as "donor:acceptor oxidoreductase." One example for alcohol dehydrogenase (EC 1.1.1.1) is shown in Eq. (1) above, in which the donor substrate is ethanol which contributes two hydrogens to NAD^+, the acceptor substrate (and cofactor) with the formation of acetal-

dehyde and $NADH_2$; $NADH_2$ then loses a proton (H^+) based on the pH of the reaction. Another example is the catalase reaction in which one H_2O_2 molecule serves as the donor substrate and the second H_2O_2 molecule serves as the acceptor substrate to form O_2 and H_2O [Eq. (2)]. The systematic name is "hydrogen peroxide:-hydrogen peroxide oxidoreductase" (EC 1.11.1.6).

$$H_2O_2 + H_2O_2 = O_2 + 2H_2O \tag{2}$$

Whitaker (2) has suggested dividing the oxidoreductases into eight subgroups based on mechanistic considerations. But the International Commission on Enzymes considers only the overall reaction in naming enzymes.

2. Transferases

Transferases are enzymes that remove groups (not including H, which belongs in group 1, the oxidoreductases) from substrate(s) and transfers the group to acceptor substrates (not including water). The systematic name is formed as "donor:acceptor group-transferred-transferase." The types of groups transferred are given by the second digit in EC 2. of Table 1. A specific example of a transferase is shown in Eq. (3).

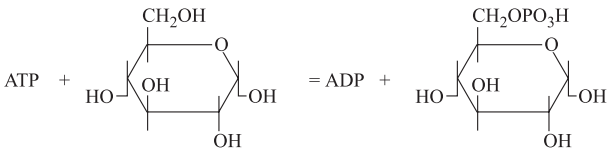

(3)

The systematic name of the enzyme that catalyzes the reaction in Eq. (3) is "ATP:D-glucose 6-phosphotransferase" (EC 2.7.1.2). The trivial name is glucokinase. The position to which the group (phosphate) is transferred to the glucose is given in the systematic name when more than one possibility exists, such as D-glucose-1-phosphate.

3. Hydrolases

Hydrolases are enzymes in which water (H_2O) is the second substrate. Water participates in the breakage of covalent bonds; for example, peptide bonds in proteins, glycosidic bonds in carbohydrates, ester bonds in lipids, and phosphodiester bonds (and others) in nucleic acids. The systematic name is formed as "substrate hydrolase." The elements (H and OH) appear in the products of the reaction as shown in Eq. (4)

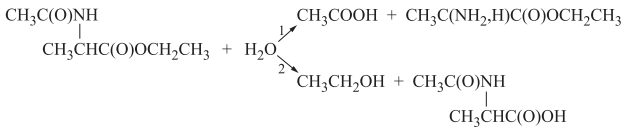

(4)

When the enzyme specificity is limited to a single group (of two or more susceptible groups), the name of the group is given as a prefix of hydrolase. For example, enzymatic hydrolysis of a compound such as N-acetyl-L-alanine ethyl ester [Eq. (4)] can occur at either the acetyl-nitrogen bond or the ethoxy-oxygen bond, depending on the specificity of the enzyme.

In reaction 1 [Eq. (4)], the enzyme is an acyl amino-hydrolase (EC 3.5.) while in reaction 2 [Eq. (4)], the enzyme is an acyl oxygenhydrolase (esterase, EC 3.1.). There is no crossreactivity between the two enzymes, as they are specific for hydrolysis of only one of the scissile bonds, unlike HCl.

4. Lyases

Lyases are enzymes that remove groups from their substrates (not by hydrolysis) to give a double bond in the product, or which conversely add groups to double bonds. The systematic name is formed as "substrate prefix-lyase." Prefixes such as "hydro-" and "ammonia-" are used to indicate the type of reaction—for example, "L-malate hydro-lyase" (EC 4.2.1.2). Decarboxylases are named as "carboxy-lases." A hyphen is always written before "lyase" to avoid confusion with hydrolases, carboxylases, etc. An example of a lyase is the removal of HOH from malic acid to give fumaric acid [Eq. (5)]:

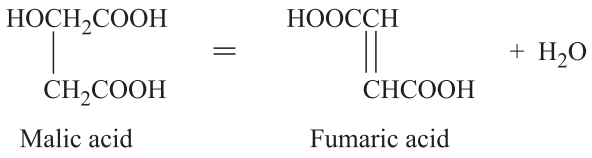

(5)

by the enzyme (s)-malate hydro-lyase (fumarate hydratase; EC 4.2.1.2; formerly known as fumarase).

5. Isomerases

Isomerases are enzymes that cause rearrangement of one or more groups on substrates without changing the atomic composition of the product. The general systematic name is formed as "substrate prefix-isomerase." The prefix indicates the type of isomerization involved, for example, "maleate *cis-trans*-isomerase" (EC 5.2.1.1) [Eq. (6)].

Table 1 Key to Numbering and Classification of Enzymes[a]

1. Oxidoreductases
- 1.1 Acting on the CH–OH group of donors
- 1.2 Acting on the aldehyde or oxo group of donors
- 1.3 Acting on the CH–CH group of donors
- 1.4 Acting on the CH–NH_2 group of donors
- 1.5 Acting on the CH–NH group of donors
- 1.6 Acting on NADH or NADPH
- 1.7 Acting on other nitrogenous compounds as donors
- 1.8 Acting on a sulfur group of donors
- 1.9 Acting on a heme group of donors
- 1.10 Acting on diphenols and related substances as donors
- 1.11 Acting on hydrogen peroxide as acceptor
- 1.12 Acting on hydrogen as donor
- 1.13 Acting on single donors with incorporation of molecular oxygen (oxygenases)
- 1.14 Acting on paired donors with incorporation of molecular oxygen
- 1.15 Acting on superoxide radicals as acceptor
- 1.16 Oxidizing metal ions
- 1.17 Acting on CH_2 groups
- 1.18 Acting on reduced ferredoxin as donor
- 1.19 Acting on reduced flavodoxin as donor
- 1.97 Other oxidoreductases

2. Transferases
- 2.1 Transferring one-carbon groups
- 2.2 Transferring aldehyde or ketone residues
- 2.3 Acyltransferases
- 2.4 Glycosyltransferases
- 2.5 Transferring alkyl or aryl groups, other than methyl groups
- 2.6 Transferring nitrogenous groups
- 2.7 Transferring phosphorous-containing groups
- 2.8 Transferring sulfur-containing groups

3. Hydrolases
- 3.1 Acting on ester bonds
- 3.2 Glycosidases
- 3.3 Acting on ether bonds
- 3.4 Acting on peptide bonds (peptidases)
- 3.5 Acting on carbon-nitrogen bonds, other than peptide bonds
- 3.6 Acting on acid anhydrides
- 3.7 Acting on carbon–carbon bonds
- 3.8 Acting on halide bonds
- 3.9 Acting on phosphorus–nitrogen bonds
- 3.10 Acting on sulfur–nitrogen bonds
- 3.11 Acting on carbon-phosphorus bonds

4. Lyases
- 4.1 Carbon–carbon lyases
- 4.2 Carbon–oxygen lyases
- 4.3 Carbon–nitrogen lyases
- 4.4 Carbon–sulfur lyases
- 4.5 Carbon–halide lyases
- 4.6 Phosphorus–oxygen lyases
- 4.99 Other lyases

5. Isomerases
- 5.1 Racemases and epimerases
- 5.2 *cis-trans*-isomerases
- 5.3 Intramolecular oxidoreductases
- 5.4 Intramolecular transferases (mutases)
- 5.5 Intramolecular lyases
- 5.99 Other isomerases

6. Ligases
- 6.1 Forming carbon–oxygen bonds
- 6.2 Forming carbon–sulfur bonds
- 6.3 Forming carbon–nitrogen bonds
- 6.4 Forming carbon–carbon bonds
- 6.5 Forming phosphoric ester bonds

[a] The third and fourth levels of classification are given in Ref. 1:v–xi.

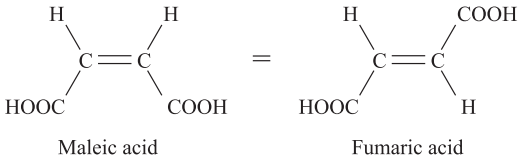

Maleic acid Fumaric acid (6)

Enzymes that catalyze an aldose-ketose interconversion are known as "ketal-isomerases (for example, "L-arabinose keto-isomerase"; EC 5.3.1.4). When the isomerization consists of an intramolecular transfer of a group, such as 2-phospho-D-glycerate to 3-phospho-D-glycerate, the enzyme is called a "mutase"; a specific example of a mutase is D-phosphoglycerate 2,3-phosphomutase (EC 5.4.2.1). Isomerases that catalyze inversions of asymmetric groups are termed "racemases" or "epimerases," depending on whether the substrate contains one or more than one center of asymmetry, respectively.

6. Ligases

Ligases are enzymes that catalyze the covalent linking together of two molecules, coupled with the breakage of a pyrophosphate bond as in ATP, UTP, or CTP. The systematic name is formed as "X:Y ligase (Z)," where X and Y are the names of the two molecules to be joined together. The compound Z is the product formed from the triphosphate (ATP, UTP, or CTP); they provide energy during the reaction. An example is:

$$\text{ATP} + \text{L}-\text{asparate} + \text{NH}_3 = \text{AMP} + \text{pyrophosphate} + \text{L-asparagine} \quad (7)$$

The systematic enzyme name is L-asparate:ammonia ligase (AMP-forming (aspartate-ammonia ligase, EC 6.3.1.1.)

Proteins, carbohydrates, and triacylglycerols are synthesized by specific ligases using ATP, UTP, and CTP, respectively.

C. Other Considerations in Naming Enzymes

1. Organism from Which the Enzyme Is Isolated

Proteins are specific to an organism. When proteins from one organism are injected into a different animal, they elicit antibodies, indicating that they differ from the proteins of the recipient animal. They have differences in amino acid sequences and therefore folding patterns. Enzymes, as proteins, are no different. Therefore, the name of the specific organism from which an enzyme is derived must be given.

2. Organ from Which the Enzyme is Isolated

No less important is the organ (of multicellular organisms) from which the enzyme is obtained. α-Amylases from human saliva are different from those produced by the human pancreas, for example. Therefore, the organ from which the enzyme is obtained must be specified.

3. Isoenzymes

Isoenzymes are different protein forms of an enzyme produced in the same organ by different genes, but qualitatively they have the same activity. Perhaps multiple gene expression of isoenzymes is protection against failure of a gene. Or they may occur due to mutation of a nucleotide base in a codon of a gene. Whatever the reason, the protein expressed is different from one gene to another, even from the same cell. The proteins have different protein properties by electrophoresis, column chromatography, and other separation methods. Quantitatively, there may be differences in catalytic efficiency of the isoenzymes.

When isoenzyme forms are present, they contain a letter (or number) indicating how they behaved by electrophoresis or the order in which they were eluted from an ion exchange column. For example, the first isoenzyme eluting from a cation exchange column would be isoenzyme-1, the second would be isoenzyme-2, etc.

One might ask whether posttranslational processing of a nascent protein (see Chapter 1) can give isoenzymes due to different levels of modification. This is a relatively easy question to answer, but it may be difficult to determine experimentally. An example often observed experimentally is that the extent of glycosylation of a seed protein (for example) is often different depending on the maturity of the seed. The glycosyl groups are covalently attached to the protein at the hydroxyl group of seryl residues and β-amino groups of asparaginyl residues, as determined by the genetic code, immediately following translation (and before the protein folds into the native form; see Chapter 1). The glycosyl groups may then be shortened by cytoplasmic carbohydrases *after folding* of the protein to the native state ("age"-related processing). Are these isoenzymes? They are not products of different genes and so do not qualify as isoenzymes. Native human hemoglobin is glycosylated over time at a level depending on its age *and* the concentration of glucose in the blood. Hemoglobin *a* levels are used clinically to determine the severity of diabetes in humans. No one would describe the age-related modified hemoglobin as an isoprotein! Multiple electrophoretic bands (> 30 sometimes) occur with peroxidase because of different levels of glycosylation. The benzoquinones formed due to the activity of polyphenol oxidase action on phenols during extraction and purification of proteins (including polyphenol oxidase itself) lead to multiple bands since the benzoquinones quickly modify the ε-amino group of lysyl residues. These different bands are not due to isoenzymes!

4. In Summary

In naming an enzyme, one must not only describe it by the overall type of reaction catalyzed (under standard conditions), but also by the source of the enzyme (organism, organ) and by isoenzyme number. With the excellent tools available today, there is no basis for publishing quantitative data on the activity of an enzyme until the degree of purity of the enzyme has

been established and one can associate the activity with one unique protein catalyst.

III. WHY ARE ENZYMES HIGHLY SPECIFIC AND EFFICIENT CATALYSTS?

A. How Efficient Are Enzymes as Catalysts?

Table 2 provides data on the relative rates of a few enzyme-catalyzed reactions in relation to the noncatalyzed and non-enzyme-catalyzed reactions at 25°C. All relative rates are based on a 1 molar concentration of catalyst for comparison. First, look at the relative rates of the reactions at 25°C. Catalase is 3.5×10^8 times more effective in conversion of H_2O_2 to H_2O and O_2 than is the noncatalyzed reaction and 1.7×10^5 times more effective than the I^- catalyst. Sucrose can be hydrolyzed by acids (by the H^+) as well as by invertase. Invertase is 5.6×10^{10} times more effective than the H^+. Carbonic anhydrase, important in our respiratory exchange of O_2 and CO_2, is 3×10^6 more effective than no catalyst. In our kidney, urease is important in the conversion of urea to ammonia and CO_2. Urease is 4.3×10^{11} times more effective than the H^+.

Table 2, column 3, gives the Arrhenius activation energy, E_a, required to convert the substrate to products. Notice that in all cases, the E_a for the enzyme-catalyzed reaction is significantly lower than for the non-enzyme-catalyzed or noncatalyzed reaction. Therefore, one can correctly conclude that the enzymes are successful in lowering the activation energy for conversion of substrate to product. To fully grasp the effectiveness of lowering E_a one must appreciate that the rate of a reaction, as controlled by the rate constant, k, is logarithmically related to E_a as shown in Eq. (8).

$$k = Ae^{-E_a/RT} \tag{8}$$

where A is the Arrhenius constant, e is the base of the natural logarithm, E_a is the Arrhenius activation energy, R is the universal gas constant, and T is Kelvin temperature.

The effect of temperature on the rate of reactions (including enzyme-catalyzed reactions) is given by the Boltzmann distribution equation:

$$n'/n = -E_a/RT \tag{9}$$

where n' is the number of molecules per unit volume of a compound having activation energy E_a or greater (see Fig. 1) and n is the total number of molecules per unit volume of a compound. The A factor in Eq. (9) is the product of the kinetic energy of the system due to Brownian movement and the probability (P) that two molecules will collide with proper orientation of reactive groups. P approaches 1 in enzyme-catalyzed reactions because the substrates are properly bound noncovalently in the active site adjacent to the catalytic group(s) required for catalysis (see Ref. 2, pages 314ff).

Figure 1 shows the change in energy (both activation energy (steps 3, 4, and 6) and thermodynamic energy (steps 1, 2, 5, and 7) as the enzyme binds with substrate and catalyzes conversion of the substrate (A) to product (P) in the reaction. The rate-limiting step requires the most energy (step 4 in Fig. 1). This energy is the activation energy, E_a, as shown in Eq. (8).

Table 2 Effect of Catalyst on E_a and on Relative Rates of Some Reactions

Substrate	Catalyst	E_a (kcal/mol)	n'/n[a] (25°C)	Relative rate (25°C)
H_2O_2	None	18.0	5.62×10^{-14}	1.00
	I^-	13.5	1.16×10^{-10}	2.07×10^3
	Catalase	6.4	1.95×10^{-5}	3.47×10^8
Sucrose	H^+	25.6	1.44×10^{-19}	1.00
	Invertase	11.0	8.04×10^{-9}	5.58×10^{10}
Carbonic acid	None	20.5	8.32×10^{-16}	1.00
	Carbonic anhydrase	11.7	2.46×10^{-9}	2.96×10^6
Urea	H^+	24.5	9.33×10^{-19}	1.00
	Urease	8.7	3.96×10^{-7}	4.25×10^{11}

[a] $n'n$ values were calculated by use of Eq. (9) and are approximate only, since differences in $\Delta S^{\ddagger}$ for the comparison reactions are ignored.
Source: Ref. 2.

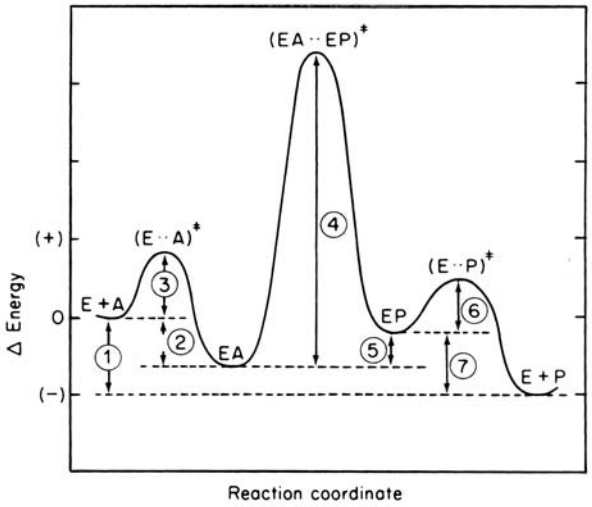

Figure 1 Change in energy along the pathway of reaction during conversion of substrate A to product P in an enzyme-catalyzed reaction. The numbers refer to steps in thermodynamic states (ground states); 1, 2, 5, and 7 and transition states (activated states); steps 3, 4, and 6 in the forward reaction pathway. (From Ref. 2.)

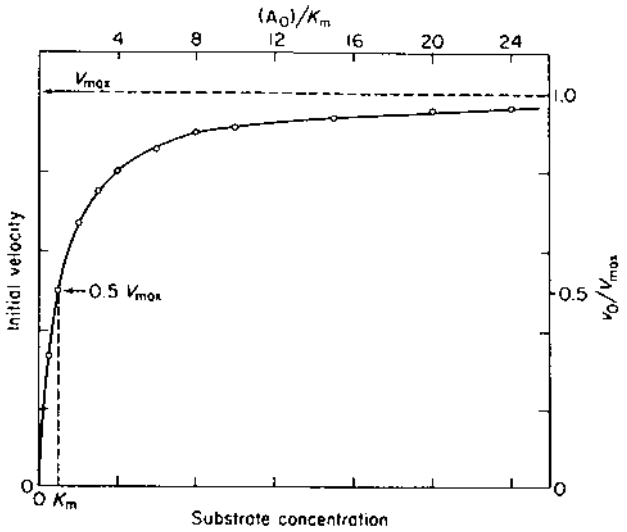

Figure 2 Variation of initial velocity with substrate concentration for an enzyme-catalyzed reaction according to Eq. (2). (From Ref. 2.)

B. Binding of Substrate by Enzyme

Very few compounds are substrates for a given enzyme. In the case of urease, really only urea is a good substrate. For other enzymes, such as alkaline phosphatase, a number of compounds serve as substrate (phenylphosphate, *p*-nitrophenyl phosphate, β-glycerol phosphate, etc.). However, all substrates for alkaline phosphatase have an ortho-phosphate group. By competitive inhibition studies with ortho-phosphate, and with different substrates, it is relatively easy to establish that the major recognition group on the substrate for the enzyme is the ortho-phosphate group. This example can be extended to most other enzymes and their recognition of substrates. Analogs of substrates are good inhibitors of enzymes, which tells us that the enzyme *must recognize and bind with the compounds*.

In 1902, Henri (3) and Brown (4) independently proposed that the observed effect of substrate concentration on the velocity of conversion of substrate to product (Fig. 2) is due to the essentiality of an intermediate substrate·enzyme noncovalent complex prior to catalysis [Eq. (10)].

$$E + S \underset{k-1}{\overset{k_1}{\rightleftharpoons}} E \cdot S \overset{k_2}{\rightarrow} E + P \tag{10}$$

When all of the enzyme is bound to substrate, the maximum velocity, V_{max}, of the reaction is achieved. Many researchers have verified by other methods that formation of the $E \cdot S$ complex is essential before conversion of substrate to product is possible. How does this binding contribute to the specificity and efficiency of enzyme-catalyzed reactions? This question is addressed in the following way.

1. Nature of the Binding Site

Table 3 lists the characteristics of the active site of an enzyme. The active site is a small area (with ~ 10 amino acid residues brought together from distant

Table 3 Active Site Characteristics of an Enzyme

1. Small area on surface of native protein
2. Shape can be crevice or hole
3. Active site binds substrate(s) and cofactors
   a. Stereospecifically with at least three points of contact
   b. Converts substrate to products
4. Ionizable groups in active site (side chains of amino acid residues)
   a. May be involved in binding
   b. Involved in catalysis
5. Active site flexible (induced fit) and can accommodate substrate(s)
6. Active site may contain cofactor(s)
7. Active site with substrate bound is hydrophobic

parts of the primary structural chain to the surface of the enzyme). The substrate can diffuse rapidly to the active site and binds stereospecifically by a minimum of three noncovalent bonds. In lysozyme, Glu35, Asn37, Asn44, Asp52, Asp59, Try63, Asp101, Arg 114, and the carbonyl oxygen of the peptide bonds between Phe34–Glu35, Gln57–Leu58, and Ala107–Try108 all appear to be in proximity in the active site (5). In ribonuclease, Lys7, Arg10, His12, Lys41, and His119 are known to be in the active site (6).

Carboxypeptidase A and lysozyme form five and 12 noncovalent contacts with the substrates benzyloxycarbonyglycyl-L-phenylalanine and hexa-N-acetylchitohexaose, respectively (2). When bound properly in the active site, the substrate is positioned in proximity to the catalytic groups that convert it to product(s), along with any cofactors that are required. On binding of substrate into the active site most of the water molecules are forced out so that the reaction takes place under hydrophobic conditions. For hydrolases, one water molecule binds stereospecifically as a second substrate in proximity to the first substrate.

Table 4 summarizes the factors accounting for the catalytic effectiveness of enzymes. Conversion of the enzyme and substrate (plus any cofactors) from an intermolecular reaction to an intramolecular reaction (the $E \cdot S$ complex) increases the rate by 10^4 for one substrate, 10^9 for two substrates, and 10^{15} for three substrates. Even five to six component reactions are possible with enzymes, such as the RNA polymerases. There is an increase in entropy of the reaction because of the highly structured nature of binding of substrate(s) and cofactors with respect to the catalytic groups, increasing the rate by a factor of $\sim 10^3$. Since water is expelled when the substrate(s) and cofactors bind in the active site, the concentration of the catalytic groups of the enzyme increase to ~ 10 M, giving a rate enhancement of 10^3–10^4.

In some cases, the scissile bonds of the substrate may be distorted during the bonding process (induced fit [8]), contributing to increase in rate. For example, in the case of lysozyme, binding of the sugar substrate to the enzyme's active site results in a glucosyl oxocarbonium ion intermediate with an enzyme-induced distortion of a glucosyl residue at the scissile bond into a half-chair conformation (5). Electrostatic stabilization of the transition state in an enzyme reaction also plays an important role. For example, the Asn155–oxyanion interaction in subtilisin contributes 3.7 kcal/mol activation energy to the transition stabilization (9). Bender et al. (10) showed that restriction of rotation of the N-acetyl-L-tryrosyl- (acyl group intermediate) chymotrypsin, in comparison with the small acetyl-L-chymotrypsin (acyl group intermediate) increased $\Delta S^{\ddagger}$ from -35.9 to -13.4 eu (cal mol^{-1} deg^{-1}), thereby increasing the rate of deacylation by 3540 times (10). In summation, the stereospecific binding of the substrate into the active site of the enzyme may increase the rate by 10^{12}- to 10^{26}-fold.

2. Catalysis

During the catalytic step(s), concerted general acid/general base catalysis or nucleophilic/electrophilic catalysis increases the overall rate enhancement by a factor of 10^2–10^3 times. The overall rate enhancement predicted for an enzyme-catalyzed reaction is $\sim 10^{18}$–10^{36}. Catalase- and peroxidase-catalyzed reactions reach values near 10^{18} enhancement.

Table 4 Factors Accounting for Catalytic Effectiveness of Enzymes

Factor	Rate enhancement[a] (approximate)
1. Formation of stereospecific enzyme·substrate complex (conversion from inter- to intramolecular reaction)	10^4; 10^9; 10^{15}[,b]
2. Increased entropy of reaction	10^3
3. Concentration of reactive catalytic groups when substrate binds	10^3–10^4
4. Distortion of substrate when bound	10^2–10^4
5. General acid/general base catalysis	10^2–10^3
6. Nucleophilic/electrophilic catalysis	10^2–10^3
7. Use of several step process	10^2–10^4
Overall rate enhancement	10^{18}–10^{36}

[a]In some cases, these values can be approximated by model experiments. In others, they are the best estimates available.
[b]For one, two, and three substrate reactions, respectively.
Source: Ref. 7.

Proteins of 25,000–100,000 molecular weight (~ 200–890 amino acid residues per molecule) are synthesized on the ribosome by polymerases in ~2–6 min at 37°C!

Figure 3 depicts the active site of ribonuclease with the substrate, cytidine 2′, 3′-phosphate bound in the active site. The catalytic groups of the enzyme are two imidazole side chains of two histidine residues. The distance between reactive groups on the enzyme and the scissile bond is ~ 2 Å, nearly covalent bond dimensions. The imidazole group on the left side of the active site functions as a general base to remove a hydrogen from a water molecule (shown as ROH in Fig. 3) to form a hydroxide ion (HO^-) in proximity to the cyclic phosphate of the substrate. The imidazole group on the right side of the active site functions as a general acid by protonating the oxygen adjacent to the P–O bond, thereby facilitating the breakage of the cyclic P–O bond. Therefore, the hydrolysis by ribonuclease is a general base/general acid–concerted mechanism. No covalent bonds are formed between the enzyme and a substrate intermediate.

In the nucleophilic/electrophilic mechanism, intermediate covalent bonds between the enzyme and a portion of the substrate are formed which are then broken in a second step. The proteolytic enzymes trypsin, chymotrypsin, papain, etc., are known to hydrolyze the substrate by nucleophilic/electrophilic catalysis. Intermediate acyl-enzymes are hydrolyzed in a second step with water as the substrate at a rate ~ 10^9 times faster than serine esters of similar structures (11).

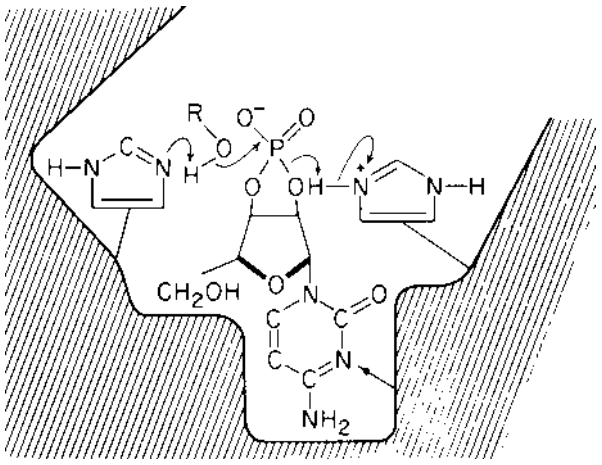

Figure 3 Proposed orientation of substrate and catalytic groups in the ribonuclease-catalyzed hydrolysis of the substrate cytidine 2′,3′-phosphate. Two imidazole groups of histidine of ribonuclease are involved in catalysis, one as a general base (left) and another as general acid (right). The arrow at the lower right corner indicates the binding site for the pyrimidine ring of the substrate which probably involves several groups on the enzyme protein, and largely determines the specificity. (From Ref. 6.)

3. Summary

Enzymes are very efficient catalysts because they bind substrates (and cofactors) into the active site with the scissile bond stereospecifically oriented in proximity to the catalytic groups that carry out the reactions. In forming the enzyme·substrate complex, most of the water is removed from the active site. Therefore the catalytic reaction is largely in a hydrophobic environment. Kato et al. (12) tested the effect of excluding water from the active site during the catalytic reaction by using glutathione synthetase, which requires the two substrates γ-glutamyl cysteine and glycine with ATP as cofactor. In the wild-type enzyme, containing a 17 amino acid loop of the peptide chain that closes the active site to exclude water when the reactants are in place, the rate constant, k_o, was 151 sec^{-1}. When the lid was removed by genetic engineering, the rate constant was 0.163 sec^{-1}, thus decreasing the rate by 930-fold by letting some water in.

The role of change in entropy on rates of enzymatic reactions was tested by use of N-acetyl-L-tyrosyl-chymotrypsin (A), where the large N-acetyl-L-tyrosyl group was tightly bound into the binding site, versus N-acetyl-chymotrypsin (B), where the small N-acetyl group can rotate freely in the binding site; the relative rate of A/B was 3540 (10). $\Delta S^{\ddagger}$ was −13.4 and −35.9 cal mol^{-1} deg^{-1} for the N-acetyl-L-tyrosyl-chymotrypsin and N-acetyl-chymotrypsin, respectively. Most of the other factors that have been proposed above to explain why enzymes are so specific and efficient have been tested by model systems.

Nature is blessed to have such efficient catalysts, the enzymes, to make life possible! But we must keep our

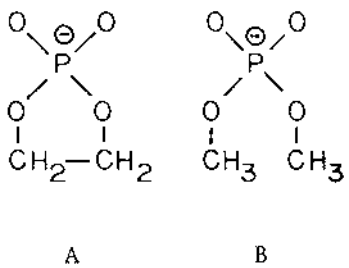

Figure 4 Ethylene phosphate (A) and dimethyl phosphate (B)

perspective and respect for very simple chemical examples of enhanced reaction rates. The relative alkaline hydrolysis rates for ethylene phosphate (A) compared to the structurally similar compound, dimethyl phosphate (B) (Fig. 4) is $\sim 1.0^8$ times (A/B). This is because of the restriction of rotation of the ethylene group in A relative to the free rotation of the methyl groups of B (Ref. 2, p. 134).

REFERENCES

1. Enzyme Nomenclature. Recommendations of the Nomenclature Committee of the International Union of Biochemistry, published for the International Union of Biochemistry. San Diego: Academic Press, 1992.
2. JR Whitaker. Principles of Enzymology for the Food Sciences. 2nd ed. New York: Marcel Dekker, 1994.
3. V Henri. Action de quelques sels neutres sur l'inversion du saccharose par la sucrase. C R Soc Biol 54:353–354, 1902.
4. AJ Brown. Enzyme action. J Chem Soc 81:373–388, 1902.
5. LN Johnson, DC Philips, JA Rupley. Activity of lysozyme: an interim review of crystallographic and chemical evidence. U.S. Atomic Energy Commission 1968 (pub. 1969); BNL 501116, Vol 1:120–138, 1969.
6. AP Mathias, A Deavin, BR Rabin. The active site and mechanism of action of bovine pancreatic ribonuclease. In: TW Goodwin, JI Harris, BS Hartley, eds. Structure and Activity of Enzymes. New York: Academic Press, 1964, pp 19–30.
7. JR Whitaker. Enzymes. In: OR Fennema, ed. Food Chemistry. 3rd ed. New York: Marcel Dekker, 1996, p 473.
8. DE Koshland Jr. Conformational changes at the active site during enzyme action. Fed Proc 23:719–726, 1964.
9. JA Wells, BC Cunningham, TP Graycar, DA Estell. Recruitment of substrate-specificity properties from one enzyme into a related one by protein engineering. Proc Natl Acad Sci USA 84:5167–5171, 1987.
10. ML Bender, FJ Kezdy, CR Gunter. XXXIII. The anatomy of an enzymatic catalysis. α-Chymotrypsin. J Am Chem Soc 86:3714–3721, 1964.
11. RL Stein, JP Elrod, RL Schowen. Correlative variations in enzyme-derived structures of catalytic transition states. Implications for the catalytic strategy of acyl-transfer enzymes. J Am Chem Soc 105:2446–2452, 1983.
12. H Kato, T Tanake, H Yamaguchi, T Haa, T Nishioka, J Oda. Flexible loop that is a novel catalytic machinery in a ligase. Atomic structure and function of the loopless glutathione synthetase. Biochemistry 33:4995–4999, 1994.

4

Enzyme-Catalyzed Reactions

Experimental Factors that Affect Rates

John R. Whitaker
University of California, Davis, Davis, California, U.S.A.

I. INTRODUCTION

A. Kinetic vs. Static Processes

There are basically two types of determinations in science. The first type is to determine the rate of change of a parameter, whether it be a chemical reaction, the enlargement of a cell, organ, or an organism, or other changes. The second determination is primarily a compositional one in which chemical or physical analyses determine one or more compounds, cells, etc., at a given time. The first example is followed by change per unit time, a kinetic process. The second example is a static process, where change with time is undesirable. Enzyme-catalyzed reactions must be investigated by a rate-of-change process.

Chapter 1 dealt with the history of development of enzyme kinetics. Undoubtedly, from the beginning researchers must have noted that the conversion of substrate to product occurred as a function of time and that the rate of change over time was not constant under all conditions as shown in Figure 1, especially when a significant amount of substrate was converted to product.

B. Pathway of Enzymatic Reactions

Before proceeding further with discussion of rates, it is important to understand the pathway by which all enzyme-catalyzed reactions occur. This was first appreciated by Brown (in 1902) and Henri (1903) independently (2, 3) when they suggested that the substrate saturation effect observed for rates of enzyme-cata-

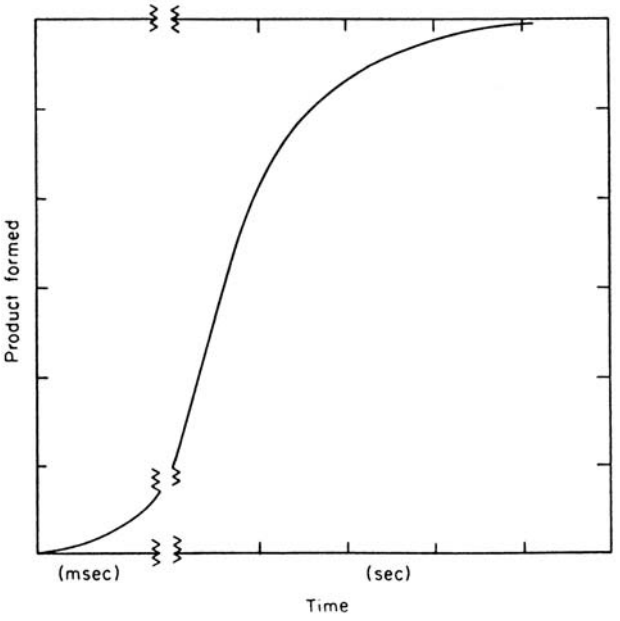

Figure 1 Typical enzyme-catalyzed reaction showing the pre-steady-state (msec), the constant rate, and the declining rate parts of the progress curve. (From Ref. 1)

lyzed reactions as a function of substrate concentration, $[A]$, resulted from an obligatory intermediate, the enzyme·substrate complex, $[EA]$, prior to product, P, formation [Eq. (1)]:

$$E + A \underset{k_{-1}}{\overset{k_1}{\rightleftharpoons}} EA \underset{k_{-2}}{\overset{k_2}{\rightleftharpoons}} E + P \tag{1}$$

Based on this premise, which has been shown now to be universal for all enzyme-catalyzed reactions, Michaelis and Menten in 1913 (4) developed an equation to numerically describe the observed relationship between velocity, v, and $[A]$. The derivation of the Michaelis-Menten equation is shown below, using the more modern concepts of initial velocity v_o, and the steady-state assumption. The EA complex has a noncovalent bond.

Let $[E]_o$ = total enzyme concentration
$[A]_o$ = total substrate concentration, which is assumed to be much larger than $[E]_o$; therefore, $[A] = [A]_o$ during initial velocity, v_o, measurements (< 5% A converted to P during time of experiment)
$[EA]$ = enzyme·substrate concentration, which is a noncovalent complex
$[P]$ = product concentration (one product is formed in the general derivation; more than one product may be formed and released in a sequential manner in many examples)
$[E]$ = free enzyme concentration

The rate of formation of EA is [see Eq. (1)]:

$$dEA/dt = k_1[E][A]_o \tag{2}$$

While the rate of disappearance of EA is

$$-\mathrm{dEA/dt} = \mathrm{k_{-1}[EA] + k_2[EA]} \tag{3}$$

When steady-state conditions are reached (within a few msec), $dEA/dt = -dEA/dt$ so that

$$k_1[E][A]_o = k_{-1}[EA] + k_2[EA] = (k_{-1} + k_2)[EA] \tag{4}$$

Rearranging:

$$[E][A]_o/[EA] = (k_{-1} + k_2)/k_1 = K_m \tag{5}$$

K_m, the Michaelis constant, is given by either $[E][A]_o/[ES]$ or $(k_{-1} + k_2)/k_1$.

The free enzyme concentration, $[E]$, cannot be measured experimentally but it is related to $[E]_o$ by the conservation equation

$$[E] = [E]_o - [EA] \tag{6}$$

Substitution of Eq. (6) for [E] in Eq (5) gives

$$([E] - [EA])[A]_o/[EA] = K_m = [E]_o[A]_o - [EA][A]_o/[EA] \tag{7}$$

Rearranging Eq. (7):

$$[E]_o[A]_o = K_m[EA] + [EA][A]_o = [EA](K_m + [A]_o) \tag{8}$$

Rearranging Eq. (8):

$$[EA] = [E]_o[A]_o(K_m + [A]_o) \tag{9}$$

$[EA]$ cannot be determined directly in most cases but it can be substituted for since the rate of formation of product, P, is

$$dP/dt = k_2[EA] = v_o \tag{10}$$

Rearranging Eq. (10):

$$[EA] = v_o/k_2 \tag{11}$$

Therefore

$$v_o = k_2[E]_o[A]_o/(K_m + [A]_o) \tag{12}$$

The maximum velocity, V_{max}, is attained when all active sites of the enzyme are combined with substrate so that $[EA] = [E]_o$. Therefore,

$k_2[E]_o$ equals V_{max} and Eq. (12) gives Eq. (13):

$$v_o = v_{max}[A]_o/(K_m + [A]_o) \tag{13}$$

C. Concept of Initial Velocity in Enzymology

The importance of determining the initial velocity of enzyme-catalyzed reactions was not fully appreciated and articulated until the early 1960s. Up to that time, rates of enzyme-catalyzed reactions were frequently based on one-point assays—i.e., at a given time of the reaction. Also, reactions often were designed so that many minutes or hours were used in the assays. Another reason is that the kinetics of non-enzyme-catalyzed reactions by chemists are designed to determine the order of reactions which must be done under conditions of several half-lives of the reaction; i.e., > 90% of the substrate must be converted to product to give four half-lives.

The order of chemical reactions is of major importance in determining the mechanisms of reactions. Often the order is not zero, first or second order, but is a fractional order (such as 1.5 for example). Not so with enzyme-catalyzed reactions, which are first, zero, or mixed order, depending on $[A]_o$ in relation to K_m for reasons explained later in this chapter.

Figure 2 shows the results of determining the velocity of an enzyme-catalyzed reaction at the same pH,

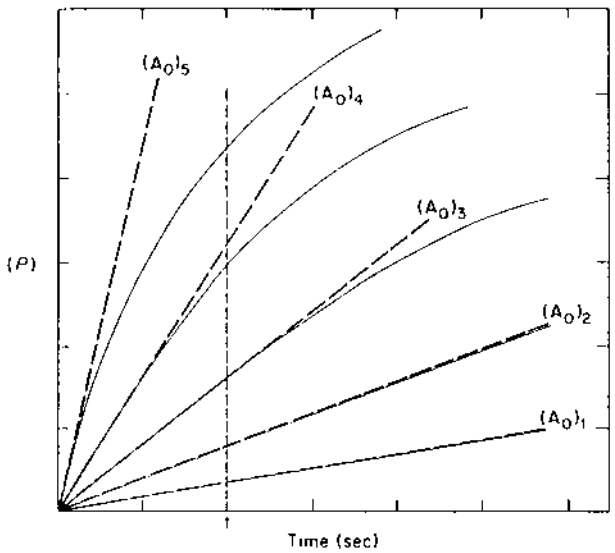

Figure 2 Method of determining initial velocities of reaction. The solid lines are the experimentally determined data; the dashed lines are tangents drawn to the initial slope of the experimental data in order to determine the initial velocity, v_o. (From Ref. 1.)

temperature, and cofactor concentration (if needed), but at different substrate concentrations. At low substrate concentrations the experimental lines (solid) and the initial velocity (v_o) lines (dashed) coincide because the concentration of product formed is < 5 % of the original substrate concentration. As the substrate concentration is increased, and the rate of formation of product increases (data for $[A]_{o3}$, $[A]_{o4}$, and $[A]_{o5}$) the experimental and v_o values diverge more and more.

There are several reasons why the experimental lines and the v_o lines are not the same and why initial velocities, v_o, are important in enzymology. Use of v_o has the advantages of (a) not being greatly affected by instability of the enzyme (the reaction should be initiated by adding the enzyme last), (b) not being influenced by product concentration since this is zero initially (product can influence the velocity by being a competitive inhibitor or by giving backward reaction), and (c) the initial substrate concentration changes very little in the reaction (when $< 5\%$ product is formed during determining of v_o).

With modern-day instrumentation, including recorders, it is possible to determine v_o with excellent precision using 5 min, or less, overall reaction times. There are no reasons why data based on single data point assays should ever be reported in enzymology.

D. Rates of Enzyme-Catalyzed Reactions

As will be shown later in this chapter, the velocities of enzyme-catalyzed reactions depend on substrate concentration, enzyme concentration, cofactor concentration, inhibitor concentration, pH, and temperature. We will discuss each of these factors separately. But at this point, it is useful to provide some data on some numerical values of the velocity constants shown in Eq. (1) calculated to 1 molar concentrations of enzymes and substrates at the pH optimum and standard temperature (usually 25–30°C).

Velocity constants (k_1) for formation of the enzyme·substrate complex are in the range of 10^4–10^9 M^{-1} sec^{-1} for the enzymes given in Table 1(5); these values are typical for many other enzymes. However, there are exceptions where the formation of the complex can be the rate-controlling step as for lactate dehydrogenase combining with the cofactor NAD^+ (~ 50 M^{-1} sec^{-1}).

The dissociation constant of the EA complex, k_{-1}, ranges from < 1.4 to 3.1 sec^{-1} for peroxidase and liver alcohol dehydrogenase, respectively, to $> 4.5 \times 10^4$ sec^{-1} for fumarase (Table 1). The overall molar catalytic rate constant k_o [k_2 in Eq. (1), often called k_{cat} because more than one step may be involved] ranges from 10^1 sec^{-1} for papain to 10^7 sec^{-1} for catalase. Therefore, one must conclude that k_1, k_{-1}, and k_2 differ markedly among enzymes. Some enzymes are more efficient than others as measured numerically by the ratio of k_o/K_m, a generally accepted measure since it includes all the rate constants of Eq. (1). The "goodness" of different substrates for the same enzyme is also measured by k_o/K_m.

II. EFFECT OF SUBSTRATE CONCENTRATION ON RATES OF ENZYME-CATALYZED REACTIONS

Section I has treated effect of substrate concentration on rates of enzyme-catalyzed reactions in a general way. Section II will deal with more specific details of how to determine K_m and k_o for one- and two-substrate enzymes, as well as allosteric behavior of enzyme–substrate interactions.

A. Initial Velocity vs. Substrate Concentration

This section will deal only with enzyme–substrate relationships obeying Michaelis-Menten kinetics. The expected relation between v_o and $[A]_o$ is shown in

Table 1 Rate Constants for Some Selected Enzymes

Enzyme	Substrate	k_1^a (M^{-1} sec^{-1})	k_1^b (sec^{-1})	k_0^c (sec^{-1})
Fumarase	Fumarate	$> 10^9$	$> 4.5 \times 10^4$	10^3
Acetylcholinesterase	Acetylcholine	10^a	—	10^3
Liver alcohol	NAD^+	5.3×10^5	74	10^3
dehydrogenase	NADH	1.1×10^7	3.1	
	Ethanol	$> 1.2 \times 10^4$	> 74	
Catalase	H_2O_2	5×10^6	—	10^7
Peroxidase	H_2O_2	9×10^6	< 1.4	10^6
Hexokinase	Glucose	3.7×10^6	1.5×10^3	10^3
Urease	Urea	$> 5 \times 10^6$	—	10^4
Chymotrypsin				10^2 to 10^3
Trypsin				10^2 to 10^3
Ribonuclease				10^2
Papain				10^1

[a]Rate constant for formation of enzyme–substrate complex.
[b]Rate constant for dissociation of enzyme–substrate complex.
[c]Order of magnitude of the turnover number in moles of substrate converted to product per second per mole of enzyme: k_0 ($= k_{cat}$) is the observed rate constant and may or may not involve a single rate-limiting step.
Source: Ref. 5.

Figure 3. At low substrate concentrations ($[A]_o \leq 0.05$ K_m) the order of the reaction with respect to $[A]_o$ is first order and fits Eq. (14).

$$dA/dt = k[A]_o = -dp/dt \tag{14}$$

At very high $[A]_o$($[A]_o \geq 100$ K_m), the enzyme is $> 90\%$ saturated with substrate. Thus, the rate is independent of $[A]_o$, and is zero order. This is described by Eq. (15).

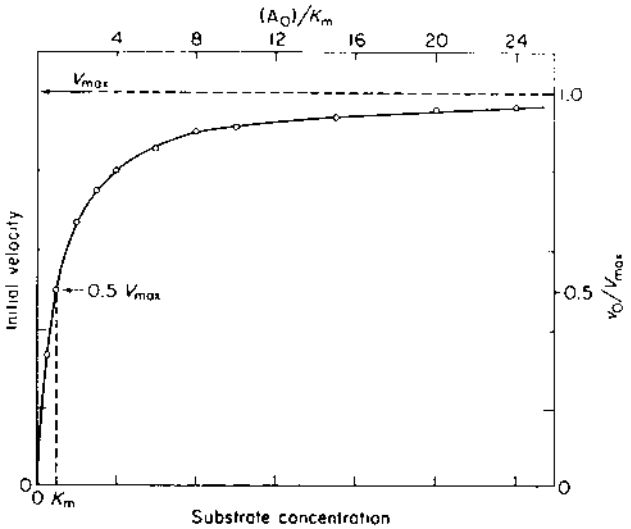

Figure 3 Variation of initial velocity, v_o, with substrate concentration for an enzyme-catalyzed reaction. (From Ref. 1.)

$$dA/dt = k = -dp/dt \tag{15}$$

It is often difficult, if not impossible, to do reactions at > 100 K_m because of (a) insolubility of the substrate, (b) cost of the substrate, or (c) the high substrate concentration becomes inhibitory of the enzyme as two molecules bind to the enzyme simultaneously, one as the substrate and the second as an inhibitor. Such behavior is observed frequently.

Between $[A]_o \leq 0.05$ K_m and $[A]_o \geq 100$ K_m is where most of the effect of $[A]_o$ on v_o is found and where most experiments are performed. Over this range of $[A]_o$, the order of the reaction is mixed order; i.e., it is the sum of first order and zero order as shown by Eq. (16), which is the differentiated form of the Michaelis-Menten equation [see Eq. (12)].

$$[E]_o k_o t = 2.3\ K_m \log[A]_o/([A]_o - [P]) + [P] \tag{16}$$

At $[A]_o < 0.05$ K_m, the first-order term, 2.3 K_m $\log[A]_o/([A]_o - [P])$ predominates, while at $[A]_o > 100$ K_m, the zero-order term $[P]$ predominates. At $[A]_o = K_m$ the two terms are equally predominate.

1. Determination of K_m and V_{max} for One-Substrate Reactions

For reasons discussed above, K_m and V_{max} cannot be precisely determined from a plot of v_o vs. $[A]_o$, primarily because V_{max} cannot be experimentally determined.

In 1934 Lineweaver and Burk (6) published a milestone paper showing that by taking the reciprocal of the Michaelis-Menten equation, a straight line relationship between $1/v_o$ and $1/[A]_o$ is obtained, which gives K_m and V_{max} as shown by Eq. (17) and Figure 4.

$$1/v_o = K_m/(V_{max}[S]_o) + 1/V_{max} \tag{17}$$

The intercept on the y-axis is $1/V_{max}$ and the slope of the line is K_m/V_{max}. The intercept on the $-$x axis is $-1/K_m$. This is one of the most cited references in the kinetics of enzymology.

Later on, Augustinsson and Eadie and Hofstee (see Ref. 1) rearranged the Lineweaver-Burk equation to two other linear transforms of the Michaelis-Menten equation. For whatever reason, these two methods are rarely used, but they can be useful analyses as in more complex reaction pathways they may give curvilinear relationships indicating the reaction may contain additional intermediates. In 1954, King and Altman (7) published a useful method for determining the equation for more complex enzyme-catalyzed reactions (see Ref. 1).

2. Determination of K_m and V_{max} for Two-Substrate Reactions

There are relatively few one-substrate reactions in enzymology. Most of these occur in the class EC 5 enzymes. (For the isomerases see Chapter 3). For the class EC 3 enzymes, the hydrolases are pseudo-first-order reactions in that the second substrate is water. At 55.4 M water concentration compared to 10^{-4}–10^{-2} M for the second substrate, the change in water concentration during the reaction is very small and is ignored.

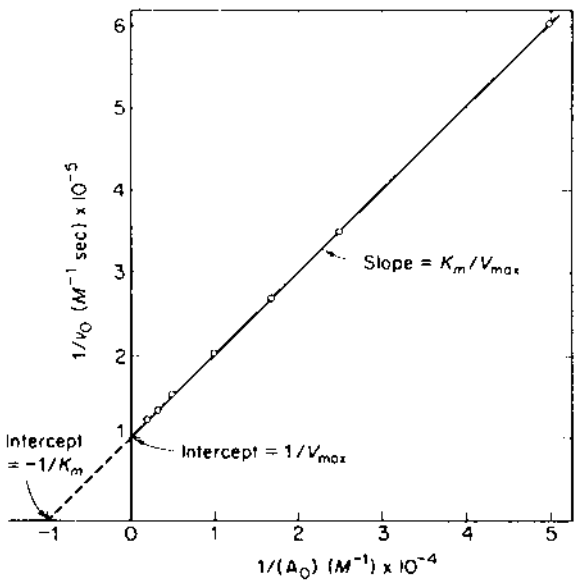

Figure 4 Plot of the reciprocal of initial velocity, v_o, versus reciprocal of initial substrate concentration, $[A]_o$, according to the Lineweaver-Burk method. (From Ref. 1.)

In the late 1950s and early 1960s, attention was given to development of equations for two and more substrate enzyme reactions (see Chapter 1 on protein structure and kinetics). Cleland, in a series of papers, provided a clear rationale for dealing with these reactions which follow the general Eq. (18) for two substrate/two product reactions.

$$A + B \rightleftharpoons P + Q \tag{18}$$

He developed equations for when A must bind in the active site of the enzyme before B can bind [Ordered Mechanism; Eq. (19)];

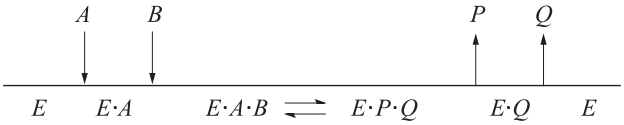

(19)

when either A or B can bind first to the enzyme active site [Random Mechanism; Eq. (20)];

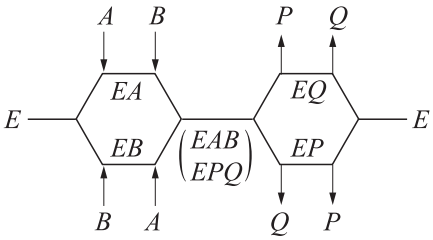

(20)

and when A binds first and is converted to product before B binds and is converted to product [Ping Pong Mechanism; Eq. (21)].

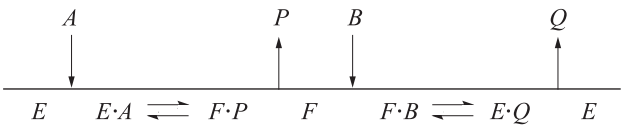

(21)

These are very important concepts and equations for the serious enzymologist. More information on this subject is found in the three key articles by Cleland (8). A detailed discussion is found in Whitaker (1) on how to experimentally translate these concepts into practice.

3. Behavior in Multisite–Multisubunit Enzymes

Many enzymes have multiple subunits, each with a substrate binding and catalytic site for substrate(s). Some enzymes have two or more domains (independent folding segments on the same polypeptide chain) that bind, and may catalyze substrates to products. If each of the active sites binds and catalyzes the substrate independently of other active sites, then the kinetics follow Michaelis-Menten behaving enzymes. On the other hand, if binding of substrate into an active site affects either binding or catalysis in a second active site, then the kinetics do not follow expected Michaelis-Menten kinetics.

a. Multiple-Subunit Enzymes. As demonstrated by Monod et al. in 1965 (9), some multiple-subunit enzymes give the kinetic behavior shown in Figure 5 for a plot of v_o vs. $[A]_o$. Note the marked difference between the curves for the allosteric-behaving enzyme and the Michaelis-Menten-behaving enzyme. The allosteric-behaving enzymes follow Eq. (22):

$$v_o = V_{max}[A]_o^n/(K + [A]_o^n) \tag{22}$$

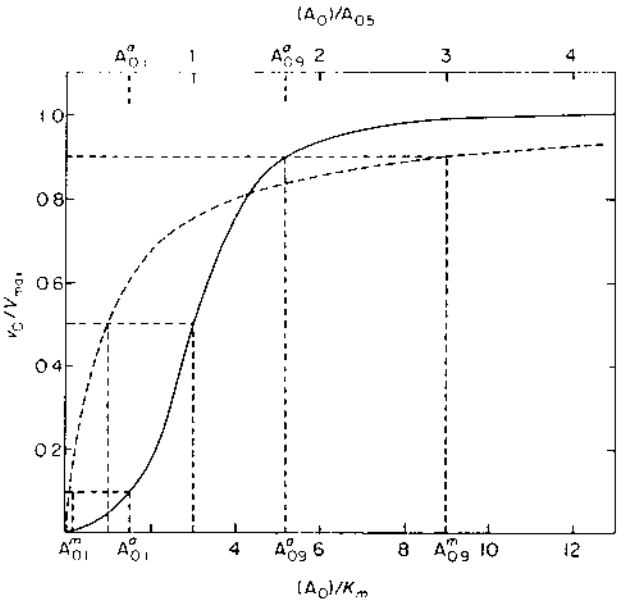

Figure 5 Comparison of effect of substrate concentration, relative to K_m, versus initial velocity, v_o, relative to V_{max} for a Michaelis-Menten-behaving enzyme (dashed line) versus a positive allosteric-behaving enzyme (solid line). The vertical and horizontal dashed lines are for calculating $R_s = [A]_o$ at 0.9 $v_o/V_{max}/[A]_o$ at 0.1 v_o/V_{max} for the Michaelis-Menten-behaving enzyme and for the allosteric-behaving enzyme. (From Ref. 1.)

where the substrate concentration is raised to power of n. For linear plotting, Eq. (22) is rearranged to Eq. (23).

$$\log v_o/(V_{max} - v_o) = n \log [A]_o - \log K \tag{23}$$

where n is the product of the number of subunits and strength of binding of substrate of interacting sites and K is the average of all the individual K_{eq} values involved in the various steps of binding and transformation of substrate to product.

Koshland et al. (10) developed an equation to measure the cooperativity of the interaction based on the experimental data. This is given in Eq. (24).

$$R_s = [A]_o \text{ at } 0.9v_o/V_{max}/[A]_o \text{ at } 0.1v_o/V_{max} \tag{24}$$

For a Michaelis-Menten-behaving enzyme, R_s is 81. For a positive allosteric-behaving enzyme, R_s is < 81 while for a negative allosteric behaving enzyme R_s is > 81 (see Fig. 5).

b. Single Active Site, Multiple-Substrate Binding Enzymes. Examples of this type of enzyme are trypsin and carboxypeptidase A. A substrate molecule that binds into the active site is converted to product. If a second substrate molecule binds at a second site and increases the rate of catalysis at the active site, it is an activator; if the rate is reduced on binding of the second substrate molecule, it is an inhibitor. Generally, K_{eq} for binding of the second substrate molecule is about 10 times larger than is K_m for the active site bound substrate molecule.

III. EFFECT OF ENZYME CONCENTRATION ON RATE OF ENZYME-CATALYZED REACTIONS

Rates of enzyme-catalyzed reactions are generally expected to be directly proportional to the enzyme concentration as shown in Figure 6. This relationship between v_o and $[E]_o$ holds whatever the $[A]_o$ is with respect to K_m as long as all other conditions are held constant and initial velocities are used.

This linear relationship between v_o and $[E]_o$ is very important from an analytical perspective. Any analysis where $[E]_o$ is important to know depends on this relationship. In the food, nutritional, and medical fields, enzyme assays are used to determine how much active enzyme is present. In the frozen food industry, for example, polyphenol oxidase, α-amylase, and protease activities affect the storage stability and storage time of the product. Levels of selected enzyme activities of blood are used in diagnostics of diseases and bacterial

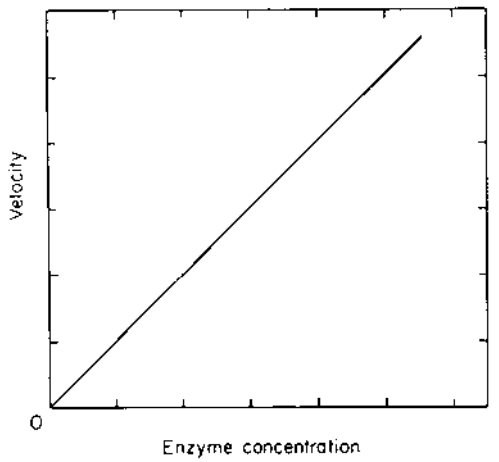

Figure 6 Expected relationship between initial velocity and enzyme concentration. Substrate concentration, pH, temperature, and buffer are kept constant. (From Ref. 1.)

infections. Purity of enzymes are based on their specific activities (activity/mg protein) and the absence of unwanted activities.

But one must not assume that the linear relationship shown in Figure 6 holds. It is the responsibility of the enzyme user to prove this relationship holds under the conditions used. There are at least five valid reasons why the relationship between v_o and $[E]_o$ can be nonlinear (1). These are listed below. More details can be found in Whitaker (1).

A. Limitations on Substrate Concentration

1. One of the Substrates is a Gas, Such as Oxygen

Oxygen has limited solubility in aqueous solution. The solubility of O_2 is 0.24 m*M* at 25°C. In such reactions, the analyst usually depends on the O_2 used to be replenished by absorption from the atmosphere to maintain a constant O_2 concentration. As the $[E]_o$ is increased, the rate of depletion of O_2 is increased. This often leads to a nonlinear relation between v_o and $[E]_o$. Only by adequate stirring rate or bubbling 100% O_2 through the solution can the O_2 concentration be kept constant.

2. The Substrate Is a Polymer

Starch, largely a homopolymer, is used often to measure α- and β-amylase activities. As hydrolysis occurs, the product fragments continue to be substrates. Initially, the molar concentration of substrates increases. As the substrate size decreases the K_m may increase so that the enzyme is less saturated with substrate. Therefore, there may be changes in v_o as a function of $[E]_o$.

Proteins are heteropolymers, being composed of 20 different amino acid residues. Proteases hydrolyze peptide bonds selectively based on their specificity for the amino acid residues on either side of the peptide bond. Trypsin will be used as a specific example of a protease. It hydrolyzes peptide bonds only where a lysyl or arginyl residue provides the carboxyl group of the peptide bond. The nitrogen side of the peptide bond can be any of the 20 amino acids. However, the relative rate of hydrolysis of the peptide bond is affected by the specific nature of the amino acid. Thus, there are a minimum of 40 different rates of hydrolysis, not counting the decreasing size of the peptides. The best peptide bonds are hydrolyzed more rapidly than the less good bonds. This leads to a decrease in v_o vs. $[E]_o$ as the enzyme concentration increases.

B. Coupled Enzyme Reactions

A coupled enzyme reaction is given by Eq. (25) where

$$\mathrm{A} \xrightarrow{E_1,k_1} \mathrm{B} \xrightarrow{E_2,k_2} \mathrm{C} \tag{25}$$

Substrate *A* is converted to product *B* by enzyme E_1. But *B* may be hard to determine analytically so E_2 is also added to the reaction to convert product *B* to product *C*, which can be more readily determined (e.g., by spectrophotometry). To be successful with the assay, *B* must be converted to *C* just as fast as it is produced, so that the rate-determining step remains *A* to *B* conversion even as $[E_1]_o$ is increased. Several commercially available enzyme kits for enzyme analyses depend on coupled reactions.

Similar problems may arise when two coupled enzyme reactions depend on a common cofactor, such as NAD^+. As the concentration of E_1 is increased it may limit the concentration of NAD^+ required by E_2.

C. Presence of Irreversible Inhibitor in Reaction System

Examples of irreversible inhibitors are Pb^{2+}, Hg^{2+}, and Ag^+ ions that might be in the water used. Sulfhydryl enzymes (where the sulfhydryl group of cysteine is essential for enzyme activity), which are 25–30% of all enzymes, would be affected. Experimentally, no enzymatic activity would be

found until sufficient enzyme is added to bind all the inhibitor. Then, enzyme activity will be seen. This case is easily recognized as the intercept on the x-axis of the v_o vs. $[E]_o$ plot would be on the right side of the zero intercept.

D. Presence of Reversible Inhibitors in the System

The amount of inhibition found would be dependent on the substrate concentration used (the lower the $[A]_o$, the greater the effect) and the enzyme concentration. In general, there would be a nonlinear response between v_o and $[E]_o$, with a downward curvature of the relationship beween v_o and $[E]_o$.

E. Need for an Essential Coenzyme (CoE)

A coenzyme is a nonenzyme compound that binds reversibly in the active site of the enzyme and is required for enzyme activity. The B vitamins, for example, are a part of a coenzyme (see Sec. IV). The example is best illustrated by use of Eq. (26).

$$E + \text{CoE} \overset{k_1}{\rightarrow} E \cdot \text{CoE} \overset{k_2}{\rightarrow} E \cdot \text{CoE} \cdot S \overset{k_3}{\rightarrow} E \cdot \text{CoE} + P \tag{26}$$

At a fixed concentration of CoE and a low $[E]_o$, not all the enzyme may be bound to CoE to give $E \cdot \text{CoE}$, which is required for the substrate to bind. As $[E]_o$ increases, more CoE will be bound owing to mass action effect, and v_o will increase. Such effects were observed as early as the 1940s and were called "dilution effects," meaning as one diluted the enzyme concentration the activity observed was less than that expected.

IV. KINETIC CONSEQUENCES OF COFACTORS

A. Nature and Essentially of Cofactors

Cofactors are small, mostly nonpeptide compounds which are required for activity of some enzymes. These include organic compounds, such as NAD^+ (nicotine adenine dinucleotide), FAD (flavin adenine dinucleotide), coenzyme B_{12}, triphosphates of adenosine (ATP), cytidine (CTP), and uridine (UTP), as well as many others (see Ref. 1 and references cited therein). They also include many inorganic cations and anions as well as metallo derivatives of organic compounds (coenzyme B_{12}, metal–porphyrin cofactors). See Table 2 for some specific examples.

The cofactors are essential components of the active site of many enzymes. They may be required for binding of the substrate into the active site and/or they may be essential for the chemical conversion of the substrate(s) to product(s). Therefore, in most cases they are absolutely essential for activity of the enzyme. Two examples, of many, explain this importance. There are > 150 enzymes in the human that require Zn^{2+} as a

Table 2 Importance of Phosphate, Ribose, and Purine and Pyrimidine Bases in Cofactors

Enzyme	Cofactor	Vitamin	Phosphate	Ribose	Base
Oxidoreductases	NAD^+	Niacin	+	+	Adenine
Oxidoreductases	$NADP^+$	Niacin	+	+	Adenine
Oxidoreductases	FMN	Riboflavin	+	+	—
Oxidoreductases	FAD	Riboflavin	+	+	Adenine
Ligases	ATP	—[a]	+	+	Adenine
Ligases	UTP	—	+	+	Uridine
Ligases	CTP	—	+	+	Cytidine
Transferases	CoA	Pantothenic acid	+	+	Adenine
Transferases	Acetyl phosphate	—	+	—	—
Transferases	Carbamyl phosphate	—	+	—	—
Tranferases	*S*-Adenosyl methionine	—	—	+	Adenine
	Adenosine-3′-phosphate-5′-phosphosulfate	—	+	+	Adenine
Transferases	Pyridoxal phosphate	Pyridoxine	+	—	—
and ligases	Thiamine pyrophosphate	Thiamine	+	—	—

[a] —, Not present.
Source: Ref. 1.

cofactor. Without adequate Zn^{2+} intake, which can be compromised by dietary compounds such as phytic acid, by pregnancy, etc., > 150 enzymes may not function at desirable rates. The second example is for the Fe^{3+}–prophyrin–containing enzymes catalase and peroxidase. The Fe^{3+}–prophyrin alone converts H_2O_2 to O_2 and water at the rate of about 10 sec^{-1}. The protein portion of the enzyme alone has no activity on H_2O_2. The complete enzyme has a catalytic rate of 10^7 moles H_2O_2 converted to product per second per mole of catalase (turnover No.). H_2O_2 is formed by metabolic processes of the cells. It has strong oxidative activity on cellular components. It is absolutely essential to convert H_2O_2 to O_2 and water as fast as it is formed.

B. Unique Features of Cofactors

Only limited examples of unique features of cofactors can be given in this chapter. The reader is referred to Whitaker (1) and specific references therein devoted to detailed treatment of this very large topic.

1. Two Types of Cofactors

Mechanistically, the cofactors can be divided into two groups, the coenzymes and the prosthetic groups. The coenzymes are loosely bound to the protein and generally act as a substrate in the catalyzed reaction. The prosthetic groups are more tightly bound, some covalently, and they are regenerated to the starting form at the end of the reaction. An example of each type will clarify these differences.

There are many enzymes that require NAD^+ or NADH as coenzymes. The reaction catalyzed by alcohol dehydrogenase is shown in Eq. (27).

$$CH_3CH_2OH + NAD^+ \underset{k-1}{\overset{k_1}{\rightleftharpoons}} CH_3CHO + NADH + H^+ \tag{27}$$

This is a reaction requiring the substrate ethanol and the coenzyme NAD^+. NAD^+ must bind to the enzyme first, followed by binding of the ethanol. After catalysis, the product acetaldehyde dissociates from the enzyme, followed by NADH. This is an ordered BiBi Mechanism (see Sec. II.A.2). The reaction is a two-substrate–three-product (counting the H^+) reaction. It is a reversible reaction with the backward reaction favored. Coenzymes, being loosely bound to the enzyme, are generally lost during purification of the enzyme. The researcher must add the coenzyme back to the inactive enzyme to restore activity. The concentration of both the apoenzyme and coenzyme will determine the overall rate of the reaction. The maximum rate, V_{max}, will be obtained when all the enzyme is in the $E \cdot CoE \cdot A$ form.

Glucose oxidase (GO-FAD) is a typical example of an enzyme that requires a prosthetic group for activity. This enzyme requires FAD (flavin adenine dinucleotide) as the prosthetic group. FAD is bound tightly to the enzyme so that it is not lost during purification or during the reaction as shown by Eqs. (28) and (29).

$$\text{Glucose} + \text{GO-FAD} \xrightarrow{k_1} \delta\text{-Gluconolactone} + \text{GO-FADH}_2 \tag{28}$$

$$\text{GO-FADH}_2 + O_2 \xrightarrow{k_2} \text{GO-FAD} + H_2O_2 \tag{29}$$

These reactions [Eqs. (28) and (29)] follow a Ping-Pong BiBi Mechanism, as described by the Cleland nomenclature (Eq. 30).

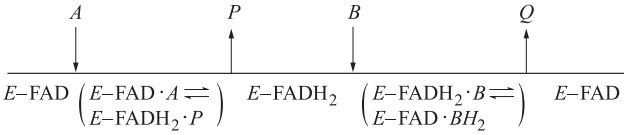

(30)

Note that the prosthetic group FAD remains bound tightly to the enzyme (*E*-FAD indicates covalent bond), the *E*-FAD is reduced to *E*-$FADH_2$ by removal of the two hydrogens from C_1 of glucose and that the *E*-$FADH_2$ is oxidized back to *E*-FAD by O_2, permitting it to be recycled catalytically in the process. The reaction takes place in two steps with only one substrate bound to the enzyme at a time.

2. Same Cofactor, Different Reactions

Earlier in this chapter, it was stated that Zn^{2+} serves as cofactor for > 150 different enzyme-catalyzed reactions. But the example chosen here to explain this concept is the prosthetic group pyridoxal phosphate. Pyridoxal phosphate is involved in amino acid conversion to different products, as shown in Figure 7. The prosthetic group binds to the amino acid in the same way, forming a Schiff base intermediate, as shown by the upper central formula. Which of the reactions is catalyzed depends on the specificity of the protein (apoenzyme) and the specific nature of the amino acid. Therefore, pyridoxal phosphate and apoenzyme together bind to the amino acid (substrate) to perform racemization, decarboxylation, deamination, α,β elimination, β,γ elimination, and addition reactions (to indole to form tryptophan) to give a variety of products.

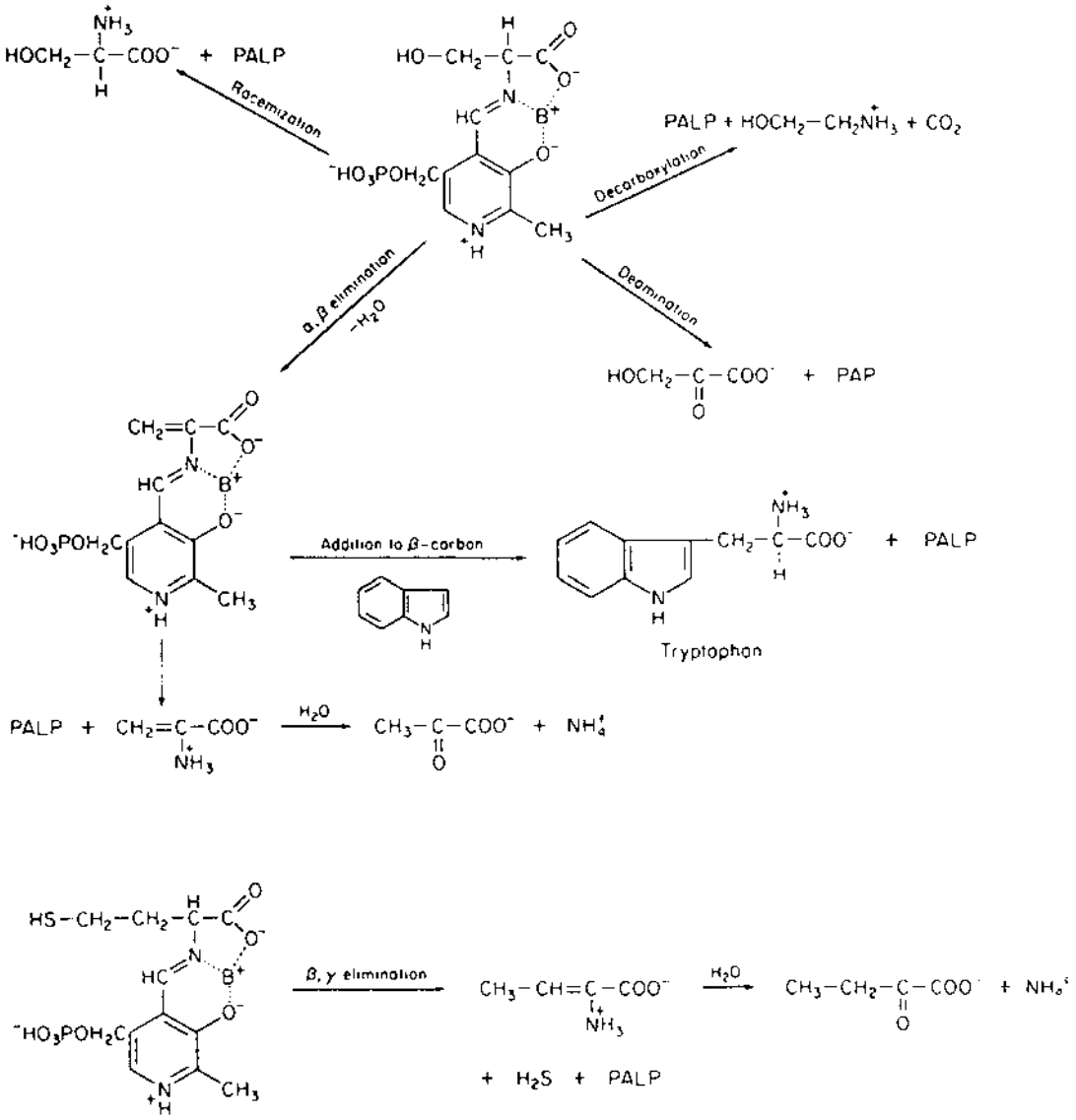

Figure 7 Schematic representation of six enzyme reactions in which pyridoxal phosphate is the cofactor. A common Schiff base intermediate between serine and pyridoxal phosphate is shown in the upper center. The type of enzyme involved determines the nature of the reaction. (From Ref. 1.)

V. KINETIC CONSEQUENCES OF ENZYME INHIBITORS

A. Nature of Inhibitors

Enzyme inhibitors are defined as any compound, except H^+ ions (see pH effects), which decrease the activity when added to an enzyme reaction. Many enzyme inhibitors are known. They are used to kill insects or unwanted plants (herbicides) or animals (rotenone). They are used to prevent browning or preserve "freshness" of fruits and vegetables. Many pharmaceutical compounds are designed to kill microorganisms by selectively inhibiting their enzyme systems.

Mechanistically, there are two major groups of enzyme inhibitors. One group inhibits enzymes by reactions involving covalent bond formation (irreversible inhibitors); the other group inhibits enzymes by reversible noncovalent bond formation (reversible inhibitors). Both types are important as they decrease or eliminate enzyme activity.

The rate and extent of inhibition of enzymes by irreversible inhibitors will depend on concentration of inhibitor, concentration of the enzyme, and the specific group modified on the enzyme, as well as pH and temperature. The rate of the inhibition will be relatively slow (minutes or hours) as a covalent bond is formed. The reaction cannot be reversed to regain enzyme activity.

$$E + I \xrightarrow{k_1} E - I \tag{31}$$

B. Reversible Inhibitors

The rate and extent of inhibition of enzymes by reversible inhibitors also depend on the factors listed above. However, the rate of inhibition is very rapid (msec) as a noncovalent complex is formed. Also, the inhibition can be reversed by removing the inhibitor (by dialysis or gel filtration). Our attention in this chapter is focused on the reversible enzyme inhibitors. Defined kinetically, a reversible inhibitor is one that reacts with an enzyme in a reversible manner as shown in Eq. (32), where K_i is an equilibrium (dissociation) constant. $K_i = [E][I]/E \cdot I$.

$$E + I \overset{K_i}{\rightleftharpoons} E \cdot I \tag{32}$$

The reaction occurs within a few msec and the extent of inhibition is controlled by the concentration of E and I and K_i. Generally, K_i for the reversible inhibitors will be in the range of 10^{-2}–10^{-7} M. If the K_i is $\leq 10^{-8}$ M, the dissociation rate is so slow that there is not a true equilibrium of the process when perturbed by addition of substrate.

Based on their different effects on the rates of enzyme-catalyzed reactions, the reversible inhibitors can be divided into three types, as shown in Figure 8. The three types are the competitive inhibitors (C), noncompetitive inhibitors (N), and the uncompetitive inhibitors (U). The competitive inhibitors (C) compete with the substrate for binding to the active site of the enzyme. Therefore, the equilibrium involves the species E, EA, and EC and the free A and C (Fig. 8). The noncompetitive inhibitors (N) affect the rate of the enzyme-catalyzed reaction by binding outside the active site in a way that permits substrate to bind into the active site but no catalysis of substrate to product occurs. As shown in Figure 8, the species E, A, EA, EA', EN, EAN, $EA'N$, and N can be present. The uncompetitive inhibitors (U) bind to the enzyme only after the substrate has bound. The uncompetitive inhibitors can also bind to other intermediate enzyme–product complexes. As shown in Figure 8, at equilibrium the species A, E, U, EAU, and $EP'U$ can exist. Actually, the three types of inhibitors are distinguishable only experimentally where different effects on the kinetics are shown. The experiments must be performed in the absence and presence of the reversible inhibitor.

Figure 9 shows the kinetic effect of a competitive inhibitor on the rate of an enzyme-catalyzed reaction, when the data are plotted by the Lineweaver-Burk method. As noted, there is no effect of inhibitor on the y-axis intercept. Therefore $V (= V_{max})$ is the same in the presence and absence of the competitive inhibitor. But the slope of the line is larger in the presence of the competitive inhibitor, reflecting the effect of the inhibitor on $K (= K_m)$ for the reaction as shown also by the difference in the $-$x intercept. The numerical difference in slopes and $-$x intercepts in the presence and absence of inhibitors is $1 + [I]_o/K_i$. Knowing the $[I]_o$ added to the reaction, K_i can be calculated. These data were determined for a linear competitive inhibitor.

Figure 10 shows the kinetic effect of a noncompetitive inhibitor when added to an enzyme-catalyzed reaction. Again, data must be obtained for a control with no inhibitor and one with a fixed concentration of the inhibitor. Figure 10 shows that both the slope and the y-intercept are changed by the term $1 + [I]_o/K_i$. There is no effect on the $-$x intercept. This is the definition of a simple linear noncompetitive inhibitor.

Figure 11 shows the effect of an uncompetitive inhibitor when added to an enzyme-catalyzed reaction. Again, a control without inhibitor must be included. There is no effect of the uncompetitive inhibitor on the slope of the lines, while there is a marked difference in the y-intercept (and the $-$x intercept). The difference in y-intercept is given by $1 + [I]_o/K_i$. The example chosen is for a linear uncompetitive inhibitor.

The examples given in Figures 9–11 are linear-behaving inhibitors, as defined in Figure 12. This is determined from a plot of slope (or intercept) vs. $[I]_o$ where experiments at several different $[I]_o$ are done. In many cases, one finds that the type of inhibition is linear. Generally, they will be linear for most competitive inhibitors. But for noncompetitive and uncompetitive inhibitors there are more opportunities for observing hyperbolic or parabolic type behavior.

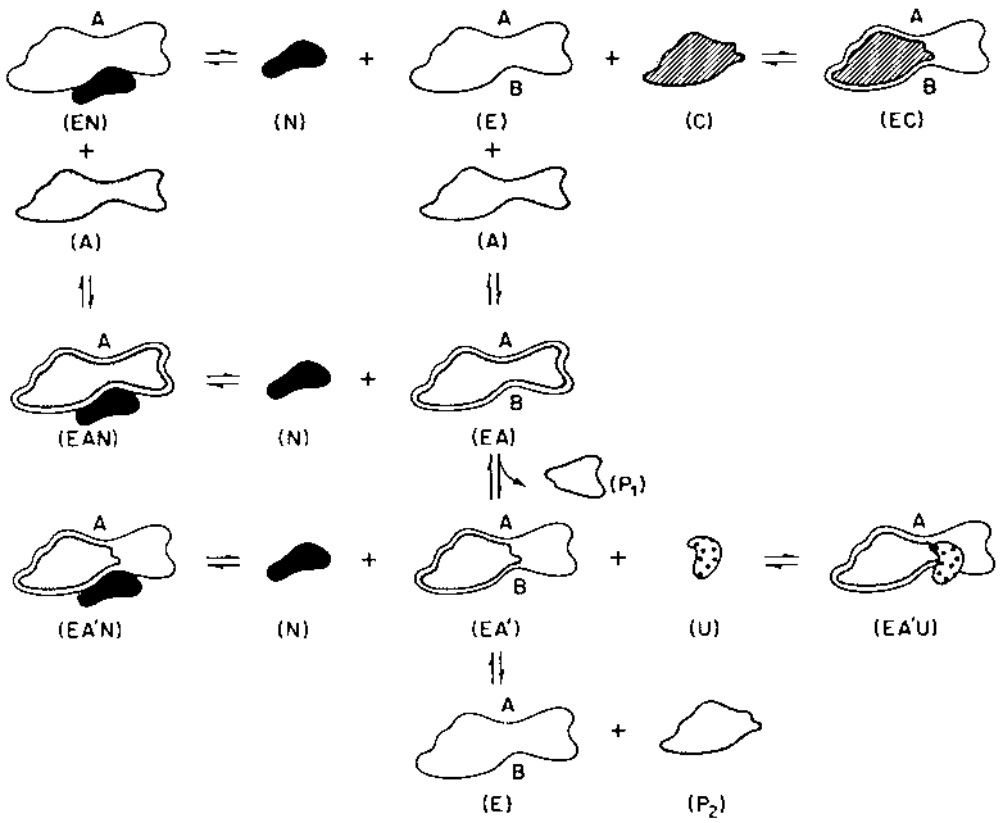

Figure 8 Schematic representation of inhibition of enzyme activity by various types of reversible inhibitors. The model for E shows only the active site with the binding locus (inner void) and the transforming locus, with catalytic groups A and B. The symbols for the species involved (in parentheses) are: E, free enzyme; EA, enzyme·substrate complex; EA′, acylenzyme intermediate; C, competitive inhibitor; N, noncompetitive inhibitor; U, uncompetitive inhibitor; P_1 and P_2 are products formed from the substrate, A, and EN, EAN, EA′N, EC, and EA′U are complexes with respective enzyme species and inhibitors. All complexes formed involve noncovalent bonds except EA′, where a covalent bond is formed with catalytic group A. (From Ref. 1.)

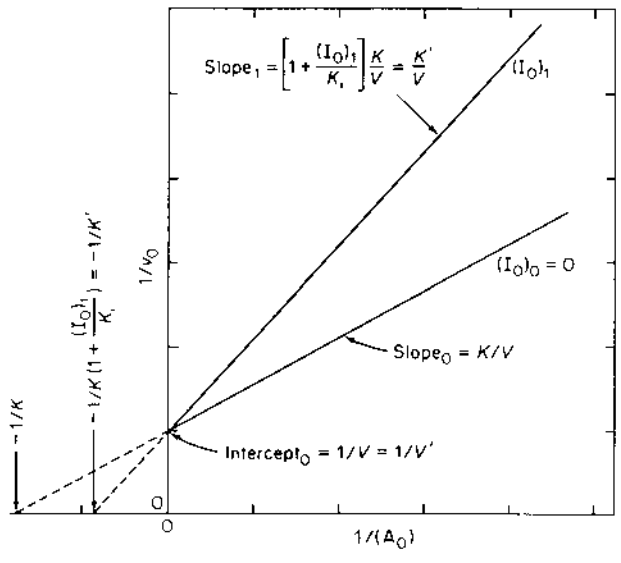

Figure 9 Linear competitive inhibition, plotted by the Lineweaver-Burk method. $V = V_{max}$ in absence of inhibitor. $V' = V_{max}(1 + (I_o)/K_i)$ in presence of inhibitor, $K = K_m$ in absence of inhibitor. $K' = (1 + (I_o)/K_i)$ in presence of inhibitor. (Ref. 1.)

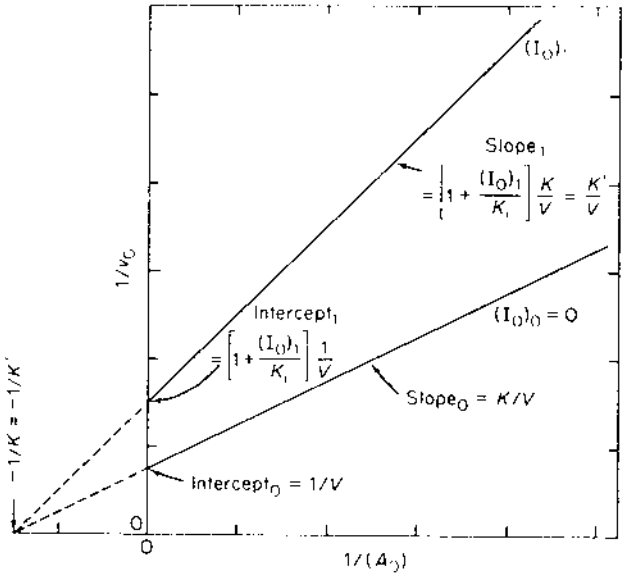

Figure 10 Simple linear noncompetitive inhibition, plotted by the Lineweaver-Burk method. See Figure 9 for additional explanation. (From Ref. 1.)

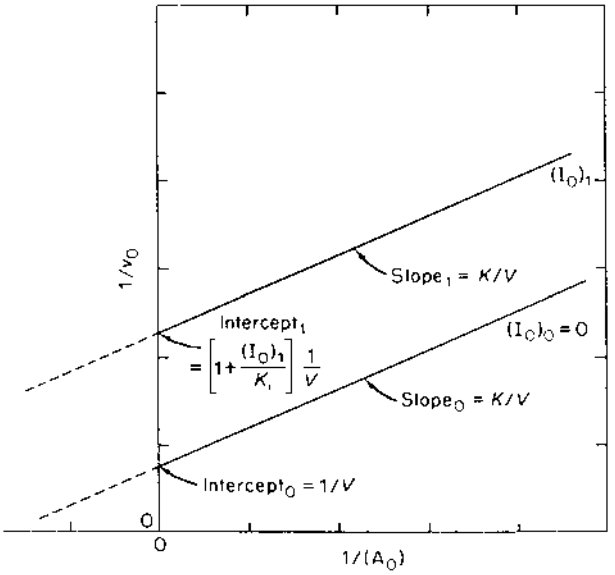

Figure 11 Linear uncompetitive inhibition, plotted by the Lineweaver-Burk method. See Figure 9 for additional explanation. (From Ref. 1.)

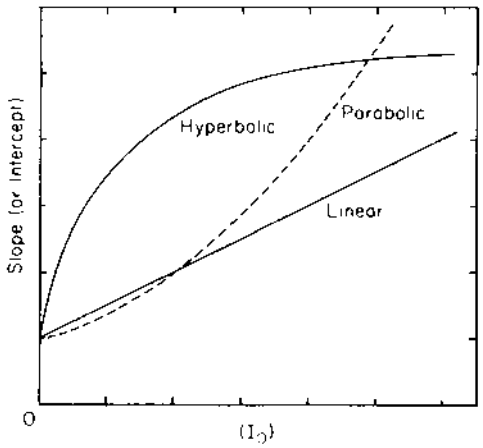

Figure 12 Linear, hyperbolic, and parabolic inhibition patterns of enzyme reactions. (From Ref. 1.)

VI. EFFECT OF pH ON ENZYME-CATALYZED REACTIONS

A. Some Data on pH Versus Activity for Enzymes

Figure 13 shows the effect of pH on activity of porcine pepsin, *Ficus glabrata* peroxidase, bovine trypsin, and milk alkaline phosphatase. The pH activity curves are

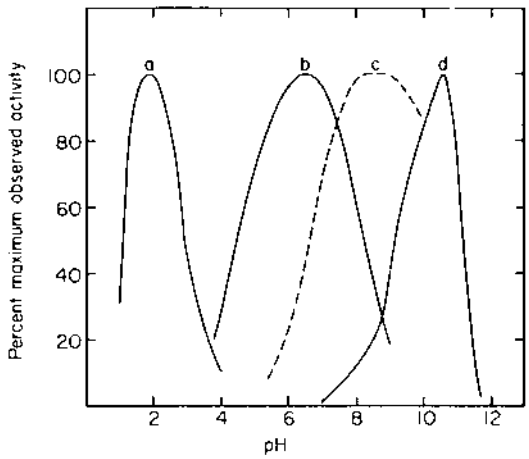

Figure 13 pH effect on activity of several enzymes. (a) Pepsin acting on acetyl-L-phenylalanyl-L-diiodotyrosine at 36.7°C with 5×10^{-4} M pepsin, reaction time 15 min (11). (b) *Ficus glabrata* peroxidase acting on 0.03 M guaiacol and 0.005 M H_2O_2 at 30.0°C (12). (c) Trypsin acting on casein (13). (d) Hydrolysis of 5×10^{-4} M *p*-nitrophenyl phosphate by crude milk alkaline phosphatase at 35°C in 0.1 M sodium glycinate buffer, reaction time 15 min (J.R. Whitaker, unpublished data). (From Ref. 1.)

generally bell-shaped, but the left side of the pH curve for pepsin and the right side of the pH curve for alkaline phosphatase are steeper than the other side. We will return to this point later. Not all pH activity curves are bell-shaped. They may be sigmoidal or they may be horizontal lines, as is the case for bovine catalase over the pH range of 3–10.

Table 3 lists the pH optima for 24 enzymes. The pH optima range from 2 to pepsin to 10 for alkaline phosphatase. A number of the enzymes have pH optima near pH 7 (in the range of 6–8). In the following section, the question of why enzymes have pH activity optima will be addressed. But it should be clear to the reader that research must determine the effect of pH on an enzyme in order to know the range in which it has activity and at which pH the maximum activity is found.

B. Why Do Enzyme-Catalyzed Reaactions Have pH Optima?

There are two reasons why pH optima are found for enzyme-catalyzed reactions. The first is because of pH instability of the enzymes. The second is because of ionization of groups in the active site of enzymes, of the substrates, or of cofactors.

Table 3 pH Activity Optimum of Several Enzymes[a]

Enzyme	pH optimum
Acid phosphatase (prostate gland)	5
Alkaline phosphatase (milk)	10
α-Amylase (human salivary)	7
β-Amylase (sweet potato)	5
Carboxypeptidase A (bovine)	7.5
Catalase (bovine liver)	3–10
Cathepsins (liver)	3.5–5
Cellulase (snail)	5
α-Chymotrypsin (bovine)	8
Dextransucrase (*Leuconostoc mesenteroides*)	6.5
Ficin (fig)	6.5
Glucose oxidase (*Penicillium notatum*)	5.6
Lactate dehydrogenase (bovine heart)	7 (forward reaction) 9 (backward reaction)
Lipase (pancreatic)	7
Lipoxygenase-1 (soybean)	9
Lipoxygenase-2 (soybean)	7
Pectin esterase (higher plants)	7
Pepsin (bovine)	2
Peroxidase (fig)	6
Polygalacturonase (tomato)	4
Polyphenol oxidase (peach)	6
Rennin (calf)	3.5
Ribonuclease (pancreatic)	7.7
Trypsin (bovine)	8

[a]The pH optimum will vary with source and experimental conditions. These pH values should be taken as approximate values.
Source: Ref. 1.

1. Effect of pH on Instability of Enzymes

The tertiary and quaternary structures of enzymes are stabilized by noncovalent electrostatic bonds, hydrogen bonds, hydrophobic bonds, and covalent disulfide bonds. The electrostatic bonds, formed between negative and positive charges on two groups of the enzyme, are affected by pH. The two predominant prototropic groups in enzymes are the side chain carboxyl groups of aspartic and glutamic acid residues (pK_a of 3–4) and the side chain ammonium groups (pK_a of $\sim$ 9–10) of the lysine side chain residues and the guanidinium groups ($pK_a \sim 12$–13) of arginine residues. In the neutral pH range the ionizable side groups are as $-COO^-$, H_3N^+-, and $H_2N-C(=N^+H_2)-NH$ groups, which can form strong electrostatic bonds (10–20 kcal/mol). But below pH 3 the carboxyl groups are protonated (–COOH) and cannot form electrostatic bonds. Above pH 10, the ammonium groups are nonprotonated ($-NH_2$) and do not form electrostatic bonds.

The active site of bovine catalase has no ionizable carboxyl or amino groups. Below pH 3 and pH 10, the electrostatic bonds are nonexistent and the enzyme loses activity owing to instability. The sharp decrease in activity of pepsin at pH < 2.0 is because of instability. The sharp decrease in activity of alkaline phosphatase at high pH is due to loss of electrostatic bonds to stabilize the enzyme.

2. Effect of pH on the Active Site Essential Ionizable Groups

Table 4 shows six ionizable groups, their ionization, pK_a, and ΔH_{ion} that can be a part of the active site of enzymes. Kinetically, ionization of one essential ionizable group gives a sigmoidal pH activity curve, while two essential ionizable groups, one in the ionized form and one in the protonated form, give a bell-shaped curve. In the case of pepsin there is an aspartic acid carboxyl group with pK_a of ~ 1 that is responsible for the left side of the pH activity curve. This group must be as $-COO^-$ for the pepsin to be active. The right side of the pH activity curve is due to ionization of another aspartic acid arboxyl group that must be in the protonated form (–COOH) for pepsin to be active. Therefore, the active site of pepsin has two ionizable carboxyl groups.

Trypsin has a pH optimum of 7.8. The left side of the activity curve is due to an imidazolium group (pK_a 5.6–7.0) in the active site that must be in the unprotonated form (Table 4) for activity of the enzyme. The right side of the bell-shaped curve is due to the ionization of the α-amino group (pK_a 8.0–8.5) of the N-terminal leucyl residue No. 16 (using the protrypsin numbering). For activity, the amino group must be in the protonated form.

Effect of pH on the observed activity of enzymes can be due to any of the components of the reactions [see Eq. (1)]. This includes ionization of groups on the free enzyme (E), the enzyme·substrate complex (EA), the substrate or any cofactor involved. To be able to interpret the effect of pH on an enzyme-catalyzed reaction, the researcher must know the stability of the enzyme at different pHs at the temperature to be used for activity measurements, the effect of pH on ionization of group(s) on the substrate and any cofactor. Equally important, the researcher must control the conditions of the experiment so that the pH effect can be on the free enzyme ($[A]_o \leq 0.05\ K_m$) or on the enzyme·substrate complex ($[A]_o \geq 100\ K_m$). The reader is

Table 4 Prototropic Groups That May Be Involved in Enzyme Catalysis

Group	Ionization		pK_a	ΔH_{ion} (kcal/mol)
Carboxyl	—COOH ⇌ —$COO^{\ominus}$ + $H^{\oplus}$	α[a]	3.0–3.2	
		β,γ,	3.0–4.7	±1.5
Imidazolium	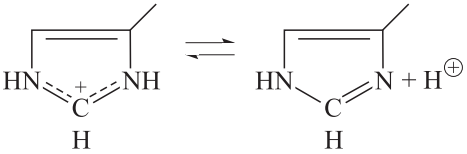		5.6–7.0	6.9–7.5
Sulfhydryl	—SH ⇌ —$S^{\ominus}$ + $H^{\oplus}$		8.0–8.5	6.5–7.0
Ammonium	—$NH_3^{\oplus}$ ⇌ —NH_2 + $H^{\oplus}$	α[a],	7.6–8.4	10–13
		ε,	9.4–10.6	
Phenolic hydroxyl	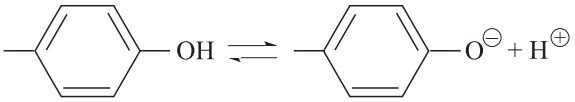		9.8–10.4	6
Guanidinium	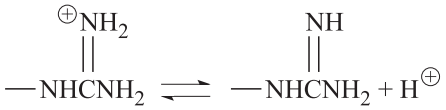		11.6–12.6	12–13

[a]Located at the end of polypeptide chain. Calories × 4.186=Joules.

referred to the detailed discussion of Whitaker (1) on this subject. Properly performed experiments are essentially the only way to determine the essential ionizable groups in the active site of an enzyme and whether they are involved in binding of substrate or in catalysis of substrate to product.

VII. EFFECT OF TEMPERATURE ON ENZYME-CATALYZED REACTIONS

A. General Discussion

Figure 14 shows (solid line) the effect of different temperatures on the velocity of an enzyme-catalyzed reaction. At 20°C, the velocity is constant over the time period used. At 40°C, there is a small deviation from a constant velocity (compare the solid experimental line and the dashed initial velocity line). At 50°C there is more deviation from a constant velocity. At 55°C and 60°C the constant velocity is maintained for only a very short time of reaction. As expected, $v_o(= dp/dt)$ will be different depending on the time of the reaction (t_o, t_1, and t_2 indicated on the x-axis of Fig. 14). These results are plotted in Figure 15 as dp/dt vs. temperature. The

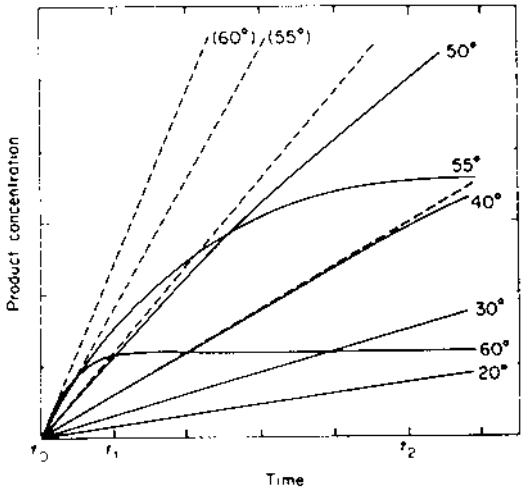

Figure 14 Effect of temperature on rate of product formation. The solid lines are for experimental data; the dashed lines are based on initial velocity, v_o. (From Ref. 1)

plot of initial velocities vs. temperature is curvilinear. As explained below, this is the expected relationship according to the Arrhenius equation. The velocities at time t_1 coincide with the expected relationship up to 50°C. Above 50°C, the velocity slows down and then

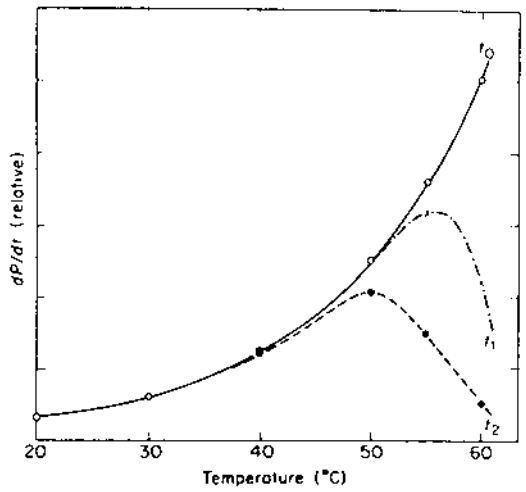

Figure 15 Velocity of formation of product as function of temperature. Data are from Figure 14, taken at time t_o, t_1, and t_2. (From Ref. 1.)

decreases. At time t_2, the data follow the expected relationship only to 40°C, slows at 50°C, and decreases at 55°C and 60°C. Therefore, the temperature optima are 60°C, 55°C, and 50°C for the reactions at times t_o t_1, and t_2, respectively. The difference between the three is due to the effect of temperature on the velocity of denaturation of the enzyme. Therefore, effect of temperature on velocity of denaturation of the enzyme is an important factor when one is studying the effect of temperature on rates of enzyme-catalyzed reactions.

Two other general factors affect the velocity of enzyme-catalyzed reactions. The factors are the effect of temperature on equilibria and on the catalytic efficiency of the enzyme.

B. Effect of Temperature on Equilibria

There are numerous equilibria in an enzyme-catalyzed reaction. These include: (a) solubility of substrates, especially gases (O_2 solubility is 2.17×10^{-3} M at 0°C and 1.12×10^{-3} M at 30°C); (b) pK_a of ionizable groups on the enzyme (see ΔH_{ion} in Table 4); (c) change in pH of buffers (Tris buffer pK_a changes 0.24 units/10°C; see also Table 4); (d) formation and dissociation of the enzyme·substrate complex and others (see Whitaker [1] for a more detailed discussion).

C. Effect of Temperature on Catalytic Rates

The catalytic rate of conversion of the substrate·enzyme complex to product is controlled by k_2 [see Eq. (1)]. To eliminate the effect of factors listed in Section VII.A and B, the enzyme should be saturated with substrate and performed at the pH optimum for the enzyme-catalyzed reaction, over a temperature range where the enzyme is stable.

The rate constant, $k_2 = V_{max}/[E]_o$, under the above conditions is plotted according to the Arrhenius equation:

$$k_2 = Ae^{-E_a/RT} \tag{33}$$

where A is the Arrhenius constant, E_a is the Arrhenius activation energy, R is the universal gas constant (1.98 cal/mol deg), and T is degrees Kelvin. The plot is shown in Figure 16. From the right-hand slope, E_a is obtained. The positive slope (left side of Fig. 16) gives E_a for denaturation of the enzyme. The relationship between E_a and $\Delta H^{\neq}$ from the Absolute Reaction Rate theory is given by Eq. (34).

$$\Delta H^{\neq} = E_a - RT \tag{34}$$

The numerical difference between $\Delta H^{\neq}$ and E_a is 0.6 kcal/mol at 25°C.

D. Effect of Catalyst on E_a and Relative Rates

Table 5 shows the effect of different catalysts on relative rates of some reactions. For example, the conversion of H_2O_2 to O_2 and H_2O relative to no catalyst is 2.07×10^3 times faster for the I^- and 3.47×10^8 times

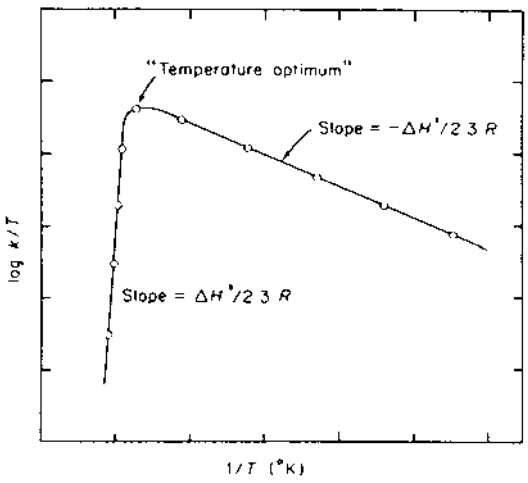

Figure 16 Effect of temperature on rate of an enzyme-catalyzed reaction, plotted according to the Absolute Reaction Rate Theory. The positive slope on the left is for rate of inactivation of the enzyme. The negative slope on the right is for effect of temperature on k_2 for conversion of EA to products. (From Ref. 1.)

Table 5 Effect of Catalyst on E_a and on Relative Rates of Some Reactions

Substrate	Catalyst	E_a (kcal/mol)	n'/n (25°C)	Relative rates[a] (25°C)
H_2O_2	None	18.0	5.62×10^{-14}	1.00
	I^-	13.5	1.16×10^{-10}	2.07×10^3
	Catalase	6.4	1.95×10^{-5}	3.47×10^8
Sucrose	H^+	25.6	1.44×10^{-19}	1.00
	Invertase	11.0	8.04×10^{-9}	5.58×10^{10}
Carbonic acid	None	20.5	8.32×10^{-16}	1.00
	Carbonic anhydrase	11.7	2.46×10^{-9}	2.96×10^6
Urea	H^+	24.5	9.33×10^{-19}	1.00
	Urease	8.7	3.96×10^{-7}	4.25×10^{11}

[a]Relative rates calculated are approximate since differences in $\Delta S^{\neq}$ are ignored.
Source: Ref. 1.

faster for catalase. n'/n, the fraction of molecules n with activation energy equal to E_a or greater, is calculated from Eq. (35):

$$n'/n = e^{-E_a/RT} \tag{35}$$

Equation (1) has been used in this chapter to describe enzyme-catalyzed reactions. Only ground state species are shown. In reality, activated state species should also be included, as shown in Figure 17. When this is done the complete equation is Eq. (36).

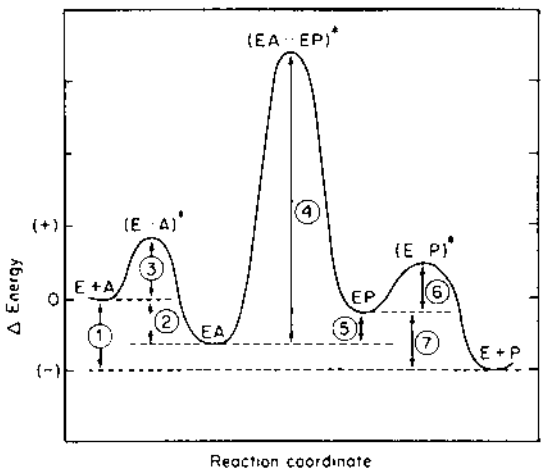

Figure 17 Change in energy along the reaction coordinate during conversion of A to P in an enzyme-catalyzed reaction according to Eq. (36). The numbers refer to steps in the thermodynamic and transition states in the forward direction. (From Ref. 1.

$$E + A \rightleftharpoons (E \cdots A)^{\neq} \rightleftharpoons EA \rightleftharpoons (EA \cdots EP)^{\neq} \rightleftharpoons EP \rightleftharpoons (E \cdots P)^{\neq} \rightleftharpoons E + P \tag{36}$$

The rate-determining step is number 4 in Figure 17. This is the step that requires the most activation energy. Activation energy is required to convert a ground state species to an activated species [Eq. (33)]. The thermodynamic energy difference between two ground state species is calculated using the Van't Hoff equation [Eq. (37)].

$$d \ln K_{eq}/dT = \Delta H/RT^2; (; \ln K_2/K_1 = \Delta H(T_2 - T_1)/T_2T_1) \tag{37}$$

E. Factors Accounting for Catalytic Efficiency of Enzymes

Enzymes are superior biological catalysts as shown in Table 5. The factors that account for their catalytic effectiveness are listed in Table 6. Factors 1–4 account for the rate enhancement due to binding of the substrate stereospecifically (at least three points of attachment) into the active site of enzymes. Factor 1 accounts for much of the rate enhancement, especially for binding of two or more substrates into the active site simultaneously (10^9 and 10^{15} enhancement for two and three substrates, respectively). The polymerases involved in biosynthesis of proteins bind five or more substrates and cofactors simultaneously into the active site. Factors 5–7 account for the rate enhancement during the chemical conversion of the substrate(s) to product(s).

Table 6 Factors Accounting for Catalytic Effectiveness of Enzymes

Factor	Rate enhancement[a]
1. Formation of stereospecific enzyme-substrate complex (conversion from inter- to intramolecular reaction)	10^4; 10^9; 10^{15}[b]
2. Decreased entropy of reaction	10^3
3. Concentration of reactive catalytic groups	10^3–10^4
4. Distortion of substrate	10^2–10^4
5. General acid/general base catalysis	10^2–10^3
6. Nucleophilic/electrophilic catalysis	10^2–10^3
7. Using several steps	10^2–10^4
Overall rate enhancement	10^{18}–10^{36}

[a]In some cases these values can be approximated by model experiments. In others, they are the best estimates available.
[b]For 1, 2, and 3 substrates, respectively.
Source: Ref. 1.

The overall theoretical rate enhancement shown in Table 6 is 10^{18}–10^{36}. The best enzymes, such as catalase and peroxidase, have rate enhancements $\sim 10^{20}$. Therefore the catalytic efficiency of enzymes can be explained by well-known chemical principles: enzymes are not magicians.

REFERENCES

1. JR Whitaker. Principles of Enzymology for the Food Sciences. 2nd ed. New York: Marcel Dekker, 1994.
2. AJ Brown. Enzyme action. J Chem Soc 81:373–379, 1902.
3. V Henri. General Laws of the Action of Diastases. Paris: Hermann, 1903.
4. L Michaelis, ML Menten. The kinetics of invertase action. Biochem Z 49:333–369, 1913.
5. M Eigen, GG Hammes. Elementary steps in enzyme reactions. Adv Enzymol 25:1–38, 1963.
6. H Lineweaver, D Burk. Determination of enzyme dissociation constants. J Am Chem Soc 56:658–666, 1934.
7. EL King, C Altman. A schematic method of deriving the rate laws for enzyme-catalyzed reactions. J Phys Chem 60:1375–1378, 1956.
8. WW Cleland. The kinetics of enzyme-catalyzed reactions with two or more substrates or products. I. Nomenclature and rate questions. II. Inhibition: nomenclature and theory. III. Prediction of initial velocity and inhibition by inspection. Biochim Biophys Acta 67:104–137, 173–187, 188–196, 1963.
9. J Monod, J Wyman, JP Changeux. On the nature of allosteric transitions: a plausible model. J Mol Biol 12:88–118, 1965.
10. DE Koshland Jr, G Nemethy, D Filmer. Comparison of experimental data and theoretical models in proteins containing subunits. Biochemistry 5:365–385, 1966.
11. LE Baker. New synthetic substrates for pepsin. J Biol Chem 193:809–819, 1951.
12. S Kon, JR Whitaker. Separation and partial characterization of the peroxidases of *Ficus glabrata* latex. J Food Sci 30:977–985, 1965.
13. JH Northrop, M Kunitz, RM Herriott. Crystalline Enzymes. New York: Columbia University Press, 1948, p 12.

5

Inactivation of Enzymes

From Experimental Design to Kinetic Modeling

Ann Van Loey, Indrawati, Chantal Smout, and Marc Hendrickx
Katholieke Universiteit Leuven, Leuven, Belgium

I. INTRODUCTION

Enzymes occur naturally in many biological raw materials and can, together with processing, affect functional properties of foods in many ways. Endogenous enzymes can have beneficial or detrimental effects on foods. Some enzymes are positively utilized during food processing for recovery of byproducts, for developing new food products, for achieving higher rates and levels of extraction, or for improving food quality in terms of, e.g., flavor, texture. On the other hand, enzymes might also have detrimental effects. Food spoilage can be caused by enzymes naturally present in the food, or by enzymes produced by certain microorganisms—for example, enzymatic browning reactions in fruits and vegetables by polyphenoloxidases, or rancidity caused by the presence of endogenous lipases and lipoxygenases.

As a consequence of the beneficial and detrimental effects of enzymes, in most food-processing steps control of enzymatic activity is required. Either one wants to promote the beneficial effects of the enzyme by enhancing the enzymatic activity during processing; in this case knowledge on enzyme stability under the relevant processing conditions is required for process design (e.g., its thermostability, resistance toward acid environments). On the other hand, in the case of detrimental enzymatic action, one wants to eliminate or retard the enzymatic reaction, which is often performed by inactivation of the enzymes by physical methods (e.g., thermal blanching) or by inhibition of the enzymatic reaction using additives, a chemical method.

The current chapter will particularly focus on the inactivation of enzymes by the processing factors temperature and pressure, discussing the experimental design and modeling of kinetic inactivation studies of enzymes, illustrated by some examples. An extended overview on thermal and pressure inactivation kinetics of enzymes is given by Ludikhuyze et al. (1).

II. A GENERAL SCHEME FOR ENZYME INACTIVATION

A general scheme for thermal enzyme inactivation was proposed by Lumry and Eyring (2): a reversible partial unfolding, followed by an irreversible reaction step

$$N \overset{K}{\longleftrightarrow} U \overset{k_{ir}}{\longrightarrow} I$$

where N represents the native, U the reversibly unfolded and I the irreversibly inactivated enzyme. K ($= [N]/[U]$) and k_{ir} symbolize the unfolding equilibrium constant and the rate constant of the irreversible reaction step, respectively. In the literature, some evidence can be found as to an analogous general scheme for pressure inactivation of enzymes (3).

If we consider this simple inactivation scheme, the rate of inactivation is given by Eq. (1):

$$v = k_{ir}[U] \quad (1)$$

Since the measurement of residual activity involves $[N] + [U]$ (U will renature upon cooling), the observed rate of inactivation (k_{obs}) is:

$$k_{ir}[U] = k_{obs}([N] + [U]) \quad (2)$$

Because $K = [N]/[U]$, assuming rapid equilibrium, the experimentally measured rate constant k_{obs} can be mathematically expressed as Eq. (3).

$$k_{obs} = \frac{k_{ir}}{1 + K} \quad (3)$$

At "high" temperature or pressure, where the concentration of the native form ($[N]$) is much smaller than the concentration of the reversibly unfolded form ($[U]$), the second step becomes rate limiting and the above equation can be simplified to Eq. (4).

$$k_{obs} = k_{ir} \quad (4)$$

i.e., when the inactivation is examined at "high" inactivation temperature or pressure (far above the denaturation temperature or pressure), the influence of the unfolding–refolding equilibrium is negligible and the inactivation is only determined by the secondary irreversible step.

III. EXPERIMENTAL DESIGN FOR KINETIC ENZYME INACTIVATION STUDIES

Enzyme inactivation kinetics can be determined using either steady-state or un-steady-state procedures (4, 5), the steady-state procedure being the most straightforward approach to study thermal or pressure inactivation kinetics. A classical steady-state experiment consists of subjecting an enzymic sample to a square wave temperature and/or pressure profile.

To study thermal inactivation, batch or flow methods can be used for sample heating and cooling. Whatever method being used, care has to be taken to ensure that heating and cooling are quasi-immediate, or else appropriate compensation for thermal lags has to be taken into account (e.g., 6, 7), especially when the heating or cooling lag is not sufficiently small relative to the half-life* of the reaction. For isothermal batch treatments, enzyme solutions are usually enclosed in small, preferably highly conductive vials or tubes (e.g., glass capillaries, thermal death tubes, thermal death cans) to minimize heating and cooling lags. The samples are immersed in a temperature-controlled heating bath at constant inactivation temperature for predetermined time intervals. Immediately upon withdrawal from the heating bath, the samples are cooled in ice water to stop the thermal inactivation, and the residual enzymatic activity is measured.

For pressure inactivation studies, today only batch methods are available. For pressure treatments, the enzymic samples should be contained in flexible containers (e.g., microtubes, plastic bags). Because of adiabatic heating, pressure buildup is inevitably associated with temperature increase. At the prevailing high pressure, this temperature increase might provoke a significant reduction of enzyme activity during pressure buildup. The temperature reached during pressure buildup can seriously be reduced by decreasing the rate of compression. To avoid problems arising from the temperature increase during pressure buildup, a possible approach is to exclude the nonisobaric/nonisothermal phase from the inactivation data by starting the time course of the experiment ("zero point") after reaching the desired pressure and an additional equilibration period to allow temperature to evolve to its desired value. At that moment, the pressure vessel is decompressed and the activity of the corresponding enzyme sample is considered as the blank. The use of this zero-point approach is merely allowed for first-order reactions (including the special cases of biphasic and first-order fractional conversion reactions). After pressure–temperature treatment, enzyme solutions are cooled in ice water to stop inactivation and reactivation, and the residual enzymatic activity is measured. To perform kinetic experiments at elevated pressure (up to 1000 MPa), specialized high-pressure equipment, consisting of several individual thermostated pressure vessels, is often used (Fig. 1). Such equipment allows submission of several samples simultaneously to treatments at the same pressure and temperature for preset times.

Upon removal of the denaturing agents (i.e., temperature or pressure), regeneration of enzyme activity might occur (see above). Hence, it should be experimentally verified whether enzyme reactivation occurs within a reasonable experimental time after treatment.

IV. MODELING ENZYME INACTIVATION KINETICS

Kinetics of the enzyme inactivation process describe its progress in time. The way in which the inactivation

*The half-life of a reaction is the time required to reduce the concentration (enzyme activity in case of enzyme inactivation studies) to half of its initial value.

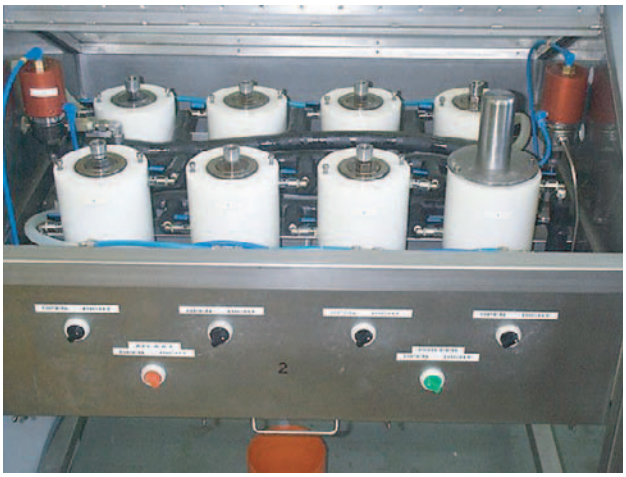

Figure 1 An example of a multivessel high-pressure equipment.

progresses as a function of time is expressed by the mathematical form of the kinetic model. The rate of inactivation is reflected by the numerical values of the kinetic parameter estimates.

Dealing with kinetic studies of thermal or pressure inactivation of enzymes, the first step of the data analysis procedure involves the identification of an adequate inactivation rate equation (e.g., first order, biphasic, *n*th order) and the identification of a temperature and/or pressure coefficient model (e.g., Thermal Death Time model, Arrhenius model, Eyring model), while the second step is the selection of a regression method to estimate kinetic parameter values with the highest probability of being correct.

A. Determination of an Inactivation Rate Equation

The general rate law to describe the decrease of enzyme activity (A) as a function of processing time (t) can be written as

$$\frac{dA}{dt} = -k_{\text{obs}} A^n \tag{5}$$

where A is the enzymatic activity at time t, k the reaction rate constant, and n the reaction order. The order of reaction can be determined by many different methods that are briefly discussed by Hill and Grieger-Block (8) and Laidler (9). Under simple initial and boundary conditions, the integration of differential Eq. (5) results in analytical solutions describing the enzymatic activity (A) as a function of time. In case of isobaric-isothermal inactivation experiments (i.e., rate constant k not varying with time), Eq. (6) or Eq. (7) is obtained depending on the reaction order (with respect to time).*

$$n = 1 \qquad A = A_0 \exp(-kt) \tag{6}$$

$$n \neq 1 \qquad A^{(1-n)} = A_0^{(1-n)} + (n-1)\, kt \tag{7}$$

By trial-and-error procedures an estimate of the reaction order n (with respect to time) can be obtained by analyzing graphically the trends and/or deviations from a linear behavior. However, a complication in determining the order of a reaction from the method of integration is that little or no distinction can be made among zero-, first-, and second-order reactions with respect to time when the response value changes only little (10). Even when a linear plot is obtained, conclusions must be drawn cautiously from the data, especially if the data points correspond to no more than 10–20% conversion because many mathematical functions are roughly linear over a sufficiently small range of variables. According to Arabshahi and Lund (7), reactions should be followed, where possible, through at least four to five half-lives (or 1–2 log reductions). If the method of analysis is not sufficient to measure response values as low as this, the longest heating times possible should be used (11). According to Hill and Grieger-Block (8), one should perform at least experimental runs in which data are taken at 40%, 50%, or higher conversions.

1. First-Order Model

Thermal or pressure inactivation of enzymes can often be described by a first-order reaction [Eq. (6)] (1). This feature is remarkable since enzyme inactivation is a complex process involving several events, such as formation and/or disruption of different interactions and/or bonds, decomposition of amino acids, aggregation, and/or dissociation. It is therefore suggested that in case of apparent first-order inactivation processes, one of these reactions predominates over the others. If several reactions occur at more or less the same rate, complex non-first-order inactivation kinetics are expected (12).

*Note that in the context of enzyme inactivation, the concept of reaction order is purely empirical and gives no direct information about the mechanism of the reaction. This procedure provides a model which describes the kinetics of a reaction, but this model should not necessarily be interpreted as representing the actual mechanism of the reaction.

Under isothermal-isobaric conditions a first-order reaction can be expressed as Eq. (6), which can be linearized by a logarithmic transformation, yielding Eq. (8).

$$\ln\left(\frac{A}{A_0}\right) = -kt \tag{8}$$

where A is enzymatic activity at time t; A_0 is initial enzymatic activity; t is treatment time; and k is the first-order inactivation rate constant. As an example, Figure 2 depicts thermal inactivation of tomato pectin methylesterase, which can be adequately described by a first-order reaction (adapted from 13). In case of a first-order inactivation model, the rate constant at a given temperature and pressure can be estimated by linear regression analysis of $\ln(A/A_0)$ versus inactivation time at constant inactivation temperature and pressure, or alternatively based on Eq. (6) by nonlinear regression analysis (see below).

In the area of food science and technology, it is common to characterize first-order reactions using the Thermal Death Time concept. The decimal reduction time (D-value) is the time, at a given temperature and pressure, needed for a 90% reduction of the initial activity. For a first-order inactivation, D-values and rate constants are directly related [Eq. (9)].

$$D = \frac{\ln(10)}{k} \tag{9}$$

Substitution of Eq. (9) into Eq. (8) yields Eq. (10).

$$\log\left(\frac{A}{A_0}\right) = -\frac{t}{D} \tag{10}$$

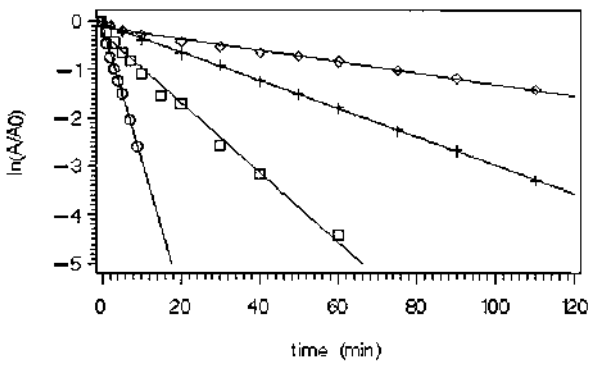

Figure 2 Thermal inactivation curves of tomato pectin methylesterase (PME) dissolved in 20 mM Tris-HCl (pH 7) at 60°C (◇), 62.5°C (+), 65°C (□), and 67.5°C (○). A_o and A are initial tomato PME activity and activity after thermal treatment, respectively. (From Ref. 13.)

The decimal reduction time at a given inactivation temperature and pressure can be calculated from the slope of a linear regression analysis of $\log(A/A_0)$ versus inactivation time at constant inactivation temperature and pressure, or alternatively by nonlinear regression analysis (see below).

The validity of a first-order inactivating behavior can be examined by plotting residual enzyme activity versus treatment time on a semilogarithmic scale and evaluation of the goodness of fit by means of, e.g., lack-of-fit test, coefficient of determination (R^2), analysis of the distribution of residuals.* Residuals of an appropriate fit represent ony the experimental error and should therefore be randomly distributed. The existence of trends in residuals (with respect to either the independent or dependent variable[s]) suggests that some systematic behavior is present in the data that is not accounted for by the model (14), in this case by a first-order inactivation.

The model for inactivation of enzymes according to first-order kinetics may be applied in many cases. However, often more complex inactivation kinetics are found, because inactivation may occur by consecutive or parallel processes, or owing to the presence of isozymes, enzyme inhibitors, or other food components. Several mathematical expressions have been suggested for modeling a non-first-order inactivation behavior. A "biphasic" inactivation behavior where a fast inactivation period is followed by a decelerated decay, eventually leading to an activity plateau, has been attributed to the occurrence of isozymes with different stabilities (~distinct isozyme model), to the presence of a resistant enzyme fraction (~fractional conversion model), or to intermediate (first-order) steps in the overall inactivation process (~consecutive step model).

2. Distinct Isozyme Model

Enzymes characterized by several isozymes can often be subdivided into two (or more) fractions with different processing stability, e.g., one more thermal (pressure) resistant than the other and both inactivating according to a first-order decay kinetic model. For constant extrinsic (e.g., pressure, temperature) and intrinsic factors and assuming that the inactivation of both fractions is independent of each other, the inactivation can be modeled according to Eq. (11).

*Residuals are the differences between experimentally observed dependent variable values and those predicted by the regression equation.

$$A = A_l \exp(-k_l t) + A_s \exp(-k_s t) \quad (11)$$

where A_s is the activity of the more stable enzyme fraction, A_l the activity of the labile enzyme fraction, k the first-order inactivation rate constant where the subscripts s and l for k denote thermostable and thermolabile, respectively. As an example of inactivation according to a distinct isozyme model, thermal inactivation of tomato polygalacturonase (PG) dissolved in 40 mM Na acetate buffer pH 4.4 is depicted in Figure 3.

By plotting the residual activity after different time intervals versus time, the inactivation rate constant of the labile fraction k_l-value), the inactivation rate constant of the stable fraction (k_s-value), and the activity of both fractions can be estimated using nonlinear regression analysis.

3. Fractional Conversion Model

Fractional conversion refers to a (first-order) inactivation process that takes into account a nonzero activity upon prolonged heating and/or pressurizing ($= A_\infty$). A fractional conversion model can be expressed mathematically as Eq. (12).

$$A = A_\infty + (A_0 - A_\infty) \exp(-kt) \quad (12)$$

This relation is valid in the temperature and/or pressure domain where only the labile enzyme fraction inactivates whereas the activity of the stable fraction (A_∞-value) does not change with respect to time. This nonzero activity may or may not be a function of applied temperature and pressure. As an example of fractional conversion, thermal inactivation of the heat-labile fraction of tomato PG dissolved in 40 mM Na acetate buffer pH 4.4 is depicted in Figure 4.

By plotting residual activity after different time intervals versus time, the inactivation rate constant (k-value) and the remaining activity after prolonged treatment (A_∞-value) can be estimated using nonlinear regression analysis.

4. Consecutive Step Model

The consecutive step model is based on a succession of (two) irreversible (first-order) reaction steps—an irreversible conversion of the native enzyme to an intermediate with lower specific activity, and the subsequent irreversible conversion of the intermediate to an inactive enzyme form. A consecutive two-step model can be mathematically expressed as Eq. (13).

$$A = \left(A_1 - A_2\left(\frac{k_1}{k_1 - k_2}\right)\right) \exp(-k_1 t) + A_2\left(\frac{k_1}{k_1 - k_2}\right) \exp(-k_2 t) \quad (13)$$

By plotting the residual activity after different time intervals versus time, the inactivation rate constants k_1 and k_2 and the activity of both fractions can be estimated using nonlinear, regression analysis. k_1 and A_1 refer to step 1, k_2 and A_2 refer to step 2.

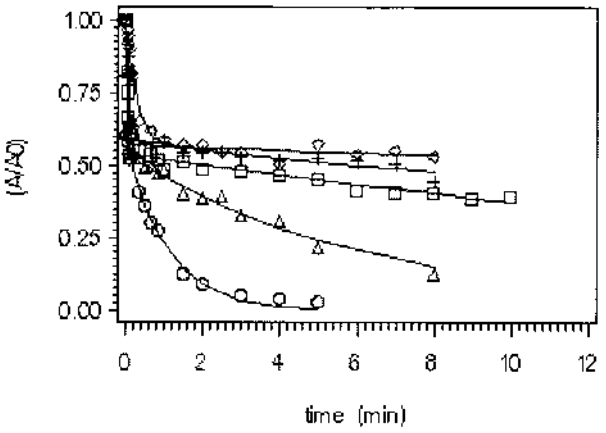

Figure 3 Thermal inactivation curves of tomato polygalacturonase (PG) dissolved in 40 mM Na acetate buffer (pH 4.4) at 70°C (◇), 75°C (+), 80°C (□), 85°C (Δ), and 90°C (○), modeled using a distinct isozyme model. A_o and A are initial tomato PG activity and activity after thermal treatment, respectively. (From Ref. 15.)

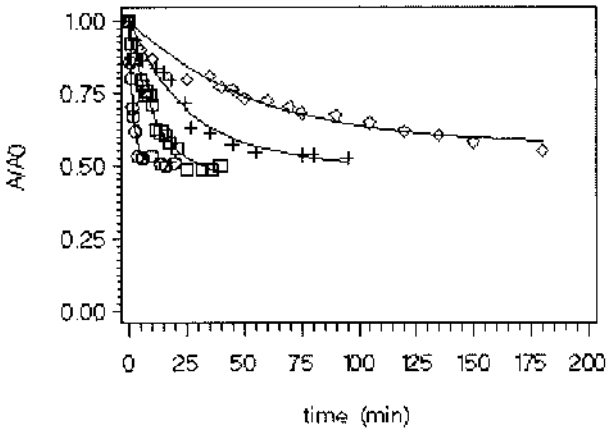

Figure 4 Thermal inactivation curves of tomato polygalacturonase (PG) dissolved in 40 mM Na acetate buffer (pH 4.4) at 58°C (◇), 60°C (+), 62°C (□), and 65°C (○), modeled using a fractional conversion model. A_o and A are initial tomato PG activity and activity after thermal treatment, respectively. (From Ref. 15.)

B. Determination of a Temperature and Pressure Coefficient Model

1. Temperature Dependence at Constant Pressure

The temperature dependence of the rate constant k is often expressed by an activation energy, E_a, as indicated in the Arrhenius relationship [Eq. (14)] (16).

$$k_{obs} = k_{obs,refT} \exp\left(\frac{E_a}{R_g}\left(\frac{1}{T_{ref}} - \frac{1}{T}\right)\right) \quad (14)$$

where $k_{obs,refT}$ is the inactivation rate constant at T_{ref}, T_{ref} the reference temperature, E_a the activation energy, and R_g the universal gas constant ($R_g = 8.314$ J/Kmol). Equation (14) can be linearized which allows the activation energy at a certain pressure to be estimated based on linear regression analysis of the natural logarithm of k versus the reciprocal of the absolute temperature (Fig. 5). Alternatively, the activation energy can be estimated based on the nonlinearized Arrhenius relationship [Eq. (14)] using nonlinear regression analysis (see below).

In the Thermal Death Time model, the temperature dependence of the D-value is given by the z_T-value [Eq. (15)]. The z_T-value equals the temperature increase necessary to obtain a 10-fold decrease of the D-value.

$$D_{obs} = D_{obs,refT} 10^{\frac{T_{ref} - T}{z_T}} \quad (15)$$

where $D_{obs,refT}$ is the inactivation rate constant at T_{ref}, T_{ref} the reference temperature, and z_T the z-value. After linearization of Eq. (15), the z-value at a certain pressure can be estimated based on linear regression analysis of the 10-based logarithm of the decimal reduction time versus temperature. Alternatively, the z-value can be estimated directly using nonlinear regression analysis based on Eq. (15).

Food technologists sometimes use the Q_{10}-factor to describe the temperature dependence of a reaction rate. The temperature dependence parameter Q_{10} is defined as the factor by which the reaction rate is increased if the temperature is raised by 10°C.

2. Pressure Dependence at Constant Temperature

The pressure dependence of the rate constant is often expressed by an activation volume (V_a), as indicated in the Eyring equation [Eq. (16)] (18).

$$k_{obs} = k_{obs,refP} \exp\left(\frac{-V_a}{R_g T}(P - P_{ref})\right) \quad (16)$$

where k_{refP} is the inactivation rate constant at P_{ref}, P_{ref} the reference pressure, V_a the activation volume at a certain temperature, T the absolute temperature, and R_g the universal gas constant ($R_g = 8.314$ cm^3 MPa/Kmol). Also the Eyring equation can be linearized by a logarithmic transformation. Hence, plotting the natural logarithm of the rate constant in function of pressure, the activation volume at a certain temperature can be derived from the slope of the regression line (Fig. 6). Alternatively, the activation volume can be estimated based on the nonlinearized Eyring relationship [Eq. (16)] using nonlinear regression analysis (see below).

Analogous to the log-linear relationshp between D-value and temperature, there is often a log-linear rela-

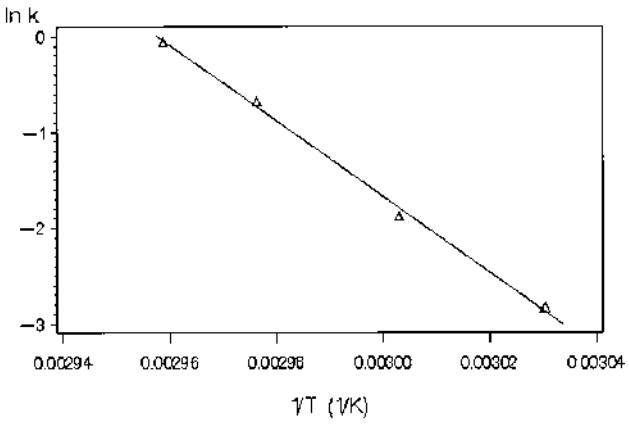

Figure 5 Arrhenius plot for thermal inactivation of orange pectinmethylesterase, dissolved in distilled water. (From Ref. 17.)

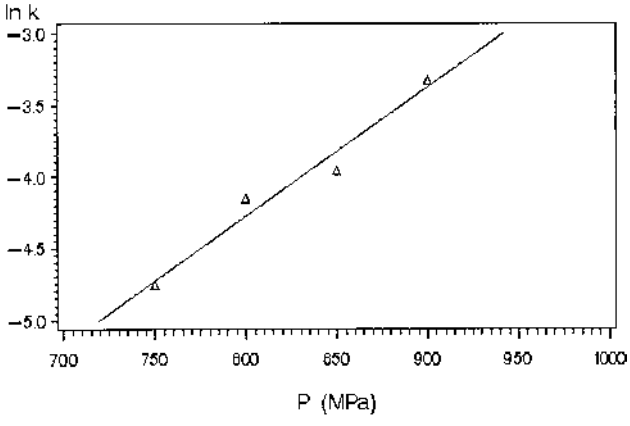

Figure 6 Eyring plot for pressure inactivation at 45°C of avocado polyphenoloxidase, dissolved in phosphate buffer (pH 7, 0.1 M). (From Ref. 19.)

tionship between D-value and pressure [Eq. (17)], whereby z_p is defined as the pressure increase necessary to obtain a 10-fold decrease of the D-value.

$$D_{obs} = D_{obs,ref} 10^{\frac{P_{ref}-P}{z_p}} \tag{17}$$

where $D_{obs,ref}$ is the decimal reduction time at P_{ref}, P_{ref} the reference pressure, and z_P the z-value at a certain temperature. Also the z_P-value can be estimated using two different regression approaches: plotting the 10-based logarithm of D in function of pressure, the z_P-value at a certain temperature can be derived from the slope of the regression line, or the z_P-value can be estimated using nonlinear regression analysis (see below).

Analogous to the validity evaluation of a first-order kinetic model, the appropriateness of the coefficient models to describe the temperature or pressure dependency of the inactivation rate constant can be evaluated by determination of the goodness of fit of ln k vs. $1/T$ (Arrhenius model), log D versus T (TDT model), ln k vs. P (Eyring model), or log D vs. P (PDT model).

3. Combined Pressure–Temperature Dependence

Based on experimentally determined inactivation rate constants for an elaborated set of pressure–temperature combinations, an iso-rate contour plot, connecting pressure–temperature combinations resulting in the same inactivation rate constant can be constructed. Iso-rate contour diagrams for pressure–temperature inactivation of enzymes as well as of microorganisms are often elliptically shaped. These elliptical pressure–temperature kinetic diagrams can be modeled on a thermodynamic basis.

The basic thermodynamic equation governing the behavior of a system during a pressure and a temperature change can be represented as Eq. (18).

$$d(\Delta G) = -\Delta S dT + \Delta V dP \tag{18}$$

Since the entropy change (ΔS) and the volume change (ΔV) vary with pressure and temperature [Eqs. (19) and (20), respectively], Eq. (18) can be reformulated as Eq. (21) (20, 21).

$$d(\Delta S) = \left(\frac{\partial \Delta S}{\partial T}\right)_P dT + \left(\frac{\partial \Delta S}{\partial P}\right)_T dP \tag{19}$$

$$d(\Delta V) = \left(\frac{\partial \Delta V}{\partial T}\right)_P dT + \left(\frac{\partial \Delta V}{\partial P}\right)_T dP \tag{20}$$

$$\begin{aligned}\Delta G = {} & \Delta G_o + \Delta V_o(P - P_o) - \Delta S_o(T - T_o) \\ & + \frac{1}{2}\Delta\kappa(P - P_o)^2 + \Delta\zeta(P - P_o)(T - T_o) \\ & - \Delta C_p\left[T(\ln\frac{T}{T_o} - 1)_+ T_o\right]\end{aligned} \tag{21}$$

where ΔCp is the heat capacity change $(T\delta\Delta S/\delta T)_P$, $\Delta\zeta$ the thermal expansibility factor $((\delta\Delta V/\delta T)_P = -(\delta\Delta S/\delta P)_T)$, and $\Delta\kappa$ the compressibility factor $(\delta\Delta V/\delta P)_T$. This thermodynamic model can be converted into a kinetic model through the transition state theory of Eyring, suggesting that enzyme inactivation is accompanied by the formation of a metastable activated state ($^{\neq}$) which exists in equilibrium with the native enzyme. This conversion is based on the substitution of Eq. (22) and Eq. (23) in Eq. (21), obtaining Eq. (24) to describe the combined pressure–temperature dependence of the inactivation rate constant.

$$\Delta G^{\neq} = -RT\ln(K^{\neq}) \tag{22}$$

$$K^{\neq} = \frac{kh}{rk_B T} \tag{23}$$

$$\begin{aligned}\ln(k_{obs}) = {} & \ln(k_0) - \frac{\Delta V_0^{\neq}}{RT}(P - P_o) \\ & + \frac{\Delta S_0^{\neq}}{RT}(T - T_o) - \frac{1}{2}\frac{\Delta\kappa^{\neq}}{RT}(P - P_o)^2 \\ & - \frac{\Delta\zeta^{\neq}}{RT}(P - P_o)(T - T_o) \\ & + \frac{\Delta C_p^{\neq}}{RT}\left[T(\ln\frac{T}{T_o} - 1) + T_o\right]\end{aligned} \tag{24}$$

The model parameters can be estimated using a nonlinear regression analysis, involving an iterative numerical procedure based on the minimal sum of squares. Figure 7 depicts an iso-rate contour diagram for pressure–temperature inactivation of soybean lipoxygenase, modeled using Eq. (24).

C. Selection of a Regression Model and Method for Kinetic Parameter Estimation

Several regression models (linear vs. nonlinear models*) and methods (two-step regression vs. one-step

*A model is linear if the first (partial) derivatives of the model with respect to the parameters are independent of the parameters and consequently higher-order derivatives are zero whereas in a nonlinear model at least one of the derivatives of the model function with respect to the parameters depends on at least one of the parameters.

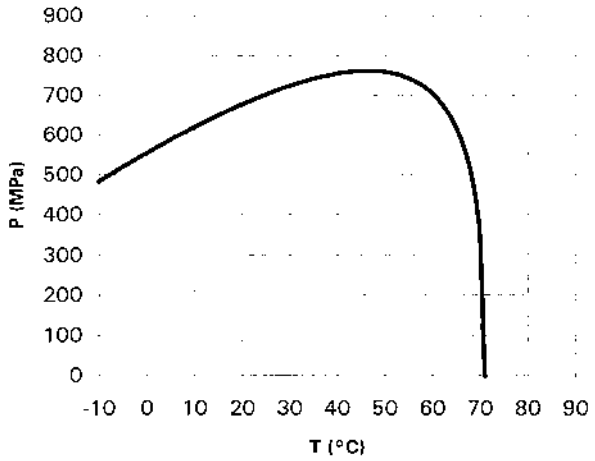

Figure 7 Iso-rate contour diagram ($k = 0.23\,\text{min}^{-1}$) for pressure–temperature inactivation of soybean lipoxygenase in Tris HCl buffer (pH 9, 0.01 M). (From Ref. 22.)

regression) can be applied to obtain kinetic parameter estimates. In this paragraph, the selection between a linear or a nonlinear kinetic model and between a two-step or a one-step regression method will be discussed.

1. Selection Between Linear Versus Nonlinear Models

Because linear least-squares fitting is easier to solve than nonlinear least-squares fitting, an approach frequently used is to perform (a) nonlinear transformation(s) of the dependent variable so that a linear model is obtained from which the least squares estimators of the linear model parameters can be calculated straight. Typical examples in the context of enzyme inactivation include linearization of the first-order rate equation by a logarithmic transformation of the inactivation data, or linearization of the temperature and pressure coefficient models by a logarithmic transformation of the rate constants. However, one of the assumptions inherent to least-squares fitting (for both linear and nonlinear) is that the experimental errors (in the dependent variables) are normally distributed (23). Hence, one should not perform any nonlinear transformation of the dependent variables (such as, e.g., a logarithmic transformation) that will alter the error distribution structure if the original data contain Gaussian uncertainties. When the model is nonlinear in the parameters no explicit analytical solutions are available for the parameters or the confidence intervals, and a solution must be found iteratively by linear approximation. Starting from an initial estimate of the parameter values provided by the user, a numerical algorithm (e.g., Gauss-Newton, Marquardt, DUD) is used to provide successively better approximations until the sum of squared residuals do not change within some specified limit (convergence criterion is met) so that finally a set of parameter values satisfying the least-squares criterion is presented. To be more certain that the minimum found is actually the global minimum desired and not a local one – it is advisable to start the nonlinear least-squares procedure at several different starting estimates of the parameters. If the final results are independent of the initial values, there is more confidence that the final parameter values describe a global minimum.

With the present availability of computing power, ease of parameter estimation is no longer a valid reason for linearizing models. It may nevertheless be useful to perform a nonlinear transformation in order (a) to produce a linear plot from which the validity of the model can easily be interpreted graphically, or (b) to be able to use a simple linear regression analysis to obtain reasonable starting values for the subsequent nonlinear regression routine of the untransformed data.

2. Selection Between Two-Step Versus One-Step Regression

It is common practice to estimate kinetic inactivation parameters by an individual, or two-step, regression method: one estimates at first inactivation rate constants (and possibly other kinetic parameters such as enzyme fraction, reaction order) from inactivation data at constant temperature or pressure by linear or nonlinear regression analysis. In a second step, one estimates temperature or pressure coefficients from regression analysis of the obtained inactivation rate constants as a function of temperature and pressure.

In a global, or one-step, regression approach, one is considering the inactivation data obtained at different inactivation temperatures or pressures simultaneously. To model a global inactivation data set, the temperature or pressure coefficient model is being incorporated in the inactivation rate equation. Using nonlinear regression analysis, one gets estimates of the inactivation rate constant at reference conditions and a temperature or pressure coefficient.

With regard to the choice between an individual or a global approach, in the literature, the effectiveness of several least-squares regression methods for the estimation of kinetic parameters has been assessed mainly based on comparison of the confidence region for the parameters estimates and on the quality of fitting (24,

25). These authors concluded that the two-step regression approach gives the least accurate estimates probably because it estimates too many intermediate values, and does not gain strength in the regression by considering the data set as a whole. Two-step regression has the disadvantage of applying regression on regression parameter estimates. Errors on the first regression estimates are not transformed to the second. On the contrary, they found a global regression procedure a very good method which yielded unbiased and precise estimates of the parameters without estimating unnecessary ones. Because of several disadvantages inherent to the two-step approach, one is advised to analyze kinetic data sets by a global fit considering the data set as a whole. Probably the use of a global fit will not provide the best individual fit at each temperature or pressure, but the whole set of results will be better described.

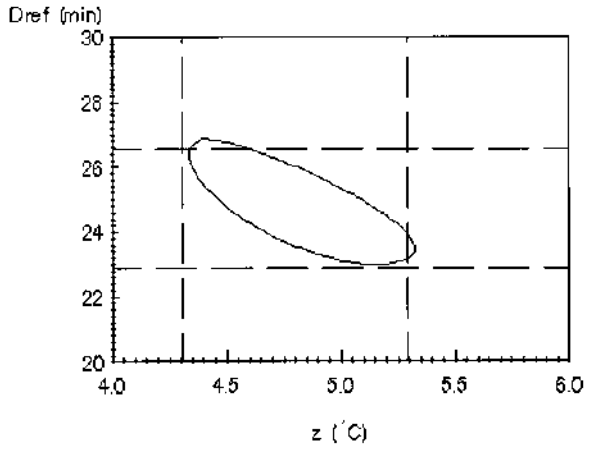

Figure 8 90% joint confidence contour of the kinetic parameter estimates for thermal inactivation of alkaline phosphatase in raw bovine milk ($T_{ref} = 60°C$) (correlation between z and D_{ref} is 0.786). (From Ref. 31).

3. Confidence Intervals of Parameter Estimates

Next to the determination of parameter values with the highest probability of being correct, it is essential to obtain a realistic measure of the statistical confidence of the estimated parameters. In the case of linear models, confidence intervals for the parameter estimates are exactly defined and symmetrical and their determination is straightforward while in case of nonlinear models confidence intervals are not symmetric and only approximate confidence intervals are provided (26). The most commonly used method for the evaluation of the confidence intervals of parameters estimated in a nonlinear regression procedure is the use of asymptotic standard errors, computed based on linearizing assumptions. However, they nearly always provide incorrect estimates of the actual confidence limits of the determined parameters because they neglect the covariances of the simultaneously determined parameters and assume normal distribution of parameters. According to several authors (23, 27–29), asymptotic standard errors should not be used in case of nonlinear least-squares analysis since there are many other published methods that provide realistic estimates of the confidence intervals of parameters determined by nonlinear least-squares methods—e.g., the construction of joint confidence regions for the parameters. Joint confidence regions take into account the correlation between the simultaneously estimated parameters. Although the use of joint confidence regions for simultaneously estimated parameters is well described in statistical handbooks, it is rarely encountered in scientific publications. $100(1–\varphi)\%$ joint confidence regions can be constructed using Eq. (25) (30).

$$SSQ \leq SSQ(\theta)\left\{1 + \frac{p}{m-p} F(p, m-p, 1-\varphi)\right\} \tag{25}$$

where $SSQ(\theta)$ represents the error sum of squares associated with the least-squares estimate θ, p the number of parameters estimated simultaneously, m the number of observations, and F the upper $1–\varphi$ quantile for an F distribution with p and $m–p$ degrees of freedom. An example of a joint confidence region for a set of parameter estimates that are highly correlated is given in Figure 8. It can be seen from Figure 8 that if the parameters are rather highly correlated no attempt should be made to interpret the individual confidence intervals simultaneously by constructing a rectangular joint confidence interval because a parameter pair may be well within the individual confidence interval but is very unlikely to occur since it is very far outside the joint confidence region. Only if the correlation between the simultaneously estimated parameters is close to zero will the rectangular region defined by the individual confidence intervals approximate to the correct joint confidence region.

REFERENCES

1. L Ludikhuyze, A Van Loey, S Denys, Indrawati, M Hendrickx. Effects of combined pressure and temperature on enzymes related to quality of fruits and

vegetables: from kinetic information to process engineering aspects. CRC Crit Rev Food Sci Nutr 2001 (submitted).
2. R Lumry, H Eyring. Conformational changes of proteins. J Phys Chem 58:110–120, 1954.
3. A Zipp, W Kauzmann. Pressure denaturation of metmyoglobin. Biochemistry 12:4217–4228, 1973.
4. JW Rhim, RV Nunes, VA Jones, KR Swartzel. Determination of kinetic parameters using linearly increasing temperature. J Food Sci 54(2):446–450, 1989.
5. RV Nunes, JW Rhim, KR Swartzel. Kinetic parameter evaluation with linearly increasing temperature profiles: integral methods. J Food Sci 56(5):1433–1437, 1991.
6. AG Perkin, H Burton, HM Underwood, FL Davies. Thermal death kinetics of *Bacillus stearothermophilus* spores at ultra high temperatures. II. Effect of heating period on experimental results. J Food Technol 12:131–148, 1977.
7. A Arabshahi, DB Lund. Considerations in calculating kinetic parameters from experimental data. J Food Process Eng 7:239–251, 1985.
8. CG Hill, RA Grieger-Block. Kinetic data: generation, interpretation, and use. Food Technol 34(2):56–65, 1980.
9. KJ Laidler. Chemical Kinetics. New York: Harper and Row, 1987.
10. MAJS van Boekel, P Walstra. Use of kinetics in studying heat-induced changes in foods. In: PF Fox, ed. Monograph on Heat-Induced Changes in Milk. Bulletin of the International Dairy Federation, Brussels, 2nd ed. IDF special issue 9501:22–50, 1995.
11. MK Lenz, DB Lund. Experimental procedures for determining destruction kinetics of food components. Food Technol 34(2): 51–55, 1980.
12. RW Lencki, J Arul, RJ Neufeld. Effect of subunit dissociation, denaturation, aggregation, coagulation and decomposition on enzyme inactivation kinetics: I. first-order behavior. Biotechnol Bioeng 40:1421–1426, 1992.
13. I Van den Broeck, L Ludikhuyze, A Van Loey, M Hendrickx. Effect of temperature and/or pressure on tomato pectinesterase activity. J Agric Food Chem 48(2):551–558, 2000.
14. M Straume, ML Johnson. Analysis of residuals: criteria for determining goodness-of-fit. Methods Enzymol 210:87–105, 1992.
15. D Fachin, A Van Loey, Indrawati, L Ludikhuyze, M Hendrickx. Thermal and high pressure inactivation of tomato polygalacturonase: a kinetic study. J Food Sci 2001 (in press).
16. S Arrhenius. Über die reaktionsgeschwindigkeit bei der inversion von rohrzucker durch säuren. Z Phys Chem 4:226–248, 1889.
17. I Van den Broeck, L Ludikhuyze, A Van Loey, C Weemaes, M Hendrickx. Thermal and combined pressure–temperature inactivation of orange pectinesterase: influence of pH and additives. J Agric Food Chem 47(7):2950–2958, 1999.
18. H Eyring, FH Johnson, RL Gensler. Pressure and reactivity of proteins, with particular interest to invertase. J Phys Chem 50:453–464, 1946.
19. C Weemaes, L Ludikhuyze, I Van den Broeck, M Hendrickx. Kinetics of combined pressure–temperature inactivation of avocado polyphenoloxidase. Biotechnol Bioeng 60(3):292–300, 1998.
20. SA Hawley. Reversible pressure–temperature denaturation of chymotrypsinogen. Biochemistry 10(13):2436–2442, 1971.
21. E Morild. The theory of pressure effects on enzymes. Adv Prot Chem 34:93–166, 1981.
22. Indrawati, A Van Loey, L Ludikhuyze, M Hendrickx. Soybean lipoxygenase inactivation by pressure at subzero and elevated temperatures. J Agric Food Chem 47(6):2468–2474, 1999.
23. ML Johnson. Review: why, when and how biochemists should use least squares. Anal Biochem 206(2):215–225, 1992.
24. E Cohen, I Saguy. Statistical evaluation of Arrhenius model and its applicability in prediction of food quality losses. J Food Proc Preserv 9:273–290, 1985.
25. SG Haralampu, I Saguy, M Karel. Estimation of Arrhenius model parameters using three least squares methods. J Food Proc Preserv 9:129–143, 1985.
26. MAJS van Boekel. Statistical aspects of kinetic modeling for food science problems. J Food Sci 61(3):477–485, 489, 1996.
27. ML Johnson, SG Frasier. Nonlinear least-squares analysis. Methods Enzymol 117:301–342, 1985.
28. HJ Motulsky, LA Ransnas. Fitting curves to data using nonlinear regression: a practical and nonmathematical review. FASEB J 1:365–374, 1987.
29. ML Johnson, LM Faunt. Parameter estimation by least-squares methods. Methods Enzymol 210:1–37, 1992.
30. NR Draper, H Smith. Applied Regression Analysis. New York: John Wiley & Sons, 1981.
31. W Claeys, L Ludikhuyze, A Van Loey, M Hendrickx. Inactivation kinetics of alkaline phosphatase and lactoperoxidase, and denaturation kinetics of β-lactoglobulin in raw milk under isothermal and dynamic temperature conditions. J Dairy Res 68:95–107, 2001.

6

Regulatory Issues of Enzymes Used in Foods from the Perspective of the E.U. Market

Danielle P. Praaning
DSM Food Specialties, Delft, The Netherlands

I. INTRODUCTION

Enzymes were used for food production 2000 years before the birth of Christ. Good examples are bread, cheese, and beer production. Of course, it was unknown at the time that it was the enzymes that were doing the job. Nowadays, the production of food enzymes has become industrialized. European enzyme manufacturers are market leaders and cater ~70% of the world's need for food enzymes, and this market is still increasing with an annual growth of about 2%.

These developments have triggered the creation of national laws and regulations to ensure both the safety of the consumer and fair trade. Although many laws in the European Union have been harmonized over the last few decades, this has not (yet) happened in the case of enzymes.

The European Association of Manufacturers of Fermentation Enzyme Products (AMFEP), which was founded in 1977, has set as one of its major aims the achieving of the widest possible harmonization of regulatory requirements for enzymes in the European Union (E.U.). To achieve this, AMFEP has initiated discussions with the European Commission, national authorities, and the food industry. This chapter presents an overview of the tangle of present regulations that are applicable for enzymes when used in food.

II. OVERVIEW OF APPLICABLE LAWS

In the European Union, there are so-called horizontal and vertical laws. Horizontal laws are those that cover all foods. Examples are the laws regarding additives and those regarding the labeling of foodstuffs. Vertical laws cover foods with a so-called standard of identity, also called compositional regulations or "recipe laws." Examples of products for which such standards exist are cheese and bread.

In both cases, vertical as well as horizontal, there are laws that have been harmonized throughout the E.U. and laws that are still subject to national legislation. This situation will probably remain so, especially in view of the fact that in the treaty signed in Maastricht in February 1992 (1), the European Union officially laid down the "principle of subsidiarity," which states that the European Commission should not regulate what could be done just as well or better at the national level.

For products regulated solely at the national level, the principle of mutual recognition applies. If a product is legally produced in one E.U. country, it can also be sold in another E.U. country, unless this country has well-founded arguments to reject the product on the grounds of protection of consumer health, or one of the other reasons listed in Article 30 of the Treaty establishing the European Community (2). Other than in this situation, member states are not allowed to create unjustified trade barriers.

If one wants to place a new enzyme on the market, any of the four cases (horizontal versus vertical, harmonized versus national) can be applicable, meaning that all possibilities have to be assessed. The following factors are of importance when establishing how a specific enzyme is regulated.

1. The purpose of its use. Is the enzyme used only during processing of the food, or does it still have a specific function in the final food that is sold to the consumer?
2. The type of food in which the enzyme is to be used. Does the food in question have a standard of identity?
3. The country in which the enzyme is to be used in food. Applicable nonharmonized regulations will differ country by country.
4. The origin or source of the enzyme. Industrial enzymes can be obtained from plant, animal, or microbial sources. These may be regulated differently. Moreover, some countries have special requirements for enzymes produced by genetically modified organisms (gmos).

III. E.U. HARMONIZED LAWS

A. Horizontal Harmonized Laws

The relevant harmonized E.U. Directive is the "Council Directive 89/107/EEC Concerning Food Additives Authorized for Use in Foodstuffs Intended for Human Consumption," also called the Additives Framework Directive (3).

According to this directive, additives are everything added to food that is not normally used as a characteristic ingredient (a characteristic ingredient would, for instance, be milk in cheese or flour in bread). In the directive, food additives are divided into those that have a technological effect in the finished product and those that do not have a technological effect in the finished product. Additives of the first category may only be used if they have been authorized and included in a positive list together with their so-called E-number and, if applicable, permitted applications. Moreover, their presence in the final food has to be declared in the ingredient list of the foodstuff. Additives of the second category are exempt from these obligations; thus they do not have to be authorized, or labeled on the final foodstuff. It is rather confusing in practice that only products in the first category are called additives, whereas products in the second category are called processing aids.

The precise definition of processing aid according to the Additives Directive is:

> "Processing aid" means any substance not consumed as a food ingredient by itself, intentionally used in the processing of raw materials, food or their ingredients, to fulfill a certain technological purpose during treatment or processing and which may result in the unintentional but technically unavoidable presence of residues of the substance or its derivatives in the final product, provided that these residues do not present any health risk and do not have any technological effect on the finished product.

In the case of enzymes, the distinction between the use as processing aid or additive (or even ingredient) is not always easy. The existing definitions in E.U. law are open to interpretation on a number of points. This makes it difficult to decide in certain applications whether an enzyme has the status of a processing aid or an additive. The lack of consistency in the legislation has already led to regulatory uncertainty and difficulties surrounding enzymes, which until now had been regarded as processing aids, suddenly being considered to be additives.

Recent attempts to bring an increasing number of enzymes within the scope of the definition of food additives have principally been based on the argument that it is only possible to speak of a "residue" when there has been a conscious effort made to remove the enzyme. However, the interpretation of the food industry, and most authorities shared this interpretation until now, has always been that if an enzyme does not have a technological function in the final food, it is a processing aid, even if it remains in the final food in the small quantity (ppm) in which it was added.

If an enzyme does have a technological function in the final food, however, it will fall under the Additives Directive. There are at present only two enzymes falling under the Additives Directive:

1. Lysozyme, when used as preservative in ripened cheese.
2. Invertase, when used for soft centered confectionery.

Confusingly, these very same enzymes may also be used as processing aids for other food applications!

Thus, in the case of enzymes, one and the same enzyme can fall under both categories, depending on its application. If the enzyme has a technological funtion in the final food, it will fall under the Additives Directive. If it does not have a function in the final

food, it is a processing aid and exempt from the Additives Directive.

Only when use of an enzyme falls under the Additives Directive does specific approval by the European Commission need to be obtained if a company wants to market a new enzyme. This means that the functionality of the enzyme product has to be proved and its safety has to be evaluated by a specific group of experts called the Scientific Committee on Food (SCF).

In 1991 the SCF published guidelines for the presentation of data on food enzymes (4). To obtain approval, toxicological data need to be submitted. According to the guidelines, two mutagenicity studies and a 90-day oral toxicity study in rat are required as a general standard. However, safety data are not required for enzymes originating from edible plants or animals. Presumably, the SCF did not think about enzymes obtained from genetically modified plants at the time these guidelines were made.

In the case of microbial enzymes, no safety data are needed if the microorganism in question has a long history of safe use in food and belongs to a species for which documented evidence exists that no toxins are produced, and the actual strain used is of well-documented origin. To date, the only such microorganism accepted by the SCF is *Saccharomyces cerevisiae* (baker's yeast).

B. Vertical Harmonized Laws

There are only two vertical harmonized directives, those on fruit juices and on wines, in which the use of certain enzymes is expressly provided for. The Fruit Juice Directive (5) states that only pectolytic, proteolytic, and amylolytic enzymes may be used in fruit juices. The Wine Regulation (6) permits the use of pectolytic enzymes and of β-glucanase from the microorganism *Trichoderma harzianum* only. No other enzymes can be used unless specific authorization, resulting in an amendment of the law, is given.

IV. NATIONAL LAWS

National laws covering the use of enzymes are:

1. The general National Food Safety Laws. Even when an enzyme is not regulated in a specific Member State, its use would be subjected to the requirements of General Food Safety Legislation, which stipulates that nothing must be added to food which renders it injurious to health.

2. Horizontal enzymes regulations. There are three E.U. countries having specific horizontal enzyme regulations: Denmark, France and the United Kingdom (see below).

3. Before Spain and Portugal had to implement the harmonized E.U. Additives Directive, these countries regarded all enzymes, whether used as additive or processing aid, as additives. As a consequence, they were mentioned on the positive additive list and had to be authorized as such. It may be confusing for these countries that only very few enzymes are mentioned on the positive list of the E.U. Additives Directive, while all other enzymes can still be used, albeit only as processing aids. These countries may see this as a legal vacuum.

4. In addition to the above-mentioned regulations, most Member States have vertical laws for cheese, flour, bread, etc., regulating the use of enzymes. These vertical legislations differ from country to country, which may not only create trade barriers but also contribute to a very complicated picture for enzyme producers and users alike.

Unfortunately, this is also an area where mutual recognition between Member States does not function properly. If an enzyme is approved for a certain use in one Member State, this does not automatically mean that it is approved for the same use in another Member State.

A. Horizontal Enzyme Regulations

In the 1970s, the Joint Expert Committee on Food Additives (JECFA) of the FAO/WHO developed toxicological requirements for enzyme products (7) based on the following classification system: enzymes from edible tissues of animals; enzymes from edible parts of plants; and enzymes from microbial origin, including microorganisms known to be present or used for food, microorganisms known to be harmless contaminants in food, and microorganisms unknown in food.

The main conclusion from this classification was that no numerical Acceptable Daily Intake or toxicity studies are necessary for enzyme preparations derived from edible tissues of animals, from edible portions of plants, or from microorganisms that are traditionally accepted as constituents of foods or are normally used in the preparation of foods.

Moreover, JECFA also established specifications to which enzyme products should comply (8). These specifications cover limits for certain heavy metals, microbial contamination, antibiotic activity, and mycotoxin con-

tent. In their guidelines, the SCF has largely followed the JECFA safety classification and specifications.

Shortly after JECFA development of specifications and toxicological requirements, the United Kingdom, France, and Denmark started developing guidelines for food enzymes. These guidelines were all largely based on the JECFA requirements and specifications. Only the French and Danish guidelines have been turned into genuine enzyme legislation. In the United Kingdom, it became a Code of Practice to ask for authorization for a new enzyme preparation on the basis of the U.K. regulations.

In principle, the French, Danish, and U.K. enzyme regulations did not mean to differentiate between the use of enzymes as additive or processing aid. However, since the use of an enzyme as additive now falls under the harmonized E.U. Additives Directive, these national laws now apply to enzymes used as processing aids only.

In all other E.U. Member States, there is no specific enzyme legislation. As a result, enzymes when used as processing aids are merely subjected to the general National Food Safety Laws if the country in question has no horizontal law regulating enzymes and if the application of the enzyme is not regulated in a vertical way. In such cases, no authorization is needed if a company wants to put a new enzyme on the market.

1. National Enzyme Law in France

The French Enzyme Decree (9) permits the use of all enzymes mentioned in an Annex to the Decree. This positive listing of enzymes is by function, enzyme name, source, foods in which the enzymes are permitted, and special conditions for use. The list is updated regularly.

The French Decree also lays down specifications of purity, which are very similar to the specifications laid down by JECFA. Furthermore, permitted preservatives and diluents for enzyme preparations are listed.

To obtain approval for a new enzyme, a dossier has to be filed with the authorities. This dossier should contain proof of the functionality of the enzyme (''case-of-need'') and the results of safety studies as described in the SCF guidelines. In case an already approved enzyme is to be marketed for a new food application, only the case-of-need is required.

2. National Enzyme Law in Denmark

In contrast to France, the Danish law (10) does not contain a positive listing system. All enzyme products and their applications are simply subjected to a notification procedure. Notification is valid only for a specific brand or trade name.

The user or importer of an enzyme preparation is responsible for such notification. It was recently decided that the information to be contained in the notification should follow the guidelines laid down by the SCF. Although the term ''notification'' is used, there is in practice no real difference between this procedure and an authorization. The authorities evaluate the dossier, and the product cannot be marketed until all questions about the dossier have been satisfactorily answered.

3. National Enzyme Regulation in the United Kingdom

In the United Kingdom, the Ministry of Agriculture, Fisheries and Food published the Food Advisory Committee's (FAC) Report on the Review of Enzyme Preparations in 1982 (11). This document was meant to form the basis for a national horizontal enzyme legislation.

The FAC recommended that food enzymes be approved only when a technical case-of-need had been established and they were considered safe for use in food. General specification requirements were also outlined. Moreover, the FAC established a positive list based on source and main enzyme activity. In this list, enzymes are divided into two groups, A and B. Group A are enzymes of vegetable or animal origin, for which no further specifications are necessary. Group B is a selection of microbial enzymes, which are temporarily approved for use in food. It was recommended that these enzymes be reviewed within 2 years of publication of the report.

As a basis for such a review, the FAC recommended the development of a nonspecific screening test to prevent the marketing of microbial enzyme preparations containing mycotoxins. However, the development of the test turned out to be impossible for technical reasons.

As an alternative, the U.K. Committee on Toxicity (COT) published Guidelines for the Safety Assessment of Microbial Enzyme Preparations in 1993 (12). These guidelines are comparable, although somewhat stricter, to those of the SCF. No U.K. guidelines exist for enzymes obtained from animals or plants.

Although these COT guidelines have not been converted into a genuine law, they have the same effect from a practical point of view. Authorization on basis of the guidelines is required to achieve marketing approval for a new enzyme preparation.

B. Regulations for Enzymes Produced by Genetically Modified Organisms (gmos)

The SCF guidelines and the national regulations in the United Kingdom, Denmark, and France also cover specific provisions for enzymes made by gmos. In simplified terms this means that the genetic modification will be evaluated by the authorities before the enzyme can be approved and that the enzyme preparation should be free of the gmo and recombinant DNA.

JECFA has also written down general considerations and specifications for enzymes from genetically modified microorganisms (13). This has not been done for enzymes obtained from genetically modified plants or animals. As has been the case for classical enzymes, these considerations might be used for future E.U. regulations.

In the Netherlands, a Novel Food Law was passed in July 1993, covering, among others, all additives and processing aids made by genetic modification. This law was issued because of the delays in the adoption of the harmonized European Novel Food Regulation, but it has now been replaced by the latter.

The E.U. Novel Food Regulation was finally adopted in January 1997 and entered into force in May of that year (14). This regulation covers novel foods and food ingredients, but, in contrast to the Dutch Novel Food Law, additives (including processing aids) are outside its scope.

During the prolonged discussions on this regulation, the European Parliament obtained a commitment from the European Commission that an investigation would be carried out as to the need to fill gaps in the area regulating the protection of public health, particularly with respect to processing aids (e.g., enzymes), and that furthermore, where necessary, these gaps would be filled by proposals for additional legislation.

As a result, the Commission added the following statement to the Novel Food Regulation:

> The Commission confirms that should it appear in the light of experience, that there are gaps in the system of protection of the public health provided for by the existing legal framework, in particular in respect of processing aids, it will formulate appropriate proposals in order to fill those gaps.

In an attempt to include gmos enzymes when used as processing aids into the scope of the E.U. Novel Food Regulation, the Dutch authorities in July 1997 wrote a proposal to regard enzymes that are not removed from the final food as ingredients instead of processing aids. In this way, such gmos enzymes would be covered by the E.U. Novel Food Regulation. Owing to strong opposition of the French authorities, the Dutch proposal has not been accepted. Instead, the European Commission was asked by the Member States to prepare a paper regarding the present legal situation for food enzymes. The European Commission transferred this task in October 1998 to a so-called Scientific Cooperation (SCOOP) task force, in which experts from various Member States participated. The four objectives of the SCOOP task force were to: make a list of food enzymes in use in E.U.; study the way they have been evaluated for their safety; make overview of the current legal situation; and find criteria for distinguishing between the use of enzymes as additives, processing aids, or ingredients.

The SCOOP task force finished its work at the end of 2000. The report however, has not yet been published at the time of this writing. One of the main conclusions the SCOOP task force drew was that the present definitions on additives and processing aids do not provide sufficient criteria to distinguish between the use of enzymes as an additive or as a processing aid. The problem on how to distinguish between additives and processing aids is also being discussed at international level, namely within the Codex Committee for Food Additives and Contaminants. The results of this discussion, which may take several years, can potentially have a great impact on the way enzymes are regulated in future in the European Union and elsewhere.

In July 2001, the European Commission adopted two new proposals for regulating products derived from gmos: (a) a proposal for regulation of genetically modified Food and Feed (15); (b) a proposal for regulation concerning traceability and labeling of gmos and traceability of food and feed products produced from gmos (16). Before becoming law, the proposals will first have to be accepted by the European Council and Parliament, a process that may take several years. The proposals will replace the abovementioned E.U. Novel Food Regulation as far as products derived from genetic modification are concerned. Again, enzymes when used as processing aids in food are explicitly exempted from the proposals. Whether this will again lead to discussions within the European Parliament remains to be seen.

V. PROBLEMS

A. Consequences of Present Regulatory Situation

Since mutual recognition among Member States does not function properly, the enzyme industry is con-

fronted with an unnecessary burden to obtain approvals for the use of a new enzyme in food in individual Member States. It goes without saying that it will potentially save cost and time if there were only one approval system. Furthermore, there is not always mutual recognition as regards the type of safety tests to be performed. This may lead to unnecessary use of laboratory animals. The approval of an enzyme is thus governed by the toughest standard in any one country.

There is no harmonized system and there are no fixed time limits for approvals resulting in uncertainty about return on R&D investments for the enzyme industry.

Member States still apply certain national rules on production within their own territory, which leads to so-called reverse discrimination. Enzyme and food producers are particularly affected by this mechanism. Enzyme producers are in principle able to *sell* their products throughout the European Union, but the remaining national rules in some Member States prevent the food producers, in their own Member State, from actually *using* the food enzyme in question, meaning that they simply will not buy the enzyme!

Nevertheless, foodstuffs produced with such enzymes can be imported into these Member States owing to the open E.U. market. Thus, such Member States discriminate against the production of particular foodstuffs in their own country.

The reverse discrimination leads to unequal starting points for food producers in the various Member States and limits their flexibility in shifting manufacturing.

The lack of consistency and clarity in the legislation, such as the different interpretations in Member States, of the terms processing aid, additive and ingredient, leads to legal insecurity for the enzyme producers as well as the food producers. In some cases, Member States use the situation as an argument for not giving approvals: ''We are waiting for Brussels.'' In other cases, Member States expressed their desire to develop their own national enzyme legislation which would result in an even more fragmented situation.

In the absence of a harmonized legal situation, the food industry creates its own rules, leading to an even more complicated and costly situation for the enzyme industry. Political parties, Parliament, and action groups are calling for enzyme regulation, especially for enzymes obtained from gmos.

Especially in countries without an enzyme legislation, like Germany, the lack of regulation can lead to low consumer confidence. Various television programs and articles have insinuated that enzymes lead to food allergy and that enzymes produced using gmos might lead to an increase in this problem.

For all these reasons, AMFEP is in favor of a clear, simple, and more harmonized regulatory regimen for food enzymes in the European Union. Such a regimen would not only solve mutual recognition problems, but also fill the perceived gap in the E.U. Novel Foods Regulation. It may also contribute to improving public confidence by increasing the transparency of the safety evaluation of food enzymes.

B. Wishes of the European Enzyme Industry for the Future

The wish of AMFEP is to have a future regulatory regimen for food enzymes which:

1. Leads to only one approval system, thus less burden, less time, less money.
2. Eliminates the present lack of mutual recognition and thus trade barriers.
3. Simplifies and clarifies the legal situation.
4. Removes present legal gaps, giving more legal security to producers and users.
5. Ensures a high level of protection of public health, leading to improved consumer confidence.
6. Ensures that legislation is primarily based on scientific evidence and risk assessment.
7. Improves the image of producers of food enzymes and its users, the food industry.

Whatever future regulatory situation is created, AMFEP would like the following five principles to be fulfilled:

1. Nondiscrimination of gmos enzymes. Gmos enzymes should not end up in a separate legislation, for instance under the E.U. Novel Food Regulation.

2. Grandfathering mechanism. Enzymes that are already on the market should be able to stay on the market.

3. Processing aid status or a category in their own right. There should be no more case-by-case discussions about whether a specific enzyme is applied as processing aid, additive, or ingredient. They should all be given the same status. That might be a category in their own right, as is the case for flavors in the E.U.

4. Application of SCF guidelines for safety testing. There should only be one standardized way to do this.

5. No fragmentation through different legislation. The complicated way enzymes are regulated now should be simplified. All food enzymes should be regulated in a uniform way.

VI. SUMMARY

There is no overall E.U. regulatory regimen for enzymes. Most enzymes are exempted from the harmonized E.U. Food Additives Directive because they are used as processing aids and not as additives with a function in the final food. Enzymes are, however, subjected to many different national legislations in the E.U. Member States. The result of these differences in legislation is a lack of consistency in the way enzymes are regulated throughout the E.U. Therefore, for the global enzyme producer, the production and marketing of an enzyme product is governed by the toughest standards in any one E.U. country. The enzyme industry is in favor of a more uniform and harmonized regulatory regimen in the European Union.

REFERENCES

1. Treaty on European Union (signed in Maastricht on 7 February 1992), consolidated version. http://europe.eu.int/eur-lex/en/treaties/livre1_c.html
2. Treaty establishing the European Community. http://europe.eu.int/eur-lex/en/treaties/dat/ec_cons_treaty_en.pdf.
3. Council Directive of 21 December 1988 on the approximation of the laws of the Member States concerning food additives authorized for use in foodstuffs intended for human consumption (89/107/EEC). Official Journal No L040 1989, p 27.
4. Guidelines for the presentation of data on food enzymes (opinion as expressed on 11 April 1991). Reports of the Scientific Committee for Food (Twenty-seventh series). EUR 14181 EN, 1992.
5. Council Directive of 21 September 1993 relating to fruit juices and certain similar products (93/77/EEC). Official Journal No L244, 1993, p 23.
6. Council Regulation of 16 March 1987 on the common organization of the market in wine (822/87/EEC). Official Journal No L084, 1987, p 1, and Commission Regulation (EC) No 2624/95 of 10 November 1995 amending Commission Regulation (EEC) No 3220/90 laying down conditions for the use of certain oenological practices provided for in Council Regulation (EEC) No 822/87. Official Journal No L269, 1995, p 1.
7. Fifteenth Report of the Joint FAO/WHO Expert Committee on Food Additives. FAO Nutrition Meetings Report Series No. 50, 1972.
8. Specifications for the identity and purity of some enzymes and certain other substances. WHO Food Additives Series, No. 2, 1972.
9. Arrété du 5 septembre 1989 relatif à l'emploi de préparations enzymatiques dans la fabrication de certaines denrées et boissons destinées à l'alimentation humaine. Journal Officiel de la République Francaise, 1er octobre 1989.
10. Bekendtgørelse om tilsætningsstoffer til levnedsmidler. Sundhedsministeriets bekendtgørelse nr. 1055 af 18 December 1995.
11. Food Additives and Contaminants Committee Review of Remaining Classes of Food Additives used as Ingredients in Food. Report on the Review of Enzyme Preparations 1982. FAC/REP/35, Ministry of Agriculture, Fisheries and Food.
12. JM Battershill. Guidelines for the safety assessment of microbial enzymes used in food. Food Additives and Contaminants 10, 5:479–488, 1993.
13. Compedium of food additive specifications. FAO Food and Nutrition Paper 52, 1988. Annex 1. General specifications for enzyme preparations. http://apps3.fao.org/jecfa/intro/Annex1.htm.
14. Regulation (EC) No 258/97 of the European Parliament and of the Council of 27 January 1997 concerning novel foods and novel food ingredients. Official Journal No L043 1997, p 1.
15. Proposal for a regulation of the European Parliament and of the Council on genetically modified food and feed. Brussels, 2001. Commission Proposal – COM (2001) 425 final. http://europa.eu.int/eur-lex/en/com/dat/2001/en_501PC0425.html.
16. Proposal for a regulation of the European Parliaments and of the Council concerning traceability and labelling of genetically modified organisms and traceability of food and feed products produced from genetically modified organisms and amending Directive 2001/18/EC. Brussels, 25.7.2001. Commission Proposal – COM (2001) 425 final. http://europa.eu.int/eur-lex/en/com/dat/2001/en_501PC0182.html.

7

Regulatory Issues of Food Enzymes Used in the United States

John R. Whitaker
University of California, Davis, Davis, California, U.S.A.

I. INTRODUCTION

Thousands of enzymes are found in all of the raw materials (plants, animals, microorganisms) produced for foods. In those consumed raw, the enzymes are active when ingested but are generally denatured by the acid pH of the stomach. They then become a (small) part of our total daily protein requirement. When foods are processed prior to eating by heating, the enzymes are denatured. In dried and freeze-dried products, the enzymes may be in active form. In fruits and vegetables, such as apricots, apples, dates, plums, potatoes, mushrooms, teas, etc., the enzymes are still active and must be inactivated by blanching ($\sim 85^{\circ}C$), or controlled by adding enzyme inhibitors such as bisulfite, ascorbic acid, or other specific inhibitors before drying. But these naturally occurring enzymes are not regulated. If an enzyme is added (by biotechnology) to a plant to increase the level of enzyme, such as overproduction of 5-enolpyruvylshikimate-3-phosphate synthase (EPSPS) or cloning a mutant gene encoding EPSPS that is insensitive to glyphosate to prevent killing of the plant by the herbicide glyphosate, while the unwanted grasses and weeds are killed, this is regulated. When an enzyme is added during the processing of a food, this is regulated.

Addition of enzymes, whether to increase the level of the enzyme or to include a new enzyme in a live plant or animal or microbe to be used as food, is regulated by the U.S. Department of Agriculture (USDA) via the Animal and Plant Health Inspection Service (APHIS), the Food Safety and Inspection Service FSIS), and the Grain Inspection, Packers, and Stockyard Administration (GIPSA) or by a state department of agriculture. Increases, or decreases, of some enzyme levels, such as polyphenol oxidase, can be done by standard breeding methods. The insertion of a new gene and its expression to change the sensory, nutrition, climate tolerance, insect resistance, or storage properties of the living organism is generally done by genetic engineering. The "inventor" must demonstrate that there are no harmful effects to humans or the environment, including other types of activities (allergenic, for example) of the food produced from such modifications. The federal and/or state departments of agriculture are responsible for enforcing such modifications to living potential food sources.

Additions of enzymes to food materials during processing are regulated by the Food and Drug Administration (FDA) unit of the Department of Health and Human Services. Specifically, the Center for Food Safety and Applied Nutrition (CFSAN) of FDA is assigned this responsibility. In carrying out its responsibility, it may request advice from the National Academy of Sciences (NAS) or other expert bodies and scientists. The regulations of FDA become binding when published in the Federal Register (published by the Office of the Federal Register, National Archives and Records Administration of the U.S. Government Printing Office).

The regulations are not only published in the Federal Register, but can be found also on several

electronic Web sites. These web sites include: http://www.fda.gov/; http://vm.cfsan.fda.gov/list.html; http://vm.cfsan.fda.gov/~dms/reg-2.html; http://vm.cfsan.fda.gov/~dms/eafus.html; http://vm.cfsan.fda.gov/~lrd/biotechm.html; http://vm.cfsan.fda.gov/cgi-bin/ws.cgi?Q...+and+food+additives+ (or use OR in place of AND); http://frwebgate.access.gpo.gov/cgi-bin/multidb.cgi.

The EAFUS ("Everything" Added to Food in the United States) Web Site (above) is an informational database maintained by the FDA Center for Food Safety and Applied Nutrition (CFSAN) under the program Priority-based Assessment of Food Additives (PAFA).

> It contains administrative, chemical and toxicological information on over 2000 substances added to food, including substances regulated by the FDA as direct, "secondary" direct, and color additives, and Generally Recognized As Safe (GRAS) and prior-sanctioned substances. In addition, the database contains only administrative and chemical information on less than 1000 other substances (without toxicological information). The more than 3000 total substances together comprise an inventory often referred to as EAFUS [quoted from EAFUS database].
>
> This list of (of some 3000) substances contains ingredients added directly to food that FDA has either approved as food additives or listed or affirmed as GRAS. Nevertheless, it contains only a partial list of all food ingredients that may in fact be lawfully added to food, because under federal law some ingredients may be added to food under a GRAS determination made independently from the FDA. The list therefore contains many, but not all, of the substances subject to independent GRAS determinations. For information about the GRAS notification program please consult the Inventory of GRAS Notifications [on the EAFUS data base].
>
> The EAFUS database is 201 pages in length.

II. ORIGIN AND HISTORY OF THE U.S. FOOD AND DRUG ADMINISTRATION

A. Origin

Regulations to prevent adulteration or sale of unfit food in Great Britain have existed since the early 13th century. The Sale of Food and Drugs Act of the United Kingdom was passed in 1875. The U.K. Act was amended by the Food and Drug Acts of 1938 and 1955. A major reason for the amendments was to improve the control of the increasingly complex process of food preparation and sale (1). The U.K. Act prohibited the sale of any food in which substances were added or deleted, or in which the food was processed in a manner that might be unsafe to human health. Other offenses included the sale of misbranded, falsely described foods, and misleading claims about the nature of the product, its substance, or its quality.

The United Kingdom in concert with other countries of the European Union (E.U.) have worked to standardize the regulations to simplify trade of foods among the European Union (see Chapter 6 of this book by Praaning).

In the United States, the first Federal Food and Drug Law was established in 1906 (2). The legislation was the basis for passage of several food standards of identity, as well as the prohibition of sale of toxic, unsanitary, adulterated, or misbranded foods. The law required the federal government to prove that suspect foods were toxic or harmful to human health. This law remained in effect until 1938, with two minor revisions in 1907 and 1912. In 1938, Congress enacted the Federal Food, Drug, and Cosmetic Act, following the death of 70 people who took the drug "Elixir Sulfanilamide." The provisions of the act were: (a) the establishment of the FDA, the primary functions of which were administrative and provided only for the prohibition of the use of known toxic substances as food additives; (b) the establishment of standards of identity and food quality, as well as (c) mandates to provide for honest labeling and safe packaging.

In 1958, the Food Additive Amendment was enacted because of increasing concern by physicians and consumers that chemical additives were a possible cause of cancer. Following deliberations of the Delaney Committee, an amendment was passed (1960) that required the FDA to consider "safety factors which, in the opinion of experts qualified by scientific training and experience to evaluate the safety of food additives, are generally recognized as appropriate for the use of animal experimentation data." This amendment required that the safety of ingredients and products be established before the consumer was exposed to them. Thus, the onus of establishing food safety was transferred to the manufacturers, along with the mandated requirement for

animal testing prior to marketing of the food. One clause of the amendment, known as the Delaney clause, caused major scientific and public controversy. It stated: ''No food additive shall be deemed to be safe if it is found to induce cancer when ingested by man or animals'' (3). The net result was that all the compounds classified as GRAS required new petitions to FDA that not only addressed the safety of the food additives but also the reagents used in preparation and use of the food additives. Since enzymes were classified as food additives in 1906, they had to be analyzed for safety, activity, and usage level in relation to the food in which they were included. Nelson (4), Hickman (5), and Roland (6) have written thorough and thoughtful reviews of the issues and problems caused by this ruling.

B. Role of the FDA in Regulation of Enzymes in Food

Food enzymes are derived from cells of living plants, animals, and microorganisms. The enzymes, known or unknown, have been a part of the food of humans, as well as animals, as long as humans have been on earth. The enzymes are an essential part of germination of seeds and reproduction of animals and microorganisms, growth of organisms, maturation, storage and utilization in producing the food and in its digestion to the building blocks for proteins, lipids, carbohydrates, and nucleic acids of all animals, including humans. From early times enzymes from plants, animals, and microorganisms were used to modify the taste, aroma, color, texture, and digestibility of agriculture products. Many major food industries (baking, brewing, dairy, meat, and fruits) are dependent on the utilization of enzymes for production of breads, beers, cheese, fruit juices, etc.

Up to 1958, enzymes were considered as food (protein) or food additives but safe, since they had been used in food since humans first appeared on earth. But since 1958, the FDA has viewed enzymes as food additives, not food. However, until 1972 when the FDA suspended the ''generally recognized as safe'' (GRAS) status, enzymes were considered to be safe, since they came from natural sources and are proteins, and a part of all raw foods. They also had an excellent safety record for many hundreds of years.

The 1958 Food Additive Amendment defined enzymes as food additives, rather than as foods, foodstuffs, or foreign substances found in very small amounts or familiar substances as some other countries did.

Food additives, as defined by the 1958 Food Additive Amendment are:

> Any substance the intended use of which results or may reasonably be expected to result, directly or indirectly, in it becoming a component or otherwise affecting the characteristics of any food (including any substance intended for use in producing, manufacturing, packing, processing, preparing, treating, packaging, transporting, or holding food; and including any source of radiation intended for such use); if such substance is not generally recognized among experts qualified by scientific training and experience to evaluate its safety as having been adequately shown through scientific procedures (or, in the case of a substance used in food prior to 1 January 1958, through either scientific procedures or experiences based on common use in food) to be safe under the conditions of its intended use.

The term food additive thus covers any substance (i.e., enzyme) directly added to food. Indirect additions to food during processing which become a component of the food are also included.

The 1958 Food Additive Amendment established three categories of food additives for foods. They were:

1. Food substances ''grandfathered'' into the category Generally Recognized as Safe (GRAS), or those substances for which prior sanctions had been previously established.
2. Substances deemed as automatically unsafe as defined by the Delaney clause, ''no additive shall be deemed to be safe if it is found to induce cancer when ingested by man or animal, or if it is found, after tests which are appropriate for the evaluation of the safety of food additives, to induce cancer in man or animals.''
3. All other food and color additives which need to be tested for safety on an individual basis.

In 1972, FDA revoked the GRAS or prior sanction status of all pre-1958 additives (which to this time were cleared under the ''grandfather clause'' of long use that had shown them to be safe, including enzymes) despite a lengthy report by the Ad Hoc Enzyme Technical Committee (AHETC), established in 1969; membership consisted of representatives from most of the firms that manufactured or marketed enzymes in the United States. The sole purpose of the AHETC was, and is, to deal with regulatory issues and requirements involving enzymes with the FAO/WHO Joint Expert

Committee on Food Additives (JECFA), a committee of outstanding scientists with experience in food toxicology from England, France, Japan, Italy, Switzerland, Holland, Australia, Russia, and the United States. After initial review the updated report was submitted to the FDA and to the Subcommittee on Codex Specifications, Committee on Food Protection, National Research Council for inclusion in the Food Chemicals Codex (published in 1974). Despite these extensive efforts by AHETC and JECFA, the FDA made it clear that further information would be required before any enzyme, even those with a long history of use, would be confirmed as GRAS.

At the 1997 Annual Meeting of the Institute of Food Technologists, Corbin Miles of the FDA's Bureau of Foods described the FDA strategy for enzyme GRAS affirmation. A summary of that report is found in Nelson (4), which is quoted here.

> FDA will again review information on enzymes and enzyme sources, particularly microbial-derived enzymes. FDA has continued to seek such information, including requests published in the Federal Register. Essentially, FDA will hew to the present requirements for food additive petitions. Any enzyme which was GRAS under the 1958 amendment will require significant safety information before it will be included in the present GRAS list. Mr. Miles stressed that the activity of the enzyme and the utilization of such activity in the manufacture or modification of foods must be described in some detail. Any GRAS regulations on enzymes must include all conditions of use which have been evaluated. Mr. Miles stated that trade secret information (if different than that publically available or proposed) must be submitted. He suggested that trade secret information be submitted via an additive petition which can be exempt from the Freedom of Information Act.

The first impression of those of us familiar with enzymes (biochemists, members of AHETC and JECFA, and perhaps the E.U. Scientific European Committee on enzyme usage in foods) was that this was a very harsh and unjustified position to take on the clearance of enzymes in food processing and manufacture. But when one recalls that commercial enzyme products are at most 1% of the desired enzyme and 99% of other materials including trace amounts of other enzymes, purification materials, etc., the view of FDA can be rationalized. Perhaps, or not, the use of higher purity enzymes produced by genetic engineering will alleviate some of the problems with extraneous materials, including fragments of microbial cells.

Nelson (4) has discussed the lengthy time required for review of petitions by FDA. The minimum time may be 18 months. But with requirements for toxicology and mutagenicity studies with animals of up to 2 years, the time can be 3 years or more, at a cost of hundreds of thousands of dollars (7). Only enzyme products with high economic value expectations are likely to be submitted for review. Anticipated revenue from food enzyme products in no way compares with that of enzyme products from drug companies, especially since the latter have to be pure!

C. GRAS Petitions to FDA

A GRAS petition for FDA review looks like the following (6).

1. Clearly state the intent of the petition to demonstrate safety, based on one common use in foods for the enzyme and/or the end product. Alternatively, establish safety through the publication of adequate supporting data.
2. Identification of the enzyme: (a) class; (b) species; (c) strain-variety; (d) enzyme source.
3. Method of preparation: (a) complete medium composition; (b) mechanical units used to produce; (c) fermentation conditions (aeration, agitation, temperature, pH).
4. Enzyme specifications: (a) single enzyme, multiple enzymes, or whole cells; (b) impurities, i.e., heavy metals, solvents; (c) comparative compositional data on a minimum of five processes of the enzyme.
5. Methods of enzyme recovery: (a) types and levels of solvents employed; (b) types of processing aids, i.e., filtration, flocculation; (c) other.
6. Toxicological data on enzyme or microorganism: (a) organism must be non pathogenic; (b) organism must not produce mycotoxins or other toxic chemicals; (c) organism must not produce antibiotics.

Ebert (8), Aunstrup (9) and Grasso (10) have designed formats for typical toxicological evaluations on animals. Table 1 is from a publication of Dr. Ebert (8).

Both FDA and USDA, in reviewing a petition, may ask advice from the National Academy of Sciences, the Federation of American Societies for Experimental Biology, Special Advisory Committees, and individual consultants.

Table 1 Typical Toxicological Evaluation of Food Additives

Study	Scope
Acute	
Oral LD_{50}	Two species (min) range find for subacute studies.
Dermal inhalation LD_{50}	As needed (OSHA requirements, etc.).
Subacute	
90-day feeding	Two species: one nonrodent, dog preferred. Three levels (min) plus control. Complete biochemical and histopathologic workup on control, highest level fed. Other levels if needed. Define no-effect level. High level to give effect.
Chronic	
2 years^{+}	Two species—rat/dog. Carry rat to 25% survival of controls. Perhaps combine with three-generation reproduction study. Three levels plus control. Complete biochemical and histopathologic workup.
Metabolic fate	Search for animal model for man. Absorption, distribution kinetics, organ/tissue concentration (if any) metabolic products defined.
Special	Carcinogenicity, teratology, cytogenicity (host mediated, dominant lethal, chick embryo).
Interaction	Special dietary restrictions, drug interactions.

Source: Ref. 8.

III. CURRENT STATUS OF ENZYME REGULATIONS (11)

Since the beginning of federal regulations involving enzymes they have been, and continue to be, classified as food additives. As noted earlier in this chapter, they were originally classified as GRAS. But after 1958, when the Food Additive Amendment was passed, safety of the enzyme-containing product had to be addressed, and in 1972, all GRAS status was revoked. As pointed out in Section II above, these changes require extensive data in the petition asking for reinstatement of GRAS status.

Regulation of food additives is covered in the Code of Federal Regulation Title 21, §170–199 (11). Enzymes are covered collectively with other food additives in Part 170—Food Additives, Chapter 1, Food and Drug Administration, Department of Health and Human Services Subchapter B, Food for Human Consumption as to regulation procedures, in §171, Food Additive Petitions; in §173, Secondary Direct Food Additives Permitted in Food for Human Consumption; and in §184, Direct Food Substances Affirmed as Generally Recognized as Safe.

A. §170—Food Additives and Food Additive Petitions

§170—Food Additives is a general section for all food additives (pp 5–10). §171—Food Additive Petitions is a general section on how to petition FDA for approval of a food additive (pp 21–26). Both *must* be consulted for the general aspects pertaining to definitions, classification of foods and ingredients, and general policies on food additive regulations. The topics covered are given in Table 2.

B. §173—Secondary Direct Food Additives

§173—Secondary Direct Food Additives Permitted in Food for Human Consumption, Subpart B—Enzyme Preparations and for a Human Consumption, Subpart B—Enzyme Preparations and Microorganisms lists those enzymes and microorganisms that have been affirmed by FDA and on what basis they were approved (Table 3). Note that all the enzymes are from microorganisms.

Table 2 Code of Federal Registrations 21. Food and Drugs. Part 170—Food Additives[a]

Subpart A—general provisions	
§170.3	Definitions
§170.6	Opinion letters on food additive status
§170.10	Food additives in standardized foods
§170.15	Adoption of regulation on initiative of Commissioner
§170.17	Exemption for investigational use and procedure for obtaining authorization to market edible products from experimental animals
§170.18	Tolerances for related food additives
§170.19	Pesticide chemicals in processed foods
Subpart B—food additive safety	
§170.20	General principles for evaluating the safety of food additives
§170.22	Safety factors to be considered
§170.30	Eligibility for classification as generally recognized as safe (GRAS)
§170.35	Affirmation of generally recognized as safe (GRAS) status
§170.38	Determination of food additive status
§170.39	Threshold of regulation for substances used in food-contact articles
Subpart C—specific administrative rulings and decisions	
§170.45	Fluorine-containing compounds
§170.50	Glycine (aminoacetic acid) in food for human consumption
§170.60	Nitrites and/or nitrates in curing premixes

[a]AUTHORITY: 21 U.S.C. 321, 341, 342, 346a, 348, 371.
Source: 42 FR 14483. Mar. 15, 1977, unless otherwise noted.

Table 3 Secondary Direct Enzymes and Microorganisms Permitted in Food for Human Consumption[a]

Subsection	Enzyme	Source
§173.110	Amyloglucosidase	*Rhizopus niveus*
§173.120	Carbohydrase and cellulase	*Aspergillus niger*
§173.130	Carbohydrase	*Rhizopus oryzae*
§173.135	Catalase	*Micrococus lysodeikticus*
§173.140	Esterase-lipase	*Mucor miehei*
§173.145	Alpha-galactosidase	*Mortierella vinaceae* var. *raffino seutilizer*
§173.150	Milk-clotting enzymes microbial	(1) *Endothia parasitica* (2) *Bacillus cereus* (3) *Mucor pusillus* Lindt (4) *Mucor meihi Cooney et Emerson* (5) *Aspergillus oryzae* (recombinant modified)
§173.160	Several enzymes (citric acid production)	*Candida guilliermondii*
	Several enzymes (citric acid production)	*Candida lipolytica*
§173.170	Aminoglycoside 3′-phosphotransferase II (CAS Reg. No. 58943-39-8)	(*Escherichia coli*, using *klan*^{r} gene)

[a]From Code of Federal Regulations 21. Food and Drugs. Part 173, Published in the Federal Register No. 21, pp 111–124, April 1, 2000.

A closer look at the approval use of microbial milk-clotting enzymes is instructive as to understanding the FDA approval process, including the conditions given in §173.150.

Milk-clotting enzymes produced by pure-culture fermentation process may be safely used in the production of cheese in accordance with the following prescribed conditions.

(a) Milk-clotting enzyme is derived from one of the following organisms by a pure-culture fermentation process.

(1) *Endothia parasitica* classified as follows: class, Ascomycetes; order, Sphaeriales; family, Diaporthacese; genus, *Endothia*; species, *parasitica*.

(2) *Bacillus cereus* classified as follows: class, Schizomycetes; order, Eubacteriales; family, Bacillaceae; genus, *Baccillus*; species, *cereus* (Frankland and Frankland).

(3) *Mucor pusillus* Lindt classified as follows: class, Phycomycetes; subclass, Zygomycetes; order, Mucorales; family, Mucoraceae; genus, *Mucor*; species, *pusillus*; variety, *Lindt*.

(4) *Mucor miehei Cooney et Emerson* classified as follows: class, Phycomycetes; subclass, Zygomycetes; order, Mucorales; family, Mucoraceae; genus, *Mucor*, species, *miehei*; variety, *Cooney et Emerson*.

(5) *Aspergillus oryzae* modified by recombinant deoxyribonucleic acid (DNA) techniques to contain the gene coding for aspartic proteinase from *Rhizomucor miehei* var. *Cooney et Emerson* as defined in paragraph (a)(4) of this section, and classified as follows: class, Blastodeuteromycetes (Hyphomycetes); order, Phialidales (Moniliales); genus, *Aspergillus*; species, *oryzae*.

(b) The strains of organism identified by paragraph (a) of this section are nonpathogenic and nontoxic in man or other animals.

(c) The additive is produced by a process that completely removes the generating organism from the milk-clotting enzyme product.

(d) The additive is used in an amount not in excess of the minimum required to produce its intended effect in the production of those cheeses for which it is permitted by standards of identity established pursuant to section 401 of the Act [42 FR 14526, Mar. 15, 1977; 42 FR 56728, Oct. 14, 1977, as amended at 62 FR 59284, Nov. 3, 1997].

C. §184—Direct Food Substances Affirmed as Generally Recognized as Safe (GRAS)

(a) The direct human food ingredients listed in this part have been reviewed by the Food and Drug Administration and determined to be generally recognized as safe (GRAS) for the purposes and under the conditions prescribed. The regulations in this part shall sufficiently describe each ingredient to identify the characteristics of the ingredient that has been affirmed as GRAS and to differentiate it from other possible versions of the ingredient that have not been affirmed as GRAS. Ingredients affirmed as GRAS in this part are also GRAS as indirect human food ingredients, subject to any limitations prescribed in parts 174, 175, 176, 177, 178 or Sec. 179.45 of this chapter or in parts 186 of this chapter. The purity specifications in this part do not apply when the ingredient is used in indirect applications. However, when used in indirect applications, the ingredient must be of a purity suitable for its intended use in accordance with §170.30 (h) (1) of this chapter.

(b) Any ingredient affirmed as GRAS in this part shall be used in accordance with current good manufacturing practice. For the purpose of this part, current good manufacturing practice includes the requirements that a direct human food ingredient be of appropriate food grade; that it be prepared and handled as a good ingredient; and that the quantity of the ingredient added to food does not exceed the amount reasonably required to accomplish the intended physical, nutrition, or other technical effect in food.

(1) If the ingredient is affirmed as GRAS with no limitations on its conditions of use other than current good manufacturing practice, it shall be regarded as GRAS if its conditions of use are consistent with the requirements of paragraph (b), (c), and (d) of this section. When the Food and Drug Administration (FDA) determines that it is appropriate, the agency will describe one or more current good manufacturing practice conditions of use in the regulation that affirms the GRAS status of the ingredient. For example, when the safety of an ingredient has been evaluated on the basis of limited conditions of use, the agency will describe in the regulation that affirms the GRAS status of the ingredient, one or more of these limited conditions of use, which may include the category of food(s), the technical

effect(s) or functional use(s) of the ingredient, and the level(s) of use. If the ingredient is used under conditions that are significantly different from those described in the regulation, that use of the ingredient may not be GRAS. In such a case, a manufacturer may not rely on the regulation as authorizing that use but shall independently establish that that use is GRAS or shall use the ingredient in accordance with a food additive regulation. Persons seeking FDA approval of an independent determination that a use of an ingredient is GRAS may submit a GRAS petition in accordance with §170.35 of this chapter.

(2) If the ingredient is affirmed as GRAS with specific limitation(s), it shall be used in food only within such limitation(s), including the category of food(s), the functional use(s) of the ingredient, and the level(s) of use. Any use of such an ingredient not in full compliance with each such established limitation shall require a food additive regulation.

(3) If the ingredient is affirmed as GRAS for a specific use, without a general evaluation of use of the ingredient, other uses may also be GRAS.

(c) The listing of a food ingredient in this part does not authorize the use of such substance in a manner that may lead to deception of the consumer or to any other violation of the Federal Food, Drug, and Cosmetic Act (the Act).

(d) The listing of more than one ingredient to produce the same technological effect does not authorize use of a combination of two or more ingredients to accomplish the same technological effect in any one food at a combined level greater than the highest level permitted for one of the ingredients.

(e) If the Commissioner of Food and Drugs is aware of any prior sanction for use of an ingredient under conditions different from those proposed to be affirmed as GRAS, he will concurrently propose a separate regulation covering such use of the ingredient under part 181 of this chapter. If the Commission is unaware of any such applicable prior sanction, the proposed regulation will so state and will require any person who intends to assert or rely on such sanction to submit proof of its existence. Any regulation promulgated pursuant to this section constitutes a determination that excluded uses would result in adulteration of the food in violation of section 402, of the Act, and the failure of any person to come forward with proof of such an applicable prior sanction in response to the proposal will constitute a waiver of the right to assert or rely on such sanction at any later time. The notice will also constitute a proposal to establish a regulation under part 181 of this chapter, incorporating the same provisions, in the event that such a regulation is determined to be appropriate as a result of submission of proof of such an applicable prior sanction in response to the proposal.

(f) The label and labeling of the ingredient and any intermediate mix of the ingredient for use in finished food shall bear, in addition to the other labeling required by the Act:

(1) The name of the ingredient, except where exempted from such labeling in part 101 of this chapter.

(2) A statement of concentration of the ingredient in any intermediate mix; or other information to permit a food processor independently to determine that use of the ingredients will be in accordance with any limitations and good manufacturing practice guidelines prescribed.

(3) Adequate directions for use to provide a final food product that complies with any limitations prescribed for the ingredient(s) [42 FR 14653, Mar. 15, 1977, as amended at 42 FR 55205, Oct. 14, 1977; 48 FR 48457, 48459, Oct. 19, 1983; 62 FR 15110, Mar. 31, 1997].

1. List of Enzymes That Have Been Affirmed as Generally Recognized as Safe

Table 4 lists the enzymes that have been affirmed as generally recognized as safe (GRAS). Note that the list includes enzymes from animals, plants, and microorganisms. The affirmation of rennet and bovine rennet (both animal derived) and chymosin (fermentation derived from microorganisms containing the prochymosin gene) (Section §84.1685) has been chosen to indicate (a) requirements for animal rennet, (b) requirements for microbial chymosin, and (c) requirements for enzymes produced by genetically engineered microorganisms.

2. §184.1685–Rennet (Animal Derived) and Chymosin (Fermentation Derived) Preparation

(a)(1) Rennet and bovine rennet are commercial extracts containing the active enzyme rennin (CAS Ref. No. 9001-98-3), also known as chymosin (International Union of Biochemistry

Table 4 Enzymes Affirmed as Generally Recognized as Safe[a]

Subsection	Enzyme (or product)	Source (or Substrate)
§184.1012	α-Amylase	*Bacillus stearothermophilus*
§184.1024	Bromelain (peptide hydrolase)	Pineapple (*Ananas comosus* and *A. bracteatus* L.)
§184.1027	Mixed carbohydrase and protease	*Bacillus licheniformis*
§184.1034	Catalase	Bovine liver
§184.1148	α-Amylase and β-glucanase	*Bacillus subtilis* or *B. amyloliquefaciens*
§184.1150	Subtilisin and neutral proteinase	*Bacillus subtilis* or *B. amyloliquefaciens*
§184.1250	Cellulase	*Trichoderma longibrachiatum*
§184.1316	Ficin	Tropical fig trees
§184.1372	Immobilized glucose isomerase (high-fructose corn syrup)	*Streptomyces rubiginosus*[b]
§184.1387	Lactase	*Candida pseudotropicalis*
§184.1388	Lactase	*Kluyveromyces lactis*
§184.1415	Lipase	From forestomach or pancreas of calves, kids, or lambs
§184.1420	Lipase	*Rhizopus nireus*
§184.1583	Pancreatin	Porcine or bovine pancreas
§184.1585	Papain	Papaya (*Carica papaya* L.)
§184.1595	Pepsin	Hog stomach glandular layer
§184.1685	Rennet (animal derived)	Fourth stomach (abomasa) of calves, kids, or lambs
	Chymosin (fermentation derived)	*Escherichia coli* K-12, *Kluyveromyces marxianus* var. *lactis*, or *Aspergillus niger* van Teighem var. *awamori* (all the microorganisms contain the calf prochymosin gene)
§184.1914	Trypsin	Bovine pancreas
§184.1924	Urease	*Lactobacillus fermentum*
§184.1985	Aminopeptidase	*Lactococcus lactis*
§184.1063	Phospholipase A_2	Gives enzyme-modified lecithin (enzyme from bovine pancreatin)
§184.1287	Lipases from milk or milk powder	Fats
§184.1857	Acids or enzymes	Corn sugar (glucose)
§184.1859	Acids or enzymes	Invert sugar (glucose + fructose)
§184.1865	Acids or enzymes	Corn syrup
§184.1866	Glucose isomerase	High-fructose corn syrup

[a]From Code of Federal Regulations 21. Food and Drugs. Part 184, sub part B, published in the Federal Register, No. 21, pp 461–556, April 1, 2000.
[b]Other microorganisms approved as a source of glucose isomerase are *Actinoplanes missouriensis*, *S. olivaseus*, *S. olivochromogenes*, and *Bacillus coagulans*.

Enzyme Commission (E.C.3.4.23.4). Rennet is the aqueous extract prepared from cleaned, frozen, salted, or dried fourth stomachs (abomasa) of calves, kids, or lambs. Bovine rennet is the product from adults of the animals listed above. Both products are called rennet and are clear amber to dark brown liquid preparations or white to tan powders.

(2) Chymosin preparation is a clear solution containing the active enzyme chymosin (E.C. 3.4.23.4). It is derived, via fermentation, from a nonpathogenic and nontoxigenic strain of *Escherichia coli* K-12 containing the prochymosin gene. The prochymosin is isolated as an insoluble aggregate that is acid-treated to destroy residual cellular material and, after solubilization, is acid-treated to form chymosin. It must be processed with materials that are generally recognized as safe, or are food additives that have been approved by the Food and Drug Administration for this use.

(3) Chymosin preparation is a clear solution containing the active enzyme chymosin (E.C. 3.4.23.4). It is derived, via fermentation, from a nonpathogenic and nontoxigenic strain of *Kluyveromyces marxianus* variety of *lactis*, containing the prochymosin gene. The prochymosin is secreted by cells into fermentation broth and

converted to chymosin by acid treatment. All materials used in the processing and formulating of chymosin must be either generally recognized as safe (GRAS), or be food additives that have been approved by the Food and Drug Administration for this use.

(4) Chymosin preparation is a clear solution containing the active enzyme chymosin (E.C. 3.4.23.4). It is derived via fermentation, from a nonpathogenic and nontoxigenic strain of *Aspergillus niger* van Tieghem variety *awamori* Nakazawa); (Al-Musallam synonym A. *awamori* Nakasawa) containing the prochymosin gene. Chymosin is recovered from the fermentation broth after the acid treatment. All materials used in the processing and formulating of chymosin preparation must be either generally recognized as safe (GRAS) or be food additives that have been approved by the Food and Drug Administration for this use.

(b) Rennet and chymosin preparations meet the general and additional requirements for enzyme preparations of the ''Food Chemicals Codex,'' 3d Ed. (1981), pp. 107–110, which is incorporated by reference in accordance with 5 U.S.C. 552(a). Copies are available from the National Academy Press, 2101 Constitution Avenue NW., Washington, DC 20418, or are available for inspection at the Office of the Federal Register, 800 North Capitol Street, NW., Suite 700, Washington, D.C.

(c) In accordance with §184.1(b)(1), the ingredient is used in food with no limitation other than current good manufacturing practice. The affirmation of this ingredient as generally recognized as safe as a direct human food ingredient is based upon the following current good manufacturing practice conditions of use:

(1) The ingredient is used as an enzyme as defined in §170.03(o)(9) of this chapter; a processing aid as defined in §170.3(o)(24) of this chapter; and a stabilizer and thickener as defined in §170.3(o)(28) of this chapter.

(2) The ingredient is used in the following foods at levels not to exceed current good manufacturing practice: In cheeses as defined in §170.3(n)(5) of this chapter; frozen dairy desserts and mixes as defined in §170.3(n)(20) of this chapter; gelatins, puddings, and fillings as defined in §170.3(n)(22) of this chapter; and milk products as defined in §170.3(n)(31) of this chapter.

(d) Prior sanctions for this ingredient different from the uses established in this section do not exist or have been waived. [FR 10935, Mar. 23, 1990, as amended at 57 FR 6479, Feb. 25, 1992; 58 FR 27202, May 7, 1993].

It is important to specifically point out that FDA has included genetically engineered enzymes as GRAS as food additives, using the same criteria as used for nongenetically engineered sources of enzymes. Under Part 173, Secondary Direct Food Additives Permitted in Food for Human Consumption, Subpart B—Enzyme Preparations, FDA permitted the genetically derived milk-clotting enzyme from *Aspergillus oryzae* to be used (§173.150).

REFERENCES

1. PP Scott. Attitudes toward regulatory control of carcinogens in food. Chem Indust 3:83–86, 1979.
2. YH Hui. United States Food Laws, Regulations, and Standards. New York: John Wiley & Sons, 1979.
3. U.S. Congress, House Committee on Appropriations. Study of the Delaney and Other Anticancer Clauses. Washington: U.S. Government Printing Office, 1974.
4. JH Nelson. Enzyme producers, food processors, and the regulators. In: JP Danehy, B Wolnak, eds. Enzymes: The Interface Between Technology and Economics. New York: Marcel Dekker, 1980, pp 137–147.
5. DH Hickman. The role of government in regulating the commercial use of enzymes. In: JP Danehy, B Wolnak, eds. Enzymes: The Interface Between Technology and Economics. New York: Marcel Dekker, 1980, pp 149–160.
6. JF Roland. Regulation of food enzymes. Enzyme Microb Technol 3:105–110, 1981.
7. General Accounting Office Report to Congress. Need for more effective regulation of direct additives to food. HRD-80-90, 1980.
8. AG Ebert. Advice to the technologist developing food additives. Food Prod Dev 10(5):40, 44, 49, 1976.
9. K Aunstrup. Industrial approach to enzyme production. In: Z Bohak, N Sharon, eds. Biotechnological Applications of Proteins and Enzymes. New York: Academic Press, 1977, pp 39–49.
10. P Grasso. Methodology in assessing carcinogenic risk. Chem Indust 3:73–76, 1979.
11. Code of Federal Regulations. 21, Food and Drugs. Part 170 to 199. Revised as of April 1, 2000. Published by the Office of the Federal Register, National Archives and Records Administration, Washington, DC.

8

Properties of Extremophilic Enzymes and Their Importance in Food Science and Technology

Magnús M. Kristjánsson and Bjarni Ásgeirsson
University of Iceland, Reykjavik, Iceland

I. INTRODUCTION

Research during the last two decades has increasingly demonstrated that various microorganisms grow and live in environments that previously were considered unimagineable for the support of life. These habitats are characterized by extreme conditions with respect to temperature, pH, salinity, and pressure. At present the apparent limits for these biologically relevant physical parameters in the biosphere are –40°C to 115°C for temperature, pressures up to 120 MPa (corresponding to hydrostatic pressure in the deep sea), water activity (a_w) of ~0.6, (as in salt lakes), and pH values between 1 and 11 (1). In order to survive and to proliferate in such hostile environments, organisms had to adapt their metabolic and other cellular functions to the persisting extreme condition. Especially important is the adaptation of stability and activity of enzymes and other proteins that have to be optimized to function under the extreme conditions. As a result of the requirement for molecular adaption, the properties of proteins, especially enzymes, from extremophiles have been a subject of much interest both for basic studies in biology and chemistry, as well as for potential use as biocatalysts in industrial applications.

Since the discovery of Archaea as a new branch on the phylogenetic tree (2), the number and variety of explored extremophilic organisms have increased enormously, as well as research on the biochemical aspects of extremophilic adaptation. An understanding of the molecular principles involved in extremophilic adaptive strategies could also be of considerable commerical interest, as the same principles could be used for example in designing industrial processes involving biocatalysts that have to withstand extreme conditions with respect to temperature and pH. Given that there are constantly expanding sources of novel and unusually stable biocatalysts from extremophiles, the prospects of expanding the limits of biocatalysis in both novel, as well as in more conventional processes, could be realized (3). Enzymes with temperature optima ranging from close to the freezing point of water and to that in excess of its boiling point have been isolated, as well as enzymes that function in extreme salinity, over a wide range of pHs, pressures, and in essentially nonaqueous solvents (3).

High thermal stability is a highly desirable trait in many industrial enzymes, as processes involving enzymes are frequently carried out at high temperatures. There are some distinct advantages in running biotechnological processes at elevated temperatures. In fact, most such industrial processes are operated at temperatures > 50°C. Benefits of higher operating temperatures include decreased viscosity, increased diffusion rates, and solubility of most organic compounds, and thus an increase in reaction rates. Higher temperatures also reduce the risks of microbial contaminations in the enzyme reactors (4–6). For these reasons, enzymes from hyperthermophiles have received great attention, as these enzymes are generally found to be

very thermostable. This also makes them ideal experimental models for answering fundamental questions regarding the molecular basis for protein stability.

Enzymes from cold-adapted organisms, or psychrophiles, have gained increasing attention by researchers during the last several years, both as subjects of basic studies on molecular origins of cold-adaptation, and as potential industrial enzymes (7, 8). These enzymes are usually found to have higher specific activities at low temperatures than their counterparts from meso- and thermophiles. That property may be beneficial in several industrial applications, such as in the processing of sensitive biological materials, including foodstuffs, that have to be carried out under chilled or refrigerated conditions. Enzymes from cold-adapted organisms are usually found to be comparatively thermolabile, which may be beneficial in operations when enzyme treatment has to be terminated rapidly, without excessive treatment of the raw material (7).

The molecular basis for function and stability of proteins from organisms living at the extremes of temperature in the biosphere is still not well understood despite extensive research effort. However, understanding which structural principles direct extreme temperature adaptation of proteins are fundamental to our general understanding of their structural stability and function. Such information on structure–function relationships in these enzymes also forms the basis for their utilization as industrial biocatalysts under different, and perhaps novel, sets of conditions.

In this chapter we will attempt to give an overview of the current status of knowledge about enzymes that originate from organisms that are adapted to extremes of temperature.

II. EFFECT OF TEMPERATURE ON STABILITY AND FUNCTION OF ENZYMES

It is important to realize when considering temperature adaptation that the native conformations of proteins are only marginally more stable than their denatured states. Free energies of stabilization of native protein structures are typically of the order 20–80 kJ mol^{-1}, or what amounts to only a few weak intramolecular interactions (1, 9, 10). The net stabilization of a native protein is the result of a delicate balance between a relatively large stabilizing and destabilizing forces, the former being a combination of the hydrophobic effect, hydrogen bonding, electrostatic interactions, and van der Waals interactions gained through close packing in the protein core, and the latter arising mainly by the increase that occurs in conformational entrophy on unfolding of the polypeptide (11, 12).

As a result of this delicate balance only minor shifts in the contributions of any of these opposing forces can in principle significantly alter the stability of a protein. The small marginal stability of the native state, and the fact that these forces are cooperative and highly dependent on environmental conditions, such as temperature and solvent exposure, make the accounting of the contributions of these different forces to the stability of a protein a highly difficult task. Partially because of the uncertainty in the magnitude of these different interactions, the free energy of stabilization for a protein cannot be calculated, even if high-resolution crystal structure for the protein is available (1). Furthermore, such calculations based on atomic coordinates from crystal structures do not consider the dynamics of protein structures, a prerequisite for their function (1). Biologically active proteins such as enzymes are dynamic molecules and need a certain degree of structural flexibility for performing their function as biocatalysts (13–15).

It appears that during the evolutionary adaptation of proteins to different environmental temperatures, preserving function through optimization of flexibility of critical regions of the protein molecules has been a priority. Thus, optimizing a function of an enzyme under given temperature conditions is expected to involve a compromise between two apparently opposing structural factors, dynamic flexibility and stability (1, 9, 15). Enzymes that perform the same catalytic function but are adapted to different habitat temperatures, appear to have about the same conformational flexibility at their respective temperature optima (1, 13, 15). This would suggest that temperature-adaptive changes of proteins would tend to conserve and optimize the functional state of the proteins, such that they are in "corresponding states," with respect to functionally important motions, under the different physical conditions to which they have adapted (1, 9). This hypothesis suggests that in order to maintain such corresponding states for efficient biological function at low temperatures, cold-adapted enzymes must have adopted a higher degree of conformational flexibility (1, 15–18).

Enzymes from thermophiles, on the other hand, require very rigid and stable conformations that have to resist excessive thermal motions that lead to their denaturation, but that can maintain optimized flexibilibity ("corresponding states") with respect to function at elevated temperatures. That the activity of enzymes

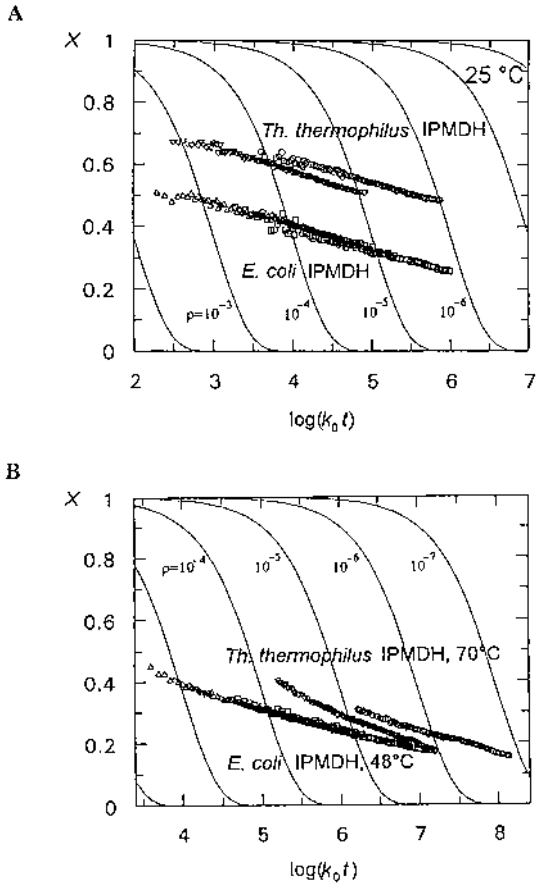

Figure 1 Hydrogen-deuterium exchange of 3-isopropylmalate dehydrogenase (IPMDH) from *E. coli*, measured at pD 7.15 (Δ) and pD 8.15 (□), and from *T. thermophilus*, at pD 7.15 (∇) and pD 8.15 (O), plotted as relaxation spectra. For experimental details see (15). (A) Measurements at 25°C for both enzymes. Increasing values of X reflect increased rigidity. Curves therefore indicate a more rigid structure for the thermophilic enzyme. (B) Measurements at the temperature optima of the enzymes: at 48°C for the *E. coli*, and at 70°C for the *T. thermophilus* IPMDH. Curves for the two enzymes show very similar flexibilities. (From Ref. 15. Copyright 1998 National Academy of Sciences, U.S.A.)

from thermophiles is greatly diminished at lower temperatures at which their mesophilic counterparts have optimal activity is a manifestation of the flexibility/function relationship, as it would imply that cooling would freeze out the molecular fluctuations at or around the active site of the enzyme that are necessary for its activity (19, 20). The role of optimized flexibility in temperature adaptation and the inverse relationship between protein stability and function have recently been supported both by results obtained in experiments where the temperature-dependent hydrogen–deuterium exchange kinetics of homologous mesophilic and thermophilic pairs of the enzymes 3-isopropylmalate dehydrogenase and glyceraldehyde phosphate dehydrogenase were compared (Fig. 1) (1, 15), and by theoretical model calculations (20). Hydrogen exchange experiments with the ultrathermostable protein rubredoxin, from the hyperthermophile *Pyrococcus furiosus*, however, did not lend support to the hypothesis that structural rigidity in the native state underlies the increased thermal stability of the protein (21). The reasons for the apparent contradictions in results obtained in these studies are not known, but have been commented on by Jaenicke (22).

On the basis of the proposed (and frequently observed) inverse correlation between enzyme stability and activity (14), much research effort has gone into explaining structural determinants of protein stability in order to gain insight into the molecular mechanisms that direct their temperature adaptation. While a global structural stabilization is essential for maintaining functional native states of thermophilic proteins at elevated temperatures, the fine adjustment of adaptive changes for activity may involve localized reversible conformational changes that would confer the necessary flexibility to critical parts of the protein molecules for function under given extreme conditions. Such local structural fluctuations within a protein structure have been defined as the microstability of proteins, as opposed to macrostability, that describes the ability of native confirmations of proteins to resist unfolding (denaturation) under given set of conditions (15). Making a distinction between micro- and macrostability of proteins may be necessary when attempting to explain the molecular origins of temperature adaptation. The noncooperative transitions that determine the microstability of a protein may occur on a different time scale and are not necessarily reflected in experiments that determine the cooperative unfolding/refolding transitions of protein molecules that define their macrostabilities.

In fact, Fields and Somero (18) found no correlation between denaturation rates and adaptation temperatures when comparing these parameters for cold-adapted orthologs of lactate dehydrogenase A4 from different fish species of Antarctic and South American origins. They suggested that increased cold activity in these orthologs involved increased flexibility in small areas of the molecule that affect mobility (hence microstability) of adjacent active site structures (18). Recent results for mutagenic studies have also shown that the stability of enzymes can be considerably increased con-

comitantly with significantly improved catalytic properties (23–25). This has not been observed, however, in enzymes from thermophiles, where lower catalytic efficiencies generally accompany higher thermal stabilities, as compared to the corresponding enzymes from mesophiles. Perhaps, the selective pressure set by the high-temperature environment imposes more restriction on the thermophilic enzymes to develop more stability at the expense of function, and are therefore not catalytically optimized enzymes, but are highly thermostable (19).

For enzymes from psychrophiles the selective pressure is probably more toward optimizing function which involves maintaining adequate molecular dynamics in spite of low thermal input from the cold habitat. This requires lowered microstability of the cold-adapted enzymes and may accompany, as is most often observed, decreased macrostability of the proteins, either as a structural consequence, or simply because it is not needed in the low-temperature environment (25).

III. THERMODYNAMIC ASPECTS OF TEMPERATURE ADAPTATION

The thermodynamic stability of a protein (that denatures in a reversible, two-state manner) as a function of temperature can be described by the modified Gibbs-Helmholtz equation (26):

$$\Delta G = \Delta H^\circ - T\Delta S^\circ + \Delta C_p[T - T^\circ - T\ln(T/T^\circ)] \quad (1)$$

where ΔC_p, the difference in heat capacity at constant pressure, is taken as a constant and is larger than zero. T° is any reference temperature (most often the melting temperature, T_m), and ΔS° and ΔH° are the changes in molar entropy and enthalpy evaluated at the reference temperature, respectively. The equation describes a parabolic curve for the temperature dependence of the free energy of unfolding (ΔG_u), defined by a slope, $\delta\Delta G/\delta T = -\Delta S$, and a curvature, $\delta^2\Delta G/\delta T^2 = -\Delta C_p/T$ (26). The curve predicts that proteins have maximum stabilities (ΔG_{max}) at a temperature T_{max}, when $\Delta S = 0$. The stability decreases on both sides of the maximum and intersects twice the x-axis (at $\Delta G = 0$), when the proteins undergo cold and heat denaturation, respectively (Fig. 2). Despite extensive research into the causes of thermal stability of (hyper-)thermophilic proteins, thermodynamic characterization in the form of protein stability curves are only available for relatively few thermophilic proteins. One major reason for this is that many thermophilic proteins, especially multidomain proteins, do not undergo reversible, two-state thermal denaturation. Competing side reactions occur, such as aggregations, that prevent proper refolding at the high temperatures at which these experiments are carried out (1).

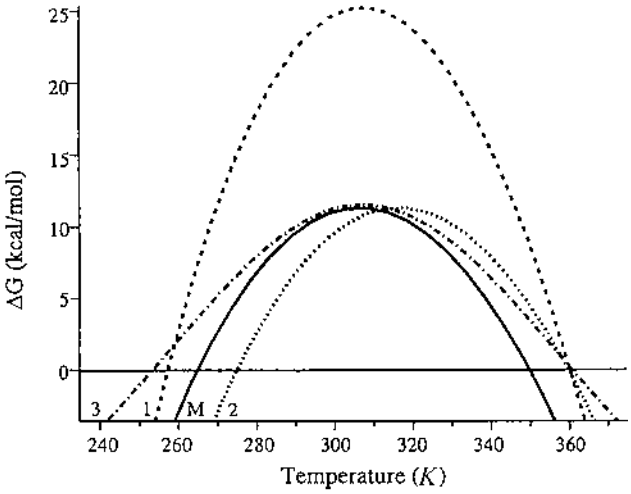

Figure 2 Three possible mechanisms for the temperature dependence of free energy of unfolding (ΔG_u) for a thermophilic protein. Curve M (solid) depicts the relation of ΔG_u and temperature (T) for a typical mesophilic protein. In curve 1 (dashed), the thermophilic protein is stabilized across the temperature range and has a greater maximum stability (mechanism 1). In curve 2 (dotted), the ΔG_u vs. T relationship is the same as for the mesophilic protein, but is shifted to a higher temperature (mechanism 2). In curve 3 (dash-dot-dash patterned), the ΔG_u of thermophilic protein depends less on T, and thus leads to flattening of the stability curve, shifting the melting temperature to higher values ($T = T_m$, when $\Delta G_u = 0$). (From Ref. 34. Copyright 1999 American Chemical Society.)

Recently, however, small, single-domain hyperthermostable proteins, which alleviate these experimental problems and fulfill the requirements for a two-state, reversible transition, have been used as models in such thermodynamic studies (27–35). More than two decades ago, Nojima et al. (36, 37) determined the thermodynamic parameters for denaturation of phosphoglycerate kinase and cytochrome c552 from the thermophile *Thermus thermophilus*, and compared them to those determined for their counterparts of mesophilic origin. From their studies they proposed three possible ways in which thermophilic proteins could thermodynamically adapt to increase their denaturation temperatures (Fig. 2). Compared to a mesophilic protein (curve M), the free energy of unfolding for the thermophilic protein could be increased over

the whole temperature range (curve 1); the stability curve (T_{max}) could be shifted to higher temperatures (curve 2); or the curve could be flattened (curve 3). In all cases the result would be to shift the melting temperature (T_m) of the thermophilic protein to a higher temperature.

In mechanism 1 the higher stability acquired would require higher absolute values for ΔH_u° and ΔS_u° at T_m than for the mesophilic protein. In the second mechanism the maximal values for ΔG_u°, ΔH_u°, and ΔS_u° would be of the same magnitude as for the mesophilic protein but would occur at different temperatures: i.e., at higher temperatures the thermophilic protein would be more stable, whereas the mesophilic protein would be more stable at lower temperatures (34). Mechanism 3 also predicts that the thermodynamic stability of the thermophilic protein would not be higher than of the mesophilic protein, but lower temperature dependence of ΔG_u° for the thermophilic protein, possibly because of lower entropy of unfolding, would lead to a flattened stability curve resulting in higher T_m values, as well as lower cold denaturation temperatures. From the relatively few cases available where the thermodynamic stability of thermophilic proteins has been characterized, it seems that mechanisms 1 and 3 most often prevail. For phosphoglycerate kinase, both from *Thermus thermophilus* and *Thermotoga maritima*, mechanisms 1 and 3 both seem to be at work in stabilizing the enzymes (36, 38), and the same seems to be the case for ribonuclease H from *T. thermophilus* (35) and ferredoxin from *T. maritima* (29).

Greater thermodynamic stability according to mechanism 1 was found to stabilize the catalytic domain of cellulase E2 from *Thermomonospora fusca* when compared to the analogous domain of cellulase CenA from the mesophile *Cellulomonas fimi* (34). The thermostability of the small DNA binding proteins Sso7d (27, 31) and Sac7d (28) from *Sulfolobus* spp. appear on the other hand to be enhanced by flattened stability curves in accordance with mechanism 3 (although data on corresponding mesophilic proteins were not provided in these studies). A lateral shift in T_{max} values to higher temperatures (mechanism 2), in concomitance with raised ΔG_u values, has also been observed in studies on thermal unfolding of cytochrome c552 from *T. thermophilus* (37) and with archaeal histones (32).

When considering protein thermal stability, it is important to observe that depending on the absolute values for the thermodynamic parameters (ΔH, ΔS, and ΔC_p), high T_m is not necessarily synonymous with larger maximum stability (39). This may be especially evident with small proteins that are unable to form a large hydrophobic core, and is reflected in low ΔC_p values (40). The small DNA-binding protein Sso7d (64 residues) from the hyperthermophilic archaeon *Sulfolobus solfataricus* has its T_{max} at 9°C with a stabilization free energy of only 7 kcal mol^{-1}, but still has a T_m of 98.9°C (at pH 5.5) (27, 31). At 80°C, or close to the optimal growth temperature of *S. solfataricus*, the protein has a marginal stability of only 2.8 kcal mol^{-1}. Similar stabilities have also been described for another related small DNA-binding protein, Sac7d from *S. acidocaldarius* (28). These proteins seem to be thermodynamically stabilized by mechanism 3 as discussed above. Since ΔC_p determines the curvature of stability curves [Eq. (1)], the small size of these proteins and the correspondingly low ΔC_ps (40), have the effect to create shallower protein stability curves, with broader ΔG maxima, that extend the T_m values to higher temperatures.

Among cold-adapted proteins only an α-amylase from the psychrophile *Alteromonas haloplanktis* has been characterized with respect to thermodynamic stability (41). The enzyme exhibits a reversible, two-state thermal unfolding with a melting temperature at 43.7°C, significantly lower than its mesophilic counterparts. The measured thermodynamic parameters were used to calculate a protein stability curve according to Eq. (1) for the enzyme, which is depicted in Figure 3, and compared to such curves for several small (< 18 kDa) proteins from meso- and thermophiles (including Sso7d and Sac7d). When the parameters were calculated and compared on per mol residue basis, to account for the different sizes of the proteins involved, it is clear that the cold-adapted enzyme is of much lower stability, characterized by lower absolute values for both enthalpy of unfolding and T_m (Fig. 3) (41).

The reverse of mechanism 1 above is apparently in effect in the cold adaptation of the enzyme, which is in line with the hypothesis that cold-adaptive mechanisms involve weakening of intramolecular interactions in order to increase flexibility (1). A most interesting feature of the stability curve for the psychrophilic enzyme, and what differs from meso- and thermophilic proteins, is that the physiological temperatures lie on different sides of T_{max} on the parabolic curve (Fig. 3). As both ΔS_u and ΔH_u change sign and become negative at or within few degrees below T_{max}, (26), low and high temperature adaptation may involve different adjustments in these thermodynamic parameters. As ΔH_u becomes negative on the "cold side" of the stability curve maximum, destabilization of the native protein occurs for enthalpic reasons, whereas it is stabilized by

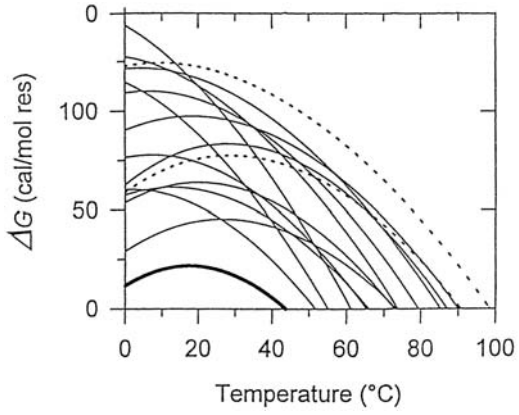

Figure 3 Protein stability curves for α-amylase from the Antarctic psychrophile *Alteromonas haloplanktis* (heavy lines), selected mesophilic proteins (continous lines), and of the thermophilic proteins Sac7d and Sso7d (dashed lines). The Gibbs free energy of denaturation is presented in specific units (per mole residue) in order to account for the different sizes of the proteins compared. By increasing order of T_m, the curves are for the proteins: psychrophilic α-amylase, T4 lysozyme, barnase, RNase T1, RNase A, spectrin SH3, barstar, phosphocarrier HPr, chymotrypsin inhibitor CI2, protein G IgG binding domain, ovomucoid third domain, thioredoxin, ubiquitin, and the thermophilic proteins Sac7d and Sso7d. (From Ref. 41. Copyright 1999 American Chemical Society.)

the negative $T\Delta S$ contribution as the temperature is lowered. At higher temperatures, entropic dissipative forces increase faster than favorable enthalpic contributions, and hence heat denaturation occurs (11).

As a result of the different thermodynamic forces involved, it is apparent that at the molecular level the causes of destabilization of native proteins to cold and heat denaturation may be quite different (42). Probably the main cause of cold denaturation is the weakening of the collective water–apolar repulsions that provide the main driving force for maintaining the folded structure under physiological conditions (42). Indeed, cold denaturation has been found to occur most readily with the most hydrophobic proteins (43, 44). An additional cause of cold destabilization of proteins is more favorable energetics of interactions of water with polar and ionic groups at low temperatures (42). In this respect favorable interactions of water with the polar peptide groups, largely buried in the native structure, but that come into contact with water on unfolding, seem to play a pivotal role (44). Thus, the fact that water increasingly becomes a good solvent for buried polar and apolar residues at low temperatures appears to be a major driving force for cold denaturation (44).

IV. MOLECULAR BASIS OF EXTREMOPHILIC TEMPERATURE ADAPTATION

It is clear from several studies that proteins from psychro- or thermophilic organisms do not exhibit any peculiarities with respect to composition, size, or complexities as compared to their counterparts adapted to moderate temperatures. They are composed of the same 20 natural amino acids and usually show high degree of sequence and structural homology with mesophilic proteins (1, 3, 31). Extremophilic adaptation is therefore an intrinsic property of the proteins, and the reasons for the striking differences observed both in stability and function at different temperatures are encoded in their gene sequences. A number of studies have therefore been carried out attempting to correlate different structural factors, at all levels of the structural hierarchy of the proteins, to differences in temperature-adaptive properties (mainly thermal stability) in comparative studies of homologous proteins from organisms isolated from different temperature habitats. By far the greatest number of such comparative studies have focused on proteins from thermo- and hyperthermophiles relative to their mesophilic counterparts in attempts to elucidate the molecular causes for their high thermal stability. In the following discussion we will attempt to summarize some of the pertinent observations made in such comparative studies on proteins from different temperature habitats.

A. Proteins from (Hyper-)thermophiles

Thermophilic organisms are conventionally classified as those having optimum growth temperatures $>60^{\circ}C$ and hyperthermophiles those with optimal growth $>80^{\circ}C$ (1, 19). While thermophiles are either bacteria or Archaea, most hyperthermophiles are Archaea (45). In earlier comparative studies on thermostabilization, attempts were made to correlate structural factors based on the content of certain amino acids and derived parameters such as hydrophobic and aliphatic indices (see 4 and reference therein for review), to thermal stability of relatively small number of meso- and thermophilic proteins.

Argos and coworkers (46) carried out the first systematic study on sequence comparison of homologous proteins from meso- and thermophiles and identified certain amino acid exchanges that occurred more frequently in going from the meso- to thermophilic representative within the three protein families they compared. The objective of these and other subsequent

studies, which have included more proteins in their database (47), has been to identify certain "traffic rules" used for thermostabilization of proteins in nature. The effect of the thermostabilizing amino acid exchanges identified in these studies showed a tendency toward increasing surface hydrophilicity, decreased flexibility, and increased hydrophobicity, mainly in α-helical regions of the proteins (46, 47). Critical evaluation of these early studies, however, showed that the data set used was too small to make predictions based on such compositional comparisons statistically significant (48).

Several recent studies, including extensive genomic comparisons of meso- and thermophiles, however, have pointed out certain trends in amino acid composition and exchanges that have correlated with temperature adaptation, some of which had also been observed in those earlier studies. These include higher content of charged amino acids, especially Arg and Glu in hyperthermophiles, often occurring concomitantly with lower content of polar uncharged amino acids (49–54). In a study where 115 protein sequences from the genome of the extreme thermophilic archaeon *Methanococcus jannaschii* were compared with their homologs from several mesophilic *Methanococcus* spp., the strongest correlation with thermophiles of observed amino acid exchanges was the decrease in the content of uncharged polar residues (Ser, Thr, Asn, and Gln), besides an increase in charged residues, increase in residue hydrophobicity, and increased residue volume (53). Nearly every other amino acid was preferred over polar uncharged amino acids in the thermophilic sequences.

A similar trend was observed in sequences deduced from the complete genome of the hyperthermophilic bacterium *Aquifex aeolicus* (50) and in a study where sequences of soluble proteins from complete genomes of eight thermophiles (including those of *M. jannaschii* and *A. aeolicus*) and 12 mesophiles (51). Moreover, Asn and Gln seem to be more discriminated against in proteins from hyperthermophiles, as compared to those from moderate thermophiles, while the decrease in Ser was apparently significant in moderate thermophiles (54). The trend to lower content of Asn and Gln likely reflects molecular adaptation in thermophilic proteins as it would tend to minimize deamidation, a reaction that may limit the thermal stability of the proteins as a result of irreversible denaturation (55, 56). A decrease in Cys, another thermolabile amino acid residue, has also been reported for thermophilic proteins when compared to their mesophilic counterparts, which may also be indicating an evolutionary pressure to reduce the number of residues that can cause irreversible thermal denaturation of the proteins (19, 52).

Some of the most frequent amino acid replacements that lead to a decrease in polar uncharged residues in the proteins of *Methanococcus jannaschii* contribute significantly to increased hydrophobicity (Ser $\rightarrow$ Ala, Thr $\rightarrow$ Ile, Ser $\rightarrow$ Pro, Thr $\rightarrow$ Val) (53). Moreover, most frequent nonpolar to nonpolar replacements (e.g., Leu $\rightarrow$ Ile, Gly $\rightarrow$ Ala, and Met $\rightarrow$ Leu) tended toward bulkier and more hydrophobic residues (53). The hydrophobic interaction has been emphasized as the major stabilizing force for the folded state of proteins (11, 12, 57). Strengthening of hydrophobic interactions and improved packing in the hydrophobic core have indeed been suggested to play an important stabilizing role in thermophilic proteins (31, 45, 49, 51, 53, 58, 59). In some other comparative studies, however, no significant correlations between hydrophobicity and thermophily have been observed (50, 52). Mutation studies have shown that increasing the bulkiness of buried nonpolar side chains, as discussed above, can significantly increase thermal stability of proteins (by $\sim$1.3 kcal mol^{-1} per $-CH_2-$ residue buried), by a direct hydrophobic effect and by reducing the size of cavities, and hence optimized core packing through, e.g., more favorable van der Waals interactions (60–64). Indeed, increased residue volume (53) and smaller cavities (54) have been found to correlate well with hyperthermophilic adaptation (see below).

The increased number of high-resolution crystal structures has allowed more direct structural comparisons, where three-dimensional structures of thermophilic proteins are being compared to corresponding structures of one or more of its mesophilic counterparts (65–83). More detailed structural data have also facilitated systematic studies where various structural parameters have been calculated on the basis of known crystal structures or computer generated homology models from related sequences, and compared within or across protein families (46–54, 59, 84–89). Querol *et al.* (58) have also surveyed the literature on studies reporting thermostabilizing mutations in several different proteins and analyzed the structural consequences of those stabilizing single amino acid replacements. They created a database comprising 195 single amino acid exchanges in 164 different positions in the proteins which had been unambigiously related to thermostability enhancement (58). The most cited physicochemical reasons for thermostabilization as observed in this survey are summarized in Table 1.

Table 1 Physicochemical Reasons for Enhanced Thermal Stability Resulting from Single Amino Acid Replacements in Several Different Enzymes as Cited in the Literature

Type	Number of citations
Better hydrogen bonding	18
Better hydrophobic internal packing	16
Enhanced secondary structure propensity	12
Helix dipole stabilization	10
Argos replacements	10
Removal of residues sensitive to oxidation or deamidation	10
Burying hydrophobic accessible area	7
Improved electrostatic interactions	6
Strengthening of intersubunit association	6
Decreased chain strain	5
Salt bridge optimization	4
Better van der Waals interactions	3
Better affinity for calcium	2
Improved ΔH upon substitution	1

Source: Ref. 58. (Copyright 1996 Oxford University Press.)

In line with these observations, Argos and coworkers (49, 85) found, when comparing several structural factors of meso- and thermophilic proteins from 16 families, that the parameter that most consistently correlated with increased thermal stability was a higher number of hydrogen bonds in the thermophilic proteins. An increase in the fractional polar surface area, reflecting added hydrogen bonding density to water, was also found to increase with the thermostability of the proteins compared (49, 85). In other extensive comparative studies of meso- and thermophilic protein structures, an increase in the number of residues involved in hydrogen bonding (51) and an increase in side chain–side chain hydrogen bonds (88) were found to correlate with thermostability. Additional hydrogen bonds have also been pointed out as a major stabilizing factor from comparisons of known crystal structures of meso- and thermophiles (70, 72, 77).

In a detailed comparative study of high-quality three-dimensional structures of 64 mesophilic and 29 thermophilic proteins (of which five were hyperthermophilic) representing 25 protein families, however, practically no difference between mesophiles and thermophiles was observed in the number of hydrogen bonds (54). There was, however, a tendency to decrease the number of unsatisfied hydrogen bond acceptors and donors as the temperature of adaptation increased. The authors attributed the discrepancy observed in their results as compared to those of Argos and coworkers (49, 85) to some bad-quality or incomplete crystal structures (five of which were mesophilic, but only one thermophilic) that had been included in the databases used in the former study that introduced a bias in the results. If these bad-quality structures had been omitted from the database used by Argos and coworkers, the observed difference in the number of hydrogen bonds between meso- and thermophilic proteins would have become insignificant (54).

Szilagyi and Zavodsky (54) calculated 13 properties in five categories (cavities, hydrogen bonds, ion pairs, secondary structure, and polarity of surfaces) from the coordinates for each of the proteins in the database, compared them using statistical methods, and correlated with optimal growth temperatures of organisms they originate from. On the basis of the optimal growth temperatures the proteins were divided into two groups; moderately thermophilic (T_{opt} = 45–80°C), and extremely thermophilic proteins ($T_{opt} \sim 100$°C). The findings of this comprehensive study are summarized in Table 2.

The most significant difference between mesophilic and thermophilic proteins was found in the number of ion pairs (salt bridges), a property that also correlated well with growth temperatures. In fact, several systematic comparative studies that have been described above (49, 51, 52, 59, 85, 88, 89), as well as comparisons of high-resolution three-dimensional structures of thermophilic and homlogous proteins (69, 72, 73, 75–77 79. 81, 90), have pointed to a prominent role of ion pairs in their stabilization, especially of hyperthermophilic proteins. The ion pairs often appear in the hyperthermophilic structures as clusters or networks at the surfaces or at interdomain interfaces in the proteins (Fig. 4). In some studies no correlation has been observed between the number of ion pairs, or ion pair networks, and stability of hyperthermophilic proteins (80, 88). Indeed, the role of ion pairs in protein stability has been controversial, as theoretical calculations have indicated that they may actually destabilize folded conformations of proteins, at least at room temperature (91).

The destabilizing effect of ion pairs or salt bridges arises primarily from desolvation penalty associated with bringing separated charged groups of the unfolded protein together to form an ion pair in the fully folded protein (92). The desolvation penalties are especially high when burying charged groups in the low dielectric environment of the hydrophobic core of proteins (52, 88, 92). Despite the favorable coulombic interaction that incurs by bringing oppositely charged

Table 2 A Summary of the Most Significant Differences Between Structural Parameters of Moderately Thermophilic and Extremely Thermophilic Proteins When Compared to Their Mesophilic Counterparts[a]

Property		Correlation with temperature	Change in moderately thermophilic proteins	Change in extremely thermophilic proteins
Cavities	Number	↓↓	0	↓↓↓
	Volume	↓	↑	↓
	Area	↓	↑	↓↓
Hydrogen bonds	Number	0	0	0
	Unsatisfied	↓	↓	↓
Ion pairs	<4.0 Å	↑↑	↑	↑↑↑
	<6.0 Å	↑↑	↑↑	↑↑↑
	<8.0 Å	↑↑↑	↑↑↑	↑↑↑
Secondary structure	α	0	↑	0
	β	↑	0	↑↑
	Irregular	↓	↓	↓
Polarity of surfaces	Exposed	↓↓	↑↑↑	0
	Buried	0	↑	↑

[a] Upward arrows refer to a positive value and downward arrow refer to a negative value for correlation with the structural parameter indicated; zeros refer to near-zero correlation values. The number of arrows (1, 2, or 3) shows whether the represented correlation is considered insignificant, moderately significant, or highly significant.
Source: Ref. 54. (Copyright 2000 Elsevier Science.)

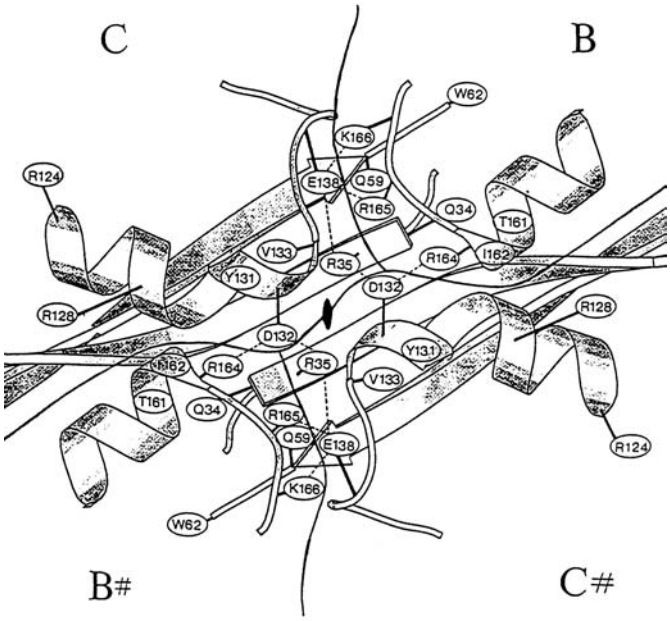

Figure 4 A schematic representation of an ion pair network cluster in glutamate dehydrogenase from *Pyrococcus furiosus*. The twofold axis relating to a CC# dimer is indicated by a diad. Potential ion pair interactions are indicated by dashed lines. The backbone of the polypeptide chain is shown as a gray ribbon. The individual amino acids are indicated by their one letter code, followed by their sequence number. (From Ref. 79. Copyright 1998 Blackwell Science Ltd.)

groups together in the folded state, it may not outweigh the unfavorable desolvation (free energy of hydration) cost. Elcock (92) has recently shown that at higher temperatures, the desolvation effect becomes less unfavorable, so ion pair formation would become increasingly favorable at higher temperatures and could provide a significant stabilization to hyperthermophilic proteins at elevated temperatures. It has also

been shown that the location of the ion pair within the protein structure, especially with respect to positioning of other ion pairs in its vicinity, is a critical determinant of the stability of these interactions, as they may in a cooperative manner facilitate the formation of ion pair networks (52, 88).

As mentioned earlier, extensive ion pair networks have been observed in three-dimensional structures of several hyperthermophilic proteins. Such cooperative electrostatic interactions offer simple means of enhancing stability without disrupting core residues, characteristics of different protein families (88). Such optimally located ion pair networks are therefore believed to be important stability determinants of proteins from hyperthermophiles.

A significant observation in the study of Szilágyi and Závodsky (54) was a decrease in the number of internal cavities in the structures of extemely thermophilic proteins, as compared to mesophilic and moderately thermophilic proteins (Table 2). A decrease in the number or the size of cavities leading to improved packing in the protein interior has also been observed in the structures of hyperthermophilic proteins (31, 67, 73, 93). However, in a study where the packing density of 80 nonhomologous proteins and 24 thermophilic ones was analyzed in context of their possible role in thermal stabilization, essentially no difference was observed in either partial specific volumes or cavity volumes in the two protein groups (86). Cavities created in the interior of proteins by use of site-directed mutagenesis have been shown to lead to significant destabilization (60–62). Creation of a cavity in barnase of the size of a $-CH_2-$ group (Ile96 $\rightarrow$Val) resulted in a destabilization of the enzyme of 1.1 kcal mol^{-1} and a cavity the size of three such groups (Ile96 $\rightarrow$ Ala) by 4.0 kcal mol^{-1} (60).

In a study of several cavity-creating mutants of T4 lysozyme, the destablization of a Leu $\rightarrow$Ala substitution amounted to a constant term, $\sim$2 kcal mol^{-1}, plus a term that increased in proportion to the size of the cavity produced by the substitution (61). The constant term is approximately equal to the transfer free energy of leucine relative to alanine as determined from their partitioning between aqueous and organic solvents (61). These results point to ways to stabilizing proteins against high temperatures, i.e., by filling cavities in their core with bulkier, more hydrophobic amino acids, leading to enhanced hydrophobic driving force and improved van der Waals contacts in the protein core. As discussed previously, amino acid replacements of this type have frequently been observed in comparative studies of mesophilic and thermophilic proteins, and optimized packing of side chains in the interiors, and the absence of cavities have been observed in crystal structures of hyperthermophilic citrate synthase (73) and lactate dehydrogenase (75).

Increasing structural compactness by decreasing cavities and increasing attractive interactions in the tightly packed protein core reflect a trend observed in structures of some hyperthermophilic proteins, i.e., to minimize their surface area-to-volume ratio (68, 72). Minimization of the ratio of surface area to volume can stabilize a protein by simultaneously reducing unfavorable surface energy and increasing the attractive interior packing interactions (68, 72, 75). Reduction of accessible surface area seems to be part of the molecular inventory that has been used in the high-temperature adaptation of hyperthermophilic proteins. At the quaternary structural level this is observed as higher states of subunit associations in oligomeric proteins from hyperthermophiles, e.g., triose phosphate isomerase (10, 71), phosphoribosyl anthranilate isomerase (76), ornithine carbamoyltransferase (78), enolase (10), and in the case of triose phosphate isomerase and phosphoglycerate kinase from *Thermotoga maritima* that are expressed as a "dimer of dimers" fusion protein (1, 10, 74). Minimizing hydrophobic surface area has also been suggested to be an important stabilizing principle in thermophilic lactate dehydrogenases (75).

Increased compactness of thermophilic proteins may also be accomplished through shortened surface loops (45, 70, 73, 74, 83, 87). Exposed surface loops and turns link successive core elements and are believed to be the regions of proteins where their unfolding begins (45, 87). Increasing the structural rigidity in such loops, either by shortening them or by stabilizing them by amino acid replacements (e.g., by increasing the number of prolines), could therefore significantly enhance protein stability (45, 87).

In some studies thermophilic proteins have also been found to be smaller than mesophilic counterparts (51, 87), reflecting truncation of loops, but also of N- and C-termini as has been observed for some thermophilic proteins (77, 80)). It has been pointed out that the apparently smaller size of thermophilic proteins may reflect a possible thermodynamical adaptive strategy of these proteins (51). As smaller proteins tend to have lower ΔC_p values of unfolding (40), the shape of the stability curve could be affected, as its curvature is determined by $\Delta C_p/T$ (see earlier). The net effect could therefore be to flatten the stability curve (Fig. 2), bringing the denaturation temperature to higher values (51).

B. Proteins from Psychrophiles

Many microorganisms and ectothermic animals live under environmental temperatures that fluctuate in the range $-2^{\circ}C$ to $10^{\circ}C$ without the opportunity to regulate their cellular temperature (94–96). The term cold-adaptation refers to the chemical and physiological mechanisms that make this possible (97, 98). Without adaptation, the chemical enzyme systems of cold-blooded animals and psychrophilic microorganisms would work too slowly. Enzymes from psychrophilic organisms (max. growth temperature at $20^{\circ}C$) or psychrotrophic organisms (max. growth temperature at $40^{\circ}C$) (6) are generally less stable structures than comparable enzymes from warm-blooded or thermophilic organisms (96). This is true for enzymes from as diverse species as bacteria (16) or fish (7, 98, 100). The need for increased "flexibility" is envisioned to call for fewer noncovalent intramolecular interactions as temperatures are lowered (16, 98, 100). This led to the concept of "corresponding states" of enzymes at the temperatures in which they find themselves in the various living forms on earth (97, 98). In recent years the study of cold adaptation of enzymes has expanded greatly. As more examples accumulate, however, few generalizations can be made as several strategies are used differently in individual cases. Here we will summarize kinetic and stability characteristics of cold-active enzymes and then give the general concepts used in an attempt to explain temperature adaptations in molecular terms. Several reviews on pyschrophilic enzymes have appeared recently (7, 16, 17, 96, 99, 101).

1. Enzyme Activity at Low Temperatures

As suggested earlier, the selective pressure for evolutionary adaptation of enzymes to low temperatures is probably geared more toward optimizing activity than stability, given that the kinetic properties are somehow related to the dynamic properties of the protein molecules. It is therefore of interest to examine how cold activity is expressed in terms of the kinetic parameters (Michaelis-Menten) for the enzymes. The final result of low temperature adaptation will surely be dependent on what properties the cold-adapted organism has to achieve from each enzyme; some extracellular enzymes presumably work at very low substrate concentrations and would benefit the organism by having low K_m values, whereas enzymes that work in abundant substrate could optimize the k_{cat} rate. Some restrictions may apply to lowering K_m values in order to increase catalytic efficiency under nonsaturating substrate conditions (k_{cat}/K_m), since for regulatory purposes most intracellular enzymes have K_m values approaching the physiological concentrations of their substrates (95). Then the rate of reaction will vary with oscillation in substrate concentration, which gives a way of controlling the reaction. Since temperature affects substrate affinity constants, cold-adapted enzymes are frequently found to have higher K_m values than mesophilic counterparts at common assay temperatures of $25^{\circ}C$ or $37^{\circ}C$.

At first sight, one might therefore expect orthologous enzymes from organisms with different temperature optima for their existence to have some obvious amino acid substitutions in their active sites. However, active-site residues are usually strictly conserved in psychrophilic enzymes (18, 102–105). This has put the focus for cold adaptation at the molecular level on the rather loose concept of "flexibility" in protein structure as a critical factor for improving catalytic efficiency. Indeed, changes in the amino acid sequence distant from the active site often seem to determine the outcome of temperature adaptation, making rational design for altered kinetic properties a much more difficult proposition than initially hoped for. Higher flexibility of an enzyme molecule should increase the available number of conformational states, and therefore the best conformations for ligand binding would become rarer than in a more rigid structure. Consequently, ligand binding would become poorer, with higher K_m values for substrates and higher K_i values for competitive inhibitors. Early studies established an inverse relationship within a group of homologous enzymes between the K_m value and the working temperature of individual enzymes (95). K_m values for enzymes from cold-adapted organisms were higher than for mesophiles, when the K_m values were determined at one common standard temperature (98). This is to be expected, since the evolution of maximal catalytic rate (high k_{cat}) can be predicted to be directed toward strong binding of the transition state and weak binding of the substrates in ground states—i.e., directing the trend toward higher K_m values (106).

As the goal is often to optimize k_{cat}/K_m, k_{cat} values must increase in psychrophilic enzymes (98, 101). This would have to occur by improving the rate-limiting step of the enzyme-catalyzed reaction under consideration, be it binding of substrates, the chemical conversion steps, or the release of products. The most common situation is a two- to fivefold increase in k_{cat}, with less prominent changes in K_m. There are, however, notable exceptions, such as in the case of

trypsins from trout, Atlantic cod, Atlantic salmon, and krill (100, 107–109). In those cases one isozyme showed 10- to 25-fold improvement in k_{cat}/K_m in comparison with bovine trypsin, that was to a large extent due to lowering of the K_m value to one-tenth the value measured for trypsin from the warm-blooded animal. Although small synthetic substrates have mostly been used in studies of many enzymes with natural polymeric substrates, being the only choice for K_m determinations, at least twofold increase in catalytic rate is also seen with natural substrates such as polypeptides (7, 110), or starch (111).

In an early study, the relative importance of the enthalpic and entropic contributions to the activation free energy of catalysis ($\Delta G^{\neq}$) was found to differ between enzymatic reactions of cold-adapted ectothermic enzymes and homologous enzymes of warm-blooded birds and mammals (112). The psychrophilic enzymes often have lower enthalpies of activation ($\Delta H^{\neq}$) and reactions are consequently less temperature driven. Furthermore, the entropic terms ($\Delta S^{\neq}$) with psychrophilic enzymes is less positive, which may indicate looser enzyme-substrate contacts, either to the ground-state *ES* complex and/or to the transition-state *ES** complex (101). As noted before, weaker net binding energy for substrate is one way to increase reaction rates in enzymes; i.e., most of the initial binding energy is offset against energetically costly preparative events, and this avoids a thermodynamic pit in front of the main energy transition curve (106). This includes events such as stopping the entropic movements of substrates present in solvent, removing hydration shells off substrates, and possibly juxtaposing charges of substrates against similar charges in the walls of the active site. Some of the catalytic power of enzymes is derived from their abilities to promote formation of reactive conformers of substrates that precede the transition state (113). Random thermal motions of the enzyme–substrate complex would eventually cause transformation of those conformers into transition states. These dynamic motions might be initiated at a distance from the active site. Although correlated motions appear to participate in catalysis, there is still little evidence as to how enzymes use such motions (113); therefore, the promotion of flexibility by amino acid substitutions in cold-adapted enzymes remains enigmatic.

k_{cat} values are expected to be higher for an enzyme isolated from organisms classified as psychrophilic, although there are exceptions. For aspartate aminotransferase from an Antarctic bacterium, k_{cat} was significantly lower than determined for the *E. coli* enzyme over a wide range of temperatures. The authors proposed that adaptation of this class of endocellular enzymes to cold environment might only have made them less stable and not more efficient (114), which is a rare outcome. Another interesting group of enzymes for consideration in the context of temperature adaptation are those which have reached the state of diffusion-controlled reaction rates, such as β-lactamase and triose phosphate isomerase (101). Such enzymes have optimized the activation energy hills throughout the reaction pathway to the extent that it is difficult to improve k_{cat} further when the organisms are challenged with low temperatures. The higher specific activity expected as a result of cold adaptation was not observed for beta-lactamase from the Antarctic psychrophilie *Psychrobacter immobilis*, although it was very thermolabile in comparison with a mesophile (115). As argued from directed evolution experiments (see below), there may be no evolutionary pressure for thermostability at low temperatures, and this last example would indicate that increasing global heat lability is not always sufficient for improving the catalytic efficiency at low temperatures (101, 115).

A kinetic comparison of three DNA ligases adapted to different temperatures (*Pseudoalteromonas haloplanktis, E. coli*, and *Thermus scotoductus*) indicated that an increase in k_{cat} is the most important adaptive parameter for enzymatic activity at low temperatures, whereas a decrease in K_m allowed *T. scotoductus* DNA ligase to work efficiently at high temperatures (116). K_m values of psychrophilic enzymes are indeed often higher compared with a matching mesophilic enzymes (101), although a number of exceptions exist. In the case of phosphoglycerate kinase from an Antarctic *Pseudomonas* sp., which notably is an intracellular metabolic enzyme, both an increase in k_{cat} and a decrease in K_m were observed. This double strategy, however, only increased catalytic efficiency twofold, compared with a mesophilic enzyme (117). For alkaline phosphatases from either a psychrophilic *Vibrio* bacterium or cold-adapted fish, faster product release (lower affinity for the phosphate reaction product) has been suggested as the underlying cause for greater catalytic rates (118, 119). The K_m values for the chosen substrate were identical in the former case and lower in the latter case, in comparisons with mesophilic enzymes. From these examples it becomes apparent that various strategies are employed in cold adaptation as reflected in K_m values, whereas k_{cat} is (nearly) always increased. The choice of substrates and/or reference mesophile may affect the outcome of such in vitro comparisons.

2. Relationship Between Cold Activity and Protein Stability

For cold-adapted enzymes, increased activity at low temperature is usually reflected in low thermal stabilities. This has been found by comparative studies of natural variants and further corroborated by site-directed mutagenesis experiments. However, it is very interesting that these two apparently interlinked phenomena can be decoupled (24, 120). Mutations have been produced that increase thermal stability while maintaining low-temperature activity (25). Although still rare, they bode well for possible development of biocatalysts for industral applications having both of those often desirable properties: high specific activity and thermal stability. Studies have shown that active-site residues may not be optimally chosen for stability as demonstrated by mutagenesis of T4 lysozyme (14), but rather have individual needs for movement, as reflected in the observation that inactivation of many enzymes precedes global conformational changes of unfolding (121). Thus, functional amino acids are likely optimized for a degree of flexibility that is appropriate for optimal effectiveness, while the rest of the protein molecule could maintain stability.

As in the case of thermophilic adaptation, there apparently are no set of "traffic rules" used for all cold-adapted proteins that are responsible for their lower conformational stabilities. By sequence comparisons researchers have attempted to spot the crucial substitutions that differentiate psychrophilic proteins from their meso- and thermophilic relatives, and lately also by tertiary structure comparisons of selected proteins. Reduced-temperature stability may not always result in improved catalytic properties, as mentioned above for aspartate aminotransferase from a psychrophilic bacterium. In contrast to the observations made with many (extracellular) psychrophilic enzymes, k_{cat} and k_{cat}/K_m were significantly lower than those for the *E. coli* enzyme over the whole temperature range, although the enzyme showed much reduced thermal stability compared with a similar enzyme from *E. coli* (114). The reduction in stability points to the fact that stability considerations may be disconnected from functional necessities and only become important as the molecule becomes too unstable for the temperature range of its operation. However, increasing the stability of a psychrophilic phosphoglycerate kinase led to drastically reduced turnover number, an indication of some link between these two properties (117).

An extensive comparison of trypsins from cold-blooded and warm-blooded animals was recently published (122). The digestive enzyme trypsin is among the most extensively studied proteins, and in this study 27 trypsin sequences were analyzed from a variety of organisms to find unique attributes. The amino acid compositions indicated a high number of charged (predominantly acidic groups) and polar residues, and fewer hydrophobic residues in the cold-adapted trypsins. All of the psychrophilic trypsins were anionic with calculated pIs of 5.5–6.6 (122). The main unique features of the cold-adapted trypsins attributable to low-temperature adaptation seemed to be: reduced hydrophobicity and packing density of the core, mainly because of a lower (Ile + Leu)/(Ile + Leu + Val) ratio; reduced stability of the C-terminal helix which cross-links to the other (N-terminal) domain; lack of one proline residue, which is conserved in temperature-stable trypsins; and a lack of one proline-plus-tyrosine stacking interaction. In addition, there was a difference in charge and flexibility of loops that extend from the substrate binding pocket, and a different conformation of the "autolysis" loop, which is likely to affect substrate binding (122).

Some of these factors have also been cited as possible structural determinants for cold adaptation in other studies. Thus, lower values of calculated hydrophobicity indices have repeatedly been observed in other studies for cold-adapted enzymes in comparison to mesophilic partners (100, 102, 111, 115, 123). For instance, the hydrophobicity index for psychrophilic bacterial α-amylase in comparison with porcine α-amylase was sharply decreased concomitantly with 25 substitutions out of the 84 residues that make up the central core in that enzyme (111). Exposure of nonpolar groups to the solvent may provide entropically driven destabilization of the protein, and hence increase the mobility within the structure. This was cited as a factor in α-amylase cold-adaptation (124). As the strength of the hydrophobic effect decreases as the temperature is lowered the cold-adapted proteins may rely less on hydrophobic interactions for stability than proteins that are adapted to higher temperatures. Reduced hydrophobicity may also protect psychrophilic proteins against cold denaturations, which may be caused in part by the diminished strength of hydrophobic interactions at low temperatures (125).

Comparisons of the relative numbers of hydrogen-bond forming residues indicate a lower proportion in some psychrophilic enzymes (102, 126). As an example, trypsin from an Antarctic fish displayed 20% less potential for hydrogen bonds than corresponding bovine trypsin (123). In the case of triose phosphate isomerase from the psychrophilic baterium *Vibrio mar-*

inus, a single amino acid substitution (Ser238→Ala), that eliminates two hydrogen bonds in a loop region of the molecule, could to a lartge extent account for the cold-adaptation of the enzyme with respect to catalytic activity and thermal stability (127).

Valuable information on the potential structural determinants of cold-adaptation has come from a few recent studies where three-dimensional crystal structures, or homology models for psychrophilic enzymes, have been compared to the corresponding structures from organisms adapted to higher temperatures. Based on such tertiary structural comparison, and corroborated with data from sequence comparisons, fewer salt bridges (111, 124, 128, 129), reduction in aromatic–aromatic interactions (11, 128, 129), extended surface loops (105, 128–130), fewer prolines in such loops (105, 115, 124, 129, 130), lower hydrophobicity (111, 115), weaker calcium bindings (104, 124, 128), improved solvent interactions through additional surface charges (105, 115, 128, 130), increased exposure of nonpolar groups to the solvent (105, 124), and reduced intersubunit ion pairs (105, 131) have all been cited as possible reasons for increased flexibility and/or decreased thermal stability of proteins from psychrophiles.

The first x-ray crystal structure of an enzyme from a cold-adapted ectothermic organism was that of salmon trypsin (102). It was followed by a structure of elastase from the same species (103) and other trypsin isozymes (132). Later, the structures of psychrophilic bacterial enzymes have been determined—those of α-amylase from *Alternomonas haloplanktis* that lives in Antarctic seawater (104), and citrate synthase from another Antarctic bacterium (105). More recently, a structure was solved for a malate dehydrogenase form a psychrophilic bacterium isolate from an Arctic sediment that grows optimally at 4°C (131).

Superposition of the α-amylase structure onto that of porcine pancreatic α-amylase showed that the 24 residues that form the binding subsites for substrate were strictly conserved. Therefore, the cause for increased catalytic efficiency had to be sought outside the catalytic center. For this enzyme, it was suggested that reduced number of salt bridges, fewer proline residues in loops, fewer arginine-mediated hydrogen bonds, and lower hydrophobicity in the core were all contributing. Also, less interdomain interactions were proposed as a determining factor for the conformational flexibility that allows efficient enzyme catalysis in cold environments (104). Structural comparison suggested that the major factors for the efficient catalytic activity of *A. arcticum* malate dehydrogenase at low temperatures were favorable surface charge distribution for substrate and cofactor binding, and reduced intersubunit ion pair interactions that increased relative flexibility of active site residues (131). The crystal structure of dimeric citrate synthase from an Antarctic bacterium revealed that the enzyme had much more accessible active site than thermophilic counterparts (105).

The surface electrostatic potential distribution was unusual, and an increased relative flexibility of the small domain compared to the large domain of the protein was noted within each monomer. Furthermore, reduced subunit interface interactions were found with no intersubunit ion pair networks, and loops were of increased length but carried fewer proline residues. Lastly, there was an increase in solvent-exposed hydrophobic residues and an increase in intramolecular ion pairs. In comparison, the thermal denaturation of hyperthermophilic dimeric citrate synthase appears to be resisted by complex networks of ion pairs at the dimer interface, a feature common to several other hyperthermophilic proteins as discussed previously. Catalytic efficiency of the cold-active citrate synthase appears to be achieved by a more accessible active site and by an increase in the relative flexibility of the small domain compared to the large domain in the enzyme (105).

Molecular modeling of various enzymes has given similar information as x-ray structures. Among features of a psychrophilic subtilisin S41 that might induce a more flexible and heat-labile conformation were four extended surface loops, a very hydrophilic surface (acidic pI of 5.3), and the lack of several salt bridges and aromatic interactions (128). The difference in the free energy of stabilization between subtilisin S41 and a mesophilic subtilisin was found to lie in the range 6–7 kJ/mol, suggesting that the balance of weak bonds is critical for the enzyme's flexibility.

Detailed model comparison of eight trypsin structures was made to seek explanations for the observed differences in properties seen with mesophilic and cold-adapted variants (132). Increased substrate affinity of the psychrophilic enzymes was traced to a lower electrostatic potential of the S1 substrate binding pocket, and the lack of five hydrogen bonds adjacent to the catalytic triad. Reduced stability of the cold-adapted trypsins might result from fewer interdomain bonds, including hydrogen bonds and salt bridges, as well as poorer packing in the core regions of the two domains.

A dimeric 3-isopropylmalate dehydrogenase that catalyzes the penultimate step in leucine biosynthesis was cloned from a psychrotrophic *Vibrio* sp., living in

Arctic seawater (129). The elements that were found to be destabilizing in this case were a smaller number of salt bridges, a reduction in aromatic interactions, fewer proline residues, and longer surface loops (129). The structural model of a psychrophilic phosphoglycerate kinase indicated the same key determinants of its low stability (117).

Some of the examples described above are of dimeric enzymes, where psychrophilic variants have reduced links between monomers. The formation of dimers, and higher multimers, has often the sole purpose of increasing stability (133), without linked effects on kinetic properties. This seems to be the case for several oligomeric enzymes from thermophiles, as we discussed earlier. Alkaline phosphatase from cold-adapted *Vibrio* bacteria is apparently monomeric (118, 134) and may thus be an example of the opposite trend, since the well-known enzyme from *E. coli*, another Gram-negative species, has a very heat-stable dimeric structure. This may be an example where pressure to form dimers was not present. Phosphoglycerate kinase is a monomeric enzyme, except in extremophilic archaea, where the enzyme has been found as a dimer or a tetramer (135, 136).

Subtle alterations in structure at dimer interfaces can produce enzymes with characteristics of being psychrophilic rather than mesophilic or thermophilic. Horse liver alcohol dehydrogenase contains two tryptophan residues per subunit, one on the surface of the catalytic domain and the second buried in the interface between the subunits of the dimer. After substituting the tryptophan at the interface with a leucine, and making two compensatory mutations that were required to obtain a stable protein, the turnover numbers for ethanol oxidation, acetaldehyde reduction, and the dissociation constants of the coenzymes increased by two- to sixfold (137). The three substitutions at the dimer interface apparently activated the enzyme by allowing more rapid conformational changes that accompany coenzyme binding, probably owing to movement of a loop. A subunit interface was also the site of a single amino acid substitution that brought different stabilities of temperature–K_m relationships to a related group of lactate dehydrogenases (95). Furthermore, many enzymes, although monomeric, can be viewed as aggregates of folding domains. Interdomain interactions could contribute to greater movement in cold-active enzymes, allowing more efficient enzyme catalysis in cold environments. In fact, fewer interdomain interactions were found in α-amylase from a psychrophilic bacterium than in porcine pancreatic amylase, which was likely a contributing factor to efficient catalysis in cold environments (124). Also, this type of adaptation has been given consideration in the case of Atlantic salmon trypsin, where the active site is divided on both sides of two relatively rigid β barrels (102). In contact regions near the catalytic residues, fewer hydrogen bonds were found in the salmon trypsin, and ion pairs might be important in the relative orientation of the two domains of the molecule, as well as contributing to greater stability of the bovine variant (102).

V. TEMPERATURE ADAPTATION BY SITE-DIRECTED MUTAGENESIS AND DIRECTED EVOLUTION

Evolution of a particular trait necessitates that a single base change can at times lead to a single amino acid substitution that brings about alterations in a protein's properties, which is beneficial to the host. Site-directed mutagenesis is therefore often employed in tandem with rational design ideas in order to understand the functioning of enzymes. Theories derived from the study of a three-dimensional model of a particular enzyme are utilized to select particular residues for mutation and predict the possible outcome. Thus, experiments with T4 lysozyme showed that even a single mutation in the hydrophobic core of an enzyme can have dramatic effects on stability (138). This may be informative, but it does not necessarily cover all the parts of the molecule that can affect its properties. Attention is often directed at the active-site region and at internal residues, whereas more distant residues may cause functional alterations, even those that reside on the outside surface of the molecule.

Studies using site-directed mutagenesis, however, have uncovered the fact that thermostability is not systematically inversely related to specific activity, one example being subtilisin excreted by an Antarctic *Bacillus* TA39 (139). The enzyme displays the usual characteristics of cold-active enzymes—i.e., a high catalytic efficiency at low temperatures and an increased thermosensitivity. The affinity for calcium is also almost 3 orders of magnitude lower than that of mesophilic subtilisins. An important stabilization of the molecular structure was achieved through a modification of one residue acting as a calcium ligand. The thermostability of the mutated product expressed in a mesophilic *Bacillus* reached that of mesophilic subtilisin, and this mutation further enhanced the specific

activity by a factor close to 2 when compared to the wild-type enzyme.

Single-base mutations do not cover a large fraction of protein sequence space since they often produce conservative substitutions. Another approach that increases nonconservative substitutions is that of directed evolution, where rapid screening procedures are combined with random mutagensis and *in vitro* recombination. Structural analysis of selected mutants can then bring about understanding of the observed phenotype, be it stability or catalytic activity, in terms of chemical function. The vast majority of possible evolutionary paths lead to poorer enzymes, so for successful directed evolution, the strategic challenge is to choose the right path that will eventually improve the desired features (140).

Recent examples can be found where the stability of enzymes from psychrophiles or mesophiles has been increased without effects on activity. A moderately stable thermolysin-like metalloprotease from *Bacillus stearothermophilus* was made hyperstable by a limited number of mutations. An eightfold mutant enzyme had a half-life of 2.8h at 100°C, but still displayed wild-type-like activity at 37°C (24, 141). Subtilisin E from a mesophilic *Bacillus subtilis* was converted into an enzyme functionally equivalent to its thermophilic counterparts by directed evolution (142). Subtilisin E differs from thermitase at 157 amino acid positions. However, only eight amino acid substitutions were sufficient to convert subtilisin E into an enzyme equally thermostable, a result from five generations of DNA alterations. Interestingly, the eight substitutions were distributed over the surface of the enzyme. Only two of those are found in thermitase. Also, thermostability could be increased without compromising enzyme activity (142).

In another study, thermoresistance was engineered into bacterial β-glucosidase by a directed-evolution strategy (143), whereas no significant alterations in kinetic parameters were observed. The main factors for increasing the thermostability were a combination of one extra salt bridge, replacement of a solvent-exposed asparagine residue, stabilization of the hydrophobic core, and stabilization of the quaternary structure. An earlier study used *in vitro* evolution to probe the relationship between stability and activity in a mesophilic esterase. Six generations of random mutagenesis, recombination, and screening, stabilized *Bacillus subtilis p*-nitrobenzyl esterase significantly without compromising its catalytic activity at lower temperatures. It was also found that mutations that increased thermostability, while maintaining low-temperature activity, were very rare. The results suggested that stability at high temperatures was not incompatible with high catalytic activity at low temperatures because of perceived mutually exclusive demands on enzyme flexibility (144).

Low-temperature activity can also be generated by mutations. It was possible to improve catalytic activity at 37°C of a thermophilic enzyme with a single or double amino acid substitution. DNA shuffling was used to mutate indoleglycerol phosphate synthase from the hyperthermophile *Sulfolobus solfataricus* (145). The parental enzyme's turnover number at room temperature was limited by the dissociation of the enzyme–product complex, apparently because the loops that obstruct the active site were not flexible enough at low temperatures. In the variants, the binding and release of product was much more rapid, and this shifted the rate-determining step to a preceding chemical step (145). Similarly, multiple random mutants of β-glucosidase from the hyperthermophile *Pyrococcus furiosus* were screened for increased activity at room temperature (146). Multiple variants were identified with up to threefold increased rates of substrate hydrolysis. Amino acid substitutions were widespread, occurring in the active-site region, at the enzyme surface, buried in the interior of the monomers, and at subunits interfaces. Interestingly, low-temperature activity was achieved in different ways, by altering substrate specificity or by overall destabilization of the enzyme. Single amino acid substitutions were sufficient to drastically alter the kinetic properties, as would be expected, if evolutionary processes are to work. The enzyme was able to accommodate in its interior amino acids with larger or smaller side chains, and with different properties without affecting thermostability. Substrate specificity was also determined by substitutions distant to the active site.

The stability of enzymes from psychrophiles can also be increased without reducing activity (25). The psychrophilic protease subtilisin S41 was subjected to two different selection pressures. The evolved subtilisin S41 retained its psychrophilic character as a catalyst in spite of its dramatically increased thermostability. These results demonstrated that it is possible to increase activity at low temperatures and stability at high temperatures simultaneously. It was concluded that the fact that enzymes displaying both properties are not found in nature, most likely reflects the effects of evolution rather than any intrinsic physico-chemical limitations on proteins (25). However, the dependence of slower thermal inactivation on calcium concentration indicated that enhanced calcium

binding was largely responsible for the increased stability.

Few studies are to be found where the kinetic characteristics of a psychrophilic enzyme have been produced by directed evolutionary methodology. A cold-adapted subtilisin has been generated by evolutionary based sequential methodology. Cold-adaptation was achieved with three mutations, and it was found that an increase in substrate affinity (i.e., decreased K_m value) was mostly responsible for the observed doubling in catalytic efficiency at 10°C (147).

This section has shown that single-residue substitutions can affect stability of enzymes considerably and influence kinetic properties. However, it may be generally a fact that more than one substitution is required to realize the full potential for temperature adaptation in an enzyme.

VI. TEMPERATURE EXTREMOPHILES AS SOURCES FOR BIOCATALYSTS FOR THE FOOD INDUSTRY

A. Thermophilic Enzymes

As mentioned earlier, it is generally advantageous to run industrial processes at elevated temperatures, as long as sensitive components in the reaction are not damaged under such conditions. It is therefore not surprising that many of the biotechnological processes involving enzymes are carried out at relatively high temperatures, and most of the enzymes used are quite thermostable, despite them being usually of mesophilic origin (148). A useful industrial enzyme must have several specific properties depending on the particular application, but thermostability is usually an absolute necessity (148). Despite the potential benefits that may be achieved by using more thermostable enzymes in several of these processes, the industrial uses of thermophilic enzymes are still very limited (19). In some industrial sectors (including the food industry), which use ''bulk'' industrial enzymes, cost is the major issue, as introducing a new enzyme is worthwhile only if the cost improvement provided by the new enzyme justifies the research and development costs as well as the required changes to production equipment (19).

Some successful biotechnological applications of thermophilic enzymes have already been developed and implemented. At present, by far the most important large-scale application of thermophilic enzymes is in the use of DNA polymerases in the polymerase chain reaction (PCR). The most commonly used enzyme in these applications is the so-called *Taq* polymerase from *Thermus aquaticus*, but several other DNA polymerases from other thermo- or hyperthermophilic bacteria and Archaea have been characterized and are commercially available (6, 149).

Improved thermal stability is a highly desirable property for the enzymes (α-amylase, glucoamylase, pullulanase, glucose isomerase) that are used in the commercial processing of starch to glucose and fructose in the production of high-fructose corn syrup. In this process the starch is typically gelatinized at 105°C for 5 min and then α-amylase is used at 95°C and pH 6–6.5 to partially cleave the α1-4-glycosidic linkages in the interior of the polymer, leading to liquefaction of the starch. For the second (saccharification) step, the temperature must be lowered to 60–62°C and the pH to 4.5, to adjust to the stability and the pH optimum of the exo-acting glucoamylase and pullulanase that further cleave the chain to smaller saccharides (95–96% glucose in glucose syrups) (6, 19, 150). In the final step the concentrated glucose syrup is again pH adjusted to 7–8.5, and is passed through a column with immobilized glucose isomerase (xylose isomerase) at 55–65°C, which converts it preferably to 55% fructose (150). The limited thermal stability of the currently used glucose isomerases determines the moderate temperatures used in this process (19).

The use of more thermostable enzymes which are active under similar temperature and pH conditions could significantly improve the starch conversion process, as it would be possible to run the liquefaction and saccharification process in one step (19, 31). Finding thermostable enzymes with similar pH characteristics (activity and stability) would also reduce costs in the process as the use of ion exchanger step could be avoided, but that is necessary to carry out to remove salts that accumulate as a result of the pH adjustments between different steps. In this respect hyperthermophilic α-amylases with lower pH optima are promising candidates (6, 151).

Studies have also shown that isomerization of glucose to fructose can be improved considerably by running this step at elevated temperatures (150). A search for more thermostable glucoamylases (or α-glucosidases), pullulanases, and glucose isomerases from hyperthermophilic Archaea and bacteria is now actively being pursued with the goal of finding enzymes with more desirable properties in the starch conversion process (see 6, 19, 31, for review). Furthermore, protein engineering has increasingly been used to improve thermal stability (152, 153), or catalytic properties (154) of glucose isomerases.

Mutant enzymes obtained with protein engineering techniques may prove to be important candidates for future industrial applications, in these and other processes.

Cyclodextrins are useful in the food industry in specific separation processes, in flavor stabilization, and in controlled release and exclusion of unwanted compounds from the bulk phase (155). They are nonreducing cyclic products of six to eight glucose units. At the industrial level they are made from starch that first is liquefied at high temperature by a thermostable α-amylase, followed by transglycosylation reaction leading to the cyclized product, a reaction catalyzed by cyclodextrin glycosyl transferase (CGTase) (6, 19). The mesophilic CTGases that are conventionally used in the process are heat-labile and the second step in the process must be run at lower temperatures. Using a thermostable CGTase would greatly improve the process, as liquefaction and cyclization could be carried out in one step (6, 19).

Several proteases from thermophiles and hyperthermophiles have been characterized (19, 48). The major large-scale use of proteases as industrial enzymes is in the detergent industry, as additives in household detergents, with alkaline serine proteinases from mesophilic *Bacillus* species (subtilisins) as the main enzymes. These enzymes are generally quite stable at moderately high temperatures (60–65°C) and under alkaline conditions (pH 9–11) (148). A number of subtilisin-like serine proteinases from extreme thermophiles have been characterized (see, e.g., 156–158) that would be expected to have properties more optimized for detergent applications, but that have not been used for that purpose. A major reason is that changing the large bulk production lines for the present detergent proteases for the more thermophilic enzymes may not be cost-effective at present.

An advantage of doing proteolysis at high temperatures is that the protein substrates are denatured, which makes them generally more accessible to proteolytic attack than when in their native states. This may be particularly important when hydrolyzing difficult proteinaceous waste materials (148). Because of their high thermal activity and stability under conditions that denature most other proteins, thermophilic proteases are good candidates for applications aimed at utilizing different protein waste materials for making protein hydrolyzates for different purposes. High-temperature treatment of such waste materials would also contribute to maintaining aseptic conditions and to prevent the growth of spoilage bacteria and pathogens during processing.

Proteases have increasingly been used in peptide synthesis, where advantage is taken of their reverse reaction under modified solvent conditions. Studies have shown that peptide synthesis is favored under controlled conditions at higher temperatures. It has therefore been suggested that, owing to their optimal activity at high temperatures and higher resistance to organic solvents than their mesophilic counterparts, thermophilic proteases should prove excellent candidates for enzymatic peptide synthesis (19). Indeed, the use of the thermophilic neutral metalloprotease thermolysin for the synthesis of the artifical sweetener aspartame (a dipeptide) has been developed into a large-scale application, and is currently the only industrial application that uses a thermophilic protease (19, 148).

B. Psychrophilic Enzymes

Depsite the fact that stability is a major criterion for the industrial application of enzymes, the use of psychrophilic enzymes in selected instances may offer advantages. Examples of the real usage of such enzymes in an industrial setting are very rare, although ideas as to the potential application of cold-active enzymes have been around for the past two decades (5, 8, 99, 159). The main advantages seen for cold-active enzymes are twofold: high activity at low temperatures, which may reduce energy consumption, and easy inactivation through moderate heating or low-pH treatment. Low processing temperatures might also work toward reducing bacterial contamination (5). Potential uses range from the use of cold-active enzymes in the detergent industry for washing or disinfecting at low temperatures (amylases, lipases, and proteinases), to various applications in food industries. Examples relating to milk processing include lactose hydrolysis by β-galactosidase, or the use of proteases to coagulate milk and accelerate cheese maturing. Also, cold-active enzymes may become useful in specific biotransformations, such as the production of oils with high polyunsaturated fatty acid content, and in whole organisms for environmental cleaning, where temperatures are generally low (e.g., removal of heavy metals or toxic materials from aqueous effluents). More specialized uses include addition to contact lens cleaning fluids, and the potential use of ice-nucleating proteins in the manufacture of ice cream or artifical snow (5, 99).

Some other examples relating to food production have been considered in the fishing industries of North Atlantic coastal nations, but large-scale use is still in its infancy (159–162). Examples where cold-

active enzymes have found use as processing aids include caviar productions (i.e., releasing roe from roe sacks), the deskinning of fish fillets or squid mantle, and the removal of membranes from cod liver or swim bladder. In some instances the task has proven virtually impossible by manual or mechanical means, thus augmenting the value of the enzymatic process. Development of several other technical processes has been a success at a laboratory scale, but not found widespread use in demanding industral environments. Also, a dependable source of speciality enzymes (i.e., cold-active enzymes) in bulk has not been there and they are still costly. Large-scale fish processing that will depend on biotechnology may still be a long way in the future.

Besides being useful for industrial application, enzymes from extremophiles have applications as fine chemicals for research laboratories. Cold-active alkaline phosphatase from shrimp (163), for example, is preferred to more heat-stable variants in DNA work, and DNA ligase from *P. haloplanktis*, which is very efficient at low temperatures, may offer a novel tool for biotechnology (116). As mentioned for thermophilic enzymes, the psychrophilic enzymes may also be well suited for biocatalysis in organic media, an emerging field of possible application (164).

REFERENCES

1. R Jaenicke, G Böhm. The stability of proteins in extreme environments. Structure 8:738–748, 1998.
2. CR Woese. Bacterial evolution. Microbiol Rev 51: 221–271, 1987.
3. MWW Adams, FB Perler, RM Kelly. Extremozymes: expanding the limits of biocatalysis. Biotechnology 13:662–668, 1995.
4. MM Kristjánsson, JE Kinsella. Protein and enzyme stability: thermodynamic and experimental aspects. Adv Food Nutr Res 35:237–316, 1991.
5. RA Herbert. A perspective on the biotechnological potential of extremophiles. TIBTECH 10:395–402, 1992.
6. F Niehaus, C Bertoldo, M Kahler, G Antranikian. Extremophiles as a source of novel enzymes for industrial applications. Appl Microbiol Biotechnol 51:711–729, 1999.
7. MM Kristjánsson, B Ásgeirsson, JB Bjarnason. Serine proteinases from cold-adapted organisms. In: S. Damodaran, ed. Food Proteins and Lipids. New York: Plenum Publishing Corporation, 1997, pp 27–46.
8. C Gerday, M Aittaleb, M Bentahir, JP Chessa, P Claverie, T Collins, S D'Amico, J Dumont, G Garsoux, D Georlette, A Hoyoux, T Lonhienne, MA Meuwis, G Feller. Cold-adapted enzymes: from fundamentals to biotechnology. Trends Biotechnol 18:103–107, 2000.
9. R Jaenicke. Protein stability and molecular adaptation to extreme conditions. Eur J Biochem 202:715–728, 1991
10. R Jaenicke, H Schurig, N Beaucamp, R Ostendorp. Structure and stability of hyperthermostable proteins: glycolytic enzymes from hyperthermophilic bacterium *Thermotoga maritima*. Adv Protein Chem 48:181–269, 1996.
11. KA Dill. Dominant forces in protein folding. Biochemistry 29:7133–7155, 1990.
12. B Honig, A-S Yang. Free energy balance in protein folding. Adv Protein Chem 46:27–58, 1995.
13. M Vihinen. Relationship of protein flexibility to thermostability. Protein Eng 1:477–480, 1987.
14. B Shoichet, WA Baase, R Kuroki, BW Matthews. A relationship between protein stability and protein function. Proc Natl Acad Sci USA 92:452–456, 1995.
15. P Závodsky, J Kardos, A Svingor, GA Petsko. Adjustment of conformational flexibility is a key event in the thermal adaptation of proteins. Proc Natl Acad Sci USA 95:7406–7411, 1998.
16. G Feller, E Narinx, JL Arpigny, M Aittaleb, E Baise, S Genicot, C Gerday. Enzymes from psychrophilic organisms. FEMS Microbiol Lett 18:189–202, 1996.
17. C Gerday, M Aittaleb, JL Arpigny, E Baise, JP Chessa, G Garsoux, I Petrescu, G Feller. Psychrophilic enzymes: a thermodynamic challenge. Biochim Biophys Acta 1342:119–131, 1997.
18. PA Fields, GN Somero. Hot spots in cold adaptation: localized increases in conformational flexibility in lactate dehydrogenase A_4 orthologs of antarctic notothenioid fishes. Proc Natl Acad Sci USA 95:11476–11481, 1998.
19. C Vielle, DS Burdette, JG Zeikus. Thermozymes. Biotechnol Annu Rev 2:1–83, 1996.
20. KES Tang, KA Dill. Native protein fluctuations: the conformational-motion temperature and the correlation of protein flexibility with protein stability. Biomol Struct Dynamics 16:397–411, 1998.
21. G Hernández, FE Jenney Jr, MWW Adams, DM LeMaster. Millisecond time scale conformational flexibility in a hyperthermophile protein at ambient temperature. Proc Natl Acad Sci USA 97:3166–3170, 2000.
22. R Jaenicke. Do ultrastable proteins from hyperthermophiles have high or low conformational rigidity? Proc Natl Acad Sci USA 97:2962–2964, 2000.
23. P Shih, JF Kirsch. Design and structural analysis of an engineered thermostable chicken lysozyme. Protein Sci 4:2063–2072, 1995.
24. B Van den Burg, G Vriend, OR Veltman, G Venema, VGH Eijsink. Engineering an enzyme to resist

boiling. Proc Natl Acad Sci USA 95:2056–2060, 1998.
25. K Miyazaki, PL Wintrode, RA Grayling, DN Rubingh, FH Arnold. Directed evolution study of temperature adaptation in a psychrophilic enzyme. J Mol Biol 297:1015–1026, 2000.
26. WJ Becktel, JA Schellman. Protein stability curves. Biopolymers 26:1859–1877, 1987.
27. S Knapp, A Karshikoff, KD Berndt, P Christova, B Atanasov, R Ladenstein, Thermal unfolding of the DNA-binding protein Sso7d from the hyperthermophile *Sulfolobus solfataricus*. J Mol Biol 264:1132–1144, 1996.
28. BS McCrary, SP Edmondson, JW Shriver. Hyperthermophile protein folding thermodynamics: differential scanning calorimetry and chemical denaturation of Sac7d. J Mol Biol 264:784–805, 1996.
29. W Pfeil, U Gesierich, GR Kleeman, R Sterner. Ferredoxin from the hyperthermophile *Thermotoga maritima* is stable beyond the boiling point of water. J Mol Biol 272:591–596, 1997.
30. F Catanzano, G Graziano, P Fusi, P Tortora, G Barone. Differential scanning calorimetry study of the thermodynamic stability of some mutants of Sso7d from *Sulfolobus solfataricus*. Biochemistry 37:10493–10498, 1998.
31. R Ladenstein, G Antranikian. Proteins from hyperthermophiles: stability and enzymatic catalysis close to boiling point of water. Adv Biochem Eng Biotechnol 61:37–85, 1998.
32. W-T Li, RA Grayling, K Sandman, S Edmondson, JW Shriver, JN Reeve. Thermodynamic stability of archaeal histones. Biochemistry 37:10563–10572, 1998.
33. D Wassenberg, C Welker, R Jaenicke. Thermodynamics of the unfolding of the cold-shock protein from *Thermotoga maritima*. J Mol Biol 289:187–193, 1999.
34. BM Beadle, WA Baase, DB Wilson, NR Gilkes, BK Shoichet. Comparing the thermodynamic stabilities of a related thermophilic and mesophilic enzyme. Biochemistry 38:2570–2576, 1999.
35. J Hollien, S Marqusee. A thermodynamic comparison of mesophilic and thermophilic ribonucleases H. Biochemistry 38:3831–3836, 1999.
36. H Nojima, A Ikai, T Oshima, H Noda. Reversible thermal unfolding of thermostable phosphoglycerate kinase. Thermostability associated with mean zero enthalpy change. J Mol Biol 116:429–442, 1977.
37. H Nojima, K Hon-nami, T Oshima, H Noda. Reversible thermal unfolding of thermostable cytochrome c-552. J Mol Biol 122:33–42, 1978.
38. M Grattinger, A Dankesreiter, H Schurig, R Jaenicke. Recombinant phosphoglycerate kinase from the hyperthermophilic bacterium *Thermotoga maritima*: catalytic, spectral and thermodynamic properties. J Mol Biol 280:525–533, 1998.
39. R Ragone, G Colonna. Do globular proteins require some structural peculiarities to best function at high temperatures? J Am Chem Soc 117:16–20, 1995.
40. JM Myers, CN Pace, JM Scholtz. Denaturant m values and heat capacity changes: relation to changes in accessible surface areas of protein unfolding. Protein Sci 4:2138–2149, 1995.
41. G Feller, D d'Amico, C Gerday. Thermodynamic stability of cold-active α-amylase from the Antarctic bacterium *Alteromonas haloplanctis*. Biochemistry 38:4613–4619, 1999.
42. F Franks. Protein destabilization at low temperatures. Adv Protein Chem 46:105–139, 1995.
43. TE Creighton. Stability of folded conformations. Curr Opin Struct Biol 1:5–16, 1991.
44. G Graziano, F Catanzano, A Riccio, G Barone. A reassessment of the molecular origin of cold denaturation. J Biochem 122:395–401, 1997.
45. C Vielle, JG Zeikus. Thermozymes: identifying molecular determinants of protein structural and functional stability. TIBTECH 14:183–190, 1996.
46. P Argos, MG Rossmann, UM Grau, H Zuber, G Frank, JD Tratschin. Thermal stability and protein structure. Biochemistry 18:5698–5709, 1979.
47. L Mendez-Arias, P Argos. Engineering protein thermal stability. Sequence statistics point to residue substitutions in α-helices. J Mol Biol 206:397–406, 1991.
48. G Böhm, R Jaenicke. Relevance of sequence statistics for the properties of extremophilic proteins. Int J Peptide Protein Res 43:97–106, 1994.
49. G Vogt, P Argos. Protein thermal stability: hydrogen bonds or internal packing. Folding Design 2:S40–S46, 1997.
50. G Deckert, PV Warren, T Gaasterland, WG Young, AL Lenox, DE Grahams, R Overbeek, MJ Snead, M Keller, M Aulay, R Huber, RA Feldman, JM Short, GJ Olsen, RV Swanson. The complete genome of the hyperthermophilic bacterium *Aquifex aeolicus*. Nature 392:353–358, 1998.
51. S Chakravarty, R Varadarajan. Elucidation of determinants of protein stability through genome sequence analysis. FEBS Lett 470:65–69, 2000.
52. S Kumar, R Nussinov. Salt bridge stability in monomeric proteins. J Mol Biol 293:1241–1255, 1999.
53. PJ Haney, JH Badger, GL Buldak, CI Reich, CR Woese, GJ Olsen. Thermal adaptation analyzed by comparison of protein sequences from mesophilic and extremely thermophilic *Methanococcus* species. Proc Natl Acad Sci USA 96:3578–3583, 1999.
54. A Szilágyi, P Závodsky. Structural differences between mesophilic, moderately thermophilic and extremely thermophilic protein subunit: results of a comprehensive survey. Structure 8:493–504, 2000.

55. TJ Ahern, AM Klibanov. The mechanism of irreversible enzyme inactivation at 100°C. Science 228:1280–1284, 1985.
56. AM Klibanov, TJ Ahern. Thermal stability of proteins. In: DL Oxender, CF Fox, eds. Protein Engineering. New York: Alan R. Liss, 1987, pp 213–218.
57. AJ Doig, DH Williams. Is the hydrophobic effect stabilizing or destabilizing in proteins? The contribution of disulfide bonds to protein stability. J Mol Biol 217:389–398, 1991.
58. E Querol, JA Perez-Pons, A Mozo-Villarias. Analysis of protein conformational characteristics related to thermostability. Protein Eng 9:265–271, 1996.
59. VZ Spassov, AJ Karshikoff, R Ladenstein. The optimization of protein solvent interactions: thermostability and the role of hydrophobic and electrostatic interactions. Protein Sci: 4:1516–1527, 1995.
60. JT Kellis Jr, K Nyberg, D Sali, AR Fersht. Contribution of hydrophobic interactions to protein stability. Nature 333:784–786, 1988.
61. AE Eriksson, WA Baase, XJ Zhang, DW Heinz, M Blaber, EP Baldwin, BW Matthews. The response of a protein structure to cavity-creating mutations and its relationship to the hydrophobic effect. Science 255:178–183, 1992.
62. CN Pace. Contribution of the hydrophobic effect to globular protein stability. J Mol Biol 226:29–35, 1992.
63. LA Lipscomb, NC Gassner, SD Snow, AM Eldridge, WA Baase, DL Drew, BW Matthews. Context-dependent protein stabilization by methionine-to-leucine substitution shown in T4 lysozyme. Protein Sci 7:765–773, 1998.
64. SM Malhauskas, SL Mayo. Design, structure and stability of a hyperthermophilic protein variant. Nat Struct Biol 5:470–475, 1998.
65. M Day, BT Hsu, L Joshua-Tor, JB Park, ZH Zhou, MWW Adams, DC Rees. X-ray crystal structures of the oxidized and reduced forms of the rubredoxin from the marine hyperthermophilic Archaeabacterium *Pyrococcus furiosus*. Protein Sci 1:1494–1507, 1992.
66. PR Blake, JB Park, ZH Zhou, DR Hare, MWW Adams, MF Summers. Solution-state structure by NMR of zinc-substituted rubredoxin from the marine hyperthermophilic Archaeabacterium *Pyrococcus furiosus*. Protein Sci 1:1508–1521, 1992.
67. KL Britton, PJ Baker, KMM Borges, PC Engel, A Pasquo, DW Rice, FT Robb, R Scandurra, TJ Stillman, KSP Yip. Insights into thermal stability from a comparison of the glutamate dehydrogenases from *Pyrococcus furiosus* and *Thermococcus litoralis*. Eur J Biochem 229:688–695, 1995.
68. MK Chan, S Mukund, A Kletzin, MWW Adams, DC Rees. Structure of a hyperthermophilic tungstopterin enzyme, aldehyde ferredoxin oxidoreductase. Science 267:1463–1469, 1995.
69. I Korndörfer, B Steipe, R Huber, A Tomschy, R Jaenicke. The crystal structure of hologlyceraldehyde-3-phosphate dehydrogenase from the hyperthermophilic bacterium *Thermotoga maritima* at 2.5 Å resolution. J Mol Biol 246:511–521, 1995.
70. S Macebo-Ribeiro, B Darimont, R Sterner, R Huber. Small structural changes account for the high thermostability of 1[4Fe–4S] ferredoxin from *Thermotoga maritima*. Structure 4:1291–1301, 1996.
71. M Kohlhoff, A Dahm, R Hensel. Tetrameric triosephosphate isomerase from hyperthermophilic archaea. FEBS Lett 383:245–250, 1996.
72. JJ Tanner, RM Hecht, KL Krause. Determinants of enzyme thermostability observed in the molecular structure of *Thermus aquaticus* D-glyceraldehyde-3-phosphate dehydrogenase at 2.5 Å resolution. Biochemistry 35:2597–2609, 1996.
73. RJM Russel, MCJ Ferguson, DW Hough, MJ Danson, GJ Taylor. The crystal structure of citrate synthase from the hyperthermophilic archaeon *Pyrococcus furiosus* at 1.9 Å resolution. Biochemistry 36:9983–9994, 1997.
74. G Auerbach, R Huber, M Grattinger, K Zaiss, H Schurig, R Jaenicke, U Jakob. Closed structure of phosphoglycerate kinase from *Thermotoga maritima* reveals the catalytic mechanism and determinants of thermal stability. Structure 5:1475–1483, 1997.
75. G Auerbach, R Ostendorp, L Prade, I Korndörfer, T Dams, R Huber, R Jaenicke. Lactate dehydrogenase from the hyperthermophilic bacterium *Thermotoga maritima*: the crystal structure at 2.1 Å resolution reveals strategies for intrinsic protein stabilization. Structure 6:769–781, 1998.
76. M Hennig, R Sterner, K Kirschner, K Jansonius. Crystal structure at 2.0 Å resolution of phosphoryl anthranilate isomerase from the hyperthermophile *Thermotoga maritima*: possible determinants of protein stability. Biochemistry 36:6009–6016, 1997.
77. G Wallon, G Kryger, ST Lovett, T Oshima, D Ringe, GA Petsko. Crystal structures of *Escherichia coli* and *Salmonella typhimurium* 3-isopropylmalate dehydrogenase and comparison with their thermophilic counterpart from *Thermus thermophilus*. J Mol Biol 266:1016–1031, 1997.
78. V Villeret, B Clantin, C Tricot, C Legrain, M Roovers, V Stalon, N Glansdorff, J van Beeumen. The crystal structure of *Pyrococcus furiosus* ornithine carbamoyltransferase reveals a key role for oligomerization in enzyme stability at extremely high temperatures. Proc Natl Acad Sci USA 95:2801–2806, 1998.
79. KSP Yip, KL Britton, TJ Stillman, J Lebbink, WM De Vos, FT Robb, C Vetriani, D Maeder, DW Rice. Insight into the molecular basis of thermal stability from the analysis of ion-pair networks in glutamate dehydrogenase family. Eur J Biochem 255:336–346, 1998.

80. KC Usher, AFA De la Cruz, FW Dahlquist, RV Swanson, R. V., MI Simon, SJ Remington. Crystal structures of CheY from *Thermotoga maritima* do not support conventional explanations for the structural basis of enhanced thermostability. Protein Sci 7:403–412, 1998.
81. C Chang, BC Park, D-S Lee, SW Suh. Crystal structure of thermostable xylose isomerases from *Thermus caldophilus* and *Thermus thermophilus*: possible structural determinants of thermostability. J Mol Biol 288:623–634, 1999.
82. S Knapp, S Kardinahl, N Hellgren, G Tibbelin, G Schafer, R Ladenstein. Refined crystal structure of a superoxide dismutase from the hyperthermophilic archaeon *Sulfolobus acidocaldaricus* at 2.2 Å resolution. J Mol Biol 285:689–702, 1999.
83. T Tahirov, H Oki, T Tsukihara, K Ogasahara, K Yutani, K Ogata, Y Izu, S Tsunasawa, I Kato. Crystal structure of methionine aminopeptidase from hyperthermophile *Pyrococcus furiosus*. J Mol Biol 284:101–124, 1998.
84. H Zuber. Temperature adaptation of lactate dehydrogenase. Structural, functional and genetic aspects. Biophys Chem 29:171–179, 1988.
85. G Vogt, S Woell, P Argos. Protein thermal stability, hydrogen bonds, and ion pairs. J Mol Biol 269:631–643, 1997.
86. A Karshikoff, R Ladenstein. Proteins from thermophilic and mesophilic organisms essentially do not differ in packing. Protein Eng 11:867–872, 1998.
87. MJ Thompson, D Eisenberg. Transproteomic evidence of a loop-deletion mechanism for enhancing protein thermostability. J Mol Biol 290:595–604, 1999.
88. L Xiao, B Honig. Electrostatic contributions to the stability of hyperthermophilic proteins. J Mol Biol 289: 1435–1444, 1999.
89. S Kumar, C-J Tsai, R Nussinov. Factors enhancing protein thermostability. Protein Eng 13:179–191, 2000.
90. MF Perutz, H Raidt. Stereochemical basis of heat stability in bacterial ferredoxins and hemoglobin A2. Nature 225:256–259, 1975.
91. ZS Hendsch, B Tidor. Do salt bridges stabilize proteins? A continuum electrostatic analysis. Protein Sci 3:211–226, 1994.
92. AH Elcock. The stability of salt bridges at high temperatures: implication for hyperthermophilic proteins. J Mol Biol 284:489–502, 1998.
93. Y-T Chang, G Loew. Homology modeling, molecular dynamics simulations, and analysis of CYP119, a P450 enzyme from extreme acidothermophile archaeon *Sulfolobus solfataricus*. Biochemistry 39:2484–2498, 2000.
94. JR Hazel, CL Prosser. Molecular mechanisms of temperature compensation in poikilotherms. Physiol Rev 54:620–677, 1974.
95. GN Somero. Proteins and temperature. Annu Rev Physiol 57:43–68, 1995.
96. G Feller, JL Arpigny, E Narinx, C Gerday. Molecular adaptations of enzymes from psychrophilic organisms. Comp Biochem Physiol 118A:495–499, 1997.
97. GN Somero, PW Hochachka. Biochemical adaptation to the environment. Am Zool 11:159–167, 1971.
98. PW Hochachka, GN Somero. Biochemical Adaptation. Princeton, NJ: Princeton University Press, 1984, pp 377–422.
99. NJ Russell. Molecular adaptations in psychrophilic bacteria: potential for biotechnological applications. Adv Biochem Eng Biotechnol 61:1–21, 1998.
100. B Ásgeirsson, JW Fox, JB Bjarnason. Purification and characterization of trypsin from the poikilotherm *Gadus morhua*. Eur J Biochem 180:85–94, 1989.
101. G Feller, C Gerday. Psychrophilic enzymes: molecular basis of cold adaptation. Cell Mol Life Sci 53:830–41, 1997.
102. AO Smalås, ES Heimstad, A Hordvik, NP Willassen, R Male. Cold adaption of enzymes: structural comparison between salmon and bovine trypsins. Proteins 20:149–166, 1994.
103. GI Berglund, NP Willassen, A Hordvik, AO Smalås. Structure of native pancreatic elastase from North Atlantic salmon at 1.61 Å resolution. Acta Cryst D51:925–937, 1995.
104. N Aghajari, G Feller, C Gerday, R Haser. Crystal structures of the psychrophilic alpha-amylase from *Alteromonas haloplanctis* in its native form and complexed with an inhibitor. Protein Sci 7:564–572, 1998.
105. RJ Russell, U Gerike, MJ Danson, DW Hough, GL Taylor. Structural adaptations of the cold-active citrate synthase from an Antarctic bacterium. Structure 6:351–361, 1998.
106. A Fersht. Structure and Mechanism in Protein Science. New York: W.H. Freeman, 1999.
107. MM Kristjánsson. Purification and characterization of trypsin from the pyloric caeca of rainbow trout (*Oncorhynchus mykiss*). J Agric Food Chem 39:1738–1742, 1991.
108. H Outzen, GI Berglund, A Smalås, NP Willassen. Temperature and pH sensitivity of trypsins from Atlantic salmon (*Salmo salar*) in comparison with bovine and porcine trypsin. Comp Biochem Physiol 115B:33–45, 1996.
109. KK Osnes, V Mohr. On the purification and characterization of three anionic, serine-type peptide hydrolyses from Antarctic krill, *Euphausia superba*. Comp Biochem Physiol 82B:607–619, 1985.
110. L Kulakova, A Galkin, T Kurihara, T Toshimura, N Esaki. Cold-active serine alkaline protease from the psychrotrophic bacterium *Shewanella* strain as 10: gene cloning and enzyme purification and characterization. Appl Environ Microbiol 65:611–617, 1999.

111. G Feller, F Payan, F Theys, M Qian, R Haser, C Gerday. Stability and structural analysis of alpha-amylase from the Antarctic psychrophile *Alteromonas haloplanctis* A23. Eur J Biochem 222:441–447, 1994.
112. PS Low, JL Bada, GN Somero. Temperature adaptation of enzymes: roles of the free energy, the enthalpy and entropy of activation. Proc Natl Acad Sci USA 70:430–432, 1973.
113. TC Bruice, SJ Benkovic. Chemical basis for enzyme catalysis. Biochemistry 39:6267–6274, 2000.
114. L Birolo, ML Tutino, B Fotanella, C Gerday, K Mainolfi, S Pascarella, G Sannia, F Vinci, G Marino. Aspartate aminotransferase from the Antarctic bacterium *Pseudoalteromonas haloplanktis* TAC 125. Cloning, expression, properties, and molecular modelling, Eur J Biochem 267:2790–2802, 2000.
115. G Feller, Z Zeknini, J Lamotte-Brasseur, C Gerday. Enzymes from cold-adapted microorganisms. The class C beta-lactamase from the Antarctic psycrophile *Psychrobacter immobilis* A5. Eur J Biochem 244:186–191, 1997.
116. D Georlette, ZO Jónsson, F Van Petegem, J-P Chessa, J Van Beeumen, U Hübscher, C Gerday. A DNA ligase from the psychrophile *Pseudoalteromonas haloplanktis* gives insights into the adaptation of proteins to low temperatures. Eur J Biochem 267:3502–3512, 2000.
117. M Bentahir, G Feller, M Aittaleb, J Lamotte-Brasseur, T Himri, J-P Chessa, C Gerday. Structural, kinetic, and calorimetric characterization of the cold-active phosphoglycerate kinase from the Antarctic *Pseudomonas* sp. TACII18. J Biol Chem 275:11147–11153, 2000.
118. JB Hauksson, ÓS Andrésson, B Ásgeirsson. Heat-labile bacterial alkaline phosphatase from a marine *Vibrio* sp. Enz Microb Technol 27:66–73, 2000.
119. B Ásgeirsson, R Hartemink, JF Chlebowski. Alkaline phosphatase from Atlantic cod (*Gadus morhua*). Kinetic and structural properties which indicate adaptation to low temperatures. Comp Biochem Physiol 110B:315–329, 1995.
120. R Hiller, ZH Zhou, MWW Adams, SW Englander. Stability and dynamics in a hyperthermophile protein with melting temperature close to 200°C. Proc Natl Acad Sci USA 94:11329–11332, 1997.
121. CL Tsou. Inactivation precedes overall molecular conformation changes during enzyme denaturation. Biochim Biophys Acta 1253:151–162, 1995.
122. HK Leiros, NP Willassen, AO Smalas. Residue determinants and sequence analysis of cold-adapted trypsins. Extremophiles 3:205–219, 1999.
123. S Genicot, F Rentierdelrue, D Edwards, J Van Beeumen, C Gerday. Trypsin and trypsinogen from an Antarctic fish — molecular basis of cold adaptation. Biochim Biophys Acta 1298:45–57, 1996.
124. N Aghajari, G Feller, C Gerday, R Haser. Structures of the psychrophilic *Alteromonas haloplanktis* alpha-amylase give insights into cold adaptation at a molecular level. Structure 6:1503–16, 1998.
125. DW Hough, MJ Danson. Extremoenzymes. Curr Opin Chem Biol 3:39–46, 1999.
126. E Gudmundsdottir, R Spilliaert, Q Yang, CS Craik, JB Bjarnason, Á Gudmundsdottir. Isolation and characterization of two cDNAs from Atlantic cod encoding two distinct psychrophilic elastases. Comp Biochem Physiol 113B:795–801, 1996.
127. M Alvarez, JP Zeelen, V Mainfroid, F Rentier-Delrue, JA Martial, L Wyns, RK Wierenga, D Maes. Triosephosphate isomerase (TIM) of the psychrophilic bacterium *Vibrio marinus*. Kinetic and structural properties. J Biol Chem 273:2199–206, 1998.
128. S Davail, G Feller, E Narinx, C Gerday. Cold adaptation of proteins. Purification, characterization, and sequence of the heat-labile subtilisin from the Antarctic psychrophile *Bacillus* TA41. J Biol Chem 269:17448-17453, 1994.
129. G Wallon, ST Lovett, C Magyar, A Swingor, A Szilagyi, P Zavodsky, D Ringe, GA Petsko. Sequence and homology model of 3-isopropylmalate dehydrogenase from the psychrotrophic bacterium *Vibrio* sp. I5 suggest reasons for thermal instability. Protein Eng 10:665–672, 1997.
130. U Gerike, MJ Danson, NJ Russel, DW Hough. Sequencing and expression of the gene encoding a cold-active citrate synthase from an Antarctic bacterium, strain DS2-3R. Eur J Biochem 248:49–57, 1997.
131. S-Y Kim, KY Hwang, S-H Kim, H-C Sung, YS Han, Y Cho. Structural basis for cold adaptation. Sequence, biochemical properties, and crystal structure of malate dehydrogenase from a psychrophile *Aquaspirillum arcticum*. J Biol Chem 274:11761–11767, 1999.
132. HKS Leiros, NP Willassen, AO Smalås. Structural comparison of psychrophilic and mesophilic trypsins. Elucidating the molecular basis of cold adaptation. Eur J Biochem 267:1039–1049, 2000.
133. KE Neet, DE Timm, Conformational stability of dimeric proteins: quantitative studies by equilibrium denaturation. Protein Sci 3:2167–2174, 1995.
134. NK Roy, RK Ghosh, J Das. Monomeric alkaline phosphatase of *Vibrio cholerae*. J Bacteriol 150:1033–1039, 1982.
135. D Hess, K Kruger, A Knappik, P Palm, R Hensel. Dimeric 3-phosphoglycerate kinases from hyperthermophilic *Archaea*. Cloning, sequencing and expression of the 3-phosphoglycerate kinase gene of *Pyrococcus woesei* in *Escherichia coli* and characterization of the protein. Structural and functional comparison with the 3-phosphoglycerate kinase of *Methanothermus fervidus*. Eur J Biochem 233:227–237, 1995.
136. CE Jones, TM Fleming, DA Cowan, JA Littlechild, PW Piper. The phosphoglycerate kinase and glyceraldehyde-3-phosphate dehydrogenase genes from the

thermophilic archaeon *Sulfolobus solfataricus* overlap by 8-bp. Isolation, sequencing of the genes and expression in *Escherichia coli*. Eur J Biochem 233:800–808, 1995.
137. F Strasser, J Dey, MR Eftink, BV Plapp. Activation of horse liver alcohol dehydrogenase upon substitution of tryptophan 314 at the dimer interface. Arch Biochem Biophys 358:369–376, 1998.
138. AE Eriksson, WA Baase, BW Matthews. Similar hydrophobic replacement of Leu99 and Phe153 within the core of T4 lysozyme have different structural and thermodynamic consequences. J Mol Biol 229:747–769, 1993.
139. E Narinx, E Baise, C Gerday. Subtilisin from psychrophilic Antarctic bacteria: characterization and site-directed mutagenesis of residues possibly involved in the adaptation to cold. Protein Eng. 10:1271–1279, 1998.
140. O Kuchner, FH Arnold. Directed evolution of enzyme catalysis. TIBTECH 15:523–530, 1997.
141. VGH Eijsink, OR Veltman, W Aukema, G Vriend, G Venema. Structural determinants of the stability of thermolysin-like proteinases. Nature Struct Biol 2:374–379, 1995.
142. HM Zhao, FH Arnold. Directed evolution converts subtilisin E into a functional equivalent of thermitase. Protein Eng 12:47–53, 1999.
143. G Gonzalez-Blasco, J Sanz-Aparicio, B Gonzalez, JA Hermoso, J Polaina. Directed evolution of beta-glucosidase A from *Paenibacillus polymyxa* to thermal resistance. J Biol Chem 275:13708–13712, 2000.
144. L Giver, A Gershenson, PO Freskgard, FH Arnold. Directed evolution of a thermostable esterase. Proc Natl Acad Sci USA 95:12809–12813, 1998.
145. A Merz, M-C Yee, H Szadkowski, G Pappenberger, AL Crameri, WPC Stemmer, C Yanowsky, K Kirschner. Improving the catalytic activity of a thermophilic enzyme at low temperatures. Biochemistry 39:880–889, 2000.
146. JH Lebbink, T Kaper, P Bron, J van der Oost, WM de Vos. Improving low-temperature catalysis in the hyperthermostable *Pyrococcus furiosus* beta-glucosidase CelB by directed evolution. Biochemistry 39:3656–3665, 2000.
147. S Taguchi, A Ozaki. T. Nonaka, Y Mitsui, H Momose. A cold-adapted protease engineered by experimental evolution system. J Biochem (Tokyo) 126:689–693, 1999.
148. MM Kristjánsson, JK Kristjánsson. Proteinases from thermophilic microorganisms. Comments Agric Food Chem 3:39–67, 1993.
149. FB Perler, S Kumar, H Kong. Thermostable DNA polymerases, Adv Protein Chem 48:377–435, 1996.
150. WD Crabb, C Mitchinson. Enzymes involved in the processing of starch to sugars. TIBTECH 15:349–352, 1997.
151. E Léveque, S Janecek, B Haye, A Belarbi. Thermophilic archaeal amylolytic enzymes. Enzyme Microbiol Technol 26:3–14, 2000.
152. NT Mrabet, A Van den Broeck, I Van den Brande, P Stanssen, Y Laroche, AM Lambeir, G Matthijssen, J Jenkins, M Chiadmi, H Van Tilbeurgh, F Rey, J Janin, WJ Quax, I Laster, M De Maeyer, SJ Wodak. Arginine residues as stabilizing elements in proteins. Biochemistry 31:2239–2253, 1992.
153. WJ Quax, NT Mrabet, RGM Luiten, PW Schuurhuizen, P Stanssens, I Lasters. Enhancing the thermostability of glucose isomerase by protein engineering. Biotechnology 9:738–742, 1991.
154. M Meng, C Lee, M Bagdasarian, JG Zeikus. Switching substrate preferences of thermophilic xylose isomerase from D-xylose to D-glucose by redesigning the substrate binding pocket. Proc Natl Acad Sci USA 88:4015–4019, 1991.
155. JR Whitaker. New and future uses of enzymes in food processing. Food Biotechnol 4:669–697, 1990.
156. WG Voorhorst, A Warner, WM de Vos, RJ Siezen. Homology modelling of two subtilisin-like proteases from the hyperthermophilic Archaea *Pyrococcus furiosus* and *Thermococcus stetteri*. Protein Eng 10:905–914, 1997.
157. H Matsuzawa, K Tokugawa, M Hamaoki, M Mizoguchi, H Taguchi, I Terada, ST Kwon, T Otha. Purification and characterization of aqualysin I (a thermophilic alkaline serine protease) produced by *Thermus aquaticus* YT-1. Eur J Biochem 171:441–447, 1988.
158. K Peek, RM Daniel, C Monk, L Parker, T Coolbear. Purification and characterization of a thermostable proteinase isolated from *Thermus* sp. strain Rt41A. Eur J Biochem 207:1035–1044, 1992.
159. G Stefansson. Fish processing. In: T Nagodawithana, G Reed, eds. Enzymes in Food Processing. San Diego, CA: Academic Press, 1993, pp 459–470.
160. NF Haard. A review of proteolytic enzymes from marine organisms and their application in the food industry. J Aquat Food Product Technol 1:17–35, 1992.
161. A Gildberg. Enymatic processing of marine raw materials. Process Biochem 28:1–15, 1993.
162. O Vilhelmsson. The state of enzyme biotechnology in the fish processing industry. Trends Food Sci Technol 8:266–270, 1997.
163. RL Olsen, A Johansen, B Myrnes. Recovery of enzymes from shrimp waste. Process Biochem 25:67–68, 1990.
164. G Sellek, JB Chaudhuri. Biocatalysis in organic media using enzymes from extremophiles. Enz Microbial Technol 25:471–482, 1999.

9

Nitrogen Fixation and the Enzyme Nitrogenase

William E. Newton
The Virginia Polytechnic Institute and State University, Blacksburg, Virginia, U.S.A.

I. INTRODUCTION

Only a very small proportion of the nitrogen present on earth is in a usable form at any one time. More than 99.9% of the nitrogen is present as the dinitrogen molecule (N_2). Most organisms cannot metabolize this abundant, but relatively inert N_2 and so they must assimilate nitrogen in a "fixed" form, such as ammonia (NH_3) or nitrate (NO_3^-). As part of the geobiochemical nitrogen cycle, nitrogen fixation drives the conversion of atmospheric N_2 to ammonia. However, the complementary processes of nitrification and denitrification convert ammonia back to dinitrogen, which is returned to the atmosphere. This constant cycling means that the pool of fixed nitrogen within the biosphere must be constantly replenished because ammonia is necessary for the formation of biologically essential, nitrogen-containing compounds, such as amino acids and nucleic acids. Dinitrogen is fixed naturally by both nonbiological processes, like lightning and combustion, and by biological processes. Natural nonbiological processes contribute $\sim 10\%$ and biological processes contribute about 65% of the total annual fixation rate. Industrial ammonia synthesis contributes the other 25% (1, 2). Thus, biological nitrogen fixation is a pivotal life-supporting process that provides the majority of the fixed nitrogen source necessary to sustain life on earth.

Animals, including man, are directly dependent on plants to supply much of the energy and many of the nitrogenous compounds required to survive. Plants, in their turn, are dependent on the availability of nitrogenous compounds produced from atmospheric N_2 either commercially or biologically by microbes. In this way, nitrogen fixation assumes significant importance in agriculture because the availability of fixed nitrogen is most often the limiting factor in crop production. Consequently, efforts to grow sufficient crops to feed the global population have led to increases in the application of commercial nitrogen fertilizers. However, applying nitrogen fertilizers has its costs. These costs, which are directly associated with the Haber-Bosch process, include: (a) consumption of nonrenewable fossil fuel resources as both feedstock and energy source; (b) significant storage costs for product manufactured year-round but applied seasonally and significant transportation costs due to the production site usually being remote from the site of use; and (c) contamination of local water systems through runoff. In fact, only about one-third of the applied nitrogen is assimilated by plants, whereas one-third is leached away (after conversion to nitrate) and one-third is denitrified and lost to the atmosphere as N_2(1). An alternative approach to using the Haber-Bosch process for producing commercial nitrogen fertilizer is to exploit the biological process and considerable effort is currently being directed at understanding the molecular mechanism of biological nitrogen fixation.

II. NITROGEN-FIXING ORGANISMS AND CROP PLANTS

Only prokaryotes, i.e., those living things without an organized nucleus (Eubacteria, Archaea, and actino-

mycetes), can perform biological nitrogen fixation. The ability to fix N_2 is widely spread among bacterial genera (3, 4) and, despite a number of claims, no eukaryote has been clearly established to fix N_2. Although farmers recognized the benefits of crop rotations centuries ago, the source of much of that benefit was unknown to them. The first report of nitrogen fixation in 1838 involved a comparison of the growth and nitrogen content of cereals with leguminous plants (mainly clover in rotations with wheat and tuber crops) in both greenhouse and field experiments. The result "that azote (nitrogen) may enter the living frame of the plants directly" (5, 6) was received with much skepticism. It was not until almost 50 years later that Boussingault's work was convincingly confirmed by Hellriegel and Wilfarth (7), who also solved the perplexing question of the source of the fixed nitrogen by localizing the activity to the bacteria-filled nodules on the roots of their pea plants (6, 8).

Most nitrogen-fixing microbes are free living and fix nitrogen for their own benefit. Except for the cyanobacteria, the free-living bacteria are generally not agriculturally important, contributing only $\sim 0.1\%$ of the fixed nitrogen of a leguminous association. The most extensively studied free-living bacterial species are *Azotobacter vinelandii* (an obligate aerobe), *Clostridium pasteurianum* (an obligate anaerobe), *Klebsiella pneumoniae* (a facultative anaerobe), *Rhodobacter capsulatus* (a photosynthetic bacterium), and *Anabaena* sp. 7120 (a heterocyst-forming cyanobacterium). However, some nitrogen-fixing microbes enter into a mutually beneficial interaction with other organisms. The most agriculturally important symbiotic relationship involves leguminous plants and rhizobial microsymbionts, but many other nitrogen-fixing, symbiotic relationships are known. These include examples with lichens, bryophytes (mosses and liverworts), pteridophytes (ferns), cycads, and other nonleguminous angiosperms, such as small shrubs and trees, like *Myrica* and alder, and larger trees, like *Casuarina* (3).

The leguminous association ensures that the plant receives fixed nitrogen directly from the rhizobia bacteria, which are harbored in nodules on its roots. In return, the bacterium receives a protected environment and a supply of energy from the plant. Another benefit arising from this association is the provision of an environment with a low O_2 tension within the root nodules. This function is vital because the enzyme, which catalyzes biological nitrogen fixation and is called nitrogenase, is extremely sensitive to the presence of O_2. Most often, the first level of protection against O_2 occurs through a physical barrier to free O_2 diffusion provided by the plant-derived, outer cortex layer of the nodule. This structure prevents O_2 from flooding the central core of the nodule where the nitrogen-fixing bacteria are located. However, some O_2 is required for bacterial respiration to provide the energy and reducing equivalents to drive its nitrogen fixation, and this low, but sufficient, concentration is delivered by an oxygen-transporting protein, called leghemoglobin.

Establishment of a symbiotic relationship is a complicated process, which most often involves specificity between the host plant and its microsymbiont (9). In the legume symbiosis, initiation of the infection process occurs when bacteria induce curling of the tip of root hairs (10, 11). These structures then envelop the bacteria and form an "infection thread," which penetrates the root cortex and along which the invading bacteria enter the host plant cells (12). As infection thread formation occurs, cell division is induced within the root cortex, resulting in formation of a nodule primordium (13). When the infection thread contacts a newly divided primordial cell, bacteria are released and they enter the cytoplasm of the primordial cell through an endocytotic process, which results in a plant-derived peribacteroid membrane that surrounds the bacteria (14). Following multiple bacterial-cell division and peribacteroid membrane proliferation, the host cell becomes filled with bacteria, which then differentiate into bacteroids that are specialized for fixing nitrogen.

The symbiotic interaction requires coordination among the partners at both the developmental and metabolic levels. This cooperation is accomplished through reciprocal communication and control of gene expression. Signaling between the partners starts when the regulatory nodulation (*nod*) genes of the rhizobia detect plant signals present in root exudates. These plant signals are usually flavanoids (15). These flavanoids specifically induce rhizobial *nodD* gene expression (16), which produces a regulatory protein (a transcriptional activator) that controls the expression of all other *nod* (and *nol*) genes. The concerted action of the products of other *nod* genes results in the synthesis and release of the bacterial signals, called Nod factors (17). Each rhizobial Nod factor is species specific. It is chitinlike, being composed of β(1-4)-linked *N*-acetylglucosamine residues. The specificity of a particular Nod factor depends on both the extent of oligomerization (usually up to five residues) and the range of chemical modification of the chitin core, such as O-acylation or N-acylation at the nonreducing end

and sulfation at the reducing end. The *nodABC* genes are called the "common" *nod* genes because their products are required for catalyzing formation of the oligosaccharide core for all Nod factors. The other *nod* genes are "host specific" and their products are responsible for oligomerization and modification of the oligosaccharide core. In some plant strains, isolated Nod factors can initiate root hair curling, infection thread development, and nodule formation.

Root nodules are the usual result of N_2-fixing symbioses involving *Rhizobium*; however, some tropical legumes, like *Sesbania*, produce stem nodules in association with *Azorhizobium caulinodans* (18). In addition, some stem nodules retain the ability for photosynthesis and contain, in the case of *Aeschynomene indica*, rhizobia themselves capable of photosynthesis (19). This close relationship of photosynthesis to nitrogen fixation may ease some of the energy demand of nodules.

Although this tight, nodule-based, symbiotic arrangement is very successful, it does not extend to most of the important food crops, like the cereal grains (rice, wheat, and corn) and root and tuber crops. None of these harbor symbiotic partners in nodules. Hence, for the productivity of these crops to reach commercially acceptable levels, extensive augmentation by commercially fixed nitrogen is usually necessary. However, other, less formal associations occur regularly in which some interdependence exists among some grasses (family Gramineae) and bacteria. The associations of tropical grasses *Paspalum* and *Digitaria* with the bacteria *Azotobacter paspali* and *Azospirillum brasilense*, respectively, are good examples of such a relationship (20). With *Paspalum*, a mucilaginous sheath forms around the root within which the bacteria live and fix N_2. The bacteria do not invade the plant tissue. In contrast, the *Digitaria–Azospirillum* association does involve root invasion but no nodule develops. The extent to which the plants benefit from these associations is uncertain. *Azospirillum lipoferum*, which occurs in temperate zones, associates with certain corn and sorghum cultivars, but the effect on the plants appears to be small (21, 22). The more formalized endophytic associations of both *Acetobacter diazotrophicus* and *Herbaspirillum* spp. with sugar cane (23) and of *Azoarcus* spp. with Kallar grass and possibly rice (24) may supply up to 100% of the fixed nitrogen required for the host plant's growth, indicating a significant agronomic and economic potential.

Nitrogen-fixing associations involving animals also exist (25). In the case of higher animals, like either man with *Klebsiella* or ruminants with *Clostridium*, it is unlikely that much is contributed to the nitrogen status of the animal because its diet likely contains sufficient fixed nitrogen, which will repress any N_2-fixing activity by the bacteria. However, with termites and shipworms, the associations are significant. *Citrobacter* infects the intestinal tract of termites and can fix N_2 there with the amount fixed and the benefit gained depending on the insect's diet (26, 27). The N_2-fixing, cellulose-decomposing bacterium that inhabits the Deshayes gland of woodboring shipworms contributes significantly to the mollusk's well-being by providing up to 35% of its fixed nitrogen requirement (28). The whole area of animal symbioses is under-researched.

III. NITROGENASES

A. Molybdenum Nitrogenase

With one exception (29), all known diazotrophs contain a nitrogenase (or nitrogenases) that is a complex of two metalloproteins (30–33). The individual nitrogenase component proteins of the most commonly occurring nitrogenase, usually referred to as Mo-nitrogenase, have been designated as the Fe protein (or component 2 or dinitrogenase reductase) and the MoFe protein (or component 1 or dinitrogenase). The trivial names for these proteins are derived from the composition of their associated metal centers. The Fe protein is a homodimer ($M_r = 64{,}000$), which contains two MgATP binding sites and a single [4Fe–4S] cluster. The MoFe protein is an $\alpha_2\beta_2$ heterotetramer ($M_r = 230{,}000$), which contains two pairs of two different metalloclusters, called P-clusters and iron-molybdenum cofactors (or FeMo cofactors). The three-dimensional structures of the Fe protein (34) and MoFe protein (35, 36) have been solved, as have the structures of their associated metal clusters (34, 37, 38). The Fe protein serves as a specific reductant for the MoFe protein, which contains the site(s) of substrate binding and reduction.

Wild-type nitrogenase catalyzes the biological nitrogen-fixation reaction, which is usually described as:

$$N_2 + 8H^+ + 8e^- + 16MgATP \rightarrow 2NH_3 + H_2 + 16MgADP + 16P_i$$

In addition, nitrogenase catalyzes the reduction of many other small molecule substrates, all of which have the same requirements for catalytic activity, namely MgATP, a low-potential reductant and an anaerobic environment (39, 40). The optimal stoichiometry for nitrogenase function is four molecules of

MgATP hydrolyzed for each pair of electrons transferred to substrate; this ratio is independent of the substrate reduced. The so-called *alternative substrates* include, for example, acetylene, which is only reduced by two electrons to ethylene, HCN, which is reduced by six electrons to methane and ammonia and by four electrons to methylamine, and azide, which is reduced by two electrons to nitrogen gas and ammonia. Carbon monoxide (CO) is a potent inhibitor of all nitrogenase-catalyzed substrate reductions with the exception of H^+ reduction (41). H_2 has a unique involvement with Mo-nitrogenase and with N_2 reduction in particular. It can play any one of four well-documented roles both *in vivo* and *in vitro*. H_2, *via* the action of hydrogenase, can be the source of reducing equivalents for nitrogenase; it is the sole product in the absence of other reducible substrates in an ATP-dependent, CO-insensitive reaction (42); it is a specific competitive inhibitor of N_2 reduction, affecting neither the reduction of any other substrate nor its own evolution (43); and, under an N_2/D_2 atmosphere, HD is formed in a CO-sensitive, MgATP-requiring reaction (44–47). These Mo-nitrogenases, from a variety of genera, exhibit a high level of primary sequence identity. The sequence conservation is particularly high in the regions of the MgATP- and metallocluster-binding sites (48). With the notable exception of *C. pasteurianum*, the component proteins from all Mo-based nitrogenases interact as heterologous crosses to form catalytically active enzymes (49).

B. Alternative Nitrogenases

With the single exception noted above and described in Section III.C below, all nitrogen-fixing organisms that have been studied at the level of the enzyme have the Mo-containing nitrogenase. There are, however, two other types of nitrogenases, which are closely related to the Mo-nitrogenase, but neither contains Mo. These so-called alternative nitrogenases (50–52) consist of two protein components, including a Fe-protein component specific for each alternative nitrogenase. The larger of the two component proteins of the first alternative nitrogenase contains a cofactor with a vanadium (V) atom substituting for the Mo atom. This replacement results in a VFe protein containing a FeV cofactor. The second type contains a cofactor where the Mo atom is substituted by Fe to produce a FeFe protein containing a FeFe cofactor. The high level of primary sequence identity recognized among the Mo-dependent nitrogenases also extends to the alternative nitrogenases. This identity strongly suggests that all nitrogenases are likely to have common structural features and mechanistic similarities. However, the larger component of these alternative nitrogenases is hexameric with three types of subunits, which are encoded by either *vnfDGK* (51, 53, 54) or *anfDGK* (52, 55), rather than the tetrameric form of the MoFe protein.

There appears to be no logic to the way in which these nitrogenases are distributed among microorganisms. For example, *Klebsiella pneumoniae* has only Mo-nitrogenase, whereas *Azotobacter chroococcum* has both Mo- and V-nitrogenase, and *Rhodobacter capsulatus* has Mo- and Fe-nitrogenase. Moreover, all three nitrogenase types are found in *A. vinelandii*. The expression of each nitrogenase is under hierarchical control through the availability of either Mo or V in the growth medium (56, 57). Whenever Mo is available, expression of the Mo-dependent nitrogenase is stimulated and the expression of the others is repressed. Similarly, when V is available and Mo is absent, expression of the V-nitrogenase only occurs. If both metals are absent, then only the Fe-nitrogenase is expressed. Such control by metal availability is physiologically reasonable because Mo-nitrogenase is the most efficient catalyst for nitrogen reduction, followed by V-nitrogenase, with the Fe-nitrogenase being the least efficient with a large majority of reducing equivalents being used to evolve H_2 rather than to produce ammonia (58, 59). Active heterologous nitrogenase results from crosses among the two-component proteins from Mo-nitrogenase and V-nitrogenase, but crosses involving either component protein from the Fe-nitrogenase are ineffective with the complementary protein from both Mo- and V-nitrogenases (59).

C. *Streptomyces thermoautotrophicus* Nitrogenase

Although this recently discovered (29), unique nitrogenase system consists of two component proteins, the larger of which contains Mo, Fe, and sulfide, that is where the similarities to the classical Mo-nitrogenase stop. The Fe-protein component of the classical nitrogenase is replaced by a manganese-containing superoxide oxidoreductase, which oxidizes superoxide to dioxygen and then transfers the electron to a MoFeS-containing protein at which each dinitrogen molecule is reduced by eight electrons to two molecules of ammonium and one molecule of dihydrogen. This reaction appears to require less MgATP per dinitrogen reduced than that required by the classical Mo-nitrogenase. In place of flavodoxin or ferredoxin as the electron donor to the Fe protein, a Mo-containing

CO dehydrogenase operates by coupling the oxidation of CO to the reduction of dioxygen to produce superoxide. The MoFeS-containing protein is a $\alpha\beta\gamma$ heterotrimer quite different from the $\alpha_2\beta_2$ composition of the classical Mo-nitrogenase. Other unique features of this nitrogenase include the insensitivity of its nitrogen fixation toward dioxygen, CO, and dihydrogen, all of which are potent inhibitors of nitrogen fixation in the classical system. Finally, this nitrogenase does not catalyze the reduction of acetylene to ethylene.

D. Mechanism of Nitrogenase Action

During catalysis, the Fe protein delivers electrons, one at a time, to the MoFe protein in a process that couples MgATP binding and hydrolysis to the association and dissociation of the two component proteins and concomitant electron transfer (33, 60). Both component proteins are required for MgATP hydrolysis, and neither component protein alone will reduce substrate.

Based on a substantial amount of kinetic data, a numerical model has been developed to describe the process by which electrons are sequentially delivered to the MoFe protein and then to substrate (60). This model treats the MoFe protein as a dimer of dimers with each $\alpha\beta$-dimer operating independently and being serviced by Fe protein. This approach involves two interconnecting processes, which are called the Fe-protein cycle and the MoFe-protein cycle. The Fe-protein cycle describes how the Fe protein's [4Fe–4S] cluster cycles between its reduced 1^+ and its oxidized 2^+ redox states as it delivers an electron to the MoFe protein, coupled with MgATP hydrolysis, and is then re-reduced by another electron transfer protein, usually either a ferredoxin or a flavodoxin.

The MoFe-protein cycle is necessarily more complex because it involves the progressive reduction of the MoFe protein by up to eight electrons for N_2 binding and reduction, which therefore requires eight turns of the Fe-protein cycle. This model is consistent with N_2 becoming bound to the active site only after three electrons have been accumulated within the MoFe protein. How and where these electrons are stored prior to the binding and reduction of substrate is unknown. However, current biochemical data suggest that intra-MoFe-protein cluster-to-cluster electron transfer occurs (61, 62). In addition, structural data supporting this thesis come from the crystallographic model for the docked complex of two Fe proteins with one MoFe protein (63) (Fig. 1). Docking occurs along the Fe protein's twofold symmetric axis, which bisects the single [4Fe–4S] cluster, and the pseudosymmetric $\alpha\beta$-interface of the MoFe protein. This arrangement places the Fe protein's [4Fe–4S] cluster in close proximity to the P-cluster of the MoFe protein and also situates the P-cluster between the Fe protein's [4Fe–4S] cluster and the FeMo cofactor. This arrangement suggests that electron transfer occurs from the [4Fe–4S] cluster through the P-cluster to the FeMo cofactor, where substrate reduction occurs.

One P-cluster is located at each $\alpha\beta$-interface of the MoFe protein. In its as-isolated form, which is believed to represent its fully reduced, all-Fe^{2+} state, the [8Fe–7S] P-cluster consists of two [4Fe–4S] subclusters that share a single, six-coordinated sulfide (P^N in Fig. 2). Upon oxidation by redox-active dyes, the P-cluster structurally rearranges through movement of two of its eight Fe atoms to P^{OX}, both of which also undergo a change in their ligand environment. This redox-dependent structural change of the P-cluster is likely to be mechanistically related to its role in accepting electrons from the Fe-protein and coupling their delivery, along with the required protons, to the FeMo cofactor and substrate (38).

The FeMo cofactor is composed of a [Mo–7Fe–9S] core plus one molecule of (R)-homocitrate (Fig. 3). This basic framework consists of two partial clusters, [Mo–3Fe–3S] and [4Fe–3S], bridged by three sulfides. Homocitrate is coordinated to the Mo atom through its 2-hydroxyl and 2-carboxyl groups. Substrate binding and reduction at the FeMo cofactor is supported by several lines of evidence. First, mutant strains, which are unable to biosynthesize FeMo cofactor, are also unable to catalyze nitrogen fixation (64) but, when isolated FeMo cofactor is added to crude extracts prepared from such mutant strains, the ability to fix nitrogen *in vitro* is restored. Second, when citrate replaces homocitrate as the organic constituent of an altered FeMo cofactor, the resulting MoFe-protein exhibits altered catalytic properties (64–66). Third, altered MoFe proteins, which have amino acid substitutions within the FeMo cofactor's polypeptide environment, also exhibit altered catalytic properties (67, 68). Although how substrates interact with FeMo cofactor during turnover is not known, both the presence of six coordinately unsaturated Fe atoms (69–73) and the homocitrate bound to Mo (74) have been suggested to be involved in substrate and inhibitor binding. For example, multiple distinct and possibly overlapping sites have been proposed involving the Fe–S framework (75). In contrast, the carboxylate group, which is coordinated to the Mo atom, has been suggested to serve as a leaving group in a mechanism that activates Mo to provide a substrate coordination site (76).

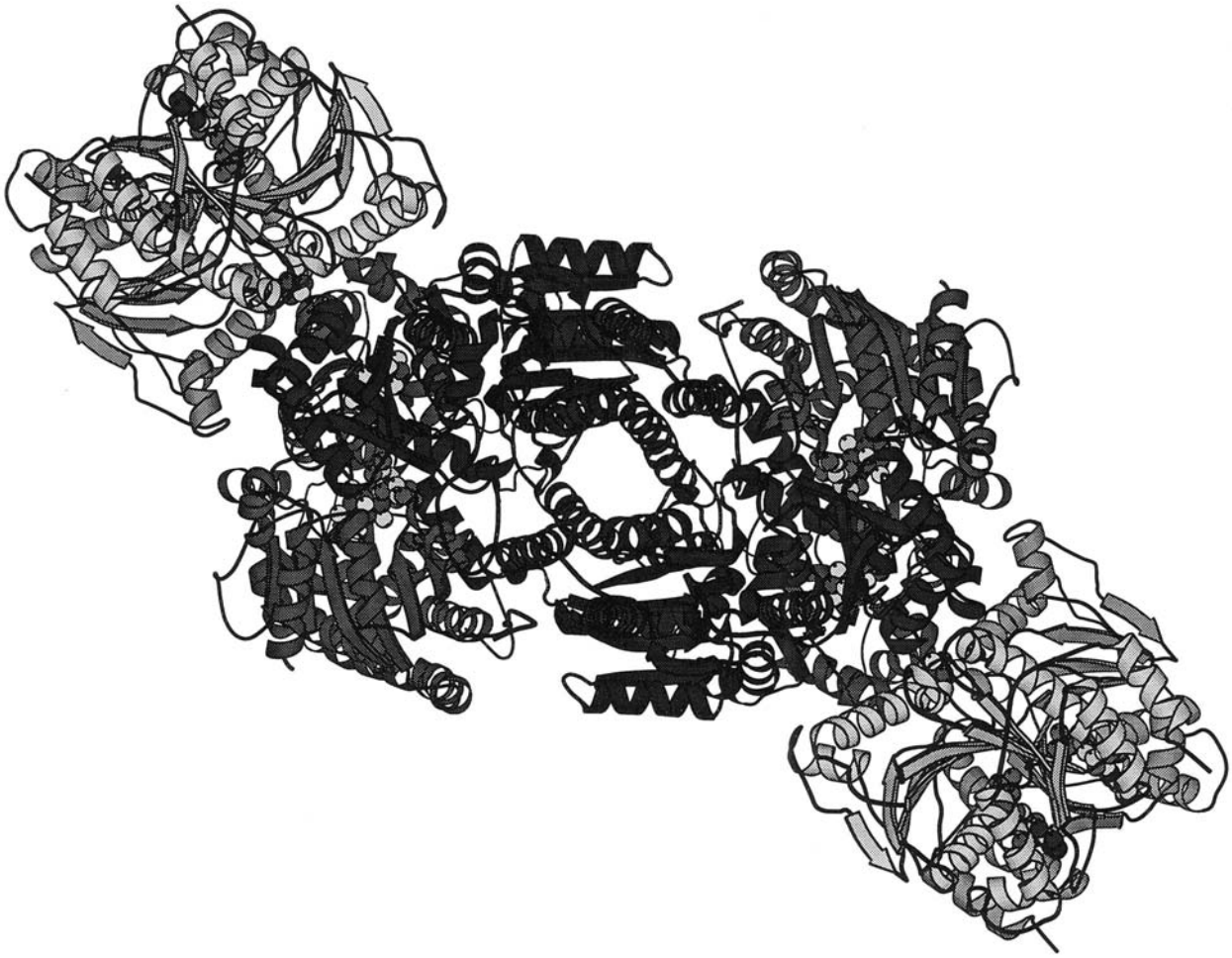

Figure 1 Ribbon diagram of the three-dimensional structure of the *A. vinelandii* Mo-nitrogenase complex, which is stabilized by using ADP-A1F_4^- as an ATP analog. The complex consists of two molecules of the Fe-protein (lightest shading), one at each end of one molecule of the MoFe-protein $\alpha_2\beta_2$ tetramer. The twofold symmetry axis of the Fe-protein aligns with the pseudo-twofold symmetry axis, which bisects the αβ-subunit interface of the MoFe-protein. Each half of the MoFe-protein molecule (which may be visualized by drawing a line through the center from the 1 o'clock to the 7 o'clock position) represents an αβ-subunit dimer, each encompassing one P-cluster and one FeMo-cofactor. The β-subunits (darkest shading) make all contacts among the two αβ-dimers. The α-subunits (medium shading), which do not contact one another, are located in the lower left and upper right (with the FeMo cofactor clearly visible in both). (Courtesy of Dr. D. C. Rees, California Institute of Technology.)

E. Role of MgATP in Nitrogenase Catalysis

The overall reduction of N_2 to yield $2NH_3$ is thermodynamically favorable, although the formation of two-electron-reduced intermediates, if they exist, is not. It appears, then, that MgATP binding and hydrolysis during nitrogenase catalysis is not a thermodynamic requirement but rather it is used to drive electron transfer toward substrate reduction and to prevent the back flow of electrons to the Fe-protein. This situation may be envisioned as the "gating" of electron flow in which MgATP binding and hydrolysis causes conformational changes in both nitrogenase proteins that ensure delivery to and accumulation within the MoFe-protein of multiple electrons prior to their delivery to substrate. In support of this concept, primary amino acid sequence and structural comparisons show that the Fe-protein is a member of a large class of signal transduction proteins that undergo conformational changes upon MgATP binding and hydrolysis.

The following sequence of events, which occur during a single turn of the Fe-protein cycle and which account for the role of MgATP in nitrogenase catalysis, is widely accepted (77). First, the reduced Fe-pro-

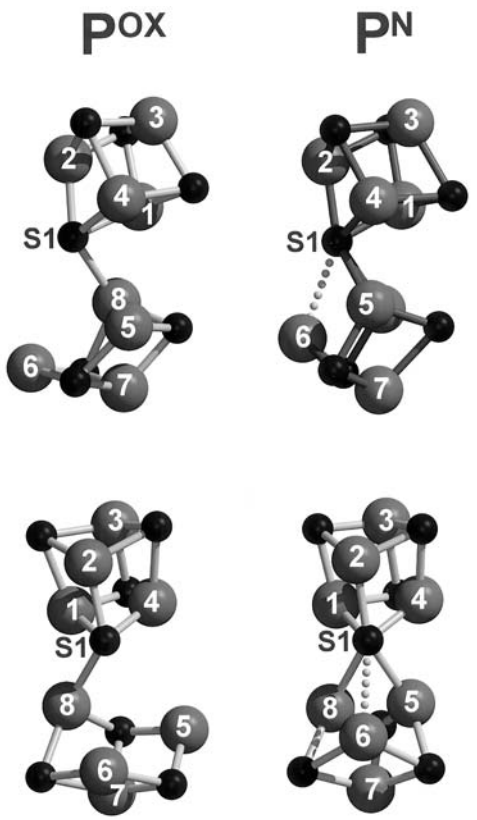

Figure 2 Ball-and-stick structural models of the two forms, P^{OX} and P^{N}, of the P-cluster of the nitrogenase MoFe-protein. Each form is shown in two orientations, which are related by a 90° rotation. The iron atoms are gray and labeled 1–8; and the S atoms are black with the S atom that is labeled as S1 being shared among the two subclusters. The length of the Fe6–S1 bond is longer than the normal Fe–S bond and is shown as a dotted line. (Figure courtesy of Dr. J.W. Peters, Utah State University.)

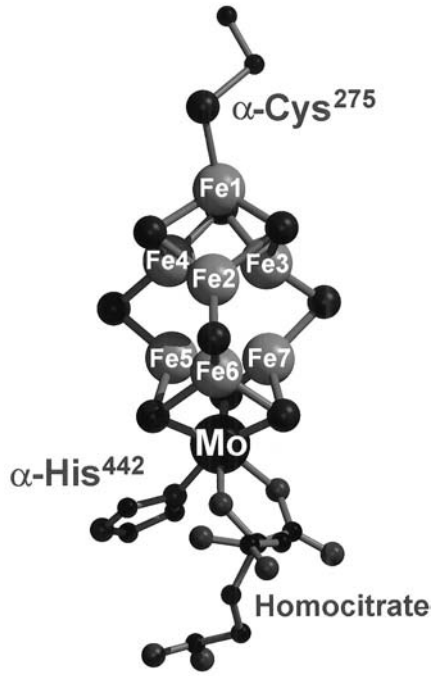

Figure 3 Ball-and-stick structural model of the FeMo cofactor of the nitrogenase MoFe–protein. Its iron atoms are gray and labeled Fe1–Fe7; the Mo atom is large and black; the S atoms are medium-size and black; and all C, N, and O atoms are small and black. Also shown are the directly bonded entities, which are R-homocitrate and the two α-subunit residues, histidinyl-442 and cysteinyl-275. (Figure courtesy of Dr. J.W. Peters, Utah State University.)

tein binds two MgATP molecules, which produces a conformational change in the Fe-protein that makes it competent for interaction with the MoFe-protein. Second, the two proteins form a complex, which induces changes in the midpoint potentials of the metal–sulfur clusters such that electron flow toward FeMo cofactor is energetically favored. In the nitrogenase complex, the redox potential of the Fe-protein's [4Fe–4S] cluster is −620 mV, that of the P-cluster is −390 mV, and the redox potential of the FeMo cofactor is −40 mV (78). Third, in addition to electron transfer, the docking of the component proteins triggers MgATP hydrolysis, although it is not clear whether this occurs shortly before, concomitantly with, or shortly after electron transfer or whether the timing varies depending on other factors. It is clear, however, that phosphate release (which is usually when energy transduction occurs) from the complex follows electron transfer and that phosphate release does not drive the dissociation of this complex into its component proteins (79). Fourth, the conversion of the Fe-protein from the MgATP-bound state to the MgADP-bound state causes complex dissociation and this process is the rate-limiting step in nitrogenase catalysis (60). This complex intercommunication between the two proteins results in the accumulation of electrons within the MoFe-protein, and the whole process appears to be synchronized by sequential conformational changes induced by MgATP binding, component protein interaction, and MgATP hydrolysis.

F. Electron Transport to Nitrogenase

A source of reducing equivalents of sufficiently low potential is required for regeneration of reduced Fe-protein after it has donated one electron to the MoFe-protein. Both flavodoxins and ferredoxins are

capable of serving this function *in vitro*. The ultimate donor of low-potential electrons has not been identified for most nitrogenases. In some bacteria, *e.g.*, *A vinelandii*, redundancy is apparent with several flavodoxins and ferredoxins capable of supporting nitrogenase turnover. However, for *K. pneumoniae*, two genes, *nifF* and *nifJ*, are involved in coupling the reduction of Fe-protein to intermediary metabolism (80, 81). The *nifF* gene product is a flavodoxin that can donate an electron to the oxidized Fe-protein. In this process, the reduced hydroquinone form of its flavin is oxidized to a semiquinone form. The re-reduction of flavodoxin is accomplished through the catalytic activity of the *nifJ* gene product, which is a pyruvate-flavodoxin oxidoreductase. It couples the oxidation of pyruvate, yielding acetyl-CoA and CO_2, to the reduction of the semiquinone form of the flavin to its hydroquinone form. The *nifJ* gene has not been found in other nitrogen-fixing genera, so other means of providing reducing equivalents to nitrogenase must be operating.

IV. *nif* GENES

In addition to the products of the *nif* genes discussed above, other genes and their products are required for the maturation of the nitrogenase component proteins and for the regulation of the expression of the nitrogenase genes. The organism that appears to have the simplest organization of nitrogen fixation–specific (*nif*) genes, and which is the one best studied at the molecular genetic level, is the facultative anaerobe, *Klebsiella pneumoniae*. This organism has 20 *nif* genes organized into seven transcriptional units. The specific designations for individual *K. pneumoniae nif* genes are also used to denote genes whose products have homologous functions in other organisms. For example, the *nif* structural genes from all diazotrophs are designated *nifH*, *nifD*, and *nifK* and they encode the Fe-protein and the MoFe-protein α- and β-subunits, respectively. Complications occur, however, in the genetic nomenclature of *nif* genes in that some organisms do not have homologues of all *K. pneumoniae nif* genes and others have nitrogen fixation–related genes that are not present in *K. pneumoniae*. A general convention is that the *nif* designation is reserved for only those genes that have functional counterparts in *K. pneumoniae*, whereas nitrogen fixation–related genes present in other organisms without functional counterparts in *K. pneumoniae* are given other designations. For example, the "*fix*" designation is used for such genes occurring in the rhizobia. A number of nitrogen fixation genes associated with both of the genetically distinct, Mo-independent "alternative" enzymes have also been identified, including the structural genes for both the V-nitrogenase (*vnfHDGK*) and the Fe-nitrogenase (*anfHDGK*) (82, 83), two *nifA*-like genes (84), and one *nifEN*-like sequence (85). The functions of the products of these last three genes is described in the next two sections.

V. MATURATION OF NITROGENASE

The primary translation products of the nitrogenase structural genes are not active. Many other *nif*-specific genes are required to activate these immature structural components. The function of the products of these *nif*-specific maturation genes is to catalyze the formation and then insertion of the individual metalloclusters into apo-forms of the Fe-protein and MoFe-protein. In the case of the Fe-protein, only the *nifM* gene product is specifically required for its maturation (86). The *nifM* gene product has not yet been isolated in an active form, but it appears to be a member of a family of peptidyl-prolyl isomerases (87), which assist protein folding by catalyzing the *cis*/*trans* isomerization of certain peptidyl-prolyl bonds. It is not obvious why such a requirement exists for the maturation of the Fe-protein, but it could be involved with the formation of a transient state of the immature Fe-protein necessary for insertion of the [4Fe–4S] cluster.

Maturation of the MoFe-protein, particularly the formation and insertion of the FeMo cofactor into an immature form of the MoFe-protein, is much more complicated. This process involves the products of, at least, the *nifH*, *nifE*, *nifN*, *nifB*, *nifV*, and *nifQ* genes. The nitrogenase Fe-protein, whose subunits are the product of *nifH*, is required for both formation and insertion of the FeMo cofactor (88, 89). The Fe-protein's specific function in these processes is unknown but neither its MgATP-binding and -hydrolysis properties nor its electron transfer capability are involved (90, 91). Biochemical complementation experiments show that the FeMo cofactor is initially synthesized elsewhere and then inserted into a FeMo cofactor–deficient MoFe-protein that contains intact P-clusters (92).

A portion of the biosynthetic process occurs within a complex of the products of the *nifEN* genes. The *nifEN* gene products bear primary sequence similarity to the products of the *nifDK* structural genes (93) and a heterotetrameric complex of the *nifEN* products likely

serves as a molecular scaffold for FeMo cofactor assembly (93, 94). In *A. vinelandii*, a second *nifEN*-like set of genes, which are called *vnfEN*, have been detected and they appear to have a common function in both the *vnf* and *anf* systems. The *vnfEN* gene products probably work similarly for both the FeV cofactor and the putative Anf cofactor (FeFe cofactor) (85). The product of the *nifB* gene catalyzes the formation of a FeMo cofactor precursor called NifB cofactor (95). NifB cofactor appears to provide the basic Fe–S framework necessary for FeMo cofactor construction and becomes accommodated within the NifEN complex (96).

The *nifV* gene product catalyzes the condensation of acetyl-CoA and α-ketoglutarate to form homocitrate, the organic constituent of FeMo cofactor (97, 98). The *nifQ* gene product has a role in providing the Mo atom for the FeMo cofactor, especially under Mo-deficient conditions, but its exact role is unknown (99). The products of the *nifX*, *nifW*, and *nifZ* genes might also have some role in FeMo cofactor biosynthesis (100, 101). With *K. pneumoniae*, a low-molecular-weight protein, encoded by *nifY*, appears to be associated with the apo-MoFe-protein produced in strains lacking either *nifB* or *nifEN* activity. The *nifY* gene product may stabilize an apo-MoFe-protein conformation that is amenable to FeMo cofactor insertion (102, 103). A different low-molecular-weight protein, which is called gamma and is not encoded by *nifY*, appears to serve the same function in *A. vinelandii* (104).

Two other *nif* gene products, those of *nifS* and *nifU*, catalyze reactions that are involved in the general mobilization of Fe and S for metallocluster assembly (98, 105, 106). The *nifS* gene product is a cysteine desulfurase that activates S for Fe–S cluster formation. The *nifU* gene product might have a role in providing Fe. Homologs to *nifU* and *nifS*, whose expression is not under *nif*-specific control, are present in many organisms and these may function in general Fe–S cluster formation and repair (107).

When the alternative nitrogenases are considered, the situation becomes complicated because the products of the *nifMBVUS* genes are essential for functional activity of the V-nitrogenase and Fe-nitrogenase as well as the Mo-nitrogenase (59, 108, 109). *The nifM* requirement indicates that all three Fe-proteins are so similar that a single NifM-protein can process them all. Because the *nifBV* gene products are involved with the biosynthesis of the FeMo cofactor of Mo-nitrogenase, their common requirement suggests similar cofactors in all three systems. Further, the *nifB* requirement supports the suggestion that its function cannot be Mo specific. The requirement for *nifB*, but not *nifEN*, is surprising because *nifB* and *nifN* are fused in *Clostridium pasteurianum* (110), which expresses a Mo-independent nitrogenase (111). Moreover, the *nifV* requirement shows that homocitrate is a constituent of all three cofactors as are S^{2-} and Fe, which would be provided through the requirement for the products of the *nifUS* genes.

VI. REGULATION OF NITROGENASE EXPRESSION

Because both nitrogenase proteins are denatured by dioxygen and because nitrogenase turnover requires consumption of considerable metabolic energy, it would make no sense to express the *nif* genes when dioxygen is present, when a fixed nitrogen source is available, or when cellular growth is limited by the availability of a carbon source. All three factors regulate *nif* gene expression. Moreover, many free-living nitrogen fixers have alternative nitrogenases and so the expression of the *nif* genes is also controlled by the availability of Mo or V.

K. pneumoniae has been most thoroughly studied in terms of the regulation of *nif* gene expression. Two of its 20 *nif*-specific genes are the regulatory genes, *nifL* and *nifA* (112), and they are contained in one of the seven transcriptional units in *K. pneumoniae*. Expression of the *nifLA* genes is controlled by the global nitrogen regulatory elements consisting of the products of the *ntrA*, *ntrB*, and *ntr*C genes. The expression of the other six *nif* transcriptional units is controlled by the products of *nifL*, *nifA*, and *ntrA*. The *ntrA* gene product, which is known as either NtrA or σ^{54}, is an alternative sigma factor that controls the expression of not only the *nif* and *ntr* genes but also that of a wide variety of gene families (113). The presence of NtrA imparts a specificity to RNA polymerase and allows it to recognize a consensus promoter sequence, CTGG-N_8-TTGCA, which is located -24 to -12 bp before the transcription initiation site. Generally, the normal RNA polymerase, which contains the abundant sigma factor called σ^{70}, recognizes a typical prokaryotic promoter sequence, TTGACA-N_{17}-TATACA, at -35 to -10 bp before the transcription initiation site. Expression of *ntrA* does not appear to be tightly controlled, and the omnipresence of NtrA apparently reserves a portion of the RNA polymerase for specialized functions like nitrogen fixation.

The specific regulation of the expression of the *nifLA* genes is controlled by the products NtrB and

NtrC of the global nitrogen regulatory genes, *ntrB* and *ntrC*. NtrB and NtrC form a two-component regulatory system in which NtrB is the phosphatase/kinase sensor protein that controls the phosphorylation state of NtrC in response to the ratio of α-ketoglutarate to ammonia in the cell (114). When this ratio is high, a condition that signals fixed-nitrogen limitation and high energy charge, NtrC is phosphorylated and, when the ratio is low, NtrC is dephosphorylated. Under the former condition, phosphorylated NtrC initiates a two-tiered regulatory cascade that first leads to activation of the *nifLA* promoter, which then results in activation of the other *nif* promoters. Phosphorylated NtrC recognizes and binds to a consensus DNA sequence that is located upstream from the σ^{54}-RNA polymerase-binding site of *nifLA*. Bound, phosphorylated NtrC catalyzes an ATP-dependent conformational isomerization at the promoter site, which ultimately results in the initiation of transcription of the *nifLA* transcriptional unit (115). Accumulation of the products of the *nifL* and *nifA* genes then specifically controls the other *nif* promoters.

NifA is structurally and functionally similar to NtrC (116, 117). It also binds to an upstream activator sequence, but one with a consensus sequence motif, TGT-N_{10}-ACA, that is different from the NtrC-binding site. This sequence is located $\sim$ 100 bp before each *nif* promoter except that for *nifLA* (118). However, unlike NtrC, NifA activity is not controlled by phosphorylation/dephosphorylation; rather, its ability to activate *nif* gene expression is controlled by NifL, which acts as an antiactivator. Although just how NifL complexes with NifA is not known, this complexation occurs when either the dioxygen level or the fixed-nitrogen level is sufficiently high and the *nif* promoters are not activated. NifL is a flavoprotein that senses the redox status of the cell by conformational changes that are controlled by the oxidation state of its FAD moiety (119, 120). In *A. vinelandii*, each of the alternative nitrogenase enzyme systems has its own specific NifA-like protein (either VnfA or AnfA), which acts as a positive regulator of *nif* gene expression (84).

The mechanism by which *K. pneumoniae* controls *nif* gene expression is not universal. Many other strategies are used. Very little is known about the regulation of *nif* gene expression in the Archaea or clostridia, for example, except that it is different from that described above. Other control mechanisms, in addition to transcriptional control, include posttranslational modifications. For example, the reversible modification of the nitrogenase Fe-protein occurs in *Rhodospirillum rubrum* and *Azospirillum brasilense*. These organisms regulate nitrogenase activity by ADP-ribosylation of a specific arginine residue on the docking surface of the Fe-protein in response to changes in environmental conditions (121, 122). In strict aerobes, nitrogenase can undergo "conformational protection" to guard against O_2 damage by forming a protein aggregate, which dissociates to resume fixation when the O_2 stress is relieved (123).

Very different examples of the control of the expression of nitrogenase activity involve the formation of specialized structures. In many cyanobacteria, for example *Anabaena* 7120, nitrogen fixation is restricted to specialized cells called heterocysts (124). The formation of heterocysts, as well as nitrogenase expression, is both temporally and spatially controlled through terminal differentiation events involving genomic rearrangements. The root nodule was discussed earlier, but here another specialized case of the control of nitrogenase gene expression occurs. Because the function of the root nodule bacteria (rhizobia) is to produce and export fixed nitrogen to its host plant, it would defeat its purpose to retain a regulatory mechanism that is sensitive to the presence of fixed nitrogen. However, control of *nif* gene expression in response to the cellular dioxygen concentration is still absolutely required. Similar to the two-component NtrB/NtrC system, dioxygen control of *nif* gene expression in rhizobia occurs through another sensor–regulator pair (125). The sensor protein, FixL, is a hemoprotein located within the cell membrane and, like NtrB, it has phosphatase/kinase activities. Under microaerobic conditions, FixL catalyzes the phosphorylation of FixJ, which then activates the expression of *nifA* similarly to NtrC activation in *K. pneumoniae*. Rhizobia do not contain a NifL analog. Therefore, control of *nif* gene expression involves no antiactivator; rather, the activity of rhizobial NifA proteins appears to be directly sensitive to the presence of dioxygen (126).

VII. SUMMARY AND OUTLOOK

Considerable progress has been made in understanding the mechanism of action of nitrogenase, particularly since 1970. In the early 1960s, only crude, cell-free preparations were available for investigating the nitrogen fixation phenomenon, whereas highly purified, crystalline preparations of the nitrogenase component proteins are now available for study. The x-ray derived structures of both protein components and a docked

complex (35, 63) have clearly defined the structural goals to add to the obvious reactivity goal for effective model building. However, there is still no detailed mechanism that describes biological nitrogen reduction in structural terms, although a very useful numerical model is available (60). Even so, purely chemical systems have been devised that bind N_2 and, in some cases, activate it sufficiently that reduced nitrogen compounds, ammonia, and/or hydrazine are produced on protonation (127–129). These chemical N_2 fixation systems, which work under ambient conditions, may in the future form the basis of a simple, low-temperature and low-pressure system, possibly operated electrochemically and driven by a renewable resource, such as solar, wind, or water power or off-peak electrical power, located near or in irrigation streams. However, they are unlikely to compete directly with commercial nitrogen fertilizer production by the Haber-Bosch process or profoundly impact our understanding of the biological system.

In the near term, exploitation of the benefits of biological nitrogen fixation will depend on an increased use of legumes and other symbiotic systems in agriculture with care to match the most effective rhizobial strains with the appropriate cultivar. If these associations could be manipulated either to start fixation earlier or to continue it longer, substantial yield, nutritional and economic benefits could accrue. Similarly, benefits would accrue if the ability to fix N_2 in the presence of fixed-nitrogen sources were conferred on bacteria. The ongoing discovery of new nonleguminous, associative symbioses indicates new avenues through which N_2 fixation and the delivery of fixed nitrogen to crop plants may be enhanced. Close scrutiny of these systems may yield information on how to engineer new associations, possibly with the principal food crops that at present do not enter into N_2-fixing symbioses. These associations could have dramatic effects on both fertilizer usage and food production.

Genetic manipulation of N_2 fixation is the ultimate solution for providing fixed nitrogen input to crop plants and for increasing global food supplies. In doing so, decreased reliance on fossil fuel energy inputs to fertilizer production will result. Recent genetic manipulation of the recognition and infection processes could result in both new and enhanced symbiotic associations because many plants appear to already have most genes necessary to produce a nodulelike structure. In addition, the success of transferring the *nif* genes from one bacterial genus to another has opened up the possibility of their transfer to crop plants (130). However, genetic transfer is not enough. If it were, nature would probably have many N_2-fixing plants already in place. Protection from dioxygen and a sufficient energy supply are also required. These needs could be satisfied if nitrogenase were relocated to the chloroplasts of leaves where, if properly protected from the O_2 evolved by photosynthesis, it could take advantage of directly available reducing equivalents produced from sunlight. Finally, at no time soon does it appear likely that the many known associations involving animals will be exploited. Therefore, man appears destined to remain dependent on plants for a supply of fixed nitrogen.

REFERENCES

1. WE Newton. Nitrogen Fixation. Kirk-Othmer Encyclopedia of Chemical Technology, Vol 17. 4th ed. New York: John Wiley & Sons, 1996, pp 172–204.
2. OC Böckman. Fertilizers and biological nitrogen fixation as sources of plant nutrients: perspectives for future agriculture. Plant Soil 194:11–14, 1997.
3. JI Sprent, P Sprent. Nitrogen Fixing Organisms: Pure and Applied Aspects. New York: Chapman & Hall, 1990.
4. JPW Young. Phylogenetic classification of nitrogen-fixing organisms. In: G Stacey, RH Burris, HJ Evans, eds. Biological Nitrogen Fixation. New York: Chapman and Hall, 1992, pp 43–86.
5. JB Boussingault. Recherches chimiques sur la végétation, enterprises dans le but d'examiner si les plantes prennet de l'azote à l'atmosphere. Ann Chim Phys 2nd Ser 67:5–54, 1838.
6. PW Wilson. The Biochemistry of Nitrogen Fixation. Madison: University of Wisconsin Press, 1940.
7. H Hellriegel, H Wilfarth. Untersuchungen über die stickstoffnahrung der Gamineen und Leguminosen. Beilageheft zu der Zeitschrift des Vereins f. d. Rübensucker-industrie d. Deutschen Reiches, 1888, pp 1–234
8. A Quispel. Hellriegel and Wilfarth's discovery of (symbiotic) nitrogen fixation hundred years ago. In: H Bothe, FJ de Bruijn, WE Newton, eds. Nitrogen Fixation: Hundred Years After. New York: Gustav Fischer, 1988, pp 3–12.
9. J Dénarié, F Debellé, C Roseberg. Signalling and host range variation in nodulation. Annu Rev Microbiol 46:497–531, 1992.
10. PY Yao, JM Vincent. Host specificity in the root hair "curling factor" of *Rhizobium* sp. Aust J Biol Sci 22:413–423, 1969.
11. FB Dazzo, A Gardiol. Host specificity in *Rhizobium*–legume interactions. In: DPS Verma, T Hohn, eds. Genes Involved in Microbe Plant Interactions. New York: Springer-Verlag, 1984, pp 3–31.

12. D Verma, S Long. The molecular biology of *Rhizobium*–legume symbiosis. In: KW Jeon, ed. Intracellular Symbiosis. New York: Academic Press, 1983, pp 211–245.
13. KR Libbenga, PAA Harkes. Initial proliferation of cortical cells in the formation of root nodules in *Pisum sativum* L. Planta 114:17–28, 1973.
14. JG Robertson, P Lyttleton, S Bullivant, GF Grayston. Membranes in lupin root nodules. I. The role of Golgi bodies in the biogenesis of infection threads and peribacteroid membranes. J Cell Sci 30:129–149, 1978
15. NK Peters, JW Frost, SR Long. A plant flavone, luteolin, induces expression of *Rhizobium meliloti* nodulation genes. Science 233:917–1008, 1986.
16. HP Spaink, CA Wijffelman, E Pees, RJH Okker, BJJ Lugtenberg. *Rhizobium* nodulation gene *nodD* as a determinant of host specificity. Nature 328:337–340, 1987.
17. P Lerouge, P Roche, C Faucher, F Maillet, G Truchet, JC Promé, J Dénarié. Symbiotic host-specificity of *Rhizobium meliloti* is determined by a sulphated and acylated obligosaccharide signal. Nature 344:781–784, 1990.
18. B Dreyfus. YR Dommergues. Nodulation of *Acacia* species by fast-growing and slow-growing tropical strains of *Rhizobium*. Appl Environ Microbiol 41:97–99, 1981.
19. ARJ Eaglesham, JM Ellis, WR Evans, DE Fleischman, M Hungria, RWF Hardy. The first photosynthetic N_2-fixing *Rhizobium*: characteristics. In: PM Gresshoff, LE Roth, G Stacey, WE Newton, eds. Nitrogen Fixation: Achievements and Objectives. New York: Chapman and Hall, 1990, pp 805–811.
20. J Döbereiner, JM Day, PJ Dart. Nitrogenase activity and oxygen sensitivity of the *Paspalum notatum*–*Azotobacter paspali* association. J Gen Microbiol 71:103–116, 1972.
21. JFW von Bülow, J Döbereiner. Potential for nitrogen fixation in maize genotypes in Brazil. Proc Natl Acad Sci USA 72:2389–2393, 1974.
22. J Döbereiner, VM Reis, AC Lazarini. New N_2 fixing bacteria in association with cereals and sugar cane. In: H Bothe, FJ de Bruijn, WE Newton, eds. Nitrogen Fixation: Hundred Years After. New York: Gustav Fischer, 1988, pp 717–722.
23. J Döbereiner, VM Reis, MA Paula, F Olivares. Endophytic diazotrophs in sugar cane, cereals and tuber plants. In R Palacios, J Mora, WE Newton, eds. New Horizons in Nitrogen Fixation. Dordrecht, Netherlands: Kluwer Academic, 1993, pp 671–676.
24. B Reinhold-Hurek, T Hurek. Capacities of *Azoarcus* sp., a new genus of grass-associated diazotrophs. In: R Palacios, J Mora, WE Newton, eds. New Horizons in Nitrogen Fixation. Dordrecht, Netherlands: Kluwer Academic, 1993, pp 691–694.
25. GJ Waughman, JRJ French, K Jones. Nitrogen fixation in some terrestrial environments. In: WJ Broughton, ed. Nitrogen Fixation, Vol 1. Oxford: Clarendon Press, 1981 pp 135–192.
26. JR Benemann. Nitrogen fixation in termites. Science 181:164–165, 1973.
27. GD Prestwich, BL Bentley. Nitrogen fixation by intact colonies of the termite *Nasutitermes corniger*. Oecologia 49:249–251, 1981.
28. JB Waterbury, CB Calloway, RD Turner. A cellulytic nitrogen-fixing bacterium cultured from the Deshayes gland in shipworms (Bivalvia: Teredinidae) Science 221:1401–1403, 1983.
29. M Ribbe, D Gadkari, O Meyer. N_2 fixation by *Streptomyces thermoautotrophicus* involves a molybdenum-dinitrogenase and a manganese-superoxide oxidoreductase that couple N_2 reduction to the oxidation of superoxide produced from O_2 by a molybdenum-CO dehydrogenase. J Biol Chem 272:26627–26633, 1997.
30. JB Howard. DC Rees. Structural basis of biological nitrogen fixation. Chem Rev 96:2965–2982, 1996.
31. BK Burgess, DJ Lowe. Mechanism of molybdenum nitrogenase. Chem Rev 96:2983–3011, 1996.
32. JW Peters, K Fisher, DR Dean. Nitrogenase structure and function: A biochemical–genetic perspective. Annu Rev Microbiol 49:335–366, 1995.
33. RV Hageman, RH Burris. Nitrogenase and nitrogenase reductase associate and dissociate with each catalytic cycle. Proc Natl Acad Sci USA 75:2699–2702, 1978.
34. MM Georgiadis, H Komiya, P Chakrabarti, D Woo, JJ Kornuc, DC Rees. Crystallographic structure of the nitrogenase iron protein from *Azotobacter vinelandii*. Science 257: 1653–1659, 1992.
35. C Kim. DC Rees. Structural models for the metal centers in the nitrogenase molybdenum-iron protein. Science 257:1677–1682, 1992.
36. JT Bolin, N Campobasso, SW Muchmore, TV Morgan, LE Mortenson. Structure and environment of metal clusters in the nitrogenase molybdenum-iron protein from *Clostridium pasteurianum*. In: EI Stiefel, D Coucouvanis, WE Newton, eds. Molybdenum Enzymes, Cofactors and Model Systems. Washington: American Chemical Society, 1993, Symp Ser 535, pp 186–195.
37. MK Chan, J Kim, DC Rees. The nitrogenase FeMo-cofactor and P-cluster pair: 2.2 Å resolution structures. Science 260:792–794, 1993.
38. JW Peters, MHB Stowell, SM Soltis, MG Finnegan, MK Johnson, DC Rees. Redox-dependent structural changes in the nitrogenase P-cluster. Biochemistry 36:1181–1187, 1997.
39. JE Carnahan, JE Castle. Nitrogen fixation. Annu Rev Plant Physiol 14:125–136, 1963.

40. WA Bulen, RC Burns, JR LeComte. Nitrogen fixation: hydrosulfite as electron donor with cell-free preparations of *Azotobacter vinelandii* and *Rhodospirillum rubrum*. Proc Natl Acad Sci USA 53:532–539, 1965.
41. RWF Hardy, E Knight Jr, AJ D'Eustachio. An energy-dependent hydrogen-evolution from dithionite in nitrogen-fixing extracts of *Clostridium pasteurianum*. Biochem Biophys Res Commun 20:539–544, 1965.
42. WA Bulen, JR LeComte, RC Burns, J Hinkson. Nitrogen fixation studies with aerobic and photosynthetic bacteria. In: A San Pietro, ed. Non-Heme Iron Proteins: Role in Energy Conversion. Yellow Springs, OH: Antioch Press, 1965, pp 261–274.
43. JL Hwang, CH Chen, RH Burris. Inhibition of nitrogenase-catalyzed reductions. Biochim Biophys Acta 292:256–270, 1973.
44. GE Hoch, KC Schneider, RH Burris. Hydrogen evolution and exchange, and conversion of N_2O to N_2 by soybean root nodules. Biochim Biophys Acta 37:273–279, 1960.
45. BK Burgess, S Wherland, WE Newton, EI Stiefel. Nitrogenase reactivity: insight into the nitrogen-fixing process through hydrogen-inhibition and HD-forming reactions. Biochemistry 20:5140–5146, 1981.
46. JH Guth, RH Burris. Inhibition of nitrogenase-catalyzed NH_3 formation by H_2. Biochemistry 22:5111–5122, 1983.
47. BB Jensen, RH Burris. Effect of high pN_2 and high pD_2 on NH_3 production, H_2 evolution, and HD formation by nitrogenases. Biochemistry 24:1141–1147, 1985.
48. DR Dean, MR Jacobson. Biochemical genetics of nitrogenase. In: G Stacey, RH Burris, HJ Evans, eds. Biological Nitrogen Fixation. New York: Chapman and Hall, 1992, pp 834–863.
49. DW Emerich, RH Burris. Complementary functioning of the component proteins of nitrogenases from several bacteria. J Bacteriol 134:936–943, 1978.
50. PE Bishop, DML Jarlenski, DR Hetherington. Evidence for an alternative nitrogen fixation system in *Azotobacter vinelandii*. Proc Natl Acad Sci USA 77:7342–7346, 1980.
51 RL Robson, RR Eady, TH Richardson, RW Miller, M Hawkins, JR Postgate. The alternative nitrogen fixation system of *Azotobacter chroococcum* is a vanadium enzyme. Nature 322:388–390, 1986.
52. JR Chisnell, R Premakumar, PE Bishop. Purification of a second alternative nitrogenase from a *nifHDK* deletion strain of *Azotobacter vinelandii*. J Bacteriol 170:27–33, 1988.
53. RL Robson, PR Woodley, RN Pau, RR Eady. Structural genes for the vanadium nitrogenase from *Azotobacter chroococcum*. EMBO J 8:1217–1224, 1989.
54. BJ Hales, EE Case, JE Morningstar, MF Dzeda, LA Mauterer. Isolation of a new vanadium-containing nitrogenase from *Azotobacter vinelandii*. Biochemistry 25:7251–7255, 1986.
55. K Schneider, A Müller, U Schramm, W Klipp. Demonstration of a molybdenum- and vanadium-independent nitrogenase in a *nifHDK*-deletion mutant of *Rhodobacter capsulatus*. Eur J Biochem 195:653–661, 1991.
56. MR Jacobson, R Premakumar, PE Bishop. Transcriptional regulation of nitrogen fixation by molybdenum in *Azotobacter vinelandii*. J Bacteriol 167:480–486, 1986.
57. F Luque, RN Pau. Transcriptional regulation by metals of structural genes for *Azotobacter vinelandii* nitrogenases. Mol Gen Genet 227:481–487, 1991.
58. RR Eady. Structure–function relationships of alternative nitrogenases. Chem Rev 96:3013–3030, 1996.
59. WE Newton. Nitrogenases: distribution, composition, structure and function. In: R Palacios, J Mora, WE Newton, eds. New Horizons in Nitrogen Fixation. Dordrecht, Netherlands: Kluwer Academic, 1993, pp 5–18.
60. DJ Lowe, RNF Thorneley. The mechanism of *Klebsiella pneumoniae* nitrogenase action: Simulation of the pH dependencies of H_2-evolution rate on component-protein concentration and ratio and sodium dithionite concentration. Biochem J 224:903–909, 1984.
61. HD May, DR Dean, WE Newton. Altered nitrogenase MoFe proteins from *Azotobacter vinelandii*. Biochem J 277:457–464, 1991.
62. JW Peters, K Fisher, WE Newton, DR Dean. Involvement of the P cluster in intramolecular electron transfer within the nitrogenase MoFe protein. J Biol Chem 270:27007–27013, 1995.
63. H Schindelin, C Kisker, JL Schlessman, JB Howard, DC Rees. Structure of ADP-AlF_4^- stabilized nitrogenase complex and its implications for signal transduction. Nature 387:370–376, 1997.
64. VK Shah, WJ Brill. Isolation of an iron-molybdenum cofactor from nitrogenase. Proc Natl Acad Sci USA 74:3249–3253, 1977.
65. TR Hawkes, PA McLean, BE Smith. Nitrogenase from *nifV* mutants of *Klebsiella pneumoniae* contains an altered form of the iron-molybdenum cofactor. Biochem J 217:317–321, 1984.
66. J Liang, M Madden, VK Shah, RH Burris. Citrate substitutes for homocitrate in nitrogenase of a *nifV* mutant of *Klebsiella pneumoniae*. Biochemistry 29:8577–8581, 1990.
67. DJ Scott, HD May, WE Newton, KE Brigle, DR Dean. Role for the nitrogenase MoFe protein α-subunit in FeMo-cofactor binding and catalysis. Nature 343:188–190, 1990.

68. MJ Dilworth, K Fisher, C-H Kim, WE Newton. Effects on substrate reduction of substitution of histidine-195 by glutamine in the α-subunit of the MoFe protein of *Azotobacter vinelandii* nitrogenase. Biochemistry 37:17495–17505, 1998.
69. I Dance. The binding and reduction of dinitrogen at an Fe_4 face of the FeMo-cofactor of nitrogenase. J Bioinorg Chem 1:581–586, 1996.
70. D Sellmann. X-ray structure analysis of FeMo nitrogenase— is the problem of N_2 fixation solved? Angew Chem Int Ed Engl 32:64–67, 1993.
71. H Deng, R. Hoffmann. How N_2 may be activated by the FeMo-cofactor of nitrogenase. Angew Chem Int Ed Engl 32:1062–1065, 1993.
72. H-I Lee, LM Cameron, BJ Hales, BM Hoffman. CO binding to the FeMo-cofactor of CO-inhibited nitrogenase. ^{13}CO and ^{1}H Q-band ENDOR investigation. J Am Chem Soc 119:10121–10126, 1997.
73. KK Stavrev, MC Zerner. Studies on the hydrogenation steps of the nitrogen molecule at the *Azotobacter vinelandii* nitrogenase site. Int J Quantum Chem 70: 1159–1168, 1998.
74. DL Hughes, SK Ibrahim, CJ Pickett, G Querne, A Laouenen, J Talarmin, A Queiros, A Fonseca. On carboxylate as a leaving group at the active site of Mo nitrogenase: electrochemical reactions of some Mo and W carboxylates, formation of mono-, di- and tri-hydrides and the detection of an $MoH_2(N_2)$ intermediate. Polyhedron 13:3341–3348, 1994.
75. J Shen, DR Dean, WE Newton. Evidence for multiple substrate-reduction sites and distinct inhibitor-binding sites from an altered *Azotobacter vinelandii* nitrogenase MoFe protein Biochemistry 36:4884–4894, 1997.
76. KLC Grönberg, CA Gormal, MC Durrant, BE Smith, RA Henderson. Why R-homocitrate is essential to the reactivity of FeMo-cofactor of nitrogenase: studies on *NifV*-extracted FeMo-cofactor. J Am Chem Soc 120:10613–10621, 1998.
77. LC Seefeldt, DR Dean. Role of nucleotides in nitrogenase catalysis. Acc Chem Res 30:260–266, 1997.
78. WN Lanzilotta, LC Seefeldt. Changes in the midpoint potentials of the nitrogenase metal centers as a result of iron protein-molybdenum-iron protein complex formation. Biochemistry 36:12976–12983, 1997.
79. DJ Lowe, GA Ashby, M Brune, H Knights, MR Webb, RNF Thorneley. ATP hydrolysis and energy transduction by nitrogenase. In: IA Tikhonovich, NA Provorov, VI Romanov, WE Newton, eds. Nitrogen Fixation: Fundamentals and Applications. Dordrecht, Netherlands: Kluwer Academic, 1995, pp 103–108.
80. D Nieva-Gomez, GP Roberts, S Klevickis, WJ Brill. Electron transport to nitrogenase in *Klebsiella pneumoniae*. Proc Natl Acad Sci USA 77:2555–2558, 1980.
81. S Hill, EP Kavanagh. Roles of the *nifF* and *nifJ* gene products in electron transport to nitrogenase in *Klebsiella pneumoniae*. J Bacteriol 141:470–475, 1980.
82. RD Joerger, MR Jacobson, R Premakumar, ED Wolfinger, PE Bishop. Nucleotide sequence and mutational analysis of structural genes (*anfHDGK*) for the second alternative nitrogenase from *Azotobacter vinelandii*. J Bacteriol 171:1075–1086, 1989.
83. RD Joerger, MR Jacobson, PE Bishop. Two nifA-like genes required for expression of alternative nitrogenases by *Azotobacter vinelandii*. J Bacteriol 171:3258–3267, 1989.
84. RD Joerger, TM Loveless, RN Pau, LA Mitchenall, BH Simon, PE Bishop. Nucleotide sequences and mutational analysis of structural genes for nitrogenase-2 of *Azotobacter vinelandii*. J Bacteriol 172:3400–3408, 1990.
85. ED Wolfinger, PE Bishop. Nucleotide sequence and mutational analysis of the *vnfENX* region of *Azotobacter vinelandii*. J Bacteriol 173:7565–7572, 1991.
86. KS Howard, PA McLean, FB Hansen, PV Lemley, KS Koblan, WH Orme-Johnson. *Klebsiella pneumonmiae nifM* gene product is required for stablization and activation of nitrogenase iron protein in *Escherichia coli*. J Biol Chem 261:772–778, 1986.
87. KE Rudd, HJ Sofia, EV Koonin, G Plunkett, S Lazar, PE Rouviere. A new family of peptidyl-prolyl isomerases. TIBS 20:12–14, 1995.
88. WA Filler, RM Kemp, JC Ng, TR Hawkes, RA Dixon, BE Smith. The *nifH* gene product is required for the synthesis of the iron-molybdenum cofactor of nitrogenase from *Klebsiella pneumoniae*. Eur J Biochem 160:371–377, 1986.
89. AC Robinson, DR Dean, BK Burgess. Iron-molybdenum cofactor biosynthesis in *Azotobacter vinelandii* requires the iron protein of nitrogenase. J Biol Chem 262:14327–14332, 1987.
90. N Gavini, BK Burgess. FeMo cofactor synthesis by a nifH mutant with altered MgATP reactivity. J Biol Chem 267:21179–21186, 1992.
91. D Wolle, DR Dean, JB Howard. Nucleotide-iron-sulfur cluster signal transduction in the nitrogenase iron-protein: The role of Asp^{125}. Science 258:992–995, 1992.
92. RA Ugalde, J Imperial, VK Shah, WJ Brill. Biosynthesis of iron-molybdenum cofactor in the absence of nitrogenase. J Bacteriol 159:888–893, 1984.
93. KE Brigle, MC Weiss, WE Newton, DR Dean. Products of the iron-molybdenum cofactor-specific genes, *nifE* and *nifN*, are structurally homologous to the products of the nitrogenase molybdenum-iron protein genes, *nifD* and *nifK*. J Bacteriol 169:1547–1553, 1987.
94. TD Paustian, VK Shah, GP Roberts. Purification and charaterization of the *nifN* and *nifE* gene products from *Azotobacter vinelandii* mutant UW45. Proc Natl Acad Sci USA 86:6082–6086, 1989.

95. VK Shah, RM Allen, NJ Spangler, PW Ludden. In vitro synthesis of the iron-molybdenum cofactor of nitrogenase. Purification and characterization of NifB cofactor, the product of the NifB protein. J Biol Chem 269:1154–1158, 1994.
96. JT Roll, VK Shah, DR Dean, GP Roberts. Characteristics of NifEN in *Azotobacter vinelandii* strains. J Biol Chem 270:4432–4437, 1995.
97. TR Hoover, AD Robertson, RL Cerny, RN Hayes, J Imperial, VK Shah, PW Ludden. Identification of the V factor needed for synthesis of the iron-molybdenum cofactor of nitrogenase as homocitrate Nature 329:855–857, 1987.
98. L Zheng, RH White, DR Dean. Purification of the *Azotobacter vinelandii* nifV-encoded homocitrate synthase. J Bacteriol 179:5963–5966, 1997.
99. J Imperial, RA Ugalde, VK Shah, WJ Brill. Role of the *nifQ* gene product in the incorporation of molybdenum into nitrogenase in *Klebsiella pneumoniae*. J Bacteriol 158:187–194, 1984.
100. MR Jacobson, VL Cash, MC Weiss, NF Laird, WE Newton, DR Dean. Biochemical and genetic analysis of the *nifUSVWZM* cluster from *Azotobacter vinelandii*. Mol Gen Genet 219:49–57, 1989.
101. VK Shah, P Rangaraj, R Chatterjee, RM Allen, JT Roll, GP Roberts, PW Ludden. Requirement of NifX and other Nif proteins for the in vitro biosynthesis of the iron-molybdenum cofactor of nitrogenase. In: C Elmerich, A Kondorosi, WE Newton, eds. Biological Nitrogen Fixation for the 21st Century. Dordrecht, Netherlands: Kluwer Academic, 1998, pp 51–52.
102. TC White, GS Harris, WH Orme-Johnson. Electrophoretic studies on the assembly of the nitrogenase molybdenum-iron protein from *Klebsiella pneumoniae nifD* and *nifK* gene products J Biol Chem 267:24007–24016, 1992.
103. MJ Homer, TD Paustian, VK Shah, GP Roberts. The *nifY* product of *Klebsiella pneumoniae* is associated with apodinitrogenase and dissociates upon activation with iron-molybdenum cofactor. J Bacteriol 175:4907–4910, 1993.
104. MJ Homer, DR Dean, GP Roberts. Characterization of the gamma protein and its involvement in the metallocluster assembly and maturation of dinitrogenase from *Azotobacter vinelandii*. J Biol Chem 270:24745–24752, 1995.
105. L Zheng, DR Dean. Catalytic formation of a nitrogenase iron-sulfur cluster. J Biol Chem 269:18723–18726, 1994.
106. W Fu, RF Jack, TV Morgan, DR Dean, MK Johnson. *nifU* gene product from *Azotobacter vinelandii* is a homodimer that contains two identical [2Fe–2S] clusters. Biochemistry 33:13455–13463, 1994.
107. D Flint. *Escherichia coli* contains a protein that is homologous in function and N-terminal sequence to the protein encoded by the *nifS* gene of *Azotobacter vinelandii* and that can participate in the synthesis of the Fe–S cluster in dihydroxy-acid dehydratase. J Biol Chem 271:16068–16074, 1996.
108. RD Joerger, PE Bishop. Nucleotide sequence and genetic analysis of the *nifB-nifQ* region from *Azotobacter vinelandii*. J Bacteriol 170:1475–1487, 1988.
109. C Kennedy, DR Dean. The *nifU*, *nifS* and *nifV* gene products are required for activity of all three nitrogenases of *Azotobacter vinelandii*. Mol Gen Genet 231:494–498, 1992.
110. J-S Chen, S-Z Wang, JL Johnson. Nitrogen fixation genes of *Clostridium pasteurianum*. In: PM Gresshoff, LE Roth, G Stacey, WE Newton, eds. Nitrogen Fixation: Achievements and Objectives. New York: Chapman and Hall, 1990, pp 483–490.
111. MJ Dilworth, RR Eady, RL Robson, RW Miller. Ethane formation from acetylene as a potential test for vanadium nitrogenase *in vivo*. Nature 327:167–168, 1987.
112. W Arnold, A Rump, W Klipp, UB Priefer, A Pühler. Nucleotide sequence of a 24,206-base-pair DNA fragment carrying the entire nitrogen fixation gene cluster of *Klebsiella pneumoniae*. J Mol Biol 203:715–738, 1988.
113. S Kustu, E Santero, D Popham, J Keener. Expression of sigma-54 (*ntrA*)-dependent genes is probably united by a common mechanism. Microbiol Rev 53:367–376, 1989.
114. BT Nixon, CW Ronson, FM Ausubel. Two-component regulatory systems responsive to environmental stimuli share strongly conserved domains with the nitrogen assimilation regulatory genes *ntrB* and *ntrC*. Proc Natl Acad Sci USA 83:7850–7854, 1986.
115. DL Popham, D Szeto, J Keener, S Kustu. Function of a bacterial activator protein that binds to transcriptional enhancers. Science 243:629–635, 1989.
116. M Drummond, P Whitty, J Wooton. Sequence and domain relationships of *ntrC* and *nifA* from *Klebsiella pneumoniae*. EMBO J 5:441–447, 1986.
117. WJ Buikema, WW Szeto, PV Lemley, WH Orme-Johnson, FM Ausubel. Nitrogen fixation specific regulatory genes of *Klebsiella pneumoniae* and *Rhizobium meliloti* share homology with the general nitrogen regulatory gene *ntrC* of *Klebsiella pneumoniae*. Nucleic Acids Res 13:4539–4555, 1985.
118. J Beynon, M Cannon, V Buchanan-Wollaston, F Cannon. The *nif* promoters of *Klebsiella pneumoniae* have a characteristic primary structure. Cell 34:665–671, 1983.
119. S Hill, S Austin, T Eydmann, T Jones, R Dixon. *Azotobacter vinelandii* NIFL is a flavoprotein that modulates transciptional activation of nitrogen-fixation genes via a redox-sensitive switch. Proc Natl Acad Sci USA 93:2143–2148, 1996.

120. R Dixon. The oxygen-responsive NifL-NifA complex: a novel two-component regulatory system controlling nitrogenase synthesis in γ-Proteobacteria. Arch Microbiol 169:371–380, 1998.
121. RG Lowery, PW Ludden. Purification and properties of dinitrogenase reductase ADP-ribosyltransferase from the photosynthetic bacterium *Rhodospirillum rubrum*. J Biol Chem 263:16714–16719, 1988.
122. LL Saari, EW Triplett, PW Ludden. Purification and properties of the activating enzyme for iron protein of nitrogenase from the photosynthetic bacterium *Rhodospirillum rubrum*. J Biol Chem 259:15502–15508, 1984.
123. S Hill. How is nitrogenase regulated by oxygen? FEMS Microbiol Rev 4:111–129, 1988.
124. JW Golden, SJ Robinson, R Haselkorn. Rearrangement of nitrogen fixation genes during heterocyst differentiation in the cyanobacterium *Anabaena*. Nature 314:419–423, 1985.
125. J Batut, M-L Daveran-Mingot, M David, J Jacobs, AM Garnerone, D Kahn. *fixK*, a gene homologous with *fnr* and *crp* from *Escherichia coli*, regulates nitrogen fixation genes both positively and negatively in *Rhizobium meliloti*. EMBO J 8:1279–1286, 1989.
126. H-M Fischer, T Bruderer, H Hennecke. Essential and non-essential domains in the *Bradyrhizobium japonicum* NifA protein: identification of indispensible cysteine residues potentially involved in redox activity and/or metal binding. Nucleic Acids Res 16:2207–2224, 1988.
127. LA Nikonova, SA Isaeva, NI Pershikova, AE Shilov. A comparison of the reduction of dinitrogen by a vanadium(II)-catechol system with that by the active centre of nitrogenase. J Mol Catal 1:367–374, 1975/76.
128. RL Richards. Reactions of small molecules at transition metal sites: studies relevant to nitrogenase, an organometallic enzyme. Coord Chem Rev 154:83–97, 1996.
129. CE Laplaza, CC Cummins. Dinitrogen cleavage by a three-coordinate molybdenum(III) complex. Science 268:861–863.
130. M Merrick, RA Dixon. Why don't plants fix nitrogen? Trends Biotechnol 2:162–166, 1984.

10

Enzymes in Amylose and Amylopectin Biosynthesis

Bruce P. Wasserman[†] **and Ying Yu**

Rutgers University, New Brunswick, New Jersey, U.S.A.

I. INTRODUCTION

Starch is the major storage carbohydrate of higher plants. In wild-type maize, starch consists of 25% amylose and 75% amylopectin. Starch and its chemically modified derivatives are of great importance to the world's food supply and economy. Starch-based products have long been used as sources for sweeteners and numerous other food and industrial ingredients, including pharmaceuticals, fat substitutes, textiles, packaging materials, and adhesives. The increasing agricultural and industrial importance of starch and its derivatives has raised interest in the possibility of producing bioengineered starches with improved functional properties.

Bioengineering of the genes encoding the major starch biosynthetic enzymes has the potential to modify starch yield and starch structure. In theory, gene alteration can be used to modify structural features such as the ratio of amylose to amylopectin, chain length and polymer size, degree of branching, the spacing between branch points, and the subsequent attachment of phosphate or sulfate groups. A detailed understanding of the enzymes that function within the starch biosynthetic pathway in higher plants is therefore vital.

II. THE STARCH BIOSYNTHETIC PATHWAY

A current view of the starch biosynthetic pathway in maize endosperm is diagrammed in Fig. 1. The immediate precursor of endosperm starch is sucrose. Sucrose is synthesized by photosynthesis in the leaf, and transported through the phloem. By the process of photoassimilate partitioning, sucrose is taken into the sink or storage tissue, which in this case is the endosperm of the kernel. Sucrose is converted into starch by a series of enzymatic steps (Fig. 1). In the cytosol, sucrose synthase and UDP-glucose pyrophosphorylase convert sucrose into Glc-1-P.*

The final three committed steps of starch biosynthesis consist of substrate formation, chain elongation, and branch point insertion. AGP catalyzes the formation of ADP-Glc from Glc-1-P and ATP. AGP is widely believed to be the major regulatory enzyme of the synthetic pathway (1, 2). One reason for this is that AGP is tetrameric and subject to allosteric regulation. A second reason is that plants carrying mutations in the AGP large or small subunits produce markedly decreased levels of starch (3, 4).

[†]Deceased.

*Abbreviations: ADP-Glc, adenosine diphosphoglucose; AGP, adenosine diphosphoglucose pyrophosphorylase; ATP, adenosine triphosphate; *ae*, amylose extender mutant; BT2, brittle-2; GBSS, granule-bound starch synthase; Glc-1-P, glucose-1-phosphate; SBE, starch branching enzyme; SDBE, starch debranching enzyme; SH2, shunken-2; SS, starch synthase; *su-1*, *sugary-1* mutant.

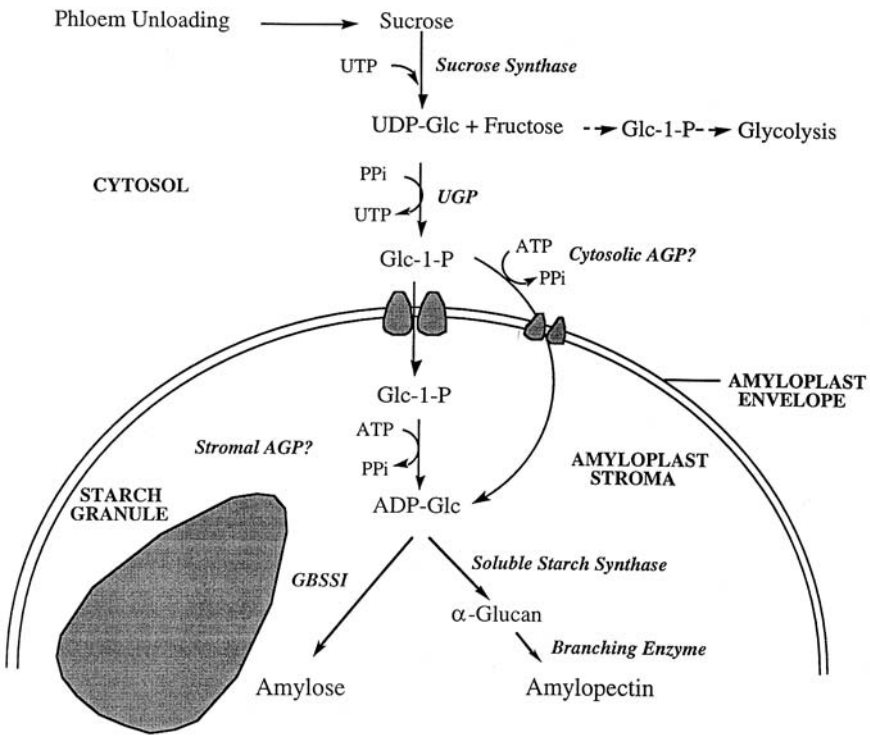

Figure 1 Starch biosynthetic pathway in maize endosperm.

Chain elongation reactions use ADP-Glc as substrate. Starch synthases are glycosyltransferases that elongate oligosaccharide chains by successive addition of (1,4)-α-linked glucose units to the nonreducing end of growing α-glucan chains. There are at least two classes of starch synthase. The GBSSI, also known as the Waxy protein, is responsible for the synthesis of amylose. The soluble starch synthases are believed to be involved in chain elongation of amylopectins. Starch chain length is thought to be controlled by specific starch synthase isoforms.

The (1,6)-α-linked branch linkages are introduced by isoforms of SBE, which are believed to operate by a cut-and-past type mechanism (5). SBE is thought to bind to the sites where adjacent starch chains are juxtaposed. The enzyme then cleaves at a (1,4)-α-linkage, and the newly generated reducing end is then attached at another site to form a (1,6)-α-branch point. Spacing between branch points may be controlled by specific SBE isoforms.

III. STARCH BIOSYNTHETIC ENZYMES AND THEIR ISOFORMS

Many isoforms of AGP, SS, and SBE have been purified, characterized, and cloned from a variety of plants. The occurrence of having multiple isoforms encoded by distinct genes may be significant for several reasons. First, each specific isoform may possess distinct catalytic properties and therefore determine parameters such as chain length or the spacing of branch points. For example, GBSSI is specifically responsible for the synthesis of amylose, and waxy mutant maize which lacks GBSSI is deficient in amylose. In addition, the isoforms of SBEI and SBEII transfer chains of different length. Second, the occurrence of multiple isoforms enables differential expression with regard to both tissue distribution, and plant growth and differentiation. Therefore, the identification and characterization of these isoforms is essential to the use of genetic engineering to improve starch yield and starch quality.

A. Adenosine Diphosphoglucose Pyrophosphorylase

AGP is a tetrameric protein composed of two large and small subunits known as SH2 and BT2, respectively. In maize, the SH2 and BT2 subunits have molecular masses of 54 and 51 kDa, respectively (Table 1) (3, 6). AGP is the only known tetrameric protein within the starch biosynthetic pathway. Most plant AGPs are subject to allosteric regulation by the activator 3-phosphoglycerate and the inhibitor inorganic phosphate (1). The AGP-catalyzed reaction is widely regarded as the rate-limiting step in the pathway. One body of evidence was obtained by expressing a regulatory variant, containing the *E. coli* AGP gene in tobacco, tomato, and potato. Since the bacterial AGP is relatively insensitive to regulatory inhibition by Pi, each of the transgenic plants exhibited significant increases in starch content (2).

The SH2 and BT2 subunits of AGP have both been purified from a variety of plants (3, 7–11). cDNA (12–16) and genomic (17) clones have been isolated and sequenced, and subunit function has been probed by site-directed mutagenesis (18).

B. Starch Synthase

Classification of starch synthases has not been straightforward because the literature groups classified the various isoforms according to three different criteria. Particular groupings may be based on solubility considerations, biochemical and catalytic properties, and deduced amino acid sequences derived from cDNA clones.

1. Granule-Bound Starch Synthase

Based on solubility, the predominant granule-bound starch synthase is referred to as GBSSI. GBSSI was identified by studies with the *waxy* mutant. This mutant lacks amylose, and is also deficient in a 60-kDa polypeptide known as the Waxy protein. *Waxy* mutants from numerous plant species are deficient in both the Waxy protein and amylose. In *waxy* mutants, the starch is exclusively amylopectin. On this basis, it has become widely accepted that the 60-kDa Waxy protein is the starch synthase responsible for chain elongation in amylose (19). Thus, the terms GBSSI and Waxy protein are now used interchangeably. The Waxy protein is solubilized by gelatinization of starch granules in the presence of a detergent such as SDS (19, 20).

GBSSI was the first maize starch synthase to be cloned (23). Mutations in the *waxy* locus result in low GBSS activities, absence of the Waxy protein, and virtually no amylose in the sink tissue of higher plants (19, 21–23). When potato plants were transformed to produce antisense RNA so that the expression of the *waxy* gene was transcriptionally inhibited, GBSS activity was greatly reduced and the tubers contained amylose-free starch (24).

2. Soluble Starch Synthases

The second major starch synthase class, based on solubility, is synthases which are partially soluble and partially granule bound (Table 1). These starch synthases have been grouped according to the order by which activity peaks from soluble extracts elute from ion exchange columns. Several soluble starch synthase iso-

Table 1 Starch Biosynthetic Isoforms from Maize

Process	Isoforms/subunits	Apparent mass (kDa)	Reference(s)
Substrate formation	AGP large subunit (SH2)	54	(12, 13, 63)
	AGP small subunit (BT2)	51	
Chain elongation	GBSSI	60	(19, 23)
	SSI	76	(28, 29)
	SSII	> 180	(30, 31)
Branch insertion	SBEI	90	(51)
	SBEIIa	89	(55)
	SBEIIb	85	(64)
Processing/trimming	SDBE (SU1)	79	(58,61)

forms have now been partially purified, characterized, and cloned from a diverse range of plants.

Ion exchange chromatography of soluble extracts from whole endosperm revealed the presence of multiple starch synthase isoforms (25–28). In maize, two soluble starch synthase isoforms have been documented. Starch synthase I exhibits maximal activity in the presence of citrate (primer independent). On the other hand, starch synthase isoform II is active in the presence of glycogen (primer dependent). The separation of the two isoforms was also achieved by size exclusion chromatography (28). Following additional purification using MonoQ and hydrophobic interaction chromatography, starch synthase I activity was correlated with a 76-kDa polypeptide (28).

A cDNA clone encoding the 76-kDa starch synthase I was subsequently obtained (29). This cDNA bears homology to a soluble starch synthase cloned from rice (25). Three isoforms of the rice synthase were isolated by anion exchange chromatography, and their N-terminal amino acid sequences were obtained. From this information, the rice cDNA phage clone was isolated using oligonucleotide probes prepared according to direct sequences. The predicted amino acid sequence of the clone contained the KXGG motif which represents the putative ADP-Glc binding domain existing in virtually all starch and glycogen synthases.

The apparent size of SSII is 180 kDa. SSII activity has not been aligned with any specific polypeptide from maize endosperm. However, isolation of a gene encoding a putative polypeptide correlating with SSII activity has been reported (30).

Moreover, two other starch synthase cDNA clones, designated *zSSIIa* and *zSSIIb*, have been isolated from a maize endosperm cDNA library (31). The deduced amino acid sequences of both clones contain the KXGGL consensus sequence. The identity of *zSSIIa* and *zSSIIb* as starch synthases has been confirmed by expression of their activities in *E. coli*. *zSSIIa* was shown to be predominantly expressed in the endosperm, while *zSSIIb* transcripts were mainly detected in the leaf at low abundance.

In potato, a third kind of soluble starch synthase, known as SSIII, has been identified. Its cDNA clone was obtained by using an antibody directed against a domain conserved in starch synthases to screen a tuber-specific expression library. The deduced amino acid sequence showed that it is a novel type of starch synthase. The immature enzyme with its transit peptide has a mass of 139 kDa (32).

3. Four Classes of Starch Synthase Genes

Based on the deduced amino acid sequences derived from cDNA clones, starch synthase genes have been divided into four classes (33). The extensively characterized GBSSI genes belong to the first class. The genes of the second class encode soluble starch synthases localized in the endosperms of monocots. Thus far, the cDNA clones of two members from this class have been isolated and characterized. These include a soluble starch synthase from rice (25) and the citrate-stimulated starch synthase I from maize (29). A third group of genes, the SSII class, bears sequence similarity to the primer-dependent SSII from pea (34) and potato (35). In addition to these three classes, starch synthases of the SSIII class, represented by a gene encoding a 139-kDa soluble starch synthase III in potato, are believed to significantly contribute to starch biosynthesis in some species (32, 33). SSIII activity is believed to account for approximately 80% of the soluble starch synthase activity present in potato tuber. The cDNA of potato SSIII exhibits greater similarity to bacterial glycogen synthases than to members of the other three classes.

The deduced amino acid sequences of starch synthase clones share several common structural features. First, they all contain the Lys-X-Gly-Gly-Leu (KXGGL) consensus sequence, which is suggested to be the putative ADP-Glc-binding site. This conserved region was first identified in *E. coli* glycogen synthase (36). The lysine residue binds to the phosphate moiety adjacent to the glycosidic linkage of ADP-Glc (37). Moreover, starch synthase genes encode transit peptides ending with a consensus cleavage site motif. It is believed that starch synthases are synthesized in the cytosol and are targeted to the amyloplast by the transit peptides, which are then proteolytically cleaved upon translocation through the amyloplast envelope into the stroma (38, 39). Finally, several conserved regions between the KXGGL site and the 3′ terminus of the coding sequence exist in most of the clones (25).

C. Starch Branching Enzymes

The functionality and economic value of starches are largely determined by the relative ratio of amylose and amylopectin. Since SBE is the enzyme which introduces α-1,6-linked branch points into the α-1,4-linked glucan chains of amylopectin, it plays an essential role in determining starch fine structure. Multiple isoforms of SBE have been identified, purified, and character-

ized from many plants including maize endosperm (40–43), wheat endosperm (44, 45), pea seed (46), and rice endosperm (47, 48).

Different SBE isoforms differ in their specificity for substrate with respect to both chain length and degree of branching. The SBE isoforms and their clones can be categorized into two groups as initially defined by the Commission on Plant Gene Nomenclature (1994) and as later suggested by Burton et al. (49). One family (SBEI or class B) includes maize SBEI, rice SBEI, pea SBEII, and potato SBE. The second family (SBEII or class A) includes maize SBEII, pea SBEI, and rice SBEIII. The establishment of the two groups was based on immunological reactivity, chromatographic and enzyme kinetic properties, and amino acid composition (46–48, 50). In vitro, maize SBEI preferentially transfers longer chains than SBEII (42). Moreover, maize SBEI preferentially adds branch points to amylose, and its activity toward amylopectin is $< 10\%$ relative to amylose (41). Conversely, maize SBEII exhibits a sixfold higher preference for amylopectin than SBEI, but lower rates in branching amylose ($\sim$ 9–12% of that SBEI) (41).

In maize, cDNA clones for SBEI (51), SBEIIa (52), and SBEIIb (53) have been isolated and their expression patterns characterized (54). Maize SBEI elutes from ion exchange columns in the pass-through fraction, whereas SBEIIa and SBEIIb require salt for eluting from the column (40). SBEIIa and SBEIIb are very similar in their immunological reactivities, enzyme kinetic properties, substrate specificity, and amino acid sequence (1, 41, 42).

For quite some time, there was a controversy as to whether or not SBEIIa and SBEIIb are encoded by a single gene. However, the isolation of SBEIIa cDNA from *ae* mutants lacking SBEIIb has clarified this question (55). Using an *ae* mutant in which SBEIIb was absent, Fisher et al. observed significant SBEIIa enzyme activity and polypeptide levels (53), suggesting that SBEIIa is encoded by an independent gene distinct from the *Sbe2b* locus. The localization of the two mRNA transcripts in maize tissues also differed. *Sbe2b* is expressed in endosperm, developing embryo and tassels (53). *Sbe2b* mRNA levels were 10-fold higher in embryo than in endosperm tissue, and were much lower than *Sbe2b* in both tissues (55).

In hexaploid wheat, the situation is more complex. Wheat is believed to contain similar classes of SBE as those found in maize and rice. Moreover, each of the three genomes of wheat may contain a unique set of SBE isoforms. The isoforms contained within each unique set are referred to as allozymes (44). Immunological evidence and substrate specificity studies indicated that wheat BEIA and BEIB are related to the SBEI class of maize and rice, while wheat BEII (45) is related to SBEII class (44).

D. Starch Debranching Enzyme

An additional putative enzyme of the starch biosynthetic pathway, SDBE, has attracted great recent interest. Ball and others have proposed an additional set of steps in the biosynthesis of amylopectin consisting of formation of a "preamylopectin" and its subsequent trimming to a "mature amylopectin" (56). SDBE is believed by some researchers to be involved in converting preamylopectin into mature amylopectin. These researchers propose that SBE and SDBE work in a concerted fashion to determine the fine structure of amylopectin (57).

Two classes of SDBE have been studied in plant systems, termed pullulanases and isoamylases. Both types can directly hydrolyze α-(1,6)-branch point linkages. Each class differs in its specificity toward distinct substrates. Pullulanases, also referred as R-enzyme, hydrolyze pullulan at a much higher rate than amylopectin, and do not act on glycogen. In contrast, isoamylases act on both amylopectin and glycogen, but do not hydrolyze pullulan or, if so, at a very low rate. Pullulanases have been characterized in maize (58), rice (59), and many other plants. Isoamylases, however, have only been reported and studied in potato tuber (60) and maize endosperm (58, 61).

In maize endosperm, the identification and characterization of SDBE, an isoamylase, was achieved using a *su1* mutant which carries mutations on the SDBE gene (61). In maize kernels, these mutations lead to increased sucrose levels, reduced amylopectin, and accumulation of the highly branched glucopolysaccharide phytoglycogen (62). The correlation between the *su* mutation and the deficiency of SDBE was first reported by Pan and Nelson (58). This study showed that SDBE activities from wild-type maize endosperm could be separated into three peaks on a hydroxyapatite chromatography column. Their key observation was that the *su1* endosperm lacked one of the three activities while the other two were greatly reduced. They also observed that SDBE activity was proportional to the number of copies of the *Su* allele, suggesting that the *Su* allele was the structural gene for SDBE. This publication classified SDBE as an R-enzyme or pullulanase, and assumed that the biochemical lesion in the *su1* mutant of maize was induced by mutations at the structural gene for the R-enzyme. Recently,

James et al. isolated part of the *su1* gene locus and a cDNA copy of the *su1* transcript using transposon tagging (61). Five new *su1* mutations were isolated. The cDNA sequence specified a polypeptide of at least 742 amino acids bearing high similarity to bacterial isoamylase. This emerging area is further discussed in a recent review paper (57).

IV. CONCLUSION

A complete understanding of amylose and amylopectin synthesis in higher plants requires full knowledge of individual enzymes catalyzing substrate formation, chain elongation, and branch point insertion. The heightened research efforts have been focused on basic biochemistry and molecular biology along the following lines:

1. Enzyme purification, characterization and polypeptide identification.
2. Isolation and characterization of cDNA and genomic clones.
3. Expression of starch biosynthetic enzymes in bacteria and transgenic plants.

These efforts will eventually lead to a complete elucidation of the molecular mechanisms underlying starch biosynthesis and thus enable the bioengineering of starch biosynthetic process in cereal plants.

DEDICATION

This chapter is dedicated to the memory of my mentor, Bruce P. Wasserman, who passed away on August 26, 1998.

ACKNOWLEDGMENTS

Funding for this research was provided by the U.S. Department of Agriculture National Research Initiative (95-02531 and 98-01235), and by the New Jersey Agricultural Experiment Station.

REFERENCES

1. J Preiss. Biology and molecular biology of starch synthesis and its regulation. Oxf Surv Plant Mol Cell Biol 7:59–114, 1991.
2. DM Stark, KP Timmerman, GF Barry, J Preiss, GM Kishore. Regulation of the amount of starch in plant tissues by ADP glucose pyrophosphorylase. Science 258:287–292, 1992.
3. LC Hannah, OE Nelson. Characterization of ADP-glucose pyrophosphorylase from *shrunken-2* and *brittle-2* mutants of maize. Biochem Genet 14:547–560, 1976.
4. CY Tsai, OE Nelson. Starch-deficient maize mutant lacking adenosine diphosphate pyrophosphorylase activity. Science 151:341–343, 1966.
5. BP Wasserman, C Harn, C Mu-Forster, R Huang. Progress toward genetically modified starches. Cereal Foods World 40:810–817, 1995.
6. DB Dickinson, J Preiss. Presence of ADP-glucose pyrophosphorylase in shrunken-2 and brittle-2 mutants of maize endosperm. Plant Physiol 44:1058–1062, 1969.
7. BY Chen, HW Janes. Multiple forms of ADP-glucose pyrophosphorylase from tomato fruit. Plant Physiol 113:235–241, 1997.
8. L Copeland, J Preiss. Purification of spinach leaf ADP-glucose pyrophosphorylase. Plant Physiol 68:996–1001, 1981.
9. LC Hannah, OE Nelson. Characterization of adenosine diphosphate glucose pyrophosphorylase from developing maize seeds. Plant Physiol 55:297–302, 1975.
10. Y Nakamura, K Kawaguchi. Multiple forms of ADP-glucose pyrophorylase of rice endosperm. Physiol Plant 84:336–342, 1992.
11. JR Sowokinos, J Preiss. Pyrophosphorylases in *Solanum tuberosum*. III. Purification, physical and catalytic properties of ADPglucose pyrophosphorylase in potatoes. Plant Physiol 69:1459–1466, 1982.
12. JM Bae, M Giroux, L Hannah. Cloning and characterization of the *Brittle-2* gene of maize. Maydica 35:317–322, 1990.
13. MR Bhave, S Lawrence, C Barton, LC Hannah. Identification and molecular characterization of shrunken-2 cDNA clones of maize. Plant Cell 2:581–588, 1990.
14. PA Nakata, TW Greene, JM Anderson, BJ Smith-White, TW Okita, J Preiss. Comparison of the primary sequences of two potato tuber ADP-glucose pyrophosphorylase subunits. Plant Mol Biol 17:1089–1093, 1991.
15. MR Olive, RJ Ellis, WW Schuch. Isolation and nucleotide sequences of cDNA clones encoding ADP-glucose pyrophosphorylase polypeptides from wheat leaf and endosperm. Plant Mol Biol 12:525–538, 1989.
16. P Villand, OA Olsen, A Kilian, LA Kleczkowski. ADP-glucose pyrophosphorylase large subunit cDNA from barley endosperm. Plant Physiol 100:1617–1618, 1992.
17. PA Nakata, JM Anderson, TW Okita. Structure and expression of the potato ADP-glucose pyrophosphorylase small subunit. J Biol Chem 269:24107–24113, 1994.

18. MJ Giroux, J Shaw, G Barry, et al. A single gene mutation that increases maize seed weight. Proc Natl Acad Sci USA 93:5824–5829, 1996.
19. S Echt, D Schwartz. Evidence for the inclusion of controlling elements within the structural gene at the *waxy* locus in maize. Genetics 99:275–284, 1981.
20. C Mu-Forster, R Huang, JR Powers, et al. Physical association of starch biosynthetic enzymes with starch granules of maize endosperm. Granule-associated forms of starch synthase I and starch branching enzyme II. Plant Physiol 111:821–829, 1996.
21. OE Nelson, PS Chourey. Nucleoside diphosphate sugar-starch glucosyl transferase activity of *wx* starch granules. Plant Physiol 62:383–386, 1978.
22. OE Nelson, HW Rines. The enzymatic deficiency in the *waxy* mutant of maize. Biochem Biophys Res Commun 9:297–300, 1962.
23. M Shure, S Wessler, N Fedoroff. Molecular identification and isolation of the *waxy* locus in maize. Cell 35:225–233, 1983.
24. RGF Visser, I Somhorst, GJ Kuipers, NJ Ruys, WJ Feenstra, E Jacobsen. Inhibition of the expression of the gene for granule-bound starch synthase in potato by antisense constructs. Mol Gen Genet 225:289–296, 1991.
25. T Baba, M Nishihara, K Mizuno, et al. Identification, cDNA cloning, and gene expression of soluble starch synthase in rice (*Oryza sativa* L.) immature seeds. Plant Physiol 103:565–573, 1993.
26. K Denyer, AM Smith. The purification and characterization of the two forms of soluble starch synthase from developing pea embryos. Planta 186:609–617, 1992.
27. FD Macdonald, J Preiss. Partial purification and characterization of granule-bound starch synthases from normal and *waxy* maize. Plant Physiol 78:849–852, 1985.
28. C Mu, C Harn, YT Ko, GW Singletary, PL Keeling, BP Wasserman. Association of a 76 kDa polypeptide with soluble starch synthase I activity in maize (cv73) endosperm. Plant J 6:151–159, 1994.
29. ME Knight, C Harn, CER Lilley, et al. Molecular cloning of starch synthase I from maize (W64) endosperm and expression in *Escherichia coli*. Plant J 14:613–622, 1998.
30. M Gao, J Wanat, PS Stinard, MG James, AM Myers. Characterization of *dull1*, a maize gene coding for a novel starch synthase. Plant Cell 10:399–412, 1998.
31. C Harn, M Knight, A Ramakrishnan, H Guan, PL Keeling, BP Wasserman. Isolation and characterization of the *zSSIIa* and *zSSIIb* starch synthase cDNA clones from maize endosperm. Plant Mol Biol 37:639–649, 1998.
32. GJW Abel, F Springer, L Willmitzer, J Kossmann. Cloning and functional analysis of a cDNA encoding a novel 139 kDa starch synthase from potato (*Solanum tuberosum* L.). Plant J 10:981–991, 1996.
33. J Marshall, C Sidebottom, M Debet, C Martin, AM Smith, A Edwards. Identification of the major starch synthase in the soluble fraction of potato tubers. Plant Cell 8:1121–1135, 1996.
34. I Dry, AM Smith, A Edwards, M Bhattacharyya, P Dunn, C Martin. Characterization of cDNAs encoding two isoforms of granule-bound starch synthase which show differential expression in developing storage organs of pea and potato. Plant J 2:193–202, 1992.
35. A Edwards, J Marshall, C Sidebottom, RGG Visser, AM Smith, C Martin. Biochemical and molecular characterization of a novel starch synthase from potato tubers. Plant J 8:183–294, 1995.
36. K Furukawa, M Tagaya, M Inouye, J Preiss, T Fukui. Identification of lysine 15 at the active site in *Escherichia coli* glycogen synthase. Conservation of a lys-X-gly-gly sequence in the bacterial and mammalian enzymes. J Biol Chem 265:2086–2090, 1990.
37. K Furukawa, M Tagaya, K Tanizawa, T Fukui. Role of the conserved Lys-X-Gly-Gly sequence at the ADP-glucose-binding site in *Escherichia coli* glycogen synthase. J Biol Chem 268:23837–23842, 1993.
38. HM Li, TD Sullivan, K Keegstra. Information for targeting to the chloroplastic inner envelope membrane is contained in the mature region of the maize Bt1-encoded protein. J Biol Chem 267:18999–19004, 1992.
39. FD Macdonald, J Preiss. Solubilization of the starch-granule-bound starch synthase of normal maize kernals. Plant Physiol 73:175–178, 1983.
40. CD Boyer, J Preiss. Multiple forms of (1,4)-a-D-glucan-6-glucosyl transferases from developing *Zea mays* L. kernels. Carbohydr Res 61:321–334, 1978.
41. H Guan, J Preiss. Differentiation of the properties of the branching isozymes from maize (*Zea mays*). Plant Physiol 102:1269–1273, 1993.
42. Y Takeda, H Guan, J Preiss. Branching of amylose by the branching isoenzymes of maize endosperm. Carbohydr Res 240:253–263, 1993.
43. BP Wasserman, JD Wagner. Determination of blanch efficacy by means of a rapid colorimetric peroxidase assay. Biochem Ed 13:84–85, 1985.
44. MK Morell, A Blennow, B Kosar-Hashemi, MS Samuel. Differential expression and properties of starch branching enzyme isoforms in developing wheat endosperm. Plant Physiol 113:201–208, 1997.
45. RB Nair, M Baga, GJ Scoles, KK Kartha, RN Chibbar. Isolation, characterization and expression analysis of a starch branching enzyme II cDNA from wheat. Plant Sci 122:153–163, 1997.
46. AM Smith. Major differences in isoforms of starch branching enzyme between developing embryos of round- and wrinkle-seeded peas (*Pisum sativum* L.). Planta 175:270–279, 1988.

47. K Mizuno, T Kawasaki, H Shimada, et al. Alteration of the structural properties of starch components by the lack of an isoform of starch branching enzyme in rice seeds. J Biol Chem 268:19084–19091, 1993.
48. Y. Nakamura, T Takeichi, K Kawaguchi, H Yamanouchi. Purification of two forms of starch branching enzyme (Q-enzyme) from developing rice endosperm. Physiol Plant 84:329–335, 1992.
49. RA Burton, JD Bewley, AM Smith, et al. Starch branching enzymes belonging to distinct enzyme families are differentially expressed during pea embryo development. Plant J 7:3–15, 1995.
50. BP Wasserman. Thermostable enzyme production. Food Technol 38(2):78–89, 98, 1984.
51. T Baba, K Kimura, K Mizuno, et al. Sequence conservation of the catalytic regions of amylolytic enzymes in maize branching enzyme-I. Biochem Biophys Res Commun 181:87–94, 1991.
52. DK Fisher, CD Boyer, LC Hannah. Starch branching enzyme II from maize endosperm. Plant Physiol 102:1045–1046, 1993.
53. DK Fisher, M Gao, KN Kim, CD Boyer, MJ Guiltinan. Allelic analysis of the maize *amylose-extender* locus suggests that independent genes encode starch branching enzymes IIa and IIb. Plant Physiol 110:611–619, 1996.
54. M Gao, DK Fisher, KN Kim, JC Shannon, M Guiltinan. Evolutionary conservation and expression patterns of maize starch branching enzyme I and IIb genes suggests isoform specialization. Plant Mol Biol 30:1223–1232, 1996.
55. M Gao, DK Fisher, KN Kim, JC Shannon, MJ Guiltinan. Independent genetic control of maize starch-branching enzymes IIa and IIb. Isolation and characterization of a *Sbe2a* cDNA. Plant Physiol 114:69–78, 1997.
56. S Ball, H Guan, M James, et al. From glycogen to amylopectin: a model for the biogenesis of the plant starch granule. Cell 86:349–352, 1996.
57. Y Nakamura. Some properties of starch debranching enzymes and their possible role in amylopectin biosynthesis. Plant Sci 121:1–18, 1996.
58. D Pan, OE Nelson. A debranching enzyme deficiency in endosperms of the *sugary-1* mutants of maize. Plant Physiol 74:324–328, 1984.
59. Y Nakamura, T Umemoto, N Ogata, Y Kuboki, M Yano, T Sasaki. Starch debranching enzyme (R-enzyme or pullulanase) from developing rice endosperm: purification, cDNA and chromosomal localization of the gene. Planta 199:209–218, 1996.
60. Y Ishizaki, H Taniguchi, Y Maruyama, M Nakamura. Debranching enzymes of potato tubers (*Solanum tuberosum* L.). I. Purification and some properties of potato isoamylase. Agric Biol Chem 47:771–779, 1983.
61. MG James, DS Robertson, AM Myers. Characterization of the maize gene *sugary1*, a determinant of starch composition in kernels. Plant Cell 7:417-429, 1995.
62. JB Sumner, GF Somers. The water soluble polysaccharides of sweet corn. Arch Biochem 4:4–7, 1944.
63. MJ Giroux, LC Hannah. ADP-glucose pyrophosphorylase in *shunken-2* and *btittle-2* mutants of maize. Mol Gen Gene 243:400–408, 1994.
64. DK Fisher, KN Kim, M Gao, CD Boyer, MJ Guiltinan. A cDNA encoding starch branching enzyme I from maize endosperm. Plant Physiol 108:1313–1314, 1995.

11

Fatty Acid Biosynthesis and Triacylglycerol Assembly

Allan Keith Stobart
University of Bristol, Bristol, England
Gareth Griffiths
Horticulture Research International, Wellesbourne, Warwick, England

I. INTRODUCTION

Vegetable oil is an economically important agricultural product with an annual production of some 90 million metric tons. It is used both as food and in a wide range of industrial applications. By using both traditional plant breeding methods and genetic engineering techniques, vegetable oils can today be modified for particular end uses. The production of so-called designer oils to suit requirements is an ever-increasing prospect, and hence it is anticipated that the world output of such commodities will increase accordingly (1).

The end use and hence value of an oil are largely dependent on the fatty acid quality and content. The wide range of fatty acids and their relative concentrations, found in oils from many plant species, have made them particularly suited for food production (e.g., confections, ice cream, mayonnaise, margarines, animal foodstuffs, etc.), cooking oils, nutraceuticals, and pharmaceuticals. Besides being used for human consumption they have many applications in the chemical industries and particularly for the manufacture of detergents and surfactants, polymers, coatings, and specialized lubricants. In the kingdom Plantae perhaps well over 800 different fatty acids have been identified (2). Many of these are uncommon and are found in only a few species. However, this enormous genetic resource is of immense commercial value as it becomes feasible to transfer the capacity to synthesize unusual and desirable fatty acids to oil-crop species such as oilseed rape, sunflower, and soy. The scientific base for the production of genetically modified oil-seeds is well established (3) and it is therefore anticipated that an ever-increasing level of oil and oil products from such sources will enter the human diet. Here we describe, therefore, the current understanding of fatty acid biosynthesis in plants, oil assembly, and the role of fatty acid oxidation in flavor generation. Where appropriate the biotechnological applications of such knowledge will be discussed.

II. FATTY ACIDS AND COMPLEX LIPIDS

Most fatty acids are monocarboxylic and consist of an unbranched chain containing an even number of carbon atoms (Table 1). The homologous series of saturated fatty acids is represented by the general structure $CH_3(CH_2)_nCOOH$ with the carboxy carbon designated carbon 1. The number of carbon atoms in the fatty acid can vary considerably from medium chain (C8–C10) to long and very long chain (C12 and up) although it is the long-chain ones that tend to predominate. The methyl and carboxy termini of the molecule are termed the omega (ω) and delta (Δ) ends, respectively. These fatty acids can be saturated or unsaturated and in some cases may have additional functional groups. A notable characteristic of plants

Table 1 Fatty Acid Structures

General structure	(omega [ω] terminus)CH3 (CH2)nCOOH (delta [Δ] terminus)
Lauric acid (C12:0)	C—C—C—C—C—C—C—C—C—C—C—C
Palmitic acid (C16:0) Hexadecanoic acid	C—C—C—C—C—C—C—C—C—C—C—C—C—C—C—C
Stearic acid (C18:0) Octadecanoic acid	C—C—C—C—C—C—C—C—C—C—C—C—C—C—C—C—C—C
Oleic acid (C18:1Δ9) Octadeca-9-monoenoic acid	C—C—C—C—C—C—C—C—C=C—C—C—C—C—C—C—C—C
Linoleic acid (C18:2Δ9,12)* Octadeca-9,12-dienoic acid	C—C—C—C—C—C=C—C—C=C—C—C—C—C—C—C—C—C
α-Linolenic acid (C18:3Δ9,12,15)* Octadeca-9,12,15-trienoic acid	C—C—C=C—C—C=C—C—C=C—C—C—C—C—C—C—C—C
γ-Linolenic acid (GLA; C18:3Δ6,9,12) Octadeca-6,9,12-trienoic acid	C—C—C—C—C—C=C—C—C=C—C—C=C—C—C—C—C—C
Stearidonic acid (C18:4Δ6,9,12,15) Octadeca-6,9,12,15-tetraenoic acid	C—C—C=C—C—C—C=C—C—C=C—C—C—C=C—C—C—C—C—C
Arachidonic acid (C20:4Δ5,8,11,14) Eicosa-5,8,11,14-tetraenoic acid	C—C—C—C—C—C—C=C—C—C=C—C—C—C=C—C—C—C=C—C—C—C—C
Eicosapentaenoic acid (EPA) C20:5Δ5,8,11,14,17	C—C—C=C—C—C—C=C—C—C—C=C—C—C—C=C—C—C—C=C—C—C—C—C
Erucic acid (C22:1Δ13)	C—C—C—C—C—C—C—C—C—C=C—C—C—C—C—C—C—C—C—C—C—C—C—C

Essential fatty acids are polyunsaturated fatty acids of the omega-6 (n-6) and omega-3 (n-3) families that are essential for life and good health, and are not produced in man and must be obtained from plants as part of the diet.

is the high incidence of unsaturated and polyunsaturated fatty acids and particularly those of 18 carbon atoms.

Unsaturation generally describes a four-electron (double bond/olefinic) linkage between carbon atoms. Polyunsaturated fatty acids (the so-called PUFAs) are polyenoic acids having more than one olefinic center, the double bonds generally of a *cis* configuration and methylene interrupted. By convention PUFAs are described as being *n3* or *n6* fatty acids depending on whether the first double bond is three or six carbon atoms from the methyl end (omega carbon), respectively. Further double bonds are separated from each other by a methylene group. Such fatty acids are also termed omega-3 and omega-6 acids. The omega-3 series are derived from α-linolenic acid (C18:3 *n3*) by chain elongation and further desaturation and include eicosapentaenoic acid (EPA; C20:5 *n3*) and docosahexaenoic acid (DHA); C22:6 *n3*). On the other hand, the omega-6 acids are derived from linoleic acid (C18:2 *n6*) and include γ-linolenic acid (GLA; C18:3 *n6*) and arachidonic acid (AA; C20:4 *n6*). Linoleic acid and linolenic acid are substances which cannot be synthesized de novo in the human body and so, like vitamins, must be provided in the diet from plant sources for the synthesis of the other *n6* and *n3* metabolites. Hence, these are the so-called essential fatty acids (EFAs) and are required for the normal structure of all membranes, for cholesterol transport, for the maintenance of normal permeability barriers and as precursors of eicosanoids (prostaglandins, thromboxanes, leukotrienes).

A further unsaturated fatty acid terminology, of particular value to biochemists, defines the position of the double bonds from carbon atom 1 (i.e., the Δ end of the molecule). The delta system is convenient for denoting all double bonds, their position in the carbon chain, and the specific desaturase enzymes which catalyze their introduction into the molecule. Hence, linoleic acid and α-linolenic acid become C18:$2^{\Delta 9,12}$ and C18:$3^{\Delta 9,12,15}$, respectively. Fatty acid structures and trivial and systemic nomenclatures are given in Table 1. Desaturases, which abstract hydrogen atoms from adjacent CH_2 groups to produce double bonds, can be specifically defined. For example, a Δ12 desaturase or a Δ5 desaturase would introduce double bonds at the Δ12 and Δ5 carbon atom in the acyl chain, respectively.

Triacylglycerols, the major constituents of the oil, consist of a glycerol backbone to which a fatty acid

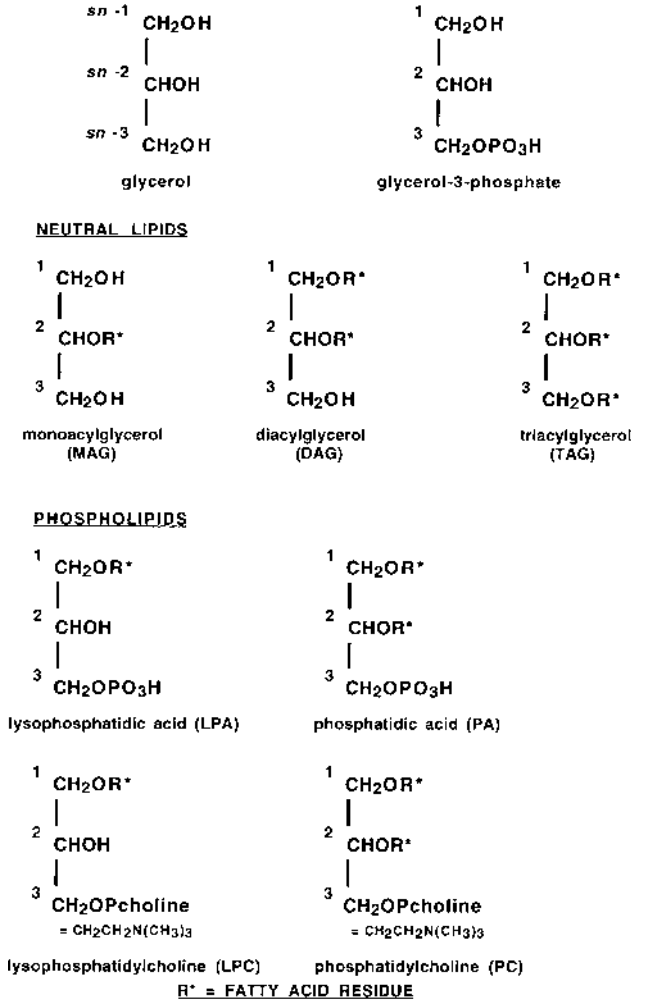

Figure 1 Glycerolipid structures.

acyl group is esterified to each of the three hydroxy groups. Each carbon atom in the glycerol molecule is defined by the stereoscopic numbering system and *sn1*, *sn2*, and *sn3* describes each carbon, respectively (Fig. 1). The glycerol carbons of the phospholipids (membrane polar lipids), important in understanding triacylglycerol biosynthesis, are similarly defined (Fig. 1). The quality of the oil, and hence its end use, is determined by the fatty acids esterified to each of the glycerol carbon atoms. Most commercial annual oil crops have seed oils largely composed of the five major fatty acids, palmitic (C16:0), stearic (C18:0), oleic ($C18:1^{\Delta 9}$), linoleic ($C18:2^{\Delta 9,12}$) and α-linolenic ($C18:3^{\Delta 9,12,15}$) acids. These are the "housekeeping" fatty acids, so called because they are also found in the membrane lipids of all plants cells. The fatty acid composition of membrane lipid in leaves and roots, however, is under strict control and differs little among plant species whereas the relative abundance of a fatty acid in the storage triacylglycerol can show distinct variations among different oil crop species.

III. FATTY ACID BIOSYNTHESIS

A. Carbon Source

Acetyl-CoA is regarded as the direct carbon source for fatty acid synthesis and can be generated by the pyruvate dehydrogenase (PDC) complex. Despite the fundamentally crucial requirements for acetyl-CoA, its biogenesis in plants is poorly understood. Both chloroplast (cPDC) and mitochondrial (mPDC) forms (4, 5) have been characterized. There has been speculation about the supply of pyruvate for acetyl-CoA formation from cPDC and whether there is sufficient activity of the glycolytic enzymes to provide pyruvate within this organelle. In mustard, for example, there appears to be a sufficient supply of pyruvate to satisfy this requirement, although in other tissues important cytosolic pyruvate may be required to support fatty acid biosynthesis (6). Studies with plastids from heterotrophic tissues indicate that the metabolites utilized for fatty acid synthesis include glucose, fructose, glucose-6-phosphate, triose phosphate, malate, pyruvate, and acetate (7). Of these only acetate has been shown to be freely permeable to the selective barrier of the plastid envelope. There is considerable variation in the efficiency with which these substrates are utilized by plastids, and the basis for this may be determined by the presence of highly selective transporter proteins on the plastid envelope.

It has recently been shown that during oil deposition in oil seed rape, fatty acid synthesis is initially supported by glucose-6-phosphate and then by pyruvate through the corresponding activities of the transporters for these metabolites (7, 8). In isolated leucoplasts from developing castor seed endosperm, however, the rate of malate-dependent fatty acid synthesis was threefold higher than that from pyruvate and evidence was presented for a malate/Pi translocator (9). Whether the expression of selective transporters on the plastid envelope determines the ability of these organelles to accumulate oils or starch requires further research. In this regard it is interesting to note the isolation of a novel *Arabidopsis* mutant producing wrinkled, incompletely filled seeds with an 80% reduction in triacylglycerols. Wild-type and homozygous *wri1* mutant plantlets or mature plants were indistin-

guishable. However, developing homozygous *wri1* seeds were impaired in the incorporation of sucrose and glucose into triacylglycerols but incorporated pyruvate and acetate at an increased rate (10). Because the activities of several glycolytic enzymes, in particular the hexokinase and pyrophosphate-dependent phosphofructokinase, are reduced in developing homozygous *wri1* seeds, it was suggested that *wri1* is involved in the developmental regulation of carbohydrate metabolism during seed filling.

B. Acetyl-CoA Carboxylase

Acetyl-CoA carboxylase (ACCase) catalyzes the formation of malonyl-CoA from acetyl-CoA and bicarbonate. Plants have two types of acetyl-CoA carboxylases; one is the multisubunit complex located in plastids, and the other a large multifunctional polypeptide localized in the cytosol (11). The plastidic form consists of four subunits, and in *Arabidopsis* these are encoded by three single copy nuclear genes (*cac1, cac2*, and *cac3*) and one plastidic gene (*accD*) (12, 13). The cytosolic ACCase generates malonyl-CoA for the biosynthesis of a variety of secondary metabolites and for the elongation of fatty acids. The enzyme is a dimer of a 260-kDa subunit and in *Arabidopsis* is encoded by two genes (*acc1* and *acc2*) which are in a tandem array within a 25-kb segment of the genome. In photosynthetic tissue the chloroplast ACCase is modulated by light/dark. Plants have a light-signal transduction pathway in chloroplasts which operates when electrons from photosystem 1 are shuttled through the electron transport chain to thioredoxins via ferredoxin and then by reducing the disulfide bonds of target enzymes (14). Enzyme activities of the reductive pentose phosphate pathway cycle in chloroplasts are regulated via this redox cascade. Recent results suggested that a redox cascade may be responsible for coordination of fatty acid synthesis with photosynthesis (14).

In mammals the ACCase consists of a single polypeptide chain containing three functional domains, while in *E. coli* the enzyme consists of four separable proteins: biotin carboxyl carrier protein (BCCP), biotin carboxylase (BC), and carboxyl transferase (CTa and CTb). Initial attempts to purify the plant ACCase generated widely differing apparent molecular weights (15, 16). These discrepancies were originally interpreted as being due to differential rates of proteolysis in different tissue extracts, and it was therefore considered that the plant acetyl-CoA carboxylase, like that from mammals, was a multifunctional protein.

It has now been established, however, that there are two forms of ACCase in plants (11, 17). In dicotyledonous species there is a low-molecular-weight (LMW) form present in the plastid and high-molecular-weight (HMW) one in the cytosol whereas in the Graminaceae the LMW form has not been detected and HMW forms are present in both the plastid and cytosol. This provides an explanation for the differential action of the monocotyledon-specific acyloxyphenoxy-propionate and cyclohexonediose group of herbicides, whose main target is the HMW ACCase in the plastid. It is currently believed that the HMW ACCase in the plastid is responsible for de novo fatty acid biosynthesis which is herbicide sensitive and a further HMW ACCase in the cytoplasm responsible for fatty acid elongation (see later) which is insensitive (11). Despite the molecular characterization of ACCases, little progress has been made on the metabolic regulation of the enzyme in plants. Unlike the mammalian enzyme where regulation by phosphorylation and intermediates of the tricarboxlic acid cycle, particularly citrate, have been shown to be involved, no evidence exists for such regulatory mechanisms in plants.

C. Fatty Acid Synthase

The molecular organization of the plant fatty acid synthase is composed of dissociable enzyme activities, similar to *E. coli* and termed type II FAS, has been recognized since the early 1980s (Fig. 2). The initial reactions of FAS are catalyzed by transacylases which transfer the acetyl and malonyl units from their CoA esters to the corresponding ACP derivatives (18). The initial condensation reaction in plant fatty acid biosynthesis takes place between acetyl (C2) ACP and malonyl (C3) ACP, resulting in the formation of acetoacetyl (C4) ACP and carbon dioxide. This reaction is catalyzed by ketoacyl ACP synthase (KAS). In the next step the acetoacetyl-ACP is reduced to hydroxybutyryl-ACP by β-ketoacyl-ACP reductase using NAD(P)H. The hydroxybutyryl-ACP is then dehydrated by hydroxyacyl-ACP dehydratase, and the crotonyl-ACP form is converted to butyryl-ACP by enoyl-ACP reductase using NAD(P)H. This completes the first round of fatty acid synthesis.

In the next round the butyryl (C4) ACP is condensed with malonyl (C3) ACP resulting in the formation of C6 ACP and carbon dioxide which then undergoes a further two reductions and dehydration step as described earlier to complete the second cycle. Subsequent additions of C2 units from malonyl-ACP results in the formation of long-chain fatty acids of

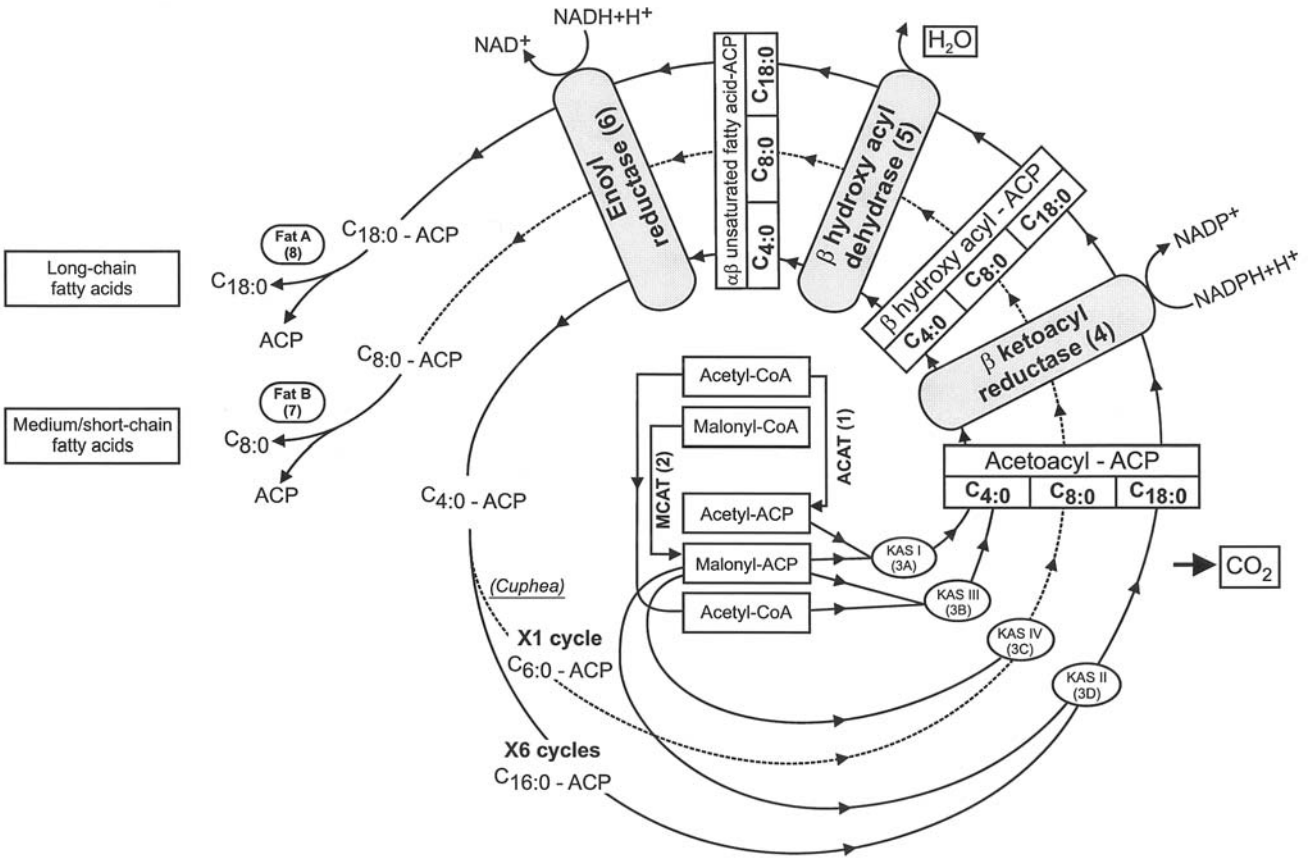

Figure 2 The fatty acid synthetase complex. Acetyl-CoA:ACP transacylase (ACAT; reaction 1) and malonyl-CoA:ACP transacylase (MCAT; reaction 2) convert acetyl-CoA and malonyl-CoA to ACP derivatives, respectively. Condensation of these products by β-ketoacyl ACP synthase (KAS I; cerulenin sensitive; reaction 3A) results in the formation of acetoacetyl-ACP (C4 on the figure) and the generation of CO_2. Acetyl-CoA can also be condensed directly with malonyl-ACP in a KAS III mediated reaction (cerulenin insensitive; reaction 3B). Acetoacyl ACPs are reduced by β-ketoacyl reductase (reaction 4) to yield the β-hydroxyacyl-ACP derivatives, which undergo dehydration, catalyzed by a β-hydroxyacyl-ACP dehydrase (reaction 5). The generated α, β-unsaturated fatty acyl-ACPs are further reduced by an NADH-specific enoyl reductase (reaction 6), resulting in the formation of the acyl-ACP product. In subsequent rounds of condensation, malonyl-ACP is used as the primer which again is followed by reduction (reaction 4), dehydration (reaction 5), and further reduction (reaction 6). In species accumulating short- to medium-chain fatty acids (e.g., *Cuphea*), a short chain–specific condensing enzyme has been identified (KAS IV; reaction 3C). In species not accumulating short-chain fatty acids, KAS I (and/or KAS III up to C6) supports these condensation reactions. A further three and four rounds of the cycle result in the formation of C8:0 and C10:0 chain length products, respectively. In species accumulating short-chain fatty acids, these products are hydrolyzed from the ACP by the action of a specific thioesterase (reaction 7; only C8 illustrated), resulting in the formation of unesterified fatty acids which are subsequently utilized for storage lipid formation. All species synthesize C16 and C18 chain length fatty acids both for membrane lipid and oil synthesis. C16:0 is elongated to C18:0 by a specific β-ketoacyl-ACP synthetase (KAS II; reaction 3D). These fatty acids are released from the ACP by thioesterase activity to yield unesterified fatty acid for use in oil assembly.

which palmitate (C16:0) and stearate (C18:0) are the principal end products. The enzyme responsible for the formation of stearate from palmitate has been shown to be an isoform of the KAS I and has been designated KAS II based on reconstitution experiments and on selective inhibitor studies using arsenite and cerulenin (19).

The transfer of acetyl groups from the CoA track to the ACP track, catalyzed by the acetyl:ACP transacylase, was considered to be the possible rate-limiting step in fatty acid synthesis (18). However, in the late 1980s studies with *E. coli* indicated the presence of a short-chain condensing enzyme whose activity was not blocked by cerulenin, and short-chain ACPs accumulated. A similar activity was subsequently reported in plants and it appeared that conversion of acetyl-CoA to acetyl-ACP could be bypassed and the acetyl-CoA and malonyl-ACP condensed directly (20). This activity has been referred to as KAS III. This has subsequently brought into question the earlier suggestion that the transacylase played a regulatory role and was the rate-limiting step in fatty acid biosynthesis. There are, however, indications that acetyl ACP:CoA transacylase is a partial activity of KAS III, but this awaits confirmation by characterization of the purified enzyme. Metabolic plasticity has been observed in many pathways, and the role of the KAS III and/or transacylase may yet be another example of this phenomenon.

Malonyl-CoA:ACP transacylases (MCAT) have been purified from a number of plant species. The enzymes usually have molecular weights determined from standard curves (MW) or by mass spectrometry (molecular mass) ~ 40 kDa, and tissue-specific isoforms have been reported (15). The gene has recently been cloned from *Brassica napus* using a complementation approach (21); the protein showed a 47% homology to the *E. coli* MCAT amino acid sequence in the coding region for the mature protein. The β-hydroxyacyl dehydratase has also been purified and partially characterized from a number of sources (see 11) and, although the plant enzyme has received little further molecular characterization, the bacterial dehydratase has recently been cloned (22).

The enzymes for the two reductive steps required in each round of fatty acid biosynthesis have been purified and shown to have a preference for the ACP-linked esters over the corresponding CoA derivatives (16). The first reductive step is catalyzed by β-ketoacyl ACP reductase, an NADPH-dependent reaction that produces hydroxyacyl-ACP. Hydroxyacyl-ACP is dehydrated by a dehydratase and then further reduced by enoylacyl-ACP reductase (ENR) to form acyl-ACP, which in developing oilseed rape, is an NADH-dependent enzyme. The *Brassica napus* ENR is tetrameric (23) and has been cloned and overexpressed in *E. coli* (24) and crystallized (25). Interestingly, the ENR is the target for antibacterial diazaborines and the front-line antituberculosis drug isoniazid. Recent structural studies have revealed the chemical basis for its molecular binding of drugs which, based on its similarity to other oxidoreductases, may have generic applications in other areas of medicinal chemistry (26).

D. Chain Termination

The principal-product of fatty acid biosynthesis in most plant tissues is palmitoyl-CoA, which can then be elongated by a specific β-ketoacyl-ACP synthase type II (KAS II) to generate stearoyl-ACP. However, since storage lipid accumulation is not under the same functional constraints imposed on membrane lipids, several plant families have evolved mechanisms for terminating fatty acid synthesis at the C8–C14 chain length stage for incorporation into triacylglycerols during seed development. The potential applications of these fatty acids has been a major driving force in the search to elucidate the mechanisms by which they are synthesized. A number of potential chain-terminating mechanisms were hypothesized (see 15) and included the presence of a medium chain–specific acyl-ACP thioesterase, specific acyl-ACP transferases, β-fatty acid synthetases, and β-ketoacyl-ACP synthetases. Other possibilities include the availability of the fatty acid metabolites malonyl-CoA and acetyl-CoA, and cofactor levels of ACP.

An important role for the medium-chain acyl-ACP thioesterase was firmly established following the expression of the Californian bay 12:0-ACP thioesterase in *Arabidopsis* resulting in the formation of laurate and the first genetically engineered rapeseed (27). Thioesterases with the potential to confer different medium-chain length phenotypes have now been isolated from a number of species, especially from the genus *Cuphea* (28–30). Although acyl-ACP thioesterases with specificities toward medium-chain substrates are requisite enzymes in plants which produce C8–C14 seed oils, they do not appear to be the sole chain length determinants. It has recently emerged that β-ketoacyl-ACP synthase also plays an important role in the production of medium-chain fatty acids and that it is the cooperation of the synthase and thioesterase which determines the phenotype, at least in *Cuphea* (28).

cDNA clones encoding the 3-ketoacyl-ACP synthase have been isolated from *Cuphea* and overexpressed in *Brassica* (29). Expression of this enzyme in transgenic *Brassica* seeds which normally do not produce medium-chain fatty acids did not result in any detectable modification of the fatty acid profile. However, coexpression of the *Cuphea* KAS with the medium chain–specific thioesterase strongly enhanced the level of C8:0–C12:0 fatty acids in the seed oil as compared with seeds expressing the thioesterase alone. By contrast, coexpression of the *Cuphea* KAS along with the 18:0/18:1-ACP thioesterase did not result in a modified fatty acid profile. These data indicated that the *Cuphea* KAS had different acyl chain specificities to the previously characterized KAS I, II, and III and was therefore designated KAS IV, a medium chain–specific condensing enzyme (29). Knowledge of this enzyme activity and its relationship with the short-chain thioesterase may be exploited in the future engineering of oilseeds to increase yields and medium-chain fatty acids or extend the range of medium-chain phenotypes.

A few plant species have been identified that accumulate significant amounts of stearate in their seed oils; these include cocoa (*Theobroma cacao*), shea (*Butyrospermum parkii*), sal (*Shorea robusta*), and kokum (*Garcinia indica*), the oils of which are valuable as cocoa butter or cocoa butter substitutes in many confectionary applications. The level of stearate available for triacylglycerol assembly is likely controlled by the combined regulation of the plastid localized enzymes β-ketoacyl-acyl carrier protein synthase II (which generates stearoyl-ACP) and stearoyl-ACP desaturase, acyl-ACP thioesterase, and acyl-ACP acytransferases, all of which use stearoyl-ACP as substrate (31). Downregulation of stearoyl-ACP desaturase resulted in the significant accumulation of stearate in the storage oil of non-stearate-accumulating species such as *Brassica rapa* and *B. napus* (32).

It should be pointed out that plant acyl-ACP thioesterases fall into two distinct but related classes known as FatA and FatB (27, 33). The FatA class includes the palmitoyl-, stearoyl-, and oleoyl-ACP thioesterases and these are regarded as ubiquitous. The fatB class contains all the specialized thioesterases (including the medium-chain thioesterases described above) as well as an apparently ubiquitous thioesterase with a broader specificity for longer-chain saturated and unsaturated substrates. Recently, Hawkins and Kridl (31) have reported the cloning and characterization of three different acyl-ACP thioesterase cDNAs from mangosteen (*Garcinia mangostana*) seed RNA—two from the fatA class, and one from the fatB class. Expression of *Garm* FatA1 in *Brassica* seeds led to the accumulation of stearate up to 22% in the seed oil. These results suggest that *Garm* FatA1 is at least partially responsible for determining the high stearate composition of mangosteen oil and that fatA, as well as fatB, thioesterases have evolved for specialized roles.

E. Unsaturated and Polyunsaturated Fatty Acids

In many oleaceous species the products of fatty acid synthesis in the plastid are palmitic (C16:0), stearic (C18:0), and oleic (C18:1) acids (see above). These are made available to the endoplasmic reticulum for triacylglycerol assembly (see below) and the formation of other fatty acids, particularly polyunsaturated fatty acids. Unsaturated fatty acids, therefore, are synthesized by the sequential insertion of double bonds into a more saturated precursor. The first double bond in the production of C18 unsaturated fatty acids is inserted at the $\Delta 9$ position of stearic acid (C18:0) and yields oleic acid ($C18:1^{\Delta 9}$). The $\Delta 9$ desaturase catalyzing this reaction is a soluble plastidic protein utilizing C18:0ACP as substrate. To date the $\Delta 9$–18:0ACP desaturase is the only desaturase to have its structure and mode of action fully characterized. A cDNA encoding this desaturase, isolated from castor bean endosperm and overexpressed in *E. coli*, generated sufficient protein for biophysical characterization (34). The desaturase contained a di-iron cluster at the active site and in this respect was similar to methane mono-oxygenase hydroxylase (35). The protein has been crystallized and its structure determined (36). A mechanism of action for the desaturase proposes that the removal of two hydrogens results in the formation of a transient di-radical that spontaneously recombines to form the $\Delta 9$ double bond (37).

Antisense constructs of the $\Delta 9$ stearoyl-ACP desaturase, with seed-specific promoters inserted into oilseed rape, brought about a dramatic increase in stearate in the rape oil from the normal $< 2\%$ to 40% and with a corresponding decrease in oleate (32). Triacylglycerols with high stearate are of commercial interest as cocoa butter substitutes in confectionary fat.

Oleate, from the plastid, is channeled into phospholipid, mainly phosphatidylcholine of the endoplasmic reticulum and there, depending on the plant species, sequentially desaturated by a $\Delta 12$ and $\Delta 15$ desaturase into linoleate and α-linolenate (38, 39). Similar desaturation steps occur in the plastid galactolipids and are catalyzed by desaturases encoded by genes which are separate from those encoding the endoplasmic reticu-

lum proteins (40). It is only the endoplasmic reticulum desaturases, however, that appear to be responsible for the production of the polyunsaturated fatty acids in the storage triacylglycerols. The Δ12 desaturation in oil seeds occurs with oleate at both the *sn1* and *sn2* positions of *sn*-phosphatidylcholine, whereas Δ15 desaturation in linseed exhibits a strong preference for substrate at position *sn2*. The oil seed endoplasmic reticulum Δ12 desaturase is cyanide sensitive and requires NAD(P)H and molecular oxygen. Spectrophotometric evidence shows that the safflower microsomal Δ12-desaturation is mediated through the cytochrome b5-cytochrome b5 reductase system (41); this was confirmed with antibodies to cytochrome b5, which inhibited desaturase activity (42). Seed microsomal cytochrome b5 has been molecularly characterized for studies on desaturation and polyunsaturated fatty acid synthesis (43–46).

Mutagenesis and conventional plant-breeding programs have produced several oil seed varieties with blocks in both oleate and linoleate desaturase activity, resulting in dramatic changes in the unsaturation level of the seed triacylglycerols (47, 48). The seeds develop normally and are viable. There were no fatty acid lesions in other parts of the plant, indicating tissue-specific Δ12 and Δ15 desaturase genes (48–50). Such observations bode well for manipulating the polyunsaturation in oil seeds by genetic engineering. The endoplasmic reticulum desaturases are integral membrane proteins and highly hydrophobic, and hence little progress has been made in their solubilization and purification. Much of our understanding of this class of desaturases has come from *Arabidopsis* mutants (40, 51). These mutants, termed FAD mutants, are each defective in a particular desaturase. For example, FAD2 and FAD3 genes have been cloned and shown to be responsible for Δ12 and Δ15 desaturation in the endoplasmic reticulum, respectively (52, 53). Examination of deduced amino acid sequences show that membrane bound desaturases from a number of sources are characterized by the presence of three regions of conserved histidine residues and that these are responsible for catalytic activity (37, 54).

Desaturation reactions involved in the synthesis of a number of other, less common polyunsaturated fatty acids are also endoplasmic reticulum–bound enzymes. Only γ-linolenic acid ($18{:}3^{\Delta 6,9,12}$), however, has been studied in detail. Polyunsaturated fatty acids with a Δ6 double bond are prevalent in the Boraginaceae. Here, the dominating Δ6 fatty acid in leaf tissue is an octadecatetraenoic acid (stearidonic acid, $18{:}4^{\Delta 6,9,12,15}$), and this is particularly enriched in the galactolipids (55). In seed oil, however, γ-linolenate predominates and in borage accounts for some 25% of the triacylglycerol fatty acids. The seed γ-linolenic acid is synthesized by a Δ6 NADH-dependent desaturation of linoleate esterified to largely microsomal phosphatidylcholine (56). The Δ6 desaturase has a strong preference for linoleate at position *sn2* of phosphatidylcholine. α-Linolenic acid acts as a substrate for the Δ6 desaturase and the formation of $18{:}4^{\Delta 6,9,12,15}$ (55).

γ-Linolenic acid is considered of therapeutic value in alleviating a wide range of clinical and atopic disorders (57), and γ-linolenate-rich oil from a number of species (borage, evening primrose, black currant, and some fungi) (58) is available for this purpose. The inclusion of a Δ6 desaturase gene in a high linoleate oil crop could yield γ-linolenate oil for medical and dietary use and at a competitive price. In borage the membrane lipids are also enriched in γ-linolenate, and the Δ6 desaturase gene appears to be expressed in the whole plant. It can be assumed, therefore, that its expression in a transgenic plant would not adversely affect membrane function and this appears to be the case.

Recently a cDNA has been isolated that encodes the Δ6 desaturase from the developing seeds of borage (59). Its function has been confirmed by ectopic expression in transgenic tobacco plants. The transformants grew well and contained appreciable quantities of γ-linolenic acid (13%) and stearidonic acid (10%). The polypeptide encoded by the Δ6 desaturase cDNA is unusual and contains diagnostic sequences related to cytochrome b5 at the N-terminus. The microsomal form of borage cytochrome b5 is 32% identical to the N-terminal extension of the Δ6 desaturase. Microsomal desaturases (Δ12, Δ15) that have been cloned from higher plants do not contain this cytochrome b5 domain (53), even though the requirement for cytochrome b5 has been demonstrated in vitro (41). The borage Δ6 desaturase therefore appears to represent a new class of fatty acid desaturases in higher plants existing as cytochrome b5 fusion proteins.

It is interesting that none of the other plant desaturases (Δ12, Δ15) (53) or the closely related hydroxylase from castor (60) have a cytochrome b5 domain and use the "free" microsomal form of the protein. It is possible that desaturation is more efficient with an endogenous heme binding domain in the protein. It may be significant that the Δ6 desaturase from borage differs from the Δ12 and Δ15 desaturases in that it introduces a center of unsaturation between an existing double bond and the carboxy carbon—i.e., a front-end desaturase (61), as opposed to double-bond formation

toward the methyl end of the carbon chain. Other-front end desaturases have now been cloned and functionally identified and include the Δ5 from the filamentous fungus, *Mortierella alpina* (62) and the nematode worm, *Caenorhabditis elegans* (63); again, these contain cytochrome b5 domains.

F. Fatty Acid Elongation

Very long chain fatty acids (VLCFAs) have chain lengths from 20 to 30 carbons or greater. For a detailed review of the biochemical and molecular characterization of elongase activity, see Postbeittenmiller (64) and Domergue et al. (65). Here we will summarize the current understanding and the recent advances in the molecular characterization of the process. The major site of VLCFA synthesis is the epidermal cells where they are used for the formation of waxes including suberin, cutin, and the epicuticular waxes which cover the aerial parts of the plant (66). The VLCFAs are either directly incorporated into waxes or else act as precursors for other aliphatic hydrocarbons which include alkanes, primary and secondary alcohols, ketones, aldehydes, and acyl esters. VLCFAs also accumulate to high levels in the seed oils of some species; they are mostly monounsaturated, belonging chiefly to the *cis* (n-9) series, i.e., higher homologs of oleic acid, e.g., erucic acid, as found in the older varieties of oilseed rape.

VLCFAs are of particular importance for the oleochemical industries, and the need for renewable raw materials has led to a significant interest in this area of research, particularly for the characterization of the so-called fatty acid elongases. The elongase activity is composed of four activities analogous to those found in de novo fatty acid synthesis and involves the sequential additions of C2 moieties from malonyl-CoA to preexisting C18 fatty acids exported from the plastid to the membranes of the endoplasmic reticulum. It is thought that each cycle of elongation comprises: (a) condensation of malonyl-CoA with a long chain acyl-CoA; (b) reduction to β-hydroxyacyl-CoA; (c) dehydration to an enoyl CoA; and (d) reduction of the enoyl-CoA, resulting in an elongated acyl-CoA. Recent work with *Arabidopsis*, which contains ~ 21% (w/w of total fatty acids) as eicosaenoic acid (20:1), has shown that a fatty acid elongation (*FAE1*) gene encodes a putative seed-specific condensing enzyme and catalyzes the first step in the cycle outlined above (67).

Introduction of the *FAE1* gene into yeast and tobacco and the vegetative tissues of *Arabidopsis* where significant quantities of VLCFAs are not found conferred the ability to accumulate these fatty acids. *FAE1* thus appears to be the rate-limiting step in *Arabidopsis* seed, and the introduction of extra copies resulted in higher levels of VLCFAs. Furthermore, it was suggested that the condensing enzyme is the activity of the elongase that determines the acyl chain length of the VLCFAs produced. In contrast, the other three enzyme activities are found ubiquitously throughout the plant and are not rate limiting and play little if any role in the control of VLCFA synthesis.

Because condensing enzymes are pivotal in the synthesis of VLCFAs, they may be useful for biotechnology. For example, the accumulation of VLCFAs in *p35S-FAE1* tobacco raises the possibility of producing VLCFAs in plant species that do not normally have them. The availability of expressed sequence tags (ESTs) may allow identification of enzyme activities that could synthesize VLCFAs up to C34 in length. Targeting of these fatty acids to seeds may eventually lead to the production of new, agronomically important VLCFAs. In a broader application, the availability of condensing enzymes with different acyl chain specificities, together with an ability to manipulate their expression in epidermal cells, could result in the generation of plant crops with enhanced performance physical barriers (waxes) and thereby show increased tolerance to environmental stresses and/or resistance to pathogens.

IV. TRIACYLGLYCEROL BIOSYNTHESIS

A. Assembly

Saturated fatty acids up to the levels of palmitic acid (C16:0), stearic acid (C18:0), and oleic acid ($18:1^{\Delta 9}$) are synthesized in the plastid (see above). All further modifications of the acyl-chain and the assembly of triacylglycerols are accomplished by membrane-bound enzymes localized in the endoplasmic reticulum (ER). The oil is released from the endoplasmic reticulum membranes and stored as discrete oil bodies in the cytoplasm. Maximum oil deposition in the seed usually occurs over a narrow time window after pollination. In species such as sunflower and safflower, > 60% of the oil is laid down over a period of a few days ~ 15 days after flowering and when the cells of the cotyledons are undergoing cell expansion. At the close of oil accumulation, the triacylglycerols constitute > 90% of the total lipid, with the remainder being phospholipids and glycolipids (68). Seed cotyledons in the active

phase of oil deposition yield microsomal membrane preparations capable of massive oil assembly in vitro. Given suitable substrates, microsomal preparations produce triacylglycerols in mass and these accumulate as visible oil droplets in the incubation medium (69).

The major pathway for triacylglycerol biosynthesis in plants is via the so-called Kennedy, or glycerol-3-phosphate, pathway (70, 71) and is catalyzed by enzymes in the endoplasmic reticulum. The assembly of the triacylglycerols proceeds through three sequential acylation steps each catalyzed by a specific acyltransferase (AT; Fig. 3). In the first reaction, the acyl moiety from acyl-CoA is transfered to the *sn1* position of *sn*-glycerol-3-phosphate to yield lysophosphatidic acid:

$$\textit{sn}\text{-glycerol 3-phosphate} + \text{acyl-CoA} \rightarrow \textit{sn1}\text{-acyl-}\textit{lyso}\text{-phosphatidic acid} + \text{CoA}$$

The glycerol-3-phosphate acyltransferase (AT1) catalyzing this reaction generally has a broad acyl specificity and will accept both saturated and unsaturated fatty acids (72, 73). In some species, however, which produce an unusual seed-specific fatty acid, the AT1 may exhibit a greater specificity for the acid than the enzyme from plants that lack it (74, 75).

The enzyme lysophosphatidic acid acyl transferase (AT2) catalyzes the acylation of lysophosphatidic acid at the *sn2* position to yield phosphatidic acid:

$$\textit{sn1}\text{-acyl-}\textit{lyso}\text{-phosphatidic acid} + \text{acyl-CoA} \rightarrow \text{phosphatidic acid} + \text{CoA}$$

In most oil seeds, AT2 exhibits a strong selectivity for unsaturated 18-carbon fatty acids (76, 77), and this results in a nonrandom distribution of the acyl groups at the *sn1* and *sn2* positions of phosphatidic acid and in other lipids derived from this such as phospholipids, diacylglycerols, and triacylglycerols (78). As a general rule, therefore, plant triacylglycerols have mainly unsaturated fatty acids at position *sn2*. Interesting exceptions are plants with triacylglycerols rich in medium-chain fatty acids (C8–C14) and especially in the genus *Cuphea* (79). The acyl specificities of the AT2 from three different *Cuphea* spp. have been investigated and have similar properties. Medium-chain acyl-CoA substrates are readily utilized. Long-chain acyl-CoA esters, however, were only used if the acyl acceptor, lysophosphatidic acid, contained a long-chain acyl group (75, 80). The AT2s from oil seed species which accumulate triacylglycerols with only long-chain fatty acids lack these properties. These enzymes poorly utilize medium-chain lysophosphatidates and acylate

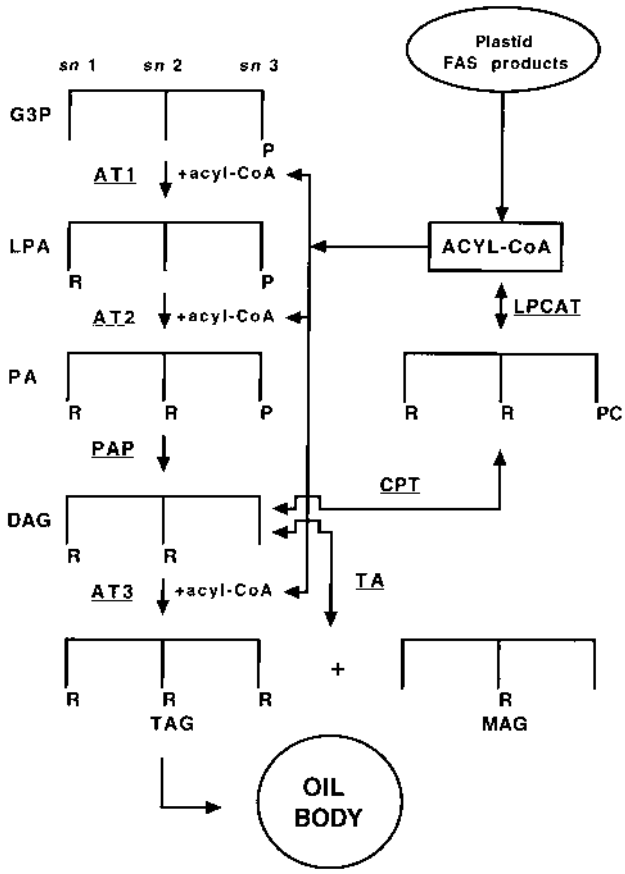

Figure 3 Glycerol-3-phosphate (G3P) undergoes acylation to yield lysophosphatidic acid (LPA) and phosphatidic acid (PA) through the action of glycerol phosphate acyltransferase (AT1) and lysophosphatidic acid acyltransferase (AT2), respectively. A phosphatidic acid phosphohydrolase (PAP) gives rise to diacylglycerol (DAG) which undergoes acylation, catalyzed by diacylglycerol acyltransferase (AT3), to form triacylglycerol (TAG). Oleic acid (18:1) from the plastid enters the acyl-CoA pool and can be transferred to the *sn2* position of *sn*-phosphatidylcholine (PC), through the activity of lysophosphatidylcholine acyltransferase (LPCAT), for desaturation to C-18 polyunsaturated fatty acids. The desaturated fatty acid products in PC enter the acyl-CoA pool by the reverse reaction of LPCAT. During the movement of glycerol backbone towards TAG through the so-called Kennedy pathway DAG can freely interconvert with PC through the forward and reverse reactions of a cholinephosphotransferase (CPT). During oil formation DAGs also give rise to TAG and monoacylglycerol (MAG) through a transacylation (TA) reaction, which is freely reversible.

them at a considerably higher rate with long-chain acyl-CoA than medium-chain acyl-CoA (81). The rather special properties of the *Cuphea* AT2 enables the cell to synthesize phosphatidic acid in two major

molecular species consisting of medium-chain and long-chain acyl groups, respectively, and with little of the mixed acyl species. This feature is probably a necessity in *Cuphea* in order to maintain correct membrane lipid assembly and function (see below).

In vitro assays have shown that the AT2 in rape seed has a poor capacity to acylate unusual fatty acids in the *sn2* position (81, 82). In line with these observations it was found that rape seed–accumulating erucic acid (C22:1) (82) and transgenic rape seed engineered to accumulate laurate (C12:0) (83, 84) nearly totally exclude these fatty acids from the *sn2* position of triacylglycerols. However, this exclusion of unusual fatty acids from the *sn2* position in rape can be surpassed by introducing other AT2s from other species. For example, transgenic laurate-producing rape transformed with a cDNA encoding coconut AT2 (which acylates medium-chain fatty acids at the *sn2* position) resulted in rape seeds with 30 mol% of laurate in the *sn2* position of triacylglycerols (85). When a cDNA encoding a *Limnanthes* AT2 was introduced into an erucate acid–producing rape, it resulted in transgenic seeds with significant erucic acid at the *sn2* position of the triacylglycerols (86). A thorough review of the molecular biology of AT1 and AT2 has been presented by Frentzen and Wolter (87). It is evident that particular cloned AT2 genes can be successfully used to manipulate fatty acid composition in transgenic seeds. It also appears that the expression of a yeast AT2 gene in transgenic rape seed improves oil yield (88, 89).

In the further reactions of triacylglycerol assembly the phosphatidic acid is converted to diacylglycerols and inorganic phosphate through the action of the enzyme, phosphatidate phosphohydrolase (PAP):

$$\text{phosphatidic acid} \rightarrow \text{diacylglycerol} + \text{inorganic phosphate}$$

In oil seeds, the enzyme appears to be present in both soluble and membrane-bound forms and these may have a regulatory function in lipid synthesis (90). Good purification of this enzyme has recently been achieved and it is currently under investigation (91).

Diacylglycerols are the precursors for the membrane lipids, phosphatidylcholine, and phosphatidylethanolamine as well as storage triacylglycerols. Consequently, diacylglycerol utilization constitutes a branch point between membrane and storage lipid synthesis. The final step in triacylglycerol biosynthesis is the acylation of the diacylglycerols at the *sn3* position catalyzed by diacylglycerol acyltransferase (AT3):

$$\text{diacylglycerol} + \text{acyl-CoA} \rightarrow \text{triacylglycerol} + \text{CoA}$$

The acylation of diacylglycerol is the only unique step in triacylglycerol assembly. There are many plant species with unusual fatty acids in their seed oil. These are often major constituents in the triacylglycerols and are almost absent in the seed membrane lipid. It is probable that the presence of many of these unusual acids in membrane lipids would severely impair proper membrane function. How particular acyl species of diacylglycerols are channeled almost exclusively to triacylglycerols is not fully understood. Although experimental data suggest that the mechanisms might differ depending on the type of "triacylglycerol-specific" fatty acid, it appears that the AT3 must play an important role in this regulation. It has been shown that AT3 in plants accumulating unusual fatty acids can exhibit acyl specificity and selectivity which enables the preferential channeling of these fatty acids into triacylglycerols (92, 93). As yet little progress has been made on the molecular biology of AT3 in plants. Recently, however, a mouse cDNA-encoding AT3 has been isolated and characterized (94). This appears to be the first successful identification of an AT3 gene and hopefully bodes well for the identification of genes with a similar function in plants.

B. Desaturation and Its Relationship to Oil Assembly

Since phospholipids are the prime substrates for the production of linoleic and linolenic acids that are designed for plant triacylglycerol assembly (see above), there must be efficient mechanisms by which the oleate is channeled into phospholipids for desaturation and the desaturated acyl groups made available for triacylglycerol biosynthesis. Among the phospholipids present in the endoplasmic reticulum, it is only phosphatidylcholine that undergoes rapid turnover and it is this lipid that is important in providing polyunsaturated fatty acids for triacylglycerol formation. An equilibration reaction between acyl groups in phosphatidylcholine and the acyl-CoA pool occurs in oil seeds and by this reaction oleate from oleoyl-CoA enters position *sn2* of phosphatidylcholine for desaturation. Concomitantly, the products from that position enter the acyl-CoA pool for the acylation of all three positions of the glycerol backbone. The reaction can be catalyzed by the combined forward and reverse reactions of an acyl-CoA:lysophosphatidylcholine acyltransferase (LPCAT) (95).

Diacylglycerol may be utilized for phosphatidylcholine synthesis by a CDP-choline:diacylglycerol cholinephosphotransferase (CPT) catalyzed reaction. In oil seeds, this appears to be reversible and thus the phosphatidylcholine can also reconvert with diacylglycerols (96). In the combined forward and reverse reactions of the cholinephosphotransferase, the oleate at both positions of diacylglycerols can enter phosphatidylcholine for desaturation and the polyunsaturated products transferred to the diacylglycerol pool for triacylglycerol synthesis (97). The relative importance of the two reactions, the acyl exchange between acyl-CoA and phosphatidylcholine and the phosphatidylcholine-diacylglycerol interconversion, in providing polyunsaturated fatty acids for triacylglycerol assembly is unclear and might differ among plant species (98, 99). The cholinephosphotransferase has recently been cloned from soybean (100), which should lead to a better understanding of the role of this enzyme in influencing oil quality.

C. Transacylation

Observations suggest that events other than those described above may also occur during oil assembly. In previous experiments with safflower microsomal membranes, triacylglycerols appeared to form from diacylglycerols, but in the absence of acyl-CoA, and hence not by the direct acylation through diacylglycerol acyltransferase activity (97). At that time no explanation was offered for this. Also it has recently been shown that preformed triacylglycerols in the embryos of sunflower at an early stage of development can become further enriched with linoleate (101), suggesting that fatty acids esterified to triacylglycerols, and presumably before stabilization in the oil body, are available to the Δ12-desaturase of the endoplasmic reticulum. Further, it has been demonstrated that there is considerable remodeling of in situ–synthesized triacylglycerol involving acyl groups from polar lipids in microsomal preparations from the developing castor bean endosperm (102).

In attempts to reconcile these observations with our present understanding of oil assembly, the utilization by microsomal membranes of radiolabeled neutral lipid substrates has been investigated. Safflower microsomes were found to catalyze the interconversion of mono-, di-, and triacylglycerols (103). From these studies it was clear that diacylglycerols gave rise to triacylglycerols and monoacylglycerols as well as phosphatidylcholine. Radioactivity was transferred from triacylglycerols to diacylglycerols and monoacylglycerols were rapidly converted to di- and triacylglycerols. These interconversions occur in the absence of acyl-CoA and hence do not involve diacylglycerol acyltransferase activity. The evidence is consistent with the operation of a diacylglycerol-diacylglycerol transacylation yielding monoacylglycerols and triacylglycerols; the reaction is freely reversible. A similar transacylase reaction has been characterized in rat intestinal microsomes where it is involved in the net synthesis of monoacylglycerols and triacylglycerols (104). The activity of the transacylase in safflower microsomes is of the same order of magnitude as the diacylglycerol acyltransferase. Hence in any diacylglycerol acyltransferase assays using radioactive diacylglycerols, it would not be possible to discriminate triacylglycerol formation via transacylation or direct acylation.

Experimental evidence also shows that the diacylglycerols, arising directly by the so-called Kennedy pathway, or via transacylation, rapidly interconvert with phosphatidylcholine, probably through the reversible action of choline phosphotransferase (96). Any oleoyl substrate entering phosphatidylcholine via choline phosphotransferase is readily desaturated and the polyunsaturated fatty acid products become incorporated into the triacylglycerol oil. Transacylation, therefore, can account for the further enrichment of preformed triacylglycerols with polyunsaturated fatty acids observed in vivo (101). It cannot be ruled out, of course, that such a desaturation can occur in vivo while the oil is still associated with the endoplasmic reticulum, and presumably before stabilization in the oil body. In this respect a solubilized Δ12-desaturase from the choloroplast was found to utilize, to some degree, other substrates (free fatty acids, acyl-CoA, and the complex lipid monogalactosyldiacylglycerol) (105). It is clear, however, that the consequence of any reaction that gives rise to diacylglycerols will also bring about the further enrichment of the glycerol backbone with C18-polyunsaturated fatty acids. Transacylation could also account for the previous observation with microsomal membranes that radioactivity in diacylglycerols would accumulate in triacylglycerols in the absence of acyl-CoA (97), and that in situ–synthesized triacylglycerols are remodeled with acyl groups from polar lipids (102).

Our current understanding of triacylglycerol assembly and turnover *in vitro* in developing oil seeds and the relationship to microsomal desaturation is outlined in Figure 3. It is also apparent that microsomal membranes catalyze the production of lysophosphatidylcholine from monoacylglycerols (103). This appears to occur via a phosphocholine transfer between phos-

phatidylcholine and the monoacylglycerol, the products being diacylglycerols and lysophosphatidylcholine. The lyso derivative can be rapidly reacylated from acyl-CoA. Such a combination of reactions could yield triacylglycerols without the participation of diacylglycerol acyltransferase and without any accumulation of monoacylglycerols.

If transacylation occurs in vivo, what might be its biological significance? Clearly, it can provide even further opportunity for desaturation and the enrichment of the oil with C18-polyunsaturated fatty acids. The reactions that channel oleate to phosphatidylcholine for its subsequent desaturation help to concentrate substrate and give a greater chance(s) for desaturation. It is possible that desaturation of complex lipids, such as phosphatidylcholine, is not an efficient process and that a number of mechanisms have evolved, including transacylation, which enables the rapid formation of polyunsaturated fatty acids for storage and membrane lipid assembly. One might also speculate that the transacylation may play some role in the assembly of triacylglycerols containing $> 70\%$ of a particular fatty acid and particularly those of an unusual nature perhaps by giving rise to species of diacylglycerols which are immediately acylated directly with the required fatty acid. Transacylation, however, could have a more profound biochemical importance. It may help to regulate the size of an active diacylglycerol pool, a possible necessity which prevents the detrimental net movement of phosphatidylcholine to diacylglycerols (via cholinephosphotransferase) and the consumption of endoplasmic reticulum structural lipid during the period of extremely rapid oil deposition that is found in the developing seed.

V. OXIDIZED FATTY ACIDS

A. Autoxidation and Antioxidants

Historically, the oxidation of fatty acids has been perceived as a deleterious process resulting in the generation of off-flavors in commercial produce. The process of oxidation can be considered as either autoxidation, a chemical reaction that usually takes place at ambient temperatures between atmospheric oxygen and an organic compound, or as an enzyme-catalyzed reaction. The complexity of the autoxidation reaction has been well documented (106). The insertion of oxygen is also accompanied by the movement of double bonds resulting in the formation of a conjugated diene with a maximal absorbance at 234 nm. Spectral measurements at this wavelength have been used to monitor hydroperoxide formation (107). An important feature of autoxidation is that it is autocatalytic, the rate of oxidation being slow at the start (the induction period) and increasing as the reaction progresses. In common with other radical chain reactions, autoxidation can be divided into three separate processes: initiation, propagation, and termination. Initiation is perhaps the process most difficult to define because of the low concentration of radicals and the likelihood of there being more than one process, since a large number of different radicals can abstract hydrogen from RH to form $R^{\bullet} + H$. The initiating species may be, for example, a transition metal ion, a radical generated by photolysis or high-energy irradiation, or a radical generated by decomposition of a hydroperoxide. In the propagative phase, further reactive species are generated as in the generation of a radical $R^{\bullet}$ from the alkene RH and its subsequent reaction with oxygen. In the termination phase there is an interaction of radicals to produce noninitiating and nonpropagating products.

Autoxidation is facilitated by pro-oxidants and inhibited by antioxidants. Pro-oxidants, such as metals or other radical initiators, operate by promoting the initiation step or else they may inhibit the activity of antioxidants. Antioxidants are frequently added to fats and fat-containing foodstuffs to prolong shelf life (108). These are often phenolic compounds which act by interferring with the propagation sequence by conserving propagating radicals into nonpropagating species (109, 110). Their effectiveness is often increased by compounds such as citric acid, ascorbic acid, or phosphoric acid (called synergists). In this regard, there is considerable evidence for a contributory, antioxidant role for vitamins E and C and the carotenoids—constituents of fruit, vegetables, beverages, and grains—in the maintenance of health and the protection from coronary heart disease, cataracts, and certain cancers (111).

Recent work indicates possible important roles of polyphenolic components (the flavonoids, phenylpropanoids, and phenolic acids) as contributors to antioxidant activities and also as agents of other mechanisms contributing to cardioprotective and anticarcinogenic actions. Epidemiological evidence suggests a negative correlation between dietary antioxidants and coronary arterial disease. Such an association may involve a mechanism whereby antioxidants delay the onset or progression of the disease by reducing oxidative reactions, downregulating thrombic mechanisms, and attenuating endothelial dysfunction.

A large range of flavonoids and phenylpropanoids found in fruit, vegetables, and beverages are more

effective antioxidants in in vitro systems than vitamin C or vitamin E (111). Examination of the antioxidant status of a number of consumables gave a hierarchy of red wine > black tea = green tea > red grape juice = blackcurrant juice > white grape juice = orange juice > white wine = apple juice. Indeed, in what has become known as the "French paradox" (their relatively high fat consumption but relatively low coronary disease) has been attributed, in part at least, to the beneficial effects derived from the consumption of red wine containing the flavonoid constituents derived from the black grape skins.

There is also increasing epidemiological evidence for an association between dietary intake of carotenoid-containing fruit and vegetables and a decreased incidence of coronary heart disease and certain cancers (111, 112). Recent studies (113) have shown that dietary intake of lycopene-rich foods was inversely associated with a risk of prostate cancer. These effects have been ascribed in part to the antioxidant activity of carotenoids. In addition to direct radical scavenging properties of some compounds given above, others such as the glucosinolates (114) (present in high amounts in vegetables such as brocolli, Brussels sprouts, and cabbage) or cysteine sulfoxides (115) in *Allium* (garlic and onion) act by stimulating the animals' own enzymic defenses (116, 117). This appears to operate via the antioxidant responsive element present in the 5′-flanking region of many antioxidant enzymes such as glutathione S-transferases, glutathione peroxidases, quinone reductase, and superoxide dismutase.

B. Oxylipin Biosynthesis (Fig. 4)

Much of the early work concentrated on characterizing lipoxygenase (LOX), a nonheme dioxygenase that catalyzes, as a primary reaction, the hydroperoxidation, by molecular oxygen, of linoleic acid and other polyunsaturated fatty acids that contain a *cis, cis*-1,4-pentadiene moiety. Unesterified fatty acids have been regarded as the principal substrates for the enzyme although LOX isoforms with activity toward complex lipid substrates have been reported (118). LOXs are ubiquitous in plants and are encoded by large gene families which may result in the presence in a given tissue of LOX isoforms differing in substrate preferences, kinetic parameters, and stereospecificity of oxygenation (119). Linoleic and linolenic acid are the major polyunsaturated fatty acids in plant tissues, and insertion of the oxygen takes place at either the $\Delta 9$ or $\Delta 12$ position to generate the corresponding 9- or 13-hydroperoxides (107, 118). While most LOXs so far characterized are soluble cytosolic enzymes, some are chloroplastic, mitochondrial, or located in the vacuoles (118). In soybean, lipoxygenases have been identified with involvement in nitrogen and assimilate partitioning and appear to be regulated in response to plant nitrogen status in both tissue-specific and developmentally controlled patterns (120). A key role for some LOX isoforms is in the generation of fatty acid hydroperoxides destined for jasmonic acid (JA), which triggers gene activation during wound response in plants (121, 122).

The fatty acid hydroperoxides generated by the activity of LOX are potentially deleterious to membrane function by causing increased rigidity and would not, therefore, be expected to accumulate (123). Hydroperoxides can be metabolized by several routes. Glutathione transferases (GSTs) exhibiting glutathione peroxidase activity toward phospholipid hydroperoxides have recently been demonstrated in mammalian tissues (124). GSTs in plants perhaps having analogous roles in hydroperoxide detoxification could be envisaged (125). Hydroperoxide fatty acids can also be metabolized by the peroxygenase cascade (126–128). This involves (a) an intramolecular transfer of one oxygen atom from fatty acid hydroperoxide yielding an epoxyalcohol and/or co-oxidation reactions such as epoxidation of double bonds of unsaturated fatty acids, and (b) an epoxide hydrolase, which preferentially hydrates the epoxides formed by the peroxygenase (127). The chloroplast envelope membranes appear to be a major site of these metabolic activities (128); it is suggested that the products of this pathway may play roles in plant defense mechanisms.

During jasmonic acid synthesis upregulation of the allene oxide synthase (AOS) gene results in the conversion of 13-hydroperoxide to 12,13-epoxylinolenic acid, and is the first committed step in jasmonic biosynthesis. This conversion step has been proposed to be the rate-limiting step in the octadecanoid pathway (129). AOS is a cytochrome P450 of the CYP74A family, and cDNA clones have been obtained from a number of species (130, 131). The protein contains a peptide leader sequence typical for chloroplast import, indicating that it is targeted to this organelle. 12,13-Epoxylinolenic acid is very unstable and rapidly cyclized to racemic 12-oxophytodienoic acid (12-oxo-PDA). In vivo, a stereospecific reaction catalyzed by allene oxide cyclase (AOC) occurs specifically yielding the 9(S), 13(S)-12-oxo-PDA isomer. The AOC gene has not been cloned to date. The 12-oxo-PDA is the first cyclopentenone in the jasmonate pathway and is

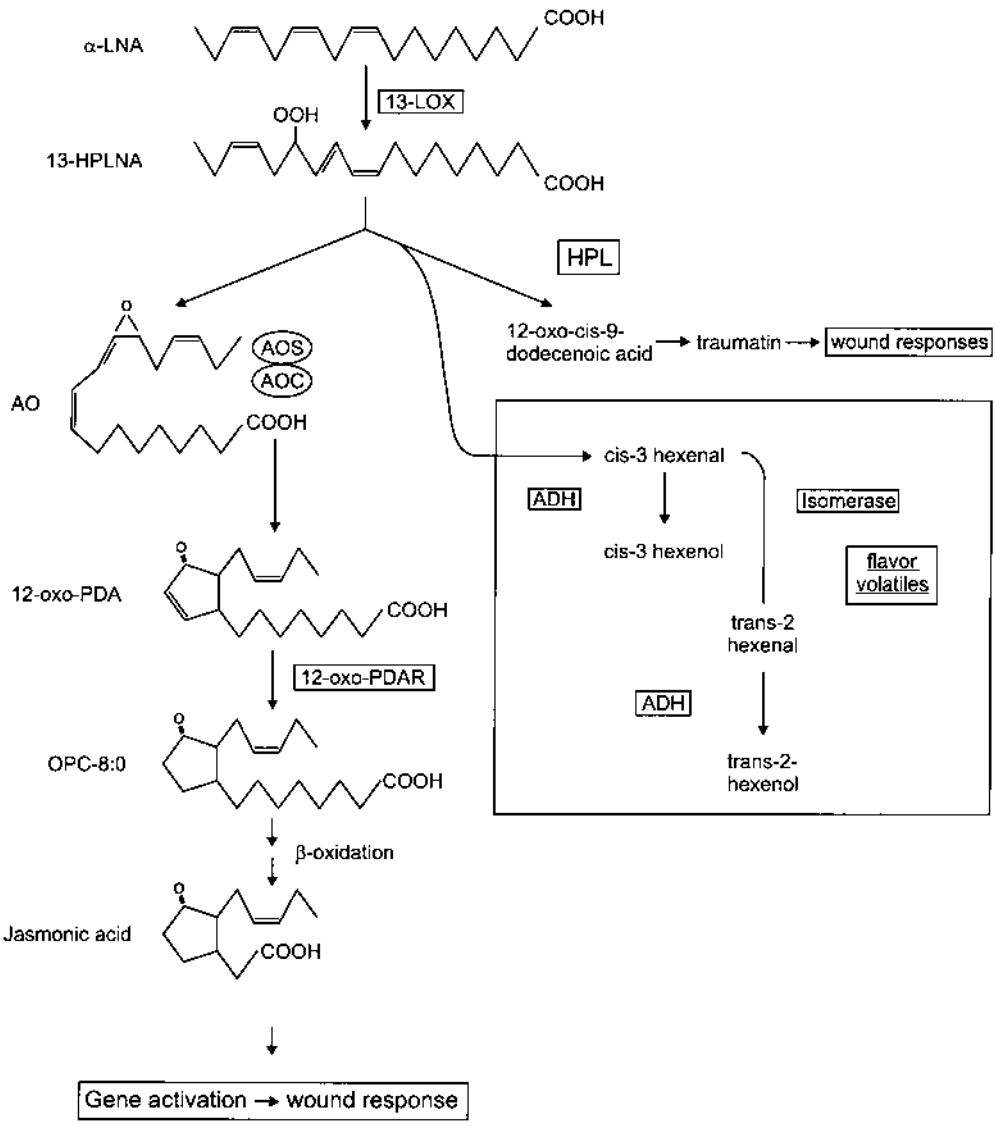

Figure 4 Oxylipin biosynthesis. α-Linolenic acid (α-LNA; C18:3$^{\Delta 9,12,15}$) is converted to 13-hydroperoxylinolenic acid (13-HPLNA) by a 13-lipoxygenase isoform. The 13-HPNLA can be metabolized by several enzymes of which the formation of jasmonic acid (JA) and flavors volatilities are illustrated. The first step in JA synthesis is catalyzed by allene oxide synthase (AOS) forming an unstable allene oxide (AO) which is converted to 12-oxo-phytodienoic acid (12-oxo-PDA) by allene oxide cyclase (AOC). These reactions are considered plastidic. The 12-oxo-PDA is likely exported to the cytosol and acts as a substrate for 12-oxo-PDA reductase (12-oxo-PDAR) forming 3-oxo-2 (2′-pentenyl)-cyclopentane-1-octanoic acid (OPC-8:0), which yields JA by β-oxidation. When 13-HPNLA is metabolized by hydroperoxide lyase (HPL), short-chain aldehydes and ω-oxo acids are generated. The figure depicts the formation of the C6 aldehyde (*cis*-3-hexenal) and the 12-oxo-*cis*-9-dodecenoic acid which in turn can be metabolized to traumatin. The chain length of the aldehydes and ω-oxo acids produced in a particular tissue is dependent on the cleavage site of the C–C bond by HPL. The downstream metabolism of the aldehydes by alcohol dehydrogenases (ADH) and isomerases generates many of the characteristic flavors and aromas of fruits and vegetables.

subsequently converted to jasmonic acid by reduction of the Δ10 double bond by 12-oxo-PDA reductase, considered to be a cytosolic enzyme (132) and is followed by three rounds of β-oxidation that may occur in the peroxisomes. Thus jasmonic acid synthesis may involve the cooperation of three subcellular compartments, the chloroplast, cytosol and peroxisomes. The 12-oxo-PDA together with its metabolite, jasmonic acid (collectively termed jasmonates), either directly or indirectly triggers gene activation in a range of responses of which the defense response has probably been the most recently well documented (119, 122, 133).

Fatty acid hydroperoxides can also serve as substrates for the fatty acid hydroperoxide lyase (HPL) resulting in the formation of aldehydes and ω-oxoacids; the former contributes to the volatile aldehydes and alcohols which are major constituents of characteristic aromas and flavors of many fruits and vegetables (107). Specificity of cleavage of the C–C bond of the hydroperoxide varies from species to species, although the most predominant products are of the C6 and C12 chain length (e.g., in soy and bell pepper) (134, 135). In pear, for example, the products are two C9 fragments (136), while in mushroom the principal products appear to be of C10 and C8 chain lengths (137), with the downstream C8 alcohol generated through the action of alcohol dehydrogenase contributing significantly to the characteristic mushroom odor. Of particular interest to the food industry is the generation of "green notes," of which hexenal is a major component used as a natural flavoring compound. Recently, a cDNA encoding the HPL from bell pepper was cloned (138). The encoded protein comprises 480 amino acids and shares similarity with P450-type proteins especially at the C-terminus. Interestingly, the most related P450 protein is AOS with 40% amino acid identity and hence the HPL is classified as a new P450 subfamily, CYP74B. It is a future possibility that crops could be engineered with enhanced or altered flavor characteristics through the introduction and expression of "foreign" lyase enzymes.

VI. CONCLUDING REMARKS

In this review we have attempted to summarize our present understanding of fatty acid biosynthesis and triacylglycerol assembly in plants. In the last decade, enormous advances have been made in lipid molecular biology with many genes cloned and characterized. This, together with biochemical studies, has made it possible to manipulate fatty acid profiles in oil seeds and even introduce the capacity to synthesize foreign fatty acids, not normally present, in transformed species. As knowledge and technology advance, it will become even more feasible to produce valuable new lipid products in plants to satisfy the demands of the food, nutraceutical, and pharmaceutical industries.

REFERENCES

1. AK Stobart, S Stymne, PR Shewry, J Napier. Triacylglycerol biosynthesis. In: JL Harwood, ed. Plant Lipid Biosynthesis. Society for Experimental Biology Seminar Series 67. Cambridge: Cambridge University Press, 1998, pp 223–245.
2. RC Badami, KB Patil. Structure and occurrence of unusual fatty acids in minor seed oils. Prog Lipid Res 19:119–153, 1981.
3. DPS Verma, ed. Control of Plant Gene Expression. Boca Raton, FL: CRC Press, 1992.
4. PJ Camp, D Randall. Purification and characterization of the pea chloroplast pyruvate dehydrogenase complex. Plant Physiol 77:571–577, 1985.
5. AH Millar, C Knorpp, CL Leaver, SA Hill. Plant miochondrial pyruvate dehydrogenase complex: purification and identification of catalytic components in potato. Biochem J 334:571–576, 1998.
6. B Liedvogel, R Bauerle. Fatty acid synthesis in chloroplasts from mustard (*Sinaosis alba* L.) cotyledons: formation and acetyl-CoA by intraplastid glycolytic enzymes and a pyruvate dehydrogenase complex. Planta 169:481–489, 1986.
7. P Eastmond, S Rawsthorne. Transporters on the plastid envelope that supply carbon skeletons for fatty acid synthesis. Proceedings of the 13th International Symposium on Plant Lipids, Seville, Spain, 1998.
8. F Kang, S Rawsthorne. Metabolism of glucose-6-phosphate and the utilization of multiple metabolites for fatty acid synthesis by plastids from developing oilseed rape embryos. Planta 199:321–327, 1996.
9. P Eastmond, DT Dennis, S Rawsthorne. Evidence that a malate inorganic phosphate exchange translocator imports carbon across the leucoplast envelope for fatty acid synthesis in developing castor seed endosperm. Plant Physiol 114:851–856, 1997.
10. N Focks, C Benning. *wrinkled1*: A novel, low-seed-oil mutant of *Arabidopsis* with a deficiency in the seed-specific regulation of carbohydrate metabolism. Plant Physiol 118:91–101, 1998.
11. AJ White, KM Elborough, SZ Hanley, AR Slabas. Down-regulation of lipid synthesis in plants implies higher orders of regulation in fatty acid biosynthesis.

In: JL Harwood, ed. Plant Lipid Biosynthesis. Society for Experimental Biology Seminar Series 67. Cambridge: Cambridge University Press, 1998, pp. 57–71.
12. J Sun, J Ke, JL Johnson, BJ Nikolau, ES Wurtele. Biochemical and molecular biological characterization of *CAC2*, the *Arabidopsis thaliana* gene coding for the biotin carboxylase subunit of the plastidic acetyl-coenzyme A carboxylase. Plant Physiol 115:1371–1383, 1997.
13. BJ Nikolau, ES Wurtele. In situ and transgenic studies of the regulation of acetyl-CoA carboxylase gene expression. Proceedings of the 13th International Symposium on Plant Lipids, Seville, Spain, 1998.
14. Y Sasaki, A Kozaki, M Hatano. Link between light and fatty acid synthesis: thioredoxin-linked reductive activation of plastidic acetyl-CoA carboxylase. Proc Natl Acad Sci USA 94:11096–11101, 1997.
15. JL Harwood. Fatty acid metabolism. Annu Rev Plant Physiol Mol Biol 39:101–138, 1988.
16. AR Slabas, T Fawcett, G Griffiths, AK Stobart. Biochemistry and molecular biology of lipid biosynthesis in plants: potential for genetic manipulation. In: D Grierson, ed. Biosynthesis and Manipulation of Plant Products. Blackie Academic and Professional, 1993, pp. 104–138.
17. C Alban, P Baldet, R Douce. Localization and characterization of two structurally different forms of acetyl-CoA carboxylase in young pea leaves, of which one sensitive to aryloxy-phenoxypropionate herbicides. Biochem J 300:557–565, 1994.
18. T Shimakata, PK Stumpf. The purification and function of acetyl-CoA: acyl carrier protein transacylase. J Biol Chem 258:3592–3598, 1983.
19. T Shimakata, PK Stumpf. Isolation and function of spinach leaf β-ketoacyl-[acyl carrier protein] synthetases. Proc Natl Acad Sci USA 79:5808–5812, 1982.
20. JG Jaworski, RC Clough, SR Barnum. A cerulenin insensitive short chain 3-ketoacyl-acyl carrier protein synthase in *Spinacia oleracea* leaves. Plant Physiol 90:41–44, 1989.
21. JW Simon, AR Slabas. cDNA cloning of *Brassica napus* malonyl-CoA:ACP transacylase (MCAT) (fabD) and complementation of an *E. coli* MCAT mutant. FEBS Lett 435:204–206, 1998.
22. TT Hoang, HP Schweizer. Fatty acid biosynthesis in *Pseudomonas aeruginosa*: cloning and characterization of the fabAB operon encoding β-hydroxyacyl-acyl carrier protein dehydratase (fabA) and beta-ketoacyl-acyl carrier protein synthase I (fabB). J Bacteriol 179:5326–5332, 1997.
23. AR Slabas, CM Sidebottom, A Hellyer, RMJ Kessell, MP Tombs. Induction, purification and characterization of NADH-specific enoyl acyl carrier protein reductase from developing seeds of oil seed rape (*Brassica napus*). Biochim Biophys Acta 877:271–280, 1986.
24. MM Kater, GM Koningstein, HJJ Nijkamp, AR Stuitje. The use of hybrid genetic system to study the functional relationship between prokaryotic and plant multi-enzyme fatty acid synthetase complexes. Plant Mol Biol 25:771–790, 1994.
25. JB Rafferty, WJ Simon, AR Stuitje, AR Slabas, T Fawcett, DW Rice. Crystallization of the NADH-specific enoyl acyl carrier protein reductase from *Brassica napus*. J Mol Biol 237:240–242, 1994.
26. C Baldock, JB Rafferty, SE Sedelnikova, PJ Baker, AR Stuitje, AR Slabas, TR Hawkes, DW Rice. A mechanism of drug action revealed by structural studies of enoyl reductase. Science 274:2107–2110, 1996.
27. T Voelker, T Cranmer, J Turner, H Davies. Genetic engineering of a quantitative trait: metabolic and genetic parameters influencing the accumulation of laurate in rapeseed. Plant J 9:229–241, 1996.
28. JM Leonard, SJ Knapp, MB Slabaugh. A *Cuphea* β-ketoacyl-ACP synthase shifts the synthesis of fatty acids towards shorter chains in *Arabidopsis* seeds expressing *Cuphea* FatB thioesterases. Plant J 13:621–628, 1998.
29. K Dehesh, P Edwards, J Fillatti, M Slabaugh, J Byrne. KAS IV: a 3-ketoacyl-ACP synthase from *Cuphea* sp. is a medium chain specific condensing enzyme. Plant J 15:383–390, 1998.
30. M Slabaugh, JM Leonard, SJ Knapp. Condensing enzymes from *Cuphea wrightii* associated with medium chain fatty acid biosynthesis. Plant J 13:611–620, 1998.
31. D Hawkins, JC Kridl. Characterization of acyl-ACP thioesterases of mangosteen (*Garcinia mangostana*) seed and high levels of stearate production in transgenic canola. Plant J 13:743–752, 1998.
32. DS Knutzon, GA Thompson, SE Radke, WB Johnson, VC Knauf, JC Kridl. Modification of *Brassica* seed oil by antisense expression of a stearoyl-acyl carrier protein desaturase gene. Proc Natl Acad Sci USA 89:2624–2628, 1992.
33. A Jones, HM Davies, TA Voelker. Palmitoyl-acyl carrier protein (ACP) thioesterase and the evolutionary origin of plant acyl-ACP thioesterases. Plant Cell 7:359–371, 1995.
34. J Shanklin, C Somerville. Stearoyl-acyl carrier protein desaturase from higher plants is structurally unrelated to the animal and fungal homologs. Proc Natl Acad Sci USA 88:2510–2514, 1991.
35. BG Fox, J Shanklin, C Somerville, E Munck. Stearoyl-acyl carrier protein Δ9 desaturase from *Ricinus communis* is a diiron-oxo protein. Proc Natl Acad Sci USA 90:2486–2490, 1993.
36. Y Lindquist, W Huang, G Schnieder, J Shanklin. Crystal structure of Δ9 stearoyl-acyl carrier protein

desaturase from castor seed and its relationship to other di-iron proteins. EMBO J 15:4081–4092, 1996.
37. J Shanklin, EB Cahoon. Desaturation and related modifications of fatty acids. Annu Rev Plant Physiol Plant Mol Biol 49:611–641, 1998.
38. S Stymne, AK Stobart. Triacylglycerol biosynthesis. In: PK Stumpf, ed. The Biochemistry of Plants: A Comprehensive Treatise. New York: Academic Press, 1987, pp 175–214.
39. S Stymne, ML Tonnet, AG Green. Biosynthesis of linolenate in developing embryos and cell-free preparations of high-linolenate linseed and low linolenate mutants. Arch Biochem Biophys 294:557–563, 1992.
40. C Somerville, J Browse. Plant lipids: metabolism, mutants and membranes. Science 252:80–87, 1991.
41. MA Smith, AR Cross, OTG Jones, T Griffiths, S Stymne, AK Stobart. Electron-transport components of the 1-acyl-2-oleoyl-*sn*-glycerol-3-phosphocholine Δ12-desaturase in microsomal preparations from developing safflower cotyledons. Biochem J 272:23–29, 1990.
42. EV Kearns, S Hugly, CR Somerville, Role of cytochrome b5 in Δ12 desaturation of oleic acid by microsomes of safflower. Arch Biochem Biophys 284:431–435, 1991.
43. MA Smith, AK Stobart, PR Shewry, JA Napier. Tobacco cytochrome b5: cDNA isolation, expression analysis and in-vitro protein targeting. Plant Mol Biol 25:527–537, 1994.
44. MA Smith, JA Napier, S Stymne, PR Shewry, AK Stobart. Expression of a biologically active plant cytochrome b5 in *Escherichia coli*. Biochem J 303:73–79, 1994.
45. JA Napier, MA Smith, AK Stobart, PR Shewry. Isolation of a cDNA encoding a cytochrome b5 specifically expressed in developing tobacco seeds. Planta 197:200–202, 1995.
46. MA Smith, AK Stobart, PR Shewry, JA Napier. Cytochrome b5 and polyunsaturated fatty acid biosynthesis. In PR Shewry, JA Napier, PJ Davies, eds. Engineering Crop Plants for Industrial Uses. London: Portland Press, 1998, pp 181–188.
47. A Green. A mutant genotype of flax containing very low levels of linolenic acid in its seed oil. Can J Plant Sci 66:499-503, 1986.
48. G Powell, A Abott, D Knauft, J Barth. Oil desaturation in developing peanut seeds. Studies of lipid desaturation in a peanut mutant that accumulates high levels of oleic acid. In: PJ Quinn, JL Harwood, eds. Plant Lipid Biochemistry, Structure and Utilization. London: Portland Press, 1990, pp 131–133.
49. P Sperling, U Hammer, W Friedt, E Heinz. High oleic sunflower: studies on composition and desaturation of acylgroups in different lipids and organs. Z Naturforsch 45:166–172, 1990.
50. ML Tonnet, AG Green. Characterization of the seed and leaf lipids of high and low linolenate flax genotypes. Arch Biochem Biophys 252:646–654, 1987.
51. C Somerville, J Browse. Dissecting desaturation: plants prove advantageous. Trends Cell Biol 6:148–153, 1996.
52. V Arondel, B Lemieux, I Hwang, S Gibson, HM Goodman, C Somerville. Map based cloning of a gene controlling omega-3 fatty acid desaturation in *Arabidopsis*. Science 258:1353–1355, 1992.
53. J Okuley, J Lightner, K Feldmann, N Yadav, E Lark, J Browse. *Arabidopsis* FAD2 gene encodes the enzyme that is essential for polyunsaturated lipid synthesis. Plant Cell 6:147–148, 1994.
54. J Shanklin, E Whittle, BG Fox. Eight histidine residues are catalytically essential in a membrane-associated iron enzyme, stearoyl-CoA desaturase, and are conserved in alkane hydroxylase and xylene monooxygenase. Biochemistry 33:12787–12794, 1994.
55. G Griffiths, F Jackson, EY Brechany, WW Christie, S Stymne, AK Stobart. Octadecatetraenoic acid (C18:4; stearidonic acid) biosynthesis in borage (*Borago officinalis*). Phytochem 43:381–386, 1996.
56. G Griffiths, AK Stobart, S Stymne. Δ6 and Δ12 desaturase activities and phosphatidic acid formation in microsomal preparations from the developing cotyledons of common borage. Biochem J 252:641–647, 1988.
57. DF Horrobin. Omega-6 Essential Fatty Acids: Pathology and Roles in Clinical Medicine. New York: Wiley-Liss, 1990.
58. FD Gunstone. γ-Linolenic acid—occurrence and physical and chemical properties. Prog Lipid Res 31:145–161, 1992.
59. O Sayanova, MA Smith, P Lapinskas, AK Stobart, G Dobson, WW Christie, PR Shewry, JA Napier. Expression of a borage desaturase cDNA containing an N-terminal cytochrome b5 domain results in the accumulation of high levels of a Δ6-desaturated fatty acids in transgenic tobacco. Proc Natl Acad Sci USA 94:4211–4216, 1997.
60. FJ Loo, P Broun, S Turner, C Somerville. An oleate 12-hydroxylase from *Ricinis communis* is a fatty acyl desaturase homolog. Proc Natl Acad Sci USA 92:6743–6747, 1995.
61. K Aitzetmuller, N Tsevegsuren. Occurrence of γ-linolenic acid in *Ranunculaceae* seed oils. Plant Physiol 143:578–580, 1994.
62. LV Michaelson, CM Lazarus, G Griffiths, JA Napier, AK Stobart. Isolation of a Δ5-fatty acid desaturase gene from *Mortierella alpina*. J Biol Chem 273:19055–19059, 1998.
63. LV Michaelson, JA Napier, M Lewis, G Griffiths, CM Lazarus, AK Stobart. Functional identification of a fatty acid Δ5 desaturase gene from *Caenorhabditis elegans*. FEBS Lett 439:215–218, 1998.

64. D Postbeittenmiller. Biochemistry and molecular biology of wax production in plants. Annu Rev Plant Physiol Plant Mol Biol 47:405–430, 1996.
65. F Domergue, J-J Bessoule, P Moreau, R Lessire, C Cassagne. Recent advances in plant fatty acid elongation. In: JL Harwood, ed. Plant Lipid Biosynthesis. Society for Experimental Biology Seminar Series 67. Cambridge: Cambridge University Press, 1998, pp 185–220.
66. Y Rhee, A Hlousek-Radojcic, J Ponsamuel, D Liu, D Postbeittenmiller. Epicuticular wax accumulation and fatty acid elongation activities are induced during leaf development of leeks. Plant Physiol 116: 901–911, 1998.
67. AA Millar, L Kunst. Very-long-chain fatty acid biosynthesis is controlled through the expression and specificity of the condensing enzyme. Plant J 12:121–131, 1997.
68. M Miguel, J Browse. Lipid biosynthesis in developing seeds. In: J Kigel, G Galili, eds. Seed Development and Germination. New York: Marcel Dekker, 1995, pp 169–193.
69. AK Stobart, S Stymne, S Hoglund. Safflower microsomes catalyse the accumulation of oil: a model system. Planta 169:33–37, 1986.
70. E Kennedy. Biosynthesis of complex lipids. Fed Proc Am Soc Exp Biol 20:934–940, 1961.
71. E Barron, P Stumpf. Fat metabolism in higher plants. Biochim Biophys Acta 60:329–337, 1961.
72. K Ichihara. Glycerol 3-phosphate acyltransferase in a particulate fraction from maturing safflower seeds. Arch Biochem Biophys 232:685–698, 1984.
73. M Bafor, AK Stobart, S Stymne. Properties of the glycerol acylating enzymes in microsomal preparations from the developing seeds of safflower and turnip rape and their ability to assemble cocoa-butter type fats. J Am Oil Chem Soc 67:217–225, 1990.
74. PC Dutta, LA Appelqvist, S Stymne. Utilisation of petroselinate (C18:1Δ6) by glycerol acylation enzymes in microsomal preparations of developing embryos of carrot, safflower and oil-seed rape. Plant Sci Lett 81:57–64, 1992.
75. M Bafor, S Stymne. Substrate specificities of glycerol acylating enzymes from developing embryos of two *Cuphea* species. Phytochemistry 31:2973–2976, 1992.
76. G Griffiths, AK Stobart, S Stymne. The acylation of *sn*-glycerol 3-phosphate and the metabolism of phosphatidate in microsomal preparations from the developing cotyledons of safflower seed. Biochem J 230:379–388, 1985.
77. K Ichihara, T Asahi, S Fujii. 1-Acyl-*sn*-glycerol-3-phosphate acyltransferase in maturing safflower seeds and its contribution to the non-random fatty acid distribution of triacylglycerol. Eur J Biochem 167:339–347, 1987.
78. A Kinney. Phospholipid headgroups. In: T Moore, ed. Lipid Metabolism in Plants. Boca Raton, FL: CRC Press, 1993, pp 259–284.
79. SA Graham, F Hirsinger, G Röbbelen. Fatty acid of *Cuphea* seed lipids and their taxonomic significance. Am J Bot 68:908–917, 1981.
80. M Bafor, L Jonsson, AK Stobart, S Stymne. Regulation of triacylglycerol biosynthesis in embryos and microsomal preparations from the developing seeds of *Cuphea lanceolata*. Biochem J 272:31–38, 1990.
81. KC Oo, AHC Huang. Lysophosphatidate acyltransferase activities in the microsomes from palm endosperm, maize scutellum, and rapeseed cotyledon of maturing seeds. Am J Plant Physiol 91:1288–1295, 1989.
82. R Bernerth, M Fentzen. Utilisation of erucoyl-CoA by acyltransferases from developing seeds of *Brassica napus* involved in triacylglycerol biosynthesis. Plant Sci 67:21–28, 1990.
83. T Voelker, T Hayes, A Crammer, J Turner, M Davies. Genetic engineering of a quantitative trait: metabolic and genetic parameters influencing the accumulation of laurate in rapeseed. Plant J 9:229–241, 1996.
84. E Wiberg, A Banas, S Stymne. Fatty acid distribution and lipid metabolism in developing seeds of laurate-producing rape. Planta 203:341–348, 1997.
85. M Davies. Engineering new oilseed crops from rapeseed. In: J Janick, ed. Progression in New Crops. Alexandria, VA: ASHS Press, 1996, pp 299–306.
86. MW Lassner, CK Levering, HM Davies, DS Knutzon. Lysophosphatidic acid acyltransferase from meadow foam mediates insertion of erucic acid at the *sn-2* position of triacylglycerol in transgenic rapeseed oil. Am J Plant Physiol 109:1389–1394, 1995.
87. M Frentzen, FP Wolter. Molecular biology of acyltransferases involved in glycerolipid synthesis. In: JL Harwood, ed. Plant Lipid Biosynthesis. Society for Experimental Biology Seminar Series 67. Cambridge: Cambridge University Press, 1998, pp 247–272.
88. JT Zoe, V Katavic, EM Giblin, DL Barton, SL MacKenzie, WA Keller, DC Taylor. Modification of seed oil content and acyl composition in the *Brassicaceae* utilizing a yeast *sn-2* acyltransferase gene. In: JP Williams, MU Khan, NW Lem, eds. Physiology, Biochemistry and Molecular Biology of Plant Lipids. Dordrecht: Kluwer Academic Publishers, 1997, pp 407–409.
89. JT Zoe, V Katavic, EM Giblin, DL Barton, SL MacKenzie, WA Keller, X Hu, DC Taylor. Modification of seed oil content and acyl composition in the Brassicaceae by expression of a yeast *sn-2* acyltransferase gene. Plant Cell 9:909–923, 1997.
90. K Ichihara, N Murata, S Fujii. Intracellular translocation of phosphatidate phosphatase in maturing safflower seeds: a possible mechanism of feedforward

control of triacylglycerol biosynthesis for fatty acids. Biochim Biophys Acta 1043:227–234, 1990.
91. M Pearce, AR Slabas. Purification and characterisation of phosphatidate phosphatase from avocado. In: JP Williams, MU Kahn, NW Lem, eds. Physiology, Biochemistry and Molecular Biology of Plant Lipids. Dordrecht: Kluwer Academic Publishers, 1997, pp 140–142.
92. JT Lin, CL Woodruff, OJ Lagouche, TA McKeon, AE Safford, M Goodrich-Tanrikulu, JA Singleton, CA Hanet. Biosynthesis of triacylglycerols containing ricinoleate in castor microsomes using 1-acyl-2-oleoyl-*sn*-glycero 3-phosphocholine as a substrate of the oleoyl-12-hydroxylase. Lipids 33:59–69, 1998.
93. G Vogel, J Browse. Cholinephosphotransfersase and diacylglycerol acyltransferase: substrate specificities at a key branch point in seed lipid metabolism. Am J Plant Physiol 110: 923–931, 1996.
94. S Cases, SJ Smith, Y Zheng, HM Myers, SR Lear, E Sande, S Novak, C Collins, CB Welch, AJ Lusis, SK Erickson, RV Farese. Identification of a gene encoding an acylCoA:diacylglycerol acyltransferase, a key enzyme in triacylglycerol synthesis. Proc Natl Acad Sci USA 95:13018-13023, 1998.
95. S Stymne, AK Stobart. Evidence for the reversibility of the acyl-CoA:lysophophatidylcholine acyltransferase in microsomal preparations from developing safflower cotyledons and rat liver. Biochem J 223:305–314, 1984.
96. CR Slack, PG Roughan, J Browse, SE Gardiner. Some properties of cholinephosphotransferase from developing safflower cotyledons. Biochim Biophys Acta 833:438–448, 1985.
97. AK Stobart, S Stymne. Interconversion of diacylglycerol and phosphatidylcholine during triacylglycerol production in microsomal preparations of developing cotyledons of safflower. Biochem J 232:217–221, 1985.
98. G Griffiths, S Stymne, AK Stobart. Utilisation of fatty acid substrates in triacylglycerol biosynthesis by tissue slices of developing safflower and sunflower cotyledons. Planta 173:309–316, 1988.
99. G Griffiths, S Stymne, AK Stobart. Phosphatidylcholine and its relationship to triacylglycerol biosynthesis in oil tissues. Phytochemistry 27:2089–2094, 1988.
100. DD Monks, JH Goode, PK Dinsmore, RE Dewey. Phosphatidylcholine biosynthesis in soybean: cloning and characterisation of genes encoding enzymes of the nucleotide pathway. In: JP Williams, MU Kahn and NW Lem, eds., Physiology, Biochemistry and Molecular Biology of Plant Lipids. Dordrecht; Kluwer Academic Publishers, 1987, pp 110–112.
101. R Garces, C Sarmiento, M Mancha. Oleate from triacylglycerols is desaturated in cold-induced developing sunflower seeds. Planta 193:507–514, 1992.
102. M Mancha, S Stymne. Remodelling of triacylglycerols in microsomal preparations from developing castor bean endosperm. Planta 203:51–57, 1997.
103. AK Stobart, M Mancha, M Lenman, A Dahlqvist, S Stymne. Triacylglycerols are synthesised and utilised by transacylation reactions in microsomal preparations of developing safflower seeds. Planta 203:58–66, 1997.
104. R Lehner, A Kuksis. Triacylglycerols synthesis by a diacylglycerol transacylase from rat intestinal microsomes. J Biol Chem 268:8781–8786, 1993.
105. H Schmidt, E Heinz. Direct desaturation of intact galactolipids by a desaturase solubilized from spinach chloroplast envelopes. Biochem J 289:777–782, 1993.
106. HW-S Chan. The mechanism of autoxidation. In: HW-S Chan, ed. Autoxidation of Unsaturated Lipids. London: Academic Press, 1987, pp 1–16.
107. HW Gardner. Analysis of plant lipoxygenase metabolites. In: WW Christie, ed. Advances in Lipid Methodology—Four. Dundee: Oily Press, 1997, pp 1–43.
108. FD Gunstone, FA Norris. Lipids in Foods. Chemistry, Biochemistry and Technology. Oxford: Pergamon Press, 1983, pp 156–164.
109. C Castelluccio, G Paganga, N Melikian, GP Bolwell, J Pridham, J Sampson, C Rice-Evans. Antioxidant potential of intermediates in phenylpropanoid metabolism in higher plants. FEBS Lett 368:188–192, 1995.
110. C Rice-Evans. Plant polyphenolics: free radical scavengers or chain-breaking antioxidants? Biochem Soc Symp 61:103–116, 1995.
111. AT Diplock, JL Charleux, G Crozier-Willi, FJ Kok, C Rice-Evans, M Roberfroid, W Stahl, J Vina-Ribes. Functional food science and defence against reactive oxidative species. Br J Nutr 80:S77–S81, 1998.
112. A Mortensen, LH Skibsted, J Sampson, C Rice-Evans, SA Everett. Comparative mechanisms and rates of free radical scavenging by carotenoid antioxidants. FEBS Lett 418:91–97, 1997.
113. SK Clinton, E Giovannucci. Diet, nutrition and prostate cancer. Annu Rev Nutr 18:413–440, 1998.
114. BA Halkier, LC Du. The biosynthesis of glucosinolates. Trends Plant Sci 2:425–431, 1997.
115. JE Lancaster, ML Shaw, WM Randle. Differential hydrolysis of alk(en)yl cysteine sulphoxides by allinase in onion macerates: Flavour implications. J Sci Food Agric 78:367–372, 1998.
116. JW Fahey, YS Zhang, P Talalay. Broccoli sprouts: an exceptionally rich source of inducers of enzymes that protect against chemical carcinogens. Proc Natl Acad Sci USA 94:10367–10372, 1998.
117. G Williamson, K Faulkner, GW Plumb. Glucosinolates and phenolics as antioxidants from plant food. Eur J Cancer Prev 7:17–21, 1998.

118. JN Siedow. Plant lipoxygenase: structure and function. Annu Rev Plant Physiol Plant Mol Biol 42:145–118, 1991.
119. J Rojo, G Vancanneyt, AG Perez, C Sanz, K Stormann, S Rosahl, JJ Sanchez-Serrano. Characterization of three potato lipoxygenases with distinct enzymatic activities and different organ-specific and wound-regulated gene expression. J Biol Chem 271:21012–21019, 1996.
120. TW Bunker, DS Koetje, LC Stephenson, RA Creelman, JE Mullet, HD Grimes. Sink limitation induces the expression of multiple vegetative lipoxygenase mRNAs while the endogenous jasmonic acid level remains low. Plant Cell 7:1319–1331, 1995.
121. I Feussner, B Hause, K Voros, B Parthier, C Wasternack. Jasmonate-induced lipoxygenase forms are localized in chloroplasts of barley leaves (*Hordeum vulgare* cv salome). Plant J 7:949–957, 1995.
122. E Titarenko, E Rojo, J Leon, JJ Sanchez-Serrano. Jasmonic acid–dependent and independent signaling pathways control wound-induce gene activation in *Arabidopsis thaliana*. Plant Physiol 115:817–826, 1997.
123. YY Leshem. Plant Membranes: A Biophysical Approach to Structure, Development and Senescence. Dordrecht: Kluwer Academic Publishers, 1192, pp 174–191.
124. R Hurst, Y Bao, P Jemth, B Mannervik, G Williamson. Phospholipid hydroperoxide glutathione peroxidase activity of human glutathione transferases. Biochem J 332:97–100, 1998.
125. KA Marrs. The functions and regulations of glutathione S-transferases in plants. Annu Rev Plant Physiol Plant Mol Biol 47:127–158, 1996.
126. E Blee, F Schuber. Efficient epoxidation of unsaturated fatty acids by a hydroperoxide-dependent oxygenase. J Biol Chem 265:12887–12894, 1990.
127. E Blee, F Schuber. Occurrence of fatty acid epoxide hydrolases in soybean (*Glycine max*). Purification and characterization of the soluble form. Biochem J 282:711–714, 1992.
128. E Blee, J Joyard. Envelope membranes from spinach chloroplasts are a site of metabolism of fatty acid hydroperoxides. Plant Physiol 110:445–454, 1996.
129. D Laudert, EW Weiler. Allene oxide synthase: a major control point in *Arabidopsis thaliana* octadecanoid signalling. Plant J 15:675–684, 1998.
130. WC Song, CD Funk, AR Brash. Molecular cloning of an allene oxide synthase: a cytochrome P450 specialized for the metabolism of fatty acid hydroperoxides. Proc Natl Acad Sci USA 90:8519–8523, 1993.
131. Z Pan, F Durst, D Werch-Reichart, HV Gardner, B Camara, K Cornish, RA Backhaus. The major protein of guayule rubber particles is a cytochrome P450. J Biol Chem 270:8487–8494, 1995.
132. F Schaller, EW Weiler. Enzymes of octadecanoid biosynthesis in plants. 12-Oxophytodienoate 10,11-reductase. Eur J Biochem 245:294–299, 1997.
133. M McConn, RA Creelman, E Bell, JE Mullet, J Browse. Jasmonate is essential for insect defense in *Arabidopsis*. Proc Natl Acad Sci USA 94:5473–5477, 1997.
134. T Matoba, H Hidaka, K Kitamura, N Kaizuma, M Kito. Contribution of hydroperoxide lyase activity to n-hexanal formation in soybean. J Agric Food Chem 33:856–858, 1985.
135. Y Shibata, K Matsui, T Kajiwara, A Hatanaka. Purification and properties of fatty-acid hydroperoxide lyase from green bell pepper fruits. Plant Cell Physiol 36:147–156, 1995.
136. I-S Kim, W Grosch. Partial purification and properties of a hydroperoxide lyase from fruits of pear. J Agric Food Chem 29:1220–1225, 1981.
137. M Wurzenberger, W Grosch. The formation of 1-octen-3-ol from the hydroperoxide isomer of linoleic acid by a hydroperoxide lyase in mushrooms (*Psalliota bispora*). Biochim Biophys Acta 794:25–30, 1984.
138. K Matsui, M Shibutani, T Hase, T Kajiwari. Bell pepper fruit fatty acid hydroperoxide lyase is a cytochrome P450 (CYP74B). FEBS Lett 394:2–24, 1996.

References Added in Proof

The following are significant publications since the writing of this chapter and not cited in text:

Dahlquist A, Stahl U, Lenman M, Banas A, Lee M, Sandager L, Ronne H, Stymne S. Phospholipid: diacylglycerol acyltransferase: an enzyme that catalyses the acyl-CoA-independent formation of triacylglycerol in yeast and plants. Proc Natl Acad Sci USA 97:6487–6492, 2000.

Griffiths G, Leverentz M, Silkowski H, Gill N, Sanchez-Serrano JJ. Lipid hydroperoxide levels in plant tissues. J Exp Bot 51:1363–1370, 2000.

Hobbs D, Hills M. Cloning of a cDNA encoding diacylglycerol acyltransferase from *Arabidopsis thaliana* and its functional expression. FEBS Lett 452:145–149, 1999.

Hornung E, Walther M, Kuhn H, Feussner I. Conversion of cucumber linoleate 13-lipoxygenase to a 9-lipoxygenating species by site-directed mutagenesis. Proc Natl Acad Sci USA 96:4192–4197, 1999.

Slabas A, Hanley Z, Schierer T, Rice D, Turnbull A, Rafferty J, Simon B, Brown A. Acyltransferases and their role in the biosynthesis of lipids-opportunities for new oils. Plant Physiol 158:505–513, 2001.

Ziegler J, Stenzel I, Hause B, Maucher H, Hamberg M, Grimm R, Ganal M, Wasternack C. Molecular cloning of allene oxide cyclase. J Biol Chem 275:19132–19138, 2000.

12

Phospholipid Biosynthetic Enzymes in Plants

Ralph E. Dewey
North Carolina State University, Raleigh, North Carolina, U.S.A.
Anthony J. Kinney
DuPont Experimental Station, Wilmington, Delaware, U.S.A.

I. PLANT PHOSPHOLIPIDS

Phospholipids are a minor (0.1–3%) but important component of all edible plant oils. They are removed during refining as a "gum" fraction but they are not discarded. Collectively known as lecithin, they are used as high-value emulsifiers and wetting agents in food manufacturing (1). The phospholipid fraction of vegetable oil, and indeed of all plant tissues, consists mainly of phosphatidylcholine (PC), phosphatidylethanolamine (PE), phosphatidylserine (PS), phosphatidylinositol (PI), phosphatidylglycerol (PG), and diphosphatidylglycerol (DPG). In addition, there are a number of less abundant phospholipids derived from phosphatidylinositol (2).

All emulsifiers can be characterized by their hydrophilic–lipophilic balance (HLB). Among plant phospholipids PC has the highest HLB value, PE is intermediate, and the other phospholipids have a low HLB. Thus, PC has the greatest value as a soluble oil-in-water emulsifier; it is used, for example, in lowering the viscosity of cocoa butter during chocolate manufacture. PE is more useful as a wetting agent—for example, in increasing fat absorption during the preparation of cake doughnuts (1). For this reason, commercial lecithin preparations are often separated into PC and PE fractions using ethanol, and there may be some value in genetically manipulating the ratio of phospholipids in plant oils for particular food applications. To achieve this it is necessary to understand the pathways of phospholipid biosynthesis in plants and have available the genes that encode phospholipid pathway enzymes.

Many of the enzymes involved in plant lipid biosynthesis are also similar to their yeast and animal counterparts (2), although there are important differences in the pathways which predominate. For example, in most animal tissues PC is predominantly synthesized from diacylglycerol and CDP-choline via a phosphoaminoalcohol pathway often referred to as the Kennedy pathway (3–5). In liver tissues and in yeast PC is synthesized mainly by the sequential methylation of PE, catalyzed by a single enzyme in animals (6) and two separate methylases in yeast (7). In many plants the first step in committed PC biosynthesis is the methylation of ethanolamine phosphate, followed by the synthesis of phosphatidylmonomethylethanolamine and then methylation to PC (see 2). The enzyme involved in this initial methylation of ethanolamine phosphate has recently been identified and its gene cloned from spinach and *Arabidopsis* (8, 9). Interestingly, no yeast or animal counterpart has been reported.

In general, however, the phospholipid pathways of all eukaryotes may be divided into those in which the glycerol backbone of the phospholipid molecule derives from CDP-diacylglycerol and those that it derives from diacylglycerol (DAG). For example,

phosphatidylethanolamine may be made from ethanolamine and diacylglycerol, by the Kennedy pathway, or by decarboxylation of phosphatidylserine, derived from CDP-diacylglycerol and free serine (Fig. 1).

The advent of modern genomics and the rapid advances in the understanding of yeast phospholipid biosynthesis has led to the cloning, heterologous expression, and characterization of many plant phospholipid biosynthetic enzymes that had previously been difficult to purify and characterize. Thus, a great deal of recent understanding of plant phospholipid biosynthetic enzymes has been derived from the molecular approaches described here. The 30 years or so of classical enzymological studies that laid the groundwork for these recent advances are described in earlier reviews (2, 10).

II. BIOSYNTHESIS OF CDP-DIACYLGLYCEROL IN PLANTS

Diacylglycerol and CDP-diacylglycerol are both derived from phosphatidic acid (PA), synthesized by the sequential acylation of glycerol-3-phosphate by two acyltransferases. These acyltransferases—**glycerol-3-phosphate acyltransferase and 1-monoacylglycerol-3-phosphate acyltransferase**—use acyl-CoA as a source of acyl moieties. PA can then be converted either to CDP-diacylglycerol or to DAG. The former reaction is catalyzed by **CDP-diacylglycerol synthase** (CTP:phosphatidate cytidylyltransferase, EC 2.7.7.41) and the latter by **phosphatidic acid phosphatase** (phosphatidate phosphohydrolase, EC 3.1.3.4).

The identification of the yeast gene encoding CDP-diacylglycerol synthase (*CDS1*) led to the construction of a null allele at this locus (11). These studies verified that CDP-diacylglycerol synthase activity is essential for cell viability and established *CDS1* as the only gene in yeast that encodes this activity. This latter observation was somewhat surprising considering that this enzyme is distributed between two very distinct organelles—the mitochondria and the endoplasmic reticulum.

Studies in animal systems reveal that, in addition to their involvement in bulk phospholipid synthesis, CDP-diacylglycerol synthase are also critical components of the phosphoinositide signal transduction cycle. A mutation in an eye-specific *Drosophila* CDP-diacylglycerol synthase resulted in the loss of IP_3-mediated light perception in photoreceptor cells (12). This defect was attributed to the inability of these cells to adequately regenerate the necessary PI pools required to maintain the signaling cascade. Multiple CDP-diacylglycerol synthase isoforms in animals may

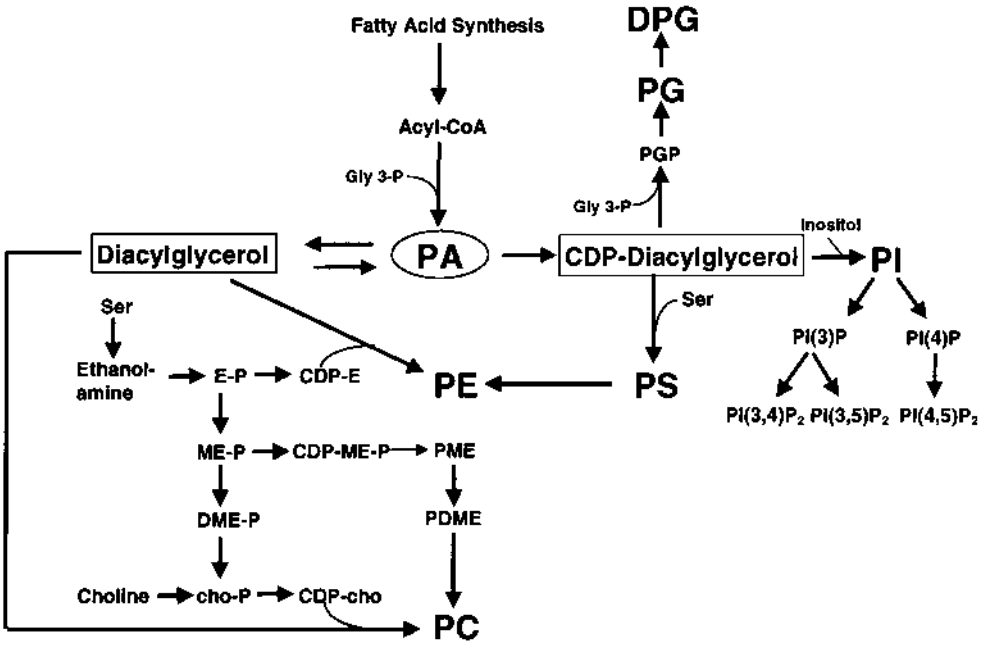

Figure 1 Major pathways of phospholipid synthesis in higher plants.

be produced from independent genetic loci (13), or derived from the alternative splicing of a single gene (12).

In plants, CDP-diacylglycerol synthase activity has been detected in a number of organelles (2, 14). The ability of researchers to identify and isolate plant cDNAs that encode enzymes involved in glycerolipid biosynthesis, based on their homology to yeast and animal genes, has been greatly accelerated by the recent proliferation of plant-derived expressed sequence tagged (EST) databases. Where sequence information for a given protein and/or gene has been elucidated in a nonplant species, computer searchers of EST databases can rapidly identify candidate plant cDNAs that are likely to encode the same function (15). Additional experimentation, such as expressing and assaying the candidate cDNA in a heterologous system that lacks the activity in question, is subsequently used to verify function.

Recently, Kopka and coworkers (14) utilized this approach to isolate cDNAs encoding CDP-diacylglycerol synthases from plants. Using the CDP-diacylglycerol synthase sequence from *E. coli* as the query sequence, a candidate *Arabidopsis* EST was identified and subsequently used as a molecular probe to obtain full-length cDNAs from both *Arabidopsis* and potato gene libraries. The deduced plant proteins had predicted molecular masses of 49 kDa and possessed eight potential membrane-spanning domains. Although the subcellular location of the encoded *Arabidopsis* and potato proteins was not established, the absence of potential mitochondrial or chloroplast targeting sequences suggested that they represent microsomal CDP-diacylglycerol synthases. To confirm the function of the putative potato CDP-diacylglycerol synthase, a GST/potato cDNA fusion construct was generated and expressed in *E. coli*. The purified fusion protein displayed CDP-diacylglycerol synthase activity when assayed in vitro.

III. SYNTHESIS OF PHOSPHOLIPIDS FROM CDP-DIACYLGLYCEROL

A. Phosphatidylglycerol and Diphosphatidylglycerol

PG in plants has been found in a number of plant organelles but is mainly associated with chloroplast thylakoids (16), whereas diphosphatidylglycerol (DPG), also known as cardiolipin, is restricted to the inner mitochondrial membrane (2, 16). In yeast the synthesis of PG is catalyzed by two enzymes, **PGP synthase** (glycerophosphate:CDP diacylglycerol phosphatidyltransferase, EC 2.7.8.5) and **PGP phosphatase** (phosphatidylglycerolphosphate phosphohydrolase, EC 3.1.3.27). The first catalyzes the reaction of CDP-diacylglycerol with glycerol phosphate to yield phosphatidylglycerolphosphate and CMP, and the second the dephosphorylation of phosphatidylglycerolphosphate to PG. In yeast both reactions are localized exclusively in the inner membranes of mitochondria (17) whereas in plants they have been reported in mitchondria, chloroplasts, and microsomes (10, 18). These enzyme activities have been well characterized in animals and yeast (19–21), and a hamster cDNA-encoding PGP synthase has been cloned and shown to complement a PGP-synthase defective mutant in CHO cells (22). In plants, however, both of these enzymes remain substantially uncharacterized and their individual activities have not been measured.

DPG is synthesized in plant mitochondria as it is in yeast, by reaction of PG with CDP-diacylglycerol (2). The reaction is catalyzed by the enzyme **phosphatidylglycerol:CDP diacylglycerol phosphatidyltranserase**, about which very little is known in plants except that the enzyme requires either magnesium, or surprisingly, cobalt, for activity (10).

Because of its ubiquitous presence in the mitochondria of eukaryotes, DPG has long been assumed to serve a critical function within the mitochondrial membrane. The observation that DGP is required for the in vitro activities of several mitochondrial enzymes, and studies indicating a need for this unique phospholipid for the import of proteins into mitochondria, further supported this presumption (23, 24). Doubts were raised concerning the essential nature of DPG when a yeast strain possessing no detectable DPG owing to a null mutation at the locus encoding cardiolipin synthase was shown to be capable of growth on both fermentable and nonfermentable carbon sources (25). A more recent report by Jiang and coworkers (26) demonstrated that although no obvious growth defects were observed when the null mutant strain was incubated at 30°C, no colony formation was observed at 37°C. Thus, there does appear to be an absolute requirement for DPG in yeast for growth at elevated temperatures.

B. Phosphatidylinositols

The enzyme **PI synthase** (CDP-diacylglycerol:myo-inositolphosphatidyltransferase, EC 2.7.8.11), which catalyzes the reaction between free inositol and CDP-diacylglycerol, to yield PI and CMP, has been charac-

terized in the membrane fractions of many different plants (2, 10, 27).

Identification of an *Arabidopsis* EST displaying homology to the yeast PI synthase sequence resulted in the first reported characterizations of a plant PI synthase cDNA (28, 29). The *Arabidopsis* cDNA encodes a protein of 227 amino acids with a predicted molecular mass of 25.9 kDa. Because *E. coli* lacks PI, it provides an ideal background for functional verification of putative PI synthases. Expression of the Arabidopsis cDNA in *E. coli* resulted in the production and accumulation of PI to levels as great as 19% of the total lipid extracted from the bacteria (28). The cDNA has also been shown to complement a yeast PI synthase mutant (29). Studies of the recombinant enzyme in heterologous systems have confirmed the requirement of Mg^{2+} ions for full activity of this enzyme (29).

In yeast and animals PI, in the presence of ATP, is converted to PI 4-phosphate [PI(4)P] and AMP, a reaction catalyzed by the enzyme **PI 4-kinase** (ATP:phosphatidylinositol 4-phosphotransferase, EC 2.7.1.67). Alternatively, PI can be phosphorylated at the D-3 position of the inositol ring by a **PI 3-kinase** (ATP:phosphatidylinositol 3-phosphotransferase) to give rise to PI(3)P. Among the bisphosphorylated PI derivatives, there is a vast body of literature documenting the cellular functions of PI(4,5)P2, a species most commonly produced by the ATP-dependent phosphorylation of PI(4)P by a **PIP kinase** (ATP:phosphatidylinositol 4-phosphate 5-phosphotransferase, EC 2.7.1.68). Although PI(4,5)P2 is clearly the best characterized of the polyphosphoinositides, PI(3,4)P2 and PI(3,5)P2 species have also been found among a diverse array of eukaryotic species, including plants (30–32). In mammals, PI(3,4)P2 is synthesized primarily through the degradation of PI(3,4,5)P3 by a 5-phosphatase, with lesser amounts generated via the 4-phosphorylation of PI(3)P and 3-phosphorylation of PI(4)P (33,34). In plants, the 4-phosphorylation of PI(3)P is the only documented route of PI(3,4)P2 synthesis (30); the 5-dephosphorylation of PI(3,4,5)P3 to produce PI(3,4)P2 is doubtful, given that PI(3,4,5)P3 has not been detected in any plant species (35). Although the specific route of PI(3,5)P2 synthesis has yet to be confirmed in plants, the 5-phosphorylation of PI(3)P has to be considered the most likely, given that both animals and yeast generate PI(3,5)P2 in this manner (31, 36).

In animal cells the synthesis and turnover of polyphosphoinositides play an essential role in the response of animal cells to various agonists (37), and in yeast polyphosphoinositides (or their breakdown products, DAG and inositol trisphosphate) are involved in the regulation of cell proliferation and membrane trafficking (38, 39). Polyphosphoinositides, and their corresponding lysophospholipids, have also been detected in many plant tissues (2, 35, 40, 41) although PIP and PIP2 species represent $< 1\%$ each of the total inositol lipid. In contrast, PI accounts for $\sim 93\%$ of the total inositol lipid but $< 10\%$ of total lipid phosphorus in plant cells (35).

PI 3-kinase, PI 4-kinase, and PIP 5-kinase activities have been measured in plasma membranes isolated from a number of plant species (2, 42–44). PI 4-kinase activity has also been characterized in soluble fractions (45) and in nuclear membranes of plant cells (46). The soluble PI 4-kinases have molecular weights in the 80-kDa range (45) whereas the membrane-associated enzymes have reported molecular weights ranging from 65 kDa to 500,000 kDa (42, 47).

The existence of both membrane and soluble PI 4-kinases has been confirmed by molecular studies. The cloning of PI 4-kinase cDNAs from animals and yeast has shown that there are two distinct isoforms that differ in size, subcellular location, and presence or absence of specific motifs (48). The smaller isoforms correspond to proteins ranging from ~ 90 to 125 kDa that are primarily found in the cytosol or associated with the Golgi. In contrast, the second class represents PI 4-kinases that are considerably larger (200–230 kDa) and are strictly membrane associated. The plant PI 4-kinase cDNAs that have been reported to date are predicted to encode products that generally fall into similar classes. An *Arabidopsis* cDNA encoding a 126-kDa PI 4-kinase was identified that showed greatest sequence homology to the smaller PI 4-kinase isoforms of animals and yeast (49). A partial cDNA corresponding to a distinct *Arabidopsis* PI 4-kinase isoform has also been identified (50). Western blot analysis using antibodies raised against the encoded partial protein sequence established the size of the complete polypeptide to be 205 kDa. The 205-kDa enzyme is associated with microsomal membranes and possesses a pleckstrin homology domain, features common to the larger PI 4-kinase isoforms of animals and yeast.

The cDNAs encoding the 126-kDa and 205-kDa PI 4-kinase isoforms described above appear to represent the complete complement of PI 4-kinase genes found in *Arabidopsis* (51). It remains to be determined if the smaller isoforms purified from plasma membranes (45, 47) represent the products of new, uncharacterized plant PI 4-kinase genes, or result from the proteolytic

cleavage or alternative splicing of either of the two documented isoforms.

Similar to the PI 4-kinases, animal and yeast PIP 5-kinases can also be categorized into two families, designated types I and II, based on their structural and biochemical properties. Type I PIP 5-kinases favor PI(4)P as the substrate, whereas type II enzymes preferentially utilize PI(5)P (each yielding PI(4,5)P2 as the end product). Both types also vary according to their ability to recognize D-3 PI substrates (reviewed in 52, 53). The *Aradidopsis* PIP 5-kinase cDNA characterized by Mikami and coworkers (54) encodes a 638–amino acid product that is equally divergent from both of these families. Furthermore, the genomic sequences of additional candidate *Arabidopsis* PIP 5-kinase genes (accession Nos. U95973, AF007269, and Y12776) are equally difficult to classify as either type I or type II enzymes based on amino acid sequence homology. Although these observations suggest that plants may possess a novel class of PI(4)P 5-kinase, an analysis of the substrate specificities and subcellular localization of individual plant isoforms is clearly warranted in order to establish their specific role within the plant cell.

Four distinct classes of PI 3-kinases have been characterized in animals that differ according to their substrate specificities and their ability to complex with specific regulatory adaptor proteins (55). Plants and yeast, in contrast, appear to possess a single type of PI 3-kinase, one that exclusively phosphorylates PI to produce PI(3)P. PI(4)P and PI(4,5)P2 are not recognized as substrates. Two soybean cDNAs encoding this class of PI 3-kinase have been characterized (44). Although closely related in size (812 and 814 amino acids) and sequence identity (98%), these two genes were differentially expressed during root module organogenesis. The modulation of gene expression for one isoform was coincident with the membrane proliferation during nodulation, lending support to the hypothesis that, similar to their yeast counterparts, plant PI 3-kinases participate in events associated with membrane trafficking. A PI 3-kinase cDNA was also characterized from *Arabidopsis* (56). Normal growth and development were severely inhibited in transgenic plants that expressed antisense constructs of this cDNA, demonstrating the essential nature of this gene in plants.

Similar to their animal counterparts, a growing body of literature suggests that polyphosphoinositides and their metabolites function as regulators of a variety of cellular processes in plants. These include responses to light, osmotic stress, and pathogen attack. In addition, polyphosphoinositides are believed to participate in the regulation of the cytoskeletal architecture of the cell and the processes controlling membrane trafficking. Some of these functions are believed to be mediated by the ability of polyphosphoinositides to alter the activities of several enzymes, including protein kinases (57), the plasma membrane ATPase (58), and certain isoforms of phospholipase D (59). For a comprehensive description of the functions of polyphosphoinositides in plants, several recent reviews are recommended (35, 40, 41, 51).

C. Phosphatidylserine and Phosphatidylethanolamine

In yeast PS is synthesized from CDP-diacylglycerol and serine, a reaction catalyzed by the enzyme CDP-diacylglycerol:L-serine O-phosphatidyltransferase (**PS synthase**, EC 2.7.8.8). Plant PS synthase activity was originally reported in spinach leaf microsomes (10) and has since been detected in many other plant tissues (2). The recent characterization of a wheat cDNA encoding a PS synthase provides definitive evidence that plants are capable of producing PS directly from CDP-diacylglycerol (60). The wheat cDNA encodes a hydrophobic 239–amino acid polypeptide that was recovered through a heterologous screening strategy intended to identify cDNAs whose expression in yeast resulted in enhanced aluminum tolerance. Although the mechanism by which PS synthase activity could serve to increase aluminum tolerance in yeast was not clear, aluminum-stressed wheat roots showed increased accumulation of PS synthase transcripts, suggesting that the enzyme also plays some role in this phenomenon in its native environment. Overexpression of the wheat PS cDNA in transgenic *Arabidopsis* proved to be very effective in increasing the cellular PS content. Though normally found only in trace quantities in plants, PS represented > 15% of the labeled phospholipid detected in the transgenic Arabidopsis after a 24-h incubation with ortho-^{32}P. Interestingly, overexpression of the wheat cDNA in both *Arabidopsis* and tobacco led to the formation of necrotic lesions on leaves. It was hypothesized that overaccumulation of PS could have resulted in increased PS on the outer surface of these cells, a condition which induces an apoptotic response in animals (61).

In yeast PS is a precursor to both PE and PC (7). PS is first decarboxylated to PE, a reaction catalyzed by **PS decarboxylase** (EC 4.1.1.65) (62), and then PE is sequentially methylated to PC by the action of two

N-methyltransferases, which utilize S-adenosylmethionine as the methyl donor. The first of these enzymes **PE N-methyltransferase** (EC 2.1.1.17) catalyzes the methylation of PE to phosphatidyl methylethanolamine (PME) and the other enzyme **phospholipid N-methyltransferase** catalyzes the two methylations necessary to convert PME to PC.

PS decarboxylase activity has also been measured in a number of plants (see 2). Thus some plant tissues, like yeast, are capable of synthesizing PE without the participation of DAG. The presence of PE methyltransferases in plants would also mean that PC could be synthesized from PE. This has led to the suggestion that all plant phospholipids could be synthesized without the involvement of DAG.

The methylation of PE to PC in plants has not been confirmed, however, although plant cDNAs encoding phospholipid N-methyltransferase activities have been isolated. Computer-based homology searches of plant EST databases resulted in the identification of *Arabidopsis* and soybean cDNAs encoding proteins (162 and 164 amino acids, respectively) that displayed low but significant sequence homology to the yeast phospholipid N-methyltransferase (R.E. Dewey, A. J. Kinney, unpublished results). The substrate specificities of the plant enzymes were established by expressing the *Arabidopsis* and soybean cDNAs in yeast mutants lacking either PE methyltransferase or phospholipid N-methyltransferase activities (or both), followed by enzymatic analysis. Similar to the yeast phospholipid N-methyltransferase, the plant enzymes were capable of methylating both PME and PDME.

Negligible activity of the plant N-methyltransferases was detected using PE as a substrate (R.E. Dewey, A. J. Kinney, unpublished results) suggesting that PE is not directly methylated in either soybean or *Arabidopsis*. This is supported by the classic radiotracer studies of Datko and Mudd in the 1980s (see reference 2 for a detailed review of these studies). More recent radiotracer evidence and some very thorough computer modeling studies (63) presented clear evidence that the major methylation flux in tobacco is via phosphoethanolamine and not CDP-ethanolamine or PE. The recent cloning and characterization of **phosphoethanolamine N-methyltransferase** cDNAs from spinach (8) and *Arabidopsis* (9) provide additional support for this pathway. Thus, while most plant phospholipids can be synthesized via CDP-diacylglycerol, it appears that the major pathway for synthesis of PC is via diacylglycerol.

IV. BIOSYNTHESIS OF DIACYLGLYCEROL IN PLANTS

Diacylglycerol, a precursor of PC and PE in plants, is made from the dephosphorylation of PA to form DAG and inorganic phosphate. The reaction is catalyzed by the enzyme **phosphatidate phosphohydrolase** (EC 3.1.3.4). This enzyme has been detected in organelle, membrane, and soluble fractions of a number of plant tissues (2, 64, 65). A microsomal phosphatidate phosphohydrolase has been purified to apparent homogeneity as a 49-kDa species from avocado (66).

Another enzyme that has the potential of influencing the flux of fatty acids through the PA, DAG, and CDP-DAG pools is **diacylglycerol kinase** (EC 2.7.1.107). Opposing the reaction catalyzed by phosphatidate phosphohydrolase, diacylglycerol kinases direct the synthesis of PA through the ATP-dependent phosphorylation of DAG. Although the influence of this enzyme is generally not considered to be of major consequence in the de novo synthesis of the major phospholipids or triacylglycerols, in animal systems it is clearly an essential component of inositol lipid signaling pathways. Similar to the CDP-diacylglycerol synthase mutant described above, retinal degeneration is observed in *Drosophila* possessing mutations in an eye-specific diacylglycerol kinase locus due to their inability to regenerate essential PI pools (67).

Diacylglycerol kinase activities have been documented in several plant species (68–70), and the isolation of their corresponding cDNAs from *Arabidopsis* and tomato has been reported (71, 72). The identification of a calmodulin-binding diacylglycerol kinase isoform from tomato lends further support to the speculation that the plant enzymes function primarily as components of signal transduction pathways (72).

V. SYNTHESIS OF PHOSPHATIDYLETHANOLAMINE AND PHOSPHATIDYLCHOLINE FROM DIACYLGLYCEROL

Flux modeling experiments in tobacco support the idea that the flux of ethanolamine into PE is split equally between PS decarboxylation (or base exchange; see below) and incorporation of phosphoethanolamine via CDP-ethanolamine and diacylglycerol (63). Phosphoethanolamine is probably derived from free or phosphorylated serine by decarboxylation (73, 74) although no enzyme operating on anything other than

phosphatidylserine has been convincingly demonstrated. In contrast, it is apparent that choline in plants is not synthesized via a free base pathway but by the methylation of phospho- and phosphatidylmonoethanolamine (see 2, 74). Furthermore, the bulk of the flux into choline compounds is likely initiated via the methylation of phosphoethanolamine (63). Free choline may then be synthesized by dephosphorylation of phosphocholine. Evidence from many different plant families supports the idea that PC is synthesized by the methylation of PME derived from methylated ethanolamine phosphate or by conversion of phosphocholine, also from methylated ethanolamine phosphate, to CDP-choline (2, 74). Both pathways utilize DAG as the source of glycerol and fatty acids (see Fig. 1). Free choline is rapidly incorporated into PC (2), suggesting that the plants can also make PC from choline reserves or exogenous choline. This hypothesis is supported by the observation that methylation of phosphoethanolamine is repressed by free choline in plant tissue cultures (75). Thus, in addition to the phosphoethanolamine methyltransferase described above, three types of enzymes are needed to make PE and PC using DAG: aminoalcohol kinases, phosphoaminoalcohol cytidylyltransferases, and aminoalcohol phosphotransferases. There is good evidence that all these activities exist in plants for both the ethanolamine and the choline pathways.

The phosphorylation of ethanolamine is catalyzed by the enzyme **ethanolamine kinase** (ATP:ethanolamine phosphotransferase, EC 2.7.1.82) and the phosphorylation of choline is mediated by an equivalent enzyme, **choline kinase** (ATP:choline phosphotransferase, EC 2.7.1.32). The yeast gene for choline kinase (CK1) was cloned by complementation of a choline kinase mutant and was shown to encode a polypeptide of about 66 kDa (76), which corresponded to the native molecular weight of a partially purified yeast choline kinase (77). However, when the CK1 gene was expressed in *E. coli*, both choline kinase and ethanolamine kinase activities were observed. Disruption of the CK1 gene in wild-type yeast resulted in the loss of both choline and most of the ethanolamine kinase activities (76). Thus it is possible that both reactions are catalyzed by the same enzyme in yeast. In contrast, the bulk of the biochemical evidence favors the hypothesis that there are separate ethanolamine and choline kinase in plants (see 2 for discussion), and this hypothesis is supported by recent molecular studies. Using an *Arabidopsis* EST that displayed homology to yeast and mammalian choline kinases, three distinct choline kinase isoforms were isolated from soybean (78). Two of the cDNAs, designated GmCK1 and GmCK2, were full-length encoding proteins of 359 and 362 amino acids, respectively. Although the third isoform, GmCK3, was reported to be considerably larger than the other two, its final predicted size was unknown because the characterized cDNA was not full length. Subsequent work, however, revealed the GmCK3 cDNA to encode a 650–amino acid protein, with most of its increase in size derived from a degenerate 11–amino acid sequence that is repeated 23 times at the N-terminus of the protein (D.E. Monks, R.E. Dewey, unpublished results). Expression of the three soybean choline kinase cDNAs in yeast and/or *E. coli* demonstrated that each functions strictly as a choline kinase; ethanolamine kinase activity was negligible (78; R.E. Dewey, D.E. Monks, unpublished results).

The discovery of two distinct size classes of soybean choline kinases may provide an explanation for discrepancies in molecular-weight estimations previously reported in the literature. A smaller, 36-kDa choline kinase from soybean reported by Wharfe and Harwood (79) may represent the product of the GmCK1 and/or GmCK2 genes, whereas larger choline kinase species (58 and 60 kDa) reported by Mellor and coworkers (80), also from soybean, may in fact be the product of GmCK3. Although computer searches could detect no entries in protein databases that displayed significant amino acid sequence homology to the large N-terminal extension found on the GmCK3-encoded protein, the 11-residue repeat structure is reminiscent of the 11-mer repeats of apolipoproteins and choline phosphate cytidylyltransferase that mediate the association of these proteins with membrane phospholipids (discussed below). Consistent with this hypothesis, a considerable amount of choline kinase activity was observed in the microsomal fraction when GmCK3 was expressed in yeast; in contrast no membrane-associated choline kinase activity was detected upon expression of GmCK1 or GmCK2 in yeast (R.E. Dewey, D.E. Monks, unpublished results).

The conversion of ethanolamine phosphate and choline phosphate to their respective CDP-aminoalcohols is catalyzed by phosphoaminoalcohol cytidylyltransferases. **Choline phosphate cytidylyltransferase** (CTP:choline phosphate cytidylyltransferase, EC 2.7.7.15) has been extensively characterized in animals (81, 82) and shown to play an important regulatory role in membrane biosynthesis in regulating the flux through the CDP-choline pathway for PC biosynthesis (5). The animal enzyme comprises four distinct subdomains: an amino-terminal nuclear localization signal; a highly conserved catalytic core; a

membrane/lipid binding domain; and a carboxyl-terminal phosphorylation domain (82). The discovery of the nuclear targeting signal is consistent with immunolocalization studies that unexpectedly revealed the nucleus, rather than the cytosol, to be the intracellular compartment where the majority of the protein resides. The lipid/membrane-binding domain consists of three 11-residue repeats that are predicted to form an amphipathic alpha helix. This region is critical not only for mediating the reversible association of the enzyme with membranes, but also for regulating enzymatic activity per se. Current models suggest that in the absence of activating lipids, the membrane/lipid-binding domain inhibits the catalytic activity of the enzyme; lipid binding increases enzymatic activity > 50-fold by ameliorating the inhibitory effects of this region (82, 83). The function of the carboxyl-terminal phosphorylation domain is less clear. Although early studies demonstrated that the membrane-associated, enzymatically active choline phosphate cytidylyltransferase was dephosphorylated, and the soluble, inactive form of the enzyme was highly phosphorylated, recent studies using phosphorylation-deficient mutants revealed that the modulation of phosphorylation does not appear to be critical either for the reversible translocation of the enzyme to membranes or in maintaining cellular growth (82).

Using an elegant yeast complementation strategy, Nishida and colleagues (84) recovered cDNAs corresponding to four distinct choline phosphate cytidylyltransferase isoforms from *Brassica napus*. Subsequently, choline phosphate cytidylyltransferase clones from *Arabidopsis* and pea were also reported (85, 86). Although extensive sequence homology between the plant enzymes and their animal and yeast counterparts is observed only across the region defined as the catalytic domain, the presence of a predicted amphipathic alpha helical motif immediately following the catalytic domain suggests that plant choline phosphate cytidylyltransferases may possess membrane/lipid binding domains that are functionally similar to those observed in animals.

Because of the polyploid nature of *Brassica napus*, the initial observation of multiple choline phosphate cytidylyltransferase isoforms in this species was not considered surprising, as functionally equivalent genes could have been derived from different ancestral parents (84). The presence of multiple isoforms is also evident in pea and soybean (86, 87). Given the recent discovery of a previously unrecognized, distinct choline phosphate cytidylyltransferase isoform in mammals, however, consideration of the possibility that different isoforms serve unique cellular functions is warranted. The newly discovered animal choline phosphate cytidylyltransferase differs from the well-characterized isoform in its subcellular location (cytoplasm as opposed to nucleus) and tissue-specific expression profile (88). With the availability of numerous plant choline phosphate cytidylyltransferase cDNAs, the tools are now available to dissect and define the function of specific structural domains of the protein and test whether different isoforms are functionally distinct.

The enzyme **ethanolamine phosphate cytidylyltransferase** (CTP:ethanolamine phosphate cytidylyltransferase, EC 2.7.7.14) has not received much attention from plant scientists but, like cholinephosphate cytidylyltransferase, it has also been well studied in yeast and animals (89, 90). Human, rat, and yeast cDNAs encoding ethanolamine phosphate cytidylyltransferases have been isolated and characterized (91–93). Not surprisingly, significant homology is observed between portions of the ethanolamine phosphate cytidylyltransferases and the catalytic domains of choline phosphate cytidylyltransferases. Uniquely found in the ethanolamine phosphate cytidylyltransferase enzymes, however, is a repeat of the first half of the catalytic domain, located adjacent to the "full-length" version of this region. Although considerable amino acid sequence homology is shared between the catalytic regions of the two aminoalcohol phosphate cytidylyltransferases, this step of the parallel PE and PC biosynthetic pathways is the only one where no functional redundancy has been reported in any biological system (89). Ethanolamine phosphate cytidylyltransferase was first reported in plants in the membrane fractions of mitochondria and ER from castor bean endosperm (94). Curiously, most of the castor bean ethanolamine phosphate cytidylyltransferase activity (80%) was in the mitochondria, whereas the choline phosphate cytidylyltransferase is found mainly in the ER and cytosol (94). The mitochondrial ethanolamine phosphate cytidylyltransferase has recently been partially purified from postgermination castor bean endosperm (95). The castor bean enzyme, predicted to have a molecular mass of 30–35 kDa, was modestly activated by the addition of phospholipids. Membrane association of both the mitochondrial and ER-localized ethanolamine phosphate cytidylyltransferases of castor bean appears to be much stronger than that observed with their mammalian counterparts, as the plant enzymes remained completely insoluble when treated with salt or detergent concentrations that completely solubilize the animal enzymes (95).

PE and PC are synthesized from their cognate CDP-aminoalcohol and DAG, reactions catalyzed by the aminoalcohol phosphotransferase enzymes **cholinephosphotransferase** (CDP-choline:1,2-diacylglycerol cholinephosphotransferase, EC 2.7.8.2) and **ethanolaminephosphotransferase** (CDP-ethanolamine: 1,2,diacylglycerol ethanolaminephosphotransferase, EC 2.7.8.1). These enzymes have been measured and characterized in many different plant tissues (see 2), but they have remained recalcitrant to solubilization and purification. The first cDNA encoding a plant aminoalcohol phosphotransferase was obtained from soybean by complementation of a double-mutant yeast strain defective in both CPT1 and EPT1 activities using a colony autoradiography assay (96). The predicted amino acid sequence of the soybean protein showed equal similarity to both the yeast CPT1 and EPT1 proteins, and inhibition studies suggested that the plant enzyme shared equal affinity for both CDP-choline and CDP-ethanolamine. These observations led to the speculation that the enzyme encoded by the soybean cDNA functions as a general aminoalcohol phosphotransferase and as a result, was designated AAPT1 (*a*mino*a*lcohol *p*hospho*t*ransferase 1). Although this report presented compelling evidence that plants possess enzymes that can function as both choline and ethanolamine phosphotransferases, Southern blot data revealed that additional isoforms of the gene were likely to residue in the soybean genome, leaving open the possibility that aminoalcohol phosphotransferases with more restrictive substrate specificities may exist, similar to the situation found in yeast.

The recent characterization of cDNAs encoding two AAPTs from *Arabidopsis* provides even further evidence that plants utilize broad-specificity aminoalcohol phosphotransferases (97). Southern blot analysis suggested that the two *Arabidopsis* AAPT cDNAs encode the complete complement of AAPT enzymes found in that species. Although subtle differences in substrate preference, and Ca^{2+} and CMP inhibition profiles were observed among the two *Arabidopsis* AAPTs and the soybean AAPT1 gene product, it was clear that all three plant enzymes could effectively utilize either CDP-choline or CDP-ethanolamine to produce PC and PE, respectively. An additional AAPT cDNA has been isolated from Chinese cabbage; however, the enzymatic properties of the encoded protein were not reported (98).

Although the cytidylyltransferase-catalyzed steps are generally recognized as the most important in regulating the net biosynthesis of PC and PE within the cell, the ease with which the reverse AAPT reactions can be detected in vitro suggests that factors altering the directionality of this activity could also influence the ultimate PC and PE composition of eukaryotic membranes. This may be particularly relevant during seed development in oil seeds, where the reverse reaction of choline phosphotransferase is believed to function in supplying polyunsaturated fatty acids directly into DAG pools destined for triacylglycerol biosynthesis (99). Consistent with previous observations using isolated plant microsomes, the activities of the soybean *AAPT1* gene and two *Arabidopsis* AAPT isoforms described above were shown to be readily reversible when expressed in yeast (97). The ability of CMP to inhibit the forward reaction and provide a necessary substrate for the reverse reaction, makes this compound a good candidate for regulating the direction of AAPT-catalyzed reactions in vivo. Further investigation of endogenous CMP pools in plants and their influence on phosphatidylamine metabolism, particularly during seed development, is warranted.

VI. PHOSPHOLIPID MODIFYING ENZYMES

There are a number of enzyme activities in plant cells that modify either the polar or lipid portion of phospholipid molecules. The best documented polar modification enzymes are those which catalyze phosphoaminoalcohol exchange of preexisting phospholipids with a similar or different heads. The best characterized of the head group exchange reactions is the synthesis of PS by the reversible exchange of serine with the headgroup of PE by the Ca^{2+}-dependent, microsomal enzyme **PE:L-serine phosphatidyltransferase** (10, 100). No progress has been reported in the characterization of this enzyme or in understanding the function of the serine/ethanolamine exchange reaction since an earlier review on the subject (2). This is also true of the PI/inositol base exchange reaction in castor bean endosperm (2) although a similar reaction has been measured in a number of animal cells (101).

Only marginally better understood than these headgroup modifying enzymes are enzymes that exchange fatty acids with phospholipids, especially PC. The activity of an enzyme capable of catalyzing the exchange of 18:1-CoA with the fatty acid at the sn-2 position of PC (LPCAT EC 2.3.1.23) (**acyl-CoA:lysophosphatidylcholine acyltransferase**) has been assayed in a number of plant tissues (102). This enzyme has a potentially important role to play in plant lipid

metabolism since PC is the substrate for fatty acid desaturation of 18:1 to linoleic acid. However, little is known about the structural and functional properties of the LPCAT protein. Recently, Tumaney and Rajasekahran (103) used photoaffinity labeling of soybean LPCAT with azidophospholipids to demonstrate molecular masses of 54 kDa and 114 kDa for putative LPCAT proteins. These relative masses are in agreement with earlier studies in castor bean endosperm using photoaffinity probes (104).

Plants also contain a **phospholipid:diacylglycerol acyltransferase** (PDAT) that can transfer the *sn*-2 acyl chain from PC to DAG, forming lyso-PC and TAG (105). This enzyme is thought to play a role in TAG biosynthesis and is related to the **lecithin:cholesterol acyltransferase** (LCAT) enzyme family found in animal cells (106). It is quite possible that other LCAT-like enzymes are present in plants since ESTs for LCAT homologs have been found in many plant cDNA libraries (A.J. Kinney, unpublished data).

Finally, there is an enzyme in animals and plants which transfers an acyl group to a polar headgroup. **N-acylphosphatidylethanolamine synthase** (NAPES) was first identified in plants in cotton seed extracts (107) and appears to be an ATP-, calcium-, and CoA-independent acyltransferase that catalyzes the direct acylation of PE with free fatty acids. This 64-kDa microsomal protein was subsequently purified from cottonseed homogenates and shown to be highly specific for PE (108). It is not known if N-acylphosphatidylethanolamine itself plays an important physiological role in plants, but NAPES is possibly involved in scavenging free fatty acids (108).

REFERENCES

1. CE Stauffer. Fats & Oils. Minnesota: Eagen Press, 1996, pp 29–46.
2. AJ Kinney. Phospholipid head groups. In: TS Moore Jr, ed. Lipid Metabolism in Plants. Boca Raton: CRC Press, 1993, pp 259–284.
3. C. Kent, GM Carman. Interactions among pathways for phosphatidylcholine metabolism: CTP synthesis and secretion through the Golgi apparatus. Trends Biochem Sci 24:146–150, 1999.
4. KA Waite, DE Vance. Why expression of phosphatidylethanolamine N-methyltransferase does not rescue Chinese hamster ovary cells that have impaired CDP-choline pathway. J Biol Chem 275:21197–21202, 2000.
5. A Lykidis, S Jackowski. Regulation of mammalian cell membrane biosynthesis. Prog Nucleic Acid Res Mol Biol 65:361–393, 2000.
6. DE Vance. Phosphatidylethanolamine N-methyltransferase: unexpected findings from curiosity-driven research. Eur J Med Res 19:182-188, 1996.
7. GM Carman, SA Henry. Phospholipid biosynthesis in the yeast *Saccharomyces cerevisiae* and interrelationship with other metabolic processes. Prog Lipid Res 38:361–399, 1999.
8. ML Nuccio, MJ Ziemk, SA Henry, EA Weretilnyk, AD Hanson. cDNA cloning of phosphoethanolamine N-methyltransferase from spinach by complementation in *S. pombe* of the recombinant enzyme. J Biol Chem 275:14095–14101, 2000.
9. CP Bolognese, P McGraw. The isolation and characterization in yeast of a gene for *Arabidopsis thaliana* SAM:phosphoethanolamine N-methyltransferase. Plant Physiol 124:1800–1813, 2000.
10. TS Moore Jr. Phospholipid biosynthesis. Annu Rev Plant Physiol 33:235–259, 1982.
11. H Shen, PN Heacock, CJ Clancey, W Dowhan. The *CDS1* gene encoding CDP-diacylglycerol synthase in *Saccharomyces cerevisiae* is essential for cell growth. J Biol Chem 271:789–795, 1996.
12. L Wu, B Niemeyer, N Colley, M Socolich, CS Zuker. Regulation of PLC-mediated signalling in vivo by CDP-diacylglycerol synthase. Nature 373:216–222, 1995.
13. S Halford, KS Dulai, SC Daw, J Fitzgibbon, DM Hunt. Isolation and chromosomal localization of two human CDP-diacylglycerol synthase (CDS) genes. Genomics 54:140–144, 1998.
14. J Kopka, M Ludewig, B Mueller-Roeber. Complementary DNAs encoding eukaryotic-type cytidine-5′-diphosphate-diacylglycerol synthases of two plant species. Plant Physiol 113:997-1002, 1997.
15. T Newman, FJ de Bruijn, P Green, K Keegstra, H Kende, L McIntosh, J Ohlrogge, N Raikel, S Somerville, M Thomashow, E Retzel, C Somerville. Genes galore. A summary of methods for accessing results from large-scale partial sequencing of anonymous *Arabidopsis* cDNA clones. Plant Physiol 106:1241–1255, 1994.
16. J Harwood. Lipid metabolism in plants. Crit Rev Plant Sci 8:1–43, 1989.
17. K Kuchler, G Daum, F Paltauf. Subcellular and submitochondrial localization of phospholipid synthesizing enzymes in *S. cerevisisiae*. J Bacteriol 165:901–911, 1986.
18. J Andrews, JB Mudd. Phosphatidylglycerol synthesis in pea chloroplasts. Plant Physiol 79:259–265, 1986.
19. SG Cao, GM Hatch. Stimulation of phosphatidylglycerolphosphate phosphatase activity by unsaturated fatty acids in rat heart. Lipids 29:475–480, 1994.

20. SA Minskoff, ML Greenberg. Phosphatidylglycerophosphate synthase from yeast. Biochim Biophys Acta 1348:187–191, 1997.
21. H Shen, W Dowhan. Regulation of phosphatidylglycerophosphate synthase levels in *Saccharomyces cerevisiae*. J Biol Chem 273:11638–11642, 1998.
22. K Kawasaki, O Kuge, SC Chang, PN Heacock, M Rho, K Suzuki, M Nishijima, W Dowham. Isolation of a Chinese hamster ovary (CHO) cDNA encoding phosphatidylglycerophosphate (PGP) synthase, expression of which corrects the mitochondrial abnormalities of a PGP synthase-defective mutant of CHO-K1 cells. J Biol Chem 274:1828–1834, 1999.
23. M Schlame, KY Hostetler. Cardiolipin synthase from mammalian mitochondria. Biochim Biophys Acta 1348:207–213, 1997.
24. M Schlame, ML Greenburg. Cardiolipin synthase from yeast. Biochim Biophys Acta 1348:201–206, 1997.
25. F Jiang, HS Rizavi, ML Greenburg. Cardiolipin is not essential for growth of *Saccharomyces cerevisiae* on fermentable or non-fermentable carbon sources. Mol Microbiol 26:481–491, 1997.
26. F Jiang, Z Gu, JM Granger, ML Greenburg. Cardiolipin synthase expression is essential for growth at elevated temperature and is regulated by factors affecting mitochondrial development. Mol Microbiol 31:373–379, 1999.
27. A-M Justin, A Hmyene, J-C Kader, P Mazliak. Compared selectivities of the PI-synthase from maize coleoptiles either in microsomal membranes or after solubilization. Biochim Biophys Acta 1255:161–166, 1995.
28. S Collin, A-M Justin, C Cantrel, V Arondel, J-C Kader. Identification of AtPIS, a phosphatidylinositol synthase from *Arabidopsis*. Eur J Biochem 262:652–658, 1999.
29. H-W Xue, K Hosaka, G Plesch, B Mueller-Roeber. Cloning *A. thaliana* phosphatidylinositol synthase and functional expression in the yeast *pis* mutant. Plant Mol Biol 42:757–765, 2000.
30. CA Brearly, DE Hanke. Pathway of synthesis of 3,4- and 4,5-phosphorylated phosphatidylinositols in the duckweed *Spirodela polyrhiza*. Biochem J 290:145–150, 1993.
31. SK Dove, FT Cooke, MR Douglas, LG Sayers, PJ Parker, RH Mitchell. Osmotic stress activates phosphatidylinositol-3,5-bisphosphate synthesis. Nature 390:187–192, 1997.
32. HJG Meijer, N Divecha, H van den Ende, A Musgrave, T Munnik. Hyperosmotic stress induces rapid synthesis of phosphatidyl-D-inositol 3,5-bisphosphate in plant cells. Planta 208:294–298, 1999.
33. A Graziani, LE Ling, G Endeman, CL Carpenter, LC Cantley. Purification and characterization of human erythrocyte phosphatidylinositol 4-kinase. Biochem J 284:39–45, 1992.
34. LK McDougall, J Domin, MD Waterfield. A family of phosphoinositide 3-kinases in *Drosophila* identifies a new mediator. Current Biol 5:1404–1415, 1995.
35. T Munnik, RF Irvine, A Musgrave. Phospholipid signalling in plants. Biochim Biophys Acta 1389:222–272, 1998.
36. JD Gary, AE Wurmser, CJ Bonangelino, LS Weisman, SD Emr. Fab1p is essential for PtdIns(3)P 5-kinase activity and the maintenance of vacuolar size and membrane homeostasis. J Cell Biol 143:65–79, 1998.
37. N Divecha, RF Irvine. Phospholipid signaling. Cell 80:269–278, 1995.
38. I Uno. Role of signal transduction systems in cell proliferation in yeast. Int Rev Cytol 139:309–332, 1992.
39. G Odorizzi, M Babst, SD Emr. Phosphoinositide signaling and the regulation of membrane trafficking in yeast. Trends Biochem Sci 25:229–235, 2000.
40. BK Drøbak. Metabolism of plant phosphoinositides and other inositol-containing lipids. In: M Smallwood, JP Knox, DJ Bowles, eds. Membranes: Specialized Functions in Plants. Oxford: BIOS Scientific, 1996, pp 195–214.
41. BK Drøbak, RE Dewey, WF Boss. Phosphoinositide kinases and the synthesis of polyphosphoinositides in higher plant cells. In: KW Jeon, ed. International Review of Cytology—A Survey of Cell Biology. San Diego: Academic Press, 1999, pp 95–130.
42. WF Boss, W Yang, Z Tan, M Cho. Regulation of PI 4-kinase by protein phosphorylation: a plasma membrane-cytoskeletal connection. In J-C Kader, P Mazliak, eds. Plant Lipid Metabolism. Dordech: Kluwer, 1995, pp 219–223.
43. A Hanenberg, JB Wissing, K Wagner. Properties of PI 4-kinase I from suspension cultured *C roseus* cells. Plant Sci 112:53–63, 1995.
44. Z Hong, DPS Verma. A phosphatidylinositol 3-kinase is induced during soybean nodule organogenesis and is associated with membrane proliferation. Proc Natl Acad Sci USA 91:9617–9621, 1994.
45. CM Okpodu, W Gross, W Burkhart, WF Boss. Purification and characterization of a soluble phosphatidylinositol 4-kinase from carrot suspension culture cells. Plant Physiol 107:491–500, 1995.
46. CM Okpodu. Characterization of a nuclear PI 4-kinase in carrot suspension culture cells. Plant Physiol Biochem 37:473–480, 1999.
47. T Westergren, L Ekblad, B Jergil, M Sommarin. Phosphatidylinositol 4-kinase associated with spinach plasma membranes. Isolation and characterization of two distinct isoforms. Plant Physiol 121:507–516, 1999.

48. K Wong, R Meyers, LC Cantley. Subcellular locations of phosphatidylinositol 4-kinase isoforms. J Biol Chem 272:13236-13241, 1997.
49. H-W Xue, C Pical, C Brearly, S Elge, B Mueller-Roeber. A plant 126-kDa phosphatidylinositol 4-kinase with a novel repeat structure. J Biol Chem 274:5738–5745, 1999.
50. JM Stevenson, IY Perera, WF Boss. A phosphatidylinositol 4-kinase pleckstrin homology domain that binds phosphatidylinositol 4-monophosphate. J Biol Chem 273:22761–22767, 1998.
51. JM Stevenson, IY Perera, I Heilmann, S Persson, WF Boss. Inositol signaling and plant growth. Trends Plant Sci 5:252–258, 2000
52. KA Hinchliffe, A Ciruela, RF Irvine, PIPkins, their substrates and their products: new functions for old enzymes. Biochim Biophys Acta 1436:87–104, 1998.
53. RA Anderson, IV Boronenkov, SD Doughman, J Kunz, JC Loijens. Phosphatidylinositol phosphate kinases, a multifaceted family of signaling enzymes. J Biol Chem 274:9907–9910, 1999.
54. K Mikami, T Katagiri, S Iuchi, K Yamaguchi-Shinozaki, K Shinozaki. A gene encoding phosphatidylinositol-4-phosphate 5-kinase is induced by water stress and abscisic acid in *Arabidopsis thaliana*. Plant J 15:563–568, 1998.
55. J Domin, MD Waterfield. Using structure to define the function of phosphoinositide 3-kinase family member. FEBS Lett 410:91–95, 1997.
56. P Welters, K Takegawa, SD Emr, MJ Chrispeels. AtVSP34, a phosphatidylinositol 3-kinase of *Arabidopsis thaliana*, is an essential protein with homology to a calcium-dependent lipid binding domain. Proc Natl Acad Sci USA 91:11398–11402, 1994.
57. GE Schaller, A Harmon, MR Sussman. Characterization of a calcium- and lipid-dependent protein kinase associated with the plasma membrane in oat. Biochemistry 31:1721–1727, 1992.
58. AR Memon, Q Chen, WF Boss. Inositol phospholipids activate plasma membrane ATPase in plants. Biochem Biophys Res Commun 162:1295–1301, 1989.
59. X Wang. The role of phospholipase D in signaling cascades. Plant Physiol 120:645–651, 1999.
60. E Delhaize, DM Hebb, KD Richards, J-M Lin, PR Ryan, RC Gardner, Cloning and expression of a wheat (*Triticum aestivum* L.) phosphatidylserine synthase cDNA. J Biol Chem 274:7082–7088, 1999.
61. K Uchida, K Emoto, DL Daleke, K Inoue, M Umeda. Induction of apoptosis by phosphatidylserine. J Biochem 123:1073-1078, 1998.
62. DR Voelker, Phosphatidylserine decarboxylase. Biochim Biophys Acta 1348:2236–2244, 1997.
63. SD McNeil, ML Nuccio, D Rhodes, BL Russell, AD Hanson. Radiotracer and computer modelling evidence that phosphobase methylation is the main route of choline synthesis in tobacco. Plant Physiol 123:945–949, 2000.
64. A Malherbe, MA Block, R Douce, J Joyard. Solubilisation and biochemical properties of phosphatidate phosphatase from spinach chloroplast envelope membranes. Plant Physiol Biochem 33:149–161, 1995.
65. MG Kocsis, RJ Weselake, JA Eng, TL Furukawastoffer, MK Pomeroy. Phosphatidate phosphatase from developing seeds and microspore derived cultures of *Brassica napus*. Phytochemistry 41:353–363, 1996.
66. M Pearce, AR Slabas. The purification and characterisation of phophatidate phosphatase from avocado. In: JP Williams, MU Khan, NW Lem, eds. Physiology, Biochemistry and Molecular Biology of Plant Lipids. Dordrecht: Kluwer Academic, 1997, pp 140–142.
67. I Masai, A Okazaki, T Hosoya, Y Hotta. *Drosophila* retinal degeneration A gene encodes an eye-specific diacylglycerol kinase with cysteine-rich zinc-finger motifs and ankyrin repeats. Proc Natl Acad Sci USA 90:11157–11161, 1993.
68. Y Kamada, S Muto. Ca^{2+} regulation of phosphatidylinositol turnover in the plasma membrane of tobacco suspension culture cells. Biochim Biophys Acta 1093:72–79, 1991.
69. Z Tan, WF Boss. Association of phosphatidylinositol kinase, phosphatidylinositol monophosphate kinase, and diacylglycerol kinase with the cytoskeleton and F-actin fractions of carrot (*Daucus carota* L.) cells grown in suspension culture. Plant Physiol 100:2116–2120, 1992.
70. J Wissing, S Heim, KG Wagner. Diacylglycerol kinase from suspension cultured plant cells: purification and properties. Plant Physiol 90:1546–1551, 1989.
71. T Katagiri, T Mizoguchi, K Shinozaki. Molecular cloning of a cDNA encoding diacylglycerol kinase (DGK) in *Arabidopsis thaliana*. Plant Mol Biol 30:647–653, 1996.
72. WA Snedden, E Blumwald. Characterization of tomato putative diacylglycerol kinases (DGKs): possible role of a calmodulin-binding isoform in Ca^{2+} and phospholipid signaling. Plant Biology '99. Baltimore: American Society of Plant Physiologists, 1999, Abstract 115.
73. AJ Kinney, TS Moore Jr. PC synthesis in castor bean endosperm: metabolism of L-serine. Plant Physiol 84:78–81, 1987.
74. D Rhodes, AD Hanson. Quaternary ammonium and tertiary sulfonium compounds in higher plants. Annu Rev Plant Physiol Plant Mol Biol 44:357–384, 1993.
75. SH Mudd, AH Datko. Synthesis of methylated ethanolamine species. Regulation by choline in soybean and carrot. Plant Physiol 90:306–310, 1989.
76. K Hosaka, T Kodaki, S Yamashita. Cloning and expression of the yeast ck1 gene encoding choline

kinase and its expression in *E. coli*. J Biol Chem 264:2053–2059, 1989.
77. MA Brostrom, ET Browning. Choline kinase from brewers yeast. Partial purification, properties and kinetic mechanism. J Biol Chem 248:2364–2371, 1973.
78. DE Monks, JH Goode, RE Dewey. Characterization of soybean choline kinase cDNAs and their expression in yeast and *Escherichia coli*. Plant Physiol 110:1197–1205, 1996.
79. J Wharfe, HL Harwood. Purification of choline kinase from soya bean. In: LA Appelqvist, C Liljenberg, eds. Advances in the Biochemistry and Physiology of Plant Lipids. Amsterdam: Elsevier, 1979, pp 443–447.
80. RB Mellor, TMIE Christensen, D Werner. Choline kinase II is present only in nodules that synthesize stable peribacteroid membranes. Proc Natl Acad Sci USA 83:659–663, 1986.
81. JM Clement, C Kent. CTP:phosphocholine cytidylyltransferase: insights into regulatory mechanisms and novel functions. Biochem Biophys Res Commun 257:643–650, 1999.
82. C Kent. CTP:phosphocholine cytidylyltransferase. Biochim Biophys Acta 1348:79–90, 1997.
83. JA Friesen, HA Campbell, C Kent. Enzymatic and cellular characterization of a catalytic fragment of CTP:phosphocholine cytidylyltransferase. J Biol Chem 274:13384–13389, 1999.
84. I Nishida, R Swinhoe, AR Slabas, N Murata. Cloning of *Brassica napus* CTP:phosphocholine cytidylyltransferase cDNAs by complementation in a yeast *cct* mutant. Plant Mol Biol 31:205–211, 1996.
85. S-B Choi, K-W Lee, SH Cho. Cloning of CTP:phosphocholine cytidylyltransferase cDNA from *Arabidopsis thaliana*. Mol Cells 7:58–63, 1997.
86. PL Jones, DL Willey, P Gacesa, JL Harwood. Isolation, characterization and expression of a cDNA for pea cholinephosphate cytidylyltransferase. Plant Mol Biol 37:179–185, 1998.
87. DM Monks, JH Goode, PK Dinsmore, RE Dewey. Phosphatidylylcholine biosynthesis in soybeans: the cloning and characterization of genes encoding enzymes of the nucleotide pathway. In: JP Williams, MU Khan, NW Lem, eds. Physiology, Biochemistry and Molecular Biology of Plant Lipids. Dordrecht: Kluwer Academic, 1997, pp 110–112.
88. A Lykidis, KG Murti, S Jackowski. Cloning and characterization of a second human CTP:phosphocholine cytidylyltransferase. J Biol Chem 273:14022–14029, 1998.
89. BA Bladergroen, LM van Golde. CTP:phosphoethanolamine cytidylyltransferase. Biochim Biophys Acta 1348:91–99, 1997.
90. BM Ross, A Moszczynska, JK Blusztajn, A Sherwin, A Lozano, SJ Kish. Phospholipid biosynthetic enzymes in human brain. Lipids 32:351–358, 1997.
91. R Min-Seok, Y Kawamata, H Nakamura, A Ohta, M Takagi. Isolation and characterization of *ECT1* gene encoding CTP:phosphoethanolamine cytidylyltransferase of *Saccharomyces cerevisiae*. J Biochem 120:1040–1047, 1996.
92. A Nakashima, K Hosaka, J Nikawa. Cloning of a human cDNA for CTP-phosphoethanolamine cytidylyltransferase by complementation in vivo of a yeast mutant. J Biol Chem 272:9567–9572, 1997.
93. BA Bladergroen, M Houweling, MJ Geelen, LM van Golde. Cloning and expression of CTP:phosphoethanolamine cytidylyltransferase cDNA from rat liver. Biochem J 343:107–114, 1999.
94. X Wang, TS Moore Jr. PE synthesis by castor bean endosperm. Intracellular distribution and characteristics of CTP:phosphoethanolamine cytidylyltransferase. J Biol Chem 266:19981–19987, 1991.
95. F Tang, TS Moore. Enzymes of the primary phosphatidylethanolamine biosynthetic pathway in postgermination castor bean. Plant Physiol 115:1589–1597, 1997.
96. RE Dewey, RF Wilson, WP Novitzky, JH Goode. The *AAPT1* gene of soybean complements a cholinephosphotransferase-deficient mutant of yeast. Plant Cell 6:1495–1507, 1994.
97. JH Goode, RE Dewey. Characterization of aminoalcoholphosphotransferases from *Arabidopsis thaliana* and soybean. Plant Physiol Biochem 37:445–457, 1999.
98. KM Min, YG Bae, JS Lee, YH Choi, YR Cha, SH Cho. Cloning of an aminoalcoholphosphotransferase cDNA from Chinese cabbage roots. J Plant Biol 40:234–239, 1997.
99. CR Slack, PG Roughan, JA Browse, SE Gardiner. Some properties of cholinephosphotransferase from developing safflower cotyledons. Biochim Biophys Acta 833:438–448, 1985.
100. S Shin, TS Moore Jr. PS synthesis by castor bean endosperm. A base exchange reaction. Plant Physiol 93:154–159, 1990.
101. AB Cubitt, MC Gershengorn. CMP activates reversal of PI synthase and base exchange by distinct mechanisms in rat pituitary GH3 cells. Biochem J 272:813–816, 190.
102. S Stymne, AK Stobart. Triacylglycerol biosynthesis. In: PK Stumpf, ed. The Biochemistry of Plants: A Comprehensive Treatise, Vol 9. Lipids: Structure and Function. Orlando: Academic Press, 1987, pp 175–214.
103. AW Tumaney, R Rajasekharan. Synthesis of azidophospholipids and labeling of lysoPC acyltransferase from developing soybean cotyledons. Biochim Biophys Acta 1439:47–56, 1999.
104. R Rajasekharan, H Roycowdhury. Photoaffinity labeling of lysoPC acyltransferase from developing

castor bean endosperm. In: J-C Kader, P Mazliak, eds. Plant Lipid Metabolism. Dordecht: Kluwer, 1995, pp 525–527.
105. A Dahlqvist, U Ståhl, M Lenman, A Banas, M Lee, L Sandager, H Ronne, S Stymme. Phospholipid:diacylglycerol acyltransferase: an enzyme that catalyzes the acyl-CoA-independent formation of triacylglycerol in yeast and plants. Proc Natl Acad Sci USA 97:6487–6492, 2000.
106. M Rosseneu. Structural and functional properties of LCAT and of natural mutants. Atherosclerosis 144:85–95, 1999.
107. KD Chapman, TS Moore Jr. N-acyl PE synthesis in plants: Occurrence, molecular origin, composition, and phospholipid origin. Arch Biochem Biophys 301:21–33, 1993.
108. S McAndrew, KD Chapman. Enzymology of N-acyl PE synthase: kinetic properties and mechanism based inactivation. Biochim Biophys Acta 1390:21–36, 1998.

13

Applications of Oxidoreductases in Foods

Colja Laane
DSM Food Specialties, Delft, The Netherlands
Yvonne Bruggeman
Unilever Research, Vlaardingen, The Netherlands
Chris Winkel
Quest International, Naarden, The Netherlands

I. INTRODUCTION

Oxidative and reductive processes play an important role in foods. They influence not only the taste but also the texture, appearance, shelf life, nutritional value, and process tolerance of food products. Both enzymatic and nonenzymatic redox processes are involved. In some cases redox processes lead to undesirable effects such as off-flavor, reduced shelf life, or textural problems. In other cases, they contribute in a positive way to the final aroma, an improved texture, a more desirable appearance, or an increased shelf life. Controlling the redox behavior in food systems during all stages of processing and storage is therefore of utmost importance.

Up until now redox reactions in foods were controlled mainly by carefully selecting raw materials, by adapting process conditions, by adding chemicals or antioxidants, or by designing air-tight packaging materials. As yet, little attention has been paid to tailor redox reactions in foods by the addition of oxidoreductases or by changing the profile or content of oxidoreductases in food raw materials by genetic tools. Presumably, the major bottleneck for the application of oxidoreductases to foods is that economically efficient enzyme production is, with a few exceptions, still not feasible. In addition, public concerns about the use of recombinant enzymes in food products is slowing down their market introduction.

In this chapter the current and potential usage of oxidoreductases in controlling the taste, texture, appearance (i.e., color), shelf life, and the nutritional value of food products will be discussed. Increasingly, redox enzymes are being used for biosensor applications in food systems. This topic will not be discussed in this chapter, however. Table 1 lists the most important redox enzymes and their functions in food systems. Most attention will be paid to the market segments bakery, beverages, and dairy and to oxidases, since relatively little is known about role and applications of reductases in food systems. Furthermore, the emphasis will be on added enzymes and not on enzymes already present in the food product constituents. For detailed information on the properties of the individual oxidoreductases the reader is referred to in Sec. IIA of this book.

II. TASTE

Many oxidoreductases play a role by influencing the taste profile of food products. They are involved in the in vivo/in situ biogenesis of desirable aroma compo-

Table 1 Overview of the Main (Potential) Applications of Oxidoreductases in Food Products

Enzymes	Taste	Texture	Appearance	Shelf life	Nutritional value
Lipoxygenases (LOX)	In situ and in vitro (off)-flavor production	Dough extensibility and strength	Flour bleaching		Destruction vitamin A
Alcohol oxidases and dehydrogenases (AO, ADH)	In situ and in vitro flavor production (I±LOX)			AO plus catalase, O_2 removal	
Sulfhydryl oxidases (SOX)	Removal of cooked flavor in UHT-milk	Dough strengthening in combination with POX			
Peroxidases (POX, LPO)	In vitro flavor production and debittering	Crosslinking biopolymers	Assisting PPO in color formation	LPO, antimicrobial agent	
(Poly)phenol oxidases (PPO)	Debittering of coffee, cacao, and olives		(Dis)coloration; in vitro production of colors	Laccase, O_2 removal	
Carbohydrate oxidases (GOX, HOX, PYROX)	GOX, mild acid production	Dough strengthening via H_2O_2; thickening agent		GOX plus catalase, O_2 removal	
Ascorbic acid oxidase (AAO)			Browning	AAO plus catalase, O_2 removal	Destruction vitamin C
Xanthine oxidases (XO)				Antimicrobial agent	
Superoxide dismutases (SOD)				Removal reactive O species with catalase	
Catalases				Removal excess H_2O_2	
Cholesterol oxidoreductases					Cholesterol reduction

nents, in the in vitro production of flavoring topnotes, and in the endogenous formation of off-flavors. The main redox enzymes are discussed below.

A. Lipoxygenases

Lipoxygenase (LOX, EC 1.13.11.12; see Chapter 43, for detailed information), formerly known as lipoxidase or carotene oxidase, is an iron-containing dioxygenase which catalyzes the oxidation of polyunsaturated fatty acids containing *cis, cis*-1, 4-pentadiene groups (linoleic, linolenic, and arachidonic acids) to the corresponding conjugated *cis, trans* dienoic monohydroperoxides. In addition LOX also accepts a relatively broad range of phenolic compounds as substrates (1) and is capable of oxidizing other substrates than the actual substrate. This process is known as co-oxidation and includes compounds like carotenoids and polyphenols (2).

LOX is one of those endogenous enzymes that play an important role in both flavor generation and off-flavor formation in virtually all food products derived from plant raw materials. Depending on the final concentration and the type of food product the same flavor component can be a desired aroma component or an off-flavor at higher concentrations. For example, C6-aldehydes and alcohols derived by the LOX-catalyzed oxidation of (poly)unsaturated fatty acids have, in most cases, a positive effect on the aroma profile (e.g., wines and juices), but in other beverages, have an undesired flavor effect (e.g., beer). Likewise, endogenous LOX is known to generate carbonyl compounds in dough systems and hence influences bread flavor (3).

The formation of C6 compounds requires the sequential action of four enzymes of which two are redox enzymes, namely an acylhydrolase, a lipoxygenase, a hydroperoxide lyase, and a yeast-derived alcohol dehydrogenase (4). Typically, off-flavor formation is prevented by using crop variants deficient in LOX isoenzymes, either by screening or by genetic tools (5) or by controlling the oxygen levels during processing (6), as well as by removing the malodorous oxidation products afterwards. The deodorization of off-flavors can be achieved by physical techniques such as adsorption, or enzymatically by converting the undesired aldehydes (e.g., with aldehyde dehydrogenase/oxidase), or alcohols (e.g., with alcohol oxidase) into their corresponding less flavorful carboxylic acid. The use of redox enzymes for this purpose has been claimed for several products such as margarine, cream, fish oil, noodles, cooked rice, and soybean products (7, 8).

LOX is also used for the in vitro production of several natural topnote flavors, which are mainly added to beverages and dairy products to tailor the flavor profile (9, 10). Typical examples include the conversion of polyunsaturated fatty acids into various short to medium-chain aldehydes/alcohols (13), or into S(-)-δ-decalactone (butter flavor; 12). Well-known fatty acid–derived flavoring aldehydes/alcohols include the above mentioned C5 and C6 compounds, as well as (E2, E6)-nonadienal (cucumber), 1-octen-3-one (field mushroom), (Z5)-octadien-3-one (geranium leaves), (E3, E5)-undecatriene (blasamic), and (E3, Z5, Z8)-undecatetraene (seaweed). Depending on the degree of unsaturation and the regioselectivity of the lipoxygenase, different hydroperoxy compounds are formed, from which the above-mentioned compounds can be derived by subsequent enzymatic reactions. For (Z3)-hexenol, linolenic acid is used as a substrate, while for most of the other aldehydes/alcohols higher unsaturated fatty acids are required. The production of (Z3)-hexenol has recently been commercialized using plant homogenates (e.g., alfalfa sprouts, green peppers) which are relatively rich in hydroperoxide lyase, the enzyme required to split the hydroperoxide fatty acid into smaller fragments. The generated (Z3)-hexenal was converted into (Z3)-hexenol using the reductive enzymatic power of bakers yeast (13). A very elegant approach has been taken recently by Givaudan-Roure. To unify all three enzymes involved in the formation of (Z3)-hexenol, they have cloned and overexpressed both soybean LOX and the hydroperoxide lyase from banana in bakers yeast. In this way they have developed a "single-step" process which produces (Z3)-hexenol in relatively high yield (14).

For the production of lactones a different strategy has to be followed after the formation of the linoleic acid hydroperoxide. It involves the fermentative β-oxidation of the hydroperoxide intermediate by the yeast *Pichia etchellsii*, and the subsequent cyclization of 5-hydroxydecanoic acid to the corresponding S(-)-δ-decalactone (10).

As shown by Quest International (1), lipoxygenases also accept a relatively broad spectrum of phenolic compounds as substrates. Of interest to the flavor industry are the LOX-catalyzed conversions of isoeugenol and coniferyl benzoate from Siam resin into vanillin. At present the commercialization of these biotransformations is hampered by the fact that isoeugenol is not readily available and that coniferyl benzoate is difficult to handle in a reactor.

Other well-known reactions of LOX include the co-oxidation reaction of carotenoids to yield, among

others, β-ionone (2, 15). More recently is the generation of a toasted or cookie-like flavor in starchy materials by a combination of LOX and an α-amylase (16).

B. Alcohol Oxidases and Dehydrogenases

In general, aldehydes are more potent flavor compounds than their alcoholic counterparts. Hence, alcohol oxidases are interesting enzymes for the in vitro production of flavoring preparations which, among others, can be applied in beverages. Typical examples include the use of methanol oxidase from *Pichia, Hansenula*, and *Candida* (17) for the production of natural acetaldehyde from ethanol. This enzyme is induced during growth on methanol. At the end of the logarithmic growth phase cells are harvested and incubated with ethanol. In this way concentrations of $\sim 1.5\%$ natural acetaldehyde can be achieved, which can be concentrated further to the desired application level. From yeast to yeast the substrate specificity of the alcohol oxidase is different. Hence, this procedure can also be used to convert other alcohols, such as hexenol and other long-chain alcohols, to their corresponding aldehyde (10, 18).

As alternatives to alcohol oxidases the corresponding dehydrogenases could in principle be used (19). A severe drawback, however, is that these dehydrogenases require the expensive cofactor $NAD(P)^+$ instead of (cheap) oxygen as an electron acceptor. Although various sophisticated $NAD(P)^+$ cofactor regenerating systems have been designed and substantial cost reductions have been realized in this way, it is evident that in commercial applications oxidases are preferred over their dehydrogenase counterparts. The use of dehydrogenases for food purposes seems to be restricted to whole-cell conversions.

Vanillyl alcohol oxidase (VAO) from *Penicillium simplicissimum* is a special type of alcohol oxidase. Recently, it has been shown that this stable, flavin-containing enzyme has a very broad substrate specificity and readily converts *para*-substituted phenols into interesting flavor precursors or flavoring compounds (20–22). Apart from natural vanillin and coniferyl alcohol, different vinylphenols (e.g., *para*-vinylguaiacol) and allylphenols can be produced from cheap raw materials and oxygen as an electron acceptor. VAO can also be used for generation of flavor building blocks. To that end a natural mix of phenolic compounds could be treated with VAO to enrich foods or flavor preparations with a range of vinylic/allylic and aldehydic substances.

C. Sulfhydryl Oxidases

Sulfhydryl oxidase (SOX, no EC number assigned; see Chapter 41 for more details) catalyzes the formation of disulfide bonds from (protein) thiols. SOX is an Fe/Cu-containing glycoprotein and has been detected in bovine, human, goat, pig, rabbit, and rat milks (23). The enzyme is capable of oxidizing the sulfhydryl groups of cysteine and glutathione, as well as milk proteins to their corresponding disulfides using molecular oxygen as electron acceptor (24). In practical applications bovine milk SOX may be added to UHT milk to reduce cooked flavors. Patents (see Refs. in 24) for this application have been issued. The enzyme has been immobilized on porous glass, and its effectiveness in ameliorating the cooked flavor has been demonstrated on a pilot scale using immobilized enzyme columns.

D. Peroxidases

Peroxidases (POX, EC 1.11.1.7; see Chapters 28 and 29 for more details) occur widely in nature and is the general name for a group of both highly specific and nonspecific enzymes which use hydrogen peroxide instead of oxygen as an electron acceptor. Peroxidases, especially the heme-containing ones, can catalyze a large number of different reactions including sulfoxidation, N-demethylation, oxidation, and hydroxylation and hence are of potential interest in the production of specific flavoring topnotes. A recent example involves the demethylation of methyl *N*-methylanthranilate (ex *Citrus*) to monomethylanthranilate (25). The latter compound is an important topnote flavor in Concord grapes. Soybean, horseradish, and microperoxidases were found to be convenient catalysts for this reaction. In addition POX gives rise to a fresh flavor profile when added to tomato paste (26).

E. Polyphenol Oxidases

Polyphenol oxidases (PPO) are a group of several enzymes. Different activities can be found within this group: tyrosinase (monophenol monooxygenase, EC 1.14.18.1; see Chapter 39) converting a phenol into a catechol group; 1,2-diphenol oxidase or catechol oxidase (EC 1.10.3.1) converting catechol into an *o*-quinone, and laccase (EC 1.10.3.2; see Chapter 40) converting a 1,4-diphenol into *p*-quinone. Usually the first two activities are linked, as catechol is much more readily oxidized than a phenol. Most enzymes that catalyze 1,4-diphenol oxidation also act on 1,2-diphenols.

The bitter taste in many food products is often the result of the presence of polyphenolic compounds such as guaiacols. PPOs are capable of oxidizing these compounds and hence can be applied to reduce bitterness. At present the debittering of coffee beans (27), Adzuki beans (28), and cacao beans (29) by PPOs have been claimed. Another application involves the use of laccase to debittering olives by treating stoned, chopped olives in the presence of air at increased temperatures (30).

III. TEXTURE

The use of oxidoreductases in texturizing food is based on their ability to crosslink proteins and/or polysaccharides. This property is of particular interest to improve the texture of dough and paste products (softness, volume, elasticity, crunchiness) or dairy products (mouth feel, appearance), and of fish and meat pastes. Basically, enzymatic crosslinking can occur via two routes:

1. Indirect via enzymatically produced hydrogen peroxide (e.g., glucose oxidase, hexose oxidase, ascorbic acid oxidase), or via the enzymatic production of radicals (e.g., peroxidase, lipoxygenase).
2. Direct via the oxidation of functional groups in the protein. Examples include the linkage of tyrosine and ferulic acid residues by tyrosinase and laccases, linkages of lysine residues by lysyl oxidase, or the formation of disulfide bridges by sulfhydryl oxidase.

An alternative, nonredox procedure for direct crosslinking is being explored using transglutaminases (see Chapter 51).

These enzymatic routes are being explored to replace chemical oxidizers, such as dehydroascorbic acid and potassium bromate. Replacement of the nonspecific chemical compounds by redox enzymes could have the benefit of more specific and better-controlled oxidation processes. Other disadvantages of the chemical substances are related to safety and labeling issues. One of the major challenges in the baking industry is to find a good replacer for potassium bromate, which is a difficult task since bromate is still more effective and cheaper than the enzymatic alternative. The most important texturizing redox enzymes will be discussed below.

A. Lipoxygenases

A rich source of LOX is soybeans. Soybean LOX contains three distinct lipoxygenase isoenzymes, designated as L1, L2, and L3. These isoenzymes have been isolated from seeds of commercial cultivars and have been well characterized (31, 32). Recent studies indicate that L2 has the greatest effect among LOX isoenzymes on dough extensibility and strength (33) and is also mostly responsible for the production of undesirable aroma compounds in bread doughs (34; see Sec. II, Chapter 43). For L3 an increase in foaming activity has been reported, as well as an overall improvement in breadmaking quality of wheat flour (35). The bakery yeast *Saccharomyces cerevisiae* also contains LOX. Recently, this enzyme was partially purified (36), but its potential, if any, on breadmaking remains to be established.

Nowadays, it is feasible to change the profile and content of LOX (iso)enzymes in plants either by classical means (5), or potentially by genetic modification. For example, by appropriate crosses, near-isogenic soybean seeds have been developed that lack either isoenzymes L1 and L3, or isoenzymes L2 and L3. These LOX-minus mutants still grow well in the field (37). In principle, transgenic plants lacking or overexpressing one or more LOX isoenzymes could be constructed and tailored to specific applications (38). To that end the heterologous expression of one or more soybean LOX isoenzymes in wheat could be of interest.

B. Sulfhydryl Oxidases

The action of SOX (see Sec. II, Chapter 41, for general information) may be the same as those of chemical oxidizing agents, provided the formation of disulfide bonds is the primary mode by which these agents function. In extensive testing (39, 40) it was found that SOX alone has no influence on loaf volume, dough strength, or mixing tolerance. Also, relatively high concentrations using recombinant SOX from *Aspergillus awamori* did not have any significant positive effect (40). One reason could be that SOX has only a limited affinity for thiol groups in gluten proteins and as a result its application in the food industry seems to be limited to the removal of small off-flavor molecules (see Sec. II, Chapter 41).

C. Peroxidases

For detailed information about POX see Section II, Chapters 28 and 29. Wheat flour contains a peroxidase that can crosslink phenolic constituents such as ferulic acid and vanillic acid. However, the pH optimum of the wheat enzyme is 4.5, and in the pH range of 5–6 of wheat doughs the activity is considerably lower than at pH 4.5 (41). Although the dough-improving effect of

peroxidase is well documented, the reactions involved in the dough are only poorly understood.

Model studies with peroxidase, glutathione, and cysteine indicate that sulfhydryl and/or lysyl groups may be involved (42). Peroxidase-catalyzed reactions result in a decreased amount of lysine recovered from proteins after acid hydrolysis. Peroxidases, or the quinones formed by the enzyme, oxidatively deaminate lysyl residues to form lysylaldehydes, resulting in the formation of protein polymers, as was revealed by gel filtration. These aggregates could not be dissociated by detergents, which indicates that covalent bonds were formed. In addition, the dough-strengthening effect of peroxidases is also ascribed to the crosslinking of carbohydrates and the coupling of carbohydrates to proteins. The gelation of wheat pentosans is due to the oxidative dimerization of ferulic acid moieties, which are covalently linked to pentosans (43).

Recently, a study has been described showing the effect of different peroxidases on the baking performance of German "Kaiser" rolls (41). Deliberately sticky doughs were prepared in order to demonstrate the effects of added peroxidases. Especially the addition of soybean POX led to strengthening of wheat doughs as determined by the stability of the dough after "shaking" the dough for 1 min in a laboratory shaker. This improving effect was observed at both short and long fermentation times. Dough volume increased after application of these peroxidases. Compared with (GOX), the results of peroxidases are better or at least equal in terms of stability and volume.

In bread dough, peroxidases seem to act without the extra addition of hydrogen peroxide in spite of their peroxide dependence. This may indicate that peroxide is present in dough at sufficient amounts, or that it is generated as a result of the peroxidase reaction. In this way, substrate radicals formed by peroxidase can react with oxygen to form hydrogen peroxide. When this reaction is occurring, catalytic amounts of peroxide present in dough are sufficient to get the cycle started, and may explain why no hydrogen peroxide has to be added together with a peroxidase. An alternative explanation is that wheat contains endogenous oxidases, which are active enough to produce some hydrogen peroxide in situ. Indeed, the addition of hydrogen peroxide–producing enzymes such as GOX has a beneficial effect on baking (44–46).

In other systems than doughs, POX has been claimed as a thickening and stabilizing agent in, for example, ice creams, deserts, sauces, and jams and jellies (47). There is also a recent patent application (48) on the POX-catalyzed gelling of hemicelluloses to form gels or viscous media for application as fat or gelatin replacer, as well as for flavor delivery, coating, or glazing.

D. Glucose Oxidases

Glucose oxidase (GOX, EC 1.1.3.4; see Chapter 30 for detailed information) catalyzes the conversion of glucose into the mild-tasting gluconic acid via glucono-δ-lactone and hydrogen peroxide. GOX complies with the FAO/WHO and GRAS requirements for food grade enzymes and is one of the few commercially available oxidases from *Aspergillus niger* and *Penicillium* strains at relatively low costs. Especially, the generation of hydrogen peroxide is believed to give the antiweakening effect in bread doughs (40). In a recent study by Hilhorst et al. (49) the effect of GOX on Dutch rusk dough was dough stiffening with a clear loss in extensibility. This made the overall effect quite undesirable. For comparison, they also tested peroxidase (see Sec. III.C above). This enzyme gave a dough-stiffening effect without loss in extensibility. The authors explain the difference by the fact that hydrogen peroxide from the GOX-catalyzed reaction oxidizes randomly and links the gluten network with the arabinoxylan network, whereas the peroxidase only increases the amount of crosslinks in the arabinoxylan fraction without affecting the gluten network or the coupling between the networks.

It has been found that synergistic effects occur when using a combination of oxidative enzymes like the combination of GOX and SOX (50). Furthermore, the dough has an increased stability.

E. Hexose Oxidases

A newcomer in the field of redox enzymes for bakery products is hexose oxidase (HOX, EC 1.1.3.5) from red seaweeds. This glycosylated flavoprotein is related to GOX but has a broader substrate specificity toward hexose sugars, including oligomers. Like GOX, it acts on the C1-position of the sugar moiety (51). Recently, the enzyme from *Chondrus crispus* has been isolated, cloned, and overexpressed in several recombinant organisms such as *Pichia pastoris, Saccharomyces cerevisiae*, and *E. coli* (51, 52). However, the production levels of active enzyme are still poor at this moment and have to be improved. For this reason, and because *C. crispus* has a long standing tradition as an edible organism, efforts have been made to develop a large-scale production method with the use

of carrageenase, which reduces the viscosity of the crude extract (51).

For HOX similar applications can be envisaged as for GOX (see above). In particular, its application in bakery products is foreseen (53), since HOX is able to generate more H_2O_2 owing to its broader substrate specificity, and hence should be more effective than GOX in dough strengthening. Likewise, combinations of HOX and H_2O_2-consuming enzymes, such as POX, may be envisaged.

Another enzyme with similar properties as HOX, isolated from *Acremonium strictum* T1, has been reported in the literature (54). The enzyme is called an oligosaccharide oxidase and is able to oxidize several di- and oligosaccharides at the anomeric site, yielding the corresponding di- and oligobionic acids. A detailed comparison between HOX and oligosaccharide oxidase performance in dough applications has not been made yet.

F. Pyranose Oxidases

Pyranose oxidase (PYROX, EC 1.1.3.10; see Refs. 55–57, 59 for more detailed information) catalyzes the oxidation of several monosaccharides at the C2-position and is therefore different from GOX, which oxidizes glucose at the C1-position. While GOX is very specific, PYROX is able to catalyze other substrates such as maltose and pentoses (e.g., xylose). As a result, the PYROX oxidation product of glucose is 2-keto-glucose and not gluconic acid. At present, this enzyme has been purified from several white rot fungi and a *Bacidiomycetous* fungus (55–57). PYROX has also been reported to show significant activity toward D-glucono-1,5-lactone, which is produced by the GOX-catalyzed oxidation of glucose (58). So if PYROX is combined with GOX, there will be more substrate available for PYROX, thereby prolonging the activity of PYROX and enhancing the total amount of hydrogen peroxide produced (59). The claimed effects in baking are gluten strengthening, reduced dough stickiness, and increased volume and crumb structure for bread (59).

IV. APPEARANCE/COLOR

Apart from texture, the appearance of food products is determined to a large extent by their color. Several redox enzymes are known to influence the color of foodstuffs. The most important ones will be discussed below.

A. Lipoxygenases

It is interesting to note that the use of soybean lipoxygenase was described in the 1930s as a means to bleach the flour in preparation of white bread. More recent experiments have shown that carotenoids present in wheat flour are destroyed by co-oxidation. Wheat flour itself contains little LOX activity, but LOX is abundantly present in, for example, soybeans. To that end wheat flour is often fortified with up to 0.5% enzyme-active soy flour (34, 60). Other applications of LOX include the bleaching of noodles, whey products, rice, and wheat bran (61–64).

B. (Poly)phenol Oxidases and Peroxidases

PPOs (see Sec. II, Chapter 39 for general information) play an important role in the browning of fresh fruits and vegetables (65, 66), in the coloring and flavoring of tea (67, 68), and in improving the quality of coffee (69).

A major concern in the food industry is to prevent the development of enzymatic browning prior to the processing of fruits and vegetables (70). This is accomplished by removing oxygen or by inhibiting PPO activity using inhibitors such as metal chelating agents, inorganic ions (e.g., halide anions), benzoic acid and some substituted cinnamic acids, reducing agents (e.g., L-cysteine, glutathione, sulfite, SO_2, ascorbic acid), small ''natural'' peptides, and combinations thereof (68). In contrast, during the fermentation of black tea PPO is used to initiate browning by oxidation of polyphenolic substances such as catechins to theaflavins.

The quality of tea, based on sensory evaluation of color and bitterness, has been correlated with total theaflavin content (71). Theaflavins, thearubigins, and caffeine are all essential ingredients in high-quality teas. The addition of microbial laccases and/or peroxidases to green tea has shown that no higher theaflavin levels can be obtained than with endogenous PPO. Addition of exogenous laccase/peroxidase to black tea, however, did yield a very significant increase in the color intensity of the tea (72).

Polyphenol oxidases also play an important role in coffee processing (69). The activity of PPO in green coffee beans has been consistently related to the quality of the coffee beverage. The exact role of PPO in cocoa beans is less well understood. There are, however, indications that it plays a role in browning during the curing of the cocoa beans (73).

In cereals, PPO is responsible for the darkening of the breadcrumb, particularly in whole-grain and rye

breads. The rate of browning is greatest in sourdough baking. Excessive discoloration can be prevented by the addition of sodium metabisulfite or ascorbic acid (41). Exogenous PPO is also reported to have a positive influence on the rheological properties of bread (74).

PPO can also be used for the in vitro production of colors. For example, Pruidze (75) reported the production of a whole range of natural colors by treating waste streams of beet and tea with PPO. Furthermore, it was claimed that safflower pigments become darker red when safflower petals were sprayed with a dilute laccase solution (76).

The role of endogenous POX in (dis)coloration is not fully understood. It seems that the oxidative role of peroxidases is useful in assisting PPOs in oxidizing the polyphenols and ultimately contributing toward the color and flavor of tea. The same seems to be true for coffee and cocoa.

C. Ascorbic Acid Oxidases

Ascorbic acid oxidase (E.C.1.10.3.3; see Ref. 77 for detailed information) plays a role in beverages such as lemon and grapefruit juices, where it is responsible for the initiation of browning and loss of vitamin C activity during storage (77). The extent of browning can be minimized by steam blanching or by the exclusion of oxygen. The rate of ascorbic acid oxidation increases markedly in the presence of metallic ions, especially copper and iron. Hence, food processed in tin cans and processing equipment should be copper free. While the loss of ascorbic acid cannot be prevented completely, it can be reduced to a minimal level during processing.

V. SHELF LIFE

The application of redox enzymes for improving the shelf life of food products includes mainly enzymes which are capable of removing oxygen or reactive oxygen species (e.g., H_2O_2 and superoxide anion), as well as enzymes that are able to generate antimicrobial agents. In this way the stability of foods can be increased significantly with respect to taste, appearance, and microbial spoilage.

A. Lactoperoxidases

Lactoperoxidase (LPO; see Ref. 78 and Chapters 19 and 20 for detailed information) is the most prominent enzyme in bovine milk, where it is found in concentrations around 30 mg/L. It is a glycoprotein with a single, covalently bound heme group (78). Lactoperoxidase requires hydrogen peroxide and thiocyanate (SCN^-) for antibacterial activity. All three components are referred to as the LP system. The growth inhibitory effect of the LP system is mediated by the generation of SCN^- oxidation products, mainly hypothiocyanate ions ($OSCN^-$), which attack sulfhydryl groups of vital metabolic enzymes of the microorganisms. Mammalian cells are not affected by the LP system. Only 10–20 ppm of lactoperoxidase is required for an effective system. The cofactor requirements are also very low: 10–25 ppm for thiocyanate and 10–15 ppm for H_2O_2. Without the enzyme H_2O_2 is also bactericidal, but at much higher concentrations: 300–900 ppm (79). Therefore LPO is often applied in combination with H_2O_2-generating enzymes. From a toxicological point of view, the levels of the cofactors in the LP system as well as the oxidation products are reported to be harmless.

The envisaged applications of the LP system are food products (e.g., liquid milk, cheese, meat, fish and poultry products, and functional foods), feed and veterinarian products (e.g., milk replacers, and antidiarrhea and antimastitis preparations), and dental products (78–80). Typically, applications have been claimed for *Lactobacillus* fermented milk products (81), pickled foods (82), fish products (LPO in combination with GOX; 83), and white mold cheeses such as Camembert (84). Also of interest is the effect of LPO on yogurt. By adding LPO to yogurt the excessive acid production of lactic acid bacteria in the yogurt is suppressed (85). These applications are becoming within reach now that it is possible to isolate lactoperoxidase from milk with high purity on an industrial scale (79). Currently, LPO is already commercially available at relatively low costs.

B. Xanthine Oxidases

Xanthine oxidase (XO, EC 1.2.3.2; see Chapters 19 and 42 for detailed information) is widely distributed in animals, plants, and microorganisms. It catalyzes the oxidation of hypoxanthine to xanthine and xanthine into uric acid. In addition XO is able to oxidize a wide range of purines, aldehydes, and pteridines with concomitant reduction of O_2 to H_2O_2. Under certain conditions XO also produces the highly reactive superoxide anion. Bovine milk is very rich in XO ($\sim$ 35 mg/L; 86). XO has been implicated in the oxidative deterioration of milk and dairy products via the

production of superoxide anion during oxidation of its substrates (87). However, Bruder et al. (88) found no evidence to support a role for native bovine milk XO in lipid oxidation. The results of Weihrauch (89) seem to indicate that in the presence of purines, XO activity generates H_2O_2 for the lactoperoxidase system in milk, making it a bactericidal or bacteriostatic agent in milk (23).

C. Superoxide Dismutases and Catalases

Superoxide dismutase (SOD; EC 1.15.1.1) and catalase (EC 1.11.1.6; see Chapters 27 and 38 for detailed information) are present in milk and are able to remove reactive oxygen species generated by other (bio)chemical processes (90). SOD catalyzes the reduction of superoxide anion, as produced, for example, by XO, to H_2O_2 and O_2. In turn, catalase is able to neutralize H_2O_2 to water and oxygen. A low level of exogenous SOD, coupled with catalase, is a very effective antioxidant in dairy products (91).

Recently, SOD has been shown to protect beer against free radical damage (92). Obviously, the commercial feasibility of SOD as an antioxidant depends on cost, particularly compared to chemical antioxidants, if permitted. As far as is known, SOD is not used commercially as an antioxidant in food systems.

Catalase is used for the cold-sterilization of milk in regions lacking refrigeration and could in principle be applied in developed countries for the treatment of cheese milk (90). Good sources for catalase are beef, liver, *Aspergillus niger*, and sweet potato. There is also interest in using immobilized catalase reactors for milk pasteurization or for glucose oxidase–catalase reactions (93). Besides the removal of reactive oxygen species by SOD and catalase, other enzymes can be applied to remove the less but still reactive oxygen. Typical examples include glucose oxidase, D-amino acid oxidase, alcohol oxidase, and ascorbic acid oxidase. The disadvantage of these oxidases is that they produce H_2O_2, which by itself is a powerful oxidant. Catalase can be added to remove H_2O_2, but then oxygen is produced again. More recently, polyphenol oxidases such as laccase have been proposed as a deoxygenation tool for beer (94) and juices (95, 96). These enzymes have the advantage that they do not produce H_2O_2, and thus the combination with catalase is not necessary. As a result PPOs allow a more efficient oxygen removal.

VI. NUTRITIONAL VALUE

Redox enzymes can have both pro- as well as antinutritional effects. For example, lipoxygenase, apart from all its other functions in food products (see Table 1), is involved in the oxidative destruction of liposoluble vitamins (provitamin A) and essential fatty acids (3). Likewise, ascorbic acid oxidase has an antinutritional effect since it oxidizes vitamin C (97).

Increasingly, redox enzymes are being claimed to improve the "healthiness" of especially beverages. For example, peroxidase and catalase have been claimed for the removal of "unhealthy" hydrogen peroxide in coffee and tea (98). Other examples include the use of cholesterol oxidase, epicholesterol dehydrogenase and cholesterol reductase to lower the cholesterol level in foods such as meat, fish, milk, and egg products (99–101).

VII. CONCLUDING REMARKS

Compared to the usage of hydrolytic enzymes such as proteases, carbohydrates, and lipases, the application of oxidoreductases as a tool to improve the processability and quality of food products is still in its infancy. Like hydrolytic enzymes, oxidoreductases are capable of tailoring the taste, texture, appearance, shelf life, nutritional value, and process tolerance of foods and the properties of all major food constituents (*e.g.*, proteins, carbohydrates, oils, fats, flavors; see Table 1). In both cases, they can exert a positive as well as a negative effect on the food quality parameters, which can be reduced or eliminated by careful selection of the raw materials, by properly controlling the process condition, by the addition of counteracting ingredients, and by genetic tools. Likewise, hydrolytic and redox-active enzymes often have more than one effect. A typical redox example is the multifunctional enzyme lipoxygenase, which can be applied to influence either taste, texture, appearance, and/or nutritional value of food products. The key difference resides in the types of reactions they catalyze. As a result, redox enzymes can be combined with hydrolytic enzymes in a variety of food products to create improved or even new functionalities, which cannot be realized by either one of them.

At present, major bottlenecks for the large-scale application of oxidoreductases include their limited availability, their safety status (not GRAS), their stability, and the fact that they often initiate radical reac-

tions, which propagate *via* redox-active food constituents such as metal ions and quinones and hence are difficult to control. In addition, many oxidoreductases require expensive cofactors for catalysis. Despite these disadvantages over hydrolytic enzymes, certain oxidoreductases are increasingly finding a home in food processing. The first generation (see Table 1) includes enzymes which are cofactor independent and thrive on oxygen (*e.g.*, oxidases) and hydrogen peroxide (*e.g.*, peroxidases). Owing to advances in recombinant DNA technology the low-cost, large-scale production of these enzymes in GRAS host microorganisms is becoming within reach, and the tools are ready to tailor redox enzymes to specific needs by site-directed mutagenesis and directed evolution. Also feasible will be the *in planta* overexpression of desired redox enzymes in food raw materials and the deletion of undesirable redox traits. The usage of cofactor-dependent oxidative enzymes seems tentatively to be confined to whole-cell systems, in which the cofactor can be regenerated, and hence to the in vitro as well as the in situ production of functional food ingredients such as flavors. The same seems to be true for reductases, since most if not all require reducing equivalents in the form of a small protein, hydrogen, and/or NAD(P)H.

Clearly, the usage of oxidoreductases in food processing is emerging. The benefits and limitations are becoming known, which allows a promising and focused search for new opportunities.

REFERENCES

1. PA Markus, ALJ Peters, R Roos. Enzymatic process for preparation of phenylacetaldehyde compounds especially vanillin by conversion of starting compounds in the presence of lipoxidase. Patent EP542348, 1991.
2. D Waldman, P Schreier. Stereochemical studies of epoxides formed by lipoxygenase-catalyzed co-oxidation of retinol, beta-ionone and 4-hydroxy-beta-ionone. J Agric Food Chem 43:626–630, 1995.
3. M Martínez-Anaya. Enzymes and bread flavor. J Agric Food Chem 44:2469–2480, 1996.
4. J Crouzet, M Nicolas, J Molina, G Valentin. Enzymes occurring in the formation of 6-carbon aldehydes and alcohols in grapes. In: J Adda, ed. Progress in Flavour Research. Amsterdam: Elsevier Science Publishers, 1985, pp 401–408.
5. DS Robinson, Z Wu, C Domoney, R Casey. Lipoxygenases and the quality of foods. Food Chem 54:33–43, 1995.
6. TE Mathiasen. Improving the storage stability of beer by fermenting wort into beer and adding a laccase to the fermented beer. Patent WO9521240.
7. RL Antrim, JB Taylor. Deodorization of a water-in-oil emulsion containing fish oil using pure alcohol and aldehyde oxidases/dehydrogenase in combinations with a cofactor. Patent US4961939, 1990.
8. Y Nomura, N Shiomi. Production of a powder of acidic acid bacteria that produce aldehyde oxidase. Patent JP10108671, 1998.
9. IM Whitehead, BL Muller, C Dean. Industrial use of soybean lipoxygenase for the production of natural green note flavour compounds. Cereal Foods World 40:193–197, 1995.
10. C Laane, I Rietjens, H Haaker, W van Berkel. Generation of taste through (redox) biocatalysis. In: KAD Swift, ed. Flavours and Fragrances. Proceedings of the 1997 RSC/SCI International Conference on Flavours and Fragrances, Royal Society of Chemistry, Special Publication No. 214, 1197, pp 137–152.
11. JC Villettaz, D Dubourdieu. Enzymes in winemaking. In: PE Fox, ed. Food Enzymology, Vol 1. London: Elsevier Science Publishers, 1991, pp 427–454.
12. PSJ Cheetham. The use of biotransformations for the production of flavours and fragrances. Tibtech 11:478–488, 1993.
13. P Brunerie (Pernod Ricard). Synthesis of *cis*-3-hexenol from unsaturated aliphatic acid—using combined action of natural enzyme system and yeast. Patent EP481147, 1991.
14. A Muheim, A Häusler, B Schilling, K Lerch. The impact of recombinant DNA-technology on the flavour and fragrance industry. In: KAD Swift, ed. Flavours and Fragrances. Proceedings of the 1997 RSC/SCI International Conference on Flavours and Fragrances, Royal Society of Chemists, Special Publication No. 214, 1997, pp 11–20.
15. M Jaren-Galan, MI Minquez-Mosquera. Beta-carotene and capsanthin co-oxidation by lipoxygenase: kinetic and thermodynamic aspects of the reaction. J Agric Food Chem 45:4814–4820, 1997.
16. JJ Desjardins, P Duby, P Dupart, RD Wood, U Zurcher. Producing of starchy material with α-amylase and lipoxygenase to produce a toasted or cookie-like flavor. Patent EP772980, 1997.
17. H Stam, M Hoogland, C Laane. Food flavours from yeast. In: BJB Wood, ed. Microbiology of Fermented Foods, 2nd ed, part 2. London: Chapman and Hall, 1998, pp 505–543.
18. WD Murray, SJB Duff. Bio-oxidation of aliphatic and aromatic high molecular weight alcohols by *Pichia pastoris* alcohol oxidase. Appl Microbiol Biotechnol 33:202–205, 1990.
19. IEM Deutz, LC Fraysse, HTWM van der Hijden. Manipulation of the aroma profile of tomato pro-

ducts—comprises adding alcohol dehydrogenase and a cofactor, electron donor or electron acceptor to tomato pieces. Patent WO9857533A1, 1998.
20. WJH van Berkel, MW Fraaije, E de Jong. Process of producing 4-hydroxycinnamyl alcohols. Patent EP0710289B1, 1997.
21. HH van den Heuvel, MW Fraaije, C Laane, WJH van Berkel. Regio- and stereospecific conversion of 4-alkylphenols by the covalent flavoprotein vanillyl-alcohol oxidase. J Bacteriol 180:5646–5651, 1998.
22. A Mattevi, MW Fraaije, A Mozzarelli, L Olivi, A Coda, WJH van Berkel. Crystal structure and inhibitor binding in the octameric flavoenzyme vanillyl-alcohol oxidase. Structure 5:907–920, 1997.
23. NY Farkye. Indigenous enzymes in milk: other enzymes. In: PF Fox, ed. Food Enzymology, Vol 1. New York: Elsevier Science Publishers, 1991, pp 107–130.
24. VG Janolino, HE Swaisgood. Isolation and characterization of sulfhydryl oxidase from bovine milk. J Biol Chem 250:2532–2538, 1975.
25. MJH van Haandel, FCE Sarabèr, MG Boersma, C Laane, Y Fleming, H Weenen, IMCM Rietjens. Characterization of different commercial soybean peroxidase preparations and use of the enzyme for N-demethylation of methyl-N-methylanthranilate to produce the food flavor methylanthranilate. J Agric Food Chem 48:1949–1954, 2000.
26. P Wilding, EM Woolner. Treatment of tomato with peroxidase to achieve a fresh flavour profile. Patent WO9738591, 1997.
27. LE Small, TN Asquith. Process for treating coffee beans with enzyme-containing solution under pressure to reduce bitterness. Patent EP337541, 1989.
28. S Okazawa, M Hashimoto, Y Hatsutori. Treatment of adzuki bean with enzymes. Patent JP05244889, 1993.
29. T Takemori, Y Ito, M Ito, M Yoshama. Flavor and taste improvement of cacao nib by enzymatic treatment. Patent JP04126037, 1992.
30. NOVO Nordisk. Debittering and darkening of olives by laccase treatment. Research Enclosure No. 37828, 1995, p 676.
31. JJ Rackis, DJ Sessa, DH Honig. Lipoxygenase and peroxidase activities of soybeans as related to the flavor profile during maturation. J Am Oil Chem 56:262–271, 1979.
32. B Axelrod, TM Cheesbrough, S Laakso. Lipoxygenases in soybean. Methods Enzymol 71:441–451, 1981.
33. B Cumbee, DF Hildebrand, K Addo. Soybean flour lipoxygenase isoenzymes effects on wheat flour dough rheological and breadmaking properties. J Food Sci 62:281–283, 294, 1997.
34. K Addo, D Burton, MR Stuart, HR Burton, DF Hildebrand. Soybean flour lipoxygenase isoenzyme mutant effects on bread dough volatiles. J Food Sci 58:583–585, 608, 1993.
35. K Shiiba, Y Negishi, K Okada, S Nagao. Purification and characterization of lipoxygenase isoenzymes from wheat germ. Cereal Chem 68:115–122, 1991.
36. B Bisakowski, S Kermasha, C Schuepp. Partial purification and some properties of lipoxygenase from *Saccharomyces cerevisiae*. World J Microb Biotechnol 11:494–496, 1995.
37. TW Pfeiffer, DF Hildebrand, DM TeKrony. Agronomic performance of soybean lipoxygenase isolines. Crop Sci 32:357–362, 1992.
38. D Shibata. Peroxidation of plant lipids and gene manipulation of plant lipoxygenases. J Am Oil Chem Soc 41:741–744, 1992.
39. SP Kaufman, O Fennema. Evaluation of sulfhydryl oxidase as a strengthening agent for wheat flour dough. Cereal Chem 64:172–176, 1987.
40. J Maat, W Musters, H Stam, PJ Schaap, PJ van der Vonderwoort, J Visser, JM Verbakel. Cloning and expression of DNA encoding of ripening form of a polypeptide having sulfhydryl oxidase activity. Patent EP565172, 1993.
41. M van Oort. Oxidases in baking. Int Food Ingredients 4:42–47, 1996.
42. G Matheis, JR Whitaker. Peroxidase catalyzed cross-linking of proteins. J Protein Chem 3:35–48, 1987.
43. T Geissmann, H Neukom. Comparison of the water-soluble wheat flour pentosans and their oxidative gelation. Lebensm Wiss Techn 6:59–62, 1973.
44. J Maat, M Roza. Novel formulation in combination with cellulase for structure, volume, appearance improvement of bread. Patent CA2012723, 1990.
45. M Roza, GHE Pieters. Bread-improving storage stable enzyme solutions. Patent EP669082, 1995.
46. PM Nielsen, P Wagner. Bread- or dough-improving composition. Patent WO9800029, 1998.
47. G Budolfsen, HP Heldt-Hansen. Oxidase promoted gelling of phenolic polymers. Patent WO9603440, 1994.
48. CS Fitchett. Production of vegetable gels. Patent WO9822513, 1997.
49. R Hilhorst, H Gruppen, R Orsel, C Laane, HA Schols, AGJ Voragen. On the mechanism of action of peroxidase in wheat dough. Proceedings, Oxidation in Foods, Viborg, Denmark, p 27–29.
50. F van Welie, B Poldermans. Enzymen gaan broodverbeteraars domineren. Voedingsmiddelen Technol 24:55–57, 1998.
51. JP van der Lugt. Evaluation of methods for chemical and biological carbohydrate oxidation. PhD dissertation, Delft University, Delft, Netherlands, 1998.
52. OC Hansen, P Sougaard. Hexose oxidase from the red alga *Chondrus crispus*: purification, molecular cloning, and expression in *Pichia pastoris*. J Biol Chem 272:11581–11587, 1997.

53. P Stougaard, OC Hansen. Recombinant hexose oxidase: a method of producing same and use of such enzyme. Patent WO9640935, 1996.
54. SF Lin, TY Yang, T Inukai, M Yamasaki, YC Tsai. Purification and characterization of a novel gluco-oligosaccharide oxidase from *Acremonium strictum* T1. Biochim Biophys Acta 1118:41–47, 1991.
55. J Volc, K-E Eriksson. Pyranose 2-oxidase from *Phanerochaete chrysosporium*. Methods Enzymol 161:316–322, 1988.
56. Y Izumi, Y Furaya, H Yamada. Purification and properties of pyranose oxidase from basidiomycetous fungus No. 52. Agric Biol Chem 54:1393–1400, 1990.
57. H-J Danneel, E Rössner, A Zeeck, F Giffhorn. Purification and characterization of a pyranose oxidase from basidiomycete *Peniophora gigantea* and chemical analyses of its reaction products. Eur J Biochem 214:795–802, 1993.
58. L Olsson, CF Mandenius. Immobilization of pyranose oxidase (*Phanerochaete chrysosporium*): characterization of the enzymic properties. Enzyme Microb Technol 13:755–759, 1991.
59. P Wagner, JQ Si. Use of pyranose oxidase in baking. Patent WO9722257, 1997.
60. HW Gardner. Lipoxygenase pathway in cereals. In: Y Pomeranz, ed. Advances in Cereal Science and Technology, Vol IX. St. Paul, MN: American Association Cereal Chemistry, 1988, pp 161–215.
61. K Kikuchi, M Enjo, S Ikeda, K Akimoto, M Imamura. Noodles containing soybean lipoxidase. Patent JP53062846, 1978.
62. SK Meiji. Improving colour, taste and flavour of processed flour foods—by adding lipoxidase and lipase. Patent JP55153549, 1980.
63. Y Isao. Production of storable noodle with good luster and color. Patent JP56131358, 1981.
64. H Fukui, D Hosokawa, H Matsuda, M Nagahama, H Morita. Bakery products and confectioneries and their manufacture using lipoxygenase-containing soybean meal as bleaching agent. Patent JP63254939, 1988.
65. G Matheis, JR Whitaker. A review: enzymatic cross-linking of proteins applicable to foods. J Food Biochem 11:309–327, 1987.
66. AM Mayer, E Harel. Phenoloxidases and their significance in fruit and vegetables. In: PF Fox, ed. Food Enzymology, Vol 1. London: Elsevier Science Publishers, 1991, pp 373–394.
67. MR Ullah. Tea. In: PF Fox, ed. Food Enzymology, Vol 2. London: Elsevier Science Publishers, 1991, pp 163–188.
68. J Zawistowski, CG Billaderis, NAM Eskin. Phenol oxidase. In: DS Robinson, NAM Eskins, eds. Oxidative Enzymes in Foods. New York: Elsevier Applied Science, 1991, pp 217–276.
69. HV Amorim, M Melo. Significance of enzymes in coffee. In: PF Fox, ed. Food Enzymology, Vol 2. London: Elsevier Science Publishers, 1991, pp 189–210.
70. NAM Eskin. Biochemistry of Foods. New York: Academic Press, 1990.
71. PJ Hilton, RT Ellis. Estimation of the market value of Central African tea by theaflavin analysis. J Sci Food Agric 23:227–232, 1972.
72. ECM Bouwens, K Trivedi, C van Vliet, C Winkel. Enhancing colour of tea-based products. Patent EP760213, 1996.
73. AS Lopez, PS Dimick. Enzymes involved in cocoa curing. In: PF Fox, ed. Food Enzymology, Vol 2, London: Elsevier Science Publishers, 1991, pp 211–236.
74. JQ Si. Laccase enzyme in bread-, dough- or pasta improvers to give improved gluten strength, increasing specific volume index and crustiness. Patent WO9428728, 1994.
75. GN Pruidze. Stable natural food-dyes of phenolic origin. Proceedings of XVth International Conference Polyphenols. Strasbourg, France: Bull. Groupe Polyphenols, 1990, pp 15, 136–139.
76. T Aso, N Sakota. Deepening of the red pigment of safflower as food colouring by spraying a dilute laccase solution on safflower petal. Patent JP08214896, 1996.
77. NAM Eskin. Biotechnology: enzymes in the food industry. In: NAM Eskin, ed. Biochemistry of Foods. New York: Academic Press, 1976, pp. 467–539.
78. IM Kooter, AJ Pierik, M Merkx, BA Averill, N Moguilevsky, A Bollen, R Wever. Difference Fourier transform infrared evidence for ester bonds linking the heme group in myeloperoxidase, lactoperoxidase, and eosinophil peroxidase. J Am Chem Soc 119:11542–11543, 1997.
79. K Kussendrager. Lactoferrin and lactoperoxidase: bio-active milk proteins. Int Food Ingredients 6:17–21, 1993.
80. SA Farrag, EH Marth. *E. coli* 0157 H7, *Y. enterocolitica* and their control in milk by the LP system: a review. Lebensm Wiss Technol 25:201–211, 1992.
81. H Kawamoto, O Ashibe. *Lactobacillus*-fermented foods. Patent JP62228224, 1987.
82. T Suguri, M Hirano, T Uchida, K Tatsumi, I Nakajima, Y Ichiro. Preservatives for pickled vegetables. Patent JP09271319, 1997.
83. L. Bernard. Control of bacteria in fish, shellfish, and seafood by using lactoperoxidase system. Patent FR2750575, 1998.
84. M Hirano, T Suguri, K Tatsumi. Lactoperoxidase for manufacturing white mold cheese. Patent JP10215767.
85. M Nakada, S Dosako, R Hirano, M Oooka, I Nakajima. Lactoperoxidase suppresses acid production in yoghurt during storage under refrigeration. Int Dairy J 6:33–42, 1996.

86. P Walstra, R Jenness. In: Dairy Chemistry and Physics. New York: John Wiley & Sons, 1984, p 128.
87. LW Aurand, NH Boone, GG Giddings. Superoxide and singlet oxygen in milk lipid peroxidation. J Dairy Sci 60:363–369, 1977.
88. G Bruder, H Heid, E-D Jorasch, TW Keenan, IH Mather. Characteristics of membrane-bound and soluble forms of xanthine oxidase from milk and endothelial cells of capillaries. Biochim Biophys Acta 701:357–369, 1982.
89. JL Weihrauch. In: NP Wong, R Jenness, M Keeney, EH Marth, eds. Fundamentals of Dairy Chemistry. New York: Van Nostrand Reinhold, 1988, pp 244–245.
90. PF Fox, MB Grufferty. Exogenous enzymes in dairy technology. In: PF Fox, ed. Food Enzymology, Vol 1. London: Elsevier Science Publishers, 1991, pp 219–270.
91. CL Hicks. Occurrence and consequence of superoxide dismutase in milk products: a review. J Dairy Sci 63:1199–1204, 1980.
92. G Yao, G Chen, J Fu. Technique for brewing beer containing SOD, hedgehog polysaccharide and theaflavin. Patent CH1145404, 1987.
93. HD Chu, JG Leeder, SG Gilbert. Immobilized catalase reactor for use in peroxide sterilization of dairy products. J Food Sci 40:641–643, 1975.
94. TE Mathiasen. Laccase and beer storage. Patent WO9521240, 1994.
95. BR Petersen, TE Mathiasen. Deoxygenation of a food item using a laccase. Patent WO9631133, 1995.
96. G Ritter, H Dietrich. The influence of modern processing techniques on the content of important plant phenols in apple juice. Fluss Obst 63:256–263, 1996.
97. GJC Bauw, MW Davey, J Ostergaard, MCE van Montagu. Production of ascorbic acid in plants. Patent WOg850558, 1998.
98. Y Suwa, T Kobayashi, N Kiyota, S Komatsubara, H Yoshizumi. Agent for inactivating the mutagenicity of coffee. Patent EP128333, 1984.
99. C Saito, H Senda, Y Yokoo. Reduction of cholesterol level by enzyme producing bacteria. Patent WO9325702, 1993.
100. DC Beitz, JW Young, SS Dehal. Plant cholesterol reductase to convert cholesterol in foods of animal origin. Patent US4921710, 1990.
101. C Aitoh, H Kumazawa, K Aisaka, T Mizakami, R Katsumata, K Ando, K Chiai, K Ouchi. Process for preparing a cholesterol-lowering compound. Patent WO9820150, 1998.

14

Transgenic Plants for Production of Enzymes

Anne S. Ponstein
Syngenta Mogen, Leiden, The Netherlands

Rob F. Beudeker
DSM Food Specialties, Delft, The Netherlands

Jan Pen
PlantZyme, Leiden, The Netherlands

I. INTRODUCTION

In terms of cost-effectiveness, plants can compete with any other production system. All that is required is a suitable plant, sunlight, mineral salts from the soil or fertilizers, and water. The overall costs of production in plants is largely determined by the existing and very efficient infrastructure and facilities in agriculture for growing, harvesting, storing, and processing of crops. Furthermore, traditional breeding has resulted in plant varieties optimized for a high yield of harvestable produce (1). Crops grown in the field can yield bulk quantities of biomass. Millions of tons of carbohydrates, lipids, and proteins for the food, feed, or processing industries are produced annually from the harvested biomass.

Biotechnology enables us to produce compounds of commercial interest in domesticated crops that were previously available only from exotic plant species, from other organisms or in limited quantities. Transgenic plants are an attractive and cost-effective alternative for the production of these biomolecules, as demonstrated by the steadily increasing number of carbohydrates (2), fatty acids (2), high-value pharmaceutical (poly)peptides (2–4), industrial enzymes (2–38), and biodegradable plastics (2) successfully produced in plants using this ''molecular farming'' approach.

Plants are gradually earning their place among other systems for production of proteins and peptides. Although research focused initially on the production of high-value pharmaceutical (poly)peptides (2), plants are equally suited as a competitive source of nonpharmaceutical enzymes (2–38). The activity and interest in this area are clearly increasing as demonstrated by existing collaborations between small plant biotechnology boutique and established enzyme or agrochemical companies, such as between Prodigene and Genencor, Sembiosys and Dow Agrosciences, Zeneca MOGEN (formerly MOGEN International) and DSM Food Specialties (formerly Gist-brocades), Agracetus (now part of Monsanto), and FinnFeeds (part of Cultor; Cultor was recently acquired by Danisco).

This chapter will summarize the method to generate transgenic plants, give an overview on what has been achieved in this area, compare plants with other methods of enzyme production, describe unique application methods for enzymes produced in plants, and finally present an illustrative example of an enzyme, phytase, applied in animal feed.

II. GENERATION OF TRANSGENIC PLANTS EXPRESSING ENZYMES

A. Transformation and Regeneration of Plants

In general, expression of (poly)peptides relies on stable integration of the encoding genes in the plant genome. An advantage of this approach is that identical offspring can be obtained by self-fertilization of the transgenic crops and consequently the stable inheritance of the trait. An alternative is production by transient expression in plants via genetically engineered viruses as CaMV (39), TMV (40–42), or CPMV (43–45).

Stable integration of genes generally consists of three phases: (a) introduction of foreign DNA into tissue amenable to transformation by methods as PEG-mediated transformation, particle bombardment, Whiskers, and *Agrobacterium tumefaciens*-mediated transformation; (b) selection of transformed material in the nontransgenic background by either selecting for tolerance to antibiotics, herbicides or another toxic chemical and/or by screening for expression of visual markers like luciferase, anthocyanin and GFP; (c) regeneration of shoots and roots after the successful selection of transgenic cells. This last phase may be quite cumbersome as cells amenable to transformation (competent cells) may not have the ability to regenerate.

Transformation of plants has developed over the last decades into a routine procedure for many crop species, including tobacco, tomato, potato, canola, soybean, alfalfa, sugar beet, lettuce, carrot, cotton, apple, rubber, rice, corn, wheat, and banana. Preference for *Agrobacterium tumefaciens*–mediated transformation exists as this generally leads to precise integration of only a limited number of copies of the gene of interest into the plant genome. However, cereals have appeared very recalcitrant to this method. Hence, the extensive use in the past of particle bombardment. With the recent development of a commercial transformation procedure for rice and the initial successes with the method in corn, wheat, and barley, it is likely that *Agrobacterium tumefaciens* will become the general vehicle for DNA delivery into plant species.

B. Expression of Enzymes in Plants

Even when using an identical expression cassette, the expression levels obtained in plants will differ from gene to gene (7, 28, 46), just as in other production systems. However, some general principles apply to achieve high-level expression of proteins in plants, like the use of promoters, enhancers, leader sequences, optimizations in codon usage, removal of mRNA-destabilizing sequences, etc. Other methods to increase the levels of heterologous proteins in plants can be found in the use of, e.g., integration-independent expression, enhancement of correct folding by coexpression of disulfide isomerases or chaperone proteins and production of polyproteins for stabilization of especially small peptides. Reduction of protein degradation by, e.g., expression in tissues, as seeds, where the level of protease inhibitors is high, by expression in tissues where the activity of the degrading enzymes is low as in seeds owing to the low water content, by targeting the enzyme to the ER or by avoiding the presence of susceptible protease-cleavage sites in the enzyme will also result in an increase of the expressed enzyme.

A unique aspect of expression in higher eukaryotes is the choice in the species, variety, and the location and timing for expression. Firstly, there is a choice in the plant species to be used for expression. A choice no longer severely limited by transformation technology (see above). If the protein content of a crop (tissue) would correlate with the accumulation of the transgene protein, crops with higher protein contents would be more cost-effective for production. However, as far as we are aware, no proof is available that this is indeed the case. Moreover, the argument may be turned around—i.e., crops that are already accumulating high levels of endogenous protein may have little capacity left for the accumulation of heterologous protein. Secondly, there may even appear to be differences among varieties of one and the same species. It is well known that different germplasms differ in agronomic characteristics as yield, disease resistance, etc. It would therefore not be surprising if they would also differ in their ability to accumulate heterologous proteins. Thirdly, the enzyme can be expressed in various organs or tissues using appropriate promoters. Fourthly, expression in the plant, tissues, or organs can be limited to certain periods of development using promoters active only during these stages. Finally, the enzyme can be targeted to specific cellular compartments as the vacuoles, the protein bodies (in seed), the chloroplasts, the mitochondria, and the ER or to the apoplast using appropriate targeting signals described in the literature (47).

Expression by integration in the plastid genome is another way to express enzymes. This can lead to dramatic increases in expression levels as demonstrated by the expression of β-glucuronidase (GUS) that accumulated to 2.5–30% of total soluble protein (20).

Combination of all these possibilities gives an almost unlimited choice. As these cellular compartments differ with regard to pH, ionic strength, and other environmental factors, these choices in fact allow the choice for a location within a plant species or a variety where active enzyme can be accumulated to the highest possible level.

No study describing the application of a range of these possibilities for enhancing the expression level has been published; there are still ample opportunities for optimization. Step increases in expression of proteins in plants can be expected, as was the case with microbial systems in their early stages of use. Competing systems are much more mature and improvements in expression levels will therefore be much more modest for the latter expression system. The fact that in its present state plants can already be competitive shows that they should have a bright future as hosts for enzyme production.

C. Downstream Processing

If purification is mandatory (which is not always the case, as shown below), rapid and economical downstream processing of the recombinant protein is essential. The benefits of the plant-based production should not be offset by increased downstream processing costs. Any decrease in these costs will increase the competitive advantage of plants. The economic feasibility of protein purification from plant biomass has not been investigated in any detail, and if at all, mainly on a lab scale, except for Austin et al. (6), who focus on extraction and purification of industrial enzymes from alfalfa; by van Rooijen et al. (48; see below), Wilcox et al. (27), who purified bovine lysozyme from transgenic tobacco to 93% homogeneity in an easily scalable process; and by Kusnadi et al. (49), who described purification of GUS and avidin from transgenic corn. Downstream processing from plant biomass is generally assumed to be difficult and expensive. One reason for this assumption is the low ratio of recombinant protein to total biomass. Concentration and purification of the protein in the first step would reduce this assumed disadvantage considerably. As only few studies have been published, no final verdict is available regarding the cost of downstream processing. With step increases in expression level still feasible (see above), the economics of production will improve. In turn this will make it easier to use plants for production, even in cases where costly purification is mandatory.

D. Exploitation of Plant Characteristics

Various production systems have been developed that are based on specific plant characteristics, on the use of plant regulatory DNA sequences, or on the exploitation of existing plant processing systems.

Prodigene (College Station, TX) used a ubiquitin promoter that preferentially directs expression of proteins to the germ portion of corn seeds. The crude protein is present in the waste fraction of the corn wet-milling process, and thus essentially produced free of charge in that process. The only costs involved in production are downstream costs for extraction and purification of the protein. A comparison of the costs for production in the germ versus the whole seed is given by Howard (50). Similarly, starch or oil crops may be interesting as hosts for production, because the enzymes may be produced as byproducts in addition to the primary product (starch or oil), thus reducing the production costs.

A very ingenious way to reduce these downstream costs was found in the use of plant seed oil bodies as carriers for proteins and peptides (48). Nonplant (poly)peptides were fused to the structural oil body protein oleosin and expressed in *Brassica napus*. The lipophilic nature of oleosins forms the basis for a highly efficient purification system for (poly)peptides. The feasibility of this approach has been demonstrated with β-glucuronidase (GUS; 19, 48) and as a first commercial example the expression and purification of the thrombin inhibitor hirudin (51). Alternatively, this system may be used to immobilize industrial enzymes as oleosin fusion proteins on the surface of oil bodies (19).

Expression during germination of seeds, using germination-specific promoters, has the advantage that a well-established process, available equipment, and factories of malt production for, e.g., the brewing industry can be used. An additional regulatory advantage is obtained, because the actual expression takes place in a contained environment; i.e., seeds are allowed to germinate in a malting factory (52, 53).

Using wound-inducible HMG2-derived promoters, expression can be effected postharvest by mechanical wounding of the leaves. An advantage is that growth of the plants is separated from the expression of the protein, which allows expression of proteins that would normally have a detrimental effect on the plant during growth or development. As the proteins are expressed in a contained environment postharvest, this approach could have regulatory advantages as well (54).

An elegant way to produce and harvest proteins is described by Boffey et al. (55). Proteins are expressed in the easily harvestable latex fraction of the rubber tree, constituting a continuous source of the protein. The relatively simple composition of the latex would allow easy purification of the protein from the tapped latex. A disadvantage may be the long generation time and consequently the long time to develop this into a commercially operating system.

Extracellular expression of proteins in the roots of hydroponically grown tobacco plants, termed rhizosecretion, is yet another way to optimize expression, as well as to facilitate purification (37).

III. ENZYMES PRODUCED IN PLANTS

A substantial number of enzymes have meanwhile been produced in plants (see Table 1) (2–38). Expression of an enzyme in the vicinity of its potential substrate does not necessarily have a negative effect on the agronomic characteristics of the plant. Endogenous cell wall degrading enzymes like glucanases, polygalacturonases, and pectin esterases are present at the same location as their substrates without a detrimental effect on the plant. Also, extracellular expression of a vacuolar glucanase—i.e., an enzyme that normally does not have access to the glucan substrate—did not result in abberations in growth or morphology (56). Xylanase can be expressed in tobacco or *Pisum sativum* without an effect on plant phenotype (9, 16, 35). In one publication (35), the authors suggest that the high temperature optimum of the enzyme prevents substantial degradation at ambient temperatures. As the enzyme exhibits considerable residual activity at this temperature, a more likely explanation may be that, for unknown reasons, the apoplastically expressed enzyme does not, or does only to a very limited degree, degrade the xylans in the plant cell wall.

Active β(1-3,1-4)glucanases can be expressed in tobacco without phenotypic alterations despite their apoplastic location (16). A thermostable β(1-3,1-4)glucanase, consisting of parts from two *Bacillus* spp. expressed in barley aleurone protoplasts and in transgenic barley under control of the germination-specific high-pI barley α-amylase promoter yielded fertile plants (17). In contrast, no viable transgenic tobacco plants could be obtained after transformation with a endo-β(1-4)glucanase gene construct. This was most likely due to degradation of cell wall β-glucans, because transient expression in tobacco protoplasts showed that cell wall synthesis was never resumed (14). A cellulase from *Thermomonospora fusca* was expressed in alfalfa, tobacco, wheat, and maize (10, 11). In one of these studies (11), the gene was put under the control of a chemically inducible promoter to prevent detrimental effects of the cellulase. Production of manganese-dependent lignin peroxidase in alfalfa severely affected plant growth and development. Affected plants showed yellowing foliage. However, they survived and set seed. In field trials the dry matter content was reduced, as was the plant height. The enzyme was most likely directed to the ER (6, 8).

GUS (β-glucuronidase) is used in molecular biological experiments as a reporter for visualizing gene expression in plants. GUS, produced in transgenic corn seed and rapeseed (18–20), is the first enzyme produced in plants that is commercially available from Sigma. The enzyme is produced by Prodigene (College Station, TX). Sigma is also selling another protein, avidin, produced by Prodigene in corn (57). Alcohol and aldehyde dehydrogenases produced in corn (5) can find application in prevention of alcohol toxicity when taken before social drinking. They should be formulated with NAD to ascertain activity in a pill, paste, or foodstuff.

Although cyclodextrin glycosyl transferase (CGTase) was produced in potato tubers for the in planta production of cyclodextrins (13), these transgenic plants could find application as a source of the enzyme as well, provided the enzyme levels can be increased considerably. Hen egg white and bovine and T-4 bacteriophage lysozymes have been expressed in tobacco (24–27). This research was partially driven by the desire to create plants resistant to bacterial pathogens. However, lysozymes produced in this way can find application as preservative in food, feed, cosmetics, and agriculture.

Other enzymes expressed in plants include lipase (22, 23), β-galactosidase (21), α-amylase (3, 6–9), β-amylase (38), and phytase (28–34 this chapter).

IV. COMPARISON OF HOSTS FOR ENZYME PRODUCTION

Bacterial and fungal cells selected for high-level expression have traditionally been used for production of industrial enzymes (58). Extraction from these nonrecombinant sources will, for some enzymes, remain the preferred method of production. For the production of commercially interesting proteins, with the use of recombinant DNA techniques, various host organisms

Table 1 Plants as Bioreactors for the Production of Enzymes

Enzyme	Origin of gene(s)	Application	Plant species	Ref
Alcohol dehydrogenase	Human	Prevention alcohol toxicity	Corn	5
Aldehyde dehydrogenase	Human	Prevention alcohol toxicity	Corn	5
Alpha-amylase	*Bacillus licheniformis*	Liquefaction of starch	Tobacco, alfalfa, *Vicia narbonensis, Pisum sativum*	3, 6–9
Beta-amylase	Barley	Brewing	Barley	38
Cellulase	*Thermomonospora fusca*	Ethanol production, paper and pulp	Alfalfa, tobacco, corn, wheat	10, 11
Chymosin	Calf	Dairy industry	Tobacco, potato	12
Cyclodextrin glycosyltransferase (CGTase)	*Klebsiella pneumoniae*	Production cyclodextrins	Potato	13
Glucanase	*Trichodema reesei*, Hybrid from two *Bacillus* spp., *Ruminococcus flavefaciens*	Brewery, feed	Barley cells	14–17
GUS (β-glucuronidase)	*Escherichia coli*	Molecular biology tool	Corn, canola	18–20
Lactase (β-galactosidase)	*Escherichia coli*	Lactose intolerance	Maize, sunflower	21
Lipase	Dog gastric preduodenal, *Rhizopus niveus*	Food, medical, fatty acid production	Tobacco, corn, canola, tomato	22, 23
Lysozyme	Hen egg white, bovine, bacteriophage T4	Food preservation	Tobacco, potato	24–27
Manganese-dependent lignin peroxidase	*Phanerochaete chrysosporium*	Bleaching and pulping of paper	Alfalfa	6, 8
Phytase	*Aspergillus niger*	Feed	Alfalfa, tobacco, canola, soybean, soybean cell suspension cultures, wheat	28–34
Xylanase	*Clostridium thermocellum, Cryptococcus albidus, Ruminococcus flavefaciens*	Feed, brewing, paper and pulp, bakery	Tobacco, *Pisum sativum*	9, 16, 35–37

are currently used: bacteria (in particular *Escherichia coli* and *Bacillus subtilis*), filamentous fungi, yeast, mammalian cells (in particular Chinese hamster ovary [CHO] cells), insect cells, transgenic animals and transgenic plants, as well as a number of other organisms that are less important. The first tier of biotechnology companies have mainly used filamentous fungi, yeast, and bacteria for production of enzymes.

Well-known industrial problems in developing systems for the production of heterologous proteins included instability and insolubility of the product, disappointing production rates, instability of selected cell lines, difficulties in scaling up, purification of the recombinant product, and complicated registration procedures (59). A specific problem for industrial enzymes is the production costs, because of the small margins on these products. Economic factors influencing the choice of production system are the rate of biomass production, equipment costs, medium composition and costs, processes for protein recovery and purification, product yields, and the potential hazard of contamination. A lot of development work is driven by the intended commercial application and by regulations set by the FDA and other organizations.

A suitable host for production is selected based on its ability to fulfill all the technical and economic requirements set by the protein of interest and its application. The production of proteins, by whatever system, remains an empirical process, making it impossible to predict the expression level. Such predictability may come with an increase in understanding of the molecular biology, biochemistry, and physiology of the expression systems and of the expressed proteins. Because expression in each organism is gene dependent, and this dependency differs from organism to organism, some proteins will express well in one system and not well in another. This argues strongly for the availability of a multitude of production systems, each having its own (dis)advantages. Plants will earn their place among these systems. A comparison of different hosts for production of enzymes is given in Table 2 (60).

V. UNIQUE APPLICATION METHODS FOR ENZYMES PRODUCED IN PLANTS

The feasibility of different methods for application of enzymes produced in plants as described below can be nicely demonstrated with α-amylase from *Bacillus licheniformis* expressed in tobacco (7). Alpha-amylases from bacterial and fungal origins find wide application in e.g. the starch processing and alcohol industry for liquefaction, in the brewing industry for production of low-calorie beer, in bakery for increasing bread volume, in the juice and wine industries for clarification and in the detergent industry for removal of starch stains (61–64). The α-amylase from *B. licheniformis* is the most commonly used enzyme in starch liquefaction, because of its extreme heat stability and its activity over a wide pH range (61, 65).

A. Production and Purification from Plants (Fig. 1a)

Bacillus licheniformis α-amylase was expressed extracellularly in tobacco at a level of maximally 0.5% of soluble protein in leaves (7, 66). The properties of the enzyme as produced in tobacco were very similar to the bacterial one. However, the protein is, in obvious contrast with the bacterial protein, glycosylated. The enzyme produced in tobacco was active and exhibited extreme thermostability, similar to the *Bacillus* enzyme. No apparent effect of the presence of the enzyme on plant phenotype was observed. Purification from tobacco has not yet been carried out for bacterial α-amylase.

B. Process-Dependent Conversion (Fig. 1b)

Enzymes produced in crops can be expressed at a sequestered location in the crop that also harbors its substrate. Alternatively, the enzyme may be expressed at the same location as the substrate, but in an active form. The conversion thus becomes process dependent. During processing of the crop, enzyme and substrate are brought into contact (or the enzyme is activated), resulting in conversion of the substrate into product. In this approach, the plant becomes equipped with the enzyme having optimal characteristics for conversion of its endogenous substrate. In planta conversion of the substrate into the desired product (Fig. 1d), by expression of active enzyme at the same location as the substrate, will have similar advantages as process-dependent conversion, but will not be suitable if the enzymatic activity has a negative effect on the plant's phenotype or its agronomic characteristics. The feasibility of this concept is exemplified by extracellular expression of α-amylase. Extracellular expression of α-amylase does not have an effect on endogenous starch, as is expected from the separated locations of enzyme and substrate. Moreover, the transgenic plants do not show any abberations in their phenotype.

Table 2 Qualitative Comparison of Hosts for Production of Industrial Enzymes

	Transgenic plants	Transgenic animals	CHO cells	Insect cells	Fungi	Yeast	Bacteria
Research and development							
Development time	Intermediate	Long	Intermediate	Intermediate	Short	Short	Short
Feasibility improvements (state of the art)	Very high	High	Limited	Intermediate	Limited	Limited	Limited
Process characteristics							
Reproducibility production	++	++	+++	+++	+++	+++	+++
Downstream processing costs	?	++	++	++	++	++	+++
Logistics							
Crude nonformulated product:	Seed	Milk	Medium	Medium	Medium	Medium	Medium
Stability	+++	±	±	±	±	±	±
Storage period	Indefinite	Limited	Limited	Limited	Limited	Limited	Limited
Upscaling time	Fast	Fast	Intermediate	Intermediate	Intermediate	Intermediate	Intermediate
Upscaling cost (capital costs)	Low	Intermediate	High	High	High	High	High
Production volume	Unlimited	Unlimited	Limited	Limited	Limited	Limited	Limited
Product characteristics—Authenticity							
Glycosylation	Yes	Yes	Yes	Yes	Yes	Yes	No
High-mannose	Yes	Yes	Yes	Yes	Yes	Yes	No
Complex	Yes	Yes	Yes	Yes/No	No	No	No
"Human"	No	Yes	Yes	No	No	No	No
Other modifications	++	+++	+++	+++	+	+	–
Folding capabilities	+++	+++	+++	+++	+++	++	–
Safety, regulations, and public acceptance							
Food use	+++	+++	–	–	+++	+++	–
Containment level	+	++	+++	+++	+++	+++	+++
Presence mammalian pathogens	–	++	++	–	–	–	–
Public acceptance level	+	±	++	++	++	++	++

Source: Ref. 60.
Key: –: absent; ±: very low or doubtful; +: low; ++: intermediate; +++: high

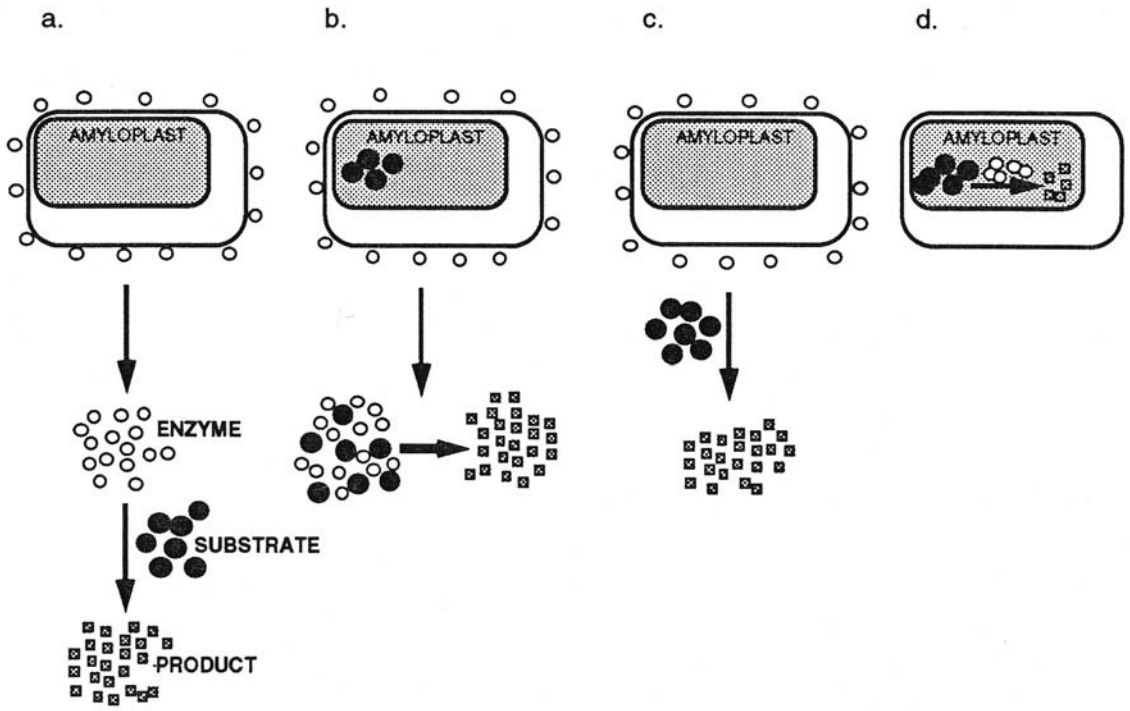

Figure 1 Application methods of industrial enzymes produced in transgenic crops. (a) Production and purification: The enzyme is purified from the plant, formulated and subsequently applied in the industrial process. (b) Process-dependent conversion; Expression of the enzyme in the crop sequestered from its substrate. Conversion of the substrate occurs during processing. (c) Seed-formulated enzymes: The transgenic seeds are directly, without any purification of the enzyme, applied in the industrial process. (d) In planta conversion: Expression of the enzyme in planta at the same location as its substrate results in conversion of the substrate and consequently accumulation of product in planta.

Homogenization of transgenic leaf material, followed by incubation at 95°C, resulted in conversion of endogenous starch by the transgene product (Table 3). In starch potatoes, the α-amylase levels as obtained in tobacco (7, 66) would be sufficient to hydrolyze all the starch present in the tuber. Similar applications for α-amylase and other enzymes may be found in other industrial processes, like for instance the application of α-amylase in the production of bioethanol, heat-stable β-glucanases for the degradation of cell wall material in the brewing industry, and the production of fatty acids in oil plants (23).

In this approach the aim is *not* producing enzymes in crops per se, but creating either a higher-quality input resource or an enabling process through expression of the enzyme inside the plant. This application has unique advantages. Firstly, enzyme manufacturing costs will be low, because there is no need for purification and formulation of the enzymes. Secondly, it obviates the necessity for separate production of enzymes. Thirdly, expression in the vicinity of the substrate assures better access to its substrate than is achieved by in vitro addition of the enzyme. In some cases as wood pulping, in vitro addition has limited success because the enzymes do not have sufficient access to the substrate. Finally, expression in the crop guarantees an optimal dispersion of the enzyme throughout the biomass; *i.e.*, an optimal homogeneous mixture of enzyme and substrate is obtained. This is less easily achieved by in vitro addition of enzymes.

C. Seed-Formulated Enzymes (Fig. 1c)

Another concept for application is the direct use of engineering plant material in the processing, food, or feed industry. The transgenic plant material serves as novel formulation for the expressed enzyme. Other plant material can be used, depending on the process, but in general seeds may be the plant organ of choice, because these create a stable environment for long-term storage of the enzymes. The potential of plants as production vehicles for enzymes is enormously increased by producing the enzyme in seeds and directly applying these in the industrial process.

Table 3 Process-Dependent Conversion of Leaf Starch by Expressed α-Amylase

Sample	Incubation time (min)		
	0	30	60
Control tobacco	+	+	+
Control tobacco + 0.02 T.A.U. *B. licheniformis* α-amylase/mg	+	+/−	+/−
Control tobacco + 0.2 T.A.U. *B. licheniformis* α-amylase/mg	+	+/−	−
Control tobacco + 2 T.A.U. *B. licheniformis*α-amylase/mg	+	−	−
Transgenic tobacco line MOG227.3	+	−	−

Homogenization of transgenic leaf material containing *Bacillus licheniformis* α-amylase, followed by incubation at 95°C for 30 min hydrolyzed starch present in the leaves. Addition of 2 T.A.U./mg *Bacillus licheniformis* α-amylase to the nontransgenic control leaf homogenate for 30 min or of 0.2 T.A.U./mg for 60 min had the same effect, while incubation of nontransgenic control leaf homogenate had no visible effect on the endogenous starch during the time of the experiment. The presence of starch, as demonstrated by I_2/KI-staining is indicated with +, intermediate staining with +/− and absence with −.

Compared with the production followed by purification, this concept has additional advantages over traditional production systems. Firstly, the formulation of the enzyme as obtained by genetic engineering of the crop is convenient; *i.e.*, it does not require an extra step in the manufacturing process, and it guarantees stable and safe storage of the enzyme. No allergenic problems due to the enzymes are to be expected, because these are contained in the seeds. Secondly, the manufacturing costs will be lower, because purification and formulation of the enzyme are no longer required. This concept is most easily applied in, but certainly not limited to, cases where enzymes are required for application in (processed) food or feed. The enzyme can then be expressed in the plants and plant organs that are the natural component in this animal feed and food. The transgenic plant material containing the enzyme is used as delivery vehicle for the protein with the same advantages as described above.

The transgenic seeds are a novel specialty enzyme product to be added in small quantities into the industrial process, provided the expression level is sufficiently high (“additive route”). This creates flexibility, because various enzymes can be engineered into plants in the same manner and used and combined according to the needs of the user. The total premium for production, transportation, etc., of transgenic plant material will be lower than in case the transgene is built into the commodity crop. Production, transportation, and marketing can be strictly and simply controlled, preventing the mingling of transgenic with nontransgenic seeds. Alternatively, the enzyme can be expressed at low levels in all (or a large part of the) seeds used in the application (“bulk route”). A comparison between these two approaches in various aspects is given in Table 4.

This enzymes-in-seed approach is exemplified by the direct application of milled transgenic α-amylase seeds in liquefaction of corn and potato starch (Fig. 2). Seeds of a transgenic plant line were milled and used without any further purification in the liquefaction of potato and corn starch. From the nature and the quality of the hydrolysis products obtained from corn and potato starch with the transgenic seeds it can be concluded that the enzyme as produced in tobacco is as suited for liquefaction of starch as the *Bacillus licheniformis* amylase. As shown in Table 5, the dextrose equivalent (DE) values, which were calculated from the HPLC patterns, were found to be similar to those obtained with the commercial preparations and within the commercially acceptable range (DE-12, preferably DE16; 67). Seeds containing α-amylase maintained full enzyme stability for at least a year. When seeds are the only organs used, seed-specific expression is preferred, because it will minimize the chance of effects on agronomic characteristics.

Table 4 Comparison of Bulk and Additive Application of Enzymes in Seed

	Additive	Bulk
Expression level	High	Low
Research costs	Medium	Low
Amount of plant material	Low	High
Importance host	Low	High
Agronomic performance	Less critical	Critical
Development costs	Low	High
IP production	+	?
Level of control	High	Low
Maintenance added value	High	Low

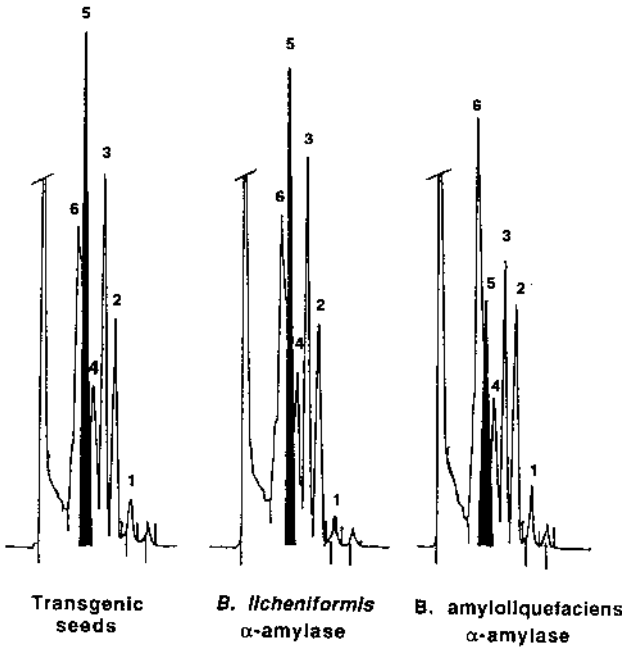

Figure 2 Liquefaction of potato and corn starch. Oligosaccharide HPLC patterns obtained from hydrolysis of corn starch by milled transgenic seeds of plant line MOG227.3 expressing α-amylase (left), *Bacillus licheniformis* α-amylase (middle), or *Bacillus amyloliquefaciens* α-amylase (right). The degree of polymerization (DP) of glucose is indicated by the numbers. The products obtained with the transgenic seeds and with *Bacillus licheniformis* amylase are virtually identical and clearly different from those obtained with *B. amyloliquefaciens* amylase. The main difference distinguishing the two specificities is the amount of DP5 (indicated in black).

Plants will often still be a competitive source, because of the low-cost production of biomass. The novel concepts of seed-formulated enzymes and process-dependent conversion will find application in various markets. For process-dependent conversion the increased access to the substrate will for some industrial processes create the required competitive advantage. For seed-formulated enzymes, application will depend on the compatibility of the seeds with the industrial process. A first commercial example of the latter concept is described below.

VI. AN EXAMPLE: PHYTASEED

A. Feed Enzymes

In livestock farming of pigs and poultry, the supplementation of animal feed with industrial enzymes to improve digestibility and utilization of nutrients has become common practice. Examples are industrial enzymes such as β-glucanase and endoxylanase which are added to diets containing high contents of barley, triticale, and wheat to improve growth, quality of eggs, and feed conversion ratio in poultry (68). Favorable effects of the inclusion of these enzymes in the diets of pigs have been reported as well. Another example is the enzyme phytase which is used to optimize phosphorus utilization in monogastric animals such as pigs, fish, and poultry.

Table 5 Dextrose Equivalent (DE) Values Obtained from Hydrolysis of Corn and Potato Starch

DE values	Potato starch	Corn starch
Transgenic tobacco seeds (MOG227.3)	16	13
Nontransgenic tobacco seeds	0	0
Bacillus licheniformis amylase	18	16
Bacillus amyloliquefaciens amylase	15	18

B. Phytase

Phytases (myoinositol hexakisphosphate phosphohydrolase, EC 3.1.3.8) are widely distributed in all classes of organisms. The enzyme catalyzes the conversion of phytate into myoinositol and phosphorus. The substrate of this reaction, phytate, is a salt of phytic acid and divalent cations of calcium, magnesium, iron, or zinc. In plant seeds up to 80% of the total phosphorus has been reported to be present in the form of phytate (69). During the germination process phytate is rapidly converted into myoinositol and phosphorus for growth and development of the seedlings.

Seeds of crops like wheat, corn, soybean, and barley are used in large amounts in animal feed. The amount of phosphorus present in these seeds would be more than sufficient to meet the animal's requirements for optimal growth. However, monogastric animals, such as pigs and chickens, are only able to use a small portion of the phosphorus present in these seeds, because the remaining part is present in the form of phytate. These animals cannot convert phytate into myoinositol and inorganic phosphate. Therefore, inorganic feed phosphate has to be added to feed. As a consequence the manure of the animals contains a huge amount of phosphate, which, released into the environment, causes pollution through eutrophication of surface waters. In many countries, especially those with inten-

sive livestock farming, there is a strong tendency to reduce the amount of phosphate. For example, in the Netherlands, farmers are taxed based on the amount of phosphate released into the environment. In Singapore, pig production is banned because of the related environmental problem. The amount of manure secreted into the environment is enormous. Even in as small a country as the Netherlands, 215 million kg of phosphate (P_2O_5) from animal manure is added to the soil per year.

Application of the enzyme phytase will optimize phosphorus utilization by pigs and poultry (70–74). Feed phosphate can be substituted by the enzyme phytase, thus reducing the environmental problems caused by phosphate considerably.

The phytase gene has been cloned successfully from *A. niger* var. van Tieghem (75, 76). The enzyme is produced on an industrial scale by means of fermentation of *A. niger*. The phytase gene is overexpressed by placing the gene under control of the *A. niger* amyloglucosidase promoter. Phytase is secreted as a large percentage of total protein by this filamentous fungus during growth in a fermenter. After fermentation, the enzyme is separated from the broth through a series of filtration steps. The final ultrafiltrate is either stabilized and sold as a liquid product or dried and formulated to a free-flowing product. The unique pH optima at 2 and 5.5 allow application of the enzyme in feed for monogastric animals because of the optimal compatibility with the environment in the gastrointestinal tract of these animals and the crop of poultry. The microbial phytase from *Aspergillus niger* is marketed by the alliance of DSM Food Specialties (former Gist-brocades) and BASF under the brand name Natuphos for use in animal feed.

C. Expression of Phytase in Tobacco

By expressing the phytase gene in plants instead of in *A. niger*, we are substituting an existing production process by a novel and innovative way of producing industrial enzymes. To demonstrate this concept, tobacco was transformed with a gene construct (28), encoding phytase from *Aspergillus niger* (75). The construct contains a DNA sequence encoding the tobacco PR-S signal peptide that will give export of the enzyme to the extracellular space (77). The cauliflower mosaic virus (CaMV) 35S promoter (78) was used that gives expression of phytase in all parts of the plants.

A total of 72 independent transgenic tobacco plants were analyzed for phytase expression in leaves and seeds. The highest expression level, measured 3 weeks after transfer of the plants to the greenhouse, was 1.7% of total soluble protein in leaves and 1% of total soluble protein in seeds. In leaves, phytase accumulated during further maturation of the plants up to a maximum level of 14.4% of soluble protein ~ 7 weeks after transfer to the greenhouse, showing the extreme stability of phytase in the extracellular space of leaves (33).

The molecular mass of tobacco-derived phytase from leaves was ~ 70 kDa and from seeds ~ 68 kDa, compared to ~ 80 kDa for the *Aspergillus* enzyme. The difference in molecular weight between phytase expressed in seeds and leaves and between plant-derived and *Aspergillus phytase* was found to be caused by differences in glycosylation, which was not unexpected because a total of 10 potential asparagine-linked sites are present in the primary structure and the *Aspergillus niger* enzyme is known to be heavily glycosylated (75). Deglycosylation experiments showed that both leaf- and seed-derived phytase contain high-mannose, as well as complex-type, carbohydrate chains. Tissue-dependent differential glycosylation of proteins, as found here for seeds and leaves, has been described before (79). Despite the differences in glycosylation, the specific activity of purified leaf-derived phytase was found to be identical with that of the purified *Aspergillus niger* enzyme.

D. PhytaSeed®

For the development of a commercially viable product, the fact that plants and plant organs are natural components of animal feed was fully exploited. PhytaSeed, the enzyme formulated by genetic engineering in canola seed, is used directly without any other post-harvest treatment than milling. In other words, the seeds are used as the packaging material and the delivery vehicle for the protein.

Aspergillus niger phytase was expressed extracellularly under control of the seed-specific cruciferin promoter in canola (*Brassica napus* cv. Westar) seeds. Canola is commonly used in animal feed, albeit in low amounts. Therefore, transgenic phytase-containing canola seeds can be simply incorporated. Transformation of canola is simple and routine, so many independent transgenic lines can be obtained. As PhytaSeed, canola seeds containing phytase, is envisioned to be marketed as an enzyme product, and since expression levels are high (see below), there is no need to incorporate the enzyme in seeds of crops that are major constituents of animal feed like soybean, corn, wheat, or barley. Small amounts of canola seed containing sufficient enzyme for the conversion of the phy-

tate present in the feed mixture will be added. The nutritional value of the seeds will be a bonus to the enzyme formulation.

A total of 95 independent transgenic canola lines were generated and grown in the greenhouse, and mature seeds were tested for phytase activity. The average phytase expression level was found to be 0.85% of total soluble protein. The highest phytase expression level obtained was 9.3%, sufficient for further development into the commercial product PhytaSeed. The application experiments described below were carried out using transgenic tobacco seeds, but similar results (to be reported elsewhere) were obtained with PhytaSeed (80–82).

E. Application of Transgenic Seeds Containing Phytase

Phytase packaged in seeds by genetic engineering techniques was found to be extremely stable. Even milled seeds did not show loss of enzyme activity when stored at room temperature for a period of a year (Fig. 3). This characteristic, brought about by the stable seed environment, is commercially very important because it generates a reliable supply to customers, as a reduced seed yield in a particular year can be replenished with stored seeds from the previous year. Packaging of the enzyme in seeds also makes it more resistant to thermomechanical processing, as for example during feed pelleting (83). The effect of addition of milled transgenic seeds on the liberation of inorganic phosphate from phytate in animal fodder was tested by first incubating a standard poultry feed sample under conditions simulating chicken crop and stomach conditions. Milled transgenic seeds released inorganic phosphate from the fodder, whereas milled control seeds had no activity (Fig. 4). This experiment shows that phytase as produced in plant seeds has retained the essential characteristics to exert its activity in the gastrointestinal tract and crop of monogastrics animals.

The effect of transgenic seeds containing phytase on animal growth was tested in vivo by milling and subsequent addition to the basal diet of broilers. Diets supplemented with nontransgenic seeds and diets with and without added phosphate were used as controls. In addition, the commercial phytase preparation from *Aspergillus niger*, Natuphos, was used for comparison. Growth during the 4-week course of the experiment was used as a measure of the effect of each supplementation. Diets supplemented with transgenic seeds resulted in significantly higher growth rates

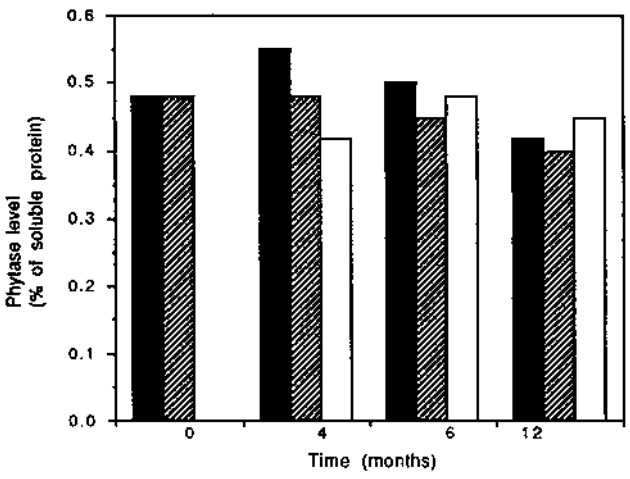

Figure 3 Stability of phytase packaged in tobacco seeds. Unmilled transgenic tobacco seeds (MOG 413.25) stored at 4°C (■) and room temperature (▨), and milled seeds stored at room temperature (□) were analyzed for phytase activity (vertical axis) at different time points during storage (horizontal axis). Milled transgenic seeds stored at 20°C were not analyzed at the first time point.

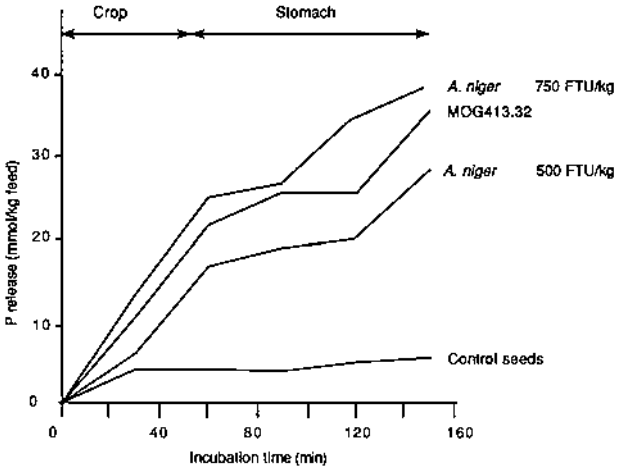

Figure 4 In vitro testing of transgenic phytase tobacco seeds under conditions simulating the digestive tract of poultry. Seeds containing phytase from a transgenic tobacco line (MOG 413.32) and from nontransgenic tobacco were used. For comparison, *Aspergillus* phytase was used in doses of 500 and 750 FTU/kg feed. During the incubation period samples were taken and analyzed for the amount of phosphate released.

than those with control seeds or without any addition (Fig. 5). Growth rates obtained with transgenic seeds were not significantly different from those obtained with *Aspergillus* phytase as a supplement or those with inorganic phosphate addition. This feeding experiment conclusively demonstrates that transgenic seeds containing phytase, added to animal feed without prior extraction of the enzymes, can compensate for the lower amount of inorganic phosphorus available to the animals.

F. Low-Phytate Mutants

Low-phytic acid mutants have been generated in several crop species such as corn and barley by Victor Raboy and coworkers (84). These mutants might be considered to become an alternative to the use of phytase for optimizing phosphorus utilization from feed components if the agronomic performance is unaltered. However, application of phytase in low-phytate corn-based diets still results in a marked improvement in the availability of phytate phosphorous from these diets in poultry. It seems likely that there is an opportunity for both technologies to reduce the phosphate contents in manure from monogastric animals.

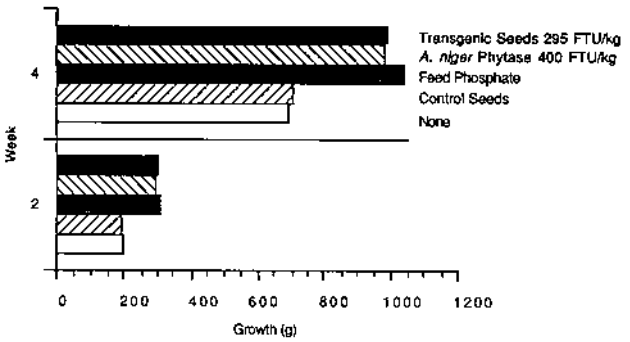

Figure 5 Effect of phytase-containing transgenic tobacco seeds on the growth of broilers. Milled transgenic seeds of line MOG413.25 was used in a concentration of 295 FTU/kg. As controls, diets supplemented with feed phosphate, nontransgenic seeds, and *A. niger* phytase (400 FTU/kg) were included. Growth was measured after 2, and 4 weeks. Growth observed for diets supplemented with *A. niger* phytase, feed phosphate, or transgenic seeds was not statistically different but better than for those with nontransgenic seeds or with no addition. This demonstrates that phytase-enriched seeds improve phosphorus utilization and can substitute for phosphate as a feed supplement.

G. Other Potential Benefits of PhytaSeed

In the processing industries, where seed and/or plant materials are used, seed-formulated enzymes may be simply incorporated in existing processes. Phytate present in corn kernels precipitates during the wet-milling process in the concentrated steep water. This causes problems in handling, transportation, and storing of the corn steep liquor. These problems may be avoided by using phytase during steeping. The addition of phytase also results in a reduction in steeping time and in an increase in starch yield (85). An efficient and elegant manner to achieve the same goal would be to package phytase in corn kernels by genetic engineering techniques.

The application of transgenic phytase seeds in food and feed may have other desirable effects. Phytate is considered to be a nutritional factor, because it chelates essential minerals like calcium, iron, and zinc, reducing their availability to monogastrics (71, 86). An increase in calcium availability by the application of microbial phytase has been demonstrated in pigs and poultry, and degradation of phytate in cereals has been shown to increase the availability of iron in vitro. Dietary addition of milled transgenic seeds containing phytase to feed or food will reduce the amount of phytate and consequently increase mineral absorption in animals as well as humans. This is especially important for infants and elderly people.

Phytate is well known to bind to proteins in general and to some digestive enzymes such as proteases and amylases in particular (87–89). Application of PhytaSeed may prevent the formation of phytate–protein complexes and thus improve digestion of feed and food.

VII. CONCLUSION

This example, as well as the other examples referred to, clearly demonstrate the advantages of using plants as a production system for enzymes. As many other applications can be envisioned, plants will certainly earn a prominent place among the various methods for producing enzymes.

REFERENCES

1. GC Whitelam, B Cockburn, AR Gandecha, MRL Owen. Heterologous protein production in transgenic plants. Biotechnol Genet Eng Rev 11:1–29, 1993.

2. OJM Goddijn, J Pen. Plants as bioreactors. Trends Biotechnol 13:379–387, 1995.
3. K Herbers, U Sonnewald. Production of new/modified proteins in transgenic plants. Curr Opin Biotechnol 10:163–168, 1999.
4. AR Kusnadi, ZL Nikolov, JA Howard. Production of recombinant proteins in transgenic plants: practical considerations. Biotechnol Bioeng 56:473–484, 1997.
5. S Hickmann, JD Loike, D Holzer. Mammalian alcohol dehydrogenase and aldehyde dehydrogenase production in plants. WO patent application 98/41616, 1998.
6. S Austin, ET Bingham, RG Koegel, DE Mathews, MN Shahan, RJ Straub, RR Burgess. An overview of a feasibility study for the production of industrial enzymes in transgenic alfalfa. Ann NY Acad Sci 721:234–244, 1999.
7. J Pen, L Molendijk, WJ Quax, PC Sijmons, AJJ van Ooyen, PJM van den Elzen, K Rietveld, A Hoekema. Production of active *Bacillus licheniformis* alpha-amylase in tobacco and its application in starch liquefaction. Bio/Technology 10:292–296, 1992.
8. S Austin, ET Bingham, DE Mathews, MN Shahan, J Will, RR Burgess. Production and field performance of transgenic alfalfa (*Medicago sativa* L.) expressing alpha-amylase and manganese-dependent lignin peroxidase. Euphytica 85:381–393, 1995.
9. L Saalbach, J Hofemeister, H Bäumlein. Plant seeds as bioreactors: use of a heat-stable, bacterial amylase in transgenic seeds of legumes for liquefaction of seed starch. In: Schriftenreihe des Bundesministeriums für Ernahrung, Landwirtschaft und Forsten. Reihe A, Angewandte Wissenschaft. Munster-Hiltrup: Landwirtschaftverlag GmbH, 1997, pp 182–184.
10. S Austin-Phillips, RR Burgess, TL German, T Ziegelhoffer. Transgenic plants as an alternative source of lignocellulosic-degrading enzymes. WO patent application 98/16651, 1998.
11. E Lebel, P Heifetz, E Ward, S Uknes. Transgenic plants expressing cellulolytic enzymes. WO patent application 98/11235, 1998.
12. L Willmitzer, U Sonnewald, M Roeber, SK Carlsen. Transgenic plants expressing industrial enzymes. Methods for commercial production and extraction of protein from seed. WO patent application 92/01042, 1992.
13. JV Oakes, CK Shewmaker, DM Stalker. Production of cyclodextrins, a novel carbohydrate, in the tubers of transgenic potato plants. Bio/Technology 9:982–986, 1991.
14. K Aspegren, L Mannonen, A Ritala, R Puupponen-Pimiä, U Kurtén, M Salmenkallio-Marttila, V Kauppinen, TH Teeri. Secretion of a heat-stable fungal β-glucanase form transgenic, suspension-cultured barley cells. Mol Breed 1:91–99, 1995.
15. BA Phillipson. Expression of a hybrid (1-3,1-4)-β-glucanase in barley protoplasts. Plant Sci 91:195–206, 1993.
16. K Herbers, HJ Flint, U Sonnewald. Apoplastic expression of the xylanase and β(1-3,1-4) glucanase domains of the *xyn*D gene from *Ruminococcus flavefaciens* leads to functional polypeptides in transgenic tobacco plants. Mol Breed 2:81–87, 1996.
17. LG Jensen, O Olsen, O Kops, N Wolf, KK Thomsen, D von Wettstein. Transgenic barley expressing a protein-engineered, thermostable (1,3-1,4)-β-glucanase during germination. Proc Natl Acad Sci USA 93:3487–3491, 1996.
18. DR Witcher, EE Hood, D Peterson, M Bailey, D Bond, A Kusnadi, R Evangelista, Z Nikolov, C Wooge, R Mehigh, W Kappel, J Register, JA Howard. Commercial production of β-glucuronidase (GUS): a model system for the production of proteins in plants. Mol Breed 4:301–312, 1998.
19. B Kühnel, LA Holbrook, MM Moloney, GJH van Rooijen. Oil bodies of transgenic *Brassica napus* as a source of immobilized β-glucuronidase. JAOCS 73:1533–1538, 1996.
20. KE McBride, DJ Schaaf, M Daley, DM Stalker. Controlled expression of plastid transgenes in plants based on a nuclear DNA-encoded and plastid-targeted T7 RNA polymerase. Proc Natl Acad Sci USA 91:7301–7305, 1994.
21. J Howard, KW Culver. Method of treating lactose intolerance. WO patent application 97/48810, 1997.
22. P Lenee, V Gruber, S Baudino, C Benicourt, C Cudrey. Recombinant preduodenal lipases and polypeptide derivatives produced by plants, processes for obtaining them and their uses. WO patent application 96/33277, 1996.
23. G Alibert, Z Mouloungui, A Boudet. Method for producing fatty acids or derivatives thereof from oil plants. European patent application 0770134, 1996.
24. A Kato, S Nakamura, H Ibrahim, T Matsumi, C Tsumiyama, M Kato. Production of genetically modified lysozymes having extreme heat stability and antimicrobial activity against Gram negative bacteria in yeast and in plant. Nahrung 42:128–130, 1998.
25. J Trudel, C Potvin, A Asselin. Expression of active hen egg white lysozyme in transgenic tobacco. Plant Sci 87:55–67, 1992.
26. K Düring, P Porsch, M Fladung, H Lörz. Transgenic potato plants resistant to the phytopathogenic bacterium *Erwinia carotovora*. Plant J 3:587–598, 1993.
27. CP Wilcox, AK Weissinger, RC Long, LC Fitzmaurice, TE Mirkov, HE Swaisgood. Production and purification of an active bovine lysozyme in tobacco (*Nicotiana tabacum*): utilization of value-added crop plants traditionally grown under intensive agriculture. J Agric Food Chem 45:2793–2797, 1997.

28. J Pen, TC Verwoerd, PA van Paridon, RF Beudeker, PJM van den Elzen, K Geerse, JD van der Klis, HAJ Versteegh, AJJ van Ooyen, A Hoekema. Phytase-containing transgenic seeds as a novel feed additive for improved phosphorus utilization. Bio/Technology 11:811–814, 1993.
29. J Li, CE Hegeman, RW Hanlon, GH Lacy, DM Denbow, EA Grabau. Secretion of active recombinant phytase from soybean cell-suspension cultures. Plant Physiol 1141:1103–1111, 1997.
30. DM Denbow, EA Grabau, GH Lacy, ET Kornegay, DR Russell, PF Umbeck. Soybeans transformed with a fungal phytase gene improve phosphorus availability for broilers. Poultry Sci 77:878–881, 1998.
31. S Austin-Phillips, M Cook, RG Koegel, RJ Straub. Animal feed composition for poultry, fish and livestock, containing the juice of transgenic alfalfa. US patent 5,900,525.
32. H Brinch-Pedersen, PB Holm, A Olesen, SR Rasmussen. Generation of transgenic wheat (*Triticum aestivum* L.) for obtaining elevated levels of phytase activity in the grain. Plant Mol Biol (Abstr. 305) Vol 15(3), 1997.
33. TC Verwoerd, PA van Paridon, AJJ van Ooyen, JWM van Lent, A Hoekema, J Pen. Stable accumulation of *Aspergillus niger phytase* in transgenic tobacco leaves. Plant Physiol 109:1199–1205, 1995.
34. J Pen, A Hoekema, PC Sijmons, AJJ van Ooijen, KR Rietveld, TC Verwoerd. The expression of phytase in plants. European patent application 0449 375, 1991.
35. K Herbers, I Wilke, U Sonnewald. A thermostable xylanase from *Clostridium thermocellum* expressed at high levels in the apoplast of transgenic tobacco has no detrimental effects and is easily purified. Bio/Technology 13:63–66, 1995.
36. J-F Laliberté, O Nicolas, S Durand, R Morsoli. The xylanase introns from *Cryptococcus albidus* are accurately spliced in transgenic tobacco plants. Plant Mol Biol 18:447–451, 1992.
37. NV Borisjuk, LG Borisjuk, S Logendra, F Petersen, Y Gleba, I Raskin. Production of recombinant proteins in plant root exudates. Nature Biotechnol 17:466–469, 1999.
38. Y Okada, N Yoshigi, K Ito, M Kihara. Tissue-specific promoter. European patent application 0 781 849, 1996.
39. GA de Zoeten, JR Penswick, MA Horisberger, P Ahl, M Schultze, T Hohn. The expression, localization and effect of human interferon in plants. Virology 172:213–222, 1989.
40. LK Grill. Tobacco mosaic virus as a gene expression vector. Agron Food Indust Hi Technol Nov/Dec:20–23, 1993.
41. H Hamamoto, Y Sugiyama, N Nakagawa, E Hashida, Y Matsunaga, S Takemoto, Y Watanabe, Y Okada. A new tobacco mosaic virus vector and its use for the systemic production of angiotensin-l-converting enzyme inhibitor in transgenic tobacco and tomato. Bio/Technology 11:930–932, 1993.
42. MH Kumagai, TH Turpen, N Weinzettl, G Della-Cioppa, AM Turpen, J Donson, ME Hilf, GL Grantham, WO Dawson, TP Chow, M Piatak Jr, LK Grill. Rapid, high-level expression of biologically active α-trichosanthin in transfected plants by an RNA viral vector. Proc Natl Acad Sci USA 90:427–430, 1993.
43. GP Lomonossoff. Plant viruses and pharmaceuticals. Agron Food Indust Hi Technol March/April:7–11, 1995.
44. C Porta, VE Spall, J Loveland, JE Johnson, PJ Barker, GP Lomonossoff. Development of cowpea mosaic virus as a high-yielding system for the presentation of foreign peptides. Virology 202:949–955, 1994.
45. R Usha, JB Rohll, VE Spall, M Shanks, AJ Maule, JE Johnson, GP Lomonossoff. Expression of an animal virus antigenic site on the surface of a plant virus particle. Virology 197:366-374, 1993.
46. PC Sijmons, BMM Dekker, B Schrammeijer, TC Verwoerd, PJM van den Elzen, A Hoekema. Production of correctly processed human serum albumin in transgenic plants. Bio/Technology 8:217–221, 1990.
47. AR Kermode. Mechanisms of intracellular protein transport and targeting in plant cells. Crit Rev Plant Sci 15:285–423, 1996.
48. GJH van Rooijen, MM Moloney. Plant seed oil-bodies as carriers for foreign proteins. Bio/Technology 13:72–77, 1995.
49. AR Kusnadi, EE Hood, DR Witcher, JA Howard, ZL Nikolov. Production and purification of two recombinant proteins from transgenic corn. Biotechnol Prog 14:149–155, 1998.
50. J Howard. Methods for commercial production and extraction of protein from seed. WO patent application 98/39461, 1998.
51. DL Parmenter, JG Boothe, GJH van Rooijen, EC Yeung, MM Moloney. Production of biologically active hirudin in plant seeds using oleosin partitioning. Plant Mol Biol 29:1167–1180, 1995.
52. RL Rodriguez. Process for protein production in plants. WO patent application 95/14099, 1995.
53. H-G Sarx, T Diefenthal, N Wolf. Process for the production of degradation and/or conversion products of storage substances present in transgenic plant material with the help of a malting process. WO patent application 97/32986, 1997.
54. CL Cramer, DL Weissenborn. HMG2 promoter expression system and post-harvest production of gene products in plants and plant cells. WO patent application 95/03690, 1995.
55. SA Boffey, H Jones, RJ Slater, P Arokiaraj, KF Cheong, WYWA Rahaman, HY Yeang. Method for

the production of proteins in plant fluids. US patent application 5,580,768, 1996.
56. LS Melchers, MB Sela-Buurlage, SA Vloemans, CP Woloshuk, JSC van Roekel, J Pen, PJM van den Elzen, BJC Cornelissen. Extracellular targeting of the vacuolar tobacco proteins AP24, chitinase and β-1,3-glucanase in transgenic plants. Plant Mol Biol 21:583–593, 1993.
57. EE Hood, DR Witcher, S Maddock, T Meyer, C Baszczynski, M Bailey, P Flynn, J Register, L Marshall, D Bond, E Kulisek, A Kusnadi, R Evangelista, Z Nikolov, C Wooge, RJ Mehigh, R Hernan, WK Kappel, D Ritland, CP Li, JA Howard. Commercial production of avidin from transgenic maize: characterization of transformant, production, processing, extraction and purification. Mol Breed 3:291–306, 1998.
58. J Hodgson. Expression systems: a user's guide. Bio/Technology 11:887-893, 1993.
59. JBL Damm. Application of glycobiology in the biotechnological production of pharmaceuticals. Pharm Technol Eur Sept:28–34, 1995.
60. J Pen. Comparison of host systems for the production of recombinant proteins. In: J Pen, MRL Owen, eds. Transgenic Plants: A Production System for Industrial and Pharmaceutical Proteins. Chichester: John Wiley and Sons, 1996, pp 149–167.
61. HJ Peppler, G Reed. Enzymes in food and feed processing. In: JF Kennedy, ed. Biotechnology, Vol 7A. Weinheim, Germany: VCH, 1987, pp 547–603.
62. JF Kennedy, VM Cabalda, CA White. Enzymic starch utilization and genetic engineering. TIBTECH 6:184–189, 1988.
63. E Schwardt. Production and use of enzymes degrading starch and some other polysaccharides. Food Biotechnol 4:337–351, 1990.
64. JR Whitaker. New and future uses of enzymes in food processing. Food Biotechnol 4:669–697, 1990.
65. T Yuuki, T Nomura, H Tezuka, A Tsuboi, H Yamagata, N Tsukagoshi, S Udaka. Complete nucleotide sequence of a gene coding for heat- and pH-stable α-amylase of *Bacillus licheniformis*: comparison of the amino acid sequences of three bacterial liquefying α-amylases deduced from the cDNA sequences. J Biochem 98:1147–1156, 1985.
66. J Pen, AJJ van Ooyen, PJM van den Elzen, K Rietveld, A Hoekema. Direct screening for high-level expression of an introduced α-amylase gene in plants. Plant Mol Biol 18:1133–1139, 1992.
67. PJ Reilly. Enzymic degradation of starch. In: GMA van Beynum, JA Roels eds. Starch Conversion Technology. New York: Marcel Dekker, 1985, pp 101–142.
68. D Cowan. Advances in feed enzyme technology. Agron Food Indust Hi Technol May/June:9, 1992.
69. M Lolas, P Markakis. Phytase of navy beans. J Food Sci 42:1094–1097, 1977.
70. R Beudeker, C Geerse, GJ Verschoor. Biotechnological products for the compound feed industry. In: K North, ed. Biotechnology International. London: Century Press, 1991, pp 340–343.
71. PCM Simons, HAJ Versteegh, AW Jongbloed, PA Kemme, P Slump, KD Bos, MGE Wolters, RF Beudeker, GJ Verschoor. Improved phosphorus availability by microbial phytase in broilers and pigs. Br J Nutr 64:525–540, 1990.
72. M Näsi. Microbial phytase supplementation for improving availability of plant phosphorus in the diet of growing pigs. J Agr Sci Finland 62:435–442, 1990.
73. H Vogt. Einsatz von Phytase im Broilermastfutter mit unterschiedlichem Phosphorgehalt. Arch Geflügelk 56:93–98, 1992.
74. J von Pallauf, D Höhler, G Rimbach, H Neusser. Einfluß einer Zulage an mikrobieller Phytase zu einer Mais-Soja-Diät auf die scheinbare Absorption von Phosphor und Calcium beim Ferkel. J Anim Physiol Anim Nutr 67:30–40, 1992.
75. W van Hartingsveldt, CMJ van Zijl, GM Harteveld, RJ Gouka, MEG Suykerbuyk, RGM Luiten, PA van Paridon, GCM Selten, AE Veenstra, RFM van Gorcom, CAMJJ van Hondel. Cloning, characterization and overexpression of the phytase-encoding gene (phyA) of *Aspergillus niger*. Gene 127:87–94, 1993.
76. RF van Gorcom, W van Hartingsveldt, PA van Paridon, AE Veenstra, RGM Luiten, GCM Selten. Cloning and expression of microbial phytase. European patent application 0420 358, 1991.
77. BJC Cornelissen, RAM Hooft van Huijsduijnen, JF Bol. A tobacco mosaic virus-induced tobacco protein is homologous to the sweet-tasting protein thaumatin. Nature 321:531–532, 1986.
78. H Guiley, RK Dudley, G Jonard, E Balazs, KE Richards. Transcription of cauliflower mosaic virus DNA, detection of promoter sequences and characterization of transcripts. Cell 30:763–773, 1982.
79. R Kornfeld, S Kornfeld. Assembly of asparagine-linked oligosaccharides. Annu Rev Biochem 54:631–664, 1985.
80. DR Ledoux, JH Broomhead, JD Firman, AJ Bermudez. Efficacy of PhytaSeed, a phytase containing transgenic canola, to improve phytase phosphorus utilization from corn-soybean meal diets fed to turkey poults from day 1 to 35. Poultry Science 77:54, 1998.
81. ZB Zhang, HP Veit, ET Kornegay. Comparison of Natuphos and PhytaSeed phytase for young pigs (1998). Report from the Department of Animal and Poultry Sciences, Virginia Polytechnic Institute and State University at Blacksburg.

82. ZB Zhang, HP Veit, CT Larsen, DM Denbow, ET Kornegay. Comparison of phytase in Natuphos and PhytaSeed for young broilers (1998). Report from the Department of Animal and Poultry Sciences Virginia Polytechnic Institute and State University at Blacksburg, V.
83. RF Beudeker. Stable compositions comprising transgenic plant materials. WO patent application 97/16981, 1997.
84. V Raboy. The genetics of seed storage phosphorus pathways. In: JP Lynch, J Deikman, eds. Phosphorus in Plant Biology: Regulatory Roles in Molecular, Cellular, Organismic and Ecosystem Processes. Am Soc Plant Physiol 1998, pp 192–203.
85. A Caransa, M Simell, A Lehmussari, M Vaara, T Vaara. A novel enzyme application of corn wet milling. Starch/Stärke 40 S409, 1988.
86. XS Zhu, PA Seib, GL Allee, YT Liang. Preparation of a low-phytate feed mixture and its bioavailability to chicks. Anim Feed Sci Technol 27:341–351, 1990.
87. SS Desphande, M Cheryan. Effect of phytic acid, divalent cations and their interaction on alpha amylase activity. J Food Sci 49:516–519, 1984.
88. BE Knuckles, DD Kuzmickuy, MR Cumbermann, AA Berschart. Effect of myoinositol phosphate esters on in vitro and in vivo digestion of protein. J Food Sci 54:1348–1349, 1989.
89. H-J Ingelmann, G Rimbach, J Pallauf. Phytinsäure-ein antinutritiver Faktor? Ernährungs-Umschau 40:400–404, 1993.

15

Enzymes in Protein Biosynthesis

John R. Whitaker
University of California, Davis, Davis, California, U.S.A.

We shall not unravel the chemistry of life in molecular detail without knowing at atomic or close to atomic resolution the structure of the biological macromolecules especially the proteins (1).

I. INTRODUCTION

Proteins perform many functions in organisms. Some of these are listed in Table 1. No other polymeric compound can perform so many functions in nature. This is because proteins are so diverse in structure. Although only 20 amino acids are used to build the primary structures, they can be arranged theoretically in 20^{19} different sequences. They also can fold in many different ways because of their ability to form secondary, tertiary, and quaternary structures and combination in macromolecular structures with different proteins. Table 2 gives a small sample of the diverse size of proteins. Each molecule of a specific protein has exactly the same size and amino acid sequence and fold in exactly the same way. Also, we will see later that proteins can be posttranslationally modified in at least 135 different ways.

The period 1925–1960 was very active for protein chemists and enzymologists. During that period James Sumner (2) crystallized urease and showed it to be a protein. In the 1930s, Kunitz and Northrop (3) at Rockefeller Institute learned how to crystallize trypsin, chymotrypsin, pepsin, and other enzymes, strengthening the argument that all enzymes are likely to be proteins. The development of ion-exchange chromatography by Moore and Stein (4, 5) for separating, identifying, and quantifying amino acids from protein hydrolysates, the Edman method of sequencing proteins (6, 7), and the development of chromatographic (4) and electrophoretic methods (8) for purification of amino acids and proteins all contributed to

Table 1 Protein Functions

Enzymes
Enzyme inhibitors
Hormones
Carriers
Hemoglobin and myoglobin (O_2 and CO_2)
Serum albumin (ions, lipids, hormones)
Protectors
Antibodies, skin, hair, nails
Blood clotting
Chaperones
Osmotic regulators (serum albumin)
Movement (contractile proteins—myosin, actin, etc.)
Connectors
Muscle to bone (elastin)
Signal transducers (nerve transmission)
Recognition
Cell-to-cell interaction (glycoproteins)
A, B, AB, O blood types
Elicitors (antigens)
Cell coating, cell "glue" (adhesion), collagen, others
Memory (brain: protein or is it DNA?)
Taste perception (tongue)
Vision (opsin, rhodopsin, alcohol dehydrogenase)

Table 2 Molecular Weights of a Few Selected Proteins

Protein	Molecular weight (daltons)	Protein	Molecular weight (daltons)
Insulin	5,737	Alkaline phosphatase	80,000
Ribonuclease	13,683	Polyphenol oxidase	128,000
Lysozyme	14,100	Fumarase	194,000
Chymotrypsinogen	23,200	Catalase	232,000
β-Lactoglobulin	35,000	Aspartate transcarbamylase	310,000
Ovalbumin	45,000	Urease	483,000
Serum albumin	65,000	β-Galactosidase	520,000
Hemoglobin	64,500	Glutamate dehydrogenase	2,000,000

rapid advances in understanding the protein nature of enzymes.

During that period, limited thought was given to protein biosynthesis. It was generally assumed that proteins were formed from activated derivatives of amino acids, probably by use of ATP for activation. But no details of the in vivo biosynthesis were known. In the late 1950s and 1960s a few publications appeared, based primarily on studies of microorganisms, that began to give evidence that protein biosynthesis at the molecular level could be more complex than originally thought. Especially, studies based on microbial genetics indicated a precise correlation between nucleotide sequences of DNAs and some RNAs and the amino acid sequences of proteins.

II. HISTORICAL BACKGROUND

There were many important contributions made in the long journey of understanding protein biosynthesis prior to the 1950s. Genes had been postulated before the turn of the 20th century based on the careful breeding studies of Gregor Mendel (8a). August Weismann in 1892 stated that "the essence of heredity is the transmission of a nuclear substance of specific molecular structure" (8b). In 1903, Walter Sutton linked chromosomes to Mendelian heredity (8c). He observed that all cell divisions producing germ cells also formed thread-like chromosomes, and that a gamete received only one of each of the chromosomes of different morphologic types. Through detailed studies of the fruit fly, *Drosophila melanogaster*, Morgan and his colleagues showed that the genes segregated as four linkage groups corresponding to the four chromosomes (8d). Similar observations followed for corn (10 chromosomes, 10 linkage groups) and peas (7 chromosomes, 7 linkage groups). By 1920, the chromosome theory of heredity became an accepted fact in genetics.

The discovery of the chemical nature of the gene resulted from the merging of genetics and biochemistry between 1930 and 1950. In 1909, Archibald Garrod determined that the human disease alkaptonuria was caused by a rare recessive mutation that was inherited according to Mendelian rules (8e). It was noticed that patients with alkaptonuria had black urine. The dark color was determined to be due to a breakdown product of phenylalanine. In his treatise on "Inborn Errors of Metabolism," Garrod wrote, "We may further conceive that the splitting of the benzene ring in normal metabolism is the work of a special enzyme, [and] that in congential alkaptonuria the enzyme is wanted."

The research of Morgan and his colleagues in the early 1900s on the inheritance of eye color in *Drosophila* (8f), together with that of Beadle and Tatum on the bread mold, *Neurospora crassa*, and its rare mutant colony development, led Beadle and Tatum to conclude that "genes somehow control protein (enzyme) structure" (8g). These findings led to studies of the chemical structure of genes, as the first step in elucidating the molecular basis for the genetic control of protein synthesis. This occurred in 1944 when Avery et al., in studying *Streptococcus pneumoniae* from patients with pneumonia, showed that DNA from "smooth" colonies can transform "rough" colonies into the smooth form (9). They proved DNA was involved. Addition of several different proteases had no effect on the transforming activity, eliminating involvement of proteins. However, small amounts of purified deoxyribonuclease (DNAase) immediately inactivated the transformation.

In 1953, Watson and Crick deduced the double-helical structure of DNA, ushering in the modern era of molecular cell biology (10). At about this same time, the electron microscope was invented. Light microscopes have a resolving power of ~ 500 nm. Electron microscopes in the early stage had resolving power of

1–5 nm; this was eventually reduced to 0.1–0.5 nm. Therefore, by the beginning of the 1960s the findings of genetists, biochemists, and structural cell biologists could be brought together, working from the molecular to the subcellular level, and vice versa. Another "principle" that developed about this same time was that the activity of genes is highly regulated. It was known that genes produced proteins, but the methods by which the gene activity was controlled was still unclear. Perhaps the principle enuciated by Jacob and Monod (11) did the most to clarify gene control. They proposed that certain genes regulate the activity of other genes. At the molecular level this transforms to an understanding that specific sets of proteins are produced that build characteristic structures, and some carry out characteristic enzymatic activities.

Further discussion in this chapter will be limited to the enzymes involved in in vivo and in vitro protein biosynthesis.

III. PROTEIN BIOSYNTHESIS

A. Differences Between Prokaryotic and Eukaryotic Protein Biosynthesis

Being unicellular, formation of bacterial mRNA is always accessible to ribosomes, as well as other components of the protein biosynthesis pathway. Even as the mRNA is being transcribed from DNA, the specific tRNAs and tRNA synthetases begin translation of the protein and transcription and translation are completed at almost the same rate and time. Therefore, the mRNA nucleotide bases are not modified (by methylation) as they are in eukaryotic cell mRNA. In eukaryotes, DNA transcription occurs in the nucleus, which contains ribosomal precursors undergoing formation (in the nucleolus), but there are no mature ribosomes that can perform protein synthesis. In eukaryotes, the mRNA is synthesized in the nucleus. The mRNA must then be secreted through the nuclear membrane into the cytoplasm for translation to occur. Therefore, transcription and translation are not coupled in eukaryotic cells.

In eukaryotes, the RNA is not a functional mRNA, tRNA, or rRNA until it is extensively modified in the nucleus before it is secreted into the cytoplasm where it associates with the ribosomes. Types of modification that occur in the nucleus are: (a) addition of chemical groups at both ends of the mRNA; (b) cutting the mRNA into segments; and (c) recombining the segments by splicing of original noncontiguous segments to produce a very different mRNA. Translation occurs only when the mRNA is in the cytoplasm. This is the major distinction between prokaryotic and eukaryotic cells (Fig. 1).

Eukaryotic RNA synthesis is carried out by three separate RNA polymerases, while RNA synthesis in prokaryotic cells is performed by a single RNA polymerase. The precursor to three of the four eukaryotic rRNAs (the 28S, 5.8S, and 18S rRNAs) is produced by RNA polymerase I in the nucleolus of the cell. The precursors of the mRNAs are made by RNA polymerase II and the small RNAs (tRNAs and the 5S rRNAs) or their precursors are made by RNA polymerase III.

There are fundamental differences between prokaryotes and eukaryotes in chromosome structure due to the core of histones wrapped around the DNA of eukaryotes. With respect to gene control of protein biosynthesis, prokaryotes are regulated at the transcription level while many eukaryotes are primarily regulated at the translation level.

B. Steps in Protein Biosynthesis

There are five steps in the biosynthesis of proteins: *transcription* phase in which mRNAs, tRNAs, and rRNAs are produced; *translation* of mRNAs to give polypeptides; *termination of translation*; *posttranslational modification* of the polypeptides; and *folding* of the polypeptides into their native structures.

1. Transcription Phase

The overall steps of transcription and translation in eukaryotes are shown in Eq. (1).

$$\mathrm{DNA} + 4\,\mathrm{NTP} \xrightarrow[\text{transcription}]{\text{RNA polymerase}} \text{mRNA, tRNA, rRNA} \xrightarrow[\text{ribosomes}]{\text{amino acids, tRNAs}} \text{Proteins} \tag{1}$$

During the transcription phase, the mRNAs, tRNAs, and rRNAs are produced. The key enzyme is RNA polymerase II. The three steps are: *initiation* signalled by the promoter recognized by RNA polymerase (in the case of prokaryotes, it is a subunit of the RNA polymerase ($\alpha_2\beta\beta'\sigma$); *elongation* involving a melting and unwinding of the double helix while sequentially attaching ribonucleotides at the 3′ end of the growing RNA molecule; *termination* by the formation of stem-loop structures of Rho-dependent terminators.

The April 28, 2000, issue of Science published a detailed crystallographic study of the protein architec-

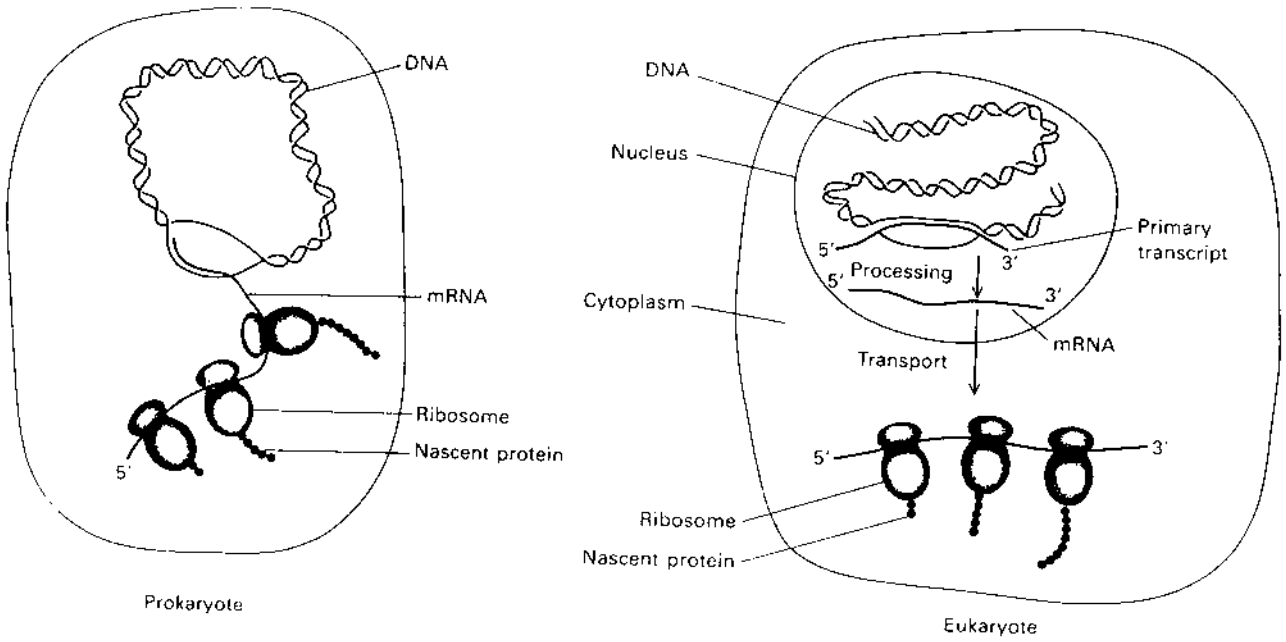

Figure 1 The production of functioning mRNA is very different in prokaryotes and eukaryotes. In prokaryotes, the RNA transcript serves directly as the mRNA, and translation begins before transcription is completed; that is, transcription and translation are coupled. In eukaryotes, the primary RNA transcript must be modified in the cell nucleus to form mRNA. Translation takes place only after the completed mRNA is delivered to the cytoplasm. (From Ref. 12.)

ture of a yeast (*Saccharomyces cerevisiae*) RNA polymerase II at 3 Å resolution (see insert, Fig. 2) in which 10 of the 12 different subunits are shown (Table 3). The yeast RNA polymerase II has a total mass of 514 kDa. Yeast and human RNA polymerase IIs are considered to be very similar since human genes for 10 of the subunits can be substituted for the yeast genes, and a very similar enzyme is produced. Also, RNA polymerases I and III of prokryotes contain nine of the 10 proteins of yeast RNA polymerase II.

RNA polymerase II is the key of the transcription process. Without help of other enzymes it can (see Fig. 3): (a) recognize the initiation codon, AUG (the regulated initiation complex contains RNA polymerase II, five transcription factors, and a multiprotein mediator; in all there are some 60 proteins involved); (b) recognize and respond to the operator complex; (c) proofread and unwind the DNA double helix; (d) produce specific mRNA, tRNAs, and rRNAs by catalyzing formation of phosphodiester bonds among nucleotides (Str. 1); proofread the nascent mRNA transcript and replace it if necessary; and (f) recognize the termination point containing the codon AUA, UAG, or UGA.

Table 3 Yeast RNA Polymerase II Subunits

Subunit	Mass (kDa)	Amino acid residues in sequence	Identity to human (%)[a]
Rpb1	191.6	1733 (1449)[b]	52
Rpb2	138.8	1224	61
Rpb3	35.3	318	46
Rpb4	25.4	221	30
Rpb5	25.1	215	45
Rpb6	17.9	155	59
Rpb7	19.1	171	61
Rpb8	16.5	146	43
Rpb9	14.3	122	37
Rpb10	8.3	70	73
Rpb11	13.6	120	50
Rpb12	7.7	70	43
Total	513.6	4565	53

[a]Percentage of identical amino acid residues, for Rpb1 excluding the COOH-terminal domain.
[b]The number in parenthesis corresponds to Rpb1 without the unstructured COOH-terminal domain (CTD).
Source: Ref. 13.

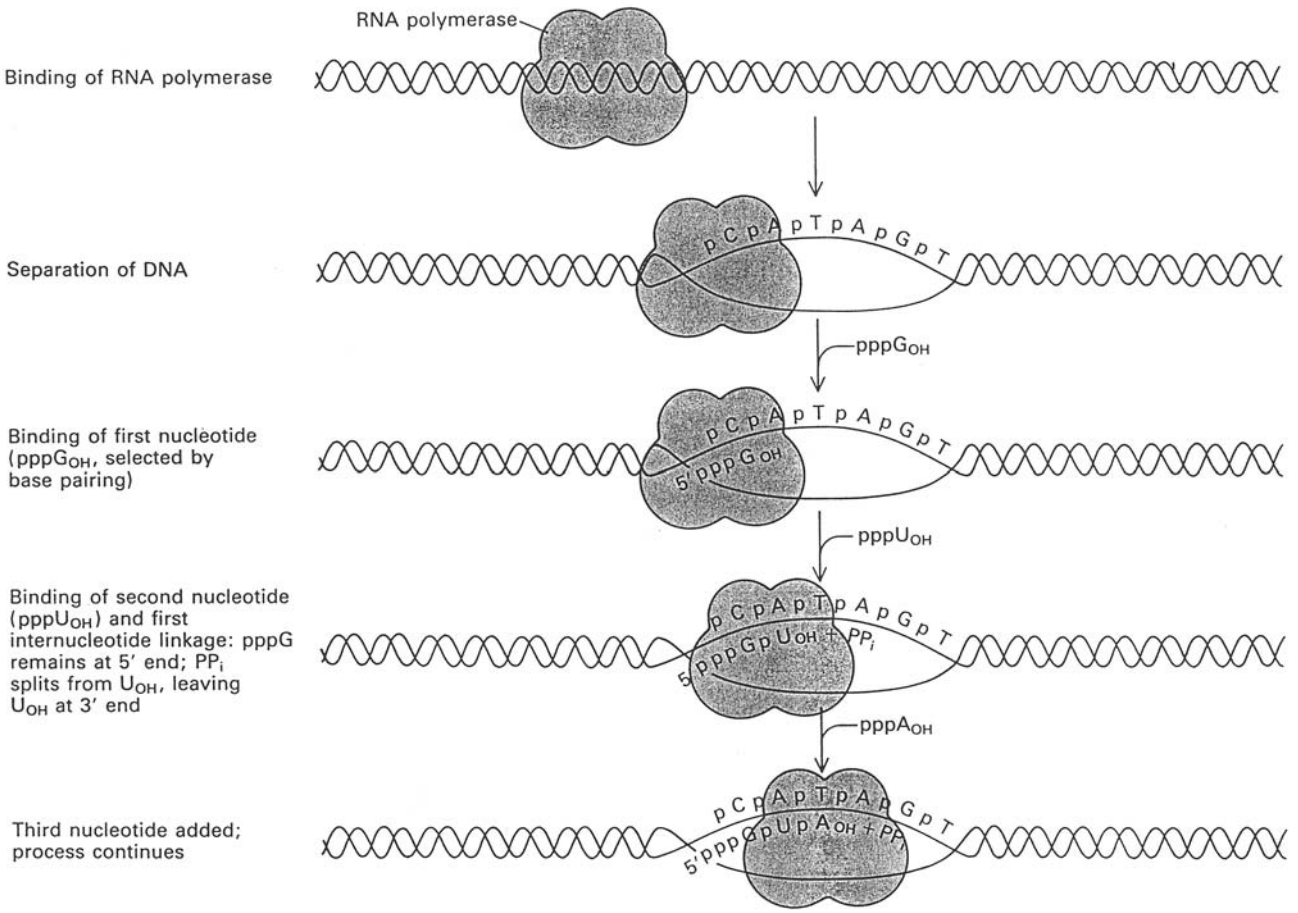

Figure 3 Transcription of a double-stranded DNA into a single-stranded RNA by an RNA polymerase. The five steps are identified on the left-hand side. Not shown is the termination step. (From Ref. 12.)

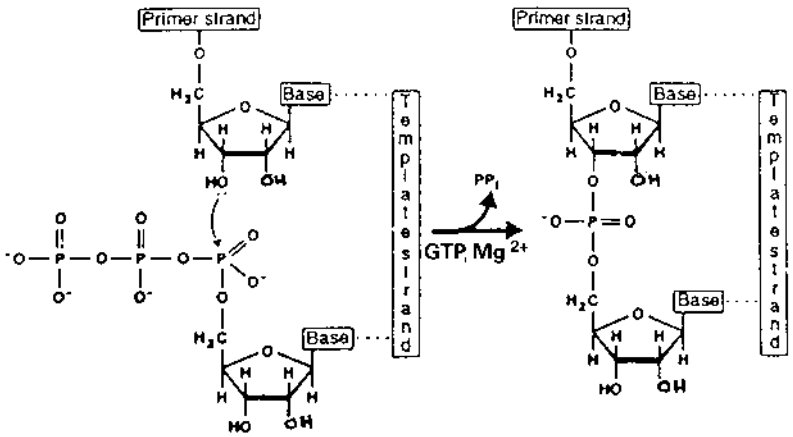

Structure 1

Table 4 The Genetic Code[a]

First position (5′ end)	Second position				Third position (3′ end)
	U	C	A	G	
U	Phe	Ser	Tyr	Cys	U
	Phe	Ser	Tyr	Cys	C
	Leu	Ser	Stop (och)	Stop	A
	Leu	Ser	Stop (amb)	Trp	G
C	Leu	Pro	His	Arg	U
	Leu	Pro	His	Arg	C
	Leu	Pro	Gln	Arg	A
	Leu	Pro	Gln	Arg	G
A	Ile	Thr	Asn	Ser	U
	Ile	Thr	Asn	Ser	C
	Ile	Thr	Lys	Arg	A
	Met	Thr	Lys	Arg	G
G	Val	Ala	Asp	Gly	U
	Val	Ala	Asp	Gly	C
	Val	Ala	Glu	Gly	A
	Val (Met)	Ala	Glu	Gly	G

[a]Bases are given as ribonucleotides, so U appears in the table instead of T. "Stop (och)" stands for the ochre termination triplet, and "Stop (amb)" for the amber. AUG is the most common initiator codon; GUG usually codes for valine, but it can also code for methionine to initiate an mRNA chain.

After synthesis of the three types of mRNAs in eukaryotes, they must be secreted from the nucleus via the cell membrane into the cytoplasm, where translation takes place. The time to produce the mRNA is estimated to be about 1–2 sec, depending on the promoter clearance time, number of RNA polymerase molecules, and size of the gene.

2. Translation Phase

The mRNA carries the genetic information for protein biosynthesis that it has transcribed from a gene located on DNA via a three-letter code (codon), complementary to that of the gene. Table 4 lists the genetic codons for each of the 20 amino acids found in proteins. The code contains some redundancies, such that 64 codons (including the "stop" codons) may be used in protein biosynthesis (Table 5).

There are tRNAs and tRNA synthetases for each one of the 20 amino acids found in nascent proteins. The $tRNA^{Ala}$ for alanine is shown in Figure 4. The tRNAs are small ribonucleotides of ~ 70–80 residues. Some of the nucleotide bases are also modified following synthesis, as shown by the shaded circles in Figure 4.

The $tRNA^{Ala}$ contains an anticodon of IGC which recognizes and binds to the GCC codon on the mRNA. At the end of the tRNA (rectangle labeled amino acid), there is an adeonsyl group to form a covalent binding site for the specific amino acid (Ala shown here). The tRNA synthetase is responsible for the reaction leading to the bound aminoacyl-tRNA [Eq. 2)].

$$\text{Amino acid} + \text{ATP} + \text{tRNA} \xrightarrow{\text{enzyme}} \text{aminoacyl-tRNA} + \text{AMP} + \text{PPi} \quad (2)$$

Table 5 Degeneracy of the Genetic Code

Number of synonymous codons	Amino acid	Total number of codons
6	Leu, Ser, Arg	18
4	Gly, Pro, Ala, Val, Thr	20
3	Ile	3
2	Phe, Tyr, Cys, His, Gln, Glu, Asn, Asp, Lys	18
1	Met, Trp	2
Total number of codons for amino acids		61
Number of codons for termination		3
Total number of codons in genetic code		64

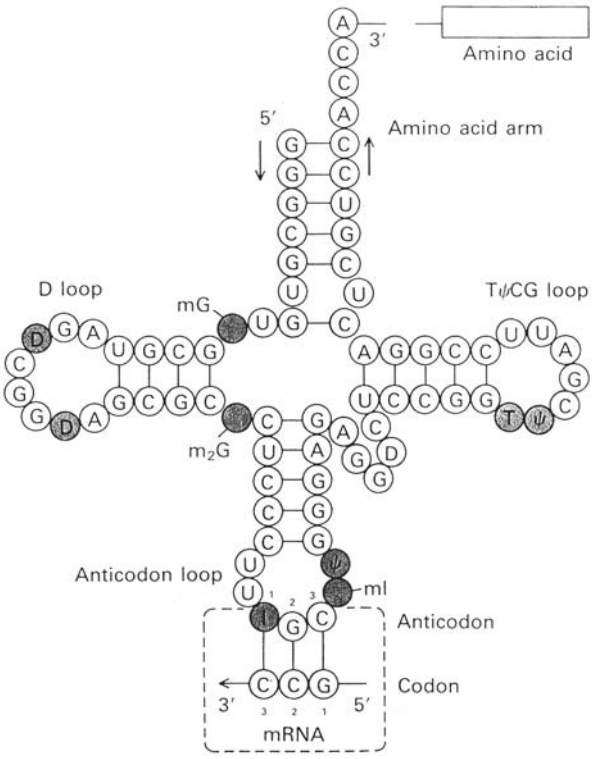

Figure 4 The primary structure of yeast alanine tRNA ($tRNA^{A1a}$). The tRNA is synthesized from the nucleotides A, C, G, and U, but some of the nucleotides are modified after synthesis (shown by labeled shaded circles) (abbreviations for labels: D = dihydrouridine, I = inosine, T = thymine, Ψ = pseudouridine, and m = methyl group). The primary structure is a cloverleaf consisting of four base-paired stems and three loops: the D loop, for dihydrouridine, a virtually constant constituent of this loop; the anticodon loop; and the TΨCG loop, so named because a sequence of thymidylate, pseudouridylate, cytidylate, and guanylate is virtually always present in this loop. (From Ref. 12.)

This chemical step is critical to protein synthesis in two major ways. The amino acid derivatives are activated via the ATP reaction as shown by Eq. (2). The amino acid products are shown in Figure 5. The amino acid is covalently attached via the 3′ oxygen of the ribose diphosphate group of the tRNA. Secondly, the specificity for binding at the right site on the mRNA is assured (see above).

Formation of the primary sequence of a protein is carried out on the ribosomes (Fig. 6). As indicated above, the eukaryotic ribosomes are located in the cytoplasm of the cells. Protein biosynthesis consists of three major stages: *initiation, elongation,* and *termination*.

Darnell et al. (12:122–123) described the entire process in great deal in the following manner (Fig. 7).

a. Initiation. An initiation factor (IF_2 in prokaryotes and eIF_2 in eukaryotes) binds a molecule of GTP and a molecule of methionyl-$tRNA_i^{Met}$ (for prokaryote *E. coli* the methionine is replaced with N-formylmethionine) to form a ternary complex. This complex binds to mRNA and the small ribosomal subunit (plus other initiation factors) to make an initiation complex (the 30S initiation complex in prokaryotes, and the 40S complex in eukaryotes). The Met-$tRNA_i^{Met}$ is now positioned correctly at the AUG initiation codon. A large ribosomal subunit then joins the complex; the bound GTP is hydrolyzed; and the initiation factors are detached. The Met-$tRNA_i^{Met}$ bearing the first amino acid is now bound to the ribosome at the P site. The initiation complex is ready to begin synthesis of the peptide chain.

b. Elongation. the met-$tRNA_i^{Met}$ is located at the P (for peptidyl-tRNA) site on the ribosome. The growing polypeptide is always attached to the tRNA that brought in the last amino acid. A new aminoacyl-tRNA (Phe-$tRNA^{Phe}$ here) binds to the ribosome at the A site (for aminoacyl site). During elongation in prokaryotes, a protein complex called Tu-Ts catalyzes the binding of each aminoacyl-tRNA to the ribosome. These are two ''elongation factors''—EF-TU and EF-TS. (A protein complex similar in action to Tu-Ts exists in eukaryotic cells.) A third elongation factor—EF-G—controls the translocation of the A to P sites. An activated Tu-GTP complex binds the TΨCG. The Tu-Ts complex probably binds to the TΨCG loop found in all tRNAs and allows the tRNA to associate with the ribosome. GTP is hydrolyzed and the Ts protein rejoins GDP-Tu and reactivates it. The complex also binds GTP, whereupon GDP and Ts dissociate from Tu. The remaining GTP-Tu complex then binds to an aminoacyl-tRNA. When the whole elongation factor complex is bound to the ribosome, the GTP is hydrolyzed to GDP, yielding energy to position the aminoacyl-tRNA in the A site. After the incoming aminoacyl-tRNA is correctly placed in the A site—that is, when the codon–anticodon pairing is correct—the peptide chain (or, here, the first methionine) is transferred to the amino group of the newly arrived amino-acyl-tRNA. This generates a peptidyl-tRNA that has acquired an additional amino acid. (In our example, the compound is methionyl-phenylalanyl-$tRNA^{Phe}$.) At this stage, the peptidyl-tRNA is bound to the ribosome at the A site. The ribosome moves one codon down the mRNA chain. (The mRNA codons

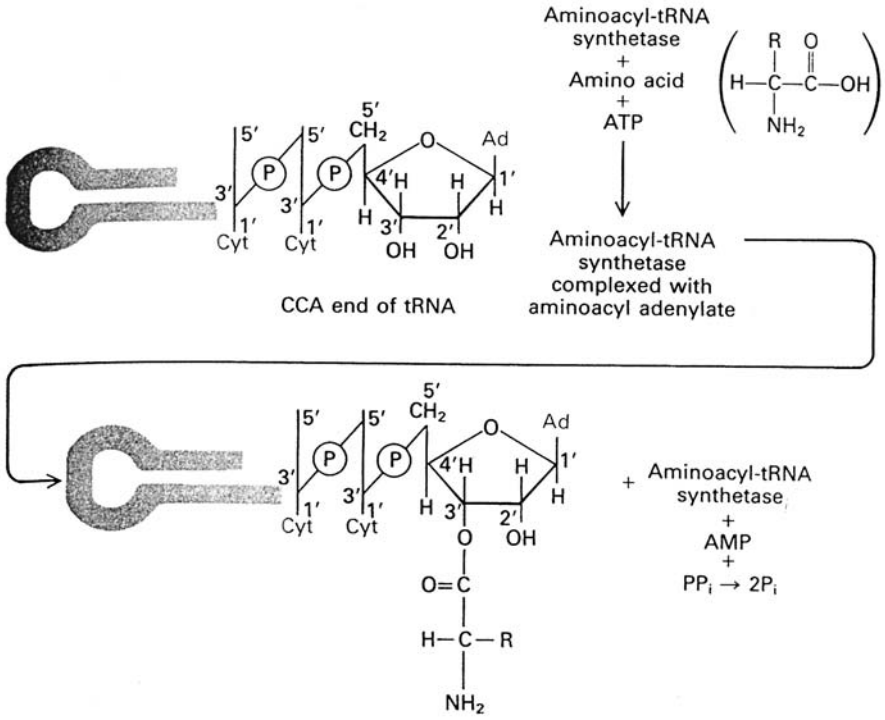

Figure 5 Translation of an mRNA strand into a protein begins with attachment of appropriate amino acids to the appropriate tRNAs (see Fig. 4). Covalent attachment requires two steps by an aminoacyl-tRNA synthetase that uniquely recognizes and binds to a specific amino acid and its cognate tRNA (see step 1). In the second step, amino acylation of tRNA occurs by ATP to attach the –COOH group of the amino acid to the 3′-hydroxy group of the terminal adenylate of the tRNA. Alternatively, the initial attachment can be to the 2′-OH group, which then rearranges to the 3′ position.

are illustrated with spaces separating them for convenience; in mRNA there are, of course, no spaces.) The translocation reaction is catalyzed in bacteria by the elongation factor G, using energy from the hydrolysis of GTP. With this movement, the empty tRNA is released from the P site, and the peptidyl-tRNA is shifted to the P site. (In eukaryotes, too, there are special proteins that serve in elongation.) The sequence of events is repeated for every amino acid added to the growing chain. Note that two molecules of GTP are used in the addition of each amino acid.

c. Termination. When the ribosome arrives at the codon UAG, the translation is completed with the aid of a terminator factor. Hydrolysis of the peptidyl-tRNA on the ribosome releases the completed polypeptide and the last tRNA, and the two ribosomal subunits separate. At least three TFs are involved in *E. coli*—RF1, RF2, and RF3. For eukaryotes, one termination factor eRF recognizes all termination codons.

IV. POSTTRANSLATIONAL COVALENT MODIFICATION OF PROTEINS

Once the primary structure of a protein is completely translated by RNA polymerase II, the protein is still biologically nonfunctional. It must undergo chemical modification involving nonhydrolytic and/or hydrolytic modification of the protein, fold into the tertiary structure, form quaternary structure (if needed) and macromolecular structure (if needed), and combine with cofactors (if needed) and often be transported to the site where it performs its function. In this section, we deal only with the posttranslational enzymatic modification.

A. Nonhydrolytic Posttranslational Enzymatic Modification

Table 6 lists examples of nonhydrolytic modification of 11 of the 20 amino acid residues, as well as the carboxy

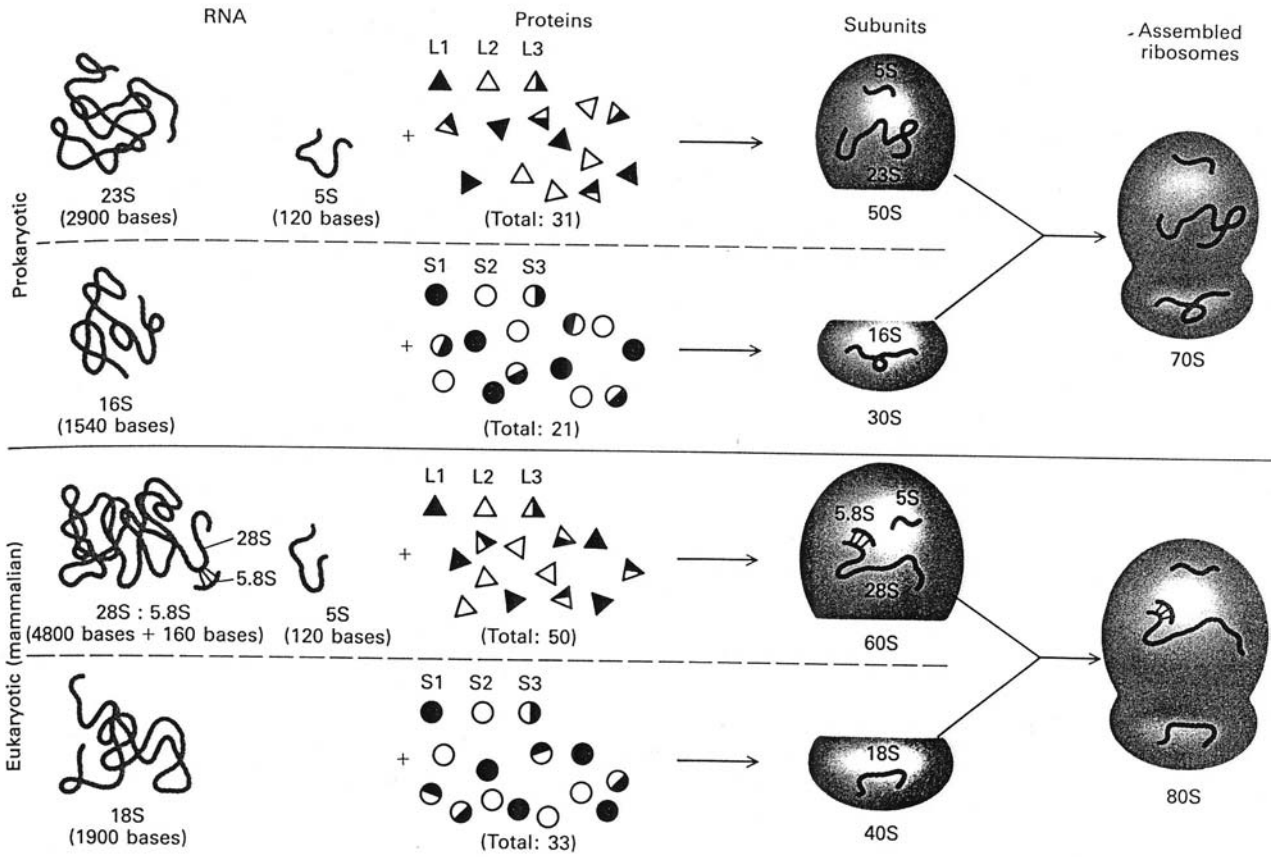

Figure 6 The composition of prokaryotic and eukaryotic ribosomes is shown, each consisting of a large and a small subunit. The different subunits contain rRNAs of different lengths and varying numbers and types of proteins (indicated by different shadings). In addition to the two major rRNA molecules, prokaryotic ribosomes have one small 5S tRNA that is ~ 120 bases long. Eukaryotic ribosomes have two small rRNAs: a 5S molecule similar to the prokaryotic 5S, and a 5.8S molecule that is 160 bases long. The proteins are named L1, L2, etc., and S1, S2, etc., depending on whether they belong to the large or small subunits. (From Ref. 12.)

and amino terminal ends of the proteins (14–16). There is a highly specific enzyme for each of these modifications. Some modifications such as glycosylation and activation of the cascade of pro-proteins in blood clotting involve a number of enzymes (see below). Most likely, nonhydrolytic modifications occur as soon as the N-terminal end of the growing protein chain emerges from the ribosomal system.

A good example of posttranslational modification of a protein is that for collagen (Fig. 8). As soon as a part of the nascent primary structure is formed on the ribosome (polysome), hydroxylation of proline and lysine (see Chapters 35 and 36) and glycosylation of hydroxylysine are known to occur (17, 18). Two pro-α1 and one pro-α2 chains are coded for by two different mRNAs. While still in the unfolded state, the two pro-α1 and one pro-α2 chains align with each other with the N-terminal amino acid all at one end and the C-terminal amino acid at the other end. This triple helix forms disulfide bonds among the three molecules. At this point the procollagen (MW ~ 115–140 kDa for each molecule) is secreted through the membrane and transported to the location where needed. Collagen is the major protein produced by animals. It forms a coating around all cells, fibrils, bundles of fibrils and, higher structures, such as the sarcomeres and fiber bundles of muscles.

At this point, highly specific and limited enzyme-catalyzed proteolysis occurs. The teleopeptides at the N-terminal end of the procollagen are removed by a specific procollagen peptidase to give molecules of ~ 95 kDa. The folded collagen molecules are aligned

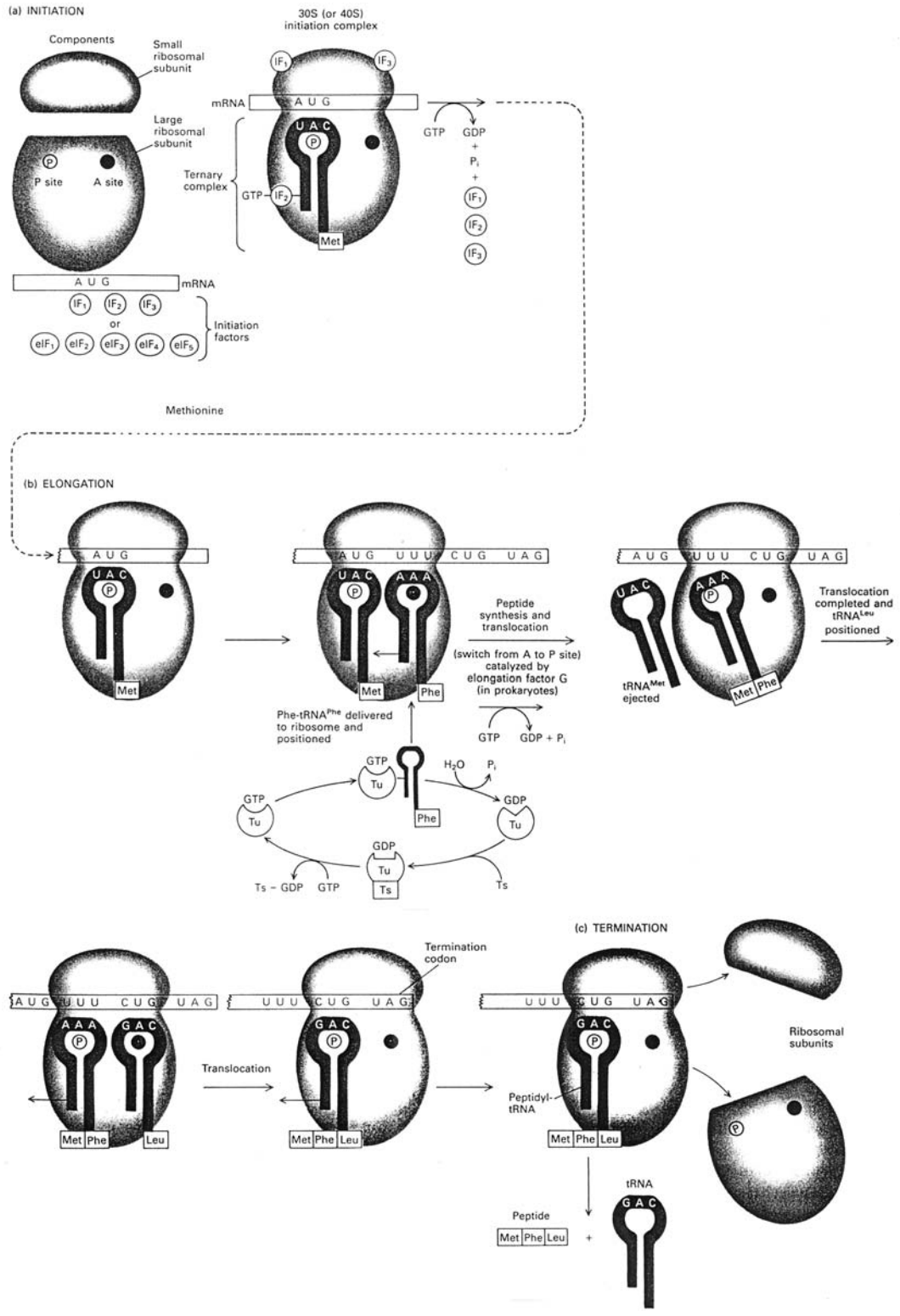

Figure 7 Cartoon diagram of the translation of tRNA-acylamino acids and mRNA to form a specific protein. The process involves: (a) the initiation phase; (b) the elongation phase; and (c) the termination phase. The chemistry involved is shown in Figure 5 and Eq. (2). (From Ref. 12.)

Table 6 In Vivo Nonhydrolytic Enzyme-Catalyzed Posttranslational Modifications of Amino Acid Residues of Proteins

Amino acid (group)	Typical modifications	Total modifications known[a]
Arginine (guanidino)	methyl-(mono- and di-)[2 b] ADP-ribosyl-[2] citrulline ornithine	6
Lysine (ϵ-NH_2)	glycosyl-[2] phospho-[2] pyridoxyl-[2] biotinyl-[2] lipoyl-[2] acetyl-[2] methyl-(mono-, di-, tri-)-[2] δ-hydroxyl-[1] δ-glycosyl-[2] crosslinks	33
Histidine (imidazole)	methyl- (1- and 3-)[2] phospho- (1- and 3-)[2] iodo- flavin-	6
Proline	4-hydroxyl-[1] 3-hydroxyl-[1] 3,4-dihydroxy-[1] 4-glycosyloxy-[2]	5
Phenylalanine (benzene ring)	β-hydroxy-[1] β-glycosyloxy-[2]	2
Tyrosine (benzene ring/ hydroxyl)	β-hydroxy-[1] β-glycosyloxy-[2] sulfono-[1] iodo- (mono-, di-)[2] brom- (mono-, di-)[2] chloro- (mono-, di-)[2] bis-ester[1] adenylyl[2] uridylyl-[2] RNA	18
Serine (hydroxyl)	phospho-[2] glycosyl-[2] methyl-[2] phophopantetheine-[2] ADP-ribosyl[2]	8
Threonine (hydroxyl)	phospho-[2] glycosyl-[2] methyl-[2]	6
Cysteine (sulhydryl)	cystine[1] glycosyl-[2] dehydroalanyl[4] heme flavin seleno-	7
Aspartic acid/ glutamic acid (carboxyl)[a]	γ-carboxyl-[1] β-phospho-[2] methyl-[2]	6
Asparagine/ glutamine (amide)[a]	glycosyl[2] R-NH- pyrrolidone	8
Carboxyl terminal residue (carboxyl)	-amide[6] -amino acid[6]	11
Amino terminal residue (amino group)	acetyl-[2] formyl-[2] glucosyl-[2] amino acyl-[2] pyruvyl-[2] α-ketobutyryl-[2] methyl-[2] glycuronyl-[2] murein[2]	19
Total modifications		135

[a]Including three each for aspartic acid and glutamic acid and four each for asparagine and glutamine.
[b]General class of enzymatic reaction: [1]oxidation/reduction; [2]transfer; [4]formation of double bond or addition to double bond; [6]ligation.
Source: Refs. 14, 16.

both end to end in a staggered array and laterally to give cylindrical fibrils with diameter range from ~ 50–2000 Å, depending on the tissue and stage of development. There are further crosslinkages, especially through desmosine formation from four lysyl side chains by lysyl oxidase (see Chapter 37).

B. Hydrolytic Posttranslational Enzymatic Modification

ins are probably modified by highly specific proteases, since most proteins are secreted from the cell for transport to other locations (organs and cells). Secretion

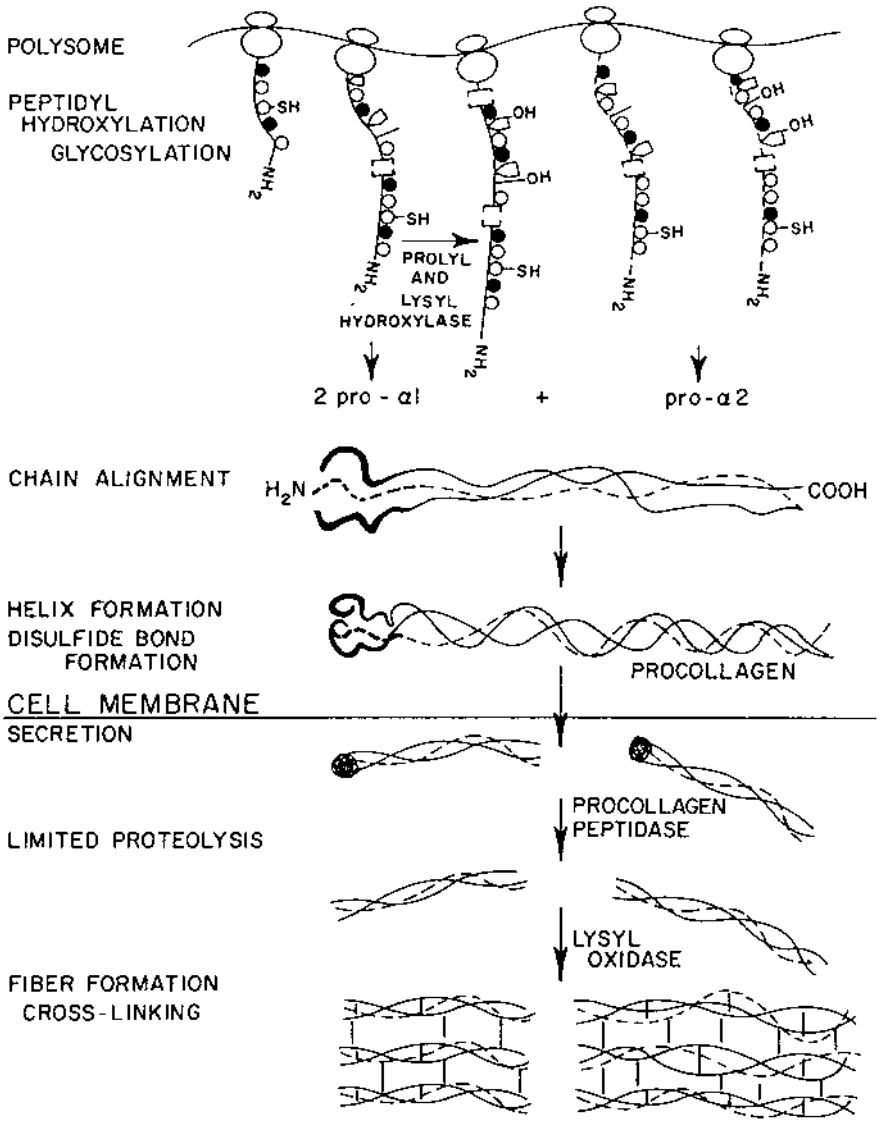

Figure 8 Proposed scheme for in vivo posttranslational enzymatic modifications involved in collagen formation. (From Refs. 17, 18.)

from the cell requires a signal peptide targeting the nascent protein for transport. The signal peptide is required to translocate the protein out of the cell. Table 7 lists a number of physiological systems controlled by posttranslational proteolysis. Table 8 gives some examples of highly specific proteases involved in physiological processes.

In addition to the posttranslational hydrolytic modifications to collagen (above), three other examples (of many) will be given for preproinsulin, chymotrypsinogen A, and preproproteins in the blood-clotting cascade.

Preproinsulin (Fig. 9) is synthesized as a 100–amino acid polypeptide. Immediately on synthesis, a highly specific protease in the luminal space of the endoplasmic reticulum removes the N-terminal signal peptide after amino acid 16 by hydrolysis. The remaining 84–amino acid proinsulin, in which two disulfide bonds have formed correctly (a posttranslational modification), is transported to the Golgi body where a 33–amino acid segment (the C segment in Fig. 9) is hydrolyzed from proinsulin by two proteolytic events at two peptide bonds (Ala^{30}–Arg^{31} and Arg^{63}–Gly^{64} of proinsulin) to give two peptides (A [21 amino acid residues]

Table 7 Physiological Systems Controlled by Limited Posttranslation Proteolysis

Physiological system	Example
Assembly	bacteriophage
	virus
	membrane
	procollagen → collagen
	fibrinogen → fibrin
Defense reactions	blood coagulation
	fibrinolysis
	complement reaction
Development	maturation of spermatozoa, release of ova, and fertilization
	(proacrosin → acrosin)
	prochitin synthetase → chitin synthetase
	prococoonase → cocoonase
Digestion	zymogen → enzyme
Hormone production	proinsulin → insulin
	angiotensinogen → angiotensin
Oncogenic transformations	division, growth, migration, and adhesion
Tissue injury	impairment of cell contact inhibition
	prekallikrein → kallikrein
	kininogen → kinin
Translocation	preprotein →protein

Source: Ref. 19.

Table 8 Some Examples of Highly Specific Proteases Involved in Physiological Processes

Group-specific proteinase of mast cells which inactivates PALP-apoenzymes
Proteinases of *B. megaterium* spores which cleave spore protein
RecA gene product from *E. coli* which cleaves bacteriophage repressor
The acid proteinase renin, which cleaves angiotensinogen to angiotensin
The carboxydipeptidase that cleaves angiotensin
The neutral proteinase enterokinase, which cleaves trypsinogen to trypsin
The albumin-degrading light subunit of rat kidney γ glutamyl transpeptidase
The plasminogen-converting streptokinase
The proteinase which cleaves the T4 prehead precursor protein
Calcium-activated protease of myofibrils
Methionine aminopeptidase

Source: Ref. 20.

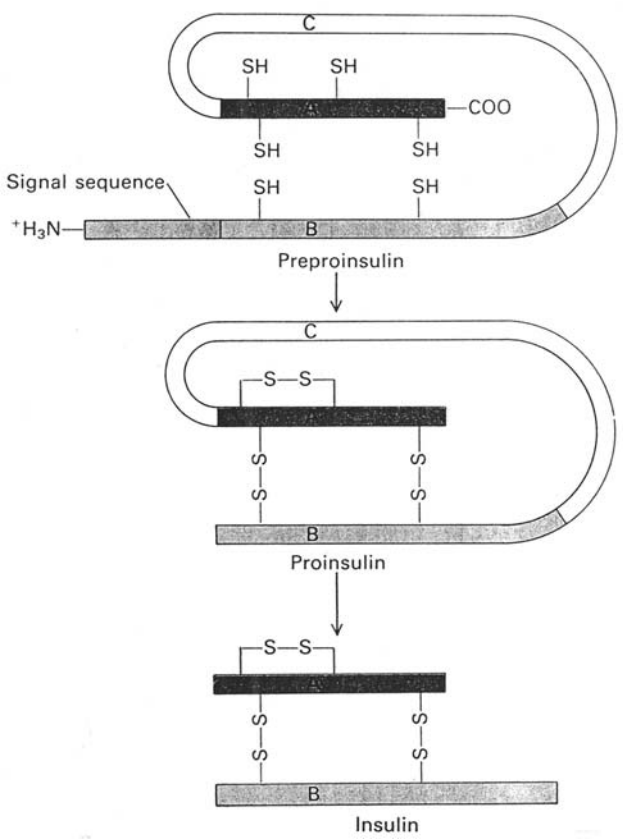

Figure 9 The processing of preproinsulin into proinsulin, and of proinsulin into insulin. The specific proteolytic cleavage of preproinsulin, which occurs immediately after the synthesis of its chain of 100 amino acids is completed, remove 16 amino acids termed the signal sequence from the amino end of the molecule. The remaining 84 amino acids constitute proinsulin, a molecule in which the correct three disulfide bonds have been formed. While the hormone is being packaged for secretion the 33 residues (of the C chain) between the A and the B chains are removed by two specific proteases to produce insulin. (From Ref. 21.)

and B [30 amino acid residues]), held together by two disulfide bonds. This is active insulin.

The proteolytic conversion of chymotrypsinogen A to α-chymotrypsin A is shown in Figure 10. Chymotrypsinogen A is stored in the pancreas as inactive protein. Following secretion into the small intestine, it is activated by trypsin (another protease). Chymotrypsinogen A is translated on ribosomes as a single polypeptide chain of 245 amino acids. The key step in activation of chymotrypsinogen A is hydrolysis of the Arg^{15}–Ile^{16} peptide bond by trypsin, thereby producing π-chymotrypsin. The active π-chymotrypsin

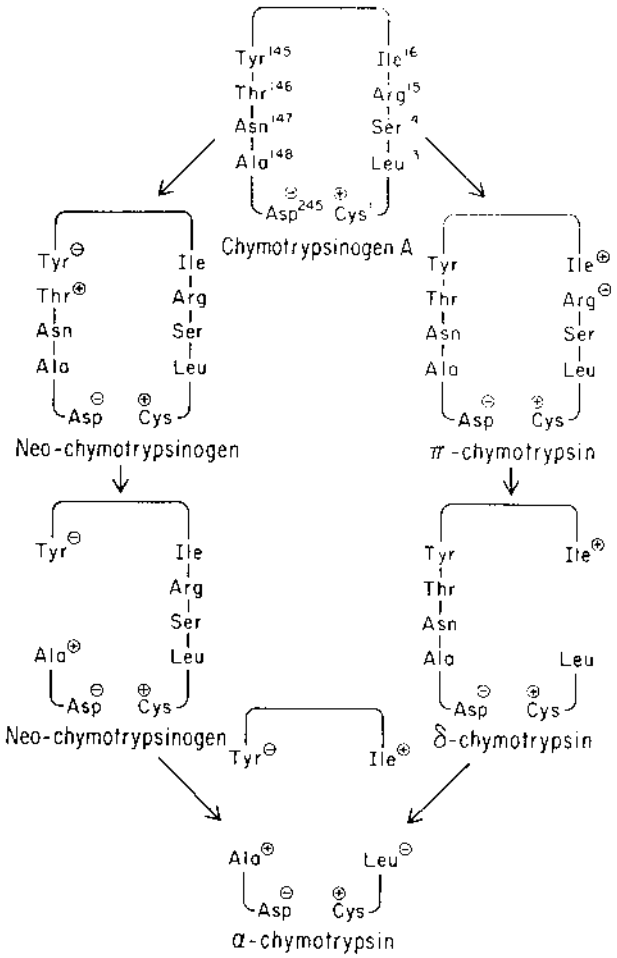

Figure 10 Schematic diagram of the role of several limited proteolytic steps in the conversion of bovine chymotrypsinogen A to π- δ-, and α-chymotrypsins. (From Ref. 22.)

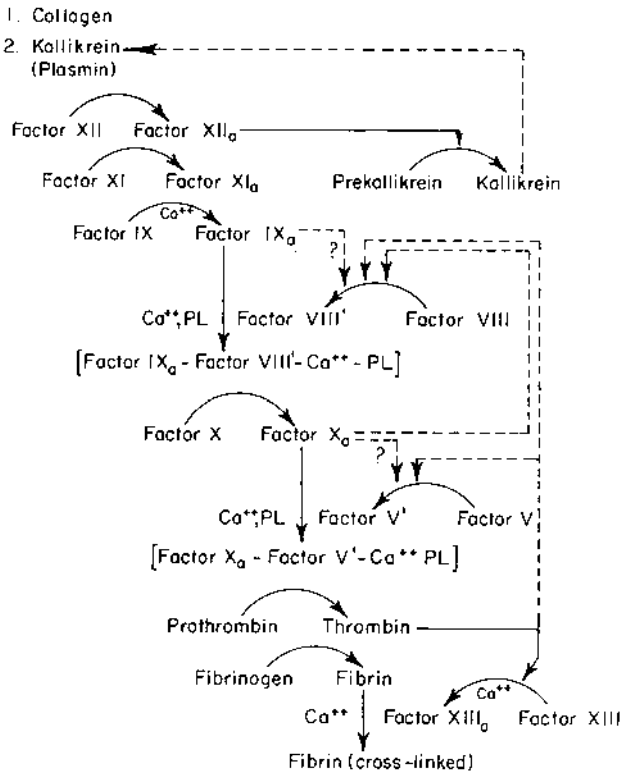

Figure 11 A proposed mechanism for blood clotting in mammalian plasma in the intrinsic system. The factor on the left side of reaction (proenzyme) is converted to active enzyme by a highly specific proteolysis. PL, phospholipids. (From Ref. 23.)

then hydrolyzes the Leu^{13}–Ser^{14} peptide bond to product active δ-chymotrypsin. δ-Chymotrypsin can then split the Tyr^{145}–Thr^{146} and Asn^{147}–Ala^{148} peptide bonds to give α-chymotrypsin, a stable enzyme. δ-Chymotrypsin can also hydrolyze the Tyr^{145}–Thr^{146} and Asn^{147}–Ala^{148} peptide bonds of chymotrypsinogen A to form inactive neochymotrypsinogen (two-step process). Proteolytic cleavage forms three large peptides and two dipeptides from the single peptide chymotrypsinogen A. The three large peptides are held together by four interchain disulfide bonds.

Posttranslational modification of the proenzymes in the blood clotting mechanism is much more complex than the two examples given above (Fig. 11). There are a total of 12 proenzymes in the activation cascade requiring 12 specific proteolytic events, along with a transglutaminase cross-linking of a glutamyl δ-carboxyl group to an ε-amino group of a lysyl residue of fibrin to form the final clot. The proenzymes are always found in the blood but the cascade of events, initiated by a cut (for example), takes < 1 min to produce a clot.

After the primary amino acid sequences of proteins are formed, they are posttranslationally modified and then folded to give the secondary and tertiary structures, as dictated by the amino acid sequence. Some proteins, such as hemoglobin, with $> 30\%$ hydrophobic amino acid residues on the surface, will form quaternary structures. Figure 12 shows the primary, secondary (α-helices) and tertiary structures of myoglobin.

C. In Vivo Turnover of Proteins

Do proteins last forever, once synthesized? The answer is no in all except one case. Table 9 shows a few exam-

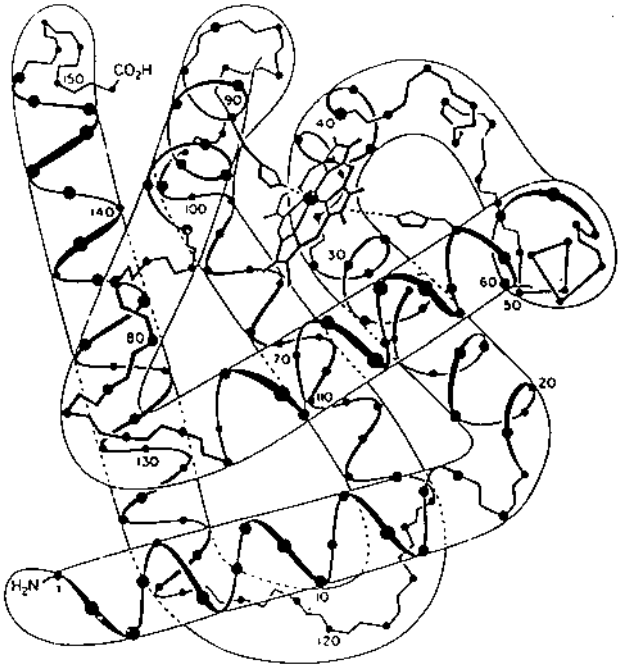

Figure 12 Schematic drawing of the primary, secondary, and tertiary structures of myoglobin as determined by x-ray crystallography. Only the α-carbons are shown. The heme is located in the upper center part of the molecule. (From Ref. 24.)

ples of turnover rates for proteins. Ornithine decarboxylase has a half-life of 10 min, while lactate dehydrogenase isoenzyme LDH_5 has a half-life of 16 days. Hemoglobin has a half-life of ~ 40 days. Elastin is thought to be stable for a lifetime.

Many studies have been done on how a protein molecule is targeted for replacement. Factors to consider include the equilibrium between native and reversible denaturated protein, the state of glycosylation, types of damage caused by metabolic events and to cofactors of enzymes. Cellular protein turnover occurs primarily in the lysosomal organelles found in the cytoplasm of cells. (See Refs. 26 and 27 for a review of in vivo protein turnover. This chapter is limited to that of protein biosynthesis.)

Table 9 Rates of Intracellular Turnover of Some Selected Proteins

Protein	Half-life
Ornithine decarboxylase	10 min
δ-Amino levulinate synthetase	60 min
Catalase	1.4 d
LDH_5	16 d
Hemoglobin	~ 40 d
Mitochondria protein as whole	4–5 d
Rat protein, 70%	4–5 d
Cultured cells	1–2 h

Source: Ref. 25.

V. COMMERCIAL UTILIZATION OF KNOWLEDGE FROM IN VIVO PROTEIN BIOSYNTHESIS

This chapter closes with a brief and incomplete look at why detailed knowledge of the pathway of protein biosynthesis is commercially important.

There is first, and foremost, the health reason for being able to potentially "fix" some 600 or so diseases and defects of humans caused by defective genes. Now that the entire human genome has been elucidated, how, and should, the defective genes be repaired in order to prolong and improve the quality of life? At what cost, in privacy, dollars, and ethical considerations?

The opportunity to use nature as an excellent "chemist" promises many rewards. Organisms, especially microoganisms, can be "reprogrammed" to concentrate most of their energy in making proteins, enzymes, and health products needed by humans and other animals. The biological process is less polluting and requires less energy and much less time, and the products are stereospecially those that can be used by other organisms, including humans. DNA shuffling and enhanced plasmid expression of a gene may lead to higher yields at faster rates than wild-type organisms can do. The change in one or a few codons may lead to more product, or a product with better properties. The Bt gene inserted into corn, cotton, and soybeans, for example, eliminates the need for highly toxic and polluting chemical pesticides.

There are several recombinant gene approaches that may be used to modify the properties of enzymes and proteins: (a) plasmid amplication; (b) selective changes in one or more nucleotides of a gene so as to modify one or a few amino acid residues in wanted proteins; (c) addition of new amino acids at the C- or N-terminal end of proteins to increase ease of purification; (d) antisense sRNAs to inhibit translation of specific genes in organisms; (e) mRNA–protein fusions to make new or modified functions (28); (f) ribosome displays to produce larger libraries for genetic cloning and improvement via combinatorial chemical techniques (28); and (g) DNA family shuffling [molecule breeding (29, 30)].

Stemmer et al. (29) are leaders in DNA family shuffling of genes. DNA shuffling can be used to great advantage for directed evolution of plants, animals, and microorganisms, in that it can select for useful mutations among similar genes from different species. Libraries of chimeric genes can be generated by random fragmentation, via specific restriction enzymes, of a pool of related genes, followed by reassembly of the fragments in a self-priming polymerase reaction. Template switching during translation causes crossovers in areas of sequence homology. Unlike traditional breeding techniques, molecular breeding by shuffling can efficiently mix gene sequences from different species of organisms. The most common uses of DNA shuffling to date are to increase specific activities of enzymes and hormones, increase stability of proteins, or improve specificity of enzymes, hormones, or drugs (29).

Some of the many examples illustrating the promise of DNA shuffling are (a) making pharmaceuticals and vaccines to target specific cells (31, 32); (b) improving starch metabolizing enzymes (33); (c) improving thymidine kinase for AZT phosphorylation (34); (d) developing humanized antibodies to ganglioside GM_2 (35); and (e) improving the specific activity and specificity of enzymes (33, 36). Specific activity increases of 50- to 150-fold have been reported in some cases.

Table 10 lists a few reasons why directed protein biosynthesis of genetic engineering of organisms has merit.

Table 10 How Can Molecular Biology Be Used for Industrial and Laboratory Purposes?

To produce needed enzymes in large, relatively pure amounts
To make needed proteins in large, relatively pure amounts
To suppress production of unwanted in vivo enzymes
To enhance production of desired in vivo enzymes
To identify and classify microorganisms
To determine amino acid sequences of proteins and enzymes
To enhance nutritional quality of food proteins
To modify proteins to improve functional properties
To increase stability of enzymes at higher temperature and pH.

REFERENCES

1. C Branden, J Tooze. Introduction to Protein Chemistry. New York: Garland Publishing, 1991, p v.
2. JB Sumner. Note. The recrystallization of urease. J Biol Chem 70:97–98, 1926.
3. M Kunitz, JH Northrop. Isolation from beef pancreas of crystalline trypsinogen, trypsin, a trypsin inhibitor and an inhibitor–trypsin compound. J Gen Physiol 19:991–1007, 1936.
4. S Moore, WH Stein. Chromatography of amino acids on sulfonated polystyrene resins. J Biol Chem 192:663–681, 1951.
5. S Moore, WH Stein. Determination of the structures of proteins. Studies on ribonuclease. Harvey Lectures 52:119–143, 1958.
6. P Edman. Determination of the amino acid sequence in peptides. Arch Biochem 22:475–476, 1949.
7. P Edman, G Begg. A protein sequenator. Eur J Biochem 1:80–91, 1967.
8. A Tiselius. Electrophoresis of serum globin. Biochem J 31:313-317, 1937.

8a. G Mendel. Versuche über Pflanzen-Hybriden. Verb Naturforshung Ver Brünn 4:3–47, 1865.

8b. A Weismann. Theory of heredity. Nature 41:317–323,373, 1890.

8c. WS Sutton. The chromosomes in heredity. Biol Bull 4:231–251, 1903.

8d. TH Morgan. Sex linked inheritance in Drosophila. Science 32: 120–122, 1910.

8e. A Garrod. Inborn Errors of Metabolism. Oxford: Oxford University Press, 1909.

8f. TH Morgan. The Theory of the Gene. New Haven: Yale University Press, 1926.

8g. GW Beadle, EL Tatum. Genetic control of biochemical reactions in *Neurospora*. Proc Natl Acad Sci USA 27: 499–506, 1941.

9. OT Avery, CM MacLeod, M McCarty. Studies on the chemical nature of the substance inducing transformation of pneumococcal types. J Exp Med 79:137–158, 1944.
10. JD Watson, FHC Crick. A structure of deoxyribonucleic acid. Nature 171:737–738, 1953.
11. F Jacob, J Monod. Genetic regulatory mechanisms in the synthesis of proteins. J Mol Biol 3:318–356, 1961.
12. J Darnell, H Lodish, D Baltimore. Molecular Cell Biology. New York: Scientific American Books, 1986, pp 105–129, 269–304.
13. P Cramer, DA Bushnell, J Fu, AL Gnatt, B Maier-Davis, NE Thompson, RR Burgess, AM Edward, PR David, RD Kornberg. Architecture of RNA polymerase and implications for the transcription mechanism. Science 288:640–648, 2000.
14. JR Whitaker, AJ Puigserver. Fundamentals and applications of enzymatic modification of proteins: an overview. In: RE Feeney, JR Whitaker, eds.

Modification of Proteins: Food, Nutritional and Pharmacological Aspects. Washington: American Chemical Society. Adv Chem Ser 198:57–87, 1982.
15. JR Whitaker. Enzymatic modification of proteins applicable to foods. In: RE Feeney, JR Whitaker, eds. Food Proteins: Improvement Through Chemical and Enzymatic Modification. Washington: American Chemical Society. Adv Chem Ser 160:95–155, 1977.
16. R Uy, F Wold. Posttranslational chemical modification of proteins. In: JR Whitaker, M Fujimaki, eds. Chemical Deterioration of Proteins. Washington: American Chemical Society. ACS Symp Ser 123:49–62, 1980.
17. P Bornstein. The biosynthesis of collagen. Annu Rev Biochem 43:567–603, 1974.
18. GJ Carinale, S Udenfriend. Prolyl hydroxylase. Adv Enzymol 41:245–300, 1974.
19. H Neurath. Limited proteolysis and zymogen activity. In: E Reich, DB Rifkin, E Shaw, eds. Proteases and Biological Control, Vol 2. Cold Spring Harbor, NY: Cold Spring Harbor Laboratory, 1975, pp 51–64.
20. H Holzer, PC Heinrich. Control of proteolysis. Annu Rev Biochem 49:63–91, 1980.
21. RE Chance, RM Ellis, WW Bromer. Porcine proinsulin: characterization and amino acid sequence. Science 161:165–167, 1968.
22. P Desnuelle. Chymotrypsin. Enzymes 4:93–118, 1960.
23. EW Davie, K Fujikawa. Basic mechanisms in blood coagulation. Annu Rev Biochem 44:799–829, 1975.
24. RE Dickerson. X-Ray analysis and protein structure. In: H Neurath, ed. The Proteins, Vol 2. New York: Academic Press, 1964, pp 603–778.
25. RT Schimke, MO Bradley. Properties of protein turnover in animal cells and a possible turnover in quality control of proteins. In: E Reich, DB Rifkin, E Shaw, eds. Proteases and Biological Control, Vol 2. Cold Spring Harbor, NY: Cold Spring Harbor Laboratory, 1975, pp 515–530.
26. AL Goldberg, JF Dice. Intracellular protein degradation in mammalian and bacterial cells. Annu Rev Biochem 43:835–869, 1974.
27. AL Goldberg, AC St. John. Intracellular protein degradation in mammalian and bacterial cells. Part 2. Annu Rev Biochem 45:747–803, 1976.
28. RW Roberts. Totally in vitro protein selection using mRNA–protein fusions and ribosome display. Curr Opin Chem Biol 3:268–273, 1999.
29. A Crameri, S-A Raillard, E Bermudez, WPC Stemmer. DNA schuffling of a family of genes from diverse species accelerates directed evolution. Nature 391:288–291, 1998.
30. J Minshull, WPC Stemmer. Protein evolution by molecular breeding. Curr Opin Chem Biol 3:284–290, 1999.
31. J Punnonen, WPC Stemmer, R Howard, PA Patten. Methods of obtaining a cell-specific binding molecule that increases uptake and/or specificity of a genetic vaccine to a target cell. PCT Int Appl WO 99 41,402, Aug 19, 1999; US Appl PV 74,294, Feb 11, 1998, 77 pp.
32. J Punnonen, WPC Stemmer, RG Whalen, R Howard. Optimization of immunomodulatory properties of genetic vaccines. PCT Int Appl WO 99, 41,368, Aug 19, 1999; US Appl 21,769, Feb 11, 1998; 105 pp.
33. WPC Stemmer, V Subramanian, SA Raillard, G Huisman. Modified starch metabolism enzymes and encoding genes for improvement and optimization of plant phenotypes. PCT Int Appl WO 00 61,731, Oct 19, 2000; US Appl PV 129,009, Apr 13, 1999; 71 pp.
34. FC Christians, L Scapozza, A Crameri, G Folkers, WPC Stemmer. Directed evolution of thymidine kinase for AZT phosphorylation using DNA family shuffling. Nat Biotechnol 17:259–264, 1999.
35. K Nakamura, M Koike, K Shitara, N Hanai, Y Kvwana, M Hasegawa. Humanized antibodies to ganglioside GM_2. US 5,939,532, Aug 17, 1999; US Appl 116,778, Sept. 7, 1993, 188 pp.
36. D Wong, G Robinson. Improving specific activity of α-amylase. Verbal communication, 2001.

16

Nucleic Acid Biosynthesis

Dominic W. S. Wong
U.S. Department of Agriculture, Albany, California, U.S.A.

I. INTRODUCTION

Biosynthesis of DNA is a biochemical process of high complexity, tightly controlled by a wide range of regulatory mechanisms. At least 30 proteins are required to replicate the chromosome of *Escherichia coli*. The overall pattern of DNA replication is semiconservative as unequivocally proved by Meselson and Stahl (1) using ^{15}N-labeling techniques. At the same time, the biochemistry and enzymology of the process of DNA replication has become the focus, since Kornberg and colleagues (2) isolated DNA polymerase I from *E. coli*. Four decades later, the general picture of DNA replication is fairly well understood, although many details remain to be filled. This chapter is not an overview of the replication process, but an attempt to describe the enzymology of the process, with emphasis on a number of relatively well-characterized enzymes critical to various stages of DNA replication in prokaryotes.

In simple genomes, DNA replication is initiated by the formation of a nucleoprotein complex formed by the association of multiple DnaA proteins with the recognition sequence at the replication origin. In *E. coli*, the origin of replication consists of a sequence of 245 bp that contains four binding sites to which DnaA can bind and initiate the stepwise assembly of all the proteins and enzymes to form a replisome necessary for replication (3). The binding of multiple dnaA proteins to the replication origin promotes denaturation of the DNA strands in an A + T-rich region adjacent to the nucleoprotein complex. In eukaryotic cells, the origin of replication consists of a core component (including an origin recognition element, a DNA-unwinding element, and an A + T-rich element) and one or more auxillary components flanking the *ori* core, that are binding sites for the activation by transcription factors (4). The opening of the strands allows several events to occur at the replication fork, each requires a unique enzyme or enzyme complex: (a) DNA helicase for progressively unwinding the parental duplex DNA; (b) primases for the synthesis of primer RNAs needed for the initiation of polymerization; (3) DNA polymerase for the continuous $5' \rightarrow 3'$ synthesis in the leading strand, and the synthesis of Okazaki fragments in the lagging strand in a discontinuous manner.

II. UNWINDING

Helicases are a family of enzymes essential to many aspects of DNA metabolism, including DNA replication, recombination, transcription, and repair and, for RNA translation, splicing and ribosomal assembly. Comparison of amino acid sequences suggests that helicases can be classified into two superfamilies, SF1 and SF2, and a smaller family consisting of DnaB-like helices (5). In the latter family, *E. coli* DnaB, RuvB, Rho, RepA, and bacteriophage T7 gp4 and T4 gp41 are helicases with a hexameric ring structure (6). This family of helicases is defined by five conserved regions. The *E. coli* DnaB and the bacteriophage T7 gp4 are the

most extensively studied replicative helicases that catalyze strand separation at the replication fork. Both are $5'-3'$ helicases which exhibit a conformational flexibility. The hexameric DnaB has been shown to exist in two different forms, with a threefold symmetry (a trimer of dimers), or sixfold symmetry, and a range of intermediate states (7). The T7 gp4 also likely involves stable dimer, trimer, and higher oligomer species (8). The functional implication of these conformations is not clear. The T7 gp4 protein, unlike DnaB, is bifunctional, consisting of a helicase domain and a primase domain, collectively known as helicase-primase.

A. Molecular Structure

The primary structure of DnaB helicase, deduced from the DNA sequence, contains 470 amino acid residues with a calculated MW of 52,265. In the mature protein, the N-terminal methionine residue is removed in vivo, leaving Ala as the N-terminal residue (9). The protein is proteolytically cleaved in a two-stage process (10). The N-terminal 14 amino acid residues are removed initially, resulting in a 50-kDa polypeptide (Fragment I), which is subsequently cleaved into two separate segments: a C-terminal 33-kDa Fragment II which contains the active site for nucleotide binding proteins, single-stranded DNA binding, DNA-dependent ATPase activity, and oligomerization to hexameric structure, and an N-terminal 12-kDa Fragment III which is essential for protein interaction with DnaC and primase in priming DNA replication in the primosome. The crystal structure of Fragment III consists of a central helix ($\alpha 1$) wrapped around by five α-helices (11).

The crystal structure of the helicase domain of the bacteriophage T7 gp4 protein has been determined (68). The T7 helicase domain has a sixfold symmetric ring with a central hole of 35 Å, that can accommodate a single-stranded DNA. The structural core is a nucleotide-binding fold consisting of a central parallel β sheet flanked by helices (Fig. 1). Four of the five motifs (H1, H1a, H2, and H3), which are conserved in the DnaB-like family, are located at the C-terminal ends of the β strands. The binding of nucleotide lies at the interface between subunits, involving interactions of residues within the four motifs. The subunits are joined with stabilization by hydrophobic and electrostatic interactions over the length of helix A intertwining between adjacent domains. Several conserved residues at the NTP binding site have been identified for interactions with the phosphates (12). Lys318 interacts with the β phosphate and also serves to stabilize

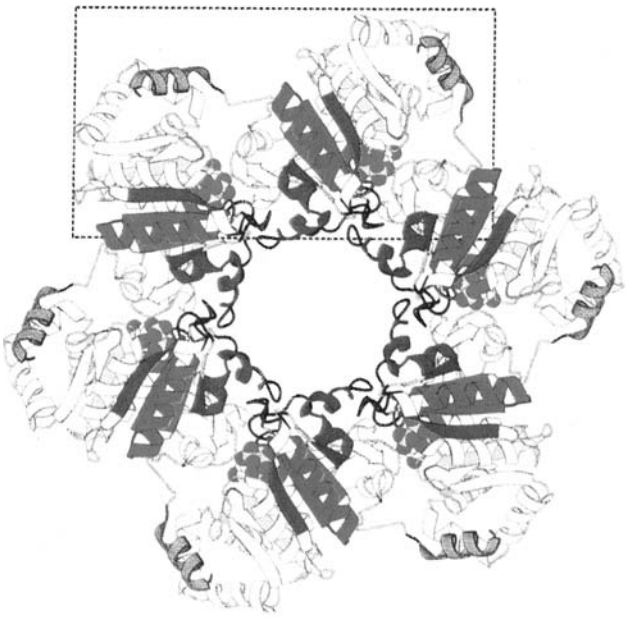

Figure 1 Ring-shaped hexamer of bacteriophage T7 gp4 helicase, with the outer diameter of 120 Å and a central hole diameter of 35 Å. The N-terminal helix of each subunit packs against the neighboring subunit of the hexamer in a swapping arrangement. (Reprinted from Ref. 68, Copyright 1999, with permission from Elsevier Science.)

the transition state during hydrolysis. Arg522 is in contact with the γ phosphate, which is linked to residues in the ssDNA binding site (located in motif H4) via His465. This arrangement may provide a switch coupling ATP hydrolysis to DNA binding. Both β and γ phosphates are coordinated by a Mg^{2+} ion that ligands to Ser319 and Asp424 sidechains.

B. NTP Binding and ATP Hydrolysis

For the unwinding of double stranded DNA, cooperative NTP binding and hydrolysis are required to induce conformational changes necessary to promote DNA binding and translocation of helicase along the DNA (13). Studies on *E. coli* DnaB suggests that all nucleotides bind with high affinity to three sites, followed by a second phase of low-affinity binding, with a negative cooperativity (14). For the bacteriophage T7 gp4, nucleotide binding at the three high-affinity sites exhibits positive cooperativity (15). The T4 helicase shows a preference with dTTP, and one to two NTPs per hexamer is sufficient for the interaction between helicase and DNA. Crystallographic studies on the T7 gp4 helicase domain indicate that NTP binding results in the

rotation of the subunits of the ring with a 15° distortion from a sixfold symmetry (12). This conformational change gives rise to the negative cooperativity of NTP binding; binding at one site confers a negative effect on the binding of the subsequent site. A model has been proposed in which the binding sites can exist in either of two conformational states—R (relaxed) when the site is filled by ADP, P_i, and T (tense) when ATP is bound to the site. Conformational changes from R to T and vice versa with each cycle of ATP binding and hydrolysis, involves three NTP binding sites at any one stage of the cycle (13). In a two-site sequential model, one catalytic NTPase site and one site for ADP + P_i, alternating among the six subunits. It is also as likely that active hydrolysis occurs at only one site in any one cycle. Nucleotide hydrolysis is mediated by Mg^{2+} coordination of the phosphates for nucleophilic attack. The metal ion also serves to stabilize the developing negative charge of the transition site. The energy released is the driving force for the helicase to unwind DNA duplex and processively translocate along the nucleic acid lattice.

C. DNA Binding

The T7 gp4 helicase, like most hexameric helicases, binds ssDNA with a much higher affinity than dsDNA. The helicase binds a 10-mer and 30-mer with a K_d value of 10 nM, and a second strand 50-fold lower in affinity (16). Similar results have been observed for *E. coli* DnaB (17). Most DNA helicases show preferences, at least in vitro, for unwinding duplex DNA with ssDNA flanking at either 5′ or 3′ ends. The *E. coli* DnaB and the T7 gp4 helicase require a forked DNA, with ssDNA primers attached to both 5′ and 3′ ends of each complementary strand (18). In the unwinding process, T7 gp4 helicase encircles the lagging strand whereas the 3′–5′ ssDNA strand (leading strand) is excluded from the central cavity (19). In this model, the helicase translocates unidirectionally along the single-stranded DNA in the direction of the DNA duplex, facilitated by ATP hydrolysis. Alternatively, an active mechanism has been proposed for the *E. coli* Rep protein, in that the helicase binds to the dsDNA at the duplex–primer junction, and plays a direct role in destabilizing the base pairs in each catalytic step (20). A recent study showed that T4 helicase can unwind unnatural substrates having the displaced DNA strand replaced by a peptide nucleic acid mimic, at similar rates as DNA-DNA substrate, indicating that unwinding is insensitive to the chemical nature of the displaced strand (21).

III. PRIMING

DNA polymerases are unable to initiate de novo polymerization, and require the priming of DNA synthesis by RNA transcription. The process involves replication-priming RNA polymerases, called primases, that synthesize short RNA primers to provide a 3′-OH onto which the first nucleotide is added. In *E. coli*, the primase, DnaG, is produced separately from the DnaB helicase, whereas in bacteriophage T7, primase and helicase activities are found in separate domains of the gp4 protein. The priming step occurs once for the leading strand, but multiple times for DNA synthesis in the lagging strand. The *E. coli* DnaG participates in protein–protein interactions with DnaB (helicase), single-stranded DNA binding protein (SSB), and DNA polymerase III holoenzyme, for cooperative synthesis of DNA. Association of primase with the replication fork is mediated by protein–protein interaction with the DnaB helicase (22), with the binding site located at the C-terminal domain of ~ 16 kDa (23). Mutations on the surfaces of interaction between the two proteins significantly reduce primer synthesis (24). The DnaG primase synthesizes primers predominantly 10–12 nucleotides in length, starting with a purine (25). This (p)ppApPu-rich sequence at the 5′ end of the primer RNAs is structurally similar to some of the eukaryotes. The primase remains stably bound to the primer RNA site via contact with the single-strand DNA-binding protein (SSB), and must be displaced before the DNA polymerase holoenzyme can attach to the DNA duplex–primer junction. It has been suggested that the χ subunit of the γ complex in the holoenzyme competitively binds to the SSB to disrupt the primase–SSB interactions, resulting in the displacement of the primase from the primer (26).

The *DnaG* gene sequence contains a coding region of 1740 nucleotides, corresponding to 580 amino acids, with the first 14 residues cleaved off in the mature protein (27). A sequence comparison of several bacterial primases reveals a conserved zinc-finger motif in the N-terminus where the catalytic domain is located, and a conserved basic region that shares with RNA polymerase large subunits (28). That the catalytic function is located in the N-terminus has been confirmed by a study on a partial proteolytic digestion of the protein, and analysis of biochemical properties of the major fragments (29). The DnaG primase is a cashew-shaped molecule consisting of three domains: an N-terminal α/β fold, a central five-stranded β sheet sandwiched by six α-helices, and a C-terminal antiparallel, three-helix bundle (Fig. 2) (30). The active site is located at a

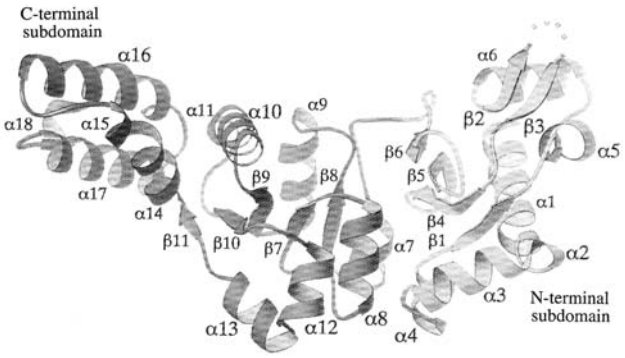

Figure 2 Structure of *Escherichia coli* DnaG primase, showing the N-terminal, central, and C-terminal subdomains from right to left. (Reprinted from Ref. 30, Copyright 2000, with permission from American Association for the Advancement of Science.)

shallow, wedge-shaped cleft formed at the interface between the N-terminal and central domains. The invariant carboxylic acids, Glu265 and Asp309, from the side formed by the central domain serve as ligands for Mg^{2+} coordination. The side covered by the N-terminal domain provides an electrostatically positive ridge for surface interaction with the template phosphodiester backbone.

IV. ELONGATION

Two modes of action are introduced in the elongation process, because of the antiparallel arrangement of the DNA duplex, and the fact that DNA polymerase can only synthesize DNA in the $5' \rightarrow 3'$ direction. DNA synthesis in the leading strand occurs in the same direction as the replication fork progress, and consequently only a single priming event is needed and DNA is synthesized continuously by DNA polymerase III holoenzyme. The leading strand synthesis is highly processive at a rate of 1000 bp/sec, owing to the action of a "sliding clamp" (β subunit) that tethers the enzyme to the DNA template. Processivity (average number of bases inserted in a single event of association, polymerization, and dissociation of the DNA polymerase on the DNA template) of 5000 (31) to even 500,000 (32) has been reported. Elongation of the lagging strands, however, consists of the formation of short DNA fragments of 1–2 kb in length, in a discontinuous process requiring repeated RNA primer synthesis, DNA extensions, primer removal, DNA repair, and gap filling. The DNA polymerase enzyme complex adapts to these various conditions by partial disassembly and reassembly of the holoenzyme structure during the synthesis of each Okazaki fragment (33, 34).

A. DNA Polymerase III

DNA polymerase III holoenzyme is a large enzyme complex (> 1 MDa) composed of 10 subunits (35), with four distinct functional components: (a) the polymerase core—α(132 kDa), ε (27 kDa), and θ (10 kDa); (b) the β subunit (38 kDa), which acts like a "sliding clamp" that confers processivity (36); (c) the γ complex ($\gamma_2\delta_1\delta'_1\chi_1\psi_1$, 47 kDa) which assembles the β subunit onto the DNA in an ATP-dependent process (37, 38); and (d) the linker protein, τ (71 kDa), which dimerizes two polymerase cores and one γ complex. The core subunits, $\alpha\varepsilon\theta$, are tightly bound and can only be dissociated by denaturation. The α subunit contains polymerase activity, while the ε subunit carries the editing function of $3'$–$5'$ exonuclease activity (39). In contrast, DNA polymerase I consists of both polymerase and $3'$–$5'$ exonuclease activities, located in the C-terminal Klenow fragment of the enzyme molecule (40).

DNA polymerases are classified into three major families—A, B, and C—based on the alignment of DNA sequences with *E. coli* polymerases (41). Family A enzymes are named for their homology to the product of the *pol*A gene encoding *E. coli* DNA polymerase I; Family B enzymes are named for homology to *pol*B gene encoding *E. coli* DNA polymerase II; and Family C for their homology to the *pol*C encoding *E. coli* DNA polymerase II α subunit. *E. coli* DNA polymerase III contains 1160 amino acid residues with a calculated MW of 129,920 daltons, and a pI of 4.93 (42). The widely investigated *E. coli* DNA polymerase I consists of 928 amino acids with a calculated MW of 103,117 and a pI of 5.37 (43, 44). Mild proteolysis of DNA polymerase I at Thr323-Val324 produces a large (Klenow) fragment of 605 amino acid residues with a MW of 68,064, and a smaller fragment of 323 amino acid residues.

B. Molecular Structure

The crystal structures of several DNA polymerases have been published, including *E. coli* DNA polymerase I Klenow fragment (40), HIV-1 reverse transcriptase (45), rat DNA polymerase β (46), *Thermal aquaticus* DNA polymerase (47), bacteriophage T7 DNA polymerase (48), bacteriophage RB69 DNA

polymerase (49), *Thermococcus gorgonarius* DNA polymerase (50), and Archaeon *Thermococcus* sp. 9°N-7 polymerase (51).

The overall structure of *E. coli* polymerase I Klenow fragment consists of a large C-terminal (polymerase) domain that has a handlike shape built by the palm, fingers, and thumb subdomains, and a smaller globular N-terminal (3′–5′ exonuclease) domain that forms a central, mostly parallel β-pleated sheet with α helices on both sides (Fig. 3) (40).

The general architecture of the polymerase domain is shared by all known polymerases. The palm subdomain contains a six-stranded antiparallel β sheet that forms the bottom of the cleft about 20–24 Å wide and 25–35 Å deep, which can accommodate $\sim 8\,bp$ of duplex DNA. The fingers subdomain contains all α helices that form one side of the wall surrounding the cleft. The other side of the wall consists of primarily two long α helices, projecting out and hanging over the cleft like a thumb. The palm subdomain is the most conserved structure among all polymerases. This is the catalytic center that contains the binding sites for the 3′ terminus of the primer and the substrate dNTP. The active site contains a cluster of three carboxylate side chains of Asp705, Asp882, and Glu883, which are ligands for two metal ions. The fingers subdomain binds the DNA template strand and directs it in a productive orientation for interactions with the primer. The thumb subdomain functions to control the accessibility of the active site to substrate binding and product release. The thumb α helices, together with numerous other protein–DNA interactions, may act as a clamp to position the template primer relative to the polymerase active site.

The small (3′–5′ exonuclease) domain contains a central mostly parallel β sheet with α helices on both sides (40). A divalent metal ion is coordinated to the carboxylate groups of Asp355, Glu357, and Asp501, and to the 5′ phosphate of dTMP, with a water molecule (or hydroxide ion) as a fifth ligand. A second metal ion at site B is observed only when dNMP is bound to the protein molecule. The meal Mg^{2+} is coordinated to the carboxylate of Asp355, Asp424, and two of the 5′ phosphate oxygens of dNMP, and three water molecules hydrogen bonded to the carboxyl oxygens of Asp424 and to backbone amides (52).

The polymerase domain and the exonuclease domain have separate DNA binding sites and can function independently. The Klenow fragment, with the polymerase active site filled by a duplex DNA, can bind and cleave a second DNA substrate at the exonuclease active site (53). Based on the crystallographic study of the Klenow fragment bound to duplex DNA (54), the duplex DNA (primer strand base-paired to the template strand) is in contact with the thumb subdomain, the single-stranded template strand beyond the site of DNA synthesis is in contact with the fingers subdomain, and the 3′ end of the primer strand lies near the carboxylates groups of the three catalytic residues in the active site. In the editing mode, the 3′ end of the primer strand is dissociated from the duplex and lies in the active site of the exonuclease domain. This particular arrangement of the substrate binding allows an interactive mechanism of DNA synthesis and

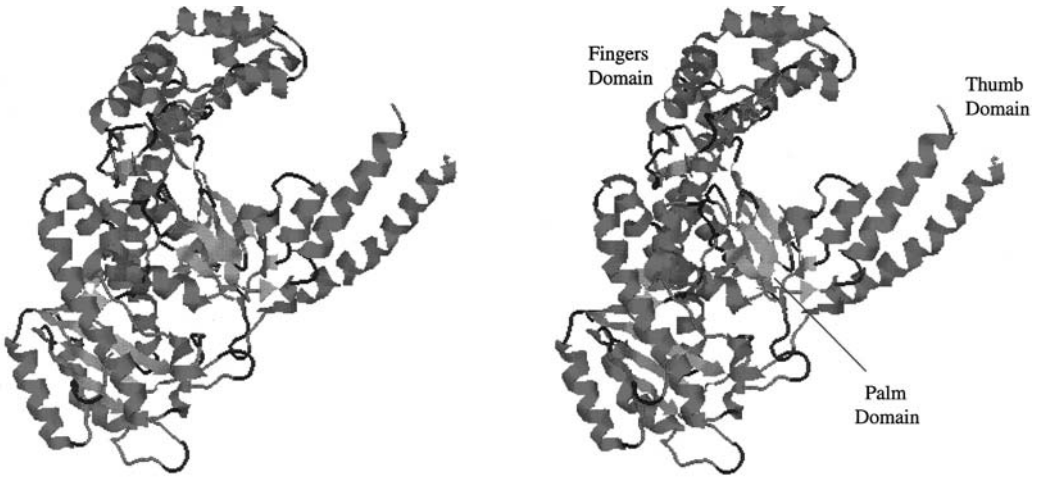

Figure 3 Schematic illustration of *Escherichia coli* DNA polymerase I Klenow fragment, showing the N-terminal, central, and C-terminal subdomains. Arrows indicate β sheet; tubes represent α helices (From PDB id: 1kfd).

proofreading (or editing) by virtue of allowing the 3′ end of the primer strand to shuttle between the two active sites, when a mismatch at the 3′ terminus occurs (55). It involves a competition between these two sites for synthesis and editing.

In *E. coli* DNA polymerase III holoenzyme, the polymerase and 3′–5′ exonuclease activities reside in separate subunits, α and ε respectively, rather than in two domains of the same subunit as in the case of DNA polymerase I described above (39). The ε subunit plays a significant role in replication fidelity by controlling the editing activity of the holoenzyme. Proofreading by DNA polymerase III depends on the cooperative interaction of the polymerase and exonuclease subunits. The efficiency and substrate specificity of the 3′–5′ exonuclease activity are markly affected when the subunit is complexed in the polymerase core. Compared with that of the free ε subunit, the activity in an $\alpha\varepsilon$ complex increased 10 to 80-fold, indicating the involvement of the α subunit in proofreading and contribution to the fidelity of DNA replication (56).

C. Reaction Mechanism

The chemical reaction at the core of DNA replication is the DNA polymerase-catalyzed nucleotidyl transfer reaction, depicted as follows:

$$\text{DNA template strand} - \text{pimer strand} + \text{dNTP} \rightarrow \text{DNA template strand} - \text{primer strand} - \text{dNMP} + \text{PPi},$$

where dTNP represents one of the four deoxynucleotides and dNMP corresponding deoxyribonucleoside 5′-monophosphate. The 3′–5′ exonuclease reaction removes the dNMP from the single-stranded primer by hydrolysis as follows:

$$\text{primer strand} - \text{dNMP} + H_2O \rightarrow \text{primer strand} + \text{dNMP}.$$

In the polymerase reaction, at least two carboxylic acid residues (Asp705 and Asp882 in DNA polymerase I Klenow fragment) serve to anchor the two metal ions which play a major role in catalysis. The Mg^{2+} at site A activates the primer's 3′-OH with one of the Asp ligands as the proton acceptor (57–59). This facilitates a nucleophilic attack on the α-phosphate of the incoming dNTP which assumes a pentacovalent transition state stabilized by both Mg^{2+} ions at sites A and B. The Mg^{2+} at site B also functions to stabilize the negative charged β and γ phosphates (Fig. 4). The high fidelity of polymerization is achieved by a large reduction in the rate of phosphodiester bond formation for incorrect nucleotides by an induced-fit conformational change, in conjunction with editing by the 3′–5′ exonuclease (60, 61). DNA polymerases have typical base substitution errors ranging from 10^{-4} to 10^{-7}. The discrimination against a wrong nucleotide insertion has been attributed to hydrogen bonding between a DNA template base and a dTNP substrate base, and more recently, to geometric selection where insertion is strongly favored by substrates with bond angles and distances that conform to the Watson-Crick model (62).

Structural and kinetic studies of 3′–5′ exonuclease reveal that phosphoryltransfer is mediated by a two-metal ionphosphoryltransfer mechanism (52, 55). One of the metal ions (site A), acting as a Lewis acid, facilitates a nucleophilic attack by a water molecule on the phosphorous atom of the terminal nucleotide, from a position opposite the 3′-OH leaving group. Metal ion B stabilizes the resulting pentacovalent transition state and facilitate the leaving of the 3′ oxyanion. Three carboxylic acid residues—Asp355, Asp501, and Glu357—serve to coordinate the metal ions and, together with Tyr497, to position the single-strand primer DNA and the H_2O molecule essential for catalysis.

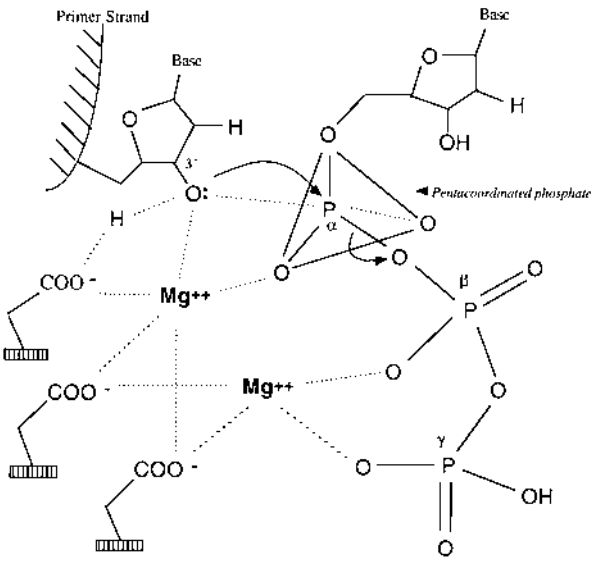

Figure 4 The two-metal ion mechanism of DNA polymerase showing the pentacoordinated transition state. (Adapted from Ref. 67, Copyright 1994, with permission from American Association for the Advancement of Science.)

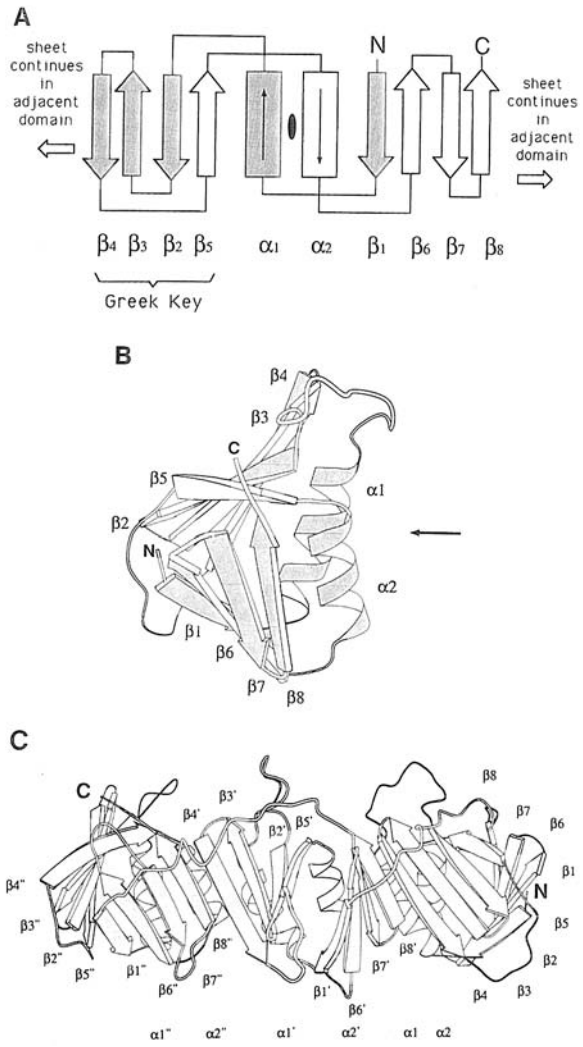

Figure 5 (A) Schematic diagram of the secondary structure of one domain of the β subunit of *Escherichia coli* DNA polymerase III holoenzyme. Arrows indicate β sheets; tubes represent a helices. (B) Ribbon diagram of a domain with the twofold symmetry axis indicated by an arrow. (C) Ribbon diagram of one monomer, consisting of three structural domains of similar architecture. (Reprinted from Ref. 63, Copyright 1992, with permission from Elsevier Science.)

D. Possessivity

E. coli DNA polymerase III holoenzyme belongs to a group of replicative polymerases which also include phage T4 DNA polymerase, and eukaryotic DNA polymerase δ. These polymerases replicate DNA processively along the entire length of the DNA template, utilizing a "sliding clamp." In *E. coli* DNA polymerase holoenzyme, the γ complex acts as a clamp loader in an ATP activation to load a β subunit ("clamp") onto the primer terminus at the single-strand/double-strand junction (or nicked duplex DNA). The association of the β clamp increases the processivity of polymerase III from polymerization of ~ 10 nucleotides to $> 50{,}000$ nucleotides per binding event, with ~ 35-fold increase in the overall rate of polymerization (32). The crystal structures of the β subunit of *E.coli* DNA polymerase III holoenzyme, and the corresponding processivity factors of T4 bacteriophage (gp45, gene 45 protein), and eukaryotic DNA polymerase (PCNA, proliferating cell nuclear antigen) have been determined (63–65). The β subunit exists as a dimer with a ring structure and a central cavity that can accommodate a DNA duplex (63). Each monomer of 366 amino acid residues consists of three domains of identical topology, each with a β sheet supporting two α-helices in a twofold symmetry (Fig. 5). A dimer formation results in 12 α-helices lining the inner surface of the ring with the β sheets on the outer layer, with an overall structure of a star-shaped ring. Once loaded by the γ complex, the β subunit ring can move freely along duplex DNA. The β subunit ring acts as a sliding clamp for the polymerase core to enable the enzyme for DNA synthesis in a processive manner. The mechanism regarding how the β dimer ring slips onto the DNA, and eventually leaves at the end of the template is not fully understood, but some involvement of breaking and closing of the ring must occur. It has been proposed that the δ subunit in the γ complex plays a major role in binding the β dimer during the loading process (66).

REFERENCES

1. M Meselson, F Stahl. The replication of DNA in *Escherichia coli*. Proc Natl Acad Sci USA 44:671–682, 1958.
2. A Kornberg. Biologic synthesis of deoxyribonucleic acid. Science 131:1503–1508, 1960.
3. D Bramhill, A Kornberg. Cell 52:743-755, 1988.
4. ML DePamphilis. Eukaryotic DNA replication: anatomy of an origin. Annu Rev Biochem 62:29–63, 1993.
5. AE Gorbalenya, EV Koonin. Helicases: amino acid sequence comparison and structure–function relationship. Curr Opin Struct Biol 3:419–429, 1993.
6. SS Patel, KM Picha. Structure and function of hexameric helicases. Annu Rev Biochem 69:651–697, 2000.
7. X Yu, MJ Jezewska, W Bujalowski, EH Egelman, 1996. The hexameric *E. coli* DnaB helicase can exist in different quaternary states. J Mol Bio 259:7–14, 1996.
8. LE Bird, K Hakansson, H Pan, DB Wigley. Characterization and crystallization of the helicase

domain of bacteriophage T7 gene 4 protein. Nucleic Acids Res 25:2620–2626, 1997.
9. N Nakayama, N Arai, MW Bond, Y Kaziro, K-i Arai. Nucleotide sequence of *dnaB* and the primary structure of the *dnaB* protein from *Escherichia coli*. J Biol Chem 259:97–101, 1984.
10. N Nakayama, N Arai, Y Kaziro, K-i Arai. Structural and functional studies of the dnaB protein using limited proteolysis. J Biol Chem 259:88–96, 1984.
11. D Fass, CE Bogden, JM Berger. Crystal structure of the N-terminal domain of the DnaB hexameric helicase. Structure 7:691–698, 1999.
12. MR Singleton, MR Sawaya, T Ellenberger, DB Wigley. Crystal structure of T7 gene 4 ring helicase indicates a mechanism for sequential hydrolysis of nucleotides. Cell 101:589–600, 2000.
13. H Xu, J Frank, T Niedenzy, W Saenger. DNA helicase RepA: cooperative ATPase activity and binding of nucleotides. Biochemistry 39:12225–12233, 2000.
14. W Bujalowski, MM Klonowska. Negative cooperativity in the binding of nucleotides to *Escherichia coli* replicative DnaB protein. Interactions with fluorescent nucleotide analog. Biochemistry 32:5888–5900, 1993.
15. MM Hingorani, SS Patel. Cooperative interactions of nucleotide ligands are linked to oligomerization and DNA binding in bacteriophage T7 gene 4 helicases. Biochemistry 35:2218–2228, 1996.
16. MM Hingorani, SS Patel. Interactions of bacteriophage T7 DNA primase/helicase protein with single-stranded and double-stranded DNAs. Biochemistry 32:12478–12487, 1993.
17. MJ Jezewska, S Rajendran, W Bujalowski, Functional and structural heterogeneity of the DNA binding site of the *Escherichia coli* primary replicative helicase DnaB protein. J Biol Chem 273:9058–9069, 1988.
18. JH Lebowitz, RM McMacken. The *Escherichia coli* dnaB replication protein is a DNA helicase. J Biol Chem 261:4738–4748, 1986.
19. KJ Hacker, KA Johnson. A hexameric helicase encircles one DNA strand and excludes the other during DNA unwinding. Biochemistry 36:14080–14087, 1997.
20. M Amaratunga, TM Lohman. *Escherichia coli* Rep helicase unwinds DNA by an active mechanism. Biochemistry 32:6815–6820, 1993.
21. AJ Tackett, PD Morris, R Dennis, TE Goodwin, KD Raney. Unwinding of unnatural substrates by a DNA helicase. Biochemistry 40:543–548, 2001.
22. K Tougu, KJ Marians. The interaction between helicase and primase sets the replication fork clock. J Biol Chem 271:21398–21405, 1996.
23. K Tougu, H Peng, KJ Marians. Identification of a domain of *Escherichia coli* primase required for functional interaction with the DnaB helicase at the replication fork. J Biol Chem 269:4675–4682, 1994.
24. Y-B Lu, PVAL Ratnakar, BK Mohanty, D Bastia. Direct physical interaction between DnaG primase and DnaB helicase of *Escherichia coli* is necessary for optimal synthesis of primer RNA. Proc Natl Acad Sci USA 93:12902–12907, 1996.
25. T Kitani, K-y Yoda, T Ogawa, T Okazaki. Evidence that discontinuous DNA replication in *Escherichia coli* is primed by approximately 10 to 12 residues of RNA starting with a purine. J Mol Biol 184:45–52, 1985.
26. A Yuzhakov, Z Kelman, M O'Donnell. Trading places on DNA—a three-point switch underlies primer handoff from primase to α the replicative DNA polymerase. Cell 96:153–163, 1999.
27. BL Smiley, JR Lupski, PS Svec, R McMacken, GN Godson. Sequences of the *Escherichia coli dnaG* primase gene and regulation of its expression. Proc Natl Acad Sci USA 79:4550–4554, 1982.
28. J Versalovic, JR Lupski. The *Haemophilus influenzae dnaG* sequence and conserved bacterial primase motifs. Gene 136:281–286, 1993.
29. W Sun, J Tormo, TA Steitz, GN Godson. 1994. Domains of *Escherichia coli* primase: functional activity of a 47-kDa N-terminal proteolytic fragment. Proc Natl Acad Sci USA 91:11462–11466, 1994.
30. JL Keck, DD Roche, AS Lynch, JM Berger. Structure of the RNA polymerase domain of *E. coli* primase. Science 287:2482–2486, 2000.
31. PJ Fay, KO Johanson, CS McHenry, R Bambara. Size class of products synthesized processively by two subassemblies of *Escherichia coli* DNA polymerase III holoenzyme. J Biol Chem 257:5692–5699, 1982.
32. M Mok, KJ Marians. The *Escherichia coli* preprimosome and DNA B helicase can form replication forks that move at the same rate. J Biol Chem 262:16644–16654, 1987.
33. PT Stukenberg, PS Studwell-Vaughan, M O'Donnell. Mechanism of the sliding β-clamp of DNA polymerase III holoenzyme. J Biol Chem 266:11328–11334, 1991.
34. Y Naktinis, J Turner, M O'Donnell. A molecular switch in a replication machine defined by an internal competition for protein rings. Cell 84:137–145, 1996.
35. H Maki, S Maki, A Kornberg. DNA polymerase III holoenzyme of *Escherichia coli*. J Biol Chem 263:6570–6578, 1988.
36. Z Kelman, M O'Donnell. DNA polymerase III holoenzyme: structure and functional of a chromosomal replicating machine. Annu Rev Biochem 64:171–200, 1995.
37. CS McHenry. DNA polymerase III holoenzyme. J Biol Chem 266:19127–19130, 1991.
38. R Onrust, PT Stukenberg, M O'Donnell. Analysis of the ATPase subassembly which initiates processive DNA synthesis by DNA polymerases. J Biol Chem 266:21681–21686, 1991.
39. RH Scheuermann, H Echols. A separate editing exonuclease for DNA replication: the ε subunit of

Escherichia coli DNA polymerase III holoenzyme. Proc Natl Acad Sci USA 81:7747–7751, 1984.
40. DL Ollis, P Brick, R Hamlin, NG Xuong, TA Steitz. Structure of large fragments of *Escherichia coli* DNA polymerase I complexed with dTMP. Nature 313:762–766, 1985.
41. DK Braithwaite, J Ito. Compilation, alignment, and phylogenetic relationships of DNA polymerases. Nucleic Acids Res 21:787–802, 1993.
42. HG Tomasiewicz, CS McHenry. Sequence analysis of the *Escherichia coli dnaE* gene. J Bacteriol 169:5735–5744, 1987.
43. CM Joyce, WS Kelly, NDF Grindley. Nucleotide sequence of the *Escherichia coli polA* gene and primary structure of DNA polymerase I. J Biol Chem 257:1958–1964, 1982.
44. WE Brown, KH Stump, WS Kelly. *Escherichia coli* DNA polymerase I. J Biol Chem 257:1965–1972, 1982.
45. LA Kohlstaedt, J Wang, JM Friedman, PA Rice, TA Steitz. Crystal structure at 3.5 Å resolution of HIV-1 reverse transcriptase complexed with an inhibitor. Science 256:1783–1790, 1992.
46. MR Sawaya, H Pelletier, A Kumar, SH Wilson, J Kraut. Crystal structure of rat DNA polymerase β: evidence for a common polymerase mechanism. Science 264:1930–1935, 1994.
47. S Koroleve, M Nayal, WM Barnes, ED Cera, G Waksman. Crystal structure of the large fragment of *Thermus aquaticus* DNA polymerase I at 2.5 Å resolution: structural basis for thermostability. Proc Natl Acad Sci USA 92:9264–9268, 1995.
48. S Doublie, S Tabor, AM Long, CC Richardson, T Ellenberger. Crystal structure of a bacteriophage T7 DNA replication complex at 2.2 Å resolution. Nature 391:251–258, 1998.
49. J Wang, AKMA Sattar, CC Wang, JD Karam, WH Konigsberg, TA Steitz. Crystal structure of a pol α family replication DNA polymerase from bacteriophage RB69. Cell 89:1087–1099, 1997.
50. K-P Hoppner, A Eichinger, RA Engh, F Laue, W Ankenbauer, R Huber, B Angerer. Crystal structure of a thermostable type B DNA polymerase from *Thermococcus gorgonarius*. Proc Natl Acad Sci USA 96:3600–3605, 1999.
51. AC Rodriguez, H-W Park, C Mao, LS Beese. Crystal structure of a Pol α family DNA polymerase from the hyperthermophilic Archaeon *Thermococcus* sp. 9°N-7. J Mol Biol 299:447–462, 2000.
52. LS Beese, TA Steitz. Structural basis for the 3′–5′ exonuclease activity of *Escherichia coli* DNA polymerase I: a two metal ion mechanism. EMBO J 10:25–33, 1991.
53. CE Catalano, S Benkovic. Inactivation of DNA polymerase I (Klenow fragment) by adenosine 2′, 3′-epoxide 5′-triphosphate: evidence for the formation of a tight-binding inhibition. Biochemistry 28:4374–4382, 1989.
54. LS Beese, V Derbyshire, TA Steitz. Structure of DNA polymerase I Klenow fragment bound to duplex DNA. Science 260:352–355, 1993.
55. PS Freemont, JM Friedman, LS Beese, MR Sanderson, TA Steitz. Cocrystal structure of an editing complex of Klenow fragment with DNA. Proc Natl Acad Sci USA 85:8924–8928, 1988.
56. H Maki, A Kornberg. The polymerase subunit of DNA polymerase III of *Escherichia coli*. J Biol Chem 260:12987–12992, 1985.
57. PMJ Burgers, F Eckstein. A Study of the mechanism of DNA polymerase I from *Escherichia coli* with diastereomeric phosphorothioate analogs of deoxyadenosine triphosphate. J Biol Chem 254:6889, 1979.
58. CM Joyce, TA Steitz. Polymerase structures and function: variations on a theme? J Bacteriol 177:6321–6329, 1995.
59. TA Steitz. DNA polymeases: structural diversity and common mechanisms. J Biol Chem 274:17395–17398, 1999.
60. RD Kuchta, P Benkovic, SJ Benkovic. Kinetic mechanism whereby DNA polymerase I (Klenow) replicates DNA with high fidelity. Biochemistry 27:6716–6725, 1988.
61. I Wong, SS Patel, KA Johnson. An induced-fit kinetic mechanism for DNA replication fidelity: direct measurement by single-turnover kinetics. Biochemistry 30:526–537, 1991.
62. MF Goodman. Hydrogen bonding revisited: geometric selection as a principal determinant of DNA replication fidelity. Proc Natl Acad Sci USA 94:10493–10495, 1997.
63. X-P Kong, R Onrust, M O'Donnell, J Kuriyan. Three-dimensional structure of the β subunit of *E. coli* polymerase III holoenzyme: a sliding DNA clamp. Cell 69:425–437, 1992.
64. I Moarefi, D Jeruzalmi, J Turner, M O'Donnell, J Kuriyan. Crystal structure of the DNA polymerase processivity factor of T4 bacteriophage. J Mol Biol 296:1215–1223, 2000.
65. TSR Krishna, X-P Kong, S Gary, PM Burgers, J Kuriyan. Crystal structure of the eukaryotic DNA polymerase processivity factor PCNA. Cell 79:1233–1243, 1994.
66. FP Leu, MM Hingorani, J Turner, M O'Donnell. The δ subunit of DNA polymerase III holoenzyme serves as a sliding clamp unloader in *Escherichia coli*. J Biol Chem 275:34609–34618, 2000.
67. H Pelletier, MR Sawaya, A Kumar, SH Wilson, J Kraut. Structures of ternary complexes of rat DNA polymerase β, a DNA template-primer, and ddCTP. Science 264:1891–1903, 1994.
68. MR Sawaya, S Guo, S Tabor, CC Richardson, T Ellenberger. Crystal structure of the helicase domain from the replicative helicase-primase of bacteriophage T7. Cell 99:167–177, 1999.

17

Protein Modification to Optimize Functionality
Protein Hydrolysates

Ton Kunst
Quest International, Naarden, The Netherlands

I. INTRODUCTION

Proteins are used abundantly in the food industries because of their nutritional value and functional properties such as emulsification, foaming, gelation, hydration, and textural properties. These functional properties of proteins are related to their molecular structures and their ability to interact with other components in the food matrix. The recently published book "Functionality of Proteins in Food" (1) reviews the results of > 50 years' extensive research to understand the factors affecting protein functionality and to develop methods to improve functionality.

Ideally, food proteins should possess a broad range of functional properties. Most commercial food proteins, however, have a limited functionality or have limitations with respect to their use in food systems. A better knowledge about structure–function relations and interactions allows the selection and/or development of optimal performing ingredients and results in the final food products with improved properties. Figure 1 schematically shows the structure–function relations in foods. Individual ingredients are combined and are processed into a final food product. The perception of the final product is determined by its sensory properties, and these are affected by the functional properties of the ingredients in the food matrix. The functional properties in turn are determined by the molecular structures and the molecular interactions of the ingredients; they are affected by the process conditions.

Food research is focused on building up knowledge on the relations between process conditions, structural properties, functional properties, and the properties of the final food product. Food product development is often based on a definition of the required properties or perception of the final products. The individual components are selected on basis of the required property in the final product and what is (often empirically) known about the properties of the individual ingredients. To modify the perception of the final product, normally one parameter in the food matrix (e.g., concentration or pH) or in the process (e.g., temperature) is altered and the effects are studied. If this does not result in the required food product, a new ingredient has to be developed on the basis of a specific functional requirement.

Food scientists can use many methods to broaden the functionality range and to improve specific functional properties of food ingredients. In case of proteins, both chemical and enzymatic methods can be applied to improve the functionality (2–5). The present review focuses on the partial enzymatic hydrolysis of proteins to make peptides with improved solubility and improved foaming, emulsifying, and nutritional properties. Aspects of both the production process and the application will be discussed.

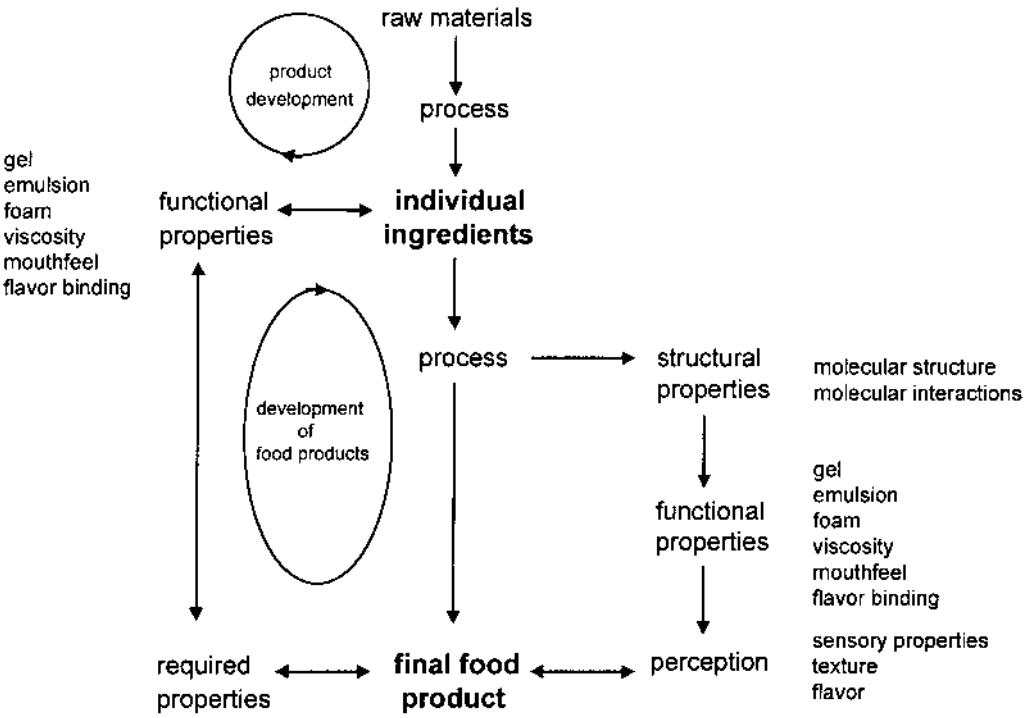

Figure 1 Structure–function relations in foods.

II. PROTEINS, PROTEIN HYDROLYSIS, AND PROTEIN HYDROLYSATES

Proteins are linear polymers of amino acids that are covalently linked via a peptide bond. The hydrolysis of proteins involves the hydrolytic degradation of this peptide bond using alkali, acid or enzyme [Eq. (1)].

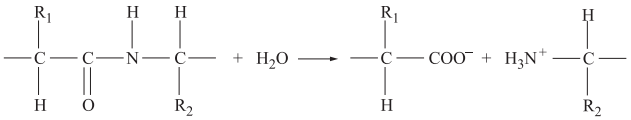

(1)

Acid hydrolysis has traditionally been used to produce flavor products (hydrolyzed vegetable protein or HVP). Most of the literature on the production of protein hydrolysates with acids is published in the form of patents. A short summary and review is given by Dave et al. (6). Today the use of acid hydrolysis of proteins is limited owing to the risk of the formation of chloropropanols during the hydrolysis.

Alkali hydrolysis of proteins has long been used to produce foaming agents to substitute egg proteins or to produce fire extinguisher foams. Also, for the alkali hydrolysis most of the literature is published in the form of patents (7, 8).

Neither alkali nor acid hydrolysis is very specific; the rate of hydrolysis of the peptide bond is mainly determined by the side chain of the amino acid residue of the peptide bond (9). In addition, a number of amino acids, e.g., cystine, serine, and threonine, are destroyed and undesired components such as lysinoalanine may be formed (10). Racemerization of amino acid residues also occurs during alkali hydrolysis (4).

Enzymatic hydrolysis is much milder than acid or alkali hydrolysis and does not lead to the destruction of amino acids. It also is much more specific. By selection of the proper enzymes the cleavage of specific peptide bonds is possible. The enzymatic hydrolysis of proteins has extensively been studied by Adler-Nissen (11).

One of the key parameters in protein hydrolysis is the degree of hydrolysis (DH). This is defined as the percentage of peptide bonds cleaved. The DH is usually approximated by the AN/TN ratio in which AN is the amount of amino nitrogen and TN is the amount of total nitrogen as determined via the Kjeldahl method. There are different methods to determine the number of amino-nitrogen groups in the hydrolysate. Well-known and often applied methods are the Formol titration (12), the determination of

free amino groups by the reaction with o-phthalic anhydride in the OPA method (13), and the determination of free amino groups by the reaction with 2,4,6-trinitrobenzene sulfonic acid in the TNBS method (14). The actual properties of a protein hydrolysate are determined by the chain length of the peptides. The average peptide chain length (PCL), given as the number of amino acids in the peptide, can be approximated from the degree of hydrolysis via $PCL = 100/DH$.

More important and more informative, however, than the average peptide chain length is the peptide chain length distribution. This can be approximated by gel filtration techniques, and can be determined by methods involving mass spectrometry or by a procedure involving the Edman degradation technique (15).

III. PRODUCTION OF ENZYMATIC PROTEIN HYDROLYSATES

A. General Aspects

For the production of protein hydrolysates with enzymes, a wide variety of endo- and exopeptidases are available as well as a great number of downstream processing techniques. A schematic overview is shown in Figure 2. A protein with a certain amino acid composition and sequence is hydrolyzed by one or more enzymes each with a certain specificity and activity. Prior to hydrolysis the protein raw material can be pretreated. The hydrolysis reaction depends on the pH, the temperature, and the concentrations of substrate and enzyme.

In industrial practice the reaction in general is carried out in batch form and takes a few hours (16). During hydrolysis the degree of hydrolysis increases and phenomena such as enzyme inactivation and product inhibition start to play a role. After hydrolysis the enzyme is inactivated (e.g., by heat treatment). The obtained hydrolysate can be subjected to a number of posttreatments such as centrifugation or (membrane) filtration to remove insoluble components or larger peptides. Finally a dried product is obtained with specific nutritional and functional properties that are determined by physicochemical properties such as the amino nitrogen (AN), the total nitrogen (TN), the free and total amino acid profile (FAA and TAA), and the peptide chain length distribution. Knowledge about the relations between the final product properties and the process conditions allows control of the reaction and makes it possible to produce hydrolysates that are optimally suited for their application.

B. The Enzymes

It will be clear that the selection of a proper enzyme is crucial for the final results. The choice of the enzyme is determined by parameters such as the required amount of free amino acids and the required degree of hydrolysis. An enzyme with a broader specificity in general results in a higher DH.

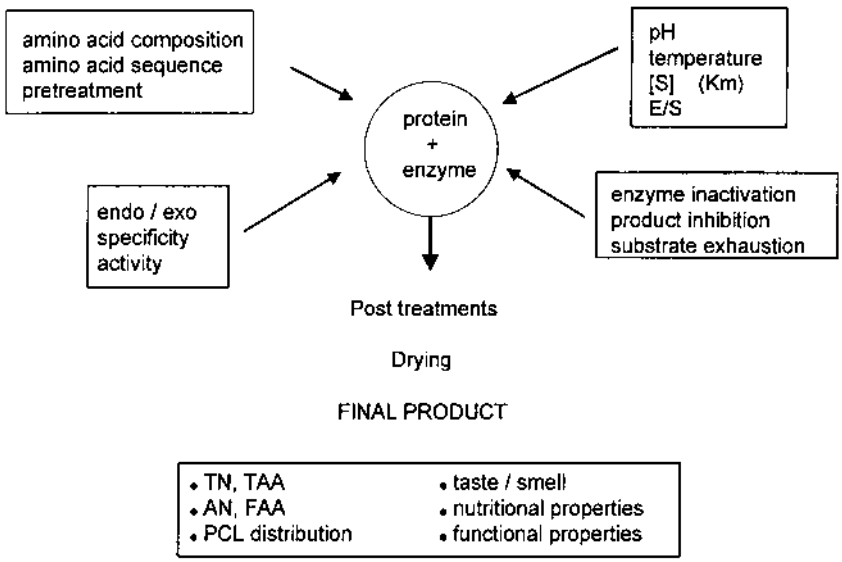

Figure 2 Production of protein hydrolysates.

Table 1 Industrially Relevant Endopeptidases

Enzyme	EC number	Preferential cleavage
Serine proteases	3.4.21	
Chymotrypsin	3.4.21.1	tyr-, trp-, phe-, leu-
Trypsin	3.4.21.4	arg-, lys-
Subtilisins	3.4.21.12	mainly hydrophobic-
Cysteine proteases	3.4.22	
Cathepsin B	3.4.22.1	arg-, lys-, phe-X-
Papain	3.4.22.2	arg-, lys-, phe-X-
Ficin	3.4.22.3	phe-, tyr-
Bromelain	3.4.22.4	lys-, arg-, phe-, tyr-
Aspartic proteases	3.4.23	
Pepsin	3.4.23.1	aromatic-, leu-, asp-, glu-
Chymosin	3.4.23.4	cleaves phe_{105}-met_{106} bond in κ-casein
Metallo proteases	3.4.24	
Thermolysin	3.4.24.27	ile-, leu-, val-, phe-
Neutral proteinase	3.4.24.28	leu-, phe-, and others

Table 2 Examples of Exopeptidases

Enzyme	EC number
leu-aminopeptidase	3.4.11.1
lys-peptidehydrolase	3.4.11.15
gly-leu dipeptidase	3.4.13.11
di-peptidyl-peptide hydrolase	3.4.14.4
gly-pro aminopeptidase	3.4.14.5
Carboxypeptidase C or Y	3.4.16.1
Glycine carboxypeptidase	3.4.17.4
Alanine carboxypeptidase	3.4.17.8
Carboxypeptidase S	3.4.17.9

There are a number of different peptidases, which can be subdivided into endo- and exopeptidases. There are four classes of endopeptidases or proteases, which differ in the nature of their catalytic center. Examples of some industrially relevant enzymes and their specificity are given in Table 1.

The exopeptidases can be subdivided into a number of classes. Important exopeptidases are the aminopeptidases and the carboxypeptidases. The carboxypeptidases are subdivided according to their catalytic center. Exopeptidases are generally not commercially available in purified form but often are used in the form of a crude extract of microorganisms such as yeast or lactobacilli or of extracts of gland materials such as pancreatin. In Table 2 some of the more important exopeptidases are listed.

C. Protein Raw Materials

The protein raw materials commonly used to produce protein hydrolysates on an industrial scale are milk proteins, meat proteins, and a number of vegetable proteins such as soy and gluten. More recently, rice protein and pea protein (17) are also being used. Fish proteins are also frequently hydrolyzed but their main application is animal feed (18).

The amino acid profile of the protein raw material not only determines the nutritional properties of the final hydrolysate, but also affects to what extent and how easily it can be hydrolyzed by a given peptidase. It has been shown that proteins with a higher content of hydrophobic amino acids were more easily hydrolyzed by an enzyme that preferably cleaves after a hydrophobic amino acid (11). The structure of the protein raw material, its solubility, and its state of denaturation all affect the hydrolysis process.

In its simplified form the hydrolysis of a protein proceeds according to the scheme originally proposed by Linderstrøm-Lang (19). It assumes that the native and denatured (reversibly unfolded) state are in equilibrium and that only the (partly) unfolded form can be hydrolyzed by an enzyme into an intermediate form which then is hydrolyzed to the final products. Basically two types of reactions can be distinguished but real hydrolysis processes will be intermediates of these two types. In the *one-by-one* type of reaction the overall rate of hydrolysis is determined by the first step in the process (the reversible unfolding of the molecule). The equilibrium lies strongly on the native side but once a native protein molecule (partly) unfolds and a peptide bond can be cleaved, the molecule becomes unstable and further unfolds; more peptide bonds are exposed and the intermediate product can be degraded rapidly into many small peptides. Since the equilibrium lies strongly on the native side, the protein molecules will be degraded one by one; no significant amounts of intermediate products will be present but only native protein and end product. In the *zipper* type of reaction, the proteins are rapidly converted into the intermediate forms. The rate-limiting step is the slow degradation into the end products.

For those hydrolysis processes that proceed according to the one-by-one reaction the denaturation of the protein (e.g., by heat treatment) will shift the equilibrium of the first step to the "denatured side," and the initial reaction rate will increase (11). Extensive denaturation, however, impairs the solubility of the protein

owing to molecular aggregation, and this slightly decreases the hydrolysis rate.

D. Reaction Conditions

The reactions conditions such as pH, temperature, hydrolysis time, and concentration of enzyme and substrate are selected on basis of the required degree of hydrolysis (DH) of the final product and the pH and temperature optimum of the enzyme. To control the hydrolysis reaction it is necessary to monitor the DH during the reaction. This can be done with a number of methods of which the most common are the pH stat, the measurement of the increase in solubilization, the measurement of the osmolarity, and the determination of the amount of amino nitrogen formed.

1. pH Stat

Upon hydrolysis of the peptide bond a free carboxyl and a free amino group are formed that are ionized depending on the pH of the reaction mixture [see Eq. (1)]. At pH values > 6 the carboxyl group will release a H^+ ion and the pH of the reaction mixture will drop. At pH values < 5 the carboxyl group will take up a H^+ ion and the pH of the reaction mixture will rise. In the range of 5–6 the pH will not vary much. Above pH 9, H^+ are released from the ammonium group of the peptide.

When the hydrolysis reaction is carried out at pH values outside the range of pH 5–6 and is kept constant during hydrolysis, the amount of alkali or acid required to maintain the pH is a measure of the amount of hydrolyzed peptide bonds. This so-called pH stat method was originally developed by Jacobsen et al. (20). A more detailed description of how to use it to determine the DH during hydrolysis is given by Adler-Nissen (11). It is an important tool in laboratory-scale experiments. On a production scale it has the disadvantages of technical difficulties and the extra minerals that are introduced into the reaction mixture.

2. Osmometry

Upon hydrolysis soluble peptides are liberated. As a consequence the freezing point of the reaction mixture is lowered. The freezing-point depression can be correlated with the DH (11). For each set of reactions, however, the osmometer has to be calibrated by a separate determination of the amount of liberated amino nitrogen (via TNBS, Formol titration, or OPA). Although it is not a continuous method it can be carried out quickly. However, the method only takes solubilized peptides into account and consequently the observed DH may be lower than the actual DH.

3. Determination of the Amount of Amino Nitrogen

The increase in the number of amino nitrogen groups can be monitored by taking samples and analyzing them as described earlier (OPA, Formol titration, TNBS). These methods also have the disadvantage of not being continuous in most laboratories; continuous measurements, however, can be done with currently available automated equipment.

Knowledge and understanding of the relationship among hydrolysis time, enzyme amount, and degree of hydrolysis allow the control of the hydrolysis reaction. Despite many attempts, however, it is still not possible to give quantitative descriptions of the hydrolysis process. This is related to the complexity of the reactions in terms of specificity and substrate composition. With 20 different amino acids, 400 different peptide bonds can be formed, for each of which the enzyme will have a different affinity and rate of hydrolysis. First the peptide bonds for which the enzyme has the highest affinity will be cleaved, followed by those for which the affinity is lower. In addition, some peptide bonds are buried inside the tertiary structure and need to be exposed to be hydrolyzed.

In kinetic studies in general only the first few minutes are taken into account to calculate parameters such as K_m and V_{max} or k_{cat}. The production of protein hydrolysates on an industrial scale, however, can take many hours. Figure 3 shows a typical relation among process time, enzyme/protein ratio, and DH as measured by the pH stat technique. The steepest increase in DH takes place in the first 30 min of the reaction. Thereafter the reaction rate slows down. Longer hydrolysis time and the use of more enzyme result in a higher DH. A number of studies are reported in the literature in which an empirical model for the hydrolysis of proteins has been developed. These models are based either on the amount of solubilized protein (21) or on the degree of hydrolysis (11, 22, 23).

From the literature data it can be concluded that substrate limitation does not play a role in industrial protein hydrolysis processes. The data in Figure 3 show that with increasing enzyme concentrations the degree of hydrolysis increases. When substrate limitation is the rate-limiting factor it is expected that the degree of hydrolysis at the end of the process is the same for all enzyme concentrations. This is clearly

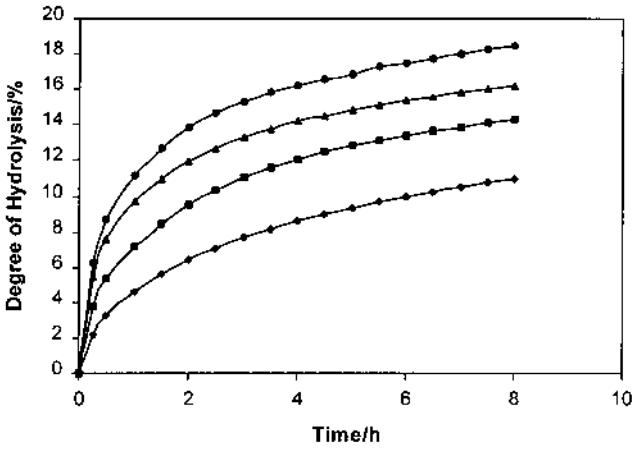

Figure 3 Relation among DH, time, and enzyme concentration. Hydrolysis conditions: temperature, 50°C; pH, 8.0; protein—soy protein, 40 g/L; enzyme—alcalase 2.4 L; enzyme concentrations—0.2 g/L (◆), 0.4 g/L (■), 0.8 gL (▲), or 1.2 g/L (●).

not the case. In industrial protein hydrolysis processes the substrate concentrations are high so that substrate saturation most likely prevails throughout most of the hydrolysis reaction (11).

The data in Figure 4 show the time course of three different hydrolysis experiments in the pH stat. Under the hydrolysis conditions as applied, enzyme inactivation was found not to be important. In the presence of 10 g/L substrate, 97% of the enzyme was still active after 48 h at 50°C. In general, enzyme inactivation does not seem to be very important provided enough

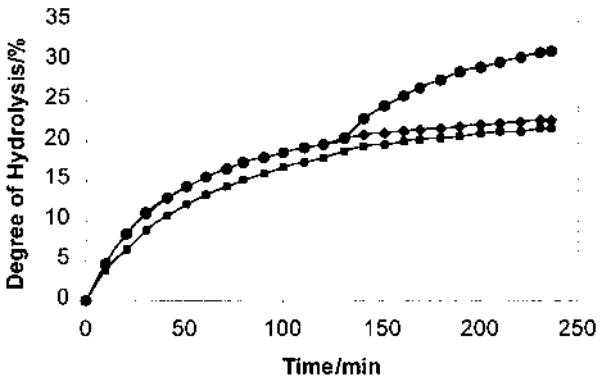

Figure 4 Product inhibition during hydrolysis. Hydrolysis conditions: temperature, 50°C; pH, 8.0; protein—potato protein, 40 g/L; enzyme—alcalase 2.4 L, 1.6 g/L. (◆) control. (●) At $t = 135$ min 20 g/L fresh substrate is added. (■) At $t = 0$ min 20 g/L peptide cocktail is added.

substrate is present (to prevent autohydrolysis of the enzyme) and the temperature is not too high (to prevent thermal denaturation).

The control hydrolysis curve in Figure 4 levels off as expected. In the second experiment, fresh substrate was added after 135 min and it was found that the rate of hydrolysis increased. In the third experiment a peptide cocktail was added at the start of the hydrolysis. This peptide cocktail was obtained by hydrolyzing the protein for 20 h, inactivating the enzyme, and removing the insolubles. It can be seen that the initial rate of hydrolysis is clearly lower than that of the control. Similar results were reported by Adler-Nissen (11), Krause et al. (24), and Haque and Antill (25). Also, the addition of fresh enzyme was found to result in an increase in the rate of hydrolysis (21, 23).

From these results it can be concluded that product inhibition is an important parameter in protein hydrolysis. The addition of fresh substrate and fresh enzyme causes a shift in the equilibrium; the addition of peptides inhibits the reaction. Adler-Nissen (26) measured the initial hydrolysis rates using hydrolysates with different DHs as substrates. It was found that the K_m was more or less independent of the DH but that V_{max} decreased with increasing DH. Similar results were obtained by Snijder and Kunst (27) as shown in Figure 5. From these results it is concluded that mixed inhibition or noncompetitive inhibition occurs (28).

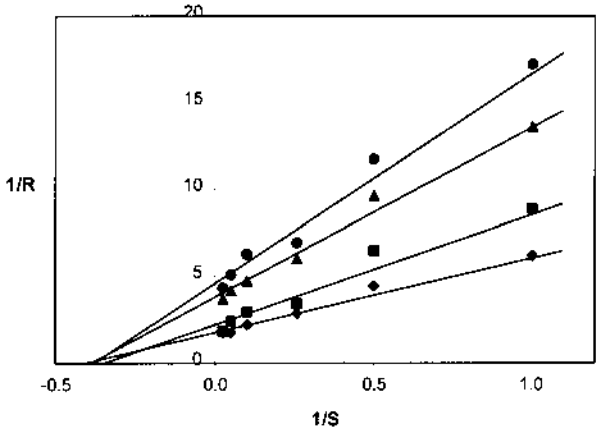

Figure 5 Effect of peptide size on enzyme kinetics. Hydrolysis conditions: temperature, 50°C; pH, 8.0; substrate—peptides obtained from potato protein. [Intact protein (◆), DH 1.8% (■), DH 4.7% (▲), DH 7.5% (●).] Substrate concentrations, 1–37.6 g/L; enzyme—alcalase 2.4 L; 0.8 g/L; R = reaction rate (meq NaOH/L/min); S = substrate concentration (g/L).

E. Downstream Processing

After the actual hydrolysis process the enzyme is inactivated via e.g. a heat treatment. The hydrolysate can be subjected to further processing steps such as separation, filtration, or treatments with charcoal or ion exchange resins (16). Charcoal nonselectively removes both high- and low-molecular-weight organic compounds and can be applied to remove off-color material and to achieve slight reductions in off-odor and bitterness. Products for patients suffering from phenylketonuria (PKU) are treated with charcoal and/or ion exchange resins to remove phenylalanine from hydrolysates (29, 30). The treatments, however, also remove tyrosine and reduce the amounts of other hydrophobic amino acids.

Filtration or separation of hydrolysates is generally applied to remove insoluble components in order to improve the clarity of the hydrolysate. Membrane filtration is often used to remove larger peptides and undigested protein fragments that are potential antigenic materials. This results in a product with a reduced allergenicity. Membrane filtration is also applied to reduce the level of endotoxins in the hydrolysate; this is important when the hydrolysate is applied in parenteral formulae or in tissue culture media. The final process step usually is drying of the hydrolysate.

F. Membrane Bioreactors

Membrane bioreactors combine the hydrolysis step and the membrane filtration step (31). The advantages of a membrane bioreactor are that the enzyme is retained (which saves costs), that the peptide size is controlled, and that peptides that inhibit the enzyme are continuously removed after formation.

The disadvantage is that the insoluble fraction in the hydrolysate is concentrated, which results in flux reduction and reduced productivity. With prolonged operation times microbiological spoilage also may become a problem; not only the insoluble protein material is retained, but also all microorganisms. Especially, the more thermophillic microorganisms may give rise to uncontrolled hydrolysis reactions. It is for these reasons that membrane bioreactors are currently not applied on an industrial scale for the production of protein hydrolysates. Further research is required to optimize the process.

G. Immobilized Enzymes

The immobilization of enzymes, including proteolytic enzymes, has been extensively studied (see Chapters 22–24 in this book). The advantage of the use of immobilized enzymes is the possibility to reuse the enzyme (which saves costs) and the possibility to produce hydrolysates in a continuous way. The application of immobilized proteolytic enzymes to produce protein hydrolysates on an industrial scale up to now is limited, however. When the immobilized enzyme is applied in a batch reactor it must be separated from the hydrolysate via e.g. a crude filtration step. The costs involved in this isolation can be higher than the savings obtained by reuse of the enzyme.

In laboratory experiments immobilized enzymes have been used in columns. Packed columns easily get blocked by the insolubles in the raw material or by the insolubles formed during hydrolysis (see Sec. IV.B.3). Expanded bed columns, therefore, have to be used. With the recently developed beads very good expanded bed columns can be made that can be applied at a production scale for adsorption of proteins from particulate-containing feedstocks (32). These beads can be used also to immobilize enzymes on the surface of the beads. The costs involved are considerable, however, and limit their application as carrier for immobilized enzymes.

In addition it is difficult to control the microbiological quality of the hydrolysate because microorganisms tend to build up on the carrier material. This requires operation at elevated temperatures, which increases the risk of protein denaturation and insolubilization. The application of immobilized enzymes in expanded bed columns thus requires a delicate balance between microbiological constraints on the one hand and protein insolubilization at the other; further research is required to establish the best conditions.

IV. APPLICATIONS

Intact, native proteins generally have well-defined three-dimensional structures that affect their functional properties. Peptides are much smaller, the molecular structure is more random, and a tertiary structure is rarely observed (33). For the secondary structure of proteins, the α-helices and the β-pleated sheets are the most important structures. Peptides in general do not have sufficient length to have enough H bonds to stabilize the helix. Upon hydrolysis of proteins the hydrophobic areas, which are normally buried inside the

folded molecule are exposed and as a consequence the properties of a protein hydrolysate strongly differ from those of the original protein.

Enzymatically hydrolyzed proteins have a wide range of both food and nonfood applications, which relate either to their nutritional or to their functional properties. Larger peptides (2–5 kDa) are mainly used as functional ingredients (aeration) or in personal-care products. Medium-size peptides (1–2 kDa) are used in clinical nutrition (34) and sports nutrition (35, 36). Smaller peptides (< 1 kDa) are used in infant food products requiring a reduced allergenicity (15) and for fermentation and tissue culture media (37).

A. Nutritional Properties

1. Nutritional Value

The nutritional value is primarily determined by the amount of essential amino acids in the protein hydrolysate and mainly depends on the amino acid composition of the protein raw material. Under some conditions a specific amino acid composition is required. For example, products for patients suffering from phenylketonuria (PKU) should be very low in phenylalanine. These products are produced from highly hydrolyzed proteins and are subjected to specific downstream processing such as treatments with charcoal or adsorption chromatography resins to remove phenylalanine (29, 30). Another example is hydrolysates with a high glutamine content. Glutamine is regarded as a conditionally essential amino acid that is required in periods of physical stress such as severe trauma, surgery, infection, starvation, or heavy training (38). Peptides rich in glutamine are also increasingly used for cell nutrition (37). In general such products are produced from wheat gluten, which contains ~ 27% glutamine.

With respect to sports nutrition it has been shown that protein hydrolysates stimulate recovery after prolonged intensive exercise (39). During high-intensity exercise, athletes use up their glycogen reserves, and the time needed to restore their muscle glycogen levels determines the time needed to recover from fatigue (40). Although the insulin release is stimulated primarily by carbohydrates, the release of insulin is further stimulated by proteins and peptides (41), resulting in an increased uptake of glucose from the blood, an increased glycogen synthesis rate, and thus an enhanced recovery after prolonged intensive exercise. Contrary to proteins, peptides are heat stable and can be applied in pasteurized, ready-to-use drinks. Furthermore, peptides are soluble over a wide pH range, which allows them to be used in refreshing drinks (36).

Not only is the nutritional value determined by the amino acid composition, but also the peptide chain length distribution seems to be an important factor. Some lactic acid bacteria for instance prefer di- and tripeptides over free amino acids (42, 43). Also, in the human small intestine most of the dietary proteins are absorbed as small peptides. There are specific carriers for small peptides that are separate from the carriers for uptake of free amino acids (44). These small peptides are more adequately absorbed in the small intestine than the equivalent free amino acids. This allows the formulation of products for enteral nutrition that gives less intestinal discomfort, as less amino acids are available for bacterial fermentation in the large intestine.

2. Reduced Allergenicity

Food allergenicity is a complex topic, and the manifestations of disease and the diagnostic methods are highly variable (45). In the majority of allergic responses a specific immunoglobulin (IgE) mediates the immediate hypersensitivity reaction. Immunoglobulins (also called antibodies) are produced by the body in response to invasions of foreign compounds such as proteins. Materials that elicit antibody production (other than IgE) in an organism are called antigens. An antigen may contain multiple antigenic determinants (epitopes), which are small regions of the antigen molecule that specifically elicits the production of antibodies to which the antigen binds. In case an antigen elicits an IgE response, the antigen is called an allergen. In order to initiate a clinical manifestation of allergenic responses, it is required that the IgE form a bridge between two epitopes; the allergen thus should have at least two epitopes at a certain distance from each other. Destroying the molecular structure of the allergen or antigen forms the basis of the application of protein hydrolysates in the control of food allergies. Decreasing the size of the molecules via hydrolysis reduces the number of protein molecules with two epitopes (and may even destroy epitopes) and will reduce the antigenicity (46).

There is, however, no definite molecular weight below which peptides are nonallergenic or above which they are allergenic. In general there appears to be a limit for antigenicity for peptides with 10–15 amino acids (47). The first products, which were marketed ~ 40 years ago, comprised > 70% free amino acids and peptides up to 8 amino acid residues long.

More recently developed products have < 10% free amino acids and peptides up to 15 amino acid residues long (15). These developments are based on a better understanding of the physiology of the small intestine (see Sec. IV.A.1).

3. Bioactive Peptides

It has long been known that proteins can be the source of bioactive peptides. Especially the milk proteins have been extensively studied (48). The main problem is how to isolate them in a commercially attractive manner. As of now only casein phosphopeptides can be manufactured on an industrial scale using a process involving ion exchange chromatography (49) or a process involving an aggregation step and an ultrafiltration step (50). Possible applications of casein phosphopeptides, which relate to their mineral binding capacity, are in the treatment of caries (51) or as mineral carriers to promote Ca^{2+} uptake (52, 53). Further research is required to design enzymes that allow the specific liberation of those sequences that are known to have a biological activity.

B. Functional Properties

Proteins and peptides are more than just a source of essential nutrients. They also have functional properties allowing them to contribute to the sensory properties of the final food product (54). Table 3 shows some functional and organoleptical properties of protein hydrolysates. The surface properties of peptides are especially important. To understand the role of protein hydrolysates it is necessary to have a general understanding of the physicochemical background of foams and emulsions. More detailed information can be found in recent reviews and textbooks on this subject (1, 55, 56).

Table 3 Important Functional and Organoleptical Properties of Protein Hydrolysates

General property	Specific property
Surface	Emulsification
	Foaming
Hydration	Solubility
Textural	Elasticity
	Viscosity
	Dough relaxation
	Gelation
Organoleptic	Taste
	Smell
	Flavor binding
	Color
	Mouth feel

1. Surface Properties

During the formation of emulsions or foams, energy is applied to disperse, deform, and break up oil droplets or air bubbles in an aqueous phase. To form a good foam or a good emulsion it is required that the newly formed air bubbles or oil droplets not (re)coalesce and that once the energy input has stopped, the obtained foam or emulsion is stable for some time. To meet these requirements surface-active agents have to be used. Surface-active agents are adsorbed at the oil–water interface (in emulsions) or air–water interface (in foams) and lower the interfacial tension. Different aspects, however, play a role in the formation on the one hand and stabilization of foams and emulsions on the other hand.

a. Formation of Foams and Emulsions. During the formation of emulsions or foams, the oil droplets or air bubbles are subjected to shear stresses and they break up when the stress exceeds the Laplace pressure difference. The Laplace pressure difference (Δp) is given by $\Delta p = 2\gamma/R$ in which γ is the surface tension and R is the radius of the oil droplet or the air bubble. From this it follows that for a given energy input smaller oil droplets or air bubbles are formed when the surface tension is lower. The (re)coalescence is prevented when the surface-active agent in the interface prevents the aggregation of oil droplets or air cells by electrostatic or steric repulsion.

The most important property for surface-active agents during the formation of foams and emulsions is the ability to quickly reduce the interfacial tension (57, 58). In the case of a protein or a peptide this requires that the molecule rapidly adsorb at the interface and rapidly unfold to maximize the reduction of the interfacial tension.

Movement to and adsorption at the interface. Much of the current knowledge on the movement to and adsorption of proteins at interfaces is collected in diffusion-driven static systems. It is important to realize that emulsification and whipping processes are highly agitated and that in such systems convection is more important. The time of movement of the protein or peptide molecule to a newly formed interface is in the order of ms. After arrival at the interface, proteins and peptides can be adsorbed. The major driving force for

adsorption is the reduction in contact area between non-polar groups and water. This reduces the free energy of the system and thus the interfacial tension. The adsorption of proteins at an interface is positively correlated with their surface hydrophobicity (55, 59).

Unfolding of the molecule and formation of films. A protein molecule that is adsorbed at an interface can unfold. The thermodynamic environment of the interface differs from that of the bulk phase, and unfolding results in a reduction of the free energy. The driving force for unfolding probably is the hydrophobic effect (56).

The surface tension of a clean air–water interface is $72\,mNm^{-1}$, which is sufficient to overcome the activation energy barrier for protein unfolding. The structure will rearrange such that the nonpolar segments are predominantly located in the gas phase and the hydrophilic parts in the aqueous phase. The foaming power is related to the rate and extent of unfolding and this depends on the flexibility of the molecule. The flexibility of the molecule is determined by the strength of the forces maintaining the structure such as S-S bridges, electrostatic interactions and repulsions, and the average hydrophobicity (59).

The surface tension of a clean oil–water interface is only $\sim 30\,mNm^{-1}$, which most probably is not enough to overcome the activation barrier for protein unfolding (55). Consequently for emulsions the surface hydrophobicity is more important than the average hydrophobicity (4, 60).

b. Stability of Emulsions and Foams. Once an emulsion or a foam is formed, its lifetime in part depends upon the viscoelastic properties of the adsorbed protein layers and their resistance to rupture. Both foams and emulsions are thermodynamically unstable systems and are subjected to various types of instabilities:

Drainage (foams) or creaming (emulsions). Drainage and creaming are caused by density differences between the phases. This process can be retarded by increasing the viscosity of the continuous phase or by gelation of the continuous phase.

Disproportionation (Ostwald ripening). This occurs when the dispersed phase is soluble in the continuous phase; it therefore only plays a role in foams. The Laplace pressure difference is greater in smaller bubbles, and as a consequence gas diffuses from small bubbles (which shrink) to large bubbles (which grow). This process is retarded when the bubbles have a uniform size and when the surface elasticity E_d exceeds $\gamma/2$ (61). The surface elasticity increases when the molecules in the interface have more intermolecular interactions.

Aggregation or flocculation. In this process air bubbles or oil droplets stick together. This process is retarded when there is more electrostatic repulsion or more steric repulsion.

Coalescence. After the aggregation of air bubbles or oil droplets the thin film separating them may break and they can flow together. The stability to coalescence can be improved by increasing the surface viscoelasticity by an increase of the intermolecular interactions.

c. General Requirements. The most important properties for a good emulsifying or foaming agent thus are the ability to rapidly reduce the interfacial tension and the ability to form a viscoelastic film that is resistant to rupture. These two properties, however, are related as can be seen for β-lactoglobulin and β-casein.

β-Lactoglobulin is a globular protein that slowly adsorbs and unfolds at the interface, but it can form strong films. It performs rather poorly in the formation of emulsions and foams but it has good stabilization properties. β-Casein, on the other hand, is a random coil molecule that quickly adsorbs at the interface; it cannot, however, form very strong films. It has good emulsification and foaming properties but poor stabilization properties.

Modifications of (globular) proteins via limited hydrolysis or by rupture of intramolecular disulfide bridges in general will result in more unfolding of the molecule. This will increase the flexibility and improve the ability to quickly reduce the interfacial tension and improve the foaming and emulsifying properties, but it will reduce the ability to form a coherent film and reduce the stabilization properties.

Figure 6 shows the interfacial properties of intact protein and protein hydrolysate on an air-water interface. The intact protein gives a surface pressure of $\sim 30\,mNm^{-1}$. The peptides obtained after hydrolysis gives a significantly higher surface pressure indicating a higher foaming capacity. The surface elasticity, which is a measure for the amount of interactions in the surface, however, is much larger for the intact protein than for the peptides. This indicates that the protein contributes more to the stability of a foam.

For good interfacial properties a peptide should have clustered hydrophobic and charged areas and a molecular weight above a certain minimum to allow this distribution (62, 63). The distribution of charge and hydrophobicity can be derived from the amino

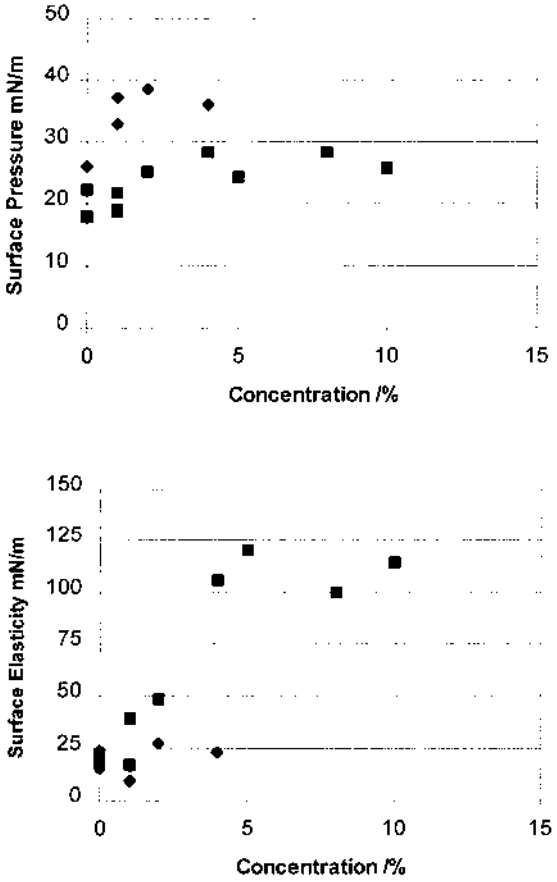

Figure 6 Surface properties of proteins and protein hydrolysates. The surface properties have been measured in a ring trough at ambient temperature. (a) Surface pressure. (b) Surface elasticity. Pea protein hydrolysate: ◆; intact pea protein: ■.

acid sequence of the protein or peptide (64, 65). An example of the distribution of the hydrophobicity in α-lactalbumin is given in Figure 7. It will be clear that hydrolysis with different enzymes will give peptides with different charge and hydrophobicity distributions, and this explains the importance of enzyme selection in the production of surface-active peptides.

Both foaming properties and emulsifying properties are strongly related to the size of the peptides. Literature reports that the optimum peptide size generally lies in the range of 15–35 amino acid residues. This corresponds to a DH of typically 3–6% (17, 66). Chobert et al. (67) and Turgeon et al. (62) report minimum peptide sizes of $\sim$ 2000 daltons. Also, Caessens (63) reported that smaller hydrophilic peptides have poor foam and emulsion stabilizing properties.

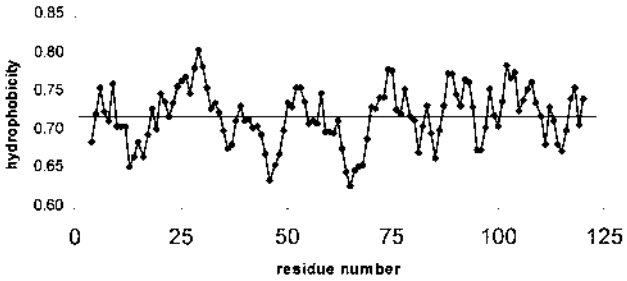

Figure 7 Hydrophobicity pattern of α-lactalbumin. The hydrophobicity is calculated using the hydrophobicity data given by Rose and Dworkin (65). The protein parts that have a hydrophobicity > 0.72 will be buried in the structure.

2. Gelation and Water Binding

The formation of a gel requires large protein molecules that can form crosslinks in all three dimensions. The strength and hardness of a gel are related to the size and shape of the molecule rather than to the amino acid composition. A very good correlation between the average molecular weight and the gel hardness was found (68). Hydrolysis of proteins, which reduces the size of the molecules, is therefore expected to reduce the ability to form a gel.

However, it has been shown that the hydrolysis of whey protein (69) or casein (70) can lead to the formation of aggregates and the formation of a gel. Electron microscopy showed that these gels have a particulate type of structure. The aggregates in the whey protein hydrolysate consist of a number of peptides with molecular weights of 2000–6000 daltons which are held together by noncovalent interactions. It is hypothesized that a limited hydrolysis causes the protein to unfold after which exposed hydrophobic areas can interact intramolecularly to form aggregates (71). The aggregates from the casein hydrolysates were found to have a higher proportion of hydrophobic amino acids. It is likely that the phenomenon of aggregate formation is sometimes misinterpreted as a plastein reaction. At this moment the potential for improvement of the texture of food products is not clear and further research will be required.

3. Solubility

Partial hydrolysis of proteins is often used to improve the solubility of a protein (Fig. 8). For optimal solubilization of soy protein a DH of $\sim$ 8% or higher is required (66). A 100% solubility, however, is never achieved; this is related partly to peptide–peptide inter-

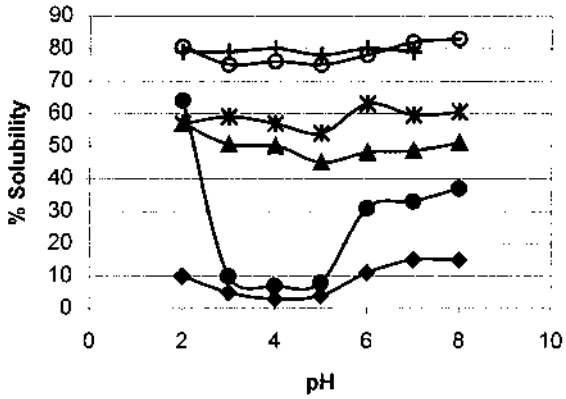

Figure 8 Effect of DH on solubility at various pH values. Intact protein (●), DH 1.0% (◆), DH 3.2 (▲), DH 5.1% (∗), DH 7.7% (+), DH 8.3% (○). The hydrolysates were obtained by hydrolyzing soy protein with alcalase 2.4 L. The solubility was measured in a 1% protein dispersion in 0.2 M NaCl. (From Ref. 66.)

actions and partly to the presence of compact structures in the protein that cannot be hydrolyzed. Further research will be required to elucidate these limiting factors and to develop methods or new enzyme preparations that allow the degradation of these compact structures.

Although peptides as such may be soluble, in a final application insoluble complexes can be formed due to interactions with other ingredients in the food matrix. In drinks, for example, peptides may associate with polyphenols or caramels, and the formed complexes can precipitate. In drinks also the concentration of the hydrolysate can be important; for soy protein hydrolysates it has surprisingly been found that at low pH the solubility is better at higher concentrations (11).

C. Organoleptic Properties

In food applications taste and smell are very important parameters. When food proteins are hydrolyzed a bitter taste and a savory taste usually develop. In addition, protein hydrolysates frequently carry the taste and smell characteristics of the raw material from which they are derived. The savory taste and smell are related to the presence of very small peptides and free amino acids. The bitterness is related to the size and the average hydrophobicity of the peptides (72). This can be calculated using the hydrophobicity values of the individual amino acids as reported in the literature (11).

Individual peptides will each have a different average hydrophobicity but also different threshold values and different bitterness intensity. The conformation of a peptide and how well it fits in the bitter receptor in the mouth will affect this. Peptides with a hydrophobic residue at the C-terminus are reported to be more bitter (73). Hydrophobic peptides are more bitter when there is another amino acid on both the N- and the C-side of the hydrophobic residue(s). Bitterness is the major limitation of the use of protein hydrolysates, and the reduction, prevention, or removal of the bitterness of protein hydrolysates has been studied extensively.

In an intact globular protein the majority of the hydrophobic side chains is hidden in the interior of the molecule and cannot interact with the taste receptors. Upon hydrolysis the protein molecule unfolds and is degraded into smaller peptides. The hydrophobic amino acids now are exposed to the solvent and can interact with the taste receptors. As the hydrolysis process proceeds, more hydrophobic amino acids are exposed and the bitterness increases. When the hydrolysis process proceeds further, the number of hydrophobic amino acids which have another amino acid at both the N- and the C-side decreases and the bitterness will pass through a maximum. At very high degrees of hydrolysis, however, a high amount of free amino acid will also be present and this will induce a savory flavor. Figure 9 shows the general relation among DH, bitterness, and savory flavor.

To reduce the bitterness, methods involving specific enzymatic treatments, selective separations, and masking can be applied (74). The bitterness of a hydrolysate can also be affected via the specificity of the enzyme. Endopeptidases that give peptides with nonpolar amino acids at the C-terminus were found to result

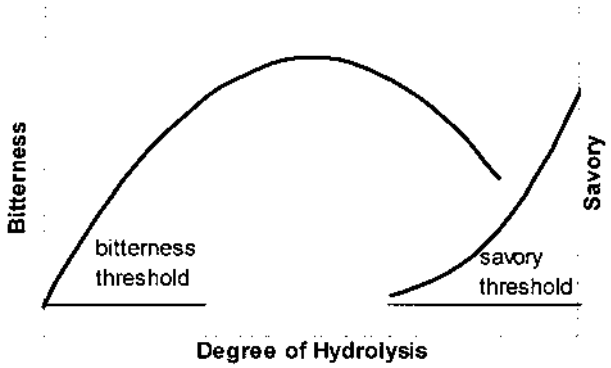

Figure 9 General relation between DH and organoleptical properties.

in hydrolysates with a relatively high bitterness (75). The application of both aminopeptidases (76) and carboxypeptidases (77) was found to reduce the bitterness of hydrolysates. Figure 10 shows the effect of using exopeptidases on the reversed-phase HPLC chromatogram of the hydrolysates. With increasing elution time, the hydrophobicity increased. The bitterness was found to be strongly correlated with the amount of material eluting after 50 min (78, 79). The neutral protease hydrolysate contains much hydrophobic material and is very bitter. When exopeptidases are used, less hydrophobic material is present and the bitterness is reduced. It should be realized, however, that the savory taste will increase owing to increased levels of free amino acids. Because of this increased level of free amino acids the osmolarity of the hydrolysate also increases. When applied in enteral feeding this may result in an influx of water into the intestine, which can cause diarrhea.

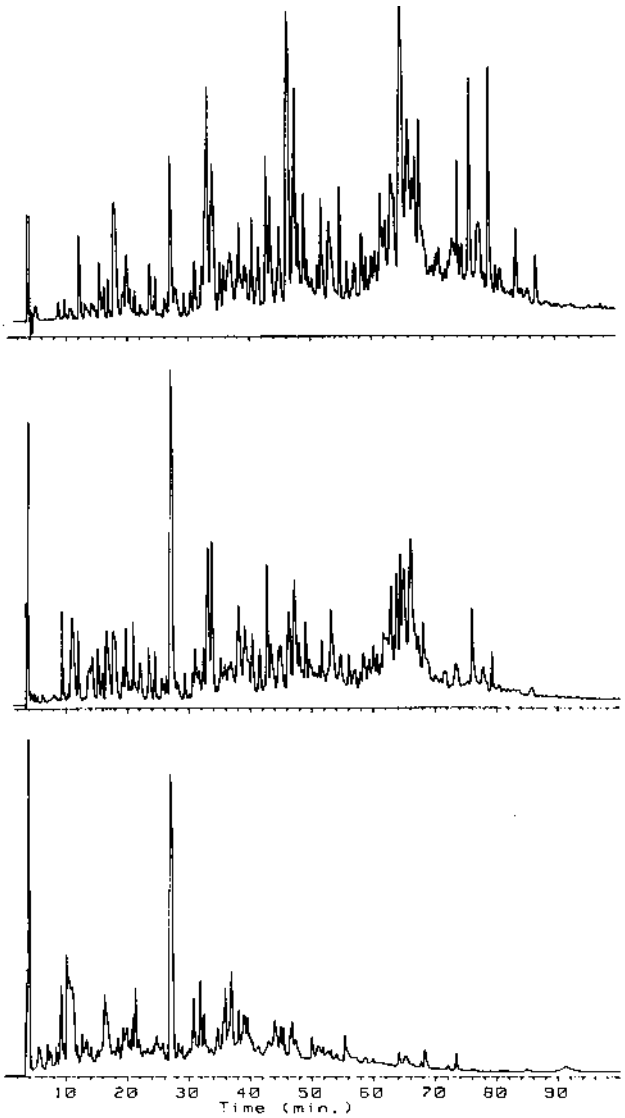

Figure 10 Reversed-phase patterns of casein hydrolysates. (Top) Casein hydrolyzed with an endopeptidase (Neutrase, NOVO). (Center) Casein hydrolyzed with an endopeptidase (Neutrase, NOVO) and a carboxypeptidase (obtained from autolysed yeast). (Bottom) Casein hydrolyzed with an endopeptidase (Neutrase, NOVO) and an enzyme mixture containing both carboxypeptidase and aminopeptidase (BioProtease P23, Quest International). The casein hydrolysates were analyzed on a C_{18} reversed-phase column using a gradient of 0.1% TFA in water to 0.1% TFA in acetonitrile as eluent.

Another method to reduce the bitterness is the plastein reaction (80). The original idea behind it is that the molecular weight is increased via a protein resynthesis but later it was thought that transpeptidation is giving the effect (81). As a result of the reduction insoluble components are formed, which are not perceived as bitter. However, it is also possible that the formation of aggregates of hydrophobic peptides (see Sec. IV.B.2) results in a reduction of the number of exposed hydrophobic side chains and consequently also results in a reduced bitterness.

Murray and Baker (82) found that treatment with activated carbon lowered bitterness. This procedure suffers from the disadvantage that the protein losses can be high (83) and that the selective removal of hydrophobic peptides negatively affects the nutritional properties (66).

Next to processing and selective separation methods, several methods to mask the bitter taste of protein hydrolysates via the addition of specific components have been reported. Polyphosphates, glycine, gelatin, gelatinized starch, cyclodextrins, glutamine, and asparagine were found to mask bitterness (74).

V. CONCLUDING REMARKS

Enzymatic hydrolysis is a valuable and flexible tool to modify and improve the functional properties of proteins. To be able to produce a specific hydrolysate it is necessary to have: (a) a detailed knowledge about the relations between process conditions and the properties of the hydrolysate obtained from a given protein and enzyme in combination, and (b) a detailed knowledge about the relations between the physicochemical properties of the hydrolysate and their functional properties.

Protein hydrolysates are complex mixtures of peptides, and this makes the task to acquire the required knowledge highly challenging. In recent years our knowledge on the kinetics of the hydrolysis reaction and the relations between structural and functional properties has increased tremendously. Information about the primary structure of proteins is very useful and for this reason in many studies on protein hydrolysis milk proteins have been used as model substrates.

With the new genetic modification techniques it will be possible to create new enzymes on the basis of increased understanding of the enzyme mechanism. This will offer new possibilities for further optimization and fine-tuning of protein hydrolysates.

REFERENCES

1. JF Zayas. Functionality of Proteins in Food. Berlin: Springer-Verlag, 1997.
2. S Arai, M Fujimaki. Enzymatic modification of proteins with special reference to improving their functional properties. In PF Fox, ed. Food Enzymology, Vol 2. London: Elsevier Applied Science, 1991, pp 83–104.
3. JS Hamada. Modification of food proteins by enzymatic methods. In: BJF Hudson, ed. Biochemistry of Food Proteins. London: Elsevier Applied Science, 1993, pp 249–270.
4. F Vojdani, JR Whitaker. Chemical and enzymatic modification of proteins for improved functionality. In: NS Hettiarachchy, GR Ziegler, eds. Protein Functionality in Food Systems. New York: Marcel Dekker, 1994, pp 261–309.
5. PM Nielsen. Functionality of protein hydrolysates. In: S Damodaran, A Paraf, eds. Food Proteins and Their Applications. New York: Marcel Dekker, 1997, pp 443–472.
6. RI Dave, NS Joshi, JR Patel, PN Thakar. Protein hydrolysates—a review. Indian J Dairy Sci 44(9):557–564, 1991.
7. K Kumetat, R Beeby. Egg substitutes from milk proteins. Dairy Indust. 730–733, 1954.
8. J Lenderink. Process for the manufacture of foam producing albuminous products and their application in food stuffs and luxuries. U.S. patent 2,522,050, 1950.
9. RIM Synge. The kinetics of low temperature acid hydrolysis of gramicidin and some related dipeptides. Biochem J 39:351–355, 1945.
10. M Sternberg, CY Kim. Lysinoalanine formation in food protein ingredients. Adv Exp Med Biol 86B:73–84, 1977.
11. J Adler-Nissen. Enzymic Hydrolysis of Food Proteins. London: Elsevier Applied Science, 1986.
12. SPL Sörensen. Enzymstudien I, Über die quantitative Messung proteolytischer Spaltungen. Die Formol Titrierung. Biochem Z 7:45–101, 1908.
13. H Frister, H Meisel, E Schlimme. OPA method modified by use of N,N-dimethyl-2-mercaptoethylammonium chloride as thiol component. Fres Z Anal Chem 330:631–633, 1988.
14. J Adler-Nissen. Determination of the degree of hydrolysis of food protein hydrolysates by trinitrobenzenesulfonic acid. J Agric Food Chem 27:1256–1262, 1979.
15. AD Siemensma, WJ Weijer, HJ Bak. The importance of peptide length in hypoallergenic infant food formulae. Trends Food Sci Technol 4:16–21, 1993.
16. WJ Lahl, SD Braun. Enzymatic production of protein hydrolysates for food use. Food Technol 48(10):68–71, 1994.
17. L Sijtsma, D Tereza, J Hustinx, JM Vereijken. Improvement of pea protein quality by enzymatic modification. Nahrung 42(3/4):215–216, 1998.
18. GM Pigott. Enzyme hydrolysis of fish waste for animal feed and fertilizer. In: F Shahidi, ed. Seafood Safety, Processing and Biotechnology. Lancaster: Technomic Publishers, 1997, pp 249–258.
19. K Linderstrøm-Lang. Proteins and enzymes. III. The initial stages in the breakdown of proteins by enzymes. In: Lane Medical Lectures. Stanford, CA: Stanford University Press, Vol VI. 1952, pp 53–72.
20. CF Jacobsen, J Léonis, K Linderstrøm-Lang, M Ottesen. The pH-stat and its use in biochemistry. Meth Biochem Anal 4:171–210, 1957.
21. A Constantinidus, B Adu-Amakwa. Enzymatic modification of vegetable protein: mechanism, kinetics, and production of soluble and partially soluble protein in a batch reactor. Biotechnol Bioeng 22:1543–1565, 1980.
22. A Margot, E Flaschel, A Renken. Empirical kinetic models for tryptic whey protein hydrolysis. Process Biochem 32(3):217–223, 1997.
23. MC Marquez Moreno, V Fernandez Cuadrado. Enzymatic hydrolysis of vegetable proteins: mechanism and kinetics. Process Biochem 28:481–490, 1993.
24. WGA Krause, E Ludwig, M Seiler. Hydrolysis of casein and casein components by acid proteases with milk clotting properties—kinetic investigations. In: KD Schwenje, R Mothes, eds. Food Proteins, Structure and Functionality. Weinheim: VCH Publishers, 1993, pp 87–91.
25. ZU Haque, P Antill. Milk peptides: effect on the enzymatic hydrolysis of sodium caseinate. Agric Sci Finl 2:371–378, 1993.
26. J Adler-Nissen. Enzymatic hydrolysis of soy protein for nutritional fortification of low pH food. Ann Nutr Alim 32:205–216, 1978.
27. MM Snijder, A Kunst. Unpublished results. Quest International, Naarden, The Netherlands, 1997.

28. JA Roels. Energetics and kinetics in biotechnology. Oxford: Elsevier Biomedial Press, 1983, pp 163–203.
29. LJ Lopez-Bajonero, P Lara-Calderon, A Galvez-Mariscal, A Velazques-Arellano, A Lopez-Munguia. Enzymatic production of a low-phenylalanine product from skim milk powder and caseinate. J Food Sci 56(4):938–942, 1991.
30. AMH Vasconcellos, CPH Oliveira, DM Grassiano, ALC Santos-Neto. Adsorption of phenylalanine from casein hydrolysates. Appl Biochem Biotechnol 37:69–80, 1992.
31. WD Deeslie, M Cheryan. Continuous enzymatic modification of proteins in an ultrafiltration reactor. J Food Sci 46:1035–1042, 1981.
32. AK Barnfield-Frey, S Johansson, P Leijon. Expanded bed adsorption at production scale: scale-up verification, process example and sanitization of column and adsorbant. Bioprocess Eng 16(2):57–63, 1997.
33. PP Bailey. An Introduction to Peptide Chemistry. Chichester: John Wiley & Sons, 1991, pp 182–203.
34. MK Schmidl, SL Taylor, JA Nordlee. Use of hydrolysate based products in special medical diets. Food Technol 48(10):77–85, 1994.
35. S Frøkjaer. Use of protein hydrolysates for protein supplementation. Food Technol 48(10):86–88, 1994.
36. A Siemensma, A Kunst. Sports nutrition. The recovery sports drink. World of Ingredients, 1999, October: 53–56.
37. WR Blom, A Kunst, BJ van Schie, GW Luli. Method for in vitro cell growth of eucaryotic cells using low molecular weight peptides. U.S. patent 5,741,705, 1998.
38. LM Castell, EA Newsholme. Glutamine and the effects of exhaustive exercise upon the immune response. Can J Physiol Pharmacol 76(5):524–532, 1998.
39. LJC van Loon, WHM Saris, M Krijgshoop, AJM Wagenmakers. Maximizing postexercise muscle glycogen synthesis: carbohydrate supplementation and the application of amino acid or protein hydrolysate mixtures. Am J Clin Nutr 72(1):106–111, 2000.
40. Plasma insulin responses following the ingestion of different amino acid/protein carbohydrate mixtures. Am J Clin Nutr 1999 (accepted for publication).
40. M Varnier, GP Leese, MJ Rennie. Effect of glutamine on glycogen synthesis in human skeletal muscle. Clin Nutr 12(suppl 2):1, 1993.
41. FQ Nuttal, AD Mooradian, MC Gannon, P Krezowski. Effect of protein ingestion of the glucose and insulin response to a standardized oral glucose load. Diabetes Care 7:465–470, 1984.
42. E Kunji. The proteolytic system of *Lactococcus lactis*. Ph.D. dissertation, Groningen University, 1997.
43. NM Loader, N Lindner, VK Pasupuleti. Proteolytic system of lactic acid bacteria and nutrients. In: TW Nagodawithana, G Reed, eds. Nutritional Requirements of Commercially Important Microorganisms. Milwaukee: Esteekay Associates Inc, 1998, pp 46–67.
44. GK Grimble. The significance of peptides in human nutrition. Annu Rev Nutr 14:419–447, 1994.
45. CT Cordle. Control of food allergies using protein hydrolysates. Food Technol 48(10):72–76, 1994.
46. MI Mahmoud, WT Malone, CT Cordle. Enzymatic hydrolysis of casein: effect of degree of hydrolysis on antigenicity and physical properties. J Food Sci 57(5):1223–1229, 1992.
47. JG Bindels. Peptiden in de Voeding. Voeding 53(10):253–257, 1992.
48. H Meisel. Overview on milk protein-derived peptides. Int Dairy J 8:363–373, 1998.
49. A Kunst. Process to isolate phosphopeptides. Patent EP0.476.199, 1992.
50. G Brule, L Roger, J Fauquant, M Piot. Phosphopeptides from casein-based material. U.S. patent 4,358,465, 1982.
51. EC Reynolds. Phosphopeptides. Patent WO87/07614, 1987.
52. DW West. Phosphopeptides and calcium absorption. Proceedings of the 23rd International Dairy Congress, 1990, pp 1208–1216.
53. D Kitts, YV Yuan. Caseinphosphopeptides and calcium bioavailability. Trends Food Sci Technol 3:31–35, 1992.
54. MI Mahmoud. Physiochemical and functional properties of protein hydrolysates in nutritional products. Food Technol 48(10):89–95, 1994.
55. S Damodaran. Protein stabilized foams and emulsions. In: S Damodaran, A Paraf, eds. Food Proteins and Their Applications. New York: Marcel Dekker, 1997, pp 57–110.
56. E Dickinson, DJ McClements. Molecular basis of protein functionality. In: Advances in Food Colloids. London: Blackie Academic & Professional, 1996, pp 27–80.
57. DE Graham, MC Phillips. The conformation of proteins at the air water interface and their role in stabilizing foams. In: RJ Akers, ed. Foams. New York: Academic Press, 1976, pp 195–215.
58. N Kitabatake, E Doi. Surface tension and foamability of protein and surfactant solutions. J Food Sci 53:1542–1569, 1988.
59. A Townsend, S Nakai. Relationship between hydrophobicity and foaming capacity of proteins. J Food Sci 48:588–594, 1983.
60. A Kato, Y Osako, N Matsudomi, K Kobayashi. Changes in the emulsifying and foaming properties of proteins during heat denaturation. Agric Biol Chem 47(1):33–37, 1983.
61. A Prins. 1988. Principles of foam stability. In: E Dickinson, G Stainsby, eds. Advances in Food

Emulsions and Foams. London: Elsevier Applied Science, 1988, pp 91–122.
62. SL Turgeon, SF Gauthier, D Molle, J Leonil. Interfacial properties of tryptic peptides of beta-lactoglobulin. J Agric Food Chem 40(4):669–675, 1992.
63. P Caessens. Enzymatic hydrolysis of β-casein and β-lactoglobulin. Foam and emulsion properties of peptides in relation to their molecular structure. Ph.D. dissertation, Wageningen University, 1999.
64. J Kyte, RF Doolittle. A simple method for displaying the hydropathic character of protein. J Mol Biol 157:105–132, 1982.
65. GD Rose, JE Dworkin. The hydrophobicity profile. In: GD Fasman, ed. Prediction of Protein Structure and the Principles of Protein Conformation. New York: Plenum Press, 1989, pp 625–634.
66. J Adler-Nissen, HS Olsen. The influence of peptide chain length on taste and functional properties of enzymatically hydrolyzed soy protein. ACS Symp Ser 92:125–146, 1979.
67. JM Chobert, C Bertrand-Harb, MG Nicolas. Solubility and emulsifying properties of caseins and whey proteins modified enzymatically by trypsin. J Agric Food Chem 36:883–892, 1988.
68. CH Wang, S Damodaran. Thermal gelation of globular proteins: weight average molecular weight dependence of gel strength. J Agric Food Chem 38:1157–1164, 1990.
69. J Otte, M Ju, M Færgemand, SB Lomholt, KB Qvist. Protease induced aggregation and gelation of whey proteins. J Food Sci 61(5):911–915, 1996.
70. PC Lorenzen, E Schlimme. Functional and structural properties of aggregates formed during plastein-like reactions. In: KD Schwenje, R Mothes, eds. Food Proteins, Structure and Functionality. Weinheim: VCH Publishers, 1993, pp 76–81.
71. J Otte, SB Lomholt, R Ipsen, H Stapelfeldt, JT Bukrinsky, KB Qvist. Aggregate formation during hydrolysis of β-lactoglobulin with a Glu and Asp specific protease from *Bacillus licheneformis*. J Agric Food Chem 45:4889–4896, 1997.
72. KH Ney. Voraussge der Bitterheit von Peptiden aus deren Aminosäurenzusammensetzung. Z Lebensm-Untersuch Forsch 147:64–71, 1971.
73. N Ishibashi, Y Arita, H Kanehisa, K Kouge, H Okai, S Fukui. Bitterness of leucine-containing peptides. Agric Biol Chem 51:2389–2394, 1987.
74. B Pedersen. Removing bitterness from protein hydrolysates. Food Technol 48(10):96–98, 1994.
75. J Adler Nissen. Relationship of structure to taste of peptides and peptide mixtures. In: RE Feeney, JR Whitaker, eds. Protein Tailoring for Food and Medical Uses. New York: Marcel Dekker, 1986, pp 97–122.
76. E Minagawa, S Kaminogawa, F Tsukasaki, K Yamauchi. Debittering mechanism in bitter peptides of enzymatic hydrolysates from milk casein by aminopeptidase T. J Food Sci 54(5):1225–1229, 1989.
77. H Umetsu, H Matsuoka, E Ichishima. Debittering mechanism of bitter peptides from milk casein by wheat carboxypepidase. J Agric Food Chem 31:50–53, 1983.
78. H Hennink, W Koelewijn. Unpublished results. Quest International, Naarden, The Netherlands, 1994.
79. H Slattery, RJ Fitzgerald. Functional properties and bitterness of sodium caseinate hydrolysates prepared with a *Bacillus* proteinase. J Food Sci 63(3):419–422, 1998.
80. M Fujimaki, M Yamashita, S Arai, H Kato. Plastein reaction—its application to debittering of protein hydrolysates. Agric Biol Chem 34:483–484, 1970.
81. M Fujimaki, S Arai, M Yamashita. Enzymatic protein degradation and resynthesis for protein improvement. Adv Chem Ser 160:156–180, 1977.
82. TK Murray, BE Baker. Studies on protein hydrolysis. I. Preliminary observations on the taste of enzymic protein hydrolysates. J Sci Food Agric 3:470–475, 1952.
83. V Cogan, M Moshe, S Mokady. Debittering and nutritional upgrading of enzymic casein hydrolysates. J Sci Food Agric 32:459–466, 1981.

18

Production and Modification of Acylglycerides

Rob M. M. Diks
Unilever Research and Development, Vlaardingen, The Netherlands

I. INTRODUCTION

Acylglycerides are important ingredients of a wide variety of food products, especially those consisting of emulsions of water and oil. Acylglycerides consist of a glycerol backbone with one, two, or three fatty acid chains attached to it, thus giving a mono-, di-, or triglyceride molecule. The delicate balance between the apolar hydrophobic fatty acids and the polar OH groups in the molecule, as well as the type of fatty acid involved, determines the physical behavior of the acylglyceride and hence its specific function in the food product.

Triglycerides can well be considered the most important class of acylglycerides. Being the major component of edible oils and fats, they serve many functions in daily food products. Apart from being an energy source, they are nutritionally important for their dietary supply of essential fatty acids, as well as fat-soluble vitamins and antioxidants. Furthermore they significantly contribute to product characteristics such as spreadability, mouth feel, and the flavor release during consumption.

Diglycerides are used generally as emulsifers, often in a mixture with monoglycerides. However, they are also known to act as crystal habit modifier in triglyceride mixtures (1, 2), and could act as a building block for the organic synthesis of, e.g., drug and phospholipids (3).

Having only one apolar fatty acid chain and two polar hydroxy groups, monoglycerides are the most surface-active type of acylglycerol. They are widely applied to stabilize water-in-oil as well as oil-in-water emulsions such as those present in spreads, dressings, and cosmetic creams (4).

In general, the physical behavior of an acylglyceride, and hence its commercial value, is related to its fatty acid composition. Hence the ability to specifically modify its composition allows the production of tailor-made acylglycerols. Using conventional organic synthesis many acylglycerols are being produced on a larger scale. These processes are generally carried out at relatively high temperatures and pressures, using rather unspecific catalysts if not fully random catalysts. As a result, complex multistep processes are required to obtain the desired product. Moreover, toxic byproducts can be formed as well as off-flavor and colors, again requiring substantial posttreatment and downstream processes, especially when food applications are concerned.

As opposed to this, enzymes are highly specific and can operate under mild conditions of temperature, pressure, and pH. In recent years much attention has therefore been focused to the exploitation of enzymes, especially lipases, for lipid modification.

In this chapter various aspects of the use of lipases for the modification of acylglycerols will be highlighted. Firstly, the general functioning of lipases, their specificities and the importance of water in lipase-catalyzed reactions are discussed. Secondly, some process engineering aspects of lipase catalyzed processes are covered. This comprises the immobiliza-

tion of lipases, reactor design, and modeling as well as the operational stability of the biocatalyst. Finally, examples of glyceride modification processes are reviewed. Though the production of monoglyerides and diglycerides is covered, the main focus in this chapter will be on the modification and processing of triglycerides, being the most important processes applied on an industrial scale.

II. LIPASES

A. General Properties

Probably the most important class of enzymes studied in general are lipases, i.e., glycerol ester hydrolases (EC 3.1.1.3), especially those that are obtained from microbial sources. In living organisms the function of lipases is to hydrolyze oils and fats into free fatty acids, a mixture of partial glycerides (mono- and di-) and glycerol. The latter products are taken up by the organism to provide energy and growth intermediates. The industrial equivalent of this process is widely employed in detergent systems for laundry cleaning (5).

In the early 1980s it was shown that under very dry conditions, such as in organic solvents, lipases remain active and sometimes even show novel characteristics such as improved stability (6). Over the years it has been shown that lipases in organic media are capable of carrying out all major reactions important for acylglycerol modification, e.g., hydrolysis, esterification (Fig. 1), and trans- or interesterification reactions (Fig. 2).

Several extensive reviews on the subject have recently been published (7, 8). It should be realized that when referring to organic media, this also covers liquid oils, i.e., solvent-free systems. For certain applications, especially those aimed at food product ingredients, this is sometimes an important benefit. Apart from the requirement of food grade solvents, its absence prevents the need for solvent removal and recovery, thus reducing processing costs.

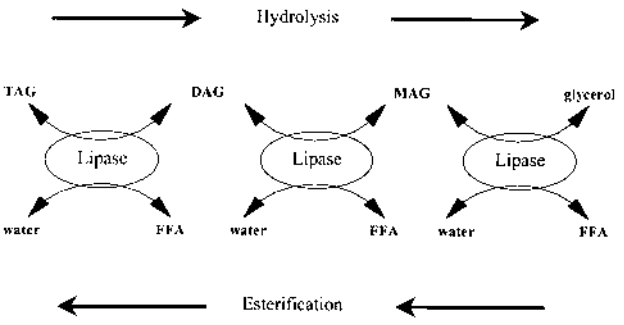

Figure 1 Reactions on acylglycerides catalyzed by lipases.

The ability of lipases to catalyze fatty acid exchange reactions on acylglycerols results from two major characteristics. Firstly, the construction of the "active site" of this class of enzymes. It consists of three amino acids forming a so-called catalytic triad (16). In close interaction, they cause the lipase to split, e.g., a triglyceride molecule in a covalent lipase–fatty acid complex and a diglyceride (Fig. 1). In a second reaction step a water molecule comes in, thereby releasing the fatty acid and returning the lipase to its native state, thus completing a full hydrolysis cycle (9). This two-substrate (triglyceride and water) two-step model is generally referred to as the Bi-Bi, Ping-Pong model (59).

In a similar manner a new ester bond can be established when a new diglyceride molecule reacts with the existing lipase–fatty acid complex, forming a new triglyceride molecule. This scheme highlights the importance of diglycerides as intermediate in trans- and interesterification reactions and hence the necessity of a minimum degree of hydrolysis to start the interesterification reaction.

Secondly, lipases are characterized by a phenomenon called *interfacial activation* (10, 11). The entrance to the active site is covered by a lid or flap when dissolved in water. However, when in contact with an interface between water and apolar phase, i.e., oil, or being dispersed in organic solvent, the flap opens, allowing substrates to enter the active site. Thus in a system of a polar and an apolar phase, lipases are highly active on substrates present in the apolar phase, whereas their activity toward water-soluble substrates is rather low. As a result of the activation in the presence of an organic phase, lipases, individually fixed on an inert carrier by adsorption, also show their activity in organic solvents and vegetable oil. In fact, the lipases here are located at the interface between the organic medium and the solid carrier material.

Though lipases are generally considered true catalysts—substances that accelerate the reaction rate but do not affect the equilibrium composition—the above-described phenomenon should be taken into account when operating in a biphasic system. For example, using *Candida rugosa* lipase for triglyceride hydrolysis $> 90\%$ free fatty acids will be formed (12), whereas $\sim 90\%$ degree of esterification is obtained when using fatty acids and long-chain alcohols ($> C_{12}$) (13) or sterols as substrates (14, 15). The latter result represents actual thermodynamic equilibrium composition.

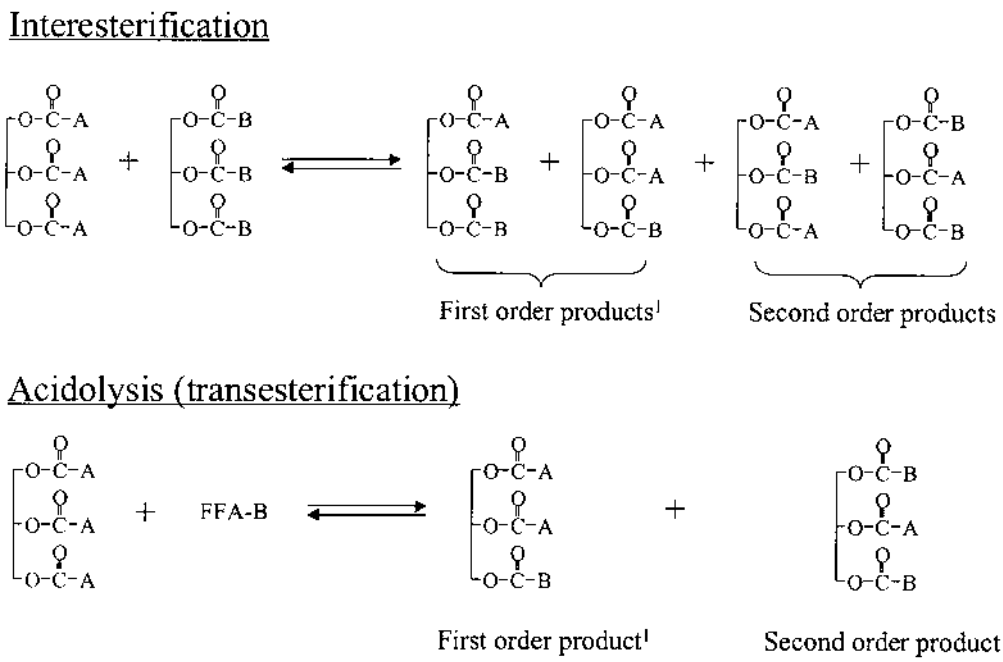

Figure 2 Interesterification and acidolysis of triglycerides with 1,3-specific lipases. The first-order products always comprise two 1,3-isomers.

However, in the former case the synthesis reaction is blocked by the fact that glycerol is strongly diluted in the aqueous phase and cannot effectively enter the active site of the lipase.

B. Lipase Specificities

Though the catalytic triad principle mentioned above is true for all lipases, the active site of lipases comes in different shapes and sizes (16, 17). This restricts the way in which acylglycerols can bind, or slows down and even prohibit certain acylglycerols from binding at all. The result is a preference of the lipase to react on certain acylglycerols or positions within, e.g., a triglyceride molecule. This is often addressed as the selectivity or specificity of a lipase.

Three major types of specificity can be distinguished (Table 1). The first type involves positional or regiospecificity, most lipases being either 1,3-specific or fully random (nonspecific). The 1,3-specificity is the most common and is displayed by, e.g., human gastric lipases, as well as microbial lipases such as from *Rhizomucor miehei*, *Thermomyces* sp., and various *Rhizopus* sp. As a result of a trough-shaped active site, triglycerides can bind only in specific positions allowing lipases to modify acylglycerols on the sn-1 and sn-3 positions, both in hydrolysis and inter- or transesterification.

It should be noted that for the *Rhizomucor miehei* lipase a surprising phenomenon was reported in that the lipase showed a preference for the sn-1 position when operating under very dry conditions (18). This property could allow for stereospecific synthesis to be carried out. As opposed to this regiospecificity, lipases, such as that from *Candida rugosa* and the one from *Geotrichum candidum*, are random and hence can modify the fatty acids on all positions of the acylglycerols.

The second type of specificity relates to the type of fatty acid being involved. For example, certain *Cuphea* lipases show a distinct selectivity for short chain fatty acids. Another important example is *Geotrichum candidum* lipase B. Though being non regiospecific, it shows a strong selectivity for fatty acids with a *cis*-Δ-9 double bond (20, 21). Both this lipase and that from *Candida rugosa* display a strong selectivity against long-chain polyunsaturated fatty acids. This property is probably related to the tunnel shape of the fatty acid binding site of both lipases (22).

The easiest way of exploiting these fatty acid selectivities in product purification or fatty acid enrichments is in single-stage reactions such as hydrolysis or esterification, in combination with a physical means of separating the desired end product and the residual unwanted fatty acid fraction (see section on fatty acid enrichment).

Table 1 Exploitation of Lipase Specificities for Acylglycerol Modification

Specificity	Lipases	Application
Regiospecificity		
sn-1, sn-3 specific	*Rhizomucor miehei*[a]	Triglycerides
	Rhizopus oryzae	interesterification/acidolysis
	Rhizopus arrhizus	synthesis by esterification
	Rhizopus delemar	Diglycerides
	Rhizopus niveus	triglyceride hydrolysis/glycerolysis (directed) fatty acid esterification
	Porcine pancreatic lipase	Monoglycerides
		triglyceride hydrolysis/glycerolysis fatty acid esterification
Nonspecific	*Candida rugosa*	Fatty acid production by hydrolysis
	Chromobacterium viscosum	Mono- and diglycerides by directed glycerolysis
	Pseudomonas fluorescens	Fatty acid production by hydrolysis
	Pseudomonas cepacia	Mono- and diglycerides by directed glycerolysis
Fatty acid specificity		
Short-chain fatty acids	*Cuphea* sp.	Production of fatty acid concentrates by selective hydrolysis
Long-chain poly-unsaturated acids	*Geotrichum candidum*	Production of enriched glycerides by selective hydrolysis or enriched fatty acids by esterification
	Candida rugosa	Production of enriched glycerides by selective hydrolysis or enriched fatty acids by esterification
Cis-Δ9 unsaturated fatty acids	*Geotrichum candidum* B	Production of enriched glycerides by selective hydrolysis or enriched fatty acids by esterification
Partial glyceride specific		
Monoglycerides	Potato acylhydrolase (patatin)	Monoglycerides by fatty acid esterification
Mono- and diglycerides	*Penicillium camembertii*[b]	Mono- and diglycerides by fatty acid esterification
	Penicillium cyclopium[b]	Mono- and diglycerides by fatty acid esterification

[a]sn-1 specific under semi-dry operating conditions (18).
[b]The selectivity for monoglycerides over diglycerides varies with the water activity (114, 115).

The third major lipase specificity is that for certain types of acylglycerols. *Penicillium camembertii* lipase is known to act upon mono- and diglycerides only, whereas other *Penicillium* lipases are reported to hydrolyze only triglycerides. Patatin, a potato acyl hydrolase, is even more specific, almost exclusively producing monoglycerides in synthesis (23). Unfortunately, details on its active site are not yet available.

C. Effect of the Thermodynamic Water Activity

Apart from being a substrate, water also has a vital function in maintaining the three-dimensional conformation of the enzyme and hence its intrinsic activity (24, 25). This effect is most conveniently expressed in terms of the thermodynamic water activity maintained in the reaction medium. It allows comparison of results of enzymatic reactions in various organic solvents, even though absolute water concentrations are significantly different (26).

It has been shown that the form of this relationship is rather lipase specific. For example, *Rhizomucor miehei* lipase has an optimum water activity ~ 0.5 and still retains 40% of its maximum activity at water activities close to zero (27, 28). On the other hand, the lipases from *Candida rugosa, Humicola*,* and *Pseudomonas cepacia* not really showed a maximum, their activity

Humicola lanuginosa, currently known as *Thermomyces lanuginosus*.

continuously increasing with the water activity up to saturation level (29). The relationship is rather independent of the type of reaction catalyzed by the lipase (30), the carrier material of the lipase (28) as well as the type of solvent applied (27). However, in polar solvents interactions with the solvent molecule itself may affect the enzyme activity (31), which may explain the low activity of certain lipases in such solvents (32).

The existence of an optimum water activity urges proper control of the water activity throughout a reaction. In fact several methods have been developed which allow accurate control of the water activity in batch as well as continuous reactor systems: e.g., vacuum, controlled air sparging (33), membrane pervaporation (34), and equilibration with concentrated salt systems (35, 36). These techniques have been shown adequate to obtain optimum performance of biocatalysts in ester synthesis.

In some cases water activity control during the process is not relevant at all. For example, in the synthesis of esters from hydrophobic fatty acids and hydrophobic alcohols degrees of synthesis in the range of 90% can easily be reached, even in the presence of free water (13, 14). Moreover, this is independent of the type of lipase applied (13).

A more general case is the interesterification or acidolysis of oils and fats. Starting with a pure triglyceride (acylglycerol) mixture, the thermodynamics of the system will cause nearly all water initially present to be used for hydrolysis (26). Though this reaction does create the diglyceride intermediates required for the interesterification reaction to proceed, it simultaneously results in a significant reduction of the water activity. Moreover, the latter may easily drop below the optimum of the lipase applied. Adding extra water to the system to increase the a_w is no solution as it will only result in further hydrolysis and hence decreased product (modified triglyceride) yield (37).

Thus, quickly losing water by hydrolysis, the major part of the interesterification reaction will proceed at a very low equilibrium water activity (38–42). As a result of this drying process, the initial water activity of the catalyst itself is of less importance, especially in a continuous reactor system. Instead, the supply of water via the feed stream to a reactor is essential in order to establish a low but constant water activity in the system, thereby preventing exhaustive drying of the catalyst and providing for fresh intermediates to keep the interesterification reaction going. It is therefore generally accepted that in interesterification reactions, the water content in the feed steam should be close to saturation (41, 43, 44).

III. REACTOR ENGINEERING ASPECTS

A. Efficiency of Free Lipases

Using free lipases in organic media, one problem to overcome is the low activity of crude enzyme powders. High lipase input obviously reduces the economic viability of the system and is hence not feasible. Both physical and chemical modification of free lipases have been developed, describing increased lipase solubility and activity.

In most cases chemical modification involves the covalent coupling of a wide variety of hydrophobic molecules onto lysine amino acid residues on the lipase (45, 46). This generally results in an enhanced activity and stability of the catalyst. It was shown that in certain cases these effects are due to an increased porosity of the lipase-aggregate structure obtained after lyophilization of the lipase (47). A similar phenomenon may explain the enhanced activities reported after physical modification of lipases. This technique often involves drying of a lipase in the presence of hydrophobic compounds, often lipids (48, 49).

An alternative ''modification'' method, referred to as in situ immobilization, is based on the conversion of an emulsion of a lipase solution in oil into a dispersion of solid particles. The latter is achieved by drying the system under reduced pressure. The intensity of mixing during the drying stage determined the average particle size of the biocatalyst thus obtained (50). Despite these developments, dispersion of the dried modified lipase preparations in hydrophobic media remains essential but difficult, especially when highly viscous oils are involved. Moreover, recovery of the suspended lipase from the reaction medium for reuse may require significant catalyst handling and operational cost.

B. Immobilization of Lipase on Inert Carriers

The use of macroscopic inert carrier materials to immobilize lipase is important, as it allows easy catalyst handling and reuse after separation of the catalyst by sedimentation or filtration. A vast amount of literature has been published on the immobilization of lipases on solid surfaces or inert carrier materials. The methods described cover covalent coupling, precipitation, entrapment, and adsorption. Moreover, many different carrier materials have been used over the years such as hydrophilic powders (celite), ion exchange resins, and hydrophobic polymers, either in the form of particles or as membranes. Extensive overviews on the details of these techniques can be found elsewhere (8).

The most widely used technique is the adsorption of lipases onto porous carrier materials. Such materials provide a huge internal surface area to immobilize individual lipase molecules from solution with high efficiency. The carrier materials should fulfill a number of criteria to deliver a proper biocatalyst (51, 52). Obviously the material should allow efficient lipase immobilization and an appropriate pore size to allow diffusion of the lipase (> 50 nm) (52). Furthermore, particle size is important in order to minimize the risk of substrate mass transfer limitations (40). However, to be able to use the biocatalyst in a packed-bed reactor, a minimum particle size (> 500 μm) should be accounted for to keep the pressure drop over the packed bed within reasonable limits.

Carrier materials such as ion exchange resins (e.g., Duolite ex Rohm-Haas, Germany (53)) and polypropylene particles (Accurel EP-100, ex Akzo-Nobel, Germany) (54, 55) are most widely used for lipase adsorption. Especially the latter material has proven to be a suitable carrier, as the immobilization of a wide variety of lipases has been shown to be very efficient and reproducible (54). Though easily immobilized on the carrier, it was reported that certain lipases gave activities much lower than could be expected based on their loading. This phenomenon is attributed to conformational changes in the structure of the lipase and hence a loss of lipase activity upon adsorption of lipase molecules onto the carrier surface. Precoating of the carrier with dummy, nonlipase protein before adsorption of the lipase has proven a reliable technique to overcome the reduction of the activity of the immobilized lipase (54, 56).

It should be noted that immobilization is mentioned as a technique to enhance the stability of lipases. Fundamental studies have revealed that indeed the flexibility of enzymes immobilized onto solid surfaces is considerably reduced (24). However, data actually comparing one and the same type of reaction with both the free and immobilized versions of one lipase are rather scarce (57). Often research measures the temperature optima of the free and immobilized enzymes in different reaction systems; for example, hydrolysis in an emulsion system for the free lipase, and an (inter)esterification in a solvent system for the immobilized lipase. However, considering effects of mass transfer, substrate solubility, and water activity as described above, comparison of results from different assays can be rather tricky, and hence the impact of immobilization itself should be evaluated with care.

C. Packed-Bed Reactor Setup

One of the major advantages of immobilization is the potential to run a continuous process with maximum exploitation but minimum handling of the biocatalyst. The simplest design of a continuous reactor is a packed-bed reactor, consisting of a cylindrical column holding a fixed bed of catalyst particles containing immobilized lipase. The reaction medium, being either liquid oil or organic solvent containing the substrates, is simply pumped through this bed of catalyst particles. During its pass through the bed the substrates are converted into the desired end-products within the pores of the catalyst. The degree of conversion is simply controlled by the time allowed in the column, i.e., the residence time. The latter is determined by the height of the fixed bed and the flow rate of the reaction medium (see Sec. III.D).

An important design parameter for a packed-bed reactor is catalyst particle size, which generally is in the range of 200–1000 μm. Too-small particles result in an unacceptable pressure drop over the packed bed, whereas too-large particles will introduce mass transfer limitation effects, thereby decreasing the efficiency of the catalyst. The latter especially holds for high-viscosity systems such as vegetable oils. Applying organic solvents as the reaction medium, pore diffusion limitation, i.e., internal mass transfer resistance, can generally be neglected (40).

External mass transfer generally is not an issue, especially when using organic solvents (40, 58). The completion of the reaction requires residence times in the packed bed from half an hour to several hours, depending on the activity of the biocatalyst applied. The oil flow rates applied are generally above the range in which external limitations become important. A detailed study of mass transfer effects in packed-bed reactors can be found elsewhere (39, 49).

D. Process Modeling

Many models have been developed to describe lipase-catalyzed reactions. The simplest models generally involve Michaelis-Menten kinetics or similar type of rate expressions describing, e.g., substrate or product inhibition. These types of models are often used to describe single reactions such as hydrolysis and esterification (59).

Acidolysis (transesterification) and interesterification of triglycerides are much more complex. Being multistep and multisubstrate reactions a full-kinetic description is highly complicated. Several models

have been developed which are based on true kinetics of the multistep process. With varying degrees of detail, these models easily contain up to five or six reaction parameters, depending on the reaction mechanism assumed (9, 42, 58). However, to limit the complexity of such a model the number of reacting species is generally reduced by assuming only two fatty acids to be involved, e.g., the one present in the triglycerides before the reaction and the fatty acids to be incorporated (9).

A second class of models lacks any mechanistic background and only describe the change in the composition of the triglyceride fraction during acidolysis and interesterification (39, 60, 61). They neglect the initial phase of the process in which water present in the starting mixture is being used for hydrolysis, thereby generating free fatty acids and diglycerides. This starting point is valid, considering the fact that the rate of hydrolysis is at least an order of magnitude faster than the rate of interesterification. As a result the hydrolysis phase is short compared to the total time required for full triglyceride conversion, and once completed, the overall glyceride composition of the mixture remains constant (38, 40–42).

The simplest approach is to consider the fatty acid exchange reactions between the triglyceride species as a purely statistical process approaching the equilibrium end composition (Sec. IV.A) for the triglyceride mixture concerned. In chemical engineering terms such a process is generally referred to as a pseudo-first-order process. Mathematically this is represented by the following one parameter equation:

$$X = 1 - e^{-\mathrm{k}\cdot\tau} \tag{1}$$

in which X is the relative degree of conversion; k is the pseudo-first-order activity constant of the biocatalyst; and τ is the incubation (batch) or average residence time (continuous) in the system.

The degree of conversion is based on the change in the composition between the start and the end of the reaction. The latter is generally characterized by the absence or presence of certain characteristic substrate or product triglycerides:

$$X = \frac{TAG_{\mathrm{t=t}} - TAG_{\mathrm{t=0}}}{TAG_{\mathrm{eq}} - TAG_{\mathrm{t=0}}} \tag{2}$$

The composition of the product triglycerides at equilibrium can be calculated from analytical data on the overall composition of the sn-1,3 and sn-2 positions in the starting triglyceride mixture (see Sec. IV.A).

When dealing with the incorporation of specific fatty acids in triglycerides, such as in an acidolysis reaction, the first-order model can still describe the change in the composition of the triglyceride fraction. However, the models fail to describe the change of the composition of the free fatty acid fraction, as well as the effect of the initial acid/oil ratio on the apparent catalyst activity. In this case a second-order model is often applied (42, 60, 62). It should be noted that the latter models can generally only describe the process for a limited number of fatty acids (61), similar to the kinetic models referred to above.

E. Stability of Immobilized Lipases

Decisive for the application of any process on industrial scale is variable cost and hence productivity of the biocatalyst. The latter is determined by the activity as well as the longer-term stability of the biocatalyst. In principle, deactivation is an inherent characteristic of any enzyme in which especially temperature is important. Also the presence of water is important as fundamental studies showed that water is involved in many enzyme deactivation reactions. This may explain the improved stability of enzymes in nonaqueous organic media (63). However, the role of water is much more complicated, as it was also reported that some water is required to sustain the enzyme activity over time in a continuous system (41, 125).

Another important mechanism causing deactivation is poisoning of the enzyme by a physical or chemical interaction with impurities in the reaction medium. A number of papers have shown that the stability of lipases in oils is related to the intrinsic quality of the feed oil (41, 43, 44, 53). More specifically, it has been shown that primary and secondary products from triglyceride auto-oxidation, such as hydroxyperoxides and their degradation products, may reduce the activity of the biocatalyst (64–66).

Deactivation is generally described as a first-order process with time (39, 43, 62), given by the following equation:

$$k = k_0 \cdot e^{-k_d \cdot t} \tag{3}$$

in which k is the catalyst activity at any time; k_0 is the catalyst activity at the start; k_d is the deactivation constant [1/time]; and t is the incubation time.

The specific deactivation constant (k_d) is actually a lump parameter, comprising all deactivation mechanisms taking place, such as the thermal deactivation and poisoning phenomena mentioned above. This parameter thus is a complex function of the reaction conditions, e.g., temperature and water activity, the

"quality" of the reaction medium, and the type of lipase involved. This complex nature of the problem generally suggests that it is rather difficult to predict the performance of a chosen lipase in a certain application and hence substantial testing is required each time a new process is being developed. This is confirmed by literature data showing half-life times varying between a few days and several months, depending on specific reaction system studied (7).

IV. MODIFICATION OF TRIGLYCERIDES

A. Modifying the Fatty Acid Composition

Chemical interesterification is one of the major modification techniques and basically involves a random rearrangement of the sn-1, sn-2, and sn-3 fatty acids over the triglycerides present in the mixture (Fig. 1). A similar result can be obtained when using a random lipase such as that from *Candida rugosa*[*] (38, 67), *Pseudomonas fluorescens* (68), or *Pseudomonas cepacia* (69). Using a 1,3-specific lipase, only the fatty acids on the outer positions of the triglyceride molecules will be randomized. In this case the sn-2 position remains intact, which implies that a different triglyceride mixture will result, as compared to the random process.

In both cases the rearrangement process can be regarded as a statistical process, and hence the final, equilibrium composition of the product can be easily calculated. For example, assuming only three fatty acids—X, Y, and Z—present in a TAG mixture, the molar concentration of an individual types of triglycerides follows from:

Random process:	XYZ	$= 6 \cdot x \cdot y \cdot z$
	X_2Y	$= 3 \cdot x \cdot x \cdot y$
	X_3	$= x \cdot x \cdot x$
1,3-specific process:	XYZ	$= 2 \cdot x_{1,3} \cdot y_2 \cdot z_{1,3}$
	XYX	$= x_{1,3} \cdot y_2 \cdot x_{1,3}$

in which x, y, z = the molar fractions of X, Y and Z in overall fatty acid composition of the trigylceride mixture; 6, 3, 1 = the number of ways in which three, two, and one type of fatty acids, respectively, can be distributed over the sn-1, sn-2, and sn-3 positions; $x_{1,3}$, $z_{1,3}$ = the molar fractions of X and Z on the sn-1 and sn-3 positions; y_2 = the molar fraction of fatty acid Y on the 2-positions; and 1, 2 = the number of ways the two and one type of fatty acids, respectively, can be distributed over the sn-1 and sn-3 positions in the triglyceride mixture.

The overall- and 2-position fatty acid composition in a triglyceride mixture can be obtained by conventional HPLC or GC analysis. The 1,3-position composition then follows by calculation. Though the above presented rules specifically refer to interesterification of triglycerides, they also apply to acidolysis—i.e., the reaction between triglycerides and fatty acids or single fatty acid esters. However, in this case the overall 1,3-positional fatty acid composition follows from the 1,3-positional fatty acid composition in the triglyceride fraction, the free fatty acid composition, and the molar ratio of free fatty acids to triglycerides.

B. Melting Properties of Triglycerides

Triglycerides are the basis for the production of spreads such as margarine and butter, as well as confectionery fats and chocolate. An important triglyceride property in this type of product is their melting behavior and contribution to product texture. The latter is easily recognized in product properties as softness, spreadability, and mouth feel.

The melting behavior of oils and fats is the result of complex interactions among large numbers of triglycerides, all different in the type and position of the fatty acids they contain. Thus modification of the fatty acid composition or distribution will result in a change in the melting behavior.

Chemical interesterification using a sodium alkoxide catalyst is widely being applied for oils and fats modification (70, 71). However, a growing interest exists for its enzymatic equivalent. This process runs under mild operating conditions of temperature and pressure. Moreover, exploiting the specificity of lipases, more specific triglyceride mixtures are obtained which cannot be produced by the random, chemical process.

To date, the main application of enzymatic TAG modification is probably the production of cocoa butterfat equivalents. Cocoa butterfat has a very special melting behavior, which is characterized by a rapid melting within a narrow temperature range. This behavior is related to its high content of POSt- and StOSt-type triglycerides (P = palmitic; O = oleic; St = stearic acid). The latter are not commonly present in vegetable oils, but can be produced by enzymatic modification of e.g. palm midfraction (a palm oil fraction rich in POP) and stearic acid. Using the 1,3-specific lipase from

[*] *Candida rugosa*, formerly referred to as *Candida cylindracea*.

Aspergillus niger in petroleum ether at 40°C, a POSt- and StOSt-rich mixture was thus obtained after 16 hours (38). Alternatively methylesters (72) or ethylester (73) have been used as stearic donor, using a 1,3-specific lipase such as *Rhizomucor miehei*, *Candida antarctica* B (74), or *Rhizopus japonicus* lipase (60).

Other liquid oils, e.g., olive oil, have also been evaluated for the production of cocoa butter equivalents. However, in this case the acidolysis product will also contain less functional tri- and di-oleyltriglycerides such as POO and StOO (75), which requires further separation of the POSt and StOSt fraction by conventional fractionation (38).

An improvement of the melting behavior has also been reported for butterfat being interesterified with a lipase. Using the 1,3-specific *Rhizopus arrhizus* lipase on Accurel interesterification during 96 h at 40–60°C resulted in significantly softer products with improved melting profiles, especially when interesterifying butter fat with canola oil (76–78). It was shown that chemical randomization yielded even more pronounced effects on fatty acid composition and spreading properties. The latter can also be obtained using a random lipase—e.g., that *from Pseudomonas fluorescens* (68).

Improved melting properties were also reported after the modification of fully vegetable oil blends. Starting with a 60/40 mixture of palm stearin and soybean oil, it was shown that the solid-fat content dropped after interesterification during 16 h using the 1,3-specific *Mucor miehei* lipase at 70°C (53). Similar results were reported for other fat blends consisting of palm stearin with coconut oil (43), palm kernel oil, and blends of palm with coconut or palm kernel oil (79). In all cases the 1,3-specific rearrangement of the fatty acids resulted in a decrease of the solids content at all temperatures.

C. Structured Triglycerides

In the last few decades it has become clear that the fatty acid composition of dietary fats has important implications for human health. Moreover, in certain cases also the position of the fatty acids, i.e., the triglyceride structure, is important (80). Much research has therefore been devoted to the production of so-called structured lipids, which are enriched in TAGs of a very specific structure and/or in a certain type of fatty acid. It is especially in this area that the selectivities of lipases become of particular interest.

Acidolysis using a 1,3-specific lipase is most commonly applied to produce structured triglycerides. A good example of such a process is the production of Betapol, an additive for infant formulas (81). This product predominantly consists of OPO, which is a major triglyceride in human milk fat (82). Hydrolysis of OPO by human pancreatic lipase will result in free oleic acid and 2-monopalmitin, which are both easily absorbed. As opposed to this, vegetable oils in infant formulas generally contain the POO-type triglycerides, the hydrolysis of which results in free palmitic acid. The latter will form insoluble calcium soaps, thereby preventing absorption of both the palmitic acid and the calcium (83).

Another example is the MLM triglycerides (M = medium-chain C_6–C_{12}; L = long-chain), preferably with an unsaturated fatty acid at the 2-position. Because of the improved digestibility of these types of triglycerides (84, 85), they are of interest for individuals suffering from pancreatic deficiency and other fat malabsorption disorders (86, 87).

Starting from liquid oils such as sunflower or soybean (88) or peanut oil (89), the desired TAGs are obtained by 1,3-specific acidolysis with a medium fatty acid donor, e.g., free fatty acids. This reaction can be carried out in batch as well as a packed-bed reactor (90).

However, in this one-step acidolysis process, MLM is not the only product. As the process is purely statistical the final mixture will also contain MLL- and LLL-type triglycerides. The concentrations of all TAG types depends on the molar excess of the fatty acids and the equilibrium composition can be calculated using the principles described above.

MLM concentrates were obtained in a two-step enzymatic process. In the first step nearly pure 2-monoglycerides were produced by ethanolysis (reaction with ethanol) of e.g. triolein or cotton seed oil using the 1,3-specific *Rhizopus delemar* lipase (Fig. 3). This reaction was carried out in organic solvent (ethers) at 40°C and 0.75 water activity. After purification by crystallization these 2-monoglycerides were reesterified with caprylic at 38°C in hexane using immobilized *Rhizomocur miehei* lipase. This process yielded ~ 90% MLM (89).

D. Fatty Acid Enrichment

Nutritionally interesting triglycerides can also be obtained by enrichment or removal of certain fatty acids from a TAG mixture, independent of the TAG structure involved. Especially in this area the fatty acid selectivity of certain lipases is rather important.

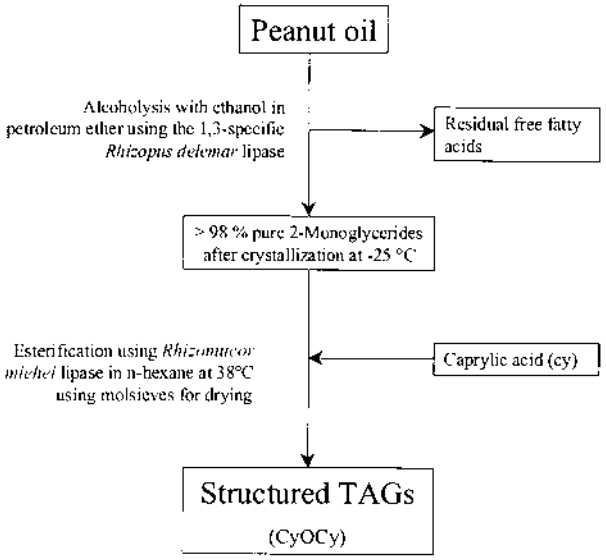

Figure 3 Two-step synthesis of structured triglycerides. (Adapted from Ref. 89.)

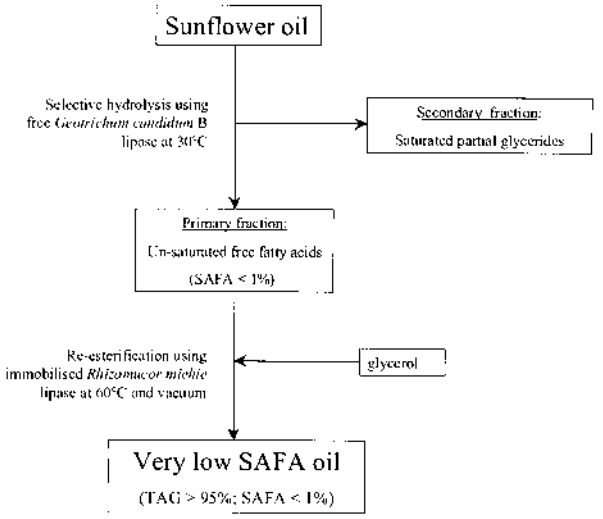

Figure 4 Fatty acid enrichment via selective hydrolysis: the production of a low-saturate oil via selective hydrolysis and nonselective enzymatic reesterification. (From Ref. 91.)

1. Low-Saturate Oils

The first example is the production of a low-saturate oil. For many decades the lowering of blood cholesterol by changing the dietary fat consumption has been a hot issue. Nowadays it is recommended to limit the intake of total fat and especially from saturated fat (127), and hence there is considerable interest in low-saturate fat products.

A two-step enzymatic process was described, exploiting the high selectivity of *Geotrichum candidum* lipase B for cis-Δ-9 unsaturated fatty acids (20, 21). In the first step of the process this lipase was used to preferentially hydrolyze oleic and linoleic acid from sunflower oil at 40°C. This resulted in > 99% unsaturated fatty acids in the free fatty acid fraction (91). After separation of the free fatty acids by conventional distillation, reesterification with glycerol was carried out using immobilized *Rhizomucor miehei* lipase (Fig. 4). Running the process at 60°C under continuous removal of water, > 95% w/w triglycerides were thus obtained with a saturated fatty acid content < 1%.

Now *Rhizomucor miehei* lipase is the most distinct 1,3-specific lipase, and hence the high yield of triglycerides in this reesterification reaction may seem rather surprising. However, whenever dealing with partial glycerides, acylmigration should be accounted for. At temperatures > 40°C monoglycerides (92) as well as diglycerides (93, 94, 126) undergo acylmigration. Thus the primary esterification products—i.e., (1(3)-monoglycerides and 1,3-diglycerides—are converted to their 2-position isomer. Subsequent esterification will result in the formation of 1,2-diglycerides and finally triglycerides (95, 96, 103). Research has shown that the presence of ionic enzyme carriers (94) and the use of apolar solvents (97) also promote acyl migration.

2. Enrichment of Long-Chain Polyunsaturated Fatty Acids

The second example of fatty acid enrichment is the production of TAGs enriched in long-chain polyunsaturated fatty acids (LPUFA). These fatty acids are now recognized to play an essential role in the human diet and have important biomedial properties. Marine oils are an important source for LPUFAs such as eicosapentaenoic acid (C20:5; EPA) and docosahexaenoic acid (C22:6; DHA). However, their individual levels are generally rather low and involve a mixture of different fatty acids. Thus enrichment and separation of these fatty acids is widely being investigated. Because of the high susceptibility of LPUFAs to oxidation, especially in this area low-temperature enzymatic processing can be a powerful tool (Fig. 5).

Glycerides enriched in LPUFAs can be produced by selective hydrolysis using the positionally nonselective but chain length–specific lipase from *Candida rugosa*

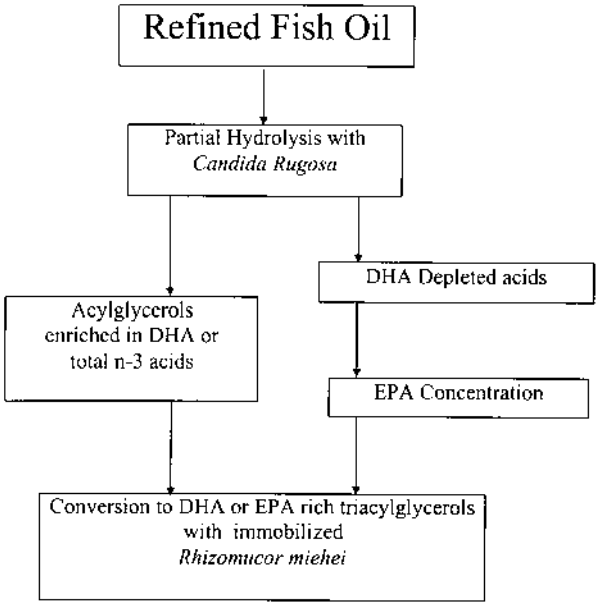

Figure 5 Production scheme for the enrichment of fish oil. (From Ref. 103.)

(Table 1). Starting with marine oils such as sardine or cod liver oil (98) or tuna oil (99, 100), partial glycerides with LPUFA levels between 45% and 65% were obtained.

It should be noted that the LPUFAs accumulate in the partial glyceride fraction because of the selectivity of the lipase against, i.e. discrimination against, these fatty acids. Using *Geotrichum candidum* lipase similar overall enrichment results were obtained. However, this lipase appears even more selective than *Candida rugosa*, as it is able to discriminate between EPA and DHA (101).

Another option for enrichment of oils is selective esterification of fish oil free fatty acids, using the conventional 1,3-specific lipases. Being also selective against LPUFAs but active in the esterification reaction, as compared to hydrolysis, reaction with simple alcohols results in free fatty acids enriched in the LPUFAs. These can be purified from the unwanted ester fraction by distillation (100, 102).

One interesting feature about the selective hydrolysis is the level of triglycerides as high as 75% in the residual glyceride mixture, even at degrees of hydrolysis as high as 70% (99, 103). This result is probably due to the ability of the *Candida rugosa* lipase to discriminate against triglycerides with a rising number of long-chain fatty acids in their structure. A model study revealed that triglycerides containing three DHA chains were hardly hydrolyzed, whereas the rate of hydrolysis increased with two or only one DHA chain in the TAG molecule (104). The phenomenon being less strong for diglycerides and absent for monoglycerides, triglycerides will always become the major compound in the product mixture.

It should be noted that processes similar to those discussed in this paragraph have been used for the enrichment of other interesting fatty acids—e.g., conjugated linoleic acid (CLA) (105), arachidonic acid (AA) (106), γ-linoleic acid (GLA) (107–109), and erucic acid (EA) (110).

V. PARTIAL GLYCERIDE PRODUCTION

A. Monoglycerides

Monoglycerides are widely applied as emulsifiers or surfactants and are normally produced by high-temperature glycerolysis using an inorganic catalyst (4). The product is a mixture of mono- and diglycerides (1:1 w/w) and residual triglycerides. Moreover, because of the reaction conditions applied, the crude product is often dark in color and has a burnt flavor. Obviously, this requires extensive purification during further down stream processing, generally involving molecular distillation. Because of the ambient reaction temperatures applied, lipase catalyzed processing has widely been investigated as the more "natural" process, with fewer byproducts and lower energy consumption.

Producing monoglycerides from oils and fats by hydrolysis would be the simplest route. It has been shown that the use of Celite immobilized porcine pancreas lipase at 40°C in a solvent-free system did result in 2-monoglyceride levels as high as 68% w/w in the residual glyceride fraction (111). This result corresponds to 67% of the theoretical molar yield. An even better result was obtained in organic solvent using *Rhizopus arrhizus* lipase at 35°C. A molar conversion of > 95% to 2-monoglycerides was obtained (89, 112). Despite this higher molar conversion, obviously the process route implies a low conversion efficiency.

Starting from free fatty acids and glycerol production of monoglycerides (predominantly the 1(3)-isomer) is much more efficient. Using the monoglyceride-specific enzyme patatin, an acylhydrolase from potato tubers (113), does offer an opportunity for a "natural" process. At temperature < 50°C this lipase was shown to produce > 95% monoglycerides in a solvent-free system (23). Though very specific, the enzyme is not commercially available.

Another option is the use of *Penicillium camembertii* lipase (lipase G), which is a mono- and diglyceride specific lipase and not able to react upon triglycerides. Moreover, it was shown that the selectivity to produce monoglycerides over diglycerides is determined by the water activity applied during the reaction. The lower the a_w, the more monoglyceride-specific the lipase. Thus at a water activity of approximately 0.1, > 90% pure monoglycerides were produced with 76% degree of conversion (114).

Even higher degrees of conversion were obtained by lowering the reaction temperature, such that the product starts to crystallize. This process is generally referred to as "directed synthesis," referring to the fact that crystallization shifts the equilibrium towards preferential synthesis of the desired solid product. Using this approach it was shown that at 40°C even solid palmitic acid could be converted to pure monoglycerides. Using *Penicillium cyclopium* lipase, nearly pure monoglycerides were produced at > 90% degree of conversion (115). It should be noted that the rate of this "solid-to-solid" conversion process is determined by the rate of diffusion of the reactants and hence the process is rather slow. Consequently the process may take 10–15 days to complete.

Similar results were reported using free lipase from *Pseudomonas fluorescens* or *Chromobacterium viscosum*. Monoglyceride yields between 70% and 90% were obtained, starting from various oils and fats (116, 117). It was shown that the high monoglyceride yield could be obtained simply by reducing the reaction temperature below a certain "critical temperature" (118). However, the latter appeared strongly dependent on the type of triglycerides involved (saturation level).

B. Diglycerides

For diglycerides processes have been developed similar to those described above, the only difference being either the optimum composition of the starting mixture, the lipase applied, or the processing conditions. Again, directed processes, i.e., applying temperature programming, have been shown to be an important tool for high purity and yield diglyceride production. Thus stepwise decreasing the reaction temperature from 62°C to 48°C, glycerolysis of hydrogenated beef tallow yielded ~90% diglycerides using a free *Pseudomonas* lipase (119).

The glycerol/triglyceride ratio was shown to affect the product purity, i.e., the level of monoglycerides formed. Optimum diglyceride yield was obtained at a glycerol/triglyceride molar ratio equivalent to its stoichiometric value for diglyceride production, i.e., 1:2 (119).

Directed esterification is another efficient means of diglyceride production. Using the 1,3-specific lipases from *Rhizomucor miehei* (116, 120) or *Rhizopus arrhizus* (94, 115), diglyceride yields of 65–85% were obtained. Applying continuous removal of water (116) during the process, yields > 90% were reported.

Comparable results were reported using the partial glyceride-specific lipase from *Penicillium camembertii*. As described above, at high water activity it loses its selectivity for monoglyceride production, yielding 60–85% diglycerides (114, 115).

It should be noted that the "directed synthesis" routes for mono- and diglyceride production prefer the use of free lipases to minimize the rate of mass transfer. Still reaction times are rather long. Moreover, recovery of the free lipase remains rather difficult if the use of solvents is to be avoided. Allowing solvents in the system, recovery of the biocatalyst obviously is much easier. Immobilizing the lipase on nonporous inorganic powders, the catalyst can be recovered after the (solvent-free) process by filtration, having dissolved the reaction medium in acetone (121). Carrying out the whole process in organic solvents, mass transfer is not an issue. For such systems other means of selective product removal also have been developed, such as in-line adsorption (122), crystallization in a separate vessel (123), and extraction (124).

VI. FUTURE PERSPECTIVE

As shown in this chapter, the use of lipases can be an important tool in the synthesis of a wide range of acylglycerides. Maximum production of a desired product can be obtained by carefully selecting the right lipase with the right selectivity under the right conditions for the process involved. Both the lipase selectivity and the relatively low reaction temperatures are important advantages over conventional organic synthesis, resulting in less byproduct formation and allowing single-step syntheses.

Despite these advantages, only a few of the processes described above are actually applied in industry at full scale. This is mainly due to the prohibitively high cost of most enzymes, as well as the relatively low operational stability encountered in certain applications. However, using modern biotechnology the cost of

enzymes is expected to decrease. Moreover, improved lipase selectivity and stability may further enhance the interest for the applications of enzymes in industry.

REFERENCES

1. S Wähnelt, D Meusel, M Tülsner. Influence of diglycerides on the phase-behaviour of edible fats. Fat Sci Technol 93:117–121, 1991.
2. DA Okiy. Interaction of triglycerides and diglycerides of palm oil. Oleagineux 33:625–628, 1978.
3. L El Kihel, J Bourass, P Richomme, JY Petit, Y Letourneux. Synthesis and evaluation of the anti-flammatory effects of niflumic acid lipophylic prodrugs in brain edema. Drug Res 46:1040–1044, 1996.
4. E Boyle. Monoglycerides in food systems: current and future uses. Food Technol 51:52–59, 1997.
5. E Boel, B Huge-Jensen. EU Patent application EP305216, 1989.
6. AM Klibanov. Enzymatic catalysis in anhydrous organic solvents. Trends Biochem Sci 14:141–144, 1989.
7. V Balcao, AL Paiva, FX Malcata. Bioreactors with immobilised lipases: state-of-the-art. Enzyme Microb Technol 18:392–416, 1996.
8. XF Malcata, HR Reyes, HS Garcia, CG Hill, CH Amundson. Immobilised lipase reactors for modification of fats and oils—review. J Am Oil Chem Soc 67:890–910, 1990.
9. HR Reyes, CH Hill. Kinetic modeling of interesterification reactions catalysed by immobilised lipase. Biotechnol Bioeng 43:171–182, 1994.
10. A Lourier, GJ Drtina, AM Klibanov. On the issue of interfacial activation of lipase in non-aqueous media. Biotechnol Bioeng 50:1–5, 1996.
11. U Derewenda, AM Brzozowski, DM Lawson, ZS Derewenda. Catalysis at the interface: the anatomy of a conformational change in a triglycerides lipase. Biochem 31:1532–1541, 1992.
12. AR Macrae, H Staines. Evaluation of microbial lipases as fat splitting catalysts. Fat Sci Technol 96:430, 1994.
13. GP Mcneill, RG Berger. Lipase catalysed synthesis of esters by reverse hydrolysis. OCL 2:359–363, 1995.
14. K Myojo, Y Matsufune. Process for preparing sterol fatty acid esters with enzymes. Yakaguku 44:883–896, 1995.
15. Y Shimada, Y Hirota, T Baba, A Sugihara, S Moriyama, Y Tominaga, T Terai. Enzymatic synthesis of sterylesters of polyunsaturated fatty acids. J Am Oil Chem Soc 76:713–716, 1999.
16. RD Schmidt, R Verger. Lipases: interfacial enzymes with attractive applications. Angew Chem Int 37:1608–1633, 1998.
17. J Pleis, M Fischer, RD Schmidt. Anatomy of lipase binding sites: the scissile fatty acid binding site. Chem Phys Lip 93:67–80, 1998.
18. IC Chandler, PT Quinlan, GP Mcneill. Lipase-catalyzed synthesis of chiral triglycerides. J Am Oil Chem Soc 75:1513–1518, 1998.
19. SA Hellyer, IC Chandler, JA Bosley. Can the fatty acid selectivity of plant lipases be predicted from the composition of the seed triglyceride? Biochem Biophys Acta 1440:215–224, 1999.
20. E Charton, AR Macrae. Specificities of immobilized *Geotrichum candidum* CMICC335426 lipase A and B in hydrolysis and ester synthesis in organic solvents. Enz Microbiol Technol 15:489–493, 1993.
21. E Charton, AR Macrae. Substrate specificities of lipases A and B from *Geotrichum candidum* CMICC-335426. Biochim Biophys Acta 1123:59–64, 1992.
22. O Lie, OG Lambertsen. Fatty acid specificity of *Candida cylindracea* lipase. Fett Seifen Anstrichm 88:365–367, 1986.
23. AR Macrae, JE Visicchio, A Lanot. Application of potato lipid acyl hydrolase for the synthesis of monoacylglycerols. J Am Oil Chem Soc 75:1489–1494, 1998.
24. A Zaks, AM Klibanov. The effect of water on enzyme action in organic media. J Biol Chem 263:8017–8021, 1988.
25. M Dolman, PJ Halling, BD Moore. How dry are anhydrous enzymes? Measurement of residual ad buried O^{18}-labelled water molecules using mass spectrometry. Biopolymers 41:313–319, 1997.
26. PJ Halling. Thermodynamic predictions for biocatalysis in non-conventional media: theory, tests and recommendations for experimental design and analysis. Enz Microbiol Technol 16:174–206, 1994.
27. RH Valivety, PJ Halling, AR Macrae. Reaction rate with lipase catalyst shows similar dependence on water activity in different solvents. Biochim Biophys Acta 1118:218–222, 1992.
28. RH Valivety, PJ Halling, AD Peilow, AR Macrae. Relationship between water activity and catalystic activity of lipases in organic media. Eur J Biochem 222:461–466, 1994.
29. RH Valivety, PJ Halling, AD Peilow, AR Macrae. Lipases from different sources vary widely in dependence of catalytic activity on water activity. Biochim Biophys Acta 1122:143–145, 1994.
30. E Wehtje, P Adlercreutz. Lipases have similar water activity profiles in different reactions. Biotechnol Lett 19:537–540, 1997.
31. G Bell, AEM Janssen, PJ Halling. Water activity fails to predict critical hydration level for enzyme activity in polar organic solvent: interconversion of water concentration and activities. Enz Microbiol Technol 20:471–477, 1997.

32. PA Claon, CC Akoh. Effect of reaction parameters on SP435 lipase-catalyzed synthesis of citronellyl acetate in organic solvent. Enz Microbiol Technol 16:835–838, 1997.
33. PE Napier, HM Lacerda, CM Rosell, RH Valivety, AM Vaiday, PJ Halling. Enhanced organic phase enzymatic esterification with continuous water removal in a controlled air-bleed evacuated-headspace reactor. Biotechnol Prog 12:47–50, 1996.
34. Z Ujang, N Al-sharbati, AM Vaidya. Organic-phase enzymatic interesterification in a hollow fiber membrane reactor with in-situ gas-phase water activity control. Biotechnol Prog 13:39–42, 1997.
35. E Wehtje, I Svensson, P Adlercreutz, B Mattiasson. Continuous control of water activity during biocatalysis in organic media. Biotechnol Technol 7:983–878, 1993.
36. CM Rosell, AM Vaiyda, PJ Halling. Continuous in-situ water activity control or organic phase biocatalysis in a packed bed hollow fiber membrane reactor. Biotechnol Bioeng 49:284–289, 1995.
37. JM Muderhwa, M Pina, J Graille. Aptitude a la transesterification de quelque lipases regioselectives 1–3. Taux de conversion et glycerides partiels en fonction de l'activite de l'eau des biocatalyseurs. Oleagineux 43:427–433, 1994.
38. AR Macrae. Lipase-catalyzed interesterification of oils and fats. J Am Oil Chem Soc 60:291–294, 1983.
39. T von Luck, W Bauer. Lipase-catalyzed interesterification of triglycerides in a solvent free process. I. Analytics and kinetics of the interesterification. Fat Sci Technol 93:41–49, 1991.
40. T von Luck, W Bauer. Lipase-catalyzed interesterification of triglycerides in a solvent free process. II. Engineering parameters for the application of a continuous process. 93:197–203, 1991.
41. P Forsell, P Paravuori, P Linko, K Poutanen. Enzymatic transesterification of rapeseed oil and lauric acid in a continuous reactor. J Am Oil Chem Soc 70:1105–1109, 1993.
42. SR Moore, J Davies. The kinetics of lipase-catalyzed interesterification of fats and oils. Inst Chem Eng Res Event 1:526–530, 1994.
43. LH Posorske, GK Lefebvre, CA Miller, TT Hansen, BL Glenvig. Process consideration of continuous fat modification with an immobilized lipase. J Am Oil Chem Soc 65:922–926, 1986.
44. RA Wisdom, P Dunhill, MD Lilly. Enzymatic interesterification of fats: laboratory and pilot-scale studies with immobilized lipase from *Rhizopus arrhizus*. Biotechnol Bioeng 29:1081–1085, 1987.
45. Y Inada, A Matsushima, K Takahashi, Y Saito. Polyethylene glycol-modified lipase soluble and active in organic solvents. Biocatalysis 3:317–328, 1990.
46. B Koops. Towards the application of lipases in organic media. PhD Thesis, Utrecht University, Utrecht, Netherlands, 1999.
47. B Koops, MH Verheij, AJ Slotboom, MR Egmond. Effect of chemical modification on the activity of lipases in organic solvents. Enz Microbiol Technol 25:622–631, 1999.
48. K Mogi, M Nakajima, S Mukataka. Surfactant modification of lipases for lipid interesterification and hydrolysis reactions. J Am Oil Chem Soc 76:1259–1264, 1999.
49. K Mogi, M Nakajima. Selection of surfactant-modified lipases for interesterification of triglyceride and fatty acid. J Am Oil Chem Soc 73:1505–1512, 1996.
50. MR Grote, PJ Geurtsen, KPAM van Putte. Immobilized enzyme and its use for the processing of triglycerides oils. Unilever patent WO 97/01632, 1997.
51. RA Wisdom, P Dunhill, MD Lilly, AR Macrae. Enzymic interesterification of fats: factors influencing the choice of support for immobilized lipase. Enz Microbiol Technol 6:443–446, 1984.
52. JA Bosley, JC Clayton. Blue print for a lipase support: use of hydrophobic controlled-pore glasses as model systems. Biotechnol Bioeng 43:934–938, 1994.
53. TT Hansen, P Eigtved. A new immobilized lipase for interesterification and ester synthesis. In: AR Baldwin, ed. Proc of the World Conf on Emerging Technologies in the Fats and Oils Industry. Champaign, IL: AOCS, 1986, pp 365–369.
54. JA Bosley, AD Peilow. Immobilization of lipases on porous polypropylene: reduction in esterification efficiency at low loading. J Am Oil Chem Soc 74:107–111, 1997.
55. T Gitlesen, M Bauer, P Adlercreutz. Adsorption of lipases on polypropylene powder. Biochim Biophys Acta 1345:188–196, 1997.
56. E Wehtje, P Adlercreutz, B Mattiasson. Improved activity retention of enzymes deposited on solid supports. Biotechnol Bioeng 41:171–178, 1994.
57. G Pencreac'h, JC Baratti. Activity of *Pseudomonas cepacia* lipase in organic media is greatly enhanced after immobilisation on a polypropylene support. Appl Microbiol Biotechnol 47:630–635, 1997.
58. DA Miller, JM Prausnitz, HW Blanch. Kinetics of lipase-catalysed interesterification of triglycerides in cyclo-hexane. Enz Microbiol Technol 13:98–103, 1991.
59. XF Malcata, HR Reyes, HS Garcia, CG Hill, CH Amundson. Kinetics and mechanisms of reactions catalyzed by immobilized lipases. Enz Microbiol Technol 14:426–446, 1992.
60. S Basheer, K Mogi, M Nakajima. Interestification kinetics of triglycerides and fatty-acids with modified lipase in n-hexane. J Am Oil Chem Soc 72:511–518, 1995.
61. S Basheer, JB Snape, K Mogi. Transesterification kinetics of triglycerides for a modified lipase in n-hexane. J Am Oil Chem Soc 72:231–237, 1995.

62. M Akimoto, Y Nagashima, D Sata. A kinetic study on lipase-catalyzed interesterification of soybean oil with oleic acid in a continuous packed-bed reactor. Appl Biochem Biotechnol 81:131–142, 1999.
63. TJ Ahern, AM Klibanov. The mechanism of irreversible enzyme inactivation at 100°C. Science 228:1280–1284, 1985.
64. Y Wang, MH Gordon. Effect of lipid oxidation products on the transesterification activity of an immobilized lipase. J Agric Food Chem 39:1693–1695, 1991.
65. D Pirrozi, PJ Halling. Lipase stability in continuous reactors for fat and oil transformation. ICHEAP4 Conference, Florence, 1999.
66. Y Ohta, T Yamane, S Shimizi. Inhibition and inactivation of lipase by fat peroxide in the course of batch and continuous glycerolysis of fat by lipase. Agric Biol Chem 53:1885–1890, 1989.
67. P Kalo, P Parviainen, K Vaara, S Ali-Yrrkö, M Antila. Changes in the triglyceride composition of butter fat induced by lipase and sodium methoxide catalysed interesterification reactions. Milchwissenschaft 41:82–85, 1986.
68. P Kalo, PH Huatori, M Antila. *Pseudomonas fluorescens* lipase-catalyzed interesterification of butter fat in the absence of solvent. Milchewissenschaft 45:281–285, 1990.
69. HR Reyes, CH Hill, CH Amundson. Interestification reactions catalysed by immobilized lipase on a hydrophobic support. J Food Process Preserv 18:199-132, 1994.
70. A Rozendaal. Interesterification of oils and fats. Inform 3:1232–1237, 1992.
71. A Rozendaal, AR Macrae. Interesterification of oils and fats. In: FD Gunstone, FB Padley, eds. Lipid Technologies and Applications. New York: Marcel Dekker, 1997, pp 223–263.
72. T Matsuo, N Sawamura, Y Hashimot, W Hashida. Method for enzymatic transesterification of lipid and enzyme used therein. Eur. patent 0035883 (Fuji Oil Company), 1981.
73. S Bloomer, P Adlercreutz, B Mattiasson. Triglyceride interesterification by lipases. 1. Cocoa butter equivalents from a fraction of palm oil. J Am Oil Chem Soc 67:519–524, 1990.
74. HMA Mohamed, S Bloomer, K Hammadi. Modification of fats by lipase interesterification. I. Changes in glyceride structure. Fat Sci Technol 95:428–431, 1993.
75 K Chang, G Abraham, VT John. Production of cocoa butter–like fat from interesterification of vegetable oils. J Am Oil Chem Soc 67:832–834, 1990.
76. D Rouseau, AG Marangoni. Tailoring the textural attributes of butter fat/canola oil blends via *Rhizopus arrhizus* lipase-catalyzed interesterification. 1. Compositional modifications. J Agric Food Chem 46:2368–2374, 1998.
77. D Rousseau, AG Marangoni. Tailoring the textural attributes of butter fat/canola oil blends via *Rhizopus arrhizus* lipase-catalyzed interesterification. 1. Modifications of physical properties. J Agric Food Chem 46:2375–2381, 1998.
78. D Roussau, AG Marangoni. The effects of interesterification of physical and sensory attributes of butter fat and butter fat-canola oil spreads. Food Res Int 31:381–388, 1999.
79. J Graille, M Pina, D Montet, JM Muderhwa. Making value-added products from palm-oil by 1,3-regioselectivity enzymatic interesterification. Elais 4:1–10, 1992.
80. U Bracco. Effect of triglyceride structure on fat absorption. J Am Clin Nutr 60:1002–1009, 1994.
81. P Quinlan, S Moore. Modification of triglycerides by lipases: process technology and its application to the production of nutritionally important fats. Inform 4:580–585, 1990.
82. WW Christie. In: RJ Hamilton, JB Rosell, eds. Analysis of Oils and Fats. Essex, UK: Elsevier Applied Science, 1986, pp. 313–340.
83. A Lucas, P. Quinlan, S Abrams, S Ryan, S Meah, PJ Lucas. Randomised controlled trial of a synthetic triglyceride milk formula for preterm infants. Arch Dis Child 77:F178–F184, 1997.
84. RJ Jandacek, JA Whiteside, BN Holcombe, RA Volpenheim, JD Taulbee. The rapid hydrolysis and efficient absorption of triglycerides with octanoic acid in the 1-position and 3-position and long-chain fatty acid in the 2-position. Am J Clin Nutr 45:940–945, 1987.
85. MM Jensen, MS Christensen, CE Hoy. Intestinal absorption of octanoic, decanoic and linoleic acids: effects of triacylglycerol structure. Ann Nutr Metab 38:104–116, 1995.
86. T Hansen, SE Godtfredsen. Triglycerdie, nutritional composition comprising such triglyceride and use of the nutritional composition for nutrition. World patent WO 90/04010 (Novo Nordinsk A/S), 1990.
87. CL Megremis. Medium-chain triglycerides: a nonconventional fat. Food Technol 45:108–110, 1991.
88. KH Huang, CC Akoh. Enzymatic synthesis of structured lipids: transesterification of triolein and caprylic acid ethyl ester. J Am Oil Chem Soc 73:345–250, 1996.
89. MM Soumanou, UT Bornscheuer, RD Schmid. Two-step enzymatic reaction for the synthesis of pure structured triacylglycerides. J Am Oil Chem Soc 75:703–710, 1998.
90. H Mu, X Xu, CE Hoy. Production of specific-structured triacylglycerols by lipase-catalyzed interesterification in a laboratory-scale continuous reactor. J Am Oil Chem Soc 75:1187–1193, 1998.
91. RMM Diks, MJ Lee. Production of a very low saturate oil based on the specificity of *Geotrichum candidum* lipase. J Am Oil Chem Soc 76:455–462, 1999.

92. G Boswinkel, JTP Derksen, K van't Riet, FP Cuperus. Kinetics of acylmigration in monoglycerides and dependence on acyl chainlength. J Am Oil Chem Soc 73:707-711, 1996.
93. DR Kodali, A Tercyak, DA Fahey, DM Small. Acyl migration in 1,2-dipalmitoyl-sn-glycerol. Chem Phys Lipids 52:163–170, 1990.
94. A Millqvist Fureby, P Adlercreutz, B Mattiasson. Glyceride synthesis in a solvent free system. J Am Oil Chem Soc 73:1489–1495, 1996.
95. R Lorti, M Trani, F Ergan. Kinetic study of the lipase catalyzed synthesis of triolein. Biotechnol Bioeng 41:1021–1026, 1993.
96. Y Dudal, R Lortie. Influence of water activity on the synthesis of triolein catalyst by immobilized *Rhizomucor miehei* lipase. Biotechnol Bioeng 45:129–134, 1995.
97. BJ Sjursness, T Anthonsen. Acyl migration in 1,2-dibutyrin dependence on solvent and water. Biocat 9:285–297, 1994.
98. T Hoshino, T Yamane, S Shimizu. Selective hydrolysis of fish oil by lipase to concentrate n-3 polyunsaturated fatty acids. Agric Biol Chem 54:1459–1467, 1990.
99. Y Tanaka, J Hirano, T Funada. Concentration of docosahexaenoic acid by glyceride by hydrolysis of fish oil with *Candida cylindracea* lipase. J Am Oil Chem Soc 69:1210–1214, 1992.
100. Y Shimada, A Sugihara, H Nakano, T Kuramoto, T Nagao, M Gemba, Y Tominaga. Purification of docosahexaenoic acid by selective esterification of fatty acids from tuna oil with *Rhizopus delemar* lipase. J Am Oil Chem Soc 74:97–101, 1997.
101. GP McNeill, RG Ackman, SR Moore. Lipase-catalyzed enrichment of long-chain polyunsaturated fatty acids. J Am Oil Chem Soc 73:1403–1407, 1996.
102. GG Haraldsson, B Kristinsson, R Sigurdardottir, GG Gudmundsson, H Breivik. The preparation of concentrates of eicosapentaenoic acid and docosahexaenoic acid by lipase catalyzed transesterification of fish oil with ethanol. J Am Oil Chem Soc 74:1419–1424, 1997.
103. SR Moore, GP McNeill. Production of triglycerides enriched in long-chain n-3 polyunsaturated fatty acids from fish oil. J Am Oil Chem Soc 73:1409–1414, 1996.
104. Y Tanaka, T Funada, J Hirano, R Hashizume. Triglyceride specificity of *Candida cylindracea* lipase: effect of docosahexaenoic acid in resistance of triglyceride to lipase. J Am Oil Chem Soc 70:1031–1034, 1993.
105. GP McNeill, C Rawlins, AC Peilow. Enzymatic enrichment of conjugated linoleic acid isomers and incorporation into triglycerides. J Am Oil Chem Soc 76:1265–1268, 1999.
106. Y Shimada, A Sugihara, K Maruyama, T Nagao, S Nakayama, H Nakano, Y Tominga. Enrichment of arachidonic acid—selective hydrolysis of a single-cell oil from *Mortierella* with *Candida cylindracea* lipase. J Am Oil Chem Soc 72:1323–1327, 1995.
107. FC Huang, YH Ju, CW Huang. Enrichment of γ-linolenic acid from borage oil via lipase-catalyzed reactions. J Am Oil Chem Soc 74:977–981, 1997.
108. MSKS Ramatulla, VKS Shukla, KD Mukherjee. Enrichment of γ-linolenic acid from evening primrose oil and borage oil via lipase-catalyzed hydrolysis. J Am Oil Chem Soc 71:569–573, 1994.
109. KD Mukherjee, I Kiewitt, MJ Hills. Substrate specificities of lipases in view of kinetic resolution of unsaturated fatty acids. Appl Microb Biotechnol 40:489–493, 1993.
110. GP McNeill, PE Sonnet. Isolation of erucic-acid from rapeseed oil by lipase-catalyzed hydrolysis. J Am Oil Chem Soc 72:213–218, 1995.
111. FJ Plou, M Barandiaran, MV Calvo, A Ballesteros, E Pastor. High-yield production of mono- and dioleylglycerol by lipase-catalyzed hydrolysis of triolein. Enz Microb Technol 18:66–71, 1996.
112. A Millqvist, P Adlercreutz, B Mattiasson. Lipase-catalyzed alcoholysis of triglycerides for the preparation of 2-monoglycerides. Enz Microb Technol 16:1042–1047, 1994.
113. D Racusen. Lipid acyl hydrolase of Patatin. Can J Bot 62:1640–1644, 1984.
114. S Yamaguchi, T Mase. High yield synthesis of monoglyceride by mono- and diacylglycerol lipase from *Penicillium camembertii* U-150. J Ferm Bioeng 72:162–167, 1991.
115. A von Weiss. Enzymatische Herstellung von festen Fettsäuremonoglyceriden. Fat Sci Technol 92:392–396, 1990.
116. R Rosu, M Yasui, Y Iwasaki, T Yamane. Enzymatic synthesis of symmetrical 1,3-diacylglycerols by direct esterification in solvent-free system. J Am Oil Chem Soc 76:839–843, 1999.
117. GP Mcneill, RG Berger. Enzymatic glycerolysis of palm oil fractions and palm oil based model mixture: relationship between fatty acid composition and monoglyceride yield. Food Biotechnol 7:75–87, 1993.
118. GP McNeill, S Shimizu, T Yamane. High-yield glycerolysis of oils and fats. J Am Oil Chem Soc 68:1–5, 1991.
119. T Yamane, ST Kang, K Kawahara, Y Koizumi. High-yield diacylglycerol formation by solid-phase enzymatic glycerolysis of hydrogenated beef tallow. J Am Oil Chem Soc 71:339–342, 1994.
120. SM Kim, JS Rhee. Production of medium chain glycerides by immobilized lipase in a solvent-free system. J Am Oil Chem Soc 68:499–503, 1991.
121. R Rosu, Y Uozaki, Y Iwasaki, T Yamane. Repeated use of immobilized lipase for monoacylglycerol pro-

duction by solid-phase glycerolysis of olive oil. J Am Oil Chem Soc 74:445–450, 1997.
122. A van der Padt, JTF Keurentjes, JJW Sewalt, EM van Dam, LJ van Dorp, K van't Riet. Enzymatic synthesis of monoglycerides in a membrane bioreactor with an in-line adsorption column. J Am Oil Chem Soc 69:748–754, 1992.
123. M Berger, MP Schneider. Enzymatic esterification of glycerol. 2. Lipase-catalyzed synthesis of regioisomerically pure 1(3)-rac-monoacylglycerols. J Am Oil Chem Soc 69:961–965, 1992.
124. DE Stevenson, RA Stanley, RH Furneaux. Glycerolysis of tallow with immobilized lipase. Biotechnol Lett 15:1043–1048, 1993.
125. JH Xu, T Kawamoto, A Tanaka. High performance continuous operation for enantioselective esterification of menthol by use of acid anhydride and free lipase in organic solvent. Appl Microbiol Biotechnol 43:639–643, 1995.
126. X Xu, ARH Skands, CE Hoy, H Mu, S Balchen, J Adler-Nissen. Production of specific structured lipids by enzymatic interesterification: elucidation of acylmigration by response surface design. J Am Oil Chem Soc 75:1179–1186, 1998.
127. American Dietetic Association. Position of the American Dietetic Association: fat replacers. J Am Dietet Assoc 98:463–468, 1998.

19

Significance of Indigenous Enzymes in Milk and Dairy Products

Patrick F. Fox
University College, Cork, Ireland

I. INTRODUCTION

About 60 indigenous enzymes have been reported in normal bovine milk (1); with the exception of α-lactalbumin, most of these have no obvious physiological role. The indigenous enzymes are constituents of the milk as excreted and arise from three principal sources: (a) the blood via defective mammary cell membranes; (b) secretory cell cytoplasm, some of which is occasionally entrapped within fat globules by the encircling fat globule membrane (MFGM); and (c) the MFGM itself, the outer layers of which are derived from the apical membrane of the secretory cell, which in turn originates from the Golgi membranes; this is probably the principal source of the enzymes. Thus, most enzymes enter milk owing to peculiarities of the mechanism by which milk constituents, especially the fat globules, are excreted from the secretory cells. Milk does not contain substrates for many of the enzymes present, while others are inactive in milk owing to unsuitable environmental conditions such as pH.

The following abbreviations are used: MFGM, milk fat globule membrane; β-CN, β-casein; α_{s2}-CN, α_{s2}-casein; LPL, lipoprotein lipase; UHT, ultra high temperature; HTST, high temperature short time; LTLT, low temperature long time; PE, pasteurization equivalent; HML, human milk lysozyme; BML, bovine milk lysozyme; EWL, egg white lysozyme; NAGase, N-acetyl-β-D-glucosaminidase; GGTP, γ-glutamyl transpeptidase; LPO, lactoperoxidase; XO, xanthine oxidase; SO, sulfhydryl oxidase; SOD, superoxide dismutase.

Many indigenous milk enzymes are technologically significant from five viewpoints:

1. Deterioration (lipase [potentially the most significant enzyme in milk], proteinase, acid phosphatase and xanthine oxidase) or preservation (lactoperoxidase, sulfhydryl oxidase, superoxide dismutase) of milk quality.
2. As indices of the thermal history of milk; these include alkaline phosphatase, γ-glutamyl transpeptidase, lactoperoxidase, and perhaps others.
3. As indices of mastitic infection; the concentration of several enzymes increases on mastitic infection, especially catalase, N-acetyl-β-glucosaminidase and acid phosphatase.
4. Antimicrobial activity, such as lysozyme and lactoperoxidase (which is exploited as a component of the lactoperoxidase–H_2O_2–thiocyanate system for the cold pasteurization of milk).
5. As commercial source of enzymes; these include ribonuclease and lactoperoxidase.

With a few exceptions (e.g., lysozyme and lactoperoxidase), the indigenous milk enzymes do not have a beneficial effect on the nutritional or organoleptic attributes of milk, and hence their destruction by heat is one of the objectives of many dairy processes.

The technologically significant indigenous enzymes in milk and their catalytic activities are listed in Table 1. All these enzymes have been isolated and well characterized. Other enzymes that have been isolated and characterized but which have little or no significance in milk are listed in Table 2. Enzymatic

Table 1 Technologically Significant Indigenous Enzymes in Milk

Enzyme	Reaction	Significance
Lipase	Triglycerides + H_2O → fatty acids + partial glycerides + glycerol	Off flavor in milk; flavor development in blue cheese
Proteinase (plasmin)	Hydrolysis of peptide bonds, particularly in β-casein	Reduced storage stability of UHT products; cheese ripening
Alkaline phosphomonoesterase	Hydrolysis of phosphoric acid esters	Index of pasteurization
Acid phosphomonoesterase	Hydrolysis of phosphoric acid esters	Cheese ripening; reduced heat stability of milk;
Lysozyme	Hydrolysis of mucopolysaccharides	Bacteriocidal agent
γ-Glutamyl transpeptidase	Transfer of γ-glutamyl residues	Index of heat treatment
N-Acetylglucosaminidase	Hydrolysis of glycoproteins	Index of mastitis
Xanthine oxidase	Aldehyde + H_2O + O_2 → Acid + H_2O_2	Pro-oxidant; cheese ripening
Sulfhydryl oxidase	$2RSH + O_2 \rightarrow RSSR + H_2O_2$	Amelioration of cooked flavor
Superoxide dimutase	$2O_2^{\bullet} + 2H^+ \rightarrow H_2O_2 + O_2$	Antioxidant
Catalase	$2H_2O_2 \rightarrow O_2 + 2H_2O$	Index of mastitis; pro-oxidant
Lactoperoxidase	$H_2O_2 + AH_2 \rightarrow 2H_2O + A$	Index of pasteurization; bactericidal agent; index of mastitis; pro-oxidant

activities that have been detected in milk but which have not been isolated and have no known significance in milk are listed in Table 3; it is possible that some of these enzymes are secreted by contaminating bacteria in milk.

The indigenous enzymes in milk have attracted the attention of researchers for > 100 years, mainly because of their potential to cause defects in milk and dairy products, especially lipase, and their usefulness as indicators of the thermal treatment of milk. More recently, they have assumed importance as indices of animal health and of the mechanisms involved in the synthesis and secretion of milk. A very extensive literature has accumulated. The general topic has been the subject of several general reviews (1–10); in addition, the literature on the principal technologically significant enzymes has been reviewed separately (see below).

In this chapter the occurrence, distribution, isolation, and characterization of the principal indigenous enzymes in bovine milk will be discussed, with emphasis on their commercial significance in milk and dairy

Table 2 Other Enzymes That Have Been Isolated From Milk and Partially Characterized but Which Are of No Known Significance in Milk

Enzyme		Reaction catalyzed	Comment
Glutathione peroxidase	EC 1.11.1.92	$GSH + H_2O \rightleftharpoons GSSH$	Contains Se
Ribonuclease	EC 3.1.27.5	Hydrolysis of RNA	Milk is a very rich source; similar to pancreatic RNase
α-Amylase	EC 3.2.1.1	Hydrolysis of starch	
β-Amylase	EC 3.2.1.2	Hydrolysis of starch	
α-Mannosidase	EC 3.2.1.24	Hydrolysis of mannan	Contains Zn^{2+}
β-Glucuronidase	EC 3.2.1.31	Hydrolysis of glucuronides	
5′-Nucleotidase	EC 3.1.3.5	5′- Nucleotides + $H_2O \rightleftharpoons$ ribonucleosides + P_i	Diagnostic test for mastitis
Adenosine triphosphatase	EC 3.6.1.3	$ATP + H_2O \rightleftharpoons ADP + P_i$	
Aldolase	EC 4.1.2.13	Fructose, 1,6 diP $\rightleftharpoons$ glyceraldehyde-3-P + dihydroxyacetone-P	

Source: Ref. 70.

products. The available information indicates that the milks of other species have an enzyme profile similar to bovine milk, although very considerable interspecies differences exist in the level of certain enzymes, e.g., the very high level of lysozyme in human and equine milks. Human milk and that of other primates contain a bile salts-activated lipase, in addition to the ubiquitous lipoprotein lipase, which is not present in the milk of other species. The indigenous enzymes in human milk have been described by Hamos et al. (11) and Hernell and Lonnerdal (12).

II. PROTEINASES (EC 3.4.–.–)

The presence of an indigenous proteinase in milk was suggested by Babcock and Russel in 1897 but because it occurred at a low concentration or had low activity in milk, it was believed until the 1960s that the proteinase in milk might have been of microbial origin. Recent changes in the dairy industry, e.g., improved hygiene in milk production, extended storage of milk at a low temperature at the farm and/or factory, and altered product profile—e.g., UHT processing of milk—have increased the significance of indigenous milk proteinase which has, consequently, been the focus of considerable research.

Milk contains at least two proteinases, plasmin (alkaline milk proteinase) and cathepsin D (acid milk proteinase) and possibly several other proteolytic enzymes, e.g., two thiol proteinases, thrombin, and an aminopeptidase. In terms of activity and technological significance, plasmin is the most important of the indigenous proteolytic enzymes and has been the subject of most attention. The relevant literature has been reviewed by Grufferty and Fox 13) and Bastian and Brown (14).

A. Plasmin (EC 3.4.21.7)

The physiological function of plasmin (fibrinolysin) is to dissolve blood clots. It is part of a complex system consisting of plasmin, its zymogen (plasminogen), plasminogen activators, plasmin inhibitors, and inhibitors of plasminogen activators (Fig. 1). In milk, there is about four times as much plasminogen as plasmin, and both, as well as plasminogen activators, are associated with the casein micelles, from which they dissociate when the pH is decreased to 4.6; the inhibitors of plasmin and of plasminogen activators are in the milk serum. It has been reported that there is a low level of plasmin activity in the milk fat globule membrane but this appears to be due to the adsorption of plasmin to casein micelles which are adsorbed on the membrane (15). The concentration of plasmin and plasminogen in milk increase with advancing lactation, mastitic infection, and number of lactations. The conversion of plasminogen to plasmin in milk increases with advancing lactation, and there is a positive correlation between plasmin activity and the level of plasminogen activator, which itself is positively correlated with somatic cell count (16). The level of plasmin in milk is also affected by diet and management practices (16). No activation of plasminogen to plasmin is reported (17) to occur during storage of milk at 4°C for 6 days; in fact, plasmin and potential plasmin (plasminogen) activity decreased under these conditions.

Bovine plasminogen contains 786 amino acids with a mass of 88.092 kDa. Its primary structure is arranged in five loops (called kringles), each stabilized by three intramolecular disulfide bonds. Plasminogen is activated in a two-step process: it is first cleaved at Arg_{557}-Ile_{558} (bovine) by plasmin (a trace of which occurs in blood) to yield Lys-plasminogen which is inactive but undergoes a conformational change

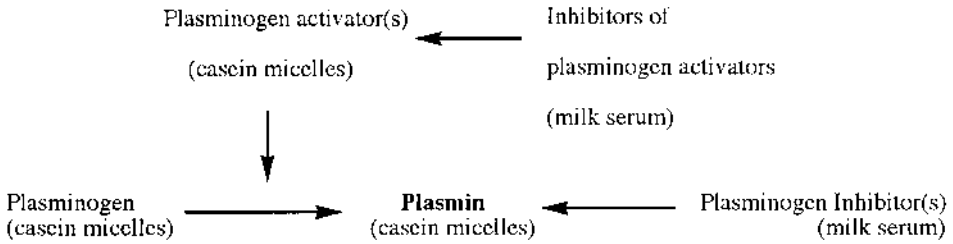

Figure 1 Schematic representation of the plasmin system in milk.

Table 3 Partial List of Minor Enzymes in Milk

Enzyme		Reaction catalyzed	Source	Distribution in milk
EC 1.1.1.1	Alcohol dehydrogenase	Ethanol+$NAD^+ \rightleftharpoons$ acetaldehyde +NADH + H^+		
EC 1.1.1.14	L-Iditol dehydrogenase	L-Iditol + $NAD^+ \rightleftharpoons$ L-sorbose + NADH + H^+	—	SM
EC 1.1.1.27	Lactate dehydrogenase	Lactic acid + $NAD^+ \rightleftharpoons$ pyruvate acid + NADH + H^+		SM
EC 1.1.1.37	Malate dehydrogenase	Malate + $NAD^+ \rightleftharpoons$ oxaloacetate + NADH + H^+	Mammary gland	SM
EC 1.1.1.40	Malic enzyme	Malate + $NADP^+ \rightleftharpoons$ pyruvate + CO_2+NADH + H^+	Mammary gland	SM
EC 1.1.1.42	Isocitrate dehydrogenase	Isocitrate + $NADP^+ \rightleftharpoons$ 2-oxoglutarate + CO_2 +NADH + H^+	Mammary gland	SM
EC 1.1.1.44	Phosphoglucuronate dehydrogenase (decarboxylating)	6-Phospho-D-gluconate + $NADP^+ \rightleftharpoons$ D-ribose-5-P + CO_2 + NADPH + H^+	Mammary gland	SM
EC 1.1.1.49	Glucose-6-phosphate dehydrogenase	D-Glucose-6-P + $NADP^+ \rightleftharpoons$ D-glucono-1,5-lactone-6-P + NADPH + H^+	Mammary gland	SM
EC 1.4.3.6	Amine oxidase (Cu-containing)	$RCH_2NH_2 + H_2O + O_2 \rightleftharpoons RCHO + NH_3 + H_2O_2$	—	SM
—	Polyamine oxidase	Spermine $\xrightarrow{O_2}$ spermidine $\xrightarrow{O_2}$ putrescine	—	SM
—	Fucosyltransferase	Catalyzes the transfer of fucose from GDP L-fucose to specific oligosaccharides and glycoproteins	—	SM
EC 1.6.99.3	NADH dehydrogenase	NADH + acceptor $\rightleftharpoons$ NAD^+ + reduced acceptor	—	FGM
EC 1.8.1.4	Dihydrolipoamide dehydrogenase (diaphorase)	Dihydrolipoamide + $NAD^+ \rightleftharpoons$ lipoamide + NADH	—	SM/FGM
EC 2.4.1.22	Lactose synthetase (A protein: UDP-galactose: D-glucose, 1-galactosyltransferase; B protein: α-lactalbumin)	UDP galactose + D-glucose $\rightleftharpoons$ UDP + lactose	Golgi apparatus	SM
EC 2.4.1.38	Glycoprotein 4-β-galactosyltransferase	UDP galactose+*N*-acetyl D-glucosaminyl-glycopeptide $\rightleftharpoons$ UDP + 4, β-D-galactosyl-N-acetyl-D-glucosaminyl glycopeptide	—	FGM
EC 2.4.1.90	*N*-Acetyllactosamine synthase	UDP galactose+*N*-acetyl-D-glucosamine $\rightleftharpoons$ UDP *N*-acetyllactosamine	Golgi apparatus	—
EC 2.4.99.6	CMP-*N*-acetyl-*N*-acetyl-lactosaminide α-2,3-sialyltransferase	CMP-*N*-acetylneuraminate + β-D-galactosyl-1,4-*N*-acetyl D-glucosaminyl glycoprotein $\rightleftharpoons$ CMP+ α-*N*-acetylneuraminyl 1-2, 3-β-D-galactosyl-1,4-*N*-acetyl-D-glucosaminyl-glycoprotein	—	SM

EC 2.5.1.3	Thiamine-phosphate pyrophosphorylase	2-Methyl-4-amino-5-hydroxymethyl/pyrimidine diphosphate + 4-methyl-5-(2-phosphonooxyethyl)-thiazole $\rightleftharpoons$ pyrophosphate + thiamine monophosphate	—	FGM
EC 2.6.1.1	Aspartate aminotransferase	L-aspartate + 2-oxoglutarate $\rightleftharpoons$ oxaloacetate + L-glutamate	Blood	SM
EC 2.6.1.2	Alanine aminotransferase	L-alanine + 2-oxoglutarate $\rightleftharpoons$ pyruvate + L-glutamate	Blood	SM
EC 2.7.7.49	RNA-directed DNA polymerase	*n* Deoxynucleoside triphosphate $\rightleftharpoons n$ pyrophosphate + DNA_n	—	
EC 2.8.1.1	Thiosulfate sulfur transferase	Thiosulfate + cyanide $\rightleftharpoons$ sulfite + thiocyanate	—	SM
EC 3.1.1.8	Cholinesterase	Acylcholine + H_2O $\rightleftharpoons$ choline + carboxylic acid anion	Blood	FGM
EC3.1.3.9	Glucose-6-phosphatase	D-Glucose 6-P + H_2O $\rightleftharpoons$ D-glucose + Pi	—	FGM
EC 3.1.4.1	Phosphodiesterase	Phosphodiester + H_2O $\rightarrow$ phosphomonoester+ alcohol	—	
EC 3.1.6.1	Arylsulfatase	Phenol sulfate + H_2O $\rightleftharpoons$ phenol + sulfate	—	—
EC 3.2.1.21	β-Glucosidase	Hydrolysis of terminal non-reducing β-D-glucose residues	Lysosomes	FGM
EC 3.2.1.23	β-Galactosidase	Hydrolysis of terminal nonreducing β-D-galactose residues in β-D-galactosides	Lysosomes	FGM
EC 3.2.1.51	α-Fucosidase	An α-L-fucoside + H_2O $\rightleftharpoons$ an alcohol + L-fucose	Lysosomes	—
EC 3.4.11.1	Cytosol aminopeptidase (leucine aminopeptidase)	Aminoacyl-peptide + H_2O $\rightleftharpoons$ amino acid + peptide	—	SM
EC 3.4.11.3	Cystyl-aminopeptidase (Oxytocinase)	Cystyl-peptides + H_2O $\rightleftharpoons$ amino acid + peptide	—	SM
EC 3.4.21.4	Trypsin	Hydrolyzes peptide bonds, preferentially Lys-X, Arg-X	—	SM
EC 3.6.1.1	Inorganic pyrophosphatase	Pyrophosphate + H_2O $\rightleftharpoons$ 2 orthophosphate	—	SM/FGM
EC 3.6.1.9	Nucleotide pyrophosphate	A dinucleotide + H_2O $\rightleftharpoons$ 2 mononucleotides	—	SM/FGM
EC 4.2.1.1	Carbonate dehydratase	H_2CO_3 $\rightleftharpoons$ $CO_2 + H_2O$	—	SM
EC 5.3.1.9	Glucose-6-phosphate isomerase	D-glucose-6-P $\rightleftharpoons$ fructose-6-P	—	SM
EC 6.4.1.2	Acetyl-CoA carboxylase	ATP + acetyl-CoA + HCO_3^- $\rightleftharpoons$ ADP + orthophosphate + malonyl-CoA	—	FGM

Source: Ref. 70.
SM = skin milk; FGM = fat globule membrane; P = phosphate.

which exposes the bond Lys_{77}-Arg_{78} to hydrolysis by urokinase or tissue-type plasminogen activator. Hydrolysis of this bond yields a mature enzyme of ~ 81 kDa, consisting of two polypeptide chains held together by a single disulfide bond. The five kringles of plasminogen are retained in plasmin; they are required for activity and are conserved in plasmins from different species. Bovine plasmin is also cleaved at Arg_{342}-Met_{343} to yield midi plasmin (15). Bovine plasminogen cDNA has been cloned (18).

Plasmin is a serine proteinase (inhibited by di-isopropylfluorophosphate, phenylmethyl sulfonyl fluoride, and trypsin inhibitors) with a high specificity for peptide bonds to which lysine or arginine supplies the carboxyl group. The active site is in the smaller of the two chains and consists of His_{598}, Asp_{641}, and Ser_{736}. It is optimally active at $\sim$ pH 7.5 and $\sim 35^{\circ}C$; it exhibits $\sim 20\%$ of maximum activity at $5^{\circ}C$ and is stable over the pH range 4–9.

Plasmin is usually extracted from casein by washing with water at pH 3.5 and purified by precipitation with $(NH_4)_2SO_4$ and various forms of chromatography, including affinity chromatography. Plasmin is quite heat stable; it is partially inactivated by heating at $72^{\circ}C$ for 15 sec, but its activity in milk increases following HTST pasteurization, probably owing to inactivation of the indigenous inhibitors of plasmin or, more likely, inhibitors of plasminogen activators. It partly survives UHT sterilization and is inactivated by heating at $80^{\circ}C$ for 10 min at pH 6.8; its thermal stability decreases with increasing pH in the range 3.5–9.2.

The inactivation of plasmin in milk follows first-order kinetics. Arrhenius plots show that inactivation is not linear with increasing temperature. In the temperature range 63–$110^{\circ}C$, E_a for inactivation is 52.75 and 74.44 kJ mol^{-1} for low and high somatic cell count (SCC) milk, respectively, while in the range 100–$130^{\circ}C$, E_a is 22.03 and 24.70 kJ mol^{-1} for low and high SCC milk, respectively (19). Plasmin is more heat stable to low-temperature treatments, e.g., thermization and HTST pasteurization, in high than in low SCC milk but the reverse is true in the UHT range (19). Milk with a high SCC has high plasminogen activator activity (19).

1. Assay of Plasmin Activity

Plasmin activity may be assayed on a wide range of substrates, including proteins, but the most widely used substrate is the synthetic fluorogenic peptide, N-succinyl-L-Ala-L-Phe-L-Lys-7-amido-4-methyl coumarin; the liberated 7-amido-4-methyl coumarin is quantified by determining the intensity of fluorescence, with excitation at 380 nm and emission at 460 nm (20). The chromogenic substrate, Val-Leu-Lys-*p*-nitroanilide, is also used (16). Plasminogen activity is measured by assaying plasmin activity before and after activation of indigenous plasminogen by an excess of added urokinase (16). Plasminogen activator activity may be assayed by the ability of an ultracentrifugal casein micelle pellet to activate exogenous (added) plasminogen (16).

2. Activity of Plasmin on Milk Proteins

β-Casein is the most susceptible milk protein to plasmin action; it is hydrolyzed rapidly at Lys_{28}-Lys_{29}, Lys_{105}-His_{106}, and Lys_{107}-Glu_{108} to yield γ^1 (β-CN f29-209), γ^2 (β-CN f106-209), and γ^3 (β-CN f108-209) caseins and proteose peptone (PP)5 (β-CN f1-105/7), and PP8 slowly (β-CN f29-105/7) and PP8 fast (β-CN f1-29). In vitro (in solution), β-casein is also hydrolyzed fairly rapidly at Lys_{113}-Tyr_{114} and Lys_{183}-Asp_{184}, but it is not known if these bonds are hydrolyzed in milk. γ-Caseins normally represent ~ 3 % of total N in milk but can be as high as 10% in late-lactation milk; as a percent of total N, the value for proteose peptones is about half that of the γ-caseins.

α_{s2}-Casein in solution is also hydrolyzed very rapidly by plasmin at bonds Lys_{21}-Gln_{22}, Lys_{24}-Asn_{25}, Arg_{114}-Asn_{115}, Lys_{149}-Lys_{150}, Lys_{150}-Thr_{151}, Lys_{181}-Thr_{182}, and Lys_{188}-Ala_{189} (see 14), but its hydrolysis in milk has not been characterized. Although less susceptible than α_{s2}- or β-caseins, α_{s1}-casein in solution is also readily hydrolyzed by plasmin (14) but it does not appear to be hydrolyzed to a significant extent in milk, although it has been suggested that λ-casein is produced from α_{s1}-casein by plasmin. Although κ-casein contains several Lys and Arg residues, it appears to be quite resistant to plasmin, presumably owing to a relatively high level of secondary and tertiary structures. The whey proteins are quite resistant to plasmin, probably owing to their compact, globular structures; in fact, β-lactoglobulin, especially when denatured, inhibits plasmin, presumably via sulfhydryl-disulfide interactions which rupture the structurally important kringles.

3. Significance of Plasmin Activity in Milk

There is sufficient plasmin in milk to cause very extensive proteolysis, but this is not realized owing to the presence of inhibitors. If the casein micelles are sedimented by ultracentrifugation and redispersed in buffer, very extensive proteolysis occurs on storage since

the inhibitors are removed in the ultracentrifugal serum. According to Guinot-Thomas et al. (17), microbial proteinases cause more proteolysis in milk than plasmin during storage at 4°C for 6 days.

Plasmin and plasminogen accompany the casein micelles on the rennet coagulation of milk and are concentrated in cheese in which plasmin contributes to primary proteolysis of the caseins, especially in cheeses that are cooked to a high temperature, e.g., Swiss and some Italian varieties, in which the coagulant is totally or extensively inactivated (21). β-Casein is the principal substrate and even in low-cooked cheeses (e.g., Cheddar, Gouda), in which the coagulant is the principal primary proteinase, proteolysis of β-casein is due mainly to plasmin action; some hydrolysis of α_{s1}-casein by plasmin also occurs.

The level of plasmin activity in cheese varies substantially with the variety; Emmental, Parmesan, and Dutch-type cheeses contain about three times as much plasmin activity as Cheddar-type cheeses (22). This is probably due to the greater activation of plasminogen in the former as a result of inactivation of inhibitors of plasminogen activators in high-cooked cheese and their removal from Dutch-type cheese curd on washing (when whey is removed and replaced by water). Plasmin activity is decreased in cheeses made from UF-concentrated milk because of the retention of inhibitors of plasmin and plasminogen activators and β-lactoglobulin in the curd. Proteolysis is less in UF cheeses than in their conventional counterparts; presumably, the lower level of plasmin activity is a contributory factor.

It has been suggested that an elevated level of plasmin activity in late-lactation milk contributes to its poor cheese-making properties; however, an elevated level of somatic cells in milk does not appear to lead to defects in cheese (13). The casein micelles in bovine milk are capable of binding ~ 10 times as much plasmin as occurs naturally in milk. Exogenous plasmin added to milk is incorporated and uniformly distributed in the cheese curd, in which it accelerates proteolysis and maturation (23). When other exogenous proteinases are added to cheese milk, much of the added enzyme is lost in the whey, increasing cost and creating potential problems for whey processors. The yield of cheese may also be decreased owing to early hydrolysis of casein in the vat. For Cheddar-type cheese, exogenous proteinases may be added to the milled curds at salting, but the enzyme is concentrated at the surface of the curd chips. Activation of indigenous plasminogen by added urokinase also accelerates proteolysis (14, 23a).

Cheese analogues are usually produced from rennet casein which may contain active plasmin. Hydrolysis of β-casein and undesirable changes in the rheological properties of cheese analogs have been attributed to plasmin action (14).

Plasmin activity may contribute to the age gelation of UHT milk produced from high-quality raw milk (which contains a low level of *Pseudomonas* proteinase). The acid precipitability of casein from late-lactation milk is poor, but evidence for the involvement of plasmin is lacking. Reduced yields of cheese and casein can be expected to result from plasmin action in milk since the proteose peptones are, by definition, soluble at pH 4.6 and are not incorporated into acid- or rennet-produced casein curd.

4. Proteinase Inhibitors in Milk

Milk contains several broad-specificity plasma-derived proteinase inhibitors: α_1-proteinase inhibitor, α_2-antiplasmin, C1 inhibitor, antithrombin-III, α_2-macroglobulin, inter-α-trypsin inhibitor, and two inhibitors analogous to human α_1-antichymotrypsin which possess inhibitory activity against trypsin and elastase, respectively. Inhibitory activity is highly elevated in mastitic milk owing to increased leakage of blood proteins into milk. It has been proposed that trypsin inhibitory activity in milk may be a useful index of mastitis in cows. Bovine colostrum contains colostrum-specific proteinase inhibitors, including trypsin-inhibitory and thiol proteinase-inhibitory activities, which protect immunoglobulins and other biologically active proteins and peptides against proteolysis by gastrointestinal enzymes in the newborn (24, 25).

Apart from the colostrum-specific inhibitors, the plasma-derived inhibitors are present in milk as a result of membrane leakage (mastitis or late lactation) and therefore might be expected to be without significance. However, they are probably quite significance: (a) The level of plasmin in milk is sufficient to cause very extensive hydrolysis of the caseins, as can be readily demonstrated by dispersing ultracentrifugally sedimented casein micelles in buffer (plasmin and plasminogen accompany the casein micelles while the inhibitors are in the milk serum). Plasmin activity is increased by pasteurization apparently because proteinase inhibitors are inactivated by heating. (b) The inhibitors are retained in cheese made from milk concentrated by ultrafiltration (UF) whereas they are lost in the whey during conventional cheese making. Consequently, proteolysis is retarded in UF cheese (14, 25).

Denatured β-lactoglobulin also inhibits plasmin, apparently owing to sulfhydryl-disulfide interchange reactions. Since β-lactoglobulin is concentrated by UF, it probably contributes to the inhibition of proteolysis in cheese made from UF-concentrated milk during ripening.

5. Plasminogen Activators

There are two types of plasminogen activators, urokinase-type plasminogen activator (uPA) and tissue-type plasminogen activator (tPA). Both types occur in milk; uPA is confined to cells in milk while tPA is associated with the casein micelles (26, 27). Both activators have been characterized and cloned (28). Lu and Nielsen (29) reported that there are five plasminogen activators in milk, with molecular weights of 93, 57, 42, 35, and 27 kDa; most were uPA-type activators. PA level increases with mastitic infection and advancing lactation (30), which explains the greater conversion of plasminogen to plasmin in such milks.

B. Cathepsin D (EC 3.4.23.5)

It has been known for ~ 30 years that milk also contains an acid proteinase (optimum pH ~ 4.0) which is now known to be cathepsin D, a lysosomal enzyme. It is relatively heat labile (inactivated by 70°C for 10 min). Its activity in milk has not been studied extensively, and its significance is unknown. At least some of the indigenous acid proteinase is incorporated into cheese curd; its specificity on α_{s1}- and β-caseins is quite similar to that of chymosin, but it has very poor milk clotting activity (31). It may contribute to proteolysis in cheese, but its activity is probably normally overshadowed by chymosin, which is present at a much higher level in cheese.

C. Other Proteinases

The presence of other minor proteolytic enzymes in milk, including thrombin and a lysine aminopeptidase, has been reported (32). In addition to cathepsin D, other proteolytic enzymes from somatic cells are probably present in milk. Verdi and Barbano (33), who studied the degradation of caseins in milk by somatic cells or plasmin, found that somatic cell proteinases and plasmin produced distinctly different peptides, and that the plasmin inhibitor 6-aminohexanoic acid was suitable for studying the action of somatic cell proteinases, without interference from plasmin. Somatic cell proteinases are capable of activating plasminogen (34), and this may influence proteolysis in cheese by elevating plasmin levels. Although leucocyte proteinases were more active on β-casein at pH 6.6 than at pH 5.2, their activity at the lower pH was such as to suggest that they may be active in cheese during ripening (35). Suzuki and Katoh (36) found two cysteine proteinases in milk (45 kDa and > 150 kDa). The authors suggested that these proteinases originated in somatic cells and their level increased during mastitic infection.

Grieve and Kitchen (37) compared the action of leucocyte proteinases, plasmin, and some psychotroph proteinases on the caseins. Leucocyte extracts hydrolyzed the caseins in order $\alpha_{s1} > \beta \gg \kappa$. Although these authors considered that neutral proteinases from leucocytes (isolated from blood) were unlikely to be important for proteolysis in milk, other authors have found considerably lower proteolytic activity in leucocytes isolated from blood than from milk (34, 35).

Kelly et al. (39), who compared proteolysis in Gouda cheeses made from milks with the same total somatic cell count but different levels of polymorphonuclear (PMN) leucocytes, found more rapid production of α_{s1}-CN f24-199 and total free amino acids in cheese made from milk with high PMN levels (α_{s1}-CN is α_{s1}-casein).

The significance of minor indigenous proteins during mastitic infections was discussed by Fang and Sandholm (40) who investigated the possibility of using specific proteinase inhibitors as therapeutic agents. Although the minor proteinases are probably less significant technologically than plasmin, more work on the subject is warranted.

III. LIPASES AND ESTERASES (EC 3.1.1.–)

Lipases catalyze the development of hydrolytic rancidity which is a serious defect in milk and some milk products, and, consequently, lipases and lipolysis in milk have been studied extensively. Milk contains three types of esterase: (a) A-type carboxylic ester hydrolase (arylesterase; EC 3.1.1.2), which hydrolyzes aromatic esters, e.g., phenylacetate. It shows little activity on tributyrin, and is not inhibited by organophosphates. (b) B-type esterase (glycerol tricarboxyl esterase, aliphatic esterase, lipase; EC 3.1.1.3). Such enzymes are most active on aliphatic esters although they show some activity on aromatic esters; they are inhibited by organophosphates. (c) C-type esterase (cholinesterase; EC 3.1.1.7; EC 3.1.1.8). These enzymes are most active on choline esters but hydrolyze some

aromatic and aliphatic esters slowly; they are inhibited by organophosphates.

In normal milk, the ratio of A : B : C types of esterase activity is about 3 : 10 : 1 but the level of A-esterase activity increases considerably on mastic infection. A and C esterases are of little technological significance in milk. Lipases hydrolyze ester bonds in emulsified esters, i.e., at a water/oil interface, although some may have limited activity on soluble esters. They are usually activated by blood serum albumin and Ca^{2+} which bind free fatty acids, which are inhibitory.

Milk lipase was first isolated and characterized by Fox and Tarassuk (41) and Patel et al. (42). The enzyme was optimally active at pH 9.2 and 37°C and was found to be a serine enzyme (inactivated by organophosphates). A lipoprotein lipase (LPL; activated by lipoprotein cofactors) was demonstrated in milk by Korn in 1962 (42a) and isolated by Egelrud and Olivecrona (43). The lipase isolated by Fox and Tarassuk (41) is, in fact, an LPL which is the principal, probably the only, indigenous lipase in bovine milk. It has been the focus of considerable research and has been characterized at the molecular, genetic, enzymatic, and physiological levels (44).

Under optimum conditions, the k_{cat} for milk LPL is $\sim 3000\,s^{-1}$ and milk contains sufficient enzymes (1–2 mg/L; i.e., 10–20 nM) to theoretically cause rancidity in 10 sec. However, this does not occur in practice because the triglycerides are protected by the MFGM while the lipase is naturally associated with the casein micelles. Also, environmental conditions, e.g., pH, are not optimal. However, if the MFGM is damaged by agitation (e.g., by milking machines, bulk tanks, pumps, etc.), homogenization or temperature fluctuations, lipolysis occurs rapidly and rancidity ensues. Milk LPL appears to be derived from blood plasma and hence any condition that increases the permeability of mammary cell membranes, e.g., physiological stress, mastitic infection, or late lactation, increases the level of LPL in milk and hence the risk of lipolysis. Some individual cows produce milk which becomes rancid spontaneously, i.e., without apparent activation. Apparently, spontaneous rancidity occurs when milk contains a high level of lipoprotein (co-lipase) from blood serum which activates the LPL. Normal milk will become spontaneously rancid if blood serum is added, suggesting that "spontaneous milks" contain a higher than normal level of blood serum. Dilution of spontaneous milk with normal milk prevents spontaneous rancidity, which, consequently, is not normally a problem with bulk herd milks. Presumably, dilution with normal milk decreases the lipoprotein content of the bulk milk to below the threshold necessary for lipase activation. Natural variations in the level of free fatty acids in normal milk and the susceptibility of normal milks to induced lipolysis may be due to variations in the level of blood serum components in milk.

In addition to LPL, human milk contains a bile salts–activated lipase, which probably contributes to the metabolism of lipids by breastfed babies who have limited pancreatic lipase activity. Bovine milk and milks from other dairy animals do not contain this enzyme.

A. Assay of Lipolytic Activity

Lipase can be assayed by incubating the sample with an emulsified lipid substrate—e.g., milk fat, olive oil, tributyrin, etc.—extraction of liberated fatty acids with diethyl ether-petroleum ether, and titration with ethanolic KOH. This method is rather tedious and tributyrin agar diffusion assays may be used when rapid screening is required. Chromogenic substrates, e.g., β-naphthyl- or *p*-nitrophenyl derivatives of fatty acids or fluorogenic substrates, e.g., coumarin derivatives of fatty acids, are very sensitive and satisfactory, especially when the enzyme has been at least partially purified.

B. Significance of Lipase

Technologically, LPL is, arguably, potentially the most significant indigenous enzyme in milk. Although LPL may play a positive role in cheese ripening, undoubtedly the most industrially important aspect of milk lipase is its role in hydrolytic rancidity which renders liquid milk and dairy products unpalatable and eventually unsaleable. Lipolysis in milk has been reviewed extensively (45). It appears to occur mainly at the farm level and the problem may be minimized by good management practices on the farm:

1. Proper installation, maintenance, and operation of milking machines.
2. Avoidance of excessive agitation by pumps or agitators in bulk tanks or risers in milk pipelines.
3. Avoidance of freezing on the walls of bulk tanks.
4. Avoidance of cooling and warming cycles in the bulk tank.
5. Culling of cows with high somatic cell counts.

The first three factors damage the MFGM, making the core triglycerides accessible to lipase. Some casein micelles probably adsorb on exposed fat surfaces. Pipeline milking machines cause more damage to the MFGM than hand milking or bucket milking machines. Suction of air at teat cups (which causes foaming), risers, and change of dimensions in the pipeline and the hose connecting the clawpiece to the receiving jar are major potential sites for damage. Homogenization causes total replacement of the natural MFGM by a membrane composed of casein micelles or submicelles and whey proteins. Unless indigenous LPL is inactivated by pasteurization before or immediately after homogenization, rancidity will develop very rapidly. Minimal high temperature short time (HTST; 72°C for 15 sec) pasteurization of milk causes extensive inactivation of LPL but pasteurization at 80°C for 10 sec is required for complete inactivation.

Freezing of milk on the walls of bulk tanks will damage the MFGM, inducing lipolysis. Temperature fluctuations, e.g., cooling to ~ 5°C, rewarming to ~ 30°C, and recooling, also activate lipolysis. Such temperature fluctuations may occur if bulk tanks are not completely emptied at each milk collection and warm milk is added at the subsequent milking. The mechanism of thermal activation is not clear, but damage to the MFGM by fat crystals seems likely.

The propensity of milk to lipolysis increases when the producing animals are under any type of stress. The mammary cell membranes become more permeable to blood constituents as a result of mastitic infection in late lactation and as the animal ages. The number of somatic cells in milk is a good index of such stress or damage, and upper limits for somatic cell count (SCC) are now frequently prescribed by milk processors. Although the potential for hydrolytic rancidity always exists in raw milk, the problem can be reduced to insignificant levels by good management practices at the farm.

IV. ALKALINE PHOSPHATASES (EC 3.1.3.1)

Milk contains several phosphatases, the principal ones being alkaline and acid phosphomonoesterases, which are of technological significance, and ribonuclease, which has no known function or significance in milk. The alkaline and acid phosphomonoesterases have been studied extensively (1, 8, 9).

The occurrence of a phosphatase in milk was first recognized in 1925. Subsequently characterized as an alkaline phosphatase, it became significant when it was shown that the time–temperature combinations required for the thermal inactivation of alkaline phosphatase were slightly more severe than those required to kill *Mycobacterium tuberculosis,* then the target microorganism for pasteurization. The enzyme is readily assayed, and a test procedure based on alkaline phosphatase inactivation was developed as a routine quality control test for the HTST pasteurization of milk.

A. Assay Methods

Several major modifications of the original assay have been developed. The usual substrates are phenyl phosphate, *p*-nitrophenyl phosphate, or phenolphthalein phosphate which are hydrolyzed to inorganic phosphate and phenol, *p*-nitrophenol, or phenolphthalein, respectively:

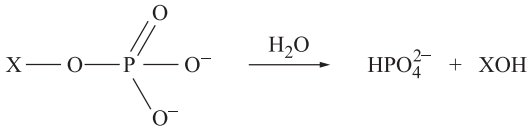

where XOH = phenol, *p*-nitrophenol, or phenolphthalein.

The release of inorganic phosphate may be assayed but the other product is usually determined. Phenol is colorless but forms a colored complex on reaction with one of several reagents, e.g., 2,6-dichloroquinonechloroimide, with which it forms a blue complex. *p*-Nitrophenol is yellow while phenolphthalein is red at the alkaline pH of the assay (~ 10) and hence these are easily quantified.

A fluorogenic aromatic orthophosphoric monoester, Fluorophos (Advanced Instruments, Needham Heights, MA), has been developed and approved for the determination of alkaline phosphatase in milk and milk products. Hydrolysis of the ester yields a fluorescent compound, Fluoroyellow, the concentration of which is determined fluorometrically (excitation, 439 nm; emission, 560 nm).

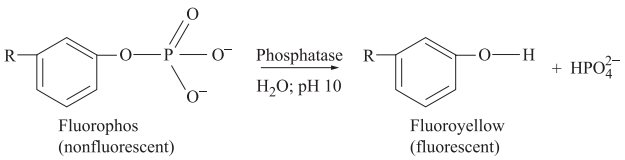

Fluorometric methods are about 100–1000 times more sensitive than colorimetric assays. A simple fluorometer has been developed for the analysis (Advanced Instruments). Comparative studies on the fluorometric and the standard colorimetric methods include those of Rocco (46) and Eckner (47).

B. Isolation and Characterization of Alkaline Phosphatase

Alkaline phosphatase is concentrated in the fat globule membrane and hence in cream. The membrane is released into the buttermilk on phase inversion; consequently, buttermilk is the starting material for most published methods for the purification of alkaline phosphatase. Later methods have used chromatography on various media to give a homogeneous preparation; up to ~7500-fold purification with a yield of ~30% have been reported (1). The characteristics of milk alkaline phosphatase are summarized in Table 4. The enzyme appears to be similar to the alkaline phosphatase of mammary tissue, which is the presumed source of the enzyme in milk.

The enzyme is a dimer of two identical 85-kDa subunits. It contains 4 Zn^{2+} per mole which are required for activity; Mg^{2+} are also strong activators, and 1 mM Mg^{2+} is usually added to the assay mixture. The enzyme is strongly but reversibly inhibited by metal chelators; the apoenzyme is reactivated by Zn^{2+}, Mg^{2+}, and other metal ions. Reaction of apoenzyme may in fact be used as a sensitive assay for available Zn^{2+} in foods. Inorganic orthophosphates are strong competitive inhibitors of the hydrolysis of *p*-nitrophenylphosphate. Alkaline milk phosphatase can dephosphorylate phosphoproteins, including casein, with a pH optimum of 6.5–7.0; however, it does not appear to do so in milk, probably owing to inhibition by the high level of orthophosphate.

Table 4 Characteristics of Milk Alkaline Phosphatase

Characteristic	Conditions
pH optimum	Casein: 6.8 *p*-nitrophenylphosphate: 9.9
Temperature optimum	37°C
K_m	0.69 mM on *p*-nitrophenylphosphate
Activators	Ca^{2+}, Mn^{2+}, Zn^{2+}, Co^{2+}, Mg^{2+}
Inhibitors	Metal chelators (EDTA, EGTA, etc.); orthophosphates
Native molecular weights	170–190 kDa
Quaternary structure	2 subunits each of molecular weights 85 kDa
Zn content	4 mol mol^{-1} enzyme
Thermal stability:	
D-value at 60°C, pH 9	27.2 min
63°C, pH 9	8.3 min

C. Reactivation of Phosphatase

Much work has been focused on a phenomenon known as "phosphatase reactivation," first recognized by Wright and Tramer in 1953, who observed that UHT-treated milk was phosphatase-negative immediately after processing but became positive on standing; microbial phosphatase was shown not to be responsible. Bulk HTST milk never showed reactivation, although occasional individual cow samples did. HTST pasteurization after UHT treatment usually prevented reactivation which was never observed in in-container sterilized milk. Reactivation can occur following heating at a temperature as low as 84°C for milk or 74°C for cream. The optimum storage temperature for reactivation is 30°C, at which reactivation is detectable after 6 h and may continue for up to 7 days. The greater reactivation in cream than in milk may be due to protection by fat, but this has not been substantiated.

A number of attempts have been made to explain the mechanism of reactivation (8). There is evidence that the form of the enzyme which becomes reactivated is membrane bound, and several factors which influence reactivation have been established. Mg^{2+} and Zn^{2+} strongly promote reactivation; Sn^{2+}, Cu^{2+}, Co^{2+} and EDTA are inhibitory, while Fe^{2+} has no effect. Sulfhydryl (SH) groups appear to be essential for reactivation; perhaps this is why phosphatase becomes reactivated in UHT milk but not in HTST milk. The role of -SH groups, supplied by denatured whey proteins, is considered to be chelation of heavy metals, which would otherwise bind to -SH groups of the enzyme (also activated on denaturation), thus preventing renaturation. It has been proposed that Mg^{2+} and Zn^{2+} cause a conformational change in the denatured enzyme, necessary for renaturation (1).

According to Murthy et al. (48), maximum reactivation occurs in products heated at ~104°C; incubated at 34°C, adjusted to pH 6.5, and containing 0.064 M Mg^{2+}; homogenization of products before heat treatment reduces the extent of reactivation. There are reports that raw milk contains three isoenzymes of alkaline phosphatase and that the zymogram patterns of raw and reactivated milk or cream are different (1, 48); however, these different forms probably represent free and bound forms of the enzyme. A mechanism for the reactivation of alkaline phosphatase was proposed by Copius-Peereboom (49); however, this mechanism of reactivation is based on a putative structure of the milk fat globule membrane which is now known to be incorrect. Linden (50)

proposed that reactivation occurs in stages and full reactivation requires Zn^{2+}, Mg^{2+}, inorganic phosphate (Pi), and substrate (S).

Reactivation of alkaline phosphatase is of considerable practical significance since regulatory tests for pasteurization assume the absence of phosphatase activity. Methods for distinguishing between renatured and residual native alkaline phosphatase are based on the increase in phosphatase activity resulting from addition of Mg^{2+} to the reaction mixture; various versions of the test have been proposed (48, 51, 52). The official AOAC method (53) is based on that of Murthy and Peeler (52). However, difficulties are experienced in the interpretation of this test applied to cream or butter (54, 55).

D. Significance

Alkaline phosphatase in milk is significant mainly because of its use as an index of HTST pasteurization and is used universally for this purpose. However, the enzyme may not be the most appropriate for this purpose (56) becomes (a) reactivation of alkaline phosphatase under certain conditions complicates interpretation of the test; (b) the enzyme appears to be fully inactivated by subpasteurization conditions (70°C for 16 sec); and (c) the relationship between $\log_{10}$% initially activity and pasteurization equivalent (PE) is less linear than the relationship of lactoperoxidase or γ-glutamyl transpeptidase (57).

Although alkaline phosphatase can dephosphorylate casein under suitable conditions, as far as is known, it has no direct technological significance in milk. Perhaps its pH optimum is too far removed from that of milk, especially acid milk products, although the pH optimum on casein is reported to be ~ 7. It is also inhibited by inorganic phosphate.

Proteolysis is a major contributor to the development of flavor and texture of cheese during ripening (58). Most of the small water-soluble peptides in cheese are from the N-terminal half of α_{s1}- or β-casein; many are phosphorylated but show evidence of phosphatase activity (i.e., they are partially dephosphorylated (59–62). In cheese made from pasteurized milk, both indigenous acid phosphatase and bacterial phosphatase are probably responsible for dephosphorylation (which is the more important is not clear), but in raw milk cheese, e.g., Parmigiano Reggiano or Grana Padano, milk alkaline phosphatase appears to be the most important (63, 64). Further work on the significance of indigenous alkaline and acid phosphatases in the dephosphorylation of phosphopeptides in cheese is warranted.

V. ACID PHOSPHOMONOESTERASE (EC 3.1.3.2)

Milk contains an acid phosphatase which has a pH optimum at 4.0 and is very heat stable. (LTLT pasteurization causes only 10–20% inactivation and 30 min at 88°C is required for full inactivation; when heated in milk at pH 6.7, the enzyme retains significant activity following HTST pasteurization but it does not survive in-bottle sterilization or UHT treatment.) The enzyme is not activated by Mg^{2+} (as is alkaline phosphatase), but it is slightly activated by Mn^{2+} and is very strongly inhibited by fluoride. The level of acid phosphatase activity in milk is only $\sim 2\%$ that of alkaline phosphatase; activity reaches a maximum 5–6 days postpartum, then decreases and remains at a low level to the end of lactation (65).

A. Isolation and Characterization

Acid phosphatase is found free in skim milk, in membrane material in skim milk and in the fat globule membrane. Kitchen (9) appears to believe that a single enzyme is involved and reported that the membrane-bound enzyme is strongly attached and is not released by nonionic detergents. The enzyme has been purified to homogeneity by various forms of chromatography, including affinity chromatography. Purification factors of 10,000 to 1 million have been reported (1). Adsorption onto Amberlite IRC50 resin is a very effective first step in purification. Andrews (65) stated that all the acid phosphatase activity in skim milk is adsorbed by Amberlite IRC50, but this is not indicated in the original papers. In an unpublished study, N.A. Flynn and P.F. Fox found that only $\sim 50\%$ of the total acid phosphatase in skim milk was adsorbed by Amberlite IRC50 even after reextracting the skim milk with fresh batches of Amberlite, suggesting that skim milk may contain two acid phosphatases. About 40% of the acid phosphatase in skim milk partitioned into the whey on rennet coagulation and this enzyme did not adsorb on Amberlite IRC50. The enzyme was partly purified from whey.

Flynn and Fox attempted to purify the alkaline phosphatase from MFGM by gel permeation chromatography; however, sonication and nonionic detergents failed to disassociate the enzyme from the membrane. The MFGM enzyme, which does not adsorb on

Amberlite IRC50, was much less heat stable than the acid phosphatase isolated from whey or from skim milk by adsorption on Amberlite IRC50. Attempts were made to confirm that the MFGM, whey, and Amberlite-adsorbed enzymes are different by studying the effects of inhibitors, but the results have been equivocal. Overall, it appears that milk contains more than one acid phosphatase. Using a zymogram technique, Andrews and Alichanidis (66) reported that milk from healthy cows contained one acid phophatase while that from mastitic cows contained two additional acid phosphatases which were of leucocyte origin. It is unlikely that the heterogeneity observed by Flynn and Fox was due to a high proportion of mastitic milk.

The acid phosphatase isolated from skim milk by adsorption on Amberlite IRC50 has been well characterized. It is a glycoprotein with a molecular weight of ~ 42 kDa and a pI of 7.9. It is inhibited by many heavy metals, F^-, oxidizing agents, orthophosphates, and polyphosphates and is activated by thiol-reducing agents and ascorbic acid. It is not affected by metal chelators. Its amino acid composition indicates a high level of basic amino acids and no methionine (65).

The enzyme is quite active on phosphoproteins, including caseins. It has been suggested that it is a phosphoprotein phosphatase. Although casein is a substrate for milk acid phosphatase, the major caseins, in the order α_s $(\alpha_{s1} + \alpha_{s2}) > \beta > \kappa$, also act as competitive inhibitors of the enzyme when assayed on *p*-nitrophenylphosphate, probably owing to binding of the enzyme to the casein phosphate groups (the effectiveness of the caseins as inhibitors is related to their phosphate content).

B. Assay

Acid phosphatase may be assayed, at pH ~ 5, on the same substrates as used for alkaline phosphatase. If *p*-nitrophenyl phosphate or phenolphthalein phosphate is used, the pH must be adjusted to > 8 at the end of the enzymatic reaction in order to induce the color of the product, i.e., *p*-nitrophenol or phenolphthalein.

C. Significance

Although acid phosphatase is present in milk at a much lower level than alkaline phosphatase, its greater heat stability and lower pH optimum may make it technologically significant. Dephosporylation of casein reduces its ability to bind Ca^{2+}, to react with κ-casein, to form micelles, and its heat stability. As discussed in Section IV.D, several small partially dephosphorylated peptides have been isolated from Cheddar and Parmigiano Reggiano and Grana Padano cheeses. However, it is not known whether indigenous or bacterial acid phosphatase is mainly responsible for dephosphorylation in cheese made from pasteurized milk. It is claimed (62–64) that alkaline phosphatase is mainly responsible for dephosphorylation in raw milk cheese. Dephosphorylation may be rate limiting for proteolysis in cheese ripening since most proteinases and peptidases are inactive on phosphoproteins or phosphopeptides. It has been suggested that phosphatase activity should be included in the criteria for starter selection.

The acid phosphatase activity in milk increases fourfold to 10-fold during mastitic infection. Three isoenzymes are then present, only one of which is indigenous milk acid phosphatase, the other two being of leucocyte origin (66). The latter isoenzymes are more thermolabile than the indigenous enzyme and are inactivated by HTST pasteurization.

The suitability of acid phosphatase as an indicator enzyme for superpasteurization of milk has been assessed (67, 68). It is not as useful for this purpose as some alternatives, e.g., γ-glutamyl transpeptidase or lactoperoxidase.

VI. LYSOZYME (EC 3.2.1.17)

Lysozyme (muramidase, mucopeptide N-acetyl-muramyl hydrolase) is a widely distributed enzyme which lyses certain bacteria by hydrolyzing the β(1-4) linkage between muramic acid and N-acetylglucosamine of mucopolysaccharides in the bacterial cell wall. Lysozyme activity is normally assayed by the lysis of cultures of *Micrococcus lysodeikticus* measured by a decrease in turbidity.

Lysozyme was isolated from human milk by Jolles and Jolles (69), who believed that bovine milk was devoid of lysozyme. Milks of many species, including bovine, have since been shown to contain lysozyme, and several have been isolated and characterized (70). Human and equine milks are exceptionally rich sources, containing 130 mg/L (3000 times the level of bovine milk) and ~ 800 mg/L, respectively.

The pH optima of human milk lysozyme (HML), bovine milk lysozyme (BML), and egg-white lysozyme (EWL) are 7.9, 6.35, and 6.2, respectively (70). BML has a molecular weight of 18 kDa compared with 15 kDa for HML and EWL. The amino acid composition of BML is considerably different from that of HML or EWL. The amino acid sequence of BML is

highly homologous with that of α-lactalbumin, a whey protein that is an enzyme modifier in the biosynthesis of lactose. All lysozymes are relatively stable to heat at acid pH values (3–4) but are relatively labile at pH > 7. More than 75% of the lysozyme activity in bovine milk survives heating at 75°C for 15 min or 80°C for 15 sec and is therefore little affected by HTST pasteurization. Low concentrations of reducing agents increase the activity of BML and HML by ~ 330% (70).

Presumably, the physiological role of lysozyme is to act as a bacteriocidal agent. In the case of milk, it may simply be a "spillover" enzyme, or it may have a definite protective role. If the latter is true, then the exceptionally high level of lysozyme in human and equine milk may be significant. Breastfed babies generally suffer fewer enteric problems than bottle-fed babies. While there are many major compositional and physicochemical differences between bovine and human milks which may be responsible for the observed nutritional characteristics, the disparity in lysozyme content may be significant. Fortification of bovine milk-based infant formulae with EWL, especially for premature babies, has been recommended but feeding studies are equivocal on the benefits of this practice, and recent trials failed to demonstrate any beneficial effect due to inactivation of EWL in the human stomach (71, 72).

One might expect that, owing to this bacteriocidal effect, indigenous milk lysozyme would have a beneficial effect on the shelf life of milk. Such effects do not appear to have been reported. Exogenous lysozyme may be added to milk for many cheese varieties, e.g., Gouda, Edam, Emmental, and Parmigiano Reggiano, as an alternative to KNO_3 to prevent the growth of *Cl. tyrobutyricum* which causes late gas blowing and off-flavors. At present, lysozyme is not widely used in commercial cheesemaking (71, 73). Since indigenous milk lysozyme is in the serum phase, very little is incorporated into cheese.

Addition of lysozyme to milk decreases the heat stability of milk, but the level of indigenous lysozyme is probably too low to contribute to the natural variations in the heat stability of milk.

VII. N-ACETYL-β-D-GLUCOSAMINIDASE (EC 3.2.1.30)

N-Acetyl-β-D-glucosaminidase (NAGase) hydrolyzes terminal, nonreducing N-acetyl-α-D-glucosamine residues from glycoproteins. It is a lysosomal enzyme which originates principally from mammary gland epithelial cells and, to a lesser extent, from somatic cells. Consequently, NAGase activity correlates highly with the intensity of mastitis. A field test for mastitis based on NAGase activity has been developed, using chromogenic *p*-nitrophenyl N-actyl-β-D-glucosamine as substrate. Hydrolysis yields *p*-nitrophenol, which is yellow at alkaline pH. NAGase activity is also high in colostrum. NAGase is optimally active at 50°C and pH 4.2 and is inactivated by HTST pasteurization (70–71°C for 15–18 sec). Andrews et al. (68) proposed that NAGase would be a suitable indicator enzyme for assessing heat treatments in the range 65–75°C for 15 sec. NAGase occurs mainly in the whey fraction, from which it has been isolated by various forms of chromatography. Two forms, A and B, differing in molecular weight, 120 and 240 kDa, respectively, and charge were obtained. Each form is dissociated to two dissimilar subunits on treatment with 2-mercaptoethanol and SDS (9, 70).

VIII. γ-GLUTAMYL TRANSPEPTIDASE (TRANSFERASE) (EC 2.3.2.2)

γ-Glutamyl transpeptidase (GGTP) catalyzes the transfer of γ-glutamyl residues from γ-glutamyl-containing peptides:

$$\gamma\text{-glutamyl-peptide} + X \rightarrow \text{peptide} + \gamma\text{-glutamyl-X} \quad (3)$$

where X is an amino acid.

The enzyme is membrane bound, being found in the membrane material in skim milk (~ 70%) or in the MFGM, from which it can be dissociated by detergents or solvents. The enzyme, which has been purified from the MFGM, has a molecular weight of ~ 80 kDa and consists of two subunits of 57 and 25 kDa, both of which are glycoproteins (74, 75). The enzyme is optimally active at pH 8.5–9 and ~ 45°C and has an isoelectric point of 3.85. It is strongly inhibited by diisopropylfluorophosphate, iodoacetamide, and metals, e.g., Cu^{2+} and Fe^{3+} (9, 70).

A. Assay

GGTP is usually assayed using γ-glutamyl-*p*-nitroanilide as substrate; the liberated *p*-NA can be determined by measuring the absorbance at 410 nm or by reaction with naphthylethylenediamine and measuring the absorbance at 540 nm (76).

B. Significance

GGTP functions in the regulation of cellular glutathione and amino acid transport via the γ-glutamyl cycle; it may be involved in the biosynthesis of milk proteins.

From a dairy technologist's viewpoint, GGTP is of interest mainly because of its heat stability characteristics. As discussed in Section IV.D, alkaline phosphatase is the test enzyme usually used to evaluate the efficiency of HTST pasteurization; however, as discussed, reactivation of this enzyme in UHT-treated products poses problems with the interpretation of the test. Based on a comparative study on the heat stability characteristics of a number of indigenous enzymes in milk, Andrews et al. 68) concluded that GGTP was appropriate for monitoring heat treatments in the range of 70–80°C for 16 sec. This conclusion has been confirmed in pilot-scale studies (77, 78). In whole or skim milk, GGTP is completely inactivated by heating at 78°C for 15 sec (77) or 77°C for 16 sec (76). No reactivation was found under a variety of conditions, and little seasonal variation occurs. As little as 0.1% raw milk could be detected in skim milk or 0.25% in whole milk (76).

Linear models for the thermal inactivation of GGTP and lactoperoxidase (LPO) in a HTST pasteurizer were developed by McKellar et al. (57). The equation for GGTP was: $\log_{10}\%$ initial activity $= 2.004 - 0.281 \times \mathrm{PE}^{0.75}$. For LPO the equation was: $\log_{10}\%$ initial activity $= 2.122 - 0.096 \times \mathrm{PE}^{0.75}$.

$$PE = \frac{t}{t_0} = \int \mathrm{e}^{\left(\frac{E_a}{R}\right)\left(\frac{1}{T} - \frac{1}{T_0}\right)} dt \qquad (4)$$

where E_a = activation energy; $R = 8.314\,\mathrm{J/mol\ ^\circ K}$; $T_0 = 345\,\mathrm{K}$ (72°C reference temperature); T = experimental temperature; $t_0 = 15\,\mathrm{sec}$ (reference holding time); t = experimental holding time, sec; and PE = pasteurization equivalent (71.6°C for 15 sec).

These equations indicate that 1 log decrease in enzyme activity can be achieved with PE values of 5.46 and 2.65 for GGTP and LPO, respectively, indicating that LPO is considerably more heat stable than GGTP. The assay for LPO (using ABTS; see Sec. XIII.A) is subject to greater variation and interference from milk proteins than the GGTP assay. The relationship between $\log_{10}\%$ initial activity and PE was more linear than the relationship for alkaline phosphatase, possibly due to more than one form of alkaline phosphatase (56). GGTP was about nine times more stable in ice cream mix than in whole milk, which had a much smaller stabilizing effect on *Listeria innocua* (79). Thus, it appears that GGTP is a suitable enzyme for estimating the intensity of heat treatment in the range 72–77°C for 15 sec to which milk was subjected.

GGTP is absorbed from the gastrointestinal tract, resulting in high levels of GGTP activity in the blood serum of newborn animals fed colostrum or early breast milk. Since GGTP is inactivated by the heat treatment to which infant formulae are subjected, the level of GGTP activity in infants can be used to distinguish breastfed from formula-fed infants (70).

γ-Glutamyl peptides have been isolated from Comté cheese (80). Since casein contains no γ-glutamyl bonds, the presence of these peptides in cheese suggests GGTP activity in cheese, but there appear to be no data on this.

IX. XANTHINE OXIDASE (EC 1.2.3.2)

It has been recognized for ~ 90 years that milk contains an enzyme capable of oxidizing aldehydes and purines with the concomitant reduction of O_2 to H_2O_2. The enzyme is now generally referred to as xanthine oxidase (XO). Milk is a very good source of XO, at least part of which is transported to the mammary gland via the bloodstream. A similar enzyme is found in various animal tissues and several bacterial species (8, 9, 70).

A. Assay

Xanthine oxidase activity can be assayed manometrically (uptake of O_2), potentiometrically using a platinum electrode, or spectrophotometrically. This last involves the conversion of the xanthine to uric acid which is quantified by measuring absorbance at 290 nm (75).

B. Isolation

The enzyme is concentrated in the MFGM, in which it is one of the principal proteins. Therefore, all isolation methods use cream as starting material, using a dissociating agent to liberate XO from membrane lipoproteins and some form of chromatography for purification.

Milk XO has a molecular weight of $\sim 300\,\mathrm{kDa}$ and consists of two identical subunits. The pH optimum is ~ 8.5 and the enzyme requires flavin adenine dinucleotide (FAD), Fe and Mo cations, and an acid-labile sulfur compound as cofactors. Cows deficient in Mo

cations have low XO activity. The amino acid composition of XO has been determined by a number of workers; at least five polymorphic forms have been reported (70).

XO can be converted to an NAD-dependent dehydrogenase by treatment with thiol-reducing agents. The enzyme reverts to an oxidase on aerobic storage, treatment with sulfhydryl oxidase, or with sulfhydryl oxidizing agents.

C. Activity in Milk

XO activity in milk varies substantially—2.5-fold (67). Various processing treatments which damage or alter the MFGM affect the XO activity of milk. Activity is increased by $\sim 100\%$ on storage at 4°C for 24 h, by 50–100% on heating at 70°C for 5 min, and by 60–90% on homogenization. These treatments cause the release of XO from the MFGM into the aqueous phase, rendering the enzyme more active. The heat stability of XO is very dependent on whether it is a component of the MFGM or is dissolved in the aqueous phase. Aging and homogenization increase heat susceptibility and explain the inconsistency of early work in which the history of the sample was unknown or unrecorded. XO is most heat stable in cream and least in skim milk. Homogenization of concentrated milk prepared from heated milk (90.5°C for 15 sec) partially reactivates XO, which persists on drying the concentrate, but no reactivation occurs following more severe heating (93°C for 15 sec). Apparently, homogenization releases potentially active, undenatured XO from the MFGM. All the major milk proteins can act as either activators or inhibitors of XO, depending on their concentration, and may have some significance in the activation, inactivation, and reactivation of the enzyme. Studies on the heat stability of XO have been reviewed by Griffiths (67), who investigated its stability in a pilot scale HTST pasteurizer. The enzyme was not completely inactivated after 120 sec at 80°C, and a Z-value of 6.8 was calculated.

D. Significance of Xanthine Oxidase

1. As an Index of Heat Treatment

The inactivation of XO parallels the conditions necessary for the production of low-heat skim milk powder (82). Andrews et al. (68) considered XO as a suitable indicator of milk heated in the temperature range 80–90°C but Griffiths (67) considered the natural variability in the level of XO activity in milk to be too high for use as a reliable index of heat treatment.

2. Lipid Oxidation

XO, which can excite stable triple oxygen ($^3O_2$) to single oxygen ($^1O_2$), is a pro-oxidant. Some individual-cow milks, which undergo spontaneous oxidative rancidity (i.e., without contamination with metals or exposure to light) contain ~ 10 times the normal level of XO, and spontaneous oxidation can be induced in normal milk by the addition of XO to about four times normal levels. Heat-denatured or flavin-free enzyme is ineffective in oxidation; the susceptibility of unsaturated fatty acids to oxidation increases with the degree of unsaturation (8).

3. Atherosclerosis

It has been suggested that XO from homogenized milk enters the vascular system and may be involved in atherosclerosis via oxidation of plasmalogens in cell membranes; this aspect of XO attracted considerable attention in the early 1970s (83). However, the experimental evidence in support of this view is very weak and the hypothesis has been disclaimed (8, 70, 84, 85).

4. Reduction of Nitrate in Cheese

Sodium nitrate is added to milk for Dutch, Swiss, and other cheese varieties to prevent the growth of *Clostridium tyrobutyricum* which causes flavor defects and late gas blowing in these cheeses. Xanthine oxidase reduces nitrate to nitrite which is necessary for the bacteriocidal effect of nitrate.

Various oxidation-reduction reactions occur in milk which affect its flavor. Perhaps XO is significant in these reactions, either directly or indirectly.

5. Production of H_2O_2

The H_2O_2 produced by the action of xanthine oxidase on oxidation of xanthine, hypoxanthine, or other substrates can serve as a substrate for lactoperoxidase in its action as a bacteriocidal agent (see Sec. XIII.B).

X. SULFHYDRYL OXIDASE (EC 1.8.3.–)

Milk contains an enzyme, sulfhydryl oxidase (SO), capable of oxidizing sulfhydryl groups of cysteine, glutathione, and proteins to the corresponding disulfide (for reviews, see 8, 70). The enzyme is an aerobic oxidase which catalyzes the following reaction:

$$2RSH + O_2 \rightarrow RSSR + H_2O_2 \quad (5)$$

It undergoes marked self-association and can be purified readily by chromatography on porous glass. The enzyme has a molecular weight of ~ 89 kDa, a pH optimum of 6.8–7.0, and a temperature optimum of 35°C. Its amino acid composition, its requirement for iron but not for molybdenum and FAD, and the catalytic properties of the enzyme indicate that sulfhydryl oxidase is a distinct enzyme from xanthine oxidase and thiol oxidase (EC 1.8.3.2).

SO is capable of oxidizing reduced ribonuclease and restoring enzymatic activity, suggesting that its physiological role may be the nonrandom formation of protein disulfide bonds, e.g., during protein biosynthesis.

SO immobilized on glass beads has the potential to ameliorate the cooked flavor arising from sulfhydryl groups exposed by protein denaturation on UHT processing of milk, but the commercial viability of this system is not known. In any case, sulfhydryl groups are effective antioxidants and may serve a beneficial role in UHT milk.

The production of sulfur compounds is believed to be very important in flavor development in Cheddar and other varieties of cheese. Residual sulfhydryl oxidase activity may play a role in reoxidizing sulfhydryl groups exposed upon heating cheesemilk; the sulfhydryl groups thus protected may be reformed during the ripening process.

XI. SUPEROXIDE DISMUTASE (EC 1.15.1.1)

Superoxide dismutase (SOD) scavenges superoxide radicals, O_2^-, according to the reaction:

$$2O_2^- + 2H^+ \rightarrow H_2O_2 + O_2 \quad (6)$$

The H_2O_2 formed may be reduced to $H_2O + O_2$ by catalase, peroxidase or suitable reducing agents. SOD has been identified in many animals and bacterial cells. Its biological function is to protect tissue against oxygen free radicals in anaerobic systems (8, 9, 70).

SOD, isolated from bovine erythrocytes, is a blue-green protein due to the presence of copper, removal of which by treatment with EDTA results in loss of activity which is restored by adding Cu^{2+}; it also contains Zn^{2+}, which does not appear to be at the active site. The enzyme, which is very stable in 9 M urea at neutral pH, consists of two identical subunits of molecular weight 16 kDa held together by one or more disulfide bonds.

Milk contains trace amounts of SOD which is present exclusively in the skim milk fraction. This enzyme has been isolated and characterized. It appears to be identical to the bovine erythrocyte enzyme. Assay methods for SOD are described by Stauffer (86).

SOD inhibits lipid oxidation in model systems. The level of SOD in milk parallels that of XO (but at a lower level), suggesting that SOD may be excreted in milk in an attempt to offset the pro-oxidant effect of XO. Attempts have been made to correlate the stability of milk to oxidative rancidity with the SOD activity in the milk, but these results have been equivocal. Milk contains several pro- and antioxidants, including exogenous factors such as light, the precise balance of which, rather than any single factor, determines overall oxidative stability. The possibility of using exogenous SOD to retard or inhibit lipid oxidation in dairy products has been considered. A marked improvement in the oxidative stability of milk with a high level of linoleic acid was achieved by adding low levels of SOD.

SOD is more heat stable in milk than in purified preparations. In milk it is stable at 71°C for 30 min (i.e., it is not affected by HTST pasteurization) but loses activity rapidly at even slightly higher temperatures. Slight variations in pasteurization temperature are therefore critical to the survival of SOD in heated milk products and may contribute to variations in the stability of milk to oxidative rancidity.

XII. CATALASE (EC 1.11.1.6)

An indigenous catalase in milk was first recognized in 1907. The catalase activity of whole milk is associated either with membranes in the skim milk phase or the MFGM. The pellet obtained from buttermilk on centrifugation at 10,000 g is a particularly rich source, from which catalase has been highly purified and crystallized (8, 9, 70).

Milk catalase is a heme protein with a molecular weight of 200 kDa and an isoelectric pH of 5.5. It is stable between pH 5 and 10 but rapidly loses activity outside the range. Heating at 70°C for 1 h at pH 7.0 causes complete inactivation. Like other catalases, it is strongly inhibited by Hg^{2+}, Fe^{2+}, Cu^{2+}, Sn^{2+}, CN^-, and NO_3^-. Analytical methods for catalase are described by Stauffer (86).

Catalase activity in milk varies with feed, stage of lactation, and especially with mastitic infection, for which it may be used as an index. However, it is not usually used for this purpose, since somatic cell count and N-acetylglucosaminidase activity are superior indices of mastitis. Catalase may act as a lipid pro-

oxidant via its heme iron (i.e., nonenzymatically), but it is probably not very significant.

There is general agreement that cheese made from raw milk ripens more quickly and develops a more intense (although not always a more desirable) flavor than cheese made from pasteurized milk (87). However, for public health reasons and in the interest of producing a consistent product, pasteurized milk is now generally used for cheese making. Many cheeses are still made from raw milk, especially in southern Europe. Many countries require that if raw milk is used for cheese making, the cheese must be ripened for at least 60 days during which it was presumed that pathogens die off, a presumption that is now considered to be invalid. Subpasteurized or thermized milk (e.g., heated at 63–65°C for 16 sec) has been considered as a compromise between raw and pasteurized milk for cheese making. The acceptance of such a practice would require an appropriate validation test, but no suitable test is available at present for identifying thermized milk. The possibility of using the inactivation of catalase as an index of thermized milk was investigated by Hirvi and Griffiths (88). Although catalase was a useful index of thermization of milk (it was almost completely inactivated by heating at 65°C for 16 sec), it was unsuitable as an index of cheese made from thermized milk owing to the production of catalase in the cheese during ripening, especially by yeasts. The thermal inactivation of catalase was also studied by Hirvi et al. (89).

XIII. LACTOPEROXIDASE (EC 1.11.1.7)

The occurrence of a peroxidase, lactoperoxidase (LPO), in milk was recognized as early as 1881. It is one of the most heat-stable enzymes in milk. Its inactivation was used as an index of flash pasteurization (now very rarely used) and is now used as an index of super-HTST pasteurization, e.g., temperatures > 75°C for 15 sec. LPO was first isolated in 1943; several isolation procedures have since been published (8, 90).

LPO is a heme protein containing $\sim 0.07\%$ Fe, with an absorbance peak (Soret band) at 412 nm ($A_{412}/A_{280} \sim 0.9$). The pH optimum is ~ 8.0, its molecular weight is 77.5 kDa, and it consists of two identical subunits. Two principal forms (A and B) occur, each of which exhibits microheterogeneity with regard to amide groups (glutamine and/or asparagine) and carbohydrate content, giving a total of 10 variants.

A. Assay of Lactoperoxidase

The principle generally used in assays for peroxidases is the use of a chromogenic or fluorogenic reducing agent, AH_2, a number of which have been used (86). A highly recommended substrate for lactoperoxidase is 2, 2′-azinobis(3-ethylbenzylthiazoline-6-sulfonic acid) [ABTS] (91).

B. Significance

1. As for many other indigenous enzymes, the level of LPO in milk increases on mastitic infection and is therefore a possible index of mastitis; however, it is not well correlated with somatic cell count, and superior methods, including enzyme-based methods (Sec. VII) are available to monitor mastitis.
2. LPO causes nonenzymic oxidation of unsaturated lipids, probably due to its heme group. The heat-denatured enzyme is more active than the native enzyme. Compared with other pro-oxidants, LPO is probably not significant in milk and dairy products.
3. LPO has been used in the Storch test for flash pasteurized milk (67), but this process is not used in modern milk processing. However, the pasteurization of milk at a temperature higher than the HTST minimum, i.e., > 72°C for 15 sec, has recently become quite common. The assay based on the inactivation of alkaline phosphatase is not applicable under such circumstances. Griffiths (67), who evaluated the suitability of several indigenous enzymes as indices of the super-pasteurization of milk, concluded that assay of LPO activity was the most promising method for detecting heat treatments in the order of 76°C for 15 sec. Andrews et al. (68) reported the results of a generally similar study, in which LPO was not included. They conclude that N-acetylglucosaminidase, γ-glutamyl transpeptidase (γ-GGTP), and α-mannosidase or xanthine oxidase may be the most suitable indicators of heat treatment of 65–75, 70–80, and 80–90°C, respectively. The relative suitability of GGTP and LPO were compared by McKellar et al. (57). The kinetics of the thermal denaturation of LPO was reported by Martin-Hernandez et al. (92).
4. Milk contains bacteriostatic or bacteriocidal substances, referred to as lactenins. One of these is LPO, which requires H_2O_2 and thiocyanate (SCN^-) to cause inhibition. The nature, mode of action, and specificity of the LPO-SCN^--H_2O_2 system have been widely studied. LPO and thiocyanate, which is produced in the rumen by enzymatic hydrolysis of thio-

glycosides from Brassicae plants, occur naturally in milk although at variable and probably suboptimal levels. Milk does not contain indigenous H_2O_2, which can be generated metabolically by catalase-negative bacteria, or produced in situ through the action of exogenous glucose oxidase on glucose which may be added to milk or produced in situ from lactose by exogenous β-galactosidase or the action of indigenous XO on added xanthine or hypoxanthine, or from added sodium percarbonate or it may be added directly.

Immobilized glucose oxidase has been used to generate H_2O_2 in situ in thiocyanate- and glucose-enriched milk or whey. A self-contained LPO-H_2O_2-SCN^- system using coupled β-galactosidase and glucose oxidase, immobilized on porous glass beads, to generate H_2O_2 in situ from lactose in milk containing 0.25 mM thiocyanate has been developed.

The bacteriocidal effect of the LPO-H_2O_2-SCN^- system has several applications which have been reviewed extensively (90, 91, 93, 94):

1. Sanitization of immobilized enzyme columns in which LPO is coimmobilized with the enzyme of interest. The requisite H_2O_2 could be generated by immobilized enzymes—e.g., xanthine oxidase, glucose oxidase, or β-galactosidase/glucose oxidase.
2. As a bacteriocidal agent in toothpaste.
3. In the therapy of mastitis during the non-lactating period.
4. For the preservation of milk in regions lacking refrigeration or pasteurization facilities.
5. To reduce the incidence of enteritis in calves or piglets fed milk replacers. The indigenous LPO is inactivated during the manufacture of these products and LPO isolated from milk or whey is added.

LPO (and lactoferrin) is cationic at the natural pH of milk at which all the principal proteins are anionic. LPO and lactoferrin can therefore be readily isolated from milk or whey by using cation exchange resins. The ion exchangers may be used as columns (95), batchwise (96), or as membranes (97). At least some of these methods are applicable on an industrial scale, making it possible to isolate LPO for use as a food ingredient.

C. Biochemistry of Lactoperoxidase System

LPO catalyzes the peroxidation of ^-SCN to products which are nontoxic to mammalian cells but which kill or inhibit the growth of many species of microorganisms. The net reaction is:

$$\underset{\text{(thiocyanate anion)}}{H_2O_2 + {}^-SCN} \xrightarrow{\text{LPO}} \underset{\text{(hypothiocyanite anion)}}{-OSCN + H_2O} \quad (7)$$

Microbial membranes have low permeability for ^-OSCN but are quite permeable to HOSCN ($pK_a = 5.3$). HOSCN or ^-OSCN oxidizes sulfhydryl groups:

$$RSH + {}^-OSCN \longrightarrow \underset{\text{(sulfenyl thiocyanate)}}{R\text{-}S\text{-}SCN + {}^-OH} \quad (8)$$

$$R\text{-}S\text{-}SCN + H_2O \longrightarrow \underset{\text{(sulfonic acid)}}{R\text{-}S\text{-}OH + H^+ + {}^-SCN} \quad (9)$$

Any reaction involving a sulfhydryl group, e.g., thiol enzymes, will be inhibited by this oxidation. The effect may be reversed by thiol compounds such as glutathione or cysteine.

XIV. OTHER ENZYMES

In addition to the enzymes described above, several other indigenous enzymes have been isolated and partially characterized (Table 2) (70). Although a fairly high level of some of these enzymes occurs in milk, they have no apparent function or significance in milk which contains no substrate for many of them. It is possible that some of these enzymes will assume importance in the future as indices of animal health or of product quality. These enzymes will not be discussed further.

Nearly 40 other enzymatic activities have been detected in milk (Table 3) but have not been isolated, and only limited information on their molecular and biochemical properties in milk is available (70). Some of these enzymes have been evaluated as indices of the heat treatment of milk (67, 68). Perhaps further study will identify some important or useful attributes of some of these enzymes.

XV. SUMMARY

Although milk contains ~ 60 indigenous enzymes, only two, lipoprotein lipase (LPL) and plasmin, are really technologically significant. LPL has the potential to cause serious problems but these can be avoided through good milking practices on the farm. The enzyme is relatively heat labile and hence does not cause problems in heat-treated products. Although milk contains considerable potential plasmin, relatively

little is expressed owing to the presence of inhibitors. The significance of plasmin is mainly negative but its action is probably positive in cheese during ripening. Acid phosphatase may be significant in the dephosphorylation of phosphopeptides in cheese. Several oxidoreductases—xanthine oxidase, lactoperoxidase, catalase, superoxide dimutase, and sulfhydryl oxidase—are, at least potentially, significant in milk stability. Lysozyme and lactoperoxidase may have antimicrobial effects in the intestine of the consumer.

Perhaps the most significant and most useful aspect of the indigenous enzymes in milk is as indicators of mastitis, especially N-acetylglucosaminidase, and of thermal treatments. The thermal stabilities of the indigenous enzymes cover quite a wide range of temperatures which make it possible to determine at what temperature milk has been heat-treated in the range 65–90°C for 15 sec. The principal advantage of enzymes compared with other heat-induced changes in analytical applications is the relative ease with which their activity can be quantified.

Most dairy products should undergo no change during storage, and hence the indigenous enzymes capable of causing undesirable changes are inactivated by heating. Cheese is an exception; a very complex series of microbiological, biochemical, and perhaps chemical reactions occur which lead to desirable characteristic taste, aroma, and texture of the finished cheese (98, 99). At least four indigenous enzymes contribute to cheese ripening—plasmin, lipoprotein lipase, acid phosphatase, and xanthine oxidase. Perhaps others contribute, but information is lacking.

Most of the indigenous enzymes in milk remain to be isolated and characterized. As for the principal enzymes, these minor enzymes probably originate from the mammary tissue. Most of these enzymes are unlikely to be technologically significant as milk contains no substrates. However, they may be significant as indicators of animal health or thermal history; if so, they will be isolated and characterized.

REFERENCES

1. AT Andrews, T Olivecrona, S Vilaro, G Bengtsson-Olivecrona, PF Fox, L Björck, NY Farkye. Indigenous enzymes in milk. In: PF Fox, ed. Advanced Dairy Chemistry, Vol. 1, Proteins. London: Elsevier Applied Science, 1992, pp 285–267.
2. RM Whitney. The minor proteins of milk. J Dairy Sci 41:1303–1323, 1958.
3. KM Shahani. Milk enzymes: their role and significance. J Diary Sci 49:907–920, 1966.
4. ML Groves. Minor milk proteins and enzymes. In: HA McKenzie, ed. Milk Proteins: Chemistry and Molecular Biology, Vol. 1. New York: Academic Press, 1971, pp 367–418.
5. KM Shahani, WJ Harper, RJG Jensen, RM Parry Jr, CA Zittle. Enzymes of bovine milk. J Dairy Sci 56:531–543, 1973.
6. BK Dwivedi. The role of enzymes in food flavors. Part I. Dairy products. CRC Crit Rev Food Technol 3:457–478, 1973.
7. HA Johnson. The composition of milk. In: BH Webb, AH Johnson, JA Alford, eds. Fundamentals of Dairy Chemistry, 2nd ed. Westport, CT: AVI Publishing, 1974, pp 1–57.
8. PF Fox, PA Morrissey. Indigenous enzymes of bovine milk. In: GG Birch, N Blakeborough, KJ Parker, eds. Enzymes and Food Processing. London: Applied Science, 1981, pp 213–238.
9. BJ Kitchen. Indigenous milk enzymes. In: PF Fox, ed. Developments in Dairy Chemistry. 3. Lactose and Minor Constituents. London: Elsevier Applied Science, 1985, pp 239–279.
10. AT Andrews, T Olivecrona, G Bengtsson-Olivecrona, PF Fox, L Björck, NY Farkye. Indigenous enzymes in milk. In: PF Fox ed. Food Enzymology. London: Elsevier Applied Science, 1991, pp 53–129.
11. M Hamos, LM Freed, JB Jones, SE Berkow, J Bitman, NR Mehta, B Happ, P Hamos. Enzymes in human milk. In: RG Jensen, MC Neville, eds. Human Lactation: Milk Components and Methodologies. New York: Plenum Press, 1985, pp 251–266.
12. O Hernell, B Lonnerdal. Enzymes in human milk. In: SA Atkinson, B Lonnerdal, eds. Proteins and Non-protein Nitrogen in Human Milk. Boca Raton, FL: CRC Press, 1989, pp 67–75.
13. MB Grufferty, PF Fox. Milk alkaline proteinase. J Dairy Res 55:609–630, 1988.
14. ED Bastian, RJ Brown. Plasmin in milk and dairy products: an update. Int Dairy J 6:435–457.
15. C Benfeldt, LB Larsen, JT Rasmussen, PA Andersen, TE Petersen. Isolation and characterization of plasminogen and plasmin from bovine milk. Int Dairy J 5:577–592, 1995.
16. A Baldi, G Savoini, F Chali, F Fantuz, E Senatare, L Bertocchi, I Politis. Changes in plasmin-plasminogen-plasminogen activator system in milk from Italian Friesian herds. Int Dairy J 6:1045–1053, 1996.
17. P Guinot-Thomas, M Al Ammoury, Y La Roux, F Laurent. Study of proteolysis during storage of milk at 4°C: effect of plasmin and microbial proteinases. Int Dairy J 5:685–697, 1995.
18. L Berglund, MD Andersen, TE Petersen. Cloning and characterization of the bovine plasminogen cDNA. Int Dairy J 5:593–603, 1995.
19. A Kennedy, AL Kelly. The influence of somatic cell count on the heat stability of bovine plasmin activity. Int Dairy J 7:717–721, 1997.

20. BC Richardson, KN Pearce. The determination of plasmin in dairy products. NZ J Dairy Sci Technol 16:209–220, 1981.
21. P Fox, PLH McSweeney. Proteolysis in cheese during ripening. Food Rev Int 12:457–509, 1996.
22. NY Farkye, PF Fox. Observations on plasmin activity in cheese. J Dairy Res 57:413–418, 1990.
23. N Farkye, PF Fox. Contribution of plasmin to Cheddar cheese ripening: effect of added plasmin. J Dairy Res 59:209–216, 1992.
23a. FM Barrett, AL Kelly, PLH McSweeney, PF Fox. Use of exogeneous urokinase to accelerate proteolysis in Cheddar cheese during ripening. Int Dairy J 9:473–479, 1999.
24. S Christensen, T Wiegers, J Hermansen, L Sottrup-Jensen. Plasma-derived protease inhibitors in bovine milk. Int Dairy J 5:439–449, 1995.
25. C Benfeldt, J Sorensen, TE Petersen. Inhibitory activity against plasmin, trypsin, and elastase in rennet whey and in cheese fortified with whey protein. J Dairy Sci 81:615–620, 1998.
26. CW Heegaard, LK Rasmussen, PA Andreasen. The plasminogen activation system in bovine milk. Differential localization of tissue-type plasminogen activator and urokinase in milk fractions is caused by binding to casein and urokinase receptor. Biochim Biophys Acta 1222:45–55, 1994.
27. JH White, B Zavizion, K O'Hare, J Gilmore, MR Guo, P Kindstedt, I Politis. Distribution of plasminogen activator in different fractions of bovine milk. J Dairy Res 62:113–122, 1995.
28. P Ravn, L Berglund, TE Petersen. Cloning and characterization of the bovine plasminogen activators uPA and tPA. Int Dairy J 5:605–617, 1995.
29. DD Lu, SS Nielsen. Isolation and characterization of native bovine plasminogen activators. J Dairy Sci 76:3369–3383, 1993.
30. JA Gilmore, JH White, B Zavizion, I Politis. Effects of stage of lactation and somatic cell count in plasminogen activator in bovine milk. J Dairy Res 62:141–145, 1995.
31. PLH McSweeney, PF Fox. Proteolysis of bovine caseins by cathepsin D: preliminary observations and comparison with chymosin. Int Dairy J 5:321–336, 1995.
32. EH Reimerdes. New aspects of naturally occurring proteases in bovine milk. J Dairy Sci 66:1591–1600, 1983.
33. RJ Verdi, DM Barbano. Preliminary investigation of the properties of somatic cell proteases. J Dairy Sci 72:534–538, 1988.
34. RJ Verdi, DM Barbano. Effect of coagulants, somatic cell enzymes, and extracellular bacterial enzymes on plasminogen activation. J Dairy Sci 74:772–782, 1991.
35. RJ Verdi, DM Barbano. Properties of proteases from milk somatic cells and blood leukocytes. J Dairy Sci 74:2077–2091, 1991.
36. J Suzuki, N Katoh. Cysteine protease in bovine milk capable of hydrolyzing casein as the substrate and elevation of the activity during the course of mastitis. Jpn J Vet Sci 52:947–954, 1990.
37. PA Grieve, BJ Kitchen. Proteolysis in milk: the significance of proteinases originating from milk leucocytes and a comparison of the action of leucocyte, bacteria and natural milk proteinases on the caseins. J Dairy Res 52:101–112, 1985.
38. AL Kelly. Variations in total and differential milk somatic cell counts and plasmin levels and their role in proteolysis and quality of milk and cheese. PhD thesis, National University of Ireland, Cork, 1995.
39. A Kelly, J Sheehan, D Tiernan, A Shattock, P Joyce, J Foley. Bovine milk with PMN content and its effects on cheese quality. Proc 3rd Mastitis Seminar, Tel Aviv, Section S-3, 1995, pp 31–35.
40. W Fang, M Sandholm. Inhibition of the proteinase activity in mastitic milk. J Dairy Res 62:61–68, 1995.
41. PF Fox, NP Tarassuk. Bovine milk lipase. I. Isolation from skimmilk. J Dairy Sci 51:826–833, 1968.
42. CV Patel, PF Fox, NP Tarassuk. Bovine milk lipase. II. Characterization. J Dairy Sci 51:1879–1886, 1968.
42a. ED Korn. The lipoprotein lipase of cow's milk. J Lipid Res 3:246–250, 1962.
43. T Egelrud, T Olivecrona. The purification of a lipoprotein lipase from bovine milk. J Biol Chem 247:6212–6217, 1972.
44. T Olivecrona, S Vilaro, G Bengtsson-Olivecrona. Indigenous enzymes in milk: lipases. In: PF Fox, ed. Advanced Dairy Chemistry. 1. Proteins. London: Elsevier Applied Science, 1992, pp 292–310.
45. HC Deeth, CH Fitz-Gerald. Lipolytic and hydrolytic rancidity in milk and milk products. In: PF Fox, ed. Advanced Dairy Chemistry. 2. Lipids, 2nd ed. London: Chapman & Hall, 1995, pp 247–308.
46. RM Rocco. Fluorometric analysis of alkaline phosphatase in fluid dairy products. J Food Protect 53:588–592, 1990.
47. KF Eckner. Fluorometric analysis of alkaline phosphatase inactivation correlated to *Salmonella* and *Listeria* inactivation. J Food Protect 55:960–963, 1992.
48. GK Murthy, S Cox, L Kaylor. Reactivation of alkaline phosphatase in ultra high-temperature, short-time processed liquid milk products. J Dairy Sci 59:1699–1710, 1976.
49. JW Copius Peereboom. Studies on alkaline milk phosphatase III: a theory for the mechanism of reactivation of alkaline milk phosphatase in a model system. Fette Seifen Anstrichmittel 72:299–308, 1970.
50. G Linden. Biochemical study of some aspects of milk alkaline phosphatase reactivation. Milchwissenschaft 34:329–332, 1979.
51. EF McFarren, RC Thomas, LA Black, JE Campbell. Differentiation of reactivated from residual phospha-

tase in high-temperature short-time pasteurized milk and cream. J Assoc Off Anal Chem 43:414–426, 1960.
52. GK Murthy, JT Peeler. Rapid methods for differentiating reactivated from residual phosphatase in milk and cream: collaborative study. J Assoc Off Anal Chem 62:822–827, 1979.
53. AOAC. Official method 961.08: phosphatase (reactivated and residual) in milk. Official Methods of Analysis, 16th ed., Vol. 2. Arlington, VA: Association of Official Analytical Chemists, 1995, p 36.
54. WS Kwee. Phosphatase reactivation in cream samples. Aust J Dairy Technol 38:160–162, 1983.
55. R Karmas, DH Kleyn. Determination and interpretation of alkaline phosphatase activity in experimental and commercial butters. J Dairy Sci 73:584–589, 1990.
56. RC McKellar, HW Modler, H Couture, A Hughes, P Mayers, T Gleeson, WH Ross. Predictive modeling of alkaline phosphatase inactivation in a high temperature short time pasteurizer. J Food Protect 57:424–430, 1994.
57. RC McKellar, S Liou, HW Modler. Predictive modeling of lactoperoxidase and γ-glutamyl transpeptidase inactivation in a high-temperature short-time pasteurizer. Int Dairy J 6:295–301, 1996.
58. PF Fox, PLH McSweeney. Proteolysis in cheese during ripening. Food Rev Int 12:457–509, 1996.
59. TK Singh, PF Fox, A Healy. Water soluble peptides in Cheddar cheese: isolation and identification of peptides in the diafiltration retenate of the water-soluble fraction. J Dairy Res 62:629–640, 1995.
60. TK Singh, PF Fox, A Healy. Isolation and identification of further peptides in the diafiltration retentate of the water-soluble fraction of Cheddar cheese. J Dairy Res 64:433–443, 1997.
61. F Addeo, L Chianese, R Sacchi, S Spagna Musso, P Ferranti, A Malorni. Characterization of the oligopeptides of Parmigiano Reggiano cheese soluble in 120 g trichloroacetic acid/L. J Diary Res 61:365–374, 1994.
62. P Ferranto, F Barone, L Chianese, F Addeo, A Scaloni, L Pellegrino, P Resmini. Phosphopeptides from Grana Padano cheese: nature, origin and changes during ripening. J Dairy Res 64:601–615, 1997.
63. L Pellegrino, G Batteli, P Resmini, P Ferranti, F Barone, F Addeo. Effects of heat load gradient occurring in moulding on characterization and ripening of Grana Padano. Lait 77:217–228, 1997.
64. I de Noni, L Pellegrino, P Resmini, P Ferranti. About presence of free phosphoserine in ripened cheese and in enzymatic hydrolysate of casein. Nahrung 41:268–273, 1997.
65. AT Andrews. Indigenous milk enzymes: phosphatases. In: PF Fox, ed. Advanced Dairy Chemistry. 1. Proteins. London: Elsevier Applied Science, 1992, pp 322–331.
66. AT Andrews, E Alichanidis. The acid phosphatases of bovine leucocytes, plasma and the milk of healthy and mastitic cows. J Dairy Res 42:391–400, 1975.
67. MW Griffiths. Use of milk enzymes as indices of heat treatment. J Food Protect 49:696–705, 1986.
68. AT Andrews, M Anderson, PW Goodenough. A study of the heat stabilities of a number of indigenous milk enzymes. J Dairy Res 54:237–246, 1987.
69. P Jolles, J Jolles. Lysozyme from human milk. Nature 192:1187–1188, 1961.
70. NY Farkye. Indigenous enzymes in milk: other enzymes. In: PF Fox, ed. Advanced Dairy Chemistry. 1. Proteins. London: Elsevier Applied Science, 1992, pp 339–367.
71. PF Fox, MB Grufferty. Exogenous enzymes in dairy technology. In: PF Fox, ed. Food Enzymology, Vol. 1. London: Elsevier Applied Science, 1991, pp 219–269.
72. PF Fox. Exogenous enzymes in dairy technology: a review. J Food Biochem 17:173–199, 1993.
73. PF Fox, L Stepaniak. Enzymes in cheese technology. Int Dairy J 3:509–530, 1993.
74. CR Baumrucker. γ-Glutamyl transpeptidase of bovine milk membranes: distribution and characterization. J Dairy Sci 62:253–258, 1979.
75. CR Baumrucker. Purification and identification of γ-glutamyl transpeptidase of milk membranes. J Dairy Sci 63:49–54, 1980.
76. RC McKellar, DB Emmons, J Farber. Gamma-glutamyl transpeptidase in milk and butter as an indicator of heat treatment. Int Dairy J 1:241–251, 1991.
77. SS Patel, RA Wilbey. Heat exchanger performance: gamma-glutamyl transpeptidase assay as a heat treatment indicator for dairy products. J Soc Dairy Technol 42:79–80, 1989.
78. HD Carter, CF Cavanagh, JL Higgins, RA Wilbey. Assessment of the heat treatment of ice cream mixes by enzyme assay. J Soc Dairy Technol 43:67–68, 1990.
79. RC McKellar. Influence of ice-cream mix components on the thermal stability of γ-glutamyl transpeptidase and *Listeria innocua*. Int Dairy J 6:1181–1189, 1996.
80. Roudot-Algaron, L Kerhoas, D Le Bars, J Einhorn, J-C Gripon. Isolation of γ-glutamyl peptides from Comte cheese. J Dairy Sci 77:1161–1166, 1994.
81. J Cerbulis, HM Farrell Jr. Xanthine oxidase activity in dairy products. J Dairy Sci 60:170–176, 1977.
82. GF Edwards. A new method for the detection of heated or reconstituted milk. J Assoc Off Agric Chem 33:855–960, 1950.
83. KA Oster. Plasmalogen diseases: a new concept of the atherosclerotic process. Am J Clin Res 2:30–35, 1971.
84. AJ Clifford, CY Ho, H Swenerton. Homogenized milk xanthine oxidase: a critique of the hypothesis relating to plasminogen depletion and cardiovascular disease. Am J Clin Nutr 38:327–332, 1983.
85. HC Deeth. Homogenized milk and atherosclerotic disease: a review. J Dairy Sci 66:1419–1435, 1983.

86. CE Stauffer, ed. Enzyme Assays for Food Scientists. New York: Van Nostrand Reinhold, 1989.
87. PF Fox, PLH McSweeney, CM Lynch. Significance of non-starter lactic acid bacteria in Cheddar cheese. Aust J Dairy Technol 53:83–89, 1998.
88. Y Hirvi, MW Griffiths. Milk catalase activity as an indicator of thermization treatments used in the manufacture of Cheddar cheese. J Dairy Sci 81:338–345, 1998.
89. Y Hirvi, MW Griffiths, RC McKellar, HW Modler. Linear transform and non-linear modelling of bovine catalase inactivation in a high-temperature short-time pasteurizer. Food Res Int 29:89–93, 1996.
90. L Björck. Lactoperoxidase. In: PF Fox, ed. Advanced Dairy Chemistry. 1. Proteins. London: Elsevier Applied Science, 1992, pp 332–338.
91. KM Pruitt, DN Kamau. Quantitative analysis of bovine lactoperoxidase system components and of the effects of the activated system on bacterial growth and survival. In: Indigenous Antimicrobial Agents of Milk: Recent Developments, Special Issue 9404. Brussels: International Dairy Federation, 1994, pp 73–87.
92. MC Martin Hernandez, BW van Markwijk, HJ Vreeman. Isolation and properties of lactoperoxidase from bovine milk. Neth Milk Dairy J 44:213–231, 1990.
93. B Reiter. The biological significance of the non-immunoglobulin protective proteins in milk: lysozyme, lactoferrin, lactoperoxidase. In: PF Fox, ed. Developments in Dairy Chemistry. 3. Lactose and Minor Constituents. London: Elsevier Applied Science, 1985, pp 281–336.
94. J Stadhouders, RR Beumer. Actual and potential applications of the natural antimicrobial agents of milk in the dairy industry. In: Indigenous Antimicrobial Agents of Milk: Recent developments, Special Issue 9404. Brussels: International Dairy Federation, 1994, pp 175–197.
95. PF Fox, DM Mulvihill. Developments in milk protein processing. Food Sci Technol Today 7:152–161, 1993.
96. R Mitchell, GW Smithers, DA Dionysius, PA Grieve, GO Regester, EA James. Extraction of lactoperoxidase and lactoferrin from cheese whey using membrane cation exchangers. In: Indigenous Antimicrobial Agents of Milk: Recent Developments, Special Issue 9404. Brussels: International Dairy Federation, 1994, pp 89–95.
97. DA Dionysius, JB Herse, PA Grieve. Extraction of lactoperoxidase and lactoferrin from cheese whey using batch ion exchange techniques. Aust J Dairy Technol 46:72–75, 1991.
98. PF Fox, TP O'Connor, PLH McSweeney, TP Guinee, NM O'Brien. Cheese: physical, biochemical and nutritional aspects. Adv Food Nutr Res 39:163–328, 1996.
99. PF Fox, JM Wallace. Formation of flavor compounds in cheese. Adv Appl Microbiol 45:17–85, 1997.

20

Exogenous Enzymes in Dairy Technology

Patrick F. Fox
University College, Cork, Ireland

I. INTRODUCTION

Milk from domesticated animals and products formed therefrom have been components of the human diet for ~ 10,000 years. Some dairy products are consumed in most or all regions of the world and they are major dietary items in many regions, e.g., Europe, North America, and South America. Total milk production is $\sim 530 \times 10^6$ metric tons per year, of which ~ 85% is bovine milk; sheep, goats, water buffalo, camels, and mares are important dairy animals in some regions. Milk is a very perishable commodity and hence there has been a strong incentive to convert it to more stable products, which is facilitated by certain properties of milk. Classically, milk has been preserved by fermentation, usually with salt addition (cheese, fermented milks, butter). Newer preservation methods include drying, pasteurization/sterilization, and freezing. Some characteristics of milk also render it very amenable to modification by enzymes; that milk is a liquid facilitates enzyme addition. Cheese production is probably the oldest, and is still the largest, application of exogenous enzymes in food processing.

Since the principal components of milk are proteins (~ 3.5%), lipids (~ 3.6%), and lactose (~ 4.8%; a disaccharide containing galactose and glucose), the principal enzymes used in dairy technology are proteinases and peptidases, lipases, and β-galactosidase (lactase). However, several oxidoreductases have significant applications.

The principal applications of enzymes in dairy technology will be considered in this review. Earlier reviews include Fox and Grufferty (1), Fox (2), Fox and Stepaniak (3), Brown (4), and Desmazeaud and Spinnler (5).

II. PROTEINASES

Bovine milk contains ~ 3.5% proteins which can be resolved into two groups based on solubility at pH 4.6 and 20°C: the caseins, which are insoluble under these conditions and which represent ~ 80% of the total protein; and the whey (serum) proteins, which are soluble. The casein fraction of bovine milk and that of the other main dairying species comprises four proteins, α_{s1}-, α_{s2}-, β-, and κ-caseins, which, although they have certain features in common, e.g., insolubility at pH 4.6, are distinctly different proteins. The whey protein fraction also comprises four main proteins—β-lactoglobulin, α-lactalbumin, blood serum albumin, and immunoglobulins—and several minor proteins, including ~ 60 indigenous enzymes. Readers are referred to Fox (6) for a detailed description of the milk protein system.

As discussed in Section II.A.1, the colloidal stability of the caseins is extensively changed by limited proteolysis, leading to gelation of the milk system, which is the first step in the production of many cheese varieties. The milk proteins can be easily separated from the other milk constituents and the caseins and whey

proteins readily separated from each other on an industrial scale. Both the caseins and whey proteins have good and diverse functional properties; consequently, milk proteins are the preferred functional food proteins for a wide range of applications (7). Some functional properties can be improved and/or modified by limited proteolysis.

Proteolytic enzymes are the most widely used enzymes in dairy technology and will be discussed below under three headings: cheese manufacture, modification of functional properties, and production of protein hydrolyzates for nutritional and other applications.

A. Cheese Manufacture

The manufacture of all cheese varieties essentially involves concentrating the protein and fat of milk six-fold to 12-fold, depending on the variety. Concentration is achieved by (a) coagulating the principal milk proteins, i.e., the caseins (if present, the milk fat is occluded in the coagulum); (b) cutting or breaking the coagulum and inducing it to synerese under the influence of heat and acid; (c) separation of curds and whey; and (d) acidification, pressing, and salting of dewheyed curd.

Coagulation of the casein is induced by one of three methods:

1. Limited proteolysis by a crude proteinase (rennet), which is exploited in the manufacture of all ripened and some fresh cheeses ($\sim$ 75% of total production).

2. Isoelectric precipitation at $\sim$ pH 4.6, used for fresh cheeses, usually by in situ production of lactic acid by a culture (starter) of lactic acid bacteria and less frequently by direct acidification with preformed acid, usually HCl, or acidogen, usually gluconic acid–δ-lactone.

3. Acid plus heat, i.e., acidification to $\sim$ pH 5.2 with acid whey, acid milk, citrus juice, vinegar, or acetic acid at 80–90°C; this method is used to produce a small number of relatively minor varieties, e.g., Ricotta.

Concentration of the total colloidal phase of milk (i.e., fat and total protein) to the level present in cheese, i.e., to a "pre-cheese," by ultrafiltration is now used commercially for the manufacture of several cheese varieties. Additions of rennet and starter to the concentrate are still necessary for texture and flavor development.

1. Enzymatic Coagulation of Milk

The principal gastric enzyme of neonatal ruminants is chymosin rather than pepsin. Chymosin has low general proteolytic activity but high milk-clotting activity. Presumably, it evolved to coagulate milk in the stomach and thus delay its discharge into the intestine and increase the efficiency of digestion. Shortly after the domestication of dairy animals ($\sim$ 8000 B.C.), humans learned to exploit the ability of chymosin and some other proteinases, collectively referred to as rennets, to coagulate milk for the production of cheese, which was probably the first application of enzymes in food processing.

The rennet coagulation of milk is a two-stage process. The first (primary) phase involves the enzymatic production of "para-casein" and TCA-soluble peptides (glycomacropeptides), while the secondary phase involves the Ca-induced gelation of para-casein at a temperature in the range of 30–35°C. Proteolysis is essentially complete before the onset of coagulation.

The enzymatic coagulation of milk exploits certain properties of the caseins. As discussed above, bovine casein consists of four proteins—α_{s1}-, α_{s2}-, β-, and κ-caseins—in the approximate ratio of 40 : 10 : 35 : 12. These contain 8–9, 10–13, 4–5, and 1–2 mol of P per mol, respectively. Owing to their high phosphate content, α_{s1}-, α_{s2}-, and β-caseins bind Ca^{2+} strongly and precipitate at $Ca^{2+} > 6$ mM. However, κ-casein binds Ca^{2+} weakly and is soluble at high Ca^{2+}. It also reacts hydrophobically with α_{s1}-, α_{s2}-, and β-caseins and can stabilize up to 10 times its weight of these Ca^{2+}-sensitive caseins against precipitation by forming colloidal aggregates, called micelles.

In milk, > 95% of the casein exists as micelles, which consist, on a dry weight basis, of $\sim$ 94% protein and 6% of other species, mainly Ca^{2+} and PO_4^{3-} with some Mg^{2+} and citrate, collectively called colloidal calcium phosphate (CCP). The micelles are spherical, 50–600 nm (mean, $\sim$ 120 nm) in diameter, with particle weights of $\sim 10^8$ daltons; i.e., a typical micelle contains $\sim$ 5000 monomers (M_r = 20–24 kDa). The micelles typically bind $\sim$ 2 g H_2O/g protein.

Within the micelles, the caseins are held together by CCP bridges, hydrophobic interactions, and hydrogen bonds. There is a widely held view that the casein monomers are organized as submicelles (spherical particles, $M_r \sim 5 \times 10^6$ daltons). The micelles dissociate when CCP is removed (e.g. by Ca^{2+} chelators or acidification/dialysis), or when the pH is increased above $\sim$ 9, or on addition of detergents (e.g., sodium dodecyl

sulfate) or urea. In most models of the casein micelle, it is envisaged that the Ca^{2+}-sensitive α_{s1}- α_{s2}-, and β-caseins interact hydrophobically to form the core of the micelles, with κ-casein located predominantly on the surface. The N-terminal two-thirds of κ-casein is hydrophobic and reacts hydrophobically with the core proteins, leaving the hydrophilic C-terminal region projecting into the surrounding environment. It has been proposed that submicelles contain variable amounts of surface κ-casein and aggregate such that κ-casein-rich submicelles predominate at the surface of the micelles with the κ-casein-deficient submicelles buried within. The micelles are stabilized by a zeta potential of ~ -20 mV and by steric factors caused by the protruding C-terminal segments of κ-casein which form a "hairy" layer, 7–10 nm thick, on the surface of the micelles, preventing close approach.

a. Primary Phase of Rennet Action. During the primary phase of rennet action, κ-casein is the only protein hydrolyzed to a significant extent. It is cleaved by chymosin, and for most of the other proteinases used as rennets, at the bond Phe_{105}-Met_{106}, which is many times more susceptible to hydrolysis by acid proteinases (which include all commercial rennets) than any other bond in the milk protein system. κ-Casein f1–105, which is referred to as para-κ-casein, remains attached to the rennet-altered micelle but the hydrophilic peptide, κ-CN f106–169, referred to as the caseino(glyco)macropeptide, diffuses into the whey and consequently the micelle-stabilizing properties of κ-casein are lost.

A number of attempts have been made to explain the unique sensitivity of the Phe-Met bond. Di-, tri-, or tetrapeptides containing a Phe-Met bond are not hydrolyzed. However, the Phe-Met bond is hydrolyzed in the pentapeptide, H.Leu-Ser-Phe-Met-Ala-OMe, i.e., a derivative of κ-CN f103–107. The length of the peptide and the sequence around the cleavage site are important determinants of enzyme-substrate interaction. Ser_{104} is particularly important and its replacement by Gly or Ala in the above pentapeptide renders the Phe-Met bond very resistant to hydrolysis by chymosin but not by pepsins. Even substituting D-Ser for L-Ser markedly reduces the sensitivity of the adjacent Phe-Met bond. Extension of the above pentapeptide from the N- and/or C-terminal to reproduce the sequence of κ-casein increases the efficiency of hydrolysis of the Phe-Met bond by chymosin; the tetradecapeptide, κ-CN f98–111, is hydrolyzed as efficiently as intact κ-casein and $\sim 66{,}000$ faster than the parent pentapeptide, κ-CN f103–107, with a k_{cat}/K_M of $\sim 2\,M^{-1}\,sec^{-1}$.

The two residues, Phe-Met, are not intrinsically essential for chymosin action. Replacement of Phe by $PheNO_2$ or cyclohexylalanine decreases k_{cat}/K_M about threefold and ~ 50-fold, respectively. Oxidation of Met_{106} decreases $k_{cat}/K_M \sim 10$-fold but substitution of Ile for Met increases this ratio about threefold. In fact, the chymosin-susceptible bond in porcine or human κ-caseins is Phe-Ile, which is readily hydrolyzed by calf chymosin. Thus, the sequence around the Phe-Met bond, rather than the bond itself, contains the important determinants of hydrolysis. The sequence Leu_{103}-Ser-Phe-Met-Ala-Ile_{108} of κ-casein, which may exist as a β-structure, fits into the active site cleft of acid proteinases. The hydrophobic residues, Leu_{103}, Phe_{105}, Met_{106}, and Ile_{108}, probably interact with hydrophobic residues along the active site cleft while the hydroxyl group of Ser_{104} forms a hydrogen bridge with a counterpart on the enzyme. Residues 98–102 and 109–111 probably form β-turns around the edges of the active site cleft in the enzyme · substrate complex; this conformation is stabilized by Pro residues at positions 99, 101, 109, and 110. One or more of the three His residues, 98, 100, 102, and Lys_{111}, are probably involved in electrostatic bonding.

Pepsins and most other acid proteinases used as rennets hydrolyze κ-casein at Phe_{105}-Met_{106} but the acid proteinase of *Cryphonectria parasitica* hydrolyzes Ser_{104}-Phe_{105}. Although the specificity of cathepsin D on α_{s1}- and β-caseins is generally similar to that of chymosin, it has very poor milk-clotting activity. The aggregation characteristics of micelles vary with the rennet used, suggesting differences in the extent and/or specificity of the hydrolysis of κ-casein or perhaps of the other caseins. Furthermore, the commonly used rennets have markedly different specific activities on synthetic κ-casein-related peptides.

Reviews on the enzymatic coagulation of milk include Dalgleish (8, 9), Fox (10–12), Fox and Mulvihill (13), and Fox and McSweeney (14).

b. Rennets. The rennets used to coagulate milk are crude preparations of selected proteinases. Many proteinases can coagulate milk but most are too proteolytic relative to their milk clotting activity and hydrolyze the coagulum too quickly, causing reduced cheese yield and/or defective, e.g., bitter cheese. Traditionally, rennets were prepared from calves', kids', or lambs' stomachs; the principal proteinase in such rennets is chymosin. The molecular and enzy-

matic properties of chymosins have been studied extensively (15–17).

Owing to increasing world production of cheese (~ 3% per year over the past 30 years), concomitant with a reduced supply of calf vells, the supply of veal rennet has been inadequate for many years, which has led to a search for rennet substitutes. Although many proteinases can coagulate milk, only six have been found to be more or less acceptable as rennets: bovine, porcine, and chicken pepsins and the acid proteinases from *Rhizomucor miehei, R. pusillus*, and *C. parasitica*. Chicken pepsin is the least suitable of these and is used only in special circumstances. Bovine pepsin gives generally satisfactory results with respect to cheese yield and quality; many commercial "calf rennets" contain a substantial proportion of bovine pepsin. Although the proteolytic specificity of the three commonly used fungal rennets on α_{s1}- and β-caseins is considerably different from that of calf chymosin, they generally yield acceptable cheese and were widely used in the United States before the introduction of microbial recombinant chymosin. Acid proteinases from flowers of the genus *Cynara* are used to coagulate sheep's milk for some artisinal cheeses in Portugal and Spain, especially Serra d'Estrala cheese; these proteinases are not generally suitable as rennets. The extensive literature on rennet substitutes has been reviewed (18–21).

The gene for calf chymosin has been cloned in selected bacteria, yeasts, and molds. Chymosin from genetically engineered *Kluyveromyces marxianus* var. *lactis* (Gist-brocades), *Escherichia coli* (Pfizer), and *Aspergillus nidulans* (Hansens) is commercially available and used extensively, with excellent results; however, these products are not yet permitted in all countries. Reviews on microbial recombinant chymosin include Teuber (22) and IDF (23).

Microbial recombinant chymosin preparations contain no pepsin whereas 5–50% of the milk-clotting activity of calf rennets may be due to pepsin; hence, some minor differences in the pattern of proteolysis in cheese made with microbial recombinant chymosin or calf rennet are observed, most notably the formation of the peptide α_{s1}-CN f110–199 in cheese made using calf rennet (owing to the action of pepsin). For those wishing to simulate the action of calf rennet more closely, blends of microbial recombinant chymosin and bovine pepsin are commercially available.

Calf chymosin contains three isoenzymes—A, B, and C. A and B are gene products that differ from each other by one amino acid; A has Asp at position 243 while B has Gly at this position. Chymosin C appears to be a degradation product of chymosin A which lacks three residues, Asp_{244}-Phe_{246}. Commercially available microbial recombinant chymosins contain only chymosin A or B; it is not known if the different forms of chymosin differ in specificity, but it is claimed by rennet manufacturers that the cheesemaking properties of chymosin A and B are not equivalent.

The primary, and probably higher, structures of commercially available microbial recombinant chymosins are identical to that of calf chymosin. However, several modified chymosins have been produced from genetically engineered microorganisms. At present, the objective of these investigations is to study the mechanism of chymosin action at the molecular level, but it is probable that chymosin with improved cheese-making properties will emerge from such studies, e.g., enzymes with increased activity on certain bonds shown to produce cheese with improved quality or reduced activity on other bonds, cleavage of which results in flavor or textural defects. It should be remembered that chymosin evolved to coagulate milk in the neonatal stomach (to improve the efficiency of digestion) and not to produce cheese. It is fortuitous that chymosin is the best proteinase for cheese production, not just for milk coagulation, but it is highly probable that it can be improved. For reference on genetically engineered chymosins, see (14, 17).

Most (70–90%) of the rennet added to cheese milk is lost in the whey. Therefore, the possibility of immobilizing rennet has been investigated as a means of extending its working life. Several rennets have been immobilized but their efficacy as milk coagulants has been questioned. There is widespread support for the view that properly immobilized enzymes can not coagulate milk owing to inaccessibility of the Phe-Met bond of κ-casein and that the apparent coagulating activity of immobilized rennets is due to leaching of enzyme from the support. Even if immobilized rennets could hydrolyze micellar κ-casein, operational difficulties would exist at the cheese factory level. Furthermore, as discussed in Section II.A.2.d, the residual rennet in cheese curd plays an essential role in cheese ripening and it would be necessary to add some chymosin or similar enzyme to the curd after coagulation, which would be difficult or impossible (see 8, 9, 24 for reviews).

c. Factors Affecting the Hydrolysis of κ-Casein. The pH optimum for chymosin and bovine pepsin is ~ 4.7 on small Phe-Met-containing peptides and 5.3–5.5 on κ-CN f98–111 or on whole κ-casein. The pH optimum for the first stage of rennet action

in milk is ~ 6.0. Milk for most cheese varieties is renneted at about pH 6.5.

Increasing ionic strength (0.01–0.11) decreases the rate of hydrolysis of κ-CN f98–112, especially if the pH is also increased. At 1 mM, NaCl, $CaCl_2$, and $MgCl_2$ stimulate the hydrolysis of κ-casein in isolated form or in sodium caseinate.

The optimum temperature for the coagulation of milk by calf rennet at pH 6.6 is $\sim 45^{\circ}C$. The temperature coefficient (Δ rate/10°C) for the hydrolysis of κ-casein in solutions of Na-caseinate is ~ 1.8, the E_a is $\sim 10{,}000$ cal mol^{-1} and the activation entropy is $\sim -39\,cal\,deg^{-1}\,mol^{-1}$; generally similar values have been reported for the hydrolysis of isolated κ-casein.

The efficacy of κ-casein as a substrate for chymosin decreases as its level of glycosylation increases. At pH 6.6, k_{cat} decreases from $\sim 43\,sec^{-1}$ for carbohydrate-free κ-casein to $\sim 25\,sec^{-1}$ for κ-casein containing 6 moles N-acetyl neuraminic acid (NANA) per mol. However, K_m is lowest for the κ-casein component containing 3 moles NANA per mol. Polymerization (aggregation) markedly increases K_m with little effect on k_{cat}.

d. Secondary (Nonenzymatic) Phase of Rennet Coagulation. Hydrolysis of κ-casein removes its highly charged, hydrophilic C-terminal segment from the surface of the casein micelles, thereby reducing their zeta potential from ~ -20 mV to ~ -7 mV and removing the steric stabilizing layer. When $\sim 85\%$ of the total κ-casein has been hydrolyzed, the casein micelles begin to aggregate and eventually form a gel. Reducing the pH or increasing the temperature from the normal (~ 6.6 and $\sim 31^{\circ}C$, respectively) induces coagulation at a lower degree of κ-casein hydrolysis.

The mechanism involved in the coagulation of rennet-altered micelles is not known precisely. Coagulation is dependent on Ca^{2+} and on colloidal calcium phosphate, which are exchangeable to a certain extent. Ca^{2+} may function by neutralizing negative charges on the caseins. Coagulation is highly temperature dependent; rennet-altered micelles do not coagulate below $\sim 20^{\circ}C$, above which the $Q_{10^{\circ}C}$ for coagulation is ~ 16. The high temperature dependence of coagulation suggests that hydrophobic bonds may be involved or that multiple bonds are formed.

The rennet coagulability of milk is adversely affected by heat treatments at temperatures $> 65^{\circ}C$ and is prevented by very severe heat treatments ($> 90^{\circ}C$ for 10 min). Although changes in the equilibria of milk salts, especially calcium phosphate, are contributory factors, complexation of κ-casein with β-lactoglobulin and/or α-lactalbumin is primarily responsible for the increased rennet coagulation time of heated milk; both the primary phase and especially the secondary phase are adversely affected. The adverse effects of heating can be reversed by acidification before or after heating or by addition of $CaCl_2$.

Rennet-coagulated milk gels are relatively stable if left undisturbed but synerese strongly if cut or broken. The rate and extent of syneresis are promoted by reducing the pH, increasing the temperature, and applying pressure, e.g., agitation. By controlling the extent of syneresis, the cheese maker can control the moisture content of cheese which is a major factor affecting the rate and pattern of ripening and the stability of cheese. Differences in moisture content are, in fact, a major factor responsible for the diversity of cheese flavor and texture.

2. Proteolysis During Cheese Ripening

Acid-coagulated cheeses are usually consumed fresh, but the vast majority of rennet-coagulated cheeses are ripened (matured) for a period ranging from ~ 3 weeks to > 2 years; the rate of ripening is directly related to the moisture content of the cheese. During ripening, numerous microbiological, biochemical, and chemical events occur, as a result of which the principal constituents of the cheese—the proteins, lipids, and lactose—are transformed to primary, and later to secondary, products. Among the principal flavor compounds present in most cheese varieties are: peptides, amino acids, amines, acids, thiols, and thioesters (derived from proteins); fatty acids, methyl ketones, lactones, esters, and thioesters (derived from lipids); organic acids (lactic, acetic, and propionic); carbon dioxide; esters; and alcohols (derived from lactose). At appropriate concentrations and combinations, these compounds are responsible for the characteristic flavor of the various cheese varieties.

The biochemistry of cheese ripening has been reviewed by Fox et al. (25, 26) and Fox and Wallace (27); only proteolysis is discussed here.

a. Significance of Proteolysis. Proteolysis is essential in all rennet-coagulated cheese varieties, especially internal- and surface-bacterially ripened cheeses in which it is probably the principal biochemical event during ripening. Proteolysis contributes to cheese ripening in at least four ways: (a) makes a direct contribution to flavor, or off-flavor, e.g., bitterness, or indirectly since free amino acids are catabolized to amines, acids, thiols, thioesters, etc.; (b) facilitates the release of sapid compounds during mastication; (c) the

production of NH_3 from amino acids released by proteolysis affects flavor and texture; (d) changes in texture due to breakdown of the protein network, increase in pH, and greater water binding by the newly formed amino and carboxyl groups. There is a good correlation between the intensity of Cheddar cheese flavor and the extent and depth of proteolysis.

Considerable information is available on the level and type of proteolysis in the principal cheese groups (14, 25, 26, 28–33).

b. Proteolytic Agents in Cheese. Four, and in some varieties five, agents contribute to proteolysis in cheese during ripening: rennet or rennet substitute; indigenous milk enzymes, especially plasmin; starter bacteria and their enzymes, released on cell lysis; nonstarter bacteria, which either survive pasteurization of the cheese milk or gain access to the pasteurized milk or curd during manufacture; and secondary inocula, e.g., propionic acid bacteria, *Brevibacterium linens*, yeasts, and molds (*Penicillium roqueforti* and *Geotricum candidum*), and their enzymes are of major importance in some varieties. Techniques have been developed which permit quantitation of the contribution of each of these five agents to the primary aspects of cheese ripening (25, 31).

Studies using these techniques have shown that primary proteolysis, as determined by gel electrophoresis or the formation of water- or pH 4.6-soluble N, is due mainly to the coagulant except in those varieties, e.g., Emmental, Parmesan, and mozzarella, cooked to a high temperature (52–55°C) in which the coagulant is extensively or completely denatured. In these latter varieties, primary proteolysis is relatively limited and is due mainly to plasmin, which also contributes to proteolysis, especially of β-casein, in low-cooked cheese. The peptides produced by the coagulant and plasmin are further hydrolyzed by the proteinases and peptidases of starter and nonstarter bacteria, leading to the formation of many small peptides and free amino acids. Proteolysis varies widely among varieties, from very limited in short-ripened cheeses such as mozzarella, to very extensive in extramature Cheddar, Parmesan, or blue cheeses. Proteolysis in cheddar cheese has been well characterized and considerable information is also available on Gouda, Emmental, and Parmesan cheeses (33).

c. Contribution of Coagulant to Proteolysis in Cheese. Most of the rennet added to cheese milk is either denatured or lost in the whey. The amount retained is influenced by the type of rennet; e.g., porcine pepsin is extensively denatured during cheese making, pH (low pH favors retention of chymosin but not microbial rennets and reduces denaturation, e.g., of pepsins), and cooking temperature, e.g., little, if any, coagulant survives the cooking conditions used for Swiss-type cheeses. About 6% of the added chymosin is retained in Cheddar cheese and up to 20–30% in high-moisture, low-cook, low-pH cheeses, such as Camembert.

The proteolytic specificity of calf chymosin on α_{s1}-, α_{s2}-, and β-caseins in solution has been established and these findings can, largely, be extended to cheese (14, 33).

The principal chymosin cleavage sites on α_{s1}-casein in cheese are: Phe_{23}-Phe_{24}, which is hydrolyzed rapidly and completely in cheese (e.g., within $\sim$ 3 months in Cheddar), and Leu_{101}-Lys_{102}, which is cleaved fairly extensively; Phe_{33}-Gly_{34} and Leu_{98}-Leu_{99} are also cleaved to some extent in cheese. Surprisingly, the Trp_{164}-Tyr_{165} bond, which is the second most susceptible bond in α_{s1} casein in solution, does not appear to be hydrolyzed in cheese. The small peptide, α_{s1}-CN f1–23, does not accumulate in cheese but is hydrolyzed rapidly by the cell envelope-associated lactococcal proteinase, with a specificity dependent on the strain (34).

Some peptide bonds in β-casein in solution are hydrolyzed quite rapidly by chymosin in the order: Leu_{192}-Tyr_{193}, Ala_{189}-Phe_{190}, Leu_{163}-Ser_{164}, and Leu_{139}-Leu_{140}. In cheese, these bonds are hydrolyzed to a very limited extent or not at all, probably because the C-terminal region of β-casein is very hydrophobic and undergoes hydrophobically driven interactions in cheese. These interactions appear to be accentuated by NaCl; even in solution, the hydrolysis of β-casein is strongly inhibited by 5% NaCl, which is the typical NaCl concentration in the aqueous phase of many cheese varieties. Inhibition of the hydrolysis of β-casein in cheese is desirable since the peptide β-CN f193–209 and fragments thereof are very bitter.

Although α_{s2}-casein in solution is fairly readily hydrolyzed by chymosin, its fate in cheese is not clear, and para-κ-casein (κ-CN f1–105) is very resistant to chymosin (and to other proteinases in cheese).

The specificity of pepsins is generally similar to that of chymosin but has not been established precisely. Bovine pepsin cleaves the Leu_{109}-Glu_{110} bond of α_{s1}-casein quite rapidly, a bond which is cleaved very slowly by chymosin. The specificity of the fungal rennet substitutes is quite different from that of chymosin (35). The principal cleavage sites of *R. miehei* proteinase in α_{s1}-casein in solution are Phe_{23}-Phe_{24}, Met_{123}-Lys_{124}, and Tyr_{165}-Tyr_{166} while those in β-casein are Glu_{31}-Lys_{32}, Val_{58}-Val_{59}, Met_{93}-Gly_{94}, and

Phe_{190}-Leu_{191} (35). *C. parasitica* proteinase is much more active on β-casein in cheese than chymosin, pepsin, or *Rhizomucor* proteinases, but its specificity on the caseins has not been determined; since it does not cause significant bitterness in cheese, its primary cleavage sites in β-casein may be in the N-terminal rather than in the C-terminal region (the N-terminal region of β-casein is quite hydrophilic, and small peptides produced from it would be expected to be nonbitter).

d. Significance of Secondary Coagulant Proteolysis. The proteolytic activity of the coagulant in cheese influences quality in four ways:

1. Some rennet-produced peptides may have a positive influence on flavor but excessive or unbalanced proteolysis, e.g., too much or excessively proteolytic rennet or unsuitable environmental conditions, e.g., too much moisture or too little NaCl, leads to bitterness. The peptide β-CN f193–209 derived from the C-terminal of β-casein and fragments thereof are particularly bitter.

2. Rennet-produced peptides serve as substrates for microbial proteinases and peptidases which produce small peptides and amino acids. These contribute at least to background flavor and perhaps to bitterness if the activity of such enzymes is excessive. Catabolism of amino acids by microbial enzymes and perhaps alterations via chemical mechanisms leads to a range of sapid compounds—amines, acids, NH_3, thiols—which are major contributors to characteristic cheese flavors.

3. Alterations in cheese texture appear to influence the release of flavorful and aromatic compounds, arising from proteolysis, lipolysis, glycolysis, and secondary metabolic changes, from cheese during mastication, and this may be the most significant contribution of proteolysis to cheese flavor.

4. Texture is an important attribute of all cheeses and is critical in some varieties. Protein forms a continuous solid matrix in cheese, and its hydrolysis leads to a softening of the texture. Chymosin is primarily responsible for textural changes during the early stages of ripening. The functionality (stretchability and meltability) of mozzarella is strongly influenced by proteolysis; a low level of proteolysis improves functionality, but quality deteriorates on further proteolysis.

3. Acceleration of Cheese Ripening

The original objective of cheese manufacture was conservation of the principal nutrients in milk (i.e., lipids and proteins) by a combination of acidification, dehydration, low E_h, and salting. Chemical and biochemical changes do occur during storage but stability was the prime objective. While still important, stability is no longer the primary objective of cheese manufacture, and since ripening is expensive, its acceleration, especially in low-moisture, slow-ripening varieties, is desirable, at least under certain circumstances, provided the whole process can be maintained in balance.

Some high-moisture cheeses develop an intense flavor through a very active secondary flora, e.g., internal blue mold, external white mold, or a bacterial surface smear; these cheeses ripen quickly, e.g., 4–16 weeks. High-moisture internal bacterially ripened cheeses also mature rapidly but develop a low flavor intensity; if the ripening of such cheeses is extended, they will probably develop off-flavors. It is possible to develop an intense flavor in internal bacterially ripened cheeses only if the moisture content is low and they are ripened for a long period, e.g., Parmesan, extramature Cheddar, or extramature Gouda, which are ripened for 2–3 years. Owing to the high cost of ripening facilities and stocks, the ripening of extramature cheeses is expensive. Consequently, there is commercial interest in accelerating the ripening of these cheeses, provided quality can be maintained. It might also be possible to apply similar techniques to medium-moisture, medium-flavor cheeses, e.g., regular Cheddar and Gouda, with the objective of accentuating their flavor. Most of the work on accelerating cheese ripening has in fact been on Cheddar. Techniques for accelerating ripening may also be applicable to reduced-fat cheeses, which tend to ripen slowly. A substantial literature on attempts to accelerate cheese ripening has accumulated and has been reviewed regularly (36).

Glycolysis is rapid in all cheeses and does not require acceleration. Lipolysis is limited in most cheeses and excessive lipolysis is undesirable. Consequently, most studies on accelerated ripening of cheese have focused on proteolysis, which contributes to flavor and is mainly responsible for changes in texture.

Methods for accelerating cheese ripening fall into six categories: elevated ripening temperature, exogenous enzymes, chemically or physically modified cells, genetically modified starters, adjunct starters, and enzyme-modified cheeses. These methods either seek to make the conditions under which indigenous enzymes function more favorable (i.e., elevated temperature) or to increase the level of certain key enzymes which are considered to be particularly important in cheese ripening.

A complex cascade of enzymes is involved in cheese ripening, and most key enzymes have not been identified. Not surprisingly, the use of single enzymes, e.g., additional coagulant (which is mainly responsible for primary proteolysis), plasmin (for which some benefits are claimed), or Neutrase (from *B. subtitis*), while accelerating proteolysis, does not accelerate flavor development and may cause off-flavors. It has been claimed that a combination of exogenous proteinases and lactococcal cell-free extracts (rich in peptidases) accelerate ripening, but the results are equivocal. Uniform incorporation of the enzyme preparation into cheese curd poses problems. For Cheddar, the enzyme preparation, diluted with salt, may be added to milled curd, but this method is not applicable to most varieties. Addition of microencapsulated enzyme(s) to cheese milk is technically feasible, but microencapsulation techniques currently available are not very efficient. At present, exogenous enzymes are not being used commercially to accelerate the ripening of natural cheese.

Exogenous lipase, traditionally pregastric esterase, is added to certain hard Italian cheeses, e.g., Romano and provolone. It has been claimed that inclusion of selected lipases in the blend of exogenous enzymes accelerates the ripening of other cheeses, e.g., Cheddar and Ras.

Most of the enzymes involved in cheese ripening are produced by microorganisms that grow in or on the cheese. By increasing the number of these organisms it should be possible to accelerate ripening. The use of whole cells should have two advantages over isolated enzymes: they contain the "natural" cocktail of enzymes found in cheese and they are cheaper to produce. Three approaches have been considered in the use of bacterial cells to accelerate cheese ripening: attenuated starter cells, genetically modified cultures, adjunct cultures.

The starter, in addition to its essential role in curd acidification, is also essential for secondary proteolysis and flavor development. Therefore, it might be expected that increasing the number of starter cells in cheese would accelerate ripening. However, increasing the level of active starter added to the cheese milk causes an excessively rapid rate of acid production which has undesirable effects, e.g., a crumbly texture and overacid flavor. The acid-producing ability of starter cells may be attenuated or destroyed by heat-shocking, freeze-shocking, or solvent treatment with very little effect on their enzyme activities. These attenuated cells are in effect packages of enzymes and their use has been reported to accelerate the ripening of a number of cheese varieties.

A simpler and probably more effective approach is the use of lactose-negative strains of *Lactococcus*, which cannot grow in milk or cheese curd but serve as a balanced "natural" source of enzymes important in cheese ripening. Such cultures are available commercially and are claimed to give satisfactory results.

Cells of selected non-lactic-acid bacteria, which do not grow in a particular cheese, either because they are aerobic, e.g., *Pseudomonas* spp. or *Brevibacterim* spp., or because they have a high growth temperature, e.g., *Propionibacterium*, might also serve as suitable "packages of enzymes" for addition to cheese curd; however, such cultures do not appear to be used commercially at present.

It is probable that certain enzymes are rate limiting in cheese ripening. At present, the key limiting enzymes are unknown, but studies are in hand with the objective of identifying these enzymes using deficient or overproducing mutants. It is possible to genetically modify *Lactococcus* to overproduce certain desirable enzymes, to delete undesirable genes, or to introduce foreign genes for putitively important enzymes. It is highly probable that genetically modified bacteria with the ability to accelerate ripening and improve cheese quality will become available in due course for use as primary or secondary cultures.

All cheese acquires an adventitious nonstarter microflora, predominantly mesophilic lactobacilli, which grow from low numbers initially (e.g., $< 10^3$ cfu/g) to 10^7–10^8 cfu/g and which dominate the microflora of cheese after ~ 3 months owing to the death of the primary starter. These nonstarter lactic acid bacteria (NSLAB) probably affect cheese ripening, and there is considerable interest in inoculating cheese milk with selected strains of NSLAB to accelerate or modify cheese flavor development (37).

An extreme form of accelerated ripening is practiced in the production of enzyme-modified cheese (EMC); the subject has been reviewed by Kilcawley et al. (38). EMCs are produced by adding a cocktail of enzymes (proteinases, peptidases, lipases) and perhaps bacterial cultures to homogenized, pasteurized fresh curd or young cheese. The mixture is incubated for a requisite period and repasteurized to terminate the microbiological and enzymatic reactions. The preparation may be spray-dried or commercialized as a paste.

Although the flavor of EMCs does not approximate that of natural cheese, they have the ability to potentiate cheeselike flavor in various food products, e.g., processed cheese, cheese analogs, cheese sauces, and dips, and products containing cheese, e.g., crackers, crisps, etc. For such applications, EMCs may replace

20–50 times their weight of natural cheese and are cheaper. Cheddar EMCs are the most important commercially, but EMCs that stimulate several varieties have been developed, e.g., blue, Swiss, and Romano.

B. Other Applications of Proteinases

In comparison with their use in cheese making, the other applications of proteinases in dairy technology are quite small but some have considerable growth potential. The more important of these are discussed below.

1. Dietary Products

Protein hydrolyzates for use in soups, gravies, flavorings, and dietetic foods are generally prepared from soy proteins, gluten, milk proteins, meat, or fish protein by acid hydrolysis. Neutralization results in a high salt content which is acceptable for certain applications but may be unsuitable for dietetic foods and food supplements. Furthermore, acid hydrolysis causes total or partial destruction of some amino acids. Enzymatic hydrolysis is a viable alternative (39), but bitterness due to hydrophobic peptides is frequently encountered. Caseins are strongly hydrophobic and yield very bitter hydrolyzates, but bitterness may be eliminated, or at least reduced, by one of several treatments (39, 40).

There is increasing interest in the production of casein-derived peptides with special nutritional or physiological properties; some of the possibilities have been reviewed (41, 42). Apart from the interest in casein hydrolyzates for the nutrition of patients with digestive problems, interest has been focused recently on phosphopeptides derived from casein which it is claimed stimulate the absorption of calcium and iron, but views on this are not unanimous (43). Methods for the production of caseinophosphopeptides for nutritional and/or medical applications have been developed (44–46).

The casein(glyco)macropeptide (CMP), κ-CN f106–169, produced from κ-casein during the enzymatic coagulation of milk for cheese or rennet casein, is lost into the whey. CMP is devoid of aromatic amino acids and hence is a suitable nutrient for patients suffering from phenylketonuria. Several biological activities have been attributed to the CMP, including inhibition of adhesion of oral actinomyces and streptococci to erythrocytes, effects on gastrointestinal motility, growth factors for *Bifidobacterium* spp., inhibition of the binding of cholera toxin, inhibition of influenza virus hemagglutinin, stimulation of cholecystokinin release from intestinal cells, and inhibition of acid secretion in the stomach (47, 48). Methods have been developed for the industrial production of CMP from whey (48, 49).

There is considerable interest in the fortification of performance-enhancing drinks with protein hydrolysates; bitterness is a problem here, and whey protein hydrolysates are preferred to casein hydrolysates.

2. Physiologically Active Peptides from Milk Proteins

Peptides with various physiological activities have been isolated from milk protein hydrolysates; at least some of these peptides are produced in vivo and may play a physiological role (50). The best-studied of these are the β-caseinomorphins, a family of peptides containing 4–7 amino acids (representing β-CN f60–63/7) with opioid activity. These peptides are produced in the intestine in vivo but it is still unclear whether or not they reach the brain. Peptides with opiate properties have also been isolated from hydrolysates of α_{s1}- and κ-caseins, lactotransferrin, α-lactalbumin, and β-lactoglobulin.

Other biologically active peptides that have been isolated from hydrolysates of milk proteins include: immunomodulating peptides, an inhibitor of angiotensin-converting enzyme, blood platelet modifiers, and stimulators of DNA synthesis (50). Whether any of these peptides are active in vivo remain to be established, but their formation has led to casein being referred to as a pro-hormone (51).

The release of biologically active peptides requires precise hydrolysis of the parent molecules at specific bonds. If the application of these peptides develops as predicted, very interesting applications for proteinases in the dairy industry will emerge.

3. Modification of Protein Functionality

Milk proteins are among the principal functional proteins used in food products (52). In general, milk proteins possess very good functional properties but suffer some limitations, notably the insolubility of casein in the pH range 3.0–5.5. The functional properties of milk proteins may be improved by limited proteolysis (1, 40, 53, 54). An acid-soluble casein, free from off-flavor and suitable for incorporation into beverages and other acid foods, has been prepared by limited proteolysis. The antigenicity of casein is destroyed by proteolysis, and the hydrolysate is suitable for use in milk protein-based foods for infants allergic to cow's milk. Controlled proteolysis improves the meltability of directly acidified cheese but excessive proteolysis

causes bitterness. Casein solutions are very viscous at concentrations > 20%, w/v, which increases the cost of drying caseinates. Viscosity may be reduced by limited proteolysis, but only a small increase in solids is possible owing to bitterness after even moderate levels of proteolysis.

The surface activity of sodium caseinate can be increased considerably by the treatment with plasmin, apparently owing to the formation of γ^2- and γ^3-caseins (β-CN f106–209, β-CN f108–209) which are very surface active. Generally, the emulsifying and foaming properties of small peptides are poor, since they form very thin interfacial layers.

Limited proteolysis of lactalbumin (heat-denatured whey protein), which is insoluble and has very poor functional properties, yields a product with greatly improved solubility and functionality. Limited proteolysis of whey protein concentrate (WPC) reduces its emulsifying capacity and increases its specific foam volume but reduces foam stability. The heat stability of WPC may be improved considerably by limited hydrolysis without concomitant impairment of other functional properties or off-flavor development.

The plastein reaction has been proposed as a mechanism by which the functional and nutritional properties of proteins may be improved. The reaction is of little relevance to milk proteins because they already have good functional and nutritional properties and yields of plastein are low.

One of the principal food applications of whey protein (WP) and whey protein isolates (WPI) is in the production of thermo-set gels. The gelation of WPCs at low temperatures has been achieved by limited proteolysis by certain enzymes (55); perhaps gelation occurs through the plastein reaction.

III. LIPASES

Lipases have a number of relatively low-volume applications in the dairy industry. Some of these applications are traditional and essential for the manufacture of particular products: others are emerging but hold considerable potential.

A. Lipases in Cheese Production

The principal application of lipases in dairy technology is in cheese manufacture, particularly, some Italian varieties, e.g., Romano and provolone. The characteristic "piquant" flavor of these cheeses is due primarily to short-chain fatty acids resulting from the action of lipase(s) in the rennet paste traditionally used in their manufacture.

Rennet pastes are prepared from the stomachs of calves, lambs, or kids slaughtered after suckling; the stomachs and contents are held for a considerable period prior to maceration. Because of possible risks to public health, the use of rennet pastes, which have proteolytic and lipolytic activities, is prohibited in some countries. The lipase in rennet paste is of oral origin and its secretion is stimulated by suckling: the secreted lipase is washed into the stomach with the ingested milk. Oral (lingual) lipase, commonly referred to as a pregastric esterase (PGE), is secreted by several species and probably makes a significant contribution to the digestion of lipids by the neonate in which the activity of pancreatic lipase is limited. The considerable literature on PGE has been comprehensively reviewed (3, 56). PGE shows a high specificity for short chain fatty acids, especially butyric, esterified on the Sn-3 position of glycerol, although some interspecies differences in specificity have been reported. They are maximally active at 32–42°C, pH 4.8–5.5, and in the presence of 0.5 M NaCl. Calf, kid, and lamb PGEs have been partially purified from commercial preparations (57). Calf PGE has been isolated from oral tissue and characterized with respect to pI (7.0), molecular weight ($\sim$ 49 kDa), and amino acid composition (58, 59). The secondary structures of rat lingual lipase and pancreatic lipase were studied and compared (60). The gene for rat lingual lipase has been cloned and sequenced, and the amino acid sequence of the enzyme has been deduced (61).

PGE-containing extracts from calf, kid, or lamb tissue are commercially available as alternatives for rennet pastes. Slight interspecies differences in specificity render one or another more suitable for particular applications. Particularly large differences in the ability of lipases to release 4-methyloctanoic acid, which exhibits a goat-muttony aroma, have been found (62). Such differences in specificity permit the generation of a range of flavors in cheese products. The propensity of PGE to synthesize triglycerides is increased in the a_w range 0.75–0.90 or by the addition of ethanol to the reaction mixture (63); this property may be exploited to modify cheese flavors.

Although PGE extract is now widely used in the manufacture of hard Italian cheese varieties, connoisseurs of Italian cheese claim that rennet paste gives superior results. Perhaps rennet paste contains enzymes in addition to chymosin and PGE. A second lipase, termed gastric lipase, was identified in an extract of cleaned gastric tissue and partially charac-

terized. A combination of calf gastric lipase and goat PGE gave Cheddar and provolone of superior quality to cheese made with PGE alone (64). However, Nelson et al. (56) expressed reservations on the occurrence of a gastric lipase distinct from PGE. Traditional rennet paste would be expected to contain both PGE and gastric lipase.

R. miehei secretes a lipase that is reported to give satisfactory results in Italian cheese manufacture (65). The enzyme has been characterized (66) and is commercially available as Piccantase. The lipases secreted by selected strains of *Penicillium roqueforti*, *P. candidum*, or *A. niger* are considered to be potentially useful for the manufacture of Romano, provolone, and other cheese varieties (67, 68). Unlike PGE, the fungal lipases do not preferentially release short-chain fatty acids. The use of different lipase preparations or blends of lipases opens possibilities for producing Italian cheeses with different degrees of sharpness.

A. oryzae secretes a lipase which has as exceptionally high specificity for C_6–C_8 acids (69). Another interesting characteristic of this enzyme is that it forms micelles, $\sim 0.2\,\mu$m in diameter, in aqueous media, as a result of which $\sim 94\%$ of the enzyme added to milk is recovered in cheese curds. The formation of short-chain fatty acids was reported to parallel flavor intensity in Cheddar cheese containing this enzyme. In contrast to the FFA profile caused by calf PGE, which liberated high concentrations of $C_{4:0}$, the FFA profile in the cheese containing *A. oryzae* lipase was similar to that in the control cheese, but the level of FFA was much higher.

Extensive lipolysis also occurs in blue cheese varieties, and in addition to making a direct contribution to flavor, the free fatty acids serve as substrates for fungal enzyme systems in the biosynthesis of methyl ketones, which are the principal contributors to the typical flavor of blue cheese (70). *P. roqueforti* lipase predominates the ripening of blue cheeses. However, blue cheese ripening may be accelerated and quality improved by the addition of exogenous lipases (71, 72).

Blue cheese is a popular ingredient for salad dressings and cheese dip. High-quality natural cheese is not normally required for these applications and there is considerable interest in the production of cheaper substitutes. Various methods have been developed for the production of blue cheese flavor concentrates; most of these methods involved the use of fungal lipases and usually *P. roqueforti* spores (1, 2, 73).

The low level of lipolysis that occurs in most other varieties is catalyzed by lipases/esterases derived from the starter or nonstarter lactic acid bacteria. Considerably more lipolysis occurs in cheeses made from raw milk than in pasteurized milk cheeses, possibly owing to the indigenous milk lipoprotein lipase and/or a more diverse nonstarter microflora in the former. It has been claimed that the flavor of many cheeses can be intensified or their ripening accelerated by incorporating PGE or fungal lipases, although their use appears to be very limited (1–3). Relatively extensive lipolysis occurs in Parmigiano-Reggiano, which can probably be attributed to the use of raw milk (which contains an indigenous lipase) and the long ripening time (2 years).

Lipases, probably mainly of fungal origin, are used in the production of some enzyme-modified cheeses (38).

B. Other Applications of Lipases

Lipases are used to hydrolyze milk fat for a variety of uses in the confectionery, candy, chocolate, sauce, and snack food industries. The partially hydrolyzed fat imparts a greater intensity of butterlike flavor to the products and delays stalling, presumably as a result of the emulsifying effect of di- and monoglycerides (56, 71, 74).

An important new application of lipases is in the trans/interesterification of fatty acids on triglycerides (75). This approach can be used to modify the melting point of triglycerides, and hence their rheological properties. An important application of this technology is in the production of cocoa butter substitutes for chocolate manufacture. Mono- or polyunsaturated fatty acids may also be introduced to relatively saturated milk lipids to improve their nutritional qualities. Immobilized lipase systems have been developed for these applications (74).

IV. β-GALACTOSIDASE

Lactose is a reducing disaccharide containing galactose and glucose linked by a β-1-4 O-glycosidic bond (O-β-D-galactopyranosyl-(1-4)-α- or β-D-glucopyranose, α- and β-lactose, respectively). Lactose is by far the dominant carbohydrate in milks which are, in turn, the only significant natural sources of lactose. The concentration of lactose in milk ranges from 0% in the milk of marine mammals to $\sim 10\%$ in milk from some species of monkey; bovine and human milk contain $\sim 4.8\%$ and 7% lactose, respectively. Lactose is an important source of energy for the newborn mammal, but when a very energy-dense milk is required (mammals in aquatic or polar environments), the lipid rather than the lactose content is increased. In fact, there is a fairly

good inverse relationship between the level of fat and that of lactose.

Among sugars, lactose possesses many fairly unique properties: low solubility ($\sim 18\,g/100\,mL$ H_2O at $20^\circ C$); a marked tendency to form supersaturated solutions which are difficult to crystallize; when crystallization does occur, the crystals are hard and sharp and, unless kept to dimensions $< 20\,\mu m$, cause a sandy texture in foods; crystallization is complicated by its mutarotation characteristics since α- and β-lactose differ considerably in solubility and degree of hydration; it has low sweetness (16% as sweet as sucrose at 1%, w/v); owing to its crystallization and mutarotation characteristics, it is hygroscopic and may cause "caking" of dairy powders; it has a strong tendency to absorb flavors and odors.

At $20^\circ C$, α-lactose is considerably less soluble ($\sim 7\,g/100\,g$ H_2O) than β-lactose ($\sim 50\,g/100\,g$ H_2O). However, the solubility of the α-anomer increases more sharply with increasing temperature than that of the β-anomer and the solubility curves intersect at $\sim 93.5^\circ C$; therefore, when lactose is crystallized at a temperature $< 93.5^\circ C$, α-lactose is obtained. α-Lactose crystallizes as a monohydrate while β-lactose crystals are anhydrous.

When milk is spray-dried, there is insufficient time for lactose to crystallize and an amorphous lactose glass is formed. If the moisture content of the powder is low, the glass is stable, but if the moisture content increases, the glass become hygroscopic, and lactose crystallizes as α-lactose monohydrate, leading to caking. In practice, the problem is solved by precrystallizing the lactose, usually induced by seeding with powdered lactose crystals.

When milk is frozen, the lactose usually does not have time to crystallize and the concentration of inorganic solutes in the liquid aqueous phase increases. On holding in the frozen state, calcium phosphate crystallizes as $Ca_3(PO_4)_2$, releasing H^+ and reducing the pH to ~ 5.8, and lactose crystallizes as α-lactose monohydrate, reducing the amount of solvent water, further increasing the concentration of inorganic solutes. The combination of low pH and high Ca^{2+} destabilizes the casein micelles which aggregate when the milk is thawed. Unless properly controlled, these characteristics of lactose may cause defects in concentrated, dehydrated, and frozen dairy products. However, some of the same characteristics may be exploited to make lactose an interesting and useful food additive—e.g., as a free-flowing agent, an agglomerating (instantizing) agent, an additive to stabilize color, flavor, and texture, especially when concomitant sweetness is undesirable, and as a reducing sugar in products in which Maillard browning is desirable as a source of color and flavor. The chemistry, properties, problems, modifications, and applications of lactose and lactose derivatives have been reviewed (76–85).

It is claimed that lactose promotes the intestinal absorption of calcium and phosphorus and hence should be nutritionally beneficial, especially in infant nutrition. However, lactose is involved in two enzyme deficiency diseases: lactose intolerance and galactosemia. There are in fact two forms of galactosemia, both arising from the congenital deficiency of an enzyme in their Leloir pathway for galactose metabolism (86). Classical galactosemia is due to a deficiency of galactose-1-phosphate:uridyl transferase. Ingested galactose (from lactose or other source) is phosphorylated to galactose-1-phosphate which is not metabolized further, leading to the accumulation of galactose and galactose-1-phosphate. Galactosemic infants appear normal at birth but develop various symptoms, including mental retardation, unless put on a galactose-free diet within 2–3 months. The second form, galactokinase-deficient galactosemia, results in the failure to phosphorylate galactose, some of which is metabolized to galactitol which accumulates in the eye, causing cataracts.

Disaccharides must be hydrolyzed to monosaccharides in the intestine prior to absorption, in the case of lactose by β-galactosidase. The vast majority of infants secrete adequate levels of β-galactosidase in the brush border of the small intestine to hydrolyze ingested lactose; however, a small minority of infants secrete an inadequate level of β-galactosidase. The level of intestinal β-galactosidase reaches a maximum shortly after birth and declines thereafter to a low level. With the exception of northwestern Europeans and a few African tribes, the level of intestinal β-galactosidase becomes so low within 6–8 years as to render the subject incapable of hydrolyzing ingested lactose at an adequate rate, leading to lactose intolerance. The unhydrolyzed lactose passes to the large intestine where it leads to flatulence, cramps, diarrhea, and possibly death. Thus, only a minority of the world's population can consume large quantities of lactose-containing foods with impunity. The subject of lactose intolerance has been reviewed extensively (87, 88).

The third feature of the lactose problem is the development of economic outlets for the large quantities ($\sim 5 \times 10^9\,kg/year$) available from cheese and casein wheys. The technology for lactose production is well developed but $< 10\%$ of the potentially available lactose is recovered as such; although lactose has a num-

ber of special food applications, the market appears to be limited. Increasing concern about environmental pollution has focused attention on more complete utilization of whey for which there are many options (76–85).

The dairy industry has developed methods for controlling the physicochemical problems posed by lactose, and lactose intolerance may not be too serious if lactose-containing products are introduced gradually to the diet. However, all the various problems posed by lactose (technological, nutritional, utilization) may be solved via hydrolysis by β-galactosidase (lactase) to the less problematic sugars, glucose and galactose.

β-Galactosidase (β-D-galactoside galactohydrolase; EC 3.2.1.23) catalyzes the hydrolysis of lactose to its component monosaccharides, glucose and galactose. The use of β-galactosidase in dairy technology has been considered as one of the most promising applications of exogenous enzymes in food processing. However, although many interesting applications have been demonstrated, the use of β-galactosidase has not yet become commercially successful for economic reasons. The voluminous literature on the preparation, properties, and uses of β-galactosidases has been the subject of several reviews (76, 81, 83, 89, 90).

Although β-galactosidase is widely distributed in plant, animal, and microbial sources, only the enzymes from *Aspergillus niger, A. oryzae, Kluyveromyces marxianus* var. *lactis, K. fragilis, Bacillus stearothermophilus*, and *Escherichia coli* are commercially available. β-Galactosidases from several sources have been isolated and characterized; the important properties have been summarized by Mahoney (89, 90). In general, β-galactosidases produced by molds have an acid pH optimum (2.5–4.5) and are therefore best suited for use in acid wheys, while yeast and bacterial β-galactosidases, with a pH optimum in the range 6–7.5, are more suitable for use in milk or rennet wheys. β-Galactosidases with high thermal stability have been isolated and are attractive because they can be used at high temperatures at which microbial growth is slow or absent. The heat stability of β-galactosidase from *K. lactis* and *Streptococcus thermophilus* is considerably greater in milk than in buffer systems owing to the combined effects of casein and lactose.

β-Galactosidases from several sources have been immobilized by encapsulation; entrapment in fibers, gels, or semipermeable membranes; adsorption or covalent attachment by a variety of techniques to various supports, e.g., porous glass, collagen, cellulose derivatives, and various resins (76, 83, 89, 90).

The principal applications of β-galactosidase in dairy technology are: (a) production of low-lactose milk and dairy products for β-galactosidase-deficient patients; (b) modification of dairy products for use in ice cream, baked goods, yogurt, etc.; (c) production of syrups and sweeteners for food applications; and (d) pretreatment of milk for freezing.

In spite of the widespread incidence of β-galactosidase deficiency among non-Caucasians, such subjects adjust to lactose-containing diets if lactose is introduced gradually and the response to lactose is moderated by other components in the diet. Researchers are divided as to the desirability of including milk in the diets of lactose-intolerant subjects (87, 88). However, it appears to be generally agreed that treatment with β-galactosidase would enhance the nutritional value of dairy products in such cases and render protein-rich dairy products suitable for supplementation of nutritionally deficient diets. Lactose-hydrolyzed milk is commercially available but is more expensive than normal milk. β-Galactosidase is also available in powder or liquid form for home use (89, 90). Direct addition of β-galactosidase to milk at mealtime ("enzyme replacement therapy") has also given satisfactory results. A promising method for reducing treatment cost is the addition of a very low level of soluble β-galactosidase to UHT milk which, during prolonged storage, induces extensive hydrolysis. This approach has been commercialized by the Tetra-Pak Company (Lund, Sweden). The increased sweetness of lactose-hydrolyzed milk does not appear to be a problem and may actually be preferred by some individuals.

β-Galactosidase can act as a transferase resulting in the synthesis of several oligosaccharides (galacto-oligosaccharides), the range and concentration of which appear to vary with the source of the β-galactosidase and the duration of treatment. Many of the oligosaccharides are β-(1 → 6) galactosides which are not hydrolyzed in the small intestine and pass into the large intestine where they are acted on by bacteria leading to intestinal disturbances, mainly flatulence. However, galacto-oligosaccharides stimulate the growth of *Bifidobacterium* spp. in the lower intestine, which is believed to be beneficial. A product (oligonate, 6′-galactosyl lactose) is produced commercially by the Yokult Company in Japan for addition to infant formulae. Some galacto-oligosaccharides have interesting functional properties and may find commercial applications (91, 92).

Hydrolysis of lactose in milk for yogurt has been suggested as a means of increasing the sweetness of yogurt without a concomitant increase in calories; it

is reported to reduce fermentation time (89, 90). Some authors have reported that lactose-hydrolyzed yogurt has superior texture and consistency, with less wheying off, than controls. Off-flavors have been reported in some lactose-hydrolyzed yogurts, perhaps owing to the action of contaminating proteinases. Yogurt and other cultured milks are well tolerated by lactose-intolerant subjects, apparently owing to the secretion of β-galactosidase by the thermophilic culture used or to slower gastric emptying (88).

It is also claimed that the manufacturing time for Cheddar and other cheeses is reduced by pretreatment of cheese milk with β-galactosidase, and, possibly more significantly, the quality of the cheese is improved and ripening accelerated. However, a proteinase present in the commercial β-galactosidase preparations used, rather than to the action of β-galactosidase, was probably responsible for the accelerated ripening.

Hydrolysis of lactose improves the functionality of milk powder in bakery products. The glucose moiety is fermentable by baker's yeast (*Saccharomyces cerevisiae*), leading to increased loaf volume, while the nonfermentable galactose contributes to flavor and crust color through Maillard browning. Prehydrolysis of lactose using β-galactosidase renders milk stable to freezing (89, 90, 93).

Dulce de Leche, a sweetened concentrated dairy product, is popular in Latin America as a dessert or spread. Lactose crystallization is a major problem in this highly concentrated product. Growth of *K. marxianus* var. *lactis* in milk for the preparation of Dulce de Leche has been recommended for the control of lactose crystallization (94). About 50% of the lactose was hydrolyzed in 12 h (at 5.2×10^7 cells/mL) or 100% in 24 h. When the delactosed milk was mixed in proportions of 1 : 2 with normal milk and concentrated, no lactose crystallization and no significant changes in flavor were noted. The use of permeabilized *K. marxianus* var. *lactis* cells for the same application was found to be very satisfactory (95). Presumably, isolated β-galactosidase could be used successfully in the preparation of Dulce de Leche.

Lactose crystallization may also be a problem in conventional sweetened condensed milk, although the problem can be controlled by appropriate manufacturing steps. Prehydrolysis with β-galactosidase offers an alternative solution.

Treatment with β-galactosidase prevented lactose crystallization in a whey retentate–buttermilk powder spread (96). Acid (mold) β-galactosidase was preferable to neutral (yeast) enzyme, and hydrolysis of 30% of the lactose was sufficient. Lactose-hydrolyzed whey appears to be suitable for incorporation into ice cream in which up to 25% of the skim milk solids may be replaced by hydrolyzed whey syrup without adverse effects on quality; 50% of the sucrose may also be replaced by whey syrup (89, 90, 97). Lactose-hydrolyzed whey may be fed in larger amounts than normal whey to animals, especially pigs.

Probably the principal commercial interest in β-galactosidase is for the production of syrups as a profitable outlet for lactose. Glucose-galactose syrups are $\sim 70\%$ as sweet as sucrose and about four times sweeter than lactose. It has been known for a long time that lactose can be hydrolyzed to glucose and galactose by strong mineral acids, and there has been renewed commercial interest in the process, using free acid or ion exchange resins, as a means of producing glucose-galactose syrups. Production costs are reported to be lower than for enzymatic hydrolysis, but acid hydrolysis is applicable only to purified lactose solutions or perhaps ultrafiltration permeates.

Numerous applications have been reported for glucose-galactose syrups (in addition to the use of lactose-hydrolyzed whey) (83, 89, 90). Although effective systems for the production of glucose-galactose syrups and other lactose-hydrolyzed products are available and continued research will undoubtedly lead to improved systems, the cost of such syrups vis-à-vis alternatives, mainly glucose syrups from starch, remains a problem.

The sweetness of glucose-galactose syrups may be increased by isomerizing the glucose to fructose (which is about twice as sweet as glucose) using glucose isomerase, which is now widely used in the commercial production of high-fructose syrups from starch. Such a system has been patented and a glucose-fructose-galactose-lactose syrup with a sweetness equal to sucrose (both at 10% solution) has been prepared by treating a glucose-fortified lactose hydrolyzate with glucose isomerase. Conversion of lactose to lactulose offers another avenue for the production of novel sugar mixtures. Lactulose is a disaccharide consisting of galactose and fructose, which can be produced from lactose by mild alkaline treatment. At least some β-galactosidases can hydrolyze lactulose, although more slowly than lactose.

It will be apparent that β-galactosidase has numerous applications in the dairy industry. However, in spite of very considerable research and demonstrated technological feasibility in pilot-scale experiments, β-galactosidase is not yet exploited commercially on a significant scale, except for lactose-hydrolyzed pasteurized and UHT milks. Zadow (98) concluded that the

markets for lactose-hydrolyzed syrups are likely to remain limited for economic reasons.

V. LYSOZYME

Lysozyme (muramidase, EC 3.2.1.17), an enzyme which causes lysis of certain bacteria by hydrolyzing cell wall polysaccharides, is widely distributed in animal tissues and secretions. Some bacteria and bacteriophage secrete similar enzymes, lysins. Egg white is a particularly rich source of lysozyme, which is the best characterized of these enzymes. The molecular and biological properties of lysozyme and its use in food preservation and as a pharmaceutical have been comprehensively reviewed by Proctor and Cunningham (99) and Cunningham et al. (100).

The milks of most species contain an indigenous lysozyme; human and equine milks are particularly rich in this enzyme. Various aspects of indigenous milk lysozyme were reviewed by Farkye (101, 102).

In view of its antibacterial activity, the large difference in lysozyme content between human and bovine milks may have significance in infant nutrition. It is claimed that supplementation of baby food formulae based on cows' milk with egg-white lysozyme gives beneficial results, especially with premature babies; however, results are equivocal (1).

Lysozyme has some other minor applications in dairy technology, but most current interest is focused on its use in Dutch, Swiss, Italian, and other cheese varieties to prevent late gas blowing and/or off-flavors caused by the growth of *Clostridium tyrobutyricum*. Contamination of cheese milk with *Clostridium* spp. can be reduced by good hygienic practices, and populations may be further reduced by bactofugation or microfiltration. However, in most countries it is normal practice to add sodium nitrate as a further precaution. The use of nitrate in foods is suspect because it leads to nitrosamine formation, and many countries have reduced permitted levels or prohibited its use.

Lysozyme is effective in killing *Clostridium* cells and preventing the outgrowth of their spores. It has been shown to be an effective alternative to nitrate in preventing the butyric acid fermentation and late gas blowing in several cheese varieties (1, 2, 99, 100, 103, 104). It was concluded (103, 104) that

> the published information indicates that for some cheese types, lysozyme is a suitable substance for the control of late blowing, provided the number of clostridial spores is low. For these cheese types, which may be considered less sensitive to late blowing, the level of lysozyme already permitted by regulatory authorities in a number of countries appears to be satisfactory until further evidence is obtained. Lysozyme appears to be of value in the control of late blowing in countries which prohibit nitrate. Published information indicates that in some cheese types which are very sensitive to late blowing, such as Gouda, lysozyme used at the current normal addition under normal manufacturing and storage conditions is less effective than the usual amount of nitrate. In this case, lysozyme can not be considered a suitable alternative to nitrate at present. More information will become available for the various cheese types about the critical number of spores in the raw milk to cause defects when lysozyme is used. Combinations of lysozyme addition and other control measures can then be evaluated further.

Lysozyme appears to be quite effective against *Listeria monocytogenes* and other bacteria involved in foodborne diseases and food spoilage (105). Considering the widespread attention now focused on *Listeria* in dairy products, especially cheeses, it is likely that this application of lysozyme will be the subject of further research. The preservative effects of lysozyme in other foods were reviewed by Proctor and Cunningham (99) and Cunningham et al. (100). It is possible that some of these may be applicable to dairy products.

VI. GLUCOSE OXIDASE

Glucose oxidase (GO) catalyzes the oxidation of glucose to gluconic acid (via gluconic acid-δ-lactone) according to the following reactions (106):

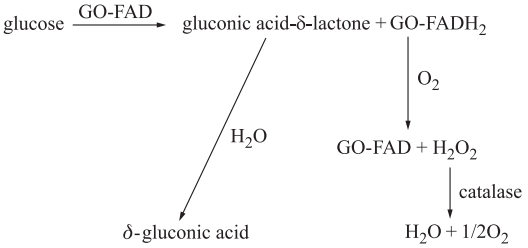

The hydrogen peroxide formed is normally reduced by catalase present as a contaminant in commercial preparations of GO (from *P. notatum, P. glaucum*, or *A. niger*) or added separately. GO, which has a pH optimum ~ 5.5, is highly specific for D-glucose and is used to assay specifically for D-glucose in the presence of other sugars, blood, urine, etc.

In the food industry, GO has four principal applications, which are not commercially very significant, especially in the dairy industry (1, 106, 107):

1. *Removal of residual, trace levels of glucose.* This application, which is particularly useful for the treatment of egg white prior to dehydration (although an alterative procedure using yeast fermentation is more commonly used), is of little if any significance in dairy technology.

2. *Removal of trace levels of oxygen.* Traces of oxygen in wines and fruit juices cause discoloration and/or oxidation of ascorbic acid. Chemical reducing agents may be used to scavenge oxygen, but enzymatic treatment with GO may be preferred. The GO system has been proposed as an antioxidant for high-fat products, such as mayonnaise, butter, and whole milk powder, but it does not appear to be used commercially for this purpose, probably because of cost vis-à-vis chemical antioxidants (if permitted) and the relative effectiveness of inert gas flushing of canned milk powder.

3. *Generation of hydrogen peroxide in situ.* The hydrogen peroxide generated by glucose oxidase has a direct bacteriocidal effect (which is a useful side effect of GO applied to egg products), but its bacteriocidal properties can be much more effectively exploited as a component of the lactoperoxidase/hydrogen peroxide/thiocyanate system (see Sec. X). Two components of this system occur naturally in milk: lactoperoxidase is present at ~ 30 mg/L, and thiocyanate, produced in the rumen by hydrolysis of thioglucosides from members of the Brassicae family, varies from 0.017 to 0.26 mM. Hydrogen peroxide does not occur naturally in bacteria-free milk, but it can be generated metabolically by catalase-negative bacteria, added directly (which is usually preferred) or produced in situ from sodium percarbonate or by the action of xanthine oxidase on added hypoxanthine or by the action of glucose oxidase on glucose, either added or produced in situ from lactose by β-galactosidase. Activation of the lactoperoxidase–hydrogen peroxide–thiocyanate system suppresses the growth of psychrotrophs in milk stored at 5°C and has given promising results as a milk preservative in tropical regions where refrigeration is lacking. It would appear that in such applications the use of exogenous hydrogen peroxide is the simplest and most appropriate.

4. *Production of acid in situ.* Direct acidification of dairy products, particularly cottage, feta-type, and mozzarella cheeses, is now fairly common. Acidification is normally performed by addition of acid or acidogen (usually gluconic acid-δ-lactone) or by a combination of acid and acidogen. In situ production of gluconic acid from added glucose or from glucose produced in situ from lactose by β-galactosidase or from added sucrose by invertase has been proposed (108). It is possible to produce gluconic acid from glucose using immobilized glucose oxidase. However, it is doubtful whether immobilized glucose oxidase could be applied to the acidification of milk because of the high probability of fouling by precipitated protein even if low temperatures at which less extensive casein precipitation occurs were used.

VII. SUPEROXIDE DIMUTASE

Superoxide dismutase (SOD) catalyzes the reduction of superoxide anions, O_2^-, according to the following:

$$2O_2^- + 2H^+ \longrightarrow H_2O_2 + O_2 \qquad (2)$$

The hydrogen peroxide formed may be reduced by catalase, peroxidase, or a suitable reducing agent. SOD occurs widely in tissues where it plays a major antioxidant role in scavenging superoxide radicals which are produced through the action of several enzymes, e.g., XO and peroxidases.

Milk contains a low level of indigenous SOD which has been isolated and characterized (101, 102); the milk enzyme appears to be identical to SOD from bovine erythrocytes. The level of indigenous SOD in milk, which is entirely in the skim phase, varies considerably among individual cows, with stage of lactation and mastitic infection. It may play a role in the oxidative stability of milk, but attempts to correlate stability with SOD activity have been inconclusive, presumably owing to the interaction of various pro- and antioxidants. The tendency of fat in milk to oxidize is directly correlated with increases in XO and negatively with increases in SOD activity. A low level of exogenous SOD, together with catalase, is a very effective antioxidant in dairy products, and it has been suggested that treatment of milk with SOD may be effective in preserving the flavor of UHT milk which is prone to lipid oxidation (1). It has been reported that a combination of SOD and catalase is a more effective antioxidant than butylated hydroxyanisole. However, it appears to be ineffective as an antioxidant in the presence of 0.1 ppm Cu^{2+}, apparently because Cu^{2+} effectively competes with SOD for O_2^- and converts it to lipid-reactive species such as $^{\bullet}OH$. The commercial feasibility of using SOD as an antioxidant depends on cost, particularly vis-à-vis chemical antioxidants, if permitted. As far as is known, SOD is not used commercially as an antioxidant in the dairy industry.

VIII. SULFHYDRYL OXIDASE

Milk contains an enzyme capable of oxidizing sulfhydryl groups to disulfides:

$$2RSH + O_2 \longrightarrow RSSR + H_2O \quad (3)$$

The enzyme, which has molecular and catalytic properties distinctly different from thioloxidase (EC 1.8.3.2), glutathione:protein disulfide oxidoreductase (EC 1.8.4.2), and protein disulfide isomerase (EC 5.3.4.1), has been isolated and well characterized (101, 102). Sulfhydryl oxidase (EC 1.8.3.–) also has been demonstrated in human milk.

It has been proposed that sulfhydryl oxidase has a physiological role in the formation of disulfide bonds in vivo to give proteins the correct three dimensional structure. Industrially, the potential of the enzyme lies in its ability to ameliorate the cooked flavor of UHT-treated milk (1, 109). The milk enzyme occurs exclusively in the serum (whey) from which it may be easily isolated by exploiting its marked tendency to aggregate, thus facilitating its isolation by chromatography on porous glass. The enzyme has been immobilized on porous glass and titanium oxide, and its effectiveness in ameliorating the cooked flavor of UHT-treated milk has been demonstrated on a pilot scale using immobilized enzyme columns. For industrial-scale use, an adequate supply of the enzyme from whey may be a limitation but production of the enzyme by genetically engineered microorganisms might be feasible.

IX. CATALASE

$$2H_2O_2 \longrightarrow 2H_2O + O_2 \quad (4)$$

Hydrogen peroxide is used for the cold-sterilization of milk in regions lacking refrigeration and perhaps in some developed countries also; e.g., it may be used to treat cheese milk in the United States (1, 107). In underdeveloped regions, treatment of milk with H_2O_2 is performed at ambient temperature and excess H_2O_2 is reduced by indigenous milk catalase or by chemical interaction with milk proteins in which it causes some physicochemical changes, principally oxidation of methionine, with adverse effects on cheese quality. Side effects can be decreased by short exposure to H_2O_2 at $\sim 65^{\circ}C$, after which the residual H_2O_2 is reduced by added catalase, usually from beef liver or *Aspergillus niger*. Most of the recent interest in the use of H_2O_2 as a preservative for milk has focused on the lactoperoxidase-H_2O_2-thiocyanate system in which low concentrations of H_2O_2 are required (see Sec. X). However, at 400 mg/kg, H_2O_2 alone is a more effective long-term bactericidal agent than 8.5 mg/kg H_2O_2 in the lactoperoxidase system. There was no significant difference in the quality of cultured milk made from either lactoperoxidase-activated or H_2O_2-treated milk. The activity of lactic starter was significantly lower in the former, but the rennet coagulability of the latter was extended.

There is interest in using immobilized catalase reactors for milk pasteurization or for glucose oxidase-catalase reactors. Although catalase may be readily immobilized, it is inactivated rapidly on exposure to hydrogen peroxide. Hydrogen peroxide appears to be an effective agent for inactivation of aflatoxin M_1. As discussed above, catalase, usually as a contaminant, is necessary for many of the applications of glucose oxidase and also to optimize the antioxidative properties of SOD.

X. LACTOPEROXIDASE

$$H_2O_2 + 2AH \longrightarrow 2H_2O + 2A \quad (5)$$

Bovine milk is rich in lactoperoxidase ($\sim 30\,\mu g/mL$), which is distinct from the myloperoxidase of leucocytes and salivary peroxidase. Lactoperoxidase has been purified by several investigators and well characterized (109–112).

The most important physiological and technological feature of lactoperoxidase is its ability, in the presence of H_2O_2 and thiocyanate, to inhibit the growth of several bacteria. Since lactoperoxidase is relatively heat resistant, there is adequate lactoperoxidase activity even in milk that has been moderately to severely heat-treated. Thiocyanate occurs in many animal tissues and fluids. It is produced endogenously during the detoxification of thiosulfates and metabolic products of sulfur amino acids and cyanide and from foods containing thioglucosides. Cows on pastures containing clover (rich in RCN) and nongrasses (e.g., Cruciferae containing thioglucosides) yield milk containing higher concentrations of thiocyanide than cows on winter feed or lay pastures. Saliva contains high levels of thiocyanate which is also secreted by gastric mucosal cells. Milk does not contain indigenous H_2O_2 but it may be added or produced in situ (see Sec. VI). Thus, bovine milk possesses an effective antibacterial system which probably affects the intestinal microflora of calves (and presumably other species). Lactoperoxidase also appears to protect the mammary

gland against mastitic infection, especially during the dry period. The antibacterial significance of lactoperoxidase in vivo has been reviewed (113, 114). Human milk appears to contain a low level of lactoperoxidase ($< 0.1\,\mu g/mL$) as well as myloperoxidase and eosinophil peroxidase. The lactoperoxidase system may be exploited in vitro to extend the shelf life of milk under conditions where refrigeration and pasteurization facilities are lacking (111–114).

While most interest in lactoperoxidase has focused on the indigenous enzyme, it may also acquire significance as an exogenous enzyme. Techniques have been developed for the commercial-scale purification of lactoperoxidase from milk (42). Large-scale trials have shown that addition of purified lactoperoxidase to calf milk replacers markedly reduces the incidence of diarrhea and increases weight gain. Although the antibacterial properties of human milk do not depend on lactoperoxidase, its addition to bovine milk-based infant formulae may have beneficial effects (111–114).

XI. TRANSGLUTAMINASE

Transglutaminase (TGase; protein-glutamine γ-glutamyltransferase; EC 2.3.2.13) catalyzes an acyl transferase reaction between the γ-carboxyamide group of peptide-bound glutamine residues (acyl donors) and a variety of primary amines (acyl acceptors), including amino acids, and the ε-amino group of lysine residues in certain proteins. In the absence of an amine, TGase catalyzes the deamination of glutamine residues, with water molecules acting as acyl acceptors. Thus, TGase can modify proteins by incorporation of (a) an amine, (b) crosslinking, or (c) deamination:

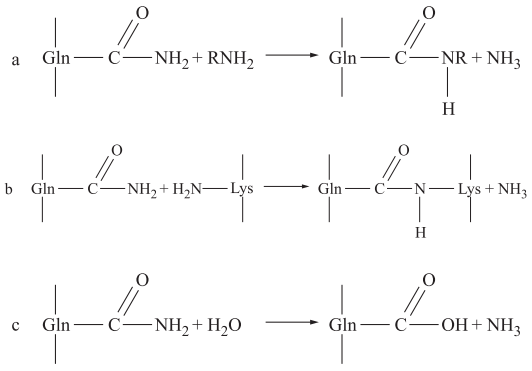

The amino group might be from a simple aliphatic or aromatic amine, an amino acid, an amino sugar, or a phospholipid (β-aminoethanol moiety).

TGase is present in several animal tissues and body fluids and is involved in several biological phenomena, including blood clotting, wound healing, keratinization of epidermal tissue, and stiffening of cell membranes. An enzyme with a similar activity has been found in the bacterium *Streptoverticillium mobaraense*; this is referred to as MTGase (M = microbial). However, TGase and MTGase differ in a number of respects, most notably in molecular weight (~ 77 and ~ 38 kDa, respectively) and dependence on Ca^{2+}; TGase requires Ca^{2+}, MTGase does not.

The activity of (M)TGase suggests several possible applications in the food industry:

1. Gelation of proteins by crosslinking
2. Formation of restructured meat and fish products from smaller pieces or comminuted meats
3. Stabilization of protein-stabilized foams or emulsions (by crosslinking proteins in the stabilizing layer)
4. Modification of the functionality, e.g., solubility or water binding, of proteins by converting glutamine to glutamic acid residues or binding of amino sugars or phospholipids
5. Modification of the nutritional value of foods by enzymatically attaching essential amino acids to proteins
6. Conjugation of the same or different proteins
7. Conjugation of amino sugars with proteins
8. Conjugation of phospholipids with proteins
9. Immobilization of enzymes

The feasibility of these applications has been demonstrated in laboratory studies, but the limited availability and cost of the enzyme to date have restricted larger-scale trials (guinea pig liver is the usual source of TGase). However, the gene for TGase has been inserted into microorganisms (115) which would be expected to increase the availability and reduce the cost of the enzyme.

Various aspects of the chemistry of TGase and its applications in foods have been reviewed by Motoki and Seguro (116) and Dickinson (117).

XII. β-LACTAMASE

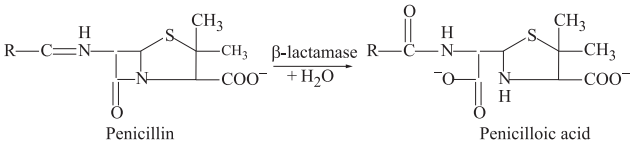

(9)

Residues of penicillin in milk, resulting from treatment of mastitis-infected cows with antibiotics, inhibit or

prevent the growth of lactic acid bacteria used in the production of cheese and fermented milks. They may also evoke an allergic response in susceptible consumers and create conditions for the selection of penicillin-resistant pathogens. The usual approach taken to prevent contamination of the milk supply with antibiotics is to withhold milk from treated cows for an adequate period after treatment; obviously, this results in economic losses to farmers.

Procedures developed for the removal of β-lactam-type antibiotics from milk include columns of activated charcoal, ultrafiltration or diafiltration (1). While these methods may be suitable under certain circumstances, they have obvious limitations. An alternative approach is the inactivation of penicillin by β-lactamase [Eq. (9)].

Korycka-Dahl et al. (118) demonstrated the ability of β-lactamase from *Bacillus cereus* to inactivate penicillin G such that Cheddar or Swiss cheeses of normal quality could be produced from the decontaminated milk. The enzyme was active at 4°C so that penicillin in milk could be inactivated during cold storage on the farm or at the factory. The enzyme lost only 50% of its activity following heating at 63°C for 30 min and hence would retain considerable activity in pasteurized milk, which may be illegal. These problems may be solved by using immobilized β-lactamase (119). This procedure appears promising and awaits further development.

An alternative approach to solving the problems caused by penicillin in fermented products is the selection of β-lactamase-producing mutants of lactic acid bacteria (120).

XIII. PERSPECTIVES

Owing to the physicochemical properties of its constituents, milk is very amenable to enzymatic modification and it will be apparent from the foregoing that many potential applications of enzymes in dairy technology exist. However, in spite of numerous studies, only a few of these applications are commercially significant. Many of the potential applications are unsuccessful commercially because the proposed application is not sufficiently significant economically or alternative solutions are available.

By far the most important application is the use of rennets in cheese making, for which no alternative exists. It is likely that rennets will remain the principal enzyme in dairy technology for the foreseeable future. An unlimited supply of chymosin from genetically engineered microorganisms is now available; it is possible that the cheese-making properties of these microbial recombinant chymosins will be improved through genetic engineering. The production of cheese is expanding worldwide, and the market for rennets will therefore continue to increase. Development of cheese-like products as food ingredients is a growth area, and it is likely that the application of proteinases and lipases in the production of such products will increase. The use of proteinases and peptidases to produce protein hydrolysates with specific functional, nutritional, or physiological properties appears to be very promising and has been attracting increasing attention.

Lipases have some traditional and novel applications in cheese technology, but the growth potential of these applications is probably limited. However, new and more effective lipases may be identified. Perhaps the greatest potential application of lipases is in the production of tailor-made lipids with superior nutritional or functional properties.

Although β-galactosidase has applications in dairy technology, most of these are not commercially viable at present, mainly for economic reasons. Niche markets exist for lactose-hydrolyzed milks and these may expand. Exploitation of the transferase activity of β-galactosidase in the production of new oligosaccharides with novel functional and/or nutritional properties appears to hold potential.

Transglutaminase should have several interesting applications in dairy technology. The availability of a cheaper enzyme should encourage work on the application of this enzyme.

With the possible exception of lactoperoxidase and lysozyme, the other enzymes discussed in this chapter appear to have very limited application in dairy technology, at least under present circumstances.

REFERENCES

1. PF Fox, MB Grufferty. Exogenous enzymes in dairy technology. In: PF Fox, ed. Food Enzymology, Vol. 1. London: Elsevier Science Publishers, 1991, pp 219–269.
2. PF Fox. Exogenous enzymes in dairy technology—a review. J Food Biochem 17:173–199, 1993.
3. PF Fox, L Stepaniak. Enzymes in cheese technology. Int Dairy J 3:509–530, 1993.
4. RJ Brown. Dairy products. In: T Nagodawithana, G Reed, eds. Enzymes in Food Processing. New York: Academic Press, 1993, pp 347–361.
5. M Desmazeaud, E Spinnler. Laits et produits laitières. In: V Larreta-Garde, ed. Enzymes en Agroalimentaire. Paris: Lavoisier, 1997, pp 48–76.

6. PF Fox, ed. Advanced Dairy Chemistry. 1. Proteins. London: Elsevier Science Publishers, 1992.
7. DM Mulvihill. Production, functional properties and utilization of milk proteins. In: PF Fox, ed. Advanced Dairy Chemistry. 1. Proteins. London: Elsevier Applied Science, 1992, pp 369–404.
8. DG Dalgleish. Enzymatic coagulation of milk. In: PF Fox, ed. Advanced Dairy Chemistry. 1. Proteins. London: Elsevier Science, 1992, pp 579–619.
9. DG Dalgleish. The enzymatic coagulation of milk. In: PF Fox, ed. Cheese: Chemistry, Physics and Microbiology, Vol. 1. London: Elsevier Applied Science, 1987, pp. 63–96.
10. PF Fox. Proteolysis and protein-protein interactions in cheese manufacture. In: BFJ Hudson, ed. Developments in Food Proteins 3. London: Elsevier Applied Science, 1984, pp 69–112.
11. PF Fox. Coagulants and their action. Proceedings of the 22nd International Dairy Congress, The Hague. Dordrecht: Reidel Publishing, 1987, pp 61–73.
12. PF Fox. Rennets and their action in cheese manufacture and ripening. Biotechnol Appl Biochem 10:522–535, 1988.
13. PF Fox, DM Mulvihill. Casein. In: P Harris, ed. Food Gels. London: Elsevier Applied Science, 1990, pp 121–173.
14. PF Fox, PLH McSweeney. Rennets and their role in milk coagulation and cheese ripening. In: BA Law, ed. Microbiology and Biochemistry of Cheese and Fermented Milk, 2nd ed. London: Blackie Academic & Professional, 1997, pp 1–49.
15. B Foltmann. General and molecular aspects of rennets. In: PF Fox, ed. Cheese: Chemistry, Physics and Microbiology, Vol. 1, 2nd ed. London: Chapman & Hall, 1992, pp 37–68.
16. B Foltmann. Chymosin: a short review on foetal and neonatal gastric proteases. Scand J Clin Lab Invest 52(suppl 210):65–79, 1992.
17. S Chitpinityol, MJC Crabbe. Chymosin and aspartic proteinases. Food Chem 61:395–418, 1998.
18. JH Nelson. Impact of new milk clotting enzymes on cheese technology. J Dairy Sci 58:1739–1750, 1975.
19. M Sternberg. Microbial rennets. Adv Appl Microbiol 20:135–157, 1976.
20. ML Green. Review of the progress of dairy science: milk coagulants. J Dairy Res 44:159–188, 1977.
21. JA Phelan. Milk coagulants: an evaluation of alternatives to standard calf rennet. PhD thesis, National University of Ireland, Cork, 1986.
22. M Teuber. Production of chymosin (EC 3.4.23.4) by microoganisms and its use for cheesemaking. Bulletin 251. Brussels: International Dairy Federation, 1990, pp 3–15.
23. International Dairy Federation. Fermentation-produced enzymes and accelerated ripening in cheesemaking. Bulletin 269. Brussels: Int Dairy Federation, 1992.
24. A Carlson, GC Hill, NF Olson. The coagulation of milk with immobilized enzymes: a critical review. Enz Microbiol Technol 8:642–650, 1986.
25. PF Fox, J Law, PLH McSweeney, J Wallace. Biochemistry of cheese ripening. In; PF Fox, ed. Cheese: Chemistry, Physics and Microbiology, 2nd ed. London: Chapman and Hall, 1993, pp 389–438.
26. PF Fox, TP O'Connor, PLH McSweeney, TP Guinee, NM O'Brien. Cheese: physical, biochemical and nutritional aspects. Adv Food Nutr Res 39:163–328, 1996.
27. PF Fox, JM Wallace. Formation of flavor compounds in cheese. Adv Appl Microbiol 45:17–85, 1997.
28. R Grappin, TC Rank, NF Olson. Primary proteolysis of cheese proteins during ripening. J Dairy Sci 68:531–540, 1985.
29. TC Rank, R Grappin, NF Olson. Secondary proteolysis of cheese during ripening: a review. J Dairy Sci 68:801–805, 1985.
30. BA Law. Proteolysis in relation to normal and accelerated cheese ripening. In: PF Fox, ed. Cheese: Chemistry, Physics and Microbiology, Vol. 1. London: Elsevier Applied Science, 1987, pp 365–392.
31. PF Fox. Proteolysis in cheese during manufacturing and ripening. J Dairy Sci 72:1379–1400, 1989.
32. IDF. Chemical methods for evaluating proteolysis in cheese maturation. Bulletin 261. Brussels: International Dairy Federation, 1991.
33. PF Fox, PLH McSweeney. Proteolysis in cheese during ripening. Food Rev Int 12:457–509, 1996.
34. ERS Kunji, I Mierau, A Hagting, B Poolman, WN Konings. The proteolytic systems of lactic acid bacteria. Antonie van Leeuwenhoek 70:187–221, 1996.
35. DM Rea. Comparison of Cheddar cheese made with chymosin, *Rhizomucor miehei* proteinase or *Cryphonectria parasitica* proteinase. MSc thesis, National University of Ireland, Cork, 1997.
36. PF Fox, JM Wallace, S Morgan, CM Lynch, EJ Niland, J Tobin. Acceleration of cheese ripening. Antonie van Leeuwenhoek 70:271–279, 1996.
37. PF Fox, PLH McSweeney, CM Lynch. Significance of non-starter lactic acid bacteria in Cheddar cheese. Aust J Dairy Technol 53:83–89, 1998.
38. KN Kilcawley, MG Wilkinson, PF Fox. Enzyme-modified cheese: a review. Int Dairy J 8:1–10, 1998.
39. J Adler-Nissen. Enzymatic Hydrolysis of Food Proteins. London: Elsevier Applied Science, 1986.
40. PF Fox, PA Morrissey, DM Mulvihill. Chemical and enzymatic modification of food proteins. In: BJF Hudson, ed. Developments in Food Proteins 1. London: Applied Science Publishers, 1982, pp 1–60.
41. JL Maubois. Separation, extraction and fractionation of milk protein components. Le Lait 64:485–495, 1984.
42. PF Fox, DM Mulvihill. Developments in milk protein processing. Food Sci Technol Today 7:152–161, 1993.

43. DD Kitts, YV Yuan. Caseinophosphopeptides and calcium bioavailability. Trends Food Sci Technol 3:31–35, 1992.
44. JL Maubois, J Leonil. Peptides du lait a activité biologique. Le Lait 69:245–269, 1989.
45. MA Juillerat, R Baechler, R Berrocal, S Chanton, J-C Scherz, R Jost. Tryptic phosphopeptides from whole casein: preparation and analysis by fast protein liquid chromatography. J Dairy Res 56:603–611, 1989.
46. D McDonagh, RJ Fitzgerald. Production of caseinophosphopeptides (CCPs) from sodium caseinate using a range of commercial protease preparations. Int Dairy J 8:39–45, 1998.
47. J Dziuba, P Minkiewiez. Influence of glycosylation on micelle-stabilizing ability and biological properties of C-terminal fragments of cow's κ-casein. Int Dairy J 6:1017–1044, 1996.
48. MH Abd El-Salam, S El-Shibiny, W Buchheim. Characteristics and potential uses of casein macropeptide. Int Dairy J 6:327–341, 1996.
49. SC Marshall. Casein macropeptide from whey—a new product opportunity. CSIRO Food Res Q 51:86–91, 1991.
50. PF Fox, A Flynn. Biological properties of milk proteins. In: PF Fox, ed. Advanced Dairy Chemistry. 1. Proteins. London: Elsevier Science, 1992, pp 255–284.
51. D Migliore-Samour, P Jolles. Casein, a prohormone with an immuno-modulating role for the newborn? Experimentia 44:188–199, 1988.
52. PF Fox, ed. Developments in Dairy Chemistry. 4. Functional Milk Proteins. London: Elsevier Applied Science, 1989.
53. A Kilara. Enzyme-modified protein food ingredients. Process Biochem 20(5):149–157, 1985.
54. S Nakai, E Li-Chan. Chemical and enzymatic modification of milk proteins. In: PF Fox, ed. Developments in Dairy Chemistry. 4. Functional Milk Proteins. London: Elsevier Applied Science, 1989, pp 347–376.
55. ZY Ju, J Otte, M Zakora, KB Qvist. Enzyme-induced gelation of whey proteins: effect of protein denaturation. Int Dairy J 7:71–78, 1997.
56. JH Nelson, RG Jensen, RE Pitas. Pregastric esterase and other oral lipases—a review. J Dairy Sci 60:327–362, 1977.
57. HJ Lee, NF Olson, DS Ryan. Characterization of pregastric esterase. J Dairy Sci 63:1834–1838, 1980.
58. BJ Sweet, LC Matthews, T Richardson. Purification and characterization of pregastric esterase from calf. Arch Biochem Biophys 234:144–150, 1984.
59. S Bernback, O Hernell, L Blackberg. Purification and molecular characterization of bovine pregastric lipase. Eur J Biochem 148:233–238, 1985.
60. IM Roberts, P Jacobson, J Cornette. Secondary structures of rat lipolytic enzymes: circular dichroism and relation to hydrophobic enzymes: circular dichroism and relation to hydrophobic moments. Biochem Biophys Res Commun 162:95–101, 1989.
61. AJP Docherty, MW Bodiner, S Angal, R Verger, C Riviere, PA Lowe, A Lyons, JS Emtage, TJR Harris. Molecular cloning and nucleotide sequence of rat lingual lipase cDNA. Nucleic Acids Res 13:1891–1903, 1985.
62. JK Ha, RC Lindsay. Release of volatile branched-chain and other fatty acids from ruminant milk fats by various lipases. J Dairy Sci 76:677–690, 1993.
63. JK Ha, RC Lindsay. Influence of a_w on volatile free fatty acids during storage of cheese bases lipolyzed by kid goat pregastric esterase. Int Dairy J 2:179–195, 1992.
64. RV Chaudhari, GH Richardson. Lamb gastric lipase and protease in cheese manufacture. J Dairy Sci 54:467–471, 1971.
65. HJ Peppler, JG Dooley, HT Huang. Flavor development in Fontina and Romano cheese by fungal esterase. J Dairy Sci 59:859–862, 1976.
66. GT Moskowitz, SS Noelck. Enzyme-modified cheese technology. J Dairy Sci 70:1761–1769, 1987.
67. K Kornacki, L Stepaniak, I Adamiec, J Grabska, K Wroma. Characteristics of lipolytic mould preparations as compared to hog pancreatic lipase. Milchwissenschaft 34:340–343, 1979.
68. M De Felice, T Gomes, T de Leonardis. Addition of animal and microbial lipases to curd. Effects on free fatty acid composition during ripening. Le Lait 71:637–643, 1991.
69. MW Arbige, PR Freund, SC Silver, JT Zelro. Novel lipase for Cheddar cheese development. Food Technol 40(4):91–98, 1986.
70. J-C Gripon. Mould-ripened cheeses. In: PF Fox, ed. Cheese: Chemistry, Physics and Microbiology, Vol. 2, 2nd ed. London: Chapman & Hall, 1993, pp 111–136.
71. RS Arnold, KM Shahani, BK Dwivedi. Application of lipolytic enzymes to flavor development in dairy products. J Dairy Sci 58:1127–1143, 1975.
72. RC Jolly, FV Kosikowski. Flavor development in pasteurized milk blue cheese by animal and microbial lipase preparations. J Dairy Sci 58:846–852, 1975.
73. A Tomasini, G Bustillo, J-M Lebault. Production of blue cheese flavour concentrates from different substrates supplemented with lipolyzed cream. Int Dairy J 5:247–257, 1995.
74. A Kilara. Enzyme-modified lipid food ingredients. Process Biochem 20(2):35–45, 1985.
75. J Grailli. Les enzymes en lipotechnie. In: V Larreta-Garde, ed. Enzymes en Agroalimentaire. Paris: Lavoisier, 1997, pp 246–257.
76. TP Shukla. β-Galactosidase technology: a solution to the lactose problem. CRC Crit Rev Food Technol 5:325–356, 1975.

77. PG Hobman. Review of processes and products for utilization of lactose in deproteinized milk serum. J Dairy Sci 67:2630–2653, 1984.
78. JG Zadow. Lactose: properties and uses. J Dairy Sci 67:2654–2679, 1984.
79. HW Modler. Functional properties of nonfat dairy ingredients—a review. Modification of lactose and products containing whey proteins. J Dairy Sci 68:2206–2214, 1985.
80. PF Fox, ed. Developments in Dairy Chemistry. 3. Lactose and Minor Constituents. London: Elsevier Applied Science, 1985.
81. International Dairy Federation. Trends in Whey Utilization. Bulletin 212. Brussels: Int Dairy Federation, 1987.
82. VH Holsinger. Lactose. In: NP Wong, ed. Fundamentals of Dairy Chemistry, 3rd ed. New York: Van Nostrand Reinhold, 1988, pp 279–342.
83. International Dairy Federation. Proceedings of the IDF Workshop on Lactose Hydrolysis. Bulletin 289. Brussels: Int Dairy Federation, 1993.
84. ST Yang, EM Silva. Novel products and new technologies for use of a familiar carbohydrate, milk lactose. J Dairy Sci 78:2541–2562, 1995.
85. PF Fox, ed. Advanced Dairy Chemistry. 3. Lactose, Water, Salts and Vitamins, 2nd ed. London: Chapman & Hall, 1997.
86. A Flynn. Nutritional significance of lactose. II. Metabolism and toxicity of galactose. In: PF Fox, ed. Developments in Dairy Chemistry. 3. Lactose and Minor Constituents. London: Elsevier Applied Science, 1985, pp 133–141.
87. DM Paige, LR Davis. Nutritional significance of lactose. I. Nutritional aspects of lactose digestion. In: PF Fox, ed. Developments in Dairy Chemistry. 3. Lactose and Minor Constituents. London: Elsevier Applied Science, 1985, pp 111–132.
88. A Mustapha, SR Hertzler, DA Savaiano. Lactose: nutritional significance. In: PF Fox, ed. Advanced Dairy Chemistry. 3. Lactose, Water, Salts and Vitamins. London: Chapman & Hall, 1997, pp 127–154.
89. RR Mahoney. Modification of lactose and lactose containing dairy products with β-galactosidase. In: PF Fox, ed. Developments in Dairy Chemistry. 3. Lactose and Minor Constituents. London: Elsevier Applied Science, 1985, pp 69–109.
90. RR Mahoney. Lactose: enzymatic modification. In: PF Fox, ed. Advanced Dairy Chemistry. 3. Lactose, Water, Salts and Vitamins. London: Chapman & Hall, 1997, pp 77–125.
91. JB Smart. Transferase reactions of β-galactosidases—new product opportunities. In: Proceedings of the IDF Workshop on Lactose Hydrolysis, Bulletin No. 289. Brussels: International Dairy Federation, 1993, pp 16–22.
92. RR Mahoney. Galactosyl-oligosaccharide formation during lactose hydrolysis: a review. Food Chem 63:147–154, 1998.
93. DD Muir. Reviews of the progress of dairy science: frozen concentrated milk. J Dairy Res 51:649–664, 1984.
94. JG Sabioni, DO Silva, AJR Pinheiro, AC Borges, JBP Chaves. Control of lactose crystallization in "Dulce de Leche" by *Kluyveromyces lactis* fermentation. J Dairy Sci 67:1694–1698, 1984.
95. JG Sabioni, AJR Pinheiro, DO Silva, JBP Chaaves, AC Borges. Control of lactose crystalization in "Dulce de Leche" by beta-D-galactosidase activity from permeabilized cells of *Kluyveromyces lactis* cells. J Dairy Sci 67:2210–2215, 1984.
96. J Patocka, P Jelen. Enzymatic lactose hydrolysis for prevention of lactose crystallization in a whey spread. J Food Sci 53:1370–1372, 1988.
97. SB Martinez, RA Speckman. β-Galactosidase treatment of frozen dairy product mixes containing whey. J Dairy Sci 71:893–900, 1988.
98. JG Zadow. Economic considerations related to the production of lactose and lactose by-products. In: Proceedings of the IDF Workshop on Lactose Hydrolysis, Bulletin No. 289. Brussels: International Dairy Federation, 1993, pp 10–15.
99. VA Proctor, FE Cunningham. The chemistry of lysozyme and its use as a food preservative and a pharmaceutical. CRC Crit Rev Food Sci Nutr 26:359–395, 1988.
100. FE Cunningham, VA Proctor, SJ Goetsch. Egg-white lysozyme as a food preservative: an overview. World's Poultry Sci J 47:141–163, 1991.
101. NY Farkye. Indigenous enzymes in milk: other enzymes. In: PF Fox, ed. Food Enzymology, Vol. 1. London: Elsevier Applied Science, 1991, pp 107–129.
102. NY Farkye. Indigenous enzymes in milk: other enzymes. In: PF Fox, ed. Advanced Dairy Chemistry. 1. Proteins. London: Elsevier Applied Science, 1992, pp 338–367.
103. International Dairy Federation. The use of lysozyme in the preservation of late blowing in cheese. Bulletin 216. Brussels: author, 1987, pp 1–16.
104. International Dairy Federation. The use of lysozyme to control butyric acid fermentation. A-Doc 112. Brussels: author, 1988, pp 40–43.
105. VL Hughey, EA Johnson. Antimicrobial activity of lysozyme against bacteria involved in food spoilage and food-borne disease. Appl Environ Microbiol 53:2165–2170, 1987.
106. FE Hammer. Oxidoreductases. In: T Nagodawithana, G Reed, eds. Enzymes in Food Processing, 3rd ed. New York: Academic Press, 1993, pp 221–277.
107. T Szalkucki. Applications of oxidoreductases. In: T Nagodawithana, G Reed, eds. Enzymes in Food

Processing, 3rd ed. New York: Academic Press, 1993, pp 279–291.
108. AG Rand, JA Hourigan. Direct conversion of lactose in milk to acid. J Dairy Sci 58:1144–1150, 1975.
109. PF Fox, PA Morrissey. Indigenous enzymes of bovine milk. In: GG Birch, N Blakeborough, KJ Parker, eds. Enzymes and Food Processing. London: Applied Science Publishers, 1981, pp 213–238.
110. BJ Kitchen. Indigenous milk enzymes. In: PF Fox, ed. Developments in Dairy Chemistry. 3. Lactose and Minor Constituents. London: Elsevier Applied Science, 1985, 239–279.
111. L Björck. Indigenous enzymes in milk. V. Lactoperoxidase. In: PF Fox, ed. Food Enzymology, Vol 1. London: Elsevier Applied Science, 1991, pp 100–106.
112. L Björck. Indigenous enzymes in milk. V. Lactoperoxidase. In: PF Fox, ed. Advanced Dairy Chemistry. 1. Proteins. London: Elsevier Applied Science, 1992, pp 332–338.
113. B Reiter. The biological significance of the non-immunoglobulin protective proteins in milk: Lysozyme, lactoferrin, lactoperoxidase. In: PF Fox, ed. Developments in Dairy Chemistry. 3. Lactose and Minor Constituents. London: Elsevier Applied Science, 1985, pp 281–336.
114. J Stadhouders, RR Beumer. Actual and potential applications of the natural antimicrobial agents of milk in the dairy industry. In: Indigenous Antimicrobial Agents of Milk, Special Issue 9404. Brussels: International Dairy Federation, 1994, pp 175–197.
115. K Seguro, N Nio, M Motoki. Some characteristics of a microbial protein cross-linking enzyme: transglutaminase. In: N Parris, A Kato, LK Creamer, and J Pearce, eds. Macromolecular Interactions in Food Technology. Washington: American Chemical Society, 1996, pp 271–280.
116. M Motoki, K Seguro., Transglutaminase and its use for food processing. Trends Food Sci Technol 9:204–210, 1998.
117. E Dickinson. Enzymatic crosslinking of milk proteins. Proc 25th Intern Dairy Congr (Aarhus), II:209–215, 1998.
118. M Korycka-Dahl, T Richardson, RL Bradley. Use of microbial β-lactamase to destroy penicillin added to milk. J Dairy Sci 68:1910–1916, 1985.
119. N-ZP Lee, T Richardson. Preparation and characterization of immobilized β-lactamase for destruction of penicillin in milk. J Dairy Sci 70:2032–2039, 1987.
120. L Khosravi, WE Sandine. β-Lactamase-producing mutants of *Streptococcus cremoris*. J Dairy Sci 70:1529–1543, 1987.

21

Flavor Enhancement in Fruit Juices and Derived Beverages by Exogenous Glycosidases and Consequences of the Use of Enzyme Preparations

Ziya Günata
University of Montpellier II, Montpellier, France

I. INTRODUCTION

Research over the past two decades has revealed that in a great number of fruit and plant tissues important flavor compounds are glycosylated and accumulate as nonvolatile and flavorless glycoconjugates (1–6). Although results in the literature had long suggested the occurrence of glycosidically bound flavor compounds in plants, the first clear evidence was found in 1969 by Francis and Allcock in rose flowers (7). The work of Cordonnier and Bayonove in 1974, suggesting the occurrence in grapes of important flavor compounds (monoterpenes) as glycoconjugates on the basis of enzymatic work (8), was later confirmed by Williams et al. in 1982 by the identification of glycosides (1). These findings opened a new field of intensive research on the chemistry of glycoconjugated flavor compounds to exploit this important flavor source present in both fruit and plant tissues. The expanding literature on the chemistry and occurrence of glycosidically bound volatiles in the plant kingdom has been recently reviewed by Vasserot et al. (9), Stahl-Biskup (4), and Winterhalter and Skouroumounis (6).

This chapter briefly presents the diversity and structure of glycosides found in fruits and plants. Attention will focus on those glycosidases involved in flavor release from glycoconjugated precursors, examining the properties and current use of these enzymes for flavor enhancement in fruit juices and derived beverages (mainly wines) and future developments. Flavor enhancement by glycosidases has been the subject of a review by the author and colleagues in 1993 (10), and brief summaries are also found in the reviews of Williams (11), Vasserot et al. (9), and Winterhalter and Skouroumounis (6).

II. STRUCTURE AND OCCURRENCE OF GLYCOCONJUGATED FLAVOR COMPOUNDS

The publication of two techniques in 1982 (12) and 1985 (2), which allow the selective retention of glycosides on hydrophobic adsorbants (C_{18} reversed-phase and Amberlite XAD-2) from the complex matrix of fruit and plant materials, replaced tedious classical techniques and greatly contributed to progress in the field of glycosidic flavor precursors. Once the glycosidic extract is obtained, different liquid chromatography techniques are applied to isolate and purify glycosides. Countercurrent chromatography, which is a liquid–liquid partition chromatography, improved separations especially by eliminating or decreasing the formation of artifacts observed on solid adsorbents (13). Various combined chromatographic and spectral

techniques (GC-MS*, GC-FTIR, HPLC-MS/MS, FAB-MS/MS) are used for identification. A recent review (6) gives general approaches to the analysis of glycosides with abundant references related to the subject.

Glycosidically bound volatiles identified in fruits and plants are highly complex and diverse, especially with regard to the aglycone moiety. The sugar parts consist of β-D-glucopyranosides and different diglycosides: 6-*O*-α-L-arabinofuranosyl-β-D-glucopyranosides; 6-*O*-α-L-arabinopyranosyl-β-D-glucopyranosides (vicianosides); 6-*O*-α-L-rhamnopyranosyl-β-D-glucopyranosides (rutinosides); 6-*O*-β-D-glucopyranosyl-β-D-glucopyranosides (gentiobiosides); 6-*O*-β-D-apiofuranosyl-β-D-glucopyranosides; and 6-*O*-β-D-xylpyranosyl-β-D-glucopyranosides (primeverosides) (Fig. 1) (1, 2, 4–7, 14–19). In rare cases trisaccharide glycoconjugates were isolated (6). As far as we are aware, only (1 → 6) intersugar linkages have been detected in plant flavor glycoconugates, while (1 → 2), (1 → 3), and (1 → 4) linkages together with (1 → 6) linkages were observed for diglycosides of flavonoids (20). Therefore, different glycosyl transferases seem to exist in plants. Recently, β-D-glucopyranosides of some volatiles of fruit and plant tissues have been shown to be acylated at the C-6 hydroxyl group of the sugar moiety with malonic acid (21, 22). Malonylated glycoconjugates of flavonoids are often detected in plants (20).

A common feature of glycosidic flavor precursors is that the aglycone moiety is always linked to β-D-glucopyranose. To date ~ 200 aglycones have been identified in 150 plant species (4, 6). The aglycone moiety is predominantly mevalonic acid (monoterpenes, C_{13}-norisoprenoids, sesquiterpenes), and shikimic acid–derived secondary metabolites. Medium-chain alkanols and alkenols have also been detected. Some abundant and important aglycones for flavor are given in Figure 1. Further information can be obtained from the reviews (4, 6).

Glycoconjugates of flavor compounds are present in several fruits, such as grape (1, 2, 19), apricot (3, 23), peach (3), yellow plum (3), quince (24), sour cherry (25), passion fruit (15, 26), kiwi 927), papaya (28, 29), pineapple (30), mango (31), lulo (32), raspberry (33), and strawberry (34). The amount of glycosidically bound volatiles is typically two to eight times greater than that of their free counterparts (2, 3, 19). Moreover, most norisoprenoids in fruit, some of which are precursors of very potent flavor compounds, have been detected mainly in glycosidic forms. This, together with the low aroma threshold and sensory properties of aglycones, makes the glycosidic compounds an important potential source of flavor volatiles during fruit juice processing.

The glycosidically bound volatiles can be released by either acid or enzyme hydrolysis (1, 2, 36). Slow acid hydrolysis takes place at fruit juice pH (35) and can be accelerated by thermal treatment (36–38). This treatment, however, can reduce the sensory quality of the products (38).

Some aglycones are already odorous when released from glycosides. They can therefore contribute to the floral aroma of some wines (36, 39), grapes (10, 36, 39), apricots (40), peaches (41), and tea (5, 7, 16, 17). This is the case, for example, of monoterpenes such as geraniol, nerol and linalol which possess mainly floral attributes and low odor thresholds (100–400 ppb in water) (39).

In contrast, polyhydroxylated monoterpenes (polyols) and the majority of norisoprenoids are odorless, but can generate potent aroma compounds due to their reactivity in the acidic medium (pH 2.8–3.8) of fruit juices (36, 37, 42). For example, some hydroxylinalool derivatives can give rise at ambient temperature and grape juice pH (3.0–3.6), to the formation of odorous monoterpenes, such as hotrienol, nerol oxide, and linalool oxides (37). The review by Strauss et al. discusses the acid catalyzed conversions of monoterpenes and role of these compounds in grape and wine flavor (36).

Potent C_{13}-norisoprenoid flavorants in fruit- and plant-derived products, such as theaspiranes, vitispiranes, edulans, and β-damascenone, are similarly generated from relevant progenitors by acid-catalyzed reactions. The major pathways leading to these flavor compounds are discussed in the review by Winterhalter (42). For example, β-damascenone, which is among the most potent flavoring substances known to date (odor threshold 2 ppt in water; floral, fruity, and iononelike odor) (43), can be generated from multiple glycosylated precursors detected in fruits and plants (42).

Glycosylated volatile compounds in plants are often considered as physiologically inactive plant storage and transport forms of secondary metabolites. However, their exact role is far from understood (4).

Abbreviations: GC, gas chromatography; MS, mass spectrometry; FTIR, Fourier transform infrared spectroscopy; HPLC, high-performance liquid chromatography; FAB, fast atom bombardment; TLC, thin-layer chromatography; *p*NP, *p*-nitrophenyl.

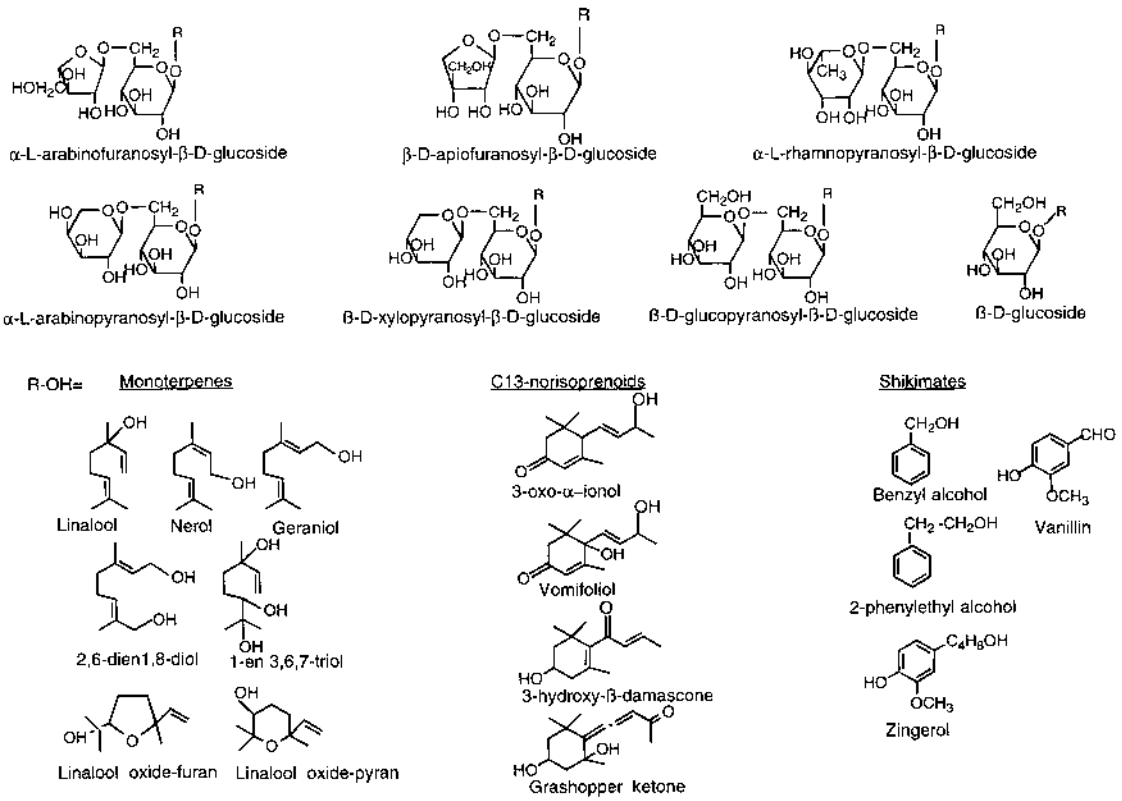

Figure 1 Structure of glycoconjugated aroma compounds from plants.

III. ENZYMES INVOLVED IN THE RELEASE OF FLAVOR COMPOUNDS FROM GLYCOSIDES

The elucidation of the enzymes responsible for the release of flavor compounds from glycosides is the first step in the development of technological applications. Glycosidases catalyze hydrolysis of the glycosidic bond of their carbohydrate substrates by two general mechanisms, leading to either the retention or inversion of the anomeric configuration at the cleavage point (44). The mechanism of hydrolysis is presumed to proceed in the same way as the acid-catalyzed cleavage of glycosicic bond, via a carbocation intermediate. Glycosidases discussed here refer to those enzymes which catalyze the hydrolysis of *O*-glycosyl compounds.

As had been suggested as early as 1913 (45) and 1924 (46), volatile compounds (monoterpenes, vanillin) can be liberated from β-D-glucosides through the action of β-glucosidase (EC 3.2.1.21). The involvement of enzymes in the release of volatiles from disaccharides, however, was shown only recently because the relevant substrates were first reported in 1982 (1). As will be later discussed, the release of the aglycone moiety may occur through two-step (sequential hydrolysis) or one-step (endoglycosidase) enzyme-catalyzed reactions. The term "endoglycosidase" is used in this chapter for glycosidases involved in flavor release as a function of their catalytic activities.

A. Sequential Hydrolysis

Preliminary work carried out on the hydrolysis of grape glycosides, by using fungal enzyme preparations (pectinases, hemicellulases, and glucanases), has shown that the release of flavor compounds depends on the presence of glycosidases as side activities in the enzyme preparations (47). With the aid of suitable analytical techniques (TLC, HPLC, GC/MS), a study using purified glycosidases and synthesized substrates was able to elucidate the sequential reaction involved in the hydrolysis of disaccharidic flavor precursors (Fig. 2) (48).

First, the inter-sugar linkage is cleaved by exoglycosidases; either an α-arabinofuranosidase (EC 3.2.1.55), an α-rhamnopyranosidase (EC 3.2.1.40), or a β-apiofuranosidase depending on the disaccharidic moiety.

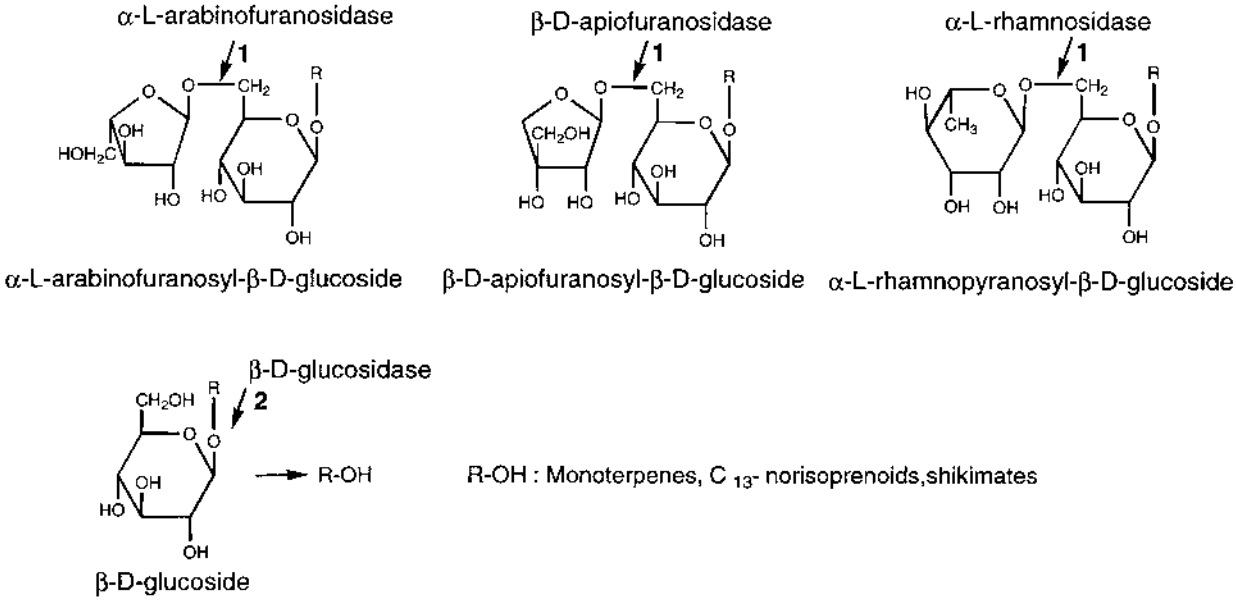

Figure 2 Sequential enzymatic hydrolysis of disaccharidic flavor precursors.

This releases terminal sugars and β-D-glucosides. Subsequently, β-glucosidase cleaves the aglyconic linkage of β-D-glucosides to liberate volatiles. This hydrolysis mechanism has been patented (49). Such two-step reactions, involving exoglycosidases (5, 6, 50, 51), are also possible in the hydrolysis of diglycosides of fruit or plant volatiles, which possess α-L-arabinopyranosyl, β-D-xylopyranosyl or β-D-glucopyranosyl as terminal sugars.

B. One-Step Hydrolysis of Disaccharide Glycosides (Endoglycosidase)

This one-step reaction occurs through the cleavage of the aglyconic linkage which yields a disaccharide and aglycone, the identity of which were confirmed by HPLC and GC/MS analysis (Fig. 3) (5, 51). The enzymes catalyzing this reaction were isolated from tea leaves (5) and grapes (51). The enzyme from tea is called primeverosidase, after primeverosides, which are the most abundant glycoconjugated flavors in this plant.

IV. OCCURRENCE OF GLYCOSIDASES

Exoglycosidases involved in flavor release are widely distributed among plants (10, 52–60) and microorganisms (61–66). The enzymes presented here mainly concern those found in fruits or plants where the occurrence of glycoconjugated flavors has been demonstrated. With regard to microbial enzymes, mainly those originating from GRAS (generally recommended as safe) will be discussed.

A. Plant-Originated Glycosidases

Most work has been devoted to grape glycosidases because the first evidence of multiple forms of glycosidic flavor precursors was found in this fruit. β-Glucosidase (55, 56, 69, 67, 68), α-arabinofuranosidase (56, 59), α-arabinopyranosidase (19), α-rhamnopyranosidase (56, 69), and β-xylosidase (51) activities were detected in grapes of various cultivars. The presence of β-apiosidase in grapes has not yet been confirmed. On the basis of glycosidase activity determinations with *p*NP-glycosylated substrates, β-glucosidase activity is considered the most important. Multiple forms of β-glucosidase exist in grape berries (51, 55, 59) and are also found in almond emulsin (69) but not in papaya fruit (54). The enzyme from papaya fruit, unlike that from grapes, is readily soluble and does not require the use of detergent for extraction.

Glycosidases are found predominantly in grape skins (67, 68), although contradictory results may arise owing to the enzyme extraction method employed (59). β-Glucosidase, α-arabinofuranosidase, and α-rhamnosidase activities have been shown to increase during the ripening of grape berries (56, 59, 67), unlike β-glucosidase activity from papaya fruit which is unaffected by the ripening stage of the fruit (54).

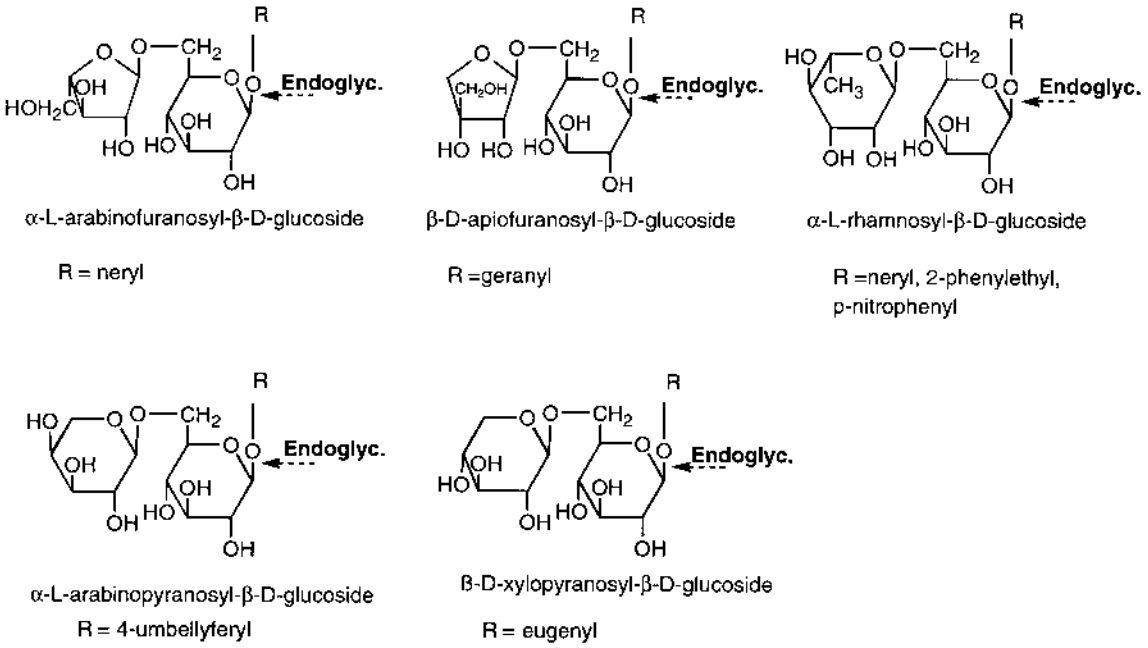

Figure 3 One-step hydrolysis of disaccharidic flavor conjugates by grape endoglycosidase.

The presence of β-glucosidase activity has also been reported in vine leaves (59, 67) where flavor glycoconjugates are abundant (70). It should be noted that glycosidases substrates other than glycosidic flavor conjugates are found in plants. Indeed, many of the secondary metabolites synthesized are glycosylated, and > 1500 flavonoid glycosides have been characterized (71).

Endoglycosidase, active on disaccharidic flavor precursors in fruits, has been recently isolated and partially characterized from grape skins (51). The extraction was only possible with the use of a detergent, the type of which greatly influenced the yield. In contrast, the extraction of tea enzyme (primeverosidase) was possible without the use of detergent (5, 72). This suggests that the structure of grape endoglycosidase differs from that obtained from tea and/or could be a membrane-bound protein. Moreover, although needing confirmation, grape endoglycosidase also seems to possess β-glucosidase activity (51).

B. Fungal-Derived Glycosidases

These can be present in fruit due to the development of fungi such as *Botrytis cinerea*. Other filamentous fungi, for example *Aspergillus* sp., and yeast are also able to produce glycosidases.

1. *Botrytis cinerea*

The ability of *B. cinerea* to produce β-glucosidase (64, 65) and α-arabinofuranosidase (62) when cultured in a suitable medium was shown. Grape berries contaminated by fungi such as *B. cinerea* were found to contain higher levels of α-arabinofuranosidase and α-rhamnosidase activities compared to uncontaminated grapes (56). This fungus has been shown to exhibit these same activities when developed on grape juice (56). In these conditions, β-glucosidase is also produced but its activity is strongly inhibited by glucono-δ-lactone which is produced from glucose through glucose oxidase activity of the fungus (10, 56). The presence of gluconolactone in grapes is one of the major limitations on flavor release by glycosidases and will be discussed later.

The development of *B. cinerea* on grapes has a very detrimental effect not only on the flavor of juice and wine, through the degradation of monoterpenes (73–75) and fatty acid esters (76), but also on the overall quality due to the action of several enzymes produced by the fungus (77–79).

2. Yeast

In wine making the alcoholic fermentation is essentially performed by yeast *Saccharomyces cerevisiae*. α-Arabinofuranosidase (80), α-rhamnosidase (80), and

β-glucosidase (80, 81) activities were only detected at low levels in juices and in cells during fermentation. β-Glucosidase activity was the most abundant, followed by α-arabinofuranosidase activity. The activities reached their maximum levels during exponential growth of the yeast population, then dropped dramatically. No differences have been observed among enological yeast (*S. cerevisiae*) strains in the production of glycosidases during fermentation (80).

Owing to the low level of glycosidases production by *S. cerevisiae*, a recombinant yeast strain, expressing β-glucosidase from *C. molischiana* (82) and α-arabinofuranosidase from *A. niger* (83), has been recently constructed. The relevant proteins were detected during grape juice fermentation, although poor secretion of the *C. molischiana* protein was observed. There is a lack of data on the contribution of these recombinant yeast strains to flavor release during fermentation. β-Glucosidases from *Kluyveromyces fragilis* (84), *A. niger* (6), and *Bacillus polymyxa* (85) have been expressed in *S. cerevisiae* in order to obtain strains able to ferment disaccharides (cellobiose and lactose).

The yeast species from the genera *Saccharomyces* (63, 86), *Dekkera* (87), *Debaryomyces* (88, 89), *Kloeckera* (90), *Hansenula* (91), and *Candida* (92–95) are able to synthesize β-glucosidase when cultured on carbon sources such as glucose, cellobiose, xylose, and alkyl thioglucosides. The lowest enzyme synthesis is generally found in the *Saccharomyces* spp. Except for *Candida* and *Debaryomyces* spp., yeast seldom secretes β-glucosidase into a growth medium. The enzyme is localized at the cell membrane and in the cytoplasm (63, 87, 93, 96).

3. Filamentous Fungi

Filamentous fungi, particularly *Aspergillus* sp., are good producers of exoglycosidases and used in industry to obtain pectic and hemicellulase enzyme preparations (61, 97, 98). These preparations are widely used in fruit juice processing and winemaking, mainly to improve juice clarification and yield. In addition to their main activities, they contain several other enzyme "side activities" including glycosidases. β-Glucosidase and α-arabinofuranosidase are often the most abundant, followed by α-rhamnosidase, while β-apiosidase is rarely detected (10) (Table 1). The production of β-apiosidase by *A. niger* appears to be inducible because, unlike β-glucosidase, which is a constitutive enzyme in fungi, it requires the presence of a carbon source inducer such as apiin (a trihydroxyflavone-apiosyl (1 → 2) glucoside) (99). Enzyme preparations shown in Table 1 differ notably in their glycosidase activity levels. Furthermore, these levels vary greatly from one batch to another, as current pectinase enzyme preparations are formulated by producers as a function of their main activities.

The production by fungi of endoglycosidase, capable of hydrolyzing disaccharidic conjugates of flavor compounds, has to date been the subject of only one paper. An *A. niger* strain was shown to produce such as enzyme (an endo-β-glucosidase) when cultured on rutin as the sole carbon source (100).

Table 1 Glycosidase Activities (nkat/mg Product) in Some Enzyme Preparations

	β-Apiosidase	β-Glucosidase	α-Arabinofuranosidase	α-Rhamnosidase
Cellulase A	—[a]	6.1	0.6	0.007
Hermicellulase	—	7.1	7.0	0.9
Pectinol VR	—	0.2	0.1	—
Rohament CW	—	3.3	0.7	0.4
Pectinol D5S	—	0.5	0.7	—
Pektolase 3PA	0.3	1.5	3.8	0.04
Ultrazym 100	0.03	0.5	0.1	—
Pectinase 263	0.2	7.2	1.4	0.3
AR 2000	1.08	5.7	14.7	0.3
Novoferm 12	0.15	8.4	0.5	0.05

Source: Ref. 10.
Commercial sources: Gist Brocades (CellulaseA, Hemicellulase, Pectinase 263, AR 2000), Röhm (Pectinol VR, Rohament CW, Pectinol D5S), Ciba-Geigy (Ultrazym 100), Grindsted (Pektolase 3PA), Novo (Novoferm 12).
[a]Undetected.

V. ENZYME ASSAY METHODS

The substrates used may be composed either of a mixture of glycosides isolated from fruits and plants by selective retention on hydrophobic adsorbents (2, 12), or of purified and synthesized natural glycosides (6, 35, 101, 102). Alternatively, artificial *p*NP-glycoconjugated substrates are often used.

Glycosidase activities can be determined by two techniques:

1. Direct analysis of glycosides by chromatographic techniques (TLC, HPLC, GC) (2, 5, 6, 19, 35, 48, 51). Before GC analysis, a derivatization step, generally involving the silylation and trifluoroacetylation of glycosides, is carried out in order to obtain their volatile forms.

2. Analysis by colorimetric or chromatographic (TLC, HPLC, CPG) techniques of aglycone or sugar moieties (monosaccharides or disaccharides) released from glycosides (2, 5, 48, 51, 103). In the case of aglycone liberated by enzymatic hydrolysis from natural glycosides, the volatiles are recovered from the enzyme assay before GC analysis, by either liquid–liquid extraction with a solvent or selective retention on hydrophobic adsorbents (2, 6, 12). A colorimetric assay of monoterpenes (aglycones) liberated from sugars has also been proposed (104).

*p*NP-glycoconjugated substrates are widely used as the standard for assaying glycosidase activities using mainly colorimetric techniques owing to their ready availability (except for certain disaccharidic substrates) and the simplicity of the analysis. Often, this analysis does not reflect the catalytic characteristics of enzymes, owing to the presence of multiple forms of glycosidases and, in some cases, the narrow aglycone specificity (see Sec. VI.C).

VI. FOOD-PROCESSING PROPERTIES OF GLYCOSIDASES

This section will examine the properties of enzymes, focusing on the specific conditions encountered in the processing of fruit juice and derived beverages. In particular, three important parameters influencing flavor release will be discussed: the effect of pH; aglycone and sugar specificity of glycosidases; and inhibition of activity by sugar and sugar analogues. A summary of the properties of β-glucosidase from some plants and microorganisms is given in Table 2.

A. Effect of pH on Activity and Stability

The optimum pH activity of plant β-glucosidase (55, 59) and endoglycosidase (51) is similar (5.0–6.0) to that of intracellular yeast β-glucosidase (63, 87, 93, 105). This value is generally lower (4.0–5.0) for extracellular yeast (63, 92, 93) and *Aspergillus* enzymes (10, 61, 106). The optimum pH of an extracellular endo-β-glucosidase from *A. niger* was found to be unusually low (3.4) (100). Most β-glucosidases exhibit only 5–15% of their maximum activity in the pH range of fruit juices (2.8–3.8).

A. niger α-arabinofuranosidase (62, 107) and α-rhamnosidase (47, 108) possess similar pH optima to that of extracellular β-glucosidase from the same fungus, while the value for *A. niger* β-apiosidase is higher (5.0–6.0). (10, 99, 106). Both -arabinofuranosidase and α-rhamnosidase exhibit $>50\%$ of their maximum activities in the pH range of fruit juices.

An important parameter that must be considered for technological applications is the stability of glycosidases in the acidic pH of fruit juices. Glycosidases differ notably in this respect (Fig. 4) (10).

β-Glucosidases from grapes, *S. cerevisiae*, and *C. wickerhamii*, are not very stable in these conditions. For example, *C. wickerhamii* β-glucosidase was able to hydrolyse β-D-glucosides of monoterpenes in a wine only when the initial pH (3.0) was adjusted to 3.5 or higher (109). Only 10% of initial β-glucosidase activity from *S. cerevisiae* was observed after 90 min incubation (20°C) in a buffer at pH 3.0. (10). This may explain the large decrease in *S. cerevisiae* β-glucosidase activity during grape juice fermentation. In fact the optimum pH stability of the enzyme corresponds to the pH of yeast cells (6.0). This decrease is also observed for α-rhamnosidase and α-arabinofuranosidase activities from *S. cerevisiae* during juice fermentation (10, 80). A β-glucosiase from *C. peltata* was fairly stable at pH 3.5–6.0 (95). The enzyme from a mutant strain of *C. molischiana* was shown to be more stable at acidic pH than an enzyme from a wild-type strain (110,111). This difference could be explained by the difference in glycosylation of the relevant proteins.

In contrast, β-glucosidase, α-arabinofuranosidase, and α-rhamnosidase from *A. niger* are remarkably stable over a pH range of 2.5–7.0 (Fig. 4) (10, 62, 106). The enzymes exhibit $>80\%$ of their maximum activity after 24 h of incubation in a buffer at pH 3.0. However, *A. niger* β-apiosidase was less stable at a pH < 4.0 (10, 106). The same trends were observed when the stability of *A. niger* glycosidases were monitored during grape juice fermentation at 20°C (pH 3.0)

Table 2 Properties of β-Glucosidases from Some Plants and Microorganisms

Origin		pH		Temperature (°C)		Glucose inhibition		Gluconolactone inhibition		Aglycone alcohol substrates	References
		Optimum	Stability	Optimum	Stability[a]	K_i (mM)	%	K_i(mM)	%		
Plant											
Grape		5.0	6.0–7.0	45	50	170	66% at 100 mM	0.22	88% at 10 mM	Primary	2, 10, 19, 55, 59
Almond		5.5	n.d.	50	65	210	12% at 100 mM	0.49	n.d.	Primary	10, 52, 59, 69, 115
Papaya		5.0	n.d.	50	n.d.	n.d.	50% at 10 mM	n.d.	n.d.	n.d.	11, 54
Yeast											
S. cerevisiae	(i)	6.0–6.8	5.0–7.0	45	45	6.7	13% at 100 mM	n.d.	42% at 10 mM	Primary	10, 80, 105
D. intermedia	(i)	5.0	n.d.	55	50	3.0	n.d.	n.d.	n.d.	n.d.	87
C. molischiana	(e)	4.0–4.5	4.0–5.0	50–60	60	7.0	n.d.	n.d.	68% at 10 mM	Primary tertiary	92, 116
C. wickerhamii	(e)	4.5	4.0–5.0	50	50	230	18% at 100 mM	n.d.	100% at 10 mM	Primary tertiary	93, 94, 116
	(i)	6.0	n.d.	50	50	9	n.d.	n.d.	100% at 10 mM	n.d.	93
C. peltata	(e)	5.0	3.5–6.0	45–50	50	1400	n.d.	n.d.	n.d.	n.d.	95
D. hansenii	(e)	4.0–5.0	n.d.	40	n.d.	n.d.	10% at 100 mM	n.d.	n.d.	Primary tertiary	89, 164
Fungus											
A. niger	(e)	4.0–6.0	2.5–7.0	60–65	60–65	3.0–3.8	90% at 100 mM	n.d.	100% at 1 mM	Primary tertiary	10, 61, 106, 113, 115
		3.4	n.d.	65	n.d.	40	81% at 250 mM	n.d.	n.d.	Primary tertiary	100, 161
		4.0–6.0	4.0–7.0	55	60	543	n.d.	n.d.	n.d.	n.d.	131
A. oryzae	(e)	4.5–6.0	3.0–7.0	n.d.	n.d.	958	10% at 100 mM	n.d.	80% at 50 mM	Primary tertiary	13, 129
B. cinerea	(i)	6.5–7.0	n.d.	50	n.d.	5.5	n.d.	0.02	n.d.	n.d.	64
	(e)	3.0	4.0–10.0	60	n.d.	n.d.	n.d.	n.d.	n.d.	n.d.	65

[a]Temperature at which rapid inactivation occurs.
n.d., not determined; (i), intracellular; (e), extracellular.

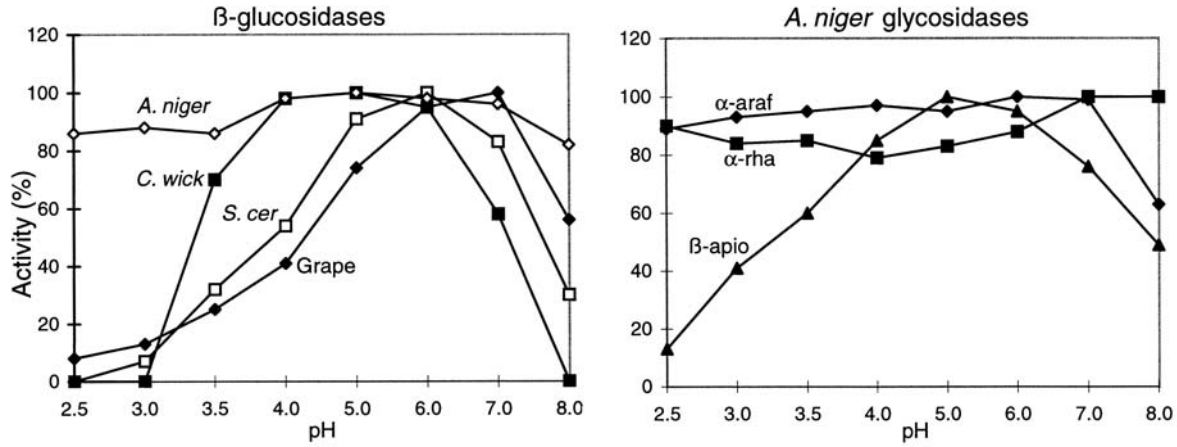

Figure 4 Effect of pH (phosphate-citrate buffer) on stability of glycosidases of *A. niger* (24 h, 30°C), *C. wickerhamii* (1 h, 30°C), *S. cerevisiae* (90 min, 20°C), and grape (24 h, 30°C). (From Ref. 10.)

(106). β-Glucosidase and α-arabinofuranosidase activities remained practically unchanged after 7 days, while only 70% of initial α-rhamnosidase and 50% of β-apiosidase activities were observed. This remarkable stability of extracellular *A. niger* enzymes is interesting for fruit juice processing and could be explained by the glycosylation of proteins (110, 112).

B. Effect of Temperature

The optimum temperature activities of plant (54, 55) and yeast β-glucosidases (63, 89, 93, 95) is generally lower (45–50°C) than that (50–60°C) of *A. niger* enzymes (61, 106, 113). At the normal temperature (20°C) of grape juice fermentation, for example, glycosidases exhibit only 10–20% of their maximum activity.

Rapid inactivation of glycosidases occurs at temperatures > 50°C, (55, 63, 99, 113), although some filamentous fungal β-glucosidases are only inactivated at temperatures > 65°C (61). The pH of the meidum plays an important role in the thermal denaturation of glycosidases. In general, glycosidases from filamentous fungi are more heat stable than those from yeasts and plants (61, 63).

C. Aglycone and Sugar Specificity of Glycosidases

The hydrolysis of monoterpenyl diglycosides by exoglycosidases—α-arabinofuranosidase (48, 107), α-arabinopyranosidase (50, 114), α-rhamnosidase (48), and β-apiofuranosidase (99, 106)—is not significantly influenced by the structure of the aglycone moiety. This is not very surprising since ^{1}H and ^{13}C NMR spectra of disaccharide glycosides show that the orientation of the terminal sugar is unaltered whether the monoterpenyl moiety is a primary or tertiary alcohol (35, 101).

The hydrolysis of monoterpenyl β-D-glucosides by plant (grape and almond; 2, 19, 55, 59, 115), fungal (yeast, *A. niger*; 10, 89, 115, 116), and bacterial (*B. polymyxa*; 117) β-glucosidases is, however, greatly influenced by the structure of the aglycone. Plant β-glucosidases showed a pronounced specificity and acted on β-D-glucosides of primary alcohols (e.g., geraniol, nerol, and citronellol) but not on those of tertiary alcohols (e.g., linalool, α-terpineol, linalool oxides) which, when hydrolyzed, can give rise to potent volatils. This shows the limitations in flavor recovery with plant endogenous β-glucosidases in fruit juice processing.

The aglycone specificity of β-glucosidases from *S. cerevisiae* and *B. polymyxa* resembled grape and almond β-glucosidases more than microbial enzymes from *Aspergillus*, *Candida*, *Debaryomyces spp*. The latter were able to catalyze the hydrolysis of both monoterpene primary and tertiary alcohol β-D-glucosides.

The rate of hydrolysis of β-D-glucosides of monoterpene primary alcohols by various β-glucosidases was found to be higher than that of β-D-glucosides of tertiary alcohols (115, 116). These results are in general agreement with the catalytic activity of almond emulsin β-glucosidase on other primary and tertiary alkyl-β-D-glucosides (118). It is interesting to note that the opposite results were obtained when the acid-catalyzed hydrolysis of these substrates was performed (119).

Furthermore, the configuration of monoterpenes has an effect on the rate of hydrolysis since diastereoisomeric monoterpenyl β-D-glucosides (linalool, α-terpineol, and citronellol) and isomeric monoterpenyl β-D-glucosides (geraniol and nerol) are hydrolyzed at different rates by enzymes (115, 116). For example, geranyl-β-D-glucoside was often hydrolyzed at a higher rate than neryl-β-D-glucoside.

The ^{1}H and ^{13}C NMR spectra of β-D-glucosides of monoterpene primary and tertiary alcohols differ in the orientation of the β-D-glucopyranosidic linkage (35, 101), which may partly explain differences observed in enzymatic hydrolysis. The conclusion reached from these results is that the source of the β-glucosidase can influence the pattern of liberated aglycones and thereby the sensory properties of products.

Little work has been devoted to the determination of the affinity of β-glucosidases for glucosidic flavor precursors. Among the substrates tested (geranyl, neryl, and citronellyl β-D-glucosides), grape enzyme showed the highest affinity for geranyl-β-D-glucoside (55). Additionally, differences were observed between two β-glucosidases isolated from grapes with regard to their affinity for monoterpenyl β-D-glucosides. Two β-D-glucosidases isolated from *A. niger* differed also significantly in their affinity toward geranyl β-D-glucoside and malvidin β-D-glucoside (participating in the red color; see Sec. VII.B) (103) and monoterpene tertiary alcohol β-D-glucosides (115). It is worthwhile to note that often multiple forms of glycosidases were detected in plants (53, 55, 120) and microorganisms such as fungi (61, 103, 106). This emphasizes the importance of the use of natural substrates to determine the catalytic properties of enzymes, as suggested by Hösel and Conn (120), instead of commonly used artificial substrates (*p*NP-glycosides).

With regard to endoglycosidase, the enzyme from grapes shows a broad specificity toward the sugar moiety of disaccharides (51). The enzyme is active against arabinofuranosyl, rhamnopyranosyl, and apiofuranosyl (1 → 6) glucosides from grapes. Arabinopyranosyl and xylopyranosyl (1 → 6) glucosides moieties from passion fruit (15) and tea leaves (5), respectively, are also substrates for the enzyme.

β-Primeverosidase from tea leaves also shows fairly broad specificity toward disaccharide glycosides. Xylopyranosyl (1 → 6) glucosides and apiofuranosyl (1 → 6) glucosides are better substrates than arabinopyranosyl and arabinofuranosyl (1 → 6) glucosides (121).

Work carried out on other plant endoglycosides has mainly focused on the hydrolysis of flavonoid glycosides. An enzyme from *Viburnum furcatum* was found to be very specific to the apiosyl (1 → 6) glucoside unit (122). Glycosides possessing rutinose and apiosyl (1 → 2) glucoside as sugar moiety were not substrates. In contrast, the latter was substrate for an enzyme from *Cicer arietinum* L. (123). An endoglycosidase from *Rhamnus* (124) and from *Fagopyrum esculentum* (125), however, showed, a broad specificity for flavonoid glycosides. Further work is needed to determine whether plants possess multiple forms of endoglycosidase differing in their catalytic activities towards glycosidic flavor precursors.

The broad substrate specificity of tea and grape endoglycosidases provides new challenges for the use of such enzymes through genetic engineering for flavor enrichment of fruit juices and other plant-derived products.

With regard to fungal endoglycosidase, an enzyme from *A. niger* was able to hydrolyze geranyl-β-rutinoside (100). We have observed in our laboratory (data not published) that *Aspergillus* sp. can produce an endoglycosidase when specific carbon souce inducers were present in the culture medium, in similar conditions to those described by Westlake et al. (126). However, the enzyme showed a distinct specificity for both the sugar and aglycone moiety of substrates. It was active on flavonoid rutinosides, such a rutin and hesperidin. Neither naringin, a flavonoid glycoside with rhamnosyl (1 → 2) glucoside as sugar moiety, nor monoterpenyl, 2-phenylethyl, or benzyl rutinosides was the substrate.

D. Inhibition of Glycosidase Activities

1. Glucose Inhibition

An important constraint for flavor release in fruit juice processing is the inhibition of β-glucosidases by glucose. This inhibition is often of a competitive type and a common characteristic of these enzymes (10, 16, 127, 128). In contrast, β-glucosidase activity is not influenced by other sugars such as fructose, galactose, arabinose, mannose, lactose, and sucrose at the concentrations occurring in food products (95, 100).

Inhibition of β-glucosidase activity by glucose has long been known to be a major problem for enzymatic debittering of citrus juices by hydrolysis of naringin (108) and for efficient enzymatic saccharification of cellulosic material (61). Cellobiose, produced by the consecutive action of cellulases (exo and endoglucanases) on cellulose, can accumulate in the medium as the consequence of end-product (glucose) inhibition of β-glucosidase, which catalyzes the hydrolysis of cello-

biose. This leads to the inhibition of cellulase activities by cellobiose. Much attention has therefore been focused on the search for glucose tolerant β-glucosidase.

Intracellular β-glucosidases from yeast are generally very sensitive to glucose inhibition. Inhibition constants vary from 3.0 to 23 mM (63, 87, 93). During grape juice fermentation, both excreted and cell β-glucosidase of *S. cerevisiae* were found to be less sensitive to glucose inhibition (80, 81). Purified β-glucosidase from *S. cerevisiae* showed, however, a low value of K_1 (6.7 mM) (105).

Some strains belonging to the genera *Candida* (92–95) and *Debaryomyces* (89) are able to produce glucose-tolerant extracellular β-glucosidase. *C. molischiana* extracellular enzyme (92) is strongly inhibited by glucose ($K_i = 7$ mM), while that from *C. wickerhamii* ($K_i = 230$ mM) (93) and particularly from *C. peltata* ($K_i = 1400$ mM) (95) were distinguished by high resistance to glucose inhibition. Rosi *et al.* (89), after screening 317 yeast strains from 20 species, selected a *D. hansenii* strain producing a highly glucose-tolerant β-glucosidase.

Bacterial and filamentous fungal β-glucosidases are generally strongly inhibited by glucose, the inhibition constant being in the range of 0.6–10 mM (95, 113, 127–129). However, we recently demonstrated that the production of highly glucose-tolerant extracellular β-glucosidase from *A. niger* and *A. oryzae* is possible (129, 130). This involves an adaptive enzyme whose production was induced by using uncommon carbon sources in the culture medium. The highest production was obtained with quercetin (a pentahydroxyflavone) as the sole carbon souce. In these conditions, two β-glucosidases were produced. The major β-glucosidase was strongly inhibitied by glucose ($K_i = 3.5$ mM) as is the case for *Aspergillus* enzymes (113, 127, 128). The minor β-glucosidase, however, was highly resistant to glucose inhibition ($K_i = 953$ mM). The molecular weight of this enzyme is quite low (30 kDa) compared to that of most *Aspergillus* enzymes. To date only one strain of *A. niger* has been reported to produce (MW = 98 kDa) a constitutive enzyme which is not very sensitive to glucose inhibition $K_i = 543$ mM) (131).

Activity enhancement by glucose was observed for an intracellular β-glucosidase from *Streptomyces* sp. (132, 133) and from *Microbispora bispora* (134). Multiple forms of β-glucosidases have been observed in *Streptomyces* sp., but only one of these forms was found to display this particular behavior. β-Glucosidase activity from one strain was stimulated by up to 0.4 M glucose, with the maximum activation occurring at 0.2 M glucose (132). That from another strain was activated only up to 0.2 M glucose concentration (133). The activity of both enzymes decreased at > 0.4 M glucose but the extent of this decline differed among the strains. No convincing explanations have emerged to account for this unusual behavior of the enzymes.

The activities of fungal exoglycosidases are not significantly affected at the usual glucose concentrations found in fruit juices (47, 135). The enzymes α-arabinofuranosidase and β-apiofuranosidase were more resistant to glucose inhibition than α-rhamnosidase (10). Glucose has been demonstrated to be a competitive inhibitor ($K_i = 120$ and 350 mM) of fungal α-rhamnosidase (66, 136).

Among plant β-glucosidases, those from grape (55) and almond (52) were resistant to glucose inhibition, with a K_i of 170 mM and 210 mM, respectively, while that from papaya fruit was more sensitive (11).

With respect to endoglycosidases, the enzyme from grapes showed a high K_i value (212 mM) (51). Glucose did not influence the activity of an endoglycosidase produced from *Aspergillus* sp. in our laboratory (data not published), which was found to be specific to flavonoid rutinosides as discussed previously. However, an *A. niger* endo-β-glucosidase able to hydrolyze geranyl β-rutinoside was found to be sensitive to glucose inhibition ($K_i = 40$ mM) (100). Furthermore, the common inhibition of glycosidases by their end product (sugar) was observed for fungal α-rhamnosidase activity (66, 136). The inhibition with rhamnose was competitive, with a K_i of 1.2 and 1.75 M.

2. Glucono-δ-Lactone

This is one of the most powerful inhibitors of β-glucosidases. Plant (52, 55) and microbiol β-glucosidases (63, 92, 93, 113, 137) are more strongly inhibited by this compound than by glucose. The high affinity of the compound for the enzyme has been explained by its structural analogy with an intermediate product in the enzymatic cleavage of β-D-glucosides (138). The inhibition is usually of the competitive type with K_i values often < 1 mM and applies equally to β-glucosidase from *Streptomyces* sp. ($K_i = 0.44$ mM), the activity of which was enhanced by glucose (133).

Gluconolactone concentration may reach levels of 5–10 mM in grape juice and wine obtained from grapes contaminated by fungi, such as *B. cinerea* (56, 139). At these levels, grape (55), *S. cerevisiae* (80), *C. wickerhamii* (93), and *A. niger* (113) β-glucosidases are strongly inhibited. However, glucose-tolerant β-glucosidase

from *Aspergillus* strains, the production of which was induced with quercetin, displays 30% of its activity at 5 mM and 20% at 50 mM of gluconolactone (129, 130).

At high concentration glucunolactone is also an inhibitor of *A. niger* α-rhamnosidase and β-apiosidase activities. For example, the former was inhibited by 50% and the latter by 85% with 100 mM gluconolactone (10). *A. niger* α-arabinofuranosidase was unaffected at this concentration.

3. Miscellaneous Compounds

a. Ethanol. Generally, fungal β-glucosidase (80, 93, 100), α-arabinofuranosidase (47, 135), α-arabinopyranosidase (47), and β-apiosidase (99) are weakly inhibited by 10% (v/v) ethanol which is the average value in wines. Inhibition often only occurs above 15% ethanol. However, *A. niger* α-rhamnosidase was found to be more sensitive to ethanol, with a loss of 20–40% of activity at a 10% ethanol concentration, depending on the enzyme preparation (47).

An enhancement of particularly microbiol β-glucosidase activity has been observed when *p*NP-β-glucoside was used as substrate, which may be due to the glucosyltransferase activity of the enzyme (47, 87, 140). Conversely, the hydrolysis of *p*NP-β-glucoside by grape (55, 59) and almond (59) β-glucosidases clearly decreased in the presence of ethanol. Grape β-glucosidase activity declined by 60% in 10% ethanol (55).

b. Sulfur Dioxide. At the usual levels (50–200 ppm) used in fruit juice processing and wine making to prevent oxidation, this compound was not found to cause an inhibitory effect on yeast β-glucosidase (80, 82) or *A. niger* endo-β-glucosidase (100).

c. Phenols and Polyphenols. Phenols (141) and polyphenols (142) display an inhibitory effect on plant β-glucosidase. The affinity of phenolic inhibitor for the enzyme increases with increasing molecular size (142). Catechin, dimeric procyanidins, and especially yellow oxidation products of catechin are powerful inhibitors of sweet almond β-glucosidase (143). Similarly, apple β-galactosidase is also inhibited by catechin, quercetin, and glycosides of quercetin (144). These polyphenols are either present in intact fruits or produced during fruit juice processing by oxidative reactions. To our knowledge, the effect of polyphenols on fungal glycosidase activities has not yet been studied.

d. Cations. Ag^{+}, Hg^{2+}, Cu^{2+}, Mg^{2+}, Ca^{2+}, Fe^{2+}, and Fe^{3+} were found to be inhibitors of plant and fungal glycosidases, the extent of inhibition depending on the source of the enzyme (55, 63, 99). The strongest inhibition was often observed with Ag^{+}, Hg^{2+}, and Cu^{2+}.

VII. USE OF GLYCOSIDASES FOR AROMA ENRICHMENT

The use of glycosidases to release flavor compounds from glycosidic precursors, was initially examined in wines. Two major reasons for this are: (i) important flavor compounds in wines of *Vitis vinifera* cultivars are accumulated in grapes as flavorless glycoconjugates, and especially (ii) the glucose inhibition of β-glucosidase in available enzyme preparations, limits the use of glycosidases to media, like wine, containing trace levels of glucose (< 1 g/L). Nevertheless, because of the occurrence of flavor glycoconjugates in several fruits, enzyme applications have been found for fruit juices.

A. Wine Flavor Enhancement

The amount of glycosidic flavor precursors decreases only slightly during grape juice fermentation (145). This phenomenon may be explained by the low levels of glycosidase activities exhibited by grapes (55, 56) and enological yeast strains (80), as discussed previously. Consequently, attention has been focused on the use of commercially available fungal enzyme preparations (pectinases, hemicellulases) containing glycosidase activities derived mainly from *Aspergillus* spp. Various enzyme preparations have been tested for flavor enhancement of wines from different cultivars by incorporating the enzymes either into the juice during fermentation or into the wine. Current regulations, however, do not allow the addition of enzymes into wine.

Muscat cultivars were often used as a model to test the effect of the enzyme treatment because of the abundance of monoterpenyl glycosides. The hydrolysis of these glycosides liberates highly odorous alcohols which can be detected by sensory analysis and easily analyzed by GC/MS. In general, the addition of enzyme preparations possessing glycosidase activities during wine making results in a significant increase in the concentration of monoterpenes, C_{13}-norisoprenoids, and shikimate derived compounds.

The total free monoterpene concentration in the treated wines increased by several fold compared to control wines (Fig. 5) (10, 109, 146–152). The concentration of free monoterpenes often exceeded their

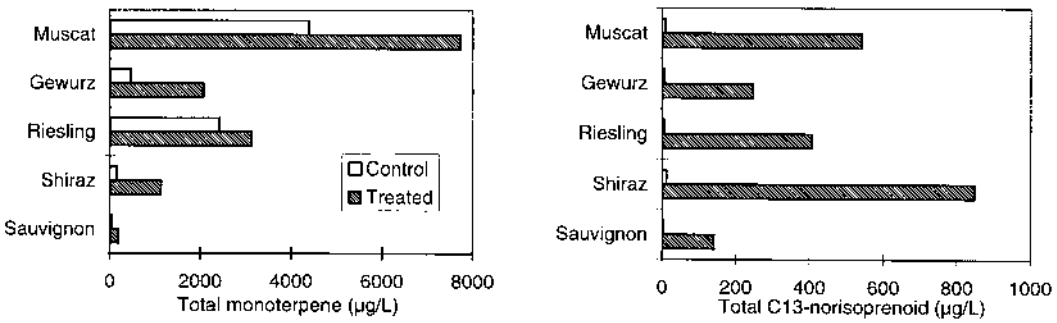

Figure 5 Total free monoterpene and C_{13}-norisoprenoid concentrations in control and glycosidase treated wines.

aroma threshold in wines made from varieties, such as Muscat and Gewürztraminer, in which large amounts of monoterpenes occur as flavorless glycoconjugates (2, 19, 109). These treated wines developed a more intense floral note owing to the abundance of monoterpenes. In nonfloral varieties, such as Sauvignon, Semillon, Shiraz, Greanche, Carignan, and Trajadura (10, 109, 148–152), the increase in monoterpenes is below the aroma threshold of these compounds. However, there is no information available about the effect of this increase on the flavor nuances that are sometimes detected in treated wines.

Among the monoterpenes, an increase was observed for geraniol, nerol, citronellol, linalool, furan, and pyran forms of linalool oxides, α-terpineol, and monoterpene polyols (e.g., 8-hydroxylinalools, *p*-menthene-7,8-diol, exo-2-hydroxy-8-cineol). The highest increase often occurred for geraniol and nerol, which impart floral attributes to the wines (10, 146, 147, 151, 152).

The concentration of linalool, and linalool oxides, and some polyols often increased to a lesser extent because of the low activity of fungal β-glucosidase toward the relevant glycoconjugates. However, mono- and diglycosides of these tertiary alcohols are more prone to acidic hydrolysis in fruit juice than those of primary alcohols (35).

Citronellol concentration increased greatly in some enzymatically treated wines (Muscat). This could not be the consequence of the enzymatic hydrolysis of related glycosidic precursors since the glycosidic conjugates of this terpenol have not been detected in grapes (153). The increase was explained by the action of yeast (*S. cerevisiae*) reductase on geraniol and nerol, which were more abundant in the enzymatically treated wines (154–156). The production of citronellol was influenced by the yeast strain (155). The high amounts of this compound resulted in the perception of citrus attributes in the wines.

It is difficult to attribute the increase in concentration of each monoterpene directly to the enzymatic release from glycoconjugate precursors. The acid-catalyzed rearrangement of released monoterpenes occurs in grape juice and wine (Fig. 6) (36–38, 157), and some monoterpenes, as mentioned above, may be involved in yeast metabolism. The ideal way to determine the effect of enzymatic release from glycoconjugate precur-

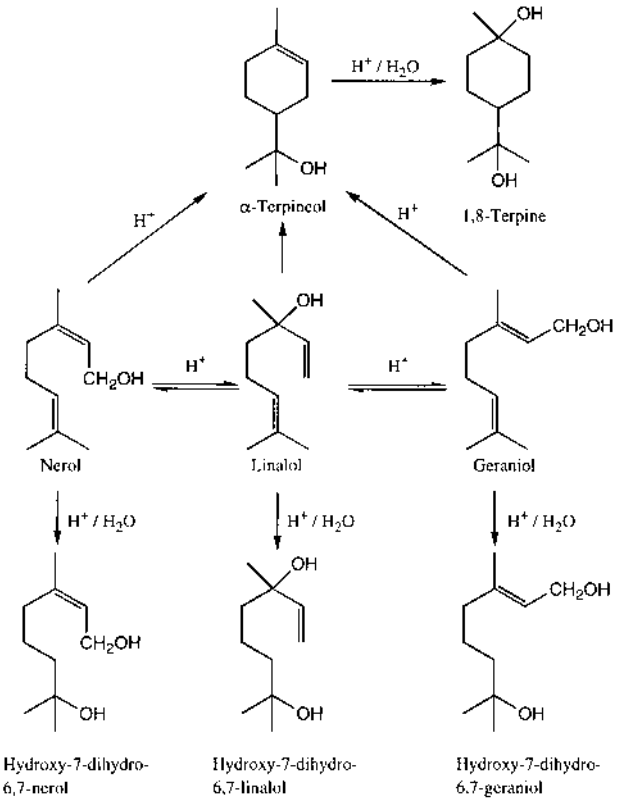

Figure 6 Acid-catalyzed rearrangement of monoterpenes. (From Ref. 157.)

sors is by direct quantitative analysis of monoterpenyl glycosides. However, this analysis requires reference glycosides which are not yet commercially available, such as certain monoterpenes. Furthermore, their synthesis, mainly for diglycosidic conjugates, is quite complex and leads generally to low yields (35, 101, 102).

In our laboratory several monoterpenyl glycosides were synthesized (35, 101), which allowed us to quantify them in control and enzymatically treated wines (10, 109, 147). An enzyme preparation, rich in glycosidase activities, was added to grape juices from different cultivars before alcoholic fermentation. The glycosides hydrolysis was measured $\sim$ 1 month after the completion of fermentation. the concentration of monoterpenyl arabinofuranosyl and rhamnopyranosyl glucosides decreased notably in treated wines, while apiosylglucosides decline less sharply (Fig. 7). This was due to the low levels of β-apiosidase activity compared to α-rhamnosidase and α-arabinofuranosidase activities in the enzyme preparation. With regard to monoglucosides, primary alcohol (geraniol and nerol) β-D-glucosides were almost totally hydrolyzed by exogenous enzymes (Fig. 8) (10, 109). In contrast, the level of tertiary alcohol (linalool) glucoside increased significantly in wines containing high levels of relevant disaccharidic conjugates. This accumulation is the result of the low activity of fungal β-glucosidase on tertiary alcohol glucosides which are generated from diglycosides by the action of exoglycosidases.

Fermentation trials with various Muscat grape juices, in the presence of different levels of glycosidase activities, showed that several hundred nanokatals of β-glucosidase, α-arabinofuranosidase, β-apiosidase, and α-rhamnosidase activities per liter of grape juice are needed to efficiently hydrolyze monoterpenyl glycosides (10, 109). These activities are much greater than those found in grape berries (55, 56) or produced by *S. cerevisiae* (80) during alcoholic fermentation.

Several C_{13}-norisoprenoids that were barely detectable in control wines were nonetheless detected in the treated wines (Fig. 5) (10, 109, 147). This is not surprising as they occur mainly in glycoconjugated forms in grapes. These compounds are not often analyzed in glycosidase-treated wines, mainly because the references compounds are not commercially available. They are not specific to any grape variety, as was found for monoterpenes in Muscat cultivars, although some cultivars, such as Chardonnay (158, 159) and Shiraz (10, 109), do seem to contain larger amounts of C_{13}-compounds.

In the enzymatically treated wines, the most abundant C_{13}-norisoprenoids were often 3-hydroxy-β-damascone, 3-oxo-α-ionol, and vomifoliol (10, 109, 147), as was also observed in the enzymatic hydrolysis

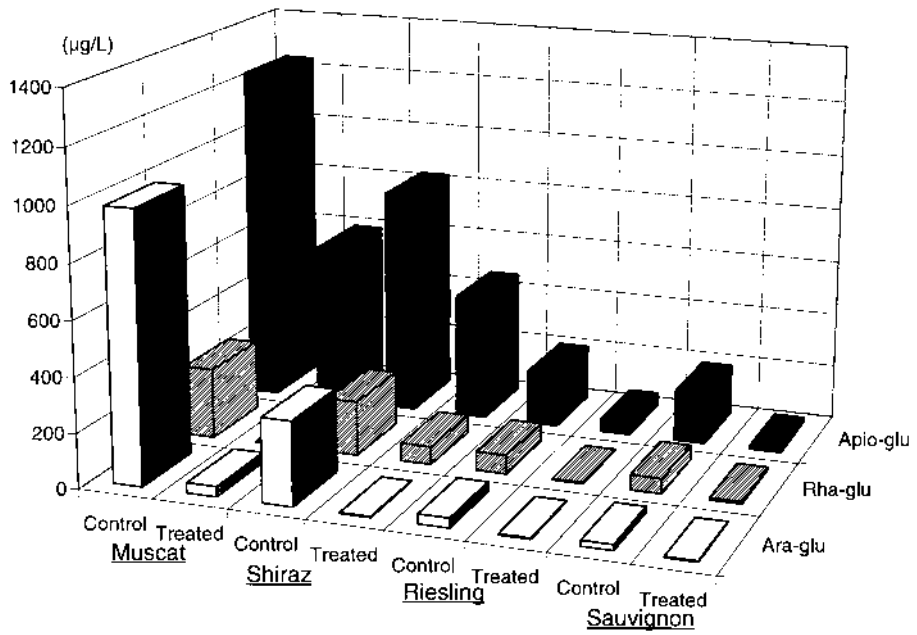

Figure 7 Monoterpenyl diglycoside concentrations in control and glycosidase-treated wines.

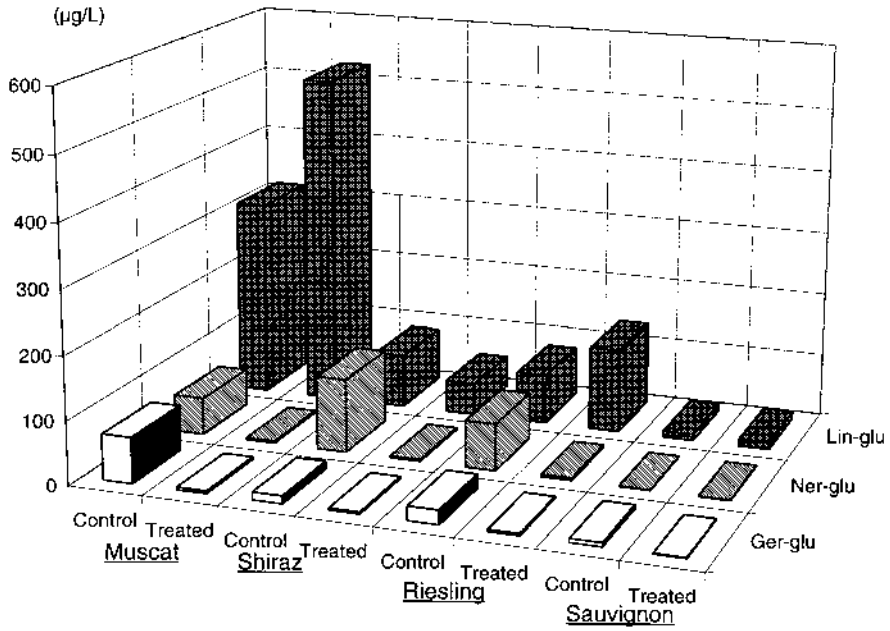

Figure 8 Monoterpenyl glucoside concentrations in control and glycosidase-treated wines.

of grape glycosidic extracts. These molecules are odorless and are considered not to generate odor-active compounds by further reactions (42, 158). In contrast, 3-hydroxy-7,8-dehydro-β-ionol, an acetylenic alcohol, detected in treated wines (10, 109) can generate a highly esteemed, flavorant, β-damascenone, along with a major product, 3-hydroxy-β-damascone, at wine pH during storage through acid catalyzed reactions (Fig. 9) (42, 70, 158). A high concentration of β-damascenone, exceeding several fold its odor threshold, has been detected in an enzymatically treated wine 1 month after the end of fermentation (147). This can be explained by the fact that glycosidase treatment may have increased the concentration of an allenic triol which is known to rearrange much faster than aforementioned acetylenic alcohol to generate β-damascenone (158, 160).

β-Damascenone, like other norisoprenoid flavorants, is generally produced in tiny amounts (in the range of ppt) (42, 158, 160) that are difficult to quantify by conventional GC/MS techniques. Nowadays, stable isotope dilution techniques are being used more and more because of their sensitivity and accuracy in quantitative analysis of trace flavorants.

Among the shikimate-derived volatiles, benzyl alcohol, 2-phenyethanol, vanillin, eugenol, and zingerone were often detected at higher concentrations in enzymatically treated wines (10, 109, 150). An enzymatically treated white wine from a nonfloral grape variety (150) contained high levels of vanillin, which is a potent flavorant usually derived from wood used in wine aging.

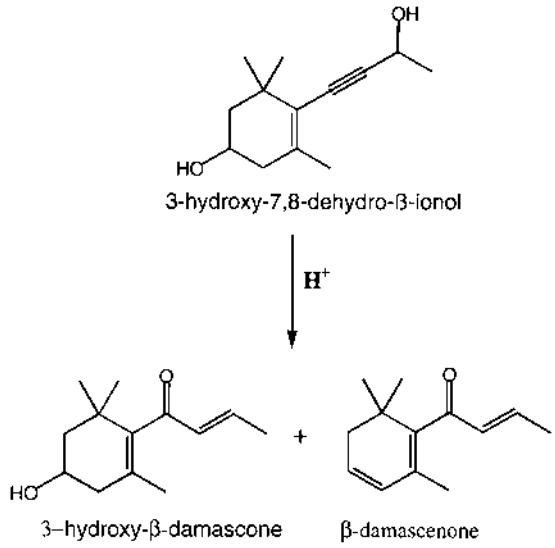

Figure 9 Products issued from 3-hydroxy-7,8-dehydro-β-ionol by acid-catalyzed reactions in fruit juice and wine. (From Ref. 158.)

The increase in flavor compounds, using the same wine and at the same dosage of enzyme preparation, is strongly influenced by the enzyme preparations used (usually from 1 to 3 g/HL) (10, 151, 152). This can be explained by the different glycosidase activities of enzyme preparations, as mentioned previously. Furthermore, the vintage had an influence on the aroma enrichment of wine, which could be explained by differences in the biosynthesis of glycosidic precursors. It has also been found that enzyme preparations were more effective when added into wine instead of grape juice (10, 109, 151).

In addition to commercial pectinase preparations, β-glucosidase preparations have been used to enhance the varietal flavor of Muscat wines, including an immobilized endo-β-glucosidase from *A. niger* (161), an immobilized β-glucosidase from *C. molischiana* (162, 163), and a β-glucosidase from *D. hasenii* (164). Monoterpenes (geraniol, nerol, linalol, linalool oxides), benzyl alcohol, and 2-phenylethanol concentrations all increased in the treated wines. Since the authors only analyzed volatiles after enzymatic treatment, it is difficult to judge the extent of glycoside hydrolysis. Furthermore, the hydrolysis of disaccharidic glycosides was probably quite limited owing to the use of an unique activity (β-glucosidase).

Finally, an important aspect in the use of glycosidases is the prevention of any contamination of the grapes or fruits by molds. As previously mentioned, such contamination may lead to the inhibition of β-glucosidase activity by gluconolactone. This was observed when glycosidases were added to a wine made from mold infected grapes (personal communication). The diglycosides were effectively hydrolyzed by exoglycosidases in the treated wine, while the resulting monoglucosides were not hydrolyzed owing to gluconolactone, of which the presence in the wine was confirmed by analysis.

Sensory difference tests often distinguished between the control and enzyme treated wines (10, 109, 147, 152, 161, 162). The difference was clearly observed in wines whose flavor is monoterpene dependent (like Muscat and Gewürztraminer) even after 2 or 3 weeks of enzyme application, due to the enhanced floral attributes. For nonfloral varieties, which constitute the greatest volume of world wine production, the effect of glycosidases can be perceived usually after several months or more. Most of the liberated aglycones, especially those corresponding to the C_{13}-norisoprenoids and monoterpene polyols, are flavorless but can generate odorous molecules during wine conservation. In contrast to the advances in our understanding of the chemistry of aglycones (6, 36), very few data are available on their effect on the formation of odor-active molecules in normal wine storage conditions.

The role of aglycones, derived from grape glycosidic precursors, in the generation of important wine aroma descriptors has been shown in mimetic conditions (165). Indeed, some important key aroma descriptors (honey, tea, lime) of white wines were detected when a glycosidic extract from nonfloral varieties (Chardonnay, Semillon, Sauvignon) was subjected to an acid hydrolysis (pH 3.2) at elevated temperature (50°C, 4 weeks, under nitrogen) in order to accelerate the acid-catalyzed conversions that slowly occur during wine conservation. The contribution of glycosidic precursors to the characteristic aroma of an important red wine cultivar (Grenache) has been recently observed in our laboratory under similar conditions.

The volatiles responsible for the key aroma descriptors have not been identified yet, most probably due to the presence of trace quantities of important flavorants.

The rapid liberation of aglycones from glycoconjugates, through the use of exogenous glycosidases, can thereby accelerate the formation of odor-active volatiles during wine storage. In fact the glycosidic flavor precursors do undergo slow hydrolysis at wine pH during storage (35, 109, 145). For example, several Muscat wines prepared without glycosidase addition and analyzed after 18 months contained from 1.2 to 1.9 times more monoterpenes in glycosylated form than in the free fraction (145). Bound forms of primary alcohols (geraniol and nerol) were 6–10 times more abundant than their free counterparts.

B. Fruit Juices

Owing to the inhibition by glucose of the "key enzyme" β-glucosidase in the available fungal derived enzyme preparations, very little work has been devoted to flavor enhancement in fruit juices.

Treating mango and passion fruit juices with a yeast β-glucosidase from *Candida cacaoi* resulted in an increase in monoterpene concentrations (166). However, the increase was much lower than that due to acid hydrolysis. The immobilized enzyme (covalently bonded to sodium alginate beads) liberated fewer terpenols than the free enzyme. The addition of β-glucosidase from *C. molischiana* (immobilized onto Duolite A-568 resin) to apricot, mango, strawberry, peach, and apple juices yielded an increase in concentration of monoterpene alcohols (linalool, α-terpineol, geraniol), benzyl alcohol, and 2-phenylethanoal (162).

No differences were observed in the flavor released using free and immobilized β-glucosidase from *C. molischiana*. The immobilized enzyme was found to be quite stable under fruit juice conditions.

An *A. niger* endo-β-glucosidase, immobilized onto acrylic beads or cellulose, increased the concentration of volatiles (linalool, benzyl alcohol and benzaldehyde) in passion fruit juice (161). In general, an aroma enhancement in the treated juice was observed (161, 162).

Although the volatile levels in fruit juices increased after the applications of β-glucosidase, two important parameters may have limited the efficiency of the process: (a) many flavor compounds occur in fruits as diglycosides which fungal β-glucosidases are, in general, unable to hydrolyze; (b) the fungal β-glucosidases tested are inhibited by glucose, which could therefore limit their action in fruit juices.

Because the authors only analyzed the volatile content of fruit juices and not the glycosides, the yield of hydrolysis cannot be evaluated. However, a paper reports how the amount of glycosides changes in a sweet wine (containing ~ 30 g/L glucose) when fungal glycosidases were used in the wine-making process (147). The level of monoterpene diglycosides decreased notably in the treated wine, which may be explained by the action of exoglycosidases. The monoterpenyl-β-D-glucosides produced were not hydrolyzed and therefore accumulated in the wine. This clearly indicates the inhibition of fungal β-glucosidase activity by glucose, which greatly limited the liberation of volatiles as confirmed by their analysis. In contrast, the hydrolysis of monoglucosides was very efficient when a dry wine was prepared using the same grape juice, enzyme dosage, and conditions (147).

VIII. POTENTIAL ADVERSE EFFECTS OF ENZYME PREPARATIONS

Certain side activities of fungal enzyme preparations can be detrimental to fruit juice and wine quality owing to the formation of off-flavors and the decolorization.

A. Off-flavor Formation

Hydroxycinnamic acids, such as *p*-coumaric and ferulic acids, occur mainly in bound forms in fruits. Quinic acid and/or glucosidic esters of these hydroxycinnamic acids have been detected in numerous fruits: apple, pear, apricot, peach, orange, grapefruit, strawberry, raspberry (167), while in grapes they are esterified with tartaric acid (167–169).

A large number of pectinase and hemicellulase preparations derived from *A. niger* used in fruit juice processing exhibit an cinnamate esterase as side activity which leads to the enrichment of the medium in free caffeic, *p*-coumaric, and ferulic acids (Fig. 10) (170–173). Free *p*-coumaric and ferulic acids can be converted to volatile high-flavorant *p*-vinylphenols, 4-vinylphenol, and 4-vinylguaiacol, respectively, by either nonenzymatic thermal (174) or enzymatic (yeast and bacteria) decarboxylations (175–179) (Fig. 10). These vinylphenols possess low detection thresholds (< 100 ppb in water) (174, 179) and spicy and medicinal odors, and they contribute positively only at low levels to the flavor of food products (180–182). Accordingly, the increase in the concentration of hydroxycinnamic acids precursors of these volatiles due to enzyme treatments can have an important consequence to the flavor of the products.

4-Vinylguaiacol (or *p*-vinylguaiacol) generated from ferulic acid through nonenzymatic decarboxylation during orange and grapefruit juices processing and storage contributes to the development of the major detrimental off-flavor (old fruit, rotten flavor) in these products (174). It has been shown that the rate of 4-vinylguaiacol formation during orange juice storage was closely dependent on the amount of free ferulic acid (183).

A phenolic off-flavor is perceived in fermented products (beer, cider, wine) when aforementioned volatile phenols are present at high levels (171–173, 181, 184). The wines made from grape juice, that was initially spiked with some pectinase preparations rich in glycosidase activities contained exceedingly high levels (> 770 ppb) of vinylphenols, masking the pleasant fruity and floral odors which were generated by hydrolysis of glycosidic flavor precursors (109, 171, 172). It was demonstrated recently that the high concentration of volatile phenols detected sometimes in wines was due to the consecutive action of cinnamate esterase activity from enzyme preparation and decarboxylase activity from yeast (*S. derevisiae*) (171–173) present in the majority of enological strains (175). Consequently, particular attention is now being directed to develop an enzyme preparation without cinnamate esterase activity and to select yeast strains with low activity toward hydroxycinnamic acids (185). Since the 1970s, pectic enzyme preparations have been widely used in wine making mainly to improve clarification and juice yield, and the problem of off-flavors has been sometimes observed without explanation (186).

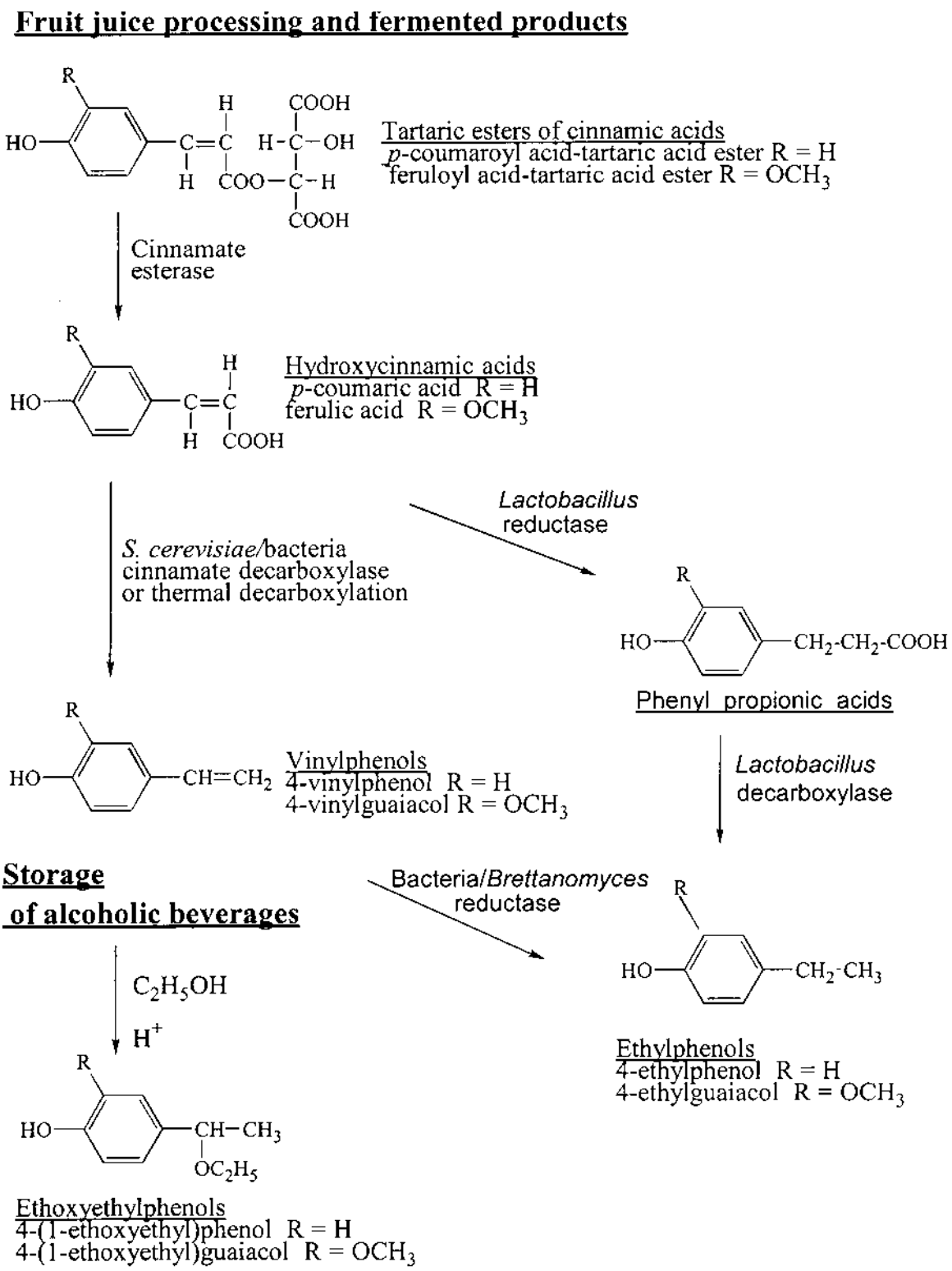

Figure 10 Some volatile phenols formation pathways during processing and storage. (Courtesy of C. Flanzy, Oenologie: fondements scientifiques et techniques, Tec-Doc, Paris, 1998.)

The formation of vinylphenols is found to be lower in red than white wines, and is explained by the inhibition of yeast decarboxylase activity by red wine polyphenols (187).

The high levels of vinylphenol and vinylguaiacol in wines dropped notably after 1 year of storage, while there was a simultaneous decrease of unpleasant odor (188). In the acidic pH of wine, these compounds were partly transformed into their corresponding ethoxyethylphenols by addition of ethanol (Fig. 10). Ethoxyethylphenols, at the levels found in wines, probably have no direct influence on flavor owing to their odor threshold (188).

Ethylphenols, 4-ethylphenol (woody, phenolic odor), and 4-ethylguaiacol (clovelike, smoky odor), which impart undesirable flavors to wine, beer, and cider are produced from 4-vinylphenol and 4-vinylguaiacol, respectively, through reductase activity from bacteria (176, 181) and more frequently from spoilage yeast, *Brettanomyces* (184, 189). The production of ethylphenols from hydroxycinnamic acids is possible by another pathway by *Lactobacillus*: firstly the double bonds of hydroxycinnamic acids were reduced, and subsequently the resultant phenyl propionic acids were decarboxylated (177, 178).

In addition to this off-flavor formation, fungal enzyme preparations cause the oxidation of C_{13}-norisoprenoids belonging to the structure of 3-hydroxymegastigmanes when they are used in assays for the determination of the aglycone moiety of glycosides (190). High enzyme concentrations are employed to ensure the complete hydrolysis of glycosides. This oxidation, by altering the structure of polyol aglycones, prevents the generation of desired aroma compounds, such as β-damascenone (6). However, at the dosage used in wine making for flavor release, the fungal-derived enzyme preparations do not provoke such oxidations (10, 109).

B. Decolorization Effect

Anthocyanins are among the most widespread natural pigments and responsible for the red, blue, and purple color of fruits (191, 192). They are composed of anthocyanidins glycosylated with mono- (usually glucose), di- or trisaccharides (193). Anthocyanidins become unstable and are readily converted to brown or colorless compounds when released from their sugar moiety (194, 195).

The hydrolytic activity of fungal enzyme preparations toward anthocyanins was reported as early as 1955 (194). β-Glucosidase (196, 197), α-arabinosidase (197, 198), and β-galactosidase (197, 199) from commercial enzyme preparations may potentially degrade anthocyanins. The decolorization effect of these enzymes has been reported for raspberry (200), strawberry (201), blackberry (202), and grape anthocyanins (197, 203, 204). Certain molds, particularly *B. cinerea*, which develop on fruits are also able to degrade anthocyanins as has been observed in strawberry juice (205), raspberry juice (206), and red wines (207, 208).

Only one in 26 enzyme preparations, used in fruit juice processing within the mean recommended dosage, degraded the anthocyanin-β-D-glucoside (cyanidin-3-glucoside) and di- and trisaccharides of cyanidin (209). Six enzyme preparations acted on disaccharidic conjugates only at high doses.

Two of four pectic enzyme preparations employed in wine making caused a significant color loss in red wine making (204). The major anthocyanin (malvidin-3-glucoside) and its acylated forms (malvidin-3-glucosylacetate and malvidin-3-glucosylcoumarate) both decreased significantly. The degradation of acylated anthocyanins requires the consecutive action of two enzymes—an esterase and β-glucosidase (170).

Accordingly, the choice of fungal enzyme preparations for flavor enhancement in fruit juices and derived beverages should be made carefully. Glycosidases that are highly active on anthocyanins may have specific applications for the decolorization of some orange juices or wines containing low levels of anthocyanin pigments.

An anthocyanin-β-glycosidase from *A. niger* has been partially purified and characterized (201). Two β-glucosidases that were isolated and characterized from an *A. niger* pectinase enzyme preparation differ mainly in their catalytic activity (103). The major one was highly active on cellobiose and geranyl-glucoside but only slowly degraded malvidin-3-glucoside. In contrast, the minor one was highly active in degrading malvidin-3-glucoside. Both enzymes were strongly inhibited by glucose. These two β-glucosidases were also observed in another pectinase enzyme preparation.

In rare cases, an oxidation of white wine color was observed in the enzyme-treated sample. This might be due to polyphenoloxidase activity from enzyme preparations or to the chemical or enzymatic oxidation of flavonoids released through the action of glycosidases.

Finally, as positive effect of glycosidases as biocatalysts, is their role in the detoxification of certain foods through the hydolysis of cyanogenetic glycosides (210) and the debittering of citrus juices by hydrolysis of narigin (211). These topics are not of the subject of this chapter.

IX. CONCLUSION AND FUTURE PROSPECTS

Major progress has been made during the past two decades in our understanding of the chemical composition of glycoconjugated flavor compounds in fruits and the biochemical characterization of glycosidases involved in flavor release. The utilization of exogenous glycosidases for aroma enrichment in fruit juices and particularly in wine processing has been clearly demonstrated.

Several approaches, through genetic engineering techniques, will doubtless be used in the near future to overcome, by using recently discovered glycosidases, the limitations (glucose inhibition, substrate specificity, pH effect) on the exploitation of the glycosylated aroma source in the processing of fruit juices and derived beverages as well as other plant-derived products. The newly identified enzymes, such as endoglycosidase, possessing a broad sugar specificity and low inhibition constant for glucose, together with highly glucose-tolerant β-glucosidases from *Aspergillus* sp. and yeasts (*Candida* and *Debaryomyces* spp.), represent important biotechnological challenges in flavor release processes.

The construction of fungal strains such as *S. cerevisiae* and *Aspergillus* sp. expressing these proteins, and/or relevant exoglycosidases involved in flavor liberation, may enable the production of "tailor-made" glycosidases without undesirable activities (such as esterase, anthocyanase, and oxydase). This would allow better control of flavor release in various processes through the use of immobilized enzymes, enzyme preparations, and recombinant yeast (*S. cerevisiae*) strains.

ACKNOWLEDGMENTS

The author thanks his colleagues identified in the literature, and Professor Christian Ambid for his helpful discussion and advice.

REFERENCES

1. PJ Williams, CR Strauss, B Wilson, RA Massy-Westropp. Novel monoterpene disaccharide glycosides of *Vitis vinifera* grapes and wines. Phytochemistry 21:2013–2020, 1982.
2. YZ Günata, CL Bayonove, RL Baumes, RE Cordonnier. The aroma of grapes. I. Extraction and determination of free and glycosidically bound fractions of some grape aroma components. J Chromatogr 331:83–90, 1985.
3. G Krammer, P Winterhalter, M Schwab, P Schreier. Glycosidically bound aroma compounds in the fruits of *Prunus species*: apricot (*P. armeniaca*, L.), peach (*P. persica*, L.), yellow plum (*P. domestica*, L. ssp. *Syriaca*). J Agric Food Chem 39:778–781, 1991.
4. E Stahl-Biskup, F Intert, J Holthuijzen, M Stengele, G Schulz. Glycosidically bound volatiles—a review 1986–1991. Flav Frag J 8:61–80, 1993.
5. K Ogawa, I Yasuyuki, W Guo, N Watanabe, T Usui, S Dong, Q Tong, K Sakata. Purification of a β-primeverosidase concerned with alcoholic aroma formation in tea leaves (Cv. *Shuixian*) to be processed to oolong tea. J Agric Food Chem 45:877–882, 1997.
6. P Winterhalter, GK Skouroumounis. Glycoconjugated aroma compounds: occurrence, role and biotechnological transformation. In: T Scheper, ed. Advances in Biochemical Engineering/Biotechnology. Heidelberg: Spring-Verlag, 1997, pp 74–105.
7. MJO Francis, C Allcock. Geraniol β-D-glucoside; occurrence and synthesis in rose flowers. Phytochemistry 8:1339–1347, 1969.
8. R Cordonnier, C Bayonove. Mise en évidence dans la baie de raisin, variété Muscat d'Alexandrie, de monoterpènes liés, révélables par une ou plusieurs enzymes du fruit. C R Acad Sci Paris 278:3387–3390, 1974.
9. Y Vasserot, A Arnaud, P Galzy. Monoterpenol glycosides in plants and their biotechnological transformation. Acta Biotechnol 15:77–95, 1995.
10. Z Günata, I Dugelay, JC Sapis, R Baumes, C Bayonove. Role of the enzymes in the use of the flavour potential from grape glycosides in winemaking. In: P Schreier, P Winterhalter, eds. Progress in Flavour Precursor Studies. Carol Stream, IL: Allured Publ, 1993, pp 219–234.
11. PJ Williams. Hydrolytic flavour release in fruits and wines through hydrolysis of nonvolatile precursors. In: TE Acree, R Teranishi, eds. Flavor Science. Sensible Principles and Techniques. Washington: American Chemical Society, 1983, pp 287–308.
12. PJ Williams, CR Strauss, B Wilson, RA Massy-Westropp. Use of C_{18} reversed-phase liquid chromatography for the isolation of monoterpene glycosides and nor-isoprenoid precursors from grape juice and wines. J Chromatogr 235:471–480, 1982.
13. P Winterhalter. Application of countercurrent chromatographic techniques in flavour precursor studies. In: P Schreier, P Winterhalter eds. Progress in Flavour Precursor Studies–Analysis, Generation, Biotechnology. Carol Stream, IL: Allured Publ, 1993, pp 31–44.
14. S Voirin, R Baumes, S Bitteur, Z Günata, C Bayonove. Novel monoterpene disaccharide glycosides of *Vitis vinifera* grapes. J Agric Food Chem 38:1373–1378, 1990.

15. D Chassagne, JC Crouzet, CL Bayonove, JM Brillouet, RL Baumes. 6-*O*-α-L-Arabinopyranosyl-β-D-glucopyranosides as aroma precursors from passion fruit. Phytochemistry 41:1497–1500, 1996.
16. W Guo, K Sakata, N Watanabe, R Nakajima, A Yagi, J Ina, S Luo. Geranyl 6-O-β-D-xylopyranosyl-β-D-glucopyranoside isolated as an aroma precursor from tea leaves for oolong tea. Phytochemistry 6:1373–1375, 1993.
17. JH Moon, N Watanabe, Y Ijima, A Nagi, K Sakata. *Cis*- and *trans*-linalool 3,7-oxides and methyl salicylate glycosides and (Z)-3-hexenyl β-D-glucopyranoside as aroma precursors from tea leaves for oolong tea. Biosci Biotechnol Biochem 60:1815–1819, 1996.
18. N Oka, M Ohki, A Ikegami, K Sakata, N Watanabe. First isolation of gernayl disaccharide glycosides as aroma precursors from rose flowers. Nat Product Lett 10:187–192, 1997.
19. YZ Günata. Recherches sur la fraction liée de nature glycosidique de l'arôme du raisin: importance des terpénylglycosides, action des glycosidases. PhD dissertation, University of Montpellier II, France, 1984.
20. JB Harborne, CA Williams. Flavone and flavonol glycosides. In: JB Harborne, ed. The Flavonoids. Advances in Research Since 1980. London: Chapman and Hall, 1988, pp 303–328.
21. JH Moon, N Watanabe, K Sakata, J Inagaki, A Nagi, K Ina, S Luo. Linalyl β-D-glucopyranoside and its 6′-*O*-malonate as aroma precursors from *Jasminum sambac*. Phytochemistry 36:1435–1437, 1994.
22. B Withopf, E Richling, R Roscher, W Schwab, P Schreier. Sensitive and selective screening for 6′-*O*-malonylated glucoconjugates in plants. J Agric Food Chem 45:907–911, 1997.
23. C Salles, JC Jallageas, F fournier, JC Tabet, JC Crouzet. Apricot glycosidically bound volatile components. J Agric Food Chem 39:1979–1983, 1991.
24. A Lutz, P Winterhalter. Isolation of additional carotenoid metabolites from quince fruit (*Cydonia oblonga* Mill.). J Agric Food Chem 40:1116–1120, 1992.
25. W Schwab, G Scheller, P Schreier. Glycosidically bound aroma components from sour cherry. Phytochemistry 29:607–612, 1990.
26. P Winterhalter. Bound terpenoids in the juice of the purple passion fruit (*Passiflora edulis* Sims). J Agric Food Chem 38:455–460, 1990.
27. H Young, VJ Paterson. Characterization of bound flavour components in kiwifruit. J Sci Food Agric 68:257–260, 1995.
28. H Heidlas, M Lehr, H Idstein, P Schreier. Free and bound terpene compounds in papaya (*Carica papaya*, L.) fruit pulp. J Agric Food Chem 32:1020–1021, 1984.
29. W Schwab, C Mahr, P Schreier. Studies on the enzymatic hydrolysis of bound aroma components from carica papaya fruit. J Agric Food Chem 37:1009–1012, 1989.
30. P Wu, MC Kuo, TG Hartman, RT Rosen, CT Ho. Free and glycosidically bound aroma compounds in pineapple (*Ananas comosus* L. Merr.) J Agric Food Chem 39:170–172, 1991.
31. M Sakho, D Chassagne, J Crouzet. African mango glycosically bound volatile compounds. J Agric Food Chem 45:883–888, 1997.
32. M Suarez, C Duque, H Wintoch, P Schreier. Glycosidically bound aroma compounds from the pulp and the peelings of Lulo fruit (*Solanum vestissimum* D.). J Agric Food Chem 39:1643–1645, 1991.
33. A Pabst, D Barron, P Etiévant, P Schreier. Studies on the enzymatic hydrolysis of bound aroma constituents from raspberry fruit pulp. J Agric Food Chem 39:173–175, 1991.
34. R Roscher, M Herderich, JP Steffen, P Schreier, W Schwab. 2,5-dimethyl-4-hydroxy-3(2H)-furanone 6′-*O*-malonyl β-D-glucopyranoside in strawberry fruits. Phytochemistry 43:155–159, 1997.
35. S Voirin. Connaissance de l'arôme du raisin: analyses et synthèses de précurseurs hétérosidiques. PhD dissertation, University of Montpellier II, France, 1990.
36. CR Strauss, B Wilson, PR Gooley, PJ Williams. Role of monoterpenes in grape and wine flavor. In: T Parliment, R Croteau, eds. Biogeneration of Aromas. Washington: American Chemical Society, 1986, pp 222–242.
37. PJ Williams, CR Strauss, B Wilson. Hydroxylated linalool derivatives as precursors of volatile monoterpenes of Muscat grapes. J Agric Food Chem 28:766–771, 1980.
38. PJ Williams, CR Strauss, B Wilson, RA Massy-Westropp. Studies on the hydrolysis of *Vitis vinifera* monoterpene precursor compounds and model monoterpene β-D-glucosides rationalizing the monoterpene composition of grapes. J Agric Food Chem 30:1219–1223, 1982.
39. P Ribéreau-Gayon, JN Boidron, A Terrier. Aroma of Muscat grape varieties. J Agric Food Chem 23:1042–1047, 1975.
40. G Chairote, F Rodriquez, J Crouzet. Characterization of additional volatile flavor components of apricot. J Agric Food Chem 46:1898–1901, 1981.
41. KH Engel, RA Flath, RG Butter, TR Mon, DW Ramming, R Teranishi. Investigation of volatile constituents in nectarines. 1. Analytical and sensory characterization of aroma components in some nectarine cultivars. J Agric Food Chem 36:549–553, 1988.
42. P Winterhalter. Oxygenated C_{13}-norisoprenoids. Important flavor precursors. In: R Teranishi, GR Takeoka, M Güntert, eds. Flavor Precursors. Thermal and Enzymatic Conversions. Washington: American Chemical Society, 1992, pp 98–115.

43. RG Buttery, R Teranishi, LC Ling. Identification of damascenone in tomato volatils. Chem Indust 7:238, 1988.
44. ML Sinnott. Catalytic mechanisms of enzymic glycosyl tranfer. Chem Rev 90:1171–1202, 1990.
45. E Bourquelot, M Bridel. Synthèse du géranyl glucoside à l'aide de l'émulsine: sa présence dans les végétaux. C R Acad Sci Paris 157:72–74, 1913.
46. MA Goris. Sur la composition chimique des fruits verts de vanille et le mode de formation du parfum de la vanille. C R Acad Sci Paris 179:70–72, 1924.
47. RE Cordonnier, YZ Günata, RL Baumes, CL Bayonove. Recherche d'un matériel enzymatique adapté à l'hydrolyse des précurseurs d'arômes de nature glucosidique du raisin. Conn Vigne Vin 23:7–23, 1989.
48. Z Günata, S Bitteur, JM Brillouet, C Bayonove, R Cordonnier. Sequential enzymic hydrolysis of potentially aromatic glycosides from grape. Carbohydr Res 184:139–149, 1988.
49. Z Günata, S Bitteur, R Baumes, JM Brilouet, C Tapiero, C Bayonove, R Cordonnier. Process for obtaining aroma components and aroma from their precursors of a glycosidic nature and aroma components and aromas thereby obtained. Institut National de la Recherche Agronomique (INRA)-Gist Brocades Patent 90202408.2-07.09.1990.
50. D Chassagne, C Bayonove, J Crouzet, R Baumes. Formation of aroma by enzymic hydrolysis of glycosidically bound components of passion fruit. In: P Etiévant, P Schreier, eds. Bioflavour 95. Paris: Ed INRA, 1995, pp 14–17.
51. Z Günata, C Blondeel, MJ Vallier, JP Lepoutre, JC Sapis, N Watanabe. An endoglycosidase from grape berry skin of cv. M. Alexandrie, hydrolyzing potentially aromatic disaccharide glycosides. J Agric Food Chem 46:2748–2753, 1998.
52. R Heyworth, PG Walker. Almond-emulsin β-D-glucosidase and β-D-galactosidase. Biochem J 83:331–335, 1962.
53. W Hösel. Glycosylation and glycosidases. In: PK Stumpf, EE Conn, eds. The Biochemistry of Plants. New York: Academic press, 1981, pp 725–753.
54. JH Schreier, P Schreier. Purification and partial characterization of β-glucosidase from papaya fruit. Phytochemistry 10:2271–2274, 1986.
55. M Lecas, YZ Günata, JC Sapis, C Bayonove. Purification and partial characterization of β-glucosidase from grape. Phytochemistry 30:451–454, 1991.
56. YZ Günata, C Biron, JC Sapis, C Bayonove. Glycosidase activities in sound and rotten grapes in relation to hydrolysis of grape monoterpenyl glycosides. Vitis 28:191–197, 1989.
57. R Bourbouze, F Percheron, JE Courtois. α-Rhamnosidase de *Fagopyrum esculentum*: purification et quelques propriétés. Eur J Biochem 63:331–337, 1976.
58. Y Shibata, K Nisizawa. Microheterogeneity of β-glycosidases in apricot emulsin. Arch Biochem Biophys 109:516–521, 1965.
59. AP Aryan, B Wilson, CR Strauss, PJ Williams. The properties of glycosidases of *Vitis viniferea* and comparison of their β-glucosidase activity with that of exogenous enzymes. An assessment of possible applications in enology. Am J Enol Vitic 38;182–188, 1987.
60. DJ Manners, DC Taylor. Studies on carbohydrate metabolising enzymes. Part XVIII. The α-L-arabinosidase activity of almond emulsin. Carbohydr Res 7:495–500, 1968.
61. J Woodward, A Wiseman. Fungal and other β-glucosidases. Their properties and applications. Enz Microbiol Technol 4:73–79, 1982.
62. A Kaji. L-arabinosidases. Adv Carbohyd Chem Biochem 42:383–394, 1984.
63. M Leclerc, A Arnaud, R Ratomahenina, P Galzy. Yeast β-glucosidases. Biotechnol Genet Eng Rev 5:269–295, 1987.
64. Y Gueguen, P Chemardin, A Arnaud, P Galzy. Purification and characterization of an intracellular β-glucosidase from *Botrytis cinerea*. Enz Microbiol Technol 17:900–906, 1995.
65. I Sasaki, H Nagayama. Purification and characterization of β-glucosidase from *Botrytis cinerea*. Biosci Biotechnol Biochem 59:100-1001, 1995.
66. C Romero, A Manjon, J Bastida, JL Iborra. A method for assaying the rhamnosidase activity of naringinase. Anal Biochem 149:566–571, 1985.
67. C Biron, R Cordonnier, O Glory, Z Günata, JC Sapis. Etude dans le raisin de l'activité β-glucosidase. Conn Vigne Vin 22:125–134, 1988.
68. R Di Stefano. The glycoside nature of terpenes of Muscat grape skins. The β-glucosidase activity of grape skins. Wein-Wissenshcaft 44:158–161, 1989.
69. P Lalégerie. La β-glucosidase de l'amande douce (*Amygdalus communis* L.). I. Isolement et purification. Biochimie 56:1163–1172, 1974.
70. P Winterhalter. The generation of C_{13}-norisoprenoïd volatiles in Riesling wine. In: C Bayonove, J Crouzet, C Flanzy, JC Martin, JC Sapis, eds. Connaissance Aromatique des Cépages et Qualité des Vins. Lattes, Hérault, France: Rev Fr Oenol, 1993, pp 65–73.
71. CA Williams, JB Harborne. Flavone and flavonol glucosides. In: JB Harborne, ed. The Flavonoids Advances in Research Since 1986. London: Chapmand and Hall, 1994, pp 337–385.
72. W Guo, K Ogawa, K Yamauchi, N Watanabe, T Usui, S Luo, K Sakata. Isolation and characterization of a β-primeverosidase concerned with alcoholic aroma formation in tea leaves. Biosci Biotechnol Biochem 60:1810–1814, 1996.
73. Shimizu, M Vehara, M Watanabe. Transformation of terpenes in grape must by *Botrytis cinerea*. Agric Biol Chem 27:141–145, 1982.

74. G Bock, I Benda, P Schreier. Biotransformation of linalool by *Botrytis cinerea*. J Food Sci 51:659–662, 1986.
75. G Bock, I Benda, P Schreier. Microbial transformation of geraniol and nerol by *Botrytis cinerea*. Appl Microbiol biotechnol 27:351–357, 1988.
76. D Dubourdieu, KH Koh, A Bertrand, P Ribéreau-Gayon. Mise en évidence d'une activité estérase chez *Botrytis cinerea*. Incidence technologique. C R Acad Sci Paris 296:1025–1028, 1983.
77. D Dubourdieu, P Ribéreau-Gayon, B Fournet. Structure of the extracellular β-D-glucan from *Botrytis cinerea*. Carbohydr Res 93:294–299, 1980.
78. JC Villettaz, D Steiner, H Trogus. The use of a β-glucanase as an enzyme in wine clarification and filtration. Am J Enol Vitic 35:253–256, 1984.
79. JJ Macheix, JC Sapis, A fleuriet. Phenolic compounds and polyphenoloxydases in relation to browning in grapes and wines. C R Food Sci Nutr 30:441–485, 1991.
80. A Delcroix, Z Günata, JC Sapis, JM Salmon, C Bayonov. Glycosidase activities of three enological yeast strains during wine making. Effect on the terpenol content of Muscat wine. Am J Enol Vitic 45:291–296, 1994.
81. D Dubourdieu, P Darriet, C Ollivier, JN Boidron, P Ribüreau-Gayon. Rôle de la levure *Saccharomyces cerevisiae* dans l'hydrolyse enzymatique des hétérosides terpéniques du jus de raisin. C R Acad Sci Paris 3:489–493, 1988.
82. P Sanzhez-Torres, L Gonzalez-Candelas, D Ramon. Heterologous expression of a *Candida molischiana* anthocyanin-β-glucosidase in a wine yeast strain. J Agric Food Chem 46:354–360, 1998.
83. P Sanchez-Torres, L Gonzalez-Candelas, D Ramon. Expression in a wine yeast strain of the *Aspergillus niger* abfB gene. FEMS Microbial Lett 145:189–194, 1996.
84. A Raynal, M Guerineau. Cloning and expression of the structural gene for β-glucosidase of *Kluyveromyces fragilis* in *Escherichia coli* and *Saccharomyces cerevisiae*. Mol Gen Genet 195:108–115, 1984.
85. AC Adam, M Rubio-Texeira, J Polaina. Induced expression of bacterial β-glucosidase activity in *Saccharomyces*. Yeast 11:395–406, 1995.
86. JD Duerksen, H Halvorson. Purification and properties of an inducible-β-glucosidase of yeast. J Biol Chem 233:1113–1120, 1958.
87. B Blondin, R Ratomahenina, A Arnaud, P Galzy. Purification and properties of the β-glucosidase of a yeast capable of fermenting cellobiose to ethanol: *Dekkera intermedia* Van der Walt. Eur J Appl Microbiol Biotechnol 17:1–6, 1983.
88. AI El-Diwany, MH Selim, AM El-Shafei. Comparison of β-glucosidase activities in different *Debaryomyces* strains. J Appl Microbiol Biotechnol 26:552–554, 1987.
89. I Rosi, M Vinella, P Domizio. Characterization of β-glucosidase activity in yeasts of enological origin. J Appl Bacteriol 77:519–527, 1994.
90. Y Vasserot, P Chemardin, A Arnaud, P Galzy. Evidence for the β-glucosidase activity and cellobiose fermentation by various *Kloeckera* strains. Acta Biotechnol 10:439–445, 1990.
91. Y Vasserot, P Chemardin, A Arnaud, P Galzy. Purification and properties of a β-glucosidase of *Hanseniaspora vineae* Van der Walt and Tscheuschner with the view to its utilization in fruit aroma liberation. J Appl Bacteriol 66:271–279, 1989.
92. P Gondé, R Ratomahenina, A Arnaud, P Galzy. Purification and properties of the exocellular β-glucosidase of *Candida molischiana* (Zikes) Meyer and Yarror capable of hydrolyzing soluble cellodextrines. Can J Biochem Cell Biol 63:1160–1166, 1985.
93. M Leclerc, A Arnaud, R Ratomahenina, P Galzy, M Nicolas. The enzyme system in a strain of *Candida wickerhamii* Meyer and Yarrow participating in the hydrolysis of cellodextrins. J Gen Appl Microbiol 30:509–521, 1984.
94. SN Freer. Purification and characterization of the extracellular β-glucosidase produced by *Candida wickerhamii*. Arch Biochem Biophys 243:515–522, 1985.
95. BC Saha, RJ Bothast. Production, purification and characterization of a highly glucose-tolerant novel β-glucosidase from *Candida peltata*. Appl Environ Microbiol 62:3165–3170, 1996.
96. JG Kaplan. An inducible system for the hydrolysis and transport of β-glucosidase in yeast. J Gen Physiol 48:873–885, 1965.
97. W Pilnik, AGJ Voragen. The significance of endogenous and exogenous pectic enzymes in fruit and vegetable processing. In: PF Fox, ed. Food Enzymology, Vol 1. New York: Elsevier Applied Science, 1991, pp 303–336.
98. JC Villettaz, D Dubourdieu. Enzymes in winemaking. In: PF Fox, ed. Food Enzymology. New York: Elsevier Applied Science, 1991, pp 427–453.
99. I Dupin, Z Günata, JC Sapis, C Bayonove, O M'Bairaroua, C Tapiero. Production of a β-apiosidase by *Aspergillus niger*. Partial purification, properties and effect on terpenyl apiosylglucosides from grape. J Agric Food Chem 40:1886–1891, 1992.
100. O Shoseyov, BA Bravdo, R Ikan, I Chet. Endo-β-glucosidase from *Aspergillus niger* grown on a monoterpene glycoside-containing medium. Phytochemistry 27:1973–1976, 1988.
101. S Voirin, R Baumes, C Bayonove, O M'Bairaroua, C Tapiero. Synthesis and NMR spectral properties of grape monoterpenyl glycosides. Carbohydr Res 207:39–56, 1990.
102. O M'Bairaroua, T Ton-That, C Tapiero. Synthèses de 6-*O*-β-D-apiofuranosyl-β-D-glucopyranosides de monoterpényle. Carbohydr Res 253:79–99, 1994.

103. MP Le Traon-Masson, P Pellerin. Purification and characterization of two β-D-glucosidase from an *Aspergillus niger* enzyme preparation: affinity and specificity toward glycosylated compounds characteristic of the processing of fruits. Enz Microbiol Technol 22:374–382, 1998.
104. E Dimitriadis, PJ Williams. The development and use of a rapid analytical technique for estimation of free and potentially volatile monoterpene flavorants of grapes. Am J Enol Vitic 34:66–71, 1984.
105. AN Inamdar, JG Kaplan. Purification and properties of an inducible β-glucosidase of bakers' yeast. Can J Biochem 44:1099–1108, 1966.
106. Z Günata, I Dugelay, MJ Vallier, JC Sapis, C Bayonove. Multiple forms of glycosidases in an enzyme preparation from *Aspergillus niger*: partial characterization of an apiosidase. Enz Microbiol Technol 21:39–44, 1997.
107. Z Günata, JM Brillouet, S Voirin, R Baumes, R Cordonnier. Purification and some properties of an α-L-arabinofuranosidase from *Aspergillus niger*. Action on grape monoterpenyl arabinofuranosyl glucosides. J Agric Food Chem 38:772–776, 1990.
108. M Roitner, T Schalkhammer, F Pittner. Preparation of prunin with the help of immobilized naringinase pretreated with alkaline buffer. Appl Biochem Biotechnol 9:483–488, 1984.
109. I Dugelay, L'arôme du raisin: étude des précurseurs hétérosidiques et des activités enzymatiques exogènes impliquées dans leur hydrolyse. Applications technologiques. PhD dissertation, University of Montpellier II, France, 1993.
110. G Janbon, J Derancourt, P Chemardin, A Arnaud, P Galzy. A very stable β-glucosidase from a *Candida molischiana* mutant strain. Enzymatic properties, sequencing and homology with other yeast strains. Biosci Biotechnol Biochem 59:1320–1322, 1995.
111. Y Vasserot, P Chemardin, A Arnaud, P Galzy. Purification and properties of the β-glucosidase of a new strain of *Candida molischiana* able to work at low pH values: possible use in the liberation of bound terpenols. J Basic Microbiol 31:301–312, 1991.
112. MH Rashid, KS Siddiqui. The stability of extracellular β-glucosidase from *Aspergillus niger* is significantly enhanced by non-covalently attached polysaccharides. Folia Microbiol 41:341–346, 1996.
113. RFH Dekker. Kinetic, inhibition and stability properties of a commercial β-D-glucosidase (cellobiase) preparation from *Aspergillus niger* and its suitability in the hydrolysis of lignocellulose. Biotechnol Bioeng 28:1438–1442, 1986.
114. D Chassagne. Les glycosides des précurseurs d'arôme du fruit de la passion: étude structural et hydrolyse enzymatique. PhD dissertation, University of Montpellier II, France, 1996.
115. Z Günata, C Bayonove, C Tapiero, R Cordonnier. Hydrolysis of grape monoterpenyl β-D-glucosides by various β-glucosidases. J Agric Food Chem 38:1232–1236, 1990.
116. Z Günata, C Bayonove, R Cordonnier, A Arnaud, P Galzy. Hydrolysis of grape monoterpenyl glycosides by *Candida molischiana* and *Candida wickerhamii* β-glucosidases. J Sci Food Agric 50:499–506, 1990.
117. Z Günata, MJ Vallier, JC Sapis, C Bayonove, V Arnaudon, A Madarro, J Polaina. Hydrolysis of monoterpenyl-β-D-glucosides by cloned β-glucosidases from *Bacillus polymyxa*. Enz Microbiol Technol 18:286–290, 1996.
118. WW Pigman. Specificity, classification and mechanism of action of the glycosidases. In: FF Nord, CH Werkman, eds. Advances in Enzymology, New York: Interscience, 1946, pp 41–74.
119. B Capon. Mechanism in carbohydrate chemistry. Chem Rev 69:407–445, 1969.
120. W Hösel, EZ Conn. The aglycone specificity of plant β-glucosidases. Trends Biochem 7:219–221, 1982.
121. Y Ijima, K Ogawa, N Watanabe, T Usui, M Ohnishi-Kameyame, T Nagata, K Sakata. Characterization of β-primeverosidase being concerned with alcoholic aroma formation in tea leaves to be processed into black tea and preliminary observations on its substrate specificity. J Agric Food Chem 46:1712–1718, 1998.
122. H Imaseki, TA Yamamoto. Furcatin hydrolyzing glycosidase of *Viburnum furcatum* blume. Arch Biochem Biophys 92:467–474, 1961.
123. W Hösel. Reinigung und characterisierung zweir β-glykosidasen mit bevorzugter Spezifität für biochanin-A-7-β-apiosylglucosid aus *Cicer arietinum* L. Hoppe-Seyler's Z Physiol Chem 357:1673–1681, 1976.
124. H Suzuki. Hydrolysis of flavonoid glycosides by enzymes (rhamnodiastase) from *Rhamnus* and other sources. Arch Biochem Biophys 99:476–483, 1962.
125. R Bourbouze, F Pratviel-Soa, F Percherorn. Rhamnodiastase and L-rhamnosidase de *Fagopyrum esculentum*. Phytochemistry 14:1279–1282, 1975.
126. DWS Westlake, G Talbot, ER Blakley, FJ Simpson. Microbial decomposition of rutin. Can J Microbiol 5:621–629, 1959.
127. YK Hoh, HH Yeoh, TK Tan. Properties of β-glucosidase purified from *Aspergillus niger* mutants USDB 0827 and USDB 0828. Appl Microbiol Biotechnol 37:590–593, 1992.
128. KS Kwon, HG Kang, YC Hah. Purification and characterization of two extracellular β-glucosidases from *Aspergillus nidulans*. FEMS Microbiol Lett 97;149–154, 1992.
129. Z Günata, MJ Vallier, R Baumes, C Bayonove. β-Glucosidase from filamentous fungi and uses thereof. Institut National de la Recherche Agronomique

(INRA) patent PCT FR96/01054, WO 97/02341 (1997).
130. Z Günata, MJ Vallier. Production of highly glucose-tolerant extracellular β-glucosidase by three *Aspergillus* strains. Biotechnol Lett 21:219–223, 1999.
131. TR Yan, CL Lin. Purification and characterization of a glucose-tolerant β-glucosidase from *Aspergillus niger* CCRC 31494. Biosci Biotech Biochem 61:965–970, 1997.
132. H Ozaki, K Yamaha. Isolation of *Streptomyces* sp. producing glucose-tolerant β-glucosidases and properties of the enzymes. Agric Biol Chem 55:979–987, 1991.
133. JA Perez-Pons, X Robordosa, E Querol. Properties of a novel glucose enhanced β-glucosidase purified from *Streptomyces* sp. (ATCC 11238). Biochim Biophys Acta 1251:145–153, 1995.
134. WM Wright, MD Yablonsky, ZP Athalita, AK Goyal, DE Eveleigh. Cloning, characterization and nucleotide sequence of a gene encoding *Microbispora bispora* BglB, a thermostable β-glucosidase expressed in *Escherichia coli*. Appl Environ Microbiol 58:3455–3465, 1992.
135. F Le Clinche, F Pinaga, D Ramon, S Vallès. α-L-Arabinofuranosidases from *Aspergillus terreus* with potential application in enology: induction, purification and characterization. J Agric Food Chem 45:2379–2383, 1997.
136. V Reyne. Isolement et caractérisation de glucosidases produites par *Aspergillus niger*. Application à l'hydrolyse d'hétérosides terpéniques. PhD dissertation, University of Montpellier II, France, 1992.
137. N Ait, N Creuzet, J Cattaneo. Properties of β-glucosidase purified from *Clostridium thermocellum*. J Gen Microbiol 128:569–577, 1982.
138. J Conchie, AL Gelman, GA Levvy. Inhibition of glucosidases by aldonolactones of corresponding configuration. The C-4 and C-6 specification of β-glucosidase and β-galactosidase. Biochem J 103:609–615, 1967.
139. LP McCloskey. Gluconic acid in California wines. Am J Enol Vitic 25:198-201, 1974.
140. MS Pemberton, RD Brown, GH Emert. The role of β-glucosidase in the bioconversion of cellulose to ethanol. Can J Chem Eng 58:723–729, 1980.
141. MP Dale, HE Ensley, K Kern, KAR Sastry, LD Byers. Reversible inhibitors of β-glucosidase. Biochemistry 24:3530–3539, 1985.
142. T Osawa, TH Lilley, E Haslam. Polyphenol interactions: astringency and the loss of astringency in ripening fruit. Phytochemistry 26:2937–2942, 1987.
143. S Guyot, P Pellerin, JM Brillouet, V Cheynier. Inhibition of β-glucosidase (*Amygdalae dulces*) by (+)-catechin oxidation products and procyanidin dimers. Biosci Biotechnol Biochem 60:1131–1135, 1996.
144. AJ Dick, R Williams, SL Bearne, PD Lidster. Quercetin glycosides and chlorogenic acid: inhibitors of apple β-galactosidase and apple softening. J Agric Food Chem 33:798–800, 1985.
145. YZ Günata, C Bayonove, R Baumes, R Cordonnier. Stability of free and bound fractions of some aroma components of grape *cv* Muscat during the wine processing. Am J Enol Vitic 37:112–114, 1985.
146. M Grossmann, A Rapp. Steigerung des sortentypischen Weinbuketts nach Enzymebehandlung. Dtsche Lebensmittel-Rundschau 84:35–37, 1988.
147. Z Günata, I Dugelay, JC Sapis, R Baumes, C Bayonove. Action des glycosidases exogènes au cours de la vinification: libération de l'arôme à partir des précurseurs glycosidiques. J Int Sci Vigne Vin 24:133–144, 1990.
148. C Bayonove, YZ Günata, JC Sapis, RL Baumes, I Dugelay, C Grassin. L'aumento degli aromi nel vino mediante l'uso degli enzimi. Vignevini 9:33–36, 1993.
149. G Nicolini, G Versini, F Mattivi, A Dalla Serra. Glicosidasi in mosti e vini. vignevini 7/8:26–32, 1994.
150. T Caboroglu. Aroma composition of grape juice and white wine of *Vitis vinifera* cv. Emir. PhD dissertation, Cukurova University, Adana, Turkey, 1995.
151. FSS Rogerson, HJ Grande, MCM Silva. Enzymatic enhancement of the free monoterpenol content of a portuguese wine from a single, native grape variety "Trajadura". Biotechnol Lett 17:35–40, 1995.
152. A Bertrand, AA Beloqui. Essais d'utilisation d'enzymes pectolytiques à activités complémentaires de type glucosidase dans les vins. Influence sur l'arôme. Rev Fr Oenol 3:157, 1996.
153. SG Voirin, RL Baumes, JC Sapis, CL Bayonove. Analytical method for monoterpene glycosides in grape and wine. Part 2. Qualitative and quantitative determination of glycosides in grape. J Chromatogr 595:269–281, 1992.
154. P Gramatica, P Manitto, BM Razi, A Delbianco, M Francavilla. Stereospecific reduction of geraniol to (R)-(+)-citronellol by *Saccharomyces cerevisiae*. Experientia 38:775–776, 1982.
155. I Dugelay, Z Günata, JC Sapis, R Baumes, C Bayonove. Etude de l'origine du citronellol dans les vins. J Int Sci Vigne Vin 26:177–184, 1992.
156. R Di Stefano, G Magiorotto, S Gianotti. Transformazioni di nerolo e geraniolo indotte dai lieviti. Rivi vitic Enol 1:43–49, 1992.
157. A Rapp, M Guntert, M Ulmeyer. Uber Veränderungen der Aromastoffe während der Flaschenlagerung von Weisweinen der Rebsorte Riesling. Z Lebensm Unters Forsch 18:109–116, 1985.
158. MA Sefton, IL Francis, PJ Williams. The volatile composition of Chardonnay juices: a study by flavor precursor analysis. Am J Enol Vitic 44:359–370, 1993.

159. PJ Williams, IL Francis, MA Sefton. Sensory and chemical analysis of hydrolysed flavour precursors from Sauvignon blanc grapes. In: P Schreier, P Winterhalter, eds. Progress in Flavour Precursor Studies. Carol Stream, IL: Allured Publ, 1993, pp 235–242.
160. GK Skouroumounis, RA Massy-Westropp, MA Sefton, PJ Williams. Precursors of damascenone in fruit juices. Tetrahedron Lett 24:3533–3536, 1992.
161. O Shoseyov, BA Bravdo, R Ikan, I Chet. Immobilized endo-β-glucosidase enriches flavor of wine and passion fruit juice. J Agric Food Chem 27:1973–1976, 1990.
162. Y Gueguen, P Chemardin, G Janbon, A Arnaud, P Galzy. A very efficient β-glucosidase catalyst for the hydrolysis of flavor precursors of wines and fruit juices. J Agric Food Chem 44:2336–2340, 1996.
163. Y Gueguen, P Chemardin, S Pien, A Arnaud, P Galzy. Enhancement of aromatic quality of Muscat wine by the use of immobilized β-glucosidase. J Biotechnol 55:151–156, 1997.
164. I Rosi, P Domizio, M Vinella, M Salicone. Hydrolysis of grape glycosides by enological yeast β-glucosidases. In: G Charalambous, ed. Food Flavors: Generation, Analysis and Process Influence. London: Elsevier Science, 1995, pp 1623–1635.
165. IL Francis, MA Sefton, PJ Williams. Sensory descriptive analysis of the aroma of hydrolyzed precursor fractions from Semillon, Chardonnay and Sauvignon blanc grape juices. J Sci Food Agric 59:511–520, 1992.
166. D Drider, G Janbon, P Chamardin, A Arnaud, P Galzy. Enzymatic hydrolysis of monoterpene glycosides of passion fruit and mango with a β-glucosidase from yeast. Bioresource Technol 49:234–246, 1994.
167. JJ Macheix, A Fleuriet, J Billot. Fruit Phenolics. Boca Raton, FL: CRC Press, 1990, pp 20–32.
168. FM Romeyer, JJ Macheix, JP Goiffon, CC Reminiac, JC Sapis. The browning capacity of grapes. 3. Changes and importance of hydroxycinnamic acid–tartaric acid esters during development and maturation of the fruit. J Agric Food Chem 31:346–349, 1983.
169. YZ Günata, M Salgues, M Moutounet. Evolution des dérivés hydroxycinnamiques au cours de l'élaboration du moût de raisin et du stockage des concentrés. Sci aliments 6:579–590, 1986.
170. GA Spanos, RE Wrolstad, DA Heatherbell. Influence of processing and storage on the phenolic composition of apple juice. J Agric Food Chem 38:1572–1579, 1990.
171. I Dugelay, Z Günata, S Bitteur, JC Sapis, R Baumes, C Bayonove. Formation of volatile phenols from cinnamic acid precursors during winemaking: role of cinnamoyl esterase activities from commercial enzyme preparations. In: P Schreier, P Winterhalter, eds. Progress in Flavour Precursor Studies. Carol Stream, IL: Allured Publ, 1993, pp 189–193.
172. I Dugelay, Z Günata, JC Sapis, R Baumes, C Bayonove. Role of cinnamoyl esterase activities from enzyme preparations on the formation of volatile phenols during winemaking. J Agric Food Chem 41:2092–2096, 1993.
173. P Chatonnet, C Barbe, RM Canal-Llauberes, D Dubourdieu, JN Boidron. Incidences de certaines preéparations pectolytiques sur la teneur en phénols volatils des vins blancs. J Int Sci Vigne Vin 26;253–269, 1992.
174. H Peleg, M Naim, U Zehavi, RL Rouseff, S Nagy. Pathways of 4-vinylguaiacol formation from ferulic acid in model solutions of orange juice. J Agric Food Chem 40:764–767, 1992.
175. G Albagnac. La décarboxylation des acides cinnamiques substitués par les levures. Ann Technol Agric 24:133–141, 1975.
176. BJ Finkle, JC Lewis, JW Corse, RE Lundin. Enzyme reactions with phenolic compounds: formation of hydroxystyrenes through the decarboxylation of 4-hydroxycinnamic acids by *Aerobacter*. J Biol Chem 237:1926–1931, 1962.
177. GC Whiting, JG Carr. Chlorogenic acid metabolism in cider fermentation. Nature 180:1479, 1957.
178. GC Whiting, JG Carr. Metabolism of cinnamic acid and hydroxy-cinnamic acids by *Lactobacillus pastorianus*, var. *quinicus*. Nature 184:1427–1428, 1959.
179. P Chattonnet, D Dubourdieu, JN Boidron, V Lavigne. Synthesis of volatile phenols by *Saccharomyces cerevisiae* in wine. J Sci Food Agric 62:191–202, 1993.
180. JA Maga. Simple phenol and phenolic compounds in food flavor. CRC Crit Rev Food Sci Nutr 10:323–372, 1978.
181. P Etiévant. Wine. In: H Maarse, ed. Volatile Compounds in Foods and Beverages. New York: Marcel Dekker, 1991, pp 483–546.
182. G Versini. Sull'aroma del vino "Traminer aromatico" or "Gewürztraminer". Vignivini 5:57–65, 1985.
183. M Naim, BJ Striem, J Kanner, H Peleg. Potential of ferulic acid as a precursor to off-flavors in stored orange juice. J Food Sci 512:500–503, 1988.
184. T Heresztyn. Metabolism of volatile phenolic compounds from hydroxycinnamic acids by *Brettanomyces* yeast. Arch Microbiol 146:96–98, 1986.
185. JC Villettaz. The use of enzymes in enology to extract colour and to extract and reveal aromas. Bull OIV 787–788;843–860, 1996.
186. CR Burkhard. Verlust des fruchteigenen Wohlgeschmacks bei verarbeiteten Lebensmitteln pflanzlicher Herkunft, der im Zusammenhang mit der Spaltung von Hydroxizimtsäureestern (Depsiden) steht. Dtsche Lebensmittel-Rundschau 74:205–208, 1978.

187. P Chatonnet, D Dubourdieu, JN Boidron. Incidences de certains facteurs sur la décarboxylation des acides phénols par la levure. Conn Vigne Vin 23:59–62, 1989.
188. I Digelay, R Baumes, Z Günata, A Razungles, C Bayonove. Evolution de l'arôme au cours de la conservation du vin: formation de 4-(1-éthoxyéthyl)-phénol et 4-(1-éthoxyéthyl)-gaïacol. Sci Aliments 15:423–433, 1995.
189. P Chatonnet, D Dubourdieu, JN Boidron, M Pons. The origin of ethylphenols in wines. J Sci Food Agric 60:165–178, 1992.
190. MA Sefton, PJ Williams. Generation of oxidation artifacts during the hydrolysis of norisoprenoid glycosides by fungal enzyme preparations. J Agric Food Chem 39:1994–1997, 1994.
191. RL Jackman, RY Yada, MA Tung, RA Speers. Anthocyanins as food colorants. A review. J Food Biochem 11:201–247, 1987.
192. FJ Francis. Food colorants: anthocyanins. Crit Rev Food Sci Nutr 28:273–314, 1989.
193. JB Harborne, RJ Grayer. The anthocyanins. In: JB Harborne, ed. The Flavonoids, London: Chapman and Hall, 1988, pp 1–18.
194. HT Huang. Fruit color destruction: decolorization of anthocyanins by fungal enzymes. J Agric Food Chem 3:141–146, 1955.
195. HT Huang. The kinetics of the decolorization of anthocyanins by fungal "anthocyanase". J Am Chem Soc 78:2390–2395, 1956.
196. T Unno, K Ide, T Yazaki, Y Tanaka, T Nakakuki, G Okada. High recovery purification and some properties of a β-glucosidase from *Aspergillus niger*. Biosci Biotechnol Biochem 57:2172–2173, 1993.
197. RE Wrolstad, JD Wightman, RW Durst. Glycosidase activity of enzyme preparations used in fruit juice processing. Food Technol 11:90–98, 1994.
198. P Lerouge, MA O'Neill, AG Darvill, P Albersheim. The purification of commercially available endo-α-L-arabinases and α-L-arabinosidase for use in the structural analysis of pectic polysaccharides. Carbohydr Res 243:373–378, 1993.
199. OP Bahl, KML Agrawal. Glycosidases of *Aspergillus niger*. I. Purification and characterization of α- and β-galactosidases and β-N-acetyl-glucosaminidase. J Biol Chem 244: 2970–2978, 1969.
200. J Jiang, A Paterson, JR Piggott. Effects of pectolytic enzyme treatments on anthocyanins in raspberry juice. Int J Food Sci Technol 25:596–600, 1990.
201. H Blom. Partial characterization of a thermostable anthocyanin-β-glycosidase from *Aspergillus niger*. Food Chem 12:197–204, 1983.
202. HY Yang, WF Steele. Removal of excessive anthocyanin pigment by enzyme. Food Technol 12:517–519, 1958.
203. C Fumian, PG Pifferi, L Setti, G Spagna, A Martino. Immobilization of an anthocyanase (β-glucosidase) from *Aspergillus niger*. Ital J Food Sci 6:31–42, 1994.
204. JD Wightman, FP Steven, BT Watson, RE Wrolstad. Some effects of processing enzymes on anthocyanins and phenolics in Pinot Noir and Cabernet Sauvignon wines. Am J Enol Vitic 48:39–47, 1997.
205. S Rwahahizi, RE Wrolstad. Effects of mold contamination and ultrafiltration on the color stability of strawberry juice and concentrate. J Food Sci 53:857–861, 1988.
206. MJ Boyles, RE Wrolstad. Anthocyanin composition of red raspberry juice: influences of cultivar, processing and environmental factors. J Food Sci 58:1135–1141, 1993.
207. R Cassignard, M Ducasse, C Barrere, M Artigau. Influence du taux de pourriture grise sur la qualité des vins produits. Vignes Vins 260:28–31, 1977.
208. Z Günata, C Olivieri, J Pineau, J Planque. Détection de la pourriture grise dans les vendanges: applications à la vinification et incidences technologiques. Rev Fr Oenol 114:7–10, 1988.
209. JD Wightman, RE Wrolstad. β-Glucosidase activity in juice processing enzymes based on anthocyanin analysis. J Food Sci 61:544–552, 1996.
210. R Birk, B Bravdo, O Shoseyov. Detoxification of cassava by *Aspergillus niger* B-1. Appl Microbiol Biotechnol 45:411–414, 1996.
211. NFF Soares, JH Hotchkiss. Naringinase immobilization in packaging films for reducing naringin concentration in grapefruit juice. J Food Sci 63:61–65, 1998.

22

Entrapment of Biocatalysts by Prepolymer Methods

Takuo Kawamoto and Atsuo Tanaka
Kyoto University, Kyoto, Japan

I. INTRODUCTION

Immobilization of biocatalysts which include enzymes, cellular organelles, microbial cells, plant cells, and animal cells is attracting worldwide attention. Immobilized biocatalysts are, in general, easier to handle and more stable than native counterparts, and they can be used either repeatedly in a long-term series of batchwise reaction or continuously in flow systems, which are useful and important features for practical applications of biocatalysts. At present, immobilized biocatalysts have contributed to a wide variety of fields including:

1. Production of useful compounds by stereospecific and/or regiospecific bioconversions.
2. Production of energy and reducing equivalent by biological processes.
3. Selective degradation or removal of pollutants.
4. Analyses of various compounds with high sensitivity and specificity.
5. Application to foods, such as hydrolysis of lactose of milk, alcohol fermentation, production of glucose from starch, and production of high-fructose corn syrup.
6. Utilization in medical fields, such as new types of drugs and artificial organs.

These processes require immobilization not only of single enzymes that catalyze simple reactions but also of multienzyme systems that mediate more complicated reactions.

There are various immobilization methods at present. In general, the immobilization methods can be classified as follows:

(a) carrier binding via covalent linkage, ionic bonds, physical adsorption, or biospecific binding; (b) cross-linking by using bi- or multifunctional reagents; (c) entrapment in gel matrices, microcapsules, liposomes or hollow fibers; and (d) combination of the above-mentioned methods (1, 2).

Of these immobilization methods developed hitherto, entrapment methods are the most promising because this method is applicable to the immobilization of not only single enzymes but also multiple enzymes, cellular organelles, microbial cells, plant cells, and animal cells.

The disadvantages of this method are: (a) high-molecular-weight substrates may not be able to access the entrapped biocatalysts, and (b) renewal of the carrier is difficult.

Among the entrapment methods, entrapment in gel matrices is the most widely used. Various types of gel materials, such as polysaccharides, proteins, and synthetic polymers, are now used to entrap biocatalysts. Because applications of immobilized biocatalysts are aimed toward a wide variety of bioreactions, including synthesis, transformation, degradation, or assay of various compounds having different chemical properties (3), it is desirable to entrap biocatalysts in gels of adequate physicochemical properties to satisfy the different demands in such a variety of applications. It is, however, difficult to select suitable gels for each pur-

pose among those prepared from natural polymers. Furthermore, it is not easy to modify natural polymers for the preparation of proper gel materials. As for synthetic materials, acrylamide and its analogs have been used widely as starting materials for gels. These monomers are, however, liable to inactivate biocatalysts in the polymerization and immobilization processes.

For these reasons, continuous efforts have been devoted to development of prepolymer methods which are new entrapment methods using synthetic prepolymers as starting materials for gels.

II. PREPOLYMER METHODS

In the case of prepolymer methods, synthetic resin prepolymers are used as gel-forming starting materials for entrapment of biocatalysts. Specific features and advantages of prepolymer methods can be summarized as follows:

1. Entrapment procedures are very simple and proceed under mild conditions.
2. Prepolymers do not contain monomers which may have a negative influence on the biocatalysts to be entrapped.
3. The network structure and strength of gels can be regulated by the chain length and the content of the reactive functional groups of the prepolymers.
4. The physicochemical properties of gels, such as hydrophilicity–hydrophobicity balance and ionic nature, can be controlled by selecting suitable prepolymers which are synthesized chemically in advance in the absence of biocatalysts.

Several examples of the prepolymer methods are described below.

A. Photocrosslinkable Resin Prepolymer Method

1. Principle

In the case of photocrosslinkable resin prepolymers, the mixture of the prepolymer and the biocatalyst is gelled by radical polymerization of the prepolymer initiated by illumination with near-ultraviolet light for several min in the presence of a proper photosensitizer (initiator) such as benzoin ethyl ether or benzoin isobutyl ether.

2. Prepolymers

The structures of some typical photocrosslinkable resin prepolymers are shown in Figure 1. The properties of the several prepolymers are summarized in Table 1.

Polyethylene glycol dimethacrylate (PEGM) was synthesized with polyethylene glycol and methacrylate. ENT and ENTP were prepared with hydroxyethylacrylate, isophoronediisocyanate, and polyethylene glycol or polypropylene glycol, respectively. Each prepolymer has a linear skeleton of optional length, at both the ends of which are attached the photosensitive functional groups, acryloyl, methacryloyl, etc. PEGM (4–6) and ENT (7, 8) containing polyethylene glycol as the main skeleton are water-soluble and form hydrophilic gels, while ENTP (9) with polypropylene glycol as the main skeleton is water-insoluble and gives hydrophobic gels. By using polyethylene glycol or polypropylene glycol of different molecular weights, prepolymers of different chain length, PEGM-1000 to PEGM-4000, ENT-1000 to ENT-6000, and ENTP-1000 to ENTP-4000, can be prepared. Chain length of the prepolymers correlates with the size of network of the gels formed from these prepolymers. Prepolymers having ionic properties can also be prepared by introducing ionic functional group(s) to the main skeleton of prepolymers. An emulsion-type photocrosslinkable resin prepolymer, ENTE-1, was prepared in the following way. Hydrophobic polyvinyl acetate was coated with hydrophilic polyvinyl alcohol to be easily dispersed in an aqueous solution. Photosensitivity was introduced by the reaction with *N*-hydroxymethyl acrylamide in the presence of an acid catalyst. After neutralization, an emulsion-type photocrosslinkable resin prepolymer

Table 1 Properties of Several Photocrosslinkable Resin Prepolymers

Prepolymer	MW of main chain	Property
PEGM-1000	~1000	Hydrophilic
PEGM-2000	2000	
PEGM-4000	4000	
ENT-1000	~1000	Hydrophilic
ENT-2000	2000	
ENT-4000	4000	
ENTP-1000	~1000	Hydrophobic
ENTP-2000	2000	
ENTP-3000	3000	
ENTP-4000	4000	
ENTE-1	—	Emulsion-type
ENTA-1	~2200	Anionic
ENTC-1	~940	Cationic

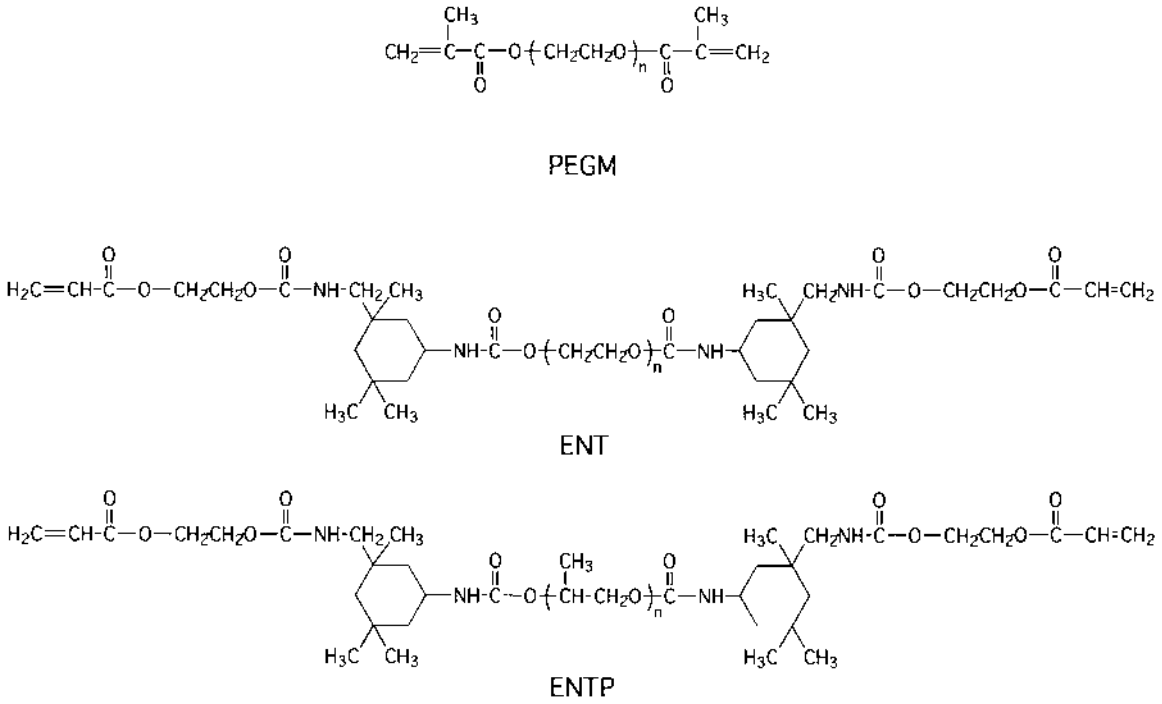

Figure 1 Structures of typical photocrosslinkable resin prepolymers.

was obtained. ENTE-1 is useful when swelling of the gels is to be avoided (10). Photocrosslinkable resin prepolymers can be autoclaved at 120°C and stored in the dark.

Among these photocrosslinkable resin prepolymers, ENT and ENTP prepolymers are commercially available from Kansai Paint Co., Tokyo, Japan.

3. Procedures

Typical procedures for entrapment with photocrosslinkable resin prepolymers are as follows: 1 g of ENT-4000 or mixture of ENT-4000 and ENTP-4000 (ENT-4000 content is above 70%) is mixed with 10 mg of a photosensitizer such as benzoin ethyl ether. The mixture is melted by warming at 60°C. An adequate buffer, such as 50 mM potassium phosphate buffer (0.5 mL) is added to the molten mixture and mixed at 60°C. The molten mixture is cooled to 4°C, and 2 mL of solution or suspension of biocatalysts is added to the mixture. The obtained mixture is layered on a sheet of transparent polyester film framed ($\sim$70 cm^2) with a plastic tape (thickness $\sim$0.5 mm). The layer is covered with a transparent thin film to eliminate air and then illuminated with near-ultraviolet light (wavelength range 300–400 nm; maximum intensity at 360 nm) for several minutes. The gel film formed is cut into small pieces and used as the entrapped biocatalyst.

Bead-type biocatalysts entrapped with photocrosslinkable resin prepolymers can also be obtained (11). Ten parts (by weight) of prepolymer are mixed with 0.08 parts of the initiator, 2 parts of 3% sodium alginate, 2 parts of distilled water, and 2 parts of the biocatalyst. The mixture obtained is dropped into 1.5% aqueous calcium chloride solution to form the beads. The beads thus formed are irradiated by near-ultraviolet light. After irradiating for 5 min, the entrapped biocatalyst beads obtained are washed with sterile water. For practical applications, the bead-type is often preferable to the cube-type or film-type.

Tube-type biocatalysts can be easily prepared by using ENTE-1. The inner surface of glass tubes (ID 2 mm) is silanized with vinyltriethoxysilane (10). ENTE-1 is mixed with photosensitizer and the solution or suspension of biocatalyst. This viscous mixture is injected at the top of each silanized glass tube to form a thin layer of biocatalyst-containing prepolymer on the inner surface of the tube. The tube is illuminated with near ultraviolet light for several minutes under an atmosphere of nitrogen to

complete the photocrosslinking of the prepolymer. The resulting tube-type biocatalysts can be used in continuous-flow systems to assay various compounds.

B. Urethane Resin Prepolymer Method

1. Principle

The urethane resin prepolymer method is very simple and convenient, because isocyanate functional groups at both terminal ends of the urethane prepolymer (Fig. 2) react with each other only in the presence of water, forming a urea linkage and liberating carbon dioxide (12). Consequently, when the prepolymers are mixed with an aqueous solution or an aqueous suspension of biocatalyst, gels are easily formed within a few minutes and gelation is complete in 30–60 min.

2. Prepolymers

Structures of typical urethane resin prepolymers are shown in Figure 2, and the properties of the prepolymers are summarized in Table 2. Urethane resin prepolymers (PU) are synthesized from toluene diisocyanate and polyether diols composed of polyethylene glycol and polypropylene glycol or polyethylene glycol alone. Prepolymers with different hydrophilic or hydrophobic properties can be obtained by changing the ratio of the polyethylene glycol and polypropylene glycol in the polyether diol moiety of the prepolymers. For example, PU-2 to PU-4 with a high content of polypropylene glycol give relatively hydrophobic gels, while PU-1 and PU-5 to PU-11 with a high content of polyethylene glycol give hydrophilic gels, although all the prepolymers are water miscible (13, 14). The chain length and the content of isocyanate group of the prepolymers, which correlate to the size of network of the gels formed from these prepolymers, can also be changed.

Urethane resin prepolymers can be sterilized at 120°C under anhydrous conditions and stored in a desiccator.

Although these urethane resin prepolymers are not currently available commercially, Hypol having a similar structure can be obtained from W. R. Grace Co., Lexington, MA.

3. Procedures

Typical entrapment procedures with urethane resin prepolymers are as follows. The urethane prepolymer (1 g) melted by incubation at 50°C (if necessary) is cooled to 4°C and mixed quickly and well with 2 mL of aqueous solution or suspension of biocatalyst in a small beaker. When gelation starts after a few minutes of mixing, the mixture is kept at 4°C for 30–60 min to complete the gelation. The gel thus formed is cut into small pieces, washed thoroughly with the buffer, and used as the entrapped biocatalyst.

If the mixture, quickly and well stirred, is immediately layered on a glass plate framed with adhesive tape with the proper dimensions before the gelation starts, a film of entrapped biocatalyst can be obtained (15).

C. Miscellaneous

Owing to the advantages of prepolymer methods mentioned above, continuous efforts have been devoted to develop new prepolymer methods.

Photosensitive resin prepolymers (PVA-SbQ) were also developed by Ichimura (16). Photosensitive resin prepolymers are derivatives of polyvinyl alcohol having styrylpyrydinium groups as photosensitive functional sites and polymerized by photodimerization with irradiation of visible or ultraviolet light. Hydrophilicity of the prepolymers can be controlled by changing the saponification degree of polyvinyl acetate.

Several prepolymers, such as polyvinyl alcohol (17), polyethylene glycol diacrylate (18), and polyethylene

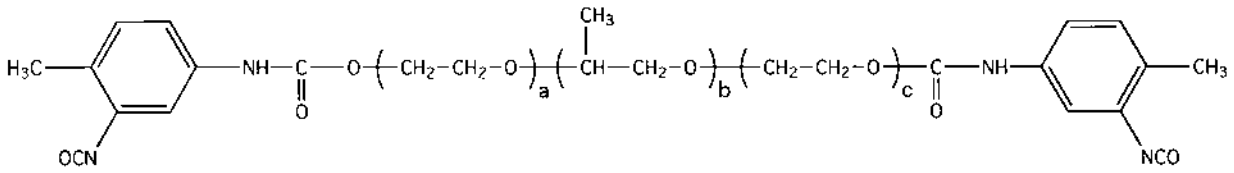

PU

Figure 2 General formula of urethane resin prepolymers.

Table 2 Properties of Urethane Resin Prepolymers

Prepolymer	MW of polyether diol	NCO content in prepolymer (%)	Polyethylene glycol content in polyether diol (%)	Property of gel formed
PU-1	1486	4.0	100	Hydrophilic
PU-2	2529	3.1	57[a]	Hydrophobic
PU-3	2529	4.2	57[a]	
PU-4	2529	5.6	57[a]	
PU-5	2627	2.7	91[a]	Hydrophilic
PU-6	2627	4.0	91[a]	
PU-7	2627	5.6	91[a]	
PU-8	2616	2.7	100	Hydrophilic
PU-9	2616	4.0	100	
PU-10	2616	5.6	100	
PU-11	4285	4.0	73[a]	Hydrophilic

[a]The remaining percentage (100–X) is polypropylene glycol.

glycol dimethacrylate (18, 19), are also useful gel materials for entrapment by radiation. In the case of 10% polyvinyl alcohol, 5–7 Mrad of radiation is sufficient to obtain rigid gels (17). The glass-forming prepolymers, such as polyethylene glycol diacrylate and polyethylene glycol dimethacrylate, are used for entrapment through radiation polymerization at low temperature. Entrapment can be carried out at -24°C with 10% prepolymer and a radiation of 1 Mrad (19). A mixture of polyvinyl alcohol and polyethylene glycol dimethacrylate is also applicable (18). This radiation method has several advantages such as possible application of a wide variety of prepolymers as gel materials and entrapment at low temperature. However, utilization of this method is limited because radiation apparatus is required.

Water-soluble linear polyacrylamide (MW 15×10^4 to 17×10^4) partially substituted with the acylhydrazide group was synthesized (20). This prepolymer can be gelled and used for entrapment of biocatalysts in the presence of a crosslinking agent such as glyoxal, glutaraldehyde, or periodate-oxidized polyvinyl alcohol.

III. BIOCATALYSTS ENTRAPPED BY PREPOLYMER METHODS

As described above, various kinds of prepolymers having different physicochemical properties have been developed for the entrapment of different kinds of biocatalysts.

A. Enzymes

Examples of enzymes entrapped with prepolymers are listed in Table 3. Some enzymes listed in Table 3 have been employed for development or appraisal of new prepolymer methods. Not many reports are available concerning the applications of enzymes entrapped by prepolymer methods.

Lipases entrapped with hydrophobic photocrosslinkable resin prepolymers (ENTP-2000 and ENTP-4000) have been applied to the hydrolysis and ester exchange reaction of triacylglycerides. Production of cacao butter-like fat from olive oil and stearic acid or palmitic acid by enzymatic ester exchange reaction has been successfully achieved with ENTP-entrapped *Rhizopus delemar* lipase in an organic solvent system (21, 22). Entrapment markedly enhanced the operational stability of the enzyme. In the case of the hydrolysis of olive oil to glycerol and fatty acids, *Candida cylindracea* lipase entrapped with ENTP showed high activity (23). Entrapment also made it possible to use the enzyme repeatedly or continuously. PU-entrapped *Candida cylindracea* lipase was used for optical resolution of *dl*-menthol through enantioselective esterification in an organic solvent (24).

Enzymes entrapped with photocrosslinkable resin prepolymers were applied to the analyses of various compounds. Tubes entrapping glutamate decarboxyl-

Table 3 Examples of Enzymes Entrapped by Prepolymer Methods

Enzyme	Polymerization method (prepolymer)	Ref.
Amino acylase	Photocrosslinking (ENT)	13
Invertase	Photocrosslinking (PEGM, etc.)	4, 5, 37
	Urea linkage (PU)	12
Lipase	Photocrosslinking (ENTP)	21, 22, 38
	Urea linkage (PU)	23, 38
Glucose isomerase	Photocrosslinking (ENT)	13
Catalase	Photocrosslinking (ENT, etc.)	8, 37
Hydrogenase	Photocrosslinking (ENT)	39
Choline oxidase	Photocrosslinking (ENT and ENTA)	13
Glucose oxidase	Photocrosslinking (ENT)	13
Uricase	Photocrosslinking (ENT)	13
Lactate oxidase	Photocrosslinking (ENT)	13
Pyruvate oxidase	Photocrosslinking (ENT)	13
Glycerophosphate oxidase	Photocrosslinking (ENT)	13
Glutamate decarboxylase	Photocrosslinking (ENTE-1)	10
Lysine decarboxylase	Photocrosslinking (ENTE-1)	25

ase (10) and lysine decarboxylase (25) were prepared with the emulsion-type photocrosslinkable resin prepolymer ENTE-1. These tubes were used in continuous-flow systems to measure the concentration of L-glutamate and L-lysine, respectively, in fermentation broths. Thin enzyme films, in which the enzymes were entrapped with photocrosslinkable resin prepolymers, were mounted on an oxygen electrode and used as enzyme electrodes (13). Several oxygen-consuming oxidases, such as choline oxidase and glucose oxidase, were employed for this purpose. These enzyme electrodes were found to be stable.

B. Cells

Applications of immobilized cells are very attractive and important because cells possess multienzyme systems which mediate complex reactions (3). In the case of immobilization of cells, it is not necessary to extract the enzymes from the cells. This avoids inactivation of the enzymes during the time-consuming and expensive purification procedures, and makes it possible to use the enzymes under more stable conditions. However, immobilized cells have some disadvantages that should be considered for practical application:

1. Byproducts may be synthesized because the cells contain many enzymes, which may catalyze undesirable reactions. Selection of a strain, mutation, or proper treatment of cells, or genetic improvement of a cell line helps to overcome this problem.

2. The cell wall and/or cell membrane of intact cells often prevents substrates, products, and other reaction components from permeating into and out of cells. In this case, appropriate treatment of cells before or after immobilization is required to eliminate the barriers to permeability.

The immobilized cells can be kept in a growing state by appropriate supply of suitable nutrients. This type of immobilized cells (immobilized growing cells) is very advantageous. Immobilized growing cells serve as self-proliferating and self-regenerating biocatalysts. However, immobilized growing cells also have some disadvantages as follows:

1. Various nutrients and energy sources are required to maintain the cells in living or growing state(s), and yield of wanted products may be lowered by the consumption of substrates and/or products as nutrients or energy sources.

2. Products are liable to be contaminated by leakage of cells from carriers.

In spite of these disadvantages, cell immobilization is a key technology to construct an efficient bioprocess because immobilized cells have many attractive characteristics, as described above. For immobilization of cells, entrapment methods have been mainly used. Especially, other immobilization methods, such as carrier binding and crosslinking methods, are difficult to use for immobilization of living or growing cells. For entrapment of cells, prepolymer methods have been also widely used. Various types of cells have been entrapped by prepolymer methods.

1. Microbial Cells

Microbial cells are thought to be excellent biocatalysts due to high growth rate, insensitivity to shear force, and a relatively low cost for cultivation. Moreover, microbial cells can synthesize and secrete not only primary metabolites but also various secondary metabolites. Thus, various conditions of microbial cells—dried, untreated, resting, living, growing, etc.—have been entrapped by prepolymer methods and employed widely. Table 4 lists examples of microbial cells entrapped by prepolymer methods. Typical applications of entrapped microbial cells are described below.

Generation of ATP by using the energy of glycolysis is very important for the production of useful compounds by biocatalysts. Dried yeast cells entrapped by photocrosslinkable resin prepolymers were employed for the phosphorylation of adenosine with glucose as an energy source (26). Such ATP-generating systems can be combined with an ATP-requiring system in the same cells.

By using growing *Saccharomyces* cells entrapped with photocrosslinkable resin prepolymers, pilot-scale production of ethanol has been successfully carried out (27).

ENT- or PU-entrapped cells of *Rhodotorula minuta* var. *texensis* were successfully employed for the enantioselective hydrolysis of a *dl*-menthyl ester, giving optically pure *l*-menthol (28).

Entrapment in suitable gels renders microbial cells significantly tolerant against unfavorable effects of organic solvents. Applications of such entrapped microbial cells to bioconversion of hydrophobic or water-insoluble compounds are very important from a practical point of view. In these cases, introduction of organic solvents into reaction systems is essential to dissolve substrates and/or products. Various reactions have been successfully carried out by using microbial cells entrapped with prepolymers in water–organic cosolvent systems and in organic solvent systems (28, 29). However, it is very difficult for the entrapped cells to live in organic solvent. Recently, we have demonstrated that doubly entrapped baker's yeast, i.e., the yeast cells entrapped with urethane resin prepolymer (PU-6) after entrapment in calcium alginate, can maintain a living state during long-term stereoselective oxidoreduction in an organic solvent (30).

Table 4 Examples of Microbial Cells Entrapped by Prepolymer Methods

Microorganism (condition)	Polymerization method (prepolymer)	Ref.
Alcaligenes eutrapus (freeze-dried or untreated)	Urea linkage (PU)	39
Brevibacterium ammoniagenes (freeze)	γ-Radiation (PEGM + PVA)	18
Brevibacterium ammoniagenes (acetone-dried)	Photocrosslinking (ENT)	40
Citrobacter freundii (acetone-dried)	Photocrosslinking (ENTE)	41
Enterobacter aerogenes (freeze-thawed)	Photocrosslinking (ENT and ENTP) and urea linkage (PU)	36
Escherichia coli (untreated)	Urea linkage (PU)	42
Escherichia coli (acetone-dried)	Photocrosslinking (ENTE)	43
Hansenura jadinii (dried)	Photocrosslinking (ENT)	44
Arthrobacter simplex (acetone-dried)	Photocrosslinking (ENT and ENTP)	9, 37
Arthrobacter simplex (acetone-dried)	Urea linkage (PU)	14, 45
Corynebacterium sp. (living)	Photocrosslinking (ENT and ENTP)	46
Norcardia rhodocrous (freeze-thawed)	Photocrosslinking (ENTP, etc.) and urea linkage (PU)	35
Nocardia rhodocrous (freeze-thawed)	Photocrosslinking (ENT and ENTP)	37, 47
Propionibacterium sp. (growing)	Photocrosslinking (ENT) and urea linkage (PU)	48
Streptomyces clavuligerus (resting)	Crosslinking with dialdehyde (water-soluble polyacrylamide having acylhydrazide group)	20
Streptomyces peucetius (growing)	Photodimerization (PVA-SbQ)	49
Streptomyces rimosus (growing)	Urea linkage (PU)	50
Streptomyces roseochromogenes (untreated)	Photocrosslinking (PEGM)	6
Curvularia lunata (living)	Photocrosslinking (ENT)	34, 51
Rhizopus stolonifer (living)	Photocrosslinking (ENT)	52
Baker's yeast (dried)	Photocrosslinking (ENT)	26
Rhodotorula minuta var. *texensis* (freeze-thawed)	Photocrosslinking (ENT) and urea linkage (PU)	28
Saccharomyces sp. (growing)	Photocrosslinking (ENT, etc.)	27

2. Plant and Animal Cells

Higher plants are important sources of numerous useful natural compounds such as pharmaceuticals, flavorings, and coloring materials, which have complicated structures and cannot be synthesized by microbial cells. Animal cells are also attractive biocatalysts for the production of vaccines and other bioactive peptides. For practical application of these cells, immobilization, especially, entrapment has received increasing interest as one of the most promising techniques. Entrapment of these cells has been carried out mostly with natural polymers such as alginate. As for prepolymer methods, cultured plant cells of *Lavandura vera* were entrapped with photosensitive resin prepolymer (PVA-SbQ) and used for production of blue pigments (31).

C. Cellular Organelles

Cellular organelles have their own organized functions for metabolizing cellular substances. This means that these organelles are useful biocatalysts for carrying out well-organized multistep reactions when they are isolated intact and immobilized without the loss of their native characteristics. Prepolymer methods have proved to be suitable for the immobilization of organelles because the immobilization can be achieved by entrapment under mild conditions (32, 33). Only a few reports have been published; the kinds of organelles immobilized with prepolymer methods are summarized in Table 5.

IV. EFFECTS OF THE PROPERTIES OF PREPOLYMERS

One of the advantages of prepolymer methods is easy preparation of gels having different properties by selecting suitable prepolymers which are synthesized chemically in advance in the absence of biocatalysts.

A. Chain Length

The chain length of prepolymers can be changed. For example, the chain length of ENT-1000-containing polyethylene glycol-1000 (average MW$\sim$1000) is $\sim$10 nm, and that of ENT-2000 containing polyethylene glycol-2000 (average MW $\sim$2000) is $\sim$20 nm.

In general, a looser network of gels prepared from longer-chain prepolymers increases the rate of diffusion of substrates and products through the gels. However, leakage of biocatalysts, especially enzymes with low molecular weights, sometimes becomes a significant problem with the gels which have a loose network (13). When invertase was entrapped with PEGM-1000 to PEGM-4000 (4) or PU of MW 2000–5000 (12), the apparent enzyme activity was highest in the case of the longest-chain prepolymer. A similar result was obtained when catalase was entrapped with ENT-1000 to ENT-6000 (8).

The loose network of gels is generally favorable to growth if the entrapped cells are allowed to grow inside gel matrices. When fungal spores (*Curvularia lunata*) were entrapped with photocrosslinkable resin prepolymers (ENT) and allowed to germinate and grow inside gel matrices, development of mycelia was abundant in gels formed from prepolymers of longer chain length, while the growth was inhibited in gels of tight network (34). Leakage of mycelia was often observed with gels prepared from longer–chain length prepolymer.

As described above, the chain length of prepolymers is an important factor affecting the activity of biocatalysts entrapped within the prepolymers. Prepolymer methods offer an easy selection of adequate chain length.

Table 5 Examples of Cellular Organelles Entrapped by Prepolymer Methods

Organelle (source)	Polymerization method (prepolymer)	Ref.
Chromatophores (*Rhodopseudomonas capsulata*)	Photocrosslinking (ENT) and urea linkage (PU)	53
Thylakoids (lettuce)	Photocrosslinking (ENT) and urea linkage (PU)	54
Chloroplasts (spinach)	γ-Radiation (polyethylene glycol diacrylate + PEGM)	19
Mitochondria (acetate-grown *Candida tropicalis*)	Photocrosslinking (ENT) and urea linkage (PU)	55
Peroxisomes or microbodies (methanol-grown *Kloeckera* sp.)	Photocrosslinking (ENT)	7
	Urea linkage (PU)	45

B. Hydrophilicity–Hydrophobicity Balance

Bioreactions with hydrophilic substrates are generally carried out in aqueous solutions. Hydrophilic properties of gels are favorable for such reaction systems. On the other hand, proper organic solvents are suitable for bioconversion of hydrophobic compounds in terms of the solubility of the compounds and of shifting the reaction equilibrium to the desired direction. In such cases, hydrophobic gels favor the transformation of hydrophobic substances owing to high affinity of the compounds to the gels. One of the most representative examples is the successful ester exchange of triglycerides with *Rhizopus delemar* lipase in water-saturated *n*-hexane, indicating the need of organic solvent and the advantage of hydrophobic gels (21). In this case, hydrolysis of triglycerides was preferential when the concentration of water was high, and the hydrophilic gel-entrapped enzyme preparation exhibited only low activity. It was also found that the activities of the entrapped biocatalysts corresponded closely to the partition of the substrates between the gels and the external solvents (35).

Prepolymer methods, especially those with photocrosslinkable resin prepolymers and urethane prepolymers, again offer easy selection of gels having an optional hydrophilicity–hydrophobicity balance by using different types of prepolymers or by mixing these prepolymers.

C. Ionic Properties

Anionic or cationic property of gels has a significant influence on the apparent activities of gel-entrapped biocatalysts through an electrostatic interaction with the charged substrates. Furthermore, the optimum reaction pH may be shifted by using gels with proper ionic properties.

When choline oxidase entrapped with photocrosslinkable resin prepolymers was used as an enzyme electrode for assay of choline, the enzyme entrapped with an anionic prepolymer exhibited significantly higher activity. On the other hand, the enzyme entrapped with a cationic prepolymer showed markedly lower activity (13). The results can be explained by different affinity of the cationic substrate choline for the gels with different ionic properties.

Shift of the optimum pH was also observed in the case of the production of adenine arabinoside through transglycosylation by *Enterobacter aerogenes* cells entrapped with the photocrosslinkable resin prepolymers of different ionic characters (36).

REFERENCES

1. K Mosbach, ed. Methods Enzymol, Vol 44. New York: Academic Press, 1976.
2. I Chibata, ed. Immobilized Enzymes. Research and Development. New York: John Wiley and Sons, 1978.
3. S Fukui, A Tanaka. Immobilized microbial cells. Annu Rev Microbiol 36:145–172, 1982.
4. S Fukui, A Tanaka, T Iida, E Hasegawa. Application of photo-crosslinkable resin to immobilization of an enzyme. FEBS Lett 66:179–182, 1976.
5. A Tanaka, S Yasuhara, S Fukui, T Iida, E Hasegawa. Immobilization of invertase by the use of photo-crosslinkable resin oligomers and properties of the immobilized enzyme. J Ferment Technol 55:71–75, 1977.
6. YY Chun, M Iida, H Iizuka. Studies on microbial transformations. XIX. Use of immobilized cells of *Streptomyces roseochromogenes* for the 16∝-hydroxylation of dehydroepiandrosterone. J Gen Appl Microbiol 27:505–509, 1981.
7. A Tanaka, S Yasuhara, M Osumi, S Fukui. Immobilization of yeast microbodies by inclusion with photo-crosslinkable resins. Eur J Biochem 80:193–197, 1977.
8. A Tanaka, N Hagi, S Yasuhara, S Fukui. Immobilization of catalase with photo-crosslinkable resin prepolymers. J Ferment Technol 56:511-515,1978.
9. K Sonomoto, A Tanaka, T Omata, T Yamane, S Fukui. Application of photo-crosslinkable resin prepolymers to entrap microbial cells. Effects of increased cell-entrapping gel hydrophobicity on the hydrocortisone Δ^1-dehydrogenation. Eur J Appl Microbiol Biotechnol 6:325-334, 1979.
10. N Itoh, N Hagi, T Iida, A Tanaka, S Fukui. Photocrosslinkable prepolymer method for immobilization of biocatalysts. Preparation of immobilized glutamate decarboxylase tubes and their application for automated analysis of L-glutamate. J Appl Biochem 1:291-300, 1979.
11. T Iida, M Sakamoto, H Izumida, Y Akagi. Characteristics of *Zymomonas mobilis* immobilized by photo-crosslinkable resin in ethanol fermentation. J Ferment Bioeng 75:28-31, 1993.
12. S Fukushima, T Nagai, K Fujita, A Tanaka, S Fukui. Hydrophilic urethane prepolymers: convenient materials for entrapment of enzymes. Biotechnol Bioeng 20:1465-1469, 1978.
13. S Fukui, K Sonomoto, N Itoh, A Tanaka. Several novel methods for immobilization of enzymes, microbial cells and organelles. Biochimie 62:381-386, 1980.
14. K Sonomoto, IN Jin, A Tanaka, S Fukui. Application of urethane prepolymer method to immobilization of biocatalysts. Δ^1-Dehydrogenation of hydrocortisone by *Arthrobacter simplex* cells entrapped with urethane prepolymers. Agric Biol Chem 44:1119-1126, 1980.

15. S Fukui, K Sonomoto, A Tanaka. Entrapment of biocatalysts with photo-cross-linkable resin prepolymers and urethane prepolymers. In: K Mosbach, ed. Methods Enzymol, Vol 135. New York: Academic Press, 1987, pp 230-252.
16. K Ichimura. A convenient photochemical method to immobilize enzymes. J Polym Sci Polym Chem Ed 22:2817-2828, 1984.
17. H Maeda, H Suzuki, A Yamauchi. Preparation of immobilized enzymes using poly(vinyl alcohol). Biotechnol Bioeng 15:607–610, 1973.
18. Y Tanaka, T Hayashi, K Kawashima, T Yokoyama, T Watanabe. Production of NADP by immobilized cells with NAD kinase. Biotechnol Bioeng 24:857-869, 1982.
19. F Yoshii, T Fujimura, I Kaetsu. Stabilization of chloroplast by radiation-induced immobilization with various glass-forming monomers. Biotechnol Bioeng 23:833-841, 1981.
20. A Freeman, Y Aharonowitz. Immobilization of microbial cells in crosslinked, prepolymerized, linear polyacrylamide gels: antibiotic production by immobilized *Streptomyces clavuligerus* cells. Biotechnol Bioeng 23:2747-2759, 1981.
21. K Yokozeki, S Yamanaka, K Takinami, Y Hirose, A Tanaka, K Sonomoto, S Fukui. Application of immobilized lipase to regio-specific interesterification of triglyceride in organic solvent. Eur J Appl Microbiol Biotechnol 14:1-5, 1982.
22. K Yokozeki, T Tanaka, S Yamanaka, K Takinami, Y Hirose, K Sonomoto, A Tanaka, S Fukui. Ester exchange of triglyceride by entrapped lipase in organic solvent. Enzyme Eng 6:151-152, 1982.
23. Y Kimura, A Tanaka, K Sonomoto, T Nihira, S Fukui. Application of immobilized lipase to hydrolysis of triacylglyceride. Eur J Appl Microbiol Biotechnol 17:107-112, 1983.
24. S Koshiro, K Sonomoto, A Tanaka, S Fukui. Stereoselective esterification of *dl*-menthol by polyurethane-entrapped lipase in organic solvent. J Biotechnol 2:47-57, 1985.
25. A Tanaka, N Hagi, N Itoh, S Fukui. Application of immobilized lysine decarboxylase tubes for automated analysis of L-lysine. J Ferment Technol 58:391-394, 1980.
26. M Asada, K Morimoto, K Nakanishi, R Matsuno, A Tanaka, A Kimura, T Kamikubo. Continuous ATP regeneration using immobilized yeast cells. Agric Biol Chem 43:1773-1774, 1979.
27. S Fukui, A Tanaka. Application of biocatalysts immobilized by prepolymer methods. Adv Biochem Eng/Biotechnol 29:1-33, 1984.
28. T Omata, N Iwamoto, K Kimura, A Tanaka, S Fukui. Stereoselective hydrolysis of *dl*-menthyl succinate by gel-entrapped *Rhodotorula minuta* var. *texensis* cells in organic solvent. Eur J Appl Microbiol Biotechnol 11:199-204, 1981.
29. A Tanaka, K Sonomoto. Immobilized biocatalysts in organic solvents. Chemtech Feb:112-117, 1990.
30. T Kanda, N Miyata, T Fukui, T Kawamoto, A Tanaka. Doubly entrapped baker's yeast survives during the long-term stereoselective reduction of ethyl 3-oxobutanoate in an organic solvent. Appl Microbiol Biotechnol 49:377-381, 1998.
31. H Nakajima, K Sonomoto, H Morikawa, F Sato, K Ichimura, Y Yamada, A Tanaka. Entrapment of *Lavandura vera* cells with synthetic resin prepolymers and its application to pigment production. Appl Microbiol Biotechnol 24:266-270, 1986.
32. A Tanaka, S Fukui. Immobilized organelles. In: B Mattiasson, ed. Immobilized Cells and Organelles, Vol 1. Boca Raton, FL: CRC Press, 1983, pp 101-119.
33. H Ochiai, A Tanaka, S Fukui. Immobilized organelles. Appl Biochem Bioeng 4:153-187, 1983.
34. K Sonomoto, MH Hoq, A Tanaka, S Fukui. 11β-Hydroxylation of cortexolone (Reichstein compound S) to hydrocortisone by *Curvularia lunata* entrapped in photo-cross-linked resin gels. Appl Environ Microbol 45:436-443, 1983.
35. T Omata, T Iida, A Tanaka, S Fukui. Transformation of steroids by gel-entrapped *Nocardia rhodocrous* cells in organic solvent. Eur J Appl Microbiol Biotechnol 8:143-155, 1979.
36. K Yokozeki, S Yamanaka, T Utagawa, K Takinami, Y Hirose, A Tanaka, K Sonomoto, S Fukui. Production of adenine arabinoside by gel-entrapped cells of *Enterobacter aerogenes* in water–organic cosolvent system. Eur J Appl Microbiol Biotechnol 14:225-231, 1982.
37. T Omata, A Tanaka, T Yamane, S Fukui. Immobilization of microbial cells and enzymes with hydrophobic photo-crosslinkable resin prepolymers. Eur J Appl Microbiol Biotechnol 6:207-215, 1979.
38. T Kawamoto, K Sonomoto, A Tanaka. Esterification in organic solvents: selection of hydrolases and effects of reaction conditions. Biocatalysis 1:137-145, 1987.
39. P Egerer, H Simon, A Tanaka, S Fukui. Immobilization and stability of the NAD-dependent hydrogenase from *Alcaligenes eutrophus* and of whole cells. Biotechnol Lett 4:489-494, 1982.
40. M Asada, K Nakanishi, R Matsuno, T Kamikubo. Continuous CoA production with immobilized *Brevibacterium ammoniagenes* cells. Agric Biol Chem 46:1687-1688, 1982.
41. A Tanaka, N Itoh, S Fukui. Assay of cephalosporin C with an immobilized microbial cell tube systems. Agric Biol Chem 46:127-134, 1982.
42. MC Fusee, WE Swann, GJ Calton. Immobilization of *Escherichia coli* cells containing aspartase activity with polyurethane and its application for L-aspartic acid production. Appl Environ Microbiol 42:672-676,1981.
43. K Watanabe, N Itoh, A Tanaka, S Fukui. Application of an immobilized *Escherichia coli* tube in analysis of L-threonine. Agric Biol Chem 46:119-126, 1982.

44. A Kimura, Y Tatsutomi, N Mizushima, A Tanaka, R Matsuno, H Fukuda. Immobilization of glycolysis system of yeasts and production of cytidine diphosphate choline. Eur J Appl Microbiol Biotechnol 5:13-16, 1978.
45. A Tanaka, IN Jin, S Kawamoto, S Fukui. Entrapment of microbial cells and organelles with hydrophilic urethane prepolymers. Eur J Appl Microbiol Biotechnol 7:351-354, 1979.
46. K Sonomoto, N Usui, A Tanaka, S Fukui. 9α-Hydroxylation of 4-androstene-3,17-dione by gel-entrapped *Corynebacterium* sp. cells. Eur J Appl Microbiol Biotechnol 17:203-210, 1983.
47. T Yamane, H Nakatani, E Sada, T Omata, A Tanaka, S Fukui. Steroid bioconversion in water-insoluble organic solvents: Δ^1-dehydrogenation by free microbial cells and cells entrapped in hydrophilic or lipophilic gels. Biotechnol Bioeng 21:2133-2145, 1979.
48. B Yongsmith, K Sonomoto, A Tanaka, S Fukui. Production of vitamin B_{12} by immobilized cells of a propionic acid bacterium. Eur J Appl Microbiol Biotechnol 15:70-74, 1982.
49. Y Takashima, H Nakajima, K Sonomoto, A Tanaka. Production of daunorubicin by immobilized growing *Streptomyces peucetius* cells. Appl Microbiol Biotechnol 27:106-109, 1987.
50. M Ogaki, K Sonomoto, H Nakajima, A Tanaka. Continuous production of oxytetracycline by immobilized growing *Streptomyces rimosus* cells. Appl Microbiol Biotechnol 24:6-11, 1986.
51. K Sonomoto, MM Hoq, A Tanaka, S Fukui. Growth of *Curvularia lunata* spores into mycelial form within various gels, and steroid 11β-hydroxylation by the entrapped mycelia. J Ferment Technol 59:465-469, 1981.
52. K Sonomoto, K Nomura, A Tanaka, S Fukui. 11α-Hydroxylation of progesterone by gel-entrapped *Rhizopus stolonifer* mycelia. Eur J Appl Microbiol Biotechnol 16:57-62, 1982.
53. VL Garde, B Thomasset, A Tanaka, G Gellf, D Thomas. Comparative stabilization of biological photosystems by several immobilization procedures. 1. ATP production by immobilized bacterial chromatophores. Eur J Appl Microbiol Biotechnol 11:133-138, 1981.
54. MF Cocoquempot, B Thomasset, JN Barbotin, G Gellf, D Thomas. Comparative stabilization of biological photosystems by several immobilization procedures. 2. Storage and functional stability of immobilized thylakoids. Eur J Appl Microbiol Biotechnol 11:193-198, 1981.
55. A Tanaka, N Hagi, G Gellf, S Fukui. Immobilization of biocatalysts by prepolymer methods. Adenylate kinase activity of immobilized yeast mitochondria. Agric Biol Chem 44:2399-2405, 1980.

23

Genetic Immobilization of Enzymes on Yeast Cell Surface

Mitsuyoshi Ueda, Toshiyuki Murai, and Atsuo Tanaka
Kyoto University, Kyoto, Japan

I. INTRODUCTION

Extensive studies have been conducted on various methods of immobilization of enzymes. Conventional methods for immobilization of enzymes through covalent bonds have some merits; the enzymes are immobilized through strong bondage, and dissociation is low in substrate or salt solution even at high concentrations. However, change in structure of the immobilized protein or in their characteristics often occurs owing to severe treatment and there are many difficulties in the determination of the immobilization reaction conditions. On the other hand, immobilization through ionic bonds does not share these disadvantages, but the enzymes are easily dissociated.

The genetic engineering method, combined with the immobilization method using cell surface as a carrier for immobilization of enzymes, overcomes the disadvantages of the above methods; enzymes are immobilized by a strong covalent bondage. They can be regenerated according to the activation of the promoter, and they are "naturally" immobilized on the cell surface. Immobilization of enzymes on cell surface saves tedious purification process of enzymes to be used in conventional immobilization. Expression of proteins on the cell surface of *S. cerevisiae* would offer more advantages than other microbial cells. First, since *S. cerevisiae* is widely used in industrial production of proteins and chemicals, enzyme-coated yeast cells could be used as novel whole-cell biocatalysts, because surface-immobilized proteins are covalently linked to glucan in the cell wall, rendering them resistant to extraction. Second, as *S. cerevisiae* is generally regarded as safe (GRAS) for oral use, it can be used in food and pharmaceutical products.

The immobilized enzyme displayed on the cell surface is also regarded as a kind of a self-immobilized enzyme on the cell surface; this phenomenon is passed on to daughter cells as long as the plasmid or the integrated gene is retained by the cells. This immobilization system could turn or remake *S. cerevisiae* into a novel and attractive microorganism as a whole-cell biocatalyst by surface expression of various enzymes, especially when target substrates are not able to be taken up by the cells.

II. PRINCIPLES OF GENETIC IMMOBILIZATION OF ENZYME ON YEAST CELL SURFACE

To immobilize protein on the cell surface of *S. cerevisiae*, molecular information of the native cell wall-anchored protein, α-agglutinin, was utilized. α-Agglutinin (1) is a mannoprotein involved in the sexual adhesion of mating-type α *S. cerevisiae* cells with mating-type **a** *S. cerevisiae* cells. α-Agglutinin has a glycosylphosphatidylinositol (GPI) anchor attachment signal (Fig. 1; Table 1), which is involved in anchoring cell wall proteins. This anchoring signal was combined with the

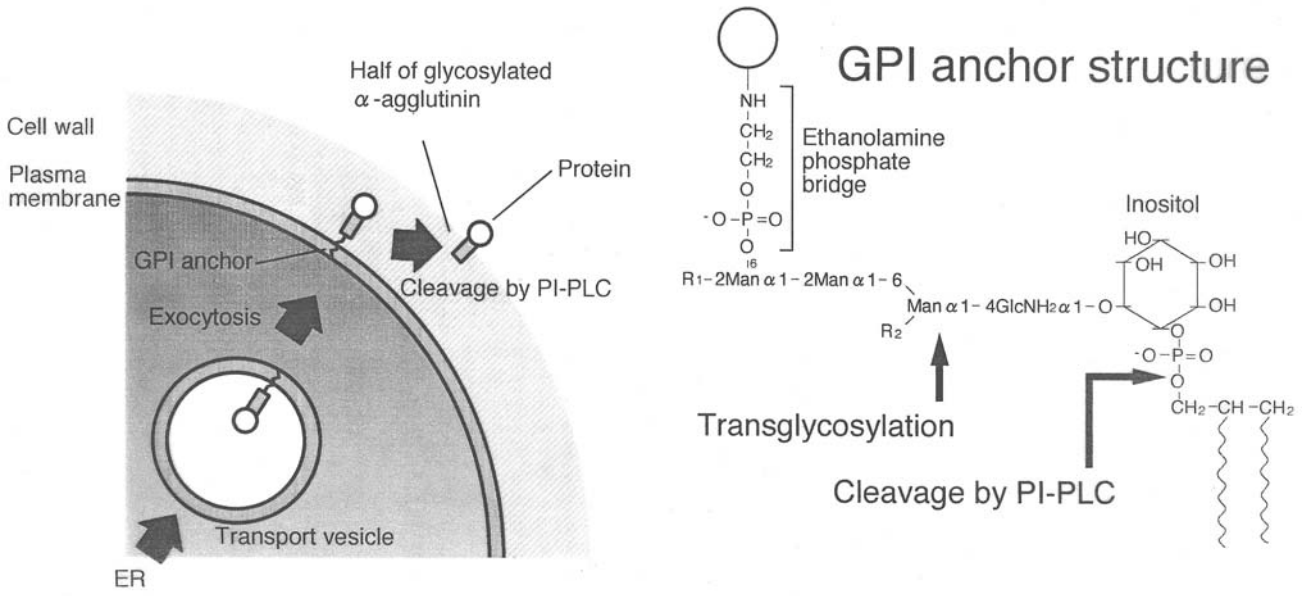

Figure 1 Transportation system of cell surface proteins in *S. cerevisiae* and GPI anchor structure. ER, endoplasmic reticulum; PI-PLC, phosphatidylinositol-specific phospholipase C; GPI, glycosylphosphatidylinositol; Man, mannose; $GlcNH_2$, glucosamine.

signal of the secreted enzymes using genetic engineering techniques. Figure 2 shows the general structure of the gene for cell surface immobilization of an enzyme (2). 3′-Half of α-agglutinin contains a glycosylphosphatidylinositol (GPI) anchor attachment signal at the C-terminal end, like other cell surface proteins.

III. GENETIC IMMOBILIZATION OF AMYLOLYTIC ENZYMES ON YEAST CELL SURFACE

Although starchy materials are available in abundance as carbon sources for cultivation, wild-type *S. cerevisiae* itself is unable to utilize starch. A number of strategies have been adopted for the construction of starch-utilizing systems, which include the addition of amylolytic enzymes in culture broth and the introduction of heterologous genes encoding amylolytic enzymes into yeast cells for secretive production of the enzymes. As one of strategies, glucoamylase (EC 3.2.1.3) from *Rhizopus oryzae* (3), an exo-type amylolytic enzyme cleaving α-1,4-linked and α-1,6-linked glucose effectively from the nonreducing end and/or α-amylase (EC 3.2.1.1) from *Bacillus stearothermophilus* CU21 (BSTA) (4), an endo-type amylolytic enzyme cleaving α-1,4-glycosidic linkage, were displayed on the yeast cell surface

Table 1 GPI Anchor Attachment Signal in *S. cerevisiae*[a]

Cell surface protein	GPI anchor attachment signal
Agα1	TSTSLMISTYEG ↑ KASIFFSAELGSIIFLLLSYLLF
Aga1	TSSMVTISQYMG ↑ SGSQTRLPLGKLVFAIMAVACNVIFS
Flo1	STASLEISTYAG ↑ SANSLLAGSGLSVFIASLLLAII
Cwp1	QAPNTVYEQTEN ↑ AGAKAAVGMGAGALAVAAAYLL
Cwp2	SSTETISQQTEN ↑ GAAKAAVGMGAGALAAAMLL
Tip1	VETASNAGQRVN ↑ AGAASFGAVVAGAAALLL
Sed1	SASSHSVVINSN ↑ GANVVVPGALGLAGVAMLFL
Tir1/Srp1	ATKAVSEQTENG ↑ AAKAFVGMGAGVVAAAAMLL

[a]The predicted cleavage sites are indicated by an arrow. The predicted ω sites are underlined.

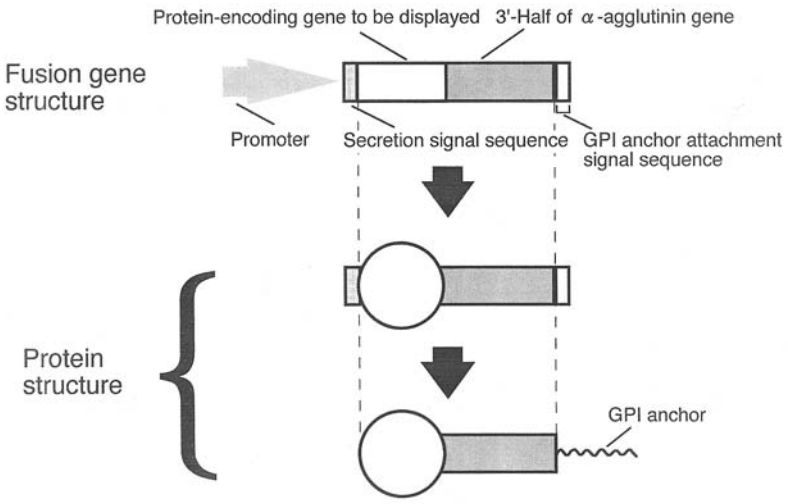

Figure 2 General strategy for cell surface immobilization of an enzyme.

(Fig. 3). The constructed strains immobilizing glucoamylase or glucoamylase and α-amylase should be able to saccharify starch on its cell wall and assimilate the released glucose to proliferate and ferment.

A. Immobilization of Glucoamylase on Yeast Cell Surface Using a Multicopy Plasmid

1. Construction of a Multicopy Plasmid

A plasmid pGA11 to immobilize glucoamylase on the yeast cell surface was constructed as a multicopy plasmid for expression of the glucoamylase/α-agglutinin fusion gene containing the secretion signal sequence of the glucoamylase under the control of the *GAPDH* promoter (2). The plasmid pGA11 was constructed as follows (Fig. 4): an *Xho*I site was generated at the end of the glucoamylase coding region on the plasmid pYGA2270 (5) by site-directed mutagenesis (U.S.E. Mutagenesis Kit, Pharmacia Biotech. Co., Uppsala, Sweden) with the primers 5′-GCACCTG CCGCTGGCTCGAGAAATTTAAATGC-3′ and 5′-CTGTGACTGGTGACGCGTCAACCAAGTC-3′ as mutation and selection primers, respectively. A DNA fragment containing glucoamylase coding region was isolated from the mutated plasmid by *Eco*RI-*Xho*I digestion. A DNA fragment of the α-agglutinin gene (*AGα1*), containing 3′-half of the coding region encoding 320 amino acids of the α-agglutinin and 446 bp of the 3′-flanking region, was prepared by PCR (primers, 5′-GTACCTCGAGCGCCAAAAGCTCTTTTATC-3′ and 5′-GCGGTACCTTTGATTATGTTCTTCTTT CTAT-3′) with genomic DNA from *S. cerevisiae* MT8-1 (*MATa ade his3 leu2 trp1 ura3*). (6) as a template, followed by digestion by *Xho*I and *Kpn*I. These two fragments were substituted for the *Eco*RI-*Kpn*I section between the *GAPDH* promoter and the *GAPDH* terminator of the yeast expression cassette vector pYE22m. The resulting plasmid was named pGA11.

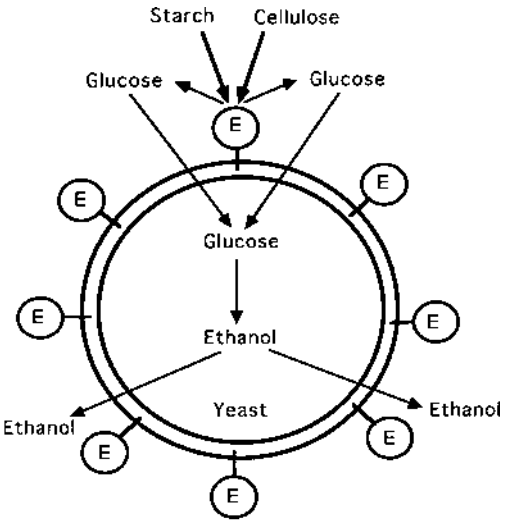

Figure 3 Model of cell surface–engineered yeast assimilating starch or cellulose. E, amylolytic or cellulolytic enzyme(s).

2. Detection of Glucoamylase Activity

The constructed plasmid was introduced into *S. cerevisiae* strain MT8-1 as a host cell. Yeast was precultivated in YPD medium (1% yeast extract, 2% peptone,

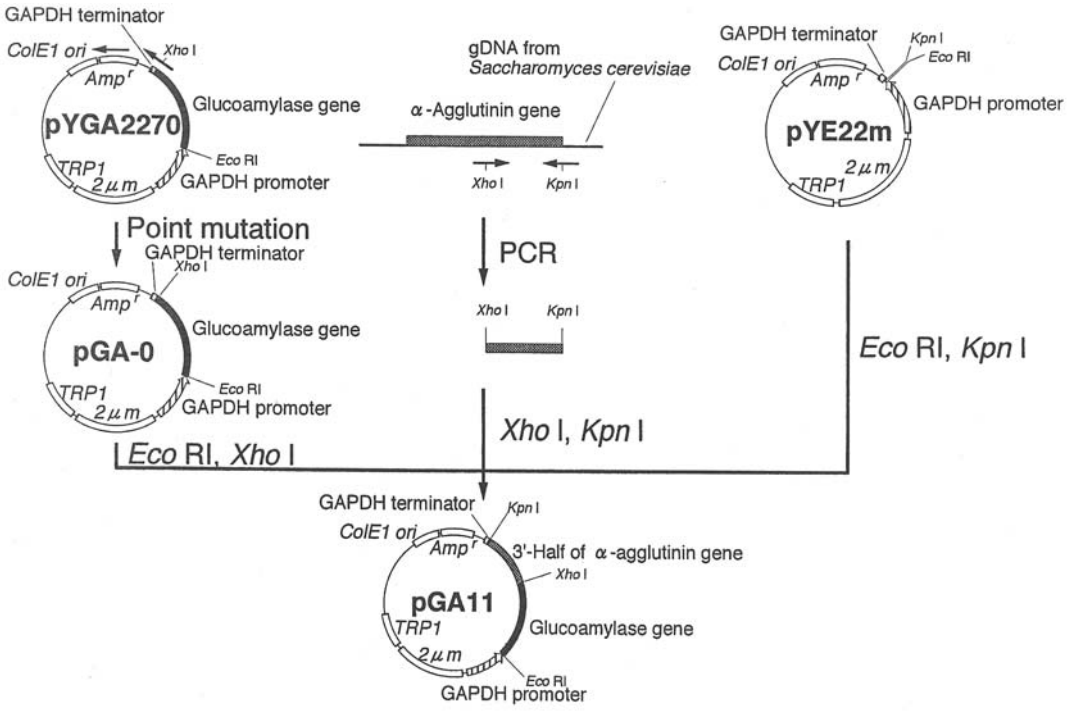

Figure 4 Construction of the multicopy plasmid pGA11 for immobilization of glucoamylase on the yeast cell surface.

2% glucose). After cells were cultivated aerobically at 30°C in modified Burkholder's medium (containing 0.002% adenine sulfate, 0.002% L-histidine·HCl, 0.003% L-leucine, 0.002% uracil, and 1% casamino acids) to which 2% glucose was added as a carbon source, culture medium and cell pellets were isolated by centrifugation to measure the glucoamylase activities in both fractions. Cell growth in the culture broth was measured by absorbance at 600 nm. For measurement of glucoamylase activity (2), the substrate for glucoamylase reaction was prepared by adding soluble starch to boiling 20 mM sodium acetate buffer (pH 4.6) to give a concentration of 0.5%. After keeping 0.9 mL of the solution at 30°C for 5 min, 0.1 mL of enzyme solution was added and the mixture was incubated at the same temperature for 15 min. The reaction was stopped by boiling the mixture for 10 min and the concentration of glucose was determined using F-kit for glucose (Boehringer Mannheim, Mannheim, Germany). One unit of glucoamylase was defined as the amount of enzyme required to release 1 μmol glucose/min from starch. As a result, the cells harboring the plasmid pGA11 had only the cell-associated glucoamylase activity without secretion of the active enzyme (2).

The cell wall of *S. cerevisiae* mainly consists of glucan and mannoproteins. Glucan is composed of β-1,3- and β-1,6-linked glucose. Some mannoproteins seemed to be covalently linked with glucan, because they can be extracted by β-1,3- or β-1,6-glucanase. The localization of the glucoamylase protein and its association with cell wall was determined. Cells were harvested by centrifugation at 3000g and washed in cooled (0°C) buffer (10 mM Tris-HCl [pH 7.8], 1 mM phenylmethylsulfonyl fluoride [PMSF]). The cells, the buffer, and glass beads (diameter 0.45–0.50 mm) were mixed in a ratio of 1:2:1 wet-w/v/w in a glass tube and agitated vigorously, using a benchtop vortex mixer, for 5 min at 0°C. The cell wall fraction was recovered by centrifugation of the homogenate at 1000g for 5 min and was washed with the same buffer. Glucoamylase was extracted from this fraction in a two-step procedure. First, noncovalently bound proteins, and proteins bound through disulfide bridges, could be extracted from cell wall with hot sodium dodecyl sulfate (SDS). Following this, the SDS-treated cell wall was further digested with laminarinase (β-1,3-glucanase). To quantify the amount of the SDS-extracted and glucanase-extracted glucoamylase protein, intensities of signals from each fraction on the filter were measured

using antiglucoamylase IgG and horseradish peroxidase protein A (2). The enzyme was almost extracted by glucanase.

The amylolytic activity was also detected by halo formation on an agar plate. Cells harboring the plasmid pGA11 or pYE22m, as a control, were inoculated on a plate of modified Burkholder's medium containing 2% glucose and 1% soluble starch. After incubation for 3 days at 30°C, the plate was stained with iodine vapor. Figure 5 shows that the cells harboring the plamid pGA11 hydrolyzed starch and produced a halo strictly around the colony, while no halo formation was observed around the cells harboring the plasmid pYE22m. This indicates that the former cells obtained amylolytic activity owing to the expression of the glucoamylase/α-agglutinin fusion gene on the cell surface.

To know the properties of the anchored enzyme, thermal stability, optimal temperature, and optimal pH of the glucoamylase anchored on the cell surface were compared with those of the secreted free glucoamylase (7). The cell wall fraction of the cells harboring the plasmid pGA11 was suspended in 20 mM sodium acetate buffer (pH 4.6). The cells harboring the plasmid for expression of the glucoamylase without being fused to α-agglutinin were cultivated in modified Burkholder's medium containing 2% glucose as a carbon source at 30°C for 24 h, and the supernatant of the culture broth was used as the source of free glucoamylase. Free glucoamylase solution was prepared by dialysis of the culture supernatant in 20 mM sodium acetate buffer (pH 4.6) at 4°C. The glucoamylase activities in the cell wall suspension and the dialyzed supernatant were measured. The properties of the anchored glucoamylase examined were similar to those of the free glucoamylase, suggesting that the enzymatic function of the anchored glucoamylase was comparable to that of the free enzyme.

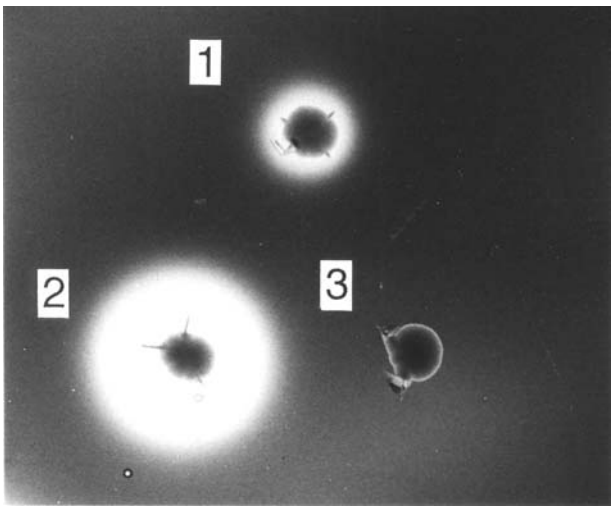

Figure 5 Plate assay for detection of amylolytic activity. 1, *S. cerevisiae* with cell surface-immobilized glucoamylase (*S. cerevisiae* MT8-1/pGA11); 2, *S. cerevisiae* secreting glucoamylase; 3, *S. cerevisiae* MT8-1 as the control (*S. cerevisiae* MT8-1/pYE22m).

3. Microscopic Observation

For immunofluorescence microscopy, immunostaining was performed as follows. As the primary antibody, the antibody against *R. oryzae* glucoamylase at the dilution rate of 1:1000 was used. Cells and the antibody were incubated at room temperature for 1.5 h. After washing of cells, the second antibody, fluorescein isothiocyanate (FITC)-conjugated goat anti-rabbit IgG diluted 1:300, was reacted with the cells at room temperature for 1 h. After washing, the image of cells was observed. Cells expressing the glucoamylase/α-agglutinin fusion gene were uniformly labeled, although not all the cells were equally intensively labeled. This is probably due to differences in expression levels among the cells. The cells harboring the control plasmid were hardly labeled (Fig. 6). For immunoelectron microscopy, yeast cells were fixed with 4% paraformaldehyde, and immunostaining was done as follows. The antibody against glucoamylase diluted 1:100, as the primary antibody, was incubated with cells at 4°C for 2 h. The second antibody, goat anti-rabbit IgG conjugating 5 nm gold diluted 1:40, was reacted with the cells at 4°C overnight, followed by fixation with 1% glutaraldehyde. Thereafter, embedding and microscopic observation were performed. Gold particles were detected on the surface of the cell wall of the cells harboring the plasmid pGA11. Few gold particles were detected in the case of the control cells (Fig. 7).

4. Assimilation of Starch

When cells were cultivated aerobically with 1% soluble starch as the sole carbon source, the cells harboring the plasmid pGA11 utilized starch and proliferated to reach an absorbance of ~ 10, which was the same level as in the case of the culture on 1% glucose.

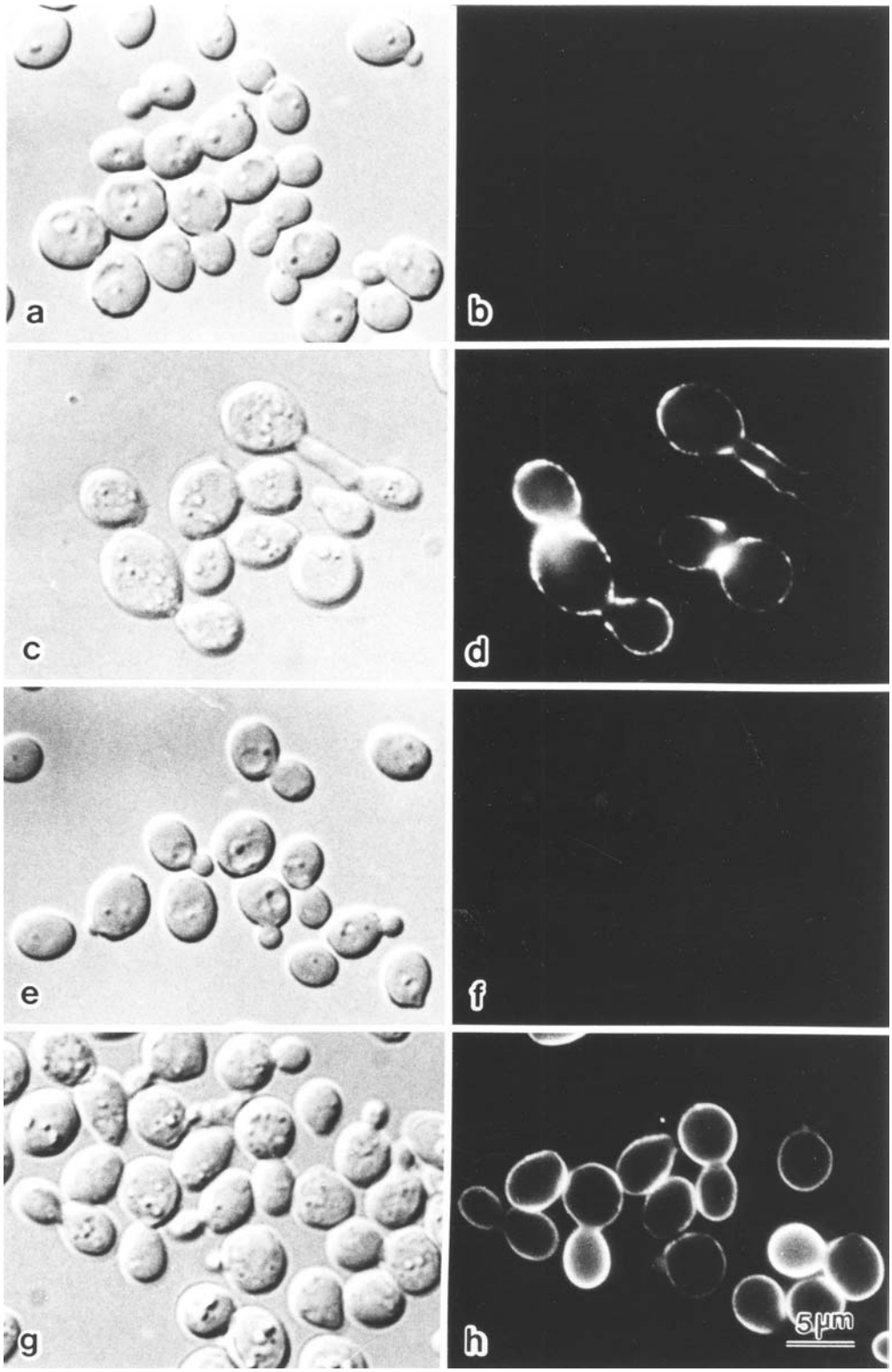

Figure 6 Immunofluorescent labeling of transformed cells. Normarsky differential interference micrographs (a, c, e, g) and immunofluorescence micrographs (b, d, f, h). a, b, e, f: *S. cerevisiae* MT8-1 harboring pYE22m (control); c, d: *S. cerevisiae* MT8-1 harboring pGA11; g, h: *S. cerevisiae* MT8-1 harboring pCMC11.

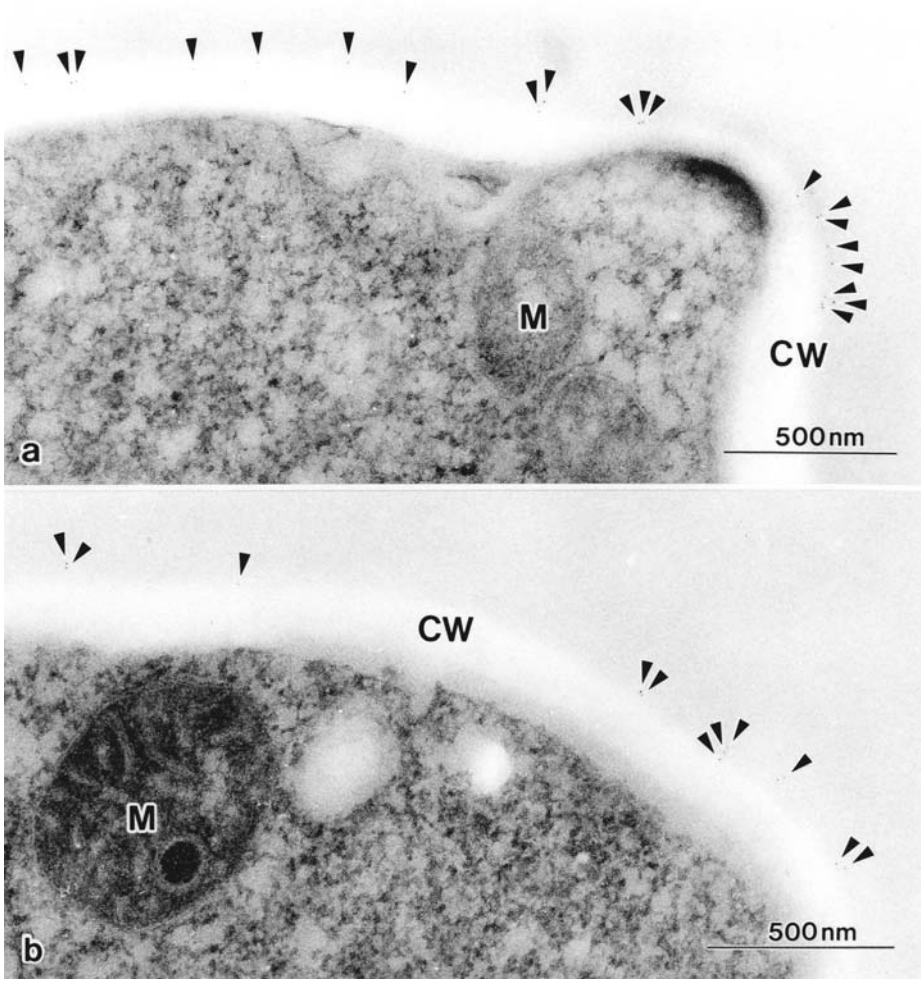

Figure 7 Immunoelectron micrographs of *S. cerevisiae* MT8-1 harboring pGA11 (a) and pCMC (b). Cells were immunogold-labeled with the respective antibodies. CW, cell wall; M, mitochondrion. Arrowheads, gold particles (diameter, 5 nm).

B. Immobilization of Glucoamylase on Yeast Cell Surface Using an Integrative Plasmid

For the stable expression of enzymes on the yeast cell surface, a gene to be integrated into the chromosome of *S. cerevisiae* was constructed using the fusion gene of glucoamylase and C-terminal half of α-agglutinin genes (8).

1. Construction of an Integrative Plasmid

An integrative plasmid for integration of the glucoamylase gene to the chromosome was constructed as follows (Fig. 8a): The yeast integration vector pRS406 (9) was digested with *Kpn*I and *Sal*I, treated with T4 DNA polymerase, and then self-ligated. The *Hin*dIII fragment containing the glucoamylase/α-agglutinin fusion gene excised from the plasmid pGA11 was inserted into the *Hin*dIII site of the self-ligated plasmid. The resulting plasmid was named pIGA11 as the integrative plasmid. The plasmid pIGA11 prepared was cut by *Apa*I and introduced into S. cerevisiae MT8-1 strain, and the transformant obtained was named IGA strain. Integration of the fusion gene was confirmed by Southern blot hybridization analysis using a full-length fragment of *URA3* as a probe.

2. Stability of the Strain Harboring the Integrative Plasmid

Mitotic stability of the integrated exogenous DNA sequence after 120 h cultivation was estimated by com-

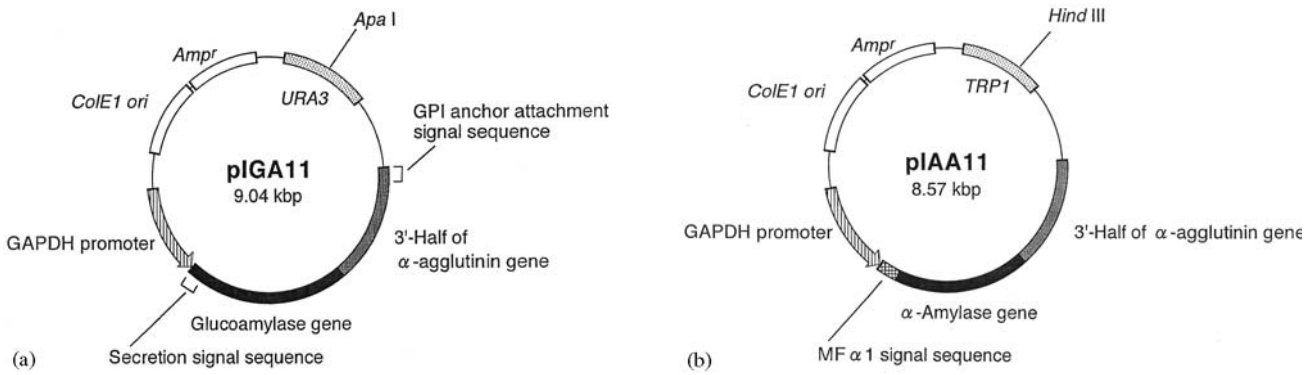

Figure 8 Construction of integrative plasmids for cell surface immobilization of glucoamylase (a, pIGA11) and α-amylase (b, pIAA11).

paring the number of colonies (cells corresponding to $A_{600} = 10$) grown on a nonselective YPD plate with that grown on a selective SD (synthetic [S] medium [0.67% yeast nitrogen base without amino acid with appropriate supplements] containing 2% glucose) plate using the replica-plate method. As for IGA strain, the number of colonies on SD plate without uracil was ~ 97% of that on YPD plate. When cultivation was repeated three times, the number of colonies of uracil nonauxotrophs was still 90%.

C. Immobilization of α-Amylase on Yeast Cell Surface Using an Integrative Plasmid

1. Construction of an Integrative Plasmid

To express the α-amylase gene from *B. stearothermophilus* CU21 (BSTA in *S. crevisiae* and display the synthesized protein on its cell surface (8), the following DNA fragments were prepared (Fig. 8b). The prepro leader sequence of the α-factor precursor (*MFα1*) was first fused to the α-amylase gene. The prepro secretion signal sequence of the *MFα1* was amplified from the plasmid pLS01 by PCR, using the primers 5′-GCAGCTCGAGATGAGATTTCCTTCAATTTTT-ACTGC-3′ and 5′-TCTCTAGAATCCAAAGATAC-CCCTTC-3′. pLS01 has a 1.7-kbp *Eco*RI-*Eco*RI fragment of the *MFα*1 inserted at *Eco*RI site of pUC13 (10). The amplified fragment was cut with *Xho*I and *Xba*I, then ligated at the *Xba*I site with the α-amylase gene fragment, which was amplified from pBR2.0A (4) by PCR using the primers 5′-CCTCTAGAGCCGCA-CCGTTTAACGGCAC-3′ and 5′-GCCTCGAGCCA-GGCCATGCCACCAACCG-3′ and digested with *XbaI* and *Xho*I. A DNA fragment of the α-agglutinin gene (*AGα1*), containing 3′-half of the coding region encoding 320 amino acids of the α-agglutinin and 446 bp of the 3′-flanking region, was prepared by the same method as the case of glucoamylase. These two fragments and *Bam*HI-*Xho*I fragment of the GAPDH promoter were inserted into the plasmid pRS404 at its *Bam*HI-*Kpn*I site.

On the constructed plasmid, introduction of the *Xba*I site changed its corresponding amino acid sequence Lys-Arg to Ser-Arg, where Lys-Arg is the recognition sequence of the Kex2 endopeptidase to cleave α-factor prosequence. Therefore, the site-directed mutagenesis was performed by PCR-based technique to change Ser-Arg to Lys-Arg. The resulting plasmid was named PIAA11. When the IAA strain harboring pIAA11 was cultivated in modified Burkholder's medium containing 2% glucose at 30°C for 24 h, ~ 60% of the total α-amylase activity was detected in the culture supernatant. This solubilization seemed to be caused by the proteolytic processing of the fusion protein.

The deduced amino acid sequence of the *BSTA* gene contains one possible processing site for the Kex2 endopeptidase, Val-Pro-Arg sequence, at amino acid residues No. 481–483. The Kex2 enzyme exhibits the substrate specificity toward each carboxyl site of Lys-Arg, Arg-Arg, and Pro-Arg sequences (11). Then, a Kex2-resistant BSTA/α-agglutinin fusion protein was constructed by eliminating 33 residues from the C-terminus of the BSTA. The C-terminal truncated BSTA/α-agglutinin fusion gene was introduced into *S. cerevisiae* (Fig. 9), using the integration plasmid pIAA12. For construction of the plasmid pIAA12, PCR was performed with primers 5′-GCAGCT-CGAGATGAGAT-TTCCTTCAATTTTTACTGC-3′ and 5′-TCCTCGA-GCCAGGAACCCAAACCGAA-ACCG-3′ and pIAA11 as a template, followed by *Xho*I digestion. The *Xho*I fragment of the plasmid

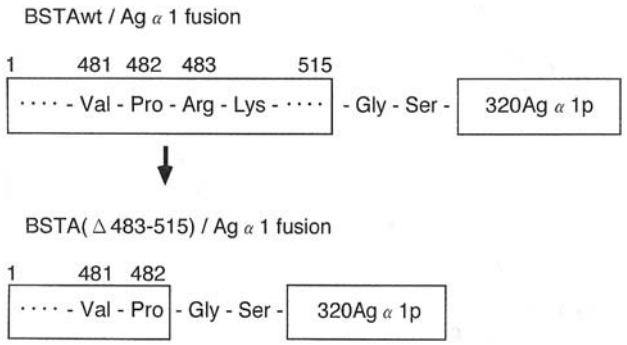

Figure 9 Strategy for the construction of the C-terminal truncated BSTA/α-agglutinin fusion protein.

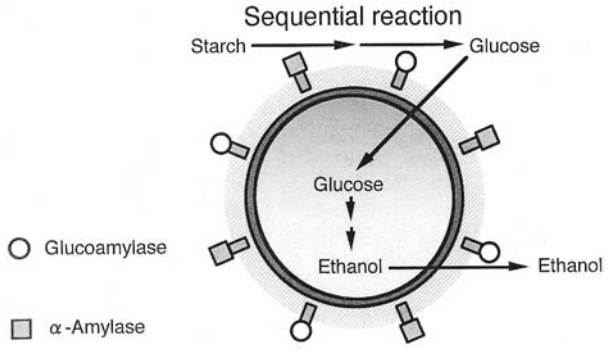

Figure 10 Model of cell surface–engineered yeast coimmobilized with glucoamylase and α-amylase.

pIAA11 was substituted for this newly synthesized fragment to produce the plasmid pIAA12 to be immobilized without cleavage by proteases. Southern blot hybridization analysis was carried out to confirm the integration into chromosomal DNA. The obtained strain was named IAAΔ strain. The IAAΔ strain exhibited α-amylase activity only in the cell pellet fraction. This indicated that the genetic immobilization of α-amylase without leaking any detectable activity to the culture medium was performed by the elimination of the possible Kex2 enzyme processing site.

D. Coimmobilization of Glucoamylase and α-Amylase on Yeast Cell Surface

Coexpression of glucoamylase and α-amylase on the cell surface was expected to be effective for efficient assimilation of starch (Fig. 10). An *S. cerevisiae* strain was constructed in which glucoamylase/α-agglutinin gene and C-terminal truncated α-amylase/α-agglutinin gene were integrated into its chromosomes (8). The plasmid pIAA12 was cut by *Hin*dIII and introduced into the IGA strain harboring pIGA11. The cell of uracil and tryptophan nonauxotrophy was picked up and named IGA/IAAΔ strain. Integration of the fusion genes was confirmed by Southern blot hybridization analysis using *URA3* and *TRP1* as probes.

1. Detection of Glucoamylase and α-Amylase

The strain IGA/IAAΔ exhibited both glucoamylase and α-amylase activities only in the cell pellet fraction. Immunofluorescent labeling and immunoelectron microscopy confirmed the location of both enzymes on the yeast cell surface. The colony of the IGA/IAAΔ strain on a starch-containing plate, unlike that of the IGA/IAA strain, formed a small halo strictly around the colony as observed in the case of the IAAΔ and IGA strains, showing the expression of both glucoamylase and α-amylase on the cell surface. These results demonstrated that glucoamylase and α-amylase were coexpressed and coimmobilized on the cell surface of the same cell.

2. Assimilation of Starch

The transformants were cultivated aerobically at 30°C in modified Burkholder's medium containing 1% soluble starch as the sole carbon source. The IGA and IGA/IAAΔ strains grew on starch and reached an absorbance of ~ 10 monitored at 600 nm, which was the same level as in the case of the culture on 1% glucose, although the growth on glucose of these strains was more rapid. No growth on starch was observed with the MT8-1 and IAA strains. The strain codisplaying glucoamylase and α-amylase, IGA/IAAΔ, grew faster than the glucoamylase-displaying strain, IGA (Fig. 11). This result demonstrated that the yeast strain armed with α-amylase in addition to glucoamylase had the enhanced ability to degrade starch by sequential hydrolytic reaction on the cell surface.

IV. GENETIC IMMOBILIZATION OF CELLULOLYTIC ENZYMES ON YEAST CELL SURFACE

Cellulose, consisting of glucose units linked together by β-1,4-glycosidic bonds, is the most abundant carbohydrate in the biosphere. An estimated synthesis rate of cellulose is ~ 4×10^7 tons/year. For a long-range

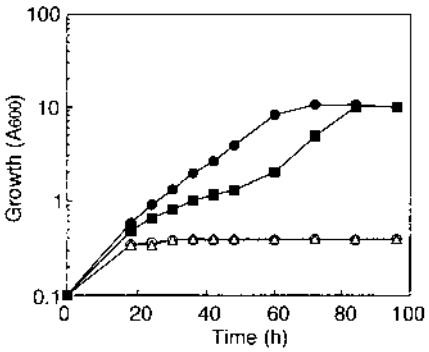

Figure 11 Time courses of cell growth (absorbance at 600 nm) during aerobic cultivation in the medium containing starch as the sole source of carbon and energy. Symbols for strains: ○, MT8-1; ■, IGA; △, IAAΔ; ●, IGA/IAAΔ.

solution to resource problems of energy, chemicals, and food, cellulose is the most promising renewable carbon source that is available in large quantity. However, the yeast *S. cerevisiae* is unable to utilize cellulosic materials in spite of its versatility in industrial fermentation. The cell surface engineering system might be applicable. The genetic immobilization on the cell surface of yeast of carboxymethylcellulase (CMCase) from *Aspergillus aculeatus*, classified as endo-1,4-β-D-glucan glucohydrolase (endoglucanase, EC 3.2.1.4), which cleaves the β-1,4-glycosidic linkage of cellulose (12) or/and β-glucosidase (1,4-β-D-glucoside glucohydrolase, EC 3.2.1.21), an exo-type enzyme (13) from the same microorganism, was carried out. It was predicted that short-chain cello-oligosaccharides formed by the endo-action of CMCase would be converted quickly to glucose by β-glucosidase. However, *S. crevisiae* lacks β-glucosidase activity and consequently is unable to utilize cellobiose as the carbon source. Thus, to construct an *S. cerevisiae* strain which is able to utilize cellulosic materials, it is necessary to endow it with β-glucosidase activity.

A. Immobilization of CMCase on Yeast Cell Surface

1. Construction of a Multicopy Plasmid

A cDNA encoding Fl-CMCase of the fungus *A. aculeatus* with its secretion signal peptide was fused with the gene encoding the C-terminal half (320 amino acid residues from the C-terminus) of yeast α-agglutinin (12). The constructed plasmid containing this fusion gene was expressed under the control of the *GAPDH* promoter from *S. cerevisiae*. The multicopy plasmid pCMC11 to immobilize CMCase was constructed as follows (Fig. 12): An *Xho*I site was generated at the end of the CMCase coding region on the plasmid YEpM93R (14) by the PCR with the primers 5′-AGTACTCGAGCCCTGTACGCTGGCAGACCA-GT-3′ and 5′-CGGTAGGTATTGATTGTAATTCT-G-3′. A DNA fragment containing CMCase coding region was isolated by *Eco*RI-*Xho*I digestion. A DNA fragment of the α-agglutinin gene (*AGα1*), containing the 3′-half of the coding region encoding 320 amino acids of the α-agglutinin and 446 bp of the 3′-flanking region, was prepared by the previously described method. These two fragments were substituted for the *Eco*RI-*Kpn*I section between the *GAPDH* promoter and the *GAPDH* terminator of the yeast expression cassette vector pYE22m. The resulting plasmid was named pCMC11.

2. Detection of CMCase

Cells were cultivated in SD medium (Sec. III.B.2) at 30°C for 24 h to the stationary phase. Culture medium and cell pellets were isolated by centrifugation to measure the CMCase activities in both fractions. The cells harboring the plasmid pCMC11 had the cell-associated CMCase activity without secretion of the active enzyme. The CMCase activity was stably maintained for 120 h at least. SDS and β-1,3-glucanase treatment indicated that the CMCase was covalently attached to the cell wall and immobilized by the genetic engineering techniques. A plate assay was carried out using Congo Red staining (15). The cells harboring the plasmid pCMC11 hydrolyzed carboxymethylcellulose and produced a halo strictly around the colony, while no halo formation was observed around the cells harboring the plasmid pYE22m (Fig. 13). Immunofluorescent labeling and immunoelectron microscopy confirmed the localization of CMCase/α-agglutinin fusion protein on the yeast cell surface (Figs. 6, 7).

B. Immobilization of β-Glucosidase on Yeast Cell Surface

1. Construction of a Multicopy Plasmid

The DNA fragment composed of the *GAPDH* promoter and the secretion signal sequence of glucoamylase gene from *R. oryzae* was prepared by PCR (primers 5′-CCGAGCTCACCAGTTCTCACACGGAACA-3′ and 5′-GCCCGCGGCAGAAACGAGCAAAGAAA-A-3′) with the plasmid pYGA2269 (3) as a template, and then cut with *Sac*I and *Sac*II. The resulting *Sac*I-

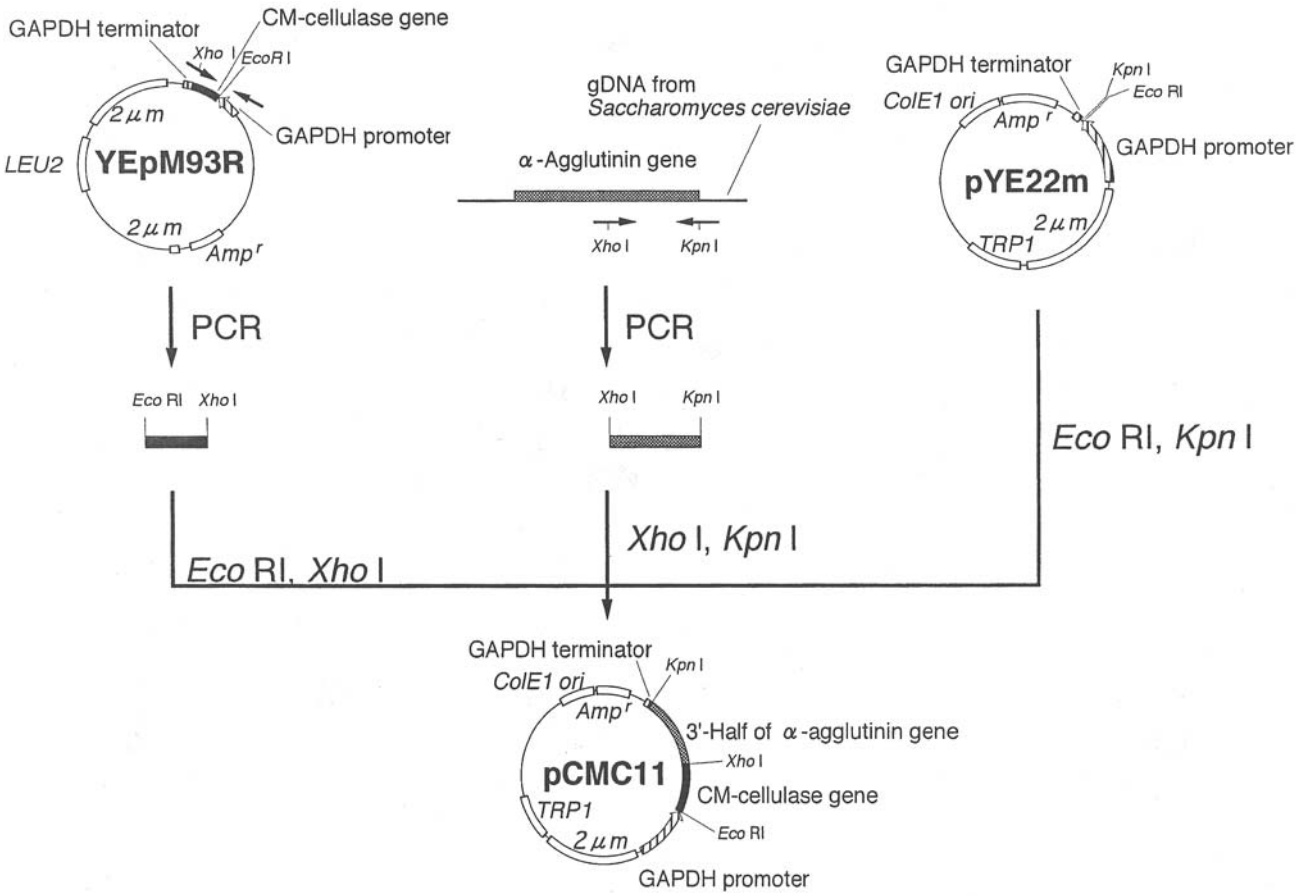

Figure 12 Construction of the multicopy plasmid pCMC11 for cell surface immobilization of CMCase.

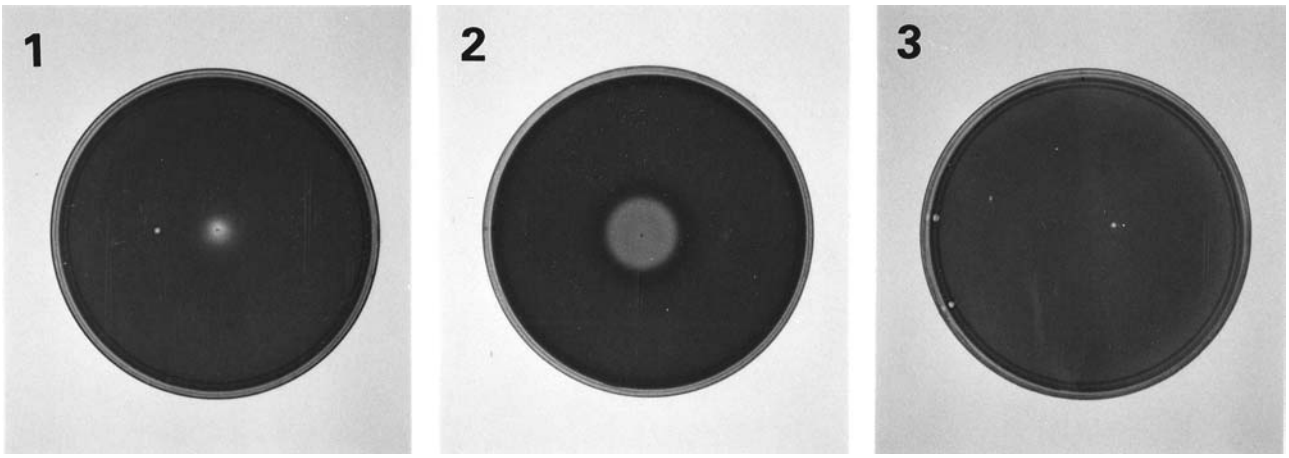

Figure 13 Plate assay for detection of CMCase activity. 1, *S. cerevisiae* with cell surface–immobilized CMCase (*S. cerevisiae* MT8-1/pCMC11); 2, *S. cerevisiae* secreting CMCase; 3, *S. cerevisiae* MT8-1 as the control (*S. cerevisiae* MT8-1/pYE22m).

*Sac*II fragment, the *Sac*II-*Xho*I fragment created by annealing two oligonucleotides 5′-GGAGATCTCCA-TGGC-3′ and 5′-TCGAGCCATGGAGATCTCCGC-3', and the *Xho*I-*Kpn*I fragment containing the 3′-half of the coding region encoding 320 amino acids of α-agglutinin and 446 bp of the 3′-flanking region excised from the plasmid pGA11, were inserted into the sections of *Sac*I-*Sac*II, *Sac*II-*Xho*I, and *Xho*I-*Kpn*I, respectively, of the plasmid pRS404 (9). The resulting plasmid was named pICAS1. The plasmid pBG211 to immobilize β-glucosidase on the yeast cell surface was constructed as follows. The yeast high-copy vector pMH1 (15) was constructed by introducing the 2.14-kbp *Eco*RI-*Eco*RI fragment of PMT34(+3) (4) containing a part of 2 μm DNA into the *Aat*II site of the plasmid pRS403 (9). The *Bgl*II-*Xho*I fragment of the cDNA encoding β-glucosidase 1 (BGL1) from *A. aculeatus* was generated by PCR (5′-GTCGAGATCTCTGATGAACTGGCGTTCTCT-3′ and 5′-TTCACTCGAGCCTTGCACCTTCGGGAG-CGCCG-3′) with the plasmid pABG7 as the template, and substituted for the *Bgl*II-*Xho*I section of pICAS1, from which the *Bss*HII-*Bss*HII fragment was transferred to the plasmid pMH1 at its *Bss*HII-*Bss*HII section. The resulting plasmid was named pBG211 (Fig. 14) (14).

2. Detection of β-Glucosidase

Yeast harboring pBG211 was precultivated in YPD medium and cultivated aerobically in the S-medium to which 2% glucose, 1% cellobiose, or 0.5% cellooligosaccharides was added as the sole carbon source. The cello-oligosaccharides contain ~11% (w/w) cellohexaose, 29% (w/w) cellopentaose, 33% (w/w) cellotetraose, 17% (w/w) cellotriose, 4% (w/w) cellobiose, and < 1% (w/w) glucose. β-Glucosidase activity was measured as follows (16): The reaction mixture was composed of 0.1 mL of 1.7 mM *p*-nitrophenyl-β-D-glucoside in 0.1 M sodium acetate buffer, pH 5.0, and 0.1 mL of enzyme solution. After incubation at 37°C for 10 min, *p*-nitrophenol released was measured spectrophotometrically as an increase of absorbance at 400 nm (molecular extinction coefficient, 17,700 M^{-1} cm^{-1}). One unit of the enzyme activity was defined as the amount of enzyme that released 1 μmol of *p*-nitrophenol from the substrate per minute. Immunofluorescence microscopy was performed the same as in other cases.

3. Analysis of Saccharides

For thin-layer chromatography of cello-oligosaccharides, aliquots (1 μL) of the culture supernatants were spotted on a silica gel 60F254 TLC plate, and developed twice with 1-butanol-pyridine-water (70:15:15, v/v). Sugars were detected by the diphenylamine-aniline method; the detection reagent, consisting of 4 mL aniline, 4 g diphenylamine, 200 mL acetone, and 30 mL 85% phosphoric acid, was sprayed on the plate, which was then heated at 105°C for 30 min.

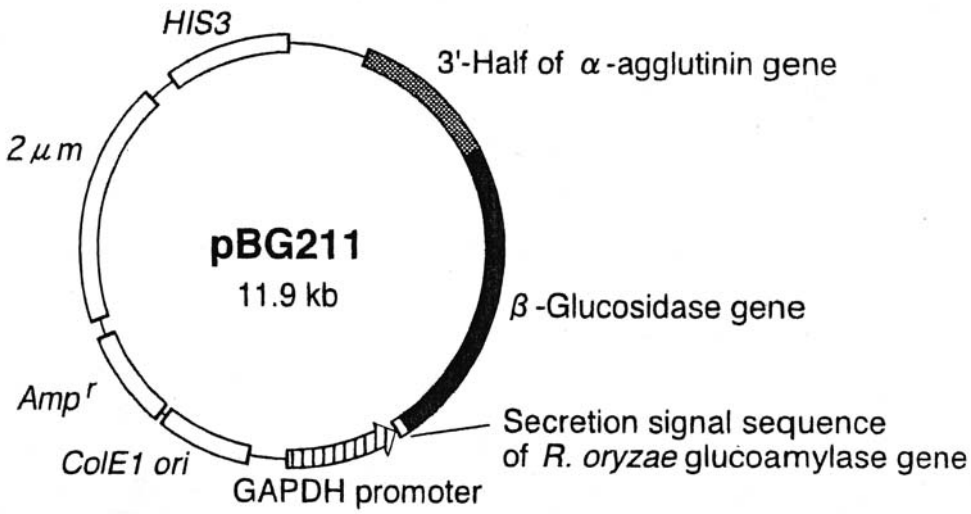

Figure 14 Construction of the multicopy plasmid pBG211 for cell surface immobilization of β-glucosidase.

C. Coimmobilization of CMCase and β-Glucosidase on Yeast Cell Surface

1. Construction of Cells for Coimmobilization of CMCase and β-Glucosidase

The plasmids pBG211 and pCMC11 described above were introduced stepwise into *S. cerevisiae* MT8-1. The resulting strain was named MT8-1/(pCMC11, pBG211) (13).

2. Detection of CMCase and β-Glucosidase

To determine the location of CMCase and β-glucosidase, yeast strains were cultivated in the SD medium (Sec. III.B.2) at 30°C for 24 h. The cells harboring the plasmid pCMC11, i.e., strain MT8-1/pCMC11 and strain MT8-1/(pCMC11, pBG211), had the cell-associated CMCase activity, and the cells harboring the plasmid pBG211, i.e., strain MT8-1/pBG211 and strain MT8-1/(pCMC11, pBG211), exhibited the cell-associated β-glucosidase activity. Moreover, the cells harboring the plasmids pCMC11 and pBG211 showed both CMCase and β-glucosidase activities. Strain MT8-1 itself exhibited neither of the activities. These results suggested that CMCase and β-glucosidase proteins were efficiently synthesized and codisplayed on the cell surface in their active forms. MT8-1/(pCMC11, pBG211) cells were labeled by fluorescence with both anti-CMCase IgG and anti-β-glucosidase IgG, confirming again that these cells coimmobilized CMCase and β-glucosidase proteins on their cell surface (Fig. 15).

3. Assimilation of Cello-oligosaccharides

The transformants were precultivated in YPD medium and cultivated aerobically in S-medium (Sec. III.B.2) containing cellobiose as the sole carbon source. The strains MT8-1/pBG211 and MT8-1/(PCMC11, pBG211) grew on cellobiose and reached an absorbance of ~ 2, which was a little lower than that in the case of the culture on 1% glucose. No growth on cellobiose was observed with strains MT8-1 and MT8-1/pCMC11. No difference was observed between the growth curves of the strains MT8-1/pBG211 and MT8-1/(pCMC11, pBG211). These results showed that the β-glucosidase genetically immobilized on the cell surface endowed the yeast with the ability of cellobiose degradation and utilization. The transformants were precultivated in YPD medium and cultivated aerobically in S-medium supplemented with cello-oligosaccharides as the sole carbon source, and the cell growth was monitored by counting colonies that appeared on YPD plates on which aliquots of the culture broth were spread. The strains MT8-1/pBG211 and MT8-1/(pCMC11, pBG211) grew on cello-oligosaccharides employed (Fig. 16).

β-Glucosidase was capable of degrading cello-oligosaccharides with glucose units of 2 to 6; the breakdown of cello-oligosaccharides by β-glucosidase seemed to be sufficient to sustain the growth of the yeast displaying this enzyme. The strain MT8-1/(pCMC11, pBG211), however, grew a little more rapidly than the strain

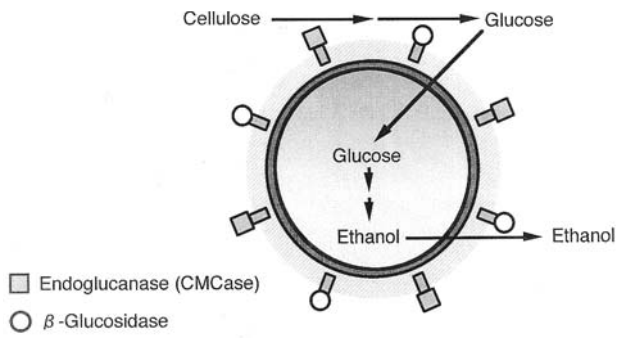

Figure 15 Model of cell surface–engineered yeast coimmobilized with CMCase and β-glucosidase.

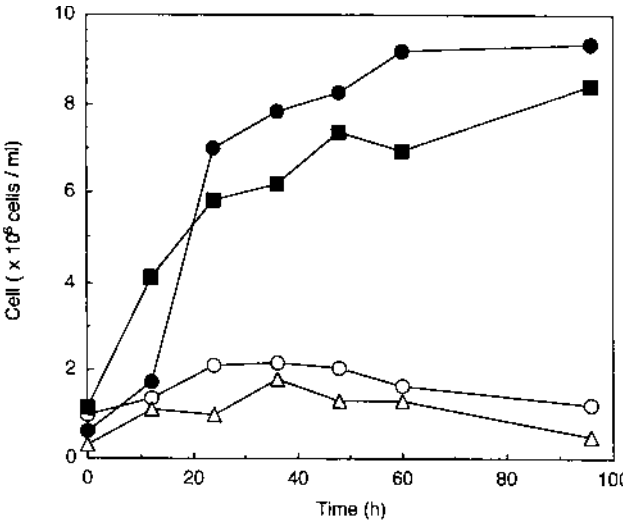

Figure 16 Time courses of the cell growth during aerobic cultivation in the medium containing cello-oligosaccharides as the sole source of carbon and energy. Symbols for strains: ○, MT8-1; △, MT8-1/pCMC11; ■, MT8-1/pBG211; ●, MT8-1/ (pBG211, pCMC11). Cell growth was monitored by counting colonies that appeared on YPD plates on which aliquots of the culture broths were spread.

MT8-1/pBG211, indicating that the yeast strain codisplaying CMCase and β-glucosidase had the enhanced ability to degrade cello-oligosaccharides. The degradation and assimilation of cello-oligosaccharides by the transformants were confirmed by thin-layer chromatography. The cello-oligosaccharides dissolved in the culture supernatants were gradually degraded and assimilated by the strains MT8-1/pBG211 and MT8-1/(pCMC11, pBG211).

The strain MT8-1/(pCMC11, pBG211) degraded cello-oligosaccharides more rapidly, especially cellopentaose (G5) and cellohexaose (G6), than the strain MT8-1/pBG211. This is probably due to the activity of CMCase displayed on the cell surface of the strain MT8-1/(pCMC11, pBG211). CMCase purified from *A. aculeatus* showed activity against G5 and G6 (17). Surely, it was confirmed that the strain MT8-1/pCMC11 degraded G5 and G6 among the cello-oligosaccharides employed, while the strain MT8-1 could not degrade any of the cello-oligosaccharides. These results gave evidence that the strain MT8-1/(pCMC11, pBG211) hydrolyzed the cello-oligosaccharides with synergistic actions of CMCase and β-glucosidase, the produced glucose being assimilated for proliferation.

V. PERSPECTIVE

The immobilization of amylolytic and cellulolytic enzymes on the yeast cell surface may facilitate the utilization of starch and cellulose by yeast. In this system, the cell surface of yeast was used as a carrier for immobilization of enzymes, and the living whole cells were remade as a "cell biocatalyst." The modified strain was named "arming yeast" (18). This system turned or remade *S. cerevisiae* into a novel and attractive microorganism as a whole-cell biocatalyst by surface expression of various enzymes, especially when target substrates are not able to be taken up by the cells. Although a lot of methods for immobilization of enzymes have been developed to construct bioreactors with effective conversion of substrates, it is still difficult to maintain the enzyme activities over the long reaction period or to perform multistep conversions. The novel cell surface-engineered cells ("arming cells"), endowed with a rapid starchy and cellulosic material-utilizing abilities by immobilizing two amylases and cellulases on their cell surface, will be employed for efficacious fermentation of starchy and cellulosic materials.

Our cell surface engineering system has a possibility of being used to construct new functional yeast strains. This may contribute to resolution of many problems concerning environmental pollution and biomass conversion at the global level.

VI. SUMMARY

We established the genetic system to immobilize enzymes as their active forms on the cell surface of yeast, *S. cerevisiae*. As a principle, a cDNA encoding enzyme with a secretion signal peptide was fused with the gene encoding the C-terminal half (320 amino acid residues from the C-terminus) of yeast α-agglutinin, a protein involved in mating and covalently anchored to the cell wall. The constructed plasmid containing this fusion gene was introduced into *S. cerevisiae* and expressed under the control of the glyceraldehyde-3-phosphate dehydrogenase (GAPDH) promoter from *S. cerevisiae*. The activity and localization of the enzyme on the cell surface was biochemically demonstrated by subcellular fractionation and glucanase treatment. Appearance of the fused protein expressed on the cell surface was further confirmed by halo formation, unlike that of secretive enzyme, and immunofluorescence and immunoelectron microscopies. Arming cells displaying glucoamylase and α-amylase, or carboxymethylcellulase and β-glucosidase, could assimilate starch or cello-oligosaccharides as the sole carbon source, although *S. cerevisiae* cannot intrinsically assimilate them. This technique endowed the cell with novel functions.

REFERENCES

1. PN Lipke, J Kurjan. Sexual agglutination in budding yeasts: structure, function, and regulation of adhesion glycoproteins. Microbiol Rev 56:180–194, 1992.
2. T Murai, M Ueda, M Yamamura, H Atomi, Y Shibasaki, N Kamasawa, M Osumi, T Amachi, A Tanaka. Construction of a starch-utilizing yeast by cell surface engineering. Appl Environ Microbiol 63:1362–1366, 1997.
3. T Ashikari, N Nakamura, Y Tanaka, N Kiuchi, Y Shibano, T Tanaka, T Amachi, H Yoshizumi. *Rhizopus* raw-starch-degrading glucoamylase: its cloning and expression in yeast. Agric Biol Chem 50:957–964, 1986.
4. R Nakajima, T Imanaka, S Aiba. Nucleotide sequence of the *Bacillus stearothermophilus* α-amylase gene. J Bacteriol 163:401–406, 1985.

5. T Ashikari, N Kiuchi-Goto, Y Tanaka, Y Shibano, T Amachi, H Yoshizumi. High expression and efficient secretion of *Rhizopus oryzae* glucoamylase in the yeast *Saccharomyces cerevisiae*. Appl Microbiol Biotechnol 30:515–520, 1989.
6. M Tajima, Y Nogi, T Fukasawa. Primary structure of the *Saccharomyces cerevisiae GAL7* gene. Yeast 1:67–77, 1985.
7. M Ueda, T Murai, Y Shibasaki, N Kamasawa, M Osumi, A Tanaka. Molecular breeding of polysaccharide-utilizing yeast cells by cell surface engineering. Ann NY Acad Sci *864:528–537, 1988*.
8. T Murai, M Ueda, Y shibasaki, N Kamasawa, M Osumi, T Imanaka, A Tanaka. Development of an arming yeast strain for efficient utilization of starch by co-display of sequential amylolytic enzymes on the cell surface. Appl Microbiol Biotechnol 51:65–70, 1999.
9. RS Sikorski, P Hieter. A system of shuttle vectors and yeast host strains designed for efficient manipulation of DNA in *Saccharomyces cerevisiae*. Genetics 122:19–27, 1989.
10. K Inokuchi, A Nakayama, F Hishinuma. Identification of sequence elements that confer cell-type-specific control of *MFα1* expression in *Saccharomyces cerevisiae*. Mol Cell Biol 7:3185–3193, 1987.
11. K Mizuno, T Nakamura, T Ohshima, S Tanaka, H Matsuo. Characterization of *KEX2*-encoded endopeptidase from yeast *Saccharomyces cerevisiae*. Biochem Biophys Res Commun 159:305–311, 1989.
12. T Murai, M Ueda, H Atomi, Y Shibasaki, N Kamasawa, M Osumi, T Kawaguchi, M Arai, A Tanaka. Genetic immobilization of cellulase on the cell surface of *Saccharomyces cerevisiae*. Appl Microbiol Biotechnol 48:499–503, 1997.
13. T Murai, M Ueda, T Kawaguchi, M Arai, A Tanaka. Assimilation of cello-oligosaccharides by cell surface-engineered yeast expressing β-glucosidase and carboxymethylcellulase from *Aspergillus aculeatus*. Appl Environ Microbiol 64:4857–4861, 1998.
14. K Minamiguchi, T Ooi, T Kawaguchi, H Okada, S Murao, M Arai. Secretive expression of the *Aspergillus aculeatus* cellulase (Fl-CMCase) by *Saccharomyces cerevisiae*. J Ferment Bioeng 79:363–366, 1995.
15. P Beguin. Detection of cellulase activity in polyacrylamide gels using Congo Red–stained agar replicas. Anal Biochem 131:333–336, 1983.
16. J Borooah, DH Leaback, PG Walker. Studies on glucosaminidase. 2. Substrates for *N*-acetyl-β-glucosaminidase. Biochem J 78:106–110, 1961.
17. S Murao, R Sakamoto, M Arai. Cellulases of *Aspergillus aculeatus*. Methods Enzymol 160:274–299, 1988.
18. Anonymous. Arming yeast with cell-surface catalysts. Chem Eng News 75(15):32, 1997.

24

Use of Immobilized Enzymes in the Food Industry

Harold E. Swaisgood
North Carolina State University, Raleigh, North Carolina, U.S.A.

1. INTRODUCTION

Most of the literature on immobilized enzymes has resulted from research and development during the past 40 years. A number of reviews have appeared (1–11) that discuss the preparation, characteristics, and uses of immobilized enzymes. Actual commercialization of immobilized enzyme bioprocesses has not occurred at a rapid pace in the food industry, perhaps owing to a natural reluctance to replace existing soluble enzyme processes and the fact that most of the industry involves low value-added products with small profit margins. Nevertheless, immobilized enzyme technology has gained acceptance in several areas. The most successful example is the production of high-fructose corn syrup using immobilized glucose isomerase, which is a unique product produced only with the immobilized enzyme.

II. WHY USE AN IMMOBILIZED ENZYME?

The commercial success of an immobilized enzyme process requires the cost per unit of product to be less than that for a comparable soluble enzyme process or that a unique product can be produced with the immobilized enzyme that cannot be obtained with the soluble enzyme. Some possible advantages of an immobilized enzyme process as compared with use of the soluble enzyme are listed in Table 1 (11). Because the same enzyme is used continuously, the amount of product obtained per unit of enzyme is much greater. For example, in the current commercial use of immobilized glucose isomerase 12,000–15,000 kg of dry product is typically obtained per kilogram of biocatalyst during its operational lifetime (J. Shetty, personal communication, 1999).

Precise control of the extent of reaction is a key advantage for many processes where a limited extent of reaction is desirable. Use of the immobilized form eliminates the need for a downstream enzyme inactivation step that could be harmful to the product. These considerations are important for processes involving protein modification or flavor generation. Even if precise control of the extent of reaction is not required, in many cases a downstream enzyme inactivation step is necessary because the commercial enzyme preparation may contain contaminating activities, e.g., proteinases, that over long periods can cause product deterioration. When the immobilized preparation is used, the short exposure time may not be detrimental.

Use of the immobilized enzyme in a bioreactor, for example, a fixed-bed or fluidized-bed reactor, allows it to be incorporated into a continuous automated bioprocess. This feature greatly reduces the materials handling and, consequently, the labor costs. For example, Tanabe-Seiyaku Co. in Japan experienced a threefold reduction in labor costs when they introduced the use of immobilized aminoacylase for L-amino acid

Table 1 Some Possible Advantages of an Immobilized Enzyme Process as Compared with Use of the Soluble Enzyme

1. Greater productivity per unit of enzyme
2. Precise control of the extent of reaction
3. Continuous operation and automation of the process is possible
4. Materials handling is minimized
5. Product does not contain the biocatalyst
6. Enzyme activity may be stabilized
7. A unique product may be produced

production (4). Another example is the Valio process for producing hydrolyzed whey syrup using immobilized β-galactosidase. One of the largest whey-processing plants in the world, operated by Dairy Crest in northern Wales and using the Valio process, is fully automated and controlled by a microprocessor, thus requiring only two operators to be present at any one time (M. Harju, personal communication, 1999).

Immobilization can also result in stabilization of the enzyme activity. Such stabilization is especially true for proteinases because autolysis is prevented (12). Moreover, in many food processes, in order to limit microbial growth it is desirable to operate at temperatures where structural stability of proteins is marginal and thus most susceptible to proteolysis. In addition, the surface microenvironment of the support may stabilize the enzyme structure; for example, many supports have a polyol type structure that is known to stabilize proteins (13).

Finally, it may be possible to produce a unique product using an immobilized enzyme. Such is the case for production of high-fructose corn syrup using immobilized glucose isomerase. Recently, the potential to design functionality by limited proteolysis has been demonstrated (14, 15). However, this requires precise control of the extent of hydrolysis, but a downstream heat inactivaction of the enzyme would also denature the polypeptides formed and thus destroy functionality. Use of immobilized proteinases would eliminate the required downsteam enzyme inactivation; consequently, functional polypeptides could be produced that have unique properties in foods.

III. ECONOMIC CONSIDERATIONS FOR AN IMMOBILIZED ENZYME BIOPROCESS

The commercial success of an enzyme process depends on its cost per unit of product balanced against the value added. The major factors that determine the cost of an enzyme process are listed in Table 2 (6, 11). For a soluble enzyme process, a major cost is that associated with its purification. The degree of purification must be balanced against the desirability of a high specific activity. Usually, costs escalate when additional purification is sought in the higher range of purity; however, higher specific activities mean less of

Table 2 Major Factors That Determine the Cost of an Enzyme Process

Purification costs	Required specific activity Required removal of contaminating activities
Immobilization costs	Characteristics of the immobilization methodology Amount of enzyme loading
Operation stability	Enzyme stability Amount of enzyme leaching Resistance of the support to attrition
Regenerative capability of the biocatalyst	Number of times the activity can be regenerated Complexity of the regeneration procedure Capability of support regeneration
Upstream processing requirements	Complexity of the process Costs of substances added
Sanitation requirements	Frequency of required cleaning Complexity of the cleaning procedure

the enzyme preparation will be required in a process. The same considerations apply to an immobilized enzyme process. Preparations with higher specific activities will result in greater loading of active enzyme and higher activities of the biocatalyst; thus, a smaller bioreactor will be required for the same production rate.

Characteristics of the immobilization procedure are very important. In general, the fewer number of steps required, the lower the costs. However, a number of factors come into play, including the effect of the procedure on enzyme activity, the efficiency of immobilization (percent of the original activity that becomes immobilized), and the cost of the support.

The productivity of the biocatalyst, i.e., the amount of product per unit of biocatalyst per half-life, is a key economic parameter. Both the specific activity and the operational stability of the biocatalyst contribute to this factor. The higher specific activities of immobilized glucose isomerase biocatalyst currently in use have a much greater (10-fold) productivity than the orginal biocatalysts that were simply crosslinked whole cells (16; J. Shetty, personal communication, 1999). Most commercial immobilized enzymes have half-lives of months or even years and typically are operated through several half-lives. Some factors that contribute to the operational stability of the biocatalyst are the stability of the enzyme, the amount of enzyme leaching (desorption), and the resistance of the support to attrition. Enzymes immobilized by adsorption, such as on ion exchange supports, will exhibit a finite desorption rate that depends on environmental conditions, including enzyme characteristics, ionic strength, and temperature. Covalently immobilized enzymes will not leach from the support but the biocatalyst cannot be regenerated. The operational stability of the bioreactor is also affected by the presence of proteinases, either those in the feed stock or those produced by microbial growth. Thus, sanitation of the bioreactor is very important. For example, immobilized glucose isomerase bioreactors are operated at 60°C to control microbial growth.

Capability of regeneration of the biocatalyst can significantly lower the cost of the bioprocess per unit of product. Thus, if the support can be regenerated many times, even an expensive support can be economical. This feature would favor the use of an adsorption immobilization procedure over the use of a covalent bond. Nevertheless, a strong adsorption interaction is most desirable because less leaching would occur and the biocatalyst could be cleansed with stronger solutions for removal of constituents adsorbed from the stock and for sanitizing the bioreactor.

IV. IMMOBILIZED ENZYME PROCESSES THAT HAVE BEEN COMMERCIALIZED IN THE FOOD INDUSTRY

A. Production of High-Fructose Corn Syrup Using Immobilized Glucose Isomerase

This industry has grown from the initial commercial production in 1970 by Clinton Corn Pocessing to become the largest industrial use of an immobilized enzyme process in the world (16, 17). Most recent data indicate that the global annual production of high fructose corn syrup is 10 million metric tons dry substance(dsb) which is produced with 1500 metric tons of immobilized enzyme (J. Shetty, personal communication, 1999). Currently, the major producers of immobilized enzyme are Novo Industry A/S and Genencor. The Genencor immobilized enzyme is produced by adsorption of substantially purified enzyme on ion exchange resins, crosslinked with polyethyleneimine and glutaraldehyde, and granulated by extrusion. This immobilized enzyme typically has a productivity of 12,000–15,000 kg dsb/kg and a half-life of 80–150 days (1920–3600 h) (J. Shetty, personal communication, 1999). The immobilized enzyme produced by Novo (Sweetzyme T) is prepared by crosslinking whole cell material from *Streptomyces murinus* with glutaraldehyde followed by extrusion (18). A typical bioprocess uses 1.5 m × 5 m fixed-bed bioreactors operated at 60–65°C to produce a 42% fructose isosyrup (16, 17). More than half of this isosyrup is converted to 55% fructose using fractionation technology. Future development of a thermostable enzyme may allow direct production of a 55% fructose isosyrup by performing the isomerization at 95°C because the equilibrium is shifted in favor of fructose.

B. Production of Hydrolyzed Whey Syrups Using Immobilized β-Galactosidase

The current commercial process, Valio Hydrolysis Process, was initiated in Finland in 1980 by Valio Ltd. (19). The biocatalyst, Valio IML, consists of a mold β-galactosidase (*Aspergillus oryzae*) adsorbed and crosslinked on a food grade resin (19, 20; M. Harju, personal communication, 1999). The major

product produced by Valio is a demineralized hydrolyzed whey syrup containing ~ 60% solids with 72% hydrolysis of the lactose, Valio Hydroval 80 (M. Harju, personal communication, 1999). Hydrolyzed whey syrups without demineralization and with 50% demineralization are also produced. Whey from cheese-making operations is received in a liquid form (6% total solids), pasteurized, passed through fixed-bed immobilized enzyme bioreactors for lactose hydrolysis, demineralized (if desired), and concentrated to ~60% total solids. The half-life and productivity of a typical bioreactor are 20 months and 2000 kg dry matter/kg enzyme, respectively. The annual production of hydrolyzed whey syrups by this process in Finland, the United Kingdom and Norway is ~ 5000–6000 metric tons.

Bioreactors containing β-galactosidase immobilized covalently on porous silica were developed at Corning Glass Co. (21) and used commercially (6, 22) in England (Specialist Dairy Ingredient Co.), the U. S. (Nutrisearch), and France (Union Laitière Normande). The Nutisearch plant used the hydrolyzed whey for production of baker's yeast; however, this plant is no longer in operation. The only plant still in operation is the SDI plant in the UK owned by Dairy Crest; however, they currently use Valio IML as the biocatalyst.

In addition to production of whey hydrolysates, immobilized enzyme also has been used commercially to hydrolyze lactose in milk. The yeast (*Kluyveromyces lactis*) enzyme, with a pH optimum near 7, was entrapped in cellulose triacetate fibers in a process developed by SNAM Progetti for production of hydrolyzed lactose milk by a plant in Milan, Italy (6, 11, 17, 23). This plant, Centrale del Latte, has a minimum capacity of 8000 L/day (23). Snow Brand Milk Products in Japan also developed an industrial process for production of hydrolyzed lactose milk using the SNAM Progetti immobilized enzyme (23). The Japanese scientists also developed a bioreactor sanitation process, involving immersion in glycerol at 10°C, that allowed them to use 60 processing cycles without an increase in microbial load.

C. Production of L-Amino Acids Using Immobilized Aminoacylase

This process for enzymatic resolution of D, L-amino acids was developed by Chibata and co-workers at Tanabe-Seiyaku Co. in Japan, and its commercialization in 1969 represented the first industrial use of an immobilized enzyme (6, 24–26). Chemically synthesized acyl-D,L-amino acids are asymmetrically hydrolyzed to produce the L-amino acid and acyl-D-amino acid that are easily separated by differences in solubility. The acyl-D-amino acid is then racemized and passed back through the bioreactor for resolution. Bioreactors are prepared by immobilization of the enzyme from *Aspergillus oryzae* by adsorption on DEAE-Sephadex. A typical half-life of a bioreactor is 65 days at 50°C. Operating as a fixed-bed bioreactor, the productivity ranges between 13 and 46 kg amino acid/L/half-life, depending on the amino acid being produced. According to Uhlig (17), the annual production in 1988 was 1000 metic tons of Phe, Met, Tyr, and Val. The overall cost of amino acid production using the immobilized enzyme was 60% of that for use of the soluble form (24).

D. Production of Specific Amino Acids

L-Aspartic acid has been produced from ammonium fumarate commercially in Japan since 1973 using immobilized L-aspartate ammonia lyase (aspartase) (EC 4.3.1.1.) prepared by entrapment of *Escherichia coli* cells in k-carrageenan (27). In 1988, ~ 1000 metric tons of L-aspartate was produced (17). The production of L-alanine from ammonium fumarate using two bioreactors with different immobilized cell preparations was successfully commercialized in 1983 in Japan by Tanabe Seiyaku Co. (28). The first bioreactor contained *E. coli* cells that were pH-treated to inactivate alanine racemase and fumarase activities and entrapped in carageenan, and the second bioreactor contained pH-treated and glutaraldehyde-crosslinked *Pseudomonas dacunhae* also entrapped in carrageenan. Thus, the first bioreactor provided the aspartase activity while the second provided L-aspartate β-decarboxylase activity. This bioprocess represents the first industrial use of sequential bioreactors.

Because of its demand as a percursor in the production of aspartame (α-L-aspartyl-L-phenylalanine methyl ester), various methods for enzymatic production of L-phenylalanine have been developed (29). Purification Engineering (Rhône Poulenc) (11,29) developed an immobilized enzyme bioprocess using phenylpyruvate as the starting material. A mutant of *E. coli* having exceptionally high activities of transaminases with the required specificities was immobilized by entrapment in a polyazetidine layer on Amberlite IRA-938 porous beads. Bioreactors typically exhibited a half-life > 8 months. A 600 metric ton per year plant was constructed (29).

Industrial processes for production of aspartame using immobilized enzymes also have been developed (10, 11, 30, 31). The process developed in Japan by Toya Soda Co. (30) utilized immobilized Thermoase (thermolysin) in a biphasic system to stereospecifically couple N-protected aspartate with D, L-phenylalanine methyl ester to give α-aspartame after hydrogenolysis to remove the protecting group. The enzymatic process eliminates the need to protect and deprotect the β-carboxyl group of aspartate to prevent formation of the bitter isomer β-aspartame and allows use of the less expensive phenylalanine methyl ester racemate. The technology has been licensed to Holland Sweetener Co., a joint venture between Tosoh Corp. and DSM. More recently, another industrial process has been reported that uses enzymes in immobilized cells to make phenylalanine from cinnamic acid and ammonia followed by direct coupling to aspartate (31).

E. Production of 5′-Ribonucleotides

A market exists for 5′-ribonucleotides as flavor enhancers in foods and as precursors for pharmaceuticals. A process was developed in Germany by Keller and co-workers at Hoechst Aktiengesellschaft for hydrolysis of RNA using 5′-phosphodiesterase immobilized on oxirane acrylic beads (Eupergit C from Röhm Pharma) (32). Elimination of the necessity of fractionation of RNA and DNA was accomplished because DNA could not penetrate the matrix and thus was not hydrolyzed. In a pilot plant operation using crude nucleic acid feed stocks at 60°C, the immobilized enzyme was used continuously for 500 days with no detectable loss of activity and produced 10 metric tons per year (32). Earlier work in Japan also resulted in a process for production of 5′-ribonucleotides, including IMP, using a mixed bed of 5′-phosphodiesterase and 5′-adenylate deaminase immobilized on porous silica (33).

F. Production of Isomaltulose

Isomaltulose (6-*O*-α-D-glucopyranosyl-D-fructofuranose) is a natural component of honey with a sweetness one-third that of sucrose. However, it appears to be noncariogenic and it encourages the growth of *Bifidobacter*. Several processes for its commercial production using immobilized enzymes have been developed (34–36). Although only one enzyme, isomaltulose synthase, is required for conversion of sucrose to isomaltulose, normally whole cells were immobilized rather than incur the cost of purification. In the process developed by Cheetham (34) in England, *Erwinia rhapontici* cells were entrapped in calcium alginate gels and formed into pellets by extrusion. The enzyme expressed by these cells was specific for sucrose and followed an unusual intramolecular mechanism in which both the glucose and fructose moieties remain enzyme bound (34). Operating as a fixed-bed bioreactor, the immobilized enzyme exhibited a half-life of 1 year and had a productivity of 1500 times its own weight in crystalline isomaltulose.

In another process developed at the South Germany Sugar Co. *Protaminobacter rubrum* cells were flocculated and crosslinked with glutaraldehyde (34, 35). Palatinit AG, a subsidiary of South Germany Sugar Co. and Bayer AG, used this process for commercial production of isomaltulose.

Using a similar procedure, except that the cells entrapped in calcium alginate gels were crosslinked with polyethyleneimine and glutaraldehyde, Mitsui Sugar Co. in Japan commercialized a process using *Serratia plymuthica or P. rubrum* cells (34, 36). The productivity of a fixed-bed bioreactor containing the immobilized *P. rubrum* enzyme was 260 kg/L of biocatalyst/half-life. The company initiated production with a 600 metric ton per year plant in Okayama, Japan.

G. Production of Invert Sugar (Hydrolysis of Sucrose)

Invertase immobilized by adsorption on ion exchangers (31) or covalently bound to a macroporous Plexiglas (17), Plexazyme IN (Röhm GmbH), has been commercialized in Europe for hydrolysis of sucrose obtained from sugar beets or cane sugar. The productivity of the Plexazyme IN bioreactor is 6000 kg dry weight/kg biocatalyst when producing a syrup with 90% conversion (17). Enzymatic hydrolysis of sucrose is less expensive than the HCl chemical process because of side reactions in the latter that lower the yield and decrease product quality. The annual production of invert sugar using immobilized invertase was 1000 metric tons in 1988 (17).

H. Production of Modified Triacyglycerols (Fats)

Chemically catalyzed interesterification results in random interchange of fatty acids among the three positions of the glycerol backbone. However, enzyme catalysis using a 1,3-specific lipase confines acyl migration to the 1- and 3-positions yielding a mixture of triacylglycerols not obtainable by any other means. Several commercial processes have been reported for

immobilization of lipase and its use for fat modification (37–40). Workers at Unilever (37, 39) immobilized lipases from *Aspergillus, Mucor* and *Rhizopus* spp. by adsorption from acetone, methanol, or ethanol solutions on inorganic matrices such as diatomaceous earth, hydroxylapatite, or alumina and used these preparations in fixed-bed bioreactors to interesterify shea oil or the mid fraction of palm oil. The substrates were dissolved in petroleum ether or hexane and passed through the bioreactor under carefully controlled water concentrations to maximize inter- or transesterification. Transesterification of the midfraction of palm oil with myristic acid produced a cocoa butter substitute from these less expensive starting materials (37). Scientists at Fuji Oil Co. Ltd, in Japan also have developed an immobilized lipase process for production of a cocoa butter–like fat using the palm midfraction as a starting material (41). Similarly, the triacylglycerols in shea oil or shea oleine have been modified by interesterification using these adsorbed lipases in two-phase systems (11, 38).

Tsukishima Kikai Co. (17, 42) developed a unique countercurrent two-phase multistage bioreactor for triglyceride hydrolysis using an immobilized thermostable lipase from a *Pseudomonas* sp. for production of glycerin and fatty acids. Workers at AKZO Chemicals (17, 43) also produced glycerin and fatty acids using a lipase from Candida sp. immobilized by adsorption on high-density polyethylene. The productivity of the CSTR bioreactor was 1100 kg of fatty acid/kg biocatalyst resulting in a cost that was competitive with the cost of steam splitting, and the product was of superior quality (43).

Eigtved (40), at Novo Industri A/S, developed an immobilized lipase bioreactor that could be used in a solvent-free system. Lipase from *Mucor miehei* was adsorbed from aqueous solution onto macroporous phenolformaldehyde resin and dried to a water content of 2–20%. The support has a relatively large particle size, allowing it to be employed with melted triglycerides in a fixed-bed bioreactor without excessive pressure drop. Operating to interesterify liquid fat (olive oil) at 60°C, the bioreactor exhibited a half-life of 3100 h and a productivity of 6.5 metric tons of modified triglyceride/kg of biocatalyst.

V. FUTURE OPPORTUNITIES

A major factor driving the commercialization of an immobilized enzyme process is the ability to produce a product that cannot be produced by other means. This may be the case for production of modified proteins designed for specific functionality in a food—for example, modification of the emulsifying, gelling, or foaming properties of a protein ingredient by limited proteolysis (14, 15, 44, 45). If the proteolysis is carefully controlled, large oligopeptides with native-like structure can be released that have more desirable functionality than the parent protein (14, 15). Use of an immobilized proteinase allows precise control of the extent of proteolysis without a downstream enzyme inactivation step such as a heat treatment. Because excellent functionality is destroyed by heat treatments that cause unfolding and aggregation, such a downstream process is often counterproductive. Another potential example is the alteration of the structural stability or gelling characteristics of a protein by limited crosslinking using transglutaminase as a catalyst (46, 47). As in the case with proteinases, use of immobilized enzyme avoids the need for a downstream enzyme inactivation step to prevent eventual gel formation and to stop reaction at the desired level of crosslinking.

Another major economic factor is the cost of enzyme purification and immobilization. Designing the enzyme for bioselective adsorption can minimize this cost. In the future, many enzymes will most likely be recombinant proteins designed with consideration of specific catalytic requirements such as specificity, thermal stability, pH optima, and cofactor requirements. In addition, it would not be difficult to design structures allowing ease of purification and immobilization. A number of fusion proteins have been genetically designed for this purpose. The cellulose-binding domain of *Cellulomonas fimi* exoglucanase has been fused to the gene for β-glucosidase allowing this fusion protein to bind to cellulose (48). Similarly, the starch-binding domain of *Aspergillus* glucoamylase was fused to β-galactosidase, resulting in a fusion protein that bound to starch (49). The streptavidin-biotin interaction represents an even stronger biospecific interaction with a dissociation constant of the order of 10^{-15} M^{-1}. Genetic constructs have been prepared that allow expression of streptavidin-β-galactosidase (50), streptavidin-lipase (51), streptavidin-transglutaminase (52), and trypsin-streptavidin (53). Biotin can be covalently attached to a variety of supports using commercially available biotinylation reagents. Streptavidin-enzyme fusion proteins were purified and immobilized in one-step from crude recombinant cell lysates (50–53). Furthermore, the biotinylated supports can be regenerated and repeatedly used by desorption of spent enzyme and readsorption of fresh recombinant fusion enzyme (54).

REFERENCES

1. K Mosbach. Immobilized Enzymes. Methods Enzymol., Vol 44. New York: Academic Press, 1976.
2. K Mosbach. Immobilized Enzymes and Cells. Methods Enzymol, Part B, Vol 135. New York: Academic Press, 1987.
3. K Mosbach. Immobilized Enzymes and Cells. Methods Enzymol, Part C, Vol 136. New York: Academic Press, 1987.
4. I Chibata. Immobilized Enzymes. New York: Halsted Press, 1978.
5. WH Pitcher Jr. Immobilized Enzymes in Food Processing. Boca Raton, FL: CRC Press, 1980.
6. HE Swaisgood. Immobilization of enzymes and some applications in the food industry. In: AI Laskin, ed. Enzymes and Immobilized Cells in Biotechnology. Menlo Park, CA: Benjamin/Cummings, 1985, pp 1–24.
7. PSJ Cheetham. Applications of immobilized enzymes and cells in the food industry. In: AT Andrews, ed. Chemical Aspects of Food Enzymes. London: Royal Society of Chemistry, 1987, pp 53–93.
8. JF Kennedy. Biotechnology, Vol. 7a. Weinheim, Germany: VCH Verlagsgellschaft, 1987.
9. WH Scouten. A survey of enzyme coupling techniques. Methods Enzymol 135:30–65, 1987.
10. HE Swaisgood, HR Horton. Immobilized enzymes as processing aids or analytical tools. In: JR Whitaker, PE Sonnet, eds. Biocatalysis in Agricultural Biotechnology, ACS Symposium Ser. 389. Washington; American Chemical Society, 1989, pp 242-261.
11. HE Swaisgood. Immobilized enzymes: applications to bioprocessing of food. In: PF Fox, ed. Food Enzymology, Vol 2. London: Elsevier Applied Science, 1991, pp 309–341.
12. HE Swaisgood, GL Catignani. Use of immobilized proteinases and peptidases to study structural changes in proteins. Methods Enzynol 135:596-604, 1987.
13. D Combes, T Yoovdihya, E Girbal, RM Willemot, P Monsan. Mechanism of enzyme stabilization. Ann NY Acad Sci 501:59-62, 1987.
14. XL Huang, GL Catignani, HE Swaisgood. Improved emulsifying properties of β-barrel domain peptides obtained by membrane-fractionation of a limited tryptic hydrolysate of β-lactoglobulin. J Agric Food Chem 44:3437–3443, 1996.
15. XL Huang, GL Catignani, HE Swaisgood. Modification of rheological properties of whey protein isolates by limited proteolysis. Nahrung/Food 43:79–85, 1999.
16. VJ Jensen, S Rugh. Industrial-scale production and application of immobilized glucose isomerase. Methods Enzymol 136:356-370, 1987.
17. H Uhlig, EM Linsmaier-Bednar. Industrial Enzymes and Their Applications. New York: John Wiley & Sons, 1998, pp 203-223.
18. S Pedersen. Industrial aspects of immobilized glucose isomerase. In: A Tanaka, T Tosa, T Kobayashi, eds. Industrial Application of Immobilized Biocatalysts NewYork: Marcel Dekker, 1993, pp 185-208.
19. M Harju. Lactose hydrolysis. Bull Int Dairy Fed 212:50–55, 1987.
20. K Hyrkas, R Viskari, YY Linko, M Linko, Hydrolysis of lactose in acid whey by immobilized β-galactosidase. Milchwissenschaft 31:129-134, 1976.
21. RA Messing, HH Weethall. U.S. Patent No. 3,519,538 (1970).
22. JL Baret. Large-scale production and application of immobilized lactase. Methods Enzymol 136:411-423, 1987.
23. Y Honda, M Kako, K Abiko, Y Sogo. Hydrolysis of lactose in milk. In: A Tanaka, T Tosa, T Kobayashi, eds. Industrial Application of Immobilized Biocatalyst. New York: Marcel Dekker, 1993, pp 209-234.
24. I Chibata. Immobilized Enzymes. New York: Halsted Press, 1978.
25. I Chibata, T Tosa, T Sato. Industrial applications of immobilized proteins. In: RF Taylor, ed. Protein Immobilization. New York: Marcel Dekker, 1991, pp 339-362.
26. I Chibata, T Tosa, T Sato, T Mori. Production of L-amino acids by aminoacylase adsorbed on DEAE-Sephadex. Methods Enzymol 44:746-759, 1976.
27. MC Fusee. Industrial production of L-aspartic acid using polyurethan-immobilized cells containing aspartase. Methods Enzymol 136:463-471, 1987.
28. I Chibata, T Tosa, S Takamatsu. Continuous L-alanine production using two different immobilized microbial cell preparations on an industrial scale. Methods Enzymol 136:472-479, 1987.
29. GJ Calton, LL Wood, ML Campbell. Phenylalanine production via polyazetidine immobilized *Escherichia coli*: Optimization of cell loading. Methods Enzymol 136:497-503, 1987.
30. K Oyama, S Irino, N Hagi. Production of aspartame by immobilized thermoase. Methods Enzymol 136:503-516, 1987.
31. D Scott. Specialty enzymes and products for the food industry. In: JR Whitaker, PE Sonnet, eds. Biocatalysis in Agricultural Biotechnology, ACS Sympopsium Series 389. Washington; American Chemical Society, 1989, pp 176-192.
32. R Keller, M Schlingmann, R Woernle. Production of 5′-ribonucleotides using immobilized 5′-phosphodiesterase. Methods Enzymol 136:517-522 1987.
33. H Samejima, K Kimura, S Noquchi, G Shimura. Production of 5′-mononucleotides using immobilized 5′-phosphodiesterase and 5′-AMP deaminase. In: EK Pye, HH Weethall, eds. Enzyme Engineering -3. New York: Plenum Press, 1978, pp 469-475.

34. PSJ Cheetham. Production of isomaltulose using immobilized microbial cells. Methods Enzymol 136:432-454, 1987.
35. W Haese, P Egerer, G. Schmidt-Kastner, H Perrey. Immobilization of Protaminobacter rubrum and use of the immobilized preparation in the transformation of sucrose into isomaltulose. European Patent No. EP0160253(1985).
36. J Shimizu, K Suzuki, Y Nakajima. Method of producing palatinose with immobilized alpha-glucosyl transferase. U.S. Patent No. 4,386,158 (1983).
37. AR Macrae, P How. Rearrangement process U.S. Patent No. 4,719,178 (1988).
38. MD Lilly, P Dunnill. Use of immobolized biocatalysts for conversions of water-insoluble reactants: interesterification of fats. Ann NY Acad Sci 8:113-118, 1987.
39. RA Wisdom, P Dunnill, MD Lilly. Enzymatic interesterification of fats: factors influencing the choice of support for immobilized lipase. Enzyme Microb Technol 6:443-446, 1984.
40. P Eigtved. Immobilized Mucor miehei lipase for transesterification U.S. Patent No. 4,798,793 (1989).
41. Y Hashimoto. Production of cocoa butter–like fats by enzymatic transesterification. In: A Tanaka, T Tosa, T Kobayashi, eds. Industrial Application of Immobilized Biocatalysts. New York: Marcel Dekker, 1993, pp 337-352.
42. Tsukishima Kikai Co., Ltd Bioprocessing Technol 9(4):3, 1987.
43. C Brady, L Metcalf, D Slaboszewski, D Frank. Lipase immobilized on a hydrophobic, microporous support for the hydrolysis of fats. J Am Oil Chem Soc 65:917-921, 1988.
44. HE Swiasgood, XL Huang, GL Catignani. Characteristics of the products of limited proteolysis of β-lactoglobulin. In: N Parris, A Kato, LK Creamer, J Pearce, eds. Macromolecular Interactions in Food Technology, ACS Symp Ser 650. Washington; American Chemical Society, 1996, pp 166-177.
45. SL Turgeon, SF Gauthier, D Mollé, J Léonil. Interfacial properties of tryptic peptides of β-lactoglobulin. J Agric Food Chem 40:669-675, 1992.
46. XL Huang, GL Catignani, HE Swaisgood. Immobilization of biotinylated transglutaminase by bioseletive adsorption to immobilized avidin and characterization of the immobilized activity. J Agric Food Chem 43:895-901, 1995.
47. CP Wilcox, DA Clare, HE Swaisgood. Utilization of immobilized recombinant fusion proteins to enhance whey protein isolate functionality. Institute of Food Technologist Annual Meeting, Abstr. 78D-11, 2000.
48. E Ong, NR Gilkes, RC Miller Jr, RAJ Warren, DG Kilburn. Enzymatic immobilization using a cellulose-binding domain of a *Cellulomonas fimi* exoglucanase. Enxyme Microb Technol 13:59-65, 1991.
49. BK Dalmia, ZL Nikolov. Characterization of a β-galactosidase fusion protein containing the starch-binding domain of *Aspergillus* glucoamylase. Enzyme Microb Technol 16:18-23, 1994.
50. MK Walsh, HE Swaisgood. An *Escherichia coli* plasmid vector system for production of streptavidin fusion proteins: expression and bioselective adsorption of streptavidin-β-galactosidase. Biotechnol Bioeng 44:1348-1354, 1994.
51. P Lee, HE Swiasgood. Cloning and expression of a streptavidin-lipase fusion gene in *Escherichia coli* and characterization of the immobilized fusion protein. Enzyme Microb Technol 22:246-254, 1998.
52. VW Valentine, DA Clare, HE Swaisgood. Engineering a protein recombinase: construction and characterization of heterologous fusions of streptavidin and transglutaminase. Am Soc Biochem Mol Biol, Annual Meeting (Abstr B 394), 1998.
53. DA Clare, VW Valentine, GL Catignani, HE Swaisgood. Molecular design, expression, and affinity immobilization of a trypsin-streptavidin fusion protein. Enzyme Microb Technol 28:483–491, 2001.
54. XL Huang, MK Walsh, HE Swaisgood. Simultaneous isolation and immobilization of streptavidin-β-lactosidase: some kinetic characteristics of the immobilized enzyme and regeneration of bioreactors. Enzyme Microb Technol 19:378-383, 1996.

25

Enzymes and Food Analysis

Philip O'Connell
National University of Ireland, Cork, Ireland
George G. Guilbault
University College, Cork, Ireland

I. ADVANTAGES AND DISADVANTAGES

The advantages of enzyme analyses are numerous, as are the disadvantages. The advantages of using enzymes must therefore be weighed against the disadvantages for each application.

The benefits of using enzyme analyses include rapid assay times (relative to most analytical assays), low cost, inherent selectivity, and simplistic systems. The disadvantages include pH and temperature dependence, a limitation to primarily aqueous analysis, limited dynamic ranges, and relatively low stability. Thus, enzymatic analyses are confined to those areas where the advantages outweigh the disadvantages.

In recent years much work has been focused on overcoming the shortcomings mentioned above and hence widening the applicability of enzymes in analyses. It has been shown that pH and temperature dependence of enzymes is significantly reduced when immobilized; this is probably due to the enforced structure induced by immobilization (1). Thus, the use of immobilization can increase the ruggedness of most enzymatic assays. Several groups (2–4) have focused on the use of enzyme sensors in organic media. They found that when using organic solvents their sensors could still work well, but that the enzyme response was dependent on both the concentration and type of solvent. Such technology allows the detection of enzymatic substrates sparingly soluble in aqueous media and enhances the thermal stability of the enzymes. Limited dynamic ranges can be extended through the use of diffusion limiting membranes (5). Gibson et al. (6) have employed polyelectrolyte backbones along with sugar alcohols to stabilize enzymes for extended periods of time, even at room temperature. Glucose oxidase was shown to have an operational stability for 5 months (7) when modified. With so much effort being focused on improving enzymatic analyses, the applications of the technology are likely to expand throughout the coming decade.

II. METHODOLOGIES AND TOOLS AVAILABLE

In science, one of the main methodologies is standardization—to be able to compare different techniques or products to a standard. However, in a relatively new area such as enzymatic analyses, such standards are rare. McAteer et al. (8) have proposed a model for shelf life prediction of stabilized commercial enzyme assays. Being able to place a well-defined shelf life on a product would make it much more viable in the commercial marketplace. Boujtita et al. (9) have concentrated on making biosensors applicable to industrial needs. They compared different modes of production of renewable carbon paste electrodes and

found that they can produce high analytical quality sensors.

Enzymes can be coupled to a myriad of detection techniques; however, some are more appropriate to food analysis than others. Commonly used techniques include visible spectrophotometry, luminescence, fluorescence, amperometry, and potentiometry. Thus, development of the tools of these assay techniques has taken place. Examples of each system used in conjunction with food analysis are shown in Table 1.

For most food samples, some pretreatment would have to take place. Solid samples would generally be dissolved or the analyte extracted from them. This is particularly the case for optical detection systems where solid particles can seriously disturb the response. The importance of pretreatment cannot be underemphasized, even in an area such as enzyme analysis where the need for pretreatment is minimized. The strong pH, ionic strength, and temperature dependence of most enzymes means that any pretreatment must be carefully considered before being applied to enzymatic analysis.

In electrochemical analysis, a major challenge has been immobilization, to make the sensors reusable. Several techniques have been developed for immobilization, but generally speaking they can be classified into two major groups.

A. Adsorption or Physical Entrapment

This method has become more important in the last decade owing mainly to the development of hydrogels (20) and sol-gels. Other methods include encapsulation of the enzyme within a growing polymer (21), entrapment behind membranes (22), encapsulation within gels (23), entrapment within carbon pastes (24), and passive adsorption of the enzyme on a suitable surface (25). Sol-gels have become important owing to the ease with which they are prepared and because they have controllable porosity, are chemically inert and physically stable, and can be produced at low temperatures under mild conditions (26). Another important property is that they can be produced as a bulk-modified electrode (27), providing simple renewal of surface by polishing, or as a coating of electrodes (28), where rapid responses are seen and a high enzyme loading can be achieved. This makes sol-gel-based enzymatic assays very versatile.

B. Covalent Binding

The use of glutaraldehyde as a crosslinking agent is perhaps the most common procedure in this area. This is due to the simplicity of the procedure. The three-dimensional structure produced allows a high enzymatic loading. Coupling to activated surfaces (29) produces a more reproducible surface coverage but at the expense of decreased enzyme loading. Other methods for covalent immobilization of enzymes include silanization (30) and multipoint covalent immobilization on epoxy-activated supports (31).

Each of these immobilization methods succeeds in making the associated assays reusable, but most decrease the activity of the enzymes and change their analytical performance such as pH optima, selectivity,

Table 1 Direct Enzyme Assays Using Various Transduction Techniques

Analyte	Detection method	Enzyme	Dynamic range	Ref.
Cyanogenic potential	Absorbance at 510 nm/linamarin	Linamarase	0.5–40 mg/kg of HCN	10
Asparagine	Absorbance/pH indicator	Asparaginase	0.2–2.3 mM	11
Glucose	Fluorimetry/FAD	GOx[a]	0.5–2 mM	12
Lactate	Fluorimetry/FMN	LMO	1.04–10 mM	13
Mannitol	Fluorimetry/NADPH	MDH/LDH	50–1500 μM	14
Lactate	Luminescence/luminol-H_2O_2	LOx	0.15 nM–0.3 μM	15
Sulfite	Luminescence/luminol-H_2O_2	SOx/HRP	3.2–320 μM	16
Biogenic amines	Amperometry/H_2O_2	DAO	1–50 μM	17
Fructose	Amperometry/O_2 redox polymer	FDH	0.2–20 mM	18
Asparagine	Potentiometry/H^+	Asparaginase	0.1–4 mM	11
Formaldehyde	Potentiometry/H^+	AOx	5–200 mM	19

[a]Glucose oxidase (GOx); lactate monooxygenase (LMO); lactate dehydrogenase (LDH); malate dehydrogenase (MDH); lactate oxidase (LOx); sulfite oxidase (SOx); horseradish peroxidase (HRP); diamine oxidase (DAO); fructose dehydrogenase (FDH); alcohol oxidase (AOx).

and temperature dependence (1). Enzyme kits, of which there are a wide variety (32), ignore this problem and use enzymes directly in solution. However, this can make the assay expensive if the enzyme cannot be produced cheaply enough. Kits are available for a wide variety of analytes, but most require optical detection by eye or through a spectrophotometer. Thus, only colorless and fully soluble samples can be assayed with this technique, which makes food analysis difficult.

III. TYPES OF ANALYSIS POSSIBLE

Enzymes are already used in a variety of assays of foods. These can be generally classified into three main areas—direct, indirect, and inhibition—as shown in Figure 1.

Direct enzyme assays use the specificity of an enzyme toward the analyte to determine the concentration of the analyte or enzyme. An example of this is a glucose assay, using glucose oxidase to oxidize the glu-

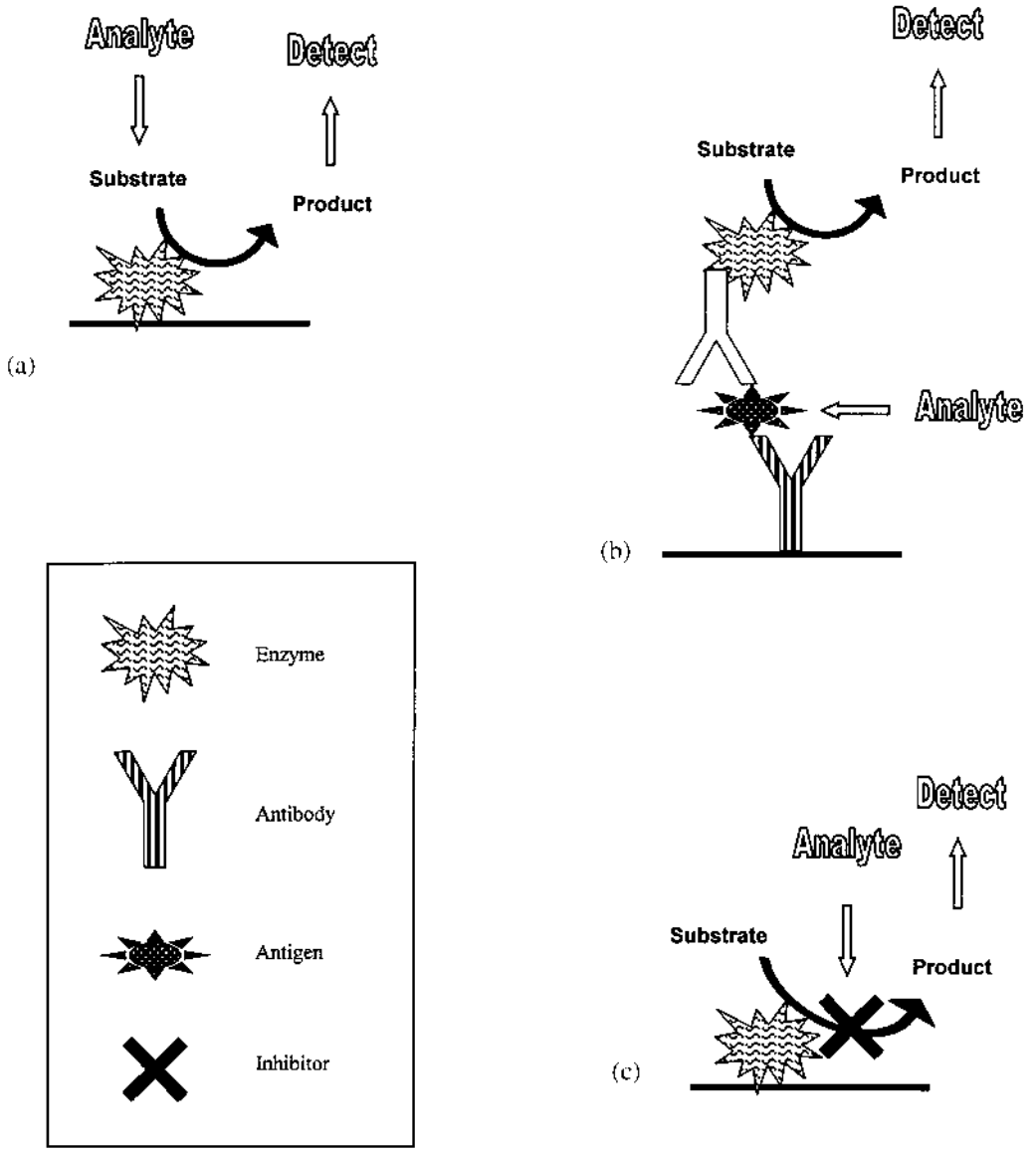

Figure 1 Schematics of direct, indirect, and inhibition enzyme assays. Example system 1 (a) is a direct enzyme assay; system 2 (b) is an ELISA, an indirect assay; and example 3 (c) is an inhibition assay.

Table 2 Summary of Sugar Analysis Through Enzymatic Methods

Analyte	Detection method	Enzyme	Application	Ref.
Glucose	Spectrophotometric	GOx[a]	Fruit juices, soft drinks, fermentation processes	33
Glucose	Amperometry (0.7 V)	GOx	Fruit juices, soft drinks	34
Galactose	Amperometry (0.1 V)	GaOx[a]/HRP	Dairy products	35
Fructose	Amperometry (0.1 V)	FDH	Honey	18
Sucrose	Amperometry	Invertase/GOx mutarotase	Juices	36
Lactose	Potentiometry (CO_2)	Lactase/*S. cerevisiae*	Milk	37

[a]Galactose oxidase (GaOx).

cose in a sample and produce a measurable response. Table 2 shows a brief list of direct enzyme assays.

Indirect enzyme assays use enzymes as a label. This means that the assay uses only the catalytic properties of an enzyme to produce an easily measured response, achieving specificity through another molecule. An example of this type of assay is ELISA, where specificity is provided by antibodies but the finally measured signal is produced by an attached enzyme.

Inhibition assays use the inhibitory effects of certain molecules or ions on enzymes to quantify their presence in samples. Heavy metals are known to inhibit most enzymes but to different extents depending on the enzyme and metal ion involved. Organophosphorous and carbamate pesticides inhibit certain cholinesterases. Depending on the pesticide and enzyme chosen, the extent of inhibition varies.

A. Direct Enzyme Analysis

Direct enzyme analysis is the simplest of the three areas. It can only be used to quantify substrates and enzymes, and is only practical when the products are readily measurable. Many modifications have been made to direct enzyme analysis, some to expand the applicability of the system, and some to overcome problems in the analysis.

1. Simple Substrates Analysis

The main applications of this system are the assays of chemical components of foods, such as sugars (Table 2) and organic acids (Table 3). This is because there are many enzymes available for these metabolic compounds. Given the inherent instability of most

Table 3 Summary of Organic Acid Analysis Through Enzymatic Methods

Analyte	Detection method	Enzyme	Application	Ref.
Lactate	Amperometry (0 V)	LOx[a]/HRP	Wine and yogurt	38
Pyruvic acid	FOB	LDH	Wine, beer, and milk	39
Formate	FOB	FDH/LDH	Fermentation of milk	14
Malate	Amperometry (0.3 V)	MDH/Diaphorase	Wine	40
Glutamate	Amperometry (0.65 V)	GluOx	Flavor enhancers	41
Ascorbate	Amperometry (0.4 V)	AscOx	Fruit juices and pharmaceutical preparations	42
Uric acid	Amperometry (0.1 V)	UOx	Fish freshness	43
Inosine monophosphate	Amperometry (0.65 V)	IMPDH/NOx	Flavor enhancers	41

[a]Lactate oxidase (LOx); glutamate oxidase (GluOx); ascorbate oxidase (AscOx); urate oxidase (UOx); inosine monophosphate dehydrogenase (IMPDH); NADH oxidase (NOx).

enzymes, these analyses are performed with a reference of known analyte concentration. Such assays are rarely applicable to analytes not commonly found in metabolic processes. An example of such a rare assay is the organophosphate pesticide sensor. Using organophosphorus hydrolase, Mulchandani et al. (44) developed a biosensor for the determination of organophosphate pesticides with no crossreactivity with carbamates or other neurotoxins. They achieved a detection limit of 2 μM for several common pesticides.

2. Enzyme Sequence Reactions

Systems employing a sequence of enzyme reactions can be used to increase the ease with which certain enzymatic products can be assayed. Peroxidase is frequently employed to detect the peroxide product of oxidase reactions at low applied potentials (45), thus avoiding electrochemical interferences that may be present in a sample. Difficulties with these systems include the possibilities that the optima for performance of the enzymes in the sequence may not be the same and that multiple enzymes decrease specificity. Such systems are therefore only used for important analytes such as sucrose (36) and aspartame (46) or to overcome major problems, such as electrochemical interference (45). Sucrose is hydrolyzed with the enzyme invertase, where the resultant glucose can be detected with glucose oxidase. Mutarotase is commonly added to such systems to speed up the conversion of α-D-glucose to β-D-glucose.

3. Multianalyte Systems

With direct enzyme sensors it is relatively easy to produce multianalyte assay systems, which can detect a range of analytes simultaneously. The main advantage of this is that the analyst can build up an accurate picture of the current state of the food product or bioprocess. This is achieved by selecting the key analytes in a given system. To define the quality of wine, Miertus et al. (47) developed a multianalyte sensor for glucose, fructose and ethanol and for lactate, malate, and sulfite. The sensors were grouped in this way to allow different fermentation processes to be analyzed. The first group would allow monitoring of any alcoholic fermentation process, while the second could be used to monitor the malolactic fermentation processes in red wine.

4. Simple Enzyme Analysis

It is possible to detect the presence of an enzyme by exposure to its substrate. This system is employed in metabolic detection, where the metabolic action of bacterial enzymes indicates their presence in a sample. It is especially useful to determine the efficiency of sterilization procedures such as pasteurization. Swain et al. (48) used this type of assay to detect foodborne pathogenic bacteria.

5. Substrate Recycling

Another modification of the direct analysis method is substrate recycling (enzyme amplification). This process can dramatically enhance the sensitivity of enzyme assays but, as it uses multiple enzymes, it suffers from the same limitations as the enzyme sequence reactions described above. One example of this system is the detection of malate (49). In the presence of malate (analyte) and oxygen, lactate mono-oxygenase produces oxaloacetate. Malate dehydrogenase then converts this back to malate, where the sequence starts again (Fig. 2). While this simple procedure amplifies the response to malate, it also makes the assay strongly susceptible to interference from lactate. Table 4 describes examples of assays for miscellaneous food analytes using direct analysis.

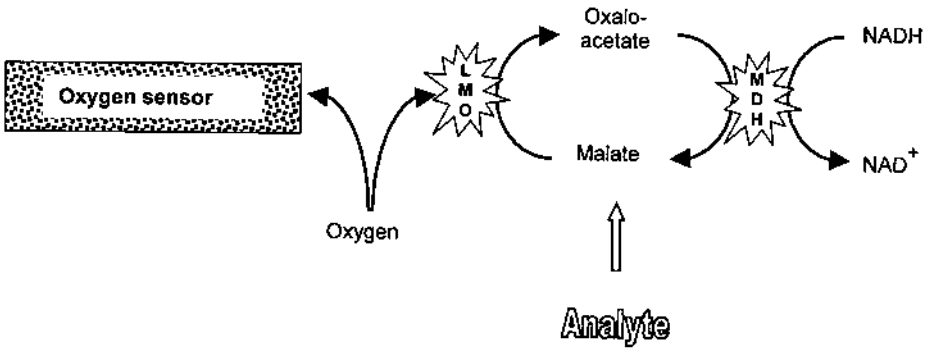

Figure 2 Schematic of a simple enzymatic amplification system for malate using an oxygen sensor.

Table 4 Summary of General Food Analytes Through Enzymatic Methods

Analyte	Detection method	Enzyme	Application	Ref.
Ethanol	Amperometry (0.7 V)	ADH[a]	Alcoholic beverages	50
Polyphenols	Amperometry for O_2 (−0.7 V)	Laccase	Catechols in tea	51
Glycerol	Amperometry (0.65 V)	GK/GPO	Alcoholic fermentation	52
Lysine	Amperometry	Lysine oxidase	Milk and pasta	53
Lecithin	Amperometry for O_2 (−0.7 V)	PL/COx	Soybean flour and chocolate	54
Asparagine	Spectrophotometric	Asparaginase	Fruits and vegetables	11
Aspartame	Amperometry for O_2 (−0.7 V)	CT/AOx	Artificial sweeteners	46

[a]Alcohol dehydrogenase (ADH); glycerokinase (GK); glycerol-3-phosphate oxidase (GPO); phospholipase D (PL); choline oxidase (COx); α-chymotrypsin (CT)

B. Indirect Enzyme Analysis Is Composed of Many Approaches

1. Immunoassays

The most commonly used indirect technique is ELISA, or enzyme-linked immunosorbant assay. An ELISA system can be designed to detect any molecule that can produce an immunogenic response, and many molecules that don't produce one on their own can be modified to generate a response. This makes the technique very versatile. While other biorecognition molecules are available, such as DNA, they are not generally coupled to enzymes. The enzyme labels are selected very carefully to fulfill defined parameters. The enzyme must be cheap, highly purified, easy to conjugate to antibodies, and have colorless substrates with a highly colored product. The main enzymes employed are horseradish peroxidase and alkaline phosphatase (55). They both meet the above requirements, but to different degrees. Given the versatility of ELISA, it is not surprising that a large number of food assays have been based on it. Primarily these have been focused upon the pathogenic bacteria and pesticides in foods, which can be difficult to detect using traditional techniques.

Bacteria analyzed by ELISA include *Listeria monocytogenes* (56), *Salmonella* sp. (57), *Escherichia coli* (58), *Staphylococcus aureus* (59), and *Bacillus cereus* (60). The popularity of the method is due to the sensitivity of the technique, which can yield results much faster than conventional techniques. Crowley et al. (61) developed a rapid immunosensor based on amperometric detection for *Listeria monocytogenes* in milk samples. The assay was performed in 3.5 h, which is an improvement over the 24 h needed to complete even the most rapid of traditional analysis. Abdel-Hamid et al. (62) developed a sensor for *E. coli* O157:H7 with a limit of detection (LOD) of 100 cells/mL. Ivnitski et al. (63) have reviewed the different techniques used for bacteriological detection using immunosensors.

It can be difficult to detect the presence of pesticides using immunoassays. Owing to their small size, the antibodies are raised against pesticides conjugated to immunogenic carriers and may thus be of low affinity/selectivity. Keay and McNeil (64) used an amperometric immunosensor to detect atrazine. Polychlorinated biphenyls (PCB) are found throughout the food chain (fish extracts, clams, milk), and Bender and Sadik (65) produced an electrochemical immunosensor to detect for them. Dankwardt and Hock (66) reviewed the use of immunoassays to detect pesticides in foods and discussed the use of immunosensors.

Marine toxins are an area of increasing interest, as their incidence of outbreaks has been rising in recent years. Kreuzer et al. (67) developed an assay for okadaic acid in shellfish. This diarrhetic toxin was detectable down to a concentration of 6×10^{-13} M in a rapid time of 90 min, far better than any HPLC system for okadaic acid. Also, a rising issue in recent times has been the use of genetically modified (GM) foods. Brett et al. (68) have concluded that antibody-based assays are the natural detector for the presence of novel proteins from GMs. Van Duijin et al. (69) have used immunoblotting to detect the presence of CP4 synthase in GM soya. Thus, ELISA and immunosensors could become powerful tools in the confirmation of GM products in our foods.

2. Induced Bioluminescence

Another type of indirect enzyme analysis is the use of luciferase-encoded bacteriophage. The bacteriophage infect specific bacteria present in the sample and

cause them to bioluminesce by forcing them to produce luciferase. A major advantage of this system, unlike ELISA, is that it distinguishes between viable and nonviable cells. *Salmonella* sp. (70) and *Listeria* were assayed (71). Loessner et al. (72) produced a system for the detection of a variety of *Listeria* strains.

C. Inhibition Enzyme Assays

There are two main groups of inhibition enzyme assays, pesticides and heavy metals.

1. Pesticide Analysis

Since pesticides are not normally present in the food chain, there are few specific enzymes that can be used for their determination, although nonspecific inhibition of cholinesterase is commonly used (73). The determination of pesticides in food and water is a particular area of interest for biosensors. This is due to the function of pesticides to inhibit cholinesterases in pests (and possibly mammals). Organophosphates have been particularly well examined as they are toxic to mammals. Carbamates are less toxic to mammals but are not very soluble in water and thus accumulate in foods if incorrectly used. Cholinesterase inhibition is used for the determination of both these pesticides. Nunes et al. (74) used a sensor based on a low charge of cholinesterase to determine carbamates in food samples. As with all sensors of this type, the sample solutions must be exposed to the sensor prior to the analysis. This slows down the analysis time. Their sensor is usable only once (74). Overcoming this problem would reduce the cost per assay. Jeanty and Martin (75) used a reactivation sequence in their pesticide assay system. Based on flow analysis, their system showed good operational stability of 3 weeks and 6 months storage stability.

The inhibition of cholinesterases by both organophosphates, carbamates, and other neurotoxins causes problems for those who wish to measure just one class of pesticides. To achieve class specificity Mulchandani et al. (44) used organophosphorus hydrolase as described in the direct enzymatic assay section. Wang et al. (76) showed that a tyrosinase-based sensor could be inhibited by carbamates as well as other phenolic compounds. They also showed that tyrosinase did not require the lengthy exposure periods that characterize most enzyme inhibition assays. Perez Pita et al. (77) used this system in conjunction with a reversed micelle as the working medium. The advantages of this system include the increased solubility of the carbamates in this medium and the low solubility of the enzyme, thus increasing the ease of immobilization.

2. Heavy Metal Analysis

Fennouth et al. (78) compared the effectiveness of heavy metal salts at inhibiting the activity of lactate dehydrogenase. They found that they could detect the presence of heavy metals below the European norms, with the exception of lead acetate. They concluded that such technology could be applicable to metal contamination in foods. Bertocchi et al. (79) found that they could detect mercury levels in the 10–60 ppb range using enzyme inhibition. Volotovsky et al. (80) showed that additions of NaI to the sample improved the selectivity of their urease-based mercury sensor by decreasing the effects of silver.

IV. ONLINE ANALYSIS

The use of enzymatic methods for continual and quasi-continual analysis is a challenge. Continual measurements require the enzymatic performance to be constant over a set period of time. Most enzyme assays cannot meet this challenge. A more applicable use would be quasi-continuous analysis, where samples are sent to an enzymatic detector at set time intervals. These intervals can be set by the need of the production process, but they are limited by the baseline recovery of the sensor. Flow injection analysis (FIA) provides a rapid means of sending a sample plug to a sensor, but after each analysis there is a recovery period when excess sample is washed away and the response returns to baseline (81). A simple flow injection system is shown in Figure 3. Such systems have two major classes—where the enzyme is contained in a reactor and the product is detected downstream at a transducer, or where the enzyme is immobilized near the surface of the transducer. The needs of the fermentation industry have led to the development of flow injection sensors for sugars (82) and ethanol (83). The versatility of this technique led to its widespread use in enzymatic analysis (84, 85).

V. QUALITY CONTROL

Production processes require quality control. The quality of food going to the consumer must always be assured. Traditionally this was performed by taking a sample and sending it to a remote laboratory. While this is successful for most samples, this was not always

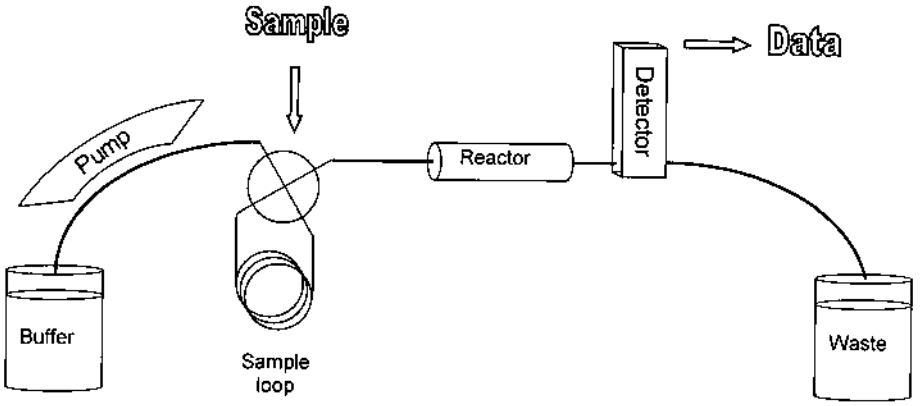

Figure 3 Schematics of a simple flow injection analysis system for use with an enzyme reactor or enzyme coated sensor (biosensor)

the case. Having remote laboratories means that the results are not instantaneous. It also means that unstable samples may have changed by the time they are analyzed. Enzyme-based systems, especially those incorporated within flow injection analyzers, overcome this problem. As the systems are small and of low cost relative to other automated analyzers, they can easily be fitted on-site. With the sensors fitted within the production process, a near instant reading can be achieved. Miertus et al. (47) developed a multianalyte sensor for quality control of red wine. By measuring a range of analytes simultaneously a picture of the true state of the product can be obtained. Since wine is liquid, there are few problems with sample pretreatment; however, there are problems with the matrix, which contains many potentially electroactive organic acids. Thus, any sensor hoping to measure in this matrix must address this problem. Minimal pretreatment was also required for a fish freshness sensor developed by Carsol et al. (86). The fish exudates were merely diluted in buffer and analyzed for the presence of inosine, inosine monophosphate, and hypoxanthine (K-value). Okuma et al. (87) developed a system to determine the initial stages of spoilage in chicken; as in the fish freshness assay, the system relies on the response of three analytes to show the spoilage. The markers selected, putrescine, cadaverine, and spermidine, allow an earlier assessment of the state of putrification of meat than the K-value. Kelly et al. (53) developed a sensor for the determination of L-lysine in heat-treated foods, but the breakdown of food proteins requires a hydrolysis step, which can be performed in 15 min. Thus, the pretreatment of the sample is the time-limiting step. The digestibility of protein is of primary importance in determining nutritional quality. Hsu et al. (88) developed a multienzyme technique for estimating protein digestibility.

REFERENCES

1. AM Klibanov. Enzyme stabilization by immobilization. Anal Biochem 93:1–25, 1979.
2. L Campanella, G Favero, MP Sammartino, M Tomassetti. Analysis of several real matrices using new mono-, bi-enzymatic, or inhibition organic phase enzyme electrodes. Anal Chim Acta 393:109–120, 1999.
3. J Wang, N Naser, D Lopez. Organic-phase biosensing of secondary alcohols with a *Ta. Brockii* alcohol dehydrogenase electrode. Biosens Bioelectron 9:225–230, 1994.
4. S Kröger, S J Setford, APF Turner. Assessment of glucose oxidase behaviour in alcoholic solutions using disposable electrodes. Anal Chim Acta 368:219–231, 1998.
5. L Gorton, E Csöregi, E Domínguez, J Emnéus, G Jonsson-Pettersson, G Marko-Varga, B Persson. Selective detection in flow analysis based on the combination of immobilised enzymes and chemically modified electrodes. Anal Chim 250:203–248, 1991.
6. TD Gibson, BLJ Pierce, JN Hulbert, S Gillespie. Improvements in the stability characteristics of biosensors using protein–polyelectrolyte complexes. Sensors Actuators B33:13–18, 1996.
7. VG Gavalas, NA Chaniotakis, TD Gibson. Improved operational stability of biosensors based on enzyme–polyelectrolyte complex adsorbed into a porous carbon electrode. Biosens Bioelectron 13:1205–1211, 1998.

8. K McAteer, CE Simpson, TD Gibson, S Gueguen, M Boujtita, N El Murr. Proposed model for shelf-life prediction of stabilized commercial enzyme-based systems and biosensors. J Mol Catalysis B: Enzymatic 7:47–56, 1999.
9. M Boujtita, M Boitard, N El Murr. Development of renewable surface biosensors to meet industrial needs for measurement of glucose in fruit juices. Biosens Bioelectron 14:545–553, 1999.
10. HH Yeoh, SV Egan. An enzyme-based dip-stick for the estimation of cyanogenic potential of cassava flour. Food Chem 60:119–122, 1997.
11. K Stein, R Shi, G Schwedt. Determination of L-asparagine using flow-injection systems with spectrophotometric and potentiometric detection. Anal Chim Act 336:113–122, 1996.
12. W Trettnak, OS Wolfbeis. Fully reversible fibre-optic glucose biosensor based on the intrinsic fluorescence of glucose oxidase. Anal Chim Acta 221:195–203, 1989.
13. W Trettnak, OS Wolfbeis. Fully reversible fibre-optic lactate biosensor based on the intrinsic fluorescence of lactate mono-oxygenase. Fresenius Z Anal Chem 334:427–430, 1989.
14. C Schelp, T Scheper, F Buckmann, KF Reardon. Fiberoptic sensors with confined enzymes and coenzymes—development and application. Anal Chim Acta 255:223–229, 1991.
15. CA Marquette, JL Blum. Luminol electrochemiluminescence-based fibre optic biosensors for flow injection analysis of glucose and lactate in natural samples. Anal Chim Acta 381:1–10, 1999.
16. J Hlavay, GG Guilbault. Determination of sulfite by use of a fiberoptic biosensor based on a chemiluminescent reaction. Anal Chim Acta 299:91–96, 1994.
17. R Draisci, G Volpe, L Lucentini, A Cecilia, R Federico, G Palleschi. Determination of biogenic amines with an electrochemical biosensor and its application to salted anchovies. Food Chem 62:225–232, 1998.
18. PA Paredes, J Parellada, VM Fernández, I Katakis, E Domínguez. Amperometric mediated carbon paste biosensor based on d-fructose dehydrogenase for the determination of fructose in food analysis. Biosens Bioelectron 12:1233–1243, 1997.
19. YI Korpan, MV Gonchar, AA Sibirny, C Martelet, AV El'skaya, TD Gibson, AP Soldatkin. Development of highly selective and stable potentiometric sensors for formaldehyde determination. Biosens Bioelectron 15:77–83, 2000.
20. H Olschewski, A Erlenkötter, C Zaborosch, GC Chemnitius. Screen-printed enzyme sensors for L-lysine determination. Enzyme Microbial Technol 26:537–543, 2000.
21. NC Foulds, CR Lowe. Enzyme entrapment in electrically conducting polymers. J Chem Soc Faraday Trans 82:1259–1264, 1986.
22. JG Zhao, RP Buck. An all-solid-state amperometric ethanol sensor. Biosens Bioelectron 6:681–687, 1991.
23. D Pfeifer, EV Ralis, A Makower, FW Scheller. Amperometric bi-enzyme base biosensor for the detection of lactose-characterization and application. J Chem Technol Biotechnol 49:255–265, 1990.
24. L Gorton. Carbon-paste electrodes modified with enzymes, tissues, and cells. Electroanal 7:23–45, 1995.
25. S Kelly, A Curulli, C O'Sullivan, GG Guilbault, G Palleschi. A new interference-free lysine biosensor using a non-conducting polymer film. Biosens Bioelectron 13:1245–1250, 1998.
26. J Wang. Sol-gel materials for electrochemical biosensors. Anal Chim Acta 399:21–27, 1999.
27. J Niu, JY Lee. Bulk-modified amperometric biosensors for hypoxanthine based on sol-gel technique. Sensor Actuat B—Chem 62:190–198, 20900.
28. U Narang, PN Prasad, F Bright, K Ramanathan, N Kumar, B Malhorta, M Kamalasana, S Chandra. Glucose biosensor based on a sol-gel-derived platform. Anal Chem 66:3139–3144, 1994.
29. JA Hamid, GJ Moody, JDR Thomas. Flow through multi-enzyme electrodes for the determination of lactose. Analyst 114:1587–1592, 1989.
30. U Bilitewski, GC Chemnitius, P Ruger, RD Schmid., Miniaturized disposable biosensors. Sensor Actuat B—Chem 7:351–355, 1992.
31. C Mateo, O Abian, R Fernandez-Lafuente, JM Guisan. Increase in conformational stability of enzymes immobilized on epoxy-activated supports by favoring additional multipoint covalent attachment. Enzyme Microbial Technol 26:509–515, 2000.
32. GG Guilbault. Analysis of substrates. In: MK Schwartz, ed. Handbook of Enzymatic Methods of Analysis. New York: Marcel Dekker, 1976, pp 189–373.
33. NG Wilson, T McCreedy, GM Greenway. In-situ immobilization of glucose oxidase on a novel microporous silica support. Analyst 125:237–239, 2000.
34. W Surareungchai, S Worasing, P Sritongkum, M Tanticharoen, K Kirtikara. Dual electrode signal–subtracted biosensor for simultaneous flow injection determination of sucrose and glucose. Anal Chim Acta 380:7–15, 1999.
35. S Mannino, MS Cosio, S Buratti. Simultaneous determination of glucose and galactose in dairy products by two parallel amperometric biosensors. Ital J Food Sci 11:57–65, 1999.
36. U Bilitewski, A Jager, P Ruger, W Weise. Enzyme electrodes for the determination of carbohydrates in food. Sensor Actuat B—Chem 15:113-118, 1993.
37. F Amarita, CR Fernandez, F Alkorta. Hybrid biosensors to estimate lactose in milk. Anal Chim Acta 349:153–158, 1997.
38. B Serra, AJ Reviejo, C Parrado, JM Pingarron. Graphite-Teflon composite bienzyme electrodes for

the determination of L-lactate: application to food samples. Biosens Bioelectron 14:505–513, 1999.
39. J Wangsa, MA Arnold. Fiber-optic biosensors based on the fluorimetric detection of reduced nicotinamide-adenine dinucleotide. Anal Chem 60:1080–1082, 1988.
40. J Katrlik, A Pizzariello, V Mastihuba, J Svorc, M Stredansky, S Miertus. Biosensors for L-malate and L-lactate based on solid binding matrix. Anal Chim Acta 379:193–200, 1999.
41. K Matsumoto, W Asada, R Murai. Simultaneous biosensing of inosine monophosphate and glutamate by use of immobilised enzyme reactors. Anal Chim Acta 358:127–136, 1998.
42. Hwang, S Mu. Bioelectrochemical response of the polyaniline ascorbate oxidase electrode. J Electroanal Chem 436:43–48, 1997.
43. T Nakaminami, S Ito, S Kuwabata, H Yoneyama. A biomimetic phospholipid/alkanethiolate bilayer immobilizing uricase and an electron mediator on an Au electrode for amperometric determination of uric acid. Anal Chem 71:4278–4283, 1999.
44. P Mulchandani, A Mulchandani, I Kaneva, W Chen. Biosensor for direct determination of organophosphate nerve agents. 1. Potentiometric enzyme electrode. Biosens Bioelectron 14:77–85, 1999.
45. DL Wang, A Heller, Miniaturizable flexible amperometric lactate probe. Anal Chem 65:1069–1073, 1993.
46. SF Chou. Amperometric biosensor for the determination of the artificial sweetener aspartame with an immobilized bienzyme system. Analyst 121:71–73, 1996.
47. S Miertus, J Katrlik, A Pizzariello, M Stredansky, J Svitel, J Svorc. Amperometric biosensors based on solid binding matrices applied in food quality monitoring. Biosens Bioelectron 13:911–923, 1998.
48. A Swain. Rapid microbial assay technology. Int Indust Biotechnol 8:11–15, 1988.
49. F Schubert, U Wollenberger, D Pfeiffer, FW Scheller. Enzymatic amplification and elimination in biosensors. In: APF Turner, ed. Advances in Biosensors. London: JAI Press Ltd, 1991, pp 77–106.
50. M Boujtita, M Chapleau, N El Murr. Biosensors for analysis of ethanol in food: effect of the pasting liquid. Anal Chim Acta 319:91–96, 1996.
51. AL Ghindilis, VP Gavrilova, AI Yaropolov. Laccase-based biosensor for determination of polyphenols: determination of catechols in tea. Biosens Bioelectron 7:127–131, 1992.
52. D Compagnone, M Esti, MC Messia, E Peluso, G Palleschi. Development of a biosensor for monitoring of glycerol during alcoholic fermentation. Biosens Bioelectron 13:875–880, 1998.
53. SC Kelly, PJ O'Connell, CK O'Sullivan, GG Guilbault. Development of an interferent free amperometric biosensor for determination of L-lysine in food. Anal Chim Acta 412:111–119, 2000.
54. L Campanella, F Pacifici, MP Sammartino, M Tomassetti. A new organic phase bienzymatic electrode for lecithin analysis in food products. Bioelectrochem Bioenerget 47:25–38, 1998.
55. RQ Thompson, M Porter, C Stuver, HB Halsall, WR Heinemean, E Buckley, MR Smyth. Zeptomole detection limit for alkaline phosphatase using 4-aminophenylphosphate, amperometric detection, and an optimal buffer system. Anal Chim Acta 271:223–229, 1993.
56. PT Feldsine, AH Lienau, RL Forgey, RD Calhoon. Assurance polyclonal enzyme immunoassay for detection of *Listeria monocytogenes* and related *Listeria* species in selected foods: collaborative study. J AOAC Int 80:775–790, 1997.
57. H Huang, MM Garcia, BW Brooks, K Nielsen, S-P Ng. Evaluation of culture enrichment procedures for use with *Salmonella* detection immunoassay. Int J Food Microbiol 51:85–94, 1999.
58. RP Johnson, RJ Durham, ST Johnson, LA Macdonald, SR Jeffrey, BT Butman. Detection of *Escherichia coli* O157:H6 in meat by an enzyme-linked immunosorbent-assay, EHEC-TEK. Appl Environ Microbiol 61:386–388, 1995.
59. A Giletto, JG Fyffe. A novel ELISA format for the rapid and sensitive detection of staphylococcal enterotoxin A. Biosci Biotechnol Biochem 62:2217–2222, 1998.
60. A Tan, S Heaton, L Farr, J Bates. The use of *Bacillus* diarrhoeal enterotoxin (BDE) detection using an ELISA technique in the confirmation of the aetiology of *Bacillus*-mediated diarrhoea. J Appl Microbiol 82:677–682, 1997.
61. EL Crowley, CK O'Sullivan, GG Guilbault. Increasing the sensitivity of *Listeria monocytogenes* assay: evaluation using ELISA and amperometric detection. Analyst 124:295–299, 1999.
62. I Abdel-Hamid, D Ivnitski, P Atanasov, E Wilkins. Flow-through immunofiltration assay system for rapid detection of *E. coli* O157:H7. Biosens Bioelectron 14:309–316, 1999.
63. D Ivnitski, I Abdel-Hamid, P Atanasov, E Wilkins. Biosensors for detection of pathogenic bacteria. Biosens Bioelectron 14:599–624, 1999.
64. RW Keay, CJ McNeil. Separation-free electrochemical immunosensor for rapid determination of atrazine. Biosens Bioelectron 13:963–970, 1998.
65. S Bender, OA Sadik. Direct electrochemical immunosensor for polychlorinated biphenyls. Environ Sci Technol 32:788–797, 1998.
66. A Dankwardt, B Hock. Enzyme immunoassays for analysis of pesticides in water and food. Food Technol Biotechnol 35:165–174, 1997.
67. MP Kreuzer, CK O'Sullivan, GG Guilbault. Development of an ultrasensitive immunoassay of rapid measurement of okadaic acid and its isomer. Anal Chem 71:4198–4202, 1999.

68. GM Brett, SJ Chambers, L Huang, MRA Morgan. Design and development of immunoassays for detection of proteins. Food Control 10:401–406, 1999.
69. G van Duijin, R van Biert, H Bleeker-Marcelis, H Peppelman, M Hessing. Detection methods for genetically modified crops. Food Control 10:375–378, 1999.
70. PE Turpin, KA Maycroft, J Bedford, CL Rowlands, EMH Wellington. A rapid luminescent phage-based MPN method for the enumeration of *Salmonella typhimurium* in environmental samples. Lett Appl Microbiol 16:24–27, 1993.
71. J Chen, MW Griffiths. *Salmonella* detection in eggs using lux^+ bacteriophages. J Food Protect 59:908–914, 1996.
72. MJ Loessner, CED Rees, GSAB Stewart, S Scherer. Construction of luciferase reporter bacteriophage A511:lux AB for rapid and sensitive detection of viable *Listeria* cells. Appl Environ Microbiol 62:1133–1140, 1996.
73. AN Ivanov, GA Evtugyn, RE Gyurcsányi, K Tóth, HC Budnikov. Comparative investigation of electrochemical cholinesterase biosensors for pesticide determination. Anal Chim Acta 404:55–65, 2000.
74. GS Nunes, P Skladal, H Yamanaka, D Barcelo. Determination of carbamate residues in crop samples by cholinesterase-based biosensors and chromatographic techniques. Anal Chim Acta 362:59–68, 1998.
75. G Jeanty, JL Martin. Detection of paraoxon by continuous flow system based enzyme sensor. Biosens Bioelectron 13:213–218, 1998.
76. J Wang, VB Nascimento, SA Kane, K Rogers, MR Smyth, L Angnes. Screen-printed tyrosinase-containing electrodes for the biosensing of enzyme inhibitors. Talanta 43:1903–1907, 1997.
77. MT Pérez Pita, AJ Reviejo, FJ Manuel de Villena, JM Pingarrón. Amperometric selective biosensing of dimethyl- and diethyldithiocarbamates based on inhibition processes in a medium of reversed micelles. Anal Chim Acta 340:89–97, 1997.
78. S Fennouh, V Casimiri, A Geloso-Meyer, C Burstein. Kinetic study of heavy metal salt effects on the activity of L-lactate dehydrogenase in solution or immobilized on an oxygen electrode. Biosens Bioelectron 13:903–909, 1998.
79. P Bertocchi, E Ciranni, D Compagnone, V Magearu, G Palleschi, S Pirvutoiu, L Valvo. Flow injection analysis of mercury(II) in pharmaceuticals based on enzyme inhibition and biosensor detection. J Pharm Biomed Anal 20:263–269, 1999.
80. V Volotovsky, YJ Nam, N Kim. Urease-based biosensor for mercuric ions determination. Sensor Actuat B—Chem 42:233–237, 1997.
81. J Ruzicka. Flow injection analysis, from test tube to integrated microconduits. Anal Chem 55:1040A-1053A, 1983.
82. F Mizutani, Y Sato, Y Hirata, S Yabuki. High-throughput flow-injection analysis of glucose and glutamate in food and biological samples by using enzyme/polyion complex-bilayer membrane-based electrodes as the detectors. Biosens Bioelectron 13:809–815, 1998.
83. AR Vijayakumar, E Csöregi, A Heller, L Gorton. Alcohol biosensors based on coupled oxidase–peroxidase systems. Anal Chim Acta 327:223–234, 1996.
84. L Pogaxnik, M Franko. Determination of organophosphate and cabamate pesticides in spiked samples of tap water and fruit juices by a biosensor with photothermal detection. Biosens Bioelectron 14:569–578, 1999.
85. NP Evmiridis, D Yao. On-line detection of nitric oxide generated by the enzymatic action of nitric oxide synthase on L-arginine using a flow injection manifold and chemiluminescence detection. Anal Chim Acta 410:167–175, 2000.
86. MA Carsol, M Mascini. Development of a system with enzyme reactors for the determination of fish freshness. Talanta 47:335–342, 1998.
87. H Okuma, W Okazaki, R Usami, K Horikoshi. Development of the enzyme reactor system with an amperometric detection and application to estimation of the incipient stage of spoilage of chicken. Anal Chim Acta 411:37–43, 2000.
88. HW Hsu, DL Vavak, LD Satterlee, GA Miller. A multienzyme technique for estimating protein digestibility. J Food Sci 42:1269–1273, 1977.

26

Recent Advances in Enzyme Development

Dominic W. S. Wong
U.S. Department of Agriculture, Albany, California, U.S.A.

I. INTRODUCTION

The important role of enzymes in food and food systems is aptly underscored by the description of some 60 enzymes in this handbook. These encompass all major six classes of enzymes—oxidoreductases, transferases, hydrolases, lyases, isomerases, and ligases–that catalyze various reactions contributing to the characterisitc features and quality attributes of a particular food. Food scientists investigate the fundamentals of enzymology, extract the information obtained from biochemical studies, and apply them to the use and control of enzymes for preserving and producing better foods. Of the ~ 4000 known enzymes, only a handful of them are currently used in industry, $\sim 45\%$ are for food processing (Table 1). The future of enzyme technology foresees an increasing use of recombinant DNA technology and biotechnological processes for the discovery and development of novel enzymes and for better utilization of our food resources. Four research areas of emerging importance are described in this chapter: The study of extremophilic enzymes will change the landscape of our current knowledge on the use of enzymes; the rapid advances in developing novel techniques in protein engineering provide an ever increasing powerful tool for tailoring enzyme structural and functional properties; the ability to manipulate metabolic enzymes in biosynthetic pathways provides new opportunities for in vivo modification of food components; and the recent development of innovative approaches in the construction of artificial enzymes results in much improved catalytic activities, and substantiates the potential of their future roles in enzyme technology.

II. EXTREMOPHILIC ENZYMES

A. Search of Enzymes from Exotic Environments

A majority of the currently known ~ 4000 enzymes have been isolated from mesophilic organisms. In terms of microbial diversity, $< 1\%$ of the world microbial species have been identified and cultured in laboratories. These enzymes have evolved to function under a narrow range of pH, temperature, ionic strength, pressure, and chemical concentration, and are not optimized for performance under industrial conditions. Considerable efforts have been devoted to harvest organisms, mostly in the Eubacterial and Archaeal phylogenetic domains (1), that thrive in extreme environments for enzymes with industrial compatible properties. Major types of extremophiles include: thermophiles (found in hot spring, deep-sea thermal vents); psychrophiles (Arctic water, Antarctic Circle); acidophiles (geothermal sulfur-rich springs, coal deposits); alkalophiles (alkaline lakes, sewage sludge); halophiles (salt lakes, mines); and barophiles (deep-sea floor). Crystal structures are available for a number of thermophilic and psychrophilic enzymes, and some of these results provide the current information on factors that might stabilize them at extreme temperatures, compared with their mesophilic counterparts.

Table 1 A List of Important Industrial Enzymes and Their Applications

α-Amylase
Conversion of starch to dextrins (liquefaction) in the production of corn syrup
Supplement to flour types low in α-amylase to ensure a continuous supply of fermentable sugar for yeast growth and gas production in dough making
Solubilization of adjuncts (nonmalt carbohydrate materials from barley and other cereal grains) used in brewing
Glucoamylase
Conversion of dextrins to glucose (saccharification) in the production of corn syrup
Conversion of residual dextrins to fermentable sugar in brewing for the production of "light" beer
β-Amylase
Production of high-maltose syrup
Xylose (glucose) isomerase
Isomerization of glucose to fructose in the production of high-fructose corn syrup
β-Glucanase
Breakdown of β-glucans in malt and other raw materials to aid filtration of wort after mashing in brewing
Lipase
Enhancing flavor development and shortening the time for cheese ripening
Production of specialty fats with improved qualities
Production of enzyme-modified cheese/butter from cheese curd or butterfat
Papain
Used as meat tenderizer
Used in brewing to prevent chill-haze formation by digesting proteins that can otherwise react with tannic substances to form insoluble colloid particles.
Chymosin
Curding of milk by specific proteolytic action on κ-caseins in cheese making
Microbial proteases
Processing of raw plant and animal proteins
Production of fish meals, meat extracts, texturized proteins, and meat extenders
Pectinase
Treatment of fruit pulp to facilitate juice extraction and for clarification and filtration of juice
Lactase
Additive for dairy products for individuals lacking lactase
Breakdown of lactose in whey products for manufacturing polyactide
Acetolactate decarboxylase
Reduction of maturation time in wine making by converting acetolactate to acetoin
(In the absence of the enzyme, acetolactate is oxidized to diacetyl that requires secondary fermentation to reduce it to acetoin)
Lysozyme
Antimicrobial preservative
Glucose oxidase
Conversion of glucose to gluconic acid to prevent Maillard reaction in products caused by high heat used in dehydration
Potential use to remove O_2 in food packaging for protection against oxidative deterioration
Cellulase
Conversion of cellulose wastes to fermentable feedstock for ethanol or single-cell protein production

Source: Ref. 24.

Protein stability can be expressed in terms of the free energy, associated with the micro- and macro-unfolding of the protein. Microunfolding represents qualitatively characteristics of the rigidity of the protein structure, and is associated with local, reversible, noncooperative unfolding reactions within the folded state. Macrounfolding represents the stability of the macroscopic state of the protein molecules and the energy required for the protein changing from the native to the unfolded macroscopic state (2). Adjustment of conformational flexibility is a key step in the thermal adaptation of proteins.

Zavodszky et al. (3) compared both the macrostability (DSC and CD measurements) and microstability (hydrogen H/D exchange and FT-IR) of *Thermus thermophilus* (a hyperthermophilic microrganism) and *E. coli* 3-isopropylmalate dehydrogenase (IPMDH), and confirmed the correlation between enzyme activity and conformational flexibility. The thermophilic IPMDH has increased conformational rigidity as compared to the mesophilic counterpart, so as to stabilize the protein against heat denaturation. However, the two enzymes show similar conformational flexibility at their corresponding physiological temperature optima. This "thermometer effect" has been previously reported by Wrba et al. (4) on the study of D-glyceraldehyde-3-phosphate dehydrogenase isolated from *Thermotoga maritima*. Maes et al. (5) compared the crystal structure of triosephosphate isomeraes (TIM) from *Thermotoga maritima* with a series of nine known TIM from a wide variety of organisms, and did not find a common theme in the adaptive mechanism for the temperature scale.

Current structural investigations indicate that mesophilic and corresponding thermophilic proteins are virtually identical in structure with the difference in free energy of stabilization in the order of 5–15 kcal mol^{-1} (6). This small energy difference is equivalent to only a few hydrogen bonds, salt bridges, or hydrophobic interactions (7). Proteins may have achieved increased thermostability by various combinations of these additional interactions. Delboni et al. (8) compared the crystal structures of six known thermophilic and mesophilic TIM enzymes, and found that hydrophobic stabilization contributes to the thermostability of the *Bacillus stearothermophilus* TIM. The enzyme shows increased hydrophobic packing with the smallest number of cavities and the total cavity surface area. The enzyme also has the largest hydrophobic surface area (314–534 Å) buried in the dimer formation compared with other TIM structures, with an energy gain of 7–13 kcal mol^{-1}. It was also shown that the *B. stearothermophilus* TIM contains 13 prolines, exceeding all other TIM enzymes, suggesting that the large number of Pro residues are responsible for thermostability by decreasing the entropy of the unfolded state. Similar effects have been achieved by introducing disulfide bridges, for example, into subtilisin (9) and lysozyme (10).

The crystal structure of several psychrophilic enzymes has been elucidated, including that of α-amylase (Antarctic *Alternomonas haloplanctis*) (11), subtilisin (Antarctic *Bacillus* TA39 and TA41) (12), trypsin (Atlantic salmon, Antarctic *Paranotothenia magellanica*) (13), and triosephosphate isomerase (psychrophilic bacterium *Vibrio marinus*) (14). The Antarctic bacteirum *A. haloplanctis* secretes a Ca^{2+} and Cl^{-}-dependent α-amylase composed of 453 amino acids with a predicted Mr of 49,340 and a pI of 5.5 (15). The enzyme is synthesized as a preproenzyme comprised of a 24-residue N-terminal signal peptide, and a 192-residue C-terminal propeptide which contains features common to β-pleated transmembrane proteins (16). The amino acid sequence displays 66% similarity with procine pancreatic α-amylase. It is characterized by a seven fold higher k_{cat} and k_{cat}/K_m values at 4°C and a lower conformation stability with the difference in free energy of 1.9 kcal mol^{-1} (17). Homology modeling reveals several features responsible for the more flexible, heat-labile conformation of the psychrophilic α-amylase: the lack of 12 surface salt bridges by replacement with Gln or Asn residues; substitution of 25 residues in the hydrophobic clusters of the porcine enzyme, causing a sharp decrease of the hydrophobicity and increase in flexibility; and deletion or substitution of 12 proline residues in loops or turns. These findings seem to substantiate the concept of local flexibility as an adaptation to thermal stability by extremophiles. The treatment of thermodynamic parameters of activation as a structure–function model accounting for local flexibility for acquiring high activity at low temperature has been described by Lonhienne et al. (18).

B. Design Enzyme Stability

1. Immobilization

Until the advent of genetic modification, immobilization was routinely used for improving the stability of enzymes in industrial processing. Immobilization anchors the enzyme onto a suitable carrier such as agarose, alginate, gelatin, or polyacrylamide either by covalent coupling, adsorption, matrix entrapment, or encapsulation. The primary advantage of immobilization is to increase the stability of the enzyme, as well as convenience in separation and recovery, and reuse of the enzyme from the product mixture. In the manufacture of high-fructose corn syrup, glucose isomerase is immobilized by direct crosslinking of lysed cells with glutaraldehyde and extruded with structural support substances, such as gelatin and polyamine (19). Although not directly relevant to food applications, immobilization of enzymes has been shown to have higher stability in reactions carried out in water-miscible organic solvents (20). Apart from the conventional approaches, Stempfer et al. (21) engineered a

fusion protein of α-glucosidase containing a hexa-arginine polypeptide stretch at the C-terminal end. The cationic peptide extension provides a strong, noncovalent attachment of the fusion protein to a polyanion matrix. Ureda and Tanaka (22) have constructed a genetic system to immobilize enzymes in their active and functional forms on the cell surface of *Saccharomyces cerevisiae*. The display of both CM-cellulase and β-glucosidase on the surface of *S. cerevisiae* results in digestion of cello-oligosaccharides as the sole carbon source. Likewise, coimmobilization of glucoamylase and α-amylase on cell surfaces has been shown to digest soluble starch as the sole source of carbon for yeast growth (23).

2. Protein Engineering

With the advent of recombinant DNA technology, enzymes have been tailored by manipulating the genetic code to target specific amino acid substitutions. Site-directed or cassette mutagenesis is rapidly becoming a routine approach in many investigations. Subtilisin, lysozyme, trypsin, and amylases are among some of the most extensively studied enzymes as models for enhancing various enzyme properties (24). Considerable work has been conducted on the contribution of disulfide bridges to the stability of proteins by decreasing the conformational entropy in the unfolded state. In T4 lysozyme, a single change of Ile3$\rightarrow$Cys creates a disulfide bridge between the new Cys3 and the native Cys97, resulting in enhancement of stability against irreversible inactivation (25) as well as reversible thermal unfolding (26). Matsumura et al. (10) have shown that mutants containing three constructed disulfide bonds (3–97, 9–164, 21–142) exhibit an additive effect with ΔT_m of 23.4°C higher than the wild type. However, mutants containing Cys90-Cys122 and Cys127-Cys154 are less stable due to the introduction of strains by the new bonds.

It has been known that salt bridges play an important role in protein stability. The introduction of His31-Asp30 in T4 lysozyme stabilizes the protein by 3–5 kcal mol^{-1} (27). Engineering Ser38$\rightarrow$Asp and Asn144$\rightarrow$Asp at the N-terminal end of the helices B and J increases stability with $\Delta\Delta G$ of 1.6 kcal mol^{-1} (28). Some investigations indicate that the contribution to stability from an engineered salt bridge is very small ($\sim$ 0.1–0.25 kcal mol^{-1}), which is largely offset by the entropic cost of localizing the ion pair on the surface of the enzyme (29). Van den Burg et al. (30) constructed a thermolysin-like protease mutant with a disulfide bridge (Asn60$\rightarrow$Cys with Gly8$\rightarrow$Cys), and several mutations to increase the rigidity of the molecule, including Ala69$\rightarrow$Pro and Ser65$\rightarrow$Pro. The resulting mutant enzyme shows a dramatic increase in stability; it is 340 times more stable than the wild type in terms of the half-life time at 100°C. All these results suggest the importance of considering the balance between favorable and unfavorable factors involved in engineering structural changes.

III. CREATING NOVEL ENZYMES BY DIRECTED EVOLUTION

In the use of rational design to engineer a protein's structural and functional properties, the change in the amino acid sequence is preconceived based on a prior knowledge of the structural and mechanistic details of the protein. In spite of some remarkable successes, prediction of the outcome of a particular amino acid substitution remains largely empirical, and explanations for the effects of site-directed mutagenesis are done in hindsight, simply because there is an enormous gap in our ability to correlate sequence structure and function. A novel approach based on the concept of combinatorial chemistry has revolutionized the way to engineering protein molecules. Initially, the concept of directed evolution was utilized in generating RNA molecules with novel binding and catalytic activities (31). Libraries of RNA can be generated by in vitro transcription of DNA by PCR with random priming. A selection step is applied to the RNA pool to isolate variants possessing the targeted function/property. The few selected RNA molecules are subjected to iterative cycles of amplification, mutation, and selection until the best-fit molecule is identified. The use of this concept for evolving proteins has been realized with the development of the DNA shuffling technique (32) and subsequent refining and expansion of this technique. The method involves random digestion of a pool of DNA sequences (typically amplified error-prone PCR products of a gene of interest) with DNaseI to a mixture of small DNA fragments. These fragments are reassembled by DNA polymerase, relying on self-priming of homologous end sequences, and in the process, recombination or crossover occcurs by template switching. This DNA shuffling step is followed by selecting the recombinant libraries for the best combination of mutations yielding the targeted properties (33).

Modification and expansion of the original DNA shuffling concept have been continuously developed and reported. One of the adaptations, called family

shuffling, allows two or more related genes to be used as the starting genetic materials (34). This approach is based on the assumption that naturally occurring genes in a family of species are already enriched for functional diversity by selection in the natural evolution process. A simplified method for in vitro recombination, called staggered extension process (StEP) recombination, eliminates the steps of DNaseI digestion and reassembly of DNA fragments (35). The key to this method is to employ very short extensions in the PCR reaction, so that in the following cycle, denaturation will free the growing fragments to anneal to different templates. Kikuchi et al. (36) developed an effective family shuffling method using single-stranded DNA of two or more related genes to avoid the problem of homoduplex formation caused by the annealing of DNA fragments derived from the same gene.

In a greater deviation from the Stemmer's shuffling method, Coco et al. (37) developed a method called random chimeragenesis on transient templates, which involves separating the gene homologs into single-stranded DNA, digesting one strand into fragments which will align with the other strand as the template. Unhybridized flaps are removed, and gaps are filled to generate a full-length heteroduplexed gene. The parental template is destroyed by uracil-DNA-glycosylase treatment, and is replaced by a homoduplex strand during PCR. Ostermeier et al. (38) described a methodology, incremental truncation for the creation of hybrid enzymes, that creates hybrid gene libraries that are independent of sequence homology. Two parent genes are truncated incrementally and the fragments are fused pairwise to generate single crossovers. A more refined method, called sequence homology-independent protein recombination (39), allows the proper sequence alignment maintained between the parent genes in the hybrid sequence. A more recent development involves exon shuffling, which is based on the fact, that in nature, genetic recombination occurs by crossover in the intron regions to produce various structure genes (40). This approach had already been successfully utilized earlier by Kumagai et al. (41) to introduce lysozyme activity to α-lactalbumin by engineering a hybrid protein by artificial exon shuffling.

Directed evolution as described above contains an in vivo step of expressing the gene variants in microorganisms. It requires an appropriate system for the transcription and translation of the DNA sequences to proteins for in vivo selection, while in the following step, the beneficial mutations are combined and subjected to in vitro mutagenesis and amplification for the next cycle. *E. coli* has been frequently used as a suitable expression system, while yeast is the choice for working with eukaryotic genes. Various techniques have been developed to allow the generation of a library of protein molecules to be displayed (anchored) on the cell surface of bacteria (42), phage (43), or yeast (44) as a fusion protein. Currently, there are two cell-free systems developed for in vitro selection and evolution of proteins. Tawfik and Griffith (45) showed that in vitro transcription/translation apparatuses can be incorporated with single genes into reverse micelles, a cell-like compartment that links genotype to phenotype. In robosome display, in vitro transcription and translation are performed on ribosomes, with a number of modification steps to retain the expressed protein on the ribosome after translation (46, 47). The ribosome-bound proteins are screened and reverse transcription and PCR of the mRNA produce the DNA sequence of the corresponding protein. Mutations in sequence can be introduced during amplification to generate a new population in the next cycle of protein synthesis and selection.

Directed evolution has been successfully employed in numerous investigations to engineer various aspects of structure–function properties of proteins and enzymes (48). However, the focus has been primarily on the improvement or alteration of existing properties. In a recent study, Alan R. Fersht's group created totally new catalytic functions in the transmutation of indole glycerol phosphate synthase (IGPS) to phosphoribozyl anthranilate isomerase (PRAI) (49). This was achieved by modification of the loops of IGPS that are differed from those in PRAI, followed by directed evolution. The final evolved enzyme loses its original IGPS activity, but acquires PRAI activity with k_{cat}/K_m value of 4.8×10^{-7} sec^{-1} M^{-1} which is sixfold that displayed by the wild-type enzyme. This study exemplifies the remarkable power of combining rational design and directed evolution in achieving novel structural and functional properties.

IV. METABOLIC ENGINEERING

Recombinant DNA technology has progressed rapidly so that foreign genes can be introduced or endogenous genes can be manipulated to redesign metabolic pathways in microbial, plant, and animal cells. For the field of agriculture and food, this means the ability of in vivo manipulation of enzymes to tailor the chemical composition and physical properties of various food components, to enhance characteristics suitable for food formulation and processing, to improve nutri-

tional values, to remove or reduce the level of antinutrients, or even to produce value-added nonfood products. The following description illustrates the application of metabolic engineering to change the quality characteristics of starch in cereal plants. The composition and molecular structure of starch have a direct impact on the rheological properties, such as gelatinization, swelling, viscosity, and retrodegradation. With the current trend of developing more processed and formulated foods, the demand for specialty starches is increasing. The ratio of amylose to amylopectin has a significant impact on the physicochemical properties of the starch, and for some applications enriched fractions of either one is desirable. Currently, most waxy mutants that produce starches with little or no amylose are created by selective breeding in maize. However, controlling the degree of branching or the ratio of amylose to amylopectin can be realized only through the use of metabolic engineering. Introduction and expression of *Escherichia coli* glycogen branching enzymes into potato tubers showed an increase in branching degree of the amylopectin (50, 51). Lloyd et al. (52) introduced a chimeric antisense construct of two starch synthase isoforms (SSII and SSIII) into potato tubers, which led to accumulation of amylopectin with an increase in short-chain branching. Antisense inhibition of starch branching enzyme (isoform SBE A) in potato increases the average chain length of amylopectin and the level of phosphorylation (53). Suppression of both SBE A and B results in very high (~ 2.5 times) amylose potato starch containing insignificant levels of highly branched amylopectin, and sixfold increase in phosphorus content (54). Other targets for genetic manipulating of starch biosynthesis include (a) increased production or alteration of storage proteins, (b) changes in size and ratio of A and B starch granules, and (c) specialty carbohydrate products, such as cyclodextrins utilizing starch as substrate (55). All these can be achieved, as future investigations continue to reveal the complex interactions and mode of action of the various enzymes involved in starch synthesis.

Metabolic pathways often employ enzyme complexes to achieve multifunctional steps of catalysis in the formation of the final product via a number of intermediates. The concept of combinatorial chemistry can be applied to biological systems by combining, changing, or shuffling the genes in a biosynthetic pathway, resulting in a whole range of novel molecules and their variants (56). For example, in polyketide biosynthesis, the multifunctional polyketide synthase enzyme complex catalyzes repeated Claisen condensation between acylthioesters (ketosynthase), followed by repeated reductive cycles comprising a ketoreduction (ketoreductase), dehydration (ketodehydratase), and enoylreduction (enol-reductase) on the β-keto group of the growing polyketide chain. After the chain has elongated through a fixed number of cycles, the polyketide product is released via the action of a thioesterase. Structural variability is introduced by variations of substitutions in the starter units, the extent of reduction, and the location of intramolecular ring closure (57). This natural process can be manipulated to produce designer polyketides by combinatorially expressing PKS subunits in modules, and a large repertoire of polyketides can be generated for screening for specific structure–function, including antibiotics and anticancer agents (58).

Recently, a wide range of structurally different carotenoids have been successfully synthesized by manipulating terpenoid pathways in bacteria and yeasts. To direct carotenoid biosynthesis in *Escherichia coli*, the terpenoid pathways need to be extended with expressing a number of genes, including phytoene synthase (for forming the C40 carotenoid phytoene), isopentenyl pyrophosphate isomerase (for the isomerization of isopentenyl pyrophosphate to dimethylallyl pyrophosphate which is the substrate for elongation), and geranylgeranyl pyrophosphate synthase (for forming geranylgeranyl pyrophosphate which is the substrate for phytoene synthase). A combination of these and several other genes for specific modifications of the phytoene chain were cloned into *E. coli* plasmids, reuslting in the synthesis of eight different hydroxy derivatives of carotenoids, including 1-hydroxylycopene, 1, 1′-dihydroxylycopene, dimethylspheroidene, 3-hydroxy-β-zeacarotene, 7,8-dihydrozeaxanthin, 3- or 3′-hydroxy-7,8-dihydro-β-carotene, and 1′-hydroxy-γ-carotene (59). Using a similar approach, but combining it with directed evolution of phytoene desaturase and lycopene cyclase, Schmidt-Dannert et al. (60) were able to introduce six double bonds into phytoene for the production of the fully conjugated carotenoid, 3,4,3′,4′-tetradehydrolycopene, and a unique cyclic carotenoid torulene.

V. ARTIFICIAL ENZYMES

The idea of replacing enzymes with synthetic biocatalysts has long been an intellectual challenge. Miniature enzymes, devoid of polypeptide backbones, offer an attractive alternative for use in processing because

they are less prone to the effects of high temperature, extreme pH, and ionic strength existing in industrial applications. Cyclodextrins have proved to be the most popular host matrix for constructing enzyme mimics, usually with the attachment of one or more reactive groups, such as a pyridoxamine to the hydrophobic binding cavity to produce selectivity for transamination of ketoacids bound into the cavity (61). Examples also include the grafting of an imidazolyl–benzoic acid moiety to achieve a chymotrypsin-like activity (62, 63). Another synthetic host that has been used quite extensively includes porphyrin or porphyrin-like structures as well as various macrocyclic compounds with built-in functions. For example, Fe^{III} and Mn^{III} (porphyrinato) complexes have been studied by several groups as superoxide dismutase mimics (64). Salvemini et al. (65) developed a Mn(II) bis(cyclohexylpyridine) macrocyclic complex that mimics superoxide dismutase catalytically and acts exclusively on superoxide, without interfering with other reactive species, such as nitric oxide, hydrogen peroxide, or peroxynitrite. An example of mimicking not only the important structural features but also the same chemistry as an enzyme was reported for the development of models of galactose oxidase, which oxidizes benzylic or allylic alcohols with O_2 to yield an aldehyde and H_2O_2 (66). In the model, the derivatized Schiff base diimine–diphenolate ligands mimics the copper coordination in the natural enzyme involving two tyrosine phenolates, two histidine imidazoles, and exogenous H_2O ligand.

Catalytic antibodies are currently the best-known enzyme mimics. These so-called abzymes are generated by screening a huge library of antibodies raised against transition state analogs for catalysts in a particular reaction of interest (67, 68). The many different reactions developed for catalytic antibodies include amide hydrolysis, ester hydrolysis, peptide cleavage, transesterification, β-elimination, cationic cyclization, Diels-Alder reaction, Claisen rearrangement, lactonization, and various chemical transformations. Esterolytic antibodies are the best characterized of the catalytic antibodies probably due to the fact that excellent transition state analogs are readily available. Several crystal structures of esterase-like antibodies have been published (69–73). All these abzymes, raised against phosphonate transition state analogs, act by stabilization of the oxyanion intermediate that results from general base-assisted or hydroxide attack on the substrate. The active site may contain a catalytic His or Ser-His dyad, and at least in one study on an abzyme with amide hydrolytic activity, a His residue at the bottom of the antigen-binding site may be involved in nucleophilic catalysis (74). Applying directed evolution techniques to evolve a hydrolytic abzyme generated by the conventional method with immunization of the transition state analog, Takahashi et al. (75) produced a variant with six- to two-fold increases in the k_{cat} value.

An alternative approach of generating catalytic antibodies has been proposed by Briboulet et al. (76) using the properties of anti-idiotypic antibodies to generate an internal image of an enzyme-binding site. This approach follows the concept of idiotypic mimicry (77) in that antienzyme antibodies generated by animal immunization are screened for those that recognize (idiotypic) the enzyme active site. The selected antienzyme antibodies are used as immunogens to induce the production of anti-idiotypic antibodies which carry the imprint of the enzyme active site and are subject to enzyme activity screening. Crystallographic studies of anti–hen egg white lysozyme antibody complexed with an anti-idiotopic antibody suggest that the mimicking is functional, involving similar binding interactions rather than exact topological "images" (78).

Another technique known as molecular imprinting deals with a very similar concept in biological recognition. The overall approach is to allow a mixture of functional monomers (of either acrylate-, styrene-, or silica-based materials) to prearrange around the selected ligand by noncovalent interactions (79, 80). The reslting complexation is immobilized by polymerization of the monomers, and subsequent extraction (or dissolution) of ligand results in the development of an "imprint" within the polymeric structure. Plastic enzyme mimics could be produced by using template-containing analogs of substrates, transition state, or product of an enzyme reaction. Several studies used phosphonate derivatives to mimic the transition of carboxylic ester hydrolysis, and the results have been very moderate. In one study, phosphonic acid monoesters were imprinted using a polymerizable amidine derivative, and the catalysts were screened for activity (81). The hydrolysis reaction follows a typical Michaelis–Menten curve with saturation kinetics.

REFERENCES

1. SM Barns, RE Fundyga, MW Jeffries, NR Pace. Remarkable archaeal diversity detected in a yellowstone national park hot spring environment. Proc Natl Acad Sci USA 91:1609–1613, 1994.
2. PL Privalov, TN Tsalkova. Micro- and macro-stabilities of globular proteins. Nature 280:693–698, 1979.

3. P Zavodszky, J Kardos, A Svingor, GA Petsko. 1998. Adjustment of conformational flexibility is a key event in the thermal adaptation of proteins. Proc Natl Acad Sci USA 95:7406–7411, 1998.
4. A Wrba, A Schweiger, V Schultes, R Jaenicke. Extremely thermostable D-glyceraldehyde-3-phosphate dehydrogenase from the Eubacterium *Thermotoga maritima*. Biochemistry 29:7584–7592, 1990.
5. D Maes, JP Zeelen, N Thanki, N Beaucamp, M Alvarez, MHD Thi, J Backmann, JA Martial, L Wyns, R Jaenicke, RK Wierenga. The crystal structure of triosephosphate isomerase (TIM) from *Thermotoga maritima*: a comparative thermostability structural analysis of ten different TIM structures. Protein Struct Funct Gen 37:441–453, 1999.
6. C Vieille, G Zeikus. Thermozymes: identifying molecular determinants of protein structural and functional stability. TIBTECH 14:183–190, 1996.
7. DC Rees, MWW Adams. Hyperthermophiles: taking the heat and loving it. Structure 15:251–254, 1995.
8. LF Delboni, SC Mande, F Rentier-Delrue, V Mainfroid, S Turley, FMD Vellieux, JA Martial, WGJ Hol. Crystal structure of recombinant triosephosphate isomerase from *Bacillus stearothermophilus*. An analysis of potential thermostability factors in six isomerases with known three-dimensional structures points to the importance of hydrophobic interactions. Protein Sci 4:2594–2604, 1995.
9. MW Pantoliano, RC Ladner, PN Bryan, ML Rollence, JF Wood, TL Poulos. Protein engineering of subtilisin BPN′: enhanced stabilization through the introduction of two cysteines to form a disulfide bond. Biochemistry 26:2077–2082, 1987.
10. M Matsumura, G Signor, BW Matthews. Substantial increase of protein stability by multiple disulfide bonds. Nature 342:291–293, 1989.
11. N Aghajari, G Feller, C Gerday, R Haser. Crystal structures of the psychrophilic α-amylase from *Alteromonas haloplanctis* in its native form and complexed with an inhibitor. Protein Sci 7:564–572, 1998.
12. S Davail, G Feller, E Narinx, G Gerday. Cold adaptation of proteins. Purification, characterization and sequence of the heat-labile subtilisin from the Antarctic psychrophile *Bacillus* TA41. J Biol Chem 269:17448–17453, 1994
13. AO Samals, ES Heimstad, A Hordvik, P Willasen, R Male. Cold adaptation of enzymes: structural comparison between salmon and bovine trypsins. Protein Struct Funct Gen 20:149–166, 1994.
14. M Alvarez, JP Zeelen, V Mainfroid, F Rentier-Delrue, JA Martial, L Wyns, RK Wierenga, D Maes. Triosephosphate isomerase (TIM) of the psychrophilic bacterium *Vibrio marinus*. J Biol Chem 273:2199, 1998.
15. G Feller, T Lonhienne, C Deroanne, C Libioulle, J Van Beeumen, C Gerday. Purification, characterization, and nucleotide sequence of the thermolabile α-amylase from the Antarctic psychrotroph *Alteromonas haloplanctis* A23. J Biol Chem 267:5217–5221, 1992.
16. G Feller, S D'Amico, AM Benotmane, F Joly, J Van Beeumen, C Gerday. Characterization of the C-terminal propeptide involved in bacterial wall spanning of α-amylase from the psychrophile *Alteromonas haloplanctis*. J Biol Chem 273:12109–12115, 1998.
17. G Feller, F Payan, F Theys, M Qian, R Haser, C Gerday. Stability and structural analysis of α-amylase from the Antarctic psychrophile *Alteromonas haloplanctis* A23. Eur J Biochem 222:441–447, 1994.
18. T Lonhienne, C Gerday, G Feller. Psychrophilic enzymes: revisiting the thermodynamic parameters of activation may explain local flexibility. Biochim Biophys Acta 1543:1–10, 2000.
19. H Uhlig. Industrial Enzymes and Their Applications. New York: John Wiley & Sons, 1998, p 208.
20. R Ulbrich-Hofmann, B Selisko. Soluble and immobilized enzymes in water-miscible organic solvents: glucoamylase and invertase. Enzyme Microb Technol 15:33–41, 1993.
21. G Stempfer, B Holl-Neugebauer, E Kopetzki, R Rudolph. A fusion protein designed for noncovalent immobilization: stability, enzymatic activity, and use in an enzyme reaction. Nat Biotechnol 14:481–484, 1996.
22. M Ueda, A Tanaka. Cell surface engineering of yeast: construction of arming yeast with biocatalyst. J Biosci Bioeng 90:125–136, 2000.
23. M Ueda, A Tanaka. Genetic immobilization of proteins on the yeast cell surface. Biotechnol Adv 18:121–140, 2000.
24. DWS Wong. Food Enzymes: Structure and Mechanism. New York: Chapman & Hall, 1995, pp 17–36.
25. LJ Perry, R Wetzel. Disulfide bond engineered into T4 lysozyme: stabilization of the protein toward thermal inactivation. Science 26:555–557, 1984.
26. R Wetzel, LJ Perry, WA Baase, WJ Becktel. Disulfide bonds and thermal stability in T4 lysozyme. Proc Natl Acad Sci USA 85:401–405, 1988.
27. DE Anderson, WJ Becktel, FW Dahlquist. pH-induced denaturation of proteins: a single salt bridge contributes 3–5 kcal/mol to the free energy of folding of T4 lysozyme. Biochemistry 29:2403–2408, 1990.
28. H Nicholson, WJ Becktel, BW Matthews. Enhanced protein thermostability from designed mutations that interact with α-helix dipoles. Nature 336:651–656, 1988.
29. D-P Sun, U Sauer, H Nicholson, BW Matthews. Contributions of engineered surface salt bridges to the stability of T4 lysozyme determined by direct mutagenesis. Biochemistry 30:7142–7153, 1991.

30. B Van den Burg, G Vriend, OR Veltman, G Venema, VGH Eusink. Engineering an enzyme to resist boiling. Proc Natl Sci USA 95:2056–2060, 1998.
31. GF Joyce. Amplification, mutation and selection of catalytic RNA. Gene 82:83–87, 1989.
32. WPC Stemmer. Rapid evolution of a protein in vitro by DNA shuffling. Nature 370:389–391, 1994.
33. WPC Stemmer. Sexual PCR and assembly PCR. In: The Encyclopedia of Molecular Biology and Molecular Medicine, New York: Wiley, 1996, pp 447–457.
34. A Crameri, S-A Raillard, E Bermudez, WPC Stemmer. DNA shuffling of a family of genes from diverse species accelerates directed evolution. Nature 391:288–291, 1998.
35. H Zhao, L Giver, Z Shao, JA Affholter, FH Arnold. 1998. Molecular evolution by staggered extension process (StEP) in vitro recombination. Nat Biotechnol 16:258–260, 1998.
36. M Kikuchi, K Ohnishi, S Harayama. An effective family shuffing method using single-stranded DNA. Gene 243:133–137, 2000.
37. WM Coco, WE Levinson, MJ Crist, HJ Hektor, A Darzins, PT Pienkos, CH Squares, DJ Monticello. DNA shuffling method for generating highly recombined genes and evolved enzymes. Nat Biotechnol 19:354–359, 2001.
38. M Ostermeier, JH Shim, SJ Benkovic. 1999. A combinatorial approach to hybrid enzymes independent of DNA homology. Nat Biotechnol 17:1205–1209, 1999.
39. V Sieber, CA Martinez, FH Arnold. 2001. Libraries of hybrid proteins from distantly related sequences. Nat Biotechnol 19:456–460, 2001.
40. JA Kolkman, WPC Stemmer. Directed evolution of proteins by exon shuffling. Nat Biotechnol 19:423–428, 2001.
41. I Kumagai, S Takeda, K Miura. Introduction of enzymatic activity to α-lactalbumin by artificial exon shuffling. Proc Jpn Acad, Series B 67, 1991, pp 184–187.
42. S Jorgensen, CE Vorgias, G Antranikian. Cloning, sequencing, characterization, and expression of an extracellular α-amylase from the hyperthermophilic archaeon *Pyrococcus furiosus* in *Escherichia coli* and *Bacillus subtilis*. J Biol Chem 272:16335–16342, 1997.
43. GP Smith. Filamentous fusion phage: novel expression vectors that display cloned antigens on the virion surface. Science 228:1315–1317, 1985.
44. T Murai, M Ueda, T Kawaguchi, M Arai, A Tanaka. 1998. Assimilation of cellooligosaccharides by a cell surface-engineered yeast expressing β-glucosidase and carboxymethylcellulase from *Aspergillus aculeatus*. Appl Environ Microbiol 64:1857–1861, 1998.
45. DS Tawfik, AD Griffiths. Man-made cell-like compartments for molecular evolution. Nat Biotechnol 16:652–656, 1998.
46. J Hanes, A Pluckthun. In vitro selection and evolution of functional proteins by using ribosome display. Proc Natl Acad Sci USA 94:4937–4942, 1997.
47. L Jermutus, A Honegger, F Schwesinger, J Hanes, A Pluckthun. Tailoring in vitro evolution for protein affinity or stability. Proc Natl Acad Sci USA 98:75–80, 2001.
48. FH Arnold. Evolutionary protein design. Adv Protein Chem 55:1–399, 2000.
49. MM Altamirano, JM Blackburn, C Aguayo, AR Fersht. Directed evolution of new catalytic activity using the α/β-barrel scaffold. Nature 403:617–622, 2000.
50. CK Shewmaker, CD Boyer, DP Wiesenborn, DB Thompson, MR Boersig, JV Oakes, DM Stalker. Expression of *Escherichia coli* glycogen synthase in the tubers of transgenic potatoes (*Solanum tuberosum*) results in a highly branched starch. Plant Physiol 104:1159–1166, 1994.
51. AJ Kortstee, AMS Vermeesch, BJ de Vries, E Jacobsen, RGF Visser. Expression of *Escherichia coli* branching enzyme in tubers of amylose-free transgenic potato leads to an increased branching degree of the amylopectin. Plant J 10:83–90, 1996.
52. JR Lloyd, V Landschutze, J Kossmann. Simultaneous antisense inhibition of two starch-synthase isoforms in potato tubers leads to accumulation of grossly modified amylopectin. Biochem J 338:515–521, 1999.
53. SA Jobling, GP Schwall, RJ Westcott, CM Sidebottom, M Debet, MJ Gidley, R Jeffcoat, R Safford. A minor form of starch branching enzyme in potato (*Solanum tuberosum* L) tubers has a major effect on starch structure: cloning and characterization of multiple forms of SBE A. Plant J 18:163–171, 1999.
54. GP Schwall, RS Roger, J Westcott, R Jeffcoat, A Tayal, Y-C Shi, MJ Gidley, SA Jobling. Production of very-high-amylose potato starch by inhibition of SBE A and B. Nat Biotechnol 18:551–554, 2000.
55. HFJ Bligh. Genetic manipulation of starch biosynthesis: progress and potential. Biotechnol Genet Eng Rev 16:177–200, 1999.
56. J Rohr. Combinatorial biosynthesis: an approach in the near future? Angew Chem Int Ed Engl 34:881–885, 1995.
57. CJ Tsoi, C Khosla. Combinatorial biosynthesis of 'unnatural' natural products: the polyketide example. Chem Biol 2:355–362, 1995.
58. H Fu, G Khosla. Antibiotic activity of polyketide products derived from combinatorial biosynthesis: implications for directed evolution. Mol Divers 1:121–124, 1995.
59. G Sandmann, M Albrecht, G Schnurr, O Knorzer, P Boger. The biotechnological potential and design of novel carotenoids by gene combination in *Escherichia coli*. TIBTECH 17:233–237, 1999.

60. C Schmidt-Dannert, D Umeno, FH Arnold. Molecular breeding of carotenoid biosynthetic pathway. Nat Biotechnol 18:750–753, 2000.
61. R Breslow, JW Canary, M Varney, ST Waddell, D Yang. Artificial transaminases linking pyridoxamine to binding cavities: controlling the geometry. J Am Chem Soc 112:5212–5219, 1990.
62. VT D'Souza, H Hanabusa, T O'Leary, RC Gadwood. Synthesis and evaluation of a miniature organic model of chymotrypsin. Biochem Biophys Res Commun 129:727–732, 1985.
63. KR Rao, TN Srinivasan, N Bhanumathi, PB Sattur. Artificial enzymes: synthesis of imidazole substituted at C(2) of β-cyclodextrin as an efficient enzyme model of chymotrypsin. J Chem Soc Chem Commun 1990:10–11, 1990.
64. DP Riley. Functional mimics of superoxide dismutase enzymes as therapeutic agents. Chem Rev 99:2573–3587, 1999.
65. D Salvemini, S-Q Wang, JL Zweler, A Samouilov, H Macarthur, TP Misko, MG Currie, S Cuzzocrea, JA Sikorski, DP Riley. A nonpeptidyl mimic of superoxide dismutase with therapeutic activity in rats. Science 286:304–306, 1999.
66. Y Wang, JL DuBois, B Hedman, KO Hodgson, TDP Stack. Catalytic galactose oxidase models: biomimetic Cu(II)-phenoxyl-radical reactivity. Science 279:537–540, 1998.
67. A Tramontano, KD Janka, RA Lerner. Catalytic antibodies. Science 234:1566–1570, 1986.
68. SJ Pollack, JW Jacobs, PG Schultz. Selective chemical analysis by an antibody. Science 234:1570–1573, 1986.
69. J-B Charbonnier, E Carpenter, B Gigant, B Golinelli-Pimpaneau, Z Eshhar, BS Green, M Knossow. Crystal structure of the complex of a catalytic antibody Fab fragment with a transition state analog: structural similarities in esterase-like catalytic antibodies. Proc Natl Acad Sci USA 92:11721–11725, 1995.
70. O Kristensen, DG Vassylyev, F Tanaka, K Morikawa, I Fujii. A structural basis for transition-state stabilization in antibody-catalyzed hydrolysis: crystal structures of an abzyme at 1.8Å resolution. J Mol Biol 281:501–511, 1998.
71. J Gao, W Huang, G Wayne Zhou, RJ Fletterick, TS Scanlan. Mechanistically different catalytic antibodies obtained from immunization with a single transition-state analog. Proc Natl Acad Sci USA 92:1694–1698, 1995.
72. GJ Wedemayer, LH Wang, PA Patten, PG Schultz, RC Stevens. Crystal structures of the free and liganded forms of an esterolytic catalytic antibody. J Mol Biol 268:390–400, 1997.
73. JL Buchbinder, RC Stephenson, TS Scanlan, RJ Fletterick. A comparison of the crystallographic structures of two catalytic antibodies with esterase activity. J Mol Biol 282:1033–1041, 1998.
74. MM Thayer, EH Olender, AS Arvai, CM Koike, IL Canestrelli, JD Stewart, SJ Benkovic, ED Getzoff, VA Roberts. Structural basis for amide hydrolysis catalyzed by the 43C9 antibody. J Mol Biol 291:329–345, 1999.
75. N Takahashi, H Kakinuma, L Liu, Y Nishi, I Fujii. In vitro abzyme evolution to optimize antibody recognition for catalysis. Nat Biotechnol 19:563–567, 2001.
76. A Fribroulet, L Izadyar, B Avalle, A Roseto, D Thomas. Abzyme generation using an anti-idiotypic antibody as the "internal image" of an enzyme active site. Appl Biochem Biotechnol 47:229–239, 1994.
77. A Nisonoff. Idiotypes: concepts and applications. J Immunol 147:2429–2438, 1991.
78. BC Braden, BA Fields, X Ysern, W Dall'Acqua, FA Goldbaum, RJ Poljak, RA Mariuzza. Crystal structure of an Fv-Fv idiotope- anti-idiotope complex at 1.9 Å resolution. J Mol Biol 265:137–151, 1996.
79. K Mosbach, O Ramstrom. The emerging technique of molecular imprinting and its future impact on biotechnology. BioTechnology 14:163–170, 1996.
80. K Haupt, K Mosbach. Plastic antibodies: developments and applications. TIBTECH 16:468–475, 1998.
81. G Wulff, T Gross, R Schonfeld. Enzyme models based on molecularly imprinted polymers with strong esterase activity. Angew Chem Int Ed Engl 36:1962–1964, 1997.

27

Catalase

Dominic W. S. Wong
U.S. Department of Agriculture, Albany, California, U.S.A.
John R. Whitaker
University of California, Davis, Davis, California, U.S.A.

I. INTRODUCTION

A. Reactions Catalyzed: Behavioral Anomalies

Catalase (hydrogen peroxide : hydrogen peroxide oxidoreductase; EC 1.11.1.6) catalyzes two different reactions and shows unusual features kinetically (1, 2). The first and best-known reaction is the decomposition of H_2O_2 to give H_2O and O_2. This is called "catalatic activity" [Eq. (1)]. But catalase also oxidizes several H donors, such as methanol, ethanol, formic acid, and phenols with the consumption of 1 mole of hydrogen peroxide. This is called "peroxidatic-like" activity [Eq. (2)].

$$2H_2O_2 \xrightarrow{\text{catalase}} 2H_2O + O_2 \quad (1)$$

$$ROOH + AH_2 \xrightarrow{\text{catalase}} H_2O + ROH + A \quad (2)$$

Which reaction predominates depends on the concentration of H donor and the steady-state concentration of H_2O_2 in the system. In both reactions the active catalase-H_2O_2 compound I is formed first. The decomposition step of H_2O_2, in which H_2O_2 serves as H donor for compound I proceeds very rapidly ($k \sim 10^7\ M^{-1}\ sec^{-1}$), while peroxidatic-like reactions [Eq. (2)] proceed much slower ($k \sim 10^2$–$10^3\ M^{-1}\ sec^{-1}$) (3).

Another anomaly of catalase-catalyzed reactions is that catalase does not obey the expected order of reaction (Michaelis-Menten) shown by most enzymes. First, it is not possible to saturate the enzyme with substrate even as high as 5 M H_2O_2. Second, there is a rapid inactivation of catalase at H_2O_2 concentrations above 0.1 M, because the active enzyme-H_2O_2 compound I is converted to the inactive compounds II and III (Fig. 1) (4). Therefore, one cannot experimentally determine V_{max} by saturating catalase with H_2O_2. As a result, the reactions must be performed at ~ 10 mM H_2O_2 Successful and reproducible assays must be performed at catalase concentrations high enough so that the half-time ($t_{1/2}$) for decomposition of the H_2O_2 is 30 sec or less (4). Temperature changes have a low effect on rate of reaction ($Q_{10} = 1.05$–1.12; about the same effect as on diffusion rates). Therefore, the activation energy, E_a, for conversion of H_2O_2 to H_2O and O_2 is ~ 0.60–1.7 kcal mol^{-1}. Conversion of H_2O_2 to products initially (0–30 sec) follows a linear reaction (first order with respect to H_2O_2 concentration) between 0.01 and 0.05 M H_2O_2.

The rate constant (k) for the overall reaction is given by Eq. (3).

$$k = (2.3/\Delta t) \log[S_1]/[S_2]\ sec^{-1} \quad (3)$$

where $\Delta t = t_2 - t_1$ near the beginning of reaction (see above), $[S_1]$ and $[S_2]$ are H_2O_2 concentrations at t_1 and t_2, respectively. In studies with purified enzyme preparations the specific activity (k_1') is given by Eq. (4).

$$k_1' = k/[E]\ M^{-1}\ sec^{-1} \quad (4)$$

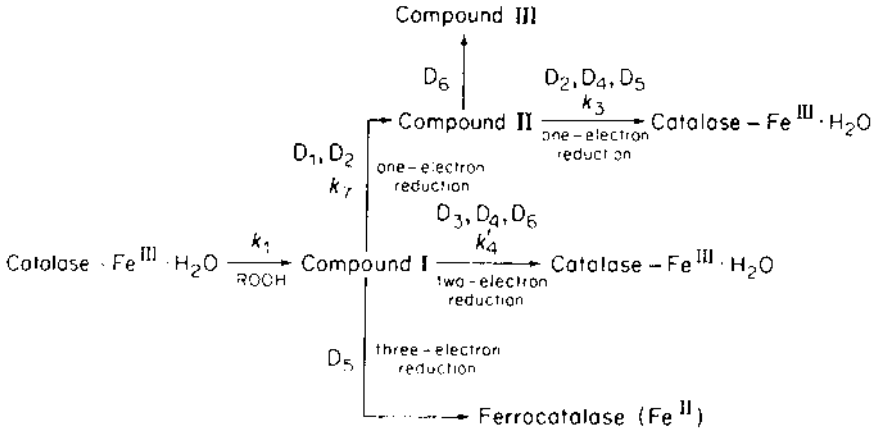

Figure 1 Reactions of catalase with hydrogen donors. The Ds refer to the donors: D_1 is ascorbate or ferrocyanide; D_2 is phenols; D_3 is alcohols or formic acid; D_4 is nitrite; D_5 is azide or hydroxamine; and D_6 is hydrogen peroxide. (From Ref. 4.)

The k_1' for pure catalase from human erythrocytes is $3.4 \times 10^7\ M^{-1}\ sec^{-1}$. This value permits estimation of the concentration of catalase in blood and tissues.

There are some problems in estimating the concentration of catalase because of molecular heterogeneity due to genetic origin (not all isozymes have the same specificity), conformational alterations due to -SH group oxidation or dissociation of the active tetramer (catalatic activity) into the dimer which has peroxidatic activity but not catalatic activity (6–8).

B. Historical Aspects

Catalase appears to be the first potential enzyme recorded (about 1812), based on the appearance of rapid bubble evolution when biological extracts were mixed with H_2O_2. The catalatic activity was regarded originally as an attribute of "protoplasm," a term shared with other general catalysts such as platinum. In 1901, Loew introduced the specific name "catalase" (9). But the true nature of catalase was overlooked by the more prevalent discussion of the actions of metals in biological oxidation. Wieland (10) considered the initial oxidation reaction to be the transfer of hydrogen to oxygen to form peroxide, and the role of the metal was to remove the peroxide so formed. Warburg (11) considered that hydrogen peroxide was not formed during biological oxidation, but that the iron of the cells activated O_2 to react directly with substrates. Therefore, he did not consider special catalatic or peroxidative roles for the heavy metals in contrast to Wieland (10). Hennichs in 1926 (12) also failed to recognize that the prosthetic group of catalase contains iron despite his partial purification of catalase. Willstätter (13) also doubted the function of iron in peroxidase.

In 1930, Zeile and Hellström (14) prepared purer catalase from liver and demonstrated the hematin nature of the prosthetic group. The analogies between catalase and other hematin compounds were soon recognized (15–17). Bray and Gorin (18) postulated the reaction with iron of the hematin prosthetic group was probably that shown in Eq. (5). This was the first formulation of a catalytic role for quadrivalent (ferryl) iron.

$$Fe^{2+} + H_2O_2 \rightarrow FeO^{2+} + H_2O \tag{5}$$

Earlier, Manchot and Lehmann (19) reported that a pentavalent iron (Fe_2O_5) could perform a catalatic reaction [Eq. (6)].

$$Fe_2O_5 + 2H_2O_2 + 2H^+ \rightarrow 2Fe(OH)_2 + 2O_2 + H_2O \tag{6}$$

But in enzymes, the theory of the enzyme-substrate complex formation was an alternate explanation to the free-radical hypothesis required by Eq. (6). Von Euler and Josephson's data (20) supported the idea that catalase formed a Michaelis complex with H_2O_2, with K_m of 0.025 M. Bonnichsen et al. (21) proved that the reaction velocity could be explained by the collision theory of reaction rates and strongly argued against the assumptions of chain mechanisms postulated earlier. At the same time Chance (22) discovered the primary compound ($FeOOH^{2+}$) formed between catalase and H_2O_2 (compound I; [Eq. (7)], which then reacts with a second H_2O_2 [Eq. (7)].

$$FeOH^{2+} + H_2O_2 \rightarrow FeOOH^{2+} + H_2O$$
$$FeOOH^{2+} + H_2O_2 \rightarrow FeOH^{2+} + H_2O + O_2 \quad (7)$$

Chance's demonstration of the similarity between the catalatic and peroxidatic behaviors of the catalase compound I required a reexamination of the hypothesis that the biological role of catalase is in fact a peroxidatic one (23).

II. IMPORTANCE OF CATALASE IN FOOD SCIENCE AND TECHNOLOGY

Catalase is widely distributed in nature. It is found in all aerobic microorganisms, and in all plant and animal cells. The catalase activity of mammalian cells varies. It is highest in liver and kidney and low in connective tissues. Catalase has been used in the food processing industry to determine the adequacy of blanching (70–105°C) of vegetables and fruits to destroy microorganisms and enzymes to preserve color, texture, flavor, taste, and aroma of the products when stored frozen up to 2 years. Early in the application of blanching for stabilization of frozen foods catalase was used especially for Birdseye peas (24–26), the best on the market. But catalase is much less heat stable than peroxidase (Fig. 2) (27), causing the U.S. Federal Drug Administration some concern about whether catalase was the best enzyme to use. In 1949, Joslyn (29), based on his research from 1933 to 1945, concluded that loss of peroxidase activity paralleled the loss of enzymes responsible for off-flavor development in blanched frozen foods more closely than the loss of catalase activity. Neither catalase nor peroxidase has been shown to be directly involved in quality deterioration of frozen blanched foods. But it is easy to determine their activities and demonstrate the conditions required to inactivate them in the blanching process.

In the dairy industry, catalase activity is a sensitive and easily detected indicator of contamination of milk by neutrophil granucytes. In biomedical research and medical clinics, catalase in liver, leukocytes, and erythrocytes has received substantial attention as to its role in oxidative metabolism and its protective role as a H_2O_2 scavenger. In maize genetics, investigation of catalase has been extensively studied in relation to human acatalasemia. Severe cases of acatalasemia in humans indicate that the catalase activity is near zero, raising the question of how such individuals deal with the metabolic destruction of H_2O_2. Catalase activity has been used as a diagnostic predictor in some haematological disorders and in determining urinary tract infections.

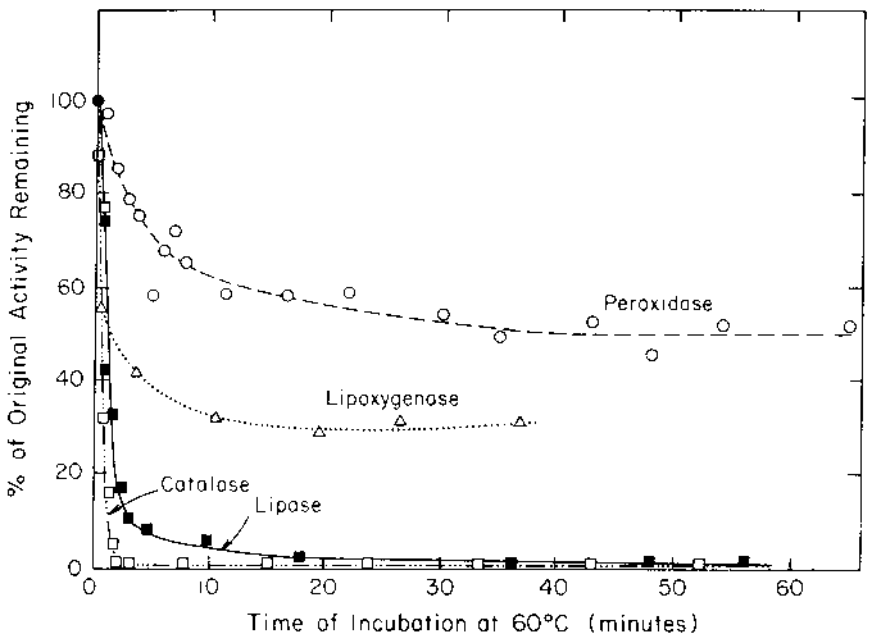

Figure 2 Rates of inactivation of catalase, peroxidase, lipoxygenase, and lipase in English green pea homogenates incubated at 60°C. (From Ref. 27.)

Following cold pasteurization of milk by H_2O_2, the residual H_2O_2 is removed by addition of catalase. Catalase has been widely used in removing O_2 from the head space of several foods, including dried egg powder, fruit juices, and wines, to prevent enzymatic browning by polyphenol oxidase. It is also used in analytical determinations of O_2 and H_2O_2 concentration in foods (30).

III. MOLECULAR STRUCTURE

A large number of amino acid sequences of catalases are known, primarily deduced from the gene sequences. These include (based on entries listed in Swiss-Prot): *Aspergillus fumigatus (Sartorya fumigata), A. niger, Arabidopsis thaliana* (mouse ear cress), *Bacillus subtilis, B. firmus, B. stearothermophilus, Bacteroides fragilis, Bordetella pertussis, Bos taurus* (bovine), *Botrytis cinerea (Botryotinia fuckeliana), Brucella abortus, Caenor habditis elegans, Campylobacter jejuni, Candida albicans, C. tropicalis, Cavia porcellus* (guinea pig), *Cucurbita pepo* (summer squash), *Deinococcus radiodurans, Desulfovibrio vulgaris* (strain Miyazaki), *Drosophila melanogaster* (fruit fly), *Emericella nidulans (Aspergillus nidulans), Glycine max* (soybean), *Gossypium hirsutum* (upland cotton), *Haemophilus influenzae, Helianthus annuus* (common sunflower), *Helicobacter pylori (Campylobacter pylon), Homo sapiens* (human), *Hordeum vulgare* (barley), *Ipomoea batatas* (sweet potato), *Lactobacillus sake, Listeria seeligeri, Lycopersicon esculentum* (tomato), *Micrococcus luteus (M. lysodeikticus), Mus musculus* (mouse), *Mycobacterium avium, M. bovis, M. intracellulare, M. tuberculosis, Neisseria gonorrhoeae, Nicotiana plumbaginifolia* (leadwort-leaved tobacco), *N. tabacum* (common tobacco), *Onchocerca volvulus endobacterium), Oryza sativa* (rice), *Penicillium janthinellum (P. vitale), Phaseolus aurens* (mung bean), *Pichia angusta (Hansenula polymorpha), Pisum sativum* (garden pea), *proteus mirabilis, Pseudomonas aeruginosa, Ps. putida, Ps. syringe, Rattus norvegicus* (rat), *Rhizobium meliloti (Sinorhizobium meliloti), Rhodobacter capsulatus (Rhodopseudomonas capsulata), Ricinus communis* (castor bean), *Saccharomyces cerevisiae), Salmonella typhimurium, Schizosaccharomyces pombe* (fission yeast), *Secale cereale* (rye), *Solanum melongena* (eggplant), *Solanum tuberosum* (potato), *Triticum aestivum* (wheat), *Vibrio fischeri*, and *Zea mays* (maize).

The primary structure of bovine liver catalase (BLC) subunit consists of 506 amino acid residues with a prosthetic group. In the homotetrameric molecule, the four Cys residues in each subunit do not form disulfides (31). BLC belongs to a family that may be referred to as true catalases (or heme catalases), corresponding to homotetrameric, heme-containing enzymes with an $\alpha + \beta$ fold, ubiquitously found in eukaryotes and also in many prokaryotes (32). These heme catalases have molecular weights (MW) in the range of 200–330 kDa. The other family of catalases consists of Mn-catalases that are nonheme hexameric enzymes with an all α-fold, and are present only in prokaryotes (33).

An interesting group of bifunctional catalase-peroxidases have been identified in *Escherichia coli, Mycobacterium tuberculosis*, and *Synechococcus* sp. These KatG enzymes are phylogenetically related to eukaryotic ascorbate peroxidases and yeast cytochrome peroxidase forming class I of the plant peroxidase superfamily (34). The *E. coli* KatG enzyme (or hydroperoxide I, or HPI) is a tetramer of 84-kDa subunits and 2 protoheme IX groups, with a primary structure of 726 amino acid residues (35).

E. coli also produces hydroperoxidase II (HPII) which has been characterized as a monofunctional catalase containing a modified heme imparting a characteristic green color to the protein (36). It is a tetramer of identical 84-kDa subunits, each encoded by the *katE* gene, with a predicted sequence of 753 amino acid residues (37). The Cys residues in HPII do not have a catalytic role. Moreover, the highly conserved Cys438 is blocked with a unique hemithioacetal structure originated from a pyruvate modification (38).

Crystal structures of several catalases have been elucidated, including bovine liver, human erythrocyte, *Penicillium vitale, E. coli, Proteus mirabilis,* and *Saccharomyces cerevisiae*. The beef liver catalase subunit consists of four domains: an N-terminal section of 70 residues forms an arm extending from the globulin region and intersects with the neighboring subunits; the second domain (residues 76–320) forms a β-barrel consisting of two topologically similar, four-stranded antiparallel sheets; the third domain (residues 321–436), also known as the wrapping domain, is a long stretch of polypeptide chain forming an outer layer; and the C-terminal domain (residues 437–506) consists of four α-helices on the external part of the molecule (32, 39–41) (Fig. 3A, B). In the tetrameric structure, most of the intersubunit interactions are confined to the N-terminal arm and the wrapping domain. The β-barrel and the C-terminal domain form a hydrophobic channel leading to the heme pocket which is ~ 20 Å below the surface. Heme protein interactions involve

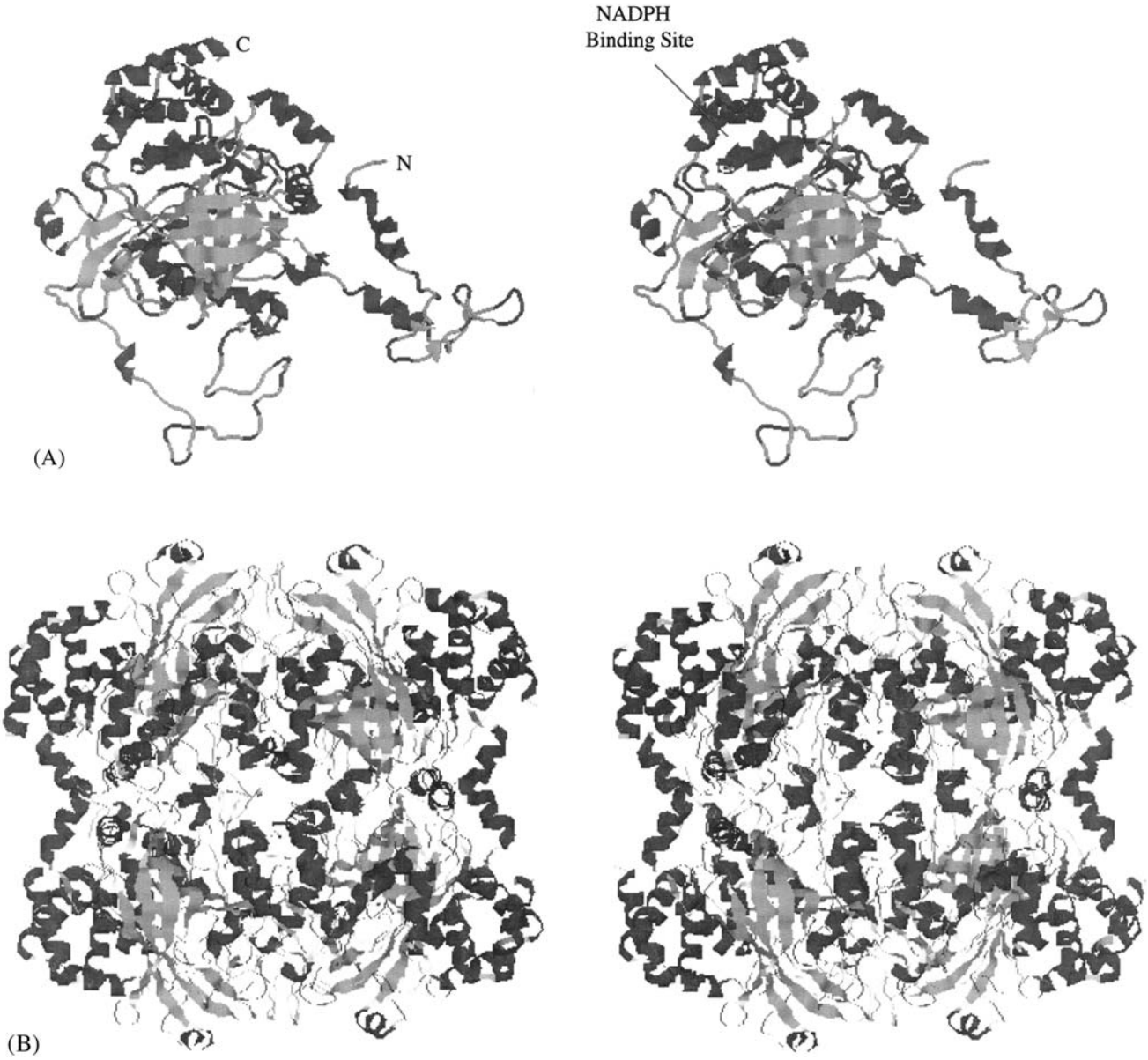

Figure 3 Stereo view of beef liver catalase (A) subunit (PDB id 7cat) and (B) tetramer (PDB id 4b1c).

mostly van der Waals contacts between the heme vinyl and methyl groups and nonpolar side chains, and a few charge interactions between the heme propionyl groups and Arg and carboxylic acid residues. At the proximal side of the heme, Tyr357 provides a protein ligand (as ligand 5) with the Fe-phenolic oxygen distance of 1.9 Å. Ionization of the Tyr-OH is assisted by interactions with the guanidinium group of Arg353. On the distal side of the heme are the essential His74 and Asn147, with their N_δ atoms at 4.3 Å and 6.2 Å from the heme iron, respectively. The ligand 6 site on the distal side of the heme is unoccupied.

The tetrameric enzyme from human and bovine contains four molecules of tightly bound NADPH located toward the carboxyl ends of α5 and α10 helices (42, 43). However, the binding of NADPH is not essential for activity, but may function to prevent the formation of compound II, an inactive intermediate in the catalatic cycle (see below). The binding site shows relative affinities in the order of: NADPH > NADH >

$NADP^+ > NAD^+$. The crystal structure of the fungal *Penicillium vitale* catalase is similar to that of the beef liver enzyme, except that there is an additional C-terminal flavodoxin-like domain (residues 520–670) (44, 45). This domain has an α/β structure with a central β-sheet of five parallel strands and four helices around it, with a topology similar to that of flavodoxin (46). *Escherichia coli* catalase HPII, encoded by the *katE* gene, shows a very close structural relationship with other catalases. It differs from BLC in that the C-terminal domain of ~ 150 residues is structurally flavodoxin-like (47). In addition, the N-terminal 60 amino acids increase the contact area between subunits. The crystal structures of *Proteus mirabilis* PR catalase and *Saccharomyces cervisiae* catalase-A show that the bound NADPH has the same conformation as in BLC, and lacks a C-terminal domain equivalent to that found in *Penicillium vitale* (48, 49).

Escherichia coli catalase HPII exhibits an unusual absorption spectrum distinctly different from that of other catalases containing heme *b* (protoporphyrin IX). The heme prosthetic group of HPII is an unusual green chromophore derived from a member of the family of *d*-type hemes, which is also found in *Penicillium vitale* catalase. The structure has been characterized as having a configuration of a *cis*-hydroxychloin γ-spirolactone at the saturated pyrrole ring III of the macrocycle in the C-6 position, which may arise from heme *b* by a self-catalyzed epoxide formation on ring III followed by hydrolysis to the *cis* diol (50–52).

IV. REACTION MECHANISM

The overall reaction catalyzed by catalases involves the conversion of two moles of H_2O_2 to yield water and oxygen as the final products. The substrate H_2O_2 participates in both oxidizing and reducing activities, with a two-electron transfer in each process.

Step. 1. Two-electron oxidation of native ferric enzyme to catalase compound I, with the substrate H_2O_2 reduced to H_2O:

$$\text{En-Fe(III)} + H_2O_2 \rightarrow \text{En-Fe(IV)} = O^+ + H_2O$$

Step 2. Two-electron reduction of compound I to native ferric enzyme, with a second molecule of H_2O_2 oxidized to O_2.

$$\text{En-Fe(IV)} = O^+ + H_2O_2 \rightarrow \text{En-Fe(III)} + O_2$$

A. Formation of Compound I

Compound I contains a π-cation radical of the heme structure of $[O = Fe(IV)porphyrin]^+$ similar to that of compound I formed by horseradish peroxidase (HRP) (53). The rate constant for the formation of compound I with H_2O_2 as substrate in the catalatic reaction is $6 \times 10^6\ M^{-1}\ sec^{-1}$ (54). Other hydroperoxide substrates, such as alkyl or acyl peroxides, can also be reduced to corresponding alcohols, albeit with much lower rate constants (Table 1).

Upon the binding of a peroxide molecule, two water molecules in the heme cavity are displaced for the substrate to form interactions with the enzyme. The peroxide α oxygen interacts with the heme Fe(III) via electrostatic interactions, and with His74-N_ϵ through hydrogen bonding (Fig. 4) (40). The net result is increasing acidity of the α-proton and the weakening of the peroxide O_α–H bond. The O_α–O_β bond is further polarized by the formation of hydrogen bonding between the β oxygen and Asn147. Finally, a charge-relay system formed between His74-N_δ and Ser113-O_γ, and the propionic carbonylic group of pyrrole III facilitates the transfer of the α-proton from O_α to O_β of the peroxide. The deprotonation of O_α in turn enhances the interaction between O_α and heme (Fe(III), delocalization of the negative charge on O_β, and development of a

Table 1 Rate Constants of Catalase in the Enzymatic Cycle

Substrate	Formation of Compound I k_1 (M^{-1} sec^{-1})	Substrate	Reduction of Compound I k_4 app (M^{-1} sec^{-1})
HOOH	6×10^6	HOH	1.8×10^7
CH_3OOH	8.5×10^5	CH_3OH	830
CH_3CH_2OOH	2×10^4	CH_3CH_2OH	1020
$CH_3(CH_2)_2OOH$	5.5×10^3	$CH_3(CH_2)_2OH$	6.5
$HOCH_2OOH$	3×10^4	$HOCH_2OH$	1200

Source: Ref. 54.

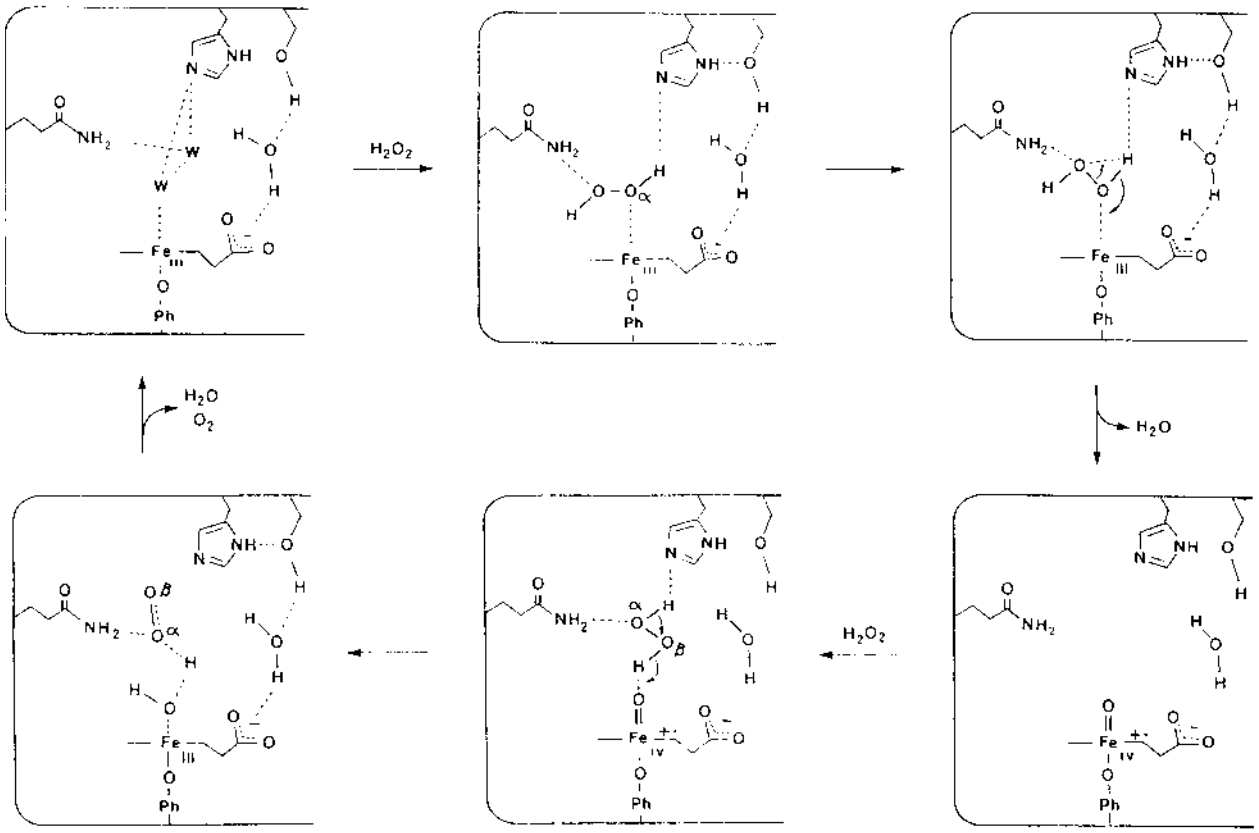

Figure 4 Reaction mechanism of catalase showing the formation and reduction of compound I. (From Ref. 70; adapted from Ref. 40.)

positive charge of the heme group, allowing the final transfer of the O_α to the heme iron.

B. Reduction of Compound I

In the second half of the cycle, catalase compound I reacts with a second molecules of H_2O_2 to yield the native enzyme with generation of O_2 and H_2O. However, compound I reacts poorly with other hydrogen donors, such as alcohol, hydroxylamine, or formic acid. Reduction of compound I occurs via a hydride transfer by abstracting the β-hydrogen by the heme ferryl oxygen (55). Deprotonation of the substrate's α-proton is unlikely to occur because the His74 is less nucleophilic as the heme in compound I is positively charged. The β-hydrogen abstraction is stereospecific for the pro-R hydrogen in the oxidation of ethanol substrate (56). A hydride transfer facilitates the development of a double-bond character at O_α–O_β, and the final transfer of the α proton to the heme ferryl oxygen (Fig. 2).

C. Formation of Compound II

Catalase can slowly form compound II by a two-step one-electron reduction of compound I under a steady low concentration of H_2O_2 or with other special substrates, such as ferrocyanide and ascorbate. Catalase compound II is an inactive form in the catalatic mode of the enzyme. This is in contrast to HRP compound II, which is an active species produced by two sequential one-electron reductions of compound I with most of its substrates. The difference in the reactivities of compound II species of catalase and HRP is probably due to protein control of the accessibility of substrates to the heme group (57). In addition, the phenoxylate oxygen of the proximal Tyr residue provides more electron density to the heme iron than the His residues of HRP, and favors a two-electron transfer instead of a sequential addition of electrons (58).

The slow inactivation of catalase by its own substrate can be prevented by experimentally limiting the exposure to H_2O_2, or reducing the concentration of compound I. However, the primary inhibition of the

formation of compound II is provided by the enzyme's cofactor, NADPH, which has been shown to prevent and reverse the process (59). It has been suggested that the initial formation of compound II involves a compound II radical intermediate, and NADPH reduces both the iron and the free radical by a two-electron transfer (60, 61).

V. MEASUREMENT OF CATALASE ACTIVITY

Catalase activity can be measured spectophotometrically, manometrically, polargraphically, and titrimetrically. The best methods are the spectrophotometric and titrimetric methods. They will be presented below.

A. Spectrophotometric Method (1, 2, 62)

Hydrogen peroxide has a molar extinction coefficient (ϵ_m) of $52\,M^{-1}\,cm^{-1}$ at 235 nm and its disappearance can be followed by continuous spectrophotometry when purified catalase preparations are used. As noted in paragraph 3 of Section I, 10 mM H_2O_2 should be used in the catalase assay so as to avoid formation of inactive compounds II and III. Therefore, the time zero absorbance reading will be 0.520. This method is the easiest to perform, is sensitive, and is the best when purified catalase is used.

1. Equipment Needed

UV spectrophotometer suitable for accurate measurements at 235 nm, connected to a high-speed recorder. Quartz cuvettes (10 mm light path).

2. Reagents and Solutions

a. Purity of Reagents. Glassware, buffer, and substrate should be free from heavy metals, as they will cause decomposition of H_2O_2. Potential problems caused by metal impurities can be determined by a control containing an equivalent volume of phosphate buffer, pH 7.0, in place of the enzyme.

b. Phosphate Buffer (50 mM, pH 7.0). (1) Dissolve 6.81 g KH_2PO_4 in water and make to 1 L. (2) Dissolve 8.90 g $Na_2HPO_4 \cdot 2\,H_2O$ in water and make to 1 L. Mix solutions (1) and (2) in the proportion of 1 : 1.5 (V/V), pH 7.0.

c. Hydrogen Peroxide (30 mM). Dilute 0.34 mL of 30% hydrogen peroxide (freshly opened) with phosphate buffer, pH 7.0 (above) to 100 mL. (Smaller volumes of reagents can be prepared by keeping the concentrations constant as given.)

d. Sample of Catalase. Prepared in the 50 mM, pH 7.0, phosphate buffer.

3. Stability of Solutions

The phosphate buffers are stable as long as bacterial contamination is avoided; store at 2°C. Prepare the buffered H_2O_2 solution fresh each day.

4. Reaction

a. Blank. Place 1.00 mL of 50 mM phosphate buffer into a quartz cuvette. Add 2.00 mL catalase sample.

b. Catalase Reaction. Place 2.00 mL catalase sample into a quartz cuvette. Add 1.00 mL of H_2O_2 solution (above). Mix rapidly ($\sim$ 5 sec) with a plastic paddle or by inversion three times using parafilm.

c. Place in Spectrophotometer. Record continuously for 30–60 sec. If a recorder is not available, take readings at 5- to 10-sec intervals. The temperature should be at 20–25°C. ΔAbs/15 sec should be no larger than 0.100 and not smaller than 0.020. If necessary, adjust concentration of enzyme solution to be within these limits and repeat the experiment.

5. Calculation of Results

As noted earlier in Section I.A, the reaction approximates a first-order reaction. Therefore, the following relations can be used for a 15-sec or other interval of reaction time.

$$\begin{aligned} k &= (2.3/15\,\text{sec})\log(A_1/A_2) \\ &= 0.153\log\,(A_1/A_2)\,\text{sec}^{-1} \end{aligned} \tag{8}$$

To calculate the catalytic concentration b of the sample (k/L) or catalytic content Z_c/m_s of the sample (unit k/g Hb) use:

$$\mathrm{b} = (\mathrm{V/v})(2.3/15)\log(\mathrm{A_1/A_2})\ k/L \tag{9}$$

$$\begin{aligned} \mathrm{b} &= (3/2)(2.3/15)\log(\mathrm{A_1/A_2})\ k/\mathrm{L} \\ &= 0.23\log(\mathrm{A_1/A_2})\ k/L \end{aligned} \tag{10}$$

where A_1 is A_{235} at time = 0; A_2 is A_{235} at $t = 15$ sec; V is total assay volume; v is enzyme sample volume in the assay mixture. The 3/2 is total reaction volume/enzyme sample volume (see Sec. V.4 above).

$$Z_c/m_s = (2.3\alpha/15\,\text{Hb}) \log (A_1/A_2)$$
$$= 0.153 \log (A_1/A_2)\,\text{sec}^{-1} \times \text{g Hb}\ (Z_c/\text{g Hb}) \quad (11)$$

where α is the quotient of weight concentration of hemoglobin (Hb; unit g/L) in blood or erythrocyte sediment, and in the cuvette.

For a difference in absorbance of 0.450 (t_0) − 0.400 (t_{15} sec) log (A_1/A_2) = 0.05115, the following relationship holds:

$$k = (2.3/\Delta t) \log (A_1/A_2) = (0.1175/\Delta t)\,\text{sec}^{-1} \quad (12)$$

6. Precision, Accuracy, and Sensitivity

With values around 300 k/g Hb, a precision of $\pm 10\,k$/g Hb was found. The coefficient of variation is 2–3%.

7. Detection Limits

The limits of this method are set by the turbidity (of tissue homogenates) or by the hemoglobin content (of the hemolysate). Whenever low catalase activity of a sample does not permit dilution of at least 1 : 100 (i.e., activity in blood is < 20 k/g Hb), use of the alternative titration technique (below) is recommended.

B. Titrimetric Method (62)

1. Method Design

The conversion of H_2O_2 to products is measured by determining the H_2O_2 left in the reaction after a certain time by back-titration with permanganate. Portions of the assay mixture are taken after 0, 10, 20, and 30 sec, and reactions are stopped immediately by addition of 1 M H_2SO_4.

2. Optimized Conditions for Measurement

See spectrophotometric method above (Sec. V.A). Titrimetric methods with incubation times > 30 sec give only comparative values. Preparation of rate curves require time and effort, with a large series of measurements. Perborate, a stabler substrate than H_2O_2, is best for routine studies. The inactivation of the enzyme is somewhat slower than with H_2O_2. The results obtained with H_2O_2 and perborate are of the same order of magnitude. The method of Feinstein (63) is suitable, insofar as the assay conditions are modified according to the recommended procedure of Bonnichsen (64) (i.e., 30 sec incubation time at pH 7.0 and 20°C).

3. Equipment

Thermostatic water bath (20°C) with rotating shaking attachment.

4. Reagents and Solutions

a. Purity of Reagents. See remarks in Section V.A.3 under spectrophotometric method.

b. Preparation of Solutions. Use repurified water.

Phosphate buffer (50 mM, pH 7.0). See Section V.A.2.b under spectrophotometric method.

Sodium perborate (100 mM, pH 7.0). Dissolve 7.694 g $NaBO_3 \cdot 4\ H_2O$ n ca. 20 ml of 2.4 M HCl, add ca. 400 ml of water, adjust pH to 7.0 with additional 2.4 M HCl and make to 500 ml with water.

Potassium permanganate (0.01 M). Dissolve 1.58 g $KMnO_4$ in water and make 1 liter.

Stability of solutions. The phosphate buffer is stable as long as bacterial contamination is avoided; store at 2°C. The perborate solution is stable for several days at 2°C; check titer with permanganate in each series of measurements.

5. Procedure

a. Assay Conditions. Incubation at 20°C; final reaction volume 5.00 mL.

b. Measurement. The blank contains 1.00 mL phosphate buffer and 3.00 mL perborate solution. After preincubation for 10 min at 20°C, add 1.00 mL water; mix. Stop the reaction after 30 sec by addition of 3.00 mL of 1 M H_2SO_4. Mix.

The sample contains 1.00 mL phosphate buffer and 3.00 mL of perborate solution. After preincubation at 20°C for 10 min, 1.00 mL catalase solution is added; mixed. Stop the reaction after 30 sec by adding 3.00 mL of 1 M H_2SO_4. Mix.

The remaining perborate in the blank and sample is determined by titrating with permanganate solution.

To construct a rate curve, prepare several assay mixtures and stop the reactions at 10, 20, and 30 sec, respectively. The concentration of the enzyme solution should be such that after 30 sec not > 50% and not < 10% of the perborate is converted to product. If the catalase activity in the sample is low, the incubation time should be increased to 1 min, or even to 5 min.

6. Calculations

The rate constant (k) for the overall reaction is given by:

$$k = (2.3/\Delta t) \log \frac{\text{titration vol for blank}}{\text{titration vol for sample}} \text{ sec}^{-1} \quad (13)$$

The specific activity (k_1') is obtained by dividing k by the molar concentration of enzyme [E].

$$k_1' = k/[E]\ M^{-1}\ \text{sec}^{-1} \quad (14)$$

Owing to the progressive inactivation of the catalase the calculated k values for the various time intervals must be plotted and extrapolated to $t = 0$. The values obtained in this way for the rate constant k are somewhat lower than nonextrapolated values.

For comparative purposes the results can also be expressed in arbitrarily defined "units"—e.g., the number of millimoles of perborate decomposed under the standard experimental conditions related to mg wet weight of tissue (or g hemoglobin, etc.) ("perborate units") (62, 63).

7. Validation of Method

According to the type of sample, the relative standard deviation is 3–5%. The source of errors includes the titration of concentrated homogenates or blood samples (because of their low catalase activity). The endpoint is not sharp since the protein in the sample slowly reacts with permanganate. If the titration is carried out rapidly and always to the same endpoint (relative excess of $KMnO_4$), the resulting error is small. A correction can be applied by titration of an additional control mixture containing no perborate or by deproteinization of the incubation reaction mixture with trichloroacetic acid. Oxidizable compounds (e.g., Tris) must not be used as components of buffers if catalase activity is determined by the titrimetric method.

VI. PURIFICATION OF CATALASE

As reported in Section III, the amino acid sequence has been determined for 63 catalases, largely by gene sequencing. Individual researchers have developed their own methods for purification. In Methods in Enzymology, Vol II, 1955, detailed methods are given for purifying catalase from beef liver (65, 66), horse and pig blood (64), bacteria [*Micrococcus lysodeikticus* (67), and spinach leaves (68).

The purification procedure for spinach leaf catalase will be described here, as being more appropriate for food enzymology (69). Freshly harvested spinach leaves are washed in tap water and stored in a cold room at 2–4°C. The leaves are transferred to large stainless steel vats, covered with commercial acetone previously chilled to −15°C, and let sit for at least 2 h at this temperature. The cold, partially dehydrated leaves are very brittle and are easily reduced to small pieces with a large Waring-type blender. The blending is complete in 30–60 sec and the slurry is gravity-filtered in the cold; the filtrate is discarded. The residue is washed several times with portions of cold acetone (−4°C), and the resulting gray-green material is dried overnight in a ventilated hood.

The acetone powder is extracted repeatedly with ice-cold 0.1 M Na_2HPO_4, yielding a filtrate of Kat.f. ~ 50 and an inactive residue, which is discarded. The filtrate is half-saturated with solid $(NH_4)_2SO_4$ and left overnight in the cold room (4°C). The precipitate, obtained by centrifugation at 0°C and containing all the activity, is redissolved in a small volume of 0.1 M Na_2HPO_4. This preparation, after clarification by filtration or centrifugation, has a Kat.f. of ~ 180. Three successive fractionations with 20%, 7%, and 20% saturated $(NH_4)_2SO_4$ are carried out, the precipitates being saved in each instance. The product has a Kat.f. of ~ 920, shows a faint absorption band at 630 nm, and gives absorption peaks at 275, 330, 405, and 625 nm in a Beckman spectrophotometer.

The catalase solution is adjusted to pH 6.5 and made 0.1 M with respect to Na acetate by addition of the solid salt. Cautious fractionation with saturated $(NH_4)_2SO_4$, also adjusted to pH 6.5, yields several precipitates varying in Kat.f. from 1200 to 10,000. The most active preparations are dialyzed for 2 days in the cold against pH 7.14 phosphate buffer of ionic strength 0.1 and then subjected to preparative free boundary electrophoresis (18 mA, 330 volts, 4 h), yielding five fractions—three on the anodic side, one in the bottom cell, and one from the cathodic side. (Note: polyacrylamide gel electrophoresis should be used today.) The Kat.f. and spectrophotometric data for these fractions, as well as Kat.f.'s and all the other fractions in the preparatory scheme, are shown in Table 2.

The cathodic fraction of Kat.f. 23,600 gives needle-like crystals after concentration, dialysis against 0.1 M Na_2HPO_4, and addition of solid $(NH_4)_2SO)4$ to ~ 12% saturation. These needles, when redissolved in

Table 2 Kat.f. Values and Spectrophotometric Characteristics of Various Fractions of the Spinach Leaf Catalase Preparation

Fraction	Kat.f.[a,b]	$\frac{E_{280\ nm}}{E_{405\ nm}}$
1. Na_2HPO_4 extract of acetone powder	50	—
2. Ppt. of Fraction 1 insol. in 50% satd. $(NH_4)_2SO_4$ redissolved in 0.1 M Na_2HPO_4	180	—
3. Ppt. of Fraction 2 insol. in 20% satd. $(NH_4)_2SO_4$ redissolved in 0.1 M Na_2HPO_4, sol. in 7% satd. $(NH_4)_2SO_4$	425	—
4. Ppt of Fraction 3 insol. in 20% satd. $(NH_4)_2SO_4$ redissolved in 0.1 M Na_2HPO_4	920	—
5. Ppts. obtained from adjusting Fraction 4 to pH 6.5, making 0.1 M with respect to Na acetate, then cautiously fractionating with solid $(NH_4)_2SO_4$	10,100	—
6. Electrophoretic fractions of redissolved Fraction 5		
Cathodic	23,600	1.54
Bottom cell	9,020	2.07
Anodic No. 2	12,100	2.07
Anodic No. 1	7,320	2.37
Anodic (top cell)	2,620	2.54

[a] $k = 1/t \log_{10}\ A_0/(A_0 - x)$, where k = 1st-order rate constant, t = time in min, A_0 = mL permanganate used at zero time and $A_0 - x$ = mL permanganate used at 3, 6, 9, and 12 min, respectively.
[b] Purity (Katalasefähigkeit) determined as Kat.f. = k/g catalase/mL.
Source: Ref. 69.

0.1 M Na_2HPO_4, give a good catalase absorption spectrum (Fig. 5).

The catalase prepared by the above method contained 0.049% iron, approximately half the value for a pure 4-hematin catalase. The prosthetic group is protohematin, as shown by preparation of a typical pyridine hemochromogen in the acetone-HCl supernatant of an aliquot of the enzyme.

The enzyme is inhibited by KCN and NaN_3, 50% inhibition being produced by 5×10^{-6} M KCN and 2×10^{-5} NaN_3; Na diethyldithiocarbamate does not affect activity.

The enzyme is completely inactivated in 10 min when incubated at 60°C but is indefinitely stable at 1° C between pH 5.3 and 8.9. The activity is optimal between pH 5.3 and 8.0, but decreases rapidly at more acid values and slowly at more alkaline values.

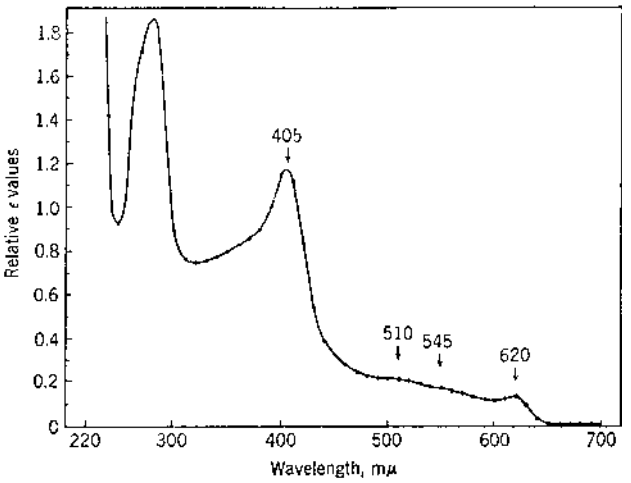

Figure 5 Absorption spectrum of electrophoretically prepared spinach leaf catalase. Kat.f. = 23,600. Concentration of the enzyme was ~ 0.5 mg/mL. (From Ref. 69.)

REFERENCES

1. B Chance, D Herbert. The enzyme-substrate compounds of bacterial catalase and peroxidases. Biochem J 46:402–414, 1950.
2. AC Maehly, B Chance. The assay of catalases and peroxidases. In: D Glick, ed. Methods of Biochemical Analysis, Vol 1. New York: Interscience Publishers, 1954, pp 357–424.
3. B Chance. An intermediate compound in the catalase-hydrogen peroxide reaction. Acta Chem Scand 1:236–267, 1947.
4. D Keilin, P Nicholls. Reactions of catalase with hydrogen peroxide and hydrogen donors. Biochim Biophys Acta 29:302–307, 1958.
5. RK Bonichsen, B. Chance, H Theorell. Catalase activity. Acta Chem Scand 1:685–709, 1947.
6. H Aebi. Erythrocytic catalase. Exposés Annu Biochim Med (Paris) 29:139–166, 1969.
7. B Scherz, EJ Kuchinskas, SR Wyss, H Aebi. Heterogeneity of erythrocyte catalase: dissociation, recombination and hybridization of human erythrocyte catalases. Eur J Biochem 69:603–613, 1976.
8. H Aebi, SR Wyss, B Scherz. Heterogeneity of human erythrocyte catalase. In: CL Market, ed. Isozymes. Proc 3rd International Conference on Isozymes. New York: Academic Press, 1975, pp 227–244.
9. O Loew. A new enzyme of general occurrence in organisms. A preliminary note. Science 11:701–702, 1900; A new enzyme of general occurrence in organisms. US Dept Agr Rep 68:47, 1901.
10. H Wieland. On the Mechanism of Oxidation. Silliman Lectures. New Haven, CT: Yale University Press, 1932.

11. O Warburg. Heavy Metal Prosthetic Groups and Enzyme Action. New York: Oxford University Press, 1949.
12. S Hennichs. Activity and iron content of highly active catalase preparations. Ber 59B:218–225, 1926.
13. R Willstätter. The isolation of enzymes. Ber 55B:3601–3623, 1922.
14. K Zeile, H Hellström. The active site of liver catalase. Z Physiol Chem 192:171–192, 1930.
15. D Keilin, EF Hartree. Inhibitors of catalase reaction. Nature 134:933–934, 1934.
16. D Keilin, EF Hartree. Mechanism of the decomposition of hydrogen peroxide by catalase. Proc R Soc B124:397–405, 1938.
17. J Weiss. Reaction mechanism of the enzymes catalase and peroxidase in the light of the theory of chain reactions. J Phys Chem 41:1107–1116, 1937.
18. WC Bray, MH Gorin. Ferry ion, a compound of quadrivalent iron. J Am Chem Soc 54:2124–2125, 1932.
19. W Manchot, G Lehmann. The action of hydrogen peroxide on ferrous salts. (Studies on oxidation processes.) Ann 460:179–201, 1928.
20. H von Euler, K Josephson. Catalase II. Ann 455:1–16, 1927.
21. RK Bonnichsen, B Chance, H Theorell. Catalase activity. Acta Chem Scand 1:685–708, 1947.
22. B Chance. An intermediate compound in the catalase-hydrogen peroxide reaction. Acta Chem Scand 1:236–267, 1947.
23. D Keilin, EF Hartree. Properties of catalase. Catalysis of coupled oxidation of alcohols. Biochem J 39:293–301, 1945.
24. HC Diehl. A physiological view of freezing preservation. Indust Eng Chem 24:661–665, 1932.
25. HC Diehl, JH Dingle, JA Berry. Enzymes can cause off-flavors even when foods are frozen. Food Indust 5:300–301, 1933.
26. HC Diehl, H Campbell, JA Berry. Freezing of Alderman peas. Food Res 1:61–71, 1936.
27. DC Williams, MH Lim, AO Chen, RM Pangborn, JR Whitaker. Blanching of vegetables for freezing: which indicator enzyme to choose. Food Technol 40:130–140, 1986.
28. JR Whitaker. Enzymes. In: OR Fennema, ed. Food Chemistry, 3rd ed. New York: Marcel Dekker, 1996, pp 431–530.
29. MA Joslyn. Enzyme activity in frozen vegetable tissue. Adv Enzymol 9:613–652, 1949.
30. JR Whitaker. Analytical uses of enzymes. In: DW Gruenwedel, JR Whitaker, eds. Food Analysis: Principles and Techniques. Vol 3, Biological Techniques. New York: Marcel Dekker, 1984, pp 297–377.
31. WA Schroeder, JR Shelton, JB Shelton, B Robertson, G Apell, RS Fang, JB Ventura. The complete amino acid sequence of bovine liver catalase and the partial sequence of bovine erythrocyte catalase. Arch Biochem Biophys 214:397–421, 1982.
32. TJ Reid II, MRN Murthy, A Sicignano, N Tanaka, WDL Musick, MG Rossmann. Structure and heme environment of beef liver catalase at 2.5 Å resolution. Proc Natl Acad Sci US 78:4767–4771, 1981.
33. SV Khangulov, VV Barynin, NV Voevodskaya, AI Grebenko. ESR spectroscopy of the binuclear cluster of manganase ions in the active center of Mn-catalase from *Thermus thermophilus*. Biochim Biophys Acta 1020:305–310, 1990.
34. M Zamocky, G Regelsberger, C Jakopitsch, C Obinger. The molecular peculiarities of catalase-peroxidases. FEBS Lett 492:177–182, 2001.
35. BL Triggs-Raine, BW Doble, MR Mulvey, PA Sorby, PC Loewen. Nucleotide sequence of *katG*, encoding catalase HPI of *Escherichia coli*. J Bacteriol 170:4415–4419, 1988.
36. P Lowen,J Switala. Purification and characterization of catalase HPII from *Escherichia coli* K12. Cell Biol 64:638–646, 1986.
37. I von Ossowski, MR Mulvey, PA Leco, A Borys, PC Loewen. Nucleotide sequence of *Escherichia coli katE*, which encodes catalase HPII. J Bacteriol 173:514–520, 1991.
38. MS Sevinc, W Ens, PC Loewen. The cysteines of catalase HPII of *Escherichia coli*, including Cys438 which is blocked, do not have a catalytic role. Eur J Biochem 230:127–132, 1995.
39. MRN Murphy, TJ Reid II, A Sicignano, N Tanaka, MG Rosmann. Structure of beef liver catalase. J Mol Biol 152:465–499, 1981.
40. I Fita, MG Rossmann. The active center of catalase. J Mol Biol 185:21–37, 1985.
41. I Fita, AM Silva, MRN Murphy, MG Rossmann. The refined structure of beef liver catalase at 2–5 Å resolution. Acta Cryst B42:497–515, 1986.
42. HN Kirkman, GF Gaetani. Catalase: a tetrameric enzyme with four tightly bound molecules of NADPH. Proc Natl Acad Sci USA 81:4343–4347, 1984.
43. I Fita, MG Rossmann. The NADPH binding site on beef liver catalase. Proc Natl Acad Sci USA 82:1604–1608, 1985.
44. BK Vainshtein, WR Melik-Adamyan, VV Barynin, AA Vagin, AI Grebenko. Three-dimensional structure of the enzyme catalase. Nature 293:411–412, 1981.
45. WR Melik-Adamyan, VV Barynin, AA Vagin, VV Borisov, BK Vainshtein. Comparison of beef liver and *Penicillium vitale* catalases. J Mol Biol 188:63–72, 1986.
46. BK Vainshtein, WR Melik-Adamyan, VV Barynin, AA Vagin, AI Grebenko, VV Borisov. Three-dimensional structure of catalase from *Penicillium vitale* at 2.0 Å resolution. J Mol Biol 188:49–61, 1986.

47. J Switala, PC Loewen, I Fita. Crystal structure of catalase HPII from *Escherichia coli*. Structure 3:491–502, 1995.
48. P Gouet, H-M Jouve, O Dideberg. Crystal structure of *Proteus mirabilis* PR catalase with and without bound NADPH. J Mol Biol 249:933–954, 1995.
49. MJ Mate, M Zamocky, LM Nykyri, C Herzog, PM Alzari, C Betzel, F Koller, I Fita. Structure of catalase-A from *Saccharomyces cerevisiae*. J Mol Biol 268:135–149, 1999.
50. JT Chiu, PC Loewen, J Switala, RB Gennis, R Timkovich. Proposed structure for the prosthetic group of the catalase HPII from *Escherichia coli*. J Am Chem Soc 111:7046–7050, 1989.
51. R Timkovich, LL Bondoc. Diversity in the structure of hemes. Adv Biophys Chem 1:203–247, 1990.
52. GN Murshudov, AI Grebenko, V Barynin, Z Dauter, KS Wilson, BK Vainshtein, W Melik-Adamyan, J Bravo, JM Ferran, JC Ferrer, J Switala, PC Loewen, I Fita. Structure of the heme *d* of *Penicillium vitale* and *Escherchia coli* catalases. J Biol Chem 271:8863–8868, 1996.
53. D Dolphin, A Forman, DC Borg, J Fajer, RH Felton. Compounds I of catalase and horse radish peroxidase: π-Cation radicals. Proc Natl Acad Sci USA 68:614–618, 1971.
54. CR Schonbaum, B Chance. Catalase. Enzymes 7:363–408, 1976.
55. AL Dounce. A proposed mechanism for the catalatic action of catalase. J Theor Biol 105:553–567, 1983.
56. RJM Corrall, HM Rodman, J Margolis, BR Landau. Stereospecificity of oxidation of ethanol by catalase. J Biol Chem 249:3181–3182, 1974.
57. W-J Chuang, J Heldt, HE van Wart. Resonance raman spectra of bovine liver catalase compound II. J Biol Chem 264:14209–14215, 1989.
58. B Chance, L Powers, Y Ching, T Poulos,GR Schonbaum, I Yamazaki, KG Paul. X-ray absorption studies of intermediates in peroxidase activity. Arch Biochem Biophys 235:596–611, 1984.
59. HN Kirkman, S Galiano, GF Gaetani. The function of catalase-bound NADPH. J Biol Chem 262:660–666, 1987.
60. A Hillar, P Nicholls. A mechanism for NADPH inhibition of catalase compound II formation. FEBS Lett 314:179–182, 1992.
61. DJ Bicout, MJ Field, P Gouet, HM Jouve. Simulations of electron transfer in the NADPH-bound catalase from *proteus mirabilis* PR. Biochim Biophys Acta 1252:172–176, 1995.
62. HU Bergmeyer. Methods of Enzymatic Analysis, 3rd ed. Enzymes 1: Oxidoreductases, Transferases, Vol III. Weinheim: Verlag Chemie GmbH, 1983, pp 277–285.
63. RN Feinstein. Perborate as substrate in a new assay of catalase. J Biol Chem 180:1197–1202, 1949.
64. RK Boonichsen. Blood catalase. In: SP Colowick, NO Kaplan, eds. Methods in Enzymology, Vol II. New York: Academic Press, 1955, pp 781–784.
65. JB Sumner, AL Dounce. Liver catalase. In: SP Colowick, NO Kaplan, eds. Methods in Enzymology, Vol II. New York: Academic Press, 1955, pp 775–781.
66. NK Sarkar, JB Sumner. Isolation, estimation, chemical nature and classification of catalases. Enzymology 14:280–283, 1951.
67. D Herbert. Catalase from bacteria. In: SP Colowick, NO Kaplan, eds Methodsin Enzymology, Vol II. New York: Academic Press, 1955, pp 784–788.
68. AW Galston. Plant catalase. In: SP Colowick, NO Kaplan, eds. Methods in Enzymology, Vol II. New York: Academic Press, 1955, pp 789–791.
69. AW Galston, RK Bonnichsen, DI Arnon. Preparation of highly purified spinach leaf catalase. Acta Chem Scand 5:781–790, 1951.
70. DWS Wong. Food Enzymes: Structure and Mechanism. Chapman & Hall, New York, 1995, p. 352.

28

Horseradish Peroxidase

Zhong Yi Yuan and Tai Jiao Jiang
Institute of Biochemistry and Cell Biology, Chinese Academy of Sciences, Shanghai, China

I. INTRODUCTION

Horseradish peroxidase (HRP; donor:hydrogen-peroxide oxidoreductase; EC 1.11.1.7) catalyzes the reaction:

$$\text{Donor} + H_2O_2 \rightarrow \text{oxidized donor} + 2H_2O \quad (1)$$

The enzyme utilizes hydrogen peroxide, some organic peroxides, or peroxy acids of the general formula ROOH as hydrogen acceptors to catalyze the oxidation of a variety of organic and inorganic hydrogen donors, such as phenols, aromatic amines, and others.

Horseradish peroxidase occupies an important position in the history of enzymology. Because of its stability and availability, the purified enzyme is often used as a typical model for the family of peroxidases. Since the 1950s, research on the reaction mechanism, structure, and function of this enzyme has drawn much attention (1–6). The practical applications of HRP in clinical, food, and industrial analyses (ELISA, etc.) (7–9) and catalysis in nonaqueous media (producing pharmaceuticals, synthesizing polymers, etc.) (10, 11) have been exploited. Horseradish peroxidases are glycoproteins, containing one polypeptide chain, one protoporphyrin IX as prosthetic group, three to eight carbohydrate chains, and two Ca^{2+} (1, 12).

II. OCCURRENCE AND PHYSIOLOGY FUNCTION

Peroxidases are widely distributed in the leaf, stem, and root of horseradish (*Armoracia rusticana, A. lapthifola, Cochlearia armracia* L., etc.); the highest activity is in the roots. The content of peroxidase not only varies with location but also with maturity and season. However, little is known about its cellular location, microenvironment, or specific participation of HRP in physiological pathways. Plant peroxidases play very important physiological roles:

1. Degrading and synthesizing lignin in cell wall damage and repair. It is also important in the elongation of plants (13).
2. Providing defense against pathogens and stress (14).
3. Catalyzing the catabolism of phyto-growth hormones, e.g., indole acetic acid (IAA) and auxin to regulate plant growth (15).
4. Controlling respiration (16).
5. Promoting formation of highly reactive species, i.e., free radicals and electronically excited states. These species may participate in cell damage or be of benefit against pathogens (17).
6. Catalyzing removal of hydrogen peroxide (18).

III. PEROXIDASE FAMILIES AND SUPERFAMILIES

Besides being found in horseradish, peroxidases are found also in other plants, microorganisms, and animals including humans. On the basis of sequence homologies, Welinder (3) proposed classification of peroxidases by families and superfamilies as shown in Table 1.

Table 1 Superfamilies and Families of Peroxidases

Superfamily	Family
Plant peroxidase	(a) Peroxidases of prokaryotic origin: yeast cytochrome C peroxidase, chloroplast and cytosolic ascorbate peroxidases, gene duplicated bacterial peroxidases. (b) Secreted fungal peroxidases: lignin peroxidase (*Phanechaete chryosporium*), manganase peroxidase (*P. chrysoporium*), ink cap mushroom peroxidase (*Coprinus sinereus*), chloroperoxidase (*Caldariomyces fumago*), cytochrome C peroxidase (*Pseudomonas aeruginosa*). (c) Classical plant peroxidases: HRP isoenzyme C is the most intensively studied.
Animal peroxidases	Myeloperoxidase, verdoperoxidase, eosinophil peroxidase, prostaglandin H synthase, glutathione peroxidase, lactoperoxidase, thyroid peroxidase.
Catalases	They are found in plants and animals. These are tetrameric proteins.

IV. PROPERTIES AS PROTEINS

A. HRP Isoenzymes

Over 40 isoenzymes of peroxidase have been found in the horseradish plant. By cloning techniques, some of the isoenzymes come from different genes and others may be produced by posttranslational modification, especially by degree of glycosylation. There are differences in amino acid composition and sequences among the isoenzymes (19). Based on the isoelectric points, the isoenzymes can be classified as shown in Table 2 (20).

Table 2 Horseradish Peroxidase Isoenzymes

FORM	pI	pH_{opt}	Carbohydrate (%)
HRP-A	4	Acid	Higher
HRP-B, -C	5.75, 9.63	Neutral[a], slightly alkaline	Low
HRP-D, -E	10.6, > 12	Strongly alkaline	Low

[a]Neutral HRP-C is the main isoenzyme in the plant.

B. Primary, Secondary, and Tertiary Structures of HRP

Determination of the complete amino acid sequence of HRP-C was largely contributed by Welinder (21). HRP-C consists of 308 amino acid residues, a hemin group, and eight neutral carbohydrate side chains attached to asparagine residues. The amino acid sequence and carbohydrate attachment points are shown in Figure 1. The molecular weight was reported to be between 40,000 and 45,000, and the carbohydrate moiety constitutes ~ 18%. HRP-C is the most extensively investigated isoenzyme in the plant peroxidase superfamily. Within the superfamily, HRP-C belongs to Class III of the plant extracellular peroxidases (22). Peroxidases from flowering plants have considerable identity of amino acid sequences (40–64%). In particular, those sequences in the regions of the two His residues (the distal His42 and proximal His170 in HRP) and Cys residues forming disulfide bonds are conserved (12, 22).

Gajhede et al. (23) published a 2.15 Å resolution structure of HRP-C, which gave complete information on overall structure and its comparison to other peroxidases. HRP-C has the same overall fold typical of the peroxidase superfamily, with the secondary structure elements (especially the 10 prominent helices A–J), heme group, and calcium-binding sites in similar positions. The secondary and the tertiary structures of HRP-C are summarized in Figure 2.

More recently, the synthetic and native HRP-C have been cloned in various microorganisms—*E. coli*, *Baculovirus*, *and Pichia pastoris*, etc. (24–26).

V. PROPERTIES AS AN ENZYME

A. Specific Mechanism of Action

The normal peroxidase cycle is shown in Figure 3. The reaction of HRP with H_2O_2 produces a two-electron oxidized species known as Compound I in which the ferric iron is oxidized to a ferryl ($Fe^{IV}=O$) species and the porphyrin to a radical cation. Stepwise reduction of Compound I by two substrate-derived electrons produces Compound II, in which the porphyrin radical cation has been quenched, and subsequently the resting ferric state form. The second-order rate constants for the reaction HRP and H_2O_2 are: k_1, $(1.58 \pm 0.05) \times 10^7\ M^{-1}\ s^{-1}$; k_2, $(9.97 \pm 0.28) \times 10^6\ M^{-1}\ sec^{-1}$; and k_3, $(3.64 \pm 0.01) \times 10^2\ M^{-1}\ sec^{-1}$ (1, 27, 28).

Generally, k_3 is always 10–20 times slower than k_2, and under most steady-state conditions is rate limiting.

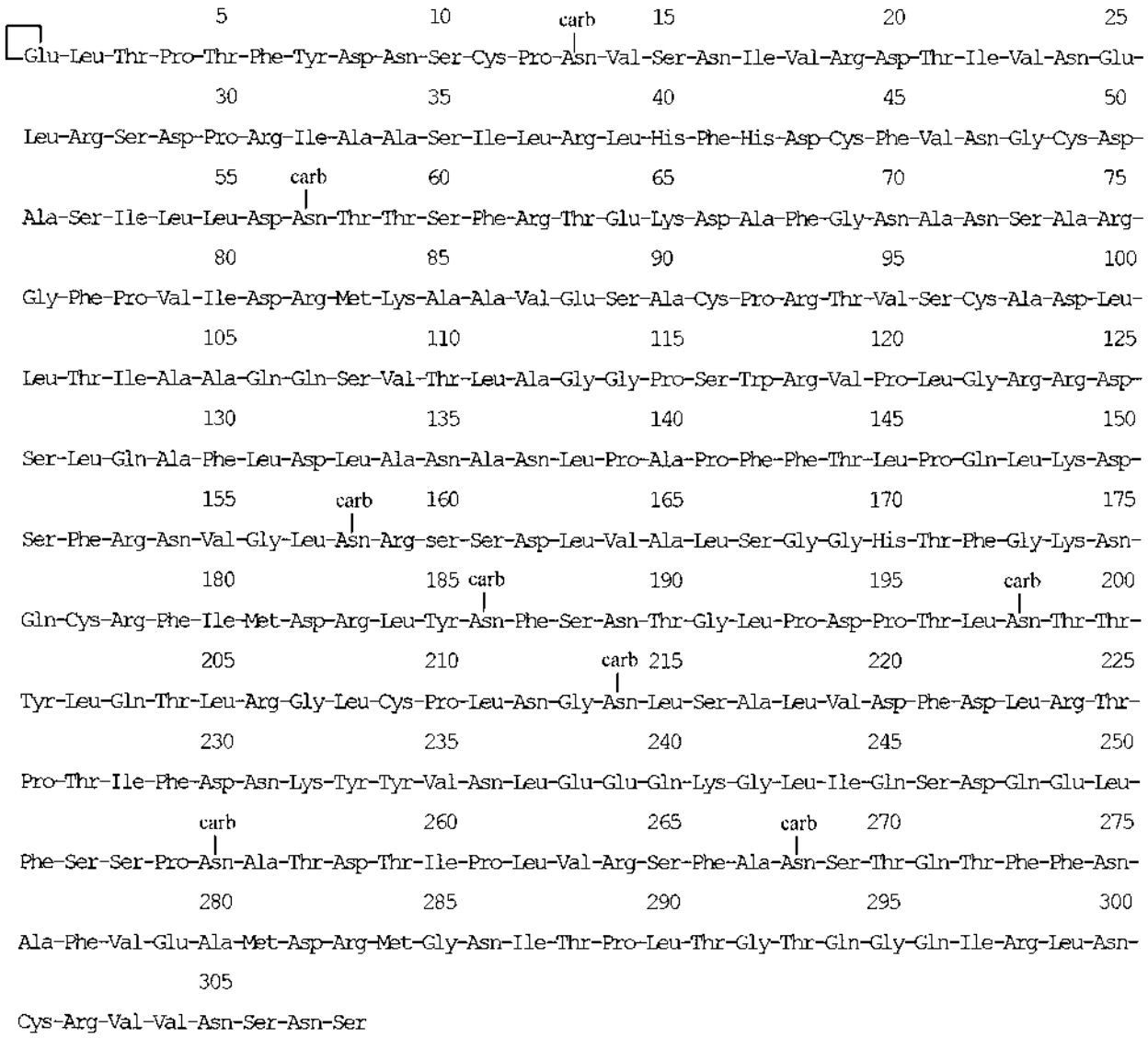

Figure 1 The amino acid sequence of horseradish peroxidase (carb = site of carbohydrate attachment). Disulfide bridges: 11–91, 44–49, 97–301, 177–209. (From Ref. 21.)

The values of k_2 and k_3 depend on the nature of the substrate.

Both competitive binding (1) and spectroscopic studies (29) have revealed that the peroxide- and substrate-binding sites are not the same. Specific-site mutation analyses (30, 31) and the high-resolution crystallographic structure of HRP-C (23) have provided detailed information on structural basis of HRP catalysis. Peroxide binding, activation, and Compound I formation occur in the distal heme pocket, where the key residues (His42 and Arg38) play a role in mediating the reactions with a general acid/base mechanism. The aromatic donor molecule interacts with a substrate accessible channel contributed by Phe residues (Phe68, Phe142, and Phe179) and the heme C18 methyl group.

B. Substrate Specificity

Peroxidase is specific to the hydrogen acceptors. Only hydrogen peroxide, methylhydroperoxide, and ethylhydroperoxide can be used as hydrogen acceptors.

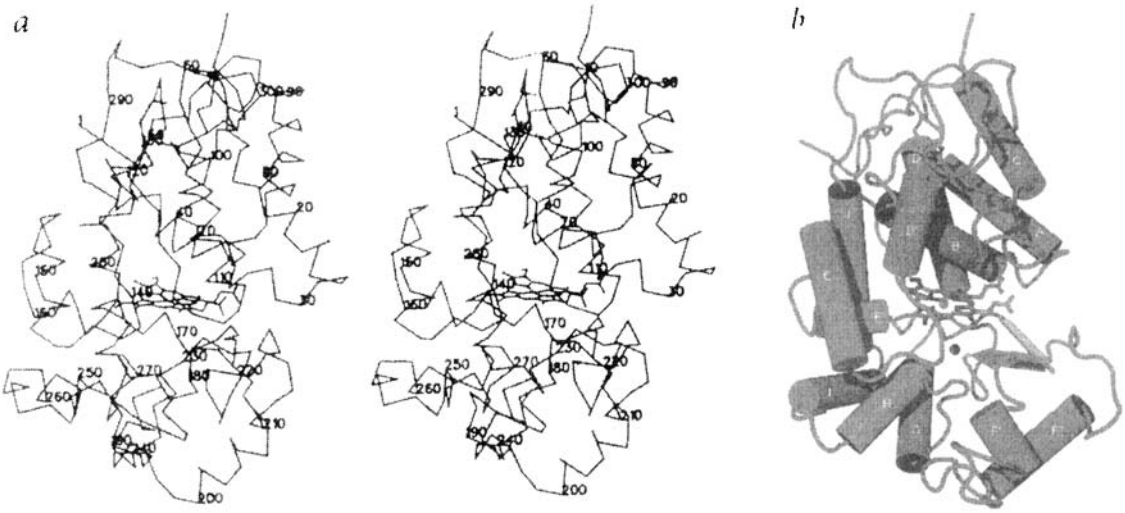

Figure 2 (a) Stereo Cα trace of HRP-C with the heme C20 edge in the foreground. Every 10th residue is labeled. This figure was prepared with program SETOR. (b) The relative positions of the secondary structural elements (α-helices and β-sheets) in HRP-C. The helices are labeled with their conventional names. (From Ref. 23.)

The enzyme is not specific to the hydrogen donor. A variety of phenols, aminophenols, diamines, indophenols, leucodyes, ascorbate, and several amino acids are hydrogen donors. In HRP kinetic studies and activity assays, guaiacol and 2, 2′-azino-bis(3-ethylbenzthiazoline-6-sulfonic acid) (ABTS) are the most commonly used hydrogen donors as shown in Table 3 (32, 33). The kinetic parameters of other substrates (including hydrogen acceptors) are also listed in Table 4 (34–36).

C. Effect of Environmental Factors

1. pH and Temperature Optima

pH optimum is 7.0 for the commercial HRP preparations. As seen from Table 2, each isoenzyme has a different optimal pH.

Temperature optimum is 40–52°C, depending on the type of isoenzyme and the substrates (1).

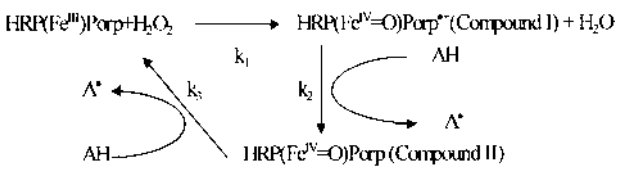

Figure 3 The catalytic cycle of horseradish peroxidase. (From Ref. 1.)

2. Inhibitors

Horseradish peroxidase is inhibited reversibly by cyanide (36, 37), sulfide, and dithionite (10^{-4}–10^{-6}M) (36). Azide fluoride, hydroxylamine, diethyldithiocarbamate, cyclopropanone hydrate, and borohydride at $\sim 10^{-3}$ M inhibit HRP (36, 38). Vanadate and hydroxymethylhydroperoxide inhibit the enzyme irreversibly (39, 40). As HRP inhibitor, 1,10-phenanthroline is used in immunoperoxidase procedures (41).

3. Stability

Horseradish peroxidase is very stable. The commercial HRP, as a lyophilized powder, may be stored at 4°C for several years without apparent loss of activity. A solution of purified HRP (1 mg/mL) is stable for 1 year at 4°C.

VI. DETERMINATION OF HRP ACTIVITY

Based on chromogenesis and chemiluminescence of products, numerous methods have been developed for determining the activity of HRP. The hydrogen donors in common use are guaiacol, pyrogallol, ABTS, 4-methoxy-α-naphthol, and phenol plus aminoantipyrine. Among them, guaiacol is easily available and simple to operate and is used very often, although its product is not stable. ABTS and phenol plus aminoantipyrine are widely used in microanalysis, enzyme-

Table 3 The Steady-State Kinetic Parameters for the Peroxidation of Guaiacol and ABTS by HRP

Substrate	Enzyme (nM)	$K_m(\mu M)$	$k_{cat}(s^{-1})$	k_{cat}/K_m ($s^{-1}\mu m^{-1}$)	Specific activity (units/mg)
ABTS[a]	0.2	8.0×10^2	4.1×10^3	5.1 ± 0.2	1.15×10^3
Guaiacol[b]	2	5.8×10^3	4.2×10^2	$(7.2 \pm 1.1) \times 10^{-2}$	—[c]

Source: Refs. 29, 30.
[a]pH 4.6, 10 mM H_2O_2.
[b]pH 6.0, 1 mM H_2O_2.
[c]Unverified.

linked immunosorbent assay (ELISA), and histochemical tracer techniques. Both methods are rather sensitive, and the chromogenic products are relatively stable. On the other hand, aromatic amines, such as *o*-dianisidine, *o*-phenylenediamine, and mesidine are less used now, because the oxidized products are carcinogenic.

A. Determination of HRP Activity Using ABTS (42, 43)

1. Reaction

The reaction catalyzed is shown in equation (2).

$$H_2O_2 + AH_2 \xrightarrow{HRP} 2H_2O + A \qquad (2)$$

$$(AH_2 = ABTS)$$

ABTS (2,2′-azinobis(3-ethylbenzthiazolin-6-sulfonate) has an absorption maximum at 340 nm (pH 4.4) and $\epsilon_{340} = 3.97 \times 10^4\ M^{-1}\ cm^{-1}$. It is oxidized by HRP to a radical cation that has an adsorption at pH 5.0 with $\epsilon_{414} = 3.6 \times 10^4\ M^{-1}\ cm^{-1}$.

Table 4 Kinetic Parameters of HRP with Different Substrates

Substrate	Rates constants (31)
(a) Hydrogen acceptors	k_1 [M^{-1} sec^{-1}]
H_2O_2	9×10^8
Methyl hydroperoxide	1.5×10^6
Ethyl hydroperoxide	3.6×10^6
(b) Hydrogen donors	K_m (mM) (32, 33)
KI	181.7
o-dianisidine	0.48
4-Aminophenazone	83.33
Pyrogallol	23.80

Source: Refs. 31–33.

2. Solutions

All solutions are prepared with deionized water and kept at 4°C.

a. ABTS. 1.5×10^{-2} M as a stock solution. Dissolve 0.077 g ABTS (diammonium salt) in 10 mL water.

b. H_2O_2. Dilute the ~ 10 M commercial solution to a stock solution of 0.01 M. Titrate the stock solution with a 0.02 M $KMnO_4$ solution. The concentration of the stock solution can be checked by its $\epsilon_{240} = 4.36 \times 10^4\ M^{-1}\ cm^{-1}$.

c. HRP. Dissolve 1.00 g lyophilized HRP in 1 mL deionized water, and dilute to 0.01 g/mL just before use. The concentration of HRP is determined by the Soret absorbance at 403 nm using $\epsilon_{403} = 1.02 \times 10^5\ M^{-1}\ cm^{-1}$.

d. Sodium Acetate Buffer. 0.2 M, pH 5.0.

3. Procedure

The method is according to Chailds and Bardsley (42) with some modification. Ten microliters of HRP sample with the appropriate dilution is added to a cuvette containing 50 μL of ABTS, and 0.1 M sodium acetate buffer in a final volume of 1.9 mL. After the mixture is preincubated at 20°C, 100 μL of H_2O_2 (0.5 mM) is added to initiate the reaction and formation of the ABTS radical cation is monitored at 414 nm for the first 5 min against a blank in which the HRP sample is replaced by deionized water. One unit of enzymatic activity is defined as the amount of HRP which causes oxidation of one μmol of ABTS per min at 25°C, pH 5. Molar absorption coefficient $\epsilon_{414} = 3.6 \times 10^4\ M^{-1}\ cm^{-1}$.

4. Calculation

Specific activity (U/mg) $= \Delta A_{414}/(3.6 \times 10^4 . d\Delta t[E])$, where d is light path = 1 cm, Δt is time of reaction in min, and [E] is enzyme concentration in mg/mL.

B. Determination of HRP Activity Using Guaiacol (35, 44, 45)

1. Reaction

$$H_2O_2 + AH_2 \rightarrow 2H_2O + A \quad (AH_2 = \text{Guaiacol}) \tag{3}$$

2. Solutions

a. Phosphate Buffer. 0.2 M sodium phosphate buffer, pH 7.0.

b. Guaiacol Solution. 18 mM (245 mg of guaiacol in 100 mL water).

c. H_2O_2 Solution. 8 mM (dilute 0.1 mL of 30% H_2O_2 solution with redistilled water to read $A_{240} = 0.400$; light path = 1 cm.

3. Procedure

The appropriately diluted HRP sample is mixed with 0.3 mM guaiacol in 0.1 M phosphate buffer in a total volume of 3.0 mL and preincubated at 25°C. Addition of 0.03 mL 8 mM H_2O_2 initiates the oxidation reaction; the oxidation of guaiacol is monitored at 470 nm ($\epsilon_{470} = 2.75 \times 10^3\ M^{-1}\ cm^{-1}$) for the first 5 min. One unit of HRP activity is the amount of enzyme that results in the oxidation of 1 μmol of guaiacol per min at 25°C, pH 7.0, under the above-described conditions.

4. Calculation

Specific activity $= 3.03\,\Delta A_{470}\,min^{-1}/(2.75 \times 10^3\ M^{-1}\ cm^{-1} \times d \times [E])$ where 3.03 is the total reaction volume in mL, d is the light path = 1 cm, [E] is the enzyme concentration in mg/mL, d is the light path and $\Delta A/min$ is the change of absorbance at 470 nm/min.

C. Determination of HRP Activity Using Phenol Plus 4-Aminoantipyrine (46)

1. Reaction

$$2H_2O_2 + \text{Phenol} + \text{4-Aminoantipyrine} \longrightarrow 4H_2O + \text{Quinol Red} \tag{4}$$

When phenol plus 4-aminoantipyrine is used as hydrogen donor, the HRP-catalyzed reaction is monitored by measuring the increase in absorbance at 510 nm due to formation of quinol in red color with extinction coefficient $\epsilon_{510} = 6.58\ M^{-1}\ cm^{-1}$.

2. Solutions

a. Phosphate Buffer. 0.2 M sodium phosphate buffer, pH 7.0.

b. H_2O_2. Dilute 1 mL of 30% H_2O_2 to 100 mL with redistilled water. Further dilute 1 mL of this solution to 50 mL with 0.2 M phosphate buffer to obtain 1.7 mM H_2O_2. Prepare fresh daily.

c. 4-Aminoantipyrine and Phenol. Dissolve 810 mg phenol and 25 mg 4-aminoantipyrine in 40 mL redistilled water and add more water to a final volume of 50 mL.

3. Procedure

Pipette 1.4 mL of phenol/4-aminoantipyrine solution and 1.5 mL of 1.7 mM H_2O_2 into each cuvette, and preincubate at 25°C for 3–4 min. Add 0.1 mL of the diluted enzyme and measure the ΔA_{510} for 4–5 min. One unit of the enzyme is defined as the amount which brings about 1 μmol of hydrogen peroxide to result in A_{510} increase per min at 25°C and pH 7.0 under the specified conditions.

4. Calculation

Specific activity (U/mg) $= (\Delta A_{510}/min/(6.58 \times$ mg enzyme/mL reaction mixture).

The RZ (Reinheitzahl) number, the absorbance ratio A_{403}/A_{275}, is used as an evaluation of enzyme purity. As an example, partially purified HRP has an RZ of 0.8–1.0 with a specific activity of 85–200 U/mg. The chromatographically purified HRP has an RZ of 3.0 with a specific activity of 650–900 U/mg. However, the RZ values for the isozymes have been found to vary from 2.50 to 4.19 (47); RZ is also pH dependent. Therefore, both the specific activity and RZ value have been given together as the criterion of purity.

VII. PREPARATION OF PEROXIDASE FROM HORSERADISH

Since the 1950s, a variety of isolation and purification methods have been developed. Preparation of HRP is generally composed of (a) initial extraction, (b) isolation and partial purification, and (c) refinement.

A. Initial Extraction

Fresh roots of horseradish plant are cut, minced, extracted with water, and filtered through cheesecloth.

The extract may contain > 40 HRP isoenzymes as harvested (47, 48).

B. Traditional Purification of HRP

In the traditional processes of HRP production pioneered by Theorell (1945) and Keilin and Hartree (1951), the common biochemical methods involved ammonium sulfate fractionation, organic solvent (acetone, ethanol, etc.) different precipitation, calcium phosphate gel adsorption, and corresponding dialysis and crystallization selected to achieve the HRP with RZ ~ 2.3–3.04 (46–48).

HRP isoenzyme C was successfully separated from isoenzyme B by using a modified elution gradient from CM-cellulose column, and further purified using a preparative isoelectric focusing to achieve HRP C as a single component (49). However, this process was time-consuming and expensive with respect to ampholyte needed.

Ion-exchange column chromatography was also used in isolating five major neutral isoenzymes of HRP from a partially purified preparation (RZ = 0.8). Three columns of SP-Sephadex C-50 combined with an improved elution system in which a stepwise increase of pH of elution buffer at a fixed low concentration was used instead of increasing the concentration of the buffer at a fixed pH (50).

In recent years, a cation-exchange column was combined with an anion-exchange column to form a simple and effective approach to purify HRP. The partially purified preparation of HRP flowed in an anion-exchange column. The acidic HRP isoenzymes and other contaminant proteins were adsorbed on the resin, whereas the neutral and basic HRP passed through. Then the effluent was applied on the second cation-exchange column to remove all the basic isoenzymes and contaminant proteins. The effluent contained neutral HRP. After being desalted and lyophilized, a purified HRP with a specific activity ~ 500 $U \cdot mg^{-1}$ and RZ = 3.0 was obtained (Zhong-Yu Ji, personal communication, 1995).

C. Reverse Micellar Purification of HRP

As an alternative to the above methods, reverse micelles were recently utilized in isolation and purification of the enzyme from the root extract (51). The reverse micellar isolation involved two stages.

The horseradish root extract with a specific activity of 1.1 $U \cdot mg^{-1}$ was diafiltrated using 10 kDA MWCO membranes against deionized water. In the first forward transfer, the anionic surfactant AOT (aerosol-OT [sodium-bis(2-ethylhexl)]sulfosuccinate]) in isooctane (110 mM) was mixed with the dialyzed extract at pH 4.15 and 0.15 M NaCl ($V_{aq}/V_{org} = 5$). In this case, HRP protein solubilized in the aqueous phase, and most contaminant proteins (~ 49% protein) were removed into the organic phase. After centrifugation, the organic phase was separated and regenerated by backtransfer. In the second stage, the forward transfer of the HRP micelles was carried out at pH 3.5, 0.15 M NaCl by mixing with AOT in isooctane ($V_{aq}/V_{org} = 10$). Finally an HRP of specific activity of 86 guaiacol $U \cdot mg^{-1}$ was obtained with 80-fold purification and 46% yield.

Comparison between the two-stage reverse micellar extraction and traditional methods (two ammonium sulfate fractionations plus two differential ethanol precipitations with the corresponding dialysis steps) gave a good efficiency of the former (see Table 5). Other techniques, such as affinity chromatography

Table 5 Peroxidase Purification Using the Traditional Biochemical Methods in Combination with Reverse-Micelle Extraction (Horseradish Peel only; Method C)[a]

Purification stage	Protein (mg)[b]	Activity (U)[c]	Specific activity ($U\ mg^{-1}$)	Purification factor	Yield (%)
Crude extract	5500	5300	1.0	1	100
Crude preparation	100	4100	41	40	76
Two-stage reverse-micelle extraction	16	2400	150	150	45

Source: Ref. 51.

[a]Values are the mean of three replicates with SE within 5% of the mean.

[b]Total protein was measured using the BCA method (32).

[c]Activity measured by the guaiacol assay (30).

and hydrophobic chromatography, were also used for peroxidase purification (52, 53).

REFERENCES

1. HB Dunford. Horseradish peroxidase: structure and kinetics. In: J Everse, KE Everse, MB Grisham, eds. Peroxidases in Chemistry and Biology, Vol II. Boca Raton, FL: CRC Press, 1991, pp 1–24.
2. HB Dunford. Heme enzymes. In: M Sinnott, ed. Comprehensive Biological Catalysis, Vol III. Radical Reactions and Oxidation/Reduction. New York: Academic Press, 1998, pp 195–237.
3. KG Welinder. Superfamily of plant, fungal and bacterial peroxidases. Curr Opin Struct Biol 2:388–393, 1992.
4. KG Welinder. Plant peroxidases: their primary, secondary and tertiary structures, and relation to cytochrome c peroxidase. Eur J Biochem 151:497–504, 1985.
5. TH Gaspar, CL Penel, T Thorpe, H Greppin, eds. *Peroxidases* 1970–1980. Geneva: Université de Genève–Centre de Botanique, 1982.
6. BC Saunders, AG Holmes-Siedle, BP Stark. Peroxidase. London: Butterworths, 1964.
7. S Avrameas, B Guilbert. Enzyme-immunoassay for the measurement of antigen using peroxidase conjugates. Biochimie 54:837–842, 1972.
8. P Tijssen. Properties and preparation of enzymes used in enzyme immunoassay. In: RH Burdon, PH Van Knippenberg, eds. Practice and Theory of Enzyme Immunoassays, Vol 15. Amsterdam: Elsevier, 1985, pp 173–219.
9. M Imagawa, S Yoshitaka, Y Hamaguchi, W Shikawa, Y Niitau, I Urushizaki, R Kanazawa, S Tachibana, N Nakazawa, H Ogawa. Characteristic and evaluation of antibody–horseradish peroxidase conjugates prepared by using a maleimide compound, glutaraldehyde and periodate. J Appl Biochem 4:41–57, 1982.
10. P Kolodziejczyk, K Reszka, JW Lown. Enzymic oxidative activation and transformation of the antitumor agent mitoxantrone. Free Radical Biol Med 5:13–25, 1988.
11. JS Dordick, MA Marletta, AM Klibanov. Polymerization of phenols catalyzed by peroxidase in nonaqueous media. Biotech Bioeng 30:31–36, 1987.
12. K Fujiyama, H Takemura, A Shinmyo, H Okada, M Tanaka. Genomic DNA structure of two new horseradish-peroxidase-encoding genes. *Gene* 89:163–169, 1990.
13. SC Fry. Phenolic components of the primary cell wall and their possible role in the hormonal regulation of growth. Planta 146:343–351, 1979.
14. CP Vance, TK Kirk, RT Sherwood. Lignification as a mechanism of disease resistance. Annu Rev Phytopathol 18:259–288, 1980.
15. J Ricard, D Job. Reaction mechanism of indole-3-acetate degradation by peroxidase. A stopped flow and low-temperature spectroscopic study. Eur J Biochem 44:359–374, 1974.
16. AK Paul, S Mukherji. Change in respiration rate of rice seedlings as affected by storage and viability and its possible relation with catalase and peroxidase activities during germination. Biol Plant 14:414–419, 1972.
17. L Frylink, IA Durbery, JC Schabort. Biochemical changes involved in stress response and ripening behaviors of γ-irradiated mango fruit. Phytochemistry 26:681–686, 1987.
18. TH Gaspar, CL Penel, T Thorpe, H Greppin, eds. Peroxidases 1970–1980. Geneva: Université de Genève, 1982, pp 89–121.
19. JHC Shih, LM Shannon, E Kay, TY Lew. Peroxidase isoenzymes from horseradish roots. IV. Structural relationships. J Biol Chem 246:4546–4551, 1971.
20. E Bartonek-Roxa, H Eriksson. Expression of a neutral horseradish peroxidase in *Escherichia coli*. J Biotechnol 37:133–142, 1994.
21. KG Welinder. Covalent structure of the glycoprotein horseradish peroxidase (EC 1.11.1.7). FEBS Lett 72:19–23, 1976.
22. KG Welinder. Plant peroxidases: structure–function relationships. In: C Penel, T Gaspar, H Greppin, eds. Plant Peroxidases 1980–1990. Topics and Detailed Literature on Molecular, Biochemical and Physiological Aspects. Geneva: University of Geneva, 1992, pp 1–24.
23. M Gajhede, DJ Schuller, A Henriksen, AT Smith, TL Poulos. Crystal structure of horseradish peroxidase C at 2.15 Å resolution. Nature Struct Biol 4:1032–1037, 1997.
24. AT Smith, N Santama, S Dacey, M Edwards, RC Bray, RN Thorneley, JF Burke. Expression of a synthetic gene for horseradish peroxidase C in *Escherichia coli* and folding and activation of the recombinant enzyme with Ca^{2+} and heme. J Biol Chem 265:13335–13343, 1990.
25. C Hartmann, PR Ortiz de Montellano. Baculovirus expression and characterization of catalytically active horseradish peroxidase. Arch Biochem Biophys 297:61–72, 1992.
26. TJ Jiang, XS Ji, RA Zhang, YH Huang, XF Wu, ZY Yuan. High-level expression of active horseradish peroxidase in methyltrophic yeast. Prog Biochem Biophys 26(6):584–587, 1999.
27. AT Smith, SA Sanders, RNF Thorneley, JF Burke, RRC Bray. Characterization of a haem active-site mutant of horseradish peroxidase, Phe41→Val, with altered reactivity towards hydrogen peroxide and

reducing substrates. Eur J Biochem 207:507–519, 1992.
28. SG Wang, W Liu, XS Ji, L Ma, TJ Li, ZY Yuan. Stopped-flow, pre-steady-state kinetic study of horseradish peroxidase catalysis in nonaqueous media. Ann NY Acad Sci 799:364–375, 1996.
29. J Sakurada, S Takahashi, TJ Hosoya. Nuclear magnetic resonance studies on the spatial relationship of aromatic donor molecules to the heme iron of horseradish peroxidase. J Biol Chem 261:9657–9662, 1986.
30. JS de Ropp, Z Chen, GN La Mar. Identification of residues in the aromatic substrate binding site of horseradish peroxidase by ^{1}H NMR studies on isozymes. Biochemistry 34:13477–13484, 1995.
31. M Tanaka, K Ishimori, M Mukai, T Kitagawa, I Morishima. Catalytic activities and structural properties of horseradish peroxidase distal His42→Glu or Gln mutant. Biochemistry 36:9889–9898, 1997.
32. MI Savenkova, LS Newmyer, PRO Montellana. Rescue of His-42→Ala horseradish peroxidase by a Phe-41→His mutation. J Biol Chem 271:24598–24603, 1996.
33. AT Smith, N Santama, S Dacey, M Edwards, RBC Bray, RNF Thorneley, JF Burke. Expression of a synthetic gene for horseradish peroxidase C in *Escherichia coli* and folding and activation of the recombinant enzyme with Ca^{2+} and heme. J Biol Chem 265:13335–13343, 1990.
34. KG Paul. Peroxidases. In: PD Boyer, HA Lardy, K Myrbäck, eds. The Enzymes. New York: Academic Press, 1963, pp 227–274.
35. K Kariya, E Lee, M Hirouchi, M Hosokawa, H Sayo. Purification and some properties of peroxidases of rat bone marrow. Biochim Biophys Acta 911:95–101, 1987.
36. JS Schindler, RE Childs, WG Bardsley. Peroxidase from human cervical mucus: the isolation and characterization. Eur J Biochem 65:325–331, 1976.
37. WD Ellis, HB Dunford. The kinetics of cyanide and fluoride binding by ferric horseradish peroxidase. Biochemistry 7:2054–2062, 1968.
38. JS Wiseman, JS Nichols, MX Kolpak. Mechanism of inhibition of horseradish peroxidase by cyclopropanone hydrate. J Biol Chem 257:6328–6832, 1982.
39. MA Serra, E Sabbioni, A Marchesini, A Pintar, M Valoti. Vanadate as an inhibitor of plant and mammalian peroxidases. Biol Trace Elem Res 23:151–164, 1989–90.
40. S Marklund. Mechanisms of the irreversible inactivation of horseradish peroxidase caused by hydroxymethylhydroperoxide. Arch Biochem Biophys 154:614–622, 1973.
41. W Straus. Phenylhydrazine as inhibitor of horseradish peroxidase for use in immunoperoxidase procedures. J Histochem Cytochem 20:949–951, 1972.
42. BE Chailds, WG Bardsley. The steady-state kinetics of peroxidase with 2,2′-azino-di-(S-ethylbenzthiazoline-6-sulphonic acid) as chromogen. Biochem J 145:93–103, 1975.
43. SL Newmeyer, PRO Montellano. Horseradish peroxidase His-42→Ala, His-42→Val, and Phe-41→Ala mutants. J Biol Chem 270:19430–19438, 1995.
44. KG Paul, T Stigbrand. Four isoperoxidases from horseradish root. Acta Chem Scand 24:3607–3617, 1970.
45. J Putter. Horseradish peroxidase. In: HU Bergmeyer, ed. Methoden der Enzymatischen Analyse. Weinheim: Verlag Chemie, 1974, pp 725–731.
46. LM Shannon, E Kay, JY Lew. Peroxidase isozymes from horseradish roots. 1. Isolation and physical properties. J Biol Chem 241:2166–2172, 1966.
47. BD Keilin, EF Hartree. Purification of horse-radish peroxidase and comparison of its properties with those of catalase and methaemoglobin. Biochem J 49:88–104, 1951.
48. BRH Kenten, PJG Mann. A simple method for the preparation of horseradish peroxidase. Biochem J 57:347–348, 1954.
49. J Carke, LM Shanuon. The isolation and characteriztaion of the glycopeptides from HRP isoenzyme. Biochim Biophys Acta 427:428–442, 1976.
50. S Aibara, H Yamashita, E Mori, M Kato, Y Morita. Isolation and characterization of five neutral isoenzymes of horseradish peroxidase. J Biochem 92:531–539, 1982.
51. C Regalado, JA Asenjo, DL Pyle. Studies on the purification of peroxidase from horseradish roots using reverse micelles. Enzyme Microb Technol 18:332–339, 1996.
52. C Chavez, WH Flurky. Biospecific adsorption of peroxidase. J Chromatogr 298:169–171, 1984.
53. VM Paradkar, JS Dordick. Affinity-based reverse micellar extraction and separation (ARMES): a facile technique for the purification of peroxidase from soybean hulls. Biotechnol Prog 9:199–203, 1993.

29

Glutathione Peroxidase

Jun-qiu Liu and Gui-min Luo
Jilin University, Changchun, China

I. INTRODUCTION

Glutathione peroxidase (GPX; EC 1.11.1.9) is a selenoenzyme that protects biomembranes and other cellular components against oxidative damage (1–3). Its activity was discovered by Mills in 1957 (1). In 1973, the stoichiometric amount of selenium was found in this peroxidase in the effort of searching for the prosthetic group of GPX and the essentiality of selenium as the trace element (4, 4a). The enzyme catalyzes the reduction of a variety of hydroperoxides including hydrogen peroxide, organic hydroperoxides, and lipid hydroperoxides using glutathione (GSH) as the reducing equivalent [Eq. (1)]:

$$2GSH + ROOH \rightarrow GSSG + ROH + H_2O \qquad (1)$$

where ROOH is the hydroperoxide such as H_2O_2, *tert*-butyl hydroperoxide, cumene hydroperoxides, etc. (Table 1), GSSG is the oxidized form of glutathione which is reverted to GSH by glutathione reductase, and ROH is the corresponding alcohol or H_2O in the case of H_2O_2 acting as substrate.

Four types of GPX have been discovered: (a) the classical cellular glutathione peroxidase, cGPX (1); (b) the phospholipid hydroperoxide glutathione peroxidase, PHGPX (5); (c) the plasma glutathione peroxidase, pGPX (6–8); and (d) the gastrointestinal glutathione peroxidase, giGPX (9). Another type of enzyme that contains GPX activity but does not depend on selenium for catalysis has been previously classified as selenium-independent GPX (10). It catalyzes glutathione-dependent nucleophilic substitution and addition reactions with endogenous and xenobiotic electrophiles as well as the reduction of organic hydroperoxides, but not hydrogen peroxide. The enzyme has subsequently been demonstrated to be glutathione S-transferase (11). Among the GPX isozymes, cGPX, pGPX, and giGPX are tetramers and have similar substrate specificity. They catalyze the reduction of H_2O_2, *tert*-butyl hydroperoxide, cumene hydroperoxide, and linoleic acid hydroperoxide with glutathione, but reduce cholesterol hydroperoxide and phospholipid hydroperoxide poorly (9–13). The giGPX displays most of the enzymatic properties of the classical cellular GPX, but shows little activity toward lipid hydroperoxides (9). Plasma glutathione peroxidase is an extracellular enzyme, which is different from other GPX enzymes in structural and enzymatic properties (7, 8). PHGPX is a membrane-bound enzyme, a monomer, and has different substrate specificity compared to cGPX, pGPX, and giGPX. It catalyzes the reduction of phospholipid hydroperoxide, linoleic acid hydroperoxide, and cholesterol hydroperoxide in biological membranes, and also shows activity on H_2O_2 and organic hydroperoxides (5, 14).

II. BIOLOGICAL DISTRIBUTION OF GPX

Glutathione peroxidase has been found in most animals but not in plants (15–17). A low level of the enzyme has been demonstrated in some insects (18), and GPX activity has been detected in yeast, *Hansenula mraki* (19). The enzyme is found chiefly in

Table 1 Substrates and Their Structures of Glutathione Peroxidase

Substrate	Chemical structure	Examples
Glutathione	γ-Glu-Cys-Gly	
Hydroperoxides	R-O-O-H	H_2O_2 **Organic hydroperoxidase:** ethyl, cumene, tert-butyl, 5-phenyl-4-pentenyl, linoleic, linoleic acid hydroperoxides, and their methyl esters: 13-hydroperoxy-9, 11-octacadienoic acid, cholesterol 7β-hydroperoxide; allopregnanolone 17α-hydroperoxide; thymine hydroperoxide. **Lipid hydroperoxide:** phosphatidylethanolamine, phosphatidyl-choline, phosphatidylserine, cardiolipin and phosphatidic acid hydroperoxides: mono- and dihydroperoxydilinoleoylphosphatidyl cholines

respiratory tissues (blood vessels, lung, heart), digestive tissues (liver, kidneys), and brain tissues where oxygen is required. In rats, a high level of the enzyme is found in the liver with lower concentrations detected in red cells, heart, lung, and kidney. In hepatocytes 70% of the GPX activity is from the cytosol and 30% is localized within the mitochondrial matrix (20).

Classical GPX is present abundantly in erythrocytes, kidney, and liver (16). The lens of different animal species contain remarkably high GPX activity (21, 22). PHGPX has been identified in all tissues in which it was searched for, namely, rat kidney, heart, lung, muscle, and brain; bull spermatozoa; and fish liver (23). A high level of GPX activity has been observed in rat testis (24). pGPX is detected in plasma, milk, and lung (6, 7). giGPX has been found in the cytosol of human and rat gastrointestinal tracts (9). It was detected in human liver and colon, but not other human tissues including kidney, heart, lung, placenta, and uterus. In rodent tissues, giGPX is only detected in the gastrointestinal tract, not in other tissues. In rat, the highest activity of the enzyme is detected in stomach followed by decreasing activities in esophagus, colon, and intestine.

The study by Godin and Ganett (25) showed that the distribution of GPX in mammalian tissues is strictly functionally related to other antioxidant enzymes such as superoxide dismutase (SOD; EC 1.15.1.1) and catalase (EC 1.11.1.6). It should be kept in mind that the level of GPX is subject to numerous influences, including dietary selenium, age and sex, and estrous cycle, and other environmental factors (26–28).It has been documented that GPX activity is subject to large species differences in all organs (20).

III. UTILITY OF GPX

The biological damage such as peroxidation of lipids and nucleic acid damage can be caused by reactive oxygen species. Antioxidant defenses consist of a number of antioxidant enzymes protecting cells and membranes against the reactive oxygen. The first line of defense seems to be governed by superoxide dismutase which acts by converting the superoxide ion O_2^- into hydrogen peroxide. Secondly, catalase, and GPX share the task of metabolizing H_2O_2 to water. In the last line of defense, the GPX is the sole enzymatic system capable of preventing lipid peroxidation. The enzyme can reduce a wide variety of hydroperoxides, and acts as an important part of the antioxidant defense of biology body.

Many studies have shown that low selenium in the diet can result in low levels of GPX activity leading to oxidative damage and several medical disorders such as Keshan disease, Kashin-Beck disease, cancer, heart disease, premature aging, and diabetes. The importance of this enzyme as an oxidant defense enzyme has led to its proposed strong possibilities to be used in treatment for these diseases (29–32).

IV. PROPERTIES AS PROTEIN

A. Molecular Weight and Physical Properties

cGPX, pGPX, and giGPX are tetrameric proteins of four identical subunits, with each subunit containing one atom of selenium in the form of selenocysteine residue. The average molecular weight is 19–25 kDa (33, 34, 42). PHGPX is a monomeric protein of 23

kDa containing a single selenocysteine residue (5, 13, 35). The properties of GPXs from different sources are listed in Table 2.

B. Protein Structure

Multiple forms of GPX exist in different animal tissues. In the cGPX family, the bovine erythrocyte cGPX was well investigated. It consists of four identical subunits each of 198 amino acids. The catalytic active selenocysteine is localized at residue 45 with four other cysteine residues present at positions 74, 91, 111, and 152 (36). The primary structures of several GPXs have been determined from their cDNA sequences (Fig. 1) (9, 37–42).

Within each GPX class high-sequence homology is found. The similarity between any two cGPXs ranges from $\sim 80\%$ to 90% (43). The mouse pGPX protein sequence is 98% identical to rat, 89% identical to human, and 88% identical to bovine pGPX protein sequences (44); the homology between different classes is much lower. The sequence homology of human pGPX is 44% identical with the human cGPX, 34% with the human giGPX, and 25% with the human PHGPX (9, 41). The homology of mouse pGPX is $< 52\%$ identical to mouse cellular cGPX (44). However, the homology is much higher in the active-site domain with the selenocysteine residue and in some regions containing residues 61–74, 93–108, 119–138, and 181–192 (41, 44).

In the GPX family, only two crystal structures have been determined—the bovine erythrocyte GPX (45) and the human plasma GPX (34). Bovine cGPX exists as a tetramer with each asymmetric unit consisting of two identical subunits. The secondary structure within each subunit contains four β-sheets, four α-helices, 12 clearly defined β-turns, and three one-turn 3_{10} helices. Two β-turns, β_1 and β_2, are parallel, and close to the N-terminus. The other two, β_3 and β_4, are antiparallel. The α-helices, α_1, α_2, and α_4, are located on the side of the central β-sheets and another one, α_3, is on the other side. The α_1 and α_4 are nearly parallel and their axes seem to parallel with β-sheets. The active selenocystine residue 45 is located at the N-terminal end of helix α_1 which forms a $\beta\alpha\beta$ substructure. The $\beta\alpha\beta$ structure may be important for catalysis and substrate binding. The structure of the other GPX, human pGPX, was proved to be similar to that of cGPX, although they belong to different species and have 42% sequence identity. No significant deviation of secondary structure was found between the two enzymes (34). The main differences in two enzyme subunits are an extended N-terminus and possible existence of a disulfide bridge in the pGPX.

cGPX exists as a rather flat, tetrahedral quaternary structure with point symmetry 222. Each asymmetric unit consists of two identical subunits in the dimer. The contact regions are extensive along two of the perpendicular twofold symmetry axes, a local axis relating the monomer of an asymmetric unit, and a crystallographic axis producing the tetrameric structure from the dimer. The interactions at each interface contain hydrogen bonds formed across the local axis by residues Glu77, Arg86, Arg286, and Glu227; hydrophobic actions; and the main-chain hydrogen bonds (45). The active-site selenocysteine residues are located on two opposite surfaces of the tetramer. The active center of GPXs is found in a flat depression on the tetramer surface surrounded by aromatic amino acid residues, with selenocysteine located at the N-terminal ends of α-helices forming $\beta\alpha\beta$ structures together with adjacent parallel β-sheets. Three residues, Arg40, Glu130, and Arg167 are involved in binding of substrate glutathione (GSH). Arg167 and Arg40 form salt bridges with the carboxyl groups of GSH, and Glu130 can form a hydrogen bond with

Table 2 Properties of GPXs from Different Sources

Enzyme	Subcellular location	Subunits molecular weight (kDa)	Subunits	Isoelectric	Activiation energy (kcal/mol^{-1})	Ref.
Bovine cGPX	Cytosolic	21	4	5.6–6.0	—	4, 56
Human cGPX	Cytosolic	23	4	4.9	8.2	60
Hamster liver cGPX	Cytosolic	23	4	5.1	3	58
Rat lunk cGPX	Cytosolic	20	4	—	—	67
Pig heart PHGPX	Membrane	22	1	—	—	5
Human pGPX	Plasma	21.5	4	—	—	64

Figure 1 Amino acid sequences of GPXs: bovine erythrocyte cGPX (37), mouse erythrocyte cGPX (38), human cGPX (39), human giGPX (9), pig PHGPX (40), human pGPX, bovine pGPX (42). The selenocysteine is indicated by an asterisk.

GSH. A proposed model of glutathione binding was given by Epp et al. (45).

Compared with cGPX, the three residues for binding GSH are mutated or deleted in pGPX. The surface of pGPX is more negatively charged, especially close to the active site. These differences may affect substrate binding and lead to different enzyme activities (34, 41).

Although there are no data on the crystal structure of PHGPX, a model has been developed by molecular dynamics calculation (43). According to this model, the shape of the core of these enzyme families comprising the pleated sheets and three of the helices is largely identical to that of cGPX. However, the deletion of several amino acids in the PHGPX sequence causes a substantial short-cut of the subunit interaction loop and an elimination of a small helix. In the PHGPX model, the active site appears more freely accessible. This allows the enzyme to attack more complex hydroperoxy lipids.

C. Isoforms

The existence of multiple forms of GPX is due to the expression of different genes (41, 46). Many mammalian cGPX genes display highly conserved sequences around the site of selenium (47). The gene for human pGPX has been found at chromosome 5q32, and contains five exons rather than two for cGPX. Rat and bovine pGPX genes have been identified similar to human pGPX (48). The gene for PHGPX has seven exons; exons 3 and 5 show homology with exons of cGPX, indicating that this gene, although related to cGPX, is distinct from it (40, 46). Multiple isoforms of PHGPX have been detected in human, rat, pig, and bovine tissues (5, 23, 24, 49–51). Another intercellular GPX is giGPX. The gene expression was found in human liver and colon and also detected in mouse and rat gastrointestinal tract (9). giGPX has been regarded as the most closely related offspring of the cGPX family (43).

An artificial GPX mimic, selenosubtilisin, was created by converting the active serine residue of the catalytic site of subtilisin into selenocysteine. It displays GPX activity but not as efficient as cGPX (52, 53). Another artificial selenium-containing enzyme has been generated by monoclonal technique and chemical modification (54). The abzyme displays a higher GPX activity compared with rabbit liver cGPX.

All the cDNA sequences of these GPX contain a UGA codon coding for selenocysteine (9, 41, 38). The UGA codon, usually functioning as a "stop" codon, was demonstrated to encode the amino acid residue selenocysteine, which could be incorporated directly during protein synthesis (46, 38).

V. ENZYMETIC PROPERTIES

A. Kinetics of GPX

The steady-state kinetics of bovine erythrocyte GPX was studied by Flohé et al. (56). The enzyme system

follows *tert uni* Ping-Pong mechanism with indefinite Michaelis constants and indefinite maximum velocities (56, 57). The double-reciprocal plots of GPX reaction with hydroperoxides in various concentrations of both GPX and hydroperoxide lead to parallel lines. The rate equation was described in Eq. (2).

$$[E_0]/v = \Phi_1/[ROOH] + \Phi_2/[GSH] \quad (2)$$

In this mechanism, $[E_0]$, [ROOH], and [GSH] are the concentrations of GPX, ROOH, and GSH, respectively, v is initial rate of the enzyme reaction, and Φ_1 and Φ_2 are Dalziel coefficients, examples of which are presented in Table 3. In double-reciprocal plot of $[E_0]/v$ vs 1/[ROOH], the slope is identical to Φ_1 and the intercepts equal $\Phi_2/[GSH]$. The Michaelis constant for one substrate depends on the other and is expressed as follows:

$$K_{m,ROOH} = (\Phi_1/\Phi_2)][GSH] \quad (3)$$

$$K_{m,GSH} = (\Phi_2/\Phi_1)[ROOH] \quad (4)$$

cGPX from bovine and ovine erythrocytes and hamster liver show no saturation for GSH, and true Michaelis constants for GSH cannot be measured (56, 58). However, the apparent Michaelis constant for ROOH and GSH can be calculated according to Eqs. (3) and (4).

The reaction kinetics of cGPX and PHGPX is in agreement with a *tert uni* Ping-Pong mechanism (5). The K_m values and other kinetic parameters for cGPX and PHGPX are listed in Tables 4 and 5.

The reaction mechanism of pGPX also displays Ping-Pong and is similar to those for cGPX and PHGPX. However, the pGPX shows saturation kinetics on both substrates (8, 60). The true K_m values can be obtained from kinetic plots. Some kinetic constants for human cGPX and pGPX are listed in Table 4 and Table 5. The value of k_{cat}/K_m are very close to the diffusion controlled limit for a bimolecular reaction, suggesting that pGPX is a very effective hydroperoxide scavenger at low concentration of plasma GSH.

B. Specific Mechanism of Action

In the catalytic cycle of the enzyme reaction with a *tert uni* Ping-Pong mechanism, the selenol form (E-SeH) of the enzyme is first oxidized by hydroperoxide to a selenenic acid (E-SeOH) which is reduced back by two GSH through an intermediate selenenyl sulfide form (E-SeSG) (5, 56).

$$ROOH + ESeH \xrightarrow{k_1} ESeOH + ROH \quad (5)$$

$$ESeOH + GSH \xrightarrow{k_2} ESeSG + H_2O \quad (6)$$

$$ESeSG + GSH \xrightarrow{k_3} ESeH + GSSG \quad (7)$$

A proposed catalytic cycle containing selenenic acid, selenenyl sulfide, and selenol has been suggested (Fig. 2), which is consistent with Ping-Pong kinetics (45, 56, 60). The seleninic acid (E-SeOOH) is not involved in the main catalytic cycle but may become important at high concentrations of hydroperoxide.

C. Substrate Specificity

The enzyme has a broad substrate specificity. The relative substrate specificity of different GPXs are presented in Table 6. All GPXs have specificity toward hydroperoxides (ROOH) but not on peroxides (ROOR). GSH is the only physiological donor substrate although GPX exhibits activities for some sulfhydryl compounds such as mercaptoethanol (5, 62). cGPX, PHGPX, pGPX and giGPX display substrate specificity for H_2O_2 and organic hydroperoxides. Although it shows lower hydroperoxide

Table 3 Dalziel Coefficients for cGPX and PHGPX

	cGPX		PHGPX	
Substrate	$\phi_1(10^{-8}$msec)	$\phi_2(10^{-6}$msec)	$\phi_1(10^{-6}$msec)	$\phi_2(10^{-4}$msec)
H_2O_2	0.56	1.27	5.5	1.3
tert-Butyl hydroperoxide	13.5	2.24	1.4	31
Cumene hydroperoxide	7.8	2.24	9.1	2.5
Linoleic acid hydroperoxide	—	—	5.5	2.3
Phosphatidyl choline hydroperoxide	—	—	1.2	1.6

Source: Refs. 5, 20, 56.

Table 4 Kinetic Constants for Human pGPX, Human cGPX, and Ovine cGPX

Enzyme	Hydroperoxide	K_m(μM) 1mM GSH	$k_{cat}(10^3 min^{-1})$	$k_{cat}/K_m 10^7 (M^{-1}min^{-1})$
Human pGPX	H_2O_2	3.3	18.4	2.3
	13-hydroperoxy-9,11-octadecadienoic	0.66	9.20	5.6
	15-hydroperoxy-5,8,11,13-eicosatetrenoic	2.1	13.2	4.8
	5-phenyl-4-pentenyl hydroperoxide	2.6	20.0	3.0
	Cumene hydroperoxide			
	t-butyl hydroperoxide			
Ovine cGPX		80	—	—
	H_2O_2	120	—	—
	5-phenyl-4-pentenyl hydroperoxide			
Human cGPX		12	—	—
		10	—	—

Source: Refs. 60, 61.

activities for phospholipid hydroperoxides than organic hydroperoxides, pGPX possesses the ability to reduce phospholipid hydroperoxides, whereas giGPX and cGPX have no activities for lipid hydroperoxides (Table 6).

Phospholipid hydroperoxides are the primary substrates for PHGPX, which is also active on H_2O_2 and organic hydroperoxides such as *tert*-butyl hydroperoxide, cumene hydroperoxide and linoleic acid hydroperoxide (5). pGPX is about one-tenth less reactive against organic and hydrogen peroxides than cGPX (63, 64). giGPX displays lower activity than pGPX against organic and hydrogen peroxides.

The second-order constants for the reduction of the hydroperoxides show that H_2O_2 is a poorer substrate for PHGPX than for cGPX, while linoleic acid hydroperoxide is reduced faster by PHGPX. PHGPX is highly active on lipid hydroperoxides (Table 7).

In cGPX, the hydrophobic effect of a bulky substrate seems important, the more hydrophobic, the faster a bulky substrate is reduced by cGPX. For small and unhindered substrate such as H_2O_2 and ethyl hydroperoxide, this effect can be negligible (63).

Table 5 K_m Values for Human pGPX and Human cGPX

Enzyme	$K_{mt,BuOOH}$(μM)	K_{mGSH}(mM)
pGPX	570	5.3
cGPX	52	4.1

Source: Ref. 8, 65.

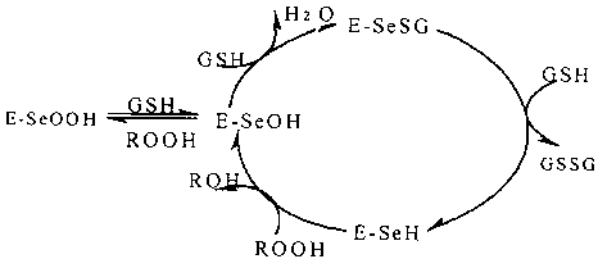

Figure 2 The proposed catalytic mechanism of GPX for reduction of ROOH by GSH.

D. Effect of Environmental Factors

1. pH Effects

GPX is relatively stable in the range of pH 7–10 (20). Enzymes from different sources have similar pH optimum > 8 (Table 8). The enzyme alone can form oxidized state (seleninic acid) in the air, but can be reactivated by incubation with GSH (45, 65).

cGPX is very stable at pH 7.0 at 4°C. The enzyme lost only 15–20% activity when stored at 4°C at pH 7.0 for 4 months. However, it is very unstable at low pH; At pH 4.0, the enzyme lost all its activity in 20 min (65). The GPX from rat lung was found to have very little activity at physiological pH 7.0, < 20% of the activity at the pH optimum of 8.8 (67).

Table 6 Activity of GPX Toward Different Hydroperoxides

Substrate	Specific activity (U/ mg enzyme)			
	cGPX[a]	pGPX[b]	PHGPX[c]	giGPX[d]
H_2O_2	216	31.3	135	2.1
tert-Butyl hydroperoxide	224	26.6	13.5	0.6
Cumene hydroperoxide	199	25.0	8.7	0.9
Linoleic acid hydroperoxide	—	—	187	1.2
Phosphatidyl choline hydroperoxide	0	8.41	226	0.004

The specific activities are defined as μmol NADPH oxidized/min/mg protein.
Data shown for GPXs: [a]human erythrocyte cGPX (63); [b]human plasma pGPX (63); [c]pig heart PHGPX(5); [d]human carcinoma MCF-7 cells giGPX (9).

2. Inhibitors

Divalent cations, sulfhydryl reagents, and iodoacetate inhibit the enzyme activity. The enzymes from human erythrocyte and human plasma exhibit similar inhibitory spectrum by divalent cations (8, 66). Cu^{2+} and Hg^{2+} completely inhibit the two enzyme activities. Zn^{2+} completely inhibits human pGPX but partly inhibits human cGPX. Ni^{2+}, Co^{2+}, Ca^{2+}, and Mg^{2+} also inhibit the two enzymes. Most enzymes from various sources are inhibited by iodoacetate in the presence of GSH or a sulfhydryl reagent such as mercaptoethanol or dithioerthritol (5, 8, 66). The active selenocysteine residue of the reduced enzyme can be alkylated by iodoacetate, but the other alkyling reagent, iodoacetamide, has no inhibitory effect. Human erythrocyte GPX was reported to be inactivated by *N*-ethylmaleimide (66, 68). In an inhibition study for hamster liver GPX, a number of mercaptocarboxylic acids and tertiary mercaptans have been found to be strong and specific inhibitors (69).

Table 7 Second-Order Rate Constants (k_1) for the Reaction Between cGPX and PHGPX with Hydroperoxidic Substrates (pH 7.6)

Substrate	cGPX $k_1 \cdot 10^5$	PHGPX ($mM^{-1}min^{-1}$)
H_2O_2	2.98	1.8
tert-Butyl hydroperoxide	7.1	0.71
Cumene hydroperoxide	10.4	1.1
Linoleic acid hydroperoxide	23.6	1.8
Phosphatidyl choline hydroperoxide	0	8.6

Source: Refs. 5, 58.

VI. DETERMINATION OF ACTIVITY

A. Methods for Determining the GPX Activity

Three methods are used for determining the GPX activity. The most commonly used assay is the GSH reductase–NADPH coupled assay (33, 70, 71). The method takes advantage of the capability of glutathione reductase to regenerate GSH from GSSG. The loss of NADPH is monitored continuously by absorbance spectrophotometry. The other two methods involve measurement of the GSH removal by the formation of thionitrobenzoate from Ellman's reagent, 5,5′-dithiobis-2-nitrobenzoic acid (DTNB) (72) and by polarographic GSH analysis (20).

1. Method 1: Coupled Enzymatic Assay

a. Reagents. 100 mM potassium phosphate buffer, pH 7.0, containing 1 mM sodium azide and 1 mM EDTA; 2.4 U/mL glutathione reductase (from yeast), prepared daily; 10 mM GSH (AR) in distilled water; 2.5 mM NADPH in 0.1% $NaHCO_3$, prepared daily; 12 mM hydroperoxide (AR) in water.

Table 8 Optimum pH of GPXs

Enzyme	Optimum pH	Ref.
Bovine erythrocyte cGPX	8.8	56
Human erythrocyte cGPX	8.5	66
Hamster liver cGPX	8.0	58
Rat lung cGPX	8.8	57
Human pGPX	8.9	64

b. Procedure. 500 μL of 100 mM phosphate buffer (pH 7.0), 100 μL of enzyme sample, 100 μL of glutathione reductase (0.24 U), 100 μL of 10 mM GSH, and 100 μL of 2.5 mM NADPH are added into a 1-mL curette. The reaction mixture is preincubated for 10 min at 37°C. The reaction is started by adding 100 μL of hydroperoxide solution. The linear decrease of NADPH absorption is monitored at 340 (or 366) nm for about 5 min. The control is assessed by replacing the enzyme with phosphate buffer.

2. Method 2: Assay of GSH Removal by DTNB

a. Reagents. 50 mM potassium phosphate buffer, pH 7.0; 10 mM GSH (AR) in distilled water; 1.5 mM DTNB in potassium phosphate buffer, pH 7.0; 12 mM hydroperoxide (AR) in water.

b. Procedure. 700 μL of potassium phosphate buffer, 100 μL of 10 mM GSH, 100 μL of enzyme solution are added into a 1-mL cuvette and preincubated for 10 min at 37°C. The reaction is started by adding 100 μL of hydroperoxide solution. Over 10 min 50 μL of the reaction mixture is taken at 1-min intervals. The solution is transferred into a cuvette containing 1.5 mM DTNB. The amount of GSH remaining in the reaction is determined by measuring the absorbance at 412 nm with an extinction of coefficient 13.0 mM^{-1} cm^{-1}.

3. Method 3: Assay of GSH Removal by Polarography

a. Reagents. 100 mM potassium phosphate buffer, pH 7.0, containing 1 mM sodium azide and 2 mM EDTA; 4 mM GSH (AR) in distilled water; 5 mM H_2O_2 in distilled water prepared from a commercial solution (30%); 0.7 M $HClO_4$.

b. Procedure. 1 mL of 100 mM phosphate buffer is incubated with 0.5 mL GSH solution for 10 min at 37°C. The reaction is started by addition of 0.5 mL of 5 mM H_2O_2 and stopped after various times by addition of 2 mL of 0.7 M $HClO_4$. The acidified assay mixture is cooled to room temperature and bubbled with nitrogen for 3 min. Polarogram is recorded between 0 and -0.5 V with 5 μA full scale, versus a mercuric sulfate reference electrode. The calibration curve is prepared by adding $HClO_4$ to a series of different GSH concentrations. The control is measured without enzyme addition.

4. Definition of Units

In the above three methods, 1 unit of the enzyme activity is defined as the amount of enzyme oxidizing 1 μmol of NADPH per min at 37°C. The specific activity expresses units/mg of protein or units/μmol of protein. Some GPX specific activities with different peroxide substrates are listed in Table 6.

B. Factors Affecting Activity Determination

The coupled enzyme method is suitable for activity determination of both purified and crude enzymes. In working with crude biological materials (e.g., liver and kidney), it is necessary to use H_2O_2 as the substrate in order to differentiate GPX from glutathione S-transferase which has similar activity on organic hydroperoxides but is unreactive toward H_2O_2. In this case, sodium azide should also be added to inhibit catalase. For blood red cells, the conversion of hemoglobin into cyanomethemoglobin prior to assay is necessary because of the interference of methemoglobin (20). PHGPX activity is measured by this method with the phospholipid hydroperoxide substrate dispersed in mixed micellar form using Triton X-100 (5).

The method for assay of GSH removal is suitable for determining only purified enzymes. Inorganic halides interfere with polarographic determination. Other sulfhydryl compounds such as mercaptoethanol and cysteine will interfere with both polarography and DTNB methods.

In all assay systems, the assay mixture should be preincubated with GSH. The inactive state of the enzyme (E-SeOOH) can be activated by GSH to the active E-Se-SG form. High concentrations of polyvalent cations (e.g., Hg^{2+}, Cu^{2+}, and Zn^{2+}) can inhibit GPX activity.

VII. PURIFICATION

Several GPXs have been purified from various sources (1, 5–14, 21, 63, 66, 67). A currently used procedure for cGPX isolation has been described by Wendel (20). This strategy includes dialysis of the hemolysate, organic solvent precipitation, ion-exchange chromatography on DEAE-Sephadex, hydrophobic chromatography on phenyl-Sepharose, gel filtration on Biogel P-100, or hydroxyapatite chromatography.

Step 1. Hemolysate. Eight liters of bovine blood is centrifuged. The erythrocytes are washed twice with 0.9% NaCl and are hemolyzed by adding water to

form 8 L of hemolysate. Six liters of 0.6 M potassium phosphate at pH 6.6 is added and the mixture is stored in the cold for 2–12 h.

Step 2. Organic solvent precipitation. A mixture of chloroform/ethanol (3:5, v/v), 4 L, cooled to −20°C, are added dropwise to the vigorously stirred hemolysate. The dark-brown precipitate is removed by centrifugation at 2000 g for 30 min at 0°C. The yellowish supernatant liquid is filtered and immediately concentrated to ~1 L with a membrane with exclusion limits of 50 kDa.

Step 3. Phosphate precipitation. One liter of concentrated enzyme solution is mixed with 2 L of 3.65 M potassium phosphate at pH 7.0. The floating precipitate is collected by filtration and dissolved in 0.7 M potassium phosphate at pH 8.0.

Step 4. Phenyl-Sepharose. The enzyme is adsorbed in a batch step to phenyl-Sepharose equilibrated with 0.7 M potassium phosphate at pH 8.0. The adsorbed gel is added to a column (2×30 cm) previously prepared with 5 mL of fresh equilibrated gel. The column is washed with 300 mL of 0.7 M phosphate buffer and then with 300 mL of 0.5 M phosphate buffer with the same pH. A linear, 300-mL gradient, from 100 to 10 mM potassium phosphate, pH 8.0, is used to elute the enzyme at a flow rate of 6 mL/h.

Step 5. DEAE-Sephadex. The pooled fraction is diluted to a final buffer concentration of 5 mM phosphate, pH 8.0, and applied to a column of DEAE-Sephadex equilibrated by the same buffer. After washing with 1 L of starting buffer, the enzyme is eluted with a linear gradient of 5–80 mM potassium phosphate containing 1 mM GSH at pH 8.0.

Step 6. S-300 Sephacryl. The active fractions are concentrated by a Diaflo cell to 15 mL and charged onto a S-300 Sephacryl column (2.0×180 cm), equilibrated with 20 mM potassium phosphate, pH 8.0, containing 0.5 M NaC1, with a rate of 12 mL/h. The enzyme is eluted as a single protein that has an apparent molecular weight of ~100 kDa.

Step. 7. The enzyme is dialyzed against 5 mM potassium phosphate at pH 7.4, adsorbed onto a hydroxyapatite column (1×100 cm), equilibrated with the same buffer, and eluted with a gradient up to 80 mM phosphate.

Purification of PHGPX from pig heart has been described by Ursinbi et al. (49). This procedure can also be used for other tissues.

Step 1. A total of 500 g of ventricular muscle is prepared from pig heart and is minced and thoroughly homogenized in a Polytron mixer, set at maximum power, for 5 min in 3 volumes of ice-cold 0.1 M Tris-HC1 (pH 7.4), 5 mM mercaptoethanol. The soluble fraction is prepared by two centrifugations of the homogenate: 30 min at 10,000 g and 45 min at 100,000 g. Before the second centrifugation, the supernatant is filtered through cheesecloth to eliminate fluffy material. The supernatant is dialyzed exhaustively against 10 mM potassium phosphate buffer (pH 7), 5 mM mercaptoethanol. During dialysis some proteins precipitate and are eliminated by centrifugation.

Step 2. The supernatant is applied to a DEAE-Sepharose 6B column (13×5.5 cm) equilibrated with 10 mM potassium phosphate buffer (pH 7), 5 mM mercaptoethanol. The column is washed with 2 L of the equilibration buffer and then eluted with 0.5 L of 0.2 M potassium phosphate buffer (pH 7), 5 mM mercaptoethanol. The active fractions are collected and pooled, and 10% (v/v) (final concentration) glycerol is added.

Step 3. The above fraction is loaded onto a Sepharose-bromosulfophthalein glutathione (BSP) affinity column. The column is equilibrated with 25 mM Tris-HCI (pH 7.2), 5 mM mercaptoethanol, and 10% (v/v) glycerol. After the sample is loaded, the column is washed with 300 mL of 25 mM Tris-HCl (pH 7.2), 100 mM KSCN, 5 mM mercaptoethanol, aand 10% (v/v) glycerol. The elution is carried out with 25 mM Tris-HCl (pH 7.6), 300 mM KSCN, 5 mM mercaptoethanol, and 10% (v/v) glycerol. The active fractions are pooled and concentrated to 5–10 mL using an Amicon ultrafiltration apparatus with a YM10 membrane.

Step 4. The above fractions are applied onto a Sephadex G-50 column (140×5.5 cm) equilibrated with 25 mM Tris-HCl (pH 7.4), 5 mM mercaptoethanol, and 10% (v/v) glycerol. The active fractions are pooled and concentrated with the same ultrafiltration apparatus as before. This fraction is dialyzed against potassium phosphate buffer (pH 6.5), 0.1 M KCl, and 5 mM mercaptoethanol.

Step 5. The final purification step is carried out by HPLC using a weak cation-exchange column, TSK CM. The chromatographic conditions are as follows: Buffer A: 10 mM potassium phosphate buffer, 100 mM KCl, 5 mM mercaptoethanol (pH 6,5); buffer B: 10 mM potassium phosphate buffer, 300 mM KCl, 5 mM mercaptoethanol (pH 6.5). The gradient from 0–100% buffer B is developed in 25 min after 3 min in isocratic conditions. Injection volume is < 0.2 mL. Peaks isolated from several runs are pooled, and 10% glycerol is added.

REFERENCES

1. GC Mills. Hemoglobin catabolism. I. Glutathione peroxidase, an erythrocyte enzyme which protects hemoglobin from oxidative damage. J Biol Chem 229:189–197, 1957.
2. C Little, PJ O'Brien. An intracellular GSH-peroxidase with a lipid peroxide substrate. Biochem Biophys Res Commun 31:145–150, 1968.
3. BO Christophersen. Formation of monohydroxy-polyenic fatty acid from lipid peroxides by a glutathione peroxidase. Biochim Biophys Acta 164: 35–46, 1968.
4. JT Rotruck, AL Pope, HE Ganther, AB Swanson, D Hafeman, WG Hoekstra. Selenium: biochemical role as a component of gluthathione peroxidase. Science 179:588–590, 1973.

4a. L Flohé, WA Gunzler, HH Schock. Glutathione peroxidase: a selenoenzyme. FEBS Lett 32: 132–134, 1973.

5. F Ursini, M Maiorini, C Gregolin. The selenoenzyme phospholipid hydroperoxide glutathione peroxidase. Biochim Biophys Acta 839:62–70, 1985.
6. KR Maddipati, C Gasparski, LJ Matnett. Characterization of the hydroperoxide-reducing activity of human plasma. Arch Biochem Biophys 254: 9–17, 1987.
7. DJ Broderick, JT Deagen, PD Whanger. Properties of glutathione peroxidase isolated from human plasma. J Inorg Biochem 30:299–308, 1987.
8. K Takahashi, N Avissar, J Within, H Cohen. Purification and characterization of human plasma glutathione peroxidase: a selenoglycoprotein distinct from the known cellular enzyme. Arch Biochem Biophys 256:677–686, 1987.
9. FF Chu, JH Doroshow, RS Esworthy. Expression, characterization, and tissue distribution of a new cellular selenium-dependent glutathione peroxidase, GSHPx-GI. J Biol Chem 268:2571–2576, 1993.
10. RA Lawrence, RF Burk. Glutathione peroxidase activity in selenium-deficient rat liver. Biochem Biophys Res Commun 71:952–958, 1976.
11. B Ketterer, LG Christodoulides. Enzymology of Cytosolic glutathione S-transferases. Adv Pharmacol 27:37–49, 1994.
12. RS Esworthy, FF Cu, RJ Paxton, S Akmen, JH Doroshow. Reactivity of plasma glutathione peroxidase with hydroperoxide substrates and glutathione. Arch Biochem Biophys 307:29–34, 1993.
13. JP Thomas, M Maiorino, F Ursini, AW Girotti. Protective action of phospholipid glutathione peroxidase against membrane damaging lipid peroxidation: in situ reduction of phospholipid and cholesterol hydroperoxide. J Biol Chem 265:454–461, 1990.
14. R Schuckelt, R Brigelius-Flohé, M Maiorino, A Roveri, J Reumkens, W Straburger, L Flohé. Phospholipid glutathione peroxidase is a selenoenzyme distinct from the classical glutathione peroxidase as evident from cDNA and amino acid sequencing. Free Rad Res Commun 14:343–361, 1991.
15. J Smith, A Shrift. Phylogentic distribution of glutathione peroxidase. Comp Biochem Physiol 63B: 39–44, 1979.
16. ME Tappel, J Chaudiene, AL Tappel. Glutathione peroxidase activity of animal tissues. Comp Biochem Physiol 73B:945–949, 1982.
17. F Mazeaud, J Marcel, AM Michelson. Distribution of superoxide dismutase and glutathione peroxidase in the carp: erythrocyte manganese SOD. Biochem Biophys Res Commun 86:1161–1168, 1979.
18. S Ahmad, MA Beilstein. RS Pardini. Glutathione peroxidase activity in insects: a reassessment. Arch Insects Biochem Physiol 12:31–49, 1989.
19. LT Tran, Y Inoue, A Kimura. Oxidative stress response in yeast: partial purification and some properties of a membrane bound glutathione peroxidase from *Hansenula markii*. Biochim Biophys Acta 1164:166–172, 1993.
20. A Wendel. Glutathione peroxidase. Methods Enzymol 77:325–333, 1981.
21. A Pierie. Glutathione peroxidase in lens and a source of hydrogen peroxide in aqueous humour. Biochem J 76:244–253, 1965.
22. RA Lawrence, RA Sunde, GL Schwartz, WG Hoelstra. Glutathione peroxidase activity in rat lens and other tissues in relation to dietery selenium intake. Exp Eye Res 18:563–569, 1974.
23. L Zhang, M Maiorino, A Roveri, F Ursini. PHGPX: specific activity in tissues of rats of different age and comparison with other GPX. Biochim Biophys Acta 1006:140–143, 1989.
24. A Roveri, A Casasco, M Maiorino, P Dalan, A Calligaro, F Ursin. Phospholipid hydroperoxide glutathione peroxidase of rat testis. J Biol Chem 267:6142–6146, 1992.
25. DV Godin, ME Garnett. Species-related variations in tissue antioxidant status. I. Differences in antioxidant enzyme profiles. Comp Biochem Physiol 103B:737–742, 1992.
26. CK Chow, AL Tappel. Response of glutathione peroxidase to dietary selenium in rats. J Nutr 104:444–451, 1974.
27. RE Pinto, W Bartley. The effect of age and sex on glutathione reductase and glutathione peroxidase activities and on aerobic glutathione oxidation in rat liver homogenates. Biochem J 112:109–115, 1969.
28. K Reddy, AL Tappel. Effect of dietary selenium and antioxidized lipids on the glutathione peroxidase system of the gastrointestinal tract and other tissues of rat. J Nutr 104:1069–1078, 1974.
29. K Ge, G Yang. The epidemiology of selenium deficiency in the etinological study of endemic diseases in China. Am J Clin Nutr Suppl 57:259–263, 1993.

30. M Välimäki, G Alfthan, J Pikkarinen, R Ylikahri, M Salaspuro. Blood and liver selenium concentrations in patients with liver disease. Clin Chim Acta 166:171–176, 1987.
31. JP Thomas, AW Girrotti. Role of lipid peroxidation in hematoporphyrin derivative sensitized photokilling of tumour cells. Protective effects of glutathione peroxidase. Cancer Res 49:1682–1686, 1989.
32. E Antilla, T Westermark. On the ethiopathogenesis and therapy of Down's syndrome. Int J Dev Biol 33:183–189, 1989.
33. L Flohé. Glutathione peroxidase. Basic Life Sci 49:663–668, 1988.
34. B Ren, WH Huang, B Akesson, R Ladenstein. The crystal structure of selenoglutathione peroxidase from human plasma at 2.9Å resolution. M Mol Biol 268:869–885, 1997.
35. SJ Chambers, N Lambert, G Williamson. Purification of a cytosolic enzyme from human liver with phospholipid hydroperoxide glutathione peroxidase activity. Int J Biochem 26:1279–1286, 1994.
36. WA Günzler, GJ Steffens, A Grossmann, S Kim, F Otting, A Wendel, L Flohé. The amino acid sequence of bovine glutathione peroxidase. Hoppe-Seyler's Z Physiol Chem 365:195–212, 1984.
37. S Yoshimura, S Takekoshi, K Watanabe, Y Fujii-Kuriyama. Determination of nucleotide sequence of cDNA coding rat glutathione peroxidase and diminished expression of the mRNA in selenium deficient rat liver. Biochem Biophys Res Commun 154:1024–1028, 1988.
38. I Chambers, J Frampton, P Goldfarb, M Affara, W Mcbain, PR Harrison. The structure of the mouse glutathione peroxidase gene: the selenocysteine in the active site is encoded by the 'termination' codon TGA. EMBO J 5:1221–1227, 1986.
39. K Ishida, T Morino, K Takagi Y, Sukenaga. Nucleotide sequence of a human gene for glutathione peroxidase. Nucleic Acids Res 15:10051, 1987.
40. RA Sunda, JA Dyer. Phospholipid glutathione peroxidase: full length pig blastocyst cDNA sequence and regulation by Se status. Biochem Biophys Res Commun 193:905–911, 1993.
41. K Takahashi, M Akasaka, Y Yamamoto, C Kobayashi, J Mizoguchi, J Koyama. Primary structure of human plasma glutathione peroxidase deduced from cDNA sequence. J Biochem 108:145–148, 1990.
42. A Wendel. Glutathione peroxidase. In WB Jakoby, ed. Enzymatic Basis of Detoxification. New York: Academic Press, Vol I 1980, pp 333–353.
43. F Ursini, M Maiorino, R Brigelius-Flohé, KD Aumann, A Roveri, D Schomburg, L Flohé. Diversity of glutathione peroxidases. Methods Enzymol 252:38–53, 1995.
44. RL Maser, BS Magenheimer, JP Calvet. Mouse plasma glutathione peroxidase. J Biol Chem 269:27066–27073, 1994.
45. O Epp, R Landenstein, A Wendel. The refined structure of the selenoenzyme glutathione peroxidase at 0.2-nm resolution. Eur J Biochem 133:51–69, 1983.
46. SC Gamble. Selenium-dependence glutathione peroxidase and other selenoproteins: their synthesis and biochemical roles. J Chem Tech Biotechnol 68:123–134, 1997.
47. M Akasaka, J Mizogushi, KA Takahashi. Human cDNA sequence of novel glutathione peroxidase related-protein. Nucleic Acids Res 18:4619, 1990.
48. JM Martin-Alonso, S Ghosh, M Coca-Prados. Cloning of bovine pGPX cDNA from the ocular ciliary epithelium: expression of the plasma and cellular forms within the mammalian eye. J Biochem 114:281–291, 1993.
49. M Maiorino, C Gregolin. Phospholipid glutathione peroxidase. Methods Enzymol 186:448–457, 1990.
50. F Ursini, M Maiorino, M Valente, C Gregolin. Purification from pig liver of a protein which protects liposomes and biomembrances from peroxidative degradation and exhibits GPX activity on phospholipid hydroperoxides. Biochim Biophys Acta 71:197–211, 1982.
51. M Maiorino, F Ursini, M Leonelli, N Finato, C Gregolin. A pig heart peroxidation inhibition protein with GPX activity on phospholipid hydroperoxides. Biochem Int 5:575–583, 1982.
52. ZP Wu, D Hilvert. Selenosubtilisin as a glutathione peroxidase mimic. J Am Chem Soc 112:5647–5648, 1990.
53. IM Bell, ML Fisher, ZP Wu, D Hilvert. Kinetic studies on the peroxidase activity of selenosubtilisin. Biochemistry. 32:3754–3862, 1993.
54. GM Luo, ZQ Zhu, L Ding, QA Sun, Z Liu, JC Shen. Generation of selenium-containing abzyme by using chemical mutation. Biochem Biophys Res Commun 198:1240–1247, 1994.
55. L Flohé, G Loschen, WA Günzeler, E Eichele. Glutathione peroxidase. V. The kinetic mechanism. Hoppe-Seyler's Z Physiol Chem 353:987–999, 1972.
56. RS Esworthy, FF Chu, P Geiger, AW Girotli, JH Doroshow. Reactivity of pGPX with hydroperoxide substrates and glutathione. Arch Biochem Biophys 307:29–34, 1993.
57. J Caudiere, AL Tappel. Purification and characterization of the selenium-glutathione peroxidase from hamster liver. Arch Biochem Biophys 226:448–457, 1983.
58. KR Maddipati, LJ Marnett. Characterization of the major hydroperoxide-reducing activity of human plasma. J Biol Chem 262:17398–17403, 1987.
59. JR Prohaska, HE Ganther. Glutathione peroxidase activity of glutathione S-transferases purified from rat liver. Biochem Biophys Res Commun 6:588–590, 1973.
60. L Flohé, B Eisele, A Wendel. Glutathione peroxidase. I. Reindarstellung und Molekulargewichtsbestimung-

en. Hoppe-Seyler's Z Physiol Chem 352:151–158, 1971.
61. Y Yamamoto, K Takahashi. Glutathione peroxidase isolated from plasma reduces phospholipid hydroperoxides. Arch Biochem Biophys 305:541–545, 1993.
62. KR Maddipati, C Gasparski, LJ Marnett. Characterization of the hydroperoxide-reducing activity of human plasma. Arch Biochem Biophys 254: 9–17, 1987.
63. HE Ganther, RJ Kraus. Glutathione peroxidase. Methods Enzymol 107:593–598, 1984.
64. YC Awasthi, E Beutler, SK Srivastata. Purification and properties of human erythrocyte glutathione peroxidase. J Biol Chem 250:5144–5149, 1975.
65. DTY Chiu, FH Stults, AL Tappel. Purification and properties of rat lung soluble glutathione peroxidase. Biochim Biophys Acta 445:558–566, 1976.
66. TC Stadtman. Selenium-dependent enzymes. Annu Rev Biochem 49:93–110, 1980.
67. J Chaudiere, EC Wilhelmsen, AL Tappel. Mechanism of selenium glutathione peroxidase and its inhibition by mercaptocarboxylic acids and other mercaptans. J Biol Chem 259:1043–1050, 1984.
68. DE Paglia, WN Valentine. Studies on the quantitative and qualitative characterization of erythrocyte glutathione peroxidase. J Lab Clin Med 70:158–169, 1967.
69. WA Guzler, H Kremers, L Flohé. An improved coupled test procedure for glutathione peroxidase in blood. Z Klin Chem Klin Biochem 12:444–448, 1974.
70. JJ Zakowski, AL Tappel. A semiautomated system for measurement of glutathione in the assay of glutathione peroxidase. Anal Biochem 89:430–436, 1978.

30

Glucose Oxidase

A. J. Vroemen
DSM Food Specialties, Delft, The Netherlands

I. INTRODUCTION

Glucose oxidase (GOX) is produced predominantly by fungi as part of an enzyme complex also containing catalase. The best-studied microorganisms are species of *Aspergillus* (1–3) and *Penicillium* (4, 5). In *Aspergillus* the enzymatic complex is located in cell compartments called peroxisomes (6), which results in the need to open the fungal cell walls before the enzyme can be released and purified. The enzyme complex of *Penicillium* is secreted into the extracellular environment (7). Almost all GOX preparations available on the market are produced by *Aspergillus niger*. These preparations are either highly or somewhat or completely exempt of catalase (see Sec. II.A.1). This chapter will focus mainly on GOX of *Aspergillus niger*.

The question can be raised why fungi like *Aspergillus niger* invest a high amount of nutrients and energy in the synthesis of the enzymatic complex. As we will see later, the catalyzed reaction of glucose to gluconic acid does not yield energy for the microorganism. Most probably the enzymatic complex gives the microorganiism an ecological advantage in the soil. In nature, GOX is produced by the fungus only when glucose is present: It is an inducible enzyme. When glucose is liberated from, for instance, starch or cellulose, the synthesis of the enzymatic complex starts and in the presence of air, glucose is oxidized to gluconic acid with simultaneous production of hydrogen peroxide. The decrease of the pH caused by the gluconic acid as well as the antibacterial effect of the hydrogen peroxide produced, are favorable for the fungus. In addition, *A. niger* is able to consume the gluconic acid produced, which is not the case for most of the competing microorganisms. Bacteria like *Gluconobacter* are also capable of converting glucose into gluconic acid, but these bacteria use a different mechanism. *Gluconobacter oxidans* contains two types of glucose dehydrogenases, one PQQ and one NADP dependent, which convert glucose to gluconic acid without formation of hydrogen peroxide. The PQQ-dependent enzyme seems to be the most important (8). This oxidation process yields energy for the bacteria concerned. It is notable that these bacteria are rather acid tolerant.

II. REACTION CATALYZED

As substrates GOX uses β(D)-glucose and oxygen. Two hydrogen atoms are first transferred from glucose to the coenzyme FAD during formation of δ-gluconolactone (9). Subsequently the enzyme transfers the two hydrogen atoms directly to molecular oxygen during formation of hydrogen peroxide. The δ-gluconolactone is hydrolyzed to gluconic acid spontaneously or by the enzyme gluconolactonase.

$$C_6H_{12}O_6 + \text{E-FAD} \rightleftharpoons C_6H_{10}O_6 + \text{E-FADH}_2 \quad (1)$$

glucose gluconolactone

$$C_6H_{10}O_6 + H_2O \longrightarrow C_6H_{12}O_7 \quad (2)$$

gluconolactone gluconic acid

$$\text{E-FADH}_2 + O_2 \longrightarrow \text{E-FAD} + H_2O_2 \quad (3)$$

$$C_6H_{12}O_6 + H_2O + O_2 \rightleftharpoons C_6H_{12}O_7 + H_2O_2$$

glucose gluconic acid hydrogen peroxide

The fact that GOX uses only β-glucose as substrate does not mean that glucose can be only partially oxidized; during the process α-glucose spontaneously mutarotates to α-,β-glucose, making all the glucose available as substrate. GOX is rather specific for glucose. There is < 1% activity on related sugars like xylose and galactose. Also, the activity on other natural mono- and disaccharides is very low. In a systematic study Whitaker showed that in the deoxyglucoses, replacement of the hydroxyl group by a hydrogen atom at successively the 6, 4, 2, 3 and 5 position resulted in respectively 10%, 4%, 3%, 1% and 0% remaining activity (10).

The hydrogen peroxide formed causes the reaction to stop since it inactivates the GOX rapidly and irreversibly. In principle, hydrogen peroxide can be hydrolyzed by the enzyme catalase, or the active oxygen can be transferred spontaneously or enzymatically to another molecule.

As mentioned before, the fungi concerned also produce catalase, which oxidizes/reduces the hydrogen peroxide produced into water and oxygen. The overall reaction of the enzyme complex becomes:

$$2C_6H_{12}O_6 + 2H_2O + 2O_2 \rightleftharpoons 2C_6H_{12}O_7 + 2H_2O_2 \quad (4)$$

$$2H_2O_2 \longrightarrow 2H_2O + O_2 \quad (5)$$

Overall reaction:

$$2C_6H_{12}O_6 + O_2 \longrightarrow C_6H_{12}O_7 \quad (6)$$

III. ENZYME CHARACTERISTICS

A. Michaelis-Menten Constants

The enzyme has two substrates: glucose and molecular oxygen. Simple Michaelis-Menten kinetics results in

$$v = k_{cat} \cdot [E] \cdot \frac{c_{glu}}{K_{m_{glu}} + c_{glu}} \cdot \frac{c_{O_2}}{K_{m_{O_2}} + c_{O_2}}$$

The K_m values as determined by Gibson et al. (11)

$K_{m_{glu}} = 110$ mM; $K_{m_{O_2}} = 0.48$ mM

(both determined at 27°C.)

Here the molarity of glucose is defined as total glucose, not as β-glucose.

The value of 110 mM mentioned by Gibson seems rather high. Other values mentioned in the literature are 37 mM (12), which is more in agreement with GOX from other microorganisms. The *Penicillium amagasakiense* enzyme has a higher affinity for glucose: a K_m value of 5.2 mM is reported (13). The problem in the determination of the Michaelis-Menten constant for glucose is that precautions must be taken to ensure that the concentration of dissolved oxygen, which is consumed during the reaction, remains constant. Technically it seems possible to maintain the dissolved oxygen concentration constant during the reaction in for instance a fermenter, enabling the determination of correct velocity values at different glucose concentrations. However, to the author's best knowledge such an approach has never been published so far. Initial velocity, v_o, can also be used to obtain correct data.

These K_m values mentioned above show that the affinities of GOX for the two substrates are rather poor. This is especially true for the substrate oxygen when we compare the K_m for oxygen with the solubility of oxygen in water. At 1 bar, 25°C, and in the presence of air, the maximum solubility of oxygen is ~6 mg/L or 0.2 mM, equaling < 50% of the K_m. Even with pure oxygen the maximum solubility of ~30 mg/L is only twice the K_m. With glucose concentrations far below the K_m value, which is between 7 to 20 g/L for the *Aspergillus* enzyme, the velocity of the reaction will be low. As a consequence it can be concluded that for the elimination of low quantities of glucose or oxygen from certain foods, high quantities of enzyme and/or long incubation times are necessary even under optimal conditions. The affinity of the enzyme catalase for its substrate hydrogen peroxide is extremely low: K_m = 1.1 M or 37.4 g/L. This aspect is very important in certain applications.

B. Determination of GOX Activity

From a theoretical point of view, the analysis of GOX is rather complicated. The enzyme has two substrates: glucose and oxygen. In principle high glucose concentrations can be chosen, far above the K_m, so that the

velocity of the reaction is no longer dependent on the glucose concentration. This is more difficult for the second substrate oxygen. To obtain oxygen concentrations in solution far above the K_m, very high oxygen pressures have to be chosen, which is not practical. The concentration of oxygen is below the K_m if the reaction is performed under normal conditions, and as a result the velocity of the reaction is below the maximum velocity.

An extra complication is that the reaction consumes oxygen. When there is insufficient supply to maintain the oxygen concentration at a saturation level, there will not be a linear production of gluconic acid in time at a fixed enzyme concentration or a linear relationship between the amount of gluconic acid produced within a fixed time and amount of enzyme. Such linear relationships are desirable for an analytical method. Therefore, an analytical method for GOX is preferably based on a system in which only very small quantities of oxygen are consumed. A sensitive method is not realized when it is based on the consumption of glucose or the formation of gluconic acid. If the analysis is based on the consumption of oxygen, the result is influenced by the presence of catalase. In this type of method high quantities of GOX-free catalase have to be added. This is the principle underlying a method described in 1953 by Scott (14) and in 1957 by Underkofler (15). In a Warburg equipment the amount of oxygen consumed under optimal conditions was determined. The unit most frequently used is the Sarrett unit, which is defined as the amount of enzyme which catalyzes the uptake of 10μL oxygen/ min at 30°C, pH 5.9, and a glucose concentration of 3%. Working with a Warburg is rather laborious, and therefore Underkofler also describes a method using a sodium hydroxide solution neutralizing the gluconic acid produced.

A very sensitive and accurate method is based on the production of hydrogen peroxide. The amount of hydrogen peroxide is determined indirectly by the oxidation of a chromogen catalyzed by a peroxidase. Owing to the very high affinity of this peroxidase for hydrogen peroxide compared to catalase, the presence of this last enzyme in GOX preparations does not influence the analytical result. As chromogen, *o*-dianisidine, *o*-toluidine, and others are used, the developed color is measured in a spectrophotometer, and by using internal standards the amount of oxidized glucose can be determined. The activity is often expressed as IU (international units), defined as micromolar glucose oxidized per min under optimal conditions. For the *Aspergillus niger* enzyme the relationship between IU and Sarrett units is determined as 1 IU = 1.12 SU (16, 18) or 1.1 SU(17). (See Annex 1 for a detailed description of a method with *o*-dianisidine.) Methods based on the oxidation of a chromogen by hydrogen peroxide are now generally used. The relationship between IU and Sarrett units can be different for glucose oxidation from different organisms. Finally, it should be mentioned that comparison of units in literature is extremely difficult owing to different incubation conditions, including saturation levels of oxygen, and different unit definitions. The best thing to do is to work with an internal standard of GOX of known activity.

C. Specific Activity

By measuring the oxygen consumption of a pure, catalase-free GOX preparation of *A. niger*, Tsuge et al. (21) found a specific activity of 172 IU/mg protein at 30°C and pH 5.6. About the same value has been reported by Hayashi and Nakamura (22). Several research groups have purified the *A. niger* enzyme by ion-exchange chromatography and obtained pure preparations with activities from 200 to 250 Sarrett units/mg protein, equaling 180–225 IU/mg protein. Pure catalase-free preparations can be obtained from compa-

Annex 1 Analysis of Glucose Oxidase

The method used by Whittington (26) is mentioned here:
Glucose solution A: 2 g/L in 0.2 *M* Tris phosphate buffer, pH 7.0.
o-Dianisidine solution B: 2 g/L in 0.2 *M* Tris phosphate buffer pH 7.0.
Horseradish peroxidase solution C: 60 units/mL in 0.2 *M* Tris phosphate buffer pH 7.0.
Glycerol.
Enzyme solution standard D: 10 IU glucose oxidase/mL.
Hydrochloric acid solution E: 5 *M*.
All reagents Sigma quality.
Preincubate all solutions at least 10 min at 30°C.
Add to 1 mL A, 0.1 mL B, 0.1 mL C, and 0.8 mL glycerol. Mix carefully.
Add 10–20 μL of an enzyme sample containing 0–10 IU/mL.
Incubate 30 min at 30°C.
Stop reaction by adding 2 mL of 5 *M* hydrochloric acid solution. Mix carefully.
Oxidized *o*-dianisidine is measured in a spectrophotometer at 525 nm.
Compare with internal standard of 0–10 IU/mL enzyme.

nies selling research chemicals, or by growing a transgenic yeast harboring a GOX gene.

The specific activity of the purified *Penicillium amagasakiense* enzyme is ~60% higher than that of the *A. niger* enzyme (22).

D. Turnover Number

Gibson et al. (11) found a turnover number of 16,200/min. Whittington et al. (27) cloned the *A. niger* enzyme in yeast and found a value of 17,000–20,000 for the yeast-derived enzyme. V_{max} values of 235/sec for the wild-type enzyme and 500 for the yeast-derived enzyme are found, but it remains unclear whether these differences are really significant.

E. pH Activity Profile

The pH activity curves for both the *Penicillium* and *Aspergillus* enzymes show a horizontal profile between pH 4.5 and 7.5, with a sharp decline on both sides (10, 20). There is almost no activity at < pH 3.0 or > pH 8.5. GOX is stabilized by its substrate glucose (32), explaining why in certain applications with a pH between 2.5 and 3.0 and with a high concentration of glucose the enzyme is still active. Also at > pH 8.0 the stability of the enzyme is improved by adding the substrate.

F. Temperature Activity Profile

In determination of the temperature activity profile of GOX, some specific complications are encountered. GOX is sensitive to the hydrogen peroxide formed especially at higher temperatures. This means that when a method is applied in which the hydrogen peroxide is not removed immediately and completely, the optimum temperature and the maximum temperature will be low as compared to a method where this is done properly (10). Moreover, long incubation times give a lower optimum. In the analytical method using perosidase and a chromogen, the hydrogen peroxide reacts immediately with the chromogen. This method gives an activity profile which is rather constant with time between 30°C and 60°C. Above 60°C activity goes down slowly with still 10% activity at 70°C but no activity at 80°C.

G. Protein Properties

The molecular weights of the enzymes from both *Aspergillus* and *Penicillium* have been determined at between 140 and 160 kDa (19–21). The enzyme consists of two identical subunits with 1 molecule FAD per subunit as coenzyme. Because of this, the color of the oxidized protein is yellow with absorption maxima at 377 and 455 nm. Under anaerobic conditions in the presence of glucose, the enzyme molecule is reduced and the color disappears. When oxygen is admitted to the system the color reappears. The FAD is not covalently linked and can easily be removed by acid, urea, or guanidine. But without these reagents, the FAD is bound to the enzyme. The apoenzyme is not active but activity is restored upon incubation with FAD (15).

GOX is a glycoprotein. The amount of carbohydrate in different preparations from *A. niger* can vary from 10% to 18% (22, 23). Mannose is by far the most important sugar with amounts of 70–80%. Galactose contributes ~5% and glucosamine ~15% to the total carbohydrate content. In the *Penicillium* enzyme Kalisz (13) found 95 residues of mannose, 12 residues of glucosamine, and five residues of galactose per molecule of enzyme, and a total carbohydrate content of 13%.

In the *A. niger* enzyme the sugar molecules are N and O linked. By selective elimination of the O-linked sugars Takegawa (12) showed that predominantly mannose monomers are linked to serine and threonine, but the exact place in the molecule is not yet known. The N-linked sugar moiety can be selectively removed by an enzyme from *Flavobacterium*, resulting in the liberation of 30% of the total carbohydrates. The partly deglycosylated enzyme has the same kinetic and biochemical properties and resistance to proteases as the native enzyme except that the native enzyme precipitates at higher concentrations of ammonium sulfate or TCA, and the deglycosylated enzyme is less stable in relation to pH and temperature. The same results were obtained with the *Penicillium* enzyme by Kalisz et al. (13). In this case 95% of the carbohydrate was split off by the enzymatic treatment. Losses in pH and temperature stability were observed as well.

The enzyme from *Phanerochaete chrysosporium* (24) was found to be a flavoprotein with a molecular weight of ~160 kDa and containing 2 mol FAD per mol protein, but it does not seem to contain any carbohydrate and its specificity is lower. Although glucose is the main substrate, considerable activity is still found on sorbose, xylose, and maltose.

The gene of the *A. niger* enzyme has been isolated and the sequence analyzed by various research groups with identical results (25–27). This sequence is now available in data bases. The gene codes for a signal peptide of 22 amino acids (1–22), followed by the 583 amino acid subunit itself (–23–605). The molecular weight of the subunit plus signal peptide is calculated

to be 65,638, and without signal peptide it is 63,250. With ~16% sugars and two molecules of FAD the total molecular weight can be calculated to be ~152 kDa. When the gene is expressed in yeast, an enzyme is obtained with a higher glycolysation level and an improved thermostability. This is in line with the observed lower thermostability the deglycosylated enzymes. The kinetic parameters of the yeast-derived enzyme and the original one are not significantly different. The yeast expression system can be used to obtain GOX completely free of catalase. The transgenic yeast must not been grown on glucose since the hydrogen peroxide formed will inactivate the enzyme and stop growth. Instead it can be grown on saccharose, since this sugar is hydrolyzed by membrane-bound invertase in the cell to fructose and glucose, which are immediately metabolized without formation of gluconic acid and hydrogen peroxide.

H. Genetic Aspects

A comparison of the mature GOX sequence with sequences present in data bases shows 26% homology with the alcohol oxidase from *Hansenula polymorpha*. The GOX's from *Aspergillus* and *Penicillium* show 66% identity and 79% similarity. The *Penicillium* enzyme consists of 587 amino acids. The two enzymes are highly conserved in the FAD-binding and substrate-binding domain, in their secondary structures and in regions at the subunit interface. The highest similarity with other oxidoreductases is observed in the FAD-binding domain. Aryloxidase, a FAD-dependent enzyme involved in lignin degradation, has been cloned from *Pleurotus eryngii*. The enzyme is composed of 593 amino acids, 27 of which form a signal peptide. It shows 33% sequence identity with GOX from *Aspergillus niger*. The predicted secondary structures of the two enzymes are very similar (28).

I. Three-Dimensional Structure

The three-dimensional structures of the two enzymes of *Aspergillus* and *Penicillium* have been determined by x-ray crystallography at 2.3 Angstrom resolution (29) and later improved to 1.9 Å resolution (30). The FAD-binding domain is very similar to other FAD-binding proteins, and 11 amino acid residues from different parts of the molecule are involved in this binding. The same is true for substrate binding. The substrate enters a deep pocket and is stabilized by 12 hydrogen bonds and hydrophobic contacts to three aromatic residues and to FAD. A detailed analysis of this substrate-binding site explains the high specificity of GOX described above. Part of the entrance to the pocket is at the interface to the second subunit and is formed by a 20-residue lid. The carbohydrate moiety attached to Asn89 at the top of this lid forms a link between the subunits of the dimer. In total, there are four N-glycosylation sites, with an extended carbohydrate moiety at Asn89. Starting from the 3D structure of the *Pencillium amagasakiense* enzyme, it could be shown by mutation of key conserved active-site residues that Arg516 is involved in the binding to the 3-OH group of the glucose molecule (31). Replacement of this arginine by another amino acid lowers the affinity for the substrate. Aromatic residues on other locations like 73, 418, and 430 are important for the correct orientation and maximum velocity of glucose oxidation.

IV. APPLICATIONS OF GOX IN FOOD

Looking at the reaction catalyzed by the enzyme, the applications are linked to four different aspects:

1. Removal of glucose
2. Removal of oxygen
3. Production of gluconic acid
4. Production of hydrogen peroxide

A separate subject is the application of glucose oxidase as an analytical agent.

A. Removal of glucose (10)

Glucose is a reducing sugar that can react with amino groups in, for instance, proteins, to form colored Maillard components that are often undesirable in food products. Additions of GOX to the food system in the presence of air or an oxygen donor like hydrogen peroxide will result in the conversion of glucose to the non-amine-reactive gluconic acid and thus prevent the formation of these Maillard components. The best known application is the prevention of nonenzymatic browning in egg white powder. A detailed description of this application is given by Scott (10). Treatment can be done up to 50°C and in the pH range from 4 to 7. Egg white is neutral at the time of laying, but the pH rises quickly as carbon dioxide is lost, such that it is generally close to 9 when the egg white is processed. The pH is brought below 7 by adding citric acid; addition of hydrogen peroxide as oxygen donor is advantageous. Owing to the low affinity of GOX for glucose, high quantities of enzyme and/or long incubation times are necessary to remove the glucose almost completely,

making this application less competitive than other systems like addition of active yeast. Canadian researchers have shown that GOX is also efficient in the reduction of nonenzymatic browning in potato products like chips and French fries (33, 34). However, complete removal of glucose is also not realized in this process. It is clear that in this type of application only glucose is converted to a nonreducing component; other sugars, such as maltose and lactose, maintain their reducing characteristics. A solution can be the application of an oxidase active on a broad range of reducing sugars. Some enzyme candidates are under investigation now.

B. Removal of Oxygen

During storage of food, oxygen can have a detrimental effect on quality. As an example, oxidation of unsaturated fatty acids can lead to rancidity of vegetable oils. Oxidation of colored components will change the color of beverages or wine. In addition, oxygen influences the taste of beer in a negative way during storage. The majority of foods contain certain quantitites of glucose. In closed systems, the quantity of oxygen to be removed, in order to prevent oxidation, is generally rather low. Therefore GOX can be used to remove oxygen. If necessary a small quantity of glucose is added. An important aspect is the stability of the enzyme under application conditions. Fruit juices and wine have a very low pH of 2.5–3, conditions in which the enzyme is neither active nor stable. However, the high glucose concentrations in fruit juices appear to have a stabilizing effect on the enzyme.

A large number of publications describe the positive effect on quality of adding GOX to food. A good review is given by Scott (10). Other publications concern: prevention of rancidity in oils, fats and fish (35–37); and prevention of off-flavors and color changes in fruit juices, fruit concentrates, white wine, and beer (10, 38, 39). Despite all these positive results, no applications of adding GOX to food has been realized on an industrial scale until now. The main reason seems to be the existence of competing technologies to prevent oxidation; for example, flushing out of oxygen by carbon dioxide or nitrogen in beverages, addition of antioxidants as BHA, ascorbic acid, sulfite, etc.

C. Production of Gluconic Acid

Milk can be directly acidified by adding glucose, GOX, and hydrogen peroxide as oxygen donor. A variant is combining lactase, which hydrolyzes the milk sugar into glucose and galactose, with GOX and hydrogen peroxide (40). Owing to the pH drop, the milk coagulates. In principle, the same can be done in cheese manufacture, where direct acidification is fairly common. However, in industrial practice, the addition of an acid or gluconolactone, which under the conditions of cheese manufacturing slowly hydrolyzes into gluconic acid, is preferred.

Until, now production of gluconic acid on an industrial scale is done by fermentation with selected strains of *Aspergillus niger* and *Gluconobacter oxydans*. Several attempts have been made toward production of gluconic acid using an enzymatic system. Until recently complete bioconversion was only obtained with glucose solutions of 10% and lower, which is not interesting from an economical point of view. Beverini and Vroemen (41) have now shown that glucose concentrations as high as 40–50% can be completely converted in a fermenter at pH 5–6 and up to 30°C, using low quantities of GOX rich in catalase in a relatively short time. The high catalase content needed is necessary owing to the low affinity of this enzyme for hydrogen peroxide. Under the conditions mentioned, the concentration of hydrogen peroxide remains low such that the two enzymes GOX and catalase are not completely inactivated before the end of the bioconversion. The advantages of this enzymatic process are that no fermentation is necessary (sterilization, nutrients, time), the yield is up to 100%, and the purification of the final product is much easier.

D. Production of Hydrogen Peroxide

Hydrogen peroxide is a potent oxidant, which can be used as an active antimicrobial agent. Based on this property of hydrogen peroxide, several applications of GOX have been developed of which some are applied on a large scale. For these applications the GOX preparations have to be exempt or poor in catalase. Unfortunately, the GOX itself risks also being inactivated by the hydrogen peroxide formed.

1. Toothpaste

In the Netherlands, toothpaste containing enzymes has been developed (42). If sufficient glucose is present, the GOX generates hydrogen peroxide, which kills plaque-forming bacteria in the mouth. To obtain sufficient glucose, amyloglucosidase can be added, which together with the amylase present in saliva, hydrolyzes starch into glucose. In addition, it is claimed that GOX stimulates the lactoperoxidase system in the mouth.

2. Milk and Milk Products

GOX can generate hydrogen peroxide for the lactoperoxidase (LPO) system naturally present in milk. This combined GOX-LPO system has been studied extensively by a number of research groups to solve severe contamination problems in milk and cheese production (43, 44). Especially in cheese made from raw nonpasteurized milk, there is an urgent need for a natural antibacterial system. Although a strong effect could be shown on a high number of pathogens, introduction of the GOX-LPO system has not yet taken place. One of the reasons is that it has not given an absolute guarantee against all pathogens.

3. Baking

An important aspect of baking is the strength or weakness of the dough. Flours with a low protein content are characterized as weak, and the gluten is very extensible under stress but does not return to its original dimensions when the stress is released. Bakers generally prefer strong doughs because of their better rheological and handling properties, which result in a better form and texture of the final bread. Bakers have used dough conditioners to strengthen the dough. These conditioners are mostly nonspecific oxidants like bromates, iodates, and ascorbic acid. In North America and Western Europe, public opinion and legislation are more and more opposed to the use of chemicals in bread. Moreover, these nonspecific oxidants can have a negative influence on the bread aroma. In the United Kingdom bromates are no longer allowed since 1990, and in France no addition of chemicals is permitted in the production of traditional bread (pain à tradition française). Therefore, a need exists to replace the nonspecific oxidants by a natural alternative. Enzymes are judged as natural and in agreement with "clean label." Already in 1957, a patent appeared (45) which describes the addition of GOX to flour to improve the dough quality and the baking properties. As a particular advantage, the combination with ascorbic acid is mentioned. This is already an indication that GOX added gives a better result than ascorbic acid or other nonspecific oxidants alone, which has been confirmed in many tests. This, together with the fact that in that era the acceptance of chemicals was still high, resulted in a low market penetration of the addition of GOX to flour.

The big breakthrough came in the beginning of the 1990s, when researchers of the Finnish company Cultor discovered the synergistic effect of combining several enzymes. The first patent (46) concerns the combination of GOX and sulfhydryl oxidase. The latter enzyme catalyzes the selective oxidation of sulfhydryl groups to disulfides by oxygen.

$$2\ RSH + O_2 \rightleftharpoons RSSR + H_2O_2 \qquad (7)$$

This leads to interprotein disulfide bonds. The role of GOX is not yet completely understood. It clearly participates in the formation of disulfide bonds between gluten proteins, but most probably it also participates in the formation of other bonds like oxidative gelation. This is the coupling of two ferulic acid residues of neighboring arabinoxylan chains by the hydrogenperoxide formed by glucose oxidase.

The second patent (47) concerns the synergistic effect of GOX and hemicellulases, like xylanases. It is believed that GOX makes stronger doughs, permitting the addition of higher amounts of hemicellulases. Addition of such amounts of hemicellulases alone often results in softer and sometimes sticky doughs. Especially, the latter combination of GOX and hemicellulases has obtained a high market acceptance. This "Hemilox" preparation, produced and commercialized by DSM Baking Ingredients under license of Cultor, permits production of clean-label breads of high quality without addition of nonspecific oxidants or emulsifiers (48).

4. Glucose Oxidase as an Analytical Agent

GOX is the most widely employed enzyme as an analytical agent, particularly for the determination of glucose in clinical laboratories, fermentation media, food, feed, etc. Different systems have been developed using glucose oxidase in soluble form, but also in immobilized form as glucose electrodes or sticks for the determination of glucose in urine, as practiced by every physician. For a good detailed review see Raba and Mottola (49).

ACKNOWLEDGMENTS

The author wants to thank his son Casper W. Vroemen of Wageningen University for valuable comments on the manuscript.

REFERENCES

1. B Drews, H Smalla. Brantweinwirtschaft 22, 1969.
2. K Zetelaki, K Vas. Biotech Bioeng 10:45, 1968.
3. W Franke, L Mochel, K Haye. Arch J Mikrobiol 51:323, 1965.

4. T Yoshimura, T Isemura. J Biochem Tokyo 1971 69:839.
4a. S Nakamura, S Hayashi. FEBS Lett 41:327, 1974.
5. JP van Dijken, M Veenhuis. Eur J Appl Microbiol, 9:275, 1980.
6. T Yoshimura, T Isemura. J Biochem (Tokyo) 69:839, 1971.
7. JT Pronk, PR Levering, W Olijve, JP van Dijken. Enzyme Microb Technol, 11:160, 1989.
8. D Keilin, EF Hartree. J Biochem 42:221–229, 1948.
9. D Scott. Enzymes in Food Processing. New York: Academic Press, 1975, p 228.
10. Q H Gibson, BEP Swoboda, V Massey. J Biol Chem 239:3927, 1964.
11. K Takegawa, K Fujiwara, S Wahora. Biochem Cell Biol 67:460, 1989.
12. HM Kalisz, J Hendle, RD Schmid. Appl Microbiol Biotechnol 47:502–507, 1997.
13. D Scott, J Agric Food Chem, 1:727, 1953.
14. LA Underkofler. Proc Int Symp on Enzyme Chemistry, Tokyo and Kyoto 1957. London: Pergamon Press, 1957, p 586.
15. G Tholey, B Wurtz. Soc Biol 159:2512, 1965.
16. Catalog PL Biochemicals 1974.
17. Catalog Serva Biochemicals 1975.
18. T Yoshimura, T Isemura. J Biochem (Tokyo) 69:839, 1971.
19. S Nakamura, S Fujiki. J Biochem (Tokyo) 63:51, 1968.
20. H Tsuge, O Natsuaki, K Ohashi. J Biochem (Tokyo) 78:835, 1975.
21. S Hayashi, S Nakamura. Biochim Biophys Acta 438:37–48, 1976.
22. S Hayashi, S Nakamura. Biochim Biophys Acta 657:40–51, 1981.
23. RL Kelley, CA Reddy. J Bacteriol 166:269, 1986.
24. M Kriechbaum et al. FEBS Lett 255:63–66, 1989.
25. KR Frederick, S Chakraborty, et al. J Biol Chem 265:3793, 1990.
26. H Whittington et al. Curr Genet 18:531–536, 1990.
27. E Varela, MJ Martinet, AT Martinez. Biochim Biophys Acta 1481:202–208, 2000.
28. HJ Hecht et al. J Mol Biol 229:153–172, 1993.
29. G Wohlfahrt et al. Acta Cryst D55:969–977, 1999.
30. S Witt, G Wohlfahrt, D Schomburg, HJ Hecht, H M Kalisz. Biochem 347:553–559, 2000.
31. P Vaha-Vahe. Food Technol Int Eur, p 139, 1994.
32. Z Jiang, B Ooraikul. J Food Prod Preserv 13:175–186, 1989.
33. N Low et al. J Food Sci 54:118–121, 1989.
34. CA Kannt et al. J Food Sci 58:104–107, 1993.
35. YH Lin. Dissertation, University of Rhode Island, 1987.
36. M Dedek, J Hanus, M Vedlich. Int Dairy Cong Sydney, 1970, p 225.
37. Ough, Mcleod. Am J Enol Viticult 26:30–36, 1975.
38. U Schobinger, P Durr, R Waldvogel. Fluss Obst 59:586–588, 1992.
39. AGJ Rand. J Food Sci 37:698–701, 1972.
40. M Beverini, AJ Vroemen. European Patent.
41. Technical Documentation Zendium. Akzo Dental Research now Sara Lee, Veenendaal, Netherlands.
42. M Sandholm et al. J Vet Med B 35:346–352, 1988.
43. M Desmazeaud et al. Food Ingredients Europe. Conf Proc Maarssen, Netherlands, 1989, pp 96–103.
44. -. Luther, U.S. Patent 2783150, 1957.
45. S Haarasilta, S Vaisanen, D Scott. U.S. Patent 136003, 1987.
46. S Haarasilta, T Pullinen, S Vaisanen, I Tammersalo-Karsten. U.S. Patent 4990343, 1991.
47. DSM-Gist, P.O. Box 1, 2600 MA Delft, Netherlands. Technical Documentation Hemilox.
48 J Raba, HA Mottola. Crit Rev Anal Chem 25:1–42, 1995.

31

Lactate Dehydrogenase

Hayao Taguchi
Tokyo University of Science, Noda, Chiba, Japan

I. INTRODUCTION

This chapter will focus on the NAD-dependent lactate dehydrogenases (LDHs), although there are NAD-independent LDHs that are usually linked to flavoproteins. There are two forms of NAD-dependent LDHs with distinct stereospecificities for lactate: L-LDHs (L-lactate:NAD oxidoreductases, EC 1.1.1.27) and D-LDHs (D-lactate:NAD oxidoreductases, EC 1.1.1.28). This chapter will mainly concern L-LDHs, D-LDHs being concomitantly mentioned. L-LDHs catalyze the following overall reaction:

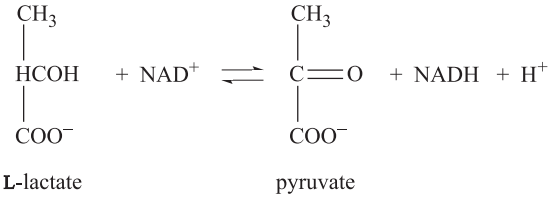

D-LDHs catalyze virtually the same reaction as L-LDH beside the distinct chirality of the lactic acid substrates (products). The physiological reaction of both types of LDHs generally comprises pyruvate reduction (NAD oxidation), the reverse reaction, in which the equilibrium is much more favorable than that of the forward reaction under physiological (neutral) pH conditions (see Sec. IV). Therefore, LDHs act in the last step of the glycolytic pathway, converting pyruvate and NADH into lactate and NAD^+. It should, however, be noted that LDHs are highly diverged enzymes during evolution, and exhibit a multiplicity in their catalytic properties in different species and tissues. The structures, properties, and relationships of various LDHs have been described in great detail by some other reviews (1–4). This chapter outlines these aspects of LDHs, with a few recent advances.

II. IMPORTANCE TO QUALITY OF FOOD

LDHs play key roles in the production of lactic acid, which gives food a sour taste, by stimulating glycolysis through the consumption of pyruvate and the recycling of NAD^+ under anaerobic conditions. It is known that muscles of exhausted animals are acidic and taste sour because of the lactic acid produced. Glycolysis from glycogen also proceeds in the meat after the death of the animal, producing ATP and lactic acid. While the ATP produced is mostly consumed, lactic acid is accumulated and reduces the pH of the meat, usually to ~5.5 (ultimate pH). The pH decrease in the meat mostly results from the lactic acid produced, and the rate differs with animal species and storage conditions. The rapid pH decrease, before cooling of the meat, tends to occur particularly in the case of pork, and causes the denaturation of some proteins in the meat, leading to the decline of meat quality. Since the isoelectric points of many meat proteins are around pH 5, the pH decrease also releases water molecules from hydrated proteins of meat and thus makes the meat watery.

In processed foods such as dairy products, lactic acid is produced through lactic acid fermentation by some bacteria, in particular, lactic bacteria.

Homofermentative lactic bacteria usually produces > 85% lactate as an end product, and heterofermentative bacteria form mixed end products containing acetic acid or ethanol besides lactic acid. Lactic bacteria ferment D- or L-lactic acid, or both, depending on the growth conditions, such as the oxygen concentration, temperature, pH, and sugars or other catabolites supplied, and also on the nature of the LDHs contained in bacterial strains. D- and L-LDHs play key roles in the fermentation of D- and L-lactic acids in lactic bacteria, respectively, and the amount and properties of each LDH greatly affect the fermentation patterns of lactic bacteria. Bacteria that possess L-LDHs activated by fructose-1,6-bisphosphate (Fru-1,6-P_2) (see below) produce mainly L-lactic acid when Fru-1,6-P_2 is accumulated in the cells, but under other growth conditions the bacteria may ferment a large amount of D-lactic acid, or some other end products, rather than L-lactic acid (3).

III. LOCATION OF LDH

L-LDHs are widely distributed in animals, plants, and bacteria. Vertebrates have L-LDH in isoforms, depending on the tissues and organs, such as the A (or M), B (or H), and X types of the enzymes, which are mainly located in skeletal and heart muscles, and testes, respectively. These isozyme subunits can also be hybridized, and form heterotetramers such as A_4, A_3B, A_2B_2, AB_3, and B_4. On the other hand, D-LDHs are widely found in invertebrates, fungi, and bacteria, and the tissue-specific izozymes of D-LDHs are found in invertebrates. It has been reported that invertebrates possess either L- or D-LDH, depending on the species (5). For example, only D-LDHs are found in horseshoe crab, arachnids, and gastropods, but insects or crustaceans only possess L-LDHs. On the other hand, some lactic bacteria contain D- or L-LDHs, or both, and therefore ferment D-, or L-, or both lactic acids (3, 6).

Activity staining with a tetrazolium salt (see below) is often used for the histological analysis of the isozymes, or phylogenic or taxonomic analysis of LDHs in lactic bacteria. LDHs are usually separated by electrophoresis of a native protein sample, and distinct bands on the electrophoresis gel are visualized by staining with D- or L-lactate, or both.

IV. UTILIZATION OF LDH IN FOODS

LDHs are used for the quantitative or qualitative determination of pyruvate, lactate, and related compounds (7). In particular, the pyruvate content can be simply determined through measurement of the reduction of NADH by the direct LDH reaction. The decrease in NADH, which can be monitored as the change in absorbance at ~340 nm, is equal to the reduction in the pyruvate content. The equilibrium constant (K_{eq}) of this reaction is shown in the following equation:

$$K_{eq} = \frac{[\text{pyruvate}] \times [\text{NADH}]}{[\text{lactate}] \times [\text{NAD}^+]} = 2.76 \times 10^{-6} (\text{pH } 7.0, 25^\circ\text{C})$$

The favorable equilibrium allows pyruvate to be quantitatively converted into lactate under conventional LDH assay conditions. The contents of some other catabolites in glycolysis, such as phosphoenolpyruvate and D-glycerate 2-phosphate, can also be quantitatively determined by means of the LDH reaction, coupling with enzyme(s), such as pyruvate kinase (EC 2.7.1.40) and/or enolase (EC 4.2.1.11). Therefore, LDHs are also useful as coupling enzymes for the determination of enolase and pyruvate kinase activities. In addition, some common LDHs exhibit low but sufficient catalytic activity on certain pyruvate analog such as hydroxypyruvate, and these substrates can also be assayed using the enzyme.

On the other hand, the L- and D-lactate contents in food can be individually determined by the use of L- and D-LDHs, respectively. To remove the pyruvate produced, appropriate coupling reagents are required for quantitative determination because of the unfavorable equilibrium. For example, L-alanine aminotransferase (EC 2.6.1.2) is used to convert pyruvate into L-alanine in the presence of L-glutamate. Assay kits for D- or L-lactate including LDHs and aminotransferase are available commercially (such as F-kits for L- and D/L-lactate from Boehringer Mannheim).

L-LDHs from many sources can be purchased from commercial source, such as the muscle, heart, and liver isozymes from rabbit, cow, and pig, and the enzymes of lobster and some bacteria. The D-LDHs of lactic bacteria, for example, *Lactobacillus leichmannii* and *Leuconostoc mesenteroides* enzymes, are also available from commercial sources.

V. STRUCTURES AND STRUCTURE–FUNCTION RELATIONSHIP

The three-dimensional structures of LDHs were first determined for vertebrate L-LDHs in apo and ligand complex forms (2, 4), and then extensively analyzed for

the bacterial L- (8–10) and D- (11) LDHs. Most L-LDHs are tetrameric enzymes composed of identical polypeptides (subunits) with three twofold symmetric axes, P- Q-, and R-axes, although some L-LDHs, such as the *Alcaligence eutrophus* enzyme (12), are homodimers. Vertebrate L-LDHs can form heterotetramers through association among the different subunits of the isozymes both in vivo and in vitro, and some bacterial enzymes may also associate in vitro, if they are closely related to each other (13). Subunits of L-LDHs, as well as those of D-LDHs, are usually composed of 310–350 amino acids (molecular weights 34,000–40,000).

The subunits of L-LDHs comprise two similar sized domains: NAD-binding and catalytic domains. The NAD-binding domain is located in the N-terminal half of the L-LDH primary structure and is folded into a typical open α/β structure (Rossmann fold), which is a highly conserved domain structure among NAD-dependent dehydrogenases. The structure of the catalytic domain in the C-terminal half appears unique in L-LDHs among these dehydrogenases, except for L-malate dehydrogenases (MDH), the catalytic domain of which quite resembles that of L-LDHs as well as the NAD-binding domain. Although MDHs are usually dimeric enzymes with a symmetric axis, their quaternary structures are quite homologous to that of the Q-axis dimer of L-LDHs. The homology of the tertiary and quaternary structures indicates that MDHs and L-LDHs appear to have recently diverged during enzyme evolution, although there is little similiarity in their primary structures. It is known that only one amino acid substitution in L-LDH (Arg102 to Gln) sufficiently alters the substrate specificity of L-LDHs to that of MDHs (14).

In the case of L-LDHs, the amino acid sequences have been systematically aligned with a standard alignment system (N-system) based on the primary structure of a vertebrate isozyme (15). Although all known L-LDHs have essentially the same overall protein structures, however, the primary structures of L-LDHs are highly divergent in different species and tissues. The vertebrate isozymes usually exhibit more than 70% amino acid identity with one another, but bacterial L-LDHs share considerably less common amino acids with one another, depending on the species, and with the vertebrate enzymes up to $< 40\%$. Evolutionary trees have been proposed for L-LDHs on the basis of the divergence of their primary structures (16, 17).

There are, in particular, marked differences in the N-terminal region between vertebrate and bacterial L-LDHs. The N-terminus of vertebrate L-LDHs is usually acetylated, while bacterial L-LDHs have a free amino group at the N-terminus. In addition, vertebrate L-LDHs possess a long additional amino acid sequence (R-arm) at the N-terminus, which is followed by the β-sheet strand of the NAD-binding domain. The R-arm ($\sim$20 amino acids) extends from the NAD-binding domain to another subunit across the R-axis subunit interface, and is responsible for intersubunit interactions on the R-axis subunit interface in vertebrate L-LDHs. On the other hand, bacterial L-LDHs, in general, exhibit no or much weaker interactions on the R-axis subunit interface, since they largely or completely lack the R-arm sequence and are thought to form tetramers mostly through P- and Q-axis interactions (9). The lack of an R-arm may be important in allosteric types of L-LDHs, which are widely distributed in bacterial cells and are usually activated by fructose 1,6-bisphosphate (see below). The 3D structures of the active and inactive forms of the *Bifidobacterium longum* enzyme indicate that the quaternary structure markedly changes through alteration of the intersubunit interactions in the allosteric transition (9). The lack of an R-arm possibly provides the enzyme sufficient flexibility for the structural change in the allosteric transition.

Unlike L-LDHs, many D-LDHs have dimeric structures comprising identical subunits and only one twofold symmetric axis in the quaternary structure, which is not homologous to the P-, Q-, or R-axis dimer of L-LDHs. But some D-LDHs, such as the *Haemophilus influenzae* enzyme, the molecular weight of which was estimated to be 35,000 and 135,000 by SDS-PAGE and gel filration, respectively (18), are possible tetrameric forms. D-LDHs have been distantly separated from L-LDHs in the enzyme evolution (19) in spite of the quite homologous catalytic functions, which possibly resulted from convergent evolution. D-LDHs exhibit little sequence similarity with L-LDHs except for only a small locus such as a Gly-X-Gly-X-X-Gly motif (X is unconserved amino acid) in the NAD-binding domain, and the 3D structure of the enzymes is very distinct from that of L-LDHs. It is known that D-LDHs constitute a dehydrogenase family distinct from that of L-LDH, together with other NAD-dependent 2-D-hydroxyacid dehydrogenases such as 2-D-glycerate dehydrogenase, 3-D-phosphoglycerate dehydrogenase, 2-D-hydroxyisocaproate dehydrogenase, and interestingly, also some NAD-dependent formate dehydrogenases, since these enzymes exhibit homologous primary and 3D structures (20–23). Recently, furthermore, it has been shown that L-alanine dehydrogenases also

resemble D-LDH in 3D structure, in spite of their poor amino acid sequence identity with D-LDH (24). The primary structure of D-LDHs appear to be also divergent among species, since even the enzymes from *Lactobacillus pentosus* and *L. bulgaricus* strains of the same genus have < 50% identical amino acids (25).

The subunits of most D-LDHs are composed essentially of two domains: NAD-binding and catalytic domains, which are connected by a hinge containing two peptides (11). The NAD-binding domain of the enzyme is folded into a typical Rossmann fold, which is quite homologous to the NAD-binding domain of the L-LDH, but is located at a different position in the primary structure from that of L-LDH, i.e., in the middle of the primary structure near the C-terminus (residues 101 to 299 in *Lactobacillus pentosus* D-LDH [total 332 amino acids]) (11).

On the other hand, the structure of the catalytic domain is composed of a large N-terminal and a small C-terminal part (residues 1–100 and 300–332, respectively, in *Lactobacillus pentosus* D-LDH), and is folded in to an α/β structure, which resembles the NAD-binding domain structure but greatly differs from the L-LDH catalytic domain structure. Two of the NAD-binding domains are tightly bound to each other with no covalent bond, and are responsible for not only the main interactions for the subunit assembly but also the rigid base that allows the catalytic domains to flexibly move during catalysis through the hinge motion of the two connecting peptides. This motion of D-LDH in catalysis is also different from the loop motion of L-LDH (see below).

VI. CATALYTIC PROPERTIES AND MECHANISMS

The kinetics of L-LDH are explained by an ordered bi-bi mechanism, in which coenzyme NADH (or NAD^+) is bound first, and subsequently the substrate, pyruvate (or L-lactate), is bound to the enzyme active site. In the L-LDH catalysis, the imidazole group of the His195 (the numbering is based on the vertebrate enzyme according to Eventof et al. [15]) residue acts as an essential acid/base catalyst, which mediates proton transfer between the substrate and the solvent. The catalytic reaction occurs through the concerted attack by the nicotinamide ring of NAD and the His195 imidazole toward the 2-carbonyl (or hydroxymethyl) group of pyruvate (or lactate). In the case of pyruvate reduction, hydride and proton hydrogens are transferred from NADH (4-H of the nicotinamide ring) and the protonated imidazole of His195 onto the 2-carbon and the carbonyl oxygen of the substrate, respectively, while NAD^+ and the unprotonated His195 act as acceptors for hydride and proton hydrogens from lactate on lactate oxidation. The carboxyl group of Asp168, which is located close to the imidazole of His195, is thought to promote the catalytic function of the imidazole, through stabilizing the protonated form of the imidazole (26). Two guanidino groups of the enzyme are known to play an essential role in promoting enzyme catalysis. The guanidino group of Arg171 undergoes strong interactions with the substrate carboxyl group, and allows the substrate to be correctly orientated in the catalytic site of the enzyme (27). The other guanidino group of Arg109 is located on a loop polypeptide (residues 98–110) over the active site of the enzyme. The substrate binding induces marked structural rearrangement in the L-LDH active site, in which the loop closes over the active site. Arg109 moves toward the active site and comes near the carbonyl oxygen of pyruvate through the rearrangement, and promotes the hydrogen transfer reaction by polarizing the substrate carbonyl group (28). The structural rearrangement, like the hydrogen transfer, is one of the slow steps in the L-LDH catalytic process. It has been indicated that the rearrangement step is fully rate-determining in the pyruvate of *Bacillus stearothermophilus* L-LDH, which exhibits a k_{cat} value of 250 sec^{-1} for pyruvate reduction, due to the primary isotope effect of an NADH deutrium derivative on the enzyme transition state kinetics, while the hydrogen transfer step is rate limiting in lactate oxidation (4).

In the case of D-LDHs, the catalytic site of the enzyme exists in a cleft between the NAD-binding and catalytic domains, and the substrate binding allows the cleft to be closed through the hinge motion of the catalytic domain. In the active site of D-LDH, the His296–Glu264 pair plays essentially the same role as the His195–Asp168 pair does, and Arg235 possibly fulfills the roles of both Arg102 and Arg171 (11, 29, 30). In spite of their distinct substrate stereospecificities, L- and D-LDHs exhibit common stereospecificity for the NADH hydrogen, which is located on the A-side (*re*-side) at the C-4 position (*pro-R* hydrogen) of the nicotinamide ring (31).

Both L- and D-LDHs are sensitive to chemical modification reagents for His imidazole and Arg guanidino groups, such as diethylpyrocarbonate and 2,3-butandione, respectively, and are protected from inactivation by coenzymes and subtrates (analogues), because the enzymes possess essential His and Arg residues in their catalytic sites. Sulfhydryl reagents,

such as *p*-hydroxymercuribenzoate and N-ethylmaleimide, also inactivate vertebrate L-LDHs by the modification of Cys165, which is highly conserved in vertebrate L-LDHs, but not in other L-LDHs. Although the D-LDHs of invertebrates (31) and *Haemophilus influenzae* (18) are also inactiviated by sulfhydryl reagents, some bacterial D-LDHs have no cysteine residue in their primary structures (19).

The pH profile of LDH activity differs markedly in the forward (from lactate to pyruvate) and reverse (from pyruvate to lactate) reactions, depending on the *pK* of the catalytic His residue, which is ~7.0 in most LDHs (6.7 in apo and binary complex L-LDHs of mammals) (2, 26), since the unprotonated and protonated forms of imidazole are required for the lactate and pyruvate binding, respectively. Therefore, the pyruvate K_m is virtually constant at < pH 6.0, and increases to > pH 8.0 in a reverse proportion to the H^+ concentration in the solvent, in usual cases, while the lactate K_m is constant at > pH 8.0, and increases to < pH 6.0. In contrast, the k_{cat} values and dissociation constants of NAD are usually much less sensitive to pH conditions. In the LDH reaction, thus, the optimal pH of the pyruvate reduction is usually lower than that of the lactate reduction.

The A- and B-types of the bovine and chicken L-LDH isozymes exhibit pyruvate K_ms of 10^{-5}–10^{-4} M, and L-lactate K_ms of $10^{-3} - 10^{-2}$ M, and the B-type of L-LDH isozymes shows several-fold lower substrate K_m values than the A-type isozymes (32). Most L-LDHs, including all known vertebrate L-LDHs, are significantly inhibited by a high concentration of the substrate, pyruvate (32), although the B-type isozyme generally shows more marked substrate inhibition than the A-type isozymes. It has been indicated that the substrate inhibition mostly results from the formation of an abortive enzyme–NAD^+–pyruvate ternary complex (1). Everse and Kaplan (1) and Holbrook et al. (2) reviewed the steady-state and transition kinetics of vertebrate L-LDHs in detail.

Vertebrate L-LDHs exhibit no apparent cooperative effects on substrate binding, and require no particular factors for their enzyme activity. On the other hand, bacterial L-LDHs show great variety in their catalytic properties, and often allosteric regulation by certain factors, as reviewed by Garvie (3) in detail. Some bacterial L-LDHs, such as the enzymes of *Lactobacillus casei* (33–35), *Thermus* spp. (36, 37), and *Bifidobacterium longum* (38), show positive cooperative effects on substrate binding. It was, in addition, particularly noted that many bacterial L-LDHs require Fru-1,6-P_2 as a specific activator for their catalytic activities. The regulations of these enzymes greatly differ, depending on the bacterial species (3,39). Some of the bacterial enzymes absolutely require Fru-1,6-P_2 and exhibit virtually no catalytic activity unless Fru-1,6-P_2 is present. On the other hand, some of the enzymes exhibit significant activity even without Fru-1,6-P_2, but much more enhanced activity in the presence of Fru-1,6-P_2, which usually improves the substrate binding. In the case of the *B. stearothermophilus* L-LDH, for example, the pyruvate K_m is reduced from 2 mM to 0.04 mM by 5 mM Fru-1,6-P_2 at pH 6.0 (28). On the other hand, the L-LDHs of *L. casei*, *Thermus* sp., and *Biffidobacterium longum* have positive cooperative effects on pyruvate binding, in the absence of Fru-1,6-P_2, shown by the sigmoidal pyruvate saturation curve, which changes into a hyperbolic one in the presence of Fru-1,6-P_2. Besides Fru-1,6-P_2, the L-LDHs of *L. casei* and *curvatus* (35) and *Enterococcus faecalis* (40), previously called *Streptococcus faecalis*, require certain divalent metal ions such as Mn^{2+} under physiological pH conditions, and thus constitute a subclass of divalent metal ion-dependent allosteric L-LDHs (35). The metal ions improve the activation function of Fru-1,6-P_2 by increasing its affinity to these enzymes. In the case of the *L. casei* enzyme, 10 mM Mn^{2+} reduces the dissociation constant for the enzyme and Fru-1,6-P_2 from 15 mM to 0.2 mM at pH 7.0 (41).

It has been demonstrated that the Arg173 and His188 residues, which are located on the P-axis subunit interface of L-LDHs, are directly involved in the Fru-1,6-P_2-binding in common allosteric L-LDHs, such as the enzymes of *L. casei* (42), B. *stearothermophilus* (8, 43), *Thermus caldophilus* (44, 45), and *B. longum* (9, 46). The side chains of these amino acids face each other across the P-axis subunit interface, and constitute the Fru-1,6-P_2-binding site with a highly positive charge. The Fru-1,6-P_2 molecule neutralizes the positive charges and thereby reduces the static repulsions, which stabilizes the inactive form of the enzyme in the absence of Fru-1,6-P_2. Thus, Fru-1,6-P_2 binding is one of the triggers for the change in the quaternary structure of the enzyme, which is closely coordinated with the structural change of the substrate-binding site (9) and the coenzyme in the enzyme (47). The *T. caldophilus* enzyme is converted into the fully active form that is independent of Fru-1,6-P_2 through chemical modifications of the Arg residues, mainly Arg173 (44) and/or Arg216 (48), which are also located on the P-axis interface of the enzyme, with protection of the catalytic site by NADH and

oxamate (49, 50). Reduction of positive charge, through the replacement of Arg173 or Arg216 by site-directed mutagenesis, also leads to partial activation of the enzyme (44, 48).

The x-ray structures revealed that one Fru-1,6-P_2 molecule, which possesses a pseudosymmetric structure, is bound per one P-axis dimer in the *B. stearothermophilus* (8) and *B. longum* (9) L-LDHs (two Fru-1,6-P_2 molecules per tetramer), although equilibrium dialysis of the *L. casei* L-LDH indicates that one Fru-1,6-P_2 molecule is bound per one of the subunits (four Fru-1,6-P_2 molecules per tetramer) (41). The pH conditions greatly influence the regulation by Fru-1,6-P_2, in the cases of usual allosteric L-LDHs, since enzyme activation highly depends on the interaction between the protonated His188 (the numbering is based on the vertebrate enzyme according to Eventof et al. [15]) and the phosphate moiety of Fru-1,6-P_2 (both pKs are ~ 6). For example, the *L. casei* enzyme shows a dissociation constant of 1 μM with Fru-1,6-P_2 at pH 5.4, but one of 15 mM at pH 7.0 (41). Usually allosteric L-LDHs are markedly stabilized, or protected from the dissociations of subunits, in the presence of allosteric ligands such as Fru-1,6-P_2, or divalent cations in some cases, as well as coenzymes, although the *E. faecalis* enzyme is unique in that it is rather labile in the presence of these ligands (51).

Nonallosteric L-LDHs of vertebrates possess a corresponding binding site at the same locus of the Fru-1,6-P_2-binding site, called the anion-binding site, where citrate ions were found to be bound on x-ray crystallographic analysis (2). In vertebrate enzymes, the active forms are sufficiently stabilized in the absence of Fru-1,6-P_2, through some intrinsic interactions, such as the R-axis interaction that is missing in bacterial enzymes. It is nevertheless thought that the anion-binding site is not involved in the regulation of the enzyme activity, but in the stabilization of the enzyme structure through binding certain organic or inorganic anions. Both Arg173 and His188 are also highly conserved in most known nonallosteric L-LDHs including vertebrate enzymes, except for the enzymes of *L. pentosus* (19, 52), *L. plantarum* (53), and *Pediococcus acidilactici* (54), in which His188 is substituted by Asp. The mutant *L. pentosus* enzyme, in which Asp188 is replaced with His by site-directed mutagenesis, is not significantly regulated, but markedly stabilized by Fru-1,6-P_2 (52).

D-LDHs of invertebrates and bacteria generally display hyperbolic saturation curves for substrates, and exhibit high activities independent of certain allosteric factors. Unlike L-LDHs, no D-LDH has been found that is regulated by Fru-1,6-P_2. Nevertheless, some D-LDHs, such as the enzymes of *Butyribacterium rettgeri* (55) and *Escherichia coli* B (56), show positive cooperativity in the substrate binding, as shown by the sigmoidal pyruvate saturation curves. The enzyme from *Pythium devaryanum*, a homolactate-fermenting fungus, is unique in that it also shows cooperativity in the NADH and D-lactate binding, but not in NAD^+ or pyruvate binding (57). In addition, GTP has an allosteric inhibition effect on the enzyme by increasing the cooperative effects on the NADH and D-lactate binding, while ATP inhibits the enzyme reaction by only competing with coenzyme NAD^+.

Adenine nucleotides such as AMP, ADP, and ATP generally inhibit the catalytic reactions of LDHs through competition with coenzymes at the NAD-binding site of the enzymes, and exhibit K_I values of $\sim 10^{-3}$ M in human L-LDH A- and B-type isozymes. On the other hand, oxamate and oxalate, the structures of which are analogous to those of pyruvate and lactate, respectively, are representative substrate-relative inhibitors that inhibit LDH reactions by competing with substrates, and exhibit particularly strong inhibitory effects on pyruvate reduction and lactate oxidation, respectively. In the case of the bovine A-type isozyme, for example, oxamate and oxalate show dissociation constants of 1.1×10^{-5} and 5.5×10^{-3} M with the enzyme-NADH binary complex, and 1.7×10^{-4} and 2.1×10^{-6} M with the enzyme-NAD^+ complex, respectively (58, 59). Nevertheless, oxamate also sometimes exhibits an apparent activation effect on the LDH reaction. In the case of LDHs that show positive cooperativity in the substrate binding, a low concentration of oxamate usually stimulates the enzyme reaction when the substrate concentration is sufficiently low through reduction of the cooperativity of substrate binding.

In the case of Fru-1,6-P_2-activated L-LDHs, inorganic phosphate usually competes with Fru-1,6-P_2 at the Fru-1,6-P_2-binding site, and has a strong inhibitory effect on the enzyme reaction, besides the coenzyme- and substrate-related inhibitors. It is nevertheless known that the *Enterococcus faecalis* L-LDH is not markedly sensitive to inorganic phosphate (40).

VII. QUALITATIVE AND QUANTITATIVE DETERMINATION OF ACTIVITY

The enzyme activity is usually assayed based on pyruvate reduction, in which the catalytic efficiency of most LDHs together with the equilibrium are much

more favorable than those of lactate oxidation. The rate of decrease of the NADH is quantitatively determined by monitoring absorbance at 340 nm (ε of NADH = 6,220 $M^{-1}cm^{-1}$ at 338 nm, pH 7.5). Pyruvate concentrations of ~2 and 0.3 mM are usually appropriate for the A_4 and B_4 isozymes of mammals, respectively, at pH 7.2 and 25°C. In general, however, the pyruvate concentrations must be chosen or searched for carefully, together with pH and temperature conditions, in particular for new or unknown LDHs, because the pyruvate K_m and inhibitory concentrations of pyruvate change greatly depending on the pH and temperature. It should be noted that the suitable concentrations of pyruvate markedly differ with individual enzymes, depending on the species and tissues containing the enzymes, in particular in bacterial L-LDHs, which often exhibit sigmoidal saturation curves for pyruvate or require Fru-1,6-P_2 for enzyme activities. The concentration of NADH which is more favorable for the reaction than NADPH in LDHs in general, and does not critically affect the enzyme activity in the usual LDH assay compared with the pyruvate concentration, because the dissociation constants between LDH and NADH are sufficiently small ($10^{-7} - 10^{-6}$ M for vertebrate A and B L-LDH isozymes) under usual assay conditions, in which the NADH concentration is ~ 0.1 mM (A_{340} is 0.62). In addition, the NADH binding is usually less sensitive to the pH condition, and the excess concentration of NADH inhibits the enzyme reaction less than in the case of pyruvate.

The concentration of Fru-1,6-P_2 must also be carefully chosen for the assay of Fru-1,6-P_2-activated L-LDHs, since it highly depends on the bacterial strain and pH. Phosphate buffer is usually unsuitable, since inorganic phosphate reduces the activation effects of Fru-1,6-P_2 on the enzymes.

Lactate oxidation is also useful for the assay of LDHs in some cases, and can also be determined by following the rate of the change in the absorbance at 340 nm. However, it is recommended that this enzyme reaction be performed in the presence of much higher coenzyme and substrate concentrations and/or under a more alkaline pH (pH > 9) than those in the pyruvate reduction, since the equilibrium is unfavorable at neutral pH, and LDHs generally show higher optimal pHs for lactate oxidation than pyruvate reduction. The NADH resulting from lactate oxidation can also be detected using a tetrazolium salt with a coupling reagent, phenazine methosulfate (PMS). Since the reduced tetrazolium salt displays a blue color as lactate oxidation proceeds, this assay is also useful for the semiquantitative or qualitative determination of the enzyme activity, and can be applied to histological staining or phylogenic or taxonomic differentiation of distinct LDHs or isozymes. For example, LDHs are separated on a native electrophoresis gel and give distinct colored bands on staining of the gel with lactate, NADH, PMS, and tetrazolium salt (35). If an enzyme hardly catalyzes the lactate oxidation, the reverse reaction (pyruvate reduction) is also available for the assay (negative staining). In the case of the reverse reaction, the sample gel is primarily treated with NADH and pyruvate (and Fru-1,6-P_2 if necessary) for the LDH reaction to proceed in the gel, and subsequently with PMS and a tetrazolium salt. Since LDHs consume NADH during the pretreatment, the tetrazolium gives clear bands for the LDHs in a blue-colored background.

VIII. PURIFICATION

Since LDHs are usually localized in the cytoplasmic fraction of cells, the first step of purification is the preparation of cell-free extract through disruption of the cells with a homogenizer, or through osmotic shock or sonication. The conventional methods for protein purification, such as ammonium sulfate precipitation, and ion exchange, or gel filtration chromatography, are generally available for both L- and D-LDH purification. The excess dilution or repeated freezing and thawing of an enzyme sample is usually undesirable during the purification or storage of the enzyme, since these promote the dissociation of the enzyme subunits. Purification of LDHs is usually performed in conventional buffers such as phosphate and Tris-HC1 buffers, around neutral pH (between 6.0 and 7.5), where the enzymes are relatively stable. However, acetate buffers of pH 5.5 are often used in the case of *Lactobacillus* LDHs. The *L. casei* and *L. curvatus* allosteric L-LDHs tend to dissociate into dimers or monomers under neutral or slightly alkaline conditions (60).

Heat-treatment is sometimes used for the purification of certain bacterial L-LDHs, although the thermostability of the enzymes greatly differs with the original source of the enzyme (3). The *L. casei* and *L. curvatus* allosteric enzymes have been three to fivefold purified from cell-free extract by heat treatment at 60°C and pH 5.5, at which the enzymes are stable in the presence of Mn^{2+} as compared with other cell proteins (35). In the case of *L. plantarum* cells, which contain both L- and D-LDHs, the former is much more thermostable

than the latter, and it alone can retain activity after heat treatment at 50° or 60°C (61), The L-LDHs from thermophilic bacteria are usually thermostable. The enzyme of *B. stearothermophilus* retains 50% of its activity after heat treatment at 90°C for 7 min (28). The *T. caldophilus* enzyme is not markedly inactivated by heating at 95°C for 1 h, and 50% of its activity remains at 100°C after 20 min (36). Heat treatment is not effective for purification of the enzymes from the orginal bacterial cells, in which other proteins are also thermostable, but effective when the recombinant proteins are produced in other host cells such as *E. coli* cells (44).

The conventional approaches alone may lead to sufficient purity if an enzyme is an abundant protein in the cell-free extract, but affinity chromatographies based on the affinity of LDH to NAD^+ and the substrate often allow very efficient and specific purification of LDHs. Columns of 5′-AMP, NAD^+, and dye-immobilized gels, such as 5′-AMP and Blue Sepharose, are promising for both L- and D-LDH purification, as in the case of general nucleotide binding proteins. After the enzymes have been adsorbed to the gel, they are usually eluted with buffers containing NADH or a high salt concentration.

Another resin for affinity chromatography, which is also specific for L-LDH, is prepared by the immobilization of oxamate on gels such as Sepharose-4B through a spacer such as diaminohexane (62). With the use of the oxamate gel, L-LDH is adsorbed to the gel in the presence of NADH, and eluted by removing NADH from the elution buffer. This purification protocol is based on the fact that the binding of a substrate (oxamate in this case) to the enzyme absolutely depends on NADH. This elution, however, sometimes gives a broad peak of the eluted enzyme. If a sharper peak of the enzyme is required, oxamate (or pyruvate) may be added to the NADH-free elution buffer. The oxamate gel gives efficient purification of usual L-LDHs, but appears to be unsuitable for D-LDH purification (63).

These affinity chromatographies are promising approaches for general LDH purification, in particular, when the enzyme is not abundant in the enzyme source. To obtain a successful result, it is recommended that one or two conventional purification steps be carried out before the affinity chromatography step, since cell-free extracts usually contain certain compounds that inhibit the adsorption of the enzyme on to the gel, such as some nucleotides and 2-keto-acids, which compete with the affinity resin in the enzyme binding.

REFERENCES

1. J Everse, NO Kaplan. Lactate dehydrogenases: structure and function. Adv Enzymol 28:61–133, 1973.
2. JJ Holbrook, A. Liljas, S J Steindel, M G Rossmann. Lactate dehydrogenase. In: PD Boyer, ed. The Enzymes. 3rd ed Vol 11. New York; Academic Press, 1975, pp 191–292.
3. EI Garvie. Bacterial lactate dehydrogenases. Microbiol Rev 44:106–139, 1980.
4. AR Clarke, T Atkinson, JJ Holbrook. From analysis to synthesis: new ligand binding sites on the lactate dehydrogenase framework. Trends Biochem Sci 14:101–105, 145–148, 1989.
5. GI Long, NO Kaplan. D-Specific pyridine nucleotide lactate dehydrogenase in animals. Science 162:685–686, 1968.
6. F Gasser, M Doudoroff, R Conotopoulos. Purification and properties of NAD-dependent lactic dehydrogenases of different species of *Lactobacillus*. J Gen Microbiol 62:241–250, 1970.
7. W Lamprecht, F Heintz, AW Holldorf, F Noll, K Gawehn. In: HU Bergmeyer, ed. Methods of Enzymatical Analysis, 3rd ed, Vol. VI, Weinheim; Verlag Chemie, 1984, pp 570–592.
8. DB Wigley, SJ Gabblin, JP Turkenburg, EJ Dobson, K Piontek, H. Muirhead, JJ Holbrook. Structure of a ternary complex of an allosteric lactate dehydrogenase from *Bacillus stearothermophilus* at 2.5 Å resolution. J Mol Biol 223:317–335, 1992.
9. S Iwata, K Kamata, T Minowa, T Ohta. T and R states in the crystals of bacterial L-lactate dehydrogenase reveal the mechanism for allosteric control. Nat Struct Biol 1:176–185, 1994.
10. G Auerbach, R Ostendorp, L Prade, I Korndørfer, T Dams, R Huber, R Jaenicke. Lactate dehydrogenase from the hyperthermophilic bacterium *Thermotoga maritima*: the crystal structure at 2.1Å resolution reveals strategies for intrinsic protein stabilization. Structure (Curr Biol) 6:769–781, 1998.
11. VS Stoll, MS Kimber, EF Pai. Insights into substrate binding by D-2-ketoacid dehydrogenases from the structure of *Lactobacillus pentosus* D-lactate dehydrogenase. Structure (Curr Biol) 4:437–447, 1996.
12 A Steinbuechel, H Schlegel. NAD-linked L(+)-lactate dehydrogenase from the strict aerobe *Alcaligenes eutrophus*. 1. Purification and properties. Eur J Biochem 130:321–328, 1983.
13. U Mayr, R Hensel, O Kandler. Factors affecting the quaternary structure of the allosteric L-lactate dehydrogenase from *Lactobacillus casei* and *Lactobacillus curvatus* as investigated by hydridization and ultracentrifugation. Eur J Biochem 110:527–538, 1980.
14. HM Wilk, KW Hart, R Feeney, CR Dunn, H Muirhead, WN Chia, DA Barstow, T Atkinson, AR Clarke, JJ Holbrook. A specific, highly active malate

dehydrogenase by redesign of a lactate dehydrogenase framework. Science 242:1541–1544, 1988.
15. W Eventoff, MG Rossmann, SS Taylor, et al. Structural adaptations of lactate dehydrogenase isozymes. Proc Natl Acad Sci USA 74:2677–2681, 1977.
16. HG Griffin, SR Swindell, MJ Gasson. Cloning and sequence of the gene encoding L-lactate dehydrogenase from *Lactococcus lactis*: evolutionary relationships between 21 different LDH enzymes. Gene 122:193–197, 1992.
17. SC-M Tsoi, SS-L Li. The nucleotide and deduced amino-acid sequences of a cDNA encoding lactate dehydrogenase from *Caenorhabditis elegans*: The evoltionary relationships of lactate dehydrogenases from mammals, birds, amphibian, fish, nematode, plants, bacteria, mycoplasma, and plasmodium. Biochem Biophys Res Commun 205:558–564, 1994.
18. A Donicola-Seoane, BM Anderson. Purification and characterization of *Haemophilus influenzae* D-lactate dehydrogenase. J Biol Chem 265:3691–3696, 1990.
19. H Taguchi, T Ohta. D-lactate dehydrogenase is a member of D-isomer-specific 2-hydroxyacid dehydrogenase family. Cloning, sequence, and expression in *Escherichia coli* of the D-lactate dehydrogenase gene of *Lactobacillus plantarum*. J Biol Chem 266:12588–12594, 1991.
20. V S Lamzin, Z Dauter, V O Popov, E H Harutyunyan, K S Wilson. High resolution structure of holo and apo formate dehydrogenase. J Mol Biol 236:759-785, 1994.
21. JD Goldberg, T Yoshida, P Brick. Crystal structure of an NAD-dependent D-glycerate dehydrogenase at 2.4 Å resolution. J Mol Biol 236:1123–1140, 1994.
22. DJ Schuller, GA Grant, LJ Banaszak. Allosteric ligand site in the V_{max}-type cooperative enzyme phosphoglycerate dehydrogenase. Nature Struct Biol 2:68–76, 1995.
23. U Dengler, K Nifind, M Kiess, D Shonburg. Crystal structure of a ternary complex of D-2-hydroxyisocaproate dehydrogenase from *Lactobacillus casei*, NAD^+ and 2-oxoisocaproate at 1.9 Å resolution. J Mol Biol 267:640–660, 1997.
24. PJ Baker, Y Sawa, H Shibata, SE Sedelnikova, DW Rice. Analysis of the structure and substrate binding of *Phormidium lapideum* alanine dehydrogenase. Nature Struct Biol 5:561–567, 1998.
25. S Kochhar, PE Hunziker, P Leong-Morgenthaler, H Hottinger. Primary structure, physicochemical properties, and chemical modification of NAD^+-dependent D-lactate dehydrogenase. Evidence for the presence of Arg-235, His-303, Tyr-101, and Trp-19 at or near the active site. J Biol Chem 267:8499–8513, 1992.
26. AR Clarke, HM Wilks, DA Barstow, T Atkinson, WN Chia, JJ Holbrook. An investigation into the contribution made by the carboxylate group of an active site histidine-aspartate couple to binding and catalysis in lactate dehydrogenase. Biochemistry 27:1617–1622, 1988.
27. KW Hart, AR Clarke, DB Wigley, et al. A strong carboxylate-arginine interaction is important in substrate orientation and recognition in lactate dehydrogenase. Biochim Biophys Acta 914:294–298, 1986.
28. AR Clarke, DB Wigley, WN Chia, DA Barstow, T Atkinson, J Holbrook. Site-directed mutagenesis reveals role of mobile arginine residue in lactate dehydrogenase catalysis. Nature 324:699–702, 1986.
29. H Taguchi, T Ohta. Histidine 296 is essential for the catalysis in *Lactobacillus plantarum* D-lactate dehydrogenase. J Biol Chem 268:18030–18034, 1993.
30. H Taguchia, T Ohta, H Matsuzawa. Involvement of Glu-264 and Arg-235 in the essential interaction between the catalytic imidazole and substrate for D-lactate dehydrogenase catalysis. J Biochem 122:802–809, 1997.
31. GL Long, NO Kaplan. Diphosphopyridine nucleotide-linked D-lactate dehydrogenases from the horseshoe crab, *Limulus polyphemus* and seaworm, *Nereis virens*. Arch Biochem Biophys 154:711–725, 1973.
32. A Pacce, TP Fondy, F Stolzenbach, F Castillo, NO Kaplan. The comparative enzymology of lactic dehydrogenases. III. Properties of the H4 and M4 enzymes from a number of vertebrates. J Biol Chem 242:2151–2167, 1967.
33 R Holland, GG Pritchard. Regulation of the L-lactate dehydrogenase from *Lactobacillus casei* by fructose-1,6-bisphosphate and metal ions. J Bacteriol 121:777–784, 1975.
34. GL Gordon, HW Doelle. Purification, properties and immunological relationship of L(+)-lactate dehydrogenase from *Lactobacillus casei*. Eur J Biochem 67:543–555, 1976.
35. R Hensel, U Mayr, KO Stetter, O Kandler. Comparative studies of lactic acid dehydrogenases in lactic acid bacteria. 1. Purification and kinetics of the allosteric L-lactic acid dehydrogenase from *Lactobacillus casei* spp. *casei* and *Lactobacillus curvatus*. Arch Microbiol 112:81–93, 1977.
36. H Taguchi, M Yamashita, H Matsuwawa, T Ohta. Heat-stable and fructose 1,6-bisphosphate-activated L-lactate dehydrogenase from an extremely thermophilic bacterium. J Biochem 91:1343–1348, 1982.
37. M Machida, H Matsuwawa, T Ohta. Fructose 1,6-bisphosphate-dependent L-lactate dehydrogenase from *Thermus aquaticus* YT-1, an extreme thermophile: activation by citrate and modification reagents and comparison with *Thermus caldophilus* GK24 L-lactate dehydrogenase. J Biochem 97:899–909, 1985.
38. S Fushinobu, T Ohta, H Matsuzawa. Homotropic activation via the subunit interaction and allosteric symmetry revealed on analysis of hybrid enzymes of

L-lactate dehydrogenase. J Biol Chem 273:2971–2976, 1998.
39. F Gøtz, KH Schleifer. Purification and properties of a fructose 1,6-bisphosphate activated L-lactate dehydrogenase from *Staphylococcus epidermidis*. Arch Microbiol 105:303–312, 1975.
40. VL Crow, GG Pritchard. Fructose 1,6-diphosphate-activated L-lactate dehydrogenase from *Streptococcus lactis*: kinetic properties and factors affecting activation. J Bacteriol 131:82–91, 1977.
41. U Mayr, R Hensel, M Deparade, HE Pauly, G Pfleiderer, W E Trommer. Structure-function relationship in the allosteric L-lactate dehydrogenases from *Lactobacillus casei* and *Lactobacillus curvatus*. Eur J Biochem 126:549–558, 1982.
42. R Hensel, U Mayr, C Woenckhause. Affinity labelling of the allosteric site of the L-lactate dehydrogenase of *Lactobacillus casei*. Eur J Biochem 135:359–365, 1983.
43. AR Clarke, DB Wigley, DA Barstow, WN Chia, T Atkinson, JJ Holbrook. A single amino acid substitution deregulates a bacterial lactate dehydrogenase and stabilizes its tetrameric structure. Biochim Biophys Acta 913:72–80, 1987.
44. H Matsuzawa, M Machida, K Kunai, K Ito, T Ohta. Identification of an allosteric site residue of a fructose 1,6-bisphosphate-dependent L-lactate dehydrogenase of *Thermus caldophilus* GK24: production of a non-allosteric form by protein engineering. FEBS Lett 233:375–378, 1988.
45. G Schroeder, H Matsuzawa, T Ohta. Involvement of the conserved histidine-188 residue in the L-lactate dehydrogenase from *Thermus caldophilus* GK24 in allosteric regulation by fructose 1,6-bisphosphate. Biochem Biophys Res Commun 152:1236-1241, 1988.
46. S Fushinobu, K Kamata, S Iwata, H Sakai, T Ohta, H Matsuzawa. Allosteric activation of L-lactate dehydrogenase analyzed by hybrid enzymes with effector-sensitive and -insensitive subunits. J Biol Chem 271:25611–25616, 1996.
47. M Machida, S Yokoyama, H Matsuzawa, T Miyazawa, T Ohta. Allosteric effect of fructose 1,6-bisphosphate on the conformation of NAD^+ as bound to L-lactate dehydrogenase from *Thermus caldophilus* GK24. J Biol Chem 260:16143–16147, 1985.
48. S Koide, S Yokoyama, H Matsuzawa, T Miyazawa, T Ohta. Conformational equilibrium of an enzyme catalytic site in the allosteric transition. Biochemistry 31:5362–5368, 1992.
49. H Taguchi, H Matsuzawa, T Ohta. L-lactate dehydrogenase from *Thermus caldophilus* GK24, an extremely thermophilic bacterium. Desensitization to fructose 1,6-bisphosphate in the activated state by arginine-specific chemical modification and N-terminal amino acid sequence. Eur J Biochem 145:283–290, 1984.
50. S Koide, S Yokoyama, H Matsuzawa, T Miyazawa, T Ohta. Conformation of NAD^+ bound to allosteric L-lactate dehydrogenase activated by chemical modification. J Biol Chem 264:8676–8679, 1991.
51. CL Wittenberger, N Angelo. Purification and properties of a fructose-1,6-bisphosphate-activated lactate dehydrogenase from *Streptococcus faecalis*. J Bacteriol 101:717–724, 1970.
52. Taguchi, T Ohta. Unusual amino acid substitution in the anion-binding site of *Lactobacillus plantarum* non-allosteric L-lactate dehydrogenase. Eur J Biochem 209:993–998, 1992.
53. T Ferain, D Garmyn, N Bernard, P Hols, J Delcour. *Lactobacillus plantarum ldhL* gene: overexpression and deletion. J Bacteriol 176:596–601, 1994.
54. D Garmyn, T Ferain, N Bernard, P Hols, J Delcour. Cloning, nucleotide sequence, and transciptional analysis of the *Pediococcus acidilactici* L-(+)-lactate dehydrogenase gene. Appl Environ Microbiol 61:266–272, 1995.
55. CL Wittenberger, JG Fulco. Purification and allosteric properties of a nicotinamide adenine dinucleotide-linked D(-)-specific lactate dehydrogenase from *Butyribacterium rettgeri*. J Biol Chem 242:2017–2024, 1967.
56 EM Tarmy, NO Kaplan. Kinetics of *Escherichia coli* B D-lactate dehydrogenase and evidence for pyruvate-controlled change in conformation. J Biol Chem 243:2587–2596, 1968.
57. HB LéJohn. D(-)-Lactate dehydrogenases in fungi. J Biol Chem 246:2116–2126, 1971.
58. AD Winer, GW Schwert. Lactic dehydrogenase. VII Fluorescence spectra of ternary complexes of lactic dehydrogenase, reduced diphosphopyridine nucleotide, and carboxylic acids. J Biol Chem 234:1155–1161, 1959.
59. WB Novoa, GW Schwert. Lactic dehydrogenase. VIII. Binding of oxamate and of oxalate by enzyme-coenzyme complexes. J Biol Chem 236:2150–2153, 1961.
60. U Mayr, R Hensel, O Kandler. Factors affecting the quaternary structure of the allosteric L-lactate dehydrogenase from *Lactobacillus casei* and *Lactobacillus curvatus* as investigated by hybridization and ultracentifugation. Eur J Biochem 110:527–538, 1980.
61. D Dennis, NO Kaplan. D- and L-lactic acid dehydrogenases in *Lactobacillus plantarum*. J Biol Chem 235:810–818, 1960.
62. P O'Carra, S Barry. Affinity chromatography of lactate dehydrogenase. Model studies demonstrating the potential of the technique in the mechanistic investigation as well as in the purification of multi-substrate enzyme. FEBS Lett 21:281–285, 1972.
63. P Tuengler, TN Stein, GL Long. Studies on the active center of D- and L-lactate dehydrogenases using oxamate-diaminohexyl-Sepharose affinity chromatography. Proc Natl Acad Sci USA 77:5832–5836, 1980.

32

Alcohol Dehydrogenase

Sabato D'Auria

Institute of Protein Biochemistry and Enzymology, Naples, Italy, and University of Maryland, Baltimore, Maryland, U.S.A.

I. INTRODUCTION

Of the estimated 25,000 enzymes present in nature, ~ 2800 have been classified and ~ 400 have been commercialized. On a larger industrial scale, in particular for detergent and food processing, only ~ 50 enzymes are used. The main impetus for the use of enzymes is the continuous growth in the demand for enantiomerically pure compounds. This trend plays an important role in the use of chiral drugs, but is also essential in the flavor industry where, besides microbial fermentation, enzyme technology is an alternative for the biotechnological production of flavor compounds (1). For example, acetaldehyde is an important low-molecular-weight flavor compound that plays a significant role in the flavor of yogurt and certain fruits, such as orange. Figure 1 shows the conversion of ethanol to acetaldehyde using alcohol dehydrogenase. This process suffers from the same drawbacks as all enzymatic oxidation reactions that rely on cofactor regeneration. Specifically, the process involves the use of alcohol dehydrogenase and its cofactor NAD^+, which during the reaction is reduced and subsequently regenerated by light-catalyzed oxidation with flavin mononucleotide (FMN). The reduced flavin mononucleotide (FMNH2) is reconverted to FMN by oxidation with molecular oxygen. The byproduct of this reaction is hydrogen peroxide, which is in turn decomposed by the action of the enzyme catalase to oxygen and water. Conversion rates in the range of 10–20% are typically obtained, and in a continuous batch reactor system the concentration of acetaldehyde is ~ 2.5 g/L after a period of 9 h (2).

Recently it has been shown that genetic manipulation of alcohol dehydrogenase levels in ripening tomato fruit affected the balance of some flavor aldehydes and alcohols. In particular, modified alcohol dehydrogenase levels in the ripening fruit influenced the balance between some of the aldehydes and the corresponding alcohols associated with flavor production. Hexanol and *Z*-3-hexenol levels were increased in fruit with increased alcohol dehydrogenase activity and reduced in fruit with low alcohol dehydrogenase activity. In some taste trials, fruits with elevated alcohol dehydrogenase activity and higher levels of alcohols were identified as having a more intense "ripe fruit" flavor (3). Moreover, the involvement of alcohol dehydrogenases in the biogenesis of six carbon alcohol constituents of the aroma of olive oil has been recently discussed (4). In yeast, ethanol is produced from acetaldehyde during anaerobic fermentation of sugar and this could represent an important process in the production of alcohol-containing beverages.

A survey of the actual use of enzymes in synthetic organic chemistry shows that 65% of all reported applications fall into the classes of hydrolytic and dehydrogenase reactions (1).

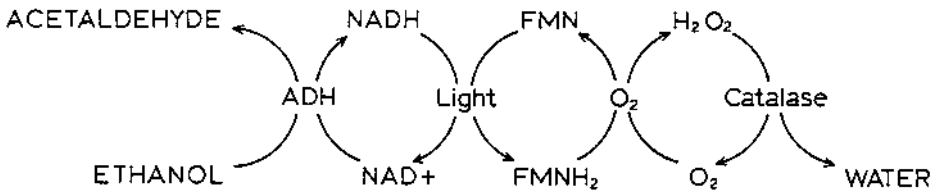

Figure 1 Enzymatic oxidation of ethanol to acetaldehyde. (From Ref. 2.)

II. PROPERTIES AS PROTEIN

Alcohol dehydrogenase (ADH) (EC 1.1.1.1) is an oxidoreductase enzyme that catalyzes the oxidation of alcohols and the reduction of carbonyl compound such as aldehydes and ketones. The enzyme displays a broad substrate specificity, being active on a variety of primary, secondary, branched, and cyclic alcohols. Alcohol dehydrogenases are widely distributed enzymes and have been found in many microorganisms, fungi, and animal cells (5). Most bacterial ADHs are so-called soluble enzymes and are located in the cytoplasmic, but some have been shown to be membrane bound. The intracellular compartmentation of eukaryotes gives rise to greater possibilities of variation in location. Thus, *Saccharomyces cerevisiae* contains three ADHs of which two are cytoplasmic and the third is mitochondrial (6). Some of these enzymes (e.g., ADHs from horse liver and yeast) have been extensively studied, because they can provide new data on the relationship between structure and function, being oligomeric, coenzyme dependent, and containing structural and functional metal atoms (5).

ADH requires a nicotinamide cofactor for the catalytic activity, and it is capable of distinguishing the diastereotopic methylene hydrogens at the dihydropyridine C-4 position of NADH or NADPH, transferring the hydride to the substrate stereospecifically (7). This interesting enzymatic feature suggests a potential use of ADHs for the production of alcohols with a 100% optical yield (7).

ADHs catalyze the interconversion of alcohols to aldehydes/ketones:

$$\text{Alcohol} + \text{NAD(P)}^+ \rightleftharpoons \text{Aldehyde/ketone} + \text{NAD(P)H} + \text{H}^+$$

This reaction is highly reversible and the direction of the reaction is influenced by pH of the reaction medium. At pH 9 the equilibrium of this reaction is directed toward aldehyde formation, while at pH 7 alcohol formation is favored. ADHs can be very effective for the conversion of the readily available aldehydes citronellal and citral for the production of (–)-citronellol and geraniol, compounds with a much higher flavor impact than the corresponding aldehydes or ketones (8). Thus, the potential applications of ADHs in industry are numerous. With mesophilic enzymes, however, limitations due to narrow specificity, instability to heat and organic solvents, and loss of activity on immobilization have been incurred. The use of these enzymes from thermophilic sources in immobilized and continuous reactor systems has also been proposed for the regeneration of NAD(P)H needed for such reactors, the lifetime of which would be extended with stable enzymes. The ADH from *Thermoanaerobium brockii* has been shown to reduce aliphatic acyclic ketones asymmetrically with an optimal purity. Furthermore, this enzyme has been used to obtain optically pure cyclic ethers, which are constituents of civet used as a fixative in the perfume industry (9).

ADHs have been subdivided into different families according to the polypeptide chain lengths: the short-chain family consisting of non-metalloenzymes with subunits of ~ 250 residues (10); the medium-chain family with subunits of 350–375 residues, often containing zinc (11); and the long-chain family with subunits of > 700 residues (12). Moreover, ADHs lacking zinc as well as alcohol dehydrogenases requiring iron for activation have been described (13). A monomeric ADH was also isolated from *Saccharomyces cerevisiae*, but its metal content is yet unknown (14).

ADHs have been classified as α/β proteins with high amounts of α-helices and β-structures. Figure 2 shows the far-UV circular dichroism spectrum of *B. acidocaldarius* ADH. The deconvolution of the spectrum resulted in $\sim 22\%$ α-helix and 45% β-structure, suggesting that ADHs from thermophilic microorganisms could also have a secondary structural organization similar to that described for mesophilic ADHs (15).

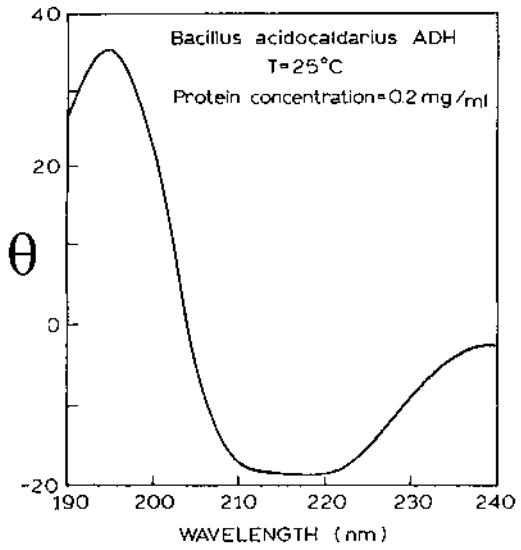

Figure 2 Far-UV circular dichroism spectrum of *Bacillus acidocaldarius* ADH. Protein concentration 0.2 mg/mL. Temperature 25°C.

Moreover, conformational variations have been reported in many ADHs on binding to coenzyme or substrate. One of the many techniques utilized to detect conformational changes in protein structure is fluorescence spectroscopy. Horse liver ADH (HLADH) contains two tryptophan residues: Trp15 located at an outer edge of the catalytic domain and accessible to solvent, and Trp314 located in the apolar intersubunit region of the catalytic domain, inaccessible to the solvent. In a detailed fluorescence study Lakowicz and coworkers showed that these two tryptophan residues displayed different emission spectra and time decay by using one- or two-photon excitation. The results suggest that the intrinsic fluorescence of HLADH can be used to probe small changes in the active site of the enzyme (16).

Zinc-dependent alcohol dehydrogenases have a dimeric or tetrameric structure. Dimeric enzymes are the ADHs from mammals (11) and from higher plants (17). Tetrameric enzymes are the ADHs from yeasts and bacteria. Recently, a detailed characterization of the ADH from *S. solfataricus* has ascertained the presence of both dimeric and tetrameric forms, with the dimeric conformation showing a lower level of catalytic efficiency than the tetrameric one (18). Moreover, mammalian ADHs have been divided into three major classes (I, II, and III) based on their electrophoretic mobility and kinetic properties (19).

Multiple sequence alignment of > 60 ADHs from different sources with that of HLADH has shown that in almost all the zinc containing ADHs studied to date, three zinc-binding amino acids (Cys46, His67, and Cys174) are highly conserved (20). However, in ADH from *Thermoanaerobacter brockii* only Cys37 and His59, which align with Cys46 and His67 of HLADH, are conserved. Although the residue corresponding to Cys174 of HLADH is absent in *Thermoanaerobacter brockii* ADH, it has been suggested that Asp150 could serve as the third Cys residue in the latter enzyme. Moreover, the absence in *Thermoanaerobacter brockii* ADH of all four amino acid residues found in HLADH to coordinate the structural zinc ions (Cys97, Cys100, Cys103, Cys111) suggests that the Cys37 is involved in the catalytic activity of *T. brockii* enzyme (21). The ADHs isolated from *Bacillus acidocaldarius* and *Sulfolobus solfataricus* have two zinc atoms per enzyme subunit, one with a catalytic role and the other with a structural role (15, 22).

The thiol groups of cysteines are important for protein structure and folding (23). As in other proteins, chemical modification of reactive cysteine residues has been used extensively to investigate the importance of cysteine residues in the structure and function of the ADHs. Figure 3 shows the structure of the E-subunit of HLADH resolved at 2.2 Å. In the same figure the cysteine residues are shown as "*spacefill*."

In zinc-containing ADHs, cysteine serves as binding site for the catalytic zinc atom (24). In most eukaryotic and prokaryotic ADHs, cysteine serves as binding site for a structural zinc atom as well (25). The role of other cysteine residues present in the ADHs has not been determined. Of the three catalytic zinc atoms that have been identified in the 3D structure of HLADH, the only enzyme for which a detailed 3D structure of an ADH with its coenzyme is available (24), two residues, Cys46 and Cys174, can be selectively alkylated by α-halo acids in an affinity-labeling type of reaction (28). Whereas carboxymethylation of Cys46 and Cys174 of HLADH, or the putative active site zinc ligand cysteines of human ADH, sheep liver sorbitol dehdyrogenase, and human liver aldehyde dehydrogenase, abrogates enzymatic activity (27), similar modification of the ADH from *S. solfataricus* significantly increases the oxidation rate of alcohols (28). Recently it has been shown that Cys283 and Cys295 of the ADH from *Thermoanaereobacter brockii*, although they are buried within the protein core and are not accessible for chemical modification, are oxidized to cystine when the enzyme is heated at 75°C, forming a disulfide bridge that was not present in the native enzyme, without affecting either enzymatic activity or thermal stability (21).

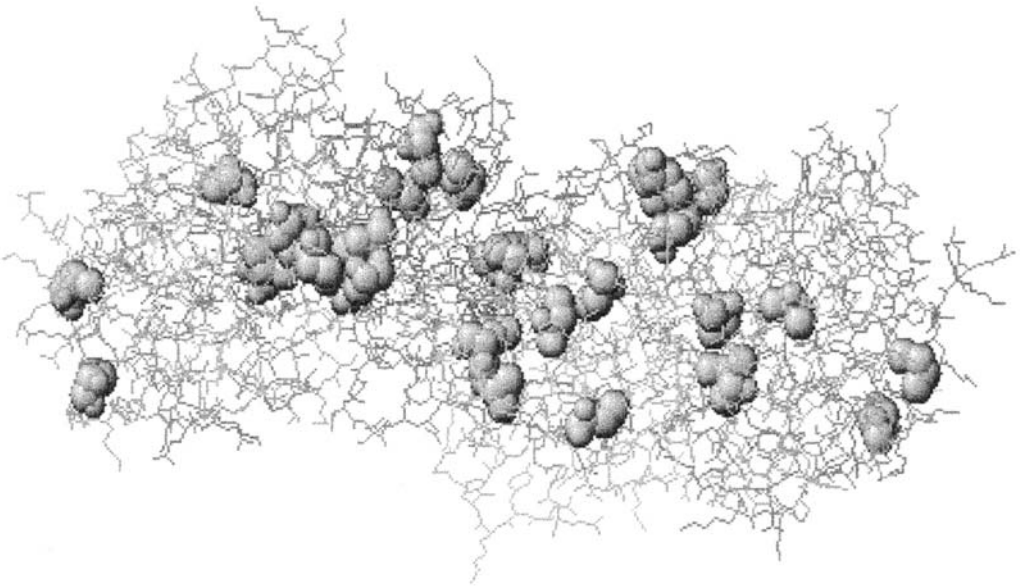

Figure 3 Structure of E-subunit of horse liver ADH solved at 2.4 Å. The cysteine residues are shown as spacefill.

Figure 4 shows the 22 amino acid residues strictly conserved in 16 ADHs from different sources (11). It is worth noting that His → Arg substitution at the position 47 (HLADH numbering) has been reported to affect both the affinity for the coenzyme and pH optimum for the activity in human ADH isoenzymes, the native enzyme displaying a lower optimum and higher K_m and V_{max} values than the mutant (18, 25).

Table 1 shows some biochemical features for some ADHs with His or Arg at position 47.

III. PROPERTIES AS ENZYMES

According to their source ADHs differ in substrate and coenzyme specificity (5). It is commonly believed that ADHs from eukaryotes are mainly NAD^+ dependent, while those from prokaryotic organisms are either NAD^+ or $NADP^+$ dependent. However, two ADHs isolated recently from thermophilic bacteria utilize $NADP^+$ as coenzyme (29, 30), while the ADHs from the eubacteria *Bacillus acidicaldarius* and *Bacillus stearothermophilus* require NAD^+ as coenzyme (15, 31). Moreover, ADHs containing pyrroloquinolin quinone (Fig. 5) as a cofactor have been isolated from various Gram-negative bacteria. Based on the cofactor requirement two classes of ADHs can be distinguished: quinoprotein alcohol dehydrogenase (containing PQR and Ca^{2+}) and quinohemoprotein alcohol dehydrogenase (containing PQQ, Ca^{2+}, and heme c). The first class includes the methanol dehydrogenases from methylotropic bacteria and alcohol dehdyrogenases occurring in *Pseudomonas* (32).

HLADH is a well-characterized zinc-containing ADH. Each subunit of the dimeric enzyme contains one catalytic and one structural zinc atom (5) and binds one ligand of NAD(P)H.

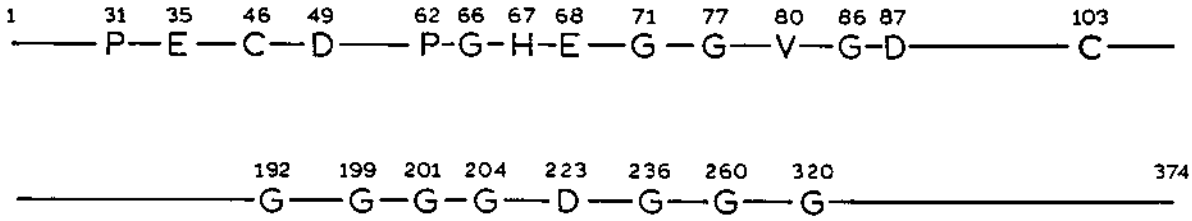

Figure 4 The 22 amino acid residues strictly conserved in several ADHs (11). The amino acids are numbered according to HLADH sequence.

Table 1 Optimal pH and K_m Values Related to Amino Acid 47 of Horse Liver (HL), Yeast (Y), $\beta_1\beta_1$ Human ($\beta_1\beta_1$h), $\beta_2\beta_2$ Human ($\beta_2\beta_2$h), and *Bacillus acidocaldarius* (Ba) ADHs

	HL ADH	Y ADH	$\beta_1\beta_1$h ADH	$\beta_2\beta_2$h ADH	Ba ADH
Amino acid residue 47	Arginine	Histidine	Arginine	Histidine	Not determined
Optimal pH activity	10	8.6	10	8.5	10
K_m (μM) (NAD^+)	53	160	7.4	180	1600

The most widely accepted reaction mechanism for alcohol dehydrogenase is indicated in Figure 6 (33) and includes: binding of NAD^+; binding of alcohol substrate by replacing a zinc-bound water molecule; deprotonation of the alcohol; hydride transfer from the alkoxide ion to NAD^+, yielding NADH and a zinc-bound aldehyde; dissociation of NADH. In applicable steps (7–9), the zinc-bound water molecule equilibrates with a zinc-bound hydroxyl ion, which gives rise to a dead-end complex. The catalytic zinc in HLADH is bound to Cys46, His67, and Cys174. The fourth ligand is a water molecule that is linked to a hydrogen-bonding network involving Ser48 and His51 (34). The four cysteine residues coordinating the noncatalytic zinc (Cys97, 100, 103, and 111) and the binding amino acids of the catalytic zinc are arranged in a distorted tetrahedral geometry (35).

The nicotinamide ring system is redox active, accepting a hydride of two electrons and a proton to form 1,4-dihydronicotinamide derivatives of NADH or NADPH. The reversible hydride transfer from a reduced substrate to NAD^+, and that from NADH to an oxidized substrate, is stereoselective and characteristic of individual enzyme. Each enzyme is able to transfer stereoselectively one of the diastereotopic methylene hydrogens at C-4 of NADH to a substrate carbonyl group or an equivalent sp^2 center with high enantiofacial or diastereofacial selectivity.

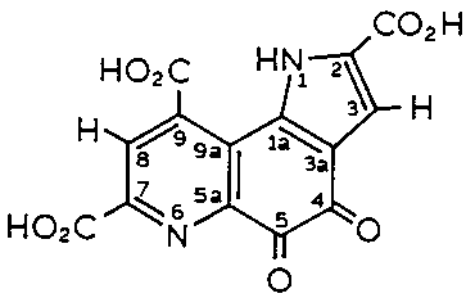

Figure 5 Structure of pyrroloquinolin quinone.

The stereospecificity of the ADH isolated from the thermoacidophilic archaeon *Sulfolobus solfataricus* (36) toward an asymmetric ketone was examined by using 3-methyl-butan-2-one as a model compound. The hydride attack, using the enzyme immobilized on Eupergit C was on *re-face* of the ketone, producing the corresponding (*s*)-3-methyl-butan-2-ol with a 100% optical yield. Moreover, the potentiality of the use of this enzyme for the preparation of chiral compounds was also pointed out by the use of resting cells of *S. solfataricus* to reduce a series of acyclic, cyclic, and aromatic ketones (37). Another interesting aspect of stereospecificity of ADH from *S. solfataricus* was discovered by studying the oxidation of secondary alcohol enantiomers (38): (*s*)-enantiomers are far better substrates than (*r*)-enantiomers. For example, (*s*)-2-butanol is oxidized about 60 times more efficiently than (*r*)-2-butanol, and (*r*)-sec-phenethyl alcohol is not oxidized at all. In a detailed study Keinan and coworkers showed that the ADH isolated from *Thermoanaerobium brockii* exhibited a high stereospecificity depending on the enzyme assay temperature (39). However, the nicotinamide cofactors are too expensive to be used as stoichiometric reagents in large-scale synthesis. Thus, recycling of the cofactors is needed if enzymes requiring nicotinamide cofactors are to be used in a preparative scale. In spite of the use of HLADH with its broad substrate acceptance, narrow stereoselectivity and bidirectional functionality, there is continuing research for novel reductases, in particular for alcohol dehydrogenases purified from thermophilic microorganisms, that are stable and active at high temperature and in the presence of organic solvents. Enzymes isolated from thermophilic sources display high levels of enzyme activity at high temperatures, being barely active at room temperature. Figure 7 shows the thermophilic behavior of two ADHs: *B. acidocaldarius* ADH (moderate thermophilic microorganism), and *S. solfataricus* ADH (hyperthermophilic microorganism). Several research groups have related these functional features to a high struc-

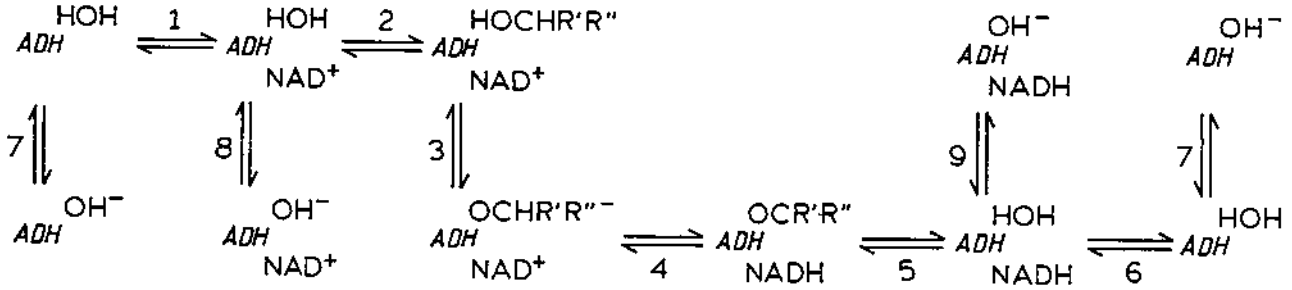

Figure 6 Reaction mechanism of ADH according to Petterson (33).

tural rigidity at room temperature (40) that could prevent the utilization of these enzymes in biotechnological applications.

IV. ENZYMATIC ASSAY

Usually alcohol dehydrogenase activity is assayed by following the increase in absorbance at 340 nm owing to the reduction of the NAD^+($NADP^+$) molecules. On the contrary, it is also possible to assay alcohol dehydrogenase activity by monitoring the decrease in absorbance at 340 nm, as a consequence of the oxidation of the NADH (NADPH) molecules.

The alcohol dehydrogenase from yeast exhibits the maximal enzymatic activity in the range of pH 8.6–9.0 at 25°C. The typical assay for measuring it is the following: 50 mM Tris-HCl (pH 8.6), 10 mM ethanol, 1.0 mM NAD^+, and 1.0 μg enzyme/mL final volume, at 20°C. The ADH activity is determined by monitoring the increase of absorbance at 340 nm. One unit of enzyme activity is defined as the amount of the enzyme that catalyzes the reduction of 1.0 μM of NAD^+ at 25°C.

For assaying enzymatic activity of thermophilic alcohol dehydrogenases it is of fundamental importance to use a sealed cuvette, in order to avoid the evaporation of the assay mixture. The alcohol dehydrogenase from the thermophilic microorganism *Bacillus acidocaldarius* shows the maximal enzyme activity at 80°C. However, *Bacillus acidocaldarius* ADH activity is usually assayed spectrophotometrically at 65°C by measuring the increase in the absorbance at 340 nm in a sealed quartz cuvette. The reaction mixture contains 50 mM glycine-NaOH (pH 10.0) and 1.0 μg protein/1.0 mL final volume. The concentrations of cofactors and substrate are 5.0 mM NAD^+ and 3.0 mM ethanol for alcohol oxidation, and 0.12 mM NADH and 3.0 mM *p*-anisaldehyde for aldehyde reduction, respectively. One unit of enzyme activity is defined as the amount of the enzyme that catalyzes the reduction of 1.0 μM of NAD^+ at 65°C, using ethanol as substrate.

It is also possible to monitor ADH activity by fluorescence spectroscopy. In this case, we follow the increase of the fluorescence emission at 450 nm (upon excitation at 340 nm) due to NADH formation. The fluorescence assay is more sensitive than the spectrophotometer one, and it is utilized when it needs the detection of low ADH activity levels.

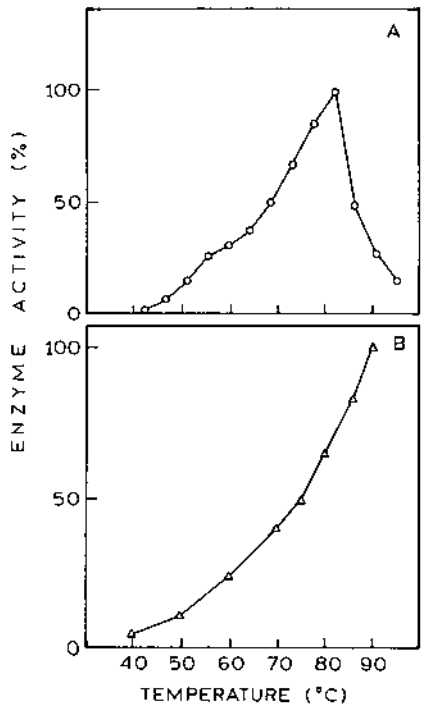

Figure 7 Thermophilic behavior of *Bacillus acidocaldarius* ADH(A) and *Sulfolobus solfataricus* ADH (B).

V. PURIFICATION

Several purification strategies have been described to isolate ADHs from different sources. However, the utilization of an affinity column has been reported as the main purification step in almost all described purification procedures. Specifically, an affinity chromatography based on the interaction of ADH coenzyme-site-blue dye molecule was used for large-scale purification of horse liver ADH. Moreover, it has recently been shown that the affinity chromatography on Matrex Gel Red A was the essential purification step for the isolation of the ADH from a novel strain of *Bacillus sterotheromphilus* (31).

Here we report the typical procedure of purification of the ADH from *Bacillus acidocaldarius* (15). However, it is worth noting that a similar method can be also used for the purification of alcohol dehydrogenases from different sources.

1. *Preparation of cell extract*. One hundred and twenty grams of wet cell pellet was suspended in 360 mL of 10 mM Tris/HCl, 0.5 mM dithiothreitol, pH 9.0 (Buffer A), and broken by five 1-min cycles of sonication at regular intervals, utilizing an MSE Soniprep 150. Cell debris was removed by centrifugation at 160,000 g for 90 min (at 4°C). The supernatant represented the crude extract.

2. *Column chromatography steps*. The crude extract was applied to a DEAE-Sepharose Fast Flow column, previously equilibrated in Buffer A. The column was washed with 1000 mL of Buffer A, and eluted with a linear gradient from 0.0 to 0.3 M NaCl in Buffer A, at a flow rate of 60 mL/h. The alcohol dehydrogenase activity was eluted at 0.1 M NaCl. The fractions containing the enzymatic activity were pooled and loaded on a Phenyl-Superose column, at a flow rate of 30 mL/h, after addition of 1.0 M ammonium sulfate. After washing with 100 mL of Buffer A, the enzymatic activity was eluted with a gradient of ammonium sulfate from 1.0 M to 0.0 M in Buffer A. Fractions containing the ADH activity were eluted at 0.3 M ammonium sulfate, pooled, and dialyzed overnight against 10 L of Buffer A, at 4°C. The active pool was loaded at a flow rate of 30 mL/h on a Mono Q FPLC column previously equilibrated with the same buffer. The column was washed with a linear gradient from 0.0 M to 0.5 M NaCl in Buffer A, at a flow rate of 60 mL/h. The enzymatic activity, eluted at $\sim$ 100 mM NaCl, was dialyzed overnight against 5 L of 10 mM Tris/HCl, pH 7.4 (Buffer B), and applied onto a Blue A affinity column, previously equilibrated with the same buffer, at a flow rate of 20 mL/h. The column was washed with 150 mL of Buffer B, and the homogeneous enzyme was eluted with a step of 2 mM NAD^+ in the same buffer. The results of the purification are summarized in Table 2.

Bacillus acidocaldarius ADH was purified to homogeneity by five steps. The crucial step in the purification procedure was the specific elution of the enzyme by NAD^+ at pH 7.4 from the affinity Blue A column. The presence of DTT in the buffers used in *Bacillus acidocaldarius* ADH purification was necessary in order to avoid the complete inactivation of the enzyme. On the other hand, no significant enzyme stabilization was observed utilizing buffers containing divalent ions (Zn^{2+}, etc.).

However, it is worth stating that the expression of thermophilic ADHs in mesophilic hosts (e.g., *E. coli*) makes the enzyme purification procedure very easy; in fact, it needs a thermoprecipitation step in order to separate the thermostable recombinant enzyme from the native proteins of the host. Moreover, the cloning and expression of thermostable ADHs in organisms generally recognized as safe (GRAS) from the U.S. Food and Drug Administration (e.g., *Saccharomyces cerevisiae*) give the opportunity to obtain large amounts of stable ADHs to use in the food industry.

In conclusion, ADHs have been isolated from different organisms and they differ according to their sources, in substrate and coenzyme specificity, as well as in their protein structural organization. Their wide substrate specificity makes this class of enzymes good biocatalysts in biotechnological applications, as well as interesting proteins in the study of evolution.

Table 2 Purification of Alcohol Dehydrogenase from *Bacillus acidocaldarius*

Purification step	Protein (mg/mL)	Specific activity	Fold purification	Yield (%)
Cell extract (homogenate)	12,200	0.3	1.0	100
DEAE-Sepharose FF	1,100	3.3	11	99
Phenyl-Superose	500	6.1	20	83
Mono-Q Sepharose	150	16	53	65
Blue Sepharose CL-6B	15	150	500	61

Source: Ref. 15.
The alcohol dehydrogenase activity was assayed spectrophotometrically by measuring the change in absorbance at 340 nm. The reaction mixture contained 50 mM glycine-NaOH, pH 10, 5.0 mM NAD^+, and 3.0 mM ethanol.

ACKNOWLEDGMENTS

I thank Professor Joseph R Lakowicz (University of Maryland), Professor Mosé Rossi (University of Naples), and Professor Carlo Fini (University of Perugia) for their stimulating scientific discussions; and Mr. Carlo Vaccaro (Italian National Research Council) for his technical assistance. Skillful assistance in the preparation of the figures by Ms. Krystyna Gryczynska is gratefully acknowledged. This work was supported by a grant from the Ministry for University and for Technological and Scientific Research (M.U.R.S.T.) 60%, and EU contract "Extremophiles," and the National Center for Research Resources, NIH RR-08119.

This chapter is dedicated to Cristina, Leandro Maria, and Gerard Joseph.

REFERENCES

1. P Schreier. Enzymes and flavor in biotechnology. Adv Biochem Eng 55:52-70, 1997.
2. WR Raymond. U.S. patent 4,481,292 (1984).
3. J Speirs, E Lee, K Holt, K Young-Duk, SN Steele, B Loveys, W Schuch. Genetic manipulation of alcohol dehydrogenase levels in ripening tomato fruit affects the balance of some flavor aldehydes and alcohols. Plant Physiol 117(3):1047–1058, 1998.
4. JJ Salas, J Sanchez. Alcohol dehydrogenases from olive (*olea europea*) fruit. Phytochemistry 48(1):35–40, 1998.
5. C-I Branden, H Jornovall, M Eklund, B Furugren. Enzymes. In: PD Boyer, ed. The Enzymes 3rd ed, Vol II. New York: Academic Press, pp. 103–190.
6. RW MacKintosh, CA Fewson. Microbial aromatic alcohol and aldehyde dehydrogenases. In: H Weiner, TG Flynn, eds. Enzymology and Molecular Biology of Carbonyl Metabolism. New York: Alan R Liss, 1987, pp. 259–273.
7. JB Jones, JF Beck. Techniques of organic chemistry. In: JB Jones, CS Sih, D Perlam, eds. Application of Biochemical Systems in Organic Chemistry. New York: Wiley Interscience, 1976, pp. 247–401.
8. W Hummel. New alcohol dehydrogenases for the synthesis of chiral compounds. Adv Biochem Eng 58:147–179, 1997.
9. T Coolebar, RM Daniel, HW Morgan. The enzyme from extreme thermophiles: bacterial sources, thermostabilities and industrial relevance. Adv Biochem Eng 45:58–90, 1992.
10. M Persson, M Krook, H Jornvall. Characterization of short-chain alcohol dehydrogenases and related proteins. Eur J Biochem 200:537–543, 1991.
11. H Jornvall, B Persson, J Jeffery. Characteristics of alcohol-polyol dehydrogenases. The zinc-containing long-chain alcohol dehydrogenases. Eur J Biochem 167:195–201, 1987.
12. PE Goodlove, PR Cunningham, J Parker, DP Clark. Cloning and sequence analysis of the fermentation alcohol dehydrogenase-encoding gene of *Escherichia coli*. Gene 85:209–214, 1989.
13. RK Scopes. An iron-activated alcohol dehydrogenase. FEBS Lett 158:303–306, 1983.
14. MR Wales, CA Fewson. NADP-dependent alcohol dehydrogenase in bacteria and yeast: purification and partial characterization of enzymes from *Acinetobacter calcoaceticus* and *Saccharomyces cerevisiae*. Microbiology 140:173–183, 1994.
15. S D'Auria, F La Cara, F Nazzaro, N Vespa, M Rossi. A thermophilic alcohol dehydrogenase from *Bacillus acidocaldarius* not reactive toward ketones. J Biochem 120:498–504, 1996.
16. JR Lakowicz, B Kierdaszuk, I Gryczynski, H Malak. Fluorescence of horse liver alcohol dehydrogenase using one- and two-photon excitation. J Fluorescence 6:51–59, 1996.
17. DJ Llewellyn, EJ Finnegan, JG Ellis, ES Dennis, WJ Peacock. Structure and expression of an alcohol dehydrogenase 1 gene from *Pisum sativum*. J Mol Biol, 115–124, 1987.
18. C Raia, S D'Auria, M Rossi. NAD^+-dependent alcohol dehydrogenase from *sulfolobus solfataricus*: structural and functional features. Biocatalysis 11:143–150, 1994.
19. JP von Warburg, JL Bethune, BL Vallee. Human liver alcohol dehydrogenase. Kinetic and physiochemical properties. Biochemistry **3**:1775–1782, 1964.
20. HW Sun, BV Plapp. Progressive sequence alignment and molecular evolution of the Zn-containing alcohol dehydrogenase family. J Mol Evol 34:522–535, 1992.
21. M Peretz, LV Weiner, Y Burstein. Cysteine reactivity in *Thermoanaerobium brockii* alcohol dehydrogenase. Protein Sci 6:1074–1083, 1987.
22. S Ammendola, C Raia, C Caruso, L Camardella, S D'Auria, M De Rosa, M Rossi. Thermostable NAD-dependent alcohol dehydrogenase from *Sulfolobus solfataricus*: gene and protein sequence determination and relationship to other alcohol dehydrogenases. Biochemistry 31:12514–12523, 1992.
23. TE Creighton. Folding pathways determined using disulfide bonds. In: TE Creighton, ed. Protein Folding. New York: W.H. Freeman, 1992, pp 301–351.
24. C-I Branden, H Eklund, B Nordstrom, T Boiwe, G Soderlund, E Zepperzauer, I Ohlsson, A Kesson. Structure of liver alcohol dehydrogenase at 2.9 angstrom resolution. Proc Natl Acad Sci USA 70:2439–2442, 1973.

25. BL Vallee, DS Auld. Zinc coordination, function and structure of zinc enzymes and other proteins. Biochemistry 29:5647–5659, 1990.
26. C Reynolds, MJ McKinley. Anion-binding to liver alcohol dehydrogenase studied by rate of alkylation. Eur J Biochem 10:474–478, 1969.
27. J Johansson, BL Vallee, H Jornvall. Closely related iso-enzymes of alcohol dehydrogenase. Carboxymethylation: gamma 1 gamma 2 differs widely from beta1 beta1 and its equine equivalence EE. FEBS Lett 279:119–122, 1991.
28. S D'Auria, C Caruso, N Vespa, M Rossi, C Raia. Selective carboxymethylation enhances the enzymatic activity and modifies the properties of *Sulfolobus solfataricus* alcohol dehydrogenase. Sixth European Congress on Biotechnology (ECB6), Florence, Italy, 1993, p 156.
29. RJ Lamed, JG Zeikus. Ethanol production by thermophilic bacteria: relationship between fermentation product yields and catabolic enzyme activities in *Clostridium thermocellum* and *Thermoanaerobium brockii*. J Bacteriol 144:569–587, 1980.
30. RJ Lamed, JG Zeikus. Novel NADP-linked alcohol-aldehyde-ketone oxidoreductase in thermophilic ethanologenic bacteria. Biochem J 195:183–190, 1981.
31. A Guagliardi, M Martino, I Iaccarino, M De Rosa, M Rossi. Purification and characterization of the alcohol dehydrogenase from a novel strain of *Bacillus stearothermophilus* growing at 70°C. Int J Biochem Cell Biol 28:239–246, 1996.
32. A Jongejan, JA Jongejan, JA Duine. Homology model of the quinohaemoprotein alcohol dehydrogenase from *Comamonas testosteroni*. Prot Eng 11(3):185–198, 1998.
33. G Petterson. Liver alcohol dehydrogenase. CRC Crit Rev Biochem 21:349–389, 1987.
34. Y Pocker, SC De Roy. The active site of liver alcohol dehydrogenase: mechanistic interferences for the binding and turnover of 2-, 3-, and 4-pyridylcarbinols. In: H Weiner, TG Flynn, eds. John Wiley & Sons, NY. The Enzymology and Molecular Biology of Carbonyl Metabolism, 1987, pp 179–187.
35. S Ramaswamy, H Eklund, BV Plapp. Structure of horse liver alcohol dehydrogenase complexed with NAD^+ and substituted benzyl alcohols. Biochemistry *33*:5230–5237, 1994.
36. M De Rosa, A Gambacorta, JD Bu'Lock. Extremely thermophilic acidiphilic bacteria convergent with *Sulfolobus acidocaldarius*. J Gen Microbiol 86:156–164, 1975.
37. A Trincone, L Lama, R Rella, S D'Auria, C Raia, B Nicolaus. Determination of hydride transfer stereospecificity of NADH-dependent alcohol-aldehyde-ketone oxidoreductase from *Sulfolobus solfataricus*. Biochim Biophys Acta 1041:94–96, 1990.
38. S D'Auria, N Vespa, A Trincone, M Rossi, C Raia. Studies on the stereospecificity of *Sulfolobus solfataricus* alcohol dehydrogenase. Second International Symposium on Chiral Discrimination, Rome, 1991, pp 111, 205.
39. E Keinan, EK Hafeli, KK Seth, R Lamed. Thermostable enzymes in organic synthesis 2. Asymmetric reduction of ketones with alcohol dehydrogenase from *Thermoanaerobium brockii*. J Am Chem Soc 108:162–169, 1986.
40. S D'Auria, M Rossi, R Nucci, G Irace, E Bismuto. Perturbation of conformational dynamics, enzymatic activity and thermostability of β-glycosidase from archeon *Sulfolobus solfataricus*. Proteins 27:71–79, 1997.

33

Alcohol Dehydrogenase

Sandrine Dallet, Marie Trovaslet, and Marie Dominique Legoy
University of La Rochelle, La Rochelle, France

I. INTRODUCTION

NAD^+-dependent alcohol dehydrogenases (AHDs) (alcohol:NAD^+) oxidoreductase E.C.1.1.1.1) are enzymes that occur widely in living organisms where they are important for the detoxification and metabolism of ethanol and other alcohols (1). ADHs catalyze the reversible oxidation of various alcohols to the corresponding aldehydes and ketones, with the concomitant reduction of NAD^+ (2). Depending on the biological source, ADHs show different substrate specificity (short-long-chain alcohols, aliphatic/aromatic alcohols, and branched alcohols).

Even though ADHs show some divergence in amino acid sequences, isoenzymes, and substrate specificity, they have certain structural and functional similarities. Three structurally and catalytically different types of ADHs are currently known (3). The medium-chain ADHs (containing ~ 350 residues per subunit) are named type I. They are zinc dependent and are characterized by a preference for primary alcohol. The short-chain ADHs (containing ~ 250 residues per subunit), named type II, are zinc independent and they display a better affinity toward secondary alcohols. Iron-activated long-chain ADHs, named type III, have an average subunit size of ~ 385 residues. Among these NAD^+-dependent ADHs, type I ADHs are the most studied with respect to structure and kinetic mechanism (4, 5). Originally, the ADHs of type I had been termed as the long-chain ADHs but were renamed as the medium-chain family after the still longer ADHs were discovered (3).

Many different type I ADHs have been characterized as subclasses based on their dimeric and tetrameric forms such as horse liver alcohol dehydrogenase (HLADH) and yeast *Saccharomyces cerevisiae* alcohol dehydrogenase (SADH or YADH), respectively. Primary structures of most ADHs are known but only the tertiary structure of HLADH is known at present (6,7). Crystallization of HLADH with or without NAD^+ has been achieved in order to understand the binding mechanism of different substrates and the kinetic mechanism (8, 9). The three-dimensional modeling of other medium chain ADHs is based on the structure of HLADH. Comparison of structure between HLADH and the other ADHs has shown that the three-dimensional structures of these enzymes must be very similar in the catalytic domains. Although the general overall sequence homology is $< 40\%$, all the structurally important residues are either homologous or conservatively substituted (Fig. 1) (4). Since HLADH and YADH are the most studied ADHs, we will present below only the state of the science concerning these two enzymes.

II. SOME UTILIZATION OF ADH IN FOOD TECHNOLOGY

The applications of ADHs as industrial catalysts are limited by the expense of the cofactors NAD(H). Many

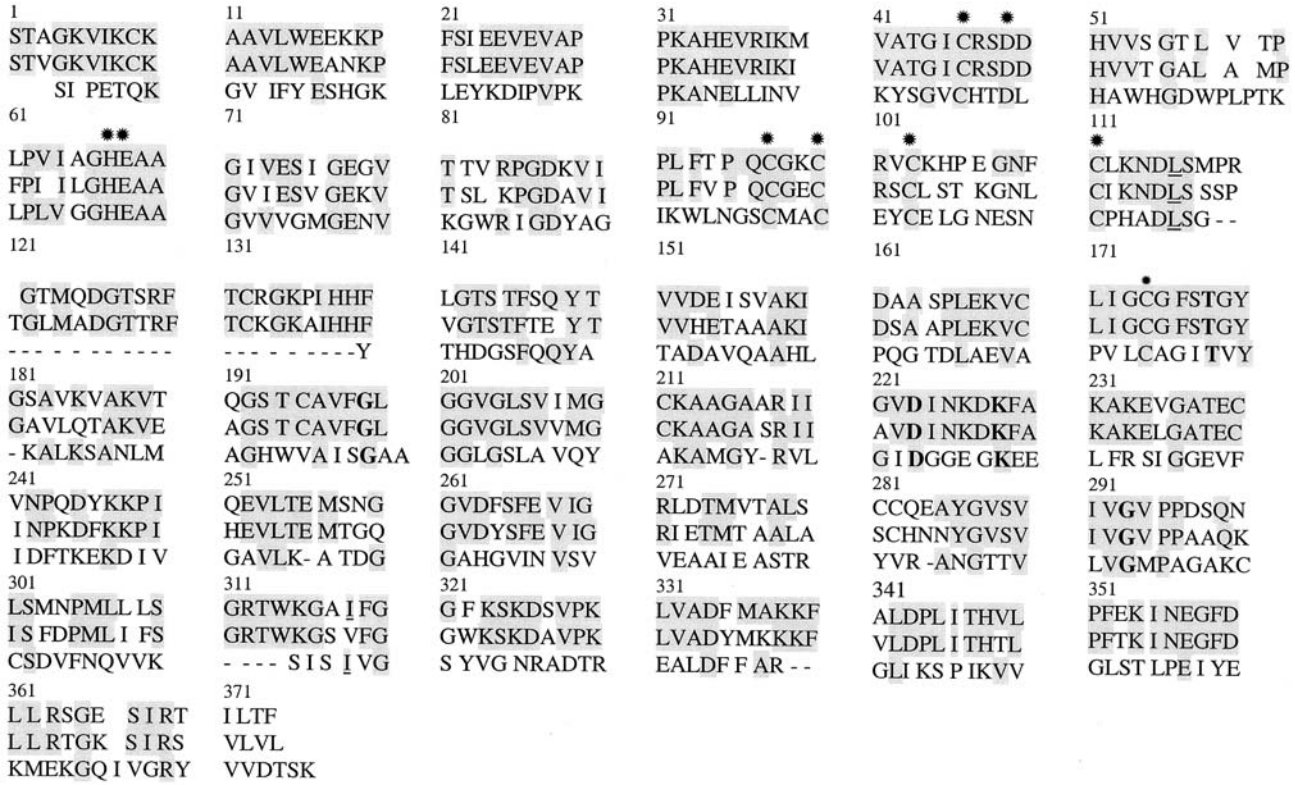

Figure 1 Alignment of the amino acid sequences of alcohol dehydrogenases from horse liver, chicken, and yeast. *Top row*, horse liver enzyme (6). *Middle row*, chicken enzyme (10). *Bottom row*, yeast enzyme (11). All residues numbering is based on alignment to HLADH, homologous residues conserved; * residue involved directly or not directly in zinc binding; **bold**: homologous residues involved in NAD$^+$ binding; underlined: homologous residues involved in substrate binding pocket.

complex methodologies have been studied for recycling the redox coenzyme, as for instance the coupling of ADH with another enzyme together with a coupled substrate in order to regenerate the coenzyme (12). An alternative approach consists in using a coenzyme mimic, bearing functional similarity to NAD$^+$ (13). Independently of the cofactor recycling, ADHs obviously have been used for the production of alcohols during the alcoholic fermentation or the production of aldehydes which represent a major source of numerous flavors.

In the case of alcoholic beverage production, it is not the enzyme that is used but the cell. The production of beverages by alcoholic fermentation is one of the oldest fermentations known. Beer and wine were probably the two earliest alcoholic drinks produced. A brief history of the knowledge in alcoholic fermentation could be summarized as follows. Until Pasteur's work in the late 19th century, little was known of the actual processes and mechanism of alcohol production. Pasteur showed that living yeast cells caused fermentation in the absence of air, converting sugar into ethanol and carbon dioxide. Research later in the 19th century showed that fermentation resulted from the action of substances contained within the yeast cells. Later, one of the major discoveries of fermentation microbiology was made by Hansen at the Carlsberg center in Copenhagen while working on "wild" yeast. These wild yeast were known to give problems during beer fermentation and, by isolating pure cultures of yeast, which he then used in the brewing process, Hansen initiated the use of pure cultures in beer production. Alcoholic beverages are produced by the alcoholic fermentation of the sugar-containing material to ethanol and carbon dioxide (see Chapter 2 for other details).

Fermentation is carried out by species of the yeast *Saccharomyces*. In some cases, sugar is present naturally, such as in grapes used in wine making; in others, sugars are produced from starches in cereals, as in beer

production. Free sugar is essential for alcoholic fermentation by *Saccharomyces* as the species is not able to hydrolyze polysaccharide material. Production of ethanol from glucose occurs via the Embden-Meyerhof-Parnas pathway. In the last reaction of this alcoholic fermentation, yeast ADHs catalyze the reduction of acetaldehyde to ethanol (14).

The yeast used in the manufacture of alcoholic beverages are strains of *Saccharomyces cerevisiae* or *S. carlsbergensis*. The definitive difference between these yeasts is that *S. carlsbergensis* ferments raffinose completely, whereas *S. cerevisiae* does not (14).

III. PROPERTIES AS PROTEIN

A. Horse Liver Alcohol Dehydrogenase

Horse liver alcohol dehydrogenase (HLADH) is generally considered to be a symmetrical dimer, composed of two identical chains of 40 kDa but with difference in amino acid sequence at six positions. One cannot ignore the different forms observed in several experiments owing to dissociation-reassociation or in other studies of the purified isoenzymes. It is known that three main isoenzymes are formed by the dimeric combination of the two different types of subunit chains, which are based on the difference in substrate specificity. There is a subunit called E for its ethanol activity and another subunit S for its steroid activity, therefore, the main isoenzymes are EE, ES, and SS. The three isoenzymes differ in that SS also has ethanol activity but lower than ES and still lower than EE and that EE has some activity toward certain steroid side chain hydroxyl groups (4).

1. Primary, Secondary, Tertiary, and Quaternary Structures

Studies of primary structure of E- and S-subunits have shown that each subunit is composed of 374 residues plus two zinc atoms. The crystal structure analysis of the apoenzyme helped to determine the position of each residue in the polypeptide chains and showed that the principal difference between these subunits is a 6 amino acid difference at positions Glu17, Thr94, Arg101, Phe110, Asp115, and Glu366 (residues listed for E-subunit). Three of the six amino acid differences observed between the E- and S-chains may be responsible for the difference in substrate specificity. These are Phe110, Asp115, and Thr94 in the E-subunit, and Leu110, Ser115, or a gap and Ile94, respectively, in the S-chain. The other three residues (Gln17, Ser101, and Lys366) that are different are all located in different regions from the catalytic domain (4).

Each subunit is divided into two domains separated by a crevice that contains a wide and deep hydrophobic pocket (active site). One of these domains, called the coenzyme-binding domain, binds the coenzyme. The two zinc atoms are bound within the second domain, called the catalytic domain. The two domains are unequal in size. The catalytic domain is larger and comprises 231 residues, whereas the coenzyme-binding domain contains 143 residues. The primary and secondary structures in the subunit of HLADH are illustrated in Figure 2 (6).

The two subunits of the dimeric enzyme are joined together mainly through noncovalent interactions within the coenzyme-binding domains. These domains thus form a core in the middle of the molecule by homologous interactions within corresponding regions of the coenzyme binding to enzyme. The catalytic domains are located on the exterior of the molecule, and the catalytic sites are found in the junction between the two domains and the core. The whole molecule has an approximate helical content of 29% of the residues while 34% are in pleated-sheet regions.

2. Coenzyme-Binding Domain

The coenzyme-binding domain of the subunit comprises residues 176–318. The amount of secondary structure in this domain is considerable; 45% of the residues are helical (mainly α-helices), 32% are in pleated-sheet structure, and 13% in reverse bends. Thus only $\sim$ 10% of the residues have no regular secondary structure. The domain is built of six parallel strands of pleated sheet (βA–βF) flanked by five helices (αA–αE) in a regular pattern. There are three hydrophobic regions in this domain. One is involved in subunit interactions; the βF strands of each subunit run in opposite directions perpendicular to the twofold axis and are joined together by hydrogen bonds forming two strands of antiparallel β structure. The other two hydrophobic regions are implicated in the folding of the domain and form hydrophobic cores between helices and the parallel pleated sheet. The unique fold of the coenzyme-binding domain creates a large cleft region between the two domains of HLADH for binding of a coenzyme molecule (4, 6, 15).

Two coenzyme molecules are bound per enzyme molecule independently of each other. The coenzyme binds to the enzyme in the central region of the carboxyl end of the parallel pleated sheet. The coenzyme binding induces different conformational changes: the active site is more shielded from the solution; the active

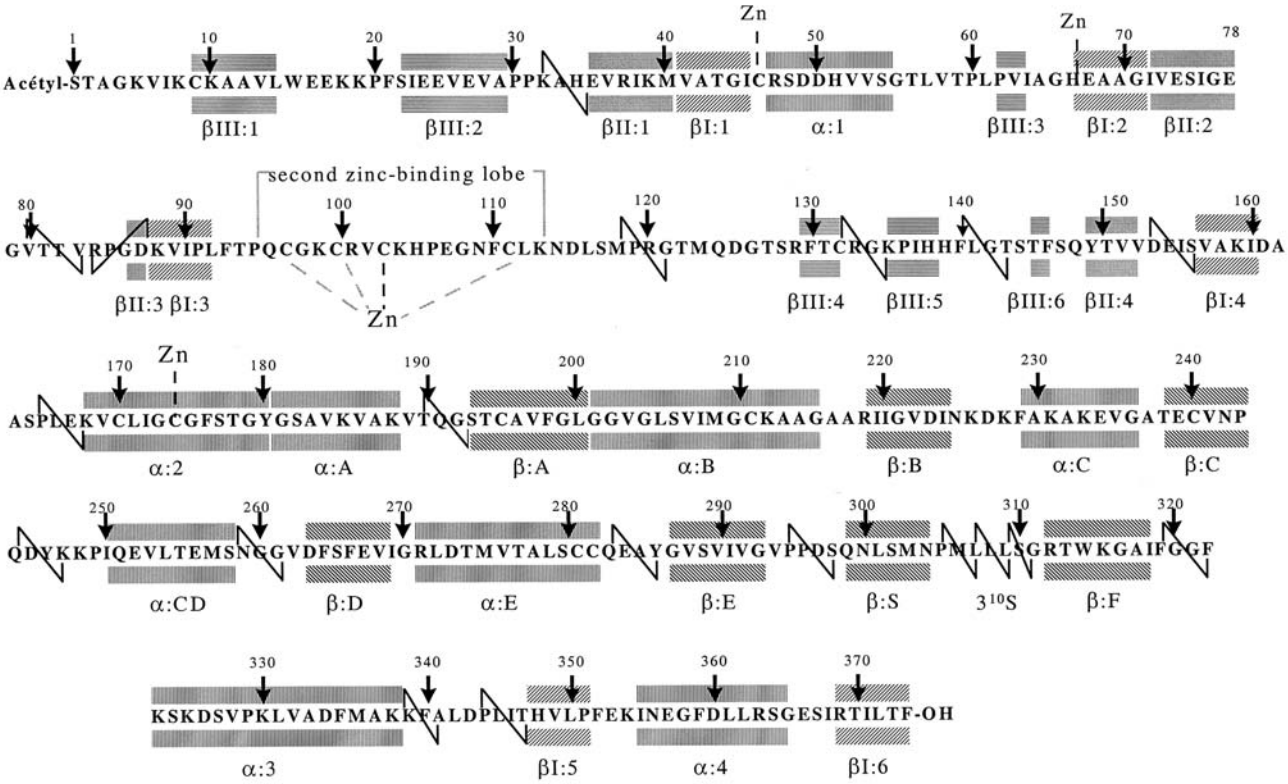

Figure 2 Primary structure and schematic diagram of the regions of secondary structure in the subunit of HLADH. Helices are called α with a numeral for those that appear in the catalytic domain and a letter for those that are in the coenzyme-binding domain. Strands of pleated sheet are called β with a similar nomenclature as for the helices. Reverse turns are denoted by the following symbol (⌐¬). ▭: indication of length of helix or strand. (From Ref. 6.)

site is then in a more hydrophobic environment in the holoenzyme than in the apoenzyme. All water molecules that are located in the active site in the apoenzyme are displaced in the ternary complex, and the catalytic reaction of the enzyme takes place in a completely water-free environment (15). The increase of hydrophobicity around the nicotinamide group in the ternary enzyme-NAD^+-alcohol complex facilitates the reaction (8).

3. Catalytic Domain

The catalytic domain comprises residues 1–175 and 319–374 plus two zinc atoms. Both ends of the polypeptide chain are within this region. The two zinc atoms of the subunit are bound to ligands from the domain; these bindings are illustrated in Fig. 2. Only the zinc atom participates in the catalytic activity; the second zinc atom is remote from the active site and may help in stabilizing protein folding (a structural zinc). Only 19% of the residues are helical (α1; α2; α3, and α4); 35% are in pleated-sheet regions (βI, βII, βIII), and 14% are in reverse bends. Thus, a large number of residues, 32%, have no regular secondary structure. An important region in the domain, necessary for the structural stability of the enzyme, is the lobe comprising residues 95–113 that binds the structural zinc atom by four sulfur atoms from cysteine residues 97, 100, 103, and 111. Although it is bound near the surface of the molecule, this zinc atom is completely surrounded by the protein and is not accessible in the native conformation of the enzyme (6).

4. Substrate-Binding Site

The substrate-binding site, lined almost exclusively by hydrophobic residues, is located in a cleft between the coenzyme-binding core and the catalytic domain. This cleft is open in the apoenzyme form, which is well suited for the initial coenzyme binding and does not hinder its entrance.

The catalytic zinc atom is situated at the bottom of this deep pocket, with a distance of ~ 20–25 Å from the exterior surface of the protein. The active-site zinc performs several functions associated with the catalytic reaction. Three of the four coordination ligands to the catalytic zinc belong to the protein; two sulfur atoms from Cys46 and Cys174 and one nitrogen atom from His67. In the apoenzyme, the fourth ligand is an ionizable water molecule that is hydrogen-bonded to the hydroxyl group of Ser48. Following the binding of the coenzyme, the water is displaced by the substrate. This is facilitated by a coenzyme-induced shift in equilibrium from an open/closed conformation of the enzyme.

B. Alcohol Dehydrogenase from Yeast (YADH)

YADH has a molecular weight of 150 kDa and contains four identical subunits of ~ 36–37 kDa. Just like in HLADH, each subunit contains two zinc atoms. They have structural and catalytic roles and are bound tetrahedrally to four sulfur atoms all close to one another in the primary sequence (structural zinc atom) or to three protein ligands (two sulfur atoms and one nitrogen atom) and a water molecule or hydroxyl ion, depending on the pH (catalytic zinc atom) (16). The primary structure of YADH has been compared to the known tertiary structure of the corresponding HLADH after proper alignment of the two proteins (17). The results show that YADH and HLADH are distantly homologous with many insertions/deletions and with only 25% of all residues conserved, but all functionally essential residues are similar or identical. Moreover, the difference in the tertiary structures of YADH and HLADH are less than the large differences in the primary structure of these proteins (Fig. 1) (17). This comparison shows that the general subunit conformations and enzymatic mechanisms of both enzymes are probably similar (Table 1). The residues in HLADH that participate in coenzyme binding, substrate binding and the catalysis are listed in Table 1, together with the equivalent residues in YADH.

Quaternary structure of YADH and residues involved in subunit contacts are not yet well known. But, in 1995, De Bolle et al. (18) suggested that a part of the subunit contacts observed in HLADH are located at homologous positions in YADH. The main difference in quaternary structure is likely to be due to surface changes of the subunits.

Four alcohol dehydrogenase isoenzymes are found in the yeast *Saccharomyces cerevisiae*. These enzymes have different substrate specificities and are differentially expressed, at least partly related to the requirement for fermentation or for oxidation of alcohols. The three chromosomally encoded isoenzymes are differentially expressed. Although YADH I and YADH II perform separate metabolic roles, they do not differ greatly in their V_{max} values for both forward and reverse reactions, but they do differ in their affinity for ethanol as a substrate. YADH I is the fermentative cytoplasmic enzyme that, when the yeasts are grown on glucose under anaerobic conditions, can account for up to 1% of cell protein. An opposite physiological role of ethanol oxidation is carried out by YADH II which converts ethanol accumulated in anaerobic growth to acetaldehyde and is expressed when ethanol is used as a carbon source. These two isoenzymes have

Table 1 Residues at Positions that Participate in Enzymatic Functions of the HLADH

Function	Horse liver[a]	Yeast
Adenine-binding pocket interior	Phe198	Ser198
	Val222	Ile222
	Ile224	Gly224
	Pro243	Phe243
	Ile250	Val250
	Thr274	Ala274
	Thr277	Ala277
Surface	Arg271	Ser271
	Asp273	Ala273
Adenosine ribose binding	**Asp223**	**Asp223**
	Gly199	**Gly199**
	Ile269	Ser269
	Asn225	Gly225
	Lys228	**Lys228**
Pyrophosphate binding	Arg47	His47
	Ile269	Ser296
Nicotinamide ribose binding	**Gly293**	**Gly293**
Nicotinamide binding	**Thr178**	**Thr178**
Substrate-binding pocket	Leu57	Trp57
	Phe93	Trp93
	Phe110	Asn110
	Leu116	**Leu116**
	Phe140	Tyr140
	Leu141	Thr141
	Pro296	Ala296
	Ile318	**Ile318**
Acid-base system	Ser48	Thr48
	His51	**His51**
Ligands to active site zinc atom	**Cys46**	**Cys46**
	His67	**His67**
	Cys174	**Cys174**

Source: Ref. 17.
[a] Numbers refer to the amino acid sequence of the horse protein.

94% sequence homology (11). YADH III is mitochondrially located and has 79% and 78% amino acid identity with YADH I and YADH II, respectively (11). The function of YADH III has not been identified, although its mitochondrial location would indicate that it may have had a role in respiration. Cells lacking YADH III isoenzyme can survive aerobically or anaerobically (11). The fourth ADH is an iron activated enzyme.

IV. PROPERTIES AS ENZYMES

A. Substrate Specificity and Activity

Alcohol dehydrogenases catalyze the reversible interconversion of a wide variety of aldehyde/alcohol substrates. The specificity of ADHs for their substrates is not the same for all enzymes. In fact, yeast alcohol dehydrogenase has more restricted specificity than horse liver alcohol dehydrogenase. The activity of YADH decreases as the chain length of the primary alcohols increases (19). YADH and HLADH also have quite different activities and stereospecificities on secondary and branched alcohols. The difference in substrate specificity between HLADH and YADH could be due to a difference in the size of the substrate binding pocket. The main differences in the substrate binding pocket are the changes from Phe93 and Ser48 in HLADH to Trp and Thr, respectively, in YADH. As a consequence YADH has a smaller substrate binding pocket (20).

The activities of HLADH and YADH on primary, secondary, and branched alcohols and the kinetic constants (*kcat* [turnover number], K_M, and k_{cat}/K_M [catalytic efficiency]) characteristic for HLADH and YADH are listed in Section V (see Tables 2–4).

Table 2 Kinetics Parameters for Oxidation of Alcohol by NAD^+ Catalyzed by HLADH

Substrates	k_{cat} (sec^{-1})	K_M (μM) coenzyme	K_M (mM) substrate	$k_{cat}/K_{M(substrate)}$ ($M^{-1}sec^{-1}$)
Primary alcohols				
Ethanol (a)	1.14	16.3	0.460	2,480
Propanol (b)	8.20		0.390	21,000
Butanol (b)	5.20		0.270	19,000
Pentanol (b)	4.30		0.150	29,000
Hexanol (b)	2.80		0.076	37,000
Heptanol (b)	2.50		0.020	125,000
Octanol (b)	2.30		0.040	58,000
Secondary and branched alcohols				
Isopropanol (c)	0.58		9.0	64
2-methyl-propanol (b)	5.30		0.4	13,000
(R)-2-butanol (c)	2.00		7.5	270
(S)-2-butanol (c)	1.00		1.35	740
2-methyl-1-butanol (S) (b)	5.70		0.31	18,000
2-methyl-1-butanol (RS) (b)	5.30		0.52	10,000
3-methyl-1-butanol (b)	2.80		0.15	19,000
(S)-2-pentanol (c)	0.87		0.73	1,200
(R)-2-pentanol (c)	1.01		31.7	32
3-pentanol (c)	2.26		1.6	1,400
(S)-2-octanol (c)	1.52		0.18	8,400
(R)-2-octanol (c)	0.053		1.92	29

Source: Refs. 20, 33, 34.
Measurements were made (a) at 25°C, in a 47 mM phosphate, 0.25 mM EDTA buffer, pH 8. Kinetics were measured with NAD^+ concentration varied from 5 to 55 μM and ethanol concentration varied from 1 to 10 mM; (b) at 30°C in a 83 mM potassium phosphate, 40 mM KCl, 0.25 mM EDTA buffer, pH 7.3. [NAD^+] was fixed at 2 mM. Concentration of substrates were varied over a 10-fold range around the corresponding K_M values; (c) at 25°C, in a 0.1 M Taps buffer, pH 8.5. Kinetics were measured with 0.5 mM NAD^+ and a substrate concentration ranging from 0.5 to 5 times the K_M.

Table 3 Kinetics Parameters for Reduction of Aldehydes Catalyzed by HLADH

Substrates	k_{cat} (sec^{-1})	K_M (μM) coenzyme	K_M (mM) substrate	$k_{cat}/K_{M(substrate)}$ ($M^{-1}sec^{-1}$)
Acetaldehyde (a)	125.00	14.37	0.46	271800
Acetone (b)	0.33		135.00	2
2-butanone (b)	0.12		15.00	8
2-pentanone (b)	0.073		14.20	5.1
3-pentanone (b)	0.36		75.00	5
Cyclohexanone (c)	26.00		5.30	4900
(3R)-3-methylcyclohexanone (c)	0.64		5.0	128
Benzaldehyde (d)	110.00	9.90	0.12	916700

Source: Refs. 22, 36.
Measurements were made (a) at 23.5°C, in a sodium phosphate buffer, pH 6. Range of concentrations of coenzyme and substrates were: [NADH] 0.5–20 μM, [acetaldehyde] 29–1440 μM; (b) at 25°C, in a 0.1 M Taps buffer, pH 8.5, with a coenzyme concentration of 0.2 mM and a substrate concentration range of 0.5 to five times the K_M; (c) at 30°C, in a 33 mM sodium phosphate buffer, pH 8, containing 0.25 mM EDTA. Range of concentrations of substrates were: [cyclohexanone] 0.2–8 mM, [(3R)-3-methylcyclohexanone] 1–9 mM, [(±)-3-methylcyclohexanone] 0.2–8 mM; (d) at 30°C, in a 50 mM sodium TES and 0.25 mM EDTA buffer, pH 7.

Table 4 Kinetics Parameters for Oxidation of Alcohol and Reduction of Aldehydes Catalyzed by YADH

Substrates	k_{cat} (sec^{-1})	K_M (μM) coenzyme	K_M (mM) substrate	$k_{cat}/K_{M(substrate)}$ ($M^{-1}sec^{-1}$)
Oxidation of alcohols by NAD^+				
Primary alcohols				
Ethanol (a)	340		17.0	20,000
Propanol (a)	120		27.0	4,400
Butanol (a)	51		55.0	930
Pentanol (a)	29		37.0	780
Hexanol (a)	16		10.0	1,700
Heptanol (a)	14		7.8	1,800
Octanol (a)	17		5.3	3,300
Nonanol (a)	8.6		1.7	5,100
Secondary and branched alcohols				
2-propanol (a)	4.8		190	25
2-butanol (R) (a)	0.05		61	0.8
2-butanol (S) (a)	1.0		55	18
2-methyl-1-propanol (a)	0.19		25	8
2-methyl-1-butanol (S) (a)	NA[a]		NA	NA
2-methyl-1-butanol (RS) (a)	NA		NA	NA
3-methyl-1-butanol (a)	NA		NA	NA
Benzyl alcohol (a)	NA		NA	NA
Cyclohexanol (a)	NA		NA	NA
Reduction of aldehydes by NADH				
Acetaldehyde (b)	3850	96	0.93	4,139,800
Butyraldehyde (b)	3450	97	27.5	125,450

Source: Refs. 19, 20.
Measurements were made (a) at 30°C in a 83 mM potassium phosphate, 40 mM KCl, 0.25 mM EDTA buffer, pH 7.3. [NAD^+] was fixed at 2 M. Concentration of substrates were varied over a 10-fold range around the corresponding K_M values; (b) at 25°C, in a sodium phosphate buffer, pH 7.05, containing bovine serum albumin. Range of coenzyme and substrate concentrations were: [NADH] 3–330 μM, [acetaldehyde] 0.027–5.5 mM, [butyraldehyde] 1.9–37 mM.
[a] NA, no measurable activity.

B. Effects of Environmental Factors

ADHs, like most enzymes, may be affected structurally and catalytically by environmental factors such as pH, temperature, and pressure.

1. pH

Alcohol dehydrogenases catalyze a reversible reaction, and forward and backward reactions occur simultaneously. The reaction of NAD^+ acidifies an unbuffered reaction medium by producing a proton while the oxidation of NADH consumes a proton (21). For YADH and HLADH, a double pH dependence for the forward and the backward directions has been established. For YADH, the optimal pH in the forward reaction (oxidation of alcohol) is 8.3 and in the backward direction 6.0 (reduction of aldehyde). These pH optima have been obtained under standard conditions (absence of buffer at high substrate concentration (100 mM), 5 mM NAD^+ or 0.5 mM NADH and zero initial product concentration). The distance between the two optimal pH values (the pH optimal distance) corresponds to two pH units. Other substrates (2-propanol/propanal) shift the optimal pH of the forward and the backward directions by about two pH units toward higher values. Moreover, whatever the substrates, the forward and the backward directions have different maximum rates, even at their corresponding optimal pH (20). In the case of HLADH, the optimal pH is 9 in the forward direction and 6 in the backward direction. The kinetic constants obtained versus pH are listed in Table 5. The K_{eq} (equilibrium constant of enzyme-coenzyme complex with substrates) decreases when pH increases. The approximate values are of 2, 1, and 0.1 nM at pH 7, 8, and 9, respectively (22).

2. Effect of Temperature on Activities of YADH and HLADH

The optimal temperature for YADH is 25°C. The optimal temperature for HLADH is 53°C. The behavior of YADH and HLADH versus temperature is opposite in direction. Whereas YADH activity decreases when temperature increases above 25°C, HLADH activity increases when temperature increases up to 53°C.

The half-life of YADH is 3.5 h when a solution of YADH at 0.1 mg/mL is stored at 25°C in 50 mM Tris-HCl buffer, pH 8.5 (23). Concerning HLADH, the half-life at 53°C is 8.5 h and it is 14.3 h at 25°C. These studies have been performed in a solution of HLADH at 0.045 mg/mL, in 50 mM Tris-HCl buffer, pH 8 (24).

3. Effect of Pressure on Activities of YADH and HLADH

In studying the effect of pressure on YADH activity at 25°C, it has been shown that pressurization of YADH

Table 5 Effect of pH on Kinetic Constants

Oxidation of ethanol[a]				
pH	k_{cat} (sec^{-1})	K_M NAD^+ (μM)	K_M substrate (μM)	k_{cat}/K_M ($M^{-1}\,sec^{-1}$)[b]
6	1.6	4.0	452	3,600
7.1	2.7	3.0	178	15,000
8	3.2	2.9	161	20,000
9	3.8	4.6	396	9,600
Reduction of aldehyde				
pH	k_{cat} (sec^{-1})	K_M NADH (μM)	K_M substrate (μM)	k_{cat}/K_M ($M^{-1}\,sec^{-1}$)[b]
6	125.0	14.4	463	270,000
7.1	125.0	12.5	413	303,000
8	47.6	6.3	186	256,000
9	7.6	1.6	97.7	78,000

Source: Ref. 32.

[a] The values have been determined in the following conditions: T = 23.5°C, in 100 mM sodium phosphate buffers (for experiments at pH 5.35–8) or in 36 mM glycine-NaOH buffer, pH 9, with 1.8–500 μM NAD^+/0.1–8.1 mM ethanol or 0.98–19.6 μM NADH/0.027–1.0 mM acetaldehyde.

[b] K_M for substrate.

resulted in a decrease of catalytic efficiencies. This phenomenon became more pronounced for pressure > 50 MPa. This loss in catalytic efficiency is mainly due to a decrease of k_{cat} (70% loss from 0.1 to 175 MPa). On the contrary, K_M for ethanol seems to be less sensitive to pressure (20% less in the same range of pressure) (25). YADH activity inhibition is therefore not due to a dissociation of the tetrameric enzyme because only the tetrameric form binds ethanol.

In contrast to YADH, HLADH activity increases with pressure up to 225 MPa at 53°C. From atmospheric pressure to 225 MPa k_{cat} increases by a factor of 13. But pressure affects the affinity of HLADH for its substrates. At the same conditions K_M for NAD^+ increases by a factor of 50 and K_M for ethanol increases by a factor of 45, but the inhibition by ethanol observed at atmospheric pressure is not observed above 150 MPa (24).

4. Some Inhibitors of ADH

There are two general classes of ADH inhibitors. One class includes analogs of alcohols and aldehydes. These compounds bind in the substrate pocket to the catalytic zinc atom displacing the zinc-bound water molecule (ex: pyrazole; $K_i = 0.22\,\mu M$ [4]). Amides and formamides are analogs of aldehydes and potent inhibitors of HLADH. These inhibitors bind preferentially to the enzyme · NADH complex. The amides inhibit alcohol metabolism and might be useful therapeutic agents—for example, to prevent oxidation of methanol or ethylene glycol to their toxic acids. The amides are uncompetitive inhibitors of ethanol and competitive of acetaldehyde (N-cyclohexylformamide; $K_i = 8.7\,\mu M$ [26]). The amides may bind to free enzyme or the enzyme · NAD^+ complex (26). The chelating agents such as 2,2-bipyridine ($K_i = 400\,\mu M$ [4]) or salicylate ($K_i = 1.25\,\mu M$ [4]) are competitive inhibitors with NAD^+ and NADH and partially competitive with alcohol. These inhibitors bind to the catalytic zinc and displace the zinc-bound water molecule at the presumed substrate binding site. Heterocyclic nitrogen bases such as imidazole form both binary and ternary complexes with HLADH. Imidazole binds to the catalytic zinc in the same way as chelating agents (4).

The second type of ADH inhibitors consists of analogs of the coenzymes NAD^+ and NADH, as well as structurally related compounds. These inhibitors bind in the coenzyme-binding cleft generally mimicking the binding of the adenosine portion of the cofactor. For instance, 5-β-D-ribofuranosylnicotinamide adenosine dinucleotide ($CNAD^+$) is an isosteric and isomeric analog to NAD^+ in which the nicotinamide ring is linked to the sugar via a C-glycosyl (C5–C1′) bond and 5-β-D-ribofuranosylnicotinamide adenosine dinucleotide ($CPAD^+$) is another one. The inhibition constant of $CNAD^+$ with respect to NAD^+ is 4 nM; this is significantly smaller than the K_i for NADH (0.4 μM). Further, $CNAD^+$ competes with both cofactor and substrate binding ($K_i = 2$ nM). The other isosteric analog of NAD^+, CPAD, shows competitive inhibition of NADH with respect to NAD^+ and does not compete with substrate binding (27).

5. Some Inhibitors for YADH (4)

Some coenzyme competitive inhibitors include N-alkyl nicotinamide derivatives (the inhibitory ability increases with increase in length of the alkyl chain), N-alkyl substituted ammonium chlorides and fluorescent dyes, and drugs such as chloroquine and propanol. Other inhibitors include chelating agents such as 1,10-phenanthroline (inhibition is considerably smaller with YADH than with HLADH), and nonchelating analogs such as 1,5-phenanthroline and 2,9-dimethyl-1,10-phenanthroline. With pyrazole, the inhibition is competitive with ethanol and uncompetitive with coenzyme and acetaldehyde and with 4-substituted pyrazole amide derivatives (weaker inhibitors than pyrazole). Thiocyanate is an inhibitor that is competitive with ethanol and noncompetitive with NAD^+. It is reversible or irreversible depending on the concentration. Urea at low concentrations inhibits the enzyme noncompetitively with respect to NAD^+, NADH, alcohol, and aldehyde, and at higher concentrations inhibits the enzyme irreversibly. Thiourea, guanidium salts, phenylisopropyl hydrazine, and canavanine are also inhibitors.

C. Reaction Mechanism of HLADH

The enzyme binds coenzyme and substrate to form a ternary complex which, in general, can be assumed to be ordered with coenzyme binding preceding substrate binding and product release preceding coenzyme release.

Aldehyde formation during the catalytic action of the enzyme requires a net removal of two hydrogen atoms from an alcohol substrate. This dehydrogenation process is known to proceed by a mechanism of combined proton and hydride ion transfer. It is well established that transfer of the hydride ion occurs directly between substrate and coenzyme in the productive ternary complex formed. The first step is an

initial binding of NAD^+. The $E \cdot NAD^+$ complex isomerizes (i.e., changes conformation) with a forward rate constant of $620\,sec^{-1}$ at pH 8 and $1100\,sec^{-1}$ at pH 7.6 (28). By isomerization of the enzyme $\cdot$ NAD^+ complex, the pK_a of the zinc bound water molecule is shifted from ~ 9.6 to ~ 7.6 (29). This isomerization is facilitated in the presence of alcohol in which case the pK_a drops to < 4.5. As a result of this isomerization, a hydroxide ion remains bound to the zinc atom, and a proton is released. It has been suggested that this proton is released through the system of hydrogen bonds involving Ser48 and His51 (28). The electric field created by the protein framework facilitates this proton tunneling along the hydrogen bonds. The presence of NAD^+ and zinc with a small positive charge further enhances this effect. It is similar to a proton pump which pumps protons from the interior hydrophobic pocket to the surface of the molecule. The transfer of the proton from the alcohol to the enzyme active site occurs simultaneously with the hydride transfer from the substrate to the coenzyme. Figure 3 presents the ordered ternary complex mechanism during HLADH catalysis.

The rate of the conformational change (isomerization) could limit the transient rate of oxidation of alcohol. The isomerization of the $E \cdot NAD^+$ complex is partially, but not fully, rate limiting for the oxidation of longer-chain alcohols. The rate of interconversion of ternary complexes can be limited by the rate of transfer of hydride ion from alcohol to NAD^+, the release of a proton to solvent, or other unimolecular steps depending on the substrate (28).

When NAD^+ concentrations are approximately stoichiometric with enzyme, HLADH catalyzes the dismutation of different aldehydes to equimolar quantities of the corresponding alcohol and acid (30). This reaction is spectrophotometrically silent because there is no net synthesis of NADH. The V_{max} for dismutation is higher than that for oxidation of the corresponding alcohol. At high concentrations of NAD^+, the enzyme catalyzes oxidation of aldehydes to acids with net NADH production with a V_{max} much less than that for alcohol oxidation (30).

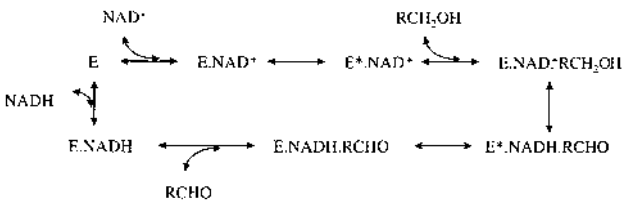

Figure 3 The ordered ternary complex mechanism usually considered for evaluation of the kinetics of HLADH catalysis. E, $E \cdot NADH$, $E^* \cdot NAD^+$, $E \cdot NAD^+ \cdot RCH_2OH$, and $E^* \cdot NAD^+ \cdot RCH_2OH$ denote enzyme, coenzyme-enzyme complex, coenzyme-enzyme complex isomerized, enzyme-coenzyme-alcohol complex, and enzyme-coenzyme-alcohol complex isomerized, respectively. (From Ref. 28.)

D. Reaction Mechanism for YADH

The main features of the reaction mechanisms for YADH are in all probability essentially the same as in HLADH (because of structural similarities of the catalytic domain of the two enzymes). Finer details of the reaction mechanism, however, are different between the two enzymes. There are differences in substrate specificity, in the rate of catalysis, and in the requirements for ordered events during the catalytic mechanism which may be random or ordered depending on substrate (31). The step of dissociation of NADH from the enzyme could be the rate-limiting step in the oxidation of alcohol.

V. QUALITATIVE AND QUANTITATIVE DETERMINATION OF ACTIVITY

A. Specific Activity with Assay Conditions

ADH activity assays for alcohol oxidation or aldehyde reduction were followed by an increase or a decrease of NADH absorption at 340 nm, respectively. As the molar absorptivity of NADH at 340 nm is dependent on the conditions of pH, ionic strength, buffer, temperature, and pressure, it must be determined for each kinetics condition (25, 32). However, some characteristics of HLADH must be known before using this enzyme. Its isoelectric point is 6.8, its optimal pH is ~ 9, its optimal temperature is 53°C. In Tables 2 and 3 some kinetic parameters obtained for oxidation of alcohol or reduction of aldehydes catalyzed by HLADH under different assay conditions are presented.

As for HLADH, some characteristics of YADH must be known before using this enzyme. Its isoelectric point is 5.4, its optimum pH is ~ 8.6 (for the alcohol oxidation), its optimal temperature is 25°C. The specific substrates and the corresponding kinetic constants are listed in Table 4.

B. Enzyme Stability

Lyophilized preparations of YADH stored at −20°C are stable for 6–12 months. Crystalline suspensions in ammonium sulfate are stable for 6 months at 2–8°C. However, preserving an active enzyme solution remains a problem. A solution of enzyme (0.1 mg/mL in 50 mM Tris-HCl buffer, pH 8.5) stored at 4°C is not stable; its half-life ($t_{1/2}$) is 4.5 h. When stored at −20°C, its half-life is 56 h. In order to increase the stability of the enzyme solution, it has been shown that storing the enzyme with NAD^+ (1.5 mM) or with NAD^+/sorbitol (1.5 mM/1 M), enhances the stability. The $t_{1/2}$ (25°C) was 28 h with NAD^+ and 16 h for NAD^+/sorbitol. The $t_{1/2}$ (4°C) increases to 82 and 68 h in the presence of NAD^+ and NAD^+/sorbitol, respectively (23).

Both lyophilized and crystalline suspensions in buffer preparations are stable for 3–6 months when HLADH is stored at −20°C. In solution, HLADH was more stable than YADH; at the same storage conditions of buffer and temperature, the $t_{1/2}$ (25°C) is 680 h and the $t_{1/2}$ (4°C) is 755 h (24). See above for stability of YADH under these conditions. To stabilize the enzymes, it is possible to add bovine serum albumin at 1 g/L.

VI. PURIFICATION OF ADH

The enzyme has been purified, and the EE and SS isoenzymes separated by affinity chromatography on an immobilized AMP analog. Commercially available preparations contain the EE isoenzyme and small amounts of the ES isoenzyme (4). The more studied YADH is a cytoplasmic protein, commercially available and usually obtained from baker's yeast. Several purification methods have been reported including toluene plasmolysis; DEAE-cellulose chromatography; fractionation with protamine sulfate and calcium phosphate gel; and purification without autolysis, heat denaturation, or use of solvents. Separation of YADH from enzyme mixtures by affinity chromatography on immobilized NAD^+ or AMP analogs has also been reported (4). It is now not necessary to purify HLADH and YADH in one's laboratory because of their commercial availability at low price and high purity. Table 6 presents the characteristics of commercially available HLADH and YADH.

Table 6 Characterization of Commercially Available Alcohol Dehydrogenase

	Yeast ADH	Horse liver ADH
Classification	medium-chain dehydrogenase	medium-chain dehydrogenase
Required coenzyme	NAD(H)	NAD(H)
Specific activity (U/mg)	300[a]	1–2[a]
Enzyme costs ($/500 units) (Sigma catalog 1998)	2	330
Stability	sensitive to O_2	stable
Limitations	low stability	

[a] oxidation of 1 μmol ethanol/min.

Figure 4 shows an example of purification of human liver alcohol dehydrogenase (which is very similar to HLADH except in regard to specificity) (37). Human liver alcohol dehydrogenase has been purified by a procedure designed to process 10- to 20-kg quantities of liver. The results are summarized in Table 7.

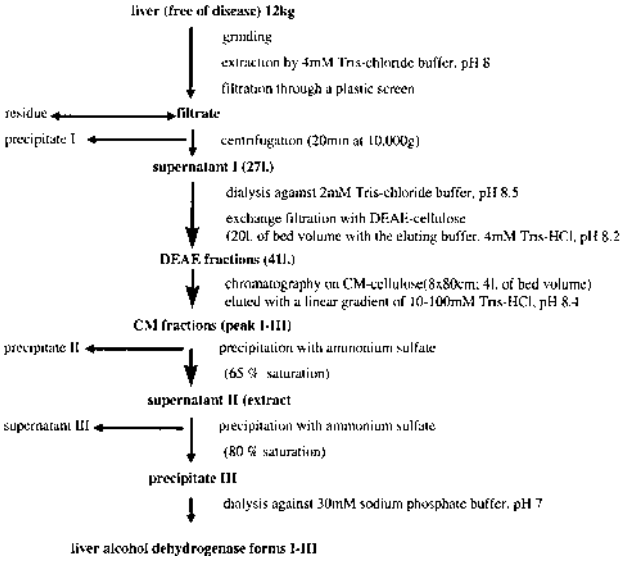

Figure 4 Example of purification: human liver alcohol dehydrogenase (which is very similar to HLADH except in regard to specificity). (From Ref. 37.)

Table 7 Large-Scale Purification of Human Liver Alcohol Dehydrogenase

Fraction	Vol (L)	Act. (ΔA_{340}nm/min)	Protein (mg)	Specific act. (ΔA_{340}nm/min/mg)
Crude extract	27	24,000	760	0.03
Dialyzed extract	32	23,300	770	0.03
DEAE-cellulose-treated extract	41	19,200	36	0.53
Concentrated CM-cellulose eluates				
Peak I	0.16	1,000	0.78	1.1
Peak II	0.19	2,700	2.6	1.0
Peak III	0.21	1,920	2.4	0.8

Source: Ref. 37.

The total activity recovered from CM-cellulose column chromatography, which represents 60–70% of that present in the DEAE-cellulose-treated extract, exceeds that exhibited by the selected fractions from peaks I–III which were combined and concentrated.

REFERENCES

1. L Ribas de Pouplana, S Atrian, R Gonzalez-Duarte, L-A Fothergill-Gilmore, S-M Kelly, N-C Price. Structural properties of long and short chain alcohol dehydrogenases. Biochem J 276:433–438, 1991.
2. H Jörnvall, B Persson, J Jeffery. Characteristics of alcohol/polyol dehydrogenases. Eur J Biochem 167:195–201, 1987.
3. W Hummel. New alcohol dehydrogenases for the synthesis of chiral compounds. Adv Biochem Eng Biotechnol 58:145–184, 1997.
4. C-I Bränden, H Jörnvall, H Eklund, B Furugren. Alcohol dehydrogenases. In: PD Boyer, ed. The Enzymes, Vol XI. New York: Academic Press, 1975, pp 103–190.
5. J Jörnvall, B Persson, J Jeffery. Alcohol and polyol dehydrogenases are both divided into two types and structural properties cross-relate the different enzyme activities within each type. Proc Natl Acad Sci USA 78:4226–4230, 1981.
6. H Eklund, B Nordström, E Zeppezauer, G Söderlund, I Ohlsson, T Boiwe, B-O Söderberg, O Tapia, C-I Bränden. Three dimensional structure of horse liver alcohol dehydrogenase. J Mol Biol 102:27–59, 1976.
7. H Eklund, B Nordström, E Zepperzauer, G Söderlund, I Ohlsson, T Boiwe, C-I Bränden. The structure of horse liver alcohol dehydrogenase. FEBS Lett 44:200–204, 1974.
8. H Eklund, JP Samana, L Wallen, C-I Bränden, A Akenon, TA Jones. Structure of a triclinic complex of horse liver alcohol dehydrogenase at 2.9 Å resolution. J Mol Biol 146:561–587, 1981.
9. R Rella, CA Raia, M Pensa, FM Pisani, A Gambacorta, M De Rosa, M Rossi. A novel archaebacterial NAD^+-dependent alcohol dehydrogenase. Eur J Biochem 167:475–479, 1987.
10. M Estonus, C Karlsson, EA Fox, J-O Hoeoeg, B Holmouist, BL Vallee, WS Davidson, H Jörnvall. Avian alcohol dehydrogenase: the chicken liver enzyme. Primary structure, cDNA-cloning, and relationships to other alcohol dehydrogenases. Eur J Biochem 194:593–602, 1990.
11. MF Reid, CA Fewson. Molecular characterization of microbial alcohol dehydrogenases. Crit Rev Microbiol 20:13–56, 1994.
12. CR Lowe. The application of coenzyme-dependent enzymes in biotechnology. Phil Trans R Soc Lond 300:335–353, 1983.
13. S Dilmaghanian, C Vivian Stead, RJ Ansell, CR Lowe. Synthesis and properties of a naphthalene-containing artificial redox coenzyme. Enzyme Microbiol Technol 20:165–173, 1997.
14. GA Beech, MA Melvin, J Taggart. Food, drink and biotechnology. In: IJ Higgins, DJ Best and J Jones, eds. Biotechnology: Principles and Applications. London: Blackwell Scientific Publications, 1985, pp. 73–110.
15. Eklund, BV Plapp, JP Samana, C-I Bränden. Binding of substrate in a ternary complex of horse liver alcohol dehydrogenase. J Biol Chem 257:14349–14358, 1982.
16. BL Vallee, DS Auld. Zinc coordination, function, and structure of zinc enzymes and other proteins. Biochemistry 29:5647–5659, 1990.
17. H Jörnvall, H Eklund, C-I Brändén. Subunit conformation of yeast alcohol dehydrogenase. J Biol Chem 253:8414–8419, 1978.
18. X De Bolle, C Vinals, D Prozzi, JY Paquet, R Leplae, E Deprierreux, J Vandenhaute, E Feytmans. Identification of residues potentially involved in the interactions between subunits in yeast alcohol dehydrogenases. Eur J Biochem 231:214–219, 1995.
19. FM Dickinson, GP Monger. A study of the kinetics and mechanism of yeast alcohol dehydrogenase with a variety of substrates. Biochem J 131:261–270, 1973.
20. DW Green, HW Sun, BV Plapp. Inversion of the substrate specificity of yeast alcohol dehydrogenase. J Biol Chem 268:7792–7798, 1993.

21. S Alexandre, I Boutelet, JC Vincent. pH control of dehydrogenase systems. Enzyme Microb Technol 10:479–485, 1988.
22. K Dalziel. Kinetic studies of liver alcohol dehydrogenase and pH effects with coenzyme preparations of high purity. J Biol Chem 238:2850–2858, 1963.
23. S Dallet. Influence of pressure of kinetic and structural behaviour of a mesostable alcohol dehydrogenase from yeast and of a thermostable alcohol dehydrogenase from *Thermoanaerobium brockii*. PhD thesis, University of Technology of Compiegne, Compiegne, France, 1995.
24. M Trovaslet. Influence of temperature and pressure on kinetic behaviour of the horse liver alcohol dehydrogenase (HLADH). MS dissertation, University of Technology of Compiegne, Compiegne, France, 1998.
25. S Dallet, MD Legoy. Hydrostatic pressure induces conformational and catalytic changes on two alcohol dehydrogenases but not oligomeric dissociation. Biochim Biophys Acta 1294:15–24, 1996.
26. S Ramaswany, M Scholze, BV Plapp. Binding of formamides to liver alcohol dehydrogenase. Biochemistry 36:3522–3527, 1997.
27. H Li, WH Hallows, JS Punzi, KW Pankiewicz, KA Watanabe, BM Goldstein. Crystallographic studies of isosteric NAD^+ analogues bound to alcohol dehydrogenase: specificity and substrate binding in two ternary complexes. Biochemistry 33:11734–11744, 1994.
28. VC Sekkar, BV Plapp. Rate constants for a mechanism including intermediates in the interconversion of ternary complexes by horse liver alcohol dehydrogenase. Biochemistry 29:4289–4295, 1990.
29. J Kvassman, G Pettersson. Unified mechanism for proton-transfer reactions affecting the catalytic activity of liver alcohol dehydrogenase. Eur J Biochem 103:565–575, 1980.
30. GTM Henehan, NJ Oppenheimer. Horse liver alcohol dehydrogenase catalyzed oxidation of aldehydes: dismutation precedes net production of reduced nicotinamide adenine dinucleotide. Biochemistry 32:735–738, 1993.
31. AJ Ganzhorn, DW Green, AD Hershey, RM Gould, BV Plapp. Kinetic characterization of yeast alcohol dehydrogenases. J Biol Chem 262:3754–3761, 1987.
32 RB McComb, LW Bond, RW Burnett, KC Keeth, GN Bowers Jr. Determination of the molar absorptivity of NADH. Clin Chem 22:141–150, 1976.
33. SAM Vanhommerig, LAAE Sluyterman, EM Meijer. Kinetic and modelling studies of NAD^+ and poly(ethylene glycol)-bound NAD^+ in horse liver alcohol dehydrogenase. Biochim Biophys Acta 1295:125–138, 1996.
34. HW Adolph, P Maurer, H Schneider-Bernlöhr, C Sartorius, M Zeppezauer. Substrate specificity and stereoselectivity of horse liver alcohol dehydrogenase. Eur J Biochem 201:615–625, 1991.
35. KM Lee, KF Dahlhauser, BV Plapp. Reactivity of horse liver alcohol dehydrogenase with 3-methylcyclohexanols. Biochemistry 27:3528–3532, 1988.
36. GL Shearer, K Kim, KM Lee, K Wang, BV Plapp. Alternative pathways and reactions of benzyl alcohol and benzaldehyde with horse liver alcohol dehydrogenase. Biochemistr 32:11186–11194, 1993.
37. AH Blair, BL Vallee. Some catalytic properties of human liver alcohol dehydrogenase. Biochemistry 5:2026–2034, 1966.

34

Amine Oxidase

Akio Ito and Jichun Ma
Kyushu University, Fukuoka, Japan

I. INTRODUCTION

Amine oxidase catalyzes the reaction $RCH_2NH_2 + O_2 + H_2O \rightarrow RCHO + H_2O_2 + NH_3$ with mono-, di-, or polyamine as substrate. Amine-oxidizing enzymes are classified by their prosthetic group(s), FAD or copper plus topaquinone, or by their sensitivity to inhibitors, 2-chlorocyclopropylamine or semicarbazide. The FAD-containing amine oxidases have monoamine-oxidizing activity, and most of the copper-containing enzymes belong to the diamine-oxidase type.

II. MONOAMINE OXIDASE (FAD-CONTAINING)

Monoamine oxidase (EC 1.4.3.4; MAO) is a flavin-containing enzyme. It catalyzes the oxidation of aliphatic and aromatic primary, secondary, and tertiary amines.

Two forms of MAO, MAOA and MAOB, are defined by their substrate and inhibitor affinities. MAOA has a higher affinity for catecholamines and 5-hydroxytryptamine (5-HT or serotonin) and is more sensitive to inhibition by clorgyline, whereas MAOB has a higher affinity for dietary amines such as phenylethylamine and is selectively inhibited by deprenyl (1, 2).

In human and animals, the enzyme plays an important role for the metabolism of biogenic monoamines in the central nervous system and peripheral tissues. MAO oxidizes neurotransmitters such as serotonin and dopamine, and the synthetic tertiary amine 1-methyl-4-phenyl-1,2,3,6-tetrahydropyridine (MPTP) has been found to be oxidized by both forms of MAO, which suggests that MAO may oxidize MPTP analogs and generate toxic effects on the central nervous system. These features make MAO an extremely important enzyme related to neuronal dysfunction in schizophrenia, Parkinson's disease, Down's syndrome, and some other neurodegenerative diseases and psychological disorders in human, and vast numbers of its inhibitor have been developed as medicines.

A. Properties as Protein

The study of MAO has a long history. However, it was at the end of 1980s that the cDNA cloning of MAOA and MAOB ended the notion that MAOA and MAOB were the same protein with different catalyzing sites or that they had different functions at different environments, and proved that they were different proteins. Essentially, all higher eukaryotic organisms express MAO (3). Both forms of MAO are localized in the outer mitochondrial membrane. They are expressed at different levels in different cell types. For example, the highest expressions of both forms are found in the liver for most species. Placenta expresses predominantly MAOA whereas platelet contains primarily MAOB. Most of the other tissue cells express both forms of MAO.

MAOA and MAOB are encoded by two very similar but different genes. In human and probably in

other mammals, the two genes are closely linked on the X-chromosome (Xp11.23–11.4) (4), suggesting that the two genes may have arisen from duplication of a common ancestral gene. Amino acid sequences of MOAO and MOAB are deduced from cDNAs for human, bovine, and rat enzymes (5–8). MAOA and MAOB contain 527 and 520 amino acid residues (rat MAOA lacks one amino acid residue at the carboxy-terminus), respectively. Molecular mass of human MAOA and MAOB are 59.7 and 58.8 kDa, respectively. Approximately 90% of the amino acid residues are identical among the same forms of MAO from different species, while there is only 70% homology between MAOA and MAOB from the same species. One highly conserved region, residues 389–460 for MAOA and 380–451 for MAOB, contains the cysteine (residue 406 for MAOA and residue 397 for MAOB) to which the FAD covalently binds as 8-α-S-cysteinyl-FAD. The N-terminus shows significant similarity to several flavoproteins. This region fulfills the criteria for a predictive fingerprint for a flavin-binding domain and contains the FAD- and ADP-binding $\beta\alpha\beta$ fold. This structure has been suggested to act as a "nucleation center." That is, during biosynthesis this domain will form first, and the rest of the protein structure forms around it. The C-termini of both forms of MAO are responsible for anchoring the enzyme to the outer membrane of mitochondria (9).

B. Properties as Enzyme

Since the crystal structures of both forms of MAO have not been established, the actual mechanism of catalysis has yet to be elucidated. A conserved region in the central parts of the proteins (residues 187–230 for MAOA and 178–221 for MAOB) is postulated as part of the active site. Chimeric and site-directed mutation studies suggest that the region between about residues 120–220 for MAOA and 111–211 for MAOB are responsible for substrate specificity (10, 11) and the phenylalanine of residue 208 for MAOA and isoleucine of residue 199 for MAOB are found to be the key amino acids responsible for substrate selectivity. Exchange of these two residues by site-directed mutation leads to an exchange of the enzyme properties; that is, F208I-MAOA shows properties of MAOB, and I199F-MAOB shows properties of MAOA (12).

MAO catalyzes many compounds. The typical substrate is 5-HT for MAOA and phenylethylamine (PEA) and benzylamine for MAOB. MPTP is found to be a substrate of MAOB, although it is oxidized by MAOA at a lower rate. The kinetic parameters for substrate specificity and inhibition from different laboratories' publications show divergence. Since the K_m value is a ratio of rate constants, it is easily varied with the purity and the lipid content of the preparation. Lipophilic substrates may be concentrated around the mitochondrial membrane to which the MAO is located, leading to a lower apparent K_m when using mitochondria than when using purified MAO for the assay (13). The same is true in the assay for reversible inhibition. Table 1 summarizes some results on the specificity of MAOA and MAOB for a number of substrates. Some are from assays using purified MAO, others from that using mitochondria or whole cell extract.

Since the discovery that MAO inhibitors are antidepressants, large numbers of inhibitors of MAOA and MAOB have been synthesized. The early MAO inhibitors were hydrazine or cyclopropylamine derivatives that showed little selectivity to the two forms of MAO. The acetylenic MAO inhibitors, clogyline and (−)-deprenyl, however, exhibit a high degree of selectivity to MAOA and MAOB, respectively. They have been found to act as mechanism-based irreversible inhibitors of MAO. These compounds first form a noncovalent complex with the active site of the enzyme, followed by the normal catalytic process to generate a reactive species, which reacts with the enzyme to form an irreversibly inhibited species. Another type of inhibitor is a selectively reversible inhibitor, which can sometimes be derived from the substitution of the hydrogen at α-carbon of MAO substrate by a methyl group. The affinity of MAO to these inhibitors is often higher than it is for its substrates, with a K_i value of 10^{-5} to 10^{-9} M vs a K_m value of 10^{-4} to 10^{-5} M. This may be a reflection of the fact that K_m is not a simple dissociation constant for the initial noncovalent complex but includes steps that may orient the α-C-H so as to optimize orbital overlap for both the electron transfer and proton abstraction processes (14). IC_{50}s of some inhibitors are summarized in Table 2.

C. Determination of Activity

The widely used methods for determination of activity of MAO are the kynuramine oxidation method and radiochemical method.

1. Kynuramine Oxidation Method

Kynuramine can be oxidized by both MAOA and MAOB to produce 4-hydroxylquinoline, which has

Table 1 Kinetic Parameters of MAOs for Some Substrates

	Turnover number (sec^{-1})		k_{cat} (sec^{-1})		K_m (μM)			
Substrate	MAOA	MAOB	MAOA	MAOB	MAOA	MOAB	Note	Ref.
Kynuramine	146				170		purified human MAO	17
			11.63		121.5		human MAO expressed in HEK293 cell	11
Serotonin					119.3		human MAO expressed in Cos cell	18
					310		rat MAO expressed in yeast cell	10
Phenylethylamine			3.07	2.57	154.4	2.4	human MAO expressed in HEK293 cell	11
						4.6	human MAO expressed in Cos cell	18
					240	8	rat MAO expressed in yeast cell	10
MTPT	20	204			140	390	purified human MAO	17

the highest absorption at 315 nm and fluorescences at 380 nm. According to the absorbance or the intensity of fluorescence, the concentration of the product can be quantitatively determined. The following protocol is a modification of Krajl's method (15). In a test tube, mix 0.25 mL of 200 mM potassium phosphate buffer, pH 7.5, and suitable volume of the enzyme sample. Add distilled water to a final volume of 0.90 mL. Incubate the test tube at 30°C for 5 min, then add 0.10 mL 1 mM kynuramine preincubated at 30°C, mix immediately, and incubate at 30°C with shaking for 20 min. Terminate the reaction by adding 0.4 mL of 20% TCA. Precipitate the protein by centrifugation at 10,000 g for 10 min. Take 0.5 mL of the supernatant and add 1.5 mL of 1 N NaOH, and measure the intensity of fluorescence at a wavelength of 380 nm with an excitation wavelength of 315 nm.

2. Radiochemical Method

This method provides more sensitive determination but needs special devices and laboratory for using radioisotopes. Many ^{14}C-labeled substrates for MAO are commercially available. For example, DuPont NEN(r) provides hydroxytrypamine binoxalate, 5-[2-^{14}C[tryptamine bisuccinate, [side chain-2-^{14}C]tyramine hydrochloride, [1-^{14}C]phenylethylamine hydrochloride, etc. MAO can oxidize these compounds and produce radioactive products. The enzyme activity can be estimated by measuring the radioactivity of the products.

Table 2 IC_{50} of Some Inhibitors for MAOs

		IC_{50} (M)			
Substrate	Inhibitor	MAOA	MAOB	Note	Ref.
Serotonin	Deprenyl	1.5×10^{-6}	5.2×10^{-5}	human MAO expressed in Cos cell	18
	Clorgyline	7.0×10^{-10}		human MAO expressed in Cos cell	18
	Ro41-1049	3.6×10^{-8}		human MAO expressed in HEK293 cell	11
	Ro41-2064	2.1×10^{-7}		human MAO expressed in HEK293 cell	11
Phenylethylamine	Deprenyl		2.7×10^{-9}	human MAO expressed in Cos cell	18
		5.0×10^{-6}	1.3×10^{-7}	rat MAO expressed in yeast cell	10
	Clorgyline		4.0×10^{-7}	human MAO expressed in Cos cell	18
		2.5×10^{-8}	7.9×10^{-5}	rat MAO expressed in yeast cell	10
	Lazabemide	1.2×10^{-4}	1.1×10^{-8}	human MAO expressed in HEK293 cell	11
	Ro41-2064		1.8×10^{-5}	human MAO expressed in HEK293 cell	11

Hot and cold substrates are mixed to a final concentration of 5 mM (usually, the hot accounts for 1/50 by concentration when using ~1.5 GBq/mmol hot substrate) to make an application solution of substrate. In each Eppendorf tube, add 10 μL of 300 mM potassium phosphate buffer, pH 7.5, and certain volume of sample (e.g., 50 μg of rat liver mitochondrial protein), and add sample buffer to make a final volume of 54 μL. Incubate the tube at 30°C for 1 min, and start the reaction by adding 6 μL of application substrate. Incubate at 30°C for 20 min and stop the reaction by adding 40 μL of 2 M HCl. Add 300 μL water-saturated ethyl acetate-toluene (1 : 1 v/v) and vortex to extract the product. Centrifuge at 10,000 g for 1 min and transfer 200 μL into a new tube. Add same volume of 0.5% PPQ; measure the radioactivity in a liquid scintillation spectrometer. Blank should be made by adding 2 N HCl before adding the substrate.

D. Purification

The Welter and Salach's procedure (16) is widely used for purification of MAOA. Briefly, mitochondrial fraction containing 140–150 units of enzyme activity is homogenized with glass/Teflon homogenizer in 0.1 M triethanolamine HCl buffer, pH 7.2, to give a final concentration of 20 mg protein/mL. The homogenate is digested with 1 mg and 670 units of phospholipases C and A, respectively, per 500 mg of the total protein in the presence of 25 mM $CaCl_2$ at 25°C for 1 h. After centrifugation of the mixture at 43,000 g for 15 min at 15°C, the pellet is resuspended in the same buffer to give a concentration of 15 mg protein/mL, solubilized with Triton X-100 at a final concentration of 1 mg detergent/3 mg protein, and centrifuged at 43,000 g for 15 min at 15°C. For each 8 mL of resulting supernatant, add 0.5 g of dextran (average Mr 500,00) and 0.4 g of PEG (average Mr 8000) and centrifuge at 9500 g for 20 min.

This produces a two-phase system. The enzyme in the upper layer is precipitated by addition of PEG to 25%, resuspended in 20 mM sodium phosphate buffer, pH 7.2, solubilized by octylglucoside at 2 mg/mg protein and subjected to DEAE-Sepharose CL-6B column chromatography. The enzyme is eluted with a linear gradient of 20–250 mM potassium phosphate buffer, pH 7.0, containing 20% glycerol (w/v), 0.8% octylglucoside, 3 mM 2-mercaptoethanol, and 1 mM D-amphetamine. The buffer should first be made anaerobic and anaerobiosis should be maintained in the gradient chambers during the elution. This will result in partially purified MAOA. Further purification by hydroxyapatite chromatography is not encouraged because it leads to obvious inactivation, although this can produce almost homogeneous MAOA.

MAOB can be purified essentially by the same method, but use Ficol, dextran, and PEG at the polymer partition step. MAOB will go to the interface between the upper (Ficol-PEG) and lower (dextran) layer, mainly in the solid material. See Salach (19) for details.

III. AMINE OXIDASE (COPPER-CONTAINING)

The copper-containing amine oxidase (EC 1.4.3.6 amine:oxygen oxidoreductase [deaminating]) is obtainable from bacteria, fungi, higher plants, blood plasma, and various mammalian organs. Most of this type of enzymes contain a cofactor possessing one or more carbonyl groups, making them sensitive to inhibition by carbonyl reagents such as semicarbazide and are classified as semicarbazide-sensitive amine oxidase (SSAO). The enzyme is relatively abundant comprising at least 0.1% total soluble protein in etiolated pea seedling, but its function(s) remain unclear despite extensive study. Amine oxidases in *Lens* and *Pisum* are absent in ungerminated seeds, and appear during the early period of germination. The enzyme activity is greatest in the growing parts of the plant and decreases with maturity and senescence.

Plasma copper-containing amine oxidase is soluble, while in most tissues the enzymes appear to be membrane bound, as plasmalemmal enzymes, which may be capable of metabolizing extracellular amines. A possible role for the cellular amine oxidase is the regulation of histamine and polyamine levels, whereas the serum proteins have been speculated to control the level of circulating biogenic amines such as dopamine and phenylethylamine. For review articles, see references (20–27).

A. Properties as Protein

Copper amine oxidases are homodimers of 70–95 kDa subunits depending on the source (Table 3) (28–33). Each subunit contains one Cu(II) and a quinone cofactor. The enzyme-bound copper is removable by treatment with diethyldithiocarbamate at acidic pH. Inactive apoprotein recovers its original activity on addition of cupric ion. A quinone cofactor was identified as 2,4,5-trihydroxyphenylalanine quinone (TPQ or TOPA quinone) first in the bovine serum enzyme.

Table 3 Molecular Properties of Some Cu-Containing Amine Oxidases

Enzyme source	Molecular weight (subunit)	Cu/mol	Absorption maxima	Yield starting material	Ref. No.	Ref. for cDNA cloning	Ref. for crystal structure
Arthrobacter	167,900 (82,250)[a]	2	480 nm $A_{480/280} = 0.0137$	92 mg/84 g wet weight	28	44 47	61
Asp. niger	150,000 (75,000)	1	490 ($\varepsilon = 5300\,M^{-1}cm^{-1}$)	427 mg/105 L culture	29	29	
Pea seedling	113,000 (77,000)	2	525 nm ($\varepsilon = 1200\,M^{-1}\,cm^{-1}$)	0.68 mg/2 kg seedling	30	48	60
Bovine plasma	180,000 (90,000)	2	480 nm	36 mg/5 L blood	31	46	
Bovine lung (membrane bound)	400,000 (100,000)	1.84	425 nm (+nitrophenyl hydrazine neutral pH)	0.9 mg/1.5 g microsomal protein	32		
Porcine aorta	200,000 (95,000, 102,000)		456 nm (+nitrophenyl hydrazine neutral pH)		33		

[a]Subunit mw.

Subsequently TPQ has been identified biochemically and its presence inferred from amino acid sequence homology in copper-containing amine oxidases from various sources (34–40).

Amine oxidase cDNA clones have been obtained from various sources, and the primary structure of the enzyme was deduced from the cDNAs (41–52). Sequence alignment of representative amino acid sequences of bacterial, yeast, plant, and mammalian amine oxidases suggests separate protein domains with a carboxyl-terminal domain encoding the cofactor consensus sequence and putative copper-binding sites, and a more divergent amino-terminal domain accommodating differing physiological functions and substrate specificities of these proteins. There are 33 completely conserved residues mainly within two regions: residues 286–459 in the pea enzyme, approximately centered on Tyr387, and the C-terminal end. In this enzyme the amino acid sequence of the phenylhydrazine-labeled peptide was determined to be VGNXDNVID, in which the X corresponds to Tyr387. TOPA quinone is posttranslationally generated by oxidation of a specific tyrosine precursor occurring in the consensus sequence of NYD/E in the active site of amine oxidases (53–57). The oxidation to TPQ is a spontaneous reaction mediated by the bound copper ion. Numerous studies point toward the presence of three histidines as ligands to copper in the enzyme. One HXH motif 40–50 residues toward the carboxyl terminus from the cofactor consensus sequence is conserved in all alignments. Crystal structures have recently been reported for several amine oxidases (58–62).

B. Properties as Enzyme

The enzyme catalyzes the oxidation by molecular oxygen of the primary amino group of di- and polyamines to corresponding amino aldehydes, hydrogen peroxide, and ammonia. The amino aldehyde products from putrescine, cadaverine, and spermidine spontaneously cyclize to Δ1-pyrroline, Δ1-piperidine, and 1,5-diazabicyclononane, respectively.

Substrate specificity varies widely among the different enzymes (Table 4) (20–32, 63, 64). The best substrates for all plant enzymes are putrescine and cadaverine. The relative reaction rates with some substrates are shown in Table 4. K_m values for putrescine seem to be of the same order of magnitude for all enzymes investigated (0.1 mM). The pH optimum is found around pH 7.0 with putrescine or cadaverine as substrate. Plasma and tissue amine oxidases also show considerable species-related variations in substrate specificity. Some endogenously occurring aromatic amines such as tyramine and tryptamine are metabolized well by copper-containing amine oxidase in homogenates of rat blood vessels, and also in vitro inhibition of the enzyme can potentiate vasoconstrictor actions of these amines in rat vascular preparations. These amines are poor substrates for human amine oxidase, thus complicating attempts to generalize possible physiological roles for these enzymes. The

Table 4 Substrate Specificity of Some Cu-Containing Amine Oxidases

Enzyme source	Kinetic parameters: Substrate	V or k_{cat}	K_m (mM)	Compound not oxidized	Ref.
Arthrobactor	methylamine	68 (μmole/min	0.20	tyramine, spermine, putrescine	28
	ethylamine	85	0.15		
	benzylamine	32	3.76		
Yeast (*Candida*	methylamine	2.41 (mmole/min/mg)	0.227	benzylamine	63
boidinii, methylamine	ethylamine	5.05	0.77		
oxidase)	phenylethylamine	0.815	0.11		
Asp. niger	n-hexylamine	100 (relative rate)		spermidine	29
	benzylamine	36.0			
	histamine	42.0			
	tyramine	109.8			
	putrescine	6.3			
Pea seedling	putrescine	165 (sec^{-1})	0.19	cyclohexylamine (competitively	30
	cadaverine	498	0.065	inhibit, $K_i = 0.045$ mM),	
	spermidine	193	5.9	diethylamine	
Bovine plasma	butylamine	0.1 (relative rate)		ethylamine, tyramine, tryptamine,	64
	amylamine	2.5		serotonin	
	heptylamine	5.4			
	benzylamine	6.1	0.025		
	spermine	10.0			
	kynuramine	1.0			
Bovine lung	benzyl amine	170 (sec^{-1})	0.05		32
	phenylethylamine	62	1.19		
	methylamine	580	0.21		
	histamine	110	1.11		

endogenously occurring aliphatic amines methylamine and aminoacetone are metabolized in vitro to formaldehyde and methyglyoxal, respectively, by amine oxidase in some animal (including human) tissues suggesting the possibility of toxicological consequences of cellular function (21–23, 25–27).

Inhibitors are common to all these enzymes. Metal chelators such as diethyldithiocarbamate, cuprizone, *o*-phenanthroline, 2,2′-bipyridil, 8-hydroxyquinoline, and CN compounds inhibit Cu-containing amine oxidases noncompetitively with different sensitivities. Carbonyl group reagents irreversibly form adducts with the enzymes with concomitant loss of catalytic activity. The most effective agents are hydrazines (phenylhydrazine and benzylhydrazine), hydrazides (semicarbazide, thiosemicarbazide, and phenylsemicarbazide), hydroxylamine, isoniazide, and iproniazid (20–27).

In addition to the protein absorbance maximum at 278 nm, the visible spectrum of the enzyme is characterized by a broad absorption peak centered around 500 nm which confers a typical pink color to purified preparations of the enzyme (28–33). The extinction coefficient at 500 nm is $4100\,M^{-1}\,cm^{-1}$ and at 278 nm is $246{,}000\,M^{-1}\,cm^{-1}$ for highly purified *Lens* enzyme. The aerobic addition of phenylhydrazine and semicarbazide to the *Lens* enzyme is followed by the formation of a strong absorption band at 445 nm ($\varepsilon = 64{,}000\,M^{-1}\,cm$), 492 nm ($\varepsilon = 8{,}600\,M^{-1}\,cm^{-1}$), and 360 nm ($\varepsilon = 34{,}800\,M^{-1}\,cm^{-1}$), respectively, concomitant with the disappearance of the absorption band at 500 nm. In anaerobiosis a stable yellow intermediate absorbing at 346, 432, and 462 nm is observed in the presence of substrates. Under this condition a Cu(I)-semiquinone state is generated by substrate reduction, and this intermediate may react directly with oxygen. The interaction of the *Lens* enzyme with primary amines gives rise to a covalent amino group quinone compound, a quinoketimine, which is converted to quinoaldimine. This releases the aldehyde product and forms a species containing Cu(II) and a reduced form of TPQ, aminocatechol, which coexists with the radical species containing Cu(I) and TPQ semiquinone. Finally, the semiquinone reacts with

oxygen and restores the oxidized enzyme, liberating ammonia and hydrogen peroxide (24, 65).

C. Determination of Activity

The enzyme activity of amine oxidase is measured by various methods, including radiochemical, spectrophotometrical, and polarographical techniques. When necessary, MAO activity is inhibited by preincubation with 1 mM clorgyline or deprenyl.

In a radiochemical method (32, 66), the reaction is carried out at 37°C in a final volume of 225 μL of 50 mM potassium phosphate buffer, pH 7.2, with radiolabeled substrates (e.g., 20 μM [^{14}C]benzylamine [3 mC/mmol], 100 μM [^{14}C]2-phenylethylamine [2.5 mCi/mmol], etc.) and is stopped by the addition of 100 μL of 2 M citric acid. Radioactively labeled products are extracted with toluene/ethyl acetate (1:1, v/v) containing 0.6% (w/v) 2,5-diphenyloxazole before liquid scintillation counting. In the assay for the activity toward methylamine (100 μM [^{14}C]methylamine [1 mCi/mmol]) as substrate, the reaction is stopped by cooling the tube in an ice bath and the reaction product ([^{14}C]formaldehyde) is separated from unchanged amine by the use of a 1-mL Amberlite C6-50 (carboxylic form) column.

In a polarographical method (67), the reaction is monitored with a Clark electrode using air as the gaseous phase. The standard reaction mixture (1 mL) contains 50 μg catalase and the reaction is started by the addition of a small volume of amine substrate (as hydrochloride) after at least 10 min preincubation.

The activity of partially purified enzyme in the presence of detergents can be determined spectrophotometrically by a peroxidase-linked method (68). Assay is conducted in 200 mM potassium phosphate buffer, pH 7.6, with 1 mM of benzylamine or putrescine as substrate, and 1 mM vanillic acid, 0.5 mM 4-aminoantipyrine, and 4 U/mL horseradish peroxidase, as chromogenic reagents. Absorbance change is monitored continuously at 498 nm ($\varepsilon_{498} = 4{,}654\,M^{-1}cm^{-1}$) by a spectrophotometer.

D. Purification

The enzyme has been purified to homogeneity from bacteria, plant, and mammalian tissues by standard methods involving homogenization, salting out, and various chromatography techniques (28–33, 67).

One representative method for the plant enzyme is as follows (30). Eight-day-old lentil seedlings are homogenized in a Waring blender with water and the homogenate is subjected to controlled heat treatment (48°C, 10 min) followed by centrifugation. To the supernatant ammonium sulfate is added to 70% saturation and centrifuged. The precipitate is dissolved in water, dialyzed, and loaded onto a DEAE-cellulose column equilibrated with 15 mM potassium phosphate buffer, pH 7, and eluted with the same buffer. The eluate containing the activity is diluted with an equal volume of water and applied to an AH-Sepharose 4B column. The enzyme is eluted with 50 mM potassium phosphate buffer, pH 7, with 43% recovery and 880-fold purification; 0.25 mg of the enzyme is obtained from 900 g of lentil seedling.

Membrane-bound amine oxidase has recently been purified from bovine lung microsomes (32). The enzyme is solubilized with Triton X-100 and purification is achieved, in the presence of detergent, by chromatography with Cibacron Blue 3GA-agarose, hydroxylapatite, *Lens culinaris* agarose, Resource Q-FPLC, and gel filtration on Superdex 200 HR-FPLC. The enzyme was purified 2320-fold from the microsomal membranes with an overall yield of 15%.

REFERENCES

1. CJ Fowler, L Oreland, BA Callingham. The acetylenic monoamine oxidase inhibitors clorgyline, deprenyl, pargyline and J-508: their properties and applications. Pharm Pharmacol 33:341–347, 1981.
2. J Knoll. History of deprenyl—the first selective inhibitor of monoamine oxidase type B. Vopr Med Khim 43:482–493, 1997.
3. W Weyler, YPP Hsu, XO Breakfield. Biochemistry and genetics of monoamine oxidase. Pharmacol Ther 47:391–417, 1990.
4. ER Levy, JF Powell, VJ Buckle, YPP Hsu, XO Breakfield, IW Craig. Localization of human monoamine oxidase-A gene to Xp11.23-11.4 by in situ hybridization: implications for Norrie disease. Genomics 5:368–370, 1989.
5. AWJ Bach, NC Lan, DL Johnson, CW Abell, ME Bembenek, SW Kwan, PH Seeburg, JC Shih. cDNA cloning of human liver monoamine oxidase A and B: molecular basis of differences in enzymatic properties. Proc Natl Acad Sci USA 85:4934–4938, 1988.
6. JF Powell, YP Hsu, W Weyler, S Chen, J Salach, K Andrikopoulos, J Mallet, XO Breakfield. The primary structure of bovine monoamine oxidase type A: comparison with peptide sequences of bovine monoamine oxidase type B and other flavoenzymes. Biochem J 259:407–413, 1989.
7. A Ito, T Kuwahara, S Inadome, Y Sagara. Molecular cloning of cDNA for rat liver monoamine oxidase

B. Biochem Biophys Res Commun 157:970–976, 1988.
8. T Kuwahara, S Takamoto, A Ito. Primary structure of rat monoamine oxidase A deduced from cDNA and its expression in rat tissues. Agric Biol Chem 54:253–257, 1990.
9. J Mitoma, A Ito. Mitochondrial targeting signal of rat liver monoamine oxidase B is located at its carboxy terminus. J Biochem (Tokyo) 111:20–24, 1992.
10. Y Tsugeno, I Hirashiki, F Ogata, A Ito. Regions of the molecule responsible for substrate specificity of monoamine oxidase A and B: a chimeric enzyme analysis. J Biochem (Tokyo) 118:974–980, 1995.
11. J Gottowik, P Malherbe, G Lang, M Da Prada, AM Cesura. Structure/function relationships of mitochondrial monoamine oxidase A and B chimeric forms. Eur J Biochem 230:934–942, 1995.
12. Y Tsugeno, A Ito. A key amino acid responsible for substrate selectivity of monoamine oxidase A and B. J Biol Chem 272:14033–14036, 1997.
13. M Krueger, TP Singer. An examination of the reliability of the radiochemical assay for monoamine oxidases A and B. Anal Biochem 214:116–123, 1993.
14. P Dostert, M Strolin Benedetti. Structure-modulated recognition of substrates and inhibitors by monoamine oxidases A and B. Biochem Soc Trans 19:207–211, 1991.
15. M Krajl. A rapid microfluorimetric determination of monoamine oxidase. Biochem Parmacol 14:1684–1685, 1965.
16. W Weyler, JI Salach. Purification and properties of mitochondrial monoamine oxidase type A from human placenta. J Biol Chem 260:13199–13207, 1985.
17. TP Singer. The colorful past and bright future of monoamine oxidase research. Prog Brain Res 106:1–22, 1995.
18. K Chen, HF Wu, JC Shih. Influence of C terminus on monoamine oxidase A and B catalytic activity. J Neurochem 66:797–803, 1996.
19. JI Salach. Monoamine oxidase from beef liver mitochondria: simplified isolation procedure, properties, and determination of its cysteinyl flavin content. Arch Biochem Biophys 192:128–137, 1979.
20. B Mondovi, P Riccio. Copper amine oxidases: structure and function. Adv Inorg Biochem 6:225–244, 1984.
21. BA Callingham. Some properties of semicarbazide-sensitive amine oxidases. J Neural Transm Suppl 23:37–54, 1987.
22. PC Waldmeier. Amine oxidases and their endogenous substrates (with special reference to monoamine oxidase and the brain). J Neural Transm Suppl 23:5–72, 1987.
23. BA Callingham. Properties and functions of the semicarbazide-sensitive amine oxidases. Biochem Soc Trans 19:228–233, 1991.
24. R Medda, G Floris. Plant copper-amine oxidases. Phytochemistry 39:1–9, 1995.
25. GA Lyles. Mammalian plasma and tissue-bound semicarbazide-sensitive amine oxidases: biochemical, pharmacological and toxicological aspects. Int J Biochem Cell Biol 28:259–274, 1996.
26. JP Klinman. New quinocofactors in eukaryotes. J Biol Chem 271:27189–27192, 1996.
27. GA Lyle, R Pino. Properties and functions of tissue-bound semicarbazide-sensitive amine oxidases in isolated cell preparations and cell cultures. J Neural Transm Suppl 52:239–250, 1998.
28. J van Iersel, RA van der Meer, JA Duine. Methylamine oxidase from *Arthrobacter* PI. A bacterial copper-quinoprotein amine oxidase. Eur J Biochem 161:415–419, 1986.
29. I Frebort, H Tamaki, H Ishida, P Pec, L Luhova, H Tsuno, M Halata, Y Hisano, Y Kato, K Matsoka, H Toyama, H Kumagai, O Adachi. Two distinct quinoprotein amine oxidases are induced by n-butylamine in the mycelia of *Aspergillus niger* AKU 3302. Purification, characterization, cDNA cloning and sequencing. Eur J Biochem 237:255–265, 1996.
30. JM Vianello, MJ Di Paolo, R Stevanato, R Gasparini, A Rigo. Purification and characterization of amine oxidase from soybean seedlings. Arch Biochem Biophys 307:35–39, 1993.
31. P Turini, S Sabatini, O Befani, F Chimenti, C Casanova, PJ Ricco, B Mondovi. Purification of bovine plasma amine oxidase. Anal Biochem 125:294–298, 1982.
32. JM Lizcano, KF Tipton, M Unzeta. Purification and characterization of membrane-bound semicarbazide-sensitive amine oxidase (SSAO) from bovine lung. Biochem J 331:69–78, 1998.
33. A Holt, G Alton, CH Scaman, GR Loppnow, A Szpacenko, I Svendsen, MM Palcic. Identification of the quinone cofactor in mammalian semicarbazide-sensitive amine oxidase. Biochemistry 37:4946–4957, 1998.
34. SM Janes, D Mu, D Wemmer, AJ Smiths, S Kaur, D Maltbg, AL Burlingame, JP Klinman. A new redox cofactor in eukaryotic enzymes: 6-hydroxydopa at the active site of bovine serum amine oxidase. Science 248:981–987, 1990.
35. DE Brown, MA McGuirl, DM Dooley, SM Janes, D Mu, JP Klinman. The organic function group in copper-containing amine oxidases. Resonance Raman spectra are consistent with the presence of topa quinone (6-hydroxydopa quinone) in the active site. J Biol Chem 266:4049–4051, 1991.
36. JP Klinman, DM Dooley, JA Duine, PF Knowls, B Mondovi, JJ Villafranca. Status of the cofactor identity in copper oxidative enzymes. FEBS Lett 282:1–4, 1991.

37. PN Turowski, MA McGuirl, DM Dooley. Intramolecular electron transfer rate between active-site copper and topa quinone in pea seedling amine oxidase. J Biol Chem 268:17680–17682, 1993.
38. YH Choi, R Matsuzaki, T Fukui, E Shimizu, T Yorifuji, H Sato, Y Ozaki, K Tanizawa. Copper/topa quinone-containing histamine oxidase from *Arthrobacter globiformis*. Molecular cloning and sequencing, overproduction of precursor enzyme, and generation of topa quinone cofactor. J Biol Chem 270:4712–4720, 1995.
39. JH Roh, Y Takenaka, H Suzuki, K Yamamoto, H Kumagai. *Escherichia coli* K-12 copper-containing monoamine oxidase: investigation of the copper binding ligands by site-directed mutagenesis, elemental analysis and topa quinone formation. Biochem Biophys Res Commun 212:1107–1114, 1995.
40. M Fontecave, H Eklund. Copper amine oxidase: a novel use for a tyrosine. Structure 3:1127–1129, 1995.
41. PC Bruinenberg, M Evans, HR Waterman, J Kuipers, AC Arnberg, G Ab. Cloning and sequencing of the peroxisomal amine oxidase gene from *Hansenula polymorpha*. Biochim Biophys Acta 1008:157–167, 1989.
42. P Barbry, M Champe, O Chossande, S Munemitsu, G Champigny, R Lingueglia, P Maes, D Frelin, A Tartar, A Ullrich, M Lanzdunski. Human kidney amiloride-binding protein: cDNA structure and functional expression. Proc Natl Acad Sci USA 87:7347–7351, 1990.
43. A Rossi, R Petruzzelli, A Finazzi Argo. cDNA-derived amino-acid sequence of lentil seedlings' amine oxidase. FEBS Lett 301:253–257, 1992.
44. X Zhang, JH Fuller, WS McIntire. Cloning, sequencing, expression, and regulation of the structural gene for the copper/topa quinone-containing methylamine oxidase from *Arthrobacter* strain P1, a gram-positive facultative methylotroph. J Bacteriol 175:5617–5627, 1993.
45. H Azakami, M Yamashita, JH Roh, H Suzuki, H Kumagai, Y Murooka. Nucleotide sequence of the gene for monoamine oxidase (maoA) from *Escherichia coli*. J Ferment Bioeng 77:315–319, 1994.
46. D Mu, KF Medzihradszky, GW Adams, P Mayer, WM Hines, AL Burlingame, AJ Smith, D Cai, JP Klinman. Primary structures for a mammalian cellular and serum copper amine oxidase. J Biol Chem 269:9926–9932, 1994.
47. K Tanizawa, R Matsuzaki, E Shimizu, T Yorifuji, T Fukui. Cloning and sequencing of phenylethylamine oxidase from *Arthrobacter globiformis* and implication of Tyr-382 as the precursor to its covalent bound quinone cofactor. Biochem Biophys Res Commun 19:1096–1102, 1994.
48. AJ Tipping, MJ McPherson. Cloning and molecular analysis of the pea seedling copper amine oxidase. J Biol Chem 270:16939–16946, 1995.
49. X Zhang, J Kim, WS McIntire. cDNA sequences of variant forms of human placenta diamine oxidase. Biochem Genet 33:261–268, 1995.
50. X Zhang, WS McIntire. Cloning and sequencing of a copper-containing, topa quinone-containing monoamine oxidase from human placenta. Gene 179:279–286, 1996.
51. NJ Morris, A Ducret, R Aebersold, SA Ross, SR Keller, G Liehard. Membrane amine oxidase cloning and identification as a major protein in the adipocyte plasma membrane. J Biol Chem 272:9388–9392, 1997.
52. Y Imamura, R Kubota, Y Wang, S Asakawa, J Kudoh, Y Mashima, Y Ogachi, N Shimizu. Human retina-specific amine oxidase (RAO): cDNA cloning, tissue expression, and chromosomal mapping. Genomics 40:277–283, 1997.
53. D Mu, SM James, AJ Smith, DE Brown, DM Dooley, JP Klinman. Tyrosine codon corresponds to topa quinone at the active site of copper amine oxidases. J Biol Chem 267:7979–7982, 1992.
54. SM Janes, MM Palcic, CH Scaman, AJ Smith, DE Brown, DM Dooley, JP Klinman. Identification of topaquinone and its consensus sequence in copper amine oxidases. Biochemistry 31:12147–12154, 1992.
55. K Tanizawa. Biogenesis of novel quinone coenzymes. J Biochem (Tokyo) 118:671–678, 1995.
56. C Anthony. Quinoprotein-catalysed reactions. Biochem J 320:697–711, 1996.
57. N Nakamura, R Matsuzaki, YH Choi, K Tanizawa, J Sanders-Loehr. Biosynthesis of topa quinone cofactor in bacterial amine oxidases. Solvent origin of C-2 oxygen determined by Raman spectroscopy. J Biol Chem 271:4718–4724, 1996.
58. JH Roh, H Suzuki, H Kumagai, M Yamashita, H Azakami, Y Murooka, B Mikami. Crystallization and preliminary x-ray analysis of copper amine oxidase from *Escherichia coli* K-12. J Mol Biol 238:635–637, 1994.
59. MR Parsons, MA Convey, CM Wilmot, KDS Yadav, V Blakeley, AS Corner, SEV Philips, MJ McPherson, PF Knowles. Crystal structure of quinoenzyme: copper amine oxidase of *Escherichia coli* at 2 Å resolution. Structure 3:1171–1184, 1995.
60. V Kumar, DM Dooley, HC Freeman, JM Guss, I Marvey, MA Mcguirk, MC Wilce, VM Zubak. Crystal structure of a eukaryotic (pea seedling) copper-containing amine oxidase at 2.2 Å resolution. Structure 4:943–955, 1996.
61. MC Wilce, DM Dooley, HC Freeman, JM Guss, H Matsunami, WS McIntire, CE Ruggiero, K Tanizawa, H Yamaguchi. Crystal structures of the copper-containing amine oxidase from *Arthrobacter globiformis*

in the holo and apo forms: implications for the biogenesis of topaquinone. Biochemistry 36:16116–16133, 1997.
62. R Li, JP Klinman, FS Mathews. Copper amine oxidase from *Hansenula polymorpha*: the crystal structure determined at 2.4 Å resolution reveals the active conformation. Structure 6:293–307, 1998.
63. GW Haywood, PJ Large. Microbial oxidation of amines. Distribution, purification and properties of two primary-amine oxidases from the yeast *Candida boidinii* grown on amines as sole nitrogen source. Biochem J 199:187–201, 1981.
64. H Yamada, KT Yasunobu. Monoamine oxidase. 1. Purification, characterization, and properties of plasma monoamine oxidase. J Biol Chem 237:1511–1516, 1962.
65. R Medda, A Padiglia, A Bellelli, P Sarti, S Santanche, AA Finazzi, G Floris. Intermediates in the catalytic cycle of lentil (*Lens esculenta*) seedling copper-containing amine oxidase. Biochem J 332:431–437, 1998.
66. CJ Fowler, KF Tipton. Concentration dependence of the oxidation of tyramine by the two forms of rat liver mitochondrial monoamine oxidase. Biochem Pharmacol 30:3329–3332, 1981.
67. G Floris, A Giartosio, A Rinaldi. Diamine oxidase from *Lens esculenta* seedlings; purifications and properties. Phytochemistry 22:1871–1874, 1983.
68. A Holt, DF Sherman, GB Baker, MM Palcic. A continuous spectrophotometric assay for monoamine oxidase and related enzymes in tissue homogenate. Anal Biochem 244:384–392, 1997.

35

Prolyl 4-Hydroxylase

Robert B. Rucker, Ana Samimi, and Jerold A. Last
University of California, Davis, Davis, California, U.S.A.

I. INTRODUCTION

A. Chemical Reactions Catalyzed

Prolyl 4-hydroxylase catalyzes the formation of 4-hydroxyproline residues in collagens and a number of other proteins in both plants and animals, e.g., acetylcholine esterase, C1q component of complement, and elastin. Equation (1) shows the conversion of L-proline to L-hydroxyproline.

B. Chemical Structure of Substrates

In vertebrate animals, an -X-Pro-Gly- triplet fulfills the minimum sequence requirement for interaction with prolyl 4-hydroxylase, wherein the Pro residue is hydroxylated (1–3). For example, the Pro residue in the central position of -Gly-Pro-Pro- or -Pro-Gly-Pro is not hydroxylated. Moreover, in vertebrate animals, single polypeptide chains serve as substrates. Useful synthetic substrates are $(Pro\text{-}Pro\text{-}Gly)_5$ or $(Pro\text{-}Pro\text{-}Gly)_{10}$. In noncollagenous proteins, such as C1q complement, 4-hydroxyproline is found in -Ala-X-4Hyp-Gly- and -Gly-X-4-Hyp-Ala- sequences. In nonvertebrate collagens, Pro in the sequence, -Pro-Y-Gly-, is the preferred site of hydroxylation (1), and in plants, Ser-Pro-Pro-Pro-Pro- is the preferred sequence, in contrast to the -X-Pro-Gly- sequences in animals (4, 5). Polyproline-enriched sequences are common to plant structural proteins, e.g., the hydroxyproline-rich glycoproteins (4). The plant enzyme also recognizes and hydroxylates substrates with distinguishable secondary and tertiary structure (5).

C. Enzyme Commission Designation

The systematic name and number for prolyl 4-hydroxylase are 4-proline:2-oxo-glutarate dioxygenase and EC 1.14.11.2, respectively.

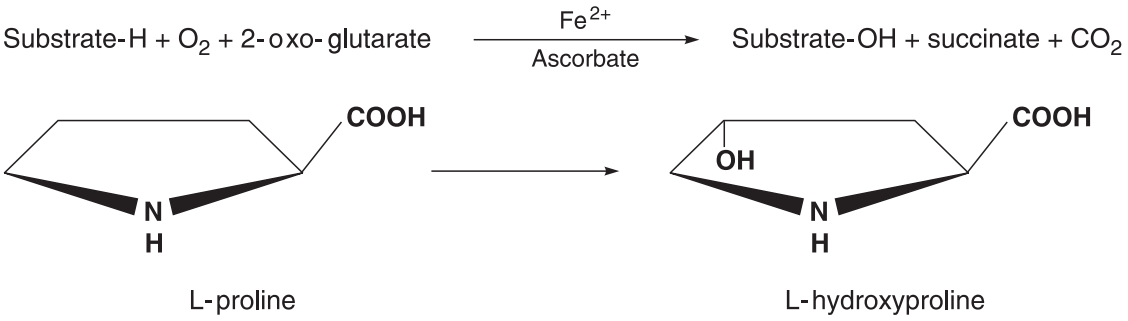

(1)

II. PHYSIOLOGICAL IMPORTANCE

The formation of hydroxyproline is necessary for the intracellular assembly of procollagen polypeptide chains into helical structures. When collagen chains are underhydroxylated, helical formation is impaired and collagen is retained within the cell. As a consequence, underhydroxylation of collagen leads to decreased collagen production (1–3, 6). In plants, increased hydroxyproline-rich glycoprotein synthesis is associated with wound healing and resistance to fungal infections. Impaired hydroxylation impairs the ability to respond to infections and wounds, particularly situations wherein encapsulation of a foreign substance is a requisite (5).

III. LOCATION IN TISSUES

Prolyl 4-hydroxylase is found in the rough endoplasmic reticulum in loose association with the cistern inner membrane. Prolyl hydroxylation takes place while the polypeptide chain is growing on the ribosome. In plants, hydroxylation also occurs within the cistern of the rough endoplasmic reticulum. The enzyme is ubiquitous, wherever collagen is found in animals or hydroxyproline-rich glycoproteins are found in plants (1–5).

IV. COMMERCIAL APPLICATIONS

There are few commercial applications for prolyl hydroxylase per se. However, inhibitors of prolyl hydroxylase are considered valuable if they can effectively modulate wound healing or abnormal collagen deposition.

V. PHYSICAL AND CHEMICAL PROPERTIES

The descriptions that follow apply mostly to vertebrate prolyl 4-hydroxylase. For additional descriptions regarding plant prolyl 4-hydroxylase or prolyl 3-hydroxylase, the reader should refer to references 3–5 and 7, respectively.

A. Molecular Weight and Structural Characteristics

The enzyme from human placenta and chick embryos exists as a heterotetramer (an $\alpha_2\beta_2$ tetramer) with a molecular weight of 240,000. The cDNA encoding the enzyme has been characterized from chicken, human, and rat (1–3). The α-subunit from mammalian sources is 64,000 daltons. The α-subunit contains the active site, but does not have detectable prolyl hydroxylase activity unless assembled as the heterotetramer. The β-subunit has a molecular weight of 60,000 daltons. Although in most animals both the α- and β-subunits are necessary for activity, prolyl 4-hydroxylase activity in algae and some plants is structurally related to only the α-subunit (7).

The β-subunit is identical to the enzyme protein disulfide isomerase (8–11). The β-subunits also provide retention and docking signals for prolyl hydroxylase within the endoplasmic reticulum (2). In addition, Wilson et al. (9) have provided data that the β-subunit acts as a chaperone for procollagen chain assembly. Of interest, there is also partial sequence homology between the β-subunit and thyroid hormone-binding protein, phospholipase C, thioredoxin, and the estrogen-binding domain of the estrogen receptor (2, 3).

B. Genes and Posttranslational Modifications

The cDNA for prolyl hydroxylase has been cloned and the active enzyme expressed in insect cells using a baculovirus vector (12). When the α- and β-subunit cDNAs are expressed separately in baculovirus, neither has prolyl 4-hydroxylase activity, but when they are expressed together, prolyl 4-hydroxylase activity is observed (12). The gene coding for the α-subunit sequence has been mapped to the human chromosome 10 (q21.3–23.1 region), while the β-subunit maps to human chromosome 17 q25, the same chromosome that contains the gene for the type I collagen α-chains (13, 14, 15).

With regard to postranslational processing, the α-subunit contains 16 residues of mannose, one residue of galactose, and two residues of N-acetylglucosamine. The β-subunit contains two residues of mannose and three residues of galactose (2, 3). Using a cell-free system, John and Bulleid (12) have shown that enzyme assembly is redox sensitive and ATP dependent. The assembled subunits are intramolecularly crosslinked by disulfide bonds.

VI. ENZYMATIC PROPERTIES

A. Substrates

As noted above, the peptides $(\text{Pro-Pro-Gly})_5$ or $(\text{Pro-Pro-Gly})_{10}$ are excellent substrates for detection

of prolyl 4-hydroxylase activity. The K_ms for these substrates are in the 1–10 μM range.

B. Effect of Environmental Factors

Mammalian prolyl 4-hydroxylase is often assayed at the physiological pH and temperature corresponding to that of the source. Activity is lost upon freeze/thawing and concentration. The enzyme is best stored at -20°C in ethylene glycol.

C. Cofactors and Proposed Mechanism

The reaction mechanism involves the following proposed sequence of scheme:

Phase I

$$E + Fe^{2+} \rightarrow E \cdot Fe^{2+} \quad (2)$$

$$E \cdot Fe^{2+} + 2\text{-OG} \rightarrow E \cdot Fe^{2+} \cdot 2\text{-OG} \quad (3)$$

$$E \cdot Fe^{2+} \cdot 2\text{-OG} + O_2 \rightarrow E \cdot Fe^{2+} \cdot 2\text{-OG} \cdot O_2 \quad (4)$$

$$E \cdot Fe^{2+} \cdot 2\text{-OG} \cdot O_2 + \text{Peptide} \rightarrow E \cdot Fe^{2+} \cdot 2\text{-OG} \cdot O_2 \cdot \text{Peptide} \quad (5)$$

Phase II

$$E \cdot Fe^{2+} \cdot 2\text{-OG} \cdot O_2 \cdot \text{Peptide} \rightarrow E \cdot Fe^{2+} \cdot \text{Succ} \cdot CO_2 + \text{Peptide-OH} \quad (6)$$

$$E \cdot Fe^{2+} \cdot \text{Succ} \cdot CO_2 \rightarrow EFe^{2+*} + \text{Succ} + CO_2 \quad (7)$$

$$E \cdot Fe^{2+*} \rightarrow E + Fe^{2+} \quad (8)$$

*Ascorbic acid is essential in keeping both iron and the enzyme in a reduced state. Enzyme activity is lost after four to six catalytic turns if a strong reducing agent, such as ascorbic acid, is not present. The K_m values for Fe^{2+}, 2-OG, and ascorbate are 2, 5, and 100 μM, respectively. 2-OG, 2-oxoglutarate; Succ, succinate.

D. Inhibitors

Several classes of inhibitors for prolyl hydroxylase have been described, including proline analogs, agents that interfere with 2-oxoglutarate or cofactor binding, and peptides containing 5-oxoproline (1–3). Table 1 lists various inhibitors and their modes of action.

VII. DETERMINATION OF ACTIVITY

The standard prolyl 4-hydroxylase assay is based on the release of tritium from underhydroxylated procollagen α-chains (1, 27). Although tedious to prepare and sometimes variable in consistency, tritiated procollagen substrate can be used in assays that are reliable in providing good relative values for enzyme activity when appropriately standardized. The procedure for substrate preparation is largely adapted from Peterkofsky and DiBlasio (28), Kivirikko and Myllyla (1) and Kivirikko et al. (2). The method may be used to prepare a [^{3}H]-L-proline labeled collagen substrate of high specific activity.

A. Substrate Preparation

Step 1. Chick embryo calvaria (15 days old) are incubated in the presence of [2,3,4,5-^{3}H]proline (16 Ci/mmol [New England Nuclear, MA] in the proline-free basal medium (Dulbecco's modified Eagle's medium [DME], GIBCO, Long Island, NY) with α-α'-dipyridyl to inhibit endogenous hydroxylation of procollagen chains. First, a basal medium is prepared containing DME with $NaHCO_3$ (3.7 g/L), penicillin (100 units/mL), streptomycin (100 μg/mL), and sodium ascorbate (50 μg/mL) added. This medium is adjusted to pH 7.6.

Step 2. From 100 to 200 calvaria should be used. The calvaria (one per 0.5 mL) are first incubated in the basal DME medium without isotope addition at 39–40°C for 1 h.

Step 3. Next, the calvaria are transferred to basal DME, but with the following additions: sodium pyruvate (1.0 mM), α, α'-dipyridyl (0.2 μM), and L-[2,3,4,5-^{3}H]proline at 5 Ci/mL. Culture flasks are flushed with 95% oxygen 5% CO_2, capped, and the incubation is continued for 12–24 h.

Step 4. The calvaria are harvested by decanting the medium. The decanted medium is saved, centrifuged (2000 g for 10 min) to remove particulate material, and dialyzed against distilled water to remove unincorporated [^{3}H]-L-proline. Following dialysis, the medium is stored (-20°C) and saved for Step 5.

Step 5. The decanted calvaria are homogenized in 0.5 M acetic acid (1:5 w/v) using a Polytron (Brinkman Instruments) and extracted twice (12 h each with agitation at 4°C). Since the dialyzed medium contains collagen, it is added to the acetic acid extracts. The combination is exhaustively dialyzed against 0.05 M Tris, pH 7.4, until < 100 dpm of [^{3}H]-L-proline is detected per mL dialysate.

Table 1 Examples of Prolyl 4-Hydroxylase Inhibitors

Inhibitor	Description	Ref.
Active-site modification		
Diethyl pyrocarbonate	Modification of active site histidine residues, $K_i \sim 10\,\mu M$	7
Substrate binding		
Mimosine	$IC_{50} \sim 100\,\mu M$	16, 17
S4682	$K_i \sim 150\,nM$	18
Iron chelation		
Pirfenidone (methyl-1-phenyl-2-[^{1}H]-pyridone)	Can be used in vivo (0.5% of diet, w/w)	19
HOE 077 (2,4-pyridine dicarboxylic acid bis[2-methoxyethyl] amide)	Can be used in vivo (200 μg/g dry food)	20
α, α'-dipyridyl and related compounds	Classical inhibitor of prolyl and other iron-requiring hydroxylases, $K_i \sim 1\,\mu M$	21, 22
2,2′-bisbipyridine-5,5′-dicarboxylic acid	Most potent inhibitor of its type, $K_i \sim 50$–100 nM. Note: 2,2′-bipyridines lacking a 5-carboxylate are poor inhibitors	23
2-Oxo-glutarate binding		
2,7,8-trihydroxyanthraquinone	Competes with 2-oxo-glutarate, $K_i \sim 40$ nM	24
Oxalylalanine and oxalylglycine	Structural analogs of 2-oxoglutarate in which the CH_2 moiety is replaced by -NH-, $K_i \sim 100$–200 nM	25, 26

Step 6. Following dialysis, the material is aliquoted and frozen until use. Note, however, that the storage of tritiated samples in the frozen state can result in some tritium exchange with water. Additional dialysis prior to use or passage through a Sephadex G-10 column equilibrated in sample buffer to remove tritiated water is often necessary. As a quality control measure, the collagenous nature of the substrate may be assessed by digestion overnight with purified bacterial collagenase (1). The digested material is divided into two portions: one that was dialyzed against 0.05 M Tris buffer at pH 7.8 and one that was not dialyzed. Loss of > 80% of the tritium following collagenase digestion and dialysis indicates that most of the labeled material is collagen.

B. Assay for Prolyl Hydroxylase

Step 1. The assay reaction mixture (0.5 mL) should contain 80 μM $FeSO_4$, 0.5 mM 2-oxo-glutarate, 0.1 mM dithiothreitol, 2.0 mM sodium ascorbate, 1 mg bovine serum albumin, and 300 units of catalase dissolved in 0.05 M Tris-HCl buffer, pH 7.8. The substrate should contain at least 100,000 dpm of tritium. Prior to its addition, the substrate should be boiled for 8–10 min to denature the collagen. Reaction mixtures are incubated at 37°C for 1 h on a rotating platform in 13×100 mm glass culture tubes, and the reaction is stopped by freezing.

Step 2. The tritiated water that is released (Step 1) is collected by vacuum distillation (60°C) and radioactivity determined (1). Hughes (27) has described a simple method for measuring release of tritium that may also be considered. A useful variant of this assay is to use ion-exchange chromatography to separate the tritiated substrate from titriated water (28), allowing one to omit the vacuum distillation step and the need for specialized equipment (see chapter on Lysyl Oxidase).

Step 3. Data are expressed as tritium released per mg protein and tissue weight of the extract or DNA in the sample. This assay is reliable when at least 10 ng of prolyl 4-hydroxylase is present in samples. The assay is also useful for semiquantification, if standardized by using purified or partially purified prolyl 4-hydroxylase as a reference. The assay is linear over the range of 5-50 ng of enzyme.

The same procedures may be used to prepare [^{14}C]-L-proline-labeled collagen as substrate. About 40,000–50,000 dpm of [^{14}C]-L-proline-labeled collagen is needed per assay. This substrate may be stored for long periods (10–16 months), in contrast to the tritiated substrate. [^{14}C]-L-hydroxyproline formed during the enzymatic reaction can be measured following hydrolysis (6 N HCl, 12–24 h, 98°C) by any procedure

that allows precise and reliable measurement of [^{14}C] as hydroxyproline.

Prolyl 4-hydroxylase activity can also be assayed by the decarboxylation of 2-oxo-[1-^{14}C]glutarate. In this case, the assay mixture can be similar to that described above, except 1 mg/mL (Pro-Pro-Gly)$_{10}$ is used as substrate (1). The reaction is followed by measuring the release of $^{14}CO_2$ (for additional details see Ref. 29).

VIII. PROLYL 4-HYDROXYLASE PURIFICATION

For purification of prolyl 4-hydroxylase, we use a procedure adapted from Kivirikko and Myllyla (1). The procedure is simple and based on the affinity of the enzyme for poly-L-proline linked to agarose, elution with a low-molecular-weight poly-L-proline peptide, and gel filtration. Using this method, prolyl 4-hydroxylase has been isolated from a number of sources, e.g., chick embryos, cultured fibroblasts, and skin. Steps in purification are as follows.

Step 1. Poly-L-proline (MW 500–20,000) may be obtained from a number of commercial sources. Poly-L-proline is coupled to agarose by cyanogen bromide activation. Commercially available forms of activated agarose are also available from a number of venders, which simplifies this process. Briefly, 100 mL of 4% agarose is used (Sepharose 4B, Pharmacia, washed twice with deionized water). Cyanogen bromide (25 g) is added, and the reaction is allowed to proceed for 15–20 min at 4–8°C with stirring. The pH is maintained at 11.0 by addition of a saturated solution of NaOH. The mixture is next washed on a Buchner funnel using a solution containing 0.14 M NaCl and 0.1 M $NaHCO_3$, pH 9.0. When the pH reaches 9.9–9.5, the coupling reaction is carried out by stirring into the gel $\sim$ 1 g of poly-L-proline (MW 30,000). The reaction is allowed to proceed overnight and the final gel product is washed extensively with water, followed by buffer containing 0.1 M NaCl, 0.1 M glycine, 10 mM dithiothreitol, and 0.01 M Tris-HCl adjusted to pH 7.8. The efficiency of coupling can be estimated by taking an aliquot of the gel, subjecting the aliquot to hydrolysis in 6 *M* HCl (98°C for 16 h), and measuring the total proline content by standard procedures for amino acid analysis. The poly-L-proline content should be 3–5 mg/mL gel.

Step 2. Next, the gel is poured into a column with a bed volume of 40–60 mL and equilibrated with enzyme buffer (1 *M* NaCl, 0.1 M glycine, 10 μM dithiothreitol, and 0.01 M Tris-HCl buffer, pH adjusted to 7.8).

Step 3. A crude enzyme extract is prepared by homogenizing from 200 to 1000 g of tissue in enzyme buffer (1 *M* NaC1, 0.1 M glycine, 10 μM dithiothreitol, and 0.01 M Tris-HCL buffer, pH adjusted to 7.8 containing 0.1% Triton X-100). The extract should be 1:4 w/v. The homogenization is usually carried out using a Waring blender. For tendon, skin, aortae, we have found that first "powdering" small pieces of the tissue (3–5 g each) in a commercial blender (appropriately vented) or with a mortar and pestle in the presence of liquid nitrogen increases the yield of enzyme.

Step 4. The homogenate is allowed to stand with occasional stirring for 15 min and then centrifuged at 15,000 g for 30 min. This and subsequent steps are carried out at 4–8°C unless stated otherwise. This step may be repeated.

Step 5. Solid $(NH_4)_2SO_4$ is slowly stirred into the supernatant fraction from Step 4 to a final concentration of 25%. After centrifugation at 15,000 g for 20 min, the pellet is discarded and solid $(NH_4)_2SO_4$ is slowly stirred into the supernatant fraction to a final concentration of 70% saturation. Following centrifugation (15,000 g for 20 min), this pellet is dissolved into buffer (see above) and aliquots (corresponding to 50 g tissue) are dialyzed to remove $(NH_4)_2SO_4$ and then stored at −20°C.

Step 6. When enzyme is needed, an aliquot of the $(NH_4)_2SO_4$ fraction is thawed and adjusted with buffer to yield $\sim$ 10 mg of soluble protein/mL. The sample is passed through the affinity column at a flow rate of about 40–60 mL/h, and the column is washed with enzyme buffer until the absorbance of the eluate (at 230 nm) is 0.05 or less. The enzyme is then eluted with 20 mL enzyme buffer containing 3 mg poly-L-proline/mL (MW < 6000). The column may be regenerated by washing with 6 M urea and re-equilibration with enzyme buffer.

Step 7. The pooled fractions containing activity are concentrated to $\sim$ 2 mL using an Amicon ultrafiltration cell.

Step 8. For further purification, this sample is centrifuged at 20,000 g for 10 min, and the clear supernatant is applied to an 8% agarose gel column (BioGel A-1.5m, 200–400 mesh, 1.5 × 90 cm, Bio-Rad, Richmond, CA). Prior to application of the sample, the column is equilibrated with enzyme buffer. Following application of the sample, the column is eluated with enzyme buffer. Fractions are collected and their absorbance is monitored (230 nm). The frac-

tions containing activity are pooled and concentrated by ultrafiltration. Since poly-L-proline eventually adsorbs to the column, after three or four uses the column packing should be discarded.

This procedure is highly specific for prolyl hydroxylase and usually results in a several thousand-fold purification.

Note added in proof: Since submission of this chapter, several relevant articles have appeared. Briefly, isoforms of prolyl hydroxylase generated by alternative splicing have been identified in both human and mouse (30). Prolyl hydroxylase α(I) gene is inducible by hypoxia (31), providing an explanation for observations made more than 20 years ago that hypoxia increases its enzymatic activity.

REFERENCES

1. KI Kivirikko, R Myllyla. Posttranslational enzymes in the biosynthesis of collagen: intracellular enzymes. Methods Enzymol 82:245–304, 1982.
2. KI Kivirikko, R Myllyla, T Pihlajaniemi. Hydroxylation of proline and lysine residues in collagens and other animal and plant proteins. In: JJ Harding, and MJC Crabbe, eds. Post-Translational Modifications of Proteins. Boca Raton: CRC Press, 1992, pp 1–51.
3. NA Guzman, GC Fuller, JE Dixon. Hydroxyproline containing proteins and their hydroxylations by genetically distinct prolyl hydroxylases. In: WS Adair, RP Mecham, eds. Organization and Assembly of Plant and Animal Extracellular Matrix. San Diego: Academic Press, 1990, pp 302–348.
4. AM Showalter, D Rumeau. Molecular biology of the plant wall hydroxyproline-rich glycoproteins. In: WS Adair, RP Mecham, eds. Organization and Assembly of Plant and Animal Extracellular Matrix. San Diego: Academic Press, 1990, pp 247–282.
5. DG Robinson, M Andreae, Blankenstein. Plant prolyl hydroxylase. In WS Adair, RP Mecham, eds. Organization and Assembly of Plant and Animal Extracellular Matrix. San Diego: Academic Press, 1990, pp 283–301.
6. EG Eleftheriades, AG Ferguson, ML Spragia, AM Samarel. Prolyl hydroxylation regulates intracellular procollagen degradation in cultured rat cardiac fibroblasts. J Mol Cell Card 27:1459–1473, 1995.
7. K Tryggvason, K Majamaa, J Risteli, KI Kivirikko. Partial purification and characterization of chick-embryo polyl 3-hydroxylase. Biochem J 286:923–927, 1992.
8. R Myllyla, V Gunzler, KI Kivirikko, DD Kaska. Modification of vertebrate and algal prolyl 4-hydroxylases and vertebrate lysyl hydroxylase by diethyl pyrocarbonate. Evidence for histidine residues in the catalytic site of 2-oxoglutarate-coupled dioxygenases. Biochem J 286:923–927, 1992.
9. R Wilson, JF Lees, NJ Bulleid. Protein disulfide isomerase acts as a molecular chaperone during the assembly of procollagen. J Biol Chem 273:9637–9643, 1998.
10. RB Freedman, NJ Bulleid, HC Hawkins, JL Paver. Role of protein disulfide-isomerase in the expression of native proteins. Biochem Soc Symp 55:167–192, 1989.
11. AR Walmsley, MR Batten, U Lad, NJ Bulleid. Intracellular retention of procollagen within the endoplasmic reticulum is mediated by prolyl 4-hydroxylase. J Biol Chem 274:14884–14892, 1999.
12. DCA John, NJ Bulleid. Intracellular dissociation and reassembly of prolyl 4-hydroxylase: the α-subunits associate with the immunoglobulin-heavy-chain binding protein (BiP) allowing reassembly with the β-subunit. Biochem J 317:659–665, 1996.
13. T Helaakoski, P Annunen, K Vuori, IA MacNeil, T Pihlajaniemi, KI Kivirikko. Cloning, baculovirus expression, and characterization of a second mouse prolyl 4-hydroxylase alpha-subunit isoform: formation of an alpha 2, beta 2 tetramer with the protein disulfide-isomerase/beta subunit. Proc Natl Acad Sci USA 92:4427–4431, 1995.
14. L Pajunen, R Myllylä, T Helaakoski, T Pihlajaniemi, K Tasanen, M Höyhtyä, K Tryggvason, E Solomon, KI Kivirikko. Assignment of the gene coding for both the beta-subunit of prolyl 4-hydroxylase and the enzyme disulfide isomerase to human chromosome region 17p11. Cytogen Cell Gen 47:37–41, 1989.
15. L Pajunen, TA Jones, T Helaakoski, T Pihlajaniemi, E Solomon, D Sheer, KI Kivirikko. Assignment of the gene coding for the alpha-subunit of prolyl 4-hydroxylase to human chromosome region 10q21.3-23.1. Am J Hum Gen 45:829–834, 1989.
16. H Ju, J Hao, S Zhao, IMC Dixon. Antiproliferative and antifibrotic effects of mimosine on adult cardiac fibroblasts. Biochim Biophys Acta 1448:51–60, 1998.
17. TA McCaffrey, KB Pomerantz, TA Sanborn, AM Spokojny, B Du, MH Park, JE Folk, A Lamberg, KI Kivirikko, DJ Falcone. Specific inhibition of eIF-5A and collagen hydroxylation by a single agent. Antiproliferative and fibrosuppressive effects on smooth muscle cells from human coronary arteries. J Clin Invest 95:446–455, 1995.
18. M Bickel, KH Baringhaus, M Gerl, V Günzler, J Kanta, L Schmidts, M Stapf, G Tschank, K

Weidmann, U Werner. Selective inhibition of hepatic collagen accumulation in experimental liver fibrosis in rats by a new prolyl 4-hydroxylase inhibitor. Hepatology 28:404–411, 1998.
19. SN Iyer, SB Margolin, DM Hyde, SN Giri. Lung fibrosis is ameliorated by perfenidone fed in diet after the second dose in a three-dose bleomycin-hamster model. Exp Lung Res 24:119–132, 1998.
20. Y Matsumura, I Sakaida, K Uchida, T Kimura, T Ishihara, K Okita. Prolyl 4-hydroxylase inhibitor (HOE 077) inhibits pig serum–induced rat liver fibrosis by preventing stellate cell activation. J Hepatol 27:185–192, 1997.
21. RI Dowell, EM Hadley. Novel inhibitors of prolyl-4-hydroxylase. J Med Chem 35:800–804, 1992.
22. YR Kim, B Peterkofsky. Differential effects of ascorbate depletion and alpha, alpha′-dipyridyl treatment on the stability, but not on the secretion, of type IV collagen in differentiated F9 cells. J Cell Biochem 67:338–352, 1997.
23. NJ Hales, JF Beattie. Novel inhibitors of prolyl 4-hydroxylase. 5. The intriguing structure–activity relationships seen with 2,2′-bipyridine and its 5,5′-dicarboxylic acid derivatives. J Med Chem 36:3853–3858, 1993.
24. TJ Franklin, M Hitchen. Inhibition of collagen hydroxylation by 2,7,8-trihydroxyanthraquinone in embryonic-chick tendon cells. Biochem J 261:127–130, 1989.
25. CJ Cunliffe, TJ Franklin, NJ Hales, GB Hill. Novel inhibitors of prolyl-4-hydroxylase. 3. Inhibition by the substrate analogue N-oxaloglycine and its derivatives. J Med Chem 35:2652–2658, 1992.
26. E Baader, G Tschank, K-H Baringhaus, H Burghard, V Guenzler. Inhibition of prolyl 4-hydroxylase by oxalyl amino acid derivatives in vitro, in isolated microsomes and in embryonic chicken tissues. Biochem J 300:525–530, 1994.
27. WL Hughes. A simple fast micromethod for measuring enzyme activities which release tritium as tritium water. Anal Biochem 161:529–532, 1987.
28. B Peterkofsky, R DiBlasio. Modification of the tritium-release assays for prolyl and lysyl hydroxylases using Dowex-50 columns. Anal Biochem 66:279–286, 1975.
29. P Annumen, P Koivunen, KI Kiviriko. Cloning of the alpha-subunit of prolyl 4-hydroxylase from *Drosophila* and expression and characterization of the corresponding enzyme tetramer with some unique properties. J Biol Chem 274:6790–6796, 1999.
30. M Nokelainen, R Nissi, L Kukkola, T Helaakoski, J Myllyharju. Characterization of the human and mouse genes for the α subunit of type II prolyl hydroxylase. Eur J Biochem 268:5300–5309, 2001.
31. Y Takahashi, S Takahashi, Y Shiga, T Yoshimi, T Miura. Hypoxic induction of prolyl 4-hydroxylase α(I) in cultured cells. J Biol Chem 275:14139–14146, 2000.

36

Lysyl Hydroxylase

Ana Samimi, Jerold A. Last, Lucas C. Armstrong, and Robert B. Rucker
University of California, Davis, Davis, California, U.S.A.

I. INTRODUCTION

A. Chemical Reactions Catalyzed

Lysyl hydroxylase catalyzes the oxidation of specific lysine residues in collagen to hydroxylysine. The reaction sequence is given in Eq. (1)

$$\begin{array}{lcl} \text{R-CH}_2\text{-CH}_2\text{NH}_2 & \rightarrow & \text{R-CHOH-CH}_2\text{NH}_2 \\ +\,\text{O}_2 + \text{2-oxoglutarate} & & +\,\text{succinate} + \text{CO}_2 \\ \text{Lysine (in collagen)} & & \text{Hydroxylysine} \\ & & \text{(in collagen)} \end{array} \qquad (1)$$

where R = (HOOC-$(CH_2)_2$-NH_2)

B. Chemical Structure of Substrates

The enzyme recognizes the sequence X-Lys-Gly. In some types of collagen, hydroxylation of lysine residues occurs at the end of α-chains in the short non-triple-helical region where there is recognition of triplet sequences, e.g., X-Lys-Ser and X-Lys-Ala. In addition to collagens, the lysine in sequences X-Lys-Ser, X-Lys-Ala, and X-Lys in arginine-rich histone proteins can also be hydroxylated (1). Evidence now points to the possibility that different isozymes of lysyl hydroxylase are responsible for catalyzing these varied substrate recognition sequences. Lysine vasopressin, which has the structure Cys-Thr-Phe-Gln-Asn-Cys-Pro-Lys-Gly-NH_2, and lysine-rich histone, which contains X-Lys-Gly sequences, also act as substrates of lysyl hydroxylase. The tripeptide Lys-Gly-Pro is not hydroxylated whereas a tripeptide Ile-Lys-Gly is hydroxylated by lysyl hydroxylase. This indicates a minimum structural requirement of an X-Lys-Gly triplet for this enzyme.

Studies with synthetic peptides have shown that the amino acid sequences, as well as the peptide chain length and peptide conformations, are critical for determining their specificity as substrates. Ile-Lys-Gly, $(\text{Ile-Lys-Gly})_2$, and $(\text{Ile-Lys-Gly})_5$-Phe have been shown to have, respectively, Lys K_ms of 4, 1, and 0.14 μM (2). The conformation of the peptide may regulate the extent of hydroxylation of the peptide. It has been suggested that a β-bend involving the lysine to be hydroxylated is required for lysyl hydroxylase recognition (3). Some amino acid sequences around the Y positioned lysine can in effect prevent hydroxylation of the lysine by exerting a conformational change not inherently recognizable to the enzyme.

C. Enzyme Commission Designation

Lysyl hydroxylase, classified as a member of the ketoglutarate-dependent dioxygenase family, has the official name of lysine:2-oxoglutarate 5-dioxygenase and an EC number of 1.14.11.4.

II. PHYSIOLOGICAL IMPORTANCE

The conversion of collagen-bound lysine to hydroxylysine alters the properties of the collagen crosslinks,

e.g., instead of Schiff-base products and simple aldimines, ketoamine derivatives also become possibilities. Further, hydroxylation provides a site for the O-glycosylation of collagen (4). Both functions are important determinants of the final structure and properties of the mature collagen fibres. The O-glycosylation results in the addition of either galactose as a monosaccharide or glucosylgalactose as a disaccharide linked to the hydroxylysyl residue(s).

Nascent collagen α-chains, not triple helical collagen, are the substrates for lysyl hydroxylase. Generally nonhelical lysyl residues are preferred sites of hydroxylation over residues occurring in the helical regions of the collagen chain. However, this property is related to the rate of folding of the collagen molecule; overhydroxylation of helical lysyl residues occurs under conditions of delayed or impaired assembly of the triple helical form of collagen (5–7). Lysyl residues in denatured (nonhelical) collagen may also be hydroxylated by the enzyme (8). There are differential hydroxylation levels in different collagens; type IV is relatively heavily hydroxylated as compared, for example, with types I or III collagens. In addition, lysyl residues in the same collagen type may be differentially hydroxylated (and glycosylated) in different tissues. Bone collagen (type I) contains relatively more hydroxylysine than type I collagen from lung, skin, or liver, and hypertrophied tendon contains relatively more hydroxylysine than does normal tendon (9). There are also apparent age-related variations in the level of lysine hydroxylation in collagen (10). Finally, hydroxylysine also occurs in noncollagenous proteins that have a triple helical collagenlike domain in their structure, such as C1q (complement component), acetyl cholinesterase, and other related proteins (1).

Evidence for the biological importance of collagen lysine hydroxylation catalyzed by lysyl hydroxylase comes from patients with Ehlers Danlos Syndrome Type VI, who exhibit thin skin, loose joints, and ocular disruption. These patients are deficient in collagen hydroxylysine and lysyl hydroxylase activity. In several such patients, defects in the lysyl hydroxylase gene have been identified (6, 7, 11). Increases in collagen lysine hydroxylation and/or lysyl hydroxylase activity have been described in a number of pathological conditions, including dimethylnitrosamine-induced liver fibrosis (12) and bleomycin-induced pulmonary fibrosis (13). Abnormal hydroxylation of lysyl residues causes changes in the ratios of hydroxylysinoleucine (HLNL) and dihydroxylysinoleucine (DHLNL), two lysine- and/or hydroxylysine-derived crosslinks, and may thereby affect the tensile strength of the collagen fibrils in the tissues involved (14, 15).

III. LOCATION IN TISSUES

Lysyl hydroxylase is an intracellular enzyme found within the lumen of the rough endoplasmic reticulum, where it comes in contact with nascent collagen chains prior to their folding. It can hydroxylate lysyl residues on unfolded nascent collagen chains, but has no demonstrable activity on triple helical collagen. This enzyme is ubiquitous, wherever collagen is found; that is, all organs of the body contain some level of this enzyme. In Northern blot analysis of total RNA or poly $(A)^+$ mRNA from various adult rat tissues, the rat lysyl hydroxylase cDNA probe (the so-called type I lysyl hydroxylase; see below) hybridizes to a 3.2-kb mRNA in all tissues, with highest levels of expression in liver, lung, heart, and cartilage.

IV. COMMERCIAL APPLICATIONS

There are none at this time. The enzyme has been notoriously difficult to purify, is sparingly soluble in aqueous buffers, and is fairly labile (16). Thus, pure enzyme is not easily prepared, and has mainly been produced by recombinant DNA techniques. Since the enzyme is a glycoprotein, its cognate DNA has to be expressed in an eukaryotic vector such as a baculovirus system (17, 18) to prepare active enzyme. Inhibitors of lysyl hydroxylase such as minoxidil (19) may have future biomedical or clinical applications as preventive agents for various fibrotic disorders, but none has yet been approved for this indication because of their toxicity.

V. PHYSICAL AND CHEMICAL PROPERTIES

The descriptions that follow apply to vertebrate lysyl hydroxylase.

A. Molecular Weight

The enzyme has been purified from human placenta and chick embryos, and it chromatographs as a homodimer of two identical 85,000-MW α-subunits on a gel filtration column (20).

B. Structural Characteristics

The cDNA encoding the enzyme has been characterized from chicken, human, and rat (17, 21, 22). Although the sequence does not closely resemble any other known protein, there is much homology in the C-terminal region between various species. The C-terminal region also contains two histidyl residues that may be conserved between different members of the α-ketoglutarate-dependent dioxygenase family (23).

The lysyl hydroxylase cDNA sequence has little similarity to the prolyl 4-hydroxylase α- or β-subunit cDNA sequences (21, 22). The rat cDNA encodes a protein of 728 amino acids, and has an overall homology at the protein level of 91% and 77% to the human and chicken lysyl hydroxylases, respectively.

Two histidyl residues in the chicken lysyl hydroxylase and other members of the α ketoglutarate-dependent dioxygenase family have been identified as possible catalytic sites (11). These histidyl residues are conserved in the rat lysyl hydroxylase, and indeed the sequence around these histidyl residues is also perfectly conserved between human and rat. It has been proposed that two histidyl residues, located 30–50 amino acids apart in the primary sequence which are conserved in different members of the α-ketoglutarate-dependent dioxygenase family, may be involved in cofactor binding (23). Conservation of the histidyl residues and surrounding residues in the rat lysyl hydroxylase supports this hypothesis. Although these enzymes can be inactivated by diethylpyrocarbonate, a histidine reactive reagent, the direct involvement of these particular residues in cofactor binding has not been demonstrated (23).

1. Genes

There are three known isoforms (from DNA sequences) arising from different, although closely related, genes (18, 24). Isoform-1 in the human gene (PLOD) has been mapped to chromosome 1p36.3-36.2 (22). Isoform-2 has been mapped in human gene (PLOD2) at 3q23-q24 (25), and isoform-3 has been mapped to the human gene (PLOD3) at chromosome 7q36 (24).

2. Posttranslational Processing

Lysyl hydroxylase is a glycoprotein wherein the asparagine-linked carbohydrate units are critical for the enzyme's activity. Four consensus sites for N-linked glycosylation are found in the rat lysyl hydroxylase. Three of these are in the same location as in the human and the chicken lysyl hydroxylases. Interestingly, Asn163 in the human lysyl hydroxylase has been replaced with a serine at the corresponding residue 164 in the rat, while Ser176 in the human enzyme has been converted to a consensus glycosylation site asparagine at residue 177 in the rat (17–19). It is not known which of these sites is glycosylated in the mature protein.

VI. ENZYMATIC PROPERTIES

A. Substrates

Several synthetic peptides have been shown to be good substrates for determining lysyl hydroxylase activity. In addition to lysine vasopressin and $(\text{Ile-Lys-Gly})_2$ (as mentioned earlier), Ala-Arg-Gly-Ile-*Lys*-Gly-Ile-Arg-Gly-Phe-Ser-Gly, Ala-Arg-Gly-Met-*Lys*-Gly-His-Arg-Gly-$(\text{Pro-Pro-Gly})_4$ and $(\text{Pro-Pro-Gly})_4$-Ala-Arg-Gly-Met-*Lys*-Gly-His-Arg-Gly-$(\text{Pro-Pro-Gly})_4$ can be used in enzymatic assays. Their respective K_ms are 1.1, 2.0, 0.4, 0.2, and 0.2 μM (2).

Underhydroxylated protocollagen substrate can also be prepared from chick calvaria or chick embryo tendon (20).

B. Effects of Environmental Factors

Vertebrate lysyl hydroxylase is assayed under physiological conditions of 37°C and pH 7.8. Activity is lost by 50% after one freeze-thaw cycle or several days at 4°C. In ethylene glycol, the enzyme is fairly stable and can be scored at −20°C for several months.

C. Proposed Mechanism

Lysyl hydroxylase and prolyl-4-hydroxylase are very similar in their substrate and cofactor requirements. Both enzymes are therefore classified as α-ketoglutarate-dependent dioxygenases, which couple hydroxylation to the conversion of oxygen and α-ketoglutarate to succinate and CO_2. These enzymes also require Fe^{2+} and ascorbate as cofactors. Furthermore, both prolyl 4-hydroxylase and lysyl hydroxylase require that the hydroxylated amino acid be in the Y position of the $(\text{X-Y-Gly})_n$ collagen motif.

The following reaction sequence is involved in the hydroxylation of lysyl residues by lysyl hydroxylase:

$$E + Fe^{2+} \rightarrow E \cdot Fe^{+2} + 2\text{-OG} \rightarrow E \cdot Fe^{2+} \cdot 2\text{-OG} + O_2 \rightarrow E \cdot Fe^{3+} \cdot 2\text{-OG} \cdot O_2^{\cdot} + \text{Peptide}$$

$$E \cdot Fe^{3+} \cdot 2\text{-OG} \cdot O_2^{\cdot}\text{Peptide} \rightarrow E \cdot Fe^{2+} \cdot \text{Succ} \cdot CO_2 + \text{Peptide-OH}$$

$$E \cdot Fe^{2+} \cdot \text{Succ} \cdot CO_2 \rightarrow E \cdot Fe^{2+} \cdot \text{Succ} + CO_2$$

$$E \cdot Fe^{2+} \cdot \text{Succ} \rightarrow E \cdot Fe^{2+} + \text{Succ}$$

$$E \cdot Fe^{2+} \rightarrow E + Fe^{2+}$$

If the enzyme is oxidized it can be reduced by ascorbic acid and is therefore regenerated to undergo further catalytic reaction cycles (see reaction below). The K_m values for Fe^{2+}, 2-OG, and ascorbate using protocollagen as a substrate are: 2, 70, and 200 μM, respectively (Table 1).

$$E \cdot Fe^{2+} \rightarrow E \cdot Fe^{3+} + \text{Ascorbate} \rightarrow E \cdot Fe^{2+} \cdot \text{Dehydroascorbate} \rightarrow E \cdot Fe^{2+} + \text{Dehydroascorbate}$$

D. Inhibitors

Inhibitors of lysyl hydroxylase can be grouped as given in Table 2 (1, 4).

VII. DETERMINATION OF ACTIVITY

A. Determination of Tritriated Water Release

Determination of lysyl hydroxylase activity by tritiated water release is conveniently performed by a modification of the method of Peterkofsky and DiBlasio (27), as described in detail elsewhere (13). For direct determination of tritiated procollagen substrate in assay mixtures, the trichloroacetic acid–precipitable material from the enzymatic reaction after addition of lysyl hydroxylase is digested with 18 units of type VII collagenase (Sigma, St. Louis, MO) for 24 h at 37°C. The reaction mixture is fractionated by passage through a Centricon 10 ultrafiltration unit (Amicon, Beverly, MA). The separated fractions are hydrolyzed in 6 N HCl at 110°C overnight. HPLC separation of hydroxylysine and lysine in hydrolysates is performed by isocratic reversed-phase HPLC. A Beckman C18 Ultrasphere column (0.46 × 25 cm) is equilibrated and run with 23% 1-propanol, 0.3% sodium dodecyl sulfate, 0.01 M phosphate, pH 2.84, as the elution solvent (28). Fractions from the HPLC are collected and mixed with an appropriate scintillation cocktail and radioactivity determined.

B. Decarboxylation of 2-Oxo[1-^{14}C]Glutarate

This assay is based on the determination of the stoichiometric release of $^{14}CO_2$ from 2-oxo[1-^{14}C]glutarate during the enzymatic assay. Synthetic peptides can be utilized as substrates instead of natural procollagen substrates, which allow for a more rapid and simple assay (20).

The procedure involves sequential addition of substrate, enzyme, and cofactors (ferrous iron, ascorbate, and 2-oxo[1-^{14}C]glutarate), as well as supplements bovine serum albumin, catalase, and dithiothreitol to the assay mixture, which is maintained at a pH of 7.8 in 0.05 M Tris-HCl buffer. The assay mixture is kept on ice until the final compound is added, after which it is immediately sealed with a rubber stopper containing a 1.5 × 3.0 cm Whatman filter paper saturated with NCS hung from a wire hook. NCS is a quaternary amine that is sold as a proprietary product of Amersham Pharmacia Biotech. Incubation is at 37°C in a shaker water bath for 30–40 min. The vials are then transferred to an ice bath where they are acidified

Table 1 Recombinant and Native Lysyl Hydroxylase Kinetics

	K_m					
	Ascorbate	α-Ketoglutarate μM	O_2 μM	Fe^{2+} μM	Procollagen pM	(cpm ^{3}H/h/mg) × 10^{-5})
Recombinant lysyl hydroxylase (rat)	122	106	ND	ND	100	60
Lysyl hydroxylase (chick embryo)	220	70	ND	2	10	20.2

Table 2 Lysyl Hydroxylase Inhibitors

Inhibitor	Description
Interference with Fe^{2+} binding	
Zn^{2+}	Competes with Fe^{2+}; 5 μm
α, α'-dipyridyl	Chelates Fe^{2+}
Interference with O_2 binding	
Zn, Cu superoxide dismutase	Dismutation of activated oxygen; 30 μm
Nitroblue tetrazolium	Scavenges activated oxygen
Interference with 2-oxoglutarate binding	
Pyridine 2,4-dicarboxylate	Competes with 2-OG; 50 μM
Pyridine 2,5-dicarboxylate	Competes with 2-OG; 150 μM
Some TCA cycle intermediates	Compete with 2-OG
Coumalic acid	Suicide substrate, 2-OG analog; > 2 mM
Active site interference	
Diethyl pyrocarbonate	A histidine reactive reagent, > 50% inhibition at 50 μM
Mechanism unclear	
Minoxidil	> 50% inhibition at > 50 μM

by injection of an equal volume of KH_2PO_4, pH 5.0, buffer. The reaction is allowed to incubate at room temperature for 30 min, after which the filters are placed in a toluene-based scintillation cocktail (20).

VIII. LYSYL HYDROXYLASE PURIFICATION

All steps are carried out at 4°C. Chick embryos (14 days old; 50–100 embryos) are homogenized (1:4) in an enzyme buffer (0.2 M NaCl, 0.1 M glycine, 10 μM dithiothreitol, 0.02 M Tris-HCl buffer, pH 7.5, containing 0.1% Triton X 100 and 60% (v/v) glycerol). This homogenate is centrifuged at 15,000g for 30 min and then subjected to ammonium sulfate precipitation. The supernatant is saturated to 17% with solid $(NH_4)_2SO_4$ and centrifuged at 15,000 g for 20 min, the pellet is discarded, and the supernatant is once again saturated to 55% with $(NH_4)_2SO_4$ and centrifuged at 15,000 g for 20 min. This pellet is dissolved in the enzyme buffer and dialyzed against two 16-L volumes of the same buffer supplemented with 0.003 M $MnCl_2$ overnight. The dialyzed fraction is adjusted to ~ 20 mg protein/mL and next passed (flow rate, 40–50 mL/h) through a concanavalin A-agarose affinity column (40–50 mL of packed gel) equilibrated with the dialysis buffer. Lysyl hydroxylase is then competitively eluted with methyl α-D-glucoside (1 M) dissolved in the enzyme buffer and ethylene glycol (40%:60%, v/v).

The effluent from chromatography on concanavalin A-agarose is next dialyzed overnight against enzyme buffer in preparation for collagen–agarose affinity chromatography. The collagen–agarose affinity column is prepared by coupling citrate-soluble calf skin collagen to cyanogen bromide-activated agarose (20). The entire dialysate is applied to the collagen–agarose column. The enzyme is eluted from the column with enzyme buffer containing 60% (v/v) ethylene glycol.

As a final step, the enzyme fractions containing activity are concentrated to 2–3 mL by ultrafiltration using an Amicon PM30 membrane. The concentrated sample is centrifuged at 20,000 g for 10 min and the supernatant fraction is loaded onto an 8% agarose gel column (Bio-Gel A 1.5 m, 200–4000 mesh, Bio-Rad, 1 × 90 cm). The final purified enzyme is subsequently eluted with enzyme buffer. This process usually results in a 5000 to 10,000-fold increase in specific activity with a recovery of 2–6%. The enzyme fractions in ethylene glycol are the most stable. There is often a large loss of activity during the gel filtration step (20).

The purified enzyme has a molecular weight of 180 kDa determined by gel filtration column chromatography under nondenaturing conditions, while it migrates at 85 kDa in polyacrylamide gels in the presence of SDS. As noted above, the enzyme is a homodimer (16). Since the protein expressed by insect cells infected with baculovirus containing the lysyl hydroxylase cDNA sequence from rat is active with the addition of cofactors such as ascorbate, α-ketoglutarate, and ferrous iron (17), it is likely that no other cofactors remain to be discovered. That insect cells infected with baculovirus containing the lysyl hydroxylase cDNA express lysyl hydroxylase with a similar specific activity to that of the chick embryo lysyl hydroxylase

confirms that lysyl hydroxylase does not require protein disulfide isomerase or any other mammalian protein for its activity (Table 2) (17).

Note added in proof: Since submission of this chapter, several relevant articles have appeared. Briefly, the lysyl hydroxylase 3 isoform not only catalyzes the hydroxylation of lysyl residues on collagen, but the pure enzyme also is a collagen glucosyltransferase, catalyzing the addition of glucose to galactosyl residues on collagen hydroxylysines (29). Thus, LH3 is also galactosylhydroxylysyl glucosyltransferase, EC 2.4.1.66. Neither LH1 nor LH2 possess this additional activity. A specific 40 amino acid-long sequence in the C-terminal end of lysyl hydroxylase has been identified that is responsible for its membrane binding and localization in the endoplasmic reticulum (30). An important role for hydroxylysine and its glycosylated forms in collagen may be regulation of the rate of fibrillogenesis and determination of the morphology of the fibers produced (31).

REFERENCES

1. KI Kivirikko, R Myllyla, T Pihlajaniemi. Hydroxylation of proline and lysine residues in collagens and other animal and plant proteins. In: JJ Harding, and MJC Crabbe, eds. Post-Translational Modifications of Proteins. Boca Raton: CRC Press, 1992, pp 1–51.
2. KI Kivirikko, K Shudo, S Sakakibara, DJ Prockop. Studies on protocollagen lysine hydroxylase. Hydroxylation of synthetic peptides and the stoichiometric decarboxylation of α-ketoglutarate. Biochemistry 11:122–129, 1972.
3. K Takahashi, YK Kang, G Nemethy, HA Scheraga. Low-energy conformations of two lysine-containing tetrapeptides of collagen: implications for post-translational lysine hydroxylation. Biopolymers 26:1781–1788, 1987.
4. KI Kivirikko, R Myllyla. The hydroxylation of prolyl and lysyl residues. In: RB Fredman, HC Hawkins, eds. The Enzymology of Post-Translational Modification of Proteins, Vol 1. London: Academic Press, 1980, pp 53–104.
5. A Ihme, T Krieg, A Nerlich, U Feldmann, J Rauterberg, RW Glanville, G Edel, PK Muller. Ehlers-Danlos syndrome type VI: Collagen type specificity of defective lysyl hydroxylation in various tissues. J Invest Dermatol 83:161–165, 1984.
6. T Hautala, J Heikkinen, KI Kivirikko, R Myllyla. A large duplication in the gene for lysyl hydroxylase accounts for the type VI variant of Ehlers-Danlos syndrome in two siblings. Genomics 15:399–404, 1993.
7. VT Ha, MK Marshall, LJ Elsas, SR Pinnell, HN Yeowell. A patient with Ehlers-Danlos syndrome type VI is a compound heterozygote for mutations in the lysyl hydroxylase gene. J Clin Invest 93:1716–1721, 1994.
8. L Ryhanen, KI Kivirikko. Hydroxylation of lysyl residues in native and denatured protocollagen by protocollagen lysyl hydroxylase in vitro. Biochim Biophys Acta 343:129–137, 1974.
9. JE Gerriets, SL Curwin, JA Last. Tendon hypertrophy is associated with increased hydroxylation of nonhelical lysine residues at two specific cross-linking sites in type I collagen. J Biol Chem 268:25553–25560, 1993.
10. MJ Barnes, BJ Constable, LF Morton, PM Royce. Age-related variations in hydroxylation of lysine and proline in collagen. Biochem J 139:461–468, 1994.
11. J Hyland, L Ala-Kokko, P Royce, B Steinmann, KI Kivirikko, and R Myllyla. A homozygous stop codon in the lysyl hydroxylase gene in two siblings with Ehlers-Danlos syndrome type VI. Nat Genet 2:228–231, 1992.
12. J Risteli, KI Kivirikko. Intracellular enzymes of collagen biosynthesis in rat liver as a function of age and hepatic injury induced by diemthylnitrosamine. Biochem J 158:361–367, 1976.
13. JA Last, JE Gerriets, LC Armstrong, TR Gelzleichter, KM Reiser. Hydroxylation of collagen by lungs of rats administered bleomycin. Am J Respir Cell Mol Biol 2:543–548, 1990.
14. KM Reiser, JA Last. Collagen crosslinking in lungs of rats with experimental silicosis. Collagen Rel Res 6:313–324, 1986.
15. KM Reiser, AF Tryka, RC Lindenschmidt, JA Last, HR Witschi. Changes in collagen cross-linking in bleomycin-induced pulmonary fibrosis. J Biochem Toxicol 1:83–91, 1986.
16. TM Turpeenniemi-Hujanen, U Puistola, KI Kivirikko. Isolation of lysyl hydroxylase, an enzyme of collagen synthesis from chick embryos as a homogeneous protein. Biochem J 189:247–253, 1980.
17. LC Armstrong, JA Last. Rat lysyl hydroxylase: molecular cloning, messenger-RNA distribution and expression in a baculovirus system. Biochim Biophys Acta 1264:93–102, 1995.
18. K Passoja, K Rautavuoma, L Ala-Kokko, T Kosonen, KI Kivirikko. Cloning and characterization of a third human lysyl hydroxylase isoform. Proc Natl Acad Sci USA 95:10482–10486, 1998.
19. S Murad, SR Pinnell. Suppression of fibroblast proliferation and lysyl hydroxylase activity by minoxydil. J Biol Chem 262:11973–11978, 1987.

20. KI Kivirikko, R Myllyla. Posttranslational enzymes in the biosynthesis of collagen: intracellular enzymes. Methods Enzymol 82:245–304, 1982.
21. R Myllyla, T Pihlajaniemi, L Pajunen, T Turpeeniemi-Hujanen, KI Kivirikko. Molecular cloning of chick lysyl hydroxylase. J Biol Chem 266:2805–2810, 1991.
22. T Hautala, MG Byers, RL Eddy, TB Shows, KI Kivirikko, R Myllyla. Cloning of human lysyl hydroxylase: complete cDNA-derived amino acid sequence and assignment of the gene (PLOD) to chromosome 1p36.3-p36.2. Genomics 13:62-69, 1992.
23. R Myllyla, V Gunzler, KI Kivirikko, D Kaska. Modification of vertebrate and algal prolyl 4-hydroxylases and vertebrate lysyl hydroxylase by diethyl pyrocarbonate. Biochem J 286:923–927, 1992.
24. M Valtavaara, C Szpirer, J Szpirer, R Myllyla. Primary structure, tissue distribution, and chromosomal localization of a novel isoform of lysyl hydroxylase (lysyl hydroxylase 3). J Biol Chem 273:12881–12886, 1998.
25. C Szpirer, J Szpirer, M Riviere, P Vanvooren, M Valtavaara, R Myllyla. Localization of the gene encoding a novel isoform of lysyl hydroxylase. Mammal Genome 8:707–715, 1997.
26. KI Kivirikko, R Myllyla, T Pihlajaniemi. Protein hydroxylation: Prolyl 4-hydroxylase, an enzyme with four cosubstrates and a multifunctional subunit. FASEB J 3:1609–1617, 1989.
27. B Peterkofsky, R DiBlasio. Modification of the tritium-release assays for prolyl and lysyl hydroxylases using Dowex-50 columns. Anal Biochem 66:279–286, 1975.
28. KM Reiser, JA Last. Analysis of collagen composition and biosynthesis by HPLC. Liquid Chromatogr 1:498–502, 1983.
29. J Heikkinen, M Risteli, C Wang, J Latvala, M Rossi, M Valtavaara, R Myllyla. Lysyl hydroxylase 3 is a multifunctional protein possessing collagen glucosyltransferase activity. J Biol Chem 275:36158–36163, 2000.
30. M Suokas, R Myllyla, S Kellokumpu. A single C-terminal peptide segment mediates both membrane association and localization of lysyl hydroxylase in the endoplasmic reticulum. J Biol Chem 275:17863–17868, 2000.
31. H Notbohm, M Nokelainen, J Myllyharju, PP Fietzek, PK Muller, KI Kivirikko. Recombinant human type II collagens with low and high levels of hydroxylysine and its glycosylated forms show marked differences in fibrillogenesis in vitro. J Biol Chem 274:8988–8992, 1999.

37

Lysyl Oxidase

Robert B. Rucker, Alyson E. Mitchell, Eskouhie Tchaparian, and Jerold A. Last
University of California, Davis, Davis, California, U.S.A.

I. INTRODUCTION

A Chemical Reactions Catalyzed

Lysyl oxidase is a copper-containing enzyme that catalyzes the oxidative deamination of amine substrates according to Eq. (1)

$$\text{R-CH}_2\text{NH}_2 + \text{O}_2 + \text{H}_2\text{O} \rightarrow \text{R-CHO} + \text{NH}_3 + \text{H}_2\text{O}_2 \quad (1)$$

B. Chemical Structure of Substrates

Substrates include simple monoamines, diamines, and/or the ϵ-amine function of lysyl and/or hydroxylysyl residues in oligopeptides and proteins that range from histone (1) to collagen and elastin (2). For polypeptides, the location and chemical properties of vicinal dicarboxylic amino acid residues adjacent to potentially oxidizable lysyl residues influence the efficiency of lysyl oxidation (3).

C. Enzyme Commission Designation

Lysyl oxidase is an amine oxidase with the numerical designation of EC 1.4.3.13.

II. PHYSIOLOGICAL IMPORTANCE

Lysyl oxidase is a key enzyme in the growth and development of all higher animals (4, 5). Both intracellular and extracellular forms of the enzyme exist. Although the mechanism(s) of action remains unclear, there is loss of expression of lysyl oxidase in malignant cells (6). It is speculated that the intracellular form(s) of lysyl oxidase targets oncogenic and growth-promoting transcription factors as substrates. Two examples are the RAS oncogene and IRF-1 transcription factor (7–9). Moreover, lysyl oxidase is also found in the cell nucleus (10).

Within the extracellular matrix (ECM), lysyl oxidase catalyzes the crosslinking of the collagens and elastin. Developmental processes beyond gastrulation are blocked when lysyl oxidase is inhibited (11–13).

For the food chemist, a general knowledge of lysyl oxidase function is essential. In general, the location and types of cross links in collagen and elastin have profound influence on their tensile and elastic properties. For example, an increase in the amount, or a change in the distribution, of crosslinked collagen in edible meats affects rheological properties (4, 14). In addition, crosslinking renders collagen and elastin less susceptible to proteolysis (15). Therefore, a decrease in lysyl oxidase activity is often associated with increased proteolysis of collagens and elastin, or altered tensile and elastic properties.

III. LOCATION IN TISSUES

Lysyl oxidase is found in highest concentrations in tissues enriched in collagen and elastin, ranging from 20 to 400 μg/g tissue (16). For cellular localization

studies, poly- or monoclonal antibodies have been used against lysyl oxidase or synthetic peptide sequences for a given form of lysyl oxidase. Methods for detection range from indirect immunofluorescence (17) to immunocytochemical approaches employing confocal microscopy (10). Four separate genes have been identified to date that may produce a distinct family of lysyl oxidase proteins (see below). Most of the comments herein apply to the forms of lysyl oxidase designated as 1 or 2 (also known as lysyl oxidase–like protein, LoxL). Lysyl oxidase 1 is usually found in tissues containing fibrillar collagens or elastin, whereas lysyl oxidase–like protein is often found in tissues enriched in nonfibrillar collagens, i.e., laminar or basement membrane collagens (2, 18).

Recently, lysyl oxidase–like 2 and 3 have also been identified as separate genes. LoxL 2 appears to be one of the lysyl oxidases that is involved in tumor suppression and is present in reproductive tissue (18–20). LoxL 3 has yet to be fully characterized, but it is expressed in response to cell senescence (21).

IV. COMMERCIAL APPLICATIONS

There are no commercial applications for the enzyme at this time. A potential long-range use of genetically engineered lysyl oxidase might be crosslinking of collagens for gelling purposes.

V. PHYSICAL AND CHEMICAL PROPERTIES

The descriptions that follow apply mostly to extracellular forms of lysyl oxidase.

A. Molecular Weight

Human lysyl oxidase is first expressed as a polypeptide of 417 amino acid residues (MW 48,000), including a signal peptide of 21 amino acids (Table 1; Fig. 1). The active form of the enzyme has a MW of $\sim$ 30,000.

B. Structural Characteristics

The translated primary amino acid sequences from human genomic, human, rat, and mouse lysyl oxidase cDNAs indicate a highly conserved primary structure. Likewise, computer-predicted secondary structure appears similar for lysyl oxidases from different animals (Fig. 1; Table 1).

C. Genes and Posttranslational Processing

1. Genes

The human lysyl oxidase gene resides on chromosome 5 while the mouse homologue is on chromosome 18 (22, 23). Three additional lysyl oxidase–like (LoxL) genes have also been identified. LoxL 1 is localized on chromosome 15 in humans (24). Its complete sequence is encoded by seven exons distributed throughout 25kb of genomic DNA. Exons 2–6 encode the region of greatest homology to lysyl oxidase. LoxL 2 maps to chromosome 8 (19). LoxL 2 (21) shares some sequence similarity to lysyl oxidase 1, e.g., 48% in protein domains transcribed and translated from exons 2–6. LoxL 3 is an 87-kDa protein and maps to human chromosome 2. This form of lysyl oxidase is also novel, since it contains four scavenger receptor cysteine-rich domains, which are not present in other known forms of lysyl oxidase.

Northern blot analysis of smooth muscle or fibroblast mRNA often results in two to four mRNA species of 5.5, 4.3, 2.4, and 2 kb in size (2) corresponding to lysyl oxidase and the lysyl oxidase–like proteins.

2. Posttranslational Processing

The "pre" part of pre-prolysyl oxidase is removed by a protease that cleaves at the peptide bond between Cys_{21} and Ala_{22} (Fig. 1), giving prolysyl oxidase. Prolysyl oxidase is N-glycosylated at two sites (residues 91–93 and 138–140 in the rat enzyme) in the region of the propeptide (Fig. 1; Table 1). These residues are lost when the propeptide is cleaved by a prolysyl-oxidase peptidase located on the external cell surface (2). For activation of lysyl oxidase, oxidation of a tyrosyl residue (Table 1) within the active site of the enzyme to peptidyl trihydroxyphenylalanine (TOPA) and eventually to the quinone, topaquinone (TPQ), or alternatively dihydroxyphenylalanine (DOPA), is essential. This cofactor is generated after copper is incorporated into the apoenzyme. In subsequent steps, a lysine derivative is formed—i.e., lysyl tyrosine quinone (Fig. 1) (25). This product is formed by the addition of the lysyl amine to topaquinone with the lost of water or by the direct addition to DOPA.

VI. ENZYMATIC PROPERTIES

A. Substrates

When synthetic oligopeptides are used as substrates, e.g. acetyl-$(Gly)_n$-Lys-$(Gly)_n$-$CONH_2$ ($n = 1$–5), the

Table 1 Rat Lysyl Oxidase: Amino Acid Sequence and Sites for Potential Posttranslational Modifications

1	NH_2-Met-Arg-Phe-Ala-Trp-Thr-Val-Leu-Phe-Leu-Gly-Gln-Leu-Gln-Phe-Cys-Pro-Leu-Leu-Arg-
21	*Cys-Als*-Pro-Gln-Ala-Pro-Arg-Glu-Pro-Pro-Ala-Ala-Pro-Gly-Ala-Trp-Arg-Gln-Thr-Ile-
41	Gln-Trp-Glu-Asn-Asn-Gly-Gln-Val-Phe-Ser-Leu-Leu-Ser-Leu-Gly-Ala-Gln-Tyr-Gln-Pro-
61	Gln-*Arg-Arg-Arg*-Asp-Ser-Ser-Ala-Thr-Ala-Pro-Arg-Ala-Asp-Gly-Asn-Ala-Ala-Ala-Gln-
81	Pro-Arg-Thr-Pro-Ile-Leu-Leu-Leu-Arg-Asp-*Asn-Arg-Thr*-Ala-Ser-Ala-Arg-Ala-Arg-Thr-
101	Pro-Ser-Pro-Ser-Gly-Val-Ala-Ala-Gly-Arg-Pro-Arg-Pro-Ala-Ala-Arg-His-Trp-Phe-Gln-
121	Val-Gly-Phe-Ser-Pro-Ser-Gly-Ala-Gly-Asp-Gly-Ala-Ser-*Arg-Arg*-Ala-Ala-*Asn-Arg-Thr*-
141	Ala-Ser-Pro-Gln-Pro-Pro-Gln-Leu-Ser-Asn-Leu-Arg-Pro-Pro-Ser-His-Val-Asp-Arg-Met-
161	Val-*Gly-Asp-Asp*-Pro-Try-Asn-Pro-Tyr-Lys-Try-Ser-Asp-Asp-Asn-Pro-Tyr-Tyr-Asn-
181	Tyr-Asp-Thr-Tyr-Glu-Arg-Pro-Arg-Ser-Gly-Ser-Arg-His-Arg-Pro-Gly-Tyr-Gly-Thr-Gly-
201	Tyr-Phe-Gln-Tyr-Gly-Leu-Pro-Asp-Leu-Val-Pro-Asp-Pro-Tyr-Tyr-Ile-Gln-Ala-Ser-Thr-
221	Tyr-Val-Gln-Lys-Met-Ser-Met-Tyr-Asn-Leu-Arg-Cys-Ala-Ala-Glu-Glu-Asn-Cys-Leu-Ala-
241	Ser-Ser-Ala-Tyr-Arg-Ala-Asp-Val-Arg-Asp-Tyr-Asp-His-Arg-Val-Leu-Leu-Arg-Phe-Pro-
261	Gln-Arg-Val-Lys-Asn-Gln-Gly-Thr-Ser-Asp-Phe-Leu-Pro-Ser-Arg-Pro-Arg-Tyr-Ser-Trp-
281	Glu-*Trp-His-Ser-Cys-His-Gln-His-Tyr-His-Ser*-Met-Asp-Glu-Phe-Ser-His-Tyr-Asp-Leu-
301	Leu-Asp-Ala-Ser-Thr-Gln-Arg-Arg-Val-Ala-Glu-Gly-His-*Lys*-Ala-Ser-Phe-Cys-Leu-Glu-
321	Asp-Thr-Ser-Cys-Asp-Tyr-Gly-Tyr-His-Arg-Arg-Phe-Ala-Cys-Thr-Ala-His-Thr-Gln-Gly-
341	Leu-Ser-Pro-Gly-Cys-Tyr-Asp-Thr-*Tyr*-Ala-Ala-Asp-Ile-Asp-Cys-Gln-Trp-Ile-Asp-Ile-
361	Thr-Asp-Val-Gln-Pro-Gly-Asn-Tyr-Ile-Leu-Lys-Val-Ser-Val-Asn-Pro-Ser-Tyr-Leu-Val-
381	Pro-Glu-Ser-Asp-Tyr-Ser-Asn-Asn-Van-Val-Arg-Cys-Glu-Ile-Arg-Tyr-Thr-Gly-His-His-
401	Ala-Tyr-Ala-Scr-Gly-Cys-Thr-Ilc-Scr-Pro-*Tyr-COOH*

Underlined and highlighted are sites associated with: leader sequence cleavage (*Cys-Ala*), glycosylations (*Ans-Arg-Thr*), prolysyl oxidase peptide cleavage to lysyl oxidase (*Gly-Asp-Asp*), potential trypsin-like proteinase cleavage sites (*Arg-Arg* and *Arg-Arg-Arg*), the proposed copper binding region (*Trp-His-Ser-Cys-His-Gln-His-Tyr-His-Ser*), and the location of the *Lys* and *Tyr* associated with lysine tyrosylquinone formation (39, 40, and Refs. cited).

k_{cat}/K_m increases with increasing peptide length. Insertion of a Glu residue immediately preceding the Lys residue causes an increase in the $k_{cat}/K_m \sim 10$-fold over that for -Lys-Glu- and about fivefold over sequences containing only Lys. Replacement of Glu with Gln increases the K_m and lowers k_{cat}/K_m. Changes in k_{cat}/K_m also respond to the carbon chain length of the vicinal amino acid at this position. In particular, decreasing the carbon chain length decreases k_{cat}/K_m (26, 27). For simple aliphatic mono- and particularly diamines, as the carbon chain length decreases, such compounds become poorer substrates; e.g., ethylenediamine is an irreversible inhibitor of lysyl oxidase (28). The K_ms for simple amine substrates are in the 100 μM to mM range (see Ref. 2 and Refs. cited within). The K_m for the oxidation of recombinant tropoelastin (MW $\sim$ 70,000, 56 residues of Lys per 1000 total residues) is $\sim 5\,\mu$M (29).

B. Effect of Environmental Factors

Lysyl oxidase is optimally active at pH 7.8–8.6 and 50–60°C. No externally added cofactors are required, since copper and TPQ are tightly associated with the enzyme.

C. Proposed Mechanism

Lysyl oxidase carries out oxidative deaminations by a classical Ping-Pong mechanism [Eqs. (2) and (3)]

$$\mathrm{A\,(RCH_2NH_2) + B(O_2) \longrightarrow P\,(RCHO) + Q\,(H_2O_2 \text{ and } NH_3)} \tag{2}$$

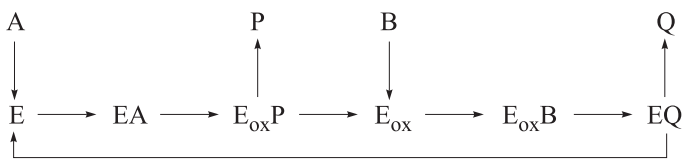

(3)

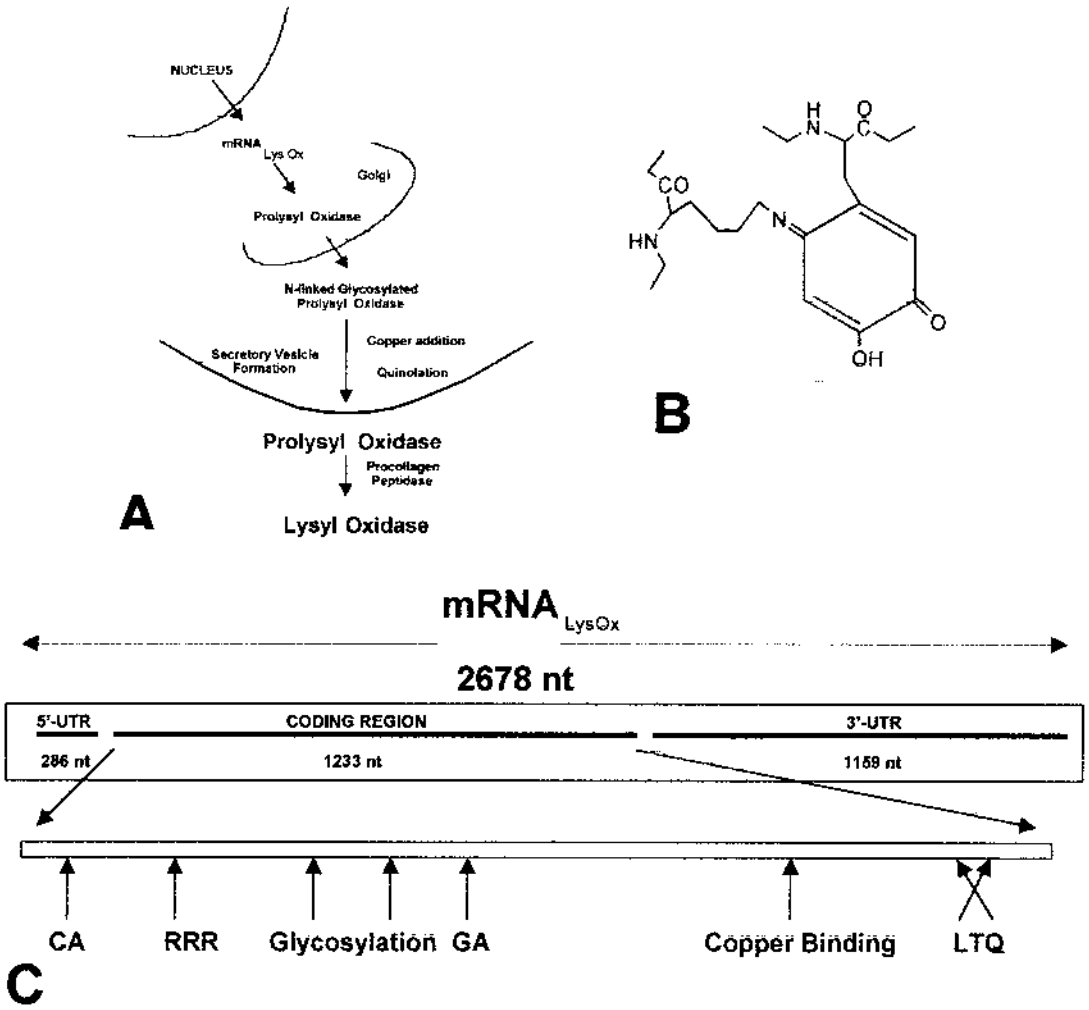

Figure 1 Lysyl oxidase processing. (A) Lysyl oxidase is first synthesized as a 46-kDa pre-proenzyme. In steps associated with Golgi and post-Golgi processing. N-linked glycosylation, copper binding, and quinone cofactor formation occur (5). A part of this process is the packaging of lysyl oxidase into vesicles for eventual secretion. At the cell surface, prolysyl oxidase is cleaved to lysyl oxidase by the same enzyme that carries out procollagen cleavage to collagen. (B) The figure insert shows the structure of lysyl tyrosine quinone. This cofactor is formed as a product of posttranslational modification following the insertion of copper into lysyl oxidase. (C) The diagram corresponds to lysyl oxidase mRNA. The size of the coding, 3′- and 5′-untranslated regions, and the approximate location of modifications that occur in pre-prolysyl oxidase are depicted. Lysyl oxidase mRNA arises from a gene that is ~ 15 kb.

Shah et al. (30) have studied selected aspects of this mechanism. To iterate, substrate efficiency often decreases with decreased carbon chain length. Regarding the two half reactions, enzyme reoxidization is the most rate-limiting step. ^{1}H NMR spectroscopy of the alcohol that is reductively derived (nonenzymatically) from the aldehyde product of the lysyl oxidase–catalyzed oxidation of deuterated tyramine indicates that the pro-S, but not the pro-R, alpha-deuteron is catalytically abstracted. As Shah et al. (30) noted, such stereospecificity and proton exchange uniquely differentiates lysyl oxidase from most of the other semicarbazide-sensitive amine oxidases.

D. Inhibitors

The most potent inhibitors are derivatives of semicarbazides and aminoallylnitriles, e.g., β-aminopropionitrile (BAPN). BAPN administration in vivo promotes

degeneration of arteries, increased friability of the skin, and bone fragility. In direct assays of lysyl oxidase activity, BAPN has a K_i of $\sim$ 10–20 μM. Other compounds that act as pseudo-substrates and/or potential inhibitors are the aminoalkylaziridines, homocysteine thiolactone, selenohomocysteine lactone, and homoserine lactone. Liu et al. (31) showed that the activities of plasma amine oxidase and diamine oxidase are only partially inhibited at concentrations of the sulfur or selenium lactones that fully inhibit lysyl oxidase. Homocysteine thiolactone, selenohomocysteine lactone, and homoserine lactone are found to be competitive, irreversible inhibitors of lysyl oxidase, with K_i values of $\sim$ 20, 8, and 420 μM, respectively. The first-order rate constants for inactivation (k_2) of the enzyme vary from 0.12 to 0.18 to 0.28 min^{-1} for the Se-, thio-, and *O*-lactones, respectively.

VII. DETERMINATION OF ACTIVITY

A. Natural Substrates

The classical substrate for assessing lysyl oxidase activity is prepared using aortae or calveria from 10- to 16-day-old chick embryos (32). Briefly, the aortae or calveria are incubated in Eagle's medium devoid of L-lysine, but containing ^{3}H-6-L-lysine or ^{3}H-4,5-L-lysine in amounts sufficient to cause 200,000–400,000 dpm ($\sim$ 3–6 kBq) of tritium to be incorporated per aorta or calveria. Standard procedures are used for the tissue culture (95/5% O_2/CO_2, 39–41°C for 18–24 h) employing vessels that allow convenient recovery of the tissue. BAPN is added at 50 μg/mL to inhibit endogenous lysyl oxidase activity. Usually 3–5 g fresh tissue (100–200 aortae) is cultured to prepare a single lot of substrate. Following incubation, the tissue is homogenized in saline containing 1 mM L-lysine. The tissue is recovered by centrifugation (10,000g, 30 min) and repeatedly washed to remove unincorporated radiochemically labeled L-lysine. Following a final wash in 0.01 M HCl, the tissue residue is lyophilized and stored at room temperature in a desiccator.

In typical assays, tissue extracts containing enzyme (equivalent of 250 ng or more of lysyl oxidase) are added to assay mixtures that contain at least one aorta or calveria equivalent of substrate suspended in 0.1 M sodium borate buffer containing 0.15 M NaCl, pH 8.0. The samples are next incubated at 45°C for 2, 4, 6, and 12 h (assay volume 1.5–2.0 mL). Assays are performed with substrate alone, with enzyme, or with enzyme preincubated for 30 min in the presence of 50 μM of β-aminopropionitrile/mL assay buffer. Released tritium is recovered by distillation.

Alternatively, the reactions may be stopped by the addition of 0.2 mL of 3 M trichloroacetic acid. Released tritium is determined after centrifugation of individual samples and passage of the supernatant fraction through a column of AG50W-X8(H) resin (1 × 4 cm). After a wash with two to three column volumes of distilled water, an aliquot of the combined fractions is assayed for radioactivity by liquid scintillation spectrometry (33). The data are expressed as radioactivity released per unit time per weight of tissue or unit of protein or DNA.

B. Simple Amine Substrates

The assay described by Trackman et al. (34) based on cadaverine oxidation is a good method for routine assays. However, the lysyl oxidase preparation must be free of endogenous inhibitors, high levels of catalase, and natural substrates (5). The assay also requires the equivalent of 1–2 μg of enzyme per assay. The oxidation of cadaverine is measured in a coupled assay system utilizing peroxidase to measure the H_2O_2 formed [see Eq. (1)]. In typical assays, samples (equivalent to 50–200 mg of tissue homogenate) are fragmented and ground in liquid nitrogen using a metal mortar and pestle. Next, readily soluble protein is extracted into 2–3 mL of phosphate-buffered (10 mM, pH 7.6) saline for 1–2 h. The tissue is recovered by centrifugation (10,000 g for 30 min), and the pellet is rehomogenized into 3 mL of 6 M urea buffered with 100 mM sodium borate at pH 8.2. This homogenate is extracted at least two times (4°C for 8–12 h) with agitation, and the supernatant fraction is collected (10,000 g for 30 min) and combined.

Assays (3 mL total volume) must contain 0.25 mg of sodium homovanillate, 40 μg horseradish peroxidase, urea extract (equivalent to $\sim$ 1 μg of lysyl oxidase; usually 0.5 mL urea extract), 3.33 mM cadaverine, and sodium borate buffer (50 mM, pH 8.2). The fluorescence resulting from homovanillate oxidation is monitored continuously at 315 nm excitation and 425 nm emission for 10–20 min at 45°C. Production of H_2O_2 is usually linear for 20–40 min. Lysine-rich peptides and proteins can also be used as substrates, if nM amounts of potentially oxidizable amine functions are present in the assay mixture. For example, if resources are available to prepare recombinant proteins, recombinant tropoelastin could be considered as a substrate (29).

Although aldehyde production and NH_3 can also be measured, the low sensitivity, inconvenience, and potential of interfering substances, e.g., NH_3 associated with the use of urea (see Sec. VIII), compromise their use for routine measurements or as endpoints for kinetic assays.

VIII. PURIFICATION

The methodological steps that follow may be applied to sources of lysyl oxidase containing > 50 μg enzyme/g tissue. In general, lysyl oxidase may be purified to homogeneity by differential extraction procedures and sequential chromatography using columns of collagen, elastin-hexylamine-Sepharose, DEAE-cellulose, and/or Sephacryl S-200. The end product is usually the activated or fully processed form of lysyl oxidase (~ 30 kDA). Lysyl oxidase from some tissues, e.g., skin, may copurify with an associated protein, a tyrosine-rich associated matrix protein (35).

A. Purification Steps (Table 2)

Step 1. To prepare connective tissue for subsequent homogenization, the tissue is frozen and pulverized in liquid nitrogen using a mortar and pestle or a blender vented to allow the escape of nitrogen. Next, the pulverized tissue (tendon, skin, aorta) is homogenized in phosphate-buffered (10 mM, pH 7.6) saline at 1 : 5 w/v. This step is repeated two or three times using the tissue pellet recovered following centrifugation (10,000g, 30 min at 4°C). At the onset of purification, it is important to remove endogenous inhibitors and native substrates that inhibit lysyl oxidase activity. Little lysyl oxidase activity is lost in these initial washes, since lysyl oxidase is tightly bound to the ECM (16 and Refs. cited within).

Step 2. The tissue is next homogenized in buffered 6 M urea (sodium borate or phosphate, 50 mM, pH 7.8–8.0). Three extractions (1 : 4 w/v) are repeated with constant agitation or stirring and are usually sufficient to extract all measurable activity. The enzyme is most easily concentrated by precipitation using ammonium sulfate. $(NH_4)SO_4$ is added to the combined urea extracts to 50% saturation. The resulting precipitate is collected by centrifugation (10,000g, 30 min).

Step 3. The product from Step 2 is next suspended in buffered 0.5 M urea to give ~ 20 mg protein per mL. $(NH_4)_2SO_4$ is removed (by dialysis against 0.5 M urea in 0.05 M sodium phosphate or borate buffer, pH 7.8–8.0) or chromatography on columns of Sephadex G-10 (Pharmacia Co., Uppsala, Sweden). Note, however, that the presence of some urea is essential in all subsequent steps to maintain lysyl oxidase in a nonaggregated state. If aggregated, there is loss of activity.

Step 4. Depending on the goal for the purification, either affinity chromatography or ion-exchange chro-

Table 2 Lysyl Oxidase Purification[a]

Steps	Volume (mL)	Total Protein (mg)	Specific activity[b]	Fold purification	Recovery (%)
1. PBS extraction[b]	150	~ 3000–6000[c]	NA[c]	—	—
2. Urea extraction	120	500–600[d]	0.8–0.9	~ 1	~ 100[d]
3. Concentration $(NH_4)_2SO_4$	10	300–400	1.1–1.5	~ 1.3	~ 100
4. Dialysis	25	300–400	0.9–1.1	~ 1.1	~ 100
5. Sephacryl S-200/elastin[e,f]	10	6	65–70	70–80	90–95
or					
6. DEAE-cellulose chromatography[e,f]	50	40–60	100–150	125–190	50–60
7. HPLC[g]	1	2–3	~ 200	~ 200	40–70

[a] The summary is based on using 10 g of chick tendon as the enzyme source, which normally contains 200 $\mu g/g$ or more lysyl oxidase.
[b] Greater than 85–90% of the total protein in tendon is collagen. This amount reflects the total protein homogenized into phosphate buffered saline, pH 7.0 (PBS). All of the extracted protein at this step is discarded.
[c] One unit of activity is the production of one nanomol of H_2O_2/min/mg protein.
[d] About 15% of the total initial protein is extracted into urea and > 90% of the total enzyme (16). For purposes of estimating indices of purification and recovery, this step is set at onefold and 100%, respectively.
[e] Affinity chromatography often results in > 50-fold purification in a single step and enzyme that is > 20% pure based on assessment using polyacrylamide gels. DEAE-cellulose chromatography may be useful in separating specific forms of isoforms of lysyl oxidase (see Fig. 2).
[f] High-performance liquid chromatography yields a product (following Step 5 or 6) that is suitable for amino acid sequencing.
[g] From Ref. 38.

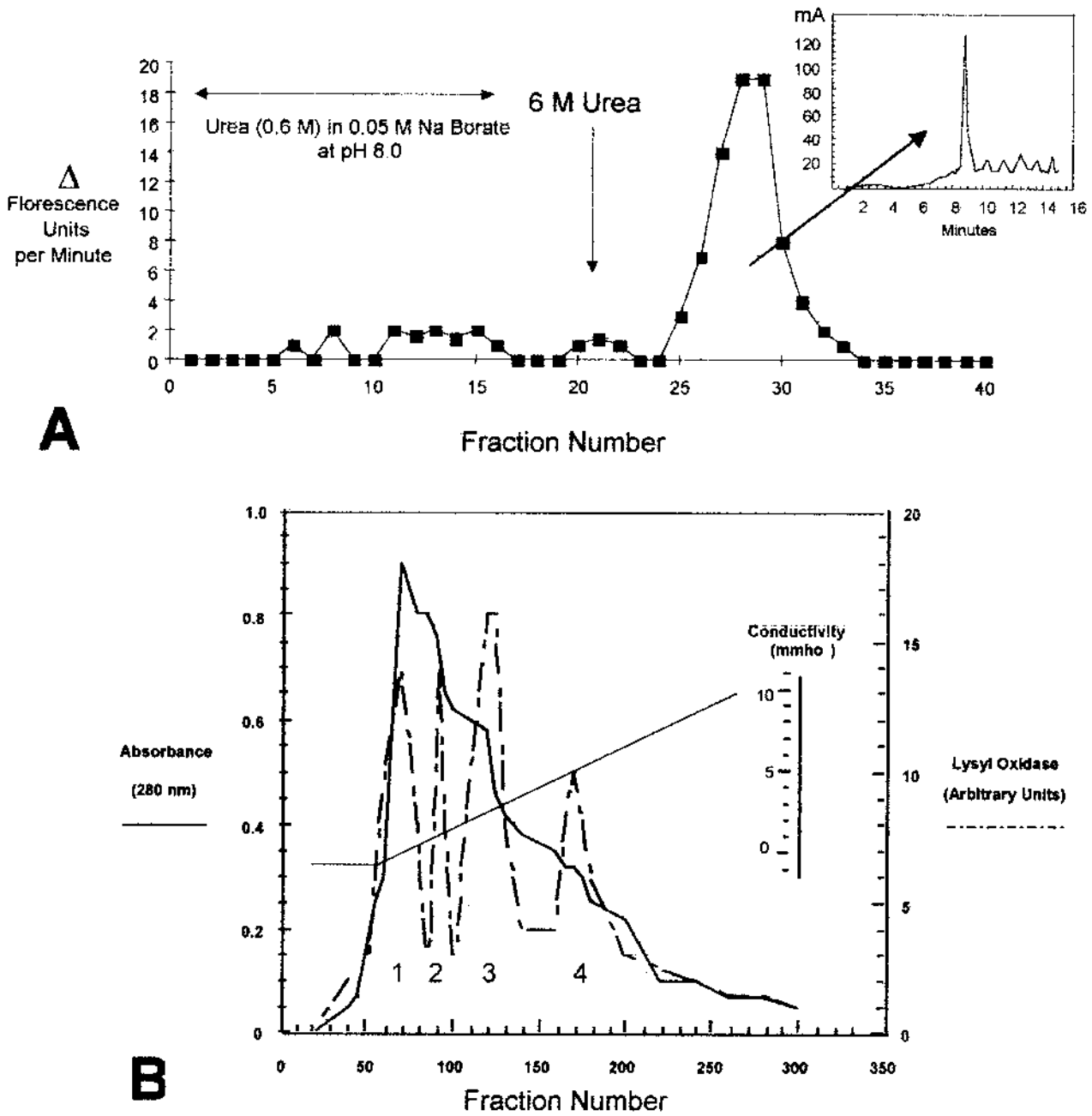

Figure 2 Lysyl oxidase purification. (A) Lysyl oxidase binds to Sephacryl S-200. An elution profile for lysyl oxidase indicates that the enzyme is released only upon addition of 6 M urea. Further purification can be achieved by reversed-phase HPLC chromatography using conventional protocols for protein and peptide elution (small insert). (B) Separation of lysyl oxidase isoforms may be achieved using ion exchange chromatography. The elution of lysyl oxidase from skin, tendon, lung, or aorta from DEAE-cellulose. Columns result in four distinct isoforms, which are immunologically indistinguishable. The protein is applied in starting buffer (0.025 M sodium phosphate, pH 7.6, containing 6 M urea). Elution is achieved with a linear gradient of NaCl (equivalent to increasing the conductivity from ~ 0 to ~ 10 mmho).

matography is useful as a next step. At urea concentrations of < 1.0 M, lysyl oxidase binds tenaciously to columns of Sephacryl S-200, and elution can only be achieved using buffers containing 4–6 M urea (see Ref. 36 for additional details). The choice of column size depends on the amount of protein applied. Approximately 3 mL of hydrated gel/10–15 mg protein is adequate. Columns composed of Sephacryl S-200 and insoluble elastin (mixed 3 : 1 w/v) further improve resolution and separation from other proteins (Fig. 2). The dialyzed urea extract is loaded onto a Sephacryl S-200/insoluble elastin column. The column is washed with 3–5 column volumes of buffered 0.5 M urea (Step 3). Lysyl oxidase is then eluted with 6 M buffered urea. Columns of collagen and hexylamine-Sepharose, which are available commercially (Elastin Products, St. Louis, MO), can also be used instead of Sephacryl. At this point the enzyme is usually sufficiently pure for enzymatic studies, such as defining inhibitor profiles.

Step 5. If further purification is required, DEAE-cellulose chromatography or reversed-phase HPLC is an option. Prior to or following Sephacryl chromatography, selected fractions may be pumped onto columns of DEAE-cellulose (see Fig. 2). Lysyl oxidase often elutes as four chromatographically different isoforms, although distinguishing features that give rise to such forms have not been fully assessed (37). Reversed-phase HPLC (Fig. 2) can yield products that are suitable for amino acid sequencing (38).

Step 6. The enzyme is best stored at 4°C in 2–4 M urea solutions at concentrations of 20–40 μg/mL. Freezing or concentration, which results in aggregation, causes rapid loss of activity, i.e., in hours to a few days (16).

REFERENCES

1. HM Kagan, MA Williams, SD Calaman, EM Berkowitz. Histone H1 is a substrate for lysyl oxidase and contains endogenous sodium borotritide reducible residues. Biochem Biophys Res Commun 115:186–192, 1983.
2. LI Smith-Mungo, HM Kagan. Lysyl oxidase: properties, regulation and multiple functions in biology. Matrix Bio 16:387–398, 1998.
3. HM Kagan, MA Williams, PR Williamson, JM Anderson. Influence of sequence and charge on the specificity of lysyl oxidase toward protein and synthetic peptide substrates. J Biol Chem 259:11203–11207, 1984.
4. L Knott, AJ Bailey. Collagen cross-links in mineralizing tissues: a review of their chemistry, function, and clinical relevance. Bone 22:181–187, 1998.
5. RB Rucker, T Kosonen, MS Clegg, AE Mitchell, BR Rucker, JY Uriu-Hare, CL Keen. Copper, lysyl oxidase, and extracellular matrix protein cross-linking. Am J Clin Nutr 67:996S–1002S, 1998.
6. K Kenyon, S Contente, PC Trackman, J Tang, HM Kagan, RM Friedman. Lysyl oxidase and rrg messenger RNA. Science 253:802–804, 1991.
7. K Kenyon, WS Modi, S Contente, RM Friedman. A novel human cDNA with a predicted protein similar to lysyl oxidase maps to chromosome 15q24-q25. J Biol Chem 268:18435–18437, 1993.
8. C Ren, G Yang, TL Timme, TM Wheeler, TC Thompson. Reduced lysyl oxidase messenger RNA levels in experimental and human prostate cancer. Cancer Res 58:1285–1290, 1998.
9. RS Tan, T Taniguchi, H Harada. Identification of the lysyl oxidase gene as target of the antioncogenic transcription factor, IRF-1, and its possible role in tumor suppression. Cancer Res 56:2417–2421, 1996.
10. W Li, K Nellaiappan, T Strassmaier, T Graham, KM Thomas, HM Kagan. Localization and activity of lysyl oxidase within nuclei of fibrogenic cells. Proc Natl Acad Sci USA 94:12817–12822, 1997.
11. E Butler, J Hardin, S Benson. The role of lysyl oxidase and collagen crosslinking during sea urchin development. Exp Cell Res 173:174–182, 1987.
12. G Wessel, D McClay. Gastrulation in the sea urchin embryo requires the deposition of crosslinked collagen with the extracellular matrix. Dev Biol 121:149–165, 1987.
13. A Di Donato, JC Lacal, M Di Duca, M Giampuzzi, G Ghigger, R Gusmano. Microinjection of recombinant lysyl oxidase blocks oncogenic p21-Ha-Ras and progesterone effects on *Xenopus laevis* oocyte maturation. FEBS Lett 419:63–68, 1997.
14. K Reiser, RJ McCormick, RB Rucker. The enzymatic and non-enzymatic crosslinking of collagen and elastin. FASEB J 6:2439–2449, 1992.
15. D Tinker, N Romero-Chapman, K Reiser, D Hyde, R Rucker. Elastin metabolism during recovery from impaired crosslink formation. Arch Biochem Biophys 278:326–332, 1990.
16. RB Rucker, N Romero-Chapman, T Wong, J Lee, J Uriu-Hare, C Keen. Modulation of lysyl oxidase by dietary copper in rats. J Nutr 126:51–60, 1996.
17. M Chanoki, M Ishii, H Kobayashi, H Fushida, N Yashiro, T Hamada, A Ooshima. Increased expression of lysyl oxidase in skin with scleroderma. Br J Dermatol 133:710–715, 1995.
18. M Decitre, C Gleyzal, M Raccurt, S Pcyrol, E Aubert-Foucher, K Csiszar, P Sommer. Lysyl oxidase–like protein localizes to sites of de novo fibrinogenesis in

fibrosis and in the early stromal reaction of ductal breast carcinomas. Lab Invest 78:143–151, 1998.
19. C Jourdan–Le Saux, O Le Saux, T Donlon, CD Boyd, K Csiszar. The human lysyl oxidase–related gene (LOXL2) maps between markers D8S280 and D8S278 on chromosome 8p21.2-p21.3. Genomics 51:305–307, 1998.
20. CJ Le Saux, H Tronccker, L Bogic, GD Bryant-Greenwood, CD Boyd, KY Csiszar. The LOXL2 gene encodes a new lysyl oxidase–like protein and is expressed at high levels in reproductive tissues. J Biol Chem 274:12939–12944, 1999.
21. H Saito, J Papaconstantinou, H Sato, S Goldstein. Regulation of a novel gene encoding a lysyl oxidase–related protein in cellular adhesion and senescence. J Biol Chem 272:8157–8160, 1997.
22. ER Hamalainen, R Kemppainen, T Pihlajanicmi, KI Kivirikko. Structure of the human lysyl oxidase gene markers D8S280 and D8S278 on chromosome 8p21.2–p21.3. Human Genet 101:198–200, 1993.
23. TJ Mariani, PC Trackman, HM Kagan, RL Eddy, TB Shows, CD Boyd, SB Deak. The complete derived amino acid sequence of human lysyl oxidase and assignment of the gene to chromosome 5 (extensive sequence homology with the murine ras recision gene). Matrix 12:242–248, 1992.
24. Z Szabo, E Light, CD Boyd, K Csiszar. The human lysyl oxidase–like gene maps between STS markers D15S215 and GHLC.GCT7C09 on chromosome 15. Hum Genet 101:198–200, 1997.
25. SX Wang, N Nakamura, M Murc, JP Klinman, J Sanders-Lochr. Characterization of the native lysine tyrosylquinone cofactor in lysyl oxidase by Raman spectroscopy. J Biol Chem 272:28841–28844, 1997.
26. N Nagan, HM Kagan. Modulation of lysyl oxidase activity toward peptidyl lysine by vicinal dicarboxylic amino acid residues. Implications for collagen cross-linking. J Biol Chem 269:22361–22367, 1994.
27. N Nagan, PS Callcry, HM Kagan. Aminoalkylaziridines as substrates and inhibitors of lysyl oxidase: inactivation of the enzyme by N-(5-aminopentyl)aziridine. Frontiers Biosci 3:23–26, 1996.
28. SN Gacheru, PC Trackman, MA Shah, CY O'Gara, P Spacciapoli, FT Greenway, HM Kagan. Structural and catalytic properties of copper in lysyl oxidase. J Biol Chem 265:19022–19027, 1990.
29. D Bedell-Hogan, P Trackman, W Abrams, J Rosenbloom, H Kagan. Oxidation, cross-linking, and insolubilization of recombinant tropoelastin by purified lysyl oxidase. J Biol Chem 268:10345–10350, 1993.
30. MA Shah, CH Scaman, MM Palcic, HM Kagan. Kinetics and stereospecificity of the lysyl oxidase reaction. J Biol Chem 268:11573–11579, 1993.
31. G Liu, K Nellaiappan, HM Kagan. Irreversible inhibition of lysyl oxidase by homocysteine thiolactone and its selenium and oxygen analogues. Implications for homocystinuria. J Biol Chem 272:32370–32377, 1997.
32. SR Pinnell, GR Martin. The cross-linking of collagen and elastin: enzymatic conversion of lysine in peptide linkage to alpha-aminoadipic-delta-semialdehyde (allysine) by an extract from bone. Proc Natl Acad Sci USA 61:708–716, 1968.
33. B Peterkofsky, R DiBlasio. Modification of the tritium-release assays for prolyl and lysyl hydroxylase using Dowex-50 columns. Anal Biochem 66:279–286, 1975.
34. PC Trackman, CG Zoski, HM Kagan. Development of a peroxidase-coupled fluorometric assay for lysyl oxidase. Anal Biochem 113:336–342, 1981.
35. C Domenicucci, HA Goldberg, J Sodek. Identification of lysyl oxidase and TRAMP as the major proteins in dissociative extracts of the demineralized collagen matrix of porcine dentine. Connec Tissue Res 36:151–163, 1997.
36. DR Shackleton, DJS Hulmes. Purification of lysyl oxidase from piglet skin by selective interaction with Sephacryl S-200. Biochem J 266:917–919, 1990.
37. HM Kagan, P Cai. Isolation of active site peptides of lysyl oxidase. Methods Enzymol 258:122–132, 1995.
38. R Ferrera, B Faris, PJJR Mogayzel, WA Gonnerman, C Franzblau. A micromethod for the purification of lysyl oxidase. Anal Biochem 126:312-317, 1982.
39. HM Kagan, PC Trackman. Lysyl oxidase. In VL Davidson, ed, Principles and Applications of Quinoprotein. New York: Marcel Dekker, 1993, pp 173–189.
40. AC Rinaldi, A Rescigno, A Rinaldi, E Sanjust. Modeling novel quinocofactors: an overview. Bioorganic Chem 27:253–288, 1999.

38

Superoxide Dismutase

Hirokazu Hara, Tetsuo Adachi, and Kazuyuki Hirano
Gifu Pharmaceutical University, Gifu, Japan

I. INTRODUCTION

Superoxide (O_2^-), a free radical generated during the monovalent metabolic reduction of oxygen, is toxic to biological systems. The major enzymatic protector against superoxide in the body is superoxide dismutase (SOD; EC 1.15.1.1) which disproportionates the superoxide to hydrogen peroxide (H_2O_2) and oxygen as follows:

$$O_2^- + O_2^- + 2H^+ \xrightarrow{SOD} H_2O_2 + O_2$$

Mitochondria and endoplasmic reticulum have been shown to produce superoxide as a consequence of autooxidation of electron transport chain components. Other sources of superoxide are cytosolic enzymes such as xanthine oxidase, and activated neutrophils. Under physiological conditions, the nonenzymatic dismutation of superoxide proceeds with a rate constant of approximately $k = 10^5\,M^{-1}\,sec^{-1}$, and the reaction is accelerated by a factor of 10^4 in the presence of SOD.

II. DISTRIBUTION OF SOD

SODs are proteins with metal ions at the active site. Four isoforms, copper,zinc-SOD (Cu,Zn-SOD), extracellular-SOD (EC-SOD), manganese-SOD (Mn-SOD), and iron-SOD (Fe-SOD), have been isolated so far from many species, and the cellular distribution pattern of these isoforms has been determined (1). Cu,Zn-SOD and EC-SOD, which are known to contain copper and zinc atoms, are found in eukaryotes. Cu,Zn-SOD has been found in many kinds of animals (vertebrates and invertebrates), fungi and slime molds, and plants, and EC-SOD has been found in mammals and in pine trees. Fe-SOD and Mn-SOD are found in prokaryotes and in eukaryotes. Mn-SOD has been found in mammals, while Fe-SOD has not.

The cellular localization of Cu,Zn-SOD is different from that of EC-SOD. Cu,Zn-SOD is located in the cytosol and the stroma of chloroplasts, while EC-SOD is mostly located in the extracellular matrix, since it is a secretory protein and has an affinity for heparin and heparan sulfate. Mn-SOD is located in the mitochondrial matrix and the thylakoids of chloroplasts. Fe-SOD is found in the cytosol of bacteria and the stroma of chloroplasts.

The contents of Cu,Zn-SOD, Mn-SOD, and EC-SOD were determined in tissues from mammalian species (2). Various tissues contain the Cu,Zn-SOD activity, and Cu,Zn-SOD activities are especially high in metabolically active organs, such as liver and kidney. The Mn-SOD content is high in organs with high respiration, such as liver, kidney, and heart. The tissue distribution of EC-SOD is different from those of other isoforms, and it is present at high levels in lung, thyroid gland, and uterus. EC-SOD is the least abundant SOD isoform in tissues, and 90–99% of the EC-SOD in the body is located in the interstitial spaces of tissues. EC-SOD is a major SOD form in extracellular fluids such as plasma, lymph, and synovial fluid. Recently, it was reported that the blood vessel walls, particularly the walls of the arteries, contain large amounts of EC-SOD (3).

III. PROPERTIES OF SOD PROTEINS

The characteristics of three SOD isoforms—Cu,Zn-SOD, Mn-SOD, and EC-SOD—are presented in Table 1. A comparison of the primary structures of several Cu,Zn-SODs are presented in Figure 1, and the sequences of human Cu,Zn-SOD and EC-SOD are shown in Figure 2.

Cu,Zn-SOD is a homodimer in which each subunit has one copper and one zinc atom. The molecular weight of Cu,Zn-SOD is ~ 32,000. The amino acid sequences of Cu,Zn-SODs have been determined in various species. Human Cu,Zn-SOD consists of 153 amino acid residues. The amino acid sequences of various mammalian Cu,Zn-SOD show > 80% identity but are significantly different from those in yeast (~ 50% identity) and spinach (~ 50% identity) (Fig. 1) (4). The amino acid residues at the active site responsible for binding Cu and Zn, and the cysteine residues of a disulfide bond, are conserved in various species. The crystal structure analysis of bovine Cu,Zn-SOD at 2 Å resolutions was reported, and the disulfide bond, the metal atoms, and the amino acid residues to which they are bound were identified (5). Each subunit of Cu,Zn-SOD is composed primarily of eight antiparallel β-strands that form a flattened cylinder, plus three external loops. The Cu atom is bound by His44, -46, -61, and -118 of bovine enzymes (His46, -48, -63, and -120 in human) with an uneven tetrahedral distortion from square planar geometry. The geometry of Zn atom ligands, His61, -69, -78, and Asp81 of bovine enzymes (His63, -71, -80, and Asp83 in human), is tetrahedral. The cysteine residues forming an intrasubunit disulfide bond Cys55-Cys144 of bovine enzyme (Cys57-Cys146 in human) are conserved in the primary structure of Cu,Zn-SODs (Fig. 1).

Table 1 Comparison of Human SOD Isoforms

	Cu,Zn-SOD	Mn-SOD	EC-SOD
Chromosomal location	21q22.1	6q25.2	4p16.3-q21
Amino acid length	153	198	222
Predicted MW	32 kDa	80 kDa	135 kDa
Subunit structure	dimer	tetramer	tetramer
Glycosylation	—	—	+
Heparin affinity	—	—	+

Recently a cDNA of EC-SOD was isolated from a human placenta cDNA library and the primary structure of the enzyme was determined (6). Human EC-SOD is a tetrametric glycoprotein containing one copper and one zinc atom per one subunit. The molecular weight of EC-SOD is ~ 135,000. EC-SOD has a putative signal sequence (18 amino acid residues), and the mature enzyme of EC-SOD consists of 222 amino acid residues. The presence of the signal sequence indicates

```
                 ** **     * *   *                 *       *** *  ** * **
HUMAN       ATKAVCVLKGDGPVQGIINFEQKESNGPVKVWGSIKGLT-EGLHGFHVHEFGDNTAGCTS 59
RAT         AMKAVCVLKGDGPVQGVIHFEQKASGEPVVVSGQITGLT-EGEHGFHVHQYGDNTQGCTT 59
BOVINE      ATKAVCVLKGDGPVQGTIHFEAK--GDTVVVTGSITGLT-EGDHGFHVHQFGDNTQGCTS 57
HORSE       ALKAVCVLKGDGPVHGVIHFEQQQEGGPVVLKGFIEGLT-KGDHGFHVHEFGDNTQGCTT 59
YEAST       -VQAVAVLKGDAGVSGVVKFEQASESEPTTVSYEIAGNSPNAERGFHIHEFGDATNGCVS 59
SPINACH     MGKAVVVLSSSEGVSGTVYFAQEG-DGPTTVTGNVSGLK-PGLHGFHVHALGDTTNGCMS 58

                 * * **    ** * *  ** ** **      * *     *  * * *     **  *
HUMAN       AGPHFNPLSRKHGGPKDEERHVGDLGNVTADKDGVADVSIEDSVISLSGDHCIIGRTLVV 119
RAT         AGPHFNPHSKKHGGPADEERHVGDLGNVAAGKDGVANVSIEDRVISLSGEHSIIGRTMVV 119
BOVINE      AGPHFNPLSKKHGGPKDEERHVGDLGNVTADKNGVAIVDIVDPLISLSGEYSIIGRTMVV 117
HORSE       AGAHFNPLSKKHGGPKDEERHVGDLGNVTADENGKADVDMKDSVISLSGKHSIIGRTMVV 119
YEAST       AGPHFNPFKKTHGAPTDEVRHVGDMGNVKTDENGVAKGSFKDSLIKLIGPTSVVGRSVVI 119
SPINACH     TGPHYNPNGKEHGAPEDDVRHAGDLGNITVGDDGTATFTIIDSQIPLSGPNSIVGRAVVV 118

                 *   **** *  * *  ***** * *** **
HUMAN       HEKADDLGKGGNEESTKTGNAGSRLACGVIGIAQ 153
RAT         HEKQDDLGKGGNEESTKTGNAGSRLACGVIGIAQ 153
BOVINE      HEKPDDLGRGGNEESTKTGNAGSRLACGVIGIAK 151
HORSE       HEKQDDLGKGGNEESTKTGNAGSRLACGVIGIAP 153
YEAST       HAGQDDLGKGDTEESLKTGNAGPRPACGVIGLTN 153
SPINACH     HAEPDDLGRGGHELSKTTGNAGGRVACGIIGLQG 152
```

Figure 1 Comparison of amino acid sequences of human, rat, bovine, horse, yeast, and spinach Cu,Zn-SODs. Asterisks indicate identical amino acid residues.

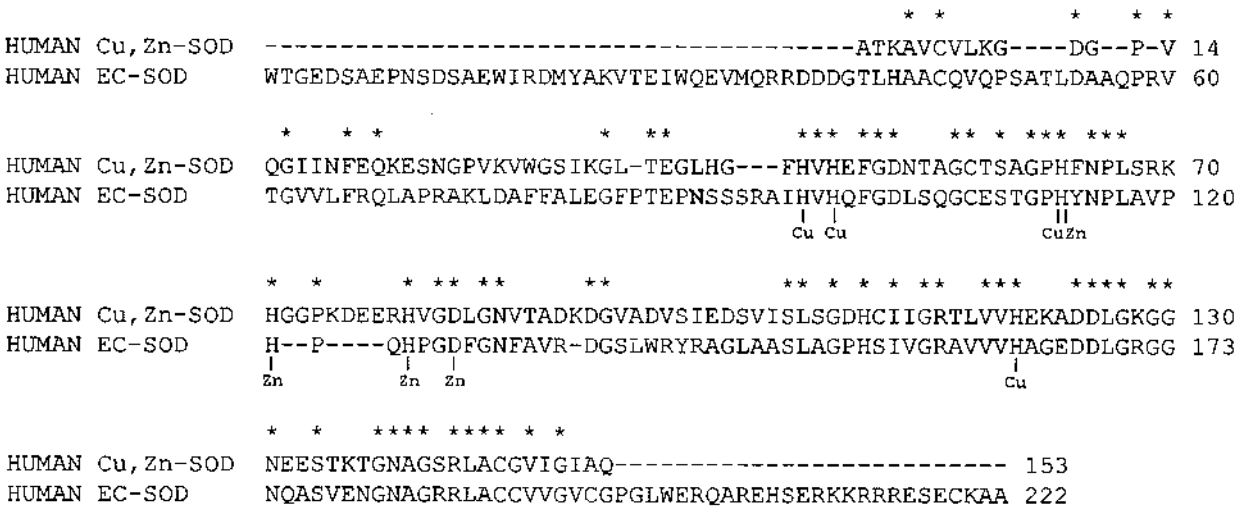

Figure 2 Comparison of amino acid sequences of human Cu,Zn-SOD and human EC-SOD. Asterisks indicate identical amino acid residues. The bold letter indicates the N-glycosylation site. Cu and Zn indicate amino acid residues binding the metals. Cysteine residues forming a disulfide bond are Cys-57-Cys-146 in Cu,Zn-SOD and Cys-107-Cys-189 in EC-SOD.

that EC-SOD is a secreted protein. The N-terminal region (amino acid residues 1–95) of the mature enzyme shows no homology with other proteins, but the region corresponding to amino acid residues 96–193 shows $\sim 50\%$ homology with the carboxyl-terminal two-thirds of the sequences of eukaryotic Cu,Zn-SODs. The amino acid residues binding the Cu and Zn atoms (Cu atom ligands His96, -98, -113, and His163; Zn atom ligands His113, -121, -124, and Asp127) and the cysteines forming the intrasubunit disulfide bridge (Cys107-Cys189) in EC-SOD can all be identified with corresponding residues in Cu,Zn-SOD (Fig. 2). The carboxyl-terminal region (194–222), including nine amino acids with a positive charge, confers the affinity of EC-SOD for heparin and heparan sulfate. There is one deduced N-glycosylation site (Asn89).

The primary structure and three-dimensional structure of Mn-SOD show no homologies with those of Cu,Zn-SOD or EC-SOD (7).

IV. PROPERTIES OF ENZYMES

The rate constants of the catalytic reactions of all of the SOD isoforms are very similar, with values of $\sim 1 \times 10^9\ M^{-1}\,sec^{-1}$(1). The enzymatic activities of Cu,Zn-SOD and EC-SOD are stable over a wide pH range, from pH 5 to 11 (8, 9). On the other hand, Mn-SOD has a lower pH resistance than other isoforms (8). SOD is a heat-stable enzyme, and Cu,Zn-SOD and EC-SOD are especially stable, up to 70°C, while Mn-SOD is stable up to 60°C (8, 9).

Since the central core active site portions of Cu, Zn-SOD and EC-SOD are conserved, the enzymatic properties of the two enzymes are very similar. However, the properties of Mn-SOD, which has no structural homology of active site with that of Cu,Zn-SOD and EC-SOD, are significantly different from those of the other two enzymes. Both Cu,Zn-SOD and EC-SOD are very sensitive to cyanide. The values of the IC_{50} of cyanide for human Cu,Zn-SOD and human EC-SOD are $10\,\mu M$ and $3\,\mu M$, respectively (10). In contrast, Mn-SOD is insensitive to cyanide and the enzymatic activity of Mn-SOD is not inhibited at 10 mM cyanide (11). All SOD isoforms are inhibited by azide. The values of the IC_{50} of azide for Cu,Zn-SOD, Mn-SOD, and EC-SOD are 21, 20, and 6.5 mM, respectively (10, 12). Cu,Zn-SOD and EC-SOD are sensitive to H_2O_2, while Mn-SOD is resistant to it (10, 11). Cu,Zn-SOD and EC-SOD are inactivated at 1 mM H_2O_2 with half-times of 9.3 and 6.2–7.1 min, respectively.

V. QUALITATIVE AND QUANTITATIVE DETERMINATION

Several methods for assaying SOD, such as the cytochrome C assay (13), nitro blue tetrazolium (NBT) assay (14, 15), nitrite assay (16), KO_2 assay (17), and enzyme-linked immunosorbent assay (ELISA) (18) have been reported. There are three SOD isozymes in eukaryotes and they have similar specific activity. The methods for assaying SOD activity (13–17) show total

SOD activity. When we want to know the activity of one of the SOD isozymes, it is necessary to separate them with reagents such as NaCN (for Mn-SOD) or pretreatment of samples with concanavalin A–Sepharose column (for EC-SOD) and/or immobilized antibodies (2). It is possible to assay one of the SOD isozymes exclusively with ELISA, because there are no immunological cross-reactivities among three SOD isozymes. ELISA is not a method for the assay of SOD activity, but rather for SOD protein measurement, while the other methods (13–17) are for the assay of activity. We describe here the procedure for the NBT assay and ELISA.

A. NBT Assay

This assay was originally reported by Beauchamp and Fridovich (14). SOD catalyzes the dismutation reaction of superoxide generated by the xanthine-xanthine oxidase reaction. However, since superoxide cannot easily be detected directly by conventional analytical tools, this assay utilizes NBT as an indicator of superoxide. The SOD activity is defined as the ability to inhibit the reduction of NBT caused by superoxide. One unit of SOD activity is defined as the amount of protein which gives half-maximal inhibition. The SOD activity is usually expressed as units per milligram protein. The following NBT assay was reported by Oberley and Spitz (15). Diethylenetriaminepentaacetic acid (DETAPAC) is used as chelator in this assay to suppress interference by metal ions. Catalase is also necessary for protection of SODs against inactivation by H_2O_2 formed in the reaction.

1. Reagents

50 mM potassium phosphate buffer, pH 7.8

Solution A: 50 mM potassium phosphate buffer, pH 7.8, containing 1.33 mM DETAPAC

Xanthine solution (prepare fresh every week): 1.8 mM xanthine in 50 mM potassium phosphate buffer, pH 7.8.

NBT solution (keep in brown bottle): 2.24 mM NBT in 50 mM potassium phosphate buffer, pH 7.8

Catalase solution: 40 units/mL catalase in 50 mM potassium phosphate buffer, pH 7.8

Xanthine oxidase solution (diluted only at time of assay): about 10^{-2} units/mL xanthine oxidase in solution A

The final concentrations of the above reagents are 1 mM DETAPAC, 1 unit/mL catalase, 56 μM NBT, and 100 μM xanthine.

2. Procedure

1. Mix the following solution for a 20-sample assay: 13 mL solution A, 0.5 mL catalase solution, 0.5 mL NBT solution, 1.1 mL xanthine solution, and 0.9 mL 50 mM potassium phosphate buffer, pH 7.8 (to measure total SOD activity), or 0.1 M NaCN in the buffer (to measure Mn-SOD activity).
2. Add 800 μL of this solution to a cuvette.
3. Add 100 μL of standard SOD or sample to the cuvette.
4. Add 100 μL xanthine oxidase solution to the cuvette.
5. Mix and monitor at 560 nm by spectrophotometer for several minutes.

3. Comments

Dilute xanthine oxidase with solution A until the change of the absorbance rate without SOD (blank) is between 0.015 and 0.025/min at 560 nm.

The change of the absorbance rate is recorded for at least 2 min after a good straight line is first obtained.

To measure the Mn-SOD activity, the xanthine oxidase solution is added after the reaction mixture is incubated in the presence of 5 mM NaCN (final concentration) for at least 30 min and no more than 2 h.

It is necessary that NBT reductase activity and xanthine oxidase inhibitory activity in tissues are checked when SOD activities in extracts of tissues are measured.

B. Enzyme-Linked Immunosorbent Assay

ELISA is a convenient and sensitive assay for the measurement of SODs. ELISAs for each of the SOD isoforms have been developed by various investigators. We describe here the procedure of ELISA for human Cu,Zn-SOD in our laboratory (19).

1. Reagents

Coating buffer: 50 mM sodium carbonate buffer, pH 9.5, containing 0.02% sodium azide

Washing buffer: 10 mM sodium phosphate buffer, pH 7.4, containing 150 mM NaCl, 0.05% Tween 20, and 0.02% sodium azide

Blocking buffer: 10 mM sodium phosphate buffer, pH 7.4, containing 150 mM NaCl, 0.05% Tween 20, 0.02% sodium azide, and 1% bovine serum albumin (BSA)

Substrate solution: 0.1 M diethanolamine hydrochloride, pH 9.8, containing 0.5 mM $MgCl_2$, 0.02% sodium azide, and 2.7 mM *p*-nitrophenylphosphate

5 N NaOH

Antibody against Cu,Zn-SOD

Alkaline phosphatase-labeled antibody against Cu,Zn-SOD

2. Procedure

1. Add 80 μL of 50 μg/mL Cu,Zn-SOD antibody dissolved in coating buffer to each well of a 96-well immunoplate, and leave the plate to stand overnight at 4°C.
2. Wash each well with washing buffer.
3. Add 300 μL blocking buffer to block the remaining protein-binding sites, and leave the plate to stand at 4°C until use. Remove the blocking buffer before use.
4. Add 70 μL sample or standard diluted with blocking buffer to the wells, and incubate the plate for 2 h at room temperature.
5. Wash three times with washing buffer.
6. Add 80 μL alkaline phosphatase-labeled Cu,Zn-SOD antibody diluted with blocking buffer to each well, and incubate the plate for 2 h at room temperature.
7. Wash three times with washing buffer.
8. Add 150 μL substrate solution to each well, and incubate the plate for 30 min at room temperature.
9. Stop the enzyme reaction by the addition of 50 μL of 5 N NaOH.
10. Measure the absorbance at 415 nm.

VI. PURIFICATION

Since Cu,Zn-SOD was first isolated from bovine erythrocytes in 1969 (13), Cu,Zn-SOD and other isoforms have been purified from various species (20–22). Generally, the purification of Cu,Zn-SOD was carried out by means of extraction with organic solvent, anion-exchange column chromatography, and gel filtration. We briefly describe a procedure for Cu,Zn-SOD preparation from spinach leaves reported by Kitagawa et al. (22). All procedures are carried out at 4°C. Spinach leaves are homogenized with 0.1 M potassium phosphate buffer, pH 7.8, using a Waring blender. The homogenate is forced through cotton cloth and centrifuged at 24,000 g by a continuous centrifugation technique. The supernatant is precipitated with 40–80% saturated ammonium sulfate. The precipitate is dissolved and dialyzed against 10 mM potassium phosphate buffer, pH 7.8. The dialyzed solution is applied to a column of DEAE-Sepharose CL-6B. The column is eluted with a linear gradient (10–60 mM) of potassium phosphate, pH 7.8. Fractions with SOD activity are collected, concentrated, and applied to a column of Sephacryl S-200. The column is eluted with 20 mM potassium phosphate buffer. Active fractions are collected and concentrated.

REFERENCES

1. K Asada, S Kanematsu, S Okada, T Hayakawa. Phylogenic distribution of three types of superoxide dismutase in organisms and in cell organelles. In: JV Bannister, HAO Hill, eds. Chemical and Biochemical Aspects of Superoxide and Superoxide Dismutase. Amsterdam: Elsevier North-Holland, 1980, pp 136–153.
2. SL Marklund. Extracellular superoxide dismutase and other superoxide dismutase isoenzymes in tissues from nine mammalian species. Biochem J 222:649–655, 1984.
3. P Strålin, K Karlsson, BO Johansson, SL Marklund. The interstitium of the human arterial wall contains very large amounts of extracellular superoxide dismutase. Arterioscler Thromb Vasc Biol 15:2032–2036, 1995.
4. *http://www.genome.ad.jp/*
5. JA Tainer, ED Getzoff, KM Beem, JS Richardson, DC Richardson. Determination and analysis of the 2 Å structure of copper,zinc superoxide dismutase. J Mol Biol 160:181–217, 1982.
6. K Hjalmarsson, SL Marklund, Å Engström, T Edlund. Isolation and sequence of complementary DNA encoding human extracellular superoxide dismutase. Proc Natl Acad Sci USA 84:6340–6344, 1987.
7. GEO Borgstahl, HE Parge, MJ Hickey, WF Beyer Jr., RA Hallewell, JA Tainer. The structure of human mitochondrial manganese superoxide dismutase reveals a novel tetrametric interface to two 4-helix bundles. Cell 71:107–118, 1992.
8. M Sugiura, T Adachi, H Inoue, Y Ito, K Hirano. Purification and properties of two superoxide dismutases from human placenta. J Pharm Dyn 4:235–244, 1981.

9. L Tibell, R Aasa, SL Marklund. Spectral and physical properties of human extracellular superoxide dismutase: a comparison with CuZn superoxide dismutase. Arch Biochem Biophys 304:429–433, 1993.
10. SL Marklund. Properties of extracellular superoxide dismutase from human lung. Biochem J 220:269–272, 1984.
11. K Asada, K Yoshikawa, M Takahashi, Y Maeda, K Enmanji. Superoxide dismutase from a blue-green alga, *Plectonema boryanum*. J Biol Chem 250:2801–2807, 1975.
12. HP Misra, I Fridovich. Inhibition of superoxide dismutase by azide. Arch Biochem Biophys 189:317–322, 1978.
13. JM McCord, I Fridovich. Superoxide dismutase. J Biol Chem 244:6049–6055, 1969.
14. C Beauchamp, I Fridovich. Superoxide dismutase: improved assays and an assay applicable to acrylamide gels. Anal Biochem 44:276–287, 1971.
15. LW Oberley, DR Spitz. Assay of superoxide dismutase activity in tumor tissue. In: L Packer, ed. Methods in Enzymology 105. New York: Academic Press, 1984, pp 457–464.
16. EF Elstner, A Heupel. Inhibition of nitrite formation from hydroxylammonium chloride: a simple assay for superoxide dismutase. Anal Biochem 70:616–620, 1976.
17. SL Marklund. Direct assay with potassium superoxide. In: RA Greenwall, ed. CRC Handbook of Methods for Oxygen Radical Research. Boca Raton: CRC Press, 1985, pp 249–255.
18. T Adachi, H Ohta, H Yamada, A Futenma, K Kato, K Hirano. Quantitative analysis of extracellular-superoxide dismutase in serum and urine by ELISA with monoclonal antibody. Clin Chim Acta 212:89–102, 1992.
19. T Adachi, Y Usami, T Kishi, K Hirano, K Hayashi. An enzyme immunoassay for cuprozinc superoxide dismutase using monoclonal antibody: application for pharmacokinetic study. J Immunol Methods 109:93–101, 1988.
20. JR Jabusch, DL Farb, DA Kerschensteiner, HF Deutsch. Some sulfhydryl properties and primary structure of human erythrocyte superoxide dismutase. Biochemistry 19:2310–2316, 1980.
21. SL Marklund. Human copper-containing superoxide dismutase of high molecular weight. Proc Natl Acad Sci USA 79:7634–7638, 1982.
22. Y Kitagawa, S Tsunasawa, N Tanaka, Y Katsube, F Sakiyama, K Asada. Amino acid sequence of copper, zinc-superoxide dismutase from spinach leaves. J Biochem 99:1289–1298, 1986.

39

Polyphenol Oxidase

Edna C. Ramírez and John R. Whitaker
University of California, Davis, Davis, California, U.S.A.
Victoria M. Virador
National Institutes of Health, Bethesda, Maryland, U.S.A.

I. INTRODUCTION

Polyphenol oxidase, also known as tyrosinase, phenolase, catechol oxidase, catecholase, *o*-diphenol oxidase, monophenol oxidase, and cresolase, was discovered in mushrooms in 1856 by Schoenbein (1). The problem with naming the enzyme is that it may act on two general types of substrates, a monohydroxyphenol (such as *p*-cresol) to hydroxylate it in the *o*-position with respect to the original hydroxyl group (monophenol, L-dopa:oxygen oxidoreductase; EC 1.14.18.1 (2) [Eq. (1)]), and on *o*-dihydroxyphenols, such as catechol, oxidizing them by removal of the hydrogens of the hydroxyl groups, forming benzoquinones (1,2-benzenediol:oxygen oxidoreductase; EC 1.10.3.1 (2) [Eq. (2)]).

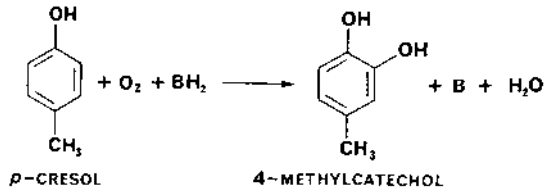

(1)

In this chapter, the first enzyme activity will be referred to as a monophenol oxidase and the second

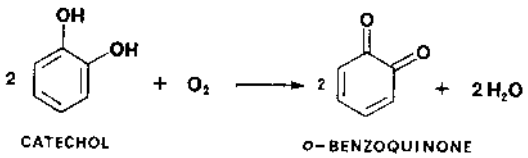

(2)

as an *o*-diphenol oxidase. The monophenol oxidases generally also act as *o*-diphenol oxidases, often at a faster rate (3). Therefore, they are sometimes classified either as monophenol oxidases, *o*-diphenol oxidases, or both depending on substrates used. But not all *o*-diphenol oxidases can act as monophenol oxidases (4, 5). This view is not shared by all researchers in this field. The benzoquinones formed by *o*-diphenol oxidases are very reactive nonenzymatically with O_2, sulfhydryl compounds, amines, amino acids, and proteins, so a variety of compounds, including melanin of the skin, are formed with colors including yellow, red, brown, and black.

A third type of "polyphenol oxidase" reaction occurs with the enzyme laccase (benzenediol:oxygen oxidoreductase EC 1.10.3.2 (2) [Eq. (3)]), acting on *p*-dihydroxy compounds, but not exclusively (Chapter 40), to give colored compounds. The laccases are also copper-containing enzymes, but the mechanistic oxidation pathway differs from that of the *o*-diphenol oxi-

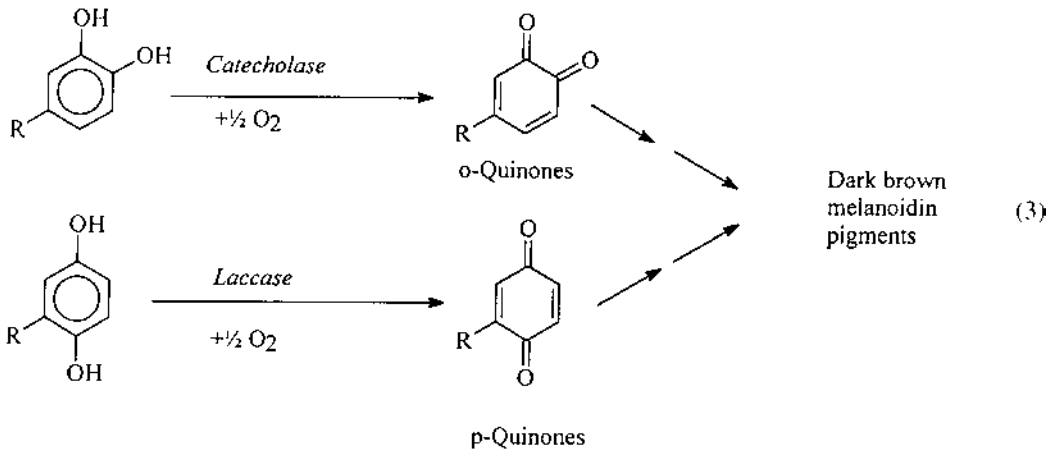

dases. The two types of enzymes can be distinguished by use of *p*-phenylene diamine or syringaldazine (these are substrates for laccase only).

Salicylhydroxamic acid and cinnamic acid inhibit only *o*-diphenol oxidases (6), while *p*-diphenol oxidases are selectively inhibited by quaternary ammonium compounds such as cetyl tetra-ammonium bromide (CTAB) (7). See also Flurkey et al. (8) and Chapter 40 on laccase in this handbook.

Polyphenol oxidases are found in many plant tissues (9, 10); in some fungi, especially those that produce brown filaments including edible mushrooms (11); and in many animals, including insects (12), mice (13), and humans (14). There are numerous genes in humans that affect pigmentation (15, 16). According to Witkop (14), there are at least 40 clinical manifestations of hypopigmentation and 27 of hyperpigmentation in humans, some leading to cancerous skin melanoma.

II. IMPORTANCE TO FOOD QUALITY AND FOOD PROCESSING

Polyphenol oxidases are very important enzymes in determining the quality and economics of fruit and vegetable harvesting, storage, and processing (17–19). Bruises, cuts, and other mechanical damage during harvest, storage, and processing that allow O_2 penetration result in rapid browning in many fruits and vegetables. Up to one-half of some tropical fruits are lost for consumer consumption owing to browning, since the off-color, off-taste, and loss of nutritional quality are unacceptable to consumers. Apricots, apples, peaches, grapes, strawberries, and bananas (among others) and several tropical fruits and juices therefrom become brown, as do Irish potatoes and some lettuces and other leafy vegetables. Black spot development in shrimp is a major economic problem.

Heat processing to inactivate polyphenol oxidase, especially in juices, is standard practice with certain fruits and vegetables. Some acceptable compounds such as ascorbic acid, thiol compounds, and sulfites may be added to prevent browning of cut fruits and vegetables (11). Cinnamic, *p*-coumaric, and ferulic acids can be added to apple juice (sometimes at $< 0.01\%$) to prevent browning due to polyphenol oxidase (20). 4-Hexyl-resorcinol is a safe and effective inhibitor of enzymatic browning, is used in shrimp processing (21, 22), and prevents apple slice browning (23) among other fruits and vegetables. Browning of foods can also be prevented by removal of O_2, acidification (if acceptability of the food permits), and removal of polyphenols by complexing with cyclodextrins and polyvinylpyrrolidone (24–26). Polyphenol oxidase levels in fruits and vegetables can be decreased by breeding and through biotechnology. An example of the use of biotechnology is the use of a specific antisense RNA to turn off expression of polyphenoloxidase in grape tissues (27).

Exclusion or decrease of O_2 and separation of polyphenol oxidase and substrate (phenols) provide excellent prevention from browning. Fruits and vegetables have "skins" (waxes and other O_2 impermeable compounds) on the surface that prevent O_2 absorption. As long as this protective skin is intact and the cellular tissue is undamaged, browning does not occur. In food processing and packaging O_2 can be excluded or reduced by use of gaseous N_2, use of O_2-impermeable coatings and films, and controlled atmospheric storage (O_2 reduced to the minimum needed to maintain cellular integrity at reduced temperature ($\sim 5^\circ C$)).

Color development due to polyphenol oxidase activity is desirable in the processing of tea, coffee, cocoa,

apple cider, prunes, black raisins, Black Mission figs, and zapote.

III. PROPERTIES OF POLYPHENOL OXIDASES AS PROTEINS

A. Primary Sequences

Several amino acid sequences of propolyphenol oxidases and polyphenol oxidases are known, primarily from sequencing the gene. Table 1 shows the similarities of nine plant PPO sequences. Another group of plant PPO sequences are depicted by a dendrogram (Fig. 1).

Whitaker (28) has compared the amino acid sequence relationships among polyphenol oxidases of higher plants, fungi, and higher animals known to 1995. The homologies (relative to potato 1) among the higher plant polyphenol oxidase gene sequences from potato 1, potato 2, tomato, and broad bean were 96.6% (potato 1 and 2), 92.2% (potato 1 and tomato), and 38.1% (potato 1 and broad bean). Among the fungi *S. glaucescens, S. antibioticus*, and *N. crassa*, the homolgies were 87.5% (*S. glaucescens* with *S. antibioticus*) and 17.0% (*S. glaucescens* and *N. crassa*). Comparison between human and mouse polyphenol oxidases showed 41.0% homology. Overall, when potato 1 sequence was compared with those of *S. glaucescens, S. antibioticus, N. crassa*, and human and mouse polyphenol oxidases, there was 19.4%, 18.8%, 13.0%, 10.4%, and 10.9% homology, respectively. Only the primary sequences of *N. crassa* and *S. glaucescens* polyphenol oxidases were determined by the Edman degradation method on the mature protein.

The amino acid sequence homologies among the nine polyphenol oxidases (Fig. 2) are much higher when compared only in the active-site regions A and B (28). In active-site region A, of 26 amino acids, there is a range from 100% to 31% homology (Table 2). In active-site region B of 56 amino acids, the homology ranges from 96% to 34% (Table 3).

B. Molecular Weights

The presumed mature molecular weights of the 12 polyphenol oxidases listed in Table 4 range from 30.7 kDa for *S. antibioticus* polyphenol oxidase to 128.0 kDa for mushroom polyphenol oxidase (with four subunits). The potato, tomato, and broad bean polyphenol oxidases have molecular weights in the range of 56.5–58.1 kDa while grape polyphenol oxidases have molecular weights of 40.7 kDa. Three of the fungi polyphenol oxidases have molecular weights of 30.9–46.0 kDa, while mushroom polyphenol oxidase is 128.0 kDa. The human and mouse polyphenol oxidases are 62.6 and 57.8 kDa, respectively. With the exception of the polyphenol oxidases from *N. crassa, S. glaucescens,* and edible mushroom (*Agaricus bisporus*) (29, 30), the molecular weights are based on the gene sequence translated to amino acid sequence. Nothing is known about posttranslational modifications.

C. Secondary, Tertiary, and Quaternary Structure

X-ray crystallography data have been published only for the sweet potato polyphenol oxidase (31, 32).

There are two isozymes of polyphenol oxidase in sweet potatoes of molecular masses 39.0 and 40.0

Table 1 Similarity of the Aligned Plant PPO Sequences

	Tomato	Tobacco	Grenache grape	Sultana grape	Apple	Bean	Pokeweed	Spinach	Sugarcane
Tomato	100	90.48	59.52	60.03	56.97	56.8	55.2	53.74	43.2
Tobacco		100	58.01	58.52	56.49	56.83	53.83	51.43	43.68
Grenache grape			100	99.18	67.17	64.42	64.22	57.83	43.16
Sultana grape				100	67.34	64.42	64.4	57.73	43.09
Apple					100	69.7	63.03	54.88	45.29
Bean						100	62.69	56.84	43
Pokeweed							100	57.58	43.44
Spinach								100	40.42
Sugarcane									100

The GCG program OldDistances was used to calculate percent similarity among the plant PPOs from a complete PileUp alignment; part of this alignment is depicted in Figure 1. Genbank accession numbers are as follows: tomato, Z12837 S61013; tobacco, Y12501; Grenache grape, U83274; Sultana grape, Z27411; apple, D87670; bean, Z11702 S45506; pokeweed, D45385; spinach, X90869; sugarcane, U46014.

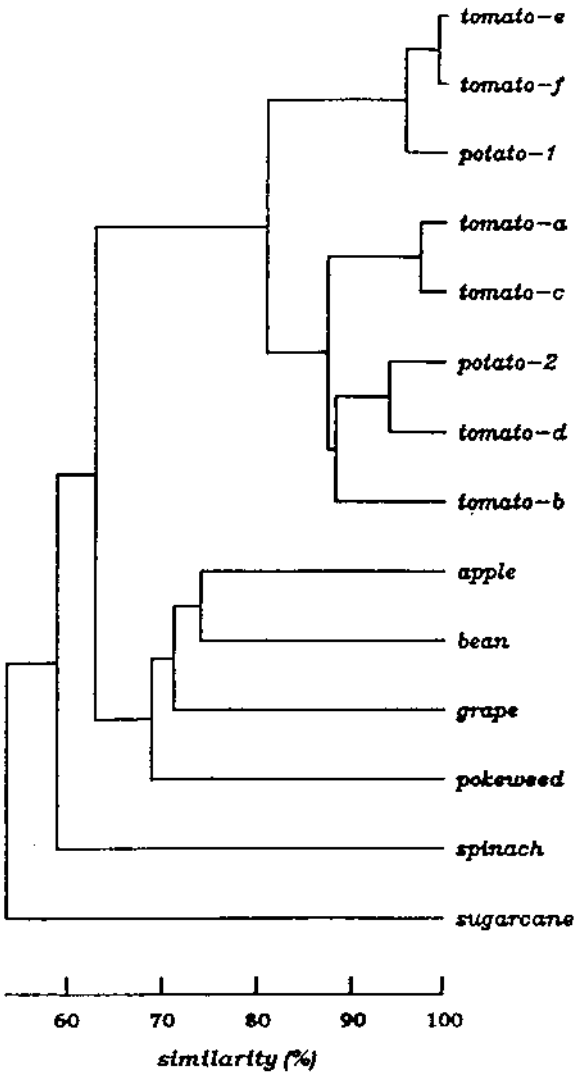

Figure 1 Dendrogram illustrating the degree of similarity between the protein sequences of reported plant PPO genes. The Genbank accession numbers are apple (L29450), bean (Z11702), grape (Z27411), potato-1 (M95196), potato-2 (U22921), tomato-a (Z12833), tomato-b (Z12834), tomato-c (Z12834), tomato-d (Z12836), tomato-e (Z12837), tomato-f (Z12838), pokeweed (D34385), spinach (Z6655), and sugarcane (U846014). Sequences were aligned using the GCG programs PILEUP and FIGURE.

kDa (determined by MALDI-MS) (20). The sweet potato polyphenol oxidase molecular weight of 39.0 kDa has 345 amino acid residues, is a monomeric, ellipsoid molecule with dimensions of $55 \times 45 \times 45$Å. The secondary structure is primarily α-helical in nature, with seven α-helices and probably four short β-sheets with β- and γ- turns and random coils in the structure (Fig. 3). It appears to be an $\alpha + \beta$ globular protein. There are two disulfide bridges (Cys11–Cys28 and Cys27–Cys89). Each of the two active-site coppers is coordinated to three histidine residues on α-helices. Copper of site A is coordinated to His88 of helix α2 and His109 and His118 of helix α3. The copper of site B is coordinated to His240 and His244 of helix α6 and His274 of helix α7.

As noted above, mushroom tyrosinase is thought to have quaternary structure (29, 30), probably composed of four subunits. The similarity of the subunits is uncertain. Based on gene sequences, there appear to be at least two isozymes of tyrosinase in mushrooms (33, 34).

IV. ENZYMATIC PROPERTIES OF POLYPHENOL OXIDASES

Some polyphenol oxidases oxidize both monophenols such as *p*-cresol, tyrosine etc. (monophenols), and diphenols such as catechol and *o*-dihydroxyphenylalanine [Eqs. (1) and (2)]. Lerch and Ettlinger (3) investigated the activity of pure *Streptomyces glaucescans* polyphenol oxidase (tyrosinase) on a large number of mono- and *o*-diphenols. In all cases, the *o*-diphenolase activity was greater than the monophenolase activity. The ratio of k_{cat} for activity on *o*-diphenol to that of k_{cat} for activity on the analogous monophenol ranged from 222 for homocatechol/*p*-cresol to 2.89 for 3,4-dihydroxyphenylacetic acid/*p*-hydroxyphenylacetic acid. The K_m values for the analogous *o*-diphenol to monophenol ranged from 1.00 to 7.88. Therefore, K_m and K_{cat} are both responsible for the large differences in activity on mono- and *o*-diphenols.

Table 5 shows some activity results of plant polyphenol oxidases on a limited number of mono- and *o*-diphenols. Polyphenol oxidase from peaches was not able to hydroxylate *p*-cresol or *p*-coumaric acid, and polyphenol oxidase from pears was not able to hydroxylate *p*-coumaric acid. The highest activities on monophenols were the 5.5% and 4% on *p*-cresol compared to that of catechol for potato and broad bean, respectively. Note also the variable relative activities on *o*-diphenols compared to that on catechol.

There is some disagreement by researchers on whether or not all polyphenol oxidases can perform the hydroxylation step [Eq. (1)]. As shown in Eq. (1) a reducing compound, BH_2, is required in the reaction. BH_2 is an *o*-diphenol such as catechol. If no BH_2 is present, some polyphenol oxidases appear to be able to slowly produce BH_2 during a lag period in the initial reaction with a monophenol (Fig. 4). The in vivo nat-

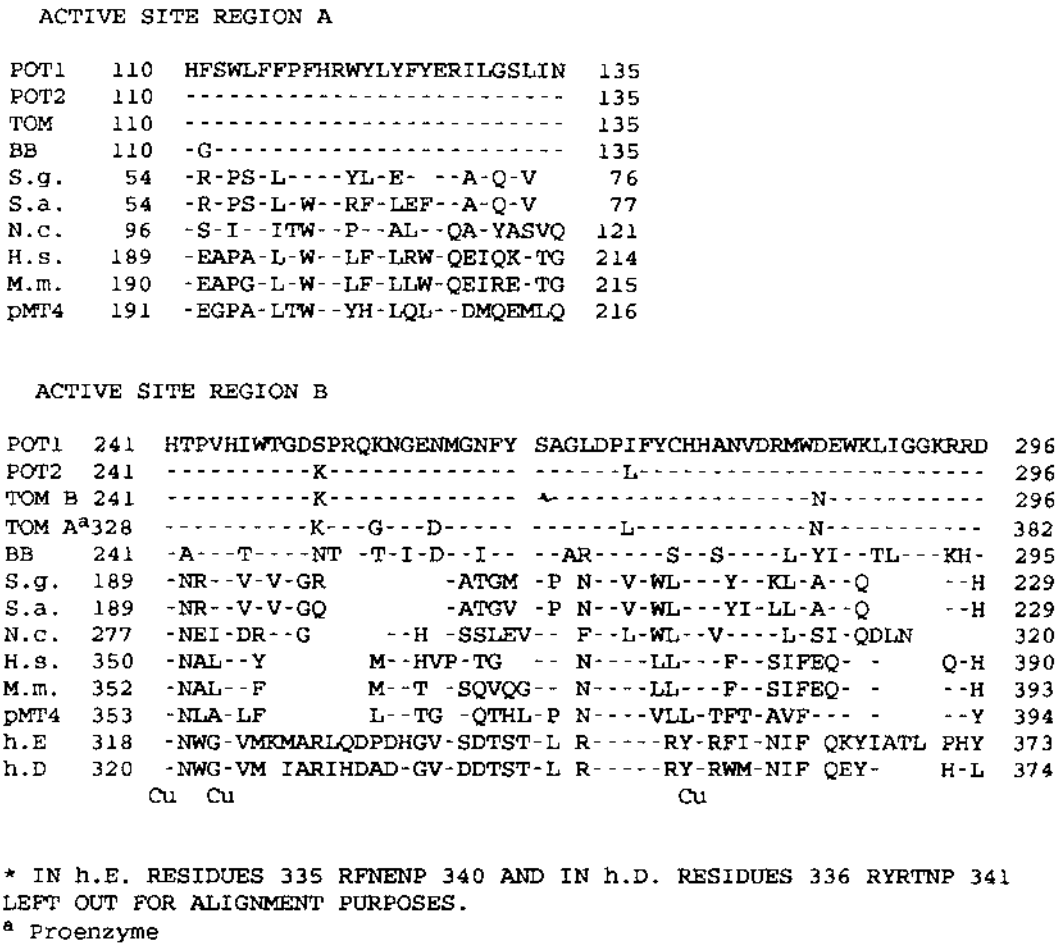

Figure 2 Amino acid sequence relationships in and near the active sites of potato (Pot 1 and Pot 2), tomato (Tom A and Tom B), broad bean (BB), *S. glaucescens* (S.g.), *S. antibioticus* (S.a.), *Neurospora crass* (N.c.), *Homo sapiens* (H.s.), *Mus musculus* (M.m.), putative mouse transcript 4 (pMT 4) polyphenol oxidases, hemocyanin E (spider, *Eurypelma californicum*) and hemocyanin D (spider, *E. californicum*). Shown are regions A and B containing the presumed copper-binding histidine residues. The Cu indicates histidines that ligand to copper in *N. crassa* polyphenol oxidase, and presumably in the other polyphenol oxidases and hemocyanins. The - indicates that the sequence is the same as for POT1. (From Ref. 28.)

ure of BH_2 is not known. Lerch and Ettlinger (3) reported lag periods of 0.32–16.0 min for *S. glaucescens* polyphenol oxidase acting on N-acetyl-L-tyrosine hydrazide and *p*-hydroxyphenylacetic acid, respectively. Whitaker (unpublished data) showed that 1×10^{-7} M 4-methylcatechol added to mushroom polyphenol oxidase, along with *p*-cresol, was able to eliminate the 9-min lag period entirely. Equation (4) shows that the BH_2 acts on the Cu(II) *met* form to reduce the two coppers to Cu(I) (*deoxy* form), which can then bind O_2 and oxidize the monophenol substrate to the *o*-diphenol. Would similar experiments with other polyphenol oxidases show that all polyphenol oxidases can do both types of reactions?

Kinetically, the mechanism of peach polyphenol oxidase (5) and *S. glaucescens* polyphenol oxidase (3) followed an ordered BiBi mechanism (Fig. 5). The O_2 must bind first to the *deoxy* form (Cu(I) state) of the enzyme followed by phenol. The ordered BiBi mechanism assumes that the products come off in the order of the benzoquinone followed by the hydrogen peroxide. This author does not know of published experimental data to support this assumption.

The overall proposed mechanism of action of polyphenol oxidase is shown in Figure 6. The top part shows the pathway for oxidation of *o*-diphenols. The *met* form (at the No. 1 position in the A cycle) is thought to be the "resting" form of the enzyme when

Table 2 Amino Acid Sequence Homologies Among Nine Polyphenol Oxidases in Active Site Region A

Source	AA sequence region	Identical AA	% Homology
Pot 1	110–135	26[a]	100
Pot 2	110–135	26	100
Tom B	110–135	26	100
BB	110–135	25	96
S.g.	54–76	13	50
S.a.	54–77	11	42
N.c.	96–121	11	42
H.s.	190–215	8	31
M.m.	191–216	8	31

[a]The number 26 amino acid residues includes amino acid residues + spaces for alignment. (Taken from Figure 2.)

no substrate is present. Addition of *o*-diphenol (catechol; BH_2) binds to the *met* Cu(II) form (#2) producing the *deoxy* [Cu(I)] form of the enzyme (and *o*-benzoquinone). The *deoxy* form binds O_2 (#3) to give the *oxy* form [Cu(II)] which then binds a molecule of *o*-diphenol (#4) to give the enzyme Cu(II) · O_2 · diphenol ternary complex. Two hydrogens are removed to give the benzoquinone (#5) and the *met* form of the enzyme in a complete cycle.

Depending on substrate available, the *oxy* form of the enzyme (produced as above from the *met* form) can bind a monophenol (Pathway B) (#1′) which is oxidized to the *o*-diphenol (#2′) and recycles through the B pathway via the diphenol intermediate to the *deoxy* form (#4′) which can bind O_2 to form the *oxy* form (#5′), etc. The *met* form, reduced to the *deoxy* form by an *o*-diphenol (Fig. 6), can also be reduced to the *deoxy* form by other reducing compounds (ascorbic acid, hydroxylamine, dithionite) and by H_2O_2 in the presence of O_2 (39). The overall mechanism indicates there are three different steps in Figure 6 leading to oxidation of *o*-diphenols to benzoquinone.

Table 3 Amino Acid Sequence Homologies Among Nine Polyphenol Oxidases in Active Site Region B

Source	AA sequence region	Identical No.	% Homology
Pot 1	241–296	56[a]	100
Pot 2	241–296	54	96
Tom B	241–296	54	96
BB	241–295	35	62
S.g.	189–229	20	36
S.a.	189–229	19	34
N.c.	277–320	20	36
H.s.	350–390	19	34
M.m.	352–393	21	38

[a] The No. 56 includes amino acid residues + spaces for alignment.

Table 4 Mature Protein Molecular Weights of Some Polyphenol Oxidases

Source	MW (kDa)
Pot 1	56.5
Pot 2	56.6
Tom	56.5
BB	58.1
GPO1	40.7
GPO2	40.7 (29.0)[a]
S.g.	30.9
S.a.	30.7
N.c.	46.0
Mushroom	128.0
H.s.	62.6
M.m.	57.9

[a] There are two peaks of polyphenol oxidase activity from a Sephadex G-100 column (40.7 and 29.0 MW). The 40.7-kDa peak has the most activity.
Source: Whitaker, 1998, unpublished data.

Polyphenol oxidases are irreversibly inactivated during the oxidation of substrate to product. Golan-Goldhirsh and Whitaker (40) calculated that inactivation of mushroom polyphenol oxidase occurs at the rate of approximately one in 5000 turnovers of the substrate to product (an efficiency of ~ 0.02%). But complete inactivation of the enzyme can occur in 2–3 min reaction with substrate (with no added reductant such as ascorbic acid). The inactivation is due to a free radical-catalyzed fragmentation of one or more of the six histidine residues that bind the two coppers at the active site. The fragmentation leads to loss of histidine and release of copper (40–42). Reaction inactivation of *N. crassa* polyphenol oxidase is due to loss of His306 in the active site (42).

Golan-Goldhirsh et al. (43) later showed that ascorbic acid, copper, and O_2 mimic the above reaction not only with polyphenol oxidase but also with ovalbumin, Kunitz trypsin inhibitor, bovine serum albumin, and small histidine-containing peptides, leading to loss of most of the histidine residues in 24 h at 25°C. In the case of mushroom polyphenol oxidase, the histidine residues of the protein are converted by the free radical process in the absence of mono- or diphenols, but require O_2, to several products including aspartic acid (major product), glycine, alanine, and urea (stoichiometric with the aspartic acid formation). Free radi-

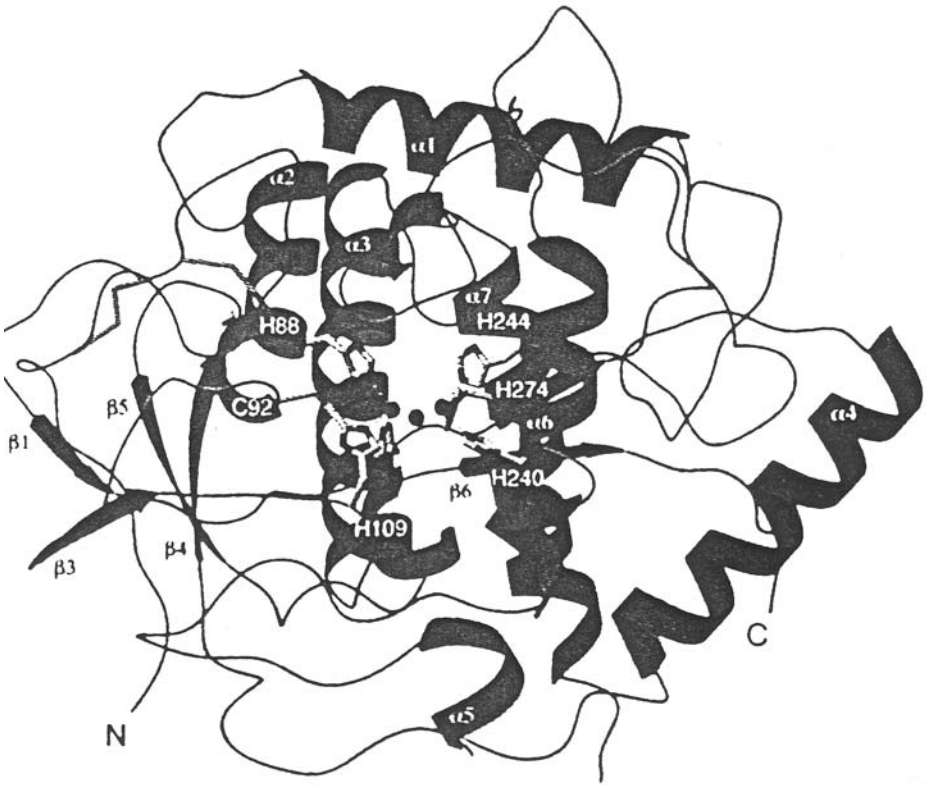

Figure 3 Ribbon drawing of sweet potato catechol oxidase, showing the front view of 39.0-kDa single polypeptide enzyme. (From Ref. 32.)

Table 5 Relative Substrate Specificities of Four Polyphenol Oxidases

	Activity relative to catechol			
Substrate	Potato[a]	Peach[b]	Broad bean leaf[c]	Pear[d]
Di- or triphenolic compounds				
Catechol	100	100	100	100
4-Methylcatechol		51.5	200–225	72.3
d-Catechin		31.8		7.79
Chlorogenic acid	140	22.2	8	71.8
Caffeic acid	76.5	0	12.5	4.41
Protocatechuic acid		16.3	0.11	
3,4-Dihydroxy-L-phenylalanine	54.3	40.5	50	
Dopamine		45.6		15.6
Gallic acid		25.7	0.22	
Pyrogallol			85–95	
Monophenolic compounds				
p-Cresol	5.5	0	4	
p-Coumaric acid	nil	0	0.05	0

[a] Ref. 35; pH 7.0.
[b] Ref. 4. For isozyme A of clingstone peach at pH 6.8 and 30°C.
[c] Ref. 36.
[d] Ref. 5; 35°C and pH 6.2; isozyme B.

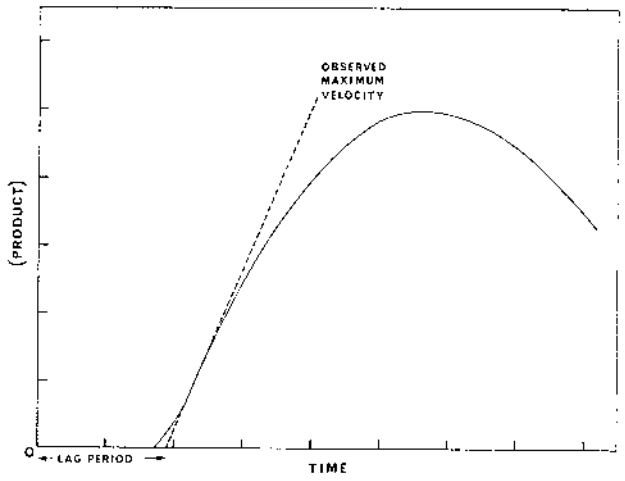

Figure 4 Theoretical graph for the velocity of product formation from oxidation of monophenols by polyphenol oxidases in the absence of BH_2. There is an initial lag period followed by maximum velocity and then slowing of the velocity as the enzyme undergoes reaction inactivation. The negative velocity phase is due to melanin formation, which absorbs at a different wavelength.

cals due to semiquinone formation of the substrate can be detected during polyphenol oxidase–catalyzed reactions (44, 45; Sugumara et al., cited in 46) in insect cuticle formation by polyphenol oxidase. Free radical formation (11) requires O_2, a reducing agent (we used ascorbic acid only), a histidine residue (histidine in small peptides are also fragmented), and Cu(II) (we could not detect Cu(I) formation by bathocuproine disulfonate in the reaction). The specific free radical formed has not been identified yet, to the authors' knowledge.

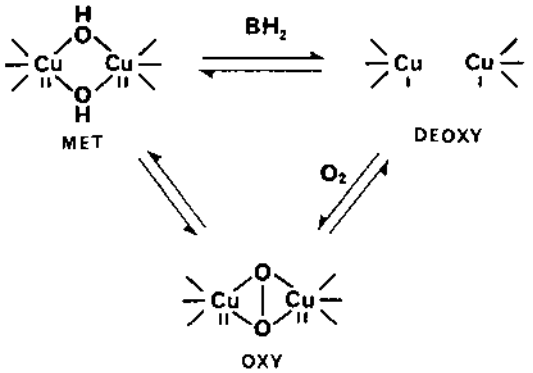

(4)

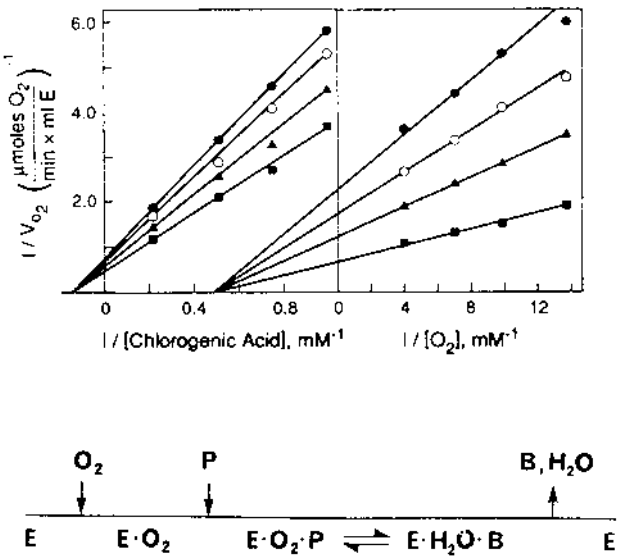

Figure 5 (Top) Effect of O_2 and chlorogenic acid concentrations on initial velocity, v_0, of pear polyphenol oxidase-B-catalyzed reactions. The reactions were followed with an oxygen electrode at pH 4.0 and 30.0°C, permitting initial v_0 to be determined. (Bottom) Kinetic mechanism for pear polyphenol oxidase-B catalysis, diagrammed according to the Cleland nomenclature for an Ordered Sequential Bi-Bi Mechanism. P is an *o*-diphenol; B is an *o*-benzoquinone; $E \cdot O_2$ is a binary enzyme $\cdot$ O_2 complex; $E \cdot O_2 \cdot P$ is a ternary enzyme $\cdot$ O_2·*o*-diphenol complex, and $E \cdot H_2O \cdot B$ is a ternary enzyme $\cdot$ H_2O·*o*-benzoquinone complex. (From Ref. 5.)

V. MEASUREMENT OF POLYPHENOL OXIDASE ACTIVITY

The two main methods of measuring polyphenol oxidase activity are spectrophotometry and polarography. There are strong advocates of each method, including statements that both methods are unreliable (47, 48). The basis of the unreliability is caused by the further nonenzymatic oxidation of the benzoquinone formed. As shown by Mayer et al. (47), results from the two are identical very early on in the reaction (Table 6), but by 54 sec the difference is 28%. Note that O_2 consumption measurements contribute primarily to the difference because of the continued nonenzymatic oxidation of benzoquinone and other intermediate products. For example, the oxidation of 4-methyl catechol to 4-methyl-2,3-benzoquinone requires 1.0 equivalent of O_2, while further reactions (generally nonenzymatic) require 1.4 additional equivalents of O_2. But, as shown by Whitaker (28), there is also a decrease in

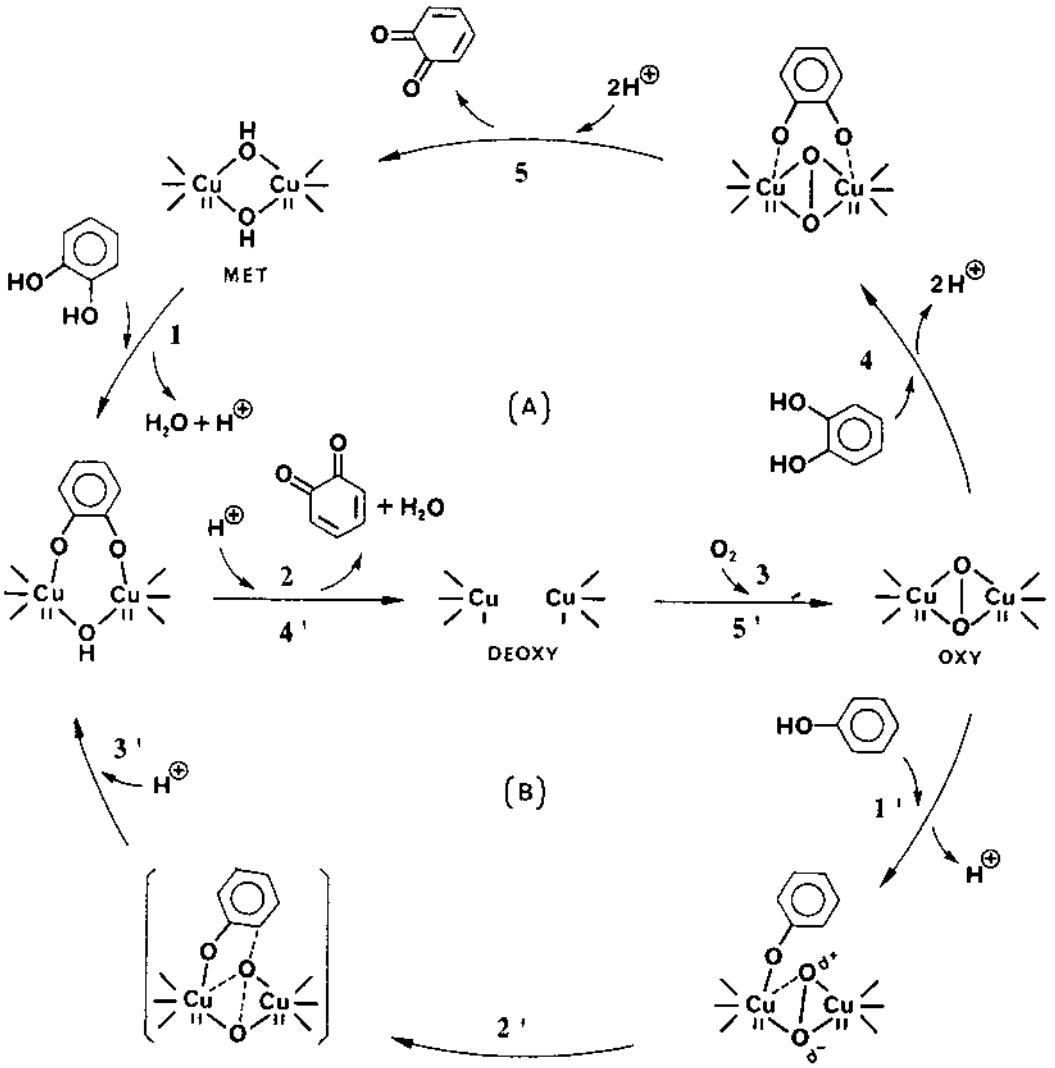

Figure 6 Proposed kinetic scheme depicting the mechanisms of oxidation of *o*-diphenol (catechol [A]) and monophenol (phenol [B]) by *Neurospora crassa* polyphenol oxidase. (From Refs. 37, 38.)

absorbance after ~ 2 min as the benzoquinone is converted to other products that do not absorb maximally at the wavelength of benzoquinones. Therefore, it is critical to obtain initial velocity (v_0) early on in the reaction. As shown by Eqs. (1) and (2), the oxidation of monophenols to benzoquinone plus H_2O requires two equivalents of oxygen, while oxidation of *o*-diphenols to benzoquinone requires one equivalent of oxygen.

In reactions involving monophenols, a lag phase is generally observed (see Fig. 4). As shown in Eq. (1) and Figure 6, BH_2 is required to reduce the *met* form of polyphenol oxidase to the *deoxy* form that can bind O_2. Addition of as little as $1 \times 10^{-7} M$ catechol to the reaction can eliminate the lag period.

In the measurement of monophenol activities, the rate of conversion of the intermediate product (an *o*-diphenol) to the benzoquinone is generally measured. But in some cases, k_{cat} values for the monophenol and product *o*-diphenol can be very similar (3). Examples are shown in Table 7.

The monophenol oxidation can be measured uniquely by use of ^{18}O-labeled O_2 or tritium-labeled substrate.

A. Measurement of Monophenolase Activity

1. Use of Tritium-Labeled Substrate

As shown in Eq. (1), one atom of oxygen (from O_2) is covalently attached to the 2 position of *p*-cresol, along

Table 6 Comparison of the Spectrophotometric and Polarographic (O_2 electrode) Methods of Measuring Apple Catechol Oxidase Using 4-Methyl Catechol as Substrate

Time (sec)	(1)[a] Quinone Formed (μmol)	(2)[b] O_2 consumption (μmol)	Ratio[c] (2)/(1)
18	0.256	0.261	1.02
54	0.512	0.653	1.28
93.6	0.768	1.133	1.48
198	1.024	1.568	1.53
480	1.408	2.464	1.75

[a] Measured spectrophotometrically.
[b] Measured polarographically.
[c] o-Benzoquinone formation from 4-methylcatechol consumes 1 gram-atom of O_2 per mole of catechol, whereas conversion of 4-methylcatechol to melanin consumes 2.4 gram-atoms O_2 per mole of catechol oxidized.
Source: Ref. 47.

with a H to give 4-methyl catechol. By the use of the 2-tritiated *p*-cresol, tritium will be released into the aqueous phase. During the initial phase of the reaction (between 0 and 60 sec), the rate of release of tritium should give a good measure of the initial velocity of the hydroxylation step. The remaining titriated *p*-cresol must be removed by chromatography or by an adsorption method.

2. Use of ^{18}O-Labeled O_2

As shown by Eq. (1), one atom of oxygen (from $^{18}O_2$) will be covalently attached to the 2 position of *p*-cresol, along with a H to give 4-methyl catechol with an ^{18}O label. The unincorporated $^{18}O_2$ can be flushed from the solution by N_2, or the water can be distilled from the solids, and the water collected to measure the increase in ^{18}O level of the water, or the 4-methyl catechol, in the presence of a reducing agent such as ascorbic acid, can be obtained. The increase in ^{18}O in the product will give a measure of the velocity of the monophenol oxidase reaction.

3. Spectrophometric Method at 280 nm

An easier method than those in 1 and 2 above is to measure the increase in absorbance at 280 nm due to the formation of 4-methyl catechol from *p*-cresol. Again, the measurements must be made within the first 30–90 sec of beginning of the reaction.

4. Use of Diphenol Conversion Rates to *o*-Benzoquinone

K_m values for monophenols are in the range of $4.5 \times 10^{-5}\,M$ (N-chloroacetyl-L-tyrosine ester ester) to $5.34 \times 10^{-3}\,M$ (glycyl-L-tyrosine) for the *S. glaucescens* polyphenol oxidase (3) and $2.62 \times 10^{-4} M$ and $4.62 \times 10^{-4}\,M$ for L-tyrosine methyl ester for the γ- and α-isozymes of mushroom polyphenol oxidase (30). When the K_m and k_{cat} values of the monophenol and *o*-diphenol substrates are similar, the observed rates of the reactions of benzoquinone formation will be contributed by both rate constants ($v_0 = k_2(E)_0(S)_0/((k_2 + k_3)/k_2k_3) + (S)_0$).

See discussion below for methodology to use.

Table 7 Ratios of k_{cat}/K_m and k_{cat}/k_{cat}, in Parentheses, for Some Monophenol/*o*-Diphenol Substrate Pairs

Substrate pairs			
Monophenol	Diphenol	(1)[a]	(2)[b]
L-Tyrosine	3,4-Dihydroxy-L-phenylalanine	7.81	(110)
p-Cresol	Homocatechol	25.7	(222)
p-Hydroxyphenylpropionic acid	3,4-Dihydroxyphenylpropionic acid	6.31	(13.6)
p-Hydroxyphenylacetic acid	3,4-Dihydroxyphenylacetic acid	2.89	(2.89)
L-Tyrosine methyl ester	3,4-Dihydroxy-L-phenylalanine	1.77	(6.17)
L-Tyrosine methyl ester (α)[c]	3,4-Dihydroxyl-L-phenylalanine (α)[a]	3.44	(2.62)
L-Tyrosine methyl ester (γ)[c]	3,4-Dihydroxy-L-phenylalanine (γ)[a]	3.41	(5.20)

[a] (k_{cat}/K_m) diphenol/(k_{cat}/K_m) monophenol.
[b] k_{cat}, diphenol/k_{cat}, monophenol.
[c] Based on kinetic constants for α- and γ-isozymes of mushroom polyphenol oxidase, using a molecular weight of 32,400.
Source: Refs. 28–30.

B. Measurement of *o*-Diphenol Oxidase Activity

Reports of K_m values for *S. glaucescens* enzyme activity on *o*-diphenols range from $3.72 \times 10^{-4}\,M$ for caffeic acid to $1.50 \times 10^{-2}\,M$ for 3,4-dihydroxy-D-phenylalanine (3). For mushroom isozymes α and γ, K_m values are $3.75 \times 10^{-4}\,M$ and $4.00 \times 10^{-4} M$, respectively (30). Other reports of K_m include those of Wong et al. (4) where K_m values for catechol and peach polyphenol oxidase were 6.6, 4.2, 7.0, and 36.0 mM for isozymes A, B, C, and D, respectively, and of Rivas and Whitaker (5) with pear isozymes A and B, where K_ms were 20.9 and 33.9 mM for pyrocatechol, 8.0 and 5.8 mM for 4-methyl catechol, 16.1 and 11.9 mM for chlorogenic acid, and 3.1 and 1.6 mM for d-catechin, respectively. These K_m values permit one to use an appropriate concentration of substrate for measuring activities.

1. Spectrophotometric Method

In the author's laboratory, *o*-diphenol oxidase activity is generally determined using catechol or 4-methyl catechol (prepared fresh daily) by mixing 4.00 mL of 0.1 *M* sodium phosphate buffer, pH 7.0, 0.50 mL of 5.00×10^{-2} M 4-methylcatechol (final concentration 5.00×10^{-3} M) and adding 0.50 mL of polyphenol oxidase of a concentration that gives a change in absorbance of ~ 0.100/min. The wavelength used is 395 nm; the ϵ_m for 4-methylbenzo-2,3-quinone is 1.350×10^3 $M^{-1}\,cm^{-1}$ at 395 nm.

Absorbance should be measured with a recording spectrophotometer so that v_0 can be determined precisely at the very early stage of the reaction for reasons discussed above. The temperature and pH should also be controlled.

2. Polarographic Method

The polarographic method, also called the O_2-electrode method, determines the rate of O_2 uptake. As shown in Figures 7 and 8 and Table 6, the O_2 electrode and spectrophotometric methods give linear relationships over a wide range of enzyme concentrations. The chronometric method measures the lag time before browning occurs or ascorbic acid is exhausted, and the manometric method (O_2 uptake) does not give linear relationships between enzyme concentration and O_2 uptake.

The concentration of enzyme, substrate, buffers, and pH used may be the same as described for the spectrophotometric method (above). Specific conditions are also given in the legends of Figures 7 and 8 (47).

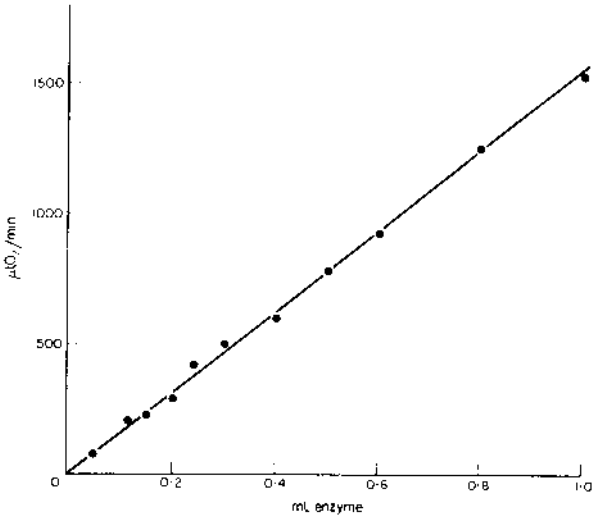

Figure 7 Relationship between enzyme concentration and μL O_2 consumed by oxidation of 4-methyl catechol by apple catechol oxidase, using an O_2 electrode. The reaction was performed in phosphate-citrate buffer, pH 5.1 with 5×10^{-3} M 4-methyl catechol and stock solution of 50 μg enzyme protein/mL. (From Ref. 47.)

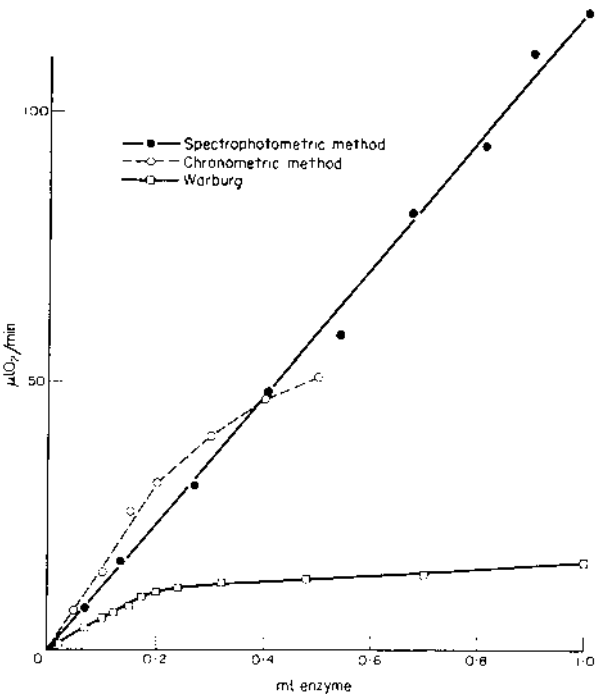

Figure 8 Relationship between enzyme concentration and μL O_2 consumed by oxidation of 4-methyl catechol by apple catechol oxidase using spectrophotometric, chronometric, and Warburg techniques. The reaction was performed under the experimental conditions given in Figure 7. (From Ref. 47.)

VI. PURIFICATION OF POLYPHENOL OXIDASES

Purification of polyphenol oxidase must be done without any development of browning. Otherwise, the polyphenol oxidase will be modified by reaction of the ϵ-amino group of lysyl residues with the *o*-benzoquinone. Modification leads artificially to several bands with activity as shown by gel electrophoresis or by column chromatography (E. Ramírez and J.R. Whitaker, unpublished data).

Several methods have been used by the authors to prevent browning. The tissue was frozen in dry ice or Freon (4, 5), lyophilized, and the powder extracted repeatedly with cold (-5 to -10°C) acetone to remove the phenolic compounds. This method of removing phenols with acetone, while used widely in the 1950s to 1970s, has been shown to modify proteins under certain conditions. We have found Freon to be a good method for rapidly freezing the tissue (5). More recently, we have used 0.03 *M* ascorbic acid and insoluble polyvinyl polypyrrolidone with frozen whole grapes to prevent browning by binding the phenols. This gave an extract that did not brown. We have also successfully used ascorbic acid and Sephadex G-25 to bind the phenols. This is done at 0°C.

The following method (E. Ramírez and J.R. Whitaker, unpublished data) was used to purify grape polyphenol oxidase to homogeneity for crystallization for x-ray structure determinations. Acceptable extraction yields were obtained only when a maximum of 250 g of grapes per batch were used as starting material. Attempts to extract PPO from larger batches were unsuccessful, owing to insufficient mechanical agitation during the second extraction step because of high viscosity of the solution. All steps were done at 4°C. In a typical extraction, 100–200 g of frozen whole Grenache grapes were blended in a Waring blender for 5 min at low speed with 2 volumes (w/v) of buffer A (100 mM sodium phosphate, 0.03 M ascorbic acid, pH 6.5) and 10% PVPP. Pulp was separated by centrifugation (23,000 g, 30 min) and the supernatant discarded. It contained no PPO activity. The precipitate was transferred to a beaker with 1 volume of buffer B (100 mM sodium phosphate, 0.1% Triton X-100, pH 6.5) and 2.5% PVPP. This suspension was mechanically stirred for 30 min. After centrifugation (23,000 g, 30 min) the precipitate was discarded and

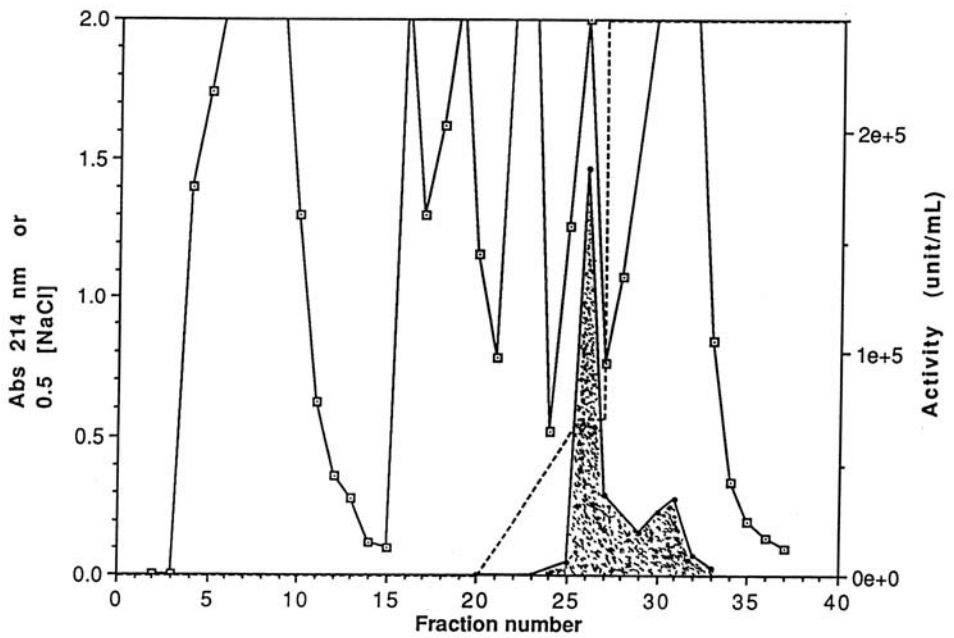

Figure 9 Mono Q [R-CH_2-$N^+(CH_3)_3$] HR 5/5 column chromatography of grape polyphenol oxidase. Protein was eluted initially with a sodium chloride linear gradient (0–0.3 M), held for 2 mL at 0.3 *M* sodium chloride, and then stepped up to 1 *M* (dashed line). Activity of polyphenol oxidase is indicated by closed circles (and shaded area). Protein is indicated by open squares. The small peak of activity at Fraction No. 30 is that designated as Mono Q II in the text.

Table 8 Purification of Grenache Grape Leaf Polyphenol Oxidase

Sample	Activity (units/mL) $\times 10^{-3}$	Protein (μg/mL)	Spec. activity (units/mg) 10^{-3}	Volume (mL)	Total protein (mg)	Total activity (units $\times 10^{-3}$)	Yield (%)	Purification (fold)
Extraction	3.64	53.1	68.5	2267	120	8250	100	1.00
40% AS (sum)	13.8	26.9	513	480	12.9	6620	80.0	7.47
95% AS (sum)	90.2	272	332	22	5.98	1980	24.0	4.82
Mono QI	164	260	631	3	0.78	492	6.75	9.19
Mono QII	33.3	105	317	14	1.47	466	5.64	4.63

the supernatant was concentrated by ultrafiltration (Amicon microconcentrator, Diaflo PM10 membrane).

The concentrated solution was brought to 40% saturation with ammonium sulfate, let stand for 30 min, centrifuged, and the precipitate discarded. The supernatant was further brought to 95% saturation with ammonium sulfate, let stand for 30 min, centrifuged, and the supernatant separated. The supernatant still contained 50% of total activity; owing to very low protein concentration, some PPO remained in solution. The precipitate was stored at 4°C (or frozen) until all extractions were done.

The precipitates from all extractions were combined, dissolved in a minimal amount of buffer (5 mM sodium phosphate buffer, pH 8.0), and dialyzed with 200 volumes of the same buffer. The sample was applied to a Mono Q [(R-CH_2-$N^+(CH_3)_3$] HR 5/5 column linked to an FPLC system and the polyphenol oxidase was eluted with 0.3 M NaCl in the 5 mM sodium phosphate buffer, pH 8.0, as shown in Figure 9 (Mono Q I peak; at Fraction No. 26). A second, smaller peak (Mono Q II) with polyphenol oxidase activity and brown color was eluted with 1 *M* NaCl at Fraction No. 31. Native PAGE of Mono Q I peak showed only one protein band (Coomassie Blue R-250 stain) and one concomitant activity band (stained with 8 mM catechol, 0.06% 3-methyl-2-benzothiazolinone hydrazone [MBTH]). Native PAGE of the Mono Q II peak gave five protein bands, all of them active. Most likely, these are modified PPO owing to reaction with PPO-produced benzoquinones. The purification of Grenache PPO is summarized in Table 8. We used the first peak (Mono Q I) for crystallization, which corresponded to unmodified polyphenol oxidase as indicated by no brown color.

Protein was determined using the 1976 Bradford assay (48) or by following the absorbance at 214 nm for column chromatography. Activity was determined by a modification of the colorimetric method described by Ponting and Joslyn (49) using 5 mM catechol as substrate and measuring the initial change in absorbance at 420 mM (pH 6.5, 25°C). One unit of activity is defined as an increase in absorbance of 0.001/min.

The M_r of the mature PPO was determined on gel filtration columns. M_r was 41.2 ± 2 kDa (replications = 4) on Sephadex G-75 (fine), 34.6 kDa on Superose 12 column (50), 28.0 kDa on TSKgel G3000 SW, and 22.9 kDa on TSKgel 2000 SW. Superose 12 columns are known to give M_r values that are too low (51). Note that the M_r values on TSK gels are even lower than those on Superose 12. All standard proteins were the same (bovine serum albumin, ovalbumin, β-lactoglobulin [dimer], chymotrypsinogen, and ribonuclease A). Based on our use of Sephadex columns for M_r determination for 37 years, we suggest the correct M_r is near 41.2 kDa.

REFERENCES

1. CF Schoenbein. On ozone and oronic actions in mushrooms. Phil Mag 11:137–141, 1856.
2. Enzyme Nomenclature. Recommendations of the Nomenclature Committee of the International Union of Biochemistry. San Diego: Academic Press, 1992.
3. K Lerch, L Ettlinger. Purification and characterization of a tyrosinase from *Streptomyces glaucescens*. Eur J Biochem 31:427–437, 1972.
4. TC Wong, BS Luh, JR Whitaker. Isolation and characterization of polyphenol oxidases of clingstone peach. Plant Physiol 48:19–23, 1971.
5. NJ Rivas, JR Whitaker. Purification and some properties of two polyphenol oxidases from Bartlett pears. Plant Physiol 52:501–507, 1973.
6. AC Allan, JRL Walker. The selective inhibition of catechol oxidases by salicylhydroxamic acid. Phytochemistry 27:3075–3076, 1988.
7. JRL Walker, RF McCallion. The selective inhibition of ortho- and para-diphenol oxidases. Phytochemistry 19:373–377, 1980.
8. WH Flurkey, B Ratcliff, L Lopez, J Kuglin, RM Dawley. Differentiation of fungal tyrosinases and lac-

cases using selective inhibitors and substrates. In: CY Lee, JR Whitaker, eds. Enzymatic Browning and Its Prevention. Washington: American Chemical Society, 1995, Symp Ser 600:81–89.
9. TD Sherman, KC Vaughn, SO Duke. A limited survey of the phylogenetic distribution of polyphenol oxidase. Phytochemistry 30:2499–2506, 1991.
10. TD Sherman, TL Gardeur, AR Lax. Implications of the phylodistribution of polyphenol oxidase in plants. In: CY Lee, JR Whitaker, eds. Enzymatic Browning and Its Prevention. Washington: American Chemical Society, 1995, Symp Ser 600:103–109.
11. D Osuga, A Van der Schaaf, JR Whitaker. Control of polyphenol oxidase activity using a catalytic mechanism. In: RY Yada, RL Jackman, JL Smith, eds. Protein Structure–Function Relationships in Foods. Glasgow: Blackie Academic & Professional, 1994, pp 62–88.
12. M Sugumaran. Molecular mechanisms for cuticular sclerotization. Adv Insect Physiol 21:179–231, 1988.
13. WK Silvers. The Coat Colors of Mice: A Model for Mammalian Gene Action and Interaction. New York: Springer-Verlag, 1979.
14. CJ Witkop Jr. Inherited disorders of pigmentation. In: RM Goodman, ed. Geno-dermatases: Clinics in Dermatology, Vol 2. Philadelphia: J.M. Lippincott, 1985, pp 70–134.
15. WC Quevedo Jr. Genetic regulation of pigmentation in mammals. In: T Kawamura, TB Fitzpatrick, eds. Biology of Normal and Abnormal Melanocytes. Baltimore: University Park Press, 1971, pp 99–115.
16 CJ Witkop Jr. Depigmentation of the general and oral tissues and their genetic foundation. Ala J Med Sci 16:331–343, 1979.
17. VL Singleton, JJL Cilliers. Phenolic browning: a perspective from grape and wine research. In: CY Lee, JR Whitaker, eds. Enzymatic Browning and Its Prevention. Washington: American Chemical Society, Symp Ser 60:23–48, 1995.
18. L Vamos-Vigyazo. Prevention of enzymatic browning in fruits and vegetables. A review of principles and practices. In: CY Lee, JR Whitaker, eds. Enzymatic Browning and Its Prevention. Washington: American Chemical Society, Symp Ser 600:49–62, 1995.
19. JRL Walker. Enzymatic browning in fruits. Its biochemistry and control. In: CY Lee, JR Whitaker, eds. Enzymatic Browning and Its Prevention. Washington: American Chemical Society, Symp Ser 600:8–22, 1995.
20. JRL Walker. The control of enzymatic browning in fruit juices by cinnamic acids. J Food Technol 11:341–345, 1976.
21. I Iyengar, A McEvily. Anti-browning agents: alternatives to the use of sulfites in foods. Trends Food Sci Technol 3:60–64, 1992.
22. RM Dawley, WH Flurkey. 4-Hexylresorcinol, a potent inhibitor of mushroom tyrosinase. J Food Sci 58:609–610, 670, 1993.
23. Y Luo, GV Barbosa-Canovas. Inhibition of apple-slice browning by 4-hexyl resorcinol. In: CY Lee, JR Whitaker, eds. Enzymatic Browning and Its Prevention. Washington: American Chemical Society, Symp Ser 600:240–250, 1995.
24. GM Sapers, RL Miller, S-W Choi. Prevention of enzymatic browning in prepeeled potatoes and minimally processed mushrooms. In: CY Lee, JR Whitaker, eds. Enzymatic Browning and Its Prevention. Washington: American Chemical Society, Symp Ser 600:223–239, 1995.
25. T Wakayama. Polyphenol oxidase activity in Japanese apples. Differences among cultivars and prevention by heat, ascorbic acid and reduced oxygen. In: CY Lee, JR Whitaker, eds. Enzymatic Browning and Its Prevention. Washington: American Chemical Society, Symp Ser 600:251–266, 1995.
26. C Billaud, E Regaudie, N Fayad, F Richard-Forget, J Nicolas. Effect of cyclodextrins on polyphenol oxidase catalyzed by apple polyphenol oxidase. In: CY Lee, JR Whitaker, eds. Enzymatic Browning and Its Prevention. Washington: American Chemical Society, Symp Ser 600:295–312, 1995.
27. MV Martinez Villar. Molecular analysis of grape (*Vitris vinifera* L., cv Gernache). Polyphenol oxidase and some aspects of grape tissue culture. PhD dissertation, University of California, Davis, 1996.
28. JR Whitaker. Polyphenol oxidase. In: DWS Wong, ed. Food Enzymes: Structure and Mechanism. New York: Chapman and Hall, 1995, pp 271–307.
29. RL Jolley Jr, DA Robb, HS Mason. The multiple forms of mushroom tyrosinase. Assocation-dissociation phenomena. J Biol Chem 244:1593–1599, 1969.
30. RL Jolley Jr, RM Nelson, DA Robb. The multiple forms of mushroom tyrosinase. J Biol Chem 244:3251–3257, 1969.
31. C Eicken, F Zippel, K Buldt-Karentzopoulos, B Krebs. Biochemical and spectroscopic characterization of catechol oxidase from sweet potatoes (*Ipomoea batatas*) containing a type-3 copper center. FEBS Lett 436:293–299, 1998.
32. T Klabunde, C Eicken, JC Sacchettini, B Krebs. Crystal structure of a plant catechol oxidase containing a dicopper center. Nature Struct Biol 5:1084–1090, 1998.
33. CEM Ebbelar, HJ Wichers, T Van den Bosch, JI Oyevaar, K Recourt. Characterization of a fruiting body expressed gene encoding a putative polyphenol oxidase in *Agaricus bisporus*. Accession No. X85113, March 6, 1995.
34. C Ebbelaar, H Wichers, T Van den Bosch, C Sarzier, J Haasjes, K Recourt. Characterization of fruiting body expressed gene encoding a putative tyrosinase in

Agaricus bisporus. Accession No. AJ223816, Jan. 30, 1998.
35. AR Macrae, RG Duggleby. Substrates and inhibitors of potato tuber phenolase. Phytochemistry 7:855–861, 1968.
36. DA Robb, T Swain, LW Mapson. Substrates and inhibitors of the activated tyrosinase of broad bean (*Vicia faba* L.). Phytochemistry 5:665–675, 1966.
37. K Lerch. *Neurospora* tyrosinase. Structural, spectroscopic and catalytic activity. Mol Cell Biochem 52:125–138, 1983.
38. EI Solomon, MJ Baldwin, MD Lowrey. Electronic structures of active sites in copper proteins: contributions to reactivity. Chem Rev 92:521–542, 1992.
39. S Gutteridge, D Robb. Catecholase activity of *Neurospora* tyrosinase. Eur J Biochem 54:107–116, 1975.
40. A Golan-Goldhirsh, JR Whitaker. k_{cat} inactivation of mushroom polyphenol oxidase. J Mol Catal 32:141–147, 1984.
41. JM Nelson, CR Dawson. Tyrosinase. Adv Enzymol 4:99–152, 1944.
42. C Dietler, K Lerch. Reaction inactivation of tyrosinase. In: TE King, HS Mason, M Morrison, eds. Oxidases and Related Redox Systems. New York: Pergamon Press, 1982, pp 305–317.
43. A Golan-Goldhirsh, DT Osuga, AO Chen, JR Whitaker. Effect of ascorbic acid and copper on proteins and other polymers. In: VT D'Souza, J Feder, eds. The Bioorganic Chemistry of Enzymatic Catalysis: An Homage to Myron L. Bender. Boca Raton: CRC Press, 1992, pp 61–76.
44. MG Peter, HB Stegmann, H Dao-Ba, K Scheffler. Detection of semiquinone radicals of N-acyldopamines in aqueous solution. Z Naturforsch 40C:535–538, 1985.
45. W Korytowski, T Sarna, B Kalyanaraman, RC Sealy. Tyrosinase-catalyzed oxidation of dopa and related catechol (amines): a kinetic electron spin resonance investigation using spin-stabilization and spin label oximetry. Biochim Biophys Acta 924:383–392, 1987.
46. M Sugumaran. Molecular mechanisms for cuticular sclerotization. Adv Insect Physiol 21:179–231, 1988.
47. AM Mayer, E Havel, R Ben-Shaul. Assay of catechol oxidase. A critical comparison of methods. Phytochemistry 5:783–789, 1966.
48. MM Bradford. A rapid and sensitive method for the quantitation of microgram quantities of protein utilizing the principle of protein-dye binding. Anal Chem 72:248–254, 1976.
49. JD Ponting, MA Joslyn. Ascorbic acid oxidation and the browning in apple-tissue extracts. Arch Biochem 19:47–63, 1948.
50. VM Martinez. Partial characterization of Chardonnay and Grenache polyphenoloxidases. Inhibitory effect of 4-hexylresorcinol. MS thesis, University of California, Davis, 1993.
51. S-C Lee. Comparative amino acid sequences, and deduced tertiary and quaternary structures of white kidney bean and black bean α-amylase inhibitors. PhD dissertation, University of California, Davis, 1996.

40

Laccase

William H. Flurkey
Indiana State University, Terre Haute, Indiana, U.S.A.

I. INTRODUCTION

Laccase was first discovered in the latex of *Rhus vernicifera*, Japanese lacquer tree, by Yoshida in 1883 (1) where it was observed to catalyze the oxidation of urushiol. The enzyme was "rediscovered" and named some 10 years later (1894–1896) by Bertrand (2), who found the enzyme in the lac trees and mushrooms. Laborde (3) also reported the existence of the enzyme in mushrooms in 1896. Laccase is a multicopper enzyme member of the blue-colored oxidase family (for reviews see 4–15). Laccase catalyzes the four-electron reduction of molecular oxygen to water. A variety of compounds, including substituted monophenols, *o*- and *p*- diphenols, methoxyphenols, aminophenols, aryl amines, and even some inorganic ions (i.e., potassium ferrocyanide), can serve as the electron donors in the reaction and are oxidized in the process (Table 1).

In general, laccases can oxidize a variety of *p*-diphenols, resulting in the production of *p*-diquinones (Fig. 1a). Oxidation of syringaldazine, a common laccase substrate, also proceeds through a free radical intermediate followed by formation of a quinone (Fig. 1b). The oxidation and formation of free radicals as semiquinones also occurs when laccase acts as a dimethyoxyphenol oxidase (Fig. 1c). With some substrates, this free radical formation leads to coupling reactions and or generation of quinone products. For example, *Rhus* laccase can act upon urushiol to yield coupled products (Fig. 1d), and plant laccases have been found to oxidize monolignols into dimers and trimers (Fig. 1e). Fungal laccases have also been found to convert syringylglycol guaiacol ethers into a variety of products containing aldehyde, carboxylic acid, ester, or quinone groups (Fig. 1f). Depending on the type of substrate and the type of laccase, a variety of products can be formed.

Chemical structures of some of the artificial substrates used to monitor laccase are shown in Figure 2. This list includes di- and tri-phenols, methoxy and amino phenols, phenylamine and phenylamine-like compounds and heterocyclic compounds. 2,2′-azino-bis-(3-ethylbenzthiazoline-6-sulfonic acid; ABTS) is currently one of the more common laccase substrates.

Laccase is classified as an oxidoreductase (benzenediol:oxygen oxidoreductase; EC 1.10.3.2). However, there is still apparent confusion over its Enzyme Commission (EC) classification number since there are recent publications about laccase using an EC number of 1.10.3.1 (*p*-diphenol:oxygen oxidoreductase) and 1.14.18.1 (*p*-diphenol:oxygen oxidoreductase) in the current literature.

II. IMPORTANCE TO QUALITY OF FOOD

The importance of laccase to the quality of food is directly related to its proposed biological function. Laccases are found in a variety of plants, fungi, and even some bacteria. In higher plants, laccases are thought to be involved in lignification and detoxification/protection. In fungi, laccases produce colored pig-

Table 1 Partial List of Natural and Artificial Substrates Used to Monitor Laccase Activity

t-butylcatechol	4-methoxy-α-naphthol	*o*- and *p*-aminophenols
catechol	4-methylcatechol	*o*- and *p*-anisidines
caffeic acid	α-naphthol	4-amino-N,N-diethylaniline
chlorogenic acid	protocatechuic acid	2,2′-azino-bis(3-ethylbenzthiazoline-6-sulfonic acid) (ABTS)
coniferyl alcohol	phloroglucinol	benzidine
p-coumaric acid	pyrogallol	3,3′-diaminobenzidine
coumaryl alcohol	resveratrol	2,7-diaminofluorene
p-cresol	resorcinol	N,N-dimethylaniline
2,6-dimethoxyphenol	quercetin	3,3′-dimethylbenzidine
dopa	toluqinol	*p*-phenylenediamine
gallic acid	urushiol	5,6-dihydroxyindole
hydroquinone	guaiacol	1,8-dihydroxynaphthalene
ferulic acid	vanillic acid	6-hydroxydopamine
hydroxycinnamic acid	sinapyl alcohol	phenylhydrazine
veratryl alcohol	sinapic acid	syringaldazine
quinol	eugenol	*o*-tolidine
ferrocyanide	ascorbic acid	1,2,4,5-tetramethoxybenzene

ments during chestnut blight pathogenic infections. Although laccases are different from lignin peroxidases, Mn peroxidases, and other peroxidases, they can utilize some of the same substrates, but they are proposed to be a less strong oxidant than these peroxidases. Because laccases can oxidize a variety of phenolic and phenolic-like compounds, they can also cause browning-like reactions in fruits and vegetables. The browning reactions decrease consumer product appeal, nutritional value, and marketability. The association of fungal laccases with many plant and fruit products poses other potential problems related to browning and crosslinking of polymeric material, and could affect product characteristics and properties during storage and processing.

III. LOCATION OF LACCASE

A. Tissue Localization

In plants, laccase has been located in lignifying xylem cells where it is associated with cell walls. Extracellular laccase is secreted by plant cell cultures. In these culture conditions, laccase was not found in the cytoplasm, but it was associated with cell walls. An epidermal location of laccase was indicated in stem tissue.

B. Methods for Determining Location

Spot tests, either of liquid culture samples or cultures grown on solid media, have relied on the use of colored products formed during enzymatic oxidations. Some of these tests have been used to distinguish white rot fungi from brown rot fungi and have been used for taxonomic classification. Immunocytochemical location of the fungal laccase from *Rigidoporous lignosus* grown on wood was carried out using antilaccase polyclonal sera and immunogold labeling (17). These studies found laccase to be located in fungal cytoplasm, in vesicle-like structures at the plasmalemma, in the cell wall, and in the extracellular slime layer connecting fungal cells to wood. In liquid-grown cultures of the fungus *Coprinus congregatus*, laccase located in the hyphal tips was suggested to be involved with sclerotia/primordia formation (18).

In plants, cytochemical localization of laccase has relied upon the use of syringaldazine, 2,7-diaminofluorene (DAF), 2,2′-azinobis(3-ethylbenzthiazoline-6-sulfonate; ABTS), and 4-methylcatechol as substrates. Laccase was localized to active lignifying zones of xylem cells in loblolly pine sections using DAF as a substrate (19). Similarly, cytochemical localization of laccase in tobacco stem cells was found in the outermost lignifying zones in xylem tissue (20). Driouch et al. (21) found laccase excreted in the extracellular medium and associated with cell walls in sycamore cell cultures by cytochemical and immunocytochemical methods. In contrast, De Marco and Roubelakis-Angelakis (22) observed laccase in areas where lignification was thought to occur in tobacco protoplasts.

Tissue printing of stem cross sections using 4-methyl catechol and syringaldazine as cytochemical substrates

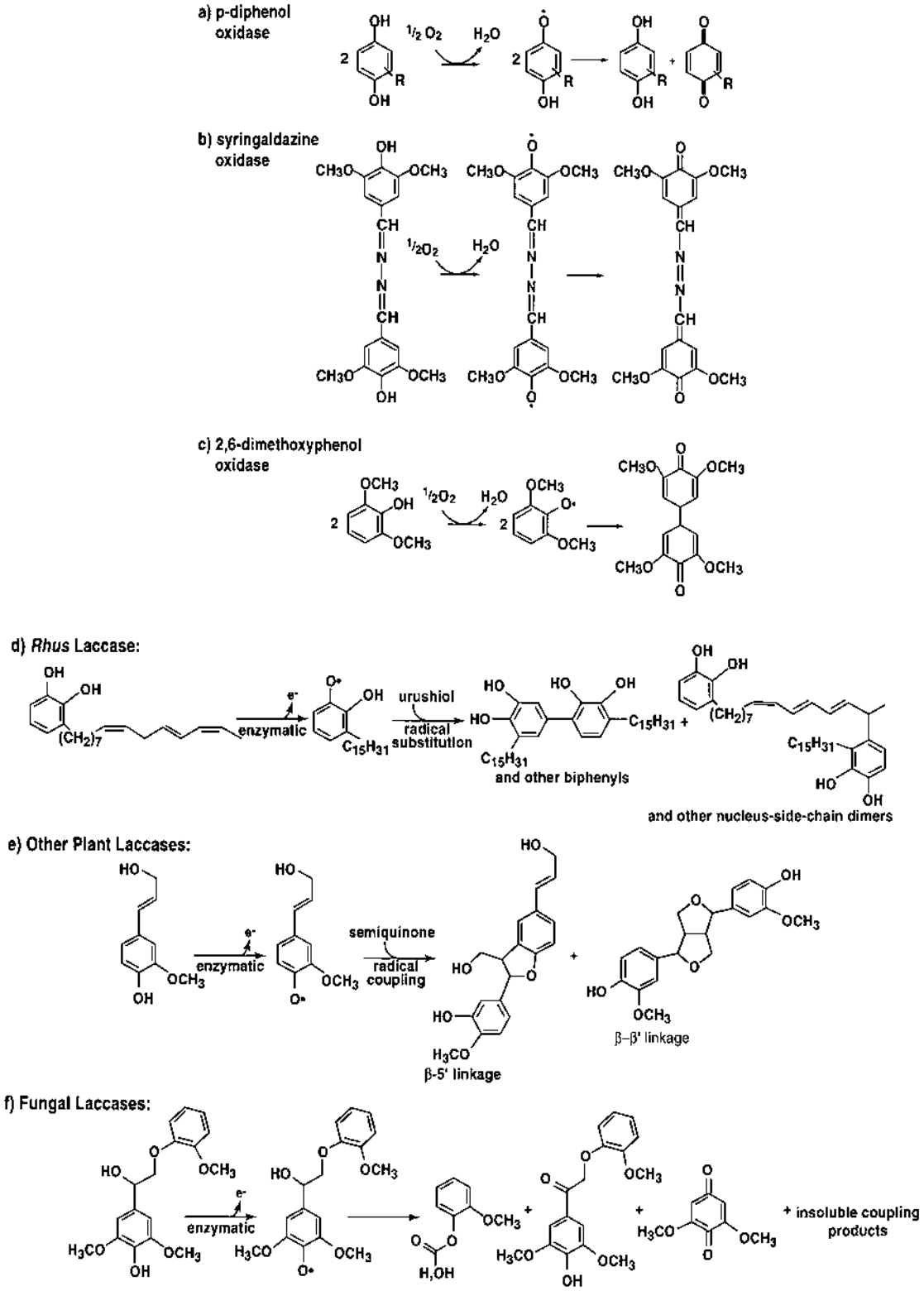

Figure 1 Types of reactions catalyzed by laccases. Reactions appearing in (a)–(c) were taken from Sanchez-Amat and Solano (16) and reactions appearing in (d)–(f) were taken from Solomon et al. (6).

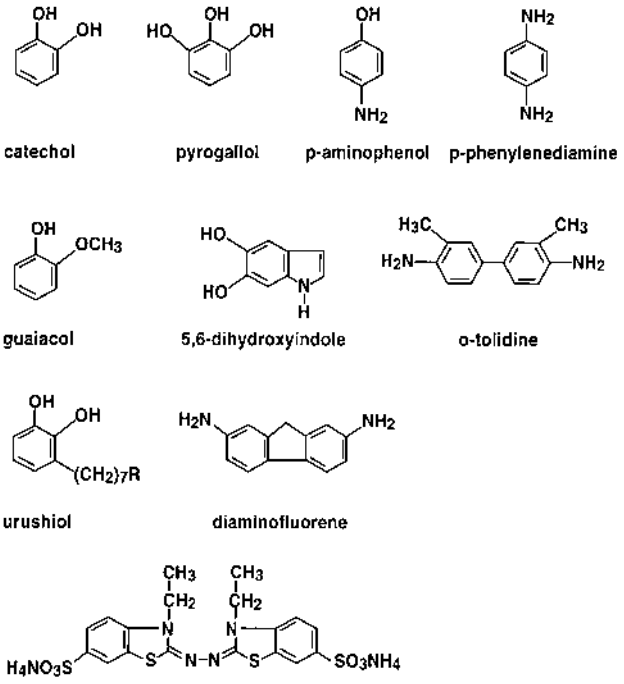

Figure 2 Chemical structures of substrates used to monitor laccase activity.

coupled with immunolabeling located laccase in the epidermal tissue (21). In petiole tissues, laccase was located in lignifying cell walls of xylem and epidermal cells. All cytochemical methods must employ some method to distinguish peroxidase and tyrosinase (catechol oxidase, phenol oxidase) from laccase. Peroxidase can be distinguished from laccase by samples treated with and without hydrogen peroxide and by including catalase in the incubation medium to remove hydrogen peroxide. A variety of tyrosinase inhibitors (i.e., tropolone, SHAM (salicylhydroxamic acid), 4-hexylresorcinol) can be included in the incubation medium to block tyrosinase activity without affecting laccase activity.

IV. UTILIZATION OF LACCASE IN FOOD

Besides its use as a bleaching agent in the wood pulp and paper industry, laccase has been used in dechlorination and for removal of phenolic compounds from wastewater. In relation to the food industry, laccase has been used in assays for phenols in natural juices (23). It has also been used as a biosensor for determination of polyphenols/catechols in tea (24). Immobilized laccase has been used to remove phenols from apple juice (25) and in must and wine (26). Lante et al. (27) also reported the use of laccase as a stabilizer during must and wine processing. Soft rot in some crop plants and gray rot in grapes are a result of *Botrytis cinerea* infection. The extracellular laccases produced by *B. cinerea* are apparently involved in pathogenesis (28). Thus, laccase may have detrimental effects on infected food products.

Laccase is extremely important for lignin degradation in providing compost material and nutrients during mushroom cultivation. Constitutively produced laccase increases during growth of *Agaricus bisporus* on compost and declines when fruit formation occurs (29). Laccase seems to be associated with vegetative growth. Extracellular laccases (ECLs) have also been used to define distinct species/strains in *Agaricus bisporus* and can be used as phylogenetic markers (30).

Recently, Figueroa-Espinoza and Rouau (31) reported the use of laccase to crosslink wheat arabinoxylans in model systems. This crosslinking affected the structure and properties of nonstarch polysaccharides, including gelation properties. The potential effects on food functionality related to this observation have yet to be determined.

Other commercial uses for laccases involve lignin degradation, bioadhesives, biosensors, bioremediation, removal of phenolic compounds from waste water, use in enzyme assays and immunosensors, and applications in organic synthesis (4).

V. MOLECULAR PROPERTIES OF LACCASE

A. Molecular Weight

Fungal and plant laccases vary considerably in size. Depending on the method of size estimation (ultracentrifugation, size exclusion, electrophoresis, predicted size from gene sequence), the molecular size of laccase ranges from 40 to 100 kDa. The more common size range is from 60 to 80 kDa, however. Most laccases are active as monomeric subunits, but dimeric and other multimeric combinations of the monomeric subunits have been reported.

B. Structure

Laccases sequenced by protein or DNA methods have been shown to be composed of a single polypeptide containing 500–580 amino acids (4, 5, and references therein). They are synthesized with an N-terminal leader peptide that is cleaved after translation. The

mature polypeptide contains N- and O-linked glycosylation sites, four copper atoms, and two or three disulfide bonds. Because laccase has not been crystallized and analyzed by x-ray crystallography, the secondary and tertiary structures are unknown. However, laccases do show some amino acid homology and similarity to ascorbate oxidase and ceruloplasmin, especially at the copper-binding sites. Because of this homology, the hypothetical secondary and tertiary structures are thought to be very similar to ascorbate oxidase.

Using this homology and similarity as model, three domains found in ascorbate oxidase are postulated to be present in laccase (4, 9). These domains in ascorbate oxidase are composed of β-barrel/β-strand motifs. By analogy to ascorbate oxidase, domain 1 should contain β–pleated sheets forming a β-sandwich motif. Domain 2 should contain β-pleated sheets and short stretches of α-helices. Domain 3 should contain two five-stranded β-pleated sheets forming a β-barrel and short α-helix stretches. Support of this comparative analogy comes from differentially scanning calorimetry, which has suggested the presence of three domains in laccase (32).

Predictive structural features would suggest that domain 1 would be connected to domain 3 by disulfide bonds. Overall, predictions suggest there would appear to be very little α-helix, a large percentage of β-sheets, and several types of turns. The C-terminal end may be blocked, buried, and/or susceptible to limited proteolysis. In general, laccase is predicted to show more homology to ascorbate oxidase than ceruloplasmin, plastocyanin, or azurin (4, 5, and references therein). Based on amino acid sequence homology, laccase has homology to ascorbate oxidase in the Cu-binding ligands, linkage of domains 1 and 3, the trinuclear Cu center, and the C-terminus. See Table 2 for a comparison of the amino acids in the copper binding sites for 10 laccases and three ascorbate oxidases. Comparisons of the blue oxidases suggest gene duplication from an ancestral blue copper protein. Even though laccase and tyrosinase both contain a type 3 copper center, this center is distinctly different in laccase (6). There is apparently little to no homology of laccase to the copper-binding regions of tyrosinase. Complete sequence information for cloned or determined sequences is available (4, 5).

C. Isoforms

Isoforms of laccase have been found in both fungi and plants. These isoforms differ in their size, charge, and kinetic properties. Some of these isoforms are due to multiple genes coding for the enzyme (33). Because many laccases are glycoproteins, isoform differences can arise from variations in carbohydrate content, linkages between carbohydrate units, and location of linkages to the polypeptide backbone. Heterogeneity due to carbohydrate content/structure can arise posttranslationally and after excretion. Other isoforms and enzyme inactivation can arise from limited proteolysis (34). Because laccases are often associated with phenolic material, the potential for artifactual protein modification during synthesis, excretion, culture conditions, and isolation also exists. Support for this comes from finding a "yellow" laccase that apparently is a modified form of the original "blue" laccase because of modification of a copper center by lignin phenolics (35).

VI. ENZYME PROPERTIES

A. Substrate Specificity

Although laccase can utilize a variety of substrates as electron donors, few recent reports have examined substrate specificity in terms of k_{cat}/K_m. In general, plant and fungal laccases have low substrate specificity (high K_m) in the mM range for organic substrates. Other studies have shown that the k_{cat}/K_m is correlated with the substrate oxidation potential (6). These observations have suggested that laccase has no phenolic substrate binding pocket and oxidation takes place by direct transfer of an electron(s) through an outer sphere mechanism to the T1 Cu-binding site (6). Physiological substrates for plant laccases include *p*-coumaryl, coniferyl, and sinapyl alcohols in which laccase can cause oxidative coupling of the substrates (6, 19). Physiological substrates for fungal laccases depend on the role laccase plays. A list of natural and artificial substrates for laccase appears in Table 1.

B. Effect of Environmental Factors

Many laccases have pH optima in the acidic pH range (pH 3–6), although some alkaline pH optima have been reported (Table 3). In general, fungal laccases usually have lower pH optima than plant laccases; however, the pH optimum is often dependent upon which substrate is chosen to assay laccase. The type of product formed also depends on the pH and the substrate. For example, at pH 3.5 two products were identified from oxidation of syringic acid by laccase while at higher pH values four different products were observed (7). The pH stability of the laccase iso-

Table 2 Comparison of Amino Acids in the Copper Centers of Laccase and Ascorbate Oxidase

	177	178	179	238	239	240	718	719	720	721	722	723	803	804	805	806	807	808	809	810	811	812	813	814
Laccase																								
Aspergillus nidulans	H	W	H	H	S	H	H	P	I	H	K	H	H	C	H	I	A	S	H	Q	M	G	G	M
Phebia radiata	H	W	H	H	S	H	H	P	F	H	L	H	H	C	H	I	D	W	H	L	E	A	A	L
Coriolus hirsutus	H	W	H	H	S	H	H	P	F	H	L	H	H	C	H	I	D	F	H	L	E	A	G	F
Neurospora crassa	H	W	H	H	S	H	H	P	I	H	L	H	H	C	H	I	A	W	H	V	S	G	G	L
Cryphonectria parasitica	H	W	H	H	S	H	H	P	I	H	L	H	H	C	H	I	A	W	H	V	S	A	G	L
Filobasidiella neoformans	H	W	H	H	S	H	H	P	Y	H	L	H	H	C	H	I	G	W	H	L	T	E	G	K
Pleurotus ostreatus	H	W	H	H	S	H	H	P	F	H	L	H	H	C	H	I	D	W	H	L	E	I	G	L
Agaricus bisporus	H	W	H	H	A	H	H	P	F	H	L	H	H	C	H	I	D	W	H	L	E	A	G	L
Basidiomycete PM1	H	W	H	H	S	H	H	P	F	H	L	H	H	C	H	I	D	F	H	L	E	A	G	F
Acer pseudoplatanus	H	W	H	H	A	H	H	P	M	H	L	H	H	C	H	F	E	R	H	T	T	W	G	M
Ascorbate oxidase																								
Cucumber	H	W	H	H	G	H	H	P	W	H	L	H	H	C	H	I	E	P	H	L	H	M	G	M
Pumpkin	H	W	H	H	G	H	H	P	W	H	L	H	H	C	H	I	E	P	H	L	H	M	G	M
Zucchini	H	W	H	H	G	H	H	P	W	H	L	H	H	C	H	I	E	P	H	L	H	M	G	M
	2	–	3	3	–	3	1	–	–	2	–	3	3	1	3	–	–	1	–	–	–	–	–	1

Numbers at the top of the columns represent alignment of amino acid residue numbers in ascorbate oxidase. Numbers at the bottom of the columns represent amino acid residues associated with the type 1, 2, or 3 copper centers of both enzymes.

Table 3 pH and Temperature Properties of Laccases

Laccase source		pH optimum	pH stability	Temperature optimum (°C)	Temperature stability (°C)
Fungal					
Coriolus hirsutus		3.5–4.5			
Schizophyllum commune		5.4–6.0			
Rhizoctonia practicola		6–7			
Coriolus versicolor		4–5			
Agaricus bisporus		3.6, 5.6			$t_{1/2}$ 40 min @ 60
Pleurotus eryngii	I	4	5–7	65	$t_{1/2}$ 30 min @ 50
Pleurotus eryngii	II	3.5	8–12	55	$t_{1/2}$ 25 min @ 55
Basidiomycete PM1		4.5	3–9	80	60 min @ 60
Trametes villosa	1,2,3	5–5.5			
Pleurotus ostreatus	POXC		$t_{1/2}$ 30 min @ pH 3	50–60	$t_{1/2}$ 30 min @ 60
	POXA1		$t_{1/2}$ 24 h @ pH 3	45–65	$t_{1/2}$ 200 min @ 60
	POXA2		$t_{1/2}$ 2 h @ pH 3	25–35	$t_{1/2}$ 10 min @ 60
Monocillium indicum		3.0, 5.0	2–6	60	$t_{1/2}$ 10 min @ 70
Cerrena unicolor		5.0–5.6	6–8	60	
Plant					
Schinus molle		6.2			
Acer pseudoplatanus		6, 6.8	4–10		

forms varies considerably. Some are stable over a wide pH range (pH 3–7) while others are more pH sensitive.

Many laccases are relatively heat stable, but specific thermal stability properties are associated with each laccase isoform (Table 3). Half-lives of 30 min at 50–65°C for laccase isoforms are not uncommon, while temperature optima are generally > 50°C.

C. Inhibitors

Laccases are inhibited by a variety of compounds that can be classified into groups such as Cu chelators, reducing agents, detergents, and free radical scavengers. Cu chelators include EDTA, CN^-, sodium azide, and diethyldithiocarbamic acid. Cetyltrimethyl–ammonium bromide (CTAB), a cationic detergent, seems to inhibit some laccases in a competitive or noncompetitive manner (36). Short-chain carboxylic acids have also been reported to inhibit some laccases (37). Desferal inhibits laccase by deactivating phenoxy radicals (38). Tiron, a superoxide ion and hydroxyl ion quinone scavenger, also decreased the activity of laccase-like oxidases in tobacco xylem (39). Halides, especially F^-, are potent inhibitors of laccase (40). N-Hydroxyglycine has been reported to be a specific inhibitor of laccase by Murao et al. (41) and later by others (42–44). However, recent work in our laboratory suggests this may be an artifact (data not shown).

D. Mechanism of Action

Laccases contain three copper centers. The type 1 copper center (T1) is responsible for the blue color of the protein because of the intense absorption at 600 nm. T1 centers also show small hyperfine splitting in an electron paramagnetic spectrum (EPR). Type 1 centers are proposed to involve the $1e^-$ oxidation of the substrate. Type 2 (T2), or normal copper centers, have no absorption to the visible spectrum and show EPR spectrum characteristic of tetragonal Cu complexes. Type 3 centers (T3) contain two copper ions and are termed coupled binuclear copper centers. They have no EPR signals but do absorb in the UV spectrum (330 nm). In laccases, T2 and T3 centers form a trinuclear copper cluster. This cluster is responsible for the $4e^-$ reduction of molecular oxygen to water.

The exact mechanism for laccase catalysis has not been elucidated. A proposed mechanism appears in the work by Solomon et al. (6). In this mechanism an electron from the substrate is transferred to the T1 copper site. The site transfers an e^- to the T2–T3 sites. Reduction of the trinuclear cluster is thought to occur by either sequential reduction of each copper in the trinuclear cluster or by reduction of the T3 copper pair by T1 and T2. Because there are a total of 4 Cu ions, a variety of intermediates with different Cu oxidation states in the copper sites have been postulated. A somewhat different mechanistic scheme is

presented in the review by Yarpolov (8). In all of the proposed mechanisms, all e^- pass through the T1 site first.

E. K_m and k_{cat} Values

K_m values for organic laccase substrates are generally in the 0.1–10 mM range for a variety of phenolic and phenolic amine-like compounds (6, 8, 40). Some hydroxyindole derivatives, such as 5,6-dihydroxyindole, have K_m values < 0.1 mM (45). For molecular oxygen as the second substrate, K_m values are in the order of 10^{-5} M and V_{max} values are 50 to $300\,M^{-1}\,sec^{-1}$ (8). k_{cat}/K_m values versus electron reduction potentials at the T1 site show a positive correlation (6). As a result, comparisons between different laccases and different substrates correspond to redox potentials between the T1 site and the electron donor substrates. k_{cat} values range from 70 to $2000\,sec^{-1}$ (8) or from 100 to $3600\,min^{-1}$ (40). According to Xu, k_{cat}/K_m differences in a variety of substituted phenolic substrates were associated with changes in k_{cat} primarily (40). Turnover numbers (expressed as k_{cat}) are generally larger than individual intramolecular electron transfer rate constants (8).

F. Inhibitors and Other Physicochemical Data

Surprisingly, there appear to be few data for E_{act}, $\Delta H^{\ddagger}$, $\Delta G^{\ddagger}$, or $\Delta S^{\ddagger}$ with regard to laccase. More data are available relating to electron reduction potential differences in native and modified laccases. Most data for inhibition of laccases are reported in terms of percent inhibition relative to some control/standard. A few reports have determined I_{50} values for selected inhibitors. Because there are few if any specific inhibitors of laccase, few data are available for K_i values. Walker and McCallion (36) examined the effect of CTAB, a cationic detergent, on several *p*-diphenol oxidases. Using CTAB, K_i values ranged from 0.25 to 23 mM depending on the substrate and source of laccase. Desferal has a high I_{50} for laccase (38), while N-hydroxyglycine was shown to have a low I_{50} for *Coriolus vesicolor* laccase of $0.1\,\mu M$ (41). Faure et al. (43) also determined the I_{50} for N-hydroxyglycine using *Pyricularia oryzae* and *A. lipoferum* laccases and *o*-aminophenol, *p*-aminophenol, and syringaldazine as substrates. These I_{50} values ranged from 50 to $800\,\mu M$. Caution must be used when interpreting data with N-hydroxyglycine because it may not inhibit the enzyme but might interact with the products of the reaction (51).

G. Unique Properties

Laccase catalyzes a variety of reactions including oxidation, coupling of free radical intermediates, carbon–carbon bond cleavage, polymerization, and crosslinking. Oxidative and nonoxidative decarboxylation of phenolic compounds have also been reported. Hydroxyindole derivatives are also acted upon by plant and fungal laccases. Laccase oxidizes ascorbic acid in the absence of a phenol-like substrate. More recently, laccase contamination in commercial tyrosinase preparations was responsible for the novel conversion of dimethoxy allyl phenol to its corresponding quinone methide instead of tyrosinase (46).

VII. QUALITATIVE AND QUANTITATIVE DETERMINATION OF ACTIVITY

A. Assay Conditions

In general, most laccases are assayed in buffers of pH 3–8 with variations in buffer concentrations from 10 to 100 mM. Changes in phenolic substrates can be monitored spectrophotometrically using continuous, fixed end points, and scanning absorption methods. Assay volumes vary from 1 to 3 mL for spectrophotometric assays and 3–4 mL for oxygen consumption assays. There is no one best method for determining laccase activity because of the differences in substrate and pH preference for each laccase isoform. A suitable substrate, pH, and buffer must be determined experimentally for each laccase.

Colorimetric assays have employed four different substrates that give uniquely colored products—2,6-dimethoxyphenol (DMP; brown), ABTS (blue-green), syringaldazine (SYR; pink), *o*-tolidine (TOL; blue). For example, 3 mL of 5 mM DMP, freshly prepared in buffer, can be monitored at 468 nm ($\epsilon = 14{,}800\ M^{-1}\ cm^{-1}$) after the addition of 5–50 μL enzyme. Likewise, 3 mL of 0.5 mM ABTS, prepared fresh in buffer, can be monitored at 420 nm ($\epsilon = 36{,}800\ M^{-1}\ cm^{-1}$). With the third substrate, stock solutions of 1–5 mM syringaldazine are dissolved in 95% ethanol. Because of the limited solubility of syringaldazine, assays for laccase usually contain 10% ethanol. Even then, syringaldazine precipitates out of solution with time. The assay solution, usually 1 mL, contains 20–50 μM concentrations of syringaldazine dissolved in buffer and is monitored at 525 nm ($\epsilon = 65{,}000\ M^{-1}\ cm^{-1}$). Because of turbidity at this wavelength, blank assays in a reference cell should contain all assay components except enzyme. With the fourth substrate, tolidine stock solu-

tions (5–40 mM) are also dissolved in 95% ethanol. Assay solutions, usually 3 mL, contain 1–5 mM tolidine when added to buffer so that the ethanol concentration remains below 10% (v/v). Five to 50 μL of enzyme is added to initiate the reaction, and the product is monitored at either 366 nm (UV) or 630 nm (VIS). Because the ϵ is not known for tolidine, units of enzyme activity are expressed in absorbance changes per min. For substrates with known ϵ values, enzyme activity is expressed in either changes in absorbance per min or μmol product formed per min.

Oxygen uptake assays can be determined using Clark-type oxygen electrodes by YSL, Hansatech, or Rankin Brothers. Air-saturated buffers are commonly used as the oxygen source and are$\sim$ 240–280 μM in oxygen. Reactions using any of the methods are normally carried out at ambient temperatures, although some reactions have been carried out at 30°C. Oxygen uptake assays must have the temperature controlled more precisely, because oxygen solubility in aqueous solutions is temperature dependent and the enzyme reaction rate is affected by temperature. Water-insoluble substrates or those with limited aqueous solubility are sometimes dissolved in a polar solvent (ethanol, methanol, dimethylsulfoxide) to make stock solutions. Oxygen has a greater solubility in some polar solvents than aqueous buffer solutions; therefore the amount of dissolved oxygen may increase with the addition of substrates dissolved in these solvents. Most laccase assays can tolerate at least 10% ethanol, but this depends on the source of laccase and its stability.

Using oxygen uptake assays for example, a 4-mL assay volume of 0.5 mM ABTS is pre-equilibrated until the percent oxygen reaches a steady value. Enzyme is added (5–25 μL) and the oxygen uptake is followed for 1–10 min, depending on the substrate and enzyme concentration. Units of enzyme are expressed in % O_2 consumed per min or μL of O_2 consumed per min. If the exact concentration of O_2 can be determined in the air-saturated buffer, then units may be expressed in μmol O_2 consumed per min.

B. Natural and Synthetic Substrates

The natural substrate for fungal laccase is presumably lignin. This lignin can originate from pulp Kraft or sulfite-type processed softwoods and hardwoods. Plant laccases, on the other hand, use monolignols (coniferyl, sinapyl, and *p*-coumaryl alcohols) as substrates to produce water-insoluble dehydrogenation polymers (DHPs). Oxidation and oligomerization of monolignols is usually monitored using high-performance liquid chromatography size exclusion chromatography (HPLC-SEC). The following method, in which production of DHPs were made from coniferyl alcohol, is a summary from Sterjiades et al. (47, 48). Coniferyl alcohol (10 mM) in 20 mM phosphate buffer (pH 6.8) was incubated for 24 h with laccase ($\sim$ 5 μg) isolated from cultured sycamore maple cells. DHPs were recovered from the reaction by centrifugation at 48,000 g for 30 min. The precipitates were resuspended in water and centrifuged again. This resuspension–centrifugation cycle was repeated for a total of three times. DHPs were dissolved in dimethylformamide and diluted to a concentration of 10 μg/mL for analysis by HPLC-SEC. DHPs were separated on an 8 × 300 mm Showdex KD-802 Millipore HPLC column (styrene divinylbenzene gels) equilibrated in dimethylformamide and 100 mM LiBr. Separations were carried out at 55°C with a flow rate of 1 mL/min. Column eluants were monitored at 280 nm. Several peaks of polymerized monomeric material larger in size than coniferyl alcohol were observed. To monitor the oxidation of coniferyl alcohol during this process, the reactions were scanned from 230 to 400 nm at various time intervals. In comparison to control reaction, mixtures that contained no enzyme, a decline in absorbance at 264 nm occurs. Depending on the choice of initial substrates, new absorption peaks sometimes appear at lower wavelengths.

Other substrates used to monitor laccase activity are listed in Table 1. Spot tests for laccase have used ABTS, gum guaiac, α-naphthol, syringaldazine, and *o*-tolidine as substrates. ABTS, *o*- and *p*-phenylenediamine, *o*-dianisidine, syringaldazine, 4-methoxy-α-naphthol, tetramethylphenylenediamine, and tetramethyl benzidine have been used for histochemical localization of laccase in plants and fungi.

C. Unique Factors That Affect Enzyme Activity

Several factors affect the ability to obtain meaningful assays for laccase. One factor is halide inhibition. Although F^- is a very potent inhibitor of laccase (I_{50} of 0.02–0.5 mM), I_{50} values for Cl^- range from 0.05 to 600 mM for plant and fungal laccases (39). Chloride ions are often found in buffers and may have some effect on the enzyme during purification and in buffer preparation. Short-chain carboxylic acids, including acetic acid, also inhibit laccase. Since acetic acid/acetate is present in some buffers used for the assay of laccase, they may also affect the enzyme. The pH affects the type of products produced (8) and kinetic

parameters (K_m, V_{max}, k_{cat}). Inhibition of the enzyme also increases as the pH is increased and when the ionic strength is increased.

Peroxidases can utilize many of the same substrates as laccase (i.e., syringaldazine, ABTS, tolidine, guaiacol, etc.). If care is not taken to eliminate or distinguish peroxidase from laccase, estimation of laccase activity or reactions attributed to laccase can be misinterpreted. The presence of peroxidase activity is usually monitored with a suitable electron donor in the presence or absence of hydrogen peroxide. Catalase can be added to laccase assays to remove any hydrogen peroxide formed, thus eliminating reactions which might arise from peroxidase.

Tyrosinase can also use many of the same substrates as laccase (i.e., catechol, dopa, phenylenediamine, pyrogallol). This activity can be eliminated by using specific tyrosinase inhibitors (tropolone, salicylhydroxamic acid, 4-hexylresorcinol) in assays for laccase (44). However, these inhibitors may react with products during the oxidation process and can possibly interfere with laccase estimations. Catalase can be added to remove endogenous hydrogen peroxide; however, oxidation of some phenolic substrates has been attributed to peroxidatic activity of catalase.

VIII. PURIFICATION OF LACCASES

A. Methods

There is no best method for the purification of laccase because of the varied number of isoforms and different characteristics. Laccases have been purified most often from extracellular fluids from fungal and plant cell cultures. In general, fungal laccase purifications employ some method for removal of cells (filtration, centrifugation) followed by concentration of the extracellular fluid using ultrafiltration or precipitation methods (ethanol, ammonium sulfate). The dialyzed and concentrated extract has been subjected to ion-exchange chromatography (IEC). IEC methods have utilized chromatography on DEAE-cellulose, QAE and mono Q columns at low salt concentrations near physiological pH. Laccase isoforms are eluted from the exchangers using increasing linear salt gradients (i.e., 0–0.5 M NaCl) depending on how tightly the enzyme binds to the exchanger. IEC can be preceded or followed by size exclusion chromatography (SEC). Typical SEC methods have used Superose-12, Superdex 75, Sephadex G-100, and Sephacryl S-200. In many cases, the enzyme is highly purified after concentration after IEC and SEC. When necessary, further purification methods have employed hydrophobic interaction chromatography (HIC) on phenyl Sepharose using initial buffers containing high ammonium sulfate concentration. Enzyme is eluted by decreasing the salt concentration stepwise or by gradient elution.

The following method is a summary of the purification of laccases from *Trametes villosa* by Yaver et al. (49). The fungus was grown in a defined medium at room temperature. The defined medium depends on the type of fungi cultured. After 4 days, 1.3 mM (final concentration) 2,5-xylidine was added to induce laccase production. Cultures were allowed to grow another 24 h before filtering, high-speed centrifugation, and concentrating the filtrate using an Amicon S1Y100 ultrafiltration membrane. After dialysis, the sample was subjected to IEC on a Q-Sepharose (Pharmacia) column equilibrated with 10 mM Tris (pH 7.7).

Some laccase activity was not adsorbed onto the IEC resin and was eluted with buffer. Two other peaks of laccase activity were adsorbed onto the column and separated by a linear 0–0.5 M NaCl gradient elution. The three laccase peaks were pooled separately, concentrated by Centricon-10 concentrators (Amicon), and subjected to SEC on a Superdex 75 column (Pharmacia). SEC columns were equilibrated in 10 mM Tris (pH 8) containing 150 mM NaCl. Active fractions were pooled, resulting in three different laccase fractions, identified as *neutral* (laccase 3), *neutral-acidic* (laccase 2), and *acidic* (laccase 1) forms (Table 4).

All three laccases showed the same apparent MW of 60–70 kDa after SDS-PAGE. SEC suggested a native size of 130 kDa. Laccase 1 consisted of a single isoform with a pI of 3.5. Laccase 2, apparently homogeneous by SDS-PAGE, consisted of five isoforms identified by isoelectric focusing with pIs of 5, 6, 6.2, 6.5, and 6.8. Laccase 3, apparently homogeneous by SDS-PAGE, contained three isoforms with pIs of 6.2, 6.5, and 6.8. While forms 1 and 3 were typical of other blue oxidases, laccase 2 showed a reduced absorbance at 605 nm. Laccase 1 had a different N-terminal sequence from laccases 2 and 3, which had similar N-terminal sequences. All forms showed differences in substrate preference and pH stability characteristics.

Extracellular plant laccases have been isolated by concentrating the extracellular fluid followed by HIC on phenyl Sepharose (2.6 × 30 cm column; 2 M potassium phosphate buffer, pH 6.7). Enzymes are typically eluted from HIC columns with a decreasing salt gradient.

Table 4 Purification of Laccases from *T. villosa* Culture Filtrates

Sample	Volume (mL)	Total protein (mg)	Total activity (μmol min^{-1})	Specific activity (μmol min^{-1}/mg protein)	Purification (fold)	Yield (%)
Culture filtrate	1500	11,000	1800	0.16	1	100
conc. culture filtrate	280	460	1500	3.3	21	83
Q-Sepharose						
neutral form	0.40	5.1	270	53	330	15
neutral-acidic form	0.42	9.6	108	11	69	6
acidic form	0.2	14.0	430	31	190	24
Superdex-75						
neutral form	4.0	1.7	122	72	450	6.8
neutral-acidic form	7.0	4.1	117	29	180	6.5
acidic form	4.5	2.0	131	66	410	7.3

Source: Dr. D. Yaver and Dr. F. Xu at Novo Nordisk Biotech Inc., Davis, CA.

Because fungal and plant laccases are glycoproteins, some purification methods have employed lectin affinity chromatography on concanavalin A (Con A) Sepharose. Following is a summary of the purification used by Drouich et al. (21) to isolate laccase from sycamore cell cultures. Proteins in the extracellular fluid were precipitated with 5 M ammonium sulfate at 4°C. After centrifugation of the precipitated protein, the pellet was dissolved in 10 mM Tris buffer (pH 7.4) containing 1 mM $MnCl_2$ and 1 mM $CaCl_2$. The sample was applied to a Con A Sepharose column (1.5×30 cm) equilibrated in the above buffer. Laccase was eluted from the column with buffer containing 50 mM methylmannoside. Laccase was precipitated from the solution with 5 M ammonium sulfate, washed with cold acetone, and dissolved in a small volume of 10 mM Tris buffer (pH 8.8), containing 10% glycerol. The sample was subjected to preparative native gel electrophoresis using the Laemmli system. After locating the laccase activity by staining the gel briefly with catechol, areas of active enzyme were excised from the gel and subjected to electroelution. Further purification of laccase for antibody production used preparative SDS-PAGE, followed by electroelution.

B. Other Aspects of Purification

Laccases are generally expressed constitutively in cell culture, but higher levels can be produced using phenolic compounds as inducers. Some of these inducers include phenolic acids, anthroquinones, or 2,5-xylidine. Chelators, such as EDTA and EGTA, in the culture medium have been found to repress laccase activity and levels. The distribution of expressed laccase isoforms is often dependent on the type of culture conditions (shake vs. stationary), culture medium, and phenolic inducer used. Many of the purified laccases have small fold purification factors (based on the specific activity of starting material compared to purified samples), indicating the laccase is a major protein in the extracellular fluid or that there is a significant loss in activity during purification. Purified laccases are typically blue in color when concentrated, but the *Agaricus bisporus* laccase was reported to be yellow in color (34) and a "white laccase" (50) has also been reported. "Yellow" laccases, modified by reactive products of lignin degradation, may be generated from blue laccases during the isolation of laccases (35). Purified laccases are usually stable for several years when stored frozen. *Rhus vernicifera* laccase is commercially available from Sigma Chemical Co.; a *Coriolus versicolor* laccase is available from Mercian Corp., Tokyo.

REFERENCES

1. H. Yoshida. Chemistry of lacquer (Urushi), part 1. J Chem Soc 43:472–486, 1883.
2. G Bertrand. Sur la presence simultanee de la laccase et de la tyrosinase dans le sue quelues champignons. C R Hebd Seances Acad Sci 123:463–465, 1896.
3. J Laborde. Sur lacasse des vins. C R Hebd Seances Acad Sci 123:1074–1075, 1896.
4. A Messerschmidt. Multi-Copper Oxidases. New Jersey: World Scientific, 1975.
5. CF Thurston. The structure and function of fungal laccases. Microbiol. 140:19–26, 1994.

6. EI Solomon, UM Sundram, TE Machonkin. Multicopper oxidases and oxygenases. Chem Rev 96:2563–2605, 1996.
7. FS Sariaslani. Microbial enzymes for oxidation of organic molecules. In: GG Stewart, I Russel, eds. Crit Rev Biotech, Vol 9. Boca Raton: CRC Press, 1989, pp 171–257.
8. AI Yarapolov, OV Skorobogatko, SS Vartanov, SD Varfolomeyev. Laccase: properties, catalytic mechanism, and applicability. Appl Biochem Biotech 49:257–280, 1997.
9. A Messerschmidt, R Huber. The blue oxidases, ascorbate oxidase, laccase, and ceruloplasmin: modeling and structural relationships. Eur J Biochem 187:341–352, 1990.
10. HP Call, I Mucke. History, overview, and application of mediated lignolytic systems, especially laccase-mediator-systems (Lignozym-process). J Biotech 53:163–202, 1997.
11. AM Mayer, E Harel. Phenoloxidases and their significance in fruit and vegetables. In: PF Fox, ed. Food Enzymology, Vol 1 London: Elsevier, 1991, pp 373–398.
12. AM Mayer. Phenol oxidases in plants—recent progress. Phytochemistry 26:11–20, 1987.
13. AM Mayer, E Harel. Phenol oxidases in plants. Phytochemistry 18:193–215, 1979.
14. B Reinhammar, BG Malstrom. "Blue" copper containing oxidases. In: TG Spiro, ed. Copper Proteins (Metal Ions in Biology, Vol 3). New York: John Wiley & Sons, 1981, pp 109–149.
15. PH Ferrar, SI Barberei, MR Ginger, JRL Walker. Laccase—new roles for an old enzyme. NZ Biosci May 7–13, 1995.
16. A Sanchez-Amat, F Solano. A pluripotent polyphenol oxidase from the melanogenic marine *Alteromonas* sp. shares catalytic capabilities of tyrosinases and laccases. Biochem Biophys Res Commun 240:787–792, 1997.
17. M Nicole, H Chamberland, JP Geiger, N Lecours, J Valero, B Rio, GB Ouellette. Immunocytochemical localization of laccase L1 in wood decayed by *Rigidoporus lignosus*. Appl Environ Microbiol 58:1727–1739, 1992.
18. HT Choi, RL Wilks, IK Ross. Formation of sclerotia in liquid cultures of *Coprinus congreatus* and their phenoloxidase isozymes. Mycologia 79:166–172, 1987.
19. W Bao, DM O'Malley, R Whetten, RR Sederhof. A laccase associated with lignification in loblolly pine xylem. Science 260:672–674, 1993.
20. A Richardson, GJ McDougall. A laccase-type polyphenol oxidase from lignifying xylem of tobacco. Phytochemistry 4:229–235, 1997.
21. A Driouich, AC Laine, B Vian, L Faye. Characterization and localization of laccase forms in stem and cell cultures of sycamore. Plant J 2:13–24, 1992.
22. A De Marco, KA Roubelakis-Angelakis. Laccase activity could contribute to cell wall reconstitution in regenerating protoplasts. Phytochemistry 46:421–425, 1997.
23. S Cliffe, MS Fawer, G Maier, K Takata, G Ritter. Enzyme assays for the phenolic content of natural juices. J Agric Food Chem 42:1824–1828, 1994.
24. AL Ghindilis, VP Gavrilova, AI Yaropolov. Laccase-based biosensor for determination of polyphenols: determination of catechols in tea. Biosensors Bioelectron 7:127–131, 1992.
25. P Piacquadio, G DeStefano, M Sammartino, V Sciancalepore. Phenols removal from apple juice by laccase immobilized on Cu^{2+}-chelate regenerable carrier. Biotech Tech 11:515–517, 1997.
26. O Brenna, E Bianchi. Immobilized laccase for phenolic removal in must and wine. Biotech Lett 16:35–40, 1994.
27. A Lante, A Crapisi, G Pasini, A Zamorani, P Spettoli. Immobilized laccase for must and wine processing. In: DS Clark, DA Estell, eds. Enzyme Engineering. New York: New York Academy of Sciences, 1992, pp 558–561.
28. N Bar-Nun, AT Lev, E Harel, AM Mayer. Repression of laccase formation in *Botrytis cinerea* and its possible relation to phytopathogenicity. Phytochemistry 27:2505–2509, 1988.
29. DA Wood. Production, purification, and properties of extracellular laccase of *Agaricus bisporus*. J Gen Microbiol 117:327–338, 1980.
30. RW Kerrigan, IK Ross. Extracellular laccases: biochemical markers for *Agaricus bisporus* systematics. Mycologia 80:689–695, 1988.
31. MC Figueroa-Espinoza, X Rouau. Oxidative cross-linking of pentosans by a fungal laccase and horseradish peroxidase: mechanism of linkage between feruloylated arabinoxylans. Cereal Chem 75:259–265, 1998.
32. M Coll, P Perez, E Villar, VL Shnyrov. Domain structure of laccase 1 from the lignin-degrading basidiomycete PM1 revealed by differential scanning calorimetry. Biochem Mol Biol Int 34:1091–1098, 1994.
33. M Mansur, T Suarez, JB Fernandex-Larrea, MA Brizuela, AE Conzalez. Identification of a laccase gene family in the new lignin-degrading basidiomycete CECT-20197. Appl Environ Microbiol 63:2637–2646, 1997.
34. CR Perry, SE Matcham, DA Wood, CF Thurston. The structure of laccase protein and its synthesis by the commercial mushroom *Agaricus bisporus*. J Gen Microbiol 139:171–178, 1993.
35. A Leontievsky, N Myasoedova, N Pozdynyakova, L Golovleva. Yellow laccase of *Panus tigrinus* oxidizes

non-phenolic substrates without electron-transfer mediators. FEBS Lett 413:446–448, 1997.
36. JRL Walker, RF McCallion. The selective inhibition of ortho- and para-diphenol oxidases. Phytochemistry 19:373–377, 1980.
37. T Kreuter., A Stuedel, H Pickert. On the inhibition of laccase by lower fatty acids. Acta Biotechnol 11:81–83, 1991.
38. MC DePinto, AR Barcelo. Inhibition of both peroxidase and laccase by desferal (desferrioxamine mesylate). Phytochemistry 42:283–286, 1996.
39. GJ McDougall, D Stewart, IM Morrison. Cell-wall-bound oxidases from tobacco (*Nicotiana tabacum*) xylem participate in lignin formation. Planta 194:9–14, 1994.
40. F Xu. Oxidation of phenols, anilines, and benzenethiols by fungal laccases: correlation between activity and redox potentials as well as halide inhibition. Biochemistry 35:7608–7614, 1996.
41. S Murao, Y Hinode, E Matsumura, A Numata, K Kawai, H Ohishi, H Jin, H Oyama, T Shin. A novel laccase inhibitor, N-hydroxylglycine, produced by *penicillium citrinum* YH-31. Biosci Biotech Biochem 56:987–988, 1992.
42. C Jacoud, D Faure, A Effosse, P Wadoux, ML Bouillant. Laccase activity in *Azospirillum lipoferum*: substrates and inhibitors. In: I Fendrik, M Del Gallo, J Vanderleyden, M Zamaroczy, eds. *Azospirillum* VI and Related Microorganisms: Genetics-Physiology-Ecology, NATO ASI Series, Vol G37. Berlin: Springer-Verlag, 1995, pp 341–345.
43. D Faure, ML Bouillant, R Bally. Comparative study of substrates and inhibitors of *Azospirillum lipoferum* and *Pyricularia oryzae* laccases. Appl Environ Microbiol 61:1144–1146, 1995.
44. WH Flurkey, B Ratcliff, L Lopez, J Kuglin, RM Dawley. Differentiation of fungal tyrosinases and laccases using selective inhibitors and substrates. In: CY Lee, JR Whitaker, eds. Enzymatic Browning and Its Prevention. Washington: American Chemical Society, 1995, pp 81–89.
45. W Cai, R Martin, B Lemaure, JL Leuba, V Petiard. Hydroxyindoles: a new class of laccase substrates. Plant Physiol Biochem 31:441–445, 1993.
46. M Sugumaran, J Bolton. Laccase—and not tyrosinase—is the enzyme responsible for quinone methide production from 2,6-dimethoxy-4-allyl phenol. Arch Biochem Biophys 353:207–212, 1998.
47. R Sterjiades, JFD Dean, G Gamble, DS Himmelsbach, KE Eriksson. Extracellular laccases and peroxidases from sycamore maple (*Acer pseudoplatanus*) cell-suspension cultures. Planta 190:75–87, 1993.
48. R Sterjiades, JFD Dean, KE Eriksson. Laccase from sycamore maple (*Acer pseudoplatanus*) polymerizes monolignols. Plant Physiol 99:1162–1168, 1992.
49. DS Yaver, F Xu, EJ Golightly, KM Brown, SH Brown, MW Rey, P Schneider, T Halkier, K Mondorf, H Dalboge. Purification, characterization, molecular cloning, and expression of two laccase genes from the white rot basidiomycete *Trametes villosa*. Appl Environ Microbiol 62:834–841, 1996.
50. G Palmieri, P Giardina, C Bianco, A Scaloni, A Capasso, G Sannia. A novel white laccase from *Plerotus ostreatus*. J Biol Chem 272:31301-31307, 1997.
51. J Zhang, R Kjonaas, WH Flurkey. Does *N*-hydroxyglycine inhibit plant and fungal laccases? Phytochemistry 52:775–783, 1999.

41

Mammalian Sulfhydryl Oxidase

Harold E. Swaisgood and Violeta G. Janolino
North Carolina State University, Raleigh, North Carolina, U.S.A.

I. INTRODUCTION

Most of the characteristics of sulfhydryl oxidase (EC 1.8.3.) reported in this chapter are those of the enzyme isolated from the skim milk membrane vesicles obtained from bovine milk (1–3). The enzyme is an integral membrane iron-containing glycoprotein found in mammary tissue, kidney, and pancreas (4). Immunofluorescent staining also indicated its location in the endothelial cells lining the capillaries of the kidney, heart, and small intestine (4). The enzyme catalyzes oxidation of sulfhydryl groups of cysteine, cysteine-containing peptides, and proteins to disulfides with molecular oxygen as the electron acceptor according to the stoichiometry given below (1, 5):

$$2RSH + O_2 \rightarrow RSSR + H_2O_2$$

This enzyme differs from thiol oxidase (EC 1.8.3.2) not only by its substrate specificity and protein characteristics but also in the fact that water is a product of the thiol oxidase–catalyzed oxidation (6), whereas, hydrogen peroxide is the product of sulfhydryl oxidase–catalyzed reactions. Also, sulfhydryl oxidase differs from glutathione oxidase (EC 1.8.3.3) because of its broader substrate specificity and it does not contain FAD (6). Hence, the enzyme is a sulfhydryl:oxygen oxidoreductase (EC 1.8.3.), but it has not been assigned a serial number as yet.

The mammalian enzyme is also distinct from microbial sulfhydryl oxidase. The microbial enzyme from *Aspergillus niger* is a soluble flavoprotein that oxidizes small thiol compounds such as dithiothreitol (DTT) but does not exhibit much activity with proteins such as reduced RNase, whereas the mammalian enzyme exhibits no activity with DTT, contains iron, and rapidly oxidizes reduced proteins (7). A mammalian flavoprotein sulfhydryl oxidase that oxidizes DTT has been isolated from the male reproductive tract (8–10).

II. IMPORTANCE TO FOOD QUALITY AND UTILIZATION IN FOOD PROCESSING

Heating of milk causes protein denaturation resulting in exposure of the sulfhydryl group, Cys121, in β-lactoglobulin and other chemical reactions of the sulfhydryl and disulfide residues of proteins yielding volatile sulfur compounds resulting in formation of a "cooked" flavor. Ultra-high-temperature (UHT) sterilized and aseptically packaged milk, typically processed at 140–150°C for 2–4 sec, initially has strong cooked flavor that slowly dissipates with storage (11). The intensity of the flavor is objectionable to most North Americans and northern Europeans who are accustomed to high-quality refrigerated pasteurized milk. UHT treatment causes extensive denaturation of the globular whey proteins and complete loss of sulfhydryl oxidase activity. Dissipation of the cooked flavor occurs concomitantly with the oxidation of sulfhydryl groups. Furthermore, sulfhydryl oxidase–catalyzed oxidation of the exposed sulfhydryls also results in elimination of cooked flavor (11–16).

A number of studies using various preparations and forms of sulfhydryl oxidase have shown that the cooked flavor of UHT milk can be immediately eliminated by treatment with the enzyme (12–16). For example, bioreactors for treatment of UHT milk have been prepared by covalent immobilization of the enzyme on succinamidopropyl porous glass beads (12–15) or by direct adsorption from whey on Spherosil QA (16). The concentration of free sulfhydryl groups in freshly processed UHT milk was rapidly depleted by treatment with sulfhydryl oxidase bioreactors operating in either a fixed-bed or a fluidized-bed configuration. Activities of the immobilized enzyme were routinely assayed using reduced glutathione (GSH) as the substrate. These data allowed a correlation to be established between the percent oxidation of GSH and the "normalized residence time" which is the ratio of units of activity/the flow rate through the bioreactor (Fig. 1) (12, 15, 16). The flavor of the enzyme-treated UHT milk was evaluated by a trained taste panel. Most significantly, a direct correlation was observed between the percent of the judges that could detect the cooked flavor and the normalized residence time in the bioreactor (Fig. 2) (16). Two patents have been issued describing preparation of the enzyme and treatment of UHT milk with the enzyme for removal of cooked flavor (17, 18).

Some evidence suggests that enzymatic oxidation of heat-liberated sulfhydryl groups may provide longer flavor stability. A major defect of UHT milk that develops during the long-term storage arises from flavors derived from oxidative reactions (19). Autoxidation of sulfhydryls produce superoxide anion that can lead to other activated oxygen species that have a pro-oxidative effect on milk lipids (20). However, sulfhydryl oxidase–catalyzed oxidation of sulfhydryls does not produce superoxide anions (5). Comparison of untreated UHT milk with UHT milk treated with soluble filter-sterilized sulfhydryl oxidase after a 10-month storage at ambient temperature indicated that the untreated milk had undergone extensive browning and was undrinkable because of its strong oxidized flavors, whereas the treated milk retained its original color and the flavor was acceptable (unpublished observations).

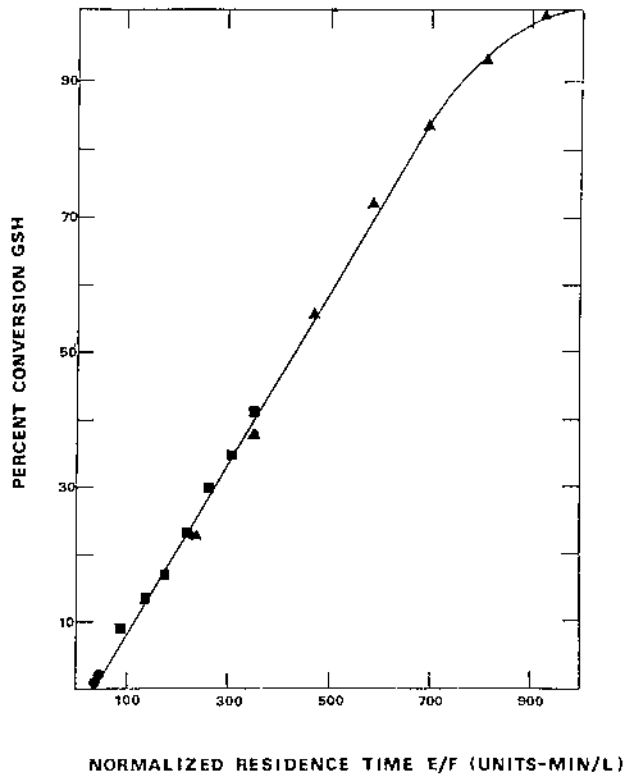

Figure 1 Conversion of GSH to GSSG as a function of normalized residence time. Column assays (●); recirculation assays (■); batch assays (▲). (From Ref. 12.)

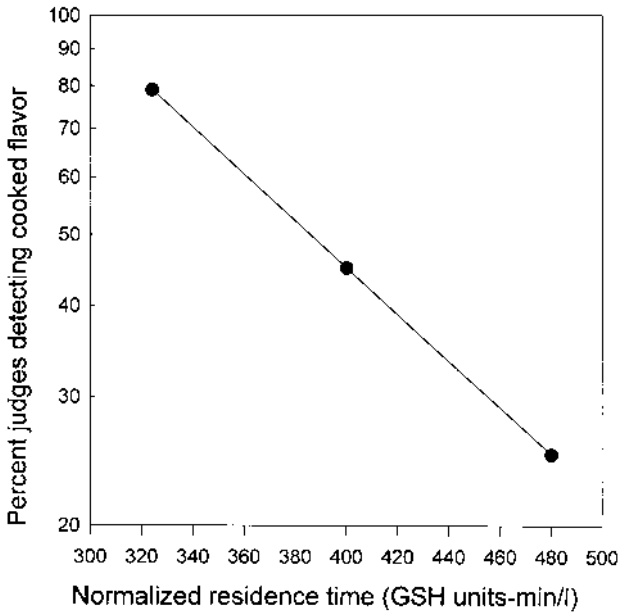

Figure 2 Relationship between the degree of cooked flavor and the extent of enzyme treatment of UHT milk. The normalized residence time in a bioreactor represents the units of enzyme activity in the bioreactor divided by the flow rate through the bioreactor. The panel consisted of trained milk judges. (From Ref. 16.)

III. PROPERTIES OF THE PROTEIN

The molecular weight of sulfhydryl oxidase determined with SDS-PAGE is 89 kDa (1). A similar value was obtained from light-scattering studies of a substantially purified preparation in 5 M guanidinium chloride (21, 22). Like other membrane proteins, preparations of the enzyme in the absence of dissociating agents are highly aggregated; thus, the size of the active protein as it exists in the membrane has not been established. The enzyme is present in skim milk in lipid vesicles $> 0.3\,\mu$m in diameter as indicated by their exclusion from Nucleopore filters (21) and their limited penetration of 0.3-μm-diameter controlled-pore glass (3, 23). Active enzyme can be solubilized with nonionic detergents. Polyoxyethylene-9-lauryl ether ($C_{12}E_9$) and β-octyl-D-glucoside are best suited for this purpose (2). More than 80% of the activity is solubilized in 1% $C_{12}E_9$; however, the complex is still quite large having limited ability to penetrate 7.5% polyacrylamide gels (2). Nevertheless, all of the solubilized enzyme was able to penetrate 0.1-μm-diameter controlled-pore glass (3). Dissociation of the aggregated enzyme with either nonionic detergent or 1 M guanidinium chloride results in increased activity (3, 21).

Analysis of a substantially purified form of the enzyme indicated that it contains 11% carbohydrate and 0.5 g-atoms of Fe/89,000. Moreover, treatment with EDTA caused removal of the Fe and complete loss of activity (1). Subsequent dialysis of the apoprotein against dilute solutions of Fe^{2+} restored 70% of the original activity. However, treatment with other divalent metals did not restore any activity, with the exception of Cu^{2+} which yielded $\sim 30\%$ of the original activity (1). The active enzyme contains two DTNB-reactive sulfhydryl groups/89,000, whereas the denatured protein contains three reactive groups (1, 24). Kinetics of activity loss due to carboxymethylation with iodoacetate indicated that modification of one sulfhydryl group/89,000 caused complete inactivation (24).

That sulfhydryl oxidase activity and γ-glutamyltransferase activity arise from distinct proteins was shown by resolution of the proteins by transient covalent chromatography on cysteinylsuccinamidopropyl glass and by specific immunoprecipitation of sulfhydryl oxidase activity (25, 26). Furthermore, the activities of sulfhydryl oxidase, γ-glutamyltransferase, xanthine oxidase, and alkaline phosphatase in detergent-solubilized skim milk membranes were resolved by isoelectric focusing (3).

IV. ENZYMATIC PROPERTIES

Cysteine, all peptides containing cysteine, and proteins with free sulfhydryl groups are all excellent substrates for mammalian membrane sulfhydryl oxidase (Table 1). Unlike the soluble flavoprotein microbial enzymes, this enzyme is not active with other simple thiol compounds such as DTT. Activity is completely lost upon treatment with EDTA (1) or reagents that react with sulfhydryl groups such as iodoacetate (24). Substrate inhibition is observed at concentrations > 5–$10\,K_m$ (1, 5, 28). With GSH as the substrate, a pH optimum of 6.8–7.0 and a temperature optimum of 35°C have been established (1). The stoichiometry of sulfhydryl oxidase–catalyzed oxidation of GSH has been confirmed by quantitation of the disappearance of GSH and O_2 and the appearance of H_2O_2 and GSSG (1, 5, 25). A number of observations, including kinetic studies (5), have indicated that catalysis follows a Bi Uni Uni Uni Ping-Pong mechanism as shown by the Cleland diagram below.

In addition to analysis of initial rate data (5), a substituted enzyme mechanism is supported by the specific covalent interaction with cysteinylsuccinamidopropyl glass and its release by reducing agents such as GSH or DTT (25). Binding of GSH prior to release of H_2O_2 is supported by the requirement of a sulfhydryl oxidase substrate for the observed oxidation of horseradish peroxidase (HRP) in the presence of the enzyme (29). Enhancement of sulfhydryl oxidase–catalyzed oxidation of GSH in the presence of HRP is thought to occur by direct transfer of peroxide from sulfhydryl oxidase to HRP, thus speeding up the rate-limiting dissociation of peroxide from the enzyme (29).

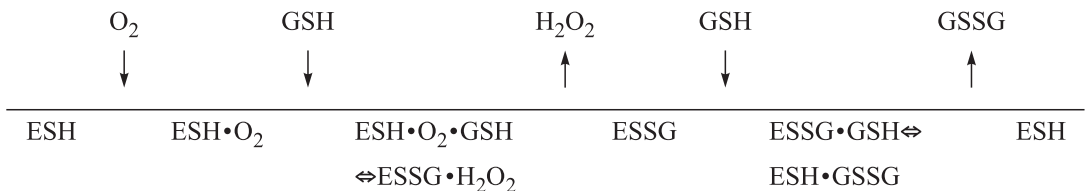

Table 1 Kinetic Characteristics of Several Sulfhydryl Oxidase Substrates

Substrates	K_m (mM)	Relative pseudo-first-order rate constant (V_{max}/K_M)
Reduced glutathione	0.1[a], 0.3[b], 0.6[c]	1.0
Gly-Gly-L-Cys	2.4[d]	~ 1[d]
L-Cysteine	0.8[c]	0.62[c]
D-Cysteine	1.33[b], 0.97[c]	0.62[c]
N-Acetyl-L-cysteine	3.85[b], 1.13[c]	0.34[c]
Cysteamine	30[b], 1.3[c]	0.68[c]
5-Nitro-5-thiobenzoic acid	100[b]	—
Reduced ribonuclease	0.14[c]	—
No activity with (5, 22):		
Dithiothreitol	Mercaptoethanol	Mercaptopopionic acid
Dithioerythritol	Mercaptoacetic acid	Lipoic acid

[a] Janolino and Swaisgood (1).
[b] Swaisgood and Horton (22).
[c] Sliwskowski et al. (5).
[d] Schmelzer et al. (27).
[e] Janolino and Swaisgood (28). This value was calculated on the basis of the sulfhydryl group concentration.

As indicated by the kinetic parameters in Table 1, reduced proteins are excellent substrates. Fully unfolded and reduced RNase A (1, 28, 30) and chymotrypsinogen A (31) are rapidly oxidized with nearly complete restoration of biological activity (Figs. 3, 4). Thus, sulfhydryl groups are oxidized and biological activity is restored within minutes in the presence of sulfhydryl oxidase, whereas > 15 h is required in its absence. Restoration of biological activity proves that native disulfide bonds are formed. Comparison of the intermediates formed during enzyme-catalyzed oxidation and air or GSH/GSSG-catalyzed oxidation

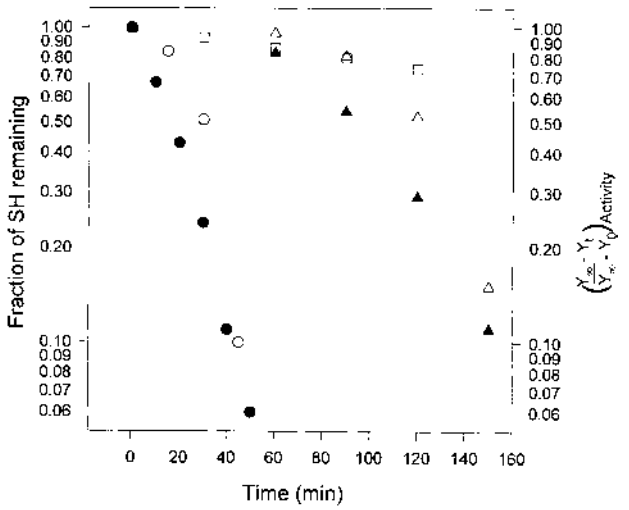

Figure 3 Comparison of the rates of sulfhydryl oxidase–catalyzed oxidation (●) and activity regeneration (○) with that observed in air (▲, △) for reduced ribonuclease. Also included are the data (□) obtained with the microbial enzyme from *A. niger* (7). Activity data are plotted as $(Y_\infty - Y)/(Y_\infty - Y_0)$ where Y_∞ and Y_0 are the activities at infinite and 0 time, respectively. Nearly 100% of the activity was restored. (From Refs. 1 and 7.)

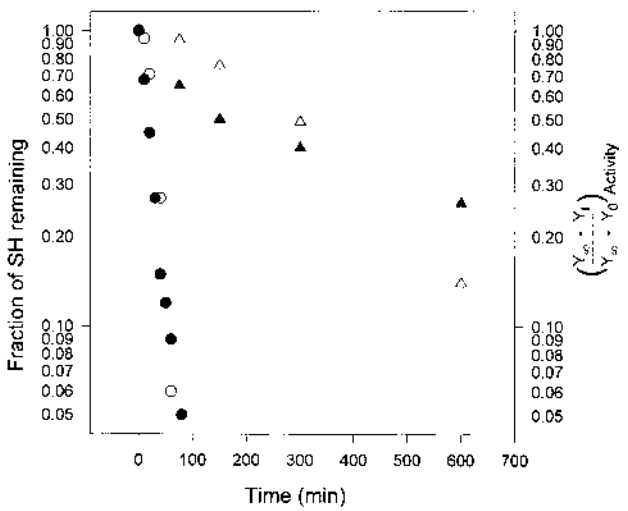

Figure 4 Comparison of the rates of sulfhydryl oxidase–catalyzed oxidation (●) and restoration of trypsin-activatable chymotryptic activity ○) with that observed in air (▲, △) for immobilized reduced chymotrypsinogen A. Activity data are plotted as $(Y_\infty - Y)/(Y_\infty - Y_0)$ where Y_∞ and Y_0 are the activities at infinite and 0 time, respectively. Nearly 50% of the original biological activity was restored. (From Ref. 31.)

of reduced RNase A (28) and bovine pancreatic trypsin inhibitor (32) suggests that the same disulfide bond formation pathway is followed in all cases. Consequently, the folding pathway of the reduced protein is determined by its structure, with the enzyme acting as a true catalyst affecting only the rate of the reaction and not the pathway.

Another reaction observed to be catalyzed in vitro by sulfhydryl oxidase that may have biological significance is the conversion of xanthine dehydrogenase to xanthine oxidase (33). The sulfhydryl groups of xanthine dehydrogenase are rapidly oxidized in the presence of the enzyme with the concomitant appearance of xanthine oxidase activity. Sulfhydryl oxidase is absent in liver where xanthine dehydrogenase is found, whereas in bovine milk xanthine oxidase is present.

V. MEASUREMENT OF SULFHYDRYL OXIDASE ACTIVITY

Typically, the enzyme is assayed with 0.8 mM GSH in 0.047 M sodium phosphate buffer, pH 7.0, at 35°C (1, 5, 25, 34). To 1.0 mL of the 0.8 mM GSH solution equilibrated at 35°C, 0.1 mL of enzyme solution is added. A blank solution is prepared using 0.1 mL of boiled enzyme solution. At 1-min intervals, 0.1 mL is removed and added to 5.0 mL of 0.1 mM DTNB solution in 0.1 M sodium phosphate buffer at pH 8.0, containing 10 mM EDTA. The absorbance of each of these solutions is read at 412 nm after a 2-min reaction. Sufficient enzyme activity must be added to complete the assay within 10 min to avoid effects of autoxidation. The initial slope of the absorbance change versus time is used to calculate the activity. Enzyme activity per milliliter of enzyme solution is calculated from the relationship

$$\mu\text{mol SH/min/mL} = 561\ (A_{412}/\text{min})/13.6\ (\text{mM}^{-1}\text{cm}^{-1})$$

where 1 μmol SH oxidized/min is defined as 1 unit of activity.

VI. PURIFICATION PROCEDURES

The procedures described have been used to obtain the enzyme from bovine milk. Because more of the enzyme exists in skim milk membranes than in the milkfat globule membranes, initially fresh raw skim milk is prepared (1). It is very important to remove all of the milkfat globules because they apparently interfere with later isolation procedures (unpublished observations). Fresh milk is centrifuged at 4100 g for 30 min at 30°C and the skim milk is carefully removed from under the fat layer. Caseins are then coagulated by addition of four units of chymosin (one unit will coagulate 10 mL of skim milk in 1 min at 30°C)/100 mL skim milk, followed by incubation at 30°C for 30 min (34). Whey is prepared by centrifugal removal of the clotted caseins at 16,300 g for 45 min at 4°C. The next step is to prepare the skim milk membrane vesicles. Several procedures have been developed for this isolation (1, 25, 35) as described in Table 2. Preparations of the membrane vesicles by chromatography on 300 nm pore diameter controlled-pore glass (CPG-3000) or by membrane fractionation using a 100,000-dalton exclusion limit membrane are more homogeneous than that obtained by ammonium sulfate fractionation. Typically, purified vesicles represent a 200- to 300-fold increase in specific activity compared to whey (35, 36).

Three procedures have been developed for purification of the enzyme from membrane vesicles. The initial procedure developed involved a differential centrifugation taking advantage of the concentration-dependent aggregation of the enzyme (1). Thus, the ammonium sulfate precipitate is made to 0.15% protein in 0.047 mM phosphate buffer, pH 7.0, and centrifuged at 2000 g for 30 min at 4°C. The supernatant is concentrated to 3% protein and recentrifuged under the same

Table 2 Three Methods for Preparing Skim Milk Membrane Vesicles from Whey

$(NH_4)_2SO_4$ fractionation (1)	Size exclusion chromatography (36)	Membrane fractionation (25)
1. Adjust the whey to 50% saturation with $(NH_4)_2SO_4$ at 4°C 2. Incubate overnight 3. Collect precipitate by centrifuging at 16,500 g for 60 min at 4°C. Represents crude vesicles.	1. Apply to a CPG-3000 column (300 nm pore diameter) equilibrated (with 0.047 mM phosphate buffer, pH 7.0. 2. Membrane vesicles are obtained in the void volume fraction.	1. Diafilter the whey against six volumes of 0.047 mM phosphate buffer, pH 7.0, using a 100,000-dalton exclusion limit membrane. 2. Concentrate the retentate containing the vesicles 10-fold.

Table 3 Two Methods for Purification of Sulfhydryl Oxidase from Detergent-Solubilized Membrane Vesicles

Transient covalent chromatography on cysteinylsuccinamidopropyl glass (25, 37)	Bioselective adsorption on monomeric avidin (35)
1. Recirculate 150 mL solubilized vesicles prepared from 1 L whey through 60 mL of the adsorbent at 30°C for 4 h.	1. The enzyme is biotinylated using 0.25 mL of biotin-HPDP[a]/mL of solubilized membrane vesicles. Incubate for 90 min at room temperature.
2. Remove adsorbed materials by washing with 1 L phosphate buffer, pH 7, containing the detergent.	2. Recirculate the biotinylated enzyme in 47 mM phosphate buffer, pH 7, through monomeric avidin beads for 20 min at room temperature. Add ~ 0.5 mg total protein/mL of adsorbent.
3. Reductively release the enzyme by recirculating 100 mL of 2 mM GSH until no thiol groups can be detected with DTNB.	3. Wash the matrix with five volumes of 47 mM phosphate buffer, pH 7, containing 1% $C_{12}E_9$.
4. Regenerate the adsorbent by recirculating 50 mL DTT in 8 M urea/1 M NaCl, followed by 0.1 M acetic acid.	4. Release the enzyme by recirculating 0.3–0.5 mL 50 mM DTT/mL matrix in 47 mM phosphate buffer for 20 min at room temperature

[a] Biotin-HPDP is N-[6-(biotinamido)hexyl]-3′(2′-pyridyldithio)propionamide.

conditions, yielding sulfhydryl oxidase activity in the pellet. Finally, the pellet is solubilized in twice the volume of the previous solution and again centrifuged under the same conditions, yielding the purified enzyme in the pellet.

The other two methods of purification are based on the catalytic mechanism or the active-site sulfhydryl group (Table 3). First, the membrane vesicles are solubilized by adjustment to 1% $C_{12}E_9$ in phosphate buffer, pH 7, and centrifuged at 100,000g to remove any insoluble material. Transient covalent chromatography on cysteinylsuccinanidopropyl glass based on the fact that sulfhydryl oxidase follows a substituted enzyme mechanism. Thus, a mixed disulfide is formed between the enzyme and the immobilized cysteinyl residue which cannot be reduced without the addition of free thiols (34). Cysteinylsuccinamidopropyl glass is prepared by reaction of cysteine with 1-ethyl-3-(3-dimethylaminopropyl)carbodiimide-activated succinamidopropyl glass as described by Sliwkowski *et al.* (25). A typical purification using this procedure results in a 4800-fold increase in the specific activity compared to that in whey (Table 4).

Bioselective adsorption on monomeric avidin is based on selective biotinylation of the active site sulfhydryl group of the enzyme with N-[6-(biotinamido)hexyl]-3′(2′-pyridyldithio)propionamide (biotin-HPDP) (35). The resulting mixed disulfide, containing a biotinyl residue, strongly binds to avidin but can be released by reduction of the disulfide bond (35). The purified enzyme obtained by this procedure exhibits a 3100-fold increase in specific activity compared to that of whey (Table 5).

Table 4 Data from a Typical Purification Using Cysteinylsuccinamidopropyl Glass

Fraction	Volume (mL)	Total protein (mg)	Total units of activity[a]	Specific activity (units/mg)	Yield (%)	Purification (fold)
Whey	910	8190	40	0.005	100	1
Solubilized skim milk membranes[b]	156	565	17	0.031	47	6.3
Purified enzyme	99	0.545	13	24.2	33	4830

[a] Assay mixtures contained 0.8 mM GSH in 50 mM sodium phosphate, pH 7.0. Activity was calculated from the rate of disappearance of sulfhydryl groups due to enzyme-catalyzed oxidation at 35°C.
[b] Prepared by membrane fractionation (see Table 2). The diafiltered whey was solubilized with 1% $C_{12}E_9$.
Source: Ref. 25.

Table 5 Purification of Sulfhydryl Oxidase by Avidin-Biotin Affinity Chromatography

Fraction	Total protein (mg/L whey)	Total units of activity[a] (U/L whey)	Specific activity (U/mg enz)	Recovery (%)	Purification (fold)
Whey	6510	53	0.008	100	1
Skim milk membranes[b]	23.6	51	2.2	96	275
Purified enzyme	0.84	21	25	39	3125

[a] Assay mixtures contained 0.8 mM GSH in 50 mM sodium phosphate, pH 7.0. Activity was calculated from the rate of disappearance of sulfhydryl groups due to enzyme-catalyzed oxidation at 35°C.
[b] Diafiltered whey was fractionated with CPG-3000 yielding the purified skim milk membrane vesicles in the void volume fraction.
Source: Ref. 35.

REFERENCES

1. VG Janolino, HE Swaisgood. Isolation and characterization of sulfhydryl oxidase from bovine milk. J Biol Chem 250:2532–2538, 1975.
2. MB Sliwkowski, HE Swaisgood, HR Horton. Solubilization of sulfhydryl oxidase, a bovine skim milk membrane enzyme. J Dairy Sci 65:1681–1687, 1982.
3. VG Janolino, HE Swaisgood. Isolation, solubilization, fractionation by electrofocusing,and immobilization of skim milk membrane. J Dairy Sci 67:1161–1168, 1984.
4. DA Clare, HR Horton, TH Stabel, HE Swaisgood, JG Lecce. Tissue distribution of mammalian sulfhydryl oxidase. Arch Biochem Biophys 230:138–145, 1984.
5. MX Sliwkowski, HE Swaisgood, DA Clare, HR Horton. Kinetic mechanism and specificity of bovine milk sulfhydryl oxidase. Biochem J 220:51–55, 1984.
6. Nomenclature Committee of the International Union of Biochemistry and Molecular Biology. Enzyme Nomenclature. San Diego, CA: Academic Press, 1992, p 110.
7. VG Janolino, HE Swaisgood. A comparison of sulfhydryl oxidases from bovine milk and from *Aspergillus niger*. Milchwissenschaft 47:143–146, 1992.
8. TSK Chang, B Morton. Epididymal sulfhydryl oxidase: a sperm-protective enzyme from the male reproductive tract. Biochem Biophys Res Commun 66:309–315, 1974.
9. MC Otrowski, WS Kistler. Properties of a flavoprotein sulfhydryl oxidase from rat seminal vesicle secretion. Biochemistry 19:2639–2645, 1980.
10. MC Otrowski, WS Kistler, HG Williams-Ashman. A flavoprotein responsible for the intense sulfhydryl oxidase activity of rat seminal vesicle secretion. Biochem Biophys Res Commun 87:171–176, 1979.
11. HE Swaisgood. New developments in UHT sterilized milk. Dairy Ice Cream Field 160:48–60, 1977.
12. HE Swaisgood, VG Janolino, MX Sliwkowski. An enzymatic approach to flavor enhancement. Proceedings of International Symposium on UHT Processing and Aseptic Packaging of Milk and Milk Products, Raleigh, NC, 1980, pp 67–76.
13. HE Swaisgood, VG Janolino, HR Horton. Immobilized sulfhydryl oxidase. AIChE Symposium Series, Vol 74, No. 172, Am Institute Chem Engr, 1978, pp 25–30.
14. HE Swaisgood. Sulphydryl oxidase: properties and applications. Enzyme Microb Technol 2:265–272, 1980.
15. HE Swaisgood, MX Sliwkowski, PJ Skudder, VG Janolino. Sulfhydryl oxidase: characterization and application for flavor modification of UHT milk. In: P Dupuy, ed. Utilisation des Enzymes en Technologie Alimentaire. Paris: Lavoisier, 1982, pp 229–235.
16. HE Swaisgood, VG Janolino, PJ Skudder. Continuous treatment of ultrahigh-temperature sterilized milk using immobilized sulfhydryl oxidase. Methods Enzymol 136:423–431, 1987.
17. HE Swaisgood. Process for removing cooked flavor from milk. U.S. patent No. 4,053,644 (1977).
18. HE Swaisgood. Purification and immobilization of sulfhydryl oxidase. U.S. patent No. 4,068,328 (1978).
19. S Rerkrai, IJ Jeon, R Bassette. Effect of various direct ultra-high temperature treatments on flavor of commercially prepared milks. J Dairy Sci 70:2046–2054, 1987.
20. JJ Lee, WF Shipe. Effects of sulfhydryl compounds on lipid oxidations catalyzed by copper and heme. J Dairy Sci 65:1414–1420, 1982.
21. VG Janolino, CS Barnes, HE Swaisgood. Dissociation and unfolding of sulfhydryl oxidase in solutions of guanidinium chloride. J Dairy Sci 63:1969–1974, 1980.
22. HE Swaisgood, HR Horton. Sulphydryl oxidase: oxidation of sulphydryl groups and the formation of three-dimensional structure in proteins. Ciba Foundation Symposium No. 72: Sulphur in Biology, Excerpta Medica, 1980, pp 205–222.

23. VG Janolino, HE Swaisgood. Effect of support size on activity of immobilized sulfhydryl oxidase. J Dairy Sci 61:393–399, 1978.
24. KB Song, HE Swaisgood, HR Horton. Requirement for a sulfhydryl group for sulfhydryl oxidase activity. J Dairy Sci 69:2589–2592, 1986.
25. MX Sliwkowski, MB Sliwkowski, HR Horton, HE Swaisgood. Resolution of sulphydryl oxidase from γ-glutamyltransferase in bovine milk by covalent chromatography on cysteinylsuccinamidopropyl-glass. Biochem J 209:731–739, 1983.
26. CH Schmelzer, HE Swaisgood, HR Horton. Resolution of renal sulfhydryl oxidase from γ-glutamyltransferase by covalent chromatography on cysteinylsuccinamidopropyl-glass. Biochem Biophys Res Commun 107:196–201, 1982.
27. CH Schmelzer, HE Swaisgood, HR Horton. Glycylglycyl-L-cysteine at a substrate for renal sulfhydryl oxidase (Glutathione oxidase). Biochim Biophys Acta 827:140–143, 1985.
28. VG Janolino, HE Swaisgood. Sulfhydryl oxidase–catalyzed formation of disulfide bonds in reduced ribonuclease. Arch Biochem Biophys 258:265–271, 1987.
29. GW Koszalka, HE Swaisgood, HR Horton. Enzymatic enhancement of the catalytic rate of sulfhydryl oxidase. Biochim Biophys Acta 915:315–329, 1987.
30. VG Janolino, HE Swaisgood, HR Horton. Renaturation of soluble and immobilized ribonuclease: are the polypeptide folding pathways for structure formation the same for soluble proteins and for proteins associated with a surface? J Appl Biochem 7:33–37, 1985.
31. VG Janolino, MX Sliwkowski, HE Swaisgood, HR Horton. Catalytic effect of sulfhydryl oxidase on the formation of three-dimensional structure in chymotrypsinogen A. Arch Biophys 191:269–277, 1978.
32. DC Chen. Coupled use of immobilized enzymes with mass spectrometry for peptide analysis including location of disulfide bonds and sulfhydryl oxidase-catalyzed formation of disulfide bonds in bovine pancreatic trypsin inhibitor. Ph.D. dissertation, North Carolina State University, Raleigh, NC, 1993.
33. DA Clare, BA Blakistone, HE Swaisgood, HR Horton. Sulfhydryl oxidase–catalyzed conversion of xanthine dehydrogenase to xanthine oxidase. Arch Biochem Biophys 211:44–47, 1981.
34. HE Swaisgood, HR Horton. Sulfhydryl oxidase from milk. Methods Enzymol 143:504–510, 1987.
35. VG Janolino, HE Swaisgood. Purification of reactive sulfhydryl enzymes by bioselective adsorption on monomeric avidin: purification of sulfhydryl oxidase. J Food Biochem 16:389–399, 1993.
36. VG Janolino, DA Clare, HE Swaisgood. Characteristics of sulfhydryl oxidase isolated by a simple chromatographic procedure. Biochim Biophys Acta 658:406–409, 1981.
37. VG Janolino, HE Swaisgood. Homogeneity of sulfhydryl oxidase preparations obtained by transient covalent affinity chromatography. J Dairy Sci 73:308–313, 1990.

42

Xanthine Oxidase

John R. Whitaker
University of California, Davis, Davis, California, U.S.A.

I. INTRODUCTION

The enzyme described in this chapter is called "xanthine oxidase," "xanthine dehydrogenase," or "xanthine oxidoreductase" by various authors. Except for the oxidation state of two sulfhydryl groups in the active site of the protein, they are the same. When the two sulfhydryl groups are present, the enzyme performs primarily as a dehydrogenase but still has some oxidase activity. When the two sulfhydryl groups (–SH) are oxidized to give a disulfide group (–S–S–), or two sulfonic acid groups ($-SO_3^{2-}$), the enzyme functions as an oxidase (1–5). Reduction of the –S–S– bond converts the oxidase back to a dehydrogenase, with a significant conformational transition in the flavin binding site (3).

A. Reactions Catalyzed

Xanthine oxidase (XO; EC 1.1.3.22) catalyzes the oxidation of hypoxanthine and xanthine to uric acid (Structure 1),

$$\text{Hypoxanthine} + H_2O + O_2 \rightarrow \text{uric acid} + H_2O_2 + (\text{some } O_2^-) \quad (1)$$

with O_2 being the second substrate (oxidant). The heavy arrows in Structure 1 show the reactions catalyzed by XO; the dashed arrows show the net result of the reactions. Note that oxidation of hypoxanthine gives the enol form of xanthine, which then spontaneously isomerizes to some keto form of xanthine that can be catalyzed by XO to the enol form of uric acid, which then spontaneously isomerizes to some keto form of uric acid. The isomeric forms of the substrates make interpretation of the kinetic results difficult, as the enol form of xanthine and the keto form of uric acid may be competitive inhibitors of XO. Other purines and adenine are oxidized more slowly (Table 1). A number of aldehydes (Table 1) are oxidized also to the corresponding carboxylic acids by XO.

Xanthine dehydrogenase (XDH; EC 1.1.1.204) reduces NAD^+ to NADH (7), as well as O_2 to H_2O_2 (8) with xanthine as the second substrate [Eqs. (2) and (3)].

$$\text{Xanthine} + NAD^+ \rightarrow \text{uric acid} + NADH + H^+ \quad (2)$$

$$\text{Xanthine} + O_2 \rightarrow \text{uric acid} + H_2O_2 \quad (3)$$

Steady-state kinetic rate constants of xanthine/O_2 and xanthine/NAD^+ reactions catalyzed by XDH are 2.1 $\pm 0.1\ \text{sec}^{-1}$ (7) and $6.3\ \text{sec}^{-1}$ (8) at 25°C and pH 7.5, respectively. For comparison, the oxidation of NADH/O_2 is $2.5 \pm 0.9\ \text{sec}^{-1}$ under the same conditions. Therefore, XDH has a significant and intrinsic xanthine oxidase activity on some substrates (7, 8).

Xanthine dehydrogenase has an NAD^+ binding site and a substantially lower reduction potential for the $FADH\cdot/FADH_2$ couple relative to XO (9, 10). In the case of the milk enzyme, the difference is 180 mV.

Xanthine oxidase has low specificity for both the substrates and the electron acceptor. More than 100 compounds are known to serve as substrates, and a

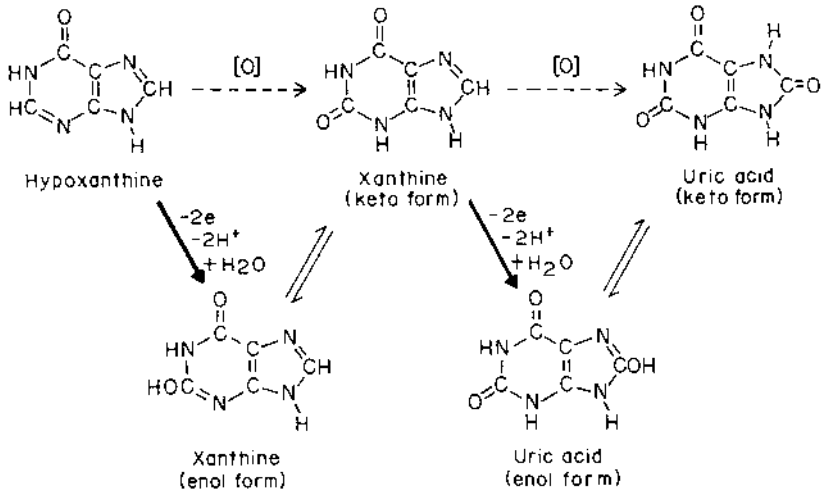

Structure 1

large number of electron acceptors are known, including O_2, NAD^+, methylene blue, 2,6-dichlorophenolindophenol, triphenyltetrazolium chloride, phenazine methosulfate, cytochrome c, and ferricyanide.

B. Historical Aspects

In 1902, Schardinger (11) determined that fresh milk decolorized Methylene Blue. In 1922, Morgan et al. (12) reported that bovine milk converted hypoxanthine and xanthine into uric acid under both aerobic and anaerobic (when Methylene Blue was included) conditions. They found the same activity in liver, spleen, and lungs of rats and cows. The activity, which they named "xanthine oxidase," was destroyed by boiling. In 1924, Dixon and Thurlow (13) partially purified XO and did kinetic studies on the rate of reduction of Methylene Blue. Dixon (14) showed that aldehydes are substrates for XO. In 1939, Ball (15) and Corran et al. (16) obtained nearly pure XO, with a golden brown color due to intrinsic flavin (FAD), plus another unknown chromophore (now known to be molybdenum) (17, 18). In 1954, Richert and Westerfeld (19) reported that addition of ferric chloride in the diet of rats substantially increased the activity of XO in rat liver; they found iron, FAD, and molybdenum to be present in the ratio of 8 : 2 : 1 in XO. In 1955, Avis et al. (20) developed an isolation procedure for XO from cow's milk which gave crystalline XO with A_{280}/A_{450} of 5.0–5.2, a level of purity that has not been increased to the current time. The ratio of iron, molybdenum, and FAD was 8.1 : 1.4 : 2.0. Later, the iron, labile sulfide, molybdenum, and FAD were found to be in the ratio

Table 1 Substrate Specificity of Xanthine Oxidase from Milk

Substrate	Relative rates	Substrate	Relative rates
Xanthine	140	Acetaldehyde	0.72
Hypoxanthine	100	Cinnamaldehyde	0.41
8-Hydroxypurine	6	Vanillin	0.01
6-Amino-2-hydroxypurine	4.5	Glyceraldehyde	0.014
6-Amino-8-hydroxypurine	7	*p*-Phthalaldehyde	0.013
Adenine	6	Decanaldehyde	0.0080
2,8-Dihydroxypurine	0.6	*n*-butyraldehyde	0.0060
p-Hydroxybenzaldehyde	1.3	Octaldehyde	0.0002
Benzaldehyde	0.8		

Source: Ref. 6.

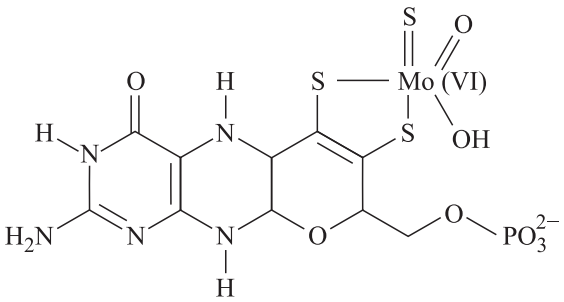

Structure 2

of 2 : 2 : 1 : 1 per subunit (21). The molecular weight of XO was determined by ultracentrifugal sedimentation and diffusion data to be 290 kDa (22), with two identical subunits.

The mechanistic aspects will be presented in Section II.

C. Importance of Xanthine Oxidase to Food Science, Nutrition, and Medicine

During metabolism of nucleic acids, animals convert the purine bases adenine and guanine to uric acid. Uric acid then forms calcium urate which is deposited in joints. As a result, XO has been implicated in a number of diseases ranging from rheumatoid pathology, ischemia-reperfusion injury, and in reactive oxidant-mediated signal transduction. The bases for these implications are due to known metabolic free radical generation by XO and correlation of XO concentrations with certain diseases. As pointed out in Section I.A, the oxidation of hypoxanthine and xanthine and of NADH/O_2 by XO leads to the formation of H_2O_2 and O_2^- (superoxide ion). In experimental animals, primarily rats and mice, there are good relationships between XO activity and the development of the pathological problems listed above. Evidence for this is well presented by the recent reviews of Nishino et al. (5), Wright and Repine (23), Bulkley (24), Harrison (25), and Blake et al. (26). In particular, the review by Blake et al. (26) details the current experimental evidence for the possible role of XO in rheumatoid pathology.

In 1977, major consumer concerns arose as to how milk was processed, in particular raw milk and lightly pasteurized milk. There was concern that active XO might pass through the small intestinal wall into the blood and lead to major problems in tissues. Special attention was given to this concern by several researchers. In particular, Dr. Clifford at U.C. Davis carefully researched this area and determined that no intact XO (active or inactive) was found in the blood of rabbits (27). His results are not surprising when one considers the size of the XO (290 kDa).

Harrison (25) reported that purified human breast milk XO has only 2–3% the specific activity of cow's milk. His data indicate that XO activity is very low in most human tissues, except for liver and intestinal tissues.

II. MECHANISM OF XANTHINE OXIDASE CATALYSIS

A. Protein Nature of Xanthine Oxidase

The complete amino acid sequences of XOs from various sources have been deduced by sequencing the respective cDNAs (genes). They are highly homologous consisting of, for example, 1332 amino acid residues for bovine milk XO and 1333 residues for human liver XO, with 90% sequence identity (28–30).

The x-ray crystallographic structure of bovine milk XO has been published (9). As reported by other methods, XO has a molecular weight of 290 kDa. It is composed of two identical subunits, each containing an active site. In addition to the several amino acid residues in the active sites there are two molecules of iron [Fe(III)], two molecules of labile sulfide, one molecule of molybdenum, one molecule of FAD per subunit (21), and one molecule of molybdopterin, a cofactor that binds the molybdenum (31) (see Structure I). In XO/XDH from prokaryotes, the dinucleotides of guanine, cytosine, adenine, or hydroxyxanthine are found. For example, in the gram-positive bacterium *Desulfouibrio gigas*, the cofactor is a molybdenum molybdopterin cytosine dinucleotide.

The dimensions of the active dimeric (two subunits) enzyme are 155 Å × 90 Å × 70 Å (Fig. 1) (9). It is butterfly shaped with the dimer interface on the smaller side of the vertically elongated subunits. Each subunit consists of three domains. The small N-terminal domain (residues 1–165) contains the two iron/sulfur cofactors. It is connected to the FAD-binding domain (residues 226–531) by a long segment of amino acid residues (166–225). The FAD domain is connected to the third domain (residues 590–1332) by the amino acid residues 532–589. This large third domain contains the Mo-pterin cofactor (Structure 2). The three domains are folded in proximity to each other so as to form the active site of the enzyme containing the

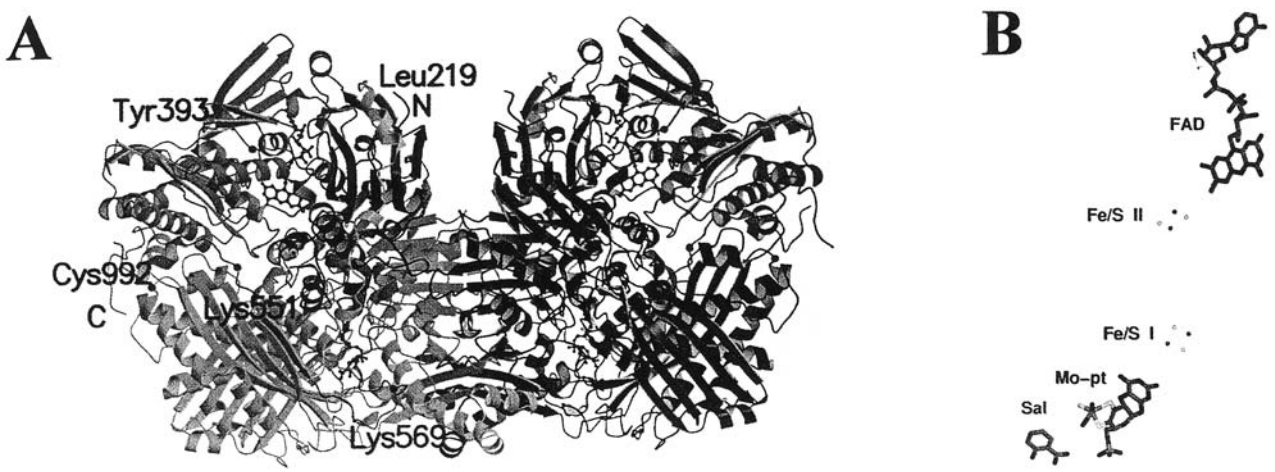

Figure 1 (A) Molecular structure of xanthine dehydrogenase (XDH) as determined by x-ray crystallography. (B) For clarity, the cofactors and salicylate (added to stabilize XDH) are shown in the same positions as found in the protein molecule. (From Ref. 9.)

two iron/sulfur cofactors, the FAD cofactor and the Mo-pterin cofactor. Each subunit functions independently of the other. The reader is referred to the publication by Enroth et al. (9) for a color-coded diagram of the XO molecule.

The tertiary structure of aldehyde oxidoreductase, a member of the xanthine oxidase family, is also known for *Desulfouibrio gigas* (32, 33); it is very similar to that of XO.

B. Mechanism of Action of Xanthine Oxidase

When xanthine and O_2 are added to XO, the reaction pathway was shown by Gutfreund and Sturtevant (34) to be that described by Fig. 2. The rate constants k_1, k_2, k_3, and k_4 for the reactions were determined by rapid reaction techniques to be $\sim 5.0 \times 10^5\,M^{-1}\,sec^{-1}$, $10.5\,sec^{-1}$, $> 4.0 \times 10^5\,M^{-1}\,sec^{-1}$, and $21.5\,sec^{-1}$, respectively. The rate constants k_1 and k_3 are for formation of the Michaelis-Menten complexes of xanthine $\cdot$ E $\cdot$ FAD and $O_2 \cdot$ E-$FADH_2$, respectively, while k_2 and k_4 are the rate constants for oxidation of xanthine to uric acid and reduction of O_2 to H_2O_2, respectively.

When the 1/(turnover numbers) are plotted versus 1/[xanthine] at three different concentrations of O_2: air saturated (0.24 mM), 60% O_2 saturated enzyme and the results of the two are extrapolated to ∞O_2 concentration, all three lines are parallel (Fig. 3) (21), indicating that the reaction follows a Ping-Pong Bi-Bi mechanism. This is diagrammed according to the Cleland Nomenclature (35) in Eq. (4) where X is xanthine and U is uric acid.

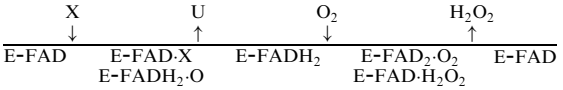

(4)

In 1964, Bray et al.(36) used electron paramagnetic resonance spectroscopy to investigate the rates of electron transfer to and decay from the several cofactors of the enzyme-substrate system. The XO and xanthine were mixed very rapidly (< 1 msec) and frozen very rapidly (< 1 msec) in liquid N_2. The Mo-δ signal,

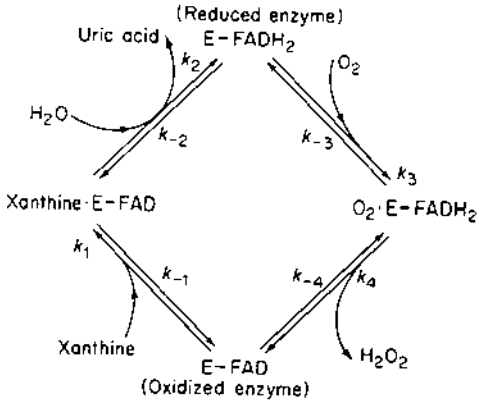

Figure 2 Mechanism of action of xanthine oxidase as determined by fast reaction kinetics. (From Ref. 34.)

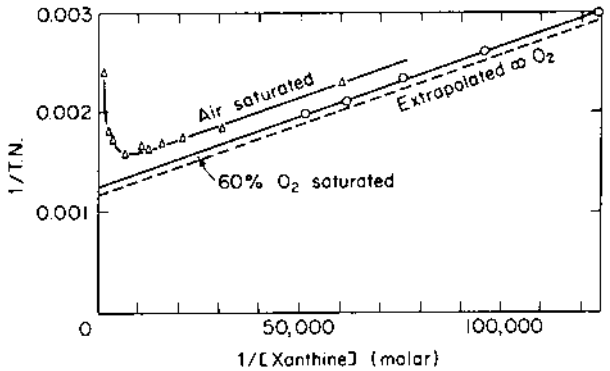

Figure 3 Effect of xanthine and O_2 concentrations on the rate of xanthine oxidation by xanthine oxidase. T.N. is the turnover number measured at pH 8.3 and 25°C. (From Ref. 21.)

believed to be conversion of Mo(VI) to Mo(V), reached a maximum in ~15 msec. The Mo-β, FADH· (FAD → FADH·), and Fe(II) [Fe(III) → Fe(II)] signals were maximum at 40, 45, and 100 msec, respectively (Fig. 4). Therefore, Bray et al. (36) suggested that the sequential steps in the reductive reaction are: xanthine → Mo → FAD → Fe → O_2. More recently, the reaction order has been shown to be: xanthine → Mo → 2Fe/2S → FAD → O_2 (21). Therefore, the overall reaction involving the flow of electrons is best described by Eq. (5).

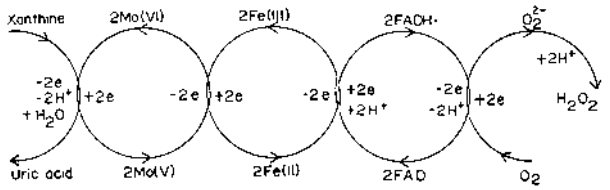

(5)

The order in which electrons and water are transferred from xanthine and oxygen to produce uric acid and hydrogen peroxide (H_2O_2) is generally agreed to be that shown in Eq. (5). However, the mechanistic pathway of the Mo-pterin cofactor and substrate in the first step is still in dispute. The key difference among scientists in the field is primarily whether the first chemical event following formation of the noncovalent enzyme-substrate complex involves an Mo-C or a Mo-O-C covalent linkage between the Mo-cofactor and substrate as shown in Eqs. (6) and (7) (37).

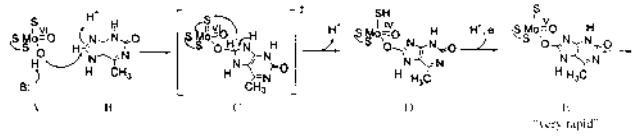

(6)

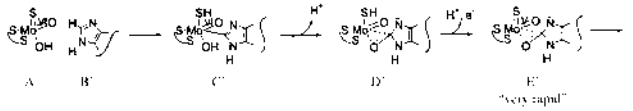

(7)

While Eqs. (6) and (7) give the same final products, the mechanisms of the reactions are fundamentally different.

In the first proposed mechanism [Eq. (6)], the product of hydroxylation of the substrate 2-hydroxy-6-methylpurine (B; in the enolate tautomeric form) is suggested to be coordinated to the molybdenum via the induced oxygen atom from the –OH group of the molybdenum cofactor (A) of the enzyme to form the bracketed intermediate/transition state compound (C). The intermediate/transition state compound is proposed to be formed in a base-assisted (B: group in the active site of the enzyme) nucleophilic attack of the Mo^{VI}–OH group on the C-8 of the substrate with a concomitant hydride transfer to the Mo═S group (bracketed structure) to give Mo^{IV}–SH (D). The "very rapid" species is formed by a one-electron oxidation and deprotonation to give the EPR-detectable $Mo^{V}OS(OR)$ species (D).

In the second proposed mechanism [Eq. (7)], the purine substrate (B′) is complexed (noncovalently) to the molybdenum cofactor (A′) of the enzyme as the keto tautomer permitting insertion of the C8–H-bond

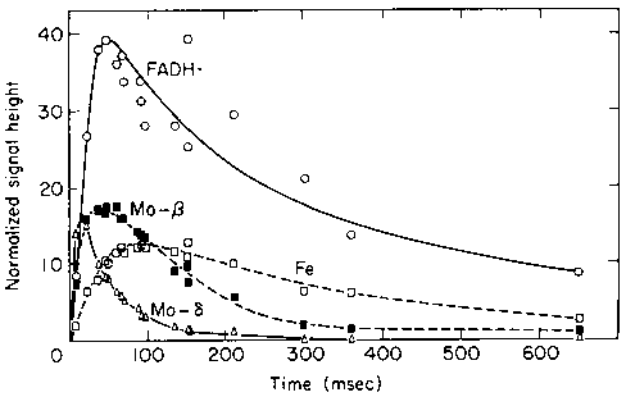

Figure 4 Electron paramagnetic resonance signals generated by xanthine oxidase in a "single turnover" experiment with xanthine as substrate. (From Ref. 36.)

across the $Mo^{VI}=S$ bond to give a species with a Mo–C(SH) bond (C′). D′ is formed by removal of a proton from the MoOH group to provide an O-bridge between the Mo and C-8 of the purine. Subsequent proton (H^+) and electron (e^-) transfers lead to the "very rapid" species (E′), with some resemblance to E in Eq. (6) (both have Mo^V–OS(OR) structure) which is EPR detectable.

III. DETERMINATION OF XANTHINE OXIDASE ACTIVITIES

A. Xanthine Oxidase Activity

A number of methods are available to determine XO activity. Using xanthine as the substrate, the rate of oxidation of xanthine to uric acid can be followed by the rate of Methylene Blue reduction (under anaerobic conditions), by cytochrome c reduction (aerobically), by oxygen uptake (oxygen electrode use), or by the rate of uric acid formation (increase in absorbance at 290 nm).

The easiest, and perhaps best assay is to follow the rate of uric acid formation from xanthine, in the presence of O_2, in a recording spectrophotometer at 290 nm, pH 8.3, 25°C (8). The molar extinction coefficient, $\epsilon_m, = 9.6 \times 10^3\ M^{-1}\,cm^{-1}$.

$$\text{xanthine} + O_2 \rightarrow \text{uric acid} + H_2O_2 \qquad (8)$$

Only initial rates should be used (< 5% conversion of xanthine to uric acid) in analyses, as H_2O_2 slowly inactivates the enzyme. Catalase can be added to remove the H_2O_2 when reaction times need to be extended (when low concentrations of XO are present).

The rate of reaction [Eq. (8)] can also be followed with cytochrome c under aerobic conditions. The rate of reduction of cytochrome c is determined by increase in absorbance at 550 nm (reduced band of cytochrome c).

B. Xanthine Dehydrogenase Activity

See Section IV.B.1.

IV. PURIFICATION OF XANTHINE OXIDASE

A. Xanthine Oxidase from Cow's Milk

An abbreviated description of the method of Avis et al. (20) for the purification of xanthine oxidase from cow's milk, published in 1955, is given below. This method is chosen for several reasons:

1. Although XO had been partially purified by other researchers, Avis et al. (20) were the first to obtain a homogeneous XO preparation *and* to crystallize it.
2. Researchers have shown this method to be the best one, even after 45 years. Some modifications of the method have been published, but all report the same maximum specific activities as Avis et al. (20).
3. Fraction M7 contained FAD, iron, and molybdenum in the ratio of 2.0 : 8.1 : 1.4 per unit of protein;' recent methods give nearly the same values.
4. Q_{O2} is 2300 units activity using xanthine as substrate at 23.5°C, indicating purity. The steps involved in purification are described below.

1. M1

Cream separated from fresh milk. The milk was cooled to 5°C overnight, skimmed, churned, and passed through a cream separator to remove additional fat. Approximately 50% of the original activity was retained; volume was 25.1 L. The buttermilk was warmed to 34°C in a pressure controlled cast-iron vessel. Calcium chloride (0.5 *M*: 250 mL) and pancreatin (40 g) were added. After 15 min a dense precipitate of casein formed and was removed by straining through nylon net to give 25 L of M2.

2. M2

Filtration was performed on type PF 40 filters and 13 sterimats precoated with Hyflo Super Cel (650 g) at ~ 5 lb/in.^{2} Hyflo Super Cel (325 g was mixed with M1). Starting pressure was 7 lb/in.^{2} using a nitrogen cylinder. The first 3 L of colorless filtrate was discarded. Filtration rate decreased after ~ 10 L was collected and a final pressure of 28 lb/in.^{2} was required. Total volume of M3 was 21 L.

3. M3

The cloudy filtrate was stored for 16 h at 5°C, then refiltered through PF 40 and 11 sterimats of grade GS to give 20 L of clear yellowish brown liquid (M4).

4. M4

M4 was chromatographed on a 6 in.×12 in. Pyrex column packed with calcium phosphate gel/Celite 545 (1 : 1) (see Ref. 38 for preparation). M4 was cooled to 5°C, adjusted to pH 6.2 with 0.1 N acetic acid, and passed through the column at 4 lb/in.^{2} pressure. The

brown enzyme bound to the calcium phosphate gel column. The column was washed with 0.02 M phosphate buffer, pH 6.2, until the washes gave a negative protein test by trichloroacetic acid addition (ppt.). The enzyme was eluted with 1 *M* phosphate buffer, pH 5.8, to give M5.

5. M5

M5 was precipitated with an equal volume of 4 *M* phosphate buffer (pH ~ 9) and the precipitate collected on a sintered-glass funnel with aid of 10 g Hyflo Super Cel. The precipitate was dissolved in a minimum amount of water and filtered using Hyflo Super Cel, which was washed with small amounts of water to give 400 mL enzyme solution. The solution was then dialyzed in a Visking cellulose casing (size 32/32) against 40 L of 0.01 *M* acetate buffer, pH 5.1, at 5°C. This treatment gave a copious, colored precipitate which was removed by centrifugation and discarded. The 450 mL of supernatant is M6.

6. M6

M6 was concentrated from 450 to 320 mL by perevaporation (air current produced by fan) in a Visking cellulose casing for 16 h at 5°C. The protein concentration was 1% as measured by absorbance at 280 nm. The solution was cooled to 0°C; 160 mL of 70% (v/v) ethanol, precooled in a carbon dioxide–acetone bath, was added to the solution from a burette fitted with a fine capillary, with sufficient stirring to ensure rapid mixing but without frothing. The solution, which began to form a small amount of precipitate, was held for 16 h at −6°C. The precipitate was collected in a refrigerated (−6°C) centrifuge at 1300g for 40 min. The precipitate was dissolved in water (88 mL), giving a total volume of 100 mL. Phosphate buffer (1 *M*; 1 mL; pH 5.8) and 10 mL of 50% (v/v) ethanol were added slowly to give a final ethanol concentration of ~ 8%. The solution was held at −1°C for 0.5 h and centrifuged. The precipitate was discarded. The supernatant liquid was seeded with crystals from a previous batch and held at −1°C. Crystals appeared after ~ 12 h. In other preparations crystals appeared within 36 h without seeding.

After 4 days at −1°C, the crystals were collected by centrifugation at −1°C and washed twice with phosphate buffer containing 7% ethanol (0.01 *M* phosphate, pH 6.2, −1°C), using 70 mL of the ethanolic buffer each time. The crystals were dissolved in aqueous 0.2 *M* sodium chloride (~ 45 mL) and the solution was dialyzed for 16 h against 1 L of 0.2 *M* sodium chloride at 5°C. The solution was diluted to 50 mL (M7).

A second crop of crystals was obtained from centrifugation of the mother liquor after 28 days at −1°C. The crystals were collected by centrifugation and dissolved in 0.2 *M* sodium chloride (15 mL) (M7a).

Part of the M7 solution (10 mL), after storage at 2° C for 28 days, was recrystallized by the following method to give M8. The enzyme was precipitated by adding 70% (v/v) ethanol (5 mL), then centrifuged, and the precipitate dissolved in water to give 10 mL of solution. Phosphate buffer (1 *M*; 0.7 mL; pH 5.8) and 50% ethanol (1.5 mL) were added. The immediate precipitate formed at 10 min was removed by centrifugation at −1°C and the supernatant liquid was seeded and left at −1°C for 16 h. The crystals formed were collected by centrifugation and dissolved in 0.2 *M* aqueous sodium chloride (final volume of 10 mL) (M8). Results of the purification are summarized in Table 2.

B. Xanthine Dehydrogenase from Cow's Milk

Hunt and Massey (8) purified cow's milk XO in a dehydrogenase form (XDH) in the presence of 2.5 m*M* dithiolthreitol. While XO reacts rapidly only with O_2 (and xanthine) and not with NAD^+, the XDH form of the enzyme reacts rapidly with NAD^+. XDH has a turnover number for the NAD^+-dependent conversion of xanthine to urate of 380 mol/NAD^+/min/mol of XDH at pH 7.5 and 25°C, with a $K_m < 1\,\mu M$ for xanthine and a K_m of $7\mu M$ for NAD^+, but very little O_2-dependent activity. XDH can be converted to the XO form by addition of three to four equivalents of the disulfide-forming reagent 4, 4′-dithiodipyridine, suggesting that in the XDH form of the enzyme disulfide bonds are reduced to –SH groups. This may create a binding site for NAD^+ that changes the protein structure near the flavin (8).

1. Enzyme Assays

Xanthine oxidase activity was measured using $165\,\mu M$ xanthine in 0.1 *M* sodium pyrophosphate buffer containing 0.3 m*M* EDTA, pH 8.5, and 25°C in an air-equilibrated solution, by monitoring production of urate at 295 nm ($\epsilon_M = 9{,}500\ M^{-1}\,cm^{-1}$) (8).

Xanthine dehydrogenase activity was measured using the same assay mixture as above, plus $530\,\mu M$ NAD^+ and determining the NADH production at 340 nm ($\epsilon_M = 6.22 \times 10^3\ M^{-1}\ cm^{-1}$) (39). Activities are expressed in turnover numbers, as moles of substrate catalyzed to product/min/mol enzyme-bound flavin.

Table 2 Summary of Purification of Xanthine Oxidase

Fraction No.	Volume (L)	Total units (XO)	Spec. Act.[a] (units/L/E_{280})	Spec. Act.[b] (units/L/E_{450})	E_{280}/E_{450} [c]	Step
M1	25	277	0.14[d]	—		Buttermilk
M2	25	275	—	—		Pancreatin treatment
M3	21	96	—	—		1st filtrate
M4	20	85	0.53	35	65	2nd filtrate (whey)
M5	1.22	96[e]	7.4	70	9.4	Eluate
M6	0.45	43	11.1	88	8.0	"Starting concentrate"
M7	0.050	17	15.2	79	5.2	Crystalline
M7a	0.015	3	10.4	66	6.3	Crystalline
M8	—	—	14.2[f]	71[c]	5.0[c]	Crystalline

[a] Equivalent to total units activity/L/total protein.
[b] Equivalent to total units activity/L/total protein.
[c] Equivalent to total protein/total flavin content.
[d] Approx. value due to turbidity of solution.
[e] Apparent increase in activity probably due to experimental error.
[f] M7 solution before 2nd crystallization gave units/L/E_{450} of 71, units/L/E_{280} of 13.3, and E_{280}/E_{450} of 5.3.
Source: Ref. 20.

Since XO/XDH have two flavins per mol, the turnover number is per active site. The XDH/XO ratio is calculated on the basis of these specific assays.

2. Enzyme Purification

Purification of XO in the reduced XDH form (8).

1. To 15 L fresh unpasteurized cow's milk, add 50 mL of 0.75 *M* dithiothreitol (DTT), 15 mL of 0.1 *M* phenylmethanesulfonyl fluoride (to inhibit serine proteases), 15 mL of 1.0 *M* sodium salicylate, 240 g of sodium bicarbonate, and 2840 g of ammonium sulfate. Stir rapidly for 1 h at 4°C (all steps below are done at 4°C).
2. Add 2.5 L chilled 1-butanol and stir for 30 min.
3. Centrifuge the suspension in 800-mL aliquots for 15 min at 4000g. Remove the top butanol layer by suction. Remove the solid lipid layer. Discard both.
4. To the 15 L of liquid, add 160 g/L of ammonium sulfate and stir for 30 min. Then let stand for 2 h to permit the precipitate to rise to the top. Skim off the brown precipitate (in ~ 1.7 L); centrifuge for 1 h at 16,000g. Remove the liquid and discard.
5. Resuspend the solid precipitate in 500 mL of 0.05 *M* potassium phosphate buffer containing 0.3 m*M* EDTA, 1 m*M* salicylate, 2.5 m*M* DTT, pH 6.0. Dialyze twice, using 6 L of the same buffer solution each time. Centrifuge the dialysate (~ 470 mL) at 16,000g for 1 h. Decant the liquid portion and save. Discard precipitate.
6. Titrate the liquid portion from above using 30 mL enzyme preparation/mL calcium phosphate gel (38). Typically, 1 L of calcium phosphate gel is stirred well with 470 mL of enzyme solution. Centrifuge for 10 min at 4,000g. Discard supernatant.
7. Resuspend the precipitate in phosphate buffer (see 5 above) and centrifuge to collect insoluble material.
8. Resuspend the precipitate in 500 mL of 10% ammonium sulfate. Centrifuge. Repeat the washing of the precipitate three more times, saving the washes.
9. To the combined washes, add ammonium sulfate to increase its concentration to 50%. Centrifuge at 16,000g for 30 min. Save the precipitate.
10. Resuspend the precipitate in a mixture of 80% of 0.05 *M* Tris, 0.3 m*M* EDTA, pH 7.8, buffer and 20% of 0.1 *M* sodium pyrophosphate, 0.3 m*M* EDTA, pH 8.5, with 2.5 m*M* DTT (Buffer A). Dialyze against 2 L of the same buffer overnight.
11. A 100-mL portion is removed from the dialysate and loaded onto a folate affinity column, prepared according to Nishino et al. (40), and equilibrated in Buffer A. The column is washed with ~ 500 mL of Buffer A until the 280 nm absorbance reaches a minimum, then elution is begun with Buffer A containing 10 m*M* salicylate. XDH moves gradually down the column and elutes as a single dark band.
12. The dark band fractions from step 11 above are pooled, concentrated, and dialyzed in 0.1 *M* sodium pyrophosphate, 0.3 m*M* EDTA, pH 7.5, buffer. The

Table 3 Purification of Milk Xanthine Dehydrogenase

Purification step	Volume (mL)	XDH/XO (total units)	Protein (mg/mL)	XDH/XO specific activity (units/mg)	XDH/XO purification (fold)	Dehydrogenase: oxidase activity (ratio)
Fresh milk	15,000	747/870	8	0.0062/0.0072	1/1	1.3
After $(NH_4)_2SO_4$/butanol fractionation and dialysis	470	800/260	7	0.24/0.79	38/11	3.1
After calcium phosphate gel	2,000	810/250	0.4	1.0/0.31	161/43	3.2
Before folate column	100	620/85	4.7	1.3/0.18	210/25	7.3
After folate column	24	450/46	12	1.56/0.16	252/22	9.7

Source: Ref. 8.

liquid fractions from step 1 are stored at 4°C in the buffer above with 1 m*M* salicylate and 2.5 m*M* DDT added. During storage there is some conversion of XDH to XO. XO can be converted back to XDH by adding fresh DTT-containing buffer.

Table 3 summarizes the results of the purification of milk XDH.

REFERENCES

1. T Nishino, T Nishino. The conversion from the dehydrogenase type of rat liver xanthine dehydrogenase by modification of cysteine residues with fluorodinitrobezene. J Biol Chem 272:29859–29864, 1997.
2. T Nishino, K Okamoto, S Nakanishi, H Hori, T Nishino. The mechanism of conversion of xanthine dehydrogenase to xanthine oxidase. Keio Univ Symp Life Sci Med (Oxygen Homeostasis and Its Dynamics), 1:333–339, 1998.
3. J Hunt, V Massey. Milk xanthine dehydrogenase. In: B Curti, S Ronchi, G Zanetti, eds. Flavins Flavoproteins Proc Int Symp, Vol 10. Berlin: de Gruyter, 1991, pp 695–698.
4. T Nishino, Y Amaya, K Noda. Cysteine residues responsible for dehydrogenase-oxidase conversion of rat liver xanthine dehydrogenase. In: B Curti, S Ronchi, G Zanetti. Flavins Flavoproteins Proc Int Symp, Vol. 10. Berlin: de Gruyter, 1991, pp 703–706.
5. T Nishino, S Nakanishi, K Okamoto, J Mizushima, H Hori, T Iwasaki, T Nishino, K Ichimori, H Nakazawa. Conversion of xanthine dehydrogenase into oxidase and its role in reperfusion injury. Biochem Soc Trans 25:783–786, 1997.
6. VH Booth. LXV. The specificity of xanthine oxidase. Biochem J 32:494–502, 1938; VH Booth. LXVI. The xanthine oxidase–aldehyde system. Biochem J 32:503–507, 1938.
7. CM Harris, V Massey. The reaction of reduced xanthine dehydrogenase with molecular oxygen. J Biol Chem 272:8370–8379, 1997.
8. J Hunt, V Massey. Purification and properties of milk xanthine dehydrogenase. J Biol Chem 267:21479–21485, 1992.
9. C Enroth, BT Eger, K Okamoto, T Nishino, T Nishino, EF Pai. Crystal structures of bovine milk xanthine dehydrogenase and xanthine oxidase: structure-based mechanism of conversion. Proc Natl Acad Sci USA 97:10723–10728, 2000.
10. A Soto, T Nihino, K Noda, Y Amaya, T Nishino. The structure of chicken liver xanthine dehydrogenase: cDNA and the domain structure. J Biol Chem 270:2818–2826, 1995.
11. F Schardinger. Ueber das Verhalten der Kuhmilch gegen Methylenblau und seine Verwendung zur Unterscheidung von ungekochter und gekochter Milch. Z Unters Nahr Genussm 5:1113–1121, 1902.
12. EJ Morgan, CP Stewart, FG Hopkins. Anaerobic and aerobic oxidation of xanthine and hypoxanthine by tissues and by milk. Proc R Soc Lond Ser B94:109–131, 1922.
13. M Dixon, S Thurlow. Studies of xanthine oxidase. I. Preparation and properties of active materials. Biochem J 18:971–975, 1924.
14. M Dixon. Studies on xanthine oxidase. VII. The specificity of the system. Biochem J 20:703–718, 1926.
15. EG Ball. Xanthine oxidase: purification and properties. J Biol Chem 128:51–67, 1939.
16. HS Corran, JG Dewan, AH Gordon, DE Green. Xanthine oxidase and flavoprotein. Biochem J 33:1694–1706, 1939.
17. EC DeRenzo, E Kaleita, P Heytler, JJ Oleson, BL Hutchings, JH Williams. The nature of the xanthine oxidase factor. J Am Chem Soc 75:753, 1953.
18. DA Richert, WW Westerfeld. Isolation and identification of the xanthine oxidase factor as molybdenum. J Biol Chem 203:915–923, 1953.

19. DA Richert, WW Westerfeld. The relation of iron to xanthine oxidase. J Biol Chem 209:179–189, 1954.
20. PG Avis, F Bergel, RC Bray. Cellular constituents. The chemistry of xanthine oxidase. Part I. The preparation of a crystalline xanthine oxidase from cow milk. J Chem Soc 1955:1100–1105, 1955.
21. V Massey, PE Brumby, H Komai, G Palmer. Milk xanthine oxidase. Some spectral and kinetic properties. J Biol Chem 244:1682–1691, 1969.
22. PG Avis, F Bergel, RC Bray, DWF James, KV Shooter. Cellular constituents. The chemistry of xanthine oxidase. Part II. The homogeneity of crystalline metalloflavoprotein fractions. J Chem Soc 1956:1212–1219, 1956.
23. RM Wright, JE Repine. The human molybdenum hydroxylase gene family: co-conspirators in metabolic free-radical generation and disease. Biochem Soc Trans 25(3):799–804, 1997.
24. GB Bulkley. Physiology of reactant oxidant-mediated signal transduction: an overview. Biochem Soc Trans 25(3):804–812, 1997.
25. R Harrison. Human xanthine oxidoreductase: in search of a function. Biochem Soc Trans 25(3):786–791, 1997.
26. DR Blake, CR Stevens, T Sahinoglu, G Ellis, K Gaffney, S Edmonds, M Benboubetrat, R Harrison, S Jawed, J Kanczler, TM Millar, PG Winyard, Z Zhang. Xanthine oxidase: four roles for the enzyme in rheumatoid pathology. Biochem Soc Trans 25(3):812–816, 1997.
27. C Ho, AJ Clifford. Bovine milk xanthine oxidase, blood lipids and coronary plaques in rabbits. J Nutr 107:758–766, 1977.
28. K Ichida, Y Ayama, K Noda, S Minoshima, T Hosoya, O Sakai, N Shimizu, T Nishino. Cloning of the cDNA encoding human xanthine dehydrogenase (oxidase): structural analysis of the protein and chromosomal location of the gene. Gene 133:279–284, 1993.
29. R Hille, T Nishino. Xanthine oxidase and xanthine dehydrogenase. FASEB J 9:955–1003, 1995.
30. L Berglund, JT Rasmussen, MD Andersen, MS Rasmussen, TE Petersen. Purification of the bovine xanthine oxidoreductase from milk fat globule membranes and cloning of complementary deoxyribonucleic acid. J Dairy Sci 79:198–204, 1996.
31. KV Rajagopalan, JL Johnson. The pterin molybdenum cofactor. J Biol Chem 267:10199–10202, 1992.
32. MJ Romao, M Archer, I Moura, JJG Moura, J LeGall, R Engh, M Schneider, P Hof, R Huber. Crystal structure of the xanthine oxidase-related aldehyde oxido-reductase from *D. gigas*. Science 270:1170–1176, 1995.
33. R Huber, P Hof, RO Duarte, JJG Moura, I Moura, M-Y Liu, J LeGall, R Hille, M Archer, MJ Romao. A structure-based catalytic mechanism for the xanthine oxidase family of molybdenum enzymes. Proc Natl Acad Sci USA 93:8846–8851, 1996.
34. H Gutfreund, JM Sturtevant. Steps in the oxidation of xanthine to uric acid catalyzed by milk xanthine oxidase. Biochem J 73:1–6, 1959.
35. WW Cleland. The kinetics of enzyme-catalyzed reactions with two or more substrates or products. I. Nomenclature and rate equations. Biochim Biophys Acta 67:104–137, 1963; II. Inhibition: Nomenclature and theory. Biochim Biophys Acta 67:173–187, 1963; III. Prediction of initial velocity and inhibition patterns by inspection. Biochim Biophys Acta 67:188–196, 1963.
36. RC Bray, G Palmer, H Beinert. Direct studies on electron transfer sequence in xanthine oxidase by electron paramagnetic resonance spectroscopy. J Biol Chem 239:2667–2676, 1964.
37. P Manikandan, E-Y Choi, R Hille, BM Hoffman. 35 GHz ENDOR characterization of the "very rapid' signal of xanthine oxidase reacted with 2-hydroxy-6-methylpurine (^{13}C8): evidence against direct Mo-C8 interaction. J Am Chem Soc 123:2658–2663, 2001.
38. SM Swingle, A Tiselius. Tricalcium phosphate as an adsorbent in the chromatography of proteins. Biochem J 48:171–174, 1951.
39. H Komai, V Massey, G Palmer. The preparation and properties of xanthine oxidase. J Biol Chem 244:1692–1700, 1969.
40. T Nishino, T Nishino, K Tsushima. Purification of highly active milk xanthine oxidase by affinity chromatography on Sepharose 48/folate gel. FEBS Lett 131:369–372, 1981.

43

Lipoxygenase and Associated Enzymes

Harold W. Gardner*
U.S. Department of Agriculture, Peoria, Illinois, U.S.A.

I. INTRODUCTION

A. Reactions Catalyzed

Lipoxygenase (LOX), a nonheme iron protein, is undoubtedly universally distributed in plants and animals. Fungal LOXs are known that give unique products and some of these LOXs apparently operate by different mechanisms (1), including a LOX with a manganese active site (2). A number of recent publications review various aspects of LOX (3–15). Although many LOXs have been thoroughly characterized, much of the literature focuses on one soybean seed isozyme, LOX-1. In this review a detailed account of soybean LOX-1 is unavoidable because the literature is too extensive to realistically review the field in its entirety.

LOXs catalyze the dioxygenation of methylene-interrupted pentadiene fatty acids to afford conjugated hydroperoxydiene fatty acids. With few exceptions, plant LOXs oxidize linoleic and linolenic acids regiospecifically at either the ω6 (C-13) or ω10 (C-9) position with (*S*)-stereospecificity (Fig. 1). In the animal kingdom LOXs oxidize linoleic and linolenic acids by mechanisms similar to those in the plant kingdom, but many of the important oxidations of physiological significance utilize arachidonic acid and other C:20 polyenoic acids as substrates. Although plant LOXs are capable of oxidizing C:20 polyenoic acids, these substrates are unnatural in plants. With some exceptions, oxidations of C:20 fatty acids occur either at ω6 (C-15), ω9 (C-12), or ω16 (C-5) position with (*S*)-stereospecificity (7). As discussed below, the list of substrates include additional natural and synthetic substrates; many of the latter give reduced activity. Generally, plant LOXs having high pH optima oxidize at the ω6 position if incubated at high pH, and those with optima at neutral or low pH mainly afford ω10 oxidation or both types of oxidation. The spatial relationship of removal of the *bis*-allylic hydrogen, and an (*S*)-oxidation at ω6 versus ω10 requires an alignment of the substrate into the active site of LOX in reverse orientations—that is, "head first" or "tail first." This can be deduced by reference to Figure 1. Since reducing the pH of the incubation has been observed to lower the ratio of ω6 to ω10 oxidation of linoleic acid by soybean LOX-1 (16) and also lowers the ratio of ω6 to ω16 oxidation of arachidonic acid by rice LOX-2 (17), this suggested that either a head-first or tail-first alignment at the active site was dependent on the charge of the carboxylate/carboxylic acid group. It is probably because of reverse orientation phenomenon that arachidonic acid is all-(*S*) doubly dioxygenated at both ends of the polyene structure (17, 18).

The rate-limiting step is an H removal from the *bis*-allylic methylene of the pentadiene on the opposite side of O_2 insertion (19, 20). The immense size of an observed kinetic isotope effect with deuterated linoleic acid indicates that hydrogen tunneling occurs in the LOX reaction (21). As shown in Figure 2, the iron

*Retired.

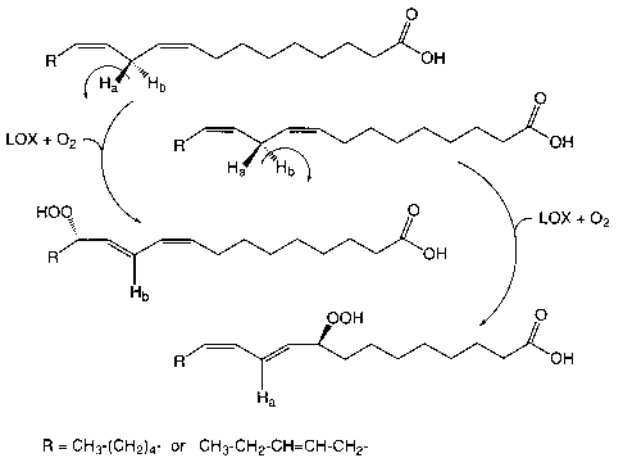

Figure 1 Oxidation of either linoleic (18:2) or linolenic (18:3) acid by plant LOXs is preceded by stereospecific removal of hydrogen followed by placement of oxygen on the opposite side of the molecule from hydrogen removal. Plant LOXs usually produce the 13(*S*)- and/or 9(*S*)-hydroperoxides of linoleic or linolenic acid as shown.

active site cycles electrons by a redox mechanism from H removal (Fe^{3+} to Fe^{2+} transition) to conversion of the fatty acid peroxyl radical to the hydroperoxide anion (Fe^{2+} to Fe^{3+} transition) (15, 22, 23). Also shown in Figure 2 is an "O_2-starved cycle" of LOX (22, 23). When LOXs become deficient in O_2 the enzyme undergoes an aberrant reaction whereby the product hydroperoxide fatty acid (ROOH) replaces ROO· as an oxidant of the active site. This results in formation of a fatty acid alkoxyl radical (RO·) from the hydroperoxide, as well as unoxidized pentadienyl radicals from substrate. From linoleic acid and its 13-hydroperoxide, a number of compounds are formed by free radical chemistry, among which are pentane, 13-oxo-9,11-octadecadienoic acid, 13-oxo-9,11-tridecadienoic acid (24), dimers (25), and racemic fatty acid hydroperoxides (26). Similarly, from linolenic acid and its 13-hydroperoxide, one obtains isomeric pentenols, 13-oxo-9,11-tridecadienoic acid, and dimers (27). It is relatively easy to obtain O_2-starved conditions, such as by using excess concentrations of LOX and substrate, and by low O_2 solubility due to increased temperatures of incubation. For good yields of hydroperoxides, one should optimize O_2 dispersal/solubility, and use optimal enzyme concentrations (6).

B. Structure of Substrates

"Natural" fatty acid substrates were discussed above. Other "natural" substrates, such as glycerides (28, 29)

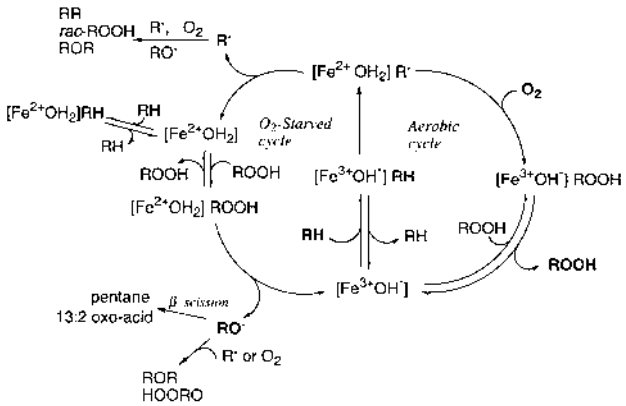

Figure 2 The iron redox cycle of the LOX active site shows the reaction of linoleic acid with O_2 under conditions of adequate aeration, as well as an aberrant reaction with linoleic acid hydroperoxide under O_2-starved conditions. Shown in bold are the entry of linoleic acid (RH) and O_2 into the cycle and products initially released from the active site—that is, linoleic acid hydroperoxide (ROOH), the alkoxyl radical of linoleic acid hydroperoxide (RO·), and the linoleic acid pentadienyl radical (R·). The alkoxyl radical (RO·) often rearranges into an epoxyallylic carbon radical which reacts with O_2 to form epoxyhydroperoxyoctadecenoic acid (HOORO), leading to epoxyhydroxyoctadecenoic acid. ROR represents dimers of epoxyoctadecenoic acid with the conjugated diene of linoleic acid. RR represents conjugated linoleic acid dimers, and *rac*-ROOH signifies racemic hydroperoxides formed by nonenzymic reaction of O_2 with the pentadienyl radical of linoleic acid. Refs. 15, 22, and 23.

and phosphoglycerides (29, 30) have been described, but the activity is often reduced compared to free polyunsaturated fatty acids. Recently, it has been found that one of the olefinic double bonds can be replaced by a carbonyl double bond, such as a ketone (31) or aldehyde moiety (32). Many unnatural substrates have been synthesized to study enzyme mechanisms, among which two detailed studies are cited here as examples of the substrate structural requirements other than those found in usual substrate fatty acids (33, 34).

C. Classification According to Enzyme Commission

According to the IUBMB (35), LOX is classified as a linoleate:oxygen 13-oxidoreductase (EC 1.13.11.12). However, many LOX isozymes that have been thoroughly characterized by sequence have been shown to catalyze other oxidations, such as linoleate:oxygen 9-oxidoreductase; thus, it would appear that classification of LOX should be amended.

II. IMPORTANCE TO QUALITY OF FOOD

LOX is known to have several detrimental effects in foods (see reviews: 36, 37), and these effects can be controlled by various methods of enzyme denaturation. By the process of cooxidation by free radicals, LOX activity is known to cause bleaching of carotenoids, chlorophyll (38, 39, and Refs. therein), and oxidation of ascorbic acid (40). LOX probably accounts for a large portion of pigment bleaching and loss of quality observed in unblanched frozen vegetables. In addition, products of LOX action, fatty acid hydroperoxides, are cleaved both enzymically and nonenzymically into odorous shorter-chain aldehydes, alcohols, and alkanes. The nonenzymic formation of odors is very detrimental leading to complex free radical products broadly defined as ''rancidity'' (see review: 41). LOX reactions can even occur in ''dry'' substrates at the lowest relative humidities examined (52%) (42). It was also demonstrated that LOX action in dry substrates initiated free radical autoxidation of polyunsaturated fatty acids.

Although LOX is often considered to be detrimental to foods, there are examples of positive uses. LOX has been used in replacing bromates to improve dough elasticity for bread making presumably by increasing disulfide bonds through oxidation (see review: 43). In addition, LOX bleaches carotenoid through cooxidation in doughs increasing the whiteness of bread. As discussed below, the LOX/hydroperoxide lyase sequence, also involving other enzymes such as alcohol dehydrogenase and double-bond isomerase, is important in imparting odors and flavors to fresh fruit and vegetables. These flavors are important enough to persuade Firmenich to develop an enzymic procedure for their biosynthesis (44).

III. ENZYMES FOUND IN RAW FOODS

A. Enzymes Acting on Hydroperoxide Products of LOX

Generally, in raw foods LOX often operates in concert with other enzymes by sequential reactions. In plants, some of the cytochrome P450 enzymes, usually membrane bound, are of considerable importance to food quality. Each raw food has its unique blend of hydroperoxide-utilizing enzymes. One of the most important of these enzymes is hydroperoxide lyase, which has been cloned, sequenced, and identified as a cytochrome P450 (CYP74B) (45). Hydroperoxide lyase cleaves 13-hydroperoxides of 18:2 and 18:3 fatty acids into C-6 aldehydes and a C-12 oxoacid, the former giving rancid-green (hexanal) and grassy (3Z-hexenal) odors. 9-Hydroperoxides cleaves into C-9 aldehydes (cucumber-like odors) and C-9 oxoacid (see review: 46). The aldehydes are then subject to further transformation by enzymes, such as reduction to alcohols. The alcohols, which generally have similar odor profiles as the aldehydes, can also be transformed into other flavor volatiles, such as the intense apple flavor hexyl acetate. The 3(*Z*)-alkenals produced by hydroperoxide lyase are susceptible to transformation by isomerase into 2(*E*)-alkenals (47) or oxidation to 4-hydroperoxy-2(*E*)-alkenals by LOX itself and possibly other enzymes (32). Most of the volatile aldehydes and alcohols are considered very desirable fresh vegetable odors, and contrast with the complex mixture of odors obtained by the free radical process of rancidity development. However, in soybean hexanal is considered to be an off-flavor, and, as described below, mutants have been developed to eliminate LOX isozymes from the seed. Also, it has been reported that a LOX/hydroperoxide lyase sequence is responsible for the odor of fresh fish (48).

In the multistep biosynthesis of an important jasmine odor, methyl 7-iso-jasmonate (49), the enzyme allene oxide synthase catalyzes the inaugural step of 12-oxo-10,15-phytodienoic acid formation from 13-hydroperoxide of linolenic acid. It is of interest to note that methyl jasmonate, the racemate of methyl 7-iso-jasmonate, is odorless (49). Allene oxide synthase, a cytochrome P450 designated as CYP74A (50), has been cloned and sequenced from a number of sources (e.g., 50). When allene oxide synthase is active, it also has the practical function of removing rancidity-causing hydroperoxide fatty acids from foods.

Another plant hemoprotein, hydroperoxide peroxygenase (not yet sequenced), utilizes one of the hydroperoxide oxygens to epoxidize a double bond intra- or intermolecularly, and in the process the hydroperoxide itself is reduced to a hydroxide (51). Hydrolysis of the epoxide by epoxide hydrolase furnishes the corresponding diol. The resulting hydroxyl/dihydroxy/trihydroxy fatty acids have been implicated in imparting bitter tastes to certain foods (52). Other hydroperoxide-metabolizing enzymes, like divinyl ether synthase (53 and Refs. therein), have little known effects on foods.

B. Location of LOXs

In plants LOXs are found in all tissues with a few exceptions. For example, soybean mutants have been

found devoid of all three LOX isozymes normally found in the seed (54), but it is likely that the absence of LOX in these mutants is only seed specific.

LOX is generally regarded as a soluble enzyme located in the cytoplasm, but recent research demonstrated a far more complex organization. Using techniques such as immunolocalization, LOX isozymes in soybean seed are generally found in the cytoplasm around the protein bodies of storage parenchyma, but LOX is also associated with aberrant protein bodies in the hypodermis and vascular bundle sheaths (55, 56). In soybean leaves, LOX isozymes also function as vegetative storage proteins being regulated by source-sink status. These isozymes differentially locate in vacuoles, in the cytosol of paravienal mesophyll and in the bundle sheath along with other storage proteins (57). Also, organ-specific expression of LOX isozymes has been observed, such as that found in potato (58).

It seems certain that membrane-associated LOXs are important. Although there are a number of reports showing LOX to be associated with microsomes and plasma membranes, there is little evidence to show specific targeting to these membranes; that is, such associations may be nonspecific binding. Numerous reports of the localization of LOXs in chloroplasts of a variety of plants (e.g., 59) have been authenticated in some cases by showing the presence of a chloroplast transit peptide (60, 61). Chloroplast LOXs have been reported to be induced by wounding, pathogenesis, and methyl jasmonate. LOX's presence in chloroplasts presumably functions to initiate a cascade of reactions through chloroplast-bound hydroperoxide-utilizing enzymes (62). There are several reports of a specific LOX being localized in lipid bodies (e.g., 63), and this type of LOX has been reported to preferentially metabolize esterified fatty acids (64).

IV. PROPERTIES AS PROTEIN

A. Protein Structure

Except for some LOXs from fungi, all are nonheme iron enzymes ranging in size from ~90 to 100 kDa. Soybean seed LOX-1, with a molecular weight of 94 kDa, serves as a model for several reasons, not the least of which are its abundance and priority of isolation in crystalline form (65). LOX-1 has been cloned and sequenced (66). As shown in Figure 3, the three-dimensional structure has been determined by x-ray crystallography (67). Numerous LOXs from plants and animals have now been cloned and sequenced, affording a pairwise sequence identity between plant and mammalian LOXs of 21–27%, among plants of 43–86%, and among mammals of 39–93% (68).

Coral LOX, which catalyzes an unusual 8*R*-specific oxidation of arachidonic acid, warrants special mention as it exists as a fusion protein with allene oxide synthase (69). The allene oxide synthase portion of the protein is not a cytochrome P450, like that found in plants, but it shares homology with catalase.

B. Isozymes

Known LOX isozymes are too numerous to review here. However, soybean can serve as an example. As discussed above, soybean seeds normally have three isozymes—LOX-1, -2, and -3 (54, 70). The process of germination gave expression of an additional three isozymes in seedlings, LOX-4, -5, and -6 (70). Multiple nonseed LOX isozymes have been identified in the soybean leaves (71). Ten isozymes of the soybean plant have now been identified (see review: 4).

Posttranslational modification of soybean seed isozymes has been studied. It has been shown that LOX-1 underwent transformation with incubation at room temperature to furnish five separable forms with different specific activity (72). Cleavage of LOX-1 and -3 by trypsin or chymotrypsin afforded two domains ~60 and 40 kDa without inactivation (73 and Refs. therein). The two domains were tightly associated, because the separated fragments did not possess activity (74).

V. PROPERTIES AS ENZYME

A. Specific Mechanism of Action

As shown by Figure 2, the mechanism of action is an iron-catalyzed one-electron redox cycle that causes free radical oxidation of polyunsaturated fatty acids. X-ray crystallography revealed many clues of the details of catalysis. Not obvious in the structural depiction of the LOX protein shown in Figure 3 is a conical hydrophobic cavity, or tunnel, that connects the bottom of the enzyme with the iron active site, which is believed to be a path for O_2. A substrate channel was identified by a long, narrow hydrophobic cavity with two bends lying to the right of the iron (75). As discussed above, the iron active site serves to cycle electrons. Iron is complexed by three histidines and one isoleucine. Higher-resolution x-ray crystallographic analysis showed that iron was additionally liganded with one water and weakly with asparagine^{694} (76), making a total of six coordinates (Fig. 4). It has been proposed that the

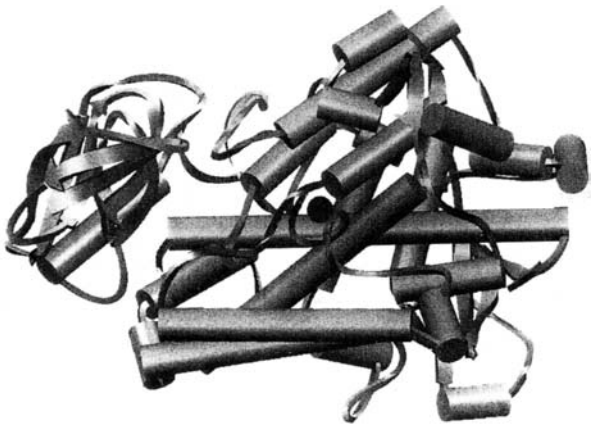

Figure 3 The three-dimensional structure of soybean lipoxygenase-1 determined by x-ray crystallography. The iron active site is shown as a sphere, α-helices by cylinders, strands in β-sheets by arrows, coils by narrow rods. (From Ref. 75.)

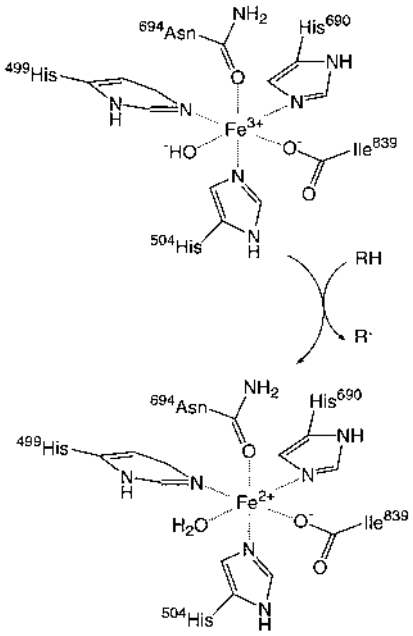

Figure 4 The six-coordinate ligands of the iron active site of soybean LOX-1 showing five amino acids with their numbered positions in the sequence; the sixth ligand (H_2O) is thought to abstract hydrogen from substrate (OH^- to H_2O transition) as shown. The position of the three histidines and isoleucine was determined by x-ray crystallography (67), and high-resolution x-ray analysis showed the presence of H_2O and asparagine as ligands (76). The OH^- to H_2O transition has been proposed by a number of investigators (e.g., see 15).

water ligand exists as a hydroxyl anion/water transition that accepts hydrogen from the substrate (see review: 15). Asparagine[694] (or its equivalent in sequential position) is mostly conserved in various LOXs, but not completely (15); replacement by histidine, as observed in certain LOXs of mammalian origin, reduced k_{cat} significantly (77).

B. Kinetics, K_m, k_{cat}, Activation Energy

A number of factors must be considered prior to determining LOX kinetics. Kinetics should be determined below the critical micelle concentration (CMC), which is dependent principally on the pH, and the presence of other hydrophobic substances, including surfactants. The CMC for linoleic acid has been reported for Na borate buffer (0.1 M) at 167, 60, and 21 μM at pH 10, 9, and 8, respectively (78). Ca^{2+} has been reported as a cofactor of LOX, but this ion is ineffective below the CMC, indicating that it affects CMC by calcium salt formation (79). However, Ca^{2+} may not be completely without effect in vivo. It has been recently reported that Ca^{2+} stimulated the membrane binding of soybean LOX-1, implying a regulatory mechanism for Ca^{2+} (80).

An initial lag in the kinetics of LOX must also be considered. The lag can be overcome simply by adding a small quantity of product hydroperoxide (81). This can be interpreted as an initial oxidation of native Fe^{2+}-LOX by hydroperoxide product to give Fe^{3+}-LOX to prime the catalytic cycle, but detailed kinetic analysis suggested a somewhat more complex interpretation (23).

The turnover rate, k_{cat}, and K_m for soybean LOX-1 with linoleic acid substrate has been variously reported at 280–350 sec^{-1} and 12–25 μM, respectively (15, 81, and Refs. therein).

The activation energy (E_a) for soybean LOX-1 and linoleic acid was determined to be 22 kcal/mol, and $\Delta H^{\neq} = 21$ kcal/mol, $\Delta S^{\neq} = 20$ e.u., and $\Delta G^{\neq} \simeq 15$ kcal/mol (82, 83).

A kinetic scheme has been developed (23 and Refs. therein) and was recently modified by Solomon et al. (15) to account for recent findings of the active site. Figure 2 essentially illustrates this scheme modified to clearly show the aerobic and O_2-starved aspects of the active site redox cycle, as well as the products obtained.

C. Effect of pH, Inhibitors, and Surfactants

Soybean LOX-1 is generally stable over a wide range of pHs. Its activity is optimum between pH 9 and 10.

Activity is negligible at pH 6.5, but it is stable at pHs as low as 4.5. Adjustment to pH 4.5 has been used with crude preparations to remove unwanted protein in LOX purification (84). However, pH 3.0 and below causes irreversible inactivation of soybean LOX activity (85).

Although many inhibitors of LOX have been investigated, only representative examples can be cited here. First, it should be emphasized that soybean LOX catalyzes its own destruction during oxidation of substrate. The destruction is greater with substrates of a higher degree of unsaturation (86). Several types of inhibitors mainly can be categorized as follows (for citations also see 86 and Refs. therein): (a) substrate suicide inhibitors, such as acetylenic fatty acids (irreversible) (87); (b) chain-breaking antioxidants (usually competitive and reversible) (88); (c) iron chelators (often reversible) (89); (d) disrupters of the active site (90); (e) reductants of the active-site iron (91); (f) free radical reactions with LOX, such as with hydroxyl radicals produced from H_2O_2 (presumably irreversible) (92); and (g) substrate mimics (usually competitive) (93). In regard to substrate mimics, such as various fatty acids, potential errors are possible because of their disruption of CMC stability (94). That is, some fatty acids actually may not be inhibitors, and exert their effect by changing the CMC of the substrate.

Nonionic surfactants, such as Tween 20 and Triton X-100, are often used by researchers to clarify substrate solutions. However, it has been found that surfactants actually decrease activity, except when concentrations of substrate and surfactant are high and low, respectively (95). Kinetic data suggested that surfactant sequestered substrate in micelles, whereas the actual substrate was indicated to be solvated monomers. That is, substrate could be oxidized only after escaping micelles in equilibrium with the aqueous phase. The rate increase at high substrate and low surfactant concentrations was interpreted as alleviating substrate inhibition by sequestering substrate in micelles. Besides surfactants, ethanol or methanol is often used to conveniently disperse fatty acid substrates, but alcohols also inhibited the activity of LOX, increased the K_m and decreased the V_{max} (96). The alcohol effect was found to be reversible.

D. Control Methods in Foods

Heat is a simple, commonly used method to inactivate enzymes, including LOX. The inactivation rate constant of soybean LOX activity at 65°C was found to be $8 \times 10^{-4}\,sec^{-1}$ at pH 5–7 (97). Greater inactivation efficiencies are obtained with combinations of heat and other treatments, such as ionizing irradiation (97), alcohol (96), sonication (98), and pressure (99). As discussed above, low pH alone inactivates LOX (85), but pH also plays a role in inactivation by heat (97) and combined treatments (98, 99).

VI. QUALITATIVE AND QUANTITATIVE DETERMINATION OF ACTIVITY

A. Class Action with Assay Conditions

Axelrod et al. (84) outlined spectrophotometric methods for assaying all three soybean seed isozymes. For assay of LOX-1, the cuvette contains 2.975 mL of 0.2 M Na borate buffer, pH 9, containing LOX-1, and then 25 μL substrate solution is added, stirred and monitored at 234 nm at 25°C. The substrate solution was Na linoleate (10 mM) containing a weight of Tween 20 equal to the weight of linoleic acid used; final concentration of Na linoleate in the reaction was 0.083 mM. The rate is the straight-line portion observed after the initial lag period. Activity is defined in units (μmol of product formed/min). Specific activity is defined as units/mg or μg protein. The μmol of product is calculated from the molar extinction coefficient of the conjugated hydroperoxydiene measured at 234 nm. Like most investigators, Axelrod et al. (84) used a molar extinction coefficient of 25,000 M^{-1} cm^{-1}, but this value is probably too low. Our lab uses a higher value of 26,800 M^{-1} cm^{-1} (6).

Several comments should be made regarding the spectrophotometric method. The method is very satisfactory for highly purified LOXs with high pH optima. However, assay of crude enzyme preparations by this method is hazardous because protein and other UV-absorbing materials may absorb all or most of the light at 234 nm, and hydroperoxide-utilizing enzymes, if present, generally destroy the conjugated diene chromophore as it is being formed. Also, when LOX concentrations are extremely high, the absorbance could increase to a maximum before the assay could be started; this could mislead the investigator to the false conclusion that no LOX activity is present. Third, inhibitory surfactants are included to clarify the solutions to avoid scatter of UV light. In our laboratory we have found that pHs below 7.5 result in artifactual absorbance changes due to imperceptible changes in micelles, even in the presence of surfactant. For these reasons, the use of O_2-electrode measurement of O_2 uptake can be a reliable and sensitive method to assay LOX activity. The method described

Table 1 Purification of LOX-1 from 200 g Defatted Soybean Meal

Purification step	Volume (mL)	Protein (mg)	Total activity (units)[a]	Specific activity (units/mg)	Fold purification
Crude extract (0.2 M Na acetate, pH 4.5)	1,160	20,800	95,900	4.72	1[b]
$(NH_4)_2SO_4$ (0.3–0.6 saturation, pH 6.8)	170	3,424	73,400	21.4	4.5
DEAE-Sephadex chromatography	172	229	24,900	101	21
Rechromatography on DEAE-Sephadex	106	81	14,600	180	38

[a] A unit is defined as 1 μmol product formed/min.
[b] The first step of extraction at pH 4.5 gave some purification from unwanted protein that would normally be extracted at higher pH. This inherent purification is not reflected in the fold purification of "1."
Source: Ref. 84.

above can be utilized, except the substrate is linoleic acid dissolved in a minimum of methanol to aid dispersal. This avoids the use of inhibitory surfactants, but alcohols are also inhibitory at high concentrations (96). Methanol can be kept to a minimum to give negligible inhibition (e.g., 2–5 μL substrate dissolved in methanol injected into 2.5 mL buffered enzyme solution).

B. Assays for Screening Purposes

In instances where seed or other material is being screened for absence or presence of LOX activity, there is need for rapid assay methods. A number of colorimetric tests have been developed that rely on the detection of either hydroperoxides or free radical cooxidation reactions (100–103). Researchers have also developed a continuous-flow amperometric detection of hydroperoxides to assay LOX activity (104).

VII. PURIFICATION

The method of Axelrod et al. (84) has been used successfully by our laboratory to isolate large quantities of soybean LOX-1. The method employs preparation of a crude extract from hexane-defatted soybean flour with 0.2 M Na acetate buffer (pH 4.5), followed by $(NH_4)_2SO_4$ fractionation and then two sequential chromatographic separations on DEAE-Sephadex (Table 1). The isolate can be stored as a concentrated suspension in 2.3 M $(NH_4)_2SO_4$ at 4°C (refrigerator) for many years. The authors (84) also outlined procedures for the isolation of LOX-2 and LOX-3.

A more recent method chromatographically separated all six isozymes found in soybean seedlings (70). Seedlings were homogenized in 50 mM Na phosphate (pH 6.8) containing 1.5% Triton X-100. The Triton X-100 was removed from the supernatant after centrifugation with Amberlite XDA-2. An initial purification was achieved by a DEAE-Toyopearl column, and final separation was accomplished with Mono Q. One isozyme that did not bind to DEAE-Toyopearl required a different purification with CM-Toyopearl and Mono S columns.

With the advent of cDNA technology, LOX is increasingly purified from *E. coli*; however, it has been found necessary to cultivate *E. coli* at low temperatures in order to obtain active LOX (105, 106).

REFERENCES

1. C Su, M Sahlin, EH Oliw. A protein radical and ferryl intermediates are generated by linoleate diol synthase, a ferric hemeprotein with dioxygenase and hydroperoxide isomerase activities. J Biol Chem 273:20744–20751, 1998.
2. M Hamberg, C Su, E Oliw. Manganese lipoxygenase: discovery of a bis-allylic hydroperoxide as product and intermediate in a lipoxygenase reaction. J Biol Chem 273:13080–13088, 1998.
3. GJ Piazza, ed. Lipoxygenase and Lipoxygenase Pathway Enzymes. Champaign, IL: AOCS Press, 1996.
4. GA Veldink, MP Hilbers, WF Nieuwenhuizen, JFG Vliegenthart. Plant lipoxygenase: structure and mechanism. In: AF Rowley, H Kühn, T Schewe, eds. Eicosanoids and Related Compounds in Plants and Animals. London: Portland Press, 1998, pp 69–96.
5. A Grechkin. Recent developments in biochemistry of the plant lipoxygenase pathway. Prog Lipid Res 37:317–352, 1998.
6. HW Gardner. Analysis of plant lipoxygenase metabolites. In: WW Christie, ed. Advances in Lipid Methodology—Four. Dundee, Scotland: Oily Press, 1997, pp 1–43.

7. S Yamamoto. Mammalian lipoxygenases: molecular structures and functions. Biochim Biophys Acta 1128:117–131, 1992.
8. BA Vick. Oxygenated fatty acids of the lipoxygenase pathway. In: TS Moore Jr, ed. Lipid Metabolism in Plants. Boca Raton, FL: CRC Press, 1993, pp 167–191.
9. HW Gardner. Recent investigations into the lipoxygenase pathway of plants. Biochim Biophys Acta 1084:221–239, 1991.
10. JN Siedow. Plant lipoxygenase: structure and function. Annu Rev Plant Physiol Plant Mol Biol 42:145–188, 1991.
11. D Shibata, B Axelrod. Plant lipoxygenases. J Lipid Mediators Cell Signalling 12:213–228, 1995.
12. BJ Gaffney. Lipoxygenases: structural principles and spectroscopy. Annu Rev Biophys Biomol Struct 25:431-459, 1996.
13. HW Gardner. Biological roles and biochemistry of the lipoxygenase pathway. HortScience 30:197–205, 1995.
14. WH Gerwick. Structure and biosynthesis of marine algal oxylipins. Biochim Biophys Acta 1211:243–255, 1994.
15. EI Solomon, J Zhou, F Neese, EG Pavel. New insights from spectroscopy into the structure/function relationships of lipoxygenases. Chem Biol 4:795–808, 1997.
16. HW Gardner. Soybean lipoxygenase-1 enzymically forms both (9S)- and (13S)-hydroperoxides from linoleic acid by a pH-dependent mechanism. Biochim Biophys Acta 1001:274–281, 1989.
17. L-Y Zhang, M Hamberg. Specificity of two lipoxygenases from rice: unusual regiospecificity of a lipoxygenase isoenzyme. Lipids 31:803–809, 1996.
18. CPA van Os, GPM Rijke-Schilder, H van Halbeek, J Verhagen, JFG Vliegenthart. Double dioxygenation of arachidonic acid by soybean lipoxygenase-1. Kinetics and regio-stereo specificities of the reaction steps. Biochim Biophys Acta 663:177–193, 1981.
19. M Hamberg, B Samuelsson. On the specificity of the oxygenation of unsaturated fatty acids catalyzed by soybean lipoxidase. J Biol Chem 242:5329–5335, 1967.
20. MR Egmond, JFG Vliegenthart, J Boldingh. Stereospecificity of the hydrogen abstraction at carbon atom n-8 in the oxygenation of linoleic acid by lipoxygenases from corn germs and soya beans. Biochem Biophys Res Commun 48:1055–1060, 1972.
21. T Jonsson, MH Glickman, S Sun, JP Klinman. Experimental evidence for extensive tunneling of hydrogen in the lipoxygenase reaction: implications for enzyme catalysis. J Am Chem Soc 118:10319–10320, 1996.
22. JJMC de Groot, GA Veldink, JFG Vliegenthart, J Boldingh, R Wever, BF van Gelder. Demonstration by EPR spectroscopy of the functional role of iron in soybean lipoxygenase-1. Biochim Biophys Acta 377:71–79, 1975.
23. MA Schilstra, GA Veldink, JFG Vliegenthart. Kinetic analysis of the induction period in lipoxygenase catalysis. Biochemistry 32:7686–7691, 1993.
24. GJ Garssen, JFG Vliegenthart, J Boldingh. An anaerobic reaction between lipoxygenase, linoleic acid and its hydroperoxides. Biochem J 122:327–332, 1971.
25. GJ Garssen, JFG Vliegenthart, J Boldingh. The origin and structures of dimeric fatty acids from the anaerobic reaction between soya-bean lipoxygenase, linoleic acid and its hydroperoxide. Biochem J 130:435–442, 1972.
26. H Berry, H Débat, VL Garde. Oxygen concentration determines regiospecificity in soybean lipoxygenase-1 reaction via a branched kinetic scheme. J Biol Chem 273:2769–2776, 1998.
27. YP Salch, MJ Grove, H Takamura, HW Gardner. Characterization of a C-5, 13-cleaving enzyme of 13(S)-hydroperoxide of linolenic acid by soybean seed. Plant Physiol 108:1211–1218, 1995.
28. J Christopher, E Pistorius, B Axelrod. Isolation of an isozyme of soybean lipoxygenase. Biochim Biophys Acta 198:12–19, 1970.
29. GJ Piazza, A Nuñez. Oxidation of acylglycerols and phosphoglycerides by soybean lipoxygenase. J Am Oil Chem Soc 72:463–466, 1995.
30. AR Brash, CD Ingram, TM Harris. Analysis of a specific oxygenation reaction of soybean lipoxygenase-1 with fatty acids esterified in phospholipids. Biochemistry 26:5465–5471, 1987.
31. AN Grechkin, RA Kuramshin, SK Latypov, YY Safonova, TE Gafarova, AV Ilyasov. Hydroperoxides of α-ketols: novel products of the plant lipoxygenase pathway. Eur J Biochem 199:451–457, 1991.
32. HW Gardner, MJ Grove. Soybean lipoxygenase-1 oxidizes 3*Z*-nonenal. A route to 4S-hydroperoxy-2E-nonenal and related products. Plant Physiol 116:1359–1366, 1998.
33. RT Holman, PO Egwim, WW Christie. Substrate specificity of soybean lipoxidase. J Biol Chem 244:1149–1151, 1989.
34. G Scheller, E Jäger, B Hoffmann, M Schmitt, P Schreier. Soybean lipoxygenase: substrate structure and product selectivity. J Agric Food Chem 43:1768–1774, 1995.
35. EC Webb, ed. Enzyme Nomenclature: Recommendations (1992) of the Nomenclature Committee of the International Union of Biochemistry and Molecular Biology. San Diego: Academic Press, 1992.
36. NAM Eskin, S Grossman, A Pinsky. Biochemistry of lipoxygenase in relation to food quality. Crit Rev Food Sci Nutr 9:1–40, 1977.

37. DS Robinson, Z Wu, C Domoney, R Casey. Lipoxygenases and the quality of foods. Food Chem 54:33–43, 1995.
38. DF Hildebrand, T Hymowitz. Carotene and chlorophyll bleaching by soybeans with and without seed lipoxygenase-1. J Agric Food Chem 30:705–708, 1982.
39. B Cohen, S Grossman, BP Klein, A Pinsky. Pigment bleaching by soybean lipoxygenase type-2 and the effect of specific chemical modifications. Biochim Biophys Acta 837:279–287, 1985.
40. P Roy, AP Kulkarni. Oxidation of ascorbic acid by lipoxygenase: effect of selected chemicals. Food Chem Toxicol 34:563–570, 1996.
41. EN Frankel. Volatile lipid oxidation products. Prog Lipid Res 22:1–33, 1983.
42. HW Gardner, MJ Grove, NP Keller. Soybean lipoxygenase is active on nonaqueous media at low moisture: a constraint to xerophilic fungi and aflatoxins? J Am Oil Chem Soc 75:1801–1808, 1998.
43. HW Gardner. Lipoxygenase pathway in cereals. In: Y Pomeranz, ed. Advances in Cereal Science and Technology, Vol 9. St Paul, MN: Am Assoc Cereal Chem 1988, pp 161–215.
44. IM Whitehead, BL Muller, C Dean. Industrial use of soybean lipoxygenase for the production of natural green note flavor compounds. Cereal Foods World 40:193–197, 1995.
45. K Matsui, M Shibutani, T Hase, T Kajiwara. Bell pepper fruit fatty acid hydroperoxide lyase is a cytochrome P450 (CYP74B). FEBS Lett 394:21–34, 1996.
46. HW Gardner. How the lipoxygenase pathway affects the organoleptic properties of fresh fruit and vegetables. In: DB Min, TH Smouse, eds. Flavor Chemistry of Lipid Foods. Champaign, IL: Am Oil Chem Soc, 1989, pp 98–112.
47. DR Phillips, JA Matthew, J Reynolds, GR Fenwick. Partial purification and properties of a *cis*-3:*trans*-2-enal isomerase from cucumber fruit. Phytochemistry 18:401–404, 1979.
48. DB Josephson, RC Lindsay. Enzymic generation of volatile aroma compounds from fresh fish. In: TH Parliament, R Croteau, eds. Biogeneration of Aromas: ACS Symposium Series 317. Washington: Am Chem Soc, 1986, pp 201–219.
49. TE Acree, R Nishida, H Fukami. Odor thresholds of the stereoisomers of methyl jasmonate. J Agric Food Chem 33:425–427, 1985.
50. W-C Song, CD Funk, AR Brash. Molecular cloning of an allene oxide synthase: a cytochrome P450 specialized for the metabolism of fatty acid hydroperoxides. Proc Natl Acad Sci USA 90:8519–8523, 1993.
51. E Blée, AL Wilcox, LJ Marnett, F Schuber. Mechanism of reaction of fatty acid hydroperoxides with soybean peroxygenase. J Biol Chem 268:1708–1715, 1993.
52. C Bauer, W Grosch, H Weiser, H Jugel. Enzymatic oxidation of linoleic acid: formation of bitter-tasting fatty acids. Z Lebensm Unters-Forsch 164:171–176, 1977.
53. AN Grechkin, FN Fazliev, LS Mukhtarova. The lipoxygenase pathway in garlic (*Allium sativum* L.) bulbs: detection of the novel divinyl ether oxylipins. FEBS Lett 371:159–162, 1995.
54. Y Nishiba, S Furuta, M Hajika, K Igita, I Suda. Hexanal accumulation and DETBA value in homogenate of soybean seeds lacking two or three lipoxygenase isozymes. J Agric Food Chem 43:738–741, 1995.
55. M Vernooy-Gerritsen, ALM Bos, GA Veldink, JFG Vliegenthart. Localization of lipoxygenases 1 and 2 in germinating soybean seeds by an indirect immunofluorescence technique. Plant Physiol 73:262–267, 1983.
56. M Vernooy-Gerritsen, JLM Leunissen, GA Veldink, JFG Vliegenthart. Intracellular localization of lipoxygenases-1 and -2 in germinating soybean seeds by indirect labeling with protein A–colloidal gold complexes. Plant Physiol 76:1070–1079, 1984.
57. LC Stephenson, TW Bunker, WE Dubbs, HD Grimes. Specific soybean lipoxygenases localize to discrete subcellular compartments and their mRNAs are differentially regulated by source-sink status. Plant Physiol 116:923–933, 1998.
58. J Royo, G Vancanneyt, AG Pérez, C Sanz, K Störmann, S Rosahl, JJ Sánchez-Serrano. Characterization of three potato lipoxygenases with distinct enzymatic activities and different organ-specific and wound-regulated expression patterns. J Biol Chem 271:21012–21019, 1996.
59. I Feussner, B Hause, K Vörös, B Parthier, C Wasternack. Jasmonate-induced lipoxygenase forms are localized in chloroplasts of barley leaves (*Hordeum vulgare* cv. Salome). Plant J 7:949–957, 1995.
60. Y-L Peng, Y Shirano, H Ohta, T Hibino, K Tanaka, D Shibata. A novel lipoxygenase from rice: primary structure and specific expression upon incompatible infection with rice blast fungus. J Biol Chem 269:3755–3761, 1994.
61. E Bell, JE Mullet. Characterization of an *Arabidopsis* lipoxygenase gene responsive to methyl jasmonate and wounding. Plant Physiol 103:1133–1137, 1993.
62. E Blée, J Joyard. Envelope membranes from spinach chloroplasts are a site of metabolism of fatty acid hydroperoxides. Plant Physiol 110:445–454, 1996.
63. M Höhne, A Nellen, K Schwennesen, H Kindl. Lipid body lipoxygenase characterized by protein fragmentation, cDNA sequence and very early expression of the enzyme during germination of cucumber seeds. Eur J Biochem 241:6–11, 1996.
64. WL Holtman, JC Vredenbregt-Heistek, NF Schmitt, I Feussner. Lipoxygenase-2 oxygenates storage lipids in

embryos of germinating barley. Eur J Biochem 248:452–458, 1997.
65. H Theorell, RT Holman, Å Åkeson. Crystalline lipoxidase. Acta Chem Scand 1:571–576, 1947.
66. D Shibata, J Steczko, JE Dixon, M Hermodson, R Yazdanparast, B Axelrod. Primary structure of soybean lipoxygenase-1. J Biol Chem 262:10080–10083, 1987.
67. JC Boyington, BJ Gaffney, LM Amzel. The three-dimensional structure of an arachidonic acid 15-lipoxygenase. Science 260:1482–1486, 1993.
68. ST Prigge, JC Boyington, BJ Gaffney, LM Amzel. Structure conservation in lipoxygenases: structural analysis of soybean lipoxygenase-1 and modeling of human lipoxygenases. Proteins Struct Funct Genet 24:275–291, 1996.
69. R Koljak, O Boutaud, B-H Shieh, N Samel, AR Brash. Identification of a naturally occurring peroxidase-lipoxygenase fusion protein. Science 277:1994–1996, 1997.
70. T Kato, H Ohta, K Tanaka, D Shibata. Appearance of new lipoxygenases in soybean cotyledons after germination and evidence for expression of a major new lipoxygenase gene. Plant Physiol 98:324–330, 1992.
71. DM Saravitz, JN Siedow. The lipoxygenase isozymes in soybean [*Glycine max* (L.) Merr.] leaves. Plant Physiol 107:535–543, 1995.
72. H Aoshima. High performance liquid chromatography studies on protein: multiple forms of soybean lipoxygenase-1. Anal Biochem 95:371–376, 1979.
73. S Ramachandran, TJ Richards-Sucheck, E Skrzypczak-Jankun, MJ Wheelock, MO Funk Jr. Catalysis sensitive conformational changes in soybean lipoxygenase revealed by limited proteolysis and monoclonal antibody experiments. Biochemistry 34:14868–14873, 1995.
74. S Ramachandran, RT Carroll, WR Dunham, MO Funk Jr. Limited proteolysis and active-site labeling studies of soybean lipoxygenase 1. Biochemistry 31:7700–7706, 1992.
75. ST Prigge, JC Boyington, BJ Gaffney, LM Amzel. Lipoxygenases: structure and function. In: GJ Piazza, ed. Lipoxygenase and Lipoxygenase Pathway Enzymes. Champaign, IL: AOCS Press, 1996, pp 1–32.
76. W Minor, J Steczko, B Stec, Z Otwinowski, JT Bolin, R Walter, B Axelrod. Crystal structure of soybean lipoxygenase L-1 at 1.4 Å resolution. Biochemistry 35:10687–10701, 1996.
77. TR Holman, J Zhou, EI Solomon. Spectroscopic and functional characterization of a ligand coordination mutant of soybean lipoxygenase-1: first coordination sphere analogue of human 15-lipoxygenase. J Am Chem Soc 120:12564–12572, 1998.
78. J Verhagen, JFG Vliegenthart, J Boldingh. Micelle and acid-soap formation of linoleic acid and 13-L-hydroperoxylinoleic acid being substrates of lipoxygenase-1. Chem Phys Lipids 22:255–259, 1978.
79. JR Galpin, JC Allen. The influence of micelle formation on lipoxygenase kinetics. Biochim Biophys Acta 488:392–401, 1977.
80. SA Tatulian, J Steczko, W Minor. Uncovering a calcium-regulated membrane-binding mechanism for soybean lipoxygenase-1. Biochemistry 37:15481–15490, 1998.
81. MJ Schilstra, GA Veldink, J Verhagen, JFG Vliegenthart. Effect of lipid hydroperoxide on lipoxygenase kinetics. Biochemistry 31:7692–7699, 1992.
82. H Aoshima, T Kajiwara, A Hatanaka, H Nakatani, K Hiromi. Kinetic study of lipoxygenase–hydroperoxylinoleic acid interaction. Biochim Biophys Acta 486:121–126, 1977.
83. MJ Gibian, RA Galaway. Steady-state kinetics of lipoxygenase oxygenation of unsaturated fatty acids. Biochemistry 15:4209–4214, 1976.
84. B Axelrod, TM Cheesbrough, S Laakso, Lipoxygenase from soybeans. Methods Enzymol 71:441–451, 1981.
85. YB Che Man, LS Wei, AI Nelson. Acid inactivation of soybean lipoxygenase with retention of protein solubility. J Food Sci 54:963–967, 1989.
86. WL Smith, WEM Lands. Oxygenation of unsaturated fatty acids by soybean lipoxygenase. J Biol Chem 247:1038–1047, 1972.
87. WF Nieuwenhuizen, A Van der Kerk–Van Hoof, JH Van Lenthe, RC Van Schaik, K Versluis, GA Veldink, JFG Vliegenthart. Lipoxygenase is irreversibly inactivated by the hydroperoxides formed from the enynoic analogues of linoleic acid. Biochemistry 36:4480–4488, 1997.
88. M Maccarrone, GA Veldink, JFG Vliegenthart, A Finazzi Agrò. Inhibition of soybean lipoxygenase-1 by chain-breaking antioxidants. Lipids 30:51–54, 1995.
89. RD Abeysinghe, PJ Roberts, CE Cooper, KH MacLean, RC Hider, JB Porter. The environment of the lipoxygenase iron binding site explored with novel hydroxypyridinone iron chelators. J Biol Chem 271:7965–7972, 1996.
90. C Pham, J Jankun, E Skrzypczak-Jankun, RA Flowers II, MO Funk Jr. Structural and thermochemical characterization of lipoxygenase–catechol complexes. Biochemistry 37:17952–17957, 1998.
91. MJ Nelson, DG Batt, JS Thompson, SW Wright, Reduction of the active-site iron by potent inhibitors of lipoxygenases. J Biol Chem 266:8225–8229, 1991.
92. M Pérez-Gilabert, GA Veldink, JFG Vliegenthart. Protection by different agents against inactivation of lipoxygenase by hydrogen peroxide. Lipids 31:1245–1250, 1996.

93. Z Zhu, MO Funk Jr. Lipoxygenase-1 inhibition with a series of half-product analogs. Bioorg Chem 24:95–109, 1996.
94. MJ Gibian, J Colanduoni. Physical state of inhibitor fatty acids and linoleate solutions under lipoxygenase assay conditions. Lipids 19:164–170, 1984.
95. MJ Schilstra, GA Veldink, JFG Vliegenthart. Effect of nonionic detergents on lipoxygenase catalysis. Lipids 29:225–231, 1994.
96. S Srinivasulu, AGA Rao. Structure and kinetic thermal stability studies of the interaction of monohydric alcohols with lipoxygenase 1 from soybeans (*Glycine max*). J Agric Food Chem 43:562–567, 1995.
97. DF Farkas, SA Goldblith. Studies on the kinetics of lipoxidase inactivation using thermal and ionizing energy. J Food Sci 27:262–276, 1962.
98. P Lopez, J Burgos. Lipoxygenase inactivation by manothermosonication: effects of sonication physical parameters, pH, KCl, sugars, glycerol, and enzyme concentration. J Agric Food Chem 43:620–625, 1995.
99. L Ludikhuyze, Indrawati, I Van den Broeck, C Weemaes, M Hendrickx. Effect of combined pressure and temperature on soybean lipoxygenase 1. Influence of extrinsic and intrinsic factors on isobaric-isothermal inactivation kinetics. J Agric Food Chem 46:4074–4080, 1998.
100. I Suda, M Hajika, Y Nishiba, S Furuta, K Igita. Simple and rapid method for the selective detection of individual lipoxygenase isozymes in soybean seeds. J Agric Food Chem 43:742–747, 1995.
101. NB Waslidge, DJ Hayes. A colorimetric method for the determination of lipoxygenase activity suitable for use in a high throughput assay format. Anal Biochem 231:354–358, 1995.
102. MV Romero, DM Barrett. Rapid methods for lipoxygenase assay in sweet corn. J Food Sci 62:696–700, 1997.
103. EG Hammond, DN Duvick, WR Fehr, DF Hildebrand, EC Lacefield, TW Pfeiffer. Rapid screening techniques for lipoxygenases in soybean seeds. Crop Sci 32:820–821, 1992.
104. R Daniel, J Dorizon, D Deprez. Determination of lipoxygenase activity by continuous flow amperometric detection. Anal Biochem 219:154–155, 1994.
105. Y Shirano, D Shibata. Low temperature cultivation of *Escherichia coli* carrying a rice lipoxygenase L-2 cDNA produces a soluble and active enzyme at a high level. FEBS Lett 271:128–130, 1990.
106. J Steczko, GP Donoho, JE Dixon, T Sugimoto, B Axelrod. Effect of ethanol and low-temperature culture on expression of soybean lipoxygenase L-1 in *Escherichia coli*. Protein Expression Purif 2:221–227, 1992.

44

Sorbitol Oxidase

Kohei Oda and Kazumi Hiraga
Kyoto Institute of Technology, Kyoto, Japan

I. INTRODUCTION

Various pathways for the use of sorbitol have been described. Sorbitol dehydrogenase (SDH; EC 1.1.1.14) is an enzyme of the polyol pathway in a wide variety of species (Fig. 1) (1-3). SDH acts on polyols such as D-sorbitol and D-xylitol but has no activity toward primary alcohols. SDH catalyzes the oxidation of D-sorbitol to form D-fructose with NAD^+ as a cofactor.

In the course of screening for glycerol oxidase-producing microorganisms, we found an enzyme that oxidized D-sorbitol in the cell-free extract of a strain isolated from soil. The enzyme is capable of oxidizing D-sorbitol to produce hydrogen peroxide and glucose without the requirement of exogenous cofactors such as NAD^+, $NADP^+$, and FAD. Apparently, this type of sorbitol-oxidizing enzyme has a different reaction mechanism from the SDHs described above. Hence, according to the reaction mechanism, we named the enzyme "sorbitol oxidase" (EC 1.1.3.–) (SOX). This enzyme contains covalently bound FAD. Moreover, when D-sorbitol is used as a substrate, the SOX does not act on the reaction product, glucose. These properties of the SOX will provide a precise and routine determination of D-sorbitol concentration even in a crude sample and may be suitable for technical applications (4).

The expression level of SOX in *Streptomyces* sp. H-7775 was very low (10 units/L culture). To obtain a large amount of SOX from H-7775, we cloned the SOX gene and succeeded in expression of the recombinant SOX with covalently bound FAD in *E. coli* with total activity about 240-fold higher than that of *Streptomyces* sp. H-7775 (5).

Sorbitol oxidase (SOX) from *Streptomyces* sp. H-7775 converts D-sorbitol to glucose in the absence of exogenous cofactors, and the other reaction product is hydrogen peroxide. SOX catalyzes the following reaction (4).

$$\text{D-Sorbitol} + O_2 \rightarrow \text{Glucose} + H_2O_2$$

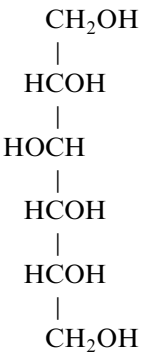

D-Sorbitol

Based on the chemical reaction catalyzed by SOX as described above, SOX is classified in a subclass of oxidoreductases (subclass 1), within six main types of enzymes. SOX can act on the CH–OH group of donors (subclass 1.1). This can be further classified in a subclass according to the acceptor, which is an

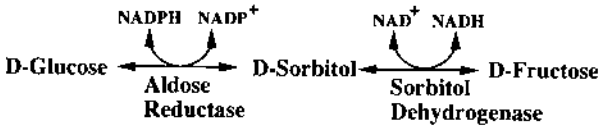

Figure 1 The polyol pathway.

oxygen. According to "Enzyme Nomenclature" (6), SOX from *Streptomyces* sp. H-7775 is classified as EC 1.1.3–.

II. IMPORTANCE TO QUALITY OF FOOD DURING GROWTH, MATURATION, STORAGE, AND PROCESSING

Applications of SOX from *Streptomyces* sp. H-7775 to quality of food during growth, maturation, storage, and processing have not been investigated. The regulation of the metabolism and transport of sorbitol in fruit may have an important influence on the accumulation of photosynthates in fruit, and consequently on their yield and quality (7–9). Sorbitol-oxidizing activity was detected in apple leaves (10).

III. RAW FOODS IN WHICH ENZYMES ARE FOUND

SOX from *Streptomyces* sp. H-7775 is localized in mycelia. The subcellular location of SOX was determined semiquantitatively in the cell-free extract, cell debris, and culture supernatant after disruption of the mycelia by ultrasonication using the method described in Section VIII. SOX activity was detected only in the cell-free extract.

IV. UTILITY/UTILIZATION OF ENZYMES IN FOODS (INCLUDING EXOGENOUS APPLICATION)

SOX from *Streptomyces* sp. H-7775 may be used for determination of D-sorbitol and D-xylitol concentration added as additives in foods. As SOX contains covalently bound FAD, the enzyme activity is not influenced by exogenous cofactors such as NAD^+, $NADP^+$, or FAD^+ in food.

V. PROPERTIES AS PROTEIN

The molecular weight of SOX purified from the cell-free extract is 45,000 daltons. The prosthetic group is a covalently bound FAD. The absorption spectrum of SOX purified from *Streptomyces* sp. H-7775 has a typical flavoprotein spectrum with the absorption maxima at 276, 358, and 455 nm and a shoulder at ~ 480 nm (Fig. 2A,B). A hypsochromic shift of the second absorption band to 358 nm relative to that of riboflavin at 372 nm has also been observed. The spectrum is similar to those of flavoproteins with covalently bound flavin (11–14). With the addition of D-sorbitol, the peaks at 358 nm and 455 nm decrease owing to the reduction of flavin (Fig. 2C). This indicates that the flavin component is functionally involved in the oxidation of D-sorbitol. The fluorescence intensity of the purified SOX is pH dependent and is similar to that of FAD as in the case for choline oxidase, but different from that of FMN and riboflavin (14). The flavin prosthetic group could not be liberated from the purified SOX protein by (a) acidification with 5% trichloroacetic acid, (b) boiling for 5 min, (c) treatment with 1% SDS, or (d) dialysis against 3 M KBr in 1 mM EDTA for 2 days at 4°C (15). It was calculated that 0.9 mol of FAD is bound to 1 mol of SOX, assuming the molecular absorption coefficient for FAD at 460 nm to be 11,300 $M^{-1}cm^{-1}$ (16).

Recombinant SOX has been expressed in *E. coli* and purified. The SOX was homogeneous by SDS-PAGE showing a strong yellowish fluorescence under UV light ($\lambda = 265$ nm) and acidic condition. The failure

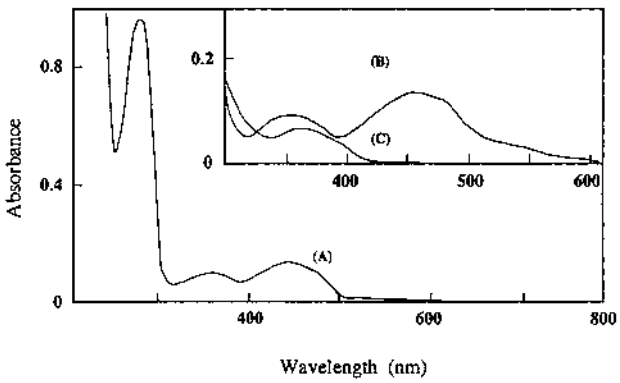

Figure 2 Absorption spectra of purified SOX. Absorption spectrum of purified SOX (A) in 20 mM potassium phosphate buffer, pH 6.0, at the final concentration of 0.64 mg/mL. The insert shows the enlarged spectrum before (B) and after (C) addition of 50 mM D-sorbitol.

to dissociate the cofactor by the same methods described above has led to the conclusion that FAD is covalently bound to the SOX even when it is expressed in *E. coli* (5).

The molecular weight of SOX from *Streptomyces* sp. H-7775 was estimated to be 45,000 daltons by both SDS-PAGE and Sephadex G-75 column chromatography. This has the same value of the molecular weight of the purified recombinant SOX expressed in *E. coli.*

The SOX gene from *Streptomyces* sp. H-7775 was cloned and sequenced (accession number for GenBank, EMBL, and DDBJ Nucleotide Sequence Database is AB000519). It consists of an open reading frame of 1260 bp encoding a protein of 420 amino acids with a molecular weight of 45,148 daltons (5). This value is in good agreement with that of an authentic SOX purified from *Streptomyces* sp. H-7775.

The deduced amino acid sequence of the SOX gene has 25.3% identity and 68.1% similarity to that of rat L-gulonolactone oxidase (EC 1.1.3.8) (10) (Fig. 3). SOX does not oxidize L-gulonolactone. One of the features of rat L-gulonolactone oxidase is that the enzyme contains a FAD covalently bound to histidine (18, 19) and has no nucleotide-binding motif (–G–x–G–x–x–G–) often found at the amino terminal region in a number of dehydrogenases (20-26). *Streptomyces* SOX also contains no nucleotide-binding motif. The cofactor that may be involved in the SOX is covalently bound FAD. Until now, five types of covalently bound flavins are known: 8-α-[*N*(1)-histidyl]-FAD, 8-α-[*N*(3)-histidyl]-FAD, 8-α-*S*-cysteinyl-FAD, 6-*S*-cysteinyl-FMN, and 8-α-*O*-tyrosyl-FAD (27). Thus, His, Cys, and Tyr residues are suggested to constitute the site for the covalently bound FAD. The SOX molecule

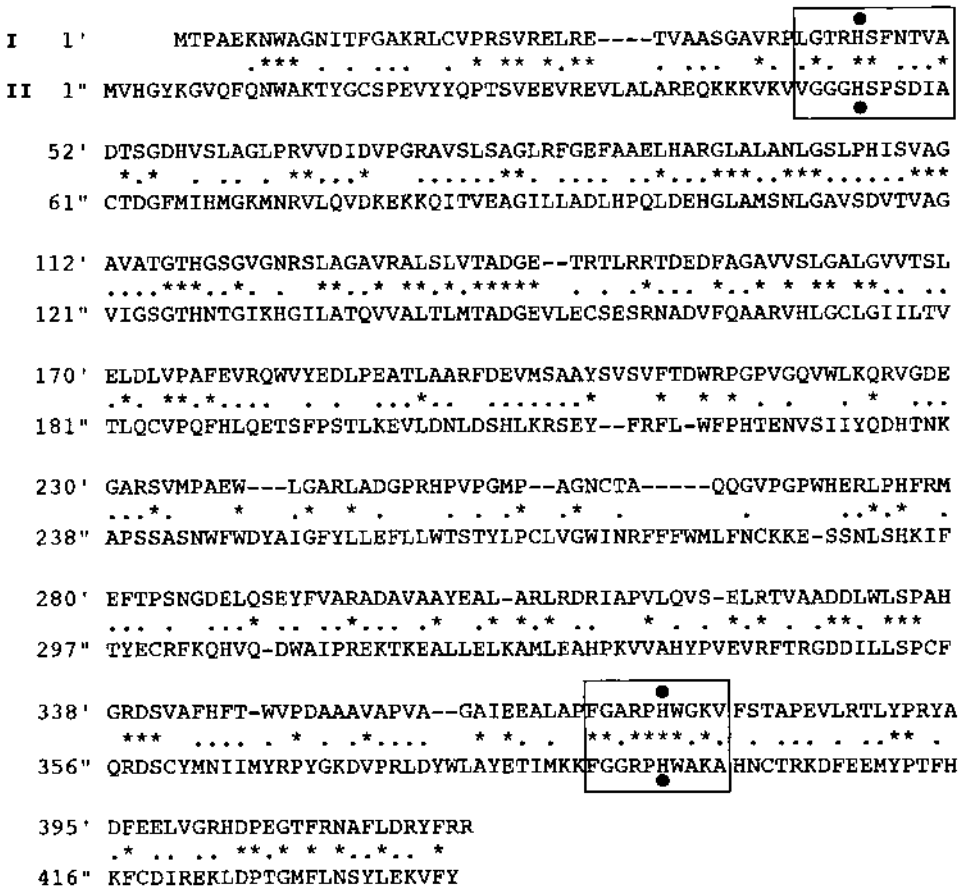

Figure 3 Comparison of the deduced amino acid sequence of SOX with that of the rat L-gulonolactone oxidase. The deduced amino acid sequence of the SOX gene (upper, I) is compared with that of rat L-gulonolactone oxidase (lower, II). Asterisks and dots indicate identical and related amino acids, respectively. Closed circles indicate the histidine residue that is possible for covalent attachment of FAD.

has 12 His, two Cys, and seven Tyr residues. The similarity between the SOX and rat L-gulonolactone oxidase shows that the similarities are mainly found around His residues (His45 and -374). These His residues occupy similar positions in the alignment as marked by a closed circle in Fig. 3. The His residue that has been suggested to be responsible for covalent attachment of FAD of the rat L-gulonolactone oxidase and mitomycin C resistance protein is located at the N-terminal region according to the sequence similarity (28). However, in the case of SOX, amino acid residues around His374 located at the C-terminal showed higher similarity than those of His45 located at the N terminal. Comparison of the amino acid sequences around Cys and Tyr residues between SOX and rat L-gulonolactone oxidase shows no possible site contributing to the binding of flavin. Moreover, Cys- and Tyr-binding regions of other flavoproteins have no sequence similarity to SOX (29, 30). From these results, it is suggested that the His374 is responsible for the binding of FAD.

There are no isoforms of SOX from different genes. There are no data about the possible formation of isozymes from posttranslational modification.

VI. PROPERTIES AS ENZYME

Substrate specificity of SOX from *Streptomyces* sp. H-7775 is summarized in Table 1. D-Sorbitol and D-xylitol were oxidized most rapidly. D-Xylitol, D-mannitol, and D-arabitol were oxidized at a rate of 93.5%, 55%, and 39%, respectively, of that for D-sorbitol. Glycerol, 1,3-propanediol, 1,3-butanediol, and 1,4-butanediol were oxidized at low rates, while D-glyceraldehyde, the dihydroxyacetone, methanol, ethanol, 1-propanol, and 1-butanol were not attacked at all at various substrate concentrations from 1 to 100 mM (Table 1). SOX did not react with glucose, a reaction product of D-sorbitol.

Enzyme characteristics of SOX are summarized in Table 2. Optimum pH is between 6.5 and 7.5 (Fig. 4A) Optimum temperature is 50°C in 10 min incubation at pH 7.5. SOX is stable below 55°C in 15 min incubation at pH 7.5 (Fig. 4B). The enzyme activity is completely lost after incubation for 15 min at pH 7.5 at 80°C. SOX is stable between pH 7.5 and 10.0 after 24 h incubation at 30°C. The enzyme activity is inhibited by 1 mM monoiodoacetate (IAA) and 1 mM *N*-ethylmaleimide (NEM) by 53.8% and 54.8%, respectively. The enzyme activity is inhibited by 1 mM of Zn^{2+} and Hg^{2+} by 96.8 and 90.7%, respectively (Table 2).

Sugar alcohols that have the *R* configuration on C3, such as D-sorbitol, D-xylitol, D-mannitol (C2 epimer of D-sorbitol), and D-arabitol (C4 epimer of D-xylitol), are good substrates of SOX. However, ribitol (C3 epimer of D-xylitol) and D-threitol, which have *S* configuration at C3 are poor substrates of SOX. The results suggest that the stereochemical requirement at position C3 of sugar alcohol is important for SOX activity.

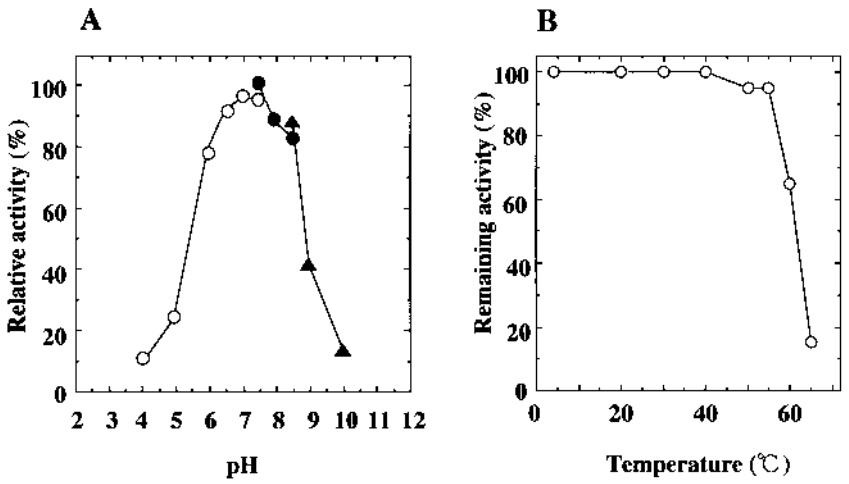

Figure 4 Optimum pH (A) and heat stability (B) of SOX. (A) SOX activity was measured at various pHs for 10 min at 37°C. Buffers used were 40 mM citrate-Na_2HPO_4 (pH 4.0–7.5, open circles), 40 mM Tris-HCl (pH 7.5–8.5, closed circles), 40 mM glycine-NaOH (pH 8.5–10.0, open triangles). (B) SOX was incubated at various temperatures for 15 min in 40 mM Tris-HCl buffer, pH 7.5, and the remaining activity was measured at 37°C.

Table 1 Substrate Specificity of Sorbitol Oxidase[a]

Compound	Relative activity (%)		Compound	Relative activity (%)
D-Sorbitol	100	(K_m 0.26 mM)	D-Fructose	0
D-Xylitol	93.5	(K_m 0.38 mM)	Saccharose	0.30
D-Mannitol	55.0	(K_m 7.38 mM)	Maltose	1.30
D-Arabitol	39.0	(K_m 7.73 mM)	Lactose	0.10
Ribitol	4.10		Methanol	0
meso-Erythritol	3.80		Ethanol	0
D-Threitol	0		1-Butanol	0
Inositol	3.30		1-Propanol	0
Glycerol	3.70		2-Propanol	0
D-Glyceraldehyde	0		1,2-Propanediol	0.80
Dihydroxyacetone	0		1,3-Propanediol	2.70
Dihydroxyacetone phosphate	0		1,2-Butanediol	0.80
D-Arabinose	0		1,3-Butanediol	3.20
D-Glucose			2,3-Butanediol	0
D-Galactose	3.50		1,4-Butanediol	7.40
D-Mannose	1.00		Ethylene glycol	0.20
L-Sorbose	0.70		PVA[b]	0.10

[a] The enzyme assay was carried out at 50 mM concentration of each compound.
[b] PVA; Polyvinyl alcohol 2000.

Table 2 Characteristics of Sorbitol Oxidase from *Streptomyces* sp. H-7775

Localization	Intracellular	Substrate specificity[a]		
Inducibility	No	D-Sorbitol	100	(K_m 0.26 mM)
		D-Xylitol	93.5	(K_m 0.38 mM)
Molecular weight		D-Mannitol	55.0	(K_m 7.38 mM)
SDS-PAGE	45 kDa	D-Arabitol	39.0	(K_m 7.73 mM)
		Glycerol	3.70	
Gel filtration	45 kDa	D-Glucose	0	
		D-Fructose	0	
Optimum pH	6.5–7.5	D-Mannose	1.00	
pH stability (for 24 h at 30°C)	7.5–10.0	Inhibitor[b]		
		Zn^{2+}	96.8	
		Hg^{2+}	90.7	
Optimum temp (pH 7.5, 10 min)	50°C	IAA	53.8	
		NEM	54.8	
Heat stability (pH 7.5, 15 min incubation)	< 55°C	Cofactor	FAD	
		Reaction products	Glucose + H_2O_2[c]	

[a] Relative activity, %.
[b] Inhibition, %.
[c] Substrate; D-sorbitol.

SOX has a K_m value of 0.26 mM for D-sorbitol, 0.38 mM for D-xylitol, 7.38 mM for D-mannitol, and 7.73 mM for D-arabitol.

A SOX-like activity that converts sorbitol to glucose was reported in an apple leaf (10). The partially purified enzyme converts sorbitol to glucose in the absence of NAD^+ or $NADP^+$. This enzyme is reported to catalyze the following reaction:

$$\text{Sorbitol} + 1/2O_2 \rightarrow \text{Glucose} + H_2O$$

One of the reaction products of this enzyme is not H_2O_2 but H_2O.

VII. QUALITATIVE AND QUANTITATIVE DETERMINATION OF ACTIVITY

The standard enzyme assay is based on the measurement of hydrogen peroxide generated during the oxidation of D-sorbitol. The hydrogen peroxide oxidatively couples with 4-aminoantipyrine and *N*-ethyl-*N*-(2-hydroxy-3-sulfopropyl)-3-methylaniline (TOOS) in the presence of peroxidase to form a quinoneimine dye, by the method of Allain et al. (31). The concentration of quinoneimine dye is measured spectrophotometrically at 555 nm. The reaction mixture in a final volume of 950 μL contains 150 mM KH_2PO_4-KOH (pH 7.0), 47.3 mM D-sorbitol, 614 μM TOOS, 158 μM 4-aminoantipyrine, 1.9 units/mL horseradish peroxidase, and a suitable amount of sorbitol oxidase. The incubation is done at 37°C for 10 min. The reaction is stopped by the addition of 2 mL of 0.5% SDS. Sorbitol oxidase activity has a linear function of both incubation time and protein concentration. One unit of the enzyme activity is defined as the amount of enzyme that catalyzes the formation of 1 μmol of H_2O_2 per min.

SOX is useful for the determination of D-sorbitol and D-xylitol concentrations in food. D-sorbitol and D-xylitol are used as sweetening agents. SOX may be used to quantitatively determine these sugar alcohols in foods. A histochemical approach elucidates the location of accumulated D-sorbitol (or D-xylitol) in vivo.

A microtiter plate assay is an easy and fast way for detection of D-sorbitol and D-xylitol in a large number of samples. At first, purple color is detected visually by the microtiter plate assay; a precise concentration of the sugar alcohols is determined spectrophotometrically.

In order to detect a reaction product directly, analysis by thin-layer chromotography is recommended. A silica get plate is soaked in 30 mM borate buffer (pH 9.0) and dried at 110°C for 1 h. Then samples are spotted on the plate. The developing system consists of: first dimension with ethyl acetate-pyridine-H_2O (3:3:2); and second dimension with 1-butanol-methanol-H_2O (5:3:2). The chromotogram is sprayed with a color reagent, 2% (w/v) diphenyl amine:2% (v/v) aniline:15% (v/v) phosphoric acid in acetone. The plate is heated at 100°C for 10 min. Reducing sugars, such as D-glucose, are detected as a dark spot.

One millimolar Zn^{2+} and Hg^{2+} strongly inhibit SOX activity. One millimolar monoiodoacetate (IAA) and *N*-ethylmaleimide (NEM) also inhibit SOX activity (Table 2).

VIII. PURIFICATION

The expression level of SOX in *Streptomyces* sp. H-7775 is very low. In contrast, we succeeded in expressing about 236-fold higher total enzyme activity in *E. coli* (production of 2360 units/L culture) (5) than that of *Streptomyces* sp. H-7775 (production of 10 units/L culture) (4). The recombinant SOX was purified as shown in Table 3; 384 mg of SOX was purified from 20 L of culture broth of *E. coli* with a yield of 37.1%. The recombinant SOX showed almost the same char-

Table 3 Purification of Recombinant Sorbitol Oxidase from *E. coli* Harboring pUCSOX

Purification step	Total activity (units)	Total protein (mg)	Specific activity (units/mg)	Yield (%)
Cell-free extract	47,200	42,000	1.1	100
Heat treatment	42,500	8,400	5.1	90.0
Q-Sepharose Big Beads	40,000	3,000	13.3	84.7
Phenyl Sepharose Fast Flow	22,000	1,200	18.3	46.6
Sephadex G-25	21,500	1,100	19.5	45.6
Q-Sepharose HP	18,000	400	45.0	38.1
Sephadex G-25	17,500	384	45.6	37.1

acteristics as those of the authentic SOX from *Streptomyces* sp. H-7775 (5). We describe below a method for the purification of recombinant SOX from *E. coli*. A method for purification of SOX from *Streptomyces* sp. H-7775 is also described in Hiraga et al. (4).

A. A Proven Method Leading to Purity

When SOX was expressed in *E. coli*, SOX activity was detected in the supernatant of a bacterial sonicate, but not in the insoluble fraction or in the culture supernatant. This suggests that SOX is localized in the cytosol or periplasmic space. In the case of *Streptomyces* sp. H-7775, SOX is localized in mycelia.

Step 1. Preparation of Cell-Free Extract

E. coli [pUCSOX] cells from 20 L of culture broth are washed with distilled water and resuspended in 4 L of 10 mM Tris-HCl, pH 7.0 (Buffer A). After the addition of 0.1% lysozyme and 20 mM EDTA, the cell suspension is incubated at 37°C for 30 min. The cell debris is removed by centrifugation at 15,000g for 15 min at 4°C.

Step 2. Heat Treatment

The cell-free extract from Step 1 is heated at 50°C for 1 h, and centrifuged at 15,000g for 15 min at 4°C.

Step 3. Q-Sepharose Big Beads Column Chromatography

The heated cell-free extract is applied onto a Q-Sepharose CL-6B Big Beads column (10 × 20 cm) equilibrated with Buffer A. The column is washed with the same buffer. The sorbitol oxidase is eluted with a linear 0–0.5 M NaCl gradient in buffer A. SOX fractions are pooled and dialyzed against Buffer A at 4°C.

Step 4. Phenyl Sepharose FF Column Chromatography

The SOX fraction obtained from Step 3 was put on a Phenyl Sepharose FF column (5 × 20 cm) equilibrated with Buffer A. The column was washed with the same buffer. SOX was eluted with a linear 0–1.0 M NaCl gradient in Buffer A and eluate was collected in fractions.

Step 5. Sephadex G-25 Column Chromatography

SOX fractions obtained at Step 4 are applied onto a Sepharose G-25 column (2 × 20 cm) equilibrated with Buffer A and eluted with the same buffer. SOX fractions are pooled and dialyzed against Buffer A overnight at 4°C.

Step 6. Q-Sepharose HP Column Chromatography

The enzyme solution is then loaded on a Q-Sepharose HP column (2.6 × 30 cm) equilibrated with Buffer A and eluted with a linear 0–1.0 M NaCl gradient. Active fractions are pooled.

Step 7. Sephadex G-25 column Chromatography

The enzyme solution is then put on a Sepharose G-25 column (2 × 20 cm) equilibrated with Buffer A and eluted with the same buffer. SOX fractions were pooled and stored at 4°C.

B. Stability

SOX is stable from pH 7.5 to 10.0 after 24 h incubation at 30°C. SOX is stable below 55°C after 10 min incubation at pH 7.5.

REFERENCES

1. J Jeffery, H Jornvall. Sorbitol dehydrogenase. Adv Enzymol 61:47–106, 1988.
2. Y Wen, I Bekhor. Sorbitol dehydrogenase. Full-length cDNA sequencing reveals a mRNA coding for a protein containing an additional 42 amino acids at the N-terminal end. Eur J Biochem 217:83–87, 1993.
3. H Wiesinger, B Hamprecht. Purification and characterization of sorbitol dehydrogenase from bovine brain. J Neurochem 52:342–348, 1989.
4. K Hiraga, M Kitazawa, N Kaneko, K Oda. Isolation and some properties of sorbitol oxidase from *Streptomyces* sp. H-7775. Biosci Biotech Biochem 61:1699–1704, 1997.
5. K Hiraga, T Eto, I Yoshioka, K Oda. Molecular cloning and expression of a gene encoding a novel sorbitol oxidase from *Streptomyces* sp. H-7775. Biosci Biotech Biochem 62:347–353, 1998.
6. JFG Vliegenthart, KF Tipton, N Sharon, W Saenger, GP Moss, C Liebecq, CR Cantor, AJ Barrett. Enzyme Nomenclature. San Diego: Academic Press, 1992, pp 24–154.

7. RL Bieleski, RL Redgewell. Synthesis of sorbitol in apricot leaves. Aust J Plant Physiol 4:1–10, 1977.
8. P Hansen. Translocation of labelled compounds from leaves to fruit and their conversion within the fruit. Physiol Plant 23:564–573, 1970.
9. RJ Redgwell, RL Bieleski. Sorbitol-1-phosphate and sorbitol-6-phosphate in apricot leaves. Phytochemistry 17:407–409, 1978.
10. S Yamaki. A sorbitol oxidase that converts sorbitol to glucose in apple leaf. Plant Cell Physiol 23:891–899, 1982.
11. A Willie, DE Edmondson, MS Jorns. Sarcosine oxidase contains a novel covalently bound FMN. Biochemistry 35:5292–5299, 1996.
12. M Fukuyama, Y Miyake. Purification and some properties of cholesterol oxidase from *Schizophyllum commune* with a covalently bound flavin. J Biochem 85:1183–1193, 1979.
13. JM McCord, I Fridovoch. Superoxide dismutase. An enzymic function for erythrocuprein (hemocuprein). J Biol Chem 244:6049–6055, 1969.
14. M Ohta-Fukuyama, Y Miyake, S Emi, T Yamano. Identification and properties of the prosthetic group of choline oxidase from *Alcaligenes* sp. J Biochem 88:197–203, 1980.
15. A Negri, V Massey, CH Williams Jr. D-Aspartate oxidase from beef kidney. Purification and properties. J Biol Chem 262:10026–10034, 1987.
16. KS Shin, HD Youn, YH Han, SO Kang, YC Hah. Purification and characterization of D-glucose oxidase from white-rot fungus *Pleurotus ostreatus*. Eur J Biochem 215:747–752, 1993.
17. T Koshizuka, M Nishikimi, T Ozawa, K Yagi. Isolation and sequence analysis of a complementary DNA encoding rat liver L-gulono-gamma-lactone oxidase, a key enzyme for L-ascorbic acid biosynthesis. J Biol Chem 263:1619–1621, 1988.
18. K Kiuchi, M Nishikimi, Y Yagi. Purification and characterization of L-gulonolactone oxidase from chicken kidney microsomes. Biochemistry 21:5076–5082, 1982.
19. WC Kenny, DE Edmondson, TP Singer, H Nakagawa, A Asano, R Sato. Identification of the covalently bound flavin of L-gulono-gamma-lactone oxidase. Biochem Biophys Res Commun 71:1194–1200, 1976.
20. RJ Cook, KS Misono, C Wagner. The amino acid sequences of the flavin-peptides of dimethylglycine dehydrogenase and sarcosine dehydrogenase from rat liver mitochondria. J Biol Chem 260:12998–13002, 1985.
21. WC Kenny, WH Walker, TP Singer. Studies on succinate dehydrogenase. XX. Amino acid sequence around the flavin site. J Biol Chem 247:4510–4513, 1972.
22. D Wood, MG Darlison, JR Guest. Nucleotide sequence encoding the flavoprotein and hydrophobic subunits of the succinate dehydrogenase of *Escherichia coli*. Biochem J 222:519–534, 1984.
23. JH Weiner, P Dickie. Fumarate reductase of *Escherichia coli*. Elucidation of the covalent-flavin component. J Biol Chem 254:8590–8593, 1979.
24. ST Cole. Nucleotide sequence coding for the flavoprotein subunit of the fumarate reductase of *Escherichia coli*. Eur J Biochem 122:479–484, 1982.
25. TD Porter, CB Kasper. Coding nucleotide sequence of rat NADPH–cytochrome P-450 oxidoreductase cDNA and identification of flavin-binding domains. Proc Natl Acad Sci USA 82:973–977, 1985.
26. J Hofsteenge, JM Vereijken, WJ Weijer, JJ Beintema, RK Wierenga, J Drenth. Primary and tertiary structure studies of *p*-hydroxybenzoate hydroxylase from *Pseudomonas fluorescens*. Isolation and alignment of the CNBr peptides; interactions of the protein with flavin adenine dinucleotide. Eur J Biochem 113:141–150, 1980.
27. K Decker. Biosynthesis and function of enzymes with covalently bound flavin. Annu Rev Nutr 13:17–41, 1993.
28. PR August, MC Flickinger, DH Sherman. Cloning and analysis of a locus (mcr) involved in mitomycin C resistance in *Streptomyces lavendulae*. J Bacteriol 176:4448–4454, 1994.
29. WH Walker, EB Kearney, RL Seng, TP Singer. The covalently-bound flavin of hepatic monoamine oxidase. 2. Identification and properties of cysteinyl riboflavin. Eur J Biochem 24:328–331, 1971.
30. W McIntire, DE Edmonson, DJ Hopper, TP Singer. 8-Alpha-(O-tyrosyl) flavin adenine dinucleotide, the prosthetic group of bacterial *p*-cresol methylhydroxylase. Biochemistry 20:3068–3075, 1981.
31. CC Allain, LS Poon, CSG Chan, W Richard, PC Fu. Enzymatic determination of total serum cholesterol. Clin Chem 20:470–475, 1974.

45

Starch Phosphorylases

Ying Yu
Rutgers University, New Brunswick, New Jersey, U.S.A.

I. INTRODUCTION

Alpha-1,4-glucan phosphorylases (EC 2.4.1.1) are widely distributed in plants and animals. Starch phosphorylase may catalyze its reversible enzymatic reaction in either a synthetic or degradative mode.

$$\text{Glc-1-P} + (\text{Glc})_n \leftrightarrow (\text{Glc})_{n+1} + \text{Pi}$$

In the synthetic reaction, a glucose unit is transferred from Glc-1-P to a growing oligoglucan chain, with release of inorganic phosphate. In the degradative mode, addition of inorganic phosphate liberates a molecule of Glc-1-P. With respect to the direction of the starch phosphorylase reaction, the precise physiological function of starch phosphorylase in higher plants remains unclear, though the predominating belief is that this enzyme catalyzes the stepwise disassembly of starches and oligoglucans. Evidence for a biosynthetic role for starch phosphorylases, within the starch biosynthetic pathway, has by no means been discounted and has been the subject of much discussion (1).

The earliest studies on starch phosphorylase focused mainly on the interconversion between starch and sugars during fruit ripening and cold-sweetening phenomenon observed in stored potatoes. More recently, there has been increasing interest in the function of starch phosphorylase in plant growth and development, particularly with respect to starch deposition and degradation within a range of higher plants.

The objective of this chapter is to provide an overview of the biochemistry, molecular biology, and putative functions of starch phosphorylases in plant tissue. The first part of this chapter focuses on the importance of starch phosphorylase to cold storage of food, specifically potato, and the putative functions of this enzyme in plant growth and starch deposition. The second part will discuss the biochemical properties of starch phosphorylases and the recent information classifying the various isoforms of starch phosphorylase present in higher plants. This information is based largely on biochemical characterization studies and the analysis of the genes and gene families encoding a range of starch phosphorylase isoforms.

II. IMPORTANCE OF STARCH PHOSPHORYLASE TO COLD STORAGE OF POTATO AND PLANT STARCH DEPOSITION

A. Starch Phosphorylase and the Cold-Induced Sweetening Phenomenon in Potato

Interconversions between starch and sucrose are of great interest, particularly with respect to a phenomenon referred to as cold-induced sweetening in potato.

This chapter is dedicated to the memory of my mentor, Professor Bruce P. Wasserman, who passed away Aug. 26, 1998.

Abbreviations: ADP-Glc, adenosine diphosphoglucose; AGP, adenosine diphosphoglucose pyrophosphorylase; Glc-1-P, glucose-1-phosphate; Glc-6-P, glucose-6-phosphate; *sh4*, *shunken4* mutant; *sh2*, *shunken2* mutant.

Cold-induced sweetening generally occurs when storage temperatures are reduced from 10°C to 2°C over the course of several days. Since starch phosphorylase acts upon oligoglucans to form hexose phosphates, which are presumed precursors to sucrose, starch phosphorylase activity has been proposed as a logical catalyst for the initial process of cold-induced sweetening of potato during storage (2). However, despite numerous efforts, a direct role for starch phosphorylase in cold-induced sweetening has yet to be demonstrated. Temperature shift experiments, either from 10°C to 2°C or vice versa, were accompanied by negligible changes in starch phosphorylase activity (3). A follow-up study (2) on the dual role of glycolytic intermediates and amyloplast envelope integrity showed that visible deterioration to the double envelope was not evident until 38 days of storage at 2°C. While these studies cannot exclude a role for starch phosphorylase in the cold-induced sweetening phenomenon, the precise function of starch phosphorylase in this process remains speculatory.

B. Putative Function in the Starch Deposition of Higher Plants

Starch phosphorylases from higher plants were initially suggested to be the primary catalysts for starch chain elongation since in the synthetic direction they catalyze the incorporation of Glc-1-P into (1,4)-α-glucan chains. This assumption began to be questioned when AGP was discovered and the starch-deficient maize mutant, *sh2*, was characterized (4). *Sh2* lacks the AGP large subunit and is thus unable to convert Glc-1-P into ADP-Glc. The deficient starch levels of this mutant implied that AGP was the enzyme regulating the flow of carbon into starch. This finding indicates that starch synthesis is predominantly controlled by transglucosylases rather than phosphorylases. Antisense inhibition of cytosolic starch phosphorylase in potato plants did not cause any significant changes of starch levels in leaves or tubers of the transgenic plants (5). In addition, no observable alterations of starch structure or tuber formation were found in the transgenic plants. This evidence suggested that cytosolic starch phosphorylase did not play an essential role in starch metabolism. Another antisense study was conducted on the potato leaf Pho 1-type starch phosphorylase. Determination of the leaf starch content revealed that the antisense inhibition of the leaf starch phosphorylase activity had no significant influence on starch accumulation in leaves (6). The effects of antisense suppression of Pho1-type starch phosphorylase genes in potato tubers or maize endosperm have not yet been reported.

In chloroplasts, starch phosphorylase is regarded as a starch degradative enzyme in the diurnal starch accumulation cycle (7). However, whether starch phosphorylase plays a similar role in the amyloplasts of storage tissues has not been determined. Since amyloplasts are actively involved in starch biosynthesis, it is conceivable that Pho 1-type starch phosphorylases could play a synthetic role using Glc-1-P as substrate. This is supported by the observation that high levels of the plastidic starch phosphorylase transcript levels as well as starch phosphorylase enzyme activity present in sink tissues of spinach. Source leaves, however, contained low amounts of plastidic starch phosphorylase transcripts. In addition, the induction of starch phosphorylase expression was observed when the leaf disks were supplied with carbohydrates (8). Some primer-independent starch phosphorylase isoforms could also be involved in the initiation of starch biosynthesis by synthesis of glucan primers. Another alternative role of starch phosphorylases suggested by some scientists is the degradation of starch-derived malto-oligosaccharides (5).

III. BIOCHEMICAL PROPERTIES OF STARCH PHOSPHORYLASE

A. Protein Structure

Phosphorylases from plants, animals, and prokaryotes exist as dimers or tetramers containing identical sets of subunits (9). It is generally accepted that glycogen phosphorylase from mammalian tissue participates in glycogen degradation and is subject to both allosteric regulation, and covalent modifications such as phosphorylation (10). Three-dimensional crystal structures of mammalian glycogen synthases, illustrating the coordinated interaction of subunits, have shed a great deal of light on the mechanism of action of glycogen phosphorylase with respect to glycogen mobilization in mammalian systems (11). X-ray crystallographic studies have revealed the three-dimensional crystal structures of mammalian glycogen synthases. For example, the subunit of rabbit muscle phosphorylase is composed of two domains. Each domain consists of a central β-sheet core surrounded by one or more layers of α-helices (Fig. 1) (11, 12).

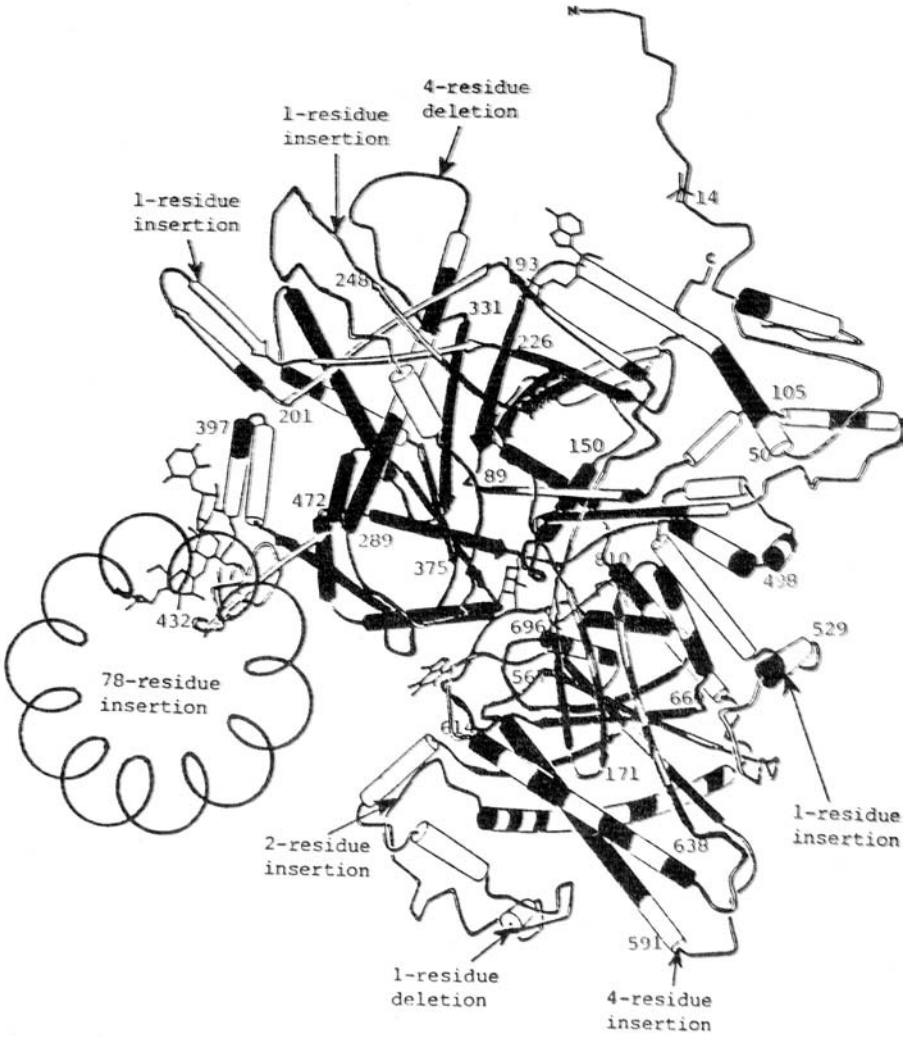

Figure 1 X-ray crystallographic model of a mammalian glycogen synthase. The "barrel-and-arrow" schematic of rabbit muscle phosphorylase *a* was compared with potato phosphorylase. The dark areas represent the regions of strong similarity. (From Refs. 11, 12.)

B. Starch Phosphorylase Isoforms

Higher-plant starch phosphorylases are classified into two groups based on their subcellular localization and affinity for various glucans (13). Members of each group can be readily distinguished by the use of zymograms (Fig. 2). The cytosolic class of starch phosphorylases has frequently been referred to as H-type phosphorylases, but more recently the term Pho2-type starch phosphorylase, based primarily upon the migration behavior on zymograms, has replaced the earlier nomenclature. In addition to their cytosolic localization, Pho2-type phosphorylases tend to exhibit high affinity for large-highly branched glucans, such as glycogen. Pho2-type starch phosphorylases have an apparent monomer size of 90 kDa (13, 14). The second distinct starch phosphorylase group, originally classified as the L-type, but now known as the Pho1-type group represents starch phosphorylases localized in plastids such as chloroplasts and amyloplasts, and are generally characterized by a monomer size of 100 kDa. Pho1-type starch phosphorylases prefer oligoglucans such as maltodextrins.

In spinach leaf or pea seed, one form of each starch phosphorylase type is present. However, the relative

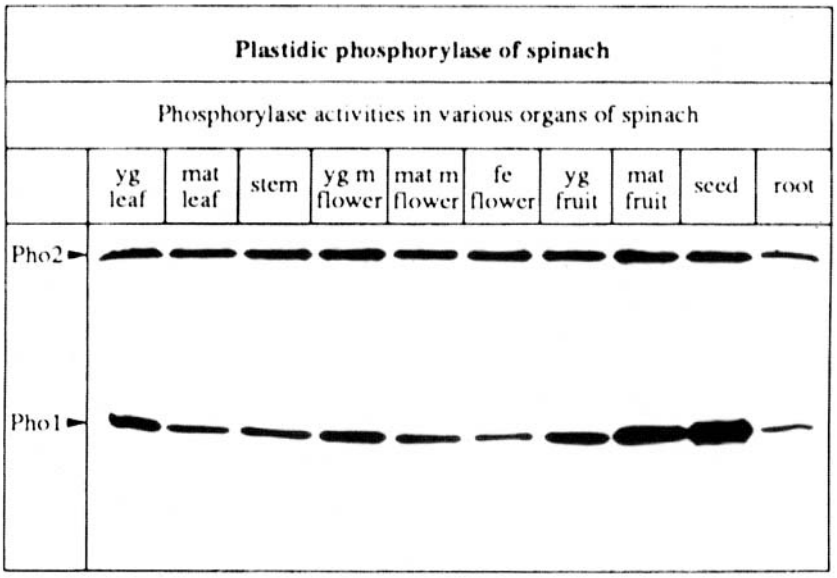

Figure 2 Classic zymogram illustrating starch phosphorylase activities in various organs of spinach. (From Ref. 8.)

ratio of the two starch phosphorylase types varies during plant development (15, 16). During seed germination, the amount of Pho2-type starch phosphorylase is increased while Pho1-type starch phosphorylase remains at a constant, lower level. The developing seeds, however, contain much higher amounts of Pho1-type starch phosphorylase than Pho2-type starch phosphorylase.

In maize, characterization of four starch phosphorylase isoforms has been reported (17, 18). The maize endosperm is rich in starch phosphorylase activity, and starch phosphorylase expression patterns correlate closely with starch deposition (19, 20). The four isoforms differ in their pH optima, primer dependence, chromatographic properties, development expression patterns, and their localization. Isoforms I, II, and III occur mainly in the endosperm, while isoform IV is localized in the embryo. The activities of isoforms I, II, and III were each reduced in the mutant *sh4*, and their enzymatic properties such as pH optima and sensitivity to activators and inhibitors were altered (18). However, the properties of isoform IV did not seem to be affected by the *sh4* mutation (21). These studies were mainly based upon separation of isoforms by ion exchange chromatography. At that time, it was not possible to prepare antibodies or to clone cDNAs. Therefore, it is not known if these starch phosphorylase isoforms represent distinct gene products.

C. Starch Phosphorylase Gene Classifications: Significance of the Species Specific Pho 1 Insertion Sequences

cDNA clones representing both Pho1- and Pho2-type isoforms of starch phosphorylase have been obtained from potato and several other plant species. In potato tuber, cDNA clones for one cytosolic (Pho2-type) (22) isoform and two plastidial (Pho1-type) isoforms (6, 23, 24) have been characterized. cDNAs for Pho1-type starch phosphorylases have also been obtained from sweet potato (25), broad bean (26), and spinach leaf (8). Predicted amino acid sequences are well conserved. For example, spinach Pho1-type starch phosphorylase has an overall amino acid sequence identity of 75% with potato (6, 8) and sweet potato (27) Pho1-type starch phosphorylases. The sequence of spinach Pho1-type starch phosphorylase has 62% identity with Pho2-type starch phosphorylases from potato (22) and broad bean (26).

Starch phosphorylase cDNAs are typified by four distinct regions (Fig. 3). Region 1, the transit peptide, exhibits low homology among species. Regions 2 and 4, at the N- and C-termini of the mature protein, respectively, are highly conserved. Region 3, distinguished by a 50- to 80-residue stretch of additional amino acids, is commonly referred to as an "insertion sequence." Insertion sequences are present only in Pho1-type starch phosphorylases. As with the transit

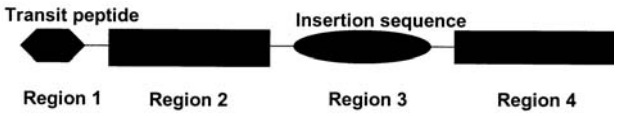

Figure 3 Schematic diagram of cDNAs encoding the four regions of a typical Pho1-type (plastidial) starch phosphorylase. Pho2-type starch phosphorylases lack the transit peptide and insertion sequence. The remaining regions of Pho1-type starch phosphorylases retain strong amino acid sequence similarity with the Pho2-type starch phosphorylases. (From Refs. 16, 17, 35.)

peptides, the insertion sequences are widely divergent from species to species; however, some common structural features are noted (28). Each insertion sequence is highly acidic, with a calculated isoelectric point of 4.0.

The presence of a transit peptide at the N-terminus of potato Pho1-type starch phosphorylase was confirmed by the sequence analysis of the cDNA clone (24). This 50 amino acid transit peptide sequence has several structural features common to transit peptides of chloroplast proteins. This sequence is rich in hydrophilic residues. It contains seven Ser and five Thr residues, representing 14% and 10% of the total amino acid content of the transit peptide. The transit sequence also contains 13 positively charged amino acids, but no acidic residues or large hydrophobic sequences. The transit peptides are required for translocation of plastidic Pho1-type starch phosphorylases from the cytosol into the plastid.

With respect to function, the insertion sequences are hypothesized to influence the affinity of starch phosphorylase for substrate. In a benchmark study designed to test the function of an insertion sequence, a chimeric potato starch phosphorylase, lacking the 78 amino acid insertion of the Pho1-type enzyme was constructed, and an extensive kinetic analysis was conducted (28). Removal of the insertion sequence resulted in a dramatic lowering of the Michaelis constant for glycogen. The authors concluded that the insertion sequence served to sterically hinder the interaction of starch phosphorylase with highly branched substrates such as glycogen. This region is therefore thought to reflect the affinity of starch phosphorylases for glucan substrate.

IV. PROPERTIES OF STARCH PHOSPHORYLASES

The enzymatic properties of several starch phosphorylases have been characterized. For example, the major starch phosphorylase of maize kernels is a homodimer with an estimated molecular weight of $223{,}000 \pm 10{,}000$ daltons (29). Pyridoxal phosphate is a cofactor of the enzyme. The estimated pyridoxal phosphate content of the purified enzyme was 112,000 g protein/mol pyridoxal phosphate (29). The purified enzyme had a K_m value of 1.0 mM for Glc-1-P when assayed in the synthetic direction at 37°C, pH 5.8. In the phosphorolytic direction, the purified enzyme had a K_m value of 4.2 mM for Pi when assayed at 25°C, pH 6.3 (29). Magnesium ion was shown to be an inhibitor of the enzyme (29). ADP-Glc was found to be an inhibitor with respect to Glc-1-P in the synthetic reaction (29). Both Pho1- and Pho2-types of starch phosphorylases have been purified and characterized from spinach leaves (13). The subunit molecular weights of Pho1- and Pho2-types spinach leaf starch phosphorylases were calculated to be 108,000 and 92,000 daltons, respectively. Based on their native molecular weights, it was suggested that both starch phosphorylases exist in dimeric form. The optimal pH values for Pho1- versus Pho2-type enzyme were shown to be 5.7 versus 6.1 in the synthetic direction, and 6.2 versus 6.5 in the phosphorolytic direction. At pH 6.6, the K_m values of Pho1-type enzyme were determined to be 3.1 mM for Glc-1-P in the presence of 10 mg/mL soluble starch in the synthetic direction and 2.2 mM for Pi in the presence of 2 mg/mL maltopentose in the phosphorolytic direction. Under the same conditions, the K_m values of Pho2-type enzyme were 6.2 mM for Glc-1-P in the synthetic direction and 6.9 mM for Pi in the phosphorolytic direction (13).

V. QUANTITATIVE DETERMINATION OF STARCH PHOSPHORYLASE ACTIVITY

The activity of starch phosphorylase can be measured either in the synthetic direction or in the phosphorolytic direction. In the synthetic direction, the amount of inorganic phosphate released from Glc-1-P can be determined by a molybdate-based colorimetric assay (30, 31). Alternatively, starch phosphorylase activity can be determined by measuring the incorporation of ^{14}C-labeled Glc-1-P into glucan primer (17). In the phosphorolytic direction, a continuous assay system is used (13, 14). Glc-1-P is converted to Glc-6-P by phosphoglucomutase. NADP reduction by Glc-6-P dehydrogenase can then be followed spectrophotometrically at 340 or 265 nm.

VI. PURIFICATION OF STARCH PHOSPHORYLASES

Starch phosphorylases have been purified from a number of sources, including spinach leaf (13), potato tuber (32), and maize kernels (29). The purification of the major starch phosphorylase of maize kernels is described below (29).

Protein extracts of maize kernels harvested at 22 days after pollination were prepared by homogenization and centrifugation. The extract was brought to 40% saturation with ammonium sulfate. Following centrifugation at 16,000g for 20 min, the supernatant was brought to 50% saturation with ammonium sulfate and centrifuged again at 16,000g for 10 min. The precipitate was resuspended and dialyzed overnight. The sample was then subjected to a step known as starch absorption. The starch absorption step was adapted from the method of Kamogawa et al. (33). Waxy maize starch was solubilized in 100 mL water by autoclaving for 1 h at 1 bar (100 kPa). The solution was chilled to $-2^{\circ}C$ and 15 mL of chilled 95% ethanol was added. The precipitate was washed once with 100 mL 11% ethanol at $-15^{\circ}C$ and resuspended in 100 mL 0.1 M EDTA, pH 7.2. The protein sample was also made 11% with ethanol and centrifuged. The chilled supernatant was then added to the starch preparation which had been chilled to incipient freezing. After mixing in an ice bath for 5 min, chilled 95% ethanol was added slowly to the mixture to a final concentration of 12.5%. The resulting precipitate was washed once with 100 mL of 11% ethanol at $-15^{\circ}C$. The precipitate was then dissolved at room temperature with 100 mL 5 mM sodium citrate buffer, pH 6.3, and applied to a DEAE-cellulose column. The protein precipitate from the fractions constituting the peak of starch phosphorylase activity was dissolved in buffer and applied onto a Sephadex G-200 column. The fractions constituting the peak of starch phosphorylase activity were pooled and stored (Table 1) (29).

VII. CONCLUSIONS

Starch phosphorylases from higher plants possess unique features with regard to their structures, catalytic properties, and subcellular localization patterns. Structurally, the phosphorylases have been classified into distinct groups based on zymograms that accurately pinpoint subcellular localization of the major isoforms. Deduced amino acid sequences show sequence conservation among a host of species. Genes corresponding to cytosolic and plastidial phosphorylase isoforms have been appropriately classified, and expression levels for transcript levels and tissue distribution have been carefully quantified. A more precise role for the insertion sequences located in the Pho2-type phosphorylases remain to be determined.

Functionally, however, the various roles of starch phosphorylase have yet to be unequivocally sorted out. Roles for starch phosphorylases in providing carbon for seed germination and photosynthetic conversions seem clear, but other functions for this enzyme remain vague. For example, the precise role of starch phosphorylase in starch deposition or degradation has remained elusive. Transformed potatoes with various forms of starch phosphorylase inserted in the antisense orientation do not appear to exhibit visible effects on starch phenotype (5, 6). Such effects could be attributed to the presence of multiple starch phosphorylase isoforms, which could require co-suppression of several genes.

Moreover, for many years, it was believed that starch phosphorylase was the primary catalyst for chain elongation of amyloses and amylopectins in monocots such as corn. This idea quickly fell from the forefront when the existence of the AGP pathway

Table 1 Purification of Maize Phosphorylase

Fraction	Volume (mL)	Activity (units/mL)	Protein (mg/mL)	Specific Activity (units/mg)	Recovery (%)
Crude homogenate	1427	0.56	5.0	0.047	100
40–50% ammonium sulfate precipitation	80	8.4	14.0	0.44	85
DEAE-cellulose peak	46	8.9	0.17	49	52
Sephadex G-200 peak	7	41	0.72	57	36

Source: Ref. 29.

for starch synthesis was finally characterized (34). Nonetheless, maize amyloplasts are rich in starch phosphorylase activity and starch phosphorylase expression patterns correlate closely with starch deposition (19, 20). Therefore, more recent thinking retains the possibility that starch phosphorylases may yet prove to be a key component of the amylose and amylopectin biosynthetic system of higher plants (1). Similar questions linger with respect to a precise biochemical function for starch phosphorylase in the cold sweetening process of potato. Continued generation of mutant cultivars deficient in the various isoforms of starch phosphorylase should play a major role toward further clarifying the potentially interesting and diverse functions of this enzyme.

ACKNOWLEDGMENTS

Funding for this research was provided by the U.S. Department of Agriculture National Research Initiative (95-02531 and 98-01235), and by the New Jersey Agricultural Experiment Station.

REFERENCES

1. O Nelson, D Pan. Starch synthesis in maize endosperms. Annu Rev Plant Physiol Mol Biol 46:475–496, 1995.
2. FA Isherwood. Mechanism of starch-sugar interconversion in *Solanum tuberosum*. Phytochemistry 15:33–41, 1976.
3. MGH Kennedy, FA Isherwood. Activity of phosphorylase in *Solanum tuberosum* during low temperature storage. Phytochemistry 14:667–670, 1975.
4. CY Tsai, OE Nelson. Starch-deficient maize mutant lacking adenosine diphosphate pyrophosphorylase activity. Science 151:341–343, 1966.
5. E Duwenig, M Steup, L Willmitzer, J Kossmann. Antisense inhibition of cytosolic phosphorylase in potato plants (*Solanum tuberosum* L.) affects tuber sprouting and flower formation with only little impact on carbohydrate metabolism. Plant J 12:323–333, 1997.
6. U Sonnewald, A Basner, B Greve, M Steup. A second L-type isozyme of potato glucan phosphorylase: cloning, antisense inhibition and expression analysis. Plant Mol Biol 27:567–576, 1995.
7. E Beck. The degradation of transitory starch granules in chloroplasts. In: R Heath, J Preiss, eds. Rockville, MD: American Society of Plant Physiologists, 1985, pp 27–44.
8. E Duwenig, M Steup, J Kossmann. Induction of genes encoding plastidic phosphorylase from spinach (*Spinacia oleracea* L.) and potato (*Solanum tuberosum* L.) by exogenously supplied carbohydrates in excised leaf discs. Planta 203:111–120, 1997.
9. T Fukui. Plant phosphorylase. In: T Akazawa, T Asahi, H Imaseki, eds. The New Frontiers in Plant Biochemistry. Tokyo: Japan Scientific Societies Press, 1983, pp 71–82.
10. MF Browner, RJ Fletterick. Phosphorylase: a biological transducer. Trends Biochem Sci 17:66–71, 1992.
11. RJ Fletterick, SR Sprang. Glycogen phosphorylase structures and function. Acc Chem Res 15:361–369, 1982.
12. K Nakano, T Fukui. The complete amino acid sequence of potato α-glucan phosphorylase. J Biol Chem 261:8230–8236, 1986.
13. S Shimomura, M Nagai, T Fukui. Comparative glucan specificities of two types of spinach leaf phosphorylase. J Biochem 91:703–717, 1982.
14. M Steup. Starch degrading enzymes. In: PJ Lea, ed. Methods in Plant Biochemistry, Vol 3. London: Academic Press, 1988, pp 103–128.
15. J van Berkel, J Conrads-Srauch, M Steup. Glucan-phosphorylase forms in cotyledons of *Pisum sativum* L: localization, developmental change, in-vitro translation, and processing. Planta 185:432–439, 1991.
16. JBW Hammond, J Preiss. Spinach leaf intra- and extrachloroplast phosphorylase activities during growth. Plant Physiol 73:709–712, 1983.
17. CY Tsai, OE Nelson. Phosphorylases I and II of maize endosperm. Plant Physiol 43:103–112, 1968.
18. CY Tsai, OE Nelson. Two additional phosphorylases in developing maize seeds. Plant Physiol 44:159–167, 1969.
19. CY Tsai, F Salamini, OE Nelson. Enzymes of carbohydrate metabolism in the developing endosperm of maize. Plant Physiol 46:299–306, 1970.
20. B Burr, OE Nelson. The phosphorylases of developing maize seeds. Ann NY Acad Sci 210:129–138, 1973.
21. CY Tsai, OE Nelson. Mutations at the shrunken-4 locus in maize that produce three altered phosphorylases. Genetics 61:813–821, 1969.
22. H Mori, K Tanizawa, T Fukui. Potato tuber type H phosphorylases isozyme: molecular cloning, nucleotide sequence, and expression of a full-length cDNA in *Escherichia coli*. J Biol Chem 266:18446–18453, 1991.
23. K Nakano, H Mori, T Fukui. Molecular cloning of cDNA encoding potato amyloplast α-glucan phosphorylase and the structure of its transit peptide. J Biochem 106:691–695, 1989.
24. N Brisson, H Giroux, A Camirand, C Simard. Maturation and subcellular compartmentation of potato starch phosphorylase. Plant Cell 1:559–566, 1989.

25. CT Lin, MT Lin, HY Chou, PD Lee, JC Su. The gene structure of starch phosphorylase from sweet potato. Plant Physiol 107:277–278, 1995.
26. P Buchner, L Borisjuk, U Wobus. Glucan phosphorylases in *Vicia faba* L.: cloning, structural analysis and expression patterns of cytosolic and plastidic forms in relation to starch. Planta 199:64–73, 1996.
27. CT Lin, KW Yeh, PD Lee, JC Su. Primary structure of sweet potato starch phosphorylase deduced from its cDNA sequence. Plant Physiol 95:1250–1253, 1991.
28. H Mori, K Tanizawa, T Fukui. A chimeric α-glucan phosphorylase of plant type L and H isozymes: functional role of 78-residue insertion in type L isozyme. J Biol Chem 268:5574–5581, 1993.
29. B Burr, OE Nelson. Maize α-glucan phosphorylase. Eur J Biochem 56:539–546, 1975.
30. CH Fiske, Y Subbarow. The colorimetric determination of phosphorus. J Biol Chem 66:375–400, 1925.
31. OH Lowry, JA Lopez. The determination of inorganic phosphate in the presence of labile phosphate esters. J Biol Chem 162:421–428, 1946.
32. YP Lee. Potato phosphorylase. I. Purification, physicochemical properties and catalytic activity. Biochim Biophys Acta 43:18–24, 1960.
33. A Kamogawa, T Fukui, Z Nikuni. Potato α-glucan phosphorylase: crystallization, amino acid composition and enzymatic reaction in the absence of added primer. J Biochim 63:361–369, 1968.
34. JL Ozbun, JS Hawker, E Greenberg, C Lammel, J Preiss, EYC Lee. Starch synthetase, phosphorylase, ADP glucose pyrophosphorylase and UDP glucose pyrophosphorylase in developing maize kernels. Plant Physiol 51:1–5, 1973.
35. E Steup. Starch degradation. In: J Preiss, ed. The Biochemistry of Plants, Vol 14. London: Academic Press, 1988, pp 255–296.

46

Amylosucrase

Volker Büttcher
Aventis CropScience GmbH, Frankfurt, Germany

I. INTRODUCTION

The enzyme amylosucrase was discovered by Hehre and Hamilton (1). The reaction demonstrated an in vitro glycogen synthesis without any activated nucleotide sugars for the first time. The reaction of amylosucrase can be described as follows:

$$\text{Sucrose} \rightarrow \text{Amylose} + \text{Fructose}$$

The amylosucrase splits off the glucosyl part from the substrate and links it covalently to an acceptor molecule. During this reaction fructose is released. The reaction mechanism is still not proven, but it is assumed that the glycosyl residue is transferred to the nonreducing end of an alpha-1,4-glucan. For the enzyme reaction no additional energy is needed but a primer seems to be necessary to trigger the reaction. The best primer is glycogen which shows enormous stimulation of the amylosucrase reaction (2).

A. Microbiology

Amylosucrase occurs only in prokaryotes and only in some genera of the genus *Neisseria* (Table 1). The amylosucrase is located in the cytoplasm of the cells, except in *N. polysaccharea*, which secretes the amylosucrase in the medium.

The genus *Neisseria* is the type genus of the family Neisseriaceae which contains 18 species that can be isolated from humans and animals. The *Neisseriaceae* are gram-negative bacteria. The morphology in this family can be diplococci, cocci, or rods. The *N. gonorrhoeae and the N. meningtidis* are the only two species that are pathogenic. All other *Neisseria* sp. are nonpathogenic and are known to be commensals.

B. Molecular Genetics

The GC content of *Neisseria* sp. ranges from 49.3 to 55.6 mol% (3). The size of the chromosome is $\sim 1.5 \times 10^6$ bp (4). The gene for amylosucrase was cloned (5, 6) and sequenced. Up to now no sequences of other amylosucrases have been published, but it is assumed that the DNA sequences among the *Neisseria* spp. are very similar. The amylosucrase gene of *N. polysaccharea* could be strongly expressed in various *E. coli* strains (6). Because of its own secretion-signal-like leader sequence in recombinant *E. coli* the enzyme is secreted into the medium, but the bulk of the protein is retained in the cytosol.

II. PROPERTIES OF THE AMYLOSUCRASE

A. Protein Data

The purified amylosucrase is a very stable enzyme. It remained active for several days in the reaction buffer (100 mM Na citrate, pH 6.7) at 37°C. The enzyme could be stored over 1 year at −20°C without significant loss of activity. The MW of the protein is around 72 kDa and the calculated isoelectric point is at pH 5.59.

Table 1 Amylosucrases Are Found in the Following *Neisseria* Strains

N. canis ATCC 31005
N. cinerea ATCC 14685
N. cuniculi ATCC 14688
N. denitrificans ATCC 14686
N. perflava
N. polysaccharea ATCC 43768
N. sicca
N. subflava ATCC 19243

The amylosucrase appears to be tightly bound to its product/substrate, which is amylose (7).

B. Detection of the Amylosucrase Activity

The simplest way to detect amylosucrase activity is in a small in vitro reaction assay. An aliquot of the enzyme sample is mixed with 100 μL reaction buffer (5% (w/v) sucrose, 50 mM Na citrate pH 6.5) and incubated for some minutes up to several days at 37°C. Very high activity samples show a white precipitate, and samples with a lower activity are mixed with Lugols solutions (0.5 mM I_2KI). This test can be used for relatively rough quantitative determination by comparing the color intensity with a calibration row.

A more accurate activity test can be done by measuring the real-time fructose release in an optically coupled enzymatic assay. The reaction cuvette contains 20% sucrose, Na citrate buffer (100 mM, pH 7), glycogen (0.05%), NAD (0.4 mM), ATP (1 mM), and the helper enzymes hexokinase (1.5 units/mL), phosphoglucose-isomerase (2 μg/mL), and glucose-6-phosphate dehydrogenase (5 μg/mL), which are added directly to the reaction mixture (200 μL). The assay is started by addition of the enzyme sample and the OD 340 is monitored. The increase of absorption at 340 nm is equivalent to the production of fructose and can be transformed mathematically in μmol of fructose released per minute (units).

C. Primer Dependence

The glucan synthesis by amylosucrase is strongly stimulated by primers. Glycogen was shown to be one of the best primers (2), but oligoglucans like maltoheptaose or branching enzymes can also trigger the glucan synthesis. From studies of MacKenzie et al. (8) it seems that the amylosucrase of *N. denitrificans* has an absolute requirement for a primer. Up to now it is not absolutely clear if the sucrose itself or an oligoglucan of a certain length is required obligatorily, because traces of glucans are enough to trigger the reactions after a very long lag phase. The reaction kinetics depends not only on primer presence or concentration. The enzyme and substrate concentrations are very important factors in the beginning of the polymerization reaction.

D. Substrate Specificity

Amylosucrase has a high substrate specificity. Several substrates like 6-desoxy-6-fluorosucrose, 6-desoxysucrose, 4,6-dideoxysucrose, 3-desoxysucrose, and α-D-allopyranosyl-β-D-fructofuranoside were used as substrates. None of the tested substrates were incorporated into a polymer, but 6-desoxy-6-fluorosucrose, 6-desoxysucrose, and 4,6-dideoxysucrose could inhibit the enzymatic reaction (9). Under optimal conditions the amylosucrase achieves nearly 100% conversion of its substrate sucrose to polymers (or oligomers) and fructose. Invertase activity (the splitting of sucrose into fructose and glucose without any glycosylation step) is negligible for the amylosucrase reaction under all reaction conditions tested. Remaud-Simeon et al. (5) showed that under special reaction conditions a transglycosylation reaction of oligomaltose may be possible. When the substrate sucrose was lacking, the amylosucrase could disproportionate oligoglucans. The glycosidic residues were mainly transferred such that the maltopentaose concentration decreased in favor of maltohexaose and maltoheptaose.

III. THE PRODUCT OF THE AMYLOSUCRASE

The product of the amylosucrase reaction is characterized as an α-1,4-glycosidic glucan (6). The molecular weight depends on substrate concentration and reaction time. The polymer molecular weights are in the range from several thousands (10^3) up to several millions (10^6) g/Mol. The molecular weights reported in the literature are often overestimated owing to the low solubility of the polymers and the preference of amylose to form strong aggregates.

Older references (10, 11) described the presence of α-1,6 linkages, which were generated by very small impurities of branching activity. The recombinant enzyme, when produced in a branching enzyme-deficient strain (glgB–), allowed the production of a pure

amylosucrase free from any branching activity. The product of the purified amylosucrase is an α-1,4-glycosidic-linked glucose polymer and no α-1,6-glycosidic (or other) linkages could be detected with NMR or methylation methods.

The naturally occurring amylose normally must contain some α-1,6-glycosidic branches, because in vivo the amylose is synthesized in the presence of a glucan branching enzyme activity. Therefore the in vitro product of amylosucrase is different from the naturally found amylose, because of the homogeneity of its glycosidic linkages. This small but important difference implies different polymer properties distinct from naturally occurring ''branched'' amylose. For clear differentiation the product is called ''Nepo-Amylose'' (*Neisseria polysaccharea*-Amylose).

IV. APPLICATIONS

The enzyme amylosucrase is not yet used in industry, because the product (Nepo-Amylose) from the pure amylosucrase is not well characterized. The formerly used crude enzyme preparations synthesized different polymers compared to the very pure recombinant amylosucrase. The reason for that is small impurities, e.g., glucans and branching enzymes, which get carried over from the crude extract. Glucans have a very high binding affinity for the amylosucrase (7). The glucans act in an uncontrolled way as primers and serve as starter molecules for the polymerization. Branching enzymes enhance the polymerization reaction by providing non-reduced ends, at which the amylosucrase elongates the growing chain and accelerates the polymerization (12).

The amylosucrase could, for example, be used in pharmaceutical formulation processes. The microcrystalline amylose could be easily synthesized around a pharmaceutical compound to change the solubility of the substance. The wrapped pharmaceutical compound could be protected after application and would release the active substance in a controlled manner. A second example is the production of indigestible amylose, which can be used as a probiotic food ingredient to improve the healthy bacterial flora in the intestine in order to prevent colon cancer. With a controlled enzymatic process, tailor-made amylose with special properties could be produced for paper coating. The coating would improve the printing quality of recycled paper used by inkjet printers.

The investigation of amylosucrase demonstrates clearly the impact that the recombinant expression of industrial enzymes can have. Only when the recombinant expression of the amylosucrase is an appropriate host strain became possible, the very pure enzyme, free of all disturbing molecules, became available. With this recombinant enzyme new products can be synthesized in a controlled method and with a reliable quality.

REFERENCES

1. EJ Hehre, DM Hamilton. Bacterial synthesis of an amylopectin-like polysaccharide from sucrose. J Biol Chem 166:777–778, 1946.
2. G Okada, EJ Hehre. New studies on amylosucrase, a bacterial alpha-D-glucosylase that directly converts sucrose to a glycogen-like alpha-glucan. J Biol Chem 249:126–135, 1974.
3. C Hoke, NA Vedros. Taxonomy of the Neisseriae: desoxyribonucleic acid base composition, interspecific transformation, and deoxyribonucleic acid hybridization. Int J Syst Bacteriol 32:57–66, 1982.
4. DT Kingsbury. Estimate of the genome size of various microorganisms. J Bacteriol 98:1400–1401, 1967.
5. M Remaud-Simeon, F Albaret, B Canard, L Varlet, P Colonna, RM Willemont, P Monsan. Studies on a recombinant amylosucrase. In: SB Peterson, B Svenson, S Pederson, eds. Carbohydrate Bioengineering. Amsterdam: Elsvier Science, 1995, pp 313–320.
6. V. Büttcher, T Welsh, L Willmitzer, J Kossmann. Cloning and characterisation of the gene for amylosucrase from *Neisseria polysaccharea*: production of a linear α-1,4-glucan. J Bacteriol 179:3324–3330, 1997.
7. CR MacKenzie, KG Johnson, IJ McDonald. Glycogen synthesis by amylosurase from *Neisseria perflava*. Can J Microbiol 23:1303–1307, 1977.
8. CR MacKenzie, JJ McDonald, KG Johnson. Glycogen metabolism in the genus *Neisseria*: synthesis from sucrose by amylosucrase. Can J Microbiol 24:357–362, 1978.
9. BY Tao, PJ Reilly, JF Robyt. *Neisseria perflava* amylosucrase: characterization of its product polysaccharide and a study of its inhibition by sucrose derivatives. Carbohydrate Res 181:163–174, 1988.
10. J-Y Riou, M Guibourdenche, MB Perry, LL MacLean, DW Griffith. Structure of the exocellular D-glucan produced by *Neisseria polysaccharea*. Can J Microbiol 32:909–911, 1986.
11. CR MacKenzie, MB Perry, IJ McDonald, KG Johnson. Structure of the D-glucans produced by *Neisseria perflava*. Can J Microbiol 24:1419–1422, 1978.
12. V Büttcher, M Quanz, L Willmitzer. Molecular cloning, functional expression and purification of a glucan branching enzyme from *Neisseria denitrificans*. Biochim Biophys Acta 1432:406–412, 1999.

47

Dextransucrase

Klaus Buchholz
Braunschweig Technical University, Braunschweig, Germany
Pierre F. Monsan
National Institute for Applied Sciences, Toulouse, France

I. INTRODUCTION

A. Chemical Reactions Catalyzed

In 1861, Louis Pasteur discovered the microbial origin of the gelification of cane sugar syrups (1). In 1874, the corresponding product was named "dextran" because of its positive rotatory power. The microorganism causing that gelification was isolated in 1878 by Van Tieghem and named *Leuconostoc mesenteroides* (2). Hehre demonstrated in 1941 that dextran could be synthesized from sucrose by a cell-free filtrate (3). The corresponding extracellular enzyme was named "dextransucrase" by Hestrin et al. (4).

Dextransucrase (DS) catalyzes the following reaction:

$$n \text{ sucrose} \rightarrow \underset{(\text{glucose})_n}{\text{dextran}} + n \text{ fructose}$$

Sucrose is the only natural D-glucosyl unit donor used as substrate by the enzyme. The energy necessary for D-glucose polymerization simply comes from the cleavage of the high-energy glycosidic bond. No activated intermediate or cofactor is needed.

Dextran is a D-glucopyranosyl polymer containing more than 50% α-1,6 glycosidic bonds, with a molecular weight ranging from 0.5 to 6.10^6 kDa (5, 6). Its type and degree of branching vary according to the origin of the dextransucrase (Table 1) (7, 8). Jeanes et al. (9) have purified and characterized the dextrans produced by 96 strains of *L. mesenteroides*, in order to select the polymers most suitable for medical applications. The structural characteristics of dextrans from several *L. mesenteroides* strains are given in Table 1. Seymour and Knapp (10) suggested classifying dextrans into three groups, according to the main type of branching: Group A, α-1,2 branching; Group B, α-1,3 branching; Group C, α-1,4 branching.

The most widely used dextran is produced by the dextransucrase of the strain *L. mesenteroides* NRRL B-512F, which synthesizes a very highly linear polysaccharide containing 95% α-1,6 bonds. Besides *Leuconostoc*, dextransucrase is also obtained from two other types of lactic bacteria—*Streptococcus* and *Lactobacillus* (7). Streptococcal glucosyltransferases, particularly from *Streptococcus mutans*, are involved in cariogenesis phenomena. These enzymes synthesize from sucrose a glucan polymer which plays a key role in the adhesion mechanism of bacteria on the tooth surface to form the dental plaque (11–13).

B. Substrates and Acceptors

The only natural substrate of dextransucrase (DS) is sucrose, which serves as a high-energy glucosyl donor for polysaccharide and oligosaccharide synthesis; the main product is dextran. In addition to sucrose, α-D-glucopyranosyl fluoride, *p*-nitrophenyl-α-D-gluco-

Table 1 Glucosidic Linkages Content in Dextran Polysaccharides from Various Strains of *L. mesenteroides* and *S. mutans*

		Osidic linkage (%)			
		α-1,6	α-1,3	α-1,2	α-1,4
Leuconostoc mesenteroides	NRRL B-512F	95	5		
	NRRL B-742	87			13
		50	50		
	NRRL B-1299	66	7	27	
		65		35	
	NRRL B-1355	95	5		
		54	46		
	NRRL B-1191	94	6		
	NRRL B-1308	95			5
	NRRL B-1415	87	1		12
Streptococcus mutans	E 49	69	18	13	
	OMZ176	9	91		
		66	33		
	HS6	94	6		
	Ingbritt	44	56		

Source: Refs. 7, 8.

pyranoside, α-D-glucopyranosyl-α-L-sorbofuranoside, and lactulosucrose serve as glucopyranosyl donors (14).

In a secondary reaction, the so called *acceptor reaction*, the glucosyl moiety is transferred from sucrose to the acceptor molecule instead of the growing dextran chain to produce the acceptor molecule elongated by one single glucosyl unit as the primary product. Usually the new bond formed is an α-1,6-glucosidic bond. In most cases, the product can itself serve as an acceptor, so that a homologous series of glucosylated oligosaccharides is formed (15, 16).

Acceptor properties have been reported for a wide variety of mono-, di-, and oligosaccharides (e.g., glucose (17), fructose (18), maltose (19), and raffinose [for overview see 14, 20]), but also for some functionalized saccharide derivatives, as for example the sugar alcohols D-sorbitol and D-glycerol (17) or the 5-O-α-D-glucopyranosyl-arabonic acid (21, 36) or even glucal, an unsaturated sugar (22, 23). This secondary reaction is therefore of special technical interest. It offers perspectives for the synthesis of new oligosaccharides, which are not accessible otherwise by feasible technical routes.

Maltose and isomaltose are the most efficient acceptors. In most acceptors, the glucose from sucrose is transferred to the 6-hydroxyl group of the nonreducing end glucose residue to give a series of isomaltooligosaccarides of degree of polymerization of 2–7 (14). A detailed kinetic analysis revealed a nearly equally high acceptor activity for the di- to tetrasaccharides in the reaction mixture (23).

C. Classification

Dextransucrase is a glucosyltransferase, and more precisely a transglucosidase, named sucrose:1,6 α-D-glucan 6-α-D-glucosyltransferase. Its Enzyme Commission nomenclature number is EC 2.4.1.5.

II. UTILIZATION

A. Synthesis of Nondigestible Oligosaccharides

The dextransucrase from the soil bacterium *Leuconostoc mesenteroides* NRRL B-1299 is known to catalyze the synthesis of dextran polymers containing α-1,2-linked branched chains (Table 1). When this specific glucosyltransferase is used in the presence of maltose as acceptor and of sucrose as D-glucosyl donor, α-gluco-oligosaccharides are obtained, which contain α-1,2 glucosidic bonds (24, 25) at their nonreducing end and a maltose residue at the reducing end.

The presence of these α-1,2 linkages results in a very high resistance of these oligosaccharides to attack by the digestive enzymes of humans and animals (26). Such α-gluco-oligosaccharides cannot be metabolized, as demonstrated by using germ-free rats. That is why such α-gluco-oligosaccharides were initially developed as low-calorie bulking agents, to be used in food formulations in complement of intense sweeteners (24).

But these α-gluco-oligosaccharides are specifically metabolized by the positive intestinal bacterial flora.

In contrast to fructo-oligosaccharides and galacto-oligosaccharides, these α-gluco-oligosaccharides are not bifidogenic, but they promote the growth of the cellulolytic intestinal flora. In addition, they induce a broader range of glycolytic enzymes than fructo-oligosaccharides and galacto-oligosaccharides, without any important side production of gases and thus any detrimental effect (27).

The prebiotic effect of α-gluco-oligosaccharides has been demonstrated for piglets, broilers, and calves (28). The addition, for example, of 0.15% (w/w) of α-gluco-oligosaccharides to young calves' feed results in a 20% decrease in veterinary costs (28). These oligosaccharides are currently marketed for human nutritional application as food complements, in combination with specific microbial flora and vitamins.

The prebiotic effect of such α-gluco-oligosaccharides has also been demonstrated at the level of skin microbial flora (29), in which lactic bacteria also play a key protective role. This has resulted in the development of dermocosmetic applications for the α-gluco-oligosaccharides, under the trade name BioEcolia.

B. Isomalto-oligosaccharides

A product manufactured in Japan as Alo mixture (Anomalously Linked Oligosaccharides) contains a range of isomalto-oligosaccharides to a major extent (glucose, isomaltose, and panose as major constituents) (30). However, it is produced from starch as substrate with α-amylase, β-amylase and a transglucosidase. It is claimed to have favorable properties for application in the food industry.

Using glucose as an acceptor, a European patent (31) describes the formation of isomalto-oligosaccharides from sucrose with 10–20 anhydroglucose units; the average molar weight may be in the range of 2000–5000. The molar ratio of sucrose to glucose is in the range of 2–5. The sucrose is added to the reaction solution of 0.2–0.5 M glucose and 1000 units dextransucrase quasi-continuously. The sucrose concentration should not exceed 25% of the total dry substance; the reaction is conducted to high conversion. The product mixture contains fructose in a molar range corresponding to that of the sucrose added and may be used as a sweetener. Some further data are presented by Pereira et al. (32) with, however, limited yields of oligosaccharides of up to 45%. Systematic investigations concerning reaction engineering were undertaken by K. Demuth (23).

C. Leucrose

Leucrose (α-5-O-[α-D-glycopyranosyl]-β-D-fructopyranose) is an isomer of sucrose which is obtained via glucosyltransfer from sucrose to fructose as an acceptor. Since fructose is a reaction product, the net reaction is an isomerization of sucrose. Basic data are: spec. rotation $[\alpha]_D^{20} - 7.5\%$, melting point 156–158°C (33).

Pilot production was reported by Schwengers (33) using dextransucrase (DS) in a 65% aqueous solution with 1/3 sucrose and 2/3 fructose (w/w) at 25°C. When the reaction was complete, the leucrose formed was separated from fructose by chromatography with a cation exchange resin, followed by an evaporation step and crystallization (30, 33). The formation of leucrose and some reaction conditions, such as the effect of fructose concentration on the formation of leucrose and dextran, were investigated also by Itoh et al. (34).

III. PROPERTIES AS PROTEIN; DS CHARACTERISTICS

A. Molecular Weight

The size of dextransucrase from *L. mesenteroides* NRRL B-512F has been debated for some time. Molecular weights of 65 kDa (35) to 190 kDa (36) have been reported. Finally, the isolation of the gene coding for this enzyme (37) suggested a protein with a total of 1527 amino acids, which corresponds to a 170-kDa molecular weight. Lower values are due to proteolytic degradation, while higher values can be attributed to dextran contamination of the protein preparation. However, one has to be careful in concluding that the gene size represents the final MW of a mature protein, since there often is proteolytic processing (to remove signal peptide and to form subunits) as well as glycosylation, phosphorylation, and other posttranslational modifications.

B. Gene Structure

The structure of the gene coding for dextransucrase from *L. mesenteroides* NRRL B-512F (37) is very similar to that of glucosyltransferases from streptococci (38–40). Starting from the N-terminal end, they consecutively contain: a signal peptide with 36 amino acids (37) allowing excretion; a variable region with 180–200 amino acids with unknown role (41); an N-terminal catalytic domain with 900 amino acids, highly conserved, which contains the catalytic groups, and parti-

cularly the Asp551 residue (41); and a C-terminal domain, with repeated units, involved in the glucan binding, but also in the dextran and oligosaccharide synthesis mechanism (42).

The site-directed mutagenesis of amino acid residues Asp511 and Asp513, which were replaced by Asn residues, completely suppresses dextran and oligosaccharide synthesis activity (43).

IV. PROPERTIES AS ENZYME

A. Mechanism

For dextran formation Ebert and Patat (45) and Ebert et al. (17, 44) were the first to propose an insertion mechanism. This concept was further developed by Kindler and Ludwig (46), who suggested the existence of a covalent intermediate glucosyl-enzyme complex. Several groups provided strong evidence for a covalent glucosyl enzyme intermediate for *S. sanguinis* and *S. sorbrinus* dextransucrase (47–50; for overview see 14). Robyt et al. (51, 52) presented further evidence for both covalent glucosyl and glucanyl enzyme intermediates, suggesting two active centers involved in the growth of the polymer chain via an insertion mechanism, questioned however by recent gene sequence data showing one active center with two Asp (511 and 551) involved in glucosyl transfer (41, 43).

In a secondary reaction, the so-called acceptor reaction, the glucosyl moiety is transferred from sucrose to the acceptor molecule instead of the growing dextran chain to give the acceptor molecule elongated by one single glucosyl unit as the primary product. A specific acceptor binding site at the active center of the enzyme has been proposed (53, 54). Usually the new bond formed is an α-1,6-glucosidic bond. In most cases, the product can itself serve as an acceptor, so that a homologous series of glucosylated oligosaccharides is formed (15, 16).

B. Kinetic Characteristics

Sucrose is the only simple carbohydrate used by dextransucrase as a D-glucosyl donor. Initial reaction rates follow Michaelis-Menten kinetics up to 200 mM sucrose concentration, but the enzyme is inhibited by higher substrate concentrations (55). The inhibitor constant for sucrose is 730 mM (56). This inhibition can be removed by acceptor or dextran addition (6, 57, 58).

Table 2 summarizes the Michaelis constant values reported in the literature for dextransucrase. Optimal pH and optimal temperature with the corresponding reaction activation energy are also given.

Dextransucrase is activated and stabilized by calcium ions (59), but they do not seem to be directly involved in the catalytic mechanism (60). The kinetic behavior of dextransucrase has been characterized and modeled to optimize the production of α-glucooligosaccharides containing α-1,2-glucosidic bonds. In fact, three families of oligosaccarides of increasing degree of polymerization are obtained (61), which respectively contain, besides a maltose residue at the reducing end (Fig. 1), only α-1,6-glucosidic bonds; α-1,6-glucosidic bonds and one α-1,2-glucosidic bond at the nonreducing end; α-1,6-glucosidic bonds and one α-1,2-glucosidic bond on the penultimate D-glucosyl unit.

Table 2 Parameter Value of *L. mesenteroides* NRRL B-512F Dextransucrase

K_M (mM)	Optimal pH	Optimal temperature (°C)	Activation energy (kCal · mol^{-1})	Reference
12–16	5.0–5.5	30	—	50, 60
46	5.0	30	—	35, 38
—	5.2	30	10.3	6
30	5.2–5.5	30	11.2	51, 62
13	4.5–5.5	30	10.5	39
28	5.0–5.6	30	10.0	29, 63
27			55 kJ/mol	20, 54
40				56
(90)[a]				56

[a] Immobilized enzyme, apparent K_M.

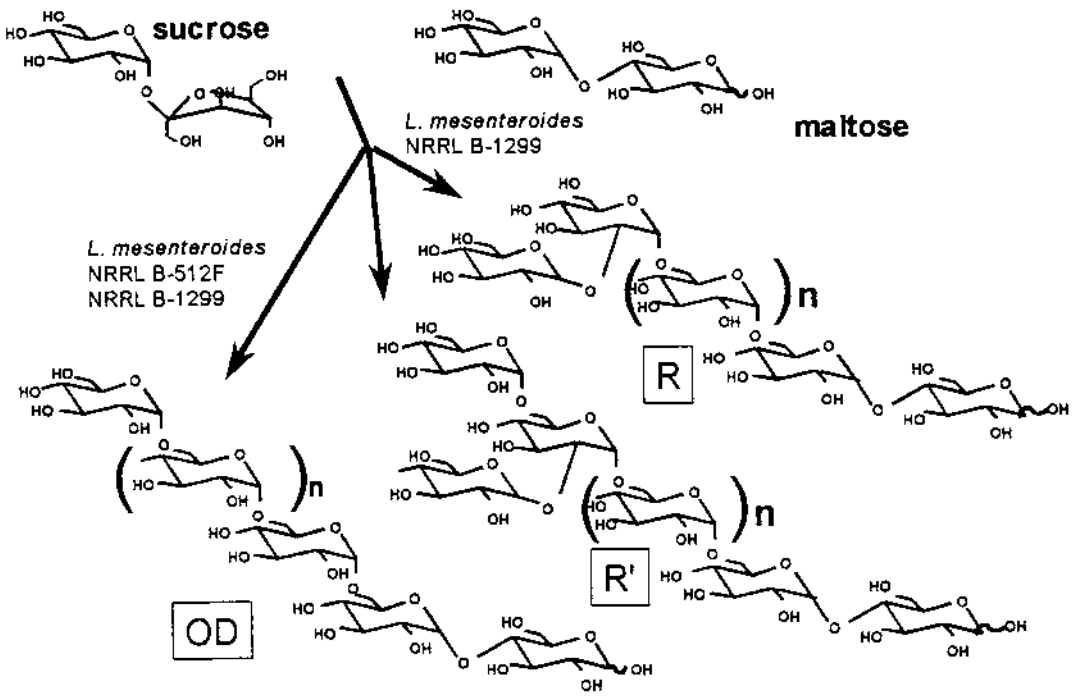

Figure 1 Types of oligosaccharides formed by dextransucrases.

It must be pointed out that Michaelis kinetics only apply in the absence of acceptors. Constants like V_{max}, K_M, and K_I are dependent on acceptor concentrations (cf. next paragraph). Thus with good acceptors, apparent V_{max} values increase with increasing acceptor concentration, from 5.8 (U/mL) with substrate only up to 19.1 (U/mL) at 600 mM maltose concentration (64). They decrease with increasing concentrations of weak acceptors like fructose, from 1.3 (U/mL) to 0.38 (U/mL) at 2.75 M fructose concentration (54). Apparent K_M values increase as well with increasing acceptor concentration, from 12 mM at zero to 163 mM at 600 mM maltose (64). A K_M value of 27 mM was obtained in the absence of an acceptor whereas this value was 40 mM at a fructose concentration of 1.39 M (54). It is obvious that in the presence of acceptors, kinetics are complex and Michaelis kinetics do not apply.

In the presence of strong acceptors, like maltose or isomaltose, several general effects may be summarized: initial overall reaction rates (sucrose consumption or sum of acceptor product and dextran formation) significantly increase both with substrate and acceptor concentration. Initial rates of acceptor product formation follow the same scheme with an even more pronounced tendency; dextran formation may be nearly suppressed at high acceptor concentration (Fig. 2) (65).

The final product concentrations depend significantly on the ratio of substrate and acceptor. The first acceptor product (panose in the presence of maltose) is favored at high maltose excess, whereas tetra- and pentasaccharides are formed in comparable amounts, as well as some higher oligosaccharides, at about equimolar substrate and acceptor concentrations.

In the presence of weak acceptors, like fructose, initial overall reaction rates decrease significantly with increasing acceptor concentration, whereas they increase with the substrate concentration. Initial rates of acceptor product formation increase with both substrate and acceptor concentration, the dextran formation being suppressed to a major extent only at very high acceptor concentration (range of 10% at 3 M fructose concentration) (Fig. 3) (66). The acceptor product of fructose, leucrose, does not act as an acceptor, so high yields can be obtained (54).

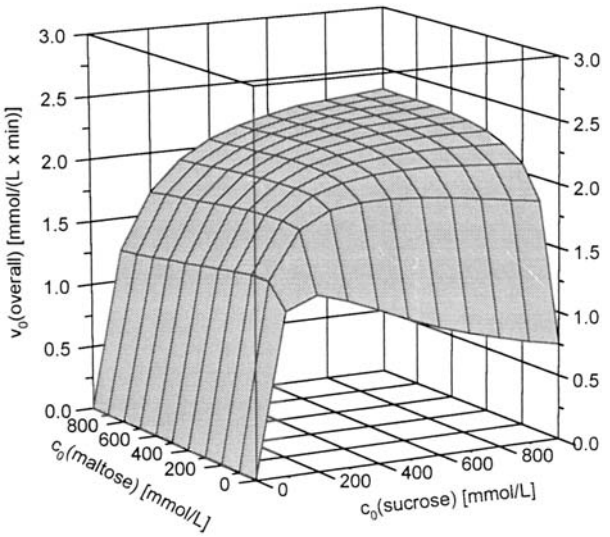

Figure 2 Overall initial reaction rates of acceptor product formation with maltose as an acceptor. (From Ref. 65.)

C. Mathematical Modeling and Reaction Engineering Considerations

The synthesis of oligosaccharides by dextransucrase is a complex series of reactions. The quantitative description of it therefore requires a model which comprises all of the relevant parameters. Such a model has been developed to predict the optimal reaction conditions and reactor configurations for different acceptors, and notably for the production of leucrose and isomalto-oligosaccharides (54, 66). The kinetic parameters of the model identified are based on a wide range of experimental data (23, 54, 56, 65, 67, 68).

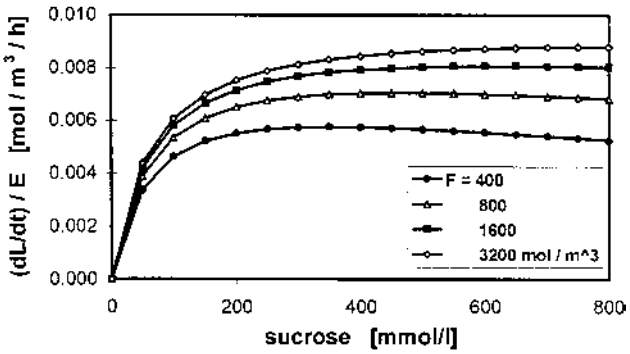

Figure 3 Initial rates of leucrose formation. (From Ref. 66.)

The acceptors considered, fructose, glucose, and maltose, represent different types; the first is a weak acceptor which slows down the overall reaction rate, the second is an acceptor of intermediate strength, and the third represents a strong acceptor which accelerates the overall reaction rate. These effects are included in the model. The scheme of reactions catalyzed by dextransucrase is shown in Figure 4 (66).

The enzyme is assumed to have three binding sites: one covalent glucosyl-, one dextran, and one acceptor (53, 54). Reactions 1, 2, and 3 represent the growth cycle of dextran formation. A sucrose molecule S is bound at the enzyme E, fructose F is released, and the glucosyl G is transferred to the dextran chain G_i, which is always linked to the enzyme. Fructose can be linked to the acceptor site, and react with G to form leucrose FG (reactions 4 and 9). The same reactions are possible with other acceptors A (reactions 6 and 13), and acceptor products (except leucrose) may again react as acceptors (reactions $6 + j$ and $13 + 2xj$). Sucrose is able to bind at the acceptor site (reaction 5) but does not react to an acceptor product, thus leading to inhibition at high concentrations. For approximate modeling, reactions 10–12 and 14 may be neglected.

The decrease of enzyme activity E with time is described by a first-order reaction (66):

$$E = E_0 \cdot \exp(-k_d \cdot t)$$

E_0 is the initial activity at the time $t_0 = 0$; E, the remaining activity after time t; and k_d, the inactivation

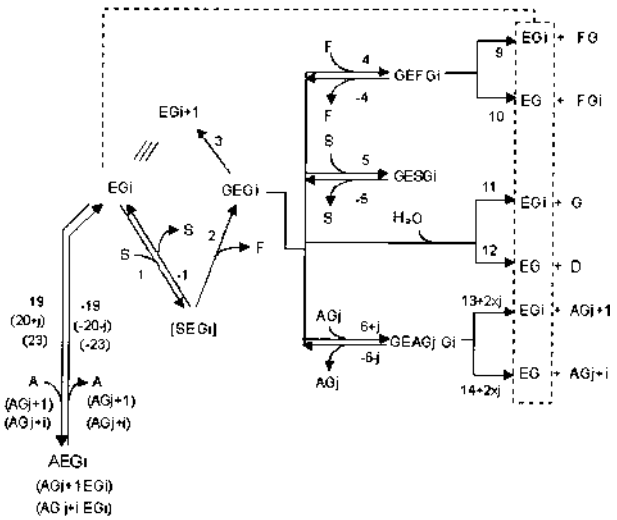

Figure 4 Scheme of reactions catalyzed by dextransucrase (see text for details). (From Ref. 66.)

parameter. For two experiments, the inactivation parameters have been calculated for the immobilized enzyme (66, 67). In these experiments, different acceptors were used: fructose in the first, and maltose in the second. The bead diameters were 0.7 and 1 mm, which have been found to be optimal. The inactivation constants k_d were 0.029 (d^{-1}) in the first and 0.0135 (d^{-1}) in the second case, respectively.

D. Kinetics of Leucrose Formation

Böker et al. (54) presented approximate kinetic correlations as well as a rational model based on the reaction mechanism for different concentration ranges of sucrose and fructose with emphasis on leucrose formation. If only sucrose and fructose are present in the reaction mixture the model may be simplified, so that it comprises only six parameters (Table 3) (54, 66). These equations are similar to an extended Michaelis-Menten equation where two substrates (sucrose and fructose as an acceptor) as well as substrate inhibition are considered.

From the model, it follows that the fructose concentration should be as high as possible; for practical reasons, it is limited by solubility and viscosity of the solution considering the sum of substrate, acceptor and product. A sucrose concentration higher than ~ 100–200 mM has little effect on leucrose production. According to the model, the ratio sucrose/fructose has no effect on the ratio of dextran formation to leucrose formation. A tubular flow reactor with immobilized enzyme is the best choice for production in a continuous mode. So with initial concentrations of 0.6 M sucrose and 2.2 M fructose the leucrose yield was in the range of 64–72% depending on the sucrose conversion (95–55%) (69). The yield can further be improved to about 85% by increasing the fructose concentration up to 3 M, however, at the expense of enhanced separation efforts. Byproducts are isomaltulose and trehalulose in the range of 4–5% each. The leucrose yield can be further improved, for example, from 70% to 75%, and the byproduct concentrations reduced at lower temperature (5°C instead of 25°C) (54). The productivity of the immobilized enzyme in a continuous tubular reactor was found to be 1.5 g leucrose formed per unit dextransucrase (test at 25°C) (69). This type of reactor proved to be optimal in model calculations, as is shown in Figure 5, where the productivity is shown as a function of the initial fructose concentration with an optimum at ~ 1.6 M and 1% residual sucrose concentration (or ~ 2.4 M and 10% residual sucrose concentration) (66).

Formation of the series of oligosaccharides from isomaltose to isomaltodecaose is shown in Figure 6 (23). The first acceptor products are much stronger acceptors themselves than glucose; therefore isomaltose up to isomaltopentaose are formed with nearly equal concentrations in the range 35–45 mM by the end of the reaction.

An overview for the acceptor activity of a range of sugars and sugar derivatives for which kinetic

Table 3 Parameters of Simplified Kinetics for Leucrose Formation[a]

Sucrose consumption rate:

$$ds = -E \cdot S \cdot (p24 + p70 \cdot F)/X$$

Leucrose formation rate:

$$dL/dt = E \cdot p70 \cdot S \cdot F/X$$

$$X = 1 + p42 \cdot S + p46 \cdot F + p47 \cdot F \cdot S + p68 \cdot S^2$$

The values of the parameter are[b]

$$p24 = 3.31 \cdot 10^{-8}\ m^3/(U \cdot min)$$

$$p42 = 1.45 \cdot 10^{-2}\ m^3/mol$$

$$p46 = 7.27 \cdot 10^{-3}\ m^3/mol$$

$$p47 = 1.11 \cdot 10^{-4}\ (m^3/mol)^2$$

$$p68 = 3.16 \cdot 10^{-5}\ (m^3/mol)^2$$

$$p70 = 1.95 \cdot 10^{-8}\ m^6/(U \cdot min \cdot mol)$$

[a] Parameters pi refer to the model as developed in Ref. 66.
[b] m^3 stands for cubic meters.

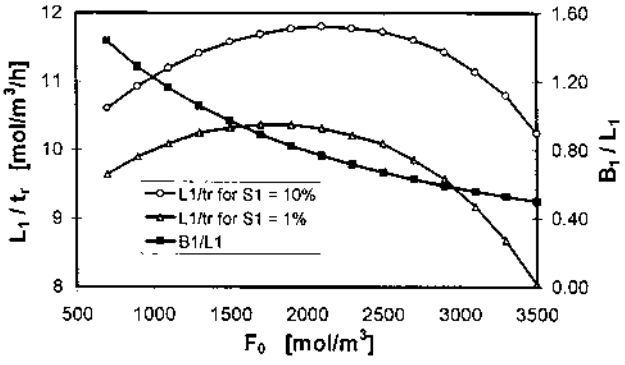

Figure 5 Modeling of the tubular flow reactor—leucrose production rate and formation of byproducts. Kinetics of the formation of isomaltooligosaccharides and different acceptor products. (From Ref. 66.)

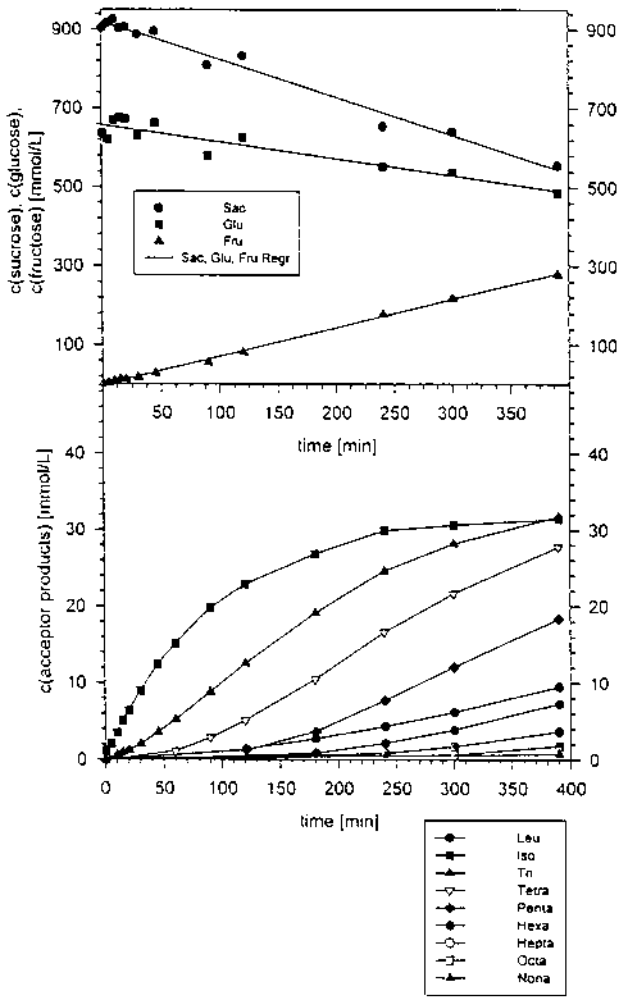

Figure 6 Acceptor production formation with glucose as an acceptor. (From Ref. 23.)

investigations were performed are given in Figure 7 (23). The acceptor activity is based on modeling so that varying concentrations of substrate, acceptor, and acceptor products during the experiments are taken into account. It is obvious that monosaccharides and their derivatives like mannitol and sorbitol are rather weak acceptors. Disaccharides, including acceptor products like isomaltose, are much better acceptors, except singular molecules like leucrose, which is not an acceptor. Surprisingly, many tri- to pentasaccharides are equally good acceptors as the disaccharides, or much better ones in the case of the mannitol and sorbitol acceptor products. It should be noted that the latter ones are nonreducing oligosaccharides with presumably increased thermal stability.

V. QUALITATIVE AND QUANTITATIVE DETERMINATION OF ACTIVITY

Dextransucrase catalyzes, using sucrose as substrate, both the synthesis of high-MW dextran polymers and the synthesis of low-MW oligosaccharides in the presence of efficient acceptors. Two different sets of reaction conditions are thus necessary to determine dextransucrase activity.

A. High-MW Dextran Synthesis

Standard reaction conditions are: 20 mM acetate buffer, pH 5.4, containing 100 g/L sucrose, 0.05 g/L calcium chloride ($CaCl_2 \cdot 2H_2O$), 1 g/L sodium azide at 30°C. Dextransucrase activity must be in the range of 0.3–1.0 U/mL (1 unit corresponds to the amount of enzyme which catalyzes the production of 1 μmol of fructose per min in the above reaction medium).

Dextransucrase activity is measured by determining the initial rate of production of reducing sugars followed by the 3,5-dinitrosalicylic acid (DNS) method (70). Reaction samples (0.1 mL) are withdrawn at various time intervals. Dextransucrase reaction is stopped by addition of 0.1 mL DNS solution (10 g/L DNS, 300 g/L sodium potassium tartarate, 16 g/L sodium hydroxide). After heating for 5 min at 95°C followed by ice cooling, 1 mL water is added and absorbance is read at 540 nm. A standard curve is prepared with standard fructose solutions ranging from 0 to 2 g/L in fructose concentration. Any catalytic activity producing reducing sugars will interfere with activity determination. HPLC for analysis of fructose can be applied as an alternative (see below).

B. Low-MW Oligosaccharide Synthesis

Standard reaction conditions are: 20 mM acetate buffer, pH 5.4, containing 100 g/L sucrose, 20–100 g/L acceptor (maltose, isomaltose, ...), 0.05 g/L calcium chloride ($CaCl_2 \cdot H_2O$), 1 g/L sodium azide at 30°C. Dextransucrase activity must be in the range of 0.3–1.0 U/mL. The key factor determining the molecular-weight distribution of the products is the sucrose donor/acceptor molecular ratio. Reaction samples (0.1 mL) are heated for 5 min at 95°C to stop the reaction. They are diluted with ultrapure water to reach a total carbohydrate concentration < 5 g/L and analyzed by HPLC using a C18 column and ultrapure water as eluent. Fructose, maltose, leucrose, sucrose, and gluco-oligosaccharides with a polymeriza-

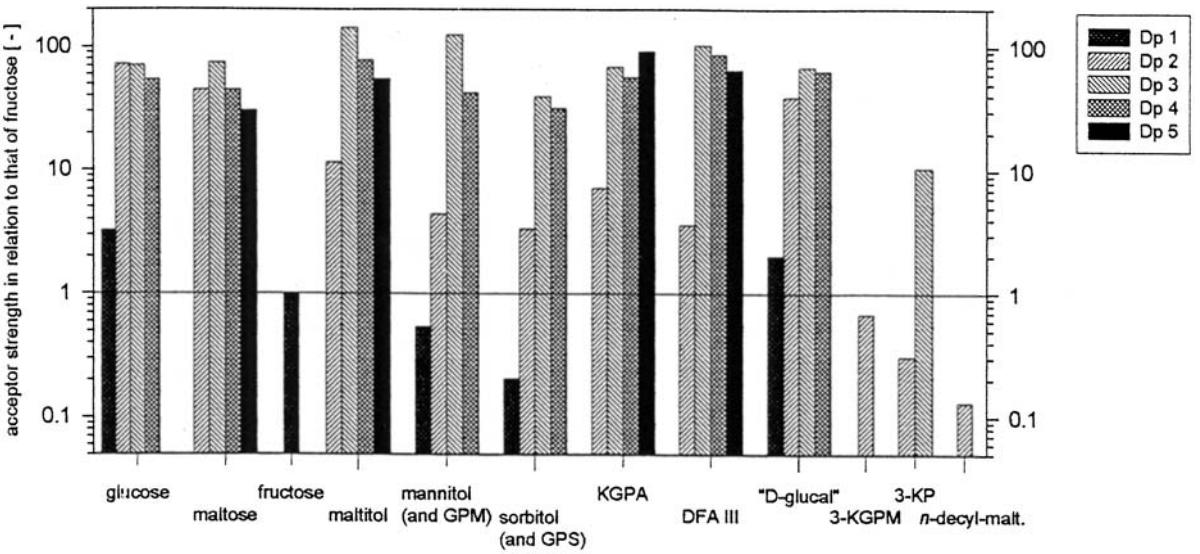

Figure 7 Acceptor strength of various mono- and disaccharides and their ensuing acceptor products in relation to the acceptor efficiency of fructose (DP1 signifies the monosaccharide, followed by the acceptor products, from di- (DP2) to pentasaccharide (DP5) (GPM: glucosylmannitol, GPS: glucosylsorbitol, KGPA: potassium glucosylarabonic acid, DFA III: difructoseanhydride III, 3-KGPM: 3-keto-glucosylmannitol, 3-KP: 3-keto-isomaltulose, n-decyl-malt: n-decyl-maltoside). (From Ref. 23.)

tion degree up to 6 are easily separated within 30 min elution time. Products are detected and quantified by measuring the refractive index of the eluent solution.

C. Immobilized Dextransucrase

For immobilized dextransucrase it is obvious that systematic errors in the activity measurement can be avoided only when dextran formation is suppressed as far as possible. This can be achieved by adding an excess of good acceptor like maltose (71). A test in which maltose was applied in fivefold excess was developed for this purpose (56, 68). However, it must be taken into account that in the presence of excess maltose the maximal activity of dextransucrase is higher by a factor of 3 at low concentrations (sucrose 28, maltose 50 mmol/L) and a factor of 2 at high concentrations (sucrose 280, maltose 150 mmol/L) (65). The test solution was composed of 730 mM maltose and 146 mM sucrose in a 0.025 M calcium acetate buffer at pH 5.4. To avoid microbial growth the solution furthermore contained 200 mg/L sodium azide and a droplet of toluene.

With native dextransucrase, 4.8 mL of this solution was incubated with 0.2 mL dextransucrase solution (activity in the range of 5–15 U/mL) at 25°C. When dextransucrase–calcium alginate beads were tested, 20 mL of the maltose test solution and 1.0 g beads (activity in the range of 5–10 U/g wet weight) were used. Samples from the reaction digests were taken after 15, 30, 45, 60, and 90 min; diluted; and heated at 100° C for 5 min to inactivate the enzyme. After cooling to ambient temperature, the samples were membrane-filtered through a 0.2-μm cellulose nitrate filter and analyzed by HPLC. [Note that prolonged storage of frozen samples prior to analysis will give wrong results due to a slowly continuing reaction (72)]. The enzyme activity is calculated from the fructose concentrations by linear regression. In case of immobilized dextransucrase, corrections must be made for the decrease in reaction volume by sampling whereas the amount of immobilized enzyme remains constant.

D. Analytical Methods: HPLC

Samples were analyzed by HPLC with the LiChrospher 100 NH_2 column (Merck, Darmstadt, Germany). Acetonitrile-water eluent mixtures from 80:20 to 70:30 (v/v) were used at 0.8 mL/min. A refractometer (Knauer, Berlin, Germany) served as detector, while data were acquired with Gynkosoft (Gynkotek, Munich, Germany). The analytical error is ±5% at low sugar concentration (< 8 g/L) and ±3 % at higher concentrations. For complex mixtures of oligosaccharides high-performance anion chromatography is the optimal method (73).

VI. PRODUCTION AND PURIFICATION

A. Dextransucrase Production and Purification

Large-scale production of dextransucrase involves only *L. mesenteroides* strains. These gram-positive, nonsporulating bacteria are heterofermentative and produce equimolar amounts of D(−) lactate and acetate or ethanol (74). Their optimal growth temperature is 25–30°C, with an optimal pH of 6.5 (75). Dextransucrase production is specifically induced by sucrose (76), but the induction mechanism has not been elucidated. Several constitutive mutants have been described for *L. mesenteroides* NRRL B-512 F (77–79), B-1355 (80, 81), B-742 (82), and B-1299 (83).

Dextransucrase is directly connected with microbial growth (84, 85). Lopez (86) obtained a linear relationship between *L. mesenteroides* NRRL B-512F growth rate and dextransucrase specific production rate. The optimization of the culture medium of *L. mesenteroides* NRRL B-512F has been reported by several groups (63, 87, 88). A pH value of 6.7 results in an improved dextransucrase activity and stability (87). The higher pH value also limits dextran production in the culture medium and thus facilitates dextransucrase purification (89). Culture temperature is generally 26°C or 27°C, although higher enzyme activities have been reported at a slower culture growth at 23°C (63, 90), corresponding to 23 units/mL. Aeration conditions poorly affect cell growth, but carbon dioxide significantly increases dextransucrase production (90). Fed-batch sucrose addition results in a sixfold increase in enzyme activity (91). This can be coupled together with pH regulation by adding an alkaline sucrose solution (63, 85). As sucrose acts simultaneously as an inducer for the enzyme production, a carbon source for the bacterial growth and a substrate for dextransucrase, enzyme preparations contain a high concentration of dextran, tightly associated to the protein.

Dextransucrase from *L. mesenteroides* NRRL B-512F can be purified from the culture medium by ammonium sulfate or ethanol precipitation (92). It can also be concentrated by ultrafiltration and purified by Biogel A-5m chromatography after dextran hydrolysis by dextranase treatment (93). The dextran associated with the enzyme allows its very efficient concentration/purification by phase partition after polyethyleneglycol (PEG 1500) addition, resulting in a one-step 20-fold concentration from the culture supernatant and a 200-fold purification (63).

The production of α-gluco-oligosaccharides at the industrial scale is achieved using immobilized dextransucrase in a continuous packed-bed reactor. The enzyme is produced by fed-batch cultivation of *L. mesenteroides* NRRL B-1299 (94, 95). Sucrose plays the simultaneous role of growth substrate for the microbial strain, specific inducer for extracellular dextransucrase production, and substrate for this enzyme. The precise characterization of the physiology of *L. mesenteroides* NRRL B-1299 has shown that the enzyme production was repressed by D-fructose accumulation in the growth medium. But it is possible to remove this repression effect in the presence of D-glucose. For that reason, the simultaneous fed-batch addition of sucrose and D-glucose to the cultivation medium has allowed an increase of 100% in the amount of dextransucrase activity present in the culture medium (96).

More than 90% of the dextransucrase activity is linked to the microbial cells and/or to the dextran polysaccharide associated to the cells. This allows a very easy recovery of the enzyme from the cultivation medium by centrifugation, as well as a very simple immobilization process by entrapping the dextransucrase activity in calcium alginate beads. Immobilized dextransucrase is used in a $1\,m^3$ packed-bed reactor.

VII. IMMOBILIZATION

High-MW dextran synthesis can be obtained using either crude *L. mesenteroides* culture medium after growth on sucrose as carbon source, or the culture supernatant after microbial cell removal. But in the case of oligosaccharide synthesis through the acceptor reaction, the continuous operation of dextransucrase involves its immobilization.

Several attempts have been made for immobilizing dextransucrase by covalent grafting onto a variety of supports, in order to study either the enzyme mechanism or the effect of diffusional limitations on enzyme kinetics. The efficiency of such methods is always relatively limited. Dextransucrase has been coupled onto BioGel activated with glutaraldehyde (51, 97). Covalent grafting onto DEAE-Sephadex or SP-Sephadex gives, under the best conditions, a 10% immobilization yield and a specific activity of 0.5 U/g support (98). Dextransucrase adsorption onto phenoxy acetylcellulose (99) or hydroxyapatite (50) results in improved immobilization yields, but the enzyme is rapidly desorbed from the support. Covalent coupling onto porous amino silica carrier activated with glutaraldehyde gives a specific activity of 40 U/g support, but with a 2% immobilization yield (100, 101).

The presence of high-MW dextran associated with the enzyme results in the possibility to very simply and efficiently immobilize dextransucrase preparations by inclusion into alginate gels. Immobilization yields $>90\%$ are obtained, with a specific activity of 1 up to 10 U/mL gel (69, 102, 103). The apparent volume of the dextranosylenzyme complex, associated with dextran/alginate interactions, allows enzyme retention within such gels, while globular enzymes are easily washed out from the gel (68).

In the case of the production of the dextransucrase from *L. mesenteroides* NRRL B-1299, $>90\%$ of the activity is associated with the bacterial cells. For that reason, the continuous industrial production of gluco-oligosaccharides containing α-1,2 linkages involves the use of the aliginate-entrapped biomass (104). The immobilization yield is 93%, with a specific activity of 4.1 U/mL gel.

VIII. CONCLUSIONS

Dextransucrase is one of the very few enzymes able to synthesize glucosidic bonds using a substrate as simple as sucrose. It has the capacity to catalyze both the production of high-MW dextran polymers, containing thousands of D-glucosyl units, and the production of low-MW oligosaccharides with <10 D-glucosyl units when efficient acceptors, like maltose for example, are added to the reaction medium.

A variety of dextransucrases have been characterized, presenting a wide range of selectivities and thus resulting in a large diversity of poly- and oligosaccharides. The main microbial sources of dextransucrases are lactic bacteria from soil (*L. mesenteroides*) and from the oral flora (*Streptococcus* sp.). It must be pointed out that *L. mesenteroides* strains can be isolated from several food products (dairy products, sauerkraut, alcoholic fermentation), and can thus be regarded as safe. In fact, dextran polysaccharides can be used as texturing agents, particularly for dairy products. In addition, dextran oligosaccharides containing α-1,2 linkages have been proven to present original prebiotic properties and are of interest for nutritional application. The simplicity of production and operation of dextransucrases, either as free or immobilized enzyme preparations, makes such enzymes very good candidates for large-scale production of both poly- and oligosaccharides.

In the near future, the diversity of dextransucrases will be significantly increased owing to both the wider screening of microbial sources using classical microbiological approaches as well as nucleic probes and genomic analysis, and the construction of modified enzymes by site-directed and random mutaganesis, combined with directed gene molecular evolution. This will result in the possibility to design improved dextransucrases with controlled selectivity in D-glucosyl residue transfer. This will allow the synthesis of a new range of poly- and oligosaccharides, and more broadly of glucoconjugates of nutritional and/or medical interest.

REFERENCES

1. L Pasteur. Sur la fermentation visqueuse. Bull Soc Chim 30–31, 1861.
2. P van Tieghem. On sugar-mill gum. Ann Sci Nat Bot Biol Veg 7:180–203, 1878.
3. EJ Hehre. Production from sucrose of a serologically reactive polysaccharide by a sterile bacterial extract. Science 93:237–238, 1941.
4. S Hestrin, S Avireni-Shapiro, M Aschner. The enzymic production of levan. Biochem J 37:450–456, 1943.
5. AJ Groenwall, BGA Ingelman. Manufacture of infusion and injection fluids. U.S. Patent 2,437,518 (1948).
6. KH Ebert, G Schenk. Mechanism of biopolymer growth: the formation of dextran and levan. Adv Enzymol 30:179–210, 1968.
7. RL Sidebotham. Dextrans. Adv Carbohydr Chem Biochem 30:371–444, 1974.
8. MD Hare, S Svensson, GJ Walker. Characterization of the extracellular, water-insoluble α-D-glucans of oral streptococci by methylation analysis, and by enzymic synthesis and degradation. Carbohydr Res 66:254–264, 1978.
9. A Jeanes, WC Haynes, CA Williams, JC Rankin, EH Melvin, MJ Austin, JE Cluskey, BE Fischer, HM Tsuchiya, CE Rist. Characterization and classification of dextrans from ninety six strains of bacteria. J Am Chem Soc 76:5041–5052, 1954.
10. FR Seymour, RD Knapp. Structural analysis of dextrans from strains of *Leuconostoc* and related genera, that contain 3-O-α-D-glucosylated-D-glucopyranosyl residues at the branched points, or in consecutive, linear position. Carbohydr Res 81:105–129, 1980.
11. H Muzaka, HD Slade. Mechanism of adherence of *Streptococcus mutans* to smooth surfaces. I. Roles of insoluble dextran-levan synthetase enzymes and cell wall polysaccharide antigen in plaque formation. Infect Immun 8:555–562, 1973.
12. S Hamada, HD Slade. Synthesis and binding of glucosyltransferase and in vitro adherence of *Streptococcus mutans* grown in a synthetic medium. Arch Oral Biol 24:399–402, 1979.
13. S Hamada, HD Slade. Biology, immunology, and cariogenicity of *Streptococcus mutans*. Microbiol Rev 44:331–384, 1980.

14. JF Robyt. Mechanism in the glucansucrase synthesis of polysaccharides and oligosaccharides from sucrose. Adv Carbohydr Chem Biochem 51:133–168, 1995.
15. JF Robyt, TF Walseth. The mechanism of acceptor reactions of *Leuconostoc mesenteroides* B-512 F dextransucrase. Carbohydr Res. 61:433–445, 1978.
16. JF Robyt, SH Eklund. Stereochemistry involved in the mechanism of action of dextransucrase in the synthesis of dextran and the formation of acceptor products. Bioorg Chem 11:115–132, 1982.
17. KG Ebert, G Schenk. Kinetik und Mechanismus der enzymatischen Dextransynthese und Wirkung der Akzeptoren auf diese Reaktion. Z Naturforsch 23b:788–798, 1968.
18. FH Stodola, HJ Koepsell, ES Sharpe. The preparation, properties and structure of the disaccharide leucrose. J Am Chem Soc 78:2514–2518, 1956.
19. M Killey, RJ Dimler, JE Cluskey. Preparation of panose by the action of NRRL B-512 dextransucrase on a sucrose-maltose mixture. J Am Chem Soc 77:3315–3318, 1955.
20. JF Robyt, SH Eklund. Relative quantitative effects of acceptors in the reaction of *Leuconostoc mesenteroides* B-512 F dextransucrase. Carbohydr Res 121:279–286, 1983.
21. D Prinz. Untersuchung ausgewählter Akzeptorreaktionen der Dextransucrase. Ph.D. thesis, Technical University, Braunschweig, Germany, 1990.
22. K Heincke, B Demuth, HJ Jördening, K Buchholz. Glucosylation by dextransucrase: modeling of reaction kinetics and unconventional products. Ann NY Acad Sci 864:203–206, 1998.
23. (a) K Demuth. Untersuchungen des Einflusses verschiedener, teils funktionalisierter nieder-molekularer Saccharide auf den Verlauf der Dextransucrase-Katalyse. Ph.D. thesis, Technical University Braunschweig, Germany, 1999. (b) K Demuth, H-J Jördening, K Buchholz. Oligosaccharide synthesis with dextransucrase. In: S Bielecki, J Tramper, J Polak, eds. Food Biotechnology. Amsterdam, Elsevier Science, 2000, pp 123–135.
24. F Paul, A Lopez Munguia, M Remaud, V Pelenc, P Monsan (1992). Process for the enzymatic preparation of oligodextrans useful in the production of sugar substitutes, and these oligodextrans. U.S. Patent 5,141,858.
25. M Remaud-Siméon, A Lopez Munguia, V Pelenc, F Paul, P Monsan. Production and use of glucosyltransferases from *Leuconostoc mesenteroides* NRRL B-1299 for the synthesis of oligosaccharides containing α(1,2) linkages. Appl Biochem Biotech 44:101–117, 1994.
26. P Valette, V Pelenc, Z Djouzi, C Andrieux, F Paul, P Monsan, O Szylit. Bioavailability of new synthesized glucooligosaccharides in the intestinal tract of gnotobiotic rats. J Sci Food Agric 62:121–127, 1993.
27. Z. Djouzi, C Andrieux. Compared effects of three oligosaccharides on metabolism of intestinal microflora in rats inoculated with a human faecal flora. B J Nutri 78:313–324, 1997.
28. PF Monsan, F Paul. Oligosaccharide feed additives. In: RJ Wallace, A Chesson, eds. Biotechnology in Animal Feeds and Feeding. Weinheim: VCH, 1995, pp 233–245.
29. JP Lamothe, Y Marchenay, P Monsan, F Paul, V Pelenc. Cosmetic compositions containing oligosaccharides. PCT International Patent WO 9300067 (1993).
30. H Takaku. Anomalously linked oligosaccharides mixture (''Alo mixture''). In: Amylase Research Society of Japan, ed. Handbook of Amylase and Related Enzymes. Oxford: Pergamon Press, 1988, pp 215–217.
31. D Schwengers. Gluco-Oligosaccharid-Gemisch und Verfahren zu seiner Herstellung. European Patent 164,656 (1985).
32. AM Pereira, FAA Cota, MI Rodrigues, F Maugeri. In vitro synthesis of oligosaccharides by acceptor reaction of dextransucrase from *Leuconostoc mesenteroides*. Biotechnol Lett 20:397–401, 1998.
33. D Schwengers. Leucrose, a ketodisaccharide of industrial design. In: Lichtenthaler, FW, ed. Carbohydrates as Organic Raw Materials. Weinheim: VCH, 1991, 183–195.
34. Y Itoh, A Ono, M Yoshiyama, S Shimura. Synthesis of leucrose by dextransucrase and some conditions for the reaction. Nippon Shokuhin Kogyo Gakkaishi 37:171–177, 1990.
35. M Kobayashi, K Matsuda. Characterization of the multiple forms and main components of dextransucrase from *Leuconostoc mesenteroides* NRRL B-512F. Biochim Biophys Acta 614:46–62, 1980.
36. RM Willemot, P Monsan, G Durand. Effects of dextran on the activity and stability of dextransucrase from *Leuconostoc mesenteroides*. Ann NY Acad Sci 542:169–172, 1988.
37. M Wilke-Douglas, JT Perchorowicz, CM Houck, BR Thomas. Methods and compositions for altering physical characteristics of fruit and fruit products. PCT Patent WO 89/12386 (1989).
38. RRB Russell. Molecular genetics of glucan metabolism in oral *streptococci*. Arch Oral Biol 35:53S–58S, 1990.
39. CL Simpson, PM Giffard, NA Jacques. *Streptococcus salivarius* ATCC 25975 possesses at least two genes coding for primer independent glucosyltransferases. Infect Immun 63:609–621, 1995.
40. MM Vickermann, MC Sulavik, JD Nowak, NM Gardner, CW Jones, DB Clewell. Nucleotide sequence analysis of the *Streptococcus gordonii* glucosyltransferase gene, *gtfG*. DNA Seq 7:83–95, 1997.
41. V Monchois, RM Willemot, M Remaud-Siméon, C Croux, P Monsan. Cloning and sequencing of a gene

coding for a novel dextransucarase from *Leuconostoc mesenteroides* NRRL B-1299 synthesizing only α(1-6) and α(1-3) linkages. Gene 182:23–32, 1996.
42. V Monchois, A Reverte, M Remaud-Siméon, P Monsan, RM Willemot. Effect of *Leuconostoc mesenteroides* NRRL B-512F dextransucrase gene carboxy-terminal deletions on dextran and oligosaccharide synthesis. Appl Environ Microbiol 64:1644–1649, 1998.
43. V Monchois, M Remaud-Siméon, RRB Russell, P Monsan, RM Willemot. Characterization of *Leuconostoc mesenteroids* NRRL B-512F dextransucrase (DSR-S) and identification of amino-acid residues playing a key role in enzyme activity. Appl Microbiol Biotechnol 48:465–472, 1997.
44. KH Ebert, G Schenk, H Stricker. Über den Mechanismus des Aufbauschrittes der enzymatischen Dextran- und Lävanbildung. Ber Bunsenges 68:765–767, 1964.
45. KH Ebert, F Patat. Kinetische Bertrachtungen über die enzymatische Dextransynthese. Z Naturforschg 17b:737–748, 1962.
46. H-P Kindler, M Ludwig. Untersuchungen zum Mechanismus der enzymatischen Dextran-Synthese mit einer Strömungsapparartur. Chem Ing Tech 24:1035, 1975.
47. RM Mayer, MM Matthews, CL Futerman, VK Parnaik, SM Jung. Dextransucrase: acceptor substrate reactions. Arch Biochem Biophys 208:278–287, 1981.
48. G Mooser, KR Iwaoka. Sucrose 6-α-D-glucosyltransferase from *Streptococcus sobrinus*: characterization of a glucosyl-enzyme complex. Biochemistry 28:443–449, 1989.
49. G Mooser, SA Hefta, RJ Paxton, JE Shively, TD Lee. Isolation and sequence of an active-site peptide containing a catalytic aspartic acid from two *Streptococcus sobrinus* α-glucosyltransferases. J Biol Chem 266:8916–8922, 1991.
50. VK Parnaik, GA Luzio, DA Grahame, SL Ditson, RM Mayer. A D-glucosylated form of dextransucrase: preparation and characteristics. Carbohydr Res 121:257–268, 1983.
51. JF Robyt, BK Kimble, TF Walseth. The mechanism of dextransucrase action. Arch Biochem Biphys 165:634–640, 1974.
52. JF Robyt, PJ Martin. Mechanism of synthesis of D-glucans by D-glucosyltransferases from *Streptococcusm utans* 6715. Carbohydr Res 113:301–315, 1983.
53. A Tanriseven, JF Robyt. Inhibition of dextran synthesis by acceptor reactions of dextransucrase and the demonstration of a separate acceptor binding-site. Carbohydr Res 225:321–329, 1992.
54. M Böker, H-J Jördeing, K Buchholz. Kinetics of leucrose formation from sucrose by dextransucrase. Biotech Bioeng 43:856–864, 1994.
55. EJ Hehre, DM Hamilton. Bacterial synthesis of an amylopectin-like polysaccharide from sucrose. J Biol Chem 166:77–78, 1946.
56. A Reischwitz. Untersuchungen zum Einschluβ von Dextransucrase. Diploma thesis, Technical University, Braunschweig, Germany, 1992.
57. RM Mayer, MM Matthews, CL Futerman, VK Parnaik, SM Jung. Dextransucrase: acceptor substrate reactions. Arch Biochem Biophys 208:278–287, 1981.
58. M Quirasco, A Lopez Munguia, V Pelenc, M Remaud, F Paul, P Monsan. Enzymatic production of glucooligosaccharides containing α(1-2) osidic bonds. Potential applications in nutrition. Ann NY Acad Sci 750:317–320, 1995.
59. RM Willemot. Etude de la dextrane saccharase de *Leuconostoc mesenteroides* NRRL B-512F. Ph D dissertation, INSA, Toulouse, France, 1993.
60. AW Miller, SH Eklund, JF Robyt. Milligram to gram scale purification and characterisation of dextransucrase from *Leuconostoc mesenteroides* NRRL B-512F. Carbohydr Res 147:119–133, 1986.
61. M Dols, M Remaud-Siméon, RM Willemot, M Vignon, P Monsan. Structural characterization of the maltose acceptor products synthesized by *Leuconostoc mesenteroides* NRRL B-1299 dextransucrase. Carbohydr Res 305:549–559, 1998.
62. WB Neely. Studies on the dextransucrase. I. The effect of pH on enzyme activity. J Am Chem Soc 80:2010-2013, 1958.
63. D Auriol. Production et purification en continu de la dextrane saccharase de *Leuconostoc mesenteroides* NRRL B-512F. Doct Ing dissertation, INSA, Toulouse, France, 1985.
64. F Paul, E Oriol, D Auriol, P Monsan. Acceptor reaction of a highly purified dextransucrase with maltose and oligosaccharides. Application to the synthesis of controlled-molecular weight dextrans. Carbohydr Res 149:433–441, 1986.
65. K Heincke, B Demuth, H-J Jördening, K Buchholz. Kinetics of the dextransucrase acceptor reaction with maltose: experimental results and modeling. Enzyme Microb Technol 24:523–534, 1999.
66. B Demuth, H-J Jördening, K Buchholz. Modelling of oligosaccharide synthesis by dextran-sucrase. Biotechnol Bioeng 62:583–592, 1999.
67. I Knop. Immobilisierung von Dextransucrase für die Oligosaccharidsynthese. Diploma thesis, Fachhochschule Ostfriesland, Emden, Germany, 1989.
68. A Reischwitz, K-D Reh, K Buchholz. Unconventional immobilization of dextransucrase with alginate. Enzyme Microb Technol 17:457–461, 1995.
69. K-D Reh, M Noll-Borchers, K Buchholz. Productivity of immobilized dextransucrase for leucrose formation. Enzyme Microbiol Technol 19:518–524, 1996.

70. JB Sumner, SF Howell. A method for determination of invertase activity. J Biol Chem 108:51–54, 1935.
71. D Su, JF Robyt. Control of the synthesis of dextran and acceptor products by *Leuconostoc mesenteroides* B-512FM dextransucrase. Carbohydr Res 248:339–348, 1993.
72. B Daum, K Buchholz. High selectivity of reactions in ice. Ann NY Acad Sci 864:207–209, 1998.
73. TJ Paskach, H-P Lieker, PJ Reilly, K Thielecke. High-performance anion-exchange chromatography of sugars and sugar alcohols on quaternary ammonium resins under alkaline conditions. Carbohydr Res 215:1–14, 1991.
74. JB Milliere, AG Mathot, P Schmidt, C Divies. Phenotypic characterization of *Leuconostoc* species. J Appl Bacteriol 67:529–542, 1989.
75. El Garvie. Genus *Leuconostoc*. In: PHA Sneath, NS Mair, ME Sharpe, JG Holt, eds. Bergey's Manual of Systematic Bacteriology. Baltimore: Williams and Wilkins, 1986, pp 1071–1075.
76. WB Neely, J Nott. Dextransucrase an induced enzyme from *Leuconostoc mesenteroides*. Biochemistry 1:1136–1140, 1962.
77. D Kim, JF Robyt. Properties of *Leuconostoc mesenteroides* B-512F MC constitutive mutant. Enzyme Microb Technol 16:1010–1015, 1994.
78. N Mizutani, M Yamada, K Takayama, M Shoda. Constitutive mutants for dextransucrase from *Leuconostoc mesenteroides* NRRL B-512F. J Ferment Bioeng 77:248–251, 1994.
79. K Funane, M Yamada, M Shiraiwa, H Takahara, N Yamamoto, E Ichshima, M Kobayashi. Aggregated form of dextransucrases from *Leuconostoc mesenteroides* NRRL B-512F and its constitutive mutant. Biosci Biotechnol Biochem 59:776–780, 1995.
80. MR Smith, J Zahnley, N Goodman. Glucosyltransferase mutants of *Leuconostoc mesenteroides* NRRL B-1355. Appl Env Microbiol 60:2723–2731, 1994.
81. D Kim, JF Robyt. Production and selection of mutants of *Leuconostoc mesenteroides* constitutive for glucansucrases. Enzyme Microb Technol 16:659–665, 1995.
82. D Kim, JF Robyt. Production, selection and properties of mutants of *Leuconostoc mesenteroides* B-742 constitutive for dextransucrases. Enzyme Microb Technol 17:689–695, 1995.
83. D Kim, JF Robyt. Dextransucrase constitutive mutants of *Leuconostoc mesenteroides* B-1299. Enzyme Microb Technol 17:1050–1056, 1996.
84. GR Lawford, A Kligerman, T Williams. Dextran biosynthesis and dextransucrase production by continuous culture of *Leuconostoc mesenteroides*. Biotechnol Bioeng 21:1121–1131, 1979.
85. DE Brown, A McAvoy. A pH controlled fed-batch process for dextransucrase production. J Chem Technol Biotechnol 48:405–414, 1990.
86. A Lopez. Production, purification et immobilisation de la dextrane-saccharase de *Leuconostoc mesenteroides*. Doct Ing dissertation, INSA, Toulouse, France, 1979.
87. HM Tsuchiya, HJ Koepsell, J Corman, G Bryant, MO Bogard, VH Feger, RW Jackson. The effect of certain factors on production of dextransucrase by *Leuconostoc mesenteroides*. J Bacteriol 64:521–527, 1952.
88. PE Barker, NJ Ajongwen. The production of the enzyme dextransucrase using non-aerated fermentation techniques. Biotechnol Bioeng 37:703–707, 1991.
89. RM Alsop. Industrial production of dextran. Prog Indust Microbiol 18:1–45, 1983.
90. NJ Ajongwen, PE Barker. Scale-up studies of non-aerated fermentation of dextransucrase and the industrial synthesis of dextran using the enzymatic route. J Chem Technol Biotechnol 56:113–118, 1993.
91. A Lopez, P Monsan. Dextran synthesis by immobilized dextransucrase. Biochimie 62:323–329, 1980.
92. HM Tsuchiya, HJ Koepsell, J Corman, G Bryant, MO Bogard, VH Feger, RW Jackson. The effect of certain cultural factors on production of dextransucrase by *Leuconostoc mesenteroides*. J Bacteriol 64:521–527, 1952.
93. JF Robyt, TF Walseth. Production, purification and properties of dextransucrase from *Leuconostoc mesenteroides*. Carbohydr Res 68:95–111, 1979.
94. M Dols, M Remaud-Siméon, P Monsan. Dextransucrase production by *Leuconostoc mesenteroides* NRRL B-1299. Comparison with *L. mesenteroides* NRRL B-512F. Enzyme Microb Technol 20:523–530, 1997.
95. M Dols, M Remaud-Siméon, RM Willemot, M Vignon, P Monsan. Characterisation of dextransucrases from *Leuconostoc mesenteroides* NRRL B-1299. Appl Biochem Biotechnol 62:47–59, 1997.
96. M Dols, W Chraibi, M Remaud-Siméon, ND Lindley, P Monsan. Growth and energetics of *Leuconostoc mesenteroides* NRRL B-1299 during metabolism of various sugars and consequences on dextransucrase production. Appl Environ Microbiol 63:2159–2165, 1997.
97. JF Robyt, H Tanigushi. The mechanism of dextransucrase action. Biosynthesis of branched linkages by acceptor reactions with dextran. Arch Biochem Biophys 174:129–138, 1976.
98. M Kaboli, PJ Reilly. Immobilisation and properties of *Leuconostoc mesenteroides* dextransucrase. Biotechnol Bioeng 22:1055–1069, 1980.
99. HN Chang, S Ghim, YR Cho. Immobilization of *Leuconostoc mesenteroides* dextransucrase to porous

phenoxyacetyl cellulose beads. Biotechnol Bioeng 23:2647–2653, 1981.
100. P Monsan, A Lopez. On the production of dextran by free and immobilized dextransucrase. Biotechnol Bioeng 23:2027–2037, 1981.
101. P Monsan, F Paul, D Auriol, A Lopez. Dextran synthesis using immobilized *Leuconostoc mesenteroides* dextransucrase. Methods Enzymol 136:239–254, 1987.
102. I Vallat (1981). Synthèse de dextranes par la dextranesaccharase libre et incluse dans un gel d'alginate. DEA dissertation, INSA, Toulouse, France.
103. D Schwengers, H Benecke, Süβungsmittel, Verfahren zur Herstellung und Verwendung desselben. German patent DPB-DE 344-6380 C1 (1986).
104. M Dols, M Remaud-Siméon, P Monsan. Optimization of the production of dextransucrase from *Leuconostoc mesenteroides* NRRL B-1299 and its application to the synthesis of non digestible glucooligosaccharides. Proceedings of the Second European Symposium on Biochemical Science, Porto, 1998, pp 86–92.

48

Levansucrase

Ki-Bang Song and Sang-Ki Rhee

Korea Research Institute of Bioscience and Biotechnology (KRIBB) and Real Biotech Co., Ltd., KRIBB, Daejeon, Korea

I. INTRODUCTION

Levansucrase is a kind of transferase which catalyzes a fructosyl transfer from sucrose to various acceptor molecules. The product, levan, consists of D-fructofuranosyl residues linked predominantly by β-(2,6) linkage as a main chain with some β-(2,1) branching points. Both linkage types are formed by the single enzyme levansucrase. The enzyme catalyzes the following reactions:

1. Polymerization reaction

$$(\text{Sucrose})_n \rightarrow (\text{Glucose})_n + \text{Levan or Oligosaccharides}$$

2. Hydrolysis reaction

$$\text{Sucrose} + H_2O \rightarrow \text{Fructose} + \text{Glucose}$$

$$(\text{Levan})_n + H_2O \rightarrow (\text{Levan})_{n-1} + \text{Fructose}$$

3. Acceptor reaction

$$\text{Sucrose} + \text{Acceptor Molecules} \rightarrow \text{Fructosyl-Acceptor} + \text{Glucose}$$

4. Exchange reaction

$$\text{Sucrose} + [^{14}\text{C}]\text{Glucose} \rightarrow \text{Fructose-}[^{14}\text{C}]\text{Glucose} + \text{Glucose}$$

5. Disproportionation reaction

$$[\text{levan}]_m + [\text{levan}]_n \rightarrow [\text{levan}]_{m-1} + [\text{levan}]_{n+1}$$

The enzyme catalyzes hydrolysis and polymerization reactions concomitantly (Reaction 1), resulting in fructose homopolymer (levan) and free glucose. This reaction occurs when sucrose exists as the sole fructosyl donor and acceptor, and involves three steps: initiation, propagation, and termination (1). Chains of levan grow in a stepwise fashion by repeated transfer of a hexosyl group from the donor to growing acceptor molecules. The enzyme primarily catalyzes a coupled reaction by a Ping-Pong mechanism, i.e., sucrose hydrolysis followed by transfructosylation involving a fructosyl-enzyme intermediate (2).

When water acts as an acceptor, a free fructose is generated from both sucrose and levan (Reaction 2). This reaction occurs in all the levansucrase-catalyzed reactions mentioned above, but the rate is much slower when compared to a sugar acceptor. Reaction 3 occurs in the presence of an acceptor in the environment. The enzyme transfers the fructosyl residue of sucrose specifically to the C-1 OH of aldose in the acceptor. Compounds containing hydroxyl groups, such as methanol, glycerol, and oligosaccharides, can act as fructosyl acceptors. The reaction mechanism yields a nonreducing sugar compound and a series of oligosaccharides, in which the sugar molecule with one more fructose moiety remains as a major reaction product. The reaction occurs predominantly in the presence of a high concentration of fructosyl donors, such as sucrose or raffinose. Reaction 4 might be considered analogous

to Reactions 2 and 3, but differs in the regeneration of sucrose, which has a high-energy bond. The enzyme also catalyzes Reaction 5, a disproportionation reaction, in which the degree of polydispersity of levan or oligomers is modified. The above five reactions compete with one another, yielding a specific major product with some minor products, but they are predominantly controlled by environmental factors.

The enzyme recognizes sugar compounds with a β-1,2 linkage between glucose and fructose residues. The most abundant substrate for the enzyme in nature is sucrose. Raffinose also serves as a substrate. Levan formed by levansucrase is hydrolyzed by the enzyme itself, and the hydrolysis ceases at the branching points. The degree of levan hydrolysis depends on the enzyme source. For example, *Rahnella aquatilis* levansucrase has strong activity, but *Zymomonas mobilis* levansucrase shows very little activity even at higher temperatures (3).

Levansucrase (sucrose:2,6-β-D fructan:6-D-fructosyltransferase, sucrose 6-fructosyltransferase) is classified EC 2.4.1.10. There are several enzymes that relate to the hydrolysis of sucrose or sucrose-originated sugar compounds: sucrase (β-D-fructofuranosidase, invertase, EC 3.2.1.26), dextransucrase (EC 2.4.1.5), levanase (EC 3.2.1.65), inulinase (EC 3.2.1.7), and alternansucrase (EC 2.4.1.140). A new fructosyltransferase (aldose β-D-fructosyltransferase, EC 2.4.1.162), which has an exceptionally high propensity to form a wide range of α-(1,2)-linked disaccharides, does not form appreciable amounts of levan (4). The enzymes involved in the biosynthesis of fructan (levan and inulin) in plants are as follows:

Sucrose:sucrose 1F-fructosyltransferase (1-SST, EC 2.4.1.99)
Fructan:fructan 1-fructosyltransferase (EC 2.4.1.100)
Sucrose:fructan 6-fructosyltransferase (6-SFT)

The last one, which has similar enzymatic functions with microbial levansucrases, is responsible for the production of levan in plants (5).

II. SOURCES AND FUNCTION OF LEVANSUCRASE

Levansucrase is found in various kinds of microorganisms and in higher plants. Levan as a product of levansucrase-type enzyme reactions is a major nonstructural carbohydrate found in plants such as barley, wheat, onions, and grass. In plants, levan accumulates in vacuoles and plays an important role in temporary storage and partitioning of assimilates and in osmoregulation. It also assists some plants in overcoming drought and cold stress (6). For example, improved drought resistance is shown upon transformation of tobacco, a species normally incapable of forming levan, with a gene encoding a bacterial levansucrase. The enzyme involved in levan biosynthesis in plants, which may be synthesized by the concerted action of a number of distinct fructosyltransferases, is not fully understood.

There are a number of microorganisms reported as levan producers beyond the genus (7). Levansucrases from some bacteria are inducible and exocellular, whereas some are constitutive and endocellular. The synthesis of levan by levansucrase in a sucrose-containing medium gives the microorganisms a mucoid morphology. Researchers have demonstrated that this mucoid structure of the microorganisms plays a role in the symbiosis (*Bacillus polymyxa*) or phytopathogenesis (*Erwinia amylovora*) of plant interactive bacteria. In addition, the enzyme also participates in the defense mechanism against environmental stress (*Bacillus subtilis*) (8). The function of levansucrase located intracellularly in some bacteria is not understood. The diversity of the enzymatic properties of levansucrase may be caused by the different biological function of each enzyme in each microorganism. Recently, the enzyme was overexpressed in *E. coli* for the mass production of levan with high yield and purity (9). An approach to produce levan in large quantity was achieved successfully in transgenic plants (10).

III. UTILIZATION OF LEVANSUCRASE

Levan, produced by levansucrase from sucrose, consists entirely of fructose and glucose at one terminal in each molecule (Fig. 1). Many potential applications of levan in food and pharmaceutical industries exist, but the use of this polymer is not yet practical due to the lack of information about its polymeric properties needed in industrial fields. Novel applications of levan include such uses as emulsifier, formulation aid, stabilizer, thickener, surface-finishing agent, encapsulating agent, and carrier for colors or flavors and fragrances in the food industry (7). It has been reported that levan has certain biological activities, such as the promotion of infection and necrosis, tumor inhibition, and an increase in cell permeability to a cytotoxic agent (11). Calazans et al. (12) postulated that levan showed antitumor activity against sarcoma 180 and Ehrlich carci-

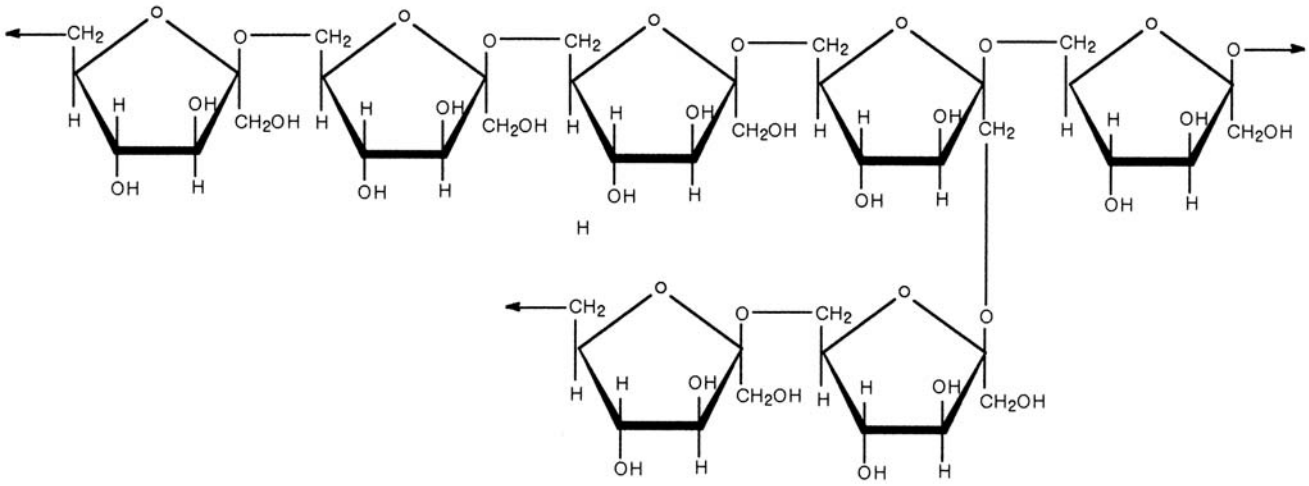

Figure 1 Chemical structure of levan.

noma in Swiss albino mice, and hypothesized that the effect might be associated with the polymer of a specific molecular size.

In addition to the above, a novel aqueous two-phase system has been developed by mixing polyethylene glycol (PEG) and levan, which offers a potential application of levan in separation and purification of biological materials, as an alternative to PEG/dextran and PEG/salt two-phase systems (13). The enzymatic or chemical hydrolytic products of levan may be used in the food industry as sweeteners or dietary fiber: ultra-high-fructose syrups (UHFS) and β-(2,6)-linked fructofuranosyl oligosaccharides (7). Several microorganisms producing various levan-assimilating enzymes such as exo- or endo-type levanase, fructose dimer- or heptamer-producing levanase, and levan fructotransferase were isolated and characterized (14). Together with the difructose anhydride compounds (DFA I and III) from inulin, which are β-(2,1)-linked fructans found in plants, DFA IV from levan is an attractive material as low-calorie sugar, non– or anti–tooth-decaying sweetener, stabilizer, and antianemic agent in the food and pharmaceutical industries (15).

Another reason for the increasing interest in levansucrase is that the enzyme can catalyze the transfer of fructosyl residue to a variety of sugar molecules. Some of the resulting hetero-oligosaccharides have potential applications as sweeteners and probiotics (16). Currently fructo-oligosaccharides and lactosucrose, which are formed using a fungal fructosyltransferase, are available in the market as a "functional food." Levansucrase enables the formation of a variety of fructosyl derivatives, alkyl fructosides, which are expected to be applicable in similar or improved uses of alkyl glucoside and used as a nonionic surfactant and as raw materials for the production of sugar esters of fatty acids (17).

IV. GENETIC PROPERTIES OF LEVANSUCRASE

The molecular weight of bacterial levansucrases is reported to be in the range of 45–64 kDa. Several analogies in their primary structures have confirmed that a close relationship exists among levansucrases from Gram-negative bacteria. The molecular weight of levansucrases from Gram-negative bacteria is nearly the same, about 45–47 kDa, while those from Gram-positive bacteria are slightly larger (54–64 kDa).

Eight levansucrase genes from microorganisms have been cloned and characterized to date (18, 19). The deduced amino acid sequences are aligned in Figure 2. All levansucrases share several conserved regions, which are thought to be important for the enzyme activity. Although conservation is observed, dissimilarity exists depending on the source of the enzyme. Levansucrases from Gram-negative origin show relatively high similarity ($> 50\%$), when compared with the Gram-positive bacterial enzymes. However, very little similarity ($< 30\%$) exists among enzymes from the two sources. In the case of protein secretion mechanisms, they are also thought to be different on the basis of the presence or absence of a signal peptide.

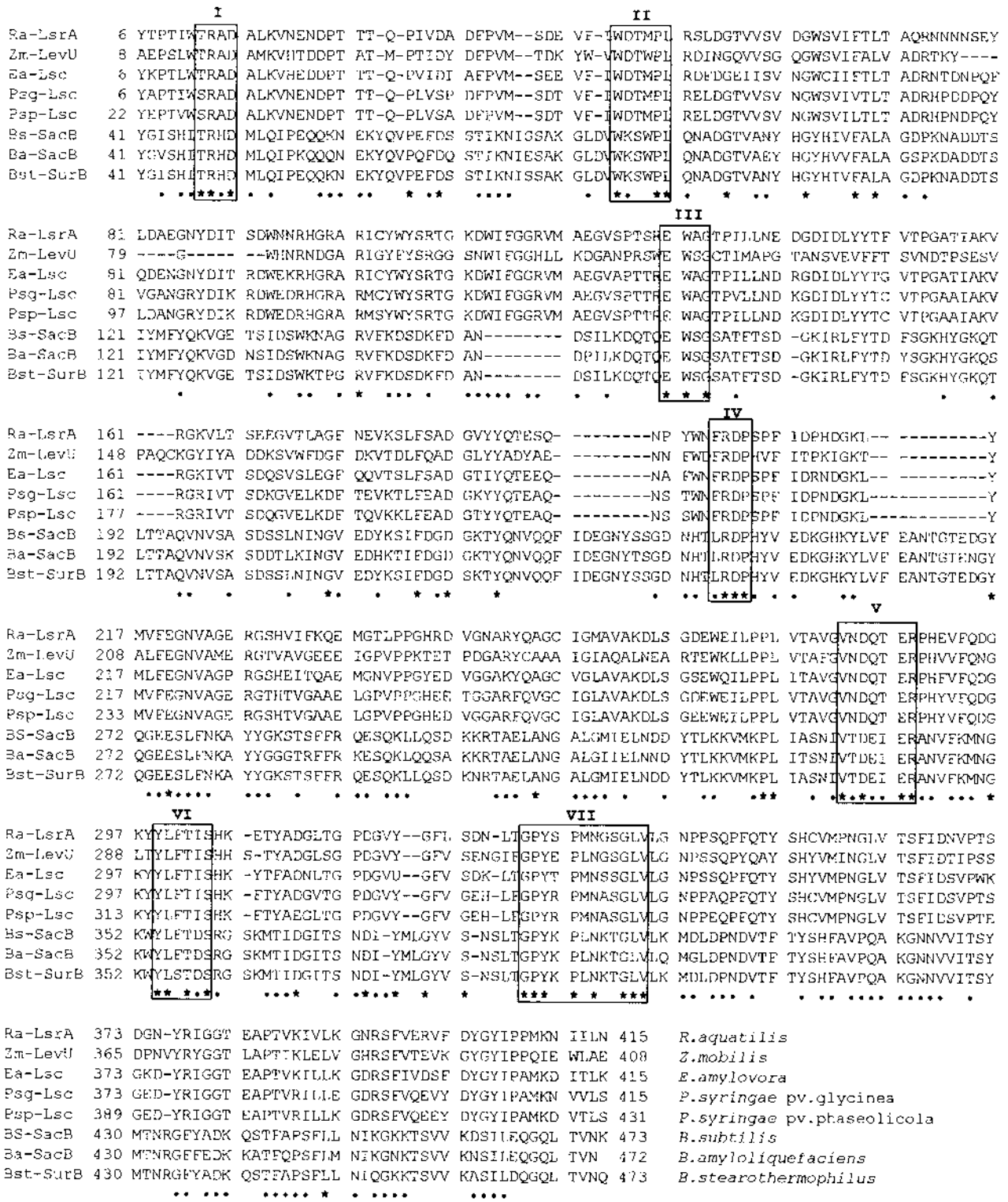

Figure 2 Multiple alignment of deduced amino acid sequences of bacterial levansucrases. Origins of levansucrases are indicated at the end of the sequences. Identical and similar residues in all levansucrases are indicated by asterisks. Regions considered to be important for activity are boxed (I–VII). Amino acid residues that are different between Gram-negative and Gram-positive origins are indicated by dots.

It is generally accepted that levansucrases from Gram-negative bacteria are secreted by a signal peptide independent pathway. It is plausible that the Gram-positive and Gram-negative genes diverged at an early stage of evolution and have separately evolved ever since. Although the amino acid sequences of levansucrases do not show any considerable homology to those of sucrose-related enzymes, the third (–EWS/AGT/SP/A–) and the fourth (–FRDP–) conserved regions are found in all fructosyl- and glucosyltransferases, sucrase, sucrose 6-phosphate hydrolase, and even in fructan-hydrolyzing enzymes. That the regions are preserved in all sucrose-related enzymes implies that they may be catalytically important regions for the hydrolysis of sucrose. The serine residue in the sixth region (–YLFTI/DS–) has been proposed as the putative residue of the catalytic site (20).

V. BIOCHEMICAL PROPERTIES OF LEVANSUCRASE

The substrate specificity of levansucrase is extremely low. Sucrose and raffinose serve as fructosyl donors. The glucose moiety of sucrose can be replaced by various sugars such as D-xylose, L-arabinose, lactose, etc. Substrate specificity for the acceptors is, however, relatively broad. Several kinds of alcohol; mono-, di- or oligosaccharides; sugar alcohols; and levan are known acceptors. The specificity toward acceptor molecules differs depending on the catalytic properties of each enzyme. In *B. subtilis* levansucrase, a turnover number of 17,000 moles of sucrose per minute per mole of enzyme at 37°C and pH 6.0 was obtained (21).

A. pH Optimum

The enzyme has a high activity at pH 5–6, and is stable at pH 4–7. No activity is observed below pH 3 and above pH 9. Thus, the enzyme has a very narrow spectrum of pH with a trapezoid-shaped curve.

B. Optimum Temperature

The range of optimal temperature for levan formation is rather uniform (18–40°C) with the exception of the psychrophilic enzyme of *Z. mobilis* (0°C), *B. subtilis* (> 10°C), and the thermostable enzyme *R. aquatilis* (50°C). One striking feature is that the synthesis of levan by levansucrase occurs far more effectively at low temperatures than at room temperature or at higher temperature, though the apparent activity determined in terms of glucose-releasing activity in the hydrolysis reaction is fairly small at lower temperatures. The enzyme is thermolabile and loses its activity at 45°C for 15 min.

Interestingly, *Z. mobilis* enzyme was most active at extreme temperatures < 10°C (9). Therefore, levan formation using *Z. mobilis* enzyme can be conducted in a stable operation and with less contamination problems.

C. Cofactors

Sucrose is directly converted to levan by the enzyme without the need of any primer, nucleotide sugar intermediate, or sugar phosphate.

D. Inhibitors and Activators

There are few reports on inhibitors and activators of the enzyme. The inhibition of the enzyme by glucose is a function of glucose concentration, and complete inhibition occurs at 16% glucose concentration. Tris-HCl buffer is an efficient inhibitor. The activity is inhibited slightly by EDTA, and no disulfide bonds are involved in the activity. Increased thermal stability and enhanced activity of the enzyme in the presence of Fe^{2+} or Ca^{2+} have been reported, with some exceptions (22). Polyethylene glycol 4000 has an activating effect by increasing the maximum velocity. The addition of levan in small quantities to the reaction mixture also stimulates the activity of levansucrase and causes the synthesis of the high molecular weight levan.

E. Kinetic Constants

The K_m values of levansucrase from *B. subtilis* are ~ 20 mM for sucrose and 50 mM for the analog glucosido-sorboside at pH 6.0 and 37°C. The affinity constant for the short-chain levan (DP 40) acting as an acceptor-activator is 5 mM under the same conditions (21).

F. Storage Property

The enzyme solution is stable at 4°C for several months without loss of activity. The enzyme was relatively resistant to freezing, thawing, and protease treatment.

G. Toxicity

Interestingly, the heterologous expression of levansucrase gene (*sacB*) from *B. subtilis* in Gram-negative bacteria appears to be toxic to the host (23). The lethality of gene expression was observed in a number of Gram-negative bacteria, but not in Gram-positive bacteria like *Streptomyces lividans* with the exception of *Corynebacterium glutamicum*, which contains mycolic acid in the outer membrane. This makes the bacterium behaves as Gram-negative bacterium. Thus, the use of the gene as a selection marker has been successful to a certain extent, although the molecular and biochemical basis of toxicity is still unclear.

VI. DETERMINATION OF LEVANSUCRASE ACTIVITY

Several analytical methods can be employed for the measurement of levansucrase activity. Isotopic procedure utilizes [^{14}C]sucrose as a substrate and measures the incorporation of isotopes into the products. This procedure is powerful when a wild-type strain with very little activity is employed as an enzyme source. The measurement of the weight of dried levan that is formed by the enzyme reaction is conducted after ethanol precipitation of the reaction mixture. Another method for the determination of levan content, which gives a linear curve at low concentrations, is to measure the optical density at visible range (450–550 nm), corresponding to the turbidity of the reaction mixture generated by the formation of levan. By paper and TLC chromatographic analyses, one can distinguish the polymeric products (nonmobile), oligomeric products, substrate, and glucose (byproducts), qualitatively or quantitatively, after visualization. Sucrose hydrolysis is commonly related to determination of levansucrase activity. The methods established are based on the fact that glucose is formed stoichiometrically in relation to the amount of fructose incorporated into products. The amount of glucose generated by enzymatic reaction can be assayed quantitatively by colorimetric enzymatic analyses (18). The enzymatic analysis, which is convenient, rapid, and highly accurate, is preferred. In this method, the reaction mixture is incubated at 37°C, at which the hydrolysis activity of levansucrase is more active than the polymerization activity (transfructosylation activity). It is followed by the coupled reactions of glucose oxidase and peroxidase toward the liberated glucose.

First reaction:

$$\text{Glucose} + H_2O + O_2 \xrightarrow{\text{Glucose Oxidase}} \text{Gluconic acid} + H_2O_2$$

Second reaction:

$$H_2O_2 + o\text{-Dianisidine (Colorless)} \xrightarrow{\text{Peroxidase}} \text{Oxidized } o\text{-Dianisidine (Brown)}$$

The assay is commercially available as a kit from many biological-product manufacturing companies. Alternatively, the Somogy-Nelson method could be employed. One unit of enzyme activity is defined as the amount or enzyme releasing 1 μmol of glucose per min. The HPLC method is commonly employed for the quantitative determination of all components in the reaction mixture, including levan, oligosaccharides, sucrose, fructose, and glucose. The method is described here in detail (24).

A. Reagents

1. Substrate solution: 100 mL solution of 1% sucrose and 0.05 M acetate buffer, pH 6.0, is prepared and stored in refrigerator. The solution is stable for several months.

2. Conditions: The analysis is conducted by HPLC (Gold Systems, Beckman) with a refractive index detector and Shodex Ionpack KS-820 column (Showa Denko Co., Japan). Deionized water is used as a mobile phase at a flow rate of 0.4 mL/min.

B. Procedure

One milliliter reaction mixture containing 1% sucrose in 0.05 M acetate buffer and enzyme (1–3 units) is incubated for 30 min. The incubation temperature depends on the enzyme source: 10°C for *Z. mobilis*, and 20°C for *R. aquatilis*. The reaction can be terminated by adjusting the pH of the reaction mixture to an alkaline range (above pH 9) with 10 mM NaOH solution. Subsequently, the mixture is filtered using a 0.45 μm pore size membrane filter and analyzed by HPLC. Oligosaccharide content is determined by using the calibration curve of raffinose as a standard. Under these conditions, a highly polymerized product (levan) and glucose are formed as major reaction products. A small amount of free fructose, oligosaccharides, and the remaining sucrose is also detected (Fig. 3). The oligosaccharide formed by levansucrase purified from *Z. mobilis* has been identified mainly as 1-ketose (25). Sugar components and linkage type of the highly poly-

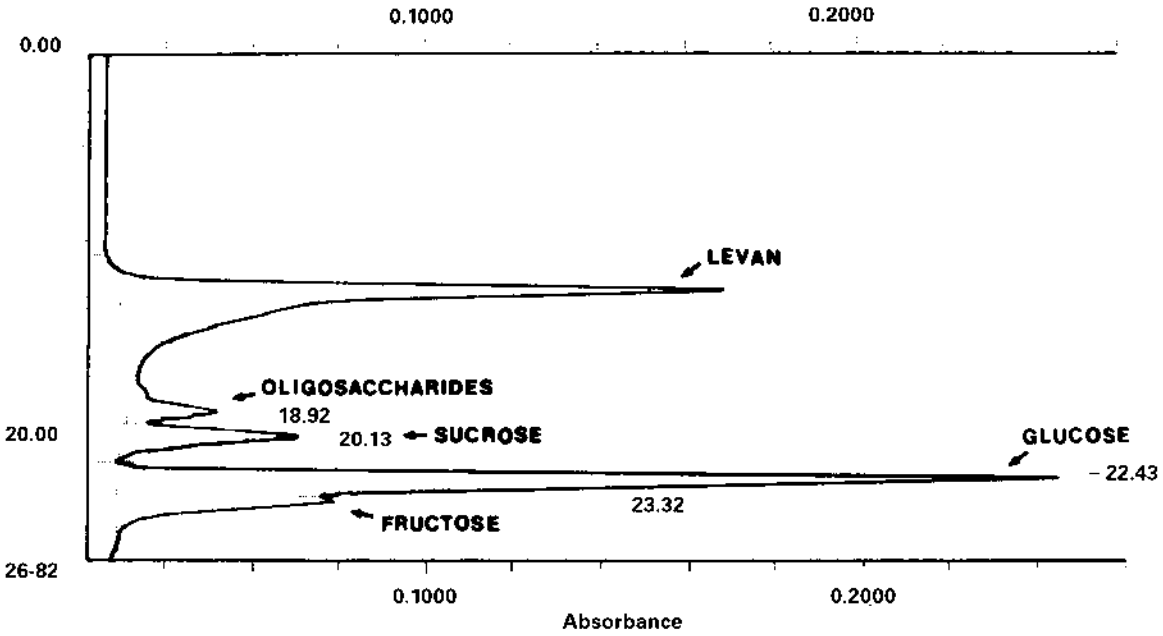

Figure 3 HPLC analysis of the reaction products formed by levansucrase with sucrose. Chromatographic conditions are described in the text. (From Ref. 9.)

merized product are determined by acid hydrolysis, methylation, and NMR shift experiments (7).

VII. PURIFICATION

Bacterial levansucrases seem to attach on the outer surface of the membrane as well as secreted extracellularly (7, 26). In some cases, the enzyme is intracellular, but its function has not been illustrated. The profile of enzyme activity from *Z. mobilis* culture shows that the activity is maximal at the late logarithmic or early stationary phase of cells grown in sucrose medium. The initial recovery of levansucrase from the supernatant of cell cultures grown at the late logarithmic phase by ammonium precipitation is somewhat difficult. This is likely due to the low yield of proteins and the presence of polymeric compound (levan) in the culture medium, in which levansucrase is inducibly produced in the presence of sucrose. To circumvent this, the preparation of cell-associated levansucrase was employed by Pabst et al. (26). The enzyme bound to levan which is encapsulated outside of the stationary-phase grown cells can be recovered in significant amounts. This method provides an additional advantage of reducing the number of contaminated proteins.

VIII. PURIFICATION OF LEVANSUCRASE FROM *Z. MOBILIS*

A. Crude Enzyme

Z. mobilis ATCC10988 is grown in a rich medium consisting of (per liter); 50 g sucrose, 20 g yeast extract and 1 g potassium phosphate (monobasic). Cells are cultivated in a 20-L jar-fermentor (working volume 15 L) at 30°C. After 24 h, cells are harvested and washed briefly with distilled water. The pellets from 1 L culture broth are resuspended in 50 mL of 100 mM phosphate buffer (pH 6.0) and incubated at 30°C for 30 min with mild shaking to release the enzyme from the cell surface and the supernatant is saved. Cell pellets are washed once and mixed with the supernatant to yield the crude enzyme.

B. Purification Procedures

The crude enzyme is purified according to the following procedure: first ammonium sulfate precipitation (80% saturation), ion exchange chromatography, hydroxyapatite chromatography, second ammonium sulfate precipitation (50% saturation), and gel filtration chromatography. Phosphate buffer (20 mM, pH 6.0) is used throughout the purification procedure. A

Table 1 Summary of Levansucrase Purification Steps from *Z. mobilis*

Step	Volume (mL)	Units (total)	Protein (mg/mL)	Spec. Act. (U/mg)	Yield (%)	Purification (fold)
Cell washed solutions	1300	—[a]	0.35	—	—	—
1st $(NH_4)_2SO_4$	115	—	1.28	—	—	—
Ion exchange	38	4.35	0.57	0.21	100	1.00
Hydroxyapatite	20	2.58	0.41	0.31	65	1.52
2nd $(NH_4)_2SO_4$	2	0.96	0.46	1.04	21	5.07
Superose 12	1.5	0.72	0.13	3.75	16.5	18.3

[a] Not determined.
Source: Ref. 24.

summary of the purity and recovery of the enzyme is given in Table 1. As a result of chromatography on DEAE-Toyopearl 650 M column, two distinct peaks of sucrose-hydrolyzing activity can be seen (Fig. 4). The first peak is responsible for levansucrase; the second one, for sucrase. After the successive purification steps of the protein by hydroxyapatite chromatography and second ammonium sulfate purification, the small amount of contaminated proteins can be eliminated from the enzyme solution by gel filtration chromatography (FPLC). A single band is observed when the purified enzyme is subjected to SDS-PAGE. The enzyme can be purified from culture broth 18.3-fold to a specific activity of 3.75 U mg^{-1} protein, with a yield of 16.5%. The molecular weight of the enzyme is ~ 91,000 by Superose 12 gel filtration, and 46,000 by SDS-PAGE, indicating that levansucrase is a dimer. The optimum pH for the enzyme activity is around pH 4.0 for sucrose hydrolysis, and is around pH 5.0 for levan formation (24).

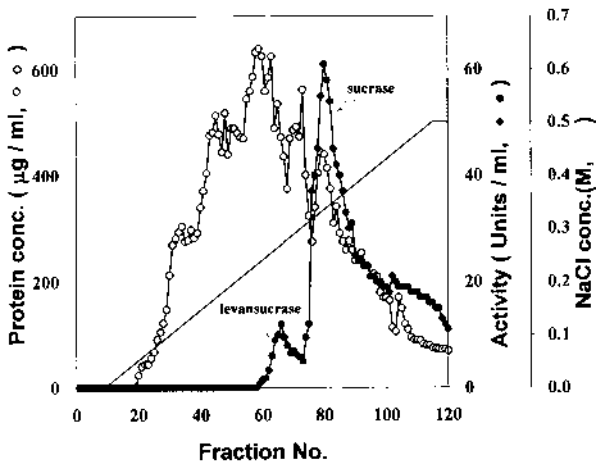

Figure 4 DEAE-anion exchange chromatogram of the extracellular saccharolytic enzymes of *Z. mobilis* ZM1. Cell washed solution from *Z. mobilis* ZM1 is put on the column (2.5 × 30 cm) pre-equilibrated with 20 mM phosphate buffer (pH 6.8), and eluted with NaCl gradient (0–0.5 M). Levansucrase activity is monitored by sucrose hydrolysis activity and the type of enzymes contained in fractions is monitored by electrophoresis and zymogram staining with TTC reagent. (From Ref. 24.)

A method monitoring the presence of sucrose-splitting enzymes has been developed using electrophoresis and zymogram staining with 2,3,5-triphenyltetrazolium chloride (TTC) reagent prior to purification (27). Levansucrase activity can be easily distinguished by the formation of a white and opalescent band. The use of periodic acid Schiff (PAS) reagent to stain levan formed by levansucrase on polyacrylamide gel has also been developed (28). Some enzymes form large aggregates in nature or during purification, causing the loss of enzymes and difficulties in purification. A small amount of unknown carbohydrates may be responsible for the formation of aggregates. This problem can be overcome by the treatment with Triton X-100 (29). In the case of the *Z. mobilis* enzyme, such aggregation is not observed during purification. To eliminate the copurification of other enzymes with sucrose-splitting activity, the levan formation activity is monitored using raffinose as a substrate, which does not normally serve as a substrate for glucosyltransferase or dextransucrase.

REFERENCES

1. RG Chambert, G Gonzy-Treboul, R Dedonder. Kinetic studies of levansucrase of *Bacillus subtilis*. Eur J Biochem 41:285, 1974.

2. RG Chambert, G Gonzy-Treboul. Levansucrase of *Bacillus subtilis*. Characterization of a stabilized frutosyl-enzyme complex and identification of an aspartyl residue as the binding site of the fructosyl group. Eur J Biochem 71:493, 1976.
3. KB Song, JW Seo, MK Kim, SK Rhee. Levansucrase from *Rahnella acquatilis*: gene cloning, expression and levan formation. Ann NY Acad Sci 864:506, 1998.
4. PJ Cheetham, AJ Hacking, M Vlitos. Synthesis of novel disaccharides by a newly isolated fructosyl transferase from *Bacillus subtilis*. Enzyme Micro Technol 11:212, 1989.
5. N Sprenger, K Bortlik, A Brand, T Boller, A Wiemken. Purification, cloning, and functional expression of sucrose:fructan 6-fructosyltransferase, a key enzyme of fructan synthesis in barley. Proc Natl Acad Sci USA 92:11652, 1995.
6. GAF Hendry. Evolutionary origins and natural functions of fructans–a climatological, biogeographic and mechanistic appraisal. New Phytol 123:3, 1993.
7. YW Han. Microbial levan. Adv Appl Microbiol 35:171, 1990.
8. F Kunst, G Rapoport. Salt stress is an environmental signal affecting degradative enzyme synthesis in *Bacillus subtilis*. J Bacteriol 177:2403, 1995.
9. KB Song, JW Seo, SK Rhee. Production of levan, a fructose polymer, using an overexpressed recombinant levansucrase. Ann NY Acad Sci 799:601, 1996.
10. MJM Ebskamp, I Van der Meer, BA Spronk, PJ Weisbeek, SJ Smeekens. Accumulation of fructose polymers in transgenic tobacco. Bio/Technology 12:272, 1994.
11. J Leibovici, Y Stark. Increase in cell permeability to a cytotoxic agent by the polysaccharide levan. Cell Mol Biol 31:337,1985.
12. GMT Calazans, CE Lopes, RMOC Lima, FP de Franca. Antitumor activities of levans produced by *Zymomonas mobilis* strains. Biotechnol Lett 19:19, 1997.
13. BH Chung, WK Kim, KB Song, CH Kim, SK Rhee. Novel polyethylene glycol/levan aqueous two-phase system for protein partitioning. Biotechnol Lett 11:327, 1997.
14. H Murakami, T Kuramoto, K Mizutani, H Nakano, S Kitahata. Purification and some properties of a new levanase from *Bacillus* sp. No. 71. Biosci Biotech Biochem 56:608, 1992.
15. K Saito, A Yokoda, F Tomita. Molecular cloning of levan fructotransferase gene from *Arthrobacter nicotinovarans* GS-9 and its expression in *Escherichia coli*. Biosci Biotech Biochem 61:2076, 1997.
16. JW Yun. Fructooligosaccharides—occurrence, preparation, and application. Enzyme Microb Technol 19:107–117, 1996.
17. MG Kim, JW Seo, KB Song, CH Kim, BH Chung, SK Rhee. Levan and fructosyl derivatives formation by a recombinant levansucrase from *Rahnella acquatilis*. Biotechnol Lett 20:333, 1998.
18. KB Song, HK Joo, SK Rhee. Nucleotide sequence of levansucrase gene (*levU*) of *Zymomonas mobilis* ZM1(ATCC 10988). Biochim Biophys Acta 1173:320, 1993.
19. J Ariesta, L Hernandez, A Coego, V Suarez, E Balmori, C Menendez, M Petit-Glatron, R Chambert, G Selman-Housein. Molecular characterization of the levansucrase gene from the endophytic sugarcane bacterium *Acetobacter diazotrophicus* SRT4. Microbiology 142:1077, 1996.
20. R Chambert, MF Petit-Glatron. Polymerase and hydrolase activities of *Bacillus subtilis* levansucrase can be separately modulated by site-directed mutagenesis. Biochem J 279:35, 1991.
21. R Dedonder. Levansucrase from *Bacillus subtilis*. Methods Enzymol 8:500, 1966.
22. L Hernandez, J Arrieta, C Menendez, R Vazquez, A Coego, V Suarez, G Selman, M Petit-Glatron, R Chambert. Isolation and enzymatic properties of levansucrase secreted by *Acetobacter diazotrophicus* SRT4, a bacterium associated with sugarcane. Biochem J 309:113, 1995.
23. W Jäger, A Schäfer, A Pühler, G Labes, W Wohlleben. Expression of the *Bacillus subtilis sacB* gene leads to sucrose sensitivity in the gram-positive bacterium *Corynebacterium glutamicum* but not in *Streptomyces lividans*. J Bacteriol 174:5462, 1992.
24. KB Song, JW Seo, HK Joo, SK Rhee. Purification and characterization of an extracellular levansucrase from *Zymomonas mobilis* ZM1(ATCC10988). Kor J Appl Microbiol Biotechnol 26:309, 1998.
25. RG Crittenden, HW Doelle. Identification and characterization of the extracellular sucrases of *Zymomonas mobilis* UQM 2716 (ATCC 39676). Appl Microbiol Biotechnol 41:302, 1994.
26. MJ Pabst, JO Cisar, CL Trummel. The cell wall–associated levansucrase of *Actinomyces viscosus*. Biochim Biophys Acta 556:274, 1979.
27. P O'Mullan, M Szakacs-Dobozi, DE Eveleigh. Identification of saccharolytic enzymes of *Zymomonas mobilis* CP4. Biotechnol Lett 13:137, 1991.
28. AW Miller, JF Robyt. Direction of dextransucrase and levansucrase on polyacrylamide gels by the periodic acid-Schiff stain: staining artifacts and their prevention. Anal Biochem 156:357, 1986.
29. MF Petit-Glatron, R Chambert, M Steinmetz. Levansucrase of *Bacillus subtilis*. Characterization of a form isolated from phenol-treated cells and activated by Triton X-100. Eur J Biochem 103:189, 1980.

49

Cyclodextrin Glycosyltransferase

Lubbert Dijkhuizen and Bart A. van der Veen
University of Groningen, Haren, The Netherlands

I. INTRODUCTION

Cyclodextrin glycosyltransferase (CGTase) is a member of the α-amylase family of glycoside hydrolases (family 13) (1). Enzymes of this family display a wide diversity in reaction specifications, catalyzing at least 18 different reactions. Whereas amylases generally hydrolyze α(1-4) glucosidic bonds in starch molecules, CGTases mainly catalyze transglycosylation reactions. Structure/function relationships in the α-amylase family have been studied extensively, clarifying the mechanistic basis of the unique activities of CGTase (2–5).

Starch and derived linear or cyclic oligosaccharides are substrates in the CGTase-catalyzed reactions. Starch consists of two types of glucan polymers: amylose and amylopectin. Potato starch for instance consists of 20% amylose and 80% amylopectin. Amylose consists mainly of linear chains of α(1-4)-linked glucose residues. Amylopectin is a highly branched α(1-4) glucan polymer (approximately α(1-6) linkage per 20 glucose residues).

Figure 1 shows an overview of enzymes of various families active on starch (amylopectin in this case). Many starch-degrading enzymes are hydrolytic, cleaving the linkages in starch; the cleavage product subsequently reacts with water, resulting in a new reducing end. These enzymes can be roughly divided into amylases, hydrolyzing α(1-4) linkages, and debranching enzymes, hydrolyzing α(1-6) linkages. Examples of debranching enzymes are isoamylase (EC 3.2.1.68) and pullulanase (EC 3.2.1.41), both members of family 13. Amylases can be further subdivided into endo- and exoacting enzymes. A typical endoacting enzyme is α-amylase (EC 3.2.1.1), cleaving α(1-4) bonds randomly in the starch molecule, producing (branched) oligosaccharides of various lengths. Exoacting amylases such as β-amylase (EC 3.2.1.2, family 14 of glycoside hydrolases) cleave α(1-4) bonds at the nonreducing end of the starch molecule and hence produce only low-molecular-weight products from starch (mostly glucose or maltose). Most of these enzymes are incapable of bypassing α(1-6) linkages; degradation of branched substrates therefore remains incomplete, leaving high-molecular-weight compounds (limit dextrins). In enzymes also able to cleave α(1-6) linkages—for instance, glucoamylase (EC 3.2.1.3, family 15 of glycoside hydrolases) and α-glucosidase (EC 3.2.1.20)—this reaction is slow compared to hydrolysis of α(1-4) bonds.

CGTase (EC 2.4.1.19) is a unique member of the α-amylase family. Its main products when acting on starch are cyclodextrins and highly branched high-molecular-weight dextrins (CGTase limit dextrins). CGTase has been identified in bacteria belonging to the genera *Bacillus, Clostridium, Klebsiella, Micrococcus, Thermoanaerobacter*, and *Thermoanaerobacterium* (6), and in a single archaeon, *Thermococcus* (7). CGTase is present as an extracellular enzyme and functions in the initial attack on this polymeric substrate. These bacteria subsequently use the cyclodextrins produced as carbon and energy

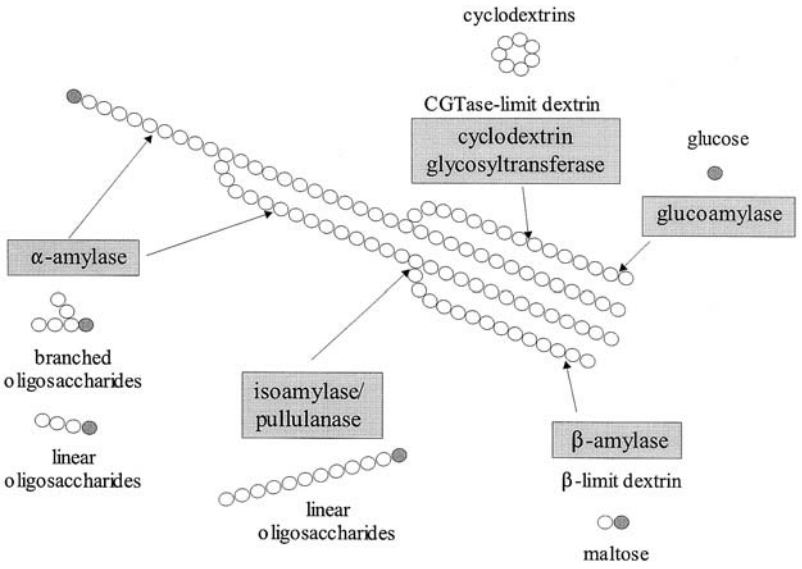

Figure 1 Action of enzymes involved in the degradation of starch. (●) Glucose molecule with a reducing end; (○) glucose molecule without a reducing end. Arrows indicate preferred cleaving point on the starch molecule. (From Ref. 70.)

sources for growth. This involves a cell-associated cyclomaltodextrinase (EC 3.2.1.54), yielding glucose, maltose, and maltotriose (8). Glucose is metabolized intracellularly via glycolysis.

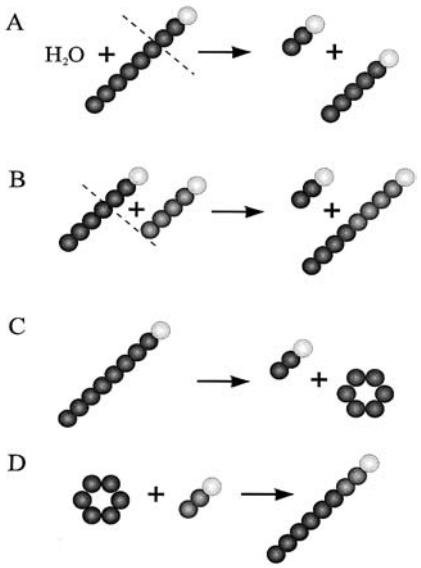

Figure 2 Schematic representation of the CGTase-catalyzed reactions. Circles represent glucose residues; the white circles indicate the reducing end sugars. (A) hydrolysis; (B) disproportionation; (C) cyclization; (D) coupling. (From Ref. 65.)

CGTase enzymes generally display only a relatively low starch hydrolytic activity (Fig. 2A). They mainly catalyze transglucosylation reactions that can be described as: $G(n) + G(m) \rightarrow G(n - x) + G(m + x)$, in which G(n) is the donor and G(m) the acceptor oligosaccharide consisting of n and m residues, respectively. Disproportionation (Fig. 2B) can be regarded as the default reaction, and is also catalyzed by several other members of the α-amylase family (e.g., 4-α-glucanotransferase, EC 2.4.1.25). The specific CGTase catalyzed reaction is the cyclization reaction (Fig. 2C) in which the part of the donor that has been cleaved off also acts as the acceptor, resulting in formation of a cyclodextrin. This reaction can be described as: $G(n) \rightarrow$ cyclic $Gx + G(n - x)$. The reverse reaction, coupling, is also catalyzed by the enzyme (Fig. 2D).

II. APPLICATIONS OF CGTASE

The cyclodextrins produced by CGTases from starch via the cyclization reaction provide the basis for most of the applications of CGTase in the food industry. The CGTase-catalyzed coupling and disproportionation reactions, allowing synthesis of modified oligosaccharides from starch or cyclodextrins and alternative acceptor substrates, are drawing increasing attention as well. Applications of CGTase limit dextrins are also being explored.

Cyclodextrins are torus-shaped molecules of cyclic α(1-4)-linked oligosaccharides mainly consisting of six, seven, or eight glucose residues (α-, β-, or γ-cyclodextrin, respectively) (Fig. 3). In cyclodextrins the secondary hydroxyl groups (C2 and C3) are located on the wider edge of the ring, and the primary hydroxyl groups (C6) on the other edge; the apolar C3 and C5 hydrogens and etherlike oxygens are on the inside of the toruslike molecules. This results in a molecule with a hydrophilic outside, which can dissolve in water, and an apolar cavity, which provides a hydrophobic matrix, described as a "microheterogeneous environment" (9). Cyclodextrins form inclusion complexes with a wide variety of hydrophobic guest molecules. One or two guest molecules can be entrapped by one, two, or three cyclodextrins (10). The most important parameter for complex formation with hydrophobic compounds or functional groups is their three-dimensional form and size. The driving force is the entropic effect of displacement of water molecules from the cavity (11). Another possibility is that this water causes strain on the cyclodextrin ring, which is released after complexation, producing a more stable, lower energy state (9, 11). Other parameters for complexation are charge or polarity of the guest compound and competition with other molecules from the medium. Because the inclusion complexes are quite stable, they can be separated from the medium by crystallization (12). Entrapment in cyclodextrins often results in changes in the chemical and physical properties of the guest molecules, suitable for applications in the food industry. Numerous other cyclodextrin applications, outside the scope of this review, are in analytical chemistry, agriculture, and the pharmaceutical field (5).

In the food industry, cyclodextrins find a range of applications. Cyclodextrins have a texture-improving

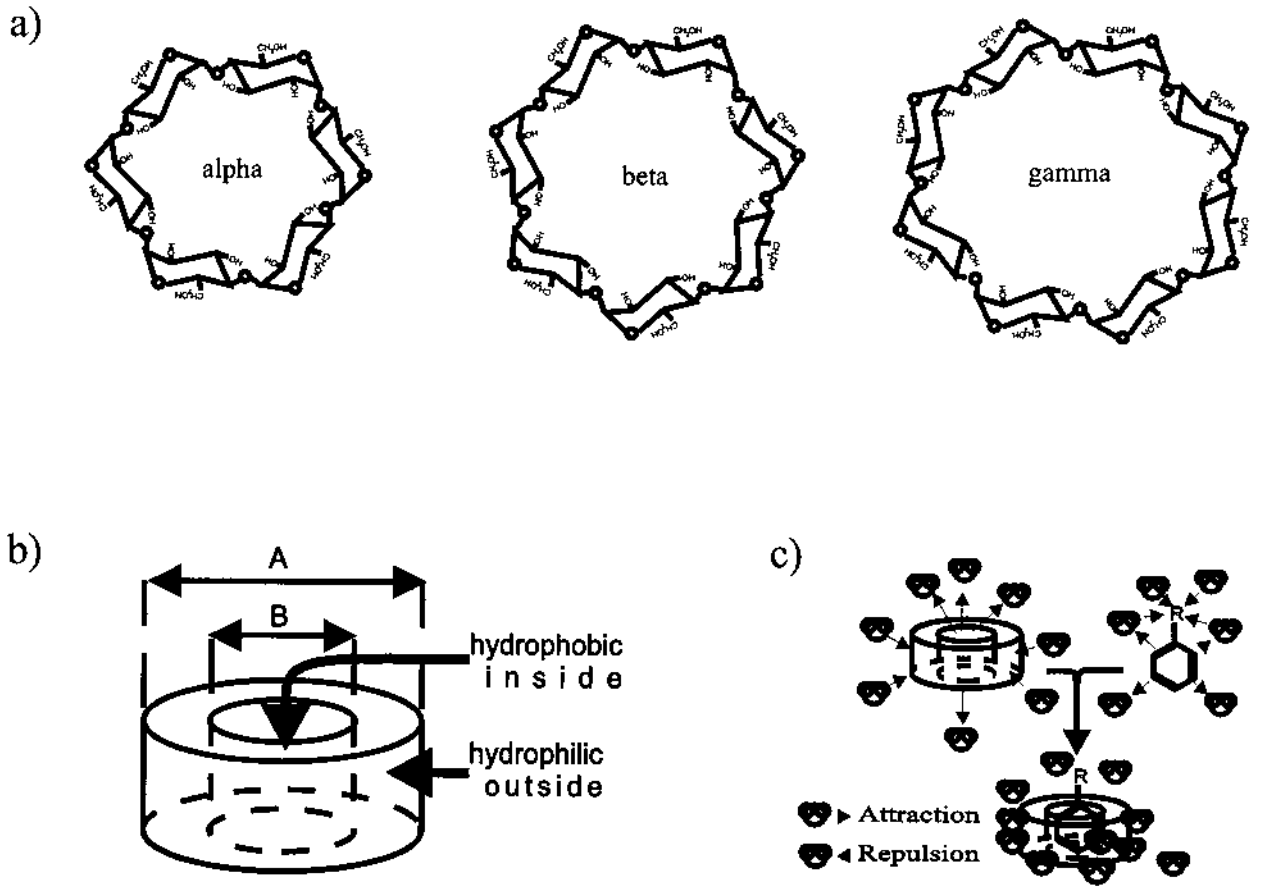

Figure 3 Structure and properties of cyclodextrins. (a) α-, β-, and γ-cyclodextrins; (b) 3D form and properties of cyclodextrins; a: 14.6, 15.4, and 17.5 Å for α-, β-, and γ-cyclodextrins, respectively; b: 4.7–5.3, 6.0–6.5, 7.5–8.3 Å for α-, β-, and γ-cyclodextrins, respectively; (c) formation of inclusion complexes of cyclodextrins and hydrophobic molecules. (From Ref. 71.)

effect on pastry and on meat products. They reduce bitterness, ill smell, and bad taste, and stabilize flavors when subjected to long-term storage. Emulsions in mayonnaise, margarine, or butter creams are stabilized with β-cyclodextrin. Furthermore, β-cyclodextrin is used to remove cholesterol from milk, yielding dairy products low in cholesterol. Marketed products involve reduced cholesterol egg yolks (Simply Eggs) by Michael Foods in the United States, cholesterol-reduced butter under *Natural* and *Ballade* trademarks by Entremont in France and Corman in Belgium, and a range of flavored salts (*Compack*) in Hungary (13). CGTase is also used in preparation of doughs for baked products; its incorporation into doughs was claimed to increase the volume of the baked product (14).

Conversion of amylose by CGTase not only yields cyclodextrins but initially also larger-size cyclic α(1-4)-glucans with a degree of polymerization ranging from nine to > 60 (15). Similar observations have been made with *B. stearothermophilus* branching enzyme (16) and potato disproportionating enzyme (17). These new starch structures combine various interesting properties—low viscosity, high solubility, and a high molecular weight—and are expected to find applications in the food industry (18).

The CGTase coupling and disproportionation reactions allow synthesis of a range of novel glycosylated compounds from starch or cyclodextrins as donor substrates and various acceptor molecules (19–21). A commercial example is glycosylation of the intense sweetener stevioside. This bitter compound is isolated from leaves of the plant *Stevia rebaudiana*; it has a low solubility. Glycosylation decreases bitterness and increases solubility (6).

Like most starch-degrading enzymes, the CGTase from *B. macerans*, which is used for the commercial production of cyclodextrins (22), is poorly active on native starch with its well-organized granular structure held together by internal hydrogen bonds. Heating in water (jet cooking) weakens these hydrogen bonds and causes swelling and gelatinization (23), resulting in a very viscous starch solution when performed at starch concentrations of industrial interest. This initial processing step is performed at temperatures up to 105-110°C, and α-amylase is added in order to liquefy the starch to make it suitable for incubation at the lower temperatures (55°C) required for the CGTase-catalyzed production of cyclodextrins. Unfortunately, the α-amylase used for liquefaction produces maltodextrins, which will act as acceptor molecules in the coupling reaction catalyzed by CGTase, severely reducing cyclodextrin yields (6). More recently, CGTases have been characterized from thermophilic anaerobic bacteria belonging to the genera *Thermoanaerobacter* (12, 24) and *Thermoanaerobacterium* (25) which are active and stable at high temperatures and low pH values and are able to solubilize starch, thereby eliminating the need for α-amylase pretreatment without any traces of low-molecular-weight oligosaccharides produced in the initial stages of the reaction (26). The use of these thermostable CGTases has the added advantage that the total cyclodextrin production time can be shortened (6). The *Thermoanaerobacter* CGTase (maximal activities at 90°C and pH 5.8) found commercial application in 1996.

III. CGTASE PROTEIN PROPERTIES

At present, at least 38 CGTases have been identified and purified, and the corresponding genes characterized. They are all monomeric enzymes, generally 680–685 amino acids in size, yielding molecular weights of ~ 75 kDa. CGTases show a clear similarity in amino acid sequence, ranging from 47% to 99% homology.

Enzymes of the α-amylase family share only ~ 30% overall amino acid sequence similarity. Four highly conserved regions have been identified in members of this family (Fig. 4). All four regions contain completely invariant amino acid residues within the α-amylase family, and the functions of most of these have been elucidated by x-ray crystallography, site-directed mutagenesis, and chemical modification of various members of this family. These residues are directly involved in catalysis, either through substrate binding, bond cleavage, transition state stabilization, or as ligands of a calcium-binding site present near the active site. Three carboxylic acid groups, one glutamic acid and two aspartic acid residues, are essential for catalytic activity in α-amylases and CGTases (Asp229, Glu257, and Asp328 in CGTase from *B. circulans*) (27, 28). Two conserved histidine residues, His140 and His327 (CGTase numbering), are involved in substrate binding and transition state stabilization (29, 30). A third histidine, present only in some α-amylases and CGTases (His233), is involved in substrate binding and acts as a calcium ligand with its carbonyl oxygen (31, 32). Arg227 is important for the orientation of the nucleophile (Asp229; see below) (30). The role of Asp135 is not clear, but it is in close proximity to the catalytic site. Asn139 again is a calcium ligand.

In contrast to the limited similarity observed in a primary structure, the three-dimensional structures of

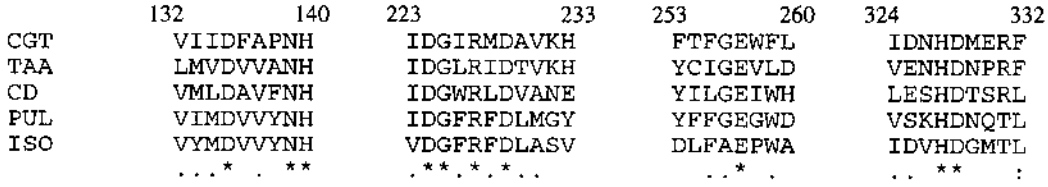

Figure 4 Amino acid sequence alignment of the four conserved regions in members of the α-amylase family. TAA: α-amylase, *Aspergillus oryzae* (Taka-amylase A) (33); CGT: CGTase, *Bacillus circulans* strain 251 (31); CD: cyclodextrinase, *Klebsiella oxytoca* (72); PUL: pullulanase, *Klebsiella aerogenes* (73); ISO: isoamylase, *Pseudomonas amyloderamosa* (74). The residues are numbered according to the CGTase from *B. circulans* strain 251. An asterisk indicates amino acid identity; a dot indicates amino acid similarity.

α-amylases (33) and CGTases (31, 34–37) are quite similar. α-Amylases generally consist of three structural domains, A, B, and C, while CGTases show a similar domain organization with two additional domains, D and E (Fig. 5). Domain A contains a highly symmetrical fold of eight parallel β-strands arranged in a barrel encircled by eight α-helices. This so-called $(\beta/\alpha)_8$-or TIM-barrel catalytic domain of 300–400 residues is present in all enzymes of the α-amylase family (38). The $(\beta/\alpha)_8$ barrel was first found in the structure of chicken muscle triose phosphate isomerase (39), but it has been shown to be widespread in functionally diverse enzymes (40). Several prolines and glycines flanking loops connecting the β-strands and α-helices have been found to be highly conserved in these enzymes (41). The catalytic and substrate-binding residues conserved in the α-amylase family are located in loops at the C-terminal of β-strands in domain A. The loop between β-strand 3 and α-helix 3 of the catalytic domain is rather large and is regarded as a separate structural domain. This B-domain consists of 44–133 amino acid residues and contributes to substrate binding. The C-domain is $\sim$ 100 amino acids long and has an antiparallel η-sandwich fold. Domain C of the CGTase from *B. circulans* strain 251 contains one of the maltose-binding sites (MBS) observed in the structure derived from maltose-dependent crystals (see below) (31). This MBS is involved in raw starch binding (42); the C-domain thus contributes in substrate binding. This C-domain may determine bond specificity, since in enzymes hydrolyzing or forming α(1,6) bonds (e.g., pullulanase, isoamylase, branching enzyme) the A-domain is followed by a different domain (Fig. 5) (43). The D-domain is $\sim$ 90 amino acids in size and is almost exclusively found in CGTases; it carries an immunoglobulin fold but its function remains unknown. The E-domain is more widespread in starch degrading enzymes. In enzymes of the α-amylase family it is present as the C-terminal domain; in glucoamylases (family 15 of glycoside hydrolases) it is attached to the C- or N-terminus of the catalytic domain via a glycosylated linker (Fig. 5). The E-domain consists of $\sim$ 110 amino acids and is responsible for the adsorption of the enzyme onto granular starch (see below).

All CGTases studied not only catalyze the three transglycosylation reactions but also display hydrolytic activity (Fig. 2). Incubation of CGTase with starch thus may not only yield cyclodextrins but also linear products. In some cases this has resulted in misidentification of CGTase enzymes. The *Thermoanaerobacterium thermosulfurigenes* EM1 CGTase was initially identified as an α-amylase because of its relatively high hydrolytic activity (44). Further studies showed that it possesses a clear cyclization activity, as in other CGTases; amino acid alignments with other CGTases also show a high overall sequence similarity, with all five domains present (25). The CGTase converts starch not only into cyclodextrins (35%) but also into linear sugars (11%) (45). In contrast, the CGTase from *B. circulans* strain 251 has minor hydrolytic activity; this enzyme exclusively forms cyclodextrins (46).

Recently the 3D structure of the *Bacillus stearothermophilus* "maltogenic" α-amylase Novamyl has been determined (47). Unlike the conventional α-amylases of family 13, Novamyl exhibits the five-domain structure associated with CGTase enzymes (Fig. 5, G2A). Its overall sequence similarity with CGTase is high, and the 3D structures are very similar. Most interestingly, Novamyl contains a 5 amino acid residue insertion in the B-domain, partially enclosing the active site at the –3 subsite. The absence of this insertion in CGTases allows for additional subsites, with up to –7 characterized crystallographically (32). Novamyl thus is either an α-amylase or a CGTase with unusual properties. Studies of evolutionary relationships within the α-amylase family have provided evidence that

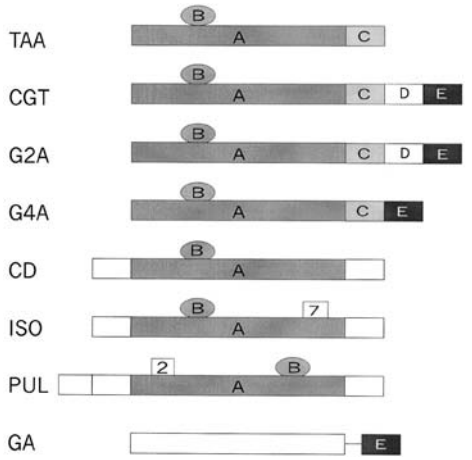

Figure 5 Domain level organization of starch degrading enzymes. CGT: CGTase, *Bacillus circulans*; G2A: maltogenic α-amylase, *Bacillus stearothermophilus*; G4A: maltotetraose forming α-amylase, *Pseudomonas stutzerl*; TAA: α-amylase, *Aspergillus oryzae* (Taka-amylase A); CD: cyclodextrinase, *Klebsiella oxytoca*; ISO: isoamylase, *Pseudomonas amyloderamosa*; PUL: pullulanase, *Klebsiella aerogenes*: GA: glucoamylase (family 15 of glycoside hydrolases) from *Aspergillus niger*. (From Ref. 43.)

CGTase enzymes evolved from α-amylases (48). Novamyl may thus be an example of an enzyme at an intermediary stage in between "true" α-amylases and "true" CGTases. It appears more likely, however, that Novamyl is a "true" CGTase with a few essential mutations modifying product specificity.

IV. PROPERTIES OF CGTASE ENZYMES

A. Catalytic Mechanism of the α-Amylase Family

The reactions catalyzed by CGTase and other enzymes of the α-amylase family proceed with retention of the substrate's anomeric (α-)configuration. Since each substitution at a chiral center results in inversion of configuration, catalysis must proceed through a double displacement reaction (49). The first step involves a protonation of the glycosidic oxygen by a general acid catalyst, creating an oxocarbonium transition state which subsequently collapses into an intermediate (50–52). This intermediate is attacked by a water nucleophile (or the C4-OH at the nonreducing end of another oligosaccharide in case of transglycosylases, e.g., CGTase) in the second step, assisted by the base form of the acid catalyst. The mechanistic roles of the three carboxylic amino acids in CGTase have been clarified by x-ray crystallographic studies with acarbose, a potent pseudotetraose inhibitor, bound in the active site (28). Glu257 (CGTase numbering) is the general acid catalyst, acting as proton donor; Asp229 serves as the nucleophile, stabilizing the intermediate; and Asp328 has an important role in substrate binding. For retaining enzymes the intermediate either could be an oxocarbonium ion which is electrostatically stabilized by a carboxylate, or involves formation of a covalent bond, in which one of the catalytic aspartates is presumed to act as a nucleophile. Although initially the nature of the intermediate was disputed, it is now generally accepted that the reaction proceeds via a covalent intermediate. Clear evidence for a covalent glycosylenzyme intermediate in family 13 has been obtained from rapid trapping studies with natural substrates. Low-temperature ^{13}C NMR experiments have provided evidence for the formation of a β-carboxylacetal ester covalent adduct between maltotetraose and porcine pancrease α-amylase (53). Conclusive evidence recently came from experiments involving trapping of a covalent intermediate with 4-deoxymaltotriosyl α-fluoride as a substrate in the virtually inactive Glu257Gln mutant of *B. circulans* 251 CGTase (54) and the x-ray crystallographic structure of the enzyme with the covalently linked intermediate (30).

B. Substrate Binding in CGTases

The first important step in enzyme catalysis is binding of the substrate. In several starch-degrading enzymes a separate domain responsible for adsorption onto raw starch has been found. Evidence for a starch-binding site in CGTases separate from the active site was presented (55), and fusion of the E-domain of the *Bacillus macerans* CGTase to β-galactosidase demonstrated that it can indeed function as a starch-binding domain (56). The function of the E-domain has been studied in more detail with the *B. circulans* strain 251 CGTase. High concentrations of maltose are required for crystallization of this protein (57). Three maltose-binding sites (MBS) were observed at the protein surface, two of which (MBS1 and MBS3) contribute to intermolecular crystal contacts. MBS1 and MBS2 are both located on the E-domain, suggesting a role in the raw starch-binding function of this domain (31). Indeed, mutational studies revealed that MBS1 is important for (raw) starch binding, while MBS2 assists in guiding the linear starch chains into the active site via a groove at the surface of the CGTase protein (see below) (31, 42). These CGTase E-domain MBS sites interact

strongly with cyclodextrins and oligosaccharides (58). Recent studies have revealed that the raw starch-binding domain also functions in the disruption of the structure of granular starch (59).

The A-domain contains the catalytic residues of CGTases, while domain B is involved in substrate binding. X-ray crystallographic studies have revealed a groove on the surface of these enzymes formed on one side by loops of the A-domain and on the other side by the B-domain. In crystal structures of CGTase from *B. circulans* strain 251 (31), where maltose molecules serve as contact points between the enzyme molecules in the crystals, the functionality of this groove in substrate binding has been shown nicely. From soaking experiments with the CGTase from *B. circulans* strain 251 the structure of this enzyme with a maltononaose inhibitor was obtained (Fig. 6), revealing in more detail the mode of substrate binding in the groove (32). The substrate binding sites are numbered +2 to −7 [numbering according to Davies et al. (60)], with the catalytic site between sites +1 and −1. The nonreducing end of the oligosaccharide is bound at subsite −7, which agrees with the formation of mainly β-cyclodextrin from starch by the enzyme. Factors determining cyclodextrin product specificity in CGTases are discussed in more detail by Van der Veen et al. (4). The glucose residue at subsite −7 is located at the end of the substrate binding groove, interacting with amino acid residues of the B-domain. The glucose residues bound at subsites +1 and −1 only interact with amino acids conserved in the whole α-amylase family.

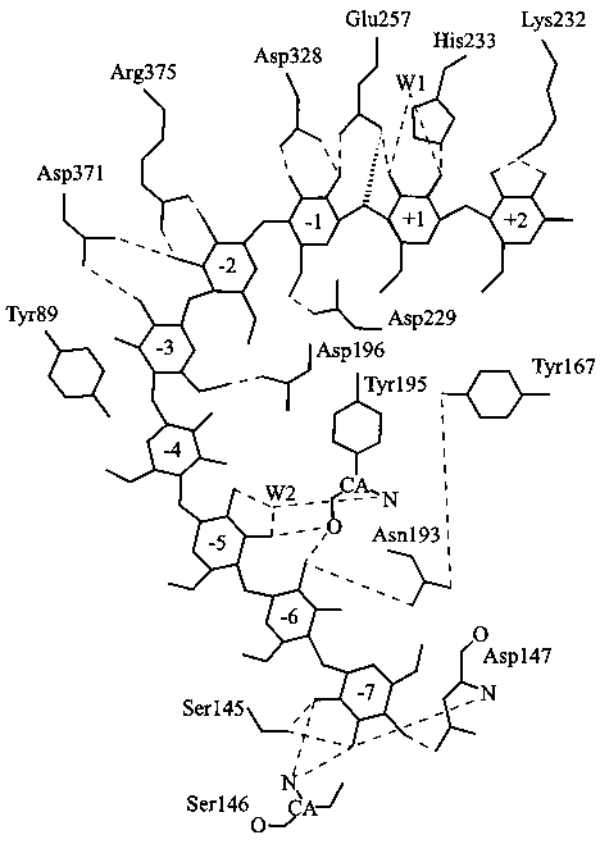

Figure 6 Schematic representation of the hydrogen bonds between the *Bacillus circulans* 251 CGTase and a maltononaose inhibitor bound at the active site. The subsites are numbered according to the general subsite labeling scheme recently proposed for all glycoside hydrolases (60). (From Ref. 32.)

C. Effects of pH and Temperature on CGTase Activity

CGTase enzymes have been found in both neutrophilic and alkaliphilic bacteria (6, 61, 62). The optimum pH for activity is generally around pH 5–6. CGTase of the alkaliphile *Bacillus* sp. 1011 also shows maximum activity at pH 5.5, but its pH activity profile is very broad; the activity at pH 8.0 is 90% of that at pH 5.5. The mutation Phe283Leu shifted the pH curve over both acidic and alkaline pH ranges (63). Mutant His327Asn has strongly reduced activity in the alkaline pH range, down to 30% of that at pH 5.5 (29). The low and the high slopes of the pH optimum curve of *T. thermosulfurigenes* EM1 CGTase clearly changed by mutations close to the catalytic residue Glu257, the proton donor in the first step of the cyclization reaction (45). The pH optimum curve of CGTase thus may be determined by the protonation state of Glu257. Changes in the environment of Glu257 before and after substrate binding can account for the broad pH optima of CGTase.

CGTase enzymes have been characterized from both mesophilic and thermophilic sources. The *Thermoanaerobacter* sp. (12) and *Thermoanaerobacterium thermosulfurigenes* (25) CGTases display maximal activities at 80–90°C and pH 5.5–6.0. The *Thermococcus* sp. strain B1001 CGTase has a temperature optimum at 90–100°C and a pH optimum at 5.0–5.5 (7). Substrate (starch) and calcium ions generally stabilize these enzymes. Fortunately, five different CGTase 3D structures have been solved (31, 34–37), with amino acid sequence similarities > 60%, of which two are thermostable enzymes. These structures were extensively compared by Knegtel et al. (36), in combination with biochemical

data, identifying many sites contributing to thermostability. Uitdehaag and Dijkstra (64) extended these studies, focusing on the atomic B factors in any of the five CGTase x-ray structures. They concluded that Nature has chosen a strategy of stabilizing flexible loops near the active site to develop more thermostable CGTase enzymes.

D. Kinetic Analysis of CGTase Transglycosylation Reactions

CGTase catalyzes three transglycosylation reactions (cyclization, coupling, disproportionation; Fig. 2) with starch and derived products. In the industrial production process for cyclodextrins, all three reactions participate in starch degradation and affect the overall efficiency and outcome of the process. Rational engineering of specific CGTases thus requires detailed knowledge of the kinetic mechanisms of the different reactions. The three transglycosylation reactions catalyzed by CGTase of *B. circulans* 251 have been analyzed in detail (65). Cyclization, coupling, and disproportionation all involve the same catalytic residues (Asp328, Glu257, and Asp229). The chemical mechanism of catalysis by CGTase is a double displacement reaction involving a covalent enzyme intermediate complex (30). Nevertheless, the transglycosylation reactions were found to proceed via different kinetic mechanisms. The kinetic data are summarized in Tables 1–3. Cyclization (cleavage of an α-glycosidic bond in amylose or starch and subsequent formation of a cyclodextrin) is a single-substrate reaction with an affinity for the high-molecular-weight substrate used (Paselli SA2, a starch derivative with an average degree of polymerization of 50) which was too high to allow elucidation of the kinetic mechanism. Michaelis-Menten kinetics, however, has been observed when using shorter amylose chains. The *B. circulans* 251 CGTase mainly produces β-cyclodextrin. Highest turnover rates were observed for this product. Coupling (cleavage of an α-glycosidic bond in a cyclodextrin ring and transfer of the resulting linear malto-oligosaccharide to the acceptor substrate methyl α-D-glucopyranoside [MaDG]) proceeds according to a random ternary complex mechanism. Thus, both substrates can bind simultaneously and in random order to the active site cleft of CGTase. This leads to two apparent affinity constants for cyclodextrins and acceptor, one in the absence (K_M) and one in the presence (K'_M) of the other substrate (see Table 2). Disproportionation (cleavage of an α-glycosidic bond of a linear malto-oligosaccharide and transfer of one part to an acceptor substrate), using 4-nitrophenyl-α-D-maltoheptaoside-4-6-)-O-ethylidene (EPS, a maltoheptasaccharide blocked at the nonreducing end and with a *p*-nitrophenyl group at its reducing end) as the donor molecule and maltose as the acceptor molecule, proceeds according to a Ping-Pong mechanism.

Despite the two-substrate character of the disproportionation reaction, its k_{cat} value is threefold higher than that for the cyclization reaction (Table 3). This may be explained by the involvement of merely linear substrates and products in the disproportionation reaction. Consequently, the reaction rates of cyclization and coupling should be determined by the rate at which the conformation changes from linear substrate to circular product and from circular substrate to linear product, respectively. This rate of conformational change presumably differs for the various cyclodextrins, explaining the variation in cyclization and cou-

Table 1 Cyclization Activities of CGTase from *Bacillus circulans* Strain 251

	α-Cyclization	β-Cyclization	γ-Cyclization
V_{max} (U/mg)	20 ± 2.0	276 ± 4.4	53 ± 3.1
k_{cat} (s^{-1})	25 ± 2.5	345 ± 5.5	66 ± 3.6

Source: Ref. 65.

Table 2 Kinetic Properties of the Coupling Reaction of CGTase from *Bacillus circulans* Strain 251

	α-CD coupling	β-CD coupling	γ-CD coupling
K_m^{CD} (mM)	2.2 ± 0.3	0.32 ± 0.02	0.13 ± 0.02
$K_m^{M\alpha DG}$ (mM)	0.45 ± 0.05	18.1 ± 1.4	16.6 ± 3.0
$K_m^{'CD}$ (mM)	5.3 ± 1.2	0.15 ± 0.04	0.12 ± 0.03
$K_m^{'M\alpha DG}$ (mM)	1.09 ± 0.26	8.25 ± 2.2	15.7 ± 6.1
V_{max} (U/mg)	192 ± 5.7	294 ± 7.6	150 ± 9.0
k_{cat} (sec^{-1})	240 ± 7.1	368 ± 9.5	188 ± 11.3

Source: Ref. 65.

Table 3 Kinetic Properties of the Disproportionation Reaction of CGTase from *Bacillus circulans* Strain 251

K_m^{EPS} (mM)	0.223 ± 0.015
$K_m^{maltose}$ (mM)	0.827 ± 0.050
V_{max} (U/mg)	970 ± 17.6
k_{cat} (sec^{-1})	1213 ± 22

Source: Ref. 65.

pling activities among the cyclodextrins. Also the rates of linearization and circularization for the individual cyclodextrins are different; especially, for α-cyclodextrin the rate of formation through cyclization is much lower than that of degradation through coupling (Tables 1–3). In view of the different kinetic mechanisms observed for the various reactions, which can be related to differences in substrate binding in the active site, it appears possible to mutagenize CGTase in such a manner that a single reaction is affected most strongly. This opens possibilities for the rational design of enzymes displaying specific activities. Recent work, based on the detailed knowledge of the active-site architecture, has led to the construction of CGTase mutants with enhanced α-cyclodextrin production (66). Current work involves rational design of mutants with decreased coupling activities and mutants with decreased transferase activities in favor of hydrolysis.

V. DETERMINATION OF CGTASE ACTIVITY

Since CGTase catalyzes four different reactions (see above), specific assays for the determination of the various activities have been developed. The assays described are used for *B. circulans* strain 251 CGTase, which requires incubation of appropriately diluted enzyme (0.1–0.2 units of specific activity for the specific reactions) at 50°C with substrate solutions in 10 mM sodium citrate (pH 6.0) (65).

Cyclization activity, resulting in formation of cyclodextrins, can be determined based on the ability of the different (α-, β-, γ-) cyclodextrins to form inclusion complexes with specific guest molecules. Paselli SA2, partially hydrolyzed potato starch with an average degree of polymerization of 50 (Avebe, Foxhol, Netherlands), is used as a substrate (up to 5% w/v). The Paselli SA2 solution is incubated in 10 mM citrate buffer (pH 6.0) for 10 min at 50°C before the reaction is started with appropriately diluted CGTase. At regular time intervals (0.25–0.5 min) 100-μL samples are taken and added to 900 μL specific detection reagent: phenolphthalein (67) or bromocresol green (68) for the detection of β- or γ-cyclodextrin, respectively. α-Cyclodextrin formation can be analyzed by complexation with Methyl Orange which is, however, not very specific and whose sensitivity is low. Therefore the use of high-performance liquid chromatography is preferred, using a 25-cm Econosphere NH_2 5-μm column (Alltech Associates) eluted with acetonitrile/water (60/40, v/v) at a flow rate of 1 mL/min. Since α-, β-, and γ-cyclodextrins are produced simultaneously from the starch substrate, the β-cyclodextrin formed (measured using the phenolphthalein method) can be used as an internal standard. One unit of activity is defined as the amount of enzyme able to produce 1 μmol of cyclodextrin per min.

Coupling activity, in which cyclodextrins (donor) are cleaved and the resulting linear oligosaccharide is linked to another (oligo)saccharide (acceptor), can be determined by measuring the amount of glucose present in the linear products formed. In this assay α-, β-, and γ-cyclodextrins are used as donors in the reaction; methyl α-D-glucopyranoside (MαDG) is used as acceptor substrate. This modified glucose does not react in the glucose detection reaction involving glucose oxidase, and therefore acceptor concentrations do not interfere with the activity measurements. Cyclodextrin and MαDG are incubated in 10 mM citrate (pH 6.0) for 10 min at 50°C before the reaction is started with appropriately dilute CGTase. At regular time intervals (0.5 min) 100-μL samples are added to 20 μL 1.2 N HCl (4°C) followed by incubation at 60°C for 10 min to inactivate the CGTase. Subsequently, the samples are neutralized with 20 μL 1.2 N NaOH and subjected to a 30-min incubation on ice with 60 μL (0.25 U) amyloglucosidase (EC 3.2.1.3; Sigma A-3514) in 167 mM NaAc (pH 4.5) to convert the products (linear oligosaccharides) to single glucose residues. The glucose concentration is determined with the glucose/GOD-Perid method (Boehringer Mannheim 124036). One unit of activity is defined as the amount of enzyme coupling of 1 μmol of cyclodextrin to MαDG per min.

Disproportionation activity can be measured using 4-nitrophenyl-α-D-maltoheptaoside-4-6-O-ethylidene (EPS) as a donor substrate and glucose or malto-oligosaccharides as acceptor substrate. EPS is a maltoheptasaccharide blocked at the nonreducing end and with a *p*-nitrophenyl group at its reducing end, which is generally used for the detection of amylase activity. The reaction mixtures are incubated for 10 min at 50°C before the reaction is started with appropriately diluted CGTase. At regular time intervals (0.5 min) 100-μL samples are added to 20 μL 1.2 N HCl (4°C) followed by incubation at 60°C for 10 min to inactivate the CGTase. Subsequently, the samples are neutralized with 20 μL of 1.2 N NaOH and incubated for 60 min at 37°C with 60 μL (1 unit) α-glucosidase (E.C.3.2.1.20; Boehringer Mannheim Biochemica 1630385) in 833 mM potassium phosphate (pH 7.0) to liberate *p*-nitrophenol from the product of the disproportionation reaction, nonblocked linear oligosac-

charide. The pH of the samples is raised above 8 by adding 1 mL of 1 M sodium carbonate, and the absorbance at 401 nm is measured ($\epsilon_{401} = 18.4\,\text{mM}^{-1}$). One unit of activity is defined as the amount of enzyme converting 1 μmol of EPS per min.

VI. PURIFICATION OF CGTASE

CGTase enzymes occur extracellularly, making purification relatively easy. The method used has been developed for *B. circulans* strain 251 wild-type CGTase enzyme and involves expression of the *cgt* gene in *B. subtilis*, which also excretes the enzyme (42). Production strains are grown in a batch fermentor to an optical density at 600 nm of 11–13 (for ~ 24 h). Under these conditions high extracellular CGTase levels generally are produced. Cultures are centrifuged at 4°C for 30 min $\times$ 16,000g and (mutant) CGTases present in the supernatants are further purified to homogeneity by affinity chromatography, using a 30-mL α-cyclodextrin Sepharose-6FF column (Pharmacia, Sweden) (69) with a maximal capacity of 3.5 mg protein/mL. After washing with 10 mM sodium acetate buffer (pH 5.5), bound CGTase is eluted with the same buffer containing 10 mg/mL α-cyclodextrin. This allows purification to homogeneity of up to 100 mg of stable (mutant) CGTase proteins, with a fivefold purification and a yield close to 90%, from 1-1 culture supernatants.

REFERENCES

1. PM Coutinho, B Henrissat. Carbohydrate active enzymes. At Url: http://afmb.cnrs-mrs.fr/~pedro/CAZY/db.html. 1999.
2. L Dijkhuizen ,D Penninga, HJ Rozeboom, B Strokopytov, BW Dijkstra. Protein engineering of cyclodextrin glycosyltransferase from *Bacillus circulans* strain 251. In: SB Petersen, B Svensson, S Pedersen, eds. Carbohydrate Bioengineering. Amsterdam: Elsevier Science, 1995, pp 165–174.
3. L Dijkhuizen, BA van der Veen, JCM Uitdehaag, BW Dijkstra. Engineering of cyclodextrin glycosyltransferase. In: Recent Advances in Carbohydrate Bioengineering. Proc 3rd Carbohydrate Bioengineering Meeting. Newcastle. London: Chemical Society, 1999, pp 263–266.
4. BA van der Veen, JCM Uitdehaag, BW Dijkstra, L Dijkhuizen. Engineering of cyclodextrin glycosyltransferase reaction and product specificity. Biochim Biophys Acta Protein Structure and Molecular Enzymology 1543:336–360, 2000.
5. RD Wind. Starch-converting enzymes from thermophilic microorganisms. Ph.D. Thesis. University of Groningen, 1997.
6. S Pederson, L Dijkhuizen, BW Dijkstra, BF Jensen, ST Jorgensen. A better enzyme for cyclodextrins. Chemtech 25:19–25, 1995.
7. Y Tachibana, A Kuramura, N Shirasaka, Y Suzuki, T Yamamoto, S Fujiwara, M Takagi, T Imanaka. Purification and characterization of an extremely thermostable cyclomaltodextrin glucanotransferase from a newly isolated hyperthermophilic archaeon, a *Thermococcus* sp. Appl Environ Microbiol 65:1991–1997, 1999.
8. H Bender. Purification and characterization of a cyclodextrin degrading enzyme from *Flavobacterium* sp. Appl Microbiol Biotechnol 39:714–719, 1993.
9. W Saenger. Structural aspects of cyclodextrins and their inclusion complexes. In: JL Atwood, JED Davies, DD MacNicol, eds. Inclusion Compounds. London: Academic Press, 1984, pp 231–259.
10. G Wenz. Cyclodextrins as building blocks for supramolecular structures and functional units. Angew Chem Int Ed 33:803–822, 1994.
11. W Saenger. Cyclodextrin inclusion compounds in research and industry. Angew Chem 19:344–362, 1980.
12. RL Starnes. Industrial potential of cyclodextrin glycosyl transferases. Cereal Foods World 35:1094–1099, 1990.
13. M Allegre, A Deratani. Cyclodextrin uses: from concept to industrial reality. Agro Food Indust Jan/Feb:9–17, 1994.
14. JH van Eijk, JHGM Mutsaers. Bread improving composition. Patent EP1995000201378 (1995).
15. Y Terada, M Yanase, H Takata, T Takaha, S Okada. Cyclodextrins are not the major cyclic alpha-1,4-glucans produced by the initial action of cyclodextrin glucanotransferase on amylose. J Biol Chem 271:15729–15733, 1997.
16. H Takata, T Takaha, S Okada, M Takagi, T Imanaka. Cyclization reaction catalyzed by branching enzyme. J Bacteriol 178:1600–1606, 1996.
17. T Takaha, M Yanase, H Takata, S Okada, SM Smith. Potato D-enzyme catalyzes the cyclization of amylose to produce cycloamylose, a novel cyclic glucan. J Biol Chem 271:2902–2908, 1996.
18. T Imanaka. Glucan having cyclic structure and method of producing same. Patent EP0710674A2 (1994).
19. T Kometani, Y Terada, T Nishimura, H Takii, S Okada. Transglycosylation to hesperidin by cyclodextrin glucanotransferase from an alkalophilic *Bacillus*

species in alkaline pH and properties of hesperidin glycoside. Biosci Biotechnol Biochem 58:1990–1994, 1994.
20. T Kometani, Y Terada, T Nishimura, T Nakae, H Takii, S Okada. Acceptor specificity of cyclodextrin glucanotransferase from an alkalophilic *Bacillus* species and synthesis of glucosyl rhamnose. Biosci Biotechnol Biochem 60:1176–1178, 1996.
21. T Kometani, T Nishimura, T Nakae, H Takii, S Okada. Synthesis of neohesperidin glycosides and naringin glycosides by cyclodextrin glucanotransferase from an alkalophilic *Bacillus* species. Biosci Biotechnol Biochem 60:645–649, 1996.
22. S Riisgaard. The enzyme industry and modern biotechnology. In: C Christiansen, L Munck, J Villadsen, eds. Proceedings of the 5th European Congress on Biotechnology. Copenhagen: Munksgaard International Publishers, 1990, pp 31–40.
23. P Nigam, D Singh. Enzyme and microbial systems involved in starch processing. Enzyme Microb Technol 17:770–778, 1995.
24. BE Norman, ST Jorgensen. *Thermoanaerobacter* sp. CGTase its properties and application. Denpun Kagaku 39:101–108, 1992.
25. RD Wind, W Liebl, RM Buitelaar, D Penninga, A Spreinat, L Dijkhuizen, H Bahl. Cyclodextrin formation by the thermostable α-amylase of *Thermoanaerobacterium thermosulfurigenes* EM1 and reclassification of the enzyme as a cyclodextrin glycosyltransferase. Appl Environ Microbiol 61:1257–1265, 1995.
26. RL Starnes, CL Hoffman, VM Flint, PC Trackman, DJ Duhart, DM Katkocin. Starch liquefaction with a highly thermostable cyclodextrin glycosyl transferase from *Thermoanaerobacter* species. In: RB Friedman, ed. Enzymes in Biomass Conversion, ACS Symposium Series. Washington: American Chemical Society, 1991, pp 384–393.
27. C Klein, J Hollender, H Bender, GE Schulz. Catalytic center of cyclodextrin glycosyltransferase derived from x-ray structure analysis combined with site-directed mutagenesis. Biochemistry 31:8740–8746, 1992.
28. B Strokopytov, D Penninga, HJ Rozeboom, KH Kalk, L Dijkhuizen, BW Dijkstra. X-ray structure of cyclodextrin glycosyltransferase complexed with acarbose. Implications for the catalytic mechanism of glycosidases. Biochemistry 34:2234–2240, 1995.
29. A Nakamura, K Haga, K Yamane. Three histidine residues in the active center of cyclodextrin glucanotransferase from alkalophilic *Bacillus* sp. 101: Effects of the replacement of pH dependence and transition-state stabilization. Biochemistry 32:6624–6631, 1993.
30. JCM Uitdehaag, R Mosi, KJ Kalk, BA van der Veen, L Dijkhuizen, SG Withers, BW Dijksra. X-ray structures along the reaction pathway of cyclodextrin glycosyltransferase elucidate catalysis in the α-amylase family. Nature Struct Biol 6:432–436, 1999.
31. CL Lawson, R van Montfort, B Strokopytov, HJ Rozeboom, KH Kalk, GE de Vries, D Penninga, L Dijkhuizen, BW Dijkstra. Nucleotide sequence and x-ray structure of cyclodextrin glycosyltransferase from *Bacillus circulans* strain 251 in a maltose-dependent crystal form. J Mol Biol 236:590–600, 1994.
32. B Strokopytov, RMA Knegtel, D Penninga, HJ Rozeboom, KH Kalk, L Dijkhuizen, BW Dijkstra. Structure of cyclodextrin glycosyltransferase complexed with a maltononaose inhibitor at 2.6 Å resolution. Implications for product specificity. Biochemistry 35:4241–4249, 1996.
33. Y Matsuura, M Kusunoki, W Harada. Structure and possible catalytic residues of Taka-amylase A. J Biochem 95:697–702, 1984.
34. M Kubota, Y Matsuura, S Sakai, Y Katsube. Molecular structure of *B. stearothermophilus* cyclodextrin glucanotransferase and analysis of substrate binding site. Denpun Kagaku 38:141–146, 1991.
35. C Klein, GE Schulz. Structure of cyclodextrin glycosyltransferase refined at 2.0 Å resolution. J Mol Biol 217:737–750, 1991.
36. RMA Knegtel, RD Wind, HJ Rozeboom, KH Kalk, RM Buitelaar, L Dijkhuizen, BW Dijkstra. Crystal structure at 2.3 Å resolution and revised nucleotide sequence of the thermostable cyclodextrin glycosyltransferase from *Thermoanaerobacterium thermosulfurigenes* EM1. J Mol Biol 256:611–622, 1996.
37. K Harata, K Haga, A Nakamura, M Aoyagi, K Yamane. X-ray structure of cyclodextrin glucanotransferase from alkalophilic *Bacillus* sp. 1011. Comparison of two independent molecules at 1.8 Å resolution. Acta Crystallogr D Biol Cryst 52:1136–1145, 1996.
38. S Janeçek. Parallel β/α-barrels of α-amylase, cyclodextrin glycosyltransferase and oligo-1,6-glucosidase versus the barrel of β-amylase: evolutionary distance is a reflection of unrelated sequences. FEBS Lett 353:119–123, 1994.
39. DW Banner, AC Bloomer, GA Petsko, DC Phillips, CI Pogson, IA Wilson, PH Corran, AJ Furth, JD Milman, RE Offord, JD Priddle, SG Waley. Structure of chicken muscle triose phosphate isomerase determined crystallographically at 2.5 angstrom resolution using amino acid sequence data. Nature 255:609–614, 1975.
40. B Svensson, M Sogaard. Protein engineering of amylases. Biochem Soc Trans 20:34–42, 1991.
41. S Janeçek. Invariant glycines and prolines flanking in loops the strand beta 2 of various (alpha/beta)(8)-barrel enzymes: a hidden homology? Protein Sci 5:1136–1143, 1996.
42. D Penninga, BA van der Veen, RMA Knegtel, SAFT van Hijum, HJ Rozeboom, KH Kalk, BW Dijkstra, L

Dijkhuizen. The raw starch binding domain of cyclodextrin glycosyltransferase from *Bacillus circulans* strain 251. J Biol Chem 271:32777–32784, 1996.
43. HM Jespersen, EA Macgregor, MR Sierks, B Svensson. Comparison of the domain-level organization of starch hydrolases and related enzymes. J Biochem 280:51–55, 1991.
44. H Bahl, G Burchhardt, A Spreinat, K Haeckel, A Wienecke, B Schmidt, G Antranikian. α-Amylase of *Clostridium thermosulfurigenes* EM1: nucleotide sequence of the gene, processing of the enzyme, and comparison to other α-amylases. Appl Environ Microbiol 57:1554–1559, 1991.
45. RD Wind, JCM Uitdehaag, RM Buitelaar, BW Dijkstra, L Dijkhuizen. Engineering of cyclodextrin product specificity and pH optima of the thermostable cyclodextrin glycosyltransferase from *Thermoanaerobacterium thermosulfurogenes* EM1. J Biol Chem 273:5771–5779, 1998.
46. D Penninga, B Strokopytov, HJ Rozeboom, CL Lawson, BW Dijkstra, J Bergsma, L Dijkhuizen. Site-directed mutations in tyrosine 195 of cyclodextrin glycosyltransferase from *Bacillus circulans* strain 251 affect activity and product specificity. Biochemistry 34:3368–3376, 1995.
47. Z Dauter, M Dauter, AM Brzozowski, S Christensen, TV Borchert, L Beier, KS Wilson, GJ Davies. X-ray structure of Novamyl, the five-domain ''maltogenic'' α-amylase from *Bacillus stearothermophilus*: maltose and acarbose complexes at 1.7 Å resolution. Biochemistry 38:8385–8392, 1999.
48. S Janeçek. Tracing the evolutionary lineages among α-amylases and cyclodextrin glycosyltransferases: the question of so-called 'intermediary' enzymes. Biologia 50:515–522, 1995.
49. DE Koshland. Stereochemistry and the mechanism of enzymatic reactions. Biol Rev 28:416–436, 1953.
50. JD Mccarter, SG Withers. Mechanisms of enzymatic glycoside hydrolysis. Curr Opin Struct Biol 4:885–892, 1994.
51. JD McCarter, SG Withers, 5-Fluoro glycosides: a new class of mechanism-based inhibitors of both alpha- and beta-glucosidases. J Am Chem Soc 118:241–242, 1996.
52. HD Ly, SG Withers. Mutagenesis of glycosidases. Annu Rev Biochem 68:487–522, 1999.
53. BY Tao, PJ Reilly, JF Robyt. Detection of a covalent intermediate in the mechanism of action of porcine pancreatic α-amylase by using ^{13}C nuclear magnetic resonance. Biochim Biophys Acta 995:214–220, 1989.
54. R Mosi, SM He, J Uitdehaag, BW Dijkstra, SG Withers. Trapping and characterization of the reaction intermediate in cyclodextrin glycosyltransferase by use of activated substrates and a mutant enzyme. Biochemistry 36:9927–9934, 1997.
55. JR Villette, FS Krzewinski, PJ Looten, PJ Sicard, SJL Bouquelet. Cyclomaltodextrin glucanotransferase from *Bacillus circulans* E-192. 4. Evidence for a raw starch-binding site and its interaction with a beta-cyclodextrin copolymer. Biotechnol Appl Biochem 16:57–63, 1992.
56. BK Dalmia, K Schutte, ZL Nikolov. Domain E of *Bacillus macerans* cyclodextrin glucanotransferase: an independent starch-binding domain. Biotechnol Bioeng 47:575–584, 1995.
57. CL Lawson, J Bergsma, PM Bruinenberg, GE de Vries, L Dijkhuizen, BW Dijkstra. Maltodextrin-dependent crystallization of cyclomaltodextrin glucanotransferase from *Bacillus circulans*. J Mol Biol 214:807–809, 1990.
58. RMA Knegtel, B Strokopytov, D Penninga, OG Faber, HJ Rozeboom, KJ Kalk, L Dijkhuizen, BW Dijkstra. Crystallographic studies of the interaction of cyclodextrin glycosyltransferase from *Bacillus circulans* strain 251 with natural substrates and products. J Biol Chem 270:29256–29264, 1995.
59. SM Southall, PJ Simpson, HJ Gilbert, G Williamson, MP Williamson. The starch-binding domain from glucoamylase disrupts the structure of starch. FEBS Lett 447:58–60, 1999.
60. GJ Davies, KS Wilson, B Henrissat. Nomenclature for sugar-binding subsites in glycosyl hydrolases. Biochem J 321:557–559, 1997.
61. H Bender. Production, characterization and application of cyclodextrins. In: Advances in Biotechnological Processes. New York: Alan R. Liss, 1986, pp 31–71.
62. K Horikoshi. Alkaliphiles: some applications of their products for biotechnology. Microbiol Mol Biol Rev 63:735–750, 1999.
63. A Nakamura, K Haga, K Yamane. Four aromatic residues in the active center of cyclodextrin glucanotransferase from alkalophilic *Bacillus* sp. 1011: effects of replacements on substrate binding and cyclization characteristics. Biochemistry 33:9929–9936, 1994.
64. JCM Uitdehaag, BW Dijkstra. A strategy for engineering thermostability: the case of cyclodextrin glycosyltransferase. In: A Ballesteros, FJ Plou, JL Iborra, PJ Halling, eds. Progress in Biotechnology 15. Stability and Stabilization of Biocatalysts. Amsterdam: Elsevier Science, 1998, pp 317–323.
65. BA van der Veen, GJWM van Alebeek, JCM Uitdehaag, BW Dijkstra, L Dijkhuizen. The three transglycosylation reactions catalyzed by cyclodextrin glycosyltransferase from *Bacillus circulans* strain 251 proceed via different kinetic mechanisms. Eur J Biochem 267:658–665, 2000.
66. BA van der Veen, JCM Uitdehaag, D Penninga, GJWM van Alebeek, LM Smith, BW Dijkstra, L Dujkhuizen. Rational design of cyclodextrin glycosyltransferase from *Bacillus circulans* strain 251 to

increase α-cyclodextrin production. J Mol Biol 296:1027–1038, 2000.
67. M Vikmon. Rapid and simple spectrophotometric method for determination of microamounts of cyclodextrins. In: J Szejtli, ed. First Int Symp on Cyclodextrins, Budapest. Dordrecht: D. Reidel, 1982, pp 69–74.
68. T Kato, K Horikoshi. Colorimetric determination of γ-cyclodextrin. Anal Chem 56:1738–1740, 1984.
69. L Sundberg, J Porath. Preparation of adsorbents for biospecific affinity chromatography. J Chromatogr 90:87–98, 1974.
70. RD Wind. Starch-converting enzymes from thermophilic microorganisms. Ph.D. dissertation, University of Groningen, 1997.
71. D Penninga. Protein engineering of cylodextrin glycosyltransferase from *Bacillus circulans* strain 251. Ph.D. dissertation, University of Gronigen, 1996.
72. G Fiedler, M Pajatsch, A Bock. Genetics of a novel starch utilisation pathway present in *Klebsiella oxytoca*. J Mol Biol 256:279–291, 1996.
73. N Katsuragi, N Takizawa,Y Murooka. Entire nucleotide sequence of the pullulanase gene of *Klebsiella aerogenes* W70. J Bacteriol 169:2301–2306, 1987.
74. A Amemura, R Chakraborty, M Fujita, T Noumi, M Futai. Cloning and nucleotide sequence of the isoamylase gene from *Pseudomonas amyloderamosa* SB-15. J Biol Chem 263:9271–9275, 1988.

50

Limonoid Glucosyltransferase

Shin Hasegawa
U.S. Department of Agriculture, Albany, California, U.S.A.

Masayuki Kita
National Institute of Fruit Tree Science, Tsukuba, Ibaraki, Japan

Mitsuo Omura
National Institute of Fruit Tree Science, Shimizu, Shizuoka, Japan

I. INTRODUCTION

Limonoids are a group of chemically related tetracyclic triterpenoids present in the plants of the Rutaceae and Meliaceae. As the bitter constituents in citrus juices, excessive limonoid levels lower the quality and value of citrus juices and have a significant negative economic impact on the citrus industry worldwide (1). However, limonoids have been shown to have anticarcinogenic activity in laboratory animals (2–5) and in cultured human breast cancer cells (6). Limonoids also have been shown to possess antifeedant activity against insects (7) and are excellent chemotaxonomic markers in the Rutaceae family plants (8). Hence, limonoids are important functional chemicals in the agriculture and food industries.

Intact citrus fruit tissues do not contain bitter limonin but contain the nonbitter precursor, limonoate A-ring lactone (LARL). In juice this precursor is gradually converted to limonin (9) (Fig. 1). This process proceeds under acidic conditions and is accelerated by the action of limonin D-ring lactone hydrolase (10). This phenomenon is generally referred to as "delayed bitterness."

Delayed bitterness is a problem in the early- to mid-season fruits, but not in the late-season fruit. As the fruit ripens, the concentration of LARL decreases. The mechanism of this natural debittering process was not determined until the discovery of limonoid glucosides in *Citrus* (11). As maturation progresses, limonoids are glucosylated to form nonbitter 17β-D-glucopyranoside derivatives (12). This reaction is catalyzed by limonoid glucosyltransferase (LGTase) (EC 2.4.1.–); UDP glucose:limonoid β-D-glucosyltransferase) (13).

A. Chemical Reaction Catalyzed

LGTase catalyzes the glucosylation of limonoid aglycones to form their respective 17β-D-glucopyranoside derivatives (12–14). Seventeen limonoid glucosides have been isolated from *Citrus* and its closely related genera (15). Each has a single glucose molecule attached to the 17-position of the limonoid molecule via a β-glucosidic linkage, such as limonin 17β-D-glucopyranoside (Fig. 1). The isolated enzyme from the albedo tissues of navel oranges takes both limonoate A-ring lactone and nomilinoate A-ring lactone as its substrates (13). This indicates that the enzyme is able to convert all limonoid aglycones present in *Citrus* sp. to their respective glucosides. Southern blot analysis of genomic DNA supports this observation—the gene for this enzyme is present only as a single copy in the citrus genome (16).

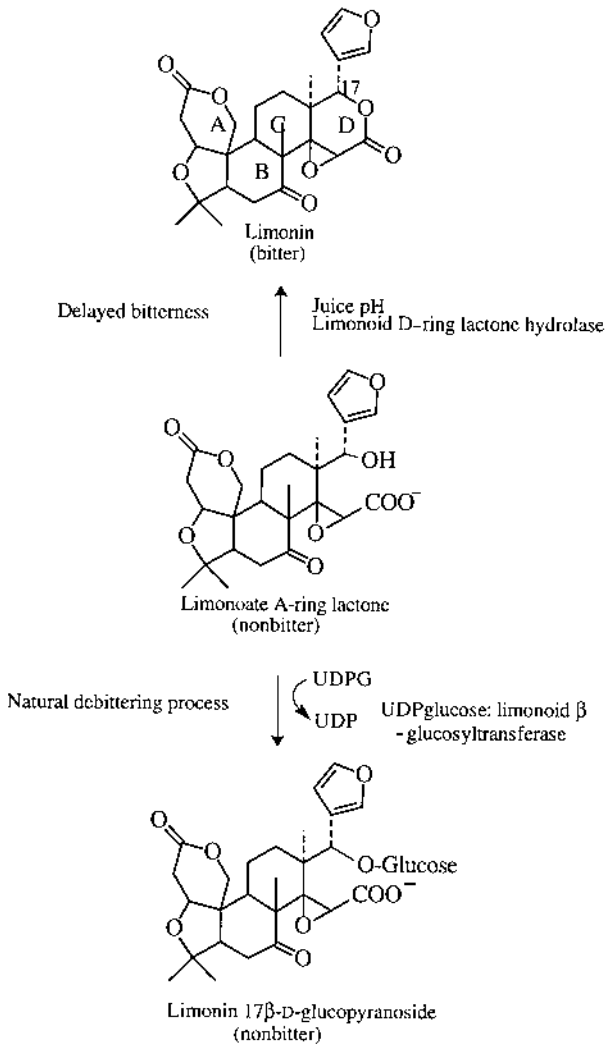

Figure 1 Mechanism of delayed bitterness in extracted citrus juice and the mechanism of glucosylation (a naturally occurring limonin debittering process) in *Citrus*.

B. Chemical Structures of Substrates

Limonoids are tetracyclic triterpenoid dilactones. Thirty-six limonoids have been isolated from *Citrus* and its closely related genera (15). An open D-ring is necessary for the glucosylation of limonoid aglycones to proceed via the LGTase reaction. In intact fruit tissue, limonoid aglycones are present in the open D-ring form, whereas in seeds they are present in both open and closed D-ring forms (1, 15). Alkaline conditions open the D-ring, whereas acidic conditions close it. The enzyme, limonoid D-ring lactone hydrolase catalyzes both the lactonization of the open D-rings and the hydrolysis of the D-ring lactones (10).

II. IMPORTANCE TO QUALITY OF CITRUS FRUIT AND PROCESSED PRODUCTS

Delayed bitterness lowers the quality and value of citrus juices. Also, under unusual conditions such as freezing or mechanical damage, the formation of the bitter forms of limonoids occurs even in the fruit tissues. Once the intact fruit tissues are disrupted, the mixture of acidic pH and limonin D-ring lactone hydrolase activity in the fruit tissues makes the conversion of limonoate A-ring (LARL) to limonin inevitable. Limonin bitterness is a major problem in the citrus industry world-wide and decreases the market value of citrus juices.

Limonin aglycones are glucosylated in the fruit tissues during late stages of fruit growth and maturation (12, 14). Figure 2 shows the changes in LARL and limonin glucoside (LG) content of California-grown navel orange during fruit growth and maturation (12). The glucosylation of LARL begins in September and continues until the fruit is harvested which begins in November. Juice from fruit harvested in November and December has a serious delayed bitterness problem due to the incomplete conversion of LARL to the glucosides. In Valencia orange, glucosylation of aglycones also begins in September and is able to continue until fruit is harvested beginning in March (14). The Valencia orange has an additional 4 months of maturation time over that of the navel orange. During this extra time, the aglycones are almost completely converted to the tasteless glucosides. As a result, the juice from Valencia orange

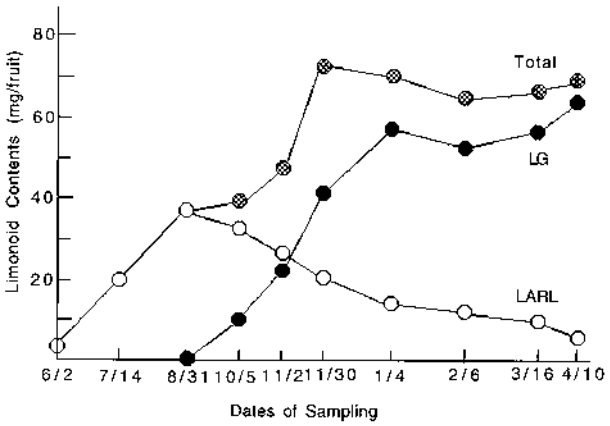

Figure 2 Changes in limonoate A-ring lactone (LARL) and limonoid glucoside (LG) contents of California-grown navel oranges during fruit growth and maturation. (From Ref 12.)

does not have the bitterness problem. Many winter citrus fruits including certain varieties of Murcott orange, Shamouti orange, Iyokan, grapefruit, Natsudaidai, pummelo, Melogold, and Oroblanco have a limonoid bitterness problem (1, 17, 18).

The rate of glucosylation of limonoid aglycones is influenced by a number of factors, but the presence of LGTase is vitally important. Any stimulation of this enzyme activity by bioregulation or genetic engineering should result in the earlier reduction of LARL concentrations via conversion to the glucoside form in the fruit tissue, and consequently reduce or eliminate limonin bitterness.

III. LGTase ACTIVITY IN COMMERCIAL CITRUS

Mandarin orange, pummelo, and citron are believed to be the three original species of *Citrus* (19). The other species and varieties are the result of centuries of natural and artificial breeding. Mandarins and citrons tend to have relatively high levels of LGTase activity, while pummels have relatively low levels. Consequently, pummelo juices, for instance, extracted from fruits harvested very late in the season have a severe limonoid bitterness problem (17). Sweet oranges, hybrids of mandarin oranges, in general have relatively high levels of LGTase activity and consequently contain high concentrations of limonoid glucosides (20). In contrast, hybrids such as grapefruit and the new varieties Oroblanco grapefruit and Melogold grapefruit more closely resemble the pummelo and have low levels of this enzyme activity (17, 18).

IV. UTILIZATION OF LGTase

An attractive approach to solving the bitterness problem at the present is through the use of genetic engineering techniques. LGTase was chosen for genetic manipulation to create transgenic citrus trees that produce fruits free from limonin bitterness. The insertion of multiple copies of a constitutively controlled gene encoding for LGTase into commercial cultivars may result in enhancing the conversion of LARL to LG (Fig. 2) and may prevent the accumulation of significant levels of any LARL at time of early season harvest. This enhancement of the LGTase activity in transgenic plants may also increase the concentration of limonoid glucosides in the fruit tissues, which are important constituents for human health and nutrition.

Limonoid aglycones are present in high concentrations in citrus seeds (1, 21). Isolated aglycones generally are water insoluble, and among 36 aglycones isolated from *Citrus* and its closely related genera, six are intensely bitter in taste (1, 22). Mass conversion of these aglycones to limonoid glucosides is pharmacologically an important future project. It would enhance the utilization of these byproducts of citrus juice processing. Limonoid glucosides are excellent candidates for new food additives as they provide anticarcinogenic activity. They are soluble in water and are practically tasteless. An approach would be to use transgenic *E. coli* cultures containing the LGTase gene to convert limonoid aglycones isolated from seeds into limonoid glucosides in fermentation tanks. The LGTase gene has been successfully expressed in *E. coli* (16).

V. ISOLATION OF THE LGTase GENE

Using a pair of degenerated oligonucleotide primers which were synthesized based on N-terminal and internal amino acid sequences of the purified LGTase isolated from albedo tissue of navel oranges, a cDNA clone encoding citrus LGTase has been isolated from Satsuma mandarin (*Citrus unshiu* Marc) (16) (Fig. 3). The isolated cDNA is 1732 bp in length encoding 511 amino acids with a predicted molecular mass of 57.5 kDa.

Figure 4 compares the amino acid sequences of the putative UDP-glucose binding domain of the LGTase gene with those of other glucosyltransferases (16). This region shows 43–68% identity in amino acid sequences to those of previously reported glucosyltransferases, indicating that the isolated clone conserves the features of the glucosyltransferase family. The coding region of the LGTase cDNA was ligated with an expression vector and transferred into *E. coli*. The transformed *E. coli* was grown and assayed for LGTase activity. The active protein fraction prepared from these cultures, when incubated with UDP-glucose and limonoate A-ring lactone, produced limonin glucoside.

Work is under way to transform and produce transgenic plants which express a constitutively controlled LGTase activity. It is hoped that the resulting transgenic citrus will produce fruit that is substantially free of LARL and delayed bitterness, but retain high levels of the limonoid glucosides.

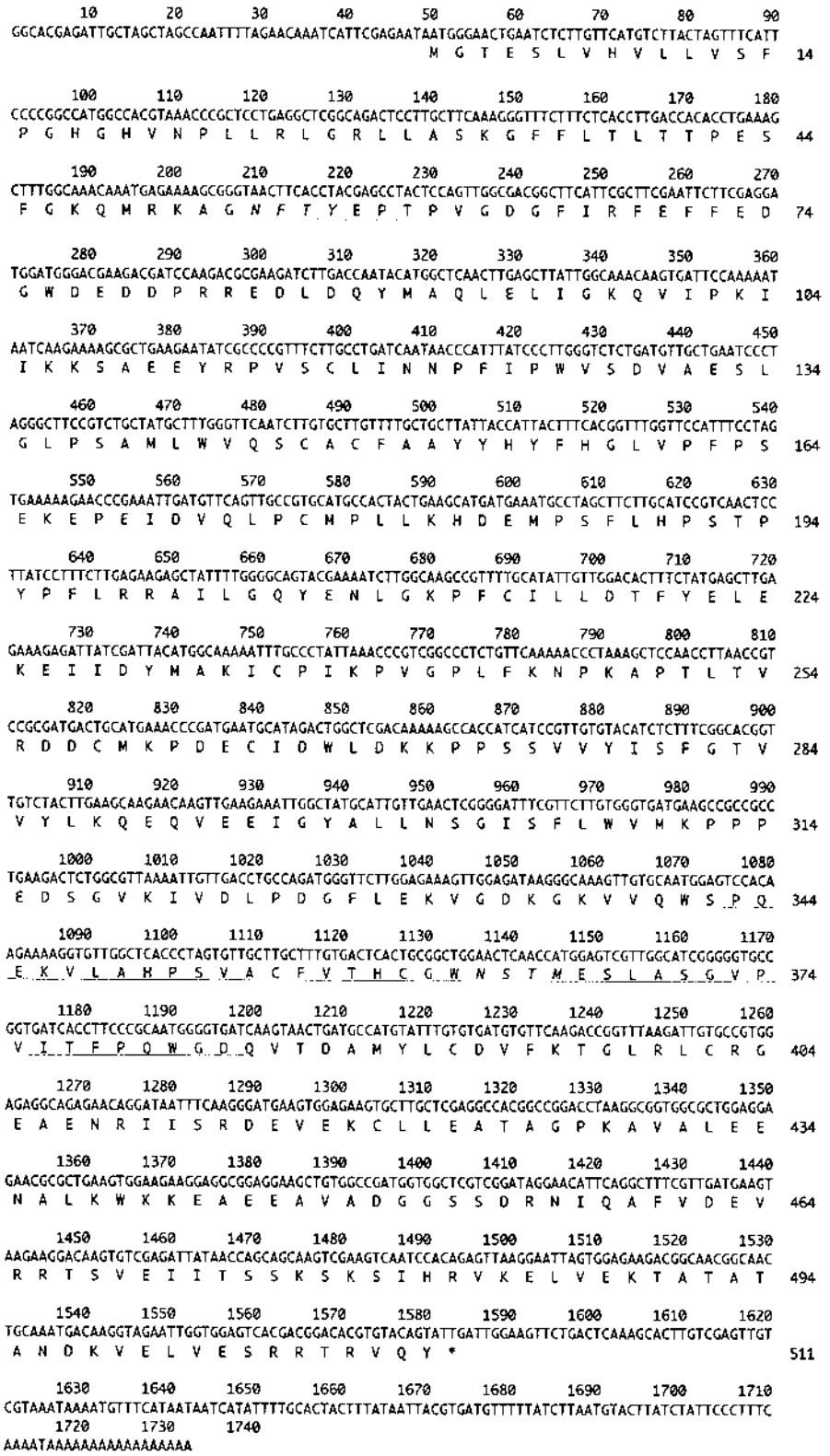

Figure 3 The nucleotide sequence of the cDNA encoding LGTase. (From Ref. 16.)

```
CTLGT          WSPQEKVLAHPSVACFVTHCGWNSTMESLASGVPVITFPQWGDQ
STSGT          WVPQLTIMEHSATGGFMTHCGTNSVLEAITFGVPMITWPLYADQ
CASGT          WSPQIHIMSHPSVGVFLSHCGWNSVLESITAGVPIIAWPIYAEQ
IPFGT          WAPQVQVLSHPGVGAFVTHCGWNSTLEAISFGVCLICRPFYGDQ
IAAGT          WCDQFRVLNHRSIGCFVTHCGWNSTLESLVSGVPVVAFRQWNDQ
PLZGT          WAPQLEILSHSSTGGFMSHCGWNSCLESITMGVPIATWPMHSDQ
```

Figure 4 Comparison of the amino acid sequences of the UDP binding domain of LGTase. STSGT: solanidine UDP-glucosyltransferase from potato; CASGT: UDP-glucosyltransferase from cassava; IAAGT: IAA glucosyltransferase from *Arabidopsis thaliana*; IPFGT: flavonoid 3-O-glucosyltransferase from *Ipomoea purpurea*; PLZGT: zeatin O-glucosyltransferase from *Phaseolus lunatus*.

VI. PROPERTIES

A. Properties as Protein

SDS-PAGE reveals a single protein band having an apparent M_r of 56–58 kDa (13), in agreement with the estimated M_r from DNA sequencing data discussed above. LGTase is a single subunit enzyme. Glucosyltransferases from citrus sources that utilize flavonoids and other small molecules as substrates are generally single-subunit enzymes. Flavanone glucosyltransferase from pummelo leaves has a M_r of 52 kDa (23) and flavanone glycosyltransferase from grapefruit seeds has M_r of 54.9 kDa (24).

B. Properties as Enzyme

The enzyme displays broad activity between pH 6.5 and 9.0 with an optimal activity at pH 8.0. Activity below pH 6.5 is completely inhibited by a closed D-ring. The enzyme requires Mn^{2+} ion for its activity, and appears to be very sensitive to Cl^-. Partially purified enzyme placed into 50 mM Tris-HCl, pH 8, and stored at -80°C showed a complete loss of activity. Replacing Tris buffer with 10 mM Mes-KOH, pH 7, allowed frozen storage of the enzyme with full recovery of activity (13).

VII. QUALITATIVE AND QUANTITATIVE DETERMINATION OF ACTIVITY

LGTase activity can be assayed at pH 7.5 in a volume of 50–100 μL. The assay solution contains 100 μM UDP-glucose, 50 μM Mn^{2+}, and 39 μM [^{14}C]nomilinoate A-ring lactone. Assays are incubated at 34°C for 15–30 min. The reaction is terminated by adding 3 μL of 1 M HCl, which also closes the D-ring of the unreacted nomilinoate A-ring lactone. Aliquots of the enzyme reaction mixture are spotted on TLC plates and developed with EtOAc–MeEtCO–H_2O–HCOOH (5:3:1:1). In this solvent system the R_f for nomilin is 0.88 and that for nomilin glucoside is 0.42. The developed plates are scanned for radioactivity with a Berthold Automatic TLC-Linear Analyser, model LB 2832 (13).

Radioactive nomilin can be produced by feeding labeled acetate to stems of lemon seedlings (25). Fresh stems are cut to 1 cm length and fed with randomly labeled [^{14}C]Na-acetate. After 2 days of incubation with a continuous supply of water, up to 5% of the original activity is incorporated into nomilin.

Recently, a liquid chromatography–mass spectrometry (LC-MS) technique has been developed to analyze limonoids in levels as low as 40 pg (26). Thus, the method could be amended to include the use of unlabeled limonoid aglycones.

VIII. PURIFICATION

The albedo tissue of navel oranges is homogenized in buffer consisting of 50 mM Tris-HCl, pH 8.0, 5 mM DTT, 15 mM KCl, 0.5% PVP (w/v) using a Polytron at low-medium speed for 4 min. The resulting slurry is centrifuged at 8000g for 20 min. The supernatant is brought to 40% saturation $(NH_4)_2SO_4$ and stirred in a 0°C bath for 1 h. The precipitate is removed by centrifugation at 20,000g for 30 min. The supernatant is taken to 80% saturation with $(NH_4)_2SO_4$ and stirred in a 0°C bath for 1 h and the precipitate is collected by centrifugation as before.

The protein precipitate is redissolved in 10 mM Mes/KOH buffer, pH 7.0, containing 15 mM 2-mercaptoethanol and 50 μM $MnCl_2$ (Buffer A). The dissolved protein is desalted on PD-10 gel filtration column (Pharmacia), equilibrated with Buffer A. The desalted, buffer-exchanged sample is loaded onto a uridine 5′-diphosphoglucuronic acid affinity column (Sigma), having a 75-mL bed volume that is pre-equilibrated with Buffer A. The column is washed with

buffer and eluted with 10 mM UDP-glucose dissolved in Buffer A. Fractionation on a UDP-glucuronic acid affinity column results in a 55-fold increase in enzyme purification over the $(NH_4)_2SO_4$ fraction.

The active fractions are pooled and loaded onto an HPLC Bio-Gel TSK-IEX DEAE 5PW (75 × 7.5 mm) column (BioRad) which has been equilibrated with 50 mM Tris-HCl, pH 7, with 2 mM DTT (Buffer B). A linear salt gradient, 0–400 mM NaCl, is used to elute the column over a 20-min period at a flow rate of 1.0 mL/min using Buffer B. The active fractions are collected, diluted 10-fold into Buffer C (50 mM/Tris-HCl, pH 8, with 2 mM DTT), and loaded onto the above DEAE column and eluted with Buffer C with a linear NaCl gradient, 0–400 mM, over a 20-min period at a flow rate of 1 mL/min. This procedure results in a 452-fold increase in enzyme purification (13).

REFERENCES

1. VP Maier, RD Bennett, S Hasegawa. Limonin and other limonoids. In: S Nagy, P Shaw, MK Velduis, eds. Citrus Science and Technology. Westport, CT: Avi Publishing, 1977, pp 335–396.
2. LKT Lam,Y Li, S Hasegawa. Effects of citrus limonoids on glutathione S-transferase activity in mice. J Agric Food Chem 37:878–880, 1989.
3. LKT Lam, S Hasegawa. Inhibition of benzo(a)pyrene-induced forestomach neoplasia in mice by citrus limonoids. Nutr Cancer 12:43–47, 1989.
4. EG Miller, AP Gonzales-Sanders, AM Couvillon, JM Wright, S Hasegawa, LKT Lam. Inhibition of hamster buccal pouch carcinogenesis by limonin 17β-D-glucopyranoside. Nutr Cancer 17:1–7, 1992.
5. T Tanaka, H Kohno, K Kawabata, S Honjo, M Miyake, K Wada. Citrus limonoids obacunone and limonin inhibit the development of a precursor lesion, aberrant crypt foci for colon cancer in rats. In: MA Berhow, S Hasegawa, GD Manners, eds. Citrus Limonoids: Functional Chemicals in Agriculture and Foods. Washington: ACS Symposium Series 758, 2000, pp 145–163.
6. N Guthrie, K Moreley, S Hasegawa, GD Manners, T Vandenberg. Inhibition of human breast cancer cells by citrus limonoids. In: MA Berhow, S Hasegawa, GD Manners, eds. Citrus Limonoids: Functional Chemicals in Agriculture and Foods. Washington: ACS Symposium Series 758, 2000, pp 164–174.
7. AR Alford, KD Murray. Prospects for citrus limonoids in insect pest management. In: MA Berhow, S Hasegawa, GD Manners, eds. Citrus Limonoids: Functional Chemicals in Agriculture and Foods. Washington: ACS Symposium Series 758, 2000, pp 164–174.
8. MA Berhow, S Hasegawa, K Kwan, RD Bennett. Limonoids and the chemotaxonomy of *Citrus* and the Rutaceae family. In: MA Berhow, S Hasegawa, GD Manners, eds. Citrus Limonoids: Functional Chemicals in Agriculture and Foods. Washington: ACS Symposium Series 758, 2000, pp 212–229.
9. VP Maier, GD Beverly. Limonin monolactone, the nobitter precursor responsible for delayed bitterness in certain citrus juice. J Food Sci 33:488–492, 1968.
10. VP Maier, S Hasegawa, E Hera. Limonin D-ring lactone hydrolase. A new enzyme from citrus seeds. Phytochemistry 8:405–407, 1969.
11. S Hasegawa, RD Bennett, Z Herman, CH Fong, P Ou. Limonoid glucosides in *Citrus*. Phytochemistry 28:1717–1720, 1989.
12. S Hasegawa, P Ou, CH Fong, Z Herman, CW Coggins Jr, DR Atkin. Changes in the limonoate A-ring lactone and limonin 17β-D-glucopyranoside content of navel oranges during fruit growth and maturation. J Agric Food Chem 39:262–265, 1991.
13. S Hasegawa, CG Suhayda, WJ Hsu, GH Robertson. Purification of limonoid glucosyltransferase from navel orange albedo tissues. Phytochemistry 46:33–37, 1997.
14. CH Fong, S Hasegawa, CW Coggins Jr, DR Atkin, M Miyake. Contents of limonoids and limonin 17-β-D-glucopyranoside in fruit tissue of Valencia orange during fruit growth and maturation. J Agric Food Chem 40:1178–1181, 1992.
15. S Hasegawa, M Miyake. Biochemistry and biological functions of citrus limonoids. Food Rev Int 12:413–435, 1996.
16. M Kita, Y Hirata, T Moriguchi, T Endo-Inagaki, R Matsumoto, S Hasegawa, CG Suhayda, M Oumra. Molecular cloning and characterization of a novel gene encoding limonoid UDP-glucosyltransferase in *Citrus*. FEBS Lett 469:173–178, 2000.
17. H Ohta, S Hasegawa, Limonoids in pummelos [*Citrus grandis* (L.) Osbeck. J Food Sci 60:1284–1285, 1995.
18. WJ Hsu, M Berhow, GH Robertson, S Hasegawa. Limonoids and flavonoids in juices of Oroblanco and Melogold grapefruit hybrids. J Food Sci 63:57–60, 1997.
19. WT Swingle, PC Reece. The botany of *Citrus* and its wild relatives In: W Reuther, HJ Webber, LD Batchelor, eds. The Citrus Industry, Vol 1. Berkeley: University of California Press, 1967, pp 190–430.
20. CH Fong, S Hasegawa, Z Herman, P Ou. Limonoid glucosides in commercial citrus juices. J Food Sci 54:1505–1506, 1989.
21. S Hasegawa, RD Bennett, CP Verdon. Limonoids in citrus seeds: origin and relative concentration. J Agric Food Chem 28:922–925, 1980.

22. S Hasegawa, M Miyake, Y Ozaki, M Berhow. Limonin: a non-volatile bitter principle in citrus juices. In: W Pickenhagen, CT Ho, A Spanier, eds. The Contribution of Low- and Nonvolatile Materials to the Flavor of Foods. Carol Stream, IL: Allured Publishing, 1996, pp 137–148.
23. M Bar-Peled, E Lewinsohn, R Fluhr, J Gressel. UDP-rhamnose:flavanone-7-glucoside-2″-0-rhamnosyltransferase. J Biol Chem 266:20953–20959, 1991.
24. CA McIntosh, L Latchinian, RL Mansell. Flavanone-specific 7-0-glucosyltransferase activity in *Citrus paradisi* seedlings: purification and characterization. Arch Biochem Biophys 282:50–57, 1990.
25. S Hasegawa, RD Bennett, VP Maier. Biosynthesis of limonoids in citrus seedlings. Phytochemistry 23:1601–1603, 1984.
26. GD Manners, S Hasegawa, RD Bennett, RY Wong. LC-MS and NMR techniques for the analysis and characterization of citrus limonoids. In: MA Berhow, S Hasegawa, GD Manners, eds. Citrus Limonoids: Functional Chemicals in Agriculture and Foods. Washington: ACS Symposium Series 758, 2000, pp 40–59.

51

Transglutaminase

Chang-Rak Ha and Ichiro Iuchi
Sophia University, Tokyo, Japan

I. INTRODUCTION

Transglutaminase (TGase, EC 2.3.2.13, γ-glutamyl-peptide, amine-γ-glutamyl-transferase) is a class of enzymes that catalyze the acyl transfer between the γ-carboxyamine group of a peptide-bound glutamine residue and the primary amino group of various substrates in a calcium-dependent reaction.

TGase was first discovered in guinea pig liver and characterized by Waelsch and coworkers (1, 2), and identified as an enzyme catalyzing incorporation of polyamines into glutamine residues of proteins or peptides. Since then, the reaction of blood-clotting Factor XIII–catalyzing polymerization of fibrin has been found to be identical to that of the liver TGase. The reaction is also involved in keratinization of epidermis (3), hair formation (4), or copulatory plug formation (5). More recently, TGase has been implicated as a widely distributed enzyme that participates in various biological phenomena such as apoptosis (6), cell growth and differentiation (7), embryonic cell differentiation (8), retinoic acid–induced abnormalities of fish embryo during the early development (9), and fertilization envelope formation (10–15, 81).

There are some studies on TGase from an aspect of food science (16, 17). The TGase reaction must be closely related to the visco-elasticity of food materials such as meat and fish eggs.

A. Classification and Nomenclature of TGase

Classification and nomenclature of TGases have been traditionally based on the function of the TGase (blood coagulation Factor XIII), on cell, tissue, or organ containing the TGase (keratinocyte TGase, liver TGase, or prostate gland TGase), or subcellular distribution of the TGase (extracellular matrix TGase, cytosolic TGase, or membrane-bound TGase). Recently, some TGases have been frequently called by abbreviations such as TGase K (18) or C (19), and TGase 1 (3), 2 (34) or 3 (19, 20). However, these recent names are somewhat inadequate to classify the many TGases from various sources including bacteria and plants. Therefore, the traditional names will be used here.

B. Reaction Catalyzed by TGase

TGase catalyzes the following reactions.

1. Formation of ϵ-(γ-glutamyl) lysine isopeptide crosslinks between proteins or peptides, resulting in polymerization (Fig. 1).
2. Incorporation of amines into proteins or peptides. This reaction plays a role in deamination or amine fixation. (Fig. 2).
3. Formation of N,N-bis-(γ-glutamyl) derivative crosslinks (Glu-CONH-R-NHCO-Glu) between proteins or peptides. (Fig. 3) (21).

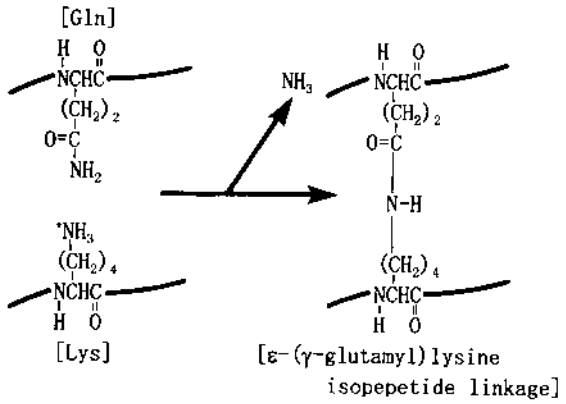

Figure 1 Formation of ϵ-(γ-glutamyl) lysine isopeptide crosslinks between proteins or peptides, resulting in polymerization.

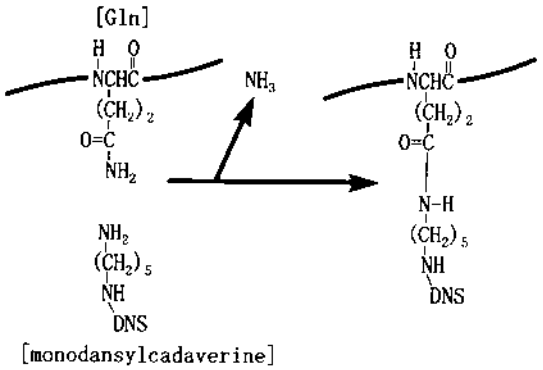

Figure 2 Incorporation of amines into proteins or peptides.

II. PROPERTIES AS PROTEIN

A. Physicochemical Properties of TGase

Properties of TGase as a protein are very variable from TGase to TGase. For example, liver TGase of guinea pig is monomeric and its molecular size is $\sim$ 75 kDa. On the other hand, human blood coagulation Factor XIII (300–350 kDa) consists of two A (or a) subunits where the catalytic site is located and two B (or b) subunits. Although more investigations are necessary, it seems reasonable to conclude that TGase belongs to a highly heterogeneous family or superfamily. Some characteristics of various TGases are shown in Table 1.

Isoelectric points of various TGases are somewhat variable. Using agarose gel electrophoresis at pH 7.4, human blood clotting Factor XIII and rat tissue TGase migrate toward the anode (22), while two isoforms of secretory TGase in rat prostate gland (coagulating gland) move toward the cathode (5, 23). Using isoelectric focusing, TGases in the crude extracts were focused at pH 7.8. On the contrary, the analysis of pure enzymes revealed an additional isoelectric point at pH 8.7 (5, 23). Rat testicular tissue TGase was focused at pH 5.25 (5). Isoelectric points of many TGases have not been accurately determined. However, they can be calculated from data of their amino acid compositions (24).

B. Primary Structure of TGase

The primary structures of various TGases have been predicted by nucleotide sequence analysis of cDNAs or genomic DNAs: blood coagulation Factor XIII [human, A subunit (25, 26); B subunit (27)'], keratinocyte TGase [rat (28); mouse (20)], rat prostate gland

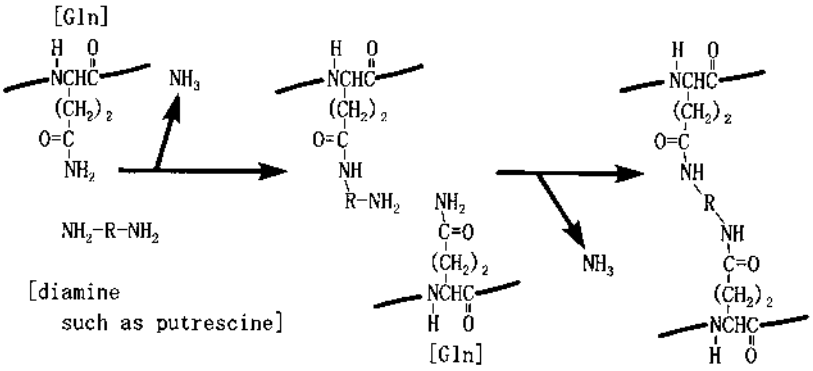

Figure 3 Formation of N,N-bis-(γ-glutamyl) derivative crosslinks between proteins or peptides.

Table 1 Some Characteristics of Various Transglutaminases (TGases)

Source (cell, tissue, organ, etc.)	Organisms	Molecular weight (daltons)	Natural substrate	Remarks	References
Blood plasma	Human		Fibrin, fibrinogen	Secretory TGase Factor XIII. Tetramer (A_2B_2; 300–350 kDa).	
				The A subunit has catalytic activity	25 26
(platelet)	Human	83231	Unknown	Zymogen form of Factor XIIIA. Dimer (A_2; 150 kDa).	
		75490	—	B subunit	27
Prostate gland	Rat	75471		Dorsal protein 1	29
			Secretion II protein.	Functions as a secretory TGase	*108
Egg envelope	Rainbow trout		Egg envelope	Extracellular matrix TGase	
P1	(*Oncorhynchus mykiss*)	82 and 76 kDa	subunit proteins (45, 56 and 65 kDa)		14
P2		76 kDa			13, 14
Keratinocytes	Human	89338		This group of TGases has been frequently called epidermal	18
			Ivolucrin	TGase or TGase K.	*109
			SKALP/Elafin		*110
(hair follicle)	Mouse	77276		TGase E, TGase 3	20
			Involucrin Small, proline-rich proteins (Cornifin B, SPR1B Cornifin A, SPR1A)		*111
Keratinocytes	Rat	90768	Involucrin Cornifin α		28
Tracheal epithelial cells	Rabbit	92 kDa (subunit)			112
			Cronifin α, β		*113
Liver	Guinea pig	77140	Unknown	This group of TGases has been frequently called tissue TGase or TGase C, and inhibited by nucleotides such as ATP and GTP.	33
Liver	Rabbit	80 kDa	Unknown		114
Liver	Rat	76889	Unknown		62
Liver	Red sea bream (*Pagrus major*)	78214	Unknown		39
Liver	Salmon (*Oncorhychus keta*)	75859	Unknown		40
Brain	Rat	75 kDa	Unknown	Tissue TGase, TGase C inhibited by GTP.	52
Brain					
(N1)	Rat	45 kDa	Unknown		115
(N2)		29 kDa	Unknown		
Macrophage	Mouse	77237	Unknown	Tissue TGase, TGase C	34
Lens	Rabbit	78 kDa	Crystallins	Not inhibited by GTP	116
Endothelial cells	Human	77256	Unknown	Tissue TGase, TGase C	34
Aortic and endothelial cells	Bovine	77111	Unknown		35
Erythrocyte	Human	76972	Unknown	Similar to band 4.2 proteins (pallidin)	30

(Continued)

Table 1 Continued

Source (cell, tissue, organ, etc.)	Organisms	Molecular weight (daltons)	Natural substrate	Remarks	References
Erythrocyte	Mouse	76738	Unknown	Pallidin	31
Erythrocyte	Chicken	78739	Unknown	Tissue TGase, TGase C	32
Muscle	Some fishes, shrimp, or molluscans	80–100 kDa	Probably muscle proteins		86
Mesenchyme cells	Embryo of an ascidian (*Ciona intestinalis*)	87193	Unknown	Tunica formation (?)	37
Hemocyte	Horseshoe crab (*Tachypleus tridentatus*)	87021	8.6-kDa protein	Membrane-bound TGase	38, 117
Boundary cells of limb segments of embryos	American grasshopper (*Schistocerca americana*)	85940	Unknown	Annulin	8
	Nematode (*Caenorhapditis elegans*)	61 kDa	Unknown	Involved in programmed cell death	66
Leaves	Soybean (*Glycine max*)	80 kDa	Unknown	Inhibited by GTP	53
	Slime mold (*Physarum polycephalum*)	77 kDa	Unknown	A probable role in the construction of spherules	54
		101 kDa	LAV1-2		65
	Bacteria (*Streptoverticillium mobaraense*)	42445	Unknown		118

The molecular weights of TGases were calculated from the amino acid sequences predicted from cDNAs or genomic DNAs. The molecular sizes (kDa) were those of the TGases isolated by ordinary biochemical methods. The complete sequences of them have not been determined. The asterisk in the column of References indicates the literature where only natural substrates for TGase are described.

TGase (29), erythrocyte band 4.2 [pallidin; human (30); mouse (31)], chicken erythrocyte tissue TGase (32), guinea pig liver TGase (33), mouse macrophage TGase (34), bovine aortic–endothelial cell TGase (35), chicken limb TGase (36), mesenchyme TGase of *Ciona intestinalis* embryo (37), *Limulus* hemocyte TGase (38), and TGase of grasshopper embryo [annulin (8)]. The amino acid sequences of liver TGases of fishes [red sea bream (39); a salmon, *Oncorhynchus keta* (40)] are available.

As shown in Figure 4, amino acid sequences of various TGases were aligned by the program CLUSTAL W ver 1.7 (41) in DNA Data Base of Japan (DDJB). The overall sequences of keratinocyte TGases, human blood clotting Factor XIIIA, and mesenchyme TGase of *Ciona intestinalis* embryo were 130–150, ~ 50, and ~ 60 amino acids longer than those of other vertebrate TGases, respectively. It may be predicted that they have a large insertion at the N-terminal regions, or at the C-terminal regions. In addition, the multiple alignment reveals that the sequence of a novel human TGase X or 5 is especially characteristic in a large deletion of about 90 amino acids at the N-terminal region and an insertion of about 50 amino acids near the central region.

We tentatively analyzed molecular phylogenetic relationships of various TGases of vertebrates. The human TGase X or 5 was removed from the analysis. In addition, the amino acids corresponding to gaps were removed from the analysis. A tree was constructed by the neighbor-joining method (42) using the program MEGA (43). The tree was rooted with

the sequence of the *Ciona* TGase (Fig. 5) or *Limulus* hemocyte TGase (data not shown). At least, five paralogous groups are definitely distinguishable in vertebrates; the groups of blood clotting Factor XIIIA, keratinocyte TGases, prostate gland TGases, erythrocyte membrane band 4.2 recently named "pallidin," and so-called tissue TGases.

A conserved amino acid sequence GQCWVF is found at the central region (e) panel of any sequence in Figure 4, which is deduced as a putative active site region for the TGase reaction. The cysteine residue in the motif is considered to be a catalytic site. However, the comparable site of the pallidin is GQAWVL for human and TQAWVS for mouse. Thus, pallidin is unique among them. The cysteine residue as a catalytic site is replaced by alanine residue. The pallidin has no TGase activity, and is considered to play a role in the regulation of erythrocyte shape and mechanical properties (30, 31). Elucidation of three dimensional structure of human blood clotting Factor XIIIA suggests that the catalytic site for its TGase activity is constructed from three residues, Cys314, His373, and Asp396 (44). Among the catalytic triad, the Cys314 corresponds to a cysteine residue in the motif GQCWVF. In addition, the His373 and the Asp396 in the Factor XIIIA are conserved in all TGase activity enzymes. However, the former is replaced by glutamine (Q) in human and mouse pallidins, the latter is by histidine (H) in mouse pallidin (Fig. 4).

The complete amino acid sequence of *Streptoverticillium* TGase has been determined (45). The TGase is a Ca^{2+}-dependent SH enzyme and contains a sole cysteine residue. The active site sequence of the TGase was predicted to be YGCVGV, which is highly homologous to that of thiol proteases such as papain and cathepsin H. The overall sequence is also significantly different from those of vertebrate TGases having the sequence GQCWVF as an active site.

Recently, three novel protein disulfide isomerases were cloned from the protozoan parasite *Giardia lamblia* (46). The enzymes are well known to be essential for forming disulfide bonds during nascent protein folding in the endoplasmic reticulum. Unlike other protein disulfide isomerases, the giardial enzymes have only one active site. The active-site sequence motif is CGHC characteristic of eukaryotic protein disulfide isomerases. Interestingly, all three enzymes have a Ca^{2+}-dependent TGase activity. There is another example like this. It has been clarified that TGase of heartworm *Dirofilaria immitis* (Filarial parasite of dog heart) has significant sequence similarity to well-characterized protein disulfide isomerases, not to any of known TGases (47).

Thus, the enzyme having TGase activity is not necessarily restricted to a distinct single type of enzyme. TGase is highly polymorphic in catalytic property, active site motif, and primary structure.

C. Three-Dimensional Structure of TGase

The three-dimensional structures of human blood coagulation Factor XIIIA and its zymogen have been determined by x-ray crystallography. The overall structure of the dimer A_2 is shown in Figure 6. The monomer molecule is characterized by the activation peptide from residues 1 to 37, domain 1 from 38 to 185, domain 2 from 197 to 503, domain 3 from 517 to 628, and domain 4 from 632 to 731. The connecting loops run between the domains (44, 48). Domain 1 (β-sandwich) contains almost exclusively β-structure consisting of two four-stranded β-sheets and forms an open barrel. Domain 3 (barrel 1) and 4 (barrel 2) contain seven β-strands and are topologically identical. Both domains interact closely with domain 2. Domain 2 (catalytic core) is constructed from a central six-stranded β-sheet, a second β-sheet of three strands, a β-hairpin, and a total of nine α-helical segments. The longest α-helix of 17 amino acid residues in the center of the molecule contains the active-site cysteine Cys314 constituting the above-mentioned motif GQCWVF. The other members of catalytic triad are His373 and Asp396. The catalytic triad is not accessible to solvent. The calcium is located in the core domain, near the surface of the protein.

The stereostructure of its catalytic site region is highly similar to that of cysteine proteinase, containing a cysteine at its catalytic site similarly to the TGase. A similar active site in the two different enzyme families catalzying a reaction in opposite directions suggests that the two enzymes are in a common evolutionary lineage (49). In addition, there is a recent report that cytosolic TGase of guinea pig liver and a coagulation factor XIIIA can hydrolyze the ϵ-γ linkage of ϵ-(γ-glutamyl) lysine isopeptides (129). TGase may play a dynamic role not only in promoting the formation of isopeptide bonds but also in the breaking of the bonds. The main calcium-binding site in each monomer involves the main chain oxygen atom of Ala457 and also the side chains from residues Asn436, Asp438, Glu485, and Glu490 (44).

In the processing of a zymogen to the mature form, an amino terminal activation peptide consisting of 37 residues is cleaved by thrombin and is released from

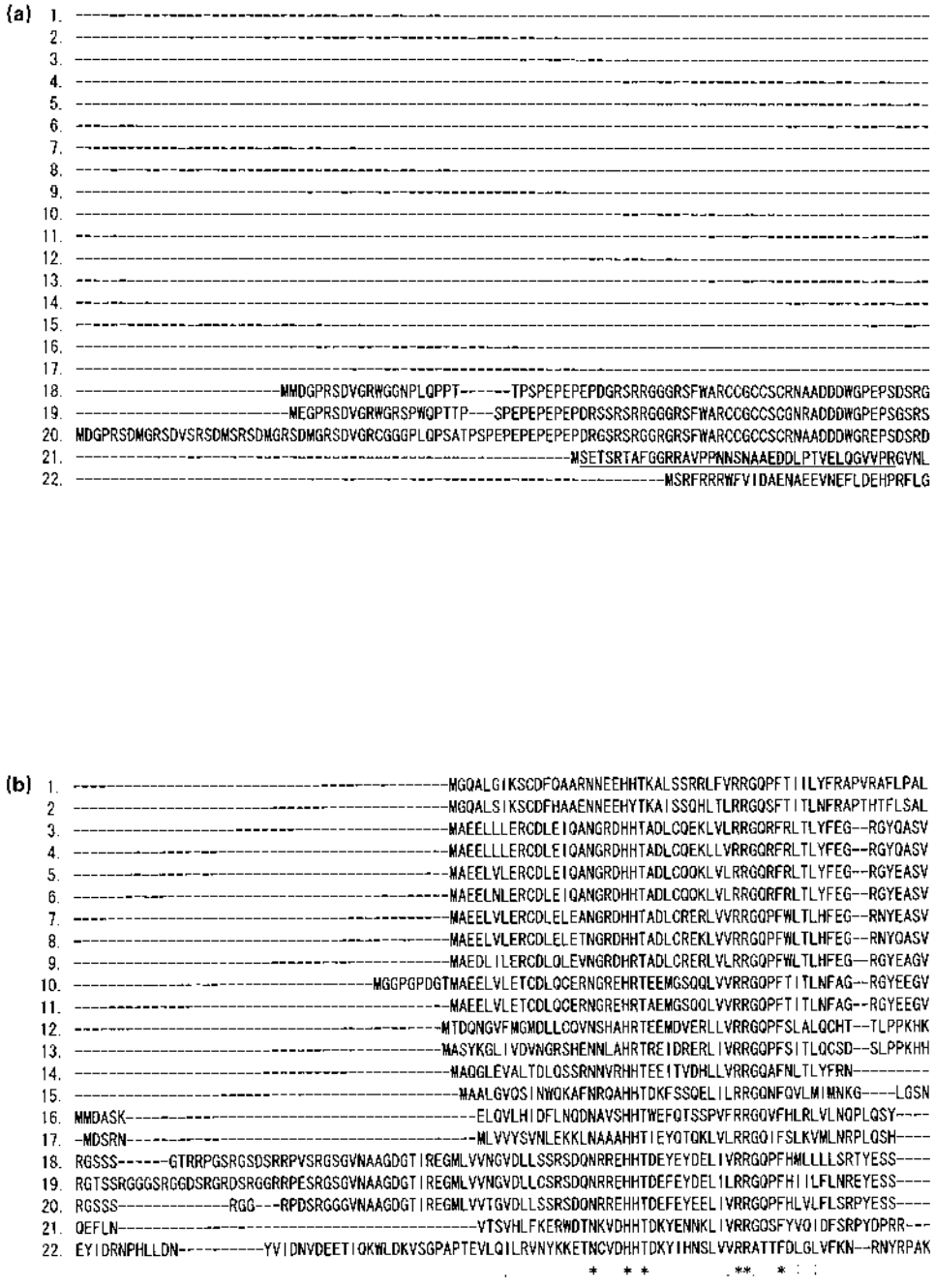

Figure 4 Alignment of amino acid sequences of various transglutaminases. A multiple alignment of the sequences was performed by the program CLUSTAL W ver 1.7 (41) in DNA Data Base of Japan (DDBJ). The identical amino acid residues in all sequences are indicated by asterisk, and conservative changes are shown by dots. In addition, the alignment gaps are expressed by hyphens. The N-terminal 37 amino acid sequence of human blood clotting factor XIIIA (underlined in the sequence 21) is the activation peptide. The C-terminal side of arginine residue (R-37) is hydrolyzed by thormbin, and the TGase activity for the Factor XIIIA becomes apparent. The active site for TGase activity in the factor consists of the amino acid residues, Cys314 in the consensus sequence GQCWVF, His373, and Asp396 (44, 48). These triad residues are conserved in TGases other than erythrocyte band 4.2 (pallidins, 1 and 2). Such active-site motif, His and Asp are boxed.

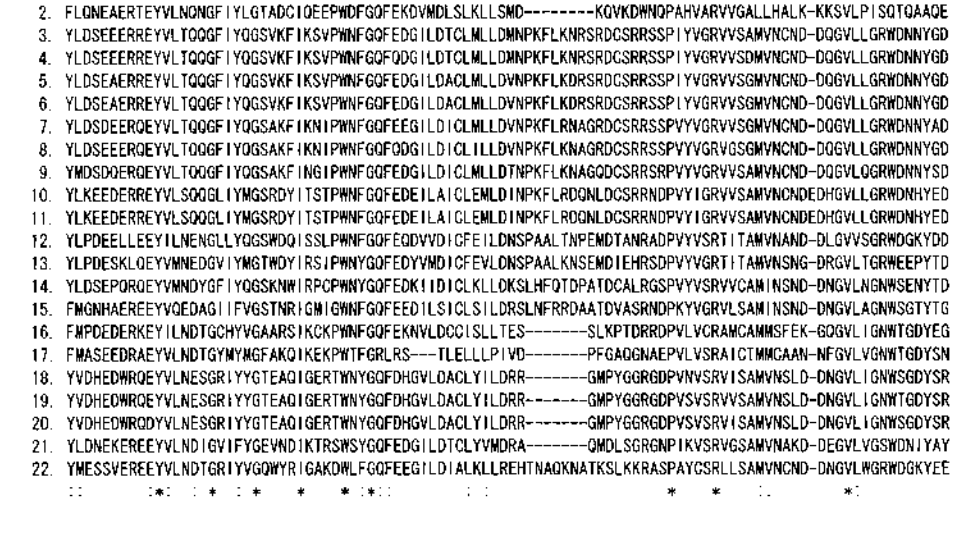

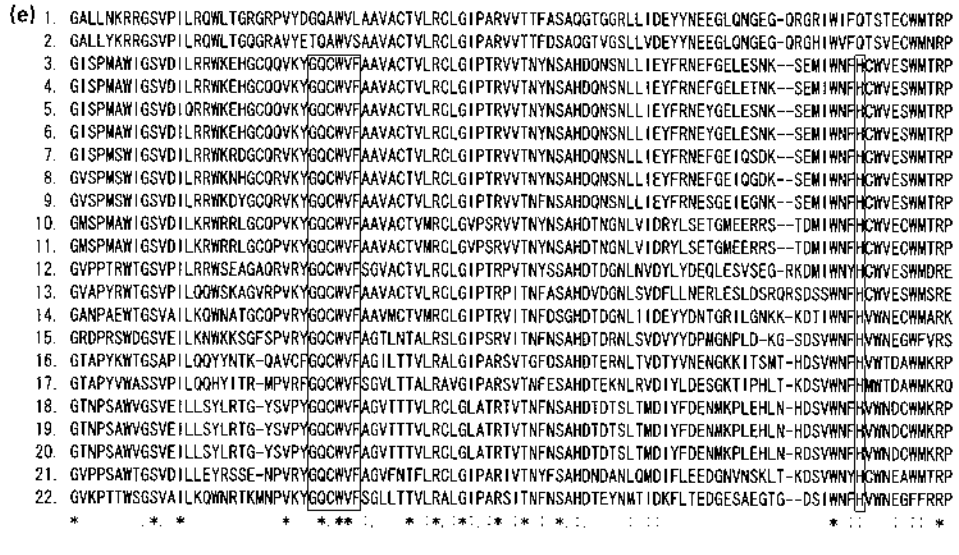

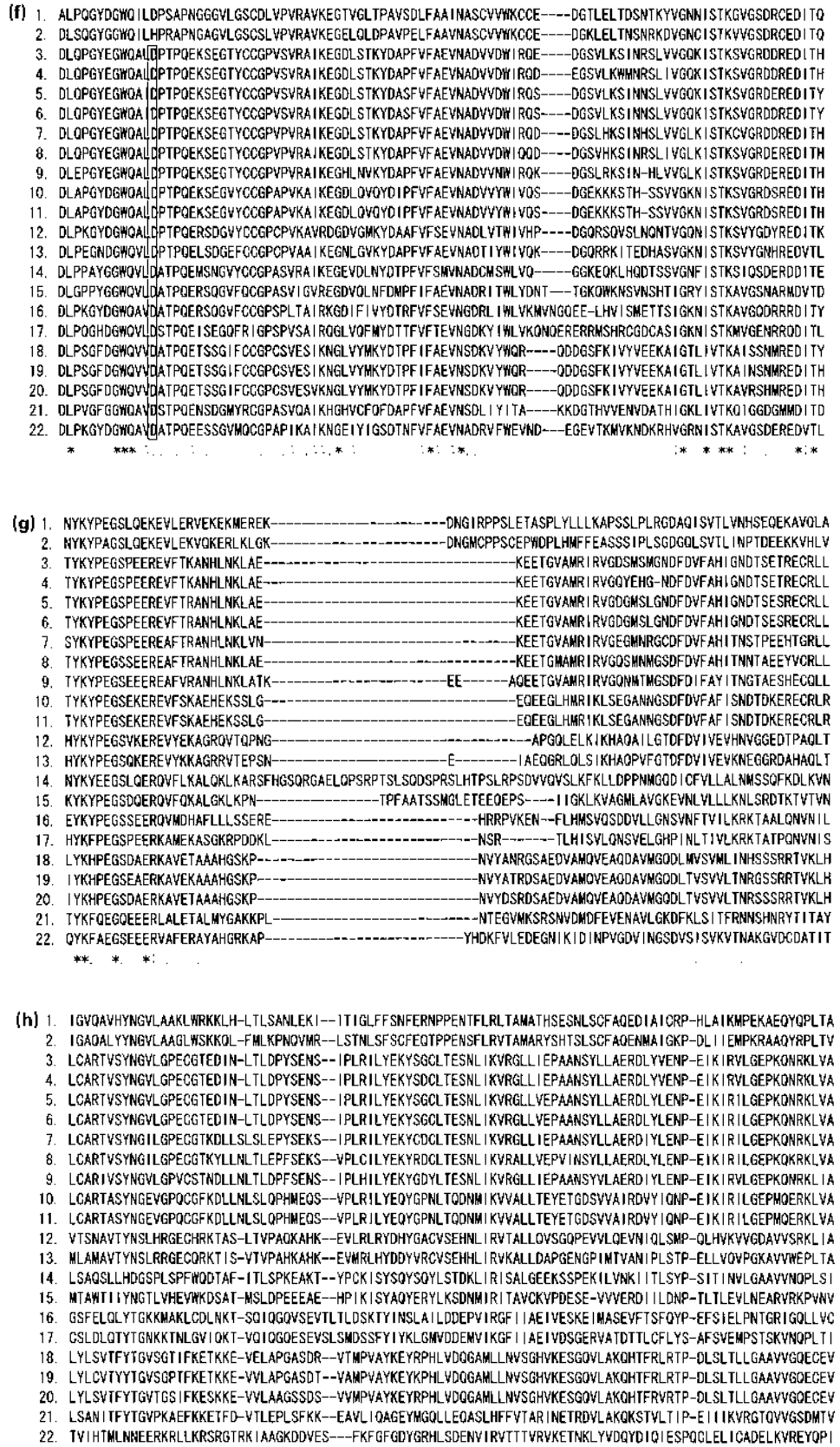

Figure 4 Continued.

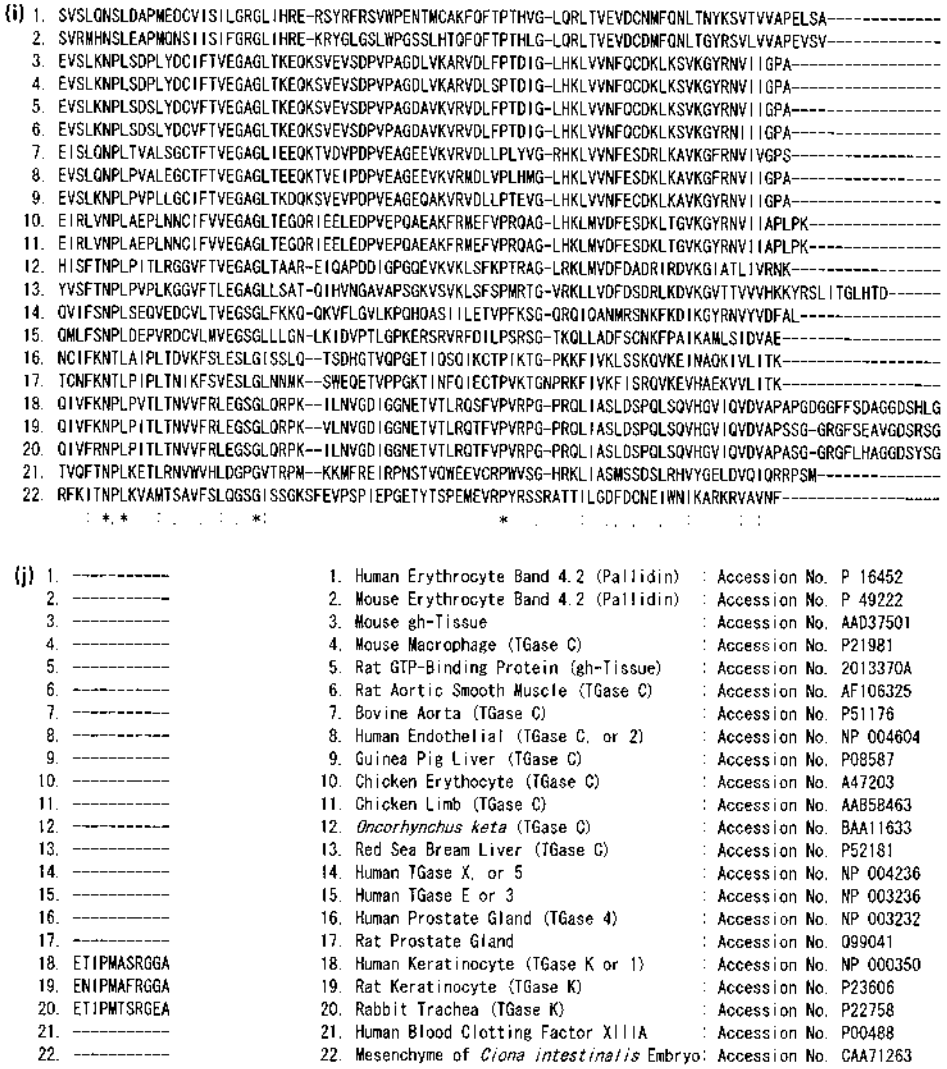

the rest of the molecule. However, the 3D structure of thrombin-cleaved Factor XIIIA is remarkably similar to that of the zymogen. The activation peptide remains associated with the rest of the molecule (50, 51).

III. PROPERTIES AS ENZYME

The main function of TGase is formation of ϵ-(γ-glutamyl) lysine isopeptide crosslinks between naturally occurring proteins or peptides, resulting in polymerization (Figs. 1, 3). Amines such as hydroxylamine, monodansylcadaverine, cadaverine, spermine, spermidine, and putrescine can be incorporated into the protein substrate by the TGase reaction to bind covalently to glutamine residues resulting in the inhibition of the polymerization of proteins (Fig. 2). Thus, amines are competitive inhibitors for the TGase reaction, and can be utilized as one of substrates as described above. For example, there is a report that K_m values of rat brain TGase for putrescine and N,N-dimethylcasein were 0.26 and 0.065 mM, respectively (52). The K_m values of muscle TGases of some animals will be described later. In a case of the TGase from soybean (*Glycine max*) leaves, the K_m values for putrescine, spermidine, and spermine were determined to be 0.109, 0.042, and 0.069 mM, respectively (53). Although this plant enzyme does not essentially require Ca^{2+}, the K_m values are similar to those of tissue TGases known in animals. Slime mold *Physarum polycephalum* TGase has K_m values of 0.049, 0.021, and 0.032 mM for [^{14}C]putrescine, [^{14}C]spermidine, and [^{14}C]spermine, respectively (54).

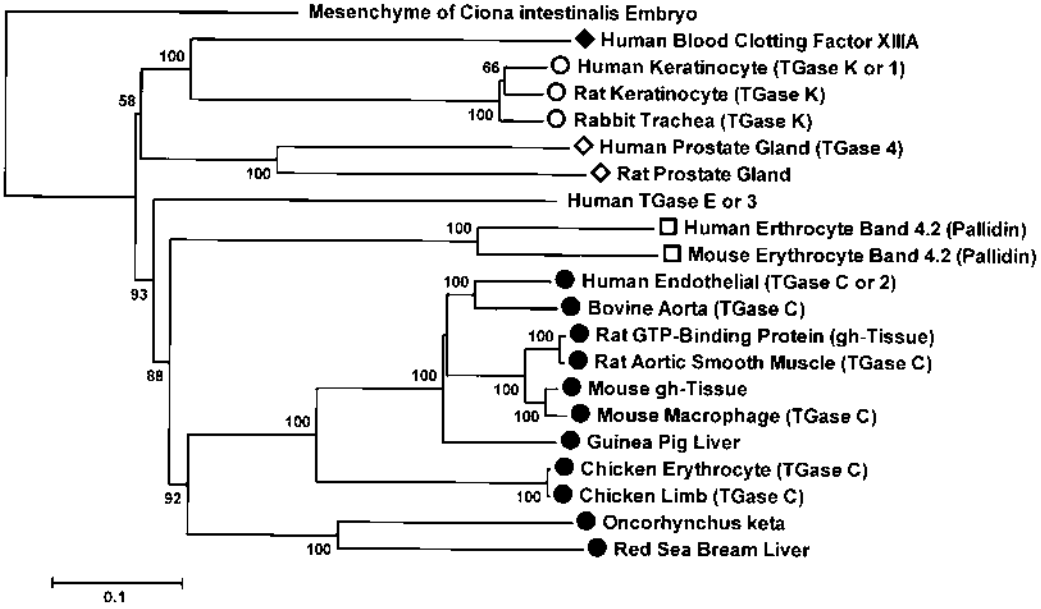

Figure 5 Molecular phylogenetic relationship among vertebrate transglutaminases. A tree was constructed by the neigbor-joining method (42) using the program MEGA (43). Bootstrap values > 50% are shown above or below branches. Filled diamond, open circle, open diamond, open square, and filled circles indicate blood-clotting Factor XIIIA, keratinocyte TGases, prostate gland TGases, erythrocyte band 4.2 (pallidin), and tissue TGases, respectively. The groups of them are considered to be paralogous to each other. The evolutionary distance is expressed in terms of amino acid substitutions per site. The tree is rooted with mesenchyme TGase of *Ciona intestinalis* embryo.

Inhibitors or cofactors were searched for mainly by an assay method utilizing amine incorporation. Metal ion chelating reagents such as EDTA and EGTA inhibit the activity of various TGases, which can be restored by the addition of Ca^{2+}. In addition, iodoacetic acid, iodoacetamide, and *p*-chloromercuribenzoate inhibit TGase activity, while 2-mercaptoethanol and dithiothreitol (DTT) stabilize the activity. Therefore, TGase is well known as a Ca^{2+}-dependent SH enzyme.

On the other hand, some synthetic compounds such as 2-[3-(diallylamino)-propionyl]benzothiophene (55), and 1,3,4,5-tetramethyl-2-[(2-oxopropyl)thio]imidazonium chloride or L-68277 (56) are well-known noncompetitive inhibitors of TGase.

Tissue TGase is inhibited by nucleotides. ATP inhibits the activity of rat liver TGase in a concentration-dependent way. Complete inhibition was obtained with 3 mM ATP. ADP inhibited the TGase activity similarly to ATP, but AMP had much less inhibition. There was no significant inhibition by adenosine and adenine. CTP possessed the same inhibitory activity as that of ATP, while GTP and UTP had $\sim$ 50% of the ATP-induced inhibition (57). Such inhibitory effect of ATP or GTP has been well elucidated for various tissue TGases [guinea pig liver TGase (5); erythrocyte TGase (59); Factor XIII (60); rat brain TGase (52)]. Moreover, it has been demonstrated that a human tissue TGase has nucleotide hydrolysis activity similar to ATPase or GTPase (61). This raises the possibility that the enzyme regulates cell receptor signaling (62). Studies show that the GTP and ATP hydrolysis sites are localized within the core domain of the tissue TGase (63). Recently, a 77-kDa GTP-binding protein, Gαh5, was isolated from pig heart membranes with a binding affinity of nucleotides in order: GTP > GDP > ITP $\gg$ ATP, which is similar to that observed for other G-proteins involved in receptor signaling. The Gαh5 also exhibits TGase activity (64).

The optimum pH of the TGase activity was highly variable as follows: 7.5 for 101-kDa *Physarum polycephalum* TGase (65); 8.0 for *Caenorhabditis elegans* TGase (66); 9.0–9.5 for red sea bream TGase (67), and 5–6 for egg envelope TGases of rainbow trout (13–15).

For guinea pig liver TGase, the optimal incorporation of amines into proteins occurs at pH 7.2–8.5 (2). However, the pH of optimal ammonia liberation (see

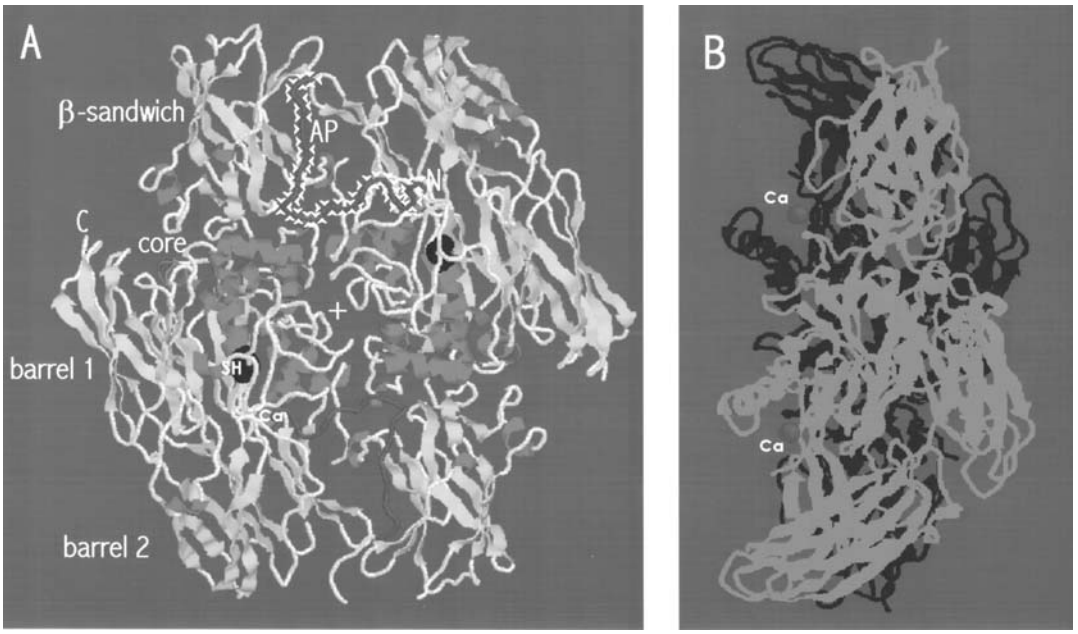

Figure 6 Three-dimensional structure of human blood-clotting Factor XIIIA. The coordinate file for the human blood clotting factor XIIIA dimer [PDB Id., 1GGU (44)], which is supported by Brookhaven Protein Databank, was obtained from National Library of Medicine (NCBI), and the 3D structure was displayed by Molecular Visualization Program, RasMol ver 2.5 (128). The overall structure is characterized by the activation peptide (AP, arrow heads) and four domains, the β-sandwich, the catalytic core, barrels 1 and 2 (44, 48). Due to unresolved problems, it appears that each monomer is missing the eight amino acid residues from the N-terminus (1–8), the linker between the activation peptides and β-sandwich (30–43), the sequence between the core and barrel 1 (508–516), and the C-termini (728–731). (A) Overall structure of the Factor XIIIA dimer. Two monomer molecules are visible in parallel, symmetrically with respect to the center of the figure (+). The cysteine residue in the catalytic site (Cys314) is represented by a solid sphere (SH). (B) Left side view of A. The left and right chains in A are displayed in light and dark, respectively. Two spheres (Ca) are Ca^{2+} ions in both molecules.

Fig. 1) varies with the substrate: 7.0–7.5 for unmodified insulin; 6.5–7.0 for acetylated insulin (68). On the other hand, there is a report for the same enzyme that the optimal incorporation of hydroxylamine into N-carbobenzoxy (CBZ)-L-glutaminylglycine occurs near pH 6.0 (69).

IV. BIOLOGICAL FUNCTION OF TRANSGLUTAMINASE

As described in the Introduction, TGase participates in various biological phenomena such as blood clotting, keratinization, hair formation, and copulatory plug formation. In the present article, we focus our attention on the following subjects to briefly review the recent development of TGase studies; apoptotic cell death, and egg envelope hardening in fish.

A. TGase, Reinoic Acid, and Induction of Apoptosis

Clarification of the compounds involved in natural cell death including apoptosis (programmed cell death) has become one of the most interesting subjects in biochemistry and molecular biology. One of the effective compounds in the death pathway is considered to be tissue TGase, because of a parallel induction of apoptosis and TGase activity [see the review of Fesus and coworkers (6)]. Tissue TGase-mediated crosslinking of some intracellular proteins occurs in cells undergoing apoptotic or programmed cell death (70, 71). Such protein crosslinking may stabilize the apoptotic bodies and prevent the leakage of cytosolic proteins into the extracellular space during fragmentation of cell (72). The induction and activation of TGase-mediated apoptosis are also supported by a recent study that TGase is involved in programmed cell death of *C. elegans* (66).

Retinoic acids, vitamin A derivatives, are known to participate in various biological phenomena by mediation of their receptors, retinoic acid receptors (RARs), and retinoid X receptors (RXRs). Especially, the findings are interesting that retinoids induce apoptotic death in various cells [human nueroblastoma cells (73): human myeloma cell line RPMI 8226 (74); embryonic stem cells (75): mouse thymocyte (76)]. For example, there is a report that apoptosis is in part inhibited by the antisense oligonucleotides for RAR message during the differentiation of mouse embryonic stem cells into neuronal cells; that is, the decreased expression of RARs may inhibit apoptosis (75).

In the pathway of apoptotic cell death, retinoids have been suggested to induce the expression of TGase in the cells; that is, the TGase gene, especially tissue TGase gene, is one of the retinoid-responsive genes. The induction is not related to binding of retinoid receptor monomers to the DNA. Homo- and heterodimeric retinoid receptor complexes bind to distinct retinoids response elements (RREs) embedded in the regulatory regions of retinoid-responsive genes (77). Recently, such RREs have been identified in the promoter regions of mouse tissue TGase gene and characterized (78). The element has been suggested to be capable of binding to and being activated by both RAR/RXR heterodimer and RXR homodimer receptor complexes.

B. Egg Envelope TGases

Recently, TGases in eggs of the rainbow trout *Oncorhynchus mykiss* have been well characterized with special reference to egg envelope (chorion) hardening. Some properties of the TGases will be described in detail because it is considered to be important in food science.

Unfertilized eggs are very fragile, while fertilized/activated eggs are very tough. An unfertilized egg of rainbow trout was broken by pressing it with the weight of less than ~ 20 g. A fertilized/activated egg incubated at 10°C overnight was resistant to the weight of 2–3 kg. Such toughness was due to the hardening of the egg envelope (chorion). During the hardening process, ϵ-(γ-glutamyl) lysine isopeptide crosslinks in the chorion increased 6 (unfertilized egg chorion) to 43 nmol/mg dry chorion (fertilized egg chorion). Moreover, 49-, 56-, and 65-kDa proteins constituting the unfertilized egg chorion were gradually polymerized, and the chorion became insoluble in protein denaturants such as 3% SDS, 8 M guanidium hydrochloride, and 12 M urea. In addition, monodansylcadaverine inhibited both the polymerization of chorion proteins and the hardening of chorion (11). These studies have raised a possibility that TGase is responsible for chorion hardening (79, 81).

Further studies showed that the activity of TGase was not localized in unfertilized egg cytoplasm but was exclusively in the egg chorion (11, 12); that is, the TGase was an extracellular matrix TGase. Thus, the chorion is a functional structure in coexistence with the enzyme and the substrate.

Two TGases, P1 and P2, were extracted and purified from the chorion and were partially characterized. They had an ability to catalyze the formation of ϵ-(γ-glutamyl) lysine isopeptide crosslinks among 49-, 56-, and 65-kDa subunit proteins of the chorion, to polymerize all the subunits, and to harden the chorion. The activity of P1 enzyme was apparent exclusively in the medium of low ionic strength such as 10 mM Tris-HCl (pH 7.2), while that of P2 was apparent both in 10 mM Tris-HCl (pH 7.2) and in isotonic saline (0.143 M NaCl-10 mM Tris-HCl, pH 7.2). P1 consisted of 82- and 76-kDa proteins, but the amino acid compositions were highly identical. P2 consisted of a homogenous 76-kDa protein (13, 14). After egg activation, P1 enzyme was processed into a 48-kDa enzyme and its activity was enhanced. As the 48-kDa TGase remains localized in the chorion, it must crosslink the subunit proteins at the restricted sites of the chorion. On the contrary, P2 enzyme was released into perivitelline space after activation of the egg. It may uniformly polymerize the chorion subunit proteins (15). The released P2 enzyme corresponds to the chorion-hardening enzyme initially suggested by Zotin (80, 81).

It has been suggested that the processing of chorion TGases after egg activation is caused by the action of an EDTA- or leupeptin-sensitive proteinase(s). In addition, the enzymes become active by Ca^{2+} released from the activated eggs (15, 81). Thus, a main biological function of chorion TGases is the fertilization/egg activation-associated hardening of the chorion to prevent the eggs from environment-derived mechanical and chemical hazard (81).

V. TRANSGLUTAMINASE STUDY IN FOOD SCIENCE

Unfertilized eggs of salmonid fishes including rainbow trout are frequently treated with a high concentration of salt ($\sim$ 7% NaCl) and are utilized as food. During food processing, the activity of the chorion TGases survives, resulting in a gradual formation of isopeptide crosslinks between egg proteins (82). It is conceivable that the

TGase reaction contributes to the viscoelastic character of salted eggs. In fact, unfertilized eggs are very fragile, while salted eggs have hardness as a desirable food.

Although more investigations are necessary, TGases have been found in unfertilized eggs of other fishes: *Oncohynchus masou, Salvelinus leucomaenis* (82), carp *Cyprinus carpio* (83), medaka *Oryzias latipes* (79, 84), cod *Gadus morhua* (85), and sea urchin *Stronglyocentrotus purpuratus* (10). TGase in fish eggs must play a role in forming a desirable texture as food as well as in the hardening of egg envelope after fertilization. However, changes of egg proteins induced by food processing remain unclear.

TGases were prepared from muscles of scallop (*Patinopecten yessoensis*), botan shrimp (*Pandalus nipponensis*), squid (*Todarodes pacificus*), carp, rainbow trout, and atka mackerel (*Pleurogrammus azonus*), and their properties were characterized (86). The K_m value of carp TGase for monodansylcadaverine was 0.33 mM, while the other enzymes had values of 0.01–0.03 mM. The K_m values for succinylated casein of scallop, botan shrimp, squid, carp, rainbow trout, and atka mackerel enzymes were 1.2, 0.3, 1.8, 0.3, 0.2, and 0.1 mg/mL, respectively. In the presence of 0.5 M NaCl or 0.5 M KCl (isotonic to sea water), the activities of TGases from marine invertebrates, scallop, botan shrimp, and squid were enhanced about 11-, two-, and sixfold, respectively. On the contrary, there was no effect of such concentrations of NaCl on the fish enzymes. Muscle TGases may play a role in food processing.

High pressure at near 300 Mpa is considered to induce gelation and denaturation of salted paste surimi, a myofibrillar concentrate of fish muscle. Endogenous TGase that survives at the high pressure promotes gelation of Alaska pollock surimi (17). In addition, there is a review article with regard to food processing that TGase is applicable for food protein deamination to improve solubility, emulsification, foaming, and other functional properties of the proteins (16). The use of the enzyme must be more desirable than other chemical treatments in speed, mild reaction conditions, and their high specificity. Especially, it may prevent foods from contamination of pollutants such as endocrine disturbers.

VI. DETERMINATION OF TRANSGLUTAMINASE ACTIVITY

A convenient assay method for measuring the TGase activity was developed by Lorand and Gotoh (87). This method is based on the incorporation of monodansylcadaverine into a protein such as N,N-dimethylcasein (Fig. 2). The standard reaction mixture, slightly modified by Ha and Iuchi (11, 12) is as follows:

Stock solution	Volume (μL)	Final concentration
Tris-HCl (pH 7.2), 200 mM	250	50 mM
2-mercaptoethanol, 200 mM	25	5 mM
$CaCl_2$, 1.0 M	5	5 mM
Monodansylcadaverine, 2.0 mM	250	0.5 mM
N,N-dimethylcasein, 1.0%	200	0.2%
Enzyme sample and some reagent	270	—

The mixture was incubated at appropriate temperature for various times, and the reaction was terminated by adding 1.0 mL of 10% trichloroacetic acid. After centrifugation, the precipitate was washed several times with ethanol-ether (1:1), dried by vacuum pump, and dissolved into 3 mL of 8 M urea-5% sodium dodecylsulfate (SDS)-50 mM Tris-HCl (pH 8.6). The intensity of fluorescence of the solution was measured by excitation at 355 nm and with emission at 525 nm, using 1 nmol/mL monodansylcadaverine as a standard. For human blood coagulation Factor XIII (fibrinoligase), the unit of TGase activity has been defined as amine incorporation unit (AIU) (87). For egg envelope TGase of rainbow trout, 1 unit of the activity was defined as 1 nmol of monodansylcadaverine incorporated into dimethylcasein per hour at 10°C (MIU: monodansylcadaverine incorporation unit) (13).

Monodansylcadaverine in the above reaction mixture can be replaced by biotinylated cadaverine (88, 89) and other amine derivatives. A novel, sensitive chemiluminescent assay was recently developed to quantitate the acyl transfer activity of blood coagulation Factor XIIIA or liver TGase, utilizing 6-[N-(4-aminobutyl)-N-ethylaminol]-2,3-dihydrophthalazine-1,4-dione as a substrate (90). As a more sensitive method, a ^{14}C- or ^{3}H-labeled putrescine or spermidine substrate has been frequently used (91, 92).

A fluorescent dipeptide compound, 1-N-(carbobenzoxy-L-glutaminylglycyl)-5-N-(5′-N′, N′-dimethylamino-1′-naphthalenesulfonyl)-diamidopentane (CBZ-Gln-Gly-C-DNS 1), was synthesized and was used as a substrate for assaying the activity of bacterial TGase or guinea pig liver TGase (93). The glutamine peptides were incorporated into lysine residues of αs_1-casein. Thus, the method is based on measuring incorporation of a glutamine residue into a protein or peptide.

A fluorometric, high-performance liquid chromatographic (HPLC) assay for TGase activity has been described (94). This method used the small synthetic

peptide benzyloxycarbonyl-L-glutaminylglycine and monodansylcadaverine as substrates. The reaction product was separated by reverse phase HPLC, and was quantitated by fluorometry. An apparent K_m of purified guinea pig liver TGase was $\sim$ 35 mM for the peptide substrate.

A microtiter plate assay using human fibrinogen as an immobilized substrate has been developed for coagulation Factor XIII (88). Factor XIII was activated by Ca^{2+} and thrombin, added to fibrinogen immobilized on a plate, and then assayed by adding biotinylated cadaverine. After the reaction was terminated by adding EDTA, the quantity of incorporated biotin was determined with streptavidin-β-galactosidase. Microtiter plates coated with N,N-dimethylcasein are also available as an immobilized substrate.

VII. ISOLATION OF TRANSGLUTAMINASE

Methods used for isolation of different types of TGases have been recently reviewed by Bergamini and Signorini (95) and by Wilhelm and coworkers (92). Some data for the purification procedures are summarized in Table 2.

In addition to secretory TGases such as blood-clotting Factor XIII and copulatory plug-forming TGase in secretions from prostate gland, tissue TGases frequently occur in cytosol and are therefore extractable by homogenization of materials such as tissue and organ with conventional buffer solutions. Some TGases bind to cell membrane, cellular particles, or extracellular matrix. As described above, egg envelope TGases of rainbow trout, extracellular matrix TGases, were nearly completely extracted by repeated homogenization with isotonic saline (0.143 M NaCl, 10 mM Tris-HCl, pH 7.2) (11–14). Rat liver particulate TGase has been partially extracted by three times homogenization of pellet fractions with a sucrose buffer. However, the extraction was not complete. The TGase was further extracted by homogenization of the remaining particulate fractions with 1% Lubrol-WX (96). In contrast to these TGases, the TGase activity in egg envelope of the fish medaka (*Oryzias latipes*) was never extracted by homogenization with 5 mM 2-mercaptoethanol, 0.5 M NaCl, 1% Tween 20 or 0.6 M CHAPS (3-[(3-cholamidopropyl)dimethylammonio]-1-propane-sulfonate) (Ha and Iuchi, unpublished data).

At the next step of purification, TGases in the extracts are frequently concentrated by various methods. A usual method for the concentration is ammonium sulfate precipitation; 25–50% saturation for TGase of secretions of coagulating glands and dorsal prostate (5), or 50–60% saturation for testicular tissue TGase of rat (5) and bovine (95). Such enrichment has been performed by protamine precipitation (liver TGases of rodents) (97) or by ethanol precipitation (Factor XII of human placenta) (98). In addition, ion exchange column chromatography may be available for concentration of TGase.

Conventional chromatographic methods such as gel filtration, ion exchange, and hydrophobic column chromatography are applicable for isolation or purification of TGases, as summarized in Table 2.

Purification methods based on isoelectric points of TGases also have been useful. Preparative isoelectric focusing in a granulated Sephadex G-75 gel bed was performed for isolation of TGase from secretions of coagulating glands and dorsal prostate of rat (5, 23). In addition, epidermal TGase from cow muzzle was finally purified using zone electrophoresis in combination with gel filtration chromatography on a Sephadex G-200 column (99).

Affinity chromatography is particularly useful for purifying various TGases. The Ca^{2+}-dependent affinity chromatography using casein-Sepharose was employed for the isolation of rat liver cytosolic TGase (100). In the presence of 5 mM Ca^{2+}, the enzyme was bound to the column, and elution was achieved using 5 mM EGTA. Recently, TSKgel Heparin-5PW (Tosoh, Tokyo) or GTP-agarose (Sigma) was used to purify rat brain TGases (52). GTP-agarose affinity chromatography was desirable because GTP has been known to bind to tissue TGases to inhibit their activities. Immunoaffinity column chromatography has been employed for one-step purification of guinea pig TGase, where the supernatants of guinea pig liver homogenates were applied to an affinity column conjugating a monoclonal antibody against guinea pig liver TGase (101).

VIII. COMMENTS

1. As shown in Table 1, natural substrates for many TGases remain unidentified. Recently, a novel histone modification was found in the testis of the starfish (*Asterina pectinifera*) (102, 103), involving formation of an ϵ-(γ-glutamyl) lysine isopeptide crosslink between a glutamine residue of histone H2B and a lysine residue of histone H4. Although a biological role of the TGase has not been well clarified, there is

Table 2 Practical Methods for the Purification of Transglutaminases (TGases)

Purification Steps		Transglutaminases	Remarks	References
Extraction	Conventional buffer	Secretory TGases, tissue TGases, and some particulate or extracellular matrix TGases		
	Detergent	Rat keratinocyte TGase (particle-associated)	Lubrol-WX (1%)	96
		Rat keratinocyte TGase (particle-associated)	NP-40 (0.3%)	119
Concentration	Ammonium sulfate precipitation	Rat prostate gland TGases (purified from the secretions)	25–50% saturation	5, 23
		Rat testicular tissue TGase	50–60% saturation	5, 23
		Coagulation factor XIII of human placenta	40% saturation	98
	Protamine precipitation	Tissue TGase of rodent liver		97
	Ethanol precipitation	Coagulation factor XIII of human placenta		98
Gel filtration column chromatography	Sephdex G-200	Rat prostate gland TGases (purified from the secretions)		5,23
	Sephacryl S-300	Tissue TGase of human erythrocyte		120
	Toyopearl SW55S	Egg envelope TGases of rainbow trout		13, 14
	TSK 125	Tissue TGase of human erythrocyte	HPLC	120
	TSK-gel	Egg envelope TGases of rainbow trout	HPLC	13, 14
Ion exchange column chromatography	DEAE-cellulose	Human blood-clotting Factor XIII	Anion exchange column chromatography [Most tissue TGases are eluted with 0.25–0.45 M NaCl using a Tris buffer containing EDTA and DTT at pH 7.5.)	98
		Rat keratinocyte TGase		96
		Guinea pig liver TGase		97
		Human epidermal TGase		121
		Limulus hemocyte TGase		117
	DEAE-Sephadex A50	Bovine epidermal TGase		99
	DEAE-Biogel A	Tissue TGase of human erythrocyte		122
	DEAE-EMD-Factogel 650	Rat prostate gland TGases (purified from the secretions)		92
	DEAE-Sepharose	Human blood-clotting Factor XIII		123
	QAE-Sephadex	Guinea pig liver TGase		124
	Q-Sepharose	Egg envelope TGases of rainbow trout		13, 14
	Mono Q	Rat liver TGase		125
	CM-cellulose	Human epidermal TGase	Cation exchange column chromatography	121
	Phosphocellulose	Rat prostate gland TGases (purified from the secretions)		126
	SP-Sepharose	Egg envelope TGases of rainbow trout	Not retained	13, 14
Hydrophobic column chromatography	Phenylalanine-Sepharose 4B	Liver TGase		124
	Phenyl-Sepharose	Rat testicular tissue TGase		5, 23, 95

(Continued)

Table 2 Continued.

Purification Steps		Transglutaminases	Remarks	References
Affinity column chromatography	Casein-Sepharose	Guinea pig liver TGase		100
	Heparin-Sepharose	Tissue TGase of human erythrocyte		120
	TSK heparin 5PW	Rat brain TGase		52
	GTP-agarose	Rat brain TGase		52
	Blue-Sepharose CL-6B	Human erythrocyte		122
	Immunoaffinity	Guinea pig liver TGase	Antibody to cytosolic TGase	125
		Guinea pig liver TGase	Monoclonal antibody to guinea pig liver TGase	101
Other column chromatography	Hydroxyapatite on Biogel-HTP	Guinea pig liver TGase		124
		Rat liver TGase		127
	Zinc-chelating Sepharose 6B	*Limulus* hemocyte TGase		117
Preparative isoelectric focusing		Rat prostate gland TGases (purified from the secretions)	pH 4.0–9.0	5, 23

a possibility that the TGase-mediated crosslink formation of nuclear proteins is closely related to some important cellular events.

2. Antibodies specific to several TGases are commercially available: antitransglutaminase II (Mono) (Quartett GmbH, Berlin, Germany); and antitransglutaminase (type II) (Upstate Biotechnology Inc., Waltham, MA., US). These antibodies may be cross-reactive to various TGases. For example, a polyclonal antibody against guinea pig liver TGase was crossreactive to human keratinocyte TGase (104), and a monoclonal antibody against guinea pig liver TGase recognized a TGase present in mouse dermal fibroblast (105).

3. Recently, a distinct enzyme cleaving ϵ-(γ-glutamyl) lysine isopeptide crosslinks between proteins or peptides was found and termed isopeptidase (106). In the medicinal leech, *Hirudo medicinalis*, this same enzyme is called destabilase (107).

ACKNOWLEDGMENTS

The authors wish to thank Dr. D. Wong U.S. Department of Agriculture, Agricultural Research Service, Western Regional Research Center, for critical reading of the present article. Our studies cited in the present article were supported in part by Grant-in-Aid from Ministry of Education, Science, Sports, and Culture of Japan to I.I. Thanks are also due Irikawa Trout Hatchery, Tokyo, and Fuji Trout Farm, Shizuoka, for supplying rainbow trout eggs.

REFERENCES

1. NK Sarkar, DD Clarke, H Waelsch. Biochim Biophys Acta 25:451–452, 1957.
2. H Waelsch, MJ Mycek. Methods Enzymol V:833–843, 1962.
3. SM Thatcher, RH Rice. Cell 40:685–695, 1985.
4. N Martinet, HC Kim, JE Girard, TP Nigra, DH Strong. SI Chung, JE Folk. J Biol Chem 263:4236–4241, 1988.
5. J Seitz, C Keppler, S Huntemann, U Raush, G. Aumuller. Biochim Biophys Acta 1078:139–146, 1991.
6. L Fesus, A Madi, Z Balajthy, Z Nemes, Z Szondy. Experientia 52:942-949, 1996.
7. PJ Davies, JP Basilion, EA Chiocca, J Johnson, S Poddar, JP Stein. Am J Med Sci 296:164–170, 1988.
8. MA Singer, M Hortsch, CS Goodman, D Bentley. Dev Biol 154:143–159, 1992.
9. T Sato. Master's thesis, Sophia University, 1999.
10. DE Battaglia, BM Shapiro. Cell Biol 107:2447–2454, 1988.
11. I Iuchi, C-R Ha, H Sugiyama, K Nomura. Dev Growth Differ 38:299–306, 1996.
12. C-R Ha, I Iuchi. Comp Biochem Physiol 118B:293–301, 1997.

13. CR Ha, I Iuchi. J Biochem (Tokyo) 122:947–954, 1997.
14. CR Ha, I Iuchi. J Biochem (Tokyo) 124:917–926, 1998.
15. CR Ha. Doctor's thesis, Sophia University, 1998.
16. JS Hamada. Crit Rev Food Sci Nutr 34:283–292, 1994.
17. Lanier TC. Adv Exp Med Biol 434:45–55, 1998.
18. HC Kim, WW Idler, IG Kim, JH Han, SI Chung, PM Steinert. J Biol Chem 266:536–539, 1991.
19. SC Park, EJ Yeo, JA Han, YC Hwang, JY Choi, JS Park, YH Park, KO Kim, IG Kim, SC Seong, SJ Kwak. J Gerontol Biol Sci Med Sci 65:B78–83, 1999.
20. IG Kim, JJ Gorman, SC Park, SI Chung, PM Steinert. J Biol Chem 268:12682–12690, 1993.
21. HG Whilliums-Ashman. Mol Cell Biochem 68:51–61, 1984.
22. J Wilson, RE Beil, M Hawkins, A Zunamon, L Lorand, HG William-Ashman. Fed Proc 38:570, 1979.
23. J Seitz, C Keppler, SB Hüntemann. Chromatogr 587:55–60, 1991.
24. B Skoog, A Wichman. Trends Anal Chem 5:(4), 1986.
25. A Ichinose, LE Hendrickson, K Fujikawa, EW Davie. Biochemistry 25:6900–6906, 1986.
26. U Grundmann, E Amann, G Zettlmeissl, HA Kupper. Proc Natl Acad Sci USA 83:8024–8028, 1986.
27. RE Bottenus, A Ichinose, EW Davie. Biochemistry 29:11195–11209, 1990.
28. MA Phillips, BE Stewart, Q Qin, R Chakravarty, EE Floyd, AM Jetten, RH Rice. Proc Natl Acad Sci USA 87:9333–9337, 1990.
29. KC Ho, VE Wuarmby, FS French, EM Wilson. J Biol Chem 267:12660–12667, 1992.
30. C Korsgren, J Lawler, S Lambert, D Speicher, CM Cohen. Proc Natl Acad Sci USA 87:613–617, 1990.
31. C Korsgren, CM Cohen. Genomics 21:478–485, 1994.
32. N Weraarchakul-Boonmark, JM Jeong, SN Murthy, JD Engel, L Lorand. Proc Natl Acad Sci USA 89:9804–9808, 1992.
33. K Ikura, T Nasu, H Yokota, Y Tsuchiya, R Sasaki, H Chiba. Biochemistry 27:2898–2905, 1988.
34. V Gentile, M Saydak, EA Chiocca, O Akande, PJ Birckbichler, KN Lee, JP Stein, PJ Davies. J Biol Chem 266:478–483, 1991.
35. K Nakanishi, K Nara, H Hagiwara, Y Aoyama, H Ueno, S Hirose. Eur J Biochem 202:15–21, 1991.
36. VA Thomazy, PJA Davies. Cell Death Differ 6:146–154, 1999.
37. L Cariello, F Ristoratore, L Zanetti. FEBS Lett 408:171–176, 1997.
38. F Tokunaga, T Muta, S Iwanaga, A Ichinose, EW Davie, K Kuma, T Miyata. J Biol Chem 268:262–268, 1993.
39. H Yasueda, K Nakanishi, Y Kumazawa, K Nagase, M Motoki, H Matsui. Eur J Biochem 232:411–419, 1995.
40. K. Sano, K Nakanishi, N Nakamura, M Motoki, H Yasueda. Biosci Biotechnol Biochem 60:1790–1794, 1996.
41. JD Thompson, DG Higgins, TJ Gibson. Nucleic Acids Res 22:4673–4680, 1994.
42. N Saitou, M Nei. Mol Biol Evol 4:406–425, 1987.
43. S Kumar, K Tamura, M Nei. MEGA: Molecular Evolutionary Genetics Analysis, Ver 1.01.University Park, PA: Pennsylvania State University, 1993.
44. BA Fox, VC Yee, LC Pedersen, I Le Trong, PD Bishop, RE Stenkamp, DC Teller. J Biol Chem 274:4917–4923, 1999.
45. T Kanaji, H Ozaki, T Takao, H Kawajiri, H Ide, M Motoki, Y Shimonishi. J Biol Chem 268:11565–11572, 1993.
46. LA Knodler, R Noiva, K Mehta, JM McCaffery, SB Aley, SG Svaerd, TG Nystul, DS Reiner, JD Silberman, FD Gillin. J Biol Chem 274:29805–29811, 1999.
47. R Candrashekar, N Tsuji, T Morales, V Ozols, K Mehta. Proc Natl Acad Sci USA 95:531–536, 1998.
48. M Weiss, HJ Metzner, R Hilgenfeld. FEBS Lett 423:291–296, 1998.
49. LC Pedersen, VC Yee, PD Bishop, I Le Trong, DC Teller, RE Stenkamp. Protein Sci 3:1131–1135, 1994.
50. VC Yee, LC Pedersen, IL Trong, PD Bishop, RE Stenkamp, DC Teller. Proc Natl Acad Sci USA 91:7296–7300, 1994.
51. VC Yee, LC Pedersen, PD Bishop, RE Stenkamp, DC Teller. Thromb Res 78:389–397, 1995.
52. H Ohashi, Y Itoh, PJ Birckbichler, Y Takeuchi. J Biochem (Tokyo) 118:1271–1278, 1995.
53. H Kang YD Cho. Biochem Biophys Res Commun 223:288–292, 1996.
54. JD Klein, E Guzman, GD Kuehn. J Bacteriol 174:2599–2605, 1992.
55. L Cariello, J Wilson, L Lorand. Biochemistry 23:6843-6850, 1984.
56. L Cariello, L Zanetti, L Loland. Biochem Biophys Res Commun 205:565–569, 1994.
57. S Kawashima. Experienta 47:709–712, 1991.
58. KE Achyuthan, CS Greenberg. J Biol Chem 262:1901–1906, 1987.
59. CM Bergamini, M Signovini, L Poltroneivi. Biochim Biophys Acta 916:149–151, 1987.
60. I Cohen, TA Blankenberg, D Borden, DR Kahn, A Veis. Biochim Biophys Acta 628:365–375, 1980.
61. TS Lai, TF Slaughter, KA Peoples, Jm Hettasch, CS Greenberg. J Biol Chem 273:1776–1781, 1998.
62. H Nakaoka, DM Perez, KJ Baek, T Das, A Husain, K Misono, MJ Im, RM Graham. Science 264:1593–1596, 1994.

63. SE Iismaa, L Chung, MJ Wu, DC Teller, VC Yee, RM Graham. Biochemistry 36:11655–11664, 1997.
64. SM Yoo, HS Jeong, KJ Han, SH Cho, HS Lee, HY Yun, NS Kwon, KJ Baek. Exp Mol Med 30:81–86, 1998.
65. J Mottahedeh, R Marsh. J Biol Chem 273:29888–29895, 1998.
66. A Madi, M Punyiczki, M Rao, M Piacentini, L Fesus. Eur J Biochem 253:583–590, 1998.
67. H Yasueda, Y Kumazawa, M Motoki. Biosci Biotechnol Biochem 58:2041–2045, 1994.
68. MJ Mycek, H Waelsch. J Biol Chem 235:3513–3517, 1969.
69. JE Folk. Methods Enzymol XVIIA:889–894, 1970.
70. L Fesus, V Thomazy, F Autuori, MP Ceru, E Tarcsa, M Piacentini. FEBS Lett 245:150–154, 1989.
71. M Piacentini, F Autuori, L Dini, MG Farrace, L Ghibelli, L Piredda, L Fesus. Cell Tissue Res 263:227–235, 1991.
72. L Fesus, PJA Davies, M Piacentini. Eur J Cell Biol 56:170–177, 1991.
73. G Melino, M Draoui, L Bellincampi, F Bernassola, S Bernardini, M Piacentini, U Reichert, P Cohen. Exp Cell Res 235:55–61, 1997.
74. BJ Joseph, O Lefebvre, C Mereau-Richard, PM Danze, B-P Belin-Plancot, P Formstecher. Blood 91:2423–2432, 1998.
75. H Okazawa, J Shimizu, M Kamei, I Imafuku, H Hamada, I Kanazawa. J Cell Biol 132:955–968, 1996.
76. Z Szondy, U Reichert, J-M Bernardon, S Micel, R Toh, P Ancian, E Ajzner, L Fesus. Mol Pharmacol 51:972–982, 1997.
77. K Umesosno, KK Murakami, CC Thompson, RM Evans. Cell 65:1255–1266, 1991.
78. L Nagy, M Saydak, N Shipley, S Lu, JP Basilion, ZH Yan, P Syka, RA Chandraratna, JP Stein, RA Heyman. J Biol Chem 271:4355–4365, 1996.
79. I Iuchi, C-R Ha, K Masuda. Fish Biol J Medaka 2:15–20, 1995.
80. AI Zotin. J Embryol Exp Morphol 6:546–568, 1958.
81. H Sugiyama, I Iuchi. Comparative Biochemistry and Physiology. Transworld Research Network, 2000 (in press).
82. A Fukuda. Master's thesis. Sophia University (in Japanese), 1996.
83. S Kudo. J Exp Zool 282:367–375, 1998.
84. K Masuda, I Iuchi, K Yamagami. Dev Growth Differ 33:75–83, 1991.
85. DO Oppen-Berntsen, JK Helvik, BT Walther. Dev Biol 137:258–265, 1990.
86. H Nozawa, S Mamegoshi, N Seki. Comp Biochem Physiol Biochem Mol Biol 118:313–317, 1997.
87. L Lorand, T Gotoh. Methods Enzymol XIX:770–782, 1978.
88. YC Song, D Sheng, SM Taubenfeld, GR Matsueda. Anal Biochem 223:8–92, 1994.
89. PA Smethurst, M Griffin. Biochem J 313:803–808, 1996.
90. KE Achyuthan. J Biolumin Chemilumin 13:1–11, 1998.
91. M Bowness. Biochem Cell Biol 65:280–285, 1987.
92. B Wilhelm, A Meinhardt, J Seitz. J Chromatogr B Biomed Appl 684:163–177, 1996.
93. R Pasternack, HP Laurent, T Ruth, A Laiser, N Schon, HL Fuchsbauer. Anal Biochem 249:54–60, 1997.
94. ML Fink, YY Shao, GJ Kersh. Anal Biochem 201:270–276, 1992.
95. CM Bergamini, M Signorini. Biochem Int 27:557–565, 1992.
96. SK Chang, SI Chung. J Biol Chem 261:8112–8121, 1986.
97. JE Folk, PW Cole. J Biol Chem 241:5518–5525, 1966.
98. CD Royer, F Traore, JC Meunier. Int J Biochem 24:91–97, 1992.
99. MM Buxmann, KD Wuepper. Biochim Biophys Acta 452:456–469, 1976.
100. DE Croall, GN DeMartino. Cell Calcium 7:29–39, 1986.
101. K Ikura, H Sakurai, K Okumura, R Sasaki, H Chiba. Agric Biol Chem 49:3527–3531, 1985.
102. T Shimizu, K Hozumi, S Horiike, K Nunomura, S Ikegami, T Takao, Y Shimonishi. Nature 380:32, 1996.
103. T Shimizu, T Takao, K Hozumi, K Nonumura, S Ohta, Y Shimonishi, S Ikegami. Biochemistry 36:12071–12079, 1997.
104. R Schmidt, S Michel, B Shroot, U Reichert. J Invest Dermatol 90:475–479, 1988.
105. AV Skalli-Trejo, PT Velasco, SN Murthy, L Lorand, RD Goldman. Proc Natl Acad Sci USA 92:8940–8944, 1995.
106. AG Loewy, JK Blodgett, FR Blase, MH May. Anal Biochem 246:111–117, 1997.
107. L Zavalova, S Lukyanov, I Baskova, E Snezhkov, S Akopov, S Berezhnoy, E Bogdanova, E Barsova, ED Sverdlov. Mol Gen Genet 253:20–25, 1996.
108. SE Harris, MA Harris, CM Johnson, MF Bean, JG Dodd, RJ Matusik, SA Carr, JW Crabb. J Biol Chem 265:9896–9903, 1990.
109. HO Molhuizen, HA Alkemade, PL Zeeuwen, GJ de Jongh, B Wieringa, J Schalwijk. J Biol Chem 268:12028–12032, 1993.
110. PL Zeeuwen, W Hendriks, WW de Jong, J Schalkwijk. J Biol Chem 272:20471–20478, 1997.
111. P Djian, M Phillips, K Easley, E Huang, M Simon, RH Rice, H Green. Mol Biol Evol 10:1136–1149, 1993.
112. AM Jetten, JE Shirley. J Biol Chem 261:15097–15101, 1986.

113. KW Marvin, MD George, W Fujimoto, NA Saunders, SH Bernacki, AM Jetten, Proc Natl Sci USA 89:11026–11030, 1992.
114. US Singh, JW Erickson, RA Cerione. Biochemistry 34:15863–15871, 1995.
115. SJ Kwak, SY Kim, YS Kim, KY Song, IG Kim, SC Park. Exp Mol Med 30:177–185, 1998.
116. SN Murthy, PT Velasco, L Lorand. Exp Eye Res 67:273–281, 1998.
117. F Tokunaga, M Yamada, T Miyata, YL Ding. M Hiranaga-Kawabata, T Muta, S Iwanaga, A Ichinose, EW Davie. J Biol Chem 268:252–261, 1993.
118. R Pasternack, S Dorsch, JT Otterbach, IR Robenek, S Wolf, HL Fuchsbauer. Eur J Biochem 257:570–576, 1998.
119. M Scott, SM Thacher. J Invest Dermatol 92:578–584, 1989.
120. M Signoini, F Bortolotti, Poltronieri, CM Bergamini. Biol Chem Hoppe Seyler 369:275–281, 1988.
121. H Ogawa, LA Goldsmith. J Biol Chem 251:7281–7288, 1976.
122. Y Ando, S Imamura, Y Yamagata, T Kikuchi, T Murchi, R Kannagi. J Biochem 101:1331–1337, 1987.
123. A Ichinose, H Kaetsu. Methods Enzymol 222:36–51, 1993.
124. PP Brookhart, PL McMahon, M Takahashi. Anal Biochem 128:202–205, 1983.
125. CR Knight, CR Rees, BM Elliot, M Griffin. FEBS Lett 265:93–96, 1990.
126. EM Wilson, FS French. J Biol Chem 255:10946–10953, 1980.
127. WC Wong, C Batt, JE Kinsella. Int J Biochem 22:53–59, 1990.
128. S Roger. RasMol version 2.6, Greenford, Middlesex, UK: Glaxo Research and Development, http://www.umass.edu/microbio/rasmol/index2.htm
129. KN Parameswaran, XF Cheng, EC Chen, PT Velasco, JH Wilson, L Lorand. J Biol Chem 272:10311–10317, 1997.

52

Feruloyl Esterases

Craig B. Faulds
Institute of Food Research, Colney, Norwich, England
Gary Williamson
Nestlé Research Centre, Lausanne, Switzerland

I. INTRODUCTION

Feruloyl esterases (ferulic acid esterase, cinnamoyl esterase, cinnamoyl ester hydrolase, FAE,* FE, etc.) belong to the class of carboxylesterases (EC 3.1.1.1). These esterases catalyze the hydrolysis of ester-linked ferulic acid groups from a wide range of substrates. The product is a phenolic carboxylic acid and an alcohol.

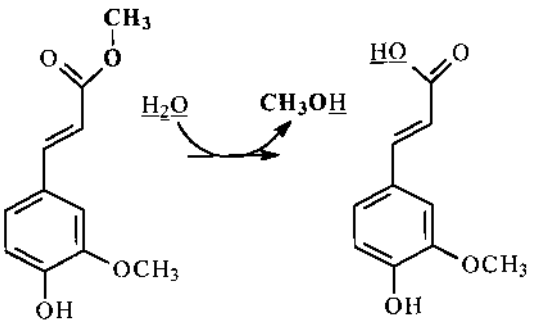

* ***Abbreviations***: AEBSF, 4-(2-amino-ethyl)-benzenesulfonyl fluoride; AraF, ferulic acid-arabinose ester; BLAST, basic local alignment search tool; CinnAE, type-B feruloyl esterase from *Aspergillus niger*; DFP, di-isofluorophosphate; EDTA, ethylenediaminetetra-acetic acid; FAE, feruloyl esterase; FAEA, type-A feruloyl esterase from *Aspergillus niger*; FE, feruloyl esterase; HPLC, high-pressure liquid chromatography; MFA, methyl ferulate; SDS-PAGE, sodium dodecylsulfate polyacrylamide gel electrophoresis.

Arabinoxylans and certain pectins contain ester-linked ferulic acid as shown in Figures 1 and 2 (1). The ferulic acid can be either monomeric or in one of several dimeric forms (2) (Fig. 3). Free ferulic acid and two of the ferulate dimers (5-5′ mainly, but also the 8-*0*-4′-linked dimer) are released from arabinoxylans in wheat bran or from pectins in sugar beet pulp by some feruloyl esterases. This activity is greatly enhanced by xylanases (3).

II. IMPORTANCE TO FOOD QUALITY AND UTILIZATION IN FOOD PROCESSING

The action, amount, and importance of endogenous feruloyl esterase in foods are unknown. Plants, especially cereals, produce feruloyl esterases (4). The role of these enzymes in plant tissue has yet to be elucidated. Endogenous activity could influence structural and textural properties during processing. Most microbial feruloyl esterases are secreted into the culture medium. Generally, monosaccharides and oligosaccharides do not induce production of feruloyl esterases but may be involved in other aspects of their regulation. Polymeric substrates such as oat spelt xylan, wheat bran, pectins, and maize bran induce production of a mixture of different forms of feruloyl esterase. Addition of free ferulic acid to the culture medium further stimulates production of feruloyl esterases (5).

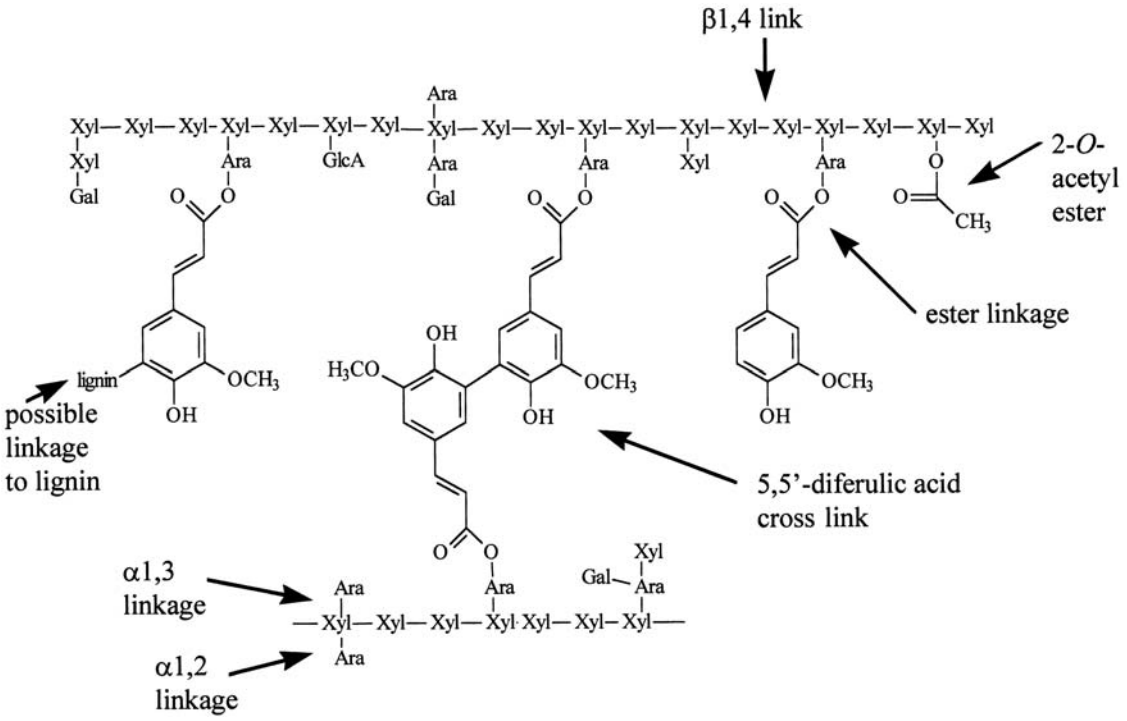

Figure 1 Simplified structure of arabinoxylan, emphasizing the attachment of ferulic acid.

The commercial production of vanillin from agro-industrial wastes such as cereal brans and sugar beet pulp requires treatment of the starting materials with enzyme mixtures containing xylanase and feruloyl esterase. The released ferulic acid is bioconverted by microbes (*Aspergillus niger, Pycnoporus cinnabarinus, Pseudomonas* spp.) into vanillin (6, 7). Other possible uses are in baking or any food process involving plant cell walls.

III. PROPERTIES OF THE PROTEIN

In recent years, the number of microbial cinnamoyl esterases identified has reached > 30, with 10 genes sequenced. Some esterases are part of a modular complex (8–9), contain cellulose-binding modules (10, 11), or exist as only a catalytic domain (12). No structural data have been published, although recently a crystal of the cinnamoyl esterase domain of XynZ from the anaerobic bacteria *Clostridium thermocellum* was obtained (13). Two feruloyl esterases will be considered here: feruloyl esterase A (FAE-III as purified from culture supernatants of *A. niger* CBS120.49 or recombinant FAEA; $M_r = 29{,}700$) (14), and CinnAE ($M_r \sim 150{,}000$ [dimer]), also from *A. niger* (15). Other enzymes that have been purified are listed in Table 1. FAEA from *A. niger* and from *A. tubingesis* show 92% homology in amino acid sequence (12), but there is very little similarity between the feruloyl esterases sequenced to date. The primary protein sequence of FAEA shows some homology to lipases. Based on this homology, FAEA possesses conserved residues at the active site: the nucleophilic serine (residue 133), the catalytic acid (Asp174), and the catalytic base (His247). Based on modeling studies using the lipase template and on chemical modification using dithiobisnitrobenzoic acid treatment of denatured enzyme, FAEA has three intramolecular disulfide bonds and one free cysteine. CinnAE has not yet been cloned, but BLAST searches of short protein sequences show no homology with any other protein.

There is limited glycosylation of FAEA, while CinnAE is extensively glycosylated, possibly up to 40% (ww). *A. tubingensis* FAEA is more susceptible to proteolysis than *A. niger* FAEA, and this can give rise to multiple bands on Western blots in culture supernatants. This susceptibility may be due to residue differences at locations on the protein surface (16). Although no more than one gene encoding feruloyl esterases have been sequenced from a single source, there is some evidence of enzymatic isoforms existing.

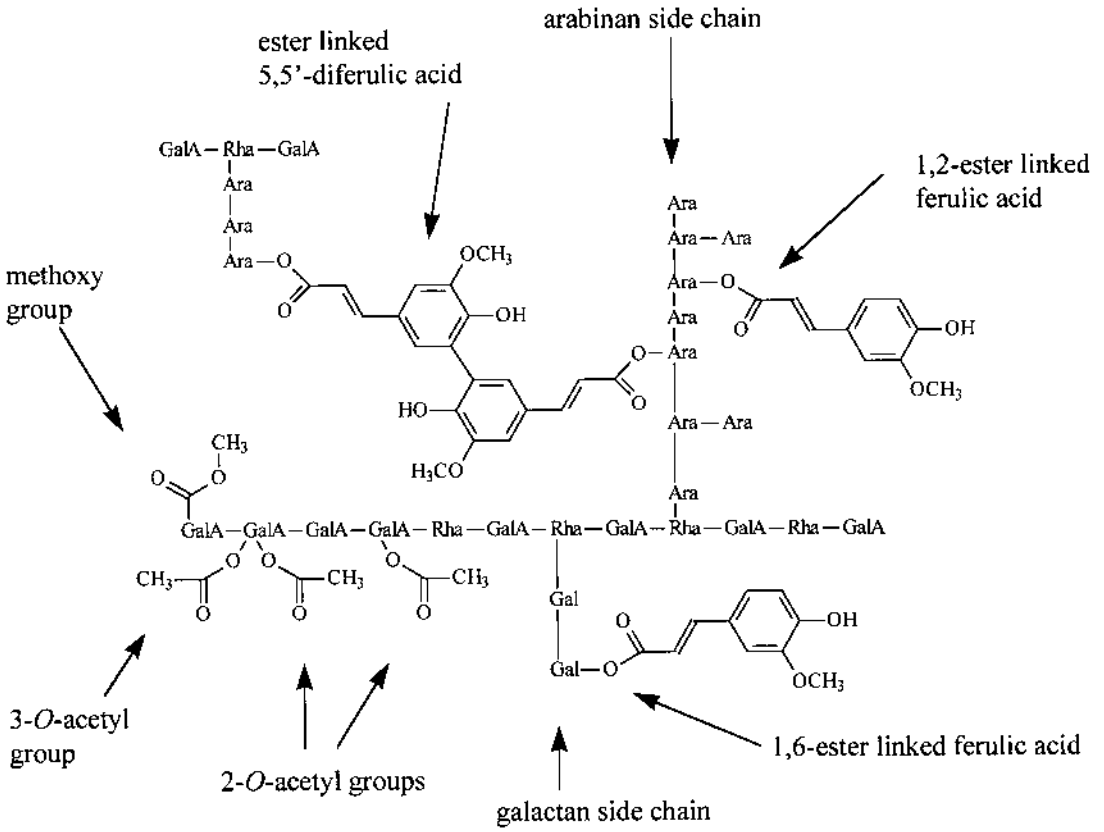

Figure 2 Simplified structure of sugarbeet pectin, emphasizing the attachment of ferulic acid.

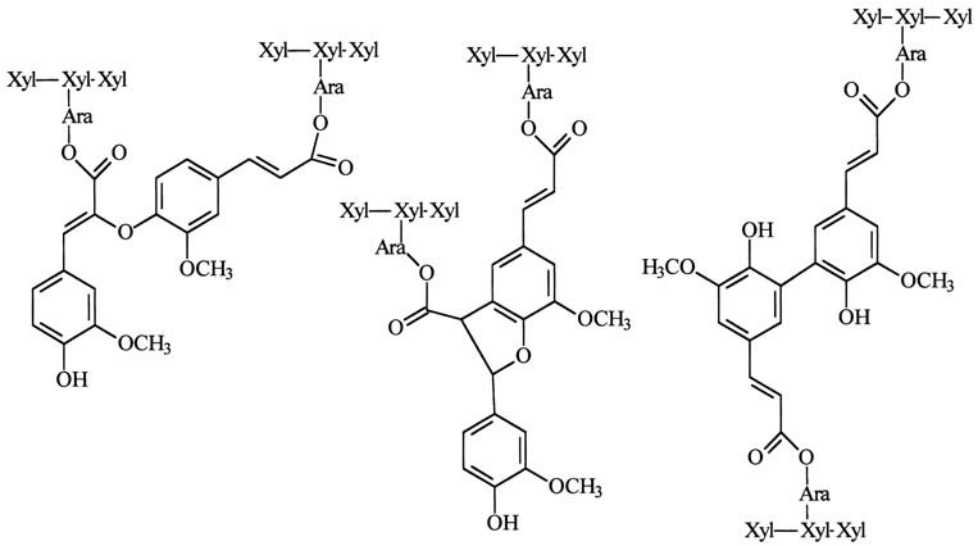

Figure 3 The most abundant diferulic acids found in plant cell walls: 8-0-4′, 8-5′ benzofuran and 5-5′ diferulic acids linked to sugars.

Table 1 Ferulic Acid Esterases Purified from Microbial Sources

Organism	Enzyme	Native M_r (kDa)	Reference
Neocallimastix MC-2	FAE-I	69	28
Neocallimastix MC-2	FAE-II	24	28
Neocallimastix MC-2	*p*CAE	11	34
P. pinophilum	*p*-CAE/FAE	57	29
P. funiculosum	FaeB	53	11
P. expansum	*p*-CAE/FAE	57.5	33
A. awamori	FAE	112	30
A. awamori	*p*-CAE	75	30
A. oryzae	FAE	30	31
A. niger	FAE-I/CinnAE	145	15, 17
A. niger	FAE-II/FAE-III/FAEA	29.7	12, 14, 17
B. fibrisolvens	CEH (*cinA*)	27	25
B. fibrisolvens	CEH (*cinB*)	31.4	32
Piromyces equis	EstA	37	10
S. olivochromogenes	FAE	29	35
Ps. fluorescens	*XYLD*	58.5	36

FAE-I was purified from a commercial source of pectinase originally obtained from *a. niger* (17). On the basis of physical properties and substrate specificity, it may be a posttranslationally modified form of CinnAE. Likewise, FAE-II was also purified from the pectinase preparation and may be a posttranslationally modified form of FAEA.

IV. ENZYMATIC PROPERTIES

Although there have yet to be any reports on active site inhibitor kinetics or active site mutagenesis of feruloyl esterases, the mechanism of action of these esterases is probably analogous to other serine esterases and lipases, and involves a nucleophilic serine (Ser133 in FAEA), which can be modified by the reagent, di-isofluorophosphate (DFP). By analogy with lipases, a catalytic acid and base are also essential. CinnAE activity is lost on modification with AEBSF, which also indicates the involvement of an active site nucelophilic serine. Feruloyl esterases isolated to date do not require the presence of a cofactor.

Tables 2–8 show the activity of FAEA and CinnAE on a range of different substrates. The substrate can be considered to be two moieties, a phenolic and an esterified group, either a sugar or alkyl substituent. A summary of the specificity of each enzyme is shown in Figures 4 and 5. Methyl caffeate is not a substrate for FAEA, but competitively inhibits it with a K_i of ~ 1.5 mM (18). Based on the selective hydrolytic activity shown in these tables, a putative classification of fer-

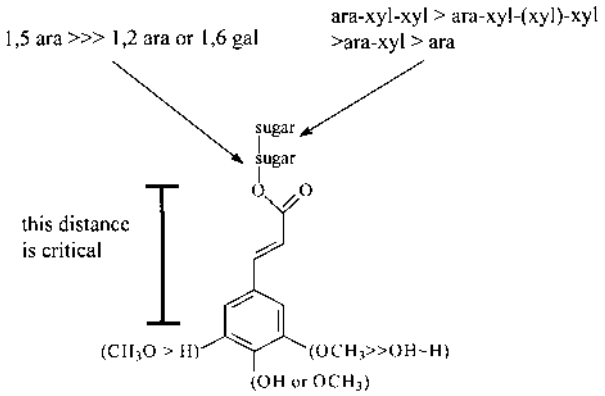

Figure 4 Summary of the specificity and preferences of FAEA for substrates.

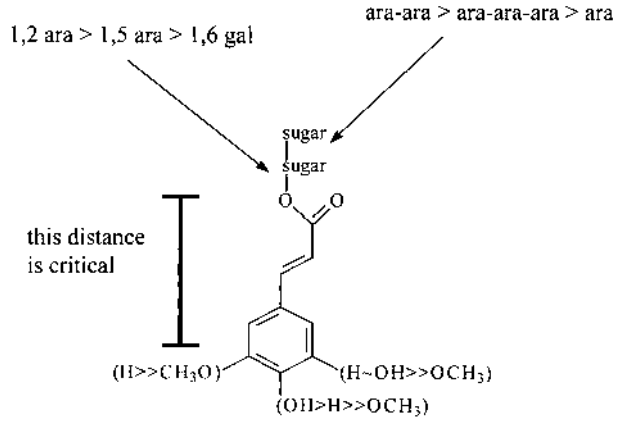

Figure 5 Summary of the specificity and preferences of CinnAE for substrates.

Table 2 Influence of Length and Saturation in the Aliphatic Chain on Activity of FAEA and CinnAE on Methyl Esters

Substrate	FAEA K_m (mM)	FAEA V_{max} (sec^{-1})	(OH^-) $k_2 \times 10^3$ ($dm^3\ mol^{-1} sec^{-1}$)	CinnAE K_m (mM)	CinnAE V_{max} (sec^{-1})
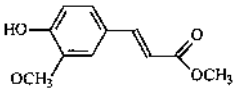	2.1	87	2.5	1.3	12
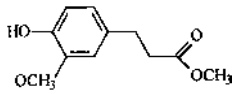	3.2	289	120	2.0	610
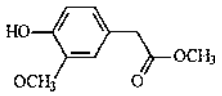	—	—	11	—	—
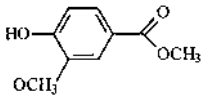	—	—	07	—	—

[a] Comparison, the rate of deesterifiation with NaOH is also shown.
Source: Ref. 18.

Table 3 Influence of Length of the Aliphatic Chain on Activity of FAEA and CinnAE on Methyl Esters

Substrate	FAEA K_m (mM)	FAEA V_{max} (sec^{-1})	(OH^-) $k_2 \times 10^3$ ($dm^3\ mol^{-1}\ sec^{-1}$)	CinnAE K_m (mM)	CinnAE V_{max} (sec^{-1})
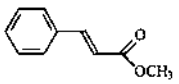	—	—	8	0.79	56
	—	—	4.4	—	—

[a] For comparison, the rate of deesterifiation with NaOH is also shown.
Source: Ref. 18.

uloyl esterases has been proposed: type A (e.g., *A. niger* FAEA) and type B (e.g., *A. niger* CinnAE, *P. funiculosum* FAEB), although there are exceptions (e.g., *P. fluorescens* XYLD), and not all enzymes displaying feruloyl esterase activity have been tested for activity using all the substrates used for FAEA and CinnAE. There is clearly a dependence of the rate of reaction on the number and nature of sugars in the substrate (Tables 6, 7) (19). However, it is not known if this is due to the presence of subsites on the esterases. The pH optimum of FAEA is 5.0, and that of CinnAE is 6.0.

The stability of FAEA to thermal and chemical denaturation has been studied. Thermodynamic parameters are shown in Table 8. FAEA is most stable at pH 5–6, where it retains ~ 50% of its catalytic activity after 1 h incubation at 60°C (20).

Like many esterases, feruloyl esterases catalyze the reverse reaction—i.e., synthesis of an ester bond (21). Although this reaction has only been reported with pentanol, the potential is there to make feruloylated esters with novel biological activities and applications.

V. MEASUREMENT OF FERULOYL ESTERASE ACTIVITY

To measure feruloyl esterase activity, a range of low-molecular-weight synthetic methyl esters can be used as substrates, as described above (Fig. 6). Suitable natural substrates, which are feruloylated, are wheat arabinoxylan or sugar beet pulp (Figs. 1, 2). The rate of

Table 4 Influence of Number of Methoxy Groups on Activity of FAEA and CinnAE on Methyl Esters

Substrate	FAEA K_m (mM)	FAEA V_{max} (sec^{-1})	(OH^-) $k_2 \times 10^3$ ($dm^3\ mol^{-1}\ sec^{-1}$)	CinnAE K_m (mM)	CinnAE V_{max} (sec^{-1})
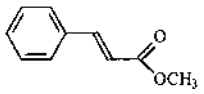	—	—	8	0.8	55
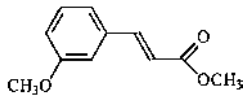	2	9.9	61	—	—
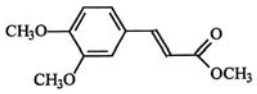	1.4	61	33	—	—
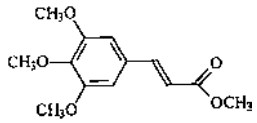	1.6	880	45	—	—

[a] For comparison, the rate of deesterification with NaOH is also shown
Source: Ref. 18.

Table 5 Influence of Position of a Single Methoxy Group on Activity of FAEA and CinnAE on Methyl Esters

Substrate	FAEA K_m (mM)	FAEA V_{max} (sec^{-1})	(OH^-) $k_2 \times 10^3$ ($dm^3\ mol^{-1}\ sec^{-1}$)	CinnAE K_m (mM)	CinnAE V_{max} (sec^{-1})
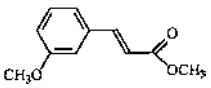	2	9.9	61	—	—
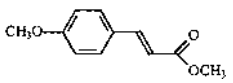	—	—	22	0.31	99
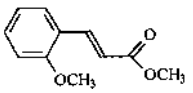	—	—	41	0.85	65

[a] For comparison, the rate of deesterification with NaOH is also shown.
Source: Ref. 18.

reaction is increased in the presence of a xylanase or arabinofuranosidase/arabinanase respectively.

Table 9 shows the activity of native FAEA and recombinant FAEA on methyl ferulate at pH 6.0, 37 °C (12). The assay for feruloyl esterases can be performed in several ways, but the most convenient is to use methyl ferulate as a substrate and monitor the reaction in a spectrophotometer (19). The limitation of this method is that the absorbance of methyl ferulate makes it difficult to use the substrate at concentrations about the K_m. As a standard method, the total assay volume is 0.6 mL in disposable semimicro cuvettes with a 1-cm path length. For higher substrate concentrations, 0.3 mL in 0.1-cm path length cuvettes can be used. Dissolve methyl ferulate in methanol and add a small amount to 100 mM MOPS, pH 6.0. Determine the A_{335} of a solution of $\sim 100\,\mu M$ ($A_{335} = 1.4$; E_{335} for MFA is $1400\,M^{-1}\,cm^{-1}$). Add 0–100 μL of the enzyme solution to appropriate volumes of assay mixture so that final volume is 0.6 mL (1-cm path length) or 0.3 mL (0.1 cm) and incubate at 37°C. Calculate the rate using ΔE of

Table 6 Influence of Number of Hydroxyl Groups on Activity of FAEA and CinnAE on Methyl Esters

Substrate	FAEA K_m (mM)	FAEA V_{max} (sec^{-1})	(OH^-) $k_2 \times 10^3$ ($dm^3\,mol^{-1}\,sec^{-1}$)	CinnAE K_m (mM)	CinnAE V_{max} (sec^{-1})
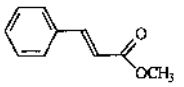	—	—	8	0.79	55
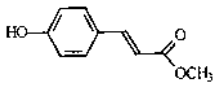	—	—	6	0.014	54
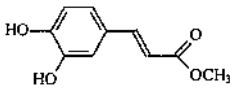	—	—	2	0.22	85

[a] For comparison, the rate of deesterifiation with NaOH is also shown.
Source: Ref. 18.

Table 7 Influence of Sugars on Activity of FAEA and CinnAE on Feruloylated Oligosaccharides; All Ferulic Acid–Sugar Linkages are $1 \rightarrow 5$ (substrates derived from limited hydrolysis of wheat or maize bran)

Substrate (all $1 \rightarrow 5$ linked)	FAEA (V_{max}/K_m)	CinnAE (V_{max}/K_m)
	1728	3.5
	2448	30
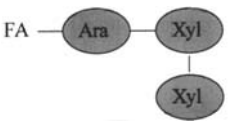	7600	34
	1086	17
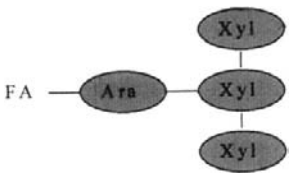	3270	nd

$9300\,M^{-1}\,cm^{-1}$ at 335 nm (19). Other assays reported include, using a microtiter plate containing AraF (22), ethyl cinnamate in agar with pH sensitive dye (23), separation of substrate and product by capillary zone electrophoresis (24) or MUTMAC (4-methylumbelliferoyl [*p*-trimethyl ammonium cinnamate chloride]) with detection by fluorescence (25).

Table 8 Influence of Sugars on Activity of FAEA and CinnAE on Feruloylated Oligosaccharides; All Ferulic Acid–Sugar Linkages are $1 \rightarrow 2$ (substrates derived from limited hydrolysis of sugarbeet pulp)

Substrate (all $1 \rightarrow 2$ linked)	FAEA (V_{max}/K_m)	CinnAE (V_{max}/K_m)
	0	14
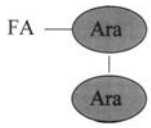	0	204
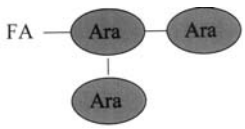	0	109

The most accurate and time-consuming assay for the measurement of the release of ferulic acid is by HPLC. This is the only assay that can be used when measuring the release of phenolic acids (ferulic acid and dimers) from insoluble plant cell wall-derived material (26). Samples of plant material (e.g., 10 mg) and enzyme preparation diluted in buffer (in a total volume of 0.5 mL) are incubated at a specific temperature for selected times. It is important to mix the reaction tube during this step to ensure complete interaction between the enzyme and the substrate. Reactions are stopped by the addition of glacial acetic acid (0.2 mL) and centrifuged, and the supernatant is filtered through a 0.22-μm filter. The

Table 9 Thermodynamic Parameters for FAEA

ΔG (H_2O) (kJ/mol) with GuHCl as denaturant (30°C, pH 6.0)	Slope (*m*) (kJ/mol.M) with GuHCl as denaturant (30°C, pH 6.0)	$[GuHCl]_{1/2}$ (M) (30°C, pH 6.0)	$k_{(unfolding)}$ (sec^{-1}) (60°C, pH 6.0)	$k_{unfolding)}$ (sec^{-1}) (60°C, pH 6.0) with 0.1 mM sinapic acid
16.5	−11.9	1.38	0.0076	0.0066

The rate of irreversible thermal denaturation is given by the first-order rate constant, $k_{(unfolding)}$, and the stability is slightly increased in the presence of sinapic acid, which is a product of the hydrolysis of methyl sinapate.
Source: Ref. 20.

Table 10 Kinetic Parameters for FAE-III and Recombinant FAEA from *A. niger* Show That the Two Enzymes Are Identical

	FAE-III	FAEA from *A. niger*
M_r (SDS-PAGE)	36000	36000
M_r (mass-spectrometry)	29740 ± 16	29738 ± 50
pI	3.3	3.3
pH optimum	5.0	5.0
temperature optimum	55–60°C	60°C
V_{max} (MFA)	147	143
K_m (MFA)	0.72	0.76

Source: Ref. 12.

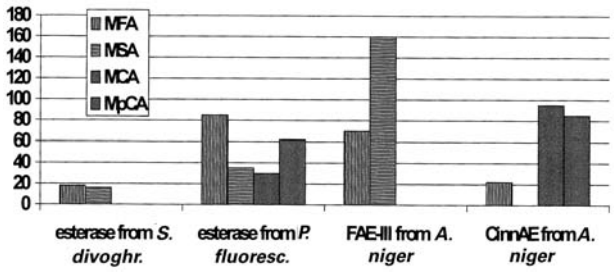

Figure 6 Using methyl esters of ferulic (MFA), caffeic (MCA), sinapic (MSA), and *p*-coumaric (MpCA) acids to fingerprint esterases from *Streptomyces olivochromogenes, Pseudomonas fluorescens,* and *Aspergillus niger*. The y axis shows specific activity (U/mg protein) for the *A. niger* enzymes, and the specific activity (U/mg) multiplied by 100-fold for the *S. olivochromogenes* and *P. fluorescens* enzymes.

supernatant is then injected onto an HPLC column (e.g., Spherisorb ODS 3), and the amount of free phenolic acid released is quantified from a standard curve (27).

VI. PURIFICATION PROCEDURES

Most microbial feruloyl esterases are extracellular. In this section, we describe the purification of FAEA from *Aspergillus niger* (14). Slight variations of these procedures have been used for a number of microbial feruloyl esterases.

Prepare 20 L of liquid media (2 L media in each 5-L conical flask) containing 1.0% (w/v) oat spelt xylan, incubate with *Aspergillus niger* (CBS, 120.49) at 25°C and 120 rpm for 4 days. At the end of the incubation, pass the culture supernatant though a double layer of muslin, and clarify by centrifugation (4000 rpm/15 min at 4°C). The culture supernatant is concentrated to 800 mL (10,000 M_r cutoff). Concentrated culture supernatant is fractionated by 50–80% saturated ammonium sulfate, and the pellet from 80% saturation is resuspended in 80–100 mL of 50 mM sodium phosphate, pH 7.0, 1 mM EDTA, the solution made up to 1 M $(NH_4)_2SO_4$ and then filtered through a 0.45-μm cellulose acetate filter. Hydrophobic interaction chromatography (HIC) is carried out using two buffers: Buffer A—50 mM phosphate, pH 7.0, 1 mM EDTA, 1.7 M $(NH_4)_2SO_4$; Buffer B—50 mM phosphate, pH 7.0, 1 mM EDTA. The prepared sample is loaded into a HiLoad column (200 mL). FAEA elutes at 100% Buffer B. The fractions containing activity are then again subjected to a repeat hydrophobic interaction chromatography step. The pooled FAEA sample from the previous step is made 1 M $(NH_4)_2SO_4$, filtered through a 0.45-μm cellulose acetate filter, and then applied again to a smaller HiLoad (50 mL) column with the same gradient. The active fractions are then applied to an anion exchange column using MonoQ (10/10) with a gradient of Buffer A: 20 mM Tris-HCl, pH 8.5, 1 mM EDTA to Buffer B: 20 mM Tris-HCl, pH 8.5, 1 mM EDTA, 1 M KCl. FAEA elutes at 35% Buffer B. At this stage, the enzyme is essentially pure

by SDS-PAGE. Feruloyl esterases are relatively stable when stored frozen between pH 5 and 6.

REFERENCES

1. G Williamson, PA Kroon, CB Faulds. Hairy plant polysaccharides: a close shave with microbial esterases. Microbiol 144:2011–2023, 1998.
2. J Ralph, S Quideau, JH Grabber, RD Hatfield. Identification and synthesis of new ferulic acid dehyrodimers present in grass cell walls. J Chem Soc Perkin Trans 1:3485–3498, 1994.
3. B Bartolomé, CB Faulds, PA Kroon, K Waldron, G Williamson. An *Aspergillus niger* esterase (FAE-III) and a recombinant *Pseudomonas fluorescens* subsp. *cellulosa* esterase (XYLD) release a 5-5′ ferulic dehydrodimer (''diferulic acid'') from barley and wheat cell-walls. Appl Environ Microbiol 63:208–212, 1997.
4. AI Sancho, CB Faulds, B Bartolomé, G Williamson. Characterization of feruloyl esterase activity in barley. J Sci Food Agric 79:447–449, 1999.
5. CB Faulds, RP de Vries, PA Kroon, J Visser, G Williamson. Influence of ferulic acid on the production of feruloyl esterases by *Aspergillus niger*. FEMS Microbiol Lett 157:239–244, 1997.
6. JF Thibault, M Asther, B Colonna-Ceccaldi, D Couteau, M Delattre, CB Faulds, HP Heldt-Hansen, PA Kroon, L Lesage-Meessen, V Micard, C Renard, M Tuohy, S Van Hulle, G Williamson. An integrated multidisciplinary approach for the fungal biotransformation of European agricultural by-products to natural vanillin. Lebensm-Wiss Technol 31:530–536, 1998.
7. NJ Walton, A Narbad, CB Faulds, G Williamson. Novel approaches to the biosynthesis of vanillin. Curr Opin Biotechnol 11:490–496, 2000.
8. JI Laurie, JH Clarke, A Ciruela, CB Faulds, G Williamson, HJ Gilbert, JE Rixon, J Millward-Sadler, GP Hazlewood. The NodB domain of a multidomain xylanase from *Cellulomonas fimi* deacetylates acetylxylan. FEMS Microbiol Lett 148:261–264, 1997.
9. DL Blum, IA Kataeva, X-L Li, LG Ljungdahl. Feruloyl esterase activity of the *Clostridium thermocellum* cellulosome can be attributed to previously unknown domains of XynY and XynZ. J Bacteriol 182:1346–1352, 2000.
10. IJ Fillingham, PA Kroon, G Williamson, HJ Gilbert, GP Hazlewood. A modular cinnamoyl ester hydrolase from the anaerobic fungus *Piromyces equi* acts synergistically with xylanase and is part of a multiprotein cellulose-binding cellulase-hemicellulase complex. Biochem J 343:215–224, 1999.
11. PA Kroon, G Williamson, NM Fish, DA Archer, NJ Belshaw. A modular esterase from *Pencillium funiculosum* which releases ferulic acid from plant cell walls and binds crystalline cellulose contains a carbohydrate binding module. Eur J Biochem 267:6740–6752, 2000.
12. RP deVries, B Michelsen, CH Poulsen, PA Kroon, RHH van den Heuvel, CB Faulds, G Williamson, JPTW van den Hombergh, J Visser. The *faeA* genes from *Aspergillus niger* and *Aspergillus tubingensis* encode ferulic acid esterases involved in degradation of complex cell wall polysaccharides. Appl Environ Microbiol 63:4638–4644, 1997.
13. DL Blum, FD Schubot, LG Lgungdahl, JP Rose, B-C Wang. Crystallization and preliminary x-ray analysis of the *Clostridium thermocellum* cellulosome xylanase Z feruloyl esterase domain. Acta Crystallogr D56:1027–1029, 2000.
14. CB Faulds, G Williamson. Purification and characterization of a ferulic acid esterase (FAE-III) from *Aspergillus niger*. Specificity for the phenolic moiety and binding to microcrystalline cellulose. Microbiol 140:779–787, 1994.
15. PA Kroon, CB Faulds, G Williamson. Purification and characterization of a novel esterase induced by growth of *Aspergillus niger* on sugar-beet pulp. Biotechnol Appl Biochem 23:255–262, 1996.
16. CB Faulds, FO Aliwan, RP de Vries, RW Pickersgill, J Visser, G Williamson. Chemical and thermal stability of ferulic acid (feruloyl) esterases from *Aspergillus*. In: A Ballesteros, FJ Plou, JL Iborra, P Halling, eds. Stability and Stabilisation of Biocatalysts, Progress in Biotechnology 15. Amsterdam: Elsevier, 1998, pp 41–46.
17. CB Faulds, G Williamson. Ferulic acid esterases from *Aspergillus niger*: purification and partial characterisation of two forms from a commercial source of pectinase. Biotechnol Appl Biochem 17:349–359, 1993.
18. PA Kroon, CB Faulds, C Brezillon, G Williamson. Methyl phenylalkanoates as substrates to probe the active site of esterases. Eur J Biochem 248:245–251, 1997.
19. MC Ralet, CB Faulds, G Williamson, J-F Thibault. Feruloylated oligosaccharides from sugar-beet cell wall polysaccharides. Part III. Degradation by ferulic acid esterases from *Aspergillus niger*. Carbohydr Res 263:257–269, 1994.
20. G Williamson, J Vallejo. Chemical and thermal stability of ferulic acid esterase-III from *Aspergillus niger*. Int J Biol Macromol 21:163–167, 1997.
21. S Giuliani, C Piana, L Setti, Hockkoeppler, PG Pifferi, G Williamson, CB Faulds. Synthesis of pentylferulate by a feruloyl esterase from *Aspergillus niger* using water-in-oil microemulsions. Biotechnol Lett 23:325–330, 2001.
22. JA McCallum, IEP Taylor, GHN Towers. Spectrophotometric assay and electrophoretic detection of trans-feruloyl esterase activity. Anal Biochem 196:360–366, 1991.

23. JA Donaghy, AM McKay. Novel screening assay for the detection of phenolic acid esterases. World J Microbiol Biotechnol 10:41–44, 1994.
24. JA Donaghy, AM McKay. Measurement of feruloyl/*p*-coumaroyl esterase by capillary zone electrophoresis. World J Microbiol Biotechnol 11:160–162, 1995.
25. BP Dalrymple, Y Swadling, DH Cybinski, GP Xue. Cloning of a gene encoding cinnamoyl ester hydrolase from the ruminal bacterium *Butyrivibrio fibrisolvens* E14 by a novel method. FEMS Microbiol Lett 143:115–120, 1996.
26. CB Faulds, PA Kroon, B Bartolomé, G Williamson. Hydrolysis of hemicelluloses using combinations of xylanases and feruloyl esterases. In: C Burke, ed. Methods Biotechnology 10, Carbohydrate Biotechnology Protocols. Totowa, NJ: Humana Press, 1998 pp 183–195.
27. KW Waldron, AJ Parr, A Ng, J Ralph. Cell wall esterified phenolic dimers: identification and quantification by reverse phase high performance liquid chromatography and diode array detection. Phytochem Anal 7:305–312, 1996.
28. WS Borneman, LG Ljungdahl, R Hartley, DE Akin. Purification and partial characterisation of two feruloyl esterases from the anaerobic fungus *Neocallimastix* strain MC-2. Appl Environ Microbiol 58:3762–3766, 1992.
29. A Castanares, SI McCrae, TM Wood. Purification and properties of a feruloyl/p-coumaroyl esterase from the fungus *Penicillium pinophilum*. Enzyme Microb Technol 14:875–884, 1992.
30. SI McCrae, KM Leith, AH Gordon, TM Wood. Xylan-degrading enzyme system produced by the fungus *Aspergillus awamori*: isolation and characterization of a feruloyl esterase and a *p*-coumaroyl esterase. Enzyme Microb Technol 16:826–834, 1994.
31. M Tenkanen, J Schuseil, J Puls, K Poutanen. Production, purification and characterisation of an esterase liberating phenolic acids from lignocellulosics. J Biotechnol 18:69–84, 1991.
32. BP Dalrymple, Y Swadling. Expression of a *Butyrivibrio fibrisolvens* E14 gene (*cinB*) encoding an enzyme with cinnamoyl ester hydrolase activity is negatively regulated by the product of an adjacent gene (*cinR*). Microbiology 143:1203–1210, 1997.
33. J Donaghy, AM McKay. Purification and characterization of a feruloyl esterase from the fungus *Penicillum expansum*. J Appl Microbiol 83:718–726, 1997.
34. WS Borneman, LG Ljungdahl, RD Hartley, DE Akin. Isolation and characterisation of *p*-coumaroyl esterase from the anaerobic fungus *Neocallimastix* strain MC-2. Appl Environ Microbiol 57:2337–2344, 1991.
35. CB Faulds, G Williamson. The purification and characterisation of 4-hydroxy-3-methoxy-cinnamic (ferulic) acid esterase from *Streptomyces olivochromgenes*. J Gen Microbiol 137:2339–2345, 1991.
36. LMA Ferreira, TM Wood, G Williamson, CB Faulds, GP Hazlewood, HJ Gilbert. A modular esterase from *Pseudomonas fluorescenes* subsp. *cellulosa* contains a non-catalytic binding domain. Biochem J 294:349–355, 1993.

53

Lipase

Dominic W. S. Wong
U.S. Department of Agriculture, Albany, California, U.S.A.

I. INTRODUCTION

Lipases (EC 3.1.1.3) are key enzymes involved in fat digestion in vertebrates by converting insoluble triacylglycerols into more soluble products, fatty acids and monoacylglycerols, that can easily be assimilated by the organism. The lipolysis process is controlled by gastric lipase in the stomach that hydrolyzes dietary fat (triacylglycerols) to fatty acids and diacylglycerols, which are further converted by pancreatic lipase in the intestine to fatty acids and monoacylglycerols for intestinal absorption. Most lipases have a basic pH optimum. Only lipase isolated from lingual or gastric tissue have an acidic pH optimum. Lipases for food processing are obtained from edible forestomach tissue of calves, kids, or lambs, and animal pancreatic tissues as purified edible tissue preparations or as aqueous extracts (1). Industrial lipases are also produced by the controlled fermentation of *Aspergillus niger* var., *Aspergillus oryzae* var., *Candida rugosa*, and *Rhizomucor miehei* as a powder or liquid. Typical applications in the food industry include lipid hydrolysis, manufacture of cheese and cheese flavors, modification of lipids, manufacture of dairy products and confectionery goods, and development of flavors in processed foods (2).

II. CLASSIFICATION

Esterases are classified under hydrolases which are subdivided according to the action on the type of ester bonds. Lipases hydrolyze carboxylic ester bonds of triacylglycerols to diacylglycerols and carboxylates. According to IUBMB nomenclature (3), triacylglycerol lipase or lipase (trivial name) has the systematic name of triacylglycerol acylhydrolase, and a code number of EC 3.1.1.3. The pancreatic enzyme acts only on an ester-water interface, with the outer ester links preferentially hydrolyzed. Other important lipolytic enzymes include phospholipases A1 (EC 3.1.1.32) and A2 (EC 3.1.1.4), which are phosphoglyceride acylhydrolases, and phospholipases C (EC 3.1.4.3) and D (EC 3.1.4.4), which are phosphoric diester hydrolases. Triacylglycerol lipases are distributed widely in animals, plants, and microorganisms. Animal lipases including pancreatic, gastric, intestinal, and milk have been investigated. Microbial lipases are found in *Rhizomucor miehei, Rhizopus delemar, R. niveus, Geotrichum candidum, Candida rugosa* (*C. cylindracea*), *C. antarctica, Humicola lanuginosa, Pseudomonas glumae, Ps. aeruginosa, Ps. cepacia, Ps. fragi*, and *Staphylococcus hyicus*. The present discussion will focus on pancreatic lipases and fungal lipases which have been extensively investigated in terms of their reaction mechanisms and known crystal structures.

III. INTERFACIAL ACTIVATION

Lipases constitute a special class of esterases that acts specifically on water-insoluble esters at oil-water interfaces. Sarda and Desnuelle (4) first demonstrated in a quantitative way that pancreatic lipase exhibits very

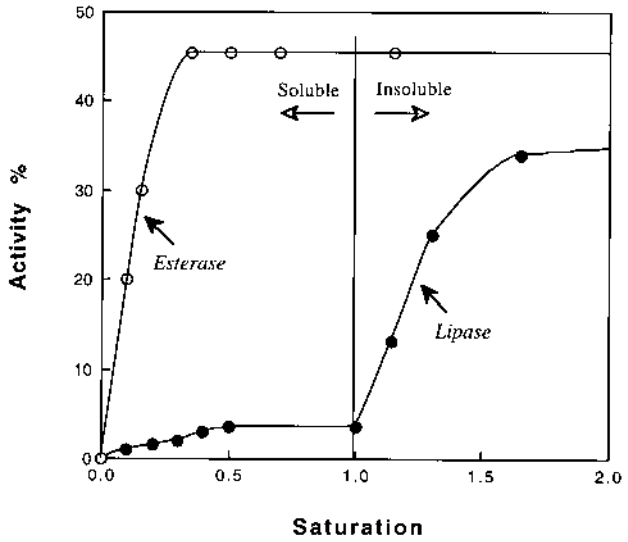

Figure 1 Hydrolysis of triacetin by pancreatic lipase and esterase. (Adapted from Ref. 4.)

little activity when triacetin, a short fatty acid chain triacylglycerol, is in a monomeric (soluble) solution (Fig. 1). However, when the triacetin concentration exceeds the solubility limit and the insoluble substrate forms emulsified particles separated from water by an interface, the lipase activity increases dramatically. Adsorption of lipase at the interface is followed by a 10^3-fold activation. This unique phenomenon of lipases in catalyzing a heterogeneous reaction that involves interfacial activation—a sharp increase in the enzyme activity once the substrate solubility is exceeded and a lipid-water interface appears—is in great contrast to esterases that act on water-soluble substrates and show a normal Michaelis-Menten-type dependence on substrate concentration. (See Sec. V for more details.)

IV. MOLECULAR STRUCTURE

Numerous amino acid sequences of lipases are known, primarily deduced from DNA sequencing. A total of 58 entries are listed in the Swiss-Prot: *Bos tauru* (bovine) pregastric, pancreatic lipase; *Rattus norvegicus* (rat) hepatic, pancreatic, lingual, pancreatic lipase related protein; *Mus musculus* (mouse) hepatic, pancreatic lipase; *canis familiaris* (dog) gastric, pancreatic lipase-related protein; *Homo sapiens* (human) hepatic, pancreatic, gastric, pancreatic lipase-related protein; *Cavia porcellus* (guinea pig) pancreatic; *Oryctolagus cuniculus* (rabbit) pancreatic; *Equus caballus* (horse) pancreatic; *Sus scrofa* (pig) pancreatic; *Candida rugosa* (yeast) (formerly *Candida cylindracea*); *C. albicans* (yeast); *Moraxella* sp; *Geotrichum candidum* (*Oospora lactis*); *Myocastor coypus* (Coypu) (Nutria) pancreatic, pancreatic lipase-related protein; *Chromobacterium viscosum; Rhizomucor miehei; Rhizopus oryzae* (R. *delemar*); *R. niveus; Staphylococcus epidermidis; S. hyicus; S. aureus; Saccharomyces cerevisiae* (baker's yeast); *Photohabdus luminescens* (*Xenorhabdus luminescens*); *Yarrowia lipolytica* (*Candida lipolytica*); *Aeromonas hydrophila* extracellular lipase; *Burkholderia cepacia* (*Pseudomonas cepacia*); *Ps. aeruginosa* lactonizing lipase; *Pseudomonas* sp. (strain KWI-56); *Ps. fluorescens*; *Ps. glumae*; *Ps. fragi; Pseudomonas* sp. (strain 109) lactonizing lipase; *Psychrobacter immobilis; Canadida antarctica* (yeast) (*Trichosporon oryzae*); *Bacillus subtilis; Vibrio cholerae* lactonizing lipase.

The crystal structures of a number of lipases have been solved, including those of *Bos taurus* (bovine) pancreatic lipase; *Sus scrofa* (pig) pancreatic lipase; *Rattus norvegicus* (rat) pancreatic lipase-related protein; *Homo sapiens* (human) gastric, pancreatic lipase, lipase complexed with colipase and phospholipid, lipase complexed with colipase and inhibited by undecane phosphonate methyl ester; *Cavia porcellus* (guinea pig) pancreatic lipase related protein; *Equus caballus* (horse) pancreatic lipase; *Canis familiaris* (dog) pancreatic lipase related protein; *Chromobacterium viscosum* lipase; *Candida antarctica* lipase with phosphonate inhibitor; *Rhizopus niveus* lipase; *R. delemar* lipase; *Candida rugosa* (formerly *C. cylindracea*) lipase, lipase complexed with (*IR*)-methyl hexyl phosphonate, lipase complexed with doecanesulfonate, lipase complexed with hexadecanesulfonate, lipase complexed with hexadecanesulfonate, lipase complexed with (*IS*)-menthyl hexyl phosphonate; *Pseudomonas cepacia* lipase; *Ps. glumae* lipase; *Candida antarctica* lipase; *Rhizomucor miehei* lipase, complex with diethylphosophate, complexed with n-hexylphosphonate ethyl ester; *Geotrichum candidum* strain atcc 34614 lipase; and *Humicola lanuginosa* lipase.

A. Pancreatic Lipases

The porcine pancreatic enzyme is a glycoprotein composed of 450 amino acids with a calculated MW of 50,084 daltons. The enzyme consists of six disulfide bridges, Cys4-Cys10, Cys91-Cys102, Cys238-262, Cys286-297, Cys300-Cys305, and Cys434-450, with two free cysteines, Cys 104 and Cys 182 (5–8) (see also Swiss-Prot). The porcine pancreatic enzyme is

N-glycosylated at Asn167. The glycosylation site Asn167-Gly168-Thr169 in the porcine enzyme is conserved in the human and canine lipases, and the glycan structure of porcine pancreatic lipase has been elucidated (9). In contrast to the human, porcine, and canine pancreatic lipases, the horse, ovine, and bovine enzymes are not glycosylated. Heterogeneity of the glycan moiety at Asn167 gives rise to 4 isoforms, L_{A1}, L_{A2}, L_B, and L_C, with the less anionic L_B the major form (70%) in the porcine enzyme (10). Unlike most of the pancreatic enzymes which are secreted as proenzymes and further activated by proteolytic cleavage in the small intestine, pancreatic lipases are directly secreted as a 50-kDa active enzyme.

The porcine lipase comprises two domains (7). The larger, N-terminal domain (residues 1–336) has an α/β structure, containing the catalytic triad: Ser153, Asp177, and His264. The C-terminal domain (residues 337–450) assumes a β-sandwich, and contains the binding site for colipase. In the human pancreatic lipase, the central parallel β-sheet of the α/β-domain has nine strands cross-connected by α-helices or loops, whereas the C-terminal β-sandwich is formed by two layers of β-sheet, each of four antiparallel strands (11). The crystal structure of the horse enzyme shows close resemblance (8). A significant discovery in the x-ray crystallographic investigation is the existence of a surface loop or flap covering the active site. This "lid" must be repositioned via a conformational change during interfacial activation to allow the substrate to enter the active site. In a lipase-colipase system, the lid, together with the colipase, forms a continuous hydrophobic surface which serves as the lipid binding site of the complex at the interface.

B. Microbial Lipases

Microbial lipases have been extensively studied owing to their potential industrial applications. The phycomycete fungus *Rhizomucor miehei* (formally *Mucor miehei*) produces an extracellular lipase that hydrolyzes a broad spectrum of lipid substrates found in animal plants. The lipase is synthesized as a precursor containing a signal peptide and a propeptide, in addition to 269 amino acid residues of the mature enzyme which has a calculated MW of 29,472 daltons (12). The secreted lipases were purified in two isoforms, A (pI = 3.9) and B (pI = 4.3), because of partial deglycosylation in posttranslational processing (13). The *Geotrichum candidum* lipase also exists in two isoforms, I (pI = 4.56) and II (pI = 4.46) (14). Both have the same chain length of 544 amino acid residues (excluding the signal peptide of 13 residues), with a calculated MW of 59,085, containing two and three N-glycosylation sites, respectively (15). However, lipases I and II, with an overall 84% identity in the two sequences, are encoded by separate genes, *lip1* and *lip2* (16, 17). The asporogenic yeast *Candida rugosa* (formerly *C. cylindracea*) produces extracellular lipase in multiple forms, five of which have been cloned and sequenced: lipase I (pI 4.5), II (pI 4.9), III (pI 5.1), IV (pI 5.7), and V (pI 5.5) (18, 19). All five genes code for 57-kDa proteins of 534 amino acid residues.

The *Rhizomucor miehei* lipase, similar to pancreatic lipases, is an α/β-type protein. The enzyme molecule consists of a central parallel eight-stranded β-sheet folded onto a highly amphipathic N-terminal helix (Fig. 2) (20–22). All the connecting loops are right-handed, and hence located on one side of the β-sheet. Three disulfide bonds, Cys29–Cys268, Cys40–Cys43, and Cys235–Cys244, provide a global stabilization to the protein. The active center containing the catalytic triad (Ser144$\cdots$His257$\cdots$Asp203) is buried under a helical "lid" that is amphipathic in nature. When the enzyme is adsorbed at the lipid-water interface, the lid undergoes conformational changes to roll back from the active site. The hydrophobic side of the lid is exposed to the interface, thereby expanding the nonpolar surface area surrounding the active site. This stabilization of the open form of the lipase at the interface in effect creates a catalytically active enzyme to attack the triacylglycerol molecule with the lipid phase.

The *Geotrichum candidum* lipase has an α/β structure with a central mixed β-sheet formed by 11 strands, seven of which are parallel (23, 24). The helices and loops connecting the strands are found on both sides of the β-sheet. Two disulfide bonds are present: Cys61–Cys105, and Cys276–Cys288. The active site, consisting of the catalytic triad Ser217–His463–Glu354 is concealed by two nearly parallel α helices.

The general molecular architecture has been observed in lipases from other microbial sources, including *Candida rugosa* (25), *C. antarctica* (26), *Rhizopus delmar* (27), *Pseudomonas glumae* (28), and *Ps. aeruginosa* (29). The major difference between the molecular structures of the pancreatic and the microbial enzymes is that the former contains a C-terminal domain serving as the binding site for colipase which is required for facilitating the interfacial catalysis in the presence of bile salts, whereas the latter is devoid of this domain. It should also be noted that lipases do not all subscribe to the phenomenon of interfacial activation. For example, the *Psedomonas aeruginosa* lipase lacks a lid-like helical loop structure covering the

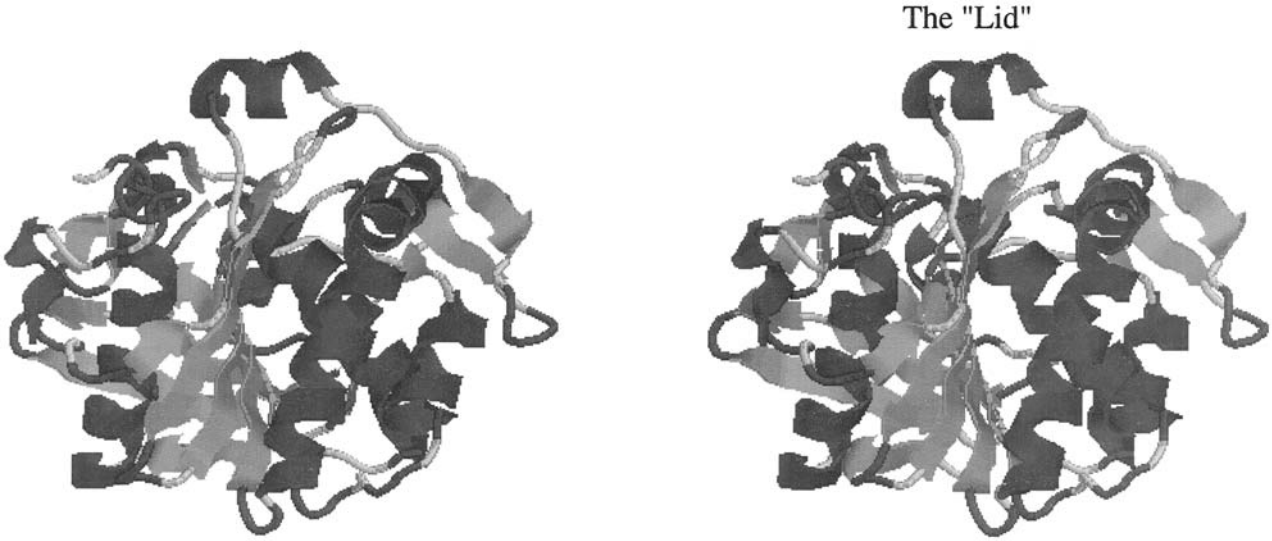

Figure 2 A stereo view of *Candida rugosa* lipase (PDBid: 1trh).

active site, and does not show interfacial activation (30). A lipase isolated from guinea pig was found to carry a deletion in the lid sequence, and shows no interfacial activation (31). In addition to providing accessibility of the active site for the substrate, the opening of the lid causes a concomitant conformational change for proper positioning of the residues forming the oxygen hole during catalysis (22, 25).

V. COLIPASE

Adsorption of protein molecules at the lipid-water interface often leads to unfolding and denaturation. For pancreatic lipases, adsorption at the interface results in decreased activity and consequently inactivation. In the physiological environment, the activity of pancreatic lipases is regulated by the presence of bile salts (cholic and chenodeoxycholic acids conjugated with glycine or taurine, such as taurodeoxycholate, glycodeoxycholate, or taurocholate) and other amphiphilic compounds, such as phospholipids and proteins. The presence of bile salts creates a negatively charged film on the triacylglycerol micelle that prevents lipase adsorption (32, 33). The cooperative formation of an enzyme–bile salt complex with a dissociation constant of 1.4×10^{-15} M prevents the adsorption to the interface (34). For a pancreatic lipase to act at the interface, the enzyme requires the binding of colipase, a 10-kDa protein also secreted by the exocrine pancreas, to facilitate adsorption of the enzyme at bile salt-coated lipid-water interface. The inhibitory action of bile salts is observed on both microbial and pancreatic lipases, but the activity of the pancreatic enzyme can only be restored by the addition of pancreatic colipase, indicating that specific interactions occur between the pancreatic lipase and colipase (35).

Porcine pancreatic colipase is a single polypeptide chain containing 96 amino acid residues with five disulfide bridges, and has an isoelectric point of 5.0 (36). Its primary structure has been determined by protein sequencing (37, 38). The protein is synthesized as a procolipase of 101 amino acid residues, and the active form, colipase$_{96}$, is produced by proteolytic (tryptic) removal of the N-terminal pentapeptide (Val-Pro-Asp-Pro-Arg) (39, 40).

Colipase consists of a small N-terminal region and a three-fingers region held together by disulfide bridges (41, 42). Colipase exhibits an overall amphipathic character with most hydrophilic residues found in the N-terminal region, whereas most of the hydrophobic residues are located at the tip of the fingers in the opposite side that constitute the lipid-binding site (43–46).

Binding of colipase to lipase occurs between two hairpin loops (residues 44–46, 65–67) in the N-terminal region of colipase, and the β-sheet of the C-terminal domain of the lipase molecule (41, 46). The interactions are mostly hydrophilic with the formation of two salt bridges and six hydrogen bonds. Porcine pancreatic lipase binds to colipase to form a 1:1 complex with a K_d of 5×10^{-7} M in the absence of an interface (34, 47, 48). In the presence of 2 mM sodium tauro-

deoxycholate and 150 mM NaCl, binding of lipase to colipase at pH 7.0 has a K_d of 2×10^{-6} M (49).

The binding of colipase to the bile salt–liquid substrate at the interface involves the three-finger region that forms a hydrophobic surface interacting with the lipid (Fig. 3) (41). The central finger consists of three highly conserved Tyr residues (Tyr55, Tyr58, Tyr59 in porcine prolipase) in a strongly hydrophobic loop (also designated as the tyrosine loop region) that has long been implicated as the lipid-binding site (50–52). The binding of colipase to the substrate, tributyrin, at pH 7.0 in the presence of 4 mM sodium taurodeoxycholate and 150 mM NaCl has a dissociation constant $K_d = 3.3 \times 10^{-7}$ M (53). The binding of colipase to an emulsion of long-chain triacylglycerols stabilized with phosphatidylcholine and glycerol showed a K_d of 1.2×10^{-6} M in the presence of 4 mM sodium taurodeoxycholate and 150 mM NaCl at pH 7.0.

Colipase also binds to the surface helix (the lid) covering the catalytic triad of lipase in its open conformation (54, 55). The interaction is mediated by three hydrogen bonds between Arg38, Leu16, and Glu15 of colipase, and Val246, Ser343, and Asn240 of the lid. The binding serves to stabilize the lid during activation, and provides an extended hydrophobic surface that constitutes the lipid-water interface binding site, which is more than 50 Å in length and has a surface area of approximately $965A^2$ (42, 56).

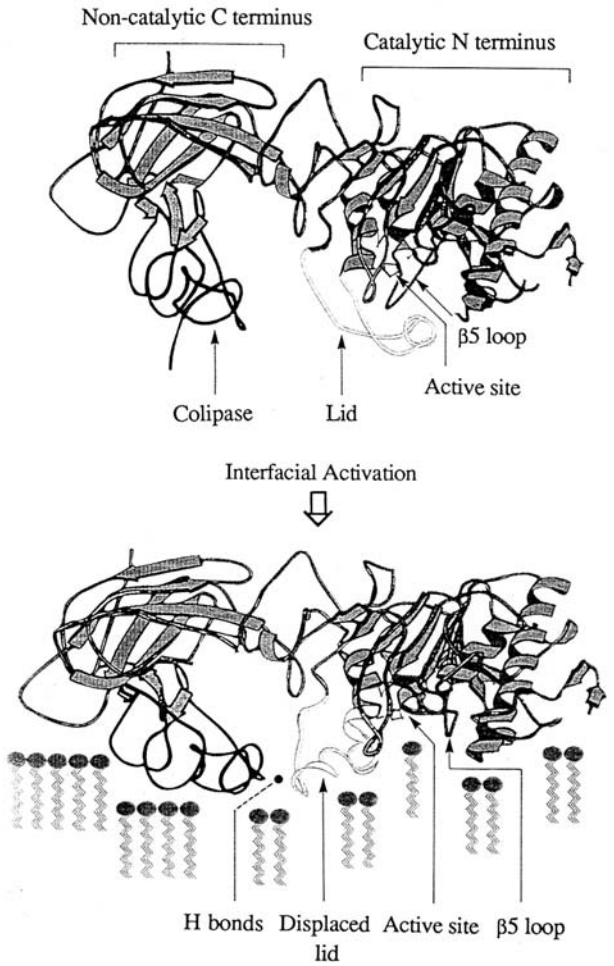

Figure 3 The structure of human pancreatic lipase-colipase complex and its comformational change in the presence of mixed phospholipid/bile salt micelles. (Reprinted from Riddihough 1993, *Nature* 362, 793, with permission. Copyright 1993 Macmillan Magazine, Ltd.)

VI. REACTION MECHANISM

All lipases and esterases contain an active Ser in a consensus sequence G-X-S-X-G which is reminiscent of the pentapeptides in serine proteases (Gly-Asp-Ser-Gly-Gly in the trypsin family, and Gly-X-Ser-X-Ala in subtilisin) (Fig. 4) (57). That most lipases are susceptible to inactivation with classic serine protease inhibitors, such as diisopropylphosphofluoridate and diethyl-*p*-nitrophenyl phosphate, has long been implicated as evidence that lipases belong to the mechanistic class of serine proteases. Recent structural analyses have been shown conclusively that lipases contain the same constellation of the catalytic triad, Ser···His···Asp, present in all serine proteases, although the topological position of the individual residue's side chain varies (11, 20). It has also been demonstrated that the

LIPASES	
Procine pancreatic	VHVIGHSLGSHAA
Canine pancreatic	VQLIGHSLGAHVA
Equine pancreatic	VHIIGHSLGSHAA
Human pancreatic	VHVIGHSLGAHAA
Rat hepatic	VHLIGYSLGAHVS
Human gastric	LHYVGHSQGTTIG
Rhizomucor miehei	VAVTGHSLGGATA
Geotrichum candidum	VMIFGESAGAMSV
Pseudomonas fragi	VNLIGHSQGALTA
Straphylococcus aureus	VHLVGHSMGGQTI
ESTERASES	
Esterase (human)	MSIFGHSMGGH
acetylcholinesterase(*Drosophila*)	MTLFGESAGSS
Thioesterase (Rat mamary gland)	FAFFGHSFGSV
SERINE PROTEASES	
Subtilisin (*Bacillus licheniformis*)	NGTSMASPHV
Subtilisin (Carlsberg)	NGTSMASPHV
Trypsin (rat)	QGDSGGPVVC
Chymotrypsin (rat)	MGDSGGPLVC

Figure 4 Active serine sequences of lipases and esterases compared with serine proteases.

hydrolysis of dissolved *p*-nitrophenyl acetate by pancreatic lipase proceeds via an acyl enzyme intermediate (Fig. 5) with $k_3 = k_{cat}$ (deacylation) $= 0.11 \pm 0.01\ min^{-1}$, k_2 (acylation) $= 7 \pm 0.7\ min^{-1}$, $K_{m(app)} = 0.22 \pm 0.02$ mM, and $K_S = 15$ mM, and that the relation k_{cat}/K_m equals k_2/K_s is consistent with an acyl-enzyme mechanism (58). Using *p*-nitrophenyl butyrate as the substrate, the k_{cat}/K_m values of *Candida cylindracea* lipases A and B have been reported to be 2.51×10^7, and 0.42×10^7 $sec^{-1}M^{-1}$, respectively (59). In the hydrolysis of *p*-nitrophenyl laurate in mixed micelles with Triton X-100, the apparent k_{cat}/K_m values are 3.0×10^5 and $5.6 \times 10^5\ sec^{-1}\ M^{-1}$, respectively for lipase A and B (60).

Since the pioneering work by Matthews et al. (61) on the 3D structure of chymotrypsin, the mechanistic nature of the catalytic triad during catalysis by serine proteases has been the focus of extensive investigations. In the original model of double proton transfer, the catalytic triad is described as a charge relay system involving a concerted double transfer of protons from Ser-OH to His-$N_{\epsilon 2}$ and from His-$N_{\delta 1}$ to Asp-$O_{\delta 2}$ with a schematic representation (Asp-COOH$\cdots$N-Im-NH$\cdots$O-Ser). The negative charge on the carboxylate anion is transferred fully to the carbonyl oxygen of the substrate (62–64). An alternative mechanism proposes that the proton of Ser-OH is transferred to His-$N_{\epsilon 2}$ without the concomitant transfer of the His-$N_{\delta 1}$ proton to the adjacent carboxylate anion (65, 66). NMR and neutron diffraction studies, as well as theoretical calculations of the energetics, suggest that the Asp residue remains ionized and the imidazole is protonated at the transition state to form a charged structure [$Asp^- \cdots His^+ \cdots Ser^-$] (67–70). In this model, positive character will develop on the His imidazole, as negative charge builds up on the carbonyl oxygen from the formation of the new carbon-oxygen bond via the nucleophilic attack of the Ser-O^- at the carbonyl carbon of the substrate.

Taking into account that the lipase-catalyzed hydrolysis of monomeric substrates involves the Ser$\cdots$His$\cdots$Asp triad and the formation of an acylenzyme, the following mechanism can be envisioned to occur based on the catalytic pathway of serine proteases (Fig. 6).

1. The enzyme first binds the substrate to form a Michaelis-Menten adsorption complex.
2. Nucleophilic attack by the essential Ser-OH on the acyl carbon of the substrate yields a covalent tetrahedral intermediate. This step is facilitated by general base catalysis by the His in the triad.
3. A collapse of the intermediate to an acylenzyme involves the His-catalyzed protonation of the ester oxygen of the leaving group.
4. In the following step, deacylation of the acylenzyme occurs with H_2O assisted by general base catalysis involving the His, resulting in the formation of a tetrahedral intermediate.
5. Finally, protonation of the Ser causes the breakdown of the intermediate, resulting in liberation of the product as a carboxylic acid.

It has been well established that oxyanion-binding sites in the proteases, for example, Ser221 and Asn155 in subtilisin, form hydrogen bonds to the carbonyl oxygen of the scissile peptide bond, contributing to the stabilization of the charge distribution and the reduction of the ground-state energy of the tetrahedral intermediate (71). In human lipase, the repositioning of the lid induces a second conformational change in the vicinity of the active site. This brings the Phe78 sided

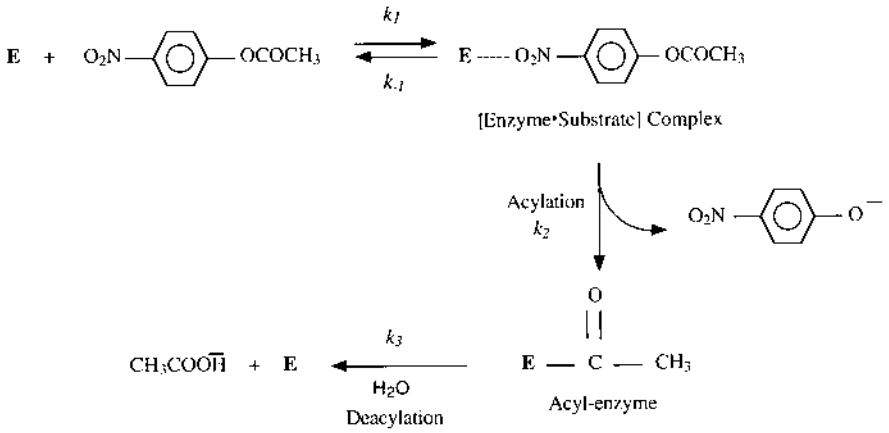

Figure 5 Lipase-catalyzed hydrolysis of *p*-nitrophenyl acetate.

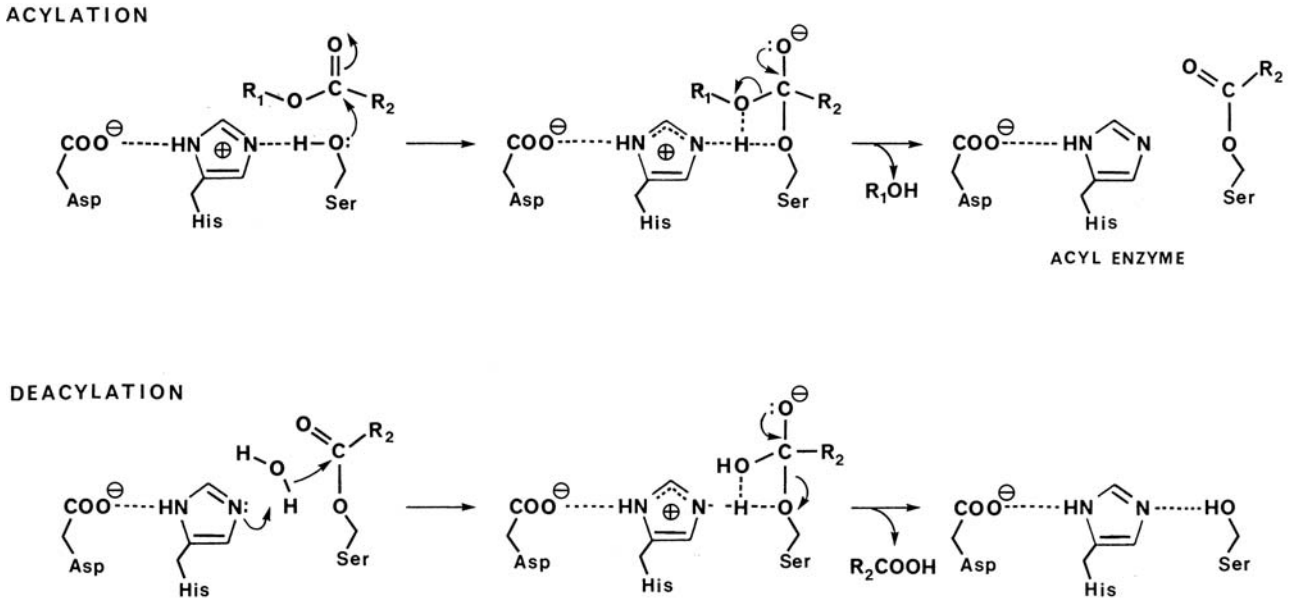

Figure 6 Proposed reaction mechanism showing acylation and deacylation via the formation of an acylenzyme intermediate. (From Ref. 122.)

chain into a position for its main chain nitrogen to stabilize the negatively charged oxyanion (Ser153-Oγ) developed in the tetrahedral intermediate (8). In the *Rhizomucor miehei* lipase, the movement of the lid in the active conformation results in the positioning of the hydroxyl and amide bond nitrogen of Ser82 for its interactions with and stabilization of the ester carbonyl oxygen of the substrate complex (22). In the *Candida rugosa* lipase, the open state involves a change in the conformation of the lid, leading to a movement of the NH of Ala132 into a proper position for the oxyanion hole (25).

The kinetic behavior of lipases at the lipid-water interface is far more complicated than what is described above for the hydrolysis of dissolved substrates. The lipase in the aqueous phase must first bind to the interface ($E \rightarrow E^*$) before it can bind to the substrate. Physically, it involves movement of the lid, and the enzyme assumes an open conformation. In addition, the lipase regenerated in the deacylation step can either diffuse from the interface or stay bound (Fig. 7). The pathway through which E^* is recycled can be described by two different models (72, 73). In the "scooting" model, E^* stays in the interface between catalytic turnovers. In the extreme situation, it remains bound to the interface until all substrate has been depleted. In the "hopping" model, only a small amount of the substrate will be hydrolyzed in each binding event. In the extreme situation, the binding and the desorption of the bound enzyme at the interface occur after each catalytic turnover cycle. The *Pseudomonas glumae* lipase exhibits a kinetic behavior which is explained by the hopping model (74). Lipoprotein lipase shows a similar mode of action (75).

VII. ACYL TRANSFER REACTIONS

In the reaction mechanism described above for lipase-catalyzed hydrolysis of lipids, deacylation involves nucleophilic attack of the acylenzyme by H_2O. This step can also be accomplished by other nucleophiles, such as alcohols and amines, resulting in an acyl transfer instead of hydrolysis. In an aqueous environment, hydrolysis is the favorable route, whereas in organic media, the acylenzyme is exposed to nucleophiles without competition from H_2O, and acyl transfer prevails. It has been shown that *Rhizomucor miehei* lipase retains high rates in esterification and transesterification at water activity < 0.0001 (76).

The acyl transfer reaction provides a novel use of lipases as catalysts in organic synthesis. Using amines as nucleophiles, esters can be converted to the corresponding amides in organic media at ambient temperature. For example, *Candida antarctica* lipase-catalyzed aminolysis of ethyl octanoate gives a 95% yield of octanamide (77). Peptide bonds can be formed

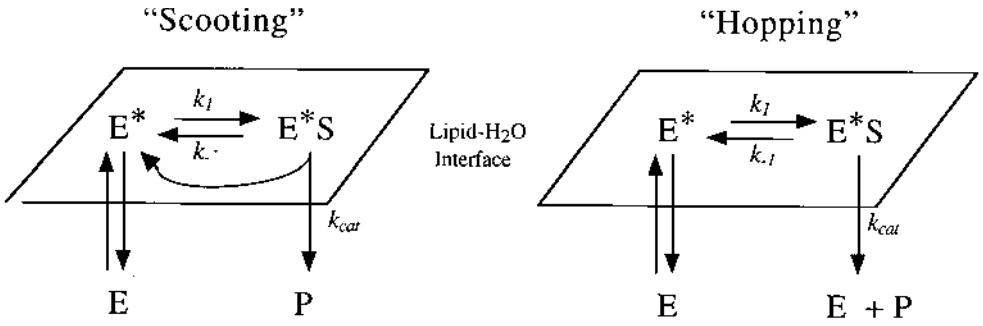

Figure 7 "Scooting" and "hopping" models of interfacial catalysis. (Adapted from Ref. 72, 73.)

between N-acetyl-L-(amino acid)-2-chloroethyl esters and amides of L or D amino acids (78). This reaction can be utilized in the production of optically active amides by taking advantage of the regio- and stereospecificity of the enzyme (79). Using hydroxyacid esters, bifunctional molecules containing both a methyl ester and an OH group as substrates, lipases can catalyze intermolecular or intramolecular condensation to give corresponding oligomers or lactones as the product (80, 81). The preference for oligomerization or lactonization depends on the chain length and degree of substitution of the substrate. This reaction has been exploited for the synthesis of optically active γ-substituted lactones from symmetrical hydroxycarboxylic acid esters (82). Lipases have been used in the regioselective acylation of sugars, the process of which can rarely be effectively performed in organic synthesis and often requires multisteps of protection and deprotection of the various hydroxyl groups. Porcine pancreatic lipase catalyzes transesterification between monosaccharides (glucose, galactose, mannose) and trichloroethyl carboxylates in pyridine resulting in the selective acylation at the C6-OH (83). Sucrose esters, used as emulsifiers in food, cosmetics, and medicines, can be synthesized by the lipase-catalyzed transesterification of sucrose with esters of fatty acids (84). In similar reactions, nucleosides and furanose and pyranose derivatives can be selectively acylated (85, 86).

One of the lipase-catalyzed reactions important to the food industry is the interesterification of triacylglycerols. In these reactions, a triacyglycerol reacts with a fatty acid, alcohol, or fatty acid alkyl ester, to produce a mixture of new triacylglycerols resulting from a rearrangement of the fatty acid moieties. Chemical catalysts such as sodium metal or sodium alkoxide can promote interesterification; however, acyl migration among the triacylglycerol molecules is nonspecific with random distribution of the acyl fatty acids. By exploiting lipases as catalysts, it is possible to generate products enriched with the new fatty acids at specific positions, thereby changing the physicochemical properties of triacylglycerols (87, 88). For example, in the interesterification of a triacylglycerol/fatty acid mixture catalyzed by 1,3-specific lipase, the product consists of novel triacylglycerols with the fatty acid selectively incorporated to the 1- and 3-positions, and no enrichment at the 2-position. Using *Geotrichum candidum* lipase which has specificity for *cis*-9 unsaturated fatty acids, linolenic acid, for example, can be selectively exchanged and enriched in an interestified triacylglycerol mixture. Miller et al. (89) studied the kinetics of interesterification of trilaurin and lauric acid catalyzed by *Candida cylindracea* lipase in cyclohexane. The reaction follows a two-step mechanism: initial hydrolysis of the trilaurin to dilaurin and lauric acid with $K_m = 7.8 \times 10^{-3}$ M, and $k_{cat} = 0.9\,sec^{-1}$, and subsequent reesterification of dilaurin and lauric acid with K_m values of 1.7×10^{-2} M (lauric acid) and 0.16 M (dilaurin), and $k_{cat} = 3\,sec^{-1}$. The use of microbial lipases in nonconventional solvents, such as supercritical fluids, has also been investigated as a means of improving the activity and stability of the enzyme for promoting acyl transfer reactions in an anhydrous environment (90).

VIII. LIPASE SPECIFICITY

The types of specificity that can be ascribed to lipases include:

1. Substrate specificity: The enzyme shows a different rate of lipolysis of various acylglycerols, tri-, di-, and monoacylglycerols, or various types of fatty acids.

2. Positional specificity: The enzyme catalyzes the release of fatty acids preferentially at the primary ester, secondary ester, or nonspecific at all esters.

3. Stereospecificity: The enzyme hydrolyzes the two primary esters (*sn*-1 or *sn*-3) at different rates (91).

Porcine pancreatic lipase has specificity for acylglycerols in the order: 1,3-triacylglycerol > 1(3)-monoacylglycerol > 2-monoacylglyercol (91). Eicosapentaenoic and docosahexaenoic acids at the 1(3)-position are resistant to the action of lipase (92). The enzyme shows the same reactivity on palmitoyl, linoleoyl, and linolenoyl groups at the 1(2)-position. However, triacylglycerols containing hydroperoxy linoleic or linolenic acids at the 1(3)-position are hydrolyzed at rates about two times higher than those of the unoxidized fatty acids in the corresponding positions (93). Lipolysis rates of the porcine pancreatic lipase on esters of saturated fatty acids increase with chain length until C9, which approaches the rates of the oleates. Substitutions or unsaturation, in particular at C2-C5, lead to increased resistance to hydrolysis (94). It has been demonstrated that human and rabbit gastric lipases have a stereospecificity for the *sn*-3 ester bond of trioctanoin or triolein (95). Pancreatic lipase cleaves the ester bonds in the *sn*-1 and *sn*-3-positions without selectivity (96).

The *Geotrichum candidum* lipase is known to show a rather unique specificity for the hydrolysis of fatty acids with a *cis*-9 or *cis,cis*-9,12 unsaturations in preference to the *trans*-isomers or corresponding saturated fatty acids (97, 98). The isoform lipase B exhibits a very high degree of specificity for monounsaturated fatty acid esters of *cis*-9 double bonds, whereas lipase A hydrolyzes a wide variety of fatty acid esters (99, 100). Similar to pancreatic lipases, a majority of the microbial lipases attack preferentially the 1(3)-position of triacylglycerols, with exceptions, such as *Corynebacterium acnes*, *Staphylococcal aureus*, and *Candida cylindracea* lipases which hydrolyze all three positions (101–103). The isoforms III and IV from *Geotrichum candidum* have been shown to cleave the 2-position ester bond of triolein at nearly twice the rate of the cleavage of the 1(3)-position (104). *Candida natarctica* lipase A shows a preference for *sn*-2 when trioctanoin and triolein are used as substrates, whereas lipase B is selective for *sn*-3 (105). The *Rhizopus arrhizus* lipase shows stereospecificity with *sn*-1 preference toward trioleoylglycerols, while the *Chromobacterium viscosum* enzyme has *sn*-3 selectivity (105). It has been demonstrated that structural variations at the *sn*-2 position cause a change in the stereoselectivity. The preference of *Chromobacterium viscosum* lipase is shifted from *sn*-3 to *sn*-1 when the *sn*-2 acylester is replaced by a non-ester alkyl chain (106).

IX. MEASUREMENT OF LIPASE ACTIVITY

Numerous methods have been used for measuring the activity of lipases, and can be classified into the following groups: (a) titrimetry based on the neutralization of the free fatty acids released with time in the hydrolysis of triacylglycerols by titration with NaOH; (b) use of chromogenic reagents to form color complexes with free fatty acids, or substrates conjugated with a chromophore or fluorophore to form fatty acid products, that can be monitored spectrophotometrically or fluorimetrically (107, 108); (c) use of radioactive triacylglycerols and measurement of the release of radiolabeled fatty acids (109); (d) chromatographic analysis of the fatty acid released (110); and (e) enzymatic conversion of the release fatty acid to products that can be measured by spectrophotometry (111). For a comprehensive review of this subject, refer to Beisson et al. (112).

The following is a procedure for measuring the rate of hydrolysis of emulsified trioleoylglycerol titrimetrically based on Vorderwulbecke et al. (113). A mixture of trioleoylglycerol (1 g) and Triton X-100 (30 mL) is heated to 55°C and added to a NaCl solution (0.9%, 200 mL H_2O, preheated also to 55°C) slowly under stirring. The final mixture is cooled to room temperature and the pH adjusted to 8.0 with 1 M NaOH. For enzyme activity assay, 25 mL of this solution is prewarmed to 37°C, adjusted to pH 8.0, before the addition of lipase. Fatty acids released are continuously titrated with 10 mM NaOH at pH 8.0 and 37°C using a recording pH stat. The lipase activity is expressed as International Enzyme Units where 1 unit corresponds to the release of 1 μmol of fatty acid per min related to the volume of the reaction mixture or to the amount of substrate transformed. The specific activity is expressed as U/mg of pure lipase.

Trioleoylglycerol (18:1/18:1/18:1) exists in a liquid form at the assay temperature and can be readily emulsified. It satisfies the definition of a "true" substrate for lipases, in particular if it is hydrolyzed in an emulsion. Emulsifiers other than Triton include Tweens, SDS, bile salts, and stabilizers such as gum arabic which can be used. The high salt in the reaction mixture is used to suppress interfacial charge effects, otherwise

causing inhibition of the enzyme. Tributyrylglycerol (4:0/4:0/4:0) is another substrate used in many investigations because of the convenience that it can be dispersed without the use of emulsifiers. However, it does not meet the definition of a substrate for lipase, and it is also hydrolyzed by some esterases. The choice of pH, temperature, substrate types, inclusion/exclusion of emulsifiers, and other parameters, depends on the aim of the investigation. Refer to Jensen (114) for a critical assessment of this subject.

Lipase activity can be screened using a zymogram procedure where the PAGE gel is overlaid with a chromogenic substrate, such as resorufin ester (1,2-*O*-dilauryl-*rac*-glycero-3-glutaric acid resorufin ester) dissolved in dioxane with deoxycholic acid. Bands containing lipase activity show up as a pink band over a white background (115). A plate assay has been used to detect lipase-producing bacteria or to quantify lipase activity in the culture (116). Lipase activity is detected by the formation of orange fluorescent halos around lipase-producing colonies when incubated in agar plates containing trioleoylglycerol and rhodamine B. The logarithm of lipase activity is linearly related to the zone diameter.

X. PURIFICATION OF LIPASE

Triacylglycerol lipase has been purified to homogeneity from pancreas of a number of species, with the porcine enzyme the most thoroughly investigated. The procedure originally developed by Verger et al. (117) essentially includes an aqueous extraction of a defatted pancreas powder, followed by DEAE-cellulose and Sephadex G-100 chromatographic steps. Various modifications of the purification have been described (10, 118, 119). The procedure, according to Brockman (119), consists of (a) delipidation of fresh porcine pancreas tissue by chloroform-*n*-butanol; (b) extraction of lipase with potassium phosphate buffer containing NaCl and diisopropylfluorophosphate; (c) affinity chromatography using hydrophobic glass beads; and (d) DEAE-cellulose chromatography (Table 1). Colipase contamination can be removed by additional chromatography on concanavalin A–Sepaharose or hydroxyapatite (120). The use of fresh pancreas is critical, as most commercial pancreatic powders may contain degraded lipase, and so is the addition of di-isopropylfluorophosphate to the buffer for inhibition of proteolytic enzymes present in the extract.

Purification of extracellular lipases from microbial sources is less cumbersome than from animal tissues. *Rhizomucor miehei* lipase is purified by passing the culture supernatant onto an anion exchange column, following by affinity chromatography on Con A–Sepharose, hydrophobic interaction chromatography (Phenyl-Sepharose), and gel filtration (12, 13). The *Geotrichum candidum* lipases I and II have been obtained by ethanol precipitation, gel filtration (Sephacryl-200 HR), anion exchange (Mono Q), and chemofocusing (Polybuffer exchanger 94) (14). A similar scheme has been used to purify multiple isoforms of *Candida rugosa* lipase (25).

Table 1 Purification of Triacylglycerol Lipase from Porcine Pancreas

	Volume (mL)	Total activity ($10^{-4} \times$ U)	Total protein (mg)	Specific activity (U/mg)	Yield (%)	Colipase (mol%)
1. Extraction of delipidated pancreas	190 ± 7	96 ± 13	$1.1 \pm 0.1 \times 10^4$	87	100	—
2. Concentration by 3.5 mM taurodeoxycholate eluate from hydrophobic beads	107 ± 16	35 ± 14	220 ± 90	1590	36	—
3. DEAE chromatography						
Fraction I (lipase B)	189	21.1	33.0	6360	7.3	≤ 1.2
Fraction II (lipase B + A)	170	9.7	17.1	5610	3.3	12.3
Fraction III (lipase B + A)	224	12.4	24.0	5120	4.3	62.0

Enzyme U = 1 mmol of butyric acid released per min. Volume, activity, and protein are expressed as average ±SD from three preparations subsequently combined for DEAE chromatography.
Source: Ref. 119.

REFERENCES

1. NAS. Food Chemical Codex, 4th ed. Washington: National Academy Press, 1996, pp 787, 803–807.
2. RD Schmid, R Verger. Lipases. Interfacial enzymes with attractive applications. Agnew Chem Int Ed 37:1608–1633, 1998.
3. IUBMB. Enzyme Nomenclature. New York: Academic Press, 1992, pp 306–307.
4. L Sarda, P Desnuelle. Action of pancreatic lipase on emulsified esters. Biochim Biophys Act 30:513–521, 1958.
5. JD De Caro, M Boudouard, J Bonicel, A Guidoni, P Desnuelle, M Rovery. Porcine pancreatic lipase. Completion of the primary structure. Biochim Biophys Acta 671:129–138, 1981.
6. F Benkouka, A Guidoni, JD De Caro, JJ Bonicel, PA Desnuelle, M Rovery. Porcine pancreatic lipase. The disulfide bridges and the sulfhydryl groups. Eur J Biochem 128:331–341, 1982.
7. J Hermoso, D Pignol, B Kerfelee, I Crenon, C Chapus, JC Fontecilla-Camps. Lipase activation by nonionic detergents. The crystal structure of the porcine lipase-colipase-tetraethylene glycol monooctyl ether complex. J Biol Chem 271:18007–18016, 1996.
8. Y Bourne, C Martinez, B Kerfelec, D Lombardo, C Chapus, C Cambillau. Horse pancreatic lipase. The crystal structure refined at 2.3 Å resolution. J Mol Biol 238:709–732, 1994.
9. B Fournet, Y Leroy, J Montreuil, J De Caro, M Rovery, JA van Kuik, JFG Vliegenthart. Primary structure of the glycans of porcine pancreatic lipase. Eur J Biochem 170:369–371, 1987.
10. M Rovery, M Boudouard, J Bianchetta. An improved large scale procedure for the purification of porcine pancreatic lipase. Biochim Biophys Acta 525:373–379, 1978.
11. FK Winkler, A D'Arcy, W Hunziker. Structure of human pancreatic lipase. Nature 343:771–774, 1990.
12. E Boel, B Huge-Jensen, M Christensen, L Thim, NP Fill. *Rhizomucor miehei* triglyceride lipase is synthesized as precursor. Lipids 23:701–706, 1988.
13. B Huge-Jensen, DR Galluzzo, RG Jensen. Partial purification and characterization of free and immobilized lipases from *Mucor miehei*. Lipids 22:559–565, 1987.
14. K Veeraragavan, T Colpitts, BF Gibbs. Purification and characterization of two distinct lipases from *Geotrichum candidum*. Biochim Biophys Acta 1044:26–33, 1990.
15. A Sugihara, Y Shimada, Y Tominaga. Separation and characterization of two molecular forms of *Geotrichum candidum* lipase. J Biochem 107:426–430, 1990.
16. Y Shimada, A Sugihara, T Iizumi, Y Tominaga. cDNA cloning and characterization of *Geotrichum candidum* lipase II. J Biochem 107:703–707, 1990.
17. T Nagao, Y Shimada, A Sugihara, Y Tominaga. Cloning and sequencing of two chromosomal lipase genes from *Geotrichum candidum*. J Biochem 113:776–780, 1993.
18. M Lotti, R Grandori, F Fusetti, S Longhi, S Brocca, A Tramontano, L Alberghina. Cloning and analysis of *Candida cylindracea* lipase sequences. Gene 124:45–55, 1993.
19. M Lotti, A Tramontano, S Longhi, F Fusetti, S Brocca, E Pizzi, L Alberghina. Variability within the *Candida rugosa* lipases family. Protein Eng 7:531–535, 1994.
20. L Brady, AM Brzozowski, ZD Derewenda, E Dodson, G Dodson, S Tolley, JP Turkenburg, L Christiansen, B Huge-Jensen, L Norskov, L Thim, U Menge. A serine protease triad forms the catalytic centre of a triacyglycerol lipase. Nature 343:767–770, 1990.
21. ZS Derewenda, U Derewenda. The crystal and molecular structure of the *Rhizomucor miehei* triacylglyceride lipase at 1.9 Å resolution. J Mol Biol 227:818–839, 1992.
22. AM Brzozowski, U Derewenda, ZS Derewenda, GG Dodson, DM Lawson, JP Turkenburg, F Bjorkling, B Huge-Jensen, SA Patkar, L Thim. A model for interfacial activation in lipases from the structure of a fungal lipase-inhibitor complex. Nature 351:491–494, 1991.
23. JD Schrag, M Cygler. 1.8 Å refined structure of the lipase from *Geotrichum candidum*. J Mol Biol 230:575–591, 1993.
24. JD Schrag, Y Li, S Wu, M Cygler. Ser-His-Glu triad forms the catalytic site of the lipase from *Geotrichum candidum*. Nature 351:761–764, 1991.
25. P Grouchulski, Y Li, JD Schrag, F Bouthillier, P Smith, D Harrison, B Rubin, M Cygler. Insights into interfacial activation from an open structure of *Candida rugosa* lipase. J Biol Chem 268:12843–12847, 1993.
26. J Uppenberg, MT Hansen, S Patkar, TA Jones. The sequence, crystal structure determination and refinement of two crystal forms of lipase B from *Candida antarctica*. Structure 2:293–308, 1994.
27. U Derewenda, L Swenson, Y Wei, Y-W Green, R Green, PM Kobos, R Joerger, MJ Haas, ZS Derewenda. Conformational lability of lipases observed in the absence of an oil-water interface: crystallographic studies of enzymes from the fungi *Humicola lanuginosa* and *Rhizopus delemar*. J Lipid Res 35:524–534, 1994.
28. MEM Noble, A Cleasby, LN Johnson, MR Egmond, LGJ Frenken. The crystal structure of triacylglycerol lipase from *Pseudomonas glumae* reveals a partially redundant catalytic aspartate. FEBS Lett 331:123–128, 1993.

29. M Nardini, DA Lang, K Liebeton, K-E Jaeger, BW Dijkstra. Crystal structure of *Pseudomonas aeruginosa* lipase in the open conformation. J Biol Chem 275:31219–31225, 2000.
30. KE Jaeger, S Ransac, HB Koch, F Ferrato, BW Dijkstra. Topological characterization and modeling of the 3D structure of lipase from *Pseudomonas aeruginosa*. FEBS Lett 332:143–149, 1993.
31. A Hjorth, F Carriere, C Cudrey, H Woldike, E Boel, DM Lawson, F Ferrato, C Cabillau, GG Dodson, L Thim, R Verger. A structural domain (the lid) found in pancreatic lipases is absent in the guinea pig (phospho)lipase. Biochemistry 32:4702–4707, 1993.
32. H Brockerhoff. Substrate specificity of pancreatic lipase: influence of the structure of fatty acids on the reactivity of esters. Biochim Biophys Acta 212:92–101, 1970.
33. A Larsson, C Erlanson-Albertsson. The importance of bile salt for the reactivation of pancreatic lipase by colipase. Biochim Biophys Acta 750:171–177, 1983.
34. WE Momsen, HL Brockman. Inhibition of pancreatic lipase B activity by taurodeoxycholate and its reversal by colipase. J Biol Chem 251:384–388, 1976.
35. P Canioni, R Julien, J Rathelot, L Sarda. Pancreatic and microbial lipases: a comparison of the interaction of pancreatic colipase with lipases of various origins. Lipids 12:393–397, 1977.
36. C Erlanson, B Borgstrom. Purification and further characterization of co-lipase from porcine pancreas. Biochim Biophys Acta 271:400–412, 1972.
37. M Charles, C Erlanson, J Bianchetta, J Joffre, A Guidoni, M Rovery. The primary structure of porcine colipase II. I. The amino acid sequence. Biochim Biophys Acta 359:186–197, 1974.
38. C Erlanson, M Charles, M Astier, P Desnuelle. The primary structure of porcine colipase II. The disulfide bridges. Biochim Biophys Acta 359:198–203, 1974.
39. B Borgstrom, T Wieloch, C Erlanson-Albertsson. Evidence for a pancreatic pro-colipase and its activation by trypsin. FEBS Lett 108:407–410, 1979.
40. C Erlanson-Albertsson. The existence of pro-colipase in pancreatic juice. Biochim Biophys Acta 666:299–300, 1981.
41. H van Tilbeurgh, L Sarda, R Verger, C Cambillau. Structure of the pancreatic lipase-procolipase complex. Nature 259:159–162, 1992.
42. H van Tilbeurgh, MP Egloff, C Martinez, N Rugani, R Verger, C Cambillau. Interfacial activation of the lipase-procolipase complex by mixed micelles revealed by x-ray crystallography. Nature 362:814–820, 1993.
43. C Chaillan, E Rogalska, C Chapus, D Lombardo. A cross-linked complex between horse pancreatic lipase and colipase. FEBS Lett 257:443–446, 1989.
44. C Chaillan, B Kerfelec, E Foglizzo, C Chapus. Direct involvement of the C-terminal extremity of pancreatic lipase (403–449) in colipase binding. Biochem Biophys Res Commun 184:206–211, 1992.
45. N Mahe-Gouhier, CL Leger. Immobilized colipase affinities for lipases B, A, C and their terminal peptide (336–449): the lipase recognition site lysine residues are located in the C-terminal region. Biochim Biophys Acta 962:91–97, 1988.
46. A Abousalham, C Chaillan, B Kerfelec, E Foglizzo, C Chapus. Uncoupling of catalysis and colipase binding in pancreatic lipase by limited proteolysis. Protein Eng 5:105–111, 1992.
47. J Donner, CH Spink, B Borgstrom. I Sjoholm. Interaction between pancreatic lipases, co-lipase, and taurodeoxycholate in the absence of triglyceride substrate. Biochemistry 15:5413–5417, 1976.
48. JS Patton, P-A Albertsson, C Erlanson, B Borgstrom. Binding of porcine pancreatic lipase and colipase in the absence of substrate studied by two-phase partition and affinity chromatography. J Biol Chem 253:4195–4202, 1978.
49. A Larsson, C Erlanson-Albertsson. The identity and properties of two forms of activated colipase from porcine pancreas. Biochim Biophys Acta 664:538–548, 1981.
50. T Wieloch, B Borgstrom, K-E Falk, S Forsen. High-resolution proton magnetic resonance study of porcine colipase and its interactions with taurodeoxycholate. Biochemistry 18:1622–1628, 1979.
51. JD De Caro, WD Behnke, JJ Bonicel, PA Desnuelle, M Rovery. Nitration of the tyrosine residues of porcine pancreatic colipase with tetranitromethane, and properties of the nitrated derivatives. Biochim Biophys Acta 747:253–262, 1983.
52. S Granon. Spectrofluorimetric study of the bile salt micelle binding site of pig and horse colipases. Biochim Biophys Acta 874:54–60, 1986.
53. C Erlanson-Albertsson. Measurement of the binding of colipase to a triacylglycerol substrate. Biochim Biophys Acta 617:371–382, 1980.
54. ME Lowe. Colipase stabilizes the lid domain of pancreatic triglyceride lipase. J Biol Chem 272:9–12, 1997.
55. KA Dugi, HL Dichek, GD Talley, B Brewer Jr, S Santamarina-Fojo. Human lipoprotein lipase: the loop covering the catalytic site is essential for interaction with lipid substrates. J Biol Chem 267:25086–25091, 1992.
56. M-P Egloff, F Marquet, G Buono, R Verger, C Cambillau, H van Tibeurgh. The 2.46 Å resolution structure of the pancreatic lipase-colipase complex inhibited by a C11 alkyl phosphonate. Biochemistry 34:2751–2762, 1995.
57. S Brenner. The molecular evolution of genes and proteins: a tale of two serines. Nature 334:528–530, 1988.
58. C Chapus, M Semeriva, C Bovier-Lapierre, P Desnuelle. Mechanism of pancreatic lipase action. I.

Interfacial activation of pancreatic lipase. Biochemistry 15:4980–4987, 1976.
59. ML Rua, T Diaz-Maurino, VM Fernandez, C Otero, A Ballesteros. Purification and characterization of two distinct lipases from *Candida cylindracea*. Biochim Biophys Acta 1156:181–189, 1993.
60. O Redondo, A Herrero, JF Bello, MG Roig, MV Calvo, FJ Plou, FJ Burguillo. Comparative kinetic study of lipases A and B from *Candida rugosa* in the hydrolysis of lipid *p*-nitrophenyl esters in mixed micelles with Triton X-100. Biochim Biophys Acta 1243:15–24, 1995.
61. W Matthews, PB Sigler, R Henderson, DM Blow. Three-dimensional structure of tosyl-α-chymotrypsin. Nature 214:652–656, 1967.
62. DM Blow, JJ Birktoft, BS Hartley. Role of a buried acid group in the mechanism of action of chymotrypsin. Nature 221:337–340, 1969.
63. MW Hunkapiller, SH Smallcombe, DR Whitaker, JH Richards. Carbon nuclear magnetic resonance studies of the histidine residue in α-lytic protease. Implications for the catalytic mechanism of serine proteases. Biochemistry 12:4732–4743, 1973.
64. S Scheiner, WN Lipscomb. Molecular orbital studies of enzyme activity: catalytic mechanism of serine proteinases. Proc Natl Acad Sci USA 73:432–436, 1976.
65. JH Wong. Facilitated proton transfer in enzyme catalysis. Science 161:328–334, 1968.
66. L Polgar, ML Bender. The nature of general base-general acid catalysis in serine proteases. Proc Natl Acad Sci USA 64:1335–1342, 1969.
67. PA Kollman, DM Hayes. Theoretical calculations on proton-transfer energies: studies of methanol, imidazole, formic acid, and methanethiol as models for the serine and cysteine proteases. J Am Chem Soc 103:2955–2961, 1981.
68. AA Kossiaskoff, SA Spencer. Direct determination of the protonation states of aspartic acid-102 and histidine-57 in the tetrahedral intermediate of the serine proteases: neutron structure of trypsin. Biochemistry 20:6462–6474, 1981.
69. FMLG Stamato, E Longo, LM Yoshioka. The catalytic mechanism of serine proteases: single proton versus double proton transfer. J Theor Biol 107:329–338, 1984.
70. A Warshel, S Russel. Theoretical correlation of structure and energetics in the catalytic reaction of trypsin. J Am Chem Soc 108:6569–6579, 1986.
71. A Warshel, G Naray-Szabo, F Sussman, J-K Hwang. How do serine proteases really work? Biochemistry 28:3629–3637, 1989.
72. R Verger. Enzyme kinetics of lipolysis. Methods Enzymol 64:340–392, 1980.
73. MK Jain, OG Berg. The kinetics of interfacial catalysis by phospholipase A2 and regulation of interfacial activation: hopping versus scooting. Biochim Biophys Acta 1002:127–156, 1989.
74. AMTJ Deveer, R Dijkman, M Leuveling-Tjeenk, L van den Berg, S Ransac, M Batenburg, M Egmond, HM Verheij, GH de Haas. A monolayer and bulk study on the kinetic behavior of *Pseudomonas glumae* lipase using synthetic pseudoglycerides. Biochemistry 30:10034–10042, 1991.
75. G Bengtsson, T Olivecrona. Lipoprotein lipase moves rapidly between lipid droplets. FEBS Lett 154:211–213, 1983.
76. RH Valivety, PJ Halling, AR Macrae. *Rhizomucor miehei* lipase remains highly active at water activity below 0.0001. FEBS Lett 301:258–260, 1992.
77. MC de Zoete, AC Kock–van Dalen, F van Rantwijk, RA Sheldon. Ester ammoniolysis; a new enzymatic reaction. J Chem Soc Chem Commun 24:1831–1832, 1993.
78. AL Margolin, AM Klibanov. Peptide synthesis catalyzed by lipases in anhydrous organic solvents. J Am Chem Soc 109:3802–3804, 1987.
79. V Gotor, R Brieva, C Gonzalez, F Rebolledo. Enzymatic aminolysis and transamidation reactions. Tetrahedron Lett 47:9207–9214, 1991.
80. A. Makita, T Nihira, Y Yamada. Lipase catalyzed synthesis of macrocyclic lactones in organic solvents. Tetrahedron Lett 28:805–808, 1987.
81. AL Gutman, D Oren, A Boltanski, T Bravdo. Enzymatic oligomerisation versus lactonisation of ω-hydroxyesters. Tetrahedron Lett 28:5367–5368, 1987.
82. AL Gutman, K Zuobi, T Bravo. Lipase-catalyzed preparation of optically active γ-butyrolactones in organic solvents. J Org Chem 55:3546–3552, 1990.
83. M Therisod, AM Klibanov. Facile enzymatic preparation of monoacylated sugars in pyridine. J Am Chem Soc 108:5638–5640, 1986.
84. H Seino, T Uchibori, T Nishitani, S Inamasu. Enzymatic synthesis of carbohydrate esters of fatty acids. 1. Esterification of sucrose, glucose, fructose and sorbitol. J Am Oil Chem Soc 61:1761–1765, 1984.
85. A Uemura, K Nozaki, J-I Yamashita, M Yasumoto. Lipase-catalyzed regioselective acylation of sugar moieties of nucleosides. Tetrahedron Lett 30:3817–3818, 1989.
86. WJ Hennen, HM Sweers, Y-F Wang, C-H Wong. Enzymes in carbohydrate synthesis: lipase-catalyzed selective acylation and deacylation of furanose and pyranose derivatives. J Org Chem 53:4939–4945, 1988.
87. AR Macrae. Lipase-catalyzed interesterification of oils and fats. J Am Oil Chem Soc 60:291–294, 1983.
88. AR Macrae. Tailored triacylglycerols and esters. Biochem Soc Trans 17:1146–1148, 1989.

89. DA Miller, M Prausnitz, HW Blanch. Kinetics of lipase-catalyzed interesterification of triglycerides in cyclohexane. Enzyme Microb Technol 13:98–103, 1991.
90. E Cernia, C Palocci. Lipases in supercritical fluids. Methods Enzymol 286:495–508, 1997.
91. RG Jensen, FA Dejong, RM Clark. Determination of lipase specificity. Lipids 18:239–252, 1983.
92. NR Bottino, GA Vandenburg, R Reiser. Resistance of certain long-chain polyunsaturated fatty acids of marine oils to pancreatic lipase hydrolysis. Lipids 2:489–493, 1967.
93. K Miyashita, T Takagi, EN Frankel. Preferential hydrolysis of monohydroperoxides of linoleoyl and linolenoyl triacylglycerol by pancreatic lipase. Biochim Biophys Acta 1045:233–238, 1990.
94. H Brockerhoff. On the function of bile salts and proteins as cofactors of lipase. J Biol Chem 246:5828–5831, 1971.
95. E Rogalska, S Ransac, R Verger. Stereoselectivity of lipases II. Stereoselective hydrolysis of triglycerides by gastric and pancreatic lipases. J Biol Chem 265:20271–20276, 1990.
96. F Paltauf, F Esfandi, A Holasek. Stereospecificity of lipases. Enzymic hydrolysis of enantiomeric alkyl diacylglycerols by lipoprotein lipase, lingual lipase and pancreatic lipase. FEBS Lett 40:119–123, 1974.
97. RG Jensen. Characteristics of the lipase from the mold, *Geotrichum candidum*: a review. Lipids 9:149–157, 1974.
98. MW Maillargeon. Purification and specificity of lipases from *Geotrichum candidum*. Lipids 25:841–848, 1990.
99. CM Sidebottom, E Charton, PPJ Dunn, G Mycock, C Davies. *Geotrichum candidum* produces several lipases with markedly different substrate specificities. Eur J Biochem 202:485–491, 1991.
100. E Charton, AR Macrae. Substrate specificities of lipases A and B from *Geotrichum candidum* CMICC 335426. Biochim Biophys Acta 1123:59–64, 1992.
101. G Benzonana, S Esposito. The positional and chain specificities of *Candida cylindracea* lipase. Biochim Biophys Acta 231:15–22, 1971.
102. GS Hassing. Partial purification and some properties of a lipase from *Corynebacterium acnes*. Biochim Biophys Acta 242:381–394, 1971.
103. J Rollof, SA Hedstrom, P Nilsson-Ehle. Positional specificity and substrate preference of purified *Staphylococcus aureus* lipase. Biochim Biophys Acta 921:370–377, 1987.
104. A Sugihara, Y Shimada, M Nakamura, T Nagao, Y Tominaga. Positional and fatty acid specificities of *Geotrichum candidum* lipases. Protein Eng 7:585–588, 1994.
105. E Rogalska, C Cudrey, F Ferrato, R Verger. Stereoselective hydrolysis of triglycerides by animal and microbial lipases. Chirality 5:24–30, 1993.
106. P Stadler, A Kovac, L Haalck, F Spener, F Paltauf. Stereoselectivity of microbial lipases. The substitution at position *sn*-2 of triacylglycerol analogs influences the stereoselectivity of different microbial lipases. Eur J Biochem 227:335–343, 1995.
107. AM Rogel, WL Stone, FO Adebonojo. A novel spectrophotometric assay for lipase activity utilizing *cis*-parinaric acid. Lipids 24:518–525, 1989.
108. HS Hendrickson. Fluorescence-based assays of lipases, phospholipases, and other lipolytic enzymes. Anal Biochem 219:1–8, 1994.
109. RG Jensen, B Daggy, A Bensadoun. Triacylglycerol lipase, monoacylglycerol lipase and phospholipase activities of highly purified rat hepatic lipase. Biochim Biophys Acta 710:464–470, 1982.
110. K-Y Tserng, RM Kliegman, E-L Miettinen, SC Kalhan. A rapid, simple, and sensitive procedure for the determination of free fatty acids in plasma using glass capillary column gas-liquid chromatography. J Lipid Res 22:852–858, 1981.
111. S Ulitzur, M Heller. Bioluminescent assay for lipase, phospholipase A_2 and phospholipase C. Methods Enzymol 72:338–346, 1981.
112. F Beisson, A Tiss, C Tiss, R Verger. Methods for lipase detection and assay: a critical review. Eur J Lipid Sci Technol 2000:133–153, 2000.
113. T Vorderwulbecke, K Kieslich, H Erdmann. Comparison of lipases by different assays. Enzyme Microb Technol 14:631–639, 1992.
114. RG Jensen. Detection and determination of lipase (acylglycerol hydrolase) activity from various sources. Lipids 18:650–657, 1983.
115. A Abousalham, R Verger. Zymogram of pancreatic lipases. Anal Biochem 281:234–236, 2000.
116. G Kouker, K-E Jaeger. Specific and sensitive plate assay for bacterial lipases. Appl Environ Microbiol 53:211–213, 1987.
117. R Verger, GH de Haas, L Sarda, P Desnuelle. Biochim Biophys Acta. Purification from porcine pancreas of two molecular species with lipase activity. 188:272–282, 1969.
118. CW Garder Jr, LC Smith. Porcine pancreatic lipase. J Biol Chem 247:561–565, 1972.
119. HL Brockman. Triglyceride lipase from porcine pancreas. Methods Enzymol 71:619–627, 1981.
120. J Rietsch, F Pattus, P Desnuelle, R Verger. Further studies of mode of action of lipolytic enzymes. J Biol Chem 252:4313, 1977.
121. G Riddihough. Picture an enzyme at work. Nature 362:793, 1993.
122. DWS Wong. Food Enzymes. NY: Chapman & Hall, 1995, pp 180–181.

54

Chlorophyllase

Roger F. McFeeters
U.S. Department of Agriculture and North Carolina State University, Raleigh, North Carolina, U.S.A.

I. INTRODUCTION

Chlorophyllase (EC 3.1.1.14) was first described in 1913 (1). When attempts have been made to detect it, chlorophyllase has been found in all green plants and algae. Chlorophyllase can hydrolyze alcohols esterified to the propionic acid side chain on C_7 of the porphyrin ring of chlorophylls, pheophytins, and various derivatives of these compounds. In addition, it can catalyze transesterification reactions (2) that result in the addition of a variety of side chains to the porphyrin ring. See Table 1 and Figure 1 for the nomenclature of chlorophyllase substrates. A previous review of this enzyme has been published by Drazkiewicz (3).

II. MEASUREMENT OF CHLOROPHYLLASE ACTIVITY

Chlorophylls or pheophytins are the usual substrates for chlorophyllase activity assays. These compounds are insoluble in water. Therefore, either reactions must be done with the substrate solubilized into an aqueous buffer system using a surfactant, or there must be sufficient organic solvent, usually acetone, added to the reaction mixture to dissolve the substrate. McFeeters et al. (4) provided an example of the aqueous buffer system adapted from the earlier procedure of Klein and Vishniac (5). Examples of the use of acetone to solubilize substrates are Weast and Mackinney

Table 1 Structures for Substrates and Inhibitors of Chlorophyllase[a]

Compound	Mg^{2+} (±)	7, 8 Position reduced (±)	R	R_1	R_2	R_3	R_4
Chlorophyll *a*	+	+	CH_3	CH_2CH_3	=O	CO_2CH_3	phytyl
Chlorophyll *b*	+	+	CHO	CH_2CH_3	=O	CO_2CH_3	phytyl
Pheophytin *a*	−	+	CH_3	CH_2CH_3	=O	CO_2CH_3	phytyl
Methyl chlorophyllide *a*	+	+	CH_3	CH_2CH_3	=O	CO_2CH_3	CH_3
Ethyl chlorophyllide *a*	+	+	CH_3	CH_2CH_3	=O	CO_2CH_3	CH_2CH_3
Methyl pheophorbide *a*	−	+	CH_3	CH_2CH_3	=O	CO_2CH_3	CH_3
9-Hydroxyl methyl pheophorbide *a*	−	+	CH_3	CH_2CH_3	OH	CO_2CH_3	CH_3
Pyropheophytin *a*	−	+	CH_3	CH_2CH_3	=O	H	phytyl
[I]Protochlorophyll *a*	+	−	CH_3	CH_2CH_3	=O	CO_2CH_3	phytyl
[I]4-Vinyl protochlorophyll *a*	+	−	CH_3	$CH=CH_3$	=O	CO_2CH_3	phytyl

[a] See Figure 1 for the ring structure common to these compounds
[I] Inhibitor

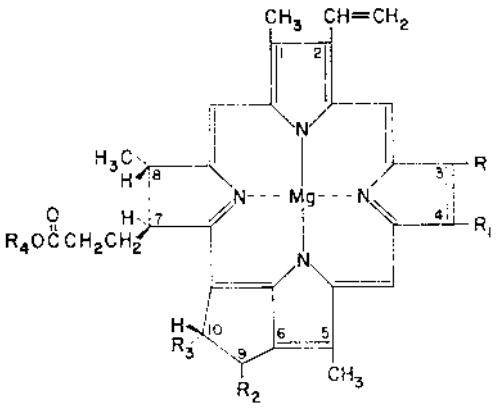

Figure 1 Ring structure for compounds that are substrates or inhibitors of chlorophyllase

(6) and Shioi et al. (7). The reaction is stopped, and the product is separated from the remaining substrate by partitioning between an organic phase and an aqueous acetone phase after KOH solution is added to raise the pH. For measurement of pheophytin or chlorophyll hydrolysis, McFeeters et al. (4) added 60% hexane:40% acetone and KOH solution to raise the reaction mixture pH to 8.5. The final proportion of solvents was 50% hexane, 33.3% acetone, and 16.7% water. After separation of the two phases, substrate depletion or, preferably, product formation is measured spectrophotometrically. To measure hydrolysis of methyl and ethyl chlorophyllides or pheophorbides, McFeeters (8) used a mixture of hexane, acetone, and 2-butanone to separate reaction products from the substrates.

III. PURIFICATION

Chlorophyllase was first purified to homogeneity by Moll and Stegwee (9). Subsequently, Shioi et al. (7) developed a somewhat simplified method. A homogeneous preparation of the enzyme was prepared from *Chlorella protothecoides* with over a 50% yield using a butanol extraction, ammonium sulfate precipitation, and chromatography on size exclusion columns (Table 2). The same procedure, except that the butanol solubilization step was unnecessary, resulted in purification of the enzyme from tea leaf sprouts but with only a 9.6% yield (10). Trebitsch et al. (11) purified chlorophyllase from the flavedo of mature green oranges, determined the N-terminal sequence of the purified enzyme, and used it for generation of antibodies to chlorophyllase. Tauchiya et al. (12) purified two chlorophyllase isozymes from mature *Chenopodium album* leaves using hydrophobic chromatography, ConA Sepharose, heparin, and ion exchange HPLC on two different columns. The presence of isozymes was confirmed by N-terminal sequencing of the separated chlorophyllases and by showing that the 10th amino acid from the N-terminus was different (Fig. 2). However, the N-terminal sequences of the *Chenopodium* isozymes had no homology with the sequence from orange chlorophyllase (11) or with any other published protein sequence (Fig. 2).

IV. PROPERTIES

The molecular weight for chlorophyllase has been reported to range from 27 to 65 kDa. Chlorophyllase from citrus fruit peel was found to be 27 kDa in one study (13) and 35 kDa in another (11). *Phaeodactylum* was reported to have two enzymes that were 43 and 46 kDa in size (14). Isozymes from *Chenopodium album* were 41.3 and 40.2 kDa (12). The largest size chlorophyllase reported to date was 65 kDa in *Chlorella regularis* (15). Most frequently, however, molecular size has been found to be near 38 kDa. This includes the chlorophyllase from *Chlorella protothecoides* (7), tea leaf sprouts (10), sugar beet leaves (16), and rye seedlings (17).

Most often, chlorophyllases have been found to have pH optima near pH 7. However, McFeeters et al. (4) and Ogura (18) found chlorophyllases from *Ailanthus altissima* and tea, respectively, had acidic optima. McFeeters et al. (4) showed a pH optimum near 7 could be obtained erroneously if the pH of the aqueous phase in the usual organic solvent/aqueous partitioning mixtures was not raised by the addition of KOH. Therefore, earlier reports of pH optima for chlorophyllases may be in error. This work indicated the absence of ionizable groups in the enzyme that affected substrate binding, but there did appear to be a pK_a 3.4 group in the active site of the enzyme involved in substrate hydrolysis. Use of acetone in the reaction mixture when determining the optimum pH of chlorophyllase could raise the apparent pK_a of this group and give a higher pH optimum in the presence of acetone than in the absence of this solvent.

The effect of different substituents of the chlorophyll *a* molecule on the ability of chlorophyllase to bind and hydrolyze potential substrates has been investigated. The picture that emerges is that of a rather high specificity esterase. First, chlorophyllase does not require the presence of a metal ion in the center

Table 2 Purification of Chlorophyllase from *Chlorella protothecoides*[a]

Purification step	Protein (mg)	Total activity (units)	Specific activity (U/mg protein)	Purification (-fold)	Yield (%)
Butanol extract	1105	1436	1.3	1	100
Ammonium sulfate (0–30% saturation)	12.4	1561	126	97	109
First Sephadex G-200	5.50	1359	247	190	95
Sepharose CL-6B	1.31	902	689	530	63
Second Sephadex G-200	0.79	758	960	738	53

[a] Chlorophyllase was extracted from 50 g (wet weight) of cells.
Source: Ref. 7.

of the tetrapyrrole ring. This is demonstrated by the fact that chlorophyllase has been found to hydrolyze chlorophylls and pheophytins with similar K_m and V_{max} value (4). Kinetic data suggested that the K_m is a binding constant for those substrates. Data have not been obtained to determine the effect of different metal ions in the porphyrin ring on chlorophyllase hydrolysis. Transesterification experiments have shown that chlorophyllase can use a variety of primary and secondary alcohols in place of phytol alcohols as substrates (2). This implies that the enzyme can also hydrolyze chlorophyllide esters of the same alcohols. Protochlorophyll and 1-vinyl protochlorophyll are not hydrolyzed by chlorophyllases, but they bind with affinities similar to pheophytin *a* (4). This showed that a double bond between C_7 and C_8 does not affect binding to chlorophyllase but that it prevents hydrolysis of phytol. Similarly, removal of the carbomethoxy group from C_{10} of pheophytin greatly reduces hydrolysis rates with little effect upon binding (4). Fiedor et al. (19) found that chlorophylls a′ and b′ were not hydrolyzed by chlorophyllase from two different plants and that the presence of these isomers did not affect the hydrolysis rates of the corresponding chlorophylls. These results suggested that a carbomethoxy group on the opposite side of ring V, as occurs in chlorophyll, prevents both binding and hydrolysis of chlorophylls a′ and b′. Comparison of the kinetics of hydrolysis of methyl pheophorbide *a* with 9-hydroxy methyl pheophorbide *a* showed that introduction of a hydroxyl group at C_9 in ring V reduced the binding affinity of substrate dramatically while, at the same time, having little effect on substrate hydrolysis rate (8).

There is little information available on the stability of chlorophyllase from different plants. In general, assays for activity have been performed at 30°C at a pH near 7. Recently, a 30°C optimal temperature was reported for chlorophyll hydrolysis by crude chlorophyllase extracts from artichoke (20). Chlorophyllase activity was nearly inactivated during a 1-h incubation

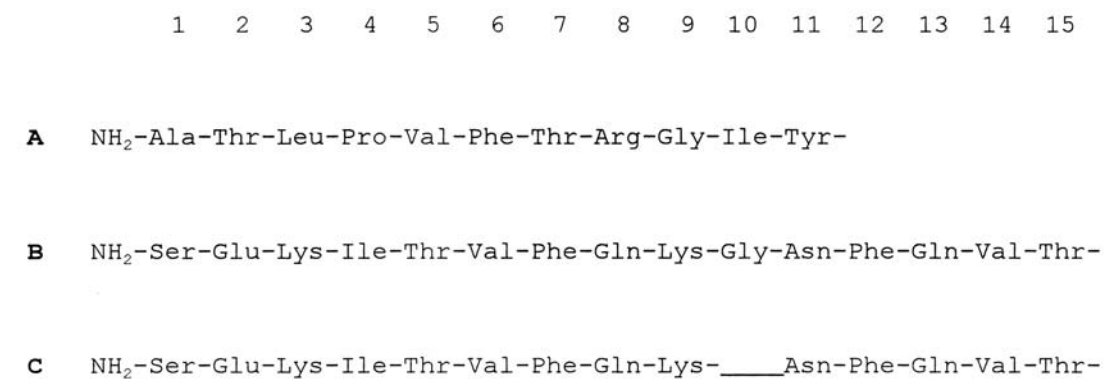

Figure 2 N-terminal sequences of chlorophyllases from orange (*Citrus sinensis* L.) (A) and *Chenopodium album* (B and C). (From Refs. 11, 12.)

at 45°C. Partially purified chlorophyllase from *Ailanthus altissima* retained > 90% of its activity during a 1-h incubation between pH 3.7 and 9.2 (4).

V. FUNCTION IN CHLOROPHYLL METABOLISM

There has been uncertainty for many years whether chlorophyllase is active in chlorophyll biosynthesis or degradation in plants. However, Rudiger et al. (21) have demonstrated the existence of a chlorophyll synthase which catalyzes esterification of chlorophyll using geranyl geranyl pyrophosphate as the substrate. The geranyl geranyl ester is then reduced to phytol, the usual side chain in the chlorophylls of higher plants. There is the possibility that "chlorophyll synthase" and "chlorophyllase" are two names given to the same enzyme investigated in different ways, as was assumed by Dogbo et al. (22).

However, the information available on the substrate specificity of chlorophyllase described above compared to the substrate specificity of chlorophyll synthase activity strongly suggests that these are different enzymes. For example, pheophorbide *a* is not a substrate for chlorophyll synthase (23), but the pheophytins are readily hydrolyzed to pheophorbides by chlorophyllase (4). In addition, pyrochlorophyllide *a* is a good substrate for chlorophyll synthase (24), but the V_{max} for pyropheophytin hydrolysis by chlorophyllase is only 2.5% as large as the V_{max} for pheophytin hydrolysis (8). Langmeier et al. (25) concluded there is little double that chlorophyllase is indispensable for chlorophyll degradation. This was based upon evidence that pheophorbide *a* is a required intermediate in the degradation of chlorophyll to fluorescent linear tetrapyrrole compounds. However, it may not be the first enzyme in the degradative pathway because Mg^{2+} removal may occur prior to phytol hydrolysis (25).

VI. LOCATION AND PHYSIOLOGICAL CHANGES

Brandis et al. (26) found chlorophyllase to be associated with the chloroplast envelope and not with chlorophyll–protein complexes, as has been reported earlier (27). This has been confirmed by Matile et al. (28). They also found that pheophorbide *a* oxygenase, the enzyme responsible for degrading the cyclic tetrapyrrole chlorophyll degradation product to a linear tetrapyrrole, is located in the chloroplast envelope. They suggest that the initiation of chlorophyll degradation must involve a mechanism to transport chlorophyll from the thylakoid pigment–protein complexes to the chloroplast envelope where chlorophyllase is located.

Trebitsh et al. (11), using chlorophyllase antibodies to detect chlorophyllase molecules, found that chlorophyllase was synthesized de novo when green oranges were exposed to ethylene to speed ripening. The senescence-delaying plant regulators gibberellin A_3 and N^6-benzyladenine inhibited the synthesis of chlorophyllase, which could be induced by ethylene.

VII. SIGNIFICANCE IN FOOD PROCESSING

Chlorophyllase appears to be of limited significance in food processing and storage. Dephytylated chlorophyll derivatives, particularly pyropheophorbide *a*, have been implicated in photosensitization reactions in humans. It has been observed that higher levels of these derivatives in food supplements prepared from leaf protein concentrate (29) or dried *Chlorella* cells (30) is correlated with chlorophyllase activity in the plant or alga.

Pheophorbides derived from chlorophylls have been observed in pickles (31), fermented olives (32), and coleslaw (33). Modeling of these data suggested that, in coleslaw, chlorophyllase converted pheophytins to pheophorbides after the chlorophylls were initially converted to pheophytins by the low pH (34). In the fermented vegetables, chlorophylls were first converted to chlorophyllides by chlorophyllase, and, as acid formed during fermentation, the chlorophylides converted to pheophorbides (34). While pheophytins and the corresponding pheophorbides have the same visible spectra in organic solvents, Heaton et al. (33) observed that the color of coleslaw changed as chlorophyllase hydrolyzed pheophytins to the corresponding pheophorbides.

Efforts have been made to promote retention of green color in processed vegetables by treating them to increase formation of chlorophyllides from chlorophylls (35). This was done on the assumption that magnesium ions would be removed more slowly from chlorophyllides than chlorophylls. However, it has been shown that chlorophyllides lose the magnesium ion more rapidly than do chlorophylls (36). Ihl et al. (20) found that inactivation of chlorophyllase in green artichokes correlated with optimum color retention for microwave and boiling-water blanching procedures.

REFERENCES

1. R Willstätter, A Stoll. Untersuchungen uber Chlorophyll. Berlin: Springer-Verlag, 1913, pp. 172–193.
2. TJ Michaelski, JR Hunt, C Bradshaw, AM Wagner, JR Norris, JJ Katz. Enzyme-catalyzed organic syntheses: transesterification reactions of chlorophyll a, bacteriochlorophyll a, and derivatives with chlorophyllase. J Am Chem Soc 110:5888–5891, 1988.
3. M Drazkiewicz. Chlorophyllase: occurrence, functions, mechanism of action, effects of external and internal factors. Photosynthetica 30:321–331, 1994.
4. RF McFeeters, CO Chichester, JR Whitaker. Purification and properties of chlorophyllase from *Ailanthus altissima* (Tree of Heaven). Plant Physiol 47:609–618, 1971.
5. AO Klein, W Vishniac. Activity and partial purification of chlorophyllase in aqueous systems. J Biol Chem 236:2544–2547, 1961.
6. CA Weast, G Mackinney. Chlorophyllase. J Biol Chem 133:551–558, 1940.
7. Y Shioi, H Tami, T Sasa. A simple purification method for the preparation of solubilized chlorophyllase from *Chlorella protothecoides*. Anal Biochem 105:74–79, 1980.
8. RF McFeeters. Substrate specificity of chlorophyllase. Plant Physiol 55:377–381, 1975.
9. WA Moll, D Stegwee. The activity of Triton X-100 soluble chlorophyllase in liposomes. Planta 140:75–80, 1978.
10. M Kuroki, Y Shioi, T Sasa. Purification and properties of soluble chlorophyllase from tea leaf sprouts. Plant Cell Physiol 22:717–725, 1981.
11. T Trebitsh, EE Goldschmidt, J Riov. Ethylene induces de novo synthesis of chlorophyllase, a chlorophyll degrading enzyme, in citrus fruit peel. Proc Natl Acad Sci USA 90:9441–9445, 1993.
12. T Tsuchiya, H Ohta, T Masuda, B Mikami, N Kita, Y Shioi, K Takamiya. Purification and characterization of two isozymes of chlorophyllase from mature leaves of *Chenopodium album*. Plant Cell Physiol 38:1026–1031, 1997.
13. K Shimokawa. Hydrophobic chromatographic purification of ethylene-enhanced chlorophyllase from *Citrus unshiu* fruits. Phytochemistry 21:543–545, 1982.
14. A Khalyfa, S Kermasha, P Marsot, J Goetghebeur. Purification and characterization of chlorophyllase from alga *Phaeodactylum tricornutum* by preparative native electrophoresis. Appl Biochem Biotech 53:11–27, 1995.
15. Y Nishiyama, M Kitamura, S Tamura, T Watanabe. Purification and substrate specificity of chlorophyllase from *Chlorella regularis*. Chem Lett 13:146–154, 1994.
16. MF Bacon, M Holden. Chlorophyllase of sugar-beet leaves. Phytochemistry 9:115–125, 1970.
17. K Tanaka, T Kakuno, J Yamshita, T Horio. Purification and properties of chlorophyllase from greened rye seedlings. J Biochem 92:1763–1773, 1982.
18. N Ogura. Studies on chlorophyllase in tea leaves. III. Properties of soluble and insoluble chlorophyllases. Plant Cell Physiol 13:971–979, 1972.
19. L Fiedor, V Rosenbach-Belkin, A Scherz. The stereospecific interaction between chlorophylls and chlorophyllase. J Biol Chem 267:22043–22047, 1992.
20. M Ihl, M Monsalves, V Bifani. Chlorophyllase inactivation as a measure of blanching efficacy and colour retention of artichokes (*Cynara scolymus* L.). Lebensm-Wiss U-Technol 31:50–56, 1998.
21. W Rudiger, J Benz, C Guthoff. Detection and partial characterization of activity of chlorophyll synthetase in etioplast membranes. Eur J Biochem 109:193–200, 1980.
22. O Dogbo, F Bardat, B Camara. Terpenoid metabolism in plastids: activity, localization and substrate specificity of chlorophyll synthetase in *Capsicum annum* plastids. Physiol Veg 22:75–82, 1984.
23. M Helfrich, W Rudiger. Various metallopheophorbides as substrates for chlorophyll synthetase. Z Naturforsch 47C:231–238, 1992.
24. J Benz, W Rudiger. Chlorophyll biosynthesis: various chlorophyllides as exogenous substrates for chlorophyll synthetase. Z Naturorsch 36C:51–57, 1981.
25. M Langmeier, S Ginsburg, P Matile. Chlorophyll breakdown in senescent leaves: demonstration of Mg-dechelatase activity. Physiol Plant 89:347–353, 1993.
26. A Brandis, A Vainstein, EE Goldschmidt. Distribution of chlorophyllase among components of chloroplast membranes in *Citrus sinensis* organs. Plant Physiol Biochem 34:49–54, 1996.
27. LG Rarasenko, EV Khodasevich, KI Orlovskaya. Location of chlorophyllase in chloroplast membranes. Photobiochem Photobiophys 12:119–121, 1986.
28. P Matile, M Schellenberg, F Vicentini. Localization of chlorophyllase in the chloroplast envelope. Planta 210:96–99, 1997.
29. M Holden. Chlorophyll degradation products in leaf protein preparations. J Sci Food Agric 25:1427–1432, 1974.
30. Y Tamura, T Maki, Y Shimamura, S Nishigaki, Y Naoi. Causal substances of photosensitivity dermatitis due to chlorella ingestion. J Food Hyg Soc Jpn 20:173–180, 1979.
31. RC White, ID Jones, E Gibbs. Determination of chlorophylls, chlorophyllides, pheophytins and pheophorbides in plant material. J Food Sci 28:431–435, 1963.

32. MI Minguez-Mosqera, J Garrido-Fernandez, G Gandul-Rojas. Pigment changes in olives during fermentation and brine storage. J Agric Food Chem 37:8–11, 1989.
33. JW Heaton, RY Yada, AG Maragoni. Discoloration of coleslaw is caused by chlorophyll degradation. J Agric Food Chem 44:395–398, 1996.
34. JW Heaton, RW Lencki, AG Maragoni. Kinetic model for chlorophyll degradation in green tissue. J Agric Food Chem 44:399–402, 1996.
35. FM Clydesdale, DL Fleischman, FJ Francis. Maintenance of colour in processed green vegetables. Food Prod Dev 4:127–138, 1971.
36. SJ Schwartz, TV Lorenzo. Chlorophylls in foods. Crit Rev Food Sci Nutr 29:1–17, 1990.

55

Phytase

Onno Misset
DSM Patents & Trademarks, Delft, The Netherlands

I. INTRODUCTION

Phytate (*myo*-inositol 1,2,3,4,5,6-hexakis dihydrogen phosphate) is the primary source of inositol and storage form of phosphorus in plant seeds. Approximately 75% of the total phosphorus in plants is in the form of phytic acid. Animal feed is primarily of vegetal origin (i.e., oilseed meals, cereal grains, and legumes) and will therefore contain a lot of phytate.

In contrast to polygastric animals such as ruminants, monogastric animals like humans, pigs, and poultry have only a limited microbial population in the upper part of the digestive tract and are not able to use phytate as a phosphorus source. Consequently, to supply these animals with phosphate, inorganic phosphate has to be added separately to the feed. Phosphorus from phytate ends up in the manure, which gives rise to serious environmental pollution. Degradation of phytate by exogenous enzymes would therefore avoid or lower the necessity to add inorganic phosphate and reduce the amount of phosphorus from phytate in the manure.

Phytate is also considered an antinutritional factor because of its strong chelating properties. The phosphate moieties of phytic acid are able to bind di- and trivalent metal ions such as calcium, magnesium, zinc, and iron. The chelating properties of inorganic phosphate are much less than those of phytate. Degradation of phytate in this case would considerably reduce the metal chelation properties of plant-derived animal feed.

Phytases are enzymes that are capable of hydrolyzing the phosphate groups from phytate. Several commercial phytase products have been developed and used as a feed additive since 1991.

For reviews of phytate and phytases, the reader is referred to (1) and (2, 3), respectively.

A. Chemical Reaction Catalyzed

Phytase catalyzes the hydrolysis of the 6-monophosphate esters in phytate (*myo*-inositol 1,2,3,4,5,6-hexakis dihydrogen phosphate) via intermediary penta-, tetra-, tri-, di-, and monophosphates ultimately to inorganic phosphate and *myo*-inositol.

B. Chemical Structure of Substrate

Phytic acid was described for the first time in 1903, and its chemical structure (Fig. 1) was elucidated in 1914 (3). The chemical formula is $C_6H_{18}O_{24}P_6$ and it has a molecular weight of 659.86 Da. Because phytate carries six phosphate groups, it can be regarded as a multisubstrate molecule. Upon successive hydrolysis, the resulting penta-, tetra-, tri-, di-, and monophosphate forms of *myo*-inositol are again substrates for phytase.

C. Classification According to Enzyme Commission Nomenclature

Two different types of phytases are known and classified accordingly: EC 3.1.3.8 and EC 3.1.3.26. They belong to the class of hydrolases (group 3), acting on

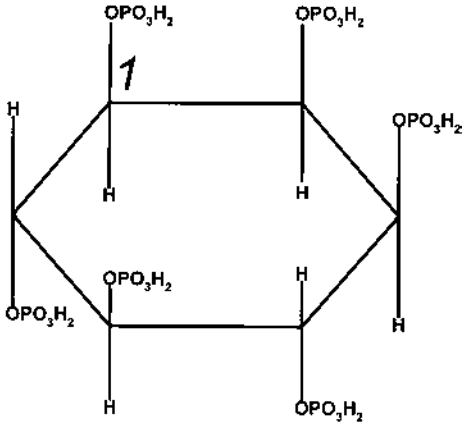

Figure 1 Structure of phytic acid. Carbon 1 of the *myo*-inositol ring has been indicated.

ester bonds (subgroup 1), in particular phosphomonoesters (subsubgroup 3).

EC 3.1.3.8 is a 3-phytase (recommended name) and hydrolyzes first the ester bond at the 3-position of the substrate. The systematic name is *myo*-inositol hexakisphosphate 3-phosphohydrolase. EC 3.1.3.26 is 6-phytase (recommended name) and hydrolyzes first the ester bond at the 6-position of the substrate. The systematic name is *myo*-inositol hexakisphosphate 6-phosphohydrolase.

II. NATURAL OCCURRENCE OF PHYTASE

Phytases are found in both the plant and microbial kingdoms. While most plant phytases belong to the class of 6-phytases (EC 3.1.3.26), most microbial phytases are considered to be 3-phytases (EC 3.1.3.8). However, not all publications mention whether the phytase involved is a 3- or 6-phytase; the reason for this is that it is rather complicated to determine the nature of the *myo*-inositol pentaphosphate (1,2,4,5,6 or 1,2,3,4,5) generated by the enzymes.

The occurrence of phytase in germinating plants has been reviewed recently (2, 5). The first phytase preparations were of plant origin; Suzuki et al. in 1907 isolated them from rice and wheat bran (3). All present-day commercial phytase products are derived from filamentous fungi, in particular from *Aspergillus* spp. For this reason this chapter will further focus on the microbial, in particular fungal, phytases.

Extensive screening programs have been carried out in the past and are still carried out today. These pro-

Table 1 Production of Intra- and Extracellular Phytases by Microorganisms

Organism	Intra- or extracellular	Reference
Fungi		
Agrocybe pediades	Extra	6
Aspergillus spp.	Extra	7
Aspergillus amstelodami	Extra	8
Aspergillus awamori	Extra	9
Aspergillus chevalieri	Extra	8
Aspergillus candidus	Extra	8
Aspergillus ficuum	Extra	8
Aspergillus fumigatis	Extra	10, 11
Aspergillus flavus	Extra	7, 8
Aspergillus niger	Extra	7, 8, 14
Aspergillus repens	Extra	8
Aspergillus sydowi	Extra	8
Aspergillus terreus	Extra	7, 12, 15
Aspergillus vesicolor	Extra	7, 8
Aspergillus wentii	Extra	8
Botrytis cinerea	Extra	8
Emericella nidulans	Extra	13
Geotrichum candidum	Extra	8
Mucor species	Extra	7
Mucor proformis	Extra	8
Mucor racemosus	Extra	8
Myceliophtora thermophila	Extra	10, 12
Neurospora crassa	Extra	16
Paxillus involtus	Extra	6
Penicillium species	Extra	7
Penicillium caseicolum	Extra	17
Peniophora lycii	Extra	6, 18
Rhizopus oryzae	Extra	8
Rhizopus oligosporus	Extra	8
Rhizopus stolonifer	Extra	8
Talaromyces fumigatus	Extra	10, 13
Thermomyces lanugosis	Extra	19, 20
Trametes pubescens	Extra	6
Ruminant microorganisms	Extra	21
Selenomonas		
Prevotella		
Treponema		
Megasphaera		
Yeast		
Saccharomyces cerevisiae	Extra	8
Schwanniomyces occidentalis	Extra	22–24
Bacteria		
Aerobacter aerogenes	Intra	25
Bacillus subtilis	Extra	26, 27
Bacillus natto N-77	Extra	28, 29
Bacillus DS11	Extra	30, 31
Escherichia coli	Intra	32
Escherichia coli B	Intra	33
Klebsiella aerogenes	Intra	34
Pseudomona species	Intra	35

grams have resulted in a long list of bacteria, yeasts, and fungi that produce 3-phytase or 6-phytase either intra- or extracellular phytase (Table 1). Many fungal phytases were identified a few decades ago (7, 8), and resulted in most of the *Aspergillus* phytases known today. There is a tendency to screen more for phytases from thermophilic strains or from microorganisms that are present in the gastrointestinal tract of ruminants. As can be seen in Table 1, fungal phytases are more abundant than phytases derived from yeasts or bacteria.

In addition to screening, protein engineering via site-directed mutagenesis of existing phytases has resulted in enzymes with increased specific activity (36) and thermostability (37).

III. INDUSTRIAL APPLICATION OF PHYTASE

The most important industrial application of phytase is in animal nutrition for reasons set out in Section I. When added to pig and poultry feed, the normal addition of inorganic phosphate can be lowered considerably, and the amount of undigested phytate in the manure of the animals is reduced substantially (30–60% depending on the type of diet composition and animal). These and other related subjects have been documented in great detail in the BASF Reference Manual entitled Phytase in Animal Nutrition and Waste Management (38) and will not be further dealt with here.

At present only a limited number of phytase products are commercially available (Table 2). The first phytase product, which entered the market in 1991, is manufactured by DSM (Gist-brocades) and sold by BASF under the trade name Natuphos. This product contains the phytase PhyA from *Aspergillus niger* (*ficuum*) NRRL3135 and is available as powder, granulate, or liquid (e.g., see www.natuphos.com).

In addition to its application as a feed additive, it has been suggested that phytase can also be used advantageously in the starch-processing industry during the liquefaction step of cornstarch (42). The function of phytase is mainly to degrade the phytate that has been shown to be an EIC (enzyme-inhibiting composition) inhibiting especially the alpha-amylase that is used in the liquefaction step.

IV. PROPERTIES AS PROTEIN

A. Molecular Weight

Most of the phytases from fungi and yeast are glycosylated. This means that their molecular weight is composed of the total of the amino acids of the (mature) protein and the molecular weight of the attached sugar chains. Furthermore, since most phytases are extracellular enzymes, their genes are encoding for a precursor protein that is slightly larger than the final mature secreted enzyme, the difference being the signal peptide that is the responsible signal for the excretion process. Therefore, we can discriminate among the following molecular weights for phytases:

1. Precursor phytase, not glycosylated—calculated from the amino acid sequence derived from the gene sequence.
2. Mature phytase, not glycosylated—calculated from the amino acids (gene) sequence and the experimentally determined maturation site (e.g., via N-terminal amino acid sequencing of the purified enzyme).
3. Mature, glycosylated phytase—experimentally determined by various methods (see below).

Table 3 summarizes the availability of amino acid sequences derived from either the corresponding gene sequences or from Edman degradation. The fungal PhyA and PhyB genes encode precursor phytases with 439–487 amino acids, corresponding to molecular weights ranging from 47 to 53 kDa (Table 4). In the

Table 2 Commercially Available Phytase Products

Company	Trademark	Produced by GMO[a]	Production organism	Phytase from	Reference
DSM (Gist-brocades)/BASF	Natuphos	Yes	*Aspergillus niger*	*Aspergillus niger ficuum NRRL 3135, van Tieghem*	39
Novozymes A/S	Phytase Novo	Yes	*Aspergillus oryzae*	*Aspergillus niger*	40
Röhm (formerly from Alko)	Finase P	Yes	*Trichoderma*	*Aspergillus awamori*	41

[a] Genetically modified organism.

Table 3 Phytase Amino Acid Sequence Entries in the Protein Information Resource (PIR) and SWISS-PROT/TrEMBL Databases Available on the Web (http://www-nbrf.georgetown.edu/pirwww/pirhome.shtml and http://www.expacy.ch respectively)

Gene	Organism	Abbr.	SWISS PROT	TrEMBL	PIR	Ref
Phy	*Bacillus strains DS11*	B.DS11	PHYT_BACSP			30, 31
Phy	*Bacillus subtilis*	B.sub	PHYT_BACSU			
PhyA	*Agrocybe pediades*	A.ped				6
PhyA	*Aspergillus awamori*	A.awa	PHYA_ASPAW		JN0889	9
PhyA	*Aspergillus ficuum*	A.nig02				46
PhyA	*Aspergillus fumigatus*	A.fum		O00092		10, 11
PhyA	*Aspergillus nidulans*	A.nid	PHYB_EMENI			14
PhyA	*Aspergillus niger (ficuum)* NRRL 3135	A.nig01	PHYA_ASPNG		JN0656	43, 44
					JN0482	45
PhyA	*Aspergillusterreus* 9A1	A.ter02		O00085		12
PhyA	*Aspergillus terreus* CBS 116.46	A.ter01		O00100		48
PhyA	*Myceliophtora thermophila*	M.the		O00107		12
PhyA	*Peniophora lycii*	P.lyc				6, 18
PhyA	*Talaromyces thermophilus*	T.the		O00096		13
PhyA	*Thermomyces lanuginosis*	T.lan				19, 20
PhyA	*Trametes pubescens*	T.pub				6
PhyA1	*Paxillus involtus*					6
PhyB	*Aspergillus awamori*	A.awa	PHYB_ASPAW		JN0890	9
PhyB	*Aspergillus niger (ficuum)* NRRL 3135	A.nig	PHYB_ASPNG		JN0715	47

case of the PhyA phytase of *Aspergillus ficum* (strain NRRL 3135), the molecular weight of the precursor phytase (51,086 daltons; Table 4) could be calculated from the gene-derived sequence (43, 44). In addition, the mature protein was also sequenced completely by Edman degradation (45). A comparison of the two sequences allowed identifying the position of the maturation site; it was found that the signal peptide consists of 23 amino acids, resulting in a mature protein of 444 amino acids with a calculated molecular weight of 48,846 daltons. The chemically and gene-derived sequences of the mature protein were found to be identical.

In a recent study, Wyss et al. (49) determined the molecular weights of several fungal phytases by SDS-PAGE, analytical ultracentrifugation, and gel filtration analysis (see Table 4 for a summary). The experimentally determined molecular weights are much larger than the values calculated on the basis of the amino acid sequences. The difference in molecular weight must be attributed to the glycosyl chains that are attached to the enzymes. The authors concluded that all phytases are monomers and that the contribution of the sugar chains to the molecular weight of the glycosylated mature enzyme could amount to 20–65%.

B. Primary, Secondary, Tertiary, and Quaternary Structures

The primary sequences of some 20–25 phytases are known. Table 2 shows that many of these sequences are available at the Web from sequence databases such as SWISS-PROT, TrEMBL, and PIR. Yet, many (new) sequences are available from the patent literature only.

Pairwise alignment of the amino acid sequences and calculation of the homology revealed that the phytase sequences can be derived into three groups: fungal phyA sequences, fungal phyB sequences, and "others" such as the sequences from *Bacillus*. The homology within a group can be as high as 45–97% as is illustrated in Table 5 for the fungal PhyA phytases. Between the groups the homology is much lower; i.e., between phyA and phyB the homology is 23–27% whereas no significant homology exists between the *Bacillus* phytases and the fungal phyA and/or phyB phytases (not shown). Figure 2 shows a multiple alignment of fungal PhyA sequences. The N-terminal residues with a gray background have been shown or are suggested to belong to the signal peptide. Residues in white with a black background are conserved in at least five sequences.

Table 4 Molecular Weights of Phytases

			Precursor		Mature					
Gene	Organism	Abbr.	#AA	Calculated MW (Da); no glycosylation	#AA	Calculated MW (Da); no glycosylation	SDS-PAGE	Analytical ultra-centrifuge	Gel filtration	References for #AA and calculated MW
PhyA	*Aspergillus awamori*	A.awa	467	51,075	444	48,851				9
PhyA	*Aspergillus ficuum*	A.nig02	467	51,164	444	48,864				46
PhyA	*Aspergillus fumigatus*	A.fum	465	50,836	439	48,270	72,360 ± 520 (49) 60,770 ± 2, 150 (49)	70,740 (49)	90,500 ± 1, 630 (49)	10, 11
PhyA	*Aspergillus nidulans*	A.nid	463	51,786	441	49,355	66,430 ± 2, 300 (49)	67,400 (49)	77,850 ± 600 (49) 86,930± 1,330 (49)	13
PhyA	*Aspergillus niger (ficuum) NRRL 3135*	A.nig01	467	51,086	444	48,846	66,360± 2,440 (49)	64,890 (49)	82,360± 1,710 (49)	43
					441	48,524 (45)	85,000 (44)			45
PhyA	*Aspergillus terreus 9A1*	A.ter02	446	51,093	447	49,128				12
PhyA	*Aspergillus terreus CBS116.46*	A.ter01	466	51,055	447	49,174				
PhyA	*Agrocybe pediades*	A.ped	454	50,030	427	47,256				6
PhyA	*Myceliophtora thermophila*	M.the	487	52,537	467	50,518	62,890± 1,210 (49)	66,150 (49)	73,800 ± 200 (49)	12
PhyA1	*Paxillus involtus*	P.inv	442	47,552	423	45,468				6
PhyA	*Peniophora lycil*	P.lyc	439	47,563	413	44,845				6, 18
PhyA	*Talaromyces thermophilus*	T.the	466	51,450	452	50,082	128,400± 1,700 (49)	137,140 (49)		13
PhyA	*Thermomyces lanuginosis*	T.lan	475	53,279	444	50,009				19, 20
PhyA	*Trametes pubescens*	T.pub	443	47,773	426	45,908				6
PhyB	*Aspergillus awamori*	A.awa	479	52,678	460	50,848				9
PhyB	*Aspergillus niger (ficuum) NRRL 3135*	A.nig	479	52,611	460	50,781				45
			476	52,595						
Phy	*Bacillus strain DS11*	B.DS11	383	41,802	357	39,230				30, 31
Phy	*Bacillus subtilis*	B.sub	382	41,946	356	39,359				

Table 5 Amino Acid Sequence Homology Between Various Fungal PhyA Phytases

	A.nig01	A.nig02	A.awa	A.fum	A.nid	A.ter01	A.ter02	T.the	T.lan	M.the	P.lyc	P.inv 1	P.inv 2	T.pub	A.ped
A.nig01															
A.nig02	96														
A.awa	97	95													
A.fum	66	65	66												
A.nid	62	62	62	67											
A.ter01	62	62	63	60	59										
A.ter02	60	60	61	59	57	87									
T.the	61	61	61	60	59	59	87								
T.lan	54	53	54	52	54	49	48	59							
M.the	46	46	46	49	48	45	47	45	46						
P.lyc	40	41	41	40	40	43	43	43	38	43					
P.inv 1	41	41	40	40	40	41	41	37	40	41	55				
P.inv 2	38	39	38	39	39	39	39	36	39	40	55	85			
T.pub	41	39	41	40	39	39	39	39	40	41	51	62	63		
A.ped	38	38	38	37	42	38	38	37	37	39	51	58	58	61	

The secondary and tertiary structures of phytase are known in great detail because the first 3-D structure of phytase from *A. niger* (*ficuum*) was recently determined by x-ray crystallography at a resolution of 2.5 Å by researchers of Hoffman–La Roche (50). To be successful in crystallizing the phytase, the enzymes had to be deglycosylated completely.

The structure has an α/β-domain similar to that of rat acid phosphatase and an α-domain with a new fold (Fig. 3). The high homology that exists between fungal PhyA phytases suggests that all these phytases (Table 5 and Fig. 2) will have the same secondary structural elements and tertiary fold and topology.

Not all the 444 amino acids could be detected in the electron density map: residues 1–6 and 249–252 (numbering of the mature protein; add 23 to obtain the precursor protein numbering) were not visible, presumably because of too high a mobility. All 10 cysteine residues are involved in a disulfide bridges: Cys8–17, Cys48–391, Cys192–442, Cys241–259, and Cys413–421. The amino acid alignment in Figure 2 shows that, with the exception of the cysteines involved in bridge Cys8–17, the eight other cysteines and therefore the four disulfide bridges are completely conserved in the fungal PhyA phytases. Amino acids involved in catalysis and substrate binding will be discussed later.

C. Isoforms

1. From Different Genes

In *Aspergillus ficuum* and *A. awamori*, two phytase genes have been identified: PhyA and PhyB (Table 3). The homology between these two types of phytases is relatively low, and the enzymological properties are very different (51).

In relation to phytases, several publications also refer to acid phosphatases (EC 3.1.3.2). However, these enzymes show no amino acid sequence homology with phytases whatsoever, and also their substrate spectrum differs from phytase since they cannot use phytate as a substrate (51, 53). Therefore, fungal PhyA phytases can be regarded as very specialized acid phosphatases because of their unique property to efficiently dephosphorylate phytic acid.

2. From Posttranslational Modification

Extracellular phytases undergo two posttranslational modifications: glycosylation and maturation. Glycosylation takes place in the Golgi apparatus of eukaryotic cells like fungi and yeast (and not in prokaryotic cells such as bacteria), and it involves only those proteins that are secreted by the cell. Glycosylation is known to generate a heterogeneous population of glycoproteins. Since the glycosyl chains contribute substantially to the molecular weight of phytase, the molecular weight will show a distribution around an average value instead of having one single value.

Glycosylation of different phytases depends on the microbial expression system (49). In *Aspergillus*, glycosylation was found to be moderate, whereas it was excessive and highly variable in *Humicola polymorpha*

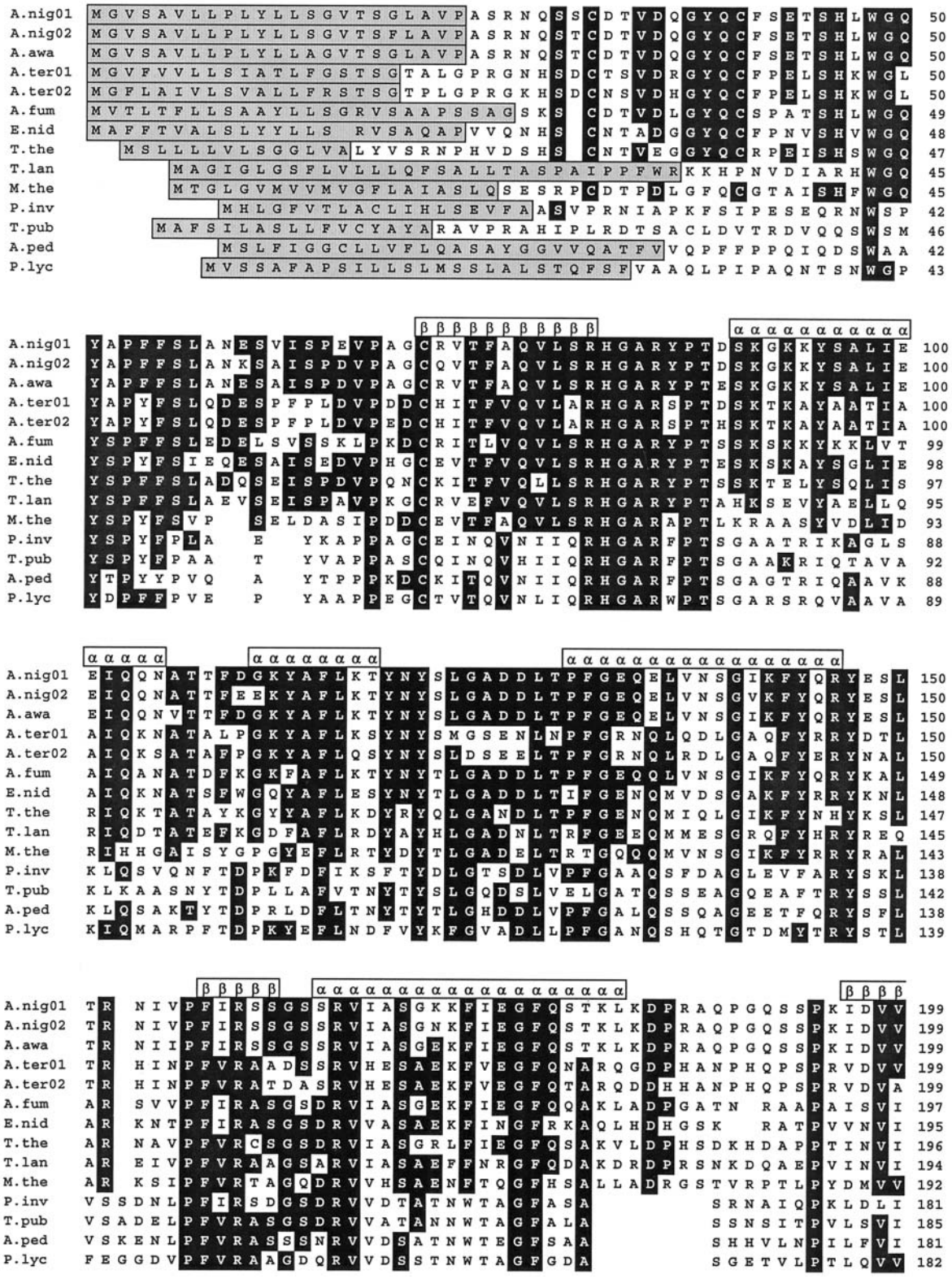

Figure 2 Amino acid sequence alignment of fungal PhyA phytases. For abbreviations and references see Table 3. The sequences were aligned using the Multiple Alignment Tool from PIR at http://www.nbrf.georgetown.edu/pirwww/search/multaln.html which makes use of Clustal W. White text and a black background mark conserved amino acid residues in at least five sequences. A gray background marks signal peptides. The α-helices and β-strands are denoted by α and β, respectively.

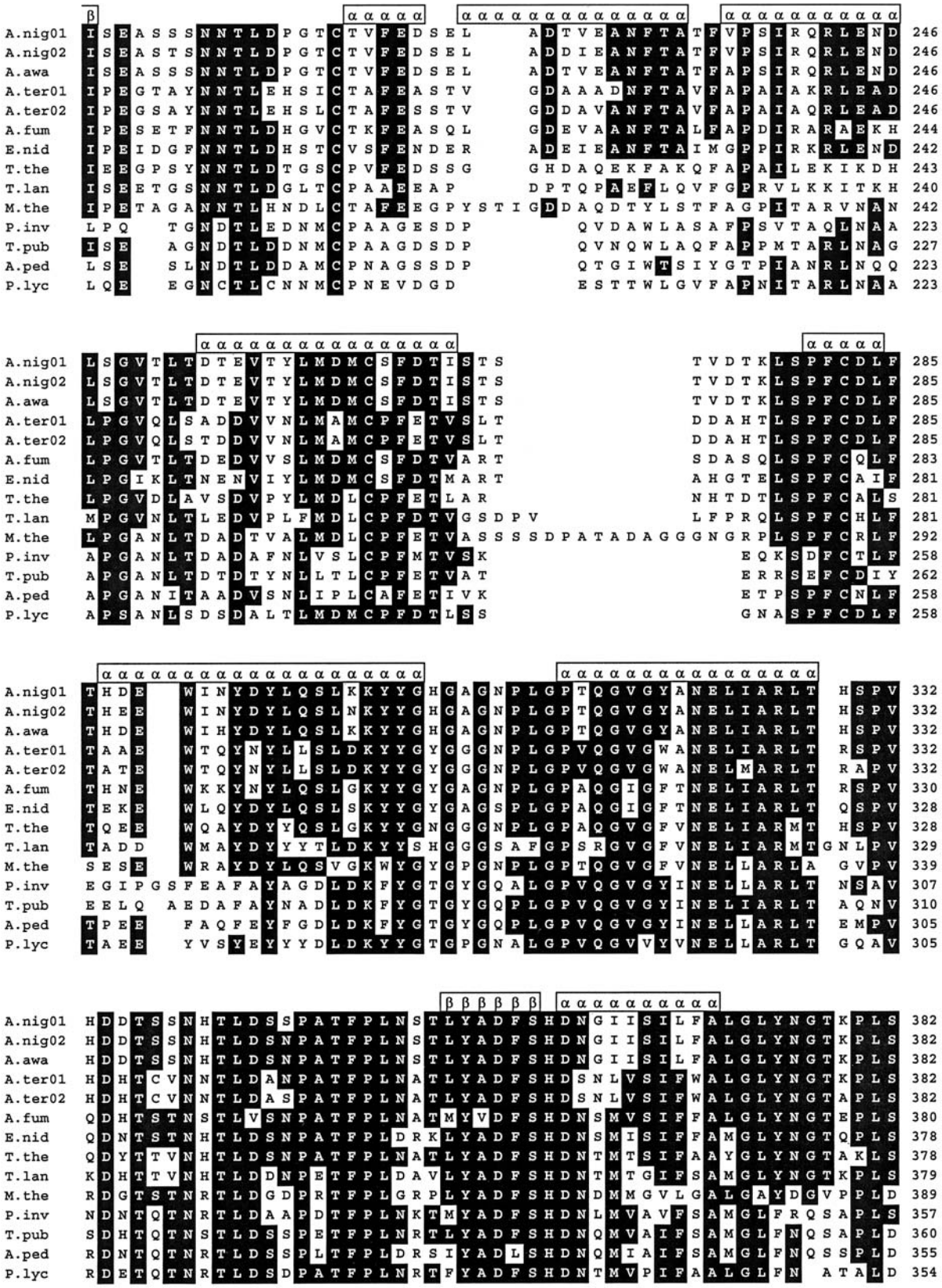

Figure 2 Continued

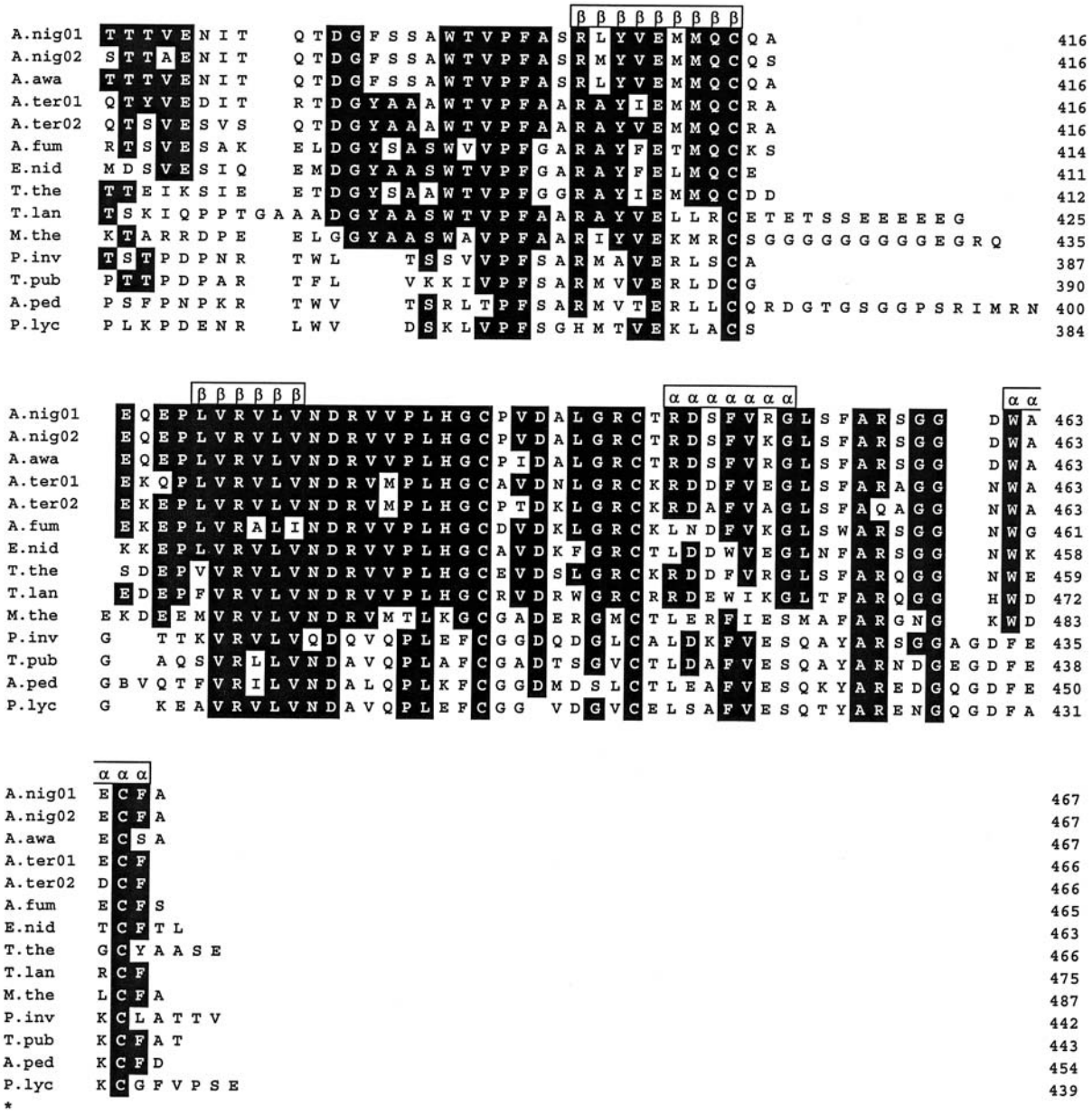

and *Saccharomyces cerevisae*. On the basis of the consensus Asn-Xxx-Ser and Asn-Xxx-Thr sequences, potential N-linked glycosylation sites in *A. niger* phytase were identified at positions 27, 59, 105, 120, 207, 230, 339, 352, 376, and 388. However, the multiple alignment of the amino acid sequences shows that only the consensus sequences at two positions: Asn207 and Asn339 are conserved. Apparently, different phytases can become glycosylated at different positions. Although the effect of glycosylation on enzyme structure and function is always under debate, the different glycosylation patterns will certainly affect properties such as molecular weight, isoelectric point, solubility, and possibly also thermostability but much less likely the enzyme activity.

Translocation of the protein over the cell membrane is mediated by the signal peptide. During this process, the signal peptide is cleaved off by signal peptidases. This process can also give rise to heterogeneity at the N-terminus of the mature protein (49). In Figure 2, a gray background marks the (putative) signal peptides of the various phytases.

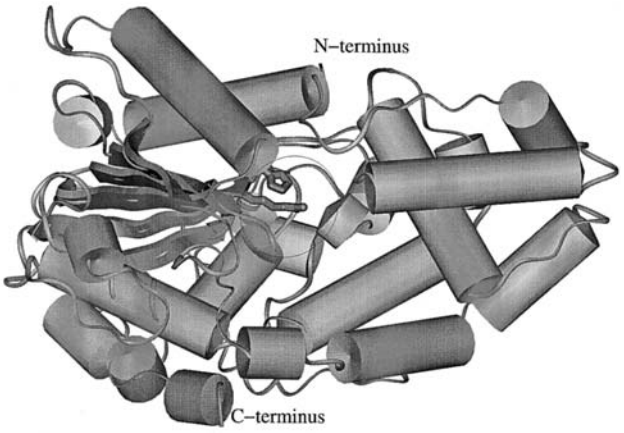

Figure 3 Schematic representation of the phytase structure. The cylinders represent the α-helices and the arrows the β-strands. The left-hand side of the molecule is the α/β-domain and the right-hand side the α-domain. (Picture courtesy of Dr. Jan-Metske van der Laan.)

3. Proteolysis

When fungal phytases were expressed in an *Aspergillus niger* strain and stored as concentrated culture supernatants, Wyss et al. (49) found that the enzymes were susceptible to limited proteolytic cleavage. In some cases, this proteolysis was accompanied with activity loss (*A. fumigatis*) but not in others (*E. nidulans*). In the latter case, the fragments remained associated with each other as was shown by gel filtration experiments, and the complex was as active as the intact enzyme. Determination of the cleavage sites was done by N-terminal sequencing of the proteolytic fragments. Comparison with the 3-D structure of the *A. niger* enzyme showed that proteolysis occurred at exposed loops on the surface of the molecule. By site-directed mutagenesis of the cleavage site amino acid residues it was possible to reduce the proteolytic susceptibility without affecting the specific activity of the mutant enzyme (49).

When expressed in *Hansenula polymorpha*, no proteolysis of the fungal phytases was observed.

V. PROPERTIES AS ENZYME

A. Substrate Specificity

Phytases are known as acid phosphatases capable of cleaving phosphate monoester bonds. In addition to phytic acid, phytases have been reported to be able to hydrolyze many other phosphate esters. Table 6 summarizes the k_{cat}, K_M, and k_{cat}/K_M values of the phytase from *A. niger* strain NRRL3135 for various phosphate ester substrates. Phytase has the highest affinity for phytate with six phosphate groups (IP6) as can be deduced from the low K_M values compared with the values for the other substrates. The highest k_{cat} values are found with the phytate substrates, in particular IP4 and IP3, for which k_{cat} is even much higher than for the IP6 substrate. The highest specificity constants (k_{cat}/K_M) are observed for the phytate substrates that are 10 to 1000-fold higher than for the other substrates. In conclusion, phytate is the "best" substrate for phytase.

In a comparative study, Wyss et al. (53) measured the specific activities of nine fungal and bacterial phytases and acid phosphatases with 14 different substrates at a fixed concentration of 5 mM and at pH 5.0 and 37°C (Fig. 4). The results clearly show that the phytases from *A. niger*, *A. terreus*, and *E. coli* have a narrow specificity compared to the other enzymes. Their highest specific activities are obtained with phytate while 30% or lower values of the phytate specific activity were found with the other 13 substrates. On the contrary, the phytases from *A. fumigatis, E. nidulans*, and *M. thermophilus*, and the acid phosphatases from *A. niger* (measured at pH 5.0 and pH 2.5) display higher activity toward a broader range of substrates. However, their activity toward phytate is much lower than the activity of *A. niger, A. terreus*, and *E. coli* phytase, or not even detectable (acid phosphatase).

B. Effect of Environmental Factors

Environmental factors such as pH and temperature exert their effect on two enzyme properties: activity and stability. Both properties are important since they determine the final application properties of the enzyme.

The pH dependence of the phytase activity has been studied extensively for various phytases from fungal and bacterial origin (Table 7). In general, the fungal phytases are active in the acid-neutral region, while the bacterial phytases behave the same (*E. coli*) or display their activity in the alkaline region (e.g., *Bacillus*). Various research groups found that the PhyA phytase from *Aspergillus niger* NRRL3135 has a broad pH optimum ranging from pH 2.5 to ~6. The profile is remarkable in the sense that two optima are found—one at pH 4 and another at pH 5.5.

To be active at the pH of the digestive tract of animals (i.e., neutral in the chicken's crop and acidic in the stomachs), a phytase is required to possess the pH activity profile as displayed by PhyA phytase from *A. niger* (*ficuum*) NRRL3135.

The activity of phytase increases with temperature until a maximum is observed. This maximum is usually caused by inactivation of the enzyme due to instability. Table 7 shows that the temperature optimum of the various phytases ranges from 45°C to 65°C.

The stability of phytase, in particular its thermostability, is an important property in view of its application as a feed additive. Namely, during the feed pelleting step, steam is injected which results in an increase of the temperature up to 65–95°C and sometimes even higher. Consequently, phytase, which has already been added to the feed at this stage, must be able to withstand these temperatures; otherwise, too much activity will be lost. This demand for thermostability explains the continuous screening efforts for more thermostable phytases and/or the protein engineering activities to improve the thermostability of existing phytases. Also, improved formulations of phytase comprising stabilizing additives are continuously developed in order to deliver stability to the enzyme during the feed pelleting step.

Wyss et al. (55) compared the thermostability of *A. niger* phytase (the currently used commercial phytase—Table 2), the *A. fumigatis* phytase, and *A. niger* acid phosphatase. Both in solution studies and in feed pelleting trials, the *A. fumigatis* enzyme proved to be more thermostable than the *A. niger* enzyme. This better thermostability, however, is counteracted by a fivefold lower specific activity of the *A. fumigatis* enzyme compared with the *A. niger* enzyme (Table 8).

The same research group also used protein engineering to improve the thermostability of phytase (37). A so-called consensus phytase was designed that has an amino acid sequence consisting of the most conserved residues found at each position in the phytases from *A. niger* (two sequences), *A. awamori*, *A. terreus* (two sequences), *A. fumigatis* (five sequences), *A. awamori, A. terreus* (two sequences), *A. fumigatis* (five sequences), *A. nidulans*, *T. thermophilus*, and *M. thermophila*. This consensus phytase proved to have the highest thermostability among all the other phytases mentioned. The temperature optimum of the activity was ~ 70°C (compare with Table 7) and also the melting temperature as measured with differential scanning calorimetry (78°C) was higher than of the other phytases (up to 63.3°C for the *A. niger* phytase).

C. Specific Mechanism of Action

Phytases hydrolyze phosphomonoester bonds in a variety of substrates and as such belong to the class of phosphatases. This class can be divided into three groups: alkaline, acid, and protein phosphatases (56). The acid phosphatases can be further subdivided into low- and high-molecular-weight (~ 18 kDa and 50–60 kDa, respectively). Examples of the last group are the extracellular fungal enzymes and the purple acid phosphatases with binuclear Fe-Fe and Fe-Zn centers in their active site.

Phytases belong to the group of histidine high-molecular-weight acid phosphatases. They hydrolyze phytate and other phosphoesters in a two-step mechanism (Ping-Pong) involving a covalent phosphorylated histidine adduct enzyme intermediate (57, 58). In the first partial reaction, the phosphorylated substrate molecule binds to the enzyme to give the noncovalent Michaelis complex which is then followed by transfer of the phosphate group to the active-site histidine. In the second partial reaction, a water molecule dephosphorylates the enzyme, resulting in free enzyme and inorganic phosphate. The consequence of this mechanism is that in case of chiral substrates, net retention of the configuration at the phosphorus atom will occur, consistent with two successive associative in-line phosphoryl transfers, each of which occurs with inversion of the configuration.

Sequence alignment of phytases shows that there is a conserved $R^{81}H^{82}G^{83}A^{84}R^{85}$ sequence (residues 81–85 in the *A. niger* precursor sequence numbering). On the basis of chemical modification studies of arginines and lysines, Ullah et al. suggested that this sequence contains an essential arginine and histidine residue (59, 60), which was confirmed by site-directed mutagenesis experiments in the *E. coli* acid phosphatase (57). The 3D structure of *A. niger* phytase indeed confirmed that this peptide was involved in substrate binding (50). Therefore, it is very likely that the histidine in the peptide mentioned is involved in the phosphorylation/dephosphorylation cycle. The conserved peptide, at least residues $R^{81}H^{82}G^{83}$, has been found to be conserved in other members of the group of acid phosphatases, some bisphosphatases, and some mutases which all make use of a phosphohistidine intermediate (59, 61).

Table 6 Substrate Specificity of PhyA Phytase from *Aspergillus niger* (*ficuum*) NRRL 3135

Substrate	k_{cat} (sec^{-1})	K_M (mM)	k_{cat}/K_M ($mM^{-1}.sec^{-1}$)	Spec. act. at V_{max} (U/mg)	Conditions	Reference
Phytate:						
Dodeca-sodium phytate (IP6)	216	0.040	5400	126	58°C, pH = 5.0	52
Dodeca-sodium phytate (IP6)	348	0.027	12888		58°C, pH = 5.0	51
Dodeca-sodium phytate (IP6)	171	0.250	684	100	37°C, pH = 5.5	44
Dodeca-sodium phytate (IP6)		< 0.005		103	37°C, pH = 5.0	53
Mono-potassium phytate (IP6)	138	0.025	5520	81	58°C, pH = 5.0	52
Dipotassium-tetramagnesium phytate (IP6)	222	0.070	3171	130	58°C, pH = 5.0	52
Myo-inositol-1,2,4,5,6-pentakisphopate (IP5)	477	0.16	2980		58°C, pH = 5.0	51
Myo-inositol-1,2,5,6-tetrakisphophate (IP4)	1554	1.00	1554		58°C, pH = 5.0	51
Myo-inositol-triphophate (IP3)	164	0.20	820		58°C, pH = 5.0	51
Myo-inositol 2-monophosphate (IP1)	12	4.50	3	7	58°C, pH = 5.0	52
Para-nitrophenylphosphate	104	0.27	385	60	58°C, pH = 5.0	52
Beta-glycerophosphate	17	1.66	10	10	58°C, pH = 5.0	52
Na_2H_2pyrophosphate	42	0.29	145	24	58°C, pH = 5.0	52
ATP	104	0.35	300	60	58°C, pH = 5.0	52
Beta-NADP	17	0.50	34	10	58°C, pH = 5.0	52
Glucose-6-phosphate	28	8.30	3	2	58°C, pH = 5.0	52
Phenylphosphate	103	0.53	194	6	58°C, pH = 5.0	52
4-nitrophenylphosphate bis	200	0.72	278	117	58°C, pH = 5.0	52
D-fructose-1,6-bisphosphate	59	1.60	37	34	58°C, pH = 5.0	52
Adenosine 5′-diphosphate	22	0.39	56	13	58°C, pH = 5.0	52
Beta-naphthylphosphate	22	0.53	42	13	58°C, pH = 5.0	52

The structure of phytase was compared with the structure of rat acid phosphatase (50). The substrate profile of phytase differs from the rat acid phosphatase in that phytase is able to hydrolyze the large phytate substrate compared to the smaller substrates of the rat enzyme. Inspection of the active site of the two enzymes reveals on one side of the substrate-binding pocket the following conserved residues (numbering of the *A. niger* precursor protein): Arg81 (Arg11 in the rat acid phosphatase), His82 (His12), Gly83 (Gly13), Arg85 (Arg15), Pro87 (Pro17) of the RHGxRxP peptide as well as Arg165 (Arg79), His361 (His257), and Asp362 (Asp258) which all belong to the α/β-domain of the enzyme. On the other side of the substrate-binding pocket (the α-domain) no similarities were found. Here, the active site of the phytase is much larger than that of the rat acid phosphatase, thus allowing the accommodation of the larger phytate substrate.

A molecular modeling study of the phytase–phytate complex showed that all conserved charged active-site residues (Arg81, His82, Arg85, Arg165, His361, and Asp362) are involved in electrostatic interactions with the scissile 3-phosphate group of the substrate. Furthermore, His82 is in a favorable position to make the nucleophilic attack at the phosphorus and Asp362 is in a position to protonate the leaving alcohol [for a further discussion see (50)].

VI. PHYTASE ASSAYS

The (specific) activity of phytase is usually determined with its natural substrate phytate or the chromogenic substitute *para*-nitrophenylphosphate. The first assay involves the detection of the liberated inorganic phosphate while the second one detects the yellow *para*-nitrophenol spectrophotometrically.

Many conditions have been reported in the literature for the phytase assay using phytate as a sub-

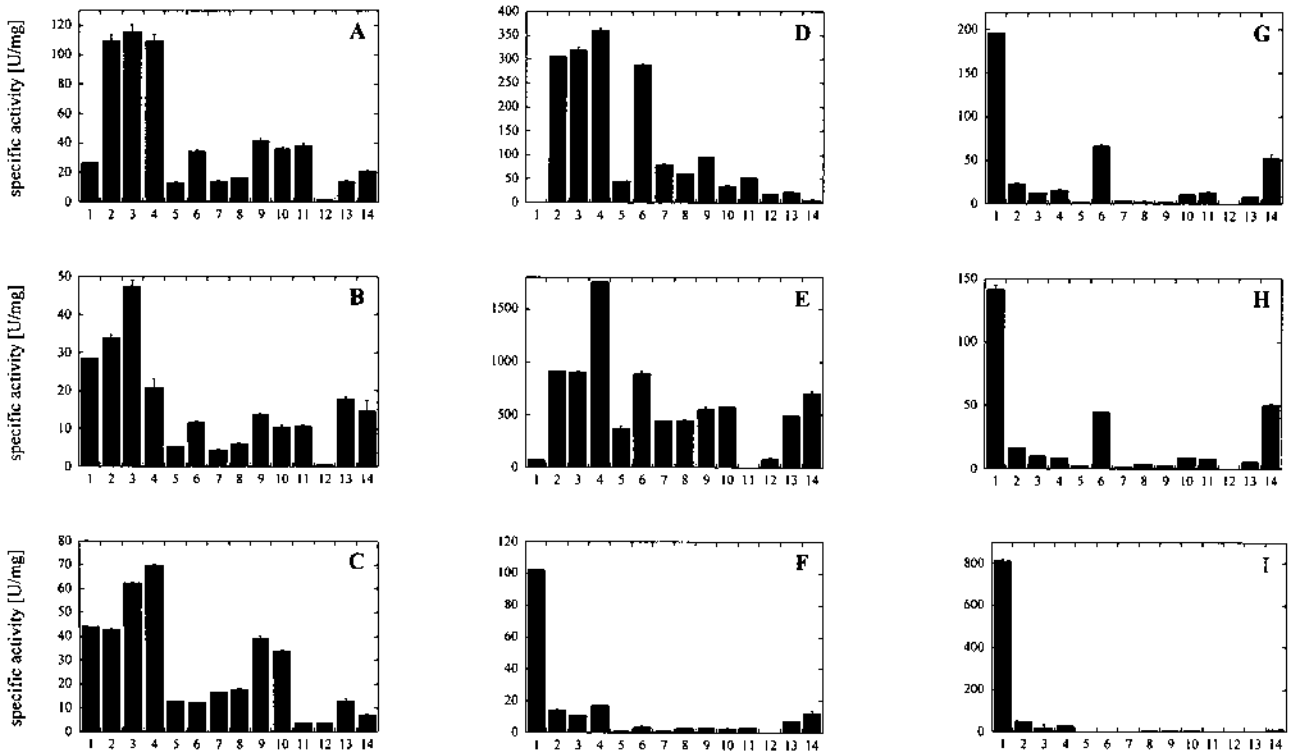

Figure 4 Substrate specificities of wild-type phytases and *A. niger* pH 2.5 acid phosphatase. All substrates were used at a concentration of 5 mM. 1, Phytic acid; 2, *para*-nitrophenyl phosphate; 3, phenyl phosphate; 4, fructose 1,6-bisphosphate; 5, fructose 6-phosphate; 6, glucose 6-phosphate; 7, ribose 5-phosphate; 8, α-glycerophosphate; 9, β-glycerophosphate; 10, 3-phosphoglycerate; 11, phosphoenolpyruvate; 12, AMP; 13, ADP; 14, ATP. (A) *A. fumigatis* phytase; (B) *A. nidulans* phytase; (C) *M. thermophila* phytase; (D) *A. niger* pH 2.5 acid phosphatase; (E) *A. niger* pH 2.5 acid phosphatase (measurements obtained at pH 2.5 instead of pH 5.0); (F) *A. niger* phytase; (G) *A. terreus* CBS phytase; (H) *A. terreus* 9A1 phytase; (I) *E. coli* phytase. (Courtesy of the American Society for Microbiology.)

Table 7 pH Profiles of Phytases[a]

Phytase from	pH optimum at 37°C	Ref.	Temperature optimum (pH)	Ref.
A. niger (*ficuum*) NRRL 3135	2.5–6	54	58 (5.0)	54
	2.5–6	44	50 (5.5)	44
	2.5–6	53	55 (5.0)	37
	2–6	19	55 (5.5)	19
A. fumigatis	3–8	53	55 (5.0)	37
	3–7.5	11, 36		
A. terreus 9A1	4–7	53	50 (5.0)	37
A. terreus CBS	4–7	53	45 (5.0)	37
E. nidulans	5.5–7	53	45 (5.0)	37
M. thermophila	3.5–6.5	53		
T. lanuginosis	3–8	19	65 (5.5)	19
A. pediades	3–6	6	50 (5.5)	6
P. lycii	3–6	18	50 (5.5)	18
B. subtilis	6–9	27		
E. coli	2.5–6	53		

[a] In all cases, phytate was used as substrate.

Table 8 Specific Activities of Various Phytases with Phytate as Substrate

Phytase from	Spec. act. (U/mg)	Conditions	Ref.
Aspergillus niger (*ficuum*)			
PhyA	103 ± 20	37°C, pH = 5.0	53
PhyA	180	37°C, pH = 5.5	19
PhyA	100	37°C, pH = 5.5	44
PhyA	126	58°C, pH = 5.0	62
Aspergillus fumigatis	27 ± 5	37°C, pH = 5.0	36, 53
Aspergillus nidulans	29 ± 4	37°C, pH = 5.0	53
Aspergillus terreus 9A1	142 ± 6	37°C, pH = 5.0	53
Aspergillus terreus CBS	196 ± 18	37°C, pH = 5.0	53
Myceliophtora thermophila	42 ± 4		53
Thermomyces lanuginosis		37°C, pH = 6.0	19
Peniophora lycii	987	37°C, pH = 5.5	6, 18
Paxillus involtus PhyA1	810	37°C, pH = 5.5	6
Paxillus involtus PhyA2	1370	37°C, pH = 5.5	6
Trametes pubescens	1450	37°C, pH = 5.5	6
Escherichia coli	811 ± 216	37°C, pH = 5.0	53
Bacillus subtilis B13	88	37°C, pH = 7.5	27

strate. The basic principle, however, is the same. Variations exist with respect to the incubation temperature, pH, and choice of buffer, substrate concentration, and the like. A suitable assay is carried out as follows (44): 100 μL enzyme solution or distilled water as a blank is added to 900 μL of a solution composed of 0.25 M sodium phosphate buffer, pH 5.5, and 1 mM phytic acid (sodium salt). The resulting mixture is incubated for 30 min at 37°C. The reaction is stopped by the addition of 1 mL of 10% trichloroacetic acid. After the reaction has terminated, 2 mL of a reagent composed of 3.66 g of $FeSO_4 \cdot 7\ H_2O$ in 50 mL of ammonium molybdate solution (2.5 g $(NH_4)_6Mo_7O_{24} \cdot 4\ H_2O$ and 8 mL H_2SO_4, diluted to 250 mL with demineralized water), is added. The intensity of the blue color is measured spectrophotometrically at 750 nm. The measurements are indicative of the quantity of phosphate released in relation to a calibration curve of inorganic phosphate in the range of 0–1 mM. One unit of phytase is defined as the amount of enzyme that is capable of forming 1 μmole of phosphate per minute. Specific activities of various phytases are summarized in Table 8.

The activity of phytase can also be determined conveniently by using *para*-nitrophenylphosphate (PNPP) as a substrate. The conditions for this determination are as follows: 10 μL of an enzyme solution is added to a solution containing 890 μL of 0.25 M sodium phosphate, pH 4.0, and 100 μL 10 mM PNPP. The absorbance of the liberated *para*-nitrophenol is measured spectrophotometrically at 30 nm as a function of time. The absorbance increase (δA/min) can be converted to a rate expressed in μM/min using an extinction coefficient of 3690 $M^{-1}\ cm^{-1}$. One unit of phytase is defined as the formation of 1 μmole of *para*-nitrophenol per minute.

VII. PURIFICATION

Numerous purification methods for the various phytases discussed here have been published in the literature; for a summary see Table 9. In general, the complexity of the method and number of steps involved depend on the expression level of the enzyme. This means that for the purification of phytase from nonrecombinant strains, more steps are required to obtain a homogeneous phytase preparation than pure phytase from overexpressing strains.

ACKNOWLEDGMENTS

I would like to acknowledge my colleagues Dr. Rob Beudeker and Dr. Jan-Metske van der Laan for helpful discussions and critically reading the manuscript.

Table 9 Overview of Phytase Purification Methods[a]

Phytase from	Original strain or overexpressed in	Method	Remarks	Reference
A. fumigatis ATCC13073	*A. niger* NW205	1. Desalting Fast-Desaltin HR 10/10 2. Cation-ion exchange chromatography Poros HS/M		11
A. niger NRRL 3135	Original strain	1. Methanol treatment of the culture filtrate 2. Cation-ion exchange chromatography over SP-Trisacryl M 3. Anion exchange chromatography over DEAE-Trisacryl M 4. Chromatofocusing	Mixture of phytase and acid phosphatase that copurified along with the phytase (42)	54
		1. Filtration of the culture broth 2. Cation-ion exchange chromatography S-Sepharose Fast-Flow 3. Anion exchange chromatography Q-Sepharose Fast-Flow 4. Isoelectric focusing (42)		44
		1. Immunoaffinity column chromatography using monoclonal antibodies against phytase that were covalently attached to to CNBr-activated Sepharose 4B. Elution of active phytase with a pH 2.5 buffer.	Simple one-step procedure	44
A. niger CB	*S. cerevisaea*	1. Hydrophobic interaction chromatography Butyl Sepharose Fast Flow 2. Gel permeation chromatography Sephacryl S-300		49
	A. niger NW205 or *H polymorpha*	1. Desalting East-Desaltin HR 10/10 or Sephadex G-25 superfine 2. Anion exchange chromatography Poros HQ/M		49
A. pediades	*S. cerevisiae* W3124	1. Anion exchange chromatography Q-Sepharose Fast flow 2. Hydrophobic interaction chromatography Phenyl Toyopearl 650s 3. Anion exchange chromatography Source 30Q 4. Anion exchange chromatography Hightrap Q		6
A. terreus	*S. cerevisaea*	1. Hydrophobic interaction chromatography Butyl Sepharose Fast Flow 2. Gel permeation chromatography Sephacryl S-300		49
	A. niger NW205 or *H. polymorpha*	1. Desalting Fast-Desaltin HR 10/10 or Sephadex G-25 superfine 2. Anion-ion exchange chromatography Poros HQ/M		49
E. nidulans	*S. cerevisaea*	1. Hydrophobic interaction chromatography Butyl Sepharose Fast Flow 2. Gel permeation chromatography Sephacryl S-300		49
	A. niger NW205 or *H. polymorpha*	1. Desalting Fast-Desaltin HR 10/10 or Sephadex G-25 superfine 2. Anion-ion exchange chromatography Poros HQ/M		49
E. coli	*E. coli* BL21	1. Sonication of cell suspension + centrifugation 2. Affinity chromatography Ni^{2+} chromatography	Enzyme expressed intracellulary	49

continued

Table 9 Continued

Phytase from	Original strain or overexpressed in	Method	Remarks	Reference
M. thermophila	*S. cerevisaea*	1. Hydrophobic interaction chromatography Butyl Sepharose Fast Flow 2. Gel permeation chromatography Sephacryl S-300		49
	A. niger NW205 or *H. polymorpha*	1. Desalting Fast-Desaltin HR 10/10 or Sephadex G-25 superfine 2. Anion exchange chromatography Poros HQ/M		49
P. involtus Phy 1	*A. cryzae* IFO4177	1. Anion exchange chromatography Q-Sepharose Fast Flow 2. Hydrophobic interaction chromatography Butyl Toyopearl 650S 3. Desalting Sephadex G25 4. Anion exchange chromatography Q- Sepharose Fast Flow 5. Desalting Sephadex G25 6. Anion exchange chromatography Source 30Q 7. Hydrophobic interaction chromatography Phenyl Toyopearl 650S		6
P. involtus Phy 2	*A. oryzae* IFO4177	1. Hydrophobic interaction chromatography Phenyl Sepharose Fast Flow 2. Hydrophobic interaction chromatography Butyl Toyopearl 650S 3. Desalting Sephadex G25 4. Anion exchange chromatography Q-Sepharose Fast Flow 5. Anion exchange chromatography Source 30Q		6

P. lycii	*A. oryzae* IFO4177	1. Anion exchange chromatography Q-Sepharose Fast Flow 2. Hydrophobic interaction chromatography Phenyl Toyopearl 650S 3. Desalting Sephadex G25 4. Anion exchange chromatography Q-Sepharose Fast Flow 5. Anion exchange chromatography Source 30Q	18
T. pubescens	*A. oryzae* IFO4177	1. Anion exchange chromatography Q-Sepharose Fast Flow 2. Hydrophobic interaction chromatography Butyl Toyopearl 650S 3. Desalting Sephadex G25 4. Anion exchange chromatography Q-Sepharose Fast Flow 5. Desalting Sephadex G25 6. Anion exchange chromatography Source 30Q	6
T. lanuginosis	*Fusarium venenatum*	1. Anion exchange chromatography Q-Sepharose Big Beads 2. Ultrafiltration 3. Anion exchange chromatography MonoQ HR10/16 column 4. Ultrafiltration 5. Cation exchange chromatography MonoS HR 5/5 column	19
T. thermophilus	*S. cerevisaea*	1. Hydrophobic interaction chromatography Butyl Sepharose Fast Flow 2. Gel permeation chromatography Sephacryl S-300	49
	A. niger NW205 or *H. polymorpha*	1. Desalting Fast-Desaltin HR 10/10 or Sephadex G-25 superfine 2. Anion exchange chromatography Poros HQ/M	49

[a] Most methods comprise as a first step the removal of the cells by centrifugation or filtration. The clear, occasionally ultrafiltrated, culture supernatant is then subjected to the further stages as indicated.

REFERENCES

1. E Graf. Chemistry and application of phytic acid: an overview. In: E Graf, ed. Phytic Acid Chemistry and Applications. Minneapolis: Pilatus Press, 1986.
2. DM Gibson, ABJ Ullah. Phytases and their action on phytic acid. In: Inositol Metabolism in Plants. New York: Wiley-Liss, 1990, pp 77–92.
3. RJ Wodzinski, AHJ Ullah. Phytase. Adv Appl Microbiol 42:263–302, 1996.
4. W Aehle, O Misset. Enzymes for industrial applications. In: HJ Rehm, G Reed, eds. Biotechnology. Weinheim: Wiley-VCH, 1999, pp 191–216.
5. NR Reddy, SK Sathe, DK Salunkhe. Phytates in legumes and cereals. Adv Food Res 28:1–92, 1982.
6. SF Lassen, L Bech, A Ohmann, J Breinholt, CC Fuglsang. Phytase polypeptides. International patent application WO 98/28409 to Novo-Nordisk. Priority date: 20 December 1996. Publication date: 2 July 1998.
7. TR Shieh, JH Ware. Survey of microorganisms for the production of extracellular phytase. Appl Microbiol 16:1348–1351, 1968.
8. SJ Howson, RP Davis. Production of phytate-hydrolysing enzyme by some fungi. Enzyme Microb Technol 5:377–382, 1983.
9. CS Piddington, CS Houston, M Paloheimo, M Cantrell, A Miettinen-Oinonen, H Nevalainen, J Rambosek. The cloning and sequencing of the genes encoding phytase (phy) and pH 2.5-optimum acid phosphatase (aph) from *Aspergillus niger* var. *awamori*. Gene 133:55–62, 1993.
10. APGM van Loon, D Mitchell. Polypeptides with phytase activity. European patent application EP0684313 to Hoffman–La Roche. Priority date 15 April 1994. Publication date 29 November 1995.
11. L Pasamontes, M Haiker, M Wyss, M Tessier, APGM van Loon. Gene cloning, purification and characterization of a heat-stable phytase from the fungus *Aspergillus fumigatus*. Appl Environ Microbiol 63:1696–1700, 1997.
12. DB Mitchell, K Vogel, BJ Weimann, L Pasamontes, APGM van Loon. The phytase subfamily of histidine acid phosphatases: isolation of genes for two novel phytases from the fungi *Aspergillus terreus* and *Myceliophthora thermophila*. Microbiol 143:245–252, 1997.
13. L Pasamontes, M Haiker, M Henriquez-Huecas, DB Mitchell, AP van Loon. Cloning of the phytases from *Emericella nidulans* and the thermophilic fungus *Talaromyces thermophilus*. Biochim Biophys Acta 1353:217–223, 1997.
14. T Skowronski. Some properties of partially purified phytase from *Aspergillus niger*. Acta Microbiol Pol 27:41–48, 1978.
15. K Yamada, Y Minoda, T Kobayashi, Y Hidaka, H Matuo, M Kobayashi. Studies on phytase of microorganisms. I. Isolation and identification of phytase producing mold. J Ferment Technol 46:858–862, 1968.
16. N Atsuhisa et al. Phytase and its production. Japanese patent application JP7059562 to Ichibiki KK. Priority date: 19 August 1993. Publication date: 7 March 1995.
17. H Matsuoka. New phytase and its production. Japanese patent application JP7067635 to Amano Pharmaceutical Co Ltd. Publication date: 14 March 1995.
18. SF Lassen, L Bech, CC Fuglsang, J Breinholt, A Ohmann, PR Ostergaard. Peniophora phytase. International patent application WO 98/28408 to Novo-Nordisk. Priority date: 20 December 1996. Publication date: 2 July 1998.
19. RM Berka, MW Rey, KM Brown, T Byun, AV Klotz. Molecular characterization and expression of a phytase gene from the thermophilic fungus *Thermomyces lanuginosus*. Appl Environ Microbiol 64:4423–4427, 1998.
20. RM Berka, K Rey, AV Klotz. Polypeptides having phytase activity and nucleic acids encoding same. International patent application WO97/35017 to Novo-Nordisk. Priority date: 18 March 1996. Publication date: 25 September 1997.
21. LJ Yanke, KJ Cheng, CW Forsberg, LB Selinger, HD Bae, L Zhou. DNA-sequences encoding phytases of ruminal microorganisms. International patent application WO 97/48812 to United Kingdom Government (Canada). Priority date: 14 June 1996; publication date 24 December 1997.
22. L Sequilha, C Lambrechts, H Boze, G Moulin, P Galzy. J Ferment Bioeng 74:7–11, 1992.
23. T Suzuki, D Mochizuki, SI Tawaki, M Shimada, J Tokuda. Novel phytase. European patent application EP0699762 to Mitsui Toatsu Chemicals. Priority date: 5 May 1994; publication date: 6 March 1996.
24. D Mochizuki, J Tokuda, T Suzuki, S Masao, S Tawaki. New phytase. Japanese patent application JP8289782 to Mitsui Toatsu Chemicals. Publication date: 5 November 1996.
25. MP Greaves, G Anderson, DM Webley. The hydrolysis of inositol phosphates by *Aerobacter aerogenes*. Biochim Biophys Acta 132:412–418, 1967.
26. VK Powar, V Jagannathan. Purification and properties of phytate-specific phosphatase from *Bacillus subtilis*. J Bacteriol 151:1102–1108, 1982.
27. J Apajalahti, P Heikkinen, M Lauraeus, A Morgan, P Nurminen, O Siikanen. Phytase. UK patent application GB2316082 to Finnfeeds Int. Priority date: 13 August 1996; publication date: 18 February 1998.
28. M Shimizu. Purification and characterization of phytase from *Bacillus subtilis* (*natto*) N-77. Biosci Biotech Biochem 56:1266–1269, 1992.

29. M Shimizu. Neutral phytase and its production. Japanese patent application JP6038745 to Zenkoku Nogyo Kyodo Kumiai Rengokai. Priority date: 18 March 1992. Publication date: 15 February 1994.
30. BK Suk, CY Woong, KH Kwon, KY Ok, LD Kyu, LS Kee, OT Kwang, PY Seo. DS11 (KCTC 0231BP) Novel *Bacillus* species strain and novel phytase produced by it. International patent application WO97/33976 to Korea Institute Science Technology. Priority date 14 March 1996. Publication date 18 September 1997.
31. YO Kim, JK Lee, HK Kim, JH Yu, TK Oh. Cloning of the thermostable phytase gene (phy) from *Bacillus* sp. DS11_ and its overexpression in *Escherichia coli*. FEMS Microbiol Lett 162:185–191, 1998.
32. R Greiner, U Konietzny, KD Jany. Purification and characterization of two phytases from *Escherichia coli*. Arch Biochem Biophys 303:107–113, 1993.
33. K Kretz. Novel phytase. International patent application WO 99/08539 to Diversa Corp. Priority date: 18 August 1997; publication date: 2 March 1999.
34. SM Tambe, GS Kaklij, SM Kelkar, LJ Parekh. Two distinct molecular forms of phytase from *Klebsiella aerogenes*: Evidence for unusually small active enzyme peptide. J Ferment Bioeng 77:123–127, 1994.
35. GCJ Irving, DJ Cosgrove. Inositol phosphate phosphatases of microbial origin. Some properties of a partially purified bacterial (*Pseudomonas*) phytase. Aust J Biol Sci 24:547–557, 1971.
36. A van Loon, M Wyss, K Vogel, L Pasamontes, D Kostrewa, A Tomschy. Modified phytases. European patent application 0 897 010 to Hoffmann–La Roche. Priority date 25 March 1997. Publication date 17 February 1999.
37. M Lehmann. Consensus phytases. European patent application 0 897 985 to Hoffman–La Roche. Priority date 24 July 1997; publication date 24 February 1999.
38. Phytase in animal nutrition and waste management. MB Coelho, T Kornegay, eds. A BASF Reference Manual DC9601, 1996. BASF Corporation, Mt. Olive, New Jersey.
39. Product sheet Finase P. Röhm enzyme gmbh January 2000.
40. GJ Verschoor. Phytase: a possible answer to phosphorus pollution. The Gist (International Quarterly of Royal Gist-Brocades NV) 34:6–7, 1987.
41. Novo-Nordisk A/S. Phytase Novo cuts phosphorus in manure by 30%. Biotimes 10:8–9, 1995.
42. RL Antrim, C Mitchinson, LP Solheim. Method for liquefaction starch. PCT application WO 96/28567. Priority date 9 March 1995, publication date 19 September 1996.
43. W van Hartingsveldt, CMJ van Zeijl, GM Harteveld, RJ Gouka, MEG Suykerbuyk, RGM Luiten, PA van Paridon, GCM Selten, AE Veenstra, RFM van Gorkum, CAMJJ van den Hondel. Cloning, characterization and overexpression of the phytase-encoding gene (phyA) of *Aspergillus niger*. Gene 127:87–94, 1993.
44. RF van Gorkum, W van Hartingsveldt, PA van Paridon, AE Veenstra, RGM Luiten, GCM Selten. European patent application 0420358 to Gist-Brocades, 1991.
45. AHJ Ullah, HC Dischinger Jr. *Aspergillus ficuum* phytase: complete primary structure elucidation by chemical sequencing. Biochem Biophys Res Commun 192:747–753, 1993.
46. RM Berka, SA Thompson. "Berka-Thompson Affidavit" in the prosecution file of European patent application EP 420358 to Gist-brocades, 14 October 1994.
47. KC Ehrlich, BG Montalbano, EJ Mullaney, HC Dischinger Jr, AHJ Ullah. Identification and cloning of a second phytase gene (phyB) from *Aspergillus niger* (*ficuum*). Biochem Biophys Res Commun 195:53–57, 1993.
48. DB Mitchell, K Vogel, B Weimann, L Pasamontes, APGM van Loon. The phytase subfamily of histidine acid phosphatases: isolation of genes for two novel phytases from the fungi *Aspergillus terreus* and *Myceliophtora thermophila*. Microbiol 143:245–252, 1997.
49. M Wyss, L Pasamontes, A Friedlien, R Rémy, M Tessier, A Kronenberger, A Middendorf, M Lehmann, L Schnoebelen, U Röthlisberger, E Kusznir, G Wahl, F Müller, H-W Lahm, K Vogel, APGM van Loon. Biochemical characterization of fungal phytases (myo-inositol hexaphosphate phosphohydrolases): molecular size, glycosylation pattern and engineering of proteolytic resistance. Appl Environ Microbiol 65:359–366, 1999.
50. D Kostrewa, F Grüninger-Leitch, A d'Arcy, C Broger, D Mitchell, APGM van Loon. Crystal structure of phytase from *Aspergillus ficuum* at 2.5 Å resolution. Nat Struct Biol 4:185–190, 1997.
51. AHJ Ullah, BQ Philippy. Substrate selectivity in *Aspergillus ficuum* phytase and acid phosphatases using myo-inositol phosphates. J Agric Food Chem 42:423–524, 1994.
52. AHJ Ullah. *Aspergillus ficuum* phytase: partial primary structure, substrate selectivity and kinetic characterization. Prep Biochem 18:459–471, 1988.
53. M Wyss, R Brugger, A Kronenberger, R Rémy, R Fimbel, G Oesterhelt, M Lehmann, and APGM van Loon. Biochemical characterization of fungal phytases (myo-inositol hexaphosphate phosphohydrolases): catalytic properties. Appl Environ Microbiol 65:367–373, 1999.
54. AHJ Ullah, DM Gibson. Extracellular phytase (EC 3.1.3.8) from *Aspergillus ficuum* NRRL 3135: purifica-

tion and characterization. Prep Biochim 17:63–91, 1987.
55. M Wyss, L Pasamontes, R Remy, J Kohler, E Kusznir, M Gadient, F Müller, APGM van Loon. Comparison of thermostability properties of three acid phosphatases from molds: *Aspergillus fumigatis* phytase, *A. niger* phytase and *A. niger* pH 2.5 acid phosphatase. Appl Environ Microbiol 64:4446–4451, 1998.
56. JB Vincent, MW Crowder, BA Averill. Hydrolysis of phosphate monoesters: a biological problem with multiple chemical solutions. Trends Biochem Sci 17:105–110, 1992.
57. K Ostanin, EH Harms, PE Stevis, R Kuciel, M-M Zhou, RL van Etten. Overexpression, site directed mutagenesis and mechanism of *Escherichia coli* acid phosphatase. J Biol Chem 267:22830–22836, 1992.
58. RL van Etten. Human prostatic acid phosphatase: a histidine phosphatase. Ann NY Acad Sci 390:27–51, 1982.
59. AHG Ullah, HC Dischinger. Identification of residues involved in active site formation in *Aspergillus ficuum* phytase. Ann NY Acad Sci 672:45–51, 1992.
60. AHJ Ullah, BJ Cummins, HC Dischinger. Cyclohexanedione modification of arginine at the active site of *Aspergillus ficuum* phytase. Biochem Biophys Res Commun 178:45–53, 1991.
61. JF Bazan, RJ Fletterick, SJ Pilkis. Evolution of a bifunctional enzyme: 6-phosphofructo-2-kinase/fructose-2,6-bisphosphatase. Proc Natl Acad Sci USA 86:9642–9646, 1989.
62. AHJ Ullah. Production, rapid purification and catalytic characterization of extracellular phytase from *Aspergillus ficuum*. Prep Biochem 18:443–458, 1998.

56

α-Amylases

Dominic W. S. Wong and George H. Robertson
U.S. Department of Agriculture, Albany, California, U.S.A.

I. INTRODUCTION

α-Amylases (EC 3.2.1.1) are endoglucanases that catalyze the cleavage of internal glucosidic bonds in starch and related polysaccharides to yield dextrins and oligosaccharides with the anomeric C1-OH in the α-configuration. The α-1,4 bonds near α-1,6 branches are resistant to hydrolysis. Extensive hydrolysis of amylopectins with α-amylases produce "α-limited dextrins," as cleavage terminates at the α-1,6 bonds. α-Amylase plays a central role in carbohydrate metabolism of microorganisms, plants, and animals. Microbial α-amylases derived from *Bacillus licheniformis* or related organisms for commercial applications are stable at temperatures $> 90^{\circ}C$, relatively less dependent on Ca^{2+} ions, and active over a wide pH range.

α-Amylase for food processing is obtained by controlled fermentation of *Bacillus stearothermophilus, Bacillus subtilis* containing a *Bacillus megaterium* or *Bacillus stearothermphilus* α-amylase gene, as an off-white to brown, amorphous powder or a liquid. Typical applications include preparation of starch syrup, dextrose, alcohol, beer, and bakery products. α-Amylase is used industrially in the liquefaction of starch to produce dextrins which are further saccharified by glucoamylase to yield glucose feed stock for corn syrup, fuel ethanol, or beverage alcohol production. In the baking industry, α-amylase is added to the dough to ensure a continuous supply of fermentable sugar for yeast growth and gas production. In the textile industry, mechanical weaving of fabrics often requires the coating of threads with a starch "size," and α-amylase is used for desizing to finish the fabric. α-Amylase is one of the enzymes incorporated into laundry detergents to remove starchy stains from fabrics, and to increase the efficiency and reduce chemical ingredients in detergents.

II. CLASSIFICATION

Glycosidases are classified under hydrolases which are subdivided into those hydrolyzing *O*-glycosyl, *N*-glycosyl, and *S*-glycosyl compounds (EC 3.2.1, 3.2.2, and 3.2.3). α-Amylase hydrolyzes internal 1,4-α-D-glucosidic linkages in oligosaccharide or polysaccharide in a random manner with the reducing groups liberated in the α-configuration. According to the IUBMB recommendation (1), α-amylase (trivial name) therefore has the systematic name of 1,4-α-D-glucan glucanohydrolase, and a code number of EC 3.2.1.1. This classification scheme is based on the type of reaction catalyzed and the substrate specificity of the individual enzyme.

More recently, an alternative classification of glycosyl hydrolases based on amino acid sequence similarities has been proposed (2–4). There are 70 families according to this classification, and most α-amylases belong to family 13, together with pullulanases (EC 3.2.1.41), cyclomaltodextrin glucanotransferase (EC 2.4.1.19), cyclomaltodextrinase (EC 3.2.1.54), and trehalose-6-phosphate hydrolase (EC 3.2.1.93). However, α-amylases from *Dictyoglomus thermophilum*, *Methanococcus jannaschii*, *Pyrococcus*

furiosus, and *Pyrococcus horikoshii* belong to family 57. This classification scheme is based on the direct relationship between sequence and folding similarities, and it provides a convenient tool to predicting mechanistic information. However, classification based on sequence and structural similarities may cause unnecessary confusion because in this scheme, an enzyme is defined by its primary sequence as a protein, but not directly by its intrinsic catalytic functions.

III. MOLECULAR STRUCTURES

Numerous amino acid sequences of α-amylases are known, primarily deduced from DNA sequencing. A total of 70 entries are listed in Swiss-Prot: *Aeromonas hydrophila, Alteromonas haloplanktis, Dictyoglomus thermophilum, Escherichia coli, Bacillus amyloliquefaciens, B. megaterium, Bacillus* sp. (strain B1018), *B. circulans, B. stearothermophilus, B. licheniformis, B. subtilis, Paenibacillus polymyxa (Bacillus polymyxa), Butryrivibrio fibrisolvens, Methanococcus jannaschii, Streptomyces lividans, S. violaceus* (*Streptomyces venezuelae*), *S. griseus, S. limosus* (*Streptomyces albidoflavus*), *S. hygroscopicus, S. thermoviolaceus, Clostridium acetobutylicum, Thermoanaerobacter thermosulfurogenes* (*Clostridium thermosulfurogenes*), *T. ethanolicus* (*Clostridium thermohydrosulfuricum*), *T. thermohydrosulfuricus* (*Clostrium thermohydrosulfuricum*), *T. saccharolyticum, Thermomonospora curvata, Pyrococcus furiosus, P. horikoshii, Salmonella typhimurium, Aspergillus niger, A awamori, A. oryzae, A. shirousami, Schizosaccharomyces pombe* (fission yeast), *Saccharomycopsis fibuligera* (yeast), *Debaryomyces occidentalis* (yeast) (*Schwanniomyces occidentalis*), *Oryza sativa* (rice), *Triticum aestivum* (wheat), *Hordeum vulgare* (barley), *Vigna mungo* (rice bean) (black gram), *Drosophila melanogaster* (fruit fly), *D. mauritiana, D. yakuba, Aedes aegypti* (yellow fever mosquito), *Dermatophagoides pteronyssinus* (house-dust mite), *Tribolium castaneum* (red flour beetle), *Pecten maximum* (king scallop) (pilgrim's clam), *Tenebrio molitor* (yellow mealworm), *Sus scrofa* (pig), *Homo sapiens* (human), *Rattus norvegicus* (rat), and *Mus musculus* (mouse).

The sequences of α-amylases from different origins have very few discernible similarities, with the exception of four short, highly conserved segments (5–15) (Fig. 1). The three catalytic residues (two Asp and one Glu), as well as residues involved in substrate binding, are located in these four highly conserved regions which are also found in GGTase (*Bacillus macerans*), pullulanase (*Klebsiella aerogenes*), isoamylase (*Psudomonas amyloderamosa*), α-glucosidase (*Saccharomyces carlsbergenesis*), and cyclodextrinase (*Thermoanaerobacter ethanolicus*), suggesting that these enzymes may participate in the same type of reaction mechanism (16). Several microbial α-amylases—*Bacillus circulans* (17), *Bacillus subtilis* (18), *Bacillus stearothermophilus* (19), *Streptomyces limosus* (20), *Chalara paradoxa* (21), *Lactobacillus amylovorus* (22), and *Cryptococcus* sp. S-2 (23)—are known to digest not only soluble starch, but raw starch granules. In addition, porcine pancreatic α-amylase (24) and barley α-amylase (25) contain C-terminal segments that have been identified to be a raw starch–binding site. The raw starch–binding sequences found

		*		*		*	
Bacillus stearothermophilus	101	DVVFDH	230	GFRLDAVKH	264	EYWS	326 FVDNHD
Bacillus amyloliquefaciens	98	FVVLNH	227	GFRIDAAKH	261	EYWQ	323 FVENHD
Bacillus licheniformis	100	DVVINH	227	GFRLDAVKH	261	EYWQ	323 FVDNHD
Aspergillus oryzae	117	DVVAAH	202	GLRIDTVKH	230	EVLD	292 FVGNHD
Micrococcus sp.207	469	DVVVNH	554	YFRVDTVKH	587	EAWG	652 FLGSHD
Saccharomycopsis fibuligera	144	DIVTNH	229	GLRIDSAKH	257	EVFQ	319 EVENHD
Hordeum vulgare L. (Barley)	112	DIVINH	138	DGRLDWGPH	229	EVWD	310 FVDNHD
Drosophila melanogaster	111	DVVFNH	200	GFRVDAAKH	241	EVID	301 FVDNHD
Yellow meal worm	94	DAVINH	181	GFRVDAAKH	222	EVID	282 FVDNHD
Porcine pancreatic	96	DAVINH	193	GFRLDASKH	233	EVID	295 FVDNHD
Human pancreatic	111	DAVINH	208	GFRLDASKH	248	EVID	310 FVDNHD

Figure 1 Comparison of regions of sequence similarities among: *Bacillus stearothermophilus* (5), *Bacillus amyloliquefaciens* (6), *Bacillus licheniformis* (7), *Aspergillus oryzae* (8), *Micrococcus* sp. 207 (9), *Saccharomycopsis fibuligera* (10), barley isozyme 1 (11), *Drosophila melanogaster* (fruit fly) (12), yellow mealworm (13), porcine pancreatic (14), human pancreatic (15). The three residues involved in catalysis are indicated by asterisks. Numbering of the sequences starts with N-terminus of the mature protein.

in α-amylases from microbial sources exhibit a high degree of similarity to the starch binding segments in a number of bacterial β-amylase and GGTases and fungal glucoamylases. The alignment suggests an evolution path according to species rather than individual enzyme specificity (26). Some microbial enzymes, for example, *Streptomyces* α-amylase, contain a glycine rich segment segregating the C-terminus from the rest of the molecule. This arrangement is reminiscent of glucoamylases where the catalytic domain and the starch-binding domain are attached via a highly glycosylated linker (27, 28). However, the domain-linker-domain architecture is not a universal requirement for raw starch digestion, because the majority of the α-amylases that are known to degrade starch granules do not contain a linker sequence.

Despite the low sequence similarities, the crystal structures of α-amylases from various organisms exhibit similar tertiary folding. The central core is an $(\alpha/\beta)_8$ barrel (domain A), consisting of eight parallel β strands alternating with eight helices joined by loops (29, 30) (Fig. 2). About 10% of all known enzymes have an α/β barrel domain, catalyzing a wide variety of reactions. The first protein discovered to contain such folding was triose phosphate isomerase, hence the name TIM barrel (31). The evolutionary history of this α/β barrel family of enzymes has been the subject of continuous interest. Arguments in support of convergence, as well as divergent evolution have been presented (32–35). For most α/β barrel proteins, including the α-amylase family, the active site is located at the C-terminus of the parallel β-strands, with the catalytic and substrate-binding residues in the loop regions. α-Amylases also contain a small structural domain (domain B) inserted between β-strand 3 and helix 3. This protruding domain B varies both in length and sequence, and is implicated in functional diversity and stability. In the *Aspergillus oryzae* enzyme, the main feature of domain B is a short, three-stranded antiparallel β-sheet (36). In the *Bacillus licheniformis* α-amylase, domain B possesses a β-sheet of six loosely connected twisted β-strands forming a twisted barrel with a large interior hole (37). For several α-amylases with known three-dimensional structures, including *Bacillus licheniformis, Aspergillus oryzae*, and porcine pancreatic, domain B contains an invariant Asp residue (equivalent to

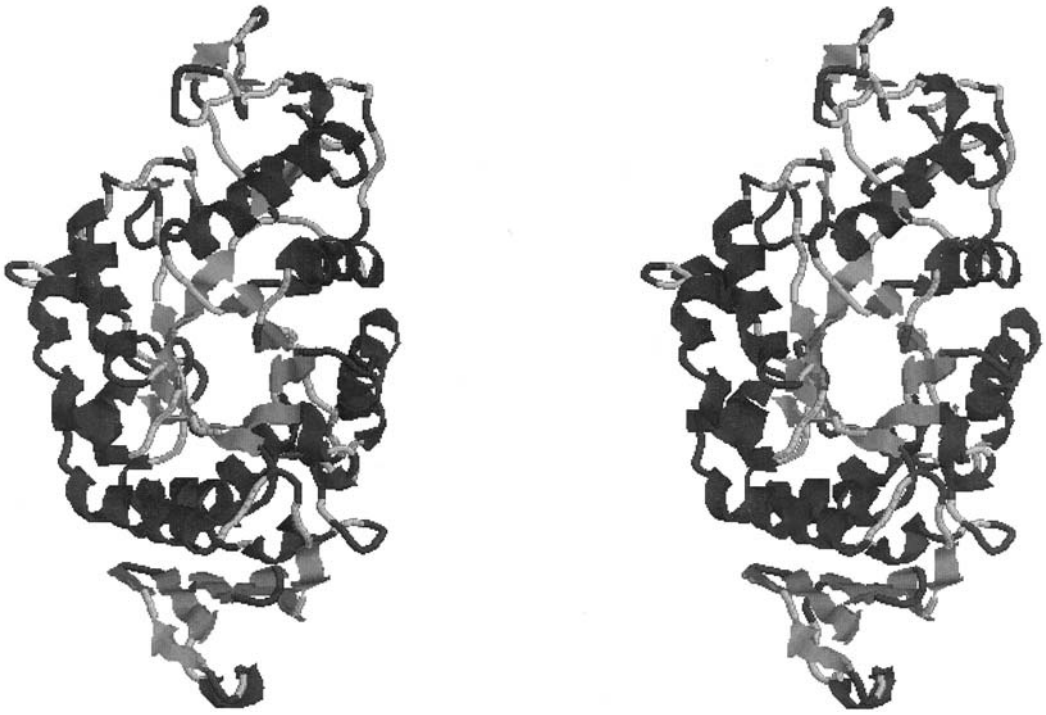

Figure 2 A stereo view of the barley α-amylase (isoform 2). The structure consists of three domains—the central $(\alpha/\beta)_8$-barrel (domain A), a five-stranded antiparallel β-sheet domain C at the bottom, and a protruding loop at the top (domain B). (From Ref. 29, PDBid: 1 amy.)

Asp175 of the *A. oryzae* enzyme) involved in calcium binding. The $(\alpha/\beta)_8$ barrel is followed by domain C, a distinct globular unit of ~ 100 amino acid residues with a folding of an antiparallel β-sandwich of the Greek key topology.

The three-dimensional structures of several α-amylases have been solved: *Aspergillus oryzae, A. niger, Bacillus licheniformis, B. subtilis, B. stearothermophilus*, yellow mealworm, porcine pancreatic, human pancreatic, *Alteromonas haloplanctis*, and barley isozyme 2. The following is a functional description of the enzyme structure of barley α-amylase (isoform AMY2) (29, 30, 38). AMY2 assumes the same basic features in the overall structure (Fig. 2). Domain A forms an $(\alpha/\beta)_8$ barrel of 286 residues, with a loop of 64 residues (domain B) protruding between β-strand 3 and helix 3. The C-terminal 53 residues form domain C with a five-stranded antiparallel β-sheet. The active site is located on the C-terminal side of the $(\alpha/\beta)_8$ barrel, with the catalytic residues Asp179, Glu204, and Asp289 positioned at A-β_4, A-β_5, and A-α_{7a}, respectively. Several invariant residues, including Tyr51, His92, Arg177, and His288, form hydrogen bonds with the substrate (39).

The α-amylase contains a calcium-binding site structurally similar to that of other amylolytic enzymes (40). The calcium atom is coordinated by amino acid side chains located in both domains A and B, providing structural stability to the enzyme. Removal of calcium from the barley enzyme results in irreversible inactivation. In addition to this high-affinity binding site, two other calcium-binding sites have been located with ligands entirely in the domain B. The calcium-binding interactions seem to contribute to the folding stability of domain B.

A surface-located starch granule–binding site characteristic of cereal α-amylase has been identified that interacts with starch granules. This site also binds β-cyclodextrin, an analog of amylose, in competition with starch granules. Chemical modification and site-directed mutagenesis suggest that two consecutive Trp residues, Trp276 and Trp277, are involved (41, 42). In a three-dimensional structure of AMY2 in complex with the inhibitor acarbose, the two Trp residues stack onto the substrate sugar rings, a typical feature of protein–carbohydrate interactions (30). However, this structural arrangement involving consecutive Trp residues protruding from the helix A-α_{6b} is not found in the microbial or animal α-amylases that also hydrolyze raw starch granules.

IV. REACTION MECHANISMS

α-Amylases hydrolyze the glucosidic bond with retention of the anomeric configuration. The retaining and inverting actions of glycosidases have been the subject of numerous investigations, and several mechanisms have been proposed to explain the stereochemistry of the catalytic process.

A. Nucleophilic Displacement Mechanism

For retaining glycosidases, the reaction proceeds via a double displacement (43–45). The protonation of the glucoside oxygen is concerted with the nucleophilic attack of a carboxylate anion at C1, resulting in the formation of a covalent glucosyl-enzyme intermediate (Fig. 3). A second displacement by a general base hydrolyzes the carboxyl-acetal bond of the glucosyl-enzyme intermediate to yield a product with α-configuration.

For inverting glycosidases, the reaction involves a single displacement. The glucosidic oxygen is protonated by a general acid, resulting in a weakened maltosyl C–O bond. The attack of a water molecule occurs at the β-side of substrate assisted by a general base. It has been suggested that both reactions involve transition states with oxocarbonium ion character. It is interesting to note that although both reactions can be called displacement, they are obviously very different. In the single displacement, one of the carboxylic catalytic residues acts as a general acid and the other as a general base, whereas in the double displacement, one residue acts as a general acid/base, and the other acts as a nucleophile. Furthermore, the covalent enzyme-substrate intermediate invoked for the double displacement is not formed in the single displacement.

B. Oxocarbonium Ion Mechanism

In this model, the reaction is described by S_N1 substitution (Fig. 4). Protonation of the glucosidic oxygen results in bond cleavage, leading to the formation of an oxocarbonium ion intermediate that is stabilized by a carboxylate anion residue (46–48). It has also been suggested that binding of the sugar substrate to the enzyme's active site induces a distortion of the sugar ring into a half-chair conformation, thereby weakening the C1–O4 bond as shown in the case of lysozyme (49). The stereoselectivity of the reaction then depends on the direction of the nucleophilic attack of the water molecule assisted by a general base. In α-amylases, the water molecule attacks from the front (original

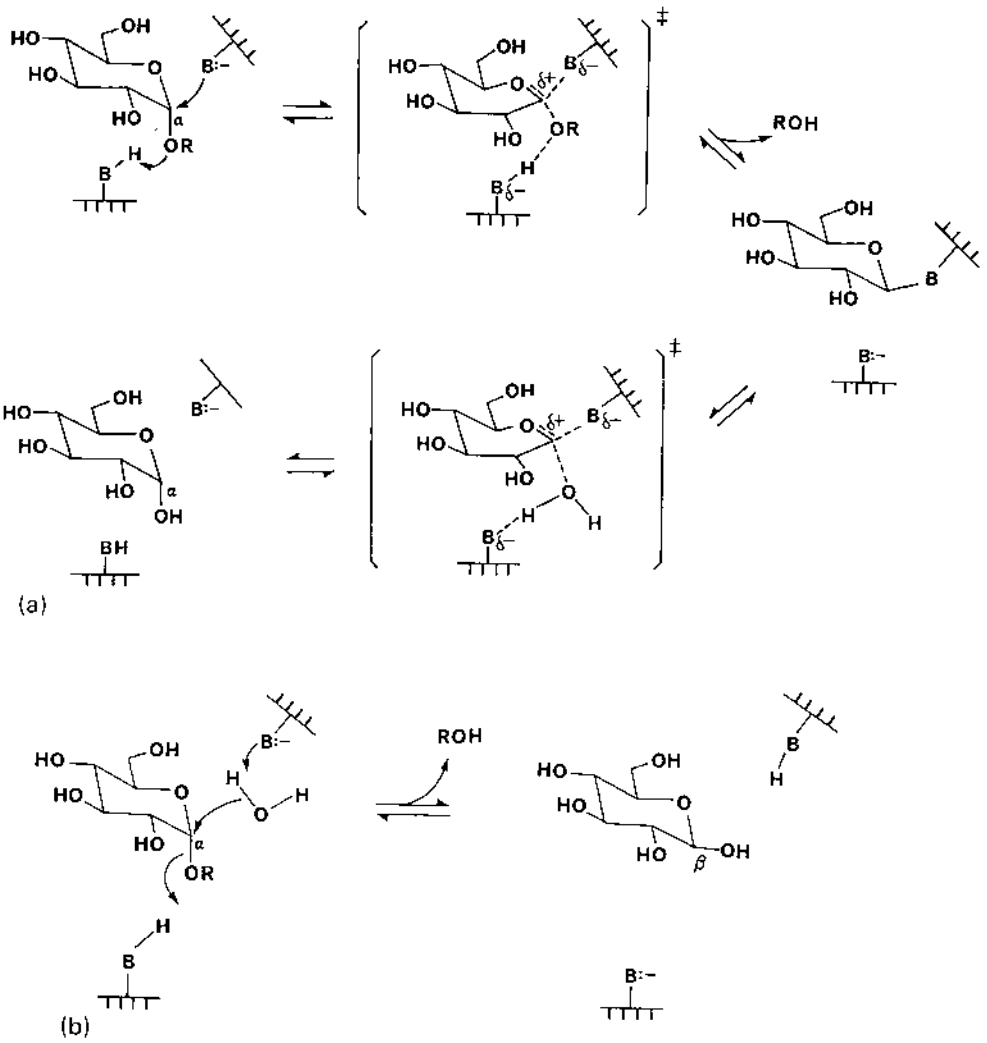

Figure 3 (A) A single-displacement mechanism. (B) A double-displacement mechanism with the formation of a glycosyl enzyme intermediate via oxocarbonium-like transition rates.

glucoside oxygen side), with the product maintaining the α-configuration. In inverting glycosidases, such as β-amylase and glucoamylase, a back-side attack results in an inversion of the configuration. The appealing aspect of this model is that the catalytic reactions of both inverting and retaining glycosidases can be explained by a single unified mechanism (50).

The main difference between this model and the displacement mechanism lies in whether a transient or stable oxocarbonium ion intermediate exists (51, 52). The formation of a stable oxocarbonium ion intermediate is preferred if bond breaking precedes the attack of water facilitated by general base catalysis. The oxocarbonium ion is readily collapsed into a covalent intermediate if nucleophilic attack occurs prior to the complete formation of the cation.

C. Ring-Opening Reaction

An alternative mechanism that is not as well received as the above two models involves endocyclic carbon–oxygen cleavage as the rate-determining step, leading to the formation of an acyclic oxocarbonium ion intermediate (44, 53). In this model, there is no distortion of the substrate into a twist-boat conformation as shown by molecular dynamics simulation. In the chair conformation of both α and β-anomers, the antiperiplanar orientation of the exocyclic O_4 lone pair fulfills the

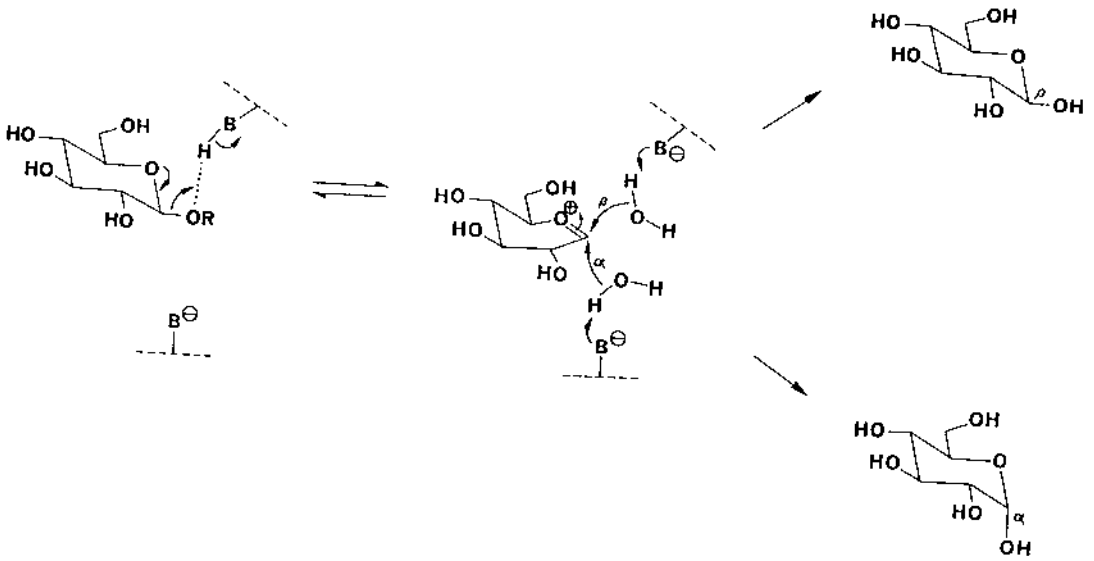

Figure 4 Reaction mechanism of carbohydrases involving a stabilized oxocarbonium intermediate.

stereoelectronic requirement in the fragmentation of the ring C–O bond (54). It has been also postulated that protonation occurs at the cyclic oxygen instead of the glucosidic oxygen, and the water nucleophilic attack is followed by a rotation of the hemiacetal center to position for cleavage (55).

V. α-AMYLASE INHIBITORS

Two families of α-amylases inhibitors (α-AI), including carbohydrate- and protein-based inhibitors, have been studied in detail. The knowledge of the inhibitory action of these compounds is of great interest in medicine in the attempt to develop therapeutics for diabetes, obesity, and hyperlipemia. Proteinaceous α-AIs are widespread in microorganisms and higher plants. Tendamistat, one of the most potent inhibitors of mammalian α-amylases, is an acidic protein of 74 amino acids isolated from the culture medium of *Streptomyces tendae* (56, 57). This class of inhibitors also includes HAIM (*S. grieseosporeus*) (58), AI-3688 (*S. aureofaciens*) (59), and PAIM (*S. griseosporeus*) (60). Tendamistat binds tightly with porcine pancreatic α-amylase with a very high inhibition constant of 9×10^{-12} M (56). The molecular structure assumes a β-barrel of two β-sheets, each consisting of three antiparallel strands. The β-strands are connected by loops and turns which contain the active-site triplet Trp18-Arg19-Tyr20 characteristics of all Tendamistat-type proteinaceous inhibitors (61, 62). Analysis of the crystal structure indicates that the head of Tendamistat containing the highly conserved triplet residues binds directly to the active site of the porcine pancreatic α-amylase, blocking the five binding subsites −3 to 2, with Arg19 forming a salt bridge with the catalytic residue, Glu233 (for subsite nomenclature, refer to Ref. 62). In the formation of the enzyme–inhibitor complex, the conformation of the enzyme active site is induced to accommodate tight binding of Tendamistat and related inhibitors.

The seeds of common beans contain a family of proteins involved in a defense mechanism, composed of phytohemaglutinin, and α-amylase inhibitor. The α-AIs inhibit the activity of some mammalian and insect α-amylases, but not of the endogenous plant enzyme. Red kidney bean α-AI has a K_D of 3.5×10^{-11} M at pH 6.9 and 30°C (63), and black bean α-AI 4.4×10^{-9} M at pH 6.9 at 37°C (64). There are at least five known sequences derived from α-AIs of common domesticated beans, wild common bean, white kidney bean, and black bean (65). The inhibitors are glycoproteins synthesized as preproproteins which require proteolytic cleavage for activation (66). Translational processes produce the active inhibitor formed by the association of two polypeptide chains, α– and β-subunits (67). In the crystal structure of the enzyme–inhibitor complex, α-AI-I exists as a dimer that binds two porcine pancreatic enzyme molecules (68). Each monomer consists of a concave

12-stranded antiparallel β-sandwich fold. Two hairpin loops protruding from the fold interact directly with the active-site region of the enzyme. A large conformational change occurs in the enzyme active site upon α-AI-1 binding, resulting in extensive interactions with the inhibitory site of α-AI. Site-directed mutagenesis studies suggest the involvement of Trp188, Arg74, and Tyr190 in αAI, analogous to the Trp-Arg-Tyr motif of Tendamistat (69). X-ray structural analysis confirms that Tyr190 forms strong contacts with the catalytic residue Asp300.

A variety of α-AIs, both endogenous and exogenous, occur in barley and wheat kernels. The α-amylase/subtilisin inhibitor (BASI) from barley has been extensively investigated and its three-dimensional structure is known. BASI is active against the plant endogenous α-amylase 2 (one of the two major barley amylase isozymes). It consists of a single polypeptide of 181 residues with a calculated MW of 19,685 daltons. Its amino acid sequence shows 26% identical residues compared to that of the soybean trypsin inhibitor (Kunitz) (70). Inhibitors with a dual function of protease and α-amylase have also been identified in wheat and ragi (71, 72). BASI forms an inactive 1:1 complex with α-amylase 2, with a dissociation constant of 2.2×10^{-10} M at pH 8 and 37°C (73) but does not inhibit α-amylase 1, the other major barley isozyme. The crystal structure of BASI is composed of a 12-stranded β-barrel, with three sets of four sequential β-strands arranged in a threefold symmetry (38). The hydrophobic core is composed of six β-strands—S1, S4, S5, S8, S9, and S12—and one end of the barrel is closed by triangular array consisting of the remaining β-strands. BASI binds tightly to domains A and B of the enzyme but does not directly interact with the catalytic residues at the enzyme active site. A calcium ion is trapped at the interface of the enzyme–inhibitor complex.

The second type of inhibitors are carbohydrate-based derived from the trestatin family and are found also in *Streptomyces*. The most common inhibitor in this class is acarbose, a pseudo-tetrasaccharide with a cyclitol unit and an amino sugar unit at the nonreducing end. Cyclitol ring exists as a half-chair resembling the conformation of the oxocarbonium ion. Binding of the inhibitor to the enzyme induces structural changes at the active site, involving extensive hydrogen bonds, hydrophobic stacking, and water-bridged contacts (74). It has been shown that pancreatic α-amylase can hydrolyze the reducing end glucose units, and several x-ray crystal structural analyses revealed that the original substrate acarbose is transformed into a more potent inhibitor via transglycosylation or condensation of the cleaved products (36, 75). The additional sugar rings of the product may be stabilized by secondary binding sites on the surface of the enzyme molecule (76). Another carbohydrate inhibitor, cyclohepta-amylose (CHA), has been known to inhibit α-amylase digestion of raw starch granule by interfering with α-amylase adsorption to raw starch granules. Hydrolysis of starch granules by wheat α-amylase is inhibited 40% by 0.88 mM CHA (41). The granular starch-binding domain of *Aspergillus niger* glucoamylase 1 binds β-cyclodextrin with a dissociation constant K_d of 1.68 μM, and a competitive inhibition constant (K_i) of 11.0 μM for raw starch adsorption showing that β-cyclodextrin and granular starch bind to the same site of the enzyme molecule (28). It has been proposed that the β cyclodextrin seven-member ring structure mimics the helical amylose with binding in the cavity (77).

VI. MEASUREMENT OF α-AMYLASE ACTIVITY

The kinetic parameters of barley α-enzyme were measured using various concentrations of the substrate ET-G_7PNP. A K_m of 0.45 mM and a k_{cat} of 1.2×10^2 sec^{-1} were obtained for the α-amylase, with k_{cat}/K_m of 2.7×10^2 $mM^{-1} \cdot sec^{-1}$. Barley malt α-amylase 1 has a k_{cat}/K_m value of 1.75×10^2 $mM^{-1} \cdot sec^{-1}$ using *p*-nitrophenyloligosaccharide (*p*-$NPGlc_7$) as the substrate (78). The catalytic efficiency is generally consistent with those obtained for α-amylases from other organisms. For example, a k_{cat}/K_m of 2.5×10^2 $mM^{-1} \cdot sec^{-1}$ has been reported for *Saccharomycopsis fibuligera* α-amylase in the hydrolysis of malto-oligosaccharides (79), and a higher value of 1.3×10^3 $mM^{-1} \cdot sec^{-1}$ has been observed for the same enzyme with amylose A as the substrate (80). Porcine pancreatic α-amylase has a k_{cat}/K_m of 5.8×10^3 $mM^{-1} \cdot sec^{-1}$ in the hydrolysis of *p*-$NPGlc_7$ (81). Increasing chain length of the substrate decreases the K_m value and increases the k_{cat}, as demonstrated in the *Aspergillus oryzae* enzyme: $K_m = 9.0 \times 10^{-4}$ and 9.5×10^{-6} mM for maltotetraose and maltodextrin VI (n = 117), respectively, and $k_{cat} = 1.2 \times 10^4$ and 9.9×10^3 min^{-1} (82).

The method of α-amylase activity measurement is characterized by the type of substrate employed in a particular procedure. All three methods described below have been used routinely by the authors for the assay of plant and recombinant α-amylases.

A. Reducing Sugar Method

Reducing sugar assays measure the increase of new reducing ends on fragments produced by the hydrolytic action of α-amylase on soluble starch. In the 3,5-dinitrosalicyclic acid method, the concentration of the nitroaminosalicyclic acid formed at the reducing hemiacetal is measured colorimetrically (83). The measurement of α-amylase activity by this method is accurate only if the sample is not contaminated with other amylolytic enzymes. A modified procedure for small-scale analysis of cereal α-amylases is described: 250 μL of enzyme in buffer (200 mM sodium acetate, pH 5.5; 10 mM $CaCl_2$) was combined with 250 μL of 1% soluble starch and incubated at 37°C for 10 min. To the reaction mixture 500 μL of dinitrosalicyclic acid reagent (1% nitrosalicyclic acid, 30% potassium sodium tartrate, 40% I N NaOH) was added, heated for 5 min in a 100°C water bath, cooled to room temperature in cold water, and then clarified by centrifugation. The absorbance at 547 nm was measured, and the activity was calculated using a maltose standard curve. One enzyme unit is defined as the amount of enzyme catalyzing the release of 1 μmole of reducing groups from soluble starch, measured as maltose, per min at 37°C. In some cases, it may be desirable to treat the starch with sodium borohydride to remove terminal reducing glucosyl residues that may interfere with the reducing sugar measurement (84). The reducing groups can also be quantitated by the alkaline ferricyanide method (85, 86), or the Nelson-Somogyi method (87, 88). Benedict's solution can detect 0.01% glucose in water.

B. Dyed Starch Substrate Method

This procedure involves the hydrolysis of dyed starch substrate by α-amylase and the measurement of absorbance at 610 nm of the soluble colored fragments released into solution from degradation of the substrate. This method is unaffected by reducing substances and is therefore particularly applicable to the measurement of α-amylase activity in cell culture media containing glucose or other reducing sugars. Two types of dyed starch substrates are available commercially.

1. Dye-Labeled Crosslinked Starch

Dye-labeled crosslinked starch is made by crosslinking partially hydrolyzed potato starch using 1,4-butandiol-diglycidether, and labeling with Cibachron Blue by covalent bonds (89). The substrate forms an insoluble network of polymers that swells in water or buffer, resulting in a suspension. The substrate is known to be very resistant to β-amylase, and is particularly suitable for the analysis of α-amylase in cereal grains which commonly contain considerable amounts of β-amylase as a common contaminant in enzyme extracts.

2. Dye-Labeled Non-crosslinked Starch

Dye-labeled non-crosslinked starch is made by labeling non-crosslinked starch with Remazol Brilliant Blue by covalent bonds. This is a soluble substrate (90). The substrate is also susceptible to β-amylase action, and therefore this assay is nonspecific for α-amylase.

A microassay has been developed using dye-labeled crosslinked starch (Phadebas, Pharmacia) for rapid screening of α-amylase activity (91). Linear correlation between the absorbance and enzyme concentrations in the 50-ng range was observed. The assay has been adapted for semiautomation and routinely used in monitoring the production of recombinant α-amylase produced in transformed yeast cells. One unit of α-amylase activity is defined as the amount of enzyme that gives an absorbance value of 0.100 (92). This definition is the most useful in the measurement of relative activities, such as monitoring chromatographic column fractions. The absorbance values obtained in the dyed-substrate-based assay can be converted to International Units using a standard curve.

C. Defined Substrate Method

The use of low-MW synthetic oligosaccharides with a defined structure has the advantage of elimination of substrate variability. However, these are not natural substrates, and activity measurement may fail to reveal some unique enzyme properties, such as raw starch binding and hydrolysis. Defined substrates have been initially developed with a chromophore such as *p*-nitrophenol group attached to the reducing-end glucose unit. These substrates, however, are nonspecific for α-amylases, since other amylases, such as β-amylase or glucoamylase, also can readily cleave the substrate. More recently, a specific substrate has been developed with the additional attachment of a chemical blocking group at the non-reducing-end glucose residue (93, 94). We use 4,6-ethylidene-(G_7)-*p*-nitrophenyl-(G_1)-α,D-maltoheptaside (Sigma) as the substrate. The ethylidene group in the 4,6-position of G7 blocks the action of exoamylases. α-Amylase hydrolyzes the substrate to G2-, G3-, and G4-*p*-nitrophenol

fragments, which are further hydrolyzed by α-glucosidase to *p*-nitrophenol and glucose. Enzyme activity corresponds to the increase in absorbance at 405 nm owing to the liberation of *p*-nitrophenol, and the chemically blocked nonreducing end renders the substrate unsusceptible to the action of β-amylase and glucoamylase.

VII. PURIFICATION OF α-AMYLASE

The following method, based on MacGregor and Morgan (95), has been used routinely in our lab to purify barley α-amylase. Barley malt (250 g) was extracted with 500 mL of 0.2 M acetate buffer containing 1 mM $CaCl_2$, pH 5.5. The suspension was centrifuged (8000g, 15 min) and the pellet was subjected to a second extraction using the same buffer. The combined extracts (supernatants) were heated at 70°C for 15 min, and denatured proteins, including β-amylase, were removed by centrifugation (8000 g, 15 min). The proteins in the supernatant were precipitated with 60% $(NH_2)_2SO_4$ at 4°C, redissolved in 200 mL of 0.02 M acetate buffer containing 1 mM $CaCl_2$, pH 4.7, and dialyzed against the same buffer. The crude enzyme preparation was loaded onto a CM Sepharose CL-6B column equilibrated with the same buffer. Elution was performed using a linear gradient from 0.02 M to 0.06 M acetate (containing 1 mM $CaCl_2$, pH 4.7), and active fractions were pooled to give a crude preparation of α-amylase isozyme 1. A second elution was performed with a salt gradient of 0.06 M acetate buffer (containing 1 mM $CaCl_2$, pH 4.7) and the same buffer containing 0.5 M NaCl, to give a crude preparation of α-amylase 2 isozyme. The enzyme preparations are concentrated by ultrafiltration (PM10 membrane) and further purified by passing through the CHA-Sepharose affinity column (96). Bound α-amylase was eluted with acetate buffer containing 8 mg/mL CHA. The CHA was removed by ion exchange chromatography as described above.

For the purification of recombinant α-amylase expressed in yeast, the following method has been used in our laboratory. Yeast cells secreting recombinant α-amylase were grown in 2 L YEPD medium for 36 h and centrifuged at 9000g for 20 min. The supernatant was filtered through a 0.2-μ filter, concentrated by ultrafiltration using Pellicon XL (10,000 mwco, Millipore, Bedford, MA) at a crossflow rate of 35 mL/min. The retentate was exchanged into 20 mM sodium acetate buffer, pH 5.0, containing 5 mM $CaCl_2$. The enzyme was separated by an affinity column of cyclohepta-amylose-substituted epoxy-Sepharose 6B according to Silvanovich and Hill (96). The concentrated enzyme preparation (100 mL) was loaded onto CHA-Sepharose affinity column (1×8 cm), followed by successive washings with 50 mL buffer, 50 mL buffer containing 4 mM NaCl, and 100 mL buffer. The adsorbed enzyme was eluted with buffer containing 8 mg/mL CHA which was subsequently removed by dialysis in 20 mM sodium acetate, pH 5.0, buffer containing 2 mM $CaCl_2$.

REFERENCES

1. IUBMB. Enzyme Nomenclature. San Diego: Academic Press, 1992.
2. B Henrissat. A classification of glycosyl hydrolases based on amino acid sequence similarities. Biochem J 280:309–316, 1991.
3. B Henrissat, A Bairoch. New families in the classification of glycosyl hydrolases based on amino acid sequence similarities. Biochem J 293:781–788, 1993.
4. B Henrissat, G Davies. Structural and sequence-based classification of glycoside hydrolases. Curr Opin Struct Biol 7:637–644, 1997.
5. GL Gray, SE Mainzer, MW Rey, MH Lamsa, KL Kindle, C Carmona, C Requadt. Structural genes encoding the thermophilic α-amylases of *Bacillus stearothermophilus* and *Bacillus licheniformis*. J Bacteriol 166:635–643, 1986.
6. K Takkinen, RF Pettersson, N Kalkkinen, I Palva, H Soderlund, L Kaarianinen. Amino acid sequence of α-amylase from *Bacillus amyloliquefaciens* deduced from the nucleotide sequence of the cloned gene. J Biol Chem 258:1007–1013, 1983.
7. T Yuuki, T Nomura, H Tezuka, A Tsuboi, H Yaagata, N Tsukagoshi, S Udaka. Complete nucleotide sequence of a gene coding for heat- and pH-stable α-amylase of *Bacillus licheniformis*: comparison of the amino acid sequences of three bacterial liquefying α-amylases deduced from the DNA sequences. J Biochem 98:1147–1156, 1985.
8. S Wirsel, A Lachmund, G Wildhardt, E Ruttkowski. Three α-amylase genes of *Aspergillus oryzae* exhibit identical intron-exon organization. Mol Microbiol 3:3–14, 1989.
9. T Kimura, K Horikoshi. The nucleotide sequence of an α-amylase gene from an alkalopsychrotrophic *Micrococcus* sp. FEMS Microbiol Lett 71:35–42, 1990.
10. T Itoh, I Yamashita, S Fukui. Nucleotide sequence of the α-amylase gene (ALPI) in the yeast *Saccharomycopsis fibuligera*. FEBS Lett 219:339–342, 1987.

11. JC Rogers, C Milliman. Isolation and sequence analysis of a barley α-amylase cDNA clone. J Biol Chem 258:8169–8174, 1983.
12. N Inomata, H Shibata, E Okuyama, T Yamazaki. Evolutionary relationships and sequence variation of alpha-amylase variants encoded by duplicated genes in the *Amy* locus of *Drosophila melanogaster*. Genetics 141:237–244, 1995.
13. S Strobl, FX Gomis-Ruth, K Maskos, G Frank, R Huber, R Glockshuber. The alpha-amylase from the yellow meal worm: complete primary structure crystalization and preliminary x-ray structures. FEBS Lett 409:109–114, 1997.
14. L Pasero, Y Mazzei-Pierron, B Abadie, Y Chicheportiche, G Marchis-Mouren. Complete amino acid sequence and location of the five disulfide bridges in porcine pancreatic α-amylase. Biochim Biophys Acta 869:147–157, 1986.
15. A Horii, M Emi, N Tomita, T Nishide, M Ogawa, T Mori, K Matsubara. Primary structure of human pancreatic α-amylase gene: its comparison with human salivary α-amylase gene. Gene 60:57–64, 1987.
16. T Kuriki, T Imanaka. The concept of the α-amylase family: structural similarity and common catalytic mechanism. J Biosci Bioeng 87:57–565, 1999.
17. H Taniguchi, CM Jae, N Yoshigi, Y Maruyama. Purification of *Bacillus circulans* F-2 amylase and its general properties. Agric Biol Chem 47:511–519, 1983.
18. S Hayashida, Y Teramoto, T Inoue. Production and characteristics of raw-potato-starch-digesting α-amylase from *Bacillus subtilis* 65. Appl Environ Microbiol 54:1516–1522, 1988.
19. B Diderichsen, L Christiansen. FEMS Microbiol Lett 56:53–60, 1988.
20. CM Long, M-J Virolle, S-Y Chang, S Chang, MJ Bibb. α-Amylase gene of *Streptomyces limosus*: nucleotide sequence, expression motifs, and amino acid sequence homology to mammalian and invertebrate α-amylase. J Bacteriol 170:5745–5754, 1987.
21. M Yamamoto, Y Monma, N Kagei, K Kainuma, T Ibaraki. Raw starch digestion by α-amylase and glucoamylase from *Chalara paradoxa*. Starch 10:382–385, 1989.
22. SH Imam, A Burgess-Cassler, GL Cote, SH Gordon, F Baker. A study of cornstarch granule digestion by an unusually high molecular weight α-amylase secreted by *Lactobacillus amylovorus*. Curr Microbiol 22:365–370, 1991.
23. H Iefuji, M Chino, M Kato, Y Imura. Raw-starch-digesting and thermostable α-amylase from the yeast *Crytococcus* sp. S-2: purification, characterization, cloning and sequencing. Biochem J 318:989–996, 1996.
24. S Hayashida, Y Teramoto, I Kira. Promotive and inhibitory effects of raw starch adsorbable fragments from pancreatic α-amylase on enzymatic digestions of raw starch. Agric Biol Chem 44:1–6, 1991.
25. DWS Wong, SB Batt, BK Tibbot, GH Robertson. Isolation of a raw starch binding fragment from barley α-amylase 1. J Protein Chem 19:373–377, 2000.
26. S Janecek, J Sevick. The evolution of starch-binding domain. FEBS Lett 456:119–125, 1999.
27. S Hayashida, S-I Kunisaki, M Nakao, PQ Flor. Evidence for raw starch affinity site on *Aspergillus awamori* glucoamylase I. Agric Biol Chem 46:83–89, 1982.
28. NJ Belshaw, G Williamson. Production and purification of a granular-starch-binding domain of glucoamylase 1 from *Aspergillus niger*. FEBS Lett 269:350–353, 1990.
29. A Kadziola, J-I Abe, B Svensson, R Haser. Crystal and molecular structure of barley α-amylase. J Mol Biol 239:104–121, 1994.
30. A Kadziola, M Sogaard, B Svensson, R Haser. Molecular structure of a barley α-amylase-inhibitor complex: implications for starch binding and catalysis. J Mol Biol 278:205–217, 1998.
31. DW Banner, AC Bloomer, GA Petsko, DC Phillips, CI Pogson, IA Wilson, PH Corrang, AJ Furth, JD Milman, RE Offord, JD Priddle, SG Waley. Structure of chicken muscle triose phosphate isomerase determined crystallographically at 2.5 Å resolution using amino acid sequence data. Nature 255:609–614, 1975.
32. D Reardon, GK Farber. The structure and evolution of α/β barrel proteins. FASEB J 9:497–503, 1995.
33. C-I Branden. The TIM Barrel—the most frequently occurring folding motif in proteins. Curr Opin Struct Biol 1:978–983, 1991.
34. HM Jespersen, EA MacGregor, B Henrissat, MR Sierks, B Svensson. Starch- and glycogen-debranching and branching enzymes: prediction of structural features of the catalytic (β/α)8-barrel domain and evolutionary relationship to other amylolytic enzymes. J Protein Chem 12:791–805, 1993.
35. S Janecek, B Svensson, B Henrissat. Domain evolution in the α-amylase family. J Mol Evol 45:322–331, 1997.
36. AM Brzozowski, GJ Davies. Structure of the *Aspergillus oryzae* α-amylase complexed with the inhibitor acarbose at 2.0 Å resolution. Biochemistry 36:10837–10845, 1997.
37. M Machius, G Wiegand, R Huber. Crystal structure of calcium-depleted *Bacillus licheniformis* α-amylase at 2.2 Å resolution. J Mol Biol 246:545–559, 1995.
38. F Vallee, A Kadziola, Y Bourne, M Juy, KW Rodenburg, B Svensson, R Haser. Barley α-amylase bound to its endogenous protein inhibitor BASI: crystal structure of the complex at 1.9 Å resolution. Structure 6:649–659, 1998.
39. M Sogaard, A Kadziolas, R Haser, B Svensson. Site-directed mutagenesis of histidine 93, aspartic acid 180, glutamic acid 205, histidine 290, and aspartic acid 291

at the active site and tryptophan 279 at the raw starch binding site in barley α-amylase 1. J Biol Chem 268:22480–22484, 1993.
40. DS Bush, L Sticher, R van Huystee, D Wagner, RL Jones. The calcium requirement for stability and enzymatic activity of two isoforms of barley aleurone α-amylases. J Biol Chem 264:19392–19398, 1989.
41. RJ Weselake, RD Hill. Inhibition of alpha-amylase-catalyzed starch granule hydrolysis by cycloheptaamylose. Cereal Chem 60:98–101, 1983.
42. RM Gibson, B Svensson. Identification of tryptophanyl residues involved in binding of carbohydrate ligands to barley α-amylase 2. Carlsberg Res Commun 52:373–379, 1987.
43. DE Koshland Jr. Mechanisms of transfer enzymes. Enzymes 1:305–346, 1959.
44. CA Vernon. The mechanism of hydrolysis of glycosides and their relevance to enzyme-catalyzed reactions. Proc Soc Lond Ser B 167:389–401, 1967.
45. ML Sinnott. Physical-organic probes of glycosidase mechanism. In: GJ Davies, HJ Gilbert, B Henrissat, B Svensson, eds. Recent Advances in Carbohydrate Bioengineering. Cambridge: Royal Soc Chem, 1997.
46. DC Phillips. The three-dimensional structure of an enzyme molecule. Sci Am 215:78–90, 1966.
47. CCF Blake, LN Johnson, GA Mair, ACT North, DC Phillips, VR Sarma. Crystallographic studies of the activity of hen egg-white lysozyme. Proc Royal Soc London Ser B 167:378–385, 1967.
48. JA Thoma. A possible mechanism for amylase catalysis. J Theor Biol 19:297–310, 1968.
49. NCJ Stryadka, MNG James. Lysozyme revisited: crystallographic evidence for distortion of an N-acetylmuramic acid residue bound in site D. J Mol Biol 220:401–424, 1991.
50. H Kaneko, T Juriki, S Handa, T Takada, H Takata, M Yanase, S Okada, H Umeyama, J Shimada. How α- and β-amylases achieve their perfect stereoselectivity. Res Commun Biochem Cell Mol Biol 2:69–89, 1998.
51. TL Amyes, WP Jencks. Lifetimes of oxocarbonium ions in aqueous solution from common ion inhibition of the solvolysis of α-azido ethers by added azide ion. J Am Chem Soc 111:7888–7900, 1989.
52. NS Banait, WP Jencks. Reactions of anionic nucleophiles with α-D glucopyranosyl fluoride in aqueous solution through a concerted, $A_ND_N(S_N2)$ mechanism. J Am Chem Soc 113:7951–7958, 1991.
53. CB Post, M Karplus. Does lysozyme follow the lysozyme pathway? An alterative based on dynamic, structural, and stereoelectronic considerations. J Am Chem Soc 108:1317–1319, 1986.
54. GWJ Fleet. An alternative proposal for the mode of inhibition of glycosidase activity by polyhydroxylated piperidines, pyrrolidines and indolizidines: implications for the mechanism of action of some glycosidases. Tetrahedron Lett 26:5073–5076, 1985.
55. AK Mazur, R Haser, F Payan. The catalytic mechanism of α-amylase based upon enzyme crystal structures and model building calculations. Biochem Biophys Res Commun 204:297–302, 1994.
56. L Vertesy, V Oeding, R Bender, K Zepf, G Nesemann. Tendamistat (Hoe467), a tight-binding α-amylase inhibitor from *Streptomyces tendae* 4158. Eur J Biochem 141:505–512, 1984.
57. K-P Killer, G Riess. Heterologous expression of the α-amylase inhibitor gene cloned from an amplified genomic sequence of *Streptomyces tendae*. J Bacteriol 171:4953–4957, 1989.
58. M Yoshida, T Nakai, K Fukuhara, S Saitoh, W Yoshikawa, Y Kobayashi, H Nakamura. Three-dimensional structure of an α-amylase inhibitor HAIM as determined by nuclear magnetic resonance methods. J Biochem 108:158–165, 1990.
59. L Vertesy, D Tripir. Isolation and structure elucidation of an α-amylase inhibitor, AI-3688, from *Streptomyces aureofaciens*. FEBS Lett 185:187–190, 1985.
60. H Murai, S Hara, T Ikenaka, A Goto, M Arai, S Murao. Amino acid sequence of protein α-amylase inhibitor from *Streptomyces griseosporeus* YM-25. J Biochem 97:1129–1133, 1985.
61. G Wiegand, O Epp, R Huber. The crystal structure of porcine pancreatic α-amylase in complex with the microbial inhibitor Tendamistat. J Mol Biol 247:99–110, 1995.
62. GJ Davies, KS Wilson, B Henrissat. Nomenclature for sugar-binding subsites in glycosyl hydrolases. Biochem J 321:557–559, 1997.
63. JR Powers, JR Whitaker. Effect of several experimental parameters on combination of red kidney bean (*Phaseolus vulgaris*) α-amylase inhibitor with porcine pancreatic α-amylase. J Food Biochem 1:239–260, 1977.
64. MM Tanizaki, FM Lajolo. Kinetics of the interaction of pancreatic α-amylase with a kidney bean (*Phaseolus vulgaris*)–amylase inhibitor. J Food Biochem 9:71–89, 1985.
65. S-C Lee. Comparative Amino Acid Sequences, and Deduced Tertiary and Quaternary Structures of White Kidney Bean and Black Bean α-Amylase Inhibitors. PhD Dissertation, University of California, Davis, 1996.
66. NM Young, P Thibault, DC Watson, MJ Chrispeels. Post-translational processing of two α-amylase inhibitors and an arcelin from the common bean, *Phaseolus vulgaris*. FEBS Lett 446:203–206, 1999.
67. JJ Pueyo, DC Hunt, MJ Chrispeels. Activation of bean (*Phaseolus vulgaris*) α-amylase inhibitor requires proteolytic processing of the proprotein. Plant Physiol 110:1341–1348, 1993.

68. C Bompard-Gilles, P Rouseau, P Rouge, F Payan. Substrate mimicry in the active center of a mammalian α-amylase: structural analysis of an enzyme-inhibitor complex. Structure 4:1441–1452, 1996.
69. TE Mirkov, SV Evans, J Wahlstrom, L Gomez, NM Young, MJ Chrispeels. Location of the active site of the bean α-amylase inhibitor and involvement of a Trp, Arg, Tyr triad. Glycobiol 5:45–50, 1995.
70. IB Svendsen, J Hejgaard, J Mundy. Complete amino acid sequence of the α-amylase/subtilisin inhibitor from barley. Carlsberg Res Commun 51:43–50, 1986.
71. J Mundy, J Hejgaard, I Svendsen. Characterization of a bifunctional wheat inhibitor of endogenous α-amylase and subtilisin. FEBS Lett 167:210–214, 1984.
72. FAP Campos, M Richardson. The complete amino acid sequence of the bifunctional α-amylase/trypsin inhibitor from seeds of ragi (Indian finger millet, *Eleusine coracana* Gaertn). FEBS Lett 152:300–303, 1983.
73. J-I Abe, U Sidenius, B Svensson. Arginine is essential for the α-amylase inhibitory activity of the α-amylase/subtilisin inhibitor (BASI) from barley seeds. Biochem J 293:151–155, 1993.
74. M Qian, R Haser, G Buisson, E Duee, F Payan. The active center of a mammalian α-amylase. Structure of the complex of a pancreatic α-amylase with a carbohydrate inhibitor refined to 2.2-Å resolution. Biochemistry 33:6284–6294, 1994.
75. M Machius, L Vertesy, R Huber, G Wiegand. Carbohydrate and protein-based inhibitors of porcine pancreatic α-amylase: structure analysis and comparison of their binding characteristics. J Mol Biol 260:409–421, 1996.
76. C Gilles, J-P Astier, G Marchis-Mouren, C Cambillau, F Payan. Crystal structure of pig pancreatic α-amylase isoenzyme II, in complex with the carbohydrate inhibitor acarbose. Eur J Biochem 238:561–569, 1996.
77. J-L Jane, JF Robyt, D-J Huang. ^{13}C-N.M.R. study of the conformation of helical complexes of amylodextrin and of amylose in solution. Carbohydr Res 140:21–25, 1985.
78. EH Ajandouz, J-I Abe, B Svensson, G Marchis-Mouren. Barley malt α-amylase. Purification, action pattern, and subsite mapping of isozyme 1 and two members of the isozyme 2 subfamily using *p*-nitrophenylated maltooligosaccharide substrates. Biochim Biophys Acta 1159:193–202, 1992.
79. I Matsui, E Matsui, K Ishikawa, S Miyairi, K Honda. A mutant α-amylase with enhanced activity specific for short substrates. FEBS Lett 310:216–218, 1990.
80. I Matsui, E Matsui, K Ishikawa, S Miyairi, K Honda. The enzymatic and molecular characteristics of *Saccharomycopsis* α-amylase secreted from *Saccharomyces cerevisiae*. Agric Biol Chem 54:2009–2015, 1990.
81. EH Ajandouz, GJ Marchis-Mouren. Subsite mapping of porcine pancreatic alpha-amylase I and II using 4-nitrophenyl-α-maltooligosaccharides. Carbohydr Res 268:267–277, 1995.
82. Y Nitta, M Mizushima, K Hiromi, S Ono. Influence of molecular structures of substrates and analogues on Taka-amylase A catalyzed hydrolyses. J Biochem 69:567–576, 1971.
83. W Rick, HP Stegbauer. α-Amylase measurement of reducing groups. In: HV Bergmeyer, ed. Methods of Enzymatic Analysis, 2nd ed, Vol 2. New York: Academic Press, 1974.
84. DH Strumeyer. A modified starch for use in amylase assays. Anal Biochem 19:61–71, 1967.
85. EA Farrand. Flour properties in relation to the modern bread processes in the United Kingdom, with special reference to alpha-amylase and starch damage. Cereal Chem 41:98–110, 1964.
86. G Guinn. An ultrasensitive chemical test for quantitative chromatography of sugars. J Cromatogr 30:178–182, 1967.
87. NA Nelson. Photometric adaptation of the Somogyi method for the determination of glucose. J Biol Chem 153:375–380, 1944.
88. M Somogyi. Notes on sugar determination. J Biol Chem 195:19–23, 1952.
89. WC Barnes, AB Blakeney. Determination of cereal alpha amylase using a commercially available dye-labelled substrate. Die Starke 26:193–197, 1974.
90. H Rinderknecht, P Wilding, BJ Haverback. A new method for the determination of α-amylase. Experientia 23:805, 1967.
91. DWS Wong, SB Batt, GH Robertson. A microassay for rapid screening of α-amylase activity. J Agric Food Chem 48:4540–4543, 2000.
92. Y-Y Linko, P Saarinen, M Linko. Starch conversion by soluble and immobilized α-amylase. Biotechnol Bioeng 17:153–165, 1975.
93. BV McCleary, H Sheehan. Measurement of cereal α-amylase: a new assay procedure. J Cereal Sci 6:237–251, 1987.
94. K-I Majima, S-I Teshima, Y Hamada, T Kikuchi, Y Kawamura, S Kitahata. Determination of α-amylase using a new blocked substrate (2-chloro-4-nitrophenol 4^4-*O*-β-D-galactopyranosyl-β-maltotetraoside). Clin Chim Acta 234:177–179, 1995.
95. AW MacGregor, JE Morgan. Determination of specific activities of malt α-amylases. J Cereal Sci 16:267–277, 1992.
96. MP Silvanovich, RD Hill. Affinity chromatography of cereal α-amylase. Anal Biochem 73:430–433, 1976.

57

β-Amylases

Dominic W. S. Wong and George H. Robertson
U.S. Department of Agriculture, Albany, California, U.S.A.

I. INTRODUCTION

The distribution of β-amylase is limited to higher plants and bacteria. It is an exoenzyme that catalyzes the hydrolysis of 1,4-α-D-glucosidic linkages in polysaccharides to remove successively β-anomeric maltose units from the nonreducing end of α-1,4-glucans such as starch and glycogen. Sweet potato contains an abundant β-amylase which accounts for 5% of the total soluble proteins in the tuber; by contrast, only a trace amount of α-amylase is present. The sweetness of sweet potato is the result of the hydrolysis of starch to maltose by the endogenous β-amylase during cooking. β-Amylase is employed by the starch industry in the production of high maltose syrups. Compared with glucose syrups, maltose syrups have a higher viscosity and lower hygroscopicity, less tendency to crystallize, and more resistance to browning. These characteristics make them particularly suitable for use in the confectionery and baking industry. β-Amylase is highly significant in determining the fermentability of worts for brewing.

II. CLASSIFICATION

Glycosidases are classified under hydrolases and are subdivided into those hydrolyzing *O*-glycosyl, *N*-glycosyl, and *S*-glycosyl compounds (EC 3.2.1., 3.2.2, 3.2.3). β-Amylase is an exoglucanase that catalyzes the hydrolysis of 1,4-α-D-glucosidic bonds in polysaccharides to cleave successively maltose units from the nonreducing end. According to the IUBMB classification (1), β-amylase has the systematic name of 1,4-α-D-glucan maltohydrolase, and a code number of EC 3.2.1.2.

A classification of glycosyl hydrolases based on similarities in amino acid sequence has been proposed and yields useful information on the structure and function of these enzymes (2–4). β-Amylase belongs to family 14 in this scheme. This classification scheme should only be used as a supplement to the IUBMB classification.

III. MOLECULAR STRUCTURE

Several amino acid sequences of β-amylases are known, primarily deduced from the gene sequences. These include (as entries are listed in Swiss-Prot): *Ipomoea batatas* (sweet potato), *Glycine max* (soybean), *Hordeum vulgare* (barley), *Triticum aestivum* (wheat), *Zea mays* (maize), *Secale cereale* (rye), *Vigna unquiculata* (cowpea), *Medicago sativa* (alfalfa), *Trifolium repens* (creeping white clover), *Arabidopsis thaliana* (mouse ear cress), *Bacillus cereus, B. firmus, B. circulans, B. polymyxa*, and *Thermoanaerobacter thermosulfurogenes* (*Clostridium thermosulfurogenes*). Several conserved regions exist in all β-amylases, although the sequences between plant and bacterial β-amylases show only 30% similarities (Fig. 1).

The three-dimensional structures of β-amylases from soybean (5–7), sweet potato (8), barley (9), and *Bacillus cereus* (10) have been reported. Soybean β-amylase consists of 495 amino acid resi-

											*
Sweet Potato	49	DGVMVDVWWGI	96	CGGNVGD	106	IPIPQWI	177	DIEVGCCAAG	**E**	LRYPSY
Soybean	48	DGVMVDVWWGI	95	CGGNVGD	105	IPIPQWV	176	DIEVGLGPAG	**E**	LRYPSY
Barley	46	DGVMVDVWWGL	93	CGGNVGD	103	IPIPQWV	174	DIEVGLGPAG	**E**	MRYPSY
Corn	46	DGVMIDVWWGL	93	CGGNVGD	103	IPIPQWV	174	DIEVGLGPAG	**E**	MRYPSY
Wheat	46	DGVMIDVWWGL	93	CGGNVGD	103	IPIPQWV	174	DIEVGLGPAG	**E**	MRYPSY
Arabidopsis	51	DGVMVDVWWGI	98	CGGNVGD	108	IPIPQWV	179	DIEVGLGPAG	**E**	LRYPSY
Bacillus cereus	74	YAITVDFWWGD	121	CGGNVGD	131	VPIPSWV	192	KIYLSGGPAG	**E**	LRYPSY
Bacillus circulans	72	YAITTDVWWGY	119	CGGNVGD	129	IPLPSWL	189	KIYLSGGPSG	**E**	LRYPSY
Bacillus polymyxa	71	YAITTDVWWGY	118	CGGNVGD	128	IPLPSWL	188	KIYLSGGPSG	**E**	LRYPSY

							#				
Sweet Potato	294	IAAKVSGIHW	341	LNFTCLEM	379	AG	**E**	NAL	417	GLTYLRLSD
Soybean	292	LAIKVSGIHW	339	LNFTCLEM	378	AG	**E**	NAL	415	GVTYLRLSD
Barley	290	LAIKISGIHW	337	INFTCAEM	376	AC	**E**	NAL	413	GFTYLRLSN
Corn	290	LAIKVSGIHW	337	MNFTCAEM	376	AC	**E**	NAL	413	GFTYLRVSD
Wheat	290	LAIKISGIHW	337	MNFTCAEM	376	AC	**E**	NAL	413	GFTYLRLSN
Arabidopsis	295	LAAKVSGIHW	342	LNFTCLEM	381	AG	**E**	NAL	418	GFTYLRLSD
Bacillus cereus	314	IGAKIAGVHW	357	VTFTCLEM	395	NG	**E**	NAL	422	GFTLLRYQD
Bacillus circulans	312	IGAKISGIHW	355	LTFTALEM	393	NG	**E**	NAL	419	GFTLLRINN
Bacillus polymyxa	311	IGAKISGLHW	354	LTFTCLEM	392	NG	**E**	NAL	418	GFTLLRINN

Figure 1 Comparison of regions of sequence similarities among nine β-amylases, including sweet potato (P10537), soybean (P10538), barley (P16098), corn (P55005), wheat (P93594), *Arabidopsis thaliana* (P25853), *Bacillus cereus* (P36924), *Bacillus circulans* (P06547), and *Bacillus polymyxa* (P21543). The catalytic Glu are marked as general acid (*) and general base (#). Numbering of sequences starts with the N-terminus of the mature protein.

dues with a molecular weight of 56 kDa. The enzyme consists of a large $(\alpha/\beta)_8$-barrel core; a smaller lobe formed by three long loops (L3, L4, and L5) extending from β3, β4, and β5 strands; and a C-terminal tail loop of $\sim$ 50 residues extending from α8 and covering the entrance of the barrel. Between the surface of the lobe region and the core is a cleft that opens into a pocket $\sim$ 18 Å deep that contains the catalytic residues Glu186 and Glu380, and an essential residue Asp101. This architecture contrasts to that of α-amylases which have the reactive center located in a long cleft open at both ends (11). The deep pocket conformation found in β-amylase is also present in glucoamylase, although the latter has an $(\alpha/\alpha)_8$-core domain (12). That the catalytic site is situated in a cavity allows endwise hydrolysis of the starch chain with the length of glucose units cleaved in a controlled manner. Substrate binding causes a movement of some segments in L3 (residues 96–103) to close over the bound substrate like a hinged lid. In the crystal structure of soybean β-amylase complexed with maltose, L3 in the closed conformation interacts with maltose forming hydrogen bonding between Asp101 and O-2 of the glucose unit 1, and Van der Waals contacts between Val99 and the substrate. The L3 lid serves to shield the active site from being exposed to the solvent, and also positions the substrate in proximity to the two catalytic residues Glu186 (acting as a general acid) and Glu380 (acting as a general base). Glu186 has been identified as the catalytic residue by affinity labeling with 2,3-epoxypropyl-α-D-glucopyranoside (13). The binding energy upon closing the lid for α-maltose estimated in an automated docking experiment is 22 kcal/mol, indicating considerable enhancement of interactions between the substrate and the subsites (14, 15). The active site of soybean β-amylase can accommodate two maltose molecules, corresponding to a maltotetraose. The two maltose molecules bind in tandem in the active site cleft occupying subsites -1, -2 and 1, 2, respectively, with the nonreducing end at the -1 subsite and cleavage occurring between subsite -1 and $+1$ (for subsite nomenclature, refer to 16). Substrates with longer chain length may have the outer glucose units anchored by hydrophobic interaction with the methyl groups of Leu383 at the cleft entrance, as revealed in the crystal structure of soybean β-amylase complex with α-cyclodextrin (6).

All plant β-amylases with known crystal structures have the same molecular architecture, except for the sweet potato enzyme which is a tetramer having a subunit MW of 55,800 daltons (598 amino acid residues) (8, 17). Each subunit consists of a central $(\alpha/\beta)_8$-barrel, a small domain formed by three long loops—L3 (residues 91–150), L4 (residues 183–258), and L5 (residues 300–327)—and a long C-terminal loop (residues 445–493). The active site is located at a deep cleft between the $(\alpha/\beta)_8$-barrel and the small domain β-amylase (Fig. 2) shows an architecture similar to that of the soybean enzyme, except that the C-terminal sequence contains Gly-rich repeats (9). Deletion of the C-terminal 45 residues led to a decrease in the thermostability of the enzyme (18). A similar extended sequence is found in endosperm-specific rye β-amylase (19).

Bacterial β-amylases share similar tertiary structure with plant β-amylases, in spite of the low sequence identity ($\sim$ 30%) with those of plant β-amylases. The crystal structure of β-amylase from *Bacillus cereus* var. *mycoides* reveals a C-terminal domain with two antiparallel β-sheets, similar to the raw starch–binding domains of glucoamylase and cyclodextrin glycosyltransferase (10, 20). The possession of this unique C-terminal domain provides bacterial β-amylases with the ability to bind and digest raw starch. In contrast, plant β-amylases do not contain a raw starch–binding site, and are incapable of digesting raw starch.

IV. REACTION MECHANISMS

In a single nucleophilic displacement mechanism, β-amylase catalyzes hydrolysis of the glucosidic bond with inversion of the anomeric configuration (21, 22). The initial step involves protonation of the glucosidic oxygen by a general acid which weakens the maltosyl C-O bond. This is followed by a general acid catalysis with a water molecule attacking from the β-side of the substrate to release a maltose unit with β-configuration. In the soybean enzyme, the carboxylic group of Glu186 acts as a general acid, and the carboxylate anion of Glu380 serves as a general base, according to affinity labeling studies and x-ray structural analysis (7, 13).

In an equally viable mechanism, protonation of the glucosidic oxygen results in a glucosyl oxocarbonium ion intermediate with an enzyme-induced distortion of the substrate in a half-chair conformation (23–25). A backside attack by a water molecule assisted by a general base produces an inversion of the configuration. (See Chapter 56, Sec. IV.)

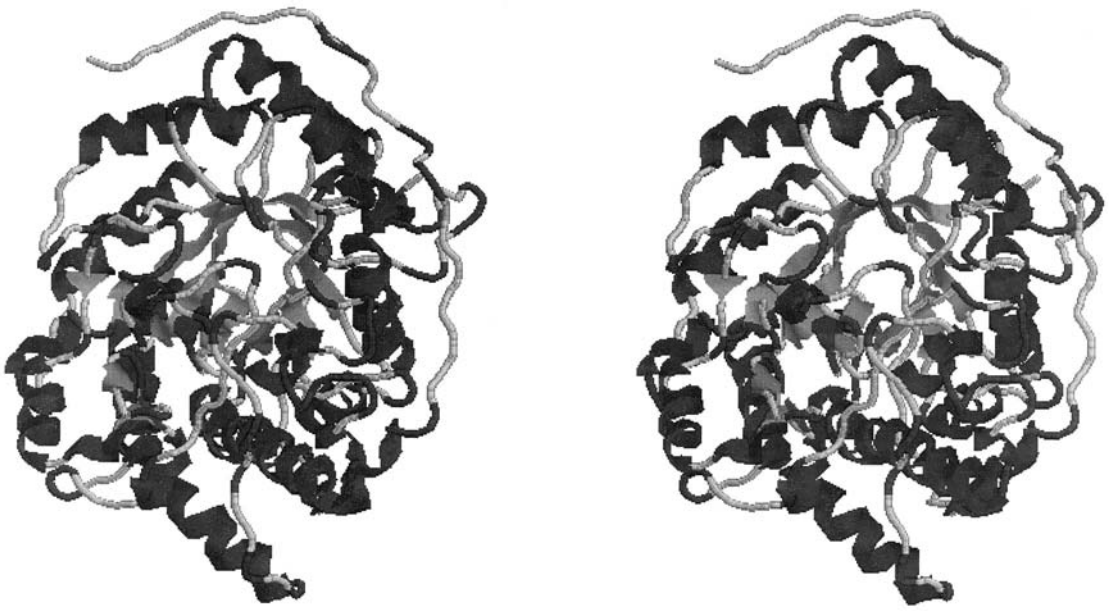

Figure 2 A stereo view of barley β-amylase (isoform 2). The structure consists of a large $(\alpha/\beta)_8$-barrel core, a smaller lobe formed by three long loops (L3, L4, and L5), and a C-terminal tail loop residues extending from α8 and covering the entrance of the barrel (Ref. 9, PDBid: 1bly).

V. INHIBITORS

α-Cyclodextrin has long been known to be a competitive inhibitor of β-amylase, and the enzyme-inhibitor binding has been postulated as evidence for the induced fit theory (26, 27). The observed K_d of soybean β-amylase for α-cyclodextrin is 0.5 mM. The three-dimensional structure of soybean β-amylase complexed with α-cyclodextrin indicates that two glucose units of the α-cyclodextrin molecule interact with the enzyme at loops L5 and L6 which form the entrance of the active-site cleft (5, 6). The inhibitor forms an inclusion complex with the methyl groups of Leu383 (28). In contrast to the binding of the maltose which is positioned deep in the cleft, α-cyclodextrin inhibits the catalytic function by physically blocking the entrance to the active site.

β-Amylases contain a conserved cysteine, and its modification by various sulfhydryl reagents, such as iodoacetamide, N-ethylmaleimide, *p*-chloromercuric-benzoate (PCMB), and 5,5′dithiobis-(2-nitrobenzoic acid) (DTNB), causes a decrease of the enzyme activity and a slight change in the Michaelis constant (29). Studies of the interaction of native and SH-modified β-amylases of soybean with α-cyclodextrin and maltose suggest that the cysteine is located near the binding site of the two substrates, but is not involved in catalysis (30–32). Selective modifications of all three cysteine residues in *Bacillus polymyxa* β-amylase yield the same conclusion (33, 34). It is believed that the attachment of bulky alkylating agents used in chemical modification introduces steric stresses that cause a structural distortion that in turn prevents the substrates from productive binding (35). This suggestion has been confirmed by the crystal structure of soybean β-amylase complexed with α-cyclodextrin where Cys95 and Cys343 are located in the L3 and L5 loops near the maltose and α-cyclodextrin binding site, respectively (5).

VI. PHYSIOCHEMICAL PROPERTIES

Plant β-amylases are $\sim$ 55 kDa, with the exception of sweet potato β-amylase, which is a tetramer of 215 kDa. Microbial β-amylases have MW of 30–160 kDa with the high value representing possible association of subunits. the tetrameric structure of the sweet potato enzyme is not essential for the catalytic function, because the monomer retains full activity (36). The pH optimum for activity ranges from 5.0 for wheat, barley malt, and sweet potato β-amylases, to 6.0 for soybean and pea enzymes. In the Triticeae (barley and wheat), β-amylase is synthesized in the endosperm in a bound form which is posttranslationally modified by proteolytic cleavage to yield a free and more active form, during germination (37, 38). Common to all cereals is the "ubiquitous" β-amylase that exhibits a transitory presence in various tissues of the developing kernels and in other seedling organs (39). All known plant β-amylases exist in several isoforms. The barley enzyme has four isozymes with pI values of 4.65, 4.75, 4.90, and 5.20 (40). All four isoforms have been shown to be products of proteolysis of the C-terminus of the full-length enzyme (MW 57 kDa), and exhibit optimal activity between pH 4.5 and 7.5, with a K_m of 2.5 $mg \cdot mL^{-1}$ (soluble starch), and V_{max} of 17 μmol maltose $\cdot$ min^{-1} (41). Soybean contains several isozymes, with isozymes 2 (pI 5.25) and 4 (pI 5.5) the most predominant. The differences between the two isozymes are due to the substitution of Glu152 and Lys399 of isozyme 2 with Lys and Arg in isozyme 4 (42). The corn enzyme consists of two isoforms with pI values of 4.25 and 4.40, with MW of 65 kDa (43). Soybean β-amylase has a K_m of 4.9×10^{-2} mM using reduced amylodextrin substrate of average degree of polymerization of 21.7 (29). Using reduced soluble starch as the substrate, Totsukan and Fukazawa (28) reported a K_m of 0.17 mM and a k_{cat} of 410 sec^{-1}, with a k_{cat}/K_m value of 2.4×10^3 sec^{-1} mM^{-1}. Shorter-chain maltooligosaccharides, such as G7, showed an increasing K_m value of 1.9×10^{-1} M, and a k_{cat} of 610 sec^{-1} (44). A k_{cat}/K_m of 1.39×10^3 sec^{-1} mM^{-1} has also been reported using a similar G7 substrate.

VII. MEASUREMENT OF ACTIVITY

Several methodologies are available for the determination of β-amylase activity. Some are based on determination of the increase in reducing groups produced by the hydrolytic action of β-amylase on suitable 1,4-α-D-glucans, such as soluble starch. In the 3,5-dinitrosalicyclic acid method, the concentration of the nitroaminosalicyclic acid formed at the reducing hemiacetal is measured colorimetrically (46). The reducing groups can also be quantitated by the alkaline ferricyanide method (47) or the Nelson-Somogyi method (48, 49). The reducing sugar assay is nonspecific, and the measurement of β-amylase activity by these methods is accurate only if the sample is devoid of α-amylase and other amylolytic enzymes. For more details, refer to Chapter 56, Sec. VI.

A specific assay for β-amylase in the presence of cereal α-amylases has been developed using a colorimetric substrate consisting of *p*-nitrophenyl oligosaccharides (50, 51). The substrate used is *p*-nitrophenyl α-maltopentaoside ($PNPG_5$), which is too short to be effectively hydrolyzed by cereal α-amylases but is readily cleaved by β-amylase to maltose and *p*-nitrophenyl maltotriose ($PNPG_3$). A subsequent reaction of the product, $PNPG_3$, with added α-glucosidase produces glucose and *p*-nitrophenol. The latter product, with a molar extinction coefficient of $1.8 \times 10^3\ M^{-1}cm^{-1}$, can be measured at 410 nm. In a standard assay (51), the enzyme preparation or extract (0.2 mL) in a buffer containing 100 mM sodium maleate, 1 mM diNaEDTA, 1 mg/mL BSA, and 3 mM NaN_3, pH 6.2, is incubated with 0.2 mL of pre-equilibrated substrate mixture containing 5 mM $PNPG_5$, 20 units of α-glucosidase, at 40°C for 10 min. The reaction is terminated and color developed by the addition of 1% w/v Tris base (3.0 mL, pH > 10). The absorbance of *p*-nitrophenol is measured at 410 nm. One enzyme unit is defined as the amount of enzyme that catalyzes the release of 1 μmol of *p*-nitrophenol per min under the assay condition. It should be noted that although $PNPG_5$ is not an effective substrate for cereal α-amylases, it has been found to be readily attacked by some other α-amylases, such as *Aspergillus niger* α-amylase. The procedure described above can therefore only be applied for the selective measurement of β-amylase in cereal flour and products. For a precise quantitation of β-amylase, it may be necessary to determine the degree of interference of α-amylase in the sample. If necessary, the α-amylase in the sample should be measured using defined substrates, such as end-blocked *p*-nitrophenol maltosaccharide, that are not susceptible to the action of β-amylase and glucoamylase (see Chapter 56). The β-amylase is then obtained by substrating the α-amylase activity (using defined substrates) from the total amylolytic activity.

VIII. PURIFICATION

β-Amylase has been prepared in a crystalline form from a variety of plant sources including germinated barley (40), sweet potato (36), and soybean (52). Purification of β-amylase from various sources reported in the literature mostly involves multisteps of fractionation by acetone, ethanol, or $(NH_4)_2SO_4$, followed by cation/anion exchange chromatography and gel filtration. The following describes a three-step procedure of cereal β-amylase purification consisting of $(NH_4)_2SO_4$ fractionation, chromatofocusing, and hydroxyapatite adsorption chromatography (Table 1) (43).

Cereal grains were sterilized for 30 min with 1% NaOCl, germinated on water-saturated cotton wool in the dark at 20–30°C for 6 days, and homogenized in 100 mM Tris buffer, pH 8.1. The extract was centrifuged at 65,000g for 20 min, to yield ~200 mL supernatant from 40 g of germinated grains. The majority of the β-amylase as precipitated by $(NH_4)_2SO_4$ at 40–60% saturation was redissolved in 25 mM histidine-HCl buffer, pH 6.2, and dialyzed in the same buffer. The dialyzed sample was applied to a 35-mL Polybuffer Exchanger Gel column, and eluted with polybuffer PB 74 diluted 10× with water, pH 4. Active fractions were pooled and dialyzed in 1 mM sodium phosphate buffer, pH 6.8, and applied onto a 4.5-mL hydroxyapatite column pre-equilibrated with the same buffer. Elution was performed using a linear gradient of sodium phosphate (1–50 mM) with a flow rate of 4 mL/h. Active fractions were pooled and the purity was analyzed by SDS-PAGE and isoelectric focusing.

Table 1 Purification of β-Amylase from 40-g Germinating Maize Grains

Purification steps	Total protein (mg)	Total activity (EU[a])	Specific activity ($EU \cdot mg^{-1}$)	Yield (%)
Crude extract	604	397	0.66	100
$(NH_4)_2SO_4$ precipitate	110	320	2.91	81
Chromatofocusing	ND[b]	192	—	48
Hydroxyapatite	0.38	105	276	26

Source: Ref. 43.
[a] EU = one enzyme unit corresponds to the release of 1 $\mu mol \cdot min^{-1}$ of *p*-nitrophenol at pH 6 at an incubation temperature of 30°C.
[b] ND = Not determined because of polybuffer interference.

Although not as frequently used as in the purification of α-amylases, the use of affinity chromatography for β-amylases has been reported. Subbaramaiah and Sharma (53) described the affinity binding of plant β-amylases (mustard, barley, and sweet potato) to soluble starch (amylose) or native starch (potato starch grains) and a rapid elution of the enzyme by 1% (w/v) white dextrin. Hoshino et al. (54) used raw rice starch for the adsorption, hence the purification of *Bacillus* β-amylases. This procedure is made possible because microbial β-amylases contain a raw starch–binding site as revealed by their sequences and crystal structures. Saha et al. (55) purified the *Clostridium thermosulfurogenes* β-amylase taking advantage of the binding of the enzyme onto raw starch granules and its desorption by soluble starch. Raw starch adsorption/desorption also provides a useful technique for separating a mixture of α- and β-amylases of plant origins. A number of investigations employed the competitive inhibitor α-cyclodextrin as a possible ligand for the affinity purification of β-amylases (56–58). Using an α-cyclodextrin Sepharose 6B column, Totsuka and Fukazawa (59) demonstrated the increase in the specific binding of soybean and barley β-amylases in the presence of 1 to 2 M $(NH_4)_2SO_4$, resulting in a 10-fold purification.

REFERENCES

1. IUBMB. Enzyme Nomenclature. San Diego: Academic Press.
2. B Henrissat. A classification of glycosyl hydrolases based on amino acid sequence similarities. Biochem J 280:309–316, 1991.
3. B Henrissat, A Bairoch. New families in the classification of glycosyl hydrolases based on amino acid sequence similarities. Biochem J 293:781–788, 1993.
4. B Henrissat, G Davies. Structural and sequence-based classification of glycoside hydrolases. Curr Opin Struct Biol 7:637–644, 1997.
5. B Mikami, M Sato, T Shibata, M Hirose, S Aibara, Y Katsube, Y Morita. Three-dimensional structure of soybean β-amylase determined at 3.0 Å resolution: preliminary chain tracing of the complex with α-cyclodextrin. J Biochem 112:541–546, 1992.
6. B Mikami, EJ Hehre, M Sato, Y Katsube, M Hirose, Y Morita, JC Sacchettini. The 2.0-Å resolution structure of soybean β-amylase complexed with α-cyclodextrin. Biochemistry 32:6836–6845, 1993.
7. B Mikami, M Degano, EJ Hehre, JC Sachettini. Crystal structure of soybean β-amylase reacted with β-maltose and maltal: active site components and their apparent roles in catalysis. Biochemistry 33:7779–7787, 1994.
8. CG Cheong, SH Eom, C Chang, DH Shin, HK Song, K Min, JH Moon, KK Kim, KY Hwang, W Suh. Crystallization, molecular replacement solution, and refinement of tetrameric β-amylase from sweet potato. Proteins Struct Funct Genet 21:105–117, 1995.
9. B Mikami, H-J Yoon, N Yoshigi. The crystal structure of the sevenfold mutant of barley β-amylase with increased thermostability at 2.5 Å resolution. J Mol Biol 285:1235–1243, 1999.
10. T Oyama, M Kusunoki, Y Kishimoto, Y Takasaki, Y Nitta. Crystal structure of β-amylase from *Bacillus cereus* var. *mycoides* at 2.2 Å resolution. J Biochem 125:1120–1130, 1999.
11. G Buisson, E Duee, R Haser, F Payen. Three-dimensional structure of porcine pancreatic α-amylase at 2.9 Å resolution. Role of calcium in structure and activity. EMBO J 6:3909–3916, 1987.
12. A Aleshin, A Golubev, LM Firsov, RB Hozaiko. Crystal structure of glucoamylase from *Aspergillus awamori* var. X100 to 2.2-Å resolution. J Biol Chem 257:19291–19298, 1992.
13. Y Nitta, Y Isoda, H Toda, F Sakiyama. Identification of glutamic acid 186 affinity-labeled by 2,3-epoxypropyl α-D-glucopyranoside in soybean β-amylase. J Biochem 105:573–576, 1989.
14. A Laederach, MK Dowd, PM Coutinho, PJ Reilly. Automated docking of maltose, 2-deoxymaltose, and maltotetraose into the soybean β-amylase active site. Proteins Struct Funct Genet 37:166–175, 1999.
15. WM Rockey, A Laederach, PJ Reilly. Automated docking of α-(1 $\rightarrow$ 4) and α-(1 $\rightarrow$ 6)-linked glucosyl trisaccharides and maltopentaose into the soybean β-amylase active site. Proteins Struct Funct Genet 40:299–309, 2000.
16. GJ Davies, KS Wilson, B Henrissat. Nomenclature for sugar-binding subsites in glycosyl hydrolases. Biochem J 321:557–559, 1997.
17. H Toda, Y Nitta, S Asanami, JP Kim, F Sakiyama. Sweet potato β-amylase: primary structure and identification of the active-site glutamyl residue. Eur J Biochem 216:25–38, 1995.
18. N Yoshigi, H Sahara, S Koshino. Role of the C-terminal region of β-amylase from barley. J Biochem 117:63–67, 1995.
19. Rorat, J Sadowski, F Grellet, J Daussant, M Delseny. Characterization of cDNA clones for rye endosperm-specific β-amylase and analysis of β-amylase deficiency in rye mutant lines. Theor Appl Genet 83:257–263, 1991.
20. B Mikami, M Adachi, T Kage, E Sarikaya, T Nammori, R Shinke, S Utsumi. Structure of raw starch-digesting *Bacillus cereus* β-amylase complexed with maltose. Biochemistry 38:7050–7061, 1999.

21. DE Koshland Jr. Mechanisms of transfer enzymes. Enzymes 1:305–346, 1959.
22. G Hanozet, H-P Pircher, P Vanni, B Oesch, G Semenza. An example of enzyme hysteresis. J Biol Chem 256:295–297, 1981.
23. CCF Blake, LN Johnson, GA Mair, ACT North, DC Phillips, VR Sarma. Crystallographic studies of the activity of hen egg-white lysozyme. Proc R Soc Lond Ser B 167:378–385, 1967.
24. JA Thoma. A possible mechanism for amylase catalysis. J Theor Biol 19:297–310, 1968.
25. NCJ Strynadka, MNG James. Lysozyme revisited: crystallographic evidence for distortion of an N-acetylmuramic acid residue bound in site D. J Mol Biol 220:401–424, 1991.
26. JA Thoma, DE Koshland Jr. Competitive inhibition by substrate during enzyme action. Evidence for the induced-fit theory. J Am Chem Soc 82:3329–3333, 1960.
27. DE Koshland Jr. The key-lock theory and the induced fit theory. Angew Chem Ind Ed Engl 33:2375–2378, 1994.
28. A Totsuka, C Fukazawa. Functional analysis of Glu380 and Leu383 of soybean β-amylase—a proposed action mechanism. Eur J Biochem 240:655–659, 1996.
29. J Spradlin, JA Thoma. β-Amylase thiol groups. J Biol Chem 245:117–127, 1970.
30. B Mikami, S Aibara, Y Morita. Chemical modification of sulfhydryl groups in soybean β-amylase. J Biochem 88:103–111, 1980.
31. B Mikami, K Nomura, Y Morita. Interaction of native and SH-modified β-amylase of soybean with cyclohexadextrin and maltose. Biochemistry 94:107–113, 1983.
32. K Nomura, B Mikami, Y Nagao. Effect of modification of sulfhydryl groups in soybean β-amylase on the interaction with substrate and inhibitors. J Biochem 102:333–340, 1987.
33. N Uozumi, T Matsuda, N Tsukagoshi, S Udaka. Structural and functional role of cysteine residues of *Bacillus polymyxa* β-amylase. Biochemistry 30:4594–4599, 1991.
34. K Nomura, I Yoneda, T Nanmori, R Shinke, Y Morita, B Mikami. The role of SH and S-S groups in *Bacillus cereus* β-amylase. J Biochem 118:1124–1130, 1995.
35. B Mikami, K Nomura, Y Morita. Two sulfhydryl groups near the active site of soybean β-amylase. Biosci Biotechnol Biochem 58:126–132, 1994.
36. Y-G Ann, MI Izuka, T Yamamoto, N Minamiura. Active monomer of sweet potato β-amylase: stabilization and an improved preparation method using α-cyclodextrin. J Ferment Bioeng 70:75–79, 1990.
37. J Daussant, J Sadowski, T Rorat, C Mayer, C Lauriere. Independent regulatory aspects and post-translational modifications of two β-amylases of rye. Plant Physiol 96:84–90, 1990.
38. C Lauriere, C Doyen, C Thevenot, J Daussant. β-Amylases in cereals. Plant Physiol 100:887–893, 1992.
39. J Daussant, J Sadowski, P Ziegler. Cereal β-amylases: diversity of the β-amylase isozyme status within cereals. Plant Physiol 143:585–590, 1994.
40. K Visuri, M Nummi. Purification and characterization of crystalline β-amylase from barley. Eur J Biochem 28:555–565, 1972.
41. R Lundgard, B Svensson. The four major forms of barley β-amylase. Purification, characterization and structural relationship. Carlsberg Res Commun 52:313–326, 1987.
42. E-S Ji, B Mikami, J-P Kim, Y Morita. Positions of substituted amino acids in soybean β-amylase isozymes. Agric Biol Chem 54:3065–3067, 1990.
43. C. Doyen, C Lauriere. β-Amylases in germinating maize grains: purification, partial characterization and antigenic relationships. Phytochemistry 31:3697–3702, 1992.
44. T Kunikata, H Yamano, T Nagamura, Y Nitta. Study on the interaction between soybean β-amylase and substrate by the stopped-flow method. J Biochem 112:421–425, 1992.
45. T Suganuma, M Ohnishi, K Hiromi, Y Morita. Evaluation of subsite affinities of soybean β-amylase by product analysis. Agric Biol Chem 44:1111–1117, 1980.
46. P Bernfeld. Amylases, α and β. Methods Enzymol 1:149–159, 1955.
47. G Guinn. An ultrasensitive chemical test for quantitative chromatography of sugars. J Chromatogr 30:178–182, 1967.
48. NA Nelson. Photometric adaptation of the Somogyi method for the determination of glucose. J Biol Chem 153:375–380, 1944.
49. M Somogyi. Notes on sugar determination. J Biol Chem 195:19–23, 1952.
50. PR Mathewson, BW Seabourn. A new procedure for specific determination of β-amylase in cereals. J Agric Food Chem 31:1322–1326, 1983.
51. BV McCleary, R Codd. Measurement of β-amylase in cereal flours and commercial enzyme preparations. J Cereal Chem 9:17–33, 1989.
52. Y Morita, S Aibara, H Yamashita, F Yagi, T Suganuma, K Hiromi. Crystallization and preliminary x-ray investigation of soybean β-amylase. J Biochem 77:343–351, 1975.
53. K Subbaramaiah, R Sharma. Affinity binding of higher plant β-amylases to starch. Starch 40:182–185, 1988.

54. M Hoshino, Y Hirose, K Sano, K Mitsugi. Adsorption of microbial β-amylase on starch. Agric Biol Chem 39:2415–2416, 1975.
55. B Saha, LW Lecureux, JG Zeikus. Raw starch and adsorption-desorption purification of a thermostable β-amylase from *Clostridium thermosulfurogenes*. Anal Biochem 175:569–572, 1988.
56. P Vretblad. Immobilization of ligands for biospecific affinity chromatography via their hydroxyl groups. The cyclohexaamylose-β-amylase system. FEBS Lett 47:86–89, 1974.
57. M Hoschke, Y Hirose, K Sano, K Mitsugi. Adsorption of microbial β-amylase on starch. Agric Biol Chem 39:2415–2416, 1976.
58. K Subbaramiah, R Sharma. Affinity purification of amylases of cyclodextrin-Sepharose columns. Starch 41:357–359, 1989.
59. A Totsuka, C Fukazawa. Affinity purification of β-amylases originating from plant using cyclomaltohexaose-immobilized sepharose 6B in the presence of ammonium sulfate. Protein Express Purif 4:333–336, 1993.

58

Glucoamylase

Peter J. Reilly
Iowa State University, Ames, Iowa, U.S.A.

I. INTRODUCTION

Glucoamylase [α-(1,4)-D-glucan glucohydrolase, EC 3.2.1.3; GA], discovered in 1951 (1) and known industrially as amyloglucosidase, attacks from the nonreducing end of starch-derived substrates to produce glucose (2). Hydrolysis is by multichain attack, different substrate molecules being more or less equally susceptible to attack after each bond cleavage (3). Although GA's natural substrates are chains of glucosyl residues linked through α-(1,4) glycosidic bonds, with branch points initiated by α-(1,6) glycosidic bonds, its action is more general, as it catalyzes the hydrolysis of α-(1,4), α, β-(1,1), α-(1,6), α-(1,3), and α-(1,2) glycosidic bonds between adjacent glucosyl residues, in order of decreasing rate (4, 5). At higher glucose concentrations, GA reforms all the glycosidic bonds that it hydrolyzes, and therefore it condenses glucose to isomaltose (6-O-α-D-glucopyranosyl-D-glucose), isomaltotriose (6-O-α-D-isomaltosyl-D-glucose), kojibiose (2-O-α-D-glucopyranosyl-D-glucose), nigerose (3-O-α-D-glucopyranosyl-D-glucose), maltose (4-O-α-D-glucopyranosyl-D-glucose), α, β-trehalose (α-D-glucopyranosyl β-D-glucopyranoside), panose (4-O-α-D-isomaltosyl-D-glucose), and isomaltotetraose (6-O-α-D-isomaltotriosyl-D-glucose) in order of decreasing equilibrium concentration (6, 7). GA catalyzes the following reactions starting with higher concentrations of starch and related substances:

$$\alpha\text{-Glc-[(1, 4), (1, 6)]-Glc}_n + H_2O \rightarrow Glc + Glc_n$$

$$Glc + Glc_n \rightleftharpoons \alpha\text{-Glc-[(1, 4), (1, 6), (}\beta\text{-1, 1), (1, 3), (1, 2)]-Glc}_n + H_2O$$

GA also can produce disaccharides of glucosyl residues linked to reducing-end arabinosyl, fructosyl, galactosyl, *myo*-inositol, lyxosyl, mannosyl, ribosyl, or xylosyl residues, as well as galactosyl-galactose, galactosyl-glucose, and mannosyl-glucose disaccharides (8). Although it was thought for many years that these so-called reversion reactions were catalyzed by glucosyltransferase impurities in GA preparations, it is now quite clear that GA itself is responsible for them (7, 8).

II. GLUCOAMYLASE IN FOODS

GA is produced by some eubacteria, a few archaea, a number of yeasts, and many filamentous fungi. Although there are reports of animal and plant GAs, these appear to be fundamentally different enzymes with kinetic properties that overlap those of true GAs. GA is therefore not a significant factor in most unprocessed foods.

GA plays a major role in food processing. In Asia, filamentous fungi from *Aspergillus* and *Rhizopus* and filamentous yeast such as *Saccharomycopsis fibuligera* that secrete GA are used to saccharify steamed rice and potato, uncooked ground grains, and amylopectin-rich

rice. In addition, black koji molds from *Aspergillus* species are employed in Japan to make many traditional foods and beverages, such as soy sauce, sake, and sochu (9).

The greatest use of purified GA has been to make glucose syrups from maltodextrins produced by α-amylase from purified starch. Originally *Rhizopus delemar* (now *R. oryzae*) and *R. niveus* GAs did this in Japan, but since the identical GAs from *Aspergillus awamori* and *A. niger* are more thermostable and have a wider optimal pH range, they are now used almost universally for starch saccharfication. Because glucose not only is used in syrup and crystalline form in foods but also serves as a raw material for high-fructose syrups, light beer, and pure fructose, as well as for fuel ethanol, GA is one of the largest-tonnage enzymes in present use.

The standard industrial saccharification process using GA starts with dextrin of DE 10-15, with DE standing for dextrose equivalent, where DE 0 is a dextrin of zero reducing power and therefore theoretically composed of infinitely long chains, and DE 100 is glucose (dextrose in industrial usage). A DE 10 dextrin has 10% the reducing power of glucose and therefore has an average chain length of 10 glucosyl residues. A lower initial DE risks retrogradation, a pseudo-crystallization of long malto-oligosaccharide chains. On the other hand, a high initial DE leads to a lower final DE and glucose yield after GA hydrolysis, because the extended α-amylase hydrolysis at pH 6–6.5 and 90–105°C required to produce high-DE starting material allows more of the glucosyl residues at the reducing ends of the malto-oligosaccharide molecules to be converted to fructosyl residues by alkaline catalysis (10).

The GA hydrolysis process is conducted batchwise in large tanks for 2 days or so at 55–60°C, a high enough temperature for microbial contamination to be insignificant but not so high that the enzyme is inactivated rapidly. The pH is 4.3–4.5, the optimal pH for GA activity and stability and, fortuitously, the pH where glucose and malto-oligosaccharides are most stable.

To reduce enzyme inactivation, microbial contamination, and the cost of boiling off large amounts of water so that the product can be economically shipped, all operations in the conversion of starch to sugars are carried out at high solids concentrations, characteristically 30–40% (w/v). This has the unwanted effect of allowing GA-catalyzed condensation reactions to proceed more rapidly and to a greater extent than at low concentrations. This occurs because the equilibrium constant of the condensation reaction

$$K_{eq} = \frac{[Glc_{n+1}]_{eq}[H_2O]_{eq}}{[Glc]_{eq}[Glc_n]_{eq}}$$

is pseudo–first order in product concentration, the water concentration being high and relatively constant during the reaction or even with substantial changes in initial reactant concentration, while the reactant concentrations are second order overall, being second order in glucose concentration if disaccharides are being produced, or first order each in glucose and oligosaccharide concentrations if higher-molecular-weight products are being formed. The reaction is stopped at peak glucose yield, when in 30% solids about 95–96% of the sugars are glucose. Glucose yield decreases thereafter because of continuing byproduct formation. It is possible to increase glucose yield slightly by adding pullulanase or isoamylase, debranching hydrolases active on α-(1,6) glycosidic bonds between adjacent glucosyl residues, to the reaction mixture. These enzymes break the branch points remaining from the α-amylase-catalyzed hydrolysis of amylopectin more rapidly than does GA. This allows the peak glucose yield to be reached earlier, before the byproducts have as much opportunity to be formed as when GA alone is present.

III. PROTEIN PROPERTIES

A. General Properties and Isoforms

The most thoroughly studied GA, that from *A. awamori* and *A. niger*, is composed of three separate structures (11): catalytic and starch-binding domains and a rigid, highly glycosylated linker between them (Fig. 1). When produced industrially, it has two common forms, the complete 616-residue mature protein (GA I) and a proteolytically cleaved form with 512 residues (GA II), missing all but a few residues of the starch-binding domain but containing the whole catalytic domain and linker. GA II has little activity on raw starch (14) but has kinetics on smaller substrates identical to those of GA I (5). A third form of 470 residues, also formed by proteolysis (15), was the one whose crystals were used to obtain the first three-dimensional structure of the GA catalytic domain (12). Crystals of GA I and GA II have never been obtained.

When expressed by yeast, the *A. awamori*/*A. niger* GA catalytic domain has a molecular weight by matrix-assisted laser desorption/ionization time-of-flight mass spectroscopy of 56.2 kDa, while those of GA II and GA I are 68.7 and 81.7 kDa, respectively

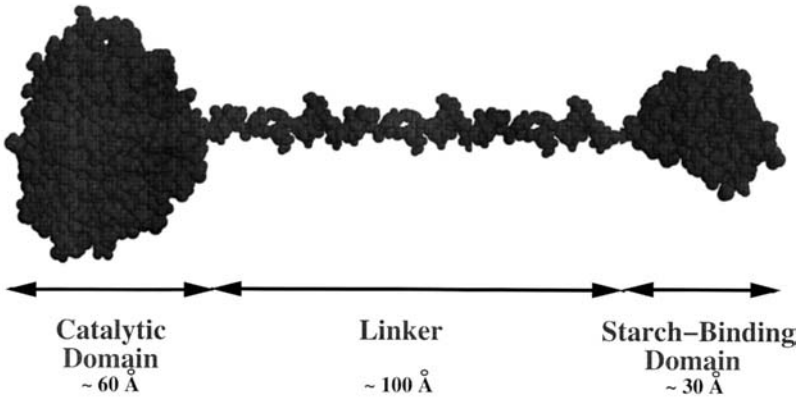

Figure 1 Space-filling model of the *A. awamori* var. *X100* GA catalytic domain (12), the linker, and the *A. niger* GA starch-binding domain (13). A postulated structure of the *A. niger* GA linker based on scanning tunneling electro micrograph (11) is shown.

(16). These values can vary slightly because of different degrees of *O*-glycosylation produced under different culture conditions. Isoelectric focusing also indicates multiple forms of GA I and GA II (17), presumably also caused by glycosylation differences. GAs from other organisms have widely varying molecular weights, depending on their primary structures and degrees of glycosylation, and more specifically on whether they possess linkers and starch-binding domains.

B. Catalytic Domain

The crystal structure of the catalytic domain of GA from a strain of *A. awamori* var. *X100*, a slightly different strain from the *A. awamori*/*A. niger* form used industrially, was the first GA structure to be elucidated (12). The domain is an $(\alpha,\alpha)_6$ barrel, with six interior α-helices surrounded by six exterior α-helices (Fig. 2), a structure found elsewhere among glycohydrolases only in *Clostridium thermocellum* endo-1,4-β-glucanases A (22) and D (23) (CelA and CelD, respectively) and in *Thermomonospora* endo/exo-cellulase E4 (24). There are 13 helices in all, with helix 11, counting from the N-terminus of the domain, peripheral to the rest. The helices form a bed supporting a network of loops, in the center of which is found the active site. This is a well $\sim$ 10 Å deep and $\sim$ 15 Å wide at its mouth, a very primitive structure ensuring that the enzyme will have a low turnover number, since the substrate chain must penetrate the well deeply and undergo cleavage, followed by the remaining chain and then the liberated glucose molecule leaving the well before the next reaction can occur. To overcome this handicap, many filamentous fungi have evolved the ability to produce very large amounts of extracellular GA. The placement of the active site in a well explains both the exo-acting nature of GA and its multichain attack pattern.

A. niger and *A. awamori* GAs were the first GAs sequenced, in 1983 and 1984, respectively (25, 26). Of the 21 archaeal, eubacterial, yeast, and filamentous fungal GAs whose full catalytic domain primary structures are known at present, computational analysis shows that all except those from *Schwanniomyces occidentalis* and *Schizosaccharomyces pombe* are substantially homologous, and have essentially the same secondary and tertiary structures as the *A. awamori* var. *X100* GA catalytic domain (18, 27, 28). α-Helices 2 and 3 are shortened and fused in the GA from the filamentous fungus *Humicola grisea* var. *thermoidea*, and the peripheral α-helix 11 is missing from the GAs from the eubacterium *Clostridium* var. *G0005* and the archaeon *Methanococcus jannaschii* (18). In addition, a number of loops vary in length in different GA catalytic domains.

GA is a member of family 15 of glycosyl hydrolases (29–32), the families being classified by primary sequence homology. Although nearly all the members of this family are GAs, a glucodextranase (EC 3.2.1.70) from *Arthrobacter globiformis* is also present (32). Of the other three glycosidases with $(\alpha,\alpha)_6$ barrel structures, *C. thermocellum* endoglucanases CelA and CelD are in families 8 and 9, respectively, and *T. fusca* endo/exocellulase E4 is in family 9, so their primary structures are not closely related to that of GA. However, they may well share a distant ancestor.

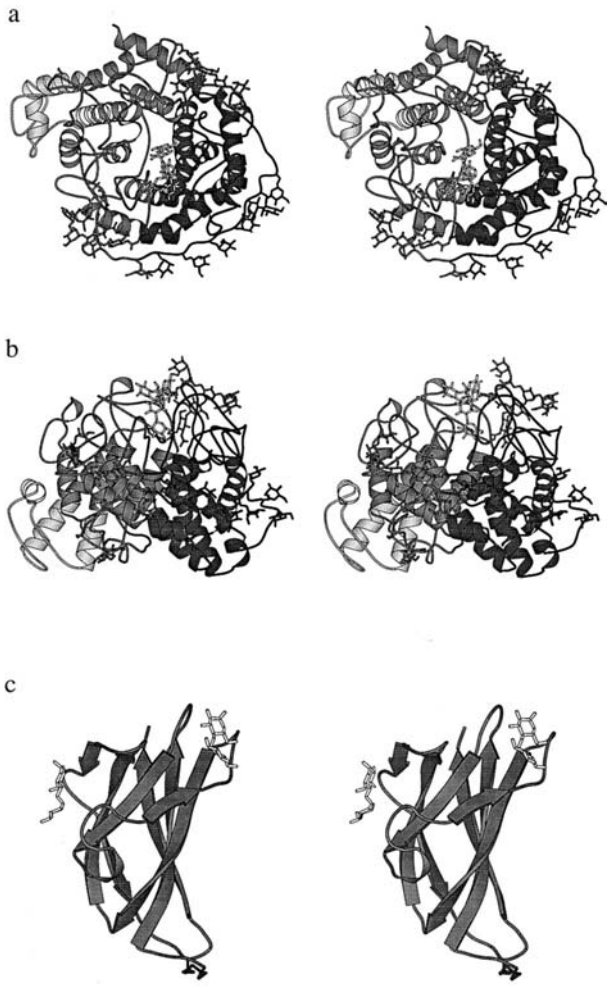

Figure 2 Stereoscopic views (18) from the front (a) and side (b) of the *A. awamori* var. *X100* GA catalytic domain and of the *A. niger* starch-binding domain (c) visualized by Molscript (19). Panels (a) and (b) show D-*gluco*-dihydroacarbose (20) in the active site (center and upper center, respectively). Increasing hydrophobicities of different folding units are denoted by increasingly dark shading. Panel (c) shows maltose in each of the two surface binding sites of the starch-binding domain (13), as found in a highly homologous cyclodextrin glucosyltransferase (21). (From Ref. 18.)

GAs from filamentous fungi other than *R. oryzae* have a highly *O*-glycoslated belt of ~ 30 amino acid residues. It extends from about residue 436 to about residue 467 (*A. awamori*/*A. niger* GA numbering), although it is shorter in *Corticium rolfsii* GA, and it appears to protect one side of the catalytic domain from proteolytic attack (18). When portions of this belt are deleted by site-directed mutagenesis, *A. awamori* GA thermostability and secretion from yeast are strongly decreased (33, 34). In addition to ~ 10 *O*-glycosylated Ser and Thr residues in the belt, many GAs have two *N*-glycosylated residues, Asn171 and Asn395 in *A. awamori*/*A. niger* GA numbering (12, 25), with *N*-acetylglucosamine residues attached in five- and eight-residue chains, respectively (35). Elimination of the latter chain by mutation of Asn395 greatly reduces enzyme secretion and thermostability (36). GAs from *Neurospora crassa, Hormiconis resinae P, R. oryzae*, and two forms of *S. fibuligera* appear to have another *N*-glycosylated chain attached to Asn72 (18).

GAs from most filamentous fungi except *R. oryzae* have catalytic domains with three disulfide bridges—Cys210–213, Cys262–270, and Cys222–449 (28). The last serves to anchor the *N*-terminal end of the belt to the rest of the catalytic domain. The GAs from *C. rolfsii* and *N. crassa* have an additional Cys20–27 bridge (18).

C. *O*-Glycosylated Linker

In GAs from filamentious fungi except *R. oryzae*, the *O*-glycosylated belt continues into an *O*-glycosylated linker between the catalytic domain and a starch-binding domain, longer in most *Aspergillus* GAs than in other fungi (18). In its longest form, ~ 40 residues to about residue 508 (*A. awamori*/*A. niger* GA numbering), it extends ~ 95 Å, as measured by scanning tunneling electron microscopy (11). Deletions of residues in this linker also decrease *A. awamori* GA secretion from yeast (34). *O*-Glycosylation of both the belt and the linker occurs on Ser and Thr residues, and in GAs secreted by *A. awamori* or *A. niger* this is composed of mannosyl residues either singly or in very short chains (37). It appears that glycosylation stiffens the linker (38, 39) and that longer linkers allow the catalytic domain in nature to attack a larger area of a starch granule while tethered to its surface by the starch-binding domain.

D. Starch-Binding Domain

Filamentous fungi except *R. oryzae* have GAs with starch-binding domains of ~ 108 residues, extending to the end of the enzyme at residue 616. *O*-Glycosylation extends into the first few residues of this domain, and a disulfide bridge is found between Cys509 and Cys604 in all starch-binding domains except that from *C. rolfsii* (18). A three-dimensional structure of the *A. niger* starch-binding domain has been elucidated (13) (Fig. 2); both its sequence and structure, with its eight β-strands, are highly homolo-

gous with *Bacillus circulans* cyclodextrin glucosyltransferase (21, 40).

The *A. awamori*/*A. niger* GA starch-binding domain has two binding sites for starch and related substances such as maltose (Fig. 2). Its binding characteristics have been most completely determined by Dalmia and Nikolov (41).

In *R. oryzae* GA, a glycosylated linker and starch-binding domain are found to the *N*-terminal side of the catalytic domain (28). The yeast *Arxula adeninivorans* has a GA with an *N*-terminal region somewhat homologous to that of *R. oryzae*, but the enzyme cannot degrade raw starch (42). The GAs from the yeasts *S. fibuligera, Saccharomyces cerevisiae,* and *S. diastaticus*, the archaeon *M. jannaschii*, and the eubacterium *Clostridium* var. *G0005* also continue beyond the *N*-termini of GAs from most filamentous fungi (18). The functions of these regions are unknown except in the *Clostrium* GA, where it links the catalytic domain to the cell wall (43, 44).

E. Evolution and Phylogenetic Tree

Seven subfamilies of GAs can be delineated through parsimony analysis (Fig. 3) (18). All members of each subfamily are closely related to each other by sequence homology. The *Aspergillus* subfamily has the most members, containing all the *Aspergillus* GAs along with single representatives from *N. crassa*, *H. grisea* var. *thermoida, H. resinae P*, and *C. rolfsii*. The secondary and tertiary structures of these GAs are very similar, with the linker becoming progressively shorter in the order listed. The *Rhizopus* and *Arxula* subfamilies each have a single member. They appear somewhat closely related, even though *Rhizopus* is a basidiomycete and *Arxula* is an ascomycete. The *Saccharomycopsis* and *Saccharomyces* subfamilies, each with two representatives, are fairly homologous with each other. Finally, the *Clostridium* and *Methanococcus* subfamilies, the only ones with nonfungal members, are more closely related to each other than to any other subfamily. It does appear that GA has an ancient eubacterial origin, not only because it is found among eubacteria, archaea, and fungi, but also because it possesses a rare tertiary structure, an $(\alpha, \alpha)_6$ barrel otherwise found at present among glycosyl hydrolases only in *C. thermocellum* and *T. fusca*, both eubacteria.

IV. ENZYME PROPERTIES

A. Enzyme Mechanism

As mentioned above, the GA active site is a well, ensuring both multichain attack and exo-action. Two residues, Glu179 (45) and Glu400 (46), are the catalytic general acid and general base, respectively, and are ~ 10 Å apart (Fig. 4). Hydrolysis is by single-displacement mechanism, with a proton being donated to the oxygen atom of the glycosidic bond by the acid, while the hydrolytic water is coordinated by the base, which accepts the proton (48) (Fig. 5). Inversion of configuration occurs, a non-reducing-end α-glycosidic bond being cleaved to yield β-glucose (6). The limiting step appears to be the release of the remaining substrate chain from the active site (49).

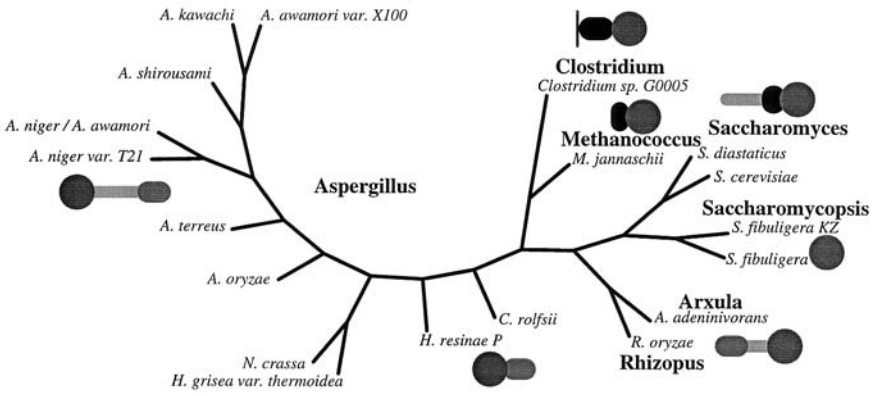

Figure 3 Phylogenetic tree (18) showing the seven subfamilies of GAs from eubacteria (*Clostridium*), archaea (*Methanococcus*), yeast (*Saccharomyces, Saccharomycopsis*, and *Arxula*), and filamentous fungi (*Rhizopus* and *Aspergillus*). Dark circles: catalytic domains; medium-light ovals: starch-binding domains; light rods: *O*-glycosylated regions or linkers; black ovals: other domains; vertical bar: cell wall. (From Ref. 18.)

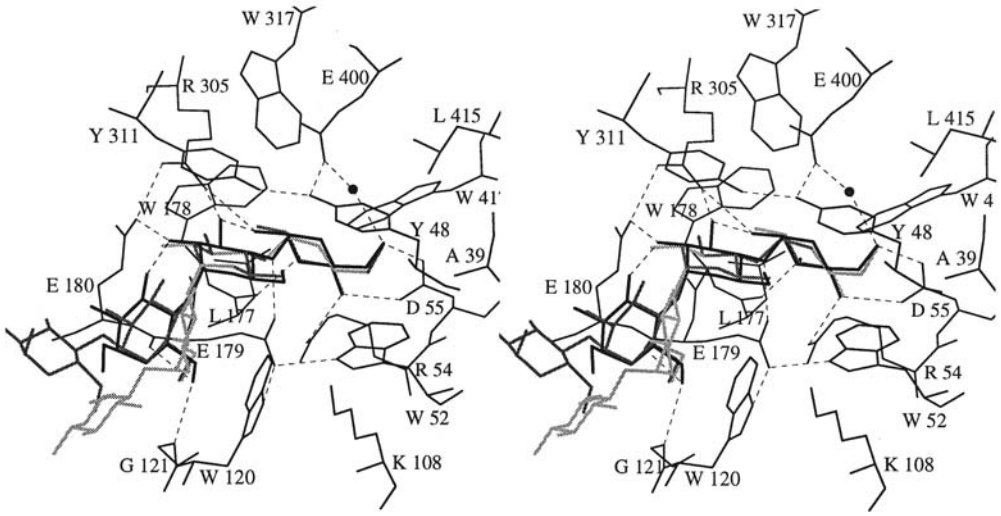

Figure 4 Stereoscopic view (47) of the crystal structure of *A. awamori* var. *X100* GA with D-*gluco*-dihydroacarbose (20) (dark gray: more abundant conformer at pH 4.0; light gray: less abundant conformer at pH 4.0) and the automated docking structure of methyl α-maltotrioside (black). Also shown is the catalytic water (filled circle). The scissile glycosidic bond is immediately to the left of the rightmost glucosidic residue. (From Ref. 47.)

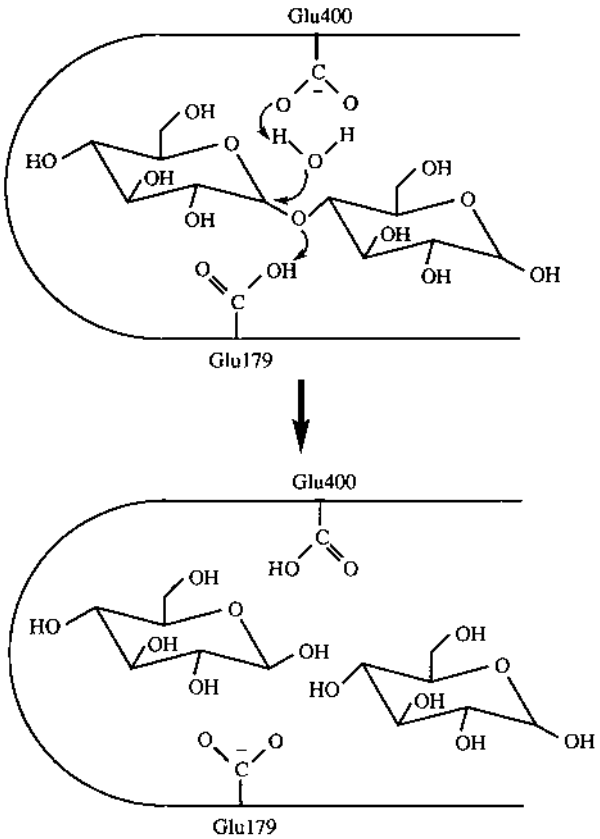

Figure 5 Schematic of GA mechanism.

All but one of the many GAs that have been subjected to subsite mapping with various substrates appear to have six or seven subsites, with the first, binding the nonreducing glucosyl residue of the substrate, having a small negative or positive binding free energy, and the five or six subsites to the other side of the cleavage point having progressively smaller but always negative binding free energies (17, 50–64). This causes substrates with more glucosyl residues to be bound more firmly and cleaved at higher rates than those with fewer residues. With all substrates and all but one GA, values of K_M decrease essentially monotonically with increasing substrate chain length, while values of k_{cat} increase until reaching a maximum at substrates with four or five glucosyl residues (Figs. 6, 7).

The reason for the uniformity of subsite structure with different GAs has now become clear, in that all have essentially the same tertiary structure, with specifically the same active-site structure and general acidic and basic catalytic residues (18). The one exception to this uniformity is the *Swanniomyces castelli* GA, which has different kinetics (65) and which is not homologous with the other GAs.

The number of substrate-binding subsites in GA, obtained by mathematical analysis of the kinetics of the hydrolysis of oligosaccharides of different lengths, does not agree with either the crystal structures of GA with various ligands or with simulated docking studies,

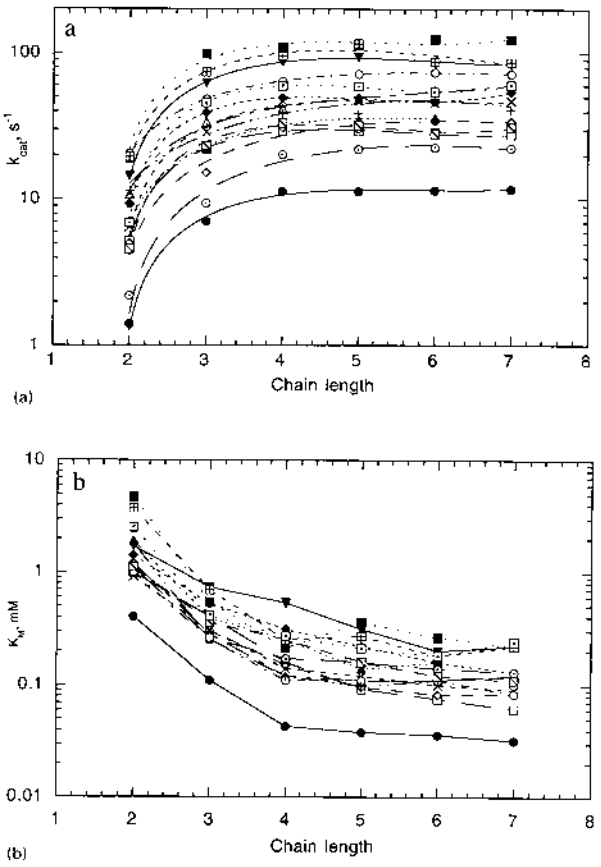

Figure 6 Kinetic parameters of different GAs as a function of chain length of maltooligosaccharide substrates. a: values of k_{cat} (sec^{-1}); b: values of K_M (mM). Symbols: — — □ — —, *A. niger* G1, pH 4.5, 35°C (17); — — ◇ — —, *A. niger* G2, pH 4.5, 35°C (17); - ⊞ -, *Clostridium G0005*, pH 4.5, 25°C (44); – – ⧅ – –, *R. delemar* (*R. oryzae*), pH 4.5, 25°C (50); ---- ▲ ----, *A. awamori*, pH 4.5, 37°C (51); — — ⊙ — —, *A. saitoi*, pH 5.0, 25°C (52); ---- × ----, *R. delemar* (*R. oryzae*), pH 4.5, 40°C (53); — ▼ —, *A. awamori* wt, pH 4.4, 50°C (54); ---- ■ ----, *A. niger*, pH 4.5, 55°C (56); — ● —, *A. niger* G2, pH 4.5, 25°C (57); --- — △ --- —, *A. niger* G1 wt, pH 4.5, 45°C (58); ---- ⊡ ----, *Clostridium G0005* wt, pH 4.5, 25°C (59); ---- ◆ ----, *A. awamori* wt, pH 4.5, 45°C (60); — --- + — ---, *A. awamori* wt, pH 4.5, 45°C (61); — - — ○ — - —, *A. awamori* wt, pH 4.4, 45°C (62).

which show that only two subsites are within the active-site well, with a third subsite being near the enzyme surface and being composed of different amino acid residues depending on the pH (20, 4) (Fig. 4). Furthermore, standard subsite theory is based on the assumption that the limiting reaction is the cleavage of the glycosidic bond (66), while instead the limiting reaction appears to be the release of cleaved substrate chain from the active site (49), as mentioned above.

B. Effect of Environmental Factors

Many studies have shown GAs from *A. awamori, A. niger*, and other filamentous fungi to have optimal pHs for activity and thermostability near 4.5. The optimal pH for activity is halfway between the pK_a of the catalytic acid Glu179, 6.0 in the presence of maltose and 5.8 when it is absent, and that of the catalytic base Glu400, 2.4 in the presence of maltose and 2.7 when it is absent (67). Substrates of higher chain length have slightly higher optimal pHs (67).

Activation energies for GA-catalyzed hydrolysis of many di- and trisaccharides range from 60 to 80 kJ/mol (5). Those for GA thermoinactivation in buffer are ~ 310 kJ/mol (36), so increasing the temperature leads to much higher rates of enzyme inactivation but only moderate increases in enzyme activities.

Increasing substrate and product concentrations strongly protect GA against inactivation, so that at 30% solids the optimal operating temperature of the *A. awamori*/*A. niger* form over 48 h is ~ 60°C. With buffer rather than substrate or product, serious inactivation occurs within 30 min at 60°C and pH 4.5, since the first order thermoinactivation rate coefficient is ~ $10^{-4}sec^{-1}$ under these conditions (36).

GA has no cofactors, nor is it stabilized by either cations or anions. It has a number of inhibitors, the most potent being the pseudo-tetrasaccharide acarbose and its various derivatives, that presumably mimic the transition-state form of the glucosyl residues about the glycosyl bond being cleaved.

C. Kinetic Properties

An exhaustive listing of the kinetic properties of many different GAs with different substrates and inhibitors is found in the doctoral dissertation of P. M. Coutinho (68). The sheer bulk of the data set (48 pages of tables) suggests that noting many specific values here would be futile. Most data have been gathered at pHs between 4 and 5 and temperatures between 25°C and 50°C (Figs. 6, 7). Substrates range from maltose through maltodecaose to various types of starch and glycogen, but also include oligosaccharides with different glycosidic bonds. Most data are on GAs from various *Aspergillus* and *Rhizopus* spp. but there are some data from virtually every GA that has been sequenced.

To concentrate on the kinetics of *A. awamori*/*A. niger* GA at 45°C and pH 4.5 (68), average values of

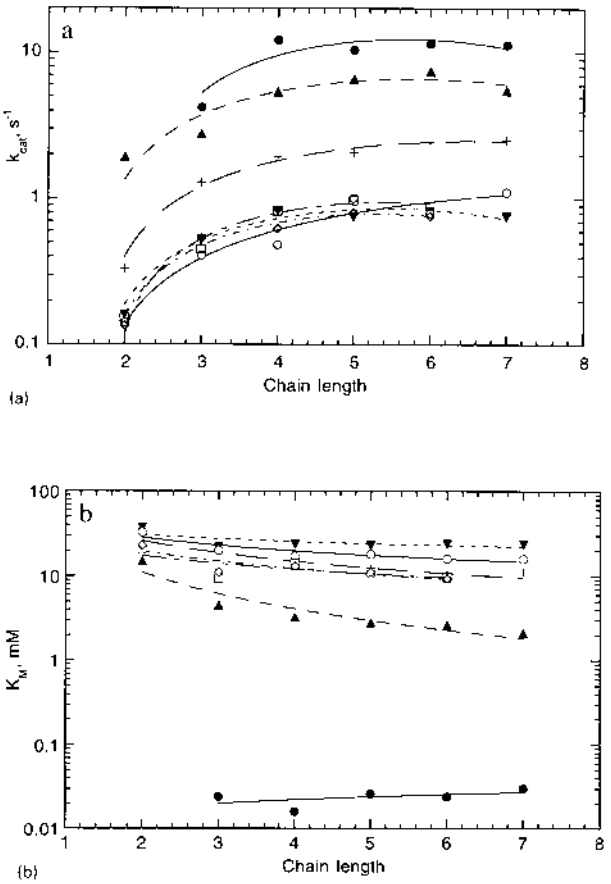

Figure 7 Kinetic parameters of different GAs as a function of chain length of isomalto-oligosaccharide substrates (except where noted). a: Values of k_{cat} (sec^{-1}); b: Values of K_M (mM). Symbols: — – □ — –, *A. niger* G1, pH 4.5, 35°C (17); — – ◇ — –, *A. niger* G2, pH 4.5, 35°C (17); — — ▲ — —, *H. resinae P*, pH 4.3, 25°C (44); – – – ▼ – – –, *H. resinae S*, pH 4.3, 25°C (55); —●—, *p*-nitrophenyl-α-D-malto-oligosaccharides, *A. niger* G2, pH 4.5, 25°C (57); — — + — —, *A. awamori* wt, pH 4.5, 45°C (61); — ○ —, *R. niveus*, pH 4.5, 25°C (63). *H. resinae* S, pH 4.3, 25°C (55); —●—, *p*-nitrophenyl-α-D-malto-oligosaccharides, *A. niger* G2, pH 4.5, 25°C (57); — — + — —, *A. awamori* wt, pH 4.5, 45°C (61); — ○ —, *R. niveus*, pH 4.5, 25°C (63).

k_{cat} and K_M for maltoheptaose hydrolysis are $60\,sec^{-1}$ and 0.13 mM, respectively, while for maltose hydrolysis they are $10\,sec^{-1}$ and 1.2 mM, respectively. For the major byproduct isomaltose the equivalent values are $0.37\,sec^{-1}$ and 23 mM, showing the large effect that decreasing substrate chain length and a change of glycosidic bond have in decreasing k_{cat} and increasing K_M. Fewer data are available for the primary product glucose, but it appears that K_i for GAs from filamentous fungi is about ~ 100 mM at pH 4.5 and a range of temperatures. Data are also rather sparse for GA kinetics on soluble starch, amylose, and amylopectin, with k_{cat} at pH 4.5 and extrapolated to 45°C being $\sim 60\,sec^{-1}$, the same value as for maltoheptaose. Values of K_M are too widely scattered for an average value to be reported, with most values being in weight percent, since substrate molecular weights were often not determined.

Among inhibitors, acarbose has a K_i of $\sim 10^{-12}$ M on *A. awamori*/*A. niger* GA at pH 4.5 and 27°C (68), while equivalent values for D-*gluco*-dihydroacarbose, methyl α-arcarviosinide, 1-deoxynojirimycin, and D-glucono-1,5-lactone are 3×10^{-8} M (64), 5×10^{-8} M (64), 3×10^{-5} M (64), and 1×10^{-3} M (68), respectively.

A general observation based on fewer kinetic and inhibition data is that values for GAs from other sources are not greatly different from those of *A. awamori*/*A. niger* GA, although there are a number of single values under different conditions, often at lower temperatures, that vary from the average values above.

Kinetic data for the GA-catalyzed condensation of glucose to di- and trisaccharides are available for *A. niger* GA at pHs 3.5, 4.5, and 5.5, at 25, 35, and 45°C, and at 20%, 30%, and 40% (w/v) initial glucose concentrations (7). Based on maltose formation as 100, the average initial rates of formation of α,β-trehalose, kojibiose, nigerose, and isomaltose across the different pHs, temperatures, and initial concentrations are 0.027, 0.010, 0.087, and 1.45, respectively, with relative rates for isomaltotrioside increasing from 0.05 to 0.085 with increasing initial glucose concentrations because of their second-order dependence on solids concentration, and that of panose being too small to measure. Equilibrium constants, defined as above (Sec. I), average 0.082 for α,β-trehalose, 0.20 for kojibiose, 0.18 for nigerose, 0.091 for maltose, 2.2 for isomaltose, 3.3 for panose, and 2.3 for isomaltotriose; little change occurs with changes of initial glucose concentration, pH, or temperature. The last three values should be similar since α-1,6 bonds are formed in each case.

V. DETERMINATION OF GLUCOAMYLASE KINETIC PROPERTIES AND THERMOSTABILITY

GA activity is easy to determine, since the enzyme exclusively produces glucose, which can be detected with minimal interference using glucose oxidase (69,

70). Assays are conducted at pH 4.4–4.5 in 0.05 M sodium acetate buffer and at 50°C or below, where enzyme inactivation over short periods is minimal. Substrates are either 4% maltose or 2% soluble starch, both concentrations being well above their corresponding K_M values, which with *A. awamori*/*A. niger* GA are 1.2 mM (0.4%) for maltose, and 0.1% or less for soluble starch near pH 4.5 and 25–50°C (68). However, both values can vary when GAs from other sources or different conditions are used, so assay substrate concentrations should be modified with this in mind so that measured activities approach their maximal values. Six or more samples are taken at short time intervals to make substrate conversions sufficiently low that increase in glucose concentration is linear with time. Samples are added to pH 7 Tris at 1 M (final concentration) buffer to stop the hydrolysis reaction (14), and the quenched sample is treated with glucose oxidase, peroxidase, and one of several chromophores, the most common being *o*-dianisidine, found in different commercial kits.

If values of k_{cat} and K_M are to be determined, substrate concentrations covering at least the range from 0.2 K_M to 5 K_M should be used. Since GA follows Michaelis-Menten kinetics with all common pure substrates, at least six activity points should be plotted against their corresponding substrate concentrations and a hyperbolic function should be fitted through them with a nonlinear regression algorithm. This is far superior to use of various linearizing routines such as Lineweaver-Burk, Eadie-Hofstee, and Hanes plots, as the data are not distorted by algebraic manipulations.

GA thermostability in buffer without substrate can be measured by incubating samples at different temperatures or different pHs. At least six samples taken at different times are treated as above to obtain residual activities. Since GA loses activity by a first-order mechanism, the slope of a ln (activity) vs. time curve gives the negative inactivation rate coefficient. Obtaining GA thermostability in substrate or glucose solutions is much more difficult, since glucose, the product being measured in the residual activity assay, is initially present. This problem can be ameliorated but not eliminated by using assay samples of very low residual activity and incubating for long periods.

VI. PURIFICATION OF GLUCOAMYLASE

GA can be brought to homogeneity in several steps. Many filamentous fungi produce GA extracellularly in high amounts, so in those cases no cell breakage is necessary unless the small amounts remaining inside the cell are to be studied. GA I and GA II can be separated from each other and from an acidic α-amylase by a linear gradient from ~pH 8 to ~pH 3 by column chromatography with DEAE or another weak base on a suitable support (71, 72), the elution order being GA II, α-amylase, and GA I. Meagher et al. (17) have completely described the purification of a sample containing both GA I and GA II by (a) precipitation of extraneous protein with $(NH_4)_2SO_4$ at 80% of saturation; (b) desalting by passage through a Sephadex G-25 column; (c) separation of the two GA forms from each other and from other proteins by DEAE-cellulose chromatography using a citrate-phosphate buffer eluant whose pH decreases linearly from 7.9 to 3.6; (d) concentration by ultrafiltration; (e) desalting of each fraction with a Sephadex G-25 column; (f) rechromatography for each fraction with DEAE-cellulose; and (g) further desalting and concentration by ultrafiltration.

Protein in a 20-g sample of a commercial preparation decreased from 1.57 g to 1.19 g after step (a), to 1.02 g after step (b), to 313 mg and 217 mg in the GA I and GA II fractions, respectively, after step (c), and to 173 mg and 94 mg for the two fractions after step (f). GA specific activities increased from 7.9 U/mg for the starting material to 9.8 U/mg after the second step, to 9.8 U/mg and 12.3 U/mg for the GA I and GA II fractions, respectively, after the third step, and to 10.8 U/mg and 13.2 U/mg for the two fractions after the sixth step. One unit was the GA activity that liberated 1 μmol/min glucose from 4% maltose at pH 4.5 and 35°C, while protein concentration was determined by UV spectroscopy using a previously measured molar extinction coefficient for GA (14).

Alternatively, complete purification of each GA form can be achieved after dialysis by acarbose-Sepharose chromatography eluted with 1.7 M Tris at pH 7.6 (73). This is especially efficient if wild-type GA containing only GA I is produced from yeast (54), but may also be used after the third step above if production is from *A. niger* or another filamentous fungus.

In some cases it is important to separately establish that seemingly homogeneous GA preparations are free of glucosyltransferase activity. This may be accomplished by measuring the conversion of panose in the presence of 0.1 g/L or more of acarbose, which completely inhibits GA but only slightly inhibits glucosyltransferase (17, 74).

ACKNOWLEDGMENT

The author thanks Pedro Coutinho for his advice during the preparation of this manuscript and for producing Figures 1–4.

REFERENCES

1. LL Phillips, ML Caldwell. A study of the purification and properties of a glucose-forming amylase from *Rhizopus delemar*, gluc amylase. J Am Chem Soc 73:3559–3563, 1951.
2. LL Phillips, ML Caldwell. A study of the action of gluc amylase, a glucose-producing amylase, formed by the mold, *Rhizopus delemar*. J Am Chem Soc 73:3563–3568, 1951.
3. SA Barker, EJ Bourne, JG Fleetwood. Studies on *Aspergillus niger*. Part IX. The mechanism of glucamylase action. J Chem Soc 4865–4871, 1957.
4. JH Pazur, K Kleppe. The hydrolysis of α-D-glucosides by amyloglucosidase from *Aspergillus niger*. J Biol Chem 237:1002–1006, 1962.
5. MM Meagher, PJ Reilly. Kinetics of the hydrolysis of di- and trisaccharides by *Aspergillus niger* glucoamylases I and II. Biotechnol Bioengin 34:689–693, 1989.
6. EJ Hehre, G Okada, DS Genghof. Configurational specificity: unappreciated key to understanding enzymatic reversions and *de novo* glycosidic bond synthesis. I. Reversal of hydrolysis by α-, β-, and glucoamylases with donors of correct anomeric form. Arch Biochem Biophys 135:74–89, 1969.
7. ZL Nikolov, MM Meagher, PJ Reilly. Kinetics, equilibria, and modeling of the formation of oligosaccharides from D-glucose by *Aspergillus niger* glucoamylases I and II. Biotechnol Bioeng 34:694–704, 1989.
8. S Pestlin, D Prinz, JN Starr, PJ Reilly. Kinetics and equilibria of condensation reactions between monosaccharide pairs catalyzed by *Aspergillus niger* glucoamylase. Biotechnol Bioeng 56:9–22, 1997.
9. K Sakaguchi, M Takagi, H Horiuchi, K Gomi. Fungal enzymes used in Oriental food and beverage industries. In: JR Kinghorn, G Turner, eds. Applied Molecular Genetics of Filamentous Fungi. Glasgow: Blackie, 1992, pp 54–61.
10. FF Dias, DC Panchal. Maltulose formation during saccharification of starch. Starch/Stärke 39:64–66, 1987.
11. GFH Kramer, AP Gunning, VJ Morris, NJ Belshaw, G Williamson. Scanning tunnelling microscopy of *Aspergillus niger* glucoamylase. J Chem Soc Faraday Trans 89:2595–2602, 1993.
12. A Aleshin, A Golubev, LM Firsov, RB Honzatko. Crystal structure of glucoamylase from *Aspergillus awamori* var. *X100* to 2.2-Å resolution. J Biol Chem 267:19291–19298, 1992.
13. K Sorimachi, AJ Jacks, M-F Le Gal–Coëffet, G Williamson, DB Archer, MP Williamson. Solution structure of the granular starch binding domain of glucoamylase from *Aspergillus niger* by nuclear magnetic resonance spectroscopy. J Mol Biol 259:970–987, 1996.
14. B Svensson, TG Pedersen, I Svendsen, T Sakai, M Ottesen. Characterization of two forms of glucoamylase from *Aspergillus niger*. Carlsberg Res Commun 47:55–69, 1982.
15. S Hayashida, T Nomura, E Yoshino, M Hongo. The formation and properties of subtilisin-modified glucoamylase. Agric Biol Chem 40:141–146, 1976.
16. SMA Khan, PJ Reilly, C Ford. Thermal and molecular characterization of *Aspergillus awamori* glucoamylase catalytic and starch-binding domains. Starch/Stärke 52:385–397, 2000.
17. MM Meagher, ZL Nikolov, PJ Reilly. Subsite mapping of *Aspergillus niger* glucoamylases I and II with malto- and isomaltooligosaccharides. Biotechnol Bioeng 34:681–688, 1989.
18. PM Coutinho, PJ Reilly. Glucoamylase structural, functional, and revolutionary relationships. Proteins Struct Funct Genet 29:334–347, 1997.
19. PJ Kraulis. MOLSCRIPT: A program to produce both detailed and schematic plots of protein structures. J Appl Crystallogr 24:945–950, 1991.
20. B Stoffer, AE Aleshin, LM Firsov, B Svensson, RB Honzatko. Refined structure of the complex of D-*gluco*-dihydroacarbose with glucoamylase from *Aspergillus awamori* var. *X100* to 2.2 Å resolution: dual conformations from extended inhibitors bound to the active site of glucoamylase. FEBS Lett 358:57–61, 1995.
21. CL Lawson, R van Montfort, B Strokopytov, HJ Rozeboom, KH Kalk, GE de Vries, D Penninga, L Dijkhuizen, BW Dykstra. Nucleotide sequence and x-ray structure of cyclodextrin glucosyltransferase from *Bacillus circulans* strain 251 in a maltose-dependent crystal form. J Mol Biol 236:590–600, 1994.
22. PM Alzari, H Souchon, R Dominguez. The crystal structure of endoglucanase CelA, a family 8 hydrolase from *Clostridium thermocellum*. Structure 4:265–275, 1996.
23. M Juy, AG Amit, PM Alzari, RJ Poljak, M Claeyssens, P Béquin, J-P Aubert. Three-dimensional structure of a thermostable bacterial cellulase. Nature 357:89–91, 1992.
24. J Sakon, D Irwin, DB Wilson, PA Karplus. Structure and mechanism of endo/exo-cellulase E4 from *Thermomonospora fusca*. Nat Struct Biol 4:810–818, 1997.

25. B Svensson, K Larson, I Svendsen, E Boel. The complete amino acid sequence of the glycoprotein, glucoamylase G1, from *Aspergillus niger*. Carlsberg Res Commun 48:529–544, 1983.
26. JH Nunberg, JH Meade, G Cole, FC Lawyer, P McCabe, V Schweikart, R Tal, VP Wittman, JE Flatgaard, MA Innis. Molecular cloning and characterization of the glucoamylase gene of *Aspergillus awamori*. Mol Cell Biol 4:2305–2315, 1984.
27. PM Coutinho, PJ Reilly. Structure-function relationships in the catalytic and starch binding domains of glucoamylase. Protein Eng 7:393–400, 1994.
28. PM Coutinho, PJ Reilly. Structural similarities in glucoamylases by hydrophobic cluster analysis. Protein Eng 7:749–760, 1991.
29. B. Henrissat. A classification of glycosyl hydrolases based on amino acid sequence similarities. Biochem J 280:309–316, 1991.
30. B Henrissat, A Bairoch. New families in the classification of glycosyl hydrolases based on amino acid sequence similarities. Biochem J 293:781–788, 1993.
31. B Henrissat, A Bairoch. Updating the sequence-based classification of glycosyl hydrolases. Biochem J 316:695–696, 1996.
32. PM Coutinho, B. Henrissat. http://afmb.cnrs-mrs.fr/~cazy/CAZY/index.html, 1999.
33. R Evans, C Ford, M Sierks, Z Nikolov, B Svensson. Activity and thermal stability of genetically truncated forms of *Aspergillus* glucoamylase. Gene 91:131–134, 1990.
34. CB Libby, CAG Cornett, PJ Reilly, C Ford. Effect of amino acid deletions in the *O*-glycosylated region of *Aspergillus awamori* glucoamylase. Protein Eng 7:1109–1114, 1994.
35. AE Aleshin, C Hoffman, LM Firsov, RB Honzatko. Refined crystal structures of glucoamylase from *Aspergillus awamori* var. *X100*. J Mol Biol 238:575–591, 1994.
36. H-M Chen, C Ford, PJ Reilly. Substitution of Asn residues in *Aspergillus awamori* glucoamylase by site-directed mutagenesis to eliminate N-glycosylation and inactivation by deamidation. Biochem J 301:275–281, 1994.
37. A Gunnarsson, B Svensson, B Nilsson, S Svensson. Structural studies of the *O*-glycosidically linked carbohydrate chains of glucoamylase G1 from *Aspergillus niger*. Eur J Biochem 145:463–467, 1984.
38. G Williamson, NJ Belshaw, MP Williamson. *O*-Glycosylation in *Aspergillus* glucoamylase. Biochem J 282:423–428, 1992.
39. G Williamson, NJ Belshaw, TR Noel, SG Ring, MP Williamson. *O*-Glycosylation and stability. Unfolding of glucoamylase induced by heat and guanidine hydrochloride. Eur J Biochem 207:661–670, 1992.
40. C Klein, GE Schulz. Structure of cyclodextrin glucosyltransferase refined to 2.0 Å resolution. J Mol Biol 217:737–750, 1991.
41. BK Dalmia, ZL Nikolov. Characterization of glucoamylase adsorption to raw starch. Enzyme Microb Technol 13:982–990, 1991.
42. DM Bui, I Kunze, S Forster, T Wartmann, C Horstmann, R Manteuffel, G Kunze. Cloning and expression of an *Arxula adeninivorans* glucoamylase gene in *Saccharomyces cerevisiae*. Appl Microbiol Biotechnol 44:610–619, 1996.
43. H Ohnishi, H Sakai, T Ohta. Purification and some properties of a glucoamylase from *Clostridium* G0005. Agric Biol Chem 55:1901–1902, 1991.
44. H Ohnishi, H Kitamura, T Minowa, H Sakai, T Ohta. Molecular cloning of a glucoamylase gene from a thermophilic *Clostridium* and kinetics of the cloned enzyme. Eur J Biochem 207:413–418, 1992.
45. MR Sierks, C Ford, PJ Reilly, B Svensson. Catalytic mechanism of fungal glucoamylase as defined by mutagenesis of Asp176, Glu179, and Glu180 in the enzyme from *Aspergillus awamori*. Protein Eng 3:193–198, 1990.
46. EMS Harris, AE Aleshin, LM Firsov, RB Honzatko. Refined structure for the complex of 1-deoxynojirimycin with glucoamylase from *Aspergillus awamori* var. X100 to 2.4-Å resolution. Biochemistry 32:1618–1626, 1993.
47. PM Coutinho, MK Dowd, PJ Reilly. Automated docking of α-(1,4)- and α-(1,6)-linked glucosyl trisaccharides in the glucoamylase active site. Ind Eng Chem Res 37:2148–2157, 1998.
48. ML Sinnott. Catalytic mechanism of enzymic glycosyl transfer. Chem Rev 90:1170–1202, 1991.
49. SK Natarajan, MR Sierks. Identification of enzyme-substrate and enzyme-product complexes in the catalytic mechanism of glucoamylase from *Aspergillus awamori*. Biochemistry 35:15269–15279, 1996.
50. K Hiromi, Y Nitta, C Numata, S Ono. Subsite affinities of glucoamylase: examination of the validity of the subsite theory. Biochim Biophys Acta 302:362–375, 1973.
51. AN Savel'ev, VR Sergeev, LM Firsov. Study of the active site of glucoamylase from *Aspergillus awamori*. Biochemistry (USSR) 47:330–336, 1982.
52. T Koyama, N Inokuchi, Y Kikuchi, H Shimada, M Iwama, T Takahashi, M Irie. Subsite affinity of a glucoamylase from *Aspergillus saitoi*. Chem Pharm Bull 32:757–761, 1984.
53. JI Abe, H Nagano, S Hizukuri. Kinetic and structural properties of the three forms of glucoamylase of *Rhizopus delemar*. J Appl Biochem 7:235–247, 1985.
54. MR Sierks, C Ford, PJ Reilly, B Svensson. Site-directed mutagenesis at the active site Trp120 of *Aspergillus awamori* glucoamylase. Protein Eng 2:621–625, 1989.

55. R Fagerström. Subsite mapping of *Hormoconis resinae* glucoamylases and their inhibition by gluconolactone. J Gen Microbiol 137:1001–1008, 1991.
56. E Nagy, EK Bélafi-Bakó, L Szabó. A kinetic study of the hydrolysis of maltodextrin by soluble glucoamylase. Starch/Stärke 44:145–149, 1992.
57. J Ermer, K Rose, G Hübner, A Schellenberger. Subsite affinities of *Aspergillus niger* glucoamylase II determined with *p*-nitrophenylmaltooligosaccharides. Biol Chem Hoppe-Seyler 374:123–128, 1993.
58. TP Frandsen, C Dupont, J Lehmbeck, B Stoffer, MR Sierks, RB Honzatko, B Svensson. Site-directed mutagenesis of the catalytic base Glu400 in glucoamylase from *Aspergillus niger*, and of tyrosine 48 and glutamine 401, both hydrogen-bonding to the γ-carboxylate group of glutamic acid 400. Biochemistry 33:13808–13816, 1994.
59. Ohnishi, H Matsumoto, H Sakai, T Ohta. Functional roles of Trp337 and Glu632 in *Clostridium* glucoamylase, as determined by chemical modification, mutagenesis, and the stopped-flow method. J Biol Chem 269:3503–3510, 1994.
60. S Natarajan, MR Sierks. Functional and structural roles of the highly conserved Trp120 loop region of glucoamylase from *Aspergillus awamori*. Biochemistry 35:3050–3058, 1996.
61. H-P Fierobe, BB Stoffer, TP Frandsen, B Svensson. Mutational modulation of substrate bond-type specificity and thermostability of glucoamylase from *Aspergillus awamori* by replacement with short homologue active site sequences and thiol/disulfide engineering. Biochemistry 35:8696–8704, 1996.
62. T-Y Fang, PM Coutinho, PJ Reilly, C Ford. Mutations to alter *Aspergillus awamori* glucoamylase selectivity. Protein Eng 11:119–126, 1998.
63. A Tanaka, T Takeda. Subsite structure of *Rhizopus* glucoamylase for the hydrolytic reaction of isomaltooligosaccharides. Biosci Biotechnol Biochem 58:1809–1813, 1994.
64. BW Sigurskjold, CR Berland, B Svensson. Thermodynamics of inhibitor binding to the catalytic site of glucoamylase from *Aspergillus niger* determined by displacement titration calorimetry. Biochemistry 33:10191–10199, 1994.
65. AM Sills, ME Sauder, GG Stewart. Amylase activity in certain yeasts and a fungal species. Dev Ind Microbiol 24:293–303, 1983.
66. SK Natarajan, MR Sierks. Minimizing nonproductive substrate binding: a new look at glucoamylase subsite affinities. Biochemistry 36:14946–14955, 1997.
67. U Bakir, PM Coutinho, PA Sullivan, C Ford, PJ Reilly. Cassette mutagenesis of *Aspergillus niger* glucoamylase near its general acid residue to probe its catalytic and pH properties. Protein Eng 6:939–946, 1993.
68. PM Coutinho. Computational studies of glucoamylase selectivity. PhD dissertation, Iowa State University, Ames, Iowa, 1996.
69. ID Fleming, HF Pegler. The determination of glucose in the presence of maltose and maltose by a stable, specific enzyme reagent. Analyst 88:967–968, 1963.
70. W Banks, CT Greenwood. Characterization of starch and its components. IV. Specific estimation of glucose using glucose oxidase. Stärke 23:222–228, 1971.
71. JH Pazur, T Ando. Action of an amyloglucosidase of *Aspergillus niger* on starch and malto-oligosaccharides. J Biol Chem 234:1966–1970, 1959.
72. DR Lineback, IJ Russell, C Rasmussen. Two forms of glucoamylase of *Aspergillus niger*. Arch Biochem Biophys 134:539–553, 1969.
73. AJ Clarke, B Svensson. Identification of an essential tryptophanyl residue in the primary structure of glucoamylase G2 from *Aspergillus niger*. Carlsberg Res Commun 49:559–566, 1984.
74. JK Shetty, JJ Marshall. Method for determination of transglucosidase. U.S. patent 4,575,487 (1986).

59

Limit Dextrinase/Pullulanase

E. Ann MacGregor
University of Manitoba, Winnipeg, Manitoba, Canada

I. INTRODUCTION

The enzymes known as pullulanase (EC 3.2.1.41) or limit dextrinase (EC 3.2.1.142) catalyze hydrolysis of α-1,6-D-glucosidic linkages in pullulan, amylopectin, and the α- and β-amylase limit dextrins of amylopectin and glycogen (Fig. 1), with limited or no action on glycogen. They are usually more active on oligosaccharide dextrins than on polysaccharide substrates—hence the systematic name α-dextrin 6-glucanohydrolase. The names limit dextrinase and R-enzyme have both been applied to enzymes of plant origin; the former name is preferred since it is related to the natural substrate. In plants, the function of the enzyme is to help bring about complete degradation of starch to glucose and maltose by hydrolyzing the α-1,6-glucosidic bonds of small branched dextrins resulting from the combined action of α- and β-amylase on starch. The name pullulanase, in contrast, has been used for many years for microbial enzymes important for the breakdown of branched polysaccharides such as the amylopectin of starch. The EC recommended name is α-dextrin endo-1-6-α-glucosidase, but it is little used.

Studies of the primary structures of limit dextrinases and pullulanases have shown appreciable sequence similarity between the plant and microbial enzymes, and it is now common to refer to plant pullulanases where the name limit dextrinase has been used in the past. There has been, however, a recommendation that "limit dextrinase" continue to be used for the plant enzymes to distinguish between these and the microbial proteins, particularly since there are some specificity differences, with plant enzymes in general being less active on glycogen than the microbial pullulanases (1).

The minimum structural requirement for a branched oligosaccharide to be a substrate for pullulanase/limit dextrinase is a maltose residue on either side of the α-1,6 linkage (Fig. 2); i.e., the enzymes cannot remove a 1,6-linked glucosyl stub from a chain of α-1,4-linked glucose residues, or remove a 1,4-linked glucose chain attached to carbon 6 of a single glucose unit. The enzymes have high activity on 6^3-α-maltosyl maltotetraose and 6^3-α-maltotriosyl maltotetraose (2, 3) (Fig. 2).

The limited activity of pullulanase/limit dextrinase on glycogen distinguishes these enzymes from another important starch-debranching enzyme, isoamylase (EC 3.2.1.68), which brings about appreciable hydrolysis of α-1,6-glucosidic bonds in glycogen but has little effect on pullulan. Furthermore pullulanase, hydrolyzing α-1,6 links in pullulan to yield maltotriose, should not be confused with neopullulanase (EC 3.2.1.135) or isopullulanase (EC 3.2.1.57), which hydrolyze the α-1,4-glucosidic bonds in pullulan to give panose or isopanose, respectively (Fig. 3). Enzymes known as amylopullulanases or α-amylase-pullulanases can bring about hydrolysis of both α-1,4 and α-1,6 linkages in glucans, and therefore can be distinguished from true pullulanases, which hydrolyze α-1,6-glucosidic bonds only. In some cases, however, an enzyme acting on pullulan is not always tested for activity on α-1,4- and α-1,6-glucosidic linkages, and confusion exists in the literature where several amylopullulanases are described as pull-

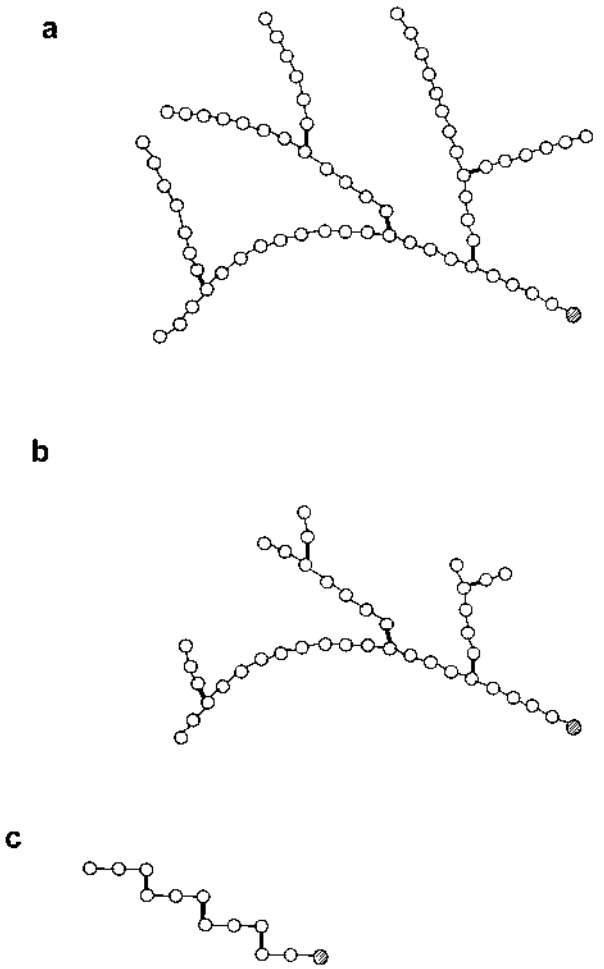

Figure 1 (a) Representation of glycogen or amylopectin molecule. ○ = glucose residue; ◍ = reducing glucose residue; – = α-1,4-glucosidic bond; ▮ = α-1,6-glucosidic bond. In glycogen there is approximately one α-1,6-linkage for every 12 α-1,4-linkages; in amylopectin the ratio is 1:25. (b) β-Limit dextrin of amylopectin or glycogen. Outer chains are trimmed to one to three glucose residues in length. (c) Pullulan.

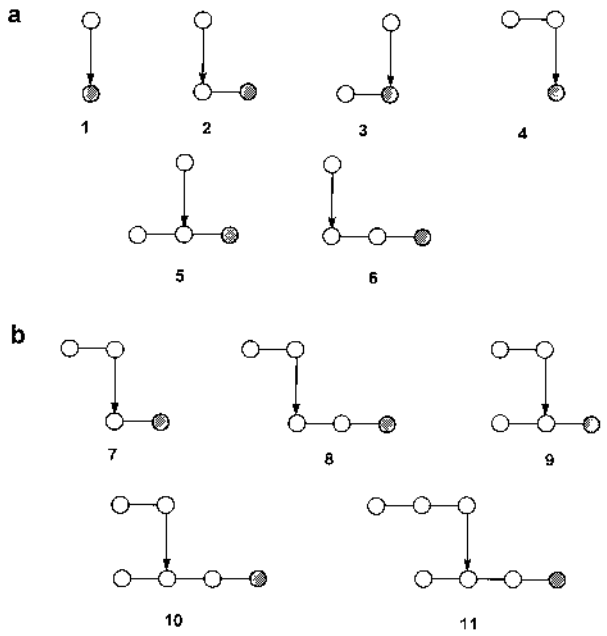

Figure 2 (a) Oligosaccharides resistant to pullulanase/limit dextrinase action. Symbols are as in Figure 1, with an arrow representing an α-1,6-glucosidic linkage. 1: Isomaltose, 2: panose, 3: 6^1-α-glucosyl maltose, 4: isopanose, 5: 6^2-α-glucosyl maltotriose, 6: 6^3-α-glucosyl maltotriose. (b) Substrates for pullulanase/limit dextrinase. 7: 6^2-α-maltosyl maltose, 8: 6^3-α-maltosyl maltotriose, 9: 6^2-α-maltosyl maltotriose, 10: 6^3-α-maltosyl maltotetraose, 11: 6^3-α-maltotriosyl maltotetraose.

ulanases (e.g., 4). In other cases, enzymes are described as type I or type II pullulanases. The type I enzymes are true pullulanases, specific for α- 1,6-glucosidic bonds, while type II pullulanases are, in fact, amylopullulanases (5).

II. IMPORTANCE IN FOOD

Microbial pullulanases are used, as purified enzymes, in the production of glucose, fructose, and maltose syrups (see Sec. IV). The plant enzyme of greatest commercial importance is the limit dextrinase of barley, which plays a role in the brewing and distilling industries (see Sec. IV). The enzyme is known to occur in mature barley kernels, and additional limit dextrinase is synthesized when barley seeds germinate. Much of the limit dextrinase activity of germinated barley is also found in brewers' malt, i.e., barley germinated under carefully controlled conditions and dried by kilning. During brewing, the enzyme, in theory, acts in conjunction with malt α- and β-amylases to break down the starch from the malt itself and any added starch to glucose and maltose, prior to fermentation with yeast to produce alcohol. In practice, however, the dextrinase has very limited action, since a potent inhibitor of the enzyme (see Secs. VI and VII) also exists in malt (6).

III. SOURCES OF PULLULANASE/LIMIT DEXTRINASE

True pullulanases have been found in, and prepared from, a variety of bacteria. The enzyme is synthesized

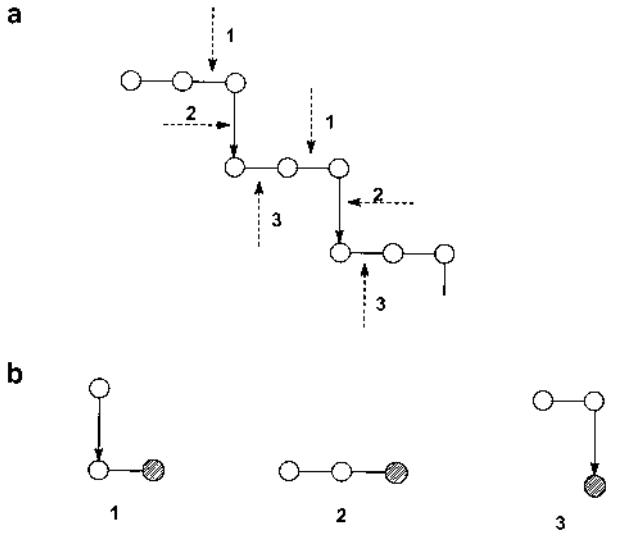

Figure 3 (a) Hydrolysis of pullulan at 1 by neopullulanase; at 2 by pullulanase; at 3 by isopullulanase. (b) 1. Panose, product of neopullulanase action; 2. maltotriose, product of pullulanase action; 3. isopanose, product of isopullulanase action. Symbols are as in Figure 1 with an arrow representing an α-1,6-glucosidic bond.

intracellularly, then is usually secreted to give an extracellular pullulanase that can be purified from the supernatant of the culture.

Bacterial pullulanases that are to be used as purified enzymes in the production of glucose syrups must act in conjunction with a fungal glucoamylase, and so are used at 60°C and pH 4.5–5.0, conditions where the glucoamylase is most active (see Sec. IV). The most widely studied pullulanases, those from *Klebsiella pneumoniae*[*] or related bacteria, lose activity at 60°C (9). The enzymes from *Bacillus acidopullulyticus* and *B. deramificans* (10, 11) are efficient under the optimum conditions for glucoamylase, but are not heat stable at temperatures much above 60°C. Enzymes from thermophilic bacteria, with potentially greater heat stability, have been investigated, but most have been found to have high activity only at pH 6.0 or higher. A pullulanase from *Fervidobacterium pennavorans* is, however, very active in the pH range 4.5–5.0 and is stable at 70°C (12).

Amylopullulanases could be used in place of pullulanases if they are active under the conditions required for dextrin hydrolysis by glucoamylase; enzymes from *Clostridium thermohydrosulfuricum* and *Thermoanaerobium* Tok6-B1 appear to have these properties (13, 14).

Limit dextrinases are known to occur in several plants, but only the enzyme of barley is of commercial importance. The enzyme is found in mature barley kernels, mainly in the endosperm (15), and additional limit dextrinase is synthesized in the aleurone cells during germination (16). The location of the enzyme within the seeds has been determined by dissection of the seeds and evaluation of enzyme levels within each tissue (15, 16).

IV. UTILIZATION OF ENZYMES IN FOODS

Before microbial pullulanases can be used in the preparation of glucose and maltose syrups, starch in a slurry must be gelatinized by heat treatment and liquefied using a heat-stable α-amylase. In the liquefaction stage, the amylose and amylopectin are hydrolyzed to oligosaccharides of average chain length of 8–12 glucose units, if a glucose syrup is required, or slightly higher chain length for production of a maltose syrup (17, 18). These oligosaccharides are a mixture of linear dextrins containing α-1,4-glucosidic linkages only, and branched dextrins containing all the α-1,6-glucosidic bonds of the amylopectin, since such bonds are not hydrolyzed by α-amylase. The second stage in glucose syrup production is saccharification, where single glucose residues are removed from the nonreducing ends of the dextrins by an exo-acting enzyme, a glucoamylase. This enzyme, however, acts slowly on α-1,6 linkages and, when glucose concentrations become high, can catalyze a reverse reaction to give isomaltose. Addition of a bacterial pullulanase to hydrolyze α-1,6-glucosidic bonds allows reaction times to be reduced, while higher substrate and lower glucoamylase concen-

[*] There is confusion about the nomenclature of bacteria in which important pullulanases can be found. The first pullulanase, studied by Bender and Wallenfels (7), was said to have been prepared from *Aerobacter aerogenes*. This is now reclassified as *Klebsiella pneumoniae* (8). The bacterium *Klebsiella aerogenes*, frequently cited as a source of pullulanase, should also, more properly, be called *Klebsiella pneumoniae* (8). In 1982, however, a new species of *Klebsiella*, *K. planticola*, was distinguished from *K. pneumoniae* (8). Thus some pullulanases, prepared before 1982 and said to have originated from *K. pneumoniae*, may actually derive from *K. planticola*. Indeed the strain of "*Aerobacter aerogenes*" used by Bender and Wallenfels (7) for the original pullulanase preparation is now believed to be *K. planticola* (Culture No. 15050, American Type Culture Collection; Web site www.atcc.org/).

trations can be used. This lowers isomaltose and increases glucose yields. Because the glucoamylase and pullulanase act simultaneously, the two enzymes must be compatible with respect to optimum pH and temperature. The saccharification reaction is usually carried out at 60°C and pH ~ 4.5 for maximum activity of the glucoamylase. Pullulanases active under these conditions can be obtained from *B. acidopullulyticus* (10, 17) and *B. deramificans* (11), and both are considered safe for food use (17, 19). If required, fructose syrup can subsequently be prepared from glucose syrup by isomerization with glucose isomerase.

For maltose syrups, the dextrins obtained by liquefaction of starch are treated simultaneously with β-amylase and pullulanase. The β-amylase produces maltose from the nonreducing ends of α-1,4-linked glucose chains, but can neither hydrolyze nor bypass α-1,6-glucosidic bonds. The pullulanase is therefore essential to convert branched dextrins in the liquefied starch mixture to linear dextrins to allow the β-amylase to have maximum effect (17, 20).

Although purified enzymes are usually added to the liquefied starch in a batch process, various studies have been carried out to investigate the feasibility of using immobilized pullulanase, or plant limit dextrinase, or pullulanase plus glucoamylase for hydrolysis (21–23).

Cyclodextrins can be used for flavor delivery in food, but limited solubility of the cyclodextrins can pose problems. Means of increasing the water solubility of cyclodextrins have been studied, and for this purpose glucosyl or maltosyl cyclodextrins have been prepared, where the glucose or maltose is attached by an α-1,6 linkage to a glucose residue of the cyclodextrin ring. Here the reversibility of the hydrolysis reaction catalyzed by pullulanase has been employed, where the enzyme synthesizes rather than ruptures α-1,6 bonds (24, 25). Such products may, in the future, acquire some commercial importance.

In the process of brewing beer, barley malt starch is gelatinized in warm water, and precooked adjunct starch, often from corn, may be added. The starches are broken down by the hydrolytic enzymes of the malt, principally α- and β-amylase, to glucose and maltose plus smaller quantities of longer α-1,4-linked linear maltodextrins and branched dextrins containing the α-1,6 bonds of the amylopectin of the original starches, since neither α- nor β-amylase attacks these latter bonds. In principle, the limit dextrinase of the malt is able to hydrolyze the α-1,6-glucosidic linkages of the branched dextrins, but the presence of a proteinaceous inhibitor (see Secs. VI and VII) in the malt limits the efficacy of the enzyme (6). Thus glucose, maltose, and linear and small branched dextrins are usually present in wort (aqueous extract of malt) before yeast is added, and since the yeast is able to utilize only glucose, maltose, and maltotriose for alcohol production, the larger dextrins appear in a traditional beer (26, 27). Lowering the inhibitor level, or raising limit dextrinase activity, would allow for greater breakdown of branched dextrins and greater fermentability of a wort, essential for the production of low-carbohydrate beers, but also of economic importance to the distilling industry (6, 28). Alternatively, an extraneous pullulanase or limit dextrinase could be added to increase hydrolysis of branched oligosaccharides (29).

V. PROTEIN PROPERTIES

The molecular weight of pullulanase/limit dextrinase varies with the source of the enzyme, and discrepancies exist in the value quoted for one pullulanase, particularly the *Klebsiella* pullulanases, depending on the method used for molecular-weight determination. Calculations from amino acid sequence for the pullulanases of *B. acidopullulyticus* and *B. deramificans* suggest the molecular weights should be ~ 100,000 daltons, while experimental determinations gave values of 116,000 and 102,000, respectively (10, 11). A molecular weight of 105,000 was found experimentally for barley limit dextrinase (30), while predictions from the sequence would lead to a value ~ 97,000 (31, 32).

Polysaccharide-hydrolyzing enzymes have been classified into families, based on amino acid sequence similarities (33). It is now thought that the enzymes of one family share a common tertiary structure. The primary structures of several pullulanases/limit dextrinases are now known, including those of *B. acidopullulyticus, B. deramificans*, and *barley* (11, 31, 32, 34), and the enzymes are believed to belong to family 13 of the carbohydrases, which includes many other starch-degrading enzymes such as α-amylase and isoamylase (35). While the three-dimensional structure of a pullulanase/limit dextrinase molecule has not been determined, it is expected to be similar to those of other family 13 enzymes for which x-ray crystallographic studies have been carried out (see, e.g., 36). The family 13 enzymes are, in general, multidomain proteins, and in pullulanase/limit dextrinase, as in isoamylase, an N-terminal domain precedes the catalytic domain. The catalytic domain itself is likely to take the form of a $(\beta/\alpha)_8$-barrel, i.e., a barrel of eight parallel β-strands, usually with at least one helix located in the primary sequence between

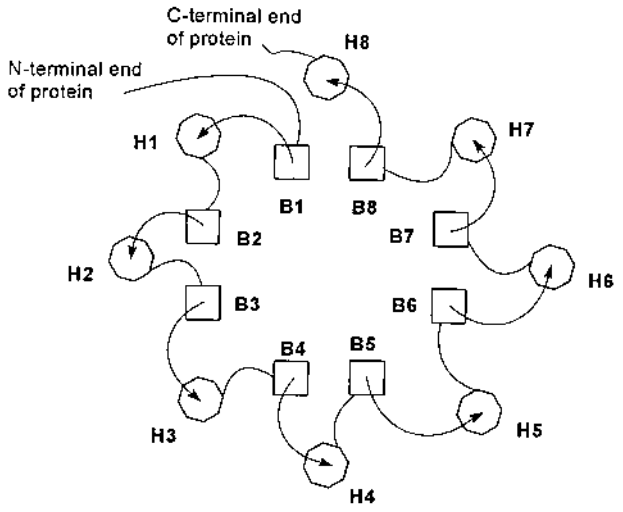

Figure 4 Secondary structure of catalytic domain of a family 13 enzyme. B1–B8 represent parallel β-strands; H1–H8 represent helices of the $(\beta/\alpha)_8$-barrel. Arrows joining a β-strand to the following helix represent loops in the enzyme structure on which are situated amino acid residues of the active site.

each pair of adjacent β-strands (Fig. 4) (37). In general, the active site of family 13 enzymes is made up of amino acid residues situated on loops linking the C-terminal end of a β-strand to the N-terminal end of the adjacent helix (36) (Fig. 4). Amino acids on β-strands 3, 4, 5, and 7, or on loops immediately following these strands, are found at the active site in all family 13 enzymes. The presence and location of active-site acids on other loops vary from one enzyme to another. An obvious characteristic of this family is a long loop between the third β-strand of the barrel and the third helix, amino acid residues on this loop making up much of one side of the active site. In the known three-dimensional structures of family 13 enzymes, at least one domain containing a β-sheet structure follows the catalytic domain, and is also likely to be found in pullulanases/limit dextrinases.

There is limited sequence homology among family 13 enzymes, but all have four well-conserved short sequence segments around β-strands 3, 4, 5, and 7 of the barrel that contain amino acid residues thought to be critically important for the catalytic action of the enzymes (Fig. 5) (38).

The amylopullulanases tend to have larger molecules than pullulanases, with polypeptide chains of up to 1500 amino acids (39), while true pullulanases usually have 700–1100 amino acid residues. Hence the molecular weights of amylopullulanases are expected to be higher than those of pullulanases, in general $>$ 140,000 daltons. These enzymes, however, also belonging to family 13, are predicted to have the characteristic $(\beta/\alpha)_8$-barrel catalytic domain, and contain the four conserved sequence segments typical of the family (Fig. 5) (35, 37, 38).

Phylogenetic trees have been constructed for family 13 enzymes in general and starch-debranching enzymes in particular (31, 35, 38). These show that the plant limit dextrinases are closely related to one another, with the bacterial pullulanases being nearest neighbors, and isoamylases next closest in a tree of the whole family. Amylopullulanases, in contrast, are much more distantly related, and are closer to neopullulanases than pullulanases.

In neither bacteria nor plants is there evidence for more than a single gene for pullulanase/limit dextrinase in each organism. Multiple forms of an enzyme can exist, however, but these have not been well characterized. *Klebsiella* pullulanases are believed to be modified by attachment of lipid at the N-terminal end (40), while the differences between two apparent forms of *B. acidopullulyticus* pullulanase have not been explained (10). Several forms of barley limit dextrinase, separated by electrophoresis and detected using antibodies (15), possibly arise because of the presence of free limit dextrinase and limit dextrinase bound to a proteinaceous inhibitor (41). In another study, three forms of purified barley limit dextrinase have been found, but the differences among them have not been elucidated (42), although they are believed to be products of a single gene (31, 32).

VI. ENZYME PROPERTIES

While pullulanase/limit dextrinase can degrade pullulan, the importance of these enzymes for food and beverages lies in their ability to hydrolyze the α-1,6-glucosidic bonds of amylopectin and branched dextrins resulting from amylopectin breakdown. It is difficult to measure quantitatively the increase in reducing power produced by limited pullulanase action on amylopectin. It is also difficult to obtain a "standard" sample of amylopectin, or a pure, small, branched dextrin to be used as substrate. Thus, absolute values of pullulanase activity are rarely determined, and it is difficult to compare results from different laboratories, since different samples of pullulan or amylopectin may have been used. It is generally agreed, however, that pullulanase/limit dextrinase is more active on small branched dextrins than on pullulan or amylopectin (Table 1).

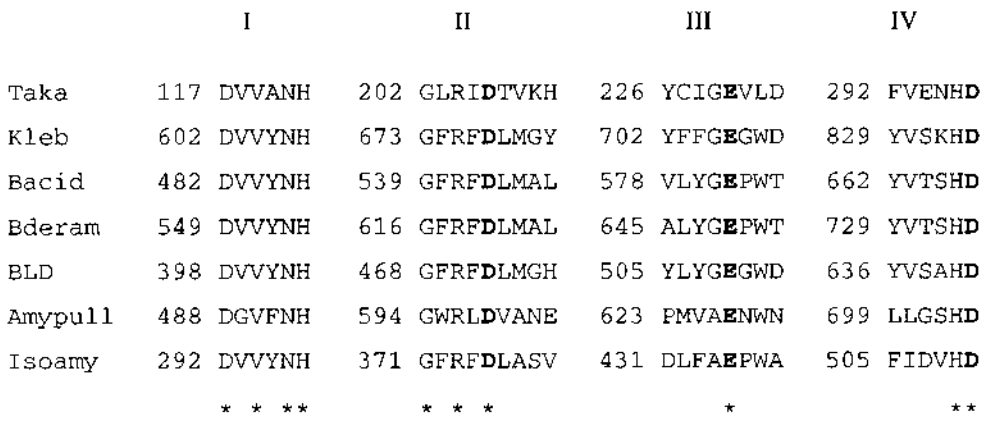

Figure 5 Four short sequence segments conserved in all members of family 13 carbohydrases. Taka: α-amylase from *Aspergillus oryzae*, Genbank sequence No. D00434; Kleb: pullulanase from *Klebsiella pneumoniae*, Genbank sequence No. M16187; Bacid: pullulanase from *Bacillus acidopullulyticus*, sequence from (34); Bderam: pullulanase from *B. deramificans*, sequence from (11); BLD: barley limit dextrinase, sequence from (31); Amypull: amylopullulanase from *Clostridium thermohydrosulfuricum*, sequence from (39); Isoamy: isoamylase from *Pseudomonas amyloderamosa*, Genbank sequence No. A10909. Amino acid residues are numbered from the N-terminal end of the protein. ∗ Indicates residues conserved in all enzymes shown. The three residues involved in catalysis are shown in bold lettering; D in sequence segment II, E in segment III, and D in segment IV.

Values of K_m for pullulan for *Klebsiella* pullulanase are given as 2.5 mM (10), 78 μM, or 21 μM (43) in glucose equivalents, and 70 μM (44) in terms of concentration of hydrolyzable α-1,6-glucosidic bonds. For the *B. acidopullulyticus* enzyme, K_m for pullulan is said to be 2.5 mM glucose equivalents (10), while barley limit dextrinase has a K_m for amylopectin of 26 mM glucose equivalents (3).

The turnover number (k_{cat}) for *Klebsiella* pullulanase has been measured as 99 sec^{-1} or 220 sec^{-1} at 30°C (43), 53 sec^{-1} at 25°C, 132 sec^{-1} at 40°C (44), and 290 sec^{-1} at 60°C, while measured values for the *B. acidopullulyticus* enzyme are 2.9×10^3 or 3.6×10^3 sec^{-1} at 60°C, all on pullulan (10). For barley limit dextrinase acting on a well-defined dextrin, 6^2-0-α-maltotriosyl maltotriose, at 40°C, the number is 90 sec^{-1} (42).

The response to pH and temperature varies with the enzyme source. *Klebsiella* pullulanase is most active between pH 5.5 and 7, and is stable in the pH range 5–12 (9); the *B. acidopullulyticus* and *B. deramificans* enzymes have maximum activity at pH 4–6 and pH 3.75–4.9, respectively, and are stable at pH 4–9 (10) and 3.5–6 (11), respectively. The limit dextrinase of barley, on the other hand, has optimum activity at pH 5.5–6.5 in the presence of bovine serum albumin, which seems to stabilize the active enzyme (30).

Temperature optima for *Klebsiella* and *B. acidopullulyticus* pullulanases are 50°C and 65°C, respectively, and both enzymes are stable at temperatures up to 55°C at pH 5 (9, 10). The enzyme from *B. deramificans* is said to retain 75% of its activity when held at 60°C for 24 h at pH 4.5, and has optimum activity at 60°C (11). The barley limit dextrinase shows maximum activity at 40–50°C (45, 46) and is stable under the mashing conditions in a brewery for at least 1 h at 60°C, but loses activity rapidly at 65°C (47).

Table 1 Relative Activity of Pullulanase/Limit Dextrinase on Different Substrates

Source of enzyme	*K. pneumoniae* (2)	*B. acidopullulyticus* (10)	Barley (3)
Activity[a] on 6^3-α-maltotriosyl maltotetraose	146	—	250
Activity[a] on amylopectin	15	15–16	13

[a] Activity on pullulan taken as 100.

Activation energies, E_a, can be calculated from published data on the variation of activity with temperature, and are shown in Table 2.

Several enzymes of family 13 are known to require Ca^{2+} for activity, but although a *Klebsiella* pullulanase was found to be activated by Ca^{2+} (48), little effect was found for barley limit dextrinase (42). EDTA gave some inhibition of both *Klebsiella* and barley enzymes (42, 48). Cyclodextrins are known to be strong inhibitors of pullulanase/limit dextrinase, with β-cyclodextrin being the most effective. K_i for this dextrin is around 1 μM at 25°C for a *Klebsiella* pullulanase (44) and 40 μM at 40°C for barley limit dextrinase (42).

No investigations of subsite structure of pullulanase/limit dextrinase have been carried out because of the difficulties of obtaining well-defined substrates. In common with other family 13 enzymes, however, these enzymes would be expected to have several subsites for glucose binding at the active site. In general, family 13 enzymes are believed to operate by a mechanism involving retention of anomeric configuration. This has been demonstrated experimentally for a bacterial pullulanase (49) and barley limit dextrinase (42). Two acid groups at the active site, one to act as proton donor and the other as catalytic nucleophile, are expected to be found in family 13 enzymes. In fact, three acid groups (Fig. 5) are found to be essential for enzymic activity; the conserved glutamic acid is thought to be the proton donor, while the conserved aspartic acid in sequence segment II acts as the nucleophile. The role of the second aspartic acid residue in sequence segment IV is not clear.

In barley, germinated barley, and malt, a proteinaceous inhibitor of barley limit dextrinase has been found. The inhibitor levels decrease at later stages of germination (6), and it therefore appears likely that the uninhibited limit dextrinase can then continue the degradation of barley starch begun by the α- and β-amylases of the grain. The resulting small linear maltodextrins can be further hydrolyzed by α-glucosidases to provide glucose for the growth of a new barley plant. Under the conditions used for brewing beer, this inhibitor severely restricts the action of limit dextrinase, since germination for malt production is stopped before inhibitor disappears (6).

VII. DETERMINATION OF ACTIVITY

Well-defined substrates for pullulanase/limit dextrinase, particularly small branched dextrins, are not readily available, and so activity is usually determined on pullulan or a commercially available modified pullulan.

There seems to be no generally accepted standard procedure for measurement of activity on pullulan. Temperature and pH conditions are usually chosen to suit the particular enzyme under study. Pullulan concentration is usually in the range 2.5–5 mg/mL in buffer, often acetate of concentration 20–100 mM and a pH in the range 5.0–5.6 (10, 44, 50). Enzyme is added to the pullulan and after a set time a sample is withdrawn and may be added to 0.1 M NaOH to stop the reaction, and reducing power in the sample is determined by the Nelson-Sömogyi method (51). Calculation of activity depends on the assumption that pullulanase/limit dextrinase converts pullulan mainly to maltotriose (Fig. 3) and that measurement of reducing power gives an indication of the amount of maltotriose present. If the pullulanase is not pure, however, and contains a glucosidase, then reducing power determination may seriously overestimate maltotriose concentration and activity of the pullulanase.

In plants, β-amylase may be present in impure samples of limit dextrinase, and in high enough concentration, β-amylase also can hydrolyze maltotriose. Methods of determining limit dextrinase activity in plant extracts have been developed based on the use of modified pullulans (50). In one method, a soluble red-dyed pullulan (Red Pullulan, Megazyme, Bray, Ireland) is dissolved in 0.5 M KCl solution to a concentration of 20 mg/mL. Enzyme solution in acetate buffer (0.2 M, pH 5.0) containing 20 mM cysteine and 0.02% sodium azide is added to substrate solution and incubated at 40°C for a set time. High-molecular-weight substrate is then precipitated by addition of

Table 2 Activation Energies

Enzyme source	*K. pneumoniae* (9)	*B. acidopullulyticus* (10)	*B. deramificans* (11)	Barley (46)
Activation energy (kJ)	33	45	23	37
Calculated over temperature range (°C)	30–50	40–55	55–60	30–50

ethanol (95% v/v), the mixture is left at room temperature for 10 min, and centrifuged at 1000g for 10 min. Small fragments of dyed pullulan, hydrolyzed by the enzyme from the original high-molecular-weight pullulan, remain in the supernatant giving a colored solution. Absorbance of this solution is measured at 510 nm against distilled water. A blank without enzyme must also be prepared. Absorbance can then be related to pullulanase activity in terms of μmoles of glucose reducing sugar equivalents released per min, using a standard curve. The standard curve is prepared by measuring reducing sugar released from pullulan by purified enzyme in acetate buffer (0.2 M, pH 5.0) at 40°C over a set time period. The Nelson-Sömogyi (51) method is used for reducing sugar determination.

In a second method involving a modified pullulan (50), enzyme solution in sodium maleate buffer (0.1 M, pH 5.5) containing 25 mM dithiothreitol and 0.02% sodium azide is incubated at 40°C for 5 min. A tablet of insoluble blue-dyed pullulan (Limit Dextri-Zyme tablet, Megazyme, Bray, Ireland) is added and the mixture is incubated for a set time. The reaction is terminated by stirring with Tris base solution (1% w/v), and the mixture is left at room temperature for $\sim$ 5 min, then stirred and filtered. In this case, the enzyme hydrolyzes some of the insoluble substrate to give soluble blue-dyed fragments that remain in the filtrate, and measurement of absorbance of the filtrate at 590 nm gives a measure of pullulanase activity. Again, a suitable blank must be prepared by adding Tris base solution to enzyme solution before addition of substrate. Limit dextrinase activity in terms of absorbance at 590 nm must be converted to glucose reducing power equivalents using a standard graph. Preparation of the standard graph differs from the method given for the red pullulan graph only in that buffer at pH 5.5 must be used.

Once standard graphs have been prepared, both methods using modified pullulan have the advantage that the assays are not affected by other enzymes such as α-amylase, β-amylase, or α-glucosidase that could be present in impure preparations of plant limit dextrinase. (Both modified pullulans are available commercially, and detailed instructions for their use are provided by the supplier.) It has been found, however, that the presence of maltodextrins in a limit dextrinase assay system (such as would occur in a malt extract) interferes with activity determinations using the dyed pullulans as substrate (52). In such cases, pretreatment of extracts with amyloglucosidase gives a more accurate estimate of limit dextrinase activity.

Screening for pullulanase/limit dextrinase activity in the presence of other starch-degrading enzymes is difficult, unless polyacrylamide gel electrophoresis is used (53). Red Pullulan (Megazyme, Bray, Ireland) can be incorporated into a gel, and after electrophoresis in e.g., Tris-HCl buffer (pH 7.4), the gel should be immersed in acetate buffer (0.2 M, pH 5.5) at 40°C to allow the enzyme to hydrolyze the pullulan and leave a yellow band on the red background. Amylopullulanase may also give a yellow band, but enzymes such as α-amylase, β-amylase, and α-glucosidase should have no effect on the red pullulan substrate.

A major problem in determining the activity of limit dextrinase in a plant extract is the possible presence of strong inhibitors. This has been demonstrated to be the case for germinated barley, for example, and it has been found that prolonged incubation (16 h) at 40°C in the presence of 25 mM dithiothreitol (30) or treatment overnight at 4°C with 5 mM ascorbic acid (42) is necessary to disrupt completely the inhibitor–limit dextrinase complex. If the complex is not destroyed, then any measure of limit dextrinase activity gives an underestimate of the amount of enzyme actually present.

VIII. PURIFICATION

Details of the method used for purification of a pullulanase/limit dextrinase depend on the source of the enzyme and the response of the enzyme to pH and temperature.

B. acidopullulyticus pullulanase, for example, can be purified from Promozyme (Novozymes North America, Inc., Franklinton, NC, U.S.A.), a commercially available source of the enzyme (10). After dialysis of Promozyme overnight against acetate buffer (50 mM, pH 5.0), the pullulanase can be precipitated by addition of cold acetone (−20°C) to a final concentration of 50% (v/v). The precipitate is collected by centrifugation at 10,000g for 30 min and dried in vacuo. The powder is dissolved in acetate buffer (20 mM, pH 5.0) and applied to a CM-Toyopearl 650 S column equilibrated with the same buffer. The enzyme is eluted with the acetate buffer containing a linear gradient of 0–0.5 M NaCl. Active fractions are pooled and concentrated, then applied to a Toyopearl HW-55S column equilibrated with acetate buffer (20 mM, pH 6.0) containing 0.8 M NaCl. Enzyme is eluted from the column using this buffer, and active fractions are pooled and concentrated, then dialyzed against phosphate buffer (20 mM, pH 7.0). Solid ammonium sulfate is added to 25% saturation, the precipitate is removed by centrifugation at 10,000g for 20 min, and the supernatant is applied to a Butyl Toyopearl 650 S

column equilibrated with phosphate buffer (20 mM, pH 7.0) containing ammonium sulfate at 25% saturation. The column is eluted with the same buffer using a linear gradient of 25% to 0% saturation of ammonium sulfate. Two active fractions are obtained from the column, but the properties of the two fractions are very similar, and apparently there is no gain in purity by use of the Butyl Toyopearl column (10). Yield of active enzyme decreases appreciably, however, when the latter column is used (10).

Barley limit dextrinase is most easily prepared from green malt, and two slightly different methods have been published (30, 42). In the procedure of MacGregor et al. (30), ground green malt is extracted with acetate buffer (0.1 M, pH 5.5) containing 25 mM dithiothreitol at 40°C for 16 h. The slurry is centrifuged at 9000g for 15 min and the supernatant collected. The pellet is re-extracted for 1 h at 40°C with buffer and recentrifuged, and the supernatants are combined. Limit dextrinase is precipitated overnight at 4°C by addition of ammonium sulfate to 80% saturation. The precipitate is obtained by centrifugation at 9000g for 15 min and dissolved in phosphate-citrate buffer (0.02 M, pH 6.0) containing 1 mM monothioglycerol. The solution is dialyzed at 4°C against the same buffer to remove ammonium sulfate and centrifuged at 8000g for 15 min, and the supernatant is filtered through glass wool. The dialyzed extract is then loaded onto a diethylaminoethyl cellulose ion exchange column (Whatman DE52) equilibrated with the phosphate-citrate buffer containing 1 mM monothioglycerol. The column is washed with this buffer until the absorbance of the eluate at 280 nm returns to baseline. The column is then eluted with the same buffer using a linear gradient of 0–0.5 M NaCl. Active fractions are pooled, concentrated, and dialyzed against acetate buffer (0.02 M, pH 5.5) containing 1 mM monothioglycerol. A β-cyclodextrin affinity column [Sepharose CL6B covalently linked to β-cyclodextrin (54)] is prepared and equilibrated with acetate buffer (0.02 M, pH 4.0) containing 1 mM monothioglycerol. The dialyzed enzyme solution is adjusted to pH 4.0 with acetic acid, centrifuged at 10,000g for 10 min, and loaded onto the affinity column. The column is washed with acetate buffer (0.02 M, pH 5.5) containing 1 mM monothioglycerol, and enzyme is eluted with the buffer using a linear gradient of 0–0.5 mg/mL β-cyclodextrin. Fractions are collected into tubes containing acetate buffer (0.02 M, pH 5.5) containing 1 mM monothioglycerol to minimize time spent by the enzyme at pH 4.0. Active fractions are pooled, concentrated, and dialyzed overnight at 4°C against the 0.02 M acetate buffer. The enzyme solution is then further concentrated and applied to a Sephacryl S-200 gel permeation column equilibrated with the same acetate buffer. The column is eluted with the buffer, and active enzyme fractions are pooled and concentrated. Typical recovery of protein and activity during the purification are given in Table 3.

In a second method (42), green malt flour is extracted with acetate buffer (0.2 M, pH 5.0) containing 5 mM ascorbic acid for 2–4 h at room temperature and allowed to settle overnight at 4°C. The supernatant is concentrated and ammonium sulfate is added to 20% saturation. The precipitate is discarded after centrifugation, and ammonium sulfate is added to the supernatant to 70% saturation. The precipitate is collected and dissolved in acetate buffer (50 mM, pH 5.0) containing 0.5 M $CaCl_2$. The solution is desalted by diafiltration and applied to a DEAE-Fractogel 650S column equilibrated in acetate buffer (20 mM, pH 5.0). The column is washed with this buffer and eluted using a linear gradient of 0–1 M NaCl. Active fractions are pooled and ammonium sulfate is added to 1.5–2 M. The solution is applied to a β-cyclodextrin Sepharose column equilibrated in

Table 3 Purification of Limit Dextrinase

Stage of purification	Total activity (mU)[a]	Total protein (mg)	Specific activity (mU/mg)	Purification (fold)
Extract	412,000	50,200	8.21	1
Ammonium sulfate precipitate	230,000	7,740	29.7	3.6
After ion exchange chromatography	161,000	144	1,120	136
After affinity chromatography	116,000	13.1	8,860	1080
After gel permeation chromatography	70,400	8.32	8,460	1030

[a] Activity was measured using Limit DextriZyme tablets and converted to glucose reducing power equivalents using a standard graph supplied with the substrate (see Sec. VII).

acetate buffer (50 mM, pH 5.0) containing 2 M ammonium sulfate. The column is washed with this buffer and then with acetate buffer without the ammonium sulfate until the absorbance of the eluate at 280 nm is < 0.05. Limit dextrinase is then eluted with the acetate buffer containing 7 mM β-cyclodextrin. Active enzyme fractions are pooled and applied to a DEAE-Fractogel 650S column in acetate buffer (20 mM, pH 5.5). The column is washed with the 20 mM acetate buffer, and enzyme is eluted using this buffer with a linear gradient of 0–0.5 M NaCl. Active fractions are pooled and may be stored at -18°C.

In each preparation, the initial presence of dithiothreitol or ascorbic acid is necessary to disrupt limit dextrinase–inhibitor complexes and release free, active limit dextrinase.

REFERENCES

1. DJ Manners. Observations on the specificity and nomenclature of starch debranching enzymes. J Appl Glycosci 44:83–85, 1997.
2. K Kainuma, S Kobayashi, T Harada. Action of *Pseudomonas* isoamylase on various branched oligo- and polysaccharides. Carbohydr Res 61:345–357, 1978.
3. DJ Manners. Debranching enzymes in plant tissues. Biochem Soc Trans 3:49–53, 1975.
4. Y Suzuki, K Hatagaki, H Oda. A hyperthermostable pullulanase produced by an extreme thermophile, *Bacillus flavocaldarius* KP 1228, and evidence for the proline theory of increasing protein thermostability. Appl Microbiol Biotechnol 34:707–714, 1991.
5. A Spreinat, G Antranikian. Purification and properties of a thermostable pullulanase from *Clostridium thermosulfurogenes* EM1 which hydrolyzes both α-1,6- and α-1,4-glycosidic linkages. Appl Microbiol Biotechnol 33:511–518, 1990.
6. AW MacGregor, LJ Macri, SL Bazin, GW Sadler. Limit dextrinase inhibitor in barley and malt and its possible role in malting and brewing. Proceedings of the 25th Congress, European Brewery Convention, Brussels, 1995, pp 185–192.
7. H Bender, K Wallenfels. Pullulan. II. Specific decomposition by a bacterial enzyme. Biochem Z 334:79–95, 1961.
8. I Orskov. Genus V. *Klebsiella* Trevisan 1885, 105^{AL}. In: NR Krieg, JG Holt, eds. Bergey's Manual of Systematic Bacteriology, Vol 1. Baltimore: Williams and Wilkins, 1984, pp 461–465.
9. R Ohba, S Ueda. Purification, crystallization and some properties of intracellular pullulanase from *Aerobacter aerogenes*. Agric Biol Chem 37:2821–2826, 1973.
10. S. Kusano, N Nagahata, S Takahashi, D Fujimoto, Y Sakano. Purification and properties of *Bacillus acidopullulyticus* pullulanase. Agric Biol Chem 52:2293–2298, 1988.
11. P Deweer, A Amory. Pullulanase producing microorganisms. U.S. patent 5817498 (1998).
12. R Koch, F Canganella, H Hippe, KD Jahnke, G Antranikian. Purification and properties of a thermostable pullulanase from a newly isolated thermophilic anaerobic bacterium, *Fervidobacterium pennavorans* Ven 5. Appl Environ Microbiol 63:1088–1094, 1997.
13. H Melasniemi. Characterization of α-amylase and pullulanase activities of *Clostridium thermohydrosulfuricum*. Biochem J 246:193–197, 1987.
14. AR Plant, RM Clemens, RM Daniel, HW Morgan. Purification and preliminary characterization of an extracellular pullulanase from *Thermoanaerobium* Tok6-B1. Appl Microbiol Biotechnol 26:427–433, 1987.
15. MJ Sissons, RCM Lance, DHB Sparrow. Studies on limit dextrinase in barley. 3. Limit dextrinase in developing kernels. J Cereal Sci 17:19–24, 1993.
16. SW Schroeder, AW MacGregor. Synthesis of limit dextrinase in germinated barley kernels and aleurone tissues. J Am Soc Brew Chem 56:32–37, 1998.
17. BF Jensen, BE Norman. *Bacillus acidopullulyticus* pullulanase: application and regulatory aspects for use in the food industry. Process Biochem 19:129–134, 1984.
18. WD Crabb, C. Mitchinson. Enzymes involved in the processing of starch to sugars. Trends Biotechnol 15:353–356, 1997.
19. JP Modderman, HH Foley. Safety evaluation of pullulanase enzyme preparation derived from *Bacillus licheniformis* containing the pullulanase gene from *Bacillus deramificans*. Regul Toxicol Pharmacol 21:375–381, 1995.
20. E Nebesny. Carbohydrate compositions and molecular structure of dextrins in enzymatic high maltose syrups. Starch 42:437–444, 1990.
21. AC Chakrabarti, KB Storey. Co-immobilization of amyloglucosidase and pullulanase for enhanced starch hydrolysis. Appl Microbiol Biotechnol 33:48–50, 1990.
22. L Furegon, ADB Peruffo, A Curioni. Immobilization of rice limit dextrinase on γ-alumina beads and its possible use in starch processing. Process Biochem 32:113–120, 1997.
23. DY Schafhauser, KB Story. Co-immobilization of amyloglucosidase and pullulanase onto granular chicken bone for enhanced starch degradation. Biotechnol Appl Biochem 17:103–113, 1993.
24. DK Yim, YH Park, YH Park. Production of branched cyclodextrins by reverse reaction of microbial debranching enzymes. Starch 49:75–78, 1997.

25. N Watanabe, K Yamamoto, W Tsuzuki, T Oya, S Kobayashi. A novel method to produce branched α-cyclodextrins: pullulanase-glucoamylase-mixed method. J Ferment Bioeng 83:43–47, 1997.
26. BS Enevoldsen. Degradation of starch by amylases in beer brewing. J Jpn Soc Starch Sci 25:89–99, 1978.
27. E Vinogradov, K Bock. Structural determination of some new oligosaccharides and analysis of the branching pattern of isomaltooligosaccharides from beer. Carbohydr Res 309:54–64, 1998.
28. AW MacGregor, SL Bazin, LJ Macri, JC Babb. Modelling the contribution of alpha-amylase, beta-amylase and limit dextrinase to starch degradation during mashing. J Cereal Sci 29:161–169, 1999.
29. IC Willox, SR Rader, JM Riolo, H Stern. The addition of starch debranching enzymes to mashing and fermentation and their influence on attenuation. MBAA Tech Q 14:105–110, 1977.
30. AW MacGregor, LJ Macri, SW Schroeder, SL Bazin. Limit dextrinase from malted barley: extraction, purification and characterization. Cereal Chem 71:610–617, 1994.
31. RA Burton, X Zhang, M Hrmova, GB Fincher. A single limit dextrinase gene is expressed both in the developing endosperm and in germinated grains of barley. Plant Physiol 119:859–871, 1999.
32. M Kristensen, F Lok, V Planchot, I Svendsen, R Leah, B Svensson. Isolation and characterization of the gene encoding the starch debranching enzyme limit dextrinase from germinating barley. Biochim Biophys Acta 1431:538–546, 1999.
33. B Henrissat. A classification of glycosyl hydrolases based on amino acid sequence similarities. Biochem J 280:309–316, 1991.
34. AP Kelly, B Diderichsen, S Jorgensen, DJ McConnell. Molecular genetic analysis of the pullulanase B gene of *Bacillus acidopullulyticus*. FEMS Microbiol Lett 115:97–106, 1994.
35. HM Jespersen, EA MacGregor, B Henrissat, MR Sierks, B Svensson. Starch- and glycogen-debranching and branching enzymes: prediction of structural features of the catalytic $(\beta/\alpha)_8$-barrel domain and evolutionary relationship to other amylolytic enzymes. J Protein Chem 12:791–805, 1993.
36. Y Katsuya, Y Mezaki, M Kubota, Y Matsuura. Three-dimensional structure of *Pseudomonas* isoamylase at 2.2 Å resolution. J Mol Biol 281:885–897, 1998.
37. HM Jespersen, EA MacGregor, MR Sierks, B Svensson. Comparison of the domain-level organization of starch hydrolases and related enzymes. Biochem J 280:51–55, 1991.
38. S Janecek. α-Amylase family: molecular biology and evolution. Prog Biophys Mol Biol 67:67–97, 1997.
39. H Melasniemi, M Paloheimo, L Hemio. Nucleotide sequence of the α-amylase-pullulanase gene from *Clostridium thermohydrosulfuricum*. J Gen Microbiol 136:447–454, 1990.
40. AP Pugsley, C Chapon, M Schwartz. Extracellular pullulanase of *Klebsiella pneumoniae* is a lipoprotein. J Bacteriol 166:1083–1088, 1986.
41. LJ Macri, AW MacGregor, SW Schroeder, SL Bazin. Detection of a limit dextrinase inhibitor in barley. J Cereal Sci 18:103–106, 1993.
42. M Kristensen, V Planchot, J Abe, B Svensson. Large-scale purification and characterization of barley limit dextrinase, a member of the α-amylase structural family. Cereal Chem 75:473–479, 1998.
43. CJ Brandt, BJ Catley, WM Awad. Extracellular and protease-released pullulanases. J Bacteriol 125:501–508, 1976.
44. H Iwamoto, M Ohmori, M Ohno, J Hirose, K Hiromi, H Fukada, K Takahashi, H Hashimoto, S Sakai. Interaction between pullulanase from *Klebsiella pneumoniae* and cyclodextrins. J Biochem (Tokyo) 113:93–96, 1993.
45. DJ Manners, KL Rowe. Studies on carbohydrate-metabolizing enzymes. Part XXV. The debranching enzyme system in germinated barley. J Inst Brew 77:358–365, 1971.
46. I Maeda, N Jimi, H Taniguchi, M Nakamura. Purification of R-enzyme from malted barley and its role in in vitro digestion of barley starch granules. J Jpn Soc Starch Sci 26:117–127, 1979.
47. K Sjoholm, AW MacGregor, L Macri. Is there a role for limit dextrinase in mashing? Proceedings of the 25th Congress, European Brewery Convention, Brussels, 1995, pp 277–284.
48. R Ohba, S Ueda. Some properties of crystalline extra- and intra-cellular pullulanases from *Aerobacter aerogenes*. Agric Biol Chem 39:967–972, 1975.
49. N Shiomi, J Yamada. α-Anomeric configuration of the saccharides produced by the action of debranching enzymes on glycogen and pullulan. Carbohydr Res 111:175–179, 1982.
50. BV McCleary. Measurement of the content of limit-dextrinase in cereal flours. Carbohydr Res 227:257–268, 1992.
51. M Sömogyi. Notes on sugar determination. J Biol Chem 195:19–23, 1952.
52. AW MacGregor, SL Bazin, SW Schroeder. Effect of starch hydrolysis products on the determination of limit dextrinase and limit dextrinase inhibitors in barley and malt. J Cereal Sci 35:17–28, 2002.
53. L Furegon, A Curioni, ADP Peruffo. Direct detection of pullulanase activity in electrophoretic polyacrylamide gels. Anal Biochem 221:200–201, 1994.
54. MP Silvanovich, RD Hill. Affinity chromatography of cereal α-amylase. Anal Biochem 73:430–433, 1976.

60

Limit Dextrinase

James Hutchison Bryce
Heriot-Watt University, Edinburgh, Scotland

I. INTRODUCTION

My aim is to provide an outline of the reactions of limit dextrinase and consider how our present knowledge about limit dextrinase will affect its use during the processing of starch in the food industry. My focus will be upon the effect of limit dextrinase in the production of alcoholic beverages from malted barley. However, my comments are relevant to anybody involved in processing starch from any cereal to produce alcoholic beverages or syrups. Furthermore, an understanding of the properties and regulation of limit dextrinase is essential to any project where the aim is to produce a genetically modified organism with altered limit dextrinase activity.

A plant with genetically modified limit dextrinase activity may have altered starch degradation and/or modified starch synthesis. Such genetically modified plants would be an important source of material for studying starch metabolism. Also, such plants have the potential to be the breeding material for new varieties of crops which could produce products with improved yields or processing properties.

Limit dextrinase (α-1,6-glucanohydrolase, EC 3.2.1.142) is a debranching enzyme which selectively catalyzes the hydrolysis of α-1,6-glucosidic linkages and has no action on α-1,4-glucosidic linkages (1). Limit dextrinase is the name commonly used for the debranching enzyme derived from plants, whereas the bacterial enzyme is known as pullulanase (EC 3.2.1.41). Both these enzymes degrade pullulan, amylopectin, and α-1,6-glucosidic bonds in branched dextrins derived from amylopectin (2). The structures of pullulan and amylopectin are shown in Figure 1.

II. IMPORTANCE TO QUALITY AND EFFICIENCY OF ALCOHOLIC BEVERAGE PRODUCTION

Limit dextrinase is necessary for complete starch breakdown because starch consists not only of amylose, linear chains of glucose, but also of amylopectin, which contains $\sim$ 4–5% of α-1,6-glucosidic linkages (3). The precise proportion of amylose to amylopectin varies with the source of the starch, but generally is in the range of 20–30% for normal cereal starches (4).

In processing cereals to produce alcoholic beverages, a wort is normally produced by mixing the ground cereal with hot water ($\sim 65^{\circ}$C) for at least 1 h. The temperature is selected to achieve gelatinization of starch granules while maintaining, at least briefly, some activity of the hydrolytic enzymes that will degrade carbohydrate and protein (5). In a wort produced entirely from malted barley, a typical carbohydrate profile following starch degradation is 75% glucose, maltose, and maltotriose, and 25% dextrins, about half of which have multiple branches (6, 7).

Limit dextrinase activity, or indeed lack of activity, is of fundamental importance in the production of wort from cereals in the brewing and distilling industries. Dextrins with α-1,6-glucosidic bonds are not fer-

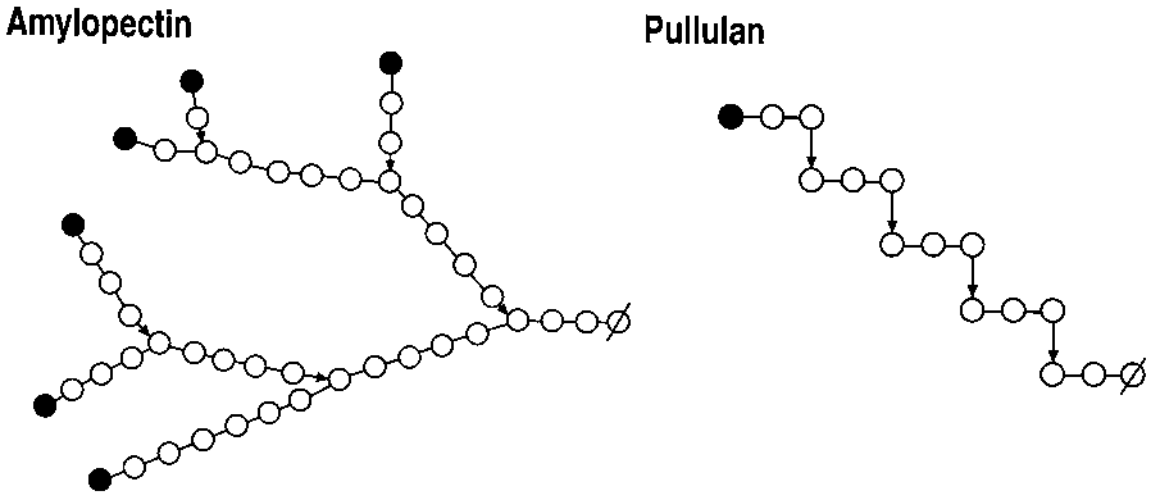

Figure 1 Representations of the structures of amylopectin and pullulan. Circular symbols denote glucose residues. A line (—) denotes an α-1,4-glucosidic bond, and line with an arrow (→) denotes an α-1,6-glucosidic bond. All glucose residues are linked via their hemiacetyl hydroxyl groups at carbon 1 except for the residues shown with a diagonal line through them (∅) (the reducing end of each molecule). The residues shown in black contain hydroxyl groups at carbon 4 which are not linked to other residues.

mented by yeast, except in the rare cases of yeast strains that secrete enzymes capable of hydrolyzing α-1,6-glucosidic bonds. Normally, therefore, if branched dextrins are present in brewer's wort, they will be found in the final beer. In beer, dextrins contribute to calorific value and may also impart fullness or body (8). In contrast, during fermentation of distiller's wort, dextrin degradation may continue because the wort is not boiled and therefore malt enzymes that survive mashing temperatures can remain active. However, dextrins remaining after fermentation will contribute nothing to the new make distilled spirit. Therefore, the requirements for limit dextrinase activity differ between brewers and distillers. A brewer may desire only limited activity of limit dextrinase to ensure that adequate fermentable sugars are produced during mashing (but sufficient branched dextrins remain), whereas a distiller would wish for complete hydrolysis of α-1,6-glucosidic bonds so that the greatest possible amount of fermentable sugar is available to yeast (9).

III. PROPERTIES OF LIMIT DEXTRINASE PROTEIN

The properties of limit dextrinase have been thoroughly reviewed by Stenholm (10). In summary, the enzyme from malted barley is reported to have a molecular weight of 103–105 kDa with a pH optimum of 5.0–5.5 (5.5–6.5 in the presence of bovine serum albumin [BSA]). The pI values reported in the literature vary from 4.2 to 4.6.

The gene-encoding limit dextrinase has been isolated (11). In an independent study, the cDNA isolated by Burton et al. (11) has been used to show that there is only one limit dextrinase gene in barley and that the gene is located on the long arm of chromosome 4H, where it has now been mapped [C-D Li, X-Q Zhang, RCM Lance, LC MacLeod, GB Fincher, P Langridge, unpublished data; cited by Burton et al. (11)].

Molecular techniques have been used to establish a clear distinction between strictly α-1,6-specific debranching enzymes, such as limit dextrinase, and dual-bond type enzymes that attack α-1,4-glucosidic and α-1,6-glucosidic bonds (12).

When amino acid sequences of debranching enzymes were examined for phylogenic relatedness using the PileUp program (13), two distinct groups were distinguished (11). Debranching enzymes that attacked pullulan were grouped together, whereas the isoamylase type fell into a second group.

Partial amino acid sequence analysis provides evidence that barley limit dextrinase belongs to the α-amylase family of multidomain amylolytic enzymes with a characteristic $(\beta/\alpha)_8$-barrel catalytic domain (12, 14, 15).

IV. SUBSTRATES, SPECIFICITY, AND ROLE OF DEBRANCHING ENZYME IN BARLEY

The specificity and nomenclature of debranching enzymes have been clarified by Manners (16). Enzymes formerly classified as EC 3.2.1.41 included limit dextrinase (from plants) which does not act on glycogen, and pullulanase of microbial origin which attacks both amylopectin and glycogen. "Isoamylase" enzymes (EC 3.2.1.68) hydrolyze interchain linkages in glycogen, amylopectin, and certain derived dextrins, but have no action on pullulan.

Barley limit dextrinase has ~50% and 85% sequence identity to bacterial pullulanases and rice starch debranching enzyme, respectively (17). This sequence similarity between barley limit dextrinase and bacterial pullulanases and the similarity of their action (18–21) added weight to the appropriateness of the former classification of barley limit dextrinase with pullulanases (EC 3.2.1.41).

It was believed in the early 1970s that there were two plant debranching enzymes, limit dextrinase and R-enzyme. R-enzyme has been found to act on amylopectin and its β-limit dextrin, and to act on α-dextrins from both amylopectin and glycogen, but it did not act on undegraded glycogen. Thus, the substrates of limit dextrinase and R-enzyme are identical. Indeed, it is now well established that limit dextrinase and R-enzyme are the same enzymes, and the name limit dextrinase is preferred since this name relates to its natural substrate (16). In the context of starch breakdown to fermentable sugars, it is important to note that the smallest substrate for limit dextrinase is 6^2-α-maltosyl-maltose (Fig. 2) (20). Limit dextrinase requires at least one α-1,4-glucosidic bond on either side of the α-1,6-glucosidic bond if it is to hydrolyze the α-1,6-bond.

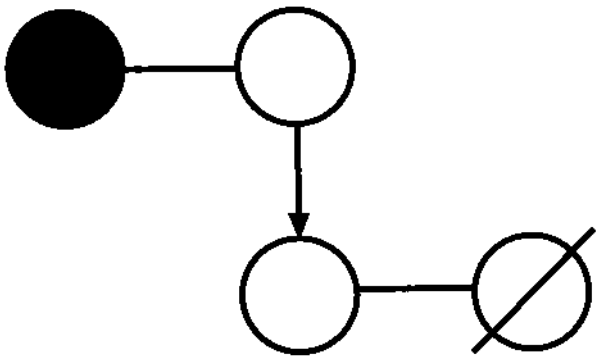

Figure 2 Structure of 6^2-α-maltosyl-maltose. (Symbols are as for Figure 1.)

The question arises as to why enzymes formerly classified as EC 3.2.1.41 should have had two names, limit dextrinase (EC 3.2.1.142) (from plants) and pullulanase (EC 3.2.1.41) (from microbes). Manners (16) suggested that the two different names were appropriate because pullulanase is capable of attacking both amylopectin and glycogen whereas limit dextrinase has very limited activity, if any, with glycogen. Furthermore, the nomen- clature maintained the subgroups of enzymes that attack pullulan in different ways, namely pullulanase that produces maltotriose, and isopullulanase and neopullulanase that act on α-1,4-linkages to produce isopanose (22) and panose (23), respectively. However, a distinction has now been drawn between these enzymes with their allocation of separate EC numbers.

Although the debranching enzyme from germinating barley grain falls into the pullulanase group of debranching enzymes; it should be emphasized that the natural substrates of the enzyme are amylopectin or oligomeric limit dextrins rather than pullulan. In vivo, the debranched oligosaccharides are susceptible to further hydrolysis by amylases and α-glucosidases (24).

In addition to a role in hydrolysis of starch degradation products during germination, limit dextrinase has been implicated in starch synthesis where it is proposed that an appropriate balance between branching and debranching enzymes is required to achieve the final degree of branching in amylopectin (25–30). Furthermore, a debranching enzyme would also be capable of producing primers for the starch synthase reaction (31), a function that could explain the presence of limit dextrinase in developing rice grain (32).

Burton et al. (11) have obtained mRNA encoding barley limit dextrinase from overlapping cDNA clones from PCR amplification. The cDNA sequence has an open reading frame that encodes a putative transit peptide of 78 amino acid residues and a mature polypeptide of 884 amino acid residues. The calculated molecular weight of the mature polypeptide is 97.4 kDa and the calculated pI is 5.0 (assuming all the acidic and basic groups are on the surface in the tertiary structure). These are values comparable to the molecular weight of 105 kDa and pI values of 4.2–4.6 reported for purified limit dextrinase (17, 33, 34). The discrepancy between the deduced and measured values of molecular weight could be due to glycosylation of the enzyme; seven potential N-glycosylation sites are present in the deduced amino acid sequence.

A number of features relating to the function of the gene stand out. First, limit dextrinase mRNA is abun-

dant in gibberellic acid (GA)-treated aleurone layers and in germinated grain. Furthermore, abscisic acid (ABA) abolishes the GA induction of limit dextrinase mRNA in isolated aleurone cells. This would be expected since ABA often acts as an antagonist to GA in plant tissues. These observations would tend to confirm that limit dextrinase should participate in starch degradation during endosperm mobilization in germinating grains. However, if this is so, then it would be expected that limit dextrinase would carry a signal peptide to target the nascent polypeptide to the endoplasmic reticulum for eventual secretion from the aleurone to the endosperm. No such signal peptide has been identified (11). Therefore, since there is no evidence that aleurone cells become leaky to metabolites as they senesce, the mechanism of limit dextrinase release into the endosperm, if it does occur, remains to be established.

The question of the potential role of limit dextrinase in starch synthesis also arises. Low levels of limit dextrinase mRNA were detected in the developing endosperm of barley until ~ 20 days post anthesis (DPA), after which time the levels rapidly declined. Limit dextrinase activity was detected in the developing grain. This expression pattern corresponds closely to the timing of starch synthesis in developing barley grains, although the precise timing in any give grain is dependent to some extent on growth temperatures (35).

Starch synthesis occurs in an organelle known as an amyloplast and limit dextrinase has a presequence typical of transit peptides that target nascent polypeptides to amyloplasts (11). In the developing endosperm of barley, limit dextrinase is thus targeted to the organelle in cells whose primary role is to synthesize starch and is expressed at a time coinciding with starch synthesis. This suggests a role for limit dextrinase in starch synthesis in the developing endosperm.

While the above molecular evidence points to a role for limit dextrinase in starch synthesis, the biochemical evidence is much less convincing. In the model of amylopectin biosynthesis involving debranching enzyme activity (28), it is proposed that there is intensive branching generating phytoglycogenlike structures. These structures are then trimmed by debranching enzymes. This requires very precise regulation of the activities of the enzymes involved. The lack of evidence for such precise regulation of these enzymes, plus the lack of limit dextrinase activity with phytoglycogen (16), means that a role of limit dextrinase in starch synthesis is as yet unresolved.

V. MEASUREMENT OF LIMIT DEXTRINASE ACTIVITY

A. Assay

The extraction and measurement of limit dextrinase have advanced recently with analytical procedures employing pullulan reacted with dye molecules (36, 37). The sensitivity of these methods is better than that of methods based on measurement of reducing sugars (10). Two commercial products, Red-Pullulan (soluble Reactive Red 120-labeled pullulan, Megazyme Ltd) and Limit DextriZyme tablets (insoluble cross-linked azurine-pullulan, Megazyme Ltd), are now widely used for assay of limit dextrinase activity in barley and malt extracts. The Limit-DextriZyme tablets have the advantage of greater sensitivity (10- to 15-fold), lower blank values, greater ease of use, and greater stability than Red-Pullulan (37).

There are other potential methods for the measurement of limit dextrinase. Sissons et al. (38) developed a rapid enzyme-linked immunosorbant assay (ELISA) for measuring limit dextrinase. The assay was supposed to be specific and sensitive and to recognize the active enzyme, but values do not correlate with the Red Pullulan assay (10).

Earlier assays were based on the measurement of maltotriose released from pullulan by limit dextrinase (24, 39). The drawback of this procedure was the production of additional reducing groups if the sample to be analyzed contained α-glucosidase. Thus, for crude extracts containing endogenous α-glucosidase, Lee and Pyler (40) developed a two-step assay method in which the limit dextrinase reaction products from pullulan were hydrolyzed to glucose by added yeast α-glucosidase, and the glucose was then assayed. Problems with this approach included (a) the fact that α-glucosidase does not hydrolyze the higher oligosaccharides, which are initial hydrolysis products of pullulan (37), and (b) the requirement to remove endogenous reducing sugars by dialysis (41).

B. Extraction

From the foregoing discussion, it should be evident that while the assay of limit dextrinase can be difficult, the use of dyed pullulan has been a significant advance. However, just as important as assaying the enzyme correctly is the correct extraction of the enzyme. It is thought that in vivo in germinating barley, the enzyme exists in three forms—bound and inactive, soluble and active (known as "free"), and soluble and inactive (42,

43). Furthermore, limit dextrinase inhibitors have been detected in barley grain extracts (44). While barley grains at maturity have a high level of limit dextrinase inhibitor, the level is lower in wheat, and the inhibitor is absent in rice and maize (45). All these factors complicate the interpretation of limit dextrinase activity measurements. However, it is currently believed that the "total" activity of limit dextrinase in germinating barley grain can be determined by extraction for 5 h with a reducing agent, whereas extraction for 5 h without a reducing agent provides a measure of the "free" activity (soluble and active).

C. Properties

1. Inhibitors and Activators

The effect of inhibitors and activators of limit dextrinase is reviewed by Stenholm (10). One potentially important feature to emerge is the inhibition of rice limit dextrinase by maltose, maltotriose, and a number of small maltosaccharides. This suggests that rice limit dextrinase contains binding sites for at least two, and probably more, adjacent α-1,4-linked glucose residues (19). If barley limit dextrinase were inhibited by these low-molecular-weight oligosaccharides during mashing in the brewing process, then it could reduce the conversion of nonfermentable branched dextrins to fermentable sugars.

Cyclodextrins inhibit limit dextrinase, with β-cyclodextrin being very significantly more inhibitory than α-cyclodextrin or γ-cyclodextrin (21, 34, 46, 47). Purified limit dextrinase (200 mU/mL) was inhibited 50% by 75 μg/mL β-cyclodextrin (34). All three cyclodextrins are competitive inhibitors of limit dextrinase.

The properties of limit dextrinase differ significantly from those of α-amylase. There is no effect of Ca^{2+} (1–100 mM) on activity and EDTA (10 mM) causes only a 15% decrease in activity. Also, the pseudo-tetrasachharide acarbose, a potent inhibitor of α-1,4-specific amylolytic enzymes such as α-amylase and glucoamylase, reduces the activity of limit dextrinase by only 30% at a high concentration of 10 mM (34).

2. Temperature Stability

In the past, there have been major differences in the reported heat stability of limit dextrinase (10). If limit dextrinase is to be active in mashing, then it must survive kilning of the grain where temperatures will normally exceed 60°C and may even exceed 80°C—for example, if an ale malt is being produced. At present, it is generally agreed that barley limit dextrinase has thermostability properties during kilning that are intermediate between α-amylase (heat stable) and β-glucanase (relatively heat labile and inactivated by kilning) (37). However, whereas in the past it was thought that limit dextrinase was denatured during mashing, there is now good evidence that limit dextrinase survives mashing temperatures of 63–65°C.

3. Measurement in Crude Extracts

The measurement of limit dextrinase is most simply done by determining the "total" activity of the enzyme (extraction with a reducing agent) and activity of the "free" enzyme (extraction without a reducing agent). In the recommended procedures, limit dextrinase is extracted from ground grain for 5 h at 40°C in 0.1–0.2 M NaOAc (pH 5.0–5.5). This extracts the "free" enzyme (soluble-active) (37), whereas "total" activity is obtained after similar extraction with a reducing agent, e.g., 25 mM dithiothreitol (DTT). Soluble-inactive enzyme is the total activity minus the free activity. Excessive extraction of limit dextrinase in the presence of DTT can start to lead to a decline in the apparent total activity of limit dextrinase, a decline that is probably due to the activation of nonspecific proteases that start to degrade limit dextrinase.

Sjöholm et al. (48) measured limit dextrinase activity during mashing. In a 1 h mash, limit dextrinase activity remained stable at 60°C, declined by 55% at 62.5°C, and declined by 65% at 65°C. Limit dextrinase was only fully inactivated in 1 h by temperatures > 65°C. Similar evidence for the stability of limit dextrinase at mashing temperatures was obtained by MacGregor et al. (45) and Bryce et al. (49). Furthermore, when MacGregor et al. (45) collected samples mashed at 63°C and incubated the sample supernatants at 40°C with 25 mM DTT (dithioltreitol) the measured activity of limit dextrinase increased dramatically. This shows that a large portion of the limit dextrinase in the malt was solubilized during mashing but had remained in the wort as inactive enzyme.

In some of the experiments just described (45, 48, 49), samples were taken directly from wort for measurement of limit dextrinase activity using dyed pullulan as substrate. The aim of this was to provide a measure of limit dextrinase activity in the wort rather than its potential activity. MacGregor et al. (45) were able to obtain much higher activities when the sample was extracted with DTT prior to assay. This makes an important point; if limit dextrinase is to be assayed, the researcher must decide whether to determine the activ-

ity present or the potential "free" or "total" activity. Potential free activity would be that obtained by further extraction in the absence of a reducing agent.

Furthermore, the presence of limit dextrinase inhibitor in certain cereals means that in any process to which limit dextrinase or pullulanase is being added, it is necessary to determine whether or not the enzyme will be inhibited upon addition to the process. Bryce et al. (49) produced a lactic malt with a "free" limit dextrinase activity of 800 mU/g. A recombination experiment was carried out in which an extract from this malt with high free activity was mixed with an equal proportion of a more typical malt where a high percentage of limit dextrinase is in the soluble but inactive form. The result was an inhibition of the free limit dextrinase from the lactic malt $> 50\%$. This shows that the typical malt contains inhibitor capable of inhibiting free limit dextrinase. It also suggests that supposedly free activity in malt could be activity of the soluble and "inactive" enzyme. However, pullulanase from *Bacillus acidopullulyticus* (Promozyme 200 L, Novo Nordisk, Denmark) was not inhibited by malt extracts (49). Therefore, it appears that pullulanase is not inhibited by limit dextrinase inhibitor.

McCafferty and Bryce (unpublished) have found activities of limit dextrinase from malted barley substantially higher than those of "free" limit dextrinase by rapid extraction (a few minutes) and assay at pH 4.4. Therefore, any analysis of limit dextrinase activities of crude extracts should be accompanied by careful checking of the optimum pH and time for extraction and assay.

4. Measurement of Purified Enzyme Activity

A further factor that should be taken into account in assaying limit dextrinase is the presence of protein. BSA (0.05 mg/mL) increased the activity of purified limit dextrinase threefold (34). This stabilization or activation effect was not specific to BSA; proteins from crude barley extracts had the same effect of boosting the activity of purified limit dextrinase (provided endogenous inhibitor was first removed from the extracts). To avoid any apparent loss of activity of limit dextrinase following purification 0.5 mg/mL BSA was added routinely to assay buffers to overcome any effects that could arise owing to variable protein levels (34).

5. Measurement in Food and Food Processing—Summary

From the above discussion, it should be apparent that there is an incomplete understanding of how limit dextrinase activity is regulated. However, present knowledge should make it possible to measure limit dextrinase activity and how it changes either during the processing of food, for example, cereal grains or following the production of genetically modified plants with altered limit dextrinase expression.

6. Extraction and Purification of Limit Dextrinase

The key to extraction of limit dextrinase from germinating barley is to do it in the presence of a reducing agent such as DTT; also, if a good yield of enzyme is desirable, it should be done after at least 8–10 days of germination. There is evidence that sulfhydryl proteases, activated by a reducing agent, are necessary during extraction to activate limit dextrinase solubilized from germinating barley grains (50), and such proteases are also necessary to solubilize bound limit dextrinase associated with the insoluble fraction of germinating barley grains (43).

The extraction process should also aim to minimize the effect of heat-stable endogenous inhibitor(s) of $\sim$ 15 kDa (44) that are reported to form soluble but inactive complexes with limit dextrinase (51). Two factors could reduce the effect of these inhibitors. First, activity of sulfhydryl proteases could "upset" the enzyme–inhibitor complex, and second, an extended period of germination could lead to breakdown of the inhibitor. MacGregor et al. (45) showed a very low level of inhibitor to be present after 6 days of germination. The problem of the inhibitor will only occur in extracts from cereal grains of barley, triticale, durum, wheat, and oats, since the inhibitor has been detected in these grains. The inhibitor has not been detected in rice, sorghum, millet, or maize.

Homogeneous barley limit dextrinase has been isolated on a large scale with a yield of 9 mg/kg from 10-day germinated green (unkilned) malt (17). This represented a 9400-fold purification with a 29% recovery of activity compared to that of a flour extracted in 0.2 M NaOAc (pH 5.0) containing 5 mM ascorbic acid. The purification protocol consisted of precipitation of limit dextrinase from an extract at 20–70% saturated ammonium sulfate (AMS), followed by diethylaminoethyl (DEAE) 650S Fractogel anion exchange chromatography, and affinity chromatography on β-cyclodextrin-Sepharose in the presence of 2 M AMS. Limit dextrinase was eluted by 7 mM β-cyclodextrin and contained a single polypeptide chain of 105 kDa (SDS-PAGE) and pI of 4.3.

MacGregor et al. (34) purified limit dextrinase by extraction of grist in 0.1 M NaOAc, pH 5.5 at 40°C for 16 h with 25 mM DTT, followed by ammonium sulfate precipitation, and chromatography on ion exchange (DEAE, pH 6.0), affinity (β-cyclodextrin Sepharose with pH 4.0 for loading and pH 5.5 for elution), and gel filtration (Sephacryl S-200, pH 5.5) columns. The enzyme had high specific activity, was homogeneous, and gave single bands of protein when examined by SDS-PAGE ($\sim$ 105 kDa) and IEF (pI 4.6).

Binding of limit dextrinase to the β-cyclodextrin column was improved in two ways. First, the affinity column was equilibrated to pH 4.0, and the pH of the DEAE purified pool was adjusted to pH 4.0 just before loading to the column. Seventy percent of the limit dextrinase applied to the column was recovered in the postaffinity pool. This degree of binding was similar to that reported by Maeda et al. (52) but higher than that reported by researchers who used a higher pH (5.5 or 6.0) for β-cyclodextrin columns (33, 43, 53). Limit dextrinase activity is lost quickly at pH 4.0; therefore it was necessary to bring the pH of the eluted enzyme back to pH 5.5 as quickly as possible by collecting column effluent into tubes containing a small volume of strong pH 5.5 buffer.

Binding of limit dextrins to the affinity column was also improved by first removing from the preparation, by DEAE chromatography, other β-cyclodextrin-binding enzymes, such as α-amylase. α-Amylase binds to β-cyclodextrin columns much more tightly than limit dextrinase (53), and would be eluted after limit dextrinase in the β-cyclodextrin gradient.

Limit dextrinase was eluted from the column by a low concentration of β-cyclodextrin. This step achieved a large increase in the specific activity of the enzyme, confirming the effectiveness of an appropriate affinity chromatography method of protein purification. Gel permeation chromatography on Sephacryl S-200 was used as the final step in the purification of the enzyme to remove β-cyclodextrin, as well as a small amount of a low-molecular-weight contaminant.

REFERENCES

1. DJ Manners. Some aspects on the metabolism of starch. Cereal Foods World 30:722–727, 1985.
2. BS Enevoldsen. Debranching enzymes in brewing. Proceedings of 15th Congress, European Brewery Convention, Zoeterwounde, 1975, pp 683–697.
3. DJ Manners. Starch degradation during malting and mashing. Brew Dig 49:56–62, 1974.
4. DJ Manners. Some aspects on the structure of starch. Cereal Foods World 30:461–467, 1985.
5. MJ Lewis, TW Young. Brewing. New York: Chapman and Hall, 1995.
6. BS Enevoldsen, F Schmidt. Dextrins in brewing. II. Distribution of oligo- and megalosaccharides during mashing, in wort and beer. Proceedings of 14th Congress, European Brewery Convention, Salzburg. Amsterdam: Elsevier Scientific, 1974, pp 135–148.
7. BS Enevoldsen, F Schmidt. Dextrins in brewing. Studies on singly-branched and multiply-branched dextrins in brewing. J Inst Brew 80:520–533, 1974.
8. CW Bamforth. Beer. Tap into the Art and Science of Brewing. London: Plenum Press, 1998.
9. GN Bathgate. Cereals in Scotch whisky production. In: GH Palmer, ed. Cereal Science and Technology. Aberdeen: Aberdeen University Press, 1989, pp 243–278.
10. K Stenholm. Malt Limit Dextrinase and Its Importance in Brewing. Espoo, Julkaisija-Utgivare, Finland: VTT Publication 323, Technical Research Centre of Finland, 1997.
11. R Burton, X-Q Zhang, M Hrmova, GB Fincher. A single limit dextrinase gene is expressed both in the developing endosperm and in germinated grains of barley. Plant Physiol 119:859-871, 1999.
12. HM Jespersen, EA MacGregor, B Henrissat, MR Sierks, B Svensson. Starch- and glycogen-debranching and branching enzymes. Prediction and structural features of the catalytic $(\beta/\alpha)_8$-barrel domain and evolutionary relationships to other amylolytic enzymes. J Prot Chem 12:791–805, 1993.
13. J Devereux, P Haeberli, O Smithies. A comprehensive set of sequence analysis programs for the VAX. Nucleic Acids Res 12:387–395, 1984.
14. HM Jespersen, EA MacGregor, MR Sierks, B Svensson. Comparison of the domain level organization of starch hydrolases and related enzymes. Biochem J 280:51–55, 1991.
15. B Svensson. Protein engineering in the α-amylase family: catalytic mechanism, substrate specificity, and stability. Plant Mol Biol 25:141–157, 1994.
16. DJ Manners. Observations on the specificity and nomenclature of starch debranching enzymes. J Appl Glycosci 44:83–85, 1997.
17. M Kristensen, V Planchot, J-I Abe, B Svensson. Large-scale purification and characterization of barley limit dextrinase, a member of the α-amylase structural family. Cereal Chem 75:473–479, 1998.
18. DG Hardie. Control of carbohydrase formation by gibberellic acid in barley endosperm. Phytochemistry 14:1719–1722, 1975.
19. G Dunn, DG Manners. The limit dextrinase from ungerminated oats (*Avena saltiva* L) and ungermi-

nated rice (*Oryzae sativa* L). Carbohydr Res 39:283–293, 1975.
20. I Maeda, N Jimi, H Taniguchi, M Nakamura. Purification of R-enzyme from malted barley and its role in in vitro digestion of barley starch granules. J Jpn Soc Starch Sci 26:117–127, 1979.
21. D Yellowlees. Purification and characterization of limit dextrinase from *Pisum sativum* L. Carbohydr Res 83:109–118, 1980.
22. Y Sakano, N Masuda, T Kobayashi. Hydrolysis of pullulan by a novel enzyme from *Aspergillus niger*. Agric Biol Chem 35:971–973, 1971.
23. T Kuriki, S Okada, T Imanaka. New type of pullulanase from *Bacillus stearothermophilus* and molecular cloning and expression of the gene in *Bacillus subtilis*. J Bacteriol 170:1554–1559, 1988.
24. EY Lee, JJ Marshall, WJ Whelan. The substrate specificity of amylopectin-debranching enzymes from sweet corn. Arch Biochem Biophys 143:365–374, 1971.
25. D Pan, OE Nelson. A debranching enzyme deficiency in endosperm of the sugary-1 mutants of maize (*Zea mays*). Plant Physiol 74:324–328, 1984.
26. MG James, DS Robertson, AM Meyers. Characterization of the *sugary*-1, a determinant of starch composition in kernels. Plant Cell 7:417–429, 1995.
27. C Martin, AM Smith. Starch synthesis. Plant Cell 7:971–985, 1995.
28. S Ball, H-P Guan, M James, A Myers, P Keeling, G Mouille, A Buleon, P Colonna, J Preiss. From glycogen to amylopectin: a model for the biogenesis of the plant starch granule. Cell 86:349–352, 1996.
29. Y Nakamura, A Kubo, T Shimamune, T Matsuda, K Harada, H Satoh. Correlation between activities of starch debranching enzyme and alpha-polyglucan structure in endosperms of *sugary*-1, mutants of rice. Plant J 12:143–153, 1997.
30. A Rahman, K Wong, J Jane, AM Myers, MG James. Characterization of SU1 isoamylase, a determinant of storage starch structure in maize. Plant Physiol 117:425–435, 1998.
31. CM Duffus, MP Cochrane. Development, structure and composition of the barley kernel. In: AW MacGregor, RS Bhatty, eds. Barley: Chemistry and Technology. St Paul, MN: American Association of Cereal Chemists, 1993, pp 31–72.
32. Y Nakamura, T Umemoto, N Ogata, Y Kuboki, M Yano, T Sasaki. Starch debranching enzyme (R-enzyme or pullulanase) from developing rice endosperm: purification, cDNA and chromosomal localization of the gene. Planta 199:209–218, 1996.
33. MJ Sissons, RCM Lance, DHB Sparrow. Studies on limit dextrinase in barley. 1. Purification of malt limit dextrinase and production of monospecific antibodies. J Cereal Sci 16:107–116, 1992.
34. AW MacGregor, LJ Macri, SW Schroeder, SL Bazin. Limit dextrinase from malted barley: extraction, purification and characterization. Cereal Chem 71:610–617, 1994.
35. LC MacLeod, CM Duffus. Temperature effects on starch granules in developing barley grains. J Cereal Sci 8:29–37, 1988.
36. L Serre, C Laurière. Specific assay of α-dextrin-6-glucanohydrolase using labelled pullulan. Anal Biochem 186:312–315, 1990.
37. BV McCleary. Measurement of the content of limit dextrinase in cereal flours. Carbohydr Res 227:257–268, 1992.
38. MJ Sissons, RCM Lance, DHB Sparrow. Studies on limit dextrinase in barley. II. Application of an ELISA and immunoblotting to studies of genetic variability and malting effects. J Cereal Sci 16:117–128, 1992.
39. DJ Manners, D Yellowlees. Studies on debranching enzymes. Part I. The limit dextrinase activity of extracts of certain higher plants and commercial malts. J Inst Brew 79:377–385, 1973.
40. WJ Lee, RE Pyler. Improved assay procedure for limit dextrinase in malt extracts. Brew Dig 57:24–26, 1982.
41. L Serre, C Laurière. Limit dextrinase in cereal seeds. Sci Aliments 9:645–663, 1989.
42. MA Longstaff, JH Bryce. Levels of limit dextrinase activity in malting barley. Proceedings of 23rd Congress, European Brewery Convention, Lisbon. Oxford: Oxford University Press, 1991, pp 593–600.
43. M Kristensen, B Svensson, J Larsen. Purification and characterization of barley limit dextrinase during malting. Proceedings of 24th Congress, European Brewery Convention, Oslo. Oxford: Oxford University Press, 1993, pp 37–43.
44. AW MacGregor, LJ Macri, SW Schroeder, SL Bazin. Purification and characterization of limit dextrinase inhibitors from barley. J Cereal Sci 20:33–41, 1994.
45. AW MacGregor, LJ Macri, SL Bazin, GW Sadler. Limit dextrinase inhibitor in barley and malt and its possible role in malting and brewing. Proceedings of 25th Congress, European Brewery Convention, Brussels. Oxford: Oxford University Press, 1995, pp 185–192.
46. TW Okita, J Preiss. Starch degradation in spinach leaves. Plant Physiol 66:870–876, 1980.
47. K Iwaki, H Fuwa. Purification and some properties of debranching enzymes of germinating rice endosperm. Agric Biol Chem 45:2683–2688, 1981.
48. K Sjöholm, LJ Macri, AW MacGregor. Is there a role for limit dextrinase in mashing? Proceedings of 25th Congress, European Brewery Convention, Brussels. Oxford: Oxford University Press, 1995, pp 277–284.
49. JH Bryce, NJ Kim, R Zammitt, CA McCafferty, MGM Pinheiro, GL Kendall. Branched dextrins in wort—is their presence inevitable? Proceedings of

25th Congress, European Brewery Convention, Brussels. Oxford: Oxford University Press, 1995, pp 285–292.
50. MA Longstaff, JH Bryce. Development of limit dextrinase in germinated barley (*Hordeum vulgare* L). Evidence of proteolytic activation. Plant Physiol 101:881–889, 1993.
51. LJ Macri, AW MacGregor, SW Schroeder, SL Bazin. Detection of a limit dextrinase inhibitor in barley. J Cereal Sci 18:103–106, 1993.
52. I Maeda, Z Nikuni, H Taniguchi, M Nakamura. Purification of debranching (R-enzyme) from malted barley, and the role of the enzyme in the digestion of starch granules during the germination of barley seeds. Carbohydr Res 61:309–320, 1978.
53. D Lecommandeur, AW MacGregor, J Daussant. Purification of germinated barley α-amylase isozymes and limit dextrinase by chromatofocussing and affinity chromatography. J Chromatogr 441:436–442, 1988.

61

Methodologies for Assaying the Hydrolysis of Cellulose by Cellulases

David Johnston
U.S. Department of Agriculture, Wyndmoor, Pennsylvania, U.S.A.

I. INTRODUCTION

This chapter does not intend to be a complete description of all cellulase assays available. The methods described here are generally regarded as the most useful or commonly employed assays. Many of the assays are useful from an empirical standpoint, but they cannot be used to compare results among laboratories. An attempt has been made to include methods applicable to a variety of research interests.

The analysis of cellulase activity presents a number of unique problems that are not typically observed in the study of other enzymes. Cellulose, the native substrate for cellulases, is insoluble and varies significantly in its structure. This complexity makes the kinetic analyses difficult since concentration and form of substrate are variable. Additionally, the presence of trace amounts of other cellulases may enhance hydrolysis in a synergistic fashion, altering experimental results. Enzymes such as β-glucosidase or cellobiose phosphorylase, which are not strictly cellulases, can also enhance cellulose hydrolysis by the removal of products that cause inhibition.

The unifying characteristic of all cellulases is their ability to hydrolyze the β-1,4-glucosidic linkage in cellulose. Cellulases are classified into four separate classes, based on their positions of hydrolysis and the products they produce.

The first class comprises the endoglucanases, which are enzymes that hydrolyze the internal bonds of the cellulose chain (endo-1,4[1,3;1,4]-β-D-glucan 4-glucanohydrolases, EC 3.2.1.4). The second class is the exocellobiohydrolases (1,4-β-D-glucan cellobiohydrolases, EC 3.2.1.91). This class of enzymes releases predominately cellobiose from cellulose molecules. Previously this group consisted of enzymes that released cellobiose from the nonreducing end; however, the class is now being subdivided into two separate groups of enzymes that release cellobiose from either the reducing or the non-reducing end of the cellulose molecule. The third class is the exoglucohydrolases (1,4-β-D-glucan glucobiohydrolase, EC 3.2.1.74). This group is composed of enzymes that release predominantly glucose from the nonreducing end of the cellulose molecule. There are some researchers who dispute the existence of these enzymes, with the contention that they are actually cellobiohydrolases contaminated with β-glucosidase or cellobiohydrolases that have some ability to hydrolyze cellobiose. The fourth class is the β-glucosidases (β-glucoside glucohydrolase, EC 3.2.1.21). This group hydrolyzes cellobiose, and to a much lesser extent cellotriose, to produce glucose. Technically these enzymes may not be considered cellulases (since they do not hydrolyze cellulose); they are included with the cellulases because they hydrolyze a β-1,4-

Mention of brand or firm name does not constitute an endorsement by the U.S. Department of Agriculture above others of a similar nature not mentioned.

glucosidic linkage and their action is important for complete hydrolysis of cellulose to glucose.

The classification above is currently under revision as increased information about cellulase specificity, hydrolytic activity, products formation, hydrolytic stereochemistry, and structural similarities is gathered. The current trend in the literature is to classify cellulases based on the comparison of their deduced amino acid sequences. In 1993 the comparison of 120 primary sequences of cellulases and xylanases defined a total of 11 families (designated A–K) (1).

Cellulases have a variety of commercial applications and many potential applications. In the food industry, cellulases are used in the processing of some fruits to aid in peeling or to increase juice yield. In the textile industry, cellulases are used to treat dyed fabrics to give a look similar to stone washing and to alter the properties of some regenerated fibers. One of the more exciting potential uses of cellulases is in the conversion of cellulosic waste material to glucose for fermentation into fuel ethanol. While cellulases are currently used in the detergent and textile industries, their application for waste conversion is still not considered economically viable because of the large quantities of enzymes necessary for the complete conversion of cellulosic material to glucose.

II. SUBSTRATE PREPARATION

A. Carboxymethyl Cellulose (CMC) and Hydroxyethyl Cellulose (HEC) (2)

Many different procedures are cited for preparation of substrates for viscosity determinations; however, most do not yield a substrate with a stable viscosity. The procedure described here is a slight modification from Garcia et al. (2) and does yield a solution with stable viscosity for several weeks. CMC or HEC can be used interchangeably without modification. Higher-molecular-weight substrates permit greater sensitivity in viscosity methods. CMC is the preferred choice when using capillary viscometry since HEC tends to form bubbles.

The substrate solution is prepared by slow addition of CMC 7H3SF from Aqualon to water heated to 80° C and stirred for 1 h to completely dissolve the substrate. After completing the addition, the solution is filtered through a sintered glass funnel (coarse) into a vacuum filtering flask and then allowed to cool to room temperature. Equal weights of the substrate and a 0.1 *M* sodium acetate buffer (pH 5.0) are weighed into a vacuum flask and degased with stirring for 1 h.

B. Phosphoric Acid Swollen Cellulose (4)

Phosphoric acid swollen cellulose (PSC) is commonly used as an example of an amorphous cellulose substrate in cellulase hydrolysis experiments. This procedure is a slight modification of Ställberg et al. (3) producing a more uniform substrate than by other methods, without requiring blending or filtering (3, 4).

A suspension of cellulose is prepared by addition of 3.00 g Sigmacell 20 to 5 mL deionized water. The cellulose suspension is then added slowly to 300 mL of cold 85% (w/v) phosphoric acid with stirring in an ice bath. The container of the cellulose suspension is rinsed with an additional 5 mL water to remove all of the cellulose. The cellulose solution is stirred on ice for 2 h. No undissolved cellulose should be visible to the naked eye. The solution is then slowly added to 4 L cold water with constant stirring on a magnetic stir plate. The precipitated cellulose is allowed to settle and the supernatant is removed by vacuum aspiration. An additional 4 L water is added with mixing, the suspension is allowed to settle, and the supernatant is removed by vacuum aspiration. This procedure is repeated a total of 10 times. After the final settling of the suspension, the cellulose is transferred to 1-L graduated cylinder. The supernatant is removed, and 500 mL of 0.10 *M* acetate buffer, pH 5.0, is added and the volume adjusted to 1 L. The final substrate concentration is determined using the Dubois method (5) for total carbohydrate.

C. Dyed Avicel (6)

Dyed Avicel is a convenient substrate for many applications. It is particularly useful for assays where reducing group measurements give excessively high blank values (e.g., inhibition by glucose or cellobiose).

A suspension of 100 g of Avicel is prepared in 1 L water. The suspension is heated to 50°C with vigorous stirring. One liter of 1% (w/v) Remazol Brilliant Blue dye is prepared in water and added to the Avicel suspension. Vigorous stirring is continued for 45 min, followed by addition of 200 g Na_2SO_4 in several portions. Following the Na_2SO_4 addition, 100 mL of a 100% solution of Na_3PO_4 is added (pH should now be 12) and the mixing continued for an additional 75 min. The suspension is now filtered through a sintered glass funnel (porosity 1) and washed with 60°C distilled water until the filtrate is colorless. While still in

the funnel, the dyed Avicel is washed with acetone and then ether. The prepared substrate is then vacuum dried.

III. METHOD TYPES

A. Viscosity (2)

1. Capillary

A 22-mL (22.00 g) aliquot (delivered by weight) of 0.5% CMC solution (prepared as described in Sec. II.A) is placed in a screw-cap tube in a 40°C water bath and preequilibrated for 15 min. After equilibration, 220 μL enzyme solution is added and the reaction timer activated. The cap is secured and the tube inverted gently 10 times. The solution is removed from the tube using a syringe, and $\sim$ 20 mL is injected into the capillary tube (Ubelode type). The reaction mixture is drawn up into the capillary using suction, and the drain time measured. This is repeated consecutively over the desired time frame. The viscosity is then calculated using the capillary tube calibration constant. The reaction time used for each measurement is the time at one-half of the drain time (reaction time at beginning of measurement plus 0.5 the drain time).

2. Rotational

A rotating spindle viscometer (Brookfield DV-III rheometer) is used to measure viscosity. Eight milliliters (8.00 g) of 0.5% CMC solution (prepared as described in Sec. II.A) is weighed into a chamber for small sample volumes (Brookfield spindle model SC4-18) and preequilibrated with the spindle at 40°C for 15 min. After equilibration, an 80 μL aliquot of CMC solution is removed and 80 μL enzyme solution is added. The sample is mixed for 1 min by moving the chamber up and down in the thermostated jacket. The spindle is then started at 60 rpm; after 2 min the first reading is taken, and subsequently each minute thereafter, in order to follow the rate of CMC hydrolysis.

B. Reducing-Group Methods

Reducing-group measurements are the best methods for general cellulase activity determinations. One of the greatest difficulties with this type of method is the nonuniform response between oligosaccharides with different degrees of polymerization (DP). Another difficulty is the incompatibility of some methods with certain substrates. Among the three reducing-group methods described here for measurement of cellulase activity, the disodium 2,2′-bicinchoninate (BCA) method gives the greatest sensitivity and little or no difference in response among different DPs.

1. BCA Method

Reagent A. The reagent is prepared by dissolving 54.28 g/L (512 mM) of Na_2CO_3, 24.2 g/L (288 mM) of $NaHCO_3$ and 1.942 g/L (5 mM) of disodium 2,2′-bicinchoninate. The solution is stored in a foil-covered bottle at room temperature. It is stable for several months.

Reagent B. The reagent is prepared by dissolving 1.248 g/L (5 mM) of $CuSO_4 \cdot 5H_2O$ and 1.262 g/L (12 mM) of L-serine. Solution is stored in a foil-covered bottle at 4°C. The solution is stable for up to 2 months. A new solution should be made when reagent blank value increases.

Sodium carbonate/bicarbonate solution. The solution is prepared by dissolving 54.28 g/L (512 mM) of Na_2CO_3, and 24.2 g/L (288 mM) of $NaHCO_3$ in the same solution. Final pH of the solution is 10.

BCA Working Reagent. Equal volumes of reagents A and B are mixed. The BCA Working Reagent solution should be prepared daily.

a. Sampling Using CMC (2). Twenty milliliters (20.00 g) of CMC solution is transferred to a 50-mL screw-cap tube gravimetrically and incubated at 40°C. Two 1-mL aliquots are taken as controls after 15 min and transferred to 13 $\times$ 100 mm test tubes containing 2 50 μL $Na_2CO_3/NaHCO_3$ solution. The enzyme reaction is initiated by addition of 180 μL enzyme solution to the 50-mL tube and mixed by gently inverting several times. One-milliliter aliquots are removed at timed intervals and transferred to tubes containing 250 μL of the $Na_2CO_3/NaHCO_3$ solution to inactivate the enzyme.

b. Sampling Using PSC (4). One milliliter of PSC suspension is transferred into a microcentrifuge tube from a flask mixing on a magnetic stir plate. The tubes are preequilibrated to 40°C for 10 min. The enzyme reaction is initiated by addition of 5–40 μL enzyme plus buffer followed by thorough mixing. The mixture is incubated at 40°C for a specified time and then inactivated by addition of 250 μL $Na_2CO_3/NaHCO_3$ solution followed by mixing.

To determine the total reducing groups formed during the enzymatic reaction, the inactivated sample is vortexed ($<$ 5 min before sampling) and hand-mixed immediately before removing a 100 μL sample. The sample is added to 900 μL of water in a 13 $\times$ 100

mm test tube. Soluble reducing groups can be determined after centrifuging for 5 min prior to removing the 100-μL sample to pellet the insoluble cellulose. Total and soluble reducing groups can be determined on the same sample by first sampling for total reducing groups followed by sampling of soluble reducing groups.

c. Determination of Reducing Group (4). Reducing groups are determined by addition of 1 mL of BCA Working Reagent to each tube containing 1 mL of sample or standard and incubated in a water bath at 80°C for 30 min. Tubes are mixed before incubation and covered with marbles to minimize evaporation. A standard curve of glucose (0–55 nmoles/mL) is prepared and incubated at the same time as the samples. Following heating, the tubes are cooled to room temperature in a water bath, sealed with Parafilm, and mixed by inverting several times. The absorbance values are measured in a spectrophotometer at 560 nm against a buffer blank. The number of glucose equivalents (nmoles of reducing groups/mL) is calculated by comparison to the standard curve. To prevent variation due to turbidity, samples using PSC as the substrate should be allowed to settle and the supernate removed for absorbance measurements using a Pasteur pipette.

2. Nelson-Somögyi Method (7, 8)

a. Somögyi Reagent. The reagent is prepared by dissolving 12.0 g $KNaC_4H_4O_6$ (potassium sodium tartrate) and 24.0 g anhydrous Na_2CO_3 in 250 mL deionized water. In a separate container, 4.0 g of $CuSO_4 \cdot 5H_2O$ is then dissolved in minimal water and added to the mixture. Sixteen grams of $NaHCO_3$ is then added and dissolved. Deionized water (500 mL) is boiled for 10 min with 180 g Na_2SO_4 to expel air and then added to the mixture. The final volume is then diluted to 1.0 L and the solution aged 1 week. The aged solution is filtered before using.

b. Nelson Reagent. The reagent is prepared by dissolving 50.0 g ammonium heptamolybdate $[(NH_4)_6Mo_7O_{24} \cdot 4H_2O]$ in 900 mL deionized water. Concentrated H_2SO_4 (42.0 mL) is then added slowly with mixing. In a separate container, 6.0 g $Na_2HAsO_4 \cdot H_2O$ is dissolved in 50 mL deionized water and added to the mixture. The final volume is adjusted to 1.0 L and aged 24 h at 37°C in the dark before use.

c. Procedure. Sampling using CMC and PSC is done as described under the BCA-reducing group assay with the modification of enzyme inactivation by heating in a boiling water bath for 5 min prior to reducing group determination.

Somögyi reagent (0.5 mL) is added to 0.5 mL of sample or standard in a 16 × 100 mm test tube. The tubes are mixed by vortexing, covered with marbles to prevent evaporation, and placed in a boiling water bath for 10 min. The tubes are removed and cooled to room temperature. After cooling, 0.5 mL of the Nelson reagent is added to each tube followed by mixing using a vortex mixer until no bubbles remain. A standard curve using glucose from 0 to 180 μg/mL is prepared and heated at the same time as the samples. The absorbance values are measured at 560 nm in a spectrophotometer, and the number of glucose equivalents (μmoles of reducing groups/mL) is calculated by comparison to the standard curve.

3. DNS Method (9)

The 3,5-dinitrosalicyclic acid reagent is prepared by dissolving 1.0 g of 3,5-dinitrosalicylic acid (DNS) in 50 mL water followed by addition of 20 mL of 2 *N* NaOH. After all the material is dissolved, 30 g of sodium potassium tartrate ($KNaC_4H_4O_6$) is added and dissolved. The solution is diluted to 100 mL with water. The solution is stable for several weeks when stored in an amber bottle protected from CO_2.

Sampling using CMC and PSC is done as described under the BCA reducing group assay (Sec. III.B.1) with the modification of enzyme inactivation by heating in a boiling water bath for 5 min prior to reducing group determination.

DNS reagent (1.00 mL) is added to 1.00 mL of sample or standard in a 18 × 150 mm test tube. The tubes are heated for 5 min in a boiling water bath and then cooled in a water bath to room temperature. The solutions are diluted to 3 mL with water and read in a spectrophotometer at 540 nm against a blank in which 1.00 mL water is used in place of the sample. The concentration of reducing groups is determined from a standard curve of glucose (0–1 mg).

4. Filter Paper Method

While this method is considered standard, many researchers have made extensive modifications to meet various needs. The method described here is based on the standard method of Mandelis et al. (10) as described by Ghose (11).

To a 25-mL or larger test tube is added 1.0 mL of 0.05 *M* sodium citrate buffer, pH 4.8. A 0.5-mL aliquot of enzyme diluted in sodium citrate buffer is added and the tube equilibrated at 50°C. (A minimum of two different dilutions is necessary for each enzyme to be tested. One dilution should produce slightly > 2 mg of glucose and the other slightly less.) A 1.0×6.0 cm (~ 50 mg) Whatman No. 1 filter paper strip is rolled around a glass rod and added to the test tube and incubated at 50°C for 60 min. The reaction is stopped by the addition of 3 mL DNS mixture. All tubes are then boiled together (including standards and blanks) for 5 min and cooled in a cold-water bath. The reactions are then diluted with 20 mL water, mixed by inverting several times, read in a spectrophotometer at 540 nm, and compared with a standard curve of glucose (1–3.35 mg).

The absolute amount of glucose released is determined after subtraction of the appropriate enzyme blank. A semilog plot (to improve linearity) of the glucose released against the fold enzyme dilution is made and the amount of enzyme necessary to release exactly 2.0 mg of glucose is determined. The filter paper units (FPU) in U/mL are calculated by dividing 0.37 by the determined enzyme concentration necessary to release 2.0 mg glucose. [*Note*: The FPU is derived from the International Unit (IU). When the product is glucose, 1 IU is equal to 0.18 mg min^{-1}. At the defined dilution (4% hydrolysis), 2 mg of glucose is produced from 0.5 mL of enzyme in 60 min. Therefore, the enzyme necessary to release 2.0 mg of glucose in the reaction contains 0.37 units (IU mL^{-1}).]

C. Chromophore and Fluorescent Group Release Methods

1. Dye Release—Cellulose Azure Method (12)

Cellulose azure (commercially available) is weighed into a test tube (100 mg), and 3 mL of 0.05 *M* sodium citrate buffer, pH 4.8, is added. The tube is equilibrated to 50°C and a stirring bar is added. Two milliliters of enzyme (equilibrated to 50°C) is added and incubated with stirring for 10 min. After incubation, the suspension is filtered through Whatman No. 1 filter paper and the OD at 595 nm is measured in a spectrophotometer.

2. Dye Release—Avicel Method (12)

A substrate suspension is prepared in 50 m*M* sodium citrate buffer, pH 4.8, using 50–100 mg/mL dyed Avicel (prepared as described in Sec.IIC). Enzyme solution 2 mL is pipetted into a test tube and equilibrated to 50°C. Three milliliters of the substrate suspension (equilibrated to 50°C) is added. The enzyme-substrate mixture is incubated for 1–2 h with or without stirring using a magnetic stirrer at 400 rpm. Following incubation, the suspension is heated in a boiling water bath for 5 min and then filtered through Whatman No. 1 filter paper. The filtrate is allowed to cool to room temperature, and the absorbance at 595 nm is determined. Activity is expressed in arbitrary units of absorbance.

3. MeUmb Method (13, 14)

The use of 4-methylumbelliferyl β-D-glycosides as substrates can be used to monitor cellulase activities. The cellobiose and cellotriose derivatives are commercially available or can be prepared according to Tilbeurgh et al. (14).

a. Continuous Method, OD. At pH 5.0, the release of 4-methylumbelliferone (MeUmb) can be followed continuously by difference absorption spectrophotometry at 347 nm. Enzyme assays are done at 25°C in 50 m*M* sodium acetate buffer, pH 5.0, using substrate concentration of 10–2000 μM. Concentrations of MeUmb glycosides can be determined using the molar absorption coefficient at 316 nm; $\epsilon_m = 13{,}600\, M^{-1}\, \text{cm}^{-1}$.

b. Fixed-Point Method, Fluorescent. Using a discontinuous method, taking samples, and adjusting the pH to 10.0, the release of MeUmb can be monitored fluorometrically. The sensitivity of the discontinuous fluorometric method is significantly greater ($< 1\, \mu M$ of MeUmb) than the continuous method at pH 5.0. The reaction conditions used are the same as in the continuous assay, but the reaction is stopped by the addition of an equal volume of 50 m*M* Na glycine, pH 10, in 50% ethanol. The relative fluorescence is then measured (excitation 366 nm, emission > 400 nm). A calibration curve is made using standard solutions of MeUmb (recrystallized from ethanol).

D. Chromatographic Methods

1. HPLC Method

Separation of substrates and products by HPLC can be used to analyze product distribution of individual cellulases for classification and to determine specificity of cellulases when using cello-oligosaccharides. Several different procedures have been used successfully with a variety of different separation procedures. Labeled

and unlabeled substrates and products have also been used.

a. Unlabeled Sugar Substrates (15). Separation of unlabeled sugars using Aminex columns with detection by refractive index is one of the more common procedures used. These columns have the distinct advantage that they use water, or in some applications, dilute sulfuric acid as the eluent. In application to cellulases analysis, the HPX-87P (Pb form) and the HPX-42A (Ag form) for monosaccharides and oligosaccharides analyses, respectively, are used most frequently.

An HPLC system using an Aminex column (ideally with a deashing guard column), a column heater, and a refractive index detector is required. Samples are prepared using an appropriate hydrolysis system followed by inactivation of the enzyme by heating (5 min in boiling water). If the final pH is not between 5 and 9 for the HPX-87P or between 6 and 8 for the HPX-42A, the pH should be adjusted to prevent loss of column performance. Samples are then filtered through 0.45-μm filters and injected (10–20 μL) into the HPLC system. Flow rates of 0.4–0.8 mL/min are used with column temperatures of 60–85°C. Quantification of results is accomplished by running external standards and constructing response factors for each sugar.

b. MeUmb-Labeled Substrates (13). MeUmb-labeled cello-oligosaccharides are prepared according to Tilbeurgh et al. (14), or they are available commercially. Enzymes are mixed with substrates in 0.05 *M* acetate buffer, pH 5.0, with substrate concentration from 300–500 μM and incubated at 25°C. Samples are taken from the reaction mixture (at 5 to 10-min intervals for 30–60 min) and diluted 1:3 in acetonitrile to stop the reaction. Inactivated samples (20 μL) are injected into an HPLC system consisting of a 25 × 0.46 cm Rsil-Polyol 5-μm particle-size column from Alltech and a UV detector monitoring at 313 nm. The eluent is a mixture of acetonitrile and water (39:11, v/v) at a flow rate of 1.5 mL/min. Quantification of results is accomplished by running external standards and constructing response factors for each sugar using integrated peak areas. Using the same column and eluent, the unmodified cello-oligosaccharides can be analyzed using a refractive index detector.

2. Enzyme Detection in Polyacrylamide Gels (16)

The detection of cellulases in polyacrylamide gels is based on the hydrolysis of 5-bromoindoxyl-β-D-cellobioside by endo-1,4-β-D-glucanases to produce 5-bromoindoxyl. The product 5-bromoindoxyl is then oxidized with nitroblue monotetrazolium (NBMT) producing an insoluble blue precipitate.

Standard gel electrophoresis is carried out using nondenaturing PAGE or isoelectric focusing systems. The incubation solution is prepared by first dissolving 5 mg of 5-bromoindoxyl-β-D-cellobioside and 20 mg NBMT in 0.5 mL dimethylformamide followed by mixing with 20 mL of 0.1 *M* sodium acetate buffer, pH 5.0. The gel is added to the solution and incubated in the dark at 40°C until dark blue bands appear. The development time is 2–15 h and is dependent on the concentration of active enzyme in the gel. Gels can be scanned or photographed for preservation. The staining solution can be used many times before discarding.

3. Gel Electrophoresis of Products (17–19)

a. ANTS Reagents. A 0.2-*M* solution is prepared by dissolving 0.086 g of 8-aminonaphthyl-1,3-6-trisulfonate (ANTS) in 5 mL of a solution of glacial acetic acid/water (3:17; v/v).

b. Reducing Agent. A 1.0-*M* solution of sodium cyanoborohydride ($NaCNBH_4$) is prepared in HPLC-grade dimethylsulfoxide (DMSO) by the addition of 2.5 mL DMSO to 0.25 g $NaCNBH_4$.

c. Procedure. Enzymatic hydrolysis reactions are carried out using 0.05 *M* ammonium acetate buffer, pH 5.0, and inactivated by a change in pH using ammonium hydroxide. The use of this volatile buffer system prevents high salt concentrations and allows samples to be dried before labeling with the ANTS reagent. Following hydrolysis, the inactivated reaction is centrifuged and the necessary volume (10–50 nmoles reducing sugar) is transferred to a microcentrifuge tube and dried using a vacuum centrifuge.

The dried sample containing 10–50 nmoles of reducing sugar is labeled by adding 5–10 μL of the ANTS reagent and 5–10 μL of the reducing agent. This mixture is vortexed for 10 sec and centrifuged briefly to bring reagents together. The reaction is incubated at 40°C for 15 h.

Electrophoresis is done using a 5–36% gradient acrylamide gel with a Tris-glycine buffer system, pH 8.3, and a 5% stacking gel, pH 6.8 (no SDS is incorporated). [The acrylamide stock solution used to prepare gels is acrylamide/bis-acrylamide (39:2 w/w).] The labeled sample is diluted with four times loading buffer (40% glycerol in 0.2 *M* Tris-HCL buffer, pH 6.8) and applied to sample wells. Current is applied and the migration monitored by use of a hand-held UV moni-

tor. The gel is removed when the fluorescent dye front reaches the bottom of the gel. Gels are documented by photography on a UV gel box. A Polaroid camera is used with a 4 × 5 film holder model 545, type 55 film, which gives a negative and a positive image, and a No. 8 filter.

4. Capillary Electrophoresis of Products (17, 19)

a. Saturated Trisodium Phosphate (TSP). An excess of TSP is added to water and mixed. Solution is kept at room temperature.

b. Phosphoric Acid. Commercial 85% phosphoric acid (8.67 *M*) is diluted to 1 *M* with deionized water.

c. Running Buffer. Phosphoric acid 100 m*M* is titrated to pH 2.5 using triethylamine (TEA). The final solution is ~ 100 m*M* phosphate, 36 m*M* TEA.

d. Procedure. Hydrolysis samples are labeled as above for gel electrophoresis but diluted with water (1:10) rather than loading buffer. A capillary electrophoresis system with an inactivated capillary column (60 cm × 50 μm) and phosphate-TEA buffer, pH 2.5, is used. Injection is done using pressure at 20 psi ∗ sec. Separation is monitored at 235 nm and samples are run at 20 kV with the polarity (−) to (+). Capillary and sample chamber temperatures are set at 35°C. Run times are ~ 15 min. The column is flushed with fresh buffer between runs.

The capillary is conditioned and cleaned before separation by sequentially flushing the column with saturated TSP, deionized water, 1 *M* phosphoric acid, deionized water, and running buffer for 5 min each. When the column performance decreases, as indicated by a change in elution times, the column is again cleaned.

E. Coupled Enzyme Methods

1. Glucose Oxidase/Peroxidase Method (20)

The enzymatic determination of glucose concentrations for estimating cellulase activity is a useful method when reducing group determinations are not possible or when total cellulose conversion determinations are required. Several variations of the glucose oxidase/peroxidase assay for the determination of glucose concentration have been published. The primary difference is the particular compound used as the indicator. Kits are available from some chemical supply companies (Sigma).

a. Glucose Reagent. Dissolve 1.5 U/mL peroxidase, 9 U/mL glucose oxidase, and 0.5 mg/mL of 2,2′-azino-di-(3-ethylbenzthiazoline)-6-sulfonate (ABTS) in 0.12 *M* phosphate buffer, pH 7.0. A few drops of chloroform can be added to avoid bacterial growth. When stored at 4°C the solution is stable for several weeks.

b. Procedure. Glucose reagent (3 mL) is added to 1.0 mL of sample or standard in a 16 × 100 mm test tube. The tubes are incubated for 30 min at room temperature and the absorbance measured at 450 nm. A standard curve of glucose (0–75 μg) is used to determine the concentration in unknown samples.

2. Cellobiose Dehydrogenase (Discussion Only)

Coupled enzyme methods using cellobiose dehydrogenase for determining cellulase activity have been published (21, 22). The methods require the use of enzymes from *Phanerochaeta chrysosporium* or *Humicola insolens* that are not commercially available and therefore their purifications will be required to use this method. These are among the few methods permitting a continuous measurement of cellulase activity and could prove extremely valuable in kinetic comparison between purified cellulases.

F. Special Methods

In a detailed study of a purified cellulase, additional details about the enzyme activity can contribute to the characterization and classification of the enzyme. Several techniques will be discussed that have been developed for determination of some important factors.

1. Inverting or Retaining—NMR Method (22, 23)

During the course of hydrolysis, the stereochemistry of the anomeric carbon formed is dependent on the structure and topology of the enzyme active site. Utilizing proton NMR, the hydrolysis of reduced cellodextrins (i.e., cellohexaitol) can be monitored for the formation of α- or β-anomers. The enzymes can then be classified as inverting or retaining based on the product stereochemistry. Dividing cellulases based on the primary sequences into families shows that there is very strong relationship between the family and the stereochemical course of hydrolysis.

2. Cellulose Chain End Determination Method (24)

Until recently it was believed that the mechanism of hydrolysis for exocellulases (cellobiohydrolases) was solely from the nonreducing end of the cellulose molecule. In 1996, Barr et al. (24) used ^{18}O and ^{14}C labeling of cellooligosaccharides in conjunction with ion-spray mass spectrometry to determine the precise position and direction of hydrolysis of five different exocellulases from *Thermonospora fusca* and *Trichoderma reesei*. Their results support the conclusion that there are two different classes of exocellulases each working from different ends of the cellulose molecules.

3. Dialysis Reactor Cell Method (25)

Synergism is an interesting observation shown with cellulases and with other enzymes, such as amylase, that have insoluble substrates and multiple types of enzymes working on the same substrate. Determination of synergism is difficult, especially using a native substrate. Baker et al. (25) developed a microdialysis device for studying synergism using native or pretreated substrates, under conditions in which product inhibition is minimized. The reactor cell is loaded with substrate and enzymes and held under constant temperature. The cell is continually flushed with fresh buffer, and the eluent is collected and assayed using HPLC sugar analysis.

REFERENCES

1. B Henrissat. Hidden domains and active site residues in β-glycanase-encoding gene. Gene 125:199–204, 1993.
2. E Garcia, DB Johnston, JR Whitaker, SP Shoemaker. Assessment of endo-1,4-beta-D-glucanase activity by a rapid colorimetric assay using disodium 2,2′-bicinchoninate. J Food Biochem 17:135–145, 1993.
3. J Stählberg, G Johansson, G Pettersson. *Trichoderma reesei* has no true exo-cellulase: all intact and truncated cellulases produce new reducing end groups on cellulose. Biochim Biophys Acta 1157:107–113, 1993.
4. DB Johnston, SP Shoemaker, GM Smith, JR Whitaker. Kinetic measurements of cellulase activity on insoluble substrates using disodium 2,2′-bicinchoninate. J Food Biochem 22:301–319, 1998.
5. M Dubois, KA Gilles, JK Hamilton, PA Rebers, F Smith. Colorimetric method for determination of sugars and related substances. Anal Chem 28:350–356, 1956.
6. T Wood. Preparation of crystalline, amorphous, and dyed cellulase substrates. In: Methods in Enzymology, Vol 160. San Diego: Academic Press, 1988, pp 19–25.
7. N Nelson. A photometric adaptation of the Somögyi method for the determination of glucose. J Biol Chem 153:375–380, 1944.
8. M Somögyi. Notes on sugar determination. J Biol Chem 195:19–23, 1951.
9. GL Miller. Use of dinitrosalicylic acid reagent for determination of reducing sugar. Anal Chem 31:426–428, 1959.
10. M Mandelis, R Andreotti. C Roche. Biotechnol Bioeng Symp 6:17, 1976.
11. TK Ghose. Measurement of cellulase activities. Pure Appl Chem 59(2):257–268, 1987.
12. M Leisola, M Linko. Determination of the solubilizing activity of a cellulase complex with dyed substrates. Anal Biochem 70:592–599, 1976.
13. H van Tilbeurgh, M Claeyssens, CK De Bruyrne. The use of 4-methylumbelliferyl and other chromophoric glycosides in the study of cellulolytic enzymes. FEBS Lett 149:152–156, 1982.
14. H van Tilbeurgh, FG Loontiens, CK De Bruyne, M Claeyssens. Fluorogenic and chromogenic glycosides as substrates and ligands of carbohydrases. In: Methods in Enzymology, Vol 160. San Diego: Academic Press, 1988, pp 45–59.
15. B Nidetzky, W Zachariae, G Gercken, M Hayn, W Steiner. Hydrolysis of cellooligosaccharides by *Trichoderma reesei* cellobiohydrolases: experimental data and kinetic modeling. Enzyme Microbiol Technol 16:43–52, 1994.
16. VM Chernoglazov, OV Ermolova, YV Vozny, AA Klyosov. A method for detection of cellulases in polyacrylamide gels using 5-bromoindoxyl-β-D-cellobioside: high sensitivity and resolution. Anal Biochem 182:250–252, 1998.
17. D Johnston. Cellulase, kinetics and synergism using insoluble substrates. PhD dissertation, University of California, Davis, CA, 1997.
18. P Jackson. The use of polyacrylamide-gel electrophoresis for the high-resolution separation of reducing saccharides labeled with the fluorophore 8-aminonaphthalene-1,3,6-trisulphonic acid. Biochem J 270:705–713, 1990.
19. C Chiesa, RA O'Neill. Capillary zone electrophoresis of oligosaccharides derivatized with various aminonaphthalene sulfonic acids. Electrophor 15:1132–1140, 1994.
20. HU Bergmeyer, E Bermt. Glucose determination with glucose-oxidase and peroxidase: method with 2,2′-azino-di-(3-ethylbenzthiazoline)-6-sulphonate (ABTS). In: Methods in Enzymatic Analysis, 2nd ed, Vol 3. New York: Academic Press, 1974, pp 1205–1215.

21. SM Kremer, PM Wood. Continuous monitoring of cellulase action on microcrystalline cellulose. Appl Microb Biotech 37:750–755, 1992.
22. C Schou, G Rasmussen, M Kaltoft, B Henrissat, M Schülein. Stereochemistry, specificity and kinetics of the hydrolysis of reduced cellodextrins by nine cellulases. Eur J Biochem 217:947–953, 1993.
23. M Claeyssens, P Tomme, CF Brewer, JE Hehre. Stereochemical course of hydrolysis and hydration reactions catalyzed by cellobiohydrolases I and II from *Trichoderma reesei*. FEBS Lett 263:89–92, 1990.
24. BK Barr, Y Hsieh, B Ganem, DB Wilson. Identification of two functionally different classes of exocellulases. Biochemistry 35:586–592, 1996.
25. JO Baker, TB Vinzant, CI Ehrman, WS Adney, ME Himmel. Use of a new membrane-reactor saccharification assay to evaluate the performance of cellulases under simulated SSF conditions. Effect on enzyme quality of growing *Trichoderma reesei* in the presence of targeted lignocellulosic substrate. Appl Biochem Biotechnol 63/65:585–595, 1997.

62

Cellulases in Food Processing

Maija Tenkanen, Marja-Leena Niku-Paavola, Markus Linder, and Liisa Viikari
VTT Biotechnology, Espoo, Finland

I. INTRODUCTION

Plant materials contain different β-glucans, mainly celluloses and mixed 1,3-1,4-β-glucans. Cellulases belong to the group of β-glucan hydrolases that have the ability to degrade cellulose. Enzymes often called β-glucanases that are able to hydrolyze β-1,4-linkages in other materials, such as in water-soluble β-glucans, but not in cellulose, are not covered in this chapter. Cellulases are not among the main enzymes used in the food industry. They are, however, applied in processing of cereal-based beverages and foods such as beer and bread. Cellulases are used in rather large amounts in animal feed. As a consequence of modern enzyme production technologies, which enable the production of more selective, tailor-made enzyme products, and owing to the increased knowledge of the structure-function relationship of food components, the use of cellulases may increase in the future in food processing.

II. CELLULOSE: A CHEMICALLY SIMPLE BUT STRUCTURALLY COMPLEX SUBSTRATE

Cellulose is the most abundant biopolymer on earth. It is mainly produced in higher plants, e.g., woods as well as annual plants in which it forms the rigid skeleton of the plant. In addition, all algae produce highly crystalline cellulose. Some bacteria, especially *Acetobacter xylinum*, are also able to synthesize cellulose.

Cellulose is chemically a very simple polymer. It is a homopolymer consisting of up to 1000 β-1,4-linked anhydroglucopyranoside units. However, its physical state makes it a very challenging substrate for enzymes. Single glucose polymers are packed onto each other to form a highly crystalline fibrillar material in which the individual cellulose chains are held together by hydrogen bonds. Cellulose microfibrils also contain some amorphous regions, the amount of which depends on the source. The most crystalline cellulose is produced by algae, and the least crystalline by plants.

Animals do not possess digestive enzymes able to degrade crystalline cellulose. However, several microorganisms, including filamentous fungi, yeast, and bacteria, existing in the intestine and colon of monogastric animals are able to hydrolyze cellulose to oligosaccharides and eventually to glucose, which they can then use as a carbon source. Ruminants, particularly, are able to fully degrade cellulose in their rumen by the wide spectrum of microorganisms present. To meet the challenge of degradation of crystalline and water-insoluble cellulose, microorganisms produce a complex mixture of several enzymes, which act synergistically. There are also several reports on plant cellulases, which are involved in plant cell expansion for loosening the cell walls during the growth of cell (1). Cellulase from different microorganisms have been thoroughly reviewed during the last decade (2–7).

III. CLASSIFICATION OF CELLULASES

All cellulases act on the chemically identical bond, i.e., the β-1,4-linkage between two anhydroglucose units. However, they differ in terms of their site of attack on the cellulose chain. Enzymes acting on cellulose have traditionally been classified by the International Union of Biochemistry (IUB) (www.expacy.ch.cg1-bin/enzyme-search-cl) into two distinct groups, endoglucanases and exoglucanases, which act in the middle of the cellulose chain or at either end of the cellulose chain, respectively (Fig. 1; Table 1). However, this classification is not very satisfactory, as some exoglucanases have also been claimed to possess endoactivity (8, 9). The classification of cellulases becomes even more complicated as some also have activity on other polysaccharides, such as xylan (10). Therefore, a new classification of these enzymes, as well as of other glycosyl hydrolases, have been suggested based on their structural similarities (11). This, however, requires information on their amino acid sequence which is not always available.

At present, the different glycosyl hydrolases are grouped according to the structures of their catalytic domains into more than 70 families (afmb.cnrs-mrs.fr/~cazy/CAZY/index.html). In addition, some of the families have further subfamilies. The classification is based on sequence alignments and hydrophobic cluster analysis (HCA) (12), but it has been proven to correlate well with the three-dimensional structures and reaction mechanisms. So far, some families contain only enzymes with the same catalytic activity, but most contain both endo- and exoglycanases being able to act on different polymers. For example, family 5 contains endoglucanases, exoglucanases, endomannanases, and endoxylanases. Currently, there are cellulases in 11 glycosyl hydrolase families (families 5–10, 12, 26, 44, 45, and 48).

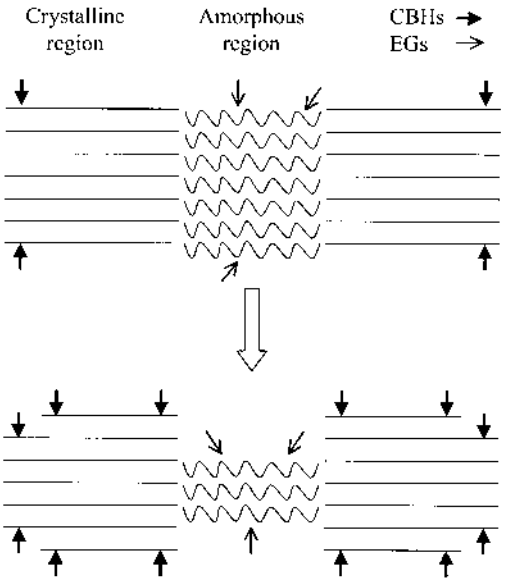

Figure 1 Hypothetical picture of cellulose degradation.

The new suggestion for the naming of different cellulases is based purely on their assignment to these glycosyl hydrolase families (11). If there is more than one enzyme belonging to the same family from one organism, the enzymes are further named with running alphabets in the order that they have been classified. For example *Trichoderma reesei* Cel7A (CBH I) and Cel7B (EG I) are two cellulose degrading enzymes in the glycosyl hydrolase family 7. In this chapter, the old naming system using endoglucanases and cellobiohydrolases is used since most publications still use this nomenclature.

The endoglucanases (EG) (1,4-β-D-glucan-4-glucanohydrolase, EC 3.2.1.4) catalyse random cuts in cellulose chains, thereby producing shorter and shorter cello-oligomers, which can be further degraded by exoglucanases. The trivial name given by the IUB for endoglucanases is cellulases, which is very misleading as cellobiohydrolases (CBH) (1,4-β-D-glucan cellobiohydrolase, EC 3.2.1.91) also act on cellulose and are actually the main enzymes responsible for the degradation of crystalline cellulose. Therefore, in this chapter the name cellulase covers all enzymes that are able to degrade polymeric celluloses, i.e., both EGs and CBHs. The final degradation of cello-oligomers produced by EGs and CBHs to glucose is accomplished by β-glucosidases (BGL) (EC 3.2.1.21). In addition to β-1,4-linkages, the latter enzymes are often also able to hydrolyze other β-glucosidic linkages, and although they are not able to hydrolyze polymeric cellulose they are, owing to their action on cello-oligosaccharides, usually considered as part of cellulolytic enzyme system.

CBHs cleave predominantly cellobiose units from either the reducing or nonreducing the ends of cellulose chains and cello-oligosaccharides (Table 1). CBHs normally produce a small amount of cellotriose when acting on cello-oligosaccharides. Substitution of cellulose chains blocks the action of CBHs, but most of them are able to hydrolyze 1,4-β-linkages in mixed 1,3-1,4-β-glucans, which exist in high quantities in the cell walls of grains (Table 2).

EGs are mainly active on amorphous cellulose, thus breaking down the less ordered amorphous parts of

Table 1 Classification of Enzymes Acting on 1,4-β-Glucans

Action	Systematic name	Trivial name(s)	EC No.	Substrate specificity	Linkage hydrolyzed	Main products formed
Endo	1,4-β-D-glucan-4-glucanohydrolase	Cellulase, endoglucanase (EG)	3.2.1.4	Cellulose, 1,3-1,4-β-glucans	1,4-β	1,4-β-dextrins, mixed 1,3-1,4-β-dextrins
	1,3-1,4-β-D-glucan-4-glucanohydrolase	Lichenase, β-glucanase	3.2.1.73	Lichenin, 1,3-1,4-β-glucans	Next 1,4-β after 1,3-β-linkage	Mixed 1,3-1,4-β-dextrins
	1,3-β-D-glucan-3/4-glucanohydrolase	Laminarinase	3.2.1.6	Laminarin, 1,3-1,4-β-glucans	Next 1,4-β- or 1,3-β-after 1,3-β-linkage	Mixed 1,3-1,4-β-dextrins
	1,3-β-D-glucan-3-glucanohydrolase	Laminarinase	3.2.1.39	Laminarin, pachyman, (1,3-1,4-β-glucans)	1,3-β	1,3-β-dextrins (1,4-β-dextrins)
Exo	1,4-β-D-glucan-cellobiohydrolase	Cellobiohydrolase (CBH)	3.2.1.91	Cellulose, 1,3-1,4-β-glucans	1,4-β	Cellobiose
	1,4-β-D-glucan-glucohydrolase	Exoglucanase	3.2.1.74	1,4-β-glucans	1,4-β	Glucose
	β-Glucosidase	Cellobiase	3.2.1.21	Wide variety of β-D-glucosides	1,4-β 1,3-β 1,6-β	Glucose

Table 2 Specific Activities of the Major *T. reesei* Cellulases Against Different Substrates

	Specific activity[a] (nkat/mg)			
Enzyme	HEC	β-GLC	XYL	MUC
EG I	540	3920	550	60
EG II	1170	6850	3	3.4
CBH I	2	12	3	3.2
CBH II	2	72	2	0

[a] Substrates used in the measurement: HEC = hydroxyethylcellulose; β-GLC = β-glucan from barley; XYL = birch xylan; MUC = methylumbelliferyl cellobiose.

cellulose fibers (13). Some bacterial EGs are also claimed to be able to degrade crystalline parts of cellulose microfibrils (14). EGs are highly active on various water-soluble cellulose derivatives such as carboxymethyl cellulose (CMC) and hydroxyethyl cellulose (HEC), which are often used as substrates for determination of the endoglucanase activity (see Chapter 61). In addition, EGs hydrolyze β-1,4 linkages in mixed 1,3-1,4-β glucans. There are also other enzymes, which are able to hydrolyze β-1,4-glucosidic linkages in soluble β-glucans (Table 1) (Fig. 2). However, as they are not able to hydrolyze cellulose, these enzymes are not discussed here (see Chapter 74).

EGs are basically able to hydrolyze all polysaccharides containing β-1,4-linked glucopyranosyl units, such as xyloglucans (1,4-β-glucan backbone with side chains made up of xylose, galactose, and occasionally fucose) (see Chapter 73). These are present in small quantities in plants but are the predominant polysaccharides in tamarind seeds. Many EGs are also able to hydrolyze polymers in which glucose is β-1,4-linked to other glycosyl units. Thus, for example, the β-1,4-linkages between glucose and mannose units in glucomannans are cleaved by EGs (see Chapter 75). Glucomannans are interesting food hydrocolloids and they exist in high quantities in some plants, such as in konjac tubers. Some EGs act also on other β-1,4-glycosidic linkages. One example of this lack of specificity is the EG I from *T. reesei* which is also able to hydrolyze β-1,4-xylosidic linkages in xylans (Table 2) (see Chapter 71).

IV. METHODS TO ASSAY CELLULASES

The determination of cellulase activities is not a very easy task, as the degradation of the water-insoluble, highly crystalline cellulose is not linear with time and different enzyme dosages. Therefore, several "nonnatural" substrates are normally used. As mentioned earlier, soluble cellulose derivatives are often used to assay EG activity. These are rather specific to EGs, as CBHs are not generally able to degrade substituted celluloses (Table 2). The international standard assay for measuring EGs is based on the hydrolysis of HEC (15). Soluble cereal, 1,3-1,4-β-glucans can also be used as substrates. They are degraded by EGs and by many CBHs. However, 1,3-1,4-β-glucans are not a specific substrate for cellulases as other β-glucanases are also able to degrade it. Amorphous cellulose has been used as a substrate mainly for EGs, but in many cases the enzymatic reaction is not linear or is linear only at the short initial reaction stage. Recently, a novel method for the preparation of totally amorphous cellulose beads has been developed (Pettersson, unpublished). These beads can also be made from dyed cellulose and were shown to be excellent substrates for EGs.

There are several ways to analyze the degree of degradation of the substrate. It can be based on the reduction in viscosity, on the formation of new reducing groups, or on the liberation of dyed oligosaccharides from chromophoric polymers. The viscosity method is the most sensitive one and can be used to measure very low levels of EGs, for example, from plant extracts. It is also highly specific to EGs, as exoglycanases do not affect the viscosity of the polymer.

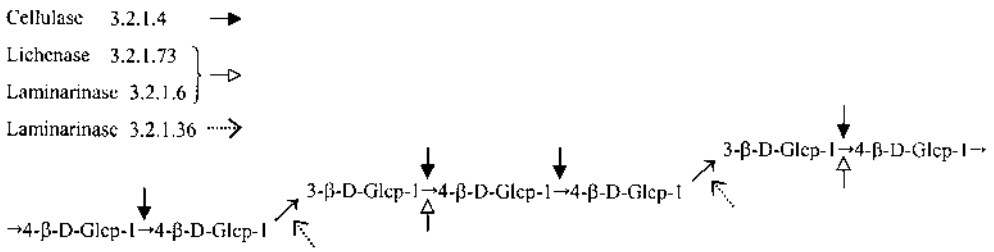

Figure 2 Endoglucanases acting on 1,3-1,4-β-glucans.

The action of EGs and CBHs is difficult to differentiate in the methods based on the formation of reducing groups.

The activity of CBHs is often measured by using small fluorogenic substrates such as methylumbelliferyl cellobioside or methylumbelliferyl lactoside. However, these substrates are specific not only to CBHs as some EGs also degrade them (Table 2). The activity of β-glucosidases is in most cases determined using *p*-nitrophenyl-β-D-glucopyranoside as a substrate and measuring the color formed by the liberated *p*-nitrophenol. EGs and CBHs do not hydrolyze this substrate.

Naturally soluble oligosaccharides up to DP 6 can be used as substrates for all cellulases, and the formed degradation products are normally analyzed by HPLC. In some cases it is important to know the overall cellulolytic capacity of the sample, i.e., how well real cellulose is degraded by a mixture of different cellulases. This is normally measured by the international standard method using filter paper as a substrate and the activity is expressed as filter paper units (FPU) (15). The different methods used for assaying the hydrolysis of cellulose by cellulases are covered in more detail in a separate chapter (see Chapter 61).

V. STRUCTURE-FUNCTION RELATIONSHIPS IN CELLULASES

A two-domain structure consisting of a catalytic domain and a separate substrate-binding domain is typical for cellulose-degrading enzymes from both bacteria and fungi. The existence of substrate-binding domains is also common in other enzymes which degrade solid substrates. In fungal enzymes the cellulose-binding domains (CBDs) are typically linked to the catalytic domain (catalytic core) by linkers which clearly separate the two domains (Fig. 3). The CBDs can be found in either the C or N terminus of the enzyme. In some cases, such as in the bacterium *Thermomonospora fusca* enzyme E4, the CBD forms a more integral part of the enzyme (16). Some bacteria have been reported to produce multidomain proteins which contain different, covalently linked catalytic domains hydrolyzing cellulose and hemicelluloses as well as several binding domains (17).

Many aerobic organisms produce large complexes called cellulosomes, which are clusters of different noncovalently linked proteins (18, 19). The assembly and action of cellulosomes have been studied by cloning the genes of the different subunits. Cellulosomes may consist of several EGs, CBHs, and other glycanases, but

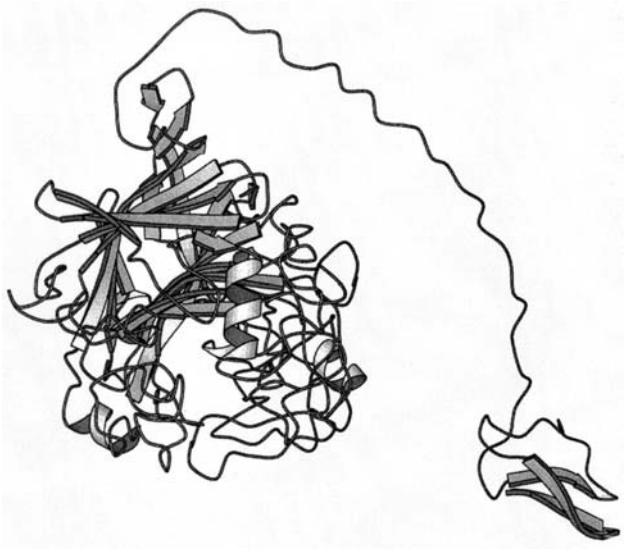

Figure 3 Model showing the two-domain structure of CBH from *T. reesei*. The larger catalytic domain is connected by the linker to the smaller cellulose-binding domain (CBD). Model coordinates provided by Christina Divne, Uppsala University.

also proteins involved in binding and targeting the cellulosome to the substrate. The individual enzymes alone in the complex normally have no significant activity against crystalline cellulose, but the cellulosome hydrolyzes it actively. Each enzyme component is attached to a nonenzymatic protein called scaffoldin, via a conserved docker sequence. The scaffoldin polypeptide contains a CBD and internal repeats (cohesins) which interact with enzymes. The molecular weight of cellulosomes can be as high as 2000 kDa.

Although 13 families of CBDs have been identified based on sequence homology, only one of them (family 1) occurs in fungi (20). The fungal CBDs are distinguished by their small size (< 40 amino acid residues). Like most other carbohydrate-binding proteins, the binding to cellulose has been shown to be largely dominated by interactions from aromatic amino acid residues. The CBDs have been shown to be important for the function of cellulases on solid substrates (Fig. 4). If they are removed either by proteolysis or protein engineering, both activity and binding to solid substrates are greatly decreased (21, 22). In many experiments the binding of cellulases to cellulose has been seen to be irreversible, which has sometimes been ascribed to the CBD. The interaction is complex, however, and is seen as interplay between the catalytic and binding domains which results in a synergistic binding to cellulose (23). At least in the case of fungal enzymes, no evidence has

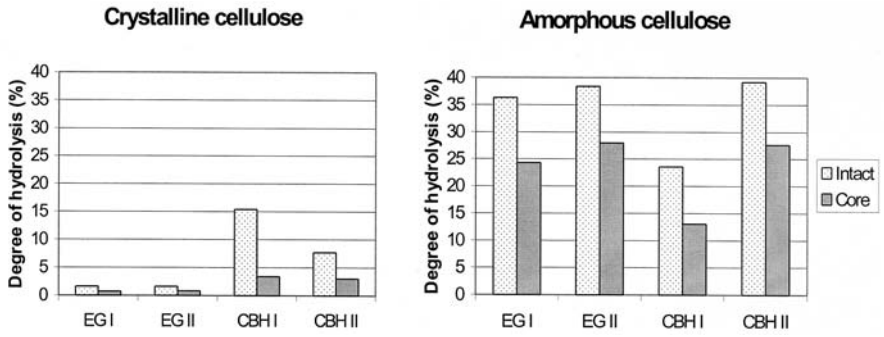

Figure 4 Hydrolysis of bacterial crystalline cellulose and amophous cellulose by *T. reesei* cellulases and the corresponding core proteins (300 nmol/g, pH 5, 50°C, 20 h).

been presented which would show that CBDs have one active role in hydrolysis of the crystalline cellulose, e.g., breaking down the hydrogen bonds. CBDs have been reported to lower the apparent K_m, but also to reduce the apparent k_{cat} probably by slowing down the mobility of the enzyme (24).

Owing to several three-dimensional protein structures of cellulases that are available together with detailed biochemical characterization, many special structural features of cellulases have been revealed. For example the EG I and the CBH I of *T. reesei* have a sequence identity of $\sim 45\%$. Comparison of their structures shows that the active site of CBH I is located in a tunnel formed by surface loops, while many of these loops are missing in EG I, which gives this enzyme a much more open active site (Fig. 5). The tunnel shape of the active site in the CBH I, as well as that found in other CBHs, gives a structural explanation for the action of the enzyme. It is thought that the long tunnel keeps the enzyme bound to the same cellulose chain by multiple interactions as it progressively moves along the chain hydrolyzing cellobiose units. The open active site groove found in EGs allows them to hydrolyze in the middle of cellulose chains (25–27). It has been speculated that cellulases can display more or less a continuum of structures with active sites covered to different degrees, giving more ''endo-like'' or ''exo-like'' enzymes, making the division unclear as mentioned earlier. The degree of endo- or exo-character can be determined by either the pre-

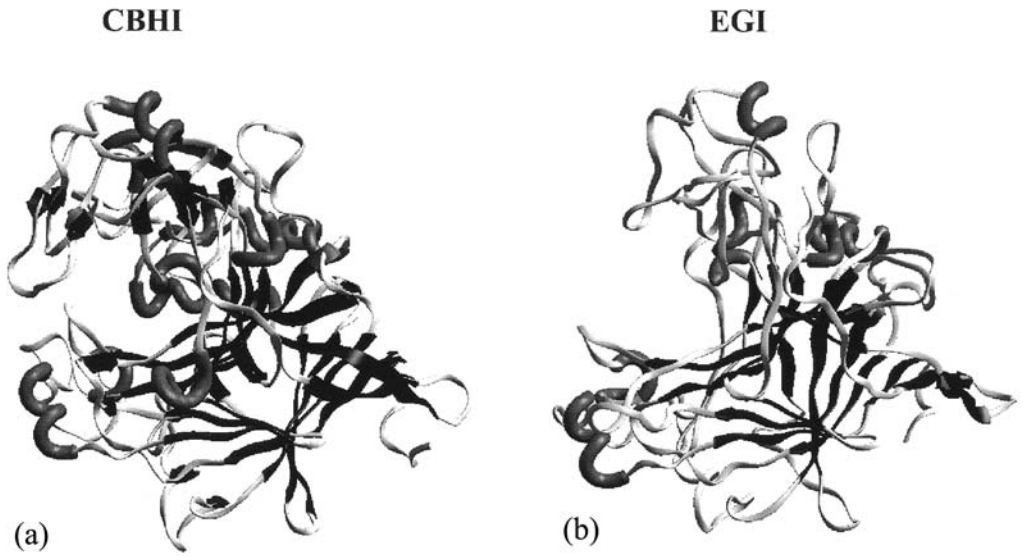

Figure 5 Comparison of the structure of endo- and exoglucanases. (A) Core domain from CBH I; (B) core domain of EG I from *T. reesei*.

sence/absence of the loops, or their flexibility. An issue, which is still not understood for CBHs is how the cellulose chain is picked up from the crystalline cellulose and how it is targeted to the tunnel. In the case for CBH II from *T. reesei*, a region on the outer side of the tunnel has been shown to be important for the hydrolysis of crystalline cellulose, but not for soluble substrates or amorphous cellulose (28).

Cellulases, like all glycosidases, catalyze the hydrolysis of the glycosidic bonds by general acid catalysis (29). The reaction involves two essential catalytic carboxylates, the proton donor and the nucleophile, which are generally located on opposite sides of the scissile bond. Depending on the structure of the active site, the cleavage proceeds by either retention or inversion of the configuration of the (β) anomeric carbon (29). Based on the structure of the active-site tunnel, some cellulases are proposed to twist the cellulose chain at the active site in order to expose the scissile bond better (25). The active sites have been shown to bind up to 10 glucose units. Since the active sites contain several sugar binding sites, it is convenient to have a common nomenclature for them. The bond cleavage occurs at the bond between the -1 and $+1$ sites so that the $+$ direction is toward the reducing end of the sugar chain and the $-$ direction is toward the nonreducing end.

VI. FUNGAL CELLULASES

Cellulolytic fungi occur in all major taxa (30, 31), but the current knowledge of fungal cellulases has been obtained mainly by studying deuteromycetes *Trichoderma* (21), *Penicillium* (13), and *Humicola* (24). Other significant fungi-producing cellulase are the plant pathogen *Fusarium solani* (32), *Aspergillus aculeatus* (33), and the asomycete *Neurospora crassa* (34). Cellulase producers have also been found among anaerobic rumen fungi, the first example of which was *Neocallimastix frontalis* (35). Studies on the white rot fungi *Sporotrichum pulverulentum* (anamorph of *Phanerochaete chrysosporium*) (36) and *Phanerochaete chrysosporium* (37) have revealed that lignin-degrading fungi are also able to produce a complete set of cellulolytic enzymes depending on the culture conditions. The studies on brown rot fungi suggest that these organisms produce only EGs and β-glucosidases (38).

Most cellulolytic fungi produce a mixture of several EGs, CBHs, and β-glucosidases to be able to degrade crystalline cellulose into glucose (Table 3). Fungal enzymes are normally glycosylated, and the isoforms, having different isoelectric points, make the purification and characterization of individual enzymes difficult. In addition, the culture filtrates often contain the catalytic core domains of cellulases as the native

Table 3 *T. reesei* and *H. insolens* Cellulases

Fungi	Enzyme	New name	Size (kDa)	pI	Remarks	Optimal pH	Reference
T. reesei	EG I	Cel7B	50–55	4.6		4.5–5.5	101
	EG II	Cel5A	48	5.5		4.5–5.5	102
	EG III	Cel12A	25	7.4	No CBD[a]	4.5–5.5	103
	EG IV	Cel61A	37	nd		4.5–5.5	104
	EG V	Cel45A	23	2.8–3.0		4.5–5.5	105
	CBH I	Cel7A	59–68	3.5–4.2		4.5–5.5	106
	CBH II	Cel6A	50–58	5.1–6.3		4.5–5.5	107
	BGL I		71	8.7	Family 3	4.6	108
	BGL II		52 (114)	4.8	Family 1 Dimer	4.0	108, 109
H. insolens	EG I	Cel7B	50	5.5	No CBD	7.0–8.5	110
	EG II	Cel5A	50	7.0		7.0–8.5	110
	EG III	Cel12	26	5.2	No CBD	7.0–8.5	110
	EG V	Cel45	43	5.2		7.0–8.5	110, 111
	EG VI	Cel6B	43	5.0		7.0–8.5	110
	CBH I	Cel7A	72	4.5		5.5	110
	CBH II	Cel6A	65	4.6–5.2		9.0	110
	BGL IV		54 (250–295)		Family 1 Multimer	5.0	109, 112

[a] CBD = cellulose binding domain.
Source: From Refs. 101–112.

enzymes are sometimes cleaved at the linker region by secreted proteases. Therefore, confusing literature exists on the number of individual enzymes produced by different fungi. After cloning the genes encoding the corresponding cellulases, the picture will become clearer.

The commercial cellulases are mainly produced with *T. reesei* and *H. insolens*. In addition, individual *H. insolens* genes have been cloned into a noncellulolytic *Aspergillus* strain and produced as monocomponent enzymes. However, these enzymes are not yet available for food use. The current *T. reesei* strains, which have been developed by classical mutagenesis from the native strain, are among the most powerful producers of extracellular proteins (39, 40). When grown on cellulose, $\sim 90\%$ of the extracellular protein consists of four major cellulases ($\sim 50\%$ CBH I, 20% CBH II, 10% EG I, and 10% EG II). Several tailor-made *T. reesei* strains have been recently developed by deleting the genes encoding nonwanted enzymes, thus leaving for example only one of the four major cellulases (40). *T. reesei* is also nowadays used as a host organism for the production of other glycosyl hydrolases (41, 42).

A. Cellulases from *T. reesei*

T. reesei is the most thoroughly studied cellulolytic organism. It is reported to produce at least five different endoglucanases (EG I through EG V), two cellobiohydrolases (CBH I and CBH II) and two β-glucanases (BGL I and BGL II) (Table 3). All EGs, except EG III, and both CBHs have a modular structure with a separate catalytic core domain and a CBD. EG I differs from the other EGs in being able to also hydrolyze xylan (10). Its specific activity on the water-soluble xylan is about the same as the activity on the soluble cellulose derivative HEC (Table 2). All EGs act mainly on amorphous cellulose (Fig. 4). However, EG II has been shown to reduce the degree of polymerization much faster than EG I (43).

CBH I and CBH II from *T. reesei* both act on the cellulose chain ends, but they clearly have different substrate specificities. CBH I acts from the reducing end of the cellulose chain whereas CBH II starts the action from the nonreducing end (7, 44). Thus, all these cellulases act on different parts of the cellulose chain and complement each other in the total hydrolysis of cellulose. CBH I has a rather unique action as most exoglycanases act from the nonreducing end. CBH I, which is clearly the major enzyme produced by *T. reesei*, has been found to be the key enzyme in the degradation of crystalline cellulose. Deletion of the gene encoding CBH I has resulted in $> 70\%$ reduction in the filter paper degrading activity, whereas deletion of other cellulases had only a minor effect (45).

Electron microscopy studies have shown that CBH I causes lateral thinning of cellulose microfibrils, whereas CBH II has been reported to sharpen the crystal ends (46, 47). CBH I seems to be a more processive enzyme than CBH II. This might be due to a longer tunnel in CBH I having 10 glucose binding sites (25). However, the action of CBHs on crystalline cellulose is at least 10 times slower than their action on soluble cellulose derivatives (28). Thus, it seems that stripping the cellulose chain from the crystal and targeting the chain end to the active site is the rate-limiting step. It might also be that the transfer of the cellulose chain along the active site for the next cut is a slow process compared to the actual hydrolytic action. *T. reesei* CBH I is also very sensitive to end-product inhibition (48). The *Trichoderma* enzymes usually exhibit the highest activity at acid pH (~ 5) and at temperatures $< 55^{\circ}$C.

B. Cellulases from *H. insolens*

The other commercially interesting fungus, *H. insolens*, produces an almost identical pattern of cellulases to *T. reesei*, having at least five EGs, two CBHs, and several β-glucosidases. These enzymes are also structurally similar, thus belonging to same glycosyl hydrolase families (Table 3). In addition, there exists remarkable homology ($> 50\%$) in the amino acid sequences between the corresponding cellulase component of *T. reesei* and *H. insolens*. However, several *H. isolens* cellulases work at higher pH and higher temperatures than *T. reesei* enzymes and have therefore found commercial applications, especially in textile treatments (49).

Two *H. insolens* cellulases, EG I and EG III, are lacking the CBD. EGs I–III show similar activity toward CMC and amorphous cellulose, while EGs V–VI have the highest catalytic activity on amorphous cellulose. None of them has been reported to be active in hydrolyzing xylan. *H. insolens* CBH I degrades crystalline cellulose, but it is clearly less sensitive to end product inhibition than CBH I from *T. reesei*.

C. Other Fungal Cellulases

Many *Aspergillus* spp. produce cellulases. *A. aculeatus* produces several cellulases (33) of which EG V, EG I, and CBH I have clear similarities to EG II, EG III, and CBH I from *T. reesei*, respectively (afmb.cnrs-mrs.fr/

~cazy/CAZY/index.html). Noncellulolytic *Aspergillus* spp., mainly *A. oryzae*, are often used as hosts for transformed cellulase genes from other fungi (50). *Penicillium* strains are also good cellulase producers. *P. pinophilum* produces an extensive set of endoglucanases (13). EG II and CBH I of *P. janthinellum* are homologous to EG II and CBH I of *T. reesei* (51).

Among anaerobic cellulolytic rumen fungi, *Neocallimastix frontalis* has been studied most extensively (35). It is reported to produce a cellulosome-like protein complex containing EG, CBH, and xylanase (52, 53). Other rumen fungi, e.g., *Piromyces* sp., produce similar cellulase complexes. It has been speculated that cellulases from anaerobic rumen fungi would hydrolyze crystalline cellulose more actively than enzymes from aerobic fungi (35).

Studies on the white rot fungi *Sporotrichum pulverulentum* (anamorph of *Phanerochaete chrysosporium*) and *Phanerochaete chrysosporium* have revealed that lignin-degrading fungi are able to produce a complete set of cellulolytic enzymes (36, 37). Four *P. chrysosporium* CBH Is are classified into family 7 and CBH II into family 6 (afmb.cnrs-mrs.fr/~cazy/CAZY/index.html). Interestingly one of the CBH Is is lacking the CBD.

The studies on the brown rot fungi suggest that these fungi possess both an oxidative and hydrolytic pathway in cellulose degradation. The initial step in the hydrolysis of crystalline cellulose is speculated to be nonenzymatic. Brown rot fungi have been reported to produce only EGs and β-glucosidases (38). The degradation of cellulose by white rot and brown rot fungi is different. The action of brown rot fungi is directed toward the whole cellulose microfibrils, whereas white rot fungi attack the surfaces of the microfibril, producing progressive erosion (54).

VII. BACTERIAL CELLULASES

Bacteria harbor several systems for cellulose degradation. They can produce extracellular EGs and CBHs, cell-bound enzymes, or powerful enzyme complexes. For example, the following bacterial species secrete low amounts of EGs and CBHs: *Clostridium, Acetovibrio, Ruminococcus, Streptomyces, Microspora*, and *Cellulomonas* (55). *Cellulomonas fimi* cellulases are among the most extensively studied bacterial cellulases. Four secreted EGs (CenA, -B, -C, -D), one CBH (CbhA), and one cellulase-xylanase (Cex) have been characterized both at the biochemical and genetic levels (56). The cellulases of *Actinomycetes, Corynebacteria, Thermomonospora fusca*, and *Microbispora bispora* have also been studied in detail (57, 58). Several *Streptomyces* spp. have been reported to produce cellulases. These filamentous bacteria are able to secrete both EGs and CBHs.

Some bacteria do not produce cellulolytic enzymes separately but rather as large cellulosomes (18). The most thoroughly studied cellulosome is from *Clostrium thermocellum*. The individual cellulase components cloned from *C. thermocellum* are three CBHs, 21 EGs, six xylanases, two β-glucosidases, and two lichenases (59). The main cellulase component is the exoglucanase CelS, which alone is able to slowly hydrolyze microcrystalline cellulose, but when linked to the anchoring protein containing the CBD it hydrolyzes this substrate extensively (60). However, none of the bacterial CBHs characterized until now belong to the family 7, but several are in the family 6 (afmb.cnrs-mrs.fr/~cazy/CAZY/index.html). Cellulosomes are also formed by the following bacteria: *Bacteroides, Acetivibrio, Bacillus, Butyrivibrio, Cellulomonas, Fibrobacter*, and *Thermomonospora* (18). Thermophilic bacterium *Caldocellulosiruptor saccharolyticus* produces an interesting multidomain enzyme that contains two catalytic domains, EG and mannanase, and two substrate-binding domains (17).

Bacterial cellulases have in many cases been reported to have much higher specific activities than fungal cellulases. However, bacteria generally produce extracellular cellulases in much lower quantities than fungi. In addition, several bacterial cellulases exist as part of a cellulosome. Therefore, their production, especially by using native strains, is difficult and uneconomic at large scale compared to the production of fungal cellulases. Individual bacterial cellulases have, however, been cloned and produced at an industrial scale in more suitable host organisms. These types of products are entering the markets, but they are still used only in nonfood applications.

VIII. ENDOGENOUS CELLULASES IN PLANTS

Several plants, for example cereals, produce endogenous enzymes acting on β-1,4-glucosyl linkages (see Chapter 74). However, these enzymes are reported to be mainly active on mixed-linked 1,3-1,4-β-glucans and do not possess activity on cellulose. There are also several reports on true cellulases in plants (1, 61). So far only EGs have been found in plants; there are no reports on CBHs. In contrast to fungal and bacterial EGs, plant enzymes lack the CBD. Plant EGs have

been found to degrade only amorphous cellulose in vitro. The exact substrate in vivo is not known, but it is thought to be xyloglucan (1). Endogenous plant EGs have been suggested to play a role in plant development, e.g., in fruit ripening and leaf abscission, or in the rearrangement of polysaccharides in growing cells. The mode of action of EGs in cell expansion could be either to promote wall loosening or to contribute to the incorporation of new microfibrils in the growing wall (61). There are several projects ongoing around the world screening different plant genomes. Owing to fast, modern screening techniques, several new enzymes, which are able to hydrolyze cellulose, will almost surely be found in the near future.

One interesting group of proteins is the expansins, which have been found in several plants (62). The action of these proteins is not well understood, but they are believed to break down the hydrogen bonds between individual cellulose chains during growth of the plant cells. Expansins are currently not classified as enzymes as they seem not to act on any covalent linkages. One study has been carried out on the production of an expansins type protein by the fungus *T. reesei* (Markku Saloheimo, unpublished).

IX. ROLE OF DIFFERENT CELLULASES IN THE HYDROLYSIS OF CELLULOSE

To study the biochemical properties of cellulases, absolutely pure enzymes are needed. The purification of individual cellulases from the mixture is often very difficult even using specific affinity chromatography techniques (63). It has been shown that minor (0.4%) contamination of an EG makes a significant difference in the action of a CBH (64). Cross-contamination can be avoided by gene cloning and expressing the individual cellulases in noncellulolytic hosts (65). Another possibility is to delete most of the cellulase genes from the cellulolytic organism and leave only the one encoding the acceptable activity (66). The enzyme preparation used in the studies must also carefully be characterized and confirmed to be a whole, intact protein since core parts are produced by proteolysis during cultivation. It has clearly been demonstrated that CBDs are necessary in the hydrolysis of both crystalline and amorphous cellulose (Fig. 4) (67). However, the hydrolysis of soluble substrates, which are often used in the activity assays, is not dependent on the presence of CBDs.

For complete hydrolysis of crystalline cellulose an effective mixture of different cellulases is needed. The key enzymes are CBHs possessing activity on crystalline cellulose. These enzymes are sometimes even able to degrade crystalline cellulose totally on their own, but the hydrolysis is very slow (60, 68). CBHs are thought to be processive enzymes, remaining bound to the substrate until it is totally degraded (69). They start their action from the ends of the cellulose chain, liberate cellobiose, and decrease the degree of polymerization (DP) of the substrate very slowly. EGs cleave bonds along the length of the cellulose chains, resulting in a faster decrease in DP of the substrate. Most EGs attack only the amorphous regions of cellulose and have different specificities toward the oligosaccharides liberated during hydrolysis. They are, however, highly active on polymeric water-soluble β-glucans such as carboxymethyl cellulose and cereal β-glucans, and even very low dosages of EGs reduce the DP rapidly.

Conventional kinetic parameters for cellulase reactions are not obtained while the substrate is changing during hydrolysis, and thus, only apparent values can be measured. Furthermore, the degradation of cellulose by individual cellulases is seldom linear, making kinetic measurements difficult. Therefore, water-soluble cellulose derivatives and cello-oligosaccharides up to DP 6 are normally used in kinetic studies for EGs and CBHs, respectively.

Cellulases have not been reported to have any specific inhibitors. Hg compounds, which inactive many glycosyl hydrolases, have been reported to affect the activity of CBH I more than EGI from *T. reesei* (70). End-product inhibition has often been considered as one reason for inefficient hydrolysis. The K_i values of cellobiose for different CBHs cannot be strictly compared because they have been estimated using different substrates. A very low K_i value (0.02 M) has been reported for *T. reesei* CBH I in the hydrolysis of methylumbelliferyl β-glucosides (48), whereas the K_i was 0.4 mM in the hydrolysis of cellodextrins (71). CBH I from *H. insolens* is less sensitive to the end-product inhibition, having a K_i value of 0.65 mM in the hydrolysis of cellotriose (24).

When the cellulase components act together in the hydrolysis of cellulose, they enhance the efficiency of each other significantly (72, 73). EGs assist the action of CBHs by liberating new chain ends from which CBHs can continue the hydrolysis towards more crystalline parts of the cellulose (Fig. 1). In general, only a small amount of EG is needed to improve the hydrolysis rate significantly. For example, the optimal mixture of *T. reesei* EG I and CBH II in the hydrolysis of crystalline cellulose is 2 : 8 (74). The synergism is com-

pleted by β-glucosidase, which is needed for the final step in the hydrolysis of cello-oligosacchares to glucose. The presence of β-glucosidase also enhances the action of other enzymes by diminishing the end-product inhibition through the hydrolysis of cellobiose, which is a strong inhibitor especially for CBHs. Cooperative action is mainly found between EGs and CBHs, but also exo-exo synergism has been reported (75). The degree of synergism is dependent on the relative amounts of the enzymes and on the substrate used. The synergy is greatest on crystalline cellulose (76). The synergy in general can be explained when differently acting enzymes provide good substrates and binding sites for each other by degrading different parts of cellulose crystals. EGs and CBHs also assist each other in the hydrolysis of soluble 1,3-1,4-β-glucans. However, the synergism is much smaller than in the case of cellulose as EGs are alone very effective in the degradation of water-soluble β-glucans (see Chapter 73).

Cross-synergism between cellulases from different organisms has also been demonstrated (76). This makes it possible to optimize the mixture of supercellulase components originating from different sources. In fact, the degradation of cellulose in nature obviously proceeds by mixed microbial populations.

X. APPLICATION OF CELLULASES IN FOOD PROCESSING

Cellulases are not among the major enzymes used in food production (Table 4). In many food applications cellulases are not used alone but are added to boost the action of other enzymes, mainly pectinases and/or xylanases. As all EGs are active on 1,3-1,4-β-glucans, they can be used in the same applications as the more specific 1,3-1,4-β-glucanases e.g., lichenases and laminarinases (Table 1; Fig. 2). 1,3-1,4-β-Glucans and arabinoxylans are the main components in cereal cell walls (see Chapter 74) and 1,3-1,4-β-glucans exist in high quantities especially in barley and oat (Table 5). Thus, cellulases are useful enzymes in the processing of cereals. Most mixed-linked β-glucans are water soluble and form viscous solutions. In some cases this is desired—for example, as soluble nondigestible fiber within the food—but in other cases they create problems during processing of cereal materials.

A. Brewing

Brewing is largely based on the action of endogenous barley and yeast enzymes which are activated during malting, mashing, and fermentation. During malting,

Table 4 Possible Uses of Cellulases in Food and Feed

	Process	Action	Benefits
Food	Baking	Degradation of cell walls	Softer dough Shorter fermentation time Increased loaf volume
	Brewing	Degradation of soluble β-glucan	Better filterability Higher production efficiency
	Wine and juice production	Degradation of cell walls	Better extraction Higher yield Enhanced color and/or aroma
	Extraction of oils	Degradation of cell walls	Better extraction Higher yield
	Extraction of starch and other polysaccharides	Degradation of cell walls	Better extraction Higher yield
	Upgrading agricultural residues	Degradation of cellulose to glucose	Better economics Less waste production Utilization of renewable materials
Feed	Animal farming	Degradation of cell walls	Better release of nutrients Enhanced feed conversion rate Less waste
	Pet animals	Degradation of cell walls	Better release of nutrients Healthier animals

Table 5 Chemical Composition of Cereal Grains

Grain	Starch (%)	β-Glucan (%)	Xylan (%)	Protein (%)	Fat (%)
Wheat	60–73	0.5–3.8	5.5–7.8	9–17	2.1–3.8
Barley	53–67	3.0–10.6	4.0–11.0	8–13	0.9–4.6
Oat	39–55	2.2–5.4	3.2–12.6	11–15	5.0–9.0
Rye	50–63	1.0–3.5	8.0–10.0	8–12	2.0–3.5

the grain polymers are mainly degraded to smaller fragments by amylases, proteases, and β-glucanases. The main separation problems during brewing processes are connected to the water-soluble cell wall polysaccharides, i.e., β-glucan and xylan. They both may increase viscosity, form gels, and cause serious problems including poor filtration of the wort, slow run-off times, low extract yields, or the development of haze in the final product. Mashing performance is determined largely by the raw materials used. In addition to malt, alternative sources of fermentable carbohydrates, such as corn, rice, and wheat starch from various origins and syrups, are used in many breweries depending on the beer type, availability of starchy raw material, and the price of the extract. There is natural seasonal variation in the quality of barley and malt, due to variations in weather conditions during growth and storage. Barley cultivars also differ from each other in the potential to produce endogenous enzymes during germination.

Plant enzymes are not very heat stable and are mostly inactivated in kilning after germination, whereas most microbial enzymes can tolerate much higher temperatures. Thus, exogenous microbial enzymes are often used in brewing. β-Glucanases (cellulases) are mainly added in the mashing (77), but they can also be used during malting (78) or after mashing in primary fermentation (77). *T. reesei* cellulases have been found to be better than other commercial β-glucanases in both pilot and industrial-scale trials in terms of higher filtration rate and overall brewhouse efficiency (79).

The other option to increase the level of β-glucanases is to enhance the level of endogenous plant enzymes by genetic engineering (see also Chapter 75) or by cloning a microbial enzyme to barley. The first enzyme to be successfully cloned into barley was the EG I from *T. reesei* (80, 81). An even more thermostable bacterial β-glucanase has later been expressed in barley (82). Another sophisticated option is to construct a glucanolytic brewer's yeast strain. *T. reesei* EG I was cloned > 15 years ago into an industrial brewer's yeast strain (83). The EG I secreted during fermentation decreased the viscosity of beer, which resulted in a markedly improved filterability with unaltered quality (84).

B. Wine and Juice Production

Even though the amount of β-glucans in grapes and fruits is significantly lower than in cereals, cellulases have also found applications in the production of wines and fruit juices where they are used in combination with pectinases and hemicellulases. In wine making, the enzymes are generally used for better skin maceration, improved color extraction, easier must clarification and filtration, and increased wine quality and stability (85). The use of β-glucosidases for aroma development from naturally present glucosylated precursors has also been described (86). Macerating enzyme cocktails with cellulases are also used in fruit juice production. In addition, the use of these enzymes offers advantages in the treatment of by products of the fruit industry by improving the extraction yield and the overall process efficiency. Cellulases and hemicellulases can be used for the isolation of pectin from citrus fruits to break down the cell walls, increasing the pectin yield. Cellulases can be used alone or in combination with other cell wall degrading enzymes in all processes in which valuable compounds such as juice, oil, polysaccharides, protein, etc., are extracted from the plant material.

C. Baking

Added enzymes are used increasingly in baking for improved processing and product quality. Traditionally, the main enzymes used in wheat baking are amylases and xylanases. β-Glucanases (cellulases) have gained less attention. Enzymes acting on cell walls are used especially in the manufacture of high-fiber bread to overcome processing problems caused by the high content of cell wall material in the dough. Addition of cell wall components decreases the bread volume, and the breadcrumb loses its elasticity. Soluble, nondigestable polysaccharides, which are often called dietary fiber, are believed to be beneficial for human health by lowering cholesterol levels (especially soluble β-glucan), preventing colon cancer, and acting as specific growth substrates (prebiotics) for beneficial intestinal bacteria (probiotics, mainly lactic acid bacteria and bifidobacteria) (87). Thus, breads with a high fiber content are gaining growing interest.

In wheat baking, the addition of water-soluble β-glucans has shown to improve breadcrumb grain (88). Treatment of the β-glucans with β-glucanase before their addition to the bread dough resulted in bread with poor crumb grain. In wheat dough supplemented with rye bran, xylanases and cellulases have been shown to make the cell wall polysaccharides more soluble and functional (89). The added enzymes made the dough softer, specific volume of the bread and crumb structure were improved, and the staling rate was reduced. Enzyme mixtures were found to be more efficient than individual enzymes.

Wholemeal rye baking differs significantly from wheat baking as rye proteins do not form a gluten matrix. Instead of gluten, the amounts of soluble xylans and endogenous enzymes are very important for the baking quality of rye since the gums in the rye dough have an important role in stabilizing the gas cells. The water-extractable xylans improve the baking quality by increasing dough viscosity. In rye meal slurries β-glucan and xylan extractability was increased by 90% and 40%, respectively, by EG II of *T. reesei* (90). Both xylanase and EG II from *T. reesei* are reported to make the rye dough softer, increase dough volume, and shorten fermentation time (91). The most marked effect of the enzymes was the reduction of proofing time. Cell wall–degrading enzymes softened the bread crumb and reduced the staling rate, but had a negative effect on oven rise. From the published reports on β-glucanases in baking it appears that the enzymes, including EGs, are useful especially when used in combination with other baking enzymes.

D. Isolation of Starch and Other Polysaccharides

The major application of food enzymes is in starch processing, i.e., hydrolysis of starch to glucose by amylolytic enzymes (see Chapters 56 and 57) and in the further isomerization of glucose to high-fructose syrup by glucose isomerase. The starch is mainly isolated from wheat or corn by milling and extraction. The isolation procedure can be further improved by cell wall degrading enzymes, i.e., by β-glucanases (cellulases), xylanases, or their mixture (92).

Several food hydrocolloids, mainly carrageenan, alginate, and agar, are isolated from algae. After initial isolation steps, the products often contain some contaminating cellulose from algae cell walls that impairs the functional properties of these polysaccharides. Cellulases are in some cases used in further purification steps to degrade the residual cellulose, after which the target polysaccharide can be further isolated. Cellulases can also be used for controlled degradation of some water-adsorbing polysaccharides used in food processing, e.g., CMC, konjac glucomannan, and some bacterial exopolysaccharides, such as xanthan, which contain β-1,4-glucosidic linkages.

E. Animal Feed Production

A large quantity of cereals or various side fractions of grains from food processing are used as animal feed. In many cereals, part of their energy content is locked up in the form of nonstarch polysaccharides, undigestible for several animals. Therefore, selected enzymes, such as cellulases and hemicellulases, can be added to break down the cell walls leading to increased metabolizable energy (93). The viscous arabinoxylan and 1,3-1,4-β-glucan also creates difficulties in the adsorption and digestion of nutrients, especially by monogastric animals such as chicken and pig. The viscosity is considered to be an important constraint to animal digestion by interfering with the diffusion of pancreatic enzymes, substrates, and reaction products (94). As a consequence, the presence of high levels of these components in feed causes poor feed conversion rates, slow weight gain, and wet droppings, particularly with poultry. The addition of enzymes, mainly xylanases and β-glucanases (cellulases), in feed enhances the breakdown of the corresponding polysaccharides and helps the adsorption of all feed components including proteins and fats, thereby improving feed conversion and weight gain. It is assumed that the beneficial effects of enzyme addition are due to both reduced intestinal viscosity and release of nutrients from grain cells. Other benefits of the cell wall–degrading enzymes are greater flexibility of diet formulations, the possibility of using cheaper raw materials, and production of less waste. In addition, with chickens the color of egg yolk is better and cleaner eggs are produced.

The liquid enzyme preparations are normally mixed in feed before pelleting. However, the current trend is to use higher pelleting temperatures to eliminate *Salmonella* contamination. Thus, normal fungal cellulases, such as those from *T. reesei*, may not survive the high temperature (95). The other option is to use granulated enzymes or to spray liquid enzyme preparations on the pellets at the cooling phase. The most advanced option is to clone new enzymes directly into animals. A transgenic mouse expressing a microbial cellulase in the exocrine pancreas has been constructed (96). The enzyme was secreted into the small intestine, demonstrating the feasibility of generating

nonruminant animals with a capacity to utilize cell wall polysaccharides.

Fungal enzymes are very suitable as feed additives owing to their acidic pH optimum which facilitates their action in the upper intestine. Some enzyme action already takes place during the feed production, especially at and after the pelleting stage, but mostly it occurs in the animal's digestive track.

The optimal enzyme mixture varies depending on the animals the feed is made for. Different enzyme cocktails are used for pigs and chickens. In addition, the xylanase : cellulase ratio is carefully designed for each diet. Broilers and laying and breeding hens fed on diets based on barley, wheat, or wheat and barley mixtures each have their own optimal enzyme formulation. Postweaning young piglets can obviously benefit most from enzyme supplementation to their diet. Cellulases and xylanases are often used in combination with proteases and amylases, and the cereal diet composition will determine the optimal enzyme mixture to be used (85). Adult pigs are less susceptible to viscose polysaccharides because of the longer retention time in their digestive system and more effective dilution of the viscose polymer (97).

F. Other Uses of Cellulases

Clearly the largest industrial use of cellulases is outside the food and feed sector in textile processing of natural textile fibers composed of cellulose (85, 98). Cellulases have also found potential applications in the pulp and paper industry (99). The textile and pulp fibers must retain their strength after cellulase treatment. Thus, novel commercial products with altered cellulase profiles have been developed. The detergent industry is the other major user of enzymes. The main enzymes used are proteases, but cellulases are also added in some detergents. Enzymes are now entering dishwashing detergents, and cellulases could also find applications there.

The total enzymatic hydrolysis of agricultural and forest residues to monosaccharides is an actively studied field. For this purpose a complete mixture of all individual cellulolytic enzymes is desired. The cellulase mixtures are capable of hydrolyzing cellulose to glucose with good yields, but the hydrolysis requires a large enzyme dosage or a very long hydrolysis time and is therefore economically not yet competitive with the enzymatic production of glucose from starch (100). However, better enzymes are being intensively developed, as the use of renewable biomaterials for raw materials in the chemical industry will increase in the future. Agricultural residues from farming and food processing, such as husks, straws, stems, brans, peels, etc., are normally fed to animals. These side fractions are rich in plant cell walls and could be upgraded with the aid of enzymes to several products including glucose. The hydrolyzed glucose can be further transformed by microorganisms to several valuable products, such as ethanol for fuel or lactic acid for bioplastics.

G. Commercial Cellulase Products

Several enzyme companies produce commercially available cellulases. The main producers are Nozymes (Denmark) and Genencor International (USA). Other companies manufacturing industrial enzymes are AB Enzymes (Germany/Finland/UK), DSM Bakery Ingredients (Netherlands), ICI-Quest (Netherlands/UK), Danisco (Denmark), Le Saffre (France), Beldem (Belgium), Frimond (Belgium), Biocatalysts (UK), Stern-Enzyme (Germany), Mühlenchemie (Germany), Enzyme Bio-Systems (USA), Valley Research (USA), Amano (Japan), Meiji (Japan), and Sankyo (Japan). However, several commercial cellulase products are not accepted for food use. Most cellulases that are now marketed for food applications are mixtures containing several EGs, CBHs, and β-glucosidases, as well as many other enzymes such as xylanases, proteases, amylases, etc., as minor components. This must be kept in mind when use of these enzymes in selective degradation of cellulose and/or 1,3-1,4-β-glucan is desidered. Some purified enzymes are also available in small quantities mainly for research purposes from Megazyme (Ireland) and Sigma (USA).

XI. CONCLUSIONS

Considering the significant variability of cellulolytic enzymes and the complexity of their substrates, it can be concluded that these enzymes still offer scientific challenges. Because of the better production techniques, complex enzyme mixtures will be in the future replaced by well-defined cellulases or tailor-made enzyme cocktails, which will enable better control the process and the quality of the end product. Modern genetic engineering techniques offer tools for improving cellulase properties to better suit different applications. As the structure-function relationships in food materials will be further understood, enzyme products

can be specifically designed to achieve targeted changes. Cellulases are very versatile enzymes and thus can offer practical solutions for several food applications.

ACKNOWLEDGMENTS

We are thankful to Martin Schülein from Novozymes for providing information on *Humicola* cellulases and to our colleagues Silja Home, Marjatta Salmenkallio-Marttila, and Anu Koivula for valuable information and comments.

REFERENCES

1. DA Brummell, CC Lashbrook, AB Bennett. Plant endo-1,4-β-D-glucanases. Structure, properties and physiological function. In: ME Himmel, JO Baker and RP Overand, eds. Enzymatic Conversion of biomass for Fuels Production. Washington: ACS, 1994, pp 100–112.
2. P Béguin, J Millet, S Chauvaux, S Salamitou, K Tokatlidis, J Navas, T Fujino, M Lemaire, O Raynaud, MK Daniel, JP Aubert. Bacterial cellulases. Biochem Soc Trans 20:42–46, 1992.
3. SSB Leschine. Cellulose degradation in anaerobic environments. Annu Rev Microbiol 49:399–426, 1995.
4. A Singh, K Hayashi. Microbial cellulases: protein architecture, molecular properties, and biosynthesis. Adv Appl Microbiol 40:1–44, 1995.
5. PJ Weimer, C Odt. Cellulose degradation by ruminal microbes: physiological and hydrolytic diversity among ruminal cellulolytic bacteria. In: JW Saddler, MH Penner, eds. Enzymatic Degradation of Insoluble Carbohydrates. San Diego: Academic Press, 1995, pp 291–304.
6. RAJ Warren. Microbial hydrolysis of polysaccharides. Annu Rev Microbiol 50:183–212, 1996.
7. A Koivula, M Linder, T Teeri. Structure-function relationships in *Trichoderma* cellulolytic enzymes. In: GE Harman, CP Kubicek, eds, *Trichoderma* and *Gliocladium*, Vol 2. London: Taylor & Francis, 1998, pp 3–23.
8. J Ståhlberg, G Johansson, G Pettersson. *Trichoderma reesei* has no true exocellulase: all intact and truncated cellulases produce new reducing end groups on cellulose. Biochim Biophys Acta 1157:107–113, 1993.
9. P Tomme, RAJ Warren, NR Gilkes. Cellulose hydrolysis by bacteria and fungi. Adv Microb Physiol 37:1–81, 1995.
10. P Biely, M Vršanská, M Claeyssens. The endo- 1,4-β-D-glucanase from *Trichoderma reesei*: action on β-1,4-oligomers derived from D-glucose and D-xylose. Eur J Biochem 200:157–163, 1991.
11. B Henrissat, TT Teeri, RAJ Warren. A scheme for designating enzymes that hydrolyse the polysaccharides in the cell walls of plants. FEBS Lett 425:352–354, 1998.
12. B Henrissat. A classification of glycosyl hydrolases based on amino acid sequence similarities. Biochem J 280:309–316, 1991.
13. TM Woods, S McCrae, M Bhat. The mechanism of fungal cellulase action. Biochem J 260:37–43, 1989.
14. K Bronnenmeier, WL Staudenbauer. Cellulose hydrolysis by a highly thermostable endo-1,4-β-glucanase (avicelase 1) from *Clostridium stercorarum*. Enzyme Microb Technol 12:431–436, 1990.
15. IUPAC. Measurement of cellulase activities. Pure Appl Chem 59:257–268, 1987.
16. J Sakon, D Irwin, DB Wilson, PA Karplus. Structure and mechanism of endo/exocellulase E4 from *Thermomonospora fusca*. Nat Struct Biol 4:810–818, 1997.
17. DD Morris, RA Reeves, MD Gibbs, DJ Saul, PL Bergqvist. Correction of the β-mannanase domain of the calC pseudogene from *Caldocellusiruptor saccharolyticus* and activity of the gene product on kraft pulp. Appl Environ Microbiol 61:2262–2269, 1995.
18. E Bayer, E Morag, R Lamed. The cellulosome—a treasure trove for biotechnology. Tibtech 12:379–386, 1994.
19. Y Shoham, R Lamed, EA Bayer. The cellulosome concept as an efficient microbial strategy for the degradation of insoluble polysaccharides. Trends Microbiol 7:275–281, 1999.
20. P Tomme, A Boraston, B McLean, J Kormos, AL Creagh, K Sturch, NR Gilkes, CA Haynes, RA Warren, DG Kilburn. Characterization and affinity applications of cellulose-binding domains. J Chromatogr Biomed Sci Appl 715:283–296, 1998.
21. P Tomme, H van Tilbeurgh, G Pettersson, J van Damme, J Vandekerckhove, J Knowles, T Teeri, M Claeyssens. Studies of the cellulolytic system of *Trichoderma reesei* QM9414. Analysis of domain function in two cellobiohydrolases by limited proteolysis. Eur J Biochem 170:575–581, 1988.
22. H van Tilbeurgh, M Clayssens, R Bhikhabnai, G Pettersson. Limited proteolysis of the cellobiohydrolase I from *Trichoderma reesei*. FEBS Lett 204:223–227, 1986.
23. H Palonen, M Tenkanen, M Linder. Dynamic interaction of *Trichoderma reesei* cellobiohydrolases Cel6A and Cel7A and cellulose at equilibrium and during hydrolysis. Appl Environ Microbiol 65:5229–5233, 1999.

24. M Schülein. Enzymatic properties of cellulases from *Humicola insolens*. J Biotechnol 57:71–81, 1997.
25. C Divine, J Stahlberg, TT Teeri, TA Jones. High-resolution crystal structures reveal how a cellulose chain is bound in the 50 Å long tunnel of cellobiohydrolase I from *Trichoderma reesei*. J Mol Biol 275:309–325, 1998.
26. GJ Kleywegt, JY Zou, C Divne, GJ Davies, I Sinning, J Stahlberg, T Reinikainen, M Srisodsuk, TT Teeri, TA Jones. The crystal structure of the catalytic core domain of endoglucanase I from *Trichoderma reesei* at 3.6 Å resolution, and a comparison with related enzymes. J Mol Biol 272:383–397, 1997.
27. TT Teeri. Crystalline cellulose degradation: new insight into the function of cellobiohydrolases. Trends Biotechnol 15:160–167, 1997.
28. A Koivula, T Kinnari, V Harjunpaa, L Ruohonen, A Teleman, T Drakenberg, J Rouvinen, TA Jones, TT Teeri. Tryptophan 272: an essential determinant of crystalline cellulose degradation by *Trichoderma reesei* cellobiohydrolase Cel6A. FEBS Lett 429:341–346, 1998.
29. G Davies, B Henrissat. Structures and mechanisms of glycosyl hydrolases. Structure 3:853–859, 1995.
30. M Coughlan. The properties of fungal and bacterial cellulases with comment on their production and application. Biotechnol Genet Eng Rev 3:39–109, 1985.
31. H Nevalainen, M Penttilä. Molecular biology of cellulolytic fungi. In: U Kück, ed. The Mycota II Genetics and Biotechnology. Berlin: Springer-Verlag, 1995, pp 303–319.
32. MP Coughlan, AP Moloney, SI McCrae, T Wood. Cross-synergistic interactions between components of the cellulase systems of *Talaromyces emersonii, Fusarium solanii, Penicillium funiculosum* and *Trichoderma koningii*. Biochem Soc Trans 15:263–264, 1987.
33. S Murao, R Sakamoto, M Arai. Cellulases of *Aspergillus aculeatus*. Methods Enzymol 160:274–299, 1988.
34. MT Yazdi, JR Woodward, A Radford. The cellulase complex of *Neurospora crassa*: activity, stability and release. J Gen Microbiol 136:1313–1319, 1990.
35. TM Wood, CA Wilson, S McCrae, K Joblin. A highly active extracellular cellulase from the anaerobic rumen fungus *Neocallimastix frontalis*—potential industrial application for cellulose saccharification. FEMS Microbiol Lett 34:370–40, 1986.
36. KE Eriksson. Enzyme mechanisms involved in cellulose hydrolysis by the rot fungus *Sporotrichum pulverulentum*. Biotechnol Bioeng 20:317–332, 1978.
37. PFG Sims, C James, P Broda. The identification, molecular cloning and characterization of a gene from *Phanerochaete chrysosporium* that shows strong homology to the exo-cellobiohydrolase I gene from *Trichoderma reesei*. Gene 74:411–422, 1988.
38. TL Highley. Cellulolytic activity of brown-rot and white-rot fungi on solid media. Holzforschung 44:211–216, 1988.
39. T Reese. History of the cellulase program at the U.S. Army Natick Development Center. Biotechnol Bioeng Symp 6:9–20, 1976.
40. A Mäntylä, M Paloheimo, P Suominen. Industrial mutants and recombinant strains of *Trichoderma reesei*. In: GE Harman, CP Kubicek, eds. *Trichoderma* and *Gliocladium*, Vol 2. Taylor & Francis, 1998, pp 291–304.
41. KMH Nevalainen, ME Penttilä, AM Harkki, TT Teeri, J Knowles. The molecular biology of *Trichoderma* and its application to the expression of both homologous and heterologous genes. In: SA Leong, R Berka, eds. Molecular Industrial Mycology, Systems and Applications for Filamentous Fungi. New York: Marcel Dekker, 1991, pp 129–148.
42. M Paloheimo, A Mäntylä, J Vehmaanperä, S Hakola, R Lantto, T Lahtinen, E Parkkinen, R Fagerström, P Suominen. Thermostabile xylanases produced by recombinant *Trichoderma reesei* for pulp bleaching. In: M Claeyssens, W Nerinckx, K Piens, eds. Carbohydrates from *Trichoderma reesei* and Other Microorganisms. Ghent: Royal Society of Chemistry, 1998, pp 255–264.
43. J Pere, M Siika-aho, J Buchert, L Viikari. Effects of purified *Trichoderma reesei* cellulases on the fibre properties of kraft pulp. Tappi J 78:71–78, 1995.
44. TT Teeri, A Koivula, M Linder, G Wohlfart, C Divne, T Jones. *Trichoderma reesei* cellobiohydrolases: why so efficient on crystalline cellulose. Biochem Soc Trans 26:173–177, 1998.
45. PL Suominen, AL Mäntylä, T Karhunen, S Hakola, H Nevalainen. High frequency one-step gene replacement in *Trichoderma reesei*. II. Effects on deletions of individual cellulase genes. Mol Gen Genet 241:523–530, 1993.
46. H Chancy, B Henrissat. Unidirectional degradation of *Valonia* cellulose microcrystals subjected to cellulase action. FEBS Lett 184:285–288, 1985.
47. B Sprey, HP Bochem. Effect of endoglucanase and cellobiohydrolase from *Trichoderma reesei* on cellulose microfibril structure. FEMS Microbiol 97:113–118, 1992.
48. H van Tilbeurgh, M Claeyssens. Detection and differentiation of cellulase components using low molecular mass fluorogenic substrates. FEBS Lett 187:283–288, 1985.
49. M. Schülein, D Tikhomirov, C Schou. *Humicola insolens* alkalene cellulases. In: T Reinikainen, P Suominen, eds. Proc 2nd Tricel Meeting. Majvik,

Finland: Foundation for Biotechnical and Industrial Fermentation Research, Vol 8, 1993, pp 109–1116.
50. T Christensen, H Woldike, E Boel, SB Mortensen, K Hjortshoj, L Thim, MT Hansen. High level expression of recombinant genes in *Aspergillus oryzae*. Biotechnology 6:1419–1422, 1988.
51. A Koch, CTO Weigel, G Schulz. Cloning, sequencing, and heterologous expression of cellulase-encoding cDNA (cbh1) from *Penicillium janthinellum*. Gene 124:57–65, 1993.
52. CA Wilson, TM Wood. The anaerobic fungus *Neocallimastix frontalis*: isolation and properties of cellulosome-type enzyme fraction with the capacity to solubilize hydrogen-bond-ordered cellulose. Appl Microbiol Biotechnol 37:125–129, 1992.
53. GP Xue, K Gobius, C Orpin. A novel polysaccharide hydrolase cDNA (celD) from *Neocallimastix patriciarum* encoding three multi-functional catalytic domains with high endoglucanase, cellobiohydrolase, and xylanase activities. J Gen Microbiol 138:2397–2403, 1992.
54. K Kleman-Leyer, E Agosin, A Conner, K Kirk. Changes in molecular size distribution of cellulose during attack by white rot and brown rot fungi. Appl Environ Microbiol 58:1266–1770, 1992.
55. TM Wood, V Garcia-Campayo. Enzymology of cellulose degradation. Biodegradation 1:147–161, 1990.
56. NR Gilkes, B Henrissat, DG Kilburn, RC Miller, RAJ Warren. Domains in microbial β-1,4-glycanases: sequence conservation, function and enzyme families. Microbiol Rev 55:303–315, 1991.
57. P Bequin. Molecular biology of cellulose degradation. Annu Rev Microbiol 44:219–248, 1990.
58. D Wilson. Biochemistry and genetics of *Actinomycete* cellulases. Crit Rev Biotechnol 12:45–63, 1992.
59. P Béquin, P Alzarit. The cellusome of *Clostridium thermocellum*. Biochem Soc Trans 26:178–183, 1998.
60. JDH Wu, WH Orme-Johnson, AL Demain. Two components of an extracellular protein aggregate of *Clostridium thermocellum* together degrade crystalline cellulose. Biochemistry 27:1703–1709, 1988.
61. F Nicol, H Höfte. Plant cell expansion: scaling the wall. Curr Opin Plant Biol 1:12–17, 1998.
62. DJ Cosgrove. Plant cell enlargement and the action of expansis. Bioessays 18:533–540, 1996.
63. P Tomme, S McCrae, TM Wood, M Claeyssens. Chromatographic separation of cellulolytic enzymes. Methods Enzymol 160:187–192, 1988.
64. T Reinikainen, K Henriksson, M Siika-aho, O Teleman, K Poutanen. Low-level endoglucanase contamination in a *Trichoderma reesei* cellobiohydrolase II preparation affects its enzymatic activity on β-glucan. Enzyme Microbiol Technol 17:888–890, 1994.
65. ME Penttilä, L Andre, M Saloheimo, P Lehtovaara, JKC Knowles. Expression of two *Trichodema reesei* endoglucanases in the yeast *Saccharomyces cerevisiae*. Yeast 3:175–185, 1987.
66. A Harkki, A Mäntylä, ME Penttilä, S Muttilainen, R Buhler, P Suominen, J Knowles, H Nevalainen. Genetic engineering of *Trichoderma* to produce strains with novel cellulase profiles. Enzyme Microbiol Technol 13:227–233, 1991.
67. A Suurnäkki, M Tenkanen, M Siika-aho, ML Niku-Paavola, L Viikari, J Buchert. *Trichoderma reesei* cellulases and their core domains in the hydrolysis and modification of chemical pulp. Cellulose 2000 (in press).
68. H Chanzy, B Henrissat, R Vuong, M Schulein. The action of 1,4-β-D-glucan cellobiohydolase on *Valonia* cellulose microcrystals. FEBS Lett 153:113–118, 1983.
69. J Rouvinen, T Bergfors, T Teeri, J Knowles, T Jones. Three-dimensional structure of cellobiohydrolase II from *Trichoderma reesei*. Science 249:380–386, 1990.
70. ET Reese, M Mandels. Stability of the cellulase of *Trichoderma reesei* under use conditions. Biotechn Bioeng 22:323–335, 1980.
71. TA Hsu, CS Gong, GT Tsao. Kinetic studies of cellodextrin hydrolysis by exocellulase from *Trichoderma reesei*. Biotechnol Bioeng 22:2305–2320, 1980.
72. W Gilligan, ET Reese. Evidence for multiple components in microbial cellulases. Can J Microbiol 1:90–107, 1954.
73. B Henrissat, H Driguez, C Viet, M Schulein. Synergism of cellulases from *Trichoderma reesei* in the degradation of cellulose. Bio/Technology 3:722-726, 1985.
74. M Bailey, M Siika-aho, A Valkeajärvi, M Penttilä. Hydrolytic properties of two cellulases of *Trichoderma reesei* expressed in yeast. Biotechnol Appl Biochem 17:65–76, 1993.
75. L Fägerstam, L Pettersson. The 1,4-β-glucan cellobiohydrolases of *Trichoderma reesei* QM9414. A new type of cellulolytic synergism. FEBS Lett 119:97–101, 1980.
76. TM Wood, S McCrae. Synergism between enzymes involved in the solubilization of native cellulose. Adv Chem Ser 181:181–209, 1979.
77. J. Oksanen, J Ahvenainen, S Home. Microbial cellulases for improving filterability of wort and beer. Proc 20th Congr Eur Brew Conv, Helsinki. Oxford: IRL Press, 1985, pp 419–425.
78. S Home, H Maunula, M Linko. Proc Eur Brew Conv London, 1983, pp 385–392.
79. AM Canales, R Garza, JA Sierra, R Arnold. The application of a β-glucanase with additional side activities in brewing. MBAA Tech Q 25:27–31, 1988.
80. L Mannonen, U Kurtén, A Ritala, M Salmenkallio, R Hannus, K Aspergren, TH Teeri, V Kauppinen. Biotechnology for the improvement of malting barley. In: Proc 24th Congr Eur Brew Conv, Oslo. Oxford: IRL Press, 1993, pp 85–93.

81. AM Nuutila, A Ritala, R Skadsen, L Mannonen, V Kauppinen. Expression of thermotolerant endo-(1,4)-β-glucanase in transgenic barley seeds during germination. Plant Mol Biol 41:777–783, 1999.
82. L Jensen, O Olsen, O Kops, N Wolf, KK Thomsen, D von Wettstein. Transgenic barley expressing a protein-engineered, thermostable (1,3-1,4)-β-glucanase during germination. Proc Natl Acad Sci USA 93:3487–3491, 1996.
83. M Penttilä. ML Suihko, U Lehtinen, M Nikkola, JKC Knowles. Construction of brewer's yeast secreting fungal endo-β-glucanases. Curr Genet 12:413–420, 1987.
84. ML Suihko, U Lehtinen, B Zurbriggen, A Vilpola, J Knowles, M Pentillä. Construction and analysis of recombinant glucanolytic brewer's yeast strains. Appl Microbiol Biotechnol 35:781–787, 1991.
85. YM Galante, A DeConti, R Monteverdi. Application of *Trichoderma* enzymes in the food and feed industries. In: GE Harman, CP Kubicek, eds. *Trichoderma* and *Gliocladium*, Vol 2. Taylor & Francis, 1998, pp 311–325.
86. C Caldini, F Bonomi, PG Pifferi, G Lanzarini, YM Galante. Kinetic and immobilization studies of fungal glycosidases for aroma enhancement in wine. Enzyme Microb Technol 16:286–291, 1994.
87. GR Gibson, MB Roberfroid. Dietary modulation of the human colonic microbiata: introducing the concept of prebiotics. J Nutr 125:1401–1412, 1995.
88. L Wang, RA Miller, RC Hoseney. Effects of (1 $\rightarrow$ 3) (1 $\rightarrow$ 4)-β-D-glucans of wheat flour on breadmaking. Cereal Chem 75:629–633, 1998.
89. T Laurikainen, H Härkönen, K Autio, K Poutanen. Effects of enzymes in fibre-enriched baking. J Sci Food Agric 76:239–249, 1998.
90. H Härkönen, P Lehtinen, T Suortti, T Parkkonen, M Siika-Aho, K Poutanen. The effects of xylanase and a β-glucanase from *Trichoderma reesei* on the non-starch polysaccharides of whole meal rye slurry. J Cereal Sci 21:173–183, 1995.
91. K Autio, H Härkönen, T Parkkonen, T Frigård, K Poutanen, M Siika-Aho, P Åman. Effects of purified endo-β-glucanase on the structural and baking characteristics of rye doughs. Lebensm-Wiss, Technol 29:18–27, 1996.
92. PL Weegels, JP Marseille, RJ Hamer. Enzymes as a processing aid in the separation of wheat flour into starch and gluten. Starch/Stärke 44:44–48, 1992.
93. WD Cowan. Animal feed. In: T Godfrey, S West, eds. Industrial Enzymology. London: Macmillan, 1996, pp 69–86.
94. A Morgan, M Bedford, A Tervila-Wilo, M Hopeakoski-Nurminen, K Autio, K Poutanen, T Parkkonen. How enzymes improve the nutritional value of wheat. Zootecnica Int April:44–48, 1995.
95. JT Piironen. Studies on the stability of β-glucanase and xylanase activities of *Trichoderma reesei* during pelleting. Proc Aust Poultry Sci Symp 8:146–148, 1996.
96. J Hall, A Simi, MA Surani, GP Hazlewood, AJ Clarck, JP Simons, BH Hirst, HJ Gilbert. Manipulation of the repertoire of digestive enzymes secreted into the gastrointestinal tract of transgenic mice. Bio/Technology 11:36–379, 1993.
97. GA Walsh, RF Power, DR Headon. Enzymes in the animal feed industry. Trends Biotechnol 11:424-430, 1993.
98. T Godfrey. Textiles. In: T Godfrey, S West, eds. Industrial Enzymology. London: Macmillan, 1996, 359–371.
99. J Buchert, T Oksanen, J Pere, M Siika-aho, A Suurnäkki, L Viikari. Applications of *Trichoderma reesei* enzymes in the pulp and paper industry. In: GE Harman, CP Kubicek, eds. *Trichoderma* and *Gliocladium*, Vol 2. London: Taylor & Francis, 1998, pp 343–363.
100. M Himmel, M Ruth, C Wyman. Cellulase for commodity products from cellulosic biomass. Curr Opin Biotechnol 10:358–364, 1999.
101. ME Penttilä, P Lehtovaara, H Nevalainen, R Bhikhabhai, JKC Knowles. Homology between cellulase genes of *Trichoderma reesei*: complete nucleotide sequence of the endoglucanase I gene. Gene 45:253–263, 1986.
102. M Saloheimo, P Lehtovaara, M Penttilä, T Teeri, J Ståhlberg, G Johansson, G Pettersson, M Claeyssens, P Tomme, J Knowles. EGIII, a new endoglucanase from *Trichoderma reesei*; the characterization of both gene and enzyme. Gene 63:11–21, 1988.
103. M Ward, S Wu, J Dauberman, G Weiss, E Larenas, B Bower, M Rey, K Clarkson, R Bott. Cloning, sequence and preliminary analysis of a small, high pI endoglucanase EGIII from *Trichoderma reesei*. In: P Suominen and T Reinikainen, eds. *Trichoderma reesei* Cellulases and other Hydrolases. Helsinki: Foundation for Biotechnical and Industrial Fermentation Research, 1993, pp 153–158.
104. M Saloheimo, T Nakari-Setälä, M Tenkanen, M Penttilä. cDNA cloning of a *Trichoderma reesei* cellulase and demonstration of endoglucanase activity by expression in yeast. Eur J Biochem 249:584–591, 1997.
105. A Saloheimo, B Henrissant, AM Hoffrén, O Teleman, M Penttilä. A novel, small endoglucanase gene, *egl5*, from *Trichoderma reesei* isolated by expression in yeast. Molec Microbiol 13:219–228, 1994.
106. S Shoemaker, V Schweickart, M Ladner, D Gelfand, S Kwok, K Myambo, M Innis. Molecular cloning of exo-cellobiohydrolase I derived from *Trichoderma reesei* strain L27. Bio/Technol 1:691–696, 1983.
107. CM Chen, M Gritzali, DW Stafford. Nucleotide sequence and deduced primary structure of cellobio-

hydrolase II of *Trichoderma reesei*. Bio/Technol 5:274–278, 1987.
108. H Chen, M Hayn, H Esterbauer. Purification and characterization of two extracellular β-glucosidases from *Trichoderma reesei*. Biochim Biophys Acta 1121:54–60, 1992.
109. S Takashima, A Nakamura, M Hidaka, H Masaki, T Uozumi. Molecular cloning and expression of the novel fungal beta-glucosidase genes from *Humicola grisea* and *Trichoderma reesei*. J Biochem 125:728–736, 1999.
110. M Schülein, D Tikhomirov, C Schou. *Humicola insolens* alkaline cellulases. In: T Reinikainen, P Suominen, eds. Proc 2nd Tricel Meeting, Majvik, Finland 1993, Foundation for Biotechnical and Industrial Fermentation Research, Vol 8, 1993, pp 109–116.
111. GJ Davies, GG Dodson, RE Hubbard, SP Tolley, Z Dauter, KS Wilson, C Hjort, JM Mikkelsen, G Rasmussen, M Schülein. Structure and function of endoglucanase V. Nature 365:362–364, 1993.
112. S Hayashida, K Ohta, K Mo. Methods Enzymol 160:274–299, 1988.

63

β-Glucosidase

Asim Esen
Virginia Polytechnic Institute and State University, Blacksburg, Virginia, U.S.A.

I. INTRODUCTION

β-Glucosidase (β-D-glucoside glucohydrolase, EC 3.2.1.21) catalyzes the hydrolysis of the β-glycosidic bond between two glycone residues (e.g., cellobiose and other β-linked oligosaccharides) or that between glucose and an aryl or alkyl aglycone (e.g., many naturally occurring substrates in plants). The enzyme constitutes a major group among glycoside hydrolases and occurs universally in all three domains (Eukarya, Archaea, and Eubacteria) of living organisms. A nomenclature system classifying glycosyl hydrolases into 82 families based on amino acid sequence similarities has been proposed (1–3) and is now widely used. A continuously updated server giving access to these families is available at URL://http://afmb.cnrs-mrs.fr/~pedro/CAZY/db.html. Under this classification scheme, β-glucosidases belong to families 1 and 3 of the clan GH-A. Unless otherwise stated, this chapter's emphasis will be family 1 enzymes.

β-Glucosidases have been the focus of much research recently because of their key roles in a variety of fundamental biological (e.g., growth and development, chemical defense, host–parasite interactions, cellulolysis, lignification, glycosylceramide and vitamin B_6 metabolism, signaling, etc.) and biotechnological (biomass conversion, food detoxification, and beverage quality enhancement) processes. For example, plant β-glycosidases have been either implicated or shown to be involved in (a) defense against pests (4–6); (b) phytohormone activation (7); (c) lignification (8); (d) cell wall degradation in the endosperm during germination (9); and (e) quality enhancement in wine, fruit juices (10; Chapter 21), and tea (12). β-Glucosidases hydrolyze either O-linked β-glycosidic bonds, as is done by β-glucosidases (β-D-glucoside glucohydrolase, EC 3.2.1.21), or S-linked β-glycosidic bonds, as is done by β-thioglucosidases (myrosinase, or β-D-thioglucoside glucohydrolase, EC 3.2.3.1). Thus, specific physiological functions and multiplicity of β-glycosidases in an organism depend on the nature and diversity of the aglycone (aryl or alkyl) or glycone (Glc, Gal, Fuc, Xyl) moiety of their substrates.

II. USE OF β-GLUCOSIDASES IN FOOD PROCESSING AND QUALITY ENHANCEMENT

The importance of β-glycosidases to food quality and processing is ably reviewed and discussed by Günata (see Chapter 21) with emphasis on flavor enhancement in fruit juices and various beverages derived from them. Therefore, the reader is referred to Chapter 21 for more information on this aspect. There are several hundred different β-glucosidic flavor precursors identified from plants whose aglycones are products of mevalonate or shikimate pathways. Obviously, there are β-glucosidases in source plant tissues that hydrolyze these flavor precursors. Thus, in each case there is need for isolating and characterizing the specific enzyme that hydrolyzes a β-glucoside whose aglycone

moiety is of interest to food quality and processing. Such biochemical data are crucial to making practical decisions as to whether or not enzymes from host plants or other sources should be added to drinks and beverages before, during, or after processing to enhance flavor, aroma, and other quality factors. Likewise, such data are essential for targeting enzymes with desirable properties for overproduction in transgenic microbial or plant hosts and improvement of their catalytic properties and stability for specific uses by genetic engineering.

Another aspect of β-glucosidases that pertains to food processing and quality is that edible portions of some plants contain compartmentalized β-glucosidase-β-glucoside systems that produce toxic aglycones and/or HCN when tissue is macerated during preparation or by chewing. This is exemplified by cassava roots and leaves, lima beans, and flax seeds. Of these, cassava is a food staple in tropical regions of Africa, Asia, and South America; consumption reaches about 1 kg/per capita per day in some parts of Africa (e.g., Congo). It contains the cyanogenic β-glucoside linamarin and the corresponding β-glucosidase linamarase. When consumed raw, cyanide poisoning can occur depending on the amount ingested, where symptoms are difficulty in breathing, paralysis, convulsion, coma, and even death. Similarly, certain processing methods (e.g., maceration of roots followed by washing) remove the components and products of cyanogenesis as well as many nutritional factors, thus reducing quality. Cooking inactivates the enzyme and eliminates the possibility of cyanogenesis. Similar symptoms can arise when bitter almonds are eaten and ingested without roasting.

The myrosinase–glucosinolate (or β-thioglucosidase–β-thioglucoside) system, which occurs in cruciferous vegetables (e.g., mustard, cabbage, kale, broccoli, rapeseed, horseradish, etc.), also has importance for food quality and processing because the aglycone moiety and its breakdown products from enzymatic hydrolysis of glucosinolates are responsible for the bitter, pungent taste and aroma associated with these vegetables, as well as the processed foods and relishes that include them (13). The distinct flavor associated with glucosinolates comes primarily from isothiocyanates and is believed to have evolved to serve as a repellent against microorganisms and herbivores. Glucosinolates and their breakdown products may impart undesirable flavors to milk, meat, and eggs when farm animals graze on cruciferous plants or when their feed includes seed meals from such plants. Besides off-odors and off-flavors in foods of animal origin associated with glucosinolates, direct ingestion of large amounts of cruciferous vegetables is thought to cause endemic goiter in man, as well as toxicity in laboratory animals. Similarly, claims have been made on anticarcinogenic effects of glucosinolates and their breakdown products in humans. Although the precise mechanism of action is not clear, studies on rodents showed that raw or cooked cruciferous vegetables (e.g., cabbage, broccoli, turnip, and cauliflower) increased aryl hydrocarbon hydroxylase activity (14).

III. BIOCHEMISTRY

A. Structure

Family 1 β-glucosidase monomers have molecular weights ranging from 55 to 65 kDa as estimated by SDS-PAGE, which is consistent with the determined polypeptide lengths ranging from 447 (e.g., *Bacillus polymyxia*) to 527 (e.g., white mustard myrosinase) amino acids long, depending on source organism of the enzyme. Not surprisingly, the longest polypeptide chains are found in eukaryotic enzymes while the shortest ones are in eubacteria and archaeabacteria (Fig. 1). All β-glucosidases isolated from animals and dicotyledonous plants (except indigo plant) so far are glycosylated and thus have estimated monomeric molecular weights 3–5 kDa larger than those calculated from sequences of mature polypeptide chains deduced from cDNA or genomic DNA sequences. The catalytically active form of β-glucosidases is a homodimer of $\sim$120 kDa or its multimers. The amino acids and sites that contribute to the dimer interface are not well conserved based on crystallographic data from eight enzymes (see below). High-molecular-weight quaternary complexes of β-glucosidases are either homocomplexes differing from each other by a dimer or its multiples as is the case for example with avenacosidase from oats, or heterocomplexes formed between β-glucosidase dimers and certain specific proteins associated with them. For example, in maize β-glucosidase forms large, insoluble or poorly soluble aggregates resulting from a specific interaction between the enzyme and a 32-kDa small heat shock protein, which is expressed at elevated levels in certain maize inbred lines (15, 16). Similarly, high-molecular-weight aggregates of β-glucosidases have been described from oat (17), flax (18), and cabbage (19) where in the case of cabbage the aggregates were shown to be due to interaction with specific myrosinase-binding proteins.

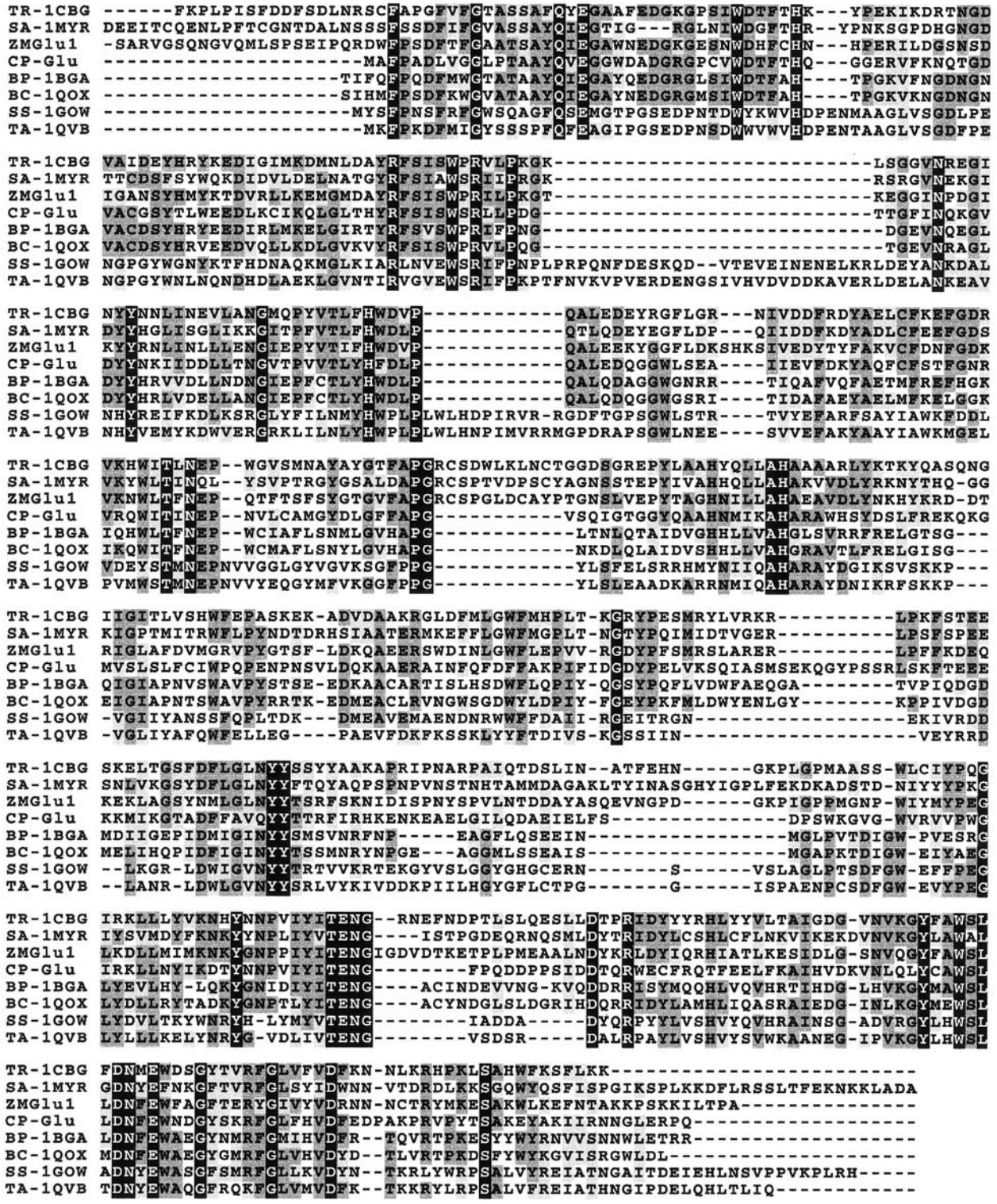

Figure 1 Sequence alignment of family 1 β-glycosidases from representative species of three organismic domains (Eukarya, Archaea, and Eubacteria). TR-1CBG, white clover (*Trifolium repens* L.) linamarase; SA-1MYR, white mustard (*Sinapis alba*) myrosinase; ZMGlu1, maize (*Zea mays* L.) Glu1; CP-Glu, guinea pig (*Cavia porcellus*) cytosolic β-glucosidase; BP-1BGA, *Bacillus polymyxa* β-glucosidase; BC-1QOX, *Bacillus circulans* sp. *alkalophilus* β-glucosidase; SS-1GOW, *Sulfolobus solfataricus* β-glucosidase; and TA-1QVB, *Thermosphaera aggregans* β-glucosidase. Regions with black background show the universally conserved sites, whereas regions with dark gray and light gray show highly conserved and moderately conserved sites, respectively. Regions with white background show variable sites, while dashes indicate the gaps (deletions) that the alignment software (ClustalW) introduced to optimize the alignment. The alignment was produced with ClustalW and formated with Boxshade, both of which are free downloads from the Web.

The primary structure of each family 1 β-glucosidase monomer contains the highly conserved peptide motifs SAYQI, YRFSI, TFNEP, LGLNYY, YITENG, and DNFEW, which serve as fingerprints to identify an unknown protein as a family 1 β-glucosidase (Fig. 1). Of these, TFNEP and YITENG are the most conserved; they make up a part of the active site and contain the two catalytic glutamates (20–23). Furthermore, the 3D structures of eight family I β-glycosidases [1CBG, white clover (*Trifolium repens*) linamarase; 1MYR, white mustard (*Sinapis alba*) myrosinase; ZMGlu1, maize (*Zea mays* L., see Fig. 2); 1BGA, *Bacillus polymyxa* β-glucosidase; 1QOX, *Bacillus circulans* sp. *alkalophilus* β-glucosidase; 1PBG, *Lactococcus lactis* phospho-β–galactosidase; 1GOW, *Sulfolobus solfataricus* β-glucosidase; and 1QVB, *Thermosphaera aggregans* β-glucosidase] have recently been solved (20–27). All eight enzymes have essentially the same basic $(\beta/\alpha)_8$-barrel fold structure (Fig. 2) although they share only 17–63% sequence identity (Fig. 1). It is remarkable that the basic catalytic machinery, reaction mechanism, and 3D structure have been rigidly retained in the three domains of living organisms in spite of large amounts of sequence divergence through eons of evolution.

B. Multiple Molecular Forms (Isoforms)

β-Glucosidase is ubiquitous, and thus a given organism is expected to have at least one molecular form of the enzyme. When the enzyme occurs in multiple molecular forms (isoforms) as detected by electrophoretic mobility or ion exchange chromatography, typically two or three forms are observed whose existence is also confirmed by molecular biological techniques (e.g., Southern blotting and Northern blotting) and DNA sequencing. However, electrophoretic and chromatographic detections are limited to those enzymes that hydrolyze the test substrate used for detection while blotting techniques are limited to those genes or mRNAs that have sufficient sequence similarity to the probe sequence. Therefore, the number of isoforms detected is very likely to be lower than the number of those that actually exist. Indeed, the data from genome sequencing projects appear to support this conclusion. For example, *Arabidopsis thaliana* genome sequence data so far indicate that there are at least 40 different genes encoding family 1 β-glucosidase in this plant, which has the smallest and most streamlined genome among plants. Whether or not all of these putative genes are actually expressed and code for a functional enzyme remains to be shown by functional genomics studies. However, it would not be too surprising if there are more β-glucosidase isoforms than expected in view of the possibility that there may be tens of different physiological substrates (β-glucosides or glucoconjugates) produced during the life of, especially, a multicellular organism in specific tissues, organs, developmental stages, and environmental stresses. Some if not all of these substrates may have a corresponding specific β-glucosidase isoform hydrolyzing them under specific conditions and with specific kinetics.

In addition to genetically determined β-glucosidase multiplicity that can be demonstrated by DNA sequencing and blotting, there are many examples of β-glucosidase multiplicity generated by posttranslational modifications (e.g., glycosylation and proteolytic modification in vitro) during isolation and subsequent manipulations of enzyme preparations. For example, as many as six different forms of the maize β-glucosidase isozyme Glu1 can be detected on zymograms in a time- and pH-dependent manner. Five of these bands are artifactual, and they result from the activity of an endogenous cysteine protease in buffers of pH 5–6 containing a reducing agent such as 2-ME (28). These data suggest that multiple forms of β-glucosidase detected on zymograms or after chromatography should not be interpreted as being distinct isozymes or allozymes without ruling out artificial heterogeneity due to proteolysis and differential posttranslational modification on the same polypeptide chain.

C. Catalytic Site and Machinery

All family 1 β-glycosidases are "retaining" enzymes in that the anomeric configuration of the glycone (e.g., glucose) is the same in the product (β-D-glucose) as it was in the substrate (a β-D-glucoside). Substrate hydrolysis involves two steps (enzyme glycosylation and deglycosylation) and requires participation of two specific glutamic acid residues in the active site.

* *Abbreviations*: AH, amygdalin hydrolase; AS, ammonium sulfate; 6BNGlc, 6-bromo-2-naphthyl-β-D-glucoside; DIMBOA, 2,4-dihydroxy-7methoxy-1,4-benzoxazin-3-one; DIMBOAGlc, 2-O-β-D-glucopyranosyl-4-hydroxy-7-methoxy-1,4-benzoxazin-3-one; HIC, hydrophobic interaction chromatography; IEF, isoelectric focusing; 2-ME, 2-mercaptoethanol; 4MUGlc, 4-methylumbelliferyl-β-D-glucoside; NP, nitrophenol; NPGlc, nitrophenyl glucoside; PAGE, polyacrylamide gel electrophoresis; PH, prunasin hydrolase; SB, *Sorghum bicolor*; SDS, sodium dodecyl sulfate; Xglc, 5-bromo-4-chloro-3-indolyl-β-D-glucoside; ZM, *Zea mays*.

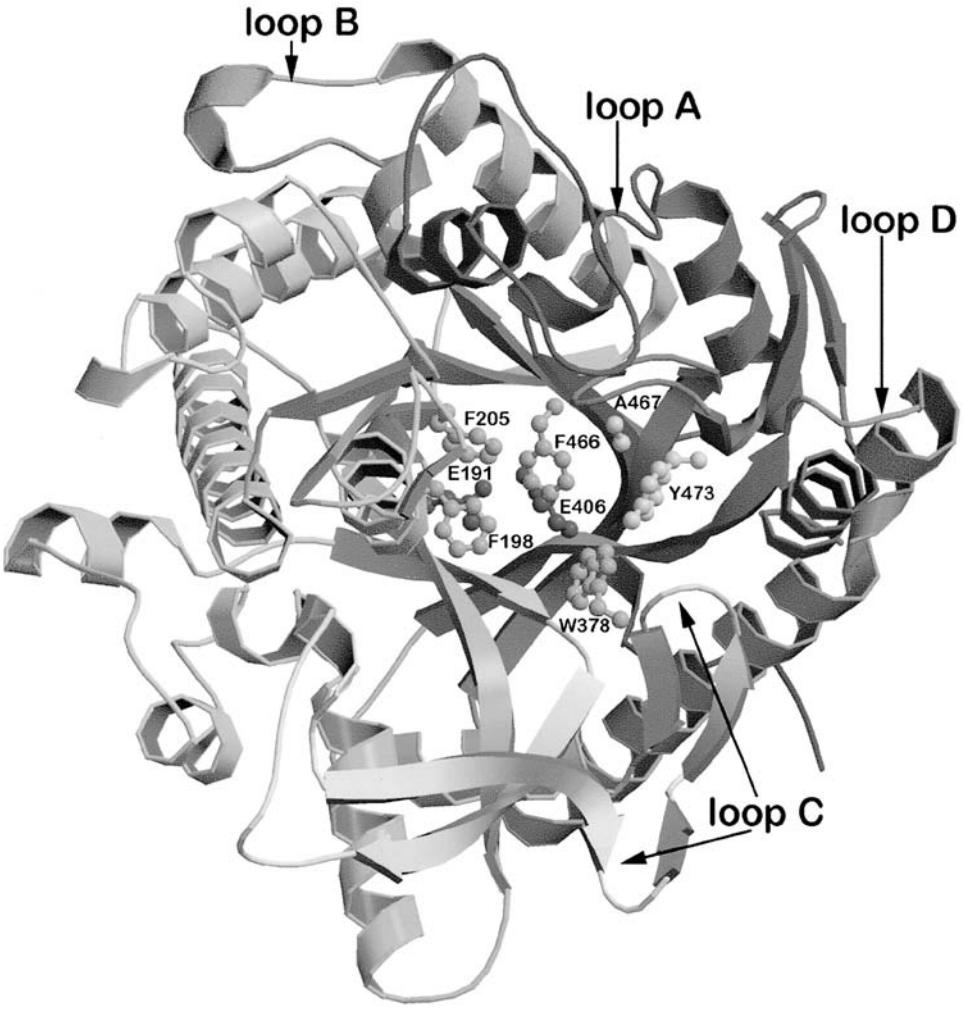

Figure 2 Ribbon diagram representation of the tertiary structure of the maize β-glucosidase Glu1 monomer, showing the catalytic glutamates E191 and E406, four residues (F198, F205, W378, and F466) forming the aglycone-binding pocket, and two other residues (A467 and Y473) that are probably important for aglycone recognition. Note the $(\beta/\alpha)_8$ fold barrel structure with alternating β-strands and α-helices and the four loops surrounding and contributing to the structure of the active site. Different colors and the color transitions in α-helices and β-strands in the original diagram trace the polypeptide backbone in the barrel-shaped 3-D structure from the N-terminal to C-terminal direction. The figure was produced with the softwares MOLSCRIPT and Raster3D.

In the glycosylation step, the nucleophilic glutamate residue in the motif YI/VTENG attacks at the anomeric carbon (C_1) of the substrate and forms a covalent glycosyl-enzyme intermediate with concomitant release of the aglycone after protonation of the glycosidic oxygen by the acid catalyst glutamic acid residue in the motif (T(F/L/M)NEP (29, 30). In the deglycosylation step, the second catalytic glutamate residue, now an anion and a base catalyst, removes a proton from water, and the resulting OH– group performs a nucleophilic attack on the covalent bond between the glycone and the enzyme, releasing the glycone and regenerating the nucleophilic glutamate residue. In all structures except myrosinase, a β-S-glucosidase, the residues of the TFNEP and I/VTENG motifs are involved in glycone binding and catalysis within a crater-shaped active site (31). The two catalytic glutamic acid residues (i.e., the nucleophile and the acid/base catalyst) are positioned within the active site at expected distances (~ 5.5 Å) (Fig. 2). In myrosinases, the motif that is homologous to TFNEP of β-O-glucosidases is TINQL, in which the acid/base catalyst glutamic acid residue is replaced by a glutamine residue. There is no need for protonic assistance for aglycone departure in

myrosinase, as the aglycone of β-glucosinolates is, by its chemical nature, an excellent leaving group.

D. Substrate Specificity

Substrate specificity in β-glycosidases literally means specificity for the chemical group attached to glycone through β-glycosidic linkage since the glycone moiety in a β-glycosidic substrate is an invariant monosaccharide (e.g., glucose in O- and S-linked β-glucosides). The group attached to glucose is either another glycone as in β-linked disaccharides (e.g., cellobiose) and oligosaccharides or an aglycone as in glucoconjugates. The aglycone moiety of the substrate is either an alkyl group (e.g., linamarin) or an aryl group (e.g., prunasin, dhurrin, and DIMBOAGlc). The subtle substrate specificity differences exhibited by β-glucosidases in general and plant β-glucosidases in particular, and the importance of the aglycone moiety in determining the specificity of β-glycosidases for their physiological substrates, have been well documented in the literature and reviewed (32, 33). The authors cited many cases of subtle substrate specificities and urged the use of physiological substrates during enzyme purification and characterization.

Conn (33) explained the historical reasons for the inaccurate perception that plant β-glycosidases have broad substrate specificity and cited as examples the popular plant β-glucosidase almond emulsin and crude plant extracts. Both of these sources contain mixtures of enzymes with β-glucosidase activity and exhibit broad specificity on artificial chromogenic (e.g., nitrophenyl-β-D-glucosides) or fluorogenic (e.g., 4MUG1c) substrates. However, examples of narrow substrate specificity can be demonstrated if one uses purified enzyme in assays. Two such examples are β-glucosidases (also called dhurrinase) of sorghum and the Glu2 isozyme of maize whose primary structures have been determined in the author's laboratory (34, 35). In the first case, one isozyme (Dhr1) represents an extreme; it hydrolyzes only the natural substrate dhurrin and shows no activity toward other aryl or alkyl β-glucosides, including the popular artificial substrate *p*NPGlc. The second dhurrinase isozyme (Dhr2) also shows narrow specificity for dhurrin but it also hydrolyzes *p*NPGl1 and 4MUGlc, albeit at a very low rate (35, 36). Similarly, the maize Glu2 isozyme hydrolyzes the natural substrate DIMBOAGlc with the same efficiency as does the other maize isozyme (Glu1) but hydrolyzes poorly or not at all other substrates that are readily hydrolyzed by the Glu1 isozyme.

As for the so-called broad-specificity plant β-glucosidase, such as almond emulsin, Poulton and associates (37) showed that the black cherry homolog of the emulsin actually includes two distinct β-glucosidases, each with multiple forms and catalyzing different steps in amygdalin hydrolysis. One of these enzymes is amygdalin hydrolase (AH), and it has four isozymes and hydrolyzes amygdalin (mandelonitrile β-1,6-gentiobioside) to prunasin (mandelonitrile β-Glc) and glucose. The second enzyme is prunasin hydrolase (PH), and it has three isozymes, each hydrolyzes prunasin to glucose and mandelonitrile. Both AH and PH hydrolyze only their own natural substrates in vivo, and each shows varying levels of activity on artificial substrates.

The above-cited examples support Conn's conclusion (33) that plant β-glycosidases exhibit narrow specificity when one uses purified enzyme in assays. Conn also points out that almost every research paper dealing with plant β-glucosidases used an NPGlc as substrate. In some studies, both artificial and natural substrates were used during enzyme purification while in others either a physiological substrate was not known or it was unavailable. In such cases two unfortunate outcomes are possible: (a) purifying and describing an enzyme that has no activity on an abundant natural substrate, and (b) failing completely to detect a physiologically relevant β-glucosidase that does not hydrolyze the artificial substrate used in the assay. Thus, the broad substrate specificity often attributed to β-glucosidases does not mean that the enzymes catalyze the hydrolysis of a large number of physiological substrates in vivo. Rather, it means that a large number of test substrates whose aglycone structure is similar to that of the physiological substrate can be hydrolyzed by an enzyme.

In fact, even some nonphysiological substrates may be hydrolyzed with a much higher catalytic efficiency than the physiological substrate. This is because the nonphysiological substrate may have better shape and functional group complementarity for binding with high affinity and its aglycone moiety may be a better leaving group in the glycosylation step of the reaction than that of the physiological substrate. For example, the maize β-glucosidase isozyme Glu1 hydrolyzes such natural and artificial substrates with aryl aglycone moieties as *p*- and *o*-NP, 4-methylumbelliferyl, 6-bromo-2-naphthyl, indoxyl, 5-bromo-4-chloro-3-indolyl, and cytokinin in addition to its abundant natural substrate DIMBOAGlc. Moreover, the maize enzyme hydrolyzes *p*NP-fucosides about 10 times more efficiently than *p*NP-glucosides. However, none of these substrates hydrolyzed by the enzyme

except DIMBOAGlc occur in maize. The only thing they have in common with the natural substrate is an aryl aglycone moiety that mimics DIMBOA. In fact, a research group (38) isolated Glu1 as an auxin-binding protein using an auxin analog as an affinity matrix because the enzyme was bound to the matrix owing to the similarity of the auxin analog to the aglycone (DIMBOA) of the natural substrate.

A simple and effective assay to search for natural substrates of β-glucosidases is to prepare an alcohol extract of the tissue of interest, concentrate, and fractionate it over a column (e.g., Sephadex LH-20) in 70% methanol. The resulting fractions are then dried and tested with a crude protein extract of the same tissue for glucose production, by a coupled PGO assay (see below) using appropriate controls. Once glucose production has been detected and confirmed in a fraction or crude organic extract, one can purify and identify the source glucoside by further analytical studies. Similarly, one can purify and identify the β-glucosidase that is hydrolyzing an isolated and identified physiological substrate by subjecting crude protein extracts of the same tissue or organ to purification by conventional biochemical procedures.

E. Mechanism of Substrate Specificity

Much progress has been made in understanding the mechanism of catalysis and defining the roles of the two catalytic glutamates within the active site that are involved in catalysis (29, 30, 39, 40). However, until recently, there was little or no information as to how β-glucosidases recognize and interact with their substrates, specifically the aglycone moiety, which is the basis of tremendous diversity in natural substrates and is responsible for the subtle substrate specificity differences among β-glucosidases. None of the seven structures published on family 1 enzymes contained either an intact substrate or an aglycone product to address the issue of substrate specificity.

Studies with reciprocal ZMGlu1/SBDhr1 chimeric enzymes indicated that the aglycone (i.e., substrate) specificity determining sites are different in maize β-glucosidase isozyme ZMGlu1 and sorghum β-glucosidase isozyme SBDhr1 (41). These data show that specificity for dhurrin hydrolysis residues in a C-terminal region octapeptide (^{462}SSGYTERF^{469}) of SBDhr1 where SBDhr1 and ZMGlu1 sequences differ from each other by four amino acid substitutions, while specificity for DIMBOAGlc hydrolysis is not within the ZMGlu1 homolog of the aforementioned octapeptide nor within the extreme 47-amino-acid-long C-terminal domain of ZMGlu1.

Questions about the mechanism and the site of substrate (i.e., aglycone) specificity and affinity could be directly addressed if it were possible to crystallize the enzyme-aglycone, inactive enzyme-substrate, or enzyme-unhydrolyzed competitive inhibitor complexes and identify the residues that are interacting with the aglycone in the 3D structure. Recently, the author's laboratory in collaboration with that of Bernard Henrissat in Marseille (AFMB-CNRS) was able to directly investigate the mechanism and the site of substrate (i.e., aglycone) recognition and specificity in maize β-glucosidase by x-ray crystallography using co-crystals of a catalytically inactive mutant (Glu1E191D) in complex with the natural substrate DIMBOAGlc, the free aglycone DIMBOA, and unhydrolyzed competitive inhibitor para-hydroxy-S-mandelonitril β-glucoside (dhurrin). The structures of these complexes and uncomplexed mutant were solved at 2.0, 2.1, and 2.2 Å resolution, respectively. The structural data from the complexes for the first time allowed us to visualize an intact substrate, free aglycone, or an unhydrolyzed competitive inhibitor in the slotlike active site of a β-glucosidase (42). These data show that the aglycone moiety of the substrate is sandwiched between W378 on one side and F198, F205, and F466 on the other. Thus, specific conformations of these four hydrophobic amino acids and the shape of the aglycone binding site they form determine aglycone recognition and substrate specificity in maize ZMGlu1. In addition to these four residues, A467 interacts with the 7-methoxy group of DIMBOA. All but W378 of these sites are variable among β-glucosidases that differ in substrate specificity, supporting the conclusion that these sites are the basis of aglycone recognition and binding (i.e., aglycone substrate specificity) in β-glucosidases. The data also provide a plausible explanation for the competitive binding of dhurrin to maize β-glucosidases with high affinity without being hydrolyzed.

F. Kinetic Constants

β-Glucosidases show variable affinity toward β-glucosides. The K_m values for good substrates, including natural substrates, are typically 1 mM or less. Similarly, β-glucosidases have, relatively speaking, low k_{cat} values ($\sim 300\,s^{-1}$ or lower). It is believed that the physiological function of these enzymes for the cell dictates slow hydrolysis of the substrates rather than "bursts" and natural selection favored such slow

rate of hydrolysis. The best way to compare substrate specificities and affinities is to compare the k_{cat}/K_m (efficiency coefficient) values, as two substrates with similar K_m values may yield as much as an order of magnitude differences in catalytic efficiency owing to the aglycone moiety (better or worse as a leaving group) or the glycone moiety. It is obvious that high k_{cat} and low K_m values would increase catalytic efficiency. When substrates differ with respect to leaving-group ability of their aglycones, the rate-limiting or enhancing step will be the glycosylation reaction. If they differ with respect to the glycone moiety, either glycosylation or deglycosylation step, or both, would be rate limiting. For example, maize β-glucosidases (along with most other β-glucosidases) hydrolyze *p*-nitrophenyl β-fucoside 10 times more efficiently than *p*NPGlc although their K_m values are similar. The difference in this case is clearly apparent in V_{max} values, although how the fucopyranosyl moiety enhances the reaction rate is not known.

G. Inhibitors and Cofactors

β-Glucosidases are inhibited by transition state sugar analogs (e.g., δ-gluconolactone), substrate analogue glucosides, free aglycones of their substrates, and substrate analogs. Since the active site has distinct aglycone- and glycone-binding pockets, sugars and sugar analogs with half-chair conformation can bind to the glycone-binding site and inhibit the enzyme, as can free aglycones, and the aglycone moiety of substrate analogs bind to the aglycone-binding site.

Free glucose is a poor inhibitor ($K_i = 100$–200 mM) because glucose must be in a half-chair conformation for binding to the glycone binding site, which it acquires after the aglycone moiety binds to the aglycone-binding site and distorts the conformation of the attached glucose to half-chair. In contrast, free aglycones are potent competitive inhibitors because their ground-state conformation is sufficient to recognize and bind to the aglycone binding site.

Metal ions, primarily Ag^+ and Hg^{2+}, are also potent β-glucosidase inhibitors. The inhibition can be completely reversed by reducing agents such as 2-ME (43). The target of these cations on the enzyme is not known although the catalytic nucleophile glutamate is a potential target. There are also reports of inhibition by Cu^{2+} and Fe^{3+} (44). A complete listing of β-glucosidase inhibitors is given in Zollner (44). There is no well-documented case of a cofactor requirement for a β-O-glucosidase, whereas the requirement of ascorbate for activity of β-S-glucosidases (myrosinases) is well known (45). Similarly, the presence of Mn^{2+} in the crystal structure of myrosinase suggests that this divalent cation might be required for activity by myrosinases.

H. Heat and pH Stability and Resistance to Proteases

β-Glucosidases are stable in the pH range 4–10 at 0–4°C, with highest stability at ~ pH 7. The sources of instability during storage are pH extremes, co-purifying proteases, and microbial contamination. Although most β-glucosidases are extremely resistant to proteases because of their tightly folded core structure, which exposes only the extreme N- and C-terminal regions to proteases, they are slowly degraded by contaminating or co-purifying proteases during prolonged storage without protease inhibitors in the medium. For example, maize Glu1 and almond emulsin lose only 10–15% of their activity after 18 h of exposure to one of the most potent proteases (proteinase K; Esen, unpublished) at room temperature. Under similar conditions, almost all of the other proteins in a crude extract are digested. β-Glucosidases are resistant to denaturation by ionic detergents such as SDS, which allows extraction with buffers containing up to 3% SDS and zymogram development after SDS-PAGE when samples are applied without heating.

As for thermostability, mesophilic β-glucosidases are irreversibly inactivated at and above 55–60°C, depending on the source, although they may show highest catalytic activity at 50–55°C (43). Increased catalytic activity at such high temperatures as 50–55°C is not physiologically and practically meaningful if the half-life of the activity is only 10 min or so due to thermal denaturation and inactivation, as is the case with maize β-glucosidase (43). However, β-glucosidases of thermophilic bacteria (e.g., *Thermosphaera* spp. and *Sulpholubus* spp.) have temperature optima ~ 85°C (46). The basis of this thermostability is attributed to the increase in the number of proline residues, internal water molecules, internal and surface electrostatic bridges, and the decrease in the solvent-accessible surface area by a tetrameric quaternary structure as opposed to the dimeric structure of mesophilic enzymes (25).

IV. ASSAYS FOR β-GLUCOSIDASE ACTIVITY

There are well-established procedures for assay of β-glucosidase activity, and they can be used to determine not only whether or not a crude tissue extract or sam-

ple has enzyme activity, but also to quantify the amount of enzyme activity present in a preparation. To this end, solution assays utilizing a substrate whose aglycone moiety is either chromogenic or fluorogenic are desirable. Almost all published solution assays use the commercially available nitrophenyl glucosides as substrate and commercially available almond emulsin as enzyme source. The assay can be performed in cuvettes or in 96-well microtiter plates and the absorbance of the nitrophenolate ion ($pK_a = 7.16$) can be read in a spectrophotometer or microtiter plate reader for quantification. A sample solution assay protocol for the microtiter plate format is give below. This procedure can be scaled up for test tube or cuvette format.

A. Spectrophotometric Assays

The following is a solution assay procedure that is applicable to any family 1 β-glucosidase after changing the pH of the buffer to one that is optimum for the enzyme of interest. All reagent chemicals and substrates mentioned are available from Sigma Chemical Company. The solutions needed are:

1. 50 mM citrate 100 mM phosphate buffer, pH 5.8 (also known as McIlvaine Buffer). Titrate 100 mM citric acid solution with 200 mM Na_2HPO_4, until pH is 5.8 (Buffer 1).
2. 5 mM *p*-nitrophenyl-β-D-glucopyranoside (*p*NPGlc) prepared in Buffer 1.
3. 0.4 M sodium carbonate (Na_2CO_3) prepared in water (stored at room temperature).
4. Tissue extracts or purified β-glucosidase preparations, diluted with Buffer 1 to yield 0.1–1.0 A_{410} units of activity in 5 min at 25°C. (Initially, tissue extracts may be diluted 10- to 100-fold in Buffer 1 and assayed to decide the appropriate dilution for quantitative assay.)

The procedure is as follows.

1. Add 70 μL of enzyme solution (Solution 4) to the wells of a 96-well microtiter plate in quadruplicate. Add 70 μL Buffer 1 to four blank wells (this is a minus enzyme control). Place the plate on rotary shaker-incubator set at 25°C for temperature equilibration ($\sim$ 5 min).
2. Pour sufficient volume of Solution 2 (substrate) in a 25-mL pipetting reservoir and leave it at 25°C for $\sim$ 5 min to equilibrate to room temperature.
3. Draw 70 μL of Solution 2 (substrate) with a multichannel pipette (if available, otherwise use a single-channel micropipette) from the trough, mark the time, and add it to the wells that had received 70 μL of enzyme solution (Solution 4) or Buffer 4 before.
4. Place in the incubator and shake at 50 rpm until exactly 5 min have elapsed from the time of substrate addition.
5. Remove the plate, add to each well 70 μL of Solution 3, and mix gently.
6. Read the absorbance at 410 nm in the microplate reader.
7. Compute the mean and standard deviation of the four values for each sample (see step 8).
8. Express (calculate) the enzyme activity as below.

One unit of enzyme activity is defined as the amount of enzyme that hydrolyzes 1 μmole of *p*NPG/h at 25°C. It has been determined that 1.69 μg (or 0.0121 μmole) *p*NP in 210 μL of volume in a 96-well microplate reader well gives an absorbance of 1000 at 410 nm. Example: A tissue extract, after diluting 100×, yielded 0.711 A_{410} units of β-glucosidase activity in 5 min at 25°C.

Enzyme activity $= a \times b \times c \times d = 0.0121 \times 0.711 \times 100 \times 12 = 10.32$ U/h/70 μL of original enzyme solution, or $10.32 \times 1000/70 = 147.5$ U/mL.*

Specific activity $= 147.5/1.5 = 98.3$ U/mg protein if the protein content of the original extract is 1.5 mg/mL.

To calculate the amount of *p*NP produced from *p*NPG by β-glucosidase activity, it is best to prepare serial dilutions of *p*NP, read their absorbance in the volume to be used in enzyme assays, and convert the reading to the amount of the *p*NP (μmoles) from the extinction coefficient ($\epsilon_{410} = 18{,}300\ M^{-1}\,cm^{-1}$) (47) of the nitrophenolate ion.

The above spectrophotometric assay may be changed to a fluorometric assay, for even higher sensitivity, using the fluorogenic substrate 4MUGlc and a fluorometer. Although most β-glucosidases hydrolyze *p*NPGlc and 4MUGlc, albeit at varying rates, some such as dhurrinase-1 of sorghum may not have any detectable activity on these popular artificial substrates. Therefore, an assay measuring the amount of glucose rather than the aglycone is desirable to detect the activity of a known or unknown enzyme on known or unknown natural substrates that are not chromogenic or fluorogenic. Coupling β-glucosidase assay to glucose oxidase/peroxidase assay meets the requirement of measuring glucose produced by β-glucosidase activity by oxidizing glucose to δ-gluconolactone by

* *a*, Amount of nitrophenolate (0.0121 μmole) yielding 1.0 A_{410}; *b*, measured A_{410} (0.711); *c*, enzyme dilution factor (100); *d*, time multiplication factor (12) to convert assay time (5 min) to 1 h.

glucose oxidase. The latter reaction produces hydrogen peroxide, which is used by peroxidase as a hydrogen acceptor to oxidize a chromogenic peroxidase substrate 2,2-azino-bis (3-ethylbenzthiazoline-6-sulfonic acid) (ABTS). The amount of oxidized peroxidase product is determined by measuring the absorbance and relating it to equivalent amount of glucose using a glucose calibration curve.

B. Solid-Phase Assays (Dot Blots and Zymograms)

Solid-phase assays are performed in the dot-blot format using nitrocellulose, polyvinyldene difluoride (PVDF), or ordinary chromatography paper. The test protein solutions are directly spotted on the matrix (sheet or strips) and incubated with a substrate whose aglycone forms an insoluble colored or fluorogenic spot at the site of enzyme activity. The most suitable chromogenic substrates for spot assay are 6BNGlc and XGlc. The aglycone of 4MUGlc may be detected by viewing under a UV lamp or on a UV box within the first 5 min or so, but it is soluble and cannot be fixed and detected later.

C. Detection of β-Glucosidase Activity on Polyacrylamide Gels

Zymogram assays are also routinely used for detection of the presence and multiplicity of β-glucosidase activity after native polyacrylamide gel electrophoresis (PAGE), isoelectric focusing gel (IEF), or sodium dodecyl sulfate–polyacrylamide gel electrophoresis (SDS-PAGE) under nondenaturing conditions. A sample protocol for native PAGE is given. The same protocol can be used for IEF and SDS gels if samples are applied to SDS gels without boiling. The following is a gel assay procedure that is applicable to all family 1 β-glucosidases after changing the pH of the buffer to the one that is optimum for the enzyme of interest (modified from 48). The solutions and reagents needed are:

1. 100 mM citrate–200 mM phosphate buffer, pH 5.8. Titrate 200 mM citric acid solution with 400 mM sodium phosphate (dibasic) until pH is 5.8.
2. 50 mM citrate–100 mM phosphate buffer. Dilute the above buffer with water at a ratio of 1 : 1.
3. 6-Bromo-2 naphthyl β-D-glucopyranoside (6BNGlc). Prepare just before using in dimethyl formamide at 100 mg/mL in a 1.5-mL microfuge tube. Usually 1 mL of 1 mg/mL solution will be sufficient for two gels.
4. Fast Blue BB salt. Dissolve 150 mg in 200 mL of 50 mM citrate–100 mM phosphate buffer, pH 5.8, in a 250-mL flask by stirring.
5. Fixative. Acetic acid methanol water mixed in 1 : 1 : 5 ratio. Store at room temperature.

Alternative substrate: 1 mM 4-methylumbelliferyl-β-D-glucoside (4 MUGlc) in 50 mM citrate–100 mM phosphate buffer, pH 5.8. This substrate is more sensitive and detects more β-glucosidases than 6BNGlc, but gels cannot be stored and dried. One needs to photograph the gel within 5–20 min under UV light.

The procedure is as follows.

1. Place the gel in a glass or clear plastic tray after electrophoresis or isoelectric focusing. Equilibrate in two changes of 50 mM citrate–100 mM phosphate buffer, pH 5.8 $\sim$ 15 min each, at room temperature.
2. Pour off the last (second) change of the equilibration buffer and then add freshly mixed substrate-coupling dye solution onto the gel in the dish. For this, add the substrate solution to the Fast Blue RR salt solution, mix in flask, and then pour onto the gel. Make sure that there is enough solution to cover the gel and permit free movement of the gel in solution during incubation and shaking.
3. Cover the tray with Saran wrap and aluminium foil; incubate in a shaker-incubator (set at $\sim$ 50 rpm) in the dark at 37°C for 2–16 h.
4. Stop the shaker-incubator at intervals, remove foil, and check for the appearance and intensity of enzyme bands. If no bands develop or they are too light after 2 h, it is best to continue incubation overnight.
5. When enzyme bands develop to a desired intensity and resolution, pour off the substrate-dye coupling solution, and rinse the gel several times with water in order to wash away the precipitated dye-substrate complex.
6. Add the fixative solution (#5) and store at room temperature for several hours before photographing, scanning, or imaging. Note that enzyme bands are completely stable in fixative solution up to several months, and the gel may be dried for long-term storage and record keeping.

When one's interest is surveying a food source for β-glucosidase activity, a simple, rapid, and inexpensive assay procedure is needed. Clearly, chromogenic solution assay in 96-well microtiter plates and dot-blot assay on nitrocellulose or ordinary chromatography paper are the best choices as long as the enzyme of

interest hydrolyzes the test substrate at detectable levels. In certain applications, one might be interested in detecting a β-glucoside present in a food sample using a specific enzyme that hydrolyzes and detects it. In this case, the PGO assay will be the choice since it measures glucose production.

D. Factors Interfering with Assays

The presence of β-glucosidase inhibitors in buffers or tissue extracts can interfere with solution assays, especially when extracts are not diluted much. In this case, endogenous substrates, substrate analog (aryl or alkyl glycosides), and glucose and its analog (e.g., δ-gluconolactone) can competitively inhibit the hydrolysis of test substrate such that the enzyme activity is neither detected nor underestimated. This problem can be alleviated by diluting crude extracts 50- to 100-fold if they have high activity levels or removing interfering substances by precipitating the enzyme with ammonium sulfate (AS) and resolubilizing to the original volume and/or dialysis.

V. PURIFICATION

When it comes to purification, every protein becomes a specific project and challenge to the skills and ingenuity of protein biochemists, although one can prescribe a general scheme for purification of related proteins. Having said that, it should be noted that β-glucosidases are relatively easier to purify than most proteins. The reader is referred to the primary literature for detailed procedures to design a protocol to purify a specific β-glucosidase of interest. In the author's laboratory, a number of maize and sorghum β-glucosidases and their chimeras and mutants have been successfully purified to homogeneity using just a combination of differential solubility and hydrophobic interaction chromatography (41, 49). Needless to say, the first step in purification protocol should start with differential solubility fractionation. To that end, a survey of buffers with different pH and ionic strengths to solubilize the β-glucosidase of interest while keeping most of the contaminating proteins insoluble or partly soluble would be worthwhile. For example, Mkpong et al. (50) were able to isolate cassava β-glucosidase by extraction with a buffer (0.1 M Na phosphate) of pH 3.5 with very high specific activity because the enzyme was stable and soluble at such a low pH, whereas contaminating proteins were not. Once conditions to extract the enzyme with high specific activity have been defined, such conditions can be used in large-scale purification projects. The next step would be to make a 40–60% ammonium sulfate (AS) cut on the crude extract (prepared with a buffer of pH 5–7) at 0–4°C as all family β-glucosidases precipitate between 40% and 60% AS concentration and can be fully recovered from the pellet by suspension in a suitable buffered solution. This step can increase specific activity significantly and serves as a stepping stone to a chromatographic separation method such as ion exchange, chromatofocusing, and hydrophobic interaction chromatography (HIC). Of these, HIC is the most effective as the pellet can be solubilized with 1.5 M AS in a buffer of pH 6–8, which itself removes a substantial amount of contaminants and then is directly loaded onto the column. In the author's laboratory HIC is performed on a Toyo-Pearl butyl column, and the eluate from this column, if necessary,

Table 1 Purification[a] of the Sorghum β-Glucosidase Isozyme Dhr2 after Expression in *E. coli*

Purification steps	Enzyme activity (μmole o-NP h^{-1})	Protein (mg/mL)	Specific activity (μmole o-NP h^{-1} mg^{-1})	Purification (fold)
1. Crude extract (before sonication)	17.54	0.98	17.90	1.0
2. Crude extract (after sonication)	82.05	4.90	16.74	0.94
3. 30% AS supernatant	82.01	4.50	18.22	1.02
4. 65% AS, pellet suspended	417.36	10.50	39.75	2.22
5. Butyl-HIC	119.70	0.74	161.76	9.04
6. Ether-HIC	68.02	0.24	283.42	15.83

[a] *E. coli* cell pellet was lysed in the extraction buffer (100 mM Tris-HCl, pH 8, and 50 mM NaCl), sonicated, and centrifuged. Ammonium sulfate (AS) was added to the supernatant (30% final concentration) and centrifuged. The supernatant was transferred to a fresh tube and sufficient AS was added to obtain 65% final concentration. The slurry was centrifuged and the resulting pellet was suspended in buffer, cleared by centrifugation, and subjected to hydrophobic interaction chromatography (HIC) on Toyopearl Butyl 650M and Toyopearl Ether 650M columns, respectively. Enzyme activity and protein content were determined after each step during purification.

may be rechromatographed on Toyo-Pearl Ether-M650. This two-step procedure after optimization of elution conditions for HIC yields homogeneous or near homogeneous preparations for characterization and crystallization studies. A summary of purification steps and increase in specific activity using the described procedure for the sorghum β-glucosidase isozyme Dhr2 expressed in *E. coli* is given as an example in Table 1.

REFERENCES

1. B Henrissat. A classification of glycosyl hydrolases based on amino acid similarities. Biochem J 280:309–316, 1991.
2. B Henrissat, A Bairoch. Updating the sequence-based classification of glycosyl hydrolases. Biochem J 316:695–696, 1996.
3. B Henrissat, GJ Davies. Structural and sequence-based classification of glycoside hydrolases. Curr Opin Struct Biol 7:637–644, 1997.
4. EE Conn. Cyanogenic glycosides. In; PK Stumpf ,EE Conn, eds. Biochemistry of Plants, Vol 7. New York: Academic Press, 1981, pp 479–500.
5. HM Niemeyer. Hydroxamic acids (4-hydroxy-1,4-benzoxazin-3-ones), defense chemicals in the Gramineae. Phytochemistry 27:3349–3358, 1988.
6. JE Poulton. Cyanogenesis in plants. Plant Physiol 94:401–405, 1990.
7. AR Smith, J van Staden. Changes in endogenous cytokinin levels in kernels of *Zea mays* L. during imbibition and germination. J Exp Bot 29:1067–1073, 1978.
8. DP Dharmawardhana, BE Ellis, JE Carlson. A β-glucosidase from lodgpole pine xylem specific for the lignin precursor coniferin. Plant Physiol 107:331–339, 1995.
9. R Leah, J Kigel, I Svendsen, J Mundy. Biochemical and molecular characterization of barley seed β-glucosidase. J Biol Chem 270:15789–15797, 1995.
10. Z Günata, I Dugelay, JC Sapis, R Baumes, C Bayonove. Role of the enzymes in the use of the flavour potential from grape glycosides in winemaking. In: P Schreier, P Winterhalter, eds. Progress in Flavour Precursor Studies. Carol Stream, IL: Allured Publ, 1993, pp 219–234.
11. Reference deleted.
12. K Ogawa, I Yasuyuki, W Guo, N Watanabe, T Usui, S Dong, Q Tong, K Sakata. Purification of a β-primeverosidase concerned with alcoholic aroma formation in tea leaves (cv. *Shuixian*) to be processed to oolong tea. J Agric Food Chem 45:877–882, 1997.
13. GR Fenwick, RK Heaney, WJ Mullin. Glucosinolates and their breakdown products in food and food plants. CRC Crit Rev Food Sci Nutr 18:123–201, 1983.
14. LW Wattenberg. Studies on polycyclic hydrocarbon hydroxylases of the intestine possibly related to cancer. Effect of diet on benzopyrene hydroxylase activity. Cancer 28:99–102, 1971.
15. A Esen, DJ Blanchard. A specific β-glucosidase-aggregating factor is responsible for the β-glucosidase null phenotype in maize. Plant Physiol 122:1–10, 2000.
16. DJ Blanchard, M Cicek, J Chen, A Esen. Identification of β-glucosidase aggregating factor (BGAF) and mapping of BGAF binding domains on maize (*Zea mays* L.) β-glucosidase. J Biol Chem 276:11895–11901, 2001.
17. A Nisius. The stromacentre in *Avena* plastids: an aggregation of β-glucosidase responsible for the activation of oat-leaf saponins. Planta 173:474–481, 1988.
18. MA Fieldes, KE Gerhardt. An examination of the β-glucosidase (linamarase) banding pattern in flax seedlings using Ferguson plots and SDS-PAGE. Electrophoresis 15:654–661, 1994.
19. A Falk, J Taipalensuu, B Ek, M Lenman, L Rask. Characterization of rapeseed myrosinase-binding protein. Planta 195:387–395, 1995.
20. C Wiesmann, G Beste, W Hengstenberg, GE Schulz. The three-dimensional structure of 6-phospho-β-galactosidase from *Lactococcus lactis*. Structure 3:961–968, 1995.
21. T Barrett, CG Suresh, SP Tolley, EJ Dodson, MA Hughes. The crystal structure of a cyanogenic β-glucosidase from white clover, a family 1 glycosyl hydrolase. Structure 3:951–960, 1995.
22. WP Burmeister, S Cottaz, H Driquez, R Iori, S Palmieri, B Henrissat. The crystal structures of *Sinapis alba* myrosinase and a covalent glyosyl-enzyme intermediate provide insights into the substrate recognition and active-site machinery of an S-glycosidase. Structure 5:663–675, 1997.
23. J Sanz-Aparicio, JA Hormoso, M Martinez-Ripoll, JL Lequerica, J Polaina. Crystal structure of β-glucosidase A from *Bacillus polymyxa*: insights into the catalytic activity in family 1 glycosyl hydrolases. J Mol Biol 275:491–502, 1998.
24. CF Aguilar, I Sanderson, M Moracci, M Ciaramella, R Nucci, M Rossi, LH Pearl. Crystal structure of the β-glycosidase from the hyperthermophilic archeon *Sulfolobus solfataricus*: resilience as a key factor in thermostability. J Mol Biol 271:789–802, 1997.
25. Y-I Chi, LA Martinez-Cruz, RV Seanson, DE Robertson, SH Kim. Crystal structure of the β-glycosidase from the hyperthermophile *Thermosphaera aggregans*: insights into its activity and thermostability. FEBS Lett 445:375–383, 1999.

26. N Hakulinen, S Paavilainen, T Korpela, J Rouvinen. The crystal structure of beta-glucosidase from *Bacillus circulans* sp. *alkalophilus*: ability to form long polymeric assemblies. J Struct Biol 129:69–79, 2000.
27. M Czjzek, M Cicek, V Zaboni, WP Burmeister, DR Bevan, B Henrissat, A Esen. Crystal structure of a monocot (maize ZMGlu1) β-glucosidase and its complex with *p*-nitrophenyl-β-D-thioglucoside. Biochem J 354:37–46.
28. A Esen, C Cokmus. pH- and temperature-dependent β-glucosidase multiplicity in maize (*Zea mays* L.) is a proteolysis artifact. Plant Sci 74:17–26, 1991.
29. SG Withers, RAJ Warren, IP Street, K Rupitz, JB Kempton, R Aebersold. Unequivocal demonstration of the involvement of a glutamate residue as a nucleophile in the mechanism of a ''retaining'' glycosidase. J Am Chem Soc 112:5887–5889, 1990.
30. QD Wang, R Trimbur, R Graham, RAJ Warren, SG Withers. Identification of the acid/base catalyst in *Agrobacterium faecalis* β-glucosidase by kinetic analysis of mutants. Biochemistry 34:14554–14562, 1995.
31. G Davies, B Henrissat. Structures and mechanisms of glycosyl hydrolases. Structure 3:858–859, 1995.
32. W Hösel, EE Conn. The aglycone specificity of plant β-glycosidases. Trends Biochem Sci 6:219–221, 1982.
33. EE Conn. β-Glycosidases in plants: substrate specificity. In: A Esen, ed. β-Glucosidases: Biochemistry and Molecular Biology .ACS Symposium Series 533. Washington: American Chemical Society, 1993, pp 15–26.
34. H Bandaranayake, A Esen. Nucleotide sequence of a cDNA corresponding to second β-glucosidase gene in maize (*Zea mays* L.) (Accession #U44087). Plant Physiol 110:1048, 1996.
35. M Cicek, A Esen. Structure and expression of a dhurrinase (β-glucosidase) from sorghum. Plant Physiol 116:1469–1478, 1998.
36. W Hösel, I Tober, SH Eklund, EE Conn. Characterization of β-glucosidase with high specificity for the cyanogenic glucoside dhurrin in *Sorghum bicolor* (L) Moench seedlings. Arch Biochem Biophys 252:152–162, 1987.
37. JE Poulton. Enzymology of cyanogenesis in rosaceous stone fruits. In: A Esen, ed. β-Glucosidases: biochemistry and Molecular Biology. ACS Symposium Series 533. Washington: American Chemical Society, 1993, pp 170–190.
38. N Campos, L Bako, B Brzobohaty, J Feldwisch, J Schell, K Palme. A protein from maize labelled with azido-IAA has novel β-glucosidase activity. Plant J 2:675–684, 1992.
39. M Moracci, L Capalbo, M Ciaramella, M Rossi. Identification of two glutamic acid residues essential for catalysis in the β-glycosidase form the thermoacidophilic archaeon *Sulfolobus solfataricus*. Protein Eng 9:1191–1195, 1996.
40. S Cottaz, B Henrissat, H Driguez. Mechanism-based inhibition and stereochemistry of glucosinolate hydrolysis by myrosinase. Biochemistry 35:15256–15259, 1996.
41. M Cicek, DJ Blanchard, DR Bevan, A Esen. The aglycone specificity determining sites are different in 2,4-dihydroxy-7-methoxy-1,4-benzoxazin-3-one (DIMBOA)-glucosidase (maize β-glucosidase) and dhurrinase (sorghum β-glucosidase). J Biol Chem 275:20002–20011, 2000.
42. M Czjzek, M Cicek, V Zamboni, DR Bevan, B Henrissat, A Esen. The mechanism of substrate (aglycone) specificity in β-glucosidases is revealed by crystal structures of mutant maize β-glucosidase-DIMBOA, -DIMBOAGlc, and -dhurrin complexes. Proc Natl Acad Sci USA 97:13555–13560, 2000.
43. A Esen. Purification and partial characterization of maize (*Zea mays* L.) β-glucosidase. Plant Physiol 98:174–182, 1992.
44. H Zollner. Handbook of Enzyme Inhibitors. Weinheim, Germany: VCH, Verlaggessalschaft, 1989, pp 94–95.
45. M Ohtsuru, T Hata. The interaction of L-ascorbic acid with the active center of myrosinase. Biochim Biophys Acta 567:384–391, 1979.
46. M Moracci, R Nucci, F Febbraio, C Vaccaro, CN Vespa, F La Cara, M Rossi. Expression and extensive characterization of a beta-glycosidase from the extreme thermoacidophilic archaeon *Sulfolobus solfataricus* in *Escherichia coli*: authenticity of the recombinant enzyme. Enzyme Microb Technol 17:992–997, 1995.
47. H-C Hung, G-G Chang. Partitioning of 4-nitrophenol in aerosol-OT reverse micelles. J Chem Soc Perkin Trans 2:2177–2182, 1999.
48. A Esen, C Cokmus. Maize genotypes classified as null as the glu locus have β-glucosidase activity and immunoreactive protein. Biochem Genet 28:319–336, 1990.
49. M Cicek, A Esen. Expression of soluble and catalytically active plant (monocot) β-glucosidases in *E. coli*. Biotech Bioeng 63:392–400, 1999.
50. OE Mkpong, H Yan, G Chism, RT Sayre. Purification, characterization, and localization of linamarase in cassava. Plant Physiol 93:176–181, 1990.

64

β-D-Fructofuranoside Fructohydrolase

Laura Cantarella
University of Cassino, Cassino, Italy
Francesco Alfani[†] **and Maria Cantarella**
University of L'Aquila, L'Aquila, Italy

I. INTRODUCTION

β-D-Fructofuranoside fructohydrolases (β-Fs) are sucrose-hydrolyzing enzymes found in microbial, plant, and animal sources. Trivial names are β-fructofuranosidase, formerly called invertase or saccharase, and sucrase. The enzyme was first isolated by Berthelot in 1860 (1). βFs occur in *Saccharomyces cerevisiae* and in strains used in brewing, distilling, wine making, and the baking of bread, as an extracellular glycoprotein, the predominant form, and an intracellular protein (2, 3). Several molecular forms exist differing in molecular weight and cell location even within the same yeast culture. Most βFs in plants and tissues (5–9) are multimeric proteins discernible on their pH optima (acid, 4.5–5.0, and neutral (alkaline), 7.0–7.8) (10–13), glycosylation state, subcellular location, and pI values. βFs from *S. cerevisiae* or *S. carsbergensis* are commercially available.

A. Chemical Reaction Catalyzed

Sucrose hydrolysis is the main reaction catalyzed by βF. Raffinose and stachyose are hydrolyzed to a lesser extent.

$$\text{Sucrose} + H_2O \xrightarrow{\beta\text{-fructofuranosidase}} \text{D-Glucose} + \text{D-Fructose}$$

Acid βFs are able to catalyze transfructosylation reactions. At high sucrose concentration (1 M), the β-D-fructofuranosyl residue is transferred to a primary alcohol (methanol, ethanol, n-propanol) and to only isopropanol as a secondary alcohol (3).

B. Chemical Structure of Substrates

1. Sucrose, α-D-glucopyranosyl [1 → 2]-β-D-fructofuranoside, also indicated as [Glc β 1,2 Fru]
2. Raffinose, O-α-D-galactopyranosyl [1 → 6]-α-D-glucopyranosyl [1 → 2]-β-D-fructofuranoside, also indicated as [Gal α 1,6 Glc β 1,2 Fru]
3. Stachyose, α-D-galactopyranosyl [1 → 6]-α-D-galactopyranosyl [1 → 6]-α-D-glucopyranosyl [1 → 2]-β-D-fructofuranoside, also indicated as [Gal α 1,6 Gal α 1,6 Glc β 1,2 Fru]
4. Substituted β-D-fructofuranosides, such as methyl-β-D-fructofuranoside, and *p*-nitrophenyl-β-D-fructofuranoside

C. Classification According to Enzyme Commission Nomenclature

All βFs are classified as EC 3.2.1.26. True βFs have to show no activity with nonsubstrates such as cellobiose [Glc β1,4 Glc], gentobiose [Glc β1,6 Glc], lactose [Gal

[†]Deceased.

β1,4 Glc], maltose [Glc α1,4 Glc], melezitose [Glc α1,3 Fru α 2,1 Glc], α-methyl-D-glucopyranoside, β-methyl-D-glucopyranoside, α,α-trehalose [Glc α1,1 Glc] or turanose [Glc α1,3 Fru], and *p*-nitrophenyl-β-glucoside (α-fructofuranosides, fructopyranosides, β-L-sorbofuranosides, β-D-xyloketofuranosides, and sugars with substituent on the β-fructofuranosyl residue).

II. IMPORTANCE TO QUALITY OF FOOD DURING GROWTH, MATURATION, STORAGE, AND PROCESSING

In plants, the different βF isoforms independently control import sucrose metabolism, sugar composition in storage organs, translocation from source tissues to sink tissues, osmoregulation, and gravitropism (6, 14–16). Compositional changes observed in several developing fruits are associated with the changes in enzyme activities related to sucrose metabolism. Acid and neutral βF activities are very high in immature fruits of *Cucumelis melo* L. and decline rapidly and concomitantly with the accumulation of sucrose, as the fruit matures (7). The activation of preexisting invertase in dormant *Helianthus tuberosus* (Jerusalem artichoke) tubers takes place at the beginning of the germination process.

The absence of βF contributes to the accumulation of sucrose rather than hexoses as a source of carbon and energy. Vacuolar βF controls the sugar composition in tomato species (15). *Lycopersicon esculentum* has high βF activity, accumulates high levels of glucose and fructose, and stores little sucrose. In contrast, *L. peruvianum* and *L. chmielewskii* (15) have low βF activity, accumulate high levels of sucrose and store little glucose and fructose. Vacuolar βFs are also involved in glucose and fructose accumulation in grape berries that is one of the main features of the ripening process and is a major commercial consideration for grape growers, wine makers, and dried-fruit producers (17). Alkaline βF activities increase during the development and maturation of tissues in sugar cane stalks, carrot, and sugar beet roots and young *versus* mature leaves of *Citrus sinensis*.

During cold storage (1–3°C), potato tuber βF isoforms cause the accumulation of reducing sugars that are responsible for the development of unpalatable flavor and texture in cooked potatoes (18). Darkening of the potatoes due to a nonenzymatic Maillard reaction also occurs. Sugarbeet roots contain an endophytic population of sucrose-hydrolyzing bacteria (*Pseudomonas fluorescens*) that possibly utilize the sucrose in stored roots awaiting processing (19). During the prestorage phase of *Vicia faba*, high levels of hexoses in the cotyledons are correlated with the activity of seed coat-associated invertases. The degradation of the thin-walled parenchyma expressing the invertase (developmentally regulated) apparently initiates the storage phase and is characterized by a switch to a low sucrose/hexose ratio (8). During the storage of raw juice extracts from healthy tubers of *Cyperus esculentus* Linn. (earth almond), yeasts possibly play a greater role than bacteria in the hydrolysis of sucrose. *Saccharomyces rouxii*, an osmophilic yeast strain, was isolated from dried prunes where the natural environment typically has a high concentration of sucrose. The species survives by initially metabolizing other components in the medium. After death of a fraction of the population, cryptic βF hydrolyzes sucrose, and the osmotic pressure is gradually lowered. Competition with other microorganisms in the ecological niche is thus delayed.

In plant intact tissue nearly all the βF activity can be attributed to alkaline βF, while in the case of injury, acid βFs are rapidly formed in response to wounding and bacterial infection, suggesting their possible role in pathogen defense mechanisms (20). The active defense response can be induced by chemical stimuli (elicitors) derived from fungi (21). α-Chymotrypsin cleavage of yeast βF generates small glycopeptides, acting as elicitors in tomato cells, inducing the biosynthesis of ethylene (plant stress hormone) and of phenylalanine ammonia-lyase. By contrast, the isolated glycan side chains act as suppressors.

Freezing-tolerant wheat cultivars may respond to subzero temperatures and increase hardiness by the conversion of fructan to cryoprotective sugars, such as fructose and sucrose, whereas snow mold-resistant cultivars continue to accumulate fructan. This difference in response to subzero temperature may depend on differences in gene expression of enzymes in fructan metabolism, which involves several enzymes (22).

III. RAW-FOODS ENZYMES FOUND

In *Saccharomyces cerevisiae*, internal βF is found in the cytoplasm whereas external βF resides on the cell wall (cw-βF), and functions to cleave extracellular sucrose to fructose and glucose, sugars that yeast can import (2, 3).

In plants, the subcellular location of soluble βF is controversial: the enzyme is described either as cytoplasmic, despite its glycoprotein nature, or as vacuolar. Spatially, βFs occur as intra- and extracellular forms.

Both soluble and cw-βFs are found (23–27). Two types of acid βF (N-linked glycoproteins) are located either as soluble proteins in the vacuole or ionically bound to the cell wall. Acid and neutral βFs may coexist even in the same tissue (11). However, acid βF is mainly found in immature tissues while neutral βF is confined to mature storage tissues of sucrose-accumulating plants. In contrast, neutral βF in the mesocarp of developing muskmelon declined with the accumulation of sucrose (7). Soluble acid βF also occurs in the apoplast of plant tissues (papaya, sugar cane, oat, radish, wheat, maize, artichoke, barley, potato, carrot, cherry, tomato, peach, strawberry). Acid βF is extremely low in the reserve cotyledon tissue throughout development, and activity appears to be correlated with the growth and differentiation of certain plant tissues, particularly involved in organ elongation and cell enlargement (6). It declines rapidly when roots begin to enlarge, and is hardly detectable in mature roots and organs. Acid cw-βF plays a key role in the generation of sink strength of storage sinks (photosynthetically less active or inactive tissues such as stems, flowers, and roots) during development of *Vicia faba* L. seeds (28). Less information is available on neutral or alkaline βFs (10) present in the cytoplasm of most living cells of higher plants.

IV. UTILITY/UTILIZATION OF ENZYMES IN FOODS

In the food industry, the main use of βF is for producing chocolate-coated candies with a soft and creamy center. A hard and firm center is prepared with sucrose and molded into the desired shape. After coating with chocolate the βF is inoculated into the center to change its consistency to a permanent and noncrystallizable cream. Purified βF is preferred to yeast since variations in both the added amount and in the strains of yeast utilized does not assure uniform quality of softer centers. Other βF uses are related to the production of artificial honey and to the enzymatic determination of glucose and sucrose in dietetic foods (29). The productivity value, the operational stability and mechanical stability of βF, the low cost of the immobilization on a variety of carrier, and the absence of undesirable reaction byproducts make the scale production of inverted syrups from sucrose and nonrefined sugars economically very attractive. In the confectionery industry fructose is preferred over sucrose because it is sweeter and does not crystallize as easily. Health and taste reasons require highly purified βF. Invertase from *S. cerevisiae* is utilized for the commercial production of invert sugars from sucrose at concentrations up to 3 M (30).

Brewing, distilling, wine making, and the baking of bread all require freshly grown, specially developed yeast strains (*S. cerevisiae*) to inoculate each fermentation. The activity of βF and of β-glucosidase determines the physical and organoleptic properties of bread. The capacity of a given strain for sugar uptake and the further conversion of the sugars present in bread dough are of primary importance for its bread-making suitability (31).

Fructo-oligosaccharides (1-kestose, nystose, and 1^F-β-fructofuranosyl nystose), produced by transferring one, two, or three molecules of fructose to the fructose residue in sucrose by the action of fungal βF (32), have been shown to decrease the levels of cholesterol and lipid in the serum and to stimulate the growth of intestinal bifidobacteria.

Transgenic tomato plants that expressed a yeast βF show a decrease in the growth rate. Accumulation of hexoses and amino acids (proline) is up to 40-fold higher than in the wild type. The fruits were ~ 30% smaller than controls. Soluble acid βF controls this differential growth which correlates with high rates of sugar accumulation during the last stage of development (33). Potato tubers expressing yeast βF in the cytosol result in a reduction in tuber size and an increase in tuber number per plant, whereas apoplastic targeting leads to an increase in tuber size and a decrease in tuber number per plant (18).

V. PROPERTIES AS PROTEIN

A. Molecular Weight

The molecular mass of βFs varies considerably: in plants from 42 kDa to 504 kDa, in microorganisms from 37–560 kDa. The glycosylated nature may lead to a lack of precision in estimating the molecular weight. Values are reported in Tables 1 and 2.

B. Primary, Secondary, Tertiary, Quaternary, and Macromolecular Structures

Internal and external yeast βFs appear with identical protein moieties. The same (SUC2) gene is translated from different start codons resulting in one or two additional amino acids (a.a.) at the N-terminus of external βFs (44). The subunit has an MW of ~ 58 kDa. Internal βF exists in its native state as a nonglycosylated active monomer. A signal sequence directs external βF into the endoplasmic reticulum, where it

Table 1 Major Structural Characteristics of Some Purified βF from Different Plants

Source	βF purified [pl]	Carbohydrate	Native protein		SDS-PAGE		Other isoforms [pI]
			Form	MW (kDa)	MW (kDa)	Protein band	
Arabidopsis thaliana L., mature green leaves (9)	acid [4.75]	positive	monomer	58	52		4 acid [4.65; 4.70; 4.85; 4.95] and 1 cw [9.0]
Avena sativa, oat seedling (5)	acid [8.6]			59		single	
	acid [4.4]			108		single	
Cichorium intybus L., roots (10)	neutral		tetramer	260	65	single	multiple peaks
Daucus carota L., cell culture (12)	neutral		octamer	456	57	single	multiple peaks
	alkaline		tetramer	504	126	single	
Seed seedling (23, 24)	acid [5.7]	positive[a]	monomer	68	68, 43, 25	3 bands	acid [3.8] cw bound
Glycine max, sprouting hypocotyl (6)	alkaline	negative[b]	tetramer	240	58	single	acid
Hordeum vulgare L., leaves (34)	acid	positive[b]	monomer	64	64	single	
			multimer	116		multi	
			multimer	155		multi	
Lycopersicon esculentum, pericarp tissue (17)	acid		monomer	52	52	single	2
Prunus avium L., mesocarp (35)	acid	positive[b]	multimeric	400	63	single	1
Solanum tuberum, tuber (36)	acid	10.9%[b]	dimer	60	30	single	
Sugar cane juice (37)	neutral	22	monomer		15		
			dimer		35		
			tetramer		66		
			decamer		160		
Vicia faba L., cotyledon (8)	alkaline [5.2]		homotetramer	238	53.4		acid

[a] N-glycosylated with high-mannose-containing and high-xylose-containing complex glycans.
[b] Is a glycoprotein as indicated by positive reaction with periodic acid–Schiff reagent and its ability to bind ConA.

Table 2 Major Structural Characteristics of Some Purified βF from Different Microorganisms

Source	Location	Carbohydrate	Native protein		SDS-PAGE		Other isoforms
			Form	MW (kDa)	MW (kDa)	Protein band	
Arthrobacter sp. K-1 (38)		2.4% Glc	monomer	51	52	single	1
			monomer	58	58	single	
Aspergillus nidulans (39)	secreted S-βF	14% Man + 5% Gal	dimer	185	78	single	3
	secreted F-βF	29% Gal 12% Man	monomer	94	110	single	3
Aspergillus niger (40)	secreted	Man, Glc, Gal, N-acetylglucosamine	dimer	250	125	single	
	secreted N-linked glycans, O-linked glycans	Man, Glc, Gal, N-acetylglucosamine	dimer	120	90		
Candida utilis (41)	secreted	positive[a]	dimer	150		single	
Pichia anomala (42)		30% Man	multimer	254	86.5	single	
Saccharomyces cerevisiae wild type X2180 (4, 43)	internal/protoplast	< 3% carbohydrate	dimer	135	60	single	6
	external cw bound/periplasm	50% Man + 3% glucosamine[b]	dimer	270	140	single	
			tetramer	360			
			hexamer	560			

[a] Positive Lecitin affinity recognition on blotting using ConA-HRP conjugate.
[b] Nine high mannose oligosaccharide chains each linked to an asparagine residue by a di-N-acetylchitobiosyl core.

is glycosylated (45). The enzyme consists of 140-kDa subunits, which are in excess of 50% by weight mannose glycan and 3% glucosamine. The carbohydrate is attached as short oligosaccharides ($Man_{8\text{-}14}GlcNAc_2$) to hydroxyamino acids or as polysaccharide chains ($Man_{>50}GlcNAc_2$) to asparagine through N-acetylglucosamine. The protein consists of 13 or 14 potential glycosylation sites with an Asn-X-Ser (or Thr) although only 9–10 appear to be glycosylated (45). Yeast βF presents a continuous spectrum of molecular forms that might represent different degrees of glycosylation during the secretion process, which culminates in the formation of the heavy extracellular enzyme (4). The oligosaccharide moiety maintains external βFs in an oligomeric equilibrium of dimer, tetramer, hexamer, and octamer, equally active, and facilitates, without affecting the active sites of βF, subunit interactions to form active oligomers. The very stable dimers present a spherical nature presumably with the two monomers tightly bound (46), occluding some oligosaccharides at the interacting subunit surfaces. Dissociation to a monomer results in the generation of a form devoid of enzyme activity (43).

In contrast to *Saccharomyces*, SUC2 βF secreted by *Pichia pastoris* is a homogeneous product of ~ 85-kDa subunits associated with 8–10 oligosaccharides of the size $Man_{8\text{-}14}GlcNAc_2$. However, the majority of component of $Man_{8\text{-}10}GlcNAc$ family has structures identical to those found associated with *Saccharomyces* βF. The protein produced by *A. niger* βF gene (SUC1) contains 14 potential glycosylation sites with equal numbers of the two sequences Asn-X-Thr and Asn-X-Ser, for N-linked glycosylation. The βF a.a. sequences from *S. cerevisiae* and *Schwanniomyces occidentalis* contain large conserved domains but do not exhibit extensive homology in any region of the protein with the predicted sequence of the *A. niger* enzyme. Six domains of *S. cerevisiae* βF and *Schw. occidentalis* are conserved in βFs from prokaryotes, *Zymomonas mobilis, Bacillus subtilis, Streptococcus mutans*, and *Vibrio alginolyticus*. By contrast, only one could be partially identified in the *A. niger* βF since only six a.a. were identical of the nine a.a. which comprised the domain.

Homologous sequences in 14 *S. cerevisiae* strains and in 10 closely related *Saccharomyces* spp. are detected by using cloned SUC2 DNA probes. The SUC DNA sequence is highly conserved within the genus *Saccharomyces*; only the DNA from *Saccharomyces kluyveri* UCD51-242 fails to hybridize with the SUC2 DNA probe. During evolution its SUC gene has diverged sufficiently to leave no detectable homology (44).

Significant sequence homologies around the catalytic residues (Asp23 and Glu204) has been shown with other fructosylhydrolases form different sources. Inulinase from *Kluyveromyces marxianus* and βF from *Pichia anomala* share 53% and 44% homology, respectively, and the inulinase contains a single cysteine residue that corresponds to Cys205 in the βF. Yeast βF is closer to levanases and fructosyltransferase from bacteria (34–35% homology) than bacterial sucrases (30–31% homology) and plant βFs (27–29% homology (47).

In plants, alkaline βFs are thought to be nonglycosylated proteins (6). The glycosylation of cytoplasmically synthesized acid βF is necessary for its transport across either the tonoplast or the plasma membrane. Nucleotide and predicted amino acid sequences of acid invertase cDNA are known for tomato fruit, carrot, potato tuber, and grape berries (17, 48–50) with the following homologies in the amino acid sequences: tomato acid βF and carrot extracellular acid βF are 40.5% identical; isoenzyme I of carrot soluble acid βF and acid βF from tomato are closely related; isoenzyme II and acid βF from bean show the highest homology; carrot extracellular cw-βF and acid βF potato share high homology. A phylogenetic tree was generated (49). Table 3 reports some identified genes producing βF in plants and microorganisms together with molecular characteristics.

C. Isoforms

Some of the identified βF isoforms in plants and microorganisms are reported in Tables 1 and 2. Growth conditions and glucose concentration determine the cellular content of internal and external forms and their distribution in yeasts. In repressed *S. cerevisiae* cells, most of the enzyme is intracellular; in derepressed cells, 95% of the total enzyme is mainly located outside the cytoplasmic membrane. In *Saccharomyces* wild type six different genes encode six isoforms of βF. The existence of multiple forms of βF is common also in fungi (40). βF isoforms are not uncommon in plants with their location in tissues well distinct, and concentration levels within cells appeared to be regulated during development.

1. From Different Genes

Six βF structural genes in unlinked loci, similar in structure and expression but not identical, are known in the yeast *S. cerevisiae*—SUC1–SUC5 and SUC7. Each SUC gene encodes both the constitutive

Table 3 Some Identified Genes Producing β-D-Fructofuranosidase in Microorganisms and Plants

Source (location)	βF encoding gene	MW	Polypeptide size	Active site[a]	Signal peptide a.a.	Glycosylation
Bacillus subtilis	SACA or IPA-50D	54,888	480	D-43	—	
Escherichia coli (cytoplasm)	CSCA	54,363	477	D-39	—	
Hansenula anomala	INV1	63,188	550	—	22	10
Klebsiella pneumoniae (cytoplasm)	SCRB	52,708	466	D-41	—	
Lactococcus lactis (cytoplasm)	SACA	54,785	473	D-47	—	
Saccharomyces cerevisiae	SUC1[b]	60,570	20–532	D-42	19	12
(external)	SUC2 or YIL 162W[b]	60,639	20–532	D-42	19	13
(internal)	SUC2[b]		21–532	D-42	19	
	SUC3[b]		20 > 74 (fragment)	D-42	19	
	SUC4[b]	60,575	20–532	D-42	19	14
	SUC5[b]		20 > 74 (fragment)	D-42	19	
	SUC7[b]		20 > 96 (fragment)	D-42	19	
Schwanniomyces occidentalis	INV	60,839	23–533[c]	D-50	22	8
Staphylococcus xylosus	SCRB	57,371	494	D-48	—	
Streptococcus mutans (cytoplasm)	SCRB	51,754	455	D-47	—	
Vibrio alginoliticus (cytoplasm)	SCRB	55,657	484	D-51	—	
Zymomonas mobilis (cytoplasm)	INVA	58,725	512	D-43	—	
(cytosplasm)	SACA	58,397	511[d]	D-43	—	
Daucus carota L.	INV1	66,813	49–592	D-74	1–31 of 39 (propeptide 32–48 or 40)	5
(cw-βF of leaves roots of young plants)						
(cw-βF II)	INV2	67,397	[e]–592	D-75	potential	5
(cw-βF)	INV3	66,381	[e]–583; insoluble isoenzyme 3		(propeptide potential)	5
Lycopersicon esculentum (tissue-fruit vacuole)	TIV1 or AIV-1	70,097	93–636	D-118	potential and propeptide from [e]–92	4
Phaseolus aurens (vacuole)	INVA	72,167	heterodimer: 102–328 (30 kDa) 329–649 (38 kDa) monomer: (70 kDa)	D-130	potential from 1–[e]	3[f]
Pisum sativum	BFRUCT1	62,655	23–555	D-140	22	3
Zea mays (vacuole)	IVR1	71,932	[e]–670	D-139	potential	5
(cw-βF)	—	65,198	29–590	D-68	28	2

[a]Conservative domain, NDPNG.
[b]SUC1, SUC3, SUC4, SUC5 compared with SUC2, SUC7, all are highly homologous within the coding region.
[c]45% identity with *S. cerevisiae*.
[d]The a.a. sequence showed strong homologies with sucrases from *Bacillus subtilis, Salmonella thyphimurium*, and *Vibrio alginolyticus*.
[e]Not identified.
[f](2 complex-type glycan and 1 high-mannose type glycan).
Source: SwissProt database.

nonglycosylated βF and the glycosylated one (4, 44). The different yeast strains contain zero, one, or several of these genes, and the possession of one active SUC gene enables a yeast strain to ferment sucrose and raffinose. Strains expressing different SUC genes reveal different specific βF activities under both repressing and derepressing conditions. SUC4 determines the highest βF activity on raffinose as carbon source. Strains expressing SUC7 are unable to grow on raffinose as the sole carbon source. SUC4 and SUC5 differ in their βF activity about fivefold. SUC2, the most extensively studied, encodes the enzyme βF, required for growth of yeast cells on sucrose. SUC2 is transcriptionally repressed in high glucose whereas it is derepressed in low glucose, and transcription is increased > 100-fold (44).

In many plants βF is encoded by a multigene family (9). The different isoforms of tomato fruit βF may originate from a single gene or from closely related genes (16). In *Daucus carota* L. different genes encode acid βF while the neutral βF is encoded either by different genes or by the same gene and is generated by differential splicing or proteolytic cleavage of alkaline βF (12, 24). Only one gene appears to encode βF in *Helianthus tuberosus*, although it is possible that several genes produce transcripts of a similar size. The transcript size (2.5 kb) is close to those shown in tomato fruit (2.4 kb), carrot (2.0 kb), and yeast (1.8 and 1.9 kb). Multiple βF cDNAs were isolated from carrot tissue and exhibited between 44% and 99.1% identity of amino acid sequence. Two cDNAs (GIN1 and GIN2) were cloned from berries; the translation products are 62% identical to each other, and both appear to be vacuolar forms of βF (17).

2. From Posttranslational Modification

The most posttranslational modification of βFs is the extensive glycosylation that could affect the efficiency of biosynthesis and secretion of both the heterologous and homologous proteins. During secretion and transport to the periplasm the signal peptide is cleaved and the external yeast βF becomes glycosylated. The polymannose chains aid the self-association of homodimer into tetramer, hexamer, and octamer (46, 47).

3. Artifacts

Freezing or addition of PEG promotes the self-association of only external yeast βF subunits. Low NaCl concentration favors the presence of internal βF dimers while concentration as high as 0.8 M yields the maximum octamer-hexamer mixture. In external βF oligosaccharides shield the subunit from large interactions with NaCl. The formation of higher oligomers is also facilitated by KCl. Concentrations up to 0.4 M of CH_3COONa, $(NH_4)_2SO_4$, K_3PO_4, and NaF have no effect, indicating that chloride ions are primarily responsible for promoting self-association. External βF exists mostly as tetramers in 0.8 M GuHCl, reflecting the opposing effects of dissociation by guanidium and association by chloride ions (46).

Soluble βF of carrot isoenzyme I (68 kDa) and tomato are cleaved into an N-terminal and a shorter C-terminal fragment, neither of which separates during protein purification (16, 24, 49). Whether this proteolytic cleavage occurs in vivo or during protein purification is not known. The monomeric nature of the carrot enzyme suggests a labile bond such as a disulfide bridge between the two polypeptide fragments. Maturation of tomato acid βF may involve additional proteolytic processing at the C-terminus (48) since the MW of predicted mature polypeptide (60 kDa) exceeds that determined by SDS (52 kDa).

VI. PROPERTIES AS ENZYME

A. K_m, V_{max}, Substrates, Nonsubstrates, and Activation Energy

Tables 4 and 5 report the Michaelis constant for sucrose, K_m^{Suc}, and raffinose, K_m^{Raf}, of βFs from several plants and microorganisms, other identified substrates and nonsubstrates, the optimal pH, and maximal velocity. In plants, K_m^{Suc} for alkaline βF is higher than that of the acid form. The activation energy, E_a of plant βF has been reported to be 57.3 kJ/mol for *Ricinus communis* (25) and 147 kJ/mol for nodules of *Cicer arietinum* L. (51). The E_a value is 37.63 kJ/mol in whole yeast cell for acid βF (56) and 29.30 kJ/mol for a soluble preparation of acid βF from yeast (57).

B. Effect of Environmental Factors

The optimal pH depends on the form and the source of βF as presented in Tables 4 and 5. *Saccharomyces cerevisiae* βF exhibits relatively high activity over a broad range of pH (3.5–5.5), with the optimum near pH 4.5. The enzyme activity reaches a maximum at ~ 55°C. Certain ions affect the pH optimum of βF. The symbol (—) in Table 6 indicates a weak inhibition, with at the most 20% loss of βF activity. Inhibition constants and inhibition mechanism, when identified, are reported in Table 7. Plant βFs are characteristically inhibited by heavy metals and reagents that react with sulfhydryl

Table 4 Some Values of K_m for Purified βF from Different Plants

Source	βF purified	K_m^{Suc} (mM)	pH	K_m^{Raf} (mM)	Other substrates	Nonsubstrates[d]	V_{max}	Optimal pH
Avena sativa cv. (5)	soluble acid	2.4	4.5	2.9	Sta	Inu		4.5
	soluble acid	6.7	5.0	17		Inu		5.0
Beta vulgaris L. (11)	soluble acid	3.8						5.0
	alkaline	33.3						
	acid $NaCl_{released}$	0.56						
	acid $EDTA_{released}$	4.2						
	extracellular acid I	12.3						
	extracellular acid II	4.4					4.8[a]	7.0
Cicer arietinum L. (51)	neutral	14.2						
Cichorium intybus (10)	neutral	10–20			Raf	Cel, Inu, Kes, Mal, Nys, Tre		7.0–7.5
Cucumis melo L. (7)	soluble acid	2.2			Raf, Sta			
	cw acid $EDTA_{released}$	3.2						
	cw acid $NaCl_{released}$	2.2						
	soluble neutral	10						6.5–7.0
Daucus carota L. (12)	neutral	18.7	7.5		Raf			
		14.3	6.8		Sta			
	alkaline	20.7	7.5		Raf, Sta			
		15.1	8					
Daucus carota L. (24)	soluble acid	5			Raf	Inu		5
Fragaria × *ananassa* (14)	soluble acid	3.5			Raf, Sta			4.6
	cw $NaCl_{released}$	3.7						5.0
	cw $EDTA_{released}$	4.4						4.2
Glycine max L. (52)	alkaline	10			Sta, Raf	Cel, Gen, Mal, Tur, Lac, Mele, Tre, α-CH_3-D-Glc, β-CH_3-D-Glc		
(6)	alkaline	10				Cel, Lac, Mal, Raf		7.0–7.6
Lycopersicon	soluble acid	7.9					9.23[b]	4.5
Esculentum (16)	soluble acid	7.7					9.08[b]	
	soluble acid	7.4					8.42[b]	
Oryza sativa (26)	alkaline	70.1				Raf, Mal		7.0
	soluble acid	0.9		4.7	Raf	Mal		3.5–4.0
	soluble acid	12.1		30.2	Raf	Mal		5.0
	acid cw- bound	4.3				Mal		4.5
Phaseolus vulgaris (53)	alkaline	8.9	7.7					
	soluble acid	2.4	5	14 [5.0]	Sta, Kes	Mele		
Prunus avium L. (35)	soluble acid	4			Sta	Tre, Mal, Lac, Mel, Mele		
Ricinus communis (25)	soluble acid	8.7	3.5		Raf	Mele, α-Gal, α- and β-Glc		
Solanum tuberum (36)	soluble acid	16	4.7					5.0
Sugar cane (37)	soluble acid	2.8					2.7[c]	
	neutral	0.32					2.8[c]	
Vicia faba L. (8)	alkaline	10.1				Lac, Mal, Raf, Sta, Tre	0.58[b]	7.4
Wheat (27)	soluble acid	3.5			Raf	Mel, Mele		
	cw acid	1.7						

[a] μmole/h.
[b] μmole/min.
[c] μmole sucrose hydrolyzed/h/mg protein.
[d] Cellobiose (cel), α-galactosides (α-Gal), gentiobiose (Gen), α- and β-glucosides (α-β-Glc), α-methyl-D-glucopyranoside (α-CH_3-D-Glc), β-methyl-D-glucopyranoside (β-CH_3-D-Glc), inulin (Inu), 1-kestose (Kes), lactose (Lac), maltose (Mal), melibiose (Mel), melezitose (Mele), 1, 1-nystose (Nys), raffinose (Raf); stachyose (Sta), turanose (Tur), α, α-trehalose (Tre).

Table 5 Some K_m Values of Purified βF from Different Microorganisms

Source	Form	K_m^{Suc} (mM)	K_m^{Raf} (mM)	Nonsubstrates[c]	V_{max}^{d} (mM min^{-1})	Optimal temperature (°C)	Optimum pH	
							Activity	Stability
Arthrobacter sp. K-1[a] (38)		9.1	15.1	Pal, Inul, Cel, Mal	100% (Suc) 49% (Raf)	55	6.5–6.8	5.5–10
Aspergillus niger (40)	Specific βF	30–160[b]		Mal, Inu, Mele			6.0	
	Nonspecific βF	40		Mal, Mele			5.0	
Candida utilis (41)		11	150		333 (Suc) 215 (Raf)		5.5	3.0–6.0
Kluyveromyces fragilis (54)	β-Mercaptoethanol$_{released}$	13.6	46.1				5.0	
Pichia anomala (42)		16	82	Inu, Mele		38	4.5	4.5–6.5
Pseudomonas fluorescens (19)	Internal	90					6.5	
Saccharomyces rouxii (55)	Internal		83				5.5	4.5–7.5
Saccharomyces cerevisiae (2)	Internal	25	150				3.5–5.5	6.0–9.0
	External	26	15				3.5–5.5	3.0–7.5

[a] Other substrates: erlose, fructosylxyloside, neokestose, lactosylfructoside, stachyose.
[b] Non-Michaelis-Menten kinetics.
[c] Cellobiose (Cel), inulin (Inu), inulobiose (Inul), maltose (Mal), melezitose (Mele), palatinose (Pal).
[d] Raffinose (Raf), sucrose (Suc).

Table 6 Inhibitory Effect on the Activity of Purified βF from Some Microorganisms and Plants

Source	βF purified	$AgNO_3$	$CaCl_2$	$CoCl_2$	$CuSO_4$	$HgCl_2$	I_2	KCl	$MgCl_2$	$MnCl_2$	NaCl	NH_4Cl	$ZnCl_2$	$MgSO_4$	EDTA	Aniline	Fructose	Glucose	Tris
Arthrobacter sp.K-1 (38)		+	—	—	+	+			—	—	—		+		—				
Aspergillus oryzae (58)		—	—		—	+									—				
Kluyveromyces fragilis (54)		+			+	+											—		
Avena sativa cv., oat seedlings (5)	soluble acid	—				—	—									+			
	soluble acid	+				+	+									—			
Cichorium intybus, chicory roots (10)	neutral	+	—	+	—	+		—		—		—		—	—		+	+	+
Cucumis melo L., mesocarp (7)	soluble acid	+	—	—	—	+				+			—	—	—				
	cw $EDTA_{released}$	—	—	—	—	—				+			—	—	—				
	cw $NaCl_{released}$	+	—	—	—	+				+			—	—	—				
	soluble neutral	+	—	—	+	+				+			+	—	—				
Daucus carota L., cell culture (12)	neutral		—		+	—			—	—							+	+	
	alkaline		+		+	—			+	+							+	+	
Fragaria × *ananassa*, fruit (14)	soluble acid	+	—	—	—	+				+			—	—	—				
	cw $NaCl_{released}$	—	—	—	—	—				+			—	—	—				
	cw $EDTA_{released}$	+	—	—	—	+				+			—	—	—				
Glycine max L., nodule (52)	alkaline		+		+	+		—	+		—	—					+		+
Prunus avium L., mesocarp (35)	soluble acid	—	—		—	+		—	—		—	—							—
Wheat, coleoptiles (27)	soluble acid	+	—	—		+	+		—						—				

Table 7 Some K_i Values (mM) for βF from Different Sources

Inhibitor	*Cichorium intybus* (5)	*Daucus carota* L. neutral (12)	*Daucus carota* L. alkaline (12)	*Glycine max* L. (6)	Potato (59)	Sugar cane (37)	Sugar cane (37)	*Vicia faba* L. (8)	*Neurospora* (59)	*Yeast* (59)
Lauryl sulfate						0.54[a]	12			
Metasilicate						0.96[b]	0.28			
Pirydoxal					4				21	29
Pyridoxine					18				24	27
Deoxypyridoxine					17				30	15
Pyridoxal phosphate	0.5			0.005	6				> 150	56
Pyridoxamine					60				> 150	> 150
Aniline					110				1.5	1.7
Fructose	16[c]	13.4[b]	16.3[b]					8.6 ± 0.6		
Glucose	16	28[b]	33[b]							
Tris	1.2			4						
$HgCl_2$				0.025						

Inhibition mechanism: [a] uncompetitive; [b] noncompetitive; [c]competitive.

groups. Hg^{2+}, *p*-chloromercuribenzoate (100 μM), and *p*-chloromercuriphenyl sulfonic acid (100 μM) completely inhibit the βF. Co^{2+} and Zn^{2+} are inhibitors to a weaker extent. Ag^{+} ions attach to the histidine side chains of the βF molecule and render it inactive. Dithiobis 2-nitrobenzoic acid and iodoacetamide, reagents known to inactive enzymes that require free sulfhydryl groups for activity, have no effect because such groups are perhaps inaccessible under the assay conditions (10). Inhibitors of plant βFs are pyridoxal, pyridoxine, and pyridoxamine (5–7, 26, 27). Yeast external βF is weakly inhibited by *p*-hydroxymercuribenzoate, N-ethylmaleimide, iodoacetic acid, and iodoacetamide. Alkaline metal ions and related cations affect alkaline βF activity from *Ipomoea batatas* in the order of $Li^{+} > Na^{+} > K^{+} > Rb^{+} > NH_4^{+} > Tris^{+}$, while anions affect the activity in order of $F^{-} > NO^{3-} > Br^{-} > I^{-} > Cl^{-}$. The interrelated effect of cations and anions on βF activity prevents distinction between activator (suggested Na^{+} and K^{+}) and inhibitor (suggested Cl^{-}) (20). Some alkaloids found in vacuoles (caffeine, berberine, strychnine, morphine, ethyl-narceine, and nornicotine) produce an inhibiting effect on βF activity of *Ricinus communis, Solanum tuberosum, Oryza sativa*, and *Carica papaya* (60). Acid βFs activity is curtailed by endogenous proteinaceous inhibitors (36) as it occurs in red beet, sugar beet, and sweet potato and in maize endosperm. Plant βFs are activated by exogenous proteins (*R. communis* βF activity is increased 30%), PVP, and dextran sulfate (25), which suppress the inhibitory action of glucose, fructose, and organic acids. Since the vacuoles contain $\sim$ 19% of the total protein of the protoplast, it appears unlikely that fructose or the other vacuolar metabolites could exert control on βF activity.

C. Specific Mechanism of Action

The mechanism of yeast βF action involves a nucleophile and a proton donor in a two-step reaction. The Glu204 residue acts as a proton donor to the glycosidic oxygen of sucrose. The C-2 of the fructose moiety is attacked by the nucleophile Asp23. A covalent fructosyl–enzyme complex is formed and glucose is released. In the second step a proton from the water molecule is abstracted by Glu204. The hydroxyl group displaces fructose, and the original active center residues are restored. Glu204 is essential for sucrose hydrolysis while Cys205 possibly plays a supportive role in catalysis by maintaining a suitable microenvironment in the active site, or perhaps in aiding substrate binding. A carboxylate group, along with histidine, methionine, and tryptophan residues, is essential for βF activity. An ester linkage of the carboxylate group with conduritol B epoxide causes an irreversible inactivation of βF. The participation of carboxyl imidazole groups in catalysis is suggested for *Neurospora* βFs and in some higher plants (47).

D. Unique Properties

Yeast βFs have a transferring activity for β-fructofuranosyl residues that is negligible under the usual assay conditions (2). βFs from barley leaves exhibit a fructosyltransferase activity, at high concentrations of sucrose, forming mainly 1-kestose (34). The action of transglycosylation or transfructosylation of different microorganisms' βF (61, 62) leads to fructosyl and oligofructosyl trehaloses. Methyl fructosides are prepared from sucrose and methanol by βFs from *S. cerevisiae* (63). Mold βFs also (*A. niger, A. syduwi, A. japonicus, A. oryzae, Penicillium oxalicum, Aureobasidium* sp.) show high transfructosylating activity (38).

The hydrolysis of inulin is also catalyzed, albeit very slowly, by βFs. Unlike that in higher plants, the majority of microbial inulinases also possess sucrose hydrolytic activity and are thus classified as nonspecific βFs. The reverse situation, that all microbial βFs possess inulinase activity, has not been verified (40). The question in debate is whether inulinase should be regarded as a special type of βF or as a different enzyme with an analogous mode of action. Inulinases are characterized by the ratio of the activities with sucrose versus inulin as substrates < 50. The physiological role of βF mainly concerns the hydrolysis of sucrose within the cell wall. The main physiological role of inulinase is the breakdown of fructans outside the cell wall. Difructose dianhydride is hydrolyzed to D-fructose in two reaction steps by the enzyme from *Arthrobacter aureafaciens* presumed to be a β-fructofuranosidase, which is markedly different from yeast enzyme. It is not clear whether *Arthrobacter* enzyme is some other fructan hydrolase.

VII. QUALITATIVE AND QUANTITATIVE DETERMINATION OF ACTIVITY

A. Assay Conditions

Approximately 0.03–0.05 units of acid βF are incubated in 0.05 M acetate buffer, pH 4.6, with 100–200 mM sucrose for 10–60 min at 30 or 37°C. Phosphate

buffer, pH 7.5, is used for alkaline βF. Crude extracts require 0.1 M buffer.

The amount of glucose or fructose released can be estimated by enzymatic quantitative assay or by any of the procedures commonly used for determining reducing sugars such as the dinitrosalicylic acid (DNS) method (64) or the Nelson-Somögyi method (65). Glucose always serves as standard in the calibration curve.

1. β-D-Glucose is determined by coupled reactions involving glucose oxidase (GOD), peroxidase (POD), and *o*-dianisidine dihydrochloride (DH_2) as chromogen.

$$\beta\text{-D-Glucose} + H_2O + O_2 \xrightarrow{\text{GOD}} \text{D-Gluconic acid} + H_2O_2$$

$$H_2O_2 + DH_2 \xrightarrow{\text{POD}} 2H_2O + D$$

The βF activity is stopped by changing the pH with the 0.5 M addition of Na_2HPO_4, pH 8.83 (which also accelerates the mutarotation of α-D-glucose), and heating in a boiling bath for 10 min. A 0.4-mL volume of GOD-POD mixture (0.4 unit of each enzyme and 400 μg of DH_2) is mixed with 0.8 mL incubation mixture and kept for 30 min at 37°C. Then 0.3 mL of 6N HCl is added. The color developed is measured at 460 nm against blanks.

2. The D-glucose and D-fructose released are determined using a commercial kit (Boehringer Mannheim) based on hexokinase (HK), phosphoglucose isomerase (PGI), and glucose-6-phosphate dehydrogenase (G6P-DH).

$$\text{D-Glucose} + \text{D-Fructose} + 2\text{ATP} \xrightarrow{\text{HK}} \text{Glucose-6-P} + \text{Fructose-6-P} + \text{P} + 2\text{ADP}$$

$$\text{Fructose-6-P} \xrightarrow{\text{PGI}} \text{Glucose-6-P}$$

$$2\text{Glucose-6-P} + 2\text{NADP}^+ \xrightarrow{\text{G6P-DH}} 2\text{Glucoonate-6-P} + 2\text{NADPH} + 2\text{H}^+$$

A 0.01-mL volume of the sample for βF activity assay is added with 2.5 mL triethanolamine buffer (0.1 M, pH 7.6), 0.1 mL $MgCl_2$ (0.2 M), 0.1 mL ATP Na salt, 0.1 mL NADP Na salt, 0.01 mL HK, 0.01 mL PGI (all 10 mg/mL), and 0.01 mL G6P-DH (5 mg/mL). The reaction is kept at 25°C for 15 min and the absorbance is read at 340 nm. Deproteinization of biological samples (e.g., food) and addition of 0.5 mM EDTA to inhibit the nonspecific reoxidation of NADPH are recommended.

3. *Dinitrosalicylic reagent* (DNS): Dissolve 40 g dinitrosalicylic acid, 8 g phenol, 2 g Na_2SO_3, 800 g Rochelle salt ($NaKC_4H_4O_6 \cdot 4H_2O$) in 2 L of 2% (w/v) NaOH solution and then dilute it to 4 L with distilled water. *Procedure*: Add 1 mL DNS reagent to 0.5 mL assay mixture, and it stops the action of βF by shifting the pH of the medium into the alkaline range. Heat 5 min in a boiling water bath, then dilute with 2–10 mL water, and measure the absorbance at 540 nm. The molar extinctions of glucose and fructose are identical.

4. **Nelson-Somögyi reagents.** *Reagent A*: Dissolve 25 g Na_2CO_3, 25 g $NaKC_4H_4O_6 \cdot 4H_2O$ (Rochelle salt), 20 g $NaHCO_3$, and 200 g anhydrous Na_2SO_4 into distilled water (1 L final volume). Store at room temperature. *Reagent B*: Dissolve 15% (w/v) of $CuSO_4 \cdot 5H_2O$ in water with few drops of concentrated H_2SO_4. *Reagent C*: Dissolve 50 g $(NH_4)_2MoO_4$ in 900 mL water. Add slowly under stirring 42 mL concentrated H_2SO_4, then add 6 g $Na_2HAsO_4 \cdot 7H_2O$ in 50 mL water. Mix, incubate at 37°C for 24–48 h, and store in a dark bottle.

Procedure: The enzyme reaction (1.0 mL) is stopped with 1 mL of a freshly prepared solution (25 mL reagent A + 1 mL reagent B) and heated for 20 min in a boiling bath. Cool on ice bath, add 1 mL reagent C with immediate mixing to develop a blue color and CO_2. Dilute with water to 25 mL and mix. Read absorbance at 520 nm against reagent blank.

B. Specific Activity

One unit of activity is defined as the amount of enzyme that hydrolyzes 1 μmol substrate (expressed as glucose equivalent) per min under the assay conditions. Alternately, units can be expressed in microkatals—i.e., the amount of enzyme catalyzing the hydrolysis of 1 μmol substrate per sec under the assay conditions. The specific activity of βF is expressed as units of katals/mg protein as measured by the method of Lowry et al. (66) with bovine serum albumin as a standard protein.

VIII. PURIFICATION

Most purification schemes of βF from different sources are adapted from the procedure of Goldstein and Lampen (3) with extensive modifications. Purification-fold, ×P, and percentage of activity recov-

Table 8 Purification Yield and Recovery of βF from Some Microorganisms and Plants

Source		Crude extract U $mg^{-1}_{protein}$	Purified βF U $mg^{-1}_{protein}$	Purification (fold)	Recovery %	Assay conditons T (°C)	pH
Aspergillus niger (66)	secreted	143	3,290	23	9.9	30	5.0
Bifidobacterium infantis (68)	internal	25.8	437	17	30.9	37	6.2
Candida utilis (41)	periplasmic	32	3,100	97	34	60	5.1
Pichia anomala (42)	internal	29	1,482	51	46	30	4.5
Saccharomyces cerevisiae (3)	internal	3	4,700	1,567	32	30	4.9
strain FH4C (3)	external	19	4,800	253	37	30	4.9
(43)	internal	0.18	3,600	19,390	19	37	5.0
Thermomyces lanuginosus (69)	internal	0.5	132	275	3.4	—	6.5
Arabidopsis thaliana (9)	soluble acid inv1	0.16	431	2,694	1.7	37	5.5
Daucus carota (24)	soluble acid Iso1	0.93	600	650	4.5	37	4.6
(13)	acid	0.001	0.62	400	6.91	—	4.5
(12)	alkaline	0.2	15	75	6.2	37	8.0
(12)	neutral	0.2	23.4	117	4.4	37	6.8
Hordeum vulgare L. (34)	soluble acid	0.14	192	1,370	1.2	25	5.6
Oryza sativa (26)	soluble acid	0.08	4.21	50	7	37	5.0
	cw	—	0.30	5.6	6.8	37	7.0
Phaseolus vulgaris (53)	alkaline	0.13	14.5	110	0.1	25	—
Ricinus communis (25)		0.038	166	4,368	23.3	37	5.5
Solanum tuberosum (36)		0.042	65.5	1,560	29	37	4.7
Glycine max (52)	alkaline	0.27	10.4	38	40	30	7.5
(6)	alkaline	0.49	48	98	11	25	7.0
Wheat (27)		7.5	1,305	174	26.4	37	5.5

ery, R, are listed in Table 8 for βF from some microorganisms and plants.

The procedure of Chu et al. (43) for internal βF from *S. cerevisiae*, leading to a 19,390-fold purification and 19% activity recovery, is hereafter outlined. All operations are carried out at 0–5°C.

1. Yeast paste is suspended in equal weight of 50 mM Tris-HCl pH 7.5, with 5 mM $MgCl_2$, 40 mM βMSH, 1 mM phenylmethylsulfonylfluoride (PMSF, a protease inhibitor), and broken in a Bead-Beater. Cell lysate is centrifuged 20 min at 30,000g (R = 100; ×P = 1).
2. 1% streptomycin sulfate is added to the supernatant and after 1 h in an ice bath; nucleic acids and ribosomes are removed by centrifugation (R = 98; ×P = 1.04).
3. A precipitate is obtained from streptomycin supernatant at 40–85% $(NH_4)_2SO_4$ saturation and is then dissolved in 10 mM Tris-HCl buffer, pH 7.3 (buffer 1) containing 1 mM βMSH and 0.5 mM PMSF, and dialyzed thoroughly against this buffer.
4. 2 M acetic acid solution is added to the dialysate to bring the pH to 4.9. A proteic precipitate is formed and is discarded. The supernatant, containing βF, is adjusted to pH 7.3 with a Trizma base solution.
5. The supernatant is loaded onto a Whatman microgranular DE 52 column (2 × 18 cm). This is developed with 1 L linear gradient of 50–350 mM NaCl in buffer 1. External βF is eluted at ~ 0.1 M NaCl, while the internal form is eluted at 0.2 M NaCl (R = 54; ×P = 1.5).
6. Fractions exhibiting internal βF activity are pooled and concentrated by precipitation with solid $(NH_4)_2SO_4$ up to 80% saturation (R = 35; ×P = 5024).
7. The precipitate is dissolved in 1–2 mL buffer 1 with 0.1 M NaCl and loaded onto a Ultrogel AcA 44 column (1.5 × 98 cm) equilibrated with the same buffer. The βF fractions are pooled and added with $(NH_4)_2SO_4$ to a final concentration of 20%, then chromatographed on a 1 × 4 cm column of phenyl-Sepharose CL-4B equilibrated with buffer 1, plus 20% $(NH_4)_2SO_4$. A linear gradient, 20–0% $(NH_4)_2SO_4$ in buffer 1, is applied for eluting internal βF in a pure form at 5% $(NH_4)_2SO_4$ (R = 22; ×P = 19,610).

8. Concentration by ultrafiltration and dialysis against 10 mM NaH_2PO_4/Na_2HPO_4, pH 7.2 (R = 19; ×P = 19,390).

The procedure suggested by Bracho and Whitaker (36) for a plant glyco-βF and outlined hereafter allows good purification-fold (1560) and enzyme recovery (29%). All steps are performed at 0–5°C.

1. Potato slices (1 kg) are homogeneized with 100 mL $NaHSO_3$ (0.1 M) in a Waring blender. The filtrate through eight-layer cheesecloth is centrifuged and the supernatant is dialyzed against water. The formed precipitate is removed by centrifugation. The supernatant is lyophilized and suspended in buffer A (20 mM Tris-HCl/500 mM NaCl, pH 7.4) containing $CaCl_2$, $MgCl_2$, and $MnCl_2$ (1 mM of each) (R = 100; ×P = 1).
2. The sample is loaded onto an affinity column (2.5 × 10 cm) Con A–Sepharose 4B equilibrated and eluted with buffer A. 30 mM of methyl α-D-mannopyranoside in buffer A allows enzyme elution. βF is concentrated by ultrafiltration and then dialyzed against buffer B (20 mM NaH_2PO_4/Na_2HPO_4, pH 6.0) (R = 110; ×P = 11).
3. The solution is chromatographed on a DEAE-Sephadex A-50-120 column (2.5 × 18 cm) equilibrated in buffer B and eluted with a linear gradient of 0–250 mM NaCl. The active fractions are pooled and concentrated by ultrafiltration. The concentrate is dialyzed three times against buffer B (R = 69; ×P = 193).
4. The sample is loaded on a Sephadex G-150 column (1.5 × 90 cm), equilibrated, and eluted with 50 mM NaH_2PO_4/Na_2HPO_4/100 mM NaCl buffer (pH 7.2). βF fractions are pooled and concentrated (R = 51; ×P = 210).
5. The purified enzyme is obtained upon a second run on a DEAE-Sephadex A-50-120 column (1.5 × 18 cm), equilibrated in buffer B, and eluted with buffer B/100 mM NaCl (R = 29; ×P = 1560).

To the memory of Prof. Francesco Alfani, our intellectual guide, who prematurely died.

REFERENCES

1. M Berthelot. Sur la fermentation glucosigne du sucre de canne. CR Acad Sci 50:980–984, 1860.
2. S Gascon, NP Neumann, JO Lampen. Comparative study of the properties of the purified internal and external invertases from yeast. J Biol Chem 243:1573–1577, 1968.
3. A Goldstein, JO Lampen. β-D-Fructofuranosidase fructohydrolase from yeast. Methods Enzymol 42:504–511, 1975.
4. F Moreno, AG Ochoa, S Gascon, JR Villanueva. Molecular forms of yeast invertase. Eur J Biochem 50:571–579, 1975.
5. R Pressey, JK Avants. Invertases in oat seedlings. Plant Physiol 65:136–140, 1980.
6. JQ Chen, CC Black. Biochemical and immunological properties of alkaline invertase isolated from sprouting soybean hypocotyls. Arch Biochem Biophys 95:61–69, 1992.
7. AP Ranwala, S Iwanami, H Masuda. Acid and neutral invertases in the mesocarp of developing muskmelon (*Cucumis melo* L. cv. *Prince*) fruit. Plant Physiol 96:881–886, 1991.
8. HA Ross, D McRae, HV Davies. Sucrolytic enzyme activities in cotyledons of faba bean. Plant Physiol 111:329–338, 1996.
9. X Tang, HP Ruffner, JD Scholes, SA Rolfe. Purification and characterisation of soluble invertases from leaves of *Arabidopsis thaliana*. Planta 198:17–23, 1996.
10. W Van den Ende, A Van Laere. Purification and properties of a neutral invertase from the roots of *Cichorium intybus*. Physiol Plant 93:241–248, 1995.
11. H Masuda, T Takahashi, S Sugawara. Acid and alkaline invertases in suspension cultures of sugar beet cells. Plant Physiol 86:312–317, 1988.
12. HS Lee, A Sturm. Purification and characterization of neutral and alkaline invertase from carrot. Plant Physiol 112:1513–1522, 1996.
13. JR Stommel, PW Simon. Multiple forms of invertase from *Daucus carota* cell cultures. Phytochemistry 29:2087–2089, 1990.
14. AP Ranwala, C Suematsu, H Masuda. Soluble and wall-bound invertases in strawberry fruit. Plant Sci 84:59–64, 1992.
15. EM Klann, RT Chetelat, AB Bennett. Expression of acid invertase gene controls sugar composition in tomato (*Lycopersicon*) fruit. Plant Physiol 103:863–870, 1993.
16. Yelle, RT Chetelat, M Dorais, JW DeVerna, AB Bennett. Sink metabolism in tomato fruit. Plant Physiol 95:1026–1035, 1991.
17. C Davies, SP Robinson. Sugar accumulation in grape berries. Plant Physiol 111:275–283, 1996.
18. R Zrenner, K Schüler, U Sonnewald. Soluble acid invertase determines the hexose-to-sucrose ratio in cold-stored potato tubers. Planta 198:246–252, 1996.
19. WM Bugbee. Partial purification and properties of an invertase from *Pseudomonas fluorescens*. Sugarbeet Research and Extension Reports 21:150–152, 1983.

20. K Matsushita, I Uritani. Change in invertase activity of sweet potato in response to wounding and purification and properties of its invertases. Plant Physiol 54:60–66, 1974.
21. CW Basse, K Bock, T Boller. Elicitors and suppressors of the defense response in tomato cells. J Biol Chem 267:10258–10265, 1992.
22. M Yoshida, J Abe, M Moriyama, T Kuwabara. Carbohydrate levels among winter wheat cultivars varying in freezing tolerance and snow mold resistance during autumn and winter. Physiol Plant 103:17–23, 1998.
23. C Laurière, M Laurière, A Sturm, L Faye, MJ Chrispeels. Characterization of β-fructosidase, an extracellular glycoprotein of carrot cells. Biochimie 70:1483–1491, 1988.
24. C Unger, J Hofsteenge, A Sturm. Purification and characterization of a soluble β-fructofuranosidase from *Daucus carota*. Eur J Biochem 204:915–921, 1992.
25. FE Prado, MA Vattuone, OL Freischmacher, AR Sampietro. Purification and characterization of *Ricinus communis* invertase. J Biol Chem 260:4952–4957, 1985.
26. YY Charng, RH Juang, JC Su, HY Sung. Partial purification and characterization of invertase isozymes from rice grains (*Oryza sativa*). Biochem Mol Biol Int 33:607–615, 1994.
27. HB Krishnan, JT Blanchette, TW Okita. Wheat invertases. Plant Physiol 78:241–245, 1985.
28. H Weber, L Borisjuk, U Heim, P Buchner, U Wobus. Seed-coat-associated invertases of fava bean control both unloading and storage functions cloning of cDNAs and cell-type-specific expression. Plant Cell 7:1835–1846, 1995.
29. J Hallfrisch. Metabolic effects of dietary fructose. FASEB J 4:2652–2660, 1990.
30. AJJ Straathof, APG Kieboom, H van Bekkum. Invertase-catalysed fructosyl transfer in concentrated solutions of sucrose. Carbohydr Res 146:154–159, 1986.
31. B Antuna, MA Martinez-Anaya. Sugar uptake and involved enzymatic activities by yeasts and lactic acid bacteria: their relationship with bread-making quality. Int J Food Microbiol 18:191–200, 1993.
32. Y Oda, K Ouchi. Construction of a sucrose-fermenting bakers' yeast incapable of hydrolysing fructooligosaccharides. Enzyme Microb Technol 13:495–498, 1991.
33. EM Klann, B Hall, AB Bennet. Antisense acid invertase (TIV1) gene alters soluble sugar composition in transgenic tomato fruit. Plant Physiol 112:1321–1330, 1996.
34. DM Obenland, U Simmen, T Boller, A Wiemken. Purification and characterization of three soluble invertases from barley (*Hordeum vulgare* L.) leaves. Plant Physiol 101:1331–1339, 1993.
35. HB Krishnan, SG Pueppke. Cherry fruit invertase: partial purification, characterization and activity during fruit development. J Plant Physiol 135:662–666, 1990.
36. GE Bracho, JR Whitaker. Purification and partial characterization of potato (*Solanum tuberosum*) invertase and its endogenous proteinaceous inhibitor. Plant Physiol 92:386–394, 1990.
37. EJ Del Rosario, V Santisopasri. Characterization and inhibition of invertases in sugar cane juice. Phytochemistry 16:443–445, 1977.
38. K Fujita, K Hara, H Hashimoto, S Kitahata. Purification and some properties of β-fructofuranosidase I from *Arthrobacter* sp. K-1. Agric Biol Chem 54:913–919, 1990.
39. J Chen, J Saxton, FW Hemming, JF Peberdy. Purification and partial characterization of the high and low molecular weight form (S- and F-form) of invertase secreted by *Aspergillus nidulans*. Biochim Biophys Acta 1296:207–218, 1996.
40. GL Wallis, FW Hemming, JF Peberdy. Secretion of two β-fructofuranosidases by *Aspergillus niger* growing in sucrose. Arch Biochem Biophys 15:214–222, 1997.
41. FP Chavez, L Rodriguez, J Diaz, JM Delgado, JA Cremata. Purification and characterization of an invertase from *Candida utilis*: comparison with natural and recombinant yeast invertases. J Biotechnol 53:67–74, 1997.
42. J Rodriguez, JA Perez, T Ruiz, L Rodriguez. Characterization of the invertase from *Pichia anomala*. Biochem J 306:235–239, 1995.
43. FK Chu, K Takase, Don Guarino, F Maley. Diverse properties of external and internal forms of yeast invertase derived from the same gene. Biochemistry 24:6125–6132, 1985.
44. M Johnston, M Carlson. Gene expression. In: EW Jones, JR Pringle, JR Broach, eds. The Molecular Biology of the Yeast *Saccharomyces*. Cold Spring Harbor, NY: Cold Spring Harbor Laboratory Press, 1992, pp 193–281.
45. VA Reddy, RS Johnson, K Biemann, RS Williams, FD Ziegler, RB Trimble, F Maley. Characterization of the glycosylation sites in yeast external invertase. J Biol Chem 263:6978–6985, 1988.
46. AV Reddy, R MacColl, F Maley. Effect of oligosaccharides and chloride on the oligomeric structures of external, internal, and deglycosylated intervase. Biochemistry 29:2482–2487, 1990.
47. A Reddy, F Maley. Studies on identifying the catalytic role of glu-204 in the active site of yeast invertase. J Biol Chem 271:13953–13958, 1996.
48. EM Klann, S Yelle, AB Bennett. Tomato fruit acid invertase complementary DNA. Plant Physiol 99:351–353, 1992.

49. C Unger, M Hardegger, S Lienhard, A Sturm. cDNA cloning of carrot (*Daucus carota*) soluble acid beta-fructofuranosidases and comparison with the cell wall isoenzyme. Plant Physiol 104:1351–1357, 1994.
50. D Zhou, A Mattoo, N Li, H Imaseki, T Solomos. Complete nucleotide sequence of potato tuber acid invertase cDNA. Plant Physiol 106:397–398, 1994.
51. B Asthir, R Singh. Purification and characterization of neutral invertase from chickpea nodules. Indian J Biochem Biophys 34:529–534, 1997.
52. M Morell, L Copeland. Enzymes of sucrose breakdown in soybean nodules. Plant Physiol 74:1030–1034, 1984.
53. RA Cooper, RN Greenshields. The partial purification and some properties of two sucrases of *Phaseolus vulgaris*. Biochem J 92:357–364, 1964.
54. WE Workman, DF Day. Purification and properties of the beta-fructofuranosidase from *Kluyveromyces fragilis*. FEBS Lett 160:16–20, 1983.
55. WN Arnold. Expression of cryptic beta-fructofuranosidase in *Saccharomyces rouxii*. J Bacteriol 120:2 886–894, 1974.
56. M Cantarella, L Cantarella, A Gallifuoco, F Alfani. Invertase activity of *Saccharomyces cerevisiae* cells entrapped in poly-(2-hydroxyethyl metacrylate) gels: kinetic and thermostability study in membrane reactors. J Biotechnol 24:159–168, 1992.
57. M Vitolo, DP Barros. Sucrose hydrolysis by invertase immobilized on chitin. Lebensm.-Wiss.U.-Technol. 25:240–243, 1992.
58. CT Chang, YY Lin, MS Tang, CF Lin. Purification and properties of beta-fructofuranosidase from *Aspergillus oryzae* ATCC 76080. Biochem Mol Biol Int 32:269–277, 1994.
59. R Pressey. Inhibition of invertases by pyridoxal and its analogues. Biochim Biophys Acta 159:414-416, 1968.
60. HP Rojo, EN Quiroga, MA Vattuone, AR Sampietro. The effects of selection of alkaloids on the invertase activity of some higher plants. Biochem Mol Biol Int 43:1331–1338, 1997.
61. M Muramatsu, T Nakakuki. Enzymatic synthesis of novel fructosyl and oligofructosyl trehaloses by *Aspergillus sydowi* beta-fructofuranosidase. Biosci Biotechnol Biochem 59:208–212, 1995.
62. YC Su, CS Sheu, JY Chien, TK Tzan. Production of beta-fructofuranosidase with transfructosylating activity for fructooligosaccharides synthesis by *Aspergillus japonicus* NTU-1249. Proc Natl Sci Counc Repub China 15:131–139, 1991.
63. M Rodriguez, A Gomez, F Gonzalez, E Barzana, A Lopez-Munguia. Selectivity of methyl-fructoside synthesis with β-fructofuranosidase. Appl Biochem Biotechnol 59:167–175, 1996.
64. GL Miller, R Blum, WE Glennon, AL Burton. Measurement of carboxymethylcellulase activity. Anal Biochem 1:127–132, 1960.
65. N Nelson. A photometric adaptation of the Somögyi method for the determination of glucose. J Biol Chem 153:375–380, 1944.
66. OH Lowry, NJ Roseburgh, AL Farr, RJ Randall. Protein measurement with the Folin phenol reagent. J Biol Chem 193:265–275, 1951.
67. LM Boddy, T Berges, C Barreau, MH Vainstein, MJ Dobson, DJ Ballance, JF Peberdy. Purification and characterisation of an *Aspergillus niger* invertase and its DNA sequence. Curr Genet 24:60–66, 1993.
68. L Imamura, KI Hisamitsu, K Kobashi. Purification of β-fructofuranosidase from *Bifidobacterium infantis*. Biol Pharm Bull 17:596–602, 1994.
69. A Chaudhuri, R Maheshwari. A novel invertase from thermophilic fungus *Thermomyces lanuginosus*: its requirement of thiol and protein for activation. Arch Biochem Biophys 327:98–106, 1996.

65

β-Galactosidase

Raymond R. Mahoney
University of Massachusetts, Amherst, Massachusetts, U.S.A.

I. INTRODUCTION

β-Galactosidase (β-D-galactoside galactohydrolase, EC 3.2.1.23) is often known as lactase because it catalyzes the hydrolysis of lactose into its constituent sugars—viz., lactose + H_2O → galactose + glucose. All lactases are β-galactosidases but some β-galactosidases, including those from plant cells and mammalian organs other than the intestine, have little or no activity on lactose because their function is to hydrolyze other galactosyl moieties, including glycolipids, glycoproteins, and mucopolysaccharides (1).

β-Galactosidase hydrolyzes O-glycosyl bonds and exhibits strict specificity for the glycone part of the substrate (Fig. 1). The only changes that allow activity (albeit reduced) are replacement of the hydroxylmethyl group on carbon 6 with a methyl group or a hydrogen atom. Consequently, the enzyme shows some activity on α-L-arabinosides and β-D-fucosides. Other changes such as methylation of the hydroxyl on carbons 2, 3, 4, or 6; loss of the pyranose ring structure; or conversion to the α-anomeric form, lead to loss of activity (1). Replacement of the glycosidic oxygen with sulfur causes loss of activity but not loss of binding affinity (1). The enzyme shows wide tolerance for the structure of the aglycone which may be another sugar, an alkyl group or an aryl group. The nature of the aglycone, however, strongly influences the kinetic parameters (1).

Activity of intestinal lactase in mammals decreases after weaning, and this leads to some degree of lactose intolerance in many population groups. Consequently, the enzyme is used in clinical settings to aid lactose digestion and in commercial operations to produce low-lactose diary products.

II. IMPORTANCE TO FOOD QUALITY

Enzymatic hydrolysis of lactose is of interest in both food science and nutrition, as well as in waste management and byproduct utilization. The product sugars are sweeter, more soluble, more easily fermented, and more readily absorbed from the intestine. Consequently, hydrolysis of lactose in milk and whey provides new functional properties for these ingredients which can be exploited in a variety of products (see Sec. IV below).

The principal reason for hydrolyzing lactose in fluid milk, however, is to overcome the problem of lactose

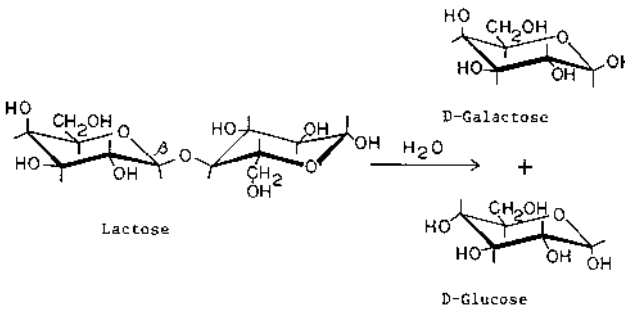

Figure 1 Hydrolysis of lactose by β-galactosidase.

intolerance, which is widespread among non-Caucasian adults and leads to reduced milk consumption. This is of concern since milk is a good source of high-quality protein and an especially good source of calcium.

Whey is the principal byproduct of cheese manufacture and contains > 70% lactose on a dry-weight basis. Hydrolysis of the lactose improves whey utilization in a variety of products and processes (see Sec. IV).

III. SOURCES

β-Galactosidases are widely distributed in nature according to their various functions, which include digestion, lysosomal degradation, and catabolism. However, lactases are found essentially only in the mammalian intestinal tract and in various microorganisms, including many fungi, yeasts, and bacteria (2).

In the intestine, the enzyme is located in the microvilli of the mucosal cells of the brush border membrane. In microorganisms, the enzyme is usually intracellular in bacteria and yeasts but may be intra- or extracellular in fungi.

For commercial use lactase is extracted from a few microbial sources, primarily yeasts and fungi, which are considered safe as hosts for food grade enzymes (see Table 1). It may be possible to use β-galactosidases from other sources by cloning them into one of these hosts. The commercial enzymes are usually classified as acid pH (pH optimum < 5) for use in acid whey, or neutral pH (pH optimum 5.5–7.0) for use in milk or sweet whey. The enzyme is also produced from *Escherichia coli* for biochemical and analytical uses.

Table 1 Commercial Sources of β-Galactosidase for Hydrolysis of Lactose in Foods

Organism	pH Optimum[a]	Molecular weight (kDa)
Bacteria		
Bacillus spp. related to *B. stearothermophilus*	5.5–6.5	116
Yeasts		
Kluyveromyces fragilis	6.5–7.5	201
K. lactis	6.5–7.0	117
Candida psuedotropicalis	6.2	—[b]
Fungi		
Aspergillus niger	2.5–4.0	109–112
A. oryzae	4.5–5.0	90

[a] Dependent on strain.
[b] Not known.

IV. USE IN FOODS

Reduction of the lactose content of milk or whey by hydrolysis with β-galactosidase leads to several products/applications, as shown in Table 2. These applications have been reviewed extensively elsewhere (2).

V. PROPERTIES AS A PROTEIN

The best-understood β-galactosidase in terms of protein structure is the enzyme from *Escherichia coli* encoded by the lac Z gene. This enzyme has a molecular weight of 464 kDa and is composed of four identical subunits (each 116 kDa), each containing 1023 residues (3). X-ray crystallography confirms that the protein is a tetramer with 222 point symmetry (4). Each subunit contains a binding site for Mg^{2+} and has five essentially independent domains. The key active site residues are located in a depression formed from loops connecting the C-terminal ends of β-strands to surrounding α-helices in an α/β barrel. Subunits and dimers of subunits are inactive whereas activity in the tetramer state is due to completion of each active site by a loop donated from a neighboring monomer (4).

At the primary sequence level, each subunit contains 16 half-cystine residues per 116-kDa monomer; virtually none of these residues appear to be involved in disulfide linkages (5).

Table 2 Applications of Lactose Hydrolysis

Product/process	Advantages
Low-lactose milk	Overcomes the problem of lactose intolerance
Sweetened condensed milk, ice cream, dulce de leche	Reduce lactose crystallization in concentrated or frozen milk products
Yogurt and cheese	Accelerates ripening by production of more easily fermented sugars
Sugars syrups from deproteinized whey	Increased sweetness of glucose and galactose allows multiple uses in ice cream, baked goods, confectionery, and soft drinks
Fermentation to ethanol	Fermentation yeasts grow more easily on the glucose produced

In contrast to the above, very little is known about the protein structure of β-galactosidase from eukaryotes. However, amino acid sequences have been established for β-galactosidase from several other bacteria and from the yeast *Kluyveromyces lactis* (6). Comparison of the yeast β-galactosidase with the subunits of β-galactosidase from prokaryotes show similarity in molecular weight (117 kDa) and extended sequence homology, suggesting close structural and evolutionary relationships (6).

Extracts of *E. coli* subjected to electrophoresis and stained histochemically for β-galactosidase show multiple bands (7), and a similar phenomenon has been seen with both crude and purified enzyme from *Kluyveromyces fragilis* (8). Purification and characterization of the isoforms from *E. coli* have shown them to be polymers and have not revealed compositional differences (9). In the case of fungal enzymes, however, isoforms have been observed which do differ in the extent of glycosylation (10).

VI. PROPERTIES AS AN ENZYME

The enzymatic properties of β-galactosidase vary with the source. These properties are summarized in Table 3 for three different β-galactosidases (one each from bacteria, yeasts, and molds).

Comparison of k_{cat}/K_m shows that the synthetic substrate ONPG (*o*-nitrophenyl β-D-galactopyranoside) is a better substrate than lactose in all cases. The fungal enzyme from *Aspergillus niger* is the most thermostable and is unaffected by cations or sulfhydryl modifiers such as *p*-chloromercuribenzoate. However, it is the most susceptible to product inhibition by galactose.

The mechanism of action is not completely understood, but the *E. coli* enzyme appears to work in a fashion analogous to that of lysozyme. Thus, one group acts as a general acid, donating a proton to the glycosidic oxygen, and another, negatively charged group stabilizes a positively charged carbonium galactosyl-enzyme intermediate for reaction with water (11). Site-directed substitutions in the *E. coli* enzyme indicate that Tyr503 functions as the general acid and that Glu461 functions as the stabilizer for the intermediate which alternates between a carbocation and a covalently bound form (12). The hydrolytic reaction [Eq. (1)] can then be described as:

$$\begin{aligned} \text{enzyme} &\Leftrightarrow \text{enzyme-lactose} \\ &\text{enzyme-lactose} \rightarrow \text{enzyme-galactose} \\ &+ \text{glucose enzyme-galactose} \rightarrow \\ &\text{enzyme-galactose}^{+} \text{enzyme-galactose}^{+} \\ &+ H_2O \rightarrow \text{enzyme} + \text{galactose} \end{aligned} \tag{1}$$

Reaction of the enzyme-galactose^{+} complex with another sugar (such as lactose, galactose, or glucose) instead of water allows for the synthesis of oligosaccharides by the transferase reaction, which can become significant at high substrate concentrations and/or when the degree of substrate conversion is high (13).

There are several substrate/product analogs which inhibit β-galactosidase. Galactose is a competitive inhibitor, but glucose is often ineffective except at very high concentrations, where it is noncompetitive (14). Thiogalactosides such as *p*-aminophenyl β-D-thiogalactoside are weak competitive inhibitors (15, 16). The most powerful inhibitors are the 1-4 and 1-5 galactonolactones, especially the latter, which, it has been suggested, may resemble the transition state form of the substrate (17).

VII. DETERMINATION OF ACTIVITY

β-Galactosidase activity can be followed quite readily by following the disappearance of substrate or the appearance of product, but it is usually easier to follow product formation.

Determination of lactose hydrolysis is complicated by transferase activity, although the latter is minimal (and can often be ignored) when the lactose concentration is 5% or less, or only initial rates are being measured. Under these conditions, it is easy to assay activity on lactose by measuring the production of glucose or galactose, preferably enzymatically. The most commonly used method is determination of glucose with glucose oxidase coupled to peroxidase (see Sec. VII.A below).

Where a large percentage of the original lactose is hydrolyzed, determination of total monosaccharides is a good practical indicator of the extent of hydrolysis, but it may underestimate the number of glycosyl bonds broken in lactose, owing to the formation of oligosaccharides by the transferase reaction.

Hydrolysis of lactose can also be followed by polarimetry due to a small change in specific rotation (from $+52.5^{\circ}$ to $+67.0^{\circ}$). However, this method is not

Table 3 Enzymatic Properties of β-Galactosidase

	Escherichia coli (14)	*Kluyveromyces fragilis* (8, 15)	*Aspergillus niger* (10, 27)
Molecular weight (kDa)	464	201	109–112
pI	4.61	5.1	4.64
pH optimum	7.2–7.4	6.2–6.4	2.5–4.0
pH stability	6–8	6.5–7.5	2–8
Temperature optimum (°C)	~ 40	~ 37	~ 55–60
Activation energy (kJ/mole)	12.6	38.1	35.1
k_{cat} ONPG[a] sec^{-1}	1.38×10^6	3.41×10^3	2.19×10^5
k_{cat} lactose sec^{-1}	5.10×10^3	1.551×10^3	1.91×10^5
K_m ONPG[a] (m*M*)	0.161	2.72	2.22
K_m lactose (m*M*)	1.9	13.9	85–125
k_{cat}/K_m PNPG[a] ($sec^{-1}\,M^{-1}$)	8.57×10^9	1.25×10^6	98.6×10^6
k_{cat}/K_m lactose ($sec^{-1}\,M^{-1}$)	2.68×10^6	1.08×10^5	1.91×10^6
K_i galactose (m*M*)	21	27.7	4
K_i PAPTG[b] (m*M*)	5	6.05	—[c]
Activators	Na^+, Mg^{2+}	K^+, Mg^{2+}, Mn^{2+}	None
Inhibitors			
Galactono-1-4-lactone	Yes	Yes	—[c]
p-Chloromercuribenzoate	Yes	Yes	No

[a] ONPG, *o*-nitrophenyl-β-D-galactoside.
[b] PAPTG, *p*-aminophenylthio-β-D-galactoside.
[c] Not known.

used much compared to chemical estimation of the products.

Synthetic substrates such as *o*-nitrophenyl β-D-galactopyranoside (ONPG) and *p*-nitrophenyl β-D-galactopyranoside (PNPG) are usually hydrolyzed faster than lactose and provide an easy, convenient, colorimetric assay since the nitrophenol released absorbs in the range 400–420 nm when in alkaline solution.

For detection of very low levels of activity, fluorimetric methods of assay can be used with substrates such as 4-methylumbelliferone β-D-galactoside (8).

The conditions for assay vary with the source of the enzyme and the substrate; representative examples are given below.

A. Assay of β-Galactosidase Activity on Lactose with Neutral-pH Enzyme

Enzyme 100 μL ($\leq$ 30 U/mL) is added to 4 mL of 5% lactose in 0.1 *M* potassium phosphate buffer, pH 6.6, containing 3.2 m*M* $MgCl_2$, at 30°C, or to 4 mL milk at the same temperature. The reaction is stopped after 10 min by adding 0.1 mL of 4 N HCl and then neutralized by adding 0.1 mL of 6.4 N NaOH. The solution is then analyzed for glucose, preferably by the use of glucose oxidase and peroxidase in conjunction with a dye such as *o*-dianisidine [Eqs. (2) and (3)].

$$\text{D-glucose} + O_2 \xrightarrow[\text{oxidase}]{\text{glucose}} H_2O_2 + \text{D-gluconolactone} \tag{2}$$

$$H_2O_2 + o\text{-dianisidine} \xrightarrow{\text{peroxidase}} \text{oxidized } o\text{-dianisdine} \quad (\lambda_{max}\ 436\,\text{nm}) \tag{3}$$

Alternatively, the galactose produced can be estimated indirectly by use of galactose dehydrogenase [Eq. (4)].

$$\text{D-galactose} + NAD^+ \xrightarrow[\text{dehydrogenase}]{\text{galactose}} \text{D-galactonolactone} + NADH + H^+ \tag{4}$$

The increase in absorbance at 340 nm is a measure of the NADH produced and of the lactose hydrolyzed.

B. Assay of β-Galactosidase Activity on *o*-Nitrophenylgalactoside (ONPG) Using Neutral-pH Enzyme

Enzyme (100 μL ($\leq$ 1 U/mL) is added to 4 mL of 2 m*M* ONPG in 0.1 *M* potassium phosphate buffer, pH 6.6, containing 0.1 m*M* $MnCl_2$ and 0.5 m*M* dithioerythritol. The reaction is stopped after 5 min by adding 1 mL of 0.5 *M* Na_2CO_3 containing 15 m*M* EDTA, and the absorbance is determined at 420 nm. Activity is calculated using a molar extinction coefficient of 4500 $M^{-1}\,cm^{-1}$ for *o*-nitrophenol at pH 10 (15). For acid-pH enzymes, the substrate buffer is changed to 100 m*M* sodium acetate buffer, pH 4.0, and the reaction is stopped as described above.

C. Other Aspects

β-Galactosidase activity in tissues can be detected by histochemical staining with 6-bromo-2-naphthyl-β-galactosidase. The product 6-bromo-2-naphthol, reacts with tetrazotized *o*-dianisidine (Diazo Fast Blue B) in alkaline solution to give a blue-purple color at the site of enzyme activity (19). The same method can be used to detect activity of β-galactosidase in electrophoresis gels (7).

Neutral-pH enzymes require Mg^{2+} or Mn^{2+} for maximum activity, but acid-pH enzymes (from fungi) do not require metal ions. Incorporation of a sulfhydryl reagent (2-mercaptoethanol or dithiothreitol) often increases activity with neutral-pH enzymes.

Activity and stability of β-galactosidase in milk and whey can be very different from that in lactose solutions. Activity is often lower in milk or whey (20, 21) owing to the high level of calcium, which exerts a strong inhibitory effect (21, 22). Stability against thermal denaturation is markedly increased—up to 100-fold in milk (23). This appears to be due to several milk constituents: salts, lactose, and proteins, acting in concert. Casein is the principal stabilizer, but its effect is markedly lactose dependent.

The β-galactosidase from *Streptoccocus thermophilus* can be stabilized by a number of proteins, such as bovine serum albumin and casein, via hydrophobic interactions (24). The β-galactosidase from *K. lactis* is stabilized by several amino acids, notably histidine, which decreases the rate of unfolding of the enzyme during heat denaturation (25).

VIII. PURIFICATION

β-Galactosidase can be purified by the conventional methods of protein separation such as gel filtration and ion exchange chromatography and also, very effectively, by affinity chromatography. Examples are shown below.

A. Purification of β-Galactosidase from *Kluyveromyces lactis* (26)

The yeast cells were disrupted in a steel press, and the ruptured cells were extracted with 50 m*M* phosphate buffer, pH 7.0, containing 10 m*M* $MgCl_2$ (Buffer 1). After centrifugation to remove cell debris, the supernatant was brought to 55% saturation with $(NH_4)_2SO_4$ to precipitate the enzyme. The precipitate was dialyzed against Buffer 1 containing 1 m*M* 2-mercaptoethanol to stabilize the enzyme against activity loss. The enzyme was then purified by gel filtration chromatography on Sephadex G-100 using Buffer 1 followed by ion exchange chromatography on DEAE-Sephadex A50. The enzyme was applied in Buffer 1 and was eluted with a gradient of 0–0.5 M NaCl in Buffer 1. A summary of the purification is shown in Table 4. Overall, this enzyme was purified 79-fold with a yield of 19% and was judged homogeneous by polyacrylamide gel electrophoresis.

Table 4 Purification of β-Galactosidase from *Kluyveromyces lactis*

Fraction	Volume (mL)	Protein (mg/mL)	Activity ($U \times 10^{-3}$)	Specific activity (U/mg)
Centrifuged cell extract	46	77	14.9	4.22
Ammonium sulfate fractionation	30	48	12.7	8.25
Sephadex G-100	123	2.7	14.5	43.7
DEAE Sephadex-A50	26	0.55	2.04	143

Source: Ref. 26

B. Purification of β-Galactosidase from *Escherichia coli* by Affinity Chromatography (16)

Cells of *E. coli* were suspended in 50 m*M* Tris-HCl, pH 7.5, containing 100 m*M* NaCl and 10 m*M* $MgCl_2$ (Buffer 2) and disrupted by sonication. After centrifigation to remove cell debris, the supernatant was brought to 50% saturation with $(NH_4)_2SO_4$ and centrifuged, and the pellet was dissolved in Buffer 2 and dialyzed against the same buffer. The enzyme solution was then applied to a column of an affinity matrix consisting of the inhibitor *p*-aminophenyl-β-D-galactopyranoside ($K_i \sim 5$ mM) attached to Sepharose 4B via a long spacer arm (3-aminosuccinyl-3-aminodipropylamine). The column was washed with Buffer 2, and the enzyme was eluted by 0.1 *M* borate buffer, pH 10; it was homogeneous as judged by gel electrophoresis. The yield was 95% compared with a yield of ~ 50% using conventional procedures (5).

REFERENCES

1. K Wallenfels, R Weil. β-Galactosidase. In: PD Boyer ed. The Enzymes, Vol 7 (3rd ed). New York: Academic Press, 1972, pp 617–663.
2. RR Mahoney. Lactose: enzymatic modification. In: PF Fox, ed. Advanced Dairy Chemistry—3. London: Chapman and Hall, 1977, pp 77–118.
3. AV Fowler, I Zabin. Amino acid sequence of β-galactosidase. XI. Peptide ordering procedures and the complete sequence. J Biol Chem 258:10204–10207, 1978.
4. RH Jacobson. The dimensional structure of β-galactosidase. PhD thesis, University of Oregon, Corvallis, OR, 1993.
5. GR Craven, E Steers Jr, CB Anfinsen. Purification, composition and molecular weight of the β-galactosidase of *Escherichia coli* K12. J Biol Chem 240:2468–2477, 1965.
6. O Poch, HL Hote, V Dallery, F Debeaux, R Fleer, R Sodoyer. Sequence of the *Kluyveromyces lactis* β-galactosidase: comparison with prokaryotic enzymes and secondary structure analysis. Gene 118:55–63, 1992.
7. SH Appel, DH Alpers, GM Tomkins. Multiple molecular forms of β-galactosidase. J Mol Biol 11:12–21, 1965.
8. RR Mahoney, JR Whitaker. Purification and physiocochemical properties of β-galactosidase from *Kluyveromyces fragilis*. J Food Sci 43:584–591, 1978.
9. SL Marchesi, E Steers Jr, S Shifrin. Purification and characterization of the multiple forms of β-galactosidase of *Escherichia coli*. Biochim Biophys Acta 181:20–34, 1969.
10. F Widmer, JL Leuba. β-Galactosidase from *Aspergillus niger*. Separation and characterization of three multiple forms. Eur J Biochem 100:559–567, 1979.
11. ML Sinnott. Ions, ion pairs and catalysis by the lacZ β-galactosidase of *Escherichia coli*. FEBS Lett 94:1–9.
12. CG Cupples, JH Miller, RE Huber. Determination of the roles of Glu-461 in β-galactosidase (*Escherichia coli*) using site-specific mutagenesis. J Biol Chem 265:5512–5518, 1990.
13. RR Mahoney. Galactosyl-oligosaccharide formation during lactose hydrolysis—a review. Food Chem 63:147–154, 1998.
14. K Wallenfels, OP Malhotra. β-Galactosidase. In: PD Boyer, H Lardy, K Myrback, eds. The Enzymes, Vol 4 (2nd ed). New York: Academic Press, 1960, p 409.
15. RR Mahoney, JR Whitaker. Stability and enzymatic properties of β-galactosidase from *Kluveromyces fragilis*. J Food Biochem 1:327–350, 1977.
16. E Steers Jr, P Cuatrecasas, HB Pollard. The purification of β-galactosidase from *Escherichia coli* by affinity chromatography. J Biol Chem 246:196–200, 1971.
17. J Conchi, AJ Hay, I Strachan, GA Levvy. Inhibition of glycosidases by aldonolactones of corresponding configuration. Biochem J 102:929–941, 1967.
18. JW Woolen, PG Walker. Fluorimetric estimation of N-acetyl beta-glucosaminidase and beta-galactosidase in blood plasma. Clin Chem Acta 12:647–665, 1965.
19. MS Burstone. Enzyme Histochemistry. New York: Academic Press, 1962, p 375.
20. NA Greenberg, RR Mahoney. The activity of lactose (*Streptococcus thermophilus*) in milk and sweet whey. Food Chem 15:307–313, 1984.
21. RR Mahoney, C Adamchuk. Effect of milk constituents on the hydrolysis of lactose by lactase from *Kluyveromyces fragilis*. J Food Sci 45:962–969, 1980.
22. EJ Guy, EW Bingham. Properties of β-galactosidase of *Saccharomyces lactis* in milk and milk products. J Dairy Sci 61:147–151, 1978.
23. RR Mahoney, T Wilder. Stabilization of lactase (*Escherichia coli*) by milk components and related compounds. J Food Sci 45:899–901, 1989.
24. BS Chang, RR Mahoney. Enzyme thermostabilization by bovine serum albumin and other proteins: evidence for hydrophobic interactions. Biotechnol Appl Biochem 22:203–214, 1995.
25. SS Surve, RR Mahoney. Thermostabilization of *Kluveromyces marxianus* β-galactosidase by histidine: physical studies. Biotechnol Appl Biochem 23:155–162, 1996.
26. J Burstone, MD Glantz. Isolation and characterization of β-galactosidase from *Saccharomyces lactis*. Biochim Biophys Acta 167:373–377, 1968.
27. YC Lee, V Wacek. Galactosidases from *Aspergillus niger*. Arch Biochem Biophys 138:264–271, 1970.

66

Pectic Polysaccharides

H. A. Schols and Alphons G. J. Voragen
Wageningen University, Wageningen, The Netherlands

I. INTRODUCTION

In the vast amount of literature on pectic enzymes an unambiguous interpretation of presented results is often hampered by the fact that ill-defined substrates and inadequate methodology have been used. The importance of the use of well-defined substrates and adequate methods is demonstrated by the facts that in the last decade more than five new enzymes active on specific structural elements of pectin have been identified and that within classes of specific enzymes a further differentiation became possible based on differences in substrate specificity. So can polygalacturonases be differentiated with respect to their tolerance of methyl esterified galacturonic acid residues in their active sites (Chapter 69). Also, to understand the technological role of a specific enzyme in an application, its action at a molecular level should be known. We therefore felt the need to devote a chapter to the description of the structural elements present in pectins, which variations are found in nature in these structural elements, and the methodology to measure the activity and mode of action of the enzyme families active on pectins.

Pectins or pectic substances are collective names for a group of closely associated polysaccharides present in plant cell walls, where they contribute to complex physiological processes like cell growth and cell differentiation and so determine the integrity and rigidity of plant tissue. They also play an important role in the defence mechanisms against plant pathogens and wounding. As constituents of plant cell walls and due to their anionic nature, pectic polysaccharides are considered to be involved in the regulation of ion transport; they determine the porosity of the walls, and they may thus control the permeability of the walls for enzymes. They also determine the water-holding capacity of the wall (1, 2).

The following groups of polysaccharides are comprised in the term pectic substances:

1. Linear homogalacturonan consisting of α-(1 $\rightarrow$ 4)-linked D-galacturonic acid units in which varying proportions of the carboxyl groups are esterified with methanol, and secondary hydroxyl groups at O-2 and O-3 with acetyl groups.
2. Linearly branched xylogalacturonan carrying single-unit xylopyranosyl residues and the rarely occurring apiogalacturonan carrying mono- and diapiosyl side chains (2).
3. Highly branched galacturonan, in the literature in retrospect wrongly termed rhamnogalacturonan II (RG-II).
4. Rhamnogalacturonan having a backbone of alternating α-(1 $\rightarrow$ 2)-linked L-rhamnosyl residues and α-(1 $\rightarrow$ 4)-linked D-galacturonosyluronic acid residues ramified at O-4 of the rhamnosyl residue with neutral sugar side chains of varying composition and size (1 to $\sim$ 50 sugar moieties).

5. Polymeric side chains of pectin usually distinctly referred to as arabinans, galactans, and arabinogalactans.

Next to the xyloglucan-cellulose network, these pectic polysaccharides are suggested to form an independent network determining, e.g., the porosity of the cell wall (3).

The texture of fruits and vegetables during growth, ripening, and storage is strongly influenced by the amount and composition of the pectic molecules present. Consequently, the structure of pectins present in fruit and vegetables depends on enzymatic and chemical modifications occurring during these processes. Endogenous as well as exogenous enzymes (processing aids) play an important role in determining the pectic structures present in plant tissues or food products at a given time.

Pectin used in the food industry as natural ingredients for their gelling, thickening, and stabilizing properties are extracted from suitable agrobyproducts like citrus peel and apple pomace (2, 4). Commercially produced pectins usually contain > 65% of galacturonic acid by weight, since the extraction conditions used remove the greatest part of the neutral side chains present in native pectin rather specifically (2, 4, 5).

The chemistry and technology of pectin are discussed extensively by Walter (6). A general representation of native pectins is given in Figure 1. This figure shows that the major part of the galacturonosyl residues is present in homoglacturonan segments (smooth regions of pectin), whereas only a relatively small part of the uronic acids is present in so-called hairy regions (7, 8).

The proportion of the various structural elements of pectin may differ strongly from one pectin to another (Table 1). The proportion of homogalacturonan can be > 65% for commercially extracted pectins but can also be zero in the case of soybean pectin. Large variations are also found for xylogalacturonan, arabinan, or galactan segments (Table 1) (8, 26).

The various different structural elements present in pectic substances will be discussed in more detail below. Enzyme systems which are able to (specifically) degrade or modify homogalacturonans, xylogalacturonans, rhamnogalacturonans, arabinans, and (arabino) galactans are covered in Chapters 67–70, 73, and 80 of this book.

II. HOMOGALACTURONAN

As described above, the linear homogalacturonan dominates in commercial pectins and plays a prominent role in plant physiology (e.g., ripening). Therefore, both the chemical fine structure of homogalacturonans (Fig. 2) and enzymes specific to (methyl esterified) galacturonans are studied in great detail. In addition to the type and amount of neutral sugars present, the major structural differences among various commercial pectins (in essence homogalacturonans) are explained by the level of methyl esters present at C6 of the galacturonic acid residues and the distribution of these esters and neutral sugar side chains over the galacturonan backbone. Usually, the degree of methyl esterification (DM) is expressed as moles of methanol present per 100 moles of galacturonic acid. When the DM is 50 or higher, pectins are called high-methoxyl (HM) pectins, whereas the term low-methoxyl (LM) pectins indicates a DM < 50.

Methyl esters may be distributed over the homogalacturonan quite differently where the two extremes are formed by a random distribution where all esters are "spread out" over the polymer in a rather statistical way or by a blockwise distribution where blocks of nonesterified galacturonic acid residues are interspersed with segments having a rather high degree of methyl esterification (2, 10). Such distributions are strongly influenced by the presence of endogenous enzymes like plant pectin methylesterase, whose activity may cause a blockwise distribution or by the conditions under which the raw material is processed or the pectin extracted (2). Pectin lyase can therefore be active on an LM pectin with a blockwise distribution and polygalacturonase on an HM pectin with blockwise distribution. In addition to methyl esterification, depending on the origin of the pectin, galacturonic acid moieties may be substituted with acetyl groups at O-2 or O-3 (e.g., sugar beet pectin, potato pectin) (2).

III. XYLOGALACTURONANS

In xylogalacturonans, the amount of β-xylose substitution to the O-3 position of galacturonic acid residues in the backbone may vary significantly (Fig. 3), depending on their origin (e.g., apple, pea hulls, watermelon,

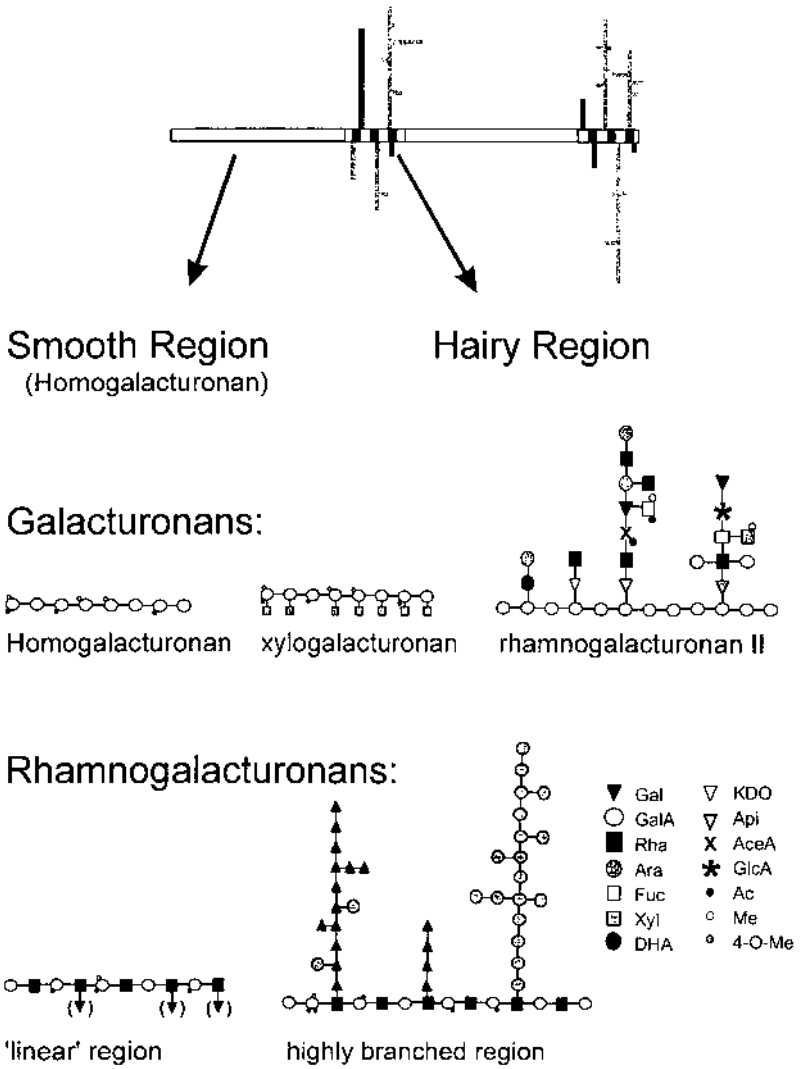

Figure 1 Structural elements of pectin. Occurrence, amount, and chemical fine structure of the individual segments may vary significantly depending on the origin of the pectin. Gal, galactose; GalA, galacturonic acid; Rha, rhamnose; Fuc, fucose, Xyl, xylose; DHA, 3-deoxy-D-lyxo-2-heptulosaric acid; KDO, 2-keto-3-deoxy-D-manno-octulosonic acid; Api, apiose; AceA, aceric acid, GlcA, glucuronic acid, Ac, acetyl group; Me, methyl ester; 4-O-Me, 4-O-methyl ether. (From Refs. 7, 8.)

soybeans). This is also the case for the amount and distribution of methyl esters present, since for apples various populations of xylogalacturonans with a rather distinctive methyl ester level have been reported (7).

IV. HIGHLY BRANCHED GALACTURONAN (HBG) OR RHAMNOGALACTURONAN II

HBG or RG-II consists of a backbone of about nine α-(1 $\rightarrow$ 4)-linked galacturonosyl residues carrying four side chains containing a number of rare sugars (e.g., apiose, aceric acid, KDO, and DHA) in a defined and rather conserved structure (Fig. 1). This structural element is involved in the crosslinking of two pectin molecules within the cell wall through a borate diester (11, 12). No enzymes able to degrade the complex HBG structure have been described in detail.

V. RHAMNOGALACTURONAN

Rhamnogalacturonan has a backbone of up to 300 repeating units of alternating α-(1 $\rightarrow$ 2)-linked rhamnosyl and α-(1 $\rightarrow$ 4)-linked galacturonosyluronic acid

Table 1 Occurrence and Proportion of the Various Structural Elements of Native Pectin in Apple, Sugar Beet, and Soybean

	Soybean meal	Sugar beat pulp	Apple
Total polysaccharide (w/w% dry matter)	16	67	20
Pectic substances (% of total polysaccharides)	59	40	42
Structural element (% of pectic substances)			
Homogalacturonan	0	29	36
Xylogalacturonan	21	< 1	4
Rhamnogalacturonan II	4	4	10
Rhamnogalacturonan backbone	15	8	4
arabinan	60	46	27
arabinogalactan I		12	20
arabinogalactan II	0	0	+

Source: Ref. 8.

residues, which may be methyl esterified and/or acetylated (Fig. 4) (7, 13, 14). Depending on the origin of the cell walls examined (type of cell wall, tissue, plant segment, etc.), the length of the side chains attached to 20–80% of the rhamnose residues can vary from one single galactose residue up to chains of 50 residues or more being composed of arabinose (e.g., sugar beet), galactose (e.g., flax, garlic, onion) or both (e.g., soy, potato) (7, 13). Taking all possible variations into account, it can be stated that rhamnogalacturonans are a family of quite complex structures with "only" the rhamnogalacturonan backbone in common.

Recently, a whole family of rhamnogalacturonan-specific carbohydrases has been recognized which is discussed in Chapter 73. Using a specific rhamnogalacturonan hydrolase, it was shown that rhamnogalacturonan contains blocks highly ramified with long neutral sugar side chains, and in addition segments of alternating rhamnose and galacturonic acid sequences with or without single-unit galactose substitution on O-4 of the rhamnosyl residues up to ~ 30 residues in length. Some rhamnogalacturonan preparations (e.g., from sycamore cells) were resistant to degradation by RG hydrolases (7), demonstrating the absence of low-substituted RG segments. A common feature of these RG structures is that they are also (highly) substituted with acetyl groups, either attached to O-2 *or* to O-3 or to both O-2 *and* O-3 of the galacturonic acid moieties (7, 14) which inhibits RG-hydrolase and -lyase (see Chap. 73).

VI. ARABINANS

Arabinans are branched homoglycans mainly composed of a backbone of α-L-(1 $\rightarrow$ 5)-linked arabinosyl residues and in native form substituted with α-arabinofuranosyl residues at O-2 and/or O-3 position. Such a substitution can be a single arabinosyl residue, but longer (branched) chains can also be present mostly one to three arabinosyl residues (see Fig. 5), resulting in complex structures (see the reviews 15–17 and references herein).

Arabinans have been described to be present in cell walls from apples, sugar beet, rapeseed, carrot, cowpea, azuki- and soybean, rape, mustard, lemon, grape, cabbage, onion, potato, and others (17). Arabinans can have molecular weights up to 10 kDa and are

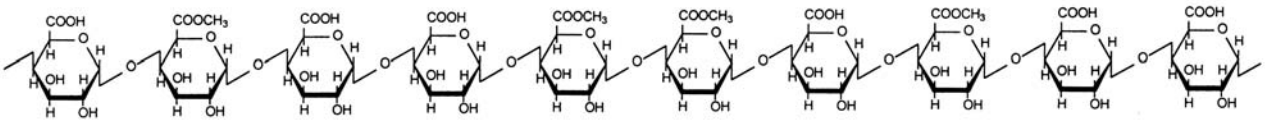

Figure 2 Homogalacturonan fragment of pectin. Acetyl groups may be present at O-2, O-3 or both at O-2 and O-3 for some pectins from some sources. (From Ref. 2.)

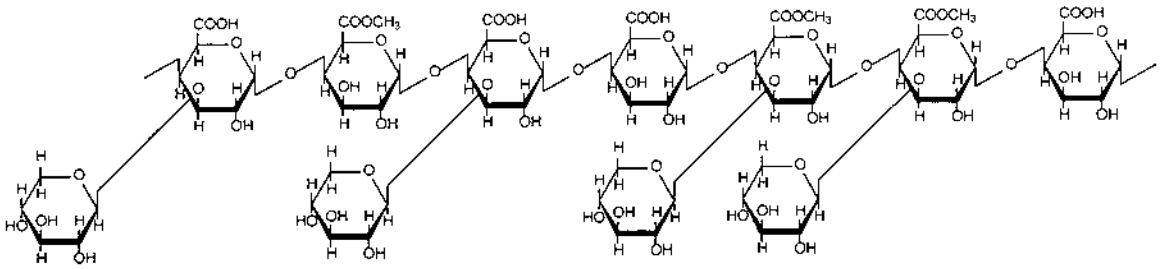

Figure 3 Schematic structure of a xylogalacturonan. The position of methyl esters is chosen arbitrarily.

often covalently linked to galacturonic acid–rich polymers. Although arabinans have been isolated in a pure form, the extraction conditions used may have resulted in chemical (β-elimination, chain peeling) or enzymatic degradation of any attached pectin structures (17 and references herein).

VII. GALACTANS

Galactans and arabinogalactans in which the galactan backbone is substituted with various amounts of arabinose or galactose have been found in a broad range of higher plants (18–20). Aspinall (21) classified the arabinogalactans as type I and type II arabinogalactans, where both types may be present as side chains of pectin or as a single polymer. Type II arabinogalactans may also be present as side chains of a protein segment and as such be referred to as arabinogalactan proteins (AGPs).

A. Arabinogalactan Type I

Arabinogalactans of type I are quite common for various types of plant tissues (20) and consist of a $(1 \rightarrow 4)$-linked linear chain of β-D-glactopyranosyl residues. Pure galactans have been isolated from lupine, potato, and tobacco, although type I galactans usually are substituted with short chains of α–$(1 \rightarrow 5)$-arabinofuranosyl residues attached through the O-3 position (20). O-6 substitution of the galactan backbone with β-galactose is also found. Figure 6 shows the schematic structure of type I arabinogalactans.

Depending on the way of extraction, remnants of the pectic backbone may still be present.

B. Arabinogalactan Type II

Arabinogalactans of type II are highly branched polysaccharides with ramified chains of β-D-galactopyranose residues joined by 1,3 and 1,6 linkages. They are more common in plants than type I and have been reported in leaves, stems, roots, floral parts, seeds, and media of suspension cultured cells (20).

In general, the interior backbone of a type II galactan consists mainly of β-$(1 \rightarrow 3)$-linked galactose moieties; β-$(1 \rightarrow 6)$-linked galactopyranosyl residues occur mainly in the exterior chains which may be terminated with an L-arabinopyranosyl residue. The $(1 \rightarrow 3)$-galactan may be branched through O-6 with arabinofuranose residues or (to a lesser extent) with arabinopyranose units, while also longer α-$(1 \rightarrow 3)$-linked arabinose chains may be present. In general, galactose is more abundantly present than arabinose, although the ratio of arabinose to galactose may differ significantly. Arabinogalactans of type II may be present within the ramified regions of pectins but are also

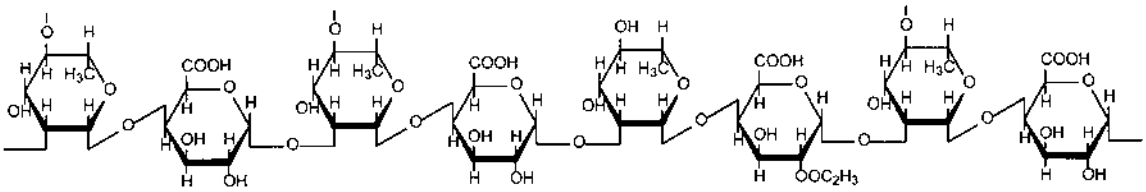

Figure 4 The alternating structure of rhamnogalacturonan segments of pectin. The number, length, and structure of the side chains may vary significantly depending on the origin of the pectin. The acetyl groups may be substituted to O-2, O-3 or both O-2 and O-3 of the galacturonic acid residues. (From Refs. 7, 13, 14.)

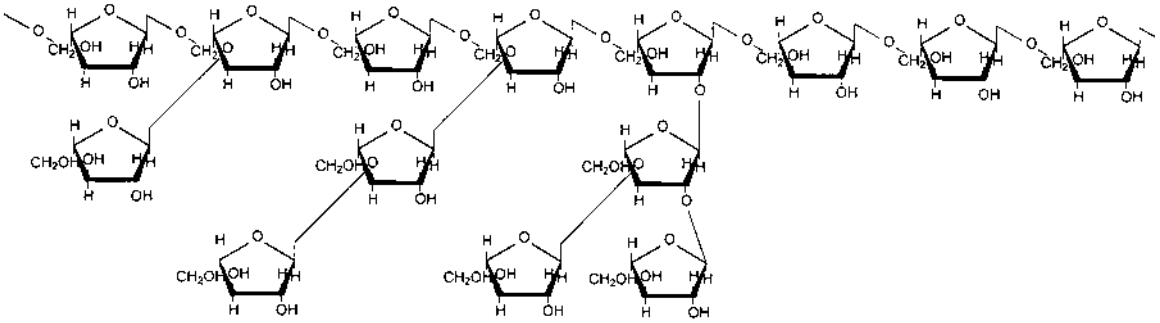

Figure 5 Schematic structure of a highly branched α-L-(1 $\rightarrow$ 5)-arabinan.

often reported to be linked to a hydroxyproline-rich protein (AGP), of which gum arabic from *Acacia senegal* is a well-known example. The hypothetical structure of a type II arabinogalactan is shown in Figure 7. It should be emphasized that many variations with respect to the model shown have been reported including substitution with glucuronic acid (22, 23).

VIII. ISOLATION OF POLYSACCHARIDE STRUCTURES

It should be realized that all commercially available polymeric substrates to be used in enzyme screening and characterization have been isolated from the complex plant material. As mentioned above, pectins with a high galacturonic acid content (> 70%) are extracted under acidic conditions from suitable raw materials, followed by precipitation with alcohol and possibly treatment with acidic alcohol to remove salts like potassium, sodium, and calcium. The precise conditions (pH, time, temperature) will determine the molecular weight, the amount of neutral sugars still present, and the degree of methyl esterification (2, 5).

Arabinans and (arabino)galactans are not yet being used routinely by the food industry. However, for research purposes, these polysaccharides are commercially available and are usually obtained by alkaline treatment at increased temperatures to enhance degradation of the pectic backbone and lowering the strength of hydrogen bridges between the neutral polysaccharides and the cellulose matrix. Further purification of neutral polysaccharides includes preparative anion exchange chromatography to remove charged "impurities."

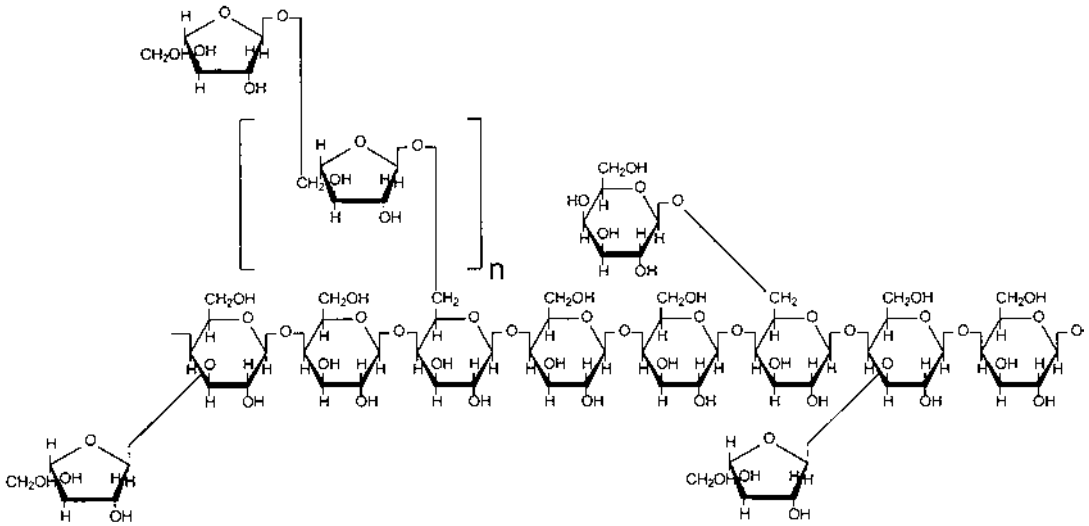

Figure 6 Schematic structure of a type I β-(1 $\rightarrow$ 4)-linked arabinogalactan.

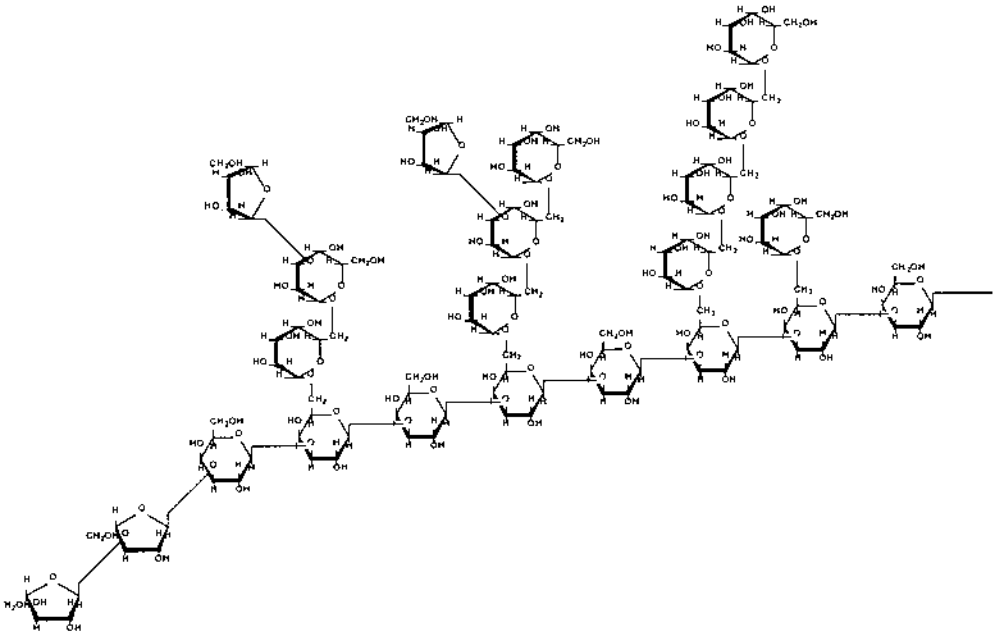

Figure 7 Hypothetical structure of type II β-(1,3,6)-arabinogalactan. (From Refs. 22, 23.)

Defined polysaccharides with various degrees of methyl esterification or branching are usually not commercially available and should be prepared in the laboratory. Purification of polysaccharides is often a compromise: extensive handling in order to obtain pure polysaccharides often changes the chemical composition (as compared to the polysaccharide in its native form), whereas mild procedures may result in the presence of "contaminating" polysaccharides, originally linked to the polysaccharide of interest. This latter phenomenon may result in the presence of galacturonic acids in an arabinan or galactan preparation. More universal assays to monitor enzyme action as based on the release of reducing end groups may so produce unreliable results because they do not given information as to which glycosidic bond in the substrate is split. Analysis of the degradation product by high-performance liquid chromatography (HPLC) or mass spectrometry (MS) will avoid such a confusion in most cases.

IX. METHODS TO MONITOR "PECTIC" ENZYMES

It should be realized that the summary of frequently used methods given below is only a short list selected from the literature and from our own laboratory and is not complete. In most cases, adequate references are given rather than extensive descriptions of the method mentioned.

A. Substrates

Pectic substrates can be purchased from several (specialized) suppliers (e.g., Megazyme, Ireland; Sigma-Aldrich Fine Chemicals, USA), but the origin, purity, and specifications are not always clear and straightforward. When monitoring crude enzyme mixtures, relatively small amounts of other polysaccharides accompanying the polysaccharide indicated on the label may give erroneous results.

A broad range of synthetic substrates like p-nitrophenyl- and p-methylumbelliferylglycosides can be obtained (e.g., Sigma-Aldrich) to assay glycosidase activity. Specific oligosaccharides may also be purchased from the same companies, although the choice and purity are limited. Alternatively, oligosaccharides can be produced and purified in the laboratory (24).

Branched polysaccharides like arabinan or arabinogalactans can be rather easily de-branched by mild acid treatment (17, 20, 25, 26) to obtain a more suitable substrate for endoacting enzymes. A wide variety of both soluble azopolysaccharides and insoluble azurine-crosslinked polysaccharides which can be used to screen for specific classes of carbohydrases are commercially available from Megazyme.

When a series of pectins is needed with various degrees of methyl esterification, it is better to prepare such a series in-house than to buy pectins with a different DM. In the former situation, relatively homogeneous substrates are obtained; in the latter situation these preparations may be very heterogeneous owing to their different history (origin, MW, neutral sugars), and these different characteristics may influence the outcome of the experiments. Lowering the DM in a random way is possible by controlled alkali treatment (27) or by using fungal pectin methylesterase (see Chapter 68). A more blockwise-distributed methyl esterification can be obtained using pectin methylesterase from plant origin (Chapter 68). Degrees of esterification up to 85–90% can be obtained by methyl esterification using a $MeOH–H_2SO_4$ treatment as described previously (28). Polygalacturonic acid can be obtained from chemical supply stores and is a rather well-defined substrate for endopolygalacturonase owing to the absence of methyl esters and neutral sugars (as a result of a bleaching step).

B. Substrate Solubility and Stability

Not all polysaccharides, when added to cold water, will readily dissolve but they may cause lump formation. This phenomenon can be avoided by premoistening the sample with a drop of ethanol prior to adding the water/buffer. Heat treatment (80–100°C) may also be helpful. However, for esterified pectins, care should be taken to avoid circumstances which allow β-eliminative degradation (ΔT; pH > 5). Especially when the solubilization of insoluble cell wall polysaccharides as consequence of enzyme action is monitored, it is important not to have inaccurate results caused by cleaving a few pectin bonds chemically. Depending on the structure of the substrate, the "history" of the sample (cold storage, freezing, etc.) may influence aggregation/association behavior of the polymeric molecules, which may result either in a rather poor solubility or in a high apparent molecular weight. When only part of the substrate is soluble and only this part is used further for enzyme assays, it is relevant to examine whether this part is representative for the desired substrate.

X. ANALYSIS OF DIGESTS OF PECTIC POLYSACCHARIDES

Enzymic digests of pectic substances can be analyzed from different points of view, each requiring its own approach and method. Some of the methods and approaches used in the characterization of enzymes are described below.

A. Reducing End Groups

Carbohydrases increase the number of reducing ends when degrading their substrates. Many methods have been described to determine the amount of reducing sugars released including the Somogyi-Nelson procedure, neocuproine assay, ferricyanide, and the 2,4-dinitrosalicylic acid test (29; Chapter 71). One has to be aware that the outcome of the different assays may depend on the type of sugar moieties present in the oligomers formed and the length of the oligomers (29, Chap. 71). Recently, the use of the very sensitive bicinchoninic acid (BCA) reducing value assay has been described to detect any carbohydrase activity degrading any polysaccharide by which both endo- and exoenzymes can be measured (30). The reaction can be carried out in wells of microtiter plates so that large numbers of samples can be analyzed simultaneously. Because of the sensitivity, several precautions should be taken to prevent too high background levels as a result of the enzyme protein itself. Furthermore, depending on the polysaccharide used, the background caused by the reducing end group of the polymer can also be too high. This can be avoided by choosing a rather low substrate concentration or, alternatively, by reducing the reducing end of the polymer by treatment with $NaBH_4$ prior to use (31).

B. Assays Using Synthetic or Dyed Substrates

The most commonly used assays to determine glycosidases and exocarbohydrases make use of synthetic substrates like *p*-nitrophenyl- and *p*-methylumbelliferylglycosides where the release of the glycosyl group results in a colored solution, which can be quantified using a spectrophotometer set at the appropriate wavelength.

Endoacting enzymes can be measured using polysaccharides to which usually an azocompound has been attached. Degradation with endoenzymes results in the release of dyed fragments which remain soluble after the addition of ethanol to precipitate the remaining polymer. The color of the supernatant (and thus the enzyme activity) is measured spectrophotometrically (Megazyme).

C. Solubilizing Activity of Carbohydrases

When enzymes are tested on insoluble substrate (e.g., cell wall polysaccharides), a relatively simple assay to monitor the solubilization of pectic material is by using (automated) colorimetric assays like the *m*-hydroxybiphenyl assay (32, 33) for uronic acids and the phenol-sulfuric acid or orcinol-sulfuric acid assay for neutral sugars (34, 35). Obviously, the latter two methods are not very discriminative for the various neutral sugars, but can be used quite satisfactorily to monitor enzyme activity. More information on the enzyme is obtained when the determination of concentration of the solubilized carbohydrates is combined with information on their size (e.g., reducing sugar assay or size exclusion chromatography).

D. Molecular-Weight Measurement

To establish whether the (purified) carbohydrase is an exo- or an endoacting enzyme, a relatively simple assay is based on the measurement of viscosity reduction during the enzymatic degradation, since endoacting enzyme activity results almost immediately in a loss of viscosity. However, using this method, quantification of the enzyme activity is rather difficult and the method is not very specific in case of mixtures of pectic enzymes (36). Using high-performance size exclusion chromatography, a more accurate impression of the mode of action of the enzyme is obtained. Although many different types of columns can be used for such HPSEC measurements (37), fairly good results to determine the enzymic degradation of pectic polysaccharides includes elution on three Bio-Gel TSK columns in series (40 XL, 30 XL, 20 XL; identical to TSK-Gel G4000, 3000, 2000 PWXL, respectively), eluted with 0.4 M acetic acid, pH 3, or 0.2 M $NaNO_3$ and monitored using a refractive index detector (38). In a time course experiment, HPSEC allows quantification of the enzyme activity fairly well, whereas also endo- and exoactivity can be distinguished rather easily (even in enzyme mixtures having both activities).

E. Assays for Specific Pectic Enzymes

1. Lyases

Enzymes acting by β-eliminative cleavage like pectin and pectate lyase or rhamnogalacturonan lyase may be monitored quite easily by measuring the absorbance at 235 nm due to the formation of Δ4,5-unsaturated products from their specific substrate ($\epsilon_{235} = 4600\,M^{-1}\,cm^{-1}$ for pectate and $5200\,M^{-1}\,cm^{-1}$ for pectin (39–41).

2. Pectin Methyl Esterase

The action of pectin methyl esterase results in the release of methanol and consequently in the formation of carboxylic acid groups, and allows two ways of monitoring the action of the enzyme. The release of the H^+ can simply be monitored in a nonbuffered system using a pH indicator which corresponds to the optimal pH range of the pectin methyl esterase assayed (42, 43). Furthermore, a more quantitative assay to measure the action of the enzyme includes an automated titration at the optimal pH (nonbuffered) where the amount of NaOH necessary to compensate the pH changes caused by the enzyme is measured (43, 44).

The release of methanol can be measured using gas-liquid chromatography (GLC) directly (45) or after conversion of the methanol to methyl nitrite (46). Although this latter method is quite sensitive and reliable, it is also quite laborious (42). Alternatively, methanol can also be determined by HPLC on an Aminex column 87H column (47) although this method may not be sensitive enough for all purposes. Colorimetric methods have been developed in which methanol is oxidized to formaldehyde (43, 48–50),but they are not easy to perform (51).

3. Acetyl Esterases

The release of acetyl groups by enzymatic action is usually followed by HPLC using the so-called organic acid column (Aminex HPX 87H) and refractive index detection (47; Chap. 71). An alternative procedure is an enzymic assay for acetic acid including a NADH/NAD^+ conversion step using a commercial test kit (Boehringer-Mannheim, Germany). Obviously, care should be taken when using the frequently applied acetate buffers when using these methods. This is less important (although product inhibition may occur) when using colorimetric assays based on *p*-nitrophenyl acetate, *p*-naphtyl acetate, or *p*-methylumbelliferylacetate (Chap. 71). Another synthetic substrate used for the determination of acetylesterases is triacetine, where the acetic acid released has to be measured by one of the methods mentioned. However, these latter substrates are usually also deesterified by nonpectin esterases.

XI. CHROMATOGRAPHY AND MASS SPECTROMETRY OF COMPLEX ENZYME DIGESTS

Chromatography in its wide variety is a powerful technique to detect activities of specific enzymes and to obtain important information on their substrate specificity and mode of action. Especially for heterogeneous carbohydrate substrates, chromatography (with or without MS detection) is almost indispensable to determine enzyme's substrate requirements. High-performance anion exchange chromatography (HPAEC) as introduced by Dionex in the late 1980s is able to separate oligosaccharides having the same size and sugar composition but differing in branching and/or linkage composition. A similar breakthrough in oligosaccharide characterization and identification as achieved by the introduction of HPAEC was obtained by the introduction of matrix-assisted laser desorption/ionization time of flight mass spectrometry (Maldi Tof MS) during the last 5 years enabling molecular-mass measurements of oligosaccharide mixtures rather accurately and easily. Nowadays, HPAEC, Maldi Tof MS, and LC-MS techniques have been developed into quick, reliable, and easy-to-operate techniques allowing a more detailed examination of the mode of action of enzymes on complex substrates by characterizing the enzymic degradation products.

A. High-Performance Anion Exchange Chromatography of Oligosaccharides

Although many different types of chromatography have been used to separate oligosaccharides (52, 53), HPAEC using alkaline elution conditions in combination with pulsed amperometric detection (PAD) is preferred for specifically monitoring oligosaccharides (55–57). The principles for both separation and detection are nicely described by Hensall (56). In principle, separation is based on interaction with a strong anion exchange resin, and usually salt (sodium acetate) gradients in 100 mM NaOH are used to elute the oligosaccharides. Since elution is usually performed in alkali, even neutral carbohydrates bind to the column and can be eluted later on. HPAEC allows separation of oligosaccharides with a DP up to 50. PAD detection is direct (no derivatization required), highly sensitive, and compatible with the gradients commonly used in HPAEC. When neutral eluents are used to separate charged oligosaccharides, alkali should be added post column prior to detection since PAD detection of (part of the) sugar residues requires a high pH (56, 57). A "disadvantage" of the method is that the separation is influenced by the size, sugar (linkage) composition, and degree of branching of the oligomer (55).

Figure 8 shows the dependency of the elution behaviour of various hololog ous series of oligosaccharides on the "elution power" of the gradient expressed as NaOAc. This can result in a rather unpredictable elution behavior when not much is known about the complexity of the oligosaccharide mixtures under investigation (55), and other methods of identification like mass spectrometry might be necessary. However, when the polymeric substrate is well defined and the (class of) enzyme is known, even complex elution patterns might be interpreted reasonably. This is illustrated in Figure 9, where a complex HPAEC elution pattern of a pectic arabinogalactan type I from soybean after digestion with arabinan- and galactan-degrading enzymes is shown (26). The more intensive peaks eluting between 10 and 25 min represent linear galactose oligomers, whereas the smaller peaks eluting in this time frame represent "mixed" oligomers consisting of both arabinose *and* galactose. Oligomers of arabinose are eluted after 25 min.

The broad applicability of HPAEC/PAD is demonstrated by the fact that also the release of the various *monomeric* sugar residues can easily be monitored using weaker elution conditions (58). In case of UV-absorbing oligosaccharides (e.g., after lyase action), degradation products can be monitored using an UV detector set to 235 nm (59). HPAEC-PAD may give some problems when quantifying "unknown" compounds where response factors are not available, since such response factors may also depend on size and structure of the analyte (55).

When the oligomeric degradation products released by the enzyme under investigation are expected to be negatively charged, HPAEC can be performed under neutral elution conditions (56, 60). Such conditions are relevant when the oligomers are substituted with alkali-labile groups (e.g., methyl-esterified galacturonic acid oligomers). Identification of these partially esterified oligomers may give information about the precise mode of action of the enzyme (10, 61–63).

B. Matrix-Assisted Laser Desorption/Ionization Time of Flight MS

Maldi Tof MS is a rather new mass-spectrometric technique, enabling collection of valuable data concerning the molecular masses of compounds present in a complex mixture of biomolecules in the range of 400–300,000 daltons (64, 65). Maldi Tof MS gives a good

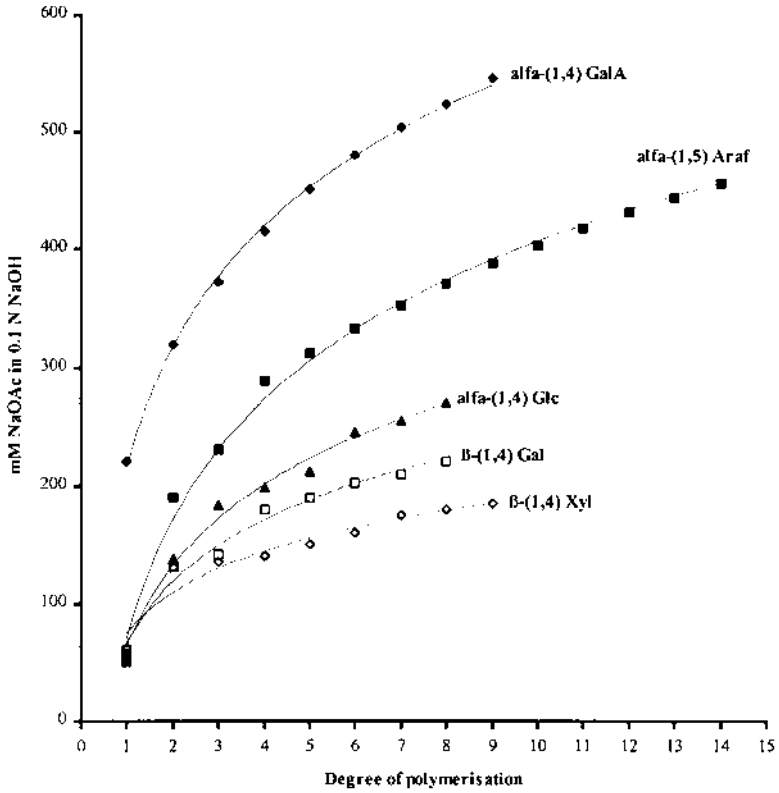

Figure 8 Total sodium concentration at which series of linear oligosaccharides elute in HPAEC as a function of the degree of polymerization (DP). Gradient: 0–600 mM NaAc in 100 mM NaOH in 40 min. CarboPac PA100 column. (From Ref. 54.)

mass accuracy, is easy to operate, and requires relatively little sample preparation. For oligosaccharides, mass determinations in the range of 400–4000 are rather easy to perform.

Figure 10 shows a Maldi Tof mass spectrum for the pentamer/hexamer fraction of enzymatically degraded soybean arabinogalactan, obtained after size exclusion chromatography of the whole digest, as shown in Figure 9. It can be seen that the different oligomers consisting of arabinose and galactose can be easily recognized. Obviously, isomers having the same molecular mass cannot be distinguished from each other. If necessary, electrospray tandem MS analysis following HPAEC analysis may be used to verify the precise structure of different isomers present (26). Kabel et al. (66) described the off-line coupling of HPAEC and Maldi Tof MS where on-line desalting by membrane suppressors, microtiterplate fraction collection, and automated sample handling followed by Maldi Tof MS analysis allow determination of the molecular mass of individual peaks within a complex HPAEC elution pattern rather routinely. The precise structure of galacturonic acid oligomers having methyl or ethyl esterification, glycosidation, or amidation, and oligomers as present in an enzyme digest have been studied by Maldi Tof MS and nanoelectrospray MS in detail (61, 63, 67–70).

C. Screening Using Plate Assays and Chromogenic Substrates

When huge amounts of enzyme samples have to be screened for specific activities (e.g., cDNA libraries), commonly used assays are based on the property of the substrate to specifically bind to a coloring agent like Congo Red (71–73) or Ruthenium Red (74), or by using polysaccharides where a chromogen is covalently attached (Megazyme catalog). In specific cases, enzyme action may result in a modified substrate which can specifically be precipitated by metal complexation in a plate assay (75). Also the use of synthetic substrates in plates like *p*-methylumbelliferylglycosides and p-nitrophenylglycosides to screen for glycosidases

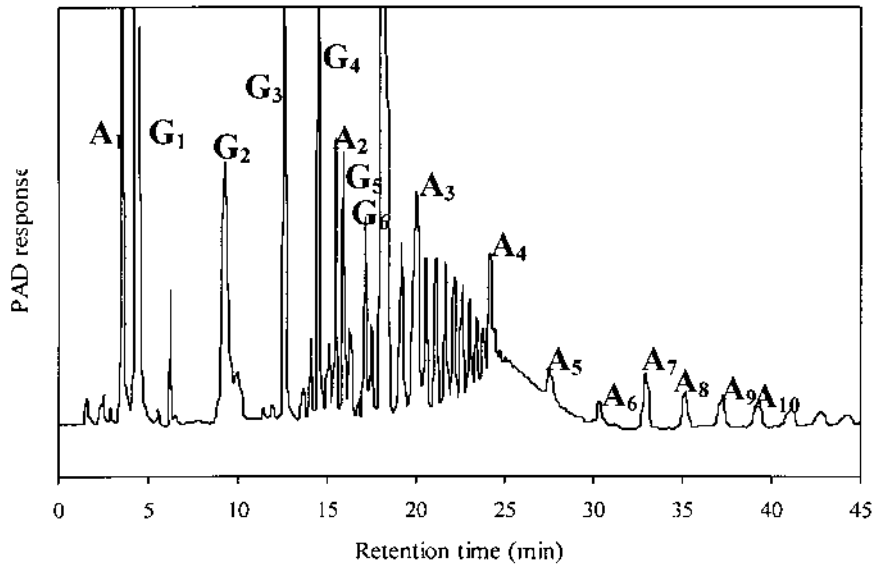

Figure 9 HPAEC elution pattern for the oligosaccharide-containing pool from digest obtained after incubation of soybean-chelating agent extractable pectin with endogalactanase, exogalactanase, endoarabinanase, and arabinofuranosidase B. G_n, linear β-1,4-linked galactose oligomers; A_m, linear α-1,5-linked arabinose oligomers. (From Ref. 26.)

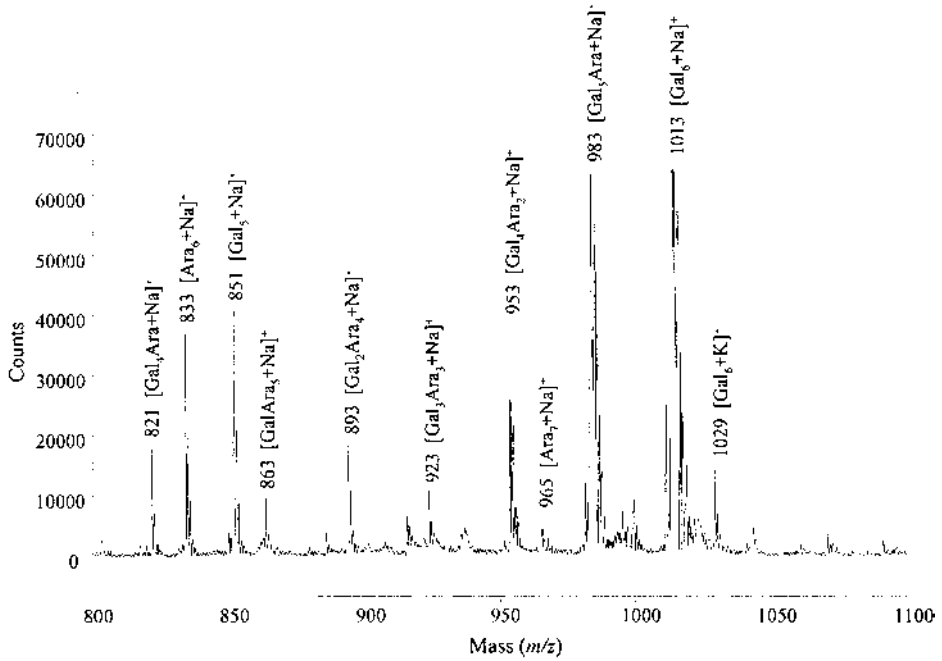

Figure 10 MALDI-Tof MS of a size exclusion chromatography fraction containing mainly pentamers and hexamers released from soybean pectic arabinogalactan type I by arabinogalactan-degrading enzymes. (From Ref. 26.)

is quite common. The same holds for the inclusion of a pH indicator to the medium to detect esterase activity.

REFERENCES

1. A Basic, PJ Harris, BA Stone. Structure and function of plant cell walls. Biochem Plants 14:297–369, 1988.
2. AGJ Voragen, W Pilnik, JF Thibault, MAV Axelos, CMCG Renard. Pectins. In: AM Stephen, ed. Food Polysaccharides and Their Applications. New York: Marcel Dekker, 1995, pp 297–339.
3. M McCann, K Roberts. Architecture of the primary cell wall. In: CW Lloyd, ed. The Cytoskeletal Basis of Plant Growth and Form. New York: Academic Press, 1991, pp 109–129.
4. CD May. Pectins. In: GO Phillips, PA Williams, eds. Handbook of Hydrocolloids. Cambridge, UK: Woodhead, 2000, pp. 69–188.
5. JF Thibault, MC Ralet. Pectins, their origin, structure and function. In BV McCleary, L Prosky, eds. Advanced Dietary Fibre Technology. London: Blackwell Science, 2001, pp 369–378.
6. RH Walter. The Chemistry and Technology of Pectins. San Diego: Academic Press, 1990.
7. HA Schols, AGJ Voragen. Complex pectins: structure elucidation using enzymes. In: J Visser, AGJ Voragen, eds. Progress in Biotechnology 14: Pectins and Pectinases. Amsterdam: Elsevier, 1996, pp 13–19.
8. AGJ Voragen, G Beldman, HA Schols. Chemistry and enzymology of pectins. In: BV McCleary, L Prosky, eds. Advanced Dietary Fibre Technology. London: Blackwell Science, 2001, pp 379–398.
9. M O'Neil, P Albersheim, A Darvill. The pectic polysaccharides of primary cell walls. Methods Plant Biochem 2:415–441, 1990.
10. PJH Daas, AGJ Voragen, HA Schols. Investigation of the galacturonic acid distribution of pectin with enzymes. Part 2. Characterization of non-esterified galacturonic acid sequences in pectin with endopolygalacturonase. Carbohydr Res 326:120–129, 2000.
11. P Pellerin, T Doco, S Vidal, P Williams, JM Brillouet, MA O'Neill. Structural characterization of red wine rhamnogalacturonan II. Carbohydr Res 290:183–197, 1996.
12. S Vidal, T Doco, P Williams, P Pellerin, WS York, MA O'Neill, J Glushka, AG Darvill, P Albersheim. Structural characterization of the pectic polysaccharide rhamnogalacturonan. II. Evidence for the backbone location of the aceric acid-containing oligoglycosyl side chain. Carbohydr Res 326:277–294, 2000.
13. M McNeil, AG Darvill, SC Fry, P Albersheim. Structure and function of the primary cell walls of plants. Annu Rev Biochem 5:625–663, 1984.
14. P Komalavilas, AJ Mort. The acetylation at O-3 of galacturonic acid in the rhamnose-rich portion of pectins. Carbohydr Res 189:261–272, 1989.
15. JR Whitaker. Pectin substances, pectic enzymes and haze formation in fruit juices. Enzyme Microb Technol 6:341–348, 1984.
16. A Kaji. L-arabinofuranosidases. Adv Carbohydr Chem Biochem 42:383–394, 1984.
17. G Beldman, HA Schols, SM Pitson, MJF Searle–Van Leeuwen, AGJ Voragen. Arabinans and arabinan degrading enzymes. In: RJ Sturgeon, ed. Advances in Macromolecular Research, Vol 1. London: JAI Press, 1997, pp 1–64.
18. AE Clarke, RL Anderson, BA Stone. Form and function of arabinogalactans and arabinogalactan proteins. Phytochemistry 18:521–540, 1979.
19. GB Fincher, BA Stone, AE Clarke. Arabinogalactan proteins: structure, biosynthesis and function. Annu Rev Plant Physiol 34:47–70, 1983.
20. JW De Vis. Characterization and mode of action of enzymes degrading galactan structures of arabinogalactans. PhD thesis, Wageningen University, 1994.
21. AO Aspinall. Carbohydrate polymers of plant cell walls. In: F Loewus, ed. Biogenesis of Plant Cell Wall Polysaccharides. New York: Academic Press, 1973, pp 95–115.
22. A Majewska-Sawka, EA Nothnagel. The multiple roles of arabinogalactan proteins in plant development. Plant Physiol 122:3–9, 2000.
23. GR Ponder, GN Richards. Arabinogalactan from western larch. Part III. Alkaline degradation revisited, with novel conclusions on molecular structure. Carbohydr Polym 34:251–261, 1997.
24. GJWM Van Alebeek, O Zabotina, G Beldman, HA Schols, AGJ Voragen. Structural analysis of (methylesterified) oligogalacturonides using post-source decay matrix-assisted laser desorption/ionization time-of-flight mass spectrometry. J Mass Spec 35:831–840, 2000.
25. GO Aspinall. The Polysaccharides, Vol 1. New York: Academic Press, 1982.
26. MMH Huisman, LP Brüll, JE Thomas-Oates, J Haverkamp, HA Schols, AGJ Voragen. The occurrence of internal (1-5)-linked arabinofuranose and arabinopyranose residues in arabinogalactan side chains from soybean pectic substances. Carbohydr Res 330:103–114, 2001.
27. EMW Chen, AJ Mort. Nature of sites hydrolyzable by endopolygalacturonase in partially-esterified homogalacturonans. Carbohydr Poly 29:129–136, 1996.
28. W Heri, H Neukom, H Deuel. Chromatographic von pektinen mit verschiedener verteilung der methylestergruppen auf den fadenmolekeln. Helv Chim Acta 44:1945–1949, 1961.
29. FJM Kormelink, JW van de Vis, MJF Searle–Van Leeuwen, AGJ Voragen. Comparison of different

reducing sugar assays in relation to their application to glycanase tests. Food Hydrocolloids 4:481–487, 1991.
30. PJA Meeuwsen, JP Vincken, G Beldman, AGJ Voragen. A universal assay for screening expression libraries for carbohydrases. J Biosci Bioengin 89:107–109, 2000.
31. H Omran, K Dorreich, K Gierschner. Some results of the isolation of discrete (exopolygalacturonase and pectinesterase) from a commercial pectic enzyme preparation. I. Isolation, purification and characterization of an exopolygalacturonase. Lebensum Wiss Technol 19:457–463, 1986.
32. N Blumenkrantz, G Asboe-Hansen. New method for quantitative determination of uronic acids. Anal Biochem 54:484–489, 1973.
33. J-F Thibault. Automisation du dosage des substances pectique par la methode au meta-hydroxydiphenyl. Lebensm Wiss Technol 11:247–251, 1979.
34. M Dubois, KA Gilles, JK Hamilton, PA Rebers, F Smith. Colorimetric method for determination of sugars and related substances. Anal Chem 28:350–356, 1956.
35. M Tollier, J Robin. Adaptation de la methode a l'orcinol sulfurique au dosage automatique des glucides neutres totaux: conditons d'application aux extraits d'origine vegetale. Ann Technol Agric 28:1–15, 1979.
36. FM Barnby, FF Morpeth, DL Pyle. Endopolygalacturonase production from *Kluyveromyces marxianus*. I. Resolution, purification, and partial characterisation of the enzyme. Enzyme Microb Technol 12:891–897, 1990.
37. CS Wu. Column Handbook for Size Exclusion Chromatography. San Diego: Academic Press, 1999.
38. HA Schols, MA Posthumus, AGJ Voragen. Structural features of hairy regions of pectins isolated from apple juice produced by the liquefaction process. Carbohydr Res 206:117–129, 1990.
39. GP MacMillan, RH Vaughn. Purification and properties of a polygalacturonate-*trans*-eliminase produced by *Clostridium multifermentans*. biochemistry 3:564–572, 1964.
40. M Mutter, IJ Colquhoun, G Beldman, HA Schols, EJ Bakx, AGJ Voragen. Characterization of recombinant rhamnogalacturonan α-L-rhamnopyranosyl-(1,4)-α-D-galactopyranosyluronide lyase from *Aspergillus aculeatus*. Plant Physiol 117:141–152, 1998.
41. C Roy, HCM Kester, J Visser, V Shevchik, N Hugouvieux-Cotte-Pattat, J Robert-Baudouy, JAE Bensen. Modes of action of five different endopectate lyases from *Erwinia chrysanthemi* 3937. J Bacteriol 181:3705–3709, 1999.
42. W Pilnik, AGJ Voragen. The significance of endogenous and exogenous pectic enzymes in fruit and vegetable processing. In PF Fox, ed. Food Enzymology, Vol 1. London: Elsevier Applied Science, 1991, pp 303–336.
43. C Versteeg. Pectinesterases from the orange fruit—their purification, general characteristics and juice cloud destabilizing properties. PhD thesis, Wageningen University, 1979.
44. M Lee, JD MacMillan. Mode of action of pectic enzymes. I. Purification and properties of tomato pectinesterase. Biochemistry 7:4005–4010, 1968.
45. RF McFeeters, SA Armstrong. Measurement of pectin methylation in plant cell walls. Anal Biochem 139:212–217, 1984.
46. MA Litchman, RP Upton. Gas chromatographic determination of residual methanol in food additives. Anal Chem 44:1497–1497, 1972.
47. AGJ Voragen, HA Schols, W Pilnik. Determination of the degree of methylation and acetylation of pectins by HPLC. Food Hydrocolloids 1:65–70, 1986.
48. PJ Wood, IR Sidiqui. Determination of methanol and its application to measurements of pectin ester content and pectin methylesterase activity. Anal Biochem 39:418–428, 1971.
49. RG Cameron, BS Bulsig, PE Shaw. Adaption of a spectrophotometric assay for pectin methylesterase to a kinetic microplate reader. J Food Sci 47:1006–1008, 1992.
50. GP MacMillan, DJ Johnston, JB Morel, MCM Perombelon. A pH-independent assay for pectin methyl esterase for use in column chromatography. Anal Biochem 209:377–379, 1993.
51. M Bordenave. Analysis of pectin methylesterase. In: HF Linskens, JF Jackson, eds. Modern Methods of Plant Analysis. Vol. 17—Plant Cell Wall Analysis. Berlin: Springer-Verlag, 1996, pp 165–180.
52. SC Churms. Recent developments in the chromatographic analysis of carbohydrates. J Chromatogr 500:555–583, 1990.
53. WMA Niessen, HA Schols, RAM van der Hoeven, AGJ Voragen, J van der Greef. Characterization of oligosaccharides derived from plant cell wall polysaccharides by on-line high-performance anion-exchange chromatography thermospray mass spectrometry. In: HF Linskens, JF Jackson, eds. Modern Methods of Plant Analysis. Vol 17—Plant Cell Wall Analysis. Berlin: Springer-Verlag, 1996, pp 147–163.
54. HA Schols, KMJ Van Laere, AGJ Voragen. Determination of oligosaccharides. In: COST 92 Metabolic and Physiological Aspects of Dietary Fibre in Food, Copenhagen, 1994. Recent Progress in the Analysis of Dietary Fibre, EC, 1995, pp 53–59.
55. YC Lee. Carbohydrate analyses with high-performance anion-exchange chromatography. J Chromatogr 720:137–149, 1996.
56. A Henshall. High performance anion exchange chromatography with pulsed amperometric detection: a powerful tool for the analysis of dietary fiber and complex carbohydrates. In: SS Cho, L Prosky, M

Dreher, eds. Complex Carbohydrates in Foods. New York: Marcel Dekker, 19999, pp 267–289.
57. AT Hotchkiss, KEI-Bahtimy, ML Fishman. Analysis of pectin structure by HPAEC-PAD. In: HF Linskens, JF Jackson, eds. Modern Methods of Plant Analysis. Vol. 17—Plant Cell Wall Analysis. Berlin: Springer-Verlag, 1996, pp 129–146.
58. E Quigly, HN Englyst. Determination of neutral sugars and hexosamines by high-performance liquid chromatography with pulsed amperometric detection. Analyst 117:1715–1718, 1992.
59. L Parenicová, JAE Benen, HCM Kester, J Visser. PgaE encodes a fourth member of the endopolygalacturonase gene family from *Aspergillus niger*. Eur J Biochem 251:72–80, 1998.
60. AT Hotchkiss, KB Hicks. Analysis of oligogalacturonic acids with 50 or fewer residues by high-performance anion-exchange chromatography and pulsed amperometric detection. Anal Biochem 184:200–206, 1990.
61. PJH Daas, PW Arisz, HA Schols, GA De Ruiter, AGJ Voragen. Analysis of partially methyl-esterified galacturonic acid oligomers by high-performance anion-exchange chromatography and matrix-assisted laser desorption/ionization time-of-flight mass spectrometry. Anal Biochem 257:195–202, 1998.
62. PJH Daas, K Meyer-Hansen, HA Schols, GA De Ruiter, AGJ Voragen. Investigation of the non-esterified galacturonic acid distribution in pectin with endopolygalacturonase. Carbohydr Res 318:120–129, 1999.
63. HCM Kester, JAE Benen, J Visser, ME Warren, R Orlando, C Bergmann, D Magaud, D Anker, A Doutheau. Tandem mass spectrometric analysis of *Aspergillus niger* pectin methyl-esterase: mode of action on fully methyl-esterified oligogalacturonates. Biochem J 346:469–474, 2000.
64. U Bahr, M Karas, F Hillenkamp. Analysis of biopolymers by matrix-assisted laser desorption/ionisation mass spectrometry. Freseniau J Anal Chem 349:783–791, 1994.
65. R Kaufmann. Matrix-assisted laser desorption ionization mass spectrometry: a novel analytical tool in molecular biology and biotechnology. J Biotechnol 41:155–175, 1995.
66. MA Kabel, HA Schols, AGJ Voragen. Mass determination of oligosaccharides by matrix-assisted laser desorption/ionization time-of-flight mass spectrometry following HPLC, assisted by on-line desalting and automated sample handling. Carbohydr Polym 44:161–165, 2001.
67. GJWM Van Alebeek, O Zabotina, G Beldman, HA Schols, AGJ Voragen. Esterification and glycosyldation of oligogalacturonides: examination of the reaction products using MALDI-TOF MS and HPAEC. Carbohydr Polym 43:39–46, 2000.
68. R Korner, G Limberg, JD Mikkelsen, P Roepstorff. Characterization of enzymatic pectin digests by matrix-assisted laser desorption/ionization mass spectrometry. J Mass Spec 33:836–842, 1998.
69. G Limberg, R Korner, HC Buchholt, TMIE Christensen, P Roepstorff, JD Mikkelsen. Analysis of different de-esterification mechanisms for pectin by enzymatic fingerprinting using endopectin lyase and endopolygalacturonase II from *A. niger*. Carbohydr Res 327:293–307, 2000.
70. G Limberg, R Korner, HC Buchholt, TMIE Christensen, P Roepstorff, JD Mikkelsen. Quantification of the amount of galacturonic acid residues in block sequences in pectin homogalacturonan by enzymatic fingerprinting with exo- and endo-polygalacturonase II from *Aspergillus niger*. Carbohydr Res 327:321–332, 2000.
71. H Dalboge, HP Heldt-Hansen. A novel method for efficient expression cloning of fungal enzyme genes. Mol Gen Genet 243:253–260, 1994.
72. S Christgau, T Sandal, LV Kofod, H Dalboge. Expression cloning, purification and characterization of a β-1,4-galactanase from *Aspergillus aculeatus*. Curr Genet 27:135–141, 1995.
73. D Kluepfel. Screening for prokaryotes for cellulose, and hemicellulose-degrading enzymes. Methods Enzymol 160:180–187, 1988.
74. RJ Taylor, GA Secor. An improved diffusion assay for quantifying the polygalacturonase content of *Erwina* culture filtrates. Phytopathology 787:1101–1103, 1988.
75. M Mutter. Application of Cu^{2+} staining for detection of rhamnogalacturonase activity towards modified hairy regions of pectin. In: New Rhamnogalcturonan Degrading Enzymes from *Aspergillus aculeatus*. PhD Thesis, Wageningen University, 1997, pp 63–73.

67

Pectic Enzymes

Jacques A. E. Benen and Alphons G. J. Voragen
Wageningen University, Wageningen, The Netherlands

Jaap Visser
Fungal Genetics and Technology Consultancy, Wageningen, The Netherlands

I. INTRODUCTION

The pectic enzymes comprise a diverse group of enzymes. In view of the complexity of the substrate, the multitude of different enzymes active toward pectin can easily be envisaged. Formally, the enzymes acting on the side chains, galactanases and arabinases, do not belong to the pectic enzymes although these substrates are in general strongly associated with pectin as side chains.

The pectic enzymes consist of main-chain depolymerases and esterases active on methyl- and acetylesters of galacturonosyl uronic acid residues in the galacturonan and rhamnogalacturonan structures. The depolymerizing enzymes comprise hydrolases as well as lyases. Both classes of enzymes contain enzymes that act on the homogalacturonan backbone or "smooth" part, and enzymes that degrade the rhamnogalacturonan part, also known as "hairy regions". The methylesterases hydrolyze the methylester at O6 of a galacturonic acid residue whereas acetylesterases hydrolyze the acetylester at O2 and/or O3 of a galacturonic acid. Acetylesterases specific for the smooth regions as well as for the hairy regions have been identified (1). It is not known whether a hairy region–specific methylesterase exists. A list of pectic enzymes is provided in Table 1.

In the literature a class of enzymes named protopectinases is described (2, 3). Protopectinases are those enzymes active on protopectin, the insoluble pectin that cannot be extracted from the plant tissue by chemical or enzymatic treatment without degradation. The action of a protopectinase results in the release of soluble pectin or pectin constituents. Several protopectinases have been studied in detail, and it turned out that most of them belong to either the polygalacturonases, rhamnogalacturonases, pectate lyases, or the pectin lyases (3). One of the protopectinases was in fact an arabinase whereas another was a galactanase. The nondiscriminative term protopectinase will therefore not be used.

In recent years knowledge about pectic enzymes has increased significantly. Numerous genes encoding pectic enzymes of all classes have been cloned from bacterial, fungal, and plant origin. Several of these genes have been overexpressed, and the corresponding enzymes have been purified and extensively characterized. Three dimensional structures have now been solved for representatives from many classes of pectic enzymes—viz., pectate and pectin lyases (4–7), polygalacturonases (8, 9), a rhamnogalacturonase (10), a pectin methylesterase (11), and a rhamnogalacturonan acetyl esterase (12). Surprisingly, except for the rhamnogalacturonan acetyl esterase, all the enzymes show the same basic β-helical architecture. This new architecture was first described for a pectate lyase by Jurnak and coworkers (4). Despite the rather low degree of sequence similarity between different classes of pectic enzymes, ranging from 10% to 25%, the common β-

Table 1 Enzymes Involved in Pectin Degradation

Hydrolases	Lyases	Esterases	Auxiliary enzymes
endopolygalacturonase	endopectate lyase	pectin methyl esterase	galactanase
exopolygalacturonase	exopectate lyase	pectin acetyl esterase	arabinanase
exo-poly-α-D-galacturonosidase	pectin lyase (endo)	rhamnogalacturonan acetyl esterase	β-galactosidase
rhamnogalacturonan hydrolase	rhamnogalacturonan lyase		α-L-arabino-furanosidase
rhamnogalacturonan rhamnohydrolase			feruloyl esterase
xylogalacturonanhydrolase			coumaryl esterase

helical structure suggests that these pectinases have evolved from one ancestral gene (13). The unique structural features of each class will be described in the corresponding chapters.

Coutinho and Henrissat (14) have classified the pectic enzymes based on amino acid sequence similarities with the intention that such similarities reflect structural features of these enzymes. The classification can be found at the following URL: http://afmb.cnrs-mrs.fr/CAZY/CAZY/db.html

II. ENDOGENOUS AND EXOGENOUS PECTIC ENZYMES IN FRUIT AND VEGETABLE PROCESSING

Pectic enzymes occur naturally in many fruits and vegetables (endogenous enzymes), but they are also added as processing aids (exogenous enzymes). The latter are mostly derived from food-grade fungi, e.g., *Aspergillus niger, A. aculeatus*. In higher plants, particularly pectin methyl esterase and polygalacturonase, both endo- and exoacting, are present. Pectin acetyl esterase has been found in citrus fruit and more recently also pectate lyase and rhamnogalacturonan hydrolase have been found in plants. The endogenous enzymes are assumed to play important roles in plant development and during ripening. The modern genomic approach will enable us to better understand their presence in plants in numerous isoforms and their roles in plant developments. Pectic enzymes are also produced by many microorganisms, and here also numerous isoforms have been described. The impact of endogenous enzymes on fruit and vegetable processing will be discussed in the chapters devoted to the various pectic enzymes (15–17).

As processing aids, pectic enzymes have predominantly found applications in the fruit juice industry. Traditional processes to manufacture fruit juices in essence consist of mechanical destruction of cells by grinding of intact tissues into a semifluid system in which cells and cell wall fragments are suspended in cell liquid. From this pulp a crude juice can be obtained by mechanical separation methods—e.g., pressing, sieving, or centrifugation. Clear juices can be obtained from the crude juice by additional clarification treatments: cloudy or pulpy juices by adjustment of the amount of fineness of the pulp particles through mechanical treatments in which large and insoluble particles are removed. Clarification is obtained through reduction of the viscosity of the cloudy and pectin-rich crude juice by treatment with enzymes, which causes coagulation and precipitation of the cloud particles. The viscosity reduction also allows the production of fruit juice concentrates which, for economic and technological reasons, can be stored and transported.

From the pulp of apples, grapes, and pears, juice can be obtained quite easily by pressing. In the manufacture of juices from berries or bananas, grinding results in a highly viscous juice which sticks as a gel to the pulp particles. A mechanical separation of juice and pulp particles is here impossible. To facilitate this separation the pulps are treated with enzymes, which are able to degrade the polysaccharides forming the gel. This enzyme treatment results in higher juice yields and improves the color of the juice. This treatment is also successfully used for grapes and for stored overripe apples.

Industrial enzymes used in these applications contain pectin methyl esterases, polygalacturonases, pectin lyases, rhamnogalacturonan hydrolases, rhamnogalacturonan lyases, and rhamnogalacturonan acetyl esterases in varying amounts, as well as arabinanases, galactanases, xylanases, β-1,4-glucanases, amylases, many glycosidases, and proteases.

The enzymes of technological relevance in the various steps of fruit juice manufacture have been identified and we are now more and more able to formulate enzyme cocktails tailored to specific applications. It

was established that enzyme mixtures able to readily degrade high esterified pectins (pectin methyl esterase, endopolygalacturonase, and/or pectin lyase) are also very suitable for improving the pressability of fruit pulps and for clarification of fruit juices. The presence of rhamnogalacturonan hydrolase or rhamnogalacturonan lyase and rhamnogalacturonan acetyl esterase in these formulations further enhances juice extraction but also the solubilization of cell wall polysaccharides (18, 19).

Food-grade fungal enzyme preparations which predominantly contain endopolygalacturonase activity and no pectin methyl esterase and pectin lyase are successfully used as macerating enzymes for the production of pulpy nectars. These nectars are characterized by a creamy consistency and have higher contents of fruit solids, more pigments, and more nutrients than nectars prepared by thermomechanical treatments. Cloudy or pulpy products can be obtained by further grinding, finishing, and homogenization. Maceration can also be achieved by endopectin lyase and endopectate lyase.

By combining pectin-degrading enzymes like endopolygalacturonase, pectin methyl esterase, and/or pectin lyase with cellulose-degrading enzymes like endoglucanases, endoxyloglucanase, cellobiohydrolase, and cellobiase plant cell walls can be almost completely degraded. As a result, the cells cannot withstand the osmotic pressure, and they collapse. The phenomenon of complete liquefaction of the fruit tissues can be observed. This process enables a new, rather simple, flexible, and economical technology for the manufacture of clear or cloudy juices with high yields (18). The liquefaction process can be further enhanced by including rhamnogalacturonan hydrolase or rhamnogalacturonan lyase and rhamnogalacturonan acetyl esterase in the formulation and by also including xylogalacturonan-, and arabinan-, and galactan-degrading enzymes. The clarification of the juices by ultrafiltration is substantially improved by avoiding fouling of the membranes (19). The liquefaction technology is particularly suitable for fruits from which no juice can be obtained by pressing or for which no presses have yet been developed, e.g., tropical fruits such as mango, guava, and banana (19–21). The liquefaction process limits losses of nutrients and makes them even more bioavailable (22). The liquefaction process can also be used for extraction of oils from oleaginous fruits and seeds or for the extraction of other valuable cell constituents. In the conversion of agricultural biomass to sugars or alcohol, enzymatic liquefaction is the first step to further saccharification. For each of these applications optimal formulations have to be established depending on the starting raw material. In the following chapters the different classes of enzymes active toward pectin are covered. In these chapters also specific application aspects as processing aids are mentioned. A separate chapter is devoted to the description of the characteristics of the structural units making up pectins and of methods to monitor activity of pectic enzymes.

Pectic enzymes	(This chapter)
Pectic polysaccharides	(Schols and Voragen, Chap. 66)
Polygalacturonases	(Benen and Visser, Chap. 69)
Pectate and pectin lyases	(Benen and Visser, Chap. 80)
Pectic esterases	(Benen, van Alebeek, Visser, and Voragen, Chap. 68)
Enzymes degrading rhamnogalacturonan and xylogalacturonan	(Vincken, Voragen, and Beldman, Chap. 73)
Enzymes releasing L-arabinose and D-galactose from the side chains of pectin	(de Vries and Visser, Chap. 70)

REFERENCES

1. MJF Searle-van Leeuwen, J-P Vincken, D Schipper, AGJ Voragen, G Beldman. Acetyl esterases of *Aspergillus niger*: purification and mode of action on pectins. In: J Visser, AGJ Voragen, eds. Progress in Biotechnology 14: Pectins and Pectinases. Amsterdam: Elsevier Science, 1996, pp 793–798.
2. T Sakai. Degradation of pectins. In: G Winkelmann, ed. Microbial Degradation of Natural Products. New York: VCH Publishers, 1992, pp 57–81.
3. T Sakai, T Sakamoto, J Hallaert, EJ Vandamme. Pectin pectinase, and protopectinase: production, properties, and applications. Adv Appl Microbiol 39:213–294, 1993.
4. MD Yoder, F Jurnak. The refined three dimensional structure of pectate lyase C from *Erwinia chrysanthemi* at 2.2 Å resolution—implications for an enzymatic mechanism. Plant Physiol 107:349–364, 1995.
5. R Pickersgill, J Jenkins, G Harris, W Nasser, J Robert-Baudouy. The structure of *Bacillus subtilis* pectate lyase in complex with calcium. Nature Struc Biol 1:717–723, 1994.
6. O Mayans, M Scott, I Connerton, T Gravesen, J Benen, J Visser, R Pickersgill, J Jenkins. Two crystal structures of pectin lyase A from *Aspergillus* reveal a pH driven conformational change and striking divergence in the substrate-binding clefts of pectin and pectate lyases. Structure 5:677:689–1997.
7. J Vitali, B Schick, HCM Kester, J Visser, F Jurnak. The three-dimensional structure of *Aspergillus niger*

pectin lyase B at 1.7-Å resolution. Plant Physiol 116:69–80, 1998.
8. R Pickersgill, D Smith, K Worboys, J Jenkins. Crystal structure of polygalacturonase from *Erwinia carotovora* ssp. *carotovora*. J Biol Chem 273:24660–24664, 1998.
9. Y van Santen, JAE Benen, K-H Schröter, KH Kalk, S Armand, J Visser, BW Dijkstra, 1.68-Å Crystal structure of endopolygalacturonase II from *Aspergillus niger* and identification of active site residues by site-directed mutangenesis. J Biol Chem 274:30474–30480, 1999.
10. TN Petersen, S Kauppinen, S Larsen. The crystal structure of rhamnogalacturonase A from *Aspergillus aculeatus*: a right-handed parallel beta helix. Structure 5:533–544, 1997.
11. RW Pickersgill, JA Jenkins. Crystal structures of polygalacturonase and pectin methylesterase. In: HJ Gilbert, GJ Davies, B Henrissat, B Svensson, eds. Recent Advances in Carbohydrate Bioengineering. Cambridge: Royal Society of Chemistry, 1999, pp 144–149.
12. A. Molgaard, S Kauppinen, S Larsen. Rhamnogalacturonan acetylesterase elucidates the structure and function of a new family of hydrolases. Struct Folding Design 8:373–383, 2000.
13. J Jenkins, O Mayans, R Pickersgill. Structure and evolution of parallel β-helix proteins. J Struct Biol 122:236–246, 1998.
14. PM Coutinho, B Henrissat. Carbohydrate-active enzymes: an integrated database approach. In: HJ Gilbert, GJ Davies, B Henrissat, B Svensson, eds. Recent Advances in Carbohydrate Bioengineering. Cambridge: Royal Society of Chemistry, 1999, pp 3–12.
15. AGJ Voragen, W Pilnik. Pectin-degrading enzymes in fruit and vegetable processing. In: JR Whitaker, PE Sonnet, eds. Biocatalysis in Agricultural Biotechnology. Washington: Symp Ser No. 389, 1989, pp 93–115.
16. W Pilnik, AGJ Voragen. The significance of endogenous and exogenous pectic enzymes in fruit and vegetable processing. In PF Fox, ed. Food Enzymology. London: Elsevier Applied Science, 1991, pp 303–336.
17. W Pilnik, AGJ Voragen. Pectic enzymes in fruit and vegetable juice manufacture. In T Nagodawithana, G Reed, eds. Enzymes in Fruit Processing. London: Academic Press, 1993, pp 363–399.
18. W Pilnik. Enzymes in the beverage industry. In D Dupuy, ed. Use of Enzymes in Food Technology. Technique et Documentation. Paris: Lavoisier, 1982, pp 425–450.
19. AGJ Voragen, HA Schols, G Beldman. Tailor-made enzymes in fruit juice processing. Fruit Processing 2:98–102, 1992.
20. C Grassin, P Fauquembergue. Application of pectinases in beverages. In: J Visser, AGJ Voragen, eds. Progress in Biotechnology 14: Pectins and Pectinases. Amsterdam: Elsevier, 1996, pp 453–463.
21. HP Heldt-Hansen, LV Kofod, G Budelfsen, PM Nielsen, S Hüttel, T Bladt. Application of tailor-made pectinases. In: J Visser, AGJ Voragen, eds. Progress in Biotechnology 14: Pectins and Pectinases. Amsterdam: Elsevier, 1996, pp 463–474.
22. JM Castenmiller, CE West, JPH Linssen, KH van het Hof, AGJ Voragen. The food matrix of spinach is a limiting factor in determining the bio-availability of β-carotene and to a lesser extent of lutein in humans. J Nutr 129:349–355, 1999.

68

Pectic Esterases

Jacques A. E. Benen, Gert-Jan W. M. van Alebeek, and Alphons G. J. Voragen
Wageningen University, Wageningen, The Netherlands

Jaap Visser
Fungal Genetics and Technology Consultancy, Wageningen, The Netherlands

I. INTRODUCTION

Pectic esterases comprise enzymes that hydrolyze the esters present in the pectin backbone (EC 3.1.1.–). Currently three classes of esterases have been identified: (a) the pectin methylesterases (EC 3.1.1.11) that hydrolyze methylesters from O6 of galacturonic acid in the homogalacturonan part; (b) the pectin acetylesterases (EC 3.1.1.6); and (c) the rhamnogalacturonan acetylesterases (3.1.1.–). The acetylesterases remove acetyl groups from O2 and/or O3 of galacturonic acid residues either in the homogalacturonan part or in the rhamnogalacturonan part. Until now, no pectin methylesterase active toward methylesters in the rhamnogalacturonan part has been identified. The pectin methylesterases belong to family 8 of the carbohydrate esterase classification (1). The microbial rhamnogalacturonan and homogalacturonan acetylesterases have been grouped into family 12 whereas the plant pectin acetylesterases make up family 13 (1). Other esterases, like feruloylesterase, which are not active on the backbone but rather on side chains, will be covered elsewhere in this volume.

II. ENDOGENOUS PECTIC ESTERASES IN PLANTS

A major part of the pectic esterase nucleotide sequences present in the databases originate from plants and represent pectin methylesterases and pectin acetylesterases. As for the endopolygalacturonases, by far the largest portion is taken by open reading frames (putative genes) from *Arabidopsis thaliana*.

A. Pectin Methylesterase

Apart from the presence of many genes encoding putative pectin methylesterases (PMEs), these enzymes have also been detected in various plants by their activity, which confirms their wide distribution. They have been identified in higher plants, particularly in apple, banana, berries, citrus (lime, orange, grapefruit, and mandarin), cherry, grape, mango, papaya, passion fruit, pear, plum, beans, carrot, cauliflower, cucumber, leek, onion, pea, potato, radish, and tomato. Within each species multiple forms of PME can be present as was shown for example for citrus fruits (2, 3), mung bean hypocotyl (4–6), and flax seedlings (7). In general, basic, neutral, and acidic isoforms are found, which differ in various biochemical properties, such as relative molecular mass and pH optimum. PMEs are found in various tissues and are mainly associated by ionic interactions with cell wall proteins, although some soluble forms have been detected as well. Their exact role is not known, but since they are able to de-esterify pectin and are often present in the cell wall, it is obvious that they are involved in pectin modification. The degree of methylesterification is very important for the gelling properties of pectin. Highly methylated pec-

tins form gels via hydrogen bonds and are generally associated with young, differentiating and elongating cells, whereas Ca^{2+}-pectate gels are formed by low-methoxyl pectins in older, elongated, and differentiated cells (8). Thus, it can be inferred that pectin methylesterases serve important developmental processes in plants by modulating the degree of methylesterification.

During growth, ripening, and storage, the texture of the fruit changes, and fruit softening occurs. These alterations are believed to be due to changes in the turgor of the cell and cell wall metabolism. In tomato these are caused by the degradation of both pectins and hemicelluloses (9, 10). Pectin degradation is caused by the combined action of PME and PG in the fruit. But since PG activity appears to be limited by some chemical or physical restrictions despite being present in high abundance, pectin degradation is limited. As a consequence, antisense suppression of PG activity or PME activity in tomato results in only a small decrease in pectin degradation and a very small increase in fruit firmness later, during ripening (11). Despite the low effect of the antisense downregulation of PG or PME, in normal tomato fruits, during processing, these enzymes are liberated and, without precautions, will degrade the pectin. This may result in either desirable or undesirable changes (11).

In the processing of tomatoes a heat shock treatment called "hot break" is used to inactivate PME and PG and keep a high consistency and viscosity of the juice. When this high consistency is not desired, a "cold break" is used during which PME and PG degrade pectin, thereby lowering the viscosity (11).

During fruit fermentation PME action is responsible for methanol release (12). To keep methanol levels below legal limits, fruit pulps have to be pasteurized before fermentation. PMEs play important roles in fruit and vegetable processing. In citrus processing they cause cloud loss due to precipitation of pectin demethylated by endogenous PME with calcium ions and negatively charged proteins. This is desirable in the production of lemon juice but causes a serious quality defect of orange juice. In orange juice concentrates strong calcium pectate gels may form which prevent reconstitution of single-strength juice. The problem can be overcome either by heat inactivation of PME, which will harm the flavor, or by keeping the concentrate at $-20^{\circ}C$. Another possibility is the addition of endopolygalacturonase, which breaks down the low-ester pectin formed before it can coagulate with calcium (13). Versteeg et al. (2) identified a high-MW isoform of PME, which was much more heat stable than the other isoforms. It was found to occur in all the component parts of the orange fruit. In the traditional French cider industry, the endogenous PME of apple was used for the self-clarification of apple juice. Today fungal PME preparations free of depolymerizing activity are available for industrial application in cider and lemon juice clarification (13).

The calcium pectate coagulation phenomenon as a result of PME action improves the pressing characteristics of citrus peel and lowers costs when the peel has to be dried for use as cattle feed. Before drying the peel is ground up together with calcium hydroxide. This limiting operation activates the enzyme, pectin coagulates as calcium pectate, and peel juice is released easily before and during pressing (13). Endogenous PME can also be used for protecting and improving the texture and firmness of several processed fruits and vegetables such as apple slices, cauliflower, carrots, potatoes, beans, and peas. Through adjustment of the blanching temperature and time, PME is activated. By the demethylation of cell wall pectin, the cation uptake is increased. Firming effects by the addition of Ca^{2+} ions are well established and have long been used to prevent excess vegetable softness. Fungal PME preparations have also been developed for these applications, for improving the consistency of tomato pastes, and also for the manufacture of low-ester pectins with reduced Ca^{2+} sensitivity (13).

B. Pectin Homogalacturonan Acetylesterase

Pectin homogalacturonan acetylesterases (PAE) have so far been purified from orange (3) and mung bean hypocotyl (14, 15). In orange the enzyme was distributed over the whole fruit, with higher levels in the outer parts of the peel (albedo and flavedo) and in the segments. In mung bean the PAE expression was shown to be tissue specific. The highest expression was found in the hypocotyl, whereas expression was significantly lower in the leaves and roots and almost absent in the cotyledons (15). PAE activity has been detected in carrots as well (16), and it is likely that this activity is more widespread among plants.

C. Rhamnogalacturonan Acetylesterase

Thus far, rhamnogalacturonan acetylesterase (RGAE) activity has been demonstrated only for the fungus *Aspergillus* (17, 18). Despite the absence of any reports describing this activity in plants, it is reasonable to assume plants have this activity, as it has recently been shown that rhamnogalacturonan degrading

enzymes, which require RGAE activity for optimal activity, are present in carrot (16).

III. APPLICATION OF ESTERASES

A. Pectin Methylesterases

Pectin enzymes find a wide application in fruit and vegetable juice manufacturing, like fruit juice clarification, enzymic pulp treatment for juice extraction, liquefaction, and maceration (19). In most of these applications pectic enzymes are used for the complex degradation of pectin. Since these juices are generally acidic, the depolymerization of the pectin is accomplished by polygalacturonases which are generally specific for low-methylated polygalacturonic acid. To convert the pectin into a PG-accessible substrate, the action of PME is required. For maceration of fruits and vegetables, complete pectin degradation is not desired. Only pectin in the middle lamella should be degraded, which can be accomplished by either PG or PL action alone. Therefore, endogenous pectin methylesterase has to be inactivated.

Pectin is widely used in industry because of its gelling properties. High-methoxyl (HM) pectins are able to form sugar acid gels (jams) in which cosolutes like sugar and acid are present to lower water activity or diminish electrostatic repulsion, respectively. LM pectins (degree of methylation [DM] < 50%) can gel in the presence of divalent ions. In food gels this ion is usually Ca^{2+}. The Ca^{2+} gel-forming ability increases with decreasing DM, although the distribution of the methylesters along the homogalacturonan backbone strongly influences the gelling properties of the pectin. LM pectins with a blockwise distribution of the carboxyl groups (long stretches of de-esterified homogalacturonan) are extremely sensitive to low calcium levels, whereas randomly de-esterified pectins are far less sensitive. This distribution of methylesters can be controlled by the manner of de-esterification of HM pectin. De-esterification of HM pectin by plant PME results in blocks of unmethylesterified galacturonic acid residues, whereas NaOH or fungal PME yields a random distribution of free carboxyl groups. Thus, pectin methyl esterases are of major importance for the preparation of pectins for specific applications. Recently, techniques like MALDI-TOF MS and HPAEC (pH 5) have been developed to discriminate among the various types of pectins and thus allow correlation of functional properties of the pectin to the degree and distribution of methylesterification (20, 21).

B. Pectin Homogalacturonan Acetylesterase

Sugar beet pectin is rich in methylated and acetylated galacturonic acid residues and hence has poor gelling properties with either acid/sugar or Ca^{2+} ions (22). PME treatment of sugar beet pectin results in partial hydrolysis of the methylesters, resulting in better gelling properties using Ca^{2+} ions. Upon addition of PAE isolated from *A. niger* (23), part of the acetyl groups are removed as well. This action in turn allows PME to further remove methylesters. This synergistic effect results in an increase of the stiffness of the Ca^{2+}-formed gel (24).

C. Rhamnogalacturonan Acetylesterase

Rhamnogalacturonan acetylesterase is essential for the breakdown of rhamnogalacturonan. After deacetylation of the galacturonic acid residues in rhamnogalacturonan, the hairy regions can be further degraded by rhamnogalacturonan hydrolase (25) and rhamnogalacturonan lyase (26), which is of technological importance for the extraction of fruit and fruit juice ultrafiltration (18).

IV. BIOPHYSICAL PROPERTIES OF PECTIC ESTERASES

Pectin methylesterases have been known and characterized for several decades, which has yielded a wealth of information compared to the recently discovered pectin and rhamnogalacturonan acetylesterases. As with many enzyme families, the more enzymes one studies, the more the variety in biochemical and biophysical properties one observes within the family. The pectic esterases are medium-size enzymes as their MWs are 25–54 kDa. These enzymes are active as monomers. Many PMEs from eukaryotic origin are glycoproteins, and there is even a report of a bacterial PME from *E. chrysanthemi* that is in fact a lipoprotein (27). The isoelectric point of the pectic esterases varies from as low as 3.1 for fungal PME to 11 for a tomato PME. The pH stability depends on the source of the enzyme, and the range for all PMEs stretches from pH 1.1 to pH 10.0. The temperature stability is moderate (40–70°C) with a slightly higher stability for the plant enzymes compared to the microbial enzymes.

A. Three-Dimensional Structures of Pectic Esterases

Currently, 3D structures are only available for the *Erwinia chrysanthemi* PME (PDB code: 1QJV) (28) and the *Aspergillus aculatus* rhamnogalacturonan acetylesterase (RGAE) (PDB codes: 1DEO and 1DEX) (29). The structure of the PME reveals a similar topology as found for the pectate and pectin lyases, and polygalacturonases/rhamnogalacturonases (30–33). This topology is characterized by a right-handed parallel beta-helix structure with loops protruding from the helix core that form the substrate-binding cleft. The conservation of the unique topology among these enzymes strongly indicates that a complete set of different pectinases have evolved from the same ancestral gene.

The structure adopted by RGAE is completely different. This enzyme folds into an $\alpha/\beta/\alpha$ structure (29), which is different from the normally observed α/β structure common to esterases and lipases. As for the α/β enzymes in the RGAE, the active-site residues are Ser, Asp, and His, in the same sequential order, but the Asp and His residues are only three residues apart instead of being located on different loops (29). Based on the strict sequence conservation in the esterase family 12 of Ser and His and two additional residues, Gly and Asn, which both act as hydrogen bond donors to the oxyanion hole, it has been proposed that this group of esterases be named the SGNH hydrolase family (29).

B. Isoforms of Pectic Esterases

The *Arabidopsis* genome sequencing project has resulted in > 50 putative pectin methylesterases and numerous pectin acetylesterases. The databases also contain multiple (putative) PME sequences from other plants. The presence of isoforms at the genetic level therefore seems a common theme among plants. Such a large variety of pectic esterases is not present in microorganisms. At the genetic level, two PME isoforms have been identified in *E. chrysanthemi* (27, 34) whereas all other microorganisms studied so far have only one *pme*, *pae*, or *rgae* gene.

Eukaryotic enzymes and proteins are prone to N- and O-linked glycosylation. Heterogeneous glycosylation can often lead to multiple isoforms of the same enzyme. There are no reports describing the analysis of (heterogeneous) glycosylation patterns of pectic esterase isoforms.

V. BIOCHEMICAL PROPERTIES OF PECTIC ESTERASES

In the pre–molecular biology era, numerous pectin methylesterases, primarily of plant origin, were characterized. In the past few years the pectin acetylesterase and rhamnogalacturonan acetylesterase activities were discovered and studied, but the number of reports on these enzymes is limited (3, 14–18).

Pectin methylesterases hydrolyze the ester bond between methanol and the carboxylic function of galacturonic acid. The action of the enzyme thus results in the formation of a free carboxylic function, methanol, and H_3O^+. In general, the plant and bacterial PMEs have pH optima between pH 6 and 8 whereas some fungal PMEs have pH optima between pH 4 and 6. The plant enzymes often require the addition of 0.1–0.2 mM NaCl for the optimal catalysis. Action of any PME on (highly) methylated pectins does not result in full demethylation. Generally, the residual DM is between 20% and 30%. In part this is due to the presence of acetyl groups in certain pectins (24). Pretreatment or simultaneous treatment with PAE increases the amount of methyl groups removed, but still not all groups will be hydrolyzed (2).

Plant and microbial PMEs differ in their mode of action. Whereas plant enzymes generally remove blocks of methyl groups on a single chain, fungal PMEs attack the methyl groups on the pectin randomly, resulting in a random distribution of the unmethylated galacturonic acid groups. Recently, three different isoforms from mung bean hypocotyls—PMEα, PMEβ, and PMEγ—were subjected to a detailed analysis of their mode of action (35). This elaborate study in which PME activities were measured at pH 5.6 and 7.6 revealed that the three isoforms have different substrate specificities and rates. Strikingly, for PMEα at pH 5.6, a sharp drop in activity was observed when the DM decreased below 70% whereas at pH 7.6 the reaction rate remained constant down to 40% DM. For PMEβ and PMEγ this effect was less pronounced. However, PMEβ showed at both pH values the strongest preference for highly methylesterified pectin. Not only in this respect did the enzymes differ; in their mode of action a clear difference was also observed. The mode of action of the enzymes was simulated and fitted to the actual distribution of methylesters after partial hydrolysis of various DM pectins as recorded by NMR (35).

For PMEβ at both pH values the reaction was best described by a single-chain mechanism. The enzyme remains attached to one substrate molecule and con-

tinues to demethylate the pectin molecule toward the reducing end until the end of the molecule is reached. Similar behavior was concluded for PMEα and PMEγ at pH 5.6, but at pH 7.6 the single-chain mechanism changed into a multiple-attack mechanism. According to this mechanism, only a limited number of methyl groups is removed during each encounter. Furthermore, the studies revealed that for catalysis the presence of an unesterified galacturonic acid residue is required for all three enzymes. For PMEα and PMEγ, this unesterified residue should be present two residues toward the nonreducing end from the methylated residue to be attacked. For PMEβ, this distance was three residues in the same direction (35).

From a practical point of view, pectins treated with either plant or microbial PME result in pectins with different gelling properties and thus are suitable for different applications. Recently, a PAE encoding gene (*pae*Y) was cloned from the phytopathogenic bacterium *Erwinia chrysanthemi*, sequenced, and overexpressed in *Escherichia coli* (36). An *E. chrysanthemi* strain with a disrupted *pae* gene showed a reduced invasion of the host plant tested, demonstrating the important role of PAEY in the soft-rot disease (36).

A. Effect of Environmental Factors

To date no pectic esterase–specific low MW inhibitory compounds have been reported. However, there are numerous compounds (Hg^{2+}, Al^{3+}, NH_4^+, sugar, gallic acid) that inhibit some PMEs, whereas other PMEs are not inhibited (reviewed in Ref. 2). Many PMEs are also inhibited by polygalacturonic acid, the product of its action. NaCl and KCl have been reported to stimulate activity of PME and it has been argued that this stimulation is a result of reduced inhibition by polygalacturonic acid in the presence of NaCl or KCl (2).

Recently, a glycoprotein inhibitor of PME has been identified in kiwi fruit (37, 38). This 16.7-kDa protein was purified by affinity chromatography using partially purified tomato PME coupled to Sepharose. The interaction between the PME and the inhibitor appeared to be a 1-to-1 complex formation. This interaction is very strong and the complex was only dissociable at high pH and high ionic strength (pH 9.5, 1.5 M NaCl). The physiological function of the protein may be in the defense mechanism of plants against phytopathogens, similar to the polygalacturonase-inhibiting proteins (PGIPs) or, alternatively, in the regulation of endogenous PME activity in relation to cell wall development. The primary sequence of the PME inhibitor was established by peptide sequencing (38), which now allows in vitro gene synthesis. Primary sequence homology searches have revealed significant sequence homology with some plant invertase inhibitors (38). Thus, the presence of a family of inhibitor proteins may be common in plants.

B. Specific Mechanism of Action

Based on the 3D structure of PME and primary sequence alignments, Pickersgill and Jenkins hypothized a possible mechanism (28). Two aspartates and one arginine are strictly conserved among PMEs. One of the Asp residues makes a hydrogen bond to the Arg and is therefore most likely unprotonated. The other Asp is likely to be protonated. A water molecule adjacent to the unprotonated Asp may be activated by transferring its proton to the Asp. The hydroxyl generated can then attack the carbonyl carbon. Simultaneous protonation of one of the oxygens results in the formation of a tetrahedral intermediate, which collapses with the release of methanol and thus results in demethylation (28).

For RGAE it can be postulated that catalysis will proceed via the general mechanism observed for lipases where the catalytic triad Asp-His-Ser, which forms a charge-relay system, will attack the ester bond via the activated serine (29).

For PAE no mechanism has been proposed yet.

C. Subsites in Binding to the Substrate

For PAE and RGAE no studies have been reported with respect to the number of subsites involved in substrate binding. For PME such studies have not been carried out either, but some reports allow inferring the number of subsites. Kester and coworkers (39) reported that the rate of de-esterification by fungal *A. niger* PME of individual fully esterified oligomers increased by a factor of 100 when the chain length increased from $n = 3$ to $n = 6$. The increase in reaction rate for $n = 5$ to $n = 6$ still amounted to a factor of 2. These results indicate that the number of subsites for *A. niger* PME is at least five and may even be six. Catoire et al. (35) simulated the mode of action of PME isoforms from mung bean hypocotyls using NMR data of (partially) de-esterified pectins. For one of the PME forms, PMEβ, successful simulation of the data was only possible by allowing an unesterified residue to interact with the enzyme at a subsite three subsites in the direction of the nonreducing end away from the active site (35). Thus, for this particular

enzyme, at least four subsites are involved in binding the substrate.

D. Synthetic Substrates

Using monomethylesterified trigalacturonides carrying the monomethyl group at a defined position (40) and fully methylesterified oligogalacturonides of chain length $n = 3$–6, Kester et al. (39) studied the mode of action of *Aspergillus niger* PME. These studies revealed that this fungal enzyme cannot remove a methyl group from a galacturonic acid residue at the nonreducing end. It was further shown that an unesterified residue somewhere along the chain is not necessary for this enzyme. *A. niger* PME preferentially attacked a methyl group in the middle of the methylesterified oligomers. The distribution of the products observed after partial saponification demonstrates that this enzyme acts according to a multiple-chain mechanism: each encounter results in the removal of only one methyl group (39).

Triacetin is often used as a substrate for esterases. For *A. niger* esterase, the substrate was specifically used by pectin acetylesterase, whereas it was not hydrolyzed by RGAE (23). Alternative substrates for acetylesterases are paranitrophenyl acetate and 4-methylumbelliferyl acetate.

VI. QUALITATIVE AND QUANTITATIVE DETERMINATION OF ACTIVITY

In order to determine the different enzymes qualitatively and/or quantitatively, specific substrates and assays are needed. This preparation of substrates, together with the assays, is described by Schols and Voragen in Section IX. in Chapter 66.

REFERENCES

1. PM Coutinho, B Henrissat. Carbohydrate-active enzymes: an integrated database approach. In: HJ Gilbert, GJ Davies, B Henrissat, B Svensson, eds. Recent Advances in Carbohydrate Bioengineering. Cambridge: Royal Society of Chemistry, 1999, pp 3–12.
2. C Versteeg. Pectinesterases from the orange fruit—their purification, general characteristics and juice cloud destabilizing properties. PhD thesis, Wageningen University, Wageningen, 1979.
3. TMIE Christensen, JE Nielsen, JD Mikkelsen. Isolation, characterization and immunolocalization of orange fruit acetylesterase. In: J Visser, AGJ Voragen, eds. Progress in Biotechnology 14: Pectins and Pectinases. Amsterdam: Elsevier Science, 1996, pp 723–730.
4. M Bordenave, R Goldberg. Purification and characterization of pectin methylesterases from mung bean hypocotyl cell walls. Phytochemistry 33:999–1003, 1993.
5. M Bordenave, R Goldberg. Immobilized and free apoplastic pectinmethylesterases in mung bean hypocotyl. Plant Physiol 106:1151–1156, 1994.
6. M Bordenave, C Breton, R Goldberg, JC Huet, S Perez, JC Pernollet. Pectinmethylesterase isoforms from *Vigna radiata* hypocotyl cell walls: kinetic properties and molecular cloning of a cDNA encoding the most alkaline isoform. Plant Mol Biol 31:1039–1049, 1996.
7. F Alexandre, O Morvan, J Gaffe, A Mareck, A Jauneau, H Dauchel, AP Balange, C Morvan. Pectin methylesterase pattern in flax seedlings during their development. Plant Physiol Biochem 35:427–436, 1997.
8. P Albersheim, AG Darvill, MA O'Neill, HA Schols, AGJ Voragen. An hypothesis: the same six polysaccharides are components of the primary cell walls of all higher plants. In J Viser, AGJ Voragen, eds. Progress in Biotechnology 14: Pectins and Pectinases. Amsterdam: Elsevier Science, 1996, pp 47–55.
9. DJ Huber, EM O'Donoghue. Polyuronides in avocado (*Persea Americana*) and tomato (*Lycopersicon esculentum*) fruits exhibit markedly different patterns of molecular weight downshifts during ripening. Plant Physiol 102:473–480, 1993.
10. G Maclachlan, C Brady. Endo-1,4-β-glucanase and xyloglucanase and xyloglucan endo-transglycosylase activities versus potential substrates in ripening tomatoes. Plant Physiol 105:965–974, 1994.
11. GA Tucker, H Simons, N Errington. Transgenic tomato technology: enzymic modification of pectin pastes. Biotechnol Genet Eng Rev 16:293–307, 1999.
12. C Frenkel, JS Peters. Pectin methylesterase regulates methanol and ethanol accumulation in ripening tomato (*Lycopersicon esculentum*) fruit. J Biol Chem 273:4293–4295, 1998.
13. AGJ Voragen, W Pilnik. Pectin-degrading enzymes in fruit and vegetable processing. In: JR Whitaker, PE Sonnet, eds. Biocatalysis in Agricultural Biotechnology. Washington: American Chemical Society, 1989, pp 93–115.
14. M Bordenave, R Goldberg, JC Huet, JC Pernollet. A novel protein from mung bean hypocotyl cell walls with acetyl esterase activity. Phytochemistry 38:315–319, 1995.
15. C Breton, M Bordenave, L Richard, JC Pernollet, JC Huet, S Perez, R Goldberg. PCR cloning and expres-

sion analysis of a cDNA encoding a pectin acetylesterase from *Vigna radiata* L. FEBS Lett 388:139–142, 1996.
16. E Stratilova, O Markovic, M Dzurova, A Malavikova, P Capek, J Omelkova. The pectolytic enzymes of carrots. Biologia 53:731–738, 1998.
17. MJF Searle–Van Leeuwen, LAM van de Broek, HA Schols, G Beldman, AGJ Voragen. Rhamnogalacturonan acetylesterase: a novel enzyme from *Aspergillus aculeatus*, specific for the deacetylation of hairy (ramified) regions of pectin. Appl Microbiol Biotechnol 38:347–349, 1992.
18. G Beldman, M Mutter, MJF Searle–Van Leeuwen, LAM van de Broek, HA Schols, AGJ Voragen. New enzymes active toward pectic structures. In J Visser, AGJ Voragen, eds. Progress in Biotechnology 14: Pectins and Pectinases. Amsterdam: Elsevier Science, 1996, pp 231–245.
19. W Pilnik, AGJ Voragen. Pectic enzymes in fruit and vegetable juice manufacture. In: T Nagodawithana, G Reed, eds. Enzymes in Food Processing. New York: Academic Press, 1993, pp 363–399.
20. PJH Daas, B Boxman, AMCP Hopman, AGJ Voragen, HA Schols. Nonesterified galacturonic acid sequence homology of pectins. Biopolymers 58:1–8, 2001.
21. PJH Daas, AGJ Voragen, HA Schols. Characterization of non-esterified galacturonic acid sequences in pectin with endopolygalacturonase. Carbohydr Res 326:120–129, 2000.
22. EL Pippen, RM McCready, HS Owens. Gelation properties of partially acetylated pectins. J Am Chem Soc 72:813–816, 1950.
23. MJF Searle–Van Leeuwen, J-P Vincken, D Schipper, AGJ Voragen, G Beldman. Acetyl esterases of *Aspergillus niger*: purification and mode of action on pectins. In: J Visser, AG Voragen, eds. Progress in Biotechnology 14: Pectins and Pectinases. Amsterdam: Elsevier Science, 1996, pp 793–798.
24. A Oosterveld, G Beldman, MJF Searle–Van Leeuwen, AGJ Voragen. Effect of enzymatic deacetylation on gelation of sugar beet pectin in the presence of calcium. Carbohydr Polymers 43:249–256, 2000.
25. HA Schols, CCJM Geraeds, MJF Searle–Van Leeuwen, FJM Kormelink, AGJ Voragen. Rhamnogalacturonase: a novel enzyme that degrades the hairy regions of pectins. Carbohydr Res 206:105–115, 1990.
26. M Mutter, IJ Colquhoun, G Beldman, HA Schols, EJ Bakx, AGJ Voragen. Characterization of recombinant rhamnogalacturonan α-L-rhamnopyranosyl-(1,4)-α-D-galactopyranosyluronide lyase from *Aspergillus aculeatus*. An enzyme that fragments rhamnogalacturonan I regions of pectin. Plant Physiol 117:141–152, 1998.
27. VE Shevchik, G Condemine, N Hugouvieux-Cotte-Pattat, J Robert-Baudouy. Characterization of pectin methylesterase B, an outer membrane lipoprotein of *Erwinia chrysanthemi* 3937. Mol Microbiol 19:455–466, 1996.
28. RW Pickersgill, JA Jenkins. Crystal structures of polygalacturonase and pectin methylesterase. In: HJ Gilbert, GJ Davies, B Henrissat, B Svensson, eds. Recent Advances in Carbohydrate Bioengineering. Cambridge: Royal Society of Chemistry, 1999, pp 144–149.
29. A Molgaard, S Kauppinen, S Larsen. Rhamnogalacturonan acetylesterase elucidates the structure and function of a new family of hydrolases. Structure 8:373–383, 2000.
30. MD Yoder, F Jurnak. The refined three dimensional structure of pectate lyase C from *Erwinia chrysanthemi* at 2.2 Å resolution—implications for an enzymatic mechanism. Plant Physiol 1076:349–364, 1995.
31. O Mayans, M Scott, I Connerton, T Gravesen, J Benen, J Visser, R Pickersgill, J Jenkins. Two crystal structures of pectin lyase A from *Aspergillus* reveal a pH driven conformational change and striking divergence in the substrate-binding clefts of pectin and pectate lyases. Structure 5:677–689, 1997.
32. R Pickersgill, D Smith, K Worboys, J Jenkins. Crystal structure of polygalacturonase from *Erwinia carotovora* spp. *carotovora*. J Biol Chem 273:24660–24664, 1998.
33. TN Petersen, S Kauppinen, S Larsen. The crystal structure of rhamnogalacturonase A from *Aspergillus aculeatus*: a right-handed parallel beta helix. Structure 5:533–544, 1997.
34. F Laurent, A Kotoujansky, G Labesse, Y Bertheau. Characterization and overexpression of the *pem* gene encoding pectin methylesterase of *Erwinia chrysanthemi* strain 3937. Gene 131:17–25, 1993.
35. L Catoire, M Pierron, C Morvan, CH du Penhoat, R Goldberg. Investigation of the action patterns of pectinmethylesterase isoforms through kinetic analysis and NMR spectroscopy. J Biol Chem 273:33150–33156, 1998.
36. VE Shevchik, N Hugouvieux-Cotte-Pattat. Identification of a bacterial pectin acetyl esterase in *Erwinia chrysanthemi* 3937. Mol Microbiol 24:1285–1301, 1997.
37. A Giovane, C Balestrieri, L Quagliuolo, D Castaldo, L Servillo. A glycoprotein inhibitor of pectin methylesterase in kiwi fruit. Eur J Biochem 233:926–929, 1995.
38. L Camardella, V Carratore, MA Ciardello, L Servillo, C Balestrieri, A Giovane. Kiwi protein inhibitor of pectin methylesterase. Eur J Biochem 267:4561–4565, 2000.
39. HCM Kester, JAE Benen, J Visser, M Esteban Warren, R Orlando, C Bergmann, D Magaud, D

Anker, A Doutheau. Tandem mass spectrometric analysis of *Aspergillus niger* pectin methylesterase: mode of action on fully methylesterified oligogalacturonates. Biochem J 346:469–474, 2000.

40. HCM Kester, D Magaud, C Roy, D Anker, A Doutheau, V Shevchik, N Hugouvieux-Cotte-Pattat, JAE Benen, J Visser. Performance of selected microbial pectinases on synthetic monomethyl-esterified di- and trigalacturonates. J Biol Chem 274:37053–37059, 1999.

69

Polygalacturonases

Jacques A. E. Benen
Wageningen University, Wageningen, The Netherlands
Jaap Visser
Fungal Genetics and Technology Consultancy, Wageningen, The Netherlands

I. INTRODUCTION

Polygalacturonases cleave the α-1,4-D-galacturonosidic linkage by hydrolysis. Whereas endopolygalacturonases (EC 3.2.1.15) hydrolyze the polymer substrate randomly, the exopolygalacturonases are confined to cleave off galacturonic acid monomers (EC 3.2.1.67) or digalacturonides (EC 3.2.1.82) from the nonreducing end. The names of these enzymes suggest that polygalacturonic acid is their sole substrate. However, as found for the pectate lyases, endopolygalacturonases are also active on pectins with a lower or moderate degree of esterification. Recently it was shown that endopolygalacturonases A and B from *Aspergillus niger* even prefer a low degree of esterification (1).

The polygalacturonases have all been grouped into family 28 of the general glycosyl hydrolase classification (2). In addition to the endopolygalacturonases, this family also comprises the rhamnogalacturonases and the recently cloned xylogalacturonase (3). Three-dimensional structures of two endopolygalacturonases (4, 5) and a rhamnogalacturonase have been solved (6), and their close resemblance indeed justifies the grouping in one family. By far the largest group of potential polygalacturonase genes (52 open reading frames) is formed by those from *Arabidopsis thaliana*. This large amount originates from the recent *Arabidopsis* genome-sequencing project. Such an abundance of genes indicates a profound developmental role of the corresponding enzymes. Contrary to plant polygalacturonases, microbial polygalacturonases serve to mobilize nutrients from pectin to support growth. For several yeasts such as *Kluyveromyces marxianus* (7) and *Saccharomyces cerevisiae* (8), polygalacturonase production has been documented and respective genes have been cloned, whereas no obvious physiological function is served since those yeasts can not utilize galacturonic acid.

II. ENDOGENOUS POLYGALACTURONASES IN PLANTS

In view of the important role of pectin in the primary cell wall of plants, it is obvious that endogenous polygalacturonases play important roles in the development of plants. Polygalacturonase activity has been demonstrated in almost any plant tissue. Based on mRNA expression studies in *Arabidopsis thaliana* (9), tomato [*Lycopersicon esculentum* (10)], and lemon [*Cucumus melon* (11)] among others, it was shown that there are at least three types of polygalacturonases: the pollen-specific polygalacturonases, the fruit-specific enzymes, and the abscission-specific polygalacturonases. For tomato it was established that the specific expression, i.e., auxin repression and ethylene and abscisic acid induction, resides in the regulatory

elements within the individual promoters of the polygalacturonase-encoding genes (10).

A phylogenetic analysis by Hadfield and coworkers (11) revealed that the plant polygalacturonases belong to three clades. Clade A comprises fruit- and abscision-specific polygalacturonases without pro-sequence, clade B consists of fruit- and abscision-specific polygalacturonases with a pro-sequence, and clade C contains all the pollen-specific polygalacturonases. It has been hypothesized that all clade C enzymes are exopolygalacturonases, as those enzymes characterized were of the exolytic type. In an excellent review Hadfield and Bennet (12) have compiled the major findings on endogenous plant polygalacturonases of the past two decades. In a more recent review Lang and Dörnenburg (13) further elaborate on this and also pay attention to the role of polygalacturonases in wounding of plants, the interaction of phytopathogenic fungi and plants, and the plant response to this.

To the food enzymologist the most interesting endogenous polygalacturonases are those present in the part of the plant that is used as or in food. One of the best-characterized subjects in this respect is the tomato. As a major food, either as the complete fruit or as puree, catsup, or juice, the influence of endogenous polygalacturonases on fruit ripening and processing has been studied extensively. To this end gene-silencing techniques have been employed that have revealed that endopolygalacturonases are not necessary for fruit ripening (reviewed in 12–14). However, owing to the gene silencing it turned out that the shelf life of the tomato increased profoundly as a result of reduced cracking of the tomato. Upon homogenization of nongenetically modified tomatoes, the deleterious effect of endogenous polygalacturonases becomes evident—i.e., a decrease in viscosity of the homogenate upon aging. To prevent the action of these enzymes, tomatoes are homogenized after heat pretreatment to inactive the enzymes and yield the so-called hot break pastes.

III. BIOPHYSICAL PROPERTIES OF POLYGALACTURONASES

Although all polygalacturonases belong to family 28 of glycosyl hydrolases, considerable variation in molecular mass (30–75 kDa) and isoelectric point (pI 3.8–8.8) can still be obtained from the databases going from enzyme to enzyme. Currently no relation has been established between molecular mass and/or isoelectric point and/or specificity.

A. Three-Dimensional Structures of Polygalacturonases

Currently, 3-D structures are only available for the *Erwinia carotovora* endopolygalacturonase [PDB code: 1 BHE (4)] and the *Aspergillus niger* endopolygalacturonase II [PDB code: 1CZF (5)]. Despite limited sequence identity between the two enzymes (19%), a striking similarity of the two β-helical structures is observed at the C-alpha trace level although certain differences can be observed as well, notably in the loop regions. Details are discussed by Van Santen et al. (5). Unfortunately, no structure is available for any enzyme-substrate complex. However, Van Santen et al. (5) and Armand et al. (15) present evidence that the substrate binds to the enzyme at the observed cleft with the reducing end of the substrate facing toward the C-terminal part of the enzyme. This orientation was also observed for the topologically highly similar pectate lyase C in complex with the substrate (16).

B. Isoforms of Polygalacturonases

The rapidly expanding family 28 of glycosyl hydrolases clearly demonstrates that many species analyzed have at least two genes encoding polygalacturonases. Thus, as for the pectic lyases, isoforms at the genetic level are plentiful. Wubben et al. (17) constructed a phylogenetic tree of 35 endopolygalacturonases of yeast and fungi which appeared to group into five monophylogenetic groups. Hadfield et al. (11) analyzed the plant polygalacturonases in this respect which appeared to group in three clades.

For eukaryotic polygalacturonases, many reports describe heterogeneity of polygalacturonase preparations as a result of glycosylation. To date, the N-glycosylation patterns of only two polygalacturonases have been analyzed in detail, viz., endopolygalacturonases I and II from *Aspergillus niger* (18, 19). The single N-glycosylation site in endopolygalacturonase II appeared to be heterogeneously glycosylated with glycans of the high mannose type (18), whereas of the two N-glycosylation sites of endopolygalacturonase I only one was similarly decorated as the one of polygalacturonase II and the other site was not glycosylated (19). For neither enzyme was O-glycosylation found.

In contrast to *A. niger* pectic lyases, the *A. niger* polygalacturonases all contain a prosequence in addition to the presequence normally found in secreted enzymes. The role of the prosequence is not clear but

is removed by a KEX-like protease in most cases (20, 21). Also, in *Botrytis cinerea* the prosequence was reported in four of the six endopolygalacturonase genes cloned (17).

Sheehy et al. 922) and DellaPenna et al. (23) were among the first to analyze processing of a tomato polygalacturonase. In addition to glycosylation, evidence for proteolytic processing was obtained. In addition to a presequence, a prosequence was reported as well. Moreover, Sheehy et al. (22) also observed C-terminal processing. It has been proposed that the prosequence is necessary for the targeting of the particular enzyme to a certain part of the cell wall (23), but it has also been hypothesized that the prosequence keeps the enzyme in an inactive state until the prosequence is processed at the proper location (12). As mentioned in Section II, the enzymes of clade B all have a prosequence in addition to the presequence.

IV. BIOCHEMICAL PROPERTIES OF POLYGALACTURONASES

In the past, several polygalacturonases have been characterized biochemically. However, the most comprehensive and in-depth analyses have been carried out for polygalacturonases from the genus *Aspergillus* and notably for the seven-membered endopolygalacturonase family from *A. niger* N400 and for exopolygalacturonase from *A. tubingensis* NW752. The variety of biochemical properties of these enzymes is such that it covers essentially most other endo- and exopolygalacturonases. The discussion of biochemical properties will therefore be confined to this group of enzymes and will be complemented with additional data for other polygalacturonases where appropriate.

A. *A. niger* endopolygalacturonases

An early investigation of a commercial *A. niger* pectinase preparation by Kester and Visser (24) revealed the presence of six different endopolygalacturonases with different specific activities and different modes of action (cleaving patterns) on oligomeric substrates. Using a ''reverse–genetics'' approach, genes encoding endopolygalacturonases I and II were cloned (21, 25), and, using the endopolygalacturonase II gene as a probe, genes encoding endopolygalacturonases A to E (1, 20, 26, 27) were cloned. All the endopolygalacturonase-encoding genes were individually overexpressed in view of their potential industrial application and to facilitate production, purification, and characterization (1, 20, 27, 28). Endopolygalacturonase D appeared quite different from the other *A. niger* endopolygalacturonases as it carries an 136 amino acid N-terminal extension whose function is not clear but which is not processed as evidenced by sequencing the N-terminus by Edman degradation (27).

Several basic biochemical properties of the seven enzymes are listed in Table 1. As can be seen, there is only little variation in pH optima. However, there is an enormous difference in maximal turnover, ranging from 25 U/mg for endopolygalacturonase C to 4000 U/mg for endopolygalacturonase II. For the three enzymes with the lowest turnover rates, endopolygalacturonase C, D, and E, it was proposed that polygalacturonic acid was not the natural substrate. All three enzymes still retain some activity on pectins with a low degree of esterification (DE), making it unlikely that these are the preferred substrates (Table 2). This in contrast to endopolygalacturonases A and B, which both prefer low-DE pectin.

For these latter two enzymes that is quite understandable since these enzymes are constitutively expressed, thus making their role as ''scouting'' enzymes which encounter primarily medium DE pectin quite likely (1). They are supposed to be involved in producing the inducers required to obtain the complete pectinase spectrum (1). The natural substrates for endopolygalacturonases C and E have yet to be identified. For endopolygalacturonase D,

Table 1 General Properties and Kinetics of *Aspergillus niger* Endopolygalacturonases

Enzyme	M_r (kDa)	pH[a]	S.A.[b] (U/mg)	K_m [b] (mg/mL)	V_{max} [b] (U/mg)
PG I	34.9	4.2	800	< 0.15	800
PG II	34.9	4.2	4000	< 0.15	4000
PG A	35.5	4.0	1030	< 0.15	1200
PG B	34.9	5.0	520	0.9	900
PG C	36.2	4.1	25	< 0.15	25
PG D	50.8	4.2	90	0.2	96
PG E	35.6	3.8	38	2.5	80

[a]Determined in McIlvaine buffers using 0.25% polygalacturonic acid at 30°C.
[b]Conditions: 50 mM sodium acetate, pH 4.2, 30°C. PG B: 50 mM sodium acetate, pH 5.0. S.A.: specific activity using 0.25% polygalacturonic acid.

Table 2 Performance of *Aspergillus niger* Endopolygalacturonases on Pectins with Various Degrees of Esterification

	Degree of esterification (%)					
Endopolygalacturonase	0	7	22	45	60	75
	Relative specific activity					
I	100	97	87	43	18	3
II	100	68	50	24	9	2
A	100	125	135	52	7	6
B	100	150	168	131	62	27
C	100	102	86	36	16	5
D	100	97	93	71	44	25
E	100	103	71	38	16	4

Enzymes were incubated with 0.25% (w/v) substrate in 50 mM sodium acetate buffer, pH 4.2, at 30°C.

it has been proposed that the enzyme is actually an oligogalacturonan hydrolase (27) based on the estimated number of subsites and other features (see below).

1. Effect of Environmental Factors

Endopolygalacturonases are generally active between pH 3.5 and pH 6.0. Some enzymes have a quite narrow pH optimum whereas others have a relatively broad pH optimum. As the majority of endopolygalacturonases have been isolated from mesophilic organisms, it is not surprising that the enzymes are also mesophilic. Many polygalacturonases tested in this respect have their highest activity between 40°C and 55°C. However, it should be noted that at these temperatures denaturation sets in. Generally, assays are performed between 25°C and 37°C.

Low-molecular-mass inhibitors for endopolygalacturonases have not been reported, although some inhibitory effect can be expected from divalent ions that interact with the substrate. The known inhibitors of polygalacturonases are the polygalacturonase inhibitor proteins (PGIPs) produced by plants.

Polygalacturonases have long been implicated in the infection process of plants by phytopathogenic microorganisms and not until recently has direct evidence of this been obtained via gene knock-out studies in *A. flavus* (29) and *B. cinerea* (30).

PGIPs belong to the leucine-rich repeat proteins and are produced by nongraminaceous monocotyledonous and dicotyledonous plants. They have been proposed to form part of the plant's "immune system" (31). It had been known for quite some time that oligogalacturonides with degree of polymerization > 10 could effectively induce phytoalexin accumulation in plants (32). Cervone and coworkers proposed that inhibition of endopolygalacturonase activity by PGIP would increase the amount of larger oligogalacturonides and hence stimulate the phytoalexin accumulation which in turn would trigger the PGIP production (33). The effect of PGIP on endopolygalacturonase activity was demonstrated in vitro (34). Bergmann et al. (35) showed that the oligogalacturonides indeed exerted such an elicitor function by analyzing PGIP mRNA accumulation. Not only were the oligogalacturonides active in this respect, but wounding as well as infection resulted in a similar observation. Devoto et al. (36) demonstrated by using a PGIP1 promoter glucuronidase (GUS) reporter construct that of the minimally five PGIP genes present in *Phaseolus vulgaris* L. at least the PGIP1 gene is only induced by wounding and not by elicitor molecules or infection.

Since phytopathogenic fungi generally have a family of endopolygalacturonases at their disposal, different specificities of PGIPs are expected. Indeed, Desiderio et al. (37), Cook et al. (38) and Stotz et al. (39) demonstrated that the inhibition depends on the type of PGIP and the type of endopolygalacturonase. The most comprehensive study in this respect so far was carried out by Leckie and coworkers (40). They studied *P. vulgaris* PGIP1 and PGIP2 of which only the former cannot interact with the *Fusarium moniliforme* endopolygalacturonase. In a loss-of-function approach they determined that Q253 of PGIP2 was important for binding to the *F. moniliforme* endopolygalacturonase. By mutagenizing K253 of PGIP1 into Q253, PGIP1 acquired inhibitory properties toward *F. moniliforme* endopolygalacturonase. By modeling studies it was shown that K253 is exposed to the surface of the protein (40).

Stotz et al. (39) not only demonstrated the differences in specificity of PGIPs and endopolygalacturonases, they also analyzed the evolution of 22 PGIP genes and 19 fungal endopolygalacturonase genes of different origin. It was demonstrated that advantageous amino acid substitutions dominate the molecular evolution of both PGIP and endopolygalacturonases and that the proteins are likely to evolve adaptively in response to natural selection. Unlike the demonstration of Q253 to be critical for *F. moniliforme* recognition (40), this residue was not significant in the evolutionary analysis (39).

2. Specific Mechanism of Action

Endo- and exopolygalacturonases hydrolyze the glycosidic bond between two adjacent α1,4-linked D-galacturonic acid residues. Biely et al. (41) demonstrated that for both exoPG and endopolygalacturonase, hydrolysis proceeds with inversion of the anomeric configuration. According to the general concept of glycosyl hydrolytic action inverting hydrolases should have two acidic residues, of which one activates the water that acts as a nucleophile and the other serves as the base, spaced 9–9.5 Å apart. In neither the *E. carotovora* endopolygalacturonase (4) and *A. niger* endopolygalacturonase II 3D structures (5) nor in the *A. aculeatus* rhamnogalacturonase 3D structure (6) are acidic residues spaced at such a distance that they could play the proposed role. By site-directed mutagenesis studies of *A. niger* endopolygalacturonase II and by comparison with the phage 22 tailspike rhamnosidase, Van Santen et al. (5) and Armand et al. (15) were able to propose the catalytic mechanism. A triad of three strictly conserved Asp residues at the bottom of the substrate-binding cleft of endopolygalacturonases forms the catalytic machinery. Two Asp residues, Asp180 and Asp202 (*A. niger* endopolygalacturonase II numbering), together activate the water that acts as the nucleophile whereas Asp201 serves as the base that protonates the leaving group (15). Asp201 is assisted in its role by an adjacent His residue (His223). A His residue has long been thought to be critical for catalysis (42–44). By chemical modification Stratilova et al. (45) demonstrated the involvement of a tyrosine in catalysis of an endopolygalacturonase. Recently, Pagès et al. (46) indeed demonstrated the indirect involvement in catalysis of a strictly conserved Tyr residue (Tyr291, *A. niger* endopolygalacturonase II numbering). Replacing Tyr291 by Phe reduced the activity to 7% of the wild-type enzyme (46).

3. Subsites in Binding to Substrate

The *A. niger* endopolygalacturonase II was the first enzyme to be characterized with respect to number of subsites, which was estimated at four (47). More recently the entire *A. niger* endopolygalacturonase family was characterized in this respect (1, 20, 27, 28). For endopolygalacturonase E the number of subsites was estimated to be at least five, stretching from -4 to $+1$ (20) and subsite affinities were calculated according to the method outlined by Suganuma et al. (48). The calculation revealed that the total contribution to the binding of the substrate by subsites -2, -1, and $+1$ was only small (1.1 kJ/mole). The major contribution of the substrate-binding energy, 14.4 kJ/mole, originated from subsite -3. The low affinity at subsites -2, -1, and $+1$ can be due to the fact that the substrates used, oligogalacturonates, are not the natural substrates for endopolygalacturonase E. For endopolygalacturonases I, II, A, B, and C, the number of subsites was estimated to be at least seven, from -5 to $+2$ (1, 28) and for endopolygalacturonase D the number of subsites is four, from -3 to $+1$ (27).

For endopolygalacturonases I and II subsite energy maps were calculated as well (28). A major difference was observed for subsite -5. At this particular subsite, quite remote from the active site, the contribution to binding of the substrate was 6 kJ/mole higher for endopolygalacturonase I than for endopolygalacturonase II. It was proposed that this higher affinity at subsite -5 is the underlying principle for the processive (or multiple attack on a single chain) behavior of endopolygalacturonase I (28). Owing to the high affinity after hydrolysis, the product remains bound from subsites -5 to -1 instead of diffusing away, and subsequently shifts to subsites -4 to $+1$ for another hydrolytic event. Thus, the processivity appears as an exolytic action from the reducing end and continues until the degree of polymerization of the substrate has reduced so far ($n = 5$ for endopolygalacturonase I) that it does not cover the remote high-affinity subsite anymore. For endopolygalacturonases A, C, and D, processive behavior was observed as well (1, 27, 28). For endopolygalacturonases A and C, the minimum chain length is 6 and for endopolygalacturonase D this is 4. Upon hydrolysis of polymeric substrates the product progression of typical endoacting enzymes such as endopolygalacturonases II, B, and E is characterized by a transient increase of oligomers with $n > 6$, which are gradually converting into smaller products whereas for the processive enzymes the product progression typically shows a strong increase of monomers from the beginning of the reaction with hardly any transient accumulation of longer oligomers.

Of the processive *A. niger* endopolygalacturonases, endopolygalacturonase D is the most extreme in this respect. Furthermore, endopolygalacturonase D is the only *A. niger* endopolygalacturonase capable of hydrolyzing dimers. This, in conjunction with only four subsites, prompted Pařenicovà et al. (27) to propose endopolygalacturonase D as an oligogalacturonan hydrolase.

B. *A. tubingensis* Exopolygalacturonase

The *A. tubingensis* exopolygalacturonase (EC 3.2.1.67) hydrolyzes monomers from the nonreducing end of the substrate (49). Like the majority of *A. niger* endopolygalacturonases, exopolygalacturonase is optimally active between pH 4 and 5. The calculated subsite map reveals four subsites, stretching from −1 to +3. Subsite +1 has a very high affinity for a galacturonic acid unit (24.5 kJ/mole) whereas subsite −1 even has some repelling force (−1.6 kJ/mole). The high affinity at subsite +1 and negative affinity at subsite −1 are probably why nonproductive complex formation occurs readily and why therefore the actual turnover, $220\,sec^{-1}$, is much lower than the potential intrinsic rate ($716\,sec^{-1}$) (49). Also, galacturonic acid appeared to be quite a strong inhibitor (K_i 0.3 mM).

Both the *A. tubingensis* and *A. aculeatus* exopolygalacturonase are able to release xylogalacturonic acid dimers (β-xylose-1,3-galacturonic acid) from apple pectin (50) or soy bean pectin (51). This ability may be a reflection of the low affinity at subsite −1. It is not known whether xylose-substituted galacturonic acid may be present at subsite +1. In view of the high affinity for galacturonic acid it is likely that this may not be the case. Körner and coworkers (52) have shown by analysis of reaction products of partially methylated galacturonic acid oligomers by mass spectrometry that *A. tubingensis* exopolygalacturonase does not hydrolyze a nonmethylated galacturonic acid from the reducing end when the following residue is methylated. However, using defined monomethylated dimers and trimers, Kester et al. (53) showed that exopolygalacturonase can accommodate such residues at subsite −1 and +1 albeit with reduced efficiency (< 20% of nonmethylated trimer and < 36% of nonmethylated dimer). The discrepancy between these two studies originates from the presence of galacturonic acid monomers, potent inhibitors of exopolygalacturonase, in the oligomer mixture used by Körner et al. (52). In practice, during pectin hydrolysis, exopolygalacturonase will cease action when a methylated galacturonic acid has to bind at subsite +1 thus leaving a nonmethylated residue at the nonreducing end.

C. Exo-Poly-α-D-Galacturonosidase

Exo-poly-α-D-galacturonosidase (EC 3.2.1.82) catalyzes the hydrolysis of digalacturonate from the nonreducing end of polygalacturonic acid (pectate). So far, the activity has only been detected in bacteria like *Erwinia chrysanthemi* (54, 55), *Clostridium thermosaccharolyticum* (56), and *Ralstonia solancearum* (57).

By using a mixture of Δ4,5-unsaturated oligomers (generated by pectate lyase action) and saturated oligomers, Collmer et al. (54) were able to deduce that the *Erwinia* enzyme preferred hydrolysis of Δ4,5-unsaturated dimers, attacked the nonreducing end, and was a single-attack enzyme. The preferred action of this enzyme on unsaturated substrates is understandable in view of the enormous amount of different pectate lyases produced by this organism (see Chapter 80). Shevchik et al. (55) demonstrated that hydrolysis of saturated oligomers indeed occurs at the nonreducing end by using reduced hexagalacturonate. In addition, Kester et al. (53) showed that on purified Δ4,5-unsaturated trigalacturonate the enzyme is slightly more active than on the saturated counterpart (0.32 U/mL vs. 0.2 U/mL) and that the enzyme can not accommodate a methylated galacturonic acid residue at subsites −2, −1, or +1.

For *C. thermosaccharolyticum*, Van Rijssel et al. (56) were able to show that the exopolygalacturonase activity is associated with a pectin methylesterase activity in a very large complex (1200 kDa). Although this enzyme primarily hydrolyzed dimers from the nonreducing end, the formation of trimers was observed as well. It is not known whether the formation of trimers is a result of a specific binding mode or is due to condensation or tranglycosylation. The latter is highly unlikely to invert. It is therefore interesting that yet another D-galacturonan, digalacturonohydrolase, has been studied that does transglycosylate (58). This enzyme, purified from *Selenomonas ruminatium*, released dimers from tri-, tetra-, and pentagalacturonates, but at high trimer concentrations bimolecular reactions were observed. This demonstrates that the particular exopolygalacturonase acts via retention of the anomeric configuration and thus should not be included in family 28 of glycosyl hydrolases.

D. Synthetic Substrates

Using monomethylesterified di- and trigalacturonides carrying the monomethyl group at a defined position (59), Kester et al. (53) studied the specificity of *Aspergillus* polygalacturonases. The data obtained for the *A. tubingensis* exopolygalacturonase were discussed above, as were the data for endopolygalacturonase D (27). For all six remaining endopolygalacturonases (I, II, A, B, C, and E) it was shown that at subsite −1 a nonmethylated galacturonate residue is mandatory

(53). At subsite +1 only endopolygalacturonase I, II, and B were able to accommodate a methylated galacturonate albeit very poorly (activities $< 0.6\%$ compared to nonmethylated trimer). At subsite −2 all six enzymes tolerated fairly well a methylated galacturonate (activities between 6% and 38%). This was also shown by Körner et al. (52), who used partially methylated oligomers mixtures as substrate and analyzed the products of endopolygalacturonase II action by mass spectrometry.

Strictly speaking, almost all commercially available pectin compounds are synthetic substrates, as they all have undergone some chemical treatment. This holds even more for pectin series of various degree of methylation that have been either methylated by chemical treatment (acidic methanol) or demethylated by sodium hydroxide treatment or pectin methylesterase action. Especially the pectin methylesterase-treated pectins can give valuable information about substrate preference of pectic depolymerases as a blockwise distribution of methyl groups can be obtained by plant pectin methylesterase action and a random distribution by fungal pectin methylesterase. By using a series of demethylated pectins which were differently prepared, Pagès et al. (46) demonstrated that endopolygalacturonase II prefers blockwise demethylated substrate but that a single mutation (Glu252Ala) can change the preference profoundly toward less block specificity or to even more block specificity (Gln186Glu). Although these studies are based on kinetic studies (initial rates), valuable information on substrate specificity is also obtained by analyzing the products after various times of hydrolysis of pectins with various degree of methylation (52, 60, 61).

V. APPLICATION OF POLYGALACTURONASES

Polygalacturonases have found widespread application in many industrial processes. The enzymes applied are mostly obtained from the filamentous fungi of the genus *Aspergillus*. These preparations generally contain a whole range of cell wall–degrading and –modifying enzymes and are predominantly applied in the fruit juice industry. Together with pectin methylesterase, endopolygalacturonases are essential in most of these applications e.g., clarification of fruit juices, enzymatic juice extraction, liquefaction of plant tissues (Chap. 67).

Fungal pectinase preparations containing predominantly endopolygalacturonases and which are free of pectin methylesterase activity are used successfully for the production of pulpy nectars. These comminuted fruit juices are viscous, pulpy drinks and are usually prepared by a mechanical-thermal dispersion process. However, products prepared with enzymes are superior in cloud stability and smooth consistency and have higher contents of soluble solids and pigments. These suspensions of loose cells from fruit and vegetable tissue are obtained by weakening the cell cohesion by a limited pectin breakdown, particularly in the middle lamella. Nutrients like vitamin A or proteins are protected inside the cells. Enzyme preparations, which have only one depolymerase system (commonly Endopolygalactronase(s)), are chosen. When endogenous pectin methylesterase is present in the fruit, blanching is indicated. Maceration can also be achieved with endopectin lyase or exopectate lyase. These enzymes might have potential application for processing of vegetables with a higher pH (62). Endopolygalacturonase(s) added to citrus concentrates will reduce the viscosity of these concentrates and contribute(s) to extend the cloud stability of citrus juices. Endopolygalacturonases can also be used for the manufacture of less calcium-sensitive pectin preparations that can be used in systems where the viscosity aspect is not important. Endopolygalacturonases will hydrolyze the galacturonan backbone preferentially in the nonesterified, calcium-sensitive regions.

Polygalacturonases are widely distributed in higher plants. They are believed to contribute to fruit softening of pears, peaches, and avocado (62, 64). Polygalacturonases and also pectin methylesterase activities are abundant in tomatoes. Ingenious systems are used in the tomato processing industry to heat-inactivate instantaneously (“hot break” process) to obtain the highly viscous juice preferred by the consumer and the high-consistency concentrated juice (tomato paste) used for sauces, soups, catsup, and similar products. When tomatoes are used for color and flavor only, and consistency is provided by other ingredients such as starch, a more easily handled, thin, “cold break” juice is the starting material for paste production. A holding time is introduced between crushing and heat treatment to ensure breakdown of the pectins by combined pectin methylesterase/polygalacturonase action (64).

VI. QUALITATIVE AND QUANTITATIVE DETERMINATION OF ACTIVITY

See Chapter 66 on pectic polysaccharides.

REFERENCES

1. L Pařenicovà, JAE Benen, HCM Kester, J Visser. *pga*A and *pga*B encode constitutively expressed members of the *Aspergillus niger* endopolygalacturonase gene family. Biochem J 345:637–644, 2000.
2. PM Coutinho, B Henrissat. Carbohydrate-active enzymes: an integrated database approach. In: HJ Gilbert, GJ Davies, B Henrissat, B Svensson, eds. Recent Advances in Carbohydrate Bioengineering. Cambridge: Royal Society of Chemistry, 199, pp 3–12.
3. CJB Van der Vlugt-Bergmans, PJA Meeuwsen, AGJ Voragen, AJJ van Ooyen. Endo-xylogalacturonan hydrolase, a novel pectinolytic enzyme. Appl Environ Microbiol 66:36–41, 2000.
4. R Pickersgill, D Smith, K Worboys, J Jenkins. Crystal structure of polygalacturonase from *Erwinia carotovora* spp. *carotovora*. J Biol Chem 273:24660–24664, 1998.
5. Y van Santen, JAE Benen, K-H Schröter, KH Kalk, S Armand, J Visser, BW Dijkstra. 1.69-Å Crystal structure of endopolygalacturonase II from *Aspergillus niger* and identification of active site residues by site-directed mutagenesis. J Biol Chem 274:30474–30480, 1999.
6. TN Petersen, S Kauppinen, S Larsen. The crystal structure of rhamnogalacturonase A from *Aspergillus aculeatus*: a right-handed parallel beta helix. Structure 5:533–544, 1997.
7. RF Schwan, AH Rose. Polygalacturonase production of *Kluyveromyces marxianus*: effect of medium composition. J Appl Microbiol 76:62–67, 1994.
8. P Blanco, C Sieiro, NM Reboredo, TG Villa. Genetic determination of polygalacturonase production in wild type and laboratory strains of *Saccharomyces cerevisiae*. Arch Microbiol 167:284–288, 1997.
9. M Torki, P Manadaron, F Thomas, F Quigley, R Mache, D Falconet. Differential expression of a polygalacturonase gene family in *Arabidopsis thaliana*. Mol Gen Genet 261:948–952, 1999.
10. SB Hong, ML Tucker. Genomic organization of six tomato polygalacturonases and 5′ upstream sequence identity with *tap*1 and *win*2 genes. Mol Gen Genet 258:479–487, 1998.
11. KA Hadfield, JKC Rose, DS Yaver, RM Berka, AB Bennett. Polygalacturonase gene expression in ripe melon fruit supports a role for polygalacturonase in ripening-associated pectin disassembly. Plant Physiol 117:363–373, 1998.
12. KA Hadfield, AB Bennett. Polygalacturonases: many genes in search of a function. Plant Physiol 117:337–343, 1998.
13. C Lang, H Dörnenburg. Perspectives in the biological function and the technological application of polygalacturonases. Appl Microbiol Biotechnol 53:366–375, 2000.
14. GA Tucker, H Simons, N Errington. Transgenic tomato technology: enzymic modification of pectin pastes. Biotechnol Genet Eng Rev 16:293–307, 1999.
15. S Armand, MJM Wagemaker, HCM Kester, P Sanchez-Torres, Y van Santen, BW Dijkstra, J Visser, JAE Benen. The active-site topology of *Aspergillus niger* endopolygalacturonase II as studied by site-directed mutagenesis. J Biol Chem 275:691–696, 2000.
16. RD Scavetta, SR Herron, AT Hotchkiss, N Kita, NT Keen, JAE Benen, HCM Kester, J Visser, F Jurnak. Structure of plant cell wall fragment complexed to PelC. Plant Cell 11:1081–1092, 1999.
17. JP Wubben, W Mulder, A Ten Have, JAL van Kan, J Visser. Cloning and partial characterization of endopolygalacturonase genes from *Botrytis cinerea*. Appl Environ Microbiol 65:1596–1602, 1999.
18. Y Yang, C Bergmann, J Benen, R Orlando. Identification of the glycosylation site and glycan structures of recombinant *Endo*polygalacturonase II (EPG-II) by mass spectrometry. Rapid Commun Mass Spec 11:1257–1262, 1997.
19. J Colangelo, V Licon, J Benen, J Visser, C Bergmann, R Orlando. Characterization of the glycosylation of recombinant endopolygalacturonase I from *Aspergillus niger*. Rapid Commun Mass Spec 13:1448–1453, 1999.
20. L Pařenicovà, JAE Benen, HCM Kester, J Visser. *pga*E encodes a fourth member of the endopolygalacturonase gene family from *Aspergillus niger*. Eur J Biochem 251:72–80, 1998.
21. HJD Bussink, HCM Kester, J Visser. Molecular cloning, nucleotide sequence and expression of the gene encoding prepro-polygalacturonase II of *Aspergillus niger*. FEBS Lett 273:127–130, 1990.
22. RE Sheehy, J Pearson, CJ Brady, WR Hiatt. Molecular characterization of tomato fruit polygalacturonase. Mol Gen Genet 208:30–36, 1987.
23. D DellaPenna, DC Alexander, AB Bennett. Molecular cloning of tomato fruit polygalacturonase: analysis of polygalacturonase mRNA levels during ripening. Proc Natl Acad Sci USA 83:6420–6424, 1986.
24. HCM Kester, J Visser. Purification and characterization of polygalacturonases produced by the hyphal fungus *Aspergillus niger*. Biotechnol Appl Biochem 12:150–160, 1990.
25. HJD Bussink, KB Brouwer, LH de Graaff, HCM Kester, J Visser. Identification and characterization of a second polygalacturonase gene of *Aspergillus niger*. Curr Genet 20:301–307, 1991.
26. HJD Bussink, FP Buxton, BA Fraaye, LH de Graaff, J Visser. The polygalacturonases of *Aspergillus niger*

are encoded by a family of diverged genes. Eur J Biochem 208:83–90, 1992.
27. L Pařenicovà, HCM Kester, JAE Benen, J Visser. *pga*D encodes a new type of endopolygalacturonase from *Aspergillus niger*. FEBS Lett 467:333–336, 2000.
28. JAE Benen, HCM Kester, J Visser. Kinetic characterization of *Aspergillus niger* N400 endopolygalacturonases I, II and C. Eur J Biochem 259:577–585, 1999.
29. M Shieh, RL Brown, MP Whitehead, JW Cary, PJ Cotty, TE Cleveland, RA Dean. Molecular genetic evidence for the involvement of a specific polygalacturonase, P2c, in the invasion and spread of *Aspergillus flavus* in cotton balls. Appl Environ Microbiol 63:3548–3552, 1997.
30. A Ten Have, W Mulder, J Visser, JAL van Kan. The endopolygalacturonase gene BcPG1 is required for full virulence of *Botrytis cinerea*. Mol Plant Microbe Interact 11:1009–1016, 1998.
31. G De Lorenzo, F Cervone. Polygalacturonase-inhibiting proteins (PGIPs): their role in specificity and defense against pathogenic fungi. In: G Stacey, NT Keen, eds. Plant-Microbe Interactions. New York; Chapman & Hall, 1997, Vol 3, pp 76–93.
32. MG Hahn, AG Darvill, P Albersheim. Host-pathogen interactions. XIX. The endogenous elicitor, a fragment of a plant cell wall polysaccharide that elicits phytoalexin accumulation in soybeans. Plant Physiol 68:1161–1169, 1982.
33. F Cervone, G De Lorenzo, L Degra, G Salvi, M Bergami. Purification and characterization of a polygalacturonase inhibiting protein from *Phaseolus vulgaris* L. Plant Physiol 85:631–637, 1987.
34. F Cervone, MG Hahn, G De Lorenzo, A Darvill, P Albersheim. Host-pathogen interactions. XXXIII. A plant protein converts a fungal pathogenesis factor into an elicitor of plant defense responses. Plant Physiol 90:542–548, 1989.
35. C. Bergmann, Y Ito, D Singer, P Albersheim, AG Darvill, N Benhamou, L Nuss, G Salvi, F Cervone, G De Lorenzo. Polygalacturonase-inhibiting protein accumulates in *Phaseolus vulgaris* L. in response to wounding, elicitors and fungal infection. Plant J 5:625–634, 1994.
36. A Devoto, F Leckie, E Lupotto, F Cervone, G De Lorenzo. The promoter of a gene encoding a polygalacturonase-inhibiting protein of *Phaseolus vulgaris* L. is activated by wounding but not by elicitors or pathogen infection. Planta 205:165–174, 1998.
37. A Desiderio, B Aracri, F Leckie, B Mattei, G Salvi, H Tigelaar, JSC van Roekel, DC Baulcombe, LS Melchers, G De Lorenzo, F Cervone. Polygalacturonase-inhibiting proteins (PGIPs) with different specificities are expressed in *Phaseolus vulgaris*. Mol Plant Microbe Interact 10:852–860, 1997.
38. BJ Cook, RP Clay, CW Bergmann, P Albersheim, AG Darvill. Fungal polygalacturonases exhibit different substrate degradation patterns and differ in their susceptibilities to polygalacturonase inhibiting proteins. Mol Plant Microbe Interact 12:703–711, 1999.
39. HU Stotz, JG Bishop, CW Bergmann, M Koch, P Albersheim, AG Darvill, JM Labavitch. Identification of target amino acids that affect interactions of fungal polygalacturonases and their plant inhibitors. Physiol Mol Plant Pathol 56:117–130, 2000.
40. F Leckie, B Mattei, C Capodicasa, A Hemmings, L Nuss, B Aracri, G De Lorenzo, F Cervone. The specificity of polygalacturonase-inhibiting protein (PGIP): a single amino acid substitution in the solvent exposed β-strand/β-turn region of the leucine rich repeats (LRRs) confers a new recognition capability. EMBO J 18:2352–2363, 1999.
41. P Biely, JAE Benen, K Heinrichová, HCM Kester, J Visser. Inversion of configuration during hydrolysis of alpha-1,4-galacturonidic linkage by three *Aspergillus* polygalacturonases. FEBS Lett 382:249–255, 1996.
42. L Rexova-Benkova, M Mrackova. Active groups of extracellular endo-D-galacturonase of *Aspergillus niger* derived from pH effect on kinetic data. Biochim Biophys Acta 523:162–169, 1978.
43. R Cooke, C Ferber, L Kanagasabapathy. Purification and characterization of polygalacturonases from a commercial *Aspergillus niger* preparation. Biochim Biophys Acta 452:440–451, 1976.
44. C Caprari, B Mattei, ML Basile, G Slavi, V Crescenzi, G de Lorenzo, F Cervone. Mutagenesis of endopolygalacturonase from *Fusarium moniliforme*: histidine residue 234 is critical for enzymatic and macerating activities and not for binding to polygalacturonase-inhibiting protein (PGIP). Mol Plant Microbe Interact 9:617–624, 1996.
45. E Stratilova, M Dzurova, O Markovic, H Jornvall. An essential tyrosine residue of *Aspergillus* polygalacturonase. FEBS Lett 382:164–166, 1996.
46. S Pagès, WHM Heijne, HCM Kester, J Visser, JAE Benen. Subsite mapping of *Aspergillus niger* endopolygalacturonase II by site-directed mutagenesis. J Biol Chem 275:29348–29353, 2000.
47. L Rexova-Benkova. The size of the substrate-binding site of an *Aspergillus niger* extracellular endopolygalacturonase. Eur J Biochem 39:109–115, 1973.
48. T Suganuma, R Matsuno, M Ohnishi, K Hiromi. A study of the mechanism of action of Taka-amylase A1 on linear oligosaccharides by product analysis and computer simulation. J Biochem 84:293–316, 1978.
49. HCM Kester, MA Kusters–Van Someren, Y Müller, J Visser. Primary structure and characterization of an exopolygalacturonase from *Aspergillus tubingensis*. Eur J Biochem 240:739–746, 1996.
50. HCM Kester, JAE Benen, J Visser. The exopolygalacturonase from *Aspergillus tubingensis* is also active on

xylogalacturonan. Biotechnol Appl Biochem 30:53–57, 1999.
51. G Beldman, LAM van den Broek, HA Schols, MJF Searle–Van Leeuwen, KMJ van Laere, AGJ Voragen. An exopolygalacturonase from *Aspergillus aculeatus* able to degrade xylogalacturonan. Biotechnol Lett 18:707–712, 1996.
52. R Körner, G Limberg, TMIE Christensen, JD Mikkelsen, P Roepstorff. Sequencing of partially methyl-esterified oligogalacturonates by tandem mass spectrometry and its use to determine pectinase specificities. Anal Chem 71:1421–1427, 1999.
53. HCM Kester, D Magaud, C Roy, D Anker, A Doutheau, V Shevchik, N Hugouvieux-Cotte-Pattat, JAE Benen, J Visser. Performance of selected microbial pectinases on synthetic monomethyl-esterified di- and trigalacturonates. J Biol Chem 274:37053–37059, 1999.
54. A Collmer, CH Whalen, SV Beer, DF Bateman, An exo-poly-α-D-galacturonosidase implicated in the regulation of extracellular pectate lyase production in *Erwinia chrysanthemi*. J Bacteriol 149:626–634, 1982.
55. VE Shevchik, HCM Kester, JAE Benen, J Visser, J Robert-Baudouy, N Hugouvieux-Cotte-Pattat. Characterization of the exo-pectate lyase PelX of *Erwinia chrysanthemi*. J Bacteriol 181:1652–1663, 1999.
56. M van Rijssel, GJ Gerwig, TA Hanse. Isolation and characterization of an extracellular glycosylated protein complex from *Clostridium thermosaccharolyticum* with pectin methylesterase and polygalacturonate hydrolase activity. Appl Environ Microbiol 59:828–836, 1993.
57. O Huang, C Allen. An exo-poly-alpha-D-galacturonosidase, PeHB, is required for wild-type virulence of *Ralstonia solanacearum*. J Bacteriol 179:7369–7378, 1997.
58. K Heinrichova, M Dzurova, L Rexova-Benkova. Mechanism of action of D-galacturonan digalacturonohydrolase of *Selenomonas ruminantium* on oligogalactosiduronic acids. Carbohydr Res 235:269–280, 1992.
59. D Magaud, C Grandjean, A Doutheau, D Anker, VE Shevchik, N Cotte-Pattat, J Robert-Baudouy. Synthesis of the two mono methyl esters of α(1-4) linked D-galacturonic acid dimer and of precursors for the preparation of higher oligomers methyl esterified in definite positions. Carbohydr Res 314:189–199, 1998.
60. AJ Mort, F Qiu, NO Maness. Determination of the pattern of methyl esterification in pectin—distribution of contiguous nonesterified residues. Carbohydr Res 247:21–35, 1993.
61. PJH Daas, K Meyer-Hansen, HA Schols, GA De Ruiter, AGJ Voragen. Investigation of the non-esterified galacturonic acid distribution in pectin with endopolygalacturonase. Carbohydr Res 318:135–145, 1999.
62. AGJ Voragen, W Pilnik. Pectin-degrading enzymes in fruit and vegetable processing. In: JR Whitaker, PE Sonnet, eds. Biocatalysis in Agricultural Biotechnology. Washington: ACS Symp Ser No. 389, 1989, pp 93–115.
63. W Pilnik, AGJ Voragen. The significance of endogenous and exogenous pectic enzymes in fruit and vegetable processing. In: PF Fox, ed. Food Enzymology. London: Elsevier Applied Science, 1991, pp 303–336.
64. W Pilnik, AGJ Voragen. Pectic enzymes in fruit and vegetable juice manufacture. In: T Nagodawithana, G Reed, eds. Enzymes in Fruit Processing. London: Academic Press, 1993, pp 363–399.

70

Enzymes Releasing L-Arabinose and D-Galactose from the Side Chains of Pectin

Ronald P. de Vries
Utrecht University, Utrecht, The Netherlands
Jaap Visser
Fungal Genetics and Technology Consultancy, Wageningen, The Netherlands

I. INTRODUCTION

Owing to the abundance of arabinose containing structures in pectin and other plant cell wall polysaccharides, arabinose-releasing enzymes (arabinanases) play an important role in the degradation of plant material. These enzymes and the polysaccharides on which they are active have recently been reviewed (1). Arabinanases can be divided into four classes:

1. Endoarabinanases (often referred to as endoarabinases) cleave the internal bonds of the arabinan chains.
2. Exoarabinanases release terminal arabinose residues or short arabino-oligosaccharides from arabinan.
3. α-L-Arabinofuranosidases release only monomeric terminal arabinose residues from arabinose containing oligo- and polysaccharides.
4. Arabinoxylan arabinofuranohydrolase, another exoacting type of enzyme specific for xylan and xylan-derived oligosaccharides. The latter enzyme will be discussed in Chapter 71.

A second group of enzymes that is important for the hydrolysis of pectin side chains are the galactose releasing enzymes (galactanases), which can be divided in three classes: endogalactanases which cleave the internal linkages in the galactans; exogalactanases; and β-D-galactosidases which remove terminal galactose residues and short galacto-oligosaccharides (in the case of the exogalactanases) from galactose containing oligo- and polysaccharides. These enzymes have been identified in both prokaryotes and lower eukaryotes, as well as in some plants, and have been studied in detail. The enzymes from microbial origin are those most commonly used in food technology, particularly enzymes from species of the filamentous fungus *Aspergillus*. Therefore the emphasis in this chapter will be on these enzymes, although enzymes from other origins will also be mentioned. An overview of arabinose- and galactose-releasing enzymes from *Aspergillus* and their encoding genes can be found in recent review on plant cell wall polysaccharide degrading enzymes from *Aspergillus* (2).

The more specific experimental procedures involved in the purification and characterization of galactanases and arabinanases will be given. The different classes of enzymes will be discussed separately, followed by information about the induction of the production of these enzymes, the cooperative or synergy of these enzymes in the degradation of the polymeric substrates, and the applications of the enzymes in food technology.

II. EXPERIMENTAL PROCEDURES FOR THE PURIFICATION AND CHARACTERIZATION OF THE ARABINANASES AND GALACTANASES

A. Purification

Since most microbial arabinanases and galactanases are extracellular enzymes, they can be isolated from culture filtrates using classical purification techniques, such as precipitation, ultrafiltration, gel filtration, ion exchange chromatography, isoelectric focussing, and adsorption. However, some materials for affinity chromatography have been developed specifically for these enzymes. Arabinanases and galactanases are commonly produced by microorganisms during growth on crude plant cell wall material. The crude enzyme preparations obtained this way also contain many other cell wall–degrading enzymes. During growth on sugar beet pulp, which is rich in pectin, polygalacturonase and arabinanase are produced abundantly. Using chromatography over a cross linked alginate column (3), these two classes of enzymes have been efficiently separated. Divinylsulfone-substituted Sepharose and chelating Sepharose have been applied to crude enzyme preparations high in both galactanases and arabinanases. Using this material an efficient separation of arabinanases and galactanases from *A. niger* was obtained (4). This column has also been used to remove contaminating arabinanase activities during the purification of a $\beta(1 \rightarrow 6)$-endogalactanase (5). Crosslinked arabinan or arabinan linked to activated Sepharose 6B (6) was demonstrated to be able to bind one of the two arabinofuranosidases commonly present in crude enzyme preparations from *Aspergillus*.

B. Qualitative and Quantitative Determination of Activity

Arabinofuranosidase and β-galactosidase activity is generally assayed by using *p*-nitrophenyl-α-L-arabinofuranoside and *p*-nitrophenyl-β-L-galactopyranoside as their respective substrates. The activity of the enzymes is determined by measuring the release of *p*-nitrophenol spectrophotometrically at 400–420 nm after adjustment of the pH to 9.0.

An assay in which both arabinofuranosidase activity and endoarabinanase activity can be determined is measuring the appearance of reducing sugars from arabinans with different degrees of branching (e.g., linear arabinan, heavily branched sugar beet arabinan, and moderately branched arabinans isolated from apple juice) (7). More advanced methods to determine arabinanase activity (including activity on polymeric substrates) use FPLC and HPLC. Methods for the analysis of the delignification activity of arabinofuranosidases (8) and action on monoterpenyl arabinofuranosylglucosides (9) have also been described but will not be discussed here.

Several methods have been described for the determination of galactanase activity. The $\beta(1-6)$-galactanase activity was derived from the amount of $\beta(1 \rightarrow 6)$-galacto-oligosaccharides liberated from grape galactan (5). The amount of $\beta(1 \rightarrow 6)$-galacto-oligosaccharides was measured by oxidizing non-reducing terminal galactose residues using the D-galactose dehydrogenase method of Finch et al. (10). Using the same method, $\beta(1 \rightarrow 3)$-exogalactanase activity was measured using a galactan prepared from acacia gum (11, 12). Recently, a wide spectrum of substrates has become commercially available. These include different arabanans, galactans and arabinogalactans, as well as arabino- and galacto-oligosaccharides. Additionally, several chromogenic substrates have been developed for the rapid analysis of arabinanase and galactanase activity. McCleary (13) developed a specific assay for endoarabinanase activity using a dye-crosslinked substrate (Azurine-crosslinked linear arabinan) which is commercially available (Megazyme, Ireland). The same company also developed a similar assay for $\beta(1 \rightarrow 4)$-galactanase activity using Azurine-crosslinked potato galactan. In both assays the enzyme activity is measured by the amount of color released from the insoluble substrate. The same company also markets an endoarabinanase, an arabinofuranosidase, a $\beta(1 \rightarrow 4)$-D-endogalactanase, and a β-galactosidase, all purified from *A. niger*.

III. α-L-ARABINOFURANOSIDASES

A. Substrate Specificity and Action Pattern

α-L-Arabinofuranosidases are exoacting enzymes that remove terminal arabinofuranose residues from the nonreducing end of arabinan and arabinose containing oligosaccharides. In pectin these residues are linked via an $\alpha(1 \rightarrow 2)$-, $\alpha(1 \rightarrow 3)$- or an $\alpha(1 \rightarrow 5)$-linkage to arabinan and arabinogalactan side chains. Arabinofuranosidases differ with respect to their ability to release $\alpha(1 \rightarrow 3)$- or $\alpha(1 \rightarrow 5)$-linked arabinose. Two distinctly different arabinofuranosidases have been described (1). Type A is not active on polymeric substrates, only on oligomeric substrates. Type B, however, is able to release arabinose from both

oligomeric and polymeric substrates. Some α-L-arabinofuranosidases are able to release arabinose not only from arabinan but also from arabinoxylan (14, 15). All arabinofuranosidases described so far are able to hydrolyze the synthetic substrate *p*-nitrophenyl-α-L-arabinofuranoside. This substrate can be used to distinguish between arabinofuranosidases and arabinoxylan arabinofuranohydrolases, since the latter enzyme is not able to hydrolyze *p*-nitrophenyl-α-L-arabinofuranoside.

B. Properties

In general, type A arabinofuranosidases in general have a molecular weight in the range of 60–80 kDa. Some gel filtration studies assessed the molecular mass to be > 120 kDa, suggesting that these enzymes may be present as homodimers (Table 1). The native form of a type A arabinofuranosidase was demonstrated to be an octamer composed of eight subunits of 62 kDa (16). The variation in molecular weight of type B arabinofuranosidases is wider (between 34 and 94 kDa; Table 1). For these enzymes, higher molecular masses were also observed suggesting that they are also present as multimeric proteins. Nearly all fungal arabinofuranosidases have an acidic pI (between 3.2 and 6.0), whereas the variation among bacterial arabinofuranosidases is much wider (from 3.8 to 9.0). No apparent correlation exists between the pI and A or B type arabinofuranosidases. Differences observed in the molecular mass and pI of arabinofuranosidases from the same (eukaryotic) organism are most likely due to posttranslational modifications of the enzymes, especially glycosylation. Differences in glycosylation of extracellular fungal enzymes have been observed depending on the culture conditions of the strain. This can explain, to some extent, the different molecular mass reported for the arabinofuranosidases from two *Aspergillus niger* strains (Table 1) but not the large difference in pI, indicating significant differences in the enzymes produced by the different strains.

A comparison of the kinetic properties of the two types of arabinofuranosidases is made for the well-studied enzymes from *A. niger* (1). Using *p*-nitrophenyl-α-L-arabinofuranoside as a substrate the K_m for AbfA and AbfB are 0.6 and 0.48 mM, respectively (Table 1). The k_{cat} for AbfA and AbfB are 262 and 243 (sec^{-1}), respectively (1). These data indicate that despite the strong differences in their ability to hydrolyze natural substrates, their activity on *p*-nitrophenyl-α-L-arabinofuranoside is nearly identical. The K_m and k_{cat} of arabinofuranosidases of other organisms show differences up to a factor of 30 compared to the *A. niger* enzymes.

Table 1 Comparison of the Properties of Some α-L-Arabinofuranosidases

Organism	Type	MW (kDa)[a]	pI	pH_{opt}[b]	K_m (mM)	Ref.
Bacterial						
Bacillus subtilus	A	61		7.0		66
Bacillus subtilus	B	65	5.3	6.5		67
Streptomyces massasporeus	B	54 (gf)		5.0	1.67	68
Streptomyces purpurascens	A	62 495 (gf)	3.9	6.5		16
Thermomonospora fusca	A	46 92 (gf)		6.0	0.1	69
Fungal						
Aspergillus niger	A	128	6–6.5	4.1	0.6	3
Aspergillus niger	B	60	5.5–6	3.7	0.48	3
Aspergillus niger	A	83	3.3	3.4	0.68	70
Aspergillus niger	B	67	3.3	3.4	0.52	70
Aurobasidium pullulans	B	105 210 (gf)		4.0–4.5		71
Trichodema reesei	B	53	7.5	4.0	1.2	72
Plant						
Daucus carota (carrot)	B	94	4.7	4.2	1.33	73

[a]MW is determined by SDS-PAGE, unless otherwise indicated (gf = gelfiltration chromatography).
[b]Determined using *p*-nitrophenyl-α-L-arabinofuranoside as a substrate.

Despite the significant differences in pI between the enzymes purified from the two *A. niger* strains (Table 1), nearly identical K_m values were observed.

C. Classification and Mechanism

Based on the classification and nomenclature of the Commission of Enzymes of the International Union of Biochemistry, α-L-arabinofuranosidases (EC 3.2.1.55) belong to the class of hydrolases (group 3), more specifically the O-glycosylases (subgroup .2.1.). The distinction between the two types of arabinofuranosidases from *Aspergillus niger* in the ability to hydrolyze polymeric substrates reflects the assignment of these enzymes to the different glycoside hydrolase families as described by Henrissat and Bairoch (17) at URL http://afmb.cnrs-mrs.fr/~cazy/cazy/index.html.

This assignment of enzymes to the different families is made based on homology of the deduced amino acid sequence derived from the genes encoding these enzymes. AbfA is assigned to family 51, whereas AbfB is assigned to family 54. The genes encoding the other purified type A or type B arabinofuranosidases have not all been isolated, so a conclusion whether this is a general correlation cannot yet be made. Families 51 and 54 contain only arabinofuranosidases, indicating that these enzymes are not very similar to other proteins. An arabinofuranosidase from family 54 has also been shown to possess β-xylosidase activity (18). The same is observed for some bacterial arabinofuranosidases (19–21), which have been assigned to family 43. This family also contains endoarabinanases and β-xylosidases.

The reaction mechanism of some members of these families has been determined Arabinofuranosidases from families 51 and 54 work via a retaining mechanism, whereas enzymes from family 43 have an inverting reaction mechanism (17). The reaction mechanism of the arabinofuranosidase from *Pseudomaonas fluorescens* subsp. *cellulosa* (22), the only member of family 62, has not been determined. This enzyme contains a putative cellulose-binding domain. Additionally, an arabinofuranosidase has been identified which contains a xylan-binding domain (23), but this enzyme has not yet been assigned to a glycosylase family.

D. Inhibitors

L-Arabinose has been demonstrated to be a compatible inhibitor ($K_I = 16.4$ mM) of arabinofuranosidase II from *Penicillium casulatum*, but did not affect arabinofuranosidase I from this fungus (24).

Inhibition of α-L-arabinofuranosidase III from *Monilinia fructigena* was demonstrated using 1,4-dideoxy-1,4-imino-L-threitol and 1,4-dideoxy-1,4-imino-L-arabinitol (25). However, the data presented there indicated that efficient inhibition will only occur when the pK_a of the iminoalditol is below that of the acid-catalytic group of the target enzyme. Consequently these compounds will not inhibit most fungal arabinofuranosidases.

IV. ENDOARABINANASES

A. Substrate Specificity and Mode of Action

Endoarabinanases act on the arabinan side chains of pectins releasing arabinose oligosaccharides. They hydrolyze the internal $\alpha(1 \rightarrow 5)$-linkages of the main chain of arabinan resulting in arabino-oligosaccharides. The activity of this enzyme significantly enhances the activity of the α-L-arabinofuranosidases and is therefore essential for an efficient degradation of arabinan. Endoarabinanases prefer unsubstituted linear substrates and therefore also benefit form the action of arabinofuranosidase (AbfB), removing the side chains from polymeric branched arabinan. Bacterial endoarabinanases produce predominantly arabinose and arabinobiose as end products (26, 27), while action of an endoarabinanase from *A. niger* results in the accumulation of arabinobiose and arabinotriose in the reaction mixture (3).

Two endoarabinanases from closely related *Aspergillus* spp. have been studied with respect to their action pattern and substrate specificity (28). The *A. aculeatus* enzyme contains six subsites, while the *A. niger* endoarabinanase contains only five subsites. Different action patterns of the two enzymes resulted in different initial hydrolysis products, but for both enzymes the predominant final hydrolysis products were arabinobiose and arabinotriose.

B. Properties

Endoarabinanases are relatively small monomeric proteins with a molecular mass between 30 and 45 kDa (Table 2). The fungal endoarabinanases have an acidic pI (3.0–3.3), whereas bacterial endoarabinanases have an alkaline pI (7.9–9.3). Although many organisms produce several arabinofuranosidases, no evidence for multiple forms of endoarabinanase has been reported for any organism.

Table 2 Comparison of the Properties of Some Endoarabinanases

Organism	MW (kDa)	pI	pH_{opt}	Ref.
Bacillus subtilis	32	9.3	6.0	67
Aspergillus nidulans	40	3.25	5.5	61
Aspergillus niger	43	3.0	4.6	70

C. Classification and Mechanism

Like the α-L-arabinofuranosidases, endo-α-L-arabinanases (EC 3.2.1.99) belong to the O-glycosylases. The systematic name of endoarabinanase is arabinan endo-1,5-α-L-arabinosidase, but this name is rarely used. In this chapter this enzyme will therefore also be referred to as endoarabinanase.

Based on the sequence of the encoding genes, all these enzymes belong to family 43 of the glycoside hydrolases (17). This is a very heterogeneous family containing also (bacterial) arabinofuranosidases and β-xylosidases. The enzymes from this family work via an inverting mechanism (17). No three-dimensional structure has been reported for an endoarabinanase, but crystals have been obtained for the endoarabinanase produced by *Pseudomonas fluorescens* (29).

V. EXO-α-L-ARABINANASES

Exoarabinanases are enzymes acting on polymeric and oligomeric substrates and have no, or very low, activity against the synthetic substrate *p*-nitrophenyl-α-L-arabinofuranoside. So far, two exoarabinanases have been identified. An exoarabinanase from *Erwinia carotovora* produced arabinotriose from sugar beet arabinan (30). The enzyme was specific for α(1 → 5)-linked arabinofuranosyl residues but did not hydrolyze linear arabinan. Therefore, this enzyme most likely releases side chains of sugar beet arabinan.

A second exoarabinanase was characterized from *A. niger* (var. *aculeatus*) (31). This enzyme produced mainly arabinobiose from sugar beet arabinan, although a small amount of arabinotriose was also detected.

Exoarabinanases have not yet been assigned a number according to the Commission on Enzymes of the International Union of Biochemistry. However, they will surely be added to the group of O-glycosylases (EC 3.2.1.–). So far no genes encoding exoarabinanases have been described, and therefore the enzyme can also not be assigned to one of the glycosyl hydrolase families.

VI. ENDO- AND EXOGALACTANASES

A. Substrate Specificity and Mode of Action

Endogalactanases cleave within the galactan chains reacting with galacto-oligosaccharides, whereas exogalactanases attack the substrate from the terminal nonreducing end–releasing galactose or short galacto-oligosaccharides. While most of these enzymes work specifically by an endo- or exomechanism, some bacterial enzymes are able to work via both mechanisms (32, 33). Different types of endo- and exogalactanases have been identified with respect to their specificity for the various β-D-galactan linkages. These enzymes therefore have different specificities with respect to naturally occurring substrates. Type I arabinogalactans only contain (β(1 → 4)-galactan linkages and can therefore only be hydrolyzed by β(1 → 4)-endo- and exogalactanases. Type II arabinogalactans contain mainly β(1 → 3)- and β(1 → 6)-galactan linkages. The hydrolysis of pectins containing both types of arabinogalactans requires the joint action of all three types of galactanases.

In general, bacterial β(1 → 4)-galactanases release mainly galactotriose or galactotetrose (32–36) from galactan, while some also release galactobiose (32, 36, 37). Eukaryotic β(1 → 4)-galactanases release predominantly galactobiose and galactose from galactan (4, 38, 39). Fewer studies have been reported on galactanases working against type II arabinogalactan. They have been shown to release mainly galactose and galactobiose from the polymeric substrate (5, 12, 40).

B. Properties

Properties of some endo- and exogalactanases are given in Table 3. The molecular mass of the enzymes differs strongly among different organisms and depends on the linkage they are active on. The β(1 → 4)-endogalactanases from *Aspergilli* all have molecular masses ~ 40 kDa and an acidic pI. The enzymes are monomers and prefer unsubstituted galactan chains as a substrate (41). The *A. niger* β(1 → 6)-endogalactanase has a higher molecular mass (60 kDa), and its activity is inhibited by the presence of arabinose residues on the β(1 → 6)-, β(1 → 3)-galactan chain. Both types of endogalactanases release predominantly galactobiose, but also release some galactose, demonstrating a different action pattern

Table 3 Comparison of the Properties of Some Endo- and Exogalactanases

Organism	Active against	Action	MW (kDa)	pI	pH_{opt}	T_{opt}	K_m (mM)	Ref.
Aspergillus aculeatus	$\beta(1 \rightarrow 4)$	endo	44	2.85	4.0–4.5	45–65		41
Aspergillus niger	$\beta(1 \rightarrow 4)$	endo	43	4–6	4.0	50–55	0.77	52
Aspergillus sojae	$\beta(1 \rightarrow 4)$	endo	39.7	3.6	4.5	50	0.82	58
Aspergillus niger	$\beta(1 \rightarrow 4)$	exo	120	3.8	3.5	60		43
			90	4.1				
Bacillus subtilis	$\beta(1 \rightarrow 4)$	exo	36	7.9	6.5–7	60		37
Lupinus angustifolius L.	$\beta(1 \rightarrow 4)$	exo	60	7.0				74
Tomato	$\beta(1 \rightarrow 4)$	exo	75	9.8	4.5			75
Aspergillus niger	$\beta(1 \rightarrow 3)$	exo	62		5.0	40	1.3	76
Irpex lacteus	$\beta(1 \rightarrow 3)$	exo	42–51	8.2	4.6		2.13	12
Aspergillus niger	$\beta(1 \rightarrow 6)$	endo	60		3.5	60	4.5	5

compared to the *Aspergillus* endoarabinases. The $\beta(1 \rightarrow 3)$-exogalactanase from *A. niger* (11) and *Irpex lacteus* (12) differ significantly in their molecular mass (66 and 51 kDa, respectively). They are both inhibited in their activity by branching of the $\beta(1 \rightarrow 3)$-galactan chain.

For some galactanases transglycosylation activity has been observed. The $\beta(1 \rightarrow 4)$-endogalactanase from *Penicillium citrinum* produced several oligosaccharides using soybean arabinogalactan as donor, and mono- or disaccharide derivatives containing β-galactosyl residues as acceptors (42). The $\beta(1 \rightarrow 4)$-exogalactanase from *A. niger* synthesized oligosaccharides with a higher degree of polymerization when incubated with short galacto-oligosaccharides (43). A comparison was made of the transfer products of glycerol formed by *Bacillus subtilis* $\beta(1 \rightarrow 4)$-exogalactanase, *E. coli* β-galactosidase, and *P. citrinum* $\beta(1 \rightarrow 4)$-endogalactanase (44). The β-galactosidase transferred 90% of the galactose residues to the primary hydroxyl group of glycerol, whereas the $\beta(1 \rightarrow 4)$-endogalactanase transferred 80% of the galactose residues to the secondary hydroxyl group. The $\beta(1 \rightarrow 4)$-exogalactanase was less specific. Both products were formed, although the amount of transfer to the secondary hydroxyl group was approximately twice as high.

C. Classification and Mechanism

So far, only $\beta(1 \rightarrow 4)$- and $\beta(1 \rightarrow 3)$-endogalactanases have been included in the classification and nomenclature of the Commission on Enzymes of the International Union of Biochemistry. Like all other enzymes discussed in this chapter, they belong to the group of O-glycosylases and are numbered EC 3.2.1.89 and EC 3.2.1.90, respectively. The exogalactanases and the $\beta(1 \rightarrow 6)$-endogalactanases should also be included in this class (EC 3.2.1.–).

For only one type of galactanases, the $\beta(1 \rightarrow 4)$-endogalactanases, have genes been characterized. On the basis of the sequence the encoded enzymes are all assigned to family 53 of the glycosyl hydrolases (17). These enzymes have a retaining mechanism, and for the *Pseudomonas fluorescens* subsp. *cellulosa* $\beta(1 \rightarrow 4)$-endogalactanase the catalytic residues have been determined (45). For the $\beta(1 \rightarrow 4)$-endogalactanase for *A. aculeatus* crystals have been obtained (46), but a three-dimensional structure has not yet been reported.

VII. β-D-GALACTOSIDASES

Endogalactanases enhance the release of monomeric galactose by β-D-galactosidases, which remove single-terminal galactose residues. β-Galactosidases have been detected in prokaryotes and lower and higher eukaryotes and are active on a wide range of substrates as discussed in other chapters of this book. This chapter will therefore only briefly mention the function of β-galactosidases in pectin hydrolysis.

Plant β-galactosidases are believed to be involved in fruit ripening. β-Galactosidase was demonstrated to increase in parallel with an increase in tissue softness (47–49). This is most likely caused by removal of the galactose residues from pectin, thus altering the cell wall structure. The β-galactosidase from *A. niger* was shown to be highly active on the side chains of sugar beet pectin (15). It enhanced the activity of the *A. niger* $\beta(1 \rightarrow 4)$-endogalactanase, resulting in an efficient hydrolysis of the galactan chains.

β-D-Galactosidases (EC 3.2.1.23) are also members of the O-glycosylases in the classification and nomenclature of the Commission on Enzymes of the International Union of Biochemistry. All β-galactosidases for which the encoding gene has been cloned have so far been assigned to family 35 of the glycosyl hydrolases (17). They work via a retaining mechanism, and contain a highly conserved region (G-G-P[LIVM]$_2$-X_2-Q-X-E-N-E-[FY]). Based on the similarity with other glycosyl hydrolases, the second glutamic acid residue most likely acts as the proton donor in the catalytic mechanism (50).

VIII. COOPERATIVELY (SYNERGY) OF THE ENZYMES IN THE DEGRADATION OF POLYMERIC SUBSTRATES

Positive interaction among enzymes, most commonly referred to as synergy, is a general phenomenon in polysaccharide biodegradation. Synergy is important for the efficient action of both arabinofuranosidases and endoarabinanases. These two classes of enzymes positively affect each other in the hydrolysis of arabinan. Additionally, the presence of β-galactosidase and endogalactanase also enhances the activity of arabinanases on sugar beet pectin (15) and arabinogalactan protein (51).

Synergy has also been reported for $\beta(1 \rightarrow 4)$-endogalactanase and β-galactosidase from *A. niger*, and for $\beta(1 \rightarrow 4)$-endogalactanase and endoarabinanase from *A. niger* (52). The first effect is mostly likely due to the removal of single-unit galactose side chains from the galactan backbone, whereas the second effect indicates that linear arabinan chains limit the activity of $\beta(1 \rightarrow 4)$-endogalactanase on galactan. A recent study (15) reported the synergy of endoarabinanase, arabinofuranosidase B, β-galactosidase, $\beta(1 \rightarrow 4)$-endogalactanase, and feruloyl esterase A from *A. niger* in the hydrolysis of the side chains of sugar beet pectin. Synergy was observed between most enzymes, although not always to the same extent. Endoarabinanase and arabinofuranosidase B positively influenced each other (Fig. 1), as did β-galactosidase and $\beta(1 \rightarrow 4)$-endogalactanase (Fig. 2). Additionally, endoarabinanase and arabinofuranosidase B strongly influenced the release of galactose by β-galactasidase and $\beta(1 \rightarrow 4)$-endogalactanase, whereas the latter two enzymes did not significantly influence arabinose release. Feruloyl esterase A, an enzyme capable of removing ferulic acid residues from the side chains of pectin positively affected the activity of all four enzymes.

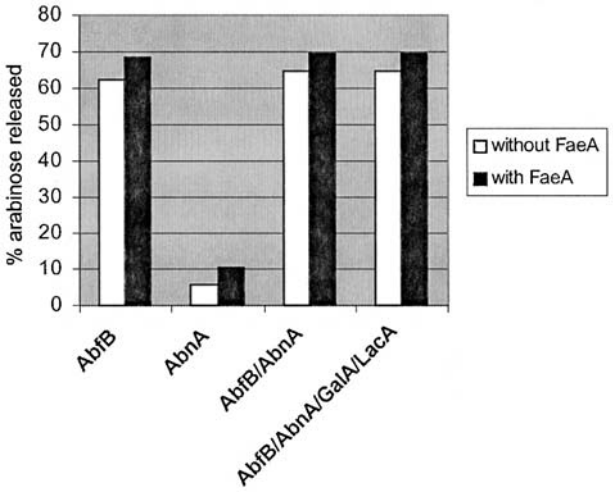

Figure 1 Synergy between *A. niger* enzymes in the release of arabinose from sugar beet pectin. AbfB, arabinofuranosidase B; AbnA, endoarabinanase; GalA, $\beta(1 \rightarrow 4)$-endogalactanase; LacA, β-galactosidase; FaeA, feruloyl esterase A. (From Ref. 15.)

Less specific interactions have also been reported. The addition of BSA (100 μg/mL) had a stimulating effect on the hydrolysis of *p*-nitrophenyl-α-L-arabinofuranosidoside by arabinofuranosidase (51), most likely by stabilizing the enzyme in the reaction mixture.

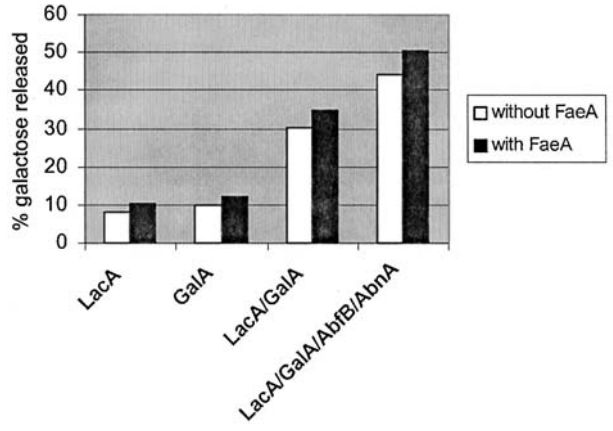

Figure 2 Synergy between *A. niger* enzymes in the release of galactose from sugar beet pectin. AbfB, arabinofuranosidase B; AbnA, endoarabinanase; GalA, $\beta(1 \rightarrow 4)$-endogalactanase; LacA, β-galactosidase; FaeA, feruloyl esterase A. (From Ref. 15.)

IX. PRODUCTION OF ARABINANASES AND GALACTANASES

Arabinanases and galactanases used in food processing are mainly of microbial origin. They are in general extracellular enzymes, and are needed for the degradation of polymeric compounds to produce monomeric sugars and small oligosaccharides, which can be imported into the cell to serve as a carbon source for the organism. Some papers report intracellular arabinofuranosidases (e.g., 53), but the method used to purify these enzymes is probably not able to distinguish between intracellular enzymes and extracellular cell wall bound enzymes.

Microorganisms produce arabinanases and galactanases when grown on complex substrates, such as sugar beet pulp, wheat bran, alfalfa, (arabino)xylan, arabinan, and gum (41, 53–59). Additionally, production of the arabinanases has been observed on L-arabinose, L-arabitol, and D-xylose (60, 61). These compounds are most likely the inducing compounds, driving the expression of the arabinanase encoding genes. In *Aspergillus* the role of L-arabitol as inducer has been confirmed using an L-arabitol-accumulating mutant (62) and by Northern blot analysis of the genes encoding the arabinanases (63). β-Galactosidase gene expression in *A. niger* was observed on arabinose, xylose, xylan, and pectin and to a less extent on galactose and galactose containing oligo- and polysaccharides other than xylan and pectin (64). The expression on xylan and xylose could be contributed to the general xylanolytic transcriptional activator protein XlnR (64, 65), indicating that β-galactosidase is produced as one of the many enzymes of the xylanolytic spectrum from *Aspergillus niger*. However, expression of the β-galactosidase encoding gene on non-xylan-related compounds (galactose, pectin) indicates that it is also under the control of other regulatory systems.

X. APPLICATION

Arabinases and galactanases are generally present in industrial enzyme preparations applied in the fruit industry. Fruit juices prepared with enzyme preparations which are short in arabinan-degrading enzymes are liable to cloud formation due to precipitation of polymeric linearized arabinan molecules. Enrichment of the preparations with arabinan-degrading enzymes will solve this problem. Depolymerization of arabinan and galactan type I and II in fruit juices with enzymes facilitates ultrafiltration processes by preventing membrane fouling. Adequate formulations of enzyme mixtures are required (77).

REFERENCES

1. G Beldman, HA Schols, SM Pitson, MJF Searle–Van Leeuwen, AGJ Voragen. Arabinans and arabinan degrading enzymes. Adv Macromol Carbohydr Res 1:1–64, 1997.
2. RP de Vries, J Visser. Enzymes from *Aspergillus* involved in the degradation of plant cell wall polysaccharides. Microbiol Mol Biol Rev. 65:497–522, 2001.
3. FM Rombouts, AGJ Voragen, MF Searle–Van Leeuwen, CCJM Geraeds, HA Schols, W Pilnik. The arabinases of *Aspergillus niger*: purification and characterization of two α-L-arabinofuranosidases and an endo-1,5-α-L-arabinase. Carbohydr Polymers 9:25–47, 1988.
4. M Lahaye, J Vigouroux, J-F Thibault. Endo-β-1,4-D-galactanase from *Aspergillus niger* var. *aculeatus*: purification and some properties. Carbohydr Polymers 15:431–444, 1991.
5. J-M Brillouet, P Williams, M Moutounet. Purification and some properties of a novel endo-β-(1-6)-D-galactanase from *Aspergillus niger*. Agric Biol Chem 55:1565–1571, 1991.
6. R Waibel, R Amado, H Neukom. Purification of an α-L-arabinofuranosidase from *Aspergillus niger* by substrate affinity chromatography. J Chromotogr 197:86–91, 1980.
7. AGJ Voragen, FM Rombouts, MF Searle–Van Leeuwen, HA Schols, W Pilnik. The degradation of arabinans by endo-arabinanase and arabinofuranosidases purified from *Aspergillus niger*. Food Hydrocolloids 1:423–437, 1987.
8. L Bezalel, Y Shoham, R Rosenberg. Characterization and delignification activity of a thermostable α-L-arabinofuranosidase from *Bacillus stearothermophilus*. Appl Microbiol Biotechnol 40:57–62, 1993.
9. Z Gunata, J-M Brillouet, S Voirin, R Baumes, R Cordonnier. Purification and some properties of an α-L-arabinofuranosidase from *Aspergillus niger*. Action on grape monoterpenyl arabinofuranosylglucosides. J Agric Food Chem 38:772–776, 1990.
10. PR Finch, R Yuen, H Schachter, MA Moscarello. Enzymic methods for the micro assay of D-mannose, D-glucose, D-galactose, and L-fucose from acid hydrolyzates of glycoproteins. Anal Biochem 31:296–305, 1969.
11. P Pellerin, J-M Brillouet. Purification and properties of anexo-(1 $\rightarrow$ 3)-β-D-galactanase from *Aspergillus niger*. Carbohydr Res 264:281–291, 1994.
12. Y Tsumuraya, N Mochizuki, Y Hashimoto, P Kovac. Purification of an exo-β-(1 $\rightarrow$ 3)-D-galactanase of *Irpex lacteus* (*Polyporus tulipiferas*) and its action on

arabinogalactan-proteins. J Biol Chem 265:7207–7215, 1990.
13. BV McCleary. Novel and selective substrates for the assay of endo-arabinanase. In: GO Phillips, DJ Wedlock, PA Williams, eds. Gums and Stabilisers for the Food Industry, Vol 5. IRL Press, pp 291–298, 1989.
14. K Tagawa, A Kaji. Preparation of L-arabinose-containing polysaccharides and the action of an α-L-arabinofuranosidase on these polysaccharides. Carbohydr Res 11:293–301, 1969.
15. RP de Vries, HCM Kester, CH Poulsen, JAE Benen, J Visser. Synergy between accessory enzymes from *Aspergillus* in the degradation of plant cell wall polysaccharides. Carbohydr Res 327:401–410, 2000.
16. K Komae, A Kaji, M Sato. An α-L-arabinofuranosidase from *Streptomyces prupurascens* IFO 3389. Agric Biol Chem 46:1899–1905, 1982.
17. B Henrissat, A Bairoch. New families in the classification of glycosidases based on amino acid sequence similarities. Biochem J 293:781–788, 1993.
18. LN Huang, TH Hseu, YJ Lee. Database submission, Acc. Nr. U38661, 1995.
19. EA Utt, CK Eddy, KF Keshav, LO Ingram. Sequencing and expression of the *Butyrivibrio fibrisolvens xylB* gene encoding a novel bifunctional protein with β-D-xylosidase and α-L-arabinofuranosidase activities. Appl Environ Microbiol 57:1227–1234, 1991.
20. K Sakka, K Yoshikawa, Y Kojima, S Karita, Kohmiya, K Shimada. Nucleotide sequence of the *Clostridiumstercorarium xylA* gene encoding a bifunctional protein with β-D-xylosidase and α-L-arabinofuranosidase activities, and properties of the translated product. Biosci Biotechnol Biochem 57:268–272, 1993.
21. TR Whitehead. Nucleotide sequences of xylan-inducable xylanase and xylosidase/arabinosidase genes from *Bacteroides ovatis* V975. Biochim Biophys Acta Gene Struct Expr 1244:239–241, 1995.
22. LE Kellett, DM Poole, LMA Ferreira, AJ Durrant, GP Hazlewood, HJ Gilbert. Xylanase B and an arabinofuranosidase from *Pseudomonas fluorescens* subsp. *cellulosa* contains identical cellulose-binding domains and are encoded by adjacent genes. Biochem J 272:369–276, 1990.
23. P Vincent, F Shareck, C Dupont, R Morosoli, D Kluepfel. New α-L-arabinofuranosidase produced by *Streptomyces lividans*: cloning and DNA sequence of the abfB gene and characterization of the enzyme. Biochem J 322:845–852, 1997.
24. EXF Filho, J Puls, MP Coughlan. Purification and characterization of two arabinofuranosidases from solid-state cultures of the fungus *Penicillium capsulatum*. Appl Environ Microbiol 62:168–173, 1996.
25. MTH Azamawaty, GWJ Fleet, KA Hannah, SK Namgoong, ML Sinnott. Inhibition of the α-L-arabinofuranosidase III of *Monilinia fructigena* by 1,4-dideoxy-1,4-imino-L-threitol and 1,4-dideoxy-1,4-imino-L-arabinitol. Biochem J 266:245–249, 1990.
26. A. Kaji, T Saheki. Endo-arabinanase from *Bacillus subtilus* F-11. Biochim Bophys Acta 410:354–360, 1975.
27. T Sakai, T Sakamoto. Purification and some properties of a protopectin-solubilizing enzyme that has potent activity on sugar beet protopectin. Agric Biol Chem 54:879–889.
28. SM Pitson, AGJ Voragen, J-P Vincken, G Beldman. Action patterns and mapping of the substrate-binding regions of endo-(1 → 5)-α-L-arabinases from *Aspergillus niger* and *Aspergillus aculeatus*. Carbohydr Res 303:207–218, 1997.
29. M Scott, RW Pickersgill, GP Hazlewood, HJ Gilbert, GW Harris. Crystallization and preliminary x-ray analysis of arabinanase A from *Pseudomonas fluorescens* subspecies *cellulosa*. Acta Cryst 55:544–546, 1999.
30. A Kaji, K Shimokawa. New exo-type arabinase from *Erwinia carotovora* IAM 1024. Agric Biol Chem 48:67–72, 1984.
31. M Lahaye, J-F Thibault. Poster presented at Third International Workshop on Plant Polysaccharides, Structure and Function, 19–21 September 1990, Le Croisic, France.
32. S Emi, J Fukumoto, T Yamamoto. Studies of hemicellulolytic enzymes of *Bacillus subtilis*. Part I. Purification, crystallization and some properties of arabinogalactanase. Agric Biol Chem 35:1891–1898, 1971.
33. JM Labavitch, LE Freeman, P Albersheim. Purification and characterization of a β-1,4-galactanase which degrades a structural component of the primary cell walls of dicots. J Biol Chem 251:5904–5910, 1976.
34. S Emi, T Yamamoto. Purification and properties of several galactanases of *Bacillus subtilis* var. *amylosaccharitiicus*. Agric Biol Chem 36:1945–1954, 1972.
35. T Yamamoto, S Emi. Arabinogalactanase of *Bacillus subtilis* var. *amylosaccharitiicus*. Methods Enzymol 160:719–728, 1988.
36. K Tsumura, Y Hashimoto, T Akiba, K Hirokoshi. Purifications and properties of galactanases from alkalophilic *Bacillus* sp. S-2 and S-39. Agric Biol Chem 55:1265–1271, 1991.
37. H Nakano, S Takenishi, S Kitahata, H Kinugasa, Y Watanabe. Purification and characterization of an exo-1,4-β-galactanase from a strain of *Bacillus subtilis*. Eur J Biochem 193:61–67, 1990.
38. H Nakano, S Takenishi, H Kinugasa, Y Watanabe. Purification and properties of two galactanases from *Penicillium citrinum*. Agric Biol Chem 49:3445–3454, 1985.

39. H Konno, Y Yamasaki, K Katoh. Characteristics of β-galactosidase purified from cell suspension cultures of carrot. Physiol Plant 68:46–52, 1986.
40. M Sekimata, K Ogura, Y Tsumuraya, Y Hashimoto, S Yamamoto. A β-galactosidase from radish (*Raphanus sativus* L.) seeds. Plant Physiol 90:567–574, 1989.
41. S Christgau, T Sandal, LV Kofod, H Dalboge. Expression cloning, purification and characterization of a β-1,4-galactanase from *Aspergillus aculeatus*. Curr Genet 27:135–141, 1995.
42. H Fujimoto, H Nakano, M Isomura, S Kitahata, K Ajisaka. Enzymatic synthesis of oligosaccharides containing Gal beta $\rightarrow$ 4Gal disaccharide at the non-reducing end using beta-galactanase from *Penicillium citrinum*. Biosci Biotechnol Biochem 61:1258–1261, 1997.
43. E Bonnin, M Lahaye, J Vigouroux, J-F Thibault. Preliminary characterization of a new exo-β-(1,4)-galactanase with transferase activity. Int J Biol Macromol 17:345–351, 1995.
44. H Nakano, S Kitahata, H Kinugasa, Y Watanabe, H Fujimoto, K Ajisaka, S Takenishi. Transfer reaction catalyzed by exo-β-1,4-galactanase from *Bacillus subtilis*. Agric Biol Chem 55:2075–2082, 1991.
45. KL Braithwaite, T Barna, TD Spurway, SJ Charnock, GW Black, N Hughes, JH Lakey, R Virden, GP Hazlewood, B Henrissat, HJ Gilbert. Evidence that galactanase A from *Pseudomonas fluorescens* subspecies *cellulosa* is a retaining family 53 glycosyl hydrolase in which E161 and E270 are the catalytic residues. Biochemistry 36:15489–15500, 1997.
46. C Ryttersgaard, J Poulsen, S Christgau, T Sandal, H Dalboge, S Larsen. Crystallization and preliminary x-ray studies of beta-1,4-galactanase from *Aspergillus aculeatus*. Acta Crystallogr D Biol Crystallogr 55:929–930, 1999.
47. ZM Ali, S Armugam, H Lazan. Regulation of cellulase biosynthesis in *Aspergillus terreus*. Phytochemistry 38:1109–1114, 1995.
48. AE Ahmed, JM Labavitch. Cell wall metabolism in ripening fruit. II. Changes in carbohydrate-degrading enzymes in ripening "bartlett" pears. Plant Physiol 65:1014–1016, 1980.
49. DM Phar, HN Sox, WB Nesbitt. Cell wall-bound nitrophenylglycosidases of tomato fruits. J Am Soc Hortic Sci 101:397–400, 1976.
50. B Henrissat, I Callebaut, S Fabrega, P Lehn, J-P Mornon, G Davies. Conserved catalytic machinery and the prediction of a common fold for several families of glycosyl hydrolases. Proc Natl Acad Sci USA 92:7090–7094, 1995.
51. Y Hirano, Y Tsumuraya, Y Hashimoto. Characterization of spinach leaf alpha-L-arabinofuranosidases and beta-galactosidases and their synergistic action on an endogenous arabinogalactan-protein. Physiol Plant 92:286–296, 1994.
52. JW van de Vis, MF Searle–Van Leeuwen, HA Silha, FJM Kormelink, AGJ Voragen. Purification and characterization of endo-1,4-β-D-galactanases from *Aspergillus niger* and *Aspergillus aculeatus*: use in combination with arabinases from *Aspergillus niger* in enzymic conversion of potato arabinogalactan. Carbohydr Polymers 16:167–187, 1991.
53. S Kaneko, T Shimasaki, I Kusakabe. Purification and some properties of intracellular α-L-arabinofuranosidase from *Aspergillus niger* 5-16. Biosci Biotechnol Biochem 57:1161–1165, 1993.
54. P van der Veen, MJA Flipphi, AGJ Voragen, J Visser. Induction, purification and characterisation of arabinases produced by *Aspergillus niger*. Arch Microbiol 157:23–28, 1991.
55. MJA Flipphi, M van Heuvel, P van der Veen, J Visser, LH de Graaff. Cloning and characterisation of the *abfB* gene coding for the major α-L-arabinofuranosidase (AbfB) of *Aspergillus niger*. Curr Genet 24:525–532, 1993.
56. P Manzanares, LH de Graaff, J Visser. Characterization of galactosidases from *Aspergillus niger*: purification of a novel α-galactosidase activity. Enzyme Microb Technol 2:383–390, 1998.
57. RR Gonzalez, P Monsan. Purification and some characteristics of β-galactosidase from *Aspergillus fonsecaeus*. Enzyme Microb Technol 13:349–352, 1991.
58. I Kimura, N Yoshioka, S Tajima. Purification and characterization of an endo-1,4-β-D-galactanase from *Aspergillus sojae*. J Ferment Bioeng 85:48–52, 1998.
59. A. Araujo, OP Ward. Extracellular mannanases and galactanases from selected fungi. J Ind Microbiol 6:171–178, 1990.
60. P van der Veen, MJA Flipphi, AGJ Voragen, J Visser. Induction of extracellular arabinases on monomeric substrates in *Aspergillus niger*. Arch Microbiol 159:66–71.
61. D Ramon, P van der Veen, J Visser. Arabinan degrading enzymes from *Aspergillus nidulans*: induction and purification. FEMS Microbiol Lett 113:15–22, 1993.
62. RP de Vries, MJA Flipphi, CFB Witteveen, J Visser. Characterisation of an *Aspergillus nidulans* L-arabitol dehydrogenase mutant. FEMS Microbiol Lett 123:83–90, 1994.
63. MJA Flipphi, J Visser, P van der Veen, LH de Graaff. Arabinase gene expression in *Aspergillus niger*: indications for co-ordinated gene expression. Microbiology 140:2673–2682, 1994.
64. RP de Vries, HC van den Broeck, E Dekkers, P Manzanares, LH de Graaff, J Visser. Differential expression of three α-galactosidase genes and a single β-galactosidase gene from *Apergillus niger*. Appl Environ Microbiol 65:2453–2460, 1999.

65. NNME van Peij, J Visser, LH de Graaff. Isolation and analysis of *xlnR*, encoding a transcriptional activator coordinating xylanolytic expression in *Aspergillus niger*. Mol Microbiol 27:131–142, 1998.
66. S Kaneko, M Sano, I Kusakabe. Purification and some properties of α-L-arabinofuranosidase from *Bacillus subtilis* 3-6. Appl Environ Microbiol 60:3425–3428, 1994.
67. L Weinstein, P Albersheim. Structure of plant cell walls. IX. Purification and partial characterization of a wall-degrading endo-arabanase and an arabinosidase from *Bacillus subtilis*. Plant Physiol 63:425–432, 1979.
68. A Kaji, M Sato, O Yoshihara, A Adachi. α-L-Arabinofuranosidase from *Streptomyces massasporeus* IFO 3841. Tech Bull Fac Agric Kagawa Univ 34:79–85, 1982.
69. SL Bachman, AJ McCartney. Purification and cooperative activity of enzymes constituting the xylan-degrading system of *Thermonospora fusca*. Appl Environ Microbiol 57:2121–2130, 1991.
70. P van de Veen, MJA Flipphi, AGJ Voragen, J Visser. Induction, purification and characterisation of arabinases produced by *Aspergillus niger*. Arch Microbiol 157:23–28, 1991.
71. BC Saha, RJ Bothast. Effect of carbon source on production of α-L-arabinofuranosidase by *Aureobasidium pullulans*. Curr Microbiol 37:337–340, 1998.
72. K Poutanen. An α-L-arabinofuranosidase of *Trichodema reesei*. J Biotechnol 7:271–281, 1988.
73. H Konno, Y Yamasaki, K Katoh. Purification of an α-L-arabinofuranosidase from carrot cell cultures and its involvement in arabinose-rich polymer degradation. Physiol Plant 69:405–412, 1987.
74. MS Buckeridge, JS Reid. Purification and properties of a novel β-galactosidase or exo-(1-> 4)-β-D-galactanase from the cotyledons of germinated *Lupinus angustifolius* L seeds. Planta 192:502–511, 1994.
75. AT Carey, K Holt, S Pickard, R Wilde, GA Tucker, CR Bird, W Schuch, GB Seymour. Tomato exo-(1-> 4)-β-D-galactanase—isolation, changes during ripening in normal and mutant tomato fruit, and characterization of a related cDNA clone. Plant Physiol 108:1099–1107, 1995.
76. JW van de Vis. Characterization and mode of action of enzymes degrading galactan structures of arabinogalactan. PhD thesis, Wageningen Agricultural University, Wageningen, Netherlands, 1994.
77. AGJ Voragen, HA Schols, G Beldman. Tailor made enzymes in fruit juice processing. Flüss Obst. 59:90–102, 1992.

71

Xylanolytic Enzymes

Peter Biely
Slovak Academy of Sciences, Bratislava, Slovakia

I. INTRODUCTION

A. Xylan—the Second Most Abundant Plant Cell Wall Component and Natural Polymer

Plant cell walls can be considered to be the main renewable resource formed in the process of photosynthetic fixation of carbon dioxide. They are composed of three major polymeric constituents: cellulose, an insoluble skeletal polysaccharide composed of β-D-glucopyranosyl residues linked β-1,4-glycosidically; hemicellulose, a series of matrix and crosslinking heteropolysaccharides that include a variety of glucans, mannans, arabinans, galactans, and xylans; and lignin, a complex polyphenol. As a part of the carbon cycle, all three constituents are degraded by specialized enzyme systems produced by microorganisms. This chapter is devoted to the enzymes that degrade the major plant hemicellulose, xylan. After cellulose, xylan is the most abundant polysaccharide in nature. Xylanolytic enzymes have been extensively reviewed in the past (1–5). Books covering xylan and xylanases exclusively have also been published (6, 7).

B. Occurrence of Xylanolytic Enzymes

Many bacteria, fungi, yeasts, and protozoa are able to degrade xylan (1, 8). Some of these are saprophytic soil or aqueous microorganisms, some grow aerobically, some grow at room temperature, and others show thermophilicity. Some occur in the digestive track of ruminant animals and in the intestines of wood-eating insects (8). Most, if not all, fungal plant pathogens produce and secrete enzymes that degrade cell wall hemicellulose (9). Xylanolytic enzymes also occur in plants. The enzymes participate in the process of cell wall extension, cell division, seed germination, and other morphological and physiological events in plants. During germination endogeneous enzymes catalyze hydrolysis of these polysaccharides to remove the physical barrier imposed by the walls on the free diffusion of starch and storage protein-degrading enzymes through the germinated grains (10–12). Enzymes degrading hemicellulose polysaccharides were also reported to be present in wheat grain (13) and wheat flour (14).

C. Application of Xylanolytic Enzymes

The past two decades have seen a growing interest in microbial enzyme systems that degrade plant xylan, a polymer of the five-carbon sugar D-xylose. Xylose can be converted to a variety of useful products, including ethanol, the engine fuel of the future (15, 16). Enzymic saccharification of agricultural, industrial, and municipal wastes may provide sugar syrups for human and animal consumption, and carbon sources for industrial fermentations. Xylo-oligosaccharides have a variety of uses as food additives (17). Plant structural polysaccharides provide the major source of nutrients for ruminal livestock and also play an important role in animal fodder. Pretreatment of forage crops with polysaccharide-degrading enzymes improves the nutritional qual-

ity and digestibility of ruminant fodder and facilitates composting (18, 19). Enzymic hydrolysis of highly viscous arabinoxylans originating in cereal endosperms improves nutrient uptake and digestion in broiler chickens (20–23). Other applications of xylanolytic enzymes include improvement of the baking process and modification of baked products (24–30). Xylanases are also important components of enzyme systems used for liquefaction of vegetables and fruit, and for clarification of juices (3, 18). In all of the above-listed processes, microbial xylanolytic systems can be applied together with other enzymes hydrolyzing plant polysaccharides such as amylases, cellulases, and pectinases. There are, however, applications in which xylanases should not be contaminated by cellulases to preserve the polymerization degree of cellulose.

Xylanases free of cellulases have applications with important ecological implications in pulp and paper industry. They facilitate lignin extraction, reducing the consumption of toxic chemicals required for pulp bleaching (31–34). The mechanism of this process, called enzymic prebleaching or bleachbusting, is not completely understood. However, it is believed that xylanase attacks the xylan moiety of lignin-carbohydrate complexes (31). Xylanases also have potential in the purification of dissolving pulp from hemicellulose (35, 36), in the recovery of cellulose textile fibers (37), and in paper recycling (38).

D. Chemical Structure of Xylan

Xylan is structurally similar to cellulose, but instead of D-glucose, its main chain is built from β-1,4-linked xylopyranosyl residues. In contrast to cellulose, however, the xylan structure is extremely variable and depends on its source. The structure ranges from an almost linear unsubstituted chain, e.g., in some grasses, to highly branched heteropolysaccharides in cereal seeds. The prefix *hetero* indicates the presence of sugars other than D-xylose. The main chain is usually substituted to various degrees by residues of 4-O-methyl-D-glucuronic acid, D-glucuronic acid, or L-arabinofuranose, and in some cases is also esterified by acetyl groups. The substituents may be also represented by oligosaccharides and esterified by cinnamic (phenolic) acids. The principal types of xylan found in plants are well known and have been extensively reviewed (39–41). They differ in the character of their side chains as indicated in Table 1.

A hypothetical fragment of a plant xylan which shows the major structural features found in this group of hemicelluloses is depicted in Figure 1. Xylan's backbone is built of β-1,4-linked D-xylopyranosyl residues. In hardwood xylans the side chains are α-1,2-linked 4-O-methyl-D-glucuronic acid residues and acetyl groups partially esterifying the two available hydroxyl groups of xylosyl residues. Owing to

Table 1 Examples of Major Types of Plant Xylans

Structural type	Source	Nature of side chains	Approximate ratio Xyl:side chain subst.
Linear β-1,4-D-xylan	Esparto grass Tobacco stalk	Substituents are rare	
O-Acetyl-4-O-methyl-D-glucuronoxylan	Hardwoods	Acetyl, 2-O-α-MeGlcA	Xyl:Ac:MeGlcA 10:7:1
O-Acetyl-4-O-methyl-D-glucuronoxylan	Gramineae Legumes	Acetyl, 2-O-α-MeGlcA Acetyl, 2-O-α-GlcA	Not specified
L-Arabino-4-O-methyl-D-glucuronoxylan	Softwoods	3-O-α-L-Ara*f*, 2-O-α-MeGlcA	Xyl:Ara:MeGlcA 10:1:3:2
O-Acetyl-L-arabinoxylan	Gramineae (monocots primary walls, flours)	2-O-α-L-Arf*a*, 3-O-α-L-Ara*f* Substitution of Xyl in the main chain: single and double	Xyl:Ara varies from 0.9 to 2.2 depending on source. Double substitution of Xyl with Ara is more frequent than single substitution.
	Pericarp	L-Arabinan oligomers	Not specified

Source: Refs. 42–44.

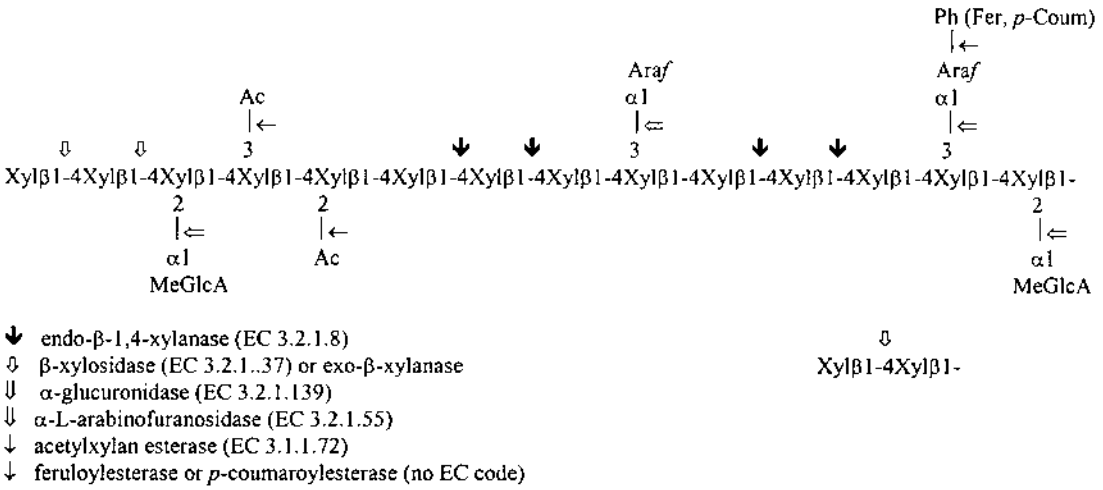

Figure 1 Hypothetical plant xylan and the enzymes required for its complete hydrolysis.

the ease of migration of acetyl groups among the hydroxyl groups, it is difficult to determine their actual distribution between positions 2 and 3. Softwood xylans are similar to hardwood xylans, but contain α-1,3-linked L-arabinofuranosyl residues instead of acetyl groups. Xylans from grasses contain a smaller proportion of uronic acids, but are more highly branched with L-arabinofuranosyl residues. As indicated in Table 1, the arabinofuranosyl residues also can be linked to the main chain by α-1,2-linkages, often to D-xylopyranosyl residues already substituted by α-1,3-linked L-arabinofuranosyl residues. In cereals, the ratio of Xyl : Ara is low, ranging from 1 to 2.2 (44). Xylans from graminaceous plants also contain 2–5% by weight of acetyl groups and 1–2% of phenolic (cinnamic) acids esterifying the C-5 position of arabinose side chains (45). In sugar beet pectins, ferulic acid esterifies the OH-2 of L-arabinofuranose or the OH-6 of D-galactose (46). Ferulic acid [3(3-methoxy-4-hydroxy phenyl)-2-propanoic] is the major cinnamic acid found in cereals and in the Gramineae (47). In wheat bran, one of 150 of xylose residues is substituted with L-arabinose esterified with ferulic acid (45).

Ferulic acid is synthesized in plants via the shikimic pathway and is an intermediate in lignin biosynthesis (48). In some plants it has been shown to be involved in the chemical linkages between xylan and lignin, contributing to integrity of the plant cell walls. Intermolecular crosslinking may result from the dimerization of feruoyl and p-coumaroyl residues or from the formation of ester linkages between polysaccharides and lignin (49, 50).

E. Xylanolytic System and Its Components

Depending on its complexity, the complete breakdown of xylan requires the action of several enzyme components which can be considered as a xylanolytic system (3). As depicted in Figure 1, the more complex the xylan structure, the more components of the xylanolytic system are required. The crucial enzyme for xylan depolymerization is endo-β-1,4-xylanase (β-1,4-xylan xylanohydrolase; EC 3.2.1.8, abbreviated EX). EX attacks the main chain most easily and therefore most rapidly at non-substituted regions, generating nonsubstituted and branched or esterified oligosaccharides. The main chain substituents are liberated by corresponding glycosidases or esterases: α-L-arabinosyl residues by α-L-arabinofuranosidases (α-L-arabinofuranoside arabinofuranosidase; EC 3.2.1.55), D-glucuronosyl and 4-O-methylglucuronosyl residues by α-glucuronidase (EC 3.2.1.139), acetic acid, and ferulic acid and p-coumaric acid residues by corresponding esterases (EC numbers not assigned). β-Xylosidase (xylobiase or exo-β-1,4-xylanase) (β-1,4-xylan xylohydrolase; EC 3.2.1.37) attacks xylo-oligosaccharides from the nonreducing end, liberating D-xylose.

The hydrolases removing xylan side chains have been referred to as "accessory" or "auxiliary" xylanolytic enzymes. Two categories of accessory enzymes can be recognized: those that operate on both polymeric and oligomeric substrates, and those that are active only on branched or substituted oligosaccharides generated by EXs. There is usually no sharp boundary between these groups. The enzymes operat-

ing on polymeric substrates can be distinguished from those of the second group by their ability to catalyze precipitation of the originally highly soluble branched polymeric xylan. This precipitation is due to removal of substituents that hinder the association of the xylan main chains by hydrogen bonding (analogous to that found in cellulose). This precipitation can be used for specific procedures to detect debranching enzymes in the absence of depolymerizing endoxylanases. Accessory enzymes further differ in their requirements for the fine structure of the xylan main chain and the position of the group to be removed.

F. Synergism of Xylanolytic Enzymes

The synergistic action of two or more enzymes during hydrolysis of xylan is evident when the rate of hydrolysis of the polysaccharide with two or more enzymes is faster than the sum of the rates of hydrolysis by individual enzymes. Several types of synergism have been recognized among the xylanolytic enzymes (51–53). The most important type concerns the cooperativity between the enzymes attacking the main chain (EXs) and enzymes that liberate side chain substituents, such as acetyl (54) and arabinofuranosyl residues (51). The action of EX releases substituted xylo-oligosaccharides, which are more readily diffusible and more favorable substrates for accessory enzymes. On the other hand, the removal of side chain substituents by accessory enzymes creates new sites on the main chain for productive binding with EX. From some accessory enzymes the cleavage of the main chain is indispensable. Individual components of xylanolytic systems are discussed below.

G. Analysis of Xylan Hydrolysates

It is always important to confirm that the apparent xylanolytic activity of any preparation is really connected with xylan depolymerization and not with degradation of some other polysaccharides present as impurities. This aspect is especially important for plant enzyme preparations which contain high levels of amylolytic enzymes. Almost all commercial xylan preparations contain a small amount of starch, which must be removed by α-amylase treatment before testing for the presence of xylanases.

The traditional method of analyzing enzymic hydrolysates of xylan is by paper and thin-layer chromatography. A suitable solvent system for separation of D-xylose and β-1,4-xylooligosaccharides (linear or substituted) on Whatman No. 1 or 3 MM paper is ethyl acetate–acetic acid–water (18:7:8, always v/v). A similar efficiency of separation can be achieved on thin layers of microcrystalline cellulose (Merck, Darmstadt, Germany) in ethyl acetate–acetic acid–water (3:2:2) or ethyl acetate–acetic acid–formic acid–water (18:3:1:5). These systems separate well neutral oligosaccharides, aldouronic acids, and partially acetylated xylo-oligosaccharides. Acetylated xylo-oligosaccharides show higher mobility than the corresponding deacetylated products. These systems may also be used to follow the liberation of 4-O-methyl-D-glucuronic acid, which migrates in all the above solvent systems ahead of D-xylose. The use of aniline-hydrogenphthalate reagent provides a color differentiation of the acid from xylose and xylo-oligosaccharides (orange-brown versus dark-brown colors). The reagent, which can be poured onto dry chromatograms, is prepared by dissolving 1 g of phthalic acid in 50 mL acetone followed by addition of 0.9 mL aniline. Visualization of reducing sugars is obtained on heating at 110°C for a few min.

Good separation of neutral products of xylan hydrolysis is obtained by thin-layer chromatography on silica gel (Merck) in such solvent systems as 1-butanol–ethanol–water (10:8:7), 1-propanol–ethyl acetate–ethanol–pyridine–water (7:3:3:2:1) or nitromethane–acetonitrile–ethanol–water (1:4:3:2), the last being the fastest system. Reducing sugars can be visualized with an aniline/diphenylamine reagent, consisting of a solution of aniline (2 mL) and diphenylamine (2 g) in acetone (100 mL) containing 15 mL of 85% H_3PO_4. Visualization of all sugars, both reducing and nonreducing, is done with 1% orcinol solution in ethanol/conc. H_2SO_4 (9:1). Both reagents can be poured onto well-dried chromatograms, which is more convenient than spraying. The solvent system 1-butanol–ethanol–water (10:5:1) is suitable to follow the reaction of xylanases with 4-nitrophenyl β-xylopyranoside. 4-Nitrophenol and 4-nitrophenyl glycosides also can be detected directly under UV light (360 nm).

Other, more up-to-date methods of monitoring the enzymic hydrolysis of xylan include a variety of liquid chromatographies, such as gel permeation chromatography, ion exchange chromatography, adsorption chromatography, reversed-phase chromatography, and partition chromatography, usually in HPLC setups. All of these methods require the proper choice of sorbents and eluent, and sophisticated equipment. Paper and thin-layer chromatography are the most simple and least expensive separation techniques for the simultaneous analysis of a large number of samples.

II. ENDO-β-1,4-XYLANASE (EC 3.2.1.8)

A. Chemical Reaction Catalyzed

$$R_1\text{-Xyl}\beta 1\text{-4Xyl}\beta 1\text{-4Xy1}\beta 1\text{-4Xyl-}R_2^* \xrightarrow{H_2O} R_1\text{-Xyl}\beta 1\text{-4Xyl}^* + \text{Xyl}\beta\text{-4Xyl-}R_2^*$$

R_1 and R_2, substituted or unsubstituted portions of the main chain of xylan; * reducing end.

B. Classification

β-1,4-Xylan xylanohydrolase, EC 3.2.1.8.

C. Properties as Proteins

1. EX Families

A careful comparison of microbial EXs on the basis of their different physicochemical properties, such as molecular mass and isoelectric point, was carried out by Wong et al. (55). This analysis indicated that these enzymes can be divided into two groups, one consisting of high-molecular-mass enzymes with low pI values, and the other consisting of low-molecular-mass enzymes with high pI values. As usual, there are exceptions, particularly concerning pI values. Interestingly, this grouping of EXs (55) was found to be in agreement with the general classification of glycanases on the basis of hydrophobic cluster analysis and sequence similarities (56–59). Hydrophobic cluster analysis is designed to predict protein folding based on hydrophobic/hydrophilic patterns and is used to compare members of a protein group of similar functions (60). Acidic high-molecular-mass EXs (> 30 kDa) were found to be assigned to glycanase family 10 (59) (formerly family F), and basic, low-molecular-mass EXs (< 30 kDa), to glycanase family 11 (formerly family G). While family 10 also contains other glycosyl hydrolases, family 11 is exclusively made up of EXs.

EXs belonging to the two glycosyl hydrolase families show remarkable differences in their tertiary structures as established by crystallography (Fig. 2). Members of individual families have a similar protein folding pattern—i.e., a similar three-dimensional structure. These tertiary structures are more conserved than amino acid sequences. The most conserved region within a family appears to be the catalytic domain. EXs of family 11 appear to be smaller, well-packed molecules, formed mainly of β-sheets (61–64). These enzymes appear very small in their native states (65, 66). The catalytic groups are present in a cleft that accommodates a chain of five to seven xylopyranosyl residues.

The tertiary structure of EXs of family 10 (Fig. 2) is typically an eightfold α/β barrel $[(\alpha/\beta)_8]$, resulting in a "salad bowl" shape (67–70). The substrate binds to a shallow groove on the bottom of the bowl, which is shallower than the substrate binding cleft of family 11 EXs (9). This feature, together with the generally greater conformational flexibility of larger enzymes, may account for the lower substrate specificity and greater catalytic versatility of family 10 EXs.

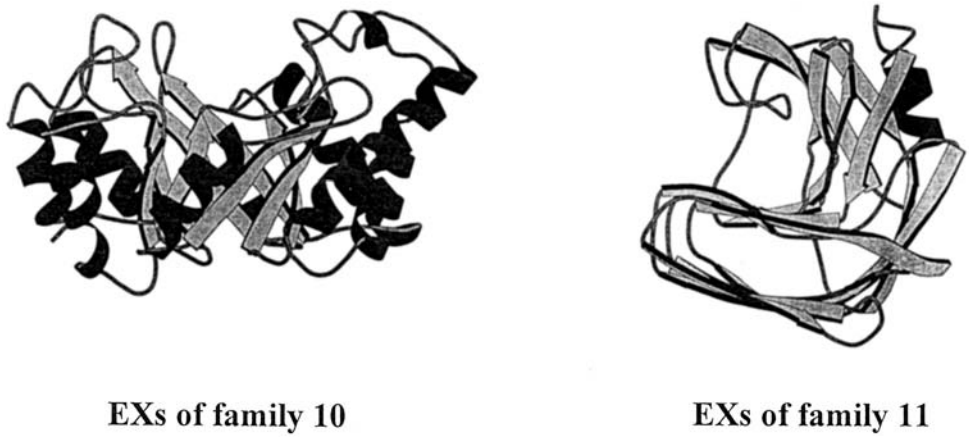

Figure 2 Tertiary structures of endoxylanases of families 10 and 11.

A comparison of the tertiary structure of EXs with other classified glycosyl hydrolases reveals that the two EX families evolved from different ancestors. EXs of family 10 are closely related to the endo-β-1,4-glucanases of family 5, with which they share some common catalytic properties (see below). Both enzyme families 5 and 10 belong to a larger clan of enzymes possessing the eightfold α/β barrel architecture (69, 71), known as clan GH-A (59). EXs of family 11 show a certain degree of similarity to the low-molecular-mass endo-β-1,4-glucanases of family 12 (formerly H) (72).

2. Multiplicity of Forms

Genetic differences are not the only source of heterogeneity among EXs. A multiplicity of forms is frequently observed among the products of one gene. Several molecular forms of enzymes purified to homeogeneity often can be revealed by isoelectric focusing. The observed multiplicity of forms may be a consequence of several factors. The most common reasons include differential mRNA processing, partial proteolysis, and variable degrees of amidation and glycosylation. Additional causes may include autoaggregation and aggregation with other proteins (51).

3. Multiple Domains

The molecular architectures of EXs range from a single catalytic domain to a complex arrangement of catalytic and noncatalytic domains (73–76), recently named modules (73, 74). The catalytic domain (module) includes the part of enzyme (Fig. 3) that contains the active site, i.e., the substrate-binding site in the classical sense, and the catalytic groups. Noncatalytic domains (modules) of EXs act independently of the catalytic domain as polysaccharide-binding domains (carbohydrate-binding modules; CBMs). Catalytic domains are connected to CBMs to which they are linked by linker sequences rich in proline and hydroxy amino acids. The linkers function as flexible, extended hinge regions between functional domains (57). Originally, it was believed that CBMs increased the catalytic rate against insoluble substrates. however, later observations suggested that binding domains may also facilitate the hydrolysis of soluble polysaccharides (75, 77).

Surprisingly, there are several EXs that contain binding modules that bind exclusively to cellulose (cellulose-binding domain; CBD) and not to xylan (57, 74). This is likely related to the biological role of these enzymes in degrading plant cell walls which are predominantly built from cellulose closely associated with hemicellulose. Targeting of EX to cellulose may bring the enzyme in proximity of its substrate. There is a family of CBMs (CBD9) that are found only in EXs (73). CBMs of EX B (XlnB) from *Streptomyces lividans* and EX D from *Cellulomonas fimi* appear to be specific for soluble and insoluble xylan (75, 77). The 3D structure of this xylan-binding domain (XBD) is very similar to that of CBD. A single amino acid change converts the protein from a XBD to a CBD (75). An example of an EX containing two CBMs has been found in *Pseudomonas fluorescens* subsp. *cellulose* (78).

Nature also has designed multifunctional enzymes with two catalytic domains connected by linker sequences. Some bacteria produce bifunctional EXs containing two identical (79) or two different EX domains (80, 81). Other enzymes possess catalytic

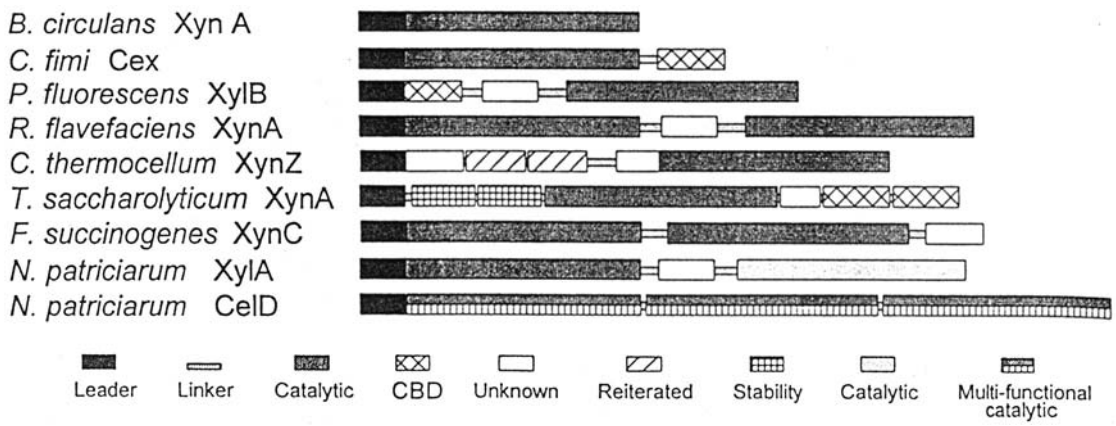

Figure 3 Molecular architecture of some endo-β-1,4-xylanases. (From Ref. 76.)

domains of two different xylanolytic enzymes—one catalyzing the xylan depolymerization, and the other deacetylation of the xylan main chain (82–84). Such bifunctional enzymes may have an advantage over enzymes containing a single catalytic domain in the hydrolysis of native acetylated xylan. Multidomain xylanases also occur as subunits of cellulosomes and xylanosomes. These supramolecular extracellular cell-associated protein complexes of thermophilic clostridia can efficiently degrade cellulose, xylan, and related plant cell wall polysaccharides (85, 86).

D. Properties as Enzymes

1. Catalytic Properties of EXs Belonging to Two Families

EXs belonging to glycanase family 10 hydrolyze heteroxylans and rhodymenan (a linear algal β-1,3-β-1,4-xylan) to a greater extent than EXs of family 11 (87, 88). The EXs of family 10 are better able to cleave glycosidic linkages in the xylan main chain that are near substituents, such as MeGlcA and acetic acid. The alteration of the xylan main chain by replacing β-1,4-linkages by β-1,3-linkages, as it is in rhodymenan, represents a more serious steric barrier for EXs of family 11 than for EXs of family 10. Consequently, EXs of family 10 liberate smaller products from 4-O-methyl-D-glucurono-D-xylan, rhodymenan, and, with some exceptions, also from acetylxylan, than do EXs of family 11. EXs of family 10 can further hydrolyze the shortest branched or isomeric xylooligosaccharides which are released by EXs of family 11 (87).

Characterization of the shortest acidic fragments released from 4-O-methyl-D-glucurono-D-xylan after a long-term hydrolysis (88, 89) suggests which linkages are accessible to hydrolysis by the two types of EXs. EXs of family 10, unlike EXs of family 11, are capable of attacking the glycosidic linkage next to the branch and toward the nonreducing end. While EXs of family 10 require two unsubstituted xylopyranosyl residues between the branches, EXs of family 11 require three unsubstituted consecutive xylopyranosyl residues (Scheme 1). Kinetic data for cleavage of individual glycosidic linkages of the xylan main chain are not available, but time course of product analyses suggest that linkages closer to substituents are hydrolyzed more slowly than more distant linkages.

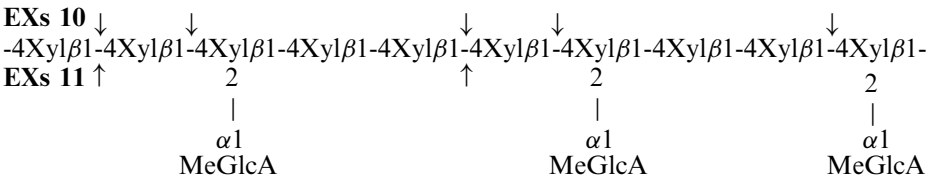

Scheme 1

The degradation of a cereal L-arabino-D-xylan with two EXs of *Aspergillus awamori* (EXI, 39 kDa, pI 5.7–6.7, most probably a member of family 10, and EXIII, 26 kDa, pI 3.3–3.5, most probably a member of family 11) (90) is shown in Scheme 2. The cleavage site specificities L-arabinosyl-D-xylan resemble those on 4-O-methyl-D-glucurono-D-xylan. The L-arabinosyl substituents represent a more serious steric hindrance for

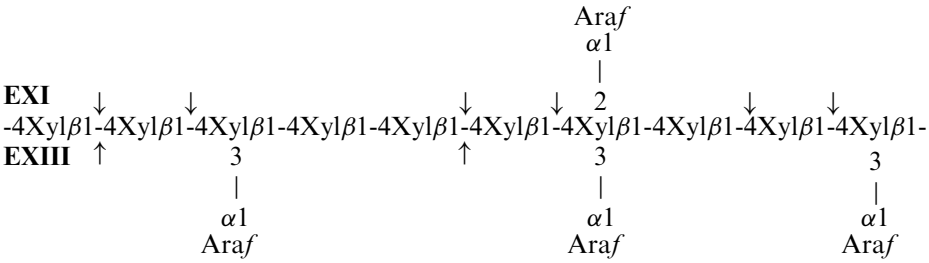

Scheme 2

the formation of productive complexes of the polysaccharide with EXIII. Only the larger type of the enzyme is capable of attacking the linkages between substituted and unsubstituted xylopyranosyl residues.

Studies of the action of EXs on rhodymenan are complicated by the fact that EXs of family 10 are also capable of cleaving β-1,3-linkages (91, 92). Generally, EXs of family 10 do not attack the polysaccharide at β-1,4-linkages which follow β-1,3-linkages toward the reducing end (91), liberating xylotriose, Xylβ1-3Xylβ-4Xyl, as the shortest isomeric product EXs of family 11 liberate from rhodymenan isomeric products larger than xylotriose.

Consistent with the fact that EXs of family 10 are related to endo-β-1,4-glucanases and some glycosidases belonging to the clan of glycosyl hydrolases GH-A (59), EXs of family 10 catalyze hydrolysis of aryl β-D-xylopyranosides and low molecular mass cellulase substrates. These include aryl β-D-cellobiosides, aryl β-D-lactosides (93, 88), and cellooligosaccharides (94). The degradation of aryl xylosides, e.g. of 4-nitrophenyl β-D-xylopyranoside, also involves a complex reaction pathway including glycosyl transfer reactions leading to xylooligosaccharides and their glycosides (94, 95). The EXs of family 11 do not possess these catalytic abilities.

2. Mechanism of Substrate Degradation

The hydrolytic reaction takes place in the active site of the enzyme consisting of the substrate-binding site and catalytic groups. Consistent with their tertiary structures, EXs of family 10 appear to have a smaller substrate-binding site than do EXs of family 11. EXs of family 11 contain a larger number of subsites (five to seven) than EXs of family 10 (four to five subsites). A subsite is a part of the binding site that interacts with one xylopyranosyl residue of the substrate. The interaction may not be only attractive, it can also be repulsive, particularly on the site of the leaving group. The number of subsites and their binding affinities can be determined by a procedure that is called subsite mapping (96–98) which is complementary to the image of the substrate binding site provided by x-ray crystallography (99).

EXs of both families catalyze the hydrolysis of glycosidic linkages with the retention of anomeric configuration (100, 101). The reaction involves a double-displacement mechanism leading to a new reducing end with β-anomeric configuration (102) (Fig. 4). The catalytic amino acids in the substrate binding site divide the subsites to the left (numbered with minus Roman numbers) and to the right of the catalytic groups (numbered with positive Roman numbers) (Fig. 5). The catalytic residues have been identified as two conserved glutamate residues (in a few cases one asparate replaces a glutamate), which are located opposite each other in the active site. One residue functions as a general acid catalyst protonating the glycosidic oxygen, while the other functions as a nucleophile, attacking the anomeric center to form a covalent enzyme-glycosyl intermediate (Fig. 4). In the second step a water molecule attacks the intermediate in a general base-catalyzed process to yield the product of retained anomeric configuration (99, 103). The catalytic residues have been identified by chemical modification, site-directed mutagenesis, and use of stabilized enzyme-glycosyl intermediate (76, 103). Glycosyl transfer reactions catalyzed by both types of EXs at high substrate concentrations are also evidence for the enzyme-glycosyl intermediate. Using linear β-1,4-xylo-oligosaccharides as substrates, it has been established that EXs utilize multiple pathways of substrate degradation (104, 105). Unimolecular hydrolysis takes place at low substrate concentrations. Different cleavage of the substrate occurs at so-called shifted binding, which is observed at higher substrate concentrations and which is, generally, accompanied by formation of products larger than the substrate. An example of such reactions of xylotriose catalyzed by EX from *Cryptococcus albidus* is shown in Figure 5.

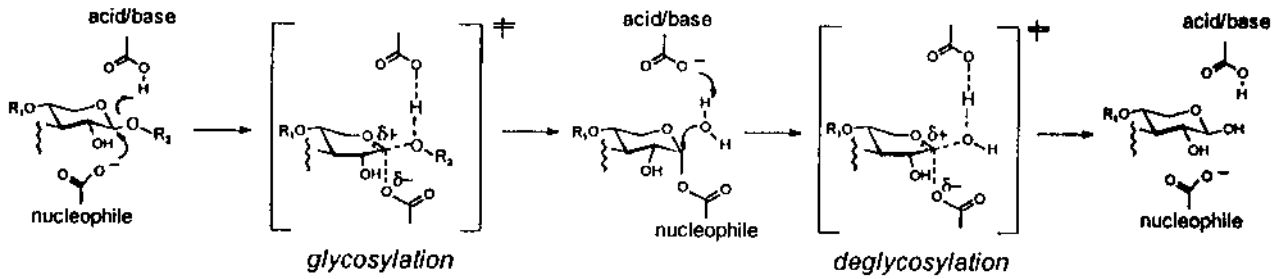

Figure 4 Mechanism of hydrolysis of glycosidic linkage with endo-β-1,4-xylanases.

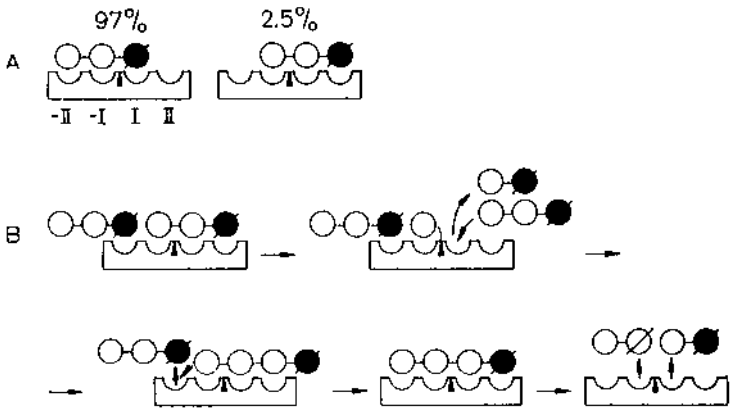

Figure 5 Possible binding and degradation of xylotriose by EX from *Cryptococcus albidus*. (A) Productive complexes at low substrate concentration and probability of their formation; (B) shifted two-one binding of xylotriose at high substrate concentration and subsequent xylosyl transfer to second xylotriose molecule to give xylotetraose, which is finally cleaved to two molecules of xylobiose. (From Ref. 104.)

At sufficiently high concentrations of xylotriose, xylobiose initially is generated as the only product of xylotriose degradation. Analogous reaction pathways are also observed with longer oligosaccharides. The main molecular and catalytic properties of EXs of families 10 and 11 are summarized in Table 2.

3. Xylan-Degrading Endo-β-1,4-Glucanases

It has been unambiguously established that at least one type of endo-β-1,4-glucanase exhibits activity on both cellulose and xylan (106, 107). The best-known enzyme in this regard is endoglucanase I from *Trichoderma reesei*, a member of family 5 glycosyl hydrolases. The enzyme catalyzes the hydrolysis of both polysaccharides in the same active site (108). Although the enzyme belongs to the same clan as EXs of family 10, the products the enzyme generates from glucuronoxylan and rhodymenan are more similar to those liberated by EXs of family 11 (87). In *T. reesei* the enzyme is coinduced as a component of the cellulolytic and not of the xylanolytic system (3).

Table 2 Properties of EXs of Families 10 and 11

Properties	EXs of family 10	EXs of family 11
Molecular mass	usually > 30 kDa	usually < 30 kDa
Isoelectric points	usually < 7	usually > 7
Protein fold (catalytic module)	$(\alpha\beta)_8$	two β-sheets and one α-helix
Substrate binding site	shallow groove	deep cleft
Catalytic amino acids	two glutamic acid residues (occasionally one glutamate and one asparate)	two glutamic acid residues (occasionally one glutamate and one aspartate)
Number of subsites	4—5	5–7
Substrate specificity	less specific	more specific
heteroxylans	active	active
aryl-β-xylosides	active	inactive
aryl-β-cellobiosides	active	inactive
aryl-β-lactosides	active	inactive
Stereochemistry of hydrolysis	retaining	retaining
Multiple reaction pathway at high substrate concentrations	yes	yes

E. Qualitative and Quantitative Determination of Activity

1. Reductometric Assays

The most common way to follow EX activity is to determine the reducing sugars formed from selected type of xylan. Two basic procedures for determination of reducing sugars have been widely used: the Somogyi-Nelson procedure (109–111), and the 2,4-dinitrosalicylic acid (DNS) test (112–114). The methods are sufficient to prove the presence of the enzyme, to assay its activity, and to evaluate the extent of polysaccharide hydrolysis, which may be the first criteria for xylanase differentiation. The two methods for the determination of reducing sugars have been compared in an interlaboratory evaluation organized by Finnish scientists (115). Although the Somogyi-Nelson procedure is almost 10 times more sensitive than the DNS method, the latter always gives higher values of xylanase activity. When standardized with respect to substrate and procedure, the assay employing the DNS method afforded reproducible results in various laboratories with a standard deviation of 17% (115). Recently Jeffries et al. (116) reported that the differences between the Somogyi-Nelson and DNS methods are due to the fact that the first method is less reactive and the second method more reactive with xylooligosaccharides than with xylose. The prevalence of oligosaccharides among the products of xylan hydrolysis is thus why the Somogyi-Nelson method underestimates, and the DNS method overestimates enzyme activity.

The most sensitive method for photometric determination of reducing sugars is that using 2,2′-bicinchoninate (117, 118). However, it has not been widely adopted for determination of xylanase activity. Nevertheless, the method should be listed here because of its potential for miniaturization to the scale of a microplate reader (119).

a. DNS Xylanase Assay (115)

Reagents

1. Birchwood 4-O-methyl-D-glucuronoxylan (Roth 7500, Germany; or Sigma, USA), 1% solution in 0.05 M citrate buffer, pH 5.3 (in the case of fungal enzymes or other buffers with bacterial enzymes). The solution is prepared under heating up to boiling point with stirring until the polysaccharide dissolves. Clarification by centrifugation is not necessary but may be useful. Cooled solution can be stored in the presence of 0.01–0.02% sodium azide.
2. D-Xylose, 10 mM calibration solution in 0.05 M citrate buffer, pH 5.3 (or other buffer).
3. DNS reagent prepared according to Sumner (112) or Miller (113).

Procedure. Preheated xylan solution (1.8 mL; 50°C) is mixed with 0.2 mL preheated enzyme solution (50°C) and incubated for 5 min at 50°C. The reaction is stopped by addition of 3 mL of the DNS reagent. The mixture is heated for 5 min at 100°C (boiling water bath) and then cooled in cold water. Absorbance of samples is measured at 540 nm against the substrate blank and the values are corrected for absorbance of the enzyme blank. Calibration samples with known amounts of xylose are prepared in the presence of the substrate.

One unit of xylanase activity is defined as the amount of enzyme liberating 1 μmol of xylose equivalent under the experimental conditions in 1 min. (*Note*: The volume of the assay can be reduced.)

b. Xylanase Assay Using the Somogyi-Nelson Method (120)

Reagents

1. Birchwood or beechwood 4-O-methyl-D-glucuronoxylan (Roth 7500, Germany; or Sigma, USA), 0.4% solution in 0.1 M acetate buffer, pH 5.4, or 0.2% solution in 0.05 M acetate buffer (or other buffer). The solution is prepared under heating up to boiling point with stirring until the polysaccharide dissolves. The solution can be stored in the presence of 0.01–0.02% sodium azide.
2. D-Xylose, 1 mM calibration solution.

Procedure. Xylan solution (0.25 mL, 0.4%) is mixed with 0.25 mL enzyme solution, or 0.5 mL of 0.2% xylan solution is mixed with 10–50 μL enzyme solution and incubated at 30°C for an appropriate time. The reaction is terminated by addition of 0.5 mL of the Somogyi reagent, mixed well, and heated for 10 min on a boiling water bath. After cooling in cold water the samples are vigorously mixed with 0.5 mL of the Nelson reagent. After 15 min standing with occasional stirring, cloudy samples are centrifuged to remove the fine precipitate. Absorbance at 560 nm of the supernatants is measured. Blanks to correct the values for reducing power of the substrate and the enzyme are run in parallel. Calibration is done in the range 0.05–0.5 μmol of xylose. One unit of xylanase is defined similarly as above. (*Note*: Exact duration of heating at 100°C with the Somogyi reagent is critical for reproducibility of results.)

2. Other Xylanase Assays and Specific EX Assays

It should be noted that reductometric assays are not specific for EXs and, when used with crude xylanolytic systems or EX preparations containing other xylanolytic enzymes, they cover the overall saccharification ability of the tested enzyme preparations. Frequently, reductometric xylanase assays may not be sufficiently sensitive or may be hampered by a high background of reducing sugars in the enzyme preparations. In such cases, a viscosimetric method of xylanase assay can be recommended. This method is based on measurement of the decrease of viscosity of a soluble xylan, e.g., arabinoxylan (121) or soluble xylan derivative, like carboxymethylxylan (122, 123). Viscosity can be measured using various viscosimeters or by modern electronic devices employing vibrating metal rods. Changes in the resistance of the medium to the vibrating or rotating rods are recorded and transformed into activity units. Viscosimetric measurements are important to establish the endocharacter of glycanases. Plots of specific fluidity ($1/\eta$) versus the amount of liberated reducing sugars give linear relationships, the slopes of which correspond to the randomness of the xylan attack by the enzymes (89).

Another specific EX assay employs a soluble covalently dyed xylan, Remazol Brilliant Blue–xylan (RBB-xylan), a substrate that is precipitable from aqueous solution by ethanol (124). The assay is based on the photometric determination of enzyme-released dyed fragments that remain soluble in the presence of ethanol. This method allows the determination of xylanase activity in the presence of larger amounts of reducing sugars, in membrane fractions of cells, and even in the presence of viable cells utilizing liberated xylan fragments. Limitations of the method are its sensitivity to temperature and ionic strength. Testing in 15 laboratories showed the method reproducible to $\sim 30\%$ relative standard deviation, suggesting that RBB-xylan assay could be a useful alternative assay for xylanases (115). A number of covalently dyed soluble and insoluble xylans are available from Megazyme (Wicklow, Ireland). The company offers also a specific tablet test for EX activity based on wheat arabinoxylan. The nephelometric assay of xylanase (125) could be suitable for differentiation of xylanases with respect to their performance on insoluble xylan.

a. RBB-Xylan Assay (115, 124)

Reagents

1. RBB-xylan, solution in 0.05 M acetate buffer, pH 5.4, 5–6 mg/mL (the concentration should correspond to 5 mg/mL of undyed xylan) or solution in 0.1 M acetate buffer (10–11 mg/mL).
2. Ethanol, 96% or absolute.

Procedure. The enzyme solution or suspension (10–50 μL) is mixed in 1.5 or 2.0 mL plastic microtest tubes with 0.5 mL of preheated (30°C) solution of RBB-xylan solution (5–6 mg/mL), or 0.25 mL of enzyme solution or suspension is mixed with 0.25 mL RBB-xylan solution in 0.1 M acetate buffer and incubated at 30°C for an appropriate time. The reaction is terminated by the addition of 1 mL ethanol to precipitate unhydrolyzed RBB-xylan and its high-molecular-weight fragments. After standing at room temperature for 20–30 min in closed test tubes, the mixtures are mixed again and centrifuged at 2500g for 1.5–3 min. The absorbance of supernatants is then measured at 595 nm against the respective substrate blank. (*Note*: The assay does not give direct data suitable for calculation of the enzyme activity. However, the assay can be calibrated by a reductometric assay carried out under the same experimental conditions with undyed xylan.

3. Synthetic Substrates

Synthetic substrates of glycosyl hydrolases usually include chromogenic and fluorogenic glycosides which are widely used to quantify particularly glycosidases. The most common substrates are 4-nitrophenyl and 4-methylumbelliferyl glycosides. Liberation of 4-nitrophenol is followed photometrically at 405–410 nm after termination of the enzymic reaction with alkaline reagents. Fluorimetry is used to follow the liberation of 4-methylumbelliferone (excitation at 365 nm and emission at 448 nm at pH 10–11). To achieve maximal sensitivity, permitting work in the nM concentration range of substrates and products, basidification of the reaction mixtures is required (126, 127).

Similar aryl glycosides of oligosaccharides derived from polysaccharides can be used as chromogenic and fluorogenic substrates of endoacting glycosyl hydrolases. Significant progress in differentiation of cellulolytic glycanases was achieved by the introduction of 4-nitrophenyl- and 4-methylumbelliferyl-β-glycosides or cellobiose, cellotriose, and lactose (93, 128). Of these substrates, only 4-nitrophenyl-β-cellobioside has been occasionally used for determination of activity of cellobiohydrolase. This assay is not specific, because aryl β-cellobiosides are attacked at the agluconic linkage also by endo-β-1,4-glucanases (128) and EXs of family 10 (88). Liberation of the aryl aglycone from cellobio-

sides occurs also after a two-step hydrolysis of the substrate by β-glucosidase.

Aryl β-glycosides of xylo-oligosaccharides have also been described as potential substrates of EXs (129–135). However, because they have not been commercialized, their use remains very limited in spite of their great analytical potential and unusually high sensitivity. 4-Nitrophenyl β-xylobioside was used for characterization of substrate requirements of a non-specific β-xylanase from *Cellulomonas fimi* (129). 4-Methylumbelliferyl -β-xylobioside and -xylotrioside were successfully used for detection of EXs in electrophoretic gels (130) and for differentiation of EXs (133).

4. Assays for Detection and Screening Purposes

A number of different procedures have been developed over the years for detection of EXs in gels. The same principles can be used both for the detection of the enzyme in electrophoretic gels and for screening of microorganisms and genetically transformed cells on solid agar media. The detection and screening techniques employ soluble xylan, insoluble xylan, soluble covalently dyed xylan, and fluorogenic β-glycosides of xylo-oligosaccharides.

In agar gels incorporating insoluble xylan, EX activity is visualized as the appearance of clearing zones (136). On solid growth media containing a soluble xylan-dye conjugate, such as RRB-xylan (124), xylanase-positive colonies are identified by pale-blue or colorless zones resulting from diffusion of dyed polysaccharide fragments generated by EXs (137, 138). The advantage of these two screening substrates is that the degradation of the substrate can be followed progressively without any further treatment which might prevent the isolation of the positive colonies directly from the screening plates. A replica plating is required in the case of screens employing the soluble xylan complexed with Congo Red (139, 138) or precipitation of soluble xylan with ethanol (140). Replica plating is avoided in plate assays with the fluorogenic glycosides 4-methylumbelliferyl β-xylobioside (Umb-Xyl_2) or β-xylotrioside (Umb-Xyl_3) (130).

a. Procedures

Detection of microbial producers of xylanase (137, 138). Solid media containing 0.15–0.2% RBB-xylan (can be autoclaved) are suitable for the detection of microbial producers of extracellular EX. Surrounding colonies of EX producers, pale-blue zones are formed as a result of diffusion of secreted enzymes and enzyme-released dyed fragments of RBB-xylan.

A soluble undyed glucuronoxylan (0.1–0.2%) can be used instead of RBB-xylan. The production of EX is revealed after an appropriate time by flooding the plate first with 1 M NaCl and then with 0.1% aqueous solution of Congo Red (C.I. 22120; Sigma, Aldrich, Calbiochem). After 15 min the dye solution is poured off and areas with hydrolyzed polysaccharides are destained for 10 min with two changes of 1 M NaCl with a 20-min treatment with 5 M NaCl.

Umb-Xyl_2 or Umb-Xyl_3 gives the best results when used in the form of solutions (0.1–0.5 mM) applied to the surface of solid growth medium after colonies are clearly visible. Incorporation of the fluorogenic substrates into the solid growth media may not give straightforward results due to the rapid diffusion of the fluorogenic aglycone in comparison with the rate of colony growth.

Semiquantitative gel diffusion assay (141, 142). A solution of 0.15–0.2% RBB-xylan in an appropriate buffer is solidified with agar or agarose in petri dishes. Wells 4 mm in diameter are cut using a cork borer or suitably shortened disposable plastic micropipette tip and the gel is removed by suction or by a needle. Enzyme solutions (10 μL) are pipetted into the wells, and closed dishes are left to incubate at appropriate temperature for several hours. Diffusion-zone diameters are proportional to the logarithm of enzyme concentrations.

A soluble glucuronoxylan in combination with the above described Congo Red complexing can be used for the same purpose. More sensitive and faster are similar plate assays with gels containing Umb-Xyl_2 or Umb-Xyl_3 (0.1–0.5 mM). Liberation of the fluorogenic 4-methylumbelliferone around the wells is observed under UV light (365 nm). Since the liberation of the aglycone can be a result of β-xylosidase action, enzyme samples should be tested in a parallel plate containing a specific β-xylosidase substrate, 4-methylumbelliferyl β-xyloside.

Detection of EX in electrophoretic gels (142). A warm 1.5% aqueous solution (10 mL) of RBB-xylan is mixed well with 3% molten agar in appropriate buffer (20 mL) and poured between two glass plates separated by 0.75 to 1.0-mm spacers and left to solidify. The glass plates can be covered by transparent plastic sheets, so the gel can be easily stored after glass removal. If not used immediately, the agar gel should be supplied with 0.01–0.02% sodium azide. Native PAGE or isoelectrofocusing gels (agarose or polyacrylamide) are washed twice for 5–10 min (depending on

their thickness) with a buffer corresponding to pH optimum of the tested EXs. They are then brought into contact with the RBB-xylan containing detection gel. The presence of EX leads to a change in the shade of the blue background, due to a diffusion of enzyme-released dyed fragments. The agar detection gel is then separated from the electrophoretic gel and, if needed, further incubated in a wet chamber. It is then dipped into the solvent ethanol–0.05 M acetate buffer (pH 5.4) 2:1 (v/v). Zones with enzyme-degraded substrate are destained as a result of the solubilization of dyed fragments. The background with unhydrolyzed substrate remains unchanged. The dyed fragments liberated from the blue detection gel diffuse into the separation gel, where they mark the position of the enzyme. Individual xylanase forms can be subsequently isolated from the separation gel, e.g., by electroelution.

The use of RBB-xylan enables visual monitoring of substrate hydrolysis, which is important for appropriate timing of contact between the substrate and enzymes. The detection of EXs by means of Congo Red (143) requires preliminary experimentation or knowledge of enzyme activity to terminate the reaction at the appropriate time.

The fastest procedure for the detection of EXs in electrophoretic gels can be achieved using Umb-Xyl_2 or Umb-Xyl_3 (130). Either fluorogenic substrate at a concentration of 0.1–0.5 mM can be incorporated into a 0.75 to 1-mm thick agar or agarose detection gel which is laid upon the rebuffered separation gel. A simpler approach is to bring the washed separation gel into contact with a solution of substrates on a flat glass plate. Fluorescence appears rapidly under UV light ($\sim$ 360 nm) in the regions of EXs. The fluorescence intensity can be enhanced by ammonium hydroxide vapors.

III. β-XYLOSIDASE (EC 3.2.1.37)

A. Chemical Reactions Catalyzed

$$\text{Xyl}\beta\text{1-4Xyl} \rightarrow 2\,\text{Xyl} \qquad \text{Xyln}_n \rightarrow \text{Xyl}_{n-1} + \text{Xyl}$$

$$\text{NPh-}\beta\text{-Xyl} \rightarrow \text{Xyl} + \text{NPh-OH}$$

β-Xylosidase hydrolyzes xylobiose and higher linear β-1,4-xylo-oligoaccharides to monomer and also releases xylose from branched or substituted xylo-oligosaccharides produced by the action of EXs. β-Xylosidases vary in their affinity toward short and long oligosaccharides. Those which prefer xylobiose as a substrate are referred to as β-xylosidase, and those which prefer longer oligosaccharides are referred to as exo-β-xylanases. A careful literature search suggests, however, that in spite of the existence of several glycosyl hydrolase families into which β-xylosidases have been assigned, and in spite of the fact that the enzymes behave as both retaining and inverting hydrolases, there is no sharp boundary between β-xylosidase and exo-β-xylanase with respect to their substrate preference. Therefore, this section considers all enzymes catalyzing successive removal of β-xylosyl residues from non-reducing termini.

B. Classification

β-1,4-Xylan xylohydrolase EC 3.2.1.37.

C. Properties as Proteins

β-Xylosidases are, with few exceptions, larger enzymes than EXs. Their molecular mass ranges between 26 and 360 kDa (144), and they are monomeric or dimeric proteins as shown by SDS-PAGE. Molecular masses exceeding 120 kDa usually correspond to dimeric/tetrameric aggregates. All thus far isolated enzyme species showed acidic pI values (3.25–6.1). The properties of these enzymes vary considerably, which complicates their classification. Moreover, β-xylosidase belongs to those xylanolytic enzymes which exhibit variable cellular localization. In several species of bacteria and yeasts, the enzyme is localized strictly intracellularly and is not glycosylated. In these organisms, xylo-oligosaccharides generated outside the cell by EXs must enter the cell by transport systems localized in plasmamembrane (3). In other organisms, like *Aureobasidium pullulans*, β-xylosidase is found outside and inside the cells. It remains to be established whether some organisms produce two different β-xylosidases. In laboratory cultures of mycelial fungi, β-xylosidase remains associated with mycelia during early stages of growth and is released into the media later either by true secretion or as a result of cell lysis.

Only a small fraction of known β-xylosidases have been classified on the basis of hydrophobic cluster analysis and comparison of amino acid sequences. They have been assigned to four glycosyl hydrolase families: 3, 39, 43, and 52 (58, 59). Family 3, which contains mainly β-glucosidases (EC 3.2.1.21), includes a nonspecific β-glucosidase/β-xylosidase from *Erwinia chrysanthemi* (145) and the best-known fungal β-xylosidases from *Aspergillus* and *Trichoderma* species (146, 147). A common feature of the members of this family is their retaining character. β-Xylosidases

of thermophilic bacteria have been assigned to family 39 (148–150). All β-xylosidases of this family are localized intracellularly and belong to retaining glycosyl hydrolases. Their molecular mass is between 55 and 60 kDa.

Family 43 contains 50 to 60-kDa β-xylosidases of several *Bacillus* spp. and from *Butyrivibrio fibrosolvens*. The latter enzyme has been shown to operate by a mechanism which results in inversion of the anomeric configuration (151). If the unequivocal relationship between family classification and molecular mechanism is valid, other members of family 43 should also operate with retention of the anomeric configuration.

The amino acid sequences of two *Bacillus stearothermophilus* (70–80 kDa of unprocessed precursor) β-xylosidases (152, 153) are so unique that they were grouped into a special family, assigned as family 52. The stereochemistry of hydrolysis by these enzymes has not been established yet. Three-dimensional structures are not available for any members of these four families. Some characteristic properties of individual β-xylosidase families are listed in Table 3.

D. Properties as Enzymes

There is limited knowledge about structure-function relationships in the glycosyl hydrolase families containing β-xylosidases. All β-xylosidases thus far described hydrolyze not only xylobiose and xylooligosaccharides but also aryl β-D-xylopyranosides. Consequently, 4-nitrophenyl β-D-xylopyranoside has become the most common substrate for β-xylosidase assay. There are, however, examples of aryl β-xylosidases which do not attack xylo-oligosaccharides. Therefore, it is always important to test the enzymes directly on xylobiose and xylo-oligosaccharides. Several β-xylosidases are reported also to attack polymeric xylan in an exofashion. Because of the limited information, it is not possible to correlate the catalytic properties of enzymes with their glycosyl hydrolase families. Therefore, only the properties of best known β-xylosidases will be described.

One of the best-characterized β-xylosidases is an intracellular enzyme from *Bacillus pumilus* (154, 155). It shows absolute specificity for β-xylopyranosyl residues but does not catalyze glycosyl transfer reactions. This suggests that the enzyme belongs to family 43 of glycosyl hydrolases (Table 3). The best-studied fungal β-xylosidases are extracellular enzymes produced by *Aspergillus* and *Trichoderma* spp., i.e., the enzymes from family 3. Their retaining character is revealed in glycosyl transfer reactions in high concentrations of xylo-oligosaccharides and 4NPh-β-Xyl (156–159). These enzymes do not show high specificity for the glycan moiety. β-Xylosidases from several *Trichoderma* strains exhibit α-L-arabinofuranosidase activity (160–162). This has been confirmed by cloning the *T. reesei* β-xylosidase gene in yeast (147). The α-L-arabinofuranosidase from *T. reesei* hydrolyzes only α-L-arabinofuranosides and is not able to liberate L-arabinose from arabinoxylan or arabinose-substituted xylo-oligosaccharides. Aryl β-xylosidase activity of *Trichoderma* strains is inhibited by D-xylose. Fungal β-xylosidases were shown to have a specific requirement for structural arrangement of branched oligosaccharides. The enzyme from *A. awamori* was tested on different arabinose-substituted xylooligosaccharides. The enzyme was able to remove terminal xylopyranosyl residues from the nonreducing end of branched oligosaccharides only when two contiguous unsubstituted xylopyranosyl residues were linked to single- or double-substituted xylopyranosyl residues (163). This is similar to the behavior of β-xylosidase from *T. reesei* (159, 164). The enzyme does not liberate β-1,4-xylopyranosyl residues linked to an α-1,3- or β-1,3-substituted xylopyranosyl residue

Table 3 Families of Glycosyl Hydrolases Containing β-Xylosidases

Enzyme family	Common microbial producers	Molecular mass range of listed enzymes	Stereochemistry of hydrolysis	Other enzymes in the family
3	*Erwinia, Aspergillus, Trichoderma*	60–122 kDa	retaining	β-glucosidase
39	Thermophilic bacteria	55–60	retaining	α-L-iduronidase
43	*Butylvibrio, Baccillus*	50–60	inverting	α-L-arabinanase EX
52	*Bacillus stearothermophilus*	70–80 (precursor)	unknown	none

Source: http://expasy.hcuge.ch/cgi-bin/list/glycosid.txt.

(compounds of the type Xyl-4[Ara-3]Xyl- or Xyl-4[Xyl-3]Xyl-). In such compounds the substituent is apparently so close to the site of the enzymic attack (i.e., glycosidic oxygen) that the formation of the enzyme-substrate complex is sterically impaired. The β-1,4-glycosidic linkage becomes susceptible to the enzyme attack only if the substituent is linked to a more distant C-2 position (Scheme 3).

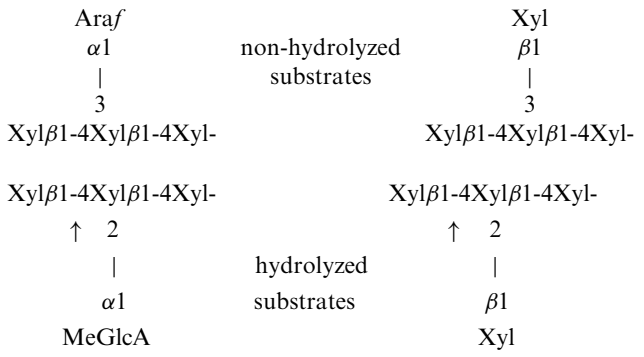

Scheme 3

E. Determination of β-Xylosidase Activity

The activity of β-xylosidases, which hydrolyze xylobiose, xylo-oligosaccharides, eventually linear portions of xylan, can be determined reductometrically using xylobiose and xylotriose, which are poor substrates for EXs. The sensitivity of assays can be increased by eliminating the background of oligosaccharides by their reduction to sugar alcohols with $NaBH_4$. The reductometric procedures described in the section devoted to EXs can be adapted for the use of xylobiitol or xylotriitol as substrates. Xylobiase activity can also be determined using xylobiose as a substrate in an enzyme-coupled assay which employs NAD^+-dependent glucose dehydrogenase. The dehydrogenase is not specific for glucose and catalyzes conversion of generated xylose to xylonolactone (165, 166). The formation of NADH is followed at 340 nm to estimate β-xylosidase activity. Two side reactions, the oxidation of xylobiose to lactone by the dehydrogenase and hydrolysis of the lactone by β-xylosidase, have to be taken into consideration.

However, the most common assay of β-xylosidase employs 4-nitrophenyl-β-D-xylopyranoside as a substrate. There are a great variety of conditions under which the assay can be done involving the substrate concentration, pH and type of the assay buffer, and various alkaline reagents to terminate the reaction and to shift the absorption maximum of liberated 4-nitrophenol to a visible region of the spectrum. In a similar assay, phenyl-β-D-xylopyranoside is used as a substrate (167). Liberated phenol is determined using the phenol reagent from the well-known Lowry procedure for protein determination.

1. β-Xylosidase Assay Using 4-Nitrophenyl-β-D-Xylopyranoside/Na_2CO_3

a. Reagents

1. 4-Nitrophenyl-β-D-xylopyranoside, 4 mM solution in 0.05 M acetate buffer, pH 4.5 (or other buffer).
2. 2 M solution of Na_2CO_3.
3. 4-Nitrophenol, 2 mM stock solution in the acetate buffer; 0.2 mM calibration solution in the acetate buffer.

b. Procedure. Preheated substrate solution (0.9 mL, e.g., at 50°C) is mixed with 0.1 mL appropriately diluted enzyme solution and incubated for suitable time at 50°C. The reaction is terminated by addition of 1 mL of 2 M Na_2CO_3. The absorbance is measured at 410 nm against the substrate blank. The values have to be corrected for enzyme blanks if they show absorbance at 410 nm. Calibration with 4-nitrophenol is done in the range of 0.02–0.2 μmol per assay mixture. One unit of β-xylosidase activity is defined as the amount of enzyme liberating 1 μmol of 4-nitrophenol in 1 min. (*Note*: The assay can be miniaturized to the scale of a microplate reader.)

2. β-Xylosidase Assay Using 4-Nitrophenyl-β-D-Xylopyranoside/$Na_2B_4O_7$

a. Reagents

1. 4-Nitrophenyl-β-D-xylopyranoside, 10 mM solution in 0.05 M acetate buffer, pH 5.0 (or other buffer).
2. Saturated solution of $Na_2B_4O_7$.
3. 4-Nitrophenol, 1 mM stock solution in the acetate buffer; 0.1 mM calibration solution in the acetate buffer.

b. Procedure. Preincubated substrate solution (0.1 mL 50°C) is mixed with 0.1 mL tested enzyme sample (50°C) in an Eppendorf test tube and incubated for appropriate time at 50°C. After addition of 1.0 mL saturated solution of $Na_2B_4O_7$, the absorbance is measured at 410 nm against a substrate blank. Calibration is done with 4-nitrophenol in the range of 0.01–0.1 μmol. One unit of β-xylosidase activity is defined as the amount of enzyme liberating 1 μmol of 4-nitro-

phenol in 1 min. (*Note*: This assay is carried out in microcentrifuge test tubes and is suitable for determination of cell-bound β-xylosidase activity. The cells used as the enzyme source must be separated by centrifugation before measurement.)

F. Assays for Screening Purposes

Detection of β-xylosidase activity in solid growth media or in electrophoretic gels usually involves incorporation of chromogenic and fluorogenic substrates, 4-nitrophenyl-β-D-xylopyranoside (1–5 mM) or 4-methylumbelliferyl-β-D-xylopyranoside (0.1–0.5 mM). Activity is revealed by flooding the growth media or gels with alkaline solutions (1 M Na_2CO_3, alkaline buffers) or exposing them to ammonium hydroxide vapors. Replica plating is required before alkalification when working in acidic pH regions. The liberation of 4-methylumbelliferone is revealed under UV light (360 nm). Alkalification of the solid medium or gel, e.g., exposure to ammonium hydroxide vapors, increases the fluorescence. As mentioned with fluorogenic substrates of EXs, fluorogenic glycosides for screening purposes give better results when applied as overlay at the later stages of colony development than when incorporated into growth media before inoculation.

IV. α-GLUCURONIDASE, 4-O-METHYL-α-GLUCURONIDASE (EC 3.2.1.139)

A. Chemical Reactions Catalyzed

Xylβ-R Xylβ-R
2
| ← → +
α1
MeGlcA MeGlcA

-R = 1-4Xyl, 1-4Xylβ1-4Xyl, 1-4Xyl$_n$

One of the best substrates

Xylβ1-4Xylβ1-4Xyl* Xylβ1-4Xylβ1-4Xyl*
2
| ← → +
α1
MeGlcA MeGlcA*
*Reducing end

B. Classification

α-D-Glucuronidase (EC 3.2.1.139).

C. Occurrence of α-Glucuronidase

α-Glucuronidase activity has been detected in cellulolytic and xylanolytic systems of a variety of fungi (168–176), actinomyces, and bacteria (177–184). Two reports mention α-glucuronidase in snail digestive juice (184, 185). There is no report on the occurrence of the enzyme in plants. In most microorganisms α-glucuronidase was found to be secreted into culture medium. However, there are examples in which the enzymes has been found confined to the cells (172, 180, 181).

D. Properties as Proteins

α-Glucuronidase has been purified from a relatively small number of microorganisms. All eukaryotic α-glucuronidases, with the exception of the enzyme from *Agaricus bisporus* (196), are monomeric enzymes with molecular masses between 91 and 150 kDa. Their isoelectric points are acidic, between values 4.6 and 5.3 (146). The α-glucuronidase purified from the snail *Helix pomatia* (185) also shares these properties. Bacterial α-glucuronidases are usually found as dimers with subunits of a molecular mass $\sim$ 70 kDa. pI values of bacterial enzymes are similar to those of fungal enzymes. α-Glucuronidase from the thermophilic bacterium *Thermotoga maritima* shows a variable oligomeric structure depending on the salt concentration (183).

So far only five amino acid sequences of α-glucuronidases are known, all based on gene sequencing (146, 176). The sequences show a high degree of similarity (40–60% identity) and have been assigned to a separate glycosyl hydrolase family 67, which does not contain any other hydrolases. A three-dimensional structure of α-glucuronidase has not been reported; however, the enzyme from *Bacillus stearophilus* has been successfully crystallized and subjected to x-ray analysis (186).

E. Properties as Enzymes

α-Glucuronidases seem to belong to those accessory xylanolytic enzymes that do not operate on polymeric substrates. With exception of α-glucuronidase from *Thermoascus aurantiacus* (170), α-glucuronidases failed to liberate 4-O-methyl-D-glucuronic (MeGlcA) acid or

D-glucuronic acid at an appreciable rate from polymeric substrates. In a few cases, an extremely low rate was found. However, it should be stressed that even a slight contamination of α-glucuronidase by EX and β-xylosidase would generate polysaccharide fragments that would serve as α-glucuronidase substrates. α-Glucuronidases, regardless of their eukaryotic or prokaryotic origin, are very selective toward the structure of aldouronic acids. They are capable of removing MeGlcA or GlcA from aldouronic acids in which MeGlcA or GlcA residues are linked to a single xylopyranosyl residue or to a nonreducing terminal xylopyranosyl residue of xylo-oligosaccharides. Such fragments can be generated from glucuronoxylan by the action of EXs of family 10 or by the action of a combination of EXs of family 11 and β-xylosidase (Scheme 4) (88, 187).

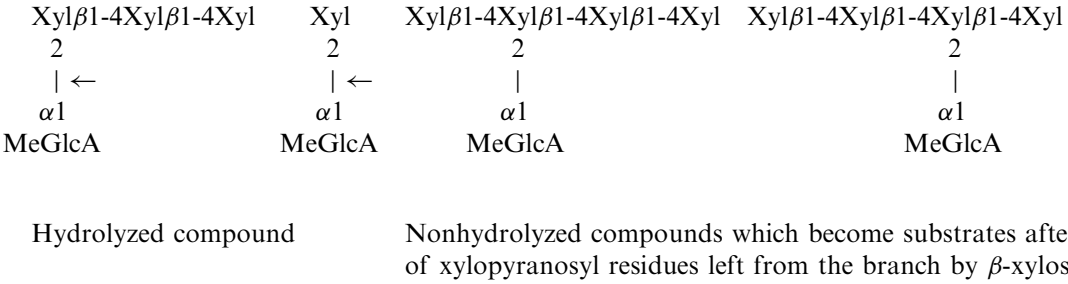

Scheme 4

An interesting question related to the substrate specificity of α-glucuronidase is whether the enzyme is specific for GlcA or MeGlcA. The enzyme from *Aspergillus niger* hydrolyzed GlcA-Xyl_3 about two times faster than $MeGlcXyl_3$ (172). This example suggests that the 4-O-methyl group in the acid is not decisive for the action of the enzymes.

A surprising property of microbial α-glucuronidases is their inability to hydrolyze 4-nitrophenyl-α-D-glucuronide, a compound that could otherwise serve as a convenient chromogenic substrate. The only α-glucuronidase capable of hydrolyzing this compound was the snail enzyme (185). Microbial α-glucuronidases require uronic acid to be linked to at least one xylopyranosyl residue, which can be in the form of an aryl glycoside as in 4-nitrophenyl-2-O-(methyl-4-O-methyl-α-D-glucuronosyl)-β-D-xylopyranoside (188).

Optimal pH values for bacterial α-glucuronidases are in the range of 5.4–6.5 and in the range of 3.5–5.0 for fungal enzymes. K_m values for aldouronic acids as substrates were reported in the range of 0.14–0.95 mM.

The stereochemistry of hydrolysis of glycosidic linkage by α-glucuronidase was recently investigated with purified *Aspergillus tubingensis* enzyme, which belongs to family 67 of glycosyl hydrolases. By NMR spectroscopy it has been established that the enzyme uses a single displacement reaction mechanism, leading to inversion of the anomeric configuration (189). Based on this finding, inverting character can be expected with other α-glucuronidases.

F. Determination of α-Glucuronidase Activity

As mentioned above, the activity of α-glucuronidase cannot be determined directly on glucuronoxylan or a related polymeric substrate. Glucuronoxylan can be used for the α-glucuronidase assay only in the presence of xylan-depolymerizing enzymes which generate aldouronic acids of the required structures (190). The most common substrate for α-glucuronidase assays are linear aldouronic acids obtained by enzymic or acid hydrolysis of glucuronoxylan. From such aldouronic acids, liberation of MeGlcA is usually followed by determination of the reducing power of the free uronic acid by a modification of the Somogyi copper reagent and the Nelson phosphomolybdenic acid reagent according to Milner and Avigad (191). The method is quite specific for uronic acids and suffers only slightly from the presence of neutral reducing sugars. The assay could be affected by some salts (citrate, phosphate), however. Alternative methods include HPLC determination of free MeGlcA (173, 174) or the equivalent amount of xylo-oligosaccharides (169), or GLC of trimethylsilyl

oxim derivatives of uronic acids (178, 179, 182, 184). Unfortunately, there is no direct α-glucuronidase assay available that would utilize a chromogenic substrate. As we have already mentioned, 4-nitrophenyl-α-glucuronide does not serve as substrate of microbial α-glucuronidases. Recently, a new β-xylosidase-coupled α-glucuronidase assay has been introduced that uses 4-nitrophenyl-2-O-(4-O-methyl-α-D-glucuronosyl)-β-D-xylopyranoside (NPh-Xyl-MeGlcA) (188). Liberation of MeGlcA from the compound yields an equimolar amount of 4-nitrophenyl-β-xylopyranoside. In the presence of excess of β-xylosidase to hydrolyze the xyloside, the amount of liberated 4-nitrophenol becomes a measure of α-glucuronidase activity (Scheme 5).

of the developed reaction mixture with water. Some authors stop the reaction by boiling and clarify the mixture by centrifugation before addition of the copper reagent (146).)

2. β-Xylosidase-Coupled Assay of α-Glucuronidase (188)

a. Reagents

1. 4-Nitrophenyl-2-O-(4-O-methyl-α-D-glucuronosyl)-β-D-xylopyranoside (NPh-Xyl-MeGlcA), prepared by alkaline deesterification of its methyl ester (191, 192), 4 mM solution in 0.05 M acetate buffer, pH 5.0.

$$\text{NPh-Xyl-MeGlcA} \xrightarrow[\alpha\text{-glucuronidase}]{} \text{MeGlcA} + \text{NPh-Xyl} \xrightarrow[\beta\text{-xylosidase}]{} \text{NPh-OH} + \text{Xyl}$$

Scheme 5

1. Determination of α-Glucuronidase Activity Using the Milner-Avigad Copper Reagent

a. Reagents

1. A mixture of aldotriuronic and aldotetrauronic acid (ratio ~ 8 : 2) (Megazyme, Ireland), a solution 2 mg/mL in 0.05 M acetate buffer pH 5.0.
2. Copper reagent prepared according to Milner and Avigad (191).
3. Arsenomolybdate reagent of Nelson reagent (110).
4. D-Glucuronic acid, 1 mM calibration solution in 0.05 M acetate buffer (calibration in the range 0.02–0.2 μmol).

b. Procedure. Enzyme (0.04 mL) is added to a preheated solution of aldouronic acids (0.16 mL, 40°C) and incubated at 40°C for an appropriate time. The reaction is stopped by adding 0.6 mL of the copper reagent. The mixture is heated in a boiling water bath for 10 min and then cooled in an ice-water bath. Subsequently 0.4 mL of the Nelson reagent is then added and after mixing the absorbance at 600 nm is measured against the substrate blank. One unit of α-glucuronidase is defined as the amount of enzyme liberating 1 μmol of glucuronic or 4-O-methylglucuronic acid per 1 min under the selected assay conditions. (*Note*: The original procedure (191) involves dilution

2. Recombinant β-xylosidase of *Aspergillus niger* produced in *Saccharomyces cerevisiae* (191), a solution 2 U/mL of 0.05 M acetate buffer, pH 5.0 (one unit of β-xylosidase is defined as the amount of enzyme liberating 1 μmol of 4-nitrophenol from 4-nitrophenyl-β-D-xylopyranoside).
3. Saturated solution of $Na_2B_4O_7$.
4. 4-Nitrophenol, 1 mM solution in the acetate buffer, calibration in the range 0.01–0.1 μmol.

b. Procedure. 0.1 mL of 4 mM solution of NPh-Xyl-MeGlcA is mixed with 0.1 mL of the β-xylosidase solution (200 mU per reaction mixture), preheated to 37°C, and the reaction is started with addition of 5–20 μL of the tested enzyme solution. After 10 min or longer incubation at 37°C 1 mL saturated solution of $Na_2B_4O_7$ is added and the absorbance is measured at 410 nm. An alternative procedure is to add 0.1 mL enzyme solution to 0.05 mL double-concentrated substrate and β-xylosidase solution in 0.1 M acetate buffer. One unit of α-glucuronidase is the amount of enzyme required to release 1 μmol of 4-nitrophenol. (*Note*: The assay was applied to three different α-glucuronidases. Their K_m values for NPh-Xyl-MeGlcA were in the range 0.21–0.58 mM, which is in the range of K_m values of α-glucuronidases for aldouronic acids. The new substrate is still not commercially available.)

G. Assays for Screening Purposes

No direct in situ detection of α-glucuronidases has been reported.

V. ACETYLXYLAN ESTERASE (3.1.1.72)

A. Chemical Reactions Catalyzed

$$\begin{array}{l} \qquad\qquad\qquad\qquad\qquad\qquad\qquad\qquad\qquad\qquad\quad H_2O \\ R_1\text{-Xyl}\beta 1\text{-4Xyl}\beta 1\text{-4Xyl}\beta 1\text{-4Xyl}\beta 1\text{-4Xyl-}R_2^* \rightarrow \\ \quad 2 \qquad\qquad\quad 3 \\ \quad | \qquad\qquad\quad | \\ \quad Ac \qquad\qquad\quad Ac \end{array}$$

$$R_1\text{-Xyl}\beta 1\text{-4Xyl}\beta 1\text{-4Xyl}\beta 1\text{-4Xyl}\beta 1\text{-4Xyl-}R_2^* + 2AcH$$

$$\begin{array}{lcl} & H_2O & \\ \text{Xyl}\beta 1\text{-4Xyl}^* & \rightarrow & \text{Xyl}\beta 1\text{-4Xyl}^* + AcH \\ 2 & & \\ | & & \\ Ac & & \end{array}$$

$$\begin{array}{lcl} & H_2O & \\ \text{Xyl}\beta 1\text{-4Xyl}^* & \rightarrow & \text{Xyl}\beta 1\text{-4Xyl}^* + AcH \\ 3 & & \\ | & & \\ Ac & & \end{array}$$

*Reducing end

Acetylxylan esterases (AcXEs) are components of microbial xylanolytic and cellulolytic systems which are able to remove acetyl groups esterifying D-xylopyranosyl residues of xylan main chain at positions 2 or 3 (193–195). AcXEs also deacetylate partially acetylated xylo-oligosaccharides. The enzyme action on polysaccharide substrates creates new sites on the xylan main chain, suitable for productive binding with depolymerizing EXs. This effect is reflected in a clear cooperativity of the two enzymes during acetylxylan degradation, a typical example of enzyme synergy (54, 196, 197). Acetylxylan degradation with EXs proceeds faster and to a higher degree in the presence of AcXEs (54). Deacetylation of xylo-oligosaccharides makes the oligosaccharides fully susceptible to the action of β-xylosidase.

B. AcXE Substrates

The substrate similar to the native O-acetyl-4-O-methyl-D-glucurono-D-xylan present in plant cell walls can be prepared by dimethylsulfoxide extraction of hardwood holocellulose, e.g., birchwood or beechwood holocellulose (198, 199). An analogous polysaccharide of a lower polymerization degree (average DP $\sim$ 25) and acetyl content of 13% can be obtained as a nondialyzable fraction of a water-soluble, noncellulosic polymer by steaming birch at 200°C for 10 min (200). An aqueous thermochemical treatment of hardwood leads to a similar material with a higher acetyl content (201). Since none of the above-mentioned AcXE substrates are commercially available and their isolation is difficult or dependent on availability of special equipments, some authors have replaced natural acetylxylan by a chemically acetylated polysaccharide. A widely used method of chemical acetylation of xylan was published by Johnson et al. (202). There are also examples of the use of fully chemically acetylated hardwood xylan as a substrate for AcXE (203, 204). As will be shown below, a majority of AcXEs can be assayed on a variety of aryl acetates which serve as substrates of nonhemicellulolytic acetylesterases and lipases.

C. Classification

Acetylxylan esterase (EC 3.1.1.72).

D. Properties as Proteins

AcXEs show the greatest diversity in molecular organization among all components of microbial xylanolytic systems. On the basis of amino acid sequence similarity AcXEs have been assigned to seven families of 13 so far recognized families of carbohydrate esterases (73, 205) (Table 4).

The best-known fungal AcXEs from *Aspergillus, Penicillium, Schizophyllum* and *Trichoderma* spp. can be found in carbohydrate esterase families 1 and 5 together with bacterial acetylxylan esterases. The majority of these represents one catalytic domain of bifunctional acetylxylan-degrading enzymes. Diverse AcXEs of the anaerobic fungus *Neocallimastix patriciarum* (214) can be found in families 2, 3, and 6. AcXEs produced by *Streptomyces* are grouped in family 4 together with similar AcXE modules of bacterial bifunctional enzymes. Their sequences are similar to those of nodulating proteins (NodB) from *Rhizobium* spp. and with some yeast enzymes, identified as chitooligosaccharide and chitin deacetylases (205).

Fungal AcXEs, and some bacterial enzymes, are usually monomeric enzymes, while some AcXEs from thermophilic anaerobic bacteria occur as oligomers of smaller subunits (224). As already mentioned, numer-

Table 4 Families of Carbohydrate Esterases Containing Acetylxylan Esterases

Family	Microbial producer of acetylxylan esterase	Mw (kDa)	pI	Other enzymes in the family	References
1	*Aspergillus niger*	30.5	3.1	None	206
	Schizophyllum commune[a]	30	3.4		203, 207
	Penicillium purpurogenum AcXE I	48	7.8		208
	Pseudomonas fluorescens				209
	Catalytic domains of bifunctional enzymes of anaerobic bacteria				210–212
2	Ruminal anaerobic bacteria and fungi			None	213, 214
3	Ruminal anaerobic bacteria and fungi			None	213–215
4[b]	*Streptomyces lividans*	34	9.0	Chitin and chito-oligosaccharide deacetylase	216, 217
	Streptomyces thermoviolaceus	34.3			218
	Catalytic domains of bifunctional enzymes of anaerobic bacteria				82, 212, 219
5	*Trichoderma reesei*	34	6, 8, 7.0	Cutinase	220, 221
	Penicillium purpurogenum AcXE II	23	7.8		208, 222
6	Anaerobic ruminal fungi				214, 223
7	*Thermoanaerobacterium Thermotoga neapolitana*	32, 26	4.2, 4.3		224, 225

[a]Assignment based on a sequence of fifty NH_2-terminal amino acids (226).
[b]This may be the only family, members of which do not attack synthetic low-molecular-mass substrates, such as aryl acetates (226).
Source: http://afmb.cnrs-mrs.fr/~pedro/CAZY/db.html.

ous enzymes have modular architecture. Some of AcXEs, such as those from *Pseudomonas fluorescens* (209) or *Trichoderma reesei* (221), contain cellulose-binding domains (CBDs) separated from the catalytic domain by linker regions. Others, like AcXE from *Streptomyces lividans* (217), contain a xylan-binding domain (77). AcXE of *Cellulomonas fimi* is a part of a bifunctional enzyme which contains both CBD and XBD (82). The two-catalytic module architecture, represented by various combinations of EXs linked to AcXEs, is very common particularly among acetylxylan-degrading bifunctional enzymes of ruminal anaerobic bacteria (212). AcXE domains of such bifunctional enzymes can be found in carbohydrate esterase families 1, 2, 3, and 4 (Table 4). With the bifunctional EX-AcXE enzyme from *Clostridium thermocellum* (83) it has been demonstrated that the two catalytic domains act synergistically in the degradation of acetylxylan. This observation again suggests that the production of an enzyme having both debranching and depolymerizing activity can be a great advantage for a microorganism competing for a carbon source with microorganisms using separate enzyme components.

AcXEs existing as single-domain enzymes have a molecular mass in the range of 23–48 kDa and acidic or neutral pI values. There does not seem to be a special relationship between these two parameters and their assignment into carbohydrate esterase families (Table 4).

Three-dimensional structures are known only for AcXEs belonging to family 5. Crystallization has been reported for AcXEII from *P. purpurogenum* (227) and AcXE from *T. reesei* (228). The protein from *P. purpurogenum* shows an α/β hydrolase fold, similar to that of cutinase (227). Cysteine residues form five S-S bridges which makes the structure very rigid and tightly packed. The substrate binding site appears to be small and able to accommodate only an acetyl group, thus giving a relatively high substrate specificity to the enzyme.

E. Properties as Enzymes

1. Substrate Specificity

Substrate specificity of AcXEs is one of the least-clarified aspects of this xylanolytic component. There is very limited knowledge on the structure-function rela-

tionship of these enzymes, particularly considering that they have been assigned to seven different families (Table 4). The situation is complicated because there are esterases and lipases which cannot be strictly considered as components of xylanolytic systems, but which could participate in the later stages of acetylxylan degradation, by deacetylation of xylooligosaccharides. It is known that nonhemicellulolytic esterases and lipases operate quite efficiently on low-molecular-mass acetylated carbohydrases (226, 229). As a consequence, we shall limit the discussion here to the catalytic properties of enzymes that deacetylate polymeric substrates as such or coinduced with other plant cell walls hydrolyzing enzymes.

Several lines of evidence suggest that there are two major types of acetylesterases that participate in acetylxylan degradation (197). They differ in their affinity toward polymeric and oligomeric substrates. The enzymes that perform well on polymeric substrates are capable of causing precipitation of xylan from solution due to deacetylation (207, 226). The removal of acetyl groups results in the association of xylan molecules into insoluble aggregates. This property is very typical of AcXEs of family 4 (Table 4), which appear to be most specific for acetyl xylan and do not hydrolyze low-molecular-mass substrates such as 4-nitrophenyl- or 4-methylumbelliferyl acetate (226). The enzymes of other families share properties compatible with general acetylesterases and acylesterases (226). They are active on a variety of synthetic aryl acetates and acylates (226). This second group of enzymes do not perform well on polymeric acetylxylan but are more active on acetylated oligosaccharides generated from acetylxylan by EXs (197, 226, 230). Thus EXs would synergistically facilitate the release of acetic acid in concert with this type of acetylesterases. Additional studies are also required to define the specificity of AcXEs with respect to the type of polysaccharide that they deacetylate. There are indications that at least some AcXEs are quite specific for acetylxylan (197, 230).

2. Specificity for the Position of the Acetyl Group in the Main Chain

Xylose residues in xylan are acetylated at positions 2 and/or 3, and the acetyl groups are more or less evenly distributed between these positions. This raises questions of whether the AcXEs are capable of releasing acetyl groups bound only at one position or at both positions, and to what extent is deacetylation influenced by the migration of acetyl groups between positions 2 and 3. Studies of three AcXEs on acetylated methyl glycosides showed the regioselective removal of acetyl group from positions 2 and 3 (229, 231, 232). AcXE from *S. commune* AcXE exhibited a preference for position 3 (229), while the *T. reesei* AcXE deacetylated the model compounds sequentially, first at position 2 and then rapidly at position 3 (231). *S. lividans* AcXE worked almost simultaneously on positions 2 and 3, essentially catalyzing a double deacetylation of compounds at both positions (232). Two methyl xylopyranoside diacetates, which had a free hydroxyl group at position 2 or 3, i.e., the derivatives that most closely mimicked monoacetylated xylopyranosyl residues in acetylxylan, were deacetylated by 1 or 2 orders of magnitude faster than 2,3,4-tri-O-acetyl- or 2,3-di-O-acetyl-β-D-xylopyranoside. These observations explained the double deacetylation. The second acetyl group was removed immediately after the first one. An implication of these results is that the deacetylation mechanism of positions 2 and 3, when the neighboring positions 3 and 2 are nonacetylated, might involve an enzyme-catalyzed formation of a five-member transition state intermediate (Scheme 6). Such intermediates are believed to be involved in the spontaneous migration of acetyl group along the glycopyranoid ring in aqueous media. If this hypothetical

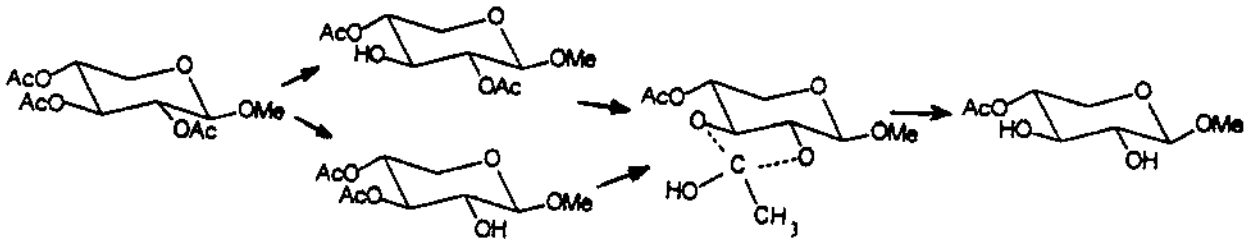

Scheme 6

mechanism is experimentally confirmed, the question of regiospecificity of AcXE at positions 2 and 3 will become irrelevant.

3. Reaction Mechanism

The inactivation of AcXEs with phenyl methyl sulfonyl fluoride (221, 227) and the occurrence of the serine sequence GXSXG in active site of AcXEs (195) suggest that AcXEs utilize a catalytic mechanism similar to lipases and serine proteases. This mechanism involves two major elements, a nucleophilic serine and a general acid-base catalyst, usually a histidine. It remains to be established whether all types of AcXEs contain the serine motif (GXSXG) in their catalytic site.

G. Determination of AcXE Activity

The most specific AcXE assay employs as substrates hardwood acetylxylans extracted either by DMSO or obtained by steaming wood. The naturally occurring acetylxylan can be replaced by chemically acetylated xylan. In the presence of EXs, both types of polysaccharides are also suitable for enzymes that prefer acetylated xylo-oligosaccharides as substrates. The amount of released acetic acid can be determined by HPLC chromatography, or enzymically using the Boeringer Test Combination No. 148,261. Practically all HPLC procedures employ for analysis of acetic acid a Bio-Rad (Richmont, CA) Aminex HPX-87H column eluted with 0.01 N H_2SO_4 (193, 202), connected to a refractometric detector. Glycerol may be recommended as internal standard. The conditions of AcXE assay on acetylxylan vary considerably among different laboratories. Typical conditions include a substrate concentration in the range of 0.2–10%, pH in the range of 5.0–7.0, and temperature in the range of 30–75°C.

Since most AcXEs exhibit general acetylesterase activity [the exception is family 4 (226)], their activity also can be determined using chromogenic or fluorogenic acetylesterase substrates such as 4-nitrophenyl acetate, α- or β-naphthyl acetate, and 4-methylumbelliferyl acetate. Examples of selected AcXE assays are given below.

1. AcXE Assay on Acetylxylan (202, 233)

a. Reagents

1. Acetylxylan obtained from hardwood by DMSO extraction or steaming, or chemically acetylated xylan, 10% solution or suspension in 0.4 M potassium phosphate buffer, pH 6.0 or 6.5.
2. 1 N H_2SO_4.
3. Acetic acid, 0.–1.0% (w/v).
4. Glycerol, 1% (w/v).

b. Procedure. One volume of acetylxylan solution or suspension is mixed with one volume of enzyme solution and incubated at 50°C. At time intervals, 0.2-mL aliquots are taken, mixed with 10 μL of 1 N H_2SO_4 to stop the reaction, clarified by a short centrifugation, and supernatants analyzed for acetic acid by HPLC. Standards of acetic acid are analyzed under the same conditions. Glycerol can be used as an internal standard at 0.1% or 0.2% concentration. One unit of AcXE is defined as the amount of enzyme liberating 1 μmol of acetic acid per minute. (*Note*: Termination of the reaction is done by heating of the sample at 100°C in case the acetic acid is determined enzymically (200).)

2. Acetylesterase Assay on 4-Nitrophenyl Acetate (233)

a. Reagents

1. 4-Nitrophenyl acetate, saturated solution in 0.2 M potassium phosphate buffer, pH 6.5 (freshly prepared solution).
2. 4-Nitrophenol, 1 mM standard solution in 0.2 M potassium phosphate buffer, pH 6.5.

b. Procedure. A volume of 10–50 μL appropriately diluted enzyme solution is mixed with 1 mL clarified saturated solution of 4-nitrophenyl acetate in a 1 cm light-path microcuvette and incubated at 22°C. Absorbance at 410 nm is measured at time intervals against a substrate blank. Alternatively, the absorbance can be followed continuously. The amount of substrate hydrolyzed is calculated from a calibration curve prepared using 4-nitrophenol in the 0.05–0.3 μmol/mL range in 0.2 M phosphate buffer. The reaction cannot be terminated chemically because of the labile nature of the substrate. One unit of acetylesterase activity is defined as the amount of enzyme liberating 1 μmol of 4-nitrophenol in 1 min.

3. Acetylesterase Assay on 4-Nitrophenyl Acetate (202)

a. Reagents

1. 4-Nitrophenyl acetate, 50 mM solution in DMSO (stable at 4°C), 2 mM solution in water prepared freshly by diluting 1 volume of the DMSO solution with 24 volumes of water.
2. 0.1 M potassium phosphate buffer, pH 6.5.

3. 4-Nitrophenol calibration solution in 0.05 M phosphate buffer.

b. Procedure. Enzyme present in 1.5 mL of 0.1 M phosphate buffer is mixed with 1.5 mL of 2 mM solution of 4-nitrophenyl acetate and incubated at 25°C. The increase in absorbance at 410 nm is measured against a substrate blank. Enzyme activity is calculated from the slopes of absorbance versus time and calibration values of 4-nitrophenol obtained under the same conditions. One unit of acetylesterase activity is defined as above.

4. Acetylesterase Assay on α-Naphthyl Acetate (234)

a. Reagents

1. α-Naphthyl acetate, 1 mM solution in 0.05 M sodium citrate buffer, pH 5.3.
2. Fast Corinth V Salt (Sigma F-6389), 0.1% solution in 1 M acetate buffer, pH 4.3, containing 10% Tween.
3. α-Naphthol, calibration solution in the citrate buffer.

b. Procedure. Enzyme solution (0.2 mL) is incubated with 1.8 mL α-naphthyl acetate solution at 50°C for 10 min, after which 1 mL dye solution is added. The absorbance at 535 nm is read exactly 10 min after addition of the dye. The calibration curve is constructed under the same conditions.

E. Fluorimetric Acetylesterase Assay on 4-Methylumbelliferyl Acetate (235)

a. Reagents. 4-Methylumbelliferyl acetate, 10 mM solution in methanol. 0.5 M potassium phosphate buffer, pH 6.5.

b. Procedure. 4-Methylumbelliferyl acetate solution (10 μL) is mixed with 10 μL phosphate buffer and made up to 100 μL with the enzyme sample and water. After an appropriate time of incubation at 40°C, the mixture is diluted with 2.9 mL distilled water. The fluorescence is measured at an excitation wavelength of 330 nm and an emission wavelength at 445 nm using 4-methylumbelliferone as the calibration standard. One unit of esterase is defined as 1 μmol of the product formed per minute. (*Note*: A much less sensitive acetylesterase assay using 4-methylumbelliferyl acetate is a photometric assay which exploits the fact that 4-methylumbelliferone shows considerable absorbance at 354 nm (not an absorption maximum) while its acetate does not absorb at this wavelength (224).)

H. Assays for Screening and Detection Purposes

All substrates used for AcXE assays can also be employed for detection of the enzyme in gels. Detection of AcXE using polymeric acetylxylan is based on the precipitation of the polysaccharide due to deacetylation (207). This approach is applicable only in those cases when the AcXEs located in the gel are free of EXs, which would prevent the precipitation by hydrolyzing the deacetylated polymer. Such a situation occurs after separation of EXs from AcXEs by electrophoretic methods. This means that precipitation of acetylxylan can be used for screening purposes only in the case of naturally occurring and recombinant strains that do not produce EXs.

For initial screens of microorganisms and transformants producing AcXEs belonging to other families than family 4 (Table 4), it is possible to use chromogenic and fluorogenic aryl acetates, such as α- or β-naphthyl acetate and 4-methylumbelliferyl acetate (214). An alternative is to screen for the production of enzymes clearing of milky solid media containing insoluble per-O-acetylated carbohydrates, e.g., penta-O-acetyl-D-glucose (236). Subsequent screening of positive colonies for the ability to deesterify acetylxylan itself is necessary. The principles outlined above can be used for detection of AcXEs in electrophoretic gels.

1. Detection of AcXE in Gels Using Acetylxylan as a Substrate (233)

An approximately 1-mm-thick flat 1.5–2.0% agarose gel containing 0.5–2.0% of acetylxylan (DMSO extracted or obtained by steaming wood) and 0.01% sodium azide in 0.1 M phosphate buffer, pH 6.5, is prepared by casting between glass plates. Visualization of AcXE is carried out by superimposing the detection and rebuffered separation gel in a plastic bag and incubating at 30–50°C until cloudy areas appear. The precipitate forms in both the separation and detection gels because of cross-diffusion of enzyme and substrate. The method fails when esterase is located close to EXs. Gels with precipitates are photographed in diffuse light similarly as immunoprecipitation bands.

2. Detection of Acetylesterase in Gels by α-Naphthyl Acetate (237)

A solution of 20 mg α-naphthyl acetate in 4 ml of N,N′-dimethylformamide is mixed with 36 mL of a solution of 20 mg of Diazo Blue R (Sigma) in 0.05

M phosphate buffer, pH 7.4. An electrophoretic or isoelectrofocusing gel is washed with 0.1 M phosphate buffer, pH 7.4, for 15 min. The gel is then placed in a freshly prepared substrate-dye solution and incubated for 1 h at 40°C. The reaction is stopped by decanting the staining solution and covering the gel with a solution of 2% acetic acid.

3. Detection of Acetylesterase Using 4-Methylumbelliferyl Acetate (233)

A flat detection agarose gel containing 0.1% 4-methylumbelliferyl acetate in 0.1 M phosphate buffer is freshly prepared. The gel is placed in contact with a washed electrophoretic gel and incubated at room temperature until a bright fluorescent zone appears under UV light at 360 nm on both separation and detection gels. An alternative procedure is to bring the separation gel into contact with a saturated solution of 4-methylumbelliferyl acetate in 0.1 M phosphate buffer on a glass plate.

VI. α-L-ARABINOFURANOSIDASE (EC 3.2.1.55)

A. Chemical Reactions Catalyzed

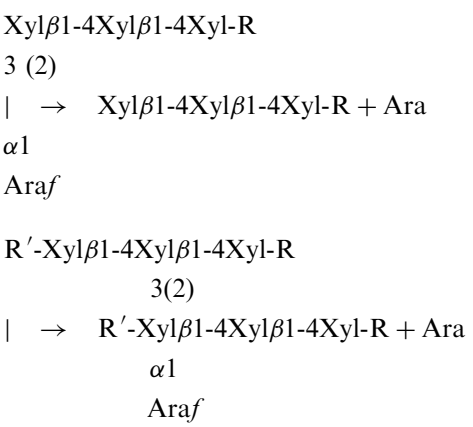

α-L-Arabinofuranosidase is a component of hemicellulolytic systems that participates in hydrolysis of plant polysaccharides built from or containing nonreducing terminal α-L-arabinofuranosyl residues (44, 238). Such polysaccharides have been recognized as part of pectic substances, gum exudates, and wood and cereal hemicelluloses (239). The pectic substances mainly include L-arabinan and various types of L-arabino-D-galactans. Other natural substrates of α-L-arabinofuranosidase are glycosylated terpenols of grape, important precursors of grape and wine aromas. Many of these terpenols are linked to disaccharide moieties in which the nonreducing terminal sugar is frequently L-arabinofuranose. Thus, α-L-arabinofuranosidase can be used for enhancement of wine flavor by the release of free terpenols (240–242).

Since the enzymes degrading arabinans and arabinogalactaus were specifically covered in Chapter 70, here we shall focus on α-L-arabinofuranosidases involved in the degradation of polysaccharides containing main chains built from β-1,4-linked xylopyranosyl residues, specifically, softwood arabinoglucuronoxylans and cereal arabinoxylans. Some of these enzymes, particularly those which attack low-molecular-mass fragments of these polysaccharides, participate in the degradation of all types of L-arabinose-containing polysaccharides. However, there are α-L-arabinofuranosidases specific for arabinoxylans. In the softwood polysaccharide the L-arabinofuranosyl residues are linked to the main chain α-1,3- or α-1,2 glycosidically as single substituents. Cereal arabinoxylans contain, in addition to α-1,3- and α-1,2-linked L-arabinofuranosyl residues as single substituents, doubly arabinosylated xylopyranosyl residues of the main chain.

B. Properties as Proteins

Fungal α-L-arabinofuranosidases occur mostly as monomeric enzymes with molecular masses between 32 and 84 kDa and pI values between 3.2 and 7.5 (44). The majority of described fungal enzymes are products of *Aspergillus* spp. (146). and have pI values ~ 3.5. Bacterial and *Streptomyces* α-L-arabinofuranosidases frequently occur as oligomers, form dimers up to octamers, with subunits of molecular mass between 33 and 75 kDa. pI values were reported in the range of 3.8–9.0.

Some α-L-arabinofuranosidases show modular architecture similar to other xylanolytic enzymes. Interesting in this regard is α-L-arabinofuranosidase from *T. reesei* (244, 245). Two different forms of the enzyme have been isolated from a culture fluid of the fungus. The 25-kDa form corresponds to the catalytic domain only (245). The 53-kDa form, the first form of the enzyme described (244), also contains a noncatalytic xylan-binding domain (245). The large 53-kDa form can be converted to the shorter one by proteolytic digestion (245). α-L-Arabinofuranosidase from *P. fluorescens* was reported to contain a cellulose-binding

domain in the N-terminal portion of the polypeptide chain (246). A xylan-binding domain was detected in C-terminal region of α-L-arabinofuranosidase B from *S. lividans* (247). The enzymes containing the noncatalytic polysaccharide-binding domains are specific for release of L-arabinofuranose from polymeric substrates.

C. Properties as Enzymes

Microbial α-L-arabinofuranosidases can be divided into three different groups according to substrate specificities (239). The groups seem to coincide with three different glycosyl hydrolase families into which α-L-arabinofuranosidases belong (Table 5).

The enzymes that perform best on short α-1,5-linked arabinooligosaccharides and are active on 4-nitrophenyl-α-L-arabinofuranoside (NPh-Ara*f*) and inactive on polymeric substrates are grouped in family 51. They include both fungal and bacterial α-L-arabinofuranosidases of molecular mass 57–72 kDa, which catalyze the hydrolysis of the glycosidic linkage with retention of the anomeric configuration (248). These are apparently the enzymes designed to degrade more arabinans rather than arabinoxylans.

Family 54 includes mainly fungal α-L-arabinofuranosidases (M.m. 49–53 kDa) which exhibit somewhat broader substrate specificities than the enzymes of family 51. The 54 family α-L-arabinofuranosidases attack not only NPh-Ara*f* and arabinose-containing oligosaccharides, but also polymeric substrates such as arabinoxylans and arabinoglucuronoxylans (239). These enzymes catalyze hydrolysis of α-1,5-, α-1,3- and also α-1,2-linked terminal L-arabinofuranosyl residues with retention of the anomeric configuration (248).

The family 62 of α-L-arabinofuranosidases (Table 5) includes enzymes which preferentially attack polymeric substrates, i.e., arabinoxylans. The best-known members of this family are enzymes from *Aspergillus* spp., assigned as AXHs (249), α-L-arabinofuranosidase B from *Streptomyces lividans* (247), and an enzyme from *Ps. fluorescens* subsp. *cellulosa* having a modular architecture (246). The enzymes show a clear preference for α-1,2-linked and α-1,3-linked α-L-arabinofuranosyl residues of arabinoxylan main chain. However, the enzymes of this family do not remove α-L-arabinofuranosyl residues from doubly substituted xylopyranosyl residues.

An arabinofuranose-releasing enzyme of novel substrate specificity was isolated from *Bifidobacterium adolescentis* DSM 20083 (250). This enzyme specifically releases terminal arabinofuranosyl residues linked α-1,3 to xylopyranosyl residues of main chains that also carry α-1,2-linked arabinofuranose. Wood and McCrea (251) reported the occurrence of a hydrolase releasing feruloylated L-arabinofuranosyl residues from wheat straw arabinoxylan. Additional evidence

Table 5 Families of α-L-Arabinofuranosidases and Differences in Their Properties

Family	Producing microorganism	Molecular mass (kDa)	Hydrolyzed substrates	Mechanism of hydrolysis	Ref.
51	*A. niger* (enz. A) *Bacillus* *Streptomyces* *Thermotoga* *Clostridium*	57–72	NPh-α-Ara*f*, arabino-oligosaccharides (enzymes are inactive on polymers)	Retaining	205
54	*A. niger* (enz. B) *T. reesei* *Ewericella nidulans* *Synchocystis* sp.	49–53	NPh-α-Ara*f*, arabino-oligosaccharides, arabinoxylan (attack mainly on α-1,3-linked Ara*f*, no attack on double arabinosylated xylopyranosyl residues.	Retaining	205, 253
62	*Aspergillus* (AXH) *Streptomyces* (enz. B), *Ps. fluorescens*	47–59	arabinoxylan (the enzymes remove α-1,3- and α-1,2-linked L-Ara*f* residues, no attack on double arabinosylated xylopyranosyl residues)	Unknown	246, 247, 249

Source: Refs. 44, 205.

for hydrolysis of substituted arabinofuranosyl residues has been reported for α-L-arabinofuranosidase from *A. terreus* (252). The mode of action of enzymes operating on high-molecular-mass arabinoxylans and their relationship to glycosyl hydrolase families is illustrated in Scheme 7. Based on the complexity of structures of plant arabinoxylan, one can anticipate the discovery of arabinofuranosidases with other substrate specificities.

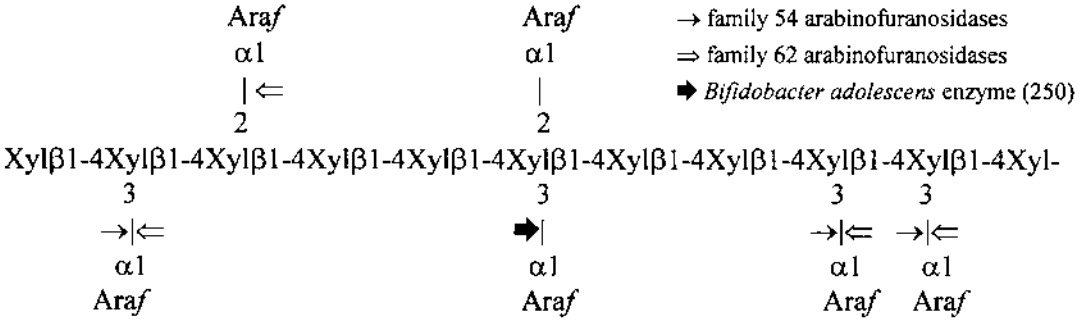

Scheme 7

D. Determination of α-L-Arabinofuranosidase Activity

As indicated in Table 5, two families of α-L-arabinofuranosidases can be assayed easily using the chromogenic substrate 4-nitrophenyl α-L-arabinofuranoside or the fluorogenic substrate 4-methylumbelliferyl α-L-arabinofuranoside. One should be aware of the fact that these substrates can also be attacked by β-xylosidases of family 43, which exhibit aryl α-L-arabinofuranosidase activity (Table 3). Therefore, it is imperative to confirm the identity of the enzyme by determining its ability to release arabinose from arabino-substituted xylans or xylooligosaccharides (5). α-L-Arabinofuranosidases of family 62 must be assayed on natural substrates, arabinoxylans, and oligosaccharides derived from arabinoxylans. Released arabinose is determined using HPLC or as reducing sugar. Examples of determination of α-L-arabinofuranosidase activity are given below.

1. α-L-Arabinofuranosidase Assay Using 4-Nitrophenyl α-L-Arabinofuranoside (244)

a. Reagents

1. 4-Nitrophenyl α-L-arabinofuranoside, 2 mM solution in 0.05 M sodium citrate phosphate buffer (pH 4.0) or in other buffer depending on the pH optimum of the assayed enzyme.
2. 1.0 M sodium carbonate.

b. Procedure. 4-Nitrophenyl α-L-arabinofuranoside solution (0.9 mL) is mixed with 0.1 mL of the enzyme sample, incubated at 50°C or an appropriate time, and the reaction is stopped by addition of 0.5 mL of 1 M solution of Na_2CO_3. Liberated 4-nitrophenol is measured spectrophotometrically at 400 nm. One unit of α-L-arabinofuranosidase activity is defined as the amount of enzyme liberating 1 μmol of 4-nitrophenol in 1 min. (*Note*: The literature offers a variety of modification of the above procedure with respect to buffer, substrate concentration, and the reaction terminating agent. Termination of the reaction using a saturated solution of sodium tetraborate is recommended.)

2. Fluorimetric Assay of α-L-Arabinofuranosidase (254)

a. Reagents

1. 4-Methylumbelliferyl α-L-arabinofuranoside, 10 mM solution in dimethyl formamide.
2. 0.02 M acetate buffer, pH 4.5.
3. 0.2 M sodium carbonate buffer, pH 10.0.
4. 4-Methylumbelliferone.

b. Procedure. Enzyme solution, 5–20 μL, is made up to 200 μL with 0.02 M acetate buffer (pH 5.5) containing 4 μL of 10 mM solution of the substrate in dimethyl formamide. To monitor the enzymic activity 20-μL aliquots of the reaction mixture are diluted with 2 mL sodium carbonate buffer, and the liberated 4-methylumbelliferone is determined fluorimetrically.

One unit is defined as the amount of enzyme that releases 1 μmol of 4-methylumbelliferone per minute.

3. Assay of 1,4-β-Arabinoxylan Arabinofuranohydrolase (249)

a. Reagent. Arabinoxylan (wheat, rye, or oats; Megazyme), 0.1% solution in 0.05 M acetate buffer, pH 5.0.

b. Procedure. The solution of oats spelt arabinoxylan is mixed with a small volume of enzyme solution, incubated at 30°C for an appropriate time, and analyzed for L-arabinose by HPLC.

4. Assay of 1,4-β-Arabinoxylan Arabinofuranohydrolase (247)

a. Reagents

1. Arabinoxylan (wheat, rye, or oats; Megazyme), 1.0% solution in 0.05 M acetate buffer, pH 5.0.
2. p-Hydroxybenzoic acid anhydride (PANBAH) reagent for determination of reducing sugars (256).

b. Procedure. 0.9 mL of 1.0% arabinoxylan solution is mixed with 0.1 mL appropriately diluted enzyme and incubated at 55°C. The reaction is stopped by transferring 0.1 mL of the sample to 0.3 mL of the PANBAH reagent and heating for 5 min at 95°C. The reducing sugars are determined spectrophotometrically at 405 nm using L-arabinose as standard. One unit if enzyme activity is defined as the amount of enzyme that releases 1 μmol of arabinose per minute.

E. Assays for Detection and Screening Purposes of α-L-Arabinofuranosidases of Families 51 and 54

α-L-Arabinofuranosidases which hydrolyze aryl α-L-arabinofuranosides can be detected in electrophoretic gels or in screening growth media using two substrates: fluorogenic 4-methylumbelliferyl α-L-arabinofuranoside (255), or chromogenic 5-bromo-3-indolyl-α-L-arabinofuranoside (254). Specific procedures how to apply these glycosides can be found in the section devoted to endo-β-1,4-xylanases. With the first substrate, which is commercially available, the presence of the enzyme results in the liberation of 4-methylumbelliferone, which shows a strong fluorescence under UV light ($\sim$ 360 nm). The fluorescence can be enhanced by alkaline agents, e.g., exposing the gels to ammonium hydroxide vapors. The hydrolysis of 5-bromo-3-indolyl glycoside results in the formation of an intensely colored indigo precipitate. The glycoside was suggested for use in cloning experiments in which α-L-arabinofuranosidase will be used as a reporter gene (254).

ACKNOWLEDGMENT

The author thanks Dr. Timothy D. Leathers from the Biopolymer Unit of the USDA, ARS, in Peoria, IL, for generous help with English in this chapter.

REFERENCES

1. RFH Dekker, GN Richards. Hemicellulases: their occurrence, purification, properties, and mode of action. Adv Carbohydr Chem Biochem 32:277–352, 1976.
2. PJ Reilly. Xylanases: structure and function. Basic Life Sci 18:11–129, 1981.
3. P Biely. Microbial xylanolytic systems. Trends Biotechnol 3:286–290, 1985.
4. K-EL Eriksson, RA Blanchette, P Ander. Biodegradation of hemicelluloses. In: TE Timell, ed. Microbial and Enzymatic Degradation of Wood and Wood Components. Berlin: Springer-Verlag, 1990, pp 181–224.
5. MP Coughlan, GP Hazelwood. β-1,4-Xylan-degrading enzyme systems: biochemistry, molecular biology and biotechnology. Biotechnol Appl Biochem 17:259–289, 1993.
6. J Visser, G Beldman, MA Kusters–Van Someren, AGJ Voragen, ed. Xylans and Xylanases. Amsterdam: Elsevier Science 1992.
7. MP Coughlan, GP Hazelwood, ed. Hemicellulose and Hemicellulases. London: Portland Press, 1993.
8. RL Uffen. Xylan degradation: a glimpse at microbial diversity. J Ind Microbiol Biotechnol 19:1–6, 1997.
9. RA Prade. Xylanases: from biology to biotechnology. Biotechnol Gen Eng Rev 13:101–131, 1995.
10. IA Preece, M MacDougal. Enzymic degradation of cereal hemicelluloses. II. Patterns of pentosan degradation. J Inst Brew 64:489–500, 1958.
11. L Taiz, RL Jones. Production of cell wall hydrolyzing enzymes in barley aleurone layers in response to gibberellic acid. Plant Physiol 58:380–386, 1972.
12. GB Fincher. Cell wall metabolism in barley. In: PR Shewry, ed. Barley: Genetics, Biochemistry, Molecular Biology and Biotechnology. Wallingford: CAB International 1992, pp 413–437.
13. G Cleemput, M Hessing, M van Oort, M Deconynck, JA Delcour. Purification and characterization of a β-D-xylosidase and an endo-xylanase from wheat flour. Plant Physiol 113:377–386, 1997.

14. G Cleemput, K Van Leare, M Hesing, F Van Leuven, S Torrekens, JA Delcour. Identification and characterization of a novel arabinoxylanase from wheat flour. Plant Physiol 115:1619–1627, 1977.
15. C-S Gong, LF Chen, MC Flickinger, GT Tsao. Conversion of hemicellulose carbohydrates. Adv Biochem Eng 20:93–118, 1981.
16. B Hahn-Hägerdahl, H Jeppsson, K Skoog, BA Prior. Biochemistry and physiology of xylose fermenting yeast. Enzyme Microb Technol 16:933–943, 1994.
17. K Koga, S Fujikawa. Xylooligosaccharides. In: T Nakakuki, ed. Oligosaccharides. Production, Properties, and Applications. Switzerland: Gordon and Breach Science Publishers, 1993, pp 130–143.
18. KKY Wong, JN Saddler. Application of hemicellulases in the food, feed, and pulp and paper industries. In; MP Coughlan, GP Hazlewood, eds. Hemicellulose and Hemicellulases. London: Portland Press, 1993, pp 127–143.
19. HJ Gilbert, GP Hazlewood. Bacterial cellulases and xylanases. J Gen Microbiol 139:187–194, 1993.
20. G Annison. The role of wheat non-starch polysaccharides in broiler nutrition. Aust J Agric Res 44:405–422, 1993.
21. G Annison, M Choet. Plant polysaccharides—their physicochemical properties and nutritional roles in monogastric animals. In: TP Lyons, KA Jacques, eds. Biotechnology in the Feed Industry. Nottingham: Alltech, 1994, pp 51–66.
22. MR Bedford, HL Classen. The influence of dietary xylanase on intestinal viscosity and molecular weight distribution of carbohydrates in rye-fed broiler chicks. In; J Visser, G Beldman, MA Kusters–Van Someren, AGJ Voragen, eds. Xylans and Xylanases. Amsterdam: Elsevier Science, 1992, pp 361–370.
23. AJ Morgan, H Graham, MR Bedford. Xylanases improve wheat and rye diets by reducing chick gut viscosity. In: C Wenk, M Boessinger, eds. Enzymes in Animal Nutrition (Proceedings of the 1st symposium, Kartause, Ittingen, Switzerland), Zurich, 1993, pp 73–77.
24. B McCleary. Enzymatic modification of plant polysaccharides. Inst J Biol Macromol 8:349–354, 1986.
25. J Maat, M Roza, J Verbakel, H Stam, MJ Santos da Silva, M Bose, MR Egmond, MLD Hagemans, RFM Gorcom, JGM Hessing, CAMJJ Hondel, C Rotterdam. Xylanases and their application in bakery. In: J Visser, G Beldman, MA Kusters–Van Someren, AGJ Voragen, eds. Xylans and Xylanases. Amsterdam: Elsevier Science, 1992, pp 349–360.
26. X Rouau. Investigations into the effects of an enzyme preparation for baking on wheat flour dough pentosans. J Cereal Sci 18:145–157, 1993.
27. X Rouau, D Moreau. Modification of some physicochemical properties of wheat flour pentosans by an enzyme complex recommended for baking. Cereal Chem 70:626–632, 1993.
28. X Rouau, M-L El-Hayek, D Moreau. Effect of an enzyme preparation containing pentosanases on the bread-making quality of flours in relation to changes in pentosan properties. J Cereal Sci 19:259–272, 1994.
29. K Autio, H Härkönen, P Aman, T Parkkonen, T Frigard, M Siika-aho, K Poutanen. Effects of purified endo-β-xylanase and endo-β-glucanase on the structural and baking characteristics of rye doughs. Lebensmittel Wissenschaft und Technologie 29:18–27, 1996.
30. A Monfort, A Blasco, JA Prieto, P Sanz. Combined expression of *Aspergillus nidulans* endoxylanase X24 and *Aspergillus oryzae* α-amylase in industrial baker's yeasts and their use in bread making. Appl Environ Microbiol 62:3712–3715, 1996.
31. L Viikari, A Kantelinen, J Sundquist, M Linko. Xylanases in bleaching: from an idea to the industry. FEMS Microbiol Rev 113:335–350, 1994.
32. J Buchert, J Salminen, M Siika-Aho, M Ranua, L Viikari. The role of *Trichoderma reesei* xylanase and mannanase in treatment of softwood kraft pulp prior to bleaching. Holzforschung 47:473–478, 1993.
33. TK Kirk, TW Jeffries. Roles for microbial enzymes in pulp and paper processing. ACS Ser 655:2–14, 1996.
34. P Baipai. Application of enzymes in the pulp and paper industry. Biotechnol Prog 15:147–157, 1999.
35. MG Paice, L Jurasek. Removing hemicellulose from pulps by specific enzyme hydrolysis. J Wood Chem Technol 4:187–198, 1984.
36. LP Christov, BA Prior. Bleaching response of sulfite pulps to pretreatment with xylanases. Biotechnol Prog 13:695–698, 1997.
37. AMF Milagres, RA Prade. Production of xylanases from *Penicillium janthinellum* and its use in the recovery of cellulosic textile fibres. Enzyme Microb Technol 15:627–632, 1994.
38. P Baipai. Enzymic deinking. Adv Appl Microbiol 45:242–269, 1996.
39. TE Timmel. Recent progress in the chemistry of wood hemicelluloses. Wood Sci Technol 1:45–70, 1967.
40. KCB Wilkie. The hemicelluloses of grass and cereals. Adv Carbohydr Chem Biochem 36:215–264, 1979.
41. KCB Wilkie. Hemicellulose. Chem Tech 13:306–319, 1983.

42. JP Joseleau, J Comtat, K Ruel. Chemical structure of xylans and their interaction in the plant cell walls. In: J Visser, G Beldman, MA Kusters–Van Someren, AGJ Voragen, eds. Xylans and Xylanases. Amsterdam: Elsevier Science, 1992, pp 1–15.
43. J Puls, J Schuseil. Chemistry of hemicelluloses: relationship between hemicellulose structure and enzymes required for hydrolysis. In: MP Coughlan, GP Hazlewood, eds. Hemicellulose and Hemicellulases. London; Portland Press, 1993, pp 1–27.
44. E Luonteri. Fungal α-Arabinofuranosidases and α-Galactosidases Acting on Polysaccharides. Espoo: VTT Publications, 1998.
45. I Mueller-Harvey, RD Hartley. Linkage of *p*-coumaroyl and feruloyl groups to cell-wall polysaccharides of barley straw. Carbohydr Res 148:71–85, 1986.
46. PA Kroon, MTG Conesa, IJ Colquhoun, G Williamson. Process for the isolation of preparative quantities of [2-O(trans-feruloyl)-α-L-arabinofuranosyl]-(1 $\rightarrow$ 5)-L-arabinofuranose from sugarbeet. Carbohydr Res 300:351–354, 1997.
47. GB Fincher, BA Stone. Cell walls and their components in cereal grain technology. In; Y Pomeranz, ed. Advances in Cereal Science and Technology. Vol. III. St. Paul, MN: American Association of Cereal Chemists, 1986, pp 207–296.
48. T Higuchi. Lignin biochemistry: biosynthesis and biodegradation. Wood Sci Technol 24:23–63, 1990.
49. A Chesson. Manipulation of fibre degradation: an old theme revisited. In; TP Lyons, KA Jacques, eds. Biotechnology in the Feed Industry. Nottingham: Alltech, 1994, pp 83–98.
50. T Watanabe, T Koshijima. Evidence for an ester linkage between lignin and glucuronic acid in lignin-carbohydrate complexes by DDQ-oxidation. Agric Biol Chem 52:2953–2955, 1988.
51. MP Coughlan, MG Tuohy, EXF Filho, J Puls, M Clayessens, M Vršanská, MH Hughes. Enzymological aspects of microbial hemicellulases with emphasis on fungal systems. In: MP Coughlan, GP Hazlewood, eds. Hemicellulose and Hemi- cellulases. London; Portland Press, 1993, pp 53–84.
52. FJM Kormelink, AGJ Voragen. Degradation of different [(glucurono)arabino]xylans by combination of purified xylan-degrading enzymes. Appl Microbiol Biotechnol 38:688–695, 1993.
53. RP de Vries, HCM Kester, CH Poulsen, JAE Benen, J Visser. Synergy between enzymes from *Aspergillus* involved in the degradation of plant cell wall polysaccharides. Carbohydr Res 372:401–410, 2000.
54. P Biely, CR MacKenzie, J Puls, H Schneider. Cooperatively of esterases and xylanases in the enzymatic degradation of acetyl xylan. Bio/Technology 4:731–733, 1986.
55. KKY Wong, LUL Tan, JN Saddler. Multiplicity of β-1,4-xylanase in microorganisms: functions and applications. Microbiol Rev 52:305–317, 1988.
56. NR Gilkes, M Claeyssens, R Aebersold, B Henrissat. A Meinke, H Morrison, DG Kilburn, RAJ Warren, RC Miller Jr. Structural and functional relationship in two families of β-1,4-glycanases. Eur J Biochem 202:367–377, 1991.
57. NR Gilkes, B Henrissat, DG Kilburn, RC Miller Jr, RAJ Warren. Domains in microbial β-1,4-glycanases: sequence conservation, function, and enzyme families. Microbiol Rev 55:303–315, 1991.
58. B Henrissat, A Bairoch. New families in the classification of glycosyl hydrolases based on amino acid sequence similarities. Biochem J 293:781–788, 1993.
59. B Henrissat, A Bairoch. Updating the sequence-based classification of glycosyl hydrolases. Biochem J 316:695–696, 1996.
60. C Gaboriaud, V Bissey, T Benchetrit, JP Mornon. Hydrophobic cluster analysis: an efficient new way to compare and analyze amino acid sequences. FEBS Lett 224:149–155, 1987.
61. I Kusakabe, S Ohgushi, T Yasui, T Kobayashi. Structures of the arabinoxylo-oligosaccharides from hydrolytic products of corncob arabinoxylan by a xylanase from *Streptomyces*. Agric Biol Chem 47:2713–2723, 1983.
62. RL Campbell, DR Rose, WW Wakarchuk, R To, W Sung, M Yaguchi. A comparison of the structure of the 20 kd xylanases from *Trichoderma harzianum* and *Bacillus circulans*. In: P Pouminen, T Reinikainen, eds. *Trichoderma* Cellulases and Other Hydrolases. Helsinki: Fagepaino Oy, 1993, pp 63–72.
63. W Wakarchuk, RL Campbell, WL Sung, J Davoodi, M Yaguchi. Mutational and crystallographic analyses of the active site residues of the *Bacillus circulans* xylanase. Protein Sci 3:467–475, 1994.
64. A Törrönen, A Harkki, J Rouvinen. Three dimensional structure of endo-1,4-β-xylanase II from *Trichoderma reesei*: two conformational states in the active site. EMBO J 13:2493–2501, 1994.
65. JED Dean, JD Anderson. Ethylene biosynthesis-inducing xylanase. II. Purification and physical characterization of the enzyme produced by *Trichoderma viride*. Plant Physiol 95:316–323, 1991.
66. AC Grabski, TW Jeffries. Production, purification and characterization of β-(1,4)-endoxylanase of *Streptomyces roseiscleroticus*. Appl Environ Microbiol 57:987–992, 1991.
67. U Derewenda, L Swenson, R Green, Y Wei, R Morosoli, F Shareck, D Kluepfel, ZS Derewenda. Crystal structure, at 2.6 Å resolution, of the *Streptomyces lividans* xylanase A, a member of the F

family of β-1,4-D-glycanases. J Biol Chem 269:20811–20814, 1994.
68. GW Harris, JA Jenkins, I Connerton, N Cummings, L Lo Leggio, M Scott, GP Hazlewood, JI Laurie, HJ Gilbert, RW Pickersgill. Structure of the catalytic core of the family F xylanase from *Pseudomonas fluorescens* and identification of the xylopentaose-binding sites. Structure 2:1107–1116, 1994.
69. R Dominguez, H Souchon, S Spinelli, Z Dauter, KS Wilson, S Chauvaux, P Beguin, AM Alzari. A common protein fold and similar active site in two distinct families of β-glycanases. Nat Struct Biol 2:569–576, 1995.
70. A Schmidt, A Schlacher, W Steiner, H Schwab, C Kratky. Structure of the xylanase from *Penicillium simplicissimum*. Protein Sci 7:2081–2088, 1998.
71. JA Jenkins, LL Legio, G Harris, R Pickersgill. β-Glucosidase, β-galactosidase, family A cellulases, family F xylanases and two barley glycanases form a superfamily of enzymes with 8-fold β/α architecture and with two conserved glutamates near the carboxy-terminal ends of β-strands four and seven. FEBS Lett 362:281–285, 1995.
72. A Törrönen, CP Kubicek, B Henrissat. Amino acid sequence similarities between low molecular weight endo-β-1,4-xylanases and family H cellulases revealed by cluster analysis. FEBS Lett 321:135–139, 1993.
73. PM Coutinho, B Henrissat. Carbohydrate-active enzymes: an integrated database approach. In: HJ Gilbert, GJ Davies, B Henrissat, S Svensson, eds. Recent Advances in Carbohydrate Bioengineering. Cambridge: Royal Society of Chemistry, 1999, pp 3–12.
74. AB Boraston, BW McLean, JM Kormos, M Alam, NR Gilkes, CA Haynes, P Tomme, DG Kilburn, RAJ Warren. Carbohydrate-binding modules: diversity of structure and function. In: HJ Gilberg, GJ Davies, B Henrissat, S Svensson, eds. Recent Advances in Carbohydrate Bioengineering. Cambridge: Royal Society of Chemistry, 1999, pp 202–211.
75. MP Williamson, PJ Simpson, DN Bolam, GP Hazlewood, A Ciruela, A Cooper, HJ Gilbert. How the N-terminal xylan-binding domain from *C. fimi* xylanase D recognizes xylan. In: HJ Gilbert, GJ Davies, B Henrissat, S Svensson, eds. Recent Advances in Carbohydrate Bioengineering. Cambridge: Royal Society of Chemistry, 1999, pp 3–12.
76. KA McAllister, L Marrone, AJ Clarke. Structure and function relationship of family 11 xylanases. In: HJ Gilbert, GJ Davies, B Henrissat, S Svensson, eds. Recent Advances in Carbohydrate Bioengineering. Cambridge: Royal Society of Chemistry, 1999, pp 89–98.
77. C Dupond, M Roberge, F Shareck, R Morosoli, D Kluepfel. Substrate-binding domains of glycanases from *Streptomyces lividans*: characterization of a new family of xylan-binding domains. Biochem J 330:41–45, 1998.
78. J Gill, JE Rixon, DN Bolan, S McQueen-Mason, PJ Simpson, MP Williamson, GP Hazlewood, HJ Gilbert. The type II and X cellulose-binding domains of *Pseudomonas* xylanase. A potentiate catalytic activity against complex substrates by a common mechanism. Biochem J 342:473–480, 1999.
79. HJ Flint, CF Forsberg. Polysaccharide degradation in the rumen: biochemistry and genetics. In: W Engelhardt, S Leonhard-Merek, G Breves, D Giesicke, eds. Ruminant Physiology: Digestion, Metabolism, Growth and Reproduction. Stuttgart: F Enke Verlag, 1995, pp 43–70.
80. JX Zhang, HJ Flint. A bifunctional xylanase encoded by the xynA gene of the rumen cellulolytic bacterium *Ruminococcus flavefaciens* 17 comprises two dissimilar domains linked by asparagine/glutamine rich sequence. Mol Microbiol 6:1013–1023, 1992.
81. HJ Gilbert, GP Hazlewood, JI Laurie, CG Orpin, GP Xue. Homologous catalytic domains in a rumen fungal xylanase: evidence for geneduplication and prokaryotic origin. Mol Microbiol 6:2065–2072, 1992.
82. JI Laurie, JH Clarke, A Ciruela, CB Faulds, G Williamson, HJ Gilbert, JE Rixon, J Millward-Sadler, GP Hazlewood. The NodB domain of a multifunctional xylanase from *Cellulomonas fimi* deacetylates acetylxylan. FEMS Microbiol Lett 148:261–264, 1997.
83. AC Fernandes, CMGA Fontes, HJ Gilbert, GP Hazlewood, TH Fernandes, LMA Ferreira. Homologous xylanases from *Clostridium thermocellum*: evidence for bifunctional activity, synergism between xylanase catalytic modules and the presence of xylan-binding domains in enzyme complexes. Biochem J 342:105–110, 1999.
84. H Hayashi, M Takehara, T Hattori, T Kimura, S Karita, K Sakka, K Ohmiya. Nucleotide sequences of two contiguous and highly homologous xylanase genes *xynA* and *xynB* from *Clostridium thermocellum*. Appl Microbiol Biotechnol 51:348–357, 1999.
85. Y Shoham, R Lamed, EA Bayer. The cellulosome concept as an efficient microbial strategy for the degradation of insoluble polysaccharides. Trends Microbiol 7:275–281, 1999.
86. A Sunna, G Antranikian. Xylanolytic enzymes from fungi and bacteria. Crit Rev Biotechnol 17:39–67, 1997.
87. P Biely, D Kluepfel, R Morosoli, F Shareck. Mode of action of three endo-β-1,4-xylanases from

Streptomyces lividans. Biochim Biophys Acta 1162:246–254, 1993.
88. P Biely, M Vršanská, M Tenkanen, D Kluepfel. Endo-β-1,4-xylanase families: differences in catalytic properties. J Biotechnol 57:151–166, 1997.
89. P Biely, M Vršanská, L Kremnický, M Tenkanen, K Poutanen, M Hayn. Catalytic properties of endo-β-1,4-xylanases of *Trichoderma reesei*. In: P Souminen, T Reinikainen, eds. *Trichoderma* Cellulases and Other Hydrolases. Helsinki: Fagepaino Oy, 1993, pp 125–135.
90. FJM Kormelink, MJF Searle–Van Leewen, TM Wood, AGJ Voragen. Purification and characterization of three endo-(1,4)-β-xylanases and one β-xylosidase from *Aspergillus awamori*. J Biotechnol 27:249–265, 1993.
91. P Biely, M Vršanská. Synthesis and hydrolysis of 1,3-β-xylosidic linkages by endo-β-1,4-xylanase of *Cryptococcus albidus*. Eur. J Biochem 129:645–561, 1983.
92. WP Chen, M Matuo, T Yasui. β-1,3-Xylanase and β-1,4-xylanase action on rhodymenan. Agric Biol Chem 50:1195–1200, 1986.
93. H van Tilbeurgh, M Claeyssens. Detection and differentiation of cellulase components using low molecular mass fluorogenic substrates. FEBS Lett 187:283–288, 1985.
94. P Biely, M Vršanská, MK Bhat. Interaction of endo-β-1,4-xylanases with compounds containing D-glucopyranosyl residues. In: M Claeyssens, W Nerinckx, K Piens, eds. Carbohydrases from *Trichoderma* and Other Microorganisms: Structure, Biochemistry, Genetics. Cambridge: Royal Society of Chemistry, 1998, pp 94–101.
95. P Biely, M Vršanská, Z Krátký. Complex reaction pathways of aryl β-xyloside degradation by β-xylanase of *Cryptococcus albidus*. Eur J Biochem 112:375–381, 1980.
96. P Biely, Z Krátký, M Vršanská. Substrate-binding site of endo-1,4-β-xylanase of the yeast *Cryptococcus albidus*. Eur J Biochem 119:559–564, 1981.
97. P Biely, M Vršanská, IV Gorbacheva. Active site of an acidic endo-1,4-β-xylanase of *Aspergillus niger*. Biochim Biophys Acta 743:155–161, 1983.
98. MR Bray, AJ Clarke. Action pattern of xylooligosaccharide hydrolysis by *Schizophyllum commune* xylanase. Eur J Biochem 204:191–196, 1992.
99. A Törrönen, J Rouvinen. Structural and functional properties of low molecular weight endo-1,4-β-xylanases. J Biotechnol 57:137–149, 1997.
100. J Gebler, NR Gilkes, M Claeyssens, DB Wilson, P Beguin, WW Wakarchuk, DG Kilburn, RC Miller JR, RA Warren, SG Withers. Stereoselective hydrolysis catalyzed by related β-1,4-glucanases and β-1,4-xylanases. J Biol Chem 267: 12559–12561, 1992.
101. P Biely, L Kremnický, J Alfödi, M Tenkanen. Stereochemistry of hydrolysis of glycosidic linkage by endo-β-1,4-xylanases of *Trichoderma reesei*. FEBS Lett 356:137–140, 1994.
102. ML Sinnott. Catalytic mechanism of enzymic glycosyl transfer. Chem Rev 90:1171–1202, 1990.
103. SG Withers. Enzymatic cleavage of glycosides: how does it happen? Pure Appl Chem 67:1673–1682, 1995.
104. P Biely, M Vršanská, Z Krátký. Mechanism of substrate digestion by endo-1,4-β-xylanase of *Cryptococcus albidus*. Lysozyme-type pattern of action. Eur J Biochem 119:565–571, 1981.
105. P Biely, M Vršanská, IV Gorbacheva. Reaction pathways of substrate degradation by an acidic endo-1,4-β-xylanase of *Aspergillus niger*. Biochim Biophys Acta 704:114–122, 1982.
106. U Hakansson, LG Fagerstam, G Pettersson, L Anderson. A 1,4-β-glucan glucanohydrolase from the cellulolytic fungus *Trichoderma viride* QM 9414. Biochem J 179:141–149, 1979.
107. S Shomaker, K Watt, G Tsisovsky, R Cox. Characterization and properties of cellulases purified from *Trichoderma reesei* strain L27. Bio/Technology 1:687–690, 1983.
108. P Biely, M Vršanská, M Claeyssens. The endo 1,4-β-glucanase I from *Trichoderma reesei*. Action on β-1,4-oligomers and polymers derived from D-glucose and D-xylose. Eur J Biochem 200:157–163, 1991.
109. M Somogyi. A reagent for the copper-iodometric determination of very small amounts of sugar. J Biol Chem 117:771–776, 1937.
110. N Nelson. A photometric adaptation of the Somogyi method for the determination of glucose. J Biol Chem 153:375–380, 1944.
111. LG Paleg. Citric acid interference in the estimation of reducing sugars with alkaline copper reagent. Anal Chem 31:1902–1904, 1959.
112. J Sumner. Dinitrosalicylic acid: a reagent for the estimation of sugar in normal diabetic urine. J Biol Chem 47:5–9, 1921.
113. GL Miller. Use of dinitrosalicylic acid reagent for determination of reducing sugar. Anal Chem 31:426–428, 1959.
114. GL Miller, R Blum, WE Glennon, AL Burton. Measurement of carboxymethylcellulase activity. Anal Biochem 2:127–132, 1960.
115. MJ Bailey, P Biely, K Poutanen. Interlaboratory testing of methods for assay of xylanase activity. J Biotechnol 23:257–270, 1992.
116. TW Jeffries, VW Yang, MW Davies. Comparative study of xylanase kinetics using dinitrosalicylic, arsenomolybdate, and ionchroma-

tographic assays. Appl Biochem Biotechnol 70–72: 257–265, 1998.
117. EM Gingler. Automated determination of glucose via reductive formation of lavende Cu(I)-2,2′-bicinchonate chelate. Clin Chem 16:519, 1970.
118. S Waffenschmidt, L Jaenicke. Assay of reducing sugars in the nanomole range with 2,2′-bicinchonine. Anal Biochem 165:337–340, 1987.
119. JD Fox, JF Robyt. Miniaturization of three carbohydrate analyses using a microscale plate reader. Anal Biochem 195:93–96, 1991.
120. P Biely, M Vršanská. Xylanase of *Cryptococcus albidus*. Methods Enzymol 160:638–648, 1988.
121. GF Fincher, AB Stone. Some chemical and morphological changes induced by gibberellic acid in embryo-free wheat grain. Aust J Plant Physiol 1:297–311, 1974.
122. IV Gorbacheva, NA Rodionova. Studies on xylan degrading enzymes. I. Purification and characterization of endo-1,4-β-xylanase from *Aspergillus niger*, str. 14. Biochim Biophys Acta 484:79–93, 1977.
123. S Sengupta, S Khowala, PK Goswami. Assay of endo--D-xylanase activity with a soluble O-carboxymethyl derivatives of larchwood xylan. Carbohydr Res 167:156–161, 1987.
124. P Biely, D Mislovičová, R Toman. Soluble chromogenic substrates for the assay of endo-1,4-β-xylanases and endo-1,4-β-glucanases. Anal Biochem 144:142–146, 1985.
125. M Nummi, JM Perrin, ML Niku-Paavola, TM Enari. Measurement of xylanase activity with insoluble xylan substrate. Biochem J 226:617–620, 1985.
126. D Robinson, P Willcox. 4-Methylumbelliferyl phosphate as a substrate for lysosomal acid phosphatase. Biochim Biophys Acta 191:183–186, 1969.
127. KR Gee, W-C Sun, MK Bhalgat, RH Upton, DH Klaubert, KA Latham, RP Hugland. Fluorogenic substrates based on fluorinated umbelliferones for continuous assays of phosphatases and β-galactosidase. Anal Biochem 273:41–48, 1999.
128. M Hrmová, P Biely, M Vršanská, Specificy of cellulase and β-xylanase induction in *Trichoderma reesei* QM 9414. Arch Microbiol 144:307–311, 1986.
129. S. Badarkar, NR Gilkes, DG Kilburn, E Kwan, DS Rose, RC Miller Jr, RAJ Warren, SG Withers. Crystallization and preliminary x-ray diffraction analysis of the catalytic domain of Cex, an exo-β-1,4-glucanase and β-1,4-xylanase from bacterium *Cellulomonas fimi*. J Mol Biol 228:693–695, 1992.
130. P Biely, M Vršanská, Š Kučár. Identification and mode of action of endo-(1-4)-β-xylanases. In: J Visser, G Beldman, MA Kusters–Van Someren, AGJ Voragen, eds. Xylans and Xylanases. Amsterdam: Elsevier Science, 1992, pp 81–95.
131. M Kitaoka, K Haga, Y Kashiwagi, T Sasaki, H Taniguchi, I Kusakabe. Kinetic studies on *p*-nitrophenyl cellobioside hydrolyzing xylanase from *Celvibrio gilvus*. Biosci Biotechnol Biochem 57:1987–1989, 1993.
132. L Ziser, SG Withers. A short synthesis of β-xylobiosides. Carbohydr Res 265:9–17, 1994.
133. P. Christakopoulos, W Nerinckx, D Kekos, B Macris, M Claeyssens. Purification and characterization of two low molecular mass alkaline xylanases from *Fusarium oxysporum* F3. J Biotechnol 51:181–189, 1996.
134. M Vršanská, W Nerinckx, P Biely, M Claeyssens. Fluorogenic substrates for endo-β-1,4-xylanase. Abstracts of 8th Bratislava Symposium on Saccharides, Smolenice, Slovakia, 1997, p 80.
135. DN Bolam, SJ Charnwood, HJ Gilbert, NA Hughes. Synthesis of 2,4-dinitrophenyl glycosides of D-xylobiose and D-mannobiose. Carbohydr Res 312:85–89, 1998.
136. B Sprey, C Lambert. Titration curve of cellulase from *Trichoderma reesei*: demonstration of a cellulase-xylanase-β-glucosidase containing complex. FEMS Microbiol Lett 18:217–222, 1983.
137. V Farkaš, M Lišková, P Biely. Novel media for detection of microbial producers of cellulase and xylanase. FEMS Microbiol Lett 28:137–140, 1985.
138. D Kluepfel. Screening of prokaryotes for cellulose- and hemicellulose-degrading enzymes. Methods Enzymol 160:180–186, 1988.
139. RM Theather, PJ Wood. Use of Congo Red–polysaccharide interactions in enumeration and characterization of cellulolytic bacteria from the bovine rumen. Appl Environ Microbiol 43:777–780, 1982.
140. B Flannigan, JEM Gilmour. A simple plate test for xylanolytic activity in wood-rotting *Basidiomycetes*. Mycologia 72:1219–1221, 1980.
141. PJ Wood, JD Erfle, RM Teather. Use of complex formation between Congo Red and polysaccharides in detection and assay of polysaccharide hydrolases. Methods Enzymol 160:59–74, 1988.
142. P Biely, O Markovič, D Mislovičová. Sensitive detection of endo-1,4-β-glucanases and endo-1,4-β-xylanases in gels. Anal Biochem 144:147–151, 1985.
143. CR MacKenzie, RE Williams. Detection of cellulase and xylanase activity in isoelectric-focusing gels using agar substrate gels supported plastic film. Can J Microbiol 30:1511–1525, 1984.
144. FJM Kormelink. Characterization and mode of action of xylanases and accessory enzymes. PhD dissertation, Agricultural University, Wageningen, Netherlands, 1992.
145. S Voremen, J Heldens, C Boyd, B Henrissat, NT Keen. Cloning and characterization of the *bgxA* gene from *Erwinia chrysanthemi* D1 which encodes a β-glucosidase/xylosidase enzyme. Mol Gen Genet 246465–477, 1995.
146. RP de Vries. Accessory enzymes from *Aspergillus* involved in xylan and pectin degradation. PhD disser-

tation, Agricultural University, Wageningen, Netherlands, 1992.
147. E Margolles-Clark, M Tenkanen, T Nakari-Setälä, M Penttilä. Cloning of genes encoding α-L-arabinofuranosidase and β-xylosidase from *Trichoderma reesei* by expression in *Saccharomyces cerevisiae*. Appl Environ Microbiol 62:3840–3846, 1996.
148. E Lüthi, DR Love, J McAnulty, C Wallace, PA Caughey, D Saul, P Berquist. Cloning, sequence analysis, and expression of genes encoding xylan-degrading enzymes from the thermophile *Caldocellum saccharolyticum*. Appl Environ Microbiol 56:1017–1024, 1990.
149. PL Bergquist, DJ Saul, MD Gibbs, DD Morris, VSJ Te'o, HW Morgan. Molecular diversity of thermophilic cellulolytic and hemicellulolytic bacteria. FEMS Microbiol Ecol 28:99–110, 1999.
150. S Armand, C Vielle, C Gey, A Heyraud, JG Zeikus, B Henrissat. Stereochemical course and reaction products of the action of β-xylosidase from *Thermoanaerobacterium saccharolyticum* strain B6A-RL. Eur J Biochem 236:449–455, 1998.
151. C Braun, A Meinke, L Ziser, SG Withers. Simultaneous high-performance liquid chromatographic determination of both the cleavage pattern and the stereochemical outcome of the hydrolysis reactions catalyzed by various glycosidases. Anal Biochem 212:259–262, 1993.
152. T Baba, R Shinke, T Nanmori. Identification and characterization of clustered genes for thermostable xylan-degrading enzymes, β-xylosidase and xylanase, of *Bacillus stearothermophilus* 21. Appl Environ Microbiol 60:2252–2258, 1994.
153. H Oh, Y Choi. Sequence analysis of β-xylosidase gene from *Bacillus stearothermophilus*. Kor J Appl Microbiol Biotechnol 22:134–142, 1994.
154. M Claeyssens, E Samen, H Kersters-Hilderson, CK De Bruyne. β-D-Xylosidase from *Bacillus pumilus*. Molecular properties and oligomeric structure. Biochim Biophys Acta 405:475–481, 1975.
155. A Shinmyo, W Panbangred, S Negoro, H Okada. Cloning of β-xylosidase gene of *Bacillus pumilus* in *Escherichia coli*. Proc Int Symp Genet Ind Microorg, 4th Meeting, 1982, p 68.
156. M Claeyssens, E Van Leemputten, FG Loontiens, CK De Bruyne. Transfer reactions catalyzed by a fungal β-D-xylosidase: enzymic synthesis of phenyl β-D-xylobioside. Carbohydr Res 3:32–37, 1966..
157. H Kizawa, H Shinoyama, T Yasui. The synthesis of new xylooligosaccharides by transxylosylation with *Aspergillus niger* β-xylosidase. Agric Biol Chem 55:671–678, 1991.
158. J Sulistyo, Y Kamiyama, T Yasui. Purification and properties of *Aspergillus pulverulentum* β-xylosidase with transxylosylation capacity. J Ferment Bioeng 79:17–22, 1995.
159. MC Herrmann, M Vršanká, M Juríčková, J Hirsch, P Biely, CP Kubicek. The β-D-xylosidase of *Trichoderma reesei* is a multifunctional β-D-xylan xylohydrolase. Biochem J 321:375–381, 1997.
160. A Lappalainen. Purification and characterization of xylanolytic enzymes of *Trichoderma reesei*. Biotechnol Appl Biochem 8:437–448, 1986.
161. M Matsuo, T Yasui. Purification and some properties of β-xylosidase from *Trichoderma viride*. Agric Biol Chem 48:1853–1860, 1984.
162. K Poutanen, J Puls. Characteristics of *Trichoderma reesei* β-xylosidase and its use in the hydrolysis of solubilized xylans. Appl Microbiol Biotechnol 28:425–432, 1988.
163. FJM Kormelink, H Gruppen, RJ Viëtor, AGJ Voragen. Mode of action of the xylan-degrading enzymes from *Aspergillus awamori* on alkali-extractable cereal arabinoxylans. Carbohydr Res 249:355–367, 1993.
164. M Tenkanen, E Luonteri, A Teleman. Effect of side groups on the action of β-xylosidase from *Trichodema reesei* against substituted xylooligosaccharides. FEBS Lett 39:303–309, 1996.
165. H Kersters-Hilderson, M Claeyssens, E Van Doorslaer, E Saman, CK De Bruyne. β-D-Xylosidase from *Bacillus pumilus*. Methods Enzymol 83:631–639, 1982.
166. WZ Xu, Y Shima, S Negoro, I Urabe. Sequence and properties of β-xylosidase from *Bacillus pumilus* IPO: contradiction of the previous nucleotide sequence. Eur J Biochem 202:1197–1203, 1991.
167. M Matsuo, T Yasui. β-Xylosidase of several fungi. Methods Enzymol 160:684–695, 1988.
168. RFH Dekker. Bioconversion of hemicellulose: aspects of hemicellulase production by *Trichoderma reesei* QM 9414 and enzymic saccharification of hemicellulose. Biotechnol Bioeng 25:1127–1146, 1983.
169. J Puls, O Schmidt, C Granzow. α-Glucuronidase in two microbial xylanolytic systems. Enzyme Microb Technol 9:83–88, 1987.
170. KM Khandke, PJ Vithayathil, SK Murthy. Purification and characterization of an α-glucuronidase from a thermophilic fungus *Thermoascus aurantiticus*. Arch Biochem Biophys 274:511–517, 1989.
171. M Siika-aho, M Tenkanen, J Buchert, J Puls, L Viikari. An α-glucuronidase from *Trichoderma reesei* RUT C-30. Enzyme Microb Technol 16:813–819, 1994.
172. H Uchida, T Nanri, y Kawabata, I Kusakabe, K Murakami. Purification and characterization of intracellular α-glucuronidase from *Aspergillus niger*. Biosci Biotechnol Biochem 56:1608–1615, 1992.
173. TM Wood, CA Wilson. α-(4-*O*-Methyl)-D-glucuronidase activity produced by the rumen anaerobic fungus *Piromonas communis*: a study of selected properties. Appl Microbiol Biotechnol 43:893–900, 1995.

174. A Castanares, AJ Hay, AH Gordon, SI McCrae, TM Wood. D-Xylan-degrading system from the fungus *Phanerochaete chrysosporium*: isolation and partial characterisation of an α-(4-*O*-Methyl)-D-glucuronidase. J Biotechnol 43:183–194, 1995.
175. E Margolles-Clark, M Saloheimo, M Siika-aho, M Pentillä. The α-glucuronidase-encoding gene of *Trichoderma reesei*. Gene 172:171–172, 1996.
176. RP de Vries, CH Poulsen, S Madrid, J Visser. *aguA*, the gene encoding an extracellular α-glucuronidase from *Aspergillus tubingensis*, is specifically induced on xylose and not on glucuronic acid. J Bacteriol 180:243–249, 1998.
177. CR MacKenzie, D Bilous, H Schneider, KG Johnson. Induction of cellulolytic and xylanolytic enzyme systems in *Streptomyces* sp. Appl Environ Microbiol 53:2835–2839, 1987.
178. KG Johnson, BA Harrison, H Schneider, CR MacKenzie, JD Fontana. Xylan-hydrolysing enzymes from *Streptomyces* spp. Enzyme Microb Technol 10:403–409, 1987.
179. DC Smith, CW Forsberg. α-Glucuronidase and other hemicellulase activities of *Fibrobacter succinogenes* S85 grown on crystalline cellulose or ball-milled barley straw. Appl Environ Microbiol 57:3552-3557, 1991.
180. W Shao, SKC Obi, J Puls, J Wiegel. Purification and characterization of the α-glucuronidase from *Thermoanaerobacterium* sp. strain JW/SL-Y485, an important enzyme for the utilization of substituted xylans. Appl Environ Microbiol 61:1077–1081, 1995.
181. K. Bronnenmeier, H Meissner, S Stocker, WL Staudenbauer. α-D-Glucuronidase from the xylanolytic thermophiles *Clostridium stercorarium* and *Thermoanaerobacterium saccharolyticum*. Microbiology 141:2033–2040, 1995.
182. DG Trudeau, CW Forsberg. Isolation of *Clostridium acetobutylicum* strains and the preliminary investigation of the hemicellulolytic activities of isolate 3BYR. Can J Microbiol 38:1120–1127, 1992.
183. P Ruille, C Winterhalter, W Liebl. Isolation and analysis of a gene encoding α-glucuronidase, an enzyme with a novel primary structure involved in the breakdown of xylan. Mol Microbiol 23:267–279, 1997.
184. JD Fontana, M Gebara, M Blumel, H Schneider, CR MacKenzie, KG Johnson. α-4-*O*-Methyl-D-glucuronidase component of xylanolytic complexes. Methods Enzymol 160:560–571, 1988.
185. Y Kawabata, K Ono, Y Gama, S Yoshida, H Kobayashi, I Kusakabe. Purification and characterization of a α-glucuronidase from snail acetone powder. Biosci Biotechnol Biochem 59:1086–1090, 1995.
186. A Teplitsky, S Shulami, S Moryles, G Zaide, Y Shoham, G Shoham. Crystallization and preliminary x-ray analysis of a α-D-glucuronidase from *Bacillus stearothermophilus* T-6. Acta Crystallogr D Biol Crystallogr 55:869–872, 1999.
187. P Biely, M Tenkanen. Enzymology of hemicellulose degradation. In: GE Harman, CP Kubicek, eds. *Trichoderma* and *Gliocladium*, Vol 2. Enzymes, Biological Control and Commercial Applications. London: Taylor & Francis, 1998, pp 25–47.
188. P Biely, J Hirsch, DC la Grange, WH van Zyl, BA Prior. A chromogenic substrate for a β-xylosidase-coupled assay of α-glucuronidase. Anal Biochem 286:289–294, 2000.
189. P Biely, RP de Vries, M Vršanská, J Visser. Inverting character of α-glucuronidase A from *Aspergillus tubingensis*. Biochim Biophys Act 1474:360–364, 2000.
190. J Puls. α-Glucuronidases in the hydrolysis of wood xylans. In: J Visser, G Beldman, MA Kusters–Van Sommeren, AGJ Voragen, eds. Xylans and Xylanases. Amsterdam: Elsevier, 1992, pp 213–224.
191. Y Milner, G Avigad. A copper reagent for the determination of hexuronic acids and certain ketoses. Carbohydr Res 4:359–361, 1967.
192. J Hirsch, M Koos, P Kovac. Improved synthesis of an aldobiuronic acid related to hardwood xylans, and preparation of a derivative thereof suitable for linking to proteins. Carbohydr Res 310:145–149, 1998.
193. P Biely, J Puls, H Schneider. Acetylxylan esterases in fungal cellulolytic systems. FEBS Lett 186:80–84, 1985.
194. LP Christov, BA Prior. Esterases of xylan-degrading microorganisms: production, properties, and significance. Enzyme Microb Technol 15:460-475, 1993.
195. G Williamson, PA Kroon, CB Faulds. Hairy plant polysaccharides: a close shave with microbial esterases. Microbiology 144:2011–2023, 1998.
196. K Poutanen, M Sundberg, H Korte, J Puls. Deacetylation of xylans by acetyl esterases of *Trichoderma reesei*. Appl Microbiol Biotechnol 33:506–510, 1990.
197. FJM Kormelink, B Lefebvre, F Strozyk, AGJ Voragen. Purification and characterization of an acetyl xylan esterase from *Aspergillus niger*. J Biotechnol 27:267–282, 1993.
198. E Hägglund, B Lindberg, J McPherson. Dimethylsulphoxide, a solvent for hemicelluloses. Acta Chem Scand 10:1160–1164, 1956.
199. HO Bouveng, PJ Garegg, B Lindberg. Position of O-acetyl groups in birch xylan. Acta Chem Scand 14:742–748, 1960.
200. K Poutanen, M Rättö, J Puls, L Viikari. Evaluation of different microbial xylanolytic systems. J Biotechnol 6:49–60, 1987.
201. AW Khan, KA Lamb, RP Overend. Comparison of natural hemicellulose and chemically acetylated xylan as substrates for the determination of acetyl-xylan

esterase activity in *Aspergilli*. Enzyme Microb Technol 12:127–131, 1990.
202. KG Johnson, JD Fontana, CR MacKenzie. Measurements of acetylxylan esterase in *Streptomyces*. Methods Enzymol 160:551–560, 1988.
203. N Halgašová, E Kutejová, J Timko. Purification and some characteristics of the acetylxylan esterase from *Schizophyllum commune*. Biochem J 298:751–755, 1994.
204. G Debrassi, BC Okeke, CL Bruschi, V Venturi. Purification and characterization of an acetyl xylan esterase from *Bacillus pumillus*. Appl Environ Microbiol 64:789–792, 1998.
205. B Henrissat, P Coutinho, http://afmb.cnrs-mrs.fr/~pedro/CAZY/db.html.
206. LH de Graaff, J Visser, HC van den Broeck, F Strozyk, FJM Kormelink, JCP Boonman. Cloning, expression and use of acetyl xylan esterases from fungal. EP 0507369-A 7 07-OCT-1992.
207. P Biely, CR MacKenzie, H Schneider. Production of acetylxylan esterase by *Trichoderma reesei* and *Schizophyllum commune*. Can J Microbiol 34:767–772, 1988.
208. L Egaña, R Gutiérrez, V Caputo, A Peirano, J Steiner, J Eyzaguirre. Purification and characterization of two acetyl xylan esterases from *Pencillium pupurogenum*. Biotechnol Appl Biochem 24:33–39, 1996.
209. LMA Ferreira, TM Wood, G Williamson, CB Faulds, GP Hazlewood, HJ Gilbert. A modular esterase from *Pseudomonas fluorescens* subsp. *cellulosa* contains a non-catalytic binding domain. Biochem J 294:349–355, 1993.
210. O Grépinet, MC Chebrou, P Béguin. Nucleotide sequence and deletion analysis of the xylanase gene (xynZ) of *Clostridium thermocellum*. J Bacteriol 170:4582–4588, 1988.
211. CM Fontes, GP Hazlewood, E Morag, J Hall, BH Hirst, HJ Gilbert. Evidence for a general role for non-catalytic thermostabilizing domains in xylanases from thermophilic bacteria. Biochem J 307:151–158, 1995.
212. GP Hazlewood, HJ Gilbert. Molecular biology of hemicellulases. In: MP Coghlan, GP Hazlewood, eds. Hemicellulose and Hemicellulases. London: Portland Press, 1993, pp 103–126.
213. J Hall, GP Hazlewood, PJ Baker, HJ Gilbert. Conserved reiterated domains in *Clostridium thermocellum* endoglucanases are not essential for catalytic activity. Gene 69:29–38, 1988.
214. BP Dalrymple, DH Cybinski, I Layton, CS McSweeney, G-P Xue, YJ Swadling, JB Lowry. Three *Neocallimastix patriciarum* esterases associated with the degradation of complex polysaccharides are members of a new family of hydrolases. Microbiology 143:2605–2614, 1997.
215. J-X Zhang, J Martin, HJ Flint. Identification of non-metabolic conserved regions in xylanases encoded by the xynB and xynD genes of the cellulolytic rumen anaerobe *Ruminococcus flavefaciens*. Mol Gen Genet 254:260–264, 1994.
216. F Shareck, P Biely, R Morosoli, D Kluepfel. Analysis of DNA flanking the xlnB locus of *Streptomyces lividans* reveals genes encoding acetylxylan esterase and the RNA component of ribonuclease P. Gene 153:105–109, 1995.
217. C Dupont, N Daignault, F Shareck, R Morosoli, D Kluepfel. Purification and characterization of an acetyl xylan esterase produced by *Streptomyces lividans*. Biochem J 319:881–886, 1996.
218. H Tsujibo, T Ohtsuki, T Ito, I Yamazaki, K Miyamoto, M Sugiyama, Y Inamori. Cloning and sequence analysis of genes encoding xylanases and acetyl xylan esterase from *Stretomyces thermoviolaceus* OPC-520. Appl Environ Microbiol 63:661–664, 1997.
219. SJ Millward-Sadler, K Davidson, GP Hazlewood, GW Black, HJ Gilbert, JH Clarke. Novel cellulose-binding domains, NodB homologous and conserved modular architecture in xylanases from the aerobic soil bacteria *Pseudomonas fluorescens* subsp. *cellulose* and *Cellvibrio mixtus*. Biochem J 312:39–48, 1995.
220. M Sundberg, K Poutanen. Purification and properties of two acetyl xylan esterases of *Trichoderma reesei*. Biotechnol Appl Biochem 13:1–11, 1991.
221. E Margolles-Clark, M Tenkanen, H Söderlund, M Penttilä. Acetyl xylan esterase from *Trichoderma reesei* contains an active site serine and a cellulose binding domain. Eur J Biochem 237:553–560, 1996.
222. R Gutiérrez, E Cederlund, L Hjelmquist, A Peirano, F Herrera, D Ghosh, W Duax, H Jörnvall, J Eyzaguirre. Acetyl xylan esterase II from *Penicillium purpurogenum* is similar to an esterase from *Trichoderma reesei* but lacks a cellulose binding domain. FEBS Lett 423:35–38, 1998.
223. DL Blum, X-L Li, H Chen, LG Ljungdahl. Characterization of an acetyl xylan esterase from the anaerobic fungus *Orpinomyces* sp. strain PC-2. Appl Environ Microbiol 65:3990–3995, 1999.
224. W Shao, J Wiegel. Purification and characterization of two thermostable acetyl xylan esterases from *Thermoanaerobacterium sp*. strain JW/SL YS485. Appl Environ Microbiol 61:729–733, 1995.
225. WW Lorenz, J Wiegel. Isolation, analysis and expression of two genes from *Thermoanaerobacterium sp*. strain JW/SL YS485: a β-xylosidase and a novel acetyl xylan esterase with cephalosporin C deacetylase activity. J Bacteriol 179:5436–5441, 1997.
226. P Biely, GL Coté, L Kremnický, RV Greene. Differences in catalytic properties of acetylxylan ester-

ase and non-hemicellulolytic acetylesterase. In: HJ Gilbert, GJ Davies, B Henrissat, S Svensson, eds. Recent Advances in Carbohydrate Bioengineering. Cambridge: Royal Society of Chemistry, 1999, pp 73–81.
227. J Eyzaguirre, D Ghosh. Acetyl xylan esterase II from *Penicillium purpurogenum*: structure and properties. In HJ Gilbert, GJ Davies, B Henrissat, S Svensson, eds. Recent Advances in Carbohydrate Bioengineering. Cambridge: Royal Society of Chemistry, 1999, pp 117–123.
228. N Hakulinen, M Tenkanen, J Rouvinen. Crystallization and preliminary x-ray diffraction studies of the catalytic core of acetyl xylan esterase from *Trichoderma reesei*. Acta Cryst D54:420–432, 1998.
229. P Biely, GL Coté, L Kremnický, D Weisleder, RV Green. Substrate specificity of acetylxylan esterase from *Schizophyllum commune*: mode of action on acetylated carbohydrates. Biochim Biophys Acta 1298:209–222, 1996.
230. M Tenkanen. Action of *Trichoderma reesei* and *Aspergillus oryzae* esterases in the deacetylation of hemicellulose. Biotechnol Appl Biochem 27:19–24, 1998.
231. P Biely, GL Coté, L Kremnický, RV Greene, M Tenkanen. Action of acetylxylan esterase from *Trichoderma reesei* on acetylated methyl glycosides. FEBS Lett 420:121–124, 1997.
232. P Biely, GL Cotém L Kremnický, RV Greene, C Dupont, D Kluepfel. Substrate specificity and mode of action of acetylxylan esterase from *Streptomyces lividans*. FEBS Lett 396:257–260, 1996.
233. P Biely, CR MacKenzie, H Schneider. Acetylxylan esterase of *Schizophyllum commune*. Methods Enzymol 160:700–707, 1988.
234. K Poutanen, M Sundberg. An acetyl esterase of *Trichoderma reesei* and its role in the hydrolysis of acetyl xylans. Appl Microbiol Biotechnol 28:419–424, 1988.
235. KP McDermit, CR MacKenzie, CW Forsberg. Esterase activities of *Fibrobacter succinogenes* subsp. *succinogenes* S85. Appl Environ Microbiol 56:127–132, 1990.
236. H Lee, RJB To, K Latta, P Biely, H Schneider. Some properties of extracellular acetylesterase produced by the yeast *Rhodotorula mucilaginosa*. Appl Environ Microbiol 53:2831–2834, 1987.
237. M Rosenberg, V Roegner, FF Becker. The quantitation of rat serum esterases by densitometry of acrylamide gels stained for enzyme activity. Anal Biochem 66:206–212, 1975.
238. FM Kormelink. Characterization and mode of action of xylanases and some accessory enzymes. PhD thesis. Agricultural University, Wageningen, Netherlands, 1992.
239. G Beldman, MJF Searle–Van Leewen, GA Deuter, HA Siliha, AGJ Voragen. Degradation of arabinans by arabinanases from *Aspergillus aculeatus* and *Aspergillus niger*. Carbohydr Polym 20:159–168, 1993.
240. Z Gunata, S Bitteur, JM Brillouet, C Bayonove, R Cordonnier. Sequential enzymic hydrolysis of potential aromatic glycosides from grape. Carbohydr Res 184: 139–149, 1988.
241. Z Gunata, JM Brillouet, S Voirin, R Baumes, R Cordonnier. Purification and some properties of an α-L-arabinofuranosidase from *Aspergillus niger*. Action on grape monoterpenyl arabinofuranosylglucosides. J Agric Food Chem 38:772–776, 1990.
242. G Spagna, F Andreani, E Salatelli, D Romagnoli, D Casarini, PG Piferi. Immobilization of the glycosidases: α-L-arabinofuranosidase and β-glucosidase from *Aspergillus niger* on a chitosanderivative to increase the aroma of wine. Enzyme Microb Technol 23:413–421, 1998.
243. Reference deleted.
244. K Poutanen. An α-L-arabinofuranosidase of *Trichoderma reesei*. J Biotechnol 7:271–282, 1988.
245. M Nogawa, K Yatsui, A Tomioka, H Okada, Y Morikawa. An α-L-arabinofuranosidase from *Trichoderma reesei* containing a noncatalytic xylan-binding domain. Appl Environ Microbiol 65:3964–3968, 1999.
246. LE Kellett, DM Poole, LM Ferreira, AJ Durant, GP Hazlewood, HJ Gilbert. Xylanase B and arabinofuranosidase from *Pseudomonas fluorescens* subsp. *cellulosa* contain identical cellulose-binding domains and are encoded by adjacent genes. Biochem J 272:369–376, 1990.
247. P Vincent, F Shareck, C Dupont, R Morosoli, D Kluepfel. New α-L-arabinofuranosidase produced by *Streptomyces lividans*: cloning and DNA sequence of the abfB gene and characterization of the enzyme. Biochem J 322:845–852, 1997.
248. SM Pitson, AGJ Voragen, G Beldman. Stereochemical course of hydrolysis catalyzed by arabinofuranosyl hydrolases. FEBS Lett 398:7–11, 1996.
249. FJM Kormelink, H Gruppen, AGJ Voragen. Mode of action of (1$\rightarrow$ 4)-β-D-arabinoxylan arabinofuranohydrolase (AXH) and α-L-arabinofuranosidase on alkali-extractable wheat-flour arabinoxylan. Carbohydr Res 249:345–353, 1993.
250. KMJ Van Laere, G Beldman, AGJ Voragen. A new arabinofuranohydrolase from *Bifidobacterium adolescentis* able to remove arabinosyl residues from double-

substituted xylose units in arabinoxylan. Appl Microbiol Biotechnol 47:231–235, 1997.
251. TM Wood, SI McCrae. Arabinoxylan-degrading enzyme system of the fungus *Aspergillus awamori*: purification and properties of an α-L-arabinofuranosidase. Appl Microbiol Biotechnol 45:538–545, 1996.
252. E Luonteri, PA Kroon, M Tenkanen, A Teleman, G Williamson. Activity of an *Aspergillus terreus* α-L-arabinofuranosidase on phenolic-substituted oligosaccharides. J Biotechnol 67:41–48, 1999.
253. E Margoles-Clark, M Tenkanen, T Nakari-Setälä, M Penttilä. Cloning of genes encoding α-L-arabinofuranosidases and β-xylosidase from *Trichoderma reesei* by expression in *Saccharomyces cerevisiae*. Appl Environ Microbiol 62:3840–3846, 1996.
254. W Berlin, B Sauer. In situ color detection of α-L-arabinofuranosidase, a "no-background" reporter gene, with 5-bromo-3-indolyl-α-L-arabinofuranoside. Anal Biochem 243:171–175, 1996.
255. MJ Renner, JA Breznak. Purification and properties of ArfI, an α-L-arabinofuranosidase from *Cytophaga xylanolytica*. Appl Environ Microbiol 64:43–52, 1998.
256. M Lever, TA Walmsley, RS Visser, SJ Ryde. Optimal conditions for 4-hydoxybenzoyl- and 2-furoylhydrazine as reagents for the determination of carbohydrates, including ketosamines. Anal Biochem 139:205–211, 1984.

72

Enzymes with Activity Toward Xyloglucan

Jean-Paul Vincken
Wageningen University, Wageningen, The Netherlands

I. INTRODUCTION

Xyloglucans are plant cell wall polysaccharides, which belong to the hemicellulose class; i.e., they can bind to cellulose. They are the most abundant hemicellulose in the walls of many nongraminaceous species. Xyloglucans can function both as a structural and as a reserve polysaccharide. In the primary cell wall, xyloglucans can crosslink cellulose fibers, yielding a network that determines to a large extent the strength of the wall. This complex usually constitutes approximately half of the amount of wall polysaccharides, the cellulose (30%) being a bit more abundant than the xyloglucan (20%). Plants possess many enzymes to remodel this network. Certain degradation products of xyloglucan may serve as signaling molecules, the activity of which can be regulated by various glycosidases. Structural xyloglucans are also important from a food industry point of view. They are an important target for fungal enzymes in applications, which aim at a complete degradation of the plant cell wall, such as the "liquefaction process" for fruit juice manufacturing. Further, xyloglucans might play a role in determining the shelf life of fruits and vegetables.

Xyloglucans can also be deposited in the secondary cell walls of seeds of several species, such as *Tamarindus indica, Tropaeolum majus, Hymenaea courbaril*, and *Copaifera langsdorffii*. The seeds can contain $> 50\%$ xyloglucan. Upon germination of these seeds, a battery of enzymes is induced to mobilize the xyloglucan food reserves of the hypocotyl. The storage xyloglucans, in particular, are used as food ingredients or in pharmaceutical applications. The decoration (or side-chain configuration) of these xyloglucans determines to a large extent their functional properties. Depending on the application, the decoration may be adjusted by using enzymes of either plant or fungal origin. With the discovery of the first enzymes in xyloglucan biosynthesis, it may be possible in the future to realize these structural modifications in the plant itself. Biosynthetic enzymes using nucleoside-diphosphate sugars will not be discussed in this chapter.

In the paragraphs below, the structural variations of xyloglucans will be reviewed first. As we will see later, substitution determines the rate at which xyloglucan molecules are degraded. Subsequently, the anchoring of xyloglucan in the plant cell wall will be discussed. Some background information on this is provided, because certain enzyme purification procedures and enzyme assays make use of these principles. The following sections deal with (plant and microbial) enzymes involved in degradation or modification of xyloglucan. After this, a number of methods for activity measurements are summarized. These methods deal predominantly with the determination of transferase activity, because these assays follow different procedures from those used for degradative enzymes. Finally, a few applications in the food industry will be described.

II. STRUCTURE AND PROPERTIES OF XYLOGLUCANS

Xyloglucans are polysaccharides with a highly branched β-(1 $\rightarrow$ 4)-Glc*p* or cellulosic backbone. Most side chains contain α-Xyl*p* residues, which are attached to the 6-position of the Glc residues (Fig. 1A). The α-Xyl*p* residues are distributed in the glucan backbone according to regular patterns. In principle, two general branching patterns can be distinguished, XXXG and XXGG (see Fig. 1B) (1). Thus, xyloglucans seem to have a subunit length of four glucosyl residues in common. In the XXXG-type xyloglucans (most nongraminaceous species), three contiguous Glc residues are branched, followed by an unbranched one. The XXGG-type xyloglucans (solanaceous plants) contain clusters of two branched Glc residues, which alternate with a sequence of two "bare" Glc residues.

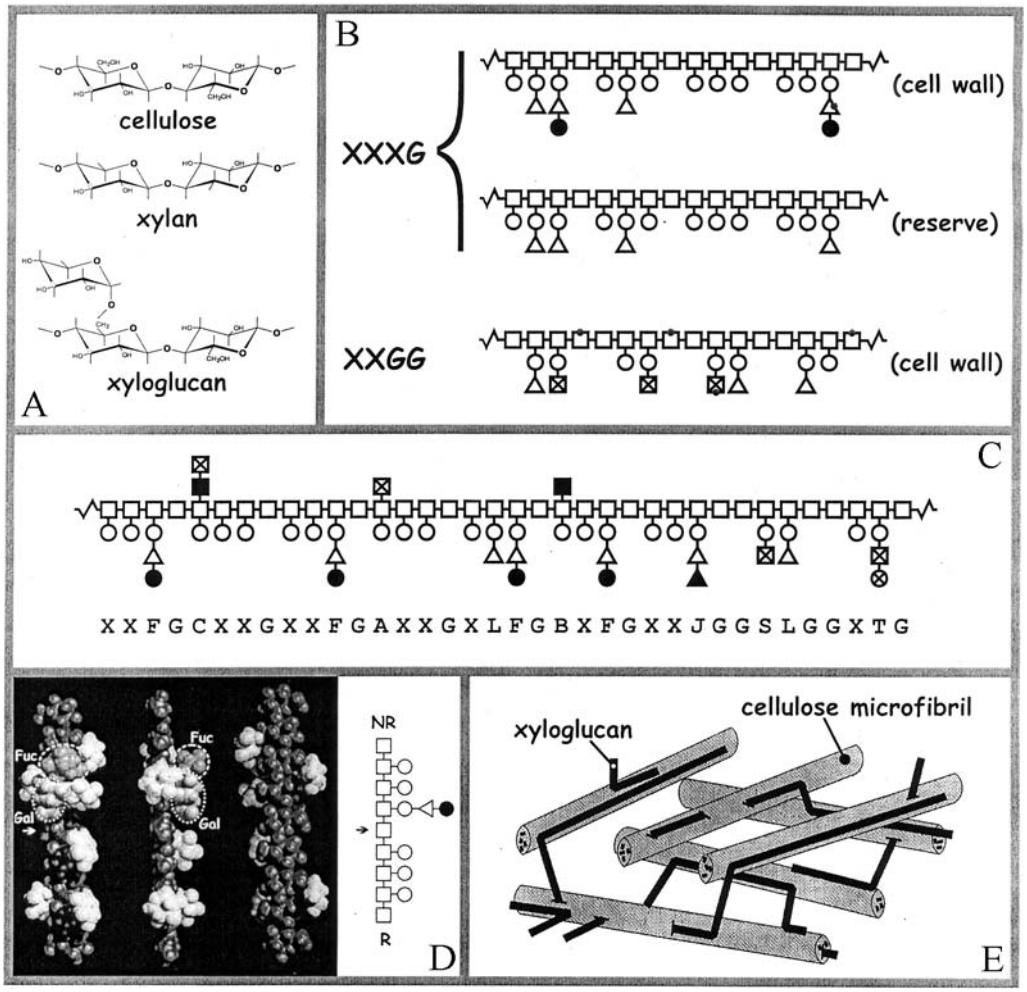

Figure 1 (A) Structure of the cellobiosyl building unit of cellulose, the xylobiosyl building unit of xylan, and a trisaccharide XG subunit of xyloglucan. Note that glucose and xylose are very similar except for *C*-6. (B) Two general branching patterns of xyloglucans, XXXG and XXGG. Small shaded circles represent acetyl groups. (C) Hypothetical (nonexisting) molecule showing the different structural elements encountered in xyloglucans. G = β-D-Glc*p*; X = α-D-Xyl*p*-(1 $\rightarrow$ 6)-β-D-Glc*p*; L = β-D-Gal*p*-(1 $\rightarrow$ 2)-α-D-Xyl*p*-(1 $\rightarrow$ 6)-β-D-Glc*p*; F = α-L-Fucp-(1 $\rightarrow$ 2)-β-D-Gal*p*-(1 $\rightarrow$ 2)-α-D-Xyl*p*-(1 $\rightarrow$ 6)-β-D-Glcp; S = α-*L*-Ara*f*-(1 $\rightarrow$ 2)-α-D-Xyl*p*-(1 $\rightarrow$ 6)-β-D-Glc*p*; A = α-D-Xyl*p*-(1 $\rightarrow$ 6)-β-D-Glc*p*-(2 $\leftarrow$ 1)-α-L-Ara*f*; B = α-D-Xylp-(1 $\rightarrow$ 6)-β-D-G1c*p*-(2 $\leftarrow$ 1)-β-D-Xyl*p*; C = α-D-Xylp-(1 $\rightarrow$ 6)-β-D-G1cp-(2 $\leftarrow$ 1)-β-D-Xyl*p*-(3 $\leftarrow$ 1)-α-L-Ara*f*; J = α-L-Gal*p*-(1 $\rightarrow$ 2)-β-D-Gal*p*-(1 $\rightarrow$ 2)-α-D-Xyl*p*-(1 $\rightarrow$ 6)-β-D-Glc*p*; T = β-L-Ara*f*-(1 $\rightarrow$ 3)-α-L-Ara*f*-(1 $\rightarrow$ 2)-α-D-Xyl*p*-(1 $\rightarrow$ 6)-β-D-*Glcp*. (D) Flat backbone conformation of the xyloglucan heptadecamer GXXFGXXXG [adapted from (4)]. NR, nonreducing end of the polymer; R, reducing end. (E) Schematic representation of a part of the cellulose-xyloglucan network in the primary cell of plants [adapted from Roberts and McCann (9)].

An exception to this rule is the xyloglucan from *Hymenaea courbaril*, which contains similar amounts of XXXG- and XXXXG-type subunits (2). Another exception might be the xyloglucan from certain graminaceous species (rice, barley), which are thought to have a degree of branching of 40% or lower (1).

The variation in xyloglucan structure is much larger than the two general branching patterns suggest. The xyloglucan skeleton can be decorated with many different residues. However, the sequence in which these residues occur in the side chain is very consistent. In 1993, a concise nomenclature was developed to unambiguously designate xyloglucan structures (3). A xyloglucan molecule is named by partitioning the backbone into segments consisting of a single glucosyl residue and its pendant side chains. Each segment is given a specific code letter, depending on the side chain configuration. For example, the letters G and X refer to the unbranched β-D-Glc*p* residue and the α-D-Xyl*p*-(1 $\rightarrow$ 6)-β-D-Glc*p* segment, respectively. The letter F refers to the α-L-Fuc*p*-(1 $\rightarrow$ 2)-β-D-Gal*p*-(1 $\rightarrow$ 2)-α-D-Xyl*p*-(1 $\rightarrow$ 6)-β-D-Glc*p* segment of the fucosylated nonasaccharide (XXFG) commonly found in xyloglucans. The different structural elements which are currently known are summarized in the hypothetical (nonexisting) xyloglucan molecule in Figure 1C.

The variation in xyloglucan structure is not only species dependent, but also relates to the physiological state of the cell wall of that particular species (1). Xyloglucans that are present as storage polysaccharides in seeds are of the XXXG type. Unlike the xyloglucan derived of the primary cell wall, these are not fucosylated (Fig. 1B). Depending on their origin, they contain different proportions of XXXG, XLXG, XXLG, and XLLG. In addition to these, the primary cell wall xyloglucan can contain the fucosylated oligosaccharides XXFG, XLFG, and XFFG, as well as larger oligosaccharides with the more rare segments A, B, and C. Smaller oligosaccharides, like FG, GFG, XFG, and XXG, also occur, but these are most likely a result of postdepositional modification by endogenous enzymes. Finally, the galactosyl residue of the F elements can be acetylated.

The XXGG-type xyloglucans have so far only been found in *solanaceous* plants (potato, tomato, tobacco) (1). Fucosylated trisaccharide side chains are not present in these xyloglucans. Instead, they possess a fair amount of arabinosyl-containing disaccharide side chains. It seems that all combinations of the elements X, L, and S can occur (XX, LX, XL, LL, SX, XS, SS, SL, and LS). The structural elements A, B, and C have not been demonstrated in the XXGG type. Acetyl groups can be attached to the *C*-6 position of Glc residues, mainly as in XX(G-ac)G, and to a minor extent as in (G-ac)XXG. Further, acetyl groups can be present on the *C*-5 of terminal arabinosyl units.

Despite their heavily branched nature, xyloglucans can interact intimately with cellulose. Molecular modeling studies with the heptadecamer GXXFGXXXG have shown that xyloglucan molecules can adopt a so-called flat-backbone conformation, which facilitates their binding to cellulose (4, 5). In this conformation, the xylosyl residues point outwards in an alternate fashion (Fig. 1D). The fucosylated side chain folds onto the backbone toward the nonreducing side, whereas the opposite face of the molecule is relatively flat. The structure of the side chains plays an important role in the interaction with cellulose. The fucosylated sidechain in particular seems to induce the flat-backbone conformation. Indeed, binding studies have shown that fucosylated xyloglucans display a higher affinity binding than nonfucosylated xyloglucans (5, 6). This may be consistent with the function of these xyloglucans in the plant cell wall. The former is encountered as a crosslinker of cellulose microfibrils in the primary wall. The latter serves as a reserve polysaccharide in the secondary wall of seeds, which needs to be easily accessible to glycanases during germination. At the moment, the binding characteristics of XXGG-type xyloglucan are unknown, as is the contribution of arabinosyl substitution to binding. Next to the side chain configuration, the length of the xyloglucan molecule is also an important parameter for interaction with cellulose. It has been shown that molecules composed of (at least) four oligosaccharide binding units (equivalent to a backbone length of 16 Glc residues) bind quantitatively to cellulose (7, 8).

The cellulose-xyloglucan network comprises $\sim$ 50% of the primary cell wall (width $\approx$ 75 nm). The wall is flanked by a plasma membrane and a middle lamella, and can accommodate three to four lamellae of cellulose microfibrils (diameter 5–12 nm; indeterminate length). The microfibrils in one layer run parallel, and no weaving between layers is observed (9). Xyloglucans coat the cellulose surface; they are also incorporated in the microfibrils during the synthesis of the wall. The length of individual xyloglucan molecules (30–400 nm) generally exceeds the distance between lamellae many times, which suggests that these polysaccharides can interlink several microfibrils (Fig. 1E). Typically, xyloglucans seem to be built of blocks of 30 nm repeats (10); one such repeat corresponds to $\sim$ 60 Glc residues (or 15 xyloglucan oligosaccharides), which is similar to the length of a

crosslink or the distance between two lamellae. The attachment of xyloglucan to cellulose provides important mechanical properties such as extensibility, which can not be realized with cellulose alone (11).

III. ENZYMIC DEGRADATION OF XYLOGLUCANS

Over the years, many xyloglucan hydrolases of both fungal and plant origin have been described. In this section, most attention will be devoted to endoglucanases, which can rapidly depolymerize xyloglucan. Next to these, a number of exoacting enzymes will be reviewed, the majority of which only act on oligosaccharides (such as xyloglucosidase, α-xylosidase, and α-fucosidase). β-Galactosidase is an exception to this, and can be used to adjust the physical properties of polymeric xyloglucan. Hydrolases with the ability to split off α-L-Ara*f* from XXGG-type xyloglucan have not been described so far.

A. Endoglucanase

In the older literature endoglucanases are sometimes referred to as cellulases or C_x factor. In principle, both cellulase and C_x are a collective noun for a group of enzymes, including endoglucanases, which have in common that they hydrolyze β-D-Glc*p*-$(1 \rightarrow 4)$ linkages. Endoglucanases have long been characterized by their activity on carboxymethyl cellulose (CMC). Unfortunately, determination of xyloglucanase activity is not a common practice, and for many well-characterized cellulases it is not known if they are able to degrade xyloglucan. However, it is important to realize that not every endoglucanase is a xyloglucanase (12). Recently, an endoglucanase with xyloglucanase, but no CMCase, activity has been described (13). This suggests that there are at least two types of xyloglucanases—a highly specific one, and one with a more promiscuous substrate specificity.

Bacteria and fungi usually possess several endoglucanases. For instance, the fungus *Trichoderma reesei* has four endoglucanases—EGI, EGII, EGIII, and EGV—of which at least two have xyloglucanase activity (EGI and EGIII; for EGV this has not been determined) (12). With this set of different endoglucanases, *Trichoderma* seems very well equipped to efficiently degrade plant cell wall cellulose, i.e., cellulose that is coated with hemicellulose (14). The variety of endoglucanases in plants is even larger than that in microbial sources. *Arabidopsis thaliana* alone already contains > 12 endoglucanases (15). Virtually nothing is known about the substrate specificity of these enzymes.

Microbial endoglucanases are often modular proteins; i.e., they are composed of separate domains, which are connected by linker peptides (16). The substrate specificity of the endoglucanase resides in the catalytic core. One or more cellulose-binding domains (CBDs) determine whether the enzyme can attach itself to, and degrade insoluble substrates like cellulose. The fact that EGI from *Trichoderma reesei* has a CBD, whereas EGIII has not, shows that xyloglucanases with and without CBD can occur naturally. So far, no plant endoglucanases with a CBD have been described (15). However, these enzymes can contain (putative) signal sequences for cell attachment or membrane anchoring. This implies that the action of the endoglucanases with a signal sequence is restricted to specific locations within the wall.

As we have seen above, the answer to the question whether an endoglucanase has xyloglucanase activity lies in the topology of the catalytic core. These catalytic cores can be grouped in families, based on similarities in apparent secondary structures of proteins (http://afmb.cnrs-mrs.fr/~pedro/CAZY/). In principle, cores with very low amino acid sequence identity can be attributed to the same glycosyl hydrolase family; i.e., the fold of the core proteins seems to be much better conserved than their sequence. Within one family, the catalytic mechanism (retaining or inverting) of the hydrolysis reaction is the same. So far, endoglucanases with xyloglucanase activity have been attributed to two families-7 and 12 (both retaining). Important characteristics of enzymes belonging to these families are summarized in Table 1.

Typically, the *Trichoderma reesei* EGI and EGIII can cleave both xyloglucan and xylan (12), suggesting that the presence of CH_2OH groups or a xylosyl residue protruding from the backbone do not matter for these enzymes (see also Fig. 1A). However, EGII from *Aspergillus aculeatus* is highly specific for xyloglucan and is unable to degrade xylan (13). This shows that activity toward xylans is not a common feature of xyloglucanases.

Another important conclusion from Table 1 is that the substrate specificity of endoglucanases is not conserved within each family. For instance, family 12 contains many different kinds of endoglucanases. Either they are mainly active on CMC, or they are active only on xyloglucan. Also, there are endoglucanases, which can degrade both substrates. This suggests that only subtle changes in the structure of endoglucanases can

Table 1 Overview of Selected Endoacting Enzymes with Activity Toward β-(1 → 4)-D-Glucans

Enzyme	Organism	EC No.	XG	CMC	Xylan	MW_{core}	Family	Cat. mech.	Cat. res.	CBD?	Anchors?
EG I	*T. reesei*	3.2.1.4	yes	yes	yes	~ 40	7	retaining	E,E	yes	no
EG	plant	3.2.1.4	??	??	??	~ 50–60	9	inverting	E,D	no	possible
EG III	*T. reesei*	3.2.1.4	yes	yes	yes	~ 25	12	retaining	E,E	no	no
EG II	*A. aculeatus*	3.2.1.4	yes	no	no	~ 25	12	retaining	E,E	no	no
EG	*S. lividans*	3.2.1.4	??	yes	??	~ 24	12	retaining	E,E	yes	no
XET	plant	2.4.1.207	yes	no	no	~ 32	16	retaining	E,E	no	no

determine whether these enzymes have xyloglucanase activity. Probably, it is important that the substrate-binding groove is lined with the appropriate amino acid residues at certain positions; this may determine whether the xylosyl side chains on the glucan backbone are tolerated in the groove. Also, xylosyl groups may be involved in the molecular recognition of the substrate by xyloglucanases. From the examples above it is clear that the family classification does not have a predictive value with respect to the substrate specificity of endoglucanases. The xyloglucanase activity of each individual endoglucanase should be verified experimentally. There are a number of reports showing that there are enzymes in plant extracts that have xyloglucanase activity. Possibly, some of these xyloglucanases will be classified in family 9. At this moment, there is no experimental evidence supporting this remark. It is interesting to note that the enzymes of family 9 act with an inverting mechanism. This means that xyloglucanase activity may not be reserved to retaining enzymes.

In the previous paragraphs it was shown that the structure of xyloglucan determines the properties of these molecules, such as binding to cellulose surfaces. Next to this, the structure also greatly influences the enzymic digestibility; i.e., the nature of the sidechains determines how fast xyloglucan is degraded by endoglucanases. It is difficult to relate the tolerance to particular side chains to individual endoglucanases, because most studies have been carried out with rather crude mixtures of enzymes from *Trichoderma*.

In Figure 2 a number of rules that seem to have a general validity are summarized. The presence of fucosylated side chains can hinder cleavage by the endoglucanase (17). Two adjacent fucosylated side chains as in XFFGXXXG can give partial resistance to endoglucanase, meaning that prolonged incubations are needed to generate the constituent oligosaccharides XFFG

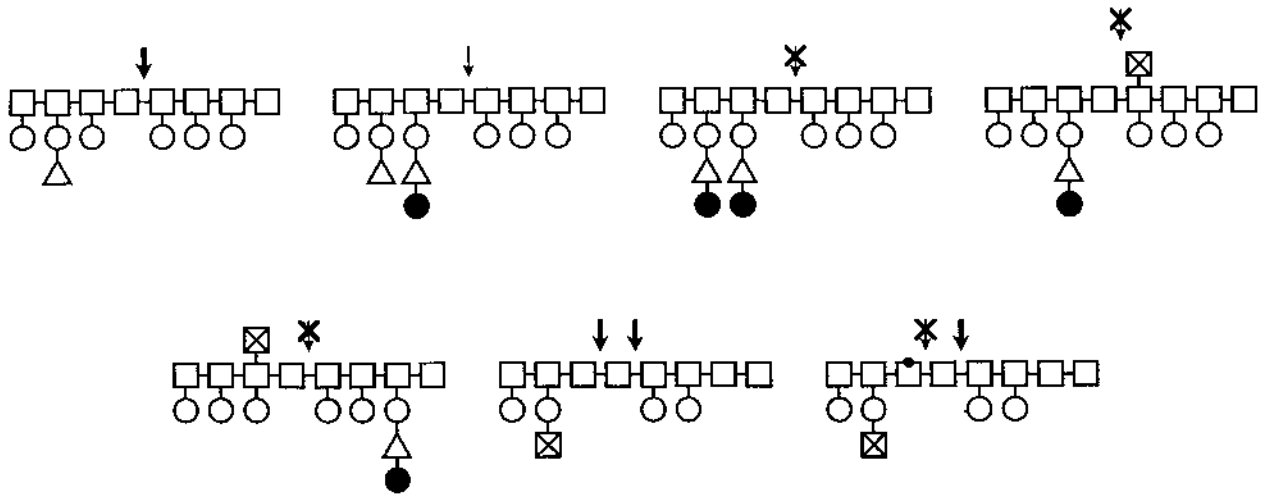

Figure 2 Overview of xyloglucan structures, which (a) are easily cleaved by endoglucanases (solid arrow), (b) are partially resistant to endoglucanase (thin arrow), and (c) are completely resistant to endoglucanases (thin arrow with cross). For details on xyloglucan structure, see Figure 1C. Small shaded circle on open box (bottom right structure) represents an acetyl group attached to a glucosyl residue.

and XXXG (18). Molecular modeling studies suggest that, in solution, the fucosylated side chain folds toward the reducing end of the molecule, i.e., over the linkage to be cleaved (4). This probably decreases the accessibility of the glucan backbone to endoglucanases.

The presence of A elements adjacent to unsubstituted glucosyl residues (as in XXFGAXXG or XXAGXXFG) blocks cleavage by endoglucanases completely (19). In *Solanaceous* spp., two vicinal unbranched glucosyl residues can occur as in XSGGXXGG (20). In this case the endoglucanase has a choice in "cleavable linkages," either XSG ↓ GXXGG or XSGG ↓ XXGG. The presence of other structural elements (L or S) at the position of the X elements probably influences the preference of the endoglucanase for a particular linkage. There is some evidence indicating that the presence of acetyl groups (as in XS(G-ac)GXXGG) inhibits cleavage of the adjacent glycosidic bond (21).

Because most xyloglucans are of the XXXG type, not many people have realized that endoglucanases may actually display differences in their mode of action towards xyloglucan. When it appeared that *solanaceous* xyloglucans were less heavily substituted than others, and that they had a regular branching pattern (XXGG type), it became possible to investigate this (20). It was demonstrated that two endoglucanases from *Trichoderma reesei*, EGI and EGIII, respond differently to substitution of the glucan backbone (Fig. 3). EGIII predominantly released an XXGG type of oligosaccharide, whereas EGI also released GXXG and XXG types of oligosaccharides (20). At this moment it is unknown whether the promiscuity of EGI and the higher specificity EGIII are common features of, respectively, family 7 and 12 endoglucanases.

From the above it is clear that the activity of endoglucanases toward xyloglucan is greatly affected by the fine structure of the polysaccharide. Much more work remains to be done to establish the structure-function relationships of endoglucanases, and to answer the important question of what determines whether an endoglucanase has xyloglucanase activity.

B. Glucosidase

Many of the glycosidases described to date play a role in mobilizing seed reserves upon germination. The β-glucosidase from *Tropaeolum majus* is probably the best-characterized one described in the literature (22). Therefore, the discussion of glucosidases will be restricted to this enzyme. The enzyme belongs to glycosyl hydrolase family 3 (retaining), and shows strong sequence homology to β-glucan exohydrolase from barley. The glucosidase contains two highly conserved motives, **SDW**—(24 aa)—**GIDM**, in which the aspartates have been implicated as the catalytic residues. Several β-linked glucose disaccharides were tested as a substrate. From this it was concluded that the enzyme hydrolyzes the various linkages at different rates: $(1 \rightarrow 3) > (1 \rightarrow 4) > (1 \rightarrow 2) > (1 \rightarrow 6)$. Xyloglucan oligosaccharides were also tested as a substrate. The glucosidase was active against GXXG, GXLG, and GXG, but not against XXXG, XXLG, XLXG, XLLG, GLXG, or GLLG. Thus, the enzyme requires an unsubstituted glucosyl residue at the nonreducing end of the oligosaccharide. Next to this, the sidechain configuration of the penultimate glucosyl residue at the

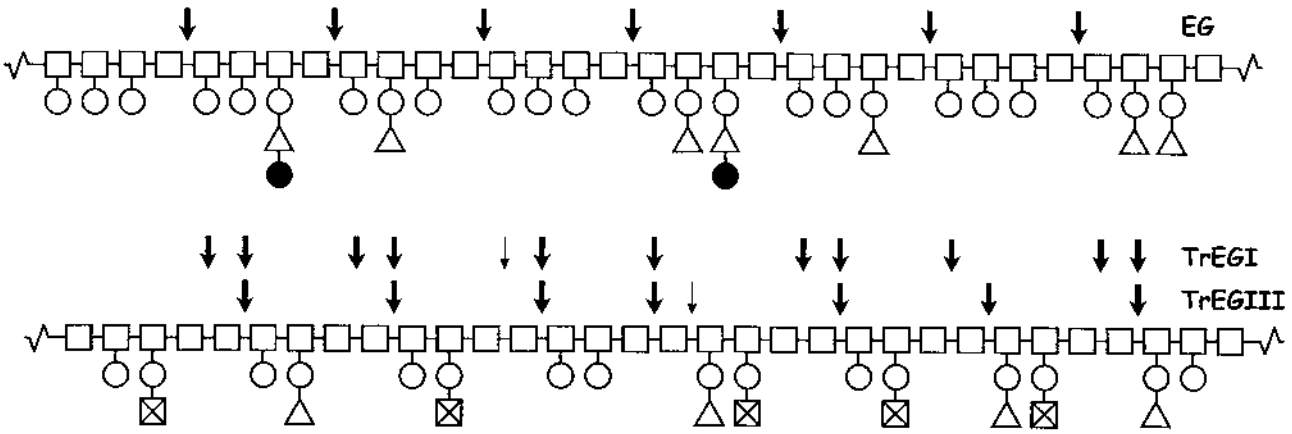

Figure 3 Schematic illustration of mode of action of endoglucanases (EGI and EGIII) from *Trichoderma reesei* on two different types of xyloglucan (XXXG and XXGG). For details on xyloglucan structure, see Figure 1C.

nonreducing end is important. Enzyme action is inhibited when this side chain contains a galactosyl residue. Another important observation is that the glucosidase shows transglycosylation activity with cello-oligosaccharides, but not with xyloglucan oligosaccharides. The cello-oligosaccharide transglycosylation products can be extended with Glc-(1 → 4)-β-, and possibly with Glc-(1 → 6)-β.

C. Xyloglucosidase

This enzyme is discussed in a separate paragraph, because contrary to glucosidase it seems to have a requirement for xylosyl side chains. Xyloglucosidase was purified from a preparation of *Aspergillus oryzae* (23) and is often used for structural characterization ("sequencing") of xyloglucan oligosaccharides. It releases isoprimeverose (α-D-Xyl*p*-(1 → 2)-β-D-Glc*p*) from the nonreducing terminus of XXXG (→ XXG + X), XXG (→ XG + X), or XG (→ G + X) oligosaccharides. Glucose release from cellotetraose is considerably slower (~ 50 times), which demonstrates that the enzyme is rather specific for xyloglucan. Also PNP-β-Glc was a very poor substrate. Xyloglucosidase is unable to by-pass galactosyl-containing side chains. It is unclear if this enzyme is active toward polysaccharides, because the polymeric substrates tested contain galactosyl residues. A similar activity is present in a preparation from *Irpex lacteus* (known under the commercial name Driselase), which is used by many plant researchers (24, 25). As of now, no such enzymes from plant origin are known.

D. Xylosidase

α-Xylosidases have been purified from *Pisum sativum* (26) as well as from *Tropaeolum majus* (27), and the two enzymes were shown to have very similar properties. The enzyme releases the xylosyl residue attached to the non-reducing glucosyl residue of a xyloglucan oligosaccharide (for instance XXXG → GXXG+ Xyl). No measurable amounts of xylose were split off from polymeric xyloglucan, which shows that no internal xylosyl residues are removed. However, the release of one xylosyl residue from the nonreducing terminus can not be excluded. The α-xylosidase may play a role in "deblocking" the nonreducing termini to facilitate β-glucosidase action. Contrary to a number of microbial α-xylosidases (28–32), PNP-α-Xyl and isoprimeverose were not substrates for the plant α-xylosidases.

E. Galactosidase

Both fungal and plant β-galactosidases have received attention. The fungal enzymes are sometimes used for structural characterization of xyloglucan oligosaccharides. The plant enzymes play a role in mobilization of seed reserves, together with the XET (see further), glucosidase, and xylosidase. York and coworkers (33) demonstrated that the β-galactosidase from *Aspergillus niger* catalyzed the following reactions: XLXG → XXXG and XLLG → XXLG. The enzyme was not capable of degalactosylating sidechains at the penultimate glucosyl residue at the reducing end, under the conditions used. Similar results have been reported for a plant β-galactosidase from *Copaifera langsdorffii* (34). The activity of this enzyme toward polymeric xyloglucan and other galactosyl-containing substrates was not further investigated. The substrate specificity of β-galactosidase from *Aspergillus oryzae* seems to be different. This preparation was successfully used to remove all galactosyl residues from three-oligo fragments of tamarind xyloglucan (8). The β-galactosidase from *Tropaeolum majus* was active toward PNP-β-Gal as well as polymeric xyloglucan (35). Unfortunately, the exact specificity was not further investigated. It is unknown if this enzyme is capable of removing both galactosyl residues from, for instance, XLLG-building blocks.

F. Fucosidase

Fucosidases have received some interest from plant researchers because it has been suggested that particular fucosylated xyloglucan oligosaccharides have biological activity (so-called oligosaccharins). The α-fucosidase from *Pisum sativum* has rather narrow substrate specificity. The enzyme recognizes α-L-Fuc*p*-(1 → 2)-β-D-Gal*p*-(1 → structures in xyloglucan oligosaccharides. No activity toward PNP-α-Fuc or polymeric xyloglucan was observed (36). It appeared that 6-*O*-acetylation of subterminal galactose of a synthetic substrate enhanced fucosidase activity. Interestingly, 6-*O*-acetylated XXFG naturally occurs as a building unit of sycamore cell wall xyloglucan (37). This enzyme probably plays a role in controlling the half-life of certain oligosaccharins (XXFG), which antagonize

auxin-induced growth. Fucosidases from other sources have also been described, but these will not be discussed here.

IV. XYLOGLUCAN ENDOTRANSGLYCOSYLASE AND RELATED ENZYMES

A separate section has been devoted to xyloglucan endotransglycosylase (XET), mainly because it is a very interesting enzyme from an enzymological point of view. The enzyme occurs throughout the plant kingdom, although some plants (for instance tomato) seem a richer source than others (38). XET or XET-related (referred to as XTR) proteins probably play a role in a number of important plant processes: (a) anchoring newly (synthesized and) deposited xyloglucan into the plant cell wall; (b) ripening; and (c) mobilization of seed reserves (39, 40). In the older literature, XET is sometimes referred to as xyloglucan-specific endoglucanase, oligosaccharide-activatable endoglucanase, or endo-xyloglucan transferase (EXT or EXGT).

XET catalyzes the cleavage of a xyloglucan molecule (**donor** substrate), and attaches the nonreducing moiety of this molecule to an **acceptor**, either water (hydrolysis reaction) or another xyloglucan molecule (transferase reaction of transglycosylation). Only XXXG-type donor molecules have been tested sofar, and these are cleaved by XET at a similar position as by endoglucanases. The acceptor can be an oligosaccharide or a polysaccharide. The three possible reactions of XET are shown in Figure 4. During polysaccharide-to-polysaccharide endotransglycosylation, the molecular-weight distribution of xyloglucan molecules broadens, but no net change in molecular weight is observed (38, 41). Polysaccharide-to-oligosaccharide transglycosylation results in a large decrease in molecular weight. This reaction has practically the same effect as endohydrolysis catalyzed by endoglucanases.

Experiments with plant extracts have shown that XET is highly specific for xyloglucan. Only xyloglucan serves as a donor substrate, whereas carboxymethyl cellulose and cellulose are not recognized (38). Several oligosaccharide have been tested as acceptor substrates. No transglycosylation was observed with cellobiose, cellotetraose to cellohexaose, laminarihexaose, FG, XGG, and GXG (38, 41–43). Some xyloglucan oligosaccharides appeared to be more efficient than others (efficiency in decreasing order XLLG, XXXG and XXFG) (38). In a separate study it was shown that XXXG was a better acceptor than XXG (42). From this it was concluded that XET requires two adjacent xylosyl residues as in XXG, which is the smallest acceptor molecule.

XET proteins can be purified relatively easily from a crude mixture of proteins, such as a plant extract. Two procedures have been described; both are based on the fact that XET can form a relatively stable enzyme-substrate complex with polymeric xyloglucan. In the first procedure, the molecular weight of XET is increased "artificially" by adding polymeric xyloglucan, which nests in the active site. Subsequently, the XET-xyloglucan complex is purified by size exclusion chromatography. Finally, XET is released from the polymer by addition of xyloglucan oligosaccharides, followed by a second chromatography step (44). The second pro-

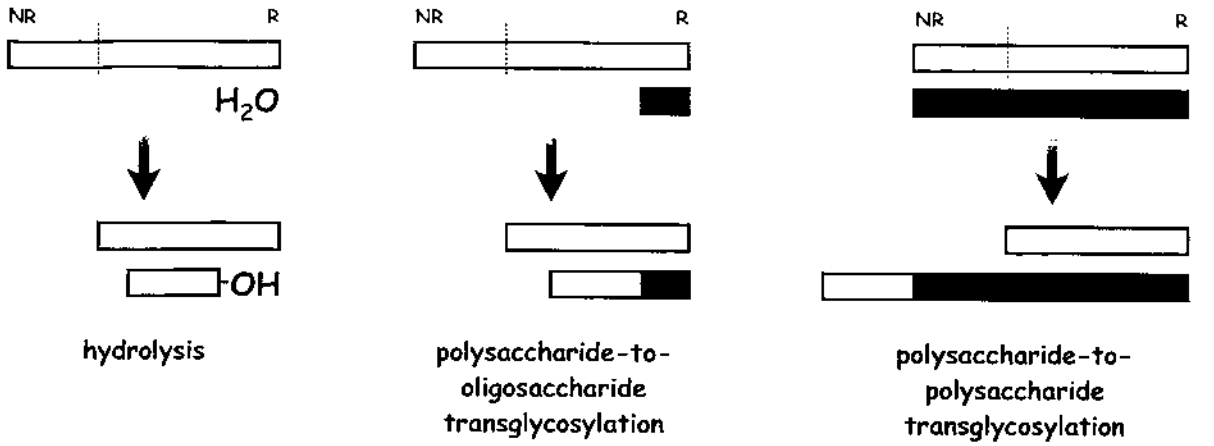

Figure 4 Schematic illustration of three reactions that can be catalyzed by XET. NR, nonreducing end of the polymer; R, reducing end. Vertical dotted line represents site of cleavage by XET.

cedure utilizes the affinity of xyloglucan for cellulose (45). The enzyme-substrate complex is adsorbed to cellulose. Subsequently, XET is released by addition of xyloglucan oligosaccharides.

Sequence comparisons have shown that the different XETs can be assigned to the same family as bacterial β-(1 $\rightarrow$ 3)(1 $\rightarrow$ 4)-glucanases, namely glycosyl hydrolase family 16 (39, 40). Reactions catalyzed by members of this family proceed with retainment of configuration, which is in line with the fact that this family contains many transferases. The three-dimensional structure of two *Bacillus* β-glucanases has been solved (46, 47). The enzymes are compact proteins with a sandwichlike jellyroll architecture. A groove, where the actual catalysis takes place, spans the concave side of the molecule. The other side of the enzyme contains a Ca^{2+}-binding site, which probably plays a role in stabilizing the protein together with one disulfide bridge. Because bacterial β-glucanases and XET have been assigned to the same family, it is expected that certain structural characteristics (e.g., fold) will also apply for XET. XET has been suggested to contain at least one disulfide bond, which appears to be important for maintaining enzyme activity. Most XETs contain a consensus sequence of **DEIDFEFLG**. Bacterial β-glucanases contain a sequence very similar to this, **DEIDIEFLG**. The DEIDIE residues are located along the bottom of the active site of these enzymes. The second glutamate (E) in this motif has been implicated as one of the catalytic residues of the enzyme. For XET it has been shown that the first glutamate is important for enzyme activity (48).

The sequence of many XETs or XET-related proteins have been described. For *Arabidopsis* it has been shown that it contains > 20 different XET (or XET-related) genes. The various XET sequences can be classified into four subgroups (I through IV) (40). Most sequence divergence is found in the carboxy terminal part of the proteins. *Arabidopsis* sequences are present in groups I–III, suggesting that plants have acquired specialized XETs to catalyze particular processes. Group III XETs differ from the enzymes in the other groups in that they have a C-terminal extension and a putative (N-linked) glycosylation site at a different position in the protein. Enzymes from these groups will be discussed in more detail below. Group IV only contains two barley XET sequences, and will not be discussed further.

The biochemical properties of two XETs in group I have been mapped. Unfortunately, different experimental procedures/conditions were used, which makes it difficult to make an extensive comparison. The enzymes have a high transferase activity in common, and they do not seem to catalyze the hydrolysis reaction (see Fig. 4). Both fucosylated and nonfucosylated xyloglucan can be used as donor. The activity of the *Vigna angularis* XET decreases dramatically when the donor substrate becomes shorter (41). Only very little activity was found on donor substrates of 10 kDa (approximately eight-oligo fragments). Possibly, this preference for high-molecular-weight xyloglucan is related to the conformation of xyloglucan in solution, but this requires further investigation. Similar observations have been made by Tabuchi et al. (49), but in this case the activity cannot be related to a sequence. The EXGT from *Arabidopsis thaliana* prefers the acceptor substrate XLLG over XXXG. XXXG seems to be preferred over XXFG (50).

Three group II XETs from *Arabidopsis thaliana* have been characterized biochemically: TCH4, Meri-5, and XTR9 (50, 51). These enzymes have a pH optimum between 6.0 and 6.5, and have low (if any) hydrolytic activity. TCH4 and XTR9 have a relatively low temperature optimum of 18°C, whereas Meri-5 is most active at 28°C. TCH4 and Meri-5 are not influenced by fucosylation of the donor substrate. In contrast to this, XTR9 has a clear preference for nonfucosylated donor substrate. The three XETs prefer XLLG over XXXG and XXFG as an acceptor substrate. However, only XTR9 seems to prefer XXFG over XXXG. Further, XTR9 has a lower K_m value for the XLLG acceptor and is significantly inhibited by high levels of XLLG. The activity of TCH4 and Meri-5 is abolished upon removal of N-linked glycosylation, whereas the activity of XTR9 is unaffected by such treatment.

The best-characterized member of group III is nasturtium (*Tropaeolum majus*) XET, often referred to as NXG1 (52). This enzyme is characterized by its relatively higher preference for water as acceptor substrate; i.e., it can catalyze hydrolysis reactions next to transglycosylation reactions. It is unlikely that NXG1 requires high-molecular-weight donor substrates. This enzyme plays a role in the mobilization of xyloglucan reserves in seeds during germination, and has long been regarded as a xyloglucan-specific endoglucanase. Typically, the highly conserved active site motif is slightly different in NXG1 (and also in other members of group III), **DELDIEFLG** instead of **DEIDFEFLG** (40). In principle, one could say that the bacterial β-glucanases hold an intermediate position between NXG1 and most other XETs with respect to this motif (compare with motif above). In addition, the

group III XETs have a small loop of three extra amino acids upstream of this motif. At the moment it is still unclear whether these special NXG1 features are responsible for its relatively high hydrolytic activity. The substrate specificity of NXG1 was investigated by Fanutti et al. (52). A xylosidase (see previously) was used to tailor the specific substrates GXXGXXXG and GLLGXLLG, which were subsequently treated with NXG1. It appeared that GXXGXXXG was converted to GXXGGXXGXXXG and XXXG. GXXG(↓)G↓XXGXXXG could be cleaved as indicated (cleavage site between brackets is likely but does not follow unambiguously from the experiments). GLLGXLLG was converted to GLLGGLLGXLLG and XLLG. GLLG(↓)GLLGXLLG was degraded in a different manner as GXXGGXXGXXXG (cleavage site between brackets is likely but does not follow unambiguously from the experiments). From these and other experiments a number of important conclusions with respect to donor and acceptor substrate specificity could be drawn:

1. NXG1 can use acceptor substrates, which do not carry a xylosyl residue on the nonreducing glucosyl residue.
2. NXG1 does not require xylosyl substitution at glucose residues −4, −2, +1, and +3 (for nomenclature see Fig. 5).
3. Xylosyl substitution at +2 (and possibly −3) is a requirement for NXG1.
4. Galactosyl substitution of a xylosyl residue at +1 prevents, and at −2 modifies, chain cleavage by NXG1.

The overview above shows that there can be important differences in the properties of XETs, even within one subgroup. Much more research is needed to understand the structure-function relationships of XETs.

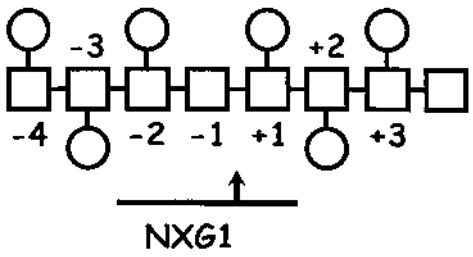

Figure 5 Xyloglucan fragment illustrating the pattern of xylose substitution of the glucan backbone around the site of chain cleavage (arrow). For details on xyloglucan structure, see Figure 1C. For significance of numbering, see text. (From Ref. 52.)

Important questions to be answered are "what determines the hydrolytic activity of some XETs?" and "what underlies the requirement for high molecular weight donor substrates for some XETs?" For family 12 endoglucanases, we have discussed already (see previous section) that subtle differences between these enzymes can determine whether or not they have xyloglucanase activity. In analogy to this, it may be expected that particular amino acid substitutions underlie donor and acceptor substrate specificity of XETs. In addition, it remains to be established whether XETs can display a different mode of action toward XXXG-type or XXGG-type xyloglucan.

V. DETERMINATION OF ENZYME ACTIVITY ON XYLOGLUCANS

Many different assays can be used for studying conversions of xyloglucans. Simple reducing end-group analysis can point out whether enzymes or enzyme extracts contain xyloglucanase activity. It should be realized that xyloglucans contain relatively few "cleavable" glycosidic linkages (less than one out of seven!). As a result of this, it may be necessary to use higher substrate concentrations than one would use for unbranched substrates (to avoid substrate limitation). High-performance size exclusion chromatography (HPSEC) with refractive index (RI) detection may be used to determine differences in molecular-weight distributions. High-performance anion exchange chromatography (HPAEC) with an electrochemical detection unit is suitable for monitoring the release of oligosaccharides from a polymer. Appropriate reference oligosaccharides cannot be obtained commercially, and should be purified by oneself. Mass spectrometry (MS) is a very useful tool in structural elucidation of reaction products. In particular, liquid chromatography/tandem–mass spectrometry (LC-MSMS) in combination with ^{18}O-labeling of reaction products may detect differences in mode of action between two endoglucanases. In this case, incubations are done in the presence of ^{18}O-labeled water; tandem-MS is used to "sequence" the individual oligosaccharides (53).

Reducing end-group assays are not applicable for determining XET activity (except for NXG1-like enzymes catalyzing hydrolysis reactions), because the number of reducing ends remains constant during transglycosylation. Several methods to quantify the transglycosylation activity of XET have been described. These protocols are all based on a polysac-

charide-to-oligosaccharide transglycosylation. Three methods are discussed below.

1. Xyloglucan oligosaccharides are radiolabeled by exchanging the hydrogen at the reducing terminus of the molecule with ^{3}H (39, 40). Radiolabeled oligosaccharides are subsequently incorporated into polymeric xyloglucan by transglycosylation. The radiolabeled products are sufficiently long to be adsorbed on a piece of filter paper (cellulose). After a washing step to remove the unreacted ^{3}H-oligosaccharides, the transglycosylation activity can be simply measured by counting the radioactivity of the filter paper with a scintillation counter.

2. In the second method, the xyloglucan (acceptor) oligosaccharides are tagged at the reducing end with a UV or fluorescent label (e.g., 2-aminopyridine) (39, 40). The transglycosylation reaction produces fluorescent xyloglucans with an increased molecular weight. These are separated by HPSEC, and quantified by a fluorescence or UV detector. It may be advantageous to couple a RI detector to the HPSEC/UV system in order to visualize a shift in molecular-weight distribution of the polymeric xyloglucan.

3. The third method is probably the easiest, because it does not involve radiolabeling or complicated derivation procedures of the acceptor oligosaccharides. The method is based on the fact that xyloglucans with a molecular weight > 10 kDa form a blue-green complex with iodine, whereas fragments < 10 kDa remain unstained (54). XET activity can be determined colorimetrically by measuring the disappearance of the blue-green-colored iodine:xyloglucan complex in the presence of xyloglucan acceptor oligosaccharides at 620 nm.

For a more qualitative analysis of XET action LC-MSMS is a valuable analytical tool (see previous paragraph) (53). This method could, for instance, be used to detect differences in mode of action of various XETs.

VI. APPLICATIONS IN THE FOOD INDUSTRY

Enzymes with activity toward xyloglucan can be used in a number of processes which are relevant for the food industry. Most applications are related to processing of vegetables and fruits. Other applications are more at the ingredient level. Some examples in which enzymic modification of xyloglucans can play a role will be discussed below.

Many processes in the food industry aim at a complete degradation of the plant cell wall (the so-called liquefaction process). For instance, in fruit juice manufacturing enzyme preparations are applied to increase juice yield. Also the recovery of important metabolites from plant material can be facilitated by using mixtures of cell wall-degrading enzymes. In many cases, xyloglucanases are an important component of these cocktails. In apple cell wall degradation, a *Trichoderma reesei* endoglucanase with xyloglucanase activity works particularly well with pectinases (55). The ratio of various endoglucanases in commercial enzyme preparations also deserves attention. It is known for quite some time that cellulose is most efficiently degraded by a mixture of glucanases: endoglucanase and cellobiohydrolase (CBH). The endoglucanase produces new chain termini for the CBH to work on. It is less known that efficient degradation of cell wall–embedded cellulose (i.e., cellulose which is coated with xyloglucan) requires (at least) one more glucanase, namely xyloglucanase. The xyloglucanase increases the accessibility of cellulose by removing its xyloglucan coating (14).

In the previous sections, we have seen that many endoglucanases and XETs can be present in plant tissues. It has been suggested that these enzymes may act in concert during fruit ripening. In this process, the EG generates xyloglucan oligosaccharides, which are subsequently used as acceptor substrates by XET in a polysaccharide-to-oligosaccharide transglycosylation (56). As a result of this, xyloglucan will be more rapidly depolymerized. This rapid breakdown of xyloglucan may be related with fruit softening, although also other enzymes like pectinases are known to play an important role in this process. It is expected that the shelf life of fruits can be extended when these enzyme activities can be kept at a low level. It has also been shown that the level of XET in apple fruit can be an important factor in the liquefaction process. The endogenous XET may act in concert with exogenous (fungal) endoglucanases (57, 58). The endoglucanases generate xyloglucan oligosaccharides on the outside of the apple tissue. These oligosaccharides diffuse into the tissue and serve as acceptor substrates for XET. "High-XET" apple fruit could be processed much faster than "low-XET" apple fruit, because it is degraded from both the inside and the outside during liquefaction. This may explain observations by the industry that the processing time can vary from one fruit batch to another.

Xyloglucans, which are stored in the secondary cell wall of seeds (for instance, tamarind seed), are often used as a viscosifyer in the food industry. The gelling

properties of these polysaccharides can be modulated by treatment with β-galactosidase from plant (59) or fungal origin (60). Removal of $\sim 40\%$ of the galactosyl residues from xyloglucan resulted in self-association of the polymers, and consequently the formation of a gel. These gels have unique properties in that they can be liquefied at low ($\sim 30^{\circ}$C) and high temperatures ($\sim 100^{\circ}$C); i.e., there are two sol-gel transition points (60). Possibly, α-xylosidases can also be useful to adjust the gelling properties of xyloglucan. However, at this moment there are no such enzymes with activity toward polymeric xyloglucan.

The special properties of XET have already been mentioned in a previous paragraph. For industrial applications the low activity of (most?) XETs toward xyloglucans with a molecular weight < 10 kDa (approximately eight oligosaccharides) is particularly interesting. These enzymes have the potential to tailor low-viscosity xyloglucan fragments, which still have the ability to bind to cellulose. Possibly, such molecules can be used in the future to engineer cellulose-xyloglucan composites with specific properties (58).

REFERENCES

1. J-P Vincken, WS York, G Beldman, AGJ Voragen. Two general branching patterns of xyloglucan, XXXG and XXGG. Plant Physiol 114:9–13, 1997.
2. MS Buckeridge, HJ Crombie, CJM Mendes, JSG Reid, MJ Gidley, CCJ Vieira. A new family of oligosaccharides from the xyloglucan of *Hymenaea courbaril* L. (Leguminosae) cotyledons. Carbohydr Res 303:233–237, 1997.
3. SC Fry, WS York, P Albersheim, A Darvill, T Hayashi, J-P Joseleau, Y Kato, EP Lorences, GA Maclachlan, M McNeil, AJ Mort, JSG Reid, HU Seitz, RR Selvendran, AGJ Voragen, AR White. An unambiguous nomenclature for xyloglucan-derived oligosaccharides. Physiol Plant 89:1–3, 1993.
4. S Levy, WS York, R Stuike-Prill, B Meyer, LA Staehelin. Simulations of the static and dynamic molecular conformations of xyloglucan. The role of the fucosylated sidechain in surface-specific side-chain folding. Plant J 1:195–215, 1991.
5. S Levy, G Maclachlan, LA Staehelin. Xyloglucan sidechains modulate binding to cellulose during in vitro binding assays as predicted by conformational dynamics simulations. Plant J 11:373–386, 1997.
6. T Hayashi, K Ogawa, Y Mitsuishi. Characterization of the adsorption of xyloglucan to cellulose. Plant Cell Physiol 35:1199–1205, 1994.
7. J-P Vincken, A de Keizer, G Beldman, AGJ Voragen. Fractionation of xyloglucan fragments and their interaction with cellulose. Plant Physiol 108:1579–1585, 1995.
8. T Hayashi, T Takeda, K Ogawa, Y Mitsuishi. Effects of the degree of polymerization on the binding of xyloglucans to cellulose. Plant Cell Physiol 35:893–899, 1994.
9. MC McCann, B Wells, K Roberts. Direct visualization of cross-links in the primary plant cell wall. J Cell Sci 96:323–334, 1990.
10. MC McCann, B Wells, K Roberts. Complexity in the spatial localization and length distribution of plant cell-wall matrix polysaccharides. J Microsc 166:123–136, 1992.
11. SEC Whitney, MGE Gothard, JT Mitchell, MJ Gidley. Roles of cellulose and xyloglucan in determining the mechanical properties of primary plant cell walls. Plant Physiol 121:657–663, 1999.
12. J-P Vincken, G Beldman, AGJ Voragen. Substrate specificity of endoglucanases: what determines xyloglucanase activity? Carbohydr Res 298:299–310, 1997.
13. M Pauly, LN Andersen, S Kauppinen, LV Kofod, WS York, P Albersheim, A Darvill. A xyloglucan-specific *endo*-β-1,4-glucanase from *Aspergillus aculeatus*: expression cloning in yeast, purification and characterization of the recombinant enzyme. Glycobiology 9:93–100, 1999.
14. J-P Vincken, G Beldman, AGJ Voragen. The effect of xyloglucans on the degradation of cell-wall-embedded cellulose by the combined action of cellobiohydrolase and endoglucanases from *Trichoderma viride*. Plant Physiol 104:99–107, 1994.
15. E del Campillo. Multiple endo-1,4-β-D-glucanase (cellulase) genes in *Arabidopsis*. Curr Top Dev Biol 46:39–61, 1999.
16. P Tomme, RAJ Warren, NR Gilkes. Cellulose hydrolysis by bacteria and fungi. Adv Microb Physiol 37:1–81, 1995.
17. J-P Vincken, G Beldman, WMA Niessen, AGJ Voragen. Degradation of apple fruit xyloglucan by endoglucanase. Carbohydr Polym 29:76–85, 1996.
18. WS York, G Impallomeni, M Hisamatsu, P Albersheim, AG Darvill. Eleven newly characterized xyloglucan oligoglycosyl alditols: the specific effects of sidechain structure and location on ^{1}H NMR chemical shifts. Carbohydr Res 267:79–104, 1995.
19. M Hisamatsu, WS York, AG Darvill, P Albersheim. Characterization of seven xyloglucan oligosaccharides containing from seventeen to twenty glycosyl residues. Carbohydr Res 227:45–71, 1992.
20. J-P Vincken, AJM Wijsman, G Beldman, WMA Niessen, AGJ Voragen. Potato xyloglucan is built from XXGG-type subunits. Carbohydr Res 288:219–232, 1996.

21. IM Sims, SLA Munro, G Currie, D Craik, A Bacic. Structural characterisation of xyloglucan secreted by suspension-cultured cells of *Nicotiana plumbaginifolia*. Carbohydr Res 293:147–172, 1996.
22. HJ Crombie, S Chengappa, A Hellyer, JSG Reid. A xyloglucan oligosaccharide-active, transglycosylating β-D-glucosidase from the cotyledons of nasturtium (*Tropaeolum majus* L) seedlings—purification, properties and characterization of a cDNA clone. Plant J 15:27–38, 1998.
23. Y Kato, J Matsushita, T Kubodera, K Matsuda. A novel enzyme producing isoprimeverose from oligoxyloglucans of *Aspergillus oryzae*. J Biochem 97:801–810, 1985.
24. M Hisamatsu, G Impallomeni, WS York, P Albersheim, AG Darvill. A new undecasaccharide subunit of xyloglucans with two α-L-fucosyl residues. Carbohydr Res 211:117–129, 1991.
25. GJ McDougall, SC Fry. Purification and analysis of growth-regulating xyloglucan-derived oligosaccharides by high-pressure liquid chromatography. Carbohydr Res 219:123–132, 1991.
26. RA O'Neill, P Albersheim, AG Darvill. Purification and characterization of a xyloglucan oligosaccharide-specific xylosidase from pea seedlings. J Biol Chem 264:20430–20437, 1989.
27. C Fanutti, MJ Gidley, JSG Reid. A xyloglucan-oligosaccharide-specific α-D-xylosidase or *exo*-oligoxyloglucan-α-xylohydrolase from germinated nasturtium (*Tropaeolum majus* L.) seeds. Planta 184:137–147, 1991.
28. J Matsushita, Y Kato, K Matsuda. Purification and properties of an α-D-xylosidase from *Aspergillus niger*. J Biochem 98:825–832, 1985.
29. N Zong, T Yasui. Purification and some properties of an α-D-xylosidase from *Bacillus* sp. No. 693-1. Agric Biol Chem 53:187–195, 1989.
30. N Zong, Y Kamiyama, T Yasui. Substrate specificity of *Bacillus* α-D-xylosidase. Agric Biol Chem 53:2129–2139, 1989.
31. K Yoshikawa, K Yamamoto, S Okada. Isolation of *Aspergillus flavus* MO-5 producing two types of intracellular α-D-xylosidases: purification and characterization of α-D-xylosidase I. Biosci Biotech Biochem 57:1275–1280, 1993.
32. K Yoshikawa, K Yamamoto, S Okada. Purification and characterization of an intracellular α-D-xylosidase II from *Aspergillus flavus* MO-5. Biosci Biotech Biochem 57:1281–1285, 1993.
33. WS York, LK Harvey, RR Guillen, P Albersheim, AG Darvill. Structural analysis of tamarind seed xyloglucan oligosaccharides using β-galactosidase digestion and spectroscopic methods. Carbohydr Res 248:285–301, 1993.
34. PHN de Alcântara, SMC Dietrich, MS Buckeridge. Xyloglucan mobilisation and purification of a (XLLG/XLXG) specific β-galactosidase from cotyledons of *Copaifera langsdorffii*. Plant Physiol Biochem 37:653–663, 1999.
35. M Edwards, YJL Bowman, ICM Dea, JSG Reid. A β-D-galactosidase from nasturtium (*Tropaeolum majus* L.) cotyledons. J Biol Chem 263:4333–4337, 1988.
36. C Augur, N Benhamou, A Darvill, P Albersheim. Purification, characterization, and cell wall localization of an α-fucosidase that inactivates a xyloglucan oligosaccharin. Plant J 3:415–426, 1993.
37. Ll Kiefer, WS York, AG Darvill, P Albersheim. Xyloglucan isolated from suspension-cultured sycamore cell walls is *O*-acetylated. Phytochemistry 28:2105–2107, 1989.
38. SC Fry, RC Smith, KF Renwick, DJ Martin, SK Hodge, KJ Matthews. Xyloglucan endotransglycosylase, a new wall-loosening enzyme activity from plants. Biochem J 282:821–828, 1992.
39. K Nishitani. The role of endoxyloglucan transferase in the organization of plant cell walls. Int Rev Cytol 173:157–206, 1997.
40. P Campbell, J Braam. Xyloglucan endotransglycosylases: diversity of genes, enzymes and potential wall-modifying functions. Trends Plant Sci 4:361–366, 1999.
41. K Nishitani, R Tominaga. Endo-xyloglucan transferase, a novel class of glycosyltransferase that catalyzes transfer of a segment of xyloglucan molecule to another xyloglucan molecule. J Biol Chem 267:21058–21064, 1992.
42. EP Lorences, SC Fry. Xyloglucan oligosaccharides with at least two α-D-xylose residues act as acceptor substrates for xyloglucan endotransglycosylase and promote the depolymerisation of xyloglucan. Physiol Plant 88:105–112, 1993.
43. EP Lorences, SC Fry. Sequencing of xyloglucan oligosaccharides by partial Driselase digestion: the preparation and quantitative and qualitative analysis of two new tetrasaccharides. Carbohydr Res 263:285–293, 1994.
44. NM Steele, SC Fry. Purification of xyloglucan endotransglycosylases (XETs): a generally applicable and simple method based on reversible formation of an enzyme substrate complex. Biochem J 30:207–211, 1999.
45. Z Sulová, V Farkaš. Purification of xyloglucan endotransglycosylase based on affinity sorption of the active glycosyl-enzyme intermediate complex to cellulose. Prot Expression Purification 16:231–235, 1999.
46. T Keitel, O Simon, R Borriss, U Heinemann. Molecular and active-site structure of a *Bacillus* 1,3-1,4-β-glucanase. Proc Natl Acad Sci USA 90:5287–5291, 1993.
47. M Hahn, O Olsen, O Politz, R Borriss, U Heinemann. Crystal structure and site-directed mutagenesis of *Bacillus macerans* endo-1,3-1,4-β-glucanase. J Biol Chem 270:3081–3088, 1995.

48. P Campbell, J Braam. Co- and/or post-translational modifications are critical for TCH4 XET activity. Plant J 15:553–561, 1998.
49. A Tabuchi, S Kamisaka, T Hoson. Purification of xyloglucan hydrolase/endotransferase from cell walls of azuki bean epicotyls. Plant Cell Physiol 38:653–658, 1997.
50. P Campbell, J Braam. In vitro activities of four xyloglucan endotransglycosylases from *Arabidopsis*. Plant J 18:371–382, 1999.
51. MM Purugganan, J Braam, SC Fry. The *Arabidopsis* TCH4 xyloglucan endo-transglycosylase. Substrate specificity, pH optimum, and cold tolerance. Plant Physiol 115:181–190, 1997.
52. C Fanutti, MJ Gidley, JSG Reid. Substrate subsite recognition of the xyloglucan *endo*-transglycosylase or xyloglucan-specific *endo*-(1 → 4)-β-D-glucanase from the cotyledons of germinated nasturtium (*Tropaeolum majus* L) seeds. Planta 200:221–228, 1996.
53. R Körner. Structural characterization of biopolymers by MS and MS/MS. PhD thesis, Department of Molecular Biology, University of Southern Denmark, Odense, Denmark, 1999.
54. Z Sulová, M Lednická, V Farkaš. A colorimetric assay for xyloglucan-endotransglycosylase from germinating seeds. Anal Biochem 229:80–85, 1995.
55. CMGC Renard, MJF Searle–van Leeuwen, AGJ Voragen, J-F Thibault, W Pilnik. Studies on apple protopectin. II. Apple cell wall degradation by pure polysaccharidase and their combinations. Carbohydr Polym 14:295–314, 1991.
56. JKC Rose, AB Bennett. Cooperative disassembly of the cellulose-xyloglucan network of plant cell walls: parallels between cell expansion and fruit ripening. Trends Plant Sci 4:176–183, 1999.
57. J-P Vincken, LAM van den Broek, DD van der Lei, G Beldman, AGJ Voragen. Fungal and plant xyloglucanases may act in concert during liquefaction of apples. J Sci Food Agric 73:407–416, 1997.
58. J-P Vincken, OA Zabotina, G Beldman, AGJ Voragen. Xyloglucan endotransglycosylase activity in apples is ripening-related: implications for fruit juice processing. J Sci Food Agric 78:46–52, 1998.
59. JSG Reid, M Edwards, ICM Dea. Enzymatic modification of natural seed gums. In: GO Phillips, DJ Wedlock, PA Williams, eds. Gums and Stabilizers for the Food Industry. Washington: IRL Press, 1988, pp 391–398.
60. M Shirakawa, K Yamatoya, K Nishinari. Tailoring of xyloglucan properties using an enzyme. Food Hydrocoll 12:25–28, 1998.

73

Enzymes Degrading Rhamnogalacturonan and Xylogalacturonan

Jean-Paul Vincken, Alphons G. J. Voragen, and Gerrit Beldman
Wageningen University, Wageningen, The Netherlands

I. INTRODUCTION

In a previous section of this book (Chap. 66), the structure of pectin was discussed in detail. Besides homogalacturonans (often referred to as the smooth regions of pectin), also branched or hairy regions occur (1). The hairy regions are composed of a collection of polysaccharides: rhamnogalacturonan (RG), xylogalacturonan (XGA), arabinan, and (arabino)galactan. This chapter deals with carbohydrases having activity toward the former two. Both polysaccharides can be referred to as heterogalacturonans. A third heterogalacturonan present in plant cell walls, rhamnogalacturonan II, has a very complex structure. At this moment, no enzymes with activity toward this polysaccharide have been characterized. Homogalacturonan-degrading enzymes, as well as arabinan- and galactan-degrading enzymes, are described elsewhere in this book (Chap. 70).

In comparison with homogalacturonan-degrading enzymes, enzymes with activity toward RG and XGA are newcomers in the field of carbohydrates. Reasons for this are the following: (a) industrial interest in these enzymes has only recently been roused by new fruit juice manufacturing techniques (see further); (b) the enzymes are usually minor components of commercial enzyme preparations used by the food industry; (c) substrates for these enzymes are often difficult to obtain from commercial resources; and (d) the enzymes produce complex mixtures of degradation products, requiring sophisticated analytical tools for identification. It is expected that the interest in these enzymes will continue to grow, because they may also be important in tailoring bioactive oligosaccharides. With the completion of the *Arabidopsis* genome-sequencing project, plant biologists have obtained clues that homologs of the enzymes discussed in this chapter are also present in plants; these enzymes may be involved in remodeling plant cell wall structure during development.

As a consequence of their fairly recent discovery, the picture of RG- and XGA-degrading enzymes is rather incomplete when compared to that of the more classical pectinases such as endopolygalacturonase (endoPG), endopectin lyase (endoPL), and endopectate lyase (endoPAL). Much less sequence information is available for these enzymes, and systematic studies to delineate the principles underlying their structure-function relationships still have to get started. Pectinases can be assigned to various enzyme families. This family classification is based on similarities in apparent secondary structure characteristics of proteins (http://afmb.cnrs-mrs.fr/~pedro/CAZY/) and is updated regularly. In principle, pectinases with very low amino acid sequence identity can be attributed to the same family; i.e., the fold of the proteins seems to be much better conserved than their sequence. Within one family, the catalytic mechanism (retaining or inverting) and the three-dimensional structure of the protein are thought to be similar.

A selection of classes of pectin-degrading enzymes is summarized in Table 1. Enzymes with activity toward

Table 1 Overview of Galacturonan-Degrading Enzymes[a]

Enzyme	Organism	Fam.	No. entries	Comments
endoPG	*Aspergillus niger*	GH28	7[b]	3D structure available
exoPG	*Aspergillus tubingensis*	GH28	1	Active toward xylogalacturonan
endoXGH	*Aspergillus tubingensis*	GH28	1	Homologous to endoPG, presumably requires xylosyl sidechains for activity
put. PG	*Arabidopsis thaliana*	GH28	~ 55	Very limited biochemical data available, sequences cluster in various groups
endoRGH	*Aspergillus niger*	GH28	2	RGHs differ in the presence of a C-terminal extension, 3D structure of *Aspergillus aculeatus* RGH is available
RG Rha-hydrolase	*Aspergillus aculeatus*	???	n.a.	No sequence information available
RG GalA-hydrolase	*Aspergillus aculeatus*	???	n.a.	No sequence information available, inverting enzyme
endoPAL	*Erwinia chrysanthemi*	L1	~ 10	3D structure available, various strains
put. endoPAL	*Arabidopsis thaliana*	L1	~ 23	Very limited biochemical data available
endoPL	*Aspergillus niger*	L1	3	3D structure available
exoPAL	*Erwinia chrysanthemi*	L2	1	
endoPAL	*Erwinia chrysanthemi*	L3	1	
endoRGL	*Aspergillus aculeatus*	L4	1	
put. endoRGL	*Arabidopsis thaliana*	L4	7	
endoPAL	*Erwinia chrysanthemi*	L9	1	
exoPAL	*Erwinia chrysanthemi*	L9	1	
endoPAL	*Pseudomonas cellulosa*	L10	1	Modular protein
endoRGL	*Pseudomonas cellulosa*	L11	1	Modular protein

[a]Enzymes with activity against rhamnogalacturonan are in boldface. For more details, see text.
[b]Number indicates that family GH28 contains seven different endoPGs from *Aspergillus niger*. EndoPGs from many other species are also members of this family, but these are not shown.

branched galacturonans are shown in boldface. Glycosyl hydrolase family 28 (GH28) is a particularly large family, comprising enzymes with a very divergent substrate specificity. Hydrolases with activity toward homogalacturonan, XGA, and RG are present within this family. Further, GH28 contains many putative proteins from plant origin. An interesting observation is that *Arabidopsis* members of GH28 outnumber those derived from one fungus (e.g., *Aspergillus niger*). It remains to be established whether these *Arabidopsis* proteins represent an array of different pectinases with activity toward the various galacturonan-containing polymers in plants. Surprisingly, galacturonan lyases are distributed over as many as seven different families (L1–L4 and L9–L11). Also in this case the *Arabidopsis* genome-sequencing effort has provided clues on the possible existence of an abundance of plant galacturonan lyases (L1 and L4). Again, at present the plant enzymes have not been characterized. Despite the large differences in substrate specificity (homogalacturonan, XGA, and RG) and catalytic mechanism (hydrolase versus lyase), it turns out that the three-dimensional structures of pectin-degrading enzymes are very similar (2). All the enzymes investigated so far possess the characteristic right-handed parallel β-helical structure, which has been discussed for homogalacturonan-degrading enzymes elsewhere in this book. In this chapter, we will focus on microbial enzymes, because there are currently no biochemical data available for the plant enzymes. XGA-degrading enzymes will be discussed first, followed by RG-degrading enzymes. Subsequently, a few words will be said on the detection of enzyme activity toward heterogalacturonans. Finally, applications with relevance to the food industry will be discussed.

II. ENZYMIC DEGRADATION OF XYLOGALACTURONANS

In the literature, there are a number of reports describing a homogalacturonan with β-D-Xyl*p*-(1 $\rightarrow$ 3) side chains (3, 4). This polysaccharide is referred to as xylogalacturonan (XGA). Besides the xylosyl branches, methoxyl groups can be attached to the *O*-6 of GalA residues (3). So far, the presence of XGA in plants seems to be confined to reproductive organs (fruits, seeds) (5), such as apple (3), pea (4), and watermelon (6), and to exudates from *Astragalus* trees (7, 8). It seems that the degree of xylosylation of the homogalacturonan backbone can differ with the origin of the XGA. For instance, in apple XGA three out of four GalA residues carry a xylosyl sidechain, whereas in watermelon XGA this is only one out of four. In apple, XGA seems to be covalently linked to RG (3); for other species, this has not been investigated in so much detail.

A. Exopolygalacturonase

Exopolygalacturonase (exoPG) from *Aspergillus aculeatus* was the first enzyme of which activity toward unesterified XGA was demonstrated (9). This enzyme is not specific for XGA, as (unesterified) homogalacturonans are also degraded, with GalA as the only product. The exoPG can release Xyl-GalA disaccharides and monogalacturonic acid from the nonreducing terminus of xylogalacturonan (see Fig. 1). Thus, it seems that the *A. aculeatus* exoPG is tolerant to xylosyl substitution of the homogalacturonan backbone, a feature also encountered in other *Aspergillus* exoPGs (10).

B. Endopolygalacturonase

EndoPGs can also show activity toward saponified XGA; however, this seems to depend greatly on its degree of xylosyl branching. Apple XGA (saponified) was resistant to all endoPGs tested, including endoPGI and edoPGII from *Aspergillus niger*. The less branched watermelon XGA can be degraded to GalA, $GalA_2$, $GalA_3$, and a series of Xyl-containing oligogalacturonides by a commercial endoPG preparation (6). Oligogalacturonides with a Xyl:GalA ratio of 1:4 and 1:5 seem to be abundant in the XGA digest. These results suggest that endoPGs are not as tolerant to xylosyl substitution as exoPG. They require a number of contiguous, unbranched GalA residues (presumably more than three) for activity.

C. Endoxylogalacturonan Hydrolase

Very recently, an endoacting enzyme with activity toward XGA was discovered by screening an

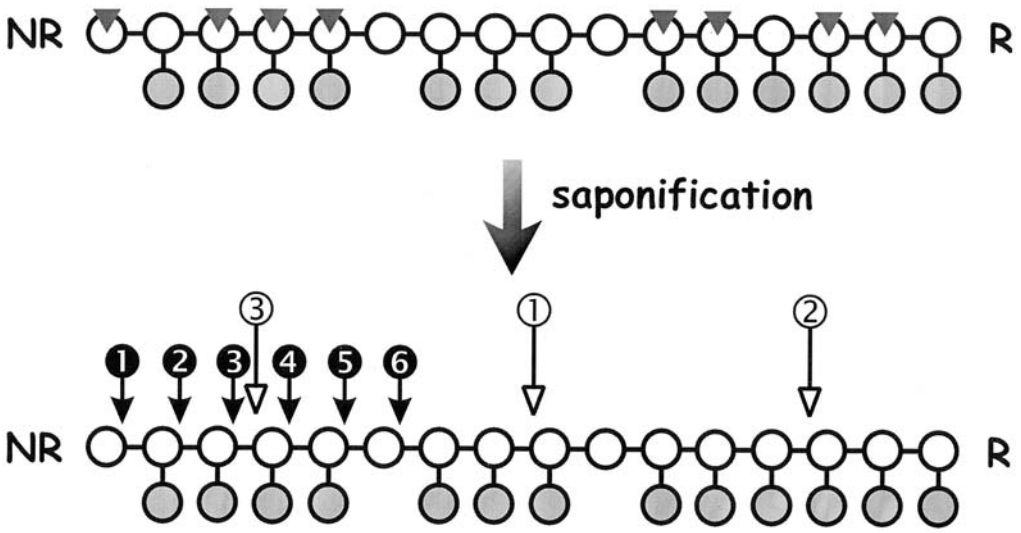

Figure 1 Schematic illustration of xylogalacturonan degradation by exopolygalacturonase (closed arrowheads) and endoxylogalacturonan hydrolase (open arrowheads). Both enzymes are hindered by the presence of methoxyl groups. Numbers indicate 1st, 2nd, 3rd, etc., cleavage of the substrate by the enzyme. Open circles represent α-D-Gal*p*A residues, shaded circles β-D-Xyl*p* residues, and small closed triangles methoxyl groups. NR indicates the nonreducing end; R, the reducing end.

Aspergillus tubingensis expression library in the yeast *Kluyveromyces lactis* (11). A modified gum tragacanth (saponified and treated with dilute acid; Xyl:GalA ratio of 1:2) was used as a substrate, and activity was detected using a reducing end-group assay (12). Amino acid sequence comparisons have shown that endoxylogalacturonan hydrolase (endoXGH) is a GH28 member, just like endoPG, exoPG, and endorhamnogalacturonan hydrolase (endoRGH). Typically, it shares the highest homology with exoPG, which is in accordance with its substrate specificity (11). EndoXGH can degrade saponified apple hairy regions (containing XGA); the disaccharide Xyl-GalA and an unknown oligosaccharide are the main end products of this treatment. Digestion of the modified gum tragacanth results in a complex mixture of many xylosylated oligogalacturonides (11). The low activity of endoXGH toward unesterified homogalacturonan and its much higher activity toward saponified XGA suggest that the enzyme has a requirement for xylosyl side chains (contrary to exoPG, which has a tolerance to xylosyl branches). Therefore, it is believed that endoXGH cleaves XGA between two xylosylated GalA residues (see Fig. 1), but this needs to be further substantiated.

D. Other Enzymes

It seems likely that more enzymes exist with activity on XGA. In apple hairy regions, XGA can be highly esterified with methoxyl groups. This polymer can not be deesterified by pectin methylesterase (PME) (3), suggesting that this enzyme is also hindered by xylosyl side chains, just like endoPG (10). At this moment it is unknown whether nature offers PMEs which are tolerant to xylosyl branching. The Xyl-GalA disaccharide can be cleaved by β-xylosidase (10). It is unknown whether this enzyme is also active toward polymeric XGA. Possibly, XGA may become digestible by endoPG after treatment with an appropriate β-xylosidase.

III. ENZYMIC DEGRADATION OF RHAMNOGALACTURONANS

Rhamnogalacturonan (RG, also referred to as RG-I) is the second heterogalacturonan of which the enzymic degradation is described in this chapter. This polysaccharide can have a backbone composed of as many as 100 repeats of the disaccharide [$\rightarrow$ 2)-α-L-Rha*p*-(1 $\rightarrow$ 4)-α-D-Gal*p*A-(1 $\rightarrow$] (5). The rhamnosyl residues can be substituted at *O*-4 with single unit [β-D-Gal*p*-(1 $\rightarrow$ 4)] or longer neutral sidechains. The latter are often referred to as the "hairs," and are mainly composed of galactosyl and/or arabinosyl residues. The GalA residues can be acetylated at the *O*-2 and/or *O*-3 position. This section will focus on the enzymes which are required to convert RG to its constituent monosaccharides.

A. Endoacting Rhamnogalacturonan-Degrading Enzymes

The first rhamnogalacturonan-degrading enzyme was discovered during fractionation of a commercial enzyme preparation derived from *Aspergillus aculeatus* (13). The enzyme acted exclusively on RG, and showed no activity on homogalacturonan. A few years later, this enzyme, as well as another rhamnogalacturonase from *A. aculeatus*, was cloned. The enzymes were termed RGaseA and RGaseB, respectively (14, 15). It appeared that the two enzymes differed in their catalytic *mechanism*. RGaseA is a hydrolase, meaning that it cleaves the RG backbone with the concomitant uptake of a water molecule. Degradation of RG by RGaseB follows a β-eliminative reaction; a double bond is formed between *C*-4 and *C*-5 of the nonreducing GalA residues of the reaction products (16, 17). This reaction can be monitored spectrophotometrically at 235 nm. Therefore, RGaseA and RGaseB were renamed to endorhamnogalacturonan hydrolase (endoRGH) and endorhamnogalacturonan lyase (endoRGL), respectively. Thus, it seems that fungi have acquired a similar set of enzymes for RG degradation as for that of homogalacturonan (endoPG, endoPAL, endoPL).

Over the years, a number of new sequences have been added to the sequence databases. The GH28 family contains four entries of endoRGHs: the one from *A. aculeatus* (14, 15); rhgA and rhgB from *A. niger* (18); and one from *Botryotinia fuckeliana* (19). Note that *A. niger* rhgB is not related to *A. aculeatus* RGaseB. Comparison of the *primary structure* of the enzymes reveals a number of regions, some of which are pectinase specific, and some of which are endoRGH specific (19). Typically, rhgB from *A. niger* and endoRGH from *B. fuckeliana* contain C-terminal extensions, which are not present in the two other RGHs. It is currently unknown whether this extension affects the properties of the enzymes. The endoRGLs have so far been assigned to two polysaccharide lyase families. The *A. aculeatus* endoRGL belongs to family L4, whereas the recently discovered *Pseudomonas cellulosa* endRGL forms a new family

(L11), together with the uncharacterized proteins YesW and YesX from *Bacillus subtilis*, and PSP from *Streptomyces coelicolor* (20). It is interesting to note that the *P. cellulosa* endoRGL is equipped with a cellulose-binding module, which is very uncommon for pectinases. The significance of this is unknown. The *P. cellulosa* endoRGL differs from the one from *A. aculeatus* in having a higher pH optimum (9.5 vs. 6) and an absolute requirement for Ca^{2+}.

The *three-dimensional structure* of the *A. aculeatus* endoRGH has been solved (21), and appears to be very similar to that of other pectinases (2). EndoRGH folds into a large right-handed parallel β helix (four parallel β sheets), with a core composed of 13 turns of β strands (see Fig. 2) (21). The potential active site is a groove, oriented almost perpendicular to the helical axis. Four amino acids with acidic side chains are located in the groove. Of these, Asp156 and Asp180 are presumably the catalytic ones. The distance between Asp156 and Asp180 is ~ 10 Å, which is consistent with the spacing between catalytic residues generally found for inverting enzymes. Another striking feature of endoRGH is its high degree of glycosylation. The enzyme contains almost 6 kDa of carbohydrates on a total molecular mass of 52 kDa. As a result of this, endoRGH is highly water soluble. *N*-glycan trees [Manα1-6(Manα1-3)Manβ1-4GlcNAcβ1-4GlcNAc] are linked to Asn32 and Asn299. The C-terminus of the molecule (amino acid residues 367–422) contains all *O*-linked glycosylation sites (Thr, Ser), which are monosubstituted with mannosyl residues. Figure 2 clearly shows that the glycosylation sites are not uniformly distributed over the enzyme. Despite the fact that the structure of endoRGH has been solved, the important question of which structure-function relationships determine whether an GH28 member has

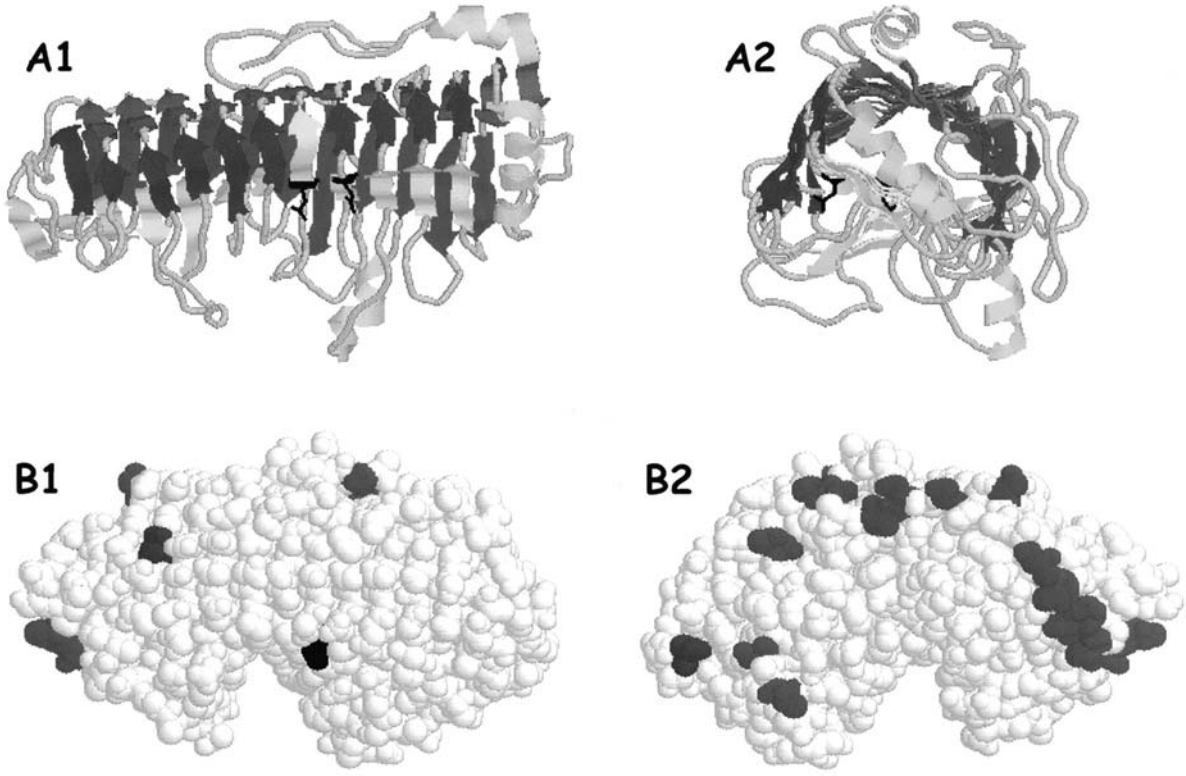

Figure 2 The three-dimensional structure of *A. aculeatus* endoRGH. (A1) Cartoon indicating the four parallel β sheets; the putative catalytic amino acids, Asp156 and Asp180, are indicated as black "sticks." (A2) View into the superhelix of the molecule at a 90° rotation to A1. (B1) Space-filling model of endoRGH (similar view as with cartoon A1) clearly showing the substrate-binding groove of the enzyme in which the catalytic residues (in black, only one visible) are located. The illustration also shows that endoRGH is heavily glycosylated. Amino acids with *O*-linked glycosylation (Thr, Ser) and those with *N*-linked glycosylation (Asn) are shown in black. (B2) View of endoRGH at a 180° rotation to B1 to show that glycosylation is confined to one side of the molecule.

endoPG or endoRGH activity remains to be answered. At this moment, no structural information is available for endoRGL.

Detailed structural characterization of reaction products has shown that endoRGH and endoRGL cleave the RG backbone at different positions (17, 22–24). The oligomeric products of *A. aculeatus* endoRGH consist of two or three Rha*p*-Gal*p*A disaccharide units, with a rhamnosyl at the nonreducing end and a galacturonosyl residue at the reducing end (22, 23). The rhamnosyl residues can be substituted with single units of galactose. The two *A. niger* endoRGHs release a similar set of oligosaccharides from saponified hairy regions (this is a RG preparation containing arabinan and galactan side chains, after treatment with alkali to remove acetyl groups) as the *A. aculeatus* enzyme (18), but the ratio between the various oligosaccharide products is different for the three enzymes. It seems as if *A. niger* rhgB accumulates the largest products of the three endoRGHs, including a number of larger oligosaccharides that have not yet been characterized. The oligosaccharides produced by *A. aculeatus* endoRGL differ from those formed by endoRGH in that they contain an unsaturated Gal*p*A residue (Δ4,5Gal*p*A) at the nonreducing end, and a Rha*p* at the reducing terminus (17, 24). Similar products are released from saponified hairy regions by the *P. cellulosa* rgl11A (20). In addition, this enzyme seems to produce smaller fragments, presumably with a Δ4,5Gal*p*A-Rha*p* disaccharide backbone. The difference in *specificity* of endoRGH and endoRGL are illustrated in Figure 3.

From the formation of oligomeric products discussed above, it might be concluded that endoRGH and endoRGL are active toward a similar part of the RG backbone. However, it is possible that the various RG-degrading enzymes recognize parts of the backbone. When the same saponified hairy regions are degraded with various RG-degrading enzymes, different shifts in the molecular-weight distribution of the polymeric products are evidenced (14, 20). Removal of the arabinan hairs from saponified hairy regions increased the catalytic efficiency of *A. aculeatus* endoRGL, whereas removal of galactan hairs decreased the efficiency (24). The *P. cellulosa* rgl11A can degrade a galactosylated oligosaccharide with a $[Rha\textit{p}\text{-}Gal\textit{p}A]_3$ backbone, whereas this oligosaccharide is not degraded anymore after treatment with a β-galactosidase (20). These examples show that side

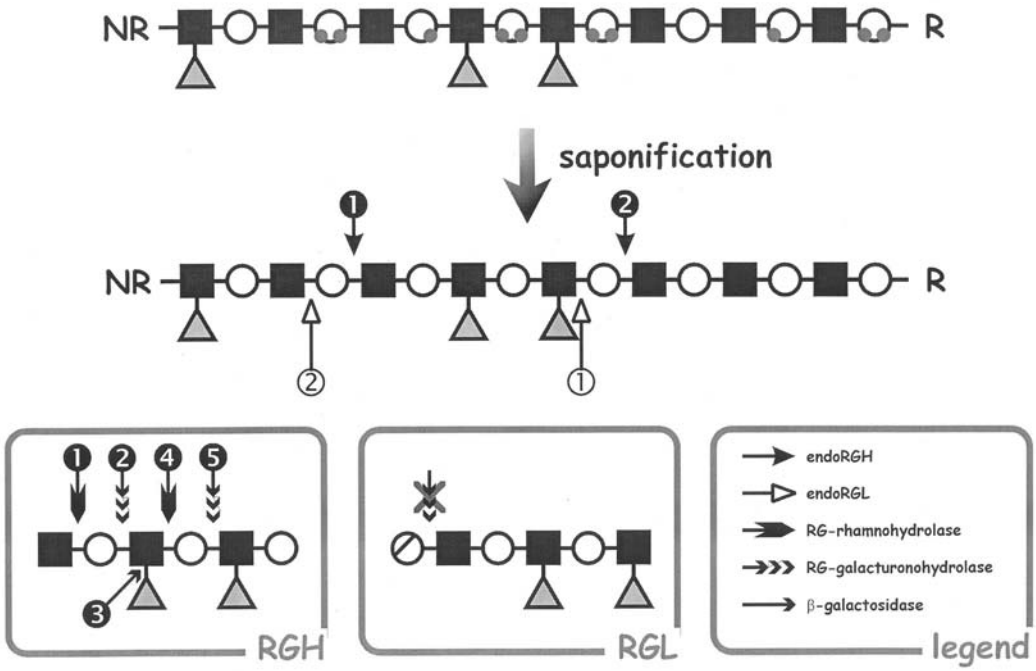

Figure 3 Schematic illustration of enzymes involved in the degradation of rhamnogalacturonan. Both endoRGH and endoRGL are hindered by the presence of acetyl groups. Numbers indicate 1st, 2nd, 3rd, etc., cleavage of the substrate by the enzyme. Open circles represent α-D-Gal*p*A residues, closed boxes α-L-Rha*p* residues, shaded triangles β-D-Gal*p*, and small shaded circles acetyl groups. NR indicates the nonreducing end; R, the reducing end.

chains may play an important role in molecular recognition. The various RG-degrading enzymes may differ considerably in their *tolerance to side chains*, or they may even have a *requirement for side chains*.

From a quantitative analysis of the total number of polymeric and oligomeric reaction products the number of splits an enzyme makes per encounter with its substrate can be estimated. It appears that endoRGH and endoRGL from *A. aculeatus* differ in their degree of multiple attack: 4.0 and 2.5, respectively (24). This implies that endoRGL is a more "randomly acting" (or less processive) enzyme than endoRGH. Linear RG oligosaccharides have been used to further substantiate the *mode of action* of RG-degrading enzymes. Such substrates can be prepared by treating pectin with dilute acid, and subsequent fractionation of the forthcoming fragments by chromatography (25).

The linkage between Rha and GalA is more easily hydrolyzed by acid than the one between GalA and Rha. As a result of this, the linear RG oligosaccharides carry a rhamnosyl residue at their reducing terminus. Figure 4 summarizes the mode of action of three different enzymes toward linear RG oligosaccharides of different length. Both endoRGHs require a backbone of at least nine or ten glycosyl residues for activity, whereas endoRGL requires longer ones (12 glycosyl residues). The *A. aculeatus* endoRGH prefers to cleave four or five glycosyl residues away from the nonreducing terminus of the oligosaccharide, and shows multiple attack toward the substrates offered (26). The *B. fuckeliana* enzyme cleaves five or seven glycosyl residues away from the reducing terminus of the substrates (19). The activity of this enzyme is distributed over a number of linkages, instead of consistently attacking the same linkage of a particular substrate (see Fig. 4). In this case, it may be more appropriate to speak of bond cleavage frequencies. The *B. fuckeliana* endoRGH does not show processivity. The *A. aculeatus* endoRGL prefers to cleave the smaller substrates four residues from the reducing rhamnose. The longest oligosaccharide (DP 16) is cleaved at 6 units from the reducing terminus. These examples demonstrate that

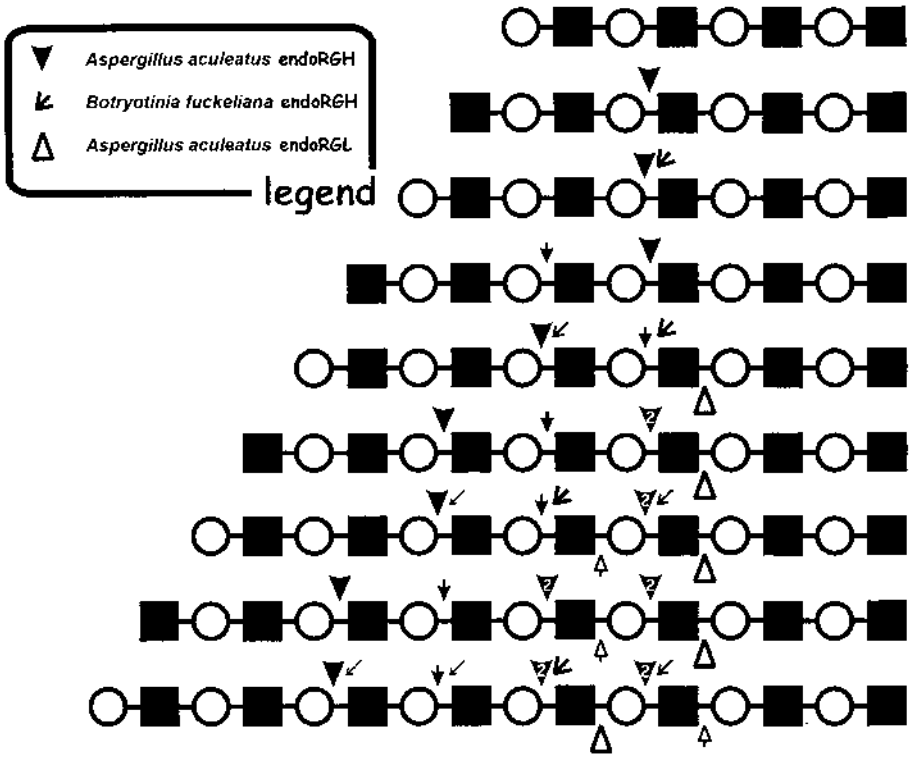

Figure 4 Mode of action of *Aspergillus aculeatus* and *Botryotinia fuckeliana* endoRGH and *Aspergillus aculeatus* endoRGL on degalactosylated rhamnogalacturonan oligosaccharides of various length. Thick arrows indicate preferred cleavage sites; less preferred sites are indicated with thinner arrows. Closed arrowheads marked with "2" indicate the second cleavage site of the enzyme. Open circles represent α-D-Gal*p*A residues; and closed boxes α-L-Rha*p* residues.

RG-degrading enzymes can differ considerably in their mode of action.

B. Rhamnogalacturonan Rhamnohydrolase

RG-rhamnohydrolase was purified from a commercial pectinase preparation (27). Characteristic of this enzyme is its absolute preference for terminal rhamnosyl residues (1,4)-linked to α-galacturonosyl residues (see Fig. 3). The enzyme was unable to split *p*-nitrophenyl-α-rhamnoside. The RG-rhamnohydrolase can degrade the products formed by endoRGH, together with the enzymes mentioned in the following paragraphs. Prior to the action of the rhamnohydrolase, removal of galactosyl residues from the RG oligosaccharides is required. At this moment, no sequence information on this enzyme is available, and consequently the enzyme has not been attributed to a glycosyl hydrolase family. The enzyme acts with inversion of the anomeric configuration (28).

C. Rhamnogalacturonan Galacturonohydrolase

The RG-galacturonohydrolase can act in concert with RG-rhamnohydrolase in the degradation of products released from hairy regions by endoRGH (see Fig. 3). This enzyme has a striking specificity for the release of galacturonosyl residues from the nonreducing end of RG oligosaccharides (29). Oligogalacturonides were not degraded by the enzyme. Also, no activity was detected toward the products released from hairy regions by endoRGL, showing that the enzyme is unable to release Δ4,5Gal*p*A residues. From kinetic experiments with linear RG oligosaccharides it could be concluded that low-molecular-weight substrates were hydrolyzed with the highest catalytic efficiency. At this moment, no sequence information for RG-galacturonohydrolase is available, and it is therefore unknown whether this enzyme has homology with for instance exoPG. The initial product of hydrolysis was β-galacturonic acid, showing that RG-galacturonohydrolase is an inverting enzyme (28).

D. Synergism in Rhamnogalacturonan Degradation

Many enzymes are involved in the degradation of hairy regions. Endogalactanase, endoarabinanase, arabinofuranosidase, and β-galactosidase may all facilitate the action of RG-degrading enzymes, as has been indicated in the paragraphs above. These enzymes are dealt with in more detail elsewhere in this book.

Another important enzyme for the degradation of RG in its natural setting is RG acetyl esterase (RGAE). This enzyme specifically can remove 70% of the acetyl groups present in hairy regions; acetyl esters present in homogalacturonans are not hydrolyzed (30). Acetyl groups hinder the action of both *A. aculeatus* endoRGH and endoRGL. When hairy regions are incubated with a combination of endoRGH and RGAE, a more extensive decrease of the molecular weight is found than with endoRGH alone (31). Similar results were obtained with endoRGL. RGAE is discussed in more detail in the esterase section of this book (Chap. 67).

IV. DETERMINATION OF ENZYME ACTIVITY ON HETEROGALACTURONANS

Many different assays can be used for studying conversion of rhamnogalacturonans. Simple reducing end-group analysis can point out whether enzymes or enzyme extracts contain RG-degrading activity. In the case of lyase activity, spectrophotometric measurements at 235 nm is a convenient option (17, 24). High-performance size exclusion chromatography (HPSEC) with refractive index (RI) detection may be used to determine differences in molecular-weight distributions (13, 14). High-performance anion exchange chromatography (HPAEC) with an electrochemical detection unit is suitable for monitoring the release of oligosaccharides from a polymer (14, 23, 24). Appropriate reference oligosaccharides cannot be obtained commercially, and should be purified by oneself. Mass spectrometry (MS) is a very useful tool in structural elucidation of reaction products. In particular, liquid chromatography/tandem mass spectrometry (LC-MSMS) in combination with ^{18}O-labeling of reaction products may detect differences in mode of action between two rhamnogalacturonases. In this case, incubations are done in the presence of ^{18}O-labeled water; tandem-MS is used to "sequence" the individual oligosaccharides (32).

V. APPLICATIONS IN THE FOOD INDUSTRY

Degradation of branched pectins, hairy regions, or heterogalacturonans is at this moment probably

mainly applied in fruit juice manufacturing, in particular when the juice is made by the so-called liquefaction process (33). In this process, fruit cell walls are extensively degraded by a mixture of pectinases, hemicellulases, and cellulases. Eventually, the cells cannot withstand the osmotic pressure anymore, and collapse. The cell content (juice) is thus released without pressing, and can be obtained by centrifugation. A final clarification step is done by ultrafiltration. Besides enormous economical benefits (juice yields up to 100%), this process has also introduced some new technological problems, which are mainly due to the fact that more soluble cell wall fragments are released into the juice. A serious problem in the liquefaction process is the membrane fouling during the final clarification step. In apple juice manufacturing, polymeric cell wall material accumulates at the membrane, and consequently the flux through the membrane is reduced.

The material causing the fouling consists predominantly of hairy regions. Experiments in our laboratory have shown that addition of endoXGH, endoRGH, and endoRGL (and RGAE) helps in maintaining the flux through ultrafiltration membranes, and minimizing the fouling (34). The exoPG, RG-rhamnohydrolase, and RG-galacturonohydrolase are less important in this respect. It has also been suggested that RG-degrading enzymes are useful for the production of cloudy apple juices and carrot macerates (35).

For the near future, it is anticipated that RG-degrading enzymes will become more important. A potential application may be the production of tailor-made bioactive RG fragments. Japanese studies suggest that pectic fragments, RG in particular, have an array of health-promoting effects (36). At this moment, efforts are directed toward unraveling the carbohydrate epitopes, which are important for certain health claims. With the various endo-type enzymes, specific structures may be generated which might be modified with appropriate glycosidases. Undoubtedly, the heterogalacturonan-specific exoenzymes will be more important in this application than in juice manufacturing. Further, it is interesting to note that soy pectin is different from that of other plants (37). Soy pectin does not seem to contain homogalacturonan, but instead consists exclusively of RG and XGA. Soy is an extremely important raw material for human and animal nutrition. We know that application of the enzymes described in this chapter is insufficient to open up the cell wall structure of this plant material. Novel auxiliary enzymes remain to be discovered for improving the recovery of valuable nutrients from soy.

REFERENCES

1. HA Schols, AGJ Voragen. Complex pectins: structure elucidation using enzymes. In: J Visser, AGJ Voragen, eds. Progress in Biotechnology 14: Pectins and Pectinases. Amsterdam: Elsevier, 1996, pp 3–19.
2. SR Herron, JAE Benen, RD Scavetta, J Visser, F Jurnak. Structure and function of pectic enzymes: virulence factors of plant pathogens. Proc Natl Acad Sci USA 97:8763–8769, 2000.
3. HA Schols, EJ Bakx, D Schipper, AGJ Voragen. A xylogalacturonan subunit present in the modified hairy regions of apple pectin. Carbohydr Res 279:265–279, 1995.
4. CMGC Renard, RM Weightman, J-F Thibault. The xylose-rich pectins from pea hulls. Int J Biol Macromol 21:155–162, 1997.
5. P Albersheim, AG Darvill, MA O'Neill, HA Schols, AGJ Voragen. An hypothesis: the same six polysaccharides are components of the primary cell walls of all higher plants. In: J Visser, AGJ Voragen, eds. Progress in Biotechnology 14: Pectins and Pectinases. Amsterdam: Elsevier, 1996, pp 47–53.
6. L Yu, AJ Mort. Partial characterization of xylogalacturonans from cell walls of ripe watermelon fruit: inhibition of endopolygalacturonase activity by xylosylation. In: J Visser, AGJ Voragen, eds. Progress in Biotechnology 14: Pectins and Pectinases. Amsterdam: Elsevier, 1996, pp 79–88.
7. GO Aspinall, J Baillie. Gum tragacanth. Part I. Fractionation of the gum and the structure of tragacanthic acid. J Chem Soc 1702–1714, 1963.
8. DMW Anderson, DAD Grant. The chemical characterization of some *Astragalus* gum exudates. Food Hydrocoll 2:417–423, 1988.
9. G Beldman, LAM van den Broek, HA Schols, MJF Searle–Van Leeuwen, KMJ van Laere, AGJ Voragen. An exogalacturonase from *Aspergillus aculeatus* able to degrade xylogalacturonan. Biotechnol Lett 18:707–712, 1996.
10. HCM Kester, JAE Benen, J Visser. The exopolygalacturonase from *Aspergillus tubingensis* is also active on xylogalacturonan. Biotechnol Appl Biochem 30:53–57, 1999.
11. CJB van der Vlugt-Bergmans, PJA Meeuwsen, AGJ Voragen, AJJ van Ooyen. Endo-xylogalacturonan hydrolase, a novel pectinolytic enzyme. Appl Environ Microbiol 66:36–41, 2000.
12. PJA Meeuwsen, J-P Vincken, G Beldman, AGJ Voragen. A universal assay for screening expression

libraries for carbohydrases. J Biosci Bioeng 89:107–109, 2000.
13. HA Schols, CCJM Geraeds, MJF Searle–Van Leeuwen, FJM Kormelink, AGJ Voragen. Rhamnogalacturonase: a novel enzyme that degrades the hairy regions of pectins. Carbohydr Res 206:105–115, 1990.
14. LV Kofod, S Kauppinen, S Christgau, LN Andersen, HP Heldt-Hansen, K Dörreich, H Dalbøge. Cloning and characterization of two structurally and functionally divergent rhamnogalacturonases from *Aspergillus aculeatus*. J Biol Chem 269:29182–29189, 1994.
15. MEG Suykerbuyk, PJ Schaap, H Stam, W Musters, J Visser. Cloning, sequence and expression of the gene coding for rhamnogalacturonase of *Aspergillus aculeatus*; a novel pectinolytic enzyme. Appl Microbiol Biotechnol 43:861–870, 1995.
16. P Azadi, MA O'Neill, C Bergmann, AG Darvill, P Albersheim. The backbone of the pectic polysaccharide rhamnogalacturonan I is cleaved by an endohydrolase and an endolyase. Glycobiology 5:783–789, 1995.
17. M Mutter, IJ Colquhoun, HA Schols, G Beldman, AGJ Voragen. Rhamnogalacturonase B from *Aspergillus aculeatus* is a rhamnogalacturonan α-L-rhamnopyranosyl-(1,4)-α-D-galactopyranosyluronide lyase. Plant Physiol 110:73–77, 1996.
18. MEG Suykerbuyk, HCM Kester, PJ Schaap, H Stam, W Musters, J Visser. Cloning and characterization of two rhamnogalacturonan hydrolase genes from *Aspergillus niger*. Appl Environ Microbiol 63:2507–2515, 1997.
19. J Fu, R Prade, A Mort. Expression and action pattern of *Botryotinia fuckeliana* (*Botrytis cinerea*) rhamnogalacturonan hydrolase in *Pichia pastoris*. Carbohydr Res 330:73–81, 2001.
20. VA McKie, J-P Vincken, AGJ Voragen, LAM van den Broek, E Stimson, HJ Gilbert. A new family of rhamnogalacturonan lyases contains an enzyme that binds to cellulose. Biochem J 355:167–177, 2001.
21. TN Petersen, S Kauppinen, S Larsen. The crystal structure of rhamnogalacturonase A from *Aspergillus aculeatus*: a right-handed parallel β helix. Structure 5:533–544, 1997.
22. IJ Colquhoun, GA de Ruiter, HA Schols, AGJ Voragen. Identification by NMR spectroscopy of oligosaccharides obtained by treatment of the hairy regions of apple pectin with rhamnogalacturonase. Carbohydr Res 206:131–144, 1990.
23. HA Schols, AGJ Voragen, IJ Colquhoun. Isolation and characterization of rhamnogalacturonan oligomers, liberated during degradation of pectic hairy regions by rhamnogalacturonase. Carbohydr Res 256:97–111, 1994.
24. M Mutter, IJ Colquhoun, G Beldman, HA Schols, EJ Bakx, AGJ Voragen. Characterization of recombinant rhamnogalacturonan α-L-rhamnopyranosyl-(1,4)-α-D-galactopyranosyl-uronide lyase from *Aspergillus aculeatus*. An enzyme that fragments rhamnogalacturonan I regions of pectin. Plant Physiol 117:141–152, 1998.
25. CMGC Renard, J-F Thibault, M Mutter, HA Schols, AGJ Voragen. Some preliminary results on the action of rhamnogalacturonase on rhamnogalacturonan oligosaccharides from beet pulp. Int J Biol Macromol 17:333–336, 1995.
26. M Mutter, CMGC Renard, G Beldman, HA Schols, AGJ Voragen. Mode of action of RG-hydrolase and RG-lyase toward rhamnogalacturonan oligomers. Characterization of degradation products using RG-rhamnohydrolase and RG-galacturonohydrolase. Carbohydr Res 311:155–164, 1998.
27. M Mutter, G Beldman, HA Schols, AGJ Voragen. Rhamnogalacturonan α-L-rhamnopyranosylhydrolase. A novel enzyme specific for the terminal nonreducing rhamnosyl unit in rhamnogalacturonan regions of pectin. Plant Physiol 106:241–250, 1994.
28. SM Pitson, M Mutter, LAM van den Broek, AGJ Voragen, G Beldman. Stereochemical course of hydrolysis catalysed by α-L-rhamnosyl and α-D-galacturonosyl hydrolases from *Aspergillus aculeatus*. Biochem Biophys Res Commun 242:552–559, 1998.
29. M Mutter, G Beldman, SM Pitson, HA Schols, AGJ Voragen. Rhamnogalacturonan α-D-galactopyranosyluronohydrolase. An enzyme that specifically removes the terminal nonreducing galacturonosyl residue in rhamnogalacturonan regions of pectin. Plant Physiol 117:153–163, 1998.
30. MJF Searle–van Leeuwen, LAM van den Broek, HA Schols, G Beldman, AGJ Voragen. Rhamnogalacturonan acetylesterase: a novel enzyme from *Aspergillus aculeatus*, specific for the deacetylation of hairy (ramified) regions of pectins. Appl Microbiol Biotechnol 38:347–349, 1992.
31. S Kauppinen, S Christgau, LV Kofod, T Halkier, K Dörreich, H Dalbøge. Molecular cloning and characterization of a rhamnogalacturonan acetylesterase from *Aspergillus aculeatus*. Synergism between rhamnogalacturonan degrading enzymes. J Biol Chem 270:27172–27178, 1995.
32. R Körner. Structural characterization of biopolymers by MS and MS/MS. PhD thesis, Department of Molecular Biology, University of Southern Denmark, Odense, Denmark, 1999.
33. AGJ Voragen, W Pilnik. Pectin-degrading enzymes in fruit and vegetables processing. Proceedings of the 195th national meeting of the American Chemical Society, Toronto, Canada, 1988. In: JR Whitaker, PE Sonnet, eds. ACS Symposium Series No. 389, Biocatalysis in Agricultural Biotechnology, Washington, DC, 1989, pp 93–115.

34. PJA Meeuwsen, CJB van der Vlugt-Bergmans, J-P Vincken, G Beldman, AGJ Voragen, MA Herweijer, AJJ van Ooijen. Novel endoxylogalacturonase. WO 99/41386.
35. HP Heldt-Hansen, LV Kofod, G Budolfsen, PM Nielsen, S Hüttel, T Bladt. Application of tailor-made pectinases. In: J Visser, AGJ Voragen, eds. Progress in Biotechnology 14: Pectins and Pectinases. Amsterdam: Elsevier, 1996, pp 463–474.
36. H Yamada. Pectic polysaccharides from Chinese herbs: structure and biological activity. Carbohydr Polym 25:269–276, 1994.
37. MMH Huisman, CTM Fransen, JP Kamerling, JFG Vliegenthart, HA Schols, AGJ Voragen. The CDTA-soluble pectic substances from soybean meal are composed of rhamnogalacturonan and xylogalacturonan but not homogalacturonan. Biopolymers 58:279–294, 2001.

74

Enzymic Hydrolysis of Cereal (1 → 3,1 → 4)-β-Glucans

Maria Hrmova and Geoffrey Fincher
University of Adelaide, Glen Osmond, South Australia, Australia

I. INTRODUCTION

The (1 → 3, 1 → 4)-β-glucans are important components of cell walls in members of the Poaceae family of higher plants (1). The (1 → 3, 1 → 4)-β-glucans consist predominantly of long, linear chains of glucosyl residues that are linked via (1 → 3)- and (1 → 4)-β-glucosidic linkages; small amounts of protein may be associated with the polysaccharide (2). Although their distribution in higher plants is restricted to cell walls of the Proaceae, the (1 → 3, 1 → 4)-β-glucans are constituents of most human diets and many animal feed formulations, because the Poaceae include key cereal species, such as wheat, rice, maize, barley, rye, sorghum, and millet. As cell wall components, the (1 → 3, 1 → 4)-β-glucans usually make a relatively minor contribution to the total weight of cereal grains, but they can have a disproportionately large impact on grain technology, utilization, and nutrition. This impact is largely attributable to the propensity of these polysaccharides to be extracted from walls with aqueous solvents and thereafter to form solutions of high viscosity. Thus, in baking with cereal flours, the (1 → 3, 1 → 4)-β-glucans and other wall polysaccharides will influence dough rheology, and in malting and brewing they can adversely affect the efficiency of malt extraction, filtration processes, and the quality of the final beer. Similarly, (1 → 3, 1 → 4)-β-glucans can have undesirable effects on the digestibility of cereal-based stockfeeds by monogastric animals such as pigs and poultry. In contrast, they are important constituents of the "dietary fiber" component of human foods, which is considered to be of salutary importance in several areas of human digestion and health (3).

Against this background, we will describe in this chapter the enzymes that are responsible for the complete depolymerization of cereal (1 → 3, 1 → 4)-β-glucans to glucose. This description will be focused on well-characterized enzymes from germinated grain and young seedlings of barley and maize and is likely to be equally relevant to the hydrolysis of (1 → 3, 1 → 4)-β-glucans from wheat, rice, and other cereals. Finally, we will present selected examples that illustrate how a detailed understanding of enzyme structures and substrate specificities can provide opportunities for the manipulation of commercially important enzymes via newly emerging technologies, which can be used to enhance performance of these enzymes in the food industry.

II. STRUCTURE AND PROPERTIES OF CEREAL (1 → 3, 1 → 4)-β-GLUCANS

Before embarking on a description of (1 → 3, 1 → 4)-β-glucan endo- and exohydrolases, it is necessary to provide a little more information on the structure and properties of the polysaccharide itself. This information will be important in subsequent discussions on substrate specificity and substrate binding of individual enzymes that are involved in (1 → 3, 1 → 4)-β-glucan depolymerization.

A. Cell Walls of the Poaceae

In the primary cell walls of higher plants, a network of cellulosic microfibrils is embedded in a matrix which consists mainly of polysaccharides, but may also contain a secondary network of structural proteins (1, 4, 5). Matrix-phase polysaccharides include xyloglucans, heteroxylans, and pectic polysaccharides. Cell walls of the Poaceae are characterized by a matrix phase which consists predominantly of $(1 \rightarrow 3, 1 \rightarrow 4)$-$\beta$-glucans and arabinoxylans; xyloglucans and pectic polysaccharides are relatively less abundant than they are in walls of many dicotyledonous plants (1, 4). The major wall polysaccharides found in the starchy endosperm of various cereal grains are compared in Table 1, where it can be seen that $(1 \rightarrow 3, 1 \rightarrow 4)$-$\beta$-glucan content generally ranges from trace amounts to 75% of the wall, and from 0.1% to 8% of total grain weight.

B. Chemical Properties of Cereal $(1 \rightarrow 3, 1 \rightarrow 4)$-$\beta$-Glucans

In considering the chemical structures of cereal $(1 \rightarrow 3, 1 \rightarrow 4)$-$\beta$-glucans it must be remembered that these polysaccharides occur as a heterogeneous family with varying molecular sizes and fine structural features. However, several $(1 \rightarrow 3, 1 \rightarrow 4)$-$\beta$-glucan fractions have been characterized in detail, and their overall structures are similar, if not identical. The $(1 \rightarrow 3, 1 \rightarrow 4)$-$\beta$-glucans from oats, wheat, and barley generally contain $\sim 70\%$ $(1 \rightarrow 4)$-β-glucosyl residues and 30% $(1 \rightarrow 3)$-β-glucosyl residues (7, 8). Adjacent $(1 \rightarrow 3)$-β-glucosyl residues are seldom if ever detected in these polysaccharides, but the single $(1 \rightarrow 3)$-β-glucosyl residues are separated by variable numbers of adjacent $(1 \rightarrow 4)$-β-glucosyl residues.

In 90% of cases, the single $(1 \rightarrow 3)$-β-glucosyl residues are separated by two or three adjacent $(1 \rightarrow 4)$-β-glucosyl residues, as shown in Figure 1, but up to 10% of the water-soluble $(1 \rightarrow 3, 1 \rightarrow 4)$-$\beta$-glucan from barley consists of blocks containing four to 14 contiguous $(1 \rightarrow 4)$-glucosyl residues (9). Similar "cellulosic" blocks of adjacent $(1 \rightarrow 4)$-β-glucosyl residues are detected in $(1 \rightarrow 3, 1 \rightarrow 4)$-$\beta$-glucans from oats (11). The linkage sequence in barley $(1 \rightarrow 3, 1 \rightarrow 4)$-$\beta$-glucans has been studied at two levels. At the first level, the absence of adjacent $(1 \rightarrow 3)$-β-glucosyl residues indicates that $(1 \rightarrow 3)$- and $(1 \rightarrow 4)$-linkages are arranged nonrandomly, because if 30% of β-glucosyl residues are $(1 \rightarrow 3)$-linked, one would expect to find frequent blocks of two or more advance $(1 \rightarrow 3)$-β-glucosyl residues. At the second level, however, mathematical analyses of the arrangement of the blocks of two or three adjacent $(1 \rightarrow 4)$-β-glucosyl residues, which together account for $\sim 90\%$ by weight of the polysaccharide, shows that these "cellotriosyl" and "cellotetraosyl" blocks (Fig. 1) are randomly distributed (10).

C. Physical Properties of Cereal $(1 \rightarrow 3, 1 \rightarrow 4)$-$\beta$-Glucans

Estimates of molecular masses of cereal $(1 \rightarrow 3, 1 \rightarrow 4)$-$\beta$-glucans vary widely, mainly because of the different polysaccharide fractions that have been examined and because of the different methods used to determine molecular mass values. Sedimentation equilibrium ultracentrifugation indicates that water-soluble

Table 1 Relative Abundance of $(1 \rightarrow 3, 1 \rightarrow 4)$-$\beta$-Glucans in Cereal Grains and in Cell Walls from the Starchy Endosperm

	Approximate cell wall composition						
Cereal species	Overall $(1 \rightarrow 3,1 \rightarrow 4)$-$\beta$-glucan content[a] (% grain weight)	$(1 \rightarrow 3, 1 \rightarrow 4)$-$\beta$-Glucan	Arabinoxylan	Pectin	Glucomannan	Xyloglucan	Cellulose
Wheat	0.5–0.75	20%	70%	—	7%	—	4%
Barley	4.5–7.7	75%	20%	—	2%	—	2%
Rice	0.13	trace	40%	10%	ND[b]	trace	48%
Oats	2.5–6.6	ND	60%	ND	ND	ND	ND
Rye	1.9–2.9	ND	65%	ND	ND	ND	20%

[a]Range of mean values from many varieties.
[b]Not determined.
Source: Ref. 6.

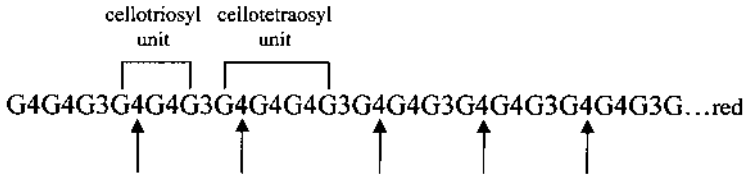

Figure 1 Distribution of linkages in barley $(1 \rightarrow 3, 1 \rightarrow 4)$-$\beta$-glucans. G = β-glucosyl residues; 3 = $(1 \rightarrow 3)$-linkages; 4 = $(1 \rightarrow 4)$-linkages; red = reducing end; arrows = sites of hydrolysis by $(1 \rightarrow 3, 1 \rightarrow 4)$-$\beta$-glucan endohydrolases (EC 3.2.1.73). (From Ref. 10.)

barley $(1 \rightarrow 3, 1 \rightarrow 4)$-$\beta$-glucans have weight average molecular weights in the range 200,000–300,000 (12, 13). These values correspond to polysaccharides containing 1200–1800 glucosyl residues.

The high viscosities of cereal $(1 \rightarrow 3, 1 \rightarrow 4)$-$\beta$-glucan solutions can be attributed not only to the high molecular masses of the polysaccharides, but also to their high degree of molecular asymmetry (Fig. 2). Woodward et al. (9) showed that the water-soluble barley $(1 \rightarrow 3, 1 \rightarrow 4)$-$\beta$-glucan has an axial ratio (average length:average width) of ~ 100. It might be anticipated that such long, extended molecules would aggregate and precipitate from aqueous solution. However, the irregular spacing of the $(1 \rightarrow 3)$-linkages along the polysaccharide chain introduces irregularly spaced links that preclude extensive intermolecular associations and prevent precipitation from solution. Thus, the arrangement of the $(1 \rightarrow 3)$- and $(1 \rightarrow 4)$-β-glucosyl residues along the polysaccharide chain accounts for the solubility of large $(1 \rightarrow 3, 1 \rightarrow 4)$-$\beta$-glucan molecules in water, their extended flexible chain conformations, and their tendency to form aqueous solutions of high viscosity (6). It is precisely these properties that enable relatively low abundance $(1 \rightarrow 3, 1 \rightarrow 4)$-$\beta$-glucans to exert such a large influence on cereal grain utilization in food and related industries.

III. OVERVIEW OF ENZYMIC HYDROLYSIS OF $(1 \rightarrow 3, 1 \rightarrow 4)$-$\beta$-GLUCANS

Enzymes that mediate the depolymerization of wall-bound $(1 \rightarrow 3, 1 \rightarrow 4)$-$\beta$-glucans and their degradation products have been mostly extracted from germinated barley grain, young barley seedlings, or maize or barley coleoptiles. Several different types of enzymes would be required to completely depolymerize $(1 \rightarrow 3, 1 \rightarrow 4)$-$\beta$-glucans to glucose. Candidate enzymes and their action patterns are summarized in Figure 3. In germinated grain, where a significant proportion of total endosperm glucosyl residues are embodied in cell wall $(1 \rightarrow 3, 1 \rightarrow 4)$-$\beta$-glucan (15), it might be expected that a battery of enzymes would catalyze the complete conversion of the polysaccharide to glucose, which could be translocated as an energy source to the developing seedling. In elongating coleoptiles, only partial hydrolysis of the $(1 \rightarrow 3, 1 \rightarrow 4)$-$\beta$-glucan might be required to "loosen" crosslinking polysaccharides in the wall during turgor-driven cell expansion.

A. Enzymes That Release Large Fragments of $(1 \rightarrow 3, 1 \rightarrow 4)$-$\beta$-Glucans

The first step involves a hypothetical endoacting enzyme (designated Endo-X in Fig. 3) that releases polymeric wall $(1 \rightarrow 3, 1 \rightarrow 4)$-$\beta$-glucan into solution, without hydrolyzing it to low-molecular-mass oligosaccharides. An enzyme with this action pattern in germinated barley grain has been the subject of persistent reports in the malting and brewing literature, and has been given the name β-glucan solubilase (16). The enzyme has not yet been purified for detailed characterization, and in one report it was suggested that the enzyme originated from microorganisms that reside on the surface of the barley grain (17). However, another $(1 \rightarrow 3, 1 \rightarrow 4)$-$\beta$-glucan endohydrolase extracted from maize coleoptiles also releases relatively high-molecular-mass $(1 \rightarrow 3, 1 \rightarrow 4)$-$\beta$-glucan from cell walls (18). It is unlikely that the maize coleoptiles would be heavily contaminated with microorganisms. Furthermore, the NH_2-terminal sequence of the maize endohydrolase (19) matches the sequences of numerous cDNAs in the rice and maize EST databases, and is clearly of plant origin.

B. $(1 \rightarrow 3, 1 \rightarrow 4)$-$\beta$-Glucan Endohydrolases

Much more precise information is available for the $(1 \rightarrow 3, 1 \rightarrow 4)$-$\beta$-glucan endohydrolases of the EC

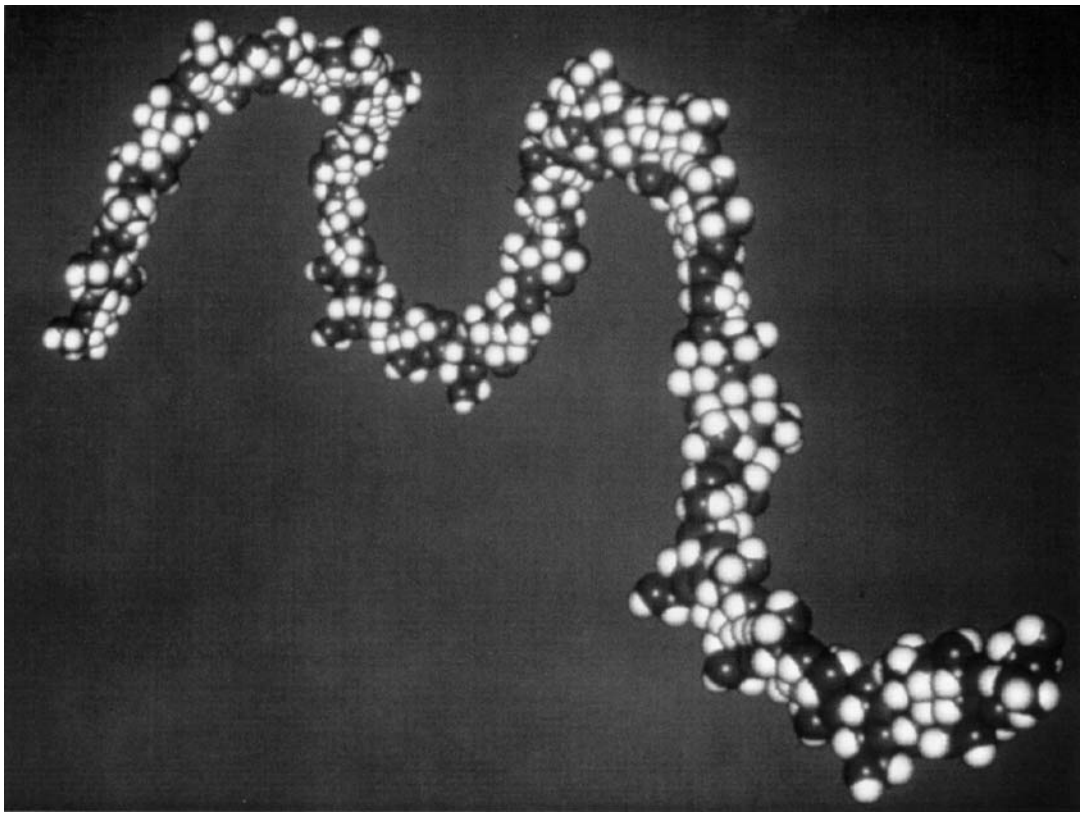

Figure 2 Computer-generated instantaneous conformation of barley (1 → 3, 1 → 4)-β-glucan. (From Ref. 14.)

3.2.1.73 group. These enzymes catalyze the hydrolysis of (1 → 4)-β-glucosyl linkages but only where these linkages are immediately adjacent, on the reducing terminal side, to (1 → 3)-β-glucosyl residues (Fig. 1). Thus, the (1 → 3, 1 → 4)-β-glucan endohydrolases of this group have a strict requirement for adjacent (1 → 3)- and (1 → 4)-β-glucosyl residues (Fig. 1), and the enzymes release a series of oligosaccharides that contain (1 → 4)-β-glucosyl residues and a single (1 → 3)-β-glucosyl residue at the reducing terminus (Figs. 1, 3). Tri- and tetrasaccharides are the most abundant products of hydrolysis, but higher oligosaccharides of up to 10 or more (1 → 4)-β-glucosyl residues, again with a single reducing terminal (1 → 3)-β-glucosyl residue, are released from the cellulosic regions of cereal (1 → 3, 1 → 4)-β-glucans (20, 21). The (1 → 3, 1 → 4)-β-glucan endohydrolases are abundant in germinated cereal grains (20, 22), where they are clearly key enzymes in the degradation of cell walls of the starchy endosperm. They are also detected in young leaves and roots, but are not detected in elongating barley coleoptiles (23).

C. Hydrolysis of Oligosaccharides

The (1 → 3, 1 → 4)-β-oligoglucosides released by (1 → 3, 1 → 4)-β-glucan endohydrolases can be further hydrolyzed to glucose (Fig. 3). This process will be particularly important in the germinated grain. The enzymes responsible for the hydrolysis of the (1 → 3, 1 → 4)-β-oligoglucosides have not been identified unequivocally, although β-glucosidases (EC 3.2.1.21) and a group of broad-specificity β-glucan exohydrolases are likely to be involved (Fig. 3). The latter enzymes can hydrolyze not only the (1 → 3, 1 → 4)-β-oligoglucosides but also polymeric (1 → 3, 1 → 4)-β-glucans and other polysaccharides (18, 24, 25).

Because the substrate specificities, action patterns, and three-dimensional structures of the (1 → 3, 1 → 4)-β-glucan endohydrolases, the β-glucosidases, and the β-glucan exohydrolases are now well defined, these will be discussed individually and in detail in the sections below. However, the definition of these enzymic properties depends on the availability

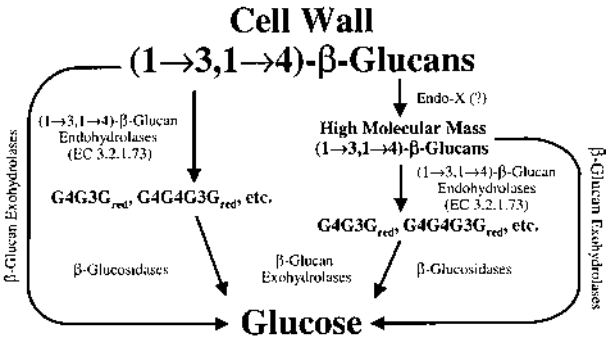

Figure 3 Enzymic hydrolysis of cell wall $(1 \rightarrow 3, 1 \rightarrow 4)$-$\beta$-glucans. For explanation see text in Section III. Symbols are as described in legend to Figure 1.

of highly purified enzyme preparations and a range of additional analytical techniques. Some methodological strategies for the purification and characterization of $(1 \rightarrow 3, 1 \rightarrow 4)$-$\beta$-glucan hydrolases are outlined in the next section.

IV. EXPERIMENTAL APPROACHES TO ENZYME CHARACTERIZATION

A. Enzyme Purification and Assay Procedures

The development of a protocol for the preparation of highly purified enzyme is considered of paramount importance for studies on the enzymic hydrolysis of cereal $(1 \rightarrow 3, 1 \rightarrow 4)$-$\beta$-glucans. Enzymes extracted from germinated barley grain and elongating coleoptiles are generally amenable to purification by fractional precipitation with ammonium sulfate, cation and/or anion exchange chromatography, and size exclusion chromatography (18, 24, 26, 27), but additional steps involving hydrophobic interaction chromatography, chromatofocusing, or affinity chromatography are usually required to achieve high levels of purity.

Enzyme purity can be rigorously demonstrated through gel electrophoresis, provided sufficient enzyme is loaded onto the gel. A single protein band on an overloaded gel, and NH_2-terminal amino acid sequence that shows a single sequence at the expected yields, are sound complementary procedures through which enzyme purity can be confidently assessed.

Another potential complication during the purification of cereal $(1 \rightarrow 3, 1 \rightarrow 4)$-$\beta$-glucan hydrolases is that assay systems may not be specific for a particular enzyme type. Thus, the cereal β-glucan exohydrolases hydrolyze polymeric $(1 \rightarrow 3, 1 \rightarrow 4)$-$\beta$-glucans, $(1 \rightarrow 3, 1 \rightarrow 4)$-$\beta$-oligoglucosides, 4′-nitrophenyl β-glucoside (4NPG), and a range of other oligo- and polysaccharides (25). The $(1 \rightarrow 3, 1 \rightarrow 4)$-$\beta$-glucan endohydrolases are absolutely specific for $(1 \rightarrow 3, 1 \rightarrow 4)$-$\beta$-glucans. Putative β-glucosidases hydrolyze not only 4NPG, but also $(1 \rightarrow 4)$-β-oligoglucosides (27). During the early stages of purification, it may therefore be necessary to assay column fractions with a number of substrates in order to monitor the activity of a particular glucan endo- and/or exohydrolase. Huber and Nevins (28) specifically measured the maize coleoptile $(1 \rightarrow 3, 1 \rightarrow 4)$-$\beta$-glucan endohydrolase by adding $HgCl_2$ to the cereal $(1 \rightarrow 3, 1 \rightarrow 4)$-$\beta$-glucan substrate; $HgCl_2$ inhibits the β-glucan exohydrolases, but not the endohydrolases.

B. Problems with Enzyme Classification

The broad specificity of certain cereal $(1 \rightarrow 3, 1 \rightarrow 4)$-$\beta$-glucan hydrolases not only presents problems for the selection of a diagnostic substrate during purification and characterization, as described above, but also creates problems for the classification of the enzyme into existing Enzyme Commission categories (29). Thus, the cereal β-glucan exohydrolases have such a broad specificity that they do not fit any EC classification.

Similarly, cereal β-glucosidases are difficult to place in existing EC categories (27), because they hydrolyze cello-oligosaccharides at significantly higher rates than synthetic aryl β-glucosidic substrates such as 4NPG. Partly because of these difficulties, a new method for the classification of glycoside hydrolases has gained considerable support in recent years. This method is based on sequence alignments and hydrophobic cluster analysis (HCA) (30), and has been used to group the glycoside hydrolases into ~ 90 families (http://afmb.cnrs-mrs.fr/CAZY) (31). It is becoming clear that HCA is particularly useful for identifying similarities in enzymes for which amino acid sequence similarities are relatively low, and that members of each family have similar three-dimensional conformation (32). Thus, the "structural" classification provided by HCA usefully complements the EC "substrate specificity" classification. For example, the HCA method shows that β-glucosidases can be classified into families 1 and 3, and this further emphasizes the inadequacies of designating an enzyme as a β-glucosidase simply because it hydrolyzes the synthetic substrate of convenience, 4NPG (27).

C. Primary Structures of Enzymes

Preliminary amino acid sequence information can be obtained by direct NH_2-terminal sequencing of the purified enzyme or by sequencing peptides generated from the purified enzyme by peptidase digestion. To define the complete primary structure of the enzyme it is usually necessary to isolate and sequence a corresponding cDNA. If the amino acid sequence deduced from the nucleotide sequence of the cDNA exactly matches the NH_2-terminal and peptide amino acid sequences determined directly from the purified enzyme, then the primary structure of the enzyme can be considered solved. However, it is often at this stage that we discover that multiple isoforms of an enzyme exist. Indeed, most enzymes involved in cereal $(1 \rightarrow 3, 1 \rightarrow 4)$-$\beta$-glucan hydrolysis are encoded by multigene families, and care must be taken to define exactly which isoenzyme is under examination.

D. Specificity and Action Pattern

Once the purity of an enzyme is clearly established, its activity on a broad range of alkyl and aryl β-glucosidic substrates, oligosaccharides, and polysaccharides can be checked quickly and easily. Analysis of the products released during hydrolysis by thin-layer chromatography or other simple procedures will reveal whether the enzyme exhibits an endo- or an exohydrolytic pattern. Proton NMR can be used to measure the anomeric configuration of released reducing-end monosaccharide residues, and hence to classify the particular enzyme into "retaining" or "inverting" groups (27, 33).

E. Three-Dimensional Structures

Perhaps the ultimate data that allow catalytic mechanisms, substrate specificity, and substrate binding to be defined in precise molecular terms are provided by detailed knowledge of the 3D structure of the enzyme of interest. Furthermore, 3D structural information can quickly reveal rational design opportunities that can be used to engineer enhanced performance into a commercially important enzyme. Increased temperature or pH stability, and altered substrate specificity are but a few examples of how 3D structural information can be applied for the manipulation of enzyme utilization in food industries. These possibilities are explored further in later sections of this chapter.

To solve the 3D structures of enzymes that participate in cereal $(1 \rightarrow 3, 1 \rightarrow 4)$-$\beta$-glucan hydrolysis, x-ray crystallography remains the method of choice; indeed, the structures of a barley $(1 \rightarrow 3, 1 \rightarrow 4)$-$\beta$-glucan endohydrolase and a barley β-glucan exohydrolase have now been solved by x-ray crystallography (34, 35). The major bottleneck in the technology is probably associated with difficulties in obtaining high-quality crystals. Crystals can take up to several months to grow to the 0.2–1 mm size required by most x-ray crystallographers (36). If a good-quality native data set can be collected from the x-ray diffraction patterns, together with data sets for heavy-metal derivatives of the enzymes, crystallographers can generally solve the structure of the enzyme.

A final point to be made here is that protein modeling is finding an increasing important place in defining "likely" 3D structures of enzymes for which no crystallographical data are available. If the complete primary structure of an enzyme can be deduced from a cDNA, and if the 3D structure of a closely related enzyme from the same family of glycoside hydrolases has been solved, it is possible to use modeling software programs to generate a likely 3D structure for the enzyme. The limitations and constraints of modeling must be acknowledged, but there are several techniques that can be used to evaluate the reliability of the model (37).

V. CEREAL $(1 \rightarrow 3, 1 \rightarrow 4)$-$\beta$-GLUCAN ENDOHYDROLASES

A. Substrate Specificity and Action Pattern

Two $(1 \rightarrow 3, 1 \rightarrow 4)$-$\beta$-glucan 4-glucanohydrolases (EC 3.2.1.73) from barley have been purified from extracts of germinated grain and characterized (20, 21). Both are members of the family 17 group of glycoside hydrolases (31). Similar enzymes are found in germinated wheat (22, 38), rye (39), sorghum (40), and other cereals (41). The properties of the two barley isoforms are compared in Table 2. Unlike other glucoside hydrolases that hydrolyze cereal $(1 \rightarrow 3, 1 \rightarrow 4)$-$\beta$-glucans, the substrate specificity of the EC 3.2.1.73 enzymes from barley is absolute; the enzymes will only hydrolyze $(1 \rightarrow 4)$-β-glucosyl linkages where these are immediately adjacent, toward the reducing end of the polysaccharide, to a $(1 \rightarrow 3)$-β-glucosyl residue, as shown in Figure 1. Reaction products are $(1 \rightarrow 3, 1 \rightarrow 4)$-$\beta$-oligoglucosides which have a single $(1 \rightarrow 3)$-β-linkage at their reducing termini (Figs. 1, 3). This indicates that the enzymes are endohydrolases,

Table 2 Properties of Barley $(1 \rightarrow 3, 1 \rightarrow 4)$-$\beta$-Glucan Endohydrolases

Property	Isoenzyme EI	Isoenzyme EII
Apparent molecular mass	30,000	32,000
Amino acids	306	306
Isoelectric point	8.5	10.6
Carbohydrate	0	4% by weight
Substrate specificity	Absolute for $(1 \rightarrow 3, 1 \rightarrow 4)$-$\beta$-glucans	Absolute for $(1 \rightarrow 3, 1 \rightarrow 4)$-$\beta$-glucans
Anomeric configuration	Retained during hydrolysis	Retained during hydrolysis
Glycosyl hydrolase classification	Family 17	Family 17
Protein fold	$(\alpha/\beta)_8$ Barrel	$(\alpha/\beta)_8$ Barrel
Catalytic acid/base	Glu93	Glu93
Catalytic nucleophile	Glu232	Glu232
Substrate binding subsites	5–8	5–8
Expression sites	Scutellum, young vegetative tissue, aleurone	Aleurone

Source: Refs. 20, 21. 23, 33, 34, 41, 42.

as does their ability to very rapidly reduce the viscosity of $(1 \rightarrow 3, 1 \rightarrow 4)$-$\beta$-glucan solutions (20). Chen et al. (33) used proton NMR to show that the anomeric configuration of released products is retained during hydrolysis.

B. Three-Dimensional Structure

The 3D structure of barley $(1 \rightarrow 3, 1 \rightarrow 4)$-$\beta$-glucan endohydrolase isoenzyme EII has been determined at $\sim$ 2.2–2.3 Å resolution by x-ray crystallography (34). The enzyme adopts a $(\alpha/\beta)_8$ TIM barrel fold. The most striking feature of the enzyme is a deep substrate-binding cleft that extends across its surface (Fig. 4). The open cleft is consistent with the enzyme's endohydrolytic pattern, because it would allow the enzyme to bind its substrate at essentially any position along the polysaccharide backbone for the hydrolysis of internal glycosidic linkages.

C. Substrate Binding

The precise details of substrate binding and the identity of amino acid residues involved have not been defined. When relatively long $(1 \rightarrow 3, 1 \rightarrow 4)$-$\beta$-oligoglucoside substrates are allowed to diffuse into crystals, they clearly bind to the enzyme. However, they are subsequently hydrolyzed and products diffuse away, even at low temperatures and suboptimal pHs, and it has therefore not been possible to generate diffraction data for the enzyme-substrate complex (M Hrmova, JN Varghese, GB Fincher, unpublished). We are now attempting to define enzyme-substrate interactions by diffusing nonhydrolyzable *S*-glycoside substrate analogs (44) into barley $(1 \rightarrow 3, 1 \rightarrow 4)$-$\beta$-glucan endohydrolase crystals, in the expectation that the substrate analogs will be bound but that their *S*-glycosidic linkages will not be cleaved by the enzyme. Thus, the substrate analogs should remain associated with the enzyme during the generation of x-ray diffraction data.

Measurements of the substrate binding cleft that runs across the surface of the barley $(1 \rightarrow 3, 1 \rightarrow 4)$-$\beta$-glucan endohydrolase indicate that it is long enough to accommodate up to eight glucosyl residues of the $(1 \rightarrow 3, 1 \rightarrow 4)$-$\beta$-glucan substrate (34).

VI. CEREAL β-GLUCOSIDASES

A. Substrate Specificity and Action Pattern

Two β-glucosidases purified from extracts of germinated barley grain have been designated isoenzymes βI and βII (26, 27, 45), and their properties are shown in Table 3. The enzymes are members of the family 1 group of glycoside hydrolases (31), although it is difficult to classify them into existing Enzyme Commission groups. The enzymes hydrolyze 4NPG and are therefore referred to as β-glucosidases of the EC 3.2.1.21 group (26, 27, 37). However, more detailed studies on their substrate specificities show that the enzymes hydrolyse a range of di- and oligosacharides. Highest activity is observed for cellodextrin substrates, for which the rate of hydrolysis increases as the length of the substrate increases from cellotriose to cellohexaose (Fig. 5) (26, 27). In all cases, the barley enzymes

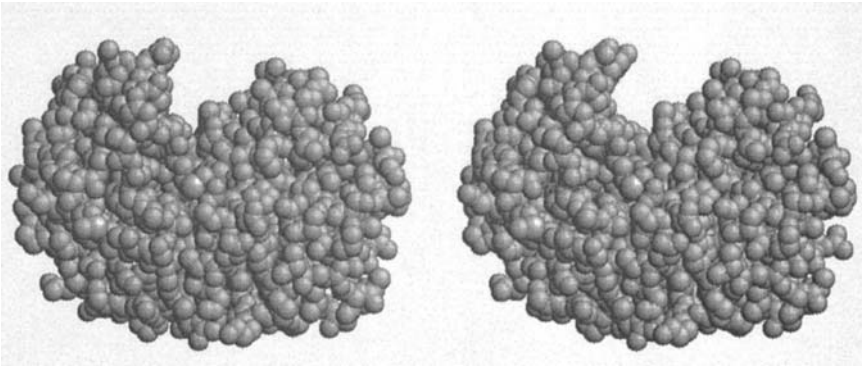

Figure 4 Three-dimensional structure of the barley $(1 \rightarrow 3, 1 \rightarrow 4)$-$\beta$-glucan endohydrolase. Stereoview space-filling representation of an $(\alpha/\beta)_8$ TIM barrel fold. The drawing was generated using RasMol (43). (From Ref. 34.)

remove single glucose units from the nonreducing ends of the substrates, and anomeric configuration is retained during hydrolysis (27). The barley β-glucosidases also catalyze glycosyl transfer reactions, through which higher oligosaccharides containing $(1 \rightarrow 3)$-, $(1 \rightarrow 4)$-, and $(1 \rightarrow 6)$-β-linkages are generated during hydrolysis of 4NPG (37). The increased activity of the enzymes as chain length of cello-oligosaccharides increase (Fig. 5) is suggestive of a polysaccharide exohydrolase rather than an enzyme that is specific for low-molecular-mass β-oligoglucosides (27). Indeed, the action patterns and specificities of the barley β-glucosidases are more typical of polysaccharide exohydrolases of the $(1 \rightarrow 4)$-β-glucan glucohydrolase group (EC 3.2.1.74). The uncertainties associated with the classification of the barley enzymes are acknowledged by Hrmova et al. (37), who propose that the enzyme be referred to as a β-glucosidase/β-glucan exohydrolase until its native substrate in germinated barley grains has been identified unequivocally. The preference of barley grain β-glucosidases for $(1 \rightarrow 4)$-β-oligoglucosides of increasing chain length suggests that it might have an extended substrate-binding region.

Table 3 Properties of Barley β-Glucosidases

Property	Isoenzyme BI	Isoenzyme BII
Apparent molecular mass	62,000	62,000
Amino acids	471	471
Isoelectric point	8.9	9.0
Carbohydrate	Not known	Not known
Substrate specificity		
4NPG	Active	Active
laminarin	Not active	Not active
$(1 \rightarrow 3, 1 \rightarrow 4)$-$\beta$-glucans	Not active	Not active
$(1 \rightarrow 4)$-β-oligosaccharides	Active	Active
Anomeric configuration	Retained during hydrolysis	Retained during hydrolysis
Glucosyl hydrolase classification	Family 1	Family 1
Protein fold	$(\alpha/\beta)_8$ Barrel	$(\alpha/\beta)_8$ Barrel
Catalytic acid/base	Glu181	Glu181
Catalytic nucleophile	Glu391	Glu391
Subsite binding subsites	6	6
Expression sites	Developing endosperm	Developing endosperm

Source: Refs. 26, 27, 37, 45.

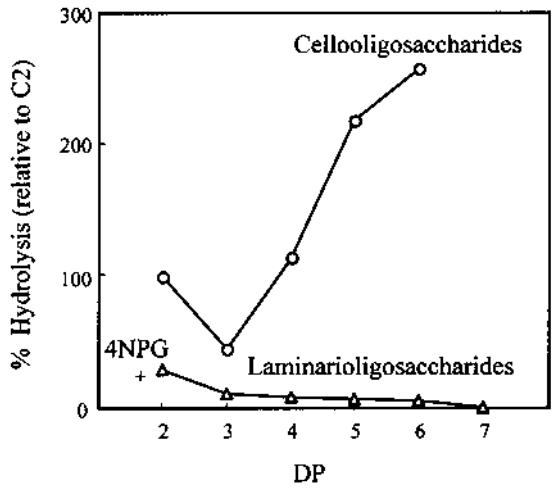

Figure 5 Relative rates of hydrolysis of β-oligoglucosides by the barley β-glucosidase. (From Ref. 27.)

B. Three-Dimensional Structure

There are no reports of 3D structures for cereal β-glucosidases. When the primary structure of the barley β-glucosidase isoenzyme βII deduced from a cDNA sequence (26) was analyzed using molecular modeling software programs (37), 3D models with very high reliability scores were built using as a template the crystal structure of a cyanogenic β-glucosidase from white clover (46) (Fig. 6). A deep, funnel-shaped pocket, or dead-end tunnel, in the barley β-glucosidase is revealed in these modeling experiments, and this can be reconciled with the substrate specificity. When $(1 \rightarrow 4)$-β-oligoglucosides were used as molecular rules in the active-site pocket, it became clear that at least six glucosyl residues would be closely associated with the enzyme surface (37). This suggests that the enzyme has five or six glucosyl-binding subsites. Furthermore, catalytic amino acid residues are located near the bottom of the pocket, and the inside surface of the pocket is lined with aromatic amino acid residues (Fig. 6) that could be involved with substrate binding, through stacking interactions with nonpolar surfaces of glucosyl residues (47). In contrast to the cleft observed on endoacting polysaccharide hydrolases (Fig. 4), the dead-end tunnel geometry (Figure 6) is consistent with an exo-action pattern, through which single glucosyl residues are released from one end of the polysaccharide.

VII. THE BROAD-SPECIFICITY β-GLUCAN EXOHYDROLASES

A. Substrate Specificity and Action Pattern

Two barley β-glucan exohydrolases, designated isoenzymes ExoI and ExoII, have been characterized in detail (24, 25, 27). Similar enzymes are found in elongating maize coleoptiles (18) and in dicotyledonous plants (48–50). Although two β-glucan exohydrolase isoenzymes have been purified from barley seedlings, Southern hybridization analyses suggest that the

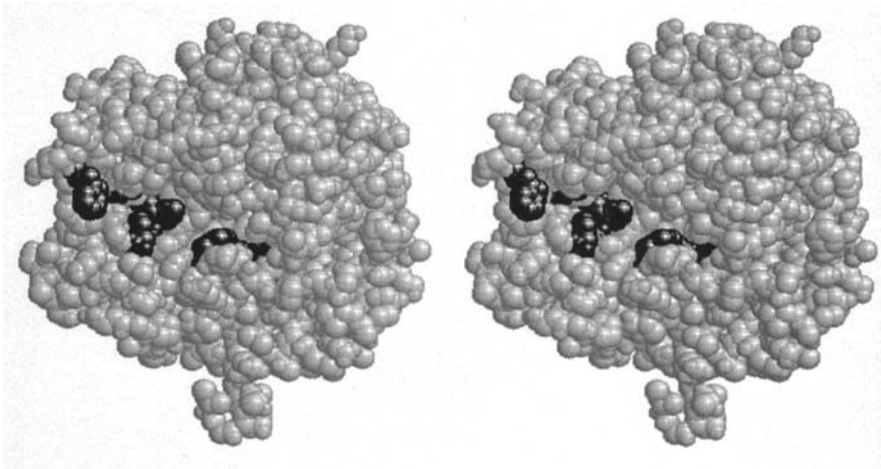

Figure 6 Three-dimensional modeled structure of the barley β-glucosidase. Stereoview space-filling representation of $(\alpha/\beta)_8$ TIM barrel fold. The aromatic amino acid residues lining the surface of the active site pocket are colored in black. The drawing was generated using RasMol (43). (From Ref. 37.)

enzymes are encoded by a family of five to six genes (AJ Harvey, M Hrmova, GB Fincher, unpublished). The properties of barley β-glucan exohydrolase isoenzymes ExoI and ExoII are shown in Table 4.

The barley β-glucan exohydrolases are exoacting enzymes that hydrolyze the nonreducing terminal glycosidic linkage in a broad range of aryl β-glycosides, β-oligoglucosides, and polymeric β-glucans. The anomeric configuration of the released glucose unit is retained, and, at high substrate concentrations, the enzymes catalyze a range of glycosyl transfer reactions (25, 27). The enzymes can be confidently classed as polysaccharide exohydrolases rather than β-glucosidases because of their ability to rapidly release glucose from a number of polysaccharide substrates, including laminarin and cereal $(1 \rightarrow 3, 1 \rightarrow 4)$-$\beta$-glucans (25). The barley β-glucan exohydrolases can be classified into the family 3 group of glycoside hydrolases (31), but again their broad substrate specificities make it difficult to assign them to existing EC groups.

The barley β-glucan exohydrolases also catalyze the hydrolysis of $(1 \rightarrow 3)$-β-glucosidic linkages at higher rates than other linkage types (Fig. 7) (25, 27). However, hydrolytic rates are relatively independent of the length of substrates, especially at degrees of polymerization of 3 and above (Fig. 7), and the enzymes have no difficulty hydrolyzing mixed linkage $(1 \rightarrow 3, 1 \rightarrow 4)$-$\beta$-oligoglucosides (25, 27). This is in marked contrast to the barley β-glucosidase, for which rates of hydrolysis increase with the chain length of cello-oligosaccharides (Fig. 5), but $(1 \rightarrow 3)$-β-oligosaccharides, $(1 \rightarrow 3)$-β-glucans, and $(1 \rightarrow 3, 1 \rightarrow 4)$-$\beta$-glucans are hydrolyzed very slowly, if at all. The small effect of substrate chain length on hydrolytic rate would suggest that the enzyme has a relatively short substrate-binding region, and indeed, subsite mapping experiments indicate that only two or three glucosyl-binding subsites are present (M Hrmova, GB Fincher, unpublished). Once these subsites are fully occupied, reaction rates would be maximal and would be expected to be unaffected by any increases in length of substrates.

B. Three-Dimensional Structure

The barley β-glucan exohydrolase isoenzyme ExoI was recently crystallized by vapor diffusion in the presence of ammonium sulfate and polyethylene glycol (36). Platinum and mercury derivatives of the crystals were subsequently obtained, and this allowed the 3D structure of the enzyme to be solved by x-ray crystallography at 1.8–2.2 Å resolution (35).

Table 4 Properties of Barley β-Glucan Exohydrolases

Property	Isoenzyme ExoI	Isoenzyme ExoII
Apparent molecular mass	69,000	71,000
Amino acids	605	602
Isoelectric point	7.8	8.0
Carbohydrate	4.7% by weight at 3 *N*-glycosylation sites	Not known
Substrate specificity		
4NPG	Active	Active
$(1 \rightarrow 3)$-, $(1 \rightarrow 3, 1 \rightarrow 4)$-, $(1 \rightarrow 3,1 \rightarrow 6)$-$\beta$-glucans	Active	Active
$(1 \rightarrow 2)$-, $(1 \rightarrow 3)$-, $(1 \rightarrow 4)$- $(1 \rightarrow 6)$-β-oligosaccharides	Active	Active
Anomeric configuration	Retained during hydrolysis	Retained during hydrolysis
Glucosyl hydrolase classification	Family 3	Family 3
Protein fold	$(\alpha/\beta)_8$ Barrel and $(\alpha/\beta)_6$ sandwich	$(\alpha/\beta)_8$ Barrel and $(\alpha/\beta)_6$ sandwich
Catalytic acid/base	Glu491	Glu491
Catalytic nucleophile	Asp285	Asp284
Subsite binding subsites	2–3	2–3
Expression sites	Mainly in scutellum and coleoptiles, also in young leaves and roots	Mainly in scutellum and coleoptiles, also in young roots and leaves

Source: Refs. 24, 25, 27, 35.

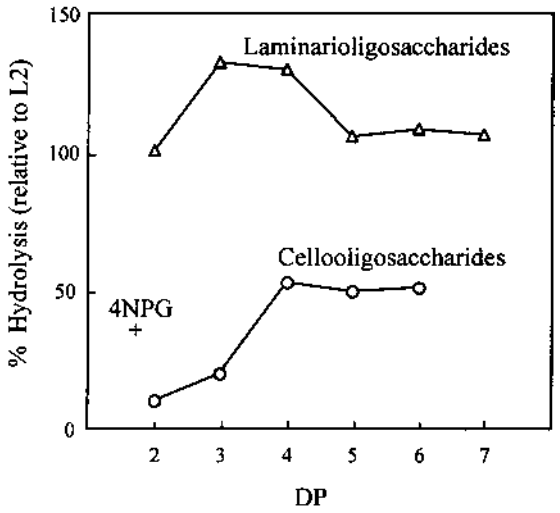

Figure 7 Relative rates of hydrolysis of β-oligoglucosides by the barley β-glucan exohydrolase. (From Ref. 27.)

The enzyme is globular in shape but has two distinct domains. The first consists of 357 amino acid residues that fold into a $(\alpha/\beta)_8$ TIM barrel. A 16 amino acid linker joins the first domain to the second domain, which consists of residues 374–599 arranged in an $(\alpha/\beta)_6$ sandwich. The $(\alpha/\beta)_6$ sandwich has a six-stranded β-sheet, with three α-helices on either side of the sheet (Fig. 8) (35). At the COOH-terminal region of the enzyme (residues 500–605) is a long, antiparallel loop. Carbohydrate can be detected on each of three potential *N*-glycosylation sites at Asn221, Asn498, Asn600 (35). Of particular interest in the crystal structure is the presence of a glucose molecule at the bottom of a surface pocket on the enzyme. The entrance to the pocket is shaped like a coin slot in a vending machine and is located near the interface of domains 1 and 2. The glucose is tightly bound to the enzyme and is likely to be the product of the enzyme-catalyzed reaction that has not been released after hydrolysis is complete (Fig. 8). It follows, therefore that the pocket occupied by the glucose represents the substrate-binding region of the enzyme.

As already noted for the barley β-glucosidase (Sec. VI.B), the 3D structure of the barley β-glucan exohydrolase (Fig. 8) and the positioning of catalytic residues in its substrate-biding pocket can be reconciled with its substrate specificity (Table 4). At 13 Å in depth, the catalytic pocket could accommodate two

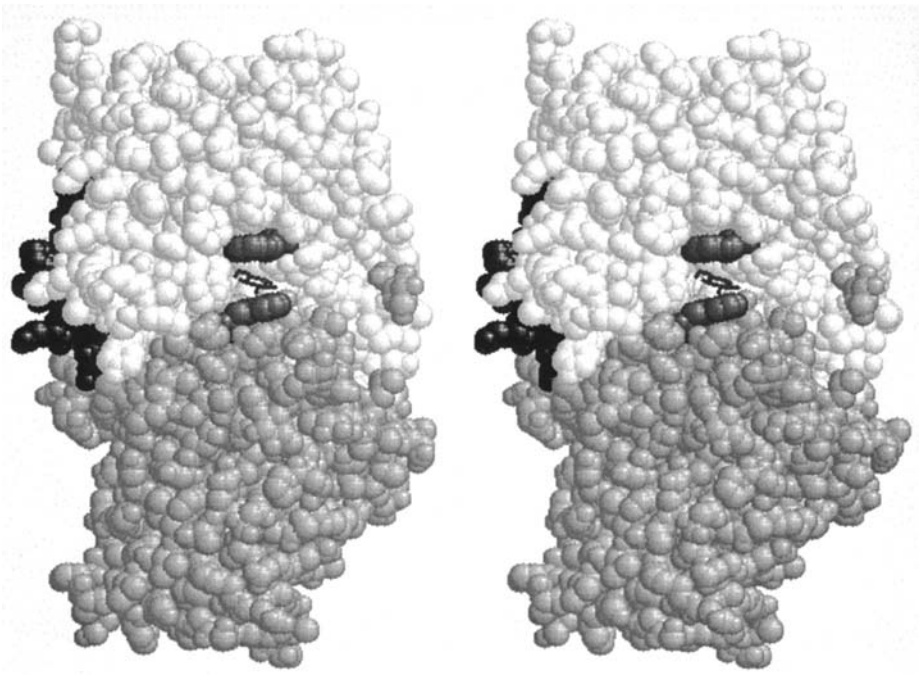

Figure 8 Three-dimensional structure of the barley β-glucan exohydrolase. Stereoview space-filling representation of the overall structure. The $(\alpha/\beta)_8$ TIM barrel (colored in white) and the $(\alpha/\beta)_6$ sandwich (colored in light gray) represent domains 1 and 2, respectively. The linker region connecting the two domains is on the left and is marked in black. Active-site region of the enzyme, which is bounded by Trp286 and Trp434 (colored in dark gray), contains a trapped glucose moiety (in a dark gray wireframe representation). The drawing was generated using RasMol (43). (From Ref. 35.)

to three glucosyl residues, given that the distance between glycosidic oxygen atoms of two adjacent residues in (1 → 3)- or (1 → 4)-β-glucans is ~ 5–6 Å (51). Furthermore, the length of the substrate-binding region estimated by subsite mapping is also two to three glucosyl residues (M Hrmova and GB Fincher, unpublished). In addition, if the pocket is deep enough for only two glycosyl residues, the remainder of the oligomeric or polymeric substrate would project out of the pocket and away from the enzyme surface. Thus, substrate binding would be relatively independent of the overall substrate shape for the β-glucan exohydrolases, in contrast to the β-glucosidases, where the substrate has to have the correct shape to fit into the much longer substrate-binding tunnel (Fig. 6). Because substrate shape is determined in large part by the type of glycosidic linkage, the lack of strict shape requirements for substrates of the β-glucan exohydrolases could explain why substrates with many different linkage types can be hydrolyzed by this broad-specificity β-glucan exohydrolase.

VIII. BIOLOGICAL ROLES OF THE DIFFERENT ENZYMES IN CEREAL (1 → 3, 1 → 4)-β-GLUCAN HYDROLYSIS

The availability of precise information on the specificity, action pattern, and kinetics of key β-glucan exo- and endohydrolases from higher plants provides important clues on the biological roles of individual enzymes during the hydrolysis of cereal (1 → 3, 1 → 4)-β-glucans. The potential roles of the enzymes in germinated grain, where cell walls of the starchy endosperm are completely degraded, are compared in the sections below with their potential roles in elongating vegetative tissues, where partial hydrolysis of cell wall polysaccharides is believed to "loosen" the wall structure sufficiently to allow turgor-driven cell expansion during normal growth and development.

A. (1 → 3, 1 → 4)-β-Glucan Endohydrolases

It can be confidently concluded that the primary function of the EC 3.2.1.73 group of (1 → 3, 1 → 4)-β-glucan endohydrolases in germinated grain is in the hydrolysis of cell wall (1 → 3, 1 → 4)-β-glucans. Both the (1 → 3, 1 → 4)-β-glucan substrate and the (1 → 3, 1 → 4)-β-glucan endohydrolases are restricted in their distribution to the Poaceae. The enzymes are expressed in germinated grain in response to the phytohormone gibberellic acid (GA). Expression occurs in the scutellar epithelium and in the aluerone layers, where it is under tight spatial and temporal control (52, 53). Isoenzyme EI is the predominant isoform found in the scutellum, while isoenzyme EII is secreted only from the aleurone layer. The genes encoding both barley isoenzymes have been isolated, and various sequence motifs that might be related to GA induction and tissue specificity of expression have been identified (54–56).

While the (1 → 3, 1 → 4)-β-glucan endohydrolases are clearly involved in depolymerization of wall (1 → 3, 1 → 4)-β-glucans in germinated grain, it is not so clear whether or not another endohydrolase might be responsible for the initial release of relatively high-molecular-mass (1 → 3, 1 → 4)-β-glucan from the walls (Fig. 3). As noted in Figure 3, the final products of hydrolysis of the endohydrolases will be a family of (1 → 3, 1 → 4)-β-oligoglucosides. These still contain a significant proportion of total grain glucose (15), but their complete hydrolysis to glucose requires the activity of other enzymes.

In barley, (1 → 3, 1 → 4)-β-glucan endohydrolase isoenzyme EI is also expressed in young leaves and roots, where transcription of the gene is mediated by auxins (23, 53). The enzyme is also found in young roots of rice (57). Auxins participate in several physiological processes that are related to wall metabolism in plants, including cell elongation, vascular differentiation, phototropic responses, and geotropism. Because (1 → 3, 1 → 4)-β-glucan endohydrolases of the EC 3.2.1.73 group appear to be completely absent from elongating barley coleoptiles (23), a role in cell elongation seems unlikely.

B. β-Glucosidases

The functional role of β-glucosidases in cereals is more difficult to define. In barley, the genes encoding the enzyme are expressed only in the maturing endosperm of the grain (26). The enzyme itself is also detected in the late stages of grain development and in ungerminated grain; activity does not increase after germination (26, 45). Possible functions of the β-glucosidases in developing and germinated grain have been reviewed by Leah et al. (26), and some of these are related to cell wall metabolism. The β-glucosidases are expressed at a time when (1 → 3, 1 → 4)-β-glucan is being deposited in the walls of starchy endosperm cells (26), and might be involved in trimming or turnover of wall (1 → 3, 1 → 4)-β-glucans during their synthesis.

Finally, the β-glucosidases could be responsible for salvaging glucose units from the (1 → 3, 1 → 4)-β-oligoglucosides released from wall (1 → 3, 1 → 4)-β-glucans by endohydrolases. The β-glucosidases are able to hydrolyze not only the more abundant tri- and tetrasaccharides released by the endohydrolases, but also the longer-chain "cellulosic" β-oligoglucosides that have single (1 → 3)-β-glucosyl residues at their reducing termini (Figs. 1, 3) (27). The detection of the β-glucosidases in germinated grain is consistent with such a role in the complete depolymerization of wall (1 → 3, 1 → 4)-β-glucans to glucose, and, based on current evidence, we believe that this might be a likely function of the barley β-glucosidases.

C. β-Glucan Exohydrolases

The β-glucan exohydrolases from barley hydrolyze polysaccharides such as laminarin and cereal (1 → 3, 1 → 4)-β-glucans, as well as a range of β-oligoglucosides, including (1 → 3, 1 → 4)-β-oligoglucosides (Table 4). This broad specificity, together with a distribution that includes not only the Poaceae but also many dicotyledons, makes it difficult to assign a single, unequivocal function to the enzyme.

Because the β-glucan exohydrolases hydrolyze (1 → 4)-β-glucosidic linkages more slowly than (1 → 3)-β-glucosidic linkages (Fig. 7), it might be argued that these enzymes are less likely to play a role in hydrolysis of (1 → 3, 1 → 4)-β-oligoglucosides in germinated grain than are the β-glucosidases. The genes encoding the β-glucan exohydrolases are transcribed in the scutellum of germinated grain, but their mRNAs are most abundant in the elongating coleoptile (AJ Harvey, M Hrmova, GB Fincher, unpublished). This latter observation has led to the suggestion that β-glucan exohydrolases function in auxin-mediated cell elongation in growing coleoptiles (24, 58: AJ Harvey, M Hrmova, GB Fincher, unpublished), where the amount of (1 → 3, 1 → 4)-β-glucan in walls decreases markedly during coleoptile growth (59) in a process that has been linked to the wall "loosening" believed to be necessary for cell elongation (60).

In concluding that the broad-specificity β-glucan exohydrolases are likely to play a role in cell elongation during normal growth and development of plants, it must be acknowledged that the actual enzymic mechanism of wall loosening cannot be precisely explained. Once can visualize wall loosening as a partial endohydrolysis of polysaccharides that noncovalently crosslink cellulosic microfibrils in the wall; turgor pressure-driven forces would allow the cellulose microfibrils to slip past each other if the strength of the crosslinking or matrix phase between the microfibrils were weakening (5). It is not easy to visualize how an exoacting hydrolase of the β-glucan exohydrolase type would be able to cleave crosslinking polysaccharides between cellulosic microfibrils. It might also be argued that this fundamental concept as to how cell wall components might behave during cell expansion is simplistic, and that our inability to describe the enzymology of the process reflects our generally inadequate understanding of the role of walls in cell expansion as a whole.

Another possible function of the β-glucan exohydrolases could be linked to defense strategies developed by plants to counter pathogen attack. The enzymes can hydrolze (1 → 3)-β- and (1 → 3, 1 → 6)-β-glucans of the type commonly found in fungal cell walls (61), and could act in synergy with the better-known pathogenesis-related (PR) proteins, (1 → 3)-β-glucan endohydrolases (EC 3.2.1.39), to degrade walls of invading fungi and thus to arrest their growth (25).

IX. APPLICATIONS IN THE FOOD INDUSTRY

Cell wall (1 → 3, 1 → 4)-β-glucans are widely recognized for their effects on extract viscosity during the commercial utilization of cereals. Although the (1 → 3, 1 → 4)-β-glucans and their highly viscous solutions are considered beneficial in human diets (3), in most commercial applications the high viscosity of (1 → 3, 1 → 4)-β-glucan solutions is undesirable.

A. Malting and Brewing Industries

Attempts by the food and beverage industries to address these problems through the application of modern technologies have been concentrated so far in the malting and brewing industries. Specifications for barley quality are tailored predominantly for these industries, and emphasis has been placed on parameters such as grain size, dormancy, malt extract, grain protein content, development of starch- degrading enzymes (diastatic power), and removal of (1 → 3, 1 → 4)-β-glucans. High levels of (1 → 3, 1 → 4)-β-glucans in barley malt are considered undesirable because they are often indicative of incomplete cell wall breakdown in the starchy endosperm and are therefore correlated with low values for malt extract (41). Further, undegraded (1 → 3, 1 → 4)-β-glucans can cause filtration difficulties in the brewery,

again because of their propensity to form solutions of high viscosity, and can contribute to the formation of undesirable hazes in the final product (62).

The quality specification relating to the removal of $(1 \rightarrow 3, 1 \rightarrow 4)$-$\beta$-glucans can clearly be tackled on two fronts. Firstly, breeders can select for barley with inherently low $(1 \rightarrow 3, 1 \rightarrow 4)$-$\beta$-glucan contents (3), or for barleys with the potential to produce high levels of $(1 \rightarrow 3, 1 \rightarrow 4)$-$\beta$-glucan hydrolases after germination. The importance of these two parameters in barley-breeding programs is underscored by the efforts to place on detailed genetic maps the quantitative trait loci (QTLs) that control$(1 \rightarrow 3, 1 \rightarrow 4)$-$\beta$-glucan content and $(1 \rightarrow 3, 1 \rightarrow 4)$-$\beta$-glucan endohydrolase activity (64, 65).

The second approach to the $(1 \rightarrow 3, 1 \rightarrow 4)$-$\beta$-glucan problem in the malting and brewing industries is to produce an improved barley through genetic engineering technologies. The genes encoding $(1 \rightarrow 3, 1 \rightarrow 4)$-$\beta$-glucan synthases have not yet been isolated, and manipulation of initial $(1 \rightarrow 3, 1 \rightarrow 4)$-$\beta$-glucan levels by downregulating this gene is therefore not possible at this stage. However, the two genes encoding barley $(1 \rightarrow 3, 1 \rightarrow 4)$-$\beta$-glucan endohydrolases have been cloned (54–56), as have $(1 \rightarrow 3, 1 \rightarrow 4)$-$\beta$-glucan endohydrolase genes from various *Bacillus* spp. (66, 67). Thus, genetic manipulation of genes encoding these endohydrolases could result in elevated levels of the enzyme in malt, and this is in turn could result in the rapid removal of residual, high-molecular-mass $(1 \rightarrow 3, 1 \rightarrow 4)$-$\beta$-glucan molecules in malt extracts.

B. Increased Levels of $(1 \rightarrow 3, 1 \rightarrow 4)$-$\beta$-Glucan Endohydrolases

There are several approaches to increasing $(1 \rightarrow 3, 1 \rightarrow 4)$-$\beta$-glucanase activity via genetic engineering. One would be to attach a more powerful promoter to the native barley $(1 \rightarrow 3, 1 \rightarrow 4)$-$\beta$-glucan endohydrolase genes. The promoter would need to be activated in the appropriate tissue at the appropriate time, so powerful constitutive promoters that were active in many tissues throughout growth and development would be of little value in this approach. However, if a barley α-amylase promoter were attached to a barley $(1 \rightarrow 3, 1 \rightarrow 4)$-$\beta$-glucan endohydrolase gene, it might be anticipated that high levels of the enzyme would be expressed in aleurone cells after germination, because the expression patterns of α-amylases and $(1 \rightarrow 3, 1 \rightarrow 4)$-$\beta$-glucanases in barley are similar (68). The major disadvantage of using more powerful promoters on the barley $(1 \rightarrow 3, 1 \rightarrow 4)$-$\beta$-glucan endohydrolase genes, even if these promoters direct appropriate tissue-specific and temporal expression patterns, is the potential to upset the metabolic balance in the germinated grain. Given that the grain has a finite energy potential and well-evolved regulatory mechanisms to ensure that the correct balance of individual hydrolytic enzymes is obtained, higher levels of $(1 \rightarrow 3, 1 \rightarrow 4)$-$\beta$-glucan endohydrolases might be achieved at the expense of other enzymes, which might then become rate limiting and cause unpredicted metabolic imbalances and associated difficulties in the malting and brewing processes.

C. Increased Stability of $(1 \rightarrow 3, 1 \rightarrow 4)$-$\beta$-Glucan Endohydrolases

A second approach to increasing $(1 \rightarrow 3, 1 \rightarrow 4)$-$\beta$-glucan endohydrolase activity for the malting and brewing industries could be to increase the stability of the existing enzyme, without trying to increase expression levels at the gene level. In this approach the enzyme itself would be engineered for increased stability, but the native $(1 \rightarrow 3, 1 \rightarrow 4)$-$\beta$-glucanase gene promoter would be retained so that the metabolic balance of the germinated grain would not be perturbed. The amount of $(1 \rightarrow 3, 1 \rightarrow 4)$-$\beta$-glucan endohydrolase in germinated barley grains will clearly meet the normal physiological requirements for starchy endosperm mobilization and successful germination of the grain. However, these enzymes are irreversibly denatured and almost completely inactivated at the temperatures used during kilning (up to 85°C) or during mashing (usually $\sim$ 65°C) (21, 69). Thus, if the stability of the enzymes could be increased at these temperatures so that more of the enzyme survived the kilning and mashing steps, the higher levels of surviving enzyme could hydrolyze residual high-molecular-mass $(1 \rightarrow 3, 1 \rightarrow 4)$-$\beta$-glucans after mashing.

How then, could the loss of $(1 \rightarrow 3, 1 \rightarrow 4)$-$\beta$-glucan endohydrolase activity at elevated temperatures be addressed? Firstly, heat-stable $(1 \rightarrow 3, 1 \rightarrow 4)$-$\beta$-glucanases occur naturally in various microbial species. An extremely thermostable $(1 \rightarrow 3, 1 \rightarrow 4)$-$\beta$-glucanase has been engineered by intragenic recombination of gene segments from *Bacillus macerans* and *B. amyloliquefaciens* (67). The gene encoding this hybrid, thermostable $(1 \rightarrow 3, 1 \rightarrow 4)$-$\beta$-glucan endohydrolase, has been expressed in barley protoplasts (70 and in transgenic barley (71).

Another approach to preventing the loss of $(1 \rightarrow 3, 1 \rightarrow 4)$-$\beta$-glucan endohydrolase activity at the temperatures encountered during malting and brewing would be to engineer enhanced thermostability into the barley enzyme itself. Random mutagenesis of the cDNA or gene encoding the barley enzyme could be used to generate thermostable mutants. Alternatively, the detailed three-dimensional structure of barley $(1 \rightarrow 3, 1 \rightarrow 4)$-$\beta$-glucan endohydrolase isoenzyme EII (34) could be used to rationally redesign the enzyme (72). In related work, a small improvement in heat stability has been engineered into the barley $(1 \rightarrow 3, 1 \rightarrow 4)$-$\beta$-glucanase isoenzyme EI through the addition of an *N*-glycosylation site to the protein (73).

D. Genetic Engineering

Perhaps the major technological bottleneck in the application of genetic engineering to improve cereal performance in the commercial arena has been the difficulty associated with transformation. Transformation procedures for wheat and barley have been developed in recent years (74, 75) but have often been plagued by very low transformation frequencies, inconsistent results, and an inability to transform the elite breeder lines. The foreign or manipulated DNA has generally been introduced into immature embryo or microspore cultures using microparticle bombardment (74) or, more recently, using methods based on *Agrobacterium tumefaciens* transformation (75).

At this stage it is important to acknowledge that genetic engineering and genetically manipulated organisms (GMOs) are not universally accepted by consumers. Indeed, considerable resistance to these new technologies has been experienced, especially where human food is derived from GMOs (76, 77). In considering whether to engineer barley with an altered barley $(1 \rightarrow 3, 1 \rightarrow 4)$-$\beta$-glucanase gene or with a naturally thermostable bacterial gene, as discussed in Section IX.C, consumer attitudes to foods derived from genetically engineered plants remain of central importance. Whether or not barley engineered with an altered barley gene would be more acceptable than a barley engineered with a bacterial gene remains to be seen.

ACKNOWLEDGMENTS

This work was supported by grants from the Australian Research Council and the Grains Research and Development Corporation. We thank Mr. Andrew Harvey and Mr. Richard Stewart for their contributions to various aspects of the work, and Dr. Jose Varghese for his patience in teaching us the principles of x-ray crystallography.

REFERENCES

1. A Bacic, PJ Harris, BA Stone. Structure and function of plant cell walls. In: J Preiss, ed. The Biochemistry of Plants. New York: Academic Press, 1988, pp 297–371.
2. IS Forrest, T Wainwright. The mode of binding of β-glucans and pentosans in barley endosperm cells walls. J Inst Brew 83:279–286, 1977.
3. RS Bhatty. Physicochemical properties of roller-milled barley bran and flour. Cereal Chem 70:397–402, 1993.
4. NC Carpita, DM Gibeaut. Structural models of primary cell walls in flowering plants: consistency of molecular structure with the physical properties of the walls during growth. Plant J 3:1–30, 1993.
5. SC Fry. Polysaccharide-modifying enzymes in the plant cell wall. Annu Rev Plant Physoil Plant Mol Biol 46:497–520, 1995.
6. GB Fincher, BA Stone. Cell walls and their components in cereal grain technology. Adv Cereal Sci Technol 8:207–295, 1986.
7. FA Parrish, AS Perlin, ET Reese. Selective enzymolysis of poly-β-D-glucans, and the structure of the polymers. Can J Chem 38:2094–2104, 1960.
8. A Bacic, BA Stone. Chemistry and organization of aleurone cell wall components from wheat (*Triticum aestivum* cultivar Insignia) and barley (*Hordeum vulgare* cultivar Clipper). Aust J Plant Physiol 8:475–495, 1981.
9. JR Woodward, GB Fincher, BA Stone. Water-soluble $(1 \rightarrow 3, 1 \rightarrow 4)$-$\beta$-D-glucans from barley (*Hordeum vulgare*) endosperm. II. Fine structure. Carbohydr Polym 3:207–225, 1983.
10. RJ Staudte, RJ Woodward, GB Fincher, BA Stone. Water-soluble $(1 \rightarrow 3, 1 \rightarrow 4)$-$\beta$-D-glucans in barley (*Hordeum vulgare*) endosperm. III. Distribution of cellotriosyl and cellotetraosyl residues. Carbohydr Polym 3:299–312, 1983.
11. PJ Wood, J Weisz, BA Blackwell. Structural studies $(1 \rightarrow 3, 1 \rightarrow 4)$-$\beta$-D-glucans by ^{13}C-nuclear magnetic resonance spectroscopy and by rapid analysis of cellulose-like regions using high-performance anion-exchange chromatography of oligosaccharides released by lichenase. Cereal Chem 71:301–307, 1994.
12. H Igarashi, Y Sakurai. Studies on the non-starchy polysaccharides of the endosperm of naked barley. Part I. Preparation of the water soluble β-glucan from naked barley endosperm and their properties. Agric Biol Chem 29:678–686, 1965.

13. JR Woodward, DR Phillips, GB Fincher. Water-soluble (1 → 3, 1 → 4)-β-D-glucans from barley (*Hordeum vulgare*) endosperm. I. Physicochemical properties. Carbohydr Polym 3:143–156, 1983.
14. GS Buliga, DA Brant, GB Fincher. The sequence statistics and solution configuration of barley (1 → 3, 1 → 4)-β-D-glucan. Carbohydr Res 157:139–156, 1986.
15. P Morrall, DE Briggs. Changes in cell wall polysaccharides of germinating barley grains. Phytochemistry 17:1495–1502, 1978.
16. CW Bamforth, HL Martin. The development of β-glucan solubilase during barley germination. J Inst Brew 87:81–84, 1981.
17. XS Yin, AW MacGregor, RM Clear. Field fungi and β-glucan solubilase in barley kernels. J Inst Brew 95:195–198, 1989.
18. E Labrador, DJ Nevins. Selected cell wall proteins from *Zea mays*: assessment of their role in wall hydrolysis. Physiol Plant 77:487–492, 1989.
19. M Inouhe, K Hayashi, DJ Nevins. Polypeptide characteristics and immunological properties of exo- and endoglucanases purified from maize coleoptile cell walls. J Plant Physiol 154:334–340, 1999.
20. JR Woodward, GB Fincher. Purification and chemical properties of two 1,3;1,4-β-glucan endohydrolases from germinated barley. Eur J Biochem 121:663–669, 1982.
21. JR Woodward, GB Fincher. Substrate specificities and kinetic properties of two (1 → 3, 1 → 4)-β-glucan endohydrolases from germinating barley (*Hordeum vulgare*). Carbohydr Res 106:111–122, 1982.
22. DML Lai, PB Høj, GB Fincher. Purification and characterization of (1 → 3, 1 → 4)-β-glucan endohydrolases from germinated wheat (*Triticum aestivum*). Plant Mol Biol 22:847–859, 1993.
23. N Slakeski, GB Fincher. Developmental regulation of (1 → 3, 1 → 4)-β-glucanase gene expression in barley. I. Tissue specific expression of individual isoenzymes. Plant Physiol 99:1226–1231, 1992.
24. T Kotake, N Nakagawa, K Takeda, N Sakurai. Purification and characterization of wall-bound exo-1,3-β-D-glucanase from barley (*Hordeum vulgare* L) seedlings. Plant Cell Physiol 38:194–200, 1997.
25. M Hrmova, GB Fincher. Barley β-D-glucan exohydrolases. Substrate specificity and kinetic properties. Carbohydr Res 305:209–221, 1998.
26. R Leah, J Kigel, I Svendsen, J Mundy. Biochemical and molecular characterization of a barley seed β-glucosidase. J Biol Chem 270:15789–15797, 1995.
27. M Hrmova, AJ Harvey, J Wang, NJ Shirley, GP Jones, BA Stone, PB Høj, GB Fincher. Barley β-D-glucan exohydrolases with β-D-glucosidase activity. Purification, characterization, and determination of primary structure from a cDNA clone. J Biol Chem 271:5277–5286, 1996.
28. DJ Huber, DJ Nevins. β-Glucans hydrolase activity in *Zea* coleoptile cell walls. Plant Physiol 65:768–773, 1980.
29. EC Webb. Enzyme Nomenclature. New York: Academic Press, 1992.
30. C Gaboriaud, V Bissery, T Benchetrit, JPH Mornon. Hydrophobic cluster analysis: an efficient new way to compare and analyse amino acid sequences. FEBS Lett 224:149–155, 1987.
31. B Henrissat. Glycosidase families. Biochem Soc Trans 26:153–156, 1998.
32. I Callebaut, G Labesse, P Durand, A Poupon, L Canard, J Chomilier, B Henrissat, JP Mornon. Deciphering protein sequence information through hydrophobic cluster analysis (HCA)—current status and perspectives [Review]. Cell Mol Life Sci 53:621–645, 1997.
33. L Chen, M Sadek, BA Stone, RTC Brownlee, GB Fincher, PB Høj. Stereochemical course of glucan hydrolysis by barley (1 → 3)- and (1 → 3, 1 → 4)-β-glucanases. Biochim Biophys Acta 1253: 112–116, 1995.
34. JN Varghese, TPJ Garrett, PM Colman, L Chen, PB Høj, GB Fincher. Three-dimensional structures of two plant β-glucan endohydrolases with distinct substrate specificities. Proc Natl Acad Sci USA 91:2785–2789, 1994.
35. JN Varghese, M Hrmova, GB Fincher. Three-dimensional structure of a barley β-D-glucan exohydrolase; a family 3 glycosyl hydrolase. Structure 7:179–190, 1999.
36. M Hrmova, JN Varghese, PB Høj, GB Fincher. Crystallization and preliminary x-ray analysis of β-glucan exohydrolase isoenzyme Exol from barley (*Hordeum vulgare*). Acta Cryst D54:687–689, 1998.
37. M Hrmova, EA MacGregor, P Biely, RJ Stewart, GB Fincher. Substrate binding and catalytic mechanism of a barley β-D-glucosidase/(1,4)-β-D-glucan exohydrolase. J Biol Chem 272:11134–11143, 1998.
38. AE Clarke, BA Stone. β-1,3-Glucan hydrolases from grape vine (*Vitis vinifera*) and other plants. Phytochemistry 1:175–188, 1962.
39. GM Ballance, DJ Manners. Structural analysis and enzymic solubilization of barley endosperm cell walls. Carbohydr Res 61:107–118, 1978.
40. AO Aisien, GH Palmer, JR Stark. The ultrastructure of germinating sorghum and millet (*Pennisetum americanum*) grains. J Inst Brew 92:162–167, 1986.
41. IM Stuart, L Loi, GB Fincher. Varietal and environmental variations in (1 → 3, 1 → 4)-β-glucan levels and (1 → 3, 1 → 4)-β-glucanase potential in barley: relationships to malting quality. J Cereal Sci 7:61–71, 1988.
42. L Chen, GB Fincher, PB Høj. Evolution of polysaccharide hydrolase substrate specificity—catalytic amino acids are conserved in barley 1,3;1,4-β-gluca-

nase and 1,3-β-glucanase. J Biol Chem 268:13318–13326, 1993.
43. R Sayle. RasMol Version 2.6 Molecular Visualisation Program. Stevenage, United Kingdom: Glaxo Wellcome Research Development, 1996.
44. V Moreau, H Driguez. Enzymic synthesis of hemithiocellodextrins. J Chem Soc Perkin Trans 1:525–527, 1995.
45. G Simos, CA Panagiotidis, A Skoumbas, D Choli, C Ouzounis, JG Georgatsos. Barley β-glucosidase-expression during seed germination and maturation and partial amino acid sequences. Biochim Biophys Acta 1199:52–58, 1994.
46. T Barrett, SG Suresh, SP Tolley, EJ Dodson, MA Hughes. The crystal structure of cyanogenic β-glucosidase from white clover; a family 1 glycosyl hydrolase. Structure 3:951–960, 1995.
47. FA Quiocho. Carbohydrate-binding proteins: tertiary structures and protein-sugar interactions. Annu Rev Biochem 55:287–315, 1986.
48. K Cline, P Albersheim. Host-pathogen interactions. XVI. Purification and characterization of a glucosyl hydrolase/transverase present in the walls of soybean cells. Plant Physiol 68:207–220, 1981.
49. Y Lienart, J Comtat, F Barnoud. A wall-bound exo-β-D-glucanase from *Acacia* cultured cells. Biochim Biophys Acta 883:353–360, 1980.
50. HJ Crombie, S Chengappa, A Hellyer, JSG Reid. A xyloglucan oligosaccharide-active, transglycosylation β-D-glucosidase from the cotyledons of nasturtium (*Tropaeolum majus* L) seedlings—purification, properties and characterization of a cDNA clone. Plant J 15:27–38, 1998.
51. I Tvaroska, K Ogawa, Y Deslandes, RH Marchessalt. Crystalline conformation and structure of lichenan and barley β-glucan. Can J Chem 61:1608–1616, 1983.
52. GI McFadden, B Ahluwalia, AE Clarke, GB Fincher. Expression sites and developmental regulation of genes encoding $(1 \rightarrow 3, 1 \rightarrow 4)$-β-glucanase in germinated barley. Planta 173:500–508, 1988.
53. N Slakeski, GB Fincher. Barley $(1 \rightarrow 3, 1 \rightarrow 4)$-β-glucanase isoenzyme EI gene expression is mediated by auxin and gibberellic acid. FEBS Lett 306:98–102, 1992.
54. JC Litts, CR Simmons, KE Karrer, N Huang, RL Rodriguez. The isolation and characterization of a barley $(1 \rightarrow 3, 1 \rightarrow 4)$-β-glucanase gene. Eur J Biochem 194:831–838, 1990.
55. N Slakeski, DC Baulcombe, KM Devos, B Ahluwalia, DNP Doan, GB Fincher. Structure and tissue-specific regulation of genes encoding barley $(1 \rightarrow 3, 1 \rightarrow 4)$-β-glucan endohydrolases. Mol Gen Gen 224:437–449, 1990.
56. N Wolf. Complete nucleotide sequence of a *Hordeum vulgare* gene encoding $(1 \rightarrow 3, 1 \rightarrow 4)$-β-glucanase isoenzyme II. Plant Physiol 96:1382–1384, 1991.
57. CR Simmons, JC Litts, N Huang, RL Rodriguez. Structure of a rice β-glucanase gene regulated by ethylene, cytokinin, wounding, salicylic acid and fungal elicitors. Plant Mol Biol 18:33–45, 1992.
58. T Hoson, DJ Nevins. β-D-Glucan antibodies inhibit auxin-induced cell elongation and changes in cell wall of *Zea* coleoptile segments. Plant Physiol 90:1353–1358, 1989.
59. N Sakurai, Y Masuda. Auxin-induced changes in barley coleoptile cell wall composition. Plant Cell Physiol 19:1217–1223, 1978.
60. E Labrador, DJ Nevins. Selected cell wall proteins from *Zea mays*: assessment of their role in wall hydrolysis. Physiol Plant 77:487–492, 1989.
61. JGF Wessels. Wall growth, protein excretion and morphogenesis in fungi. New Phytol 123:397–413, 1993.
62. CW Bamforth, HL Martin. The development of β-glucan solubilase during barley germination. J Inst Brew 87:81–84, 1981.
63. S Aastrup. Selection and characterization of low β-glucan mutants from barley. Carlsberg Res Commun 43:307–316, 1983.
64. M Hahn, O Olsen, O Politz, R Borriss, U Heinemann. Crystal structure and site-directed mutagenesis of *Bacillus macerans* endo-1,3-1,4-β-glucanase. J Biol Chem 270:3081–3088, 1995.
65. L Loi, B Ahluwalia, GB Fincher. Chromosomal location of genes encoding barley $(1 \rightarrow 3, 1 \rightarrow 4)$-β-glucan 4-glucanohydrolases. Plant Physiol 87:300–302, 1988.
66. R Boriss, R Manteuffel, J Hoffmeister. Molecular cloning of a gene for thermostable β-glucanase from *Bacillus macerans*. J Basic Microbiol 28:3–10, 1988.
67. O Olsen, R Borriss, O Simon, KK Thomsen. Hybrid *Bacillus* $(1 \rightarrow 3, 1 \rightarrow 4)$-β-glucanases: engineering thermostable enzymes by construction of hybrid genes. Mol Gen Genet 225:177–185, 1991.
68. GB Fincher. Molecular and cellular biology associated with endosperm mobilization in germinating cereal grains. Annu Rev Plant Physiol Plant Mol Biol 40:305–346, 1989.
69. L Loi, PA Barton, GB Fincher. Survival of barley $(1 \rightarrow 3, 1 \rightarrow 4)$-β-D-glucanase isoenzymes during kilning and mashing. J Cer Sci 5:45–50, 1987.
70. BA Phillipson. Expression of a hybrid (1-3,1-4)-β-glucanase in barley protoplasts. Plant Sci 91:195–206, 1993.
71. L Jensen, O Olsen, O Kops, N Wolf, KK Thomsen, D von Wettstein. Transgenic barley expressing a protein-engineered, thermostable (1,3-1,4)-β-glucanase during germination. Proc Natl Acad Sci USA 93:3487–3491, 1996.
72. BW Matthews. Structural and genetic analysis of the folding and function of T4 lysozyme [Review]. FASEB J 10:35–41, 1996.

73. DNP Doan, GB Fincher. Differences in the thermostabilities of barley $(1 \rightarrow 3, 1 \rightarrow 4)$-$\beta$-glucanases are only partly determined by *N*-glycosylation. FEBS Lett 309:265–271, 1992.
74. Y Wan, PG Lemaux. Generation of large numbers of independently transformed fertile barley plants. Plant Physiol 104:37–48, 1994.
75. S Tingay, D McElroy, R Kalla, S Fieg, M Wang, S Thornton, R Brettel. *Agrobacterium tumefaciens*–mediated barley transformation. Plant J 6:1369–1376, 1997.
76. A Dove. Pulling green biotechnology out of the red. Nature Biotechnol 16:1022–1024, 1999.
77. A Persidis. Agricultural biotechnology. Nature Biotechnol 17:612–614, 1999.

75

Enzymology of Endo-1,4-β-Mannanases

Henrik Stålbrand
Lund University, Lund, Sweden

I. INTRODUCTION

Mannan-based polysaccharides are abundant in nature; galactoglucomannan is the major softwood hemicellulose, and galactomannans are common storage polysaccharides in certain plant seeds. The major depolymerazing enzyme of these and similar polysaccharides is endo-1,4-β-mannanase (β-mannanase, EC 3.2.1.78), which hydrolyzes randomly internal 1,4-β-D-mannosidic linkages within the backbone of the polysaccharide (see Secs. VI and VII). Further hydrolysis into monomeric sugars is accomplished by the exohydrolases α-galactosidase (EC 3.2.1.22) and β-mannosidase (EC 3.2.1.25). Heteromannan degradation is important in exogenous and endogenous conversion of plant polysaccharides.

Several β-mannanase-encoding genes from bacteria, fungi, and plants have been isolated. Generally, β-mannanase catalytic modules have molecular masses of 30–45 kDa. Like many glycoside hydrolases, β-mannanases may be modular proteins with molecular masses up to or even above 100 kDa. β-Mannanases (i.e., their catalytic modules) are retaining enzymes classified in family 5 and family 26 of glycoside hydrolases (see Sec. IX).

II. THE SUBSTRATES

Hemicellulose is a collective term for a group of diverse plant cell wall polysaccharides, consisting of several different monomeric sugar units linked with *O*-glycosidic linkages (1, 2). The two major groups of hemicellulose, heteroxylans and heteromannans, have, respectively, predominantly xylose units or mannose units in the main chain. The major softwood hemicellulose is acetylated galactoglucomannan which comprises up to ~ 20% of the softwood content (2). It has β-1,4-linked mannose and glucose residues in the main chain and is substituted with α-1,6-linked galactosyl sidegroups. Two major types of acetyl galactoglucomannans occur in softwoods, one which can be solubilized in water and one which is alkali soluble (mannosyl:glucosyl:galactosyl ratio of 3:1:1 and 3:1:0.1, respectively) (1). Hardwoods contain 3–5% unsubstituted glucomannan (2). The degree of polymerization (DP) of galactoglucomannan and glucomannan hemicellulose is ~ 100– 200 (1, 2).

Certain plants contain other types of mannan and heteromannans present especially in seeds as storage polysaccharides (3). Leguminous seeds from several species contain galactomannan, which has a backbone of β-1,4-linked mannose residues with α-1,6-galactosyl side groups. Carob (*Ceratonia siliqua*) seed galactomannan (contained in locust bean gum) and guar galactomannan have a DP of ~ 1500 and 900, respectively (4). The mannosyl to galactosyl ratio is ~ 5/1 for locust bean gum and 2/1 for guar gum (4). The galactomannans can be extracted from the milled seeds (5). These polysaccharides can form highly viscous solutions and are important owing to their use as thickeners in the food industry and other industrial sectors.

They are also used in combination with xanthan gum to form strong gels and in combination with kappa carrageenan to form stronger and more elastic gels (6–8). Ivory nut (*Phytelephas macrocarpa*) mannan is a linear β-1,4-linked insoluble mannan (9).

III. OCCURRENCE OF β-MANNANASES

Both aerobic and anaerobic microorganisms produce plant cell wall polysaccharide-degrading enzymes, reviewed in Warren (10). Some of these microorganisms are present in decaying plant material, in soil, or in the rumen; others are plant pathogens, reviewed in Warren (10) and Klein and Eveleigh (11).

β-Mannanases are produced by species of bacteria, fungi, and plants, and several β-mannanase genes from these organisms have been cloned (12–21). Furthermore, β-mannanase activity has been purified from a gut preparation of the snail *Helix pomatia* (22). Also, some extremophiles produce β-mannanase; the genes have been cloned from thermophilic bacteria (23–25).

β-Mannanase activity has also been detected in several plant seeds, which is correlated to their germination (26, 27). For example, β-mannanase activity has been detected in seeds of tomato (28–30), *Coffea arabica* (31) carob, and fenugreek (32). Low levels of β-mannanase activity were detected in banana fruits during ripening (33). The β-mannanase encoding gene from tomato (*Lycopersicon esculentum*) has been isolated (17). Several tomato β-mannanase isoforms have been observed during germination (29).

IV. PRODUCTION OF MICROBIAL β-MANNANASES

Expression of hemicellulases and cellulases among fungi like *Trichoderma* and *Aspergillus* spp. is commonly glucose repressed (34–37). However, variations even within a species have been observed, partly due to the development of mutant strains, reviewed by Kubicek and Penttilä (37). β-Mannanases are extracellular proteins, but may be cell associated as indicated for anaerobes.

The most commonly used carbon sources for microbial β-mannanase production are galactomannan and other mannans. Fungal β-mannanases have been produced in submerged cultures on locust bean gum by, for example, *Aspergillus niger* (38), *Trichoderma harzianum* (39), and *Aspergillus awamori* for which also wheat bran was used (40). Reese and Shibata (9) screened for and detected β-mannanase activity in cultures of several fungi using ivory nut mannan or carob galactomannan as carbon source. In this study, two fungi produced moderate β-mannanase activity when grown on cellulose. Media containing cellulose have also been used for β-mannanase production by *Trichoderma reesei* (41). Higher levels of β-mannanase were produced on cellulose when compared to locust bean gum (42). *Trichoderma reesei* β-mannanase production appears to increase when glucose is depleted (36). The plant-pathogenic fungi *Sclerotsium rolfsii* produced β-mannanase when grown on several carbon sources, including sorbose, cellulose, mannan, and heteromannans (43). β-Mannanase was produced by the yeast *Aureobasidium pullulans* in media containing either galactomannan, galactoglucomannan, β-1,4-manno-oligosaccharides, or a synthetic nonmetablized glycoside: methyl β-D-mannopyranoside (44).

V. β-MANNANASE MULTIPLICITY

Frequently, polysaccharidases are produced in multiple forms, which at least in some cases, is a reflection of the composition and complexity of naturally occurring substrates. As an example, usually several genetically distinct endoglucanases and cellobiohydrolases are secreted by cellulolytic organisms (10, 45). β-Mannanases are commonly extracellularly produced in multiple forms as observed for some bacteria (20, 46), several plant seeds (26, 29), and several fungi, including *Scelortium rofsii* (47) and *Trichoderma* spp. (39, 41). β-Mannanase isoforms may be post-translationally modified products of the same gene (16) or products of separate genes (21).

VI. CATALYTIC MECHANISM AND MANNAN HYDROLYSIS

β-Mannanases hydrolyze randomly internal 1,4-β-D-mannosidic linkages in mannan and heteromannan polysaccharides. The *A. niger* and the *T. reesei* β-mannanases can efficiently hydrolyze manno-oligosaccharides with a DP of 4 or higher; the major hydrolysis products of ivory nut mannan after extensive incubation are mannobiose and mannotriose (38, 41). Mannotriose can only be slowly hydrolyzed and, owing to secondary hydrolysis of mannotriose (38, 48, 49) mannose may also be produced from ivory nut mannan hydrolysis (50).

Glycoside hydrolases acting on polymeric substrates often have several substrate binding subsites. Each subsite binds one backbone monosaccharide unit. The kinetics of oligosaccharide hydrolysis suggest at least four subsites for the *T. reesei* (48) and the *A. niger* (49) β-mannanases

Each glycoside hydrolase family comprises enzymes that hydrolyze the glycosidic bond by either of two catalytic mechanisms—one that yields a net retention of the anomeric configuration, and one that yields a net inversion (51, 52). Two catalytic residues participate in the mechanism: a nucleophile and an acid/base catalyst. The retaining mechanism is a two-step process. A covalent glycosyl enzyme intermediate is formed, which is hydrolyzed in the second step (51, 52). Retaining glycoside hydrolases may perform transglycosylation (53). Hitherto β-mannanases have been classified in glycoside hydrolase families 5 and 26 (see Sec. IX), which have the retaining mechanism. Accordingly, transglycosylation has been observed for several β-mannanases including those from *T. reesei* and *A. niger* (38, 48, 49).

VII. HETEROMANNAN HYDROLYSIS

β-Mannanases also hydrolyze heteromannans. However, their activity is generally restricted by the galactosyl sidegroups and the main-chain glucose residues of the substrate (22). The subsite-binding properties may vary among enzymes of different origin. The major hydrolysis products from incubation of fungal as well as bacterial β-mannanase with heteromannans are mixed oligosaccharides, mannotriose, and mannobiose, sometimes with the production also of mannose (49, 54, 55), as reviewed by Viikari et al. (56). These products are hydrolyzed further by exohydrolases, also secreted by the microorganisms. Thus, the cooperation of several enzymatic activities is needed for the degradation of heteromannans. In addition to β-mannanase (EC 3.2.1.78), α-galactosidase (EC 3.2.1.22) and β-mannosidase (EC 3.2.1.25) are also needed for the complete hydrolysis of galactoglucomannan into monomeric sugars (57, 58). β-Mannosidases hydrolyze terminal nonreducing mannose residues, and α-galactosidases hydrolyze α-1,6-linked galactosyl side groups from oligomeric and sometimes polymeric substrate (59–62). β-Glucosidase (EC 3.2.1.21) may be needed for the hydrolysis of non-reducing-end glucose residues. For the complete hydrolysis of acetylated galactoglucomannan, acetyl esterase is also needed (63, 64).

The pattern of galactomannan hydrolysis and the apparent subsite-binding requirements have been interpreted from structural analysis by NMR of isolated hydrolysis products from the galactomannan and glucomannan incubated with *A. niger* β-mannanase (49). It is suggested that the enzyme has five substrate binding subsites—α, β, γ, δ, and ϵ—which is equivalent to −3, −2, −1, +1, and +2, according to the nomenclature given by Davies et al. (52). Binding to at least four subsites is required for efficient hydrolysis. Substitution of the substrate monomers at two of the subsite positions (but not at the other) restricted hydrolysis, most likely by preventing binding (49). The hydrolysis of pine kraft pulp galactoglucomannan by the *T. reesei* β-mannanase was also studied by NMR analysis of the produced mixed oligosaccharides (55). Judging from this study, the *T. reesei* enzyme also appears to be restricted by galactosyl sidegroups in a similar way to the *A. niger* enzyme. Also, the restriction by the substrate main-chain glucose residues has been studied for some β-mannanases (49, 55).

VIII. MODULAR STRUCTURE OF β-MANNANASES

Glycoside hydrolases like cellulases and hemicellulases commonly have a modular structure. The catalytic modules may be attached to other module(s), such as carbohydrate-binding modules (10). The modules are often connected by linker peptides. Furthermore, as reviewed (10, 45), anaerobic cellulolytic organisms like *Clostridium* spp. frequently form large cell-associated multienzyme complexes. Although several β-mannanases are sole catalytic modules of ∼30–45 kDa (13, 15, 18), some β-mannanases are modular proteins with molecular masses from 50 kDa up to 100 kDa (12, 14, 16, 19, 20, 23, 25, 65). Examples of modular β-mannanases from anaerobes are enzymes which carry an additional endoglucanase catalytic module and cellulose binding modules (12) or putative protein binding modules which may be involved in the formation of multienzyme complexes (19, 65).

Also, some aerobic organisms produce modular β-mannanases (14, 16, 20). The *T. reesei* family 5 β-mannanase has a C-terminal cellulose-binding module (16, 38, 66). Biely and Tenkanen (58) discussed the possibility that the presence of a cellulose-binding module on the *T. reesei* β-mannanase is part of the reason for the superior performance in bleaching experiments for this enzyme (67). The *Cellulomonas fimi* enzyme is the

first β-mannanase reported to contain a mannan-binding module (68). It interacts with galactomannan.

IX. CATALYTIC MODULES OF β-MANNANASES

On the basis of sequence and, where available, structural similarities, the catalytic modules of glycoside hydrolases has been classified into different families by Henrissat et al. (69) (see also http://afmb.cnrs-mrs.fr/~pedro/CAZY/ghf.html). Enzymes in a particular family have a conserved overall fold, conserved catalytic mechanism and conserved catalytic and other residues. Known β-mannanases belong to family 5 or family 26 of glycoside hydrolases; both contain enzymes which have the retaining mechanism. Family 5 and family 26 enzymes belong to the clan GH-A (4/7 β/α-barrel superfamily) of glycoside hydrolases (70).

A. Glycoside Hydrolase Family 5

Family 5 includes several enzymatic activities for which the corresponding genes have been cloned. These are, for example, several endo-1,4-β-glucanases and cellobiohydrolases in addition to β-mannanases. The genes of family 5 β-mannanase have been isolated both from prokaryotes (12–14, 24) and eukaryotes, i.e., from fungi (15, 16) and from a plant—tomato (17). The three-dimensional structure of two β-mannanases of family 5 has been determined (Sec. X) (71, 72). Structures of family 5 enzymes are $(\beta/\alpha)_8$-barrels. Eight residues are conserved, including two catalytic glutamates (73, 74).

B. Glycoside Hydrolase Family 26

Family 26 contains several β-mannanases from bacteria (18–20) and from one species of anaerobic fungi (21) for which the genes have been isolated. Two glutamates have been identified as the putative catalytic residues (75). At least two additional residues are conserved. Crystallization and preliminary x-ray diffraction studies have been reported for a β-mannanase of *Pseudomonas fluorescence* subsp. *cellulosa* (76). Family 26 enzymes have been predicted to belong to the clan GH-A and thus to have the $(\beta/\alpha)_8$-barrel structure (75).

X. STRUCTURES OF β-MANNANASE CATALYTIC MODULES

Generally, endoacting cellulases and hemicellulases are expected to have an active site which is present in a quite open cleft, as is the case for structurally determined family 5 endoglucanases. Judging from the three β-mannanase structures available (71, 72, 76), these enzymes also have roughly this general architecture. These catalytic modules form the *Thermomonospora fusca* and *Trichoderma reesei* β-mannanases belong to family 5 of glycoside hydrolases, and thus both structures are $(\beta/\alpha)_8$-barrels and share the same overall fold. In both β-mannanase structures the two catalytic glutamates are situated in a groove across the surface of the enzymes. As expected, the conserved tryptophan in family 5, probably forming the −1 subsite, is present in both structures. It is unclear if the other subsites also are conserved or similar for the two β-mannanases. For the *T. fusca* enzyme complex structures with mannotriose enabled the identification of subsites −3 and −2 (71). The +1 and +2 subsites were identified for the *T. reesei* β-mannanase (72).

XI. β-MANNANASE ASSAYS

A. Conditions for Catalysis

As previously reviewed (22, 56), generally, compared to bacterial mannanases, fungal β-mannanases have lower pH optima, between ~ 3.0 and 5.5. Among the highest yet reported pH optima for a β-mannanase is pH 9, for the enzyme from an alkalophilic *Bacillus* sp. (46). In many cases, β-mannanases are stable for hours at their optimal pH up to a temperature of at least 50°C. The K_m values reported for *Trichoderma* and *Aspergillus* β-mannanases on locust bean gum varies between 0.0015 to 0.7 g/L (15, 22, 42).

B. Assays Based on Detection of Reducing Sugars Produced by Hydrolysis

The following assay procedure is used for the *Trichoderma reesei* β-mannanase (41), and can be used generally (adjustments of buffer and pH may be needed depending on the enzyme). β-Mannanase activity is assayed using 0.5% (w/v) locust bean gum (SIGMA G-0753). The substrate is suspended in 50 mM citrate or acetate buffer, pH 5.3, by homogenizing at 80°C and heating to the boiling point, cooled, and stored overnight with continuous stirring, then centrifuged and the pellet discarded. The enzyme sample (0.2

mL) is incubated with 1.8 mL substrate solution at 50°C for 5–30 min. The reducing sugars liberated in the enzymatic reaction are assayed by the addition of 3 mL DNS-reagent, boiling for 5 min, cooling, and measuring the absorbance at 540 nm. Recipe for the DNS reagent can be found in Meth Enzymol, Vol 160 (1988), pp 87–112. A standard curve is prepared with D-mannose. The enzymatic activity is given in nanokatals (nkat). An assay based on the quantification of the released reducing sugars using the Somogyi-Nelson copper agent has also been described (22).

C. Assay Based on Detection of Dyed Oligosaccharides Produced by Hydrolysis

Carob galactomannan dyed with Remazol Brilliant Blue R (AZO-carob galactomannan, Megazyme, Wicklow, Ireland) is used as the substrate. After enzyme substrate incubation for 10 min, ethanol is added to stop the reaction and to precipitate high-molecular-weight galactomannan. Low-molecular-weight fragments stay soluble and can be spectrophotometrically quantified at 590 nm, due to the attached dye (22). This assay is relative. To relate to enzyme activity units, a standard curve (supplied by Megazyme for each batch of substrate) with known enzyme amounts should be prepared.

D. Zymogram

After running a protein sample with isoelectric focusing (IEF), bands with β-mannanase activity can be identified by the use of 2% agar overlay gel (2 mm thick) containing 0.5% locust bean gum (41). When the IEF is done the overlay gel is incubated with the separation gel at 50°C for 45 min; then the overlay gel is stained with 0.1% Congo Red solution and destained with 1 M NaCl. β-Mannanase activity appears as clearing zones. The overlay gel should be made in a 50-mM buffer with a pH suitable for enzyme activity and stability (50 mM citrate, pH 5.3, for the *T. reesei* and *A. niger* β-mannanases). The method also works with native polyacrylamide gel electrophoresis. Zymograms can also conveniently be made with AZO-carob galactomannan (20).

E. Plate Assays

β-Mannanase activity secreted from bacterial or yeast colonies can be detected by growing the microorganisms on agar plates containing 0.5% locust bean gum (16). After making replicas, the microorganism is carefully washed off and the plate is incubated with 0.1% Congo Red solution, then destained with 1 M NaCl. β-Mannanase activity is detected as clear halos. Locust bean gum dyed with Remazol Brilliant Blue R can also be used for detection of clones with β-mannanase (24). β-Mannanase activity in single plant seeds can be detected by the plate assay using locust bean gum and Congo Red staining (77).

F. Assays of Other Enzymes Active on Heteromannans

The exoglucosidases α-galactosidase, β-mannsosidase, and β-glucosidase can be assayed using colorimetric detection using nitrophenylglycosides as the substrate, as described for example by Rättö and Poutanen (40).

XII. APPLICATIONS OF β-MANNANASES

β-Mannanases have several potential and existing applications in particular in the food and feed, pulp, and paper industries. The industrial applications have been reviewed by several authors (56, 78, 79). β-Mannanase can solubilize softwood pulp mannan (80, 81) and can be used as an aid in pulp bleaching (67, 80, 82). Improvement of animal feed with β-mannanase has been reported (83). Coffee beans contain heteromannan which is extractable with hot water from the roasted bean (84). Extracted green coffee bean mannan has been hydrolyzed with β-mannanase (85). A potential application for β-mannanase is to reduce the viscosity of the extract during production of instant coffee (78). β-Mannanase and other hemicellulases may also be used to reduce the viscosity of pineapple juice during processing (86). Over the past few years, attention has been directed toward endogenous β-mannanase in plant seed germination (27). Furthermore, β-mannanases may be used in the conversion of biomass and for the hydrolysis and modification of polysaccharides. The potential application of β-mannanase in the hydrolysis of galactomannan-based fluids used in oil and gas well stimulation has been shown (87).

Other hemicellulases, endo-1,4-β-xylanases, have after a relatively short time of research and development, reached major applications especially in pulp bleaching (88) and in cereal processing (89). Increased attention for β-mannanases will likely open up new applications for these enzymes.

REFERENCES

1. TE Timell. Recent progress in the chemistry of wood hemicellulose. Wood Sci Technol 1:45–70, 1967.
2. E Sjöström. Wood Chemistry. Fundamentals and Applications, 2nd ed. San Diego: Academic Press, 1993.
3. H Meier, JSG Reid. Reserve polysaccharides other than starch in higher plants. In FA Loewus, W Tanner, eds. Encyclopaedia of Plant Physiology, Vol 13A. Berlin: Springer-Verlag, 1982, pp 418–471.
4. PA Hui, H Neukom. Properties of galactomannas. Tappi 47:39–42, 1964.
5. BV McCleary. Carob and guar galactomannans. Methods Enzymol 160:523–527, 1988.
6. AM Goldstein, EN Alter, JK Seaman. Guar gum. In: RL Whistler, ed. Industrial Gums, Polysaccharides and Their Derivatives, 2nd ed. New York: Academic Press, 1973, pp 303–321.
7. E Rol. Locust bean gum. In: RL Whistler, ed. Industrial Gums, Polysaccharides and Their Derivatives, 2nd ed. New York: Academic Press, 1973, pp 323–337.
8. ER Morris. Mixed polymers gels. In: P Harris, ed. Food Gels. London: Elsevier Applied Science, 1990, pp 291–359.
9. ET Reese, Y Shibata. β-Mannanases of fungi. Can J Microbiol 11:167–183, 1965.
10. RAJ Warren. Microbial hydrolysis of polysaccharides. Annu Rev Microbiol 50:183–212, 1996.
11. D Klein, DE Eveleigh. Ecology of *Trichoderma*. In; GE Harman, CP Kubicek, eds. *Trichoderma* and *Gliocladium*, Vol 1. Basic Biology, Taxonomy and Genetics. London: Taylor and Francis, 1998, pp 57–74.
12. MD Gibbs, DJ Saul, E Luthi, PL Bergquist. The beta-mannanase from '*Caldocellum saccharolyticum*' is part of a multidomain enzyme. Appl Environ Microbiol 58:3864–3867, 1992.
13. N Arcand, D Kluepfel, FW Paradis, R Morosoli, F Shareck. β-Mannanase of *Streptomyces lividans* 66: cloning and DNA sequence of the manA gene and characterization of the enzyme. Biochem J 290:857–863, 1993.
14. A Sunna, MD Gibbs, CWJ Chin, PJ Nelson, PL Bergquist. A gene encoding a novel multidomain beta-1,4-mannanase from *Caldibacillus cellulovorans* and action of the recombinant enzyme on kraft pulp. Appl Environ Microbiol 66:664–670, 2000.
15. S Christgau, S Kauppinen, J Vind, LV Kofod, H Dalboge. Expression cloning, purification and characterisation of a β-1,4-mannanase from *Aspergillus aculeatus*. Biochem Mol Int 33:917–925, 1994.
16. H Stålbrand, A Saloheimo, J Vehmaanperä, B Henrissat, M Penttilä. Cloning and expression in *Saccharomyces cerevisiae* of a *Trichoderma reesei* β-mannanase gene containing a cellulose binding domain. Appl Env Microbiol 61:1090–1097, 1995.
17. JD Bewley, RA Burton, Y Morohashi, GB Fincher. Molecular cloning of a cDNA encoding 1,4-β-mannan endohydrolase from the seeds of germinated tomato (*Lycopersicon escolentum*). Planta 203:454–459, 1997.
18. KL Braithwaite, GW Black, GP Hazlewood, BR Ali, HJ Gilbert. A non-modular endo-β-1,4-mannanase from *Pseudomonas fluorescens* subspecies *cellulosa*. Biochem J 305:1005–1010, 1995.
19. JR Halstead, PE Vercoe, HJ Gilbert, K Davidson, GP Hazlewood. A family 26 mannanase produced by *Clostridium thermocellum* as a component of the cellulosome contains a domain which is conserved in mannanases from anaerobic fungi. Microbiology 145(Pt 11):3101–3108, 1999.
20. D. Stoll, H Stålbrand, RAJ Warren. Mannan-degrading enzymes from *Cellulomonas fimi*. Appl Env Microbiol 65:2598–2605, 1999.
21. SJ Millward-Sadler, J Hall, GW Black, GP Hazlewood, HJ Gilbert. Evidence that the *Piromyces* gene family encoding endo-1,4-mannanases arose through gene duplication. FEMS Microbiol Lett 141:183–188, 1996.
22. BV McCleary. β-D-mannanase. Methods Enzymol 160:596–610, 1988.
23. MD Gibbs, AU Elinder, RA Reeves, PL Bergquist. Sequencing, cloning and expression of a β-1,4-mannanase gene, manA, from the extremely thermophilic anaerobic bacterium, *Caldicellulosiruptor* Rt8B.4. FEMS Microbiol Lett 141:37–43, 1996.
24. N Ethier, G Talbot, J Sygusch. Gene cloning, DNA sequencing, and expression of thermostable β-mannanase from *Bacillus stearothermophilus*. Appl Env Microbiol 64:4428–4432, 1998.
25. JK Cann,S Kocherginskaya, MR King, BA White, RI Mackie. Molecular cloning, sequencing, and expression of a novel multidomain mannanase gene from *Thermoanaerobacterium polysaccharolyticum*. J Bacteriol 181:1643–1651, 1999.
26. LMA Dirk, AM Griffen, B Downie, JD Beweley. Multiple isozymes of endo-β-mannanase in dry and imbibed seeds. Phytochemistry 40:1045–1056, 1995.
27. GE Welbaum, KJ Bradford, KO Yim, DT Both, MO Oluoch. Biophysical, physiological and biochemical processes regulating seed germination. Seed Sci Res 8:161–172, 1998.
28. PE Toorop, JD Bewley, HWM Hilhorst. Endo-β-mannanase isoforms are present in the endosperm and embryo of tomato seeds, but are not essentially linked to the completion of germination. Planta 200:153–158, 1996.
29. B Boigt, JD Bewley. Developing tomato seeds when removed from the fruit produce multiple forms of germinative and post-germinative endo-β-mannanase.

Responses to desiccation, abscisic acid and osmoticum. Planta 200:71–77, 1996.
30. H Nonogaki, Y Morohashi. An endo-β-mannanase develops exclusively in the micropylar endosperm of tomato seeds prior to radivle emergence. Plant Physiol 110:555–559, 1996.
31. JF Giorgini, E Comoli. Effect of embryo and exogenous GA3 on endospermic endo-β-mannanase activity of *Coffea arabica* L. during germination and early seedling growth. Rev Bras Fysiol Veg 8:43–49, 1996.
32. F Kontos, CG Spyropoulos. Effect of linoleic, linolenic and jasmonic acid on the production of α-galactosidases and endo-β-mannanase in the endosperms of carob and fenugreek seeds. J Plant Physiol 149:629–632, 1996.
33. TN Prabha, N Bhagylakshmi. Carbohydrate metabolism in ripening banana fruit. Phytochemistry 48:915–919, 1998.
34. LH de Graaff, HC van den Broeck, AJ van Ooijen, J Visser. Regulation of the xylanalase-encoding *xlnA* gene of *Aspergillus tubigensis*. Mol Microbiol 12:479–490, 1994.
35. J Strauss, RL Mach, S Zeilinger, G Hartler, G Stöffler, M Wolshek, CP Kubicek. Cre1, the carbon catabolite repressor protein from *Trichoderma* reesei. FEBS Lett 376:103–107, 1995.
36. E Margolles-Clark, M Ilmen, M Penttilä. Expression patterns of ten hemicellulase genes of the filamentous fungus *Trichoderma reesei* on various carbon sources. J Biotechnol 57:167–179, 1997.
37. CP Kubicek, ME Penttilä. Regulation of production of plant polysaccharide degrading enzymes by *Trichoderma*. In: GE Harman, CP Kubicek, eds. *Trichoderma* and *Gliocladium*, Vol 2, Enzymes, Biological Control and Commercial Applications. London: Taylor and Francis, 1998, pp 49–72.
38. P Ademark, A Varga, J Medve, V Harjunpää, T Drakenberg, F Tjerneld, H Stålbrand. Soft-wood hemicellulose-degrading enzymes from *Aspergillus niger*: purification and properties of a β-mannanase. J Biotechnol 63:199–210, 1998.
39. Torrie, JP, DJ Senior, JN Saddler. Production of β-mannanase by *Trichoderma harzianum* E58. Appl Microbiol Biotechnol 34:303–307, 1990.
40. M Rättö, K Poutanen. Production of mannan-degrading enzymes. Biotechnology Lett 10:661–664, 1988.
41. H Stålbrand, M Siika-aho, M Tenkanen, L Viikari. Purification and characterization of two β-mannanases from *Trichoderma reesei*. J Biotechnol 29:229–242, 1993.
42. I Arisan-Atac, R Hodits, D Kristufek, CP Kubicek. Purification and characterization of a β-mannanase of *Trichoderma reesei* C-30. Appl Microbiol Biotechnol 39:58–62, 1993.
43. A Sachslehner, B Nidetsky, KD Kulbe, D Haltrich. Induction of mannanase, xylanase, and endoglucanase activities in *Sclerotium rofsii*. Appl Environ Microbiol 64:594–600, 1998.
44. L Kremnicky, P Biely. β-Mannanolytic system of *Aureobasidium pullulans*. Arch Microbiol 167:350–355, 1997.
45. P Beguin, JP Aubert. The biological degradation of cellulose. FEMS Microbiol Rev 13:25–58, 1994.
46. T Akino, N Nakamura, K Horikoshi. Characterisation of three β-mannanases of an alkalophilic *Bacillus* sp. Agric Biol Chem 52:773–779, 1988.
47. GM Gubitz, W Schnitzhofer, Balakrishnan, W Steiner. Two mannanases from *Sclerotium rolfsii* in total chlorine free bleaching of softwood kraft pulp. J Biotechnol 50:181–188, 1996.
48. V Harjunpää, A Teleman, M Siika-aho, T Drakenberg. Kinetic and stereochemical studies of manno-oligosaccharide hydrolysis catalysed by β-mannanase from *Trichoderma reesei*. Eur J Biochem 234:278–283, 1995.
49. BV McCleary, NK Matheson. Action patterns and substrate-binding requirements of β-D-mannanase with mannosaccharides and mannan-type polysaccharides. Carbohydr Res 119:191–219, 1983.
50. N Torto, G Marko-Varga, L Gorton, H Stålbrand, F Tjerneld. On-line quantitation of enzymatic mannan hydrolysates in small-volume bioreactors by microdialysis sampling and column liquid chromatography-integrated pulsed electrochemical detection. J Chromatogr 725:165–175, 1996.
51. G Davies, B Henrissat. Structures and mechanisms of glycosyl hydrolases. Structure 3:853–859, 1995.
52. G Davies, ML Sinnott, SG Withers. Glycosyl transfer. Comp Biol Catal 1:119–209, 1998.
53. GJ Davies, LF MacKenzie, A Varrot, M Dauter, AM Brzozowski, M Schuelein, SG Withers. Snapshots along an enzymatic reaction coordinate: analysis of a retaining β-glycoside hydrolase. Biochemistry 37:11707–11713, 1998.
54. GG Park, HG Chang. Separation and preparation of galactosylmanno-oligosaccharides from copra galactomannan by mannanase from *Penicillium purpurogenum*. J Microbiol Biotechnol 2:204–208, 1992.
55. M Tenkanen, M Makkonen, M Perttula, L Viikari, A Teleman. Action of *Trichoderma reesei* mannanase on galactoglucomannan in pine kraft pulp. J Biotechnol 57:191–204, 1997.
56. L Viikari, M Tenkanen, J Buchert, M Rättö, M Bailey, M Siika-aho, M Linko. Hemicellulases for industrial applications. In: JN Saddler, eds. Bioconversion of Forest and Agricultural Plan Residues. Wallingford: CAB International, 1993, pp 131–182.
57. K-EL Eriksson, RA Blachette, P Ander. Microbial and Enzymatic Degradation of Wood and Wood Components. Berlin: Springer-Verlag, 1990.

58. P Biely, M Tenkanen. Enzymology of hemicellulose degradation. In: GE Harman, CP Kubicek, eds. Trichoderma and Gliocladium, Vol 2. Enzymes, Biological Control and Commercial Applications. London: Taylor and Francis, 1998, pp 25–47.
59. E Margolles-Clark, M Tenkanen, E Luonteri, M Penttilä. Three α-galactosidase genes of *Trichoderma reesei* cloned by expression in yeast. Eur J Biochem 240:104–111, 1996.
60. P Manzanares, LH de Graaff, J Visser. Characterisation of galactosidase from *Aspergillus niger*, purification of novel α-galactosidase activity. Enz Microb Technol 22:383–390, 1998.
61. P Ademark, J Lundqvist, P Hägglund, M Tenkanen, N Torto, F Tjerneld, H Stålbrand. Hydrolytic properties of a β-mannosidase purified from *Aspergillus niger*. J Biotechnol 75:281–289, 1999.
62. P Ademark, R de Vries, H Stålbrand, J Visser. Cloning and characterisation of *Aspergillus niger* genes encoding an α-galactosidase and a β-mannosidase involved in galactomannan degradation. Eur J Biochem 268:2982–2990, 2001.
63. J Puls, J Schuseil. Chemistry of hemicelluloses: relationship between hemicellulose structure and enzymes required for hydrolysis. In: MP Coughlan, GP Hazlewood, eds. Hemicellulose and Hemicellulases. Portland Press Research Monograph IV. London: Portland Press, 1993, pp 1–27.
64. M Tenkanen, J Thornton, L Viikari. An acetylglucomannan esterase of *Aspergillus oryzae*; purification, characterization and role in the hydrolysis of O-acetyl-galactoglucomannan. J Biotechnol 42:197–206, 1995.
65. C Fanutti, T Ponyi, GW Black, GP Hazlewood, HJ Gilbert. The conserved noncatalytic 40-residue sequence in cellulases and hemicellulases from anaerobic fungi functions as a protein docking domain. J Biol Chem 270:29314–29322, 1995.
66. M Tenkanen, J Buchert, L Viikari. Binding of hemicellulases on isolated polysaccharide substrates. Enzyme Microb Technol 17:499–505, 1994.
67. A Suurnäkki, T Clark, R Allison, J Buchert, L Viikari. Mannanase aided bleaching of soft-wood kraft pulp. In K Messner and E Srebotnik, eds. Biotechnology in Pulp and Paper Industry—Advances in Applied and Fundamental Research. Vienna: WUA Universitäts Verlag, 1996, pp 69–74.
68. D Stoll, A Boraston, H Stålbrand, BW McClean, DG Kilburn, RAJ Warren. Mannanase Man 26A from *Cellulomonas fimi* has a mannan binding module. FEMS Microbiol Lett 183:265–269, 2000.
69. B Henrissat, A Bairoch. New families in the classification of glycosyl hydrolases based on amino-acid sequences similarities. Biochem J 293:781–788, 1993.
70. J Jenkins, LL Legio, G Harris, R Pickersgill. β-Glucosidase, β-galactosidase, family A cellulases, family F xylanases, and two barley glycanases form a superfamily of enzymes with 8-fold β/α architecture and with two conserved glutamates near the carboxy terminal ends of β-strands four and seven. FEBS Lett 362:281–285, 1995.
71. M Hilge, SM Gloor, W Rypniewski, O Sauer, TD Heightman, W Zimmerman, K Winterhalter, K Piontek. High resolution native and complex structures of thermostable β-mannanase from *Thermomonospora fusca*—substrate specificity in glycosyl hydrolase family 5. Structure 6:1433–1444, 1998.
72. E Sabini, H Schubert, G Murshudov, KS Wilson, M Siika.aho, M Penttilä. The three-dimensional structure of a *Trichoderma reesei* β-mannanase from glycoside hydrolase family 5. Acta Cryst D56:3–13, 2000.
73. R Macarron, J van Beeuman, B Henrissat, I de la Mata, M Claeyssens. Identification of an essential glutamate residue in the active site of endoglucanase III from *Trichoderma reesei*. FEBS Lett 316:137–140, 1993.
74. Q Wang, D Tuyll, A Meinke, NR Gilkes, RAJ Warren, R Aebersold, SG Withers. Glu280 is the nucleophile in the active site of *Clostridium thermocellum* CelC, a family A endo-β-1,4-glucanase. J Biol Chem 268:14096–14102, 1993.
75. DN Bolam, N Hughes, R Virden, JH Lakey, GP Hazlewood, B Henrissat, KL Braithewaite, HJ Gilbert. Mannanase A from *Pseudomonas fluorescens* ssp. *cellulosa* is a retaining glycosyl hydrolase in which E212 and E320 are the putative catalytic residues. Biochemistry 35:16195–16204, 1996.
76. D Hogg, EJ Woo, DN Bolam, VA McKie, HJ Gilbert, RW Pickersgill. Crystal structure of mannanase 26A from *Pseudomonas cellulosa* and analysis of residues involved in substrate binding. J Biol Chem 276:31186–31192, 2001.
77. DW Still, P Dahal, KJ Bradford. A single seed assay for endo-β-mannanase activity from tomato endosperm and radicle tissues. Plant Physiol 113:13–20, 1997.
78. KKY Wong, JN Saddler. Applications of hemicellulases in the food, feed and pulp and paper industries. In: MP Coughlan, GP Hazlewood, eds. Hemicellulose and Hemicellulases. Portland Press Research Monograph IV. London: Portland Press, 1993, pp 127–144.
79. J Buchert, T Oksanen, J Pere, M Siika-aho, A Suurnäkki, L Viikari. Applications of *Trichoderma reesei* enzymes in the pulp and paper industry. In: GE Harman, CP Kubicek, eds. *Trichoderma* and *Gliocladium*, Vol 2. Enzymes, Biological Control and Commercial Applications. London; Taylor and Francis, 1998, pp 343–363.
80. TA Clark, AG McDonald, DJ Senior, PR Mayers. Mannanase and xylanase treatment of softwood chemical pulps: effects on pulp properties and bleachabil-

ity. In: KT Kirk, H-M Chang, eds. Biotechnology in the Pulp and Paper Manufacture. Boston: Butterworth-Heinemann, 1990, pp 153–167.
81. M Rättö, M Siika-aho, J Buchert, A Valkeajärvi, L Viikari. Enzymatic hydrolysis of isolated and fibre-bound galactoglucomannans from pine-wood and pine kraft pulp. Appl Microbiol Biotechnol 40:449–454, 1993.
82. J Buchert, J Salminen, M Siika-aho, M Ranua, L Viikari. The role of *Trichoderma reesei* xylanase and mannanase in the treatment of softwood kraft pulp prior to bleaching. Holzforschung 47:473–478, 1993.
83. R James, J McNaughton, D Fodge. Improved use by turkeys of corn-soy diets with β-mannanase. Poult Sci 77:153, 1998.
84. L Navarini, R Gilli, V Gombac, A Abatangelo, M Bosco, R Toffanin. Polysaccharides from hot water extracts of roasted *Coffea arabica* beans: isolation and characterisation. Carbohydr Polym 40:71–81, 1999.
85. A Sachlehner, G Foidl, G Foidl, G Gubitz, D Haltrich. Hydrolysis of isolated coffee mannan and coffee extract by mannanases of *Sclerotium rolfsii*. J Biotechnol 80:127–134, 2000.
86. C Grassin, P Fauquembergue. Application of pectinases in beverages. In: J Visser, AGJ Voragen, eds. Progress in Biotechnology 14: Pectin and Pectinases. Amsterdam: Elsevier, 1996, pp 453–462.
87. CM McCutchen, GD Duffaud, P Leduc, ARH Petersen, A Tayal, A Khan-Saad, RM Kelly. Characterization of extremely thermostable enzymatic breakers (α-1,6-galactosidase and β-1,4-mannanase) from the hyperthermophilic bacterium *Thermotoga neapolitana* 5068 for hydrolysis of guar gum. Biotechnol Bioeng 52:332–339, 1996.
88. L. Viikari, A Kantelinen, J Sundquist, M Linko. Xylanases in bleaching: From an idea to the industry. FEMS Microbiol Rev 13:335–350, 1994.
89. K Poutanen. Enzymes: an important tool in the improvement of the quality of cereal foods. Trends Food Sci Technol 8:300–306, 1997.

76

Lysozyme

Akio Kato
Yamaguchi University, Yamaguchi, Japan

I. INTRODUCTION

Fleming found the lytic action of human nasal mucus and tear on *Micrococcus* cells in 1922 and he reported the similar lytic action of egg white constituent on Gram-positive bacteria. He proposed the name lysozyme for the enzyme and *Micrococcus lysodeikticus* for the organism serving as the substrate (1). Lysozyme cleaves the β-(1,4)-glycoside linkages between N-acetylglucosamine and muramic acid in bacterial cell wall and chitin or other oligomers. In addition to glycosidase activity, this enzyme has transglycosylation activity (2) and esterase activity (3). Thus, numerous names have been proposed for this enzyme. The Commission on Enzyme Nomenclature in 1964 recommended "E.C. 3.2.1.17. Systematic name: mucopeptide N-acetylmuramyl hydrolase; trivial name: mucopeptide glucohydrolase, lysozyme." Lysozyme is easily crystallized from chicken egg white, and a large amount of the enzyme can be obtained. Therefore, lysozyme has been one of the most intensively investigated and characterized enzymes.

II. LYSOZYME IN FOODS

Lysozyme exists abundantly in chicken egg white and constitutes 3.5% of the total egg white proteins when calculated on the basis of lytic activity. Since lysozyme interacts with ovomucin gel in egg white, the content may be $> 3.5\%$. The lysozyme activity in hen egg white decreases during storage of egg dependent on the temperature, as shown in Figure 1. The activity is retained $> 80\%$ during storage at low temperature for 1 week, while it is decreased $< 60\%$ during storage at room temperature for 1 week (4). The loss of lysozyme activity results from the increases in pH during storage of egg. The pH increases up to 9.3 within several days' storage at room temperature. On the other hand, lysozyme is stable in acidic pH in the presence of CO_2 gas, as shown in Figure 1. Lysozyme interacts with ovomucin in thick egg white. It is well known that the interaction is responsible for the gel structure of thick egg white (5). The ovomucin-lysozyme interaction decreases with egg white thinning.

III. UTILIZATION OF LYSOZYME IN FOODS

Hen egg white lysozyme is utilized as a food preservative with antimicrobial effects without any food toxicities. The bactericidal action of lysozyme is intensive on Gram-positive bacteria but much weaker on Gram-negative bacteria, because the former expose the cell wall consisting of peptidoglycan, while the latter has a unique cell envelope, which consists of the outer membrane, inner membrane, and peptidoglycan layer. Therefore, the perturbation of the outer membrane structure is needed to enhance the susceptibility to lysozyme of the peptidoglycan layer in Gram-negative bacteria. Despite this disadvantage, lysozyme is generally used as a food antiseptic. The antimicrobial action may be efficient on Gram-positive bacteria but ineffi-

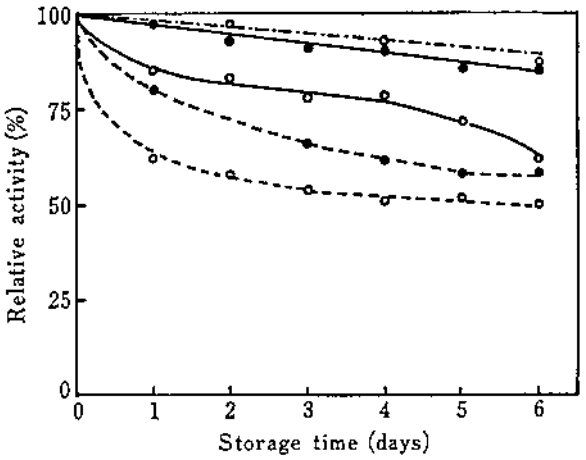

Figure 1 Effects of the temperature and pH on the relative activity of lysozyme in egg white during storage. ●—●, 5°C (final pH 9.0); ○—○, 20°C (final pH 9.3); ●- - -●, 30°C (final pH 9.4); ○- - -○, 40°C (final pH 9.5); ○— - —○, stored in an atmosphere of CO_2 at 30°C (final pH 6.5). (From Ref. 4.)

cient on Gram-negative bacteria. Some attempts to enhance the antimicrobial action for Gram-negative bacteria have been done by our colleagues. Ibrahim et al. in 1991 found that the covalent attachment of palmitic acid residues to the lysyl residues of lysozyme greatly enhanced the bactericidal action on *E. coli* (6). Nakamura et al. in 1991 reported that the Maillard-type lysozyme-polysaccharide conjugate also enhanced the bactericidal action on various Gram-negative bacteria (7). The antimicrobial action of lysozyme-dextran conjugate is shown in Figure 2. The bactericidal action is enhanced by heating at 50°C. The polysaccharide attachment seems to stabilize lysozyme and to have stronger affinity to the outer membrane of Gram-negative bacteria. These modified lysozymes can be used as food antiseptics effective on various bacteria.

IV. PROPERTIES AS PROTEIN

Lysozyme consists of 129 amino acids and the molecular weight is 14,307 daltons. The protein contains many more basic amino acids (11 arginines and six lysines) than acidic amino acids (six aspartic acids and two glutamic acids), and the isoelectric point is 11.2. The amino acid and nucleotide sequences of prelysozyme are shown in Figure 3. The sequence −1 to −18 is the signal peptide, and the N-terminus of mature lysozyme is the position 1 (lysine). Lysozyme has four disulfide bonds: Cys6–127, Cys30–115, Cys64–80, and Cys76–94. Human lysozyme, which consists of 130 amino acids, is very similar to hen egg white lysozyme in its primary and tertiary structures and the positions of

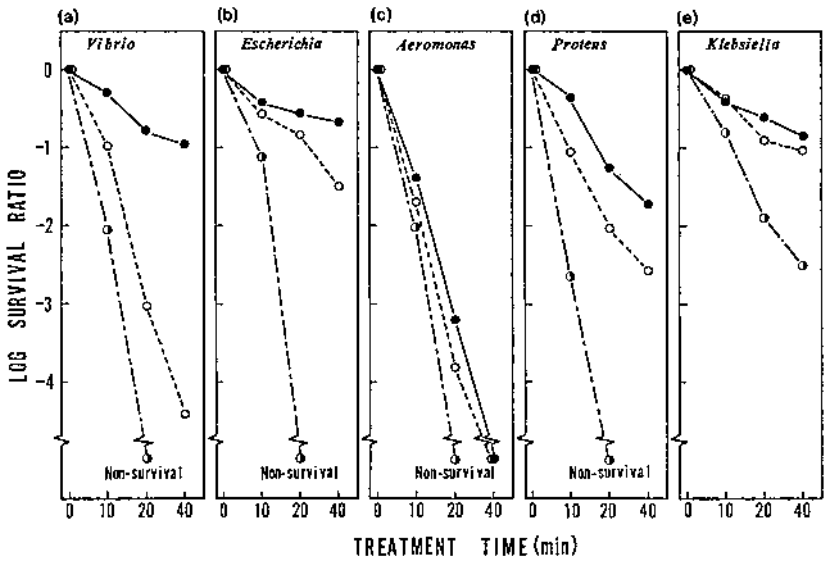

Figure 2 Antimicrobial activity of lysozyme-dextran conjugate for five Gram-negative bacteria. (a) *V. parahaemolyticus* IFO 12713; (b) *E. coli* IFO 12713; (c) *A. hydrophila* IFO 13286; (d) *P. mirabilis* IFO 12668; (e) *K. pneumoniae* IFO 14438. ●, Control (medium without lysozyme or conjugate); ○, addition of 0.05% lysozyme; ◑ addition of 0.05% lysozyme-dextran conjugate. The abscissa is the heating time at 50°C. (From Ref. 7.)

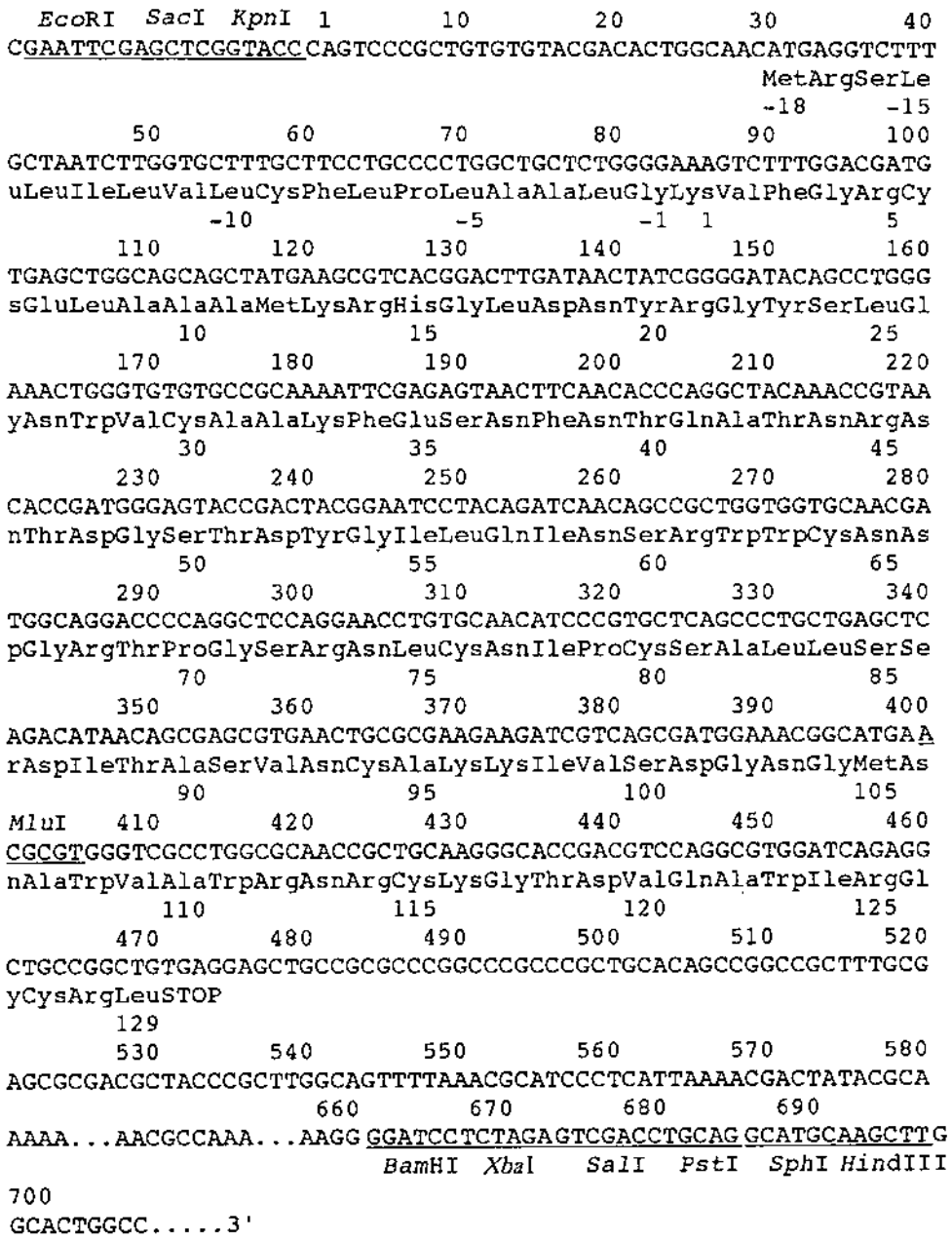

Figure 3 Amino acid and nucleotide sequences of hen egg white pre-lysozyme. The cDNA is inserted between *Kpn*1 and *Bam*H1 in pUC18. Numbering of the nucleotide sequence starts at the most likely position for the 5′ end of mRNA derived from the sequence of the genomic clone. The Met (−18) to Gly (−1) is the signal peptide and correctly processed in eukaryote cell, resulting in the N-terminal lysine.

disulfide bonds. α-Lactalbumin, which consists of 123 amino acids, is also homologous to lysozyme in its primary and tertiary structure and in the position of disulfide bonds. The x-ray analysis of hen egg white lysozyme was carried out by Blake et al. in 1965 as the first enzyme to have its tertiary structure determined by x-ray crystallography (8). The ribbon drawing model is shown in Figure 4. As shown in Figure 4, it divides the molecule into two parts—a predominantly helical core, and an irregular β-strand core. The helical core consists of four α-helices (5–15, 25–35, 88–99, and 108–115), and the β-strand core consists of three β-

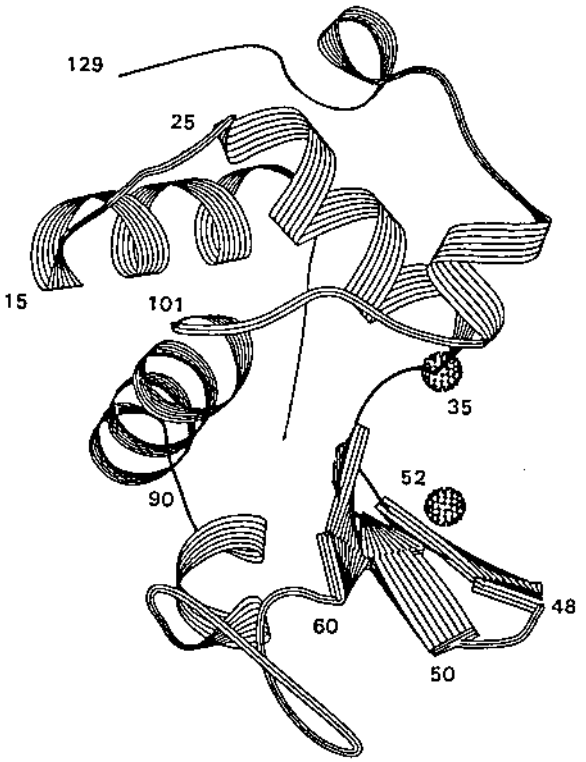

Figure 4 Ribbon drawing model of hen egg white lysozyme. The two catalytic residues, glutamic acid 35 and aspartic acid 52, are represented as small spheres.

strand regions (38–46, 50–54, and 57–60). The two structural domains (α and β) of lysozyme appears to be formed prior to docking of the domains to generate the native closed-packed structure (9). The α domain forms persistent structure during folding more rapidly than the β domain. In addition to a α-helical domain, lysozyme contains two 3^{10} helices (79–84 and 119–124).

V. PROPERTIES AS ENZYME

The most striking feature of the molecule is the crevice running across the waist of the egg-shaped molecule. The crevice is the active site of lysozyme which has the binding area for the substrate of hexasaccharide (N-acetylglucosamine/N-acetylmuramic acid)$_3$. The space-filling CPK model of lysozyme (left) and its interaction with substrate are shown in Figure 5 (10). The substrate is compactly bound to the crevice of the lysozyme molecule. A schematic view of the substrate hexamer, NAG-NAM-NAG-NAM-NAG-NAM, and its interactions with the enzyme are shown in Figure 6 (10). The view is nearly straight into the crevice, with the heavy edges of the sugar rings on the exterior. The site of catalysis was identified to be between D and E rings. When a search was made in the vicinity of the D/E ring for possible cat-

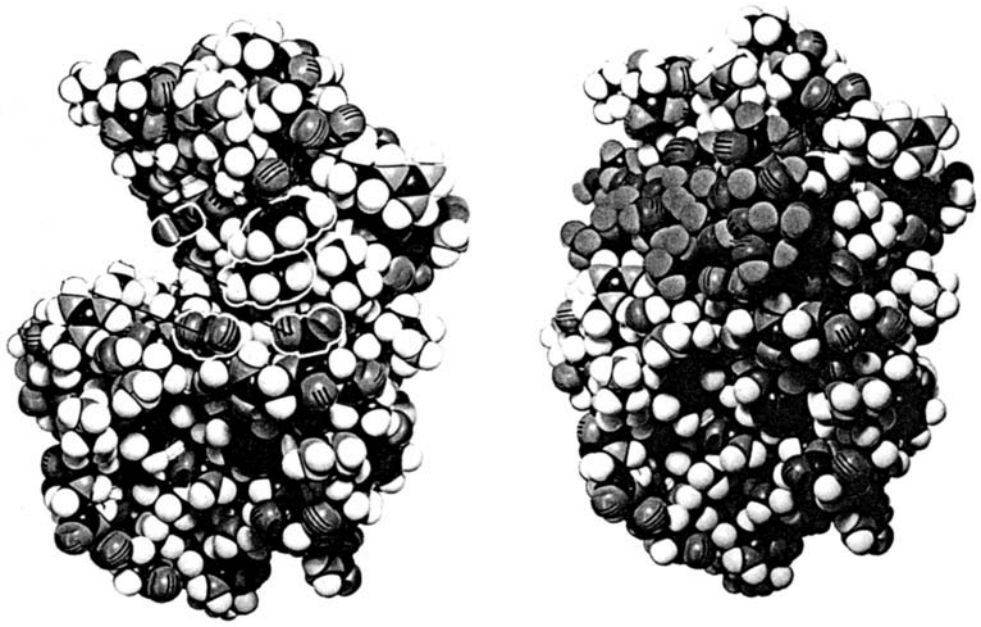

Figure 5 Space-filling CPK model of hen egg white lysozyme. Left: Enzyme without substrate, showing active site crevice. Right: Enzyme-substrate complex, with hexamer NAG substrate. (From Ref. 10.)

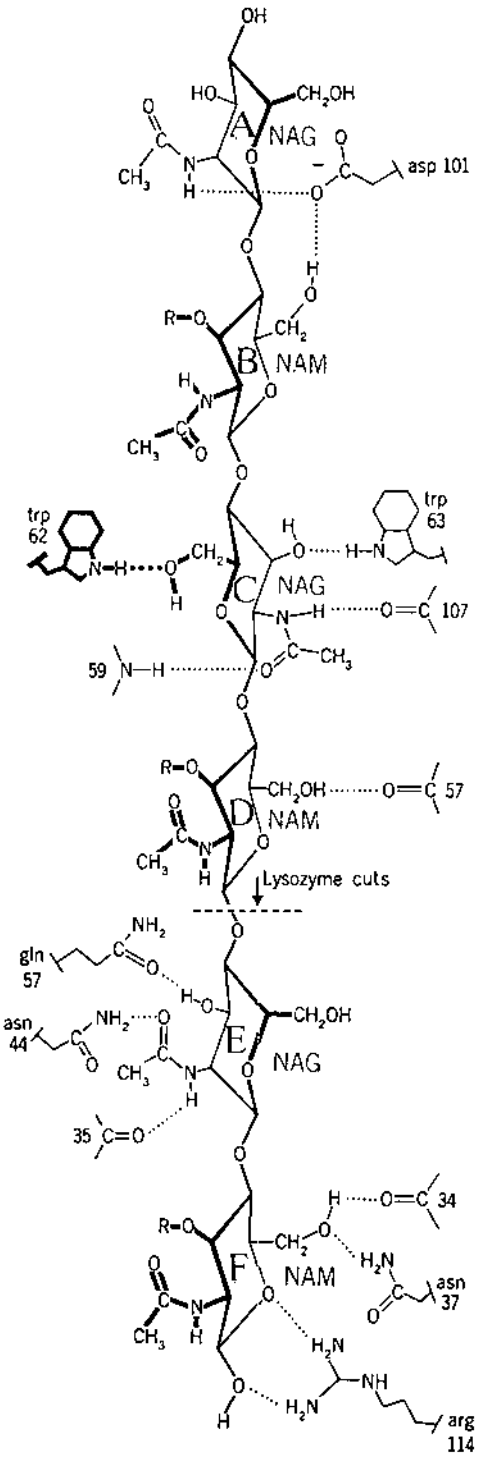

Figure 6 Substrate interactions with the active crevice in lysozyme. The dark edges of the carbohydrate rings are exposed to the outside, and the lighter ones are buried at the crevice bottom. (From Ref. 10.)

alytic groups, two candidates came to light: Asp52, in a polar environment where it will be ionized, and Glu35, in largely hydrophobic surroundings where it might easily remain protonated. The mechanism of cleavage of the polysaccharide bond in lysozyme is suggested as shown in Figure 7 (10). The proton of Glu35 first attacks the linkage oxygen and weakens the C_1-O bond (a). If the bond is cleaved, ring D forms a carbonium ion. The nearby charged Asp52 helps to stabilize the carbonium ion (b). The Glu35 proton is replaced by another from an ionizing water molecule, and the resultant hydroxyl ion then attacks the carbonium ion and completes the reaction (c). This proposal of Phillips and coworkers (11–13) has been supported by a number of chemical and kinetic experiments.

The enzyme activity of lysozyme can be easily measured by the lytic action on *M. lysodeikticus* (*M. luteus*). However, the change in the turbidity of *M. luteus* does not necessarily reflect the real enzyme activity, because the lysis is a rupture of the bacterial cell wall and is not equal to the cleavage of glycosidic bonds. Nevertheless, the lytic action is generally used for the measurement of lysozyme activity because of the ease of the assay. The decrease in the turbidity of the suspension of *M. luteus* cell wall is followed by the absorbance at OD_{450} and the enzyme activity can be represented as the initial rate. In order to get a linear curve for the decrease, a small amount of lysozyme (4 μg) should be added into the cell suspension ($OD_{450} = 0.7$). When the enzyme reaction is done at room temperature for 1 min, a linear decrease curve is obtained and used to determine the initial rate. The optimal pH is ~ 7.0 using lytic activity. On the other hand, when the activity is measured using synthetic substrates, *p*-nitrophenyl N-acetylglucosamine oligomer (14) and glycol chitin (15), the optimal pH is 5 and 5.3, respectively. Therefore, the optimal pH of lytic activity is different from that of the glycosidic activity. The glycosidic activity is determined by measuring the reducing power produced by the glycolysis of ethylene glycol chitin (15). One milliliter of 0.5% ethylene glycol chitin is added to 0.5 mL lysozyme solution in sodium acetate buffer (pH 4.5). The mixture is incubated at 40°C for 30 min. After the reaction, 2 mL of the color reagent (prepared by dissolving 0.5 g potassium ferricyanide in 1 L of 0.5 M sodium carbonate) is added and the mixture is immediately boiled for 15 min to estimate the reducing power resulting from the hydrolysis of ethylene glycol chitin.

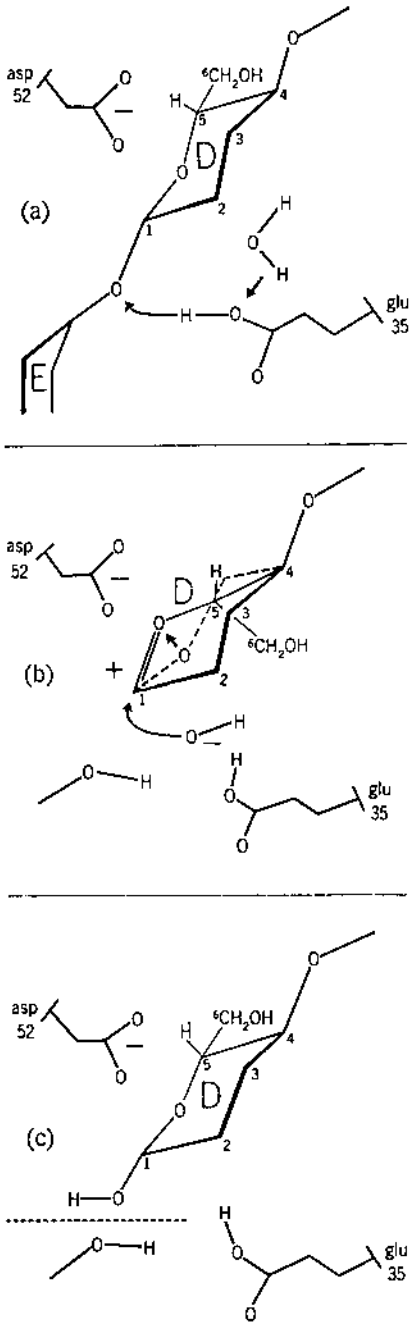

Figure 7 Mechanism of cleavage of the polysaccharide bond in lysozyme. (From Ref. 10.)

VI. PURIFICATION OF LYSOZYME

Lysozyme is easily crystallized from fresh chicken egg white. A 5% sodium chloride (w/w) is added to the homogenized egg white adjusted to pH 9.5–9.8. The egg white is stirred for 48 h at 4°C. The resulting crystals are collected and solubilized in a half-volume of acetate buffer (pH 4.5). The solution is recrystallized at least five times. Thus, the purified lysozyme is obtained and the purity is 100%. On the other hand, lysozyme can be purified by cation exchange chromatography, because the enzyme is a basic protein. For example, when the recombinant lysozyme is expressed in *S. cerevisiae*, the yeast medium is applied to CM-toyopearl equilibrated with a buffer of low ionic strength, and the adsorbed basic proteins are eluted in a gradient manner.

VII. RECENT BREAKTHROUGH STUDIES ON LYSOZYME

Since lysozyme is easily obtained in a purified form, it has been studied comprehensively as a model protein for structure, dynamics, and folding. The recent development of recombinant techniques has enabled elucidation of the molecular mechanism of structural and functional properties of lysozyme. In early studies, recombinant lysozyme was investigated in the *E. coli* expression system. However, since the prokaryotic cells have a different secretion system from eukaryotic for correct foldings cells, the correctly folded lysozyme could not be expressed. It seems likely that the folding of disulfide-rich protein such as lysozyme is difficult in *E. coli* because of the absence of endoplasmic reticulum (ER) in which proteins are posttranslationally folded. Although the enzyme is obtained as an inclusion body, the yield of refolding is at a very low level. The N-terminus of recombinant lysozyme is methionine, while that of native lysozyme is lysine. Since the N-terminus lysine is essential for correct folding, the substitution of N-terminus lysine with another amino acid results in a significant decrease in the stability of lysozyme. Kumagai et al. in 1987 found that hen egg white lysozyme was correctly processed and folded in *S. cerevisiae* (16). The N-terminus of recombinant lysozyme is lysine and the stability is the same as the native lysozyme. Since *S. cerevisiae* is a typical eukaryotic cell with an ER system, lysozyme is correctly processed and folded in the yeast. Taniyama et al. in 1992 reported the folding mechanism of disulfide bond–deficient human lysozyme C77/95A mutant secreted in *S. cerevisiae* (17). Although the deficient mutants of other disulfide bonds could not be secreted, only C77/95A mutant secreted by eightfold greater than wild-type in yeast. The stability of

C77/95A mutant greatly decreased despite the correct folding. These observations show that the disulfide bond Cys77–95 contributes to the stabilization of the folded form of human lysozyme.

Recently, the identification of human lysozyme as an amyloidogenic protein which causes serious diseases is of particular interest. The two unknown natural mutations (Ile56Thr and Asp67His) in the human lysozyme gene both cause autosomal-dominant hereditary amyloidosis (18). It has been suggested that the lysozyme amyloid fibril may be formed by the intermolecular β-sheet association due to β-strand exposed to the molecular surface by a single amino acid substitution.

We have developed new approaches for industrial application using genetic modifications of lysozyme. Nakamura et al. (19) reported that the large molecular size of N-glycosylated lysozyme with a polymannose chain was predominantly expressed in yeast carrying the lysozyme gene modified to have N-linked signal sequence Asn-X-Thr/Ser at the position of the molecular surface. The polymannosyl lysozyme showed remarkable heat stability in that no coagulation was observed by heating at 100°C. In addition to heat stability, the lysozyme revealed excellent emulsifying properties, superior to the commercial emulsifiers (20).

On the basis of the idea that the covalent attachment of palmitic acid residues to the lysysl residues of lysozyme stabilizes it and makes it more active (6), Ibrahim et al. (21) attempted the genetic fusion of a hydrophobic pentapeptide (Phe-Phe-Val-Ala-Pro), which forms a β-strand conformation with the same length as a palmitic acid residue, to its C-terminus. As expected, the hydrophobic peptide fusion greatly enhanced the bactericidal action to *E. coli*. These modified lysozymes having antimicrobial action against both Gram-positive and Gram-negative bacteria and can be used for industrial applications in future.

REFERENCES

1. A Fleming. On a remarkable bacteriolytic element found in tissues and secretions. Proc R Soc Lond Ser B 93:306–317, 1922.
2. DM Chipman, N Sharon. Mechanism of lysozyme action. Science 165:454–465, 1969.
3. D Pirzkiewiez, TC Bruice. Interaction of cellodextrins with lysozyme: the necessity of the 2-acetamide group for binding and hydrolysis. Arch Biochem Biophys 129:317–320, 1969.
4. A Kato, T Wakinaga, N Matsudomi, K Kobayashi. Changes in lysozyme during egg white thinning. Agric Biol Chem 42:175–176, 1978.
5. OJ Cotterill, AR Winter. Egg white lysozyme. 3. The effect of pH on the lysozyme-ovomucin interaction. Poultry Sci 37:679–686, 1955.
6. HR Ibrahim, A Kato, K Kobayashi. Antimicrobial effects of lysozyme against Gram-negative bacteria due to covalent binding of palmitic acid. J Agric Food Chem 39:2077–2088, 1991.
7. S Nakamura, A Kao, K Kobayashi. New antimicrobial characteristics of lysozyme-dextran conjugate. J Agric Food Chem 39:647–650, 1991.
8. CCF Blake, DF Koenig, GA Mair, ACT North, DC Phillips, VR Sarma. Structure of hen egg-white lysozyme. A three-dimensional Fouier synthesis at 2 Å resolution. Nature 206:757–761, 1965.
9. SE Radford, CM Dobson, PA Evans. The folding of hen lysozyme involves partially structured intermediates and multiple pathways. Nature 358:302–307, 1992.
10. RE Dickerson, I Geis. The Structure and Action of Proteins. New York: Harper & Row, 1969, pp 69–78.
11. RU Rupley, V Gates. Studies on the enzymic activity of lysozyme. II. The hydrolysis and transfer reactions of N-acetylglucosamine oligosaccharides. Proc Natl Acad Sci USA 57:496–510, 1967.
12. TY Lin, DE Koshland Jr. Carboxyl group modification and the activity of lysozyme. J Biol Chem 244:505–508, 1969.
13. SM Parsons, MA Raftery. The nature of amino acid side chains which are critical for the activity of lysozyme. Biochemistry 8:700–712, 1969.
14. MA Raftery, FW Dahlquist, SM Parsons, RG Wilcott. The use of nuclear magnetic resonance to describe relative modes of binding to lysozyme of homologous inhibitors and related substrates. Proc. Nat. Acad. Sci. USA 62:44–51, 1969.
15. T Imoto, K Yagishita. A simple activity measurement of lysozyme. Agric Biol Chem 35:1154–1156, 1971.
16. I Kumagai, S Kojima, E Tamaki, K Miura. Conversion of Try 62 of hen egg-white lysozyme to Tyr by site-directed mutagenesis. J Biochem 102:733–740, 1987.
17. Y Taniyama, K Ogasawara, K Yutani, M Kikuchi. Folding mechanism of mutant human lysozyme secretion efficiency in yeast. J Biol Chem 267:4619–4624, 1992.
18. DR Booth, M Sunde, V Bellotti, CV Robinson, WL Huchinson, PE Fraser, PN Hawkins, CM Dobson, SE Radford, CCF Blake, MB Pepys. Instability, unfolding and aggregation of human lysozyme variants underlying amyloid fibrillogenesis. Nature 385:787–793, 1997.

19. S Nakamura, H Takasaki, K Kobayashi, A Kato. Hyperglycosylation of hen egg white lysozyme in yeast. J Biol Chem 268:12706–12712, 1993.
20. S Nakamura, K Kobayashi, A Kato. Novel surface functional properties in polymannosyl lysozyme constructed by genetic modification. FEBS Lett 328:259–262, 1993.
21. HR Ibrahim, M Yamada, K Matsushita, K Kobayashi, A Kato. Enhanced bactericidal action of lysozyme to *Escherichia coli* by inserting a hydrophobic pentapeptide into its C terminus. J Biol Chem 269:5059–5063, 1994.

77

Ribonucleases

Jaap J. Beintema and Wei Zhao
University of Groningen, Groningen, The Netherlands

I. INTRODUCTION

A. Chemical Reactions Catalyzed

Ribonucleases depolymerize ribonucleic acids by cleavage of phosphoric diester bonds between nucleotide residues. This means that they are specialized phosphotransferases or phosphoric diester hydrolases. A further specification is that they are endonucleases, as exonucleases degrade nucleic acids from one of the two termini, which results in little depolymerization. Cleavage may occur between phosphate and the 3′-oxygen of the ribose, producing 5′-phosphomonoesters (EC 3.1.26) or between phosphate and the 5′-oxygen of the ribose, producing 3′-phosphomonoesters (EC 3.1.27). Enzymes with the latter cleavage specificity often are transferases producing 2′,3′-cyclic phosphate as intermediates, which generally are hydrolyzed in a second reaction catalyzed by the same enzyme. Figure 1 shows as an example the two successive reactions catalyzed by bovine pancreatic ribonuclease.

B. Chemical Structure of Substrates

Generally, nucleases are specific for either desoxyribonucleic acids (deoxyribonucleases) or ribonucleic acids (ribonucleases), although nucleases also occur which cleave both substrates producing either 5′-phosphomonoesters (EC 3.1.30) or 3′-phosphomonoesters [micrococcal nuclease (1); EC 3.1.31.1].

C. Classification According to Enzyme Commission Nomenclature

Section II of this handbook is organized according to the classification of enzymes as presented in Enzyme Nomenclature (2). In this classification "hydrolases (EC group 3)" are listed separately from "transferases (EC group 2)." However, for several enzymes this distinction is not correct as they are transferases reacting with compounds with general formula R-OH in which R may also be H, (H-OH) as will be discussed below.

The best-characterized ribonucleases belong to the endoribonucleases producing 3′-phosphomonoesters, with 2′, 3′-cyclic phosphate as intermediates. This feature indicates that they will not be active on deoxyribonucleic acids. These ribonucleases have been classified earlier also as nucleotidyl transferases (EC 2.7.7) or phosphoric diester hydrolases (EC 3.1.4). Three superfamilies with this cleavage pattern are those of ribonucleases A (3–11), T_1 (12, 13), and T_2 (12), respectively. Mammalian pancreatic ribonucleases belong to the ribonuclease A superfamily and the two successive catalyzed reactions are shown in Figure 1. Enzymes belonging to this family have a strict specificity for a pyrimidine base at the 3′-side of the cleaved phosphoric diester bond and a general preference for a purine base at the 5′-side. Taking into account the reversibility of chemical reactions, the second reaction with H-OH as reacting molecule can be considered as the reverse of the first reaction with R-OH as leaving group. Generally the second (hydroly-

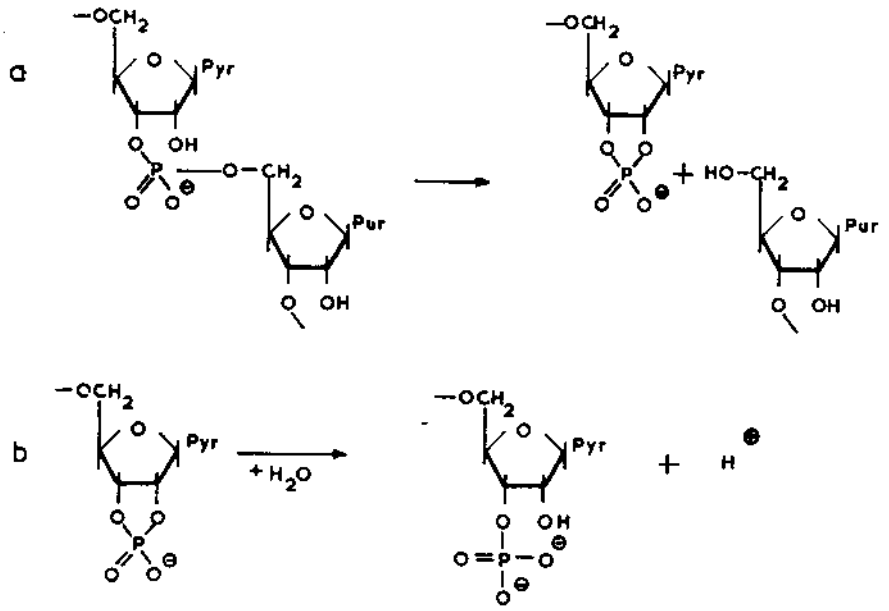

Figure 1 The two successive reactions catalyzed by bovine pancreatic ribonuclease. This ribonuclease belongs to the ribonuclease A superfamily, which has a strict specificity for a pyrimidine base at the 3′-side of the cleaved phosphoric diester bond. Within the superfamily this ribonuclease belongs to the family of pancreatic-type, secretory ribonucleases 1, which have a higher preference for cytosine than uracil as pyrimidine. These enzymes have a general preference for a purine base at the 5′-side of the diester bond, with highest activities with an adenine at that side. The pyrimidine-binding site includes a disulfide-linked loop structure in the molecule, which is absent in mammalian angiogenins and in non-mammalian members of the superfamily. These enzymes do not have a strong adenine preference and in several cases even prefer guanine over adenine.

sis) reaction is much slower than the first (transferase), and several members of the ribonuclease A superfamily do not even hydrolyze the intermediate cyclic phosphates (6). This example shows that the classification of these ribonucleases as hydrolases (EC 3.1.27) is less correct and that the previous classification as transferases (EC 2.7.7) is more appropriate.

II. IMPORTANCE OF RIBONUCLEASES TO QUALITY OF FOOD AND IN FOOD DIGESTION

Enzymes to be included as topics in a Handbook of Food Enzymology should have either a role (or potential role) in food production or processing, or be important in digestion of food components in the human species, in its domesticated animals, or in biotechnology. In this respect the history of ribonuclease research is a disappointing one. One of the first enzymes to be isolated and purified in crystalline form has been ribonuclease, a digestive enzyme which could be isolated in relatively large amounts from bovine pancreas, a major product of the beef industry (14). This enzyme has played a key role in the development of the study of proteins, with four Nobel Prizes in chemistry (in 1972 and 1984) awarded for research on it. However, it was later found that ribonuclease is only present in high amount in the pancreas of ruminants and species that have a ruminantlike digestion, and in a number of species with cecal digestion (15, 16). For instance, the ribonuclease content in human pancreas is $< 1\%$ of that in bovine pancreas, and in the 1970s ribonuclease disappeared again as an important digestive pancreatic enzyme in textbooks for medical students.

Ribonuclease was considered around 1980 as a dull enzyme, without a relevant biological function and not very interesting for chemical investigations. However, since then the enzyme underwent a renaissance by the discovery of proteins with novel biological actions, which after structural studies proved to be homologs of ribonucleases with their ribonuclease activities being a condition of these special actions (17, 18).

III. RIBONUCLEASES ARE PROTEINS OR CATALYTICALLY ACTIVE NUCLEIC ACIDS

Not all ribonucleases are proteins. Catalytically active nucleic acids include predominantly ribonucleases, among which ribonucleases P are very well characterized ones. Ribonucleases P (EC 3.1.26.5) consist of a protein and a ribonucleic acid component, of which the latter is the catalytically active part, requiring a metal ion for its activity, and producing 5′-phosphomonoesters (19).

IV. OCCURRENCE OF RIBONUCLEASES

A. Digestion of Extracellular RNA

The three best-characterized superfamilies of ribonucleases are those of the already-mentioned ribonuclease A, T_1, and T_2. All members of these superfamilies are extracellular ones, have sequences coding for signal peptides at the DNA level, and are primarily digestive enzymes for foreign RNA, originating from dead cell material.

The ribonuclease A superfamily has a strong specificity for endonucleolytic cleavage with a pyrimidine at the 3′-side of the cleaved phosphodiester bond (EC 3.1.27.5) and includes homologous enzymes isolated from many mammalian, avian, reptilian, and amphibian sources. No representatives have yet been found in fishes or nonvertebrate taxa. Other enzymes mentioned under EC 3.1.27.5 in Enzyme Nomenclature (2) are not well characterized and probably are not homologous. Several representatives have specific functions and have a very low or no apparent activity with more conventional ribonuclease substrates (10).

Nine separate families with sequences that are > 50% identical in each family can be distinguished in the ribonuclease A superfamily:

1. Mammalian (pancreatic-type or secretory) ribonucleases 1. This family, with a rather high preference for cytidine relative to uridine, includes digestive pancreatic enzymes (4), but also paralogous ribonucleases isolated from bovine semen (20) and brain (21).

2. Mammalian (nonsecretory or neurotoxin-type) ribonucleases 2 (7, 22). This family includes both enzymes isolated from tissues such as liver and kidney, and more specialized ones, isolated from eosinophil cells, such as the enzymatically active human eosinophil derived neurotoxin (EDN), which has also been isolated from other human sources, and the enzymatically inactive human eosinophil cationic protein (ECP; also called ribonuclease 3). EDN and ECP are the products of a gene duplication which occurred in an ancestor of Old World monkeys and apes after their divergence from the ancestor of New World monkeys. Recently, another human enzyme (ribonuclease 6) belonging to this family with low enzymatic activity has been discovered and characterized.

3. Mammalian ribonucleases 4 (8). These are basic uridyl-preferential enzymes, isolated from the liver of several mammalian species.

4. Mammalian angiogenins (or ribonucleases 5) (9, 23). These proteins stimulate blood vessel formation. They are virtually inactive toward RNA. However, their biological activity requires intact enzymic active sites and involves very specific cleavage of RNA molecules.

5 and 6. Ribonucleases from chicken liver (24) and chicken transformed bone marrow cells (25, 26).

7 and 8. Pancreatic ribonucleases from the pancreas of reptiles [turtle (27) and iguana (28)].

9. Several amphibian ribonucleases (5, 29).

Ribonucleases T_1 and T_2 were discovered originally in the commercial digestive Taka-Diastase from *Aspergillus oryzae* (30). Enzymes homologous with RNase T_1 with a preference for guanine have been isolated from several fungi (EC 3.1.27.3; EC 3.1.27.4) (12), but this superfamily also includes homologous prokaryotic representatives such as enzymes from several *Bacillus* spp.[EC 3.1.27.2; barnase and binase (13)], which have a less strict preference for guanine. A specialized fungal member of this superfamily isolated from *Aspergillus* spp. is α-sarcin (EC 3.1.27.10), which has cytotoxic properties resulting from a very specific cleavage pattern of ribosomal RNA (31).

The ribonuclease T_2 superfamily is the most ubiquitous one in living nature. Members of this superfamily (EC 3.1.27.1) with a preference for purines (A or G) have been isolated, sequenced, and characterized from a large number of fungi, plants, and animals (including mammals) (12). The active site of members of this superfamily consists of two very diagnostic cassettes with primary structures: I/L-H-G-L-W-P and W-X-H-E-W/Y-X-K/T-H-G, respectively. Similar cassettes can be recognized even in the sequences of prokaryote and virus ribonucleases, which show no recognizable homology to the eukaryote enzymes in the remainder of the sequences. These prokaryote and virus ribonucleases, but also several animal members of the RNase T_2 superfamily, are not purine preferential anymore (12).

Pancreatic enzymes in the ribonuclease A superfamily and microbial (especially fungal) representatives in

the other two may be classified as digestive enzymes, depolymerizing foreign RNA. Also an extracellular T_2 ribonuclease from tomato (RNase Le) has a digestive role, as its expression and excretion from cells are stimulated by shortage of inorganic phosphate in the extracellular environment, necessitating digestion of organic phosphate sources (32).

However, even pancreatic ribonucleases do not have only a digestive function as they have been identified in other tissues and body fluids as well, often in comparable quantities as observed in the pancreas (see Sec. IV.B). Other ribonucleases are synthesized exclusively in tissues which have no digestive function. Highly interesting are proteins which were isolated and characterized at first because of specific biological properties (18). Surprisingly, sequence analyses showed them to be members of one of the three extracellular ribonuclease superfamilies, which was confirmed by demonstrating ribonuclease activity, often at a low level or only with very specific cleavage patterns. Generally these ribonuclease activities were found to be a condition of the specific biological actions. Ribonucleases endowed with these special bioactions [RISBases (18)] are angiogenins (9, 23), the cytotoxic and aspermatogenic bovine seminal ribonuclease (20), amphibian members of the ribonuclease A superfamily such as onconase (33) and lectins from frog oocytes (5), self-incompatibility proteins in plants, which belong to the ribonuclease T_2 superfamily (12), and the already-mentioned α-sarcin, which is a ribonuclease T_1 superfamily member (31).

A general feature of these ribonucleases endowed with special bioactions is that available evidence indicates that they exert their cytotoxic actions by cleavage of intracellular RNA in their target cells. This means that in some way these extracellular enzymes are internalized again, for which several specific receptor-mediated processes have been proposed and also experimentally demonstrated (23, 33). Members of the ribonuclease A superfamily bind cytoplasmic protein ribonuclease inhibitors (RI) with very high affinities (34). In a previous review we pointed to the paradox that these cytoplasmic inhibitors bind to non-cytoplasmic ribonucleases (35), but recent studies about uptake in foreign cells point to a biological function of these inhibitors. Within mammals there is little specificity in ribonuclease inhibitor interactions, also not with respect to the different ribonuclease families occurring in this vertebrate class. But ribonucleases from one vertebrate class (mammals, birds, amphibians) and inhibitors from another one do not bind to each other (5, 36).

B. Role of Pancreatic Ribonucleases as Digestive Enzymes in Mammals

In Section II of this chapter it has already been mentioned that pancreatic ribonuclease is only present in high amounts in the pancreas of a limited number of mammalian taxa. Large quantities of this enzyme are found in ruminants and species that have a ruminant-like digestion, and in a number of species with cecal digestion (Fig. 2). However, there are also herbivores with cecal digestion with extremely low ribonuclease contents in the pancreas, such as lagomorphs (rabbit), hyraxes, manatee, and elephant (16). Barnard (15) proposed that an elevated level of pancreatic ribonuclease is the response to the necessity of digesting large amounts of ribonucleic acid derived from the microflora of the stomach of ruminants. This explanation agrees with the elevated level of stomach lysozyme in several ruminants and species that have a ruminantlike digestion (37). As far as we know, however, these roles of ribonuclease and lysozyme have never been investigated by comparative physiologists studying digestive systems of mammals.

The most striking differences between pancreatic ribonucleases concern the presence or absence of covalently attached carbohydrate. These differences may be related to the digestive system and the diet of the species involved. A number of pancreatic ribonucleases have carbohydrate attached to asparagine residues at positions 21, 22, 34, 62, 76, and/or 88 (Fig. 3). These positions are part of highly variant sequences at the surface of the molecule, far from the active site.

Only asparagine residues in Asn-X-Ser/Thr sequences have been found to act as attachment sites, where X may be any residue except proline (Fig. 3). However, not all Asn-X-Ser/Thr sequences possess carbohydrate chains. Other features of the ribonuclease molecule and/or the effectiveness of the carbohydrate-attaching system apparently influence the glycosylation process.

Figure 4 summarizes the occurrences of an Asn-X-Ser/Thr sequence in several investigated mammalian ribonucleases and their glycosylation states. The sugar composition of the carbohydrate chains is also indicated schematically in this figure. Both simple-type chains containing only glucosamine and mannose, and complex-type chains also containing fucose, galactose, and sialic acid occur.

All six carbohydrate sites in ribonucleases are located at external bends of the folded chain. This localization ensures maximal exposure of the carbohydrate moieties to the external solvent. In Figure 5 a

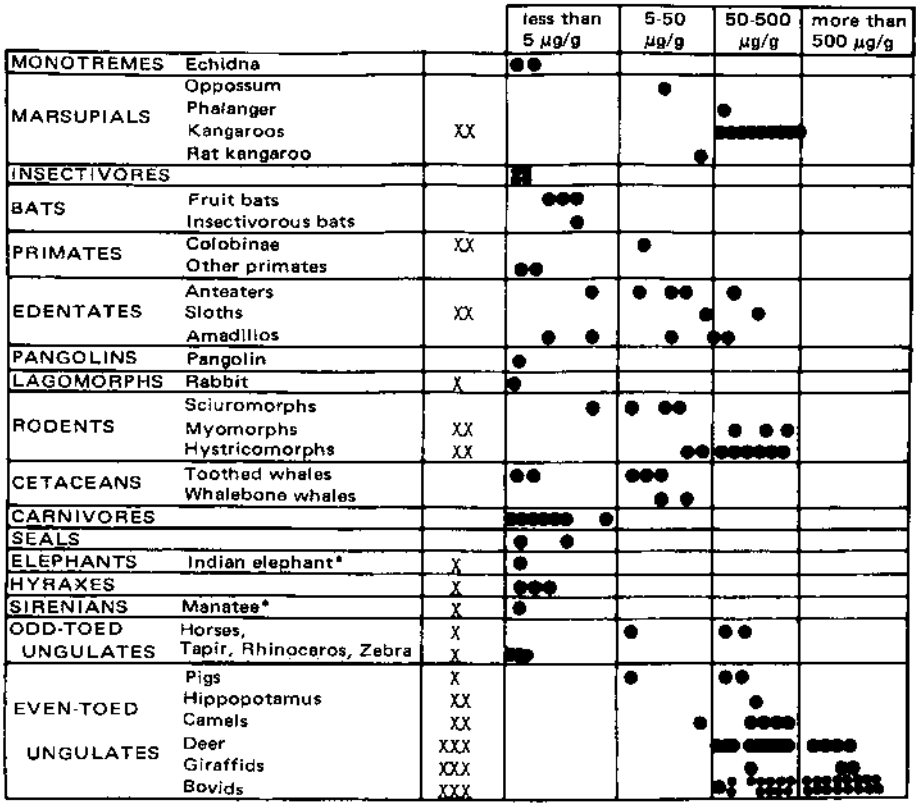

Figure 2 Pancreatic ribonuclease content in mammalian taxa. XXX, ruminants; XX, ruminantlike digestion; X, (mainly) herbivorous. *Pancreas badly autolyzed.

space-filling model of carbohydrate-free bovine ribonuclease is compared with the same model with three biantennary complex-type oligosaccharide chains attached at positions 22, 34, and 62, representing the minor glycosylated component of horse ribonuclease. Probably the carbohydrate moieties do not occupy fixed positions because of the presence of a number of flexible bonds, but the latter model shows the increase in volume as a result of the addition of carbohydrate.

The glycosylation states of the ribonucleases investigated were correlated with the type of fermentation (stomach or cecal) used by the species involved (Fig. 4). It was found that species with cecal digestion, such as pig, horse, and the hystricognath rodents (guinea pig and relatives), produce ribonucleases with large carbohydrate chains attached to several positions at the surface. Therefore, it was suggested that the presence of carbohydrate protects ribonuclease from absorption in the gut, enabling it to be transported to the large intestine where it should hydrolyze the ribonucleic acid derived from the cecal microflora (40). This would be analogous to the function of ribonucleases in the digestion of ribonucleic acid from the stomach microflora in ruminants and herbivores with ruminantlike digestion postulated by Barnard (15).

Ruminants and species with ruminantlike digestion (camel, hippopotamus, sloth, kangaroo) have less carbohydrate attached to their ribonucleases. Therefore, it seems that glycosylation of pancreatic ribonuclease may not be advantageous for species with stomach fermentation. These species escaped glycosylation of their ribonucleases not only by amino acid replacements in the protein (camel, reindeer), but probably also by developing a much less effective carbohydrate-attaching enzyme system in the pancreas than encountered in other species. Hippopotamus ribonuclease is an example of the second solution. This enzyme has four carbohydrate attachment sites, with carbohydrate attached to only one of them in only a fraction of the molecules.

If glycosylation of a ribonuclease is avoided by amino acid replacements, the enzyme will also not be glycosylated if its gene is expressed at other sites of the

	76 77 78
rat	-Ser-Ser-Thr-
mouse	-Ser-Ser-Ala-
hamster	-His-Ser-Ala-
muskrat	-Arg-Ser-Ala-
porcupine	-Asn-Ser-Leu-
chinchilla	-Asn-Ser-Asn-
casiragua	-Thr-Ser-Asn-
coypu	-Asn-Ser-Asn-
capybara	-Tyr-Ser-Ser-
guinea pig A	-Tyr-Ser-Ser-
guinea pig B	-Tyr-Ser-Arg-
cuis	-His-Ser-Ser-
horse	-Ser-Ser-Ser-
whale	CHO* -Asn-Ser-Thr-
pig	CHO -Asn-Ser-Thr-
hippopotamus	-Asn-Ser-Thr-
camels	-Ser-Thr-Thr-
bovidae	-Tyr-Ser-Thr-
pronghorn	-Tyr-Ser-Thr-
giraffe	-Tyr-Ser-Ala-
deer	-Asn-Ser-Ala-
ox semen	-Lys-Ser-Thr-
man	CHO* -Asn-Ser-Ser-
sloth	-Arg-Ser-Asn-
kangaroo	-Asn-Ser-Arg-
turtle	-Asn-Ala-Ser-

Figure 3 Amino acid sequence of the carbohydrate attachment site 76–78 in ribonucleases. CHO, carbohydrate. *Partially glycosylated.

body, but other pancreatic enzymes may be glycosylated extensively in the species involved. However, a less effective carbohydrate-attaching enzyme system in the pancreas will result in a general scarcity of glycosylated secretory pancreatic proteins, but the same gene product may be extensively glycosylated at other sites of the body. An example is human ribonuclease, which has three carbohydrate attachment sites, one being completely and one partially glycosylated in the pancreatic enzyme (41). The urinary enzyme, which is not synthesized in the pancreas, is glycosylated completely at all three sites (42).

These examples show dramatic secondary effects of apparently neutral replacements. Strong positive or negative selection may influence the presence of Asn-X-Ser/Thr sequences in proteins. However, the presence of a short oligosaccharide chain in bovine ribo-

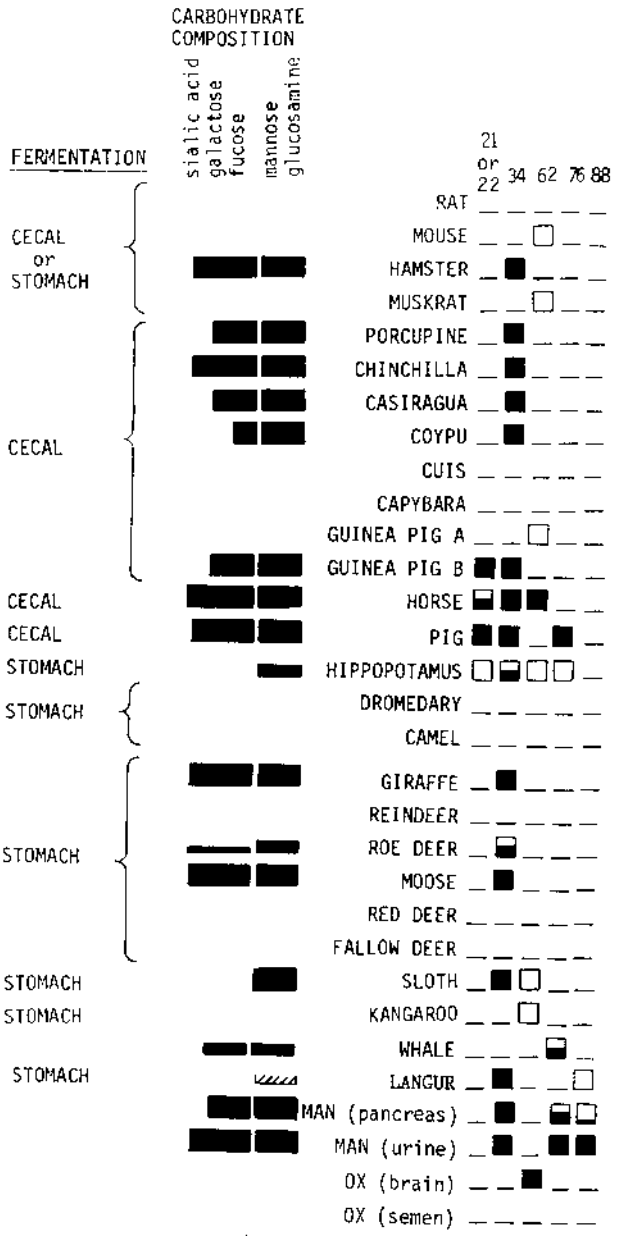

Figure 4 Occurrence of Asn-X-Ser/Thr sequences at the six carbohydrate sites (residues 21–23 or 22–24, 34–36, 62–64, 76–78, and 88–90) in ribonuclease and compositions of carbohydrate moieties. ■, completely glycosylated Asn-X-Ser/Thr sequence; ⬓, part of the molecules are glycosylated; □, Asn-X-Ser/Thr sequence without carbohydrate attached; —, no Asn-X-Ser/Thr sequence present. Carbohydrate compositions: ■, present in all molecules; ▬, present in all glycosylated molecules (only part of the molecules are glycosylated); ▁, only present in a minor glycosylated component, not present in the major glycosylated component; ▨, carbohydrate present, but composition not determined.

Figure 5 Space-filling models of bovine ribonuclease (left) and of a glycosylated ribonuclease with three biantennary complex-type oligosaccharide chains attached to the surface (right). This figure is a collage of the figure on p. 81 in Ref. 38 (ribonuclease) and Fig. 11B in Ref. 39 (spatial conformation of a biantennary glycan of the N-acetyllactosamine type in the T-conformation).

nuclease B, the minor glycosylated component, may be a neutral property. The three-dimensional structure of this protein was found to be identical to that of bovine ribonuclease A, with the carbohydrate chain extending into the solvent. This chain is disordered for most part and exerts no influence on the structure of the protein (43, 44).

Evolutionary selection against the occurrence of Asn-X-Ser/Thr sequences should occur if glycosylation is disadvantageous for the stability or function of the protein. Evidence of this has been presented by Hunt and Dayhoff (45) and Sinohara and Maruyama (46), who observed that Asn-X-Ser/Thr sequences occur less frequently than expected by chance in extracellular proteins from eukaryotes.

Similar glycosylation requirements for ribonucleases from different taxa may explain convergences in functional and structural characteristics. The pancreatic ribonuclease of giraffe is positioned with that of pronghorn and not with those of deer in most parsimonious trees of the sequences (21) as a consequence of a number of rather rarely observed amino acid replacements. However, since these shared replacements occur at internal positions, the relationship does not come to clear expression in many of the properties of these enzymes. Thus, giraffe ribonuclease is very similar to that of moose (a deer species) in glycosylation and other properties. It may be significant that in a classification of ruminants based on feeding ecology and stomach structure (47), moose and giraffe are grouped together as large "concentrate selectors" with a diet containing relatively little cellulose fiber and a simple (primitive) stomach.

Strongly positively charged ribonucleases are considerably more active on double-stranded RNA than ribonucleases with a smaller excess of positive charges on the surface (48). We do not know whether the activity of the ribonucleases on double-stranded RNA has any function. The ribonucleases with the larger excess of positive charges are the ribonucleases from human and whale pancreas, bovine semen, and ruminant brain. These enzymes have no function in the digestion of microfloral RNA from the stomach or cecum of herbivores. This suggests that there is a relationship between the excess of positive charges of ribonucleases and nondigestive functions.

Man and langur monkey are two species in the same mammalian order, of which the latter possesses all features of having ruminantlike digestion. The amino acid sequence of their ribonucleases differ at 14 (11%) of the positions (49). This leaves no doubt that they are located on the same branch in a most parsimonious tree. The hypothesis that species with ruminantlike digestion not only have a higher ribonuclease content in their pancreas, but also have less excess of positive charge and fewer attached carbohydrates, is in agreement with data presented in Table 1.

C. Intracellular RNA Processing and Turnover

Many RNA species in living cells are continuously synthesized, processed and degraded, in which ribonucleases should play a major role. However, disappointingly much less is known about these ribonucleases than about those discussed in the previous sections.

Deutscher (50) and Nicholson (51) list endoribonucleases identified and characterized in the prokaryote *Escherichia coli*. These lists include the excreted periplasmic enzyme ribonuclease I (EC 3.1.27.6), which is a member of the ubiquitous ribonuclease T_2 superfamily (12) discussed in the previous section. Interestingly, there occurs a modified form of this ribonuclease, ribonuclease I^*, which has no signal peptide sequence on its coding DNA, is not secreted through the cytoplasmic membrane, and may exert its function intracellularly. Less well characterized enzymes are ribonucleases M and R, which are similar to ribonuclease I.

The major participant in mRNA decay in *E. coli* is ribonuclease E. This enzyme also plays a role in rRNA maturation. This is a divalent metal requiring enzyme, producing 5′-phosphomonesters (EC 3.1.26). It has a

Table 1 Several Characteristics of Human and Langur Pancreatic Ribonucleases

	Man	Langur
μg/g Tissue	5	280
(Lys + Arg)–(Asp + Glu)	+6	+1
Number of possible glycosylation Sites (Asn-X-Ser/Thr sequences)	3	2
Extent of glycosylation	All molecules; extensive glycosylation of one site in all molecules and of another site in about half of the molecules	Part of the molecules; one simple[a] chain

[a]Simple-type carbohydrate chains only contain glucosamine and mannose.

polypeptide sequence of 1061 amino acids, much longer than the extracellular enzymes discussed in the previous section. A similar activity is exhibited by the already mentioned ribonuclease P (EC 3.1.26.5), of which the ribonucleic acid component is the catalytically active one.

More specialized *E. coli* ribonucleases are ribonucleases III (EC 3.1.26.3) and H1 and H3 (EC 3.1.26.4), which cleave double-stranded (ds) RNA molecules and the RNA strand of RNA-DNA hybrids, respectively. Other, less well characterized ribonucleases in *E. coli* are ribonucleases IV and F (producing 3′-phosphate termini; EC 3.1.27.7), P2, O, PIV, PC and N.

Few intracellularly synthesized eukaryotic ribonucleases have been identified and characterized. Two of the few examples are the 2-5A (= oligoadenylate with $2' \rightarrow 5'$ internucleotide linkages)–dependent human and murine ribonucleases L (52) which cleave RNA with the production of 3′-phosphoryl and 5′-hydroxyl groups. The polypeptide chains of these enzymes have chain lengths of ~ 750 residues, and each includes a ribonuclease domain of ~ 200 residues, with some sequence similarity with ribonuclease E. This suggested homology, however, is not in agreement with the different cleavage specificities of these mammalian and *E. coli* enzymes. Another ribonuclease E–related activity in mammalian cells is the product of the human ard-1 gene, which encodes a basic, proline-rich 13.3-kDa molecular-weight protein (53). Expression of this gene in *E. coli* can complement a mutant of the ribonuclease E gene, but there are no indications that this gene product represents a ribonuclease. Wennborg et al. (54) have isolated from human cell extracts a ribonuclease with the same specificity as ribonuclease E. Antibodies to ribonuclease E recognize this human protein, which has, however, not yet been structurally characterized.

Moiseyev et al. (55, 56) have isolated, characterized and sequenced two plant ribonucleases isolated from ginseng calluses. These enzymes, with polypeptide lengths of ~ 150 residues, are homologous with cytotoxic intracellular pathogenesis-related proteins (IPR or PR-10) from several plants such as parsley (57) and bean (58), and with pollen allergens from tree species such as birch (59) and alder (60). This suggests that the cytotoxic properties of these latter proteins are caused by their ribonuclease activities. However, this hypothesis is still being met with skepticism. In addition, this protein family does not contain any conserved histidine residues, a universal active-site residue in all other investigated ribonuclease families so far investigated.

So, although much knowledge has already been collected about intracellular RNA processing and degrading activities in eukaryotes (61, 62), little is known about the responsible enzymes. Part of these enzymes will be proteins, but many others may be enzymatically active RNA molecules (ribozymes). Penny and coworkers recently published a model for the evolution of life from an RNA world to the emergence of eukaryotes and prokaryotes (63), and summarized the presence of RNAs in modern organisms that are relics from the ancient RNA world. Proteins have gradually replaced RNAs in catalysis by virtue of their superior catalytic properties. However, in the case of large substrates such as RNA the rate of diffusion is the slowest reaction step, and catalytic perfection will not help much in speeding up the reaction rate. Therefore, it is not surprising that in intracellular RNA metabolism still many catalytically active RNAs are used. These authors also propose that the prokaryote genome organization was derived from a "eukaryotelike" one, which is supported by the fact that prokaryotes use proteins for many activities in RNA processing, for

which eukaryotes use RNA-protein (RNP) complexes (64).

V. DETERMINATION OF RIBONUCLEASE ACTIVITY

Methods for the determination of ribonuclease activities measure either the depolymerization of RNA or of homopolyribonucleotides (poly(C), poly(G), etc.), the cleavage of dinucleotides of defined structure, or the hydrolysis of cyclic nucleotides. Table XXIII on p. 751 in Richards and Wyckoff (65) summarizes methods used at that time, which have not changed much since then. As discussed before (Sec. I.C), the hydrolysis of cyclic nucleotides is the second reaction catalyzed by ribonucleases (Fig. 1); it generally is a rather slow one and in several cases even does not occur. Measurement of the depolymerization of RNA is the most sensitive method and can even be used for determination of the activity of family members discussed in Section IV.A with hardly any ribonuclease activity. However, these methods only give qualitative or relative quantitative data (e.g., relative to the activity of bovine pancreatic ribonuclease). Depolymerization of RNA is often measured by the formation of acid-soluble nucleotides, which, however, generally requires construction of nonlinear standard curves with known quantities of, e.g., pure bovine pancreatic ribonuclease.

Nevertheless, using one of the latter methods is most suitable for a first characterization of ribonuclease activity in biological samples and may be performed as follows (66): 0.01–0.05 mL sample solution is incubated for 30 min at 37°C with 0.5 mL RNA (e.g., commercial purified yeast RNA) solution (0.4 mg/mL) in a buffer containing 100 mg gelatin, 0.1 mM EDTA, 0.1 M NaCl in 0.05 M Tris/HCl buffer, pH 7.5. The reaction is terminated by adding 0.5 mL precipitant which contains 0.1 g $UO_2(C_2H_3O_2)_2 \cdot 3H_2O$ in 100 mL of 2.5% trichloroacetic acid. After keeping on ice for 30 min and centrifugation, the absorbance at 260 nm of the 10 times diluted supernatant is measured. The readings of the absorbance are not proportional to the enzymatic activity and produce an S-shaped curve, which requires the construction of a standard curve with a ribonuclease with similar specificity properties.

VI. PROPERTIES AS ENZYMES

The extracellular representatives of the ribonuclease A, T_1, and T_2 superfamilies are generally very stable enzymes, especially at low pH values. High temperatures are required for inactivation. They do not require cofactors or metal ions for activity. Pancreatic ribonucleases (ribonucleases 1) are inhibited by Zn^{2+} and Cu^{2+} ions. These latter enzymes depolymerize RNA with a pH optimum ~ 8.0 at ionic strength values of 0.1. However, the pH optimum for cleavage of dinucleotides or the hydrolysis of cyclic nucleotides is ~ 6.5–7.0.

In Table 2 several kinetic parameters of reactions catalyzed by bovine and turtle pancreatic ribonucleases are shown (67). The k_{cat} values for the cleavage of dinucleotide are several orders of magnitude higher than those for the hydrolysis of cyclic nucleotides.

Table 2 Several Kinetic Parameters of Bovine and Turtle Pancreatic Ribonucleases

	Bovine ribonuclease		Turtle ribonuclease	
Substrate	K_m (mM)	k_{cat} (sec^{-1})	K_m (mM)	k_{cat} (sec^{-1})
cyclic 2′, 3′-UMP	1.58	1.4	4.50	0.05
UpU	2.10	2.0	1.20	0.11
UpC	0.66	4.1	—[a]	—[a]
UpG	0.47	12.3	0.63	2.0
UpA	0.22	405	0.42	0.72
cyclic 2′, 3′-CMP	0.43	1.5	0.82	0.45
CpU	1.05	8.7	0.52	0.97
CpC	0.58	10.8	0.28	0.38
CpG	0.42	43.3	0.28	15.2
CpA	0.18	675	0.34	6.3

[a]Too slowly hydrolyzed under the experimental conditions to obtain kinetic constants.
Source: From Ref. 67.

k_{cat}/K_m values (relative to the activity of the bovine enzyme) observed for the hydrolysis of cyclic nucleotides by a large number of pancreatic ribonucleases from mammalian species vary from 0.2 (mouse; cyclic 2′, 3′—CMP) to 2.9 (kangaroo; cyclic 2′, 3′—UMP) (68).

VII. PURIFICATION OF A RIBONUCLEASE

As will be clear from the previous sections, there is no universal method for the isolation of a molecular entity with ribonuclease activity. Below, we shall summarize, as an example, our efforts to purify ribonucleases occurring in rat liver (66). As we intended to isolate members of the ribonuclease A superfamily, which are stable at low pH, while cytoplasmic inhibitors which bind to these ribonucleases are not stable at this pH, we have used homogenization of liver tissue with 0.125 M sulfuric acid as first step in the isolation procedure. After centrifugation, cold acetone (−20°C) was slowly added to the supernatant (4°C) to a concentration of 30% (v/v). After stirring for 4 h, the supernatant was obtained by centrifugation. More cold acetone was added to a concentration of 60% acetone (v/v). The suspension was kept overnight (at 4°C). After centrifugation, the pellet was dissolved in 0.2 M sodium acetate buffer, pH 5.0, for further purification by gel filtration on a Sephadex G-75 column (4°C). Ribonuclease activities were determined as described in Section V. One major peak with enzymatic activity was obtained (Fig. 6). A small shoulder of earlier eluting ribonuclease activity probably indicates the presence of a ribonuclease T_2 representative (12). Pooled fractions from the gel filtration on Sephadex G-75 were further fractionated on an SP-Trisacryl column as illustrated in Figure 7. Three fractions with enzymic activity were obtained—RL1, RL2, and RL3—which were further purified by reversed-phase HPLC, using a C18 column and elution with a linear gradient of 0–60% acetonitrile (v/v) in 0.1% trifluoroacetic acid in 60 min. The flow rate was 1 mL/min. Pure ribonuclease 1 (the pancreatic enzyme) was obtained from RL1. Partial degradation at the N-terminus explains the shape of fraction RL1 in Figure 7. A homolog of human ribonucleases 2 and 6 was isolated from RL2, while RL3 contained ribonuclease 4, with some contamination of ribonuclease 5 (angiogenin). Approximately 20 μg ribonuclease 1 (RL1), 5 μg ribonuclease 2/6 (RL2), and 80 μg ribonuclease 4 (RL3) were recovered from 1 kg rat liver. As these ribonucleases have very different specific activities (66), it is not possible to calculate enzyme recoveries during each step of the purification procedure.

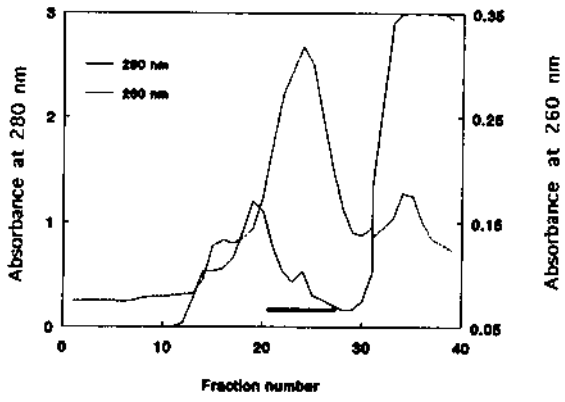

Figure 6 Sephadex G-75 gel filtration of a crude extract of rat liver. The column (2.5 × 75 cm) was equilibrated at 4°C with 0.05 M sodium acetate buffer, pH 5.0, and eluted with the same buffer. The flow rate was 1 mL/min. Fractions of 10 mL were collected. Ribonuclease activity was expressed as the reading of the absorbance at 260 nm (see Sec. V). Fractions indicated by a bar were pooled.

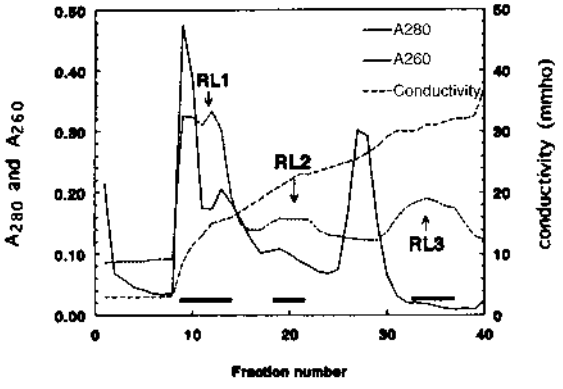

Figure 7 SP-Trisacryl column chromatography of the active fractions of the Sephadex G-75 column. The column (1 × 10 cm) was equilibrated at 4°C with 0.05 M sodium acetate buffer, pH 5.0, and washed with 0.04 M KNa phosphate buffer, pH 7.0, and developed with a gradient of 0–1.0 M ammonium acetate in 0.05 M KNa phosphate buffer. Fractions of 2.0 mL were collected. Three active fractions indicated by bars are marked RL1, RL2, and RL3, respectively, and were collected separately.

REFERENCES

1. CB Anfinsen, P Cuatrecasas, H Taniuchi. Staphylococcal nuclease. Chemical properties and catalysis. In: PD Boyer, ed. The Enzymes, 3rd ed, Vol 4. New York: Academic Press, 1971, pp 177–204.
2. Enzyme Nomenclature. San Diego: Academic Press, 1992.
3. JJ Beintema. The ribonuclease A superfamily: introduction. Cell Mol Life Sci 54:763–765, 1998.
4. MV Nogués, M Moussaoui, E Boix, M Vilanova, M Ribó, CM Cuchillo. The contribution of noncatalytic phosphate-binding subsites to the mechanism of bovine pancreatic ribonuclease A. Cell Mol Life Sci 54:766–774, 1998.
5. M Irie, K Nitta, T Nonaka. Biochemistry of frog ribonucleases. Cell Mol Life Sci 54:775–784, 1998.
6. S Sorrentino. Human extracellular ribonucleases: multiplicity, molecular diversity, and catalytic properties of the major RNAse types. Cell Mol Life Sci 54:785–794, 1998.
7. HF Rosenberg. The eosinophil ribonucleases. Cell Mol Life Sci 54:795–803, 1998.
8. J Hofsteenge, A Vicentini, O Zelenko. Ribonuclease 4, an evolutionarily highly conserved member of the superfamily. Cell Mol Life Sci 54:804–810, 1998.
9. DJ Strydom. The angiogenins. Cell Mol Life Sci 54:811–824, 1998.
10. JJ Beintema, RG Kleinedam. The ribonuclease A superfamily: general discussion. Cell Mol Life Sci 54:825–832, 1998.
11. RT Raines. Ribonuclease A. Chem Rev 98:1045–1065, 1998.
12. M Irie. RNase T_1/RNase T_2 family RNases. In: G D'Alessio, JF Riordan, eds. Ribonucleases. Structures and Functions. San Diego: Academic Press, 1997, pp 101–130.
13. RW Hartley. Barnase and barstar. In: G D'Alessio, JF Riordan, eds. Ribonucleases, Structures and Functions. San Diego: Academic Press, 1997, pp 51–100.
14. G D'Alessio, JF Riordan. Preface. In: G D'Alessio, JF Riordan, eds. Ribonucleases, Structures and Functions. San Diego: Academic Press, 1997, pp xv–xix.
15. EA Barnard. Biological function of pancreatic ribonuclease. Nature 221:340–344, 1969.
16. JJ Beintema, AJ Scheffer, H van Dijk, GW Welling, H Zwiers. Pancreatic ribonuclease: Distribution and comparisons in mammals. Nature (New Biol) 241:76–78, 1973.
17. SA Benner, RK Allemann. The return of pancreatic ribonucleases. TIBS 14:396–397, 1989.
18. G D'Alessio. New and cryptic biological messages from RNases. Trends Cell Biol 3:106–109, 1993.
19. NR Pace, JW Brown. Evolutionary perspective on the structure and function of ribonuclease P, a ribozyme. J Bacteriol 177:1919–1928, 1995.
20. G D'Alessio, A Di Donato, L Mazzarella, R Piccoli. Seminal ribonuclease: The importance of diversity. In: G D'Alessio, JF Riordan, eds. Ribonucleases, Structures and Functions. San Diego: Academic Press, 1997, pp 383–423.
21. JJ Beintema, HJ Breukelman, A Carsana, A Furia. Evolution of vertebrate ribonucleases: ribonuclease A superfamily. In: G D'Alessio, JF Riordan, eds. Ribonucleases, Structure and Functions. San Diego: Academic Press, 1997, pp 245–269.
22. MR Snyder, GJ Gleich. Eosinophil-associated ribonucleases. In: G D'Alessio, JF Riordan, eds. Ribonucleases, Sructures and Functions. San Diego: Academic Press, 1997, pp 425–444.
23. JF Riordan. Structure and function of angiogenin. In: G D'Alessio, JF Riordan, eds. Ribonucleases, Structures and Functions. San Diego: Academic Press, 1997, pp 445–489.
24. K Hayano, M Iwama, H Sakamoto, H Watanabe, A Sanda, K Ohgi, M Irie. Characterization of Poly C preferential ribonuclease from chicken liver. J Biochem (Tokyo) 114:156–162, 1993.
25. TH Graf, T Nakano. Identification of genes differentially expressed in two types of v-myb transformed myelomonocytic cells. Oncogene 7:527–534, 1992.
26. EM Klenova, I Botezato, V Laudet, GH Goodwin, JC Wallace, VV Lobanenkov. Isolation of a cDNA clone encoding the RNase-superfamily-related gene highly expressed in chicken bone marrow cells. Biochem Biophys Res Commun 185:231–239, 1992.
27. JJ Beintema, J Broos, J Meulenberg, C Schüller. The amino acid sequence of snapping turtle (*Chelydra serpentina*) ribonuclease. Eur J Biochem 153:305–312, 1985.
28. W Zhao, J Hofsteenge, JJ Beintema. The amino acid sequence of iguana (*Iguana iguana*) pancreatic ribonuclease. Eur J Biochem 219:641–646, 1994.
29. N Kinoshita, J Minshull, MW Kirschner. The identification of two novel ligands of the FGF receptor by a yeast screening method and their activity in xenopus development. Cell 83:621–630, 1995.
30. K Sato, F Egami. Studies on ribonuclease in Takadiastase. J Biochem (Tokyo) 44:753–767, 1957.
31. IG Wool. Structure and mechanism of action of the cytotoxic ribonuclease α-sarcin. In: G D'Alessio, JF Riordan, eds. Ribonucleases, Structures and Function. San Diego: Academic Press, 1997, pp 131–162.
32. W Jost, H Bak, K Glund, P Terpstra, JJ Beintema. Amino acid sequence of an extracellular phosphate-starvation-induced ribonuclease from cultured tomato (*Lycopersicon esculentum*) cells. Eur J Biochem 198:1–6, 1991.

33. RJ Youle, G D'Alessio. Antitumor RNases. In: G D'Alessio, JF Riordan, eds. Ribonucleases, Structures and Functions. San Diego: Academic Press, 1997, pp 491–514.
34. J Hofsteenge. Ribonuclease inhibitor. In: G D'Alessio, JF Riordan, eds. Ribonucleases, Structures and Functions. San Diego: Academic Press, 1997, pp 621–658.
35. JJ Beintema, C Schüller, M Irie, A Carsana. Molecular evolution of ribonuclease superfamily. Prog Biophys Mol Biol 51:165–192, 1989.
36. J Dijkstra, J Touw, I Halsema, M Gruber, G AB, Estradiol-induced synthesis of vitellogenin. Biochim Biophys Acta 521:363–373, 1978.
37. DE Dobson, EM Prager, AC Wilson. Stomach lysozymes of ruminants. J Biol Chem 259:11607–11616, 1984.
38. RE Dickerson, I Geis. The Structure and Action of Proteins. Menlo Park, CA: Benjamin, 1969.
39. J Montreuil. Spatial structures of glycan chains of glycoproteins in relation to metabolism and function. Survey of a decade of research. Pure Appl Chem 56:859–877, 1984.
40. JJ Beintema, W Gaastra, AJ Scheffer, GW Welling. Carbohydrate in pancreatic ribonucleases. Eur J Biochem 63:441–448, 1976.
41. M Ribó, JJ Beintema, M Osset, E Fernández, J Bravo, R De Llorens, CM Cuchillo. Heterogeneity in the glycosylation pattern of human pancreatic ribonuclease. Biol Chem Hoppe-Seyler 375:357–363, 1994.
42. JJ Beintema, A Blank, GL Schieven, CA Dekker, S Sorrentino, M Libonati. Differences in glycosylation pattern in human secretory ribonucleases. Biochem J 255:501–505, 1988.
43. RL Williams, SM Greene, A McPherson. The crystal structure of ribonuclease B at 2.5 Å resolution. J Biol Chem 262:16020–16031, 1987.
44. HC Joao, RA Dwek. Effects of glycosylation on protein structure and dynamics in ribonuclease B and some of its individual glycoforms. Eur J Biochem 218:239–244, 1993.
45. LT Hunt, MO Dayhoff. The occurrence in proteins of the tripeptides asparagine-X-serine and asparagine-X-threonine and of bound carbohydrate. Biochem Biophys Res Commun 39:757–765, 1970.
46. H Sinohara, T Maruyama. Evolution of glycoproteins as judged by the frequency of occurrence of the tripeptides Asn-X-Ser and Asn-X-Thr in proteins. J Mol Evol 2:117–122, 1973.
47. RR Hofmann, G Geiger, R König. Vergleichend-anatomische Untersuchungen an der Vormagen-schleimhaut von Rehwild und Rotwild. Z Saugetierk 41:167–193, 1976.
48. M Libonati, A Furia, JJ Beintema. Basic changes on mammalian ribonuclease molecules and the ability to attack double-stranded RNA. Eur J Biochem 69:445–451, 1976.
49. JJ Beintema. The primary structure of langur (*Presbytis entellus*) pancreatic ribonuclease: adaptive features in digestive enzymes in mammals. Mol Biol Evol 7:470–477, 1990.
50. MP Deutscher. Ribonuclease multiplicity, diversity, and complexity. J Biol Chem 268:13011–13014, 1993.
51. AW Nicholson. *Escherichia coli* ribonucleases: paradigms for understanding cellular RNA metabolism and regulation. In: G D'Alessio, JF Riordan, eds. Ribonucleases, Structures and Functions. San Diego: Academic Press, 1997, pp 1–49.
52. RH Silverman. 2-5A-dependent RNase L: a regulated endoribonuclease in the interferon system. In: G D'Alessio, JF Riordan, eds. Ribonucleases, Structures and Functions. San Diego: Academic Press, 1997, pp 515–551.
53. M Wang, SN Cohen. ard-1: a human gene that reverses the effects of temperature-sensitive and deletion mutants in the *Escherichia coli rne* gene and encodes an activity producing RNase E-like cleavages. Proc Natl Acad Sci USA 91:10591–10595, 1994.
54. A Wennborg, B Sohlberg, D Angerer, G Klein, A von Gabain. A human RNase E–like activity which cleaves RNA sequences involved in mRNA stability control. Proc Natl Acad Sci USA 92:7322–7326, 1995.
55. GP Moiseyev, JJ Beintema, LI Fedoreyeva, GI Yakovlev. High sequence similarity between a ribonuclease from ginseng calluses and fungus-elicted proteins from parsley indicates that intracellular pathogenesis-related proteins are ribonucleases. Planta 193:470–472, 1994.
56. GP Moiseyev, LI Fedoreyeva, YN Zhuravlev, E Yasnetskaya, PA Jekel, JJ Beintema. Primary structures of two ribonucleases from ginseng calluses. New members of the PR-10 family of intracellular pathogenesis-related plant proteins. FEBS Lett 407:207–210, 1997.
57. IE Somssich, E Schmelzer, P Kawalleck, K Hahlbrock. Gene structure and in situ transcript localization of pathogenesis-related protein 1 in parsley. Mol Gen Genet 213:93–98, 1988.
58. MH Walter, JW Liu, J Wünn, D Hess. Bean ribonuclease-like pathogenesis-related protein genes (Ypr_{10}) display complex patterns of developmental, dark-induced and exogenous-stimulus-dependent expression. Eur J Biochem 239:281–293, 1996.
59. I Swoboda, A Jilek, F Ferreira, E Engel, K Hofmann-Sommergruber, O Scheiner, D Kraft, H Breiteneder, E Pittenauer, E Schmid, O Vicente, E Heberle-Bors, H Ahorn, M Breitenbach. Isoforms of Bet v 1, the major birch pollen allergen, analyzed by liquid chromatography, mass spectrometry, and cDNA cloning. J Biol Chem 270:2607–2613, 1995.

60. H Breiteneder, F Ferreira, A Reikerstorfer, M Duchene, R Valenta, K Hoffmann-Sommergruber, C Ebner, M Brietenbach, D Kraft, O Scheiner. Complementary DNA cloning and expression in *Escherichia coli* of *Aln g* 1, the major allergen in pollen of alder (*Alnus glutinosa*). J Allergy Clin Immunol 90:909–917, 1992.
61. J Ross. RNA-processing RNases in mammalian cells. In: G D'Alessio, JF Riordan, eds. Ribonucleases, Structures and Functions. San Diego: Academic Press, 1997, pp 553–587.
62. CE Brown, AB Sachs. Messenger RNA ribonucleases and mRNA turnover in *Saccharomyces cerevisiae*. In: G D'Alessio, JF Riordan, eds. Ribonucleases, Structures and Functions. San Diego: Academic Press, 1997, pp 589–620.
63. AM Poole, DC Jeffares, D Penny. The path from the RNA world. J Mol Evol 46:1–17, 1998.
64. DC Jeffares, AM Poole, D Penny. Relics from the RNA world. J Mol Evol 46:18–36, 1998.
65. FM Richards, HW Wyckoff. Bovine pancreatic ribonuclease. In: P Boyer, ed. The Enzymes, 3rd ed, Vol 4. New York: Academic Press, 1971, pp 647–806.
66. W Zhao, Z Kote-Jarai, Y Van Santen, J Hofsteenge, JJ Beintema. Ribonucleases from rat and bovine liver. Purification, specificity and structural characterization. Biochim Biophys Acta 1384:55–65, 1998.
67. H Katoh, M Yoshinaga, T Yanagita, K Ohgi, M Irie, JJ Beintema, D Meinsma. Kinetic studies on turtle pancreatic ribonuclease: A comparative study of the base specificities of the B_2 and P_0 sites of bovine pancreatic ribonuclease A and turtle pancreatic ribonuclease. Biochim Biophys Acta 873:367–371, 1986.
68. JJ Beintema. Structure, properties and molecular evolution of pancreatic-type ribonucleases. Life Chem Rep 4:333–389, 1987.

78

Proteolytic Enzymes

John R. Whitaker
University of California, Davis, Davis, California, U.S.A.

I. INTRODUCTION

A. General Aspects, Including Importance for Food Science and Technology

Proteolytic enzymes hydrolyze peptide bonds in proteins and peptides [Eq. (1)]

$$\text{-HN-CHR}_1\text{-CO-NH-CHR}_2\text{-CO-} + \text{H}_2\text{O} \rightarrow$$
$$\text{NH-CHR}_1\text{-COOH} + {}^{+}\text{H}_3\text{N-CHR}_2\text{-CO-} \qquad (1)$$

They are found in all living organisms (animals, plants, and microorganisms). They are essential for digestion of food proteins to peptides and amino acids. The amino acids then are used for resynthesis of proteins unique for a specific organism. In the human gastrointestinal tract, the proteolytic enzyme pepsin (stomach) and a large group of small-intestinal proteolytic enzymes—trypsin, chymotrypsin, carboxypeptidases, leucine aminopeptidases, tripeptidases, and dipeptidases—convert the proteins of our ingested foods to amino acids. Humans have two internal digestive systems to hydrolyze proteins when they are no longer needed or are "worn out." These involve the lysosomal organelles of the cell containing the catheptic enzymes and the general proteolytic enzymes of the blood system. The liver is also very active in hydrolysis and in biosynthesis of proteins for numerous cells.

Many proteins are produced as zymogens; i.e., they are inactive until limited specific proteolysis transforms them into active enzymes. Examples include propepsin, protrypsin and prochymotrypsin, prolipases, proamylases, etc. In the blood-clotting mechanism, some nine pro-proteolytic enzymes need to be catalytically cleaved via a cascade process to form the active enzymes that permit blood clotting to occur (1). Proinsulin is initially synthesized in vivo and then converted to insulin by two proteolytic enzymes cleaving two different peptide bonds of pro-insulin (2). Several other examples are given in Table 1 and in Roberts and Herbert (3).

Proteins are synthesized in the endoplasmic reticulum on the m-DNA of the cell. Often, they are chemically modified following biosynthesis in numerous ways (4) and are transported outside the cell in to the blood system, where they are delivered to the host cells or other locations where they function. Transport out of the cell requires an N-terminal segment of amino acid residues (called the signal peptide), which is removed by highly specific proteolytic enzymes after the proprotein crosses the cell membrane (or wall in bacteria or plants). Proteins are continually synthesized and hydrolyzed at different rates, depending on the protein (Table 2) (5).

Some of the proproteins of glandular secretions are cleaved in the digestive tract to form specific peptides that have various physiological effects, such as the formation of adrenocorticotropic hormone (ACTH), β-lipotropic hormone (β-LP), β-melanocyte-stimulating hormone (β-MSH), β-endorphin, and enkephalin resulting from the specific proteolytic cleavage of a precursor protein of $\sim$ 8000 daltons (Fig. 1) (2, 3, 5).

Table 1 Physiologically Important Proteolysis

Conversion of food proteins to peptides and amino acids
Activation of zymogens to active enzymes
Blood coagulation
Collagen formation
Milk clotting in infant's stomach
Mammalian reproduction
Intracellular digestion of proteins
Protein translocation
Formation of hormones
Virus assembly
Immune response
Fibrinolysis
Blood pressure control
Sporulation of microorganisms
Germination of spores and plant seeds
Oncogenic transformation
Extracellular protein transport
Lysosomal protein degradation
Assembly of proteins, including tertiary and quaternary structures
Transfer of proteins across membranes
Inborn errors of amino acid metabolism and transport
Complement activation

Major physical property changes occur as the result of a single polypeptide bond cleavage by a highly specific protease. In the case of chymosin, hydrolysis of the -Phe105-Met106- bond of kappa-casein causes milk to clot (6). In the case of blood, sequential activation of the cascade of some ten pro-proteases leads to clotting of blood at the source of a wound in < 1 min (7). Table 3 lists a number of food products in which proteolysis is important (8).

Table 2 Rates of Intracellular Turnover of Some Selected Proteins

Protein	Half-life
Ornithine decarboxylase	10 min
δ-Amino levulinate synthetase	60 min
Catalase	1.4 d
LDH_5	16 d
Mitochrondria protein as whole	4–5 d
Rat protein (%)	4–5 d
Cultured cells	1–2% h

Source: Ref. 6.

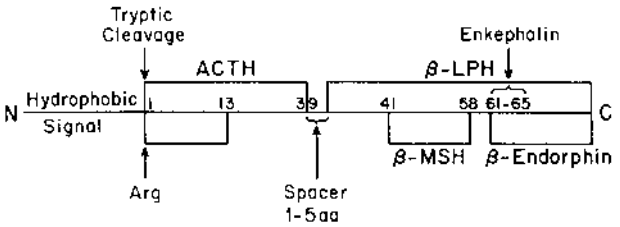

Figure 1 Pituitary gland protein precursor proteolytically cleaved to produce the hormones ACTH (adrenocorticotropic hormone), β-LPH (β-lipotropic hormone), β-MSH (β-melanocyte-stimulating hormone), β-endorphin, and enkephalin. (From Ref. 5.)

B. Specificity

Each proteolytic enzyme is very specific for a few peptide bonds of proteins. First, a protein must be denatured (unfolded) in order to be hydrolyzed. The proteins in our food are denatured by cooking and/or processing. The proteins of foods consumed raw are generally denatured by the high acidity of the stomach (pH 1–2 due to hydrochloric acid). Some physiologically important proteins, such as zymogens, have small segments that do not fold and thereby are hydrolyzed at nonfolded locations (between domains) to give active enzymes, hormones, etc.

Proteolytic enzymes are also specific in terms of being endoproteases or exoproteases. The endoproteases, such as trypsin, chymotrypsin, and chymosin, hydrolyze peptide bonds in the interior of the polypeptide chains. The exo-proteases act on peptide bonds at the N-terminal (aminopeptidases) or the C-terminal (carboxypeptidases) of the protein. The di- and tripeptidases act on di- and tripeptides produced by endoproteases to convert them to amino acids. The various types of proteases of the small intestine can, working together, convert proteins to their constituent amino acids in 2–4 h at 37°C. The human body must receive the essential amino acids (lysine, tryptophan tyrosine + phenylalanine, valine, leucine, isoleucine, threonine, histidine, methionine + cysteine) from food, as they cannot be produced in the body.

Proteolytic enzymes are also absolutely specific for one or few of the amino acid residues at the scissile peptide bond. For example, trypsin hydrolyzes peptide bonds only at lysyl and argininyl residues that furnish the carbonyl moiety of the peptide bond. Chymotrypsin hydrolyzes peptide bonds only when tyrosine, phenylalanine, or tryptophan residues provide the carbonyl group of the peptide bond. The amino acid residue at the N-side of the peptide bond

Table 3 Use of Proteolytic Enzymes in Food Processing

Food	Purpose of action
Baked goods	Softening action in doughs. Cut mixing time, increase extensibility of doughs. Improve texture, elasticity and loaf volume. Liberate β-amylase.
Brewing	Body, flavor, and nutrient development during fermentation. Aid in filtration and clarification. Chill-proofing.
Cereals	Modify proteins to increase drying rate, improve product handling characteristics. Production of miso and tofu.
Cheese	Casein coagulation. Characteristic flavor development during aging.
Chocolate, cocoa	Action on beans during fermentation.
Egg, egg products	Improve drying properties
Feeds	Waste product conversion to feeds. Digestive aids, particularly for pigs.
Fish	Solubilization of fish protein concentrate. Recovery of oil and proteins from inedible parts.
Legumes	Hydrolyzed protein products. Removal of flavor. Plastein formation.
Meats	Tenderization. Recovery of protein from bones.
Milk	Coagulation in rennet puddings. Preparation of soybean milk.
Protein hydrolysates	Condiments such as soy sauce and tamar sauce. Bouillon. Dehydrated soups. Gravy powders. Processed meats. Special diets.
Antinutrient factor removal	Specific protein inhibitors of proteolytic enzymes and amylases. Phytate. Gossypol. Nucleic acid.
Wines	Clarification[a]
In vivo processing[b]	Conversion of zymogens to enzymes. Fibrinogen to fibrin. Collagen biosynthesis. Proinsulin to insulin. Macromolecular assembly.

[a]In large part caused by other than proteolytic enzymes
[b]Representative examples given.

determines the relative rate at which the peptide bond is hydrolyzed. Some other proteolytic enzymes are even more specific, as chymosin will hydrolyze only the Phe105-Met106 peptide bond of kappa-casein.

C. Health Aspects Related to Metabolism of Proteins and Amino Acids

There are > 100 human diseases related to defects of protein and amino acid metabolism (9). These studies began as early as 1810, when Wollaston (10) discovered that defective cystine metabolism leads to cystine stones in the urinary tract due to high levels of cystine, lysine, ornithine, and arginine. The full extent and effect of these diseases are still not known.

One of the best known diseases is phenylketoneuria due to the routine testing of newborns (10). This disease is caused by deficiency of the enzyme phenylalanine hydroxylase, which converts phenylalanine to tyrosine. To date, the only medical intervention available is to exclude phenylalanine from the diet by use of protein hydrolysates from which phenylalanine has been removed. When the conversion of phenylalanine to tyrosine is blocked, the urine is dark in color, pigmentation of the skin is reduced (albinism), and neurological disturbances may occur since the levels of neurotransmitters dopamine and norepinephrine are reduced. At least eight diseases can result from failure in conversion of phenylalanine to formic acid and acetoacetic acid (9).

In babies, chymosin is a key enzyme in the stomach (replacing pepsin). Chymosin clots milk, causing it to remain longer in the stomach, where it is digested. Lack of adequate chymosin activity leads to a number of abnormalities.

Some adult humans are unable to digest some of the proteins in foods, such as glutin in wheat. These can lead to allergic reactions. To date, the only remedy is to avoid such foods.

II. TYPES OF PROTEOLYTIC ENZYMES

Given the large numbers of proteolytic enzymes (Sec. I), it is surprising that there are only four different types based on the active site. These are the serine proteases (EC 3.4.21), the cysteine proteases (EC 3.4.22), the aspartic proteases (EC 3.4.23), and the metalloproteases (EC 3.4.24), based on the catalytic group of the enzyme involved in the nucleophilic attack at the carbonyl carbon of the scissile peptide bond of the substrate.

A. Serine Proteases

The serine protease family includes trypsin, chymotrypsin, elastase, subtilisin, the nine proteases involved in blood coagulation (1), collagenase, and others.

1. Binding of Substrates and Inhibitors

Proteinwise, the serine proteases are a diverse group having different physical properties. However, at the active site they are essentially identical, except for the detail of the binding sites. The best-known binding sites are those for trypsin, chymotrypsin, elastase, and subtilisin. As shown in Figure 2, the binding sites of trypsin, chymotrypsin, and elastase are very similar except for one amino acid difference. In trypsin, there is a lysine (Lys residue) at the bottom of the pocket. In chymotrypsin, there is a tyrosine (Tyr residue) at the bottom of the pocket in place of a Lys residue. In elastase, there is a valine (Val residue) on one side of the pocket, which blocks assess of the substrate to most of the pocket.

Because of these modifications in the pocket, only lysyl and argininyl amino acid residues of protein and peptide substrates can bind stereospecifically to the active site of trypsin so that the peptide bond is oriented properly for hydrolysis [Eq. (2)].

$$\text{-HN-Lys}^{+}\text{-CO-NH-X-CO-} + \text{H}_2\text{O} \rightarrow \text{-HN-Lys}^{+}\text{-COOH} + {}^{+}\text{H}_3\text{N-X-CO-} \quad (2)$$

In chymotrypsin, the binding pocket is hydrophobic; therefore, the tyrosyl, phenylalanyl, and tryptophanyl amino acid residues of proteins and peptides can bind into the pocket stereospecifically so that hydrolysis occurs, as shown in Eq. (3) for tyrosine.

$$\text{-HN-Tyr-CO-NH-X-CO-} + \text{H}_2\text{O} \rightarrow \text{-HN-Tyr-COOH} + {}^{+}\text{H}_3\text{N-X-CO-} \quad (3)$$

In elastase, the available binding pocket is small, such that only small hydrophobic side chain amino acid residues, such as alanyl, can be bound and hydrolyzed [Eq. (4)].

$$\text{-HN-Ala-CO-NH-X-CO-} + \text{H}_2\text{O} \rightarrow \text{-HN-Ala-COOH} + {}^{+}\text{H}_3\text{N-X-CO-} \quad (4)$$

In 1967, Schechter and Berger (12) introduced the enzyme subsite concept to explain the binding of substrates into the active site of sulfhydryl proteases (Fig. 3). This concept has been extended to include the other three types of proteases. For example, in subtilisin (a serine protease), similar in specificity to chymotropsin, the binding site is at least six subsites in length – S_4, S_3, S_2, S_1, S_1', S_2' (13, 14), and eight subsites are found with some substrates and competitive inhibitors. These enzyme subsites are not sequentially located but exist on several of the secondary structural β-strands (strands 1–8) (Fig. 4). The enzyme subsites interaction strengths with substrates are not equal. In subtilisin the subsite S_1 and S_4 are the strongest; the S_1' and S_2' subsites binding is relatively weak. In subtilisin BPN′, S_1, S_2, and S_3 have been identified as Ser125-Leu126-Gly127 (16), while S_1', S_2' and S_3' are Gly102-Gln103-Tyr104 (17). In subtilisin produced by other strains, the subsites may show differences.

The native structures of subtilisin and trypsin are stabilized by calcium ions. However, the calcium ions do not participate in the binding and catalytic steps. They provide additional electrostatic binding with anionic bonds of the enzyme.

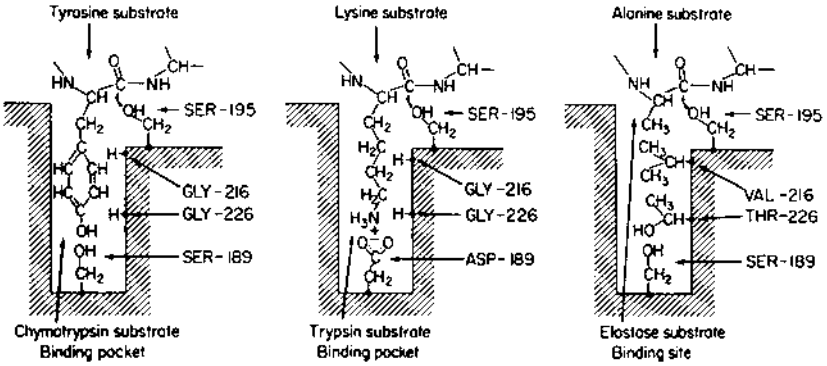

Figure 2 Schematic substrate binding sites in chymotrypsin, trypsin, and elastase. (From Ref. 11.)

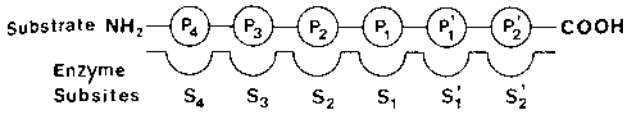

Figure 3 Schematic representation of complex of enzyme-substrate binding at subsites. (From Ref. 12.)

2. Catalytic Mechanism

The serine proteases generally hydrolyze both peptide and ester bonds of substrates, provided the enzyme substrate binding requirements are met as described above. Ester bonds of substrates are hydrolyzed much faster than peptide bonds since ΔH^* is ~ 7 kcal/mol for ester bonds vs. 20 kcal/mol for amide bonds. Therefore, small ester substrates, such as N-acetyl-L-tyrosine methyl (or ethyl) esters (for chymotrypsin and subtilisin) and N-benzoyl L-arginine methyl (or ethyl) esters (for trypsin) are used for mechanistic studies.

The serine proteases hydrolyze substrates by a two-step catalytic mechanism as shown by Eq. (5).

$$E + S \underset{k_{-1}}{\overset{k_1}{\rightleftharpoons}} E{\bullet}S \xrightarrow{k_2} EP_2 \xrightarrow{k_3} E + P_2 \qquad (5)$$
$$\qquad\qquad\qquad\qquad\quad \searrow P_1$$

The first step, controlled by k_1 and k_{-1} is the noncovalent binding of enzyme (E) and substrate (S) to form the Michaelis-Menten complex. Step 2, controlled by k_2, is the acylation step in which the acyl group (specificity side) of the substrate is transferred to the active site Ser oxygen of the enzyme active site (see Ser221 of Fig. 4) to form an ester bond [EP_2 in Eq. (5)]. Product P_1, the HN side of the peptide bond (or OR side of ester bond), dissociates from the enzyme active site. This step is controlled by the pH-dependent ($pK_a \sim 7$) protonated/deprotonated state of His64 of subtilisin (see Fig. 4). When the imidazole group of the catalytic site is protonated, the enzyme is inactive; when the imidazole group is unprotonated, the enzyme is active. The pH dependence of the acylation step can be sigmoidal (controlled by one pK_a for subtilisin) or bell shaped (controlled by two pK_as, the histidine residue, and the ionization of an N-terminal isoleucyl residue in trypsin and chymotrypsin). The N-terminal isoleucyl residue, in the ^+H_3N-isoleucyl form, is essential for maintaining the native structure of the enzyme via an electrostatic bond. Therefore, for amide substrates, the pH dependence of k_2 is bell shaped while for ester substrates it is sigmodial with a pK_{a1} of ~ 7 for trypsin and chymotrypsin.

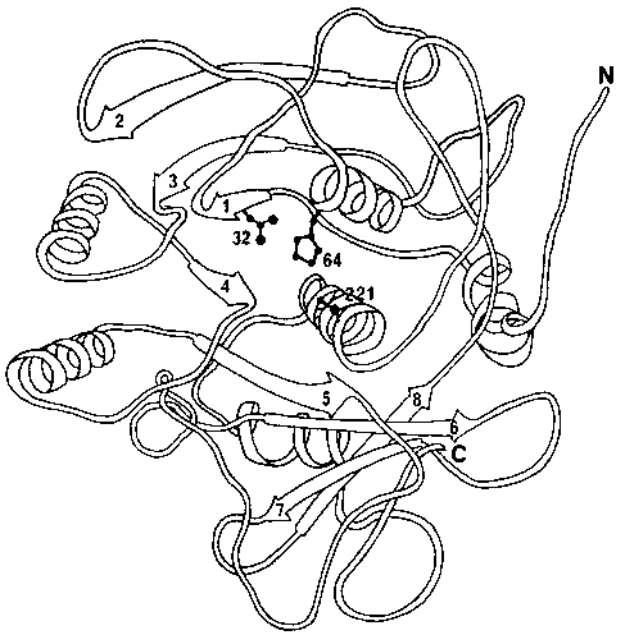

Figure 4 Schematic diagram of the three-dimensional structure of subtilisin viewed down the central parallel β-sheet. The catalytic site is composed of Ser32, His64, and Asp221. The eight β-strands are number 1–8; the six α-helices are coiled segments. (From Ref. 15.)

The step controlled by k_3 is due to deacylation (hydrolysis) in which the acyl group of the acyl-enzyme is removed by hydrolysis, eliminating the second product, P_2, as an acid. A single ionizable group, that of the imidazole group of His64 (of subtilisin), controls the deacylation step, giving a sigmodial curve with a pK_a of ~ 7 for all serine proteases. The pH and temperature dependencies of the k_3 step are identical for both amide and ester substrate hydrolyses.

Mechanistic details of the acylation and deacylation steps for subtilisin catalysis are shown in Figure 5. The acylation and deacylation half-reactions (Fig. 5) consist of the following steps: (a) formation of the Michaelis complex (ES) between the enzyme and substrate [k_1 and k_{-1} of Eq. (5)] that is noncovalent and reversible; (b) formation of a covalent tetrahedral intermediate via nucleophilic attack by the reactive Ser221-O_χ on the carbonyl carbon of the scissile bond of the substrate (this step is facilitated by a general base catalysis by His64); (c) conversion of the tetrahedral intermediate to the covalent acyl enzyme via protonation of the leaving group $R'NH_2$

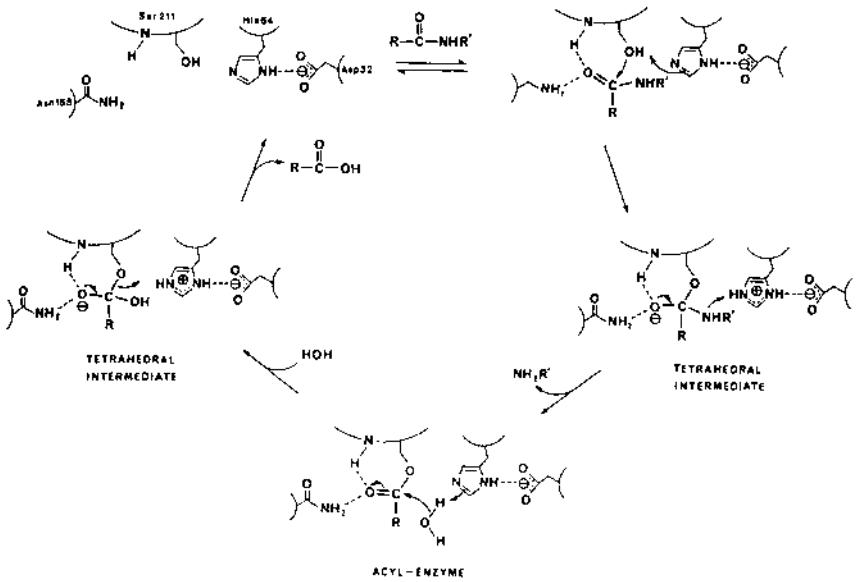

Figure 5 Reaction mechanism of subtilisin showing the catalytic pathway of acylation and deacylation via the formation of tetrahedral intermediates. (From Ref. 18.)

(P_1) of the substrate by His64; (d) nucleophilic attack by a water molecule, assisted by general-base catalysis involving His64 (this leads to a second tetrahedral intermediate); and (e) breakdown of the tetrahedral intermediate via His64-catalyzed protonation of the Ser221-O_χ, liberating the acyl group of the substrate as an acid (P_2).

The steady-state reaction equations resulting from Eq. (5) are:

$$k_{cat} = k_2k_3/(k_2 + k_3) \quad (6)$$

$$K_m = K_sk_3/(k_2 + k_3) \quad (7)$$

where $K_s = k_{-1}/k_1$.

For the reactive ester substrates, the rate of acylation is higher than deacylation ($k_2 \gg k_3$) so that K_m is $\sim K_sk_3/k_2$ and the rate-limiting step is that controlled by k_3 (deacylation). For amide and peptide substrates, $k_2 \ll k_3$. Therefore, k_2 approximates k_{cat} and $K_m \sim K_s$.

B. The Cysteine (Sulfhydryl) Proteases

Typical cysteine proteases include papain from the latex of unripe fruit of the *Carica papaya* tree, ficin from the fig tree (*Ficus carica*), actinidin from kiwi fruit (*Actinidia chinensis*), and bromelain from the pineapple (*Ananus comosus*) as well as the mammalian calpains (Ca^{2+} dependent) and some cathepsins (lysosomal).

The best-studied typical cysteine protease is papain, which will be discussed here because of its major uses in the food industry for chill proofing of beer and meat tenderization, as well as synthesis of peptides and other organic compounds. The lysosomal cathepsins are important because of their physiological roles in turnover of proteins in the body and their possible role in diseases, such as muscular dystrophy, osteoporosis, inflammatory heart diseases, and tumor invasion (19).

1. Protein Characteristics of Papain

Papain is a single polypeptide of 212 amino acids with a molecular weight of 23,350 daltons (20). It contains three disulfide bonds. Papain has exceptional stability to heat at neutral pH and to some organic solvents. It is the major protein in the aqueous phase of papaya latex, at $\sim$ 5% concentration. It can be spray dried at $\sim$65°C without loss of activity.

The primary sequence of amino acids in papain is known and the tertiary structure has been determined by x-ray crystallography (21). The molecule is folded into an ellipsoid with a dimension of $50 \times 37 \times 37$ Å. As shown in Figure 6, the polypeptide chain is folded into two domains, L and R. The L domain (N-terminal end of papain) includes amino acid residues 10–100, consisting of helices A, B, and C. The folding of the

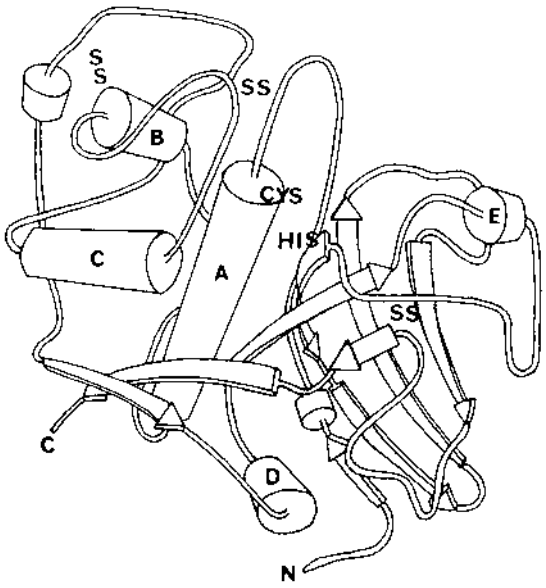

Figure 6 Schematic diagram showing the polypeptide folding in papain (actinidin folding is identical). The native molecule consists of two domains with a long cavity between the two. The left domain contains helices A, B, and C, while the right domain is formed from double β-sheet structures with helices D and E at opposite ends. The three SS's are disulfide bonds. The catalytic group Cys is on helix A while catalytic group His is on one of the β-strands. The third catalytic group is Asn (not shown). The substrate binds in the cavity formed by helix A and the pleated sheets to the right side (22).

three helices form a central core of high hydrophobicity. The R domain (C-terminal end) includes amino acid residues 113–207 and consists primarily of seven β strands which form a twisted antiparallel β-sheet producing a barrel with a large hydrophobic core. The two domains are covalently bound together only by three crossovers of the folded polypeptide chain. The interface of the two domains forms a groove (crevice) between the two domains which contains the active site of the enzyme.

2. Active Site of Papain

The active site, consisting of the binding and catalytic loci, is located in the groove formed by the two parallel R and L domains. The catalytic locus of papain consists of Cys25, (on the L domain), His159 (on R domain) [both shown at top of the groove (Fig. 6)], and Asn175 (not shown but located on the random chain within 5 Å of His159 on the R domain). The Cys25 lies adjacent to the N_1 of the His159 imidazole ring. The other His nitrogen, N_2, is hydrogen bonded to the side chain oxygen (R-CO-NH_2) of Asn175, which lies just above the His imidazole ring. During the covalent formation of the acyl enzyme, the imidazole rotates $\sim 30^\circ$, moving the His159-N_1 to a position coplaner with the leaving group nitrogen (23).

The binding locus of the active site of papain consists of seven subsites extending over 25 Å in the groove formed at the interface of the L and R domains. These subsites for binding are represented as -$S_4S_3S_2S_1$ $S_1'S_2'S_3'$- that interact with the peptide substrate amino acid side chains -H_2N-P_4, $P_3P_2P_1'1P_2'P_3'$- (12). Substrate specificity of the enzyme is largely determined by the acylating side (the -H_2N-$P_4\cdots$ side). The S_1 subsite of the enzyme is relatively nonselective, but it cannot accommodate P_1-containing substrates with branched chains, such as valine. The S_2 subsite of the enzyme is primarily responsible for the selectivity of the substrate. It consists of contributions from the hydrophobic side chains of Tyr67, Pro68, Trp69, Phe207, Ala160, Val133, and Val157 (24). Thus, subsite S_2 has a strong preference for the hydrophobic amino acid side chains of Phe, Tyr, Val, and Leu of substrates (25). The S_1' specificity is expressed in the deacylation step, similar to that for the serine proteases. The S′ subsite has a preference for the hydrophobic residues Leu and Trp. Therefore, the S_1'-P_1' interaction makes considerable contribution to binding and to the rate of hydrolysis (26, 27).

3. Catalytic Mechanism of Papain

The pathway of hydrolysis of substrates by papain, and other sulfhydryl proteases, follows that of the serine proteases [Eq. (5)]. Following formation of the Michaelis complex, a covalent acyl enzyme intermediate is formed in the second step controlled by k_2, releasing the first product. In the k_3-controlled step, water is activated to hydrolyze the thionyl enzyme intermediate to give free enzyme and the acid product. Therefore, the rate-limiting steps are controlled by k_2 and k_3, respectively, for amides and esters (24, 28). However, in contrast to the large differences found for ester vs. amide hydrolysis observed for subtilisin, trypsin, and chymotrypsin, the rates of ester and amide hydrolysis are similar for papain and the other cysteine proteases. This means that the cysteine proteases have a more efficient mechanism of lowering the activation energy, E_a, for forming the acyl enzyme intermediate or the amide substrate.

Figure 7 summarizes the reaction mechanism for hydrolysis of substrates by papain and the other sulf-

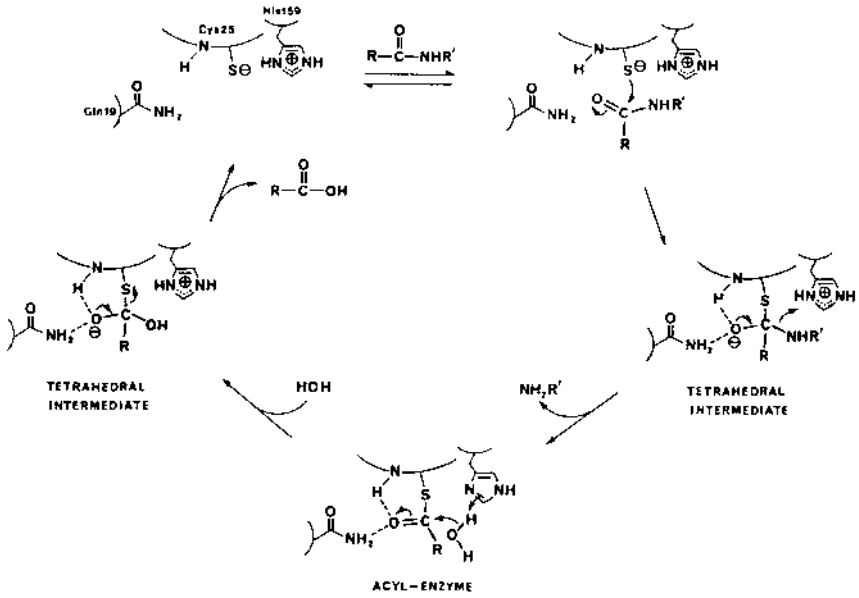

Figure 7 Reaction mechanism of papain showing the acylation and deacylation steps involving formation of tetrahedral intermediates. (From Ref. 18.)

hydryl proteases. The papain-catalyzed reaction pathways (Fig. 7) consists of the following steps: (a) the enzyme binds reversibly with the substrate to form a Michaelis complex, ES; (b) nucleophilic attack by the Cys25 thiolate anion on the carbonyl carbon of the scissile peptide bond of the substrate leads to the formation of a tetrahedral intermediate; (c) a collapse of the tetrahedral intermediate to an acyl enzyme is facilitated by protonation of the leaving group (amide nitrogen in the case of a peptide substrate) by the His159 imidazolium cation; (d) nucleophilic attack by a H_2O molecule assisted by His159 acting as a base catalyst results in deacylation of the acyl enzyme (which is a thiolester in the cysteine proteases). As shown, the pathway and mechanism are similar to those for the serine proteases.

C. Aspartic Proteases

The aspartic proteases have two aspartic acid residues in the catalytic locus of the active site, thus the name of aspartic proteases.

Calf chymosin (older name ''rennin''), porcine pepsin, cathepsin D, renin, penicillopepsin (*Penicillium* sp.), and the *Mucor pusillus* and *Mucor miethei* protease have been studied the most intensively. Calf chymosin and the *Mucor* proteases are very important in cheese making. The calf chymosin gene has been cloned and expressed in *Escherichia coli* (29, 30), *Saccharomyces cerevisiae* (31), *Aspergillus ridulans* (32), and *A. awamori* (32). Recombinant calf chymosin produced in genetically modified *E. coli* (a bacterium; 33), *A. awamori* (a fungus; 32), and *Kluyveromyces lactis* (yeast; 34) are approved by FDA for use in cheese making. While the proteolytic pH optima for these enzymes are pH $\sim$ 3–4, they are used at pH $\sim$ 5.2 for coagulation of the caseins of milk for cheese manufacture. At pH 5.2, the major peptide bond hydrolyzed is the $-Phe_{105}Met_{106}$ bond of kappa-casein.

1. Protein Structure of Chymosin

Calf chymosin, because of its commercial importance in cheese manufacture, is chosen for future detailed discussion in this chapter. Calf chymosin is produced as a prochymosin, without activity. Prochymosin is a single polypeptide chain of 365 amino acid residues. It is cleaved at the peptide bond between Phe42Gly43 by pepsin to give mature chymosin with 323 amino acid residues (35, 36). There are two chymosin isozymes. Chymosin A and B differ by a single amino acid residue, Asp or Gly difference at position 244, respectively (35, 36). The pH optimum of chymosin A is 4.2, while that of chymosin B is 3.7.

The single polypeptide chain of chymosin has an MW of 35 kDa, with three disulfide bonds. Its second-

ary structure is primarily a β-sheet protein with very little α-helix structure (Fig. 8) (37b).

Chymosin, similar to other aspartic proteases, has two domains separated by a deep substrate binding cleft, with a pseudo-twofold symmetry (Fig. 8). The N-terminal (1–175 amino acid residue sequence) and C-terminal (176–323 amino acid residue sequence) domains are topographically equivalent. Each of the domains is composed of two repeating motifs of four antiparallel β-strands and a helix. The two motifs pair to form two interlocked, four-stranded sheets that are packed orthogonally in each domain, giving a total of six antiparallel β-sheets (37b).

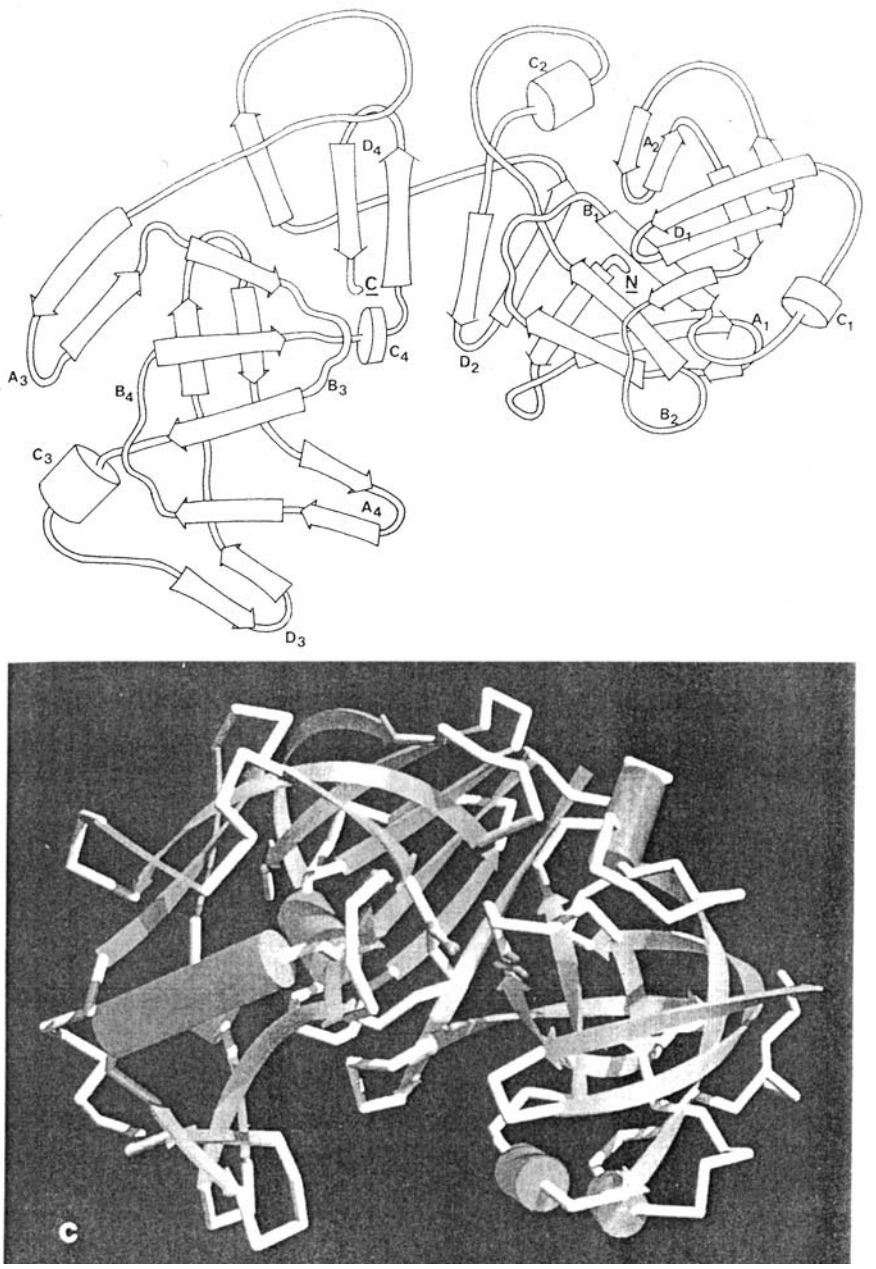

Figure 8 (Top) The general secondary structures of acid proteases showing the location of the first β hairpin turn A_1, wide loop B_2, helix C_1, and second hairpin turn D_2 in the right domain (37a). (Bottom) Recombinant bovine chymosin (37b). More details are in Ref. 37b.

2. Substrate Binding Locus of Chymosin

The extending binding locus is along the cleft between the two domains, containing up to seven subsites designated as $S_4S_3S_2S_1S_1'S_2'S_3'$ with the catalytic site (see below) located between S_1 and S_1'. The corresponding substrate units matching the binding site are NH_2-$P_4P_3P_2P_1P_1'P_2'P_3'$-COOH. Much research has been done on the effect of size and amino acid sequence of synthetic peptides as well as of bovine kappa-casein on K_m and k_{cat} for hydrolyzing the Phe105Met106 bond. A minimum of five amino acids including -SerPheMetAla- are required for hydrolysis of the PheMet bond. Addition of Leu to the N-terminal end and Ile to the C-terminal end to give substrate LeuSerPheMetAlaIle increases k_{cat} and decreases K_m. Addition of Pro further to either the N- or C-terminal end increased k_{cat}/K_m to 22 $mM^{-1}s^{-1}$ (38). The 15-amino acid residue tryptic peptide from *k*-casein (residues 98–112) with a sequence of HisProHisProHisLeu SerPheMetAlaIleProProLysLys used as a substrate for bovine chymosin gave k_{cat}/K_m of 4715 $mM^{-1}s^{-1}$ at pH 5.3–5.5 and 2123 $mM^{-1}s^{-1}$ at pH 6.6 (39). Kinetic studies using bovine k-casein as substrate gave k_{cat}/K_m of 1413 $mM^{-1}s^{-1}$ (pH 6.2, 30°C) with k_{cat} of 68.5 s^{-1} and K_m of 0.048 mM (40). Therefore, the results for the 15-amino acid residue tryptic peptide as substrate for bovine chymosin is considered to represent the maximal cleavage rate of the Phe105Met106 bond by chymosin.

3. Catalytic Locus of Chymosin

The catalytic locus is located at the base of the cleft between the N- and C-terminal domains (Fig. 8). It consists of the essential Asp34 and Asp216 amino acid residues, with the two carboxyl groups oriented toward the cleft. The distance between the carboxyl oxygens of the two aspartic acid residues is 3.1 Å. The two essential aspartic acid residues are located at the ends of the B_1 and B_2 loops formed by two homologous segments, N-terminal Asp34Thr35Gly36Ser37Ser38 and C-terminal Asp216Thr217Gly218Thr219Ser220. These two loops overlap each other such that the O of the OH group of Thr35 of the N-terminal loop hydrogen bonds with the N of the peptide bond of Thr217G218. A β-loop of 12 sequential amino acid residues (residues 71–82: -Lys71 Pro72Leu73Ser74Ieu75His76Tyr77Gly78Thr79Gly80 Ser81Met82) forms a "flap" over the cleft, such that the substrate is enclosed in a hydrophobic environment especially at the scissile bond P_1P_1' (41).

Calf chymosin, like all the aspartic proteases, gives a bell-shaped pH-V_{max} plot, with pKs of 3.2 and 4.7 for the synthetic substrate LysProA1aGluPhePhe(NO_2) AlaLeu (42) and pKs of 2.3 and 4.7 if acid-denatured hemoglobin is the substrate (43). The pH optimum is 3.7, where one aspartic acid carboxyl group involved in catalysis is ionized and the second aspartic acid carboxyl group is protonated.

The proposed mechanism of hydrolysis by bovine chymosin is shown in Figure 9 (44, 45). It is a general acid/general base catalysis with no covalent intermediate. The peptide bond carbonyl oxygen of the substrate is protonated by the Asp diad proton. This protonation increases polarization of the carbonyl peptide bond ($> C = O \cdots H^+$), resulting in a more positive carbon center for nucleophibic attack of a H_2O molecule. The nucleophilic attack of H_2O occurs at the peptide carbonyl carbon of the substrate by base catalysis (^-OH) assisted by the Asp carboxylate anion. This results in the formation of a noncovalent tetrahedral intermediate. The peptide bond nitrogen atom of the tetrahedral intermediate accepts a proton from a water molecule of the Asp diad. The N-protonation facilitates cleavage of the C-N bond of the tetrahedral intermediate.

D. Metalloproteases

Most of the metalloproteases are exopeptidases. These include the carboxypeptidases A (peptidyl-L-amino acid hydrolase, EC 3.4.17.1) and B (peptidyl-L-lysine hydrolases, EC 3.4.17.2), glycyl-glycine dipeptidase (dipeptide hydrolase, EC 3.4.13.11), carnosinase (acts on β-alanyl-L-histidine and related compounds; amino-acyl-histidine hydrolase, EC 3.4.13.3), and cytosol aminopeptidase (α-amino-acyl-peptide hydrolase, EC 3.4.11.1). All require Zn^{2+} as cofactor. Prolidase (where proline or hydroxyproline is the carboxyl terminal residue; aminoacyl-L-proline hydrolase, EC 3.4.13.9) and iminodipeptidase (in which proline or hydroxyproline is the N-terminal residue; L-propyl-amino-acid hydrolase, EC 3.4.13.8-9) require Mn^{2+}. These are just a few representatives of the many exoproteases known. Thermolysin (EC 3.4.24.4) is a metalloendoprotease, with similar active site, specificity, and mechanism to carboxypeptidase A (see Chap. 79). Other metallopeptidases include the collagenases of microorganisms and the hemorrhagic proteinases of snake venoms.

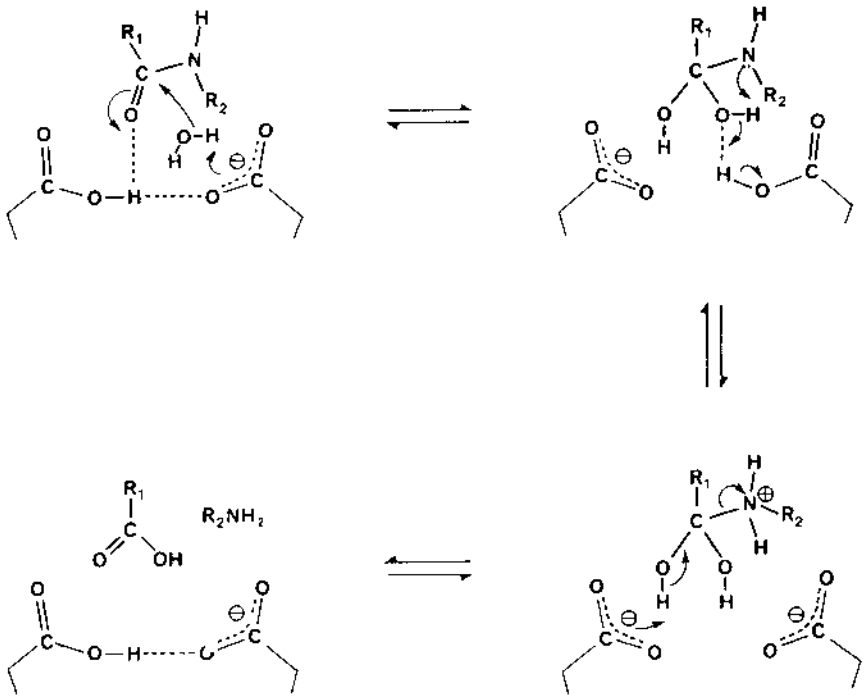

Figure 9 Proposed reaction mechanism of chymosin. (From Refs. 44, 45.)

1. Carboxypeptidase A

Bovine carboxypeptidase will be described as a prototype metalloproteolytic enzyme.

Most proteolytic enzymes are synthesized as proenzymes and are then activated by cleavage of one or more peptide bonds. This is a protective mechanism to prevent premature proteolysis. Bovine procarboxypeptidase A has a molecular weight of 87,000 and consists of three noncovalently linked polypeptide (subunits I, II, and III) (46).

Controlled trypsin treatment initially gives an enzymatically active product with one or a few peptide bonds hydrolyzed in subunit II and activity on N-acetyl-L-tyrosine ethyl ester similar to that of α-chymotrypsin (a serine protease). Further treatment with trypsin hydrolyzes a peptide bond in subunit I, giving carboxypeptidase A–like activity on hippuryl-L-β-phenyllactic acid (HPLA). The molecular weight is still $\sim$ 87,000 daltons, and both chymotrypsin and HPLA activities are present. More extensive treatment with trypsin destroys (inactivates and degrades) both subunits II and III, leaving only the 34,500-dalton subunit I with carboxypeptidaselike activity on the synthetic substrates benzyloxycarbonylglycyl-L-phenylalanine (CGP) and benzoylglycyl-β-L-phenyllactic acid (HPLA) as well as on the C-terminal ends of proteins and peptides containing any amino acid residue other than arginine or lysine (these C-terminal ends are susceptible to carboxypeptidase B hydrolysis).

During conversion of procarboxypeptidase A to carboxypeptidase A, several different peptide bonds at the N-terminal end of subunit I are hydrolyzed, giving at least four different active forms of carboxypeptidase A. These are A_α (307 amino acid residues), A_β (305 residues), A_χ (300 residues), and A_δ (300 residues, but with different physical properties. The x-ray crystallographic structure of carboxypeptidase A_α, A_β, and A_χ have been determined (Fig. 10). The N-terminal is an alanyl residue (No. 1), while the C-terminal is an asparagine residue (No. 307). Some 55 amino acid residues (18% of total) are involved in a twisted β-pleated sheet structure, made up of four pairs of parallel and three pairs of antiparallel strands that form one side of the pocket which extends into the molecule and forms the active site. The helical regions of the enzyme involve 92 amino acid residues (30% of total) and are primarily α-helices. The remaining 160 amino acid residues (52%) are in randon coils.

Figure 10 Secondary and tertiary structures of carboxypeptidase A determined by x-ray crystallography. The small open circles along the protein chain represent the α-carbon atoms of the 307 amino acid residues. The active site is indicated by the large circle in the center of the molecule. (From Ref. 47.)

The region around the active site is not a cleft, as described for subtilisin, papain, and chymosin earlier in this chapter, but rather is a hole in the enzyme. This is shown diagramatically in Figure 11, where the hole is shown at the top of the figure in a zig-zag nature with the C-terminal tyrosine residue (S_1') of the substrate enclosed. The remainder of the substrate is vertically oriented with the other amino acid residues S_1, S_2, S_3, and S_4 pointing downward. The peptide bond hydrolyzed is between S_1' and S_1. As the substrate is oriented, on the left side the Zn^{2+} (cofactor) of the enzyme is bound to His69, Glu72, and His196 residues of the enzyme and to the carbonyl O of the first peptide bond of the substrate; the Glu^{-} 270 of the enzyme is coordinated with the C of the carbonyl group of the substrate; and on the right side $Arg^{+}145$ of the enzyme is electrostatically bound to the carboxylate group of residue 1 (phenylalanyl); the hydroxyl group of Tyr248 of the enzyme is coordinated to the N's of peptide bond one and peptide bond two of the substrate and $Arg^{+}71$ to the carbonyl O of peptide 3 of the substrate. Depending on the size and nature of the substrate, reactive groups of the substrate may also interact with $Arg^{+}124$, Tyr198, and Phe279 of the enzyme.

Lipscomb et al. (47) proposed the following mechanism for the action of carboxypeptidase A. The most probable steps in the mechanisms that we slightly favor at present for polypeptide substrates, not necessarily in the order given, are as follows:

1. Water is displaced as the C-terminal side chain of the substrate moves into the (hydrophobic) pocket, the carboxylate group of the substrate saltlinks to Arg145, the carbonyl group of S_3 and perhaps S_4 bind to Arg71, and sidechains particularly of S_3 but also of S_2 and S_4 associate with Tyr198 and Phe279. (Residues S_2 and S_3 and S_4 are amino acid residues 1, 2, and 3 removed from the terminal amino acid residue of substrate.) The oxygen of the carbonyl group of the susceptible peptide (bond) probably coordinates to Zn, but the alternative in which this carbonyl is directed away from Zn has also been discussed. Large conformational changes associated with the binding step are the movement of the guanidinium group of Arg145 by ~ 2 Å to bind the terminal carboxyl group of the substrate, the coordinated movement of the OH of Tyr248 by 12 Å to donate a hydrogen bond to the NH of the (strained) susceptible peptide bond and to receive a hydrogen bond from the penultimate peptide bond,

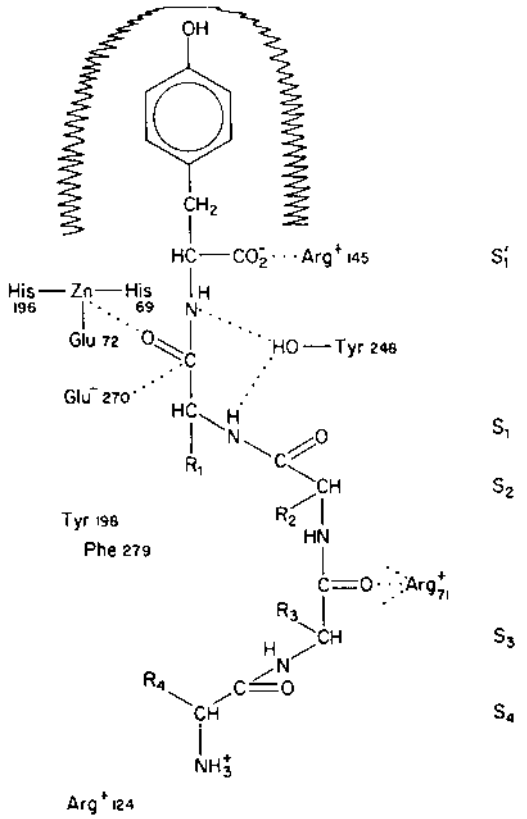

Figure 11 Schematic drawing of a substrate bound in the active site of carboxypeptidase A. The NH and CO groups of the scissile peptide bond are in a plane perpendicular to that of the drawing. The substrate is arranged vertically and center of the diagram. The amino acid residues of the enzyme surround the substrate and are numbered. (From Ref. 47.)

and the movement of the carboxylate group of Glu270 ~ 2 Å away from the region of the susceptible peptide bond in order to preserve normal Van der Waals contact in the binding step.

2. Tyr248 donates H^+ to the NH of the peptide bond, forming a phenoxide ion (of Tyr248) which is stabilized by the hydrogen bond donated from the penultimate peptide bond, and in the case of the "Zn-carbonyl" mechanism, Glu270 forms an anhydride with the carbon of the polarized $C^{\delta+} \cdots O^{\delta-} \cdots$ Zn carbonyl bond of the susceptible peptide (or Glu270 promotes the attack of water on this carbon atom).

3. After the peptide bond is split, a water molecule can cleave the anhydride (if formed) in a step which may be facilitated by the nearness of the phenoxide ion of Tyr248.

4. The remainder of the polypeptide chain moves away, the conformational changes are reversed, the C-terminal residue leaves the pocket, and the water molecules reenter (47).

Whether or not the details of the mechanism are correct in all aspects, the complexity of the enzyme action is not likely to be any less complicated than described above. For the substrate, benzyloxycarbonylglycyl-L-phenylalanine, k_{cat} is $106\,s^{-1}$ at pH 7.50 and 25.0°C, which means that one molecule of enzyme converts 106 molecules substrate to product in 1 sec (9.4 msec per substrate molecule converted to product). Truly, an enzyme is a very efficient catalyst!

Subsequent research, including x-ray crystallography, showed that the substrate benzyloxycarbonylglycyl-L-phenylalanine (CGP) can bind into the active site of the enzyme in four different ways (Fig. 12). Binding in modes (a), (b), and (c) leads to inhibition of the enzyme, rather than catalysis as shown for mode (d).

III. MEASUREMENT OF PROTEOLYTIC ACTIVITY

The activity of a protease is determined by whether it hydrolyzes peptide bonds in a protein. Its catalytic specificity is determined by which peptide bonds it hydrolyzes in the protein. Its catalytic efficiency is determined by how fast it hydrolyzes peptide bonds under standard conditions of pH, temperature, and enzyme concentration. Whether it is an endo- or exoprotease is determined by the products formed near the beginning of a reaction. Endoproteases hydrolyze the protein in the interior of the molecule, giving large polypeptide fragments. Exoproteases hydrolyze the N-terminal amino acid(s) from the protein (aminopeptidases) or from the C-terminal end (carboxypeptidases).

Proteases do not hydrolyze native protein molecules, i.e., those which are folded properly in the native state. An exception to this rule is that of a native protein folded into two or more independent domains. In this case the protease may hydrolyze peptide bonds in the random segment between the domains for which it has specificity. If a dissolved protein has both native and random structures in equilibrium ($N \rightleftharpoons R$), a protease may hydrolyze the R form, thereby permitting all the protein to be hydrolyzed. Therefore, the rate of hydrolysis may be controlled by the rate at which N is converted to R in the reaction.

Two protein substrates are generally used to determine the presence of proteases in plant, animal, and

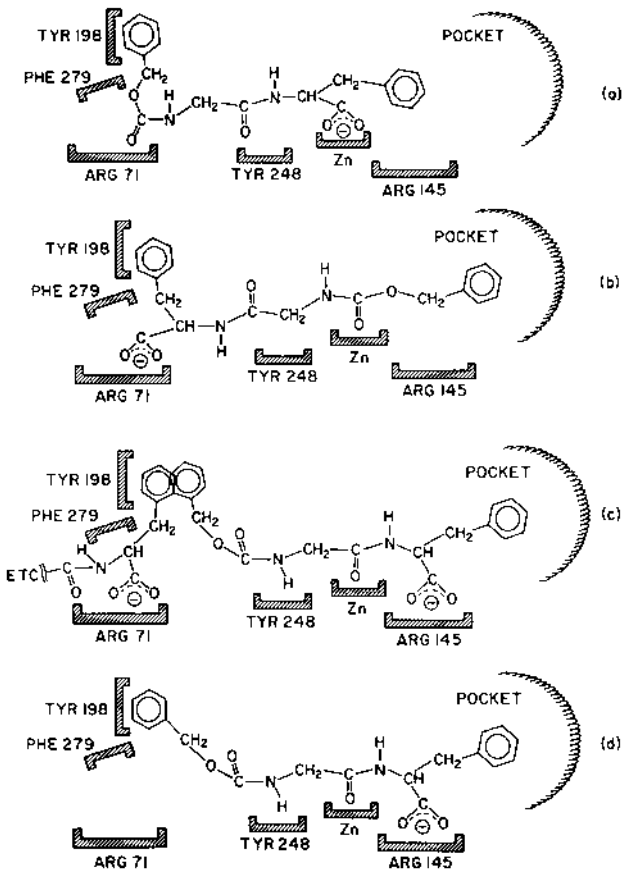

Figure 12 Proposed modes of binding of the substrate benzyloxycarbonylglycyl-L-phenylalanine into the active site of carboxypeptidase A. Only (d) is properly oriented to be converted to product. Substrate bound as shown in (a), (b), and (c) are competitive inhibitors. (From Ref. 47.)

microbial extracts. These proteins are bovine casein (generally mixture of α_s, β, and κ-caseins or purified α_s-casein) and bovine hemoglobin. The caseins are flexible molecules and readily hydrolyzed by proteases without need for denaturation by urea, heat, or temperature treatment. On the other hand, hemoglobin must be denatured, usually with 6 M urea treatment, prior to use as substrate. One difficulty with casein is that it precipitates near its isoelectric point (pH 5.1), making it difficult to use in the pH range of 5 ± 1. Denatured hemoglobin is soluble in this acid pH range.

The protein assay methods generally depend on increase in trichloroacetic acid–soluble products from proteolysis or by milk-clotting activity (48).

A. Casein Hydrolysis Method (49)

The Kunitz method is probably the most frequently used method to determine general proteolysis, applicable for all proteases (with modification of pH and presence of a sulfhydryl compound for activation of cysteine proteases). The following procedure is a modification used for many years with great success (50).

A stock solution of casein is prepared by suspending 5 g casein (preferably made by the Hammarstein method (51) in 100 mL distilled water, adding 0.5 mL of 5 N NAOH with mixing and incubating at 90° C for 15 min. This solution can be stored in the refrigerator and can be used for up to a week. Just before use, the stock casein solution is adjusted to 1% concentration and to desired pH (depending on protease) and buffer concentration (usually 0.1 or 0.2 M). For cysteine proteases sufficient stock cysteine solution (prepared fresh each day) is added to give 25 m*M* cysteine concentration in the final reaction.

At the time of use, aliquots of the 1% casein solution (1–4 mL) are incubated for at least 5 min at the temperature of the experiment. Sufficient aqueous solution (used to prepare the enzyme) is added that the overall volume will be reached when the enzyme solution is added (any constant volume needed based on activity). A timer is started after mixing the enzyme with substrate for two or three inversions of the tube. Multiple tubes can be run by starting the reactions at 30-sec intervals. At the chosen time, 3 mL of 5% trichloroacetic acid (e.g., 3 mL for a 2.00-mL reaction of enzyme and substrate) is added and mixed immediately, to stop the reaction. The stopped reaction(s) are held for 1 h (this time can be shortened to 10–20 min by placing the tubes in a 40–50°C water bath). The holding time is to complete the precipitation of TCA-insoluble products (casein and large polypeptides). The samples are centrifuged for 5–20 min depending on the centrifugal force. The clear solution is removed and read at 280 nm. Blanks are prepared by adding the TCA solution *prior* to adding the enzyme.

The results can be reported as increase in A_{280nm} with time or can be converted to phenol equivalents by use of a tyrosine standard solution (stock solution of 289.7 mg pure, dry tyrosine, dissolved in 1.00 L of 0.2 *M* HCl; working solution diluted 10-fold in 0.2 *M* HCl for use) to give 0.161 m*M* solution. One unit of protease is defined as the amount of enzyme which yields absorbance (or color value in phenol color method (below)) of 1 mmole of tyrosine per minute under the conditions used (reaction volume, pH, temperature).

A standard activity/trypsin activity curve is shown in Figure 13. Note that the data are linear only at low trypsin concentrations. This is because of limitations imposed by substrate concentration and limitation of "best" peptide bonds to hydrolyze. Absolute specificity of trypsin is for arginine and lysine residues of the substrate on the carboxyl side of the susceptible peptide bond, and relative specificity for the 20 different amino acid residues on the nitrogen side of the susceptible peptide bond.

Other methods are available for determining activity of proteases on casein. These include the phenol color method (52, 53), using the Folin-Ciocalteau phenol reagent to determine the TCA-soluble tyrosine concentration (54). This is less useful than the method above, since phenolic compounds in plant tissues also react with this reagent. The TNBS (2,4,6-trinitrobenzenesulfonic acid (picric acid) reagent is probably the best since it determines the number of peptide bonds hydrolyzed per unit time (55). However, this reagent is difficult to obtain, as it is explosive under some conditions. Ninhydrin can be used to determine the number of peptide bonds hydrolyzed, but it is not as accurate as the TNBS reagent.

Urea-denatured hemoglobin (53) can be used in place of casein under conditions similar to those described for use of casein. As noted above, casein cannot be used in the range of pH 5 ± 1 because it is insoluble. Denatured hemoglobin is soluble in this pH range and is used.

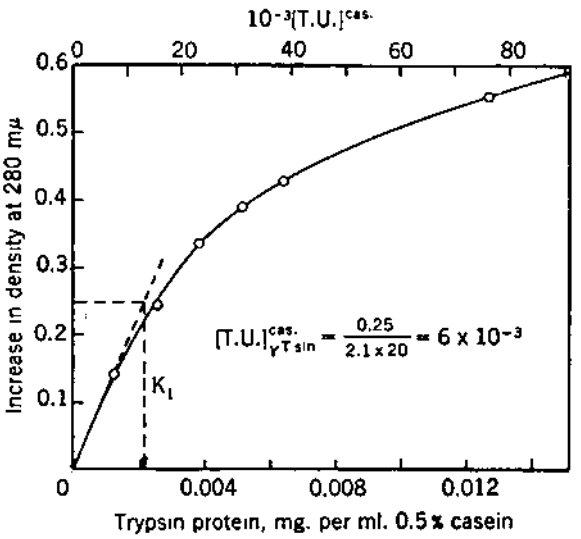

Figure 13 Standard activity curve for trypsin hydrolysis of casein. (From Ref. 49.)

B. Milk-Clotting Method (56)

The milk-clotting method is done in the pH range of 5.3–6.3. The original Balls and Hoover (56) method is described here, followed by some results by Whitaker (1998, unpublished).

Twenty grams of whole powdered milk (nonfat powder is better in the opinion of this author since storage time has less effect on results) is ground (or stirred to a smooth paste with a small amount of 0.05 *M* acetate buffer, pH 4.6 (stock solution prepared by mixing two volumes of 1 *M* acetic acid with one volume of 1 *M* sodium hydroxide). Stock buffer, 10 mL, is diluted to 85 mL with water and, when added to 20 g added milk powder gives 100 mL substrate. The reconstituted milk is filtered through cheesecloth for use. It is stable for several weeks in the refrigerator under a small layer of toluene.

Portions (1 mL) of serial dilutions of the enzyme are incubated in 15-mm-diameter test tubes with 10 mL milk preparation. When the milk preparation shows a thickening on tilting, the time is recorded. Sulfhydryl proteases (papain, ficin, bromelain) are activated with cysteine or dithiothreitol before use.

My laboratory has made some modifications to this milk-clotting procedure over the years. These include use of nonfat dry milk powder, a pH of 5.3, and the use of total reaction volume of 1 or 2 mL in small test tubes. The tubes are continuously rolled by hand at a 45° angle with a lamp placed immediately over the sample. The time of clotting is when the first granular precipitate occurs on the wall of the tube. Replications are within 0.5-sec of each other.

C. Gelatin Digestion Method

Papain is a major industrial protease produced from papaya fruit. The proteases are primarily papain and chymopapain, but there are low levels of other proteases. The proteases make up the bulk of the protein ($\sim 5\%$ of the liquid which also contains water insoluble latex). The juice is extracted, filtered, and spray-dried at $\sim 65°C$ without any loss of activity. Several methods for determining activity include the casein digestion method (CDM), the milk-clotting method (MCM), and the gelatin digestion method (GDM). The last method is followed by measuring rate of decrease of viscosity. The United States Pharmacopeia National Formulary (57) and the Food Chemical Codex (FCC; 58, 59) have attempted to standardize the methods used to

measure papain activity to encourage comparison among suppliers and users.

In 1998, Whitaker was asked to compare the three methods using proteins as substrate on a single sample of papain. Triplicate determinations were done under established conditions. The results were obtained within 16 h contiguous time using samples prepared in triplicate. The papain solutions were stored in an ice bath. The results are shown in Figures 14–16, using conditions indicated in the figure legends. In summary, the results, expressed on per-mg papain and per-min basis were: Casein Digestion Method, 590 mg^{-1} min^{-1}; Gelation Digestion Method, 8.34 mg^{-1} min^{-1}; and Milk-Clotting Method, 0.125 mg·min.

D. Synthetic Substrates

The above methods only determine that protease activity is present. To determine the type of protease—chymotrypsinlike or trypsinlike, for example—or endo- or exosplitting, it is necessary to use synthetic substrates. For example, N-acetyl-L-tyrosine ethyl ester (ATEE) is used for chymotrypsinlike enzymes. N-tosyl-L-arginine methyl ester (TAME) is used for trypsinlike enzymes. The ester derivatives are hydrolyzed at a faster rate than the equivalent amide substrates and measured by easier methodology. In many laboratories, there is also a tendency to use the equivalent nitrophenyl esters, which are hydrolyzed even faster, and the reaction can be followed spectrophotometrically by change in absorbance at 420 nm (pH > 7; the pK_a of the nitrophenol product is 7.16). At pHs > 7, controls must be done to substract the hydroxide ion–catalyzed hydrolysis of nitrophenyl esters and other ester substrates. Only one method will be described here. Other sources should be consulted for details of other enzymes and synthetic substrates (61, 62).

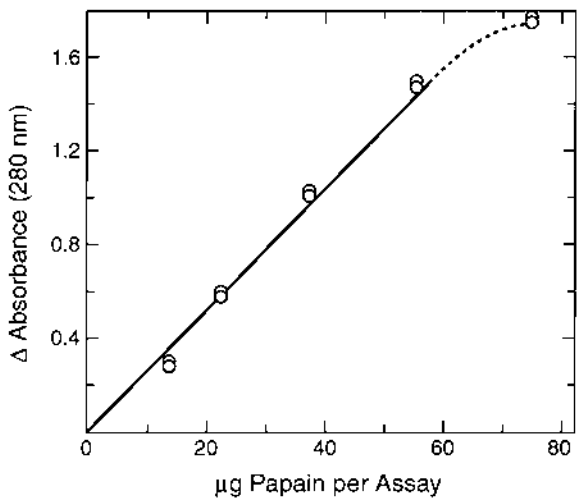

Figure 14 Results of the Casein Digestion Method for determining papain activity (57, 58). Plot of change in absorbance at 280 nm after 60 min reaction at 40°C, pH 6.0. Different amounts of papain used per assay (10 mL vol). The USP method (57, 58) was used. (From Whitaker, unpublished data, 1998.)

Chymotrypsin activity can be assayed by spectrophotometry at 256 nm using N-benzoyl-L-tyrosine ethyl ester (BTEE) or N-acetyl-L-tyrosine ethyl ester (ATEE), or N-benzoyl-L-tyrosine-*p*-nitroanilide. It can also be assayed using N-carbobenzoxy-L-tyrosine *p*-nitrophenyl ester at 420 nm. All the reactions for the above substrates are generally done at pH 7.8 and 25° C (61).

There are also fluorometric methods for the assay of chymotrypsin using N-acetyl-L-tryptophan ethyl ester (63), N-acetyl-L-tyrosine ethyl ester (64), and fluorescein dibutryrate (64) as substrates. Unfortunately, the fluorescein butyrate is also hydrolyzed by lipases, so the substrate should be used only for purified chymotrypsin solutions.

In the potentiometric method of determining chymotrypsin activity, the total reaction volume is generally 3–5 mL and the temperature is 25–35°C. The reaction includes 0.02–0.04 M BTEE or ATEE, 0.01–0.02 M phosphate buffer, pH 7.0–7.5, and sufficient enzyme to produce ~ 0.02 meq carboxyl groups per min. The reaction is performed for 5–10 min only as the initial velocity is determined. In the potentiometric method, the reaction rate is determined by titrating the acid formed by standard NaOH (0.02–0.05 M) so as to keep the pH constant. This can be done manually or with a pH Stat.

In the spectrophotometric method the change in absorbance at 256 nm is recorded during the reaction time. The absorbance is converted to umoles substrate hydrolyzed per min by use of the Beer-Lambert equation (Abs = $\Delta\epsilon_M$cl) where $\Delta\epsilon_M$ = change in extinction coefficient between AT-ATEE (or BT-BTEE) on hydrolysis, c is concentration of product formed and l is light path through cuvette (usually 1.0 cm). The change in extinction coefficient, $\Delta\epsilon_M$, between acetyl-L-tyrosine (AT) and acetyl-L-tyrosine ethyl ester (ATEE) = 1.05×10^3 M^{-1} cm^{-1}. The same $\Delta\epsilon_M$ is found for BT-BTEE.

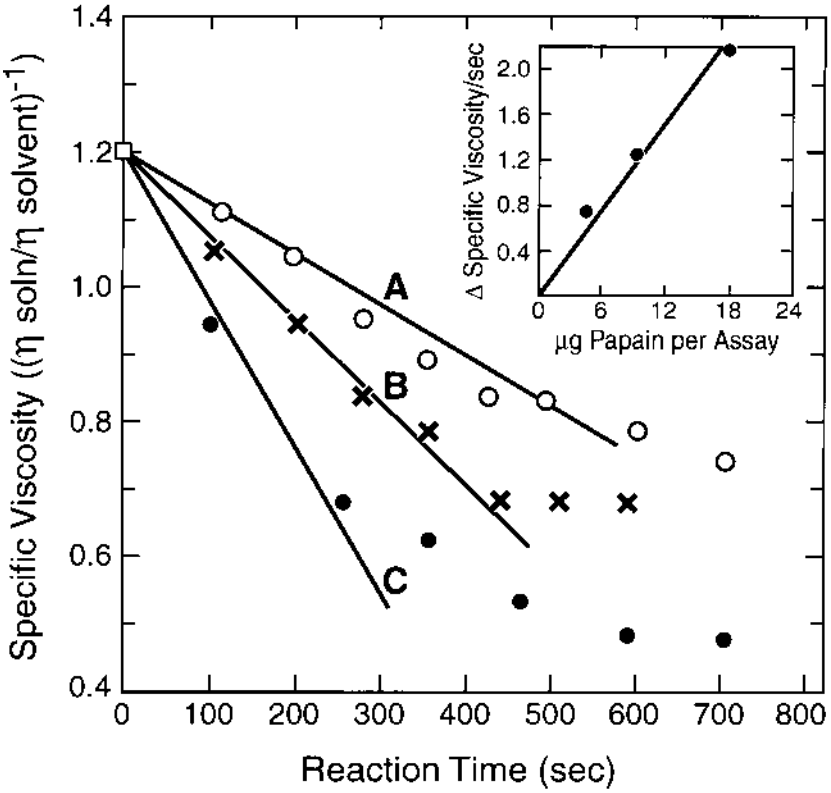

Figure 15 Results of the Gelatin Digestion Method for determining papain activity (60). The reaction used 4.5 mL of 2.5% gelatin plus 0.50 mL papain solution in acetate buffer, pH 6.0, 40°C. A, B, C: Specific viscosity change as function of time with 4.73, 9.46, or 18.9 μg papain in the reactions of 5.0 mL. Insert: replot of slope of initial specific viscosity change as function of time vs μg papain used in the assay. (From Whitaker, unpublished data, 1998.)

Crude samples containing chymotrypsin must be solubilized and clarified before the spectrophotometric method can be used. One of the best methods is that of Schlaeger and Roehr (64a)

IV. PURIFICATION OF PROTEASES

Purification of proteases began by classical techniques in the 1930s by Northrup, Kunitz, and Anson at the Rockefeller Institute in New York City and was very successful (65). Classical techniques include selective extraction procedures, followed by ammonium sulfate or acetone precipitation leading eventually to purification or crystallization of the protease.

More modern techniques include cation and anion column chromatography, size exclusion chromatography, inverse-phase chromatography, affinity chromatography, hydrophobic chromatography, electrophoresis, etc. Recent methods for the purification of subtilisin, papain, chymosin, and carboxypeptidase A will be presented here.

A. General Purification of Proteases as a Class

Stepanov and Rudenskaya (66) reported that a bacitracin-Sepharose column is effective for the affinity chromatography of aspartyl, serine, metallo- and cysteine proteases (ficin, papain, and bromelain) from various sources. The yield of purified enzyme varied from 50% to 180%. Bacitracin (Fig. 17), a cyclic peptide antibiotic produced by *Bacillus licheniformis*, contains 11 amino acid residues of which four are D- and six are L-isomers and one is a cyclic amino acid. It is resistant to proteolysis. In solution, it inhibits papain, subtilisin, leucinaminopeptidase and pepsin with K_is of 5, 4.5, 2, and 2.3 mM, respectively (67, 68).

The conditions used and the results are shown in Figures 18–20. Expanded methodology and discussions are found in Stepanov and Rudenskaya (66). No indication of purity of the preparations were given.

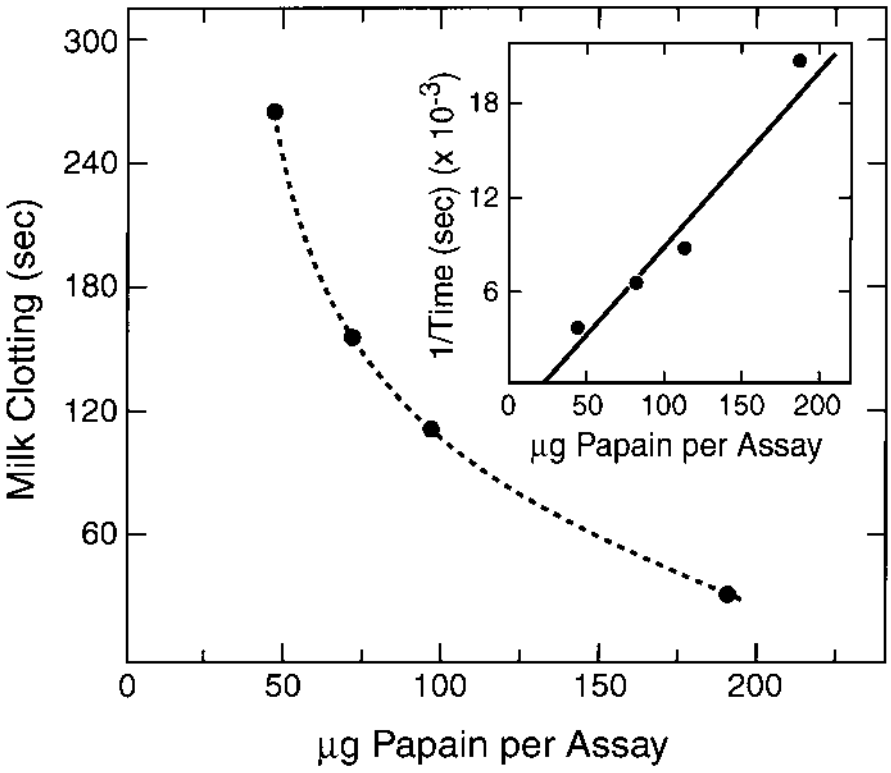

Figure 16 Results of the Milk-Clotting Method for determining papain activity. The large graph shows plot of time of milk clotting vs. μg papain in assay. The insert graph is a plot of 1/(clotting time, t) vs. μg papain per assay, which is linear but does not go through zero as reported by Greenberg (48). The reason is due to inhibitory effect of one or more compounds in the milk. The reaction contained 5.0 mL of 12% substrate (milk) + 0.20 mL papain solution and was performed at pH 6.3 and 30°C, as recommended by the Chemical Code Method (59).

B. Purification of Subtilisin

Chandrasekaran and Dhar (69) found that subtilisin can be purified in a single step by affinity chromatography. The affinity matrix was activated CH-Sepharose 4B coupled to the dye 4-(4-aminophenylazo)-phenylarsonic acid. The coupling conditions are given in the paper.

For chromatography, purified crystalline subtilisin (5 mg/mL) was dialyzed overnight against 20 mM acetate buffer, pH 5.9, containing 5 mM $CaCl_2$. The dialyzed solution (4.8 mL) was loaded to the column (1 × 51 cm). The column was washed with the starting buffer (used in dialysis) until the A_{280} returned to the baseline. The bound subtilisin was eluted with 10 mM Tris-HCl buffer containing 5 mM $CaCl_2$ and 0.1 M NaCl, pH 9 (Fig. 21, top). The enzyme was purified 1.4-fold (specific activity: 41 U/mg proteins; 98% recovery).

Purification of crude subtilisin used the product Alcalase 2.0 T. Product (2 g/mL) was dissolved in the starting buffer (above) and centrifuged at 10,000 g for 20 min. The supernatant was dialyzed overnight against the same buffer and 5 mL was loaded onto the column (1 × 51 cm). The chromatography was performed as above (Fig. 21, top). The crude enzyme was purified 211-fold (specific activity of 58 U/mg protein) with 94.4% recovery of activity.

Protease activity was determined by the Kunitz method (49; see Sec. III). Protein concentration was measured by the Lowry method (70) using bovine serum albumin (Sigma) as the standard. The column

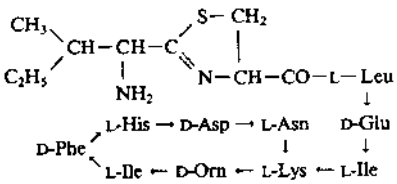

Figure 17 Bacitracin A.

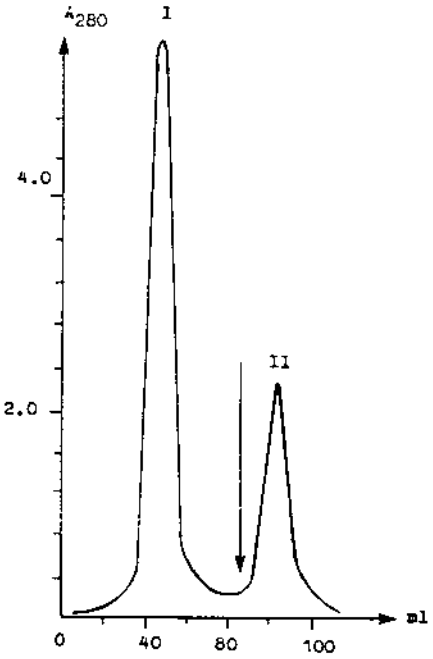

Figure 18 Chromatography of crude subtilisin 72 on bacitracin-Sepharose column. Preparation (400 mg) in 20 mL of 0.1 *M* ammonium acetate, pH 6.5, containing 1 m*M* $CaCl_2$ was applied to the bacitracin-Sepharose column (1 × 12 cm) equilibrated with the same buffer. The arrow shows the start of elution with 25% isopropanol in 1 *M* NaCl, pH 6.5. Fraction I contains inert materials; Fraction II, subtilisin (66).

used was estimated to contain ~ 40 mg of adsorbant. The column binding capacity for subtilisin A was determined to be 190 mg. The eluted subtilisin was determined to be pure by polyacrylamide slab gel electrophoresis.

C. Purification of Papain (71)

Papain might be purified by the method of Stepanov and Rudenskaya (66) on a bacitracin-Sepharose column, but this has not been proved since crude papain contains papain, chymopapain, and an aminopeptidase, which may not be separated by this method.

The Kimmel and Smith method (71) described here is an improved method of that of Balls and Lineweaver (72) and gives crystalline papain. They started with hard particles of commercial latex that had to be ground to a fine powder to permit extraction. Currently, papain is separated from the insoluble latex by filtration and dried at ~65°C in a spray drier. The dried material is soluble at 20% and retains

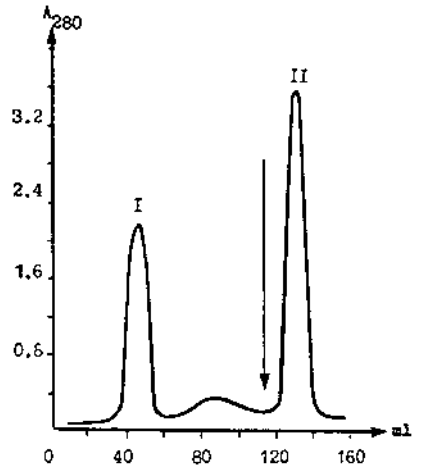

Figure 19 Chromatography of commercial papain preparation on bacitracin-Sepharose. Papain (70 mg) in 7 mL of 0.1 *M* phosphate buffer, pH 7.0, containing 0.1 *M* Na_2EDTA and 3 m*M* dithiothreitol was applied to the bacitracin-Sepharose column (1 × 12 cm) equilibrated with the same buffer. The arrow indicates start of elution with 25% isopropanol in 1 *M* NaCl. Fraction I contained inert material; Fraction II, papain (activity measured against azocasein). (From Ref. 66.)

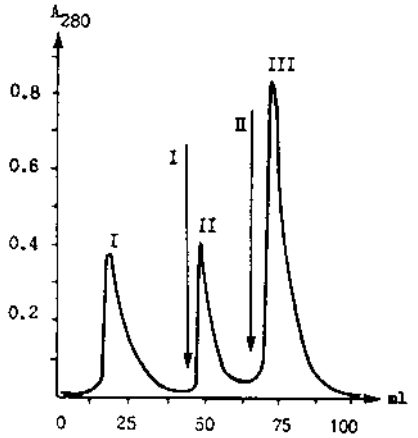

Figure 20 Separation of serine proteinase and carboxypeptidase T from *Thermoactinomyces* sp. Enzyme mixture (17.5 mg) dissolved in 7 mL of 0.1 *M* ammonium acetate, pH 6.5, containing 1 m*M* $CaCl_2$, was applied to the bacitracin-Sepharose column (1 × 12 cm). Arrow I indicates start of elution with 20 m*M* Na_2EDTA; arrow II, elution with 25% isopropanol in 1 *M* NaCl, pH 6.5. Fraction I contained inactive material; Fraction II, carboxypeptidase T (activity measured after reactivation by Ca^{2+}); Fraction III serine thiol–dependent proteinase (active against substrate Z-Ala-Ala-Leu-$NHC_6H_4NO_2$). (From Ref. 66.)

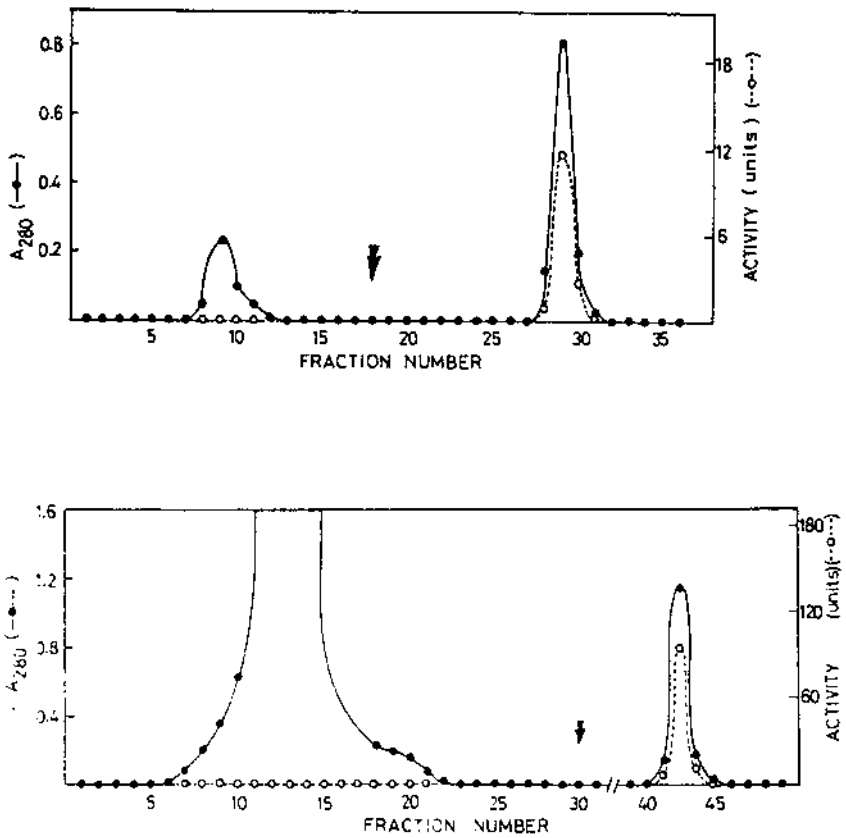

Figure 21 (Top) Affinity chromatography of crystalline subtilisin on a 4-(4-aminophenylazo)phenylarsonic acid–CH–Sepharose column. See text for experimental details. (Bottom) Purification of subtilisin from a crude preparation. See Top and text for details. (From Ref. 69.)

full activity. In water, it has a pH of ~ 5.5 (Whitaker, unpublished data).

The soluble papain (1 L) was carefully adjusted to pH 9.0 with ~ 110 mL of 1 N NaOH which is added slowly with stirring (Fraction 1; Table 4). A fine grayish denatured precipitate formed, which was removed by centrifugation at 2600 rpm for 1 h. The solution should be clear (Fraction 2).

Fraction 2 was cooled to 4°C and brought to 0.4 saturation with solid ammonium sulfate (250 g/L). A white precipitate formed. After 1–2 h at 4°C, the precipitate (Fraction 3) was recovered by centrifugation at 2500 rpm for 1 h. The supernatant fraction was saved for preparation of chymopapain. The precipitate was washed over with 400–500 mL cold (4°C) 50% saturated ammonium sulfate, and the precipitate was separated by centrifugation as above.

Fraction 3 was redissolved in 600 mL of 0.02 M cysteine (pH 7–7.5; freshly prepared), and 60 g of solid sodium chloride was slowly added. Papain was precipitated as a fine white solid. After standing for 1 h at 4°C, it was centrifuged in the cold for 1 h at 2500 rpm. The supernatant liquid was discharged. The precipitate was Fraction 4.

Fraction 4 was suspended in 400 mL of 0.02 *M* cysteine at pH 6.5 and adjusted to pH 5 with 1 *M* HCl as needed. At room temperature, the suspension developed a marked crystalline sheen in ~ 30 min. It was then placed in a cold room (or refrigerator) at 4°C overnight. The light crystals (Fraction 5) were removed by centrifugation at 2000–2500 rpm for 4–5 h. The supernatant liquid may be discarded. After several hours a small, insignificant amount of crystals formed.

Recrystallization was by dissolving Fraction 5 in the minimum amount of distilled water at room temperature and adding very slowly, with stirring 10 mL saturated sodium chloride per 300 mL protein solution. Crystallization began when ~ 75% of the 10-mL of saturated sodium chloride was added at room temperature. The suspension was then moved to a 4°C room

Table 4 Preparation of Crystalline Papain from Dried Papaya Latex[a]

Fraction No.[b]	Volume (ml)	Total protein (g)	C_1 [c]	Total activity (units)
1	770	45	0.19	1300
2	860	43	0.23	1500
3		13	0.30	580
3a	735	36	0.25	1470
4a	530	8	0.18	215
5	Crystals	2.1	0.84	270
5a	400	3.8	0.12	72
6	2 recrystallizations	1.2	1.06	190

[a]180 g dried latex used as starting material.
[b]Fractions 4a and 5a were discarded. Fraction 3a was saved for the isolation of chymopapain.
[c]The proteolytic coefficients (C_1) were determined with benzoyl-L-argininamide as substrate at 39°C, pH 5.5, in the presence of 0.005 *M* cysteine and 0.001 *M* EDTA. The units of activity are calculated by multiplying the C_1 value by the total amount of protein N in the fraction

overnight and the crystals were collected as described for Fraction 5. They were dissolved and recrystallized again as for Fraction 5.

The second crystallization is Fraction 6 in Table 4. About 1.2 g of crystals was obtained with a specific activity of 1.06. If desired, they may be recrystallized as mercuripapain with a specific activity of 1.15–1.20. This is done by dissolving the twice-recrystallized papain at room temperature in 70% ethanol/water containing 0.001 M $HgCl_2$. The protein concentration should be 1.5–2.0% for best results. If the solution is slightly turbid, the solution is filtered (before crystals form) and then stored at 4°C. Within 24 h a white crystalline precipitate forms, and after 3–4 days 90% of the activity crystallizes from solution. The large, heavy crystals are easily removed by centrifugation.

The mercuripapain has no activity. Activity is restored by treatment with a solution of 1 mM EDTA-5 mM cysteine. Specific activity was 1.19.

D. Purification of Calf Chymosin

1. Affinity Chromatography Method (73)

An affinity chromatographic column was used to purify crude chymosin (73). The 1.5-mL affinity column was packed with succinyl-Val-dLeu-Pro-Phe-Phe-Val-dLeucinamido-propyl Perloza. The column was equilibrated with buffer A (10 m*M* citrate, pH 4.4). A 5-mL sample of liquid containing chymosin ~0.3 mg/mL was diluted with 10 mL water, and the pH was adjusted to 4.4 using 1 *M* HCl. The chymosin-containing solution was loaded onto the column, which was then washed with buffer A until the A_{280} returned to baseline. The chymosin was eluted with buffer B (10 m*M* citrate, pH 6.0). The column was washed with 0.1 *M* NaOH to remove remaining protein. The results are shown in Figure 22; chymosin was eluted in buffer B. No chymosin activity was present in peaks 1 or 3. The purity of the chymosin is shown in Figure 23, lane 2. The nature of the small lower peak was not explained. Crude recombinant chymosin is shown in lane 4, as a single band. The binding capacity of the affinity column resin was determined to be 27 mg/mL of chymosin per ml of resin (column support material).

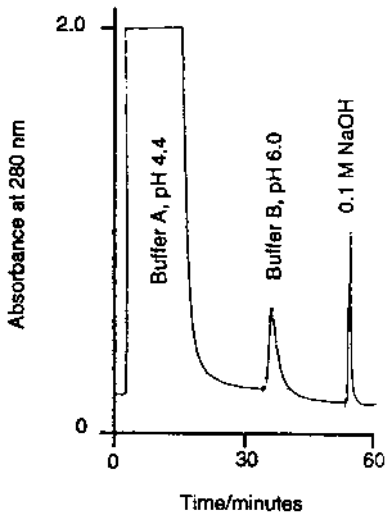

Figure 22 Chromatography of crude recombinant chymosin using succinyl-Val-dLeu-Pro-Phe-Phe-Val-dLeucinamido-propyl Perloza column. (From Ref. 73.)

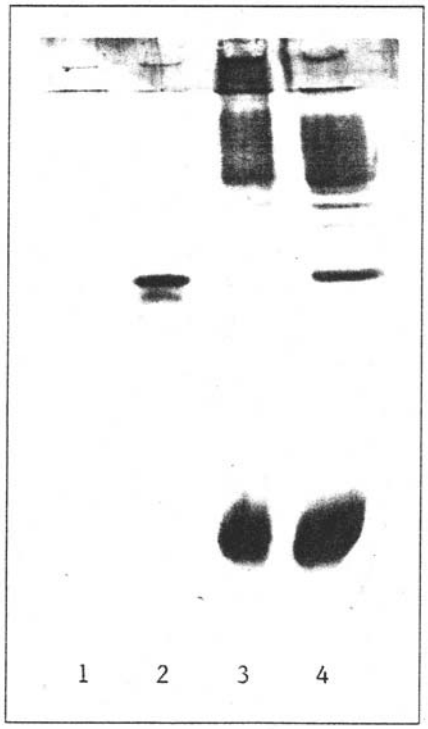

Figure 23 SDS-PAGE analysis of fractions from chromatography of crude recombinant chymosin. Lane 1, 0.1 M NaOH wash; lane 2, pH 6.0 buffer B elution; lane 3, pH 4.4 buffer A breakthrough; lane 4, unchromatographed crude recombinant chymosin. (From Ref. 73.)

2. Purification of Recombinant Calf Chymosin (74)

Prochymosin produced by *Escherichia coli* following insertion of the calf prochymosin gene is insoluble and denatured. The cell lysis procedure (75), based on lysozyme/sodium deoxycholate and ultrasonic treatment, was used to disrupt the cells. The chymosin inclusions were pelleted by centrifugation (6000g, 5 min, 5°C) and were washed with 50 m*M* Tris-HCl, pH 8.0, containing 1 *M* EDTA, and then with 50 m*M* $CaCl_2$ containing 0.5% (v/v) Trition X-100 and 1.0 *M* EDTA. The inclusions were collected by centrifugation. Solubilization was achieved by holding the prochymosin for 1 h at 31°C, pH 10.4, in 8 *M* urea or 50 m*M* KH_2PO_4, 1 m*M* EDTA, 50 m*M* NaCl, 8 *M* urea, pH 10.7. After 40 min the pH was adjusted with HCl to pH 8 within 10 min. If turbid, it was centrifuged at 12,000g for 10 min at 5°C.

The crude prochymosin was purified by ion exchange chromatography at room temperature (figure not shown in publication). The urea/alkaline extract was diluted approximately two times with distilled water to $\sim 38\,\mu$s, the same as the conductivity of the 20 m*M* Tris-HCl, 1 m*M* EDTA, 50 m*M* NaCl, pH 8.0 buffer (Buffer B). The diluted extract was applied to the DEAE-Sephacel (Pharmacia) column (0.9×1.6 cm; equilibrated with Buffer B above at a flow rate of 100 mL/h). The column was washed with four volumes of Buffer B with the NaCl concentration raised to 100 m*M*. The prochymosin was eluted with four volumes of Buffer B when the salt concentration was raised to 500 m*M* at the flow rate above. Fractions were collected.

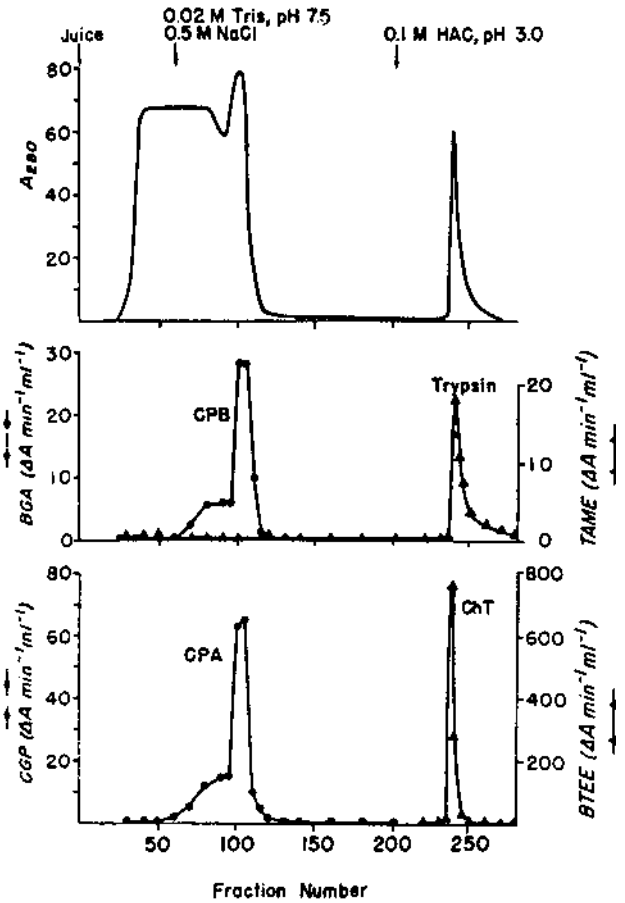

Figure 24 Chromatography of activated bovine pancreatic juice on soybean trypsin inhibitor–Sepharose column. Fraction volume was 25 mL. CPB, carboxypeptidase B (activity determined by substrate benzoylglycyl-L-arginine); CPA, carboxypeptidase A (activity determined by substrate carbobenzoxyglycyl-L-phenylalanine); trypsin (activity determined with substrate *p*-tosyl-L-arginine methyl ester); chymotrypsin (activity determined by N-benzoyl-L-tryosine ethyl ester). (From Ref. 79.)

The prochymosin was activated to chymosin by acidification to pH 2.0 (76). The activity of chymosin was assayed by a modified turbidimetric milk-clotting activity assay of McPhil (77) calibrated with crystalline calf chymosin prepared by the method of Foltmann (78). A typical recovery of correctly refolded chymosin was ~ 2 mg/33 mg applied protein.

E. Purification of Carboxypeptidases A and B (79)

Earlier sections of this chapter have not included carboxypeptidase B. Carboxypeptidase B is a metal-containing exopeptidase similar to carboxypeptidase A, but it is specific only for arginine and lysine residues at the carboxy-terminal end of proteins and peptides. Carboxypeptidase A can remove C-terminal amino acids other than arginine or lysine residues.

These two exopeptidases are found in the pancreas of animals. Figure 24 and Table 5 show the chromatography of activated proenzymes (converted to enzymes) from bovine pancreatic juice on a column of soybean trypsin inhibitor–Sepharose. The pancreatic juice (160 mL) was applied to the column. The column was then equilibrated with starting 0.02 *M* Tris buffer, pH 7.5, containing 0.5 *M* NaCl. The two carboxypeptidases were eluted together from the column under these conditions. Trypsin and chymotrypsin were eluted only when a 0.1 *M* sodium acetate, pH 3.0, buffer was applied.

The concentrated (to 210 mL volume by ultrafiltration) initial eluate from the column containing carboxypeptidases A and B was dialyzed for 36 h against a large excess of 0.02 *M* Tris, pH 7.5. A precipitate formed containing 91% of the carboxypeptidase A activity, while only 1% of the carboxypeptidase B activity precipitated. The carboxypeptidase A precipitate was collected by centrifugation, dissolved in 10% LiCl, and crystallized by dialysis against distilled water (80). Chromatography of the crystalline enzyme on a column of DE-52 cellulose by the method of Petra and Neurath (81) resulted in a single symmetrical peak corresponding to carboxypeptidase A_{β}^{Val} (Fig. 25).

The solution from dialysis for 36 h against 0.02 *M* Tris buffer, pH 7.5, contained carboxypeptidase B. It was dialyzed overnight against 0.02 *M* Tris, pH 8.0, at a protein concentration not exceeding 0.5 mg/mL. It was then applied to a 2.5×40 cm column of DE-52 cellulose which had been equilibrated with the same 0.02 *M* Tris buffer, pH 7.5, except $ZnCl_2$ was added to give 1 0^{-4} *M* concentration. After adding all the solution to the column, elution was achieved with a linear salt gradient from 0.0 to 0.1 M NaCl in a total volume of 2000 mL of 0.02 *M* Tris, pH 8.0, containing 10^{-4} M $ZnCl_2$. Carboxypeptidase B eluted in three peaks; they are labeled Native CPB, CPBI, and CPBII (Fig. 26).

The overall purification of carboxypeptidase B is summarized in Table 5. The purification sequence resulted in a 56-fold purification of carboxypeptidase B, with a yield of 71% of the original enzyme activity in the pancreatic juice.

In summary, the procedure permitted the purification of carboxypeptidase A from the supernatant from Fraction 2 on the soybean trypsin inhibitor–Sepharose column. Carboxypeptidase B was purified from

Table 5 Purification of Bovine Carboxypeptidase B

Preparative step	Volume (mL)	Enzyme conc; $\Delta A\ min^{-1}\ ml^{-1}$	Total units ($\Delta A\ min^{-1}$)	Protein ($mg \cdot mL^{-1}$)	Specific activity ($\Delta A\ min^{-1}\ mg^{-1}$)	Yield (%)	Purification (fold)
1. Pancreatic juice	1600	0.784	1254	3.87	0.097	100	1.0
2. Carboxypeptidase fraction from soybean trypsin inhibitor–Sepharose column (concentrated by ultrafiltration)	210	5.51	1157	5.86	0.448	92	4.6
3. Supernatant from dialysis against 0.02 M Tris, pH 7.5	230	4.62	1063	1.21	1.82	85	21
4. Sample for DE-52 column	73	13.4	978	1.37	4.65	78	48
5. Carboxypeptidase B fractions from DE-52 column	1000	0.889	889	0.078	5.45	71	56

Protein concentration was determined by absorbance at 280 nm assuming $A^{0.1\%} = 2.1$.
Source: Ref. 79.

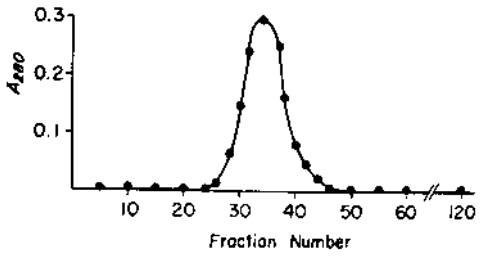

Figure 25 Chromatography of carboxypeptidase A obtained from step 2, Table 5 (from soybean trypsin inhibitor–Sepharose chromatography and dialysis) run on DE-52 cellulose column. The column was developed by flowing 0.05 *M* Tris, pH 7.5, containing 5 m*M* β-phenylpropionate and 0.04 *M* LiCl, at a flow rate of 39 mL/h on a 1.5×100 cm column. The fraction volume was 13 mL. (From Ref. 79.)

Fraction 2 dialysis as described above. Trypsin and chymotrypsin could also be purified from the first step of the procedure. Unfortunately, not all purification procedures are so rewarding.

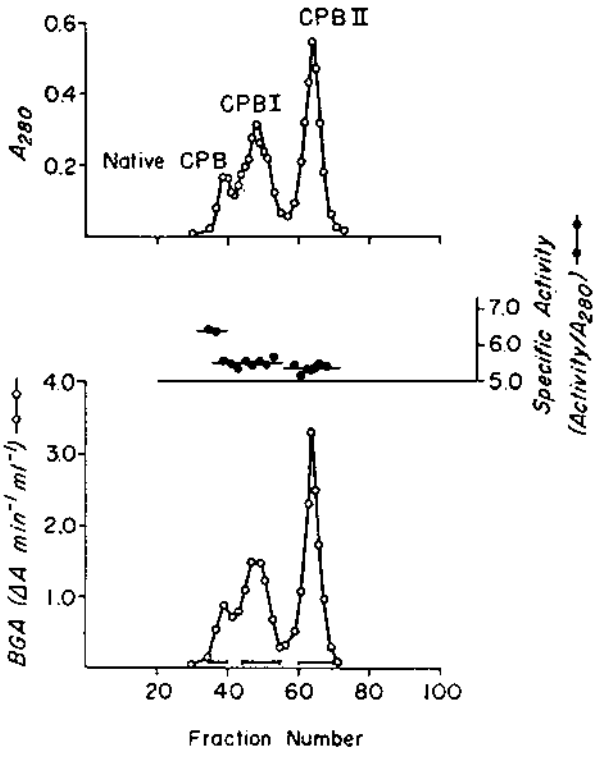

Figure 26 Chromatography of carboxypeptidase B (purified to step 5, Table 5, from activated bovine pancreatic juice) on a DE-52 cellulose column. The fraction volume was 25 mL. (From Ref. 79.)

REFERENCES

1. EW Davie, K Fujikawa. Basic mechanisms in blood coagulation. Annu Rev Biochem 44:799–829, 1975.
2. RE Chance, RM Ellis, WW Bromer. Porcine proinsulin: characterization and amino acid sequence. Science 161:165–167, 1968.
3. JL Roberts, E Herbert. Characterization of a common precursor to corticotropin and β-lipoprotein: identification of β-lipotropin peptides and their arrangement relative to corticotropin in the precursor synthesized in a cell-free system. Proc Natl Acad Sci USA 74:5300–5304, 1977.
4. JR Whitaker, AJ Puigserver. Fundamentals and application of enzymatic modifications of proteins: an overview. In: RE Feeney, JR Whitaker, eds. Modification of Proteins: Food, Nutritional and Pharmacological Aspects. Adv Chem Ser 198:57–87, 1982.
5. RT Schimke, MO Bradley. Properties of protein turnover in quality control of proteins. In: E Reich, DB Rifkin, Shaw, eds. Proteases and Biological Control. Cold Spring Harbor Conference on Cell Proliferation, 1975, Vol 2, pp 515–530.
6. HE Swaisgood. Primary sequence of κ-casein. J Dairy Sci 58:583–592, 1975.
7. H Holzer, PC Heinrich. Control of proteolysis. Annu Rev Biochem 49:63–91, 1980.
8. JR Whitaker. Enzymatic modification of proteins applicable to foods. In: RE Feeney, JR Whitaker, eds. Food Proteins: Improvement Through Chemical and Enzymatic Modification. Adv Chem Ser 160:95–155, 1977.
9. D Wellner, A Meister. A survey of inborn errors of amino acid metabolism and transport in man. Annu Rev Biochem 50:911–968, 1981.
10. WH Wollaston. ON cyctic oxide, a new species of urinary calculus. Ann Chim Paris 76:21–23, 1810.
11. D Shotton. The molecular architecture of the serine proteinases. In: H Fritz, H Tschesche, eds. Proc Intern Res Conf Proteolytic Enzymes. Berlin: Walter de Gruyter, 1971, pp 53–55.
12. I Schechter, A Berger. On the size of the active site in proteases. I. Papain. Biochem Biophys Res Commun 27:157–162, 1967.
13. K Morihara, T Oka. Inactivation by chloromethyl ketone derivatives of peptide substrates. Arch Biochem Biophys 138:526–531, 1970.
14. K Morihara, H Tsuzuki, T Oka. Comparison of various types of subtilisins in size and properties of the active site. Biochem Biophys Res Commun 42:1000–1006, 1971.
15. C Brandon, J Tooze. Introduction to Protein Structure. New York: Garland Publishing, 1991, p 242.

16. JD Robertus, RA Alden, JJ Birktoft, J Kraut, JC Powers, PE Wilcox. An x-ray crystallographic study of the binding of peptide chloromethyl ketone inhibitors to subtilisins. Biochemistry 11:2439–2449, 1972.
17. S Hirono, H Akagawa, Y Mitsui, Y Iitaka. Crystal structure at 2.6 Å resolution of the complex of subtilisin BPN′ with *Streptomyces* subtilisin inhibitor. J Mol Biol 178:389–413, 1984.
18. DWS Wong. Food Enzymes: Structure and Function. New York: Chapman & Hall, 1995, pp 131, 145.
19. AR Poole, KJ Tiltman, AD Recklies, TAM Stoker. Differences in secretion of the proteinase cathepsin B at the edges of the human breast carcinomas and fibroadenomas. Nature 273:545–547, 1978.
20. REJ Mitchell, IM Chaiken, EL Smith. The complete amino acid sequence of papain. J Biol Chem 245:3485–3492, 1970.
21. J Drenth, JN Jansonius, R Koekoek, BG Wolthers. Papain, x-ray structure. Enzymes 3:485–499, 1971.
22. EN Baker, J Drenth. The thiol proteases: structure and mechanism. In: FA Jurnak, A McPherson, eds. Biological Macromolecules and Assembles, Vol 3. Active Sites of Enzymes. New York: John Wiley & Sons, 1987, pp 313–368.
23. IG Kamphius, KH Kalk, MBA Swarte, J Drenth. Structure of papain refined at 1.65 Å resolution. J Mol Biol 179:233–256, 1984.
24. G Lowe, Y Yuthavong. Kinetic specificity in papain-catalyzed hydrolyses. Biochem J 124:107–115, 1971.
25. I Schechter, A Berger. On the active site of proteases. III. Mapping of the active site of papain. Biochem Biophys Res Commun 32:898–902, 1968.
26. A Williams, E Lucas, AR Rimmer, HC Hawkins. Proteolytic enzymes. Nature of binding forces between papain and its substrates and inhibitors. J Chem Soc Perkin Trans II: 627–633, 1972.
27. MR Alecio, ML Dann, G Lowe. The specificity of the S_1' subsite of papain. Biochem J 141:495–501, 1974.
28. AN Glazer, EL Smith. Papain and other plant sulfhydryl proteolytic enzymes. Enzymes 3:501–547, 1971.
29. K Nishimori, Y Kawaguchi, M Hidaka, T Uozumi, T Beppu. Expression of cloned calf prochymosin gene sequence in *Escherichia coli*. Gene 19:337–344, 1982.
30. JS Emtage, S Angel, MT Doel, TJR Harris, B Jenkins, G Lilley, PA Lowe. Synthesis of calf prochymosin (prorennin) in *Escherichia coli*. Proc Natl Acad Sci USA 80:3671–3675, 1983.
31. CG Goff, DT Moir, T Kohno, TC Gravius, RA Smith, E Yamasaki, A Taunton-Rigby. Expression of calf prochymosin in *Saccharomyces cerevisiae*. Gene 27:35–46, 1984.
32. KJ Hayenga, D Crabb, L Carlomagno, R Arnold, H Heinsohn, B Lawlis. Protein chemistry and recovery of calf chymosin from *Aspergillus nidulans* and *Aspergillus awamori*. The 18th Linderstrom-Lang Conference, Elsinore, Denmark, July 4–8, 1988.
33. EL Flamm. How DFA approved chymosin: a case history. Bio/Technology 9:349–351, 1991.
34. T Yamashita, N Tonouchi, T Uozymi, T Beppu Secretion of *Mucor* rennin, a fungal aspartic protease of *Mucor pusillus*, by recombinant yeast cells. Mol Gen Genet 210:462–467, 1987.
35. B Foltmann, VB Pedersen, H Jacobsen, D Kauffman, G Wybrandt. The complete amino acid sequence of prochymosin. Proc Natl Acad Sci USA 74:2321–2324, 1977.
36. B Foltmann, VB Pedersen, D Kaufman, G Wybrandt. The primary structure of calf chymosin. J Biol Chem 254:8447–8456, 1979.
37. NS Andreeva, AE Gustchina. On the supersecondary structure of acid proteases. Biochem Biophys Res Commun 87:32–42, 1979.
37a. GL Gilliland, EL Winborne, J Nachman, A Wlodawer. The three-dimensional structure of recombinant bovine chymosin at 2.3 Å resolution. Proteins: Struct Funct Gen 8:82–101, 1990.
37b. M Newman, M Safro, C Frazao, G Khan, A Zdanov, IJ Tickle, TL Blundell, N Andreeva. X-ray analyses of aspartic proteinases. IV. Structure and refinement at 2.2 Å resolution of bovine chymosin. J Mol Biol 221:1295–1309, 1991.
38. S Visser, PJ van Rooijen, C Schattenkerk, KET Kerling. Peptide substrates for chymosin (rennin). Kinetic studies with peptides of different chain length including parts of the sequence 101–112 of bovine κ-casein. Biochim Biophys Acta 438:265–272, 1976.
39. S Visser, PJ van Rooijen, CJ Slangen. Peptide substrates for chymosin (rennin). Isolation and substrate behavior of two tryptic fragments of bovine κ-casein. Eur J Biochem 108:415–521, 1980.
40. C Carles, P Martin. Kinetic study of the action of bovine chymosin and pepsin A on bovine κ-casein. Arch Biochem Biophys 242:411–416, 1985.
41. TL Blundell, JA Jenkins, BT Sewell, LH Pearl, JB Cooper, IJ Tickle, B Veerapandian, SP Wood. X-ray analysis of aspartic proteinases. The three-dimensional structure at 2.1 Å resolution of endothia-pepsin. J Mol Biol 211:919–941, 1990.
42. D Mantafounis, J Pitts. Protein engineering of chymosin. Modification of the optimum pH of enzyme catalysis. Protein Eng 3:605–609, 1990.
43. J Suzuki, K Sasaki, Y Sasao, A Hamu, H Kawasaki, M Nishiyama, S Horinouchi, T Beppu. Protein Eng 2:563–569, 1989.
44. R Bott, E Subramanian, DR Davies. Three-dimensional structure of the complex of the *Rhizopus chinensis* carboxyl proteinase and pepstatin at 2.5 Å resolution. Biochemistry 21:6956–6962, 1982.
45. K Suguna, EA Padlan, CW Smith, WD Carlson, DR Davies. Binding of a reduced peptide inhibitor to the asparatic proteinase from *Rhizopus chinensis*: implica-

tions for a mechanism of action. Proc Natl Acad Sci USA 84:7009–7013, 1987.
46. JR Brown, M Yamasaki, H Neurath. A new form of bovine pancreatic procarboxypeptidase A. Biochemistry 2:877–886, 1963.
47. WN Lipscomb, JA Hartsuck, GN Reeke Jr, FA Quiocho, PH Bethge, ML Ludwig, TA Steitz, M Muirhead, JC Coppola. Structure of carboxypeptidase A. VII. The 2.0-Å resolution studies of the enzyme and of its complex with glycyltyrosine, and mechanistic deductions. US Atomic Energy Commission 1:24–90, 1969.
48. DM Greenberg. Plant proteolytic enzymes. Methods Enzymol 2:54–63, 1955.
49. M Kunitz. Crystalline soybean trypsin inhibitor. II. General properties. J Gen Physiol 30:291–310, 1947.
50. JR Whitaker. Properties of the proteolytic enzymes of commercial ficin. Food Res 22:483–493, 1957.
51. MS Dunn. Casein. Biochem Preparations 1:22–24, 1949.
52. ML Anson. Estimation of papain with hemoglobin. J Gen Physiol 20:561–563, 1937.
53. ML Anson. Estimation of pepsin, trypsin, papain and cathepsin with hemoglobin. J Gen Physiol 22:79–89, 1938.
54. O Folin, V Ciocalteau. Tyrosine and tryptophan determinations in proteins. J Biol Chem 73:627–650, 1927.
55. AFSA Habeeb. Determination of free amino groups in proteins by trinitrobenzenesulfonic acid. Anal Biochem 14:328–336, 1966.
56. AK Balls, SR Hoover. The milk-clotting time of papain. J Biol Chem 121:737–745, 1937.
57. United States Pharmacopeia National Formulary. Papain [9001-73-4]. United States Pharmacopeial Convention, MD: Rockville, 1995, p 1012.
58. Food Chemical Codex, 3rd ed. Plant Proteolytic Activity. Washington: National Academic Press, 1981, p 495.
59. Food Chemical Codex, 3rd ed. Milk-Clotting Activity. Washington: National Academic Press, 1981, p 493.
60. JH Northrup. Pepsin activity units and methods for determining peptic activity. J Gen Physiol 16:41–58, 1932.
61. GG Guilbault. Handbook of Enzymatic Methods. New York: Marcel Dekker, 1976.
62. HU Bergmeyer. Methods of Enzymatic Analysis, 3rd ed. Vol V. Enzymes 3: Peptidases, Proteinases and Their Inhibitors. Weinheim: Verlag-Chemie, 1984.
63. BHJ Bielski, S Freed. Fluorometric assay of α-chymotrypsin. Anal Biochem 7:192–198, 1964.
64. GG Guilbault, DN Kramer. Fluorometric determination of lipase, acylase, α- and γ- chymotrypsin and inhibitors of these enzymes. Anal Chem 36:409–412, 1964.
64a. R Schlaeger, A Roehr. Faecal chymotrypsin—a new photometric method using N-acetyl-L-tyrosine ethyl ester as substrate. J Clin Chem Clin Biochem 20:147–150, 1982.
65. SP Colowick, NO Kaplan. Methods in Enzymology, Vol II. New York: Academic Press, 1955, pp 3–169.
66. VM Stepanov, GN Rudenskaya. Proteinase affinity chromatography on bacitracin-Sepharose. J Appl Biochem 5:420–428, 1983.
67. KK Mäkkinen. Inhibition by bacitracin of some hydrolytic enzymes. Int J Protein Res 4:21–28, 1972.
68. VM Stepanov, MV Gonchar, GN Rudenskaya. Bacitracin and Gramicidin as inhibitors of carboxylic proteinases. Khim Prir Soedin 385–389, 1978.
69. S Chandrasekaran, SC Dhar. Purification of subtilisin by single-step affinity chromatography. Anal Biochem 150:141–144, 1985.
70. OH Lowry, NK Rosebrough, AL Farr, RJ Randall. Protein measurement with the Folin phenol reagent. J Biol Chem 193:265–275, 1951.
71. JR Kimmel, EL Smith. Crystalline papain. I. Preparation, specificity, and activation. J Biol Chem 207:515–531, 1954.
72. AK Balls, H Lineweaver. Isolation and properties of crystalline papain. J Biol Chem 130:669–686, 1939.
73. DR Englebretsen, DRK Harding. Solid-phase synthesis of a peptide-ligand affinity matrix for isolation of chymosin. Peptide Res 6:320–329, 1993.
74. PJ Tichy, F Kaprálek, P Jecmen. Improved procedure for a high-yield recovery of enzymatically active recombinant calf chymosin from *Escherichia coli* inclusion bodies. Protein Express Purificat 4:59–63, 1993.
75. FAO Marston, PA Lowe, MT Doel, JM Schoemaker, S White, S Angal. Purification of calf prochymosin (prorennin) synthesized in *Escherichia coli*. Bio/Technology 2:800–804, 1984.
76. JS Emtage, S Angal, MT Doel, TJR Harris, B Jenkins, G Lilley, PA Lowe. Synthesis of calf prochymosin (prorennin) in *Escherichia coli*. Proc Natl Acad Sci USA 80:3671–3675, 1983.
77. P McPhie. A turbidimetric milk-clotting assay for pepsin. Anal Biochem 73:258–261, 1976.
78. B Foltmann. Prochymosin and chymosin (prorennin and rennin). Methods Enzymol 19:421–436, 1970.
79. GR Reeck, KA Walsh, H Neurath. Isolation and characterization of carboxypeptidases A and B from activated pancreatic juice. Biochemistry 10:4690–4698, 1971.
80. ML Anson. Carboxypeptidase. I. The preparation of crystalline carboxypeptidase. J Gen Physiol 20:663–669, 1937.
81. PH Pétra, H Neurath. Heterogeneity of bovine carboxypeptidase A. I. Chromatographic purification of carboxypeptidase A (Anson). Biochemistry 8:2466–2475, 1969.

79

Thermolysin

Kuniyo Inouye
Kyoto University, Kyoto, Japan

I. INTRODUCTION

A. History

Thermolysin is a natural metalloproteinase produced in culture broth of *Bacillus thermoproteolyticus Rokko* (1) which was isolated from a hot spa (Arima Onsen, Hyogo-ken) in Japan in 1962. Thermolysin is very heat stable, and is one of the first thermophilic enzymes reported. This enzyme has been extensively characterized; its amino acid sequence (Fig. 1) (2), nucleotide sequence (3), and three-dimensional structure by x-ray crystallography at 1.6 Å (Fig. 2) (4,5) are known. The heat stability (6, 7) and substrate specificity (8) have been studied.

B. Chemical Reactions Catalyzed

1. Peptidase Activity

Thermolysin catalyzes specifically hydrolysis of peptide bonds (-X-Y-) containing hydrophobic amino acid residues, especially at the P1′ site (the nomenclature used for the amino acid residues (P) of the substrate and for naming the subsites (S) of the active site is that of Schechter and Berger (9). In the peptide bond (-X-Y-), the amino acid residue (X) of the amino terminal side of the cleavable bond is at the P1 site, and (Y) is at the carboxyl terminal side, the P1′ site. Thermolysin is an endopeptidase, and does not act on the peptide bonds next to free amino- or carboxyl-terminal amino acid residues.

The specificity constant (k_{cat}/K_m) in the hydrolysis of *N*-[3-(2-furyl)acryloyl](FA)-Gly-Y amide is, in the order of the Y residue: L-Phe = L-Leu > L-Val > L-Ala. The enzymatic rate in the hydolysis of FA-X-L-Ala amide is, in the order of the X residue: L-Phe >L-Leu > Gly (10). Themolysin has been shown not to hydrolyze a number of esters, e.g., hippuryl phenyllactate, α-N-benzoyl-L-arginine ethyl ester, α-N-tosyl-L-arginine methyl ester, α-N-acetyl-L-tyrosine ethyl ester, or carbobenzoxy-glycine *p*-nitrophenyl ester. On the other hand, a series of aliphatic alkyl esters, esters in the form of depsipeptides, such as *N*-benzoyl(Bz)-Gly-OPhe-L-Ala, Bz-Gly-OLeu-L-Ala, and FA-Gly-OLeu amide, are hydrolyzed at rates three- to eightfold slower than their peptide analogs (11). It is noted that OLeu is 2-hydroxylisocaproic acid, OPhe, 2-phenyllactic acid, and OGly, glycolic acid.

2. Peptide Synthesis

Thermolysin catalyzes effectively the reverse reaction of the hydrolysis of peptide bonds, resulting in the synthesis of peptides such as the precursor of an artificial sweetener, aspartame (L-Asp-L-Phe methyl ester) (12, 13). In the case of the thermolysin-catalyzed hydrolysis of *N*-carbobenzyloxy (Z)-L-Asp-L-Phe methyl ester (Z-Asp-Phe-OMe),

$$\text{Z-Asp-Phe-OMe} + \text{H}_2\text{O} \underset{k_{-1}}{\overset{k_1}{\rightleftharpoons}} \text{Z-Asp} + \text{Phe} - \text{OME}$$

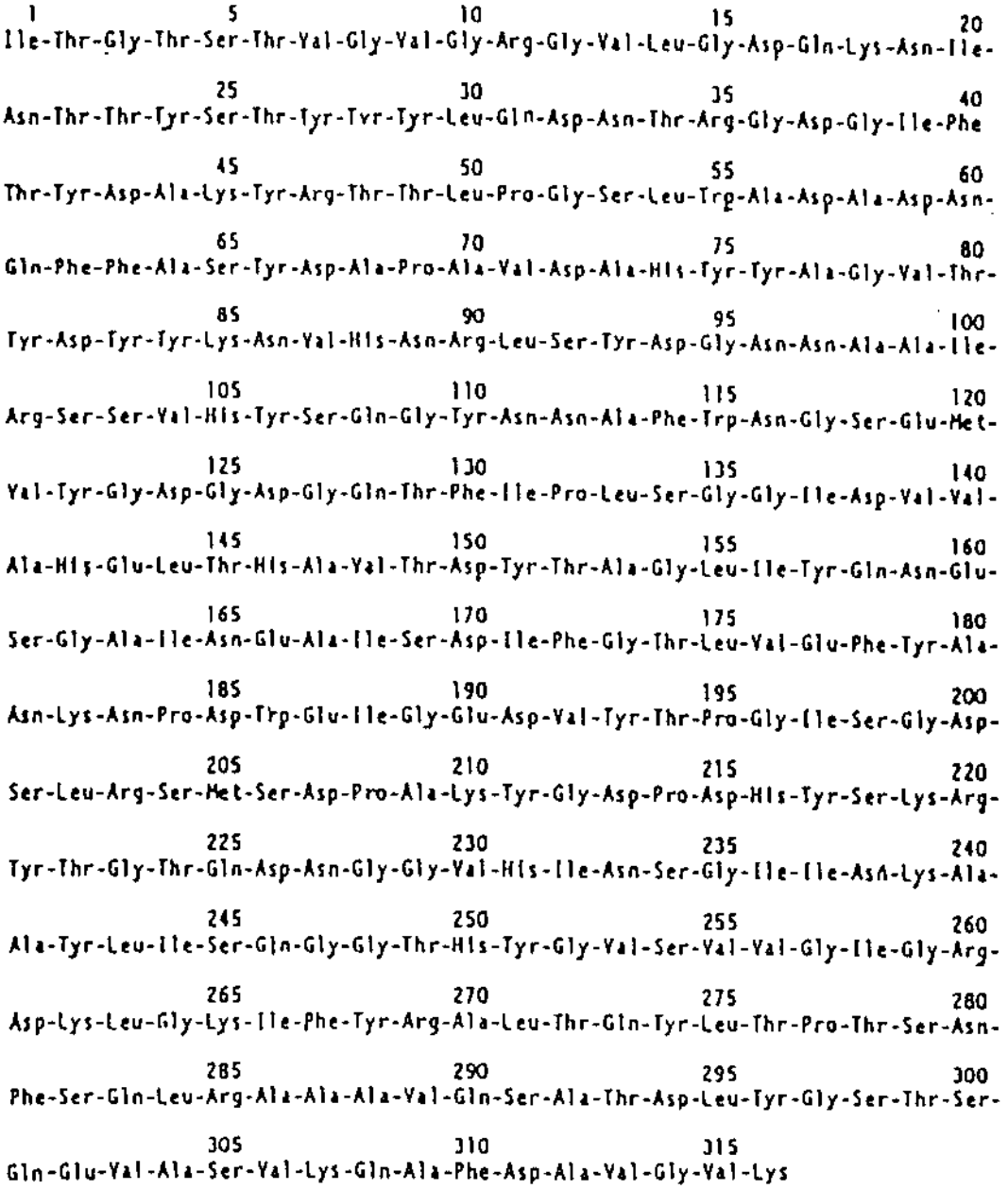

Figure 1 Primary structure of thermolysin. (From Ref. 2.)

the equilibrium constant, K_{eq}, is given by the following equation:

$$K_{eq} = \{[\text{Z-Asp}][\text{Phe-OMe}]\}/\{[\text{Z-Asp-Phe-OMe}][\text{H}_2\text{O}]\} = k_1/k_{-1}$$

The K_{eq} value is not changed in the absence or presence of catalysts. When thermolysin enhances the reaction rate (k_1) of the hydrolysis, the reaction rate (k_{-1}) of the peptide synthesis can be also enhanced by the same degree as the hydrolysis.

C. Chemical Structure of Substrates

The substrate specificity of thermolysin is primarily for an aromatic amino acid residue in P1′, although it is

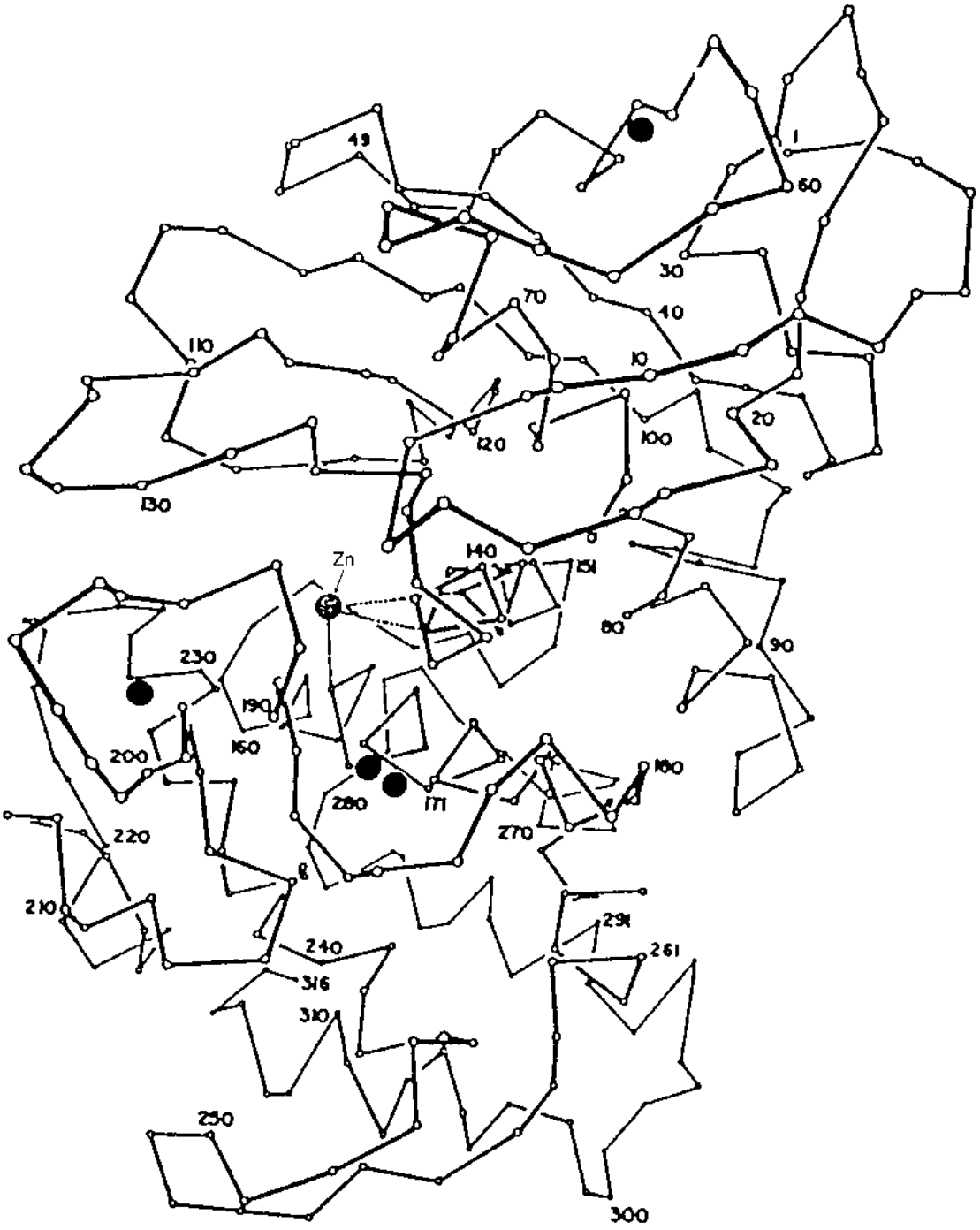

Figure 2 Three-dimensional structure of thermolysin. The catalytic zinc atom (Zn) is coordinated with three ligands (His142, His146, and Glu166). The linkages are shown diagrammatically as broken lines. The four calcium atoms are shown as solid black spheres. (From Ref. 4.)

somewhat broad, and it may be attributable to the wider substrate binding site.

D. Classification According to Enzyme Commission Nomenclature

Thermolysin is classified as a metalloendopeptidase, and the Enzyme Commission number is EC 3.4.24.27 (14).

II. IMPORTANCE TO FOOD INDUSTRY

The most remarkable quality of thermolysin is its application to the synthesis of peptides especially the artificial peptide sweetener, aspartame (L-Asp-L-Phe-OMe). Sweetener peptides L-Asp-L-Phe-OEt and L-Asp-L-Tyr-OMe are also synthesized by thermolysin. Thermolysin has been used to digest animal and plant proteins, and the hydrolysates are used as seasonings and condiments and for production of amino acids. Soy protein hydrolysates are used as raw materials in production of soy sauce and as an alternative to soy sauce. It has been reported that peptides produced by digesting soy proteins, fish proteins, etc., with thermolysin show some physiological effects such as hypotensive effect, opioidlike effect, bowel contraction, repression of Alzheimer's disease, etc. By hydrolysis of dried bonito muscle by thermolysin, eight inhibitory peptides against angiotensin-I converting enzyme have been isolated. Among them, L-Leu-L-Lys-L-Pro-L-Gln-L-Met shows the most potent inhibitory activity ($IC_{50} = 2.4\,\mu M$) (15). Based on these results, designer foods containing physiologically active peptides have come on the market.

III. PROPERTIES AS A PROTEIN

A. Molecular Weight

The molecular weight is 34,600 based on the amino acid composition (316 amino acids) plus one zinc atom and four calcium atoms (2, 4, 5). Thermolysin is a monomeric protein (34.6 kDa) in the concentration range up to 1.0 mg/mL in the presence of 0–4 M NaCl as determined by a low-angle laser light-scattering photomer (16).

B. Primary, Secondary, Tertiary, Quaternary, and Macromolecular Structures

1. Homology with Other Proteins

Thermolysinlike neutral metalloproteinases have been isolated from the culture broth of various *Bacillus* spp. (17–20). The gene *nprM* coding for a thermostable proteinase, NprM, in *B. stearothermophilus* MK232 has been cloned, and the nucleotides have been sequenced (17). The amino acid sequence of protein NprM predicted on the basis of the nucleotide sequence is identical to that found by the Edman method of sequencing of the mature thermolysin except for two amino acid substitutions (Asp37 of thermolysin is asparagine, and Glu119 of thermolysin is glutamine) in the 316 residues of the entire sequence. The amino acid sequence of thermolysin predicted on the basis of its nucleotide sequence has been reported to be the same as that of NprM (3). The residues at positions 37 and 119 of thermolysin have now been found to be asparagine and glutamine, respectively (21). Accordingly, thermolysin and NprM seem to be the same despite their different origins. Recently, we have found two mutant forms of thermolysin from thermolysin-producing *Bacillus thermoproteolyticus* which has been treated with chemical mutagens (Japan patent No. H9-255, 1997). In a mutant enzyme, Ala73 is converted to valine, and in another one, Val 140 is converted to alanine. Substrate specificity of the mutant enzymes is changed slightly from the wild-type enzyme, suggesting these two residues have some involvement in the substrate recognition, although both of them are located some distance from the active site of the native enzyme.

2. Domain Structure of Thermolysin

Thermolysin is composed of two domains, an N-terminal domain (residues 1–135) and a C-terminal domain (residues 136–316) (see Fig. 1). Both domains have characteristic domain structures; namely, the N-terminal domain is composed mainly of β-sheets (all β-domain), and the C-terminal domain is composed mainly of α-helices (all α-domain) (4, 5). The active site is in the crevice formed between the two domains. Interestingly, residues supposed to be involved in the catalysis are located in the C-terminal domain (see Sec. IV.B). It has been shown that the spatial relationship of the two domains changes on substrate binding to the enzyme, suggesting an allosteric phenomenon in a single-chain protein (22).

3. Isoforms

Thermolysin was formerly classified as EC 3.4.24.4 (1984 Recommendations of the Nomenclature Committee) but is now reclassified to EC 3.4.24.27 (14). This is in keeping with reclassification of other bacterial neutral metalloproteinases such as aeromolysin (EC 3.4.24.25) from *Aeromonas proteolytica*, pseudolysin (EC 3.4.24.26) from *Pseudomonas aeruginosa*, bacillolysin (EC 3.4.24.28) from *Bacillus subtilis*, aureolysin (EC 3.4.24.29) from *Staphylococcus aureus*, coccolysin (EC 3.4.24.30) from *Staphylococcus thermophilus*, and mycolysin (EC 3.4.24.31) from *Streptomyces griseus*.

Aeromolysin is thermostable and shows preferential cleavage of bonds with bulky hydrophobic amino acids in the P2 and P1′ positions (23). Pseudolysin (or *Pseudomonas* elastase) causes tissue damage by degrading proteins including elastins, collagen types III and IV, and fibronectin generally with bulky hydrophobic groups at the P1′ position. The cleavage pattern of insulin B chain by pseudolysin is similar to that of thermolysin (24–26). The cleavage pattern of substrates by bacillolysin is similar but not identical to that of thermolysin (27, 28). Variants of this enzyme have been found in species of *Bacillus* including *B. subtilis, B. amyloliquefaciens, B. cereus*, and *B. stearothermophilus* (29). The cleavage pattern of insulin B chain by aureolysin is similar to that of thermolysin, and it prefers a hydrophobic residue at the P1′ position (30). Coccolysin is found intracellularly in *Streptococcus thermophilus* and *S. diacetilactis*, and extracellularly in *S. faecalis* (31, 32). It cleaves preferentially hydrophobic bulky residues (L-Leu, L-Phe, and L-Tyr) at the P1′ position. Mycolysin is a component of pronase, and is produced by *Streptomyces griseus, S. naraensis*, and *S. cacaoi* (27, 33, 34). The substrate specificity is similar to that of thermolysin and preferential to bonds with hydrophobic residues at the P1′ position.

Recently, the classification of metalloproteinases into five distinct subfamilies has been proposed on the basis of the active-site sequence and metal ligands (35, 36). Thermolysin belongs to the M4 family (thermolysin family) of the MA clan. The MA clan proteases contain a Glu residue which completes the zinc-binding site in addition to two histidines of the active-site consensus sequence His-Glu-Xaa-Xaa-His (or HEXXH) (37, 38). According to the amino acid sequence of thermolysin, His142, His146, and Glu166 are the zinc ligands. It is noted that enzymes from pathogens (e.g., *Legionella, Listeria, Pseudomonas, Vibrio*) are members of this family (23, 25). Thermolysin and its precursor lack Cys residues, but this is not the case for all members of this family. Although amino acid sequence and enzymatic properties are different among the families, all families except for the thermolysin family have the consensus sequence HEXXHXXGXXH, where the three histidines are zinc ligands.

4. Small Metalloproteinases

Metalloproteinases related to thermolysin, which have been described above, have molecular weights ~35,000. On the other hand, there are reports of metalloproteinases with considerably small molecular sizes. *Streptomyces caespitosus* neutral proteinase is composed of 132 amino acids, and its molecular weight is 15,000 (39, 40). This enzyme belongs to the *Streptomyces* extracellular neutral protease (M7) family (35), and specifically hydrolyzes the peptide bond at the amino side of aromatic residues. *Penicillum citrinum* metalloprotease, penicillolysin, is composed of 177 amino acids with a molecular weight of 18,000 (41).

Aspergillus oryzae neutral proteinase II is a zinc proteinase with three disulfide bonds. It consists of 177 amino acids, and its molecular weight is 19,000 (42). Penicillolysin has a sequence 68% homologous with that of *Aspergillus oryzae* neutral proteinase II. The zinc ligands of both metalloproteinases are considered to be His128, His132, and Glu65, suggesting that their zinc ligands correspond to those of thermolysin (41). Topological diagrams of these small metalloproteinases are similar to that of the C-terminal domain of thermolysin, notwithstanding differences in amino acid sequence (40). It should be mentioned that a matrix metalloproteinase (MMP), MMP7 or matrilysin, isolated from human colon cancer cells has a molecular weight of 19,000 (43). MMPs, except MMP7, contain the C-terminal hemopexinlike domain, and their molecular weights are in the range of 28,000~84,000. These single-domain metalloproteinases with molecular weights of 15,000–19,000 might be accepted as a new type of proteinase.

IV. PROPERTIES AS ENZYME

A. Substrate Specificity

The k_{cat}/K_m values at 0 M NaCl are 43 $M^{-1}sec^{-1}$ for *N*-[3-(2-furyl)acryolyl](FA)-Gly-L-Ala amide, 2.2×10^4 $M^{-1}sec^{-1}$ for FA-Gly-L-Leu amide, and 6.9×10^2

$M^{-1}sec^{-1}$ for FA-L-Leu-L-Ala amide in 40 mM Tris-HCl buffer containing 10 mM $CaCl_2$, pH 7.5, at 25°C (10, 44). For FA-Gly-L-Leu amide, the specificity constant, k_{cat}/K_m, is 2.2–3.0 × 10^4 $M^{-1}sec^{-1}$, and K_m and k_{cat} are estimated to be > 3 mM and > 66–90 sec^{-1}, respectively. For *N*-carbobenzyloxy (Z)-L-Asp-L-Phe methylester (Z-Asp-Phe-OMe), K_m is 0.35 mM and k_{cat} is 2.73 sec^{-1} (44). With FA-L-Leu-L-Ala amide, K_m is 0.80 mM and k_{cat} is 0.56 sec^{-1}, and with FA-L-Phe-L-Ala amide, K_m is 83 μM and k_{cat} is 5.7 sec^{-1} (10). The K_m and k_{cat} values for the degradation of [L-Leu 5]-enkephalin are 0.50 mM and 95 sec^{-1} (3). A fluorescent substrate, 7-methoxycoumarin-4-yl)acetyl-L-Pro-L-Leu-Gly-L-Leu-[N^3-(2,4-dinitrophenyl)-L-2,3-diamino-propionyl)-L-Ala-L-Arg-NH_2 (MOCAc-PLG(Dpa)AR) is used for thermolysin assay (43, 45). The specificity constant, k_{cat}/K_m, is 8.0 × 10^4 $M^{-1}sec^{-1}$ in 40 mM Tris-HCl buffer containing 10 mM $CaCl_2$, pH 7.5, at 25°C (Inouye, unpublished data).

B. Effect of pH and Temperature on Activity and Reaction Mechanism

Using FA-Gly-L-Leu amide as substrate, at 0 M NaCl, the optimal pH was 6.7–7.0, the pK_{a1} and pK_{a2} value were 5.4 and 7.9 (46). The imidazole of His231 is considered to be the dissociable residue with pK_{a2}, and the carboxyl group of Glu143 might be the pK_{a1} group (47). Recently, a water molecule coordinated to the active site zinc has been considered to be responsible for pK_{a1} instead of Glu143 (46, 48). The temperature at which a 30-min incubation reduces the enzyme activity by half is 86.9°C (49, 50). The optimum temperature is 80°C when casein is used as a substrate, and thermolysin is stable in the temperature range of 30–90°C.

C. Effect of Environmental Factors

1. Role of Zinc

A zinc ion is essential for activity, but it can be replaced with a cobalt ion (51). The activity of the cobalt thermolysin is 200–250% higher than that of the native (zinc) enzyme.

2. Effect of Salts on Activity

The activity of thermolysin in the hydolysis and synthesis of peptide substrates such as *N*-[3-(2-furyl)acryloyl] (FA)-Gly-L-Ala amide (FA-Gly-L-Leu amide) and *N*-carbobenzyloxy (Z)-L-Asp-L-Phe methyl ester (Z-Asp-Phe-OMe) is enhanced markedly in the presence of high concentrations (1–5 M) of neutral salts such as NaCl, NaBr, KCl, or KBr (44). The activity increases in an exponential fashion with increasing salt concentration; in the presence of *x*M NaCl at pH 7 and 25°C, the degree of activation is expressed by 1.9^x. Accordingly, at 4 M NaCl, the activity is enhanced 13–14 times. The salt activation has been shown to increase the molecular activity, k_{cat}, while the Michaelis constant, K_m is not altered (10). The salt-dependent activation is dependent on pH and temperature and on organic solvents added to the reaction mixture (46). Activation by addition of NaCl shows a bell-shaped pH dependence with the peak at pH 7, and is only twofold at pH 5 and 10 with 4 M NaCl. Activation is greater at lower temperatures; it is 20-fold at 5°C and fivefold at 45°C in the reaction medium at pH 7.

3. Solubility of Thermolysin

The solubility of thermolysin is low, being 1.0–1.2 mg/mL in conventional buffers at low ionic strength (e.g., 40 mM Tris-HCl buffer, pH 7.5) in the temperature range between 0 and 60°C. The solubility increases on addition of salts (16). With NaCl, the solubility shows a bell-shaped curve with increasing NaCl concentration; the maximum solubility (10–12 mg/mL) is at 2.0–2.5 M NaCl. With LiCl and NaI, solubility increases to 20–50 mg/mL with increasing salt concentration up to 5 M. Thermolysin is a cold-soluble protein only in the presence of salts; it decreases in solubility with increasing temperature from 0 to 60°C. In the presence of 4 M NaCl, it is 6–7 mg/mL at 0°C and 2 mg/mL at 60°C. In the absence of NaCl, the temperature dependence is not observed.

D. Halophilic Properties of Thermolysin

Neutral salts increase not only the solubility of thermolysin but also its activity and stability. Addition of salts permits preparation of enzyme solutions of high concentration with enhanced activity. These conditions reduce reaction time and enhance industrial application of the enzyme. With maximally solubilized thermolysin solution using 4 M NaCl or NaBr, the total activity is enhanced 55 and 360 times, respectively, compared with that in the absence of salts. In the case of 1 M NaSCN, the solubility of enzyme is 88 mg/mL at 25°C, and the activity enhancement is 3.2-fold. Thus, the total activity could be enhanced 280-fold. Industrial application of thermolysin is limited

because of its low solubility. This limitation can be overcome by adding a high concentration of salts.

E. Inhibitors

Divalent metal chelators such as EDTA and *o*-phenanthroline (52) inhibit thermolysin by removing the catalytic zinc ion. Phosphonamidate transition-state analogs such as *N*-carbobenzyloxy (Z)-Gly^{P}-L-Leu-L-Leu and Z-L-Phe^{P}-L-Leu-L-Ala, where Gly^{P} shows Gly in which the carbonyl carbon is replaced with phosphorus, and naturally occurring phosphonamidates, *N*-(α-L-rhamnopyranosyloxyphospho)-L-Leu-L-Trp (or phosphoramidon) and *N*-(6-deoxy-α-L-talopyranosyloxyphospho)-L-Leu-L-Trp (or talopeptin), are tight-binding inhibitors. Z-L-Phe^{P}-L-Leu-L-Ala is the tightest-binding inhibitor described to date ($K_i = 0.068$ nM) (53). Inhibition of thermolysin by phosphoramidon and talopeptin is much weaker ($K_i = 60$ nM) (54).

Z-Gly-D-Phe is a competitive inhibitor, and it is used as an affinity ligand for affinity chromatography of thermolysin (45, 55). Reagents which ligate to the catalytic zinc ion have been shown to be good inhibitors. Representative monodendate ligands containing a thiol group, i.e., thiorphan, and bidentate hydroxamate ligand, i.e., hydroxyamino-carbonyl-2-benzyl-1-oxopropyl-glycine, have K_i values of 1.6 and 3.1 μM, respectively (56). Inhibition by Ag^{+}, Hg^{2+}, Zn^{2+}, and other metals, citrate, phosphate, mercaptoethylamine, cyanide, thioglycolate, 2,2′-bipyridine, imidazole, and β-phenylpropionyl-L-Phe have been observed (57).

F. Subsite Structure

Subsite structure in the active site of thermolysin has been proposed on the basis of the 3D structure (53, 54). The substrate is fixed in the active site with the aid of hydrogen bonds formed between peptide chains of the substrate and the subsites. Trp115 forms the S2 subsite, Ala113 and Arg203 form the S1′ subsite, and Asn112 forms the S2′ subsite. The α-carbonyl group of the P1 residue of the substrate coordinates with the catalytic Zn, and the α-NH group of the P1′ residue coordinates with Ala113. The peptide bond between these α-position groups is cleaved in the catalysis. Not only the main chain but also the side chain of Trp115 is essential for catalysis (48). Site-directed mutagenesis of Trp115 indicated that aromatic amino acids such as Trp, Tyr, and Phe are essential for enzyme activity, and the mutant enzymes containing Leu, Ile, Val, Ala, etc., do not show any activity.

G. Superactivation by Chemical Modification

Acylation of thermolysin with amino acid *N*-hydroxysuccinimide esters enhances the activity markedly. Thermolysin covalently modified with acetyl L-Phe shows 100 times higher activity toward the substrate FA-Gly-L-Ala-Gly (59). It has been considered that an acetyl L-Phe moiety binds to a tyrosyl residue in the active site to form an ester bond, although the targeted residue has not been identified because of instability of the modified residue.

V. ASSAY AND PURIFICATION

A. Thermolysin Assay

Two assay methods are described. One is based on casein digestion, and the other is based on the digestion of synthetic peptides (52).

Casein 3 mL (1.33%, w/v) and 1 mL of thermolysin (4–120 nM) are mixed in 40 mM Tris-HCl buffer, pH 7.5, at 25°C. After digestion of casein by thermolysin at 25°C for 10 min, the hydrolysate (4 mL) is treated with a solution (4 mL) consisting of 0.11 M trichloroacetic acid (TCA), 0.22 M Na acetate, and 0.33 M acetic acid, to remove undigested casein. The precipitate is removed by centrifugation at 3000g or filtration on a Whatman paper filter. The extent of digestion is measured by the amount of unprecipitated products measured at 280 nm or by the Lowry method. One unit of thermolysin activity is defined as an amount of the enzyme producing 1 μg tyrosine per min (1). Practically, when the solution (filtrate or supernatant) gives an absorbance of 0.83 at 280 nm, the tyrosine concentration is 0.1 mg/mL—namely, 1000 units of enzyme in 1 mL of the solution.

Thermolysin is assayed using synthetic substrates such as carbobenzoxy (Z)-Gly-L-Phe amide, Z-L-Thr-L-Leu amide, and furylacryloyl (FA)-Gly-L-Leu amide. The extent of hydrolysis is measured by a colorimetric ninhydrin method which estimates the number of α-amino groups liberated after hydrolysis of the peptide bonds, Gly-L-Phe, L-Thr-L-Leu, and Gly-L-Leu. The products of the peptide substrates can be determined by reversed-phase HPLC (35). Typical reaction conditions are 5–10 nM thermolysin and 1–20 mM substrates in 40 mM Tris-HCl buffer containing 10 mM $CaCl_2$, pH 7.5, at 25°C (standard conditions). In the case of FA-dipeptides, especially FA-Gly-L-Leu amide (FAGLA), the hydrolysis is measured by following the decrease in absorbance at 345 or 322 nm (44, 60). The molar absorptivity differences at 345 nm and 322 nm

due to hydrolysis are -3.10×10^2 and $-2.05 \times 10^3\ M^{-1}cm^{-1}$, respectively, in the standard conditions. Hydrolysis of Z-Asp-L-Phe methyl ester (Z-Asp-Phe-OMe) can be measured by following the decrease in absorbance at 224 nm, which is due to peptide bonds (44). The molar absorptivity difference on the hydrolysis of Z-Asp-L-Phe-OMe into Z-L-Asp and L-Phe-OMe is $-4.93 \times 10^2\ M^{-1}\ cm^{-1}$, under the standard conditions described above.

Fluorogenic substrates for thermolysin have been reported (43, 45). The K_m and k_{cat} values of dansyl (Dns)-Gly-L-Phe-L-Ala are 0.080 mM and 1.6 sec^{-1}. Those for 2-aminobenzoyl-anthraniloyl (Abz)-L-Ala-Gly-L-Leu-L-Ala- (4-nitrobenzylamide) are 0.14 mM and 290 sec^{-1}, respectively (61).

B. Purification of Thermolysin

The purification procedure of thermolysin is essentially that described by Endo (1). The culture broth (sample I; 10 L) of *Bacillus thermoproteolyticus* is filtered with the aid of Celite, and the enzyme in the filtrate (sample II; 9.7 L) is precipitated by 45% saturation with ammonium sulfate, pH 7.0, at 4°C. After centrifugation, the precipitate is dissolved in 20 mM Ca-acetate buffer (1.5 L), pH 7.0, and the solution (sample III) is brought to 30% saturation with ammonium sulfate. The precipitate is removed by centrifugation, and the supernatant is brought to 45% saturation with ammonium sulfate. After centrifugation, the precipitate is dissolved in 20 mM Ca-acetate buffer (1.0 L), pH 7.0. The solution (sample IV) is dialyzed overnight against 10 mM Ca-acetate buffer, pH 7.0, at 5°C. To the dialyzed solution (sample V; 1.1 L), chilled acetone (0.88 L, 0°C) is added and the precipitate formed is removed. Chilled acetone (1.88 L, at 0°C) is added slowly, and the precipitate is collected. The precipitate is dissolved in 20 mM Ca-acetate buffer (0.2 L), pH 7.0; the enzyme activity in the solution should be 100×10^3 U/mL. The solution is kept at 4°C. Crystals of thermolysin appear within 30 min. The solution is held overnight. Crystals (sample VI; 1.55 g) are collected by centrifugation. A lyophilized preparation of these crystals shows an activity of 6.5×10^3 U/g. In the same manner, crystallization is repeated three times. The activities of the two-times- and three-times-crystallized preparations (samples VII and VIII) are 8.5×10^3 and 10.0×10^3 U/g, respectively. Crude preparations (lyophilized acetone precipitate of culture broth) and three-times-crystallized preparations of thermolysin are available from Daiwa Kasei (Osaka, Japan). The purification process is summarized in Table 1.

Table 1 Purification of Thermolysin

Sample No.	Volume or weight	Activity	Total activity ($\times 10^6$ units)	Yield (%)
I	10 L	3.5×10^3 U/mL	35	100
II	9.7L	3.3×10^3 U/mL	32	91
III	1.5 L	19.0×10^3 U/mL	29	83
IV	1.0 L	25.0×10^3 U/mL	25	71
V	1.1 L	21.0×10^3 U/mL	23	66
VI	1.55 g	6.5×10^3 U/g	14	40
VII	1.25 g	8.5×10^3 U/g	12	34
VIII	1.10 g	10.0×10^3 U/g	11	31

Chromatographic procedures for purification of thermolysin from the crude preparation have been reported. Ion exchange chromatography with DEAE-Sephadex A-25 and A-50 has been used (62). Affinity chromatographic procedures using acetyl-D-Phe, succinyl-D-Leu (63), and Gly-D-Phe (64) covalently attached to Sepharose matrix, and Bacitracin-silica (65) have been used successfully in a one-step purification of thermolysin.

REFERENCES

1. S Endo. Studies on protease produced by thermophilic bacteria. J Ferment Technol 40:346–353, 1962.
2. K Titani, MA Hermodson, LH Ericsson, KA Walsh, H Neurath. Amino-acid sequence of thermolysin. Nat New Biol 238:35–37, 1972.
3. MJ O'Donohue, BP Roques, A Beaumont. Cloning and expression of *Bacillus subtilis* of the npr gene *Bacillus thermoproteolyticus* Rokko coding for the thermostable metalloprotease thermolysin. Biochem J 300:599–603, 1994.
4. BW Matthews, JN Jansonius, PM Colman, BP Schoenborn, D Dupourque. Three-dimensional structure of thermolysin. Nat New Biol 238:37–41, 1972.
5. MA Holmes, BW Matthews. Structure of thermolysin refined at 1.6 Å resolution. J Mol Biol 160:623–639, 1982.
6. M Tajima, I Urabe, K Yutani, H Okada. Role of calcium ions in the thermostability of thermolysin and *Bacillus subtilis* var. *amylosaccharitiicus* neutral protease. Eur J Biochem 64:243–247, 1976.
7. S Toma, S Campagnoli, I Margarit, R Gianna, G Grandi, M Bolognesi, V De Filippis, A Fontana. Granting of a calcium-binding loop of thermolysin to *Bacillus subtilis* neutral protease. Biochemistry 30:97–106, 1991.
8. K Morihara, H Tsuzuki. thermolysin: kinetic study with oligopeptides. Eur J Biochem 15:374–380, 1970.

9. I Schechter, A Berger. On the size of the active site in proteases. I. Papain. Biochem Biophys Res Commun 27:157–162, 1967.
10. K Inouye, S-B Lee, B Tonomura. Effect of amino acid residues at the cleavable site of substrates on the remarkable activation of thermolysin by salts. Biochem J 315:133–138, 1996.
11. B Holmquist, BL Vallee. Esterase activity of zinc neutral proteases. Biochemistry 15:101–107, 1976.
12. Y Isowa, H Ohmori, T Ichikawa, K Mori, Y Nonaka, K Kihara, K Oyama, H Satoh, S Nishimura. The thermolysin-catalyzed condensation reactions of N-substituted aspartic and glutamic acids with phenylalanine alkyl esters. Tetrahedron Lett 30:2611–2612, 1979.
13. K Nakanishi, T Kamikubo, R Matsuno. Continuous synthesis of N-(benzyloxycarbonyl)-L-aspartyl-L-phenylalanine methyl ester with immobilized thermolysin in an organic solvent. Bio/Technology 3:459–464, 1985.
14. Nomenclature Committee of the International Union of Biochemistry and Molecular Biology. Enzyme Nomenclature, Recommendations. New York: Academic Press, 1992.
15. H Fujita, M Yoshikawa. LKPNM: a prodrug-type ACE-inhibitory peptide derived from fish protein. Immunopharmacology 1256:123–127, 1999.
16. K Inouye, K Kuzuya, B Tonomura. Effects of salts on the solubility of thermolysin: a remarkable increase in the solubility as well as the activity by the addition of salts without aggregation or dispersion of thermolysin. J Biochem 123:847–852, 1998.
17. M Kubo, T Imanaka. mRNA secondary structure in an open reading frame reduces translation efficiency in *Bacillus subtilis*. J Gen Microbiol 134:1883–1892, 1988.
18. G Signor, C Vita, A Fontana, F Frigerio, M Bolognesi, S Toma, R Gianna, E De Gregoriis, G Grandi. Structural features of neutral protease from *Bacillus subtilis* deduced from model-building and limited proteolysis experiments. Eur J Biochem 189:221–227, 1990.
19. B van den Burg, HG Enequist, ME van der Haar, VGH Eijsink, BK Stulp, G Venema. A highly thermostable neutral protease from *Bacillus caldolyticus*: cloning and expression of the gene in *Bacillus subtilis* and characterization of the gene product. J Bacteriol 173:4107–4115, 1991.
20. DR Wetmore, S-L Wong, RS Roche. The role of the pro-sequence in the processing and secretion of the thermolysin-like neutral protease from *Bacillus cereus*. Mol Microbiol 6:1593–1604, 1992.
21. Y Miki. Reassignment of the 37th and 119th amino-acid residues in thermolysin. J Ferment Bioeng 77:457–458, 1994.
22. OR Veltman, VG Eijsink, G Vriend, A De Kreij, G Venema, B van den Burg. Probing catalytic hinge bending motions in thermolysin-like proteases by glycine—alanine mutations. Biochemistry 37:5305–5311, 1998.
23. SH Wilkes, ME Bayliss, JM Prescott. Critical ionizing group in *Aeromonas* neutral protease. J Biol Chem 263:1821–1825, 1988.
24. RA Bever, BH Iglewski. Molecular characterization and nucleotide sequence of the *Pseudomonas aeruginosa* elastase structural gene. J Bacteriol 170:4309–4314, 1988.
25. WJ Black, FD Quinn, LS Tompkins. *Legionella pneumophia* zinc metalloprotease is structurally and functionally homologous to *Pseudomonas aeruginosa* elastase. J Bacteriol 172:2608–2613, 1990.
26. K Morihara, H Tsuzuki. *Pseudomonas aeruginosa* elastase: affinity chromatography and some properties as a metallo-neutral proteinase. Agric Biol Chem 39:1123–1128, 1975.
27. K Morihara, H Tsuzuki, T Oka. Comparison of the specificities of various neutral proteinases from microorganisms. Arch Biochem Biophys 123:572–588, 1968.
28. J Millett, R Acher. Specificity of megateriopeptidase: an amino-endopeptidase with hydrophobic character. Eur J Biochem 9:456–462, 1969.
29. S Stoeva, T Kleinschmidt, B Mesrob, G Braunitzer. Primary structure of a zinc protease from *Bacillus mesentericus* strain 76. Biochemistry 29:527–534, 1990.
30. J Potempa, Z Porwit-Bobr, J Travis. Stabilization vs. degradation of *Staphylococcus aureus* metalloproteinase. Biochim Biophys Acta 993:301–304, 1989.
31. RAG Smith, J Green, PH Kopper. The purification and properties of a fibrolytic neutral metalloendopeptidase from *Streptococcus faecalis*. Arch Biochem Biophys 202:629–638, 1980.
32. P-L Makinen, DB Clewell, F An, KK Makinen. Purification and substrate specificity of a strongly hydrophobic extracellular metalloendopeptidase ("gelatinase") from *Streptococcus faecalis* (strain OG1-10). J Biol Chem 264:3325–3334, 1989.
33. A Hiramatsu, T Ouchi. A neutral proteinase from *Streptomyces naraencis* III. An improved purification and some physicochemical properties. J Biochem 71:767–787, 1972.
34. S Blumberg, Z Tauber. Inhibition of metallopeptidases by 2-mercaptoacetyl-dipeptides. Eur J Biochem 136:151–154, 1983.
35. ND Rawlings, AJ Barrett. Evolutionary families of metallopeptidases. In: AJ Barrett, ed. Methods in Enzymology, Vol 248. New York: Academic Press, 1995, pp 183–28.
36. W Jiang, JS Bond. Families of metalloendopeptidases and their relationships. FEBS Lett 312:110–114, 1992.
37. BL Callee, DS Auld. Zinc coordination, function, and structure of zinc enzymes and other proteins. Biochemistry 29:5647–5669, 1990.
38. BL Vallee, DS Auld. Active-site ligands and activated H_2O of zinc enzymes. Proc Natl Acad Sci USA 87:220–224, 1990.

39. Y Yokote, K Kawasaki, J Nakajima, Y Noguchi. Studies on enzymes produced by *Streptomyces caespitosus*. Part I. Production conditions and some properties of neutral protease. Nippon Nogeikagaku Kaishi 43:125–131, 1969.
40. G Kurisu, T Konoshita, A Sugimoto, A Nagara, Y Kai, N Kasai, S Harada. Structure of the zinc endoprotease from *Streptomyces caespitosus*. J Biochem 121:304–308, 1997.
41. K Matsumoto, M Yamaguchi, E Ichishima. Molecular cloning and nucleotide sequence of the complementary DNA for penicillolysin gene, *plnC*, and 18 kDa metalloendopeptidase gene from *Penicillium citrinum*. Biochim Biophys Acta 1218:469–472, 1994.
42. H Tatsumi, K Ikegaya, S Murakami, H Kawabe, E Nakano, H Motai. Elucidation of the thermal stability of the neutral proteinase II from *Aspergillus oryzae*. Biochim Biophys Acta 1208:179–185, 1994.
43. H Oneda, K Inouye. Refolding and recovery of recombinant human matrix metalloproteinase 7 (matrilysin) from inclusion bodies expressed by *Escherichia coli*. J Biochem 126:905–911, 1999.
44. K Inouye. Effects of salts on thermolysin: activation of hydrolysis and synthesis of *N*-carbobenzoxy-L-aspartyl-L-phenylalanine methyl ester, and a unique change in the absorption spectrum of thermolysin. J Biochem 112:335–340, 1992.
45. AG Gershkovich, VV Koholodvych. Fluorogenic substrates for proteases based on intramolecular fluorescence energy transfer (IFETS). J Biochem Biophys Methods 33:135–162, 1996.
46. K Inouye, S-B Lee, K Nambu, B Tonomura. Effects of pH, temperature, and alcohols on the remarkable activation of thermolysin by salts. J Biochem 122:358–364, 1997.
47. BW Matthews. Structural basis of the action of thermolysin and related zinc peptidases. Acc Chem Res 21:333–340, 1988.
48. WL Mock, DJ Stanford. Arazoformyl dipeptide substrates for thermolysin. Biochemistry 35:7369–7377, 1996.
49. FW Dahlquist, JW Long, WL Bigbee. Role of calcium in thermal stability of thermolysin. Biochemistry 15:1103–1111, 1976.
50. VG Eijsink, OB Veltman, W Aukema, G Vriend, G Venema. Structural determinants of the stability of thermolysin-like proteinases. Nat Struct Biol 2:374–379, 1995.
51. B Holmquist, BL Vallee. Metal substitution and inhibition of thermolysin: spectra of the cobalt enzyme. J Biol Chem 249:4601–4607, 1974.
52. H Matsubara. Purification and assay of thermolysin. In: GE Perlmann, L Lorand, eds. Methods in Enzymology, Vol 19. New York: Academic Press, 1970, pp 642–651.
53. HM Holden, DE Tronrud, AF Monzingo, LH Weaver, BW Matthews. Slow- and fast-binding inhibitors of thermolysin display different modes of binding: crystallographic analysis of extended phosphonamidate transition-state analogues. Biochemistry 26:8542–8553, 1987.
54. K Inouye, K Kuzuya, B Tonomura. A spectrophotometric study on the interaction of thermolysin with chloride and bromide ions, and the state of tryptophyl residue 115. J Biochem 116:530–535, 1994.
55. JJ Yang, HE Van Wart. Kinetics of hydrolysis of dansyl peptide substrates by thermolysin: analysis of fluorescence changes and determination of steady-state kinetic parameters. Biochemistry 33:6508–6515, 1994.
56. C Marie-Claire, E Ruffet, G Tiraboschi, M-C Fournie-Zaluski. Differences in transition state stabilization between thermolysin (EC 3.4.24.27) and neprilysin (EC 3.4.24.11). FEBS Lett 438:215–219, 1998.
57. H Matsubara, J Feder. Other bacterial, mold, and yeast proteinases. In: PD Boyer, ed. The Enzymes, 3rd ed, Vol 3. New York: Academic Press, 1971, pp 721–795.
58. K Inouye, N Mazda, M Kubo. Need for aromatic residue at position 115 for proteolytic activity found by site-directed mutagenesis of tryptophan 115 in thermolysin. Biosci Biotechnol Biochem 62:798–800, 1998.
59. S Blumberg, BL Vallee. Superactivation of thermolysin by acylation with amino acid N-hydroxysuccinimide esters. Biochemistry 14:2410–2424, 1975.
60. J Feder. A spectrophotometric assay for neutral protease. Biochem Biophys Res Commun 32:326–332, 1968.
61. N Nishino, JC Powers. *Psedomonas aeruginosa* elastase. Development of a new substrate, inhibitors and an affinity ligand. J Biol Chem 255:3482–3486, 1980.
62. H Uehara, K Yamane, B Maruo. Thermosensitive, extracellular neutral proteases in *Bacillus subtilis*: isolation, characterization, and genetics. J Bacteriol 139:583–590, 1979.
63. MK Pangburn, Y Burstein, PH Morgan, KA Walsh, H Neurath. Affinity chromatography of thermolysin and of neutral proteases from *B. subtilis*. Biochem Biophys Res Commun 54:371–379, 1973.
64. KA Walsh, Y Burstein, MK Pangburn. Thermolysin and other neutral metalloendopeptidases. In: WB Jakoby, M Wilchek, eds. Methods in Enzymology, Vol 34. New York: Academic Press, 1974, pp 435–440.
65. B van den Burg, VG Eijsink, BK Stulp, G Venema. One-step affinity purification of *Bacillus* neutral proteases using Bacitracin-silica. J Biochem Biophys Methods 18:209–220, 1989.

80

Pectate and Pectin Lyases

Jacques A. E. Benen
Wageningen University, Wageningen, The Netherlands
Jaap Visser
Fungal Genetics and Technology Consultancy, Wageningen, The Netherlands

I. INTRODUCTION

Pectate lyases (EC 4.2.2.2) cleave the α-1,4-D-galacturonosidic linkage by β-elimination resulting in the formation of a Δ4,5-unsaturated newly formed nonreducing end as is shown in Figure 1. Pectin lyases (EC 4.2.2.10) perform the same reaction. However, this class of enzymes requires the galacturonic acid residues adjacent to the scissile bond to be methylesterified. Based on their names and the Enzyme Commission classification one would expect a strict separation of the substrate specificities for the pectate and pectin lyases. However, this is not true. Indeed for several pectin lyases the specific activity increases with increasing degree of methylesterification (DM) whereas for many pectate lyases highest specific activity was recorded using pectins of moderate DM (20–50%) instead of pectin with 0% DM. The only discriminating factor between pectate and pectin lyases is the absolute requirement for Ca^{2+} ions for catalysis by pectate lyases. In some cases, as for the cytosolic *Erwinia chrysanthemi* 3937 PelW (formerly known as KdgC), Ca^{2+} is substituted by Mn^{2+} (15).

Despite the classification into two groups (EC 4.2.2.2 and EC 4.2.2.10), the classification based on the amino acid similarity by Coutinho and Henrissat (14) groups most of the pectate lyases and all known pectin lyases into family 1 of polysaccharide lyases. So far, five additional families (polysaccharide lyase families 2, 3, 9, 10, and 11) of pectate lyases have been recognized. These additional families each contain only a small number of pectate lyases.

Unfortunately there is a large discrepancy between the rapidly expanding number of pectate and pectin lyases encoding nucleotide sequences available nowadays, and the actual number of corresponding enzymes thoroughly characterized biochemically. For many pectate and pectin lyases which have been biochemically characterized in the past no nucleotide sequences are available. This makes it difficult to relate certain biochemical properties to a particular family. However, biochemical data are available for at least one member of each of the six pectate lyase families. These will be discussed later.

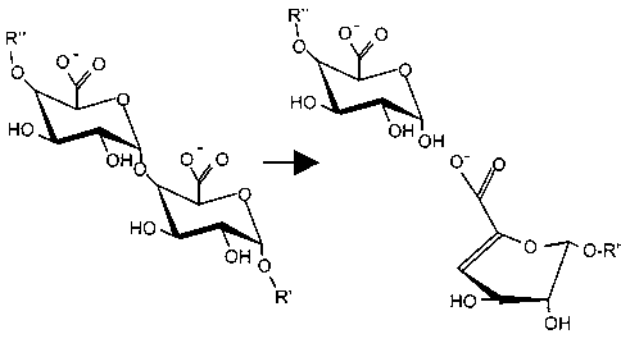

Figure 1 Elimination reaction carried out by pectate (and pectin) lyases.

A. Pectate Lyases

Initially, pectate lyases were only isolated from bacteria and fungi. Notably phytopathogenic microorganisms appeared to possess one or more pectate lyases. For several bacteria, systematic mutagenesis programs have been carried out aimed at making knockouts of the pectate lyase genes. These studies have revealed that particular pectate lyases have an important role in the infection process whereas other pectate lyases secreted by the same organism have only limited impact on infection. The bacteria *Erwinia chrysanthemi* and *E. carotovora* are among the best-studied microorganisms in this respect (16, 17). Recently, through cDNA sequencing of plant tissue specific cDNA libraries, putative pectate lyases have been identified in plants (19–22), and one of these cDNAs, obtained from *Zinnia elegans* and expressed in *Escherichia coli*, indeed encoded Ca^{2+}-dependent pectate lyase activity (22).

In *E. chrysanthemi* strain 3937 at least eight endoacting pectate lyases (PelA–PelE, PelI, PelL, and PelZ (23–26) have been identified, cloned, individually overexpressed, and biochemically characterized. In addition, an oligogalacturonan lyase (EC 4.2.2.6) and an exopectate lyase (EC 4.2.2.9) were identified and characterized (15, 27, 28).

B. Pectin Lyases

Pectin lyases (EC 4.2.2.10) have so far only been identified in and isolated from microorganisms. Unlike the pectate lyases, which have predominantly been isolated from bacteria, the pectin lyases have mostly been identified in fungi such as *Neurospora, Botrytis,* penicillia, and aspergilli. Currently, only endoacting pectin lyases are known.

II. ENDOGENOUS PECTATE LYASES IN PLANTS

As mentioned above, so far, only (putative) pectate lyases have been identified in plants. The first clear-cut demonstration of plant pectate lyase activity was reported by the group of McCann for *Zinnia elegans* (22). The gene encoding the pectate lyase (ZePel) appeared to be induced by auxin in a *Zinnia* mesophyll cell system at the onset of *trans*-differentiation into tracheary elements. It was proposed that the enzyme is involved in remodelling the cell wall during cell elongation and differentiation (22).

Based on the presence of cDNA-encoding putative pectate lyases, these activities have also been inferred in the ripening of strawberries (20) and bananas (19) and in the development of pollen in lily (18), tobacco, and *Arabidopsis* (21). Thus, although endogenous pectate lyases seem to be important for plant and fruit development, the appreciation of their role(s) is in its infancy.

III. APPLICATION OF PECTATE AND PECTIN LYASES

Pectate lyases have not found any application in the food industry owing to their high pH optima, which generally are above pH 8.0, and their calcium requirement. It should be pointed out, however, that pectate lyases may well be present in commercial pectic enzyme preparations used in the food industry. Such preparations may contain various pectic activities such as pectin methylesterases, polygalacturonases, rhamnogalacturonases, rhamnogalacturonan lyases, and pectate and pectin lyases. Although pectin lyases generally have lower pH optima than the pectate lyases and do not require calcium for activity, they are not applied in the food industry as individual enzymes. Rather, these enzymes are part of pectic enzyme preparations.

IV. BIOPHYSICAL PROPERTIES OF PECTATE AND PECTIN LYASES

As mentioned before, Coutinho and Henrissat (14) have classified the pectate and pectin lyases. The pectic lyases were classified in six families. To date the largest is family 1 which contains > 50 members with established activity and > 30 members based on sequence identity. Surprisingly, all known pectin lyases are part of family 1, which primarily contains pectate lyases. The molecular masses of the enzymes in family 1 range from 33 to 49.4 kDa. Family 2 so far contains only four members (three from *Erwinia* sp. and one from *Yersinia pseudoturberculosis*), and their molecular masses are virtually the same (60–64 kDa). Family 3 is the second largest and contains at present 14 members. Most of the pectate lyases in this family are fairly small (22.8–25.6 kDa) with two exceptions: pectate lyase B from *E. carotovora* (37.4 kDa), and pectate lyase I from *E. chrysanthemi* (36.8 kDa). The four members of family 9 are the largest pectate lyases with molecular masses of 45.5, 72.6, 79.6, and 82.3 kDa. The latter two enzymes are the only known exopectate lyases. The smaller one is from *E. chrysanthemi* strain 3937 (28),

and the larger one is from *E. chrysanthemi* strain EC16 (27). Finally, family 10 of pectate lyases contains only two very recently described genes, one from *Azospirillum irakense* (29) encoding a 47-kDa enzyme, and the other, *pel*E, from *Bacillus* sp. KSM-P15 (30) encoding a 35.6-kDa enzyme. Family 11 contains one rhamnogalacturon lyase and is, strictly speaking, neither pectate nor pectin lyase.

A. Three-Dimensional Structures of Pectate and Pectin Lyases

Currently, 3D structures are only available for family 1 lyases although the structure of PelL from *E. chrysanthemi* (family 9) was recently solved as well (J. Jenkins, personal communication). For pectate lyase from *Pseudomonas fluorescens*, which belongs to family 10, a structure has also been solved; however, the coordinates are not yet publicly available.

The *E. chrysanthemi* strain EC16 PelC structure (PDB code 2PEC) was the first to be solved by Jurnak and coworkers (4). Soon, the structure of the *Bacillus subtilis* pectate lyase (PDB code 1BN8) followed (5). In this structure a Ca^{2+} atom was found to be coordinated by three acidic residues at the bottom of the proposed substrate binding cleft, thus providing the first indication of a role for Ca^{2+}. The third structure (PDB code 1PCL) that became available was for PelE from *E. chrysanthemi* EC16 (31). Following the pectate lyase structures, three pectin lyases structures were solved. Mayans and coworkers (6) solved two structures of pectin lyase A (PLA) from *Aspergillus niger*. One of these structures (PDB code 11DJ) was solved at pH 6.5 (strain CBS120.49), and the other (PDB code 11DK) at pH 8.0 (strain 4m-147). Apart from some amino acid substitutions, the main difference between the two structures centers around Asp186, which is in a completely different position in the two structures. At pH 8.0 this residue is in an outward position and has been implicated in the reversible inactivation of the enzyme at pH 8.0 (6). Pectin lyase (PLB) (PDB code 1QCX) is the latest pectin lyase for which the structure has been solved (7).

The pectic lyases for which structures are known all have the same topology; the enzymes consist of a right-handed parallel β-helix. When it was first described for PelC this structure was unique. The unique properties of β-helical proteins and the origin of their stability were discussed by Jurnak and coworkers (32). The most recent pectate lyase structure is PelL from *E. chrysanthemi* 3937. This enzyme belongs to family 9, and it appears that the topology is the same as found for the family 1 pectic lyases (J. Jenkins, personal communication). Nowadays this β-helical structure is considered to be common among pectic enzymes except for the rhamnogalacturonan acetyl esterase which has an alpha-beta-alpha structure (12). The β-helix conformation was found for a rhamnogalacturonase (10), for two polygalacturonases (8, 9), and very recently for a bacterial pectin methylesterase (11). The evolutionary relationship between pectate and pectin lyases and tail spike protein (another right-handed β-helical enzyme) was discussed by Jenkins et al. (13). The reasoning they follow for the significant sequence variation between the enzymes with concomitant conservation of the topology can easily be extrapolated to the other pectic enzymes. Surprisingly, the family 10 *P. fluorescens* pectate lyase does not adopt the β-helical topology (G. Davies and G. Black, personal communication).

The main difference between the pectate and pectin lyases is found in the substrate-binding cleft as a result of the difference in charge of the preferred substrates. Whereas pectate lyases preferentially attack the charged polygalacturonic acid or pectin with a very low degree of esterification, with still a high degree of charges, pectin lyases prefer to act on fully or highly methylesterified pectin. As a result, the substrate binding cleft of the pectin lyases contains a very high number of aromatic (Trp, Tyr, Phe) and apolar residues (Val, Leu, Ile, Ala). In contrast, the substrate-binding cleft of the pectate lyases is occupied by polar (Ser, Thr, Asn) and charged (Asp, Glu, Arg, Lys) residues.

Recently, Scavetta and coworkers (33) solved the 3D structure of pectate lyase C from *E. chrysanthemi* EC16 in complex with a pentagalacturonide. This structure is the first of a pectic enzyme in complex with its substrate and clearly shows that the initially proposed substrate binding cleft indeed accommodates the substrate. In addition, the structure provides insight into the necessity of Ca^{2+} for catalysis by pectate lyases. This will be discussed below in Section V, on biochemical properties of pectate and pectin lyases.

B. Isoforms of Pectate and Pectin Lyases

The advances in molecular-biology techniques and tools in the past decade have allowed the rapid accumulation of nucleotide sequences of genes encoding pectate and pectin lyases. Comparison of the number of pectate lyase sequences and pectin lyase sequences present in databases shows that the pectate lyases strongly outnumber the pectin lyases. This is exemplified by an organism like *E. chrysanthemi* 3937. For this organism so far only one pectin lyase and nine pectate

lyases have been identified which have representatives in families 1, 2, 3, and 9 of polysaccharide lyases. However, *A. niger* appears to harbor at least six pectin lyase genes (34) and only one pectate lyase gene (Benen, unpublished). For other organisms, e.g., *Fusarium solani* (35–38), families of pectate lyases have been identified as well. Thus, from a genetic point of view there are many isoforms. This is not surprising in view of the complexity of the pectin molecule.

There has been no report to date of isoforms of pectinases as a result of proteolytic processing. Of course, since most of the pectinases are extracellular enzymes, they are processed by the proteases of the secretory pathway during export.

Eukaryotic organisms have the option to glycosylate secreted proteins either via N-linked glycosylation of Asn residues, provided the N- linked sequon Asn-X-Ser/Thr is present, or via O-linked glycosylation of serine residues. So far, only one detailed analysis of the glycosylation patterns of a pectate lyase has been published (39). For the overexpressed *A. niger* pectate lyase two forms were obtained. Although the two isoforms did not differ with respect to specific activity, they differed with respect to glycosylation: whereas one isoform was not N-glycosylated, the other isoform carried an N-glycon of the high mannose type (39). It is not known whether the N-glycosylation is involved in the stability of the enzyme.

V. BIOCHEMICAL PROPERTIES OF PECTATE AND PECTIN LYASES

A. Substrate Specificity

As mentioned in the introduction of this chapter, there is no strict separation of the substrate specificity between pectate and pectin lyases. Rather, the pectate lyases prefer pectin with a low DM or 0% DM whereas the pectin lyases prefer pectin with a high DM. One other property distinguishes the pectate lyases from the pectin lyases: the pectate lyases require calcium ions for catalysis.

1. Pectate Lyases

The 3D structure of the *B. subtilis* PEL revealed the presence of a Ca^{2+} ion tightly bound to the enzyme (5). However, the kinetic analysis of pectate lyases where Ca^{2+} is used as the varied substrate in many cases reveal sigmoidal curves instead of rectangular hyperbolic curves (upward curvature in Lineweaver-Burk plots instead of straight lines). If Ca^{2+} would only serve as a tightly bound cofactor, then the plots would be normal. Atallah and Nagel (40) analyzed the role of Ca^{2+} ions for a pectate lyase from a *Cephalosporium* sp. Using tetragalacturonide and Ca^{2+} in a two-substrate kinetic analysis, they concluded that the substrate binds as a Ca^{2+} tetragalacturonide complex and that Ca^{2+} might act as an activator of the enzyme. The 3D structure of the *E. chrysanthemi* EC16 PelC-pentagalacturonide complex (33), in which only four sugar moieties were seen, showed that in addition to the Ca^{2+} ion coordinated by four acidic amino acid residues, three more Ca^{2+} ions were present, each making contact to one of the carboxylic functions of the substrate and an acidic residue of the enzyme. Thus, kinetic studies as well as the 3D structure now demonstrate that Ca^{2+} is indeed involved in the binding of the substrate to pectate lyases. It is obvious that the number of Ca^{2+} ions involved in the binding will depend on the preferred DM of the substrate. The preference of the substrate will be based on the actual architecture of the subsites. A subsite which accommodates a methylesterified galacturonate residue will be different from one which accommodates a nonesterified galacturonate. Thus, by variation of the subsite composition numerous pectate lyases can be made with different substrate specificity.

The *E. chrysanthemi* 3937 pectate lyases, although not the first enzymes studied, represent the most complete set of pectate lyases from one organism thoroughly characterized (23–26, 28, 41).

Table 1 provides an overview of the biochemical properties of these enzymes. This table clearly shows the preferred DM of the substrate for the individual enzymes. Although six of the lyases belong to family 1, a considerable variation in substrate preference and reaction rates exists within this group of enzymes. It is even questionable whether polygalacturonic acid or even the partially methylesterified pectins are the natural substrates for PelA and PelZ (41). Moreover, although PelA, PelB, and PelD belong to family 1, they differ with respect to tissue maceration: PelA is devoid of this activity, PelB is moderately active, and PelD is very active in tissue maceration (16). This again demonstrates that the enzymes differ in their substrate specificity. The actual pectin structure(s) preferentially attacked during tissue maceration have not been identified.

For PelX, PelW, and oligogalacturonan lyase (OGL), it has been shown that the preferred substrates are oligogalacturonides rather than polymeric substrates (15, 28). From the localization of these enzymes

Table 1 Biochemical Properties of *E. chrysanthemi* 3937 Pectate Lyases (Kinetic Parameters Determined Using Polygalacturonic Acid)

Enzyme	Family	Mode of Action	pH opt.	% DM (range)	Cofactor(s)	K_m (mg/mL)	V_{max} (U/mg)	Ref.
PelA	1	endo	8.5	0 (0–30)	0.1 mM Ca^{2+}	0.3	46	23
PelB	1	endo	9.3	31 (0–50)	0.1 mM Ca^{2+}	0.03	2448	23
PelC	1	endo	9.2	31 (0–45)	0.1 mM Ca^{2+}	0.02	762	23
PelD	1	endo	8.8	0 (0–25)	0.1 mM Ca^{2+}	0.28	670	23
PelE	1	endo	8.0	0 (0–25)	0.1 mM Ca^{2+}	0.42	3803	23
PelI	3	endo	9.2	31 (10–55)	0.6 mM Ca^{2+}	0.12	230	26
PelL	9	endo	8.5	31 (0–70)	0.1 mM Ca^{2+}		5	25
PelZ	1	endo	8.5	7 (0–45)	0.2 mM Ca^{2+} 0.2 mM Mn^{2+}	0.15	9	46
PelX	9	exo	8.0	0 (0–25)	0.1 mM Ca^{2+}	0.25	90	28
PelW	2	exo	8.5	45 (0–60)	0.1 mM Mn^{2+} or Zn^{2+}	0.01	6	15

this is logical. PelX is localized in the periplasmic space where polymeric substrates are unlikely to be present (27). This enzyme is most active on tetragalacturonic acid (G4): K_m (G4) 25 μM and V_{max} 520 U/mg. PelW and OGL are both intracellular enzymes. The preferred substrates are trigalacturonate (G3) and digalacturonate (G2) for PelW and OGL, respectively (15). The kinetic parameters are: PelW K_m (G3) 7 μM and V_{max} 30 U/mg; OGL K_m (G2) 150 μM and V_{max} 80 U/mg. PelX and PelW both retain activity on polymeric substrates and their mode of action is exolytic on such substrates, cleaving off unsaturated dimers from the reducing end. An early report on an OGL from *Pseudomonas* sp. described an exolytic activity that cleaved off unsaturated monomers from the reducing end which were spontaneously converted into 2-keto-4-deoxygluconate (42). So far, no representative of family 10 lyases has been found in *E. chrysanthemi* 3937.

Recently, the *Azospirillum irakense* PelA which belongs to family 10 was characterized (29). It appeared that this endoacting enzyme prefers pectin with 28% methylesterification. The kinetic parameters for this enzyme using polygalacturonic acid as a substrate are: K_m 0.076 mg/mL and V_{max} 23 U/mg. The V_{max} is of the same order as found for the *E. chrysanthemi* PelA although the K_m is lower for the *Azospirillum irakense* PelA. Furthermore, the pH optimum and the Ca^{2+} concentration for optimal activity are similar to the family 1 enzymes as is the preference for low-DM pectin. Thus, although the pectate lyases can be grouped into five different families based on their primary sequences, no correlation is found with the kinetic data obtained so far.

2. Pectin Lyases

This interesting group of enzymes has recently received little attention. Only few detailed biochemical studies have been carried out in the past. The most exhaustively characterized enzymes are those obtained from *Aspergillus* pectinase preparations (43, 44). From *A. niger* N400 six genes were cloned encoding pectin lyases (34) among which are two genes, *pel*A and *pel*D, encoding pectin lyase A and D, respectively. These enzymes correspond to pectin lyase II and I, enzymes previously characterized by Van Houdenhoven (44). Kester and Visser (45) characterized PLB, the third pectin lyase from *A. niger*. This enzyme was obtained via overexpression of the *pel*B gene.

All these pectin lyases prefer high-DM pectins. The pH optima are ~ pH 6, with the exception of PLB for which a pH optimum of 8.5 was recorded. PLB was also greatly stimulated by the presence of a high salt concentration (0.5 M NaCl). Furthermore, the activity of PLB on 95% DM pectin, K_m 9.4 mM and V_{max} 1288 U/mg, is much higher than those reported for PLI (K_m 10.0 mM and V_{max} 125 U/mg) and PLII (K_m 1.5 mM and V_{max} 44 U/mg) (45). Voragen, studying three different pectin lyases, showed that using pectins with lower DM not only lowered the activities but the pH optima also shifted to lower pH. The shift of the pH optimum and the decrease in activity were also related to the distribution of the methyl groups (43). Detailed kinetic studies revealed that upon lowering DM V_{max} remained constant whereas K_m increased (43). However, by lowering the pH, the affinity for the lower DM pectins increased. It was also noted that

lyase activity was higher, using pectins of the same DM, when the pectin was deesterified by a pectin methylesterase instead of alkaline treatment. The alkaline treatment results in a random removal of methyl groups whereas the enzymic saponification results in a blockwise removal of methyl groups (see also Chap. 68 on the pectin methylesterases).

Although pectin lyases do not require Ca^{2+} for activity, Ca^{2+} appears to influence the activity of the enzymes. At pH values above the optimum, Ca^{2+} stimulated the activity, notably on partially alkaline deesterified substrates. Addition of Ca^{2+} to the reaction mixtures also resulted in a lowering of the pH optima (43).

Since pectin lyases prefer high-DM pectin as substrate, it is plausible that V_{max} remains constant and K_m increases using blockwise deesterified substrates since the actual concentration of the "high-DM" substrate decreases. Using alkaline treatment the high-DM nature of the substrate is lowered, so the substrate changes and therefore V_{max} also changes. Upon lowering the pH of the reaction mixture, more of the deesterified groups become protonated and thus the net charge of the substrate decreases. Therefore, the affinity for the substrate will increase at lower pH. A similar effect can be expected from Ca^{2+} which interacts with the carboxylates of the substrate. This effect will be stronger at higher pH as was observed.

B. Effect of Environmental Factors

Obviously, chelating compounds like EDTA dramatically reduce the activity of pectate lyases. For some pectate lyases it has been shown that other divalent ions can partially substitute for Ca^{2+}, i.e., PelX from *E. chrysanthemi* (28), or even require Mn^{2+} in addition to Ca^{2+} as has been observed for *E. chrysanthemi* PelZ (46). However, the five major *E. chrysanthemi* pectate lyases (A–E) (22) and the *A. irakense* PelA are inhibited by other divalent ions (29). The cytoplasmic *E. chrysanthemi* lyases PelW and OGL require Mn^{2+} or Mg^{2+} instead of Ca^{2+} (15). This is plausible since the actual concentration of Ca^{2+} in the cell is very low (μM range).

Ca^{2+} is apparently not only required for catalysis but it also renders the pectate lyases more resistant to thermal inactivation. The pectate and the pectin lyases are generally stable up to 50°C, their activity increasing with increasing temperature.

For the pectin lyases, so far no inhibitor molecules have been identified. The major *E. chrysanthemi* 3937 pectate lyases as well as a pectate lyase from *Colletotrichum gloeosporioides* were inhibited by epicatechin with K_i between 0.1 and 0.2 mM (23, 47). The *E. chrysanthemi* pectate lyases were also inhibited by salicylic acid (K_i between 0.2 and 0.4 mM) (23). Both compounds generally occur in plants and may be involved in the protection against attack of phytopathogenic microorganisms.

The pectin lyases from *A. niger* appear quite sensitive to the pH and the ionic strength of the medium. Both PLA and PLB reversibly inactivate at low ionic strength and higher pH (44, 45). For PLB this was accompanied by a change in the surface charge as inferred from the change in chromatographic behavior (45), and for PLA this was accompanied by changes in fluorescence (44) and in a structural change observed by x-ray crystallography (6).

C. Specific Mechanism of Action

The pectate and pectin lyases cleave the substrate by β-elimination (see Fig. 1). It is not known whether the anomeric configuration of the newly formed reducing end is retained or inverted. To initiate the reaction the proton must be removed from C5. This is to be accomplished by a base. The electron-withdrawing power of the methylesterified carboxyl group is much stronger than a carboxylic function without esterification. Thus, the pK_a of the proton at C5 will be lower in pectin than in pectate. Hence, a weaker base is necessary to initiate the reaction for pectin lyases. This may correlate with the observation that pectin lyases generally have lower pH optima than pectate lyases. Next, the glycosidic linkage must be broken, which has to be accomplished by an acid. The nature of the base and the acid were unknown until recently, when the 3D structure of the *E. chrysanthemi* EC16 PelC R218K-substrate complex was solved (33). The 3D structure of the complex could only be solved for this mutant enzyme PelC R218K which appeared strongly impaired in catalysis (48).

To lower the pK_a of the C5 proton the carboxylic acid of the substrate interacts with two Ca^{2+} ions and a Lys residue. In the mutant enzyme no obvious base is present. However, superposition of the wild-type structure revealed that Arg218 may serve as the base: one of the guanidium nitrogens is at 2.6 Å from the C5 proton while the other is at 2.7 Å from an oxygen of the carboxylic group (33). It was suggested that the latter interaction can be responsible for the lowering of the pK_a of the C5 proton and the former acts as the base (33). The nature of the acid is still unknown. Either a water molecule can be activated by one of the Ca^{2+} ions or the proton abstracted from C5 by Arg218

can be transferred to the glycosidic bond. This may be tested experimentally by kinetic isotope studies.

For the pectin lyases, a similar mechanism may be operating as the Arg218 counterpart is strictly conserved among pectate and pectin lyases. Furthermore, a site-directed mutagenesis studies on pectin lyase A and B from *A. niger* have shown that mutagenesis of this conserved Arg residue completely abolishes activity (Sanchez-Torres et al., unpublished).

D. Subsites in Binding to the Substrate

Polysaccharide-depolymerizing enzymes generally have multiple subsites, each interacting with one sugar residue of the polymer. As a rule of thumb, the exoacting enzymes have only a small number of subsites, and the endoacting enzymes have a larger number. By convention, subsites are consecutively numbered starting from the active site. Toward the reducing end the subsites are numbered starting from +1. Toward the nonreducing end the numbering starts at −1 at the subsite adjacent to subsite +1.

As mentioned above, the actual amino acids that constitute a subsite define its binding characteristics. A first partial study on pectate lyase was reported by Preston et al. (49) who analyzed *E. chrysanthemi* EC16 pectate lyases. Their data show that the four enzymes studied each have a distinct product progression profile during polygalacturonic acid degradation. Initially, larger oligomers are formed, distinctive for endocleaving enzymes, which are subsequently converted into typical smaller oligomers like unsaturated dimers and/or trimers; for instance PelC primarily generated unsaturated trimers and a smaller fraction of unsaturated dimers (49, 33). In fact, these studies helped to identify the actual active site in the PelC-substrate complex (33). A more detailed characterization of five *E. chrysanthemi* 3937 pectate lyases (PelA, PelB, PelD, PelI, and PelL) was carried out by Roy and coworkers (41). In addition to the product progression, the bond cleavage frequencies and cleavage rates of oligogalacturonides (degree of polymerization [DP] 2–8) of defined length were studied as well. These latter studies provide insight into the number of subsites and the location of the active site in the array of subsites. As a rule of thumb, endoacting enzymes show increasing rates of turnover as a function of the length of the oligomers used until the full array of subsites is filled. Actually a plot of log V_{max} vs. n (n = chain length) shows a plateau or peak when n equals or exceeds the number of subsites (50). This is also reflected in Table 2, where the bond cleavage frequencies and the rates of the five pectate lyases are presented.

The easiest to interpret are the data for PelD. The product progression on polygalacturonate is characterized by a strong accumulation of unsaturated dimer from the beginning of the reaction and only a small transient increase of oligomers with DP > 3. For all oligogalacturonides used the second bond from the reducing end is the preferred bond cleaved, and the highest reaction rate was recorded for tetragalacturonide. From this it was concluded that PelD most likely has only four subsites which stretch from −2 to +2 (41).

More complex was the behavior of PelA. For this enzyme a peak in rate was recorded at DP 4 and even higher activities at DP 7 and 8. Also, a shift in the preferred bond cleaved was observed depending on the chain length. Based on these observations it was concluded that PelA is composed of more than four subsites of which subsites −2 to +2 have the highest affinity for the homogalacturonan substrate (41). For PelB the array of subsites stretches from −3 to +3, with a strong preference to cleave off unsaturated trimers from the reducing end (41). Thus, despite PelA, PelB, and PelD belonging to the same family of lyases, their subsite compositions are quite different. This is further strengthened by the observation that for pectin lyase A from *A. niger*, belonging to the same family, 10 subsites were rationalized based on kinetic studies, stretching from −7 to +3 (44), which were recently confirmed by molecular modeling (P. Swaren, personal communication).

E. Synthetic Substrates

Applying complex carbohydrate synthesis chemistry Magaux and coworkers (51) and Kester and coworkers (52) generated monomethylesterified di- and trigalacturonides carrying the monomethyl group at a defined position. These substrates were used to test 11 different pectinases for the effect of the presence of a methylated galacturonate at subsites −2, −1, +1, or +2. This study included the *E. chrysanthemi* 3937 PelX, PelW, and Ogl, enzymes known to prefer small substrates. It was confirmed that OGL was five times more active on the unmethylated dimer than on the unmethylated trimer (15, 52). In addition it was shown that OGL can accommodate a methylated galacturonate at subsite + 1 and still retain high activity (78% on 1-Me-Gal$p$A)$_2$ and 51% on 1-Me(Gal$p$A)$_3$) at the substrate concentration used, whereas the presence of methylated galacturonate at subsite −1 was not tolerated (52). For PelX

Table 2 Bond Cleavage Frequencies and Specific Activities of *Erwinia chrysanthemi* 3937 Endopectate Lyases PelA, PelI, PelL, PelD, and PelB Acting on Oligogalacturonates of Defined Chain Length[a]

Enzyme	*n*																Activity (U mg^{-1})
PelA	3											G	– 100	G	–	**G**	0.6
	4									G	–	G	– 100	G	–	**G**	17
	5							G	–	G	– 23	G	– 77	G	–	**G**	12
	6					G	–	G	– 33	G	– 6	G	– 61	G	–	**G**	15
	7			G	–	G	– 70	G	– 9	G	– 2	G	– 19	G	–	**G**	23
	8	G	–	G	– 62	G	– 19	G	– 6	G	– 2	G	– 11	G	–	**G**	25
PelI	3											G	– 100	G	–	**G**	0.6
	4									G	– 62	G	– 38	G	–	**G**	11
	5							G	– 43	G	– 22	G	– 34	G	–	**G**	87
	6					G	–	G	– 74	G	– 23	G	– 3	G	–	**G**	252
	7			G	–	G	– 4	G	– 91	G	– 5	G	–	G	–	**G**	504
	8	G	–	G	– 2	G	– 33	G	– 61	G	– 4	G	–	G	–	**G**	630
PelL	3											G	–	G	–	**G**	0
	4									G	–	G	– 100	G	–	**G**	0.02
	5							G	–	G	– 28	G	– 72	G	–	**G**	0.22
	6					G	–	G	– 64	G	– 34	G	– 2	G	–	**G**	2.2
	7			G	–	G	– 4	G	– 91	G	– 5	G	–	G	–	**G**	3.5
	8	G	–	G	– 3	G	– 38	G	– 57	G	– 2	G	–	G	–	**G**	3
PelD	3											G	– 100	G	–	**G**	13
	4									G	–	G	– 100	G	–	**G**	418
	5							G	–	G	– 8	G	– 92	G	–	**G**	310
	6					G	–	G	– 3	G	– 3	G	– 94	G	–	**G**	268
	7			G	–	G	– 4	G	– 7	G	– 16	G	– 73	G	–	**G**	250
	8	G	–	G	–	G	– 1	G	– 14	G	– 10	G	– 75	G	–	**G**	222

Table 2 Continued

Enzyme	*n*																	Activity (U mg^{-1})
PelB	3														G	– 100	G	–	**G**	40
	4											G	– 43	G	– 57	G	–	**G**	2400
	5							G	–	G	– 69	G		G	– 31	G	–	**G**	3660
	6					G	–	G	– 10	G	– 52	G		G	– 38	G	–	**G**	4070
	7			G	–	G	– 2	G	– 6	G	– 62	G		G	– 30	G	–	**G**	3780
	8	G	–	G	–	G	–	G	– 11	G	– 67	G		G	– 22	G	–	**G**	3160

[a]Conditions: 0.5 mM oligogalacturonate ($n = 3$–8), 1 mM $CaCl_2$, 20 mM Tris/HCl, pH 8.0 (PelA, PelD, and PelL) or 20 mM amino-methyl-propanol/HCl pH 9.0 (PelB and PelI) at 37°C. Bond cleavage frequencies are given in percentages. The reducing end of the oligogalacturonates is printed in bold. *n*, degree of polymerization.

and PelW, both cleaving off unsaturated dimers, it was shown that none of the dimers were substrates. Furthermore, it was demonstrated that at subsite +2 a methylated galacturonate was tolerated, 33% and 39% activity remaining on 1-Me-(Gal*p*A)$_3$ for PelX and PelW, respectively, whereas subsite +1 absolutely required an unmethylated galacturonate. Only PelW was able to cleave 3-Me-(Gal*p*A)$_3$, albeit at a very low rate, demonstrating that for PelX and PelW an unmethylated galacturonate at subsite −1 is important as well (52).

VI. QUALITATIVE AND QUANTITATIVE DETERMINATION OF ACTIVITY

A. Substrate Preparation

Pectate and notably pectin show β-elimination at elevated pH. Any activity determination should therefore be corrected for this chemical breakdown by running the proper control reactions. A second, very important aspect is the fact that demethylation occurs quite readily at higher pH. To increase the shelf life of stock solutions of substrates, these are best prepared at pH values < 7 in distilled water rather than buffers. Since pectin in solution is viscous, for ease and accuracy of pipetting stock solutions, they can best be prepared at concentrations < 1% w/v. Before pectate or pectin can be dissolved in water, they should be hydrated. Therefore, 96% ethanol is added to the powder until the resulting slurry has a glossy shine. Next, an amount of water is added to allow pH adjustment, and then final volume adjustment should be done. In their acidic form pectate and to a lesser extent high-DM pectin do not readily dissolve as the starting pH will be < 4. Only after careful pH adjustment to a pH value > 4 will the pectate or pectin completely dissolve. Care should be taken to avoid pH overshoot (spontaneous quick demethylation). Pectate or pectin forms a buffer with a pK_a between 3.5 and 4. Initially quite large volumes of hydroxide are needed (use 1 M NaOH or less!), but when the pH reaches 4 the amount needed drastically decreases. To obtain solutions with minimal substrate interference in spectrophotometric assays the resulting solutions should be centrifuged for 15 min at 5000–7000g and decanted into a fresh container.

When selecting commercial pectin sources to be used as polymers, the product with the highest molecular mass and highest anhydrogalacturonic acid content should be chosen. The choice of DM is dependent on the purpose. When partially demethylated pectins are needed, attention should be paid to the method of demethylation which can be either enzymatic (plant or fungal pectin methylesterase) or an alkaline treatment. These methods result in different distributions of the methyl groups.

Oligogalacturonides are not commercially available. They should be prepared from polygalacturonic acid by partial digestion with either an endopolygalacuronase or a pectate lyase in case unsaturated oligogalacturonides are wanted. Methods to separate oligomer mixtures have been described (43, 53). The preparation

of methylated oligogalacturonides has also been described (54) as has the method to obtain reduced oligogalacturonides (55).

B. Assay Conditions

Pectate and pectin lyase activity are most conveniently measured spectrophotometrically at 235 nm in 1-cm light-path quartz cuvettes (1 or 3 mL). The unsaturated bond that results from the action of the lyases specifically absorbs UV light of this wavelength. For pectate the molar extinction coefficient (ϵ_{235}) is 4800 $M^{-1}cm^{-1}$ and for pectin ϵ_{235} is 5200 $M^{-1}cm^{-1}$ (56). By using the spectrophotometric method instead of a method based on the reducing sugar content, only the lyase activity is determined rather than all pectin-degrading activities like polygalacturonase activity that can be present as a contaminant.

For pectate lyase attention should be paid to the choice of the buffer as many anions interact with Ca^{2+}. In addition, for both the pectate and the pectin lyases the buffer should not absorb at 235 nm. Suggested buffers are: for pectin lyases McIlvaine buffers (pH 2.5–8.0), and for pectate lyases Tris/glycine/HCl or 2-amino-methyl propanol/HCl. It is known that Tris can have an inhibitory effect on some pectate lyases.

The amount of substrate to be used should ensure straight traces during the early stages of the reaction to allow the calculation of reaction rates. For kinetic analysis substrate concentration can vary between 0.01 and 5 mg/mL. For a standard assay any concentration between 0.2 and 3 mg/mL is adequate. For pectate lyase it should be kept in mind that Ca^{2+} will form gels with the substrate when the Ca^{2+} concentration is too high.

There are two methods to determine whether the enzyme is endolytic or exolytic. The first method relies on the reduction of the viscosity in relation to the reducing sugars formed. The second method is based on the analysis of the reaction mixture by thin-layer chromatography (TLC) or by high-performance anion exchange chromatography (HPAEC). The latter method allows accurate quantification. For the preparation of samples the reaction can be stopped either by boiling the sample or by lowering the pH below the activity region (to pH 4–5 for pectate lyase or to pH 3 for pectin lyase) by the addition of a predetermined adequate volume of acetic acid (pectate lyase) or hydrochloric acid (pectin lyase). Boiling the sample can sometimes lead to inaccurate data, as the enzyme activity initially increases until inactivation occurs.

C. Assay for Screening Purposes

To screen larger numbers of colonies (bacteria, fungi) for the production of pectate lyase, plates should be prepared in duplicate and include, in addition to all necessary compounds, 0.25% polygalacturonic acid and 0.1 mM $CaCl_2$. One of the plates serves as the master plate, and the second will be stained with Ruthenium Red. After growth in a 0.1% solution of Ruthenium Red, water has to be poured over the plate. Ruthenium Red will stain polygalacuronic acid but not degradation products thereof. The entire plate will therefore turn red/purple with a lighter halo around colonies that produce a pectate lyase. The method will not work for pectin lyases.

VII. PURIFICATION

Microbial pectic enzymes are generally secreted; they can therefore easily be recovered from the culture fluid by adsorption to an appropriate ion exchange resin. The choice of the resin depends on the isoelectric point of the enzyme, which is known to vary extensively from one enzyme to the other. For an individually overproduced enzyme, two or three chromatography steps are generally sufficient (57). When *Escherichia coli* is used to produce a recombinant pectinase, for initial characterization, no purification is necessary, as *E. coli* itself does not produce any pectinases. For the purification of a single enzyme from a pectinase preparation, many chromatography steps, including anion and cation exchange and gel filtration, may be necessary. In the past, crosslinked pectate and crosslinked alginate have successfully been applied for the purification of pectate lyases (58, 59).

REFERENCES

1. MJF Searle–Van Leeuwen, J-P Vincken, D Schipper, AGJ Voragen, G Beldman. Acetyl esterases of *Aspergillus niger*: purification and mode of action on pectins. In: J Visser, AGJ Voragen, eds. Progress in Biotechnology 14: Pectins and Pectinases. Amsterdam: Elsevier Science, 1996, pp 793–798.
2. T Sakai. Degradation of pectins. In: G. Winkelmann, ed. Microbial Degradation of Natural Products. New York: VCH, 1992, pp 57–81.
3. T Sakai, T Sakamoto, J Hallaert, EJ Vandamme. Pectin, pectinase, and protopectinase: production, properties, and applications. Adv Appl Microbiol 39:213–294, 1993.

4. MD Yoder, F Jurnak. The refined three dimensional structure of pectate lyase C from *Erwinia chrysanthemi* at 2.2 Å resolution—implications for an enzymatic mechanism. Plant Physiol 107:349–364, 1995.
5. R Pickersgill, J Jenkins, G Harris, W Nasser, J Robert-Baudouy. The structure of *Bacillus subtilis* pectate lyase in complex with calcium. Nat Struct Biol 1:717–723, 1994.
6. O Mayans, M Scott, I Connerton, T Gravesen, J Benen, J Visser, R Pickersgill, J Jenkins. Two crystal structures of pectin lyase A from *Aspergillus* reveal a pH driven conformational change and striking divergence in the substrate-binding clefts of pectin and pectate lyases. Structure 5:677–689, 1997.
7. J Vitali, B Schick, HCM Kester, J Visser, F Jurnak. The three-dimensional structure of *Aspergillus niger* pectin lyase B at 1.7-Å resolution. Plant Physiol 116:69–80, 1998.
8. R Pickersgill, D Smith, K Worboys, J Jenkins. Crystal structure of polygalacturonase from *Erwinia carotovora* spp. *carotovora*. J Biol Chem 273:24660–24664, 1998.
9. Y van Santen, JAE Benen, K-H Schröter, KH Kalk, S Armand, J Visser, BW Dijkstra. 1.68-Å Crystal structure of endopolygalacturonase II from *Aspergillus niger* and identification of active site residues by site-directed mutagenesis. J Biol Chem 274:30474–20480, 1999.
10. TN Petersen, S Kauppinen, S Larsen. The crystal structure of rhamnogalacturonase A from *Aspergillus aculeatus*: a right-handed parallel beta helix. Structure 5:533–544, 1997.
11. RW Pickersgill, JA Jenkins. Crystal structures of polygalacturonase and pectin methylesterase. In: HJ Gilbert, GJ Davies, B Henrissat, B Svensson, eds. Recent Advances in Carbohydrate Bioengineering. Cambridge: Royal Society of Chemistry, 1999, pp 144–149.
12. A Molgaard, S Kauppinen, S Larsen. Rhamnogalacturonan acetylesterase elucidates the structure and function of a new family of hydrolases. Struct Folding Design 8:373–383, 2000.
13. J Jenkins, O Mayans, R Pickersgill. Structure and evolution of parallel β-helix proteins. J Struct Biol 122:236–246, 1998.
14. PM Coutinho, B Henrissat. Carbohydrate-active enzymes: an integrated database approach. In: HJ Gilbert, GJ Davies, B Henrissat, B Svensson, eds. Recent Advances in Carbohydrate Bioengineering. Cambridge: Royal Society of Chemistry, 1999, pp 3–12.
15. VE Shevchik, G Condemine, J Robert-Baudouy, N Hugouvieux-Cotte-Pattat. The exopolygalacturonate lyase PelW and the oligogalacturonate lyase Ogl, two cytoplasmic enzymes of pectin catabolism in *Erwinia chrysanthemi* 3937. J Bacteriol 181:3912–3919, 199.
16. F Barras, F van Gysegem, AK Chatterjee. Extracellular enzymes and pathogenesis of soft rot *Erwinia*. Annu Rev Phytopathol 32:221–234, 1994.
17. N Hugouvieux-Cotte-Pattat, G Condemine, W Nasser, J Robert-Baudouy. Regulation of pectinolysis in *Erwinia chrysanthemi*. Annu Rev Microbiol 50:213–257, 1996.
18. SR Kim, D Finkel, YY Chung, G An. Abundance patterns of lily pollen cDNAs: characterization of three pollen-preferential cDNA clones. Sex Plant Reprod 7:76–86, 1994.
19. E Dominguez-Puigjaner, I Llop, M Vendrell, S Prat. A cDNA clone highly expressed in ripe banana fruit shows homology to pectate lyases. Plant Physiol 114:1071–1076, 1997.
20. N Medina-Escobar, J Cardenas, E Moyano, JL Caballero, J Monoz-Blanco. Cloning, molecular characterization and expression pattern of a strawberry ripening–specific cDNA with sequence homology to pectate lyase from higher plants. Plant Mol Biol 34:867–877, 1997.
21. R Kulikauskas, S McCormick. Identification of the tobacco and *Arabidopsis* homologues of the pollen-expressed LAT59 gene of tomato. Plant Mol Biol 34:809–814, 1997.
22. C Domingo, K Roberts, NJ Stacey, I Connerton, TF Ruiz, MC McCann. A pectate lyase from *Zinnia elegans* is auxin inducible. Plant J 13:17–28, 1998.
23. F Tardy, W Nasser, J Robert-Baudouy, N Hugouvieux-Cotte-Pattat. Comparative analysis of the five major *Erwinia chrysanthemi* pectate lyases: enzyme characteristics and potential inhibitors. J Bacteriol 179:2503–2511, 1997.
24. C Pissavin, J Robert-Baudouy, N Hugouvieux-Cotte-Pattat. Regulation of *pelZ*, a gene of the *pelB-pelC* cluster encoding a new pectate lyase of *Erwinia chrysanthemi* 3937. J Bacteriol 178:7187–7196, 1996.
25. E Lojkowska, C Masclaux, M Boccara, J Robert-Baudouy, N Hugouvieux-Cotte-Pattat. Characterization of the *pelL* gene encoding a novel pectate lyase of *Erwinia chrysanthemi* 3937. Mol Microbiol 16:1183–1195, 1995.
26. VE Shevchik, J Robert-Baudouy, N Hugouvieux-Cotte-Pattat. Pectate lyase PelI of *Erwinia chrysanthemi* 3937 belongs to a new family. J Bacteriol 179:7321–7330, 1997.
27. AD Brooks, SY He, S Gold, NT Keen, A Collmer, SW Hutcheson. Molecular cloning of the structural gene for exopolygalacturonate lyase from *Erwinia chrysanthemi* EC16 and characterization of the enzyme product. J Bacteriol 172:6950–6958, 1990.
28. VE Shevchik, HCM Kester, JAE Benen, J Visser, J Robert-Baudouy, N Hugouvieux-Cotte-Pattat. Characterization of the exo-pectate lyase PelX of

Erwinia chrysanthemi. J Bacteriol 181:1652–1663, 1999.
29. MA Bekri, J Desair, V Keijers, P Proost, M Searle–Van Leeuwen, J Vanderleyden, A van de Broek. *Azospirillum irakense* produces a novel type of pectate lyase. J Bacteriol 181:2440–2447, 1999.
30. K Sawada, A Ogawa, T Ozawa, N Sumitomo, Y Hatada, T Kobayashi, S Ito. Nucleotide and amino-acid sequences of a new-type pectate lyase from an alkaliphilic strain of *Bacillus*. Eur J Biochem 267:1510–1515, 2000.
31 SE Lietzke, RD Scavetta, MD Yoder, F Jurnak. The refined three-dimensional structure of pectate Lyase E from *Erwinia chrysanthemi* at 2.2 Å resolution. Plant Physiol 111:73–92, 1996.
32. F Jurnak, MD Yoder, R Pickersgill, J Jenkins. Parallel β-domains: a newfold in protein structures. Curr Opin Struct Biol 4:802–806, 1994.
33. RD Scavetta, SR Herron, AT Hotchkis, N Kita, NT Keen, JAE Benen, HCM Kester, J Visser, F Jurnak. Structure of plant cell wall fragment complexed to PelC. Plant Cell 11:1081–1092, 1999.
34. JAE Benen, L Pařenicovà, HCM Kester, J Visser. Molecular genetic and biochemical aspects of pectin degradation in *Aspergillus*. In: J Visser, AGJ Voragen, eds. Pectins and Pectinases, Progress in Biotechnology Vol 14. Amsterdam: Elsevier, 1996, pp 331–346.
35. MS Crawford, PE Kolattukudy. Pectate lyase from *Fusarium solani* f. sp. *pisi*: purification, characterization, in vitro translation of the mRNA, and involvement in pathogenesis. Arch Biochem Biophys 258:196–205, 1987.
36. W Guo, L Gonzalez-Candelas, PE Kolattukudy. Cloning of a novel constitutively expressed pectate lyase gene *pel*B from *Fusarium solani* f. sp. *pisi* (*Nectria haematococca*, mating type VI) and characterization of the gene product expressed in *Pichia pastoris*. J Bacteriol 177:7070–7077, 1995.
37. W Guo, L Gonzalez-Candelas, PE Kolattukudy. Cloning of a new pectate lyase gene *pel*C from *Fusarium solani* f. sp. *pisi* (*Nectria haematococca*, mating type VI) and characterization of the gene product expressed in *Pichia pastoris*. Arch Biochem Biophys 323:352–360, 1995.
38. W Guo, L Gonzalez-Candelas, PE Kolattukudy. Identification of a novel *pel*D gene expressed uniquely in planta by *Fusarium solani* f. sp. *pisi* (*Nectria haematococca*, mating type VI) and characterization of its protein product as an endo-pectate lyase. Arch Biochem Biophys 332:305–312, 1996.
39. J Colangelo, V Licon, J Benen, J Visser, C Bergmann, R Orlando. Characterization of the N-linked glycosylation site of recombinant pectate lyase. Rapid Commun Mass Spec 13:2382–2387, 1999.
40. MT Attalah, CW Nagel. The role of calcium ions in the activity of an endo-pectic acid lyase on oligogalacturonides. J Food Biochem 1:185–206, 1979.
41. C Roy, HCM Kester, J Visser, VE Shevchik, N Hugouvieux-Cotte-Pattat, J Robert-Baudouy, JAE Benen. Mode of action of five different endo-pectate lyases from *Erwinia chrysanthemi*. J Bacteriol 181:3705–3709, 1999.
42. C Hatanaka, J Ozawa. Oligogalacturonide transeliminase of a *Pseudomonas*. Agric Biol Chem 35:1617–1624, 1971.
43. AGJ Voragen. Characterization of pectin lyases on pectins and methyl oligogalacturonates. PhD dissertation, Wageningen University, Wageningen, Netherlands, 1972.
44. FEA van Houdenhoven. Studies on pectin lyase. PhD dissertation, Wageningen University, Wageningen, Netherlands, 1975.
45. HCM Kester, J Visser. Purification and characterization of pectin lyase B, a novel pectinolytic enzyme from *Aspergillus niger*. FEMS Microbiol Lett 120:63–68, 1994.
46. C Pissavin, J Robert-Baudouy, N Hugouvieux-Cotte-Pattat. Biochemical characterization of the pectate lyase PelZ of *Erwinia chrysanthemi* 3937. Biochim Biophys Acta 1383:188–196, 1998.
47. C Wattad, A Dinoor, D Prusky. Purification of pectate lyase produced by *Colletotrichum gloeosporioides* and its inhibition by epicatechin: a possible factor involved in the resistance or unripe avocado fruits to anthracnos. Mol Plant-Microbe Interact 7:293–297, 1994.
48. N Kita, CM Boyd, MR Garret, F Jurnak, NT Keen. Differential effect of site-directed mutations in PelC of pectate lyase activity, plant tissue maceration, and elicitor activity. J Biol Chem 271:26529–26535, 1996.
49. JF Preston, JD Rice, LO Ingram, NT Keen. Differential depolymerization mechanisms of pectate lyases secreted by *Erwinia chrysanthemi* EC16. J Bacteriol 174:2039–2042, 1992.
50. JA Thoma, C Brothers, J Spradlin. Subsite mapping of enzymes. Studies on *Bacillus subtilis* amylase. Biochemistry 9:1768–1775, 1970.
51. D Magaud, C Grandjean, A Doutheau, D Anker, VE Shevchik, N Cotte-Pattat, J Robert-Baudouy. Synthesis of the two mono methyl esters of α(1-4) linked D-galacturonic acid dimer and of precursors for the preparation of higher oligomers methyl esterified in definite positions. Carbohydr Res 314:189–199, 1998.
52. HCM Kester, D Magaud, C Roy, D Anker, A Doutheau, V Shevchik, N Hugouvieux-Cotte-Pattat, JAE Benen, J Visser. Performance of selected microbial pectinases on synthetic monomethyl-esterified di- and trigalacturonates. J Biol Chem 274:37053-37059, 1999.
53. HCM Kester, J Visser. Purification and characterization of polygalacturonases produced by the hyphal fungus *Aspergillus niger*. Biotechnol Appl Biochem 12:150–160, 1990.

54. HCM Kester, M Esteban Warren, R Orlando, JAE Benen, C Bergmann, J Visser. Tandem mass spectrometric analysis of *Aspergillus niger* pectin methylesterase; mode of action on fully methylesterified oligogalacturonates. Biochem J 346:469–474, 2000.
55. H Omran, K Dörreich, K Gierscher. Some results of the isolation of discrete enzymes (exopolygalacturonase and pectinesterase) from a commercial pectic enzyme preparation. Lebensm Wiss Technol 19:457–463, 1986.
56. JD MacMillan, RH Vaughn. Purification and properties of a polygalacturonic acid transeliminase produced by *Clostridium multifermentans*. Biochemistry 3:564–572.
57. L Pařenicovà, JAE Benen, HCM Kester, J Visser. *pga*E encodes a fourth member of the endopolygalacturonase gene family from *Aspergillus niger*. Eur J Biochem 251:72–80, 1998.
58. J Visser, R Maeyer, R Topp, F Rombouts. Purification of pectate lyases on cross linked pectate. Colloq Inserm Affinity Chromatog 86:51–62, 1979.
59. FM Rombouts, CCJM Geraeds, J Visser, W Pilnik. Purification of various pectic enzymes on cross-linked polyuronides. In: TCJ Gribnau, J Visser, RJF Nivard, eds. Affinity Chromatography and Related Techniques. Amsterdam: Elsevier Scientific, 1982, pp 255–260.

81

Alliinases

Edna C. Ramírez
University of California, Davis, Davis, California, U.S.A.

I. INTRODUCTION

Alliinases [S-alk(en)yl-L-cysteine sulfoxide lyase; alliin lyase; EC 4.4.1.4] cleave S-alk(en)yl-L-cysteine sulfoxides by β-elimination producing thiosulfinates, pyruvate, and ammonia (Fig. 1). This enzyme requires pyridoxal-5′-phosphate (PALP) as a cofactor. The pungent flavors and aromas of a number of species in the Amaryllidaceae family are due to the action of this enzyme. As is the case with other lyases, the enzyme is separated from the substrate in the intact tissue, and the reaction takes place upon rupture of cells.

The first alliinase to be described was from garlic bulbs by Stoll and Seebeck (1). They determined the effect of pH and temperature on the alliinase reaction from a crude extract of garlic and conducted studies on specificity based on substrate structure and configuration. Since then, alliinases from Chinese chive (2), garlic (3), leek (4), onion (5, 6), and Welsh onion (7) have been purified. Although they belong to the same genus, their individual alliin lyases are different in their physical and chemical properties.

II. IMPORTANCE TO QUALITY OF FOOD

Garlic and onion have been used for centuries by many cultures as foods, medicines, spiritual objects, etc. (8). Although they have nutritional and therapeutic values in diets, they are consumed around the world for their flavor and their ability to enhance the flavors of other foods. In garlic, diallylthiosulfinate (allicin) is the principal sulfur compound which gives its characteristic aroma. This thiosulfinate is the result of the β-elimination reaction on S-2-propenyl-L-cysteine sulfoxide (alliin) by alliinase, through the intermediary 2-propenesulfenic acid (9). In onions, there are three flavor precursors: S-1-propenyl-L-cysteine sulfoxide, S-methyl-L-cysteine sulfoxide, and S-propyl-L-cysteine sulfoxide (in the order of concentration abundance). The different thiosulfinates formed by the action of alliinase on these substrates give the distinct flavor of onions, depending on their concentrations (8). Other *Allium* spp. have different mixtures of these substrates as well as S-2-propenyl-L-cysteine sulfoxide; this last compound is absent in onion (9). The lachrymatory

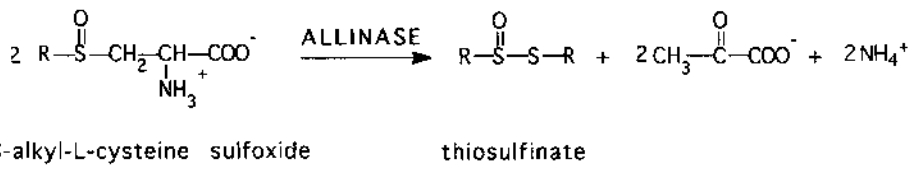

Figure 1 Alliinase general reaction.

factor in onion (propanethial sulfoxide) is derived from S-1-propenyl-L-cysteine sulfoxide (10).

Although the metabolic role of alliinase in plants has not been conclusively determined, the importance of this enzyme in defense mechanisms has been proposed by many researchers.

III. LOCATION

It is generally accepted that alliinases and their substrates are separated in vivo and only react upon wounding of the cells. High concentrations of alliinases are typically found in the bulbs of members of the genus *Allium*. In the onion bulb (*Allium cepa*), this enzyme is found in the vacuoles (11). In this study, the alliinase activity in vacuoles was found to be comparable to the total alliinase activity in protoplasts. Furthermore, vacuoles contained negligible amounts of alkyl-cysteine sulfoxides, but a considerable amount was found in cytoplasm of the protoplasts.

In garlic (*Allium sativum*), alliinases and lectins are the major proteins found in the clove (12). The total alliinase activity in the bulb of a mature plant of garlic is 10 times higher than that in the leaves (13). Ellmore and Feldberg (14) studied the location of alliinase deposits in garlic cloves through general histology, autofluorescence, and immunoblotting with enzyme-specific antibodies. Their results show alliinase to be concentrated in bundle sheaths, near phloem, scattered among storage mesophyll cells.

Analysis of the nectar from leek (*Allium porrum* L.) flowers also reveals the occurrence of two major proteins: lectin and alliinase (15). Researchers have not reported an explanation for the protein composition resemblance between garlic cloves (specialized storage tissue) and leek nectar. The discovery of the metabolic role of alliinases could provide some insight into this question.

IV. UTILITY OF THIS ENZYME IN FOODS

Alliinases are responsible for the initial reaction that produces characteristic flavors and aromas in vegetables of the genus *Allium*. The retention of full enzymatic flavor potential is the main challenge of food processors dealing with garlic and onion. To maintain this flavor potential, the retention of active alliinase and, especially, of the substrates must be considered during processing design and evaluation. Some pre- and postharvest practices are followed to increase the flavor potential of alliaceous foods; environmental factors affecting flavor intensity include sulfur content of soil, growing temperature, and water supply (8). In the case of onions, flavor potential increases with storage of the ripe bulb for a few months (10). In nature, as much as half of the S-1-propenyl-L-cysteine sulfoxide is bound as a peptide, γ-L-glutamyl-S-allyl-L-cysteine sulfoxide. It has been suggested that during storage, the substrate is released by the action of γ-glutamyl transferase.

During dehydration of onions, most of the flavor potential is lost because of the disappearance of the substrate rather than the enzyme. Thirty percent of the potential alliinase substrate is converted to cycloalliin during the initial dehydration stages (Fig. 2). Neither cycloalliin nor the S-alkyl-L-cysteines are substrates for alliinase. Reconstituted onion powder contains only a third of the onion aroma of fresh onion juice (10). Careful consideration of the drying speed is important during the design of the dehydration process to minimize substrate loss; a longer process usually results in better yields.

The action of alliin lyase may also result in the formation of unwanted pigments in alliaceous vegetables, such as pinking of onions and leek, and green pigment development in garlic (16). Although alliinase catalyzes the initial reaction and formation of thiopropanal-S-oxide (in the case of onion), the pigment formation depends on the carbonyl concentration and could vary from pink to red depending on the composition (Fig. 3).

Diallylthiosulfinate (allicin) is the antibacterial compound which has been used (as garlic extract) for thousands of years by many cultures (1). This and other medicinal properties attributed to garlic and onion are due to sulfurous compounds produced through enzymatic and nonenzymatic reactions following the reaction of alliinase on S-alk(en)yl-L-cysteine sulfoxides (10). Current research is focused on the specific compounds which give extracts from alliaceous plants their properties as antimicrobial, anticancer, anti–blood clotting, and hypoglycemic agents, as well as

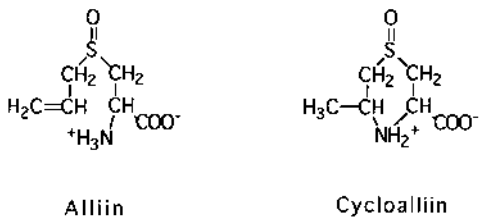

Figure 2 Structure of alliin and cycloalliin.

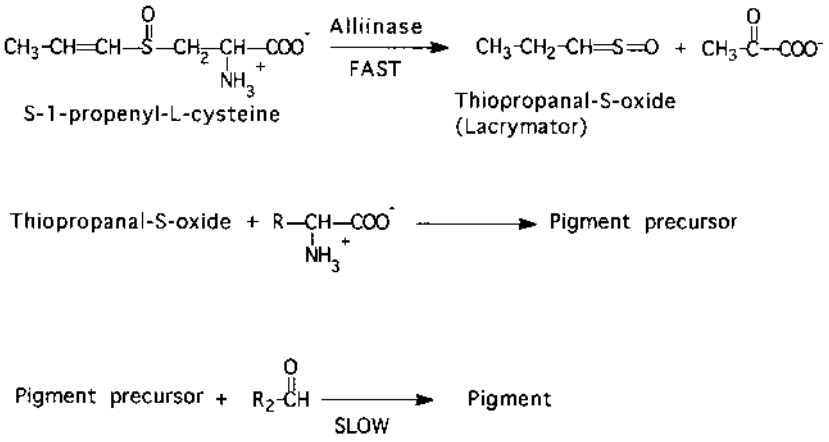

Figure 3 Formation of pigments in onion.

heavy-metal poisoning antidote and reductor of serum cholesterol and serum triglycerides (17). Garlic extract pills claiming extraordinary health benefits are very popular in the "nutraceutical" industry. Most of these extracts, however, depending on the methods used for preparation, may or may not contain the desired *Allium* organosulfur compounds due to their instability (thermodynamic) and reactivity (kinetic) (9).

V. PROPERTIES AS PROTEIN

Alliin lyases vary in molecular weight depending on the source of the enzyme. Reported values of alliinase molecular weight include 67 kDa for Chinese chive (2); 85 kDa for garlic (3); 150 kDa (5) and 59, 170, and 393 kDa for onion (6); 220 kDa for Welsh onion (7); and 386 and 580 kDa for leek (4).

The number of subunits of alliin lyase is different depending on the source, but a common characteristic among the alliin lyases is that all the subunits have approximately the same size. All reports, with the exception of Clark et al. (6), indicate that the individual proteins have subunits of the same molecular weight, showing only one band by SDS-PAGE. The number of subunits (and MW) reported to date are 1 (48 kDa) for Chinese chive (2); 2 (42 kDa) for garlic (3); 3 (50 kDa) (5) and 1, 3, and 6 or 7 (53.5 and 51.6 kDa) for onion (6); 4 (52 kDa) for Welsh onion (7); and 8 and 12 (48 kDa) for leek (4).

Pyridoxal-5′-phosphate (PALP) is a known cofactor of alliinase. The molar ratio of PALP to alliin lyase has been determined as one mole of PALP per subunit for Chinese chive, garlic, and onion (2, 3, 5). The amino acid residue involved in the PALP binding site of the onion and Chinese chive alliinase has been identified as Lys285 (18) and Lys280 (2), respectively.

Information has been reported on the amino acid composition and primary structure of alliinase by several groups. In 1992, Van Damme et al. (19) reported the cDNA sequence for alliinase from garlic, onion, and shallot, and other groups have recently obtained deduced sequences for garlic (13) and Chinese chive (2) alliinases. Onion and shallot alliinases primary sequences have the highest degree of homology (98%); those from onion and garlic showed 88% similarity (19). Deduced amino acid sequence of alliinase from Chinese chive showed homologies with those from garlic (64.3%), onion (69.1%), and shallot (69.2%) (2) (Fig. 4). No information has been reported on the secondary or tertiary structure of alliinase.

Results using the Dubois method or by staining of PAGE by periodic acid-Schiff base reagent indicate that garlic (3), leek (4), onion (5, 6), and Welsh onion alliin lyases (7) are glycoproteins. Alliinase from garlic contains 6% natural sugars and can form a complex with garlic mannose-specific lectin, the second-most-abundant protein from garlic. Asn146 has been identified as the glycosylation site of garlic alliinase (20).

Importance of glycosylation of this enzyme is apparent through the study of the degree of homology of the alliinases from garlic, onion, and leek, and the β-cystathionase from spinach based on the cross-reactivity of rabbit polyclonal antibodies raised against the enzymes (21). Results showed that glycosylated garlic alliinase antibodies reacted not only with glycosylated and deglycoslated garlic enzyme, but also with the

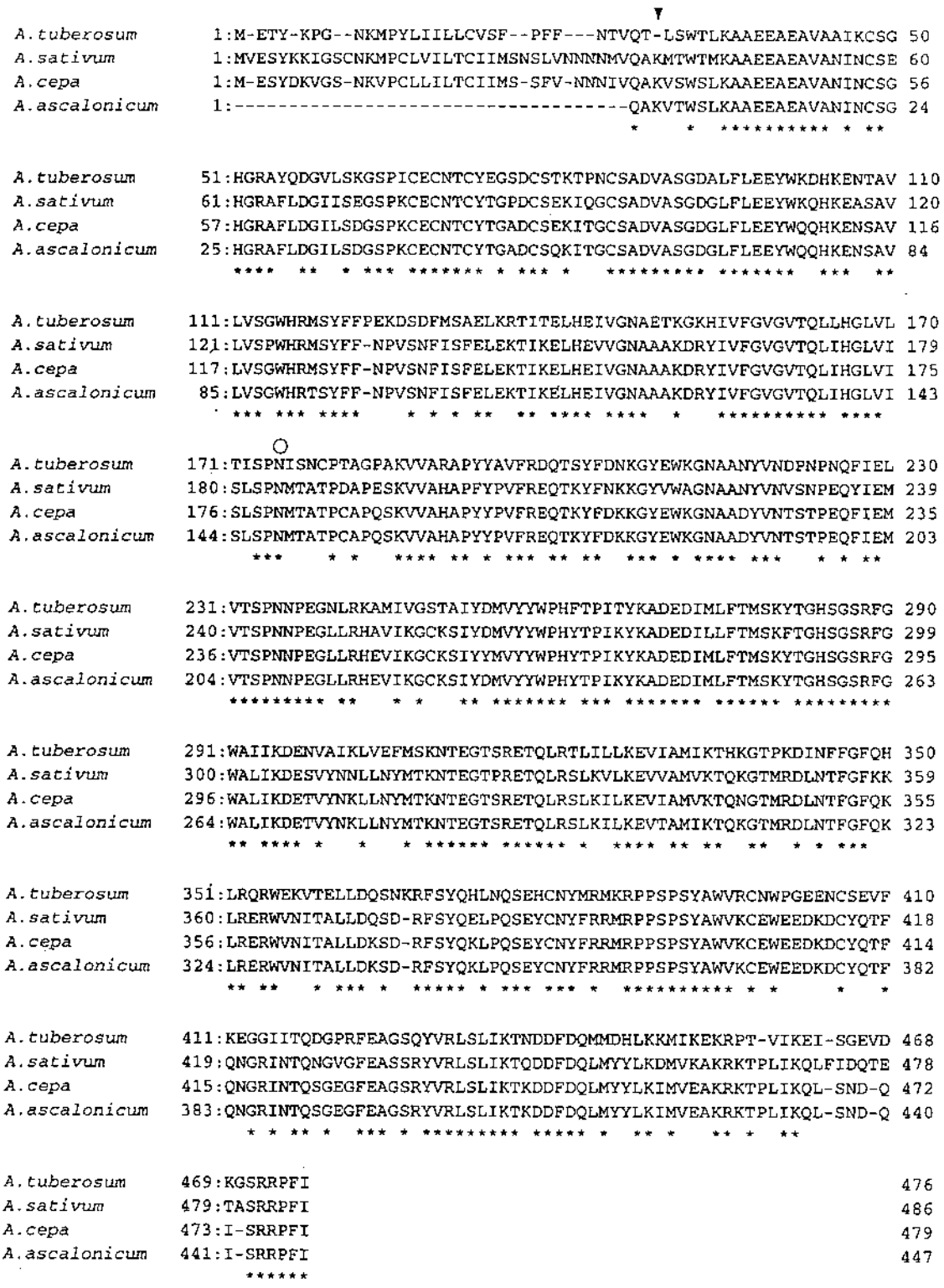

Figure 4 Comparison of deduced primary sequences of alliin lyase from Chinese chive (*Allium tuberosum*), garlic (*A. sativum*), onion (*A. cepa*), and shallot (*A. ascalonicum*). (From Ref. 2.)

native onion, leek, and spinach enzymes. Antibodies to the deglycosylated garlic enzyme reacted strongly with both native and deglycosylated garlic enzymes, less strongly with the native onion enzyme, and weakly, if at all, with native leek and spinach enzymes. Antibodies produced by deglycosylated onion enzyme reacted exclusively with native and deglycosylated onion enzyme.

VI. PROPERTIES AS ENZYME

Although alliinases are able to catalyze reactions using many S-alk(en)yl-L-cysteine sulfoxides, the pool of sulfur amino acids is different depending on the *Allium* sp. It is presumed that this difference in accumulation of S-alk(en)yl-L-cysteine sulfoxides results in the different aromas and flavors of these group of plants. The predominant natural substrate in onion is S-(1-propenyl)-L-cysteine sulfoxide, but also present are other S-alkyl-L-cysteine sulfoxides. Garlic accumulates S-(2-propenyl)-L-cysteine sulfoxide predominantly, with presence of S-alkyl derivatives. Chinese chive contains all the S-alk(en)yl-L-cysteine sulfoxides previously mentioned (2), and in leek, methyl, allyl, and propyl derivatives have been identified (4).

The affinity for substrate, expressed as K_m, is typically determined for S-ethyl-L-cysteine sulfoxide; reported values are 2.7 mM for the alliinase from Chinese chive (2), 5.7 mM for garlic (3), 5.8 mM for Welsh onion (7), 6 mM for onion (5), and 13 mM for leek (4). Alliinase is inhibited by hydroxylamine, sodium cyanide, and amino-oxyacetate (2, 5), as expected for enzymes requiring PALP as a cofactor.

There has been no report on the temperature optimum for this enzyme; however, room temperature is universally used by the different research groups for activity assays. The pH optimum varies depending on the species and the buffer used, ranging from 6.5 (garlic) (3) to 8.5 (Chinese chive in Tris-HCl buffer) (2). The pH optimum of alliinase from Chinese chive changes to 6.5 in phosphate buffer; onion also shows a pH optimum of 7.6 in phosphate buffer and 8–8.5 in tricine buffer (5).

VII. DETERMINATION OF ACTIVITY

The major substrate in garlic for alliin lyase is alliin (S-allyl-L-cysteine sulfoxide). Although the enzymatic activity could be determined by measuring any of the products of the reaction, most researchers measure the pyruvate production by a modification of the method by Friedemann and Haugen (22) for keto acids. The pyruvate reacts with dinitrophenylhydrazine to produce pyruvyl hydrazone which absorbs at 450 nm. In general, S-ethyl-L-cysteine sulfoxide is used as the substrate to determine enzymatic activity. S-ethyl-L-cysteine is commercially available, and the sulfoxide can be synthesized by oxidation with H_2O_2 as described (1).

Recently, a simple and rapid spectrophotometric method has been developed for determination of alliinase activity (23). It is based on the reaction of 2-nitro-5-thiobenzoate (NTB) with allicin (diallylthiosulfinate). The reaction is followed spectrophotometrically at 412 nm, measuring the consumption of NTB and the formation of S-allylmercapto-NTB. This method has the advantages of being direct, quantitative, and dependent on the initial velocity rather than the activity at fixed times. It requires the synthesis of NTB and alliin (S-allyl-L-cysteine sulfoxide). Both methods will be described in this chapter.

A. Pyruvate Measurement by Dinitrophenylhydrazone Formation

1. Enzymatic Reaction

The reaction mixture contains 40 mM S-ethyl-L-cysteine sulfoxide, 100 mM phosphate buffer, pH 6.5 (for garlic), 25 μM PALP, and 50–500 μg (protein) of enzyme in a total volume of 1 mL. Appropriate buffer adjusted to pH 8.0 (tricine, bicine) should be used when assaying alliinase from onion or leek. The mixture is incubated for 5–15 min (depending on enzyme concentration) at 23°C, and the reaction is stopped by the addition of 1 mL of 10% (612 mM) trichloroacetic acid (TCA). The precipitated protein is removed by centrifugation, and pyruvate is measured in the supernatant. A blank is prepared by adding 1 mL of 10% TCA solution to reaction mixture prior to enzyme addition.

2. Pyruvate Determination

Supernatant (0.5 mL) from the enzyme reaction is added to a mixture containing 2.5 mL of 10% TCA solution and 1 mL of 0.1% (5.10 mM) dinitrophenylhydrazine (DNPH) in 2 M HCl. The mixture is incubated for 5 min at 30°C and stopped with the addition of 5 mL of 2.5 M NaOH. Absorbance at 450 nm is measured after 10 min. A standard curve is made with known concentrations of sodium pyruvate. A unit of activity corresponds to the production of 1 μmol of pyruvate per min.

B. Allicin Measurement Using 2-Nitro-5-Thiobenzoic Acid

1. Preparation of NTB

2-Mercaptoethanol (5 mL) is added to a solution of 5,5′-dithiobis-(2-nitrobenzoic acid) (DTNB) (1.0 g in 50 mL of 0.5 M Tris-HCl buffer, pH 8.0). After 5 min the solution is acidified to pH 1.5 by the addition of 6 N HCl and kept overnight at 4°C. The orange crystals formed are filtered, washed with diluted HCl, and vacuum-dried over P_2O_5. NTB (dry powder) can be stored in the dark at room temperature for > 10 years. The yield is 57%.

2. Preparation of Alliin

It can be synthesized by oxidation of S-allyl-L cysteine with H_2O_2 as described (1).

3. Enzymatic Reaction

The reaction mixture contains 0.1 mM NTB, 50 mM phosphate buffer, pH 6.5, 1 mM EDTA, 20 μM PALP, 10 mM alliin, and 0.0025–0.01 units of enzyme in a total volume of 1 mL. Reaction is started by the addition of alliin, and the initial velocity is recorded by the decrease in absorbance at 412 nm. The concentration of NTB consumed in the reaction is calculated using the molar extinction coefficient ($\epsilon = 14{,}150\ M^{-1}\ cm^{-1}$). A unit of activity corresponds to the production of 1 μmol of pyruvate per min (1 mol of NTB is equivalent to 0.5 mol of allicin and thus 1 mol of pyruvate).

VIII. PURIFICATION

Alliinases have been purified from Chinese chive, garlic, leek, onion, and Welsh onion. The steps used for the purification vary depending on the plant source and research groups. There are certain common operations in most protocols such as ammonium sulfate precipitation and size exclusion and cation exchange chromatographies. The fact that alliinase is a glycoprotein is used by some researchers to purify the enzyme using a Concavalin A–Sepharose column. The addition of PALP and glycerol in buffers is recommended to help stabilize the enzyme during purification. Table 1 illustrates the steps used by different groups to purify alliinase from different plant materials.

In this chapter we will describe the conditions used for the purification of alliin lyase from garlic cloves (3). Peeled garlic cloves are blended with buffer A (0.02 M Na phosphate/10% glycerol/5% NaCl, 0.05% 2-mercaptoethanol/1 mM phenylmethylsulfonyl fluoride (PMSF), pH 7.0), 1:1 (w/v) and 5% insoluble polyvinylpolypyrrolidone (PVPP) for 1 min, and the homogenate is filtered through two layers of cheesecloth. The homogenate is centrifuged and the supernatant is decanted and saturated to 35% with $(NH_4)_2SO_4$ with constant stirring for 30 min, followed by centrifugation. The precipitate is redissolved in a minimal amount of buffer B (0.05 M Na phosphate/10% glycerol/20 μM PALP/1 mM PMSF, pH 7.0), and the suspension is dialyzed against the same buffer. The solution is clarified by centrifugation to remove insoluble materials.

The enzyme solution is fractionated through a fast-flow hydroxyapatite column and the active enzyme is

Table 1 Purification Steps Used for Alliin Lyases

Step	Chinese chive[e]	Garlic[b]	Leek[c]	Onion	Welsh onion[d]
Aqueous extraction	1	1	1	1[a,f]	1
Protamine sulfate precipitation			2	2[a]	
SDS treatment				3[a]	
$(NH_4)_2SO_4$ precipitation	2	2	3	4[a], 2[f]	2
Hydroxyapatite chrom.		3	4		
Affinity chrom. (ConA-Sepharose)		4	5	4[f]	
Size exclusion chrom.	4			5[a], 3[f]	5
Hydrophobic chrom. (Phenyl-Sepharose)				5[f]	
Alumina Cγ gel				6[a]	
Cation exchange chrom.	3			7[a], 6[f]	3,4

The numbers indicate the order of the steps used for the purification; the letters indicate the source of information. [a]Ref. 5. [b]Ref. 3. [c]Ref. 4. [d]Ref. 7. [e]Ref. 2. [f]Ref. 6.

Table 2 Purification Table for Alliinase from Garlic

Fraction	Volume (mL)	Total protein (mg)	Total activity (μmol/min)	Sp. activity (μmol/min mg)	Recovery (%)	Purif. (fold)
Homogenate[a]	350	2675	75,492	20.5[b]	100	1.00
35% $(NH_4)_2SO_4$	64	1005	40,904	40.7	54	1.99
Hydroxyapatite	20	283	20,662	73.0	27	3.56
Concavalin A-Sepharose	17	25	3,150	126.0[c]	4	6.15

[a]From 250 g of peeled garlic cloves.
[b]With S-allyl-L-cysteine sulfoxide, the specific activity was 30.8 μmol/min mg.
[c]With S-allyl-L-cysteine sulfoxide, the specific activity was 214 μmol/min mg.
Source: Ref. 3.

eluted with three volumes of buffer (3 M Na phosphate/10% glycerol/20 μM PALP/1 mM PMSF, pH 7.0). Active fractions are pooled, concentrated by ultrafiltration, and dialyzed. The dialysate is applied to a Concavalin A–Sepharose 4B column. The enzyme is eluted from the column with buffer B, using a linear methyl α-D-mannopyranoside gradient (0–100 mM). Active fractions are pooled. Table 2 shows the quantitation of each step in purifying alliin lyase from garlic.

REFERENCES

1. A Stoll, E Seebeck. Chemical investigation of alliin, the specific principle of garlic. Adv Enzymol 11:377–400, 1951.
2. T Manabe, A Hasumi, M Sugiyama, M Yamazaki, K Saito. Alliinase [S-alk(en)yl-L-cysteine sulfoxide lyase] from *Allium tuberosum* (Chinese chive). Purification, localization, cDNA cloning and heterologous functional expression. Eur J Biochem 257:21–30, 1998.
3. LP Nock, M Mazelis. The C-S lyases of higher plants. Preparation and properties of homogeneous alliin lyase from garlic (*Allium sativum*). Arch Biochem Biophys 249:27–33, 1986.
4. T Won, M Mazelis. The C-S lyases of higher plants. Purification and characterization of homogeneous alliin lyase of leek (*Allium porrum*). Physiol Plant 77:87–92, 1989.
5. HE Tobkin, M Mazelis. Alliin lyase: preparation and characterization of the homogeneous enzyme from onion bulbs. Arch Biochem Biophys 193:150–157, 1979.
6. SA Clark, ML Shaw, D Every, JE Lancaster. Physical characterization of alliinase, the flavor generating enzyme in onions. J Food Biochem 22:91–103, 1998.
7. M Fujita, M Endo, M Sano. Purification and characterization of alliin lyase from Welsh onion, *Allium fistulosum* L. Agric Biol Chem 54:1077–1079, 1990.
8. WM Randle. Onion flavor chemistry and factors influencing flavor intensity. In: SJ Risch, CT Ho, eds. Spices. Flavor Chemistry and Antioxidant Properties. ACS Symp Ser 660:41–52, 1997.
9. E Block, EM Calvey. Facts and artifacts in *Allium* chemistry. In: CJ Mussinan, ME Keelan, eds. Sulfur Compounds in Foods. ACS Symp Ser 564:63–79, 1994.
10. S Schwimmer. Enzyme action and aroma genesis in vegetables. In: Source Book of Food Enzymology. Westport, CT: Avi Publishing, 1981, pp 373–381.
11. JE Lancaster, HA Collin. Presence of alliinase in isolated vacuoles and of alkyl cysteine sulfoxides in the cytoplasm of bulbs of onion (*Allium cepa*). Plant Sci Let 22:169–176, 1981.
12. K Smeets, EJM Van Damme, WJ Peumans. Developmental regulation of lectin and alliinase synthesis in garlic bulbs and leaves. Plant Physiol 113:765–771, 1997.
13. A Rabinkov, XZ Zhu, G Grafi, G Galili, D Mirelman. Alliin lyase (alliinase) from garlic (*Allium sativum*). Biochemical characterization and cDNA cloning. Appl Biochem Biotechnol 48:149–171, 1994.
14. GS Ellmore, RS Feldberg. Alliin lyase localization in bundle sheaths of the garlic clove (*Allium sativum*). Am J Bot 81:89–94, 1994.
15. WJ Peumans, K Smeets, K Van Nerum, F Van Leuven, EJM Van Damme. Lectin and alliinase are the predominant proteins in nectar from leek (*Allium porrum* L.) flowers. Planta 201:298–302, 1997.
16. S Schwimmer. Color changes induced by enzyme action on nonphenolic substrates. In: Source Book of Food Enzymology. Westport, CT: Avi Publishing, 1981, pp 312–314.
17. CJ Mussinan, ME Keelan. Sulfur compounds in foods. An overview. In: CJ Mussinan, ME Keelan, eds. Sulfur Compounds in Foods. ACS Symp Ser 564:1–6, 1994.
18. N Kitamura, N Shimomura, J Iseki, M Honma, S Chiba, S Tahara, J Mizutani. Cysteine-S-conjugate beta-lyase activity and pyridoxal phosphate binding

site of onion alliin lyase. Biosci Biotechnol Biochem 61:1327–1330, 1997.
19. EJ Van Damme, K Smeets, S Torrekens, F Van Leuven, WJ Peumans. Isolation and characterization of alliinase cDNA clones from garlic (*Allium sativum* L.) and related species. Eur J Biochem 209:751–757, 1992.
20. A Rabinkov, M Wilchek, D Mirelman. Alliinase (alliin lyase) from garlic (*Allium sativum*) is glycosylated at Asn(146) and forms a complex with a garlic mannose-specific lectin. Glycoconjugate J 12:690–698, 1995.
21. F Ho, M Mazelis. The C-S lyases of higher plants, determination of homology by immunological procedures. Phytochemistry 34:625–629, 1993.
22. TE Friedemann, GE Haugen. The determination of keto acids in blood and urine. J Biol Chem 147:415–442, 1943.
23. T Miron, A Rabinkov, D Mirelman, L Weiner, M Wilchek. A spectrophotometric assay for allicin and alliinase (alliin lyase) activity: reaction of 2-nitro-5-thiobenzoate with thiosulfinates. Anal Biochem 265:317–325, 1998.

82

Cystine Lyases in Plants

Edna C. Ramírez
University of California, Davis, Davis, California, U.S.A.

I. INTRODUCTION

Cystine lyases (cystathionine L-homocysteine-lyase; EC 4.4.1.8) cleave L-cystine through a β-elimination reaction producing thiocysteine (cysteine persulfide), pyruvate, and ammonia (Fig. 1). Although this enzyme has been studied in detail, its substrate specificity remains controversial. In fungi and bacteria, cystine lyase and β-cystathionase activities are found together. In plants, however, cystine lyase does not recognize β-cystathionine as a substrate.

Cystine lyase activity was first detected in plants in 1966 by Tishel and Mazelis (1). They observed the ability of homogenates of cabbage leaves to degrade L-cystine, but not L-cystathionine, to pyruvate. The requirement for pyridoxal-5′phosphate (PALP) as a cofactor for this enzyme was also noted.

II. IMPORTANCE TO QUALITY OF FOOD

Cystine lyases are responsible for the initial reaction that produces characteristic flavors and aromas in important vegetables of the genus *Brassica*. Cruciferous vegetables (broccoli, Brussels sprouts, cabbage, cauliflower, etc.) have characteristic sulfurous flavors and aromas as a result of these enzymatic reactions following the maceration of tissue. In broccoli, cystine lyase was determined to be the principal enzyme responsible for the off-aroma deterioration (2). Purified cystine lyase added to blanched broccoli and presented to a panel reproduced the aroma descriptors characteristic of unblanched broccoli.

In 1993, Chin and Lindsay (3) identified the sulfur compounds formed in disrupted tissues of cabbage as methanethiol (MT), dimethyl disulfide (DMDS), and dimethyl trisulfide (DMTS). All of these compounds, although characteristic of *Brassica* vegetables, are undesirable to the consumer. This presents a problem, particularly in the use of modified atmospheres, where the unpleasant sulfurous odors limit consumer acceptance. The mechanisms of formation of these sulfur compounds in cabbage, following the activity of cystine (cystine sulfoxide) lyase, were elucidated (4). They found no significant difference in the formation of DMDS under aerobic and anerobic conditions; however, DMTS was detected only in the absence of oxygen.

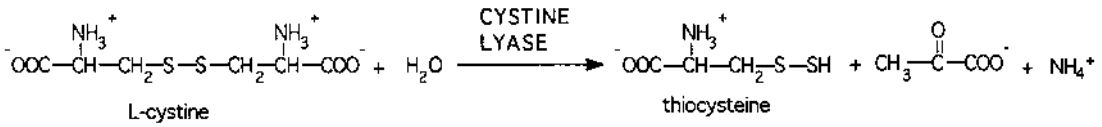

Figure 1 Cystine lyase general reaction.

Several treatments have been used to reduce the amounts of these objectionable volatiles in broccoli stored under modified atmospheres, including dipping the vegetable in caraway (*Carum carvi*) seed extract, tertiary butylhydroquinone (TBHQ), ascorbic acid (500 ppm), phosphoric acid (0.1 M), and sodium hydroxide (0.01 M) (5). Although all these treatments reduced the sulfurous aroma intensity, the alkaline treatment had the highest effect on the intensity and on suppressing the formation of dimethyl disulfide. Obenland and Aung (6) found that the formation of DMDS and MT in intact broccoli florets could be enhanced 2.8 times over the control by the infiltration of S-methyl cysteine sulfoxide prior to anaerobiosis, and nearly eliminated by infiltration of hydroxylamine (a cystine lyase inhibitor).

III. LOCATION

Location of cystine lyase in the cells has not been determined. In broccoli and cauliflower, the activity of cystine lyase in the florets is, on average, three to five times higher than in the stalks of the vegetables (Ramírez, personal observation).

IV. UTILIZATION OF THIS ENZYME IN FOODS

The metabolic role of cystine lyase in plants has not been determined. β-Cystathionase is involved in the methionine cycle, cleaving L-cystathionine to produce homocysteine.

Currently, in the frozen food industry, peroxidase is the enzyme used as the indicator for proper blanching in most vegetables, including broccoli. Results from experiments on blanching broccoli in water showed that cystine lyase is less heat stable than peroxidase (7). The use of a proper indicator enzyme could lead to blanching optimization; cystine lyase would be the logical choice in the case of broccoli. The employment of this enzyme by the frozen food industry could potentially reduce blanching times and therefore decrease the detrimental changes associated with blanching (loss in texture, color, flavor, and nutritional quality), as well as conserve energy.

V. PROPERTIES AS PROTEIN

Molecular weights of cystine lyases vary depending on the source of the enzyme. Reported values of cystine lyase molecular weight include 150,000 (8), 400,000, and 440,000 (9) for turnip cystine lyase; 110,000 (10) and 152,000 (11) for the broccoli enzyme; and 150,000 and 240,000 (12) for cabbage cystine lyase.

The number of subunits of cystine lyase varies depending on the source, but a common characteristic among the cystine lyases is that all the subunits have approximately the same size. The number of subunits (and MW) reported to date are 2 (48,000) (10) and 3 subunits (49,000) for broccoli (11), and 12 subunits (34,000 and 38,000) for turnip (9).

Results from our laboratory (10) for subunit molecular weight agree with those reported by Hamamoto and Mazelis (11); the molecular weight of the complete holoenzyme found is, however, different and therefore also the conclusion on the number of subunits. We found evidence by three different techniques that the molecular weight of cystine lyase is 100,000 ($\pm$10,000), and therefore the enzyme is a dimer. Supportive evidence that the enzyme has only two subunits comes from the results of the molar ratio of PALP to cystine lyase (2 moles of PALP/mol protein).

No information has been reported to date on the structure of cystine lyase, other than amino acid composition for broccoli (10, 11) and turnip root (9).

Results using the Dubois method indicate that broccoli (10, 11) and turnip root (9) cystine lyases are glycoproteins.

VI. PROPERTIES AS ENZYME

The substrate specificity of cystine lyase in plants is controversial. In fungi and bacteria (*Neurospora, Saccharomyces, Paracoccus denitrificans, E. coli*, etc.), β-cystathionase activity has been found together with cystine lyase activity (13, 14). These enzymes show a higher specificity for L-cystathionine than for L-cystine. While some researchers propose that a single enzyme is responsible for both the cystine lyase and the β-cystathionase activities and according to this criterion it is reported as such by the Enzyme Commission (15), others have found that highly purified protein peaks from plants only have cystine lyase activity. The only exception in plants is the β-cystathionase in spinach (16). This enzyme used L-cystathionine, L-djenkolic acid, and L-cystine as substrates with a relative activity of 100:126:17, respectively, but not L-cystine or its alkyl sulfoxides. All other cystine lyases from plants purified to date show negligible activity toward L-cystathionine.

Cystine lyase activity was first detected in plants in 1966 by Tishel and Mazelis (1). The requirement of pyridoxal-5′-phosphate (PALP) as a cofactor for this enzyme was noted. A year later (17), other species of the *Brassica* genus were investigated for the presence of cystine lyase activity and partial purification of cystine lyase from rutabaga (*Brassica napobrassica*) was achieved. It was noted the enzyme required PALP for activity and the stimulation of activity by exogenous PALP was dependent on the species. While addition of PALP was essential for rutabaga lyase activity, activity was present in the case of turnip roots (*B. rapa*) and mustard leaves (*B. hirta*), but specific activity doubled in the presence of exogenous PALP. No difference in specific activity was found in the absence or presence of exogenous PALP for varieties of the *Brassica olearacea* species (cabbage, cauliflower, and kale). Table 1 summarizes the properties of cystine lyases purified from different plant sources.

VII. DETERMINATION OF ACTIVITY

The true substrate in nature for cystine lyase has not been determined. L-Cystine is used as the substrate to determine enzymatic activity. Although the enzymatic activity could be determined by measuring any of the products of the reaction (pyruvate, thiocysteine, and ammonia), most researchers measure the pyruvate production by a modification of the method of Friedemann and Haugen (21) for keto acids. The pyruvate reacts with dinitrophenylhydrazine to produce pyruvyl hydrazone which absorbs at 450 nm. Another method for measuring cystine lyase activity by pyruvate formation is the coupling of the reaction with lactate dehydogenase.

The author chose to follow enzymatic activity during our purification by measuring thiocysteine by a modification of the method by Ellman (22) for sulfhydryl groups. This method provides advantages over other methods. Activity can be measured fast in many samples, and the method relies on initial velocity rather than activity at fixed times; this is particularly important in this reaction since it has been reported by early investigations that the formation of pyruvate is not linear with time (17). Both methods will be described in this chapter.

A. Pyruvate Measurement by Dinitrophenylhydrazone Formation

1. Reagents

a. Bicine Buffer. 37.54 g/L of bicine (230.0 mM). pH to 8.4 adjusted with 2.5 M NaOH.

Table 1 Properties of Cystine Lyase as an Enzyme

Source	K_m (mM)	T opt.	pH opt.	Substrate specificity	Inhibitors (K_i mM)
Broccoli	1.9[f] 1.0[h]	35°C	9.1[h]	L-cystine[f,h], L-cysteine-S-SO_3 [h], S-alkyl-L-cysteines[f,h], S-alkyl-L-cysteine sulfoxides[f,h], L-djenkolic acid[f,h]	*p*-hydroxymercuribenzoate[h], ethylmaleimide[h], NH_2OH [h], NaCN[h], L-cysteine (5.0)[h], DL-homocysteine (1.5)[h], pyridoxal[h], pyruvic acid[h]
Cabbage leaves	0.3[e]	ND	8.5–8.9[a] 8.5–9.0[e]	L-cystine[a,e], L-cysteine[e], L-cysteine-S-SO_3 [a], S-methyl-L-cysteine[e], S-methyl-L-cysteine sulfoxide[e], O-acetylserine[e], L-djenkolic acid[e]	NaCN[a], NH_2OH[a], L-cysteine[a], L-homocysteine[a], NaN_3 [e]
Rutabaga root[b]	1.0	ND	8.5–9	L-cystine, L-cysteine-S0SO_3, S-methyl-L-cysteine sulfoxide	L-cysteine (0.15), mercaptoethanol, glutathione (0.14), coenzyme A, cystamine
Turnip roots	0.94[c] 1.3[d] 0.54 & 0.42[g]	ND	8.5[c] 8.7–9.0[d] 8.4[g]	L-cystine[c,d,g], L-cystathionine[c], L-cysteine-S-SO_3 [c,d,g], alkyl-L-cysteines[c], S-alkyl-L-cysteine sulfoxides[c,d,g], L-djenkolic acid[c], O-acetylserine[g]	KCN[c], NH_2OH [c], mercaptoethanol[c], cystathionine (0.7)[d], L-cysteine[g], glutathione[g], dithiothreitol[g]

[a]Ref. 1. [b]Ref. 17. [c]Ref. 8. [d]Ref. 19. [e]Ref. 20. [f]Ref. 11. [g]Ref. 9. [h]Ref 10.

b. Cystine Solution. 96 mg of L-cystine dissolved in 0.60 mL of 1.5 M NaOH and diluted to 10 mL with water (9.6 g/L, 40 mM). Cystine undergoes β-elimination in the presence of high concentrations of NaOH (23), so only the minimum amount of NaOH (2 moles of NaOH/mol of cystine) was used to solubilize it.

c. PALP Solution. 0.25 g/L (1.0 mM) of pyridoxal phosphate (PALP).

d. TCA Solution. 100 g/L (612 mM) of trichloroacetic acid (TCA).

e. Sodium Pyruvate Standard Solution. 0.11 g/L (1.0 mM) of sodium pyruvate.

f. HCl Solution. 167 mL/L (2.00 M) of concentrated hydrochloric acid.

g. DNPH Solution. 1.00 g/L (5.10 mM) of dinitrophenylhydrazine dissolved in 2.00 M HCl.

2. Procedure

a. Enzymatic Reaction. The reaction mixture contains 12 mM L-cystine, 150 mM bicine, 25 μM PALP, and 10–300 μg (protein) of sample in a total volume of 1 mL. The mixture is incubated for 5–10 min (depending on enzyme concentration) at 30°C, and the reaction is stopped by addition of 1 mL TCA solution. The precipitated protein is removed by centrifugation, and pyruvate is measured in the supernatant. A blank is prepared by adding 1 mL TCA solution to the reaction mixture prior to enzyme addition.

b. Pyruvate Determination. 2.5 mL of TCA solution and 1 mL DNPH solution are added to 0.5 mL of the supernatant from enzymatic reaction. Reaction is incubated for 5 min at 30°C and stopped with the addition of 5 mL NaOH. Absorbance at 450 nm is read after 10 min. Amount of pyruvate is determined using a standard curve (pyruvate range: 0–300 nmoles). A unit of activity corresponds to the production of 1 μmol of pyruvate per min.

B. Thiocysteine Measurement Using 5,5′-Dithiobis-(2-Nitrobenzoic Acid)

1. Reagents

a. Borate Buffer. 30.92 g/L of boric acid (0.500 M). pH adjusted to 8.4 with 2.5 *M* NaOH.

b. Cystine Solution. 96 mg L-cystine dissolved in 0.60 mL of 1.5 M NaOH and diluted to 10 mL with water (9.6 g/L, 40 mM).

c. PALP Solution. 0.25 g/L (1.0 mM) of pyridoxal phosphate (PALP).

d. DTNB Solution. 3.964 g/L of 5,5′-dithiobis-(2-nitrobenzoic acid) (DTNB) (10.00 mM) in borate buffer. DTNB is insoluble in water and it is reduced by bicine or Tris buffers.

2. Procedure

The reaction mixture contains 12.00 mM L-cystine, 312.5 mM borate, 250.0 μM DTNB, 25.00 μM PALP, and 10–300 μg (protein) of enzyme sample in a total volume of 1 mL. All reagents are mixed except for the enzyme and let stand for 2 or 3 min (while nonenzymatic reduction of DTNB takes place). Enzyme is added and mixed quickly, and the increase in absorbance at 412 nm is recorded for 60 sec (formation of colored aryl mercaptan). Blank is prepared by mixing all reagents except enzyme. The thiocysteine production is calculated using the molar extinction coefficient determined for these conditions ($\epsilon = 8000\,M^{-1}cm^{-1}$). A unit of activity corresponds to the production of 1 μmol of thiocysteine per min.

VIII. PURIFICATION FROM BROCCOLI FLORETS

The steps used for the purification of cystine lyase vary depending on the plant sources and research groups. There are certain common operations in most protocols such as ammonium sulfate precipitation and anion exchange chromatography. The addition of PALP in all buffers is used universally to help stabilize the enzyme during purification. Table 2 illustrates the steps used by different groups to purify cystine lyase from different plant materials.

In this section we will describe the conditions used for the purification of cystine lyase from broccoli florets (10). Broccoli florets are blended with buffer (0.05 M phosphate/0.05 M citric acid/5% NaCl, pH 6.4), 1:1 (w/v) and 5% insoluble polyvinylpolypyrrolidone (PVPP) for 30 sec, and the homogenate is filtered through two layers of cheesecloth. The pH of the homogenate is adjusted to 4.0 by slow addition of HCl (6 N) with thorough stirring continued for 15 min at 25°C. The homogenate is centrifuged and the supernatant is decanted and saturated to 40% with $(NH_4)_2SO_4$, constantly stirring for 30 min, followed by centrifugation. Supernatant is then saturated to 60% $(NH_4)_2SO_4$, constantly stirring for 30 min and centrifuged. The precipitate is redissolved in a mini-

Table 2 Purification Steps Used for Cystine Lyases in Plants

Step	Rutabaga[a]	Turnip	Cabbage[d]	Broccoli
Aqueous extraction	1	1[b,c,f]	1	1[e,g]
Acid precipitation				2[e,g]
$(NH_4)_2SO_4$ precipitation	2	2[b,c,f], 4[b]	2	3[e,g]
Anion-exchange chrom.		5[b], 4[f]	3	4[e], 5[g]
Size exclusion chrom.		5[f]	4	6[e], 4[g]
Hydroxyapatite chrom.		3[b,f]		5[e]

The numbers indicate the order of the steps used for the purification; the letters indicate the source of information. [a]Ref. 17. [b]Ref. 18. [c]Ref. 19. [d]Ref. 20. [e]Ref. 11. [f]Ref. 9. [g]Ref. 10.

Table 3 Purification Table for Cystine Lyase from Broccoli

Step	Activity (U/mL)	Protein (mg/mL)	Sp Activity (U/mg)	Volume (mL)	Total activity (units)	Recovery (%)	Purif. (fold)
Extract[a]	1.39	17.1	0.08	1200	1668	100	1.00
Acid precip.	1.26	8.0	0.16	1100	1386	83	2.00
40% A.S.	0.93	6.9	0.13	1200	1116	67	1.63
40–60% A.S.	20.14	28.0	0.72	33	664	40	9.00
G.F.	6.60	1.4	4.71	53	350	21	58.88
DEAE	10.76	1.4	7.69	22	237	14	96.13

[a]From 1000 g of fresh broccoli.
Source: Ref. 10.

mal amount of buffer (0.02 M phosphate/20 μM PALP buffer, pH 6.4) and the suspension is dialyzed against the same buffer (Spectrapor membrane, MW cutoff 12,000–14,000). The solution is clarified by centrifugation and concentrated by ultrafiltration (Amicon microconcentrator, Diaflo PM10 membrane).

The enzyme solution is fractionated based on size through a Fractogel TSK HW 55(S) column with buffer (0.02 M phosphate/20 μM PALP/0.1 M NaCl/ 0.02% NaN_3 pH 6.4) using a peristaltic pump. Active fractions are pooled, concentrated, and dialyzed. The dialysate is applied to a LKB DEAE-Trisacryl M column connected to an FPLC system. The enzyme is eluted from the column with 0.02 M phosphate buffer, pH 6.4, using a linear NaCl gradient (0–1 M). Active fractions are pooled. Table 3 shows the quantitation of each step in purifying cystine lyase from broccoli.

Enzyme purification is monitored with activity determination by thiocysteine measurement using DTNB and protein quantification by biuret method (24). Temperature was controlled at 4°C and purity of enzyme is assessed by native PAGE at two different pHs.

REFERENCES

1. M Tishel, M Mazelis. Enzymatic degradation of L-cystine by cytoplasmic particles from cabbage leaves. Nature 211:745–746, 1966.
2. M Lim, P Velasco, R Pangborn, J Whitaker. Enzymes involved in off-aroma formation in broccoli. In: J Jen, ed. Quality Factors of Fruits and Vegetables. ACS Symp Ser 405:72–83, 1989.
3. HW Chin, RC Lindsay. Volatile sulfur compounds formed in disrupted tissues of different cabbage cultivars. J Food Sci 58:835–839, 1993.
4. HW Chin, RC Lindsay. Mechanisms of formation of volatile sulfur compounds following the action of cysteine sulfoxide lyases. J Agric Food Chem 42:1529–1536, 1994.
5. HW Chin, RC Lindsay. Modulation of volatile sulfur compounds in cruciferous vegetables. In: C Mussian, M Keelan, eds. Sulfur Compounds in Foods. ACS Symp Ser 564:90–104, 1994.

6. DM Obenland, LH Aung. Cystine lyase activity and anaerobically-induced sulfur gas emission from broccoli florets. Phyton 58:147–156, 1996.
7. EC Ramírez, JR Whitaker. Cystine lyase as blanching indicator in broccoli. Ital J Food Sci 10:171–176, 1998.
8. N Anderson, J Thompson. Cystine lyase: β-cystathionase from turnip roots. Phytochemistry 18:1953–1958, 1979.
9. K Wongpaibool, M Mazelis. Purification and characterization of cystine lyase isozymes from turnip (*Brassica rapa*) roots. J Food Biochem 18:103–121, 1994.
10. EC Ramírez, JR Whitaker. Biochemical characterization of cystine lyase from broccoli (*Brassica oleracea* var. *italica*). J Agric Food Chem 47:2218–2225, 1999.
11. A Hamamoto, M Mazelis. The C-S lyases of higher plants: isolation and properties of homogeneous cystine lyase from broccoli buds. Plant Physiol 80:702–706, 1986.
12. I Smith, D Hall. Cystine lyase from cabbage. Methods Enzymol 143:439–443, 1987.
13. JN Burnell, FR Whatley. Sulphur metabolism in *Paracoccus denitrificans*. Purification, properties and regulation of serine transacetylase, O-acetylserine sulphydrylase and β-cystathionase. Biochim Biophys Acta 418:246–265, 1977.
14. CM Dwivedi, RC Ragin, JR Uren. Cloning, purification and characterization of β-cystathionase from *Escherichia coli*. Biochemistry. 21:3064–3069, 1982.
15. International Union Biochemistry and Molecular Biology. Nomenclature Committee. Enzyme Nomenclature 1992: Recommendations of the Nomenclature Committee of the International Union of Biochemistry and Molecular Biology on the Nomenclature and Classification of Enzymes. New York: Academic Press, 1992.
16. A Stanton, M Mazelis. The C-S lyases of higher plants: Homogeneous β-cystathionase of spinach leaves. Arch Biochem Biophys 290:46–50, 1991.
17. M Mazelis, N Belmer, R Creveling. Cleavage of L-cystine by soluble enzyme preparations from *Brassica* species. Arch Biochem Biophys 120:371–378, 1967.
18. N Anderson, J Thompson. Cystine lyase: β-cystathionase from turnip roots. Phytochemistry 18:1953–1958, 1979.
19. M Mazelis, K Scott, D Gallie. Non-identity of cystine lyase with β-cystathionase in turnip roots. Phytochemistry 21:991–995, 1982.
20. D Hall, DI Smith. Partial purification and characterization of cystine lyase from cabbage (*Brassica oleracea* var. *capitata*). Plant Physiol 72:654–658, 1983.
21. TE Friedemann, GE Haugen. The determination of keto acids in blood and urine. J Biol Chem 147:415–442, 1943.
22. G Ellman. Tissue sulfhydryl groups. Arch Biochem Biophys 82:70–77, 1959.
23. AS Nashef, DT Osuga, HS Lee, Al Ahmed, JR Whitaker, RE Feeney. Effects of alkali on proteins. Disulfides and their products. J Agric Food Chem 25:245–251, 1977.
24. AG Gornall, CS Bardawill, MM David. Determination of serum proteins by means of the Biuret reaction. J Biol Chem 177:751–766, 1949.

83

Xylose (Glucose) Isomerase

Onno Misset
DSM Patents & Trademarks, Delft, The Netherlands

I. INTRODUCTION

Xylose (glucose) isomerase (EC 5.3.1.5) is one of the "oldest" industrial enzymes. Since its introduction in the starch-processing industry in the mid-1960s, it has been the subject of extensive research involving its biochemical and enzymological properties. As a consequence, there exists an enormous amount of literature. Much of the information summarized here was taken from the recent (1995) review (with 188 literature references therein) by Bhosale et al. (1) and the one by Chen (2). Other sources for information include the Enzyme Handbook (much quantitative data from 23 references; 3) and the SWISS-PROT and TrEMBL databases that are publicly available on the INTERNET (http://expasy.hcuge.ch). These databases contain the most updated information on amino acid sequences as well as links and references to the Brookhaven Protein Data Bank for the three-dimensional structures.

A. Chemical Reaction Catalyzed

Xylose isomerase catalyzes the reversible isomerization of monomeric keto sugars to their enol isomers. The natural substrate of this enzyme is D-xylose that is isomerized to D-xylulose. In the food industry, only the isomerization of D-glucose to D-fructose is of importance since this is the final step in the production of high–fructose corn syrups (HFCS; for the industrial application of glucose isomerase see Sec. II.B) (4–6). These HFCSs are used as sweeteners in soft drinks and other food products. Therefore, the enzyme is usually referred to as glucose isomerase in both the industry and the scientific community. Other sugars that are substrates for this enzyme are L-arabinose, L-rhamnose, D-ribose, and others (1–6).

B. Chemical Structure of Substrate

Figure 1 shows the open and closed configurations of D-xylose, D-xylulose, D-glucose, and D-fructose, respectively. In aqueous solution, glucose and fructose exist as an equilibrium mixture of several tautomeric structures as depicted in Table 1 (7, 8). The importance of the different configurations of substrates and products will be described in Section IV.C.

C. Classification According to Enzyme Commission Nomenclature

Xylose isomerase is classified as EC 5.3.1.5. The enzyme belongs to the class of isomerases (group 5), catalyzing intramolecular redox reactions (subgroup 3), involving aldose and ketose substrates (sub-subgroup 1). The systematic name for the enzyme is D-xylose ketol-isomerase, and the recommended name is xylose isomerase. Nevertheless, since the usage of the name glucose isomerase is so common and widespread, it will be used preferentially in this review.

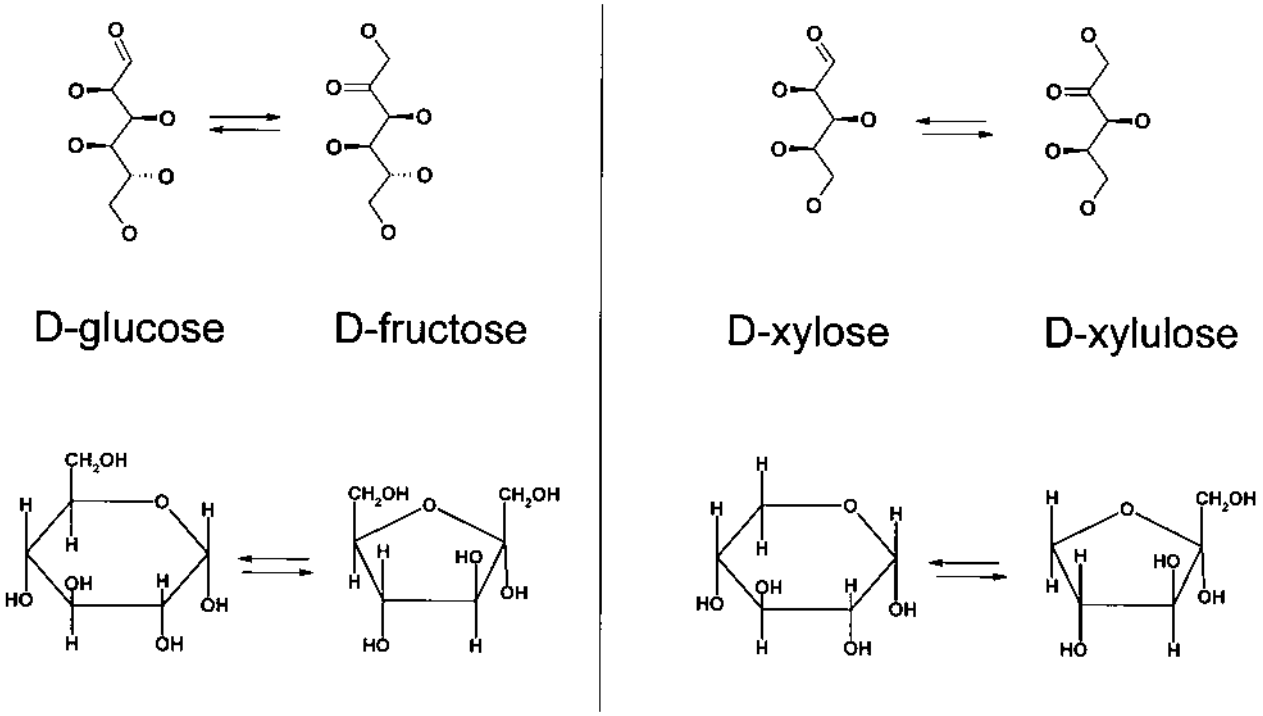

Figure 1 Chemical structures of various sugars.

II. IMPORTANCE TO QUALITY OF FOOD DURING GROWTH, MATURATION, STORAGE, AND PROCESSING

A. Natural Occurrence of Glucose Isomerase

Glucose isomerase is a microbial enzyme and widely distributed in prokaryotes (1–3, 6). The majority of enzymes are located intracellularly. The glucose isomerases that are used in the industry are derived from only a few selected microorganisms (Table 2). These enzymes exhibit the best performance under application conditions. Because of the recent acquisitions that took place among manufacturers of industrial enzymes, the number of enzyme products has been reduced considerably.

B. Production of High-Fructose Corn Syrups

High-fructose corn syrup is a mixture of glucose and fructose produced from cornstarch (4–6). HFCSs find widespread use in the food industry. Their most important application is as a sweetener in soft drinks where they replace beet and/or cane sugar. They have the advantage that at an equal sweetener level (see Table 3), they are some 10–20% cheaper than sucrose and are less caloric because of the lower resorption of fructose. A technical advantage of HFCS is the better solubility of glucose and fructose compared to sucrose and therefore the lesser tendency to crystallize in a wide range of food products. This has led to their application in confectionery, jam and jellies, ice cream, canned products, baking, pickles, sauces, meat products, etc. (5).

High-fructose corn syrups are produced in a process that comprises three consecutive enzymatic steps (Fig. 2). The raw material used in this process is starch, mainly derived from corn. Starch consists of two polymers of D-glucose: the linear amylose and the branched amylopectin (Fig. 3). In amylose and in the

Table 1 Occurrence of Tautomeric Forms of Glucose and Fructose in Aqueous Solution at 25°C

Configuration	Glucose (mole %)	Fructose (mole %)
Closed		
α-pyranose	38.8	traces
β-pyranose	60.9	73
α-furanose	total furanose =	5
β-furanose	0.3	22
Open	traces	traces

Source: Refs. 7, 8.

Table 2 Commercially Available Immobilized Glucose Isomerase Products

Manufacturer	Trade name	Microorganism	Immobilization method
Genencor[a]	Spezyme GI	*Streptomyces rubiginosus*	Purified enzyme adsorbed on DEAE-cellulose agglomerated with polystyrene and TiO2
	GC 180	Genetically modified strain of *Streptomyces rubiginosus*	Crosslinked
Novo-Nordisk	Sweetzyme T	*Streptomyces murinus*	Glutaraldehyde crosslinked cell material and subsequently extruded
CPC (Enzyme Biosystems)	G-zyme	*Streptomyces olivochromogenes*	Purified enzyme adsorbed on an ion exchanger
Godo Shusei	AGI S 600	*Streptomyces griseofuseus*	Chitosan-treated glutaraldehyde crosslinked cells and granulated
Nagase	Sweetase	*Streptomyces phaechromogenes*	Binding of heat treated cells to an anion exchange resin, granulated
UOP	Ketomax 100	*Streptomyces olivochromogenes*	PEI-treated ceramic alumina with glutaraldehyde crosslinked, purified GI

[a]Genencor acquired the industrial enzyme activities of Gist-brocades in 1995 and that of Solvay in 1996. These acquisitions included the transfer of the (immobilized) glucose isomerase products Maxazyme GI (Gist-brocades) and Optisweet and Takasweet (Solvay). These enzyme products are no longer commercially available (personal communication, H. Messchendorp).
Source: Refs. 1, 3.

main chain of amylopectin, the glucose moieties are linked through α-1,4-glycosidic bonds. The branches are made up of α-1,6 linkages. The relative amounts of amylose and amylopectin in starch vary with the source of starch.

In the first enzymatic process step, the starch, produced by wet milling of the corn grains, is subjected to liquefaction by using a thermostable bacterial α-amylase (EC 3.2.1.1) from *Bacillus* spp. such as *B. licheniformis* or *B. stearothermophilus* (see Fig. 2 for the process conditions). This enzyme cleaves the α-1,4 linkages in an endo-fashion and produces a dextrin solution with a DE (dextrose equivalent) of ~ 10 (starch has a DE of zero and glucose has a DE of 100 by definition).

In the subsequent step, glucoamylase (also named amyloglucosidase; EC 3.2.1.3) further hydrolyzes the dextrins in an exo-fashion, liberating single glucose moieties from the nonreducing end. Since glucoamylase displays a higher activity toward the α-1,4-glycosidic bonds compared to the 1,6-branch points, in some processes a debranching enzyme (e.g., pullulanase—EC 3.2.1.41) is used as well. The resulting glucose solution has a DE of ~ 95.

In the third enzymatic process step, glucose isomerase converts glucose into fructose until a concentration of 42% (molar fraction based on total sugars). This reaction is unique in that it is carried out in a column reactor using the enzyme in an immobilized form. As such, glucose isomerase was one of the first enzymes to be used as immobilized biocatalyst on an industrial scale. Typical glucose isomerase processes operate with the enzyme encapsulated in 1- to 2-mm particles in a packed-bed column reactor (5). Columns can be 1.5 m in diameter and 4–5 m in height. Such a system would contain up to 4000 kg enzyme and would produce up to 500,000 kg fructose (dry weight) per day. High-glucose syrup (DE = 95) resulting from the previous glucoamylase reaction and which has been

Table 3 Relative Sweetness of Sugars and Sugar Compositions (on weight basis)

Sugar	Relative sweetness
Lactose	0.4
Glucose syrup (42 DE)	0.3
Maltose	0.5
Sorbitol	0.5
Glucose syrup (64 DE)	0.6
Mannose	0.6
Galactose	0.6
Xylose	0.7
Mannitol	0.7
Glucose (dextrose)	0.7
Glycerol	0.8
Invert sugar	1.0
Sucrose	1.0
HFCS (42% fructose)	1.0
HFCS (55% fructose)	1.1
Fructose	1.3

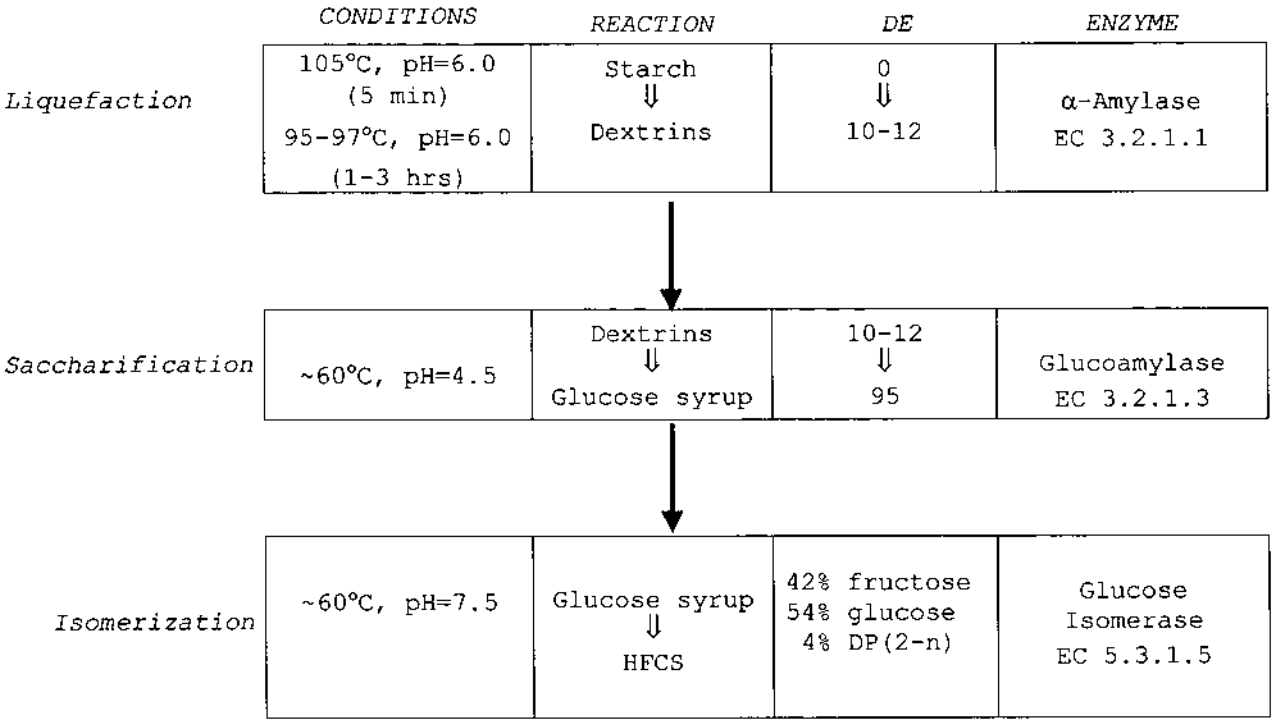

Figure 2 Scheme of HFCS production.

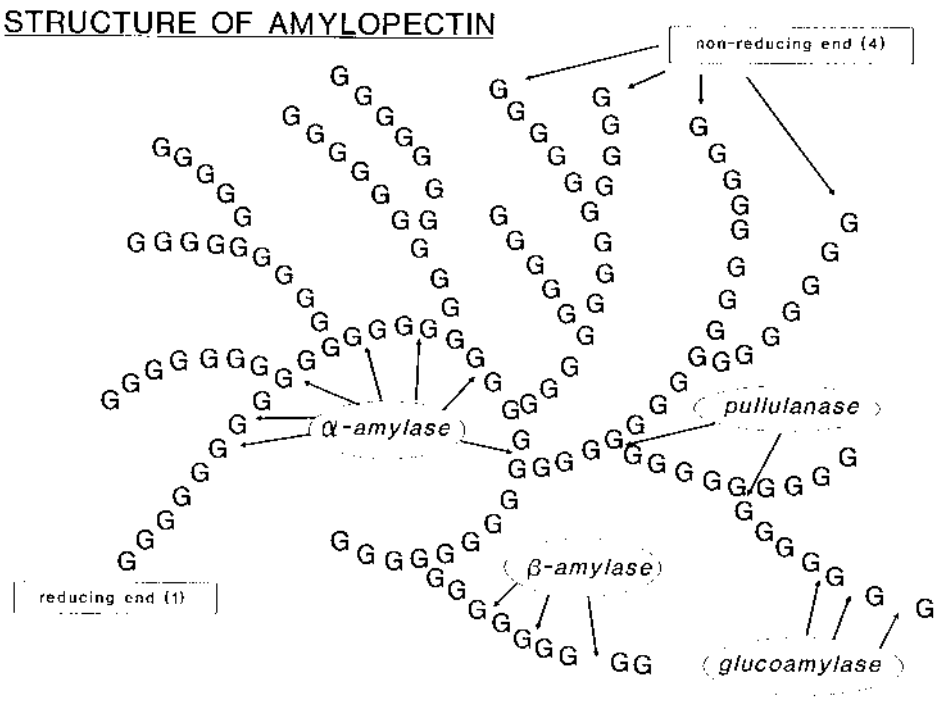

Figure 3 Schematic structure of the starch components amylose and amylopectin.

concentrated to 45% solids and adjusted to pH 7.5, is pumped continuously through the column. The flow rate and the temperature of the system are determined by several factors. The flow rate must be appropriate to give sufficient residence time to allow production of 42% fructose. Low flow rates increase the risk of microbial contamination, and too-high rates do not give enough conversion and cause channeling through the support material. Temperatures < 55–$60^{\circ}C$ increase the viscosity of the syrup and increase the risk of microbial contamination. High temperatures reduce the stability of the enzyme and cause the formation of undesired byproducts through chemical reactions (i.e., Maillard reactions). In practice, temperatures ~ 55–$60^{\circ}C$ are used.

The inactivation of the enzyme is compensated for by adjusting the flow rate of the glucose stream so as to maintain the desired conversion. Under the conditions mentioned, these processes can run for several weeks until the activity of the enzyme has become too low. After reaching that point, the columns are dismantled and repacked with a batch of fresh biocatalyst or, in the case of ion exchange columns, regenerated by washing off the enzyme and adsorbing a new batch.

The sugars present in the final HFCS comprise fructose (42%), glucose (54%), and oligosaccharides up to 4%.

III. PROPERTIES AS PROTEIN

A. Molecular Weight

The XYLA genes in the various microorganisms code for a variety of glucose isomerase subunits that can roughly be divided into two groups based on the number of amino acids and derived molecular weights (Table 4).

Group I includes the enzymes from actinomycetes like *Actinoplanes*, *Streptomyces*, and the like, and can be regarded as ''small'' enzymes with an average of 390 ± 4 amino acids. This corresponds to calculated subunit molecular weights ranging from 42,675 to 43,900 daltons. Group II includes the ''large'' enzymes from *Bacillus, Escherichia, Clostridium, Lactobacilli*, and others. The subunits of these enzymes have some 442 ± 7 amino acids, resulting in calculated molecular weights ranging from 49,700 to 50,893 daltons.

Almost all glucose isomerases are tetramers, built up of four identical subunits as was concluded from experimental techniques and 3D structure determinations. Therefore, the native molecular weights are in the order of 170,000 and 200,000 daltons for the group I and group II enzymes, respectively. Only the glucose isomerase from *Streptomyces olivochromogenus* was found to be a dimer (38).

Experimentally, the molecular weights can be determined under either non-dissociating or dissociating conditions. Subunit molecular weights are obtained under dissociating conditions using techniques such as polyacrylamide gel electrophoresis (PAGE) in the presence of the denaturant sodium dodecyl sulfate. Native molecular weights are obtained under non-dissociating conditions such as gel exclusion chromatography, sedimentation coefficients, or density gradient centrifugation. It was found that the experimental molecular weights for various glucose isomerases correspond reasonably well with the calculated values mentioned.

B. Primary, Secondary, Tertiary, and Quaternary Structures

The primary (amino acid) sequences of many xylose isomerases are known. Figure 4 shows in total 28 aligned sequences for Group I and Group II glucose isomerases. Table 5 shows that within groups I and II there exists a high amino acid sequence homology ($> 50\%$) whereas the overall homology between the groups is low (25–30%). It will be explained later that amino acids involved in substrate and metal ion binding, as well as catalysis, are completely conserved. The ~ 50 additional amino acids in the Group II glucose isomerases are located mainly at the N-terminus (Fig. 4).

The secondary and tertiary structures of glucose isomerases are known in great detail, because many 3D structures have been determined by x-ray crystallography. Table 6 summarizes the 3D structures that are currently available in the public domain (Brookhave Protein Databank). In the late 1980s and early '90s, several research groups focused on the structure elucidation of a few, mainly *Actinomycete*, glucose isomerases (12, 14, 15, 39–48). Only recently are structures from glucose isomerases originating from thermophilic bacteria becoming available (50). Today, some 60 different structural datasets are available in the Brookhaven Protein Databank, representing 11 different glucose isomerases. Per enzyme, multiple structures were determined under different experimental conditions, e.g., presence of ligands (substrates, substrate analogs, metal ions, etc.). In addition to 3D structures of the wild-type enzymes, various structures have also been determined of mutant enzymes that

Table 4 Glucose Isomerase Amino Acid Sequence Entries in the PIR and SWISS-PROT Databases Available on the Web (http://www-nbrf.georgetown.edu/pirww/pirhome.html and http://expacy.hcuge.ch, respectively)

		Organism	Abbr.	PIR-code	Swiss-Prot	# aa	MW daltons	Ref
Group I	1	*Actinoplanes missouriensis*	A.mi	ISMAXM	XYLA_ACTMI	394	43,367	9
	2	*Ampullariella* sp.	Amp	ISMAXA	XYLA_AMPSP	394	43,395	10
	3	*Arthrobacter* sp.	Arth	S16214	XYLA_ARTS7	395	43,160	11
	4	*Streptomyces murinis*	S. mur		XYLA_STRMR	388	42,772	14
	5	*Streptomyces violaceusniger*	S. vio	ISSMXV	XYLA_STRVO	389	43,013	18
	6	*Streptomyces albus*	S. alb		XYLA_STRAL	391	43,289	12
	7	*Streptomyces rubiginosus*	S. rub	B41339	XYLA_STRRU	388	43,096	17
	8	*Streptomyces diastaticus*	S. dia	JC1031	XYLA_STRDI	388	42,675	13
	9	*Streptomyces olivochromogenes*	S. oli	S28986	XYLA_STROL	388	42,792	15
	10	*Streptomyces rochei*	S. roc	ISSMXR	XYLA_STRRO	396	43,512	16
	11	*Thermus aquaticus* subsp. *caldophilus*	T. cal		XYLA_THECA	388	43,859	
	12	*Thermus aquaticus*	T. aqu	A39404	XYLA_THETH	388	43,906	19
		Average group I				390	43,180	
Group II	13	*Bacillus megaterium*	B. meg		XYLA_BACME	445	50,279	23
	14	*Bacillus subtilis*	B. sub		XYLA_BACSU	440	49,703	24
				ISBSXS		445	50,252	25
	15	*Bacillus* species LW2	B.1w2		XYLA_BACSP	441	50,169	20
	16	*Bacillus stearothermophilus*	B. ste		XYLA_BACST	441	50,141	21
	17	*Bacillus licheniformis*	B. lic		XYLA_BACLI	448	50,905	22
	18	*Thermoanaerobacter saccharolyticus*	T. sac		XYLA_THESA	439	50,477	34
	19	*Thermoanaerobacterium thermosulfurigenes*	T. the	ISCLXM	XYLA_THETU	439	50,475	35
	20	*Clostridium thermosaccharolyticum*	C. the	I40806	XYLA_CLOTS	439	50,229	26
	21	*Thermoanaerobacter ethanolithicus* = *Thermoanaerobacter thermohydrosulfuricus*	T. eth	ISCLXH	XYLA_THEET	438	50,158	33
	22	*Thermotoga neapolitana*	T. nea		XYLA_THENE	444	50,893	37
	23	*Staphylococcus xylosus*	S. xyl	S16530	XYLA_STAXY	440	50,104	32
	24	*Pediococcus halophilus*	P. hal		XYLA_TETHA	435	49,411	36
	25	*Lactobacillus brevis*	L. bre	JC1137	XYLA_LACBR	449	50,756	30
	26	*Lactobacillus pentosus*	L. pen	S18561	XYLA_LACPE	449	50,704	31
	27	*Escherichia coli*	E. coli	ISECX1	XYLA_ECOLI	440	49,742	27
	28	*Klebsiella pneumoniae*	K. pne	ISKBX	XYLA_KLEAE	440	49,919	29
	29	*Haemophilus influenzae*	H. inf	ISHIX	XYLA_HAEIN	439	49,896	28
		Average group II				442	50,200	

The number of amino acids (# aa) and calculated subunit molecular weights were taken from the SWISS-PROT database.

were considered for different purposes (e.g., stability improvement, role in mechanism).

The 3D structures of the different enzymes appear to be very similar which is also suggested by the high amino acid sequence homology. Figure 5 shows a schematic representation of the subunit structure of the *Actinoplanes missouriensis* enzyme. The monomeric subunit consists of two domains. The N-terminal domain is the catalytic domain and consists of an eight-stranded parallel β-barrel with eight connecting α-helices also known as the TIM barrel, referring to the first enzyme (TIM = triose phosphate isomerase) in which this topology was found (51). The smaller, C-terminal domain only contains α-helices and forms a looplike structure away from the larger N-terminal domain. It overlaps ("embraces") the larger N-terminal domain of an adjacent subunit so that a tightly bound dimer is formed. Two of these dimers form the tetramer which therefore can be regarded as a dimer of dimers (41). With the exception of the enzyme from *Actinoplanes missourienses* where the dimer is inactive, all other dimers tested possess enzymatic activity. The monomers are enzymatically inactive.

C. Isoforms

All the different microbial glucose isomerases known today are encoded by a single XylA gene per host organism (Table 4). This means that within one microorganism, no isoforms of the enzyme are found.

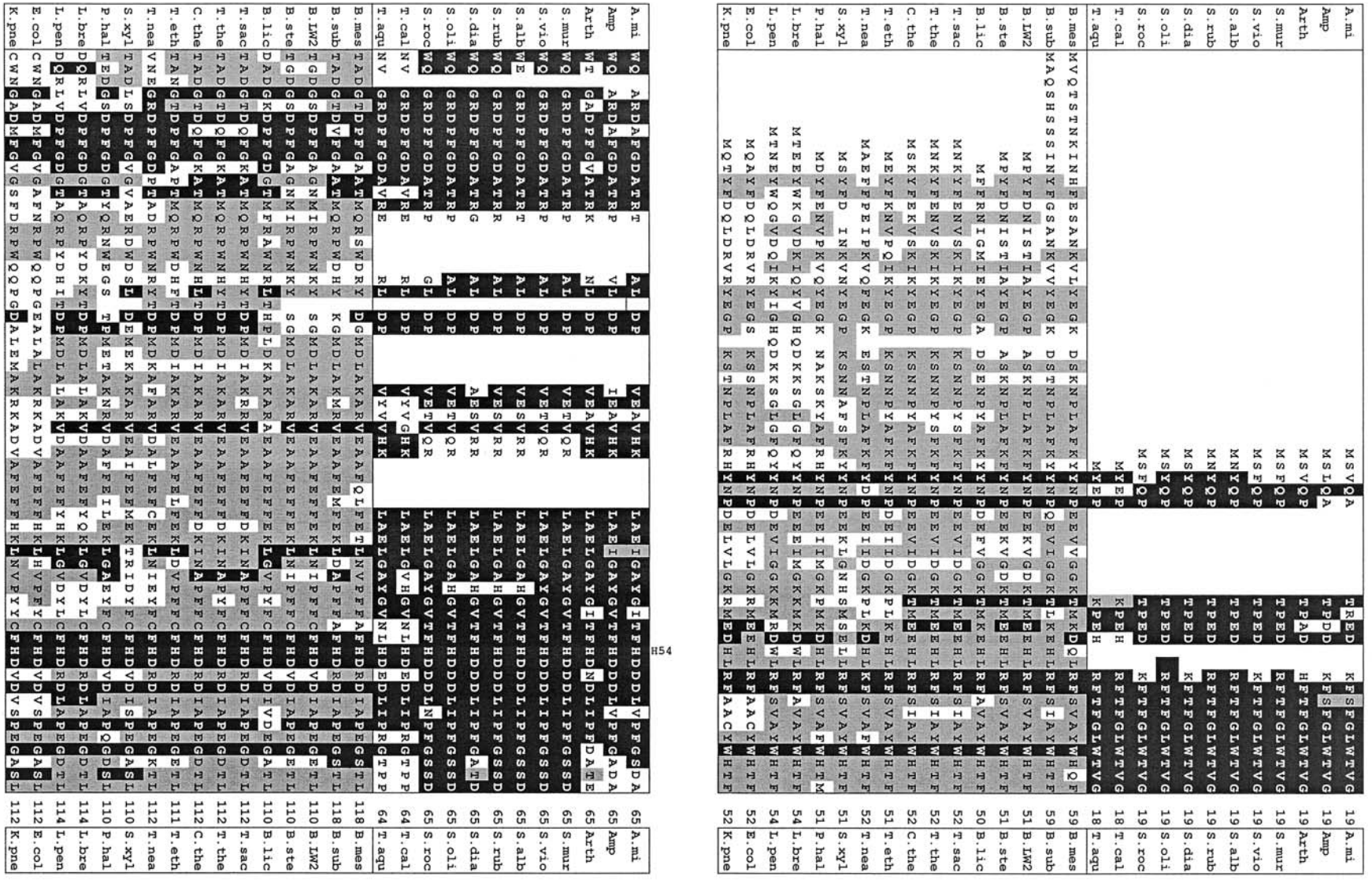

Figure 4 Amino acid sequence alignment of group I and group II glucose isomerases. For abbreviations and references see Table 4. Group I and group II sequences were aligned as separate groups using the Multiple Alignment Tool from PIR at http://www.nbrf.georgetown.edu.pirwww/search/multaln.html which makes use of ClustalW. Subsequently, sequences 8–12 from group I and 13–18 from group II were aligned in order to establish the alignment between the two groups. Residues that are highly conserved in group I (and also found in group II) are indicated by white letters and a black background. Residues that are highly conserved in group II (and also found in group I) are indicated by black letters and a gray background.

Table 4 Glucose Isomerase Amino Acid Sequence Entries in the PIR and SWISS-PROT Databases Available on the Web (http://www-nbrf.georgetown.edu/pirww/pirhome.html and http://expacy.hcuge.ch, respectively)

		Organism	Abbr.	PIR-code	Swiss-Prot	# aa	MW daltons	Ref
Group I	1	*Actinoplanes missouriensis*	A.mi	ISMAXM	XYLA_ACTMI	394	43,367	9
	2	*Ampullariella* sp.	Amp	ISMAXA	XYLA_AMPSP	394	43,395	10
	3	*Arthrobacter* sp.	Arth	S16214	XYLA_ARTS7	395	43,160	11
	4	*Streptomyces murinis*	S. mur		XYLA_STRMR	388	42,772	14
	5	*Streptomyces violaceusniger*	S. vio	ISSMXV	XYLA_STRVO	389	43,013	18
	6	*Streptomyces albus*	S. alb		XYLA_STRAL	391	43,289	12
	7	*Streptomyces rubiginosus*	S. rub	B41339	XYLA_STRRU	388	43,096	17
	8	*Streptomyces diastaticus*	S. dia	JC1031	XYLA_STRDI	388	42,675	13
	9	*Streptomyces olivochromogenes*	S. oli	S28986	XYLA_STROL	388	42,792	15
	10	*Streptomyces rochei*	S. roc	ISSMXR	XYLA_STRRO	396	43,512	16
	11	*Thermus aquaticus* subsp. *caldophilus*	T. cal		XYLA_THECA	388	43,859	
	12	*Thermus aquaticus*	T. aqu	A39404	XYLA_THETH	388	43,906	19
		Average group I				390	43,180	
Group II	13	*Bacillus megaterium*	B. meg		XYLA_BACME	445	50,279	23
	14	*Bacillus subtilis*	B. sub		XYLA_BACSU	440	49,703	24
				ISBSXS		445	50,252	25
	15	*Bacillus* species LW2	B.1w2		XYLA_BACSP	441	50,169	20
	16	*Bacillus stearothermophilus*	B. ste		XYLA_BACST	441	50,141	21
	17	*Bacillus licheniformis*	B. lic		XYLA_BACLI	448	50,905	22
	18	*Thermoanaerobacter saccharolyticus*	T. sac		XYLA_THESA	439	50,477	34
	19	*Thermoanaerobacterium thermosulfurigenes*	T. the	ISCLXM	XYLA_THETU	439	50,475	35
	20	*Clostridium thermosaccharolyticum*	C. the	I40806	XYLA_CLOTS	439	50,229	26
	21	*Thermoanaerobacter ethanolithicus* = *Thermoanaerobacter thermohydrosulfuricus*	T. eth	ISCLXH	XYLA_THEET	438	50,158	33
	22	*Thermotoga neapolitana*	T. nea		XYLA_THENE	444	50,893	37
	23	*Staphylococcus xylosus*	S. xyl	S16530	XYLA_STAXY	440	50,104	32
	24	*Pediococcus halophilus*	P. hal		XYLA_TETHA	435	49,411	36
	25	*Lactobacillus brevis*	L. bre	JC1137	XYLA_LACBR	449	50,756	30
	26	*Lactobacillus pentosus*	L. pen	S18561	XYLA_LACPE	449	50,704	31
	27	*Escherichia coli*	E. coli	ISECX1	XYLA_ECOLI	440	49,742	27
	28	*Klebsiella pneumoniae*	K. pne	ISKBX	XYLA_KLEAE	440	49,919	29
	29	*Haemophilus influenzae*	H. inf	ISHIX	XYLA_HAEIN	439	49,896	28
		Average group II				442	50,200	

The number of amino acids (# aa) and calculated subunit molecular weights were taken from the SWISS-PROT database.

were considered for different purposes (e.g., stability improvement, role in mechanism).

The 3D structures of the different enzymes appear to be very similar which is also suggested by the high amino acid sequence homology. Figure 5 shows a schematic representation of the subunit structure of the *Actinoplanes missouriensis* enzyme. The monomeric subunit consists of two domains. The N-terminal domain is the catalytic domain and consists of an eight-stranded parallel β-barrel with eight connecting α-helices also known as the TIM barrel, referring to the first enzyme (TIM = triose phosphate isomerase) in which this topology was found (51). The smaller, C-terminal domain only contains α-helices and forms a looplike structure away from the larger N-terminal domain. It overlaps ("embraces") the larger N-terminal domain of an adjacent subunit so that a tightly bound dimer is formed. Two of these dimers form the tetramer which therefore can be regarded as a dimer of dimers (41). With the exception of the enzyme from *Actinoplanes missourienses* where the dimer is inactive, all other dimers tested possess enzymatic activity. The monomers are enzymatically inactive.

C. Isoforms

All the different microbial glucose isomerases known today are encoded by a single XylA gene per host organism (Table 4). This means that within one microorganism, no isoforms of the enzyme are found.

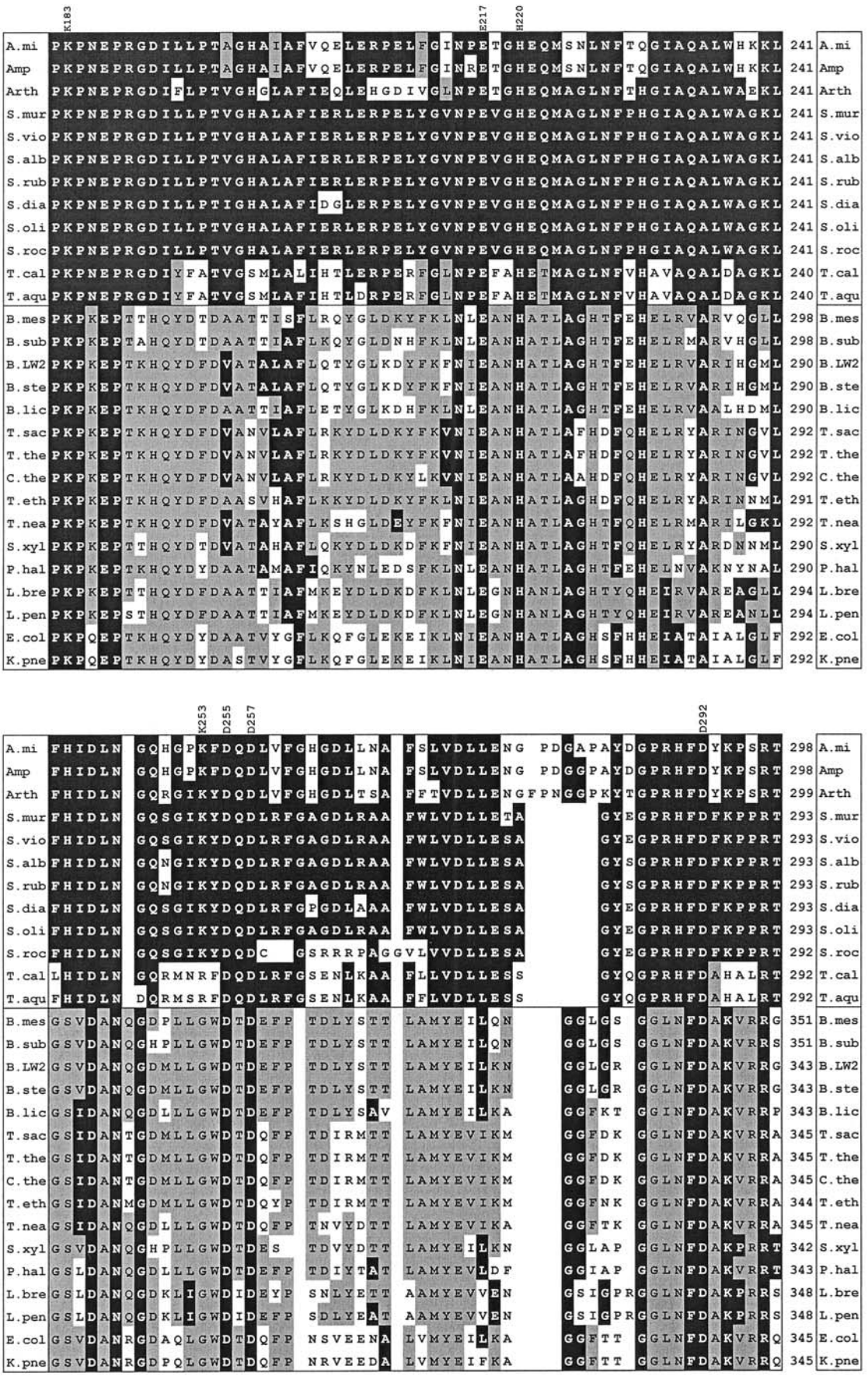

Figure 4 Continued.

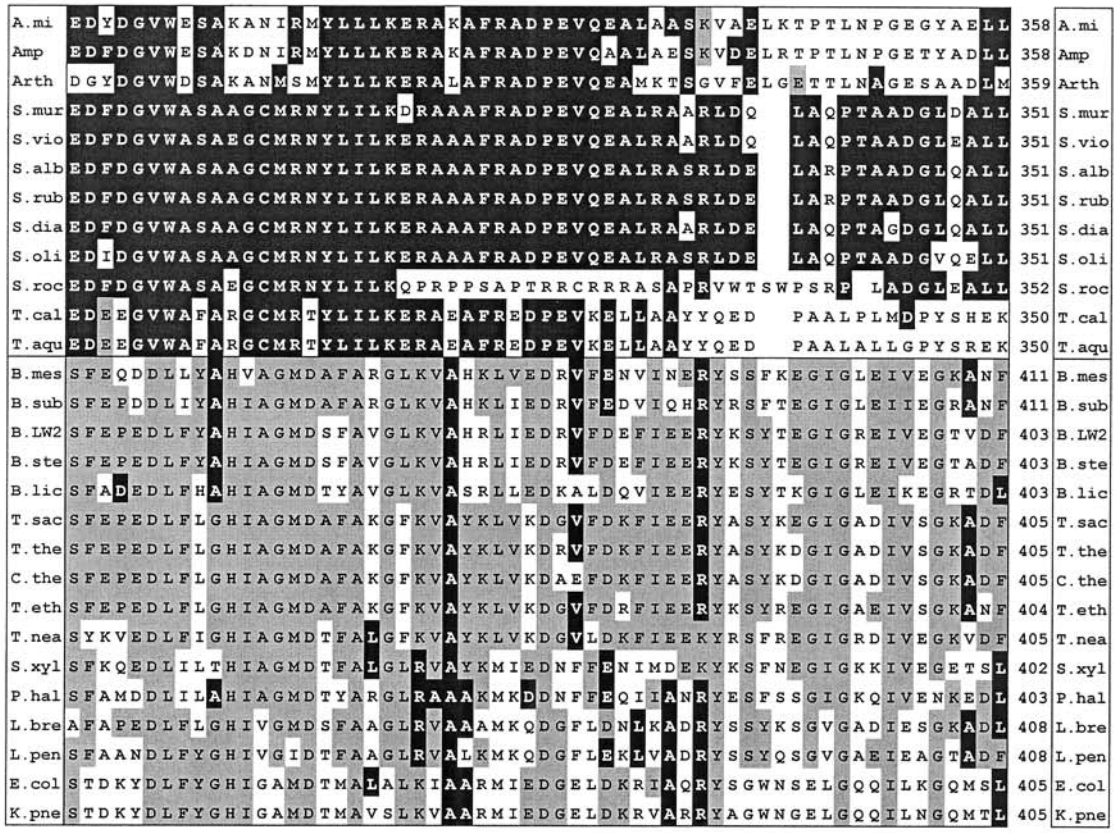

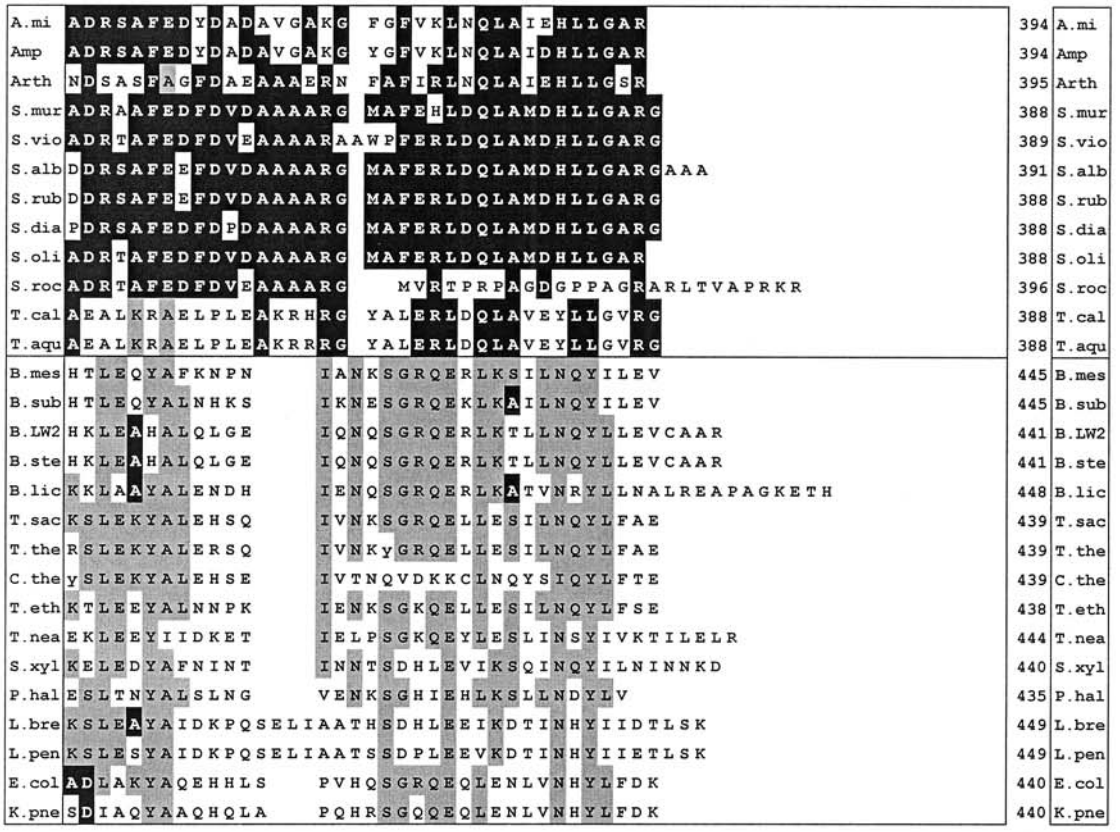

Figure 4 Continued

Table 5 Homology Matrix of Glucose Isomerase Amino Acid Sequences

		Group I												Group II																
		A.mi	Amp	Arth	S.mur	S.vio	S.alb	S.rub	S.dia	S.oli	S.roc	T.cal	T.aqu	B.mes	B.sub	B.LW2	B.ste	B.lic	T.sac	T.the	C.the	T.eth	T.nea	S.xyl	P.hal	L.bre	L.pen	E.col	K.pne
1	A.mi																													
2	Amp	93																												
3	Arth	67	66																											
4	S.mur	67	67	64																										
5	S.vio	67	67	64	96																									
6	S.alb	67	66	64	92	91																								
7	S.rub	66	66	65	92	92	99																							
8	S.dia	66	67	62	89	83	91	92																						
9	S.oli	65	65	61	92	93	90	91	88																					
10	S.roc	60	60	57	85	87	80	81	79	81																				
11	T.cal	54	53	51	57	57	59	58	56	56	58																			
12	T.aqu	55	54	52	58	57	59	59	56	56	59	94																		
13	B.mes	29	28	29	30	29	31	31	30	28	28	29	29																	
14	B.sub	27	29	30	30	29	30	31	30	29	30	27	27	84																
15	B.LW2	29	28	30	31	30	29	29	31	27	30	29	29	76	75															
16	B.ste	29	28	30	31	30	29	29	31	27	30	29	29	76	75	99														
17	B.lic	27	30	29	29	28	28	28	30	27	29	28	28	68	74	74	74													
18	T.sac	25	28	28	30	29	30	29	28	30	29	29	30	70	69	74	74	63												
19	T.the	25	28	29	30	29	29	29	28	30	28	28	28	69	69	74	74	65	98											
20	C.the	25	27	29	28	29	26	26	25	29	28	30	30	67	66	72	72	63	93	93										
21	T.eth	26	26	29	29	28	29	29	28	28	28	30	30	71	70	73	73	66	87	86	83									
22	T.nea	27	26	31	30	28	31	31	30	29	30	31	31	65	63	68	68	63	70	70	71	72								
23	S.xyl	29	29	30	30	28	31	31	29	29	28	27	27	64	63	67	67	59	61	60	60	62	60							
24	P.hal	26	28	27	29	30	29	29	30	28	30	27	27	61	60	61	61	60	58	58	55	59	58	60						
25	L.bre	26	27	28	28	27	27	27	27	26	29	28	27	57	55	56	56	54	57	57	56	57	55	56	53					
26	L.pen	29	30	32	30	28	28	28	29	28	30	30	30	57	57	56	56	54	56	56	55	57	53	55	53	88				
27	E.col	28	26	29	26	27	26	26	28	26	27	25	25	49	51	52	52	53	50	50	49	51	50	46	49	44	44			
28	K.pne	27	27	27	27	27	27	27	28	25	27	25	25	48	49	51	51	51	49	49	48	50	51	45	47	44	44	89		

The figures indicated are the %-identity determined using the gapped-BLAST similarity search tool from PIR at http://www-nbrf.georgetown.edu/pirwww/search/similarity.html or via the pairwise sequence alignment tool also from PIR at http://www-nbrf.georgetown.edu/pirwww/search/pairwise.html. For abbreviations see Table 4.

Table 6 Overview of Available 3D Structures of Glucose Isomerase in the Brookhaven Protein Databank

Source	Resolution (Å)	Code (mmyy)	Reference
Group I			
Actinoplanes missouriensis			
Wild-type enzyme			39, 40
$+Co^{2+}$	2.30	4XIM (0392)	
+ xylitol + Co^{2+}	2.20	1XIM (0591)	
+ sorbitol + Mg^{2+}	2.60	5XIM (0392)	
+ xylose + Mg^{2+}	2.50	6XIM (0492)	
demetallized	2.40	7XIM (0492)	
Mutant enzymes			
H220N + xylose + Mg^{2+}	2.40	1XIN (0492)	
K253R + xylitol + Mg^{2+}	2.30	2XIM (0591	
H290N + sorbitol + Co^{2+}	2.30	2XIN (0492)	
[K309R + K319R + K323R] + sorbitol + Co^{2+}	2.30	3XIM (0591)	
E181Q + xylose + Mg^{2+}	2.30	3XIN (0492)	
D255A + xylose + Mg^{2+}	2.30	5XIN (0492)	
E186N + xylose + Mg^{2+}	2.40	8XIM (0492)	
E186N + xylose + Mn^{2+}	2.40	9XIM (0492)	
Arthrobacter strain NRRL B3728			
Wild-type enzyme			41, 42
Native	2.30	1XIA (0288)	
+ sorbitol	2.30	4XIA (0789)	
+ xylitol	2.50	5XIA (0789)	
+ 2, 5-dideoxy-2, 5-imino-D-glucitol	2.50	1DID (0692)	
+ 1-deoxy-nojirimycin	2.50	1DIE (0692)	
apo form	2.30	1XLA (1091)	
$+Mg^{2+}$	2.50	1XLB (1091)	
+ xylose + Mg^{2+}	2.50	1XLC (1091)	
+ xylose + Mn^{2+}	2.50	1XLD (1091)	
$+Mn^{2+}$	2.50	1XLE (1091)	
+ gluconate + Mn^{2+}	2.50	1XLF (1091)	
+ xylose + Mg^{2+} + Al^{3+}	2.50	1XLG (1091)	
Al^{3+}	2.50	1XLH (1091)	
5-thio-alpha-D-glucose+ Mn^{2+}	2.50	1XLI (1091)	
+ xylitol + Mn^{2+}	2.50	1XLJ (1091)	
$+Mn^{++}$	2.50	1XLK (1091)	
$+Zn^{2+}$	2.50	1XLL (1091)	
Mutant enzyme			
[D254E + D256E] + xylitol + Al^{3+}	2.40	1XLM (0797)	
Streptomyces albus			
Wild-type enzyme	1.65	6XIA (0990)	12, 43
Streptomyces murinus			
Wild-type enzyme	2.60	1DXI (0993)	14
Streptomyces olivochromogenus			
Wild-type enzyme			15, 44, 45
$+Mg^{2+}$	1.81	1XYA (0194)	
+ glucose + Mg^{2+}	1.96	1XYB (0194)	
+ 3-methylfructose + Mg^{2+}	2.19	1XYC (0194)	
+ HYA + Mg^{2+}	1.60	2GYI (0994)	
Mutant enzyme			
E180K + Mg^{2+}	1.80	1XYL (1293)	
E180K + glucose + Mg^{2+}	1.80	1XYM (1293)	

Table 6 Continued

Source	Resolution (Å)	Code (mmyy)	Reference
Streptomyces rubiginosis			
$+Mn^{2+}$	1.60	1XIS (0391)	46
+ xylitol + Mg^{2+}	1.71	2XIS (0391)	
+ xylose	1.60	3XIS (0391)	
+ xylose + Mn^{2+}	1.60	4XIS (0391)	
$+Mn^{2+}$	1.60	1XIB (0394)	42, 47, 48
xylose + Mn^{2+}	1.60	1XIC (0394)	
+ ascorbic acid + Mn^{2+} + Mg^{2+}	1.70	1XID (0394)	
+ 1, 5-di-anhydrosorbitol	1.70	1XIE (0394)	
+ glucose + Mn^{2+} + Mg^{2+}	1.60	1XIF (0394)	
+xylitol + Mn^{2+} + Mg^{2+}	1.70	1XIG (0394)	
+sorbitol	1.70	1XIH (0394)	
xylulose + Mn^{2+}	1.70	1XII (0394)	
+threonate + Mn^{2+}	1.70	1XIJ (0394)	
+ xylose	1.90	8XIA (1090)	
+DFR + Mn^{2+}	1.90	9XIA (1090)	
Thermus aquaticus subsp. *Thermophilus*	2.20	1BXB (1098)	49
Thermus aquaticus subsp. *Caldophilus*	2.30	1BXC (1098)	49
Group II			
Thermotoga neapolitana			
$+Co^{2+}$	2.7	1A0E (1197)	50
Thermoanaerobacterium thermosulfurogenes			
$+Co^{2+}$	2.5	1A0C (1997)	50
Bacillus stearothermophilues	3.0	1A0D (1997)	50

Since glucose isomerase seems to be exclusively found in prokaryotes, none of the enzymes are glycosylated as a result of a secretory pathway. In addition, no other forms of (chemical) posttranslational modification during biosynthesis has been reported. Since glucose isomerases are predominantly intracellular enzymes, no pre- or pro-enzyme intermediates exist in the biosynthetic pathway that require a proteolytic step for maturation. Also, no other proteolytic events have been reported as posttranslational modification.

In the presence of high concentrations of glucose the glucose isomerase from *Actinoplanes missouriensis* loses its tetrameric structure and dissociates into dimers and monomers which is accompanied by inactivation (Misset et al., unpublished data). It has been postulated that this inactivation, which also occurs during its industrial application, is caused by a process called glycation. Glucose from the substrate stream may then react with one or more lysine residues in the subunit interface. During this reaction, initially Schiff-base intermediates are formed that subsequently undergo rearrangement to Amadori products. Finally, dissociation of the subunits occurs (52–54).

Stabilization of this enzyme could be achieved by applying rational protein engineering. By site-directed mutagenesis of the *Actinoplanes missouriensis* enzyme, the lysines were mutated to arginine since this residue is much less sensitive to glycation. One of the mutants thus constructed, K253R (i.e., K = lysine at position 253 substituted with R = arginine), indeed showed an increased half-life under application conditions (52). In addition, the specific activity of the mutant enzyme was the same as that of the wild-type enzyme, and pH optimum was only slightly shifted. Researchers at Gist-brocades developed a new production process for the enzyme, and the new product was tested on an industrial scale (Misset et al., unpublished data). The stability increase found in laboratory application

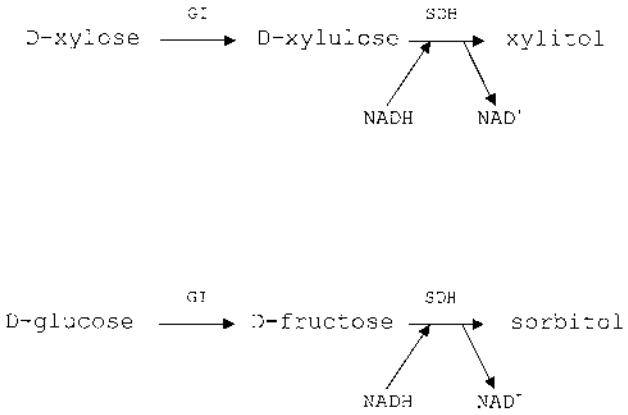

Figure 5 Schematic representation of the subunit structure of the *Actinoplanes missouriensis* enzyme.

tests was also found on industrial scale. Therefore, this mutant enzyme is a very good second-generation enzyme and a potential substitute for the original product.

Lysine at position 253 is well conserved in Group I glucose isomerases (see Fig. 4). Therefore, it is very likely that also these enzymes will undergo glycation in the presence of high glucose concentrations under the conditions employed during the industrial isomerization step. Consequently, the protein engineering solution found for the *A. missouriensis* enzyme can serve as a general solution (55). Glucose isomerase from *T. aquaticus* is the only group I enzyme in which nature has already substituted the lysine with an arginine (Fig. 4).

IV. PROPERTIES AS ENZYME

A. Substrate Specificity

Glucose isomerase catalyzes the reversible isomerization of monomeric keto sugars to their enol isomers. The natural substrate of this enzyme is D-xylose that is isomerized into D-xylulose. Other substrate/product combinations are: D-glucose/D-fructose, L-arabinose/L-ribulose, L-rhamnose/L-rhamnulose, D-ribose/D-ribulose, and others (2, 3).

The kinetic properties of the wild-type glucose isomerase from *Actinoplanes misouriensis* with xylose, glucose, and fructose were investigated (56–64). The results from Hosteaux (56) are summarized in Table 7. The data clearly show that the enzyme has a preference for xylose compared to glucose. The K_M values for xylose are, independent of the metal ion used, almost 2 orders of magnitude smaller than those for glucose or fructose. This means that the apparent affinity for xylose is 2 orders of magnitude higher. Furthermore, the k_{cat} values with xylose are twofold to 10-fold higher than with glucose or fructose (depending on the metal ion).

Consequently, the specificity constant (k_{cat}/K_M) for xylose is also much larger than for glucose. This means that in a solution containing equal concentrations of xylose and glucose, glucose isomerase will convert xylose at a much faster rate than glucose. Similar results were obtained for glucose isomerases from other sources (2, 3).

B. Effect of Environmental Factors

Under industrial conditions, glucose isomerase is used for several months at elevated temperatures (55–60°C) and at given pH. Therefore, the effects of the temperature and of the pH on both the activity and the stability of the enzyme are equally important parameters that determine the overall performance of the enzyme. The performance can be regarded as the product of the initial activity of the enzyme product times its stability as a function of time.

In general, the rate of an enzyme catalyzed reaction increases with temperature until a point where it starts to decrease again (temperature optimum). The reasons for this decrease may be twofold. First, the enzyme becomes so flexible at these temperatures that binding of the substrate (expressed by the K_M) becomes weaker. Secondly, the enzyme becomes unstable and starts to denature at a rate comparable with the time scale of the reaction. Most glucose isomerases have their temperature optimum ~ 75–85°C (2, 3). Table 6 shows that the k_{cat} values of glucose isomerase from *Actinoplanes missouriensis* with the different sugars are much higher at 60°C than at 35°C. However, the K_M values also increase, which may counteract the effect on the k_{cat} in case the substrate concentration is below the K_M values.

The rate of an enzyme-catalyzed reaction depends also on the pH. This is caused by titratable groups present on the amino acid residues in the enzyme and in the substrate and product. In the case that these groups are involved in substrate/product binding or the catalytic event, the change in charge will affect the rate. On the other hand, the stability of the enzyme may be affected by the pH as well. The pH optimum for glucose isomerases varies from microorganism to microorganism but is in general between 7 and 9.

Table 7 Kinetic Parameters for the Wild-Type Glucose Isomerase from *Actinoplanes missouriensis*

			T = 60°C			T = 35°C		
	Me^{2+}	pH	k_{cat} sec^{-1}	K_M mM	k_{cat}/K_M	k_{cat} sec^{-1}	K_M mM	k_{cat}/K_M
D-xylose	Mg^{2+}	7.2	64	22	2.9	17	4.8	3.6
		7.5						
	Mn^{2+}	5.0	8	73	0.10			
		5.2	16	59	0.27			
		5.4	22	58	0.38			
		6.0	27	60	0.45			
		6.4	29	58	0.50			
		6.9	31	57	0.54			
		7.5	—	—	—			
	Co^{2+}	5.0	23	56	0.41			
		6.9	33	46	0.71			
		7.5	—	—	—			
D-glucose	Mg^{2+}	7.3	30	290	0.10	5.1	230	0.022
	Mn^{2+}	5.0	0.8	300	0.003			
		6.0	2.4	740	0.003			
		6.9	4.8	1300	0.004	0.79	1400	5×10^{-4}
	Co^{2+}	5.0	12	1320	0.009			
		6.0	23	1320	0.017			
		6.9	23	1500	0.015			
D-fructose	Mg^{2+}	7.1	15.5	600	0.026	1.9	136	0.014
	Mn^{2+}	5.0				n.d.	$\gg$ 1M4	n.d.
		7.0				0.33	70	7×10^{-4}
	Co^{2+}	5.0				n.d.	$\gg$ 1M3	n.d.
		7.0				7	600	0.002

Initial rates were measured according to the procedures described in Section V. The metal ion concentrations were 10 mM for Mg^{2+} and 1 mM for Mn^{2+} and Co^{2+}.
Source: Ref. 56.

Table 7 shows that for the enzyme of *Actinoplanes missouriensis* k_{cat} increases when the pH increases from 5 to 7.5.

Since the pH dependence of the stability is more toward the acidic side and that for the activity more toward the alkaline side, the pH optimum for the industrial performance (= productivity) is somewhere between the optima for activity and stability (6).

Glucose isomerase has been the subject of extensive protein engineering studies. Not only has site-directed mutagenesis been used to determine the role of many amino acids in the mechanism of the reaction, but also it was used to increase the operational stability of the enzyme (52–55) and to modify the substrate specificity (60, 61) as well as the pH activity profile (62–64). Today, however, no mutant glucose isomerases are used in industrial processes.

C. Specific Mechanism of Action

The currently accepted pathway for the isomerization reaction involves the preferential binding of the sugar in the closed configuration (α-pyranose form for xylose and glucose and α-furanose form for fructose), followed by ring opening, extension of the substrate, and then proton transfer on the substrate (65). Because glucose isomerase is a metalloenzyme and requires Mg^{2+}, Mn^{2+} or Co^{2+} for its activity, in contrast to triose phosphate isomerase, which does not require metal ions for its activity and uses base catalysis to shuttle the proton between the C_1 and C_2 position of its linear substrate, it is now generally believed that glucose isomerase uses an alternative mechanism based on a 1,2-hydride shift as proposed by Farber et al. (15).

From the various 3D structures of the enzyme that were determined in the presence of metal ions and substrate, product, or their analogs, it has been concluded that there are two metal ion binding sites (15, 44). The role of these metal ions is to form a bridge between the enzyme and the sugar in the enzyme:substrate complex.

Metal site 1 is four-coordinated and tetrahedral in the absence of substrate and is six-coordinated and octahedral in its presence. Ligands are the carboxylates of Glu181, Glu217, Asp245, and Asp292 according to the *Actinoplanes missouriensis* numbering (59). Oxygen atoms O_2 and O_4 of the substrate bind to this metal ion 1. Metal site 2 is octahedral in all cases and is involved in the binding of oxygen atoms O_1 and O_2 of the substrate. Ligands are Glu217, Asp255, Asp257, and His220 (59).

Figure 4 shows that the amino acid residues that are the ligands for both metal ions are highly conserved in all glucose isomerases known today. Table 8 summarizes the conserved amino acid residues that play a role in the kinetic mechanism.

V. FACILITATION OF ACTIVITY DETERMINATIONS BY OTHER ENZYMES

The most convenient assay method for glucose isomerase is the one-step reaction using glucose or xylose as a substrate and sorbitol dehydrogenase and NADH in a coupled reaction (Fig. 6) (58, 67). The activity of xylose isomerase is measured at 35°C in a solution containing 0.028 M veronal-acetate buffer pH 7.0, 0.12 M NaCl, 10 mM $MgCl_2$, 0.15 mM NADH, and 0.06–0.6 units of sorbitol dehydrogenase (SDH). Depending on the type of experiment, the sugar concentration can be varied (for k_{cat} and K_M determinations) or is fixed at, e.g., 50 mM (for specific activity measurements). The disappearance of NADH is measured spectrophometrically

Table 8 Role of Amino Acid Residues in Glucose Isomerases

No.	AA	Conserved in group I/II	Role	Ref.
54	His	yes/yes	Not essential for catalysis Involved in anomeric selection and stabilization of the acyclic transition state by hydrogen bonding to O5	66
94	Phe	yes/yes	Not essential for catalysis Stabilizes the acyclic extended transition state directly by hydrophobic interactions and/or indirectly by interactions with Trp137 and Phe26	66
181	Glu	yes/yes	Ligand for metal binding site 1	59
183	Lys	yes/yes	Functions structurally by maintaining the position of Pro187 and Glu186 and catalytically by interacting with acyclic-extended sugars Mutants have little or no activity; no ring opening occurs	66
217	Glu	yes/yes	Ligand for meal binding site 1 and 2	59
220	His	yes/yes	Ligand for metal binding site 1 Mutants have little or no activity no ring opening occurs	66
245	Asp	yes/yes	Ligand for metal binding site 1	59
253	Lys	no/no	Stabilization of dimer interface Subject to glycation	66
255	Asp	yes/yes	Ligand for metal binding site 2	59
257	Asp	yes/yes	Ligand for metal binding site 2	59
292	Asp	yes/yes	Ligand for metal binding site 1	59

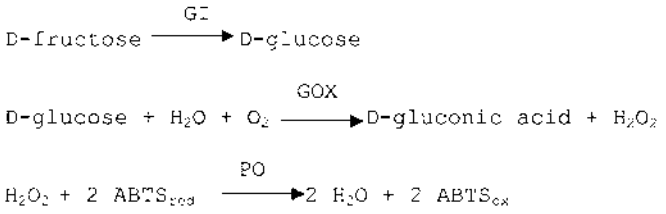

Figure 6 One-step assay for glucose isomerase using glucose or xylose as a substrate.

at 340 nm and quantified using an extinction coefficient of $6220\,M^{-1}\,cm^{-1}$.

The thermostability of sorbitol dehydrogenase prohibits carrying out this assay at more elevated temperatures (e.g., $> 40^{\circ}C$). Under these conditions, the same assay is carried out in two separate steps: first the isomerization reaction at high temperature, then dilution with cold buffer and subsequent measurement of the product formed with sorbitol dehydrogenase and NADH.

For the assay with fructose as a substrate (the "reverse reaction"), a two-step assay has been developed (Fig. 7) (68). In the first step, glucose isomerase isomerizes fructose to glucose. In the second step, glucose oxidase oxidizes the glucose formed to gluconic acid with the formation of hydrogen peroxide, while in the same step peroxidase is reducing hydrogen peroxide and oxidizing ABTS (2,2′-azino-di(3-ethylbenzthiazoline)-6-sulphonate, which can be measured and quantified spectrophotometrically at 420 nm. The activity of xylose isomerase is measured at $35^{\circ}C$ (or higher temperatures) in a solution containing 0.028 M veronal-acetate buffer, pH 7.0, 0.12 M NaCl, and 10 mM $MgCl_2$. Depending on the type of experiment, the fructose concentration is varied for k_{cat} and K_M determinations or fixed at, e.g., 50 mM for specific activity measurements. The reaction is stopped by adding $50\,\mu L$ mixture to 1 mL of a GOX-PO-ABTS solution that contains per 1 mL 0.1 M acetate buffer, pH 5, 9.5 units GOX (Sigma), 1.5 units PO (Boehringer), and 0.5 mg ABTS. After 30 min incubation at $35^{\circ}C$, the absorbance is read at 420 nm and $25^{\circ}C$, and the concentration of glucose is calculated using an extinction coefficient of $2220\,M^{-1}\,cm^{-1}$.

VI. PURIFICATION

Many different purification methods have been developed and published in order to obtain pure glucose isomerase for crystallization. In general, the complexity of the purification method and the number of steps involved depend on the expression level of the enzyme. This means that for the purification of xylose isomerase from non-recombinant strains, more steps are required to obtain a homogeneous preparation than from over-expressing strains. The various procedures comprise established techniques such as selective precipitation and chromatography on hydrophobic, ion exchange, or gel filtration resins. In addition, elegant procedures involving affinity chromatography have been shown to be very powerful.

A successful one-step purification procedure has been developed for glucose isomerase of *Actinoplanes missouriensis* (69) using immobilized metal affinity chromatography with copper as the affinity agent. This copper complexes strongly with the surface histidines of the enzyme. Cell-free supernatants containing the enzyme were applied to a column packed with Chelating Sepharose Fast Flow (Pharmacia) that was saturated before with copper ions using a 10 mg/mL $CuSO_4$ solution. Elution of the bound enzyme was provoked by lowering the pH of the elution buffer (MMA=20 mM MOPS + 20 mM MES + 20 mM acetate) from 7 to 5. This change in pH protonates the histidines and destroys the interaction with the copper ions. The resulting pure enzyme still contains some scavenged copper ions that are removed in a "polishing" step involving anion exchange chromatography on Mono-Q.

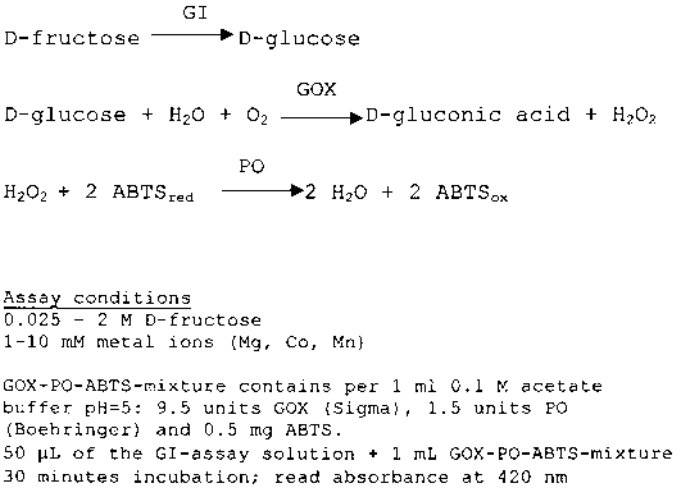

Figure 7 Two-step assay for glucose isomerase using fructose as a substrate.

ACKNOWLEDGMENT

I would like to thank my colleague Dr. Jan-Metske van der Laan for critically reading the manuscript, helpful suggestions, and preparing Figure 5.

REFERENCES

1. SH Bhosale, MB Rao, VV Deshpande. Molecular and industrial aspects of glucose isomerase. Microbiol Rev 60:280–300, 1996.
2. WP Chen. Glucose isomerase (a review). Process Biochem 15:30–41, 1980.
3. Xylose isomerase EC 5.3.1.5. In: D Schomburg, ed. Enzyme Handbook. Berlin: Springer-Verlag, 1990.
4. S Pederson. Industrial aspects of immobilized glucose isomerase. In: A Tanaka, T Tosa, T Kobayashi, eds. Industrial Application of Immobilized Biocatalysts. New York: Marcel Dekker, 1993, pp 185–208.
5. O Misset, J Labout, J Wilms, WJ Quax, CAG van Eekelen, HA Busnach. High fructose corn syrup. In: Biotechnological Innovations in Food Processing. Oxford: Butterworth-Heinemann, 1991, pp 145–187.
6. R Van Tilburg. Engineering aspects of biocatalysts in industrial starch conversion technology. PhD thesis, Technical University of Delft, 1983.
7. SR Marple, A Allerhand. Detailed tautomeric equilibrium of aqueous D-glucose. Observation of six tautomers by ultrahigh resolution carbon-13 NMR. J Am Chem Soc 109:3168–3169, 1987.
8. WJ Goux. Complex isomerization of ketoses: ^{13}C NMR study of the base-catalyzed ring-opening and ring-closing rates of D-fructose isomers in aqueous solution. J Am Chem Soc 107:4320–4327, 1985.
9. R Amore, CP Hollenberg. Xylose isomerase from *Actinoplanes missouriensis*: primary structure of the gene and the protein. Nucleic Acids Res 17:7515, 1989.
10. GC Saari, AA Kumar, GH Kawasaki, MY Insley, PJ O'Hara. Sequence of the *Ampullariella* sp. strain 3876 gene coding for xylose isomerase. J Bacteriol 169:612–618, 1987.
11. T Lovink-Anderson, PC Shaw, MK Shin, BS Hartley. D-Xylose (D-glucose) isomerase from *Arthrobacter* strain NRRL B3728. Gene cloning, sequence and expression. Biochem J 277:263–271, 1991.
12. Dauter, H Terry, H Witzel, KS Wilson. Refinement of glucose isomerase from *Streptomyces albus* at 1.65 Å with data from an imaging plate. Acta Crystallogr B 46:833–845, 1990.
13. Y Wang, Z Huang, X Dai, J Liu, T Cui, L Niu, C Wang, X Xu. The sequence of xylose isomerase gene from *Streptomyces diastaticus* No. 7 M1033. Chin J Biotechnol 10:97–103, 1994.
14. H Rasmussen, T La Cour, J Nyborg, M Schülein. Structure determination of glucose isomerase from *Streptomyces murinus* at 2.6 Å resolution. Acta Crystallogr D 50:124–131, 1994.
15. GK Farber, A Glasfeld, G Tiraby, D Ringe, GA Petsko. Crystallographic studies of the mechanism of xylose isomerase. Biochemistry 28:7289–7297, 1989.

16. T Kikuchi, Y Itoh, T Kasumi, C Fukazawa. Molecular cloning of the xylA gene encoding xylose isomerase from *Streptomyces griseofuscus* S-41: primary structure of the gene and its product. Agric Biol Chem 54:2469–2472, 1990.
17. HC Wong, Y Ting, HC Lin, F Reichert, K Myambo, KW Watt, PL Toy, RJ Drummond. Genetic organization and regulation of the xylose degradation genes in *Streptomyces rubiginosus*. J Bacteriol 73:6849–6858, 1991.
18. D Drocourt, S Bejar, T Calmels, J-P Reynes, G Tiraby. Nucleotide sequence of the xylose isomerase gene from *Streptomyces violaceoniger*. Nucleic Acids Res 16:9337–9337, 1988.
19. K Dekker, H Yamagata, K Sakaguchi, S Udaka. Xylose (glucose) isomerase gene from the thermophile *Thermus thermophilus*: cloning, sequencing, and comparison with other thermostable xylose isomerases. J Bacteriol 173:3078–3083, 1991.
20. WX Liao, L Earnest, SL Kok, K Jeyaseelan. Molecular cloning and characterization of the xylose isomerase gene from a thermophilic *Bacillus* species. Biochem Mol Biol Int 36:401–410, 1995.
21. R Jackson, J Brannigan, M Taylor. Submitted to the EMBL/GenBank/DDBJ databases (May 1996).
22. A Scheler, T Rygus, R Allmansberger, W Hillen. Molecular cloning, structure, promoters and regulatory elements for transcription of the *Bacillus licheniformis* encoded regulation for xylose utilization. Arch Microbiol 155:526–534, 1991.
23. T Rygus, A Scheler, R Allmansberger, W Hillen. Molecular cloning, structure, promoters and regulatory elements for transcription of the *Bacillus megaterium* encoded regulation for xylose utilization. Arch Microbiol 15:535–542, 1991.
24. M Wilhelm, CP Hollenberg. Nucleotide sequence of the *Bacillus subtilis* xylose isomerase gene: extensive homology between the *Bacillus* and *Escherichia coli* enzyme. Nucleic Acids Res 13:5717–5722, 1985.
25. F Kunst et al. (total 150). The complete genome sequence of the gram-positive bacterium *Bacillus subtilis*. Nature 390:249–256, 1997.
26. PG Meaden, J Aduse-Opoku, J Reizer, A Reizer, YA Lanceman, MF Martin, WJ Mitchell. The xylose isomerase-encoding gene (xylA) of *Clostridium thermosaccharolyticum*: cloning, sequencing and phylogeny of XylA enzymes. Gene 141:97–101, 1994.
27. VB Lawlis, MS Dennis, EY Chen, DH Smith, DJ Henner. Cloning and sequencing of the xylose isomerase and xylulose kinase genes of *Escherichia coli*. Appl Environ Microbiol 47:15–21, 1984.
28. RD Fleischmann, MD Adams, O White, et al. Whole-genome random sequencing and assembly of *Haemophilus influenzae* Rd. Science 269:496–512, 1995.
29. SD Feldmann, H Sahm, GA Sprenger. Cloning and expression of the genes for xylose isomerase and xylulokinase from *Klebsiella pneumoniae* 1033 in *Escherichia coli* K12. Mol Gen Genet 234:201–210, 1992.
30. Y-C Bor, C Moraes, SP Lee, WL Crosby, AJ Sinskey, CA Batt. Cloning and sequencing the *Lactobacillus brevis* gene encoding xylose isomerase. Gene 114:127–131, 1992.
31. BC Lokman, P van Santen, JC Verdoes, J Kruese, RJ Leer, M Posno, PH Pouwels. Organization and characterization of three genes involved in D-xylose catabolism in *Lactobacillus pentosus*. Mol Gen Genet 230:161–169, 1991.
32. C Sizemore, E Buchner, T Rygus, C Witke, F Goetz, W Hillen. Organization, promoter analysis and transcriptional regulation of the *Staphylococcus xylosus* xylose utilization operon. Mol Gen Genet 227:377–384, 1991.
33. K Dekker, H Yamagata, K Sakaguchi, S Udaka. Xylose (glucose) isomerase gene from the thermophile *Clostridium thermohydrosulfuricum*; cloning, sequencing, and expression in *Escherichia coli*. Agric Biol Chem 55:221–227, 1991.
34. Y-E Lee, RMV Amesh, JG Zeikus. Cloning, sequencing and biochemical characterization of xylose isomerase from *Thermoanaerobacterium saccharolyticum* strain B6A. J Gen Microbiol 139:1227–1234, 1993.
35. CY Lee, M Bagdasarian, MH Meng, JG Zeikus. Catalytic mechanism of xylose (glucose) isomerase from *Clostridium thermosulfurogenes*. Characterization of the structural gene and function of active site histidine. J Biol Chem 265:19082–19090, 1990.
36. Y Takeda, K Takase, I Yamato, K Abe. Sequencing and characterization of the xyl operon of a Gram-positive bacterium, *Tetragenococcus halophila* (*Pediococcus halophilus*). Appl Environ Microbiol 64:2513–2519, 1998.
37. C Vieille, JM Hess, RM Kelley, JGJ Zeikus. xylA cloning and sequencing and biochemical characterization of xylose isomerase from *Thermotoga neapolitana*. Appl Environ Microbiol 61:1867–1875, 1995.
38. M Suekane, M Tamura, C Tomimura. Physico-chemical and enzymatic properties of purified glucose isomerase from *Streptomyces olivochromogenes* and *Bacillus stearothermophilus*. Agric Biol Chem 42:909–917, 1978.
39. F Rey, J Jenkins, J Janin, I Lasters, P Alard, M Claessens, G Matthyssens, SJ Wodak. Structural analysis of the 2.8 Å model of xylose isomerase from *Actinoplanes missouriensis*. Proteins 4:165–172, 1988.
40. J Jenkins, J Janin, F Rey et al. Protein engineering of xylose (glucose) isomerase from *Actinoplanes missour-*

iensis. 1. Crystallography and site-directed mutagenesis of metal binding sites. Biochemistry 31:5449–5458, 1992.
41. K Henrick, CA Collyer, DM Blow. Structures of D-xylose isomerase from *Arthrobacter strain* B3728 containing the inhibitors xylitol and D-sorbitol at 2.5 Å and 2.3 Å resolution, respectively. J Mol Biol 208:129–157, 1989.
42. K Henrick, DM Blow, HL Carell, JP Glusker. Comparison of backbone structures of glucose isomerase from *Streptomyces* and *Arthrobacter*. Protein Eng 1:467–469, 1987.
43. Z Dauter, M Dauter, J Hemker, H Witzel, KS Wilson. Crystallization and preliminary analysis of glucose isomerase from *Streptomyces albus*. FEBS Lett 247:1–8, 1989.
44. A Lavie, K Allen, GA Petsko, D Ringe. X-ray crystallographic structures of D-xylose isomerase-substrate complexes position the substrate and provide evidence for metal movement during catalysis. Biochemistry 33:5469–5480, 1994.
45. GK Farber, GA Petsko, D Ringe. The 3.0 Å crystal structure of xylose isomerase from *Streptomyces olivochromogenes*. Protein Eng 1:459–466, 1987.
46. M Whitlow, AJ Howard, BC Finzel, TL Poulos, E Winborne, GL Gilliland. A metal-mediated hydride shift mechanism for xylose isomerase based on the 1.6 Å *Streptomyces rubiginosis* structures with xylitol and D-xylose. Proteins 9:153–173, 1991.
47. HL Carrell, BH Rubin, TJ Hurley, JP Glusker. X-ray crystal structure of D-xylose isomerase at 4 Å resolution. J Biol Chem 259:3230–3236, 1984.
48. HL Carrell, JP Glusker, V Burger, F Manfre, D Tritsch, J-F Biellmann. X-ray analysis of D-xylose isomerase at 1.9 Å: native enzyme in complex with substrate and with a mechanism-designed in activator. Proc Natl Acad Sci USA 86:4440–4444, 1989.
49. C Chang, BC Park, D-S Lee, SW Suh. Crystal structures of thermostable xylose isomerases from *Thermus caldophilus* and *Thermus thermophilus*: possible structural determinants of thermostability. J Mol Biol 288:623–634, 1999.
50. O Gallay, R Chopra, E Conti, P Brick, R Jackson, B Hartley, C Vieille, JG Zeikus, D Blow. Crystal structures of class II xylose isomerases from two thermophiles and a hyperthermophile. (Submitted to the PPB data bank [Nov. 97].)
51. DW Banner, AC Bloomer, GA Petsko, et al. Structure of chicken muscle triose phosphate isomerase determined at 2.5 Å resolution using amino acid sequence data. Nature 255:609–614, 1975.
52. WJ Quax, NT Mrabet, RGM Luiten, PW Schuurhuizen, P Stanssens, I Lasters. Enhancing the thermostability of glucose isomerase by protein engineering. BioTechnology 9:738–742, 1991.
53. NT Mrabet, A Vandenbroeck, I Vandenbrande et al. Arginine residues as stabilizing elements in proteins. Biochemistry 31:2239–2253, 1992.
54. WJ Quax. Thermostable glucose isomerases. Trends Food Sci Technol 4:31–34, 1993.
55. RGM Luiten, WJ Quax, PW Schuurhuizen, M Nadir. Novel glucose isomerase enzymes and their use. European patent 0351029 to Gist-brocades and Plant Genetic Systems, 1990.
56. P Hosteaux. D-xylose isomerase uit *Actinoplanes missouriensis*: katalytische eigenschappen na mutagenese van het actief centrum. PhD thesis, University of Ghent, 1992.
57. P Vanbastelaere. Wild type en mutant D-xylose isomerasen: invloed van de metaalionbinding op de katalytische eigenschappen. PhD thesis, University of Ghent, 1994.
58. M Callens, H Kersters-Hilderson, O Vanopstal, CK de Bruyne. Catalytic properties of D-xylose isomerase from *Streptomyces violaceoruber*. Enzyme Microb Technol 8:696–700, 1986.
59. J Jenkins, J Janin, F Rey et al. Protein engineering of xylose (glucose) isomerase from *Actinoplanes missouriensis*. 1. Crystallography and site-directed mutagenesis of metal binding sites. Biochemistry 31:5449–5458, 1992.
60. A-M Lambeir, M Lauwereys, P Stanssens, et al. Protein engineering of xylose (glucose) isomerase from *Actinoplanes missouriensis*. 2. Site directed mutagenesis of the xylose binding site. Biochemistry 31:5459–5466, 1992.
61. A-M Lambeir, I Lasters, WJ Quax, JM van der Laan. Glucose isomerases having altered substrate specificity. US patent 5310665 to Gist-brocades and Plant Genetic Systems, 1994.
62. H van Tilbeurgh, J Jenkins, M Chiadmi, J Janin, SJ Wodak, NT Mrabet, A-M Lambeir. Protein engineering of xylose (glucose) isomerase from *Actinoplanes missouriensis*. 3. Changing metal specificity and the pH profile by site directed mutagenesis. Biochemistry 31:5467–5471, 1992.
63. A-M Lambeir, I Lasters, N Mrabet, WJ Quax, JM van der Laan, O Misset. Modified prokaryotic glucose isomerase enzymes with altered pH-activity profiles. US Patent 5340738 to Gist-brocades and Plant Genetic Systems, 1994.
64. A-M Lambeir, I Lasters, N Mrabet, WJ Quax, JM van der Laan, O Misset. Glucose isomerases with an altered pH optimum. US Patent 5384257 to Gist-brocades and Plant Genetic Systems, 1994.
65. KN Allen, A Lavie, GK Farber, A Glasfeld, GA Petsko, D Ringe. Isotopic exchange plus substrate and inhibition kinetics of D-xylose isomerase do not support a proton-transfer mechanism. Biochemistry 33:1481–1487, 1994.

66. RD Whitaker, Y Cho, J Cha, HL Carrell, JP Glusker, PA Karplus, CA Batt. Probing the role of active site residues in D-xylose isomerase. J Biol Chem 270:22895–22906, 1995.
67. H Kersters-Hilderson, M Callens, O Vanopstal, W Vangrysperre, CK de Bruyne. Kinetic characterization of D-xylose isomerase by enzymatic assays using D-sorbitol dehydrogenase. Enzyme Microb Technol 9:145–148, 1987.
68. W Werner, H-G Rey, H Wielinger. Uber die Eigenschaften eines neuen chromogens für die Blutzuckerbestimmung nach der GOD/POD-Methode. Z Anal Chem 252:224–225, 1970.
69. NT Mrabet. One-step purification of *Actinoplanes missouriensis* D-xylose isomerase by high-performance immobilized copper-affinity chromatography: functional analysis of surface histidine residues by site-directed mutagenesis. Biochemistry 31:2690–2702, 1992.